

CHEMICALLY MODIFIED ELECTRODES IN LIQUID CHROMATOGRAPHY DETECTION: A REVIEW

RICHARD P. BALDWIN*

Department of Chemistry, University of Louisville, Louisville, KY 40292, U.S.A.

KARSTEN N. THOMSEN

Environmental Engineering Laboratory, Department of Civil Engineering, University of Aalborg, Sohngaardsholmsvej 57, DK 9000 Aalborg, Denmark

(Received 6 April 1990. Accepted 28 June 1990)

Summary—Recent trends in the use of chemically modified electrodes (CMEs) in electrochemical detection systems used in flow-injection analysis or high-performance liquid chromatography are reviewed, with the objective of indicating the most promising approaches for practical CME applications. Four specific application areas of CMEs are identified: (1) those using perm-selective coatings to enhance selectivity and inhibit surface fouling, (2) those using immobilized electron-transfer mediators to catalyse slow electrode reactions, (3) those using enzymes as modifiers to provide biological activity on the electrode surface and (4) those using ion-exchange coatings for the electrochemical detection of non-electroactive anions and cations. By virtue of these approaches, the judicious use of CMEs has already had a significant impact on the performance and scope of electrochemical detection in flow systems. The most important improvements have been in CME selectivity, which produces simpler assay procedures with less need for sample treatment, and increased usefulness for complex samples, and in CME reactivity, which expands the range of analytes amenable to electrochemical monitoring.

Although the idea of chemically modified electrodes (or CMEs) was first demonstrated systematically only in the early 1970s, this approach has assumed a dominant position in modern electrochemistry. These electrodes, which are made by incorporating specific chemical groupings or "microstructures" on otherwise conventional electrode surfaces, are of interest because their responses have two completely separate components: the usual electrochemical component determined by the potential at which the electrode is maintained instrumentally and an additional chemical component determined by the reactivity of the attached group. Consequently, CMEs offer not only easily variable redox characteristics but also the possibility of adjustable physical and chemical properties (such as charge, polarity, chirality, permeability). Therefore, to a much greater extent than is possible with classical or "unmodified" electrodes, CMEs can be targeted for a specific application or investigation and rationally designed to provide an optimal environment for that task.

Pioneering studies demonstrating the varied synthetic approaches by which modifiers can be

incorporated and the useful properties and applications that can result from modification have been the subject of several reviews.¹⁻⁵ In addition, hundreds of papers per year are published on CMEs. Of the disciplines directly affected by these developments, analytical chemistry is certainly one of the foremost; and virtually all the important analytical properties of electrodes—sensitivity, selectivity, reproducibility and even applicability—have been shown to be capable of enhancement by the judicious use of chemical modification. For example, CMEs capable of extremely selective binding and preconcentration of trace metals have been developed by utilizing well-known chelating agents such as EDTA and dimethylglyoxime as modifiers. Alternatively, effective rates of electron transfer have been improved for numerous compounds by attachment of electrocatalytic functional groups to the electrode surface. A few specific modifications—for example, the deposition of a polymer film such as Nafion—have been so successful that their use has become nearly routine. However, most modifications, although often well-conceived, offer advantages which have not yet been exploited in practical analysis.

*Author for correspondence.

The applications in which CMEs are probably closest to success in solving practical analytical problems are as amperometric detectors in flow-injection analysis (FIA) and liquid-chromatography (LCEC) systems. Over the past 20 years, the use of conventional electrodes for this purpose has become well established as an analytical technique offering extremely high sensitivity for analytes that are electroactive at modest potentials.⁶ For example, LCEC with glassy-carbon electrodes has become the method of choice for the determination of many easily oxidized biochemical compounds such as catechols, phenols and aromatic amines. As a result, LCEC instrumentation has become commercially available from several companies and is commonly used in analytical and clinical laboratories throughout the world.

Recently a diverse range of CMEs has begun to be applied in both flow-injection and liquid-chromatography systems to achieve impressive enhancements in electrode performance. The most important of these studies to date have involved the use of perm-selective coatings to enhance selectivity or inhibit electrode fouling, the use of bound electron-transfer mediators to catalyse slow electrode processes, the use of protein and enzyme modifiers to provide biological activity and the use of ion-exchange coatings for the electrochemical detection of non-electroactive ions. In this survey we will review some of the most interesting recent work and attempt to indicate some of the most important directions which the field is likely to take. We will begin by briefly examining the fabrication of CMEs and the most important CME characteristics for quantitative flow-stream applications, and then summarize specific applications from the past few years. As will be seen, the capabilities of CMEs can be imaginatively employed to enhance the analytical performance and scope of electrochemical detection in flow systems.

CONSTRUCTION OF THE ELECTRODES

Over the past 15 years, dozens of individual procedures have been reported for the immobilization of hundreds of different species on various electrode materials.^{1,2} However, virtually all these procedures are based on only a few approaches:

(1) direct adsorption of the modifier onto the bare electrode surface;

- (2) covalent binding of the modifier to a specific surface site;
- (3) physical coating of the electrode surface with a polymer that contains the modifier grouping;
- (4) mixing of a slightly soluble modifier with a conductive matrix (such as a carbon paste).

Each of these general approaches has been well characterized experimentally and thoroughly reviewed and discussed in the literature, so detailed description is not necessary here. Suffice it to say that several synthetic routes are likely to be available for the surface attachment of most modifiers and that some flexibility in choosing or designing an attachment method should usually be possible. This is especially important in usage of CMEs in analytical applications, because of the stringent demands on electrode stability and reproducibility if the electrode is to be of use in routine determinations.

The ideal CME for analytical applications involving continuous, long-term operation in a flow system should possess most of the following characteristics: good mechanical and chemical stability of the electrode substrate, the modifier and the electrode-modifier linkage; good short-term reproducibility and long-term stability of the modifier's activity towards the analyte; flexible modifier loading levels; a wide dynamic range (ideally linear) of response; low and stable background currents over the potential range required; compatibility with a wide range of aqueous and organic matrices; simple and reliable fabrication that results in consistency of response from one electrode to another. These properties are mainly those desired for a conventional electrode, plus the requirements regarding the attachment and activity of the modifier. Obviously, a CME that takes longer to prepare than it lasts in use, or has an activity which is fleeting or irreproducible, possesses very limited appeal for the analyst.

Of the four methods listed above, the last two—mixing with carbon paste and coating with a functionalized polymer—seem to approach most closely this set of ideal characteristics. The carbon-paste approach is undoubtedly the easiest method of fabrication and provides for rapid and acceptably reproducible generation of fresh modified surfaces. Relatively large batches of modified paste can be prepared in a few minutes by

simply hand-mixing appropriate portions of modifier, graphite powder and organic binder. Moreover, such mixtures can be packed into an electrode assembly, used and then provided with a new surface by extrusion and repolishing to give the same reproducibility (2–5% variation) as ordinary carbon paste. In practice, this method is limited to use in predominantly aqueous solvents (to keep the carbon paste intact) and to use of modifiers possessing only slight solubility in water. An interesting variation, suggested initially as a means of overcoming the solubility limitation, involves mixing the modifier with solid matrices such as graphite epoxy⁹ and polystyrene containing either carbon particles¹⁰ or carbon fibres.¹¹ Although this method for the construction of solid composite CMEs has not yet become widely used, its potential utility for flow applications in both aqueous and organic solvent systems is readily apparent.

The polymer-based approach is somewhat more difficult to execute, because it requires a means of including the modifier group in the polymer to be deposited on the electrode. However, once this has been accomplished, the CMEs can usually be formed from the bare electrode and functionalized polymer by simple and straightforward procedures such as dip-coating and evaporative deposition. In some instances, the polymerization and modification steps can be conveniently combined in a single electro-polymerization operation involving oxidation or reduction of the monomer at the bare electrode. The resulting polymer CMEs often have much greater chemical and mechanical stability than analogous carbon-paste CMEs and are able to operate in a wider range of aqueous and organic matrices. Furthermore, it is usually possible to control the thickness of the modifying polymer film, and thus the loading level of the modifier on the electrode surface, by relatively straightforward procedures. However, the ease and reproducibility of regeneration of polymer surfaces are likely to be somewhat less than for carbon-paste CMEs. When the modifier of interest (*e.g.*, metal particles^{12,13} or enzymes^{14,15}) can be stably trapped inside the polymer network, polymer-based CMEs can be constructed by simply depositing the polymer onto the electrode surface from a solution containing a dispersion of the modifier.

We have employed both these approaches with considerable success for making CMEs to be used for detection in flowing streams. Incorporation of the modifier into carbon paste can

often be used for evaluation of modifiers; but once optimization has been completed, the polymer method may be preferred for long-term applications.

APPLICATIONS

The principal improvements resulting from application of CMEs in FIA and LCEC have generally involved the use of (1) perm-selective coatings that restrict access of solute to the electrode surface, (2) electrocatalytic redox modifiers that activate the electrode toward solutes that exhibit substantial overpotentials, (3) enzymes and related biomolecules as modifiers as a means of incorporating specific biological activity and (4) electroactive polymer films for the electrochemical detection of non-electroactive ionic analytes. Each of these application areas will be considered in turn. While striving for a degree of completeness in this survey, our primary goal has been to focus on very recent CME applications that appear to have immediate potential for use in practical analysis. With this emphasis in mind, we have chosen to omit consideration of several CMEs which, despite exhibiting interesting properties, seem unlikely to offer useful FIA or LCEC applications.

Perm-selective mass transport

Two related ideas, both of which derive from coating the electrode with a thin semi-permeable membrane, form the basis of the applications included under this classification. First, this kind of modification may improve the selectivity of response if the membrane coating preferentially excludes some electroactive species from the electrode surface. Secondly enhanced stability and reliability can be obtained if the solutes excluded would otherwise be adsorbed on the bare surface and foul it; in these cases, electrochemical methods may be applied directly to samples which would normally require extensive pretreatment for removal of the adsorbable material.

The membranes concerned consist of polymer films coated onto electrodes made from conventional materials. The films themselves must be relatively thin (a few μm in thickness) so that transport of the analyte to the electrode surface is not too restricted. However, as even monolayers will decrease transport of the analyte to some degree, the optimal thickness

always reflects a compromise between the efficient exclusion of interfering species and the free and rapid diffusion of the analyte that is required to avoid peak broadening and tailing effects detrimental to practical analysis in flow systems. Most important, of course, are the particular structural features of the membrane that determine its permeability and, therefore, the CME selectivity. Most commonly, these include the presence of fixed anionic or cationic sites in the membrane, the existence of well defined hydrophobic or hydrophilic regions and the maximum pore size available for internal diffusion through the film. As a result, the selectivity of transport at the CME can normally be related to solute charge, polarity and molecular size or shape. Thus, the frequently studied Nafion, which is a non-crosslinked perfluorinated polymer containing strongly acidic sulphonate groups, is permeable to cationic and neutral species and excludes anions rather well. This capability, which has most notably been taken advantage of to facilitate the *in vivo* determination of catecholamines in the presence of high levels of ascorbate,¹⁶ has been thoroughly studied in terms of the effects of buffer cation and concentration, pH, polymer film thickness and concentration of organic solvent in the medium.¹⁷ Conversely, the use of cationic polymers such as polyvinylpyridine (protonated at $\text{pH} < 6$) has been shown to alter the CME selectivity to favour negatively charged analytes.¹⁸

Perhaps the most interesting CMEs in this category are those utilizing a coating of cellulose acetate. This polymer, initially suggested for use in LCEC applications by Sittampalam and Wilson¹⁹ and subsequently exploited extensively by Wang and co-workers^{18,20-22} is uncharged and therefore shows no preference for anions or cations. However, it undergoes slow hydrolysis and pore formation when exposed to alkaline media. Thus, by variation of the pH and duration of the hydrolysis, the pore size of the polymer coating can be controlled so that access to the electrode surface is restricted to molecules smaller than a limiting size (or with suitable shape). For example, only small species such as H_2O_2 may be able to pass an unhydrolysed cellulose film efficiently,¹⁹ whereas substantially larger analytes such as phenol, acetaminophen and ascorbic and uric acids are able to reach the electrode surface and contribute to the current through a coating hydrolysed for 30 min in dilute potassium hydroxide solution.²⁰ In both

cases, however, the ability of the cellulose polymer to resist fouling by macromolecules is sufficiently preserved in a flow-stream for repeated exposure of the coated electrode to the levels of proteins found in physiological matrices to result in little or no decrease in sensitivity. In a very recent report²³ it was shown that a poly(3-methylthiophene) coating formed by electro-polymerization of the monomer onto glassy carbon largely eliminated the electrode fouling problem that occurs upon electro-oxidation of phenols. Two explanations for the success of this CME were offered. One was that the polymeric products formed by oxidation of phenols tend to be less adsorbed than on a bare metal or carbon electrode. Alternatively, the structure of the coating might be such that processes leading to dimerization (and eventual polymerization) of the initially formed phenoxy radicals are substantially hindered. In either case, extremely stable responses to relatively high concentrations of phenol were obtained at this CME in static and flow experiments.

Selectivity can be enhanced by combining charge, size and other CME effects in bi- and multilayer electrode systems. For example, the size selectivity of a cellulose acetate coating can be supplemented by the activity of additional catalyst- or enzyme-containing layers similar to those discussed below. Examples of these and other perm-selective CME applications are given in Table 1.

Electrocatalysis by bound mediators

The basic principle involved in CME electrocatalysis by a surface-confined electron-transfer mediator is illustrated in Fig. 1 for a generalized oxidation process. In this sequence, the analyte diffuses from the bulk solution to the electrode surface, where it is oxidized in a purely chemical reaction with the oxidized form of the mediator (M_{ox}). However, the potential of the electrode is maintained at a value sufficiently positive for M_{ox} to be the stable state of the mediator and its reduced form (M_{red}) to be rapidly re-oxidized to the catalytically active form. Thus the heterogeneous electron transfer takes place between the electrode and mediator and not directly between the electrode and analyte. In essence, then, the mediator can be considered to function

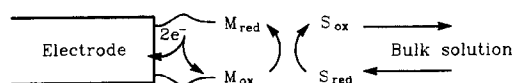


Fig. 1

Table 1. CME applications based on perm-selective coatings

CME	Analyte	Summary
Cellulose acetate on platinum ¹⁹	H ₂ O ₂	The cellulose film prevented adsorption of proteins and other surface-active substances. Although the currents observed were only a twentieth of those for an equivalent bare electrode, the calibration curve for H ₂ O ₂ at the CME remained essentially constant in the presence of bovine serum albumin or undiluted serum, compared to a 50% decrease over time with an uncoated Pt electrode. In addition, the H ₂ O ₂ oxidation current was not affected by the presence of glucose and ascorbic acid at physiological levels.
Cellulose acetate on glassy carbon ²⁰	Various small electroactive compounds	The permeability of the cellulose membrane toward analytes of different molecular size was varied by hydrolysis in KOH for different times up to 50 min. In FIA the detection of phenol and acetaminophen at a partially hydrolysed cellulose film was virtually unaffected by the presence of nitrophenols and ferrocyanide, respectively. Urine samples, pretreated only by filtration and dilution, gave simplified chromatograms suitable for the direct determination of ascorbic and uric acids. In addition, the cellulose coating improved the stability of the electrode towards exposure to bovine serum albumin and passivation by phenol oxidation products.
Cellulose acetate on glassy carbon ²¹	Various small electroactive compounds	One of a pair of glassy-carbon electrodes was coated with a cellulose acetate polymer film, the permeability of which was varied by alkaline hydrolysis for different times. When both electrodes were held at the same potential and operated in the parallel-opposed configuration, the CME detection gave simplified chromatograms, showing a response for only the smaller analyte species in diluted urine samples and beer extracts. Ratios of the peak current from the coated and uncoated surfaces were used to increase selectivity and aid in peak identification.
Nafion on glassy carbon ²⁴	Catecholamine neurotransmitters	Coating the electrode with a layer of the cation-exchanger Nafion caused it to favour cationic analytes rather than anionic or neutral ones, <i>e.g.</i> , catecholamine neurotransmitters relative to ascorbic and uric acids, bilirubin and chlorpromazine. In addition to this charge selectivity, the CMEs had a decreased flow-rate dependence and therefore less noise. By combining the Nafion film with an outer cellulose acetate coating, a bilayer electrode offering both cation preference and antifouling properties was obtained. The CME was applied to the analysis of urine samples.
Nafion on glassy carbon ²⁵	Catechols and related compounds	The response of dual glassy-carbon electrodes, one bare and the other coated with a Nafion film, was examined with respect to selectivity for charged and neutral analytes and stability in flow systems. The current observed for cationic species (dopamine and epinephrine) was only slightly diminished at the Nafion CME, while that for neutral molecules (catechol and hydroquinol) was decreased to a greater extent and that for anions (3,4-dihydroxybenzoate and ascorbate) was very small. Signal dependence on Nafion film thickness, flow-rate and pH was characterized. The Nafion CME was stable in methanol (30%) and CH ₃ CN (10%) and showed no passivation from exposure to albumin.
Poly(4-vinylpyridine), PVP, on glassy carbon ¹⁸	Chlorpromazine, uric and ascorbic acids, acetaminophen	PVP films, which are cationic at pH < 6, showed highly attenuated responses to catecholamines and other positively charged species, but still exhibited large currents for anionic and neutral analytes. This effect was illustrated by LCEC of ascorbic and uric acids in human urine. Bilayer CMEs containing both PVP and cellulose films rejected both cations and large surfactant molecules such as gelatin.
Cobalt phthalocyanine and cellulose acetate on glassy carbon ²	Oxalic and ascorbic acids, N ₂ H ₄ , cysteine	A CME exhibiting both size-selective and electrocatalytic response was obtained by co-depositing sparingly soluble cobalt phthalocyanine and a cellulose film. The bifunctional CME retained the electrocatalytic activity of the cobalt complex for the oxidation of N ₂ H ₄ , oxalic acid, and cysteine, while the permeability of the modifier coating was determined by the extent of alkaline hydrolysis of the cellulose. In FIA, lower potentials could be used for detection; decreased fouling by surface-active agents such as gelatin and albumin was observed), and increased selectivity to small analytes was confirmed. As the detection limit estimated for N ₂ H ₄ was 1 μM, the presence of the coating did not significantly affect the trace analysis capabilities of the system.
Poly(ester sulphonic acid) on glassy carbon ²⁶	Catechols and related compounds	Films of the poly(ester sulphonic acid) cation-exchanger Eastman-AQ55D excluded anions while allowing and sometimes enhancing transport of cationic and neutral compounds. Stable response was obtained in FIA for acetaminophen in the presence of an excess of bovine serum albumin.
Bilayers of Nafion and collagen on gold ²⁷	Glucose	The determination of glucose at physiological levels was possible by FIA and pulsed amperometric detection at polymer-coated Au electrodes. An inner Nafion layer acted to retain OH ⁻ at the Au surface while excluding normal levels of Cl ⁻ , amino-acids and ascorbic and uric acids. An outer collagen film prevented protein penetration and adsorption. Excellent glucose response was obtained for blood serum samples.
Poly(3-methylthiophene) on glassy carbon ²³	Phenols	These CMEs exhibited good resistance to the fouling normally caused in FIA by high concentrations of phenol.

simply as an electron shuttle between the electrode and the analyte. Of course, this sequence of events represents an idealized picture, that may often be more complex in practice. For example, if the CME has a thick or multilayered modifier coating, electron transport may take place either by direct conduction through the film or by "hopping" from one modifier group to another; in either case, the mediator group specifically reacting with the analyte does not need to be in the immediate vicinity of the electrode surface. Finally, it should be apparent that corresponding, but converse, processes would be involved in an electrocatalysed reduction.

The need for mediation of this sort arises whenever the rate of direct electron transfer is slow. When this happens at an ordinary electrode, a potential in excess of the analyte's thermodynamic potential, *i.e.*, an overpotential, must be applied in order for the desired redox process to proceed at an appreciable rate. Unfortunately, in flow-injection and liquid-chromatography applications, the use of more extreme potentials affects both the selectivity and the detection limit, to an extent depending on the overpotential required. With an electrocatalytic CME, however, the oxidation (or reduction) of the analyte is made to take place at the redox potential of the mediator. This must, of course, be higher than the analyte's thermodynamic potential, but in favourable cases can be 500 mV or more lower than that needed when the bare electrode is used. Decreases of this magnitude in the applied potential can substantially improve the analytical performance. In particular, decreased detection potentials can be expected to result in improved detection limits and greater selectivity, because of the lower noise levels and restricted range of sample components electrolysable at the lower potentials. More important, however, are the instances where the changes in potential made possible by electrocatalytic effects permit electrode processes that would normally occur at potentials near or beyond those for solvent breakdown to be shifted to a practically useful range of applied potential. In these cases, the advantages of LCEC can be extended by electrocatalytic CMEs to new groups of compounds that give no analytically useful response at ordinary electrodes.

The solution-phase electrocatalysis of many important substrates has been studied quite extensively, and a great deal of chemical

information relevant to the selection of electrocatalytic mediators as electrode modifiers is available. Certainly, CMEs applied to electrocatalysis studies in static media have successfully employed mediators of all varieties, both organic and inorganic.^{1,2} However, studies involving FIA or LCEC have been much more limited, primarily employing a few well-known metal-based catalysts as modifiers. These include, most notably, cobalt phthalocyanine in carbon paste²⁸⁻³⁷ and inorganic ruthenium polymer electro-deposited onto either platinum or glassy carbon.³⁸⁻⁴² These particular modifiers have been the most frequently used because, in addition to their catalytic activity towards a wide variety of analytes, both possess very limited solubility and therefore can be placed very stably onto electrode surfaces for flow applications. For the cobalt phthalocyanine CME, the response of which is initiated by electro-oxidation of the Co(II) centre to Co(III), analytes determined by FIA or LCEC have included hydrazine, thiols, oxalic acid, α -keto-acids, carbohydrates (mono- and polysaccharides), ribonucleosides, alditols and aldonic, uronic and aldaric acids. At the ruthenium-based CME, where the mediator redox process is the oxidation of Ru(II) to Ru(III), analytes have included As(III), thiocyanate, hydrazine and, most recently, several thiols, including cysteine, glutathione and the 50-amino-acid hormone insulin. A strength of all the electrocatalytic CME systems summarized in Table 2 is that they typically offer very low detection limits, usually in the nanogram range.

Finally, some mention should be made of a group of metal oxide electrodes which, although not technically CMEs, bear some similarity to them in their very extensive LCEC applications. The metals of interest here include Pt,⁴⁸⁻⁵⁰ Au,⁵¹⁻⁵⁴ Ni,⁵⁵⁻⁵⁸ Cu⁵⁹⁻⁶² and Ru.⁶³ With the noble metals Pt and Au, the major function of the oxide or hydroxide layer is thought to be to provide a catalytic surface capable of dehydrogenation or oxygenation reactions with the analyte species. Invariably, the products of these anodic processes are strongly adsorbed on the metal and lead to a rapid loss of signal by blocking the surface sites necessary for further oxidations. Removal of the passivating film and re-activation of the electrode is most easily accomplished by applying an oxidizing potential. Thus, stable long-term operation of Pt and Au electrodes nearly always requires the use of regularly pulsed potential waveforms that must

be supplied by the control instrumentation. With Ni, Cu and Ru, the oxide layer apparently serves both electrocatalytic and passivating functions and allows the operation of the electrode at potentials where the bare metals would undergo rapid oxidation. Fouling by oxidation products is generally not a significant problem here, and detection can be done at constant potential. Thus, in a very broad sense, these oxide films, generated *in situ* by a combination of potential and solution conditions, might be considered as electrode modifications designed to impart catalytic and passivating properties. Inclusion of these "CMEs" in this survey is justified for this reason and because of the impressive success of this approach in producing highly sensitive amperometric detection for several families of compounds not otherwise amenable to electrochemical monitoring. The most notable analytes detectable with the metal oxide electrode systems are the carbohydrates and related chemical families. However, attractive detection capabilities for other important analytes (*e.g.*, amino-acids) have also been observed.^{49,50,54,56,59} Metal oxide electrodes nearly always provide their optimum performance in strongly basic solution, often giving detection at or below the nanogram level.

Biological activity

Recent advances in the study of biological molecules and processes have had an enormous impact on many areas of chemistry, not the least of which is electroanalysis. First, there is an immediate need to devise and develop analytical methods suitable for the identification and quantification of a vast array of biologically important molecules. At the same time, there is a great opportunity for improving the analysis by taking advantage of the unique reactivity and recognition properties possessed by these same biomolecules. Thus, it is not surprising that recent years have witnessed a great deal of activity related to the design and application of electrochemical sensors, often incorporating biologically active molecules or structures, for use in a wide variety of bio-assays. The principal approaches, including those utilizing CMEs, have been reviewed by Frew and Hill.⁶⁴

The focus of virtually all CME utilization for bioanalysis has been the development of electrodes exhibiting improved electrochemical activity towards biomolecules, especially enzymes. When coupled with FIA or LCEC, this "improved reactivity" has been directed to

the determination of either the enzymes themselves or their substrates. These studies, listed in Table 3, will be considered in this section.

In the simplest approach, a CME with a surface-bound moiety capable of promoting or catalysing the oxidation or reduction of the protein of interest is used to determine it. Modification is necessary because, in spite of the fact that many enzymes and proteins contain functional groups that can readily be oxidized or reduced by purely chemical agents, most such molecules do not undergo facile oxidation or reduction at conventional electrodes. The electroactive centre is often shielded within the protein's extended three-dimensional structure and cannot gain access to the electrode surface. Alternatively, strong adsorption of the protein can occur and cause the electrode surface to become passivated. In both cases, the problem may often be solved by the use of CMEs. For example, in an extension of work on static systems by Eddowes and Hill⁶⁵ and Taniguchi *et al.*,⁶⁶ Schlager and Baldwin⁶⁷ showed that a gold electrode coated with a 4,4'-dipyridyl disulphide film can be used at very low potentials for the LCEC of cytochrome *c*. Apparently, the pyridyl groups on the CME can promote the protein redox reaction by interacting with positively charged lysine residues on cytochrome *c* and orienting the protein's haem group favourably for direct electron transfer to the electrode surface. The same research group later demonstrated that incorporation of traditional organic electron-transfer mediators can be used to make electrocatalytic CMEs for the haem-containing proteins myoglobin and haemoglobin⁶⁸ and for the copper protein ceruloplasmin.⁶⁹ In these studies, stable and sensitive detection with limits in the 1–10 pmole range was generally obtained. On the basis of these results, it would appear that CMEs tailored for other redox proteins might be similarly conceived and constructed for flow applications. A straightforward approach to protein detection would be to employ the dozens of electron-transfer mediators already in use for solution-phase oxidation or reduction of these biomolecules.⁷⁰

Apart from the above-mentioned work, which was focused on detection of the proteins themselves, several other studies have attempted to incorporate the enzymes into CME systems for the purpose of detecting the enzyme substrate. The principal attraction of this approach is that it allows the inherently high *sensitivity* of electrochemical detection to be combined with

Table 2. CME applications using electrocatalytic modifiers

CME	Analyte	Summary
Cobalt phthalocyanine (CoPC) in carbon paste ²⁸	N ₂ H ₄	The catalytic oxidation of hydrazine at this electrode was employed in FIA. Detection was performed at -0.1 V vs. Ag/AgCl in 0.20 M NaOH, which is several hundred mV less than that required at an unmodified carbon electrode. Linear response was observed for N ₂ H ₄ concentrations from 10^{-8} to 10^{-3} M, giving a detection limit of less than 1 pmole. The CME response in NaOH was stable for 7–8 hr and was not seriously degraded by operation in 10% CH ₃ OH or CH ₃ CN.
CoPC in carbon paste ^{29,30}	Thiols, including cysteine, homocysteine, N-acetylcysteine and glutathione	The CME catalysed the electro-oxidation of thiols at $+0.75$ – 0.85 V vs. Ag/AgCl. Used in conjunction with reverse-phase chromatography, the CME exhibited linear response for cysteine from 2.7 to 270 pmole. Individual electrodes were sufficiently stable for a full day of continuous use and surfaces could be reproduced with a relative standard deviation of 7%. LCEC assay procedures using the CME were developed for cysteine and glutathione in whole blood and plasma. The levels of these compounds determined by the CME approach fell within the expected ranges for normal blood samples. The only sample treatment steps required were protein precipitation and filtration.
Glassy carbon coated with (a) a ruthenium oxide/hexacyanoruthenate film or (b) a poly(4-vinylpyridine) film containing hexachloroiridate ^{31,43}	(a) As(III) (b) NO ₂ ⁻	In (a) the CME catalysed the oxidation of As(III). In FIA, linear calibration from 5×10^{-6} to 2×10^{-4} M and a detection limit $< 1 \mu$ M were obtained. Excellent reproducibility and stability were observed. In (b), NO ₂ ⁻ oxidation at CMEs containing a quaternized poly(4-vinylpyridine) film impregnated electrochemically with hexachloroiridate catalyst was examined. Short-term instability due to surface passivation was improved at the CME. However, day-to-day stability and reproducibility were less than desired.
CoPC in carbon paste ³¹	Thiopurines	Assay procedures were developed for 6-mercaptopurine, 6-thioguanine and related thiopurines in blood plasma. Sample preparation was minimal and total analysis time (including reversed-phase chromatography) was less than 10 min. Detection limits were 1.5–8 pmole, approximately an order of magnitude better than those obtained with UV absorption or fluorescence detection.
CoPC in carbon paste ^{32,33}	Oxalic acid and α -keto-acids including pyruvic, phenylpyruvic, α -ketobutyric, α -ketoglutaric, and α -ketoisocaproic acids.	The CME catalysed the oxidation of oxalic acid and α -keto-acids over the range $+0.75$ – 0.9 V vs. Ag/AgCl, which represents a roughly 500 mV decrease in overpotential compared with use of an unmodified electrode. At $+0.75$ V, the response for oxalic acid was linear from 10^{-7} to 2×10^{-3} M and gave a detection limit of 0.3 pmole. The detection limits for the α -keto-acids varied from 0.15 to 1 nmole. Assay procedures using the CME in reverse-phase chromatography were developed for oxalic acid and pyruvic acids in plasma and urine samples. Results for samples from healthy volunteers and kidney-stone patients fell within the expected ranges for both analytes. The assay procedures were attractive because relatively low detection limits were possible, and the only sample treatment required was dilution and filtration.
CoPC in carbon paste ³⁴	Carbohydrates	The electro-oxidation of sugars occurred at low potentials in strongly basic solution. The carbohydrates examined included mono- and disaccharides, pyranose and furanose rings, and reducing and non-reducing sugars. Use of this phenomenon in LCEC required that the applied potential was pulsed between $+0.4$ V (for detection) and -0.3 V (for electrode re-activation) vs. Ag/AgCl. Coupled with anion-exchange chromatography in 0.15 M NaOH, the CME provided detection limits of 100–500 pmole. The stability of the pulsed detection was such that the relative standard deviation for 40 injections over 5 hr was only 2%.
Nickel hexacyanoferrate electrochemically deposited on glassy carbon ⁴¹	Fe(III)	Fe(III) reduction, which is generally irreversible and irreproducible at bare glassy carbon, was catalysed at a CME and used for the determination of Fe(III) following separation on a chelate-loaded anion-exchange column. Because detection was at $+0.2$ V vs. SCE, there was no interference from dissolved O ₂ . The separation prevented interferences from most metal cations and common anions. The detection limit was 4×10^{-8} M, and the linear range extended from 2×10^{-7} to 9×10^{-4} M.
CoPC in carbon paste ³⁵	Carbohydrates and other polyhydroxy compounds	Electrocatalysis of carbohydrates was extended to include oligosaccharides, deoxy sugars and simple polyalcohols. Detection (with pulsed applied potential) was performed in strongly basic solution following anion-exchange chromatography. Detection limits were in the 10–50 pmole range. Sample matrices included soft drinks, beer and urine.

(a) Pt with adsorbed I ⁻ and coated with cellulose and (b) glassy carbon coated with a ruthenium cyanide film. ³⁹	SCN ⁻	Both CMEs catalysed the oxidation of SCN ⁻ at +0.7-0.8 V vs. Ag/AgCl and prevented fouling of the electrode surface by oxidation products and sample constituents. The Pt-CME had a linear response for SCN ⁻ from 5×10^{-6} to 1×10^{-4} M and was stable for several days. The Ru-based CME gave a response that was linear only over $0.2 - 4 \times 10^{-6}$ M, but was stable for more than 300 injections over 3 months. FIA of urine samples was evaluated at both CMEs; interferences by uric and ascorbic acids had to be eliminated by prior controlled potential electrolysis of the sample at +0.55 V.
Tris(4,7-diphenyl-1,10-phenanthroline)iron(II) in carbon paste ⁵	NO ₂	Attempts were made to incorporate several iron complexes into a carbon-paste CME. Of the complexes examined, tris(4,7-diphenyl-1,10-phenanthroline)iron(II) formed the most stable and reproducible CME and was chosen for further study. When used in FIA, the CME yielded anodic peaks for air samples doped with gaseous NO ₂ . The NO ₂ response, which was only 3-4 times greater than that observed at an unmodified surface, occurred at potentials more positive than +0.6 V vs. Ag/AgCl and was assigned to an electrocatalytic process involving redox mediation by the modifier. NO ₂ concentrations as low as 15 nl/l were reproducibly detected.
Glassy carbon coated with an Ru-containing poly(4-vinylpyridine) polymer ⁴⁶	NO ₂ and Ni dithiocarbamate	The CME was made by wetting a glassy-carbon surface with a solution of [Ru(bipy) ₂ (PVP) ₂ Cl]Cl and allowing the solvent to evaporate [PVP = poly(4-vinylpyridine) and bipy = 2,2'-bipyridyl]. In FIA, the CME was able to promote the oxidation of NO ₂ and several metal dithiocarbamates at high positive potentials. Although it is unclear whether simple electrocatalysis occurred, 4-10 times larger currents were obtained at the CME than at an uncoated electrode. Problems included poor electrode-to-electrode reproducibility and slow loss of the polymer in the flow-stream.
CoPC in carbon paste ⁴⁶	Ribonucleosides	The CMEs were able to catalyse the oxidation of the ribonucleosides cytidine, uridine, adenosine and guanine in strongly basic solution. Neither the purine and pyrimidine bases themselves nor 2-deoxyribonucleosides such as thymidine gave similar activity. When used in LCEC with a pulsed applied potential, the activity of the CME was very stable and reproducible. Detection limits were at the nmole level and roughly comparable to those for detection by UV absorption. Because of the selectivity of the CME, chromatograms of an RNA hydrolysate were much simpler with electrochemical detection than with UV detection at 280 nm.
CoPC in carbon paste ³⁷	Carbohydrates, alditols and acidic sugars	CoPC CMEs catalysed the oxidation of alditols and aldonic, uronic and aldaric acids similarly to that of simple carbohydrates. ^{34,35} For LCEC, detection was at +0.42 V vs. Ag/AgCl, but the potential was continually pulsed to -0.3 V to regenerate the active form of the CoPC catalyst. For anion-exchange chromatography in strongly alkaline solution, detection limits ranged from 10 pmole for the alditols up to the nmole level for some of the aldaric acids.
A mixed-valence Ru(II,III) cyanide film electro-deposited onto glassy carbon ⁴⁶	N ₂ H ₄ and mono- and dimethylhydrazines	The oxidation of hydrazine and mono- and 1,2-dimethylhydrazine was catalysed at +0.9-1.0 V vs. Ag/AgCl. For N ₂ H ₄ , FIA response was linear for concentrations from 5 to 50 μM and gave a detection limit of 2×10^{-7} M. Compared to detection of N ₂ H ₄ at CoPC-CMEs, the operation of the Ru-CME was not restricted to strongly alkaline solution and appeared to be much longer-lived. When polyaniline was co-deposited with the Ru cyanide film, the resulting CME exhibited size-selective as well as electrocatalytic properties.
Glassy carbon coated with an Ru cyanide film ⁴¹	Insulin	The CME catalysed the electro-oxidation of insulin by a mechanism presumably involving oxidation of one or more of the disulphide bonds. The catalysis, which occurs at potentials more positive than +0.9 V vs. Ag/AgCl, permitted FIA detection at or below the 10 ⁻⁷ M level.
Mn(III) meso-tetraphenylporphyrin adsorbed onto glassy carbon ⁴⁷	Ascorbic acid, acetaminophen, hydralazine, epinephrine and other biologically relevant compounds	The Mn porphyrin coated on glassy carbon promoted the oxidation of several compounds. Because the effect occurred at different potentials for different analytes, the catalysis probably involved specific interactions between analyte and modifier rather than direct charge-transfer mediation. In FIA, the primary effect of the CME consisted of 50-360 mV decreases in the potential required for oxidation of the compounds examined (relative to the unmodified electrode). A 5% decrease in response occurred over 60 injections of acetaminophen, and a linear response was obtained for hydralazine between 5 and 40 μM. The CME was used for the analysis of urine samples, where its lower operating potential should be advantageous.
Glassy carbon coated with a mixed-valence Ru oxide/cyanide film ⁴²	Cysteine and glutathione	The CME catalysed the oxidation of cysteine and glutathione between +0.9 and +1.0 V vs. Ag/AgCl. In FIA, detection limits for these compounds were below the μM level and the response was linear over about three orders of magnitude. Long-term stability was excellent, with no change in sensitivity for > 200 injections over a 2-week period.

Table 3. CME applications involving bio-active molecules

CME	Analyte	Summary
Reticulated vitreous carbon with covalently attached glucose oxidase ⁷⁷	Glucose	Glucose oxidase was immobilized onto the surface of a flow-through reticulated vitreous carbon electrode by reaction with a water-soluble carbodi-imide. In FIA, injections of glucose samples resulted in the enzymatic production of H ₂ O ₂ at the CME surface. By holding the CME at +0.9 V vs. SCE and monitoring the anodic current due to oxidation of the H ₂ O ₂ , so produced, glucose could be quantified over the 10 ⁻⁴ -10 ⁻¹ M range. The CME response was linear for glucose concentrations from 2.5 to 10mM, with a relative standard deviation of less than 2%.
Meldola Blue adsorbed on graphite ⁷¹	Glucose	NADH was oxidized electrocatalytically at the CME at 0 V vs. SCE, which was at least 300 mV less than the potential required at a bare graphite electrode. Glucose was quantified by inserting a packed-bed glucose dehydrogenase reactor ahead of the CME in a flowstream containing NAD ⁺ and measuring the NADH produced upon sample injection. The detection limit was 0.25mM, and the response was linear up to 1mM. Because of the low potential possible with the CME, potential interferences, such as ascorbic acid, uric acid and catechols, posed no problem.
4,4'-Dipyridyl disulphide adsorbed on polyvinyl-ferrocene-treated gold ⁶⁷	Cytochrome c	By use of the promoting effect of 4,4'-dipyridyl disulphide, cytochrome c could be oxidized and reduced almost reversibly. LCEC following size-exclusion chromatography gave a detection limit of 3 pmole for the reduced form of cytochrome c and a linear response over three orders of magnitude. Both redox forms of the protein were detected in human plasma pretreated only by dilution and filtration.
Meldola Blue adsorbed on graphite ⁷²	L-Lactate	The CME was used to oxidize NADH electrocatalytically at 0 V vs. Ag/AgCl. L-Lactate was determined by placing an enzyme reactor containing immobilized lactate dehydrogenase and glutamic-pyruvic transaminase ahead of the CME in the FIA flow-stream and monitoring the NADH generated upon sample injection into a mobile phase containing NAD ⁺ and glutamate. Linear response was observed in the concentration range 10μM-1.5mM. System response was rather stable, the limiting factor being the slow loss of modifier from the CME surface over the course of a few days.
Nile Blue adsorbed on graphite ⁷³	Xylose and xylulose	In the presence of xylose or xylulose, NAD ⁺ could be converted into NADH by means of a mixed-bed enzyme reactor containing xylose isomerase, mutarotase and glucose dehydrogenase. The NADH so generated was detected by oxidation to NAD ⁺ at 0 V vs. SCE at the electrocatalytic CME. In FIA, this system exhibited a linear response to both sugars from 5μM to 2mM and gave a maximum throughput of 30 samples/hr.
Carbon paste containing banana pulp ⁷⁹	Dopamine	A carbon-paste CME constructed by mixing a measured amount of banana tissue into the paste matrix illustrates a simple and effective approach for building enzymatic activity into an electrode surface without the use of isolated enzymes. Polyphenoloxidase in the banana catalysed the conversion of dopamine into dopamine quinone, which was detected amperometrically by its reduction to dopamine. In FIA, a detection limit of 1.3 × 10 ⁻⁹ M was realized, and the response was linear over nearly two orders of magnitude. In addition to its high selectivity, the principal strength of this CME was that, by incorporating the biocatalyst so intimately at the electrode surface, analyte diffusion requirements were greatly reduced compared to those with conventional tissue-based electrodes; therefore, response times were of the order of seconds rather than minutes.

Methylene Blue adsorbed on graphite ⁶⁸	Myoglobin and haemoglobin	Phenothiazine mediators, including Methylene Blue and thionine, were adsorbed on spectroscopic graphite electrodes and used to catalyse the reduction of haem-containing proteins at potentials from -0.1 to -0.2 V <i>vs.</i> Ag/AgCl. In FIA, the detection limit for myoglobin was 10 pmole, and response was linear between 20 and 2800 pmole. For haemoglobin, the limit of detection was slightly higher and the linear range somewhat smaller. In size-exclusion chromatography, detection with the CME, which maintained 90% of its activity over an 8-hr period of use, was comparable to that by UV absorption.
Carbon paste containing horseradish root tissue ⁶⁹	H ₂ O ₂	Mixing horseradish root into carbon paste produced an electrode surface that could perform the horseradish-peroxidase-catalysed reduction of H ₂ O ₂ . The reaction also requires the presence in solution of a suitable reducing agent such as <i>o</i> -phenylenediamine. In FIA, H ₂ O ₂ levels were determined by amperometric reduction of the di-imine oxidation product at 0.2 V <i>vs.</i> Ag/AgCl. A detection limit of 3×10^{-7} M H ₂ O ₂ and a linear range up to 1.2×10^{-4} M were observed. Excellent reproductibility and response times of the order of 10 sec were obtained.
Anthracene-ferrocene ester and glucose oxidase adsorbed on graphite ⁷²	Glucose	The modifier had a dual function: the anthracene group was strongly adsorbed on the graphite substrate to immobilize the modifier, while the ferrocene moiety was able to mediate the electron transfer with glucose oxidase. Subsequently, glucose oxidase itself was adsorbed on top of the anthracene-ferrocene derivative. In FIA, the CME exhibited an anodic response for glucose at the redox potential of the ferrocene compound. This response was suitable for glucose detection from 50 μ M up to 1.5 mM. Because the enzyme itself was electroactive at this CME surface, detection could be performed without the addition of an oxidizing agent or co-factor to the mobile phase.
Bis(benzophenoxazine) derivative adsorbed on graphite ⁷⁴	Mono- and oligosaccharides	A CME containing an immobilized phenoxazine gave electrocatalytic oxidation of NADH at 0 V <i>vs.</i> Ag/AgCl. Carbohydrate samples were first separated on a Ca-loaded ion-exchange column and then passed through two enzyme reactors containing amyloglucosidase and glucose dehydrogenase/mutarotase. NADH formed in the latter enzymatic process was detected at the CME located downstream. Sugars up to maltohexose were quantified at the 100–300 ng level in samples including soft drinks, beer and fermentation broths.
Polyaniline electro-deposited onto glassy carbon ⁶⁹	Ceruloplasmin	The similarity of the structure of polyaniline to that of several phenylenediamine compounds used as solution-phase electron-transfer mediators for redox proteins suggested that a CME containing this easily formed polymer might display useful electrocatalytic behaviour in FIA and LCEC. This prediction was upheld for the copper protein ceruloplasmin, which underwent reduction at approximately 0 V <i>vs.</i> Ag/AgCl. The reduction, which was greatly enhanced by the addition of modest Fe ²⁺ concentrations to the mobile phase, permitted quantification of as little as 2 pmole of ceruloplasmin. In conjunction with size-exclusion chromatography, the CME was able to determine physiological levels of the protein in human serum.
Glucose oxidase and platinum particles co-deposited onto carbon fibres ⁸¹	Glucose	This CME was constructed by electrochemically reducing hexachloroplatinate from a solution also containing glucose oxidase. In the presence of glucose, the enzymatic reaction at the CME resulted in the production of H ₂ O ₂ , which was oxidized with low overpotential at the platinum metal. Glucose concentrations as low as 1.3×10^{-7} M were accessible with a relative standard deviation of 3%, and continued monitoring with the same surface was possible for at least 20 days.
Horseradish peroxidase adsorbed on spectroscopic graphite ⁷³	H ₂ O ₂	Horseradish peroxidase was adsorbed strongly onto a spectroscopic graphite surface to form a functional CME. Upon addition of H ₂ O ₂ , broad reduction at peak potentials from $+0.6$ to -0.2 V <i>vs.</i> Ag/AgCl were observed at the CME without the addition of any solution-phase mediator. From this, it was concluded that efficient reduction of the oxidized form of the peroxidase must be possible at the bare graphite surface. In FIA, linear response was obtained at 0 V for H ₂ O ₂ concentrations from 0.5 to 250 μ M. After an initially rapid decline in activity, the CME lost its response only slowly as H ₂ O ₂ injections continued.
Horseradish peroxidase covalently attached to tin oxide ⁷⁸	H ₂ O ₂	H ₂ O ₂ was reduced at the CME in the presence of a dissolved ferrocene or ferrocyanide mediator. In FIA, determination of H ₂ O ₂ was possible down to 10^{-7} M.

the unparalleled *selectivity* of enzyme reactions in a single relatively simple sensing unit. In the simplest of these approaches, the enzyme is immobilized in a packed-bed reactor placed in the flow-stream ahead of the CME. When the enzyme substrate passes through the reactor (along with appropriate co-factors), the products of the enzymatic reaction are carried to the sensing electrode for detection. The role of the CME is to provide an electrocatalytic response to the product or co-factor, that will be related to the initial substrate concentration. Most commonly, the species detected has been the co-enzyme nicotinamide adenine dinucleotide (NADH) which exhibits a large overpotential at ordinary carbon electrodes. In particular, β -D-glucose has been detected by use of immobilized glucose dehydrogenase and a CME containing the phenoxazine dye Meldola Blue,⁷¹ L-lactate by use of immobilized L-lactate dehydrogenase and a Meldola Blue CME,⁷² xylose and xylulose by use of immobilized xylose isomerase, mutarotase, and glucose dehydrogenase and a CME containing the phenoxazine Nile Blue,⁷³ and glucose, xylose and several maltose oligomers by use of immobilized amyloglucosidase, glucose dehydrogenase and mutarotase and a bis(benzophenoxazinyl)-containing CME.⁷⁴

A similar, but more sophisticated, approach has been explored in several studies in which the enzyme is bound directly on the CME surface instead of separately in a preceding reactor bed. This is directly analogous to the numerous "enzyme electrodes" that have been developed and have become commercially available over the past 10–15 years.^{75,76} In both cases, a bio-active component, initially an enzyme but more recently an intact organism or tissue sample, is used to transform the analyte with a high degree of selectivity into a product that is easily measured potentiometrically or amperometrically. The primary differences in the CME approach are that the detection mode is always amperometric and that the enzyme or organism is always incorporated as an integral part of the active electrode surface and not just held in the vicinity of the electrode by a membrane or polymer sheath. The earliest example of the CME method, reported by Yacynych, involved the determination of glucose by oxidation of the H_2O_2 produced at a CME with covalently attached glucose oxidase.⁷⁷ Subsequently, Tatsuma *et al.* were able to detect H_2O_2 with a tin oxide electrode coated with covalently

attached horseradish peroxidase. Wang and Lin described stable, easily fabricated carbon-paste CMEs with added banana⁷⁹ and horseradish root⁸⁰ tissues, which were suitable for the FIA detection of dopamine and H_2O_2 , respectively; these electrodes, analogous to the bacteria- and tissue-based probes developed by Rechnitz's group⁷⁶ made use of the enzyme systems present naturally in the plant tissues to metabolize the target analytes and generate electroactive products. Finally, Wang *et al.*⁸¹ have recently reported a glucose-responsive micro-CME constructed by co-depositing glucose oxidase enzyme and platinum particles onto 7- μ m diameter carbon fibres.

The ultimate enzyme-based CME would combine these two approaches by not only immobilizing the enzyme at the sensing electrode surface but also incorporating an electrocatalyst capable of mediating the enzyme's own redox process. This arrangement would not only provide a relatively rapid measurement procedure but, more importantly, would eliminate the need for addition of any co-enzyme or solution-phase redox agent to the mobile phase. Such CME systems, suitable for glucose and H_2O_2 detection, have been developed by Gorton and his group.^{82,83} These electrodes consist of the familiar glucose oxidase adsorbed onto graphite along with a ferrocene/anthracene adduct that serves to mediate the enzyme's charge transfer reaction at the graphite surface,⁸² and horseradish peroxidase also adsorbed onto graphite but with no added mediator.⁸³

Detection of non-electroactive analytes

In these detection schemes, the analytes are ions which are electrochemically inactive but can, under properly controlled conditions, influence the electrochemical behaviour of redox pairs attached to a CME surface. Anions, for example, can be detected at polymer films containing fixed redox centres which acquire a positive charge upon oxidation. For oxidation of the polymer to occur to an appreciable extent, the associated build-up of positive charge in the film must be counterbalanced by the migration of anions across the electrode-solution interface. This ion-doping process and the corresponding undoping that occurs when the oxidized sites are reduced are shown in Fig. 2 for a polypyrrole film.

Application of this phenomenon in FIA or LCEC is straightforward. If such an electrode is

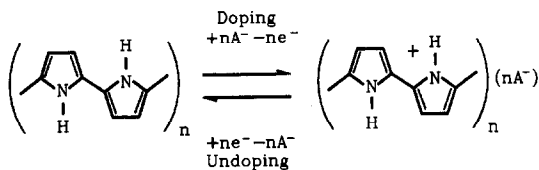


Fig. 2

placed in a flow-stream and an oxidizing potential is applied, oxidation of the film occurs only when anions capable of penetrating it are present in the surrounding solution. Thus, a transient anodic current, or chromatographic peak, results upon passage of a sample containing such anions. In the ideal case, the magnitude of this current is related directly to the concentration of the anion concerned. Furthermore, if the film exhibits unequal permeability toward different anions, its response may provide some selectivity; this is often the case, with small singly-charged ions generally giving the best sensitivity. In order to ensure that oxidation of the film does not take place prematurely, the mobile-phase electrolyte should not be capable of effectively penetrating the film. This is normally accomplished by using electrolytes with anions that are either zwitter-ions or very bulky.

For this purpose, CMEs formed with two different polymers, polypyrrole^{84,85} and polyaniline,⁸⁶ have been utilized for anion detection. Both of these CMEs enable the quantification of micromolar levels of common anions, including halides, acetate, carbonate and phosphate. However, the polyaniline-based system appears preferable in that it is more stable, operates at a considerably lower potential, and allows the undoping process to take place spontaneously without application of a strongly reducing potential.

The detection of non-electroactive cations can be realized by the analogous scheme involving the formation of negatively charged sites in a reducible polymer film and the subsequent migration of cations from solution. In fact, the first demonstration of the potential analytical utility of the ion doping/undoping process utilized an Ag(I)-Mo(CN)₈ film for the determination of potassium by cyclic voltammetry.⁸⁷ Very recently, electrodes coated with zeolite-like hexacyanoferrate deposits have been shown to be very effective for the uptake and detection of alkali-metal and ammonium ions in both static and flow experiments.⁸⁸⁻⁹¹ On reduction of the hexacyanoferrate, these films act as cation-exchangers and preferentially incorporate cations with the smallest hydrated radii. This

coupling between ion-exchange and the redox state of the film allows sensitive detection of passing cations when the electrode is placed in a flow-stream. A unique aspect of these systems is that the nature of the incorporated cation noticeably alters the redox potential of the hexacyanoferrate centres, most likely because of changes in the microstructure of the film induced by intercalation of specific ions.⁸⁸ Thus the potential required for detection is less negative for Cs⁺ than for K⁺ and a significant degree of selectivity among these ions can be achieved in flow systems by control of the potential.^{90,91}

Examples of this approach for both anion and cation detection are summarized in Table 4. Its most attractive application appears to be in ion-chromatography, as a simple alternative to conductivity detection. Although not yet able to match the highest sensitivities reported for the conductivity method, the amperometric CME-based approach described here clearly renders unnecessary the use of secondary suppressor columns ordinarily recommended for optimum conductivity detection. Furthermore, any selectivity in ion uptake demonstrated by the CME should clearly have the effect of minimizing possible interferences and easing somewhat the demands on the chromatographic separation.

CONCLUSIONS

It is clear that the development and popularization of practical CMEs has created a variety of new and potentially powerful detection opportunities in FIA and LCEC. As our ability to manipulate precisely and imaginatively the chemical nature of the electrode/solution interface continues to grow, it can be expected that applications in the areas considered above will expand and completely new applications be developed.

The most intriguing possibilities for new work are the detection of analytes not readily sensed at conventional electrodes and the detection of conventional analyte with increased selectivity. Many of the CME studies above had these objectives as their driving force and the continued use of biologically active agents as electrode modifiers will undoubtedly have increased selectivity as a principal focus. In this regard, recent work by Wang and Lin^{79,80} in which plant tissues are used intact for electrode modification is noteworthy in that it offers a simple and successful route for fabricating biologically-derived CMEs. In addition, complex

Table 4. CME applications involving the detection of non-electroactive ions

CME	Analyte	Summary
Polypyrrole on platinum ⁸⁴	Acetate, carbonate and phosphate	Oxidation of the polypyrrole film at +0.9 V vs. Ag/AgCl was accompanied by formation of positively charged sites in the film and migration of anions from solution. In FIA with the glycine zwitter-ion as the mobile phase electrolyte, injection of sample plugs containing anions such as CH ₃ COO ⁻ , CO ₃ ²⁻ and PO ₄ ³⁻ produced transient anodic currents related to oxidation of the film and uptake of the anion. After each injection, the anions were expelled from the film by application of a reducing potential (-0.3 V). The doping current was linearly dependent on anion concentration from 10 ⁻⁵ to 10 ⁻³ M. The CME response was stable as long as O ₂ was excluded from the flow-stream.
Polypyrrole on platinum ⁸⁵	Halides and other non-electroactive anions	Anodic doping of polypyrrole enabled the detection of halides, particularly Cl ⁻ , over the range 10 ⁻⁶ -10 ⁻³ M. Of various electrolytes containing bulky anions, glycine buffer gave the best response and lowest background current. Variations in applied potential indicated two linear regions, one on either side of the polypyrrole oxidation potential.
Polyaniline on platinum ⁸⁶	Non-electroactive anions in general	Polyaniline CMEs were able to give responses to anions by an anodic doping mechanism involving uptake of the anions upon oxidation of the polymer film. The anions examined were classified according to the responses obtained in mobile phases of different composition. Cl ⁻ , Br ⁻ , NO ₃ ⁻ and ClO ₄ ⁻ gave large signals in acetate buffer and even larger signals in glycine buffer. SO ₄ ²⁻ , CO ₃ ²⁻ and PO ₄ ³⁻ gave small responses in acetate and large responses in glycine. Thus some selectivity was possible by appropriate choice of mobile-phase electrolyte. The potential dependence was sigmoidal in shape and centred at the polyaniline redox wave. Undoping of the film, indicated by the presence of a shallow cathodic trough immediately following the initial anodic peak, was effected by operating at a potential (e.g., +0.2 V vs. Ag/AgCl) where the film was neither fully oxidized nor fully reduced. For NO ₃ ⁻ , linear response was obtained from 10 ⁻⁶ to 10 ⁻⁵ M. The same CME surface could be used for 2 weeks without loss of activity.
Ferric hexacyanoferrate (Prussian Blue) on the quartz crystal of a piezoelective microbalance ⁸⁹	K ⁺ and NH ₄ ⁺	Reduction of the Prussian Blue required the availability of cations, such as K ⁺ and NH ₄ ⁺ , with hydrated radii small enough to permit migration into the film and counterbalancing of the negative sites associated with the reduction process. Thus, this CME was useful for the FIA of these ions by following their uptake into the Prussian Blue film either amperometrically or by the change in mass (or frequency) of the quartz crystal. Both the current and mass responses for reduction of the film in dilute HNO ₃ gave non-linear calibrations from 10 ⁻⁴ to 10 ⁻² M for both K ⁺ and NH ₄ ⁺ .
Cupric hexacyanoferrate on glassy carbon ⁹⁰	K ⁺ and NH ₄ ⁺	Reduction of the cupric hexacyanoferrate deposit was facilitated by the availability of K ⁺ , NH ₄ ⁺ and other ions capable of transport into and out of the film. In FIA and cation-exchange chromatography, this phenomenon gave rise to transient signals at the CME, consisting of cathodic peaks for the uptake of the cations, followed by anodic troughs corresponding to their release back into solution. At an applied potential of only +0.45 V vs. Ag/AgCl, detection limits of 5 × 10 ⁻⁷ M and linear ranges over three orders of magnitude were obtained for both K ⁺ and NH ₄ ⁺ . Reproducibility (1-5% relative standard deviation) and stability (several hours) in the flow-stream were improved by adding a layer of Nafion to the CME surface. The electrode operation was fully compatible with the low ionic-strength mobile phases typically employed in ion-chromatography.
Cupric hexacyanoferrate on glassy carbon and nickel(II) hexacyanoferrate on nickel ⁹¹	K ⁺ , NH ₄ ⁺ , Rb ⁺ and Cs ⁺	Both Ni and Cu hexacyanoferrate CMEs exhibited responses in FIA and LCEC for the alkali-metal and NH ₄ ⁺ ions, but only the latter electrode was sufficiently stable for routine use. The response of the Cu-CME to K ⁺ , NH ₄ ⁺ , Rb ⁺ and Cs ⁺ was rather selective. Within this group, the selectivity could be controlled from general to almost specific for Cs ⁺ by adjusting the applied potential (from +0.4 to +0.7 V vs. Ag/AgCl). The CME gave detection limits of 2 × 10 ⁻⁷ M and was tested for determination of K ⁺ and NH ₄ ⁺ in urine and K ⁺ in blood serum.

CMEs incorporating more than one level of modification may prove extremely interesting. Several examples of such multifunctional CMEs have been reported. Most notably, Wang's group has explored bilayer cellulose/Nafion and cellulose/poly(vinylpyridine) CMEs which offer both size and charge selectivity^{18,24} and cellulose/cobalt phthalocyanine CMEs which combine both perm-selective and electrocatalytic properties.²²

As CME systems continue to develop, completely new kinds of applications can be expected. Perhaps the best illustration of this is provided by recent innovations that have demonstrated how electrochemical detection may be used in gas chromatography (GC) and supercritical fluid chromatography (SFC). The central idea behind these approaches is the use not simply of a single chemically modified or controlled electrode, but of an entire chemically controlled electrochemical cell. For GC, Pons and co-workers^{92,93} employed a micro-assembly consisting of two concentric ring electrodes separated by a thin insulating film of epoxy resin. When this cell was placed at the outlet of the GC column, eluted electroactive species were electrolysed at the inner microelectrode (either carbon or gold). Because the currents involved were only of the order of 10^{-16} – 10^{-10} A, the corresponding flow of charge to the auxiliary electrode could be sustained by the limited number of charge carriers present naturally in the epoxy resin. Applied potentials from +3.0 to -3.0 V (*vs.* the auxiliary electrode) were employed and a wide variety of organic analytes could be oxidized or reduced. However, the linear response range and sensitivity varied considerably with sample type. Subsequently, Parcher *et al.*⁹⁴ reported the use of a micro-electrode assembly coated with a solid poly(ethylene oxide) film made conductive by the addition of lithium trifluoromethanesulphonate and containing a fixed concentration of an electroactive probe such as a ferrocene. Partition of the analyte (in the GC eluate) into the polymer film altered its degree of plasticization and hence the diffusion coefficient of the probe and the resulting microelectrode current. Note that unlike the Pons technique, which requires the analyte to be electroactive, detection by this approach was also possible for non-electroactive species. Finally, in an attempt to adapt amperometric detection to SFC, Michael and Wightman^{95,96} were able to deal with the requirement of a non-conductive

mobile phase in SFC by using a cell consisting of a pair of platinum microelectrodes coated with a Nafion overlayer. In this system, ferrocenes, catechols and other electroactive substrates eluted in the supercritical fluid were partitioned into the ionically conducting Nafion film, where diffusion to the working electrode produced the expected redox current.

Acknowledgement—The authors gratefully acknowledge the support of the National Science Foundation through EPSCoR Grant 86-10671-01.

REFERENCES

1. R. W. Murray, *Acc. Chem. Res.*, 1980, **13**, 135.
2. *Idem*, in *Electroanalytical Chemistry*, Vol. 13, A. J. Bard (ed.), p. 191. Dekker, New York, 1984.
3. L. R. Faulkner, *Chem. Eng. News*, 1984, **62**, No. 9, 28.
4. R. W. Murray, A. G. Ewing and R. A. Durst, *Anal. Chem.*, 1987, **59**, 379A.
5. S. Dong and Y. Wang, *Electroanalysis*, 1989, **1**, 99.
6. P. T. Kissinger, in *Laboratory Techniques in Electroanalytical Chemistry*, P. T. Kissinger and W. R. Heineman (eds.), pp. 611–635, Dekker, New York, 1984.
7. G. T. Cheek and R. F. Nelson, *Anal. Lett.*, 1978, **11**, 393.
8. K. Ravichandran and R. P. Baldwin, *J. Electroanal. Chem.*, 1981, **126**, 293.
9. J. Wang, T. Golden, K. Varughese and I. El-Rayes, *Anal. Chem.*, 1989, **61**, 508.
10. B. R. Shaw and K. E. Creasy, *ibid.*, 1988, **60**, 1241.
11. K. E. Creasy and B. R. Shaw, *ibid.*, 1989, **61**, 1460.
12. R. N. Dominey, N. S. Lewis, J. A. Bruce, D. C. Bookbinder and M. S. Wrighton, *J. Am. Chem. Soc.*, 1982, **104**, 467.
13. K. M. Kost, D. E. Bartak, B. Kazee and T. Kuwana, *Anal. Chem.*, 1988, **60**, 2379.
14. M. Umaña and J. Waller, *ibid.*, 1986 **58**, 2979.
15. N. C. Foulds and C. R. Lowe, *ibid.*, 1988, **60**, 2473.
16. G. Nagy, G. A. Gerhardt, A. F. Oke, M. E. Rice, R. N. Adams, R. B. Moore III, M. N. Szentirmay and C. R. Martin, *J. Electroanal. Chem.*, 1985, **188**, 85.
17. A. J. Tüdös, W. J. J. Ozinga, H. Poppe and W. Th. Kok, *Anal. Chem.*, 1990, **62**, 367.
18. J. Wang, T. Golden and P. Tuzhi, *ibid.*, 1987, **59**, 740.
19. G. Sittampalam and G. S. Wilson, *ibid.*, 1983, **55**, 1608.
20. J. Wang and L. D. Hutchins, *ibid.*, 1985, **57**, 1536.
21. L. D. Hutchins-Kumar, J. Wang and P. Tuzhi, *ibid.*, 1986, **58**, 1019.
22. J. Wang, T. Golden and R. Li, *ibid.*, 1988, **60**, 1642.
23. J. Wang and R. Li, *ibid.*, 1989, **61**, 2809.
24. J. Wang, P. Tuzhi and T. Golden, *Anal. Chim. Acta*, 1987, **194**, 129.
25. H. Ji and E. Wang, *J. Chromatog.*, 1987, **410**, 111.
26. J. Wang and T. Golden, *Anal. Chem.*, 1989, **61**, 1397.
27. D. S. Bindra and G. S. Wilson, *ibid.*, 1989, **61**, 2566.
28. K. M. Korfhage, K. Ravichandran and R. P. Baldwin, *ibid.*, 1984, **56**, 1514.
29. M. K. Halbert and R. P. Baldwin, *ibid.*, 1985, **57**, 591.
30. *Idem*, *J. Chromatog.*, 1985, **345**, 43.
31. *Idem*, *Anal. Chim. Acta*, 1986, **187**, 89.

32. L. M. Santos and R. P. Baldwin, *Anal. Chem.*, 1986, **58**, 848.
33. *Idem*, *J. Chromatog.*, 1987, **414**, 161.
34. *Idem*, *Anal. Chem.*, 1987, **59**, 1766.
35. *Idem*, *Anal. Chim. Acta*, 1988, **206**, 85.
36. A. M. Tolbert, R. P. Baldwin and L. M. Santos, *Anal. Lett.*, 1989, **22**, 683.
37. A. M. Tolbert and R. P. Baldwin, *Electroanalysis*, 1989, **1**, 389.
38. J. A. Cox and K. R. Kulkarni, *Talanta*, 1986, **33**, 911.
39. J. A. Cox, T. Gray and K. R. Kulkarni, *Anal. Chem.*, 1988, **60**, 1710.
40. J. Wang and Z. Lu, *Electroanalysis*, 1989, **1**, 517.
41. J. A. Cox and T. J. Gray, *Anal. Chem.*, 1989, **61**, 2462.
42. *Idem*, *Electroanalysis*, 1990, **2**, 107.
43. J. A. Cox and K. R. Kulkarni, *Analyst*, 1986, **111**, 1219.
44. P. J. Kulesza, K. Brajter and E. Dabek-Zlotorzynska, *Anal. Chem.*, 1987, **59**, 2776.
45. C. J. Hynes, M. Bonakdar and H. A. Mottola, *Electroanalysis*, 1989, **1**, 155.
46. J. N. Barisci, G. G. Wallace, E. A. Wilke, M. Meaney, M. R. Smyth and J. G. Vos, *ibid.*, 1989, **1**, 245.
47. J. Wang and T. Golden, *Anal. Chim. Acta*, 1989, **217**, 343.
48. S. Hughes and D. C. Johnson, *J. Agric. Food Chem.*, 1982, **30**, 712.
49. J. A. Polta and D. C. Johnson, *J. Liq. Chromatog.*, 1983, **6**, 1727.
50. D. S. Austin, J. A. Polta, T. Z. Polta, A. P.-C. Tang, T. D. Cabelka and D. C. Johnson, *J. Electroanal. Chem.*, 1984, **168**, 227.
51. R. D. Rocklin and C. A. Pohl, *J. Liq. Chromatog.*, 1983, **6**, 1577.
52. P. Edwards and K. K. Haak, *Am. Lab.*, 1983, **15**, No. 4, 78.
53. G. G. Neuberger and D. C. Johnson, *Anal. Chem.*, 1987, **59**, 150.
54. L. E. Welch, W. R. LaCourse, D. A. Mead, Jr., D. C. Johnson and T. Hu, *ibid.*, 1989, **61**, 555.
55. K. G. Schick, V. G. Magearu and C. O. Huber, *Clin. Chem.*, 1978, **24**, 448.
56. J. B. Kafil and C. O. Huber, *Anal. Chim. Acta*, 1985, **175**, 275.
57. W. Buchberger, K. Winsauer and Ch. Breitwieser, *Z. Anal. Chem.*, 1983, **315**, 518.
58. R. E. Reim and R. M. Van Effen, *Anal. Chem.*, 1986, **58**, 3203.
59. W. Th. Kok, U. A. Th. Brinkman and R. W. Frei, *J. Chromatog.*, 1983, **256**, 17.
60. S. V. Prabhu and R. P. Baldwin, *Anal. Chem.*, 1989, **61**, 852.
61. *Idem*, *ibid.*, 1989, **61**, 2258.
62. P. Luo, S. V. Prabhu and R. P. Baldwin, *ibid.*, 1990, **62**, 752.
63. J. Wang and Z. Taha, *ibid.*, 1990, **62**, 1413.
64. J. E. Frew and H. A. O. Hill, *ibid.*, 1987, **59**, 933A.
65. M. J. Eddowes and H. A. O. Hill, *J. Chem. Soc., Chem. Commun.*, 1977, 771.
66. I. Taniguchi, K. Toyosawa, H. Yamaguchi and K. Yasukouchi, *J. Electroanal. Chem.*, 1982, **140**, 187.
67. J. W. Schlager and R. P. Baldwin, *J. Chromatog.*, 1987, **390**, 379.
68. J. Ye and R. P. Baldwin, *Anal. Chem.*, 1988, **60**, 2263.
69. J. Ye, R. P. Baldwin and J. W. Schlager, *Electroanalysis*, 1989, **1**, 133.
70. M. L. Fultz and R. A. Durst, *Anal. Chim. Acta*, 1982, **140**, 1.
71. R. Appelqvist, G. Marko-Varga, L. Gorton, A. Torstenson and G. Johansson, *ibid.*, 1985, **169**, 237.
72. L. Gorton and A. Hedlund, *ibid.*, 1988, **213**, 91.
73. E. Dominguez, B. Hahn-Hägerdahl, G. Marko-Varga and L. Gorton, *ibid.*, 1988, **213**, 139.
74. G. A. Marko-Varga, *Anal. Chem.*, 1989, **61**, 831.
75. G. A. Rechnitz, *ibid.*, 1982, **54**, 1194A.
76. *Idem*, *Science*, 1981, **214**, 287.
77. H. J. Wieck, G. H. Hieder and A. M. Yacynych, *Anal. Chim. Acta*, 1984, **158**, 137.
78. T. Tatsuma, Y. Okawa and T. Watanabe, *Anal. Chem.*, 1989, **61**, 2352.
79. J. Wang and M. S. Lin, *ibid.*, 1988, **60**, 1545.
80. *Idem*, *Electroanalysis*, 1989, **1**, 43.
81. J. Wang, R. Li and M. S. Lin, *ibid.*, 1989, **1**, 151.
82. G. Jonsson, L. Gorton and L. Pettersson, *ibid.*, 1989, **1**, 49.
83. G. Jonsson and L. Gorton, *ibid.*, 1989, **1**, 465.
84. Y. Ikariyama and W. R. Heineman, *Anal. Chem.*, 1986, **58**, 1803.
85. Y. Ikariyama, C. Galiatsatos, W. R. Heineman and S. Yamauchi, *Sens. Actuators*, 1987, **12**, 455.
86. J. Ye and R. P. Baldwin, *Anal. Chem.*, 1988, **60**, 1979.
87. J. A. Cox and B. K. Das, *ibid.*, 1985, **57**, 2739.
88. L. J. Amos, A. Duggal, E. J. Mirsky, P. Ragonesi, A. B. Bocarsly and P. A. Fitzgerald-Bocarsly, *ibid.*, 1988, **60**, 245.
89. M. R. Deakin and H. Byrd, *ibid.*, 1989, **61**, 290.
90. K. N. Thomsen and R. P. Baldwin, *ibid.*, 1989, **61**, 2594.
91. K. N. Thomsen and R. P. Baldwin, *Electroanalysis*, 1990, **2**, 263.
92. Y. Ghoroghchian, F. Sarfarazi, T. Dibble, J. Cassidy, J. J. Smith, A. Russell, G. Dunmore, M. Fleischmann and S. Pons, *Anal. Chem.*, 1986, **58**, 2278.
93. R. B. Brina, S. Pons and M. Fleischmann, *J. Electroanal. Chem.*, 1988, **244**, 81.
94. J. F. Parcher, C. J. Barbour and R. W. Murray, *Anal. Chem.*, 1989, **61**, 584.
95. A. C. Michael and R. M. Wightman, *ibid.*, 1989, **61**, 270.
96. *Idem*, *ibid.*, 1989, **61**, 2193.

MICROBAND ELECTRODES FABRICATED BY SCREEN PRINTING PROCESSES: APPLICATIONS IN ELECTROANALYSIS

DEREK H. CRASTON, CHRISTOPHER P. JONES and DAVID E. WILLIAMS*

Materials Development Division, Harwell Laboratory, AEA Technology, Didcot,
Oxfordshire OX11 0RA, U.K.

NABIL EL MURR

Laboratoire de R.M.N. et Réactivité Chimique-C.N.R.S.-U.R.A. 472 Groupe Electrochimie et
Bioconversion Electro-assistées, 2, Rue de la Houssinière, 44072 Nantes Cedex 03, France

(Received 6 November 1989. Accepted 26 February 1990)

Summary—A novel method for the simple and cheap manufacture of microband and multiple microband electrodes is described. The construction technique is based entirely on the screen printing of the surface of alumina tiles with conducting and insulating ink materials. The range of potentials over which the electrodes may be used has been determined by basic electrochemical studies. These electrode systems have been used successfully for the measurement of vitamin C, vitamin B₁ and paracetamol, which illustrates their potential as useful tools in the field of electroanalysis.

Microelectrodes have attracted much interest from workers in the field of electroanalysis. Their physical size allows both the exploration of microscopic domains¹⁻³ and the analysis of very small volumes of solution.⁴⁻⁶ In addition, microelectrodes exhibit a number of electrochemical properties that offer advantages over their macroscopic counterparts, namely, enhanced rates of mass transport of electroactive species to the electrode surface, reduced double layer capacitance (surface area greatly diminished) and, because of the small size of the faradaic currents that are passed, less susceptibility to ohmic losses.⁷ These characteristics make it possible to perform analyses on short time scales (μsec),^{8,9} under time-independent conditions, or in highly resistive media.¹⁰⁻¹³ Also, the increased rates of mass transport provide a greater sensitivity in the electrochemical measurements.

The only drawback, a slight one, of microelectrodes is that the currents obtained are very small. For measurement purposes this places high demands on instrumental precision. Nowadays, however, circuitry of the required sensitivity can be constructed fairly routinely. Much larger current responses are observed at electrodes that are macroscopic in one direction (*e.g.*, microband or microcylinder electrodes) and at closely spaced arrays of micro-

electrodes.¹⁴⁻²⁶ With regard to electrochemical properties, these electrodes possess many of the same advantages over macroscopic electrodes as described above, although the currents observed at microband and microcylinder electrodes do not approach a steady-state value. One advantage associated with the use of microelectrode arrays is the possibility of operating groups of electrodes separately, allowing simultaneous detection of a number of different species or "ring-disc" type electrochemical measurements^{22,27} to be performed.

Despite all the advantages that microelectrodes offer in the area of electroanalysis they have not yet been used on a large scale, owing to the problem of their fabrication, especially the sealing around the electrode. Although the methods of manufacture have improved considerably over the last 10 years, these electrodes are still, in general, hand-made one at a time by researchers who have by necessity become skilled in the art. The recent application of lithographic techniques^{16,18,20-25} to solve the fabrication problem shows promise, but there is still a need for novel approaches that will allow identical microelectrodes, either singly or in arrays, to be manufactured quickly, easily and at low cost.

Recently, Bond and co-workers^{23,28} described a method for the production of microband and microelectrode arrays which was based on a screen printing process²⁹ which

*Author for correspondence.

involves squeezing a specially prepared ink through a masked thin metal gauze onto the surface of a substrate beneath. This substrate is then fired in a furnace at high temperature to leave a thin pattern ($\sim 10 \mu\text{m}$ thick) of an insulating or conducting material on its surface. The technique used by Thormann and Bond involved organically based gold and platinum ink materials which were printed and fired on the surface of a pyrex glass plate. Conversion into microelectrodes was achieved by gluing a glass slide on top of the printed metal pattern. In this paper we describe a new method for the cheap and simple mass production of microband and multiple microband electrodes, which, unlike the process above, utilizes screen printing in all stages of manufacture.

Screen printing methods and materials have been highly developed for the manufacture of capacitors, resistors and conductors on alumina substrates for use in hybrid electronic circuits. Formulations are also available for printing onto glass, steel and plastic substrates, for making decorative patterns and electrical components. Their use in the fabrication of electrical components means that the multilayer patterns deposited are repeatable in thickness and geometry in mass production. In conjunction with the fact that screen printing is a simple process which does not require expensive specialist equipment, it would seem that the idea of adapting materials and methods to mass-produce electroanalytical tools and particularly microelectrodes is very attractive. For example, since the analytical response of a microelectrode is determined only by its geometry, any method of manufacture which gives repeatable geometry would lead to devices which did not require individual calibration. Of the inks available, conductor (Au, Pt, Ag, Pd/Ag, Cu) and resistor (C, RuO_2) formulations would seem suitable for electrodes, and dielectric formulations (typically lead-containing glasses filled with barium titanate) seem suitable for insulation and masking. Because these inks have been highly developed, problems of mutual compatibility, sealing at the interface and adhesion to substrates should already have been solved. In this paper the electrochemical behaviour of electrodes fabricated by these methods is discussed, and their potential for electroanalysis is demonstrated.

EXPERIMENTAL

Electrodes were made by screen-printing patterns of conductors and insulators on the

surface of an alumina tile. For this purpose a DEK65 (DEK Ltd, Weymouth, UK) printer was used, with the different patterns defined by precision screens which were also obtained from DEK. The alumina tiles (50 cm^2 ; NGK, Japan) used as the substrates for the screen-printing processes were cleaned prior to use by boiling in demineralized water (Milli Q) for 10 min. The inks were purchased from Agmet Ltd (Reading, UK) and are described in Table 1. Each ink was applied separately, with the appropriate pattern of screen. Between each printing step the tiles were passed through an infrared drier (DEK 1209) at about 120° for 10 min, and then fired in a belt furnace (DEK 840). The firing time (entry into the furnace at 15 mm/min and removal at 70 mm/min) and the temperature of the furnace varied according to the type of ink (see Table 1). In most cases the screens were 220-mesh made of stainless-steel wire ($45 \mu\text{m}$ thickness) with the print mask patterned in a layer of emulsion ($50 \mu\text{m}$) added on the underside. The print thickness is the sum of the mesh and emulsion layer thicknesses. The resulting patterns had a thickness of about $10\text{--}15 \mu\text{m}$ after firing (except for the organogold ink: thickness $\sim 2 \mu\text{m}$). In some of the experiments involving platinum ink electrodes the fabrication process utilized 325-mesh stainless-steel screens with a $23\text{-}\mu\text{m}$ thick layer of emulsion (resulting electrode thickness $< 10 \mu\text{m}$).

Investigations of the electrochemistry of the various ink materials were performed on macroscopic electrodes which were produced by first printing a line of a conducting ink and then defining the active area with one of the dielectric materials (Fig. 1a). To fabricate a microband electrode, a line of the conducting ink $2\text{--}8 \text{ mm}$ wide and $\sim 10 \mu\text{m}$ thick was printed on the surface of the tile. This was then coated with a layer of a dielectric material. An electrode $2\text{--}8 \text{ mm}$ long and approximately $10 \mu\text{m}$ wide could then be exposed by cutting the tile perpendicularly to the direction of the line, with a diamond saw. Multiple band arrangements were

Table 1. Inks and firing conditions

Ink material	Catalogue number	Firing temperature, $^\circ\text{C}$	Firing time, <i>min</i>
Platinum	5545	1200	15–60
Gold (fritted)	8836	850	15
Organogold	8081-A	850	15
Carbon	1116-S	300–500	10
Silver	9912	850	15
Dielectrics	4905	850	15
	4901	850	15

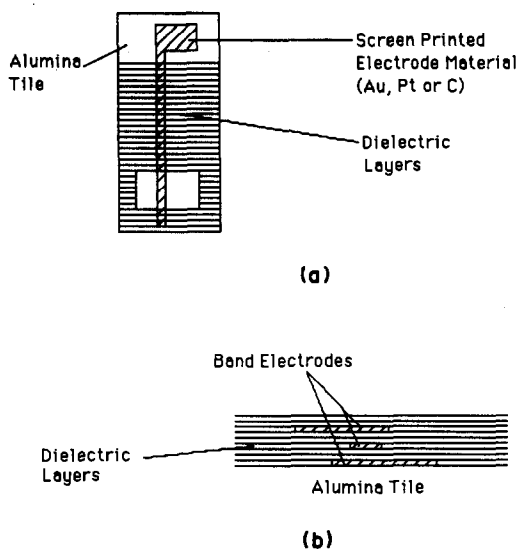


Fig. 1. Schematic diagram of two types of screen-printed electrodes: (a) a macroscopic electrode achieved by successive printing of metal and dielectric patterns and (b) a triple-band electrode (side view) made by successive printing of metal and dielectric layers and then cutting across the tile to reveal a cross-section.

prepared in a similar way: a series of alternating layers of conducting ink lines and dielectrics was printed prior to cutting the tile. The lines of the conductors were arranged so that they overlapped as illustrated in Fig. 1b. It was found that two separate layers of the insulating material had to be printed between each of the individual electrodes to prevent them from shorting together. The electroanalysis experiments involved the use of band electrodes in conjunction with a silver/silver chloride³⁰ reference/counter electrode (two-electrode arrangement). The latter electrodes were prepared by first printing a high surface-area silver electrode on the opposite side of the alumina tile. Subsequent conversion of these into silver/silver chloride electrodes was achieved by anodization in 3.5M potassium chloride.

Electrochemical measurements were performed with a potentiostat (PAR, type 173) in

conjunction with a triangular wave generator or by use of a simple 2-terminal arrangement in which the counter-electrode was powered directly from the output of the waveform generator and the working electrode was returned to ground through a sensitive current-follower (Keithley, type 427). Unless otherwise stated, all potentials are quoted with respect to a standard calomel electrode (SCE). Aqueous solutions were made up with demineralized water (Milli Q). All chemicals were obtained commercially and used without further purification. To prevent excessive oxidation, ascorbic acid solutions were prepared immediately prior to use.

RESULTS AND DISCUSSION

Electrochemistry of the ink materials

Electrodes fabricated by screen-printing processes are by their nature less pure than those constructed from base metal because the inks used contain components that facilitate interparticle binding and attachment to a substrate. This point is illustrated in Table 2, which shows surface analysis data obtained for Au and Pt screen-printed electrodes. In these cases, the native metal accounts for less than 80% of the bulk composition. It might be expected that the presence of these high levels of impurities would cause the electrochemistry of these materials to be radically altered, but this is not the case and within certain potential regions the electrochemical behaviour of the screen-printed and "pure" metal electrodes are practically identical. Taking first the example of platinum, Fig. 2 shows typical cyclic voltamperograms (CV) of printed ink and wire electrodes in phosphate buffer (pH 7.4). Here the only differences between the CVs are that for the printed electrode; a small anodic peak is present at the onset of oxide formation (approx. +350 mV) and the resolution of the hydrogen adsorption and desorption peaks is slightly poorer. This similarity in the CVs extends to those for solutions of a

Table 2. Surface analysis of screen-printed electrodes

Electrode material		Element (atom %)													
		Pt	Au	Si	O	C	Pb	Bi	Na	Al	Zn	Cu	Rh	Ag	N
Pt	surface*	20.2	—	5.9	45.1	2.8	4.9	1.9	0.3	13.7	0.8	—	—	—	—
	bulk	33.0	—	11.5	35.6	0	2.9	0.7	0.5	14.5	1.0	—	—	—	—
Au fritted	surface*	—	48.9	—	34.0	8.3	1.6	—	—	—	0.1	5.7	—	1.1	—
	bulk	—	69.7	—	28.0	0	0	—	—	—	0	2.1	—	0	—
Au organo	surface*	—	38.5	—	43.2	7.6	1.9	0.1	—	—	2.3	—	3.3	—	2.7
	bulk	—	61.2	—	38.7	0	0	0	0	—	0	—	0	—	0

*Surface refers to values obtained after 1–2 nm of the material had been removed by argon ion beam bombardment.

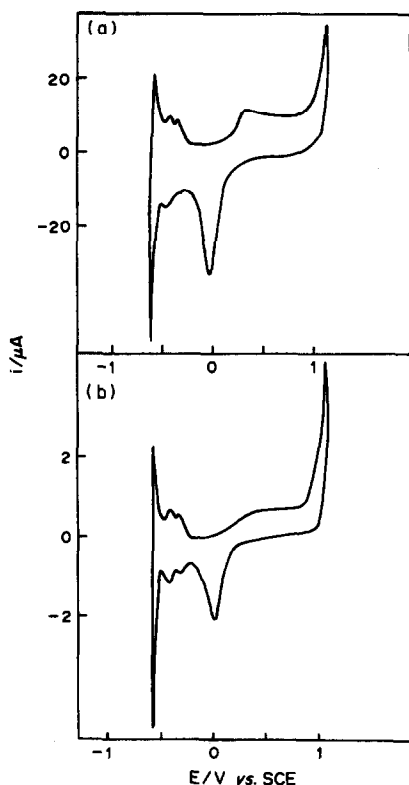


Fig. 2. Cyclic voltamperograms obtained with platinum screen-printed (a) and platinum wire (b) electrodes in 0.1M phosphate buffer (pH 7.4): sweep rate 200 mV/sec area of the printed electrode approximately 0.04 cm².

lower pH (*e.g.*, 0.1M sulphuric acid). The electrode impurities do not appear to hinder oxidation and reduction of electroactive species in solution. This is demonstrated by the cyclic voltamperogram (Fig. 3) obtained for phosphate buffer containing 5mM potassium ferrocyanide. A reversible peak is obtained at the

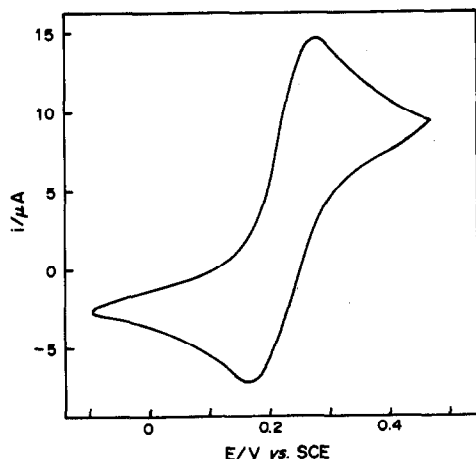


Fig. 3. Cyclic voltamperogram obtained with an ~0.04 cm² Pt printed ink electrode in phosphate buffer (0.1M, pH 7.4) containing 5mM potassium ferrocyanide: sweep rate 10 mV/sec.

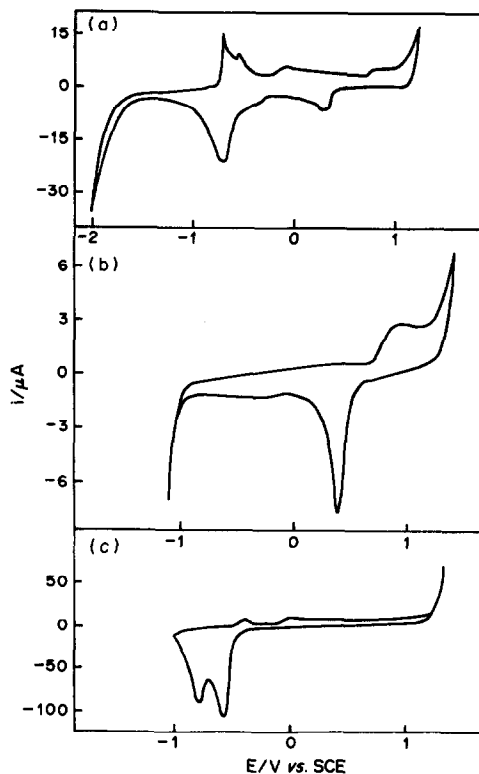


Fig. 4. Cyclic voltamperograms obtained with a gold fritted ink electrode [(a) initial scan, (c) steady-state voltamperogram obtained after about 10 scans] and a gold wire electrode (b) in 0.1M phosphate buffer (pH 7.4): sweep rate 200 mV/sec; area of the printed electrode approximately 0.04 cm².

thermodynamic potential of the redox couple, the same as that observed when a "pure" platinum electrode is used. Similarly, in the case of the gold fritted-ink electrodes (Figs. 4a and b) in the anodic region (>0 mV), the electrochemistry is virtually the same as that obtained on gold wire electrodes. In both cases the only observable features are an oxidation wave (at +700 mV) representing the formation of gold oxide and the associated reduction peak for the reverse process at between +300 and +400 mV. The kinetics of the ferricyanide/ferrocyanide redox couple is also reversible on these gold electrodes. The electrochemical behaviour, at potentials above 0 mV, of organogold electrodes in background electrolyte solutions is much the same as that observed for the fritted-ink electrodes.

In contrast to the anodic region, at potentials below -500 mV the CVs of the gold wire and gold fritted-ink electrodes are very different (Figs. 4a and b). For example, the hydrogen evolution wave is suppressed by as much as 500 mV with the printed electrodes, compared to the

gold wire. Moreover, whereas the CV obtained with the gold wire is relatively featureless, many peaks are observed with the printed electrodes between around -500 and -800 mV. These peaks appear to contain contributions from four or more different redox processes, which, because of their similarity in E^0 , are difficult to resolve. The very sharp oxidation peak at about -550 mV is not observed unless the potential is swept beyond the stable solvent limit in the cathodic direction. This probably represents the desorption of hydrogen from sites on the electrode surface. A further peculiarity regarding the cathodic electrochemistry of the gold fritted-ink electrodes is that initially the CV varies between repeated potential scans. Figure 4a represents the final CV obtained after several tens of cycles. The first potential scan is shown in Fig. 4c and is characterized by the presence of two very large reduction peaks at -650 and -850 mV. On subsequent scans both of these peaks are absent.

The voltamperograms in Fig. 4 were obtained for phosphate buffer (pH 7.4). Similar measurements were also made for solutions containing other background electrolytes (KCl, Na_2SO_4 , CH_3COONa) at neutral pH. In all cases the electrodes exhibited slow kinetics for hydrogen evolution and gave a large number of peaks in the cathodic region. It was hoped that changing the background electrolyte from one which forms insoluble salts of some of the impurity metals (*e.g.*, phosphate) to one forming soluble salts (*e.g.*, chloride) would result in a reduction in the number of peaks. This, however, was not the case and thus a more rigorous analysis of the electrochemistry of the electrodes is required to identify the nature of the electroactive impurities.

Most of the impurities present in the gold printed electrodes are electroactive only at potentials below about -500 mV. Hence, for the conditions of Fig. 2, if electroactive species with similar values of E^0 are present on the surface of the printed platinum electrodes their electrochemistry will be masked by the current associated with hydrogen evolution.

In terms of analysis, these results suggest that screen-printed electrodes can be used effectively to determine concentrations of redox-active species that can be either reduced or oxidized at potentials more anodic than -500 mV *vs.* SCE. At more cathodic potentials than this, certainly in the case of the gold fritted-ink electrodes, any technique involving stepping or sweeping

of the potential will not be feasible, because of the large currents associated with the redox properties of the electrode impurities.

In the case of the screen-printed carbon electrodes, if the firing temperature is the same as that recommended by the manufacturer, the electrodes have a high internal resistance and hence the electrochemistry is dominated by iR effects. At firing temperatures above 300° the resistance of the electrode is greatly reduced and normal electrochemical behaviour is observed. Electrodes of this type give practically featureless CVs in solutions of background electrolytes when the potential is scanned between the solvent limits. These CVs are characterized by high capacitive currents, which suggests that the electrodes are porous in nature, with a correspondingly large surface area. The dramatic increase in electrode conductivity at higher firing temperatures is most likely due to the decomposition of the epoxy-based polymer which is present as a binder for the carbon particles. A natural consequence of this decomposition is that the electrodes show poor adhesive properties and are mechanically weak. If these two problems could be overcome, the carbon ink would provide the added bonus of allowing electroanalysis to be performed at reducing potentials.

Microband electrodes

Single-band electrodes. Microband electrodes have been constructed with both gold and platinum printing inks. In the absence of electroactive species in the surrounding environment these electrodes exhibit electrochemical behaviour identical to that of their macroscopic counterparts described above. They also exhibit the general characteristics of microelectrodes (having low capacitive currents, which allows use at high sweep rates and in media of high electrical resistance). The gold microbands showed no sign of leakage around the seal with the insulator, but the platinum microbands did, evidenced in solution by a gradual increase in the observed capacitive currents with time (faradaic currents over the same period remained constant) and indicating a need for further attention to detail in the choice of materials and preparation conditions.

Figure 5 shows cyclic voltamperograms obtained with fritted gold and organogold electrodes (band length 6.5 mm in each case) in a solution containing ferrocyanide ions. The thicknesses of the bands (estimated by

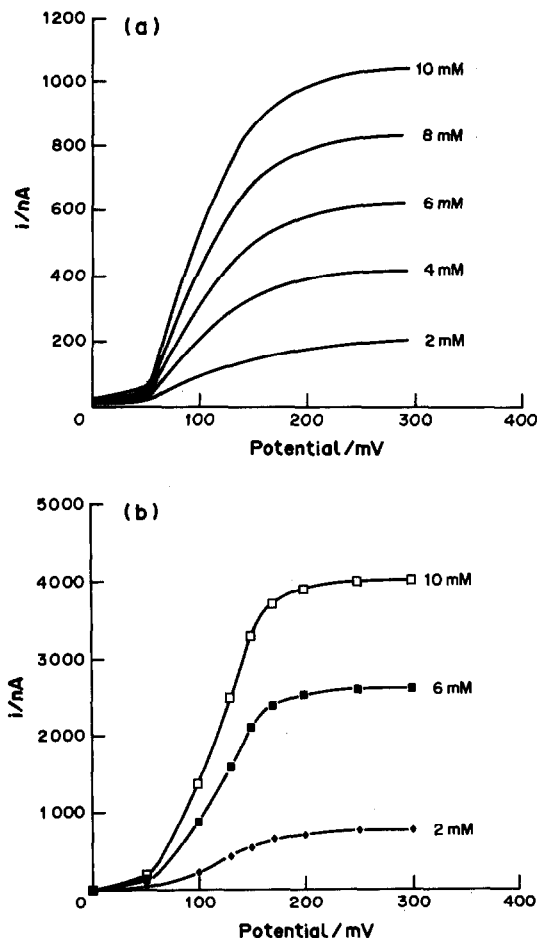


Fig. 5. Cyclic voltamperograms obtained with (a) an organogold-based microband electrode and (b) a fritted ink microband electrode in $0.1M$ KNO_3 containing $K_4Fe(CN)_6$ (concentrations indicated). Sweep rate 20 mV/sec.

inspection under a high-power optical microscope) were approximately 12 and $2 \mu m$ for the fritted and organogold electrodes respectively. The shape of the voltammetric curve, shown in Fig. 5, is characteristic of that obtained at microband electrodes, *i.e.*, at sufficiently low sweep rates the oxidation wave levels off to a quasi-steady-state limiting current and the corresponding reduction peak is greatly reduced. For both of these band electrodes the magnitudes of the limiting current are proportional to the concentration of the electroactive species.

The quasi-steady-state current (A) is given by²⁷

$$i = nFDCl \left[\frac{5.553}{\ln \theta} - \frac{6.791}{(\ln \theta)^2} \right] \quad (1)$$

where n is the number of electrons, F the Faraday constant, D the diffusion coefficient (cm^2/sec), C the bulk concentration ($mole/cm^3$)

of the electroactive species and l the length of the band (cm), and θ is $4Dt/W^2$, t being time (sec) and W the width of the band (cm).

By use of this equation, theoretical values for the steady-state currents of $0.43C$ (fritted gold) and $0.29C$ (organogold) can be calculated for the experimental conditions described in Fig. 5 ($D = 6.3 \times 10^{-6} cm^2/sec$, $t \sim 1.25$ sec ($\sim RT/Fv$, where v is the scan rate)). From Fig. 5, a value of $0.4C$ is obtained for the fritted gold electrode, which is in good agreement with theory. For the organogold ink electrode a value of $0.1C$ is obtained, which is much less than would be expected from purely theoretical considerations. However, examination of this band electrode under an optical microscope indicated that it was not continuous and hence this low value is not unexpected. The reason for the discontinuous nature of these electrodes is not known, but is likely to be due to smearing of the dielectric layer over the surface of the electrode during the cutting process (see Experimental).

One advantage of using screen printing methods with commercial inks is that the prints should be repeatable in thickness. The inter-electrode repeatability for a set of ten different microbands prepared with the fritted gold ink was checked by cyclic voltammetry of ferrocene in ethanol (containing $0.1M$ $LiBF_4$). The variation in the limiting current values obtained with the set of electrodes was less than $\pm 5\%$ around the mean.

Ascorbic acid sensors. Determination of vitamins in foodstuffs and biological fluids is generally time-consuming and expensive.³¹ Vitamin C can be measured electrochemically since it can be oxidized relatively easily to dehydroascorbic acid; the redox potential of this process is pH-dependent.

The system we have used for ascorbic acid determination consists of a fritted gold microband electrode with an associated printed silver/silver chloride auxiliary electrode (see experimental). A series of cyclic voltamperograms taken with one of these sensors in a solution containing ascorbic acid in phosphate-buffered saline at pH 7 ($0.1M$ phosphate buffer, $0.15M$ sodium chloride) is shown in Fig. 6a. The quasi-steady-state current was found to vary linearly with acid concentration. From the slope of this line a value of $5.7 \times 10^{-6} cm^2/sec$ (in good agreement with the literature value³²) can be calculated for the diffusion coefficient of ascorbic acid by equation (1).

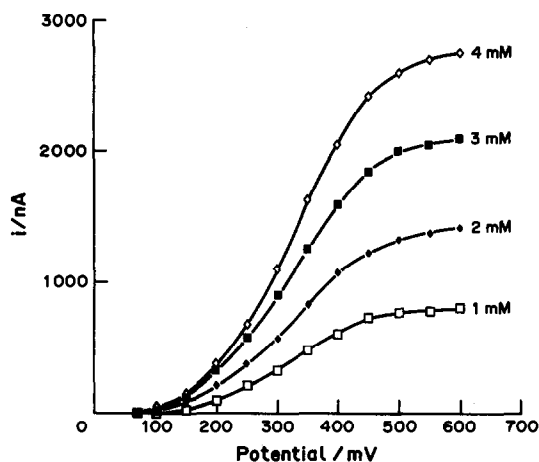


Fig. 6. Cyclic voltamperograms obtained with a fritted gold microband electrode in phosphate-buffered saline (0.1M pH 7, 0.15M NaCl) for various concentrations of ascorbic acid. Sweep rate 20 mV/sec.

This electrode system was also placed in a proprietary orange drink. Figure 7 shows the linear sweep voltamperograms obtained with and without addition of ascorbic acid. Since the position of the oxidation wave is the same for both CVs, we conclude that the current for the orange drink alone is due to the presence of ascorbic acid. Analysis of the steady-state current gave a concentration of 1.6mM, which is within the limits quoted by the manufacturer.

The electrode has also been used to measure the concentration of ascorbate in apples (Granny Smith's). Figure 8 shows voltamperograms obtained at two separate locations: one at the surface, the other near the centre. The results indicate a decrease in concentration of ascorbate with depth, as reported previously.³³ The concentration at the surface was estimated

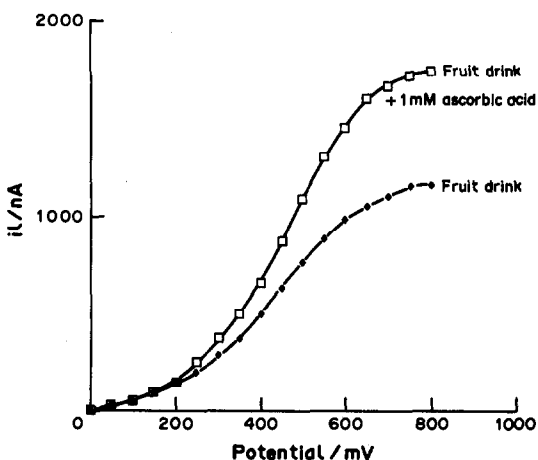


Fig. 7. Cyclic voltamperograms obtained with a fritted gold microband electrode in a proprietary fruit drink with and without added ascorbic acid. Sweep rate 20 mV/sec.

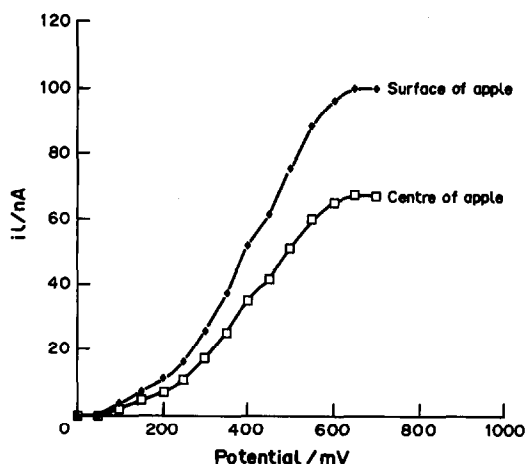


Fig. 8. Cyclic voltamperograms obtained with a fritted gold microband electrode in a Granny Smith's apple. Sweep rate 20 mV/sec.

to be approximately 3 mg/100 g of fruit, which is in line with results obtained by other techniques.³³ We have also used the method successfully for potatoes, oranges, strawberries and kiwi fruit.³⁴

Paracetamol sensor. Paracetamol can also be oxidized electrochemically. Figure 9 shows once again that a quasi-steady-state is observed, the magnitude of which is linearly dependent on the concentration of the electroactive species. Increasing the pH of the background electrolyte from 6.2 to 10.5 resulted in oxidation at a more cathodic potential. Linear calibration plots were also obtained at this higher pH.

Multiple band electrodes

In general it was found that multiple microband electrodes became less uniform as the

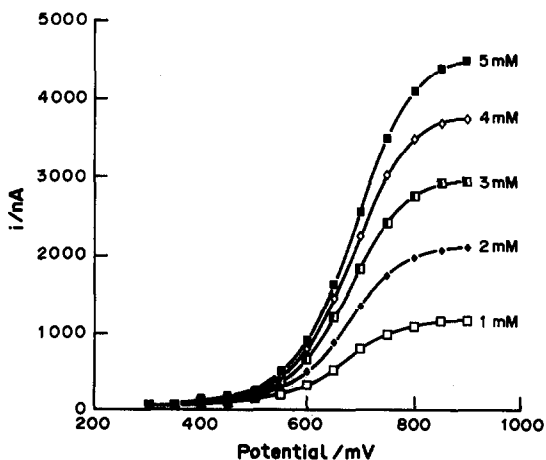


Fig. 9. Cyclic voltamperograms obtained with a fritted gold microband electrode in 0.1M NaClO₄ with various concentrations of paracetamol. Sweep rate 100 mV/sec.

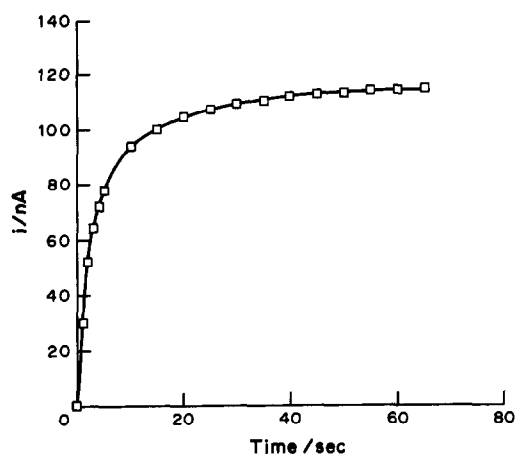


Fig. 10. Current-time transient measured on a dual microband system. Ferricyanide electrogenerated on an organogold microband electrode is measured on an adjacent fritted gold microband electrode. Electrolyte used was 0.1M KNO₃ containing 12mM K₄[Fe(CN)₆]. The potential of the fritted gold microband electrode was maintained at -0.1 V (vs. SCE). The generating current on the organogold microband electrode was supplied from a dry-cell battery.

number of printed bands was increased. This is presumably due to problems associated with the repeated firing and cooling processes used in their manufacture.

Multiple band electrodes have been operated in ring-disc mode, where the product of the electrochemical reaction at one of the electrodes is measured on the others. Taking first the example of a dual-band system, Fig. 10 shows the results of experiments where one of the electrodes was made with the fritted gold ink and the other with the organogold material. Here the transient response is shown for the case where ferricyanide produced by the oxidation of ferrocyanide at the organogold electrode is measured on the fritted gold electrode. As can be seen, the current becomes constant after slightly less than 1 min. Increasing the generator current results in a corresponding increase in the current obtained at the fritted ink electrode. The proportion of current measured, defined by $\Phi = \text{collector current} / \text{generator current}$, is called the collection efficiency.

Figure 11 shows a plot of the collector current *vs.* the generator current for the same system as in Fig. 10. The collection efficiency was 42%. Figure 11 also shows data obtained with a dual-band electrode where both of the bands were made with the fritted ink. Here a reduced collection efficiency of 29% was observed. This is in line with the findings of Shea and Bard²⁷,

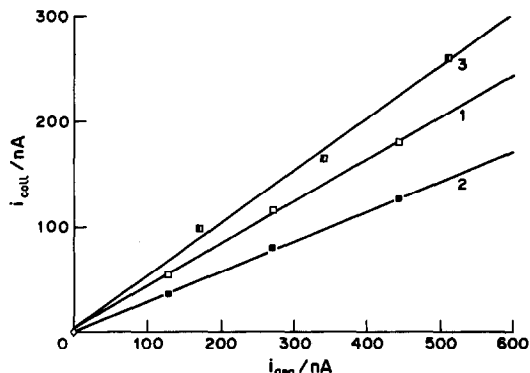


Fig. 11. Relationship between the generating current and the detected current for dual (1, 2) and triple (3) microband electrodes. Conditions as for Fig. 10. For the dual-band electrode systems a fritted gold collector microband electrode was used with both organogold (1) and fritted gold (2) generator microband electrodes.

who suggested that to maximize the collection efficiency the collector band should be much wider than the generator band.

Shea and Bard²⁷ used a computer simulation to calculate the collection efficiencies of this type of system. With θ_{gap} defined by

$$\theta_{\text{gap}} = 4Dt / (W_{\text{gap}})^2 \quad (2)$$

where W_{gap} is the width between bands (cm), the quasi-steady-state collection efficiency, Φ_{ss} , can be calculated from

$$\Phi_{\text{ss}} = 0.033 + 0.21 \log \theta_{\text{gap}} - 0.016 (\log \theta_{\text{gap}})^2 \quad (3)$$

With an average gap of 30 μm (estimated by inspection under an optical microscope), the collection efficiency for ferro/ferricyanide, for the case where the generator band was constructed from the organogold ink, was calculated to be 42%. This is in excellent agreement with the experimental value (42%).

Electrodes of triple-band configuration have been constructed with the gold fritted material (*i.e.*, all electrodes 12 μm thick). It was found that if adjacent electrodes were used in dual-band generator/collector mode then the collection efficiencies obtained were similar to those described above (29%). When both outer electrodes were used to measure the product electrogenerated at the inner electrode, the combined collection efficiency rose to 50% (Fig. 11). This is less than the sum of the individual collection efficiencies, which is again in agreement with the results obtained by Bard *et al.*²²

Thiamine sensor. For the purpose of analysis it is possible to measure non-electroactive species by monitoring their reaction with an electrogenerated reagent.³⁵ A convenient way of doing this is to use a multiple-band system where the reagent is generated at one electrode and measured at the others. In transit between the generator and collector electrodes this reagent can react with the substance of interest, which is present in the bulk solution. The reaction means that a smaller current than expected will be measured at the collector electrodes. This technique, which measures a reduction in the collection efficiency, can be operated as a type of amperometric titration.

Thiamine, vitamin B₁, when in its pyrophosphate form (cocarboxylase) is a cofactor which is utilized in a number of enzyme systems.³⁶ It is possible to oxidize this species in the presence of alkaline ferricyanide to thiochrome. The amperometric titration of thiamine, in a solution of ferrocyanide, has been performed by using triple-band electrodes. Here the central generator band is used to oxidize ferrocyanide to ferricyanide, which is subsequently measured at the two outer band electrodes. It was found that for a given current the collector current decreases with increasing thiamine concentration (an alternative method would have been to measure the collection efficiency as a function of generator current³⁶). Figure 12 shows a calibration curve which relates the collection efficiency to the concentration of thiamine.

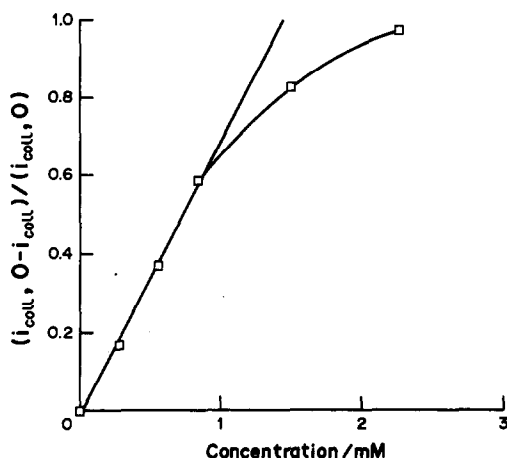


Fig. 12. Calibration graph for thiamine; i_{col} is the collection current for electrogenerated ferricyanide reduction measured on the outer fritted gold microband electrodes (generator current 320 nA) and $i_{\text{col}, 0}$ is the collector current in the absence of thiamine. Experimental conditions as for Fig. 10.

CONCLUSIONS

A new simple and cheap method for the manufacture of microband and multiple-band electrodes has been described. Despite the presence of high levels of impurities, these electrodes demonstrate good electrochemical behaviour and are therefore suitable for use in electro-analytical applications. We believe that electrodes made in this way can be inserted into complex environments (both solid and liquid) to provide information on concentrations of chemical species. The potential in this area has already been demonstrated by the measurement of ascorbic acid levels in fruit and vegetables and an orange drink. Further investigations in this area are in progress. We are also extending our studies to look at new measurement techniques and to ascertain the different species that can be analysed by use of these electrode systems.

Acknowledgements—This work was funded by the AEA Technology speculative funding programme. The authors would like to thank Vic Moore for the surface analysis measurements and Paul Fennell and Prof. Martin Fleischman for helpful discussions.

REFERENCES

1. R. N. Adams, *Anal. Chem.*, 1976, **48**, 1126A.
2. R. M. Wightman, *ibid.*, 1981, **53**, 1125A.
3. A. G. Ewing, J. C. Bigelow and R. M. Wightman, *Science*, 1983, **221**, 169.
4. A. S. Baranski, *Anal. Chem.*, 1987, **59**, 662.
5. J. G. White, R. L. St. Claire and J. W. Jorgenson, *ibid.*, 1986, **58**, 293.
6. J. G. White and J. W. Jorgenson, *ibid.*, 1986, **58**, 2992.
7. R. M. Wightman and D. O. Wipf, in *Electroanalytical Chemistry*, A. J. Bard (ed.), Vol. 15, p. 267. Dekker, New York, 1989.
8. T. Hapel and J. Osteryoung, *J. Phys. Chem.*, 1982, **86**, 1406.
9. J. O. Howell and R. M. Wightman, *ibid.*, 1984, **88**, 3915.
10. *Idem*, *Anal. Chem.*, 1984, **56**, 524.
11. A. M. Bond, M. Fleischmann and J. Robinson, *J. Electroanal. Chem.*, 1984, **168**, 299.
12. *Idem*, *ibid.*, 1984, **180**, 257.
13. J. Ghoroghchian, F. Sarfarazi, T. Dibble, J. Cassidy, J. J. Smith, A. Russell, G. Dunmore, M. Fleischmann and S. Pons, *Anal. Chem.*, 1986, **58**, 2278.
14. D. E. Weisshaar, D. E. Tallman and J. L. Anderson, *ibid.*, 1981, **53**, 1809.
15. W. L. Caudill, J. O. Howell and R. M. Wightman, *ibid.*, 1982, **54**, 2532.
16. D. G. Sanderson and L. B. Anderson, *ibid.*, 1985, **57**, 2388.
17. N. Sleszynski, J. Osteryoung and M. Carter, *ibid.*, 1984, **56**, 130.
18. T. Hapel and J. Osteryoung, *J. Electrochem. Soc.*, 1986, **113**, 752.
19. F. Belal and J. L. Anderson, *Talanta*, 1986, **33**, 448.

20. G. P. Kittlesen, H. S. White and M. S. Wrighton, *J. Am. Chem. Soc.*, 1984, **106**, 7389.
21. H. S. White, G. P. Kittlesen and M. S. Wrighton, *ibid.*, 1984, **106**, 5375.
22. A. J. Bard, J. A. Crayston, G. P. Kittlesen, T. Varco Shea and M. S. Wrighton, *Anal. Chem.*, 1986, **58**, 2321.
23. W. Thormann, P. van den Bosch and A. M. Bond, *ibid.*, 1985, **57**, 2764.
24. L. E. Fosdick, J. L. Anderson, T. A. Baginski and R. C. Jaeger, *ibid.*, 1986, **58**, 2750.
25. C. E. Chidsey, B. J. Feldman, C. Lundgren and R. W. Murray, *ibid.*, 1986, **58**, 601.
27. T. V. Shea and A. J. Bard, *ibid.*, 1987, **59**, 2101.
28. A. M. Bond, T. L. E. Henderson and W. Thormann, *J. Phys. Chem.*, 1986, **90**, 2911.
29. P. J. Holmes and R. G. Loasby (eds.), *Handbook of Thick Film Technology*. Electrochemical Publications, Ayr, 1976.
30. I. W. Burns and C. I. Nylander, *Anal. Proc.*, 1986, **23**, 289.
31. H. Varley and A. H. Gowenlock (eds.), *Practical Clinical Biochemistry, Vol. 2 Hormones, Vitamins, Drugs and Poisons*. Heinemann, London, 1976.
32. I. M. Kolthoff and J. J. Lingane, *Polarography*, Vol. 2, 2nd Ed., p. 729. Interscience, New York.
33. A. A. Paul and D. A. T. Southgate (eds.), *McCance and Widdowson's The Composition of Foods*, 4th Ed., p. 196. Elsevier, Amsterdam, 1978.
34. D. E. Williams, N. El Murr and C. P. Jones, in *World Biotech Report 1988*, p. 369. Online Publications, London, 1988.
35. S. P. Colowick, N. O. Kaplan and D. B. McCormick (eds.), *Methods in Enzymology*, Vol. 66, Part D, *Vitamins and Coenzymes*. Academic Press, New York, 1980.
36. W. J. Albery, P. N. Bartlett, A. E. G. Cass, D. H. Craston and B. G. D. Haggett, *J. Chem. Soc., Faraday Trans. 1*, 1986, **82**, 1033.

ANALYTICAL IMPLICATIONS OF ZEOLITES IN OVERLAYERS AT ELECTRODES

DEBRA R. ROLISON*, ROBERT J. NOWAK†, TIMOTHY A. WELSH and CATHERINE G. MURRAY
Code 6170, Surface Chemistry Branch, Naval Research Laboratory, Washington, DC 20375-5000, U.S.A.

(Received 30 May 1990. Accepted 6 July 1990)

Summary—A review is given of past and potential analytical and other applications of electrodes overlaid with zeolites.

The aluminosilicate zeolites, when incorporated into an electrochemical interphase, offer a number of chemical, physical, and structural characteristics of interest in the design of electro-analytical schemes. Several recent reviews cover the general interest in zeolites as materials useful in electrochemical environments.¹⁻³ The electro-analytically relevant characteristics of such zeolites will be described briefly below; the implications for electroanalysis inherent in these zeolite properties will be illustrated with examples from the literature and the work of our group. Potential zeolite-based electro-analyses will also be described.

The aluminosilicate zeolites

Many (but not all⁴) zeolites are formed from tetrahedrally oxygen-linked silicon and aluminum atoms in varying Al to Si ratios. The resulting crystalline aluminosilicate lattice has three predominant characteristics,⁵ each with electroanalytical and other implications. These characteristics are:

- (i) molecular sieve selectivity based on the size and shape of the molecules interacting with the zeolite;
- (ii) cation-exchange capacity;
- (iii) inherent catalytic properties due to the strong-acid nature of the zeolite as well as the ability to modify catalytic properties by cation-exchange with or without subsequent redox reactions.

Figure 1 summarizes the chemical/structural nature of the aluminosilicate zeolites. The two-

dimensional representation of the oxygen-linked tetrahedra (Fig. 1) illustrates characteristics (ii) and (iii). Every Al atom in the lattice results in a fixed negative charge; electroneutrality is achieved with mobile cations, frequently alkali-metal ions. These cations can be exchanged for others, depending on their specific site in the zeolite lattice and the size of the exchanging cation.⁵ The strong-acid nature of the aluminosilicate zeolites, responsible for their wide use in acid-catalyzed reactions of technological significance⁶ arises from the terminal hydroxyl groups at the crystal faces. The aluminum-rich aluminosilicate zeolites can decompose in the presence of strong acid, through removal of aluminum atoms from the lattice,⁵ so the pH of the medium needs to be considered when using these materials for electro-analysis.

The three-dimensional zeolite lattice, which arises from the linking of the various ring structures that can be formed from conjoining the oxygen-linked tetrahedra, offers a cage-and-channel architecture of molecular size; the molecular sieve character of zeolites is derived from the pore, void space, and cage aspects of this architecture. Figure 1b shows a framework representation for zeolite A, a synthetic zeolite with the ideal formula $(M^{(I)})_{12}(AlO_2)_{12}(SiO_2)_{12}$, and the zeolite of choice for our work.

Zeolite A belongs to the faujasite structure class, as do types X and Y; the channels and cages of these zeolites intersect in three dimensions, so that diffusion of sorbed species in such zeolites is three-dimensional. Figure 1b shows the supercages for the faujasitic zeolites A, X, and Y, with their pore openings in three dimensions, and as is evident from this figure, the size of the pore openings and the size of the supercages can differ as a function of the structure.

*Author for correspondence.

†Chemistry Division, Code 1113ES, Office of Naval Research, Arlington, VA 22217, U.S.A.

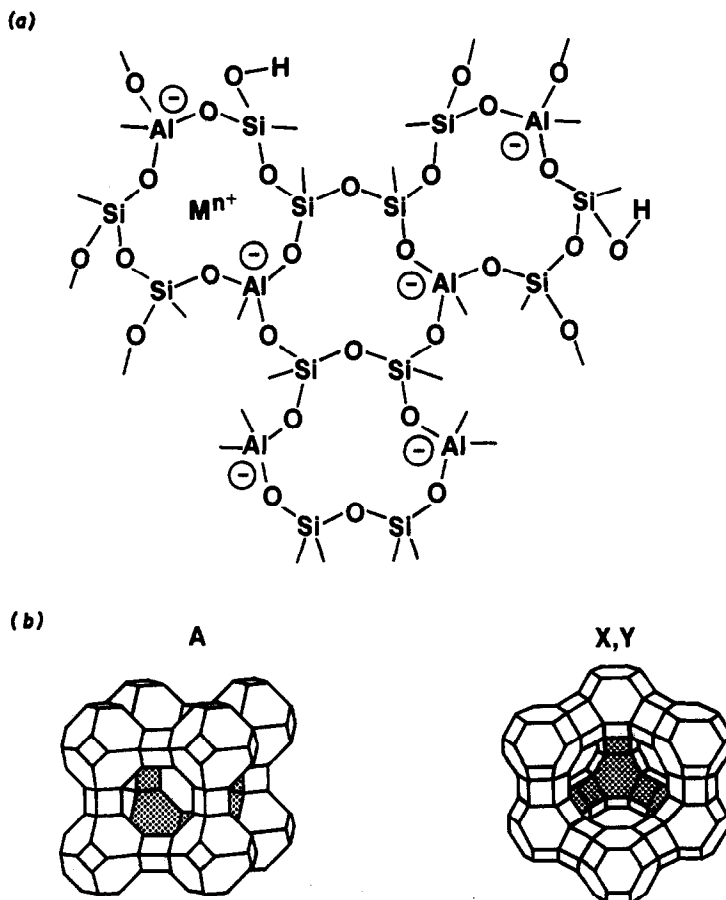


Fig. 1. The chemical and structural nature of aluminosilicate zeolites. (a) A two-dimensional representation of the Al-O-Si linkages that create the framework of aluminosilicate zeolites, illustrating the fixed anionic sites (one per Al atom), charge-compensating cations, and terminating hydroxyl groups (adapted from Rolison²); (b) three-dimensional representation of the faujasitic geometry for zeolites A (Al:Si = 0.7-1.2) and X (Al:Si = 1.0-1.5)/Y (Al:Si = 1.5-3).

Zeolites X and Y have pore openings of about 0.74 nm, whereas zeolite A has pore openings of about 0.4 nm. Zeolites in which diffusion is one- or two-dimensional along the channels also exist.^{3,5,7}

Zeolites and their electroanalytical possibilities

Combining a zeolite-containing overlayer on (or as part of) an electrode surface allows both electrochemical stimulus of the zeolite (*e.g.*, by electrogeneration of a reactant capable of interacting with the zeolite) and electrochemical detection (or reaction) of a zeolite-entrained reactant or a zeolite-reacted product. Electroanalytical consequences accrue from all of the zeolitic characteristics described above, in that any electroanalytical scheme which relies on ion-exchange, or analyte preconcentration, or size/shape/charge selectivity, or catalyst-assisted reactivity, or any combination of these features,

can be designed for use of a zeolite-modified electrode.

EXPERIMENTAL

All electrochemical experiments reported are for zeolite A, either in pure powder form (NaA, Linde; sized as less than 10 μm) or from ground and sieved 4A (NaA) or 3A (KA) molecular sieves (Linde, containing a clay extruder to form pellets or beads). The supporting electrolyte was 0.1M Et₄NClO₄ (Southwestern Chemicals, vacuum dried at 50°) in CH₃CN (Burdick & Jackson, high purity, used as received). Ferrocene, 1,4-dinitrobenzene and 1,4-benzoquinone were sublimed before use. Pyrrole (Aldrich) was purified before use, by passage through activated alumina.

Voltammetric experiments were performed with an EG&G PAR Model 173 potentiostat/

galvanostat. Pine Instruments Rotators, Models PIR and MSR, were used to electrodeposit zeolite overlayers on Pt and glassy-carbon disk electrodes (Pine Instruments) generally by a previously described procedure.⁸ Potentials are referred to a NaCl-saturated calomel electrode (SSCE), unless otherwise noted; platinum wire was used as the auxiliary electrode.

ELECTROANALYSIS WITH ZEOLITE-MODIFIED ELECTRODES

Preconcentration of electroactive solutes—amperometric detection

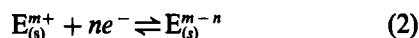
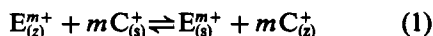
The molecular size and shape selectivity (and the high internal surface area⁵) of zeolites can be used for preferentially adsorbing appropriately sized neutral species or cations in the zeolite on the basis of the size of its pore openings. When a zeolite is coupled to an electrode (*e.g.*, by mixing with carbon paste or casting from a polymer suspension—see Rolison² for a summary of preparatory methods for zeolite-modified electrodes), species preconcentrated in it can be subsequently detected at their characteristic potentials or made available for coupled chemical and electron-transfer reactions.

An electroanalytical approach based on adsorption of cationic analytes by the zeolite in a zeolite-modified electrode, followed by electrochemical detection, has been applied in a number of instances; a few will be described here as examples. Zeolite-modified carbon pastes have been used to sorb cations such as Hg^{2+} ,⁹ or Ag^+ ,¹⁰ at $\mu\text{g/ml}$ levels from aqueous solution at open circuit and then, at a suitable applied potential, give a signal corresponding to the amounts adsorbed and hence (by calibration) to those present in the initial solutions.

Though zeolites can provide size and shape selectivity at an electrode interphase, they do not provide specificity; competing adsorbates in the analyte solution can affect the amperometric response, and this must be considered when performing electroanalysis with zeolite-modified electrodes. Wang and Martinez¹⁰ showed that the magnitude of the reduction current for Ag^+ adsorbed by zeolite-modified carbon-paste electrodes from $1 \mu\text{g/ml}$ Ag^+ solutions, was unaffected by the presence in the initial solution of $10 \mu\text{g/ml}$ amounts of Co(II) , Mn(II) , Ca(II) , Pb(II) , Cu(II) , and Ti(IV) , but completely suppressed by $10 \mu\text{g/ml}$ Fe(III) ; reduction currents were enhanced when the cationic interferents in solution were Bi(III) , U(IV) , Ni(II) , Zn(II) , and Tl(I) .

Shaw *et al.*¹¹ have explored competitive cation adsorption by zeolite Y of methylviologen (MV^{2+}) and $\text{Ru(NH}_3)_6^{3+}$ and by Cu(II)-Y for electrolyte cations of various hydrated sizes. Their work also highlights the importance of understanding the nature of the mass transport of electron-transfer species in the zeolite interphase in order to explain the observed voltammetry. Zeolite Y was shown to adsorb $\text{Ru(NH}_3)_6^{3+}$ preferentially, but the current response was greater with MV^{2+} -exchanged Y, indicating that the mobility into and out of Y was greater for MV^{2+} than for $\text{Ru(NH}_3)_6^{3+}$. The current observed for the reduction of zeolite-adsorbed Cu^{2+} increased when Cu(II)-Y was exposed to solutions of cations with small hydrated radius, showing that the smaller cations displaced the zeolite-adsorbed Cu^{2+} more readily.

The mechanism first proposed by Shaw *et al.*¹¹ to explain the amperometric response of a zeolite-modified electrode containing adsorbed electroactive solutes involves ion-exchange of the adsorbed electroactive cations with different cations in the electrolyte solution and the subsequent reduction of the liberated electroactive cations at the electrode, *e.g.*,



where E^{m+} is the electroactive cation, C^+ is the electrolyte cation, and the subscripts (z) and (s) refer to the zeolite and solution phases, respectively. The amperometric response observed for $\text{E}_{(s)}^{m+}$ thus depends on the mobility of E^{m+} within and out of the zeolite (the latter in turn being influenced by the mobility of the displacing cation) and the nature of mass transport of the species in the zeolite-electrode interphase. Zeolite overlayers at electrode surfaces provide edge effects and high interfacial concentrations of electroactive species, conditions which affect mass transport and have been shown to affect the voltammetric response of MV^{2+} -modified zeolite Y.^{11,12}

The ability of a zeolite-modified electrode to discriminate on the basis of the size of the sorbed analyte and the size of competing adsorbates can be a subtle effect, as we have shown for adsorption of oxygen by zeolite A electrodeposited as a compact coating on platinum or glassy-carbon rotating disk electrodes.⁸ In this system, both the sodium form of zeolite A (NaA , with pore openings of 0.4 nm) and the

potassium form (KA, with pore openings of 0.3 nm) sorb oxygen when the zeolite-coated electrode is exposed to air or an oxygenated solution. When these oxygen-loaded zeolite-modified electrodes were placed in deoxygenated acetonitrile/tetra-alkylammonium electrolyte, the reductive voltammetry was dominated by oxygen reduction. Attempting to purge oxygen from the coatings by bubbling nitrogen through the electrolyte solution worked only for the NaA coatings, as the nitrogen molecules were too large to enter into the pores of KA. The use of argon (with a diameter <0.3 nm) instead of nitrogen could purge oxygen from both coatings.⁸

Zeolites sandwiched between an anode and cathode have also been used to determine sorbed oxygen amperometrically, but in the dry state and at elevated temperatures (>200°).^{13,14} The voltammetric responses of adsorbed^{14,15} and occluded inorganic species^{13,16} in dry zeolite films have also been studied. Although it is not an example of amperometric detection, the work of Bein *et al.*¹⁷ is interesting: they used a mixed zeolite-silica thin film coated on a surface acoustic wave device to discriminate vapor-phase organic molecules that were small enough to be sorbed in the zeolite from those too large to penetrate it. The large surface area of the zeolite in the thin film resulted in a large change in the frequency of the device when adsorption occurred.

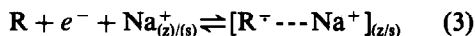
Preconcentration of electron-transfer interactive species—amperometric detection

Direct analytical application of zeolite-modified electrodes relies on adsorption of the electroactive analyte of interest by the zeolite but the zeolite can also act as a repository for reactants that can be used to affect the electrochemical response of a desired analyte. The loading of zeolite with a chemical reagent needed in an electroanalytical scheme is quite feasible and provides the reagent where it is most effective, *i.e.*, at the electrode interface during electron transfer. This aspect of electroanalysis with zeolites has yet to be exploited.

It should be remembered that a zeolite, by its inherent nature, provides an interactive electron-transfer species. The word zeolite derives from the Greek for "boiling stone" owing to the great uptake of water by a zeolite and its (reversible) release upon heating. Fully dehydrated zeolites will start to become hydrated upon exposure to ambient air, so the presence of

water in the zeolite-electrode interphase is ensured unless precautions are taken. For analyses in aqueous solutions, this would not be a primary concern, whereas in analyses for water-sensitive electroactive solutes in non-aqueous media, it could either cause difficulty or be an exploitable variable in the system. Also, as observed with regard to oxygen, the ability of zeolites to sorb appropriately sized gases can also influence the observed voltammetric response of zeolite-modified electrodes.

Another overlooked, but inherent reactive species in the zeolite is the mobile counter-ion, often Na⁺. Besides being replaceable by cationic reactants or analytes, such alkali-metal ions, when present in the zeolite-electrode interphase for a zeolite used in an aprotic electrochemical solvent of low donicity, will affect the electroreductive response to oxidants (designated as R), through ion-association reactions, *e.g.*,



The mobile counter-ions will be present in high concentrations in the zeolite-electrode interphase since zeolites are solid solutions of about 1 molal concentration and the cation-exchange reactions with electrolyte cations release these counter-ions into solution. The magnitude of their effect on organic reductions is related to the equilibrium constant for the ion-association reaction. This is the interaction which led to our discovery of the co-electrodeposition of organic oxidants and zeolite A as compact coatings on rotated Pt or glassy-carbon disk electrodes.^{8,18}

Zeolite overlayers on electrodes, however deposited, retain this ability to influence electroreductions of organic oxidants in low-donicity solvents by providing a high activity of strongly associating alkali-metal ions in the electrochemical interphase; this can be seen in Fig. 2 for the two one-electron reductions of 1,4-benzoquinone in 0.1M Et₄NClO₄/CH₃CN electrolyte. At an uncoated platinum electrode (Fig. 2a) the two reversible reductions are seen; scanning the potential at a platinum electrode with a compactly coated NaA/1,4-dinitrobenzene overlayer in the same solution shifts the second reduction (R^{•-} + e⁻ = R²⁻) to more positive voltages (see Fig. 2c), consistent with ion-pairing of the anion radical with a strongly associating cation, such as Na⁺.^{19,20} A similarly coated platinum electrode, but with visible regions of exposed metal, also shows a shift to more positive potentials for the second

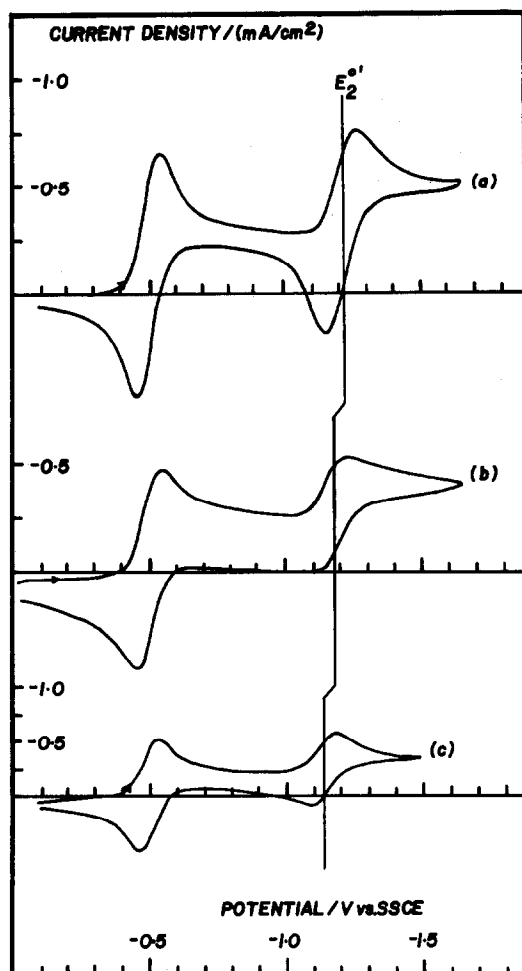


Fig. 2. The two one-electron reductions for 1,4-benzoquinone in 0.1M $\text{Et}_4\text{NClO}_4/\text{CH}_3\text{CN}$ at (a) Pt; (b) Pt partially coated with a co-electrodeposited overlayer of NaA/1,4-dinitrobenzene; (c) Pt compactly coated with a co-electrodeposited overlayer of NaA/1,4-dinitrobenzene. The standard potential for the reduction of the anion radical is marked with a solid line to show the shift to more positive potentials when the reduction occurs through a zeolite overlayer.

reduction (Fig. 2b), but less than that occurring with a compactly coated electrode (Fig. 2c).

If ion-association reactions during electroanalysis in low-donicity electrolytes are undesirable, prior ion-exchange of the zeolite with a less strongly associating cation is necessary. Lithium and sodium type zeolites should certainly be avoided in such a situation.

One design involving zeolite-modified electrodes containing preconcentrated electron-transfer interactive species that could be applied to electroanalysis, but so far has not, is based on the manipulation of vectorial electron-transport chains. In this design concept, as pioneered by Mallouk and co-workers,^{21,22} the zeolite is used

as a size- and charge-discriminating support for spatial array of donor and acceptor pairs which can respond to light or electrochemical potential. This provides a rectifying interface with charge-trapping and untrapping characteristics.

For instance, MV^{2+} -exchanged zeolite Y was partially capped by ion-exchange of the bulky porphyrin derivative, cobalt(II) tetrakis(*N*-methyl-4-pyridyl)porphyrin chloride, for Na^+ ions on the external surface of zeolite Y; this modified zeolite was cast onto SnO_2 from a zeolite-polystyrene suspension. The porphyrin blocked direct reduction of the entrained viologen, but could itself be directly reduced at the electrode; in turn the reduced porphyrin ring could reduce the entrained viologen.²³ The proper choice of the sizes and standard potentials of redox species arranged on a zeolite for vectorial transport, could provide a detection system based on the electron-flow (charge untrapping) produced by exposure of such a zeolite-electrode interphase to an analyte of appropriate standard potential.

Conductive composites—amperometric detection

Zeolite-modified electrodes can be readily prepared by casting from polymer solutions or by mixing well with carbon paste, but one of the more robust and rapidly responsive (and hence analytically useful) preparations was developed by Shaw and Creasy.²⁴ A mixture of carbon and zeolite powders is bound by a radical-initiated copolymerization of styrene and divinylbenzene; the result is a "hard" composite with a surface which can be polished. Comparing the voltammetric responses for MV^{2+} and $\text{Ru}(\text{NH}_3)_6^{3+}$ at the "hard" composites with those previously obtained with zeolite/carbon-paste composites¹¹ showed that the "hard" composites were more sensitive to these cations in solution, gave more reproducible currents and shorter response times, and were more convenient to use.

A different approach to a conductive zeolite-containing composite employs encapsulation within a conducting polymer. The possible advantage of this approach is to extend the electrochemically reactive zone beyond the boundary defined by the electrode surface and the first layer of zeolite particles, so that all the zeolite particles are available for electronic communication. In a modification of our co-electrodeposition procedure,^{8,18} a zeolite-polypyrrole composite was formed on rotated platinum or

glassy-carbon disk surfaces by oxidizing pyrrole in a slurry containing zeolite powder. Surprisingly, more uniform zeolite-polypyrrole coatings could be formed in an "upside-down" configuration which maximized incorporation of zeolite in the forming polymer. In this latter procedure, a drop of the pyrrole/zeolite/electrolyte slurry is placed on the face of a disk electrode mounted face-up, and two platinum wires (as auxiliary and reference electrodes) are positioned at the edge of the drop; as the assembled "cell" is not protected against vibration, enough vibration is transmitted through the electrode mount to prevent settling of the particles. The zeolite is gravitationally encapsulated as the pyrrole is oxidized and polypyrrole is electrodeposited. This procedure also works for other particulates; good composite coatings could be formed with ion-exchange resin beads encapsulated in polypyrrole.

The voltammetric behavior of such composites (in our work) in electrolyte solutions in acetonitrile has the broad capacitive background usually observed for electrodeposited polypyrrole films. Polypyrrole encapsulation of NaA provides yet another example of the tenacious adsorption of oxygen by zeolite A and its dominance of the amperometric response of overlayers containing zeolite. This is demonstrated in Fig. 3 for the response (in aqueous solution) of a polypyrrole/NaA composite coated on platinum (Fig. 3b) in comparison with that of a polypyrrole coating prepared similarly on glassy carbon (Fig. 3a). For both aqueous and acetonitrile electrolyte solutions, the qualitative character of the voltammetric response of polypyrrole and polypyrrole/NaA composite coatings in a blank solution becomes similar after sufficient deoxygenation of the zeolite-containing coating [compare Fig. 3a

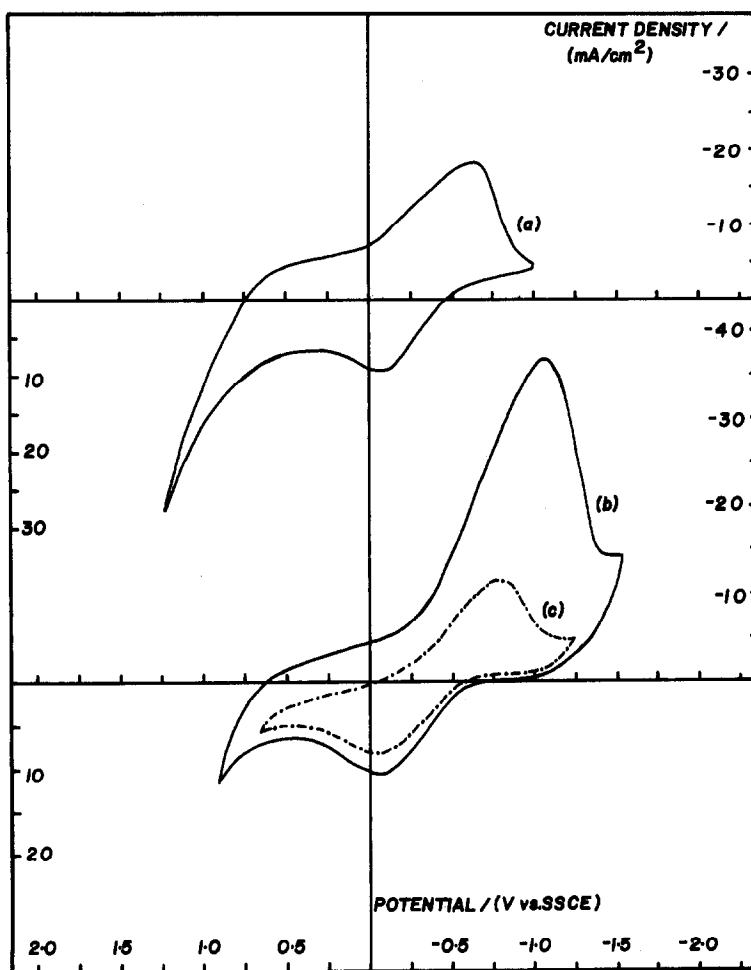


Fig. 3. Voltammetric response at 100 mV/sec in 10mM NaOH/0.1M Na₂SO₄ electrolyte for (a) polypyrrole electrodeposited (from CH₃CN) onto glassy carbon; (b) and (c) polypyrrole-NaA composite electrodeposited (from CH₃CN) onto Pt [(b) second scan; (c) sixth scan].

with the voltamperogram obtained with the polypyrrole/NaA composite after exhaustion of the zeolite-entrained oxygen (Fig. 3c)].

The obverse approach to making zeolite-conducting polymer composites, *i.e.*, encapsulating the conducting polymer within the zeolite, has also been explored. Synthesizing conducting polymer chains inside a zeolite offers two unique materials-science opportunities: (i) if growth is constrained so that bulk conducting polymer cannot form, the properties of oriented small-dimension conducting polymers can be studied; (ii) wiring the interior of a zeolite with an electronic conductor allows molecular electronic designs and constrained electron-transfer chemistry to be explored. The ability of zeolites modified with transition metals to polymerize adsorbed acetylene^{25,26} and pyrrole²⁷ has demonstrated the feasibility of this approach; recent work by Bein and Enzel (on polyaniline,^{28,29} polythiophene³⁰ and polypyrrole³¹) has expanded the chemistry and the characterization of such systems to bring the possibilities above closer to realization. Successful preparation of such molecular wiring inside zeolites will certainly create electroanalytical possibilities.

Cation-selective electrodes—potentiometric detection

The most obvious analytical application of the aluminosilicate zeolites is as ion-selective membranes for the potentiometric determination of cations. This is such a natural application that the use of zeolites in ion-selective electrodes dates back to 1939.³² In subsequent work Barrer and James demonstrated the importance of the size of the cations in competitive adsorption by zeolites, by their observation of complete selectivity of NaA membranes for Na^+ relative to Et_4N^+ ;³³ these membranes were formed by pressing zeolite microcrystals with polymer powders (such as polystyrene, the polymer of choice for casting zeolite-polymer suspensions on electrode surfaces^{2,3}) or casting with thermosetting resins.^{33,34}

Johansson *et al.* studied mordenite-type zeolite embedded in low-viscosity resin as a Cs^+ -selective membrane³⁵ and found near-Nernstian responses for Cs^+ and selectivity relative to the other alkali-metal ions and Ba^{2+} , Ca^{2+} and Cu^{2+} . Work by Demertzis and Evmiridis with Fe(III)- and Cu(II)-exchanged zeolites A and X, also in epoxy-embedded membranes, emphasized the necessity of good zeolite/epoxy ad-

hesion to achieve ideal Nernstian behavior from zeolite membranes.³⁶ Likewise, Barrer and James also found their zeolite membranes had improved selectivities after impregnation with silicone oil to seal cracks in the membrane and minimize alternative solution paths for ion transport.^{33,34}

Our study of the potentiometric response of NaA-polymer films to Cd^{2+} also highlighted the nature of the binder on the stability of the measurement. Near-Nernstian response to Cd^{2+} (33 mV/decade) was achieved for NaA-polysulfone films cast on glassy carbon, in contrast to the flat background response of polysulfone-coated glassy carbon to 10^{-5} – $10^{-2} M$ Cd^{2+} . Erratic results were obtained for both polymer and NaA-polymer coatings in Cd^{2+} solutions when the polymer was polystyrene or polycaprolactone. Sub-Nernstian (11 mV/decade), but linear, response was obtained for an NaA-polysulfone coating exposed to 10^{-5} – $10^{-1} M$ Al^{3+} .

Kinetic possibilities and electroanalysis with zeolite overlayers

Because the size of the zeolite particles placed in overlayers on electrodes can be varied, the compactness or porosity of the coating can be varied. When the residence time of an analyte in the zeolite layer needs to be considered, possibly to increase its interactive or reaction time with the zeolite, prior to its detection at an imposed potential at the electrode, the porosity of the coating can be exploited as one of the variables of the method.

We observed this for our co-electrodeposited coatings of NaA and 1,4-dinitrobenzene, in which the zeolite particle size could be varied from that of the pure powder, $<10 \mu\text{m}$ (as determined by scanning electron microscopy¹⁸), to larger size ranges obtained by sieving ground Linde 4A pellets. As would be expected, coatings formed from larger particles, though visibly compact, were more open to electroactive solute in solution than those formed with the pure NaA powder. This can be seen in Fig. 4, where the limiting current obtained at a zeolite-coated platinum electrode for an electroactive species in solution is contrasted with that at an uncoated platinum electrode of equivalent area. Compact coatings formed from pure NaA powder typically blocked 70–80% of the electrode surface (compare Fig. 4d with Fig. 4c), while compact coatings formed from 4A sieve ground to 88–125 μm typically blocked only 30–40% of the surface (compare Figs. 4a and 4b).

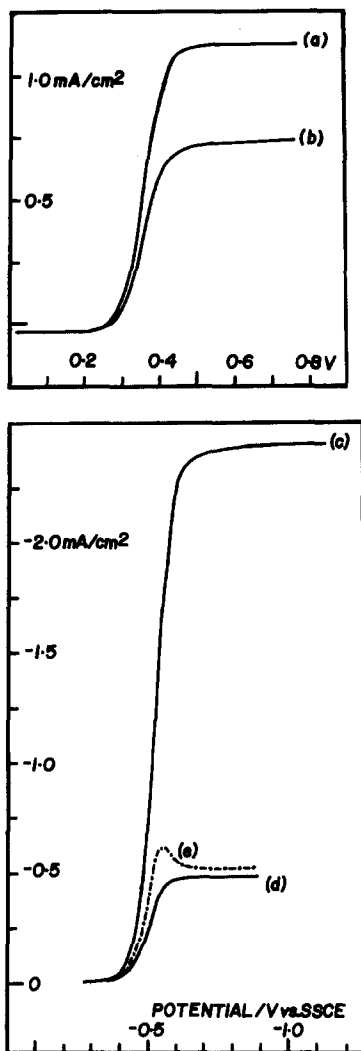


Fig. 4. Limiting current density as a function of potential for rotated Pt disk electrodes [(a), (c)] and Pt disk electrodes compactly coated with a co-electrodeposited layer of NaA/1,4-dinitrobenzene [(b), (d), (e)], for (a) and (b) 1mM ferrocene in 0.1M $\text{Et}_4\text{NClO}_4/\text{CH}_3\text{CN}$, $\omega = 1600$ rpm, sweep rate = 50 mV/sec; (c–e) 0.2mM 1,4-benzoquinone in 0.1M $\text{Et}_4\text{NClO}_4/\text{CH}_3\text{CN}$, $\omega = 900$ rpm; (c) and (e) sweep rate = 50 mV/sec; (d) sweep rate = 5 mV/sec; (b) 4A sieve ground to 88–125 μm ; (d) and (e) NaA powder, <10 μm particle size.

The pure NaA powder coatings were so compact that loss of hydrodynamic control of mass transport occurred if the electrode potential was swept too rapidly—as seen in Fig. 4e, a voltamperogram indicative of surface-confined mass transport results. Though ferrocene and 1,4-benzoquinone (the electroactive solutes used in obtaining Fig. 4) are not analytes that would necessarily benefit from manipulation of the duration of their interaction with the zeolite, they demonstrated that the porosity of the zeolite overlay can be readily changed without

altering the nature of the chemical and physical characteristics of the zeolite.

CONCLUSION

Our characterization of zeolite A coatings electrodeposited on rotated disk electrodes (and understanding of the variables controlling the electrodeposition¹⁸) has given us an appreciation of the subtle and overwhelming influences zeolites can have on an electrochemical interphase. As described in this paper, especially through the results of other workers, the analytical implications of these zeolitic influences can be discerned. The electroanalytical promise of the size/shape selectivity and cation-exchange capacity of the aluminosilicate zeolites as described here is great, but also two-edged in that unexpected consequences (e.g., entrainment of apparently “spectator” species, such as oxygen or water; potential ion-association reactions between charge-compensating zeolite cations and the analyte, the mobility of cations in and out of the zeolite) can affect what seemed to be a straightforward analysis. As with analytical chemistry in general, the characteristics of the analyte, the medium, other components of the solution, and the sensor, must be known before successful analyses can be obtained.

Acknowledgement—Funding for our research on the effects of zeolites on electrode processes has been provided by the Office of Naval Research.

REFERENCES

1. G. A. Ozin, A. Kuperman and A. Stein, *Angew. Chem., Int. Ed. Engl.*, 1989, **28**, 359.
2. D. R. Rolison, *Chem. Rev.*, 1990, **90**, 867.
3. A. J. Bard and T. E. Mallouk, in *Molecular Design of Electrode Surfaces*, R. W. Murray (ed.), in the press.
4. E. M. Flanigen, B. Lok, R. L. Patton and S. T. Wilson, *Pure Appl. Chem.*, 1986, **58**, 1351.
5. D. W. Breck, *Zeolite Molecular Sieves: Structure, Chemistry and Use*, Wiley-Interscience, New York, 1974.
6. P. A. Jacobs, *Carbonogenic Activity of Zeolites*, Elsevier, Amsterdam, 1977.
7. J. V. Smith, *Chem. Rev.*, 1988, **88**, 149.
8. C. G. Murray, R. J. Nowak and D. R. Rolison, *J. Electroanal. Chem. Interfacial Electrochem.*, 1984, **164**, 205.
9. P. Hernández, E. Alda and L. Hernández, *Z. Anal. Chem.*, 1987, **327**, 676.
10. J. Wang and T. Martinez, *Anal. Chim. Acta*, 1988, **207**, 95.
11. B. R. Shaw, K. E. Creasy, C. J. Lanczycki, J. A. Sargeant and M. Tirhado, *J. Electrochem. Soc.*, 1988, **135**, 869.
12. H. A. Gemborys and B. R. Shaw, *J. Electroanal. Chem. Interfacial Electrochem.*, 1986, **208**, 95.

13. M. Šušić and N. Petranović, *Electrochim. Acta*, 1978, **23**, 1271.
14. K. E. Creasy and B. R. Shaw, *J. Electrochem. Soc.*, 1990, **137**, 2353.
15. N. Petranović and M. Šušić, *Zeolites*, 1983, **3**, 271.
16. M. Šušić, *Electrochim. Acta*, 1979, **24**, 535.
17. T. Bein, K. Brown, G. C. Frye and C. J. Brinker, *J. Am. Chem. Soc.*, 1989, **111**, 7640.
18. D. R. Rolison, manuscript in preparation.
19. M. E. Peover in *Electroanalytical Chemistry*, A. J. Bard (ed.), Vol. 2, p. 1. Dekker, New York, 1967.
20. P. Zuman, *Electrochim. Acta*, 1976, **21**, 687.
21. Z. Li and T. E. Mallouk, *J. Phys. Chem.*, 1987, **91**, 643.
22. J. S. Krueger, C. Lai, Z. Li, J. E. Mayer and T. E. Mallouk, *Proc. 5th Intern. Symp. Inclusion Phenomena and Molecular Recognition*, Orange Beach, AL, 1988.
23. Z. Li, C. M. Wang, L. Persaud and T. E. Mallouk, *J. Phys. Chem.*, 1988, **92**, 2592.
24. B. R. Shaw and K. E. Creasy, *J. Electroanal. Chem. Interfacial Electrochem.*, 1988, **243**, 209.
25. J. Heaviside, P. J. Hendra, P. Tsai and R. P. Cooney, *J. Chem. Soc., Faraday Trans. I*, 1978, **74**, 2542.
26. P. K. Dutta and M. Puri, *J. Catal.*, 1988, **111**, 453.
27. T. H. Chao and H. A. Erf, *ibid.*, 1986, **100**, 492.
28. T. Bein and P. Enzel, *Synth. Metals*, 1989, **29**, E163.
29. P. Enzel and T. Bein, *J. Phys. Chem.*, 1989, **93**, 6270.
30. *Idem*, *J. Chem. Soc., Chem. Commun.*, 1989, 1326.
31. T. Bein and P. Enzel, *Angew. Chem. Int. Ed. Engl.*, 1989, **28**, 1692.
32. C. E. Marshall, *J. Phys. Chem.*, 1939, **43**, 1155.
33. R. M. Barrer and S. D. James, *ibid.*, 1960, **64**, 421.
34. *Idem*, *ibid.*, 1960, **64**, 417.
35. G. Johansson, L. Risinger and L. Fäilth, *Anal. Chim. Acta*, 1977, **119**, 25.
36. M. Demertzis and N. P. Evmiridis, *J. Chem. Soc., Faraday Trans. I*, 1986, **82**, 3647.

IMMOBILIZATION OF LACTATE OXIDASE IN A POLY(VINYL ALCOHOL) MATRIX ON PLATINIZED GRAPHITE ELECTRODES BY CHEMICAL CROSS-LINKING WITH ISOCYANATE

KIAMARS HAJIZADEH, H. BRIAN HALSALL and WILLIAM R. HEINEMAN*

Edison Sensor Technology Center and Department of Chemistry, University of Cincinnati, Cincinnati, OH 45221-0172, U.S.A.

(Received 15 November 1989. Accepted 27 March 1990)

Summary—A new method for development of an electrochemical sensor based on lactate oxidase is described. Platinized spectroscopic-grade graphite electrodes were modified by chemically cross-linking L-lactate oxidase from *Pediococcus species* into a poly(vinyl alcohol) network through reaction with a tri-isocyanate. The immobilized enzyme exhibits high activity and long-term stability. The sensor provides a linear response to L-lactate over a concentration range of 2×10^{-5} – $4 \times 10^{-3} M$ and a sensitivity of $1.71 \mu A.l. mmole^{-1}$. The response time of the sensor is 10–45 sec and the detection limit is $10 \mu M$. Stable response to the substrate was obtained over a period of 3 months. The new sensor was also used for the analysis of some dairy products without any special pretreatment.

The last decade has seen unprecedented interest in the development of probes for the qualitative and quantitative monitoring of biological samples of analytical interest.^{1,2} Many of these are based on enzymes and a number of different procedures are available for enzyme immobilization.³ Whereas much enzyme-sensor development is devoted to glucose oxidase, because of its recognized importance in glucose assay as a diagnostic monitor for diabetes,⁴⁻⁶ there is also a growing interest in the development and application of other sensors.

One of the enzymes that has attracted a considerable degree of attention is lactate oxidase (LOD). Blood lactate concentration is indicative of certain pathological states such as shock, respiratory insufficiencies and heart disease.⁷ The lactate concentration in blood rises rapidly as a result of anaerobic glucose metabolism when delivery of oxygen to body tissues is insufficient (Fig. 1). The fact that the hydrogen ions produced from dissociation of lactic acid are effectively buffered by bicarbonate makes pH measurements less useful than direct lactate determination. Also, though transcutaneous oxygen measurements and the arterial-venous pO_2 difference (measured with oxygen sensors) may have some utility as indicators of blood flow, lactate measurement is more convenient and useful.⁸ This becomes especially important

when the tissue oxygen is adequate but aerobic metabolism is inhibited.

In sports medicine, the lactate concentration is a very useful indicator for assessing the general physical condition of an athlete or racing animal.⁸ Highly trained individuals produce less lactate than unconditioned ones for a given exercise.

The involvement of lactate in the metabolism of glucose poses more demand on the use of a lactate sensor in conjunction with a glucose sensor for diabetic patients;⁹ the applicability of such a combination has been demonstrated in the evaluation of an endocrine artificial pancreas.

In the food industry, measurement of lactate in dairy products and for the control of additives (in wines *etc.*) is also of considerable importance. The lactic acid content of food products influences their flavor, stability and keeping quality.¹⁰

Several different methods are available for the electrochemical determination of lactic acid by use of immobilized lactate oxidase, but the three below have been most widely used.

Lactate oxidase from *Mycobacterium smegmatis*, which acquires flavin adenine mononucleotide as a co-factor in the consumption of oxygen, converts lactate into acetate and carbon dioxide. The measurement of oxygen depletion is used as an indirect means of estimating the lactate level.^{11,12}

*Author for correspondence.

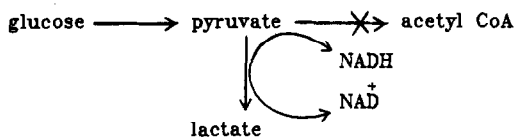


Fig. 1. Anaerobic glucose metabolism.

Lactate oxidase from *Pediococcus species*, an enzyme dependent on flavin adenine dinucleotide (FAD), catalyses the conversion of lactate into pyruvate and hydrogen peroxide by consumption of oxygen.^{12,13} In this case, the production of hydrogen peroxide can be measured as an indicator of the lactate concentration.^{14,15}

In the third approach, the catalytic activities of LOD and lactate dehydrogenase (LDH) are coupled, the LOD being enzymatically regenerated by the LDH. This enzymatic cycling reaction greatly amplifies the response.¹⁶⁻¹⁸ Although this system is conceptually attractive and yields low detection limits, it suffers from slow response time (4-9 min). Also, the preparation of the enzyme support involves some complicated steps and takes several days.

Isocyanates have been used extensively as cross-linking agents¹⁹ in polyurethane technology. Their reactions generally involve chain extension and network formation through interaction of nucleophilic groups (*e.g.*, hydroxyl, amino) with the isocyanate electrophilic carbon atoms. Some isocyanates have also been used as cross-linking agents for enzymes such as ribonuclease and chymotrypsin.²⁰

The ability to prepare well-defined model networks of the polyurethane type by end-linking hydroxyl-terminated chains by means of aromatic tri-isocyanates (TIC)²¹ has made their use attractive in the preparation of enzyme-based biosensors.²² Poly(vinyl alcohol) is a neutral partially water-soluble²³ and biocompatible polymer²⁴ and is, therefore, an appropriate matrix for consideration in sensor preparation.

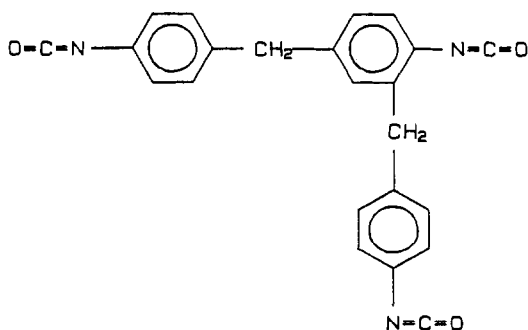


Fig. 2. Chemical structure of TIC.

In the present work we report incorporation of FAD-dependent LOD into a poly(vinyl alcohol) (PVAL) network prepared by cross-linking the available reactive nucleophilic groups (hydroxyl, amino *etc.*) with TIC (Fig. 2). Hydrogen peroxide, a product of the enzymatic reaction, was detected amperometrically at an electro-platinized spectrographic graphite electrode, which has been shown to lower the oxidation overpotential of hydrogen peroxide considerably.^{5,25}

EXPERIMENTAL

Reagents

PVAL [hydrolysed from poly(vinyl acetate)] of average molecular weight 8.6×10^4 , and Nafion solution (5% solution in a mixture of aliphatic alcohols and 10% water) were obtained from the Aldrich Chemical Company, Inc.

Lactate oxidase (L-lactate: oxygen oxidoreductase E.C. No. 1.1.3.2), from *Pediococcus species*, was purchased from Boehringer Mannheim Biochemicals.

L(+)-Lactic acid (lithium salt) was obtained from the Sigma Chemical Company. The high-reject polymer was provided by Yellow Springs Instruments (YSI).

TIC (triphenylmethane isocyanate) was generously provided by Dr. D. H. Chadwick of Mobay Chemical Company, New Martinsville, WV.

Dimethylsulfoxide (DMSO; Fisher Scientific) and other chemicals were of reagent grade and used without further purification unless otherwise stated.

Demineralized organic-free water was used for the preparation of all solutions.

Apparatus

Amperometric experiments were performed with a Bioanalytical Systems CV-27 voltammograph and recorded with a Houston Instruments series 5000 $x-t$ recorder.

A thermostatically controlled circulating-water bath (Lauda Model S-1) was used for controlled-temperature experiments.

Scanning electron micrographs (SEMs) were obtained with a Cambridge Stereo Scan 600 scanner at the Materials Science Department, University of Cincinnati.

Sensor preparation

The cylindrical surfaces of the rod-shaped spectrographic graphite electrodes (Poco

Graphite, Inc., grade AXF-SQBL-1, lot 430, Cat. No. 366-BD) were sprayed with "Krylon" as a protective coating and the flat ends were fine-polished on 600-grit emery paper. After sonication in an ultrasonic bath (Branson Ultrasonics Corp.) in "nano-pure" water to remove any loosely attached material, they were dried at room temperature in a dust-free atmosphere. Chronocoulometric measurements in 1mM potassium ferricyanide/0.5M potassium chloride/0.02M phosphate at pH 7 were used to calculate the surface area of the electrode before coating.²⁶ The average electrode area was 0.17 cm².

Electro-deposition of platinum onto the polished surface of the graphite electrodes was done from a 10mM hexachloroplatinic acid solution by holding the potential at -200 mV vs. Ag/AgCl for 10 min.

Different approaches were used for enzyme immobilization on the platinized area of the electrode.

PVAL-LOD. This electrode was made in layered form, with 5 μ l of PVAL solution (3.0% in water), 11 activity units of LOD, and 10 μ l of the PVAL solution added successively, with drying between additions. The electrode was used without any cross-linking treatment.

LOD-ISO. This electrode was simply made by covering the platinized graphite electrode with 11 activity units of LOD, letting it dry, and then treating it with 1.1 μ l of the isocyanate solution (0.045 g in 0.25 ml of DMSO).

PVAL-LOD-ISO-1. This approach is based on that developed for alkaline phosphatase.²² First, the equivalent of 11 activity units of LOD (in 5 μ l of solution) was placed at the middle of the active surface of the electrode and spin-dried, and 2.5 μ l of PVAL solution (3.0% w/w in DMSO) were placed on this layer. Finally, 1.1 μ l of TIC solution (0.045 g in 0.25 ml of DMSO) was applied and mixed in by spinning the electrode. A gel was formed in a few seconds, indicating cross-linking of the PVAL-LOD system. The electrode was then immersed in stirred water for 5 min to remove unreacted material. The cross-linked polymer and/or polymer-enzyme shrinks to the middle part of the electrode surface, looking like a small disk (\approx 0.2 mm in diameter).

PVAL-LOD-ISO-2. In this approach the cross-linking was performed with the polymer and enzyme both in the dry state; 5 μ l of the PVAL solution were applied on the electrode and spin-dried, then 5 μ l of LOD solution (11

units of activity) were added and dried similarly. The electrode was finally covered with 10 μ l of PVAL solution, dried by spinning, and left in a dust-free atmosphere for 3 hr. Finally, the dried film was treated with 1.1 μ l of TIC solution for 45-60 sec. During this period the color of the electrode surface changed to white, indicative that the cross-linking process had taken place. The electrode tip was then immersed in DMSO for 5-10 sec and agitated to ensure removal of the unreacted ingredients. Finally, it was rinsed in stirred, demineralized organic-free water for 5 min and kept in phosphate buffer at pH 7 until use.

PVAL-LOD-ISO-3. This electrode was prepared identically to PVAL-LOD-ISO-2 except that a total of 25 μ l of PVAL solution was used.

PVAL-LOD-ISO-4. In this procedure, cross-linking was performed with all the reacting components mixed together in solution on the electrode surface.

The electrodes' responses were determined by hydrodynamic amperometry. This was done by immersing the sensors in stirred phosphate buffer and applying the required oxidative potential. When the background current had stabilized, an appropriate amount of concentrated lactate solution was introduced to give a preselected concentration. The faradaic current increased as a function of time and eventually reached a limiting value. The difference between the limiting and the background current was taken as the sensor response to any particular lactate concentration.

In accordance with previous reports,^{5,25} electrochemical deposition of platinum on the graphite lowered the oxidation potential of H₂O₂ to +0.300 V vs. Ag/AgCl, compared with 1.2 V on an unplatinized graphite electrode, which is advantageous in that the sensor response is then less susceptible to electrochemical interferences. The platinized graphite surface retained its catalytic properties for over five months when stored in phosphate buffer at room temperature or 4° or in the dry state at room temperature.

RESULTS AND DISCUSSION

Assessment of the cross-linking procedure

An important aspect of sensor development is finding reaction conditions that effectively immobilize a sufficient concentration of the enzyme in an active, accessible and stable form to provide adequate sensor performance. For

this purpose five different procedures for the immobilization of LOD were evaluated with respect to lactate response. Sensor performance for each of these electrode types is summarized in Table 1 and the important features of each are discussed below. Performance was evaluated with respect to the amperometric response to an aliquot of lactate injected into a stirred solution. A representative response is shown in Fig. 3.

PVAL-LOD. Electrodes coated with successive layers of PVAL, LOD and PVAL exhibited a high initial sensitivity to lactate. The active enzyme is immobilized for a short time in the slightly soluble polymer film. However, slow dissolution of PVAL over the course of several hours of immersion in aqueous samples releases LOD and the sensitivity decreases dramatically. Similar behavior has been observed for glucose oxidase in PVAL.²² Whereas this arrangement gave the highest response to lactate, the short lifetime renders it impractical for preparation of a stable sensor. However, the strong initial response was used as a standard (100% in Table 1) against which the performance of electrodes prepared by other procedures was compared. The loss of enzyme activity in this case can also be attributed to the generally accepted fact that non-cross-linked proteins are less stable than their corresponding cross-linked forms.^{20,27}

LOD-ISO. Enzyme cross-linked with TIC directly on the electrode surface without PVAL gave a response to lactate. A thin, white and somewhat swollen film with a lustrous appearance was formed. Microscopic examination revealed a web-like network of cross-linked enzyme. This electrode lost most of its activity within several hours and the response remained at only 3% of that of the standard electrode. Addition of TIC solution to a solution of LOD

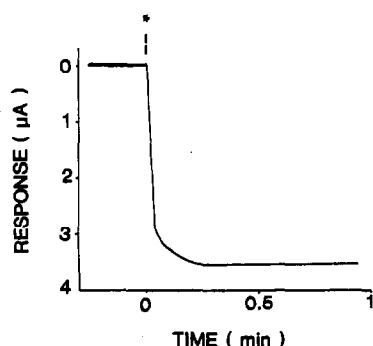


Fig. 3. Typical hydrodynamic amperogram of a chemically cross-linked PVAL-LOD-ISO-2 electrode in 2mM lactate solution in phosphate buffer (pH 7.0). Applied potential 300 mV vs. Ag/AgCl.

Table 1. Properties of lactate sensors made by different methods

Electrode	Relative response,* %	Response time, sec	R.S.D.,† %
PVAL-LOD	100	>45	6.4
LOD-ISO	28	~30	—
PVAL-LOD-ISO-1	14	6	5.2
PVAL-LOD-ISO-2	72	10-45	1.3
PVAL-LOD-ISO-3	79	60	3.2
PVAL-LOD-ISO-4	56	>20	6.0

*Relative to the LOD-PVAL electrode in 2mM lactate at pH 7 (0.1M phosphate buffer).

†Five measurements.

in DMSO results in the formation of an insoluble clump which is believed to be inactivated cross-linked enzyme.

PVAL-LOD-ISO-1. This electrode gave the poorest sensitivity to lactate. The cross-linked film was condensed as a clump on the middle of the electrode surface. The faster response of this sensor can be attributed to the fact that the area surrounding the clump, although appearing to be bare, is actually covered by a very thin layer of enzyme, which will make the electrode surface more readily accessible to the products of enzymatic reaction.

The considerable loss of enzyme activity in PVAL-LOD-ISO-1 is presumably due to extensive intra- and inter-molecular cross-linking of LOD molecules. The results are consistent with the work of other investigators on other enzyme systems with various cross-linking procedures, including isocyanate reactions.^{20,28,29}

PVAL-LOD-ISO-2. The procedure in which the enzyme and polymer were in the dry state on the electrode surface before cross-linking with TIC gave a sensor with good sensitivity, reasonably fast response and the best precision for lactate. This sensor was very smooth and homogeneous in appearance.

The lower response of PVAL-LOD-ISO-2 compared to the PVAL-LOD standard sensor is believed to be a result of the cross-linking process rather than of denaturation caused by the presence of DMSO. As a test, TIC-free DMSO was applied to the active surface of a PVAL-LOD electrode. After 1-4 min of contact with DMSO, which is longer than the cross-linking period of less than 1 min, no loss of enzyme activity was observed.

PVAL-LOD-ISO-3. This electrode differs from the previous one only in the amount of PVAL used, which was almost doubled. The resulting increase in polymer-film thickness

caused an increase in response time, which is most likely due to the greater distance through which the substrate/product must diffuse in the polymer film.

PVAL-LOD-ISO-4. Although this electrode provided a relatively good sensitivity to lactate, it had an irregular clumpy appearance with some loose particles, which led to a relatively poor precision compared with the *PVAL-LOD-ISO-2* electrode.

The *PVAL-LOD-ISO-2* electrode was adopted for the rest of this work, because of its better properties and performance overall.

Microscopic observations

The scanning electron micrograph (SEM) of the end of a spectroscopic graphite rod (Fig. 4A) reveals a very porous surface. The SEM of an electro-platinized graphite electrode (Fig. 4B) shows that the surface retained the roughness and porosity, but was essentially coated with platinum. Energy-dispersive X-ray analysis spectra obtained during the SEM study of the platinized surface clearly showed the presence of platinum.

The porosity of the electrode material is advantageous in that some polymer soaks in and anchors the film.³⁰ The adhesion and mechanical strength of the cross-linked film on the electrode were found to be excellent.

Although the platinized graphite electrode that was coated with polymer and lactate oxidase (*PVAL-LOD-ISO-2*) had a smooth and continuous visual appearance, SEM showed a web-like network with aggregates in the middle part of the electrode where the enzyme was originally placed (Fig. 4C). The film thickness was about 50–80 μm in the dry state. This was estimated from an SEM of the side of an electrode coated with PVAL film.

The aggregates were fairly uniform in size and roughly spherical, with an average diameter of about 0.5 μm . These aggregates were not observed in a chemically cross-linked PVAL film in the absence of LOD (Fig. 4D). The surface of the latter coating appears to be smooth. Since we have already observed some indications of enzyme cross-linking and do not see a similar network in the absence of the lactate oxidase, we can ascribe these aggregates to cross-linked LOD and/or cross-linked

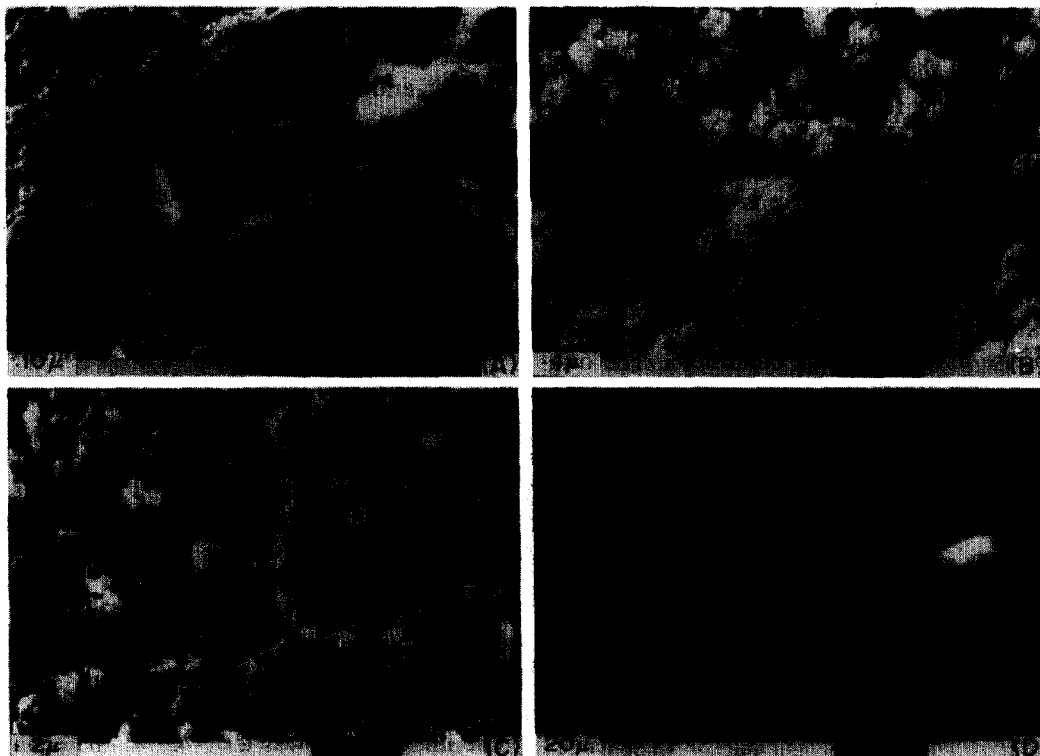


Fig. 4. Scanning electron micrographs of A, polished graphite electrode (2000 \times), B, platinized graphite electrode (2000 \times), C, platinized graphite *PVAL-LOD-ISO-2* electrode (10000 \times) and D, platinized *PVAL* graphite electrode cross-linked with TIC (1000 \times).

PVAL-LOD. Similar observations have been made when gamma-irradiation was used for enzyme immobilization.^{5,31}

Effect of DMSO on enzyme activity

Since DMSO is one of the constituents used in the cross-linking process, its effect on enzyme activity was evaluated. Hydrodynamic amperometry was used for direct measurement of the hydrogen peroxide produced by the free enzyme in solution. The initial rate of hydrogen peroxide formation was taken as a good estimate of the enzyme activity.

The response for free LOD in aqueous solution or 50% v/v water-DMSO was 1.6 $\mu\text{A}/\text{min}$, whereas that of the enzyme incubated in 100% DMSO was zero.

These results are consistent with our previous results showing the need for the presence of water to maintain greater enzyme activity for glucose oxidase.²² This effect becomes important when the enzyme is immobilized by cross-linking in the presence of DMSO.

Effect of pH and solution matrix

The effect of pH on the activity of the lactate sensor was also studied. Table 2 shows the sensor response to lactate solution in phosphate buffer in the pH range 6.0–11.1. Phosphate buffer of pH 7.0 was chosen as optimal for the rest of this work. The reported optimum pH range for the free enzyme is 6–7,³² which is comparable to that found for the immobilized LOD. The free enzyme is known to be stable in the pH range 6–9, but the cross-linked LOD was found to be stable from pH 6 to 11.1. The background current increased significantly at pH values above 8. When the lactate sensor was then returned to pH 7 it gave 95% of its original response under the same conditions. The orig-

Table 2. Effect of pH on the activity of the PVAL-LOD-ISO-2 electrode in 1mM lactate solution plus 0.1M phosphate buffer

pH	Response, μA
6.0	2.6
6.5	3.4
6.7	3.8
7.0	4.1
7.85	4.1
8.58	3.9
9.36	3.5
10.12	3.2
11.2	2.2

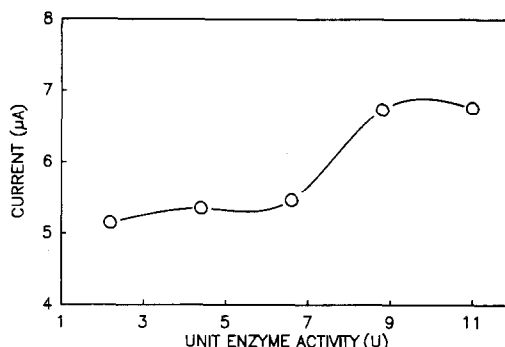


Fig. 5. Effect of the amount of immobilized LOD, on the sensor response.

inal loss of response at high pH values can be attributed, in part, to partial unfolding of the enzyme, which refolds when it is brought into contact with the solution of pH 7. Thus the sensor is reversibly inactivated by high pH. The optimum pH value reported for lactate oxidase immobilized by a different method is 7–7.5.¹³

The presence of 4.6mM azide in 0.1M phosphate buffer (pH 7), used initially as a bacteriostat, attenuated the electrode response by about 60%. Azide was therefore omitted from the buffer solution for lactate measurements. In contrast to an earlier report,¹³ the presence of potassium chloride, magnesium chloride and FAD had no significant effect on the sensitivity of the sensor, except for a higher background current and increased stabilization time.

Effect of the amount of immobilized LOD

LOD (from 2.2 to 11 activity units) was immobilized by the cross-linking process on five electrodes. As the amount of LOD increased, a larger response to the addition of substrate was obtained (Fig. 5); a loading of 5.5 activity units (260 μg) of LOD was chosen for economy.

Response to lactate

To construct a calibration curve, various amounts of L-lactate solution were added while the sensor was immersed in the stirred buffer, and hydrodynamic amperograms were recorded.

Figure 6 represents the calibration curve for lactate, obtained from the average responses of five electrodes. The sensors' responses increased with the concentration of lactate up to 14mM. The linear range was 0.02–4mM, the equation being $Y (\mu\text{A}) = 1.71X (\text{mM}) + 0.097$, with a correlation coefficient of 0.9994. The average relative standard deviation over the linear range

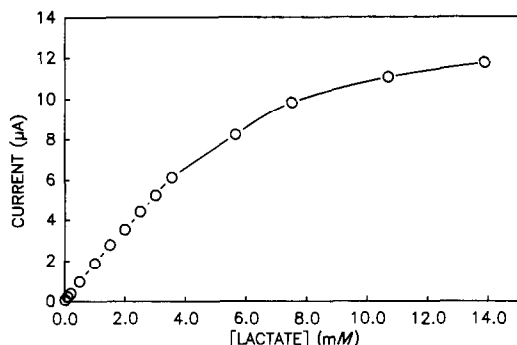


Fig. 6. Calibration curve for different concentrations of L-lactate on chemically cross-linked PVAL-LOD-ISO-2 sensors.

was 3.6%. The average detection limit of the sensors was $10\mu M$.

The loss of linearity at higher concentrations is attributed to oxygen limitation. Oxygen is a co-substrate in enzymatic degradation by oxidases and its limiting effect on the rate of reaction has already received considerable theoretical treatment.^{33,34} It has been shown that regeneration of oxygen at the electrode where the oxidase is located significantly increases the sensitivity of the electrode to the substrate. We have also observed that passing oxygen into a $5mM$ lactate solution in the presence of the LOD electrode leads to a sharp rise of $\sim 15\%$ in the stabilized current, which falls to a stable increase of $\sim 7\%$ after the oxygen flow is turned off. We have shown³⁵ that a lactate sensor prepared by gamma-irradiation immobilization of LOD in PVAL has an upper linear response limit of $8mM$ lactate when used under continuous oxygen flow.

The upper limits for these sensors are comparable to or better than those for many other amperometric lactate sensors: $3mM$ for LOD entrapped in a cellulose-based dialysis membrane in the presence of polyurethane on a

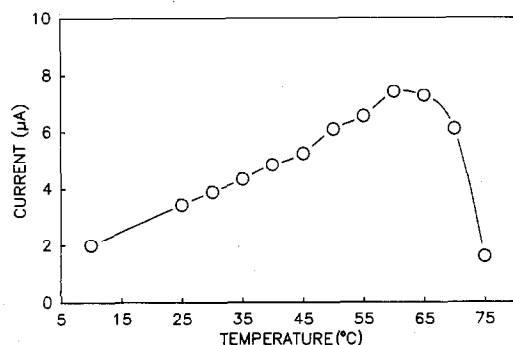


Fig. 7. Effect of temperature on the activity of the LOD electrode.

Pd/Au-sputtered carbon electrode,³⁶ $0.2mM$ for LOD from *Mycobacterium smegatis* cross-linked on chemically treated nylon nets by glutaraldehyde,⁷ and $0.5\mu M$ by enzymatic cycling procedures designed for the detection of very low lactate concentrations.¹⁵

By incorporation of a membrane of low permeability on top of a high-reject lactate membrane (Yellow Springs Instrument Co.) the diffusion of the analyte to the underlying enzyme layer was restricted and, as a result, the upper limit of the linear range extended to $10mM$.³⁷

The Michaelis-Menten constant, K_m (apparent), for the immobilized LOD was $9.75mM$, as measured by Cornish-Bowden plots.³⁸ The K_m value for the free enzyme was $0.7mM$.³² This change in K_m is likely to be due to a combination of the effect of diffusion of the substrate(s) to the active sites being modified by the microenvironment of the enzyme,³⁹⁻⁴¹ and of the effect of structural changes in the enzyme as a result of the chemistry of cross-linking. It has been demonstrated that, for a two-substrate enzyme reaction in which the relative affinities of the substrates are significantly different, the Michaelis-Menten constant increases as the diffusion is more efficiently restricted.³⁹

Temperature effects

The temperature dependence of the sensor response was measured between 10 and 75° in $1mM$ lactate solution (Fig. 7). The sensor was held at each temperature for 15 min, including the rise-time. The probe response gradually increased to a maximum at 60° and then fell more sharply. The background current and the noise increased with increasing temperature. On cooling to 35° , the electrode gave the same response as before heating. Since the optimum temperature for the free enzyme is 35° , with activity retained up to 45° ,³¹ it appears that the enzyme has been stabilized by the cross-linking.

Electrochemical interferences

Since hydrogen peroxide can be detected very efficiently at 0.3 V vs. Ag/AgCl on a platinized graphite electrode, the number of potential electrochemical interferences will be minimal. Uric acid and acetaminophen, two commonly encountered interferents in biological samples, do not interfere significantly with the detection of hydrogen peroxide at a platinized electrode.⁴² Ascorbic acid, however, may interfere because it can be oxidized at potentials lower than

300 mV. To minimize the effect of ascorbate, an additional layer of Nafion or YSI high-reject polymer was incorporated in the sensor preparation. The electrodes were prepared identically. First Nafion or the high-reject polymer was coated onto the bare electrode and then the PVAL enzyme and PVAL layers were applied in turn, following the method of preparation used for the PVAL-LOD-ISO-2 sensor. After each layer had been applied, the response of the electrode to ascorbic acid was recorded. Figure 8 shows the normalized responses of the modified sensors to ascorbic acid compared with that of the bare platinized graphite electrode. An electrode (B) covered with only a layer of chemically cross-linked PVAL gives an ascorbate signal 87% lower than that of the bare platinized electrode (A). Incorporation of LOD into the cross-linked PVAL (by sandwiching it between two PVAL layers and then cross-linking) attenuates the relative ascorbate response even more, by 90.5% (C). Therefore, the normal preparation of cross-linked PVAL-LOD-ISO-2 in the absence of a Nafion or high-reject polymer layer attenuates the ascorbate response considerably. The addition of a Nafion layer (D) reduces the interfering response by 98.4%, and the high-reject polymer (E) provides 96.2% attenuation. Although this seems to be only a small change relative to the attenuation by the cross-linked PVAL-LOD-ISO-2 electrode (90%), because in both cases the response is compared with that of the bare platinized electrode, the actual current produced by ascorbate at the high-reject polymer or Nafion PVAL-LOD-ISO-2 electrode is less

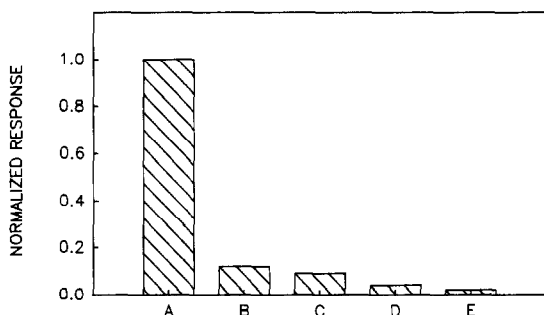


Fig. 8. Attenuation of ascorbate interference by incorporation of Nafion or high-reject polymer films. Electrodes: A, platinized graphite, B, platinized graphite/cross-linked PVAL, C, platinized graphite/cross-linked PVAL-LOD-ISO-2, D, platinized graphite/Nafion/cross-linked PVAL-LOD-ISO-2 and E, platinized graphite/high-reject polymer/cross-linked PVAL-LOD-ISO-2. Ascorbic acid concentration 200 μ M.

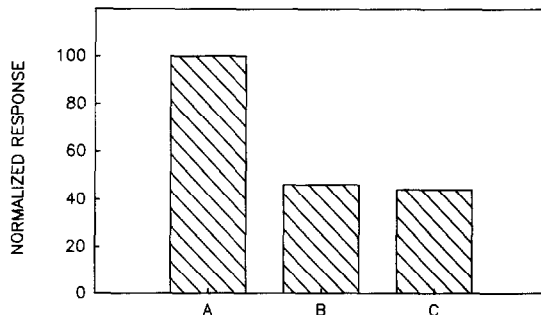


Fig. 9. Relative responses of PVAL-LOD-ISO-2 electrodes in 2mM lactate. A, Uncoated; B, coated with 500 μ g of Nafion, C, coated with high-reject polymer.

than half of that produced at the PVAL-LOD-ISO-2 electrode.

Although Nafion or high-reject polymer reduces the ascorbate response, it also lowers the response to lactate (Fig. 9). The electrodes with Nafion or high-reject polymer coated with cross-linked PVAL-LOD had a sensitivity to lactate that was only \sim 45% of that of the cross-linked PVAL-LOD electrode, probably because of the restricted diffusion of hydrogen peroxide in the thicker films.

To investigate this effect in more detail, a series of systematic studies was conducted. The amperometric responses of three sets of platinized graphite electrodes to 4.6mM hydrogen peroxide were recorded before (A) and after coating with Nafion (B) high-reject polymer (C) and cross-linked PVAL (D). The results are summarized in Fig. 10.

Electrodes B and C gave relative signals of only 4.3 and 5.7%, respectively. The response of these two modified electrodes was instantaneous. Electrode D, on the other hand, produced a response of 8.6%, with a response time of 9.6 sec. This clearly shows that the Nafion and high-reject layers restrict the diffusion of

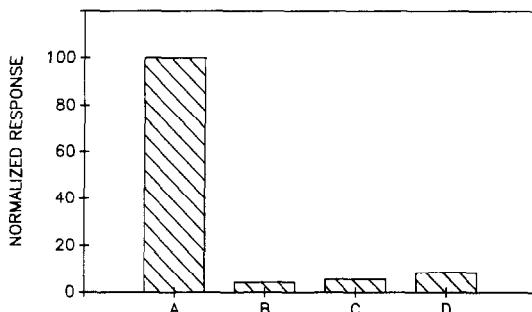


Fig. 10. Hydrogen peroxide response on platinized graphite electrodes coated with A, no film; B, Nafion; C, high-reject polymer; D, cross-linked PVAL. H_2O_2 concentration 4.6mM.

Table 3. Hydrogen peroxide response on platinized graphite electrodes coated with Nafion

[H ₂ O ₂], mM	Relative response,* %	
	Nafion 167 μ g	Nafion 83 μ g
2.2	7.0	44.3
4.4	6.0	31.2
8.8	5.1	36.4

*Relative to the response of the same electrode before being coated with Nafion.

hydrogen peroxide to a great extent, and the sensitivity of the sensor can be substantially impaired.

If the Nafion film thickness could be optimized so that ascorbate is excluded but the hydrogen peroxide flux through the film is increased, the sensitivity of the Nafion cross-linked PVAL-LOD-ISO-2 electrode could be enhanced.

Table 3 shows the response to hydrogen peroxide of two sets of platinized graphite electrodes before and after coverage with (A) 167 and (B) 83 μ g of Nafion. For electrode A, the response to different hydrogen peroxide concentrations varies from 5.1 to 7.0% relative to that of the uncovered electrode. On the other hand, sensor B, which is covered with half as much Nafion, provides a 31–44% relative response for the same range of hydrogen peroxide concentration.

Table 4 gives the responses of electrodes A and B to different ascorbate concentrations. As expected, electrode A has a lower response than electrode B to ascorbate, but this is outweighed by the greater sensitivity of the electrode B to hydrogen peroxide.

This result could be used to advantage in the preparation of an LOD-based sensor, featuring both the desired sensitivity to peroxide and the lower interference by ascorbic acid. On this basis, an LOD-based electrode was prepared with 83 μ g of Nafion coating. This sensor shows essentially no loss of sensitivity to lactate, compared with the LOD sensor without Nafion, but

Table 4. Ascorbic acid response on platinized graphite electrodes coated with Nafion

[Ascorbic acid], μ M	Relative response,* %	
	Nafion 167 μ g	Nafion 83 μ g
132	2.3	7.0
260	2.3	7.5
385	2.0	8.5
506	1.7	8.9

*Relative to the response on the bare platinized graphite electrodes before they were coated with Nafion.

Table 5. Ascorbic acid response on a platinized graphite electrode coated with 83 μ g of Nafion and cross-linked PVAL-LOD-ISO-2

[Ascorbic acid], μ M	Relative response,* %
132	5.0
260	5.2
385	4.8
506	4.9

*Relative to the response on the bare electrode before it was coated.

the response to ascorbic acid (Table 5) is only 5% of that of the bare electrode. The response time of this Nafion PVAL-LOD-ISO-2 electrode was 40–60 sec.

Lifetime

Figure 11 shows the effect of storage of the electrodes under various conditions. The buffer was renewed before each measurement. The electrodes show good stability over a period of two months. The PVAL-LOD-ISO-3 electrode stored dry in phosphate salt continued to give a stable response to lactate for another 100 days, with 2.3% R.S.D. and a total lifetime in excess of 5 months.

Analysis of dairy products

The concentrations of L-lactate in different kinds of dairy products (sour cream, plain yoghurt and milk) were determined. Table 6 summarizes the results and the pooled relative standard deviation obtained for six readings on each of four LOD-based electrodes. The dairy products were diluted by a factor of 150–500 for amperometric analysis, with no other pre-treatment. The lactate concentration in plain

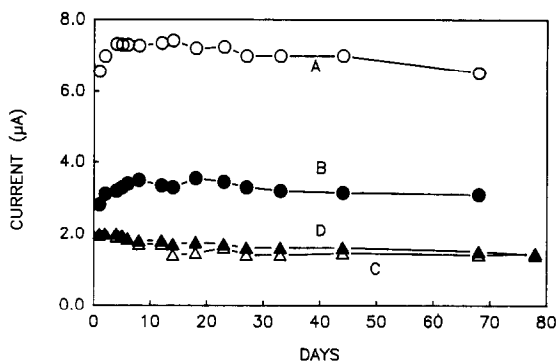


Fig. 11. Lifetime of the LOD electrodes stored under different conditions. A, PVAL-LOD-ISO-2; B, PVAL-LOD-ISO-3; C, PVAL-LOD-ISO-2; D, PVAL-LOD-ISO-2: A and B in phosphate buffer (pH 7.0) at 5°, C dry in phosphate-sodium azide salt mixture at room temperature.

Table 6. Determination of lactate in dairy products

	Plain yoghurt		Sour cream	Milk
	A	B		
Lactate found, mM	61	81.5	87.8	2.8
R.S.D., %	4.0	0.1	0.12	—

*Average of six readings on four PVAL-LOD-ISO-2 sensors.

yoghurt B, which was a commercially available product, matches very well with the values reported in the literature (83.7 and 80.6mM) and obtained by using a different immobilization method for preparing the electrode.¹³ To assess the accuracy of the results obtained by these sensors, a standard-addition method was used with two lactate sensors. For yoghurt of two different dilutions (195 and 390), and six readings, the recovery was $95.6 \pm 2.7\%$ and for sour cream $93.1 \pm 3.6\%$. These results show good accuracy and the reliable measurement of lactate in more complex matrices.

CONCLUSIONS

Chemical cross-linking based on isocyanate chemistry is a feasible method for the immobilization of lactate oxidase and has several important and advantageous characteristics. The immobilization method is very simple, making it especially useful for the manufacture of an LOD-based sensor. The sensors can be fabricated in 1–3 hr if all the reagents are prepared beforehand.

The present results compare very well with those reported by others. The response of the chemically cross-linked sensors to lactate is fast (less than 1 min), whereas for the tedious enzyme-cycling methods, which usually need several days for preparation of the sensor,¹⁴ it ranges from 4 to 9 min. The electrodes prepared here have longer lifetimes than those made by other workers. The modified films are relatively rugged; no cracks were observed when the electrodes were stored in the dry state. The linear range of the sensors includes the physiological concentrations (1–2.7mM),³⁶ which may be useful for diagnostic purposes. Extension of the upper limit of the linear range to even higher values is currently under investigation. Owing to the relatively high sensitivity of the sensor, samples may be diluted by several orders of magnitude and it is possible to use very small sample volumes (100–250 μ l).

Acknowledgements—The authors acknowledge support of this research by the Edison Sensor Technology Center and the University of Cincinnati Research Council.

REFERENCES

- G. G. Guilbault, in *Analytical Uses of Immobilized Enzymes*, Chap. 1, Dekker, New York, 1984.
- C. R. Lowe, *Biosensors*, 1985, **1**, 3.
- M. Mascini and G. G. Guilbault, *ibid.*, 1986, **2**, 147.
- D. R. Mathews, R. R. Holman, E. Brown, J. Steeman, A. Watson and S. Hughes, *Lancet*, 1987, *i*, 778.
- C. Galiatsatos, Y. Ikariyama, J. E. Mark and W. R. Heineman, *Biosensors*, 1990, **5**, 47.
- A. Genshaw and J. E. Jones, *J. Electrochem. Soc.*, 1988, **136**, 414.
- M. Mascini, D. Moscone and G. Palleschi, *Anal. Chim. Acta*, 1984, **157**, 45.
- J. G. Toffaletti, *Clin. Chem. News*, 1989, **9**, 14.
- M. Mascini, S. Fortunati, D. Moscone, G. Palleschi, M. M. Benedetti and P. Fabietti, *Clin. Chem.*, 1985, **31**, 451.
- S. H. Ashoor and J. Weily, *J. Chromatog.*, 1984, **287**, 452.
- E. B. Makovos and C. C. Liu, *Biotechnol. Bioeng.*, 1985, **27**, 167.
- M. Mascini, P. Palleschi and D. Moscone, in *Chemical Sensors*, T. Seijama (ed.), p. 603. Kodansha, Tokyo and Elsevier, Amsterdam, 1983.
- G. Bardeletti, F. Sechaud and P. R. Coulet, *Anal. Chim. Acta*, 1986, **187**, 47.
- M. H. Weil, J. A. Leavy, E. C. Rackow, C. J. Hoffman and S. J. Bruno, *Clin. Chem.*, 1986, **32**, 2175.
- J. J. Cannon, M. C. Flickinger and G. T. Tsao, *Biotechnol. Bioeng.*, 1984, **26**, 167.
- F. Mizutani, T. Yamanaka, Y. Tanabe and K. Tsuda, *Anal. Chim. Acta*, 1985, **177**, 153.
- F. Mizutani, K. Sasaki and Y. Shimura, *Anal. Chem.*, 1983, **55**, 35.
- F. Scheller, U. Wollenberger, F. Schubert, D. Pfeiffer and V. A. Bogdanovskaya, *GBF Monogr.*, 1987, No. 10, 39; *Chem. Abstr.*, 1988, **108**, 18715v.
- K. C. Frisch and H. C. Vogt, in *Chemical Reactions of Polymers*, Part C, pp. 927–1001. Dekker, New York, 1984.
- H. Ozawa, *J. Biochem.*, 1967, **62**, 419.
- P. H. Sung and J. E. Mark, *Polymer J.*, 1980, **12**, 835.
- C. Galiatsatos, K. Hajizadeh, J. E. Mark and W. R. Heineman, *Biosensors*, 1989, **4**, 393.
- J. G. Pritchard, in *Poly(vinyl alcohol), Basic Properties and Uses*. Beach Science, New York, 1975.
- H. Maeda, *Biotechnol. Bioeng.*, 1975, **17**, 1571.
- L. Gorton, *Anal. Chim. Acta*, 1985, **178**, 247.
- L. A. Coury, E. M. Birch and W. R. Heineman, *Anal. Chem.*, 1988, **60**, 553.
- F. Wold, *J. Biol. Chem.*, 1961, **236**, 106.
- B. Kozulic, I. Leustek, B. Pavlovic, P. Mildner and S. Barbaric, *Appl. Biochem. Biotechnol.*, 1987, **15**, 265.
- E. Stellwagen, *Ann. N.Y. Acad. Sci.*, 1984, **434**, 1.
- E. W. Huber and W. R. Heineman, *Anal. Chem.*, 1988, **60**, 2467.
- B. J. Radola and H. Delincee, *Ann. Technol. Agr.*, 1972, **21**, 473.
- Information from the technical department at Boehringer Mannheim Biochemicals Co.

33. J. K. Leypoldt and D. A. Gough, *Anal. Chem.*, 1984, **56**, 2896.
34. J. Rishpon, *Biotechnol. Bioeng.*, 1987, **29**, 204.
35. K. Hajizadeh, H. B. Halsall and W. R. Heineman, unpublished work.
36. F. Scheller, F. Schubert, B. Olsson, L. Gorton and G. Johansson, *Anal. Lett.*, 1986, **19**, 1691.
37. B. A. Petersson, *Anal. Chim. Acta*, 1988, **209**, 231.
38. A. Cornish-Bowden, in *Fundamentals of Enzyme Kinetics*, Chap. 2. Butterworths, London, 1979.
39. S. B. Lee and D. D. Y. Ryu, *J. Theor. Biol.*, 1980, **84**, 259.
40. F. P. Greenfield and L. R. Laurence, *Enzyme Eng.*, 1978, **4**, 381.
41. L. Goldstein, in *Methods in Enzymology*, Vol. 44, K. Mosbach (ed.). Academic Press, New York, 1976.
42. C. Galiatsatos, *Evaluation of Electrode Surface Modification Techniques for Development of Chemical Sensors*, Dissertation, pp. 82–84. University of Cincinnati, 1988.

AMPEROMETRIC ENZYME ELECTRODES FOR THE DETERMINATION OF L-GLUTAMATE

RHODORA L. VILLARTA,^{1,2} DAVID D. CUNNINGHAM^{2,*} and GEORGE G. GUILBAULT^{1,2,†}

¹Department of Chemistry, University of New Orleans, New Orleans, LA 70148 and

²Universal Sensors Inc., P.O. Box 736, New Orleans, LA 70148, U.S.A.

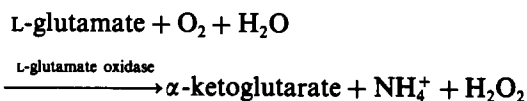
(Received 19 February 1990. Accepted 30 April 1990)

Summary—Electrodes for amperometric measurement of L-glutamate were prepared by immobilization of L-glutamate oxidase on an Immobilon-AV Affinity membrane and attachment to an oxygen/hydrogen peroxide sensor. The response of the hydrogen peroxide sensor was linear over the concentration range 5.0×10^{-8} – $5.0 \times 10^{-4} M$ L-glutamate, with a limit of detection of 35 nM. Attachment of a size-exclusion membrane (cut-off for molecular weight > 100) or of a hydrophobic oxygen membrane eliminated electro-oxidizable interferences, but the response was attenuated by a factor of 2–3. The response may be amplified 10-fold by co-immobilizing L-glutamate dehydrogenase with the L-glutamate oxidase. The electrode initially lost 25% of its activity but was then stable for more than 320 days and at least 200 assays. The electrode was successfully used to assay glutamate in a protein tablet and in several food products. A flow-injection system was assembled for the continuous assay of L-glutamate.

There is considerable interest in the rapid determination of glutamate, which is found in many kinds of foods and biological materials. Glutamate is a potent neuroexcitatory amino-acid¹ associated with the neurological pathways involved in a variety of behavior patterns. For example, the modulation of pupil diameter,^{2,3} morphine-induced muscular rigidity,⁴ retrograde amnesia⁵ and visual-task learning⁶ have all been shown to be glutamate-dependent. Monosodium glutamate (MSG) is a popular flavor enhancer linked to the Chinese-restaurant syndrome.⁷ In addition, the determination of L-glutamic acid is important in monitoring the transamination reaction, assay of protein hydrolysate, and detection of disease states associated with abnormalities of L-glutamic acid levels.⁸

Glutamate has been determined by chromatographic methods,^{9–12} potentiometric titrations^{13,14} and other indirect methods.¹⁵ However these methods are time-consuming and tedious. Enzyme-based methods are more selective, and several electrodes for potentiometric glutamate assay have been prepared from glutamate decarboxylase and glutamate dehydrogenase,^{16–23} but these systems proved to be unstable.

L-Glutamate oxidase, from *Streptomyces sp.* X119-6 has been found to react exclusively with L-glutamate, with few inhibitors.²⁴ The enzyme reacts with glutamate according to the equation



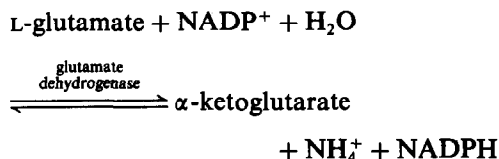
An electrode for amperometric determination of glutamate was prepared by immobilizing L-glutamate oxidase on a cellophane membrane sandwiched between Teflon and dialysis membranes.²⁵ The electrode response was linear over the concentration range 0.01–1.0 mM and suffered from interference by L-glutamine, L-aspartate, and L-asparagine.

In this paper, we report amperometric enzyme electrodes based on the immobilization of L-glutamate oxidase on pre-activated Immobilon-AV Affinity membranes. Oxygen or hydrogen peroxide may be monitored amperometrically, and the resulting change in steady-state current or its derivative with respect to time is directly proportional to the glutamate concentration. The base membrane material is a hydrophilized fluorocarbon polymer with the entire surface chemically treated for covalent immobilization of protein through the ϵ -amino groups of lysine.²⁶ The membranes are easy to handle, require very small

*Abbott Laboratories, Department 93N, Building AP9A, Abbott Park, IL 60064, U.S.A.

†Author for correspondence.

quantities of the expensive enzymes and allow fast and simple enzyme immobilization. To eliminate interferences from electro-oxidizable substances, a hydrophobic oxygen membrane or a size-exclusion membrane (cut-off for molecular weight > 100; "100 m.w. cut-off membrane") was inserted between the electrode and the enzyme membrane. The response was further amplified by co-immobilizing L-glutamate dehydrogenase [EC 1.4.1.4] with the L-glutamate oxidase. The reaction catalysed by glutamate dehydrogenase is



The two-enzyme system causes cycling of L-glutamate, α -ketoglutarate, and NH_4^+ between the two enzymatic reactions, in the presence of NADPH, resulting in an increase in the rate of oxygen consumption. The electrode thus prepared was included in a flow-injection system for the continuous assay of glutamate.

The electrode is more selective, sensitive and stable than any previously reported.

EXPERIMENTAL

Instrumentation and materials

Steady-state currents were measured with a Bioanalytical Systems (BAS) LC-4B Amperometric Detector (BioAnalytical Systems, Inc., W. Lafayette, IN). Rate measurements were made with a Gould Differentiator Amplifier Model 13-4615-71 and Gould Medium Gain Preamplifier Model 13-4615-10 (Gould Inc., Cleveland, OH). All measurements were recorded by a Houston Microscribe Strip Chart Recorder, Model 4521 (The Recorder Co., San Marcos, TX).

Immobilon-AV Affinity Membranes, 0.65 μm pore size, (Millipore Corporation, Bedford, MA), Pall Immunodyne ImmunoAffinity Membranes (Pall Biosupport Division, East Hills, NY), Nuclepore Polycarbonate Membranes, 0.03 μm pore size, (Nuclepore Corporation, Pleasanton, CA) and UltraBind Affinity Membranes, 0.45 μm pore size, (Gelman Sciences, Inc., Ann Arbor, MI) were purchased. The 100-m.w. cut-off membrane was cast from a solution of cellulose acetate in cyclohexanone, and propan-2-ol according to the procedure of Taylor *et al.*,²⁷ The hydrophobic polyethylene

oxygen membrane, amperometric oxygen electrode and internal-filling solution were from Universal Sensors, Inc., Metairie, LA.

Figure 1 shows a schematic diagram of the flow-injection system utilized for the continuous assay of L-glutamate. The flow-injection system included a Rainin Rabbit Peristaltic Pump and a Rheodyne 4-way sample injection valve. The flow-through cell was constructed in our laboratory from a plastic cuvette machined to fit the electrode tip exactly.

Reagents

L-Glutamate oxidase from *Streptomyces sp.* X119-6 was a gift from Yamasa Shoyu Co., Japan. L-Glutamic dehydrogenase [EC 1.4.1.4] from *Proteus sp.* was purchased from Toyobo Co., Ltd., Japan. L-Glutamic acid (monosodium salt, Sigma No. G-1626, 99–100%), bovine serum albumin (98–99%) and glutaraldehyde (Grade II, 25% aqueous solution) were from Sigma Chemical Co., St. Louis, MO. All reagents not listed were of analytical grade.

Regular and spicy "Season All", seasoned and unseasoned meat-tenderizer, (McCormick and Co., Inc., Baltimore, MD), "Your Life" multi amino-acid tablets (P. Leiner Nutritional Products, Inc., Torrance, CA), "Mrs. Dash" extra-spicy seasoning (Alberto-Culver Co., Melrose Park, IL), and "Accent" (Pet Inc., St. Louis, MO) were purchased from a local grocery store.

Measurements were made on samples in Dulbecco's buffer, which was prepared with demineralized water and stored at 5°. Dulbecco's buffer, pH 7.4, contains the following salt concentrations: 137mM NaCl, 2.7mM KCl, 8.0mM Na_2HPO_4 , and 1.5mM KH_2PO_4 .

Solutions of L-glutamate were prepared in Dulbecco's buffer, pH 7.4, containing 5mM sodium azide.

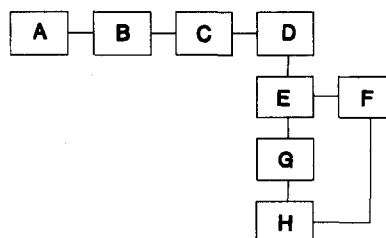


Fig. 1. Block diagram of flow system: (A) carrier solution reservoir [carrier solution: Dulbecco's buffer], (B) peristaltic pump, (C) sample injector, (D) L-glutamate oxidase electrode, (E) amperometric detector, (F) recorder, (G) amplifier, (H) differentiator.

Electrode preparation

The pre-activated membrane was attached to an inverted electrode jacket, (0.78 cm² tip area) with a rubber O-ring. 10 μ l of 72 units/ml L-glutamate oxidase solution were pipetted onto the membrane for the single-enzyme system and 5 μ l of 72 units/ml glutamate oxidase and 5 μ l of 400 units/ml glutamate dehydrogenase for the two-enzyme membrane. The membranes were allowed to dry at room temperature for 1–2 hr and were kept immersed in Dulbecco's buffer at 4° when not in use.

Procedure

The electrode jacket was filled with an internal filling solution, after which the electrode body was carefully inserted. A constant potential of +650 mV *vs.* Ag/AgCl was applied to the Pt working electrode. Electrode responses were then measured after addition of various amounts of standard L-glutamate solution to 10.00 ml of stirred Dulbecco's buffer. For the oxygen-based sensor, a hydrophobic oxygen membrane was inserted between the electrode tip and enzyme membrane. A constant potential of –650 mV *vs.* Ag/AgCl was applied to the Pt working electrode. The steady-state current change was read directly from the detector. The maximum rate of response was determined either from the peak height of the first derivative of current change with respect to time, or calculated from the slope of the line drawn through the maximum rate of current change with time, on the chart recording.

The electrode was included in a flow-injection system for the continuous assay of L-glutamate. Dulbecco's buffer, which served as the carrier solution, was pumped at a flow-rate of 0.80 ml/min. Injections of 100 μ l of standard solutions of L-glutamate were made after the electrode had attained a constant baseline potential.

To measure the glutamate content of a solid, the sample was weighed and then ground and homogenized by use of mortar and pestle. The samples were all dissolved and diluted with Dulbecco's buffer and the solutions were aerated for 5 min before testing.

The extent of enzyme retention on the membranes was determined by colorimetric assay of the storage buffer solutions for glutamate oxidase.²⁸ Two ml of 0.0025M dye solution, 0.50 ml of 16 units/ml peroxidase, 0.50 ml of 15% L-glutamate solution and 0.30 ml of dilute L-glutamate oxidase solution were pipetted into a

cuvette and mixed for a few seconds by use of a vortex mixer. The increase in absorbance at 510 nm was monitored for 3–4 min and the rate of absorbance change was calculated from the linear portion of the plot.

RESULTS AND DISCUSSION

Electrode response

The steady-state current of the electrodes was determined by the reduction of oxygen or oxidation of hydrogen peroxide at the Pt working electrode. Before the addition of glutamate, the electrodes exhibited steady-state currents of 160–220 and 0.1–0.3 nA when polarized at –650 and +650 mV respectively. The background noise at +650 mV was about 7 pA. Figure 2 shows the calibration of the hydrogen peroxide sensor, as a logarithmic plot. The response is linear from $5 \times 10^{-8}M$ up to about $5 \times 10^{-4}M$ L-glutamate. The response of the electrodes levelled off at glutamate concentrations above 1mM, owing to the nearly complete consumption of oxygen at the electrode tip. With substrate recycling, the response levelled off at a much lower concentration, $1.0 \times 10^{-4}M$. The detection limit of the hydrogen peroxide sensor is 30nM for steady-state measurements and 90nM for rate measurements (Fig. 3). The detection limit is defined as the substrate concentration which gives a signal $Y_{DL} = Y_{blank} + 3s$, where s is the standard deviation of y_{blank} .²⁹ Generally, steady-state measurements are more sensitive than rate measurements. However, rate measurements have a larger linear range and the maximum rate occurs at about 14 sec after sample injection, in comparison to 2 min for steady-state measurements.

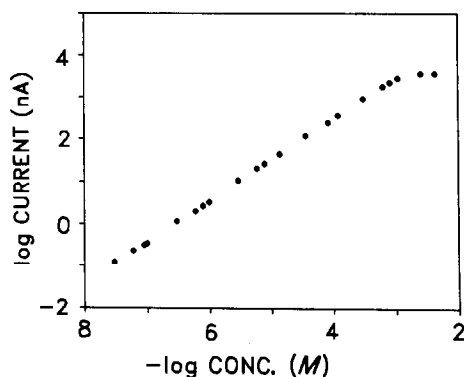


Fig. 2. Calibration of hydrogen peroxide sensor (logarithmic plot). Response is shown as the log of steady-state current change *vs.* -log (L-glutamate concentration).

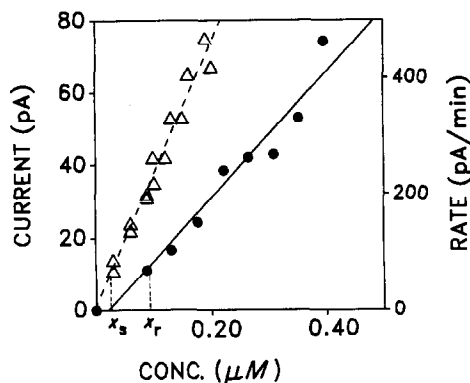


Fig. 3. Calibration plots for ● initial rate and △ steady-state measurements for low concentrations of L-glutamate. Left-hand scale is change in steady-state current. Right-hand scale is the time derivative of current. X_s = DL for steady-state measurements. X_r = DL for initial rate measurements.

Figure 4 shows the correlation of rate of current change, peak current and assay time with flow-rate. A relative response of 100 corresponds to 350 nA/min and 150 nA for maximum rate and peak height, respectively. The rate response is optimum at 0.80 ml/min, and the peak current and assay time decrease non-linearly with flow-rate. Thus, 0.80 ml/min was chosen as giving the best compromise with regard to response and assay time and was used for subsequent studies. Between 50 and 60 100- μ l samples may be assayed per hour under these conditions.

Figure 5 shows a comparison of the responses of the hydrogen peroxide sensors with and without the 100-m.w. cut-off membrane and of the oxygen sensors with and without substrate recycling. Without a second membrane, the

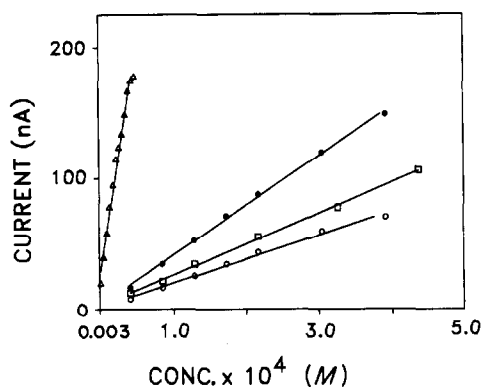


Fig. 4. Comparison of steady-state current response of L-glutamate electrodes. ● H_2O_2 -based sensor which consists of the enzyme membrane only. ○ H_2O_2 -based sensor with 100-m.w. cut-off membrane. □ O_2 -based sensor which consists of the enzyme membrane and hydrophobic oxygen membrane. △ O_2 -based sensor with substrate recycling.

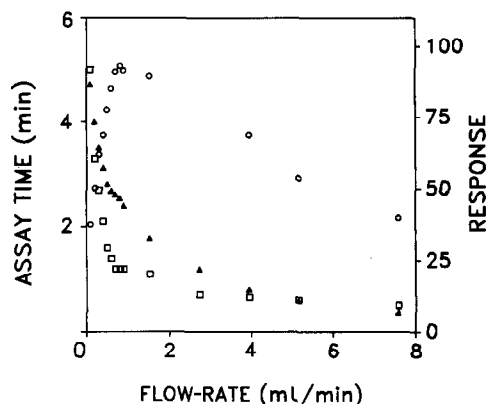


Fig. 5. Correlation of ○ initial rate, ▲ peak current, and □ assay time, with flow rate at 25°. Right-hand scale is the relative response for initial rate and peak current. A relative response of 100 corresponds to 350 nA/min and 150 nA for initial rate and peak current respectively. Left-hand scale is the assay time for one measurement, which includes response time and time for baseline recovery. Carrier solution—Dulbecco's buffer, substrate—0.439mM L-glutamate; base sensor—oxygen electrode.

steady-state current slope is 0.36 nA/ μ M (correlation coefficient 0.995). Addition of the 100-m.w. cut-off membrane reduced the sensitivity by about 50%, owing to the slower diffusion of hydrogen peroxide through the less porous membrane. With the addition of a hydrophobic oxygen membrane, and with the electrode polarized at -650 mV, the current slope is reduced by about 60%, with a detection limit of approximately $4 \times 10^{-6}M$. The linearity range of the oxygen sensor is regulated by the solubility of oxygen in the sample matrix and by the diffusion of oxygen across the membranes. A much higher detection limit is expected since the signal is measured against a high background current.

Amplification of response current was attained by substrate recycling. In the absence of NADPH and excess of ammonium ions, the responses of the single-enzyme and two-enzyme electrodes to L-glutamate are similar, indicating that the co-immobilization of the two enzymes does not cause any major drawbacks. In the presence of 5mM ammonium chloride and 1mM NADPH, the response of the two-enzyme system was amplified 10-fold (Fig. 4). Since oxygen is not produced in the reaction, substrate recycling leads to a shift of the linear range of the sensor to lower glutamate concentrations.

Optimization of parameters

The performance was evaluated for the electrodes made with Immobilon-AV Affinity

membranes, Pall Immunodyne ImmunoAffinity membranes, UltraBind Affinity membranes, and Nuclepore membranes. The immobilization on Pall and UltraBind membranes was similar to that on Immobilon, as described earlier. The best electrode constructed with the two other pre-activated membranes was only half as sensitive as the electrode prepared with Immobilon, and the membrane lost 50% of its activity after 20 days when stored in buffer at 4°. The enzyme was also immobilized on a Nuclepore polycarbonate membrane with the inert protein bovine serum albumin (BSA) and cross-linked with glutaraldehyde in aqueous medium. The much larger amount of 3.6 units of glutamate oxidase, with an immobilization matrix of 1 μ l of 2.5% glutaraldehyde solution and 10 μ l of 10% BSA solution, was needed to construct an electrode with the same performance as that of an electrode with 0.36 units of enzyme immobilized on Immobilon. When stored in Dulbecco's buffer at room temperature, the electrode was totally inactive after 100 days. The loss of activity is probably due to microbial degradation of the protein in the matrix.

The effects of varying the amount of enzyme load and the immobilization time, on the performance of the electrode constructed from Immobilon, were evaluated. The response increased with enzyme load up to 0.30 units of L-glutamate oxidase per 0.78 cm² of membrane and up to 60 min immobilization time, then started to level off. It was also found that the response varies linearly with the square of percentage of immobilization between 36 and 72%, with a correlation coefficient of 0.990.

Analytical characteristics of the electrode

The effect of pH on the electrode response was studied for four buffer systems with pH ranging from 3.70 to 11.0. The results are shown in Fig. 6. The response does not vary much with the type of buffer used. The response of the immobilized enzyme is optimum at pH 6–8, which is similar to the optimum for the free enzyme, reported to be pH 7–8 at 5°.¹⁹

D-Glutamic acid, various L-amino-acids (aspartic acid, tyrosine, alanine, arginine, glycine, isoleucine, valine, serine, tryptophan, histidine, leucine, proline, methionine, glutamine, cysteine, lysine, asparagine, threonine, and phenylalanine), various compounds containing glutamate (gly-glu, glu-glu and glutamic acid diethyl ester), and several species found in the brain extra-cellular fluid (ascorbic acid, gluta-

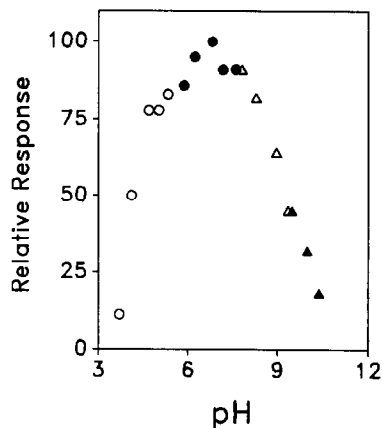


Fig. 6. Effect of pH on the L-glutamate electrode at 25°. Response was measured with 0.439mM L-glutamate as substrate in the following buffers: ○ acetate, ● phosphate, △ tris and ▲ carbonate.

thione, dopamine, norepinephrine, 3,4-dihydroxyphenylacetic acid, homovanillic acid and 5-hydroxyindoleacetic acid) were tested as possible interferents. At -650 mV, with the hydrophobic oxygen membrane, no interference from 10mM solutions of these compounds was observed. The oxygen-based sensor is totally specific for L-glutamate, except for samples which contain volatile electroactive compounds (e.g., volatile amines from hydrolysed protein). These compounds diffuse across the hydrophobic membrane to give a positive interference. At +650 mV, a number of amino-acids such as cysteine, tyrosine, dihydroxyphenylalanine, and tryptophan and the neurotransmitters and their metabolites are electro-oxidizable. The incorporation of the 100-m.w. cut-off membrane effectively removes or at least reduces the interference from these compounds to at most 2% when they are present in amounts equal to the glutamate concentration. In addition, the second, less porous, membrane is needed to protect the electrode from fouling by deposition of macromolecules from the sample matrix. In certain applications such as *in vivo* determinations, the monitoring of hydrogen peroxide has advantages. The initial oxygen content of tissues can vary, and this would make electrode calibration difficult and the net current change low. The sensitivities of the oxygen sensor or of the hydrogen peroxide sensor with a 100-m.w. cut-off membrane are enough for most of the intended applications of the device. For example, the calculated *in vivo* concentrations of glutamate in rat brain, determined by microdialysis and voltammetry, range from 1.9 to 22 μ M.³⁰ Substrate recycling increases the

Table 1. Stability of membrane in various conditions at room temperature

Solute ^a	Relative response after 50 days, %
None	90
L-Glutamate*	72
Benzoate	90
EDTA ^b	100
Amino-acid mixture*	100
Sodium azide	100
Thimerosal ^c	36
Peroxide	5
Acetate ^d	86

^a5mM solute in Dulbecco's buffer, pH 7.4.

^bEthylenediaminetetra-acetic acid (disodium salt).

^cSodium ethylmercurithiosalicylate.

^dAcetate buffer, pH 4.

*Also contains 5mM azide and 20 free-form amino acids.

sensitivity of the sensor but α -ketoglutarate and NADPH must be added to the sample matrix. This procedure is not strongly recommended, because NADPH is a cofactor for many enzymatic reactions, and might introduce unpredictable interferences.

The stability of the enzyme membrane in different solutions at room temperature is shown in Table 1. The electrode response was considerably inhibited by 5mM hydrogen peroxide and 5mM thimerosal. When stored in Dulbecco's buffer at 4°, the membrane lost 25% of its activity after 7 days, but was then stable at that level for 320 days and at least 200 assays. The stability of the electrode under operating conditions depends on the sample matrix.

Matrices which contain reducing agents or heavy metals such as mercury will rapidly deactivate the enzyme membrane. In buffered solutions of glutamate and other amino-acids, the enzyme membrane remains usable for a long time, depending on the operating temperature, required sensitivity and exposure time of the membrane to the test solution.

Table 2 shows the experimentally determined L-glutamate content of a protein tablet and some food seasonings. The values obtained are in close agreement with the manufacturer's specification within an acceptable range of error.

The immobilization of enzymes on pre-activated membranes has many advantages over the conventional methods of polymerization of the protein by use of a cross-linking agent, and attachment onto a porous membrane. The former procedure is a one-step process and should be more reproducible. Ready-to-use probes utilizing very small amounts of enzymes could be prepared routinely in 1 hr. This is especially important for industrial applications. In the L-glutamate electrode prepared, immobilization of the enzyme on an Immobilon-AV Affinity membrane gave an electrode with better sensitivity and stability than those prepared in the conventional way.

Acknowledgements—The authors wish to thank Dr. G. Lubrano of Universal Sensors, Inc., Dr. A. Suleiman of the University of New Orleans, and Dr. G. Palleschi of the University of Rome "Tor Vergata" for helpful discussions. Financial support from USDA Small Business Innovative Research grant no. 86-SBIR-8-0096 is also gratefully acknowledged.

Table 2. Determination of monosodium glutamate content of protein tablet and food products

Product	Experimental value ^a , %	Manufacturer's specification, %	Relative error, %
"Accent"	95 ± 3	100	-5
McCormick "Regular Season All"	5.5 ± 0.1	5.8	-5.2
McCormick "Spicy Season All"	5.5 ± 0.1	5.8	-5.2
McCormick "Seasoned Meat Tenderizer"	10.0 ± 0.2	10.0	0
McCormick "Unseasoned Meat Tenderizer"	0	0	0
Adolph's "Seasoned Meat Tenderizer"	0	0	0
Morton "Nature's Season"	0	0	0
Mrs. Dash "Extra-spicy Seasoning"	0	0	0
"Your Life" protein tablet ^b	8.9 ± 0.2	8.2	+8.5

^aAssay values represent the average of 5 determinations with 95% confidence level.

^bMeasured as L-glutamic acid.

REFERENCES

1. J. T. Coyle, in *Neurotransmitter Receptors. Part I: Amino Acids, Peptides and Benzodiazepines*, p. 3. Chapman & Hall, New York, 1980.
2. D. J. Albert, *Pharm. Biochem. Behav.*, 1981, **14**, 67.
3. A. Van Harreveld and E. Fikova, *J. Neurobiol.*, 1970, **2**, 13.
4. L. Turski, U. Havemann and K. Kuschinsky, *Pharm. Biochem. Behav.*, 1982, **17**, 715.
5. J. L. Davis, A. Cherkin and M. D. Hewitt, *ibid.*, 1981, **14**, 919.
6. R. Sdraulig, L. J. Rogers and A. L. A. Boura, *Physiol. Behav.*, 1980, **24**, 493.
7. J. J. Schaumburg, R. Byck, R. Gerstl and J. H. Mashman, *Science*, 1969, **163**, 826.
8. M. D. Hilty, C. A. Romshe and R. V. Delamater, *J. Pediat.*, 1974, **84**, 362.
9. E. Fernandez-Flores, A. R. Johnson and V. H. Blomquist, *J. Assoc. Offic. Anal. Chem.*, 1969, **52**, 744.
10. B. W. Bailey and H. L. Swift, *ibid.*, 1970, **53**, 1268.
11. E. D. Coppola, S. N. Christie and J. G. Hanna, *ibid.*, 1975, **58**, 58.
12. *Official Methods of Analysis of the Association of Official Analytical Chemists*, 12th Ed., Sections 20.184–20.186. AOAC, Washington, DC, 1975.
13. M.-L. Wen and C.-Y. Wang, *Anal. Chim. Acta*, 1987, **198**, 325.
14. T. Gündüz, N. Gündüz, E. Kiliç, F. Köseoğlu and S. G. Öztas, *Analyst*, 1988, **113**, 715.
15. E. Athanasiou-Malaki and M. A. Koupparis, *Analyst*, 1987, **112**, 757.
16. B. K. Ahn, S. K. Wolfson, Jr. and S. J. Yao, *Bioelectrochem. Bioenerg.*, 1975, **2**, 142.
17. S. J. Yao, S. K. Wolfson, Jr., J. M. Tokarsky and S. B. Weiner, *ibid.*, 1976, **3**, 106.
18. M. Hikuma, H. Obana, R. Yasuda, I. Karube and S. Suzuki, *Anal. Chim. Acta*, 1980, **116**, 61.
19. S. Kuriyama and G. A. Rechnitz, *ibid.*, 1981, **131**, 92.
20. J. I. Korenbrot, R. Perry and D. Copenhagen, *Anal. Biochem.*, 1987, **161**, 187.
21. D. P. Nikolelis, *Analyst*, 1987, **112**, 763.
22. G. G. Guilbault and F. R. Shu, *Anal. Chim. Acta*, 1971, **56**, 333.
23. K. Riedel and F. Scheller, *Analyst*, 1987, **112**, 341.
24. H. Kusakabe, Y. Midorikawa, T. Fujishima, A. Kuninaka and H. Yoshino, *Agri. Biol. Chem.*, 1983, **47**, 1323.
25. H. Yamauchi, H. Kusakabe, Y. Midorikawa, T. Fujishima and A. Kuninaka, *Eur. Congr. Biotechnol.*, 1984, **1**, 705.
26. *Immobilon Tech. Protocol*, Lit. No. (TP003) TP015., Millipore Corp., Bedford, MA, 1987.
27. P. J. Taylor, E. Kmetec and J. M. Johnson, *Anal. Chem.*, 1977, **49**, 789.
28. *Cholesterol Oxidase*, Toyobo Enzymes, Toyobo Co., Ltd., Japan, 1987.
29. J. C. Miller and J. N. Miller, *Statistics for Analytical Chemistry*, 1st Ed., Horwood, Chichester, 1984.
30. H. Benveniste, *J. Neurochem.*, 1989, **52**, 1667.

ENZYME ELECTRODE STUDIES OF GLUCOSE OXIDASE MODIFIED WITH A REDOX MEDIATOR

P. N. BARTLETT*, V. Q. BRADFORD and R. G. WHITAKER†

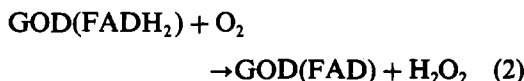
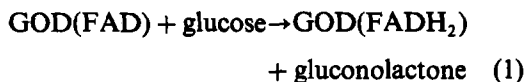
Department of Chemistry, University of Warwick, Coventry CV4 7AL, U.K.

(Received 30 October 1989. Revised 12 December 1989. Accepted 18 December 1989)

Summary—Glucose oxidase modified by the covalent attachment of ferrocenecarboxylic acid or ferroceneacetic acid groups undergoes direct oxidation at metal electrodes. Studies of the comparative stability of the two modified enzymes on storage and on electrochemical cycling show that the material modified with ferroceneacetic acid is the more stable. Amperometric studies of enzyme electrodes based on these modified forms of glucose oxidase show that their application in practical biosensors is severely limited by the poor stability of the oxidized form of the covalently attached ferrocene mediator. A comparison of the results obtained with the native enzyme and with that modified with ferroceneacetic acid, for the oxidation of glucose, D-mannose, 2-deoxy-D-glucose, D-xylose and D-galactose, suggests that the modification procedure has little effect on the selectivity of the enzyme.

The amperometric use of enzyme electrodes has been extensively studied over the past decade. The combination of the selectivity offered by enzyme catalysis with the simplicity and low cost of an amperometric detector is an attractive approach to the production of chemical sensors for a range of biomedical and biotechnological applications.

The coupling of the electron-transfer reactions of the biological component with electron transfer at the electrode poses a major problem. For example, glucose oxidase (GOD) catalyses the oxidation of glucose by molecular oxygen in a two-step process:



In the first step the flavin group (FAD) in the enzyme is reduced by reaction with glucose to give the reduced form of the enzyme, GOD(FADH₂). In the second step molecular oxygen reoxidizes the flavin to regenerate the oxidized form of the enzyme, GOD(FAD). To make use of this in an enzyme electrode for glucose we must detect either hydrogen peroxide production or oxygen consumption, or we must

replace the reoxidation with oxygen by anodic reoxidation of the enzyme.



Very similar considerations apply to the development of biosensors based on other flavoproteins, including D-amino-acid oxidase, L-amino acid oxidase, xanthine oxidase and choline oxidase.

A number of approaches to this general problem have been investigated.¹⁻³ Monitoring the production of hydrogen peroxide or consumption of oxygen,^{9,10} although quite successful, can suffer from oxygen limitation, particularly when used *in vivo*. An alternative is to replace the reaction with oxygen in the second step, by reaction with an artificial mediator:



The reduced form of the mediator, M, can then be reoxidized at the electrode. This approach has been used very successfully, with a ferrocene derivative as the mediator, in a range of applications¹¹⁻¹⁵ and is the basis of a commercial glucose monitor.¹⁶ Another approach is to use a conducting organic salt, such as TTF.TCNQ, as the working electrode in the amperometric sensor,¹⁷ the reduced form of the enzyme being oxidized at the conducting salt electrode. The mechanism of this reaction is not well understood.¹⁸⁻²⁰ Conducting polymers have also been

*Author for correspondence.

†Present address: EMS Ltd., Odd Fellows House, 2 Queen Victoria Road, Coventry, U.K.

used to entrap glucose oxidase at electrode surfaces²¹⁻²³ and it has recently been suggested that direct oxidation of glucose oxidase is possible in polypyrrole films²⁴ or in films of *N*-alkylferrocene derivatives of pyrrole.²⁵

Studies by Hill,²⁶ Degani and Heller^{27,28} and ourselves²⁹ have shown that direct oxidation of the flavin centre of glucose oxidase at unmodified electrodes can be achieved if the enzyme is first modified by the covalent attachment of ferrocene groups to amino-acid residues within the protein. This observation has been rationalized²⁷ by the suggestion that the covalently bound ferrocenes act as "stepping stones" allowing electrons to tunnel between the electrode and the active site in a number of consecutive steps.

Hill²⁶ describes the coupling of an average of 8 ferrocenecarboxylic acid groups to glucose oxidase by use of isobutyl chloroformate. In their initial work Degani and Heller²⁷ also describe the modification of glucose oxidase with ferrocenecarboxylic acid, although they employed a different coupling procedure. In a subsequent paper the same authors²⁰ extended this work to include the modification of D-amino-acid oxidase and the use of ferroceneacetic acid and ruthenium pentamine complexes as alternative mediators. In preliminary studies they found that the stability of the modified enzymes varied, depending on the oxidation state of the ruthenium, with the Ru(III) form being more stable than the Ru(II) of the bound mediator. For enzymes modified with ferrocenecarboxylic acid and ferroceneacetic acid they reported a 10% loss of current, determined by cyclic voltammetry, after incubation of the enzyme for 2 hr with 0.03M glucose. In our previous work²⁹ we studied glucose oxidase modified with ferrocenecarboxylic, ferroceneacetic, and ferrocenebutanoic acids. We found differences in the stability of the different modified enzymes on storage (at 4° and pH 7.0, in 0.085M phosphate buffer); the enzyme modified with ferroceneacetic acid was the most stable and that modified with ferrocenebutanoic acid the least.

The covalent attachment of mediators to redox enzymes is interesting for a number of reasons. First, it offers the prospect of reagentless biosensors. Secondly, such modified enzymes might be well suited to *in vivo* applications (because the mediator is covalently bound, the enzymes should not be dependent on oxygen). Thirdly, modified enzymes of this type

may prove useful in the development of bio-electronic devices based on the localization of enzymes on microelectronic substrates. Finally they are of interest in the study of the interactions between enzymes and electrodes and in the study of electron transfer to biomolecules.

In this paper a study of glucose oxidase modified with ferrocenecarboxylic acid (FCA) and ferroceneacetic acid (FAA) is presented. Their behaviour is compared with that of the native enzyme and results for membrane electrode studies with glucose and several other substrates are also given.

EXPERIMENTAL

Ferrocenecarboxylic acid and ferroceneacetic acid were obtained from Aldrich. All other chemicals were AnalaR grade from B.D.H. Glucose oxidase (E.C. 1.1.3.4) from *Aspergillus niger* was purchased from Sigma (type VII, activity 1.769×10^5 U/g). The enzyme was modified by the method of Degani and Heller^{27,28} and the products were purified by gel filtration chromatography on Sephadex G-15. The concentration of modified enzyme in each fraction was estimated from the absorbance at 450 nm and a molar absorptivity³⁰ of 14.1×10^3 l.mole⁻¹.cm⁻¹. The enzyme activity was estimated by a dye-linked spectrophotometric assay based on an earlier procedure.^{31,32} The iron contents of the modified enzymes were determined by atomic-absorption spectrophotometry. Measurements were made in duplicate at two or more concentrations, the buffers used were found to be essentially iron-free. The number of iron atoms per enzyme molecule was found to be 2 for the native enzyme, 13 for the enzyme modified with ferrocenecarboxylic acid and 22 for the one modified with ferroceneacetic acid.

All electrochemical experiments were carried out in 0.15M phosphate buffer (pH 7.0), containing 0.20M sodium chloride. Buffer solutions were freshly prepared with water from a Whatman WR50 water-purification system. Sugar solutions were allowed to equilibrate at room temperature for 24 hr before use. An Oxford Electrodes potentiostat and a Gould Bryans 60,000 series XY/t recorder were used. All potentials are reported with respect to the saturated calomel electrode (SCE).

Membrane electrodes were constructed from glassy-carbon rod (David Feckenham, diameter 0.4 cm) press-fitted into a Teflon mantle and then polished to a mirror finish with alumina

slurry. Solutions of the native or modified enzyme were applied to the glassy-carbon electrode with a micropipette (typical volumes 10–30 μl). The droplets of solution were allowed to evaporate at room temperature (ca. 2 hr) before the membrane was applied. The membranes were made from Medicell dialysis tubing pretreated according to the manufacturer's instructions and held in place by silicone rubber 'O'-rings. The assembled electrodes were kept in buffer solution for at least 30 min and then transferred to the electrochemical cell (kept at $25 \pm 0.1^\circ$) and held at a potential of 0.50 V vs. SCE (this is in the limiting-current region for the oxidation of the ferrocenecarboxylic and ferroceneacetic acids). The background current was allowed to become stable (typically in 20 min) before portions of stock glucose solution were added. On addition of glucose, and after mixing, the enzyme membrane electrode responses became steady in less than 20 sec. All solutions were deoxygenated by passage of oxygen-free nitrogen through them for at least 15 min.

RESULTS

Native enzyme

The initial membrane electrode studies were done with the native enzyme, with 1mM ferrocenecarboxylic acid in the bulk solution. Figure 1 shows typical results for the variation of the current at a membrane electrode of this type with increasing glucose concentration.

These results can be analysed in terms of our model for amperometric membrane enzyme electrodes, and assuming no product inhibition.^{20,33,34} In this model the electrode response is characterized by two parameters, the effective electrochemical rate constant for the enzyme

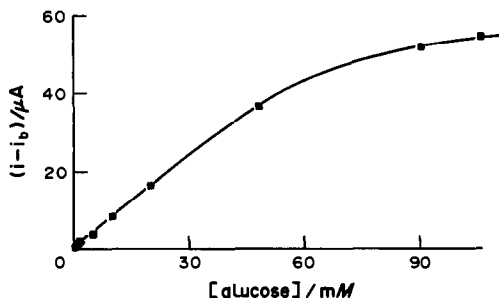


Fig. 1. Plot of the current, corrected for the background, as a function of glucose concentration for a membrane enzyme electrode based on native GOD (0.15 mg, 27.4 U) entrapped behind the membrane with 1mM ferrocenecarboxylic acid in the bulk solution.

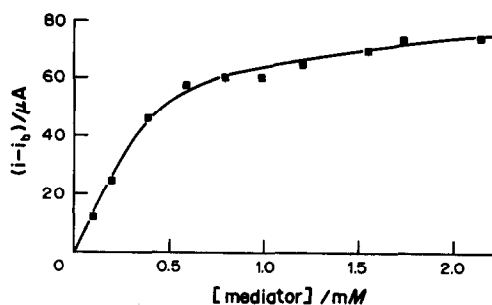


Fig. 2. Plot of the current, corrected for background, as a function of the concentration of ferrocenecarboxylic acid added to the bulk solution for a membrane enzyme electrode based on native GOD (0.15 mg, 27.4 U) placed in 0.108M glucose.

electrode, k'_{ME} (cm/sec), and the equivalent of the Michaelis constant for the enzyme electrode, K_{ME} (M), where

$$1/k'_{\text{ME}} = K_{\text{M}}/(e_{\text{z}}Lk_{\text{cat}}) + 1/k'_{\text{s}} \quad (5)$$

and

$$K_{\text{ME}} = [K_{\text{M}}/Lk_{\text{cat}} + e_{\text{z}}/k'_{\text{s}}]/[1/Lk_{\text{cat}} + 1/k'] \quad (6)$$

In these equations K_{M} and k_{cat} are the normal Michaelis–Menten terms describing the reaction of glucose with GOD, e_{z} is the concentration of enzyme behind the membrane, L is the thickness of the enzyme layer, k'_{s} is the mass-transport rate constant for the diffusion of glucose through the membrane, and k' is the heterogeneous rate constant (cm/sec) describing the rate of electrochemical reoxidation of the enzyme. When free mediator is present in solution, k' is given by $Lk_{\text{a}}m$, where k_{a} is the rate constant for the reaction between the mediator and the enzyme and m is the mediator concentration. A full discussion of the model can be found in the review by Albery and Craston.²⁰

In Fig. 1, the solid line represents the best fit of the data to this model. From this analysis we find that, at low glucose concentrations, the response is determined by diffusion of glucose through the dialysis membrane. From this and similar data we obtain a mean value for k'_{s} , the mass-transport rate constant for diffusion of glucose through the membrane, of 4.75×10^{-5} cm/sec, in excellent agreement with values in the literature.²⁰ At high glucose concentrations the response reaches a plateau limited either by the rate of the reaction between enzyme and mediator or by the enzyme kinetics. Figure 2 shows the effect of increasing the concentration of ferrocenecarboxylic acid in the bulk solution at a

constant (and enzyme-saturating) glucose concentration. At low ferrocenecarboxylic acid concentrations ($<0.5\text{mM}$) the current depends upon the mediator concentration and hence reaction of the mediator with the enzyme is the limiting factor. At high ferrocenecarboxylic acid concentrations the current is limited by the saturated-enzyme kinetics.

Stability of ferrocene-modified enzymes

The stability of glucose oxidase modified with ferrocenecarboxylic acid or ferroceneacetic acid on storage in deoxygenated aqueous buffer at 4° was monitored by a spectrophotometric assay of the activity in glucose oxidation by molecular oxygen. Figure 3 shows results for the two types of modification. The enzyme modified with ferroceneacetic acid is the more stable, retaining 88% of its activity after storage for 6 days.

To find the cause of the loss of activity, the possibility of loss of FAD from the modified enzyme during storage was first investigated. Gel permeation chromatography of "aged" samples of the enzymes gave no evidence of free FAD in solution and also the absorption spectra of freshly prepared and "aged" modified enzymes were identical. Finally, the addition of free FAD at $1\mu\text{M}$ concentration was found to have no effect on the glucose oxidation activity. We therefore concluded that the loss of activity did not arise from loss of FAD from the active site.

The effect of storage on the number of ferrocene units attached to the enzyme was also investigated. "Aged" samples were purified by gel permeation chromatography after cold storage for 13 days and then assayed for iron content by atomic-absorption spectrometry. The results showed that for the enzyme modified with ferroceneacetic acid the iron content had

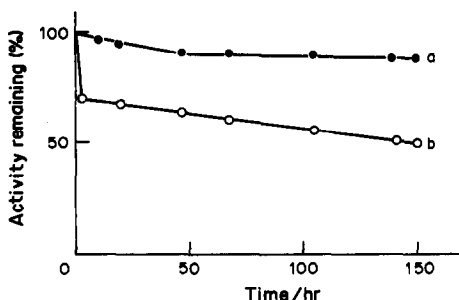


Fig. 3. Comparison of the storage stability at 4° in oxygen-free phosphate buffer (pH 7.0) of GOD modified with (a) ferroceneacetic acid and (b) ferrocenecarboxylic acid. The activity of the enzyme for glucose oxidation by molecular oxygen was assayed spectrophotometrically.

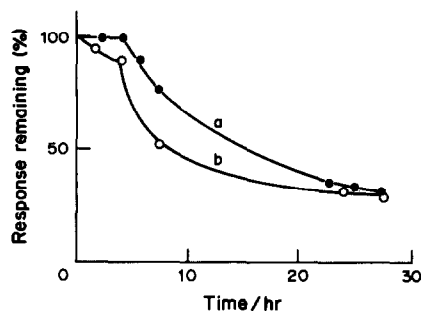


Fig. 4. Comparison of the stability of GOD modified with (a) ferroceneacetic acid and (b) ferrocenecarboxylic acid, determined electrochemically by continuous potential cycling at a glassy-carbon electrode at 20° in a 2-ml cell.

fallen from an initial value of 22 ± 2 to a final value of 6.5 ± 1 iron atoms per enzyme molecule.

In use, the ferrocene groups attached to the enzyme will cycle between the ferrocene and ferricinium oxidation states. To investigate the effect of this, the stability of the enzymes towards continuous potential cycling at a glassy-carbon electrode was also monitored in a small-volume (2 ml) electrochemical cell containing 80mM glucose. The electrode was polished before each current measurement, to eliminate any problems caused by fouling of the electrode. The results are shown in Fig. 4. In this experiment there is little difference in the stability of the two modified enzymes.

Thus there appear to be two aspects to the problem of stability: (i) cold storage produces a loss of enzyme activity for glucose oxidation, accompanied by some loss of iron from the modified enzyme and (ii) there is a much more rapid loss of activity during cycling in the electrochemical assay. We believe that the latter is associated with the loss of iron from the ferrocene groups attached to the modified enzyme, and that this process occurs much more rapidly for the ferricinium form of the mediator, which is generated during the electrochemical measurement.

Membrane electrode studies of modified GOD

To assess the suitability of the modified enzymes for use in sensors we investigated their use in membrane enzyme electrodes. The reproducibility of response of electrodes made with glucose oxidase modified with the ferrocenecarboxylic acid was poor. Curves (a) and (b) in Fig. 5 show results for two membrane electrodes prepared from different batches of the modified enzyme at nominally identical loadings. In both

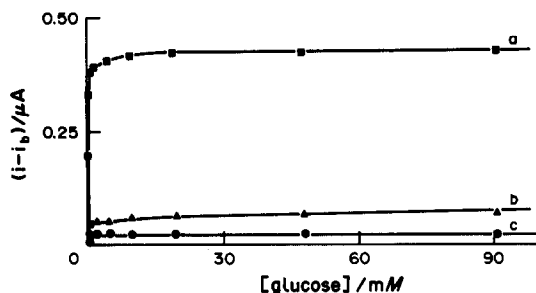


Fig. 5. Plots of the corrected current vs. glucose concentration for two membrane enzyme electrodes based on GOD modified with ferrocenecarboxylic acid: (a) 0.04 mg (7.08 U) of enzyme, (b) 0.041 mg of enzyme and (c) response in fresh solution, recorded directly after (a).

cases the steady-state responses reached saturation at very low glucose concentrations. We have analysed the results of a number of membrane electrode experiments, using our model,³³ and the results for three different batches of modified enzyme are presented in Table 1. For these electrodes k'_{ME} is smaller than the diffusion-limited value for glucose through the membrane, k'_S , as already determined with the native enzyme. Hence, the response at low glucose concentrations is determined by the enzyme kinetics. From equation (5), by using the values of k'_{ME} and K_{ME} in Table 1, the enzyme loading and the value of k'_S , we can estimate k_{cat} for the modified enzyme to be in the range 10^{-3} – 10^{-2} sec^{-1} . These values are unrealistically small when compared with the values of 5 sec^{-1} measured in homogeneous solutions.²⁹ We be-

lieve that this is because we have grossly overestimated the active enzyme loading and that much of the modified enzyme becomes inactive during preparation of the electrode for use. The poor reproducibility observed can then be attributed to the poor stability of the modified enzyme once it is placed behind the membrane (whether the enzyme is from the same batch or different batches).

If the electrode is removed from the glucose solution and placed in fresh buffer and the calibration is then repeated, we find an almost total loss (> 90%) of response [Fig. 5, curve (c)]. This was the case for all the ferrocenecarboxylic-acid type modified membrane electrodes used, and is not due to a loss of enzyme activity towards glucose oxidation, because when free mediator (1mM ferrocenecarboxylic acid) is added to the bulk solution, a large response to glucose is obtained, consistent with our results for the native enzyme (Table 1). Thus the loss of response from the glucose oxidase modified with ferrocenecarboxylic acid is due to the decomposition of covalently bound mediator rather than loss of enzyme activity for glucose oxidation.

The response of the modified glucose oxidase membrane electrode during continuous operation in 0.10M glucose (Fig. 6) declines almost exponentially over a period of approximately 1 hr.

The electrodes made with the enzyme modified with ferroceneacetic acid give much larger responses and appear to be better behaved and more reproducible. Figure 7 shows results for three different enzyme loadings. The results of the analysis of data from these and related experiments are presented in Table 2. In this case the k'_{ME} values are much closer to the value for k'_S and consequently the response is determined both by diffusion of glucose through the membrane and by the enzyme kinetics. The

Table 1. Analysis of glucose results for GOD membrane enzyme electrodes modified with ferrocenecarboxylic acid

Enzyme loading, mg	k'_{ME} , cm/sec	K_{ME} , mM
Batch I		
0.079	9.9×10^{-7}	4.65
0.119	3.8×10^{-6}	1.75
0.158	8.5×10^{-7}	4.76
Batch II		
0.055	1.1×10^{-6}	1.28
0.083	5.7×10^{-6}	1.25
0.111	1.0×10^{-6}	1.03
0.138	1.2×10^{-6}	2.56
Batch III		
0.041	2.8×10^{-6}	1.12
0.061	2.8×10^{-6}	0.32
0.082	4.3×10^{-6}	0.52
0.102	4.1×10^{-6}	0.18
Batch III with 1mM FCA added to the bulk		
0.041	3.7×10^{-5}	87.0
0.061	2.5×10^{-5}	14.3
0.082	4.3×10^{-5}	83.3
0.102	2.3×10^{-5}	52.1
0.123	4.9×10^{-5}	105.0

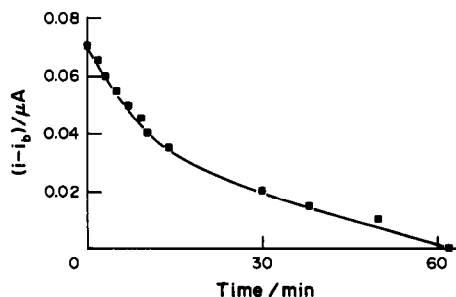


Fig. 6. Decrease in the current as a function of time for a membrane enzyme electrode based on GOD modified with ferrocenecarboxylic acid and held at 0.5 V in 0.091M glucose solution.

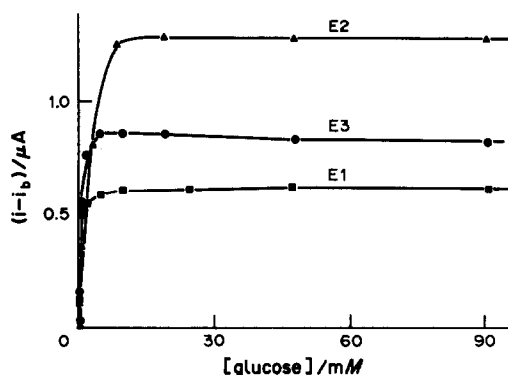


Fig. 7. Plots of the corrected current *vs.* glucose concentration for three different membrane enzyme electrodes based on GOD modified with ferroceneacetic acid. Enzyme loadings: E1 0.138 mg (24.5 U), E2 0.208 mg (36.8 U), E3 0.277 mg (49.0 U).

stability of these electrodes is also much better than that of those made with ferrocenecarboxylic acid as the enzyme modifier. After 20 hr at room temperature in glucose-free buffer the electrode still showed some response towards glucose (the response decreased by approximately 90% over this period). The analysis of these results is also given in Table 2. After 20 hr the k'_{ME} values were smaller by a factor of approximately 10, so the enzyme kinetics became rate-limiting. This was presumably the result of a loss in electrochemical activity of the enzyme over this period.

Selectivity

To investigate the effects of redox modification of the enzyme on selectivity, four other substrates (2-deoxy-D-glucose, D-mannose, D-

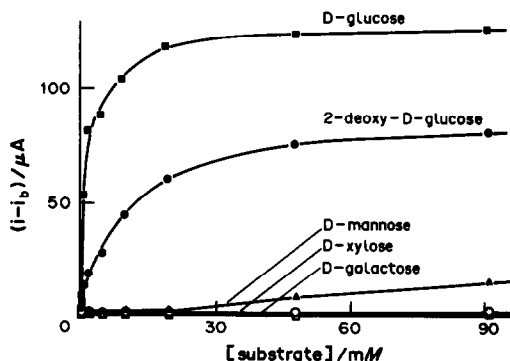


Fig. 8. Plots of the corrected current *vs.* substrate concentration for the homogeneous reaction with native GOD (0.976 mg/ml) mediated by 1mM ferrocenecarboxylic acid, for five different substrates.

galactose and D-xylose) were studied. The selectivity of the native enzyme was investigated in homogeneous solution, with ferrocenecarboxylic acid as the mediator. Figure 8 shows that the responses for the five sugars are consistent with rate data given in the literature:³⁵ glucose > 2-deoxy-D-glucose > D-mannose > D-xylose = D-galactose.

Figure 9 shows a set of results for the corresponding ferroceneacetic-acid type modified enzyme electrode and the same sugars. The results are similar to those for the native enzyme.

CONCLUSIONS

Our studies show that, although glucose oxidases modified with ferrocenecarboxylic acid and ferroceneacetic acid undergo direct unmediated oxidation at metal electrodes, they are not suitable for sensor applications because of their poor stability, which is due to the loss of the covalently bound ferrocene mediator from the

Table 2. Analysis of glucose results for GOD enzyme membrane electrodes modified with ferroceneacetic acid

Enzyme loading, mg	k'_{ME} , cm/sec	K_{ME} , mM
Batch I, identical loadings		
0.208	1.4×10^{-5}	3.57
0.208	2.8×10^{-5}	1.19
0.208	1.4×10^{-5}	1.67
0.208	2.1×10^{-5}	1.85
Batch II, freshly prepared		
0.138	2.6×10^{-5}	1.03
0.208	1.1×10^{-5}	1.20
0.277	2.6×10^{-5}	2.17
0.415	6.9×10^{-6}	1.64
Batch II, after 20 hr at room temperature		
0.138	4.2×10^{-6}	3.57
0.208	1.0×10^{-6}	1.19
0.277	4.1×10^{-6}	1.67
0.415	1.1×10^{-6}	1.09

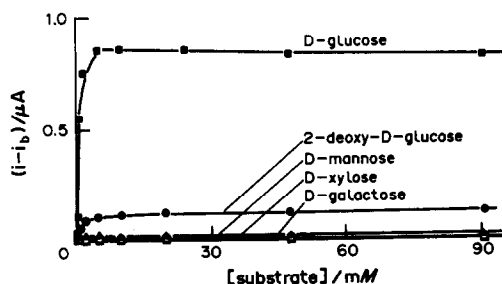


Fig. 9. Plots of the corrected current *vs.* substrate concentration for membrane enzyme electrodes based on GOD modified with ferroceneacetic acid (0.208 mg, 36.8 U), for five different substrates.

enzyme. This occurs more rapidly for the oxidized form and is a more severe problem for the enzyme modified with ferrocenecarboxylic acid. Szentrimay *et al.*³⁶ studied the stability of ferricinium ions in buffered aqueous solution (pH 7.0, phosphate) and found half-lives of 0.50 and 4.3 hr for the ferricinium forms of the carboxylic acid and acetic acid derivatives respectively. They suggested that the oxidized ferrocenes undergo a hydrolysis reaction involving disproportionation to give hydrous ferric oxide.

The results of Szentrimay *et al.* are consistent with our own observations. In the case of the membrane enzyme electrodes, where there is a small quantity of modified enzyme held at the electrode surface, with the ferrocenes in the oxidized form, the stability is very poor. This is especially true of the enzyme modified with ferrocenecarboxylic acid, where much of the bound mediator is presumably lost during the stabilization period, before the measurements of glucose response start. Similar problems may be expected if these modified enzymes are immobilized within a membrane at, or covalently attached to, an electrode surface. To overcome this problem it is necessary to replace the ferrocenecarboxylic acid or acetic acid derivatives used in this study, by more stable mediators.

Acknowledgement—We thank SERC and MediSense (U.K.) Inc. for financial support.

REFERENCES

1. D. A. Gough, J. Y. Lucisano and P. H. S. Tse, *Anal. Chem.*, 1985, **57**, 2351.
2. G. Dryhurst, K. M. Kadish, F. Scheller and R. Renneberg, *Biological Electrochemistry*, Vol. 1, p. 398. Academic Press, New York, 1982.
3. P. N. Bartlett and R. G. Whitaker, *Biosensors*, 1987/1988, **3**, 359.
4. J. Y. Lucisano and D. A. Gough, *Anal. Chem.*, 1988, **60**, 1272.
5. L. Gorton and G. Jönsson, *J. Mol. Catal.*, 1986, **38**, 157.
6. G. Jönsson and L. Gorton, *Anal. Lett.*, 1987, **20**, 839.
7. F. Scheller, F. Schubert, B. Olsson, L. Gorton and G. Johanson, *ibid.*, 1986, **19**, 1691.
8. E. Adamowicz and C. Burstein, *Biosensors*, 1987/1988, **3**, 27.
9. J. E. Frew and H. A. O. Hill, *Anal. Chem.*, 1987, **59**, 933A.
10. L. C. Clark and C. Lyons, *Ann. N.Y. Acad. Sci.*, 1962, **102**, 29.
11. A. E. G. Cass, G. Davis, H. A. O. Hill and D. J. Nancarrow, *Biochim. Biophys. Acta*, 1985, **828**, 51.
12. A. E. G. Cass, G. Davis, G. D. Francis, H. A. O. Hill, W. J. Aston, I. J. Higgins, E. V. Plotkin, L. D. L. Scott and A. P. F. Turner, *Anal. Chem.*, 1984, **56**, 667.
13. A. E. G. Cass, G. Davis, M. J. Green and H. A. O. Hill, *J. Electroanal. Chem.*, 1985, **190**, 117.
14. E. G. D'Costa, I. J. Higgins and A. P. F. Turner, *Biosensors*, 1986, **2**, 71.
15. J. M. Dicks, W. J. Aston, G. Davis and A. P. F. Turner, *Anal. Chim. Acta*, 1986, **182**, 103.
16. D. R. Matthews, R. R. Holman, E. Bown, A. Watson, S. Hughes and D. Scott, *Lancet*, 1987, *i*, 778.
17. W. J. Albery, P. N. Bartlett, and D. H. Craston, *J. Electroanal. Chem.*, 1985, **194**, 223.
18. M. S. Freund and A. Brajter-Toth, *Anal. Chem.*, 1989, **61**, 1048.
19. N. K. Cenas and J. J. Kulys, *Bioelectrochem. Bioenerg.*, 1981, **8**, 103.
20. W. J. Albery and D. H. Craston, in *Biosensors: Fundamentals and Applications*, A. P. F. Turner, I. Karube and G. S. Wilson (eds.), p. 180. OUP, Oxford, 1987.
21. P. N. Bartlett and R. G. Whitaker, *J. Electroanal. Chem.*, 1987, **224**, 37.
22. N. C. Foulds and C. R. Lowe, *J. Chem. Soc., Faraday Trans. 1*, 1986, **82**, 1259.
23. M. Umaña and J. Waller, *Anal. Chem.*, 1986, **58**, 2979.
24. S. Yabuki, H. Shinohara and M. Aizawa, *J. Chem. Soc., Chem. Commun.*, 1989, 945.
25. N. C. Foulds and C. R. Lowe, *Anal. Chem.*, 1988, **60**, 2473.
26. H. A. O. Hill, *European Patent Application No.* 84303090, 1984.
27. Y. Degani and A. Heller, *J. Phys. Chem.*, 1987, **91**, 1285.
28. *Idem*, *J. Am. Chem. Soc.*, 1988, **110**, 2615.
29. P. N. Bartlett, R. G. Whitaker, M. J. Green and J. Frew, *J. Chem. Soc., Chem. Commun.*, 1987, 103.
30. B. E. P. Swoboda and V. Massey, *J. Biol. Chem.*, 1965, **210**, 2209.
31. P. Trinder, *Ann. Clin. Biochem.*, 1969, **6**, 24.
32. D. Barham and P. Trinder, *Analyst*, 1972, **97**, 142.
33. W. J. Albery and P. N. Bartlett, *J. Electroanal. Chem.*, 1985, **194**, 211.
34. W. J. Albery and P. N. Bartlett, A. E. G. Cass and K. W. Sim, *ibid.*, 1987, **218**, 127.
35. M. Dixon and E. C. Webb, *The Enzymes*, p. 243. Longmans, London, 1979.
36. R. Szentrimay, P. Yeh and T. Kuwana, in *Electrochemical Studies of Biological Systems*, D. Sawyer (ed.), p. 143. ACS, Washington, DC, 1977.

DETERMINATION OF TOCOPHEROLS BY REVERSE-PHASE LIQUID CHROMATOGRAPHY AND ELECTROCHEMICAL DETECTION AT A SURFACE-OXIDE MODIFIED PLATINUM MICROELECTRODE, WITHOUT ADDED ELECTROLYTE

DARRYL L. LUSCOMBE and ALAN M. BOND*

Department of Chemical and Analytical Sciences, Deakin University, Geelong, Victoria 3217, Australia

(Received 30 May 1989. Revised 11 September 1989. Accepted 18 September 1989)

Summary—The reverse-phase separation and electrochemical detection of α -, γ -, and δ -tocopherol at a potential of +0.90 V vs. a gold pseudo-reference electrode is possible down to $10^{-7}M$ concentrations, with surface-modified platinum microdisc electrodes in a methanol/water (95:5) solvent mixture. The use of microelectrodes with radii of 10–70 μm , rather than electrodes of conventional size, minimizes problems associated with iR drop and obviates the need for deliberately added electrolyte. These features simplify the analytical procedure. The background response of an untreated platinum microelectrode in the methanol/water (95:5) system at positive potentials is characterized by processes arising from adsorption/oxidation of methanol and formation of surface oxides. Amperometric detection is of little use under these conditions. However, preoxidation of the electrode surface in 2M nitric acid inhibits the methanol adsorption/oxidation reaction but not the tocopherol response and therefore allows highly sensitive amperometric detection.

When electrochemical detection (ECD) is employed in conjunction with separation by liquid chromatography, it is generally considered necessary to have a sufficiently high concentration of an inert supporting electrolyte in the mobile phase, to ensure that this is electrically conducting and to reduce the cell/solution resistance, *i.e.*, reduce the so-called iR (voltage) drop across the cell. It is also considered necessary, although less importantly for flow systems, to add electrolyte to overcome the effects of the migration current of charged electroactive species in the solution. A useful rule is that to eliminate the effects of migration, the concentration of the supporting electrolyte should be 100 times that of the analyte,¹ *e.g.* with $10^{-6}M$ analyte being present, a $10^{-4}M$ electrolyte concentration is required. However, such a concentration of supporting electrolyte would not usually be regarded as high enough to reduce the cell resistance to a functional level in conventional ECD, and much higher concentrations of the electrolyte are usually added.

The need to add electrolyte is a distinct disadvantage, adding to the risk of contamination and increasing the cost of experiments. Methods for eliminating this need are therefore

desirable. It has been demonstrated that when microelectrodes are used instead of conventional electrodes, addition of a supporting electrolyte may not be necessary.³ Dissociation of the solvent (or impurities) will provide the necessary background conductivity in such experiments. The ability to combine liquid chromatography or flow-injection analysis with electrochemical detection at microelectrodes, without addition of large quantities of supporting electrolyte, makes electrochemical detectors more economical.³ If a buffer is added to the solvent system to aid either the chromatography or the electrochemical detection of a particular species, it also serves as the background electrolyte.

Electrochemical detection at positive potentials is usually done with solid electrodes constructed from platinum, gold, or various forms of carbon.⁴ The background response of noble metal electrodes, particularly of platinum in aqueous media, is characterized by surface oxide formation and hydrogen sorption/desorption.⁵ The nature of the surface oxide layer on platinum electrodes has been a subject of considerable debate over the last thirty years. Particular interest has centred on both the catalytic properties of the oxide layer with respect to electrochemical oxidation of the compounds of

*Author for correspondence.

interest, and conversely, the ability of the oxide layer to inhibit the oxidation of organic compounds.⁶⁻⁸ It is now generally agreed that the surface oxide layer initially consists of a reversibly chemisorbed hydroxo species, probably in the form of PtOH. This species may be stabilized by exchange reactions with the platinum surface, and converted into the irreversibly bound PtO.⁹ Though the exact nature of the surface oxide phases is not yet settled, it should be noted that the PtOH phase has been implicated in the catalytic oxidation of a number of species [e.g., As(III), carbohydrates, alcohols, amino-acids],¹⁰ whereas the PtO phase appears to inhibit many oxidation reactions.⁶ Thus while some of the surface properties induced at positive potentials by oxide film formation restrict the analytical usefulness of platinum electrodes, others can advantageously passivate the surface towards interfering species.¹¹

In the present work the analytical utility of the selectivity produced by a surface oxide phase at a platinum microelectrode is demonstrated by the electrochemical detection of tocopherols in a reverse-phase HPLC separation with a methanol/water mobile phase containing no electrolyte. Preoxidizing the electrode surface to form a PtO surface layer inhibits the methanol adsorption/oxidation process which overlaps the tocopherol electrode process. If this modified platinum electrode is used as a microelectrode, α -, γ - and δ -tocopherol (Fig. 1) can be oxidatively detected in a methanol/water (95:5 v/v) mobile phase without deliberate addition of a supporting electrolyte.

Ikenoya *et al.*,¹² using a conventional glassy-carbon electrode for electrochemical detection in the chromatographic separation of tocopherols with methanol as eluent, were obliged to add a supporting electrolyte and chose sodium perchlorate for the purpose. They found that the detector signal initially rose very rapidly with increase in sodium perchlorate concentration, reached a maximum at about 0.05M perchlorate

and then decreased at higher concentrations of the supporting electrolyte. It was found that the retention time and capacity factor were constant for use of eluents containing up to 0.05M perchlorate, but band-broadening and increased retention times were observed when higher concentrations were used. Thus it is desirable to minimize the perchlorate concentration, which is readily done by the use of microelectrodes.

EXPERIMENTAL

Reagents

The three tocopherol isomers (α , γ , δ) were obtained from Kodak, and used as received. Methanol and water were both of chromatographic solvent grade, and supplied by Waters Associates. Tetraethylammonium perchlorate (Southwestern Chemicals) was recrystallized from ethanol/water, then dried in a vacuum desiccator over phosphorus pentoxide.

Chromatographic system

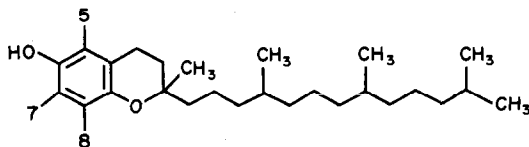
The chromatographic system was assembled from the following components: an ICI LC1500 HPLC pump (ICI Scientific Instruments, Australia), a Rheodyne 7125 sample injector fitted with a 20 μ l loop (Rheodyne Corp.), a Spherisorb ODS2 15 cm \times 4.6 mm column, an ICI TC1900 temperature controller, a Metrohm 656 electrochemical detector (Metrohm, Herisau, Switzerland), a Keithley 614 digital electrometer (Keithley Instruments), an ICI SD2100 photometric detector, and an ICI DP600 dual-pen chart-recorder.

Electrochemical detection measurements were made with a two-electrode system, with a platinum disc microelectrode as the working electrode and either an Ag/AgCl (3M KCl) reference electrode, or a gold disc (radius 1.5 mm) acting as pseudo-reference electrode. Ultraviolet detection was performed at 296 nm, and all chromatographic determinations were done at $30 \pm 0.5^\circ$.

Microelectrodes

The microelectrodes were fabricated according to previously published methods,¹³ and their radii were calculated from the steady-state (slow scan-rate) voltamperograms obtained with a conventional cell, for oxidation of ferrocene ($1.05 \times 10^{-3}M$) in acetonitrile (containing 0.10M Et₄NClO₄), and use of the relationship.¹⁴

$$i_d = 4nFDcR \quad (1)$$



α - tocopherol	5,7,8 trimethyl
β - tocopherol	5,8 dimethyl
γ - tocopherol	7,8 dimethyl
δ - tocopherol	8 methyl

Fig. 1. Structures of α -, β -, γ -, and δ -tocopherol.

where i_d = diffusion-controlled limiting current, n = number of electrons transferred (1 for ferrocene), F = the Faraday constant, C = bulk concentration, D = diffusion coefficient (2.3×10^{-5} cm²/sec),¹⁵ and r = radius of the microelectrode.

Electrode pretreatment

The platinum disc microelectrodes were given the following oxidative pretreatment before use

in the detector cell. Each electrode was placed in a beaker containing 2M nitric acid, and a potential of +1.80 V vs. Ag/AgCl was applied for the requisite time. Oxygen was evolved at the electrode surface during the pretreatment. After the oxidation, the electrode was rinsed several times in distilled water, then several times in methanol/water (95:5) solution before being placed in the electrochemical detector cell. No attempt was made to polish or dry the electrode.

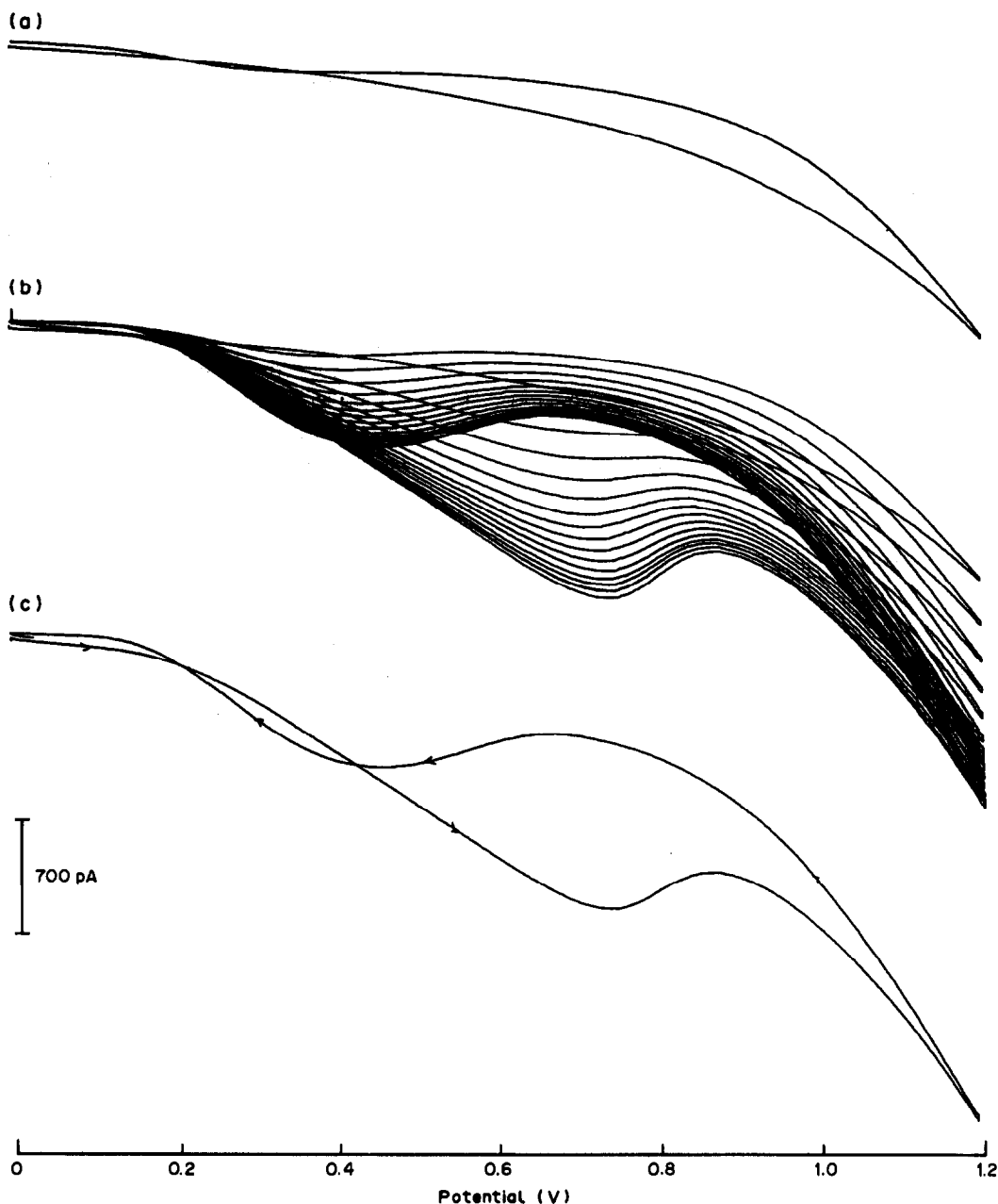


Fig. 2. Cyclic voltamperograms obtained at positive potentials (V vs. Ag/AgCl) applied in methanol/water (95:5) containing no added electrolyte, with a 12.5 μ m radius platinum microdisc electrode: (a) initial scan, (b) response observed with repeated cycling of the potential, (c) equilibrium response obtained after approximately 30 scans. Scan rate 100 mV/sec, temperature 22°.

RESULTS AND DISCUSSION

Stationary cell voltammetry

The ability of voltammetric microelectrodes to provide useful information with a minimum of distortion when used in high-resistance solvents has been demonstrated.² This feature has been used to study the mechanism of adsorption processes, in the absence of deliberately added electrolyte.¹⁶

Cyclic voltamperograms obtained with a platinum microelectrode (radius 12.5 μm) in methanol/water (95:5) without added supporting electrolyte are shown in Fig. 2. On repeated scanning there is growth of the wave at 0.75 V *vs.* Ag/AgCl on the forward (increasingly positive potential) scan, and of a wave at 0.45 V *vs.* Ag/AgCl on the reverse scan. Both waves have the same current sign despite the different scan direction. This anomalous behaviour has been reported for the oxidation of methanol in acidic solution at conventional-size electrodes,^{17,18} but not for reactions at microelectrodes, or without electrolyte being present.

The forward scan can be divided into a number of distinct potential regions (E *vs.* Ag/AgCl). On the basis of the work by Hamp-

son *et al.*,¹⁹ the following assignments can be made:

- (a) $0.0 < E < 0.2$ V double-layer region,
- (b) $E > 0.2$ V region where oxygen and methanol are adsorbed at the electrode surface, and an oxidation wave is observed,
- (c) $E > 0.75$ V region where a peak is formed owing to displacement of methanol by the more strongly bound oxide film,
- (d) $E > 0.90$ V region where the current increases because of oxide formation and possible methanol oxidation on the oxide film.

It should be noted that the initial scan [Fig. 2(a)], when PtOH is absent from the electrode surface, shows almost no oxidation taking place. The oxidation response grows as the surface coverage of oxide increases [Fig. 2(b)] up to an equilibrium value [Fig. 2(c)].

The behaviour displayed in the reverse scan has also been described for conventional-size

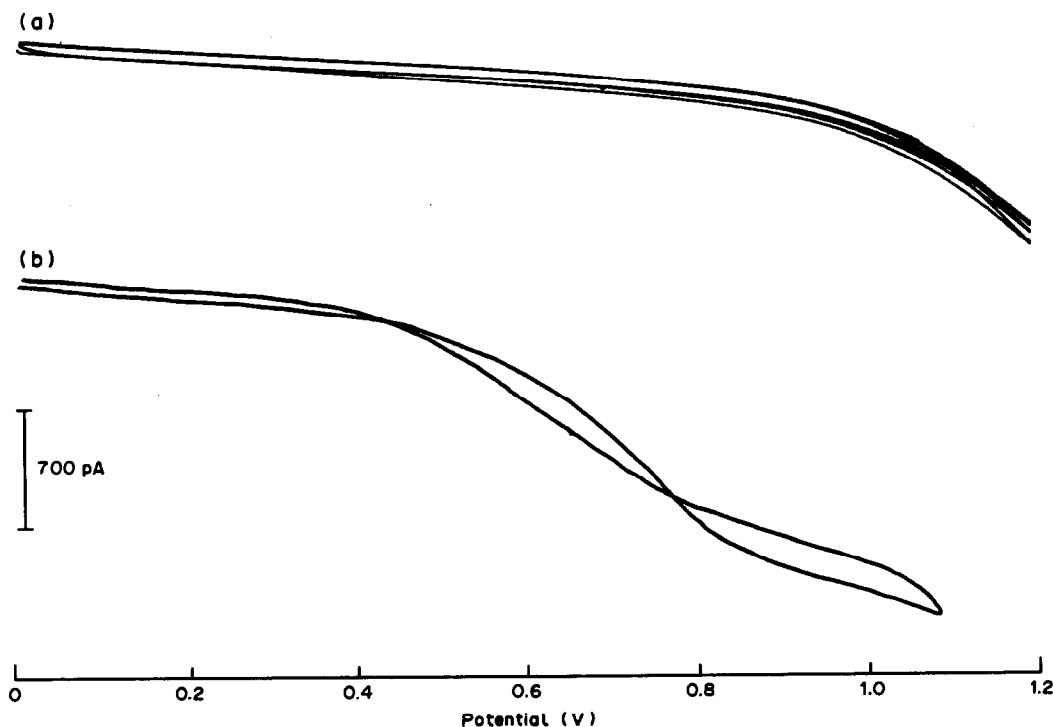


Fig. 3. Cyclic voltamperogram obtained at positive potentials (V *vs.* Ag/AgCl) applied in methanol/water (95:5) containing no added electrolyte, with a 12.5 μm radius platinum microdisc electrode preoxidized for 60 sec in 2M nitric acid at a potential of 1.80 V *vs.* Ag/AgCl: (a) blank, (b) $1.33 \times 10^{-3}M$ α -tocopherol. Scan rate 100 mV/sec, temperature 22°.

electrodes in acidic methanol solutions, the most fully substantiated explanation being that presented by Giner.¹⁷ In the reverse scan some of the oxide film formed at positive potentials is reduced, which leads to an increasing number of sites free from inhibiting oxide and adsorbed methanol. This in turn leads to an increased rate of oxidation of methanol, shown by the increased oxidative current observed in the reverse scan.

It therefore appears that at a platinum microelectrode, even in the absence of electrolyte, the oxide layer inhibits the oxidation of methanol at potentials >0.75 V *vs.* Ag/AgCl. However, since no oxidation of methanol is observed at a clean electrode [Fig. 2(a)], the formation of an oxide layer can also be said to catalyse the response over a limited potential range. At a

potential <1.2 V *vs.* Ag/AgCl the most likely oxidized phase giving rise to the catalysis is PtOH.⁹ Scanning to very positive potentials, which is likely to lead to the formation of PtO, also appears to inhibit the response for oxidation of methanol.

Since the application of very positive potentials appeared to inhibit the potentially interfering background process, the response of an electrode which had previously been oxidized at 1.80 V *vs.* Ag/AgCl in 2M nitric acid was examined. The results obtained in methanol/water (95:5) after the electrode had been held at this potential in 2M nitric acid for 60 sec and then transferred to the methanol/water solvent mixture are shown in Fig. 3(a). Repeated cycling over the potential-range of interest had little effect on the response, indicating

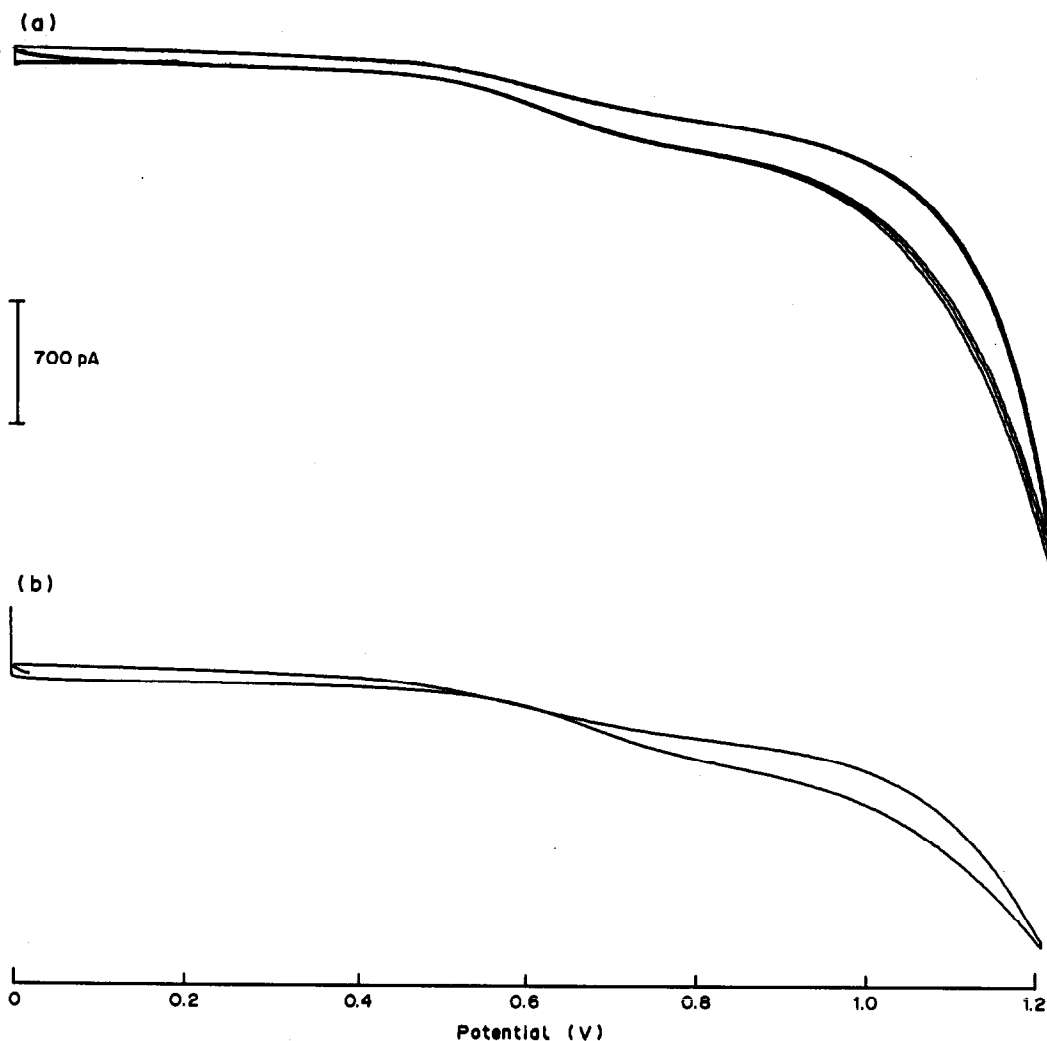


Fig. 4. Cyclic voltamperograms obtained with a $12.5 \mu\text{m}$ radius platinum microdisc electrode, for the oxidation of $2.66 \times 10^{-4} M$ α -tocopherol in methanol/water (95:5) containing (a) $10^{-3} M$ tetraethylammonium perchlorate, (b) no added electrolyte. Other conditions as for Fig. 3.

that the coating is strongly bound to the surface, and effectively inhibits the response for methanol adsorption/oxidation. The most likely composition of the surface film formed at very positive potentials would be PtO_2 ,⁹ which, unlike the PtOH film, is deposited irreversibly.

Although the background response is reduced to an acceptable level by the preoxidation at 1.8 V *vs.* Ag/AgCl, this is of little use if the response of the species to be detected at the platinum microelectrode is also inhibited. A cyclic voltamperogram for $1.33 \times 10^{-3} M$ α -tocopherol in methanol/water (95:5) at a surface-modified platinum microelectrode is shown in Fig. 3(b). The sigmoidal response expected for a faradaic process at a microelectrode is observed, showing that the tocopherol oxidation process is not inhibited. However, the response for tocopherol at the mM concentration level is slightly distorted by iR -drop effects in the absence of electrolyte. Hysteresis effects commonly occur with this type of coated electrode.²⁰ The extent to which iR -drop was the cause of this hysteresis in the absence of electrolyte was determined by experiments in $10^{-3} M$ tetraethylammonium perchlorate methanol/water (95:5). Figure 4 shows that with electrolyte present there is no hysteresis in the response of the tocopherol oxidation, which shows that iR -drop is the most likely cause of the hysteresis.

These results demonstrate that the pretreatment of the platinum surface effectively favours the tocopherol response over the methanol adsorption/oxidation reaction. The utility of

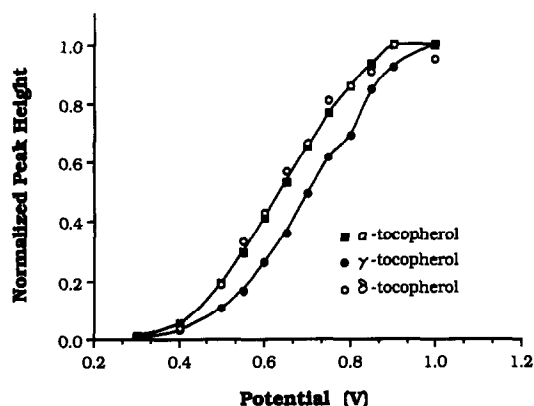


Fig. 5. Hydrodynamic voltamperograms for the oxidation of approximately $10^{-3} M$ α -, γ -, and δ -tocopherol solutions in methanol/water (95:5) (no added electrolyte), at a pre-oxidized $65.7 \mu\text{m}$ radius platinum microdisc electrode, in a wall-jet flow-cell with data recorded under HPLC conditions. Flow-rate 2 ml/min, temperature 30.0° , sample volume $20 \mu\text{l}$. Electrode stabilized for 30 min prior to determination.

this preoxidized microelectrode was then examined in a high-performance liquid chromatographic separation of a number of tocopherols with a methanol/water mobile phase without added electrolyte.

High-performance liquid chromatography

Normalized hydrodynamic voltamperograms for α -, γ - and δ -tocopherol in 95:5 methanol/

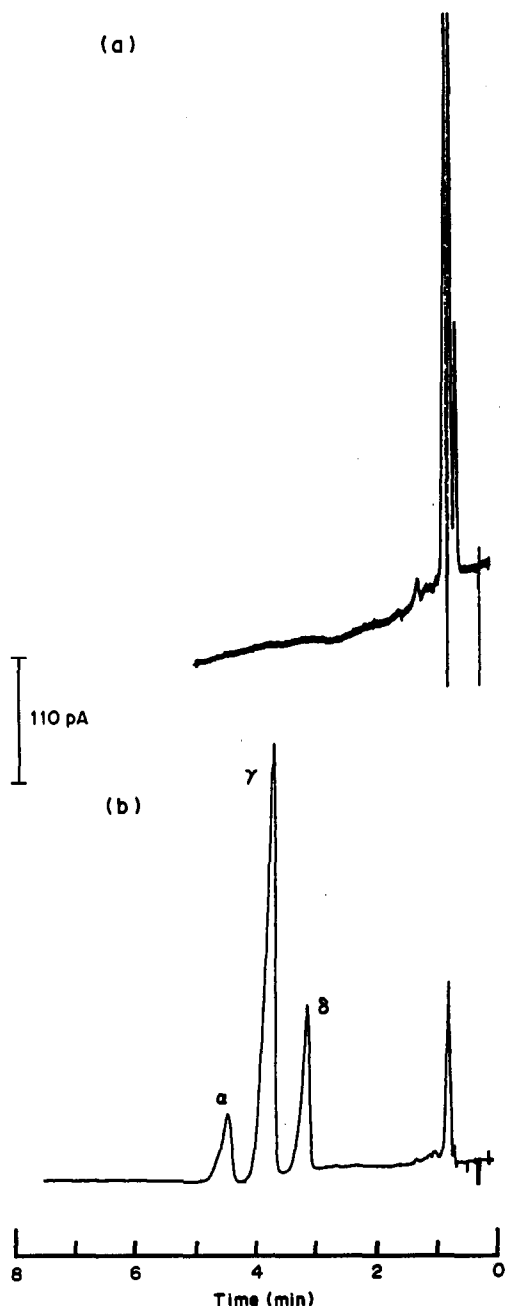


Fig. 6. Amperometric detection of α -, γ -, and δ -tocopherol at an applied potential of 0.9 V *vs.* Au following chromatographic separation in methanol/water (95:5) at (a) a polished $65.7 \mu\text{m}$ radius platinum microdisc electrode, and (b) a preoxidized electrode. Other conditions as for Fig. 5.

water in a flow cell, obtained with a microelectrode which had been preoxidized for 30 sec in nitric acid are shown in Fig. 5. Although the oxidation waves are somewhat drawn out, over a 600-mV range, they are well defined sigmoids. The half-wave potential for oxidation of α -tocopherol (0.63 V *vs.* Au) in the absence of electrolyte was found to be 70 mV less positive than that for γ -tocopherol (0.70 V *vs.* Au), which agrees with data reported for a glassy-carbon electrode in methanol.¹² The half-wave potential for oxidation of δ -tocopherol is almost the same as that of α -tocopherol. Apart from slight differences in oxidation potentials, in contrast to previously published data, the tocopherols show essentially the same voltammetric behaviour.^{12,21,22}

On the basis of data obtained from the hydrodynamic voltamperograms, the reversed-phase chromatographic separation and electrochemical detection of α -, γ - and δ -tocopherol was examined in detail. Amperometric detection without added electrolyte was used, at an applied potential of 0.90 V *vs.* Au, and the mobile phase consisted of methanol/water (95:5). The electrode was a platinum microdisc (radius 65.7 μ m). Figure 6(a) shows that the response for the tocopherol oxidation at a freshly polished platinum electrode is masked by the methanol adsorption/oxidation background reaction. In contrast, Fig. 6(b) shows that an electrode which has been preoxidized for 60 sec as described in the experimental section gives an excellent response for all three tocopherol compounds. Pre-oxidation of the electrode surface reduces the background current observed in the methanol/water mobile phase from 5.2 nA with the polished electrode, to 600 pA with the pre-treated electrode.

Pretreatment of microelectrodes at a very positive applied potential (*e.g.*, +1.80 V *vs.* Ag/AgCl) in the methanol/water (95:5) mobile phase proved a much less efficient method of preparation than pretreating the electrodes in 2M nitric acid at an applied potential of +1.80 V *vs.* Ag/AgCl. Part of the reason for this may be that the *iR*-drop in the methanol/water mixture reduces the effective applied voltage. Pretreatment in 2M nitric acid at an applied potential less than that for oxygen evolution was found to give higher background currents and a lower response for tocopherol, indicating a thinner coating of PtO. Pretreatment in acid solution (for up to 2 hr) without an applied

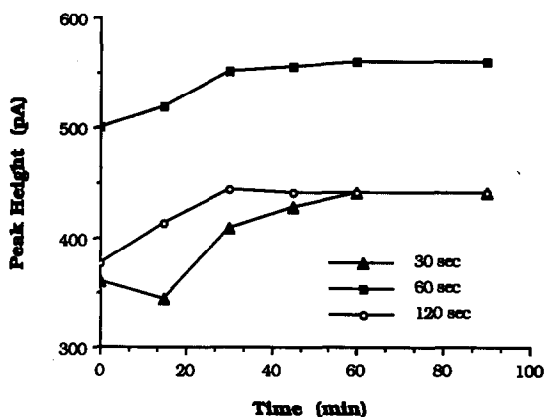


Fig. 7. Initial variation of the chromatographic peak height observed in electrochemical detection of α -tocopherol with a 65.7 μ m radius platinum microdisc electrode preoxidized for 30, 60 and 120 sec. Other operating conditions as for Figs. 5 and 6.

voltage had little effect on the response obtained at a freshly polished electrode.

The stability of the preoxidized platinum microelectrode, maintained at a potential of 0.90 V *vs.* Au, was monitored by means of the response to repeated chromatographic injections of α -tocopherol. The response of a freshly prepared electrode was found to increase over a period of about 30 min (Fig. 7) until a constant peak height was obtained. This behaviour may be attributed to the influence (on the oxide film) of the lower applied potential used in the amperometric detection (+0.90 V *vs.* Au) compared with the pretreatment potential (+1.80 V *vs.* Ag/AgCl), a mixture of PtOH and PtO probably being produced.

The long-term stability was good, the responses varying by less than 8% over 10 hr (Fig. 8). Thus reproducible measurements may be obtained over extended periods from a single electrode without the need for further treatment. However, the electrochemical response for α -tocopherol was found to decrease significantly if the electrode was left in the cell at open circuit for extended periods of time. This implies that the applied potential of +0.90 V *vs.* Au stabilizes the oxide coating in the methanol/water system.

The response at platinum microelectrodes was also found to be critically dependent on the duration of the pretreatment. An optimum pretreatment time of 60 sec was established from the data shown in Fig. 9. A plausible explanation of these data is that a certain thickness of this PtO layer is required to inhibit the methanol adsorption/oxidation reaction, and

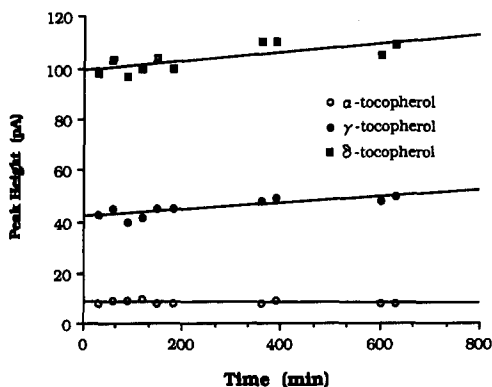


Fig. 8. Long-term stability of chromatographic peak height observed in electrochemical detection of α -, γ -, and δ -tocopherol with a 65.7 μm radius platinum microdisc electrode preoxidized for 60 sec. Other operating conditions as for Figs. 5 and 6.

that after an oxidation time of 60 sec the surface layer is so thick that it begins to inhibit the oxidation of the tocopherols.

Linear plots of peak-height vs. concentration were obtained from about 2×10^{-7} to $2 \times 10^{-5}M$. The limit of detection for the three tocopherols was calculated to be $1 \times 10^{-7}M$, or 2 pmole on the column for a 20 μl injection, based on a signal to noise ratio of 2:1 for the 67.5 μm platinum microdisc electrode with a pretreatment time of 60 sec. Detection limits (2:1 signal to noise ratio) with ultraviolet detection were found to be $2 \times 10^{-7}M$. This slightly greater sensitivity of electrochemical detection of tocopherols has been noted previously.¹² The relative standard deviation for ten 20- μl injections of $5 \times 10^{-6}M$ α -tocopherol, with the same electrode used for detection, was found to

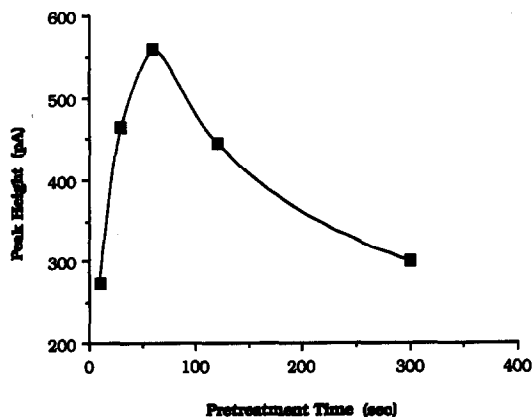


Fig. 9. Variation of the chromatographic peak current for α -tocopherol with duration of preoxidation of the micro-disc electrode. The electrode was stabilized in the flow-cell for 30 min prior to the determination. Other operating conditions as for Figs. 5 and 6.

be 5%. A similar reproducibility was obtained with ultraviolet detection, implying that the variation is due to the chromatographic system, not the detector response. The variation in the peak height for $5 \times 10^{-6}M$ α -tocopherol from electrode to electrode, or pretreatment to pretreatment, was always better than 10%. Application of electrochemical detection has been reported at glassy carbon electrodes.^{12,23,24} The present method appears to be equally sensitive.

Acknowledgement—The financial support of ICI Instruments, Australia, is gratefully acknowledged.

REFERENCES

1. A. M. Bond, *Modern Polarographic Methods in Analytical Chemistry*, p. 77. Dekker, New York, 1980.
2. A. M. Bond, M. Fleischmann and J. Robinson, *J. Electroanal. Chem.*, 1984, **168**, 299.
3. D. L. Luscombe, A. M. Bond, D. E. Davey and J. W. Bixler, *Anal. Chem.*, 1990, **62**, 27.
4. G. Dryhurst and D. L. McAllister, in *Laboratory Techniques in Electroanalytical Chemistry*, P. T. Kissinger and W. R. Heinmann (eds.), p. 289. Dekker, New York, 1984.
5. R. N. Adams, *Electrochemistry at Solid Electrodes*, Dekker, New York, 1969.
6. S. Gilman, *Electroanal. Chem.*, 1967, **2**, 111.
7. B. E. Conway, N. Marincic, D. Gilroy and E. Rudd, *J. Electrochem. Soc.*, 1966, **113**, 1144.
8. V. D. Parker, G. Sundholm, U. Svanholm, A. Ronlan and O. Hammerich, in *Encyclopedia of Electrochemistry of the Elements*, Volume XI, A. J. Bard and H. Lund (eds.), p. 182. Dekker, New York, 1978.
9. T. D. Cabelka, D. S. Austin and D. C. Johnson, *J. Electrochem. Soc.*, 1985, **132**, 359.
10. D. C. Johnson, J. A. Polta, T. Z. Polta, G. G. Neuburger, J. Johnson, A. P.-C. Tang, I.-H. Yeo and J. Baur, *J. Chem. Soc. Faraday Trans. I*, 1986, **82**, 1081.
11. J. A. Cox and K. R. Kulkarni, *Talanta*, 1986, **33**, 911.
12. S. Ikenoya, K. Abe, T. Tsuda, Y. Yamano, O. Hiroshima, M. Ohmae and K. Kawabe, *Chem. Pharm. Bull.*, 1979, **27**, 1237.
13. A. M. Bond, D. L. Luscombe, K. B. Oldham and C. G. Zoski, *J. Electroanal. Chem.*, 1988, **249**, 1.
14. A. M. Bond, K. B. Oldham and C. G. Zoski, *Anal. Chim. Acta*, 1989, **216**, 177.
15. J. W. Bixler and A. M. Bond, *Anal. Chem.*, 1986, **58**, 2859.
16. A. M. Bond and F. G. Thomas, *Langmuir*, 1988, **4**, 341.
17. J. Giner, *Electrochim. Acta*, 1964, **9**, 63.
18. M. W. Breiter, *ibid.*, 1963, **8**, 973.
19. N. A. Hampson, M. J. Willars and B. D. McNicol, *J. Chem. Soc. Faraday Trans. I*, 1979, **75**, 2535.
20. L. D. Burke and O. J. Murphy, *J. Electroanal. Chem.*, 1979, **101**, 351.
21. K. Mukai, Y. Kageyama, T. Ishida and K. Fakuda, *J. Org. Chem.*, 1989, **54**, 552.
22. K. Mukai, K. Okaba and H. Hosose, *ibid.*, 1989, **54**, 557.
23. M. Vandewoude, M. Claeys and I. De Leeuw, *J. Chromatog.*, 1984, **311**, 176.
24. P. P. Chou, P. K. Jaynes and J. L. Balley, *Clin. Chem.*, 1985, **31**, 880.

AMPEROMETRIC DETECTION AT A CARBON-FIBRE ARRAY RING/GLASSY-CARBON DISK ELECTRODE IN A WALL-JET CELL

HUAMIN JI and ERKANG WANG*

Laboratory of Electroanalytical Chemistry, Changchun Institute of Applied Chemistry,
Chinese Academy of Sciences, Changchun, Jilin 130022, People's Republic of China

(Received 27 June 1989. Accepted 25 October 1989)

Summary—A wall-jet cell incorporating a carbon fibre array ring/glassy-carbon disk electrode has been constructed, and characterized by the cyclic voltammetry and flow-injection techniques. The ring (composed of several microdisks) and glassy-carbon disk electrode, can be used separately for different purposes, e.g., detection in solution without a supporting electrolyte, collection/shielding detection with dual-electrode and voltammetric/amperometric detection with series dual-electrode. The electrode shows better collection and shielding effects than the usual ring-disk electrode in quiescent solution and the series dual-electrode in a thin-layer flow-through cell. The detection limit at the ring electrode is comparable with that at a conventional-size electrode, and has been used in the mobile phase without a supporting electrolyte, proving to be a promising detector for normal-phase liquid chromatography.

Electrochemical (EC) detection has been of continuing interest^{1,2} since the pioneer work by Kissinger *et al.*³ Amperometric and voltammetric detectors with conventional-size electrodes of mm or greater dimensions are frequently used as detectors in liquid chromatography (LC) and flow-injection analysis (FIA) because of their high sensitivity, low dead volume, simplicity and reasonable selectivity towards electroactive compounds. There have been many reports on the improvement in selectivity, stability, signal to noise (S/N) ratios and other detection properties obtained by using multiple working electrodes,^{4–8} modified electrodes,^{9–12} scanning of the potential at the electrode,^{13–15} and microelectrodes.^{16–37} There are some aspects of EC detection that can be improved by using a microelectrode detector, e.g., flow-rate effects, iR drop, S/N ratio and time-constant.

Microelectrodes have attracted great interest in the fundamental investigation of mass transport, kinetics and analytical applications since the initial interest in detection of catecholamines *in vivo*,^{16–18} and recently they have been incorporated into flow-through cells. These electrodes fall into two categories: (a) single microelectrodes (microdisk,²⁸ microring^{31,34} and microcylinder^{20–37}) and (b) multiple active units (bundles of carbon fibres,¹⁹ ordered array elec-

trodes^{29–31,35,36} and random-array electrodes^{32,33}). The first group have the advantage of easy construction and convenient use, and can be combined with columns of very small dimensions, such as open-tube capillary columns,²⁰ microcolumns²⁴ or capillary-zone electrophoresis columns.²⁶ However, femtoampere currents must then be measured at low analyte concentration, which is difficult unless one electrode dimension is large.³⁴ The bundle or array type of electrode has the advantage of simple instrumentation, and can be used with a modified or commercially available potentiostat.¹⁹

Although most reports still describe the use of amperometric detectors with only a single working electrode, dual-electrode amperometric detectors are becoming more popular and have been used in a variety of configurations such as series, parallel-adjacent and parallel-opposed, to achieve different modes of operation.¹ The main advantages of all the dual-electrode techniques are better selectivity and lower detection limit. Recently, Lunte *et al.*^{38–40} reported a different mode of operation for series dual-electrodes, called voltammetric/amperometric detection, in which the potential is scanned at the upstream electrode and the electrode product reaction is monitored amperometrically at the downstream electrode. Two detection modes, called collection and shielding, were described. In the former, the downstream

*Author for correspondence.

electrode is kept at a potential which reverses the reaction which has taken place at the upstream electrode, and in the latter it is kept at the same potential as the upstream electrode (and thus detects any of the analyte that has *not* reacted at the upstream electrode. The technique is similar to voltammetry at the ring-disk electrode⁴¹ except that the current/voltage/time relationship in the flowing stream is continuously monitored.⁴⁰ There are two problems with such a configuration, however. One is the low efficiency of collection and shielding, which depends on the cell configuration, the areas of the two electrodes and the gap between. It can be improved by reducing the gap and increasing the area of the downstream electrode, but this may be difficult to implement and may increase the dead volume. The other is the serious cross-talk effect due to the large solution resistance in the thin-layer flow-through cell, which limits the potential scan-rate at the upstream electrode. For these reasons, we now report a wall-jet cell which has been proved to have superior current sensitivity⁴² and minimum solution-resistance,⁴³ in which the solutions impinge on the reaction electrode (upstream), and flow through the collection or shielding electrode (downstream), which is a carbon-fibre array ring placed very close to the upstream electrode.

Although there have been reports about the use of a ring-disk electrode for EC detection,^{44,45} we describe one which is simple and easily constructed. The carbon-fibre array ring (CFAR) and glassy-carbon disk (GCD) electrodes have also been used for different purposes, *e.g.*, detection in a solution without supporting electrolyte, amperometric detection with a series dual-electrode, and voltammetric/amperometric detection.

EXPERIMENTAL

Construction of the electrode

The CFAR electrode was similar to that used by Khoo *et al.*³¹ except that the inner support material was a glassy-carbon rod instead of a glass tube. A 5.0-cm length of glassy-carbon rod (Beijing Institute of Artificial Crystal Material, China), 6.0 mm diameter, was first insulated with a very thin layer of epoxy resin. Sixteen carbon fibres, 33 μm in diameter, were stretched lengthwise and parallel on the rod, about 1 mm apart to ensure that the current responses of the individual fibres were independent of each other, and then fixed in position with a layer of

epoxy resin. To make electrical contact the carbon fibres at one end of the rod were embedded in silver cement, to which a copper wire was sealed. The electrode was then heated at 70° for 2 hr to cure the epoxy resin and silver cement. To expose the ends of the microfibrils, the other end of the electrode was polished on abrasive papers, and then with 1.0, 0.3, 0.03 μm α -alumina on a polishing cloth, and finally ultrasonicated in water for 5 min. The electrode was fitted into the wall-jet cell by a screw as shown in Fig. 1.

Apparatus

The LCP-350 injection pump (JASCO, Japan) was used with a home-made six-port valve with changeable sample loops (10 μl –1 ml) for FIA. Chromatographic experiments were done with a Nucleosil C18 (7 μm) column (200 \times 5 mm) (Dalian Institute of Chemical Physics, China). A home-made cyclic voltammetric analyser with triangular wave output into the bipotentiostat for simultaneously recording voltamperograms for the ring and disk electrodes, was used with a conventional three-electrode cell for cyclic voltammetry in quiescent solution. A laboratory-built bipotentiostat was used for FIA with voltammetry at the CFAR-GCD electrode, to measure pA–mA

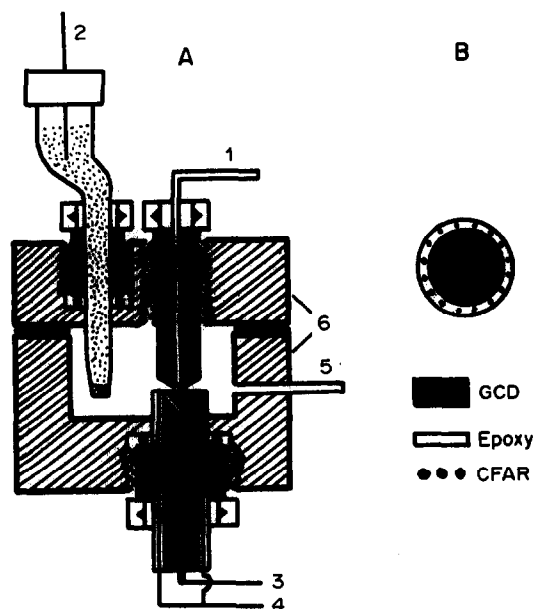


Fig. 1. Schematic illustration of the wall-jet cell with the CFAR-GCD electrode. (A) Side view of the cell; (B) top view of the electrode. 1, Solution inlet; 2, reference electrode; 3, glassy-carbon disk (GCD); 4, carbon fibre array ring (CFAR); 5, outlet, auxiliary electrode; 6, cell body (Plexiglas).

currents by changing the feedback resistance in a current-to-voltage converter. A Pine Instrument RDE 4 bipotentiostat was used with the Pt-ring/GC-disk electrode for the ring-disk experiment. An Ag/AgCl (satd. potassium chloride) reference electrode was used for cyclic voltammetry in quiescent solution, and a saturated calomel electrode (SCE) for FIA.

Reagents

All reagents were as reported previously.⁹ All solutions were prepared with doubly-distilled water, and all experiments were done at ambient temperature ($20 \pm 2^\circ$).

RESULTS AND DISCUSSION

Cyclic voltammetry at the CFAR-GCD electrode

Voltammetry in quiescent solution is an effective way to characterize microelectrodes and assess the quality of their fabrication.^{16,46} The cyclic voltamperogram for the oxidation of ferrocyanide (1 mM in 2M potassium chloride) at the CFAR electrode is shown in Fig. 2A. A sigmoidal voltamperogram was obtained, with a limiting current of 64.5 nA at a scan-rate of 10 mV/sec. This is a typical steady-diffusion voltamperogram for microdisk electrodes.¹⁶ A value of 58 mV was obtained for $E_{3/4} - E_{1/4}$, in good agreement with the theoretical value of 56.4 mV for a one-electron transfer. According to the equation²⁹

$$i = 4nFDCr$$

where r is the radius of the electrode, C the bulk concentration of the analyte, D the diffusion

coefficient and the other symbols have the usual meaning, the sum of the limiting currents at the individual microfibre disk electrodes was 64.1 nA for the 16 microdisks, in good agreement with the experimental measurement. This indicates that none of the fibres was broken during construction of the electrode, that all are active, and also that the fibres and the disk are well insulated, and that diffusion takes place independently at individual microfibre disks.

Figure 2B shows the collection effect at the CFAR-GCD electrode, when the potential was scanned from 0 to 0.7 V vs. Ag/AgCl at the GCD electrode to oxidize the ferrocyanide and the CFAR electrode was kept at 0 V to reduce the oxidized product from the GCD electrode. The product reached the CFAR electrode only by diffusion, without the convection that occurs with the conventional ring-disk electrode. The voltamperogram shows that even in quiescent solution the CFAR electrode is an effective collector, whereas the conventional ring-disk electrode is not (Fig. 2C). The remaining experiments were done in flowing solution.

Amperometric detection at the CFAR-GCD electrode

The improvement of detectors based on use of conventional-size electrodes, by such means as modification of the electrode surface to increase the EC activity^{10,12} or enhance the selectivity or stability,^{9,11} and incorporation of microelectrodes into the detector, is an active area in EC detection. So far, however, no reports have been published on the use of combinations of these

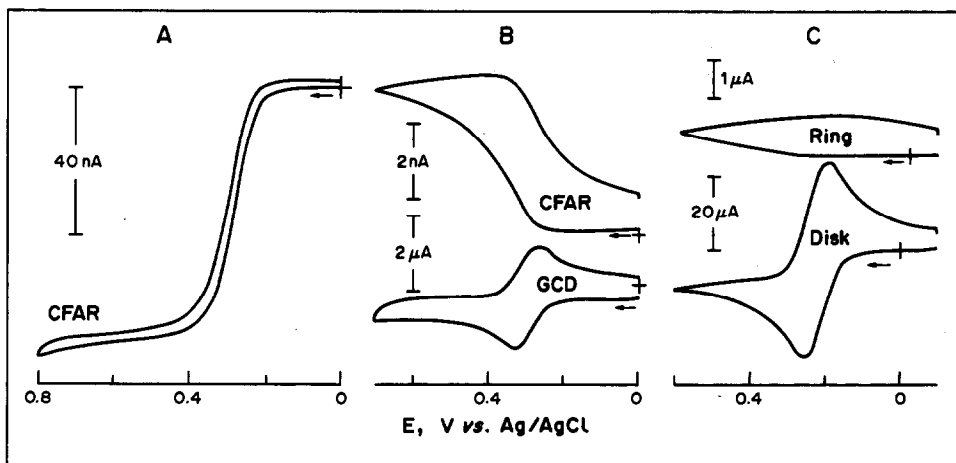


Fig. 2. Cyclic voltamperograms for ferrocyanide at the CFAR-GCD electrode and ring-disk electrode in quiescent solutions. Scan-rate, 10 mV/sec; (A) 1mM $K_4Fe(CN)_6 + 2M$ KCl at the CFAR electrode; (B) 50 μ M $K_4Fe(CN)_6 + 2M$ KCl at the CFAR-GCD electrode with $E_{CFAR} = 0$ V; (C) 1mM $K_4Fe(CN)_6 + 0.1M$ KH_2PO_4 at Pine's ring-disk electrode with $E_{ring} = 0$ V.

electrodes. In earlier papers^{27,47} we reported the use of a flow-through carbon-fibre electrode in a poly(vinyl chloride) tube, combined with an LC column, which was used successfully for the determination of vitamin B₆. The experiments with dilute supporting electrolyte showed that the flow-through cell had a large solution-resistance arising in the connecting tube between the working electrode and the reference electrode. We have therefore changed the cell to one of wall-jet type, and attempted to combine microelectrodes with a conventional-size sensor, into one electrode.

An advantage of the CFAR-GCD electrode in the wall-jet cell is that the ring and the disk can be used independently for different purposes. It was found that the hydrodynamic voltamperograms (HDVs) obtained at the two electrodes were the same as those for the conventional thin-layer cell in FIA, and that the new electrode (Fig. 1) was easier to recondition and more convenient to operate than the thin-layer cell. The coefficient of variation of FIA peak currents at the CFAR electrode for replicate injections of 5 ppm hydroquinone (HQ) over a period of 12 hr was 1.5%, indicating that the electrode was very stable and suitable for analytical application. Good linearity between FIA peak current (nA) and HQ concentration was obtained over the range 0.1–20 ppm, the regression equation being $i = -0.10 + 0.774C$, $r = 0.9998$. The baseline noise was found to be about 0.8 pA, so the detection limit was estimated to be 2.6 ng/ml (26 pg) at $S/N = 3$. Although experiments at such low concentrations were not done, owing to the FIA injection peak, we may still conclude that the CFAR is a sensitive electrode.

In the wall-jet cell, the distance between the nozzle and the electrode has a remarkable influence on the sensitivity and the dead volume of the detector, owing to mass transport at the electrode,⁴³ especially the CFAR-GCD electrode. In a wall-jet cell the current is not uniformly generated over the electrode, especially when the wall-jet ring-disk electrode is used.⁴⁴ Figure 3 shows the influence of the distance between the nozzle and electrode on the FIA peak current and peak width. The peak current decreases greatly and the peak width increases slightly at the GCD electrode and more so at the CFAR electrode, with increasing distance. These observations differ from those of Gunasingham,⁴⁵ who reported a slight increase of the LC peak width obtained by detection at the ring

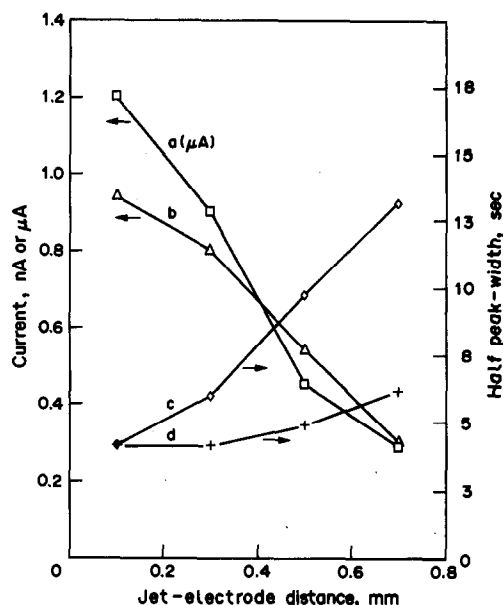


Fig. 3. Influence of the distance of the jet-electrode separation on the FIA peak current (a,b) and half-peak width (sec) (c,d) at the GCD (a,d) and CFAR (b,c) electrodes: 10 μ l of 5 ppm HQ injected every time; potential 0.7 V; mobile phase 0.1M KH_2PO_4 + 50 μM EDTA; flow-rate 0.8 ml/min.

electrode over that for detection at the disk electrode, and of Alberly *et al.*⁴⁴ who reported that the current increased with separation distance. This difference may be due to either the very small jet and electrode separation in our cell, or the different configuration. Therefore, in subsequent experiments we kept the jet and electrode as close as possible, but the distance had to be optimized for each analyte system.

The detection limits are very dependent on flow-rate. In microelectrode detectors, however, this dependence is considerably reduced by the enhanced radial diffusion due to the large edge-to-area ratios. We have reported that practically no dependence was found on flow-rate for the flow-through carbon fibre detector.²⁷ As expected, a lower dependence on flow-rate was found for the new electrode when used in FIA; the peak current at the CFAR electrode changed only from 0.567 to 0.570 nA with change in flow-rate from 0.2 to 0.5 ml/min, but from 1.96 to 2.80 μA at the GCD electrode over the same flow-rate range. Higher flow-rates were not examined, owing to the time-constant limitations of the potentiostat and recorder. However, a different dependence was found for the limiting currents in the voltamperograms. With injection of 1 ml of 1 mM HQ and recording of the voltamperogram during retention of the

analyte on the electrode, the slopes of log-log plots of limiting current *vs.* flow-rate (from 0.2 to 1.2 ml/min) were found to be 0.133 at the CFAR electrode and 0.353 at the GCD electrode. A similar dependence for peak currents and equilibrium currents at ultra-thin ring and band microelectrodes was obtained by Bixler *et al.*³⁴ In the present case we are concerned only with the peak currents.

Collection/shielding effects at the CFAR-GCD electrode

The collection and shielding efficiencies at the CFAR-GCD electrode detector were determined in a way slightly different from that used by Roston and Kissinger.⁴ In the dual-electrode detector, the upstream and downstream electrodes had almost the same area, and the collection efficiency was defined as the ratio of the current at the indicator (downstream) electrode to that at the generator (upstream) electrode, and a similar ratio for the shielding efficiency. The maximum collection efficiency found was 0.37 for hydroquinone as test compound.⁴ (Below this value it was termed the effective collection efficiency, which is related to the reaction mechanism). Even when the distance between the electrodes was varied from *ca.* 10 to 100 μm , the collection efficiency did not exceed 0.38. Various expressions have been derived for describing the collection efficiency,⁴⁸⁻⁵⁰ and although they have not been completely experimentally validated, they do indicate which detector dimensions are critical factors. The expressions contain two parameters based on cell dimensions: the ratio of the distance between the two electrodes to the length of the upstream electrode along the flow axis, and the ratio of the lengths of the two electrodes along the flow axis. Roosensaal and Poppe⁵⁰ derived a diffusion-limited current expression for the dual-electrode which could be applied at different potentials, in which the reconverted fractions (collection efficiency) and shielding factors were described. The two effects are maximal when the distance between the electrodes is zero. With a relatively long upstream electrode and a very short downstream electrode, a shielding factor of over 0.80 is observed when the gap is less than the length of the downstream electrode.⁵⁰ No attempts were made to improve the collection and shielding efficiencies experimentally.

The shielding mode of detection was not paid much attention until Lunte *et al.*³⁹ reported its

utility as a general method for electrochemical detection of compounds giving electrochemically reversible or irreversible reactions. The shielding efficiency is an important factor affecting the detection limit.

Since the ring electrode (CFAR) is much smaller than the disk electrode, we cannot use the Roston and Kissinger method to determine the collection efficiency. For the CFAR-GCD detector, the collection efficiency N_c is defined as

$$N_c = \frac{i(\text{ring})}{i'(\text{ring})} \quad (1)$$

where $i(\text{ring})$ and $i'(\text{ring})$ are the currents at the CFAR electrode with and without potential applied at the GCD electrode. The shielding efficiency is defined as

$$N_s = 1 - \frac{i(\text{ring})}{i'(\text{ring})} \quad (2)$$

In both cases, the potentials at the two electrodes are sufficiently positive or negative for the currents to be limited solely by mass transport.

Figure 4 shows the hydrodynamic voltamperogram for the CFAR electrode over the applied potential range from -0.2 to 0.8 V when the upstream (GCD) electrode is kept at 0.7 V to generate oxidized products for detection at the CFAR electrode. Figure 5 shows that when the CFAR electrode was kept at limiting-current potential (-0.15 V) and the potential of

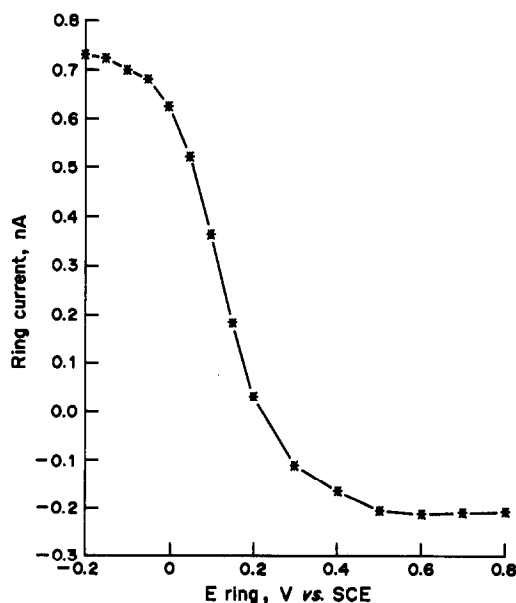


Fig. 4. Hydrodynamic voltamperogram of HQ at the CFAR electrode with the GCD electrode at 0.7 V. Experimental conditions as for Fig. 3.

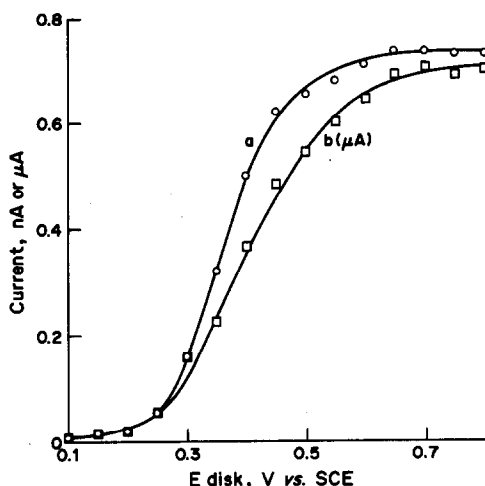


Fig. 5. Hydrodynamic voltamperograms of HQ at the CFAR electrode (a) and the GCD electrode (b) when the CFAR electrode is kept at -0.15 V and the potential at the GCD electrode is changed. Experimental conditions as for Fig. 3.

the GCD electrode was scanned from 0.1 to 0.8 V, the hydrodynamic voltamperograms for the two electrodes had the same general pattern. Figure 6 shows the electrode currents for the different applied-potential modes in FIA with the CFAR–GCD electrode detector. For the collection mode, the GCD was kept at 0.7 V and the CFAR at -0.15 V, which are both in the limiting-current potential range. In the shielding mode, both electrodes were kept at 0.7 V. From Fig. 6 the collection efficiency was measured as 0.869 and the shielding efficiency as 0.75, by use of equations (1) and (2). These values are larger than those reported for the thin-layer dual-electrode.^{4,39} The high collection efficiency at the CFAR–GCD electrode has the advantages that

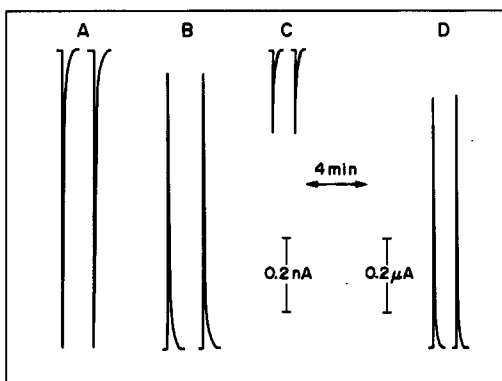


Fig. 6. FIA peaks at the CFAR (A, B, C) electrode and GCD (D) electrode with different applied-potential modes. Potentials: CFAR electrode: A, B -0.17 V; C, 0.7 V; GCD electrode: A, 0.7 V; B, 0 V; C, 0 V; D, 0.7 V. Other conditions as for Fig. 3.

the downstream electrode is a sensitive indicator electrode, and the selectivity is greatly improved because compounds giving electrochemically irreversible reactions are not detected at the downstream electrode.

The influence of the cell dimensions (*e.g.*, distance between jet and electrode) on the collection and shielding efficiencies are more complex than in the thin-layer flow-through cell. Additionally, the flow-rate, which has no influence in the thin-layer cell, affects the two efficiencies because of its different effects at the two electrodes, as described above. It was found that the collection efficiencies decreased with increasing flow-rate, but the shielding efficiencies were unchanged.

Detection in a mobile phase containing no supporting electrolyte

EC detection with conventional-size electrodes has not been generally extended to normal-phase LC, although it could be achieved by adding electrolyte pre- or post-column.^{51,52} When a low-polarity solvent (*e.g.*, *n*-hexane) is used as the mobile phase in normal-phase LC, it is difficult to find an electrolyte that is sufficiently soluble in it, and the presence of the electrolyte may affect the retention times of the analytes.

An EC detector which could be operated without the presence of a background electrolyte would be desirable. The very small currents measurable with microelectrodes make it possible for an EC detector made with them to be used in normal-phase LC.

In the previous report,²⁷ we examined the detection behaviour of the flow-through carbon-fibre detector in dilute supporting electrolyte, and found that the *S/N* values decreased with dilution of the electrolyte, owing to the large solution-resistance. Bixler and co-workers^{28,34} have described the use of microdisk and microring electrodes as detectors for use with a low electrolyte concentration in an acetonitrile mobile phase. Here we describe applications of our CFAR electrode in reversed-phase LC without supporting electrolyte, but have not yet tested its use in normal-phase LC.

A mixture of hydroquinone and catechol was chosen as a test model for reversed-phase LC separation with a mixture of water and methanol as mobile phase without supporting electrolyte. Figure 7 shows the hydrodynamic voltamperograms of HQ at the CFAR and GCD electrodes, measured independently, with

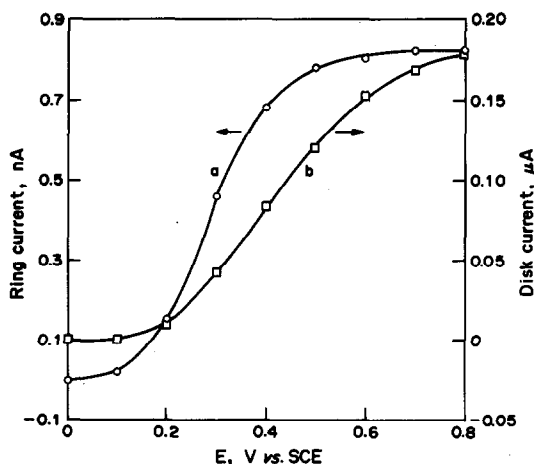


Fig. 7. Hydrodynamic voltamperograms at the CFAR electrode (a) and GCD electrode (b), with 30% v/v methanol in water as mobile phase without supporting electrolyte; 10 μ l of 5 ppm HQ injected.

30:70 v/v methanol–water mixture as mobile phase. It can be seen that the voltamperogram at the CFAR electrode is the same as that obtained with supporting electrolyte present (Fig. 5), but the one at the TCD electrode is flatter. As shown in Fig. 8, good linearity was found between LC peak current and HQ concentration with the CFAR electrode but not with the GCD electrode.

Thus the CFAR electrode would be the detector of choice for use with a wide concentration range of analyte in normal-phase LC with a mobile phase containing no background electrolyte, but the GCD electrode would be more useful at very low μ l concentrations.

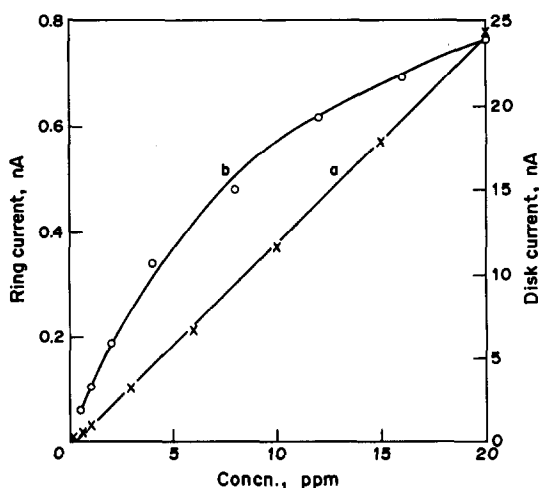


Fig. 8. Calibration curves for peak current at the CFAR electrode (a) and GCD electrode (b) vs. concentration of HQ, without the addition of supporting electrolyte to the mobile phase. Injection volume 10 μ l; potential 0.7 V; mobile phase: 30% v/v methanol in water.

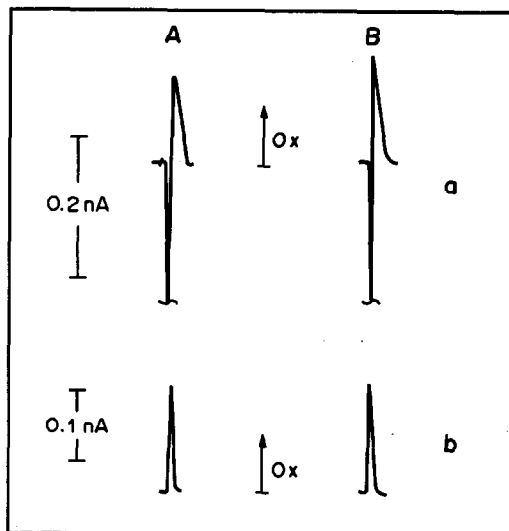


Fig. 9. FIA peaks at the CFAR electrode (a) and GCD electrode (b) for collection-mode (A) and shielding-mode (B) detection, with water as mobile phase without supporting electrolyte. (A) $E_{CFAR} = 0$ V, $E_{GCD} = 0.7$ V; (B) $E_{CFAR} = 0.8$ V, $E_{GCD} = 0.7$ V; 10 μ l of 5 ppm HQ injected.

Moreover, the CFAR–GCD electrode system has lower solution-resistance than any of the microelectrode cells reported,^{19,20,24,28–30,34} because of the narrow electrode gap possible with the wall-jet configuration.

Another interesting phenomenon was found when the dual-electrode was operated with the CFAR–GCD electrode in a mobile phase without added electrolyte (Fig. 9). Figure 9A shows that at the CFAR electrode used in the collection mode an irregular cathodic current and a small anodic current were observed. Similar peaks were obtained in the shielding mode but with a more rapid increase of cathodic current (Fig. 9B). A regular peak was observed at the GCD electrode in both cases. This can be explained as due to the large change in potential distribution in the flow, because of the high solution-resistance in pure water–methanol solution. When a large peak current is produced at the GCD electrode, then the large iR drop between the reference electrode and the CFAR and GCD electrodes may act as a potential step making the potential of the CFAR electrode more negative, so that a large cathodic current is produced at the CFAR electrode. When the current at the GCD electrode returns to the baseline, a corresponding potential step is applied to the CFAR electrode, making its potential more positive, and producing a rapid fall of cathodic current and appearance of a small anodic current at the CFAR electrode; this anodic current then returns slowly to the

baseline. This is similar to the cross-talk effect in dual-electrode detection.³⁹ Care must therefore be taken to avoid such effects in the dual-electrode detection.

CONCLUSION

Microelectrodes and conventional-size electrodes can be successfully combined for EC detection and also used independently. When they are combined as a ring-disk electrode in a wall-jet cell, some special advantages are obtained, such as high collection and shielding efficiencies. This electrode is promising for voltammetric/amperometric detection, but the electrode gap must be optimized for each application.

Acknowledgements—The support of the National Natural Sciences Foundation of China was highly appreciated, and Professor R. N. Adams, University of Kansas, is thanked for his kind gift of the carbon fibres.

REFERENCES

- D. C. Johnson, S. G. Weber, A. M. Bond, R. M. Wightman, R. E. Shoup and I. S. Krull, *Anal. Chim. Acta*, 1986, **180**, 187.
- P. Jandik, R. Haddad and P. E. Sturrock, *CRC Crit. Rev. Anal. Chem.*, 1988, **20**, 1.
- P. T. Kissinger, C. Refshauge, R. Dreiling and R. N. Adams, *Anal. Lett.*, 1973, **6**, 465.
- D. A. Roston and P. T. Kissinger, *Anal. Chem.*, 1982, **54**, 429.
- D. A. Roston, R. E. Shoup and P. T. Kissinger, *ibid.*, 1982, **54**, 1417A.
- M. Goto, G. Zou and D. Ishii, *J. Chromatog.*, 1983, **275**, 271.
- L. A. Allison and R. E. Shoup, *Anal. Chem.*, 1983, **55**, 8.
- C. E. Lunte, P. T. Kissinger and R. E. Shoup, *ibid.*, 1985, **57**, 1541.
- H. Ji and E. Wang, *J. Chromatog.*, 1987, **410**, 111.
- J. Ye, R. P. Baldwin and J. W. Schlager, *Electroanalysis*, 1989, **1**, 133.
- J. Wang and L. D. Hutchins, *Anal. Chem.*, 1985, **57**, 1536.
- L. M. Santos and R. P. Baldwin, *Anal. Chim. Acta*, 1988, **206**, 85.
- R. Samuelsson, J. O'Dea and J. Osteryoung, *Anal. Chem.*, 1980, **52**, 2215.
- D. C. Johnson and T. Z. Polta, *Chromatog. Forum*, 1986, **1**, 37.
- P. A. Reardon, G. E. O'Brien and P. E. Sturrock, *Anal. Chim. Acta*, 1984, **162**, 175.
- R. M. Wightman, *Anal. Chem.*, 1981, **53**, 1125A.
- T. E. Edmonds, *Anal. Chim. Acta*, 1985, **175**, 1.
- S. Pons and M. Fleischmann, *Anal. Chem.*, 1987, **59**, 1391A.
- K. Štulík, V. Pacáková and M. Poddak, *J. Chromatog.*, 1984, **298**, 225.
- L. A. Knecht, E. J. Guthrie and J. W. Jorgenson, *Anal. Chem.*, 1984, **56**, 479.
- R. L. St. Claire, III and J. W. Jorgenson, *J. Chromatog. Sci.*, 1985, **23**, 186.
- J. G. White, R. L. St. Claire, III and J. W. Jorgenson, *Anal. Chem.*, 1986, **58**, 293.
- J. G. White and J. W. Jorgenson, *ibid.*, 1986, **58**, 2992.
- M. Goto and K. Shimada, *Chromatographia*, 1986, **21**, 631.
- M. Goto, K. Shimada, T. Takeuchi and D. Ishii, *Anal. Sci.*, 1988, **4**, 17.
- R. A. Wallingford and A. G. Ewing, *Anal. Chem.*, 1988, **60**, 258.
- H. Ji, J. He, S. Dong and E. Wang, *J. Electroanal. Chem.*, 1991, **290**, 93.
- J. W. Bixler and A. M. Bond, *Anal. Chem.*, 1986, **58**, 2859.
- W. L. Caudill, J. O. Howell and R. M. Wightman, *ibid.*, 1982, **54**, 2532.
- F. Belal and J. L. Anderson, *Analyst*, 1985, **110**, 1493.
- S. B. Khoo, H. Gunasingham, K. P. Ang and B. T. Tay, *J. Electroanal. Chem.*, 1987, **216**, 115.
- D. J. Chesney, J. L. Anderson, D. E. Weisshaar and D. E. Tallman, *Anal. Chim. Acta*, 1981, **124**, 321.
- J. L. Anderson, K. K. Whiten, J. D. Brewster, T.-Y. Ou and W. K. Nonidez, *Anal. Chem.*, 1985, **57**, 1366.
- J. W. Bixler, M. Fifield, J. C. Poler, A. M. Bond and W. Thormann, *Electroanalysis*, 1989, **1**, 23.
- L. E. Fosdick, J. L. Anderson, T. A. Baginski and R. C. Jaeger, *Anal. Chem.*, 1986, **58**, 2750.
- L. E. Fosdick and J. L. Anderson, *ibid.*, 1986, **58**, 2481.
- J. W. Bixler, A. M. Bond, P. A. Lay, W. Thormann, P. van den Bosch, M. Fleischmann and S. Pons, *Anal. Chim. Acta*, 1986, **187**, 67.
- C. E. Lunte, S.-W. Wong, T. H. Ridgway, W. R. Heineman and K. W. Chan, *ibid.*, 1986, **188**, 263.
- C. E. Lunte, T. H. Ridgway and W. R. Heineman, *Anal. Chem.*, 1987, **59**, 761.
- C. E. Lunte, J. F. Wheeler and W. R. Heineman, *Anal. Chim. Acta*, 1987, **200**, 101.
- A. J. Bard and L. R. Faulkner, *Electrochemical Methods*, pp. 298–304. Wiley, New York, 1980.
- J. Yamada and H. Matsuda, *J. Electroanal. Chem.*, 1973, **44**, 189.
- H. Gunasingham, *TrAC*, 1988, **7**, 217.
- W. J. Albery and C. M. A. Brett, *J. Electroanal. Chem.*, 1983, **148**, 211.
- H. Gunasingham, *Anal. Chim. Acta*, 1984, **159**, 139.
- W. Thormann, J. W. Bixler, T. F. Mann and A. M. Bond, *J. Electroanal. Chem.*, 1988, **241**, 1.
- W. Hou, H. Ji and E. Wang, *Anal. Chim. Acta*, 1990, **230**, 207.
- R. Braun, *J. Electroanal. Chem.*, 1968, **19**, 23.
- H. Matsuda, *ibid.*, 1968, **16**, 153.
- E. M. M. Roosensaal and H. Poppe, *Anal. Chim. Acta*, 1984, **158**, 323.
- H. Gunasingham and B. Fleet, *J. Chromatog.*, 1983, **261**, 43.
- H. Gunasingham, B. T. Tay and K. P. Ang, *Anal. Chem.*, 1984, **56**, 2422.

ELECTROANALYSIS AT MODIFIED CARBON-PASTE ELECTRODES CONTAINING NATURAL IONIC POLYSACCHARIDES

JOSEPH WANG*, ZIAD TAHA and NAJIB NASER

Department of Chemistry, New Mexico State University, Las Cruces, NM 88003, U.S.A.

(Received 28 April 1989; Accepted 21 July 1989)

Summary—The strong affinity of natural ionic polysaccharides for certain metal ions is exploited in the design of a new class of voltammetric sensing devices. In particular, carbon-paste electrodes containing pectic and alginic acids are used for the nonelectrolytic collection and subsequent voltammetric determination of copper and lead, respectively. Cyclic and differential pulse voltammetry are used to quantify the accumulated ions. The response is characterized with respect to modifier loading, preconcentration period, metal concentration, reproducibility, possible interferences and other variables. Titrimetric experiments illustrate the potential of polysaccharide electrodes for speciation work. Preliminary data are also given for analogous measurements of copper at heparin-modified electrodes. Detection limits are 1 $\mu\text{g/ml}$ and the relative standard deviation is 4.8%.

Chemically modified electrodes (CMEs) hold great promise for use as electrochemical sensors. The electrode surfaces can be tailored to meet the needs of many sensing problems. One promising direction is to use surfaces capable of preferentially preconcentrating target analytes from solutions.¹⁻³ In this approach, a non-electrochemical preconcentration step is employed, followed by voltammetric quantification of the surface-bound analyte. Most popular schemes used to collect analytes are based on coordination reactions^{4,5} and electrostatic attraction^{6,7} at surfaces carrying an appropriate ligand or ion-exchanger. Bioaccumulation at electrodes based on micro-organisms can also be used.⁸ The preconcentrating agent is commonly incorporated into the surface by mixing it with carbon-paste matrices or by forming derivatives of polymeric films. The reactivity obtained by proper choice of the surface modifier can greatly enhance the selectivity and sensitivity of voltammetric devices (compared to those of conventional bare surfaces that utilize electrolytic preconcentration).

This paper describes a new class of modifying species, natural ionic polysaccharides, for use in making CMEs for preconcentrations. The strong interaction of ionic polysaccharides with various bivalent ions has been the subject of several investigations.⁹⁻¹² Electrochemical techniques such as polarography⁹ or potentiometry¹²

have been used, along with other methods, for exploring the binding of copper and lead to ionic polysaccharides. Such binding occurs by electrostatic interaction with carboxylate groups as well as other specific interactions. Important applications (based on this), ranging from removal and recovery of metal ions from polluted water¹³ to protection of people and animals against toxic metals¹⁴ have been reported. Preconcentrating CMEs based on the strong affinity of biopolyelectrolytes for certain metal ions have not been reported. The characteristics, advantages and analytical performance of carbon-paste electrodes containing pectic and alginic acids are described in this paper.

EXPERIMENTAL

Apparatus

Polysaccharide-modified carbon-paste electrodes were prepared by thoroughly hand-mixing the polysaccharide with graphite powder (Acheson 28) and mineral oil (40% w/w). Electrodes containing 21% pectic acid or 20% alginic acid (w/w) were used in most experiments. A portion of the paste was packed into the end of a glass tube (3 mm i.d.), and its inner end was connected to a copper wire.

Three 10-ml cells were used for the preconcentration, measurement and "cleaning" (renewal) steps; these contained the metal test solution, the supporting electrolyte solution and the acid "cleaning" solution, respectively.

*Author for correspondence.

An Ag/AgCl reference electrode (Model RE-1, Bioanalytical Systems) and a platinum wire auxiliary electrode completed the three-electrode system in the measurement cell. A Princeton Applied Research Corp. (PARC) Model 264A voltammetric analyzer, in conjunction with a PARC Model 0073X-Y recorder, was used to obtain the voltamperograms.

Reagents

Doubly distilled water was used to prepare all solutions. Pectic acid (75% purity, Kodak), alginic acid (Fluka) and heparin (Sigma) were used as surface modifiers. Sodium acetate (Mallinckrodt) and sodium perchlorate (Fisher) were used for preparing the supporting electrolyte solutions. Copper and lead solutions were prepared from their analytical grade nitrates. Atomic-absorption standard solutions of other metals (1000 ppm), used in the interference studies, were from Aldrich.

Procedure

All experiments were performed by using the preconcentration/medium-exchange/voltammetry/regeneration scheme. For the preconcentration step, the modified electrode was immersed in the stirred sample solution for a given period of time; the preconcentration proceeded at open circuit. The electrode was then removed from the preconcentration cell, briefly rinsed with doubly distilled water, and placed in the electrochemical cell containing a deaerated sodium perchlorate solution. The initial potential (-0.9 and -0.6 V for lead and copper, respectively) was then applied and after

15 sec a positive-going scan was initiated. After the scan the electrode was transferred to the cleaning (acid) cell for regenerating a "metal-free" surface (as indicated by a subsequent voltammetric run). Several such collection/measurement/cleaning cycles were required to precondition virgin surfaces. Specific details of the experimental procedure are summarized in Table 1.

RESULTS AND DISCUSSION

Three model substances, pectic and alginic acids and heparin, were used as surface modifiers to illustrate the potential of natural polysaccharides for analytical sensing.

Electrodes modified with pectic acid

Pectic acid (polygalacturonic acid) is a natural polyacid obtained from pectins. Its incorporation into the carbon-paste matrix results in effective accumulation and subsequent quantification of copper ions. Figure 1 compares cyclic voltamperograms obtained with the plain (A) and pectic acid (B) carbon-paste electrodes for 25 ppm copper, following 1-min stirring (open-circuit conditions) and transfer of the electrode to a blank/electrolyte solution. The scans were run by initially holding the electrode at -0.6 V to reduce the complexed copper to the metal. Voltammetric peaks are not observed when the unmodified electrode is used, as expected in the absence of copper collection. In contrast, the first scan (designated as 1) at the modified electrode exhibits a distinct current response ($E_{p,a} = +0.05$ V). The peak clearly corresponds to the oxidation of the copper

Table 1. Summary of experimental conditions

Analyte	copper	lead
CME	pectic acid (21%) in carbon paste	alginic acid (20%) in carbon paste
Preconditioning	five preconcentration/voltammetry/regeneration cycles with 25 ppm copper solution	two scans, between -0.9 and -0.2 V in blank solution, followed by two preconcentration/voltammetry/regeneration cycles with 10 ppm lead solution
Preconcentration solution	stirred $0.10M$ acetate buffer, pH 5.4	stirred $0.05M$ $NaClO_4$, pH 5.0
Voltammetric measurement	deaerated $0.05M$ $NaClO_4$ solution; potential range from -0.6 to $+0.2$ V; differential pulse waveform, 25 mV amplitude and 10 mV/sec scan rate	deaerated $0.05M$ $NaClO_4$ solution; potential range from -0.9 to -0.2 V; differential pulse waveform, 25 mV amplitude and 10 mV/sec scan rate
Surface regeneration	immersion in HNO_3 (pH 1.8) for 60 sec	immersion in HCl (pH 1.5) for a time equal to the preconcentration period

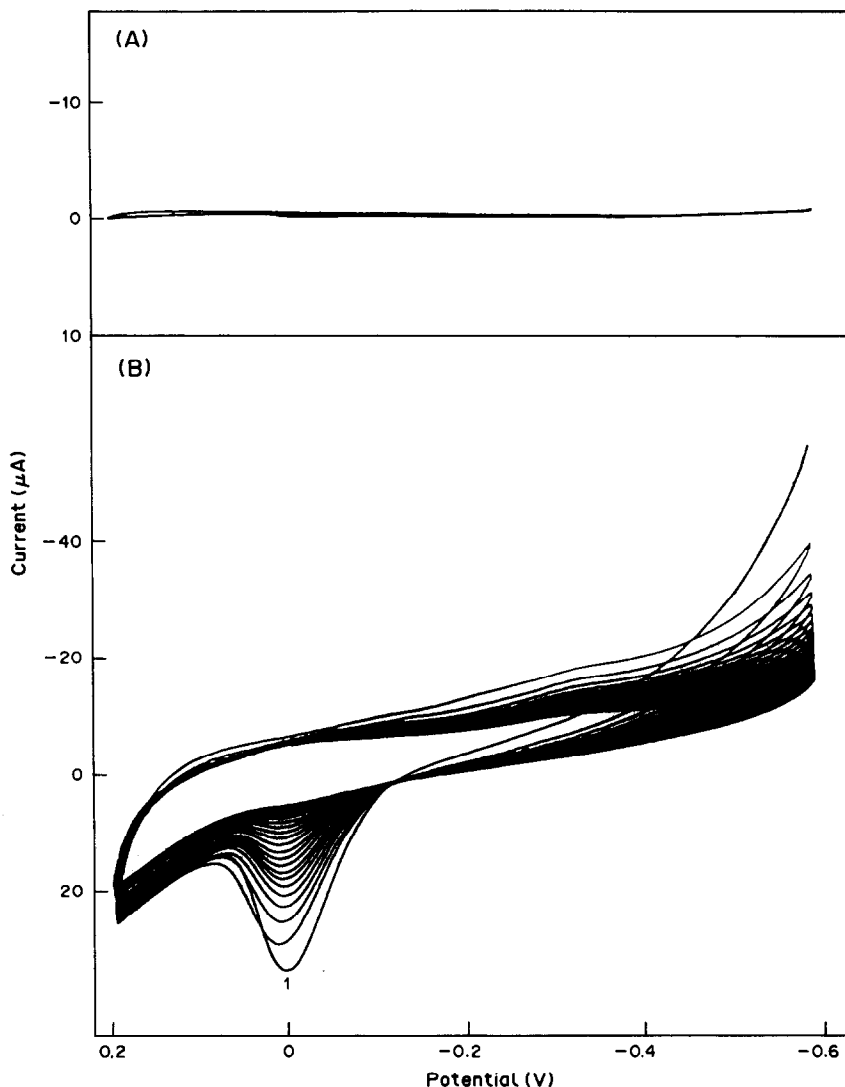


Fig. 1. Cyclic voltamperograms for unmodified (A) and pectic acid modified (B) carbon-paste electrodes after immersion for 1 min in a stirred 25 ppm copper solution and transfer to the blank/electrolyte solution. Open circuit during accumulation. Scan rate, 50 mV/sec; solutions as in Table 1.

metal arising from reduction of the copper(II) taken up electrostatically by the pectic acid. Subsequent voltamperograms, recorded by continued scanning, yield smaller and smaller peaks. With a 50 ppm copper solution, full surface coverage was attained by stirring for 120 sec. The steady-state (saturation) response corresponded to a charge of $66.1 \mu\text{C}$ and surface coverage of 1.75×10^{-9} mole/cm². The cyclic voltammetric peak current at saturation increased nonlinearly (from 21 to 52 nA) on increase in scan rate from 10 to 200 mV/sec. The peak potential shifted from 0.00 to 0.06 V on increase in scan rate, yielding a linear plot of peak potential *vs.* log (scan rate).

Figure 2 shows the dependence of the peak current on the accumulation time for (a) 9 and

(b) 18 ppm copper. As the accumulation time increases, the response rises rapidly at first and then more slowly. Apparently, the binding reaches equilibrium in accumulation for 3 min. The uptake of metal ions by the pectic acid electrode is strongly dependent on the pH. The effect of pH on the copper response is shown in Fig. 3(a). The peak increases rapidly with increase of pH between 2 and 5, and then starts to level off. Such a profile reflects the proton competition for the carboxylate binding sites. Accordingly, reversal of the metal ion binding, *i.e.*, surface regeneration after the voltammetric scan, can easily be accomplished by exposure to an acidic medium. The effect of the paste composition is shown in Fig. 3(b). The copper response increases as the pectic-acid loading is

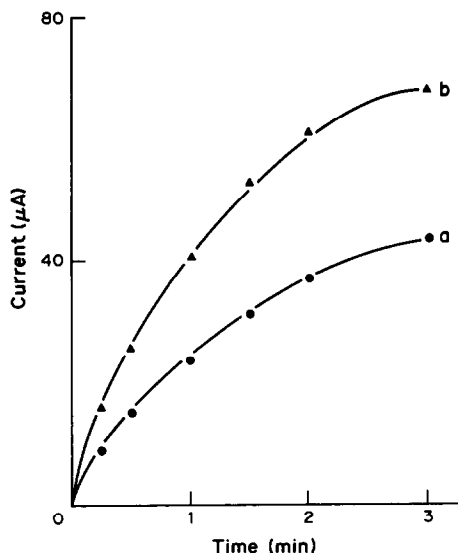


Fig. 2. Response of the pectic acid modified electrode as a function of accumulation time for (a) 9 and (b) 18 ppm copper. The electrode was immersed for different periods in the stirred copper solution, washed, and placed in the blank/electrolyte solution. Conditions as in Table 1.

increased between 0 and 21% (w/w), as expected from the increased binding capacity of the electrode. Increased electrode resistance accounts for the marked decrease in response at higher modifier loadings.

Virgin polysaccharide-modified electrodes were found to be less efficient for the collection of metal ions, compared to "old" surfaces (that had already undergone several measurement cycles). A preconditioning step, involving several such cycles was thus required (see

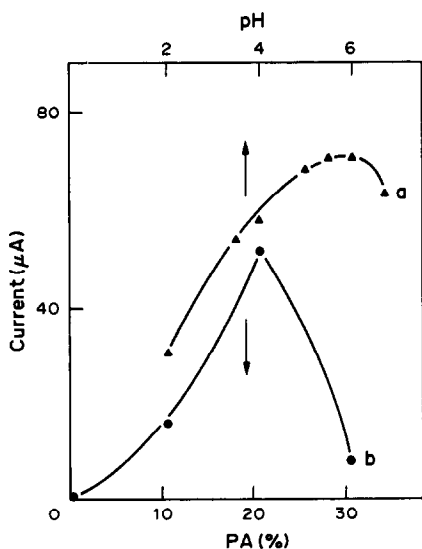


Fig. 3. Effect of (a) pH and (b) pectic acid content on the differential-pulse copper response. Solution of 18 ppm copper stirred for 60 sec. Other conditions as in Table 1.

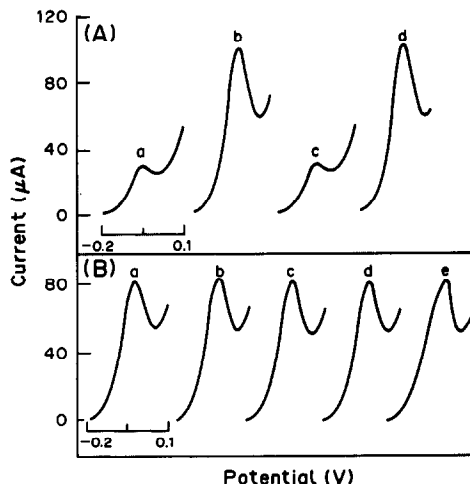


Fig. 4. Carry-over (A) and precision (B) experiments. Copper concentrations: (A) a, c, 9; b, d, 27 ppm; (B), a-e, 25 ppm. Accumulation for 30 sec; other conditions as in Fig. 2. Initial potential positions displaced for clarity.

Table 1 for details). A similar process was reported earlier for carbon-paste electrodes modified with various ligands,^{4,15} and was attributed to a certain degree of ordering of the surface ligand molecules after the metal binding.

The sensing potential of pectic-acid modified electrodes is indicated by Fig. 4, which shows voltamperograms obtained by sequential exposure to copper solutions differing in concentration (A) and for repetitive measurements at a given concentration (B). Well defined differential-pulse peaks are observed ($E_p = 0.05$ V), after short (30 sec) accumulation times. The electrode responds rapidly to the switching between the 9 and 27 ppm copper solutions. Modified electrodes conditioned and renewed as described in the experimental sections could be employed for numerous accumulation/reduction/cleaning cycles. For example, the voltamperograms shown in Fig. 4B are from a series of ten repetitions with a 25 ppm copper solution. This series yielded a mean peak current of $80.3 \mu\text{A}$, a range of $76\text{--}85 \mu\text{A}$ and a relative standard deviation of 4.8%. Such precision compares favorably with that reported for various preconcentrating CMEs.² The precision might be improved by use of flow-injection preconcentration schemes.¹⁶ The same electrode surface was used throughout each day, with no noticeable loss in activity.

Figure 5 shows calibration plots for copper, over the 1×10^{-4} – 8×10^{-4} M (6–48 ppm) range, after (a) 30 and (b) 60 sec preconcentration. In both cases the response is linear up to 4×10^{-4} M, with curvature at higher

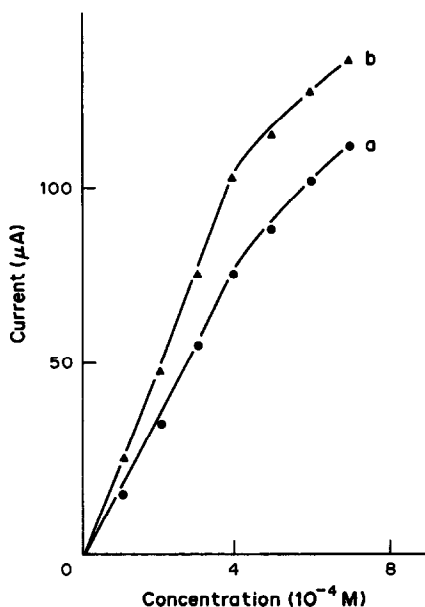


Fig. 5. Voltammetric response of the pectic acid modified electrode as a function of copper concentration for (a) 30 and (b) 60 sec accumulation times. Other conditions as in Fig. 2.

concentrations (as saturation of binding sites is approached). Least-squares treatment of the initial linear portions yielded slopes of $0.19 \mu\text{A} \cdot \text{l} \cdot \mu\text{mole}^{-1}$ (deposition for 30 sec) and $0.22 \mu\text{A} \cdot \text{l} \cdot \mu\text{mole}^{-1}$ (deposition for 60 sec), with correlation coefficients of 0.998 and 0.997, respectively. A detection limit of about 1 ppm copper was estimated from the signal-to-noise characteristics ($S/N = 3$) of the response following 5 min accumulation (not shown). Clearly, the detectability is not as low as that of conventional stripping measurements at mercury surfaces.

The advantages of the preconcentrating-CME approach lie in the selectivity of the accumulation process (which is derived from the reactivity patterns of the surface modifier), the use of "mercury-free", low-cost, surfaces, and suitability for speciation work. Surfaces containing natural polysaccharides exhibit reactivity different from that provided by modified electrodes based on common ligands or ion-exchangers. The following metal ions were tested at the 50 ppm level and found not to interfere in the determination of 25 ppm copper: Cd(II), Co(II), Ni(II), Zn(II), Cr(III) and Ca(II) (60 sec accumulation; other conditions as in Fig. 2). Minor changes in the 25 ppm copper response were observed in the presence of 50 ppm Mn(II), Pb(II), Ag(I), Bi(III) and Sn(IV) (8, 9 and 20% increases, 6 and 20% decreases, respectively). Such interference is expected to

increase at higher concentrations of these ions. The transfer of the electrode, with the collected analyte, to a blank electrolyte solution precludes interference from solution-phase species.

Preconcentrating CMEs based on natural ionic polyelectrolytes provide an interesting opportunity to explore the binding of metal ions with these materials and can serve as useful tools for metal speciation studies. Preliminary experiments indicated the potential of the pectic acid CME for speciation work. For example, a gradual decrease of the peak for $4 \times 10^{-4} M$ copper was observed when the concentration of EDTA or NTA was increased from 0.5×10^{-4} to $4 \times 10^{-4} M$ (accumulation for 30 sec). Complete disappearance of the copper response was observed for $4 \times 10^{-4} M$ EDTA, in agreement with the 1:1 stoichiometry of the Cu-EDTA complex. Work is in progress to obtain better understanding of the speciation data obtained with this and other preconcentrating electrodes, and particularly to identify the metal species measured.

Electrodes modified with alginate acid or heparin

Alginate acid is a copolymer of α -L-glucuronic acid and β -D-mannuronic acid. It has a very high binding capacity ($50 \mu\text{g}/\text{ml}$) for lead.¹⁴ The ability of alginate acid modified carbon-paste electrodes to take up lead ions from solutions prior to voltammetric analysis is illustrated below. Figure 6 compares cyclic voltammograms of (A) unmodified and (B) alginate acid modified electrodes following a 60-sec immersion in a 30 ppm lead solution, rinsing with water and placement in the blank (sodium perchlorate) solution. No distinct redox processes are observed at the plain carbon surface. In contrast, a sharp anodic peak, corresponding to the oxidation of the surface-bound lead, is observed when the modified electrode is used ($E_p = -0.46 \text{ V}$). Continuing to scan the CME in the blank solution causes the peak to decrease gradually. The oxidation peak (in Fig. 6B) reflects a full surface coverage, and corresponds to a charge of $61.7 \mu\text{C}$ and coverage of $1.63 \times 10^{-9} \text{ mole}/\text{cm}^2$.

The binding of lead by the surface-bound alginate acid can be utilized for effective preconcentration prior to voltammetric analysis. Figure 7 shows current *vs.* accumulation-time plots for (a) 5 and (b) 15 ppm lead. At both levels the peak rises rapidly at first and then more slowly. The effects of the solution pH and modifier loading were examined with a 10 ppm

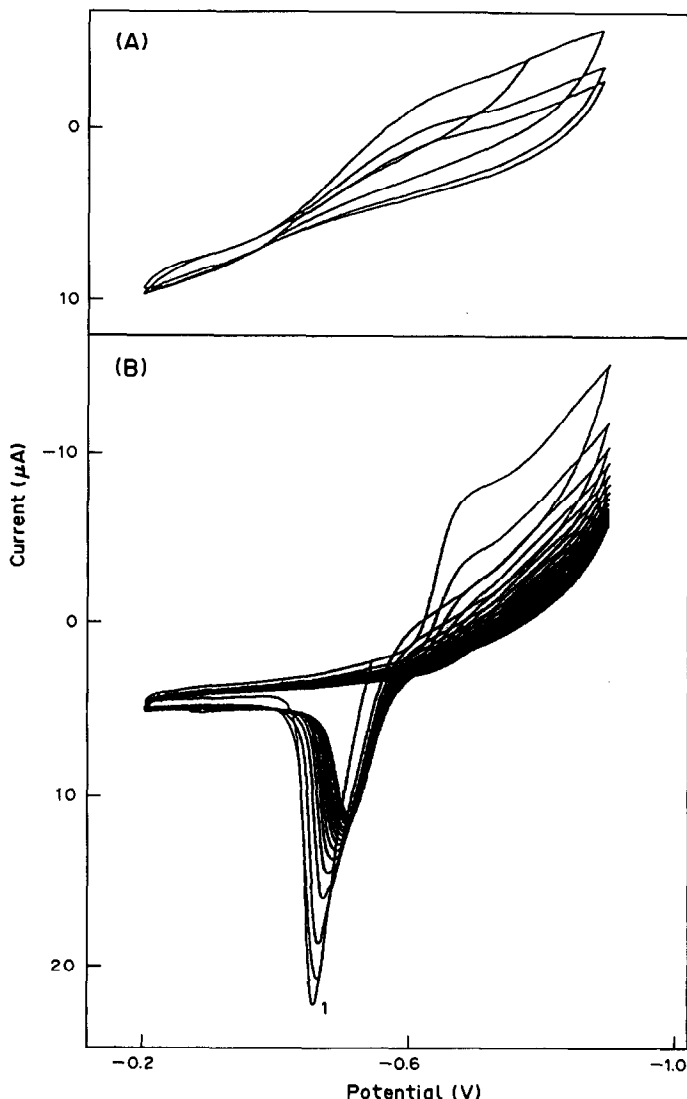


Fig. 6. Cyclic voltamperograms for unmodified (A) and alginic-acid modified (B) carbon-paste electrodes after immersion for 1 min in a stirred 30 ppm lead solution and transfer to the blank/electrolyte solution. Open circuit during accumulation. Scan rate, 50 mV/sec; solutions as in Table 1.

lead solution and stirring for 30 sec. The profiles obtained are similar to the trends shown for pectic acid (in Fig. 3), with a gradual increase in the response between pH 1 and 5, and maximal response at 20% alginic acid loading (not shown). Acid treatment was found effective for stripping the lead at the end of each cycle.

The alginic acid CME exhibits a well defined concentration dependence and reproducible response. Figure 8 shows voltamperograms for solutions with lead concentration increasing from 5 to 20 ppm, after accumulation for 20 sec and transfer to a blank solution. Well-defined peaks are observed ($E_p = -0.48$ V, $b_{1,2} = 90$ mV). A detection limit of 1 ppm can be

estimated from the 5 ppm response. Calibration plots obtained with accumulation for 20 and 60 sec were linear up to 30 and 25 ppm, respectively (slopes, 3.4 and 5.5 $\mu\text{A}\cdot\text{ml}\cdot\mu\text{g}^{-1}$, respectively; correlation coefficients, 0.998). The reproducibility was estimated from twelve successive measurements of stirred 10 ppm lead solution (30 sec accumulation). The mean peak current was 51.9 μA , range 48.4–55.2 μA , relative standard deviation 4.8%.

Interference studies were performed with 10 ppm lead in the presence of 20 ppm of different metals. The lead response was not affected by the presence of Cd(II), Ni(II), Mn(II), Ag(I) or Ca(II). In contrast, competition for surface binding sites was indicated by the 20, 26, 29 and

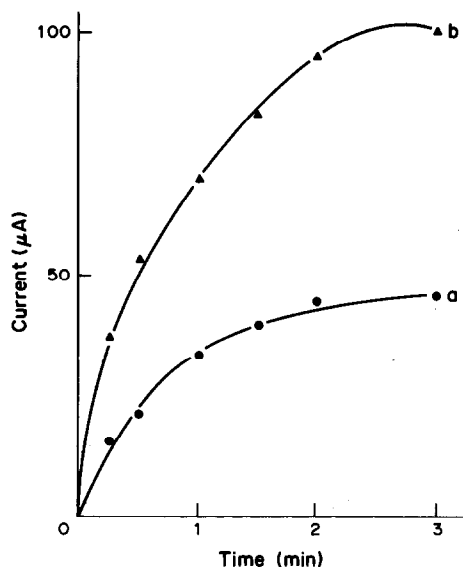


Fig. 7. Response of the alginic acid modified electrode as a function of accumulation time for (a) 5 and (b) 15 ppm lead. The electrode was immersed for different periods in the stirred lead solution, washed and placed in the blank/ electrolyte solution. Conditions as in Table 1.

33% decrease of the peak height in the presence of Zn(II), Cr(III), Fe(III) and Cu(II), respectively. The standard additions method or the use

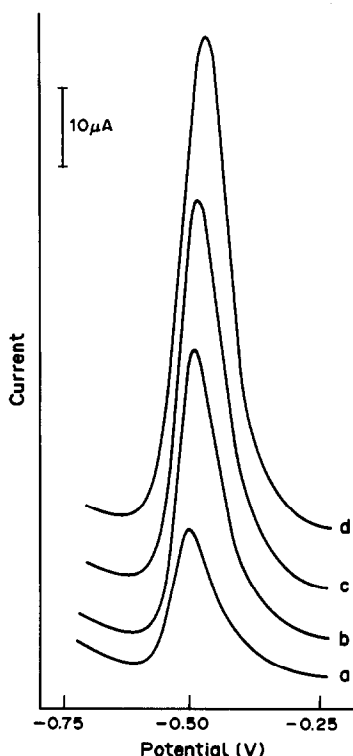


Fig. 8. Voltamperograms for solutions containing increasing levels of lead, 5–20 ppm (a–d). Accumulation for 20 sec; other conditions as in Table 1. Initial current positions displaced for clarity.

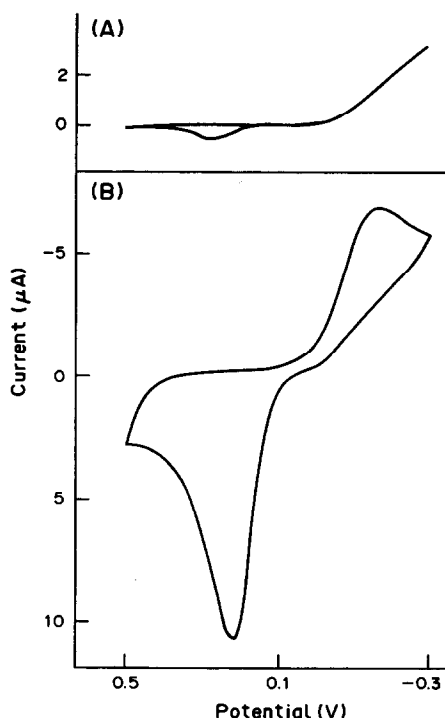


Fig. 9. Cyclic voltamperograms for unmodified (A) and heparin-modified (B) carbon-paste electrodes after immersion for 5 sec in a 25 ppm copper solution. Scan rate 50 mV/sec; electrolyte 0.1M acetate buffer (pH 6.8). Electrode composition: 30% heparin/38% graphite powder/ 32% high-vacuum silicone grease.

of selective masking agents should overcome these interferences.

In addition to electrodes modified with pectic and alginic acids, carbon-paste electrodes modified with the mucopolysaccharide heparin were used for some preliminary experiments. Physicochemical studies have demonstrated the binding of copper ions to this anticoagulant.¹⁷ Figure 9 compares cyclic voltamperograms recorded for a 25 ppm copper solution, after 5 sec immersion of the unmodified (A) and 30% heparin (B) carbon-paste electrodes. The collection of copper at the modified electrode is evident from the 25-fold enhancement of the copper oxidation peak and 50 mV negative shift in the peak potential.

In conclusion, the binding of metal ions by the negatively-charged sugar units of the polysaccharide chain was exploited for designing novel polysaccharide-modified electrodes for preconcentration/voltammetry. Because they give biological collection of metals, such surface modifiers offer unique reactivity patterns. New insights into the interaction of polysaccharides with metal ions can also be obtained. The carbon paste is shown to be a

useful matrix for the incorporation of these modifiers in a stable, responsive and reproducible form. While the work presented here is within the context of natural polysaccharides, other biological materials (*e.g.*, selected fungi and bacteria¹⁸) offer considerable promise for use as surface modifiers in connection with bioaccumulation/voltammetric sensing. These CMEs, however, cannot compete with the sensitivity of the mercury electrodes used in stripping voltammetry.

Acknowledgements—This work was supported by the National Institutes of Health (Grant No. GM-30913-06) and the U.S. Department of the Interior, through the New Mexico Water Resources Research Institute.

REFERENCES

1. A. R. Guadalupe and H. Abruna, *Anal. Chem.*, 1985, **57**, 142.
2. J. Wang, in *Electroanalytical Chemistry*, A. J. Bard (ed.), Vol. 16, p. 1. Dekker, New York, 1989.
3. D. M. T. O'Riordan and G. G. Wallace, *Anal. Proc.*, 1985, **22**, 199.
4. R. P. Baldwin, J. K. Christensen and L. Kryger, *Anal. Chem.*, 1986, **58**, 1790.
5. K. H. Lubert and M. Schnurrbusch, *Anal. Chim. Acta*, 1986, **186**, 57.
6. J. Wang, B. Green and C. Morgan, *ibid.*, 1984, **158**, 15.
7. J. Cox and P. J. Kulesza, *ibid.*, 1983, **154**, 71.
8. J. Gardea-Torresdey, D. Darnall and J. Wang, *Anal. Chem.*, 1988, **60**, 72.
9. E. Reisenhofer, A. Cesaro, F. Delben, G. Manzini and S. Paoletti, *Bioelectrochem. Bioenerg.*, 1984, **12**, 455.
10. A. Malovíková and R. Kohn, *Collecton Czech. Chem. Commun.*, 1981, **47**, 702.
11. R. Kohn, *Pure Appl. Chem.*, 1975, **42**, 371.
12. G. Manzini, A. Cesaro, F. Delben and E. Reinehofer, *Bioelectrochem. Bioenerg.*, 1984, **12**, 443.
13. H. H. G. Jellinek and S. P. Sangal, *Water Res.*, 1972, **6**, 305.
14. H. E. Rose and J. Quarterman, *Environ. Res.*, 1987, **42**, 166.
15. S. W. Prabhu, R. P. Baldwin and L. Kryger, *Anal. Chem.*, 1987, **59**, 1074.
16. J. Wang and B. A. Freiha, *ibid.*, 1983, **55**, 1285.
17. S. S. Stivala and P. A. Liberti, *Arch. Biochem. Biophys.*, 1967, **122**, 40.
18. N. Kuyucak and B. Volesky, *Biotech. Bioeng.*, 1989, **33**, 809.

EFFECTS OF COMPETITIVE BINDING ON THE AMPEROMETRIC DETERMINATION OF COPPER WITH ELECTRODES MODIFIED WITH CHROMOTROPE 2B

SEONG K. CHA, KASEM K. KASEM and HÉCTOR D. ABRUÑA*

Department of Chemistry, Baker Laboratory, Cornell University, Ithaca, NY 14853-1301, U.S.A.

(Received 17 July 1989. Accepted 6 November 1989)

Summary—Electrodes modified with Chromotrope 2B incorporated by ion-exchange into a polycationic film of electropolymerized $[Ru(v-bpy)_3]^{2+}$ ($v-bpy = 4\text{-vinyl-4'-methyl-2,2'-bipyridyl}$) have been employed in the amperometric determination of copper in solution and exhibit very high sensitivity as well as linear calibration curves in the concentration range 7×10^{-8} – $1 \times 10^{-4}M$. The effects of competing ligands, including chloride, bromide, oxalate, ammonia, acetate, citrate, borate, humic and fulvic acids, or the presence of competing metal ions such as cobalt or nickel on the uptake of copper by the modified electrodes have also been studied. The presence of competing ligands or metal ions decreases the analytical signal due to copper incorporation. The magnitude of this effect is dependent on the relative strength of coordination of the competing ligands for copper ions or of Chromotrope 2B for the competing metals, and also on the concentration of the interferents. The relevance of this work to speciation studies is discussed.

Chemically modified electrodes¹⁻⁸ are of great use in the development of analytical strategies and sensors, owing to the high specificity that can be achieved by appropriate choice of modifier, and the high sensitivity that can be achieved by preconcentration of the analyte at the surface-modified electrode. In addition, the methodologies and instrumentation involved are relatively simple. A large number of analytical applications of chemically modified electrodes have been reported.⁹⁻²⁶

In our work, we have sought to exploit the advantages of polymer-modified electrodes for the determination of transition metal ions¹⁸⁻²³ and organic functional groups.²³⁻²⁶ The methods have been based on preconcentration of the analyte (metal ion or organic species) at an electrode surface modified with polymers carrying reagents for the selective and sensitive determination of the species of interest.

For the determination of transition metal ions we employ bifunctional or multifunctional polymer films containing electroactive centers and coordinating groups. The internal redox center is used to induce precipitation of the polymer on the electrode surface and thus allows precise control of the coverage and also serves in the determination of the number of immobilized

ligand sites, which is important as it allows *a priori* determination of the saturation response. A coordinating group is chosen that will bind strongly and selectively to the metal ion of interest. In addition, we have also employed carbon-paste electrodes, in which the polymer containing the ligand is mixed with the pasting material. This approach allows rapid renewal of the electrode surface.

The analysis is based on the electrochemical determination of the amount of immobilized metal/ligand complex and can employ either a metal or ligand redox process to provide the analytical signal which is related to the concentration of the analyte in solution. We have demonstrated the applicability of this approach to the determination of iron, copper, cobalt, nickel and calcium.¹⁸⁻²³

We are also interested in assessing the utility of chemically modified electrodes in speciation studies, which are of great importance in analysis of environmental samples since the toxicity of metal ions is often strongly dependent on the form in which they are present. Speciation studies are difficult because the concentration levels are low, the given ion may be present in numerous forms, and the method of analysis must not only be sufficiently sensitive, but also not perturb the species distribution.

Fundamentally, speciation involves analysis of the competitive equilibria between the metal

*Author for correspondence.

ion of interest and the ligands present in solution. We have therefore initially investigated the response of electrodes modified with Chromotrope 2B (for structure see Fig. 1) for the determination of copper ions in solution in the presence of competing ligands or metal ions.

EXPERIMENTAL

Reagents

Chromotrope 2B (C2B) (Aldrich) was purified by three recrystallizations from an ethanol/water mixture. The water was purified by a Hydro water purification train or a Millipore Milli-Q system. Buffer solutions and standard copper solutions were prepared from reagent grade materials. Acetonitrile (Burdick and Jackson distilled in glass) and dried over molecular sieves (4 Å). Tetra-*n*-butylammonium perchlorate (TBAP) (G. F. Smith) was recrystallized three times from ethyl acetate and dried under vacuum at 75° for 72 hr. $[\text{Ru}(\text{v-bpy})_3]^{2+}(\text{PF}_6)_2^*$ was prepared as previously described.²⁷ All other reagents were of at least reagent grade quality and were used without further purification.

Instrumentation

Prior to use, platinum or glassy-carbon disk electrodes sealed in glass or teflon, respectively, were polished with 1 μm diamond paste (Buehler), rinsed with water, placed in an ultrasonic bath (in water) for 1 min and rinsed with acetone.

Electrochemical cells of conventional design with three compartments separated by medium porosity sintered-glass disks were used throughout.

Electrochemical experiments were performed with either an IBM Instruments EC 225 Voltammetric Analyzer or a BAS 100 Electrochemical Analyzer. Data were recorded on a Soltec X-Y recorder. Differential pulse voltammetric experiments were done with a 50 mV pulse amplitude and a sweep rate of 10 mV/sec. All potentials are referred to the sodium chloride saturated calomel electrode (SSCE) without regard to the liquid-junction potential.

Procedures

Electrodes were modified with a polymeric film of $[\text{Ru}(\text{v-bpy})_3]^{2+}$ by reductively initiated

polymerization from acetonitrile/0.1M TBAP solution as previously described.²⁷ The exact coverage was determined from the charge under the voltammetric wave for the Ru(III/II) process at about +120 V. Typical coverages were 2–3 equivalent monolayers. The modified electrodes were immersed in a stirred 10mM aqueous solution of Chromotrope 2B for 15 min. After rinsing with water, the electrodes were placed in contact (for 15 min, with stirring) with aqueous solutions of Cu(I) [obtained by the addition of a fivefold excess of hydroxylamine hydrochloride to Cu(II) chloride solutions] at various concentrations and in the presence (or absence) of other metal cations or ligands, also at various concentrations. Afterwards, the electrodes were rinsed with water.

Determinations (by differential pulse voltammetry) were performed in either aqueous trifluoroacetate buffer (pH 5.25) or in acetonitrile/0.1M TBAP. The currents were normalized with respect to the surface coverage, which was determined as described above. At least five replicate determinations were performed.

RESULTS AND DISCUSSION

Preliminary voltammetric characterization

In the absence of copper, C2B did not exhibit any redox response in trifluoroacetate buffer at a glassy carbon electrode in the potential range between -0.5 and +1.0 V. Upon addition of copper ions, a well defined wave was observed, which had a conditional potential of -0.05 V and that we ascribe to formation of a stable C2B/Cu complex.

The electrochemical behavior of electrodes modified with poly- $[\text{Ru}(\text{v-bpy})_3]^{2+}$ and loaded with C2B was also investigated before and after its exposure to an aqueous copper solution. Prior to exposure (Fig. 1,A), the only electrochemical response observed between -0.50 and +1.40 V was that of the poly- $[\text{Ru}(\text{v-bpy})_3]^{2+}$ at about +1.20 V. After exposure, however, an additional redox response with a formal potential of -0.05 V was observed (Fig. 1,B); consistent with the results in solution.

When the electrochemical response of modified electrodes (again prior to and after exposure to copper-containing solution) was measured in acetonitrile medium, analogous results were obtained except that the wave for the C2B/Cu complex was at a formal potential of +0.45 V.

*v-bpy = 4-vinyl-4'-methyl-2,2'-bipyridyl.

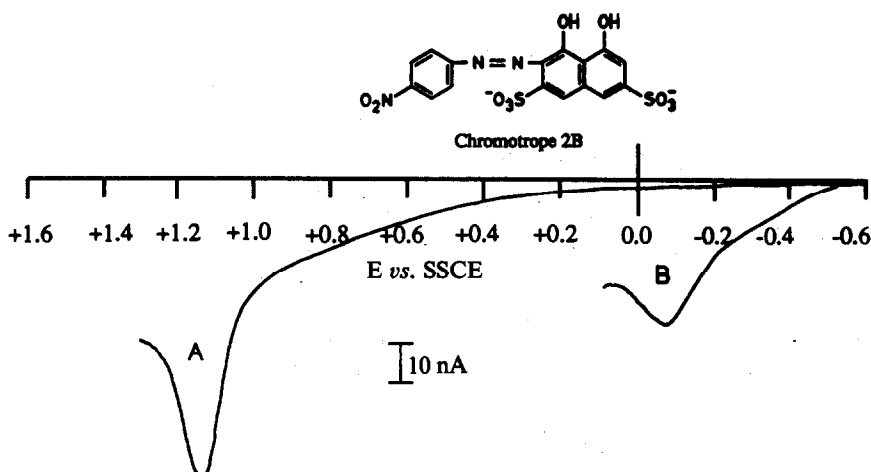


Fig. 1. Differential pulse voltamperograms for a glassy-carbon electrode modified with poly- $[\text{Ru}(\text{v-bpy})_3]^{2+}$ loaded with C2B prior to (A) and after (B) exposure to a $50\mu\text{M}$ solution of copper. Inset: structure of C2B.

Copper determination studies

Electrodes modified with C2B were exposed to aqueous copper solutions (pH 5.25) at various concentrations, as described in the experimental section. Subsequently, the electrochemical response of the surface-immobilized C2B/Cu complex in either aqueous pH 5.25 buffer or acetonitrile/ $0.1M$ TBAP was obtained, with the waves at formal potentials of -0.05 and $+0.45$ V respectively, as the analytical signal.

Figure 2 shows a plot of the logarithm of the normalized current (for the determination in acetonitrile medium) *vs.* the logarithm of the copper concentration in solution. A fairly good correlation ($r = 0.98$) was obtained over the concentration range 7.2×10^{-8} – $1.1 \times 10^{-4}M$. This illustrates the sensitivity of the method and its wide dynamic range. A saturation response is obtained as shown by the levelling of the curve at the higher concentrations,

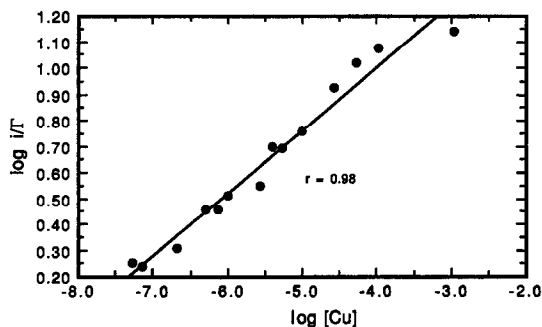


Fig. 2. Calibration curve for the determination of copper with electrodes modified with poly- $[\text{Ru}(\text{v-bpy})_3]^{2+}$ loaded with C2B.

because of coordination of all the available surface sites. This was corroborated by the fact that the current for the immobilized C2B/Cu complex did not increase with further increase in the solution concentration of copper. In addition, the observed currents correlated very well with our estimates for a completely metalated film, calculated from the experimentally determined surface coverage of the polymer on the electrode surface assuming complete neutralization of the charge due to the pendant $[\text{Ru}(\text{v-bpy})_3]^{2+}$ groups, by the sulphonate side-chains in C2B. This is based on the fact that we could precisely determine the amount of surface-immobilized $[\text{Ru}(\text{v-bpy})_3]^{2+}$ (from its voltammetric response) and from this, determine the maximum amount of C2B that could be incorporated by ion-exchange. Since the Cu/C2B stoichiometry is known, the measurement of the redox response due to the immobilized metal/ligand complex for an ostensibly metal-saturated film yields the amount of C2B incorporated. The experimental and calculated values were always in good agreement. We have also previously shown¹⁸ that for similar ligands there is virtually no loss of ligand or complex from the electrode surface upon potential cycling or in the presence of high ($1.0M$) electrolyte concentrations for extended time periods.

At the low-concentration end, the response appears to level off at a copper concentration of about $5.4 \times 10^{-8}M$. This, however, appears to be due not to the limit of detection of the technique, but to background levels of copper in the reagents employed.

Competitive binding studies

We have studied the effects of competitive binding of copper ions by other ligands or of other metals by the surface-immobilized ligand (C2B). These studies will be helpful in trying to apply the approaches described here to speciation studies since speciation fundamentally involves competitive equilibria.

Competitive binding of copper by other ligands.

In the investigation of the effects of competing ligands on the determination of copper, the modified electrode was exposed to solutions of copper at a fixed concentration of $1 \times 10^{-5} M$, which also contained a competing ligand at various concentrations. In this manner, we studied the effects of chloride, bromide, oxalate, ammonia, acetate, citrate, borate, humic and fulvic acids as competing ligands. Figure 3 shows representative results obtained when the competing ligands were chloride, bromide, oxalate and humic acid. In all cases there was a diminution in the response for the surface-immobilized C2B/Cu complex and the magnitude of this effect was proportional to the solution concentration of the competing ligand. The linearity of the $\log(i/\Gamma)$ vs. $\log[\text{competitive ligand}]$ plots strongly suggests that indeed the observed effects are due to competitive binding between the surface-immobilized C2B and the

ligand in solution. In addition, for the cases where there are reliable values for the conditional stability constants (β') of the copper complexes with the competitive ligands, we find that a plot of $\log(i/\Gamma)$ vs. $\log \beta'$ is also linear. In other words, the response depends on the conditional formation constants for the copper complexes under the specific conditions used.²⁸ This supports our assertion that competitive binding effects are responsible for the observed diminution in the analytical signal, and more importantly, establishes that the relative strengths of coordination of the various ligands are maintained under the experimental conditions employed. This implies that the coordination properties of an interface (a modified electrode in this case) can be systematically and deliberately controlled by choice of the immobilized ligand as well as by the presence of other competitive ligands in solution. This should have significant implications for speciation studies, which we are currently exploring.

Competitive binding of other metals by surface-immobilized Chromotrope 2B. We have also performed some preliminary studies on the effects of other metal cations on the determination of copper by electrodes modified with C2B. The electrodes were exposed to solutions containing copper at a concentration of $50 \mu M$

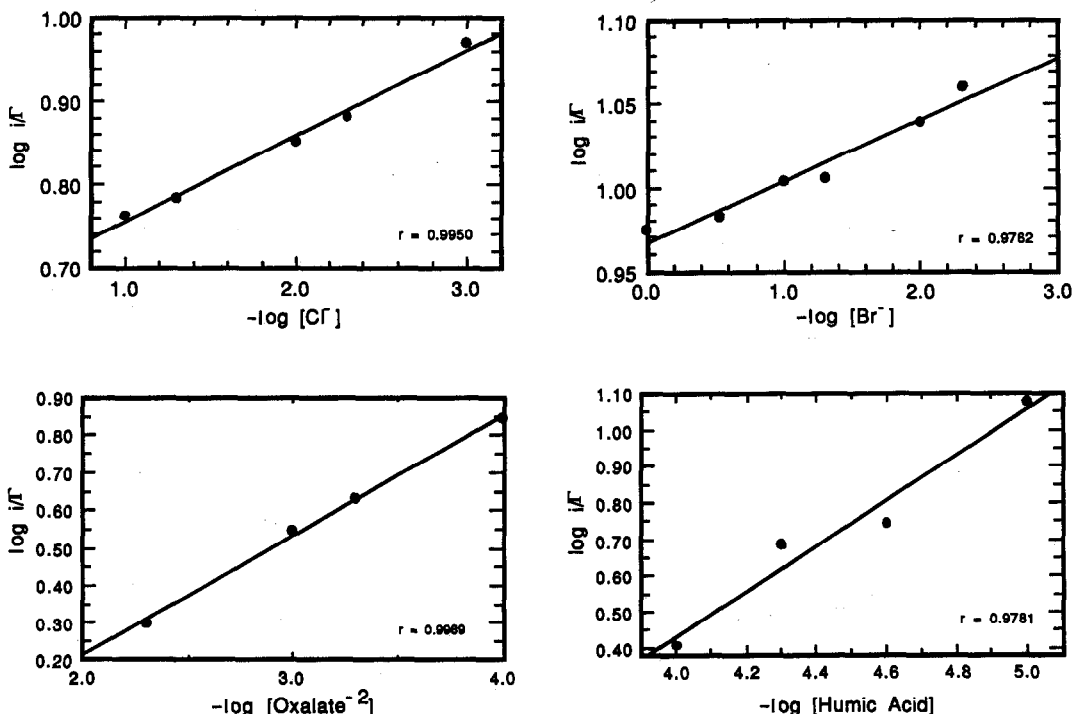


Fig. 3. Effects of competing ligands at various concentrations on the determination of copper at a solution concentration of $1 \times 10^{-5} M$ at electrodes modified with poly-[Ru(v-bpy)₃]²⁺ loaded with C2B.

Table 1. Effects of competing metal ions on the determination of copper* at electrodes modified with C2B

	[M]/[Cu]*	i_p , arbitrary units
M' = cobalt	0.0	5.55
	1.0	4.00
	5.0	3.90
M' = nickel	0.0	5.55
	0.2	2.73
	1.0	1.05

*[Cu] held constant at 50 μ M.

as well as either Co(II) or Ni(II) at various concentrations. The signal due to the immobilized C2B/Cu complex was then obtained. The results (Table 1) show that Ni(II) had a more dramatic effect on the signal than Co(II) did, which is consistent with the higher formation constant for the nickel complex. (The formation constants obtained in the literature were for Chromotrope 2R²⁹ and we have assumed that the trends in coordination strength are the same for the closely related C2B.) The lack of additional data on formation constants precludes any further analysis, but the trends are consistent with differences in the strength of coordination.

The presence of nickel gave rise to an additional redox response at -0.29 V. Thus, electrodes modified with C2B could be employed in the determination of nickel in solution.

CONCLUSIONS

We have demonstrated that electrodes modified with C2B can be employed in the determination of copper in solution at concentrations down to $7 \times 10^{-8}M$, with a wide dynamic range. The presence of competing ligands or other metal ions affects the analytical signal in proportion to the strength of coordination of the other ligands with copper ions or of other ions with the surface-immobilized C2B. The presence of competitive equilibria suggests that this analytical approach might be applicable to speciation studies, and this is currently under investigation.

Acknowledgements—This work was supported in part by the National Science Foundation. HDA is a recipient of a Presidential Young Investigator Award (1984–1989) and an A. P. Sloan Fellowship (1987–1991). SKC acknowledges support by the Korean Ministry of Education.

REFERENCES

1. R. W. Murray, in *Electroanalytical Chemistry*, A. J. Bard (ed.), Vol. 13, p. 191. Dekker, New York, 1984.
2. *Idem*, *Ann. Rev. Mater. Sci.*, 1984, **14**, 145.
3. *Idem*, *Acc. Chem. Res.*, 1980, **13**, 135.
4. L. R. Faulkner, *Chem. Eng. News*, 27 February 1982, 28.
5. H. D. Abruña, *Coord. Chem. Rev.*, 1988, **86**, 135.
6. *Idem*, in *Electroresponsive Molecular and Polymeric Systems*, T. A. Skotheim (ed.), p. 92. Dekker, New York, 1988.
7. M. Fujihira, in *Topics in Organic Chemistry*, A. J. Fry and W. R. Britton (eds.) p. 255. Plenum Press, New York, 1986.
8. R. W. Murray, A. G. Ewing and R. A. Durst, *Anal. Chem.*, 1987, **59**, 379A.
9. R. P. Baldwin, J.-K. Christensen and L. Kryger, *ibid.*, 1986, **58**, 1790.
10. S. V. Prabhu, R. P. Baldwin and L. Kryger, *ibid.*, 1987, **59**, 1074.
11. J. A. Cox and P. J. Kulesza, *J. Electroanal. Chem.*, 1983, **159**, 337.
12. J. Gardea-Torresdey, D. Darnall and J. Wang, *ibid.*, 1988, **252**, 197.
13. Y. Ikariyama and W. R. Heineman, *Anal. Chem.*, 1986, **58**, 1803.
14. J. A. Cox and B. K. Das, *ibid.*, 1985, **57**, 2739.
15. N. Oyama and F. C. Anson, *J. Electrochem. Soc.*, 1980, **127**, 247.
16. M. W. Espenscheid, A. R. Ghatak-Roy, R. B. Moore III, R. M. Penner, M. N. Szentirmay and C. R. Martin, *J. Chem. Soc. Faraday Trans. I*, 1986, **82**, 1051.
17. G. Nagy, G. A. Gerhardt, A. F. Oke, M. E. Rice, R. N. Adams, R. B. Moore III, M. N. Szentirmay and C. R. Martin, *J. Electroanal. Chem.*, 1985, **188**, 85.
18. A. R. Guadalupe and H. D. Abruña, *Anal. Chem.*, 1985, **57**, 142.
19. L. M. Wier, A. R. Guadalupe and H. D. Abruña, *ibid.*, 1985, **57**, 2009.
20. A. R. Guadalupe, L. M. Wier and H. D. Abruña, *Am. Lab.*, 1986, **18**, No. 8, 102.
21. L. L. McCracken, L. M. Wier and H. D. Abruña, *Anal. Lett.*, 1987, **20**, 1521.
22. H. C. Hurrell and H. D. Abruña, *Anal. Chem.*, 1988, **60**, 254.
23. K. K. Kasem and H. D. Abruña, *J. Electroanal. Chem.*, 1988, **242**, 87.
24. A. R. Guadalupe and H. D. Abruña, *Anal. Lett.*, 1986, **19**, 1613.
25. A. R. Guadalupe, S. S. Jhaveri, K. E. Lui and H. D. Abruña, *Anal. Chem.*, 1987, **59**, 2436.
26. S. K. Cha and H. D. Abruña, *ibid.*, 1990, **62**, 274.
27. H. D. Abruña, P. Denisevich, M. Umaña, T. J. Meyer and R. W. Murray, *J. Am. Chem. Soc.*, 1981, **103**, 1.
28. H. A. Laitinen and W. E. Harris, *Chemical Analysis*, 2nd Ed., McGraw-Hill, New York, 1975.
29. O. Prakash and S. P. Mushran, *Chim. Anal. Paris*, 1967, **49**, 473.

ANION-EXCLUDING POLYPYRROLE FILMS

M. FREUND, L. BODALBHAI and A. BRAJTER-TOTH*

Department of Chemistry, University of Florida, Gainesville, FL 32611, U.S.A.

(Received 27 July 1989. Accepted 12 September 1989)

Summary—A new method for modifying polypyrrole films is described. It involves complete oxidation of the film. The film produced is electronically non-conductive but ionically conductive, and has ion-selective properties based on the exclusion of anionic species. The effective pH within the film can be controlled by the choice of supporting electrolyte used during the oxidative treatment, without loss of selectivity. Cyclic voltammetry is used to demonstrate the effect of film pH on the rate of dopamine oxidation in a neutral supporting electrolyte.

Since the discovery of electrochemical polymerization of pyrrole at electrode surfaces,^{1,2} there has been considerable interest in the manipulation of polypyrrole (PPY) films to produce selective and catalytic surfaces for use as sensors. Because PPY films can be produced easily and with widely varying electrochemical characteristics, they have been the focus of several papers.³⁻⁸ Such films have been produced by electropolymerization of suitable *N*-substituted pyrroles,⁹⁻¹² by physically trapping catalysts,^{5,9} and by choosing counter-ions with desired characteristics.^{6,7}

In this study we report a new method for treating PPY to produce analytically useful films. It involves irreversibly oxidizing the films, which changes their characteristics, according to the supporting electrolyte used in the treatment. It has been reported that oxidation of PPY films at potentials $> +1.0$ V *vs.* SCE results in loss of the electrical conductivity of the film.^{13,14} This irreversible oxidation is attributed to nucleophilic attack by anions and/or water on the cationic pyrrole nuclei in the polymer, resulting in loss of conjugation and hence conductivity.¹³ Redox reactions at the underlying electrode still occur in spite of the loss of conductivity, contrary to what has been reported.¹⁴ This indicates that the film is porous enough to allow diffusion of analyte and electrolyte to the underlying electrode surface. The response of the films depends on the charge of the redox couple. The cyclic voltammetry responses of anionic redox couples are suppressed, whereas those of neutral and cationic redox couples are not.

The pH of the supporting electrolyte used during preparation of the film determines the effective pH within the film, as well as the peak shifts in oxidation of pH-sensitive biological molecules. For example, the use of basic electrolytes produces films that give greater reversibility in the oxidation of dopamine in pH 7 phosphate buffer.

This new treatment can produce ion-selective PPY films, the effect of which on pH-sensitive responses of biological molecules can be controlled by the method of preparation of the film. Development of such surfaces is currently of considerable interest.¹⁵⁻¹⁷ In this paper, we discuss the effects of the treatment on the responses of ferricyanide and small biological molecules involved in 2-electron 2-proton oxidations, and show how the reversibility of these redox couples can be manipulated by choice of the supporting electrolyte used in preparation of the film.

EXPERIMENTAL

Reagents and methods

All chemicals were reagent grade, and used as received. Pyrrole, acetonitrile (MeCN), and tetrabutylammonium perchlorate (TBAP) were from Kodak. Potassium ferricyanide, ascorbic acid, and disodium hydrogen phosphate and trisodium phosphate were from Mallinckrodt. Potassium chloride, sodium dihydrogen phosphate and sodium hydroxide were from Fisher, and dopamine was from Sigma.

All electrochemical experiments were performed with a Bioanalytical Systems Analyzer

*Author for correspondence.

(BAS-100) at $25 \pm 2^\circ$. A saturated calomel electrode (SCE) was used as a reference, a 1-cm² platinum foil as an auxiliary electrode, and glassy carbon was used to make the working electrode, either alone or coated with PPY films. Glassy-carbon electrodes (GCE) freshly polished with grade B γ -alumina (Fisher) on an Alpha A cloth (Mark V Laboratory) followed by ultrasonication for 5 min were used for each electrochemical measurement, and for the production of each PPY film. The GCE electrode areas were determined by chronocoulometry. The potential was stepped from +0.400 to +0.100 V *vs.* SCE in 1mM potassium ferricyanide (1M KCl, $D_{ox} = 7.63 \times 10^{-6}$ cm²/sec), with a pulse width of 500 msec. Typical electrode areas were *ca.* 0.068 cm². All solutions were deoxygenated by bubbling nitrogen through them for 5 min.

Preparation of polypyrrole films

Polypyrrole electrodes were made by electropolymerizing pyrrole on polished glassy carbon-electrodes at +0.950 V *vs.* Ag.³ The solution used for polymerization was 50mM pyrrole and 0.1M TBAP in MeCN. The film thickness was controlled by measuring the charge passed during the electropolymerization. Film thicknesses of 0.1 μ m were deposited by passage of 24 mC per cm² of electrode area.³ The amount of charge passed was always within 2% of the required amount calculated from the electrode area. The electrodes were then washed with distilled water and allowed to dry.

The PPY films were then cycled ten times, in aqueous solution, between +0.900 and -0.300 V *vs.* SCE. The supporting electrolytes used were all 0.5M and the scan rate was 20 mV/sec. The electrodes were finally washed with distilled water.

RESULTS AND DISCUSSION

When 0.1- μ m thick perchlorate-doped PPY films were oxidized in the presence of 0.5M sodium perchlorate by cycling as described above, the background signals obtained in 0.5M phosphate buffer (pH 7) were much smaller than those obtained with untreated polypyrrole (see Fig. 1). During oxidation of the PPY film, it is likely that the ratio of pyrrole units to perchlorate decreases, which may convert the PPY film from an electronic/ionic conductor¹⁸ into a non-electronic but purely ionic conductor. The decreased back-

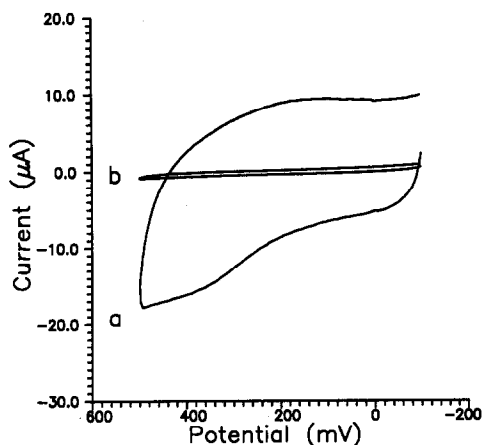


Fig. 1. Cyclic voltammograms (20 mV/sec) of (a) an untreated PY and (b) a sodium perchlorate treated PPY film in 0.5M phosphate buffer, pH 7. Areas of the GC substrate are (a) 0.0696 ± 0.0009 and (b) 0.0612 ± 0.0016 cm².

ground, which is comparable to that obtained with a glassy-carbon electrode, supports this conclusion.

The response of ferricyanide on the new film formed by oxidative treatment is suppressed relative to that on glassy carbon or on untreated PPY. Figure 2 shows voltammograms of 1mM ferricyanide in 0.5M phosphate buffer (pH 7) obtained with a GCE and the treated PPY film; in both cases the geometric electrode areas were approximately the same. The response of ascorbic acid in pH 7 phosphate buffer is also suppressed at the treated PPY electrode, in accord with the ferricyanide response, since the ascorbic acid ($pK_a = 4.2$)¹⁹ will be present as ascorbate at pH 7. The oxidation of dopamine, which is positively charged at pH 7,⁸ results in a

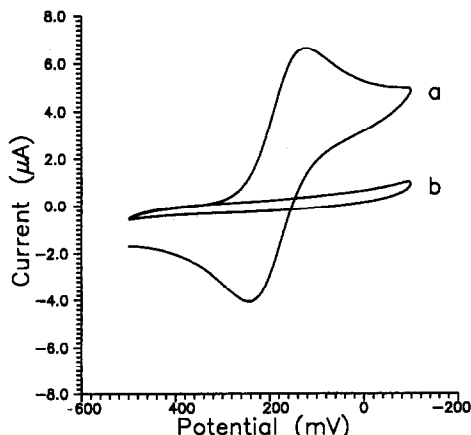


Fig. 2. Cyclic voltammograms (20 mV/sec) of 1mM ferricyanide in 0.5M phosphate buffer, pH 7, on (a) a GCE electrode and (b) a sodium perchlorate treated (pH 5.8) PPY film. Geometric areas of the GC substrate are (a) 0.0794 ± 0.0004 and (b) 0.0612 ± 0.0016 cm².

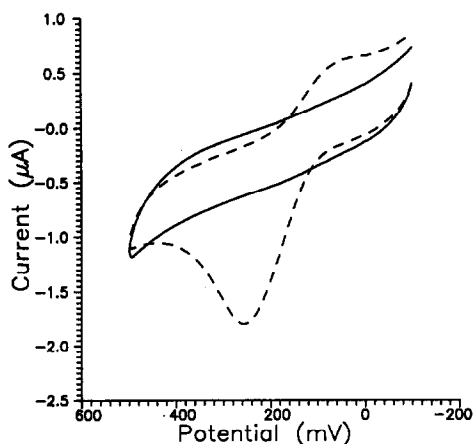


Fig. 3. Cyclic voltammograms (20 mV/sec) of 1mM ascorbic acid (solid line) and 1mM dopamine (dashed line) in 0.5M phosphate buffer (pH 7) obtained with a sodium perchlorate treated (pH 5.8) PPY film. Geometric area of the GC substrate is $0.0612 \pm 0.0016 \text{ cm}^2$.

significantly higher faradaic response than that of the two negatively-charged species. Figure 3 shows the responses of 1mM ascorbic acid and 1mM dopamine in 0.5M phosphate buffer (pH 7) on the same electrode, and illustrates the effect of the charge of the redox couple.

To determine whether this effect depended on the anion present in the supporting electrolyte during film preparation, PPY electrodes were treated in several different supporting electrolytes, as described in the experimental section, because the electrical conductivity of PPY films is known to be dependent on the anion present during the electropolymerization.^{20,21} The electrolytes used included 0.5M sodium hydroxide (pH 13.3), sodium phosphate (pH 12.7), sodium chloride (pH 6.5), sodium perchlorate (pH 5.8), and sodium dihydrogen phosphate (pH 4.4) (Table 1). In every case the anion-response was suppressed, irrespective of the supporting electrolyte used. This suggests that a PPY film with increased electronegative

character may be produced, resulting in reduction of the faradaic current produced by anionic redox species.

The response of positively charged analytes on treated PPY films is lower than that observed on GC and depends on the electrolyte anion used in the treatment (Table 1). This difference in response suggests that the effective electrode area is decreased by the presence of the film. As mentioned above, this could result from the formation of ionically conductive but electronically non-conductive films of fairly low porosity.

The reversibility of the oxidation of dopamine depends on the pH of the supporting electrolyte used in the oxidation of the film. Films treated in basic supporting electrolytes have surfaces which increase the reversibility of dopamine oxidation. Several electrodes were made by treating PPY films in the presence of 0.5M sodium hydroxide (pH 13.3), trisodium phosphate (pH 12.7), sodium chloride (pH 6.5), sodium perchlorate (pH 5.8), or sodium dihydrogen phosphate (pH 4.4). Figure 4 shows the shift in anodic peak potential for the oxidation of 1mM dopamine in 0.5M phosphate buffer (pH 7) on films prepared in the different supporting electrolytes. At low pH, the pH-dependence of the anodic peak potential of dopamine is linear and has a slope of 64 mV/pH, in fair agreement with that expected from the Nernst equation for a reaction involving a $2e^- - 2H^+$ transfer. The pK_a of dopamine is 8.92,²² and the oxidation of dopamine

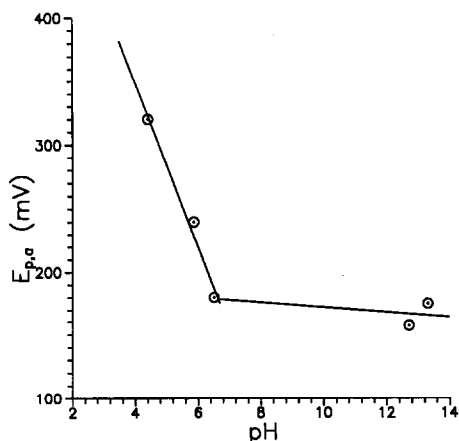


Fig. 4. Plot of anodic peak potential for the oxidation of 1mM dopamine in 0.5M phosphate buffer (pH 7) as a function of pH of the electrolyte used during treatment of the PPY film. Each point represents a different supporting electrolyte used during treatment (see text). Scan rate 20 mV/sec.

Table 1. Effect of supporting electrolyte on response for 1mM dopamine in 0.5M phosphate buffer (pH 7); scan rate 20 mV/sec

Electrolyte	pH	$\mu A.l.cm^{-2}.mmole^{-1}$
NaH ₂ PO ₄	4.4	36.75
NaClO ₄	5.8	17.01
NaCl	6.5	31.5
Na ₃ PO ₄	12.7	54.1
NaOH	13.3	141.7
GCE	—	169.1

becomes pH-independent as the pH of the film increases, as shown in Fig. 4.

The response observed for dopamine is determined by the type of film used and suggests that the internal pH of the film is controlled by the pH of the electrolyte used during oxidation, and controls the response, irrespective of the bulk solution pH. Typical responses for dopamine in 0.5M phosphate buffer (pH 7) at two electrodes of different effective pH are shown in Fig. 5.

Change in the internal pH of the film can lead to an improvement in sensitivity, which is not simply a result of improved electrochemical kinetics of the analyte. Table 1 shows peak currents, normalized for concentration and electrode area, for the oxidation of 1mM dopamine in 0.5M phosphate buffer (pH 7). Films oxidized in 0.5M sodium hydroxide (pH 13.3) yielded the largest and most reversible responses, which were close to those obtained with unmodified GC, indicating that diffusion of dopamine through the film must be fast under these conditions. No peaks were observed for ferricyanide or ascorbate, as expected from the difference in response to cations and anions, already mentioned. After some use (10 complete scans), the magnitude of the response decreased by 23% but a well defined current-potential curve was maintained, with no shifts in peak potentials. This was contrary to the observed poisoning of untreated GC by dopamine oxidation products, which resulted in anodic peak shifts and a decrease in oxidation current. This poisoning effect of catecholamines is common with solid electrodes.²³ Therefore, this reduction

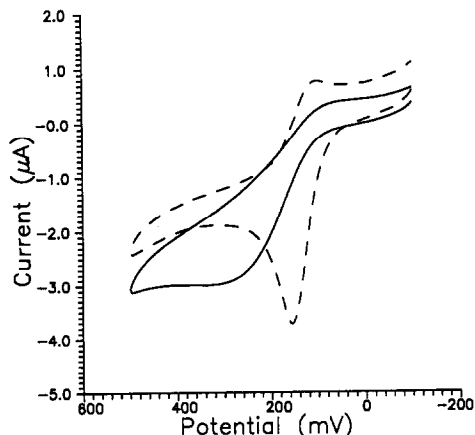


Fig. 5. Cyclic voltammograms (20 mV/sec) of 1mM dopamine in 0.5M phosphate buffer (pH 7) on a PPY electrode treated in 0.5M NaH_2PO_4 (solid line) and in 0.5M Na_3PO_4 (dashed line). Geometric areas of the GC substrate are 0.0676 ± 0.0006 and 0.0618 ± 0.0008 cm^2 respectively.

in response could be a result of changes in film structure, and in turn porosity, over long periods of use.

A plot of $\log i_{p,a}$ vs. $\log v$ (scan rate) was made for the oxidation of 1mM dopamine in 0.5M phosphate buffer (pH 7) at a film oxidized in the presence of 0.5M sodium hydroxide, to determine whether the responses were diffusion-controlled. The plot had a slope of 0.499 ± 0.004 with a correlation coefficient (R^2) of 0.9998. For oxidation at an untreated GCE the slope was 0.460 ± 0.054 ($R^2 = 0.9867$). The GCE was resurfaced and ultrasonicated between each measurement. A slope of 0.5 indicates that the redox process is diffusion-controlled.²⁴

The results thus far obtained indicate that the anions present in the supporting electrolyte during oxidation of the film may in fact control the structure and chemical properties of the resulting PPY film. More experiments are necessary to elucidate the film structure. Further experiments are currently under way to quantify the responses of several redox couples on these surfaces. Other applications of these films are also being explored.

Acknowledgements—This work was supported, in part, by grants from the National Institutes of Health (Grant No. GM 35451-02) and the Interdisciplinary Center for Biotechnology Research at the University of Florida.

REFERENCES

1. A. F. Diaz, K. K. Kanazawa and G. P. Gardini, *J. Chem. Soc. Chem. Commun.*, 1979, 635.
2. K. K. Kanazawa, A. F. Diaz, R. H. Geiss, W. D. Gill, J. F. Kwak, A. Logan, A. F. Rabolt and G. B. Street, *ibid.*, 1979, 854.
3. R. A. Bull, F. F. Fan and A. J. Bard, *J. Electrochem. Soc.*, 1982, **129**, 1009.
4. F. F. Fan and A. J. Bard, *ibid.*, 1986, **133**, 301.
5. F. Mizutani, S. Iijima, Y. Tanabe and K. Tsuda, *Synth. Meth.*, 1987, **18**, 111.
6. G. G. Wallace and Y. P. Lin, *J. Electroanal. Chem.*, 1988, **247**, 145.
7. G. Lian and S. Dong, *ibid.*, 1989, **260**, 127.
8. R. A. Saraceno, J. G. Pack and A. G. Ewing, *ibid.*, 1986, **197**, 265.
9. N. C. Foulds and C. R. Lowe, *Anal. Chem.*, 1988, **60**, 2473.
10. A. J. Downard, N. A. Surridge, T. J. Meyer, S. Cosnier, A. Deronzier and J. C. Moutet, *J. Electroanal. Chem.*, 1988, **246**, 321.
11. P. Moisy, F. Bedioui, Y. Robin and J. Devynck, *ibid.*, 1988, **250**, 191.
12. C. P. Andrieux and P. Audebert, *ibid.*, 1989, **261**, 443.
13. S. Asavapiryanont, G. K. Chandler, G. A. Gunawardena and D. Pletcher, *ibid.*, 1984, **177**, 229.
14. A. Haimerl and A. Merz, *ibid.*, 1987, **220**, 55.
15. M. Freund and A. Brajter-Toth, *Anal. Chem.*, 1989, **61**, 1048.

16. K. McKenna and A. Brajter-Toth, *ibid.*, 1987, **59**, 954.
17. L. A. Coury, Jr., E. M. Birch and W. R. Heineman, *ibid.*, 1988, **60**, 553.
18. P. Burgmayer and R. W. Murray, *Handbook of Conducting Polymers*, Vol. 1, pp. 507-523. Dekker, New York, 1986.
19. S. Steenken and P. Neta, *J. Phys. Chem.*, 1979, **83**, 1134.
20. S. Kuwabata, K. Okamoto, O. Ikeda and H. Yoneyama, *Synth. Meth.*, 1987, **18**, 101.
21. M. Yamaura, T. Hagiwara and K. Iwata, *ibid.*, 1988, **26**, 209.
22. M. D. Hawley, S. V. Tatawawadi, S. Pierkarski and R. N. Adams, *J. Am. Chem. Soc.*, 1967, **89**, 447.
23. R. F. Lane and A. T. Hubbard, *Anal. Chem.*, 1976, **48**, 1287.
24. A. J. Bard and L. R. Faulkner, *Electrochemical Methods*, p. 718. Wiley, New York, 1980.

PRECONCENTRATION AND DETERMINATION OF BISMUTH(III) AT A CHEMICALLY MODIFIED ELECTRODE CONTAINING 1-(2-PYRIDYLAZO)-2-NAPHTHOL

KONG LING DONG*, LARS KRYGER†, JOAN K. CHRISTENSEN and KARSTEN N. THOMSEN
Department of Chemistry, Aarhus University, Langelandsgade 140, DK-8000 Aarhus C, Denmark

(Received 9 August 1990. Accepted 7 September 1990)

Summary—A chemically modified electrode (CME) containing 1-(2-pyridylazo)-2-naphthol is evaluated for its ability to preconcentrate bismuth(III) prior to quantification by voltammetry. The CME approach is shown to be sufficiently sensitive for sub-nanomolar concentrations to be determinable after chemical deposition for 60 sec. Further, when the bismuth is deposited from iodide-containing sulphuric acid media, the discrimination against interference by copper(II) is significantly better than that obtained with conventional stripping analysis. The results obtained for Bi(III) in an NBS reference solution agree well with the recommended value.

Stripping voltammetry is a sensitive approach to the determination of traces of Bi(III) in aqueous media.^{1,2} Nanomolar concentrations, for example, can be determined after just a few minutes of electrolytic deposition at a mercury film electrode.³ However, the advantage of the highly sensitive stripping technique is often overshadowed by difficulties encountered in practical applications. One problem is that the diffusion-controlled electro-reduction of Bi(III) takes place at a potential which is considerably more negative than the stripping potential. This implies that Cu(II), which behaves more reversibly, and is electroactive at near the Bi(III) reduction potential, is likely to interfere. In addition, since amalgamated Bi(III) is stripped at near the mercury oxidation potential, a significant current due to oxidation of the electrode material is typically superimposed on the Bi(III) stripping signal. In this work we survey a different technique for determination of traces of Bi(III). Like conventional stripping methods, the technique includes a deposition step and a voltammetric measurement step. The difference is that the analyte is accumulated by non-electrochemical attachment to a chemically modified electrode (CME).⁴⁻⁶ The CME is based

on carbon paste and a reagent with chemical affinity for Bi(III). In most respects, the analytical approach is analogous to that for nickel(II),^{7,8} and Cu(I),⁹ which were determined with carbon-paste CMEs containing highly selective modifiers (dimethylglyoxime and 2,9-dimethyl-1,10-phenanthroline, respectively). However, no selective reagent for Bi(III) is available. Instead, the CMEs are constructed from graphite paste containing 1-(2-pyridylazo)-2-naphthol (PAN). PAN is a commercially available reagent for solvent extraction of metal chelates, and is used in many extractive procedures for a wide variety of metal species.¹⁰ PAN is non-selective, but its preference for extraction of the individual metals can be controlled through the pH of the metal solution, and the concentration of a competing water-soluble reagent, such as iodide. A study of this has revealed that chemical deposition and voltammetric determination of Bi(III) is feasible. Furthermore, subnanomolar concentrations can be determined following chemical deposition for 60 sec from dilute sulphuric acid media. Equally important, when excess of iodide is added to the deposition medium, the selectivity for Bi(III) is such that the signal for 53nM Bi(III) is not affected by the presence of 0.53mM of Cu(II). Moreover, the CME results for Bi(III) in a well defined reference solution, containing twenty different metal species, agree well with the recommended concentration.

*Present address: Water Pollution Control Research Centre, Harbin Architectural and Civil Engineering Institute, 144 Dazhi Street, Harbin, People's Republic of China.

†Author for correspondence.

EXPERIMENTAL

Reagents

Mineral acids of suprapur (Merck) grade and triply distilled water were used throughout the study. Standard solutions of metal ions were prepared by dissolving analytical grade AgNO_3 , $\text{Bi}(\text{NO}_3)_3 \cdot 5\text{H}_2\text{O}$, $\text{CoCl}_2 \cdot 6\text{H}_2\text{O}$, $\text{CuSO}_4 \cdot 5\text{H}_2\text{O}$, Fe_2O_3 , $\text{Pb}(\text{NO}_3)_2$, $\text{NiCl}_2 \cdot 6\text{H}_2\text{O}$, $\text{ZnSO}_4 \cdot 7\text{H}_2\text{O}$ and $\text{SnCl}_2 \cdot 2\text{H}_2\text{O}$ in dilute H_2SO_4 medium (pH 0.75). Graphite pastes were prepared with PAN (Merck 7531), graphite powder (*purum*), silicone oil (Merck 9762, type 550), and anhydrous ethyl alcohol. The reference sample Trace Elements in Water (NBS 1643b) was obtained from National Bureau of Standards, Washington, D.C. All solutions were kept in polyethylene bottles.

Graphite-paste electrodes

PAN/graphite mixtures (29, 38, 44, 46, and 50% PAN w/w) were prepared in the following fashion. About 3 g of PAN was accurately weighed, and warm ($\sim 45^\circ$) anhydrous ethyl alcohol was added slowly, until complete dissolution was achieved. The warm solution was placed on a hot-plate ($\sim 50^\circ$), the appropriate weight of graphite powder was added, and the resulting slurry stirred until a dry PAN-coated graphite powder was obtained. Plain (unmodified) and modified carbon pastes were prepared by hand-mixing 5 g of graphite or graphite/PAN mixture with 2 ml of silicone oil. Plain carbon paste electrodes (PCPE) and modified carbon paste electrodes were prepared from the pastes by a technique which has been described elsewhere.⁷

Table 1. Voltammetric waveforms

Linear sweep cyclic voltammetry
Initial potential: +1000 mV
Switching potential: -100 mV
Sweep rate: 40 mV/sec
Delay at switching potential: 60 sec
Programmed pulse stripping voltammetry
Initial potential: -100 mV
Delay at initial potential: 60 or 4 sec
Waveform generated by repetition of the sequence:
(a) 2 mV potential step
(b) 1 msec delay
(c) addition of the results of 40 A/D conversions of the cell current (100 μsec per conversion)
(d) 25 mV potential step
(e) 1 msec delay
(f) addition of the results of 40 A/D conversions of the cell current (100 μsec per conversion)
(g) -25 mV potential step
(h) current computed as the difference of (f) and (c)

Apparatus

Voltammetric measurements were made by using a computerized analyser.¹¹ The cells used for chemical deposition and for voltammetric measurements were 50-ml lidded polyethylene beakers, in which solutions were stirred from below by means of magnetic stirrer bars. In addition to the beaker and the carbon-paste working electrode, the voltammetric assembly included a saturated calomel reference electrode (Radiometer K401) and a counter-electrode (a platinum wire, 1 cm long and 0.5 cm thick). Prior to use, all bottles and beakers were soaked in 2M nitric acid for 7 days, washed three times with triply distilled water, and finally kept in 1M sulphuric acid. The solutions used for chemical deposition and for voltammetric measurements were freed from dissolved oxygen by passage of argon for at least 60 sec.

Procedure

First, the Bi(III) was chemically deposited on a CME (or PCPE), simply by immersing the electrode for a specified period of time in 20 ml of the deposition solution. Next, the electrode was transferred to the electrochemical cell and connected to the working electrode terminal of the potentiostat and the current *vs.* potential curve was recorded. Finally the electrode surface was regenerated.

Several variations of the basic procedure were tested. The chemical deposition was performed from solutions of Bi(III) (and potentially interfering metals) in 1M potassium sulphate, 0.1M hydrochloric acid, dilute sulphuric acid (pH 1.50, 1.32, 0.85, 0.75 and 0.62) and 5mM potassium iodide in dilute sulphuric acid (pH 0.75). The voltammetric measurement was made with dilute sulphuric acid (pH 0.75) in the electrochemical cell. The voltammetric waveforms are specified in Table 1.

Three different methods of regeneration of the CME surface were tested: polarization of the CME at +700 mV for 120 sec, exposure of the disconnected CME for 120 sec to $10^{-2}M$ EDTA in borax medium (pH 9.0), and scraping off the exposed CME surface and polishing the new surface on paper until it was shiny.

RESULTS AND DISCUSSION

The cyclic voltamperograms obtained after exposure of the unmodified electrodes for 60 sec

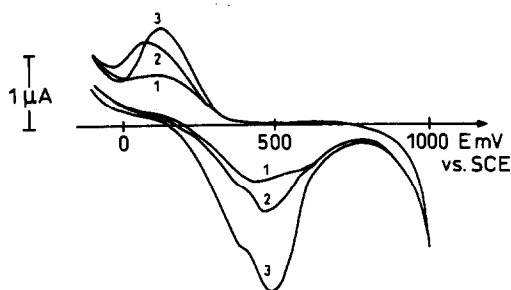


Fig. 1. Linear sweep cyclic voltamperograms recorded after 10-sec CME exposures to the blank sulphuric acid medium (1) and to this medium spiked with 2×10^{-7} (2) and $10^{-6}M$ (3) Bi(III).

to $1 \mu M$ Bi(III) in neutral to acidic media ($1M$ K_2SO_4 , $0.1M$ HCl , and $0.1M$ H_2SO_4) were featureless. Thus there were no signs of attachment of Bi(III) to the plain carbon paste. All the modified pastes, on the other hand, accumulated Bi(III), but their suitability as electrode materials depended on the modifier loading. The highest sensitivity was observed with CMEs based on the 38% (w/w) PAN/graphite mixture. Therefore such CMEs were used in all subsequent work. The experiments showed that Bi(III) could be deposited both from $1M$ potassium sulphate and from $0.1M$ hydrochloric acid. However, the highest sensitivity was observed for deposition from dilute sulphuric acid media. Figure 1 shows the cyclic voltamperograms recorded after a 10-sec exposure of the CME to a blank sulphuric acid medium (pH 0.75) (1), and to this medium spiked with $2 \times 10^{-7}M$ (2) and $10^{-6}M$ (3) Bi(III). Clearly, electroactivity was observed both for the unspiked and the spiked sulphuric acid medium. Furthermore, the oxidative voltammetric signal obtained for the blank medium overlapped the signals recorded after spiking with Bi(III). This blank response was attributed to metal impurities in the sulphuric acid medium. Such impurities—especially Co(II), Cu(II), Fe(III), Ni(II), and Sn(II)—can be extracted by PAN from acidic media,¹⁰ and CME experiments revealed

that all five species could be accumulated and exhibit electroactivity at potentials ranging from 300 to 500 mV vs. SCE. The CME-sensitivity for Ni(II) was almost as high as that for Bi(III), but the sensitivities for Cu(II), Co(II), Fe(III), and Sn(II) were about 25, 48, 28, and 16%, respectively, of that for Bi(III). Thus all five metal species presented a potential source of interference in the determination of traces of Bi(III). However, when iodide was added to the sulphuric acid medium, the blank signal decreased drastically, and the selectivity for Bi(III) was considerably improved. The sensitivity and selectivity for Bi(III) depended somewhat on pH and the concentration of potassium iodide. However, at pH 0.75 and $5mM$ iodide in the sulphuric acid medium the sensitivities for Co(II), Cu(II), Fe(III), Ni(II), and Sn(II) were all below 1% of the sensitivity for Bi(III). The most efficient CME regeneration was achieved by squeezing out a 2-mm column of the carbon paste, scraping off the excess, and polishing the electrode surface on paper. This procedure left no evidence of previous CME-exposure to Bi(III). Both the electrochemical (positive polarization), and the chemical (exposure to EDTA) treatment of the CME-surface removed part of the analyte deposit, but neither was satisfactory for repeated determinations of Bi(III) at sub-micromolar concentration levels. Table 2 summarizes the recommended experimental conditions.

These experimental conditions allowed the determination of ultratrace concentrations of Bi(III), e.g., in the unspiked deposition medium. In fact, a well defined programmed pulse voltammetric Bi(III) signal of 150 nA was observed after exposure of the CME to the blank medium for 60 sec. Furthermore, when the blank deposition medium was spiked with $10^{-10}M$ Bi(III), the mean and standard deviation of the signals recorded in 11 consecutive deposition/voltage scanning experiments were 450 and 55 nA, respectively. Thus the reagent blank concentration was lower than $10^{-10}M$, and the limit of detection for a 60-sec chemical deposition was of the order of $10^{-10}M$. The sensitivity of the CME procedure increased with the duration of chemical deposition. For instance, with $10^{-7}M$ Bi(III) in the deposition solution, the analytical signal increased linearly (correlation coefficient >0.99) with deposition time from 4 to 120 sec. The signal vs. concentration behaviour was studied with four CMEs and chemical deposition for 60 sec. In all four

Table 2. CME procedure for Bi(III); recommended experimental conditions

CME composition	5 g of PAN/graphite mixture (38% w/w) + 2 ml of silicone oil
Medium used for chemical deposition	Dilute H_2SO_4 (pH 0.75) spiked with $5mM$ KI
Medium used for voltammetric analysis	Dilute H_2SO_4 (pH 0.75)
CME surface regeneration	Manual

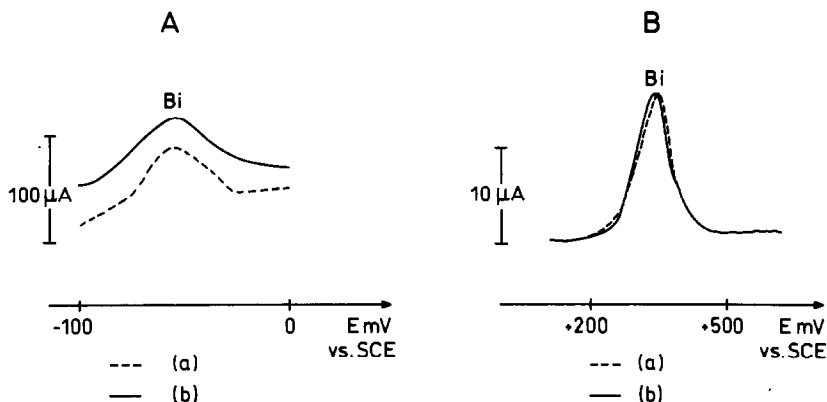


Fig. 2. A: Programmed pulse stripping voltamperograms recorded by using a thin mercury film electrode. Electrolytic deposition for 60 sec at -100 mV *vs.* SCE. Medium: NBS-SRM 1643 b (curve a), NBS-SRM 1643 b spiked with $25 \mu\text{M}$ Cu(II). B: Programmed pulse stripping voltamperograms recorded by using the CME. Chemical deposition for 60 sec. Medium: NBS-SRM 1643 b (curve a), NBS-SRM 1643 b spiked with $600 \mu\text{M}$ Cu(II).

cases the blank deposition medium could be spiked with more than 10^{-8}M Bi(III) before the signal *vs.* concentration plot became non-linear (correlation coefficient < 0.99). Linear behaviour was also observed from 10^{-9} to 10^{-7}M , with chemical deposition for 4 sec. Thus standard addition afforded a viable means of quantification.

Compared with the conventional stripping procedure, which is based on electrolytic deposition, the CME procedure discriminated well against interference from Cu(II). This aspect was demonstrated by experiments in which the influence of Cu(II) additions on the Bi(III) signal was studied by the conventional stripping procedure and the CME procedure. The solution investigated was the NBS 1643 b reference solution Trace Elements in Water. According to NBS, this solution contains 53nM Bi, 345nM Cu(II), and 18 other known metal species. In addition, the solution contains 0.5M nitric acid. For the present purpose a 20-ml volume of the solution was spiked with 5mM potassium iodide, and further acidified (to pH 0.75) by addition of a few drops of concentrated sulphuric acid.

The conventional stripping analyses revealed that the deposition of Bi(III) required a potential which was equal to or more negative than that used in the CME procedure for reduction of the Bi-PAN deposit (-100 mV *vs.* SCE).

After electrolysis at this potential Cu(II) did not produce a distinct stripping peak. However, the experiments showed that Cu(II) was in fact deposited, and that its subsequent stripping gave rise to currents at the Bi(III) stripping peak potential. This effect is demonstrated in Fig. 2A,

which shows the stripping voltamperograms obtained following 60-sec electrolytic deposition from the NBS water (a) and from the NBS water spiked with $25 \mu\text{M}$ Cu(II) (b).

In contrast, the analytical CME response was insensitive to addition of Cu(II). As shown in Fig. 2B, the Bi response obtained from the unspiked sample (a) was not significantly different from that obtained after addition of $600 \mu\text{M}$ Cu(II) (b).

In order to study the CME-performance in a practical analytical situation, the CME-procedure was used to determine traces of Bi(III) in tap water and in NBS-SRM 1643 b solution. In the latter determination, quantitative results were obtained first by a standard-additions approach, then from a calibration graph obtained by CME-analysis of standard Bi(III) solutions. The results are shown in Table 3. Clearly, despite manual regeneration of the CME the results obtained were mutually consistent. Furthermore, the results for the NBS water agreed well with the NBS recommended value. The use of calibration plots requires a selective sensing device. Thus the agreement of the calibration and standard-addition results gave additional evidence of a selective analytical approach.

We conclude that the CME approach is sufficiently sensitive for nanomolar concentrations of Bi(III) to be determined after chemical deposition for 60 sec.

The recommended regeneration method requires manual skill on the part of the experimenter. However, this disadvantage is overshadowed by the discrimination against Cu(II), which is considerably higher than that obtained by using electrolytic analyte deposition.

Table 3. CME analysis of water samples

Sample*	Bismuth concentration found, nM	Mean concentration found, nM	Recommended concentration, nM
NBS-SRM 1643 b	52†	51	53
	44†		
	51†		
	57†		
Traces Elements in Water	53§	48	
	44§		
	48§		
Tap water	75§	79	
	83§		

*Acidified to pH 0.75 with concentrated H₂SO₄ and spiked with 5mM KI.

†Standard-additions method.

§Calibration method,

Acknowledgements—The authors wish to thank Richard P. Baldwin for useful discussions and Anne-Lise Mikkelsen for typing the manuscript.

REFERENCES

1. J. Wang, *Stripping Analysis*, VCH, Deerfield Beach, 1985.
2. G. Henze and R. Neeb, *Elektrochemische Analytik*, Springer, Heidelberg, 1986.
3. T. M. Florence, *J. Electroanal. Chem.*, 1974, **49**, 255.
4. R. W. Murray, in *Electroanalytical Chemistry*, A. J. Bard (ed.), Vol. 13A, pp. 191–368. Dekker, New York, 1984.
5. L. R. Faulkner, *Chem. Eng. News*, 27 February 1984, p. 28.
6. R. W. Murray, A. G. Ewing and R. A. Durst, *Anal. Chem.*, 1987, **59**, 379A.
7. R. P. Baldwin, J. K. Christensen and L. Kryger, *ibid.*, 1986, **58**, 1790.
8. K. N. Thomsen, L. Kryger and R. P. Baldwin, *ibid.*, 1988, **60**, 151.
9. S. V. Prabhu, R. P. Baldwin and L. Kryger, *ibid.*, 1987, **59**, 1074.
10. J. Stary, *The Solvent Extraction of Metal Chelates*, Pergamon Press, Oxford, 1964.
11. K. N. Thomsen, H. J. Skov and L. Kryger, *Anal. Chim. Acta*, 1989, **219**, 105.

AMPEROMETRIC BIOSENSORS FOR GLUCOSE BASED ON CARBON PASTE MODIFIED ELECTRODES

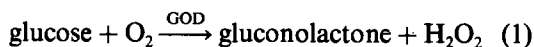
A. AMINE, J.-M. KAUFFMANN and G. J. PATRIARCHE*

Université Libre de Bruxelles, Institut de Pharmacie, Campus Plaine, CP 205/6,
Bd. du Triomphe, 1050 Bruxelles, Belgium

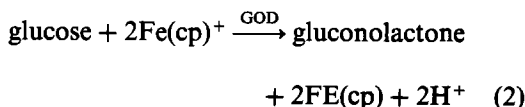
(Received 26 October 1989. Accepted 6 February 1990)

Summary—The modification of carbon-paste electrodes by incorporation of the enzyme glucose oxidase (GOD) is described. The resulting probes can be operated as amperometric glucose sensors in the presence or absence of a mediator (1,1'-dimethylferrocene) mixed into the paste. Extended linear calibration ranges have been obtained up to 90 and 50mM glucose respectively. The electrode responses were rapid, reaching steady-state values within 30–40 sec. Advantages of using a GOD–paste formulation are suggested. Plasma glucose assays were correlated with spectrophotometric determinations based on glucose oxidase ($y = 1.07x - 0.16$, $r = 0.973$, $n = 17$).

The characteristics and performances of enzyme-based electrochemical sensors for glucose measurements have been extensively studied and reviewed.¹⁻³ Selectivity, extended linearity and short response times are generally regarded as the main criteria for the applicability of glucose probes in "real sample" analysis. Amperometric detection systems employing glucose oxidase (GOD) as a natural catalyst have mainly been developed.



Non-mediated and redox-mediated systems can be considered for construction of glucose sensors. The former monitor either oxygen consumption or hydrogen peroxide production, or the electrochemical behavior of the two FADH₂ redox centers of the enzyme.⁴ The mediated biosensors generally couple small electron-carriers with redox proteins to facilitate electron transfer between the enzyme and the electrode material. Sensors based on the ferrocene/ferricinium couple have been shown to be quite useful in this respect.



The ferricinium ion [Fe(cp)⁺] competes favorably with the natural mediator oxygen to oxidize the reduced GOD. The reoxidation of the

reduced ferricinium [Fe(cp)] is monitored at the electrode at low potential (+160 mV vs. SCE) to minimize interferences. These devices require close proximity of the mediator to the electrode surface and the enzyme redox centers or its rapid diffusion between them. Several recent strategies, which combine GOD and mediator immobilization on or in the electrode material have been reported.^{5,6} The enzyme GOD may be entrapped in a thin ferrocene-containing polymer film electropolymerized onto the electrode⁵ or it can be incorporated into a carbon-paste matrix (graphite particles in liquid paraffin) in the presence of a ferrocene–polysiloxane backbone.⁶ There has been a growing interest in incorporating enzymes⁷⁻⁹ or mediators⁹⁻¹³ into carbon-paste electrodes (CPE) to enhance mechanical and electrochemical properties. In the present work both the mediated and non-mediated systems have been investigated and the resulting probes tested for glucose assays.

EXPERIMENTAL

Apparatus

Cyclic voltammetry measurements were performed with a BAS CV 27 voltamperograph connected to a Hewlett-Packard 7090 A X-Y recorder. A BAS three-electrode cell was used with the carbon-paste working electrode, saturated calomel reference electrode (SCE) and a platinum wire auxiliary electrode.

Amperometric measurements were made with a Bruker E 100 polarograph connected to a

*Author for correspondence.

Servogor X–Y recorder. The 50-ml electrochemical cell used to test the enzyme electrodes was operated in a three-electrode configuration. The temperature of the cell was controlled at $24.0 \pm 0.2^\circ$ by a Haake F thermostatic bath. The pH of the solution was measured with a Tacussel Mini 80 pH-meter.

Reagents

All reagents were of analytical grade and supplied by Sigma or Merck. The solutions were prepared with demineralized water. The supporting electrolyte was 0.1M phosphate buffer (pH 7.0). Glucose oxidase, type X–S, activity 150,000 U/g was from Sigma. Standard solutions of glucose (1M) were prepared one day before use by dissolution in 0.1M phosphate buffer and stored at 4° for no longer than one week. Liquid paraffin was from Sigma (spectroscopic grade). Colloidal graphite powder was from Marly and purified by lixiviation with chloroform. The carbon paste was from Metrohm (EA 207C).

Electrode preparation

The enzyme electrode was made by pressing the active paste into the well of the body of the BAS electrode (3 mm in diameter, 2 mm deep). The paste surface was manually smoothed on clean paper. Paste I was prepared by careful mixing of 100 mg of carbon paste (Metrohm) and 6 mg of GOD in a mortar. Paste II was prepared by mixing graphite and 1,1'-dimethylferrocene [DMFe(cp)] in a mortar with a minimum amount of chloroform, evaporating the solvent, adding GOD and paraffin oil, and blending the mixture into a paste. The best mechanical and electrochemical stability and signal to noise ratio (amperometric background current 300 nA) were obtained with 125 mg of graphite, 11 mg of DMFe(cp), 18 mg of GOD and 66 mg of oil. The pastes were stored at room temperature.

Procedures

Enzyme electrodes made with paste I were conditioned for 2 hr in quiescent phosphate buffer (pH 7.0) containing 10mM glucose, with the electrode at +1.1 V *vs.* SCE. After conditioning, the electrodes gave more stable responses and extended linear ranges. Between experiments the electrode was stored in 1mM glucose solution in pH 7.0 phosphate buffer at room temperature and at open circuit. Enzyme electrodes made of paste II were conditioned for

12 hr in similar conditions but with the electrode at +0.16 V *vs.* SCE. Between experiments the probe was kept in the buffer, at +0.16 V *vs.* SCE and at room temperature.

Assay of plasma glucose. Plasma samples, stored in fluoride/oxalate-treated tubes, were obtained from a routine clinical laboratory. The electrode was covered by a Nuclepore 0.22- μ m membrane prior to plasma assays. Measurements were made on 2.5 ml of phosphate buffer plus 0.5 ml of plasma. After the potential was applied the background current was allowed to decay to a constant value before plasma samples were added to the stirred solution.

RESULTS AND DISCUSSION

The incorporation of GOD alone or GOD and ferrocene-linked polymers into graphite pastes has already been described.^{6,7} The pastes used were home-made and contained relatively small amounts of oil, approximately 8 and 13% w/w respectively. Since mechanical instability along with large background currents may be encountered with such pastes,^{14,15} it was of interest to prepare carbon pastes with higher amounts of binder.

Paste I modified electrode (GOD–CPE)

The amperometric response to glucose was investigated in the concentration range 1–30mM and at three different applied potentials (+0.16, +0.90 and +1.1 V *vs.* SCE). At +1.1 V, evolution of oxygen started to occur. More positive potentials were therefore avoided, as high background currents and unstable signals were observed. No electrochemical response was detected at +0.16 V *vs.* SCE but currents linearly related to glucose concentration were obtained at the two other potentials; the slope of the response at +1.1 V was four times that at +0.90 V *vs.* SCE. By studying the amperometric oxidation of hydrogen peroxide solutions at the carbon paste electrode (CPE), it was possible to detect its electroactivity at potentials higher than +0.60 V *vs.* SCE. At +1.1 V *vs.* SCE and in the presence of 1mM H₂O₂ the signal obtained at the CPE was approximately 10 times that obtained under identical conditions with 1mM glucose at the GOD–CPE. Further experiments at +1.1 V *vs.* SCE indicated that the linear range of response at the GOD–CPE was extended up to 50mM glucose ($r = 0.9992$) with 90% response times of 20–30 sec. Figure 1 shows a typical calibration plot for

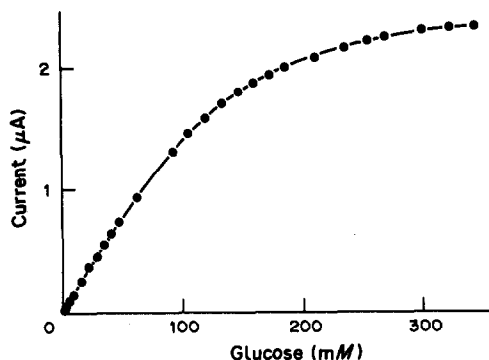


Fig. 1. Calibration curve for glucose enzyme electrode (GOD-CPE). Steady-state current measured at +1.1 V vs. SCE, pH 7.0, 24°.

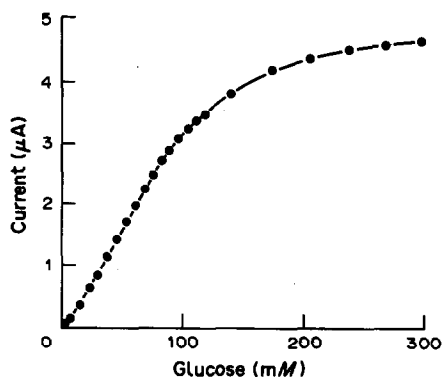


Fig. 3. Calibration curve for mediated glucose enzyme electrode [GOD-DMFe(cp)-CPE]. Steady-state current measured at +0.16 V vs. SCE, pH 7.0, 24°.

the GOD-CPE. The electrode responded up to 300mM glucose with an analytically useful range up to ~130mM. The apparent Michaelis constant was 75mM. Such an extended range of electrode response may be attributed to the slight evolution of oxygen at +1.1 V vs. SCE and the presence of a relatively high amount of liquid paraffin in the paste formulation (~30% w/w).¹⁶ The oily phase containing GOD and surrounding the graphite particles may act as a barrier restricting substrate diffusion at the electrode-solution interface. Such effects of the CP binder have already been pointed out in connection with investigation of organic substrates at carbon paste electrodes.^{13,14}

Paste II modified electrode [DMFe(cp)-GOD-CPE]

Ferrocene mixed into carbon paste electrodes has been shown by cyclic voltammetry to be-

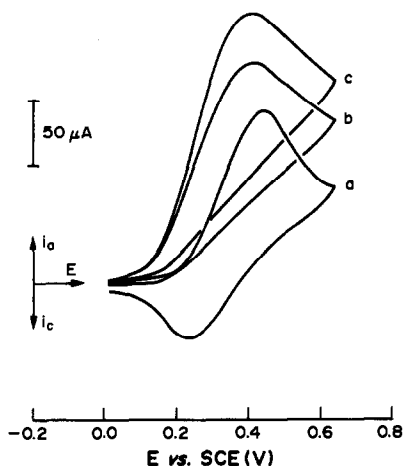


Fig. 2. Cyclic voltamperograms taken with the GOD-DMFe(cp) modified carbon paste electrode in 0.1M phosphate buffer, pH 7.0, scan rate 10 mV/sec: (a) no glucose present; (b) with 100mM glucose, (c) with 200mM glucose.

have reversibly.¹⁰ Figure 2 shows a typical cyclic voltamperogram of DMFe(cp) mixed into the Metrohm CPE. By addition of glucose to the solution, the quasi-reversible behavior of the DMFe(cp)-DMFe(cp)⁺ couple was altered. The presence of glucose induced an increase in the DMFe(cp) oxidation current and concomitant lowering of the DMFe(cp)⁺ reduction current. This behavior is indicative that the regeneration of DMFe(cp) is catalyzed by the incorporated GOD.¹⁷ Amperometric measurements were made with the electrode at +0.16 V vs. SCE in order to minimize interferences from easily oxidized compounds. A typical calibration graph of the steady-state current vs. glucose concentration (Fig. 3) was linear over the range 20-90mM ($r = 0.9982$) then non-linear up to concentrations as high as 300mM. The apparent Michaelis constant was again 75mM. Variation of the stirring speed had no significant effect on the DMFe(cp)-GOD-CPE signal. The response times of freshly prepared electrodes (90% of total current) were 10 sec during the first 2 days of use and 30 sec for older probes. The electrode stability was checked daily by obtaining calibration plots over the concentration range 0.5-10mM glucose. Linear plots were obtained in all cases, with 10, 70 and 90% decrease in response on days 2, 4 and 8 respectively. The limited electrode lifetime may be related to progressive leaching out of the ferricinium ion from the electrode, which is permanently kept at +0.16 V vs. SCE. The extended linearity obtained may again be attributed to diffusion-limited conditions through and within the oily electrode interface. Leaching of ferricinium from the electrode was detected by recording cyclic voltamperograms in the absence of glucose and with and without stirring

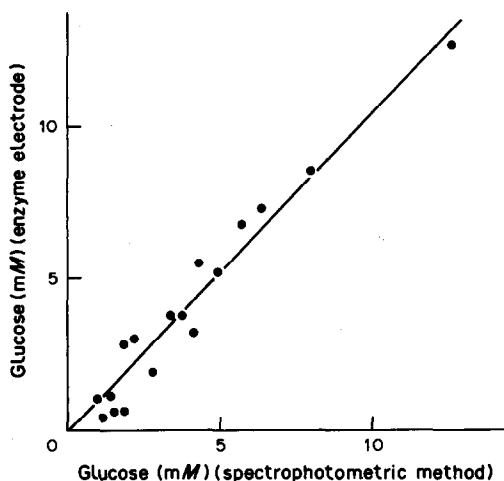


Fig. 4. Correlation between results for plasma glucose by the mediated enzyme electrode [GOD-DMFe(cp)-CPE] method and routine spectrophotometric assay.¹⁸

of the solution. The oxidation peak was not affected by stirring, whereas the reverse peak was completely removed.

Assay of plasma glucose

Correlation of the results (y) of glucose assays of plasma samples with probes based on paste II with the results (x) from a routine spectrophotometric method¹⁸ based on glucose oxidase gave a linear regression of $y = 1.07x - 0.16$ ($r = 0.973$, $n = 17$) (Fig. 4).

CONCLUSION

The incorporation of the enzyme GOD and redox mediators into a paste formulation may offer significant advantages for construction of glucose biosensors. The ease of paste preparation, handling and storage, along with possible miniaturization of the probes¹⁹⁻²¹ is highly advantageous, allowing various probe compositions and configurations. Further developments, which would additionally mix appropriate phospholipids into the enzyme-modified carbon paste,^{22,23} can be considered.

Acknowledgements—Thanks are expressed to le Fonds National de la Recherche Scientifique (FNRS Belgium) for partial support of this work and to the SPPS (Belgium Politic Research, A.R.C.), Contract No. 86/91-89.

REFERENCES

1. G. G. Guilbault, *Analytical Uses of Immobilized Enzymes*, Dekker, New York, 1984.
2. A. P. F. Turner, I. Karube and G. S. Wilson, *Biosensors, Fundamentals and Applications*, Oxford Press, New York, 1987.
3. G. G. Guilbault and J.-M. Kauffmann, *Biotechnol. Appl. Biochem.*, 1987, **9**, 95.
4. Y. Degani and A. Heller, *J. Am. Chem. Soc.*, 1989, **111**, 2357.
5. N. C. Foulds and C. R. Lowe, *Anal. Chem.*, 1988, **60**, 2473.
6. P. D. Hale, T. Inagaki, H. I. Karan, Y. Okamoto and T. A. Skotheim, *J. Am. Chem. Soc.*, 1989, **111**, 3482.
7. W. Matuszewski and M. Trojanowicz, *Analyst*, 1988, **113**, 735.
8. J. Wang and M. S. Lin, *Electroanalysis*, 1989, **1**, 43.
9. M. Bonakdar, J. L. Vilchez and H. A. Mottola, *J. Electroanal. Chem.*, 1989, **266**, 47.
10. J. M. Dicks, W. J. Aston, G. Davis and A. P. F. Turner, *Anal. Chim. Acta*, 1986, **182**, 103.
11. T. Ikeda, H. Hamada and M. Senda, *Agric. Biol. Chem.*, 1986, **50**, 883.
12. T. Ikeda, T. Shibata and M. Senda, *J. Electroanal. Chem.*, 1989, **261**, 351.
13. E. S. Takeuchi and R. W. Murray, *ibid.*, 1985, **188**, 49.
14. M. E. Rice, Z. Galus and R. N. Adams, *ibid.*, 1983, **143**, 89.
15. C. Urbaniczky and K. Lundström, *ibid.*, 1984, **176**, 169.
16. H. Monien, H. Specker and K. Zinke, *Z. Anal. Chem.*, 1967, **225**, 342.
17. A. E. G. Cass, G. Davis, G. D. Francis, H. A. O. Hill, W. J. Aston, I. J. Higgins, E. V. Plotkin, L. D. L. Scott and A. P. F. Turner, *Anal. Chem.*, 1984, **56**, 667.
18. D. Barham and P. Trinder, *Analyst*, 1972, **97**, 142.
19. J. Wang and J. M. Zadelli, *J. Electroanal. Chem.*, 1988, **249**, 339.
20. I. F. Cheng and C. R. Martin, *Anal. Chem.*, 1988, **60**, 2163.
21. J. Wang and A. Brennstainer, *Anal. Lett.*, 1988, **21**, 1773.
22. O. Chastel, J.-M. Kauffmann, G. J. Patriarche and G. D. Christian, *Talanta*, 1990, **37**, 213.
23. A. Amine, J.-M. Kauffmann, G. J. Patriarche and G. G. Guilbault, *Anal. Lett.*, 1989, **22**, 2403.

AN ELECTROCHEMICAL MICROSENSOR FOR CHLORIDE

SHAOJUN DONG* and GUANGLI CHE

Laboratory of Electroanalytical Chemistry, Changchun Institute of Applied Chemistry, Chinese Academy of Sciences, Changchun, Jilin 130022, People's Republic of China

(Received 6 November 1989. Revised 12 March 1990. Accepted 28 March 1990)

Summary—The potential-response of a microdisk electrode made with a chloride-doped polypyrrole (PPY) film on a carbon fibre (CF) has been examined. The effect of the polymerization conditions on the response characteristics is discussed. The optimum conditions for preparing the electrode are: cycling potential from +0.8 to +1.0 V in 0.1–0.2M pyrrole (Py) containing 0.1M LiCl, electropolymerization time 15–20 min. The electrode gives a Nernstian response of 56–58 mV/pCl and a detection limit of 3.6×10^{-5} M chloride. It has the advantages of low resistance, short conditioning time and fast response. It has been used satisfactorily for detection of chloride in serum.

The development and application of potentiometric chloride sensors remains an active area of investigation, particularly in clinical analysis. Hansen *et al.*, and Dahms and co-workers^{2,3} have used an Ag/AgCl electrode to detect chloride in sweat and serum. Coetzee and Freiser^{4,5} have developed another kind of chloride-sensitive electrode. In recent years, several groups have attempted to attach active species directly to a polymer to prepare ion-selective electrodes. Oka *et al.*⁶ prepared a chloride ion-selective electrode by grafting quaternary ammonium groups onto a polymer, and Sun and Zhang⁷ used a polymer doped with an alkylpyridine. Dong *et al.*⁸ studied a conventional electrode prepared with a chloride-doped conducting polymer. So far, a chloride-selective microsensor has not been reported. This paper describes such a sensor, prepared by electrochemical polymerization of pyrrole (Py) on a carbon fibre (CF) microdisk electrode in a chloride solution. This microsensor has been used to detect chloride in serum. It has some advantages over conventional electrodes, such as fast response, short conditioning time and lower detection limits. It is expected to be able to detect chloride *in vivo*.

EXPERIMENTAL

Reagents

Pyrrole (Fluka) was purified by distillation from calcium hydride and was stored under a nitrogen atmosphere at low temperature, and

protected from light. Lithium chloride, sodium sulphate, acetonitrile and other reagents used were of analytical reagent grade. Serum was taken from fresh blood. Doubly distilled water was used throughout.

Apparatus

All electrochemical experiments were done with a PAR model 370 Electrochemistry System, and potentials were measured with a PHS-400 pH-meter. Glass capillaries were prepared with a laboratory-made capillary puller.

Carbon fibre (CF) microdisk electrode. Carbon fibres, 30 μ m in diameter, were washed with acetone, dried and cut into pieces 1.5 cm long. One such piece was fixed on a copper wire (0.3 mm diameter) with solder, and the wire was inserted into a dry glass capillary, which was then drawn to a tip (diameter 35–50 μ m) with the capillary puller. The other end was dipped into epoxy resin, and then cured in an oven at 70° for 2 hr. The tip where the carbon fibre was exposed was cut off and the exposed wire and fibre surface was polished with alumina powder and cleaned.⁹ From the microdisk electrodes thus prepared, one with low resistance (< 1 k Ω) was chosen, and its characteristics were examined by cyclic voltammetry in acetonitrile solution containing 5×10^{-3} M ferrocene and 0.1M lithium perchlorate.

Chloride-doped polypyrrole (PPy) film CF microdisk electrode. The PPy film was prepared on the CF microdisk electrode surface by constant-potential electrolysis of an aqueous solution containing 0.1–0.2M pyrrole (Py)

*Author for correspondence.

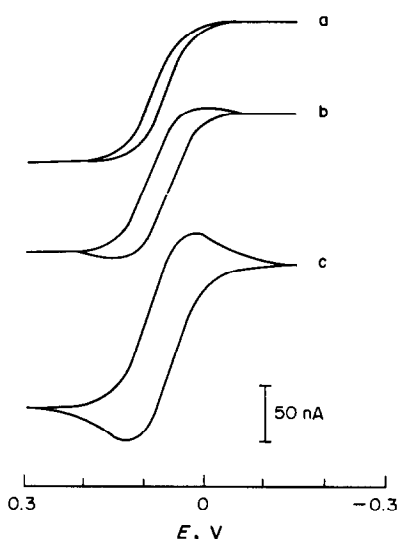


Fig. 1. Cyclic voltamperograms of 5mM ferrocene in acetonitrile containing 0.1M LiClO₄, at a CF microdisk electrode and various scan rates: (a) 100, (b) 200, (c) 500 mV/sec.

monomer and 0.1M lithium chloride. The film thickness was controlled by the electropolymerization time. A conventional single-compartment cell equipped with a platinum wire as counter-electrode, a saturated calomel reference electrode with double salt-bridges (external tubes filled with 0.1M sodium sulphate



Fig. 2. Scanning electron micrographs of CF microdisk electrode (a) and PPy-coated CF microdisk electrode (b).

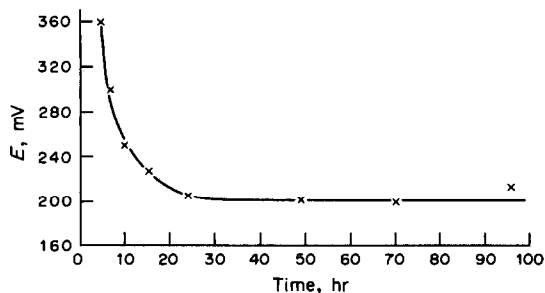


Fig. 3. Effect of conditioning time on the response of the Cl⁻-doped PPy film CF microdisk electrode to 0.1M Cl⁻.

solution), and the CF microdisk electrode as working electrode was employed for the electrochemical polymerization. The potential of the PPy film CF microdisk electrode was measured with the PHS-400 pH-meter.

RESULTS AND DISCUSSION

Electrochemical behaviour of the CF microdisk electrodes and their surface characterization

Figure 1 shows cyclic voltamperograms obtained with a CF microdisk electrode. At slow scan rates (<100 mV/sec), the voltamperograms exhibit the sigmoidal shape expected for steady-state behaviour, with little change of current. The limiting current depends only on the number of electrons transferred (n), the analyte concentration (C) and diffusion coefficient (D), and the electrode radius (r), and not on time. The results obtained are consistent with the equation⁹ $i = 4nFDCr$. Figure 2 shows scanning electron micrographs of a CF microdisk with and without a PPy film on the surface. Many holes are observed on the surface of the CF microdisk electrode (Fig. 2a), whereas the CF microdisk electrode modified with a PPy film has a smooth surface (Fig. 2b). It has been verified that a good response to chloride is obtainable only when the holes are completely covered with the PPy film.

Chloride-response of the CF microdisk electrodes

The chloride-doped PPy-coated CF microdisk electrode gives a stable response to chloride after conditioning for a sufficient period of time. As with conventional electrodes, the response of a newly made electrode drops rapidly with time,⁸ but becomes stable after conditioning for 24 hr, in contrast to the 2–3 days needed for a conventional electrode.⁸ Figure 3 shows the response curves after different conditioning times. The response is also more rapid (<30 sec) than that of a conventional electrode,⁸ owing to

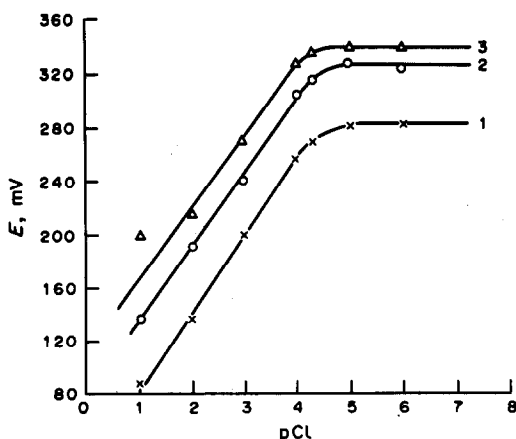


Fig. 4. Potential response of Cl^- -doped PPy film CF microdisk electrodes prepared with a cycling potential of +1.0 V, in 0.2M Py in 0.1M LiCl, and electrochemical polymerization for 20 min. Conditioning time: (1) 24, (2) 48, (3) 96 hr (three electrodes).

the low resistance. Figure 4 shows that the response of the chloride-doped PPy-coated CF microdisk electrode conditioned for >24 hr is Nernstian.

Effect of preparation conditions on response

Effect of the applied potential. The cycling potential has a direct influence on the structure of the PPy film.^{8,10-12} The film electrode prepared at 0.5–1.1 V shows a stable Nernstian response to Cl^- , but films prepared at lower (<0.5 V) or higher (>1.0 V) cycling potential give unstable responses, and electrodes prepared at the higher cycling potentials show high resistance. Non-Nernstian response occurs with electrodes made at lower cycling potential if the conditioning time is long. The optimum cycling potential is 0.8–1.0 V.

Effect of pyrrole concentration. When the Py concentration used is low (<0.1M), the PPy film formed is thin and the response is not a linear function of pCl^- . When the conditioning time is too long, the film can be lost from the surface of the PPy-coated CF microdisk electrode, resulting in no response at all to Cl^- . A Py concentration in the range 0.1–0.2M is found suitable.

Effect of doping chloride concentration. The concentration of the doping ion used in the electrochemical polymerization is important. At 1.0 V the polymerization takes 20 min. When the chloride concentration used is less than 0.1M, the response of the electrode is unstable and the slope decreases with time. The chloride-doped PPy-coated CF microdisk electrode ex-

hibits good Nernstian response with a low detection limit when prepared in 0.1M lithium chloride.

Effect of electrochemical polymerization time. Provided that the PPy film covers the surface of the electrode completely, a good response to chloride is obtained. As the PPy film thickness is mainly controlled by the polymerization time, this needs to be long enough. It is found that the PPy electrode response is unstable and non-Nernstian if the polymerization time is too short, and if it is too long (>40 min) the electrode shows slow response owing to its high resistance, and linear response to chloride can be obtained only with a longer conditioning time (>24 hr). Normally, the electrochemical polymerization time is 15–20 min.

The conditions recommended for preparing the chloride-doped PPy-coated CF microdisk electrode are therefore cycling potential 0.8–1.0 V, polymerization time 15–20 min, Py concentration 0.1–0.2M, and supporting electrolyte 0.1M lithium chloride.

The PPy-coated electrode thus prepared gives a stable Nernstian response to 10^{-4} –0.1M chloride, with a slope of 56–58 mV/pCl and a detection limit of 3.6×10^{-5} M chloride. It also has faster response and shorter conditioning time than a conventional electrode. It may be used to detect chloride *in vivo* and in organic solvents.

Figure 5 shows that the response to 10^{-3} M chloride is almost constant over the pH range 3–5–7.0.

Table 1 gives the selectivity coefficients for various anions. The electrode is not particularly selective for chloride, and several ions cause considerable interference.

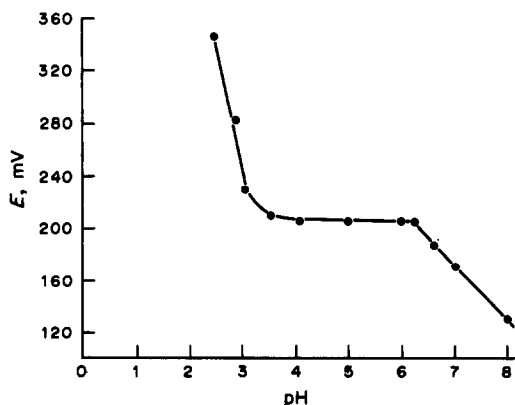


Fig. 5. Relationship between pH and response of Cl^- -doped PPy film CF microdisk electrode in 0.1M LiCl.

Table 1. Selectivity coefficients K_{ij} of the Cl^- -doped PPy film CF microdisk electrode

Interfering anions	Selectivity coefficients, K_{ij}
SO_4^{2-}	1.1×10^{-3}
F^-	4.0×10^{-1}
CH_3COO^-	2.2×10^{-2}
IO_4^-	4.5×10^{-1}
ClO_4^-	6.3×10^{-2}
NO_3^-	5.0×10^{-1}
Br^-	2.5×10^{-1}
I^-	2.8×10^{-1}
HCOO^-	5.0×10^{-1}
SCN^-	1.3×10^{-1}

Table 2. Reproducibility experiments for 100mM chloride

No.	Found, mM	No.	Found, mM
1	99	5	99
2	94	6	105
3	104	7	89
4	96		
Average		98 ± 5.6	

Table 3. Determination of chloride in serum, and recovery of a 100mM spike

No.	Without added Cl^- , mM	With added Cl^- , mM	Recovery of spike, %	Reference value,* mM
1	87	196	109	96
2	105	214	108	105
3	98	193	95	98
4	88	177	88	93
5	95	184	89	94

*Values obtained with a C-200AP Chlor Meter by the hospital.

Human body fluids contain chloride, generally at about 96–106mM level in healthy cases. Therefore, the determination of chloride is important in clinical medicine, and the utility of the chloride-doped PPy-coated CF microdisk electrode for determination of chloride in serum has been examined.

Table 2 shows the results obtained by diluting 0.5 ml of serum 100-fold with doubly distilled water, and determining the chloride content by the standard-addition method. The relative standard deviation was 5.6%.

Analysis of five patients' serum gave the results shown in Table 3, together with the results obtained by an independent method, and the recoveries for a 100mM chloride spike added to the serum.

REFERENCES

1. L. Hansen, M. Buechele, J. Koroshec and W. J. Warwick, *Am. J. Clin. Pathol.*, 1968, **49**, 834.
2. H. Dahms, *Clin. Chem.*, 1967, **13**, 437.
3. H. Dahms, R. Rock and D. Seligson, *ibid.*, 1968, **14**, 859.
4. C. J. Coetzee and H. Freiser, *Anal. Chem.*, 1968, **40**, 2071.
5. *Idem, ibid.*, 1969, **41**, 1128.
6. S. Oka, Y. Sibazuki and S. Tahara, *ibid.*, 1981, **53**, 588.
7. Z. Su and Y. Zhang, *Yingyong Hauxue*, 1985, **2**, No. 3, 45.
8. S. Dong, Z. Sun and Z. Lu, *Analyst*, 1988, **113**, 1525.
9. R. M. Wightman, *Anal. Chem.*, 1981, **53**, 1125A.
10. S. Dong and J. Ding, *Synth. Meth.*, 1987, **20**, 119.
11. M. Salmon, A. F. Diaz, A. J. Logan, M. Krounbi and J. Borgon, *Mol. Cryst. Liq. Cryst.*, 1982, **83**, 1297.
12. G. Tourillon and F. Garnier, *J. Electroanal. Chem.*, 1982, **135**, 173.

CALIBRATION OF A SOLID-STATE COPPER ION-SELECTIVE ELECTRODE IN CUPRIC ION BUFFERS CONTAINING CHLORIDE

BOY HOVER

Department of Chemistry, Aarhus University, Langelandsgade 140, DK-8000 Aarhus C, Denmark

(Received 5 February 1990. Accepted 15 March 1990)

Summary—It is shown that near-Nernstian calibration slopes can be obtained with a $\text{Cu}_{1,8}\text{Se}$ electrode in a range of cupric ion buffers in spite of a high chloride content. Best results are obtained with the ligands ethylenediamine, glycine and histidine. The onset of cupric ion toxicity towards marine organisms falls within the pCu calibration range obtained with glycine, and the $\text{Cu}_{1,8}\text{Se}$ electrode could, therefore, be useful for monitoring cupric ion activity in bioassays in sea-water media.

Cupric ion is of great environmental concern in natural waters, owing to its high toxicity towards aquatic organisms. Bioassays based on a range of growth-rate parameters and aquatic organisms (especially algae) have shown that the toxicity is a function of the activity of the cupric ion.¹⁻⁴ Thus, the overall toxicity of copper(II) is generally lowered by complexation, but lipid-soluble copper complexes are an important exception.⁵

Potentiometry with a cupric ion-selective electrode (Cu-ISE) is the only technique that allows selective determination of the cupric ion activity without disturbing equilibria in the sample. Therefore, a Cu-ISE seems to be the obvious choice for monitoring cupric ion activity in toxicity studies and environmental control. In practice, however, the utility of a Cu-ISE is limited by several factors. In media containing no bound copper(II), the lower limit of Nernstian response towards cupric ion is 10^{-7} – $10^{-6}M$,⁶ which is too high for studies of natural waters. However, with cupric ion buffers the electrode can be calibrated⁷ down to cupric ion activities as low as $10^{-19}M$, provided that the total concentration of copper(II) species is above $10^{-6}M$. Therefore, a Cu-ISE may still be useful in toxicity studies performed with cupric ion buffers.² The other major limitation to the utility of a Cu-ISE is the chloride interference,⁶ which researchers hitherto have regarded as an *a priori* obstacle to its use in sea-water studies. Although the chloride interference can be suppressed in media containing high concentrations of free cupric ion by polymer coating of the electrode,⁸ no attempts have been made to calibrate Cu-

ISEs in sea-water media containing cupric ion buffers.

This paper demonstrates that it is possible to obtain near-Nernstian calibration slopes for a Cu-ISE in a range of cupric ion buffers with high chloride content. The experiments were done in a manner which could easily be adapted to bioassays and the media employed closely resembled sea-water. Moreover, the range of cupric ion activities within which the onset of toxic effects of this ion towards aquatic microorganisms occurs¹⁻⁴ is included in the Nernstian calibration ranges obtained.

EXPERIMENTAL

Apparatus

The Cu-ISE was a Radiometer F1112Cu Selectrode, which employs a single crystal of $\text{Cu}_{1,8}\text{Se}$ as the sensing element. The reference electrode was a Radiometer K701 double-junction saturated calomel electrode with $2M$ potassium nitrate as the bridging solution. Potential readings were taken with a Radiometer PHM64 pH-meter (0.1 mV resolution). The cell was kept at $28 \pm 2^\circ$ with a water-jacket. Solutions were stirred with a Teflon-coated magnetic bar during measurement.

Reagents

Analytical grade chemicals and triply distilled water were used throughout. All calibration experiments were performed at pH 8.4 ($10^{-2}M$ boric acid/ $2.5 \times 10^{-3}M$ sodium hydroxide buffer). The complexing agent solutions (mostly standardized by complexometric

titration with cupric ion, monitored with the Cu-ISE) were ethylenediamine (en), diethylenetriamine (dien), tris(2-aminoethyl)amine (tren) and nitrolotriactic acid (NTA) at pH 8.4 and EDTA at pH 4.7 in 0.1M acetate buffer. Iminodiacetic acid (IDA), histidine and glycine were standardized by acid-base titration. The purities of en, dien and tren were checked by gas chromatography and found to be adequate.

Procedure

Prior to each calibration run, the Cu-ISE was polished with Radiometer D709 abrasive agent and 0.25 μm diamond paste, followed by rinsing with ethanol. Between experiments, the electrode was stored in distilled water.

Calibrations were performed by adding cupric ion from $[\text{Cu}^{2+}]_{\text{total}} = 2 \times 10^{-6} \text{M}$ up to the stoichiometric equivalent of the ligand concentration. Concentration increments were chosen so that approximately evenly spaced values of $\log[\text{Cu}^{2+}]_{\text{total}}$ were obtained. Calibrations were performed with 10^{-4} and 10^{-3}M ligand present, with and without addition of 0.5M sodium chloride to the medium. Potential readings were taken when electrode drift was below 0.2 mV/min, which occurred after a waiting period of at most 5 min [at low Cu(II) concentrations]; usually, a waiting period of 1 min sufficed.

After introduction of sample solution, the measurement cell was closed with plastic film and oxygen was removed by continuous passage of argon. In the calibration experiments, measurements were made in order of increasing copper concentration. The cell and the electrodes were carefully rinsed twice with 0.02M nitric acid and once with water before a solution

with a lower copper content than the previous one was introduced into the cell.

The theoretical equilibrium values of $[\text{Cu}^{2+}]$ were calculated by use of the program MINEQL⁹ with equilibrium constants from Smith and Martell.¹⁰

RESULTS

Figure 1 shows a typical calibration curve for the Cu-ISE in the presence of a Cu(II)-binding ligand. Clearly, a highly significant linear relationship between pCu and the electrode potential holds in most of the pCu range covered. The theoretical (Nernstian) slope of the calibration line is $(RT/nF) \ln 10 = (29.9 \pm 0.2) \text{ mV/pCu}$ at $(28 \pm 2)^\circ$. At high pCu values, the calibration curve levelled off in most cases, indicating that the total concentration of Cu(II) was insufficient to give a Nernstian electrode response. This part of the curve was always discarded in the calculation of the linear regression data. In the calibration experiments with NTA and EDTA, the electrode potential was almost independent of the Cu(II) concentration and no regression data for the calibration curve could be obtained. Table 1 summarizes the regression data for the calibration experiments.

It has previously been shown that coating the Cu-ISE with the perfluorosulphonate polymer Nafion greatly suppresses chloride interference in media containing high concentrations of free copper(II).⁸ However, this approach did not prove to be feasible for the copper(II)-binding media in this study, because the response times were too long.

DISCUSSION

From Table 1 it can be seen that addition of chloride to the media containing Cu(II)-binding ligands did not have any large or unequivocal effect on the calibration data for the Cu-ISE. Moreover, chloride addition did not significantly change the absolute values of the electrode potential. In the tren system, the slope of the calibration line was increased by addition of chloride, whereas the opposite effect was observed for dien. For the other ligands, the slope was not significantly affected by addition of chloride. The sub-Nernstian calibration data for IDA and the unsuitability of the NTA and EDTA media for electrode calibration is in agreement with previous results.^{11,12} The explanation of the distinctly super-Nernstian slopes

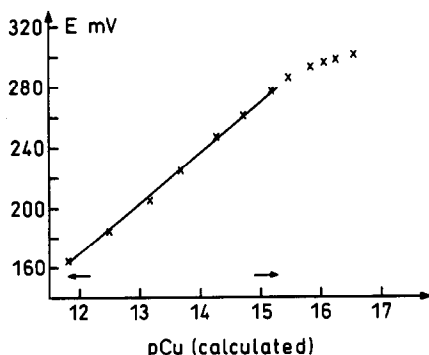


Fig. 1. Calibration curve for the Cu-ISE, obtained by titration of 10^{-3}M dien with Cu(II). Medium: 10^{-2}M boric acid buffer + 0.5M NaCl; range of total copper concentrations: 2×10^{-6} – $9 \times 10^{-4} \text{M}$. Arrows indicate the part of the calibration curve used for calculation of the regression line.

Table 1. Effect of chloride on the calibration data for the Cu-ISE in media containing copper(II)-binding ligands

Ligand	Approximate concn., M*	C _{NaCl} , M	Range of [Cu(II)] _T , M†	pCu range	Slope, mV/pCu	Regression coefficient	n‡
tren	10 ⁻⁴	0	0.6–8 × 10 ⁻⁵	14.8–16.7	26.4	0.999	6
	10 ⁻⁴	0.5	1–8 × 10 ⁻⁵	13.8–15.6	30.1	0.999	6
	10 ⁻³	0	0.2–8 × 10 ⁻⁴	14.6–17.1	39.6	0.997	8
	10 ⁻³	0.5	0.6–9 × 10 ⁻⁴	13.6–15.9	43.5	0.999	7
dien	10 ⁻⁴	0	0.4–8 × 10 ⁻⁵	13.0–15.2	31.7	0.999	8
	10 ⁻⁴	0.5	0.1–1 × 10 ⁻⁴	12.2–14.6	27.4	0.998	7
	10 ⁻³	0	0.2–9 × 10 ⁻⁴	12.1–15.8	36.9	0.999	9
	10 ⁻³	0.5	0.4–9 × 10 ⁻⁴	11.8–15.2	33.7	0.999	9
en	10 ⁻⁴	0	0.4–4 × 10 ⁻⁵	12.0–14.2	28.6	0.998	6
	10 ⁻⁴	0.5	0.4–4 × 10 ⁻⁵	11.8–14.1	30.6	0.999	5
	10 ⁻³	0	0.06–4 × 10 ⁻⁴	13.0–16.1	32.6	0.997	9
	10 ⁻³	0.5	0.1–5 × 10 ⁻⁴	11.1–15.8	29.4	0.998	9
glycine	10 ⁻⁴	0	0.2–3 × 10 ⁻⁵	8.8–10.6	29.6	0.997	6
	10 ⁻⁴	0.5	0.2–2 × 10 ⁻⁵	8.9–10.3	28.9	0.992	6
	10 ⁻³	0	0.02–4 × 10 ⁻⁴	9.0–12.7	32.3	0.998	10
	10 ⁻³	0.5	0.04–4 × 10 ⁻⁴	8.7–12.0	30.4	0.997	9
histidine	10 ⁻⁴	0	0.6–4 × 10 ⁻⁵	11.8–14.1	32.8	0.998	5
	10 ⁻⁴	0.5	1–4 × 10 ⁻⁵	11.5–13.4	28.7	0.999	4
	10 ⁻³	0	0.1–4 × 10 ⁻⁴	12.9–16.0	32.9	0.999	8
	10 ⁻³	0.5	0.2–4 × 10 ⁻⁴	12.4–15.2	31.6	0.998	7
IDA	10 ⁻⁴	0	0.4–6 × 10 ⁻⁵	10.1–12.1	21.2	0.985	5
	10 ⁻⁴	0.5	0.4–8 × 10 ⁻⁵	8.9–11.8	20.4	0.994	6
	10 ⁻³	0	0.2–6 × 10 ⁻⁴	9.8–13.3	18.0	0.989	7
	10 ⁻³	0.5	0.2–6 × 10 ⁻⁴	9.2–13.0	24.4	0.999	6

*Actual ligand concentrations were within 10% of this value.

†Data in this and the following columns refer to the linear part of the E -pCu curve.

‡Number of data points in linear regression.

obtained in the 10⁻³ M tren medium with and without chloride and in the 10⁻³ M dien medium without chloride is not known.

For the ligands en, glycine and histidine, near-Nernstian calibration slopes were obtained in media having approximately the same chloride content as sea-water. This result could be of great utility in studies on the toxic effect of Cu(II) towards marine organisms. In particular, the onset of toxic effects of Cu(II) towards micro-organisms occurs in the pCu range 9–11,¹⁻⁴ which lies within the Nernstian calibration range for glycine, making this ligand the most suitable for such studies.

Non-stoichiometric copper selenide sensors are far more sensitive towards copper(I) than copper(II), and the sensitivity towards copper(II) is attributed to the exchange reaction^{6,13}



The equilibrium constant for this reaction is

$$K_{\text{ex}} = \frac{a_{\text{Cu}^+}^2}{a_{\text{Cu}^{2+}}} \quad (2)$$

and the electrode potential is given by

$$E = E^0 + \frac{RT}{F} (a_{\text{Cu}^+} + K_{\text{Cu}^+, \text{Cu}^{2+}}^{\text{pot}} a_{\text{Cu}^{2+}}^{1/2}) \quad (3)$$

where $K_{\text{Cu}^+, \text{Cu}^{2+}}^{\text{pot}} = K_{\text{ex}}^{1/2}$. Thus, the contribution of copper(II) to the electrode potential will be governed solely by the surface concentration of copper(I) generated by reaction (1), if this reaction is fast enough to establish the equilibrium at the electrode surface. However, several complicating factors may contribute to the overall response of the Cu-ISE,^{6,14} such as reaction (1) not reaching equilibrium, the rates of transport of copper(II) and copper(I) species to and from the electrode surface, dissolution of the Cu_{1.8}Se, causing an intrinsic contribution to the copper(I) concentration at the electrode surface, the rates of the complexation and dissociation reactions of copper(I) and copper(II) species in the vicinity of the electrode surface, all of which can produce kinetic effects on the response. Although it is beyond the scope of this paper to investigate these effects in detail, it is interesting to note that addition of chloride to the copper(II)-binding media did not shift the absolute values of the electrode potential significantly. For those ligands for which the stability constants of their copper(I) complexes could be found (en, glycine and histidine), equilibrium calculations showed that the activity of copper(I) was dramatically reduced by addition of chloride (assuming a large excess of ligand). In all cases, the

complexes formed between copper(II) and the added ligands are so strong that addition of chloride has no effect on the activity of copper(II). On a kinetic basis, it would be expected that chloride, because of its smaller size, will react much faster with copper(I) than the copper(II)-binding ligands do. In view of the mechanisms listed it seems likely that transport of copper(I) from the electrode surface governs the electrode potential in the en, glycine and histidine media.

REFERENCES

1. W. G. Sunda and R. R. L. Guillard, *J. Mar. Res.*, 1976, **34**, 511.
2. W. G. Sunda and J. A. M. Lewis, *Limnol. Oceanog.*, 1978, **23**, 870.
3. D. M. Anderson and F. M. M. Morel, *ibid.*, 1978, **23**, 283.
4. R. D. Guy and A. R. Kean, *Water Res.*, 1980, **14**, 891.
5. T. M. Florence and J. L. Stauber, *Aquat. Toxicol.*, 1986, **8**, 11.
6. J. Gulens, *Ion-Selective Electrode Rev.*, 1987, **9**, 127.
7. A. Avdeef, J. Zabronsky and H. H. Stuing, *Anal. Chem.*, 1983, **55**, 298.
8. B. Hoyer and M. Loftager, *ibid.*, 1988, **60**, 1235.
9. J. C. Westall, J. L. Zachary and F. M. M. Morel, *MINEQL*, Technical Note No. 18, Ralph M. Parsons Laboratory, Massachusetts Institute of Technology, 1975.
10. R. M. Smith and A. E. Martell, *Critical Stability Constants*, Vols. 1-6, Plenum Press, New York, 1974-1989.
11. M. Neshkova and H. Sheytanov, *Talanta*, 1985, **32**, 937.
12. E. H. Hansen, C. G. Lamm and J. Růžička, *Anal. Chim. Acta*, 1972, **59**, 403.
13. M. Neshkova and H. Sheytanov, *Talanta*, 1985, **32**, 654.
14. A. Hulanicki and A. Lewenstam, *ibid.*, 1976, **23**, 661.

FLOW-REVERSAL FLOW-INJECTION ANALYSIS ENHANCEMENT OF FLOW-INJECTION TITRATIONS

GREGORY D. CLARK*, JOHN ZABLE, JAROMIR RŮŽIČKA and GARY D. CHRISTIAN†

Center for Process Analytical Chemistry, Department of Chemistry, BG-10, University of Washington,
Seattle, WA 98195, U.S.A.

(Received 3 January 1990. Revised 19 April 1990. Accepted 30 May 1990)

Summary—Most FIA applications involve simple unidirectional continuous-flow regimes. This paper continues the development of the flow-reversal (frFIA) approach and its applications. Flow-reversal flow programming achieves flexibility in operation without requiring manifolds to be refitted. The sensitivity of FIA titrations can be increased by use of frFIA.

Flow-injection analysis (FIA) has demonstrated its utility in the automation of serial assays^{1,2} and sample pretreatment³ and as a method for achieving higher orders of analytical information.⁴⁻⁶ A common characteristic of these three classes of application is their use of flow programming, *i.e.*, the use of pumps and valves to propel, manipulate and chemically treat the sample according to a preset scheme. Flow-programming techniques range from simple single-line, uninterrupted flow systems to much more complicated arrangements. For instance, by stopping the flow at an appropriate time it is possible to measure the rate constants of enzymatic reactions,⁷ enzymatic activity,^{8,9} or the substrate concentration.¹⁰ Flow programming can also be used for steps such as dilution,^{11,12} extraction¹³ and preconcentration.¹⁴

Another technique using flow programming is flow-reversal FIA (frFIA), which employs repetitive reversals of flow to achieve various tasks.¹⁵⁻¹⁹ For example, frFIA can allow a variable amount of mixing between the sample and carrier,^{15,16,18} increase the efficiency of solvent extraction,¹⁷ lead to multiple detection capabilities¹⁸ and allow sampling and preconcentration of gaseous analytes.¹⁹

Two variables are often used separately to describe the extent of mixing or equilibration of the sample with the carrier/reagent. The dispersion coefficient, D , is the ratio of the concen-

tration of analyte detected to the concentration injected, and is therefore indicative of the amount of mixing between the sample and carrier in the element of fluid on which the measurement is made.

The overall equilibration of sample with carrier is often treated by the classical theory of mixing,^{20,21} which relates the degree of mixing to the number, N , of mixing stages in the FIA system. The length of such a mixing state is a fundamental parameter of the type and geometry of the FIA reactor and flow system (in formal analogy to plate-height theory in chromatography). Thus for a particular conventional FIA manifold with a reactor of length, L , N is fixed since the equivalent theoretical plate height, H , is also fixed. Adjustment of the reactor length is the technique most often used to adjust the amount of mixing in the FIA apparatus.¹¹⁻¹³ Thus, varying L in a flow-reversal experiment provides an additional means of varying the number of mixing stages.

An application that benefits from the use of frFIA to vary the number of mixing stages is FIA titration. The FIA titration theory was developed by using the one-tank model.^{22,23} It follows, from the equation for FIA titration,²⁴ that adjusting the number of mixing stages allows versatile control of the sensitivity of the determination. This paper is concerned primarily with developing a capillary-based FIA titration system which allows easy adjustment of the mixing conditions by avoiding the need for physical reconfiguration of the flow manifold.

*Present address: Department of Laboratory Medicine, SB-10, University of Washington, Seattle, WA 98195, U.S.A.

†Author for correspondence.

EXPERIMENTAL

Apparatus

A home-made FIA analyzer based in part on the FIALab system (Alitea U.S.A.) was used. The design of the components and software is discussed elsewhere.²⁵

Hardware. A single-line manifold was used (Fig. 1). The reaction-coil length, a , was varied, typically being 50, 93 or 250 cm, the reactor tubing (0.5 mm bore) being coiled round a metal framework. FIALab Teflon spacers served as connectors. A Rheodyne pneumatically actuated injection valve was used, with an injection volume of 25 μl (0.8 mm bore tubing).

Alitea C-6V peristaltic pumps were used to propel the carrier, reagent and sample streams. A Z-shaped flow-cell with a volume of 10 μl was used. Optical fibers were used to guide light from a tungsten lamp into the flow-cell and hence to the detector.

A Milton Roy Spectronic Mini 20 Spectrophotometer served as the monochromator and detector. The analog signal was amplified from 50 mV to 10 V full scale by a home-made linear-gain amplifier, which employed an Analog Devices AD625 programmable-gain amplifier. The signal from the amplifier was filtered with a 4-pole filter, which removed any periodic noise with a frequency above 2 Hz, and was then directed to an IBM Data Acquisition and Control Adapter (DACA). The amplifier-filter and DACA configuration is described elsewhere.²⁵

In addition, a Radiometer REA 112 chart recorder was connected in parallel with the amplifier to provide real-time signal output. The signal was split before entering the amplifier, being converted into absorbance by a logarithmic converter before being recorded.

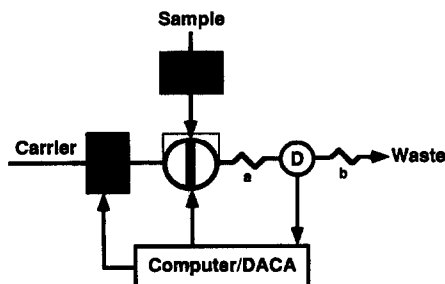


Fig. 1. Flow-reversal single-line flow-injection manifold for the titration of strong acids (HCl , H_2SO_4 , H_3PO_4): a and b are coils of Microline tubing. D is the flow cell. An IBM-compatible AT computer was used for experimental control and data acquisition.

Automated operation. A computer program was used to control operation of the pumps and injection valve to acquire data.²⁵ Before the beginning of an experiment, the appropriate pump sequence was entered into the program. The experiment was started by loading the valve and injecting the sample. The program, upon receiving an interrupt generated from the DACA board, read the 12-bit analog-to-digital converter and stored the data in memory. Each time the interrupt pulse was received by the program, a counter was incremented. This counter was used as a timer for control of the pumps, with an accuracy of 30 msec for a 60-sec FIA experiment.

Reagents

A 0.01M solution of borax (sodium tetraborate decahydrate) was used as the carrier for part of the study. A Bromothymol Blue (BTB) solution was prepared by adding 0.4 g of BTB to 25 ml of 96% ethanol and diluting to 100 ml with the borax solution; a 100 $\mu\text{g/ml}$ solution prepared by further dilution with borax solution was used as the test sample in the dye tracer experiments. The titrations were done with 0.001M sodium hydroxide as carrier, containing 100 $\mu\text{g/ml}$ BTB.

Procedure

The reactor length was held constant (see Apparatus). The flow-rates were measured by collecting the carrier for 3 min in a graduated cylinder. After injection, the sample was allowed to travel part-way in the coiled reactor. At the appropriate time the direction of pump rotation was instantaneously reversed. After an appropriate period of reversed flow the pump was again reversed and the sample propelled in the forward direction. The number of flow-reversal periods was preset according to the extent of mixing desired. After the final flow-reversal period, the sample was propelled to the flow-cell. Absorbance measurement was made at 620 nm, at which the base form of the indicator is monitored.

The parameters of the flow program were the flow-time up to the first reversal, the duration of the reversed-flow cycle, and the number of flow-reversal cycles. In general, two types of experiments were performed. In one, the effect of flow-reversals on the peak shape for a tracer dye was examined. In the other, the effect of flow-reversals on FIA titrations was studied.

RESULTS AND DISCUSSION

Some investigators^{15,16,18} allow the sample bolus to pass through the flow-cell before the flow is reversed, so that the sample passes through the detector twice. This approach has several obvious advantages, *e.g.*, the opportunity to repeat measurement of the analyte several times in one run, by repeated reversals. If the reaction kinetics is suitable, the rate of formation of the reaction product may be calculated. However, most flow-cells have flow paths greater in diameter than the bore (0.5 mm) of the tubing commonly used in FIA systems, so passage through the detector on each flow-reversal cycle may then cause band broadening. In such a case, the flow-cell acts like a gradient device. In this study, the effects of changing the length of sample travel, L , on FIA titrations and on bolus shape were examined by not using flow reversal after the sample had passed through the flow-cell (and, as far as possible, while it was still partly in the injection loop).

Effect of flow reversal on tracer dyes

An experiment was performed to determine the effect of carrier-flow reversal on the peak shape. The bolus was retained in the reaction and injection loop. A series of flow reversals, each lasting 4.5 sec in each direction, was used. Since the flow-rate was set at 3.36 ml/min, the volume moved in each pulse was 252 μ l. The injection volume was 25 μ l and the reactor was 215 cm long, corresponding to a volume of 430 μ l. Other flow-rates were examined, although not systematically, because the primary interest was in the effects of flow-reversal. Other factors which may contribute to the degree of mixing, including flow-rate, injection volume and reactor length, were held constant. The dispersion during each flow-reversal period in each direction would be expected to vary with the flow-rate, as in conventional flow-injection analysis.¹

The total volume (excluding the flow-cell volume and neglecting the connector dead volume) was 455 μ l, so the bolus was retained primarily in the reactor and to a lesser extent in the injection loop. The responses for 0–4 flow-reversal periods are shown in Fig. 2. The time axis refers to the duration of the signal measurement: the recorder was started immediately before the calculated appearance of the peak, *i.e.*, the separate peaks are not related to the flow-reversal periods. It is clear that the peak undergoes a transition from a skewed to a more

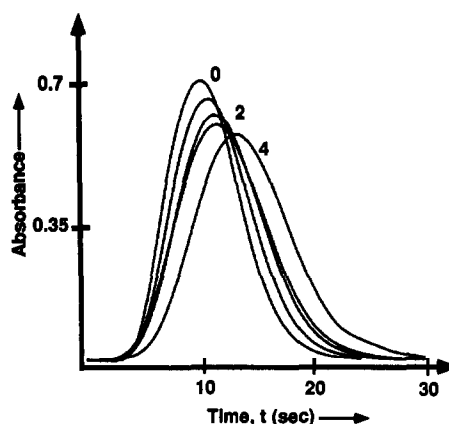


Fig. 2. Effect of flow-reversal on peak shape: 0–4 flow-reversal periods are used in the five runs.

symmetrical and almost Gaussian form, as reported by Betteridge *et al.*¹⁵ As would be expected, the peak heights are reduced by increasing the number of flow-reversals, as a result of the increased length of travel of the bolus. Other experiments (data not shown) demonstrated that the residence time of the peak after one or several flow-reversal cycles is the sum of the residence time in the absence of flow-reversal, plus the sum of the times of each complete flow-reversal cycle.

The absorbance values at the maxima of the peaks are plotted in Fig. 3 as a function of the residence time of the peaks. The residence time was used since it is one of the contributing factors in the dispersion of the analyte bolus. It is important to remember that the same reactor was used, and the number of flow reversals was increased. The peak height decreased as the residence time increased. Rule 3 of Růžička and Hansen¹ states that “the dispersion of the sample zone increases with the square root of the distance travelled through the tubular conduit.” Therefore, D is proportional to the square root of the residence time, τ , since $L = \tau U_{ave}$, where U_{ave} is the linear flow velocity. The dispersion coefficient was plotted as a function of the square root of the residence time and the linearity was confirmed by a regression coefficient, R^2 , of 0.996.

Effect of flow-reversal on titrations

The effect of the flow-reversal on peak shape and dispersion is clear. The sample bolus undergoes dispersion proportional to the square root of the length of travel. Another feature is the transition from the skewed peak, which is characteristic of a system with a single mixing

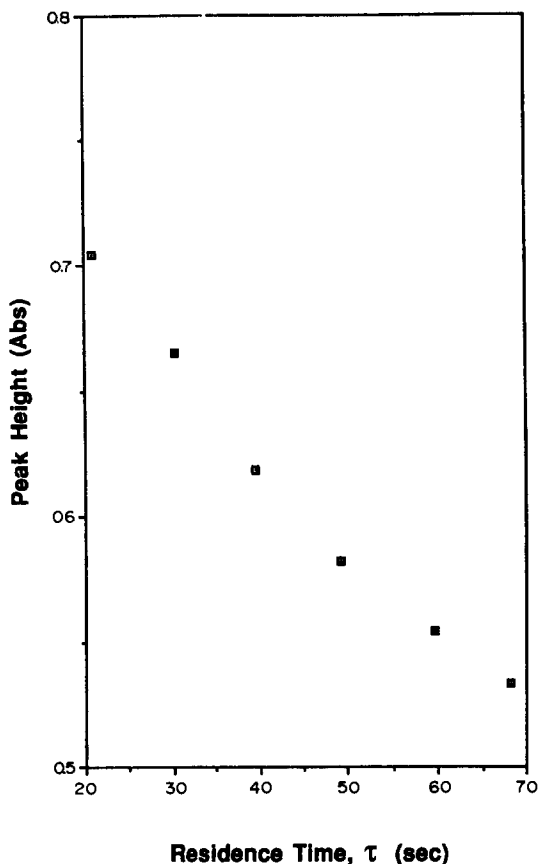


Fig. 3. Absorbance at peak maximum as a function of the total residence time for 0-5 flow-reversal periods of 4.5-sec duration.

stage, to a curve which is more symmetrical, because of more complete axial mixing. The question is whether data generated by using frFIA will be as useful as data generated by traditional techniques.

Number of flow-reversal periods. A simple, unidirectional FIA titration of hydrochloric acid with sodium hydroxide solution gives peaks

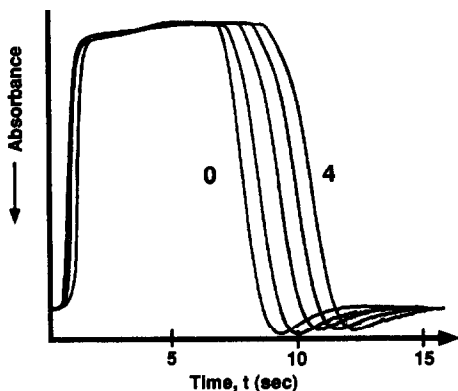


Fig. 4. Effect of 0-4 flow reversals on the titration of 0.1M HCl with 0.001M NaOH.

which increase in width with increasing acid concentration.²⁶ With the single-line manifold shown in Fig. 1, the effect of flow-reversal on the titration of 0.1M hydrochloric acid with 0.001M sodium hydroxide was examined; the results are shown in Fig. 4. The peak width was measured at a constant absorbance (half the steady-state absorbance).²² As expected, increasing the number of flow-reversal periods increased the time corresponding to equivalence (peak width, Δt).

Five concentrations of hydrochloric acid ranging from 0.01 to 0.1M were titrated, with 0-4 flow-reversal periods. The results are plotted in Fig. 5 and the regression data are given in Table 1. The salient features of the graph are the increasing slope and the increased intercept at $\log[\text{HCl}] = 0$, with increasing number of reversals. It is also seen that increasing the number of flow-reversal periods increases the peak width for a given acid concentration, and hence the sensitivity.

Other experiments, in which the length of the flow-reversal cycle was varied, confirmed that the increase in sensitivity was due to the increase in total residence time. The flow-reversal time of 4.5 sec was the longest which allowed the sample

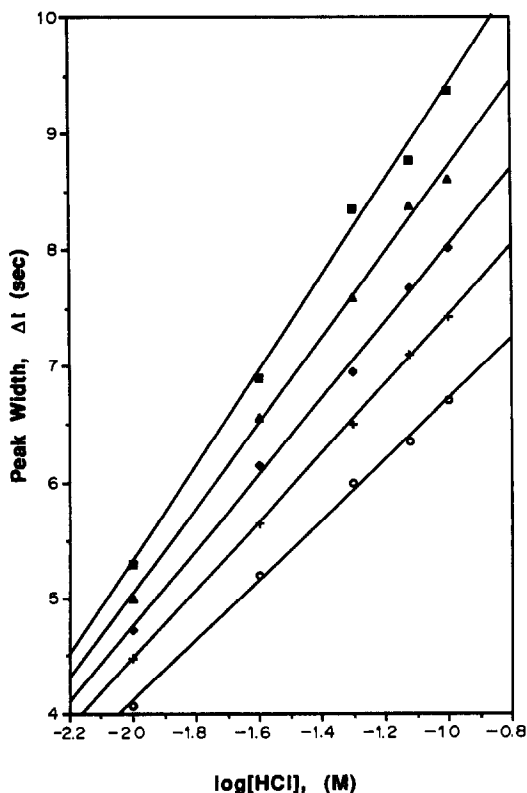


Fig. 5. Plots of peak width, Δt , vs. $\log[\text{HCl}]$ for different numbers of flow-reversal periods: (○) 0; (+) 1; (◆) 2; (▲) 3; (■) 4.

Table 1. Regression data for peak width as a function of $\log[\text{HCl}]$ for different numbers of flow-reversals

Number of reversals	Intercept	Slope	R^2
0	9.3	2.70	0.998
1	10.4	2.96	0.999
2	11.3	3.28	0.997
3	12.4	3.68	0.996
4	16.5	4.08	0.996

bolus to remain within the reactor used, thereby yielding the largest enhancement of sensitivity (while excluding mixing effects from the detector and injector) and was therefore used in the remainder of the experiments.

Concentration dependence. Intuitively, the frFIA titration of a strong acid would be expected to behave similarly to the "normal", unidirectional FIA titration. Figure 7 shows the titration curves for several concentrations of hydrochloric acid, ranging from 0.01 to 0.1M. They are very similar to those for unidirectional titrations.²⁶ Figure 6 shows that the peak widths in Fig. 7 are linearly proportional to the logarithm of the acid concentration.

Dependence on neutralization stoichiometry. Polyprotic acids are often titrated by use of FIA titration devices. The effect of neutralization stoichiometries on the titration curve was examined. Strong acids of equal concentration but different proticity would intuitively be expected to give identical FIA titration curves for a given degree of neutralization. In a potentiometric FIA titration, the steps for the titration of the first two protons of phosphoric acid can be differentiated. In a dye-based FIA system, however, where the dye changes color at a fixed pH, the two steps cannot be distinguished. If the dye

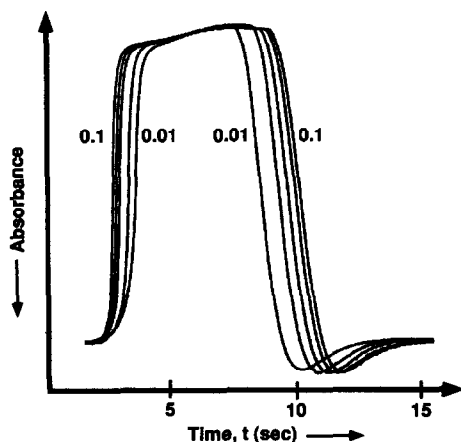


Fig. 6. FIA traces for the titration of 0.01–0.1M HCl with one flow-reversal period.

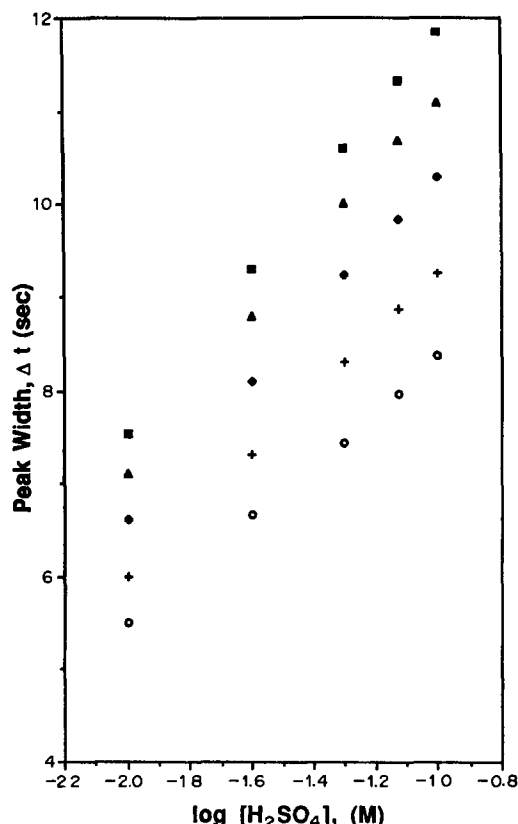


Fig. 7. Plots of the peak width, Δt , vs. $\log[\text{H}_2\text{SO}_4]$ for the titration of H_2SO_4 with different numbers of flow-reversals (key as for Fig. 5).

has a sufficiently low $\text{p}K_a$ only the first step will be observed, and if it has a high enough $\text{p}K_a$ the sum of the two steps will be obtained. The latter is the case with sulfuric acid titrations. Figure 7 shows excellent linearity for the relation of peak width to the logarithm of the acid concentration. The plots also exhibit the expected increase in slope for increasing number of flow-reversal periods. Titrations of phosphoric acid showed similar behavior.

Empirical equation. The equation²⁴ for the titration of an analyte was derived by using the single mixing-tank model. It has been shown here that both the slope and intercept of the calibration line increase with increasing number of flow-reversal periods (Table 1). Thus an appropriate empirical equation might be:

$$\begin{aligned} \Delta t &= 2.303k_1(V_m/Q) \log(C_S^0/C_R^0n) \\ &\quad + 2.303k_2(V_m/Q) \log(S_V/V_m) \\ &= 2.303k_1(V_m/Q) \log C_S^0 + 2.303(V_m/Q) \\ &\quad \times [k_2 \log(S_V/V_m) - k_1 \log(C_R^0n)] \end{aligned} \quad (1)$$

where V_m is the volume of the mixer/reactor, Q is the volumetric flow-rate, C_S^0 is the concentration of the analyte, C_R^0 is the concentration of the titrant and S_v is the sample volume. The different slopes and intercepts for different numbers of flow-reversal cycles are reflected by change in k_1 and in both k_2 and k_1 , respectively. Since these variables are an integral part of the calibration curve, the calibration is accomplished by plotting the peak width against the logarithm of the analyte concentration.

CONCLUSIONS

The primary advantage cited by Betteridge *et al.*¹⁵ for the use of frFIA was the increased travel length of the sample, which in turn increases the sample dispersion. Increasing the dispersion beyond that attainable by unidirectional flow allows alteration of the reaction conditions without reconfiguration of the entire system. In this work, it is demonstrated that the use of flow-reversal enhances FIA titrations by allowing the analyst to control the amount of mixing. In flow-reversal FIA, the dispersion and extent of axial mixing are increased, leading to greater sensitivity of FIA titrations.

Both the capillary and gradient-chamber approaches have benefits and difficulties. The capillary-based system has the advantage of speed, but lacks the dispersive power for dealing with highly concentrated solutions, whereas gradient-chamber devices permit the necessary expansion of concentration range, but often provide too large a dilution, causing the analyte concentration to be indeterminate.¹⁰ By its nature, the gradient chamber also has a long wash-out time, which lowers the sampling frequency.¹⁵ Neither approach is particularly easily adjustable to allow optimization of the technique.

Flow-programming is a fairly novel FIA technique. So far only six papers^{11,15-19} utilizing flow-reversal FIA have come to the attention of the authors. The reasons for this scarcity are as follows.

(1) Many FIA practitioners have used chromatographic intuition in their design of FIA manifolds and techniques and, except for column back-flushing,²⁷ chromatographic techniques do not utilize flow reversal.

(2) The technique requires the use of pumps designed for instantaneous flow reversal, and of computer programs or sophisticated timers to

control them. Until recently, these tools were not readily available.

The motivation for employing flow-reversal is that, as with chromatographic flow programming,²⁸ it provides another adjustable experimental parameter. Control of the analyte bolus and its dispersion is critical in FIA and this technique supplies another means of manipulating the sample zone.

REFERENCES

1. J. Růžička and E. H. Hansen, *Flow Injection Analysis*, 2nd Ed., Wiley, New York, 1988.
2. *Idem*, *Anal. Chim. Acta*, 1975, **78**, 145.
3. G. D. Clark, D. Whitman, J. Růžička and G. D. Christian, *CRC Crit. Rev. Anal. Chem.*, 1990, **21**, 357.
4. W. Lindberg, G. D. Clark, D. A. Whitman, C. Hannah, J. Růžička and G. D. Christian, *Anal. Chem.*, 1990, **62**, 849.
5. D. A. Whitman, *Ph.D. Dissertation*, University of Washington, Seattle, 1989.
6. D. A. Whitman, M. B. Seasholtz, J. Růžička, B. Kowalski and G. D. Christian, unpublished work.
7. J. M. Hungerford, G. D. Christian, J. Růžička and J. C. Giddings, *Anal. Chem.*, 1985, **57**, 1794.
8. S. Olsen, J. Růžička and E. H. Hansen, *Anal. Chim. Acta*, 1982, **136**, 101.
9. J. Růžička and J. Flossdorf, *ibid.*, 1989, **218**, 291.
10. J. Růžička and E. H. Hansen, *ibid.*, 1980, **114**, 19.
11. G. D. Clark, J. Růžička and G. D. Christian, *Anal. Chem.*, 1989, **61**, 1773.
12. M. B. Garn, M. Gisin, H. Ross, P. King, W. Schmidt and C. Thommen, *Anal. Chim. Acta*, 1988, **207**, 225.
13. B. Karlberg and S. Thelander, *ibid.*, 1978, **98**, 1.
14. N. Lacy, J. Růžička and G. D. Christian, *Anal. Chem.*, 1990, **62**, 1483.
15. D. Betteridge, P. B. Oates and A. P. Wade, *ibid.*, 1987, **59**, 1236.
16. A. Ríos, M. D. Luque de Castro and M. Valcárcel, *ibid.*, 1988, **60**, 1540.
17. F. Cañete, A. Ríos, M. D. Luque de Castro and M. Valcárcel, *ibid.*, 1988, **60**, 2354.
18. M. Valcárcel, M. D. Luque de Castro, F. Lazaro and A. Ríos, *Anal. Chim. Acta*, 1989, **216**, 275.
19. F. Cañete, A. Ríos, M. D. Luque de Castro and M. Valcárcel, *ibid.*, 1989, **224**, 127.
20. O. Levenspiel, *Reaction Engineering*, 2nd Ed., Wiley, New York, 1972.
21. J. M. Reijn, H. Poppe and W. E. Van der Linden, *Anal. Chim. Acta*, 1983, **145**, 59.
22. J. Růžička, E. H. Hansen and H. Mosbaek, *ibid.*, 1977, **92**, 235.
23. A. U. Ramsing, J. Růžička and E. H. Hansen, *ibid.*, 1981, **129**, 1.
24. J. Růžička and E. H. Hansen, *op. cit.*, p. 57.
25. G. D. Clark, G. D. Christian, J. Růžička, G. A. Anderson and J. A. van Zee, *Anal. Instr.*, 1989, **18**, 1.
26. J. Růžička and E. H. Hansen, *op. cit.*, p. 236.
27. J. Růžička and G. D. Christian, *Anal. Chim. Acta*, 1990, **234**, 31.
28. B. L. Karger, L. R. Snyder and C. Horvath, *An Introduction to Separation Science*, Wiley, New York, 1973.

DETERMINATION OF RATE CONSTANTS AND REACTION ORDERS WITH AN OPEN-CLOSED FLOW-INJECTION CONFIGURATION

S. D. KOLEV*, A. RIOS, M. D. LUQUE DE CASTRO and M. VALCARCEL

Department of Analytical Chemistry, Faculty of Sciences, University of Córdoba,
14004 Córdoba, Spain

(Received 21 December 1989. Revised 5 July 1990. Accepted 10 July 1990)

Summary—A new, very useful application of open-closed configurations to kinetic studies is reported. The multipeak recordings provided by the manifold used, which features a single conventional photometric detector, were used to calculate the rate constants and reaction orders of a chemical system, namely the ligand displacement reaction between the cobalt(II)-EGTA complex and PAR.

Since its inception, flow-injection analysis (FIA) has gained increasing popularity, both for routine analyses and for research purposes. Among the latter, the determination of different physicochemical constants (*e.g.*, viscosity,¹ diffusion coefficients,² kinetic parameters³) makes the technique a very useful tool for scientific research.

Flow-injection analysis combines the advantages of continuous-flow mixing methods and stopped-flow methods^{4,5} and overcomes their disadvantages, *e.g.*, it allows faster reactions to be investigated and ensures continuous flushing of the measuring cell (it resembles the continuous-flow mixing methods in this respect), and a single experiment provides information on the reaction kinetics through the recorded concentration/time curve. The main disadvantages of the traditional open manifold are the high reagent consumption and the limited amount of information that can be obtained from development of the reaction in a single injection. These drawbacks could be efficiently eliminated by using an open-closed system.⁶⁻⁸ In this way, multipeak detection could be accomplished without the need to install a series of detectors along the manifold, which could prove rather expensive. An additional advantage of open-closed systems is the possibility of reaching reaction equilibrium, which is not always feasible with open systems. Because of the intensive mixing in open-closed flow systems when

the system volume considerably exceeds the injected volume, static reaction conditions (*i.e.*, constant concentration of one of the reactants), which otherwise require sophisticated equipment,⁴ can be readily accomplished.

Open-closed systems have already been applied for determination of partial reaction orders and rate constants of different reactions widely used in chemical analysis.⁶⁻⁸ The results are most likely to be affected by the hydrodynamic regime of the flow system and cannot be considered "pure" chemical kinetic parameters. One approach to the determination of true reaction orders and rate constants irrespective of the flow pattern in the manifold involves finding a relation between the signals obtained under the same hydrodynamic conditions in the absence and presence of the chemical reaction investigated.

This paper reports on the theoretical development of such an approach and its application to the study of the ligand-displacement reaction between the cobalt(II)-EGTA complex and PAR.

THEORETICAL FOUNDATION

The dispersion of the analyte in traditional open FIA systems can be described on the basis of an axially-dispersed plug flow model,⁹ which is represented mathematically by the equation:

$$dC/dt = D_L d^2C/dx^2 - u dC/dx \quad (1)$$

where t is time, x the axial distance, C the concentration, u the mean linear flow-rate and D_L the axial dispersion coefficient. This last

*Permanent address: Department of Analytical Chemistry, Faculty of Sciences, University of Sofia, 1126 Sofia, Bulgaria.

parameter depends on the extent of convective mixing and on the molecular diffusion, and can be calculated theoretically when this type of mixing is prevalent.¹⁰

When the analyte is involved in a first or pseudo-first order reaction, equation (1) becomes:

$$dC/dt = D_L d^2 C/dx^2 - u dC/dx - kC \quad (2)$$

However, it can be shown that substitution of $C^0 \exp(-kt)$ into equation (2) yields equation (1), with a new dependent variable, C^0 replacing C . Obviously, C^0 is the analyte concentration which would be detected in the absence of chemical reaction. On the basis of the reasoning above, if the injected analyte is involved in a first (or pseudo-first) order reaction, the actual rate constant can be determined by processing the data obtained by injecting the analyte into the carrier without $[C^0(t)]$ and with reactant $[C(t)]$ according to the equation:

$$C(t) = C^0(t) \exp(-kt) \quad (3).$$

If the reaction product rather than the analyte itself is monitored, then we may write:

$$dC_p/dt = D_{Lp} d^2 C_p/dx^2 - u dC_p/dx + kC \quad (4)$$

where C_p is the concentration of the product and D_{Lp} its axial dispersion coefficient.

If, in addition, we assume the axial dispersion coefficients of the analyte (D_L) and the product (D_{Lp}) to be similar, then the following relationship will hold:

$$C_p + C = C_p^0 = C^0 \quad (5)$$

where C_p^0 is the concentration of product that would arise if all the analyte reacted immediately after injection.

By using the equations

$$C = (C_p^0 - C_p) = C_p^0 \exp(-kt) \quad (6)$$

and

$$C_p = C_p^0 [1 - \exp(-kt)] \quad (7)$$

equation (4) can be transformed into a form of equation (1) in which the variable C_p^0 replaces C . Further, if the product is monitored, the rate constant can be calculated from equation (6) provided the shape of the concentration/time curve obtained by injection of the product or the analyte in the absence of chemical reaction is known in advance. The assumption that the axial dispersion coefficients of the analyte and the product are very similar imposes no substantial limitations as long as the dispersion pro-

cesses in the flow system are governed by convective mass-transfer, since any difference between the diffusion constants of the analyte and the product would result in no substantial differences between the corresponding axial dispersion coefficients. In fact, the flow pattern of an open-closed flow system is convectively controlled because of the intensive mixing resulting from the use of the peristaltic pump.

According to these considerations, the concentration of the monitored chemical species (*i.e.*, the analyte or the product) at the detection point in the absence of a chemical reaction can be taken as the initial or final (steady-state) value under batch conditions, while the concentrations monitored in the event of a chemical reaction can be regarded as the transient concentrations corresponding to these initial or final concentrations.

It may be assumed that, if the condition involving the equality of the axial dispersion coefficients of all the chemical species taking part in the reaction is valid, this reasoning could also be applied to reactions other than those of first or pseudo-first order. In this respect, the following reaction stoichiometry and kinetic equation are a representative example:



$$dC_p/dt = kC_1 C_2 \quad (9)$$

where C_1 and C_2 are the concentrations of reactants R_1 and R_2 , respectively. If the concentration/time curves for at least two of the chemical species involved in the reaction in the absence of chemical interaction (*e.g.*, C_1^0 and C_2^0) are known, then, taking into account that $C_1 = C_1^0 - C_p$ and $C_2 = C_2^0 - C_p$, the corresponding solution of equation (9) allows the rate constant to be calculated. Assuming the product is the chemical species monitored:

$$\frac{1}{(C_2^0 - C_1^0)} \ln \left[\frac{C_1^0(C_2^0 - C_p)}{C_2^0(C_1^0 - C_p)} \right] = kt \quad (10)$$

If only the stoichiometry is known and both the rate constant and the reaction orders are to be determined, then the following approach could be applied: (i) the time-dependence of C_1^0 , C_2^0 and C_p should be obtained; (ii) among the kinetic equations with solutions similar to equation (10), *i.e.*, $f(C_1^0, C_2^0, C_p) = kt$, that yielding the same k value for all time points should be selected as the most likely kinetic equation; (iii) such an equation should be

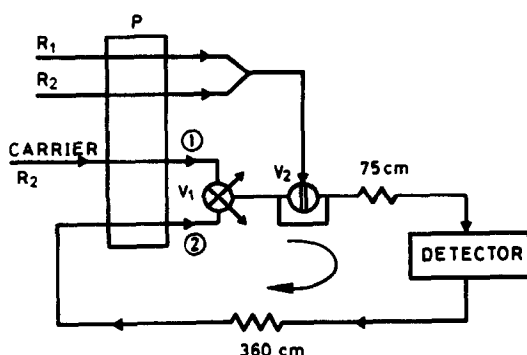


Fig. 1. Scheme of the open-closed FIA manifold. R_1 , R_2 , reagents; P, peristaltic pump; V_1 , selecting valves for channels (1) and (2); V_2 , injection valve.

checked at different initial concentrations (*i.e.*, C_1^0 and C_2^0 should be varied).

EXPERIMENTAL

Reagents

Aqueous solutions of ethyleneglycol bis-(β -aminoethyl ether)- N,N,N',N' -tetra-acetic acid (EGTA), 4-(2-pyridylazo)resorcinol monosodium salt monohydrate (PAR), cobalt(II) nitrate (guaranteed reagent grade) and boric acid/sodium hydroxide buffer¹¹ (pH = 8.8) were used.

Apparatus

A Hewlett-Packard 8452A diode-array spectrophotometer furnished with a Hellma 178.12QS flow-cell (18 μ l) and interfaced to a Hewlett-Packard Vectra ES/12 personal computer was used. A Gilson Minipuls-2 peristaltic pump, Tecator L 100-1 and Rheodyne 5041 injection valves, and a Tecator TM-III chemifold were also used.

Manifold

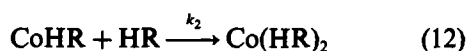
The manifold used is depicted in Fig. 1. Valve V_1 is an ordinary valve that can be switched between channels 1 and 2, while the other channels lead to waste. The sample containing both reagents, mixed at a confluence point upstream of the injection valve V_2 , is introduced into the flow system previously closed by valve V_1 . The reagent concentration in the carrier stream, and the pH, are the same as in the injected sample. Pump P ensures the flow circulation in the closed system. The lengths of the two reactors are 75 and 360 cm, respectively. Teflon tubes of 0.5 mm bore are used. The flow-rate in the closed system is measured from its total volume (2.08 ml) and

the mean residence time is taken as the time difference between two adjacent peaks. The volume of sample injected is 77 μ l. All volumes are determined from the weight of doubly distilled water required to occupy them. The volume of the sample loop is also checked on the basis of the injected analyte concentration, the volume of the closed system and the equilibrium analyte concentration in the absence of chemical reaction.

Chemical reactions and spectral data

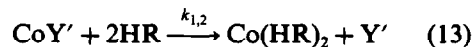
Under the experimental conditions, *viz.* pH = 8.8, the predominant species of PAR is the singly charged species, HR^- ,¹² and the complex of cobalt(II) with EGTA occurs in the forms CoY^{2-} , $CoHY^-$, and CoH_2Y , the stability constants of which are $10^{12.3}$, $10^{4.9}$ and $10^{3.3}$, respectively.¹³ Cobalt(II) forms a red complex with PAR with a metal-ligand ratio of 1:2 in slightly alkaline media.¹⁴ The stability constants of the complexes $CoHR^+$ and $Co(HR)_2^+$ are $10^{10.0}$ and $10^{7.1}$,¹⁵ respectively. It should be noted that magnetic susceptibility measurements have revealed that cobalt occurs as cobalt(III) in its complexes with PAR and PAN.¹⁶ According to Funahashi and Tanaka,¹³ the oxidation of cobalt(II) occurs immediately after the incorporation of the second PAR molecule.

The ligand-substitution reaction can be represented schematically in two stages:



where Y' denotes all forms of EGTA, irrespective of their extent of protonation.

The overall reaction can be obtained by adding equations (11) and (12):



The electrical charges of all chemical species in equations (11)–(13) have been omitted for clarity and simplicity. The proton mass-balance has not been taken into account, because all the chemical reactions take place in a buffered medium.

The kinetics of reaction (11) on the one hand, and of reactions (12) and (13) on the other, can be elucidated if CoY' is in excess in the first case, and PAR in the other two. Calculations based on the stability constants of $CoHR$ and

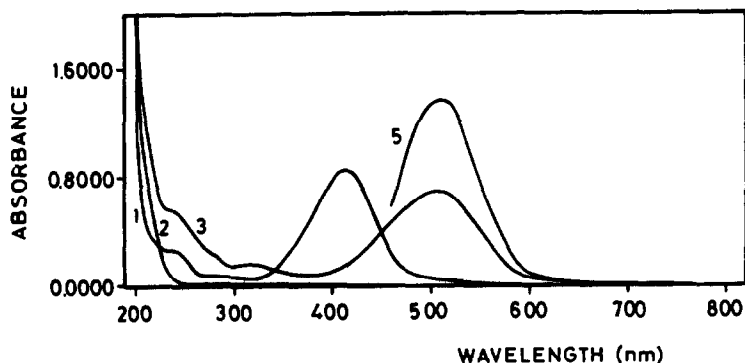


Fig. 2. Spectra of $2.50 \times 10^{-5} M$ solutions of: (1) PAR; (2) CoY'; (3) CoHR; (4) EGTA (coinciding with the spectrum of CoY'); (5) Co(HR)₂. The spectrum of Co(HR)₂ was recorded with excess of PAR present.

Co(HR)₂ showed that if equal volumes of equimolar solutions of cobalt(II) and PAR are mixed, the 1:1 complex obtained is predominant (>99.9%), whereas if the concentration of PAR is twice that of cobalt(II) the Co(PAR)₂ complex should predominate. On the basis of this, solutions of CoHR and Co(HR)₂ were prepared. By mixing equal volumes of equimolar solutions of cobalt(II) and EGTA, the corresponding complex (CoY') was obtained.

The spectra of CoY', PAR, CoHR, Co(HR)₂, and EGTA are shown in Fig. 2. All solutions were prepared in boric acid/sodium hydroxide buffer (pH 8.8).

The ligand-displacement reaction was investigated by monitoring the absorbance of the flowing solution at 410 nm (λ_{\max} for PAR), 448 nm (isosbestic point for PAR and CoHR), 505 nm (maximum for CoHR) and 515 nm, where the absorbance was due almost exclusively to CoHR. Concentration *vs.* absorbance plots obtained at these wavelengths over the concentration range $0-5.00 \times 10^{-5} M$ for PAR, CoHR, and Co(HR)₂ were all linear.

Procedure

During the experiments, the following injections were made:

(i) $5.00 \times 10^{-4} M$ solutions of PAR and CoHR into a carrier containing only buffer.

(ii) $5.00 \times 10^{-4} M$ solution of CoHR into a carrier containing $2.50 \times 10^{-4} M$ PAR or 1.25×10^{-5} , 2.50×10^{-5} , 5.00×10^{-5} , 1.25×10^{-4} or $2.50 \times 10^{-4} M$ CoY'.

(iii) $5.00 \times 10^{-4} M$ solution of CoY' into a carrier containing 1.25×10^{-4} or $2.50 \times 10^{-4} M$ PAR.

In all cases, the corresponding confluent solutions of CoY' and PAR were twice as concentrated as the carrier. This resulted in a

reagent concentration in the sample loop of valve V₂ (Fig. 1) equal to that in the carrier.

The experiments were repeated for three different carrier flow-rates (1.7, 2.5 and 3.1 ml/min).

RESULTS AND DISCUSSION

In the first series of experiments the ligand-displacement reaction was investigated under pseudo-first-order kinetic conditions. For that purpose, solutions of CoHR (Fig. 3B) and CoY' (Fig. 3C) were injected into carrier solutions in which PAR was in large excess. The axial dispersion coefficients of all reagents and products of the reactions studied were assumed to be equal, and the absorbances for individual species were assumed to be additive. The dispersion of CoHR was calculated from the recordings shown in Fig. 3A. The recordings in Fig. 3B allowed calculation of the extent of the reaction $\text{CoHR} + \text{HR} \rightleftharpoons \text{Co(HR)}_2$, by solution of the simultaneous equations for the total absorbances at 510 and 550 nm, and the corresponding molar absorptivities of CoHR and Co(HR)₂. The extent of the displacement reaction was similarly calculated from Fig. 3C.

Under the experimental conditions above, only reaction (12), the interaction of CoHR with excess of PAR, and reaction (13), the overall ligand-displacement reaction, again in excess of PAR, were investigated. In both cases, the rate law could be expressed by means of first-order kinetic equations.

$$dC_{\text{CoHR}}/dt = -k_2 C_{\text{CoHR}} \quad (14)$$

$$dC_{\text{CoY'}}/dt = -k_{1,2} C_{\text{CoY'}} \quad (15)$$

This was supported by the good linearity of the corresponding first-order plots (Fig. 4). The k_2 and $k_{1,2}$ values, determined by the least-

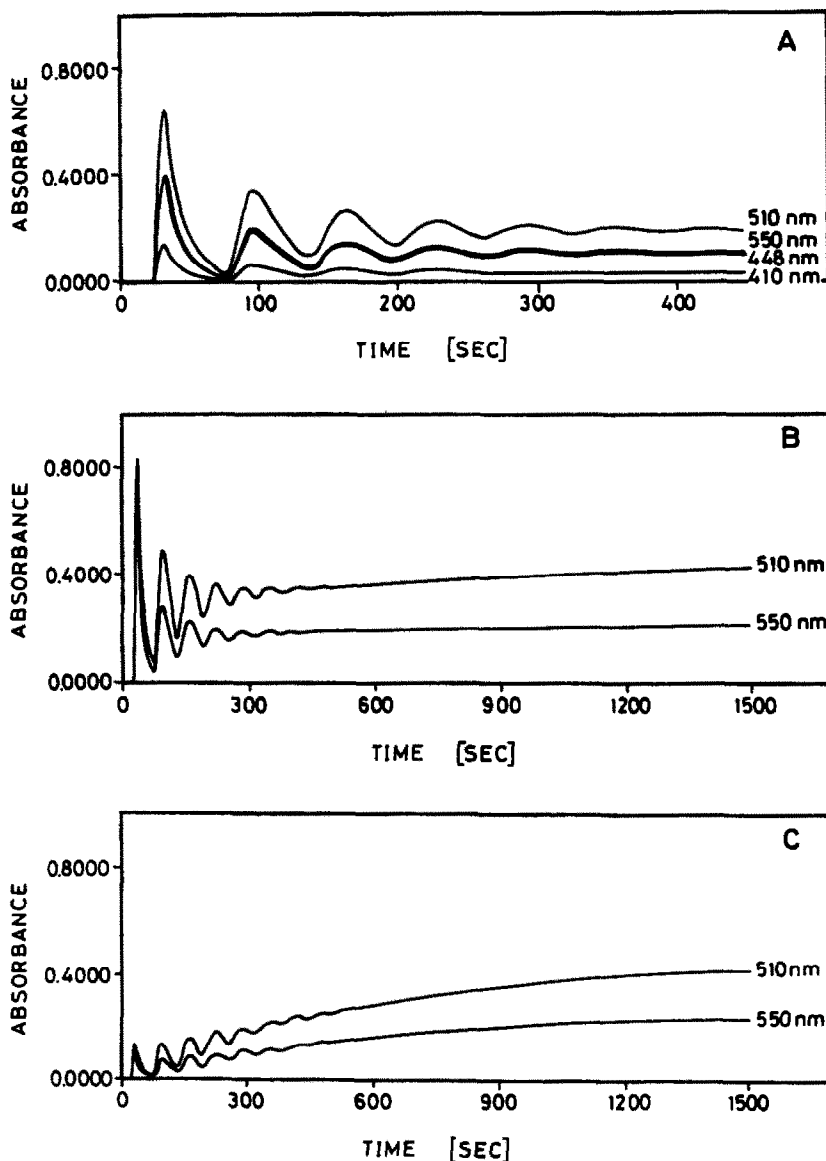


Fig. 3. Recordings obtained upon injection of CoHR into a carrier containing buffer only (A) or $2.50 \times 10^{-4}M$ PAR (B), and of CoY' into a carrier containing $2.50 \times 10^{-4}M$ PAR (C). The flow-rate was 1.7 ml/min in all cases.

squares method, were 8.85×10^{-3} and $2.41 \times 10^{-3} \text{ sec}^{-1}$, respectively.

A PAR solution ($5.00 \times 10^{-4}M$) was injected into a carrier containing only buffer or CoY' at various concentrations (1.25×10^{-5} – $2.50 \times 10^{-4}M$) for investigation of reaction (11). The concentration/time curve obtained by injecting PAR into a carrier containing buffer only was almost identical to that obtained on injection of CoHR into the same carrier. This shows that the assumption involving the equality of the axial dispersion coefficients of the reagents, on which the proposed method relies, is valid for the CoHR/PAR/CoY'/EGTA system. Con-

centrations of CoY' in the carrier above $2.50 \times 10^{-5}M$ ensured completion of the ligand-displacement reaction in a few seconds, and the recordings showed only the dispersion of the already obtained CoHR complex (Fig. 3A). The absorbance/time recordings obtained for 2.50×10^{-5} and $1.25 \times 10^{-5}M$ CoY' in the carrier solution are shown in Fig. 5A and B, respectively. In both cases, the concentrations of CoHR, CoY, and PAR were of the same order of magnitude, so the pseudo-first order simplification may not be applied. The concentrations of PAR and CoHR at each peak maximum were determined from the molar absorptivities of

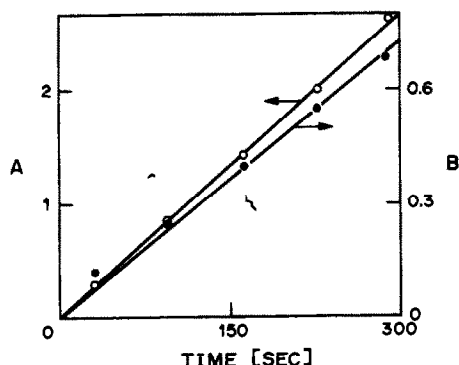


Fig. 4. First-order plots corresponding to equation (14) (○) and equation (15) (●), where $A = \ln(C_{\text{CoHR}}^0/C_{\text{CoHR}})$ and $B = \ln(C_{\text{CoY}}^0/C_{\text{CoY}})$.

PAR and CoHR (Table 1) at the wavelengths monitored and the absorbance values at the same wavelengths. Only the first five peaks were processed. As only the data for 2 wavelengths were required, 410 and 448 nm were chosen. Good agreement with the data found at 510 and 550 nm was observed. The data obtained were processed by using the kinetic equations listed in Table 2. First, an initial CoY' concentration of $1.25 \times 10^{-5} M$ in the carrier was used, as it allowed the first four peaks to be processed. The

reaction was completed before the appearance of the fifth peak. At an initial CoY' concentration of $2.50 \times 10^{-5} M$, the reaction was completed by the time the third peak was recorded, so only the first two peaks could be used. For all calculations, the initial concentration of PAR at each peak maximum was determined by injection into a carrier containing buffer only, while the initial concentration of CoY' was assumed to be that in the carrier prior to introduction of the PAR sample.

The results obtained are plotted in Fig. 6. Parameter R is the term on the left-hand side in the solution of a given kinetic equation (Table 2), divided by its maximum value (*i.e.*, that corresponding to the last peak used in the calculations). Parameter T is the time, divided by that of the appearance of the last peak maximum used. According to this normalization, the co-ordinates of the last peak used in the calculations will be $T = 1$; $R = 1$, irrespective of the kinetic equation used. The following kinetic equation provided the best fit to the experimental data at a CoY' concentration in the carrier of $1.25 \times 10^{-5} M$:

$$dC_p/dt = k \sqrt{C_1 C_2} \quad (16)$$

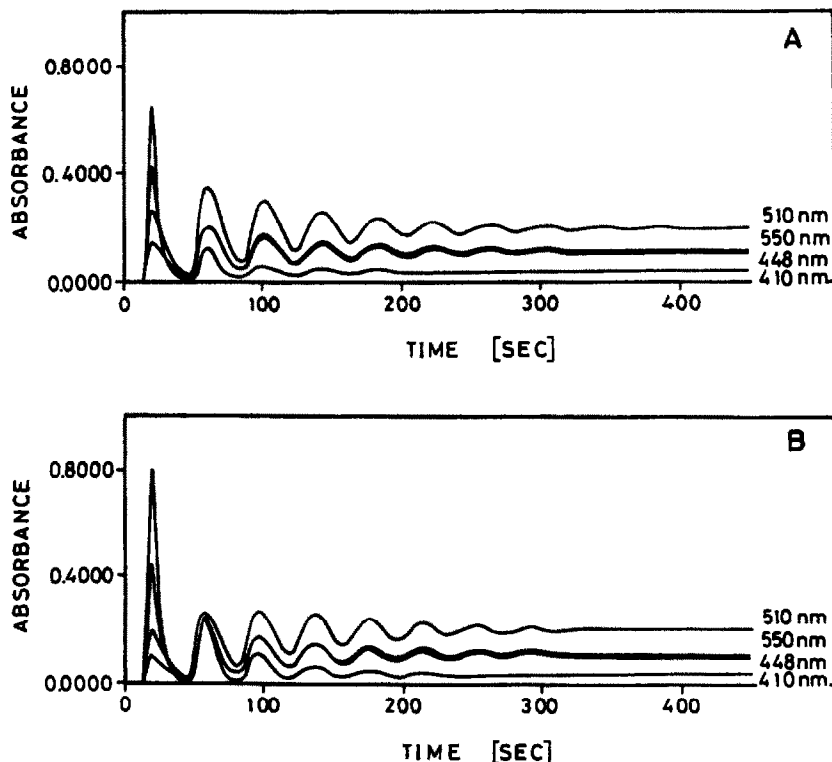


Fig. 5. Recordings obtained for injection of $5.00 \times 10^{-6} M$ PAR into a carrier containing CoY' at a concentration of $2.50 \times 10^{-5} M$ (A) and $1.25 \times 10^{-5} M$ (B). The flow-rate was 3.1 ml/min.

Table 1. Molar absorptivities ($l. mole^{-1}. cm^{-1}$) of PAR, CoHR and $Co(HR)_2$

Compound	Wavelength, nm			
	410	448	510	550
PAR	3.23×10^4	1.54×10^4	1.26×10^3	650
CoHR	6.31×10^3	1.59×10^4	2.84×10^4	1.67×10^4
$Co(HR)_2^*$			5.57×10^4	2.36×10^4

*The spectral features of $Co(HR)_2$ were investigated with excess of PAR present. Under such conditions, the molar absorptivities of $Co(HR)_2$ could not be determined at 410 and 448 nm because of the very high absorbance of the PAR.

Table 2. Kinetic equations used for the calculations

No.	Equation	Solution
(1)	$dC_p/dt = kC_1 C_2$	$\frac{1}{C_2^0 - C_1^0} \ln \frac{C_1^0(C_2^0 - C_p)}{C_2^0(C_1^0 - C_p)} = kt$
(2)	$dC_p/dt = kC_1 C_2^2$	$\frac{1}{C_1^0 - C_2^0} \left[\frac{C_p}{C_2^0(C_2^0 - C_p)} - \frac{1}{C_2^0 - C_1^0} \ln \frac{C_1^0(C_2^0 - C_p)}{C_2^0(C_1^0 - C_p)} \right] = kt$
(3)	$dC_p/dt = kC_1 C_2^{1/2}$	for $A > 0$: $\frac{1}{\sqrt{A}} \left[\ln \frac{(\sqrt{A+X} - \sqrt{A})(\sqrt{C_2^0} + \sqrt{A})}{(\sqrt{A+X} + \sqrt{A})(\sqrt{C_2^0} - \sqrt{A})} \right] = -kt$ for $A < 0$: $\frac{2}{\sqrt{-A}} \left[\arctan \sqrt{\frac{A+X}{-A}} - \arctan \sqrt{\frac{C_2^0}{-A}} \right] = -kt$
	$A = C_2^0 - C_1^0$ $X = C_1^0 - C_p$	
(4)	$dC_p/dt = kC_1^{1/2} C_2$	the same as the solution for equation (3) but C_2^0 replaced everywhere by C_1^0
	$A = C_1^0 - C_2^0$ $X = C_2^0 - C_p$	
(5)	$dC_p/dt = kC_1^{1/2} C_2^2$	for $A > 0$: $\frac{1}{A} \left\{ \frac{\sqrt{A+X}}{X} - \frac{\sqrt{C_1^0}}{C_2^0} + \frac{1}{2\sqrt{A}} \ln \left[\frac{(\sqrt{A+X} - \sqrt{A})(\sqrt{C_1^0} + \sqrt{A})}{(\sqrt{A+X} + \sqrt{A})(\sqrt{C_1^0} - \sqrt{A})} \right] \right\} = -kt$ for $A < 0$: $\frac{1}{A} \left\{ \frac{\sqrt{A+X}}{X} - \frac{\sqrt{C_1^0}}{C_2^0} + \frac{1}{\sqrt{-A}} \left[\arctan \sqrt{\frac{A+X}{-A}} - \arctan \sqrt{\frac{C_1^0}{-A}} \right] \right\} = -kt$
	$A = C_1^0 - C_2^0$ $X = C_2^0 - C_p$	

Subscripts 1 and 2 refer to PAR and CoEGTA, respectively.

where C_1 and C_2 are the concentrations of PAR and CoY' respectively.

However, the equation

$$dC_p/dt = k \sqrt{C_1} C_2^2 \quad (17)$$

cannot be completely discarded as a possible approximation to the true kinetic equation for the ligand-displacement reaction studied. The values of both rate constants obtained by a least-squares method were $6.53 l^{0.5}. mole^{-0.5}. sec^{-1}$ for equation (16) and $1.15 \times 10^6 l^{1.5}. mole^{-1.5}. sec^{-1}$ for equation (17).

Processing the results obtained with a CoY' concentration of $2.50 \times 10^{-5} M$ in the carrier solution yielded the following values for the two rate constants above: $5.11 l^{0.5}. mole^{-0.5}. sec^{-1}$ for equation (16) and $2.55 \times 10^5 l^{1.5}. mole^{-1.5}. sec^{-1}$ for equation (17). These results allow us to conclude that the most likely kinetic equation for reaction (11) is equation (16). Accordingly, the reaction must

be much faster in the presence of excess of CoY' than excess of PAR. This was experimentally confirmed, which is an additional proof for the validity of equation (16).

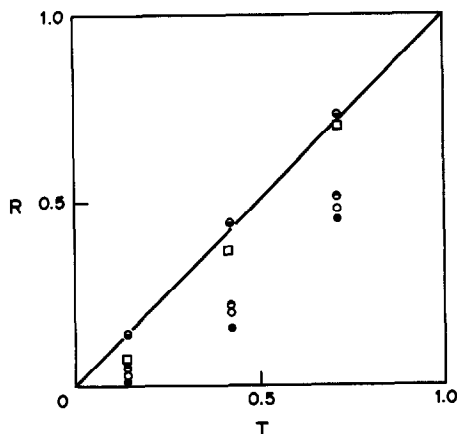


Fig. 6. Plots of R vs. T for equations (1) ○; (2) ●; (3) ⊙; (4) ⊖; and (5) □.

CONCLUSIONS

The proposed method for the determination of kinetic constants and reaction orders of chemical reactions can be successfully applied to kinetic studies, and can be implemented most efficiently in open-closed flow-injection systems where several peak maxima can be obtained from a single injection, and where the course of the chemical reaction from the beginning to equilibrium can be monitored with a single detector. These two major advantages make open-closed systems superior to traditional open flow-injection systems for this purpose.

Acknowledgement—The authors are grateful to Pergamon Press (*Talanta*) for financial support accorded to Dr. Spas D. Kolev by the Ronald Belcher Memorial Award.

REFERENCES

1. D. Betteridge, W. C. Cheng, E. L. Dagless, P. David, T. B. Goad, D. R. Deans, D. A. Newton and T. B. Pierce, *Analyst*, 1983, **108**, 1.
2. D. Betteridge, E. L. Dagless, B. Fields, P. Sweet and D. R. Deans, *Anal. Proc.*, 1981, **18**, 26.
3. J. M. Hungerford, G. D. Christian, J. Růžička and J. C. Giddings, *Anal. Chem.*, 1985, **57**, 1794.
4. H. A. Mottola, *Kinetic Aspects of Analytical Chemistry*, Wiley, New York, 1988.
5. D. Pérez-Bendito and M. Silva, *Kinetic Methods in Analytical Chemistry*, Horwood, Chichester, 1988.
6. A. Ríos, M. D. Luque de Castro and M. Valcárcel, *Anal. Chem.*, 1985, **57**, 1803.
7. *Idem*, *Anal. Chim. Acta*, 1986, **179**, 463.
8. J. M. Fernández-Romero, M. D. Luque de Castro and M. Valcárcel, *ibid.*, 1989, **219**, 191.
9. S. D. Kolev and E. Pungor, *Anal. Chem.*, 1988, **60**, 1700.
10. G. Taylor, *Proc. Roy. Soc. A*, 1953, **219**, 186.
11. D. D. Perrin and B. Dempsey, *Buffers for pH and Metal Ion Control*, Chapman & Hall, London, 1974.
12. W. J. Geary, G. Nickless and F. H. Pollard, *Anal. Chim. Acta*, 1962, **26**, 575.
13. S. Funahashi and M. Tanaka, *Bull. Chem. Soc. Japan*, 1970, **43**, 763.
14. D. Nonova and B. Evtimova, *Anal. Chim. Acta*, 1972, **62**, 456.
15. W. J. Geary, G. Nickless and F. H. Pollard, *ibid.*, 1962, **27**, 71.
16. T. Iwamoto and M. Fujimoto, *ibid.*, 1963, **29**, 282.

AUTOMATED DETERMINATION OF TOTAL PHOSPHORUS IN AQUEOUS SAMPLES

SHEN DONG and PURNENDU K. DASGUPTA*

Department of Chemistry and Biochemistry, Texas Tech University, Lubbock, TX 79409-1061, U.S.A.

(Received 30 July 1990. Accepted 13 August 1990)

Summary—The determination of total phosphorus in an automated microbatch analyzer system is described. The procedure combines persulfate digestion of the sample and colorimetric detection of orthophosphate by the ascorbic acid reduction of phosphomolybdate in a single processing chamber. Approximately 9 min are required per sample; ~1.7 ml of sample and 0.17 ml of total reagent are consumed. The limit of detection is $\leq 10 \mu\text{g/l}$. phosphorus. The method is tolerant of variations in salinity of the sample. Good agreements with ASTM procedures are shown for a variety of test compounds, lake water, wastewater and urine samples.

The microdetermination of phosphorus is of major importance in clinical and environmental contexts. Two publications on this topic^{1,2} are among the ten most cited papers in the analytical literature.³

Conversion of phosphorus into inorganic orthophosphate enables its straightforward determination. The first option listed in the current American Society for Testing and Materials (ASTM) standards⁴ is the ascorbic acid reduction of phosphomolybdate to molybdenum blue, originally due to Chen *et al.*¹ It is, however, the conversion of other forms of phosphorus into orthophosphate that is the tedious and time-consuming step. Acid-hydrolyzable phosphorus is operationally defined by ASTM as that which can be completely converted into orthophosphate by boiling for 30 min in dilute sulfuric acid; The acid-hydrolyzable phosphorus compounds are most notably inorganic meta-, pyro- and polyphosphates. Total phosphorus also includes the organically bound element; its conversion into orthophosphate is accomplished by including persulfate in the sulfuric acid digestion medium.

Determination of total P rather than orthophosphate or acid-hydrolyzable phosphorus is the parameter usually required by regulatory agencies. The persulfate digestion method for total phosphorus in sea-water was introduced by Menzel and Corwin⁵ and subsequently developed for general application by Gales *et al.*⁶ In lieu of boiling on a hot-plate, autoclaving the

digestion mixture (30–60 min at 120°) is frequently advocated,^{7–9} but is not easily automated. Attempts to automate continuous flow systems have been made with a UV-aided in-line flow digester (85°) in an air-segmented system¹⁰ or with a 10-m long PTFE capillary digester (at 160°, with an inserted platinum wire of equal length serving as a catalyst) in a flow-injection system.¹¹ Although both of these methods have advantages and their applicability to the determination of total phosphorus in natural waters has been demonstrated, complete conversion of certain degradation-resistant compounds, *e.g.*, thiophosphorus insecticides, into orthophosphate has not been established, and this can often only be achieved by conventional block- or autoclave-digestion methods as required by the ASTM.

We have recently introduced the automated microbatch analyzer (AMBA) and demonstrated its utility for a number of different applications.^{12–15} The present work describes a unique application of the AMBA system—the determination of total phosphorus by adaptation of the ASTM procedure. Digestion at elevated temperature and pressure is followed by colorimetric measurement in the same cavity, requiring less than 9 min per sample.

EXPERIMENTAL

Apparatus

The AMBA system was similar to that in previous descriptions^{14,15} except as detailed below. The cavity was machined from 1½ in. diameter poly(vinylidene fluoride) (Kynar®,

*Author for correspondence.

Pennwalt Corp.) and has a rounded bottom, 9.2-mm inner diameter and a 34.6-mm deep well. The heater element is contained within a 1.2-mm diameter, 16-mm long ceramic sleeve and is capable of generating 25 W at 30 V (Watlow Inc., St. Louis, MO). This is inserted within a thin-walled pyrex tube (*ca.* 1.8-mm outer diameter) sealed at one end, and packed with magnesium oxide as heat-transfer agent. The heater is inserted through a hole in the cavity lid, offset from the center, to such a depth that its bottom tip is several mm above the stirrer bar when the cavity is sealed with the lid and its attendant O-ring, and the top of the heating element is several mm below the sample level. The glass tube encasing the heater is sealed into the lid with a compression fitting. The light source is a high radiant-intensity infrared light-emitting diode (LED) (CN-305, 8 mW at 880 nm and 50 mA, Stanley Electric, Tokyo, Japan) coupled to a silica fiber as shown in the inset of Fig. 1. The LED is inserted within a $\frac{1}{4}$ -28 to 10-32 compression-fitting union commonly used in liquid chromatography (an all-plastic black version is available from Dionex Corp., Sunnyvale, CA). A small infrared photodiode, R, is placed immediately behind the LED, L. The leads are suitably insulated from each other with sleeves and the assembly is fixed in place with a $\frac{1}{4}$ -28 fitting (not shown). The silica fiber

F (1-mm core, Ensign-Bickford Optics, Avon, CT) butts against L (the connecting passage between the two sides of the fitting is enlarged by drilling) and is held in place by a plastic compression fitting. L is powered by a constant-current source at 50 mA and the photodiode R receives enough light reflected off the front surface of L to make the arrangement practical and avoid the need for a bifurcated fiber optic. The receiving and transmitting optical fibers are both sealed into the cavity with compression fittings, diametrically opposite to each other, and both protrude slightly into the cavity, resulting in an optical path-length of ~ 6 mm. The receiving fiber optic is coupled to an infrared photodiode and the output of this and the reference detector R are in turn processed by a log ratio amplifier (AD757N, Analog Devices, Norwood, MA) to provide an output of 1 V for an absorbance of 1.0.

The fluid system is also schematically shown in Fig. 1. All liquid reservoirs are pressurized by the same nitrogen supply at 15 psig. The different flow-rates of the individual liquids are achieved by use of appropriate lengths and diameters of the standard wall thickness (SW) PTFE tubing (Zeus Industrial Products, Raritan, NJ) connecting the liquid reservoirs to the cavity. The sample and pressure/vent lines enter the cavity through 23 gauge tubes, and the

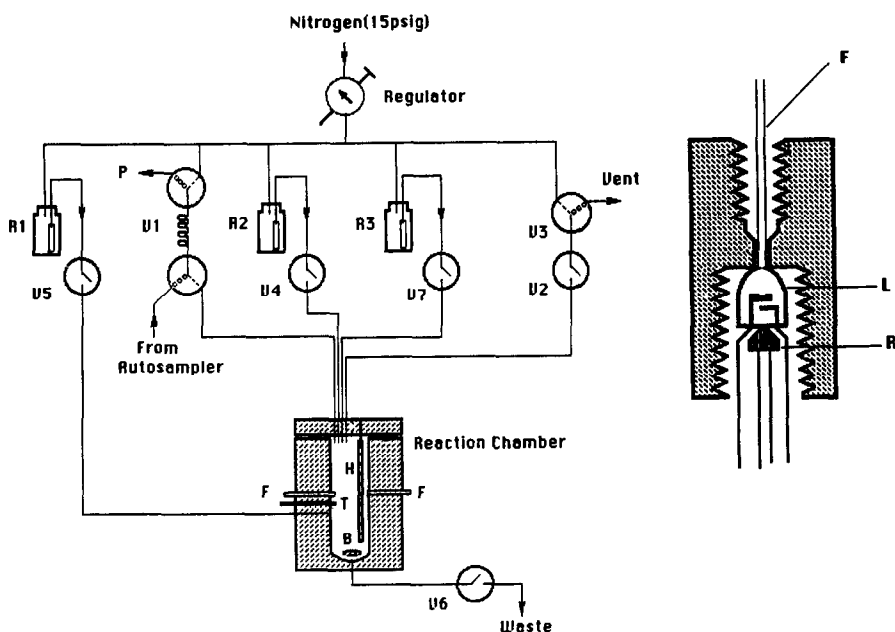


Fig. 1. Schematic of AMBA. V1, Sample valve; P, peristaltic pump; R2, digestion reagent; R3, wash water; R1, color reagent; V4-V7, liquid dispensing valves; V2, V3, cavity closure/vent/pressurization valves; V6, bottom outlet valve; H, heater; F, fiber optic; T, thermistor; B, stirrer. Inset shows IR light-emitting diode L, reference photodiode R and fiber optic F in a chromatography union; retaining nuts are not shown.

acid/persulfate, color reagent and wash lines have ~30 cm of 30 gauge, ~15 cm of 30 gauge and ~40 cm of 20 gauge tubing, respectively, as primary restrictions. Only the color development reagent enters through the side of the cavity (below the digested liquid level), and all the other connections, except for the waste line, are made through the cavity lid as shown. The sample loop was made from 18 gauge tubing and the volume delivered was found gravimetrically to be 1.66 ± 0.09 ml.

Reagents

Except as mentioned below, all chemicals were obtained from Aldrich. Adenosine-5'-monophosphate and α -D-glucose-1-phosphate were obtained from Sigma, sodium metaphosphate from Fisher Scientific, analytical-reagent grade potassium dihydrogen phosphate from Mallinckrodt, disodium phenyl phosphate dihydrate from Fluka and *O,O*-diethyl-*O*-(3,5,6-trichloro-2-pyridyl)phosphorodithioate (Chlorpyrifos®) was obtained as an analytical standard from the Dow Chemical Company. The pesticide Dursban® (Gro-Tec Inc.) was purchased locally.

The acid/persulfate reagent contained 2.5 g of ammonium persulfate dissolved in 10 ml of 2.75M sulfuric acid. The mixed reagent, as used here, is unstable and should be prepared daily. A 66.0- μ l volume of this reagent is dispensed under our operational conditions. If the acid and the oxidant are kept separate, the usable lifetime can be greatly improved. The color development reagent was prepared by dissolving 390 mg of potassium antimonyl tartrate (J. T. Baker), 16.8 g of ammonium heptamolybdate tetrahydrate (Fisher) and 106 ml of concentrated sulfuric acid in water and diluting to 1000 ml, and then dissolving 1.50 g of ascorbic acid (Merck) in 100 ml of this solution. A 100- μ l aliquot of the reagent is dispensed. The formulations of the acid/persulfate and the color development reagents are adaptations of the ASTM recipes to provide the same acidity and reducing power in the present method. Note that if the sample contains very substantial amounts of acid or base, this recipe will need adjustment.

Aqueous solutions of all compounds were directly used except for the Dursban®, for which an aqueous extract was used. Recovery of total phosphorus from the test compounds was investigated in the concentration range 100–1000

μ g/l., with 2–8 replicates per sample for the test compounds as well as for the urine and environmental samples.

Operational procedure

The timing and functional sequence of the analyzer are shown in Table 1. The operational status is described by an 8-bit number (1 = ON, 0 = OFF), the first (most significant) through to the seventh bit representing valves V1–V7 [2-way valves allow fluid flow when on; for 3-way valves, the common port (solid line) is connected to the dashed-line port when the valve is on], and the last bit representing the heater status. A major time-consuming step is the cool-down period; this is necessary to avoid the loss of ebullient liquid that would occur if the cavity were vented at temperatures $> 100^\circ$. Conceivably, this period can be reduced by using a thinner-walled cavity that will allow faster cooling.

RESULTS AND DISCUSSION

The system gives linear response in the range 0–1 μ g/ml phosphorus, and may be described by the equation $A = (0.187 \pm 0.002) C + (0.002_1 \pm 0.001_1)$, $r^2 = 0.9991$, where A is the absorbance and C the phosphorus concentration in μ g/ml. The standard error of estimate for A is 0.002₂. Because the color reagent is added when the solution is still very hot, color development is very rapid. As may be evident from the system output shown for blanks and samples containing 0.025 μ g/ml P (Fig. 2), the analytical signal is best taken as the sharp absorbance change that occurs immediately upon addition of the color reagent when

Table 1. AMBA operational sequence for total phosphorus determination

Time, sec	System status	Function
000–012	11010000	Deliver sample (1.66 ml) and digestion reagent (66 μ l)
013–312	00000001	Heat sealed enclosure to 140°
313–460	00000000*	Let sealed enclosure cool to $< 100^\circ$ Load next sample in loop
461–475	01000000	Pressure release
476–483	01001000	Add color reagent (100 μ l)
484–493	01000000	Develop and measure color
494–498	01100100	Discard contents
499–501	01000010	Add wash water (2 ml)
502–506	01100100	Discard contents
507–511	01000010	Add wash water (2 ml)
511–515	01100100	Discard contents

*Sampling pump is set to turn on under this condition.

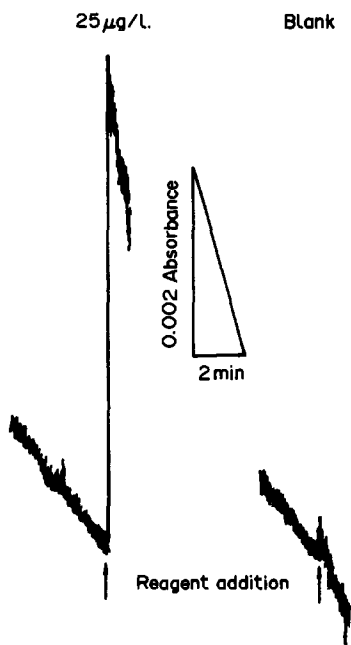


Fig. 2. Recorder trace showing the system output from a sample containing 25 $\mu\text{g/l}$. P and from a blank.

phosphorus is present. The detector signal drifts for thermal reasons. When the heater is turned off, the temperature decreases continuously and the associated change in refractive index causes the signal drift, especially with the more sensitive detector settings. The drift rate is increased further upon addition of the relatively cool reagent. However, as may be obvious from Fig. 2, the drift is slow relative to the sample-induced signal and no significant problems are encountered in interpreting the results.

Table 2. Recovery of total phosphorus from test compounds, with reference to the ASTM method

Compound	Recovery \pm s.d., %
Sodium pyrophosphate	98.1 \pm 0.4
Sodium metaphosphate	95.9 \pm 1.0
Sodium tripolyphosphate	102.8 \pm 0.8
Disodium phenyl phosphate	98.7 \pm 1.0
Diethyl phosphate	98.2 \pm 0.4
Trimethyl phosphate	97.2 \pm 0.4
Trimethyl phosphite	99.6 \pm 0.4
Adenosine-5'-monophosphate	99.2 \pm 0.8
α -D-Glucose-1-phosphate	97.8 \pm 0.8
Ethylchlorothiophosphate	102.9 \pm 1.7
α -Carboxyethylphosphonic acid	98.8 \pm 0.4
Hexyltriphenylphosphonium bromide	94.6 \pm 0.8
Chlorpyrifos [®]	87.0 \pm 3.4
Dursban [®]	90.2 \pm 2.4
Potassium dihydrogen phosphate	100.0 \pm 0.7
KH ₂ PO ₄ in 0.6M sodium chloride	97.5 \pm 1.8
KH ₂ PO ₄ in 200 mg/l. sucrose	96.6 \pm 2.5
KH ₂ PO ₄ in 200 mg/l. Triton X-100	93.0 \pm 0.2

Table 3. Results for natural water and wastewater samples

Sample	P, $\mu\text{g/ml}$	
	ASTM	AMBA
Lake 1	0.067 \pm 0.002	0.063 \pm 0.001
Lake 2	0.141 \pm 0.002	0.135 \pm 0.001
Lake 3	0.056 \pm 0.002	0.055 \pm 0.0
Wastewater		
City of Post	0.976 \pm 0.012	1.000 \pm 0.007
Treatment plant influent,		
City of Levelland	7.52 \pm 0.29	7.76 \pm 0.03
Raw sewage,		
City of Wofforth	4.00 \pm 0.06	4.13 \pm 0.00 ₄

Interestingly, this procedure obviates the need for using calibrants that are exactly matrix-matched with the sample, e.g., sea-water, to prevent the refractive index effects common to flow-through detectors. The limit of detection in our system may be estimated from Fig. 2 to be $\leq 10 \mu\text{g/l}$. phosphorus.

Recovery of phosphorus from a number of disparate test compounds is shown in Table 2, relative to the value obtained by the ASTM method (assumed to be 100%). With the exception of Chlorpyrifos[®] (this is also the active ingredient in Dursban[®]), the recovery is $\geq 95\%$, adequate for most purposes. If the digestion time is increased from 5 to 9 min, the recovery for the more difficult samples increases considerably, that for metaphosphate, for example, to $98.3 \pm 1.0\%$. The presence of sodium chloride at salinities typical of ocean water has no marked effect on the result, nor is there any major interference from organic compounds or surface-active agents, which have been reported to cause problems.¹¹ The results for a number of environmental samples appear in Table 3 and those for urine samples in Table 4; in all cases good agreement with the ASTM method is observed.

Table 4. Results for urinary phosphorus*

Sample†	ASTM	AMBA
M	754 \pm 18	760 \pm 27
M	114 \pm 6	107 \pm 3
M	145 \pm 4	144 \pm 6
F	330 \pm 7	338 \pm 10
F	890 \pm 29	885 \pm 5
F	403 \pm 25	380 \pm 8
M	475 \pm 5	452 \pm 5
F	537 \pm 9	535 \pm 2
M	416 \pm 12	417 \pm 5
M	1410 \pm 18	1403 \pm 25
M	800 \pm 14	820 \pm 29

*Large dilutions, up to a factor of 2500, were used for these samples.

†M = male; F = female.

Acknowledgements—We gratefully acknowledge the help of Steve Gluck, Dow Chemical Co., Midland, MI and Steve Garner, Watlow, Inc., St. Louis, MO. This research was supported by a cooperative agreement with the Dow Chemical Co., Midland, MI.

REFERENCES

1. P. S. Chen, Jr., T. Y. Toribara and H. Warner, *Anal. Chem.*, 1956, **28**, 1756.
2. R. J. L. Allen, *Biochem. J.*, 1940, **34**, 858.
3. T. Braun, A. Schubert and S. Zeindely, *Trends Anal. Chem.*, 1989, **8**, 1.
4. *ASTM Annual Book of Standards*, Vol. 11.01, Method D515-82, American Society for Testing and Materials, Philadelphia, 1989.
5. D. W. Menzel and N. Corwin, *Limnol. Oceanog.*, 1965, **10**, 280.
6. M. E. Gales, Jr., E. C. Julian and R. C. Kroner, *J. Am. Water Works Assoc.*, 1966, **58**, 1363.
7. D. S. Jeffries, F. P. Dieken and D. E. Jones, *Water Res.*, 1979, **13**, 275.
8. J. Ebina, T. Tsutsui and T. Shirai, *ibid.*, 1983, **17**, 1721.
9. M. Hosomi and R. Sudo, *Int. J. Environ. Stud.*, 1986, **27**, 267.
10. P. Goulden and P. Brooksbank, *Anal. Chim. Acta*, 1975, **80**, 183.
11. M. Aoyagi, Y. Yasumasa and A. Nishida, *ibid.*, 1988, **214**, 229.
12. J. A. Sweileh, J. L. Lopez and P. K. Dasgupta, *Rev. Sci. Instrum.*, 1988, **59**, 2609.
13. J. A. Sweileh and P. K. Dasgupta, *Anal. Chim. Acta*, 1988, **214**, 107.
14. L. Ping and P. K. Dasgupta, *Anal. Chem.*, 1990, **62**, 85.
15. P. K. Dasgupta and K. Petersen, *ibid.*, 1990, **62**, 395.

SIMULTANEOUS DETERMINATION OF CALCIUM AND MAGNESIUM BY USING A FLOW-INJECTION SYSTEM WITH SIMULTANEOUS INJECTION OF TWO SAMPLE PLUGS AND A MASKING AGENT PLUG

TAKESHI YAMANE* and EIICHI GOTO

Department of Chemistry, Faculty of Education, Yamanashi University, Takeda-4, Kofu 400, Japan

(Received 24 May 1990. Revised 6 July 1990. Accepted 13 July 1990)

Summary—A flow-injection system is described for the simultaneous determination of calcium and magnesium with simultaneous injection of two sample plugs and a masking agent plug and with a single detector. The system utilizes the simultaneous injection of an ethylene glycol-bis(2-aminoethylether)-*N,N,N',N'*-tetra-acetic acid plug and two small sample plugs into the same carrier stream and which are merged downstream with 3,3'-bis[*N,N*-bis(carboxymethyl)aminomethyl]-*o*-cresolphthalein solution for spectrophotometric determination of calcium and magnesium. The results for the analysis of natural waters by the proposed method correspond well with those obtained by the conventional titration method with ethylenediaminetetra-acetic acid, and showed good reproducibility. The rate of analysis is about 15 samples/hr.

Calcium and magnesium are often determined for environmental and biological monitoring. Titrimetry, spectrophotometry and atomic-absorption spectrometry are the most frequently used techniques for such determinations.

Flow-injection analysis (FIA) has proved to be a suitable tool for rapid, simple and reproducible analysis with rather inexpensive apparatus. FIA has also been found useful for simultaneous determination of two or more components in a sample. Reviews of such determinations and speciation measurements with FIA have appeared in the literature.^{1,2} We previously reported an approach to a simple FIA system which allows the simultaneous determination of two components with a single detector.³

This paper extends this FIA system to the simultaneous determination of calcium and magnesium in natural waters. Several FIA methods with spectrophotometric detection have been proposed for calcium⁴⁻⁷ or magnesium^{8,9} with various chromogenic reagents. These are, however, focused on single component determination, with the exception of the total hardness determination. FIA spectrophotometric methods with one detector, with Chlorophosphonazo III¹⁰ or murexide and Eriochrome Black T (EBT),¹¹ so far described

for the simultaneous determination of calcium and magnesium, should be better described as sequential,¹ because two consecutive injections are required along with switching of the reagent solution for the determination of the two components. Such methods also require a switching valve and therefore would lead to a complicated and troublesome system. A sequential FIA determination of calcium and magnesium with EBT as reagent has also been reported.¹² The FIA system described here exploits a simple configuration which does not need switching or splitting of the flow stream, and allows a simple and rapid simultaneous determination. Natural waters such as river water, ground water and sea-water were satisfactorily analysed by the proposed method.

EXPERIMENTAL

Manifold and procedure

A Jasco UVIVDEC-320 spectrophotometer equipped with a flow cell, a Hitachi 655A-13 pump, and a Hitachi K-1600 16-port valve were used. All pieces of tubing, including a 4-m long separation coil (SC), a 15-cm masking agent loop (R, 31 μ l) and two 15-cm sample loops (S1, S2, 31 μ l) which were connected to a 16-port valve, were made of Teflon (0.5 mm i.d.). The flow-injection manifold used is shown in Fig. 1. Two small sample plugs and a masking agent

*Author for correspondence.

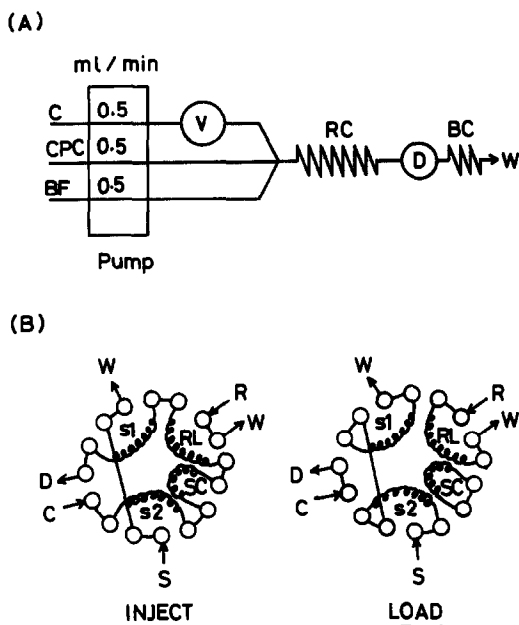


Fig. 1. (A)—Schematic diagram of FIA system for simultaneous determination of calcium and magnesium; (B)—16-port valve and loop configuration. For further details see text. C, Carrier (water); CPC, 0.050% CPC solution; BF, ammonia buffer solution (pH 10.1); V, 16-port valve with two sample loops, separation coil and a masking reagent loop; s1, s2, sample loop (15 cm long, 31 μ l); SC, separation coil (4 m); RC reaction coil (1-m long); RL, masking reagent loop (15 cm long, 31 μ l); R, $3.0 \times 10^{-3}M$ EDTA solution; S, sample loading; D, spectrophotometric detection (575 nm); BC, back-pressure coil (0.25 mm i.d., 2.5 m); W, waste.

plug are simultaneously injected into the same carrier stream by making effective use of the 16-port valve. In one of the sample plugs (s1), calcium is complexed with ethylene glycol-bis(2-aminoethylether)-*N,N,N',N'*-tetra-acetic and (EGTA) by penetration of the s1 and R plugs during transport to the reaction coil (RC). Calcium and in the other sample plug (s2), are kept as they were in the original sample. The mixing of these sample plugs with the 3,3'-bis[*N,N*-bis(carboxymethyl)]-*o*-cresolphthalein (CPC) solution causes two peaks to be observed in the spectrophotometric measurement at 575 nm, as shown in Fig. 2(b). The first peak corresponds to magnesium and the second to the sum of calcium and magnesium. The concentration of calcium can be calculated by difference. The peaks in Fig. 2(b) were recorded for a single injection of a mixture of calcium and magnesium. Calibration graphs, two for magnesium (one for the first peak, the other for the second, which is more dispersed) and one for calcium, were prepared separately.

Reagents

Unless otherwise noted, all reagents were of analytical grade and were used as received. The standard solutions of calcium and magnesium were prepared from 100- μ g/ml stock solutions (Wako Pure Chemical Industries, Osaka, Japan). The CPC solution (0.05%) was prepared by dissolving the reagent (Dojindo Laboratories, Kumamoto, Japan) in water, adding 50 ml of ammonia buffer solution (pH 10.1) and diluting to 100 ml with water. The EGTA solution ($1.0 \times 10^{-2}M$) was prepared by dissolving the reagent (Dojindo Laboratories) in a dilute solution of ammonia and then diluting to volume with water. More dilute solutions were prepared by dilution of this stock solution with water. The ammonia buffer solution was prepared by mixing 2.0M ammonia solution (50 ml) and 1.0M ammonium chloride solution (25 ml), adding one of the components to adjust the pH to 10.1 and finally diluting to 100 ml with water.

RESULTS AND DISCUSSION

FIA manifold for simultaneous determination

In the present approach, a long coil (separation coil) filled with carrier solution between two sample plugs was used. This configuration prevents any overlap of the two zones. The effect of the length of the separation coil on the efficiency of peak separation was investigated by injecting a 20- μ g/ml magnesium solution, with use of the manifold in Fig. 1. Good separation of the two peaks was observed with separation coils longer than 2 m. Longer coils resulted in better separation but caused a decrease in peak height and an increase in the width of the second peak. The height of the first peak was independent of the separation coil length, as expected. A 4-m coil was used in this study to avoid any penetration of the reagent R into sample plug s2. With a 4-m coil the height of the second peak for calcium and/or magnesium did not change when the $3.0 \times 10^{-3}M$ EGTA solution in R was replaced by water. This indicated that EGTA did not affect the complex formation of calcium and magnesium with CPC in plug s2. The length of the reaction coil is important for controlling the dispersion of the sample zone (s1) and the masking reagent zone (R), because there must be effective penetration of these zones. A 1-m reaction coil was found to be suitable both for the masking of calcium and for obtaining good separation of the two peaks as

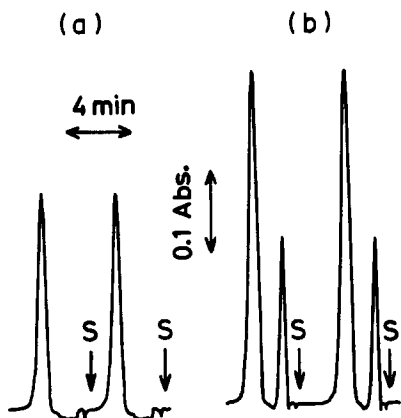


Fig. 2. Typical recordings for calcium and magnesium with injection of the solutions containing (a) 10 $\mu\text{g/ml}$ calcium alone and (b) 10 $\mu\text{g/ml}$ calcium and 20 $\mu\text{g/ml}$ magnesium in a mixture.

shown in Fig. 2. It is of interest to note that increasing the sample coil length (*s1*) from 15 cm to 30 cm improved the peak height about twofold, but the masking capacity of $3.0 \times 10^{-3}M$ EGTA was limited to 20 $\mu\text{g/ml}$ calcium in the *s1* plug.

Detection of calcium and magnesium with CPC

CPC reacts with both calcium and magnesium in alkaline medium to form red complexes which have similar absorption spectra, with broad maxima at about 570 nm for magnesium and 575 nm for calcium. Thus, a wavelength of 575 nm was chosen so that both analytes could be detected with a single detector. For this simultaneous determination, it was desirable for the signal for one component to be obtained separately, in addition to the signal for the sum of the two components. It was decided to mask one component (calcium) in the sample with EGTA, because there is a considerable difference between the log *K* values for the EGTA complexes of calcium and magnesium.¹³ Experiments at pH 10.1 with ammonia buffer solution indicated that calcium (up to 30 $\mu\text{g/ml}$) could be masked by addition of $3.0 \times 10^{-3}M$ EGTA since only one peak was found when the solution containing only calcium was injected [Fig. 2(a)]. A smaller concentration ($1.0 \times 10^{-3}M$) of EGTA resulted in incomplete masking. Thus, a $3.0 \times 10^{-3}M$ solution was adopted.

The effect of the CPC concentration on the peak height was studied by injecting a 10- $\mu\text{g/ml}$ calcium solution and 0.010, 0.025, 0.050 and 0.075% CPC solutions. The peak height was found to be almost independent of the CPC

concentration in the range 0.025–0.075%, but it slightly decreased at 0.010%. The baseline absorbance increased almost linearly with increase in CPC concentration. The 0.050% solution was chosen for this study.

The pH dependence of the complex formation of calcium and magnesium with CPC was studied. The pH was adjusted with ammonia–ammonium chloride buffer solutions. The peak height for calcium increased gradually from pH 9.5 to 10.7, whereas a maximum peak height was observed for magnesium at about pH 10.4 (Fig. 3). This effect may be due to the hydrolysis and precipitation of magnesium in more alkaline media. Experiments with higher concentrations of buffer solutions at constant pH or with more alkaline solutions buffered with ammonia or borate–sodium hydroxide caused too much baseline disturbance. As a result, a pH of 10.1 for complex formation and a buffer solution of 1.0M ammonia–0.25M ammonium chloride were employed in this FIA system. Only small changes in the baseline caused by changes in refractive index still appeared in the first peak region under these conditions (Fig. 2). This, however, is not a serious drawback in measuring the peak height, because of the low noise and good stability in the baseline.

Calibration

Under the conditions described, calibration graphs were linear up to at least 30 $\mu\text{g/ml}$ for each analyte as shown in Fig. 4. Slopes obtained by least squares for two series of solutions with successively increasing magnesium concentrations (5.0, 10, 20, and 30 $\mu\text{g/ml}$) and fixed 10 $\mu\text{g/ml}$ calcium concentration and solutions

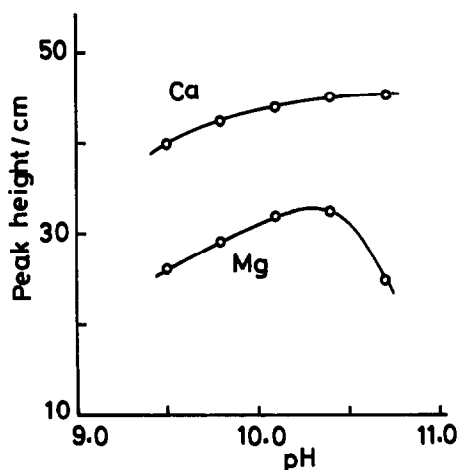


Fig. 3. Effect of pH on the second peak for 10 $\mu\text{g/ml}$ of calcium and magnesium.

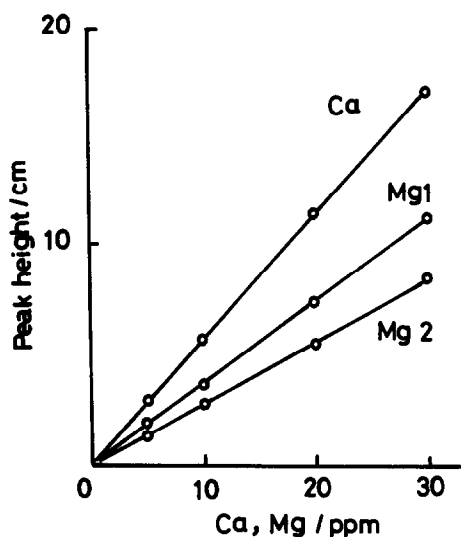


Fig. 4. Calibration graphs for calcium and magnesium. Mg1 and Mg2 indicate the heights of the first and second peaks, respectively, for magnesium.

containing successively increasing calcium (5.0, 10, 20, and 30 $\mu\text{g/ml}$) and fixed 10 $\mu\text{g/ml}$ magnesium were in good agreement with those of the corresponding calibration graphs for the individual elements. This indicates good recoveries of calcium and magnesium in synthetic mixtures even at differing ratios. The relative standard deviations for 10 $\mu\text{g/ml}$ of both calcium and magnesium in a synthetic mixture were 0.4 and 0.8%, respectively. The limit of detection (signal three times the standard deviation of the average blank signal) was 0.2 and 0.3 $\mu\text{g/ml}$ for calcium and magnesium, respectively.

At a flow-rate of 0.5 ml/min for each channel in Fig. 1, an injection rate of 15 samples/hr could be achieved.

Interferences

The interference study involved focusing on some metals that may be found occasionally at

levels up to several $\mu\text{g/ml}$ in natural waters, and some anions that might cause precipitation of calcium and magnesium. Solutions were prepared which contained 10 $\mu\text{g/ml}$ of both calcium and magnesium, together with the other ions to be examined. These were injected exactly as in the experiments described above. In order to investigate interferences in the calcium determination in more detail, solutions from which magnesium was omitted were injected. No significant interference was observed for the following ions ($\mu\text{g/ml}$); Fe(III) (5), Al(III) (5), Cu(II) (5), Zn(II) (1), Ni(II) (1), Mn(II) (1), Co(II) (1), PO_4^{3-} (20), SO_4^{2-} (500), tartrate (500), citrate (20), oxalate (20). Significant interference was defined as causing a deviation of more than 3%. Phosphate, citrate and oxalate at levels of several hundred $\mu\text{g/ml}$ affected the determination of both analytes, especially that of calcium (negative interference). This interference is probably caused by the formation of complexes or low solubility species. The concentrations of these ions in most natural waters is usually low enough for no interference in the present method to be expected. It is important to note that the sample solution to be injected must be nearly neutral, or at least have a $\text{pH} > 4$, because the colour development for detection with CPC is sensitive to pH variation.

Analysis of natural waters

The proposed FIA method was applied to the analysis of natural waters such as river water, ground water and sea-water. The ground water and sea-water were diluted until the concentrations would fit into the linear range of the calibration graphs. As shown in Table 1, the results obtained by the FIA method compare well with those found by the conventional EDTA titration method. Differences in most

Table 1. Analysis of natural waters by the proposed FIA method

Sample	Dilution	Metal ion found, $\mu\text{g/ml}$			
		FIA method		Titration method	
		Ca	Mg	Ca	Mg
Ground water					
Tohkohji	2/5	29.6 (0.5)*	9.8 (1.3)*	31.3	10.1
Kunado	1/5	57.3 (1.0)	9.6 (2.5)	61.0	9.6
River water					
Fuefuki river		7.8 (0.6)	1.4 (2.0)	—	—
Kamanashi river		13.3 (0.5)	2.1 (7.0)	14.6	2.2
Sea-water					
Numazu coast	1/100	435 (0.5)	11.6×10^2 (1.0)	436	12.0×10^2

*Values in parentheses are the relative standard deviations of 3–5 determinations.

results for calcium are less than 6%, and better agreement is observed in the magnesium determination. The concentrations of calcium and magnesium obtained by the FIA method for the sea-water sample are comparable with the average concentrations published in the literature. The reproducibilities of this method are satisfactory for both calcium and magnesium, with relative standard deviations of less than 3% for most water samples, except for a value of 7% in the determination of magnesium in river water. These results indicate that the proposed FIA approach can provide a simple and rapid procedure for simultaneous determination of calcium and magnesium, with good precision and accuracy. Although the sensitivity of the proposed method is lower than for flame atomic-absorption spectrometry (but much higher than that for conventional titrimetry), it should be applicable to the analysis of most common natural waters.

REFERENCES

1. M. D. Luque de Castro and M. Valcárcel, *Analyst*, 1984, **109**, 413.
2. M. D. Luque de Castro, *Talanta*, 1986, **33**, 45.
3. T. Yamane and E. Goto, *Anal. Sci.*, 1989, **5**, 783.
4. E. H. Hansen, J. Růžička and A. K. Ghose, *Anal. Chim. Acta*, 1978, **100**, 151.
5. W. D. Basson and J. F. van Staden, *Analyst*, 1979, **104**, 419.
6. G. Nakagawa, H. Wada and C. Wei, *Anal. Chim. Acta*, 1983, **145**, 135.
7. K. Uchida, M. Tomoda and S. Saito, *Bunseki Kagaku*, 1985, **34**, 568.
8. T. Yamane and M. Kamijo, *ibid.*, 1984, **33**, 110.
9. H. Wada, A. Yuchi and G. Nakagawa, *Anal. Chim. Acta*, 1983, **149**, 291.
10. Yuan Youxian, *ibid.*, 1988, **212**, 291.
11. F. Cañete, A. Ríos, M. D. Luque de Castro and M. Valcárcel, *Analyst*, 1987, **112**, 267.
12. A. T. Haj-Hussein and G. D. Christian, *Microchem. J.*, 1986, **34**, 67.
13. J. Kragten, *Atlas of Metal-Ligand Equilibria in Aqueous Solutions*, Ellis Horwood, Chichester, 1978.

IMPROVEMENTS IN THE *N,N*-DIETHYL-*p*-PHENYLENEDIAMINE METHOD FOR THE DETERMINATION OF FREE AND COMBINED RESIDUAL CHLORINE THROUGH THE USE OF FIA

G. GORDON, D. L. SWEETIN, K. SMITH and G. E. PACEY
Miami University, Oxford, OH 45056, U.S.A.

(Received 27 April 1990. Revised 13 June 1990. Accepted 21 June 1990)

Summary—In the determination of free and combined chlorine, the reaction of permanganate standards with *N,N*-diethyl-*p*-phenylenediamine (DPD) exhibits nonlinearity presumably because both the colored semiquinoid product and the colorless quinoid product are both formed. The titrimetric DPD method titrates both of the products while the colorimetric method monitors only the colored semiquinoid products. This results in a nonlinear response for the colorimetric method above 1.0 mg/l. as Cl₂. Under FIA conditions, the nonlinearity of the DPD colorimetric method is eliminated in the 0.1–5.0 mg/l. (as Cl₂) range and the linear range is expanded to 0.1–8.0 mg/l. as Cl₂. Also, relative standard deviations are improved by 0.5–11% relative to the colorimetric method and 1.5–4.0% relative to the titrimetric method. The FIA method was developed further to sequentially determine both free and combined chlorine, since chloramine was found to have a negligible interference in the free chlorine determination.

Although the 1986 Safe Drinking Water Amendments will reduce the use of chlorine for disinfection of water and wastewater, an accurate spectrophotometric method for the determination of free chlorine (Cl₂, HOCl, OCl⁻) and combined chlorine (chloramines) is needed, especially as the use of monochloramine (NH₂Cl) as a disinfectant residual may increase. Because free and combined chlorine have different germicidal capabilities and health effects, it is important to differentiate these species in order to assess contact time (CT) values properly.¹⁻³

The most widely accepted methods for measuring free chlorine (Cl₂, HOCl, OCl⁻) and combined chlorine (NH₂Cl, NHCl₂) are based on use of *N,N*-diethyl-*p*-phenylenediamine (DPD).^{4,5} DPD can be used as an indicator for both acid-base and oxidation reactions.⁶⁻⁸ The initial oxidation products formed are highly colored semiquinoid free radicals which are relatively stable owing to resonance stabilization,⁷ but are susceptible to further oxidation to less stable colorless quinoid products.⁷ This oxidation of the semiquinoid product is responsible for the apparent "fading" in the DPD colorimetric reaction.

DPD undergoes oxidation by both free chlorine and monochloramine to form the colored

semiquinoid free radical. The semiquinoid radical may be reduced to the colorless diamine by titration with ferrous ammonium sulfate (FAS) or its absorbance may be measured.

Because monochloramine also reacts with DPD, it is considered to be a major interferent in the free chlorine measurement.⁶ However, whereas free chlorine species react almost instantaneously with DPD, chloramines react much more slowly. At pH 6.3, the monochloramine reaction has a rate constant of about 10 l.mole⁻¹.sec⁻¹.⁸ However, if potassium iodide is added in a catalytic amount, monochloramine will react with it to produce iodine, which in turn reacts with DPD to produce the colored semiquinoid product almost instantaneously.⁴ The kinetic difference between the reactions of free chlorine and monochloramine with DPD can be exploited by flow-injection analysis (FIA).

The highly reproducible mixing and timing in FIA allow analytical measurements to be made before equilibrium is reached, and the free chlorine species can react with DPD and be measured before the monochloramine has had time to react.⁹

This paper describes a method for the determination of free chlorine and total chlorine, and hence also the amount of combined chlorine.

EXPERIMENTAL

Reagents

Reagent grade chemicals and triply distilled water (resistivity 18.6 M Ω /cm) were used throughout. The DPD titrimetric method and colorimetric method were followed as described in the literature⁴ except where otherwise stated.

A standard permanganate stock solution was prepared, and standardized with dried sodium oxalate.¹⁰ Anhydrous DPD sulfate (Sigma) was used to make DPD solutions of various concentrations. A 137 mg/l. ammonium chloride solution was prepared and used to make the chloramine solutions. A 50 mg/ml solution of sodium hypochlorite was used as a free-chlorine stock solution.

Apparatus

An HP 8450A spectrophotometer was used to measure absorbances at 510 nm, with 1-cm fused-silica cells. Metrohm Herisau Dosimat E535 and Multi-Dosimat E415 autoburets were used for all titrations and to make the standard permanganate solutions. The flow-injection system was made up of a Tecator 5020 FIA unit with an internal dual injector, and two Tecator 5023 detectors with 1-cm flow cells and 520 nm filters. Teflon tubing with 0.5 mm bore was used throughout.

FIA manifold and experimental conditions

A CHEMIFOLDTM type II manifold was used throughout. For the free chlorine determination, the DPD stream (1.2 ml/min) was merged with pH 6.3 buffer (1.2 ml/min) in a 60° T-piece. The mixture was pumped through a 10-cm coil and merged with the water carrier stream (2.2 ml/min) and sample in a second 60° T-piece. The sample (200 μ l) was injected into a water carrier stream to minimize reagent depletion. The reaction mixture then went

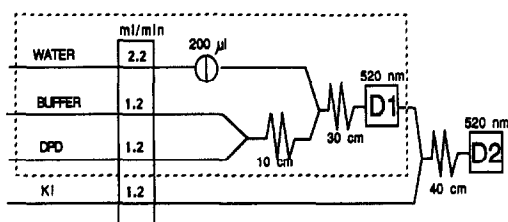


Fig. 1. Schematic diagram of FIA system for free and combined chlorine. The free chlorine system includes all components in the portion enclosed in the broken line. The KI and second detector, D2, are for the determination of total chlorine.

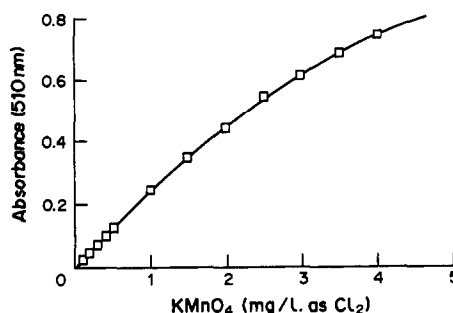


Fig. 2. Nonlinear response curve of permanganate standards in the DPD colorimetric method, $4.29 \times 10^{-3} M$ DPD.

through a 30-cm mixing coil to detector D1. The portion of Fig. 1 enclosed in a dashed line shows the FIA system used for the free chlorine determination.

For the determination of total chlorine, the flow from detector D1 was merged with potassium iodide solution (1.2 ml/min) in a 90° T-piece before going on to detector D2 (Fig. 1).

RESULTS AND DISCUSSION

Permanganate standards were made that were equivalent to a concentration range of 0.100–4.000 mg/l. Cl_2 and analysed by the DPD titrimetric and colorimetric methods. For the titrimetric method a plot of concentration of permanganate found *vs.* the known concentration was linear with a slope of 1.005, a *y*-intercept of -6×10^{-4} mg/l., and a correlation coefficient of 0.99998.

For the colorimetric method the concentration of permanganate found by titration was plotted *vs.* absorbance. The plot was nonlinear at concentrations equivalent to >1 mg/l. Cl_2 (with a DPD concentration of $4.29 \times 10^{-3} M$.) A typical plot is shown in Fig. 2. Table 1 lists the linear regression data for different concentration ranges of permanganate standards. The DPD colorimetric method is reported⁴ to be applicable up to 5 mg/l. Cl_2 , but true linearity, without a significant *y*-intercept, is observed only up to 1 mg/l. Cl_2 .

Table 1. Linear regression data for different concentration ranges of permanganate standards

Concentration range, mg/l. Cl_2	Slope, l./mg	<i>y</i> -Intercept	Correlation coefficient
0.10–4.00	0.1891	0.032 ₂	0.9948
0.10–3.00	0.2070	0.018 ₀	0.9977
0.10–2.00	0.2212	0.009 ₇	0.9987
0.10–1.00	0.2431	0.001 ₃	0.9993

Table 2. Linear regression data for increasing DPD concentration (colorimetric method)

[DPD], M	Slope, l./mg	y-Intercept	Correlation coefficient	Linear range, mg/l.Cl ₂
4.22×10^{-3}	0.1817	0.034 ₅	0.9936	0.10-1.50
4.52×10^{-2}	0.2287	0.031 ₀	0.9950	0.10-2.50
4.51×10^{-1}	0.2417	0.003 ₇	0.9999 ₅	0.10-4.00

To find the reason for the deviation from linearity, an additional study was made with DPD solutions of different initial concentrations. In the colorimetric method, as the DPD concentration was increased, the response became linear with a smaller y -intercept (Table 2). Figure 3 shows that in the FIA system, as the concentration of the DPD solution increased, the linearity range of the response curve also increased.

The results indicate that in the standardization procedure, permanganate reacts with DPD to form both the semiquinoid product and the quinoid product. The formation of the quinoid product occurs if the semiquinoid is further oxidized, and the formation of this quinoid product explains the decolorization. In the titrimetric procedure with ferrous ammonium sulfate, both the semiquinoid and quinoid forms are titrated. As a result, an accurate determination of oxidant concentration can be made in the titration method. In the colorimetric method only the absorbance of the semiquinoid is measured, but if any of the quinoid product is present owing to further oxidation by the oxidizing species as described above, the calibration plot will not be linear.

However, if the FIA method is used, even with concentrations of DPD ($4.29 \times 10^{-3}M$) that cause error in the manual procedure, the curvature is eliminated because in the FIA system the DPD to sample ratio is much higher, so the oxidant is less likely to react with the

colored radical to form the unwanted quinoid product, and the calibration is linear. This problem with nonlinearity in the colorimetric batch standardization procedure with permanganate should be considered as a potential source of error in the determination of free and combined chlorine at higher concentrations.

Measurement of free chlorine

The FIA system for the free chlorine measurements is shown in the dashed portion of Fig. 1. A linear response, with a slope of 3.28×10^{-3} l./mg, a y -intercept of 0.042 mg/l. and a correlation coefficient of 0.9999, was obtained in the FIA method for the permanganate concentration range equivalent to 0.1-8.0 mg/l. Cl₂. Solutions of varying concentrations of NaOCl were used to compare the standard titration method⁴ with the FIA method. As expected, the FIA method was more precise and the results agreed well with those from the titrations (Table 3). A plot of titration data against FIA data was linear with a slope of 1.007, a y -intercept of -0.037 mg/l., and a correlation coefficient of 0.9997.

In additional experiments, chloramine was introduced into the FIA system in order to determine the extent of chloramine interference in the free chlorine reading. By varying the starting ratio of the 137 mg/l. ammonium ion solution to the OCl⁻ solution, different proportions of free chlorine to chloramine were obtained. These solutions were also titrated to determine the concentrations of free chlorine and chloramine. Once the concentrations of each were known, appropriate dilutions were made to achieve the desired concentrations of each species. A series of solutions was made with a constant free chlorine concentration (1.83

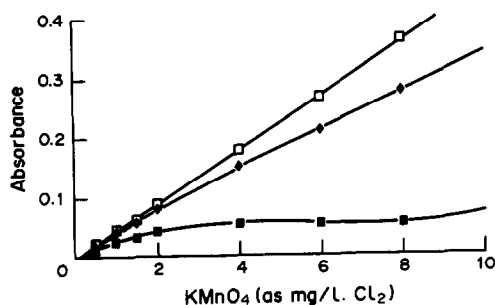


Fig. 3. Effect of increasing concentration of DPD with KMnO₄ standards: □ $4.29 \times 10^{-3}M$ DPD; ◆ $4.29 \times 10^{-4}M$ DPD; ■ $4.29 \times 10^{-5}M$ DPD.

Table 3. Mean \pm standard deviation of free chlorine concentration (mg/l.) for the titration ($n = 3$) and FIA ($n = 10$) systems

Titration	FIA	Titration	FIA
5.65 ± 0.07	5.63 ± 0.02	0.95 ± 0.03	1.03 ± 0.01
4.37 ± 0.03	4.36 ± 0.02	0.64 ± 0.02	0.67 ± 0.01
1.89 ± 0.03	1.98 ± 0.01	0.36 ± 0.01	0.31 ± 0.00

Table 4. Data (mg/l. Cl₂) from sequential detection (*n* = 10); "actual" values are from triplicate titrations⁴

Free chlorine		Combined chlorine	
Measured	Actual	Measured	Actual
5.63 ± 0.02	5.65 ± 0.07	3.88 ± 0.04	3.89 ± 0.02
4.36 ± 0.02	4.37 ± 0.03	1.55 ± 0.03	1.53 ± 0.04
1.98 ± 0.01	1.89 ± 0.03	1.32 ± 0.02	1.35 ± 0.02
1.02 ± 0.01	0.95 ± 0.03	1.05 ± 0.03	1.04 ± 0.02
0.31 ± 0.00	0.36 ± 0.02	0.09 ± 0.03	0.10 ± 0.01

mg/l. as Cl₂) and a steadily increasing concentration of monochloramine (0–1.86 mg/l. as Cl₂). The absorbance values, when measured with the FIA system, were constant (0.383 ± 0.001). Thus, no significant monochloramine interference was observed.

Measurements of free and total chlorine

The FIA system for free and total chlorine determination is also shown in Fig. 1. Chloramines react with iodide to produce iodine, which is reactive with DPD.⁴ A potassium iodide stream was added to the system to allow determination of total chlorine concentration. After measurement of the amount of free chlorine and total chlorine, the amount of chloramine in the solution could be calculated. In the context of our experiments, introduction of the iodide stream to catalyze the chloramine reaction with DPD produced correspondingly more of the colored semiquinoid radical but also diluted the sample as it came from the free chlorine determination. Therefore, the absorbance reading at the second detector was not simply the sum of the free chlorine absorbance reading and the chloramine absorbance reading. The absorbance reading at the second detector required correction by a dilution factor dependent on the volume of iodide solution added to the reaction stream from the first detector.

Absorption measurements were made for permanganate standards at both the first and second detectors in order to determine the degree of dilution in the system. The response curves that correspond to the absorbances at each detector can be used to calculate the dilution factor from the ratio of the slopes. Once the dilution factor is known, it can be applied for correcting the second absorbance measurement. The absorbance (*y*) measurements at the first detector gave a line with the equation $y = -0.0059 + 0.0667x$; $r = 0.998$, where *x* is the equivalent Cl₂ concentration (mg/l.). The ratio of the slopes is 0.0667/0.0420, which gives a dilution factor of 1.59. Results for free chlor-

Table 5. Comparison of detection limits and rsd for DPD methods⁶

Method	Detection limit,	
	mg/l. Cl ₂	rsd, %
Titration	0.05	2–7
Colorimetric	0.05	1–14
FIA	0.07	0.5–3

ine and calculated chloramine concentrations from sequential detection are given in Table 4. The detection limits and relative standard deviations⁶ are shown in Table 5.

CONCLUSIONS

The ferrous ammonium sulfate titrimetric method reduces all the oxidation products. Therefore, both the quinoid and semiquinoid are titrated, giving an accurate measure of oxidant. However, in the colorimetric method, any colorless quinoid present is not detectable but causes the absorbance to be lower than that corresponding to the amount of oxidant than is actually present. When using the DPD colorimetric method to measure the amounts of free chlorine and monochloramine in solution, it must be recognized that if the concentrations of these species are high (*i.e.*, ≥ 1 mg/l. as Cl₂) or if the initial mixing is poor, there may be formation of the unwanted quinoid product, resulting in nonlinearity of the response curve, and low results.

The use of FIA, with a thorough understanding of the chemistry involved, has been shown to improve the DPD chlorine method by minimizing the formation of the colorless quinoid species and by minimizing the interference of monochloramine in the free chlorine reading, by kinetic discrimination. The FIA method has a much higher throughput than either the titration or colorimetric method because there are no sample-transfer steps and all mixing is done during flow through the FIA system. This ability to analyze more samples in a short time period and hence run more replicates in a given time allows for greater statistical confidence in the results. The FIA system also exhibits a greater linear range than either of the other methods (0.1–8.0 mg/l.).

REFERENCES

1. Environmental Protection Agency, *National Primary Drinking Water Regulations; Filtration and Disinfection; Turbidity, Giardia Lamblia, Viruses, Legionella, and Heterotrophic Bacteria; Proposed Rule, Federal Register*, 1987, 42178.

2. Environmental Protection Agency, *National Primary Drinking Water Regulations; Total Coliforms; Proposed Rule, Federal Register*, 1987, 42224.
3. Environmental Protection Agency, *National Primary Drinking Water Regulations, Filtration and Disinfection; Proposed Rule, Federal Register*, 1988, 16348.
4. *Standard Methods for the Examination of Water and Wastewater*, 17th Ed., APHA, AWWA, WPCF, Washington, D.C., 1985.
5. A. T. Palin, *J. Inst. Water Eng. Sci.*, 1986, **40**, 501.
6. G. Gordon, W. J. Cooper, R. G. Rice and G. E. Pacey, *Disinfectant Residual Measurement Methods*, AWWA Research Foundation, Denver, CO, 1987.
7. L. Michaelis, M. P. Schubert and S. Granick, *J. Am. Chem. Soc.*, 1939, **61**, 1981.
8. H. E. Moore, M. J. Garmendia and W. J. Cooper, *Environ. Sci. Technol.*, 1984, **18**, 348.
9. D. J. Leggett, N. H. Chen and D. S. Mahadevappa, *Z. Anal. Chem.*, 1983, **315**, 47.
10. A. I. Vogel *A Textbook of Quantitative Inorganic Analysis*, 3rd Ed., Longmans, London, 1961.

THE SPECIATION OF ARSENIC(V) AND ARSENIC(III), BY ION-EXCLUSION CHROMATOGRAPHY, IN SOLUTIONS CONTAINING IRON AND SULPHURIC ACID

M. J. HEMMINGS* and E. A. JONES

Analytical Science Division, Mintek, Private Bag X3015, Randburg 2125, Republic of South Africa

(Received 30 May 1990. Revised 26 June 1990. Accepted 6 July 1990)

Summary—Arsenic(V) and arsenic(III) can be separated, by ion-exclusion chromatography, in solutions containing iron and sulphuric acid. Iron is removed by ion-exchange before the speciation of arsenic, with phosphoric acid as the eluent. The separated arsenic(V) and arsenic(III) are measured spectrophotometrically in the ultraviolet region at a wavelength of 195 nm. Arsenic(V) and arsenic(III) can be determined at concentrations ≥ 3 mg/l. The relative standard deviations are 1.3% for arsenic(V) and 0.9% for arsenic(III), at the 10 mg/l. level. The time required for the separation of the inorganic arsenic species is 11 min.

The measurement of inorganic arsenic species in metallurgical solutions allows the easy monitoring of their oxidation levels in various processes. In several commercial processes, such as the Giammarco-Vetrocoke and Thylox processes,¹ arsenate is used to oxidize hydrogen sulphide to elemental sulphur and as an intermediate oxygen-transfer reagent.

The behaviour of arsenic species during the leaching of sulpharsenide materials such as tennantite ($\text{Cu}_{12}\text{As}_4\text{S}_{13}$) and arsenopyrite (FeAsS) is relevant from both the processing and environmental points of view. The presence of arsenite in solutions that result from the bio-leaching of arsenopyrite samples slows down the autocatalytic reaction caused by *Thiobacillus ferrooxydans*, which is the most common ore-leaching bacterium.

There is a great variation in the toxicological activity of the various arsenic species present in foodstuffs and therefore a knowledge of the actual forms present is required in order to assess the dietary risk. Of the two arsenic species, arsenite is considered to be a potentially far greater hazard than arsenate.²

The determination of these species by ion chromatography in simple matrices is already well established³ but a different approach is required for more complicated matrices. Analytical methods using ion chromatography (IC) with conductivity detection have been reported previously for the determination of arsenic

species.^{4,5} In solutions containing large amounts of iron and sulphuric acid,⁴ a pre-separation of cations is performed; the arsenic species are then separated on an ion-exchanger, and arsenic(V) is detected by conductivity detection. A second portion of the sample is oxidized with *aqua regia* so that the arsenic(III) can be determined by difference. A similar system is described for the separation of arsenic species in the presence of iron and hydrochloric acid.⁵ The same authors describe the simultaneous detection of both arsenic species by the combination of electrochemical and conductivity detection.⁶

The use of ion-exclusion chromatography (IEC) for the separation of weak-acid anions from strong-acid anions is an old technique that has been attracting renewed attention. As a result of Donnan exclusion, strong inorganic mineral acids are not retained by the stationary phase, and are eluted as a single peak within the dead-volume time. Weakly dissociated species can penetrate through the solid resin network into the resin bead; this retards their passage through the column, and allows separation to take place. Ion-exclusion work has been extensively documented elsewhere.⁷⁻⁹ Butler¹⁰ determined arsenic(III) species in bottled mineral water by use of ion-exclusion chromatography coupled with amperometric detection. Total arsenic was determined as arsenic(III) after arsenic(V) had been reduced by sulphur dioxide.

The main disadvantages were that arsenic(V) and arsenic(III) cannot be determined simultaneously and the detection system is complex,

*Author for correspondence.

i.e., two detectors in series are required. In addition, Tan and Dutrizac⁴ established that the pH value of the solutions containing ferric sulphate and sulphuric acid affects the conductivity measurements. The presence of large amounts of chloride and sulphate in solutions to be analysed could result in overloading of the column, and an exact knowledge of the concentration of the matrix is therefore required before the analysis.

The suitability of ultraviolet detection for inorganic ions, even for those without suitable chromophores, has been demonstrated repeatedly.^{8,11-13} Williams¹³ describes the application of variable-wavelength detection in series with a conductivity detector. He highlights various advantages, such as the ability to detect anions that cannot normally be detected by conductivity (sulphide and arsenite), the elimination of problems associated with the carbonate "dip", the identification of unknown peaks, and the resolution of overlapping peaks.

The present investigation describes the separation and determination of arsenic(V) and arsenic(III) in solutions containing iron and sulphuric acid at levels as high as 30 g of iron and 100 g of total sulphate per litre. The iron was removed by a cation-exchange procedure before the separation of the arsenic species. After the separation, the species were monitored by means of an ultraviolet detector.

EXPERIMENTAL

Apparatus

Chromatographic separations were obtained by use of a Dionex model 2010i ion chromatograph fitted with a 50 μ l sample loop and an HPICE-AS1 ion-exclusion column. The photometric detector (Linear UVIS 200 detector) was set at 195 nm, and the absorbance output data were recorded with a Spectra-Physics SP4200 computing integrator.

Reagents

All the solutions were prepared from analytical-grade reagents, and distilled water was used. A standard stock solution of 1 g/l. arsenic(III) was prepared by dissolving 0.1320 g of arsenious oxide (As_2O_3) in 10 ml of 10% sodium hydroxide solution. The solution was acidified with dilute sulphuric acid and diluted to 100 ml. A stock solution of 1 g/l. arsenic(V) was prepared by dissolving 0.4160 g of sodium arsenate heptahydrate in water and diluting the solution

to 100 ml. These solutions were standardized by standard atomic-absorption spectrophotometric measurements. The eluent was 0.01M phosphoric acid.

Sample preparation

On dilution, to avoid the precipitation of matrix cations and hence co-precipitation of arsenic, which would produce low results, the acidity had to be maintained at 0.05M sulphuric acid. A sample clean up procedure is recommended to prevent the poisoning of the separation column by cations.

A series of Monoject 20-ml plastic syringes (20 mm \times 85 mm), the ends of which were sealed with a borosilicate disc, were filled to the 10-ml mark with a slurry of Bio-Rad AG 50W-X8 H⁺ form (50-100 mesh) resin, and assembled in clamps in a rack. The resin beds were equilibrated with 0.05M sulphuric acid, and each syringe was placed above a suitable standard flask. The required volume of sample was transferred to the resin bed in the syringe (care being taken not to disturb the surface of the resin), and iron and other cations were sorbed. The arsenic species and other anions were eluted by washing the resin with three 10-ml portions of 0.05M sulphuric acid.

Between samples the resin was regenerated by passing three 10-ml portions of 1M sulphuric acid through the syringe, followed by equilibration with 0.05M sulphuric acid.

Chromatographic procedure

A flow-rate of 0.7 ml/min was selected for the eluent, and the Dionex ion-exclusion column was equilibrated with 0.01M phosphoric acid until a stable baseline was obtained. The chart speed was set at 2.5 mm/min, and a suitable attenuation was selected. The sample was then injected, and the arsenic species were separated. The eluted species were monitored at 195 nm. A set of calibration standards was run, ranging from 10 to 30 mg/l. for arsenic(V) and from 5 to 10 mg/l. for arsenic(III). Calibration graphs were constructed. Arsenic(V) and arsenic(III) were identified by their retention times, and their concentrations were determined by measuring their peak heights, and comparing these with those in the calibration graphs.

RESULTS AND DISCUSSION

The separation of the arsenic species was initially attempted by means of a Dionex AS-4A

anion-separator column, which was coupled to a conductivity detector and an electrochemical detector in series. After separation, arsenic(V) was determined conductometrically, and the weakly dissociated arsenic(III) was determined amperometrically. Owing to the complex matrix of the samples that had to be analysed, this approach presented a number of problems, most notably the overlap of the arsenic(V) peak by that of the large amounts of sulphate present. Arsenious acid is a very weak acid and, as a result of its low dissociation constant, cannot be detected at low levels by conductivity measurements. When electrochemical detection was used, the electrode surface used for the detection of arsenic(III) showed a dark coating, indicating that the electrode was susceptible to poisoning. This was accompanied by a reduction in peak size when consecutive injections of the same sample were made.

Instead, it was decided to use ion-exclusion chromatography with photometric detection for the determination of arsenic species. Ion-exclusion columns for use in the separation of weak-acid anions contain totally sulphonated

cation-exchange resins consisting of beads of polystyrene cross-linked with divinylbenzene. The proportion of divinylbenzene cross-linkage determines, to some extent, the rate of diffusion into the resin beads.⁷ Arsenic species, as well as weak-acid anions such as sulphide and sulphite, enter the resin phase, whereas strong-acid anions such as sulphate, nitrate and chloride are excluded, passing through the column and being eluted with the solvent front.

At a wavelength of 195 nm most anions—including chloride and nitrate—absorb light. Since phosphate does not absorb at the wavelength used, phosphoric acid was chosen as the eluent.

A chromatogram of the separation of arsenic(V) and arsenic(III) is shown in Fig. 1. The two species are clearly separated, with arsenic(V) and arsenic(III) eluted with an adjusted retention time of 1.2 and 4.8 min, respectively. Interfering anions such as chloride and nitrate are elute with the solvent front in 5 min. Use of ultraviolet detection showed that arsenic(III) was more sensitive than arsenic(V).

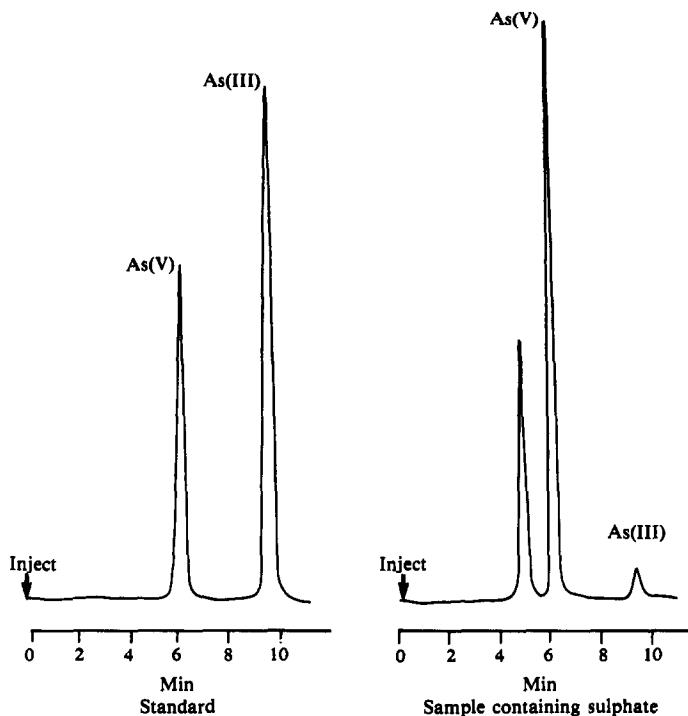


Fig. 1. Separation of arsenic(V) and arsenic(III) with a DIONEX AS-1 ion exclusion column. Elution with 0.01M H_3PO_4 at 0.7 ml/min. Detection at 195 nm.

Table 1. Retention times for arsenic(V), arsenic(III) and various sulphur species

Species	Adjusted retention time, <i>min</i> ($t_0 = 5.3$ min)
As(V)	1.2
SO ₃ ²⁻	2.5
As(III)	4.8
S ²⁻	13.3
SO ₄ ²⁻	Not detected
SCN ⁻	} Eluted with the solvent front
S ₂ O ₃ ²⁻	
S ₄ O ₆ ²⁻	

The presence of sulphate in quantities equal to or less than 120 g/l. did not pose a problem when an ion-exclusion column was used.

Sulphate is eluted with the solvent front and does not absorb light at the wavelength used for speciation of arsenic. Therefore, it will not interfere with the detection of the arsenic species. Sulphur species known to have absorption characteristics at 195 nm, such as thiocyanate, thiosulphate, and tetrathionate, do not affect the speciation of arsenic since they are eluted with the solvent front. Both sulphide and sulphite absorb at the same wavelength, but have retention times different from those of the arsenic species (Table 1).

Several common anions were tested. Nitrate was eluted with the solvent front. Under the conditions chosen, cyanide was not detected, and chloride was detected but with very low sensitivity.

The pre-separation of iron(II) and iron(III), and other cations, such as cobalt(II), nickel(II) and copper(II), that are present in the sample, is required to avoid the co-precipitation of arsenic during dilution, which would cause low arsenic results. The removal of hydrolysable cations also prevents the deterioration of the column. Iron was removed by means of a cation-exchanger in the hydrogen form.

In order to establish the validity of the proposed method, samples containing arsenic species in a high-sulphate matrix were analysed by ion-exclusion chromatography, and total arsenic was determined by atomic-absorption spectrophotometry. Table 2 gives a summary of the results obtained for samples with a matrix consisting of approximately 30 g/l. iron, 10 g/l. sulphuric acid, and a total sulphate concentration ranging from 50 to 100 g/l. The agreement between both sets of results is good at both the mg/l. and the g/l. levels.

The arsenic species can be determined in the concentration range 10–30 mg/l. for arsenic(V) and 5–20 mg/l. for arsenic(III). Linear calibration graphs were obtained over these ranges.

The relative standard deviation for the method, which was calculated from 13 replicate analyses of a synthetic sample containing 10 mg/l. arsenic(V) and arsenic(III), was found to be 1.3% for arsenic(V) and 0.9% for arsenic(III).

RECOMMENDATIONS

The coupling of the chromatographic separation of inorganic anions with instrumental techniques other than conductimetric, amperometric, or UV/VIS detection is not a new concept.^{2,3} Because of the lack of sensitivity of the ultraviolet detector for the determination of arsenic species at trace levels, atomic-absorption spectrophotometry (AAS) could be considered for their low-level detection. Since AAS does not suffer interference from common anions, the separation of the arsenic species can be achieved on a less efficient, but much faster, column (250 mm in length and 5 mm in diameter), packed with conventional cation-exchange particles. At an eluent concentration of 0.005M phosphoric acid and a flow-rate of 0.4 ml/min, the separation time for the arsenic species could

Table 2. Comparative results for arsenic(V) and arsenic(III), obtained by ion-exclusion chromatography and atomic-absorption spectrophotometry

Sample	Ion-exclusion chromatography			Atomic-absorption spectrophotometry
	As(V) g/l.	As(III) g/l.	Total As g/l.	Total As g/l.
1	5.10	4.51	9.61	9.93
2	2.30	2.79	5.09	4.90
3	2.09	2.40	4.49	4.09
4	—	0.003	0.003	0.003
5	9.7	0.18	9.88	9.70
6	1.88	2.50	4.38	4.22

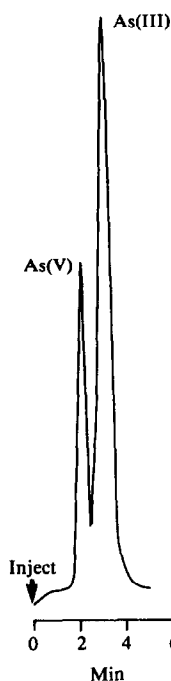


Fig. 2. Separation of arsenic(V) and arsenic(III) with a 250×5 mm Bio-Rad AG 50-X8 (200–400 mesh) column. Elution with $0.005M$ H_3PO_4 at 0.4 ml/min.

be reduced to less than 4 min (Fig. 2). Because of its speed, such an arrangement can be easily coupled to an AAS instrument, and both arsenic species can be conveniently, and much more sensitively, determined in the hydride form.

Acknowledgement—This paper is published by permission of Mintek.

REFERENCES

1. A. L. Kohl and F. C. Riesenfeld, *Gas Purification*, 3rd Ed., Gulf Publ. Co., Houston, TX, 1979.
2. L. Ebdon, S. Hill, A. P. Walton and R. W. Ward, *Analyst*, 1988, **113**, 1159.
3. L. D. Hansen, B. E. Richter, D. K. Rollins, J. O. Lamb and D. J. Eahough, *Anal. Chem.*, 1979, **51**, 633.
4. L. K. Tan and J. E. Dutrizac, *ibid.*, 1985, **57**, 2615.
5. *Idem, ibid.*, 1985, **57**, 1027.
6. *Idem, ibid.*, 1986, **58**, 1383.
7. C. Pohlandt, *Report*, NIM-2107, 1981.
8. D. J. Gjerde and J. S. Fritz, *Ion Chromatography*, 2nd Ed., Hüthig, Heidelberg, 1987.
9. J. Weiss, *Handbook of Ion Chromatography*, Dionex.
10. E. C. V. Butler, *J. Chromatog.* 1988, **450**, 353.
11. R. P. Buck, S. Singhadeja and L. B. Rogers, *Anal. Chem.*, 1954, **26**, 1240.
12. H. Small and T. E. Miller, Jr., *ibid.*, 1982, **54**, 462.
13. R. J. Williams, *ibid.*, 1983, **55**, 851.

ARRHENIUS PLOTS FOR ACTIVATION ENERGY OF ATOMIZATION IN GRAPHITE-FURNACE ATOMIC- ABSORPTION SPECTROMETRY

C. L. CHAKRABARTI* and S. J. CATHUM

Centre for Analytical and Environmental Chemistry, Chemistry Department, Carleton University,
Ottawa, Ontario, Canada K1S 5B6

(Received 20 November 1989. Revised 13 July 1990. Accepted 25 July 1990)

Summary—Activation energy plots drawn by use of various Arrhenius-type equations for atomization reactions in graphite-furnace atomic-absorption spectrometry (GFAAS) do not give reliable kinetic information about the atomization mechanism of the analyte element beyond a few data-points located near the very beginning of the absorbance signal profile. These plots are non-linear if they are drawn with data points near the maximum of the absorbance signal profile. This paper presents two Arrhenius-type equations which give linear plots over a long range of data-points, and hence reliable values for the activation energy. Also, a simple method is proposed for calculating the activation energy from the data-points anywhere from the initial appearance of the absorbance signal to its maximum. Activation energy values given by these two equations and by the method of calculation are compared with each other and with those given by the commonly used methods. The calculated activation energy values obtained can be used to verify those obtained experimentally. The three proposed methods also provide reliable kinetic information on atom-formation reactions in GFAAS. A mechanism for the atomization of copper, based on the experimentally determined activation energy and reaction order is proposed.

Arrhenius plots constructed from absorbance data from electrothermal atomization have been widely used since their introduction by Tessari and co-workers,¹⁻³ and the more extensive study by Sturgeon *et al.*,⁴ and later by Smets.⁵ Frech *et al.*,⁶ and Chung⁷ compared several methods for extracting kinetic parameters. Recently, Yan Xiuping *et al.*⁸ have reported an improvement of the Smets method. Holcombe⁹ and Bass and Holcombe¹⁰ have reported that the use of Arrhenius-type plots, which are often non-linear, to obtain energies characterizing the atom formation reaction in graphite-furnace atomic-absorption spectrometry (GFAAS) is likely to be erroneous and have attributed the non-linearity in Arrhenius plots obtained at 1 atm pressure to the finite residence time of analyte atoms.

Most commercially available electrothermal atomizers have a common feature in that the atom formation in the analysis volume and the atom removal from it are temperature-dependent. It may therefore be possible to determine rates of atom formation from the effect of temperature on the atom release in these atomizers. According to the Arrhenius law, the rate

constant, k , for atom formation can be expressed as

$$k = k_{\infty} \exp(-E_a/RT) \quad (1)$$

where k_{∞} is the pre-exponential factor, E_a is the activation energy, R is the gas constant and T is the absolute temperature. The activation energy is determined by plotting $\ln k$ vs. $1/T$; the slope ($-E_a/R$), yields the activation energy, E_a .

The methods reported in the literature^{5,7,11} for obtaining the Arrhenius plots do not satisfactorily account for the noticeable curvature in these plots when data points are taken near the absorbance maximum. The problem of large uncertainties in the determination of activation energy,^{6,9,10} and the possibility that atomization reactions do not necessarily follow first-order kinetics¹² have hindered progress in the application of activation energy for elucidating atomization mechanisms. Most studies on atomization mechanisms have been done by using data points near the very beginning of the absorbance signal profile, and have ignored the later part of the absorbance signal profile, which also contains useful information on atomization mechanisms. Also, the widely used Smets method⁵ does not provide reliable kinetic information on atomization reactions except near

*Author for correspondence.

the appearance of the absorbance signal profile.^{5,10}

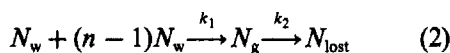
The objectives of this work were to provide a method for activation energy calculation that is valid for any order of reaction; to develop Arrhenius-type equations that are useful for extracting kinetic parameters such as the activation energy, and to increase the range of data points usable for Arrhenius plots, utilizing data from the appearance of an absorbance signal to the absorbance maximum.

THEORY

Arrhenius-type equations

The following simplifying assumptions are made: (a) all unatomized analyte atoms are at the same temperature at the time of atomization; (b) the rate of atom removal in the gas flow mode of atomization is faster than the rate of atom supply; (c) there is no activation energy for the analyte atom diffusion through the gas phase; (d) the rate constant for atom formation is approximated by the Arrhenius law at a constant heating rate and (e) atomization of the sample occurs at a constant, low heating rate.

With these assumptions, the time-dependence of the analyte atom population in a graphite furnace can be described by consecutive reactions as follows:¹³



where n is the order of reaction (assumed constant), N_w is the number of analyte entities left unatomized at time t , N_g is the number of analyte entities that are in the gas phase at time t (not to be confused with the number of analyte atoms in the analysis volume), N_{lost} is the number of analyte atoms lost from the atomizer at time t , and k_1 and k_2 are the temperature-dependent rate constants for the supply and removal functions, respectively. The time-dependent variation of N_g is expressed as a convolution:¹⁴

$$[N_g] = \int_0^t S(t')R(t-t') dt' \quad (3)$$

where $S(t)$ is the supply function defining the supply rate of analyte atoms, $R(t)$ is the mass transport or removal function for analyte atoms and t' is a variable of integration. The square brackets in equation (3) and subsequent equations have been used simply to enclose certain terms in the equations, and do not stand

for molar concentrations of the enclosed terms. If the removal rate is very rapid compared to the supply rate,¹⁴ then

$$[N_g] = S(t) \int_0^\infty R(t) dt = S(t) \tau, \quad (4)$$

where τ , is the overall time constant of the removal function. Thus the shape of a plot of N_g or absorbance A vs. time will reflect the time-dependence of the supply function. Conversely, if the removal rate is very slow compared to the supply rate the shape of the absorbance signal profile is determined by $R(t)$.¹⁴

From reaction scheme (2), we may write the following for the release of analyte atoms N_g :

$$d[N_g]/dt = nk_1[N_w]^n - k_2[N_g] \quad (5)$$

Equation (5) has been reported earlier for $n = 1$.¹⁵ With forced convection at low heating rates and no activation energy for the removal of analyte atoms, the loss by diffusion and convection is fast and therefore cannot be the rate-determining step. We will discuss this in greater detail in the Results and Discussion section. Under these conditions, the supply function is approximated by:

$$\begin{aligned} A &= \beta Q d[N_g]/dt = -\beta Q d[N_w]/dt \\ &= \beta Q nk_1 [N_w]^n = \beta Q S(t) \end{aligned} \quad (6)$$

where Q is a proportionality constant which relates the absorbance, A , to the number of analyte atoms present in the analysis volume at time t , and β is the atomization efficiency, defined by Smets⁵ as the fraction of analyte atoms which are atomized.

The next step in developing the new method is to find a mathematical relationship between the rate constant for atom formation and the absorbance. This can be done by integrating both sides of equation (6) to find an expression for $[N_w]$, which is then substituted back into equation (6) subject to the boundary condition that the number of unatomized analyte atoms is $[N_w^0]$ at $t = 0$ and $[N_w]$ at time t :

$$-\int_{N_w^0}^{N_w} [N_w]^{-n} d[N_w] = \int_0^t nk_1 dt$$

which can be solved for $n \neq 0$ and $n \neq 1$ to yield¹⁶

$$\begin{aligned} [N_w]^n &= [N_w^0]^n \\ &\times \left(1 + (n-1)[N_w^0]^{n-1} \int_0^t nk_1 dt \right)^{n/(1-n)} \end{aligned} \quad (7)$$

and, for $n = 1$ to yield

$$[N_w] = [N_w^0] \exp\left(-\int_0^t k_1 dt\right) \quad (8)$$

Substituting equation (7) into equation (6) and arranging terms yields

$$A = \beta Q n k_1 [N_w^0]^n \times \left(1 + (n-1)[N_w^0]^{n-1} \int_0^t n k_1 dt\right)^{n(1-n)} \quad (9)$$

Substituting equation (8) into equation (6) gives

$$A = \beta Q k_1 [N_w^0] \exp\left(-\int_0^t k_1 dt\right) \quad (10)$$

At the very beginning of the absorbance signal profile $\int_0^t k_1 dt \rightarrow 0$. Hence, applying the Arrhenius law to k_1 in equations (9) and (10) and taking natural logarithms of both sides of the resulting two equations we obtain the following expression (for $n \neq 0$):

$$\ln A = -E_a/RT + Z \quad (11)$$

where $Z = \ln(\beta Q [N_w^0] k_\infty)$ and is a constant, R is the gas constant, and T is the absolute temperature. By use of the transition-state theory Sturgeon *et al.*⁴ have derived equation (11) from a general relationship between k_1 and $T^a \exp(-\Delta G^{0*}/RT)$, where ΔG^{0*} is the standard free energy change of activation and $a = 1$. Equation (11) is valid for any order of reaction for atom release except for $n = 0$, whereas the other methods are valid only when atom formation follows a first-order reaction.

L'vov¹⁷ has reported that with the Massmann-type graphite furnace integrated absorbance has a much greater potential than peak-height absorbance for giving absolute measurement of absorbance. Use of integrated absorbance in an Arrhenius-type equation will increase the temperature range usable for collecting absorbance data for Arrhenius plots. For this, equation (6) is used to obtain integrated absorbance. Rearranging and integrating this equation, subject to the boundary condition that $[N_w] = 0$ at $t = \infty$ and $[N_w]$ at time t , gives

$$[N_w] = (1/\beta Q) \int_t^\infty A dt \quad (12)$$

Similarly, equation (6) can be integrated, subject to the boundary condition that $[N_w] = [N_w^0]$ at $t = 0$ and $[N_w]$ at time t , to yield

$$[N_g] = (1/\beta Q) \int_0^t A dt \quad (13)$$

Equations (13) and (14) were also derived by Smets⁵ and used by Bass and Holcombe.¹⁰ Substituting equation (13) into equation (6) gives:

$$k_1 = cA \left(\int_t^\infty A dt\right)^{-n} \quad (14)$$

where

$$c = n^{-1}(\beta Q)^{n-1}$$

It is of interest to note that β will appear in equation (14) only for $n \neq 1$. We will describe later in this paper how equation (14) can be used to determine E_a from the absorbance signal profile by a method (named the method of calculation) without recourse to Arrhenius plots, provided that the value of n is known. The value of n can be determined at the absorbance maximum by the method reported in another publication from this laboratory.¹⁶ For $n = 1$, equation (14) reduces to:

$$k_1 = A \left(\int_t^\infty A dt\right)^{-1} \quad (15)$$

which is another form of the Smets equation.⁵ Other forms of equation (15) have been developed by Frech *et al.*,⁶ Bass and Holcombe,¹⁰ L'vov *et al.*,¹⁸ and Guerrieri *et al.*¹⁹ Application of the Arrhenius law equation (1) to k_1 in equation (15) allows E_a to be determined from a plot of $\ln(A/\int_t^\infty A dt)$ vs. $1/T$; the slope equals $-E_a/R$, yielding the value of E_a .

Absorbance profile obtained with a constant heating rate of the atomizer. Mathematical treatment of atomization under non-isothermal conditions is simplified if the atom release process follows first-order kinetics and the temperature is increased at a constant heating rate, α , from an initial temperature, T_i (kelvin) to the final temperature T (kelvin):

$$T = \alpha(t_0 + t'') = \alpha t \quad (16)$$

where t_0 is the time when the temperature of the tube wall is T_i , t'' is the time required for the temperature to increase from T_i to T , and t is the time that would elapse if the heating were started at absolute zero.

Substituting equation (16) into equation (1) (the Arrhenius law) gives

$$k_1 = k_\infty \exp(-\epsilon/t) \quad (17)$$

where

$$\epsilon = E_a/\alpha R \quad (18)$$

In the integrated form equation (17) becomes

$$\int_0^t k_1 dt = \int_0^t k_\infty \exp(-\epsilon/t) dt \quad (19)$$

If high heating rates are excluded, the integral $\int_0^t k_\infty \exp(-\epsilon/t) dt$ in (19) can be approximated by the expression (see Appendix A):

$$\int_0^t k_1 dt = t^2 \epsilon^{-1} k_\infty \exp(-\epsilon/t) \quad (20)$$

Substituting (15) into (20) and taking into account equations (16) and (18) yields

$$-\ln \left(\frac{\int_t^\infty A dt}{\int_0^\infty A dt} \right) = T^2 (\alpha^2 \epsilon)^{-1} k_\infty \exp(-E_a/RT) \quad (21)$$

which can be rearranged to give

$$y = v \exp(-E_a/RT) \quad (22)$$

where

$$y = -\ln \left(\frac{\int_t^\infty A dt}{\int_0^\infty A dt} \right) / T^2 \quad (23)$$

and $v = k_\infty (\alpha^2 \epsilon)^{-1}$, which is a constant.

The terms on the right-hand side of (23) are experimentally measurable. Taking natural logarithms of both sides of (22) gives

$$\ln y = -E_a/RT + \ln v \quad (24)$$

A plot of $\ln y$ vs. $1/T$ should be linear with a slope $-E_a/R$ and an intercept $\ln v$.

Determination of activation energy. As a by-product of the mathematical formulation above, the activation energy, E_a , can be determined directly with any data points from the initial appearance of the absorbance signal to its maximum, by using equation (21), provided that atom formation follows first-order kinetics. This method allows a cross-check of the activation energy values that are obtained graphically from Arrhenius plots. From equation (21) for a constant heating rate of the atomizer, the activation energy, E_a , can be expressed by (see Appendix B):

$$E_a = -(ART^2)(\gamma \ln \Psi)^{-1} \quad (25)$$

where

$$\gamma = \alpha \int_t^\infty A dt$$

and

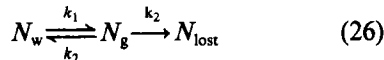
$$\Psi = \int_t^\infty A dt / \int_0^\infty A dt$$

A , T and the other terms (except R , which is the gas constant) on the right-hand side of equation (25) are experimentally measurable.

An Arrhenius-type equation developed by taking atom redeposition into account

The following approximations are used to simplify the mathematical treatment: (a) all unatomized analyte atoms are at the same temperature at the time of atomization; (b) atom formation and redeposition of gaseous atoms on the graphite surface follow first-order kinetics; (c) the rate of release and the redeposition of analyte atoms in the gas flow interrupt mode of operation are equal;¹⁹ (d) rate constants of both atom formation and redeposition are approximated by the Arrhenius law; (e) the atomization occurs at a constant low heating rate.

With these assumptions the following reaction scheme is proposed:



where N_w is the number of analyte entities on the graphite surface at time t , and N_g is the number of gaseous analyte atoms, k_1 and k_2 are first-order rate constants for atom release from and redeposition of atoms on the graphite surface, respectively, N_{lost} is the number of analyte atoms lost from the analysis volume at time t , and k_3 is the first-order rate constant for analyte atom loss. In the gas flow interrupt mode of operation we assume that the transformation of N_g into N_{lost} is much slower than the rate of formation of N_g and the rate of the reverse reaction (back to N_w). Hence, as a first approximation, k_3 may be ignored in the rate equation for N_g :

$$d[N_g]/dt = k_1[N_w] - k_2[N_g] \quad (27)$$

Using assumption (c), at equilibrium we can rewrite (27) as

$$0 = k_1[N_w] - k_2[N_g]$$

or,

$$k_1/k_2 = [N_g]/[N_w] \quad (28)$$

For the gas flow interrupt mode of operation, $[N_g]$ and $[N_w]$ can be expressed by the following two equations:

$$[N_g] = (1/\beta Q) \langle k_2 \rangle \int_0^t A dt \quad (29)$$

and

$$[N_w] = (1/\beta Q) \langle k_2 \rangle \int_t^\infty A dt \quad (30)$$

where $\langle k_1 \rangle$ and $\langle k_2 \rangle$ are the mean values of k_1 and k_2 over the indicated time interval. Substituting (29) and (30) into (28) and rearranging terms gives

$$k_1/k_2 = \int_0^t A dt / \int_t^\infty A dt \quad (31)$$

Here it is assumed that $\langle k_1 \rangle = \langle k_2 \rangle$ as done by Smets.⁵ Applying the Arrhenius law [equation (1)] to k_1 and k_2 in (31), and taking natural logarithms of both sides of the resulting equation, yields

$$\ln \varphi = -\Delta E_a/RT + X \quad (32)$$

where

$$\varphi = \left(\int_0^t A dt / \int_t^\infty A dt \right)$$

and

$$X = \ln(k_{1\infty}/k_{2\infty})$$

and ΔE_a is the difference between the energy of activation for release of analyte atoms from the graphite surface and the energy of activation for redeposition of analyte atoms on the graphite surface, and $k_{1\infty}$ and $k_{2\infty}$ are pre-exponential factors in the Arrhenius law corresponding to rate constants k_1 and k_2 , respectively. A plot of $\ln \varphi$ vs. $1/T$ should be linear with a slope of $-\Delta E_a/R$ and intercept X .

EXPERIMENTAL

Apparatus

A Perkin-Elmer model 503 atomic-absorption spectrophotometer, equipped with a deuterium-arc background corrector and a model 76B heated graphite atomizer (HGA) was used. The atomic-absorption spectrophotometer was modified in our laboratory to allow signals to be registered with a time constant of 20 msec. The graphite furnace was heated with a laboratory-made power supply capable of supplying variable heating rates up to 7 K/msec. Pyrolytically-coated graphite tubes (Perkin-Elmer part No. BOO91-504) were used. The signals were measured with a programmable model 4094 digital oscilloscope (Nicolet Instrument Corporation, Madison, WI, USA). The integrated absorbance was measured by use of a software package provided by Nicolet Instrument Corporation. A copper hollow-cathode lamp (Perkin-Elmer) was used and operated at a lamp current of 10 mA. The experimental parameters are given in Table 1.

Table 1. Experimental and instrumental parameters for atomization of copper from a pyrolytically-coated graphite-tube surface

Wavelength	324.8 nm
Charring temperature	800 K
Atomization temperature	2300 K
Heating rate	477 K/sec
Mass of copper (interrupt mode)	5 ng
Mass of copper (flow mode)	200 ng
Volume of test solution	10 μ l

Standard solutions

A stock 1000 μ g/ml copper solution was prepared by dissolving 0.5005 g of copper foil of 99.90% purity in 10 ml of Baker "Ultrex" nitric acid (1 + 1); the solution was boiled, cooled and diluted accurately to 500 ml with ultrapure water. Ultrapure water of resistivity 18.3 M Ω .cm was obtained direct from a Milli-Q2 water purification system (Millipore Corporation). Test solutions containing 5.00 ng/ml copper were prepared by serial dilution of the stock solution just before use. In all cases, 10 μ l of the test solution were injected into the graphite furnace with an Eppendorf micropipet fitted with a disposable plastic tip.

Gas

Argon (99.995% pure) was used as sheath gas and purge gas for the graphite furnace.

RESULTS AND DISCUSSION

Figure 1 shows a plot of the absorbance signals, both the peak-height and the integrated absorbance, given by 200 ng of copper as a function of the flow-rate argon (purge gas) through the graphite furnace. The signals fall

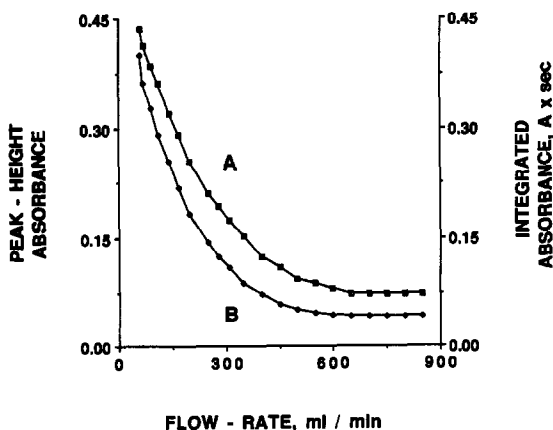


Fig. 1. Absorbance signals of 200 ng of copper (as the nitrate) at a constant heating rate as a function of the flow-rate of argon: (A) peak-height absorbance; (B) integrated absorbance.

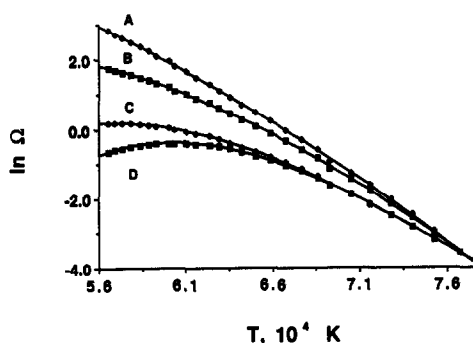


Fig. 2. Arrhenius-type plots from this work compared with those of Sturgeon *et al.*⁴ and Smets.⁵ The ordinate, $\ln \Omega$, stands for: (A) $\ln \phi$ vs. $1/T$, equation (32); (B) $\ln y$ vs. $1/T$, equation (24); (C) $\ln(A/\int_0^\infty A dt)$ vs. $1/T$, equation (15); (D) $\ln A$ vs. $1/T$, equation (11).

rapidly before levelling off at high flow-rates, which can be explained as follows. At low flow-rates of argon, the supply function is much larger than the removal function; at high flow-rates of argon, the removal function is much larger than the supply function. Therefore, at the high argon flow-rate of 625 ml/min (*i.e.*, under the increased forced convection) the supply of atoms is much slower than their removal, and hence is the rate-determining step.

Figure 2 shows curves of two Arrhenius-type plots (curves A and B) from this work compared with those of Sturgeon *et al.*,⁴ curve C, and Smets,⁵ curve D. The plots from the four equations [(11), (15), (24) and (32)] were drawn by normalizing all data points to equation (15). Figure 2 shows that curves A and B obtained from equations (24) and (32) are closer to linearity over a greater range of data points (from the beginning to the maximum of the absorbance signal profile) than curves C and D obtained from equations (11) and (15). However, the data points (near extreme right of Fig. 2) taken at the beginning of the absorbance signal profile give practically linear curves for all four equations.

In Fig. 2, the plot of $\ln A$ vs. $1/T$, curve D, was drawn by using data points from the very beginning of the absorbance signal profile to its maximum. In order to test the reproducibility, three replicate determinations of the activation energy were made from Fig. 2, by use of the first few data points taken from the very beginning of the absorbance signal profile. The choice of these data points was based on the assumption that this plot ($\ln A$ vs. $1/T$, curve D) was valid only for these data points, as explained in the theory section (equation (11)). Table 2 (first horizontal row) summarizes the E_a values from these three replicate determinations.

The activation energy determined from the plot of $\ln(A/\int_0^\infty A dt)$ vs. $1/T$, (Fig. 2) curve C, with the data points taken from the very beginning of the absorbance signal profile are also shown in Table 2 (second horizontal row) for three replicate determinations. It should be noted here that in Fig. 2, both methods *i.e.*, $\ln A$ vs. $1/T$ and $\ln(A/\int_0^\infty A dt)$ vs. $1/T$ plots, curves D and C, respectively, have been developed with the same mathematical treatment except for the order of reaction. In spite of the different assumptions for the order of reaction, good agreement between the two plots is observed, in Fig. 2, at the onset of the Arrhenius-type plot. The activation energy values obtained by the two methods above lead to the following conclusion about the order of reaction for the atomization of copper. Since both plots give closely agreeing values for E_a , and the order of reaction for one plot is assumed to be unity, the order of reaction for the other plot must also be unity. Thus, it may be concluded that the order of reaction has no effect on the determination of activation energy for atomization of copper by these two equations under these experimental conditions provided that the data are taken from the very beginning of the absorbance signal profile. It should be noted that one of the

Table 2. Activation energy values for atomization of copper calculated by using different Arrhenius plots

Equation used for Arrhenius plot	Fig. 2, curve	E_a , kJ/mole		
		Test No. 1	Test No. 2	Test No. 3
Equation (32)	A	348,* 274†	339,* 269†	346,* 286†
Equation (24)	B	346,* 238†	342,* 224†	339,* 229†
Equation (15)	C	344*	338*	340*
Equation (11)	D	348*	326*	346*
Reference 7	—	329*	316*	323*

*Calculated by using data from the initial segment, *i.e.*, near the appearance temperature of the absorbance signal.

†Calculated by using data from the top segment of the absorbance signal, *i.e.*, long after the appearance temperature of the absorbance signal.

serious limitations of using the $\ln A$ vs. $1/T$ plots, curve D (Fig. 2) to obtain activation energy is that the condition that the integral $\int_0^t k_1 dt \rightarrow 0$ in equations (9) and (10) is fulfilled only by the data points near the very beginning of the absorbance signal profile, where the value of the integral is extremely small and can be taken as equal to zero. Activation energy plots drawn with data points corresponding to longer times do not fulfill this condition, and hence such plots bend towards the abscissa soon after the initial data points (*i.e.*, after the very beginning) of the absorbance signal profile. However, the method based on the $\ln A$ vs. $1/T$ plot can be used to obtain activation energy for an atomization reaction of any order provided that the data are taken near the very beginning of the absorbance signal profile. The method is also useful when the order of reaction for the atomization reaction is not known.

The activation energy values obtained from the three replicate determinations by using a plot of $\ln y$ vs. $1/T$, curve B (Fig. 2) are also given in Table 2 (third horizontal row). The increase in the range of data points for linear plots for obtaining the activation energy by using $\ln y$ vs. $1/T$, curve B, results from using integrated absorbance in developing the method. The reliability of the activation energy values obtained from curve B can be tested by using the proposed method of calculation by equation (25). The activation energy values from the two methods [equations (24) and (25)] should be comparable. Table 3 shows the repro-

ducibility [of activation energy values obtained from equation (25)] of three replicate determinations; these values may be compared with those obtained graphically (Table 2). The following conclusions can be drawn from Tables 2 and 3: the data taken from the very beginning of the absorbance signal profile to the absorbance maximum and used in the Arrhenius plots give activation energy values in agreement with those obtained graphically; the results marked with a superscript dagger (and obtained from the data points from the high-temperature parts of the Arrhenius plots) agree among themselves. These results show the usefulness of equation (25) for obtaining the activation energy by using any data points from the beginning of the absorbance signal profile to its absorbance maximum.

The plot of $\ln \phi$ vs. $1/T$, curve A, Fig. 2, shows a longer linear range of data points than that of the other Arrhenius plots. This improvement is probably the result of taking atom redeposition into account. Analyte atoms initially generated from the sample are redeposited onto the graphite surface, and are subsequently released at higher temperatures, as reported by Black *et al.*²⁰ This may cause a curvature in the Arrhenius plot if the atom redeposition is not taken into account. For the data points taken from the beginning of the absorbance signal profile, this plot agrees very well with the other Arrhenius plots (Fig. 2). This agreement may be attributed to insignificant redeposition of copper, and hence, insignificant

Table 3. Activation energy values for atomization of copper, obtained by using equation (25)

E_a , kJ/mole				Location on the absorbance signal profile of the data points used for calculation of E_a
Determination number				
1	2	3	Average	
355	325	344	341	At or immediately after the appearance temperature, <i>i.e.</i> , at "low" temperatures.
349	343	325	339	From the "transition region" temperature, <i>i.e.</i> , between the "low" and the "high" temperature. At longer times after the appearance temperature <i>i.e.</i> , when the temperature is "high". The temperature to which the data refer increases from the top to the bottom of Table 3.
328	355	338	340	
337	343	343	341	
338	311	343	336	
304	284	321	303	
271	254	296	274	
242	230	268	247	
217	219	220	216	

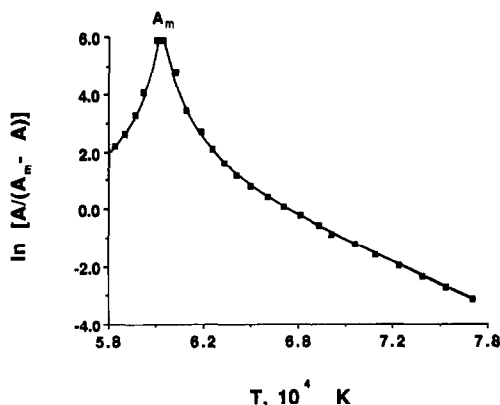


Fig. 3. A plot of $\ln[A/(A_m - A)]$ vs. $1/T$ used by Chung.⁷

desorption of copper atoms near the appearance temperature. Table 2, first horizontal row (curve A, Fig. 2) shows that closely agreeing values of the activation energy are obtained from the data points taken at longer times *i.e.*, some time after the appearance of the absorbance signal.

For comparison, a plot of $\ln[A/(A_m - A)]$ vs. $1/T$ is shown in Fig. 3. This kind of Arrhenius plot was used by Chung⁷ for elucidating atomization mechanisms in GFAAS. Figure 3 shows that the slope increases asymptotically for the data points taken after the initial few data points of the absorbance signal profile, making kinetic information on the absorbance signal profile after the initial few data points questionable. Several research workers^{4,5,10,19} have reported that the Arrhenius plots bend towards the abscissa as they approach the data for the absorbance maxima. However, the activation energy values obtained by using the data near the very beginning of the absorbance signal profile (Table 3) are satisfactory and can be used to elucidate atomization mechanisms which are valid for atomization reactions occurring near the beginning of an absorbance signal profile.

MECHANISMS OF ATOMIZATION

From published reports^{4,5,7,10,20,21} on activation energy for copper in GFAAS, it is clear that the reported activation energy values are widely divergent and the reason for this divergence still remains unclear. The difference in the reported values of E_a for copper atomization is in many cases due to curvatures in the Arrhenius plots used by the workers to obtain the activation energy values. Arthur and Cho²¹ obtained an E_a value of 265 kJ/mole under vacuum conditions; Smets⁵ reported 310

kJ/mole; Sturgeon *et al.*,⁴ 322 and 184 kJ/mole (for two different atomization mechanisms) and Chung⁷ 338 and 202 kJ/mole (for two different atomization mechanisms) under normal operating conditions. Using the Monte Carlo simulation technique, Black *et al.*²⁰ obtained 126 kJ/mole for a first-order release process for copper from a sub-monolayer coverage on the graphite tube surface.

The E_a values above range from the low value of 126 kJ/mole obtained from the Monte Carlo simulation technique, through 202 kJ/mole obtained from a higher-temperature region, to a still higher value, 338 kJ/mole, obtained from a lower-temperature region of the Arrhenius plots. This highest value correlates with the heat of sublimation of copper, $\Delta H_s = 338$ kJ/mole,²² whereas the lower values of E_a have been accounted for differently by different workers.^{4,5,7,20,21}

In this work, by deriving Arrhenius-type equations that are capable of giving data points covering a wider range of temperatures for linear activation energy plots, we have attempted to eliminate some of factors that cause curvatures in Arrhenius-type plots. Also, we have given a method which enables the E_a value to be determined by using any data points from the beginning of the absorbance signal profile to its absorbance maximum; this also allows a cross-check of the E_a value obtained graphically.

The E_a values in Tables 2 and 3 obtained by using data points corresponding to the appearance time of the absorbance signal and some later times can be used to elucidate the mechanism of copper atomization reaction as follows. Copper nitrate (taken as an aqueous solution) is reduced to free copper metal atoms on being heated in the graphite furnace.^{4,7,20,21} The energy required to release copper atoms from the graphite tube surface is not known for certain. Some authors⁴ have assumed that this energy is the heat of vaporization of the pure copper metal, which can be equated with the energy of desorption of copper from the graphite tube surface. However, the energy of desorption of an analyte metal from rough surfaces, such as graphite surfaces, may have different values because the analyte atoms may be trapped inside the surface at different depths and inside tortuous channels, resulting in a multitude of different energies being required to release them. Even though the pyrolytically-coated graphite tube possesses a smooth surface on a macroscopic scale, the surface is rough on a

Table 4. Correlation of ΔH_{273}^0 for sublimation of copper, carbon reduction of copper oxide, and dissociation of copper oxide, with the experimental activation energy

$\Delta H_{273}^0, \text{kJ/mole}^{5,22}$					$E_a, \text{kJ/mole}$
$\text{Cu}_{(s)} \rightarrow \text{Cu}_{(g)}$	$\text{CuO}_{(s)} + \text{C}_{(s)} \rightarrow \text{Cu}_{(s)} + \text{CO}$	$\text{CuO}_{(s)} + \text{C}_{(s)} \rightarrow \text{Cu}_{(g)} + \text{CO}$	$\text{CuO}_{(s)} \rightarrow \text{Cu}_{(s)} + \text{O}$	$\text{CuO}_{(g)} \rightarrow \text{Cu}_{(g)} + \text{O}$	
338	46	389	402	343	338

microscopic scale, and it is reasonable to conclude that the energies required to release copper atoms from such a rough surface will have different values, depending on the barrier encountered by the copper atoms in diffusing to the surface and being released from it. If the surface is molecularly flat and there is no significant interaction between the copper atoms and the surface, the activation energy for release of copper atoms from that surface should have a single value.

Interpretation of activation energy values

Tables 2 and 3 show that the E_a values obtained in this work can be subdivided into two classes, depending on the time (*i.e.*, the temperature) on the absorbance signal profile at which the data for calculating the E_a values were taken. Regardless of the method for determining the activation energy, the E_a values corresponding to data points at or immediately after the appearance temperature of copper, *i.e.*, at low temperatures, are consistently high, and those corresponding to data points at longer times after the appearance temperature, *i.e.*, at high temperatures, are consistently low (Tables 2 and 3). There is also a set of E_a values in Table 3 that are shown as corresponding to data points which are in between the "low" and the "high" temperature region (the so-called "transition region").

As can be seen from Table 4, the low-temperature value of the experimental activation energy (the median value is 338 kJ/mole, Table 3) correlates very well with the sublimation enthalpy of pure copper metal and also with the dissociation energy of $\text{CuO}_{(g)}$ (343 kJ/mole), whereas the high-temperature E_a values are quite different from any values in Table 4. In order to consider the possibility of the reaction, $\text{CuO}_{(g)} \rightarrow \text{Cu}_{(g)} + \text{O}$, as a pathway for $\text{Cu}_{(g)}$ it is necessary to know the energy required to sublime $\text{CuO}_{(s)}$ and the thermal stability of $\text{CuO}_{(g)}$ at elevated temperatures. The high-temperature decrease in the experimental activation energy values may be attributed to the desorption of copper from a graphite tube

surface which was initially clean. Copper has been reported^{5,12} to undergo short-range adsorption-desorption with increasing time (temperature) of atomization, which is particularly important in the long (28 mm), pyrolytically-coated graphite tubes used in this work. It should be noted that the low-temperature E_a values have been obtained by using data points near the appearance time (*i.e.*, appearance temperature) of copper, at which the loss of $\text{Cu}_{(g)}$ is assumed to be almost nil, whereas the high-temperature E_a values have been obtained by using the data points corresponding to much longer times, at which the loss of $\text{Cu}_{(g)}$ by condensation onto the graphite tube surface is substantial. The E_a values shown in Table 3, which have been obtained by using the data points from the "transition region" reflect the increasing contribution of the adsorbed Cu atoms to the $\text{Cu}_{(g)}$ as the atomization time (temperature) increases. As rightly pointed out by Holcombe⁹ and Bass and Holcombe¹⁰ there should be no single value for the activation energy except within strictly defined limits.

Acknowledgements—The authors are grateful to the Natural Sciences and Engineering Research Council of Canada for financial support of this project. They are also grateful to Professor M. Rahman, Department of Mathematics and Statistics, Carleton University, for helpful discussions. One of the authors (Shamil J. Cathum) is grateful to the Government of Iraq for a graduate scholarship

REFERENCES

1. S. L. Paveri-Fontana, G. Tessari and G. Torsi, *Anal. Chem.*, 1974, **46**, 1032.
2. G. Torsi and G. Tessari, *ibid.*, 1975, **47**, 839.
3. *Idem*, *ibid.*, 1975, **47**, 842.
4. R. E. Sturgeon, C. L. Chakrabarti and C. H. Langford, *ibid.*, 1976, **48**, 1792.
5. B. Smets, *Spectrochim. Acta*, 1980, **35B**, 33.
6. W. Frech, N. G. Zhou and E. Lundberg, *ibid.*, 1982, **37B**, 691.
7. Chan-Huan Chung, *Anal. Chem.*, 1984, **56**, 2714.
8. Yan Xiuping, Lin Tiezheng and Liu Zhijun, *Talanta*, 1990, **37**, 167.
9. J. A. Holcombe, *Spectrochim. Acta*, 1989, **44B**, 975.
10. D. A. Bass and J. A. Holcombe, *ibid.*, 1988, **43B**, 1473.
11. S. Akman, O. Genc, A. R. Ozdural and T. Balkis, *ibid.*, 1980, **35B**, 373.

12. J. A. Holcombe, G. D. Rayson and N. Akerlind, Jr., *ibid.*, 1982, **37B**, 319.
13. C. L. Chakrabarti, S. B. Chang, S. R. Lawson and S. M. Wong, *ibid.*, 1983, **38B**, 1287.
14. W. M. G. T. van den Broek and L. de Galan, *Anal. Chem.*, 1977, **49**, 2176.
15. C. W. Fuller, *Analyst*, 1974, **99**, 739.
16. S. J. Cathum, C. L. Chakrabarti and C. J. Hutton, *Spectrochim. Acta*, **44B**, 1991, in the press.
17. B. V. L'vov, *ibid.*, 1978, **33B**, 153.
18. B. V. L'vov, P. A. Bayunov and G. N. Ryabchuk, *ibid.*, 1981, **36B**, 397.
19. A. Guerrieri, L. Lampugnani and G. Tessari, *ibid.*, 1984, **39B**, 193.
20. S. S. Black, M. R. Riddle and J. A. Holcombe, *Appl. Spectrosc.*, 1986, **40**, 925.
21. J. R. Arthur and A. Y. Cho, *Surface Science*, 1973, **36**, 641.
22. R. C. Weast (ed.), *Handbook of Chemistry and physics*, 66th Ed., CRC Press, Boca Raton, 1985-1986.
23. E. Koch, *Non-isothermal Reaction Analysis*, p. 93, Academic Press, London, 1977.

APPENDIX A

Solving the integral $\int_0^t k_\infty \exp(-\epsilon/t) dt$ in equation (19)

Let

$$x = \epsilon/t \quad (1A)$$

then

$$dx = -\epsilon/t^2 dt \quad (2A)$$

Substitute equation (1A) in equation (2A) for t

$$dt = -\epsilon/x^2 dx \quad (3A)$$

Taking into account (1A) and (3A) gives

$$\int_0^t k_\infty \exp(-\epsilon/t) dt = \epsilon k_\infty \int_x^\infty x^2 e^{-x} dx \quad (4A)$$

From mathematical tables,

$$\int_x^\infty x^{\nu-1} e^{-\mu x} dx = \mu^{-\nu} \Gamma(\nu, \mu x) \quad (5A)$$

Therefore,

$$\begin{aligned} \int_0^t k_\infty \exp(-\epsilon/t) dt \\ = \epsilon k_\infty \int_x^\infty x^{-2} e^{-x} dx = \epsilon k_\infty \Gamma(-1, x) \end{aligned} \quad (6A)$$

Again, from mathematical tables,

$$\Gamma(-n, x) =$$

$$(-1)^n/n! \left(E_1(x) - e^{-x} \sum_{n=0}^{n-1} [(-1)^n n! / x^{n+1}] \right) \quad (7A)$$

where

$$E_1(x) = \Gamma(0, x) \quad (8A)$$

For $n = 1$, (7A) becomes

$$\Gamma(-1, x) = E_1(x) - x^{-1} e^{-x} \quad (9A)$$

The solution for $E_1(x)$ can be obtained from mathematical tables as follows:

$$E_1(x) = x^{-1} e^{-x} \sum_{j=0}^{\infty} ((-1)^j j! / x^j) \quad (10A)$$

Substituting (10A) into (9A) gives

$$\Gamma(-1, x) = x^{-1} e^{-x} \sum_{j=0}^{\infty} ((-1)^j j! / x^j) - x^{-1} e^{-x} \quad (11A)$$

If $x \gg 1$

$$\Gamma(-1, x) = x^{-2} e^{-x} \quad (12A)$$

Substituting (12A) into (6A) and considering (1A) gives

$$\int_0^t k_\infty \exp(-\epsilon/t) dt = (t^2/\epsilon) k_\infty \exp(-\epsilon/t) \quad (13A)$$

A similar treatment has been published in the literature.²³

APPENDIX B

Starting with equation (21) in the theory section:

$$\begin{aligned} \ln \left(\int_t^\infty A dt / \int_0^\infty A dt \right) \\ = T^2 (\alpha^2 \epsilon)^{-1} k_\infty \exp(-E_a/RT) \end{aligned} \quad (1B)$$

The Arrhenius law is

$$k_1 = k_\infty \exp(-E_a/RT) \quad (2B)$$

All the terms above have been defined previously. Substituting (2B) into (1B) for $k_\infty \exp(-E_a/RT)$ yields

$$-\ln \left(\int_t^\infty A dt / \int_0^\infty A dt \right) = T^2 (\alpha^2 \epsilon)^{-1} k_1 \quad (3B)$$

k_1 can be expressed by the following equation [see equation (15) in the theory section]:

$$k_1 = A \left(\int_t^\infty A dt \right)^{-1} \quad (4B)$$

Substituting (4B) into (3B) for k_1 gives

$$\ln \left(\int_t^\infty A dt / \int_0^\infty A dt \right) = T^2 (\alpha^2 \epsilon)^{-1} A \left(\int_t^\infty A dt \right)^{-n} \quad (5B)$$

Taking into account (18) (theory) and rearranging terms in (5B) gives the following expression for the activation energy, E_a :

$$E_a = -(ART^2) \left(\alpha \int_t^\infty A dt \ln \left[\int_t^\infty A dt / \int_0^\infty A dt \right] \right)^{-1} \quad (6B)$$

$$= -(ART^2) (\gamma \ln \Psi)^{-1} \quad (7B)$$

where

$$\gamma = \alpha \int_t^\infty A dt$$

and

$$\Psi = \int_t^\infty A dt / \int_0^\infty A dt$$

ON-LINE PHOTO-OXIDATION FOR THE DETERMINATION OF ORGANOARSENIC COMPOUNDS BY ATOMIC-ABSORPTION SPECTROMETRY WITH CONTINUOUS ARSINE GENERATION

RAJA H. ATALLAH and DAVID A. KALMAN*

Department of Environmental Health, SC-34, University of Washington, Seattle, WA 98195, U.S.A.

(Received 10 May 1990. Revised 19 June 1990. Accepted 21 June 1990)

Summary—A method has been developed for on-line conversion of organoarsenicals into arsenate, which is readily detected by atomic-absorption spectrometry with continuous arsine generation. The photo-reactor consists of a mercury lamp wrapped with 5 m of PTFE tubing (0.5 mm i.d.). The photo-oxidation conditions were optimized, with a flow-injection analysis procedure, for arsenobetaine, monomethylarsonic acid, dimethylarsinic acid, *o*-arsanilic acid, and phenylarsonic acid, all organoarsenicals of biological and environmental importance. Solutions were continuously pumped at a flow-rate of 2.0 ml/min and combined with a stream of potassium persulfate (flow-rate 0.6 ml/min) before entering the photo-reactor. With reactor dwell times of 36 sec, conversion efficiencies for these compounds were above 95% under these conditions. Interfacing of this flow-through conversion and detection system with a chromatographic inlet permits real-time analysis of mixtures of these organoarsenic compounds, in a manner suitable for environmental or biomedical samples.

Arsine-generation atomic-absorption spectrometry (AG/AAS) offers a highly sensitive, selective and simple technique for the determination of arsenic in solutions, at the nanogram level.¹ The technique can be used to differentiate between arsenic species that form volatile arsenic compounds,^{2,3} and can be easily combined with continuous flow systems.⁴⁻⁶

In speciation methods where a chromatographic separation scheme precedes the arsenic determination, detection by atomic-absorption spectrometry or inductively-coupled plasma atomic-emission spectrometry (ICP/AES) based on continuous flow is preferable to batch methods. Graphite-furnace atomic-absorption spectrometry (GFAAS), although permitting sensitive determination of all forms of arsenic, is not convenient as a detector for use with chromatographic eluents, owing to the large number of GFAAS measurements that are needed for each chromatogram, and the inability to monitor the separations in real time.⁷

Currently, ICP/AES is the most widely used method of detection in liquid chromatography arsenic speciation studies,⁸⁻¹⁰ though this technique lacks the high sensitivity of AG/AAS. In

recent studies, liquid chromatography coupled with ICP/AES and mass spectrometry (LC-ICP-MS) has been used to achieve higher sensitivities for arsenic,¹¹⁻¹³ but because of the high cost of ICP-MS equipment the technique is still beyond the reach of most laboratories.

The determination of organoarsenicals in environmental and biological samples has been of interest to various research groups.¹⁴⁻¹⁶ The major naturally occurring arsenic compounds that can be found in these sample types are the two inorganic forms of arsenic, As(III) and As(V), plus organic forms such as monomethylarsonic acid (MMA), dimethylarsinic acid (DMA), and other organoarsenicals such as arsenobetaine (AsB).¹⁷ The toxicity of these compounds decreases in the order As(III) > As(V) > MMA > DMA. Several studies have revealed that arsenobetaine is the major arsenic compound found in many sea-foods,¹⁷ and is non-toxic.¹⁸ Since many of these forms of organic arsenic, including arsenobetaine, would not be detected in an assay based on arsine, such as AG/AAS, the presence of these arsenic species in foodstuffs or tissues must be inferred by comparing the amount of total arsenic with that of arsine-forming species when such methods are used. The significance of the question of arsenic species in foodstuffs is illustrated

*Author for correspondence.

by the U.S. Environmental Protection Agency 1984 assessment of arsenic exposure in the U.S. population, which considered the bulk of dietary arsenic intake as being comprised of organoarsenic species that are not thought to have any toxic properties,¹⁴ without citing any detailed evidence for this assumption. An arsenic speciation assay having the sensitivity and specificity of arsine methods and the ability to detect all of the major arsenic species found in food and human biological samples is therefore of interest.

In order to utilize the AG/AAS technique for the determination of all soluble arsenic species, conversion of organoarsenicals into hydride-reactive arsenic is required. This might be achieved by acid or base batch digestion procedures, in which all arsenic species are converted into inorganic arsenic,¹ but these procedures are laborious, slow, and impractical when large numbers of samples are to be analyzed. In addition, batch digestion is not compatible with speciation assay, and is subject to contamination from digestion reagents. Andreae has reported¹⁶ that some organoarsenicals such as arsenobetaine are unusually resistant to acid digestion and require heating with magnesium oxide in a muffle furnace for complete decomposition. Organoarsenicals have been reported to be completely decomposed by wet oxidation with a nitric-sulphuric-perchloric acid mixture.¹⁹

Previous studies have shown that organoarsenicals can be made to undergo photo-oxidation in the presence of different mineral acids²⁰ or a combination of nitric acid and hydrogen peroxide.²¹ Cullen and Dodd reported the batch photo-oxidation of organoarsenic compounds to arsenate,²⁰ by ultraviolet irradiation in fused-silica tubes for 1 hr with a medium-pressure mercury lamp. The samples were analyzed by batch hydride generation and graphite-furnace AAS.

On-line ultraviolet irradiation procedures have been employed to improve the selectivity and sensitivity of detection of many organic compounds. The first commercially available flow-through photo-reactor was recently introduced.²² All of these systems have been used for post-column derivatization of HPLC effluents to enhance the detection of a variety of organic compounds with fluorometric,^{23,24} and electrochemical detectors.^{24,25}

The use of continuous flow methods in hydride generation makes it possible to interface a liquid chromatography effluent stream with AAS⁶ or ICP/AES⁸ detectors. These systems allow continuous and direct transfer of the generated volatile arsine products to the detector. In previous studies of arsenic species distribution, we found that organic arsenic species exhibit different responses from those of inorganic arsenic in batch or continuous flow AG/AAS detection. This is due to differences in reaction kinetics, volatilities, and efficiency of flame conversion of the corresponding arsines into elemental arsenic. Such differences affect the sensitivity of detection for each species and may introduce bias for some species. These considerations led us to develop a procedure that would allow the on-line formation of volatile arsine species from organoarsenicals that are resistant to hydride formation.

In this paper we report the successful on-line photo-oxidation of organoarsenicals to inorganic arsenic. The reaction is used within a flow-injection analysis (FIA) system. The arsenate generated by oxidation of organoarsenicals is reduced to arsine and continuously detected by AAS.

EXPERIMENTAL

Apparatus

A schematic diagram of the on-line photo-oxidation hydride generation/atomic-absorption detection system is shown in Fig. 1.

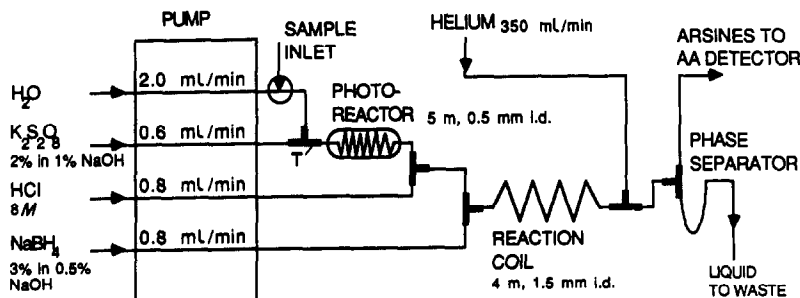


Fig. 1. On-line photo-oxidation/hydride generation/atomic-absorption system.

The components are a flow-injection hydride generation manifold, photo-reactor, gas-liquid phase-separator, and arsenic detector.

The FIA manifold is made with PTFE tubing and Kel-F T-fittings. Tubing lengths and diameters are shown in Fig. 1. A six-port Rheodyne type 50 low-pressure sample injection valve with a sample loop volume of 100 μ l is used to inject samples. Two Ismatec peristaltic pumps (Cole-Parmer) are used to pump the sample and reagent streams. The glass phase-separator used in the continuous arsine generation is similar to that described by Vijan and Wood.⁵

The photo-reactor unit is made from the mercury lamp of a portable ultraviolet light-source used for viewing samples of TLC plates (o.d. 1.5 cm, length 20 cm, Alltech). The lamp is wrapped with 5 m of 0.56-mm i.d. PTFE tubing. The source emits short wavelength light with $\lambda_{\text{max}} = 254$ nm. The unit is enclosed in aluminum foil to increase the light intensity reaching the coil and to prevent eye exposure to ultraviolet radiation.

The detector is a Perkin-Elmer atomic-absorption spectrometer Model 305 B, equipped with an arsenic electrodeless discharge lamp, monitored at 193.7 nm, and a hydrogen-flame combustion detection cell.² Absorption signals are recorded with a Hewlett-Packard model HP 3396A integrator. Peak heights and areas are obtained.

Batch photo-oxidation is performed with a photo-oxidation unit (Ace Glass, Vineland, NJ) which contains a high-pressure mercury lamp, 1200 W (o.d. 2.5 cm, length 45 cm, Hanovia), and an air fan to cool the unit and the sample tubes. Samples are placed in 150-ml fused-silica tubes and positioned around the lamp at a distance of 10 cm from it.

Reagents

The oxidizing solution, 20 mg/ml potassium persulfate (Fisher, purity 99.9%) in 10 mg/ml sodium hydroxide solution was freshly prepared before use. The reducing solution, prepared daily, was 30 mg/ml sodium tetrahydroborate (Alfa) in 5 mg/ml sodium hydroxide solution, and filtered before use.

Calibration standard stock solutions were prepared from sodium arsenate (Matheson, Coleman & Bell, OH, U.S.A.); sodium monomethylarsonate (MMA; Battelle NW, Sequim, WA); dimethylarsinic acid, (DMA; Sigma); phenylarsonic acid, (PAsA; Alfa); and *o*-arsanilic acid (*o*AsA; Aldrich). Arsenobetaine

was synthesized according to the method of Edmonds *et al.*²⁶ Diluted solutions were standardized against an inorganic arsenic(III) standard (NIST, SRM 3103) by graphite-furnace atomic-absorption spectrometry. All calibration and method development test solutions were prepared in 0.1M hydrochloric acid made with distilled demineralized water.

Method development

Photo-oxidation conditions were optimized by batch reactor tests. In each test, 10 ml of 2.5 ppm arsenobetaine solution containing the appropriate concentrations of oxidizing reagents were placed in fused-silica tubes and irradiated with the 1200 W source for 15 min. The initial selection of reagents was based on the mineral acids and oxidizing agents (such as hydrogen peroxide and persulfate) used earlier in lengthier batch photo-oxidation procedures.^{20,21} In later experiments, neutral and basic solutions were tested in the presence and absence of oxidizing agents. Photo-oxidation products were identified as inorganic arsenic, MMA, DMA, and trimethylarsine (TMA) by a previously described arsenic speciation scheme based on batch arsenic reduction and sparging, cryogenic trapping, thermal desorption and AAS detection.³

Conditions for the continuous flow generation of volatile arsines after the photo-oxidation were optimized with an arsenate solution and held constant throughout the photo-reactor optimization experiments. The stream leaving the photo-reactor (carrier flow 2.0 ml/min and oxidant flow 0.6 ml/min) was acidified by merging with a 0.8 ml/min flow of 8M hydrochloric acid before merging with a 0.8 ml/min flow of sodium borohydride solution. The concentration of sodium borohydride was kept high (30 or 40 mg/ml) as it was necessary to reduce excess of persulfate as well as the arsenate. The reduction reaction occurred in the reaction coil (4 m) and the arsine vapor generated was stripped with a 350 ml/min flow of helium before it reached the gas-liquid phase-separator. The separated gas was combined with hydrogen and air just before entering the combustion cell of the AAS detector. The resulting transient signals were recorded and integrated. In all the following experiments, the values obtained were the average peak areas of at least three sample injections of each test solution.

The photo-reactor system parameters were optimized with a 1 ppm AsB solution. The effect

of potassium persulfate concentration, photo-reactor coil length, and flow-rate of the carrier stream on the response signal were evaluated independently. The flow-rates of potassium persulfate solution, hydrochloric acid, and sodium borohydride solution were kept constant at 0.6, 0.8 and 0.8 ml/min, respectively.

The concentrations of persulfate solutions tested were 1, 5, 10, 20, and 45 mg/ml in 10 mg/ml sodium hydroxide solution. A 45 mg/ml solution was also prepared in distilled water. A saturated potassium persulfate solution contains approximately 50 mg/ml. The carrier stream flow-rate was kept at 2.0 ml/min; the reactor coil length was 5 m.

The effect of photo-reactor coil length was studied by wrapping 0.4, 0.75, 1.5, 2, 3.2, and 5 m of the PTFE tubing around the mercury lamp. The experiment was repeated at overall flow-rates of 1.0, 2.2, and 3.2 ml/min, with 20 mg/ml potassium persulfate. Standard As(V) solution was injected for comparison with AsB solution to correct for small variations in detection system response occurring with changes in the photo-reactor parameters.

The system response for several arsenic species under the optimum conditions found for the AsB solution was determined by using injections of 1 ppm solutions with the following conditions: (a) ultraviolet source off, without persulfate; (b) source on, with persulfate solution; (c) source off, with persulfate.

On-line detection of separated arsenic species was demonstrated by merging an ion-chromatograph effluent with the persulfate stream at point T in Fig. 1. AsB, MMA, DMA and As(V) were separated on a strong base anion-exchange column (Macherey-Nagel, Nucleosil 10 SB column, 250 mm × 4.6 mm i.d.) with 0.05M sodium phosphate buffer (pH = 7.4) at a flow-

rate of 1.5 ml/min. The sample volume injected was 200 μ l.

RESULTS AND DISCUSSION

The results of batch photo-oxidation reaction experiments are shown in Table 1. The arsenobetaine photo-oxidation products were identified as inorganic arsenic, monomethylarsonate, dimethylarsenate, and trimethylarsine. Little or no photo-conversion occurred in the presence of nitric acid and/or hydrogen peroxide. The best photo-oxidation was obtained in neutral or basic solutions with potassium persulfate present. Persulfate in basic medium converted AsB completely into inorganic arsenic, a specie that can easily be reduced to arsine and quantitatively measured. Results from batch photo-oxidation of 2.5 ppm solutions of MMA, DMA, PAsA and oAsA in 20 mg/ml persulfate solution in 50 mg/ml sodium hydroxide solution indicated complete decomposition of these compounds to give arsenate.

Basic sodium persulfate solution, which gave a single product in the batch procedure, was selected as the photo-oxidation medium of choice. On-line conversion was observed for injected AsB solutions mixed with basic persulfate solution when the photo-reactor was switched on. No signal was observed for AsB when the ultraviolet source was switched off and the response was reduced by 90% when the persulfate solution was prepared in distilled water instead of a basic solution.

The efficiency of photo-oxidation under the given experimental conditions was found to increase with increasing persulfate concentration, reaching a constant response of $97 \pm 2\%$ of that of As(V) at persulfate concentrations above 10 mg/ml. The efficiency of the

Table 1. Arsenobetaine batch photo-oxidation products in different solutions (arsenobetaine solutions were irradiated with ultraviolet light for 15 min)

Reaction medium	Yield of arsenic species, %				
	InAS	MMA	DMA	TMA	Total
Distilled water, pH 6	4	4	93	—	101
HCl, 0.6M	—	0.4	1.3	16	18
H ₂ O ₂ , 1.4% in H ₂ O	—	—	—	—	0
H ₂ O ₂ , 1.4% in 0.3M HCl	—	—	—	5	5
HNO ₃ , 1.3M	—	—	—	—	0
H ₂ O ₂ , 1.4% in 1.2M HNO ₃	—	—	—	—	0
K ₂ S ₂ O ₈ , 0.05% in 1.3M HNO ₃	1	0.3	4	2	7
K ₂ S ₂ O ₈ , 0.05% in 0.3M HCl	1	0.3	1	8	10
K ₂ S ₂ O ₈ , 0.05% in H ₂ O	35	60	4	—	99
K ₂ S ₂ O ₈ , 0.05% in 0.1M NaOH	101	—	—	—	101

— Not detected below 0.2% (5 ng/ml in solution).

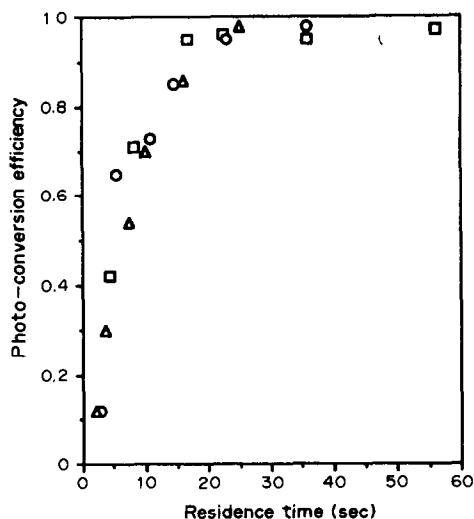


Fig. 2. Photo-conversion efficiency *vs.* residence time of analyte in the photo-reactor, at three different sample flow-rates: □, 1 ml/min; ○, 2 ml/min; △, 3 ml/min.

photoconversion reaction decreased when old persulfate solutions were used. Throughout this work, freshly prepared 10 or 20 mg/ml oxidant solutions were found necessary to maintain constant and optimal photo-conversion. The persulfate solution decomposed with time and was stable for only one day.

The effect of coil length or carrier flow on photoconversion efficiency showed a similar threshold effect, as shown in Fig. 2. Varying the residence time in the photo-reactor had the same effect, whether the variation was due to changes in reactor coil length or in pumping speed.

As an example, the 36 sec residence time for the 2 ml/min flow-rate was achieved by using a coil length of 5 m. For the experimental conditions studied, the optimal photo-reactor residence time was found to be 20–25 sec with coil lengths of 2 m or more, and pumping speeds of 1 ml/min.

The flow-through photo-reactor conversion efficiency for five arsenic species is shown in Table 2. Some of these species, such as MMA, DMA, and PAsA, are capable of direct detection by the arsine generation system, with responses different from that for arsenate. Without the presence of oxidant or the ultraviolet light source, the largest response was for As(III) and the lowest for oAsA. Because the continuous flow hydride system is optimized for rapid conversion of arsenate, arsine-forming species that react more slowly with borohydride, such as DMA, are detected with reduced response. For this reason, detection of DMA is only 23% as efficient as that of an equivalent amount of arsenate. oAsA response increased by 45% when persulfate was added, even without the ultraviolet light on. The decomposition of this compound to arsenate in the presence of persulfate was reported by Ricci *et al.*⁶ As(III) gave a higher response than As(V), owing to the ease of its reduction to arsine. The responses of the same solutions with ultraviolet irradiation indicated that As(III), MMA, oAsA and PAsA were completely converted into arsenate, and the DMA response increased from 23% to 92% of that for arsenate. Arsenobetaine, a species that could not be detected by conventional arsine assay, was found to give a response $\geq 97\%$ of that for arsenate.

The observed differences in the responses of the different arsenic species led us to assay the photo-reaction products of the different species formed by use of photo-reactor coil lengths of 3 and 5 m and 40 mg/ml persulfate solution. This was done by assaying the collected arsenic solutions pumped through the photo-reactor, for arsenic species. Speciation was achieved by means of an ion-chromatographic separation, as illustrated in Fig. 3. The results shown in Table 3 confirm that As(III), PAsA, and oAsA

Table 2. Response signals of 1.0 ppm arsenic solutions, with and without ultraviolet irradiation

Conditions	I	II	III
NaOH, %	1%	1%	1%
Persulfate, %	0%	2%	2%
Light source	off	off	on
Species	Detection efficiency [response relative to response for As(V)]		
As(V)	1.00 ± 0.02	1.00 ± 0.03	0.99 ± 0.01
As(III)	1.10 ± 0.01	1.00 ± 0.01	0.99 ± 0.02
MMA	0.96 ± 0.01	0.97 ± 0.02	0.98 ± 0.01
DMA	0.23 ± 0.02	0.25 ± 0.01	0.92 ± 0.03
oAsA	0.02 ± 0.01	0.45 ± 0.01	1.00 ± 0.02
PAsA	0.90 ± 0.01	1.00 ± 0.01	1.00 ± 0.02
AsB	—	—	0.97 ± 0.02

— Not detected below 0.01 $\mu\text{g/ml}$.

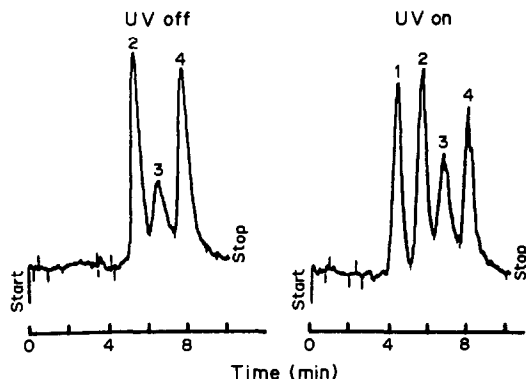


Fig. 3. Separation of four arsenic species by strong base anion-exchange LC with photo-oxidation/hydride generation/AAS. Each peak corresponds to 20 ng of As. Sample volume 200 μ l; mobile phase 0.05M phosphate buffer at a flow-rate of 1.5 ml/min. 1, AsB; 2, MMA; 3, DMA; 4, As(V).

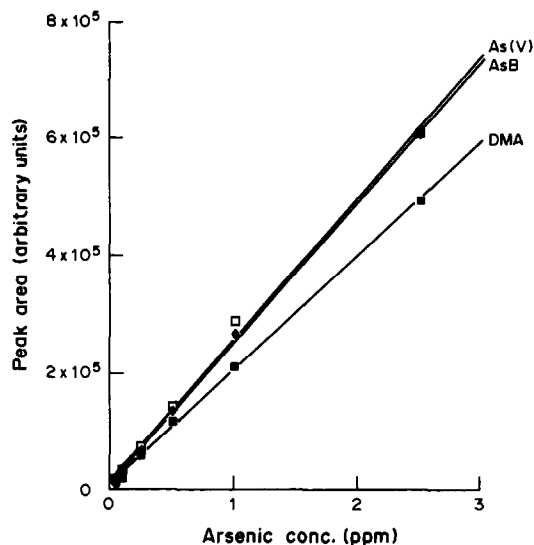


Fig. 4. Calibration curves for As(V), AsB and DMA.

are completely converted into arsenate; MMA and DMA shows incomplete conversion into arsenate, which increases with increase in the coil length. Photo-oxidation of AsB produces arsenate, DMA and MMA. The different response of these intermediate photo-oxidation products during arsine generation can therefore account for the differences in detection efficiency presented in the last column of Table 2.

By use of a series of diluted calibration solutions and the flow-through detection system, response curves were obtained for standard As(V), AsB, and DMA solutions over the concentration range 0.1–2.5 ppm, as shown in Fig. 4. The linearity of response and the good precision at each calibration level demonstrate the suitability of this technique for quantitative multi-component analysis. As would be expected from the conversion efficiencies observed (Tables 2 and 3), the AsB plot overlapped the As(V) line, but the slope for DMA was lower.

Persulfate solution absorbs strongly in the ultraviolet region (maximum absorbance at

235 nm). It has been reported that persulfate solution under ultraviolet irradiation undergoes a photo-decomposition reaction giving highly reactive hydroxyl radicals which can result in the conversion of organic compounds into carbon dioxide.²⁷ We suggest here that photo-induced persulfate oxidation of organoarsenicals, giving arsenate, water, and carbon dioxide, is similarly mediated by hydroxyl radicals. A decrease in photoconversion was observed when ammonium persulfate was used instead of potassium persulfate. Interference from ammonium ions was examined for AsB solution prepared in ammonium phosphate solution. Other solutions were prepared in methanol and urea solution. Decreases of 67, 57, and 42% in signal response were observed for 1 ppm AsB solutions prepared in 0.05M ammonium phosphate, 95% v/v methanol and 10 mg/ml urea solutions, respectively. These results indicate that the photo-decomposition reaction is hindered by the presence of certain species. Therefore, to apply the photoconversion reaction to biological and environmental samples, evaluation of the

Table 3. On-line photo-oxidation products of 5.0 μ g/ml organoarsenic solutions at two different coil lengths, with 4% persulfate solution: products identified by ion-chromatography; carrier flow-rate 1.0 ml/min

Species	Coil length 3 m, % As detected as			Coil length 5 m, % As detected as		
	As(V)	MMA	DMA	As(V)	MMA	DMA
As(III)	100	—	—	100	—	—
MMA	84	16	—	92	7	—
DMA	90	5	6	95	6	—
oAsA	100	—	—	100	—	—
PAsA	100	—	—	100	—	—
AsB	41	58	2	90	8	3

sample matrix for possible interferences is essential and sample pretreatment to remove these interferences may be needed.

CONCLUSIONS

Application of the arsine generation technique is limited to aqueous solutions of those arsenic species that undergo reduction with sodium borohydride to form volatile arsenic hydrides. Thus, many naturally occurring arsenic compound found in biological and environmental samples cannot be detected by this method. This study has demonstrated the feasibility of determination of selected organoarsenicals in solution by using on-line photo-conversion followed by a continuous flow arsine-generation/atomic-absorption system. A photo-oxidation conversion efficiency of above 95% was achieved for all arsenic species tested. Efficiencies can be further improved by increasing the reaction coil length, and using lower reagent flow-rates or (possibly) a higher intensity ultraviolet source.

The continuous flow photo-oxidation system has the advantage of being simple, fast, and free from cross-contamination. When used with liquid chromatography and AAS or ICP/AES detection, continuous flow photo-oxidation will increase the sensitivities for assay of organoarsenicals. The system might be adapted to other organohydride-forming elements, such as tin, selenium, and antimony, and organomercury compounds of environmental and biological importance. The photo-conversion of methylmercury into inorganic mercury has been demonstrated in our laboratory and will be the subject of a future paper.

REFERENCES

1. T. Nakahara, *Prog. Anal. Atom. Spectrosc.*, 1983, **6**, 163.
2. M. O. Andreae, *Anal. Chem.*, 1977, **49**, 820.
3. E. A. Crecelius, *ibid.*, 1978, **50**, 826.
4. R. J. Watling and A. R. Collier, *Analyst*, 1988, **113**, 345.
5. P. N. Vijan and G. R. Wood, *At. Abs. Newsl.*, 1974, **13**, 33.
6. G. R. Ricci, L. S. Shepard, G. Colovos and N. E. Hester, *Anal. Chem.*, 1981, **53**, 610.
7. F. E. Brinckman, K. L. Jewett, W. P. Iverson, K. J. Irgolic, K. C. Ehrhardt and R. A. Stockton, *J. Chromatog.*, 1980, **191**, 31.
8. C. J. Cappon, *LC-GC*, 1988, **6**, 584.
9. W. D. Spall, J. G. Lynn, J. L. Andersen, J. G. Valdez and L. R. Gurley, *Anal. Chem.*, 1986, **58**, 1340.
10. M. Morita, T. Uehiro and K. Fuwa, *ibid.*, 1981, **53**, 1806.
11. D. Beauchemin, M. E. Bednas, S. S. Berman, J. W. McLaren, K. W. M. Siu and R. E. Sturgeon, *ibid.*, 1988, **60**, 2209.
12. D. Heitkemper, J. Creed and J. Caruso, *J. Anal. Atom. Spectrom.*, 1989, **4**, 279.
13. Y. Shibata and M. Morita, *Anal. Sci.*, 1989, **5**, 107.
14. Environmental Protection Agency, *Health Assessment Document for Inorganic Arsenic*, PB 84-190891, pp. 2-5. EPA, Research Triangle Park, NC, 1984.
15. *Medical and Biologic Effects of Environmental Pollutants, Arsenic*, National Academy of Sciences, Washington, DC, 1977.
16. M. O. Andreae, in *Organometallic Compounds in the Environment*, J. Craig (ed.), pp. 198-228. Longmans, Harlow, 1986.
17. M. Burow and M. Stoeppler, in *Trace Element Analytical Chemistry in Medicine and Biology*, Vol. 4, P. Bratter and P. Schramel (eds.), pp. 145-150. De Gruyter, Berlin, 1987.
18. M. Vahter, E. Marafante and L. Dencker, *Sci. Tot. Environ.*, 1983, **30**, 197.
19. K. Jin, H. Ogawa and M. Taga, *Bunseki Kagaku*, 1983, **32**, E171.
20. W. R. Cullen and M. Dodd, *Appl. Organomet. Chem.*, 1988, **2**, 1.
21. C. E. Stringer and M. Attrep, *Anal. Chem.*, 1979, **51**, 731.
22. *Beam Boost*, Advance Separation Technologies Inc., Whippany, NJ.
23. C. Miles and H. Moye, *Anal. Chem.*, 1988, **60**, 220.
24. J. Stewart and W. J. Bachman, *Trends Anal. Chem.*, 1988, **7**, 106.
25. C. M. Selavka and I. S. Krull, *Anal. Chem.*, 1987, **59**, 2699.
26. J. S. Edmonds, K. A. Francesconi, J. R. Cannon, C. L. Raston, B. W. Skelton and A. H. White, *Tetrahedron Lett.*, 1977, **18**, 1543.
27. R. Rosset, M. Caude and P. Sassi, *Intern. J. Environ. Anal. Chem.*, 1982, **13**, 19.

A SOLVENT EXTRACTION-ATOMIC ABSORPTION TECHNIQUE FOR THE SIMULTANEOUS DETERMINATION OF LOW CONCENTRATIONS OF IRON, NICKEL, CHROMIUM AND MANGANESE IN DRINKING WATER

D. RAMESH BABU and P. R. NAIDU*

Department of Chemistry, Sri Venkateswara University, Tirupati 517502, India

(Received 9 May 1989. Revised 12 February 1990. Accepted 21 July 1990)

Summary—A simple and rapid method has been developed for the extraction of Fe, Ni, Cr and Mn in drinking water samples with a new reagent, pentamethylene dithiocarbamate, into methyl isobutyl ketone (MIBK) and their subsequent determination by atomic-absorption spectrometry. The extraction has been carried out at a high aqueous:organic phase ratio to achieve a 35-fold preconcentration factor. Extraction parameters and interference factors are discussed. The precision based on replicate analyses is between 3 and 10% for a concentration range of 2–250 $\mu\text{g/l}$. of the four metals. The detection limits (3σ) for Fe, Ni, Cr and Mn are 0.30, 0.36, 0.40 and 0.22 $\mu\text{g/l}$., respectively, corresponding to a metal concentration of 0.50 $\mu\text{g/l}$.

The determination of trace elements, particularly the heavy metals, has received increasing attention in pollution studies. The development of atomic-absorption spectrometry (AAS) by Walsh,^{1,2} however, provided a technique which has been particularly useful in the determination of trace metals because of its reduced susceptibility to interference. A number of techniques, including co-precipitation and co-crystallization,³ chelation-solvent extraction,⁴⁻⁹ chelating ion-exchange resins¹⁰⁻¹³ and electrolysis¹⁴⁻¹⁶ have been used for the preconcentration of metals. Solvent extraction of trace metals from water samples is a powerful technique for accomplishing preconcentration of trace metals to levels well above the normal instrumental detection limit and enhancement factors as high as 100 can easily be achieved. In addition, this technique is simple, fast, easy to manipulate, eliminates matrix effects and provides matrix normalization (*i.e.*, making the matrix of samples the same as that of the standard).

Most separation methods in use, however, are based on the formation of metal-dithiocarbamate complexes and their subsequent extraction into an organic solvent. The chelating agents, ammonium pyroolidinedithiocarbamate (APDC) and sodium diethyldithiocarbamate (NaDDC) are the two reagents most generally used for the complexation. Of these, APDC has

been found to be more suitable than NaDDC especially at low pH values.^{17,18} However, the use of APDC has certain disadvantages. Many workers have reported that the Mn-complex of APDC in MIBK (methyl isobutyl ketone) is extremely unstable and recovery is very poor.^{9,18-21} According to Sturgeon *et al.*⁹ determination of chromium is most imprecise at low concentration when APDC is used as a complexing reagent, owing to its poor extraction characteristics. Hence, we have attempted to overcome these difficulties by choosing pentamethylene dithiocarbamate (PMDTC), also known as piperidine dithiocarbamate (pipDTC), as a complexing reagent for the extraction of four trace elements (Fe, Ni, Cr, Mn) in natural drinking water supplies.

EXPERIMENTAL

Apparatus

Atomic-absorption measurements were recorded on a model 2380 Perkin-Elmer atomic-absorption spectrometer equipped with a standard burner for use with an air-acetylene flame. Standard hollow-cathode lamps were used as a line source for all elements.

An Elico Model LI-120 pH meter with combined glass electrode was used for pH measurements. Polyethylene 1-litre screw-cap bottles were used as the containers for water samples. All extraction studies were done in 500-ml borosilicate glass separatory funnels fitted with

*Author for correspondence.

Teflon stopcocks and polyethylene stoppers. Organic extracts were collected in 15-ml glass-stoppered borosilicate glass centrifuge tubes. MIBK was added with a 10-ml pipette. Other reagents were added with adjustable micro-pipettes with polypropylene tips. All the glass-ware was cleaned by the method described by Danielsson *et al.*⁷

Reagents and solutions

High-purity water was obtained by double distillation of demineralized water in a quartz still. This was used for cleaning and for preparation of standard solutions used for calibration.

Stock metal solutions which contained 1 mg/ml of each metal, were prepared with the pure metal for Fe and Ni. BDH AnalaR potassium dichromate and manganese sulphate were used for preparing Cr(VI) and Mn(II) solutions.

Mixed standards were prepared from stock solutions by progressive dilution and the concentrations were similar to those in the water samples.

Preparation of the sodium salt of pipDTC. Carbon disulphide (80 g) was slowly added to a solution of piperidine (85 g) in 25 ml of water at 5°, with constant stirring, followed by 40 g of sodium hydroxide dissolved in 20 ml of water.

The reagent solution was prepared by dissolving 1 g of the reagent in 100 ml of water, and contaminants, if any, were removed by shaking with 50 ml of MIBK.

A 0.5M ammonium acetate buffer was prepared and purified by addition of 5 ml of a 1% solution of purified pipDTC and extraction with 25 ml of MIBK. This was repeated until the aqueous layer was free from trace metal impurities and it was then stored in a clean 1-litre polyethylene bottle.

Redistilled commercial grade methyl isobutyl ketone and analytical reagent grade nitric acid were used.

Preservation and pretreatment of the samples were done as described in the literature.²²

Procedure

Water samples (350 ml) were transferred to 500-ml separatory funnels. Acetate buffer (2 ml) was added and the pH was adjusted to 4.0 ± 0.5 , followed by the addition of 5.0 ml of 1% pipDTC solution. The funnel was shaken well, 17 ml of MIBK were added and the mixture was shaken for 3 min. At equilibrium 7 ml of the solvent entered the aqueous phase owing to its

solubility, resulting in a 357:10 phase ratio. The organic phase was separated and analysed by AAS.

Standardization

Standard solutions were prepared with extracted water samples, to match the matrix of the standards to that of the samples. These samples were extracted two or three times with 10 ml of MIBK to ensure that the water was as free as possible from the trace metals under investigation. They were then combined and 350 ml portions were transferred to each of four separating funnels. The pH was adjusted and increasing amounts of the four metal solutions were added to give concentrations of 0, 2, 5 and 10 $\mu\text{g/l}$. The standards were then extracted by the recommended procedure with 10 ml of MIBK. The resulting extracts were used for calibration.

RESULTS AND DISCUSSION

Procedure optimization

The effect of pH on extraction efficiency was evaluated by performing extractions on 350 ml of water at different pH values ranging from 1 to 8 and containing 15 μg of Fe, Ni or Cr, or 50 μg of Mn the results are shown in Fig. 1.

The absorbance remains constant over the pH ranges 3.0–4.5 for Fe, 3.0–7.0 for Ni, 3.0–5.0 for Cr and 3.5–6.0 for Mn. Hence, extractions have been carried out over these pH ranges for the maximum recovery of the metals. A pH of 4.0 ± 0.5 was chosen for the simultaneous extraction of the four metals.

The solubility of MIBK in the aqueous phase was determined from the solubility data used for construction of a solubility curve, of the type described by Brooks *et al.*⁵ It was observed that 2.0 ml of MIBK dissolved in 100 ml of the aqueous phase on equilibration.

The stability of the complexes was measured by preparing a pipDTC extract in MIBK and comparing the absorbance of the "aged" samples to freshly extracted samples. The minimum times for which no appreciable loss of absorbance was noted are shown in Table 1.

Precision and recovery

The precision (expressed as the RSD) of the method was established by individually preparing ten solutions each containing the same amount of each of the four metals. The results are shown in Table 2 for a sample spiked

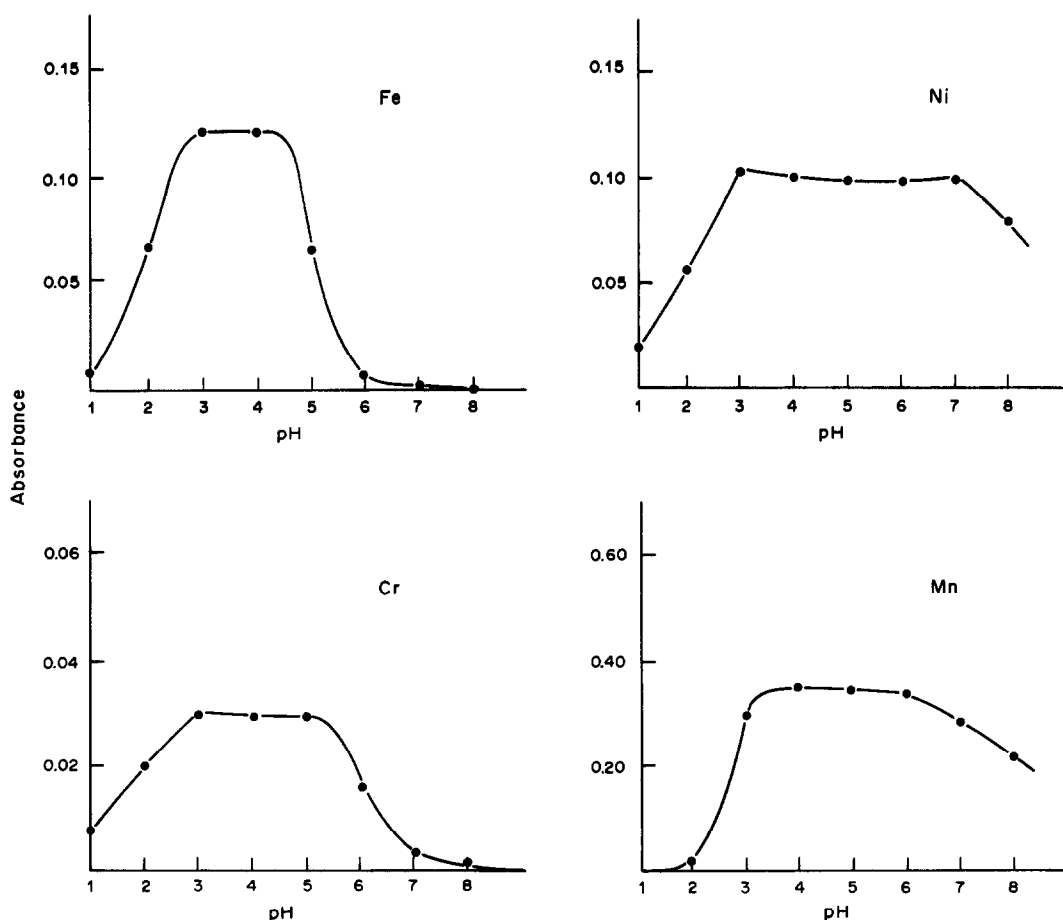


Fig. 1. Dependence of absorbance on pH of extraction.

with 2, 5, 25 and 250 $\mu\text{g/l.}$ of the metals and indicate that the precision ranges from 3 to 10%. This is comparable to that reported in the literature.⁴⁻¹¹

The recovery was computed by the method of Sturgeon *et al.*⁹ The results (Table 3) show that the extraction efficiency decreases considerably at concentrations of 250 $\mu\text{g/l.}$ for all four metals. Because a single extraction gives only partial recovery, it is essential to apply the complete procedure in preparing the calibration graph.

Table 1. Analytical parameters

Parameter	Fe	Ni	Cr	Mn
Minimum time for which complex is stable, <i>hr</i>	5	9	12	3
Limits of detection, $\mu\text{g/l.}$	0.30	0.36	0.40	0.22
Sensitivity, $\mu\text{g/l.}$	1.20	1.60	2.80	0.80
Linear working range, $\mu\text{g/l.}$	1-300	1.0-250	1.5-300	0.5-250

Sensitivity, detection limit and range of linearity

The sensitivity is expressed as the concentration which produces 1% absorption. The linear working range was determined by preparing a series of standards (0, 2, 5, 10, 25, 100, 250, 500 and 5000 $\mu\text{g/l.}$ of the metal) and after extraction their absorbance values were measured. The results are shown in Table 1.

The detection limits (based on 3 times the standard deviation of the blank) for Fe, Ni, Cr and Mn were evaluated for a concentration of 0.50 $\mu\text{g/l.}$ with a scale expansion of $A \times 10$ and an instrumental noise suppression of 4. The values are given in Table 1.

Table 2. Precision of the method for a spiked water sample

Concentration of spike, $\mu\text{g/l.}$	<i>n</i> *	RSD, %			
		Fe	Ni	Cr	Mn
2.0	10	8	9	10	6
5.0	10	6	7	9	4
25.0	10	5	6	7	3
250.0	10	3	6	3	6

*Number of observations.

Table 3. Recovery from a spiked water sample

Concentration of spike, $\mu\text{g/l.}$	Recovery*, %			
	Fe	Ni	Cr	Mn
2.0	92.0	92.7	92.0	92.5
5.0	93.0	91.0	92.0	94.0
25.0	91.0	90.8	91.0	94.7
250.0	90.4	90.5	90.7	93.4
500.0	82.7	74.3	78.5	73.7

*Calculated from $R = 100A_1/(A_1 + A_2 + A_3)$, where, A_1 , A_2 and A_3 are the signals from three successive extractions of an aliquot.

Table 4. Trace elements in drinking water

Water sample	Concentration, $\mu\text{g/l.}$			
	Fe	Ni	Cr	Mn
1	6.0	1.2	4.0	0.5
2	4.6	0.8	1.5	—
3	12.5	—	0.8	0.8
4	19.0	1.0	1.5	3.0
5	11.0	—	1.0	—
6	8.0	0.5	1.6	1.2

Effect of foreign ions

Interferences were studied for samples containing 10 and 25 $\mu\text{g/l.}$ of each of the metals.

No interference is observed from SO_4^{2-} , HCO_3^- , PO_4^{3-} , NO_3^- , F^- , Cl^- , Br^- and I^- up to 250 mg/l. ; from CN^- , EDTA up to 40 mg/l. ; and from Ca^{2+} , Mg^{2+} , Na^+ , K^+ up to 300 mg/l.

Interference from heavy metals, *viz.* Pb, Cd, Zn, Co and Cu was studied. Up to 3 mg/l. concentrations of these do not interfere to any

significant extent in the determination of Fe and Ni. However, in the extraction of Cr and Mn, these metals interfere at 2.5 mg/l. level.

Application of the method

Six untreated water samples collected at different places have been analysed for trace metals by the recommended procedure (Table 4). An alternative analysis for chromium and manganese by the method of Brooks *et al.*⁵ was also performed and the results are compared in Table 5.

Table 6 gives some of the physicochemical characteristics of the six water samples.

CONCLUSION

The results of the present investigation show that the reagent pipDTC could be successfully used for the quantitative extraction of manganese into an organic solvent (MIBK) in which the chelate is sufficiently stable (3 hr) for a routine determination. The determination of chromium is more precise with the pipDTC method than the APDC method, for all six samples. This is an added advantage of the method described here.

Considering the range of precision (3–20%) and recoveries (>90%), this method could be successfully applied to any water sample in the concentration range 2.0–250 $\mu\text{g/l.}$ of the metals being determined in a single extraction, if applied under the conditions used here.

Table 5. Comparison of extraction methods

Sample	Chromium				Manganese			
	Present		Brooks <i>et al.</i> ⁵		Present		Brooks <i>et al.</i> ⁵	
	Mean*	RSD, %	Mean	RSD, %	Mean	RSD, %	Mean	RSD, %
1	4.0	9	2.8	16	0.5	14	0.5	37
2	1.5	11	1.0	36	—	—	ND	—
3	0.8	19	ND	—	0.8	13	0.5	29
4	1.5	14	1.0	43	3.0	6	1.0	21
5	1.0	16	0.5	47	ND	—	ND	—
6	1.6	12	1.0	31	1.2	11	0.5	24

*Mean value of 10 replicate determinations.

ND = Not detected.

Table 6. Physicochemical characteristics of the water samples

Sample	pH	Hardness as CaCO_3 , mg/l.	Total solids, mg/l.	Ca^{2+} , mg/l.	Mg^{2+} , mg/l.	Cl^- , mg/l.	F^- , mg/l.	NO_3^- , mg/l.	SO_4^{2-} , mg/l.
1	7.1	76	210.0	18.9	5.6	71.5	0.60	22.1	0.66
2	7.8	249	591.4	72.0	16.2	91.0	0.42	1.3	0.34
3	7.2	181	298.6	56.0	9.7	116.3	0.46	56.0	0.83
4	7.4	224	266.0	48.5	24.5	40.8	1.2	5.6	1.3
5	7.1	259	329.8	48.7	8.4	150.4	0.99	21.0	1.5
6	7.4	281	420.3	99.4	7.6	50.2	0.36	2.8	0.33

The error ranges between 10 and 20% when the metal concentration is below 2.0 $\mu\text{g/l.}$, as indicated by the results in the Table 5.

Acknowledgement—This research was sponsored by the Department of Environment and Forests, Government of India. The generous support from this organization is gratefully acknowledged.

REFERENCES

1. A. Walsh, *Spectrochim. Acta*, 1955, 7, 108.
2. B. J. Russell, J. P. Shelton and A. Walsh, *ibid.*, 1957, 8, 317.
3. V. H. S. Gomišček and B. Gorenć, *Anal. Chim. Acta*, 1978, 98, 39.
4. T. N. Tweeten and J. W. Knoeck, *Anal. Chem.*, 1976, 48, 64.
5. R. R. Brooks, B. J. Presley and I. R. Kaplan, *Talanta*, 1967, 14, 809.
6. T. K. Jan and D. R. Young, *Anal. Chem.*, 1978, 50, 1250.
7. L. Danielsson, B. Magnusson and S. Westerlund, *Anal. Chim. Acta*, 1978, 98, 47.
8. J. D. Kinrade and J. C. Van Loon, *Anal. Chem.*, 1974, 46, 1894.
9. R. E. Sturgeon, S. S. Berman, A. Desaulniers and D. S. Russell, *Talanta*, 1980, 27, 85.
10. J. P. Riley and D. Taylor, *Anal. Chim. Acta*, 1968, 40, 479.
11. M. M. Guedes da Mota, M. A. Jonker and B. Griepink, *Z. Anal. Chem.*, 1979, 296, 345.
12. T. M. Florence and G. E. Batley, *Talanta*, 1976, 23, 179.
13. B. Holynska, *Radiochem. Radioanal. Lett.*, 1974, 17, 313.
14. C. Fairless and A. J. Bard, *Anal. Chem.*, 1973, 45, 2289.
15. W. Lund and B. V. Larsen, *Anal. Chim. Acta*, 1974, 72, 57.
16. G. E. Batley and J. P. Matousek, *Anal. Chem.*, 1977, 49, 2031.
17. R. J. Everson and H. E. Parker, *ibid.*, 1974, 46, 1966.
18. R. F. Roberts, *ibid.*, 1977, 49, 1862.
19. J. Nix and J. Goodwin, *At. Absorpt. Newsl.*, 1970, 9, 119.
20. M. Yanagisawa, M. Suzuki and T. Takeuchi, *Anal. Chim. Acta*, 1968, 43, 500.
21. R. E. Mansel, *At. Absorpt. Newsl.*, 1965, 4, 276.
22. *Standard Methods for the Examination of Water and Waste-Water*, 15th Ed., APHA-AWWA-WPCF, New York, 1980.

ANALYSIS OF POLYNUCLEAR AROMATIC HYDROCARBON MIXTURES IN VARIOUS ENVIRONMENTS BY TIME-RESOLVED FLUORESCENCE SPECTROSCOPY

KI-MIN BARK* and R. KEN FORCÉ†

Department of Chemistry, University of Rhode Island, Kingston, RI 02881, U.S.A.

(Received 30 May 1990. Revised 3 July 1990. Accepted 10 July 1990)

Summary—Time-resolved molecular fluorescence spectroscopy is presented as a sensitive and selective method for the characterization of mixtures of polynuclear aromatic hydrocarbons in the collision-free vapor phase at elevated temperature, in the condensed phase at room temperature, and at 77 K in a Shpol'skii matrix. This technique is applicable for all three conditions and the quantitative analysis for each component in mixtures has a fairly small error. Also the advantages and disadvantages are discussed for these different environments. Anthracene, pyrene and fluoranthene are used as model compounds.

Polynuclear aromatic hydrocarbons (PAH) are multi-aromatic ring systems produced at high temperatures by the incomplete combustion of fossil fuel or as the result of synthesis by some plants and formation during natural forest and prairie fires.^{1,2} A high correlation between the photodynamic action of certain PAH and their ability to induce carcinogenic responses has been found,³⁻⁵ and recently it was shown that PAH can be transformed into reactive cytotoxic and mutagenic intermediates by exposure to sunlight and other sources of radiation.⁶ A comparison of the mutagenicity of several PAH following exposure to sunlight or an artificial source of ultraviolet light has been made.⁷

Laser-induced molecular fluorescence (LIMF) spectroscopy has been shown to be one of the more sensitive techniques for quantifying PAH^{8,9} and also allows their dynamic measurement while they are in the vapor phase.⁹ Because many PAH compounds exhibit substantially different fluorescence emission spectra, spectral interference from other PAH present can be minimized through careful selection of emission wavelengths. This selectivity can be greatly improved by fluorescence line-narrowing techniques such as Shpol'skii spectroscopy.¹⁰⁻¹²

The measurement of fluorescence emission is inherently a multiparametric technique because

even the simplest such measurements involve the exploitation of more than one parameter. Obviously the introduction of additional parameters has advantages, increased selectivity being cited as the most important benefit. The multiparametric approach has been used most often in systems where the fluorescence intensity is observed as a function of excitation and emission.¹³⁻¹⁹ Time-resolved fluorescence measurements can also be incorporated into a multidimensional analysis technique. Because fluorescent molecules possess a characteristic fluorescence lifetime (the time for the decay to reach $1/e$ times its initial value), in many cases spectral interferences can be substantially minimized in this way, allowing an individual component in a mixture of PAH to be determined.

In this paper, we present results for the use of time-resolved LIMF (TRLIMF) spectroscopy as a sensitive and selective method for the determination of PAH in the collision-free vapor phase at elevated temperature, in the condensed phase at room temperature, and at 77 K in a Shpol'skii matrix. The advantages and disadvantages are also discussed for these three different environments. Pyrene, anthracene and fluoranthene are used as model compounds.

EXPERIMENTAL

The fluorescence emission spectra and the lifetime of PAH in a collision-free vapor state, a condensed phase at room temperature, and at

*Present address: Department of Chemical Education, Kyungsang University, GaJwa-dong, Jin Ju, South Korea.

†Author for correspondence.

77 K have been obtained with a system described previously.^{9,20} The excitation source used was a laboratory-built pulsed nitrogen laser having output at 337.1 nm ($29,665\text{ cm}^{-1}$) with a nominal pulse width of 12 nsec (FWHM), an average power of 4 mW and a pulse rate of 10 pulse/sec. A Schott WG360 or GG375 cut-off filter was placed in front of the monochromator to absorb the scattered light from the excitation source. To remove the laser plasma lines, an interference filter, with a transmission maximum at 337 nm and 10 nm band width (FWHM), was positioned in front of the laser output.

The vapor phase fluorescence cell was operated as a dual chamber oven to prevent the condensation of PAH on the windows. The temperature of the cell's main body, including the windows, was higher than that of the sample chamber. The fluorescence cell was connected to a vacuum pump (Model 25, Precision Scientific Co.) so that a constant back pressure of 0.005 torr could be maintained within the cell. The temperature of the cell was regulated by a tube furnace and was measured to $\pm 2^\circ$ with an iron-constantan thermocouple. The vapor phase cell has an optical path length of 1.90 cm and has been described in detail elsewhere.⁹

Low concentrations ($\sim 10^{-5}M$) were used to avoid any solute-solute interaction and self-absorption in the condensed phase experiments. The samples were held in 6 mm o.d. (4 mm i.d.) glass tubes for room temperature and 1.2 mm o.d. glass capillary tubes for low temperature (77 K) fluorescence measurements. Since Pyrex is transparent down to about 320 nm, a shorter wavelength than that of the nitrogen laser line (337.1 nm), it was not necessary to use fused silica vessels. Sample solutions were degassed by the freeze-pump thaw method at 0.005 torr a minimum of three times. A laboratory built Dewar flask with a transparent window was used in measurement of the low temperature fluorescence signal.

The fluorescence was focused into an ISA Model H-20 monochromator with 2 nm slits and detected by an RCA-1P28 photomultiplier tube (PMT). The signal from the PMT was processed by a PAR model 162/164/165 boxcar integrator with a 5 nsec window, in the model 165 module, and displayed on a X-Y recorder or strip chart recorder. A small portion (about 10%) of the laser output was split off with a microscope slide and routed to a fast photodiode to provide a triggering pulse for the

boxcar integrator. Data were passed to an IBM-XT compatible computer (10 MHz MEGA-XT) for analysis. Data and graphical analysis and three dimensional plotting were carried out with ASYSTANT[®] software. The time-dependent spectra shown in Figs. 1-3 were generated by acquiring spectra at different delay times and laminating them by using matrix manipulation routines available in ASYSTANT[®]. The concentrations of the PAH in the mixtures were calculated by the internal standard method. Since pyrene had the longest fluorescence lifetime, it was used the most frequently as the internal standard. For the determination of pyrene, fluoranthene, which differs from pyrene in emission profile, was used as the internal standard.

Reagent-grade anthracene (MC&B) and fluoranthene (Aldrich) were used without further purification. These compounds were analyzed for impurities by high performance liquid chromatography and were found to contain no impurities that would significantly interfere with either the spectral emission or decay profiles. Reagent-grade pyrene (Aldrich) was purified twice by recrystallization from reagent-grade toluene (Aldrich). The recrystallized solid was then washed with HPLC grade methanol (Fisher Scientific). HPLC grade n-hexane (Fisher Scientific) was used as the solvent in condensed phase experiments.

The fluorescence lifetimes of the different PAH were obtained by the deconvolution technique known as least-squares iterative reconvolution.¹⁹ All measurements were made at least three times.

RESULTS AND DISCUSSION

The fluorescence emission spectra of pyrene, anthracene and fluoranthene at room temperature, at 77 K, and in the vapor phase at elevated temperature are shown in Fig. 4. The large Stokes loss and broad emission band of fluoranthene have been discussed previously.²⁰ For all three compounds, no significant shift in the emission bands is caused by changing the environmental conditions, as is expected since the fluorophores and solvents are nonpolar. For anthracene there was a small red shift (~ 10 nm) in the room-temperature solution spectrum relative to the vapor phase spectrum, but for pyrene, a slight blue shift (~ 5 nm) was observed. The latter is an unusual property and needs further investigation, since a red shift, due

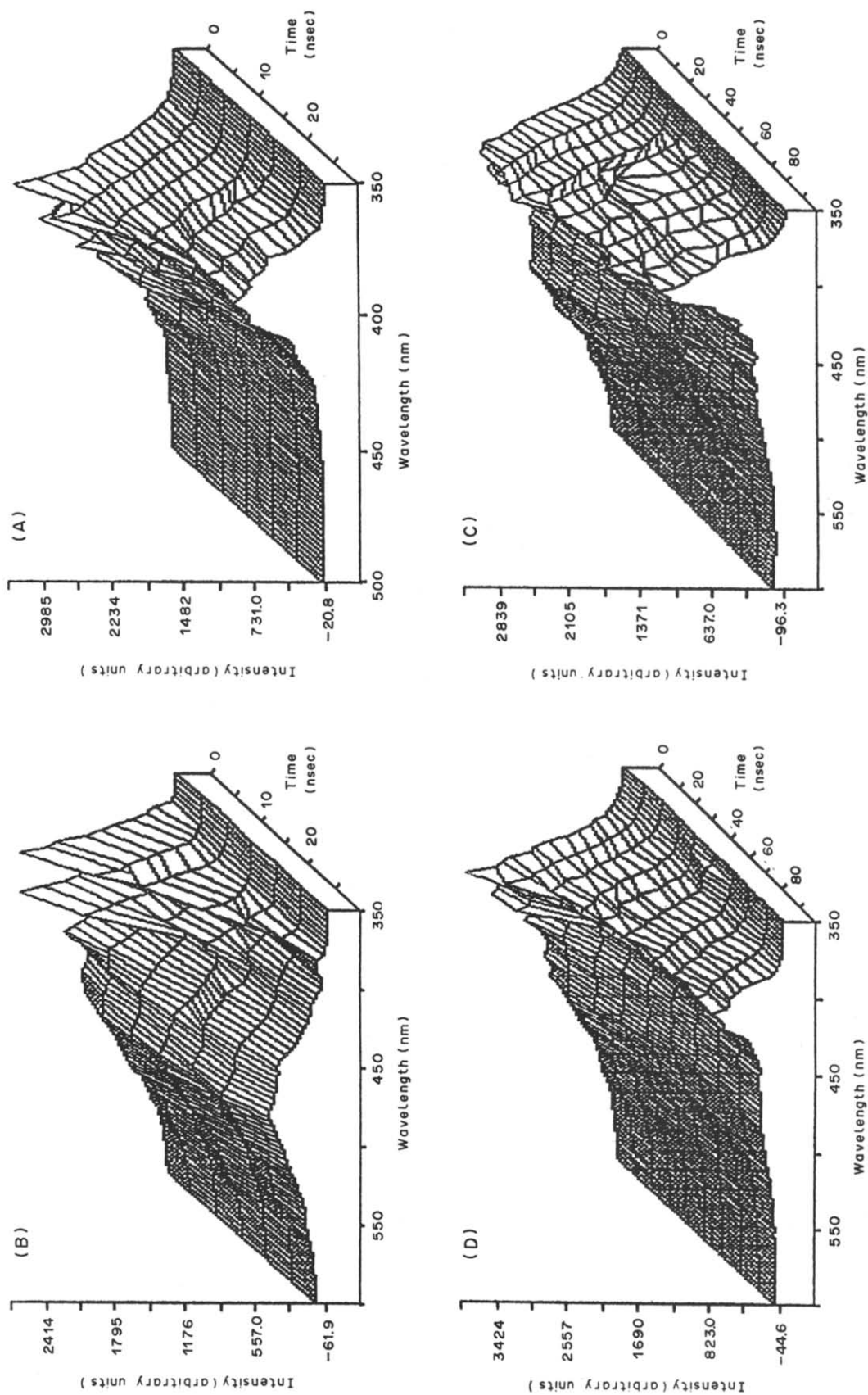


Fig. 1. Time-resolved fluorescence emission spectra (TRFES) in hexane at room temperature. The mixtures are (A) anthracene ($1 \times 10^{-6} M$) and pyrene ($1 \times 10^{-5} M$), (B) anthracene ($1 \times 10^{-6} M$) and fluoranthene ($1 \times 10^{-5} M$), (C) pyrene ($1 \times 10^{-5} M$) and fluoranthene ($1 \times 10^{-6} M$), (D) anthracene ($1 \times 10^{-6} M$) and fluoranthene ($1 \times 10^{-5} M$).

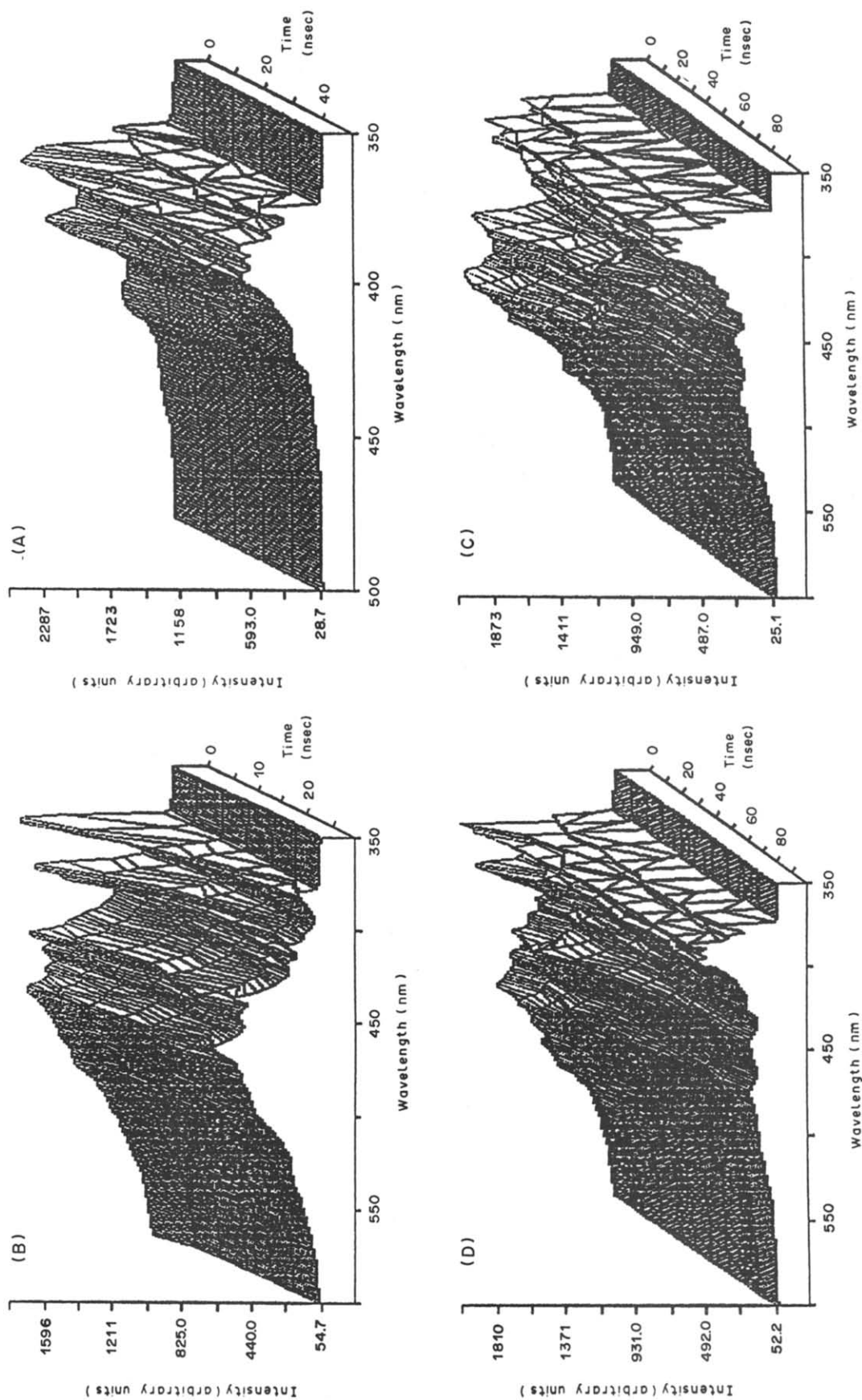


Fig. 2. TRFES in hexane at low temperature (77 K). The mixtures are (A) anthracene ($1 \times 10^{-5} M$) and pyrene ($1 \times 10^{-5} M$), (B) anthracene ($5 \times 10^{-5} M$) and fluoranthene ($5 \times 10^{-5} M$), (C) pyrene ($3.5 \times 10^{-5} M$) and fluoranthene ($5 \times 10^{-5} M$), (D) anthracene ($5 \times 10^{-5} M$) and fluoranthene ($5 \times 10^{-5} M$).

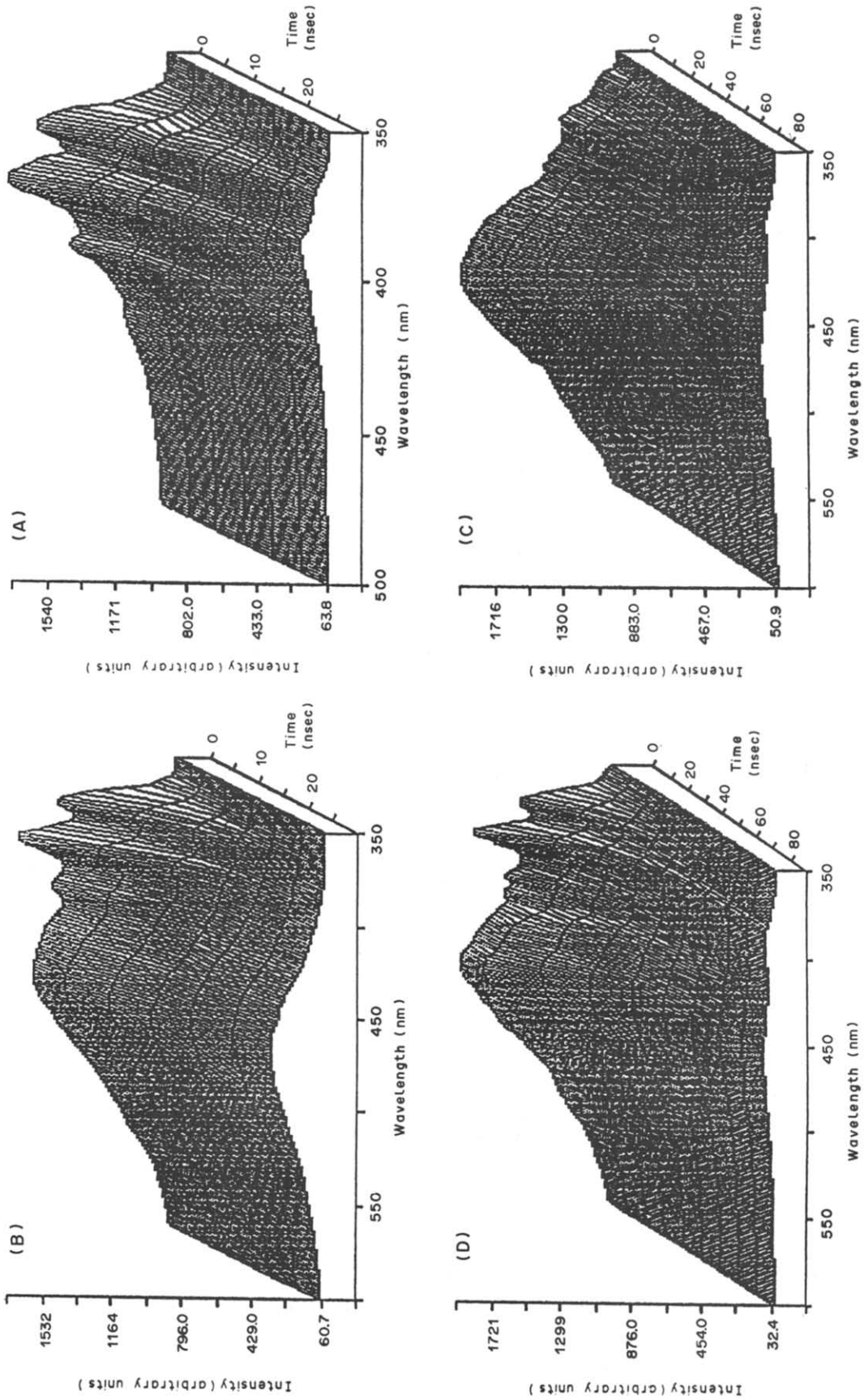


Fig. 3. TRFES in vapor phase. The mixtures are (A) anthracene and pyrene at 120°, (B) anthracene and fluoranthene at 135°, (C) pyrene and fluoranthene at 115°, (D) anthracene, pyrene and fluoranthene at 138°.

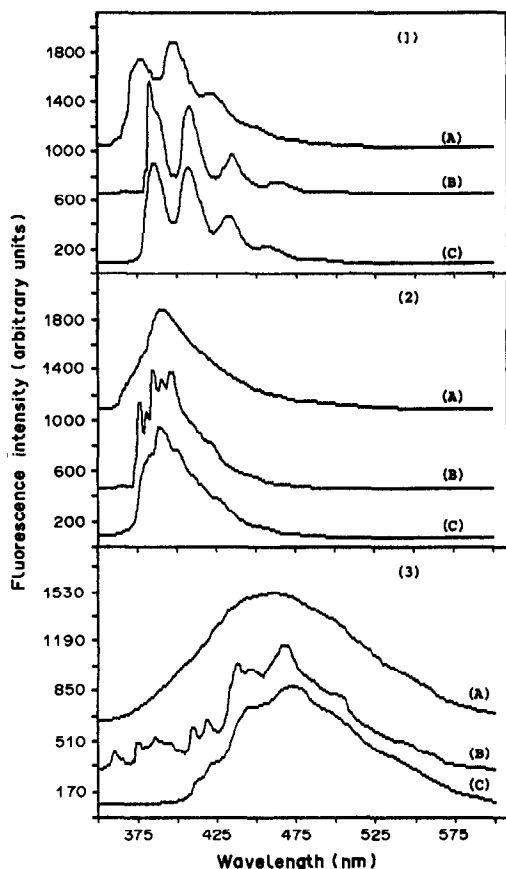


Fig. 4. Fluorescence emission spectra of PAH. (1) Anthracene, (A) vapor phase at 150°, (B) low temperature (77 K) in hexane, (C) room temperature in hexane. (2) pyrene, (A) vapor phase at 150°, (B) low temperature (77 K) in hexane, (C) room temperature in hexane. (3) Fluoranthene (A) vapor phase at 150°, (B) low temperature (77 K) in hexane, (C) room temperature in hexane.

to solvent effects, would be expected. For fluoranthene, a small red shift is also expected but the band change observed did not exceed the experimental error. At 77 K, pyrene exhibits significant vibrational structure due to the Shpol'skii effect^{11,12} but anthracene does not show any significant line-narrowing. Although the Shpol'skii effect is due to a reduction in the inhomogeneity of the environment for molecules trapped in low-temperature *n*-alkane crystals, whether or not highly resolved spectra are obtained for a particular combination of guest molecule and *n*-alkane depends on a number of experimental parameters. This effect is not clearly understood, even though the physical interpretation has invariably been based on some dimensional and geometrical correlations between the solute and host molecules. The composition and the mode of preparation of the sample appear to be important in this respect.²¹

Hexane and heptane are the best solvents for pyrene and anthracene, respectively.²¹ Some vibrational structure was also observed for fluoranthene at 77 K.

In the fluoranthene spectrum at 77 K (Fig. 4) the emission between 350 and 400 nm has been the subject of much controversy.²⁰⁻²⁴ These signals were not observed in mixtures of the PAH at 77 K. Further investigation is required to identify the origin of these bands.

The emission maximum of fluoranthene occurs at a different wavelength than the emission maxima of pyrene and anthracene. In the mixtures of these three compounds, the signals are not well resolved, especially for the pyrene and anthracene mixture, and each compound cannot be identified with any certainty without a pre-separation step. A new parameter, lifetime, was introduced to analyze these mixtures directly. The fluorescence lifetimes of anthracene, pyrene and fluoranthene are shown in Table 1. Figure 1 shows the time-resolved spectrum of various PAH mixtures at room temperature. The sensitivity for anthracene is about 10 times that for pyrene and fluoranthene, mainly due to the larger molar absorptivity at 337.1 nm, the laser line. Time zero was taken as corresponding to the emission maximum in the fluorescence decay curve at the principal band wavelength. As shown in Fig. 1A, at time zero, the two components of the mixture cannot be distinguished. When the signal acquisition is delayed, the anthracene signal decays very quickly owing to the short lifetime. As a result, these two compounds become more clearly resolved in this time-resolved spectrum. The fluoranthene band is separated from that of anthracene or pyrene relatively well at time zero because of the different emission band positions. In the time-resolved spectra as shown in Fig. 1B and 1C, the separation becomes much clearer. In Fig. 1D, the time-resolved spectra of the three-compound mixture is shown. At time zero, the anthracene and pyrene bands are completely mixed and the presence of fluoranthene is also

Table 1. Fluorescence lifetimes (nsec) of PAH; the solvent in the condensed phase is *n*-hexane

PAH	Room temperature	77 K	Vapor phase
Pyrene	430	860	420 (160°)
Anthracene	8	14	7 (150°)
Fluoranthene	77	82	*32 (150°)

*Refer to reference 20 for more details on this unusually small value.

not clear because a large part of its band is buried by the strong combined bands of anthracene and pyrene. As the time is delayed, the anthracene signal disappears, and the pyrene and fluoranthene become well resolved.

The same experiment was repeated at 77 K. At this temperature the fluoranthene signal is very weak compared to the anthracene and pyrene signals, owing to its small molar absorptivity at 337.1 nm. To observe the fluoranthene signal, it is necessary to increase its concentration by at least a factor of ten relative to that of anthracene and pyrene. As shown in Fig. 2, the resolution of each component is much clearer than in the room temperature spectra. This is due to the increased fine structure from the Shpol'skii effect. Therefore, it should be possible to analyze complex samples, owing to the improved selectivity at low temperature.

In the vapor phase, as shown in Fig. 3, the benefit of time-resolved spectra can be seen even though the emission bands for each component have very little fine structure. With 337.1 nm excitation, pyrene gives very weak emission and its presence in the mixture is not very evident. However, the pyrene signal can be identified with careful observation. This phenomenon is mainly due to the small molar absorptivity of pyrene at 337.1 nm in the vapor phase, since the vapor pressures for the three compounds are similar at elevated temperature.

By utilizing the time-resolved signal, the spectrum of each component can be reconstructed from the spectra of mixtures and used to calculate the concentration of each component. A representative example is shown in Fig. 5. The solid line in Fig. 5A is the spectrum of an anthracene and pyrene mixture in hexane at zero delay time and room temperature. The broken line in Fig. 5A is the spectrum of the same mixture at 30 nsec delay, multiplied by the decay factor for pyrene at 30 nsec, and is actually the pyrene spectrum at zero delay time because all of the anthracene signal is gone after 30 nsec delay. The decay factor (the ratio of the relative pyrene fluorescence intensity at the two delay times) is derived from the fluorescence decay curve for pure pyrene. The spectrum in Fig. 5B is obtained as the difference between the spectra in Fig. 5A and is the reconstructed anthracene spectrum. The intensity ratio of the anthracene and pyrene spectra at their principal emission wavelengths was used to calculate the anthracene concentration in the spectrum of the three-component PAH mixture, with the known

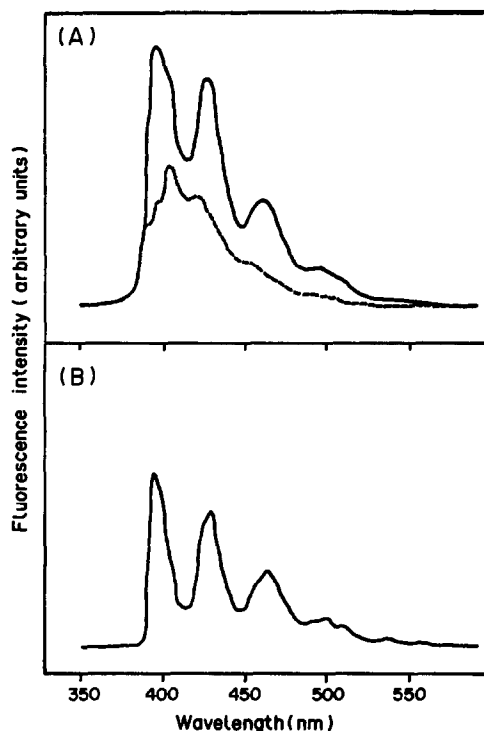


Fig. 5. Fluorescence emission spectra at room temperature. (A) (—): pyrene and anthracene mixture in hexane at zero delay time (---): pyrene and anthracene mixture in hexane at 30 nsec delay. (B) Reconstructed spectrum obtained by subtraction of broken line from solid line in (A).

concentration of pyrene as the reference. The concentrations of other components in the PAH mixture were calculated by the same procedure, with an appropriate known reference, preferably a long lifetime component. This technique can be applied for all three conditions. The results of these calculations are shown in Table 2. The uncertainty of this method is

Table 2. Concentrations of PAH in mixtures, calculated by the internal standard method

PAH	Known concentration	Calculated concentration	Relative error, %
Room temperature in hexane solution			
Anthracene	$1.0 \times 10^{-6}M$	$9.7 \times 10^{-7}M$	-3
Pyrene	$1.0 \times 10^{-5}M$	$8.9 \times 10^{-6}M$	-11
Fluoranthene	$1.0 \times 10^{-5}M$	$1.1 \times 10^{-5}M$	+10
Low temperature (77 K) in hexane solution			
Anthracene	$5.0 \times 10^{-6}M$	$4.1 \times 10^{-6}M$	-18
Pyrene	$3.5 \times 10^{-6}M$	$2.9 \times 10^{-6}M$	-17
Fluoranthene	$5.0 \times 10^{-5}M$	$5.9 \times 10^{-5}M$	+18
Vapor phase at 138°			
Anthracene	$6.3 \times 10^{-6}M$	$6.0 \times 10^{-6}M$	-5
Pyrene	$4.4 \times 10^{-6}M$	$4.0 \times 10^{-6}M$	-9
Fluoranthene	$4.3 \times 10^{-6}M$	$4.7 \times 10^{-6}M$	+9

*The % error is the percentage difference between the known concentration and the calculated concentration, determined from the time resolved spectra, divided by the known concentration.

fairly good considering that there was a 5–10% error in the pulse-to-pulse laser intensity. The increased error in the low temperature experiments is due, in large part, to non-reproducibility of positioning in the Dewar flask which results in a decreased reproducibility of the spectra low temperature spectra.

Time-resolved fluorescence measurements can be applied to analyze PAH mixtures in all three different environments. At room temperature in hexane, the mixtures can be well resolved even though this is relatively unsuitable for the analysis of complex mixtures, owing to the rather broad emission signals. The experimental procedures are the simplest and the calculated concentrations in the mixture have relatively small error. This room temperature technique would be effective for the analysis of relatively simple mixtures.

Time-resolved fluorescence spectroscopy in a low temperature Shpol'skii matrix would be excellent for the analysis of more complex mixtures. Vibrational structure and time-resolved spectra can provide highly detailed information for the analysis of complex samples, but this technique requires more specialized apparatus and effort. Also the quantitative analysis has a higher uncertainty. If this technique is combined with some simple preliminary fractionation, PAH in environmental samples should be clearly identifiable.

Time-resolved fluorescence in the vapor phase is also more complicated but this method allows dynamic measurement of the PAH directly while they are in the vapor phase. If this technique is combined with use of a temperature programmed furnace or any other precise vaporization device, rapid characterization of many types of samples could be done directly, especially samples often difficult to analyze by gas chromatographic methods, such as heavy oils, tar residues and resinous materials. It also holds considerable promise as a technique that can be applied to the study of combustion dynamics.

In summary, time-resolved fluorescence spectroscopy is a good technique for mixture

analysis with applicability to the condensed phase at room temperature, a solid phase at 77 K, and the vapor phase.

REFERENCES

1. J. C. Means, S. G. Wood, J. J. Hassett and W. L. Banwart, *Environ. Sci. Technol.*, 1980, **14**, 1524.
2. N. T. Edwards, *J. Environ. Qual.*, 1983, **12**, 427.
3. S. S. Epstein, M. Small, H. L. Falk and N. Mantel, *Cancer Res.*, 1964, **24**, 855.
4. D. D. Morgan, D. Warshawsky and T. Atkinson, *Photochem. Photobiol.*, 1977, **25**, 31.
5. D. D. Morgan and D. Warshawsky, *ibid.*, 1977, **25**, 39.
6. G. F. Strniste and R. J. Brake, in *Polynuclear Aromatic Hydrocarbons*, M. Cooke and A. J. Dennis (eds.), Vol. 5, pp. 109–118. Battelle Press, 1981.
7. R. T. Okinaka, J. W. Nickols, T. W. Whaley and G. F. Strniste, in *Polynuclear Aromatic Hydrocarbons*, M. Cooke and A. J. Dennis (eds.), Vol. 8, pp. 961–971. Battelle Press, 1985.
8. J. H. Richardson and M. E. Ando, *Anal. Chem.*, 1977, **49**, 955.
9. L. J. Jandris and R. K. Forcé, *Anal. Chim. Acta*, 1983, **151**, 19.
10. D. Bolton and J. D. Winefordner, *Talanta*, 1983, **30**, 713.
11. A. P. D'Silva and V. A. Fassel, *Anal. Chem.*, 1984, **56**, 985A.
12. E. L. Wehry and G. Mamanotov, *Modern Fluorescence Spectroscopy*, E. L. Wehry (ed.), Vol. 4, pp. 193–250. Plenum Press, New York.
13. J. W. Hofstraat, H. J. M. Janson, G. Ph. Hoornweg, C. Gooijer and N. H. Velthorst, *J. Mol. Struct.*, 1986, **142**, 279.
14. G. Patonay, G. Nelson and I. M. Warner, *Prog. Anal. Spectrosc.*, 1987, **10**, 561.
15. I. M. Warner, G. Patonay and M. P. Thomas, *Anal. Chem.*, 1985, **57**, 463A.
16. D. W. Millican and L. B. McGown, *ibid.*, 1989, **61**, 580.
17. A. E. Elsaid, A. P. D'Silva, V. A. Fassel and R. L. M. Dobson, *ibid.*, 1987, **59**, 970.
18. C.-N. Ho, G. D. Christian and E. R. Davidson, *ibid.*, 1981, **53**, 92.
19. M. Thomas, G. Patonay and I. M. Warner, *Rev. Sci. Instrum.*, 1986, **57**, 1308.
20. K. M. Bark and R. K. Forcé, *J. Phys. Chem.*, 1989, **93**, 7985.
21. J. W. Hofstraat, I. L. Freriks, M. E. J. de Vreeze, C. Gooijer and N. H. Velthorst, *ibid.*, 1989, **93**, 184.
22. J. B. Birk, *Photophysics of Aromatic Molecules*, p. 169. Wiley, New York, 1970.
23. R. V. Nauman, H. E. Holloway and J. H. Wharton, *Chem. Phys. Lett.*, 1985, **122**, 523.
24. J. W. Hofstraat, G. Ph. Hoornweg, C. Gooijer and N. H. Velthorst, *Spectrochim. Acta*, 1985, **41A**, 801.

PRECAPACITIVE PROCESSES IN SINGLE POTENTIAL-STEP CHRONOAMPEROMETRY

XIANG YUAN and RAY VON WANDRUSZKA*

Department of Chemistry, University of Idaho, Moscow, ID 83843, U.S.A.

(Received 28 February 1990. Revised 26 June 1990. Accepted 5 July 1990)

Summary—Extremely short-lived anodic currents were observed in the early parts of the transient response following the application of a cathodic potential step to a mercury working electrode. It is proposed that this phenomenon is due to the existence of a brief precapacitive period, which precedes full development of the double-layer charging current, and which allows momentary reaction (reduction) of species present at the electrode surface. The observed anodic currents are explained in terms of a re-oxidation of such “resident” species that were reduced during this precapacitive period. The subsequent capacitive surge produced by the charging of the electrical double layer leads to an anodic shift of the electrode potential that can be sufficient for the re-oxidation of the precapacitive amalgam. The anodic peak is linearly related to depolarizer concentration and varies with supporting electrolyte concentration, ion mobility and potential step size. Cathodic preconcentration of the depolarizer enhances the effect.

The behaviour of transient faradaic currents produced by a single potential step has been described theoretically by Miaw and Perone,¹ and Miaw.² They used the classical treatment of Feldberg³ to develop algorithms that allowed them to generate digitally simulated chronoamperometric curves. In subsequent work in this laboratory, high-speed instrumentation was used to produce experimental transient currents in simple reversible electrochemical systems.⁴ It was shown that the faradaic peak current varied with depolarizer concentration, yielding a calibration curve with two distinct linear regions. The temperature effect was found to be significant, giving a concentration-dependent “switch temperature”.

The application of a potential step to an electrode in an electrolyte solution gives rise to a relatively high initial current, due to the charging of the electrical double layer at the electrode–electrolyte interface. This capacitive current is given by

$$i = \frac{\Delta E}{R_u} \exp\left(\frac{-t}{R_u C_{dl}}\right) \quad (1)$$

where ΔE is the size of the potential step, R_u the uncompensated cell resistance, t the time, and C_{dl} the double-layer capacitance.

During the charging of the double layer, as the capacitive current decays the potential of

the working electrode “scans” toward its final value, as indicated by equation (1).¹

Faradaic processes can only occur when the potential reaches the decomposition potential of the active species in the course of this “pseudo-scan”. Double-layer charging currents are normally regarded as interferences in electroanalytical work and various steps are taken to minimize them. In the present investigation, their property of effectively generating a fast scan of the electrode potential is utilized as such. We have shown in previous work^{4,5} that the similarity of this process to ultra-fast linear-sweep voltammetry gives it the potential for interesting analytical applications. However, the fundamental phenomena are not well understood and further research is needed before a feasible technique can be developed.

Algorithms developed by Miaw² show that a chronoamperometric plot of the faradaic current component flowing during the first 10 time constants of the cell is peak-shaped (Fig. 1), not unlike a conventional linear-sweep voltamperogram. Laitinen and Kolthoff⁶ have described the transient faradaic response represented by the area beyond the peak, which decays with time, t , as a function of $t^{-1/2}$. In this region, the current is under diffusion control and is described by the well-known Cottrell equation:

$$i = nFA(D/\pi t)^{1/2}C \quad (2)$$

where the symbols have their usual electrochemical significance. During the period

*Author for correspondence.

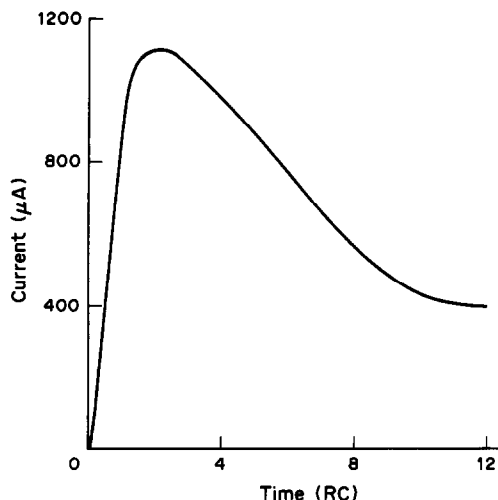


Fig. 1. Theoretical shape of a transient faradaic chronoamperogram produced by a single potential step.

preceding the faradaic peak, the rising current is caused by the potential pseudo-scan; to explain the peak shape of the chronoamperometric curve, it is useful to invoke depolarizer depletion effects, commonly discussed with reference to linear-sweep voltammetry.^{4,7}

The previous theoretical treatment¹ indicates that linearity of the current-concentration curve should not be expected for relatively high-level and wide-ranging analyte concentrations. This leaves the relationships at lower concentrations and within narrower concentration ranges to be investigated. Digital simulation also predicts that current-concentration behaviour will vary significantly at different measurement times during the existence of the transient. In our previous investigation,⁴ we chose to obtain our measurements at the peak of the faradaic transient, which occurs after about one cell time constant. This point is easily identifiable and does not vary significantly among solutions giving similar time constants.

In the present work, unexpected faradaic behaviour manifested itself at the very beginning of the cathodic potential step, at times less than approximately 0.3 times the cell time constant. A reproducible "dip" appeared in the faradaic current curve, indicating an oxidative process that briefly precedes the reductive one. The magnitude of this reverse current was found to be proportional to the depolarizer concentration in low concentration ranges and to increase with supporting electrolyte concentration. An explanation for the phenomenon is proposed.

EXPERIMENTAL

Electrodes and control/data system

A three-electrode cell was used, with a hanging mercury drop working electrode (Metrohm Herisau AG CH-9100), a calomel reference electrode, and a platinum counter-electrode.

The control/data system has been discussed in detail elsewhere⁸ and will be described only briefly here. It consists of three interactive parts: a potential-step generator and a high-speed data-acquisition module, both linked to an Apple IIe microcomputer. The instrument is capable of taking current readings (12-bit resolution) at a rate of 500 kHz after application of the potential step. A block diagram is shown in Fig. 2.

The digital portion of the potential-step generator is built around a 12-bit digital-to-analogue converter (DAC) and data are provided by the computer through a custom-built interface.⁸

The data-acquisition circuit comprises a high-speed 12-bit analogue-to-digital converter (Datel ADC-817) with a maximum conversion time of 2 μ sec. The digital data generated by the ADC are stored in 768 on-board memory locations. After application of the potential step, the data-acquisition system cycles at maximum speed, the ADC restarting itself after each conversion. When 768 current readings have been gathered in this way, the system shuts itself off and control is returned to the computer for data reduction and storage.

Chemicals

Distilled, demineralized water treated with a Millipore purification system to give 10^{18}

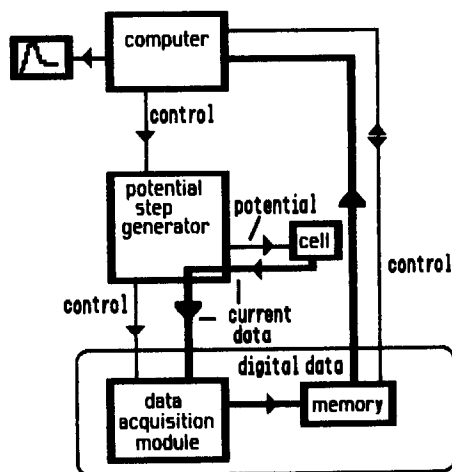


Fig. 2. Diagram of instrumentation used for measurement of faradaic transients.

M Ω .cm resistivity was used for all solutions. All electrolytes were of analytical grade from EM Science and were used without further purification. The mercury used in the working electrode was high quality electronic grade (Aldrich). Triton X-405 was obtained from Sigma as a 70% aqueous solution.

Procedure

All solutions were deaerated by passage of nitrogen for at least 10 min. A single cathodic potential step, from 0.0 to -1.0 V *vs.* SCE, was applied to the working electrode. The length of time the electrode was held at the starting potential generally varied from 5 to 10 sec. The total current readings (capacitive + faradaic) for a sample were first recorded in the data module memory, then transferred to the computer memory and committed to disk. The reported data are averages of triplicate determinations and a fresh mercury drop electrode was used for each experiment. The same procedure was followed for a blank solution, containing only supporting electrolyte. The latter data, consisting of capacitive current readings only, were digitally subtracted from the sample readings, yielding the faradaic current produced by the depolarizer. Induced charging-current effects may be operative during the period of changing faradaic current, but the focus of this investigation is on the precapacitive section of the transient, which precedes the flow of substantive charging current of any type.

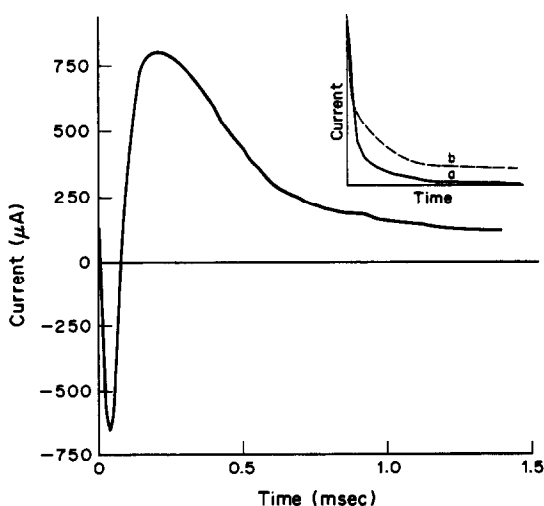


Fig. 3. Actual shape of a faradaic chronoamperogram produced by a single potential step from 0.0 to -1.0 V on a mercury electrode in $0.5M$ KCl with $2.0 \times 10^{-6}M$ Cd $^{2+}$. Inset: total component currents for; a, blank and b, sample.

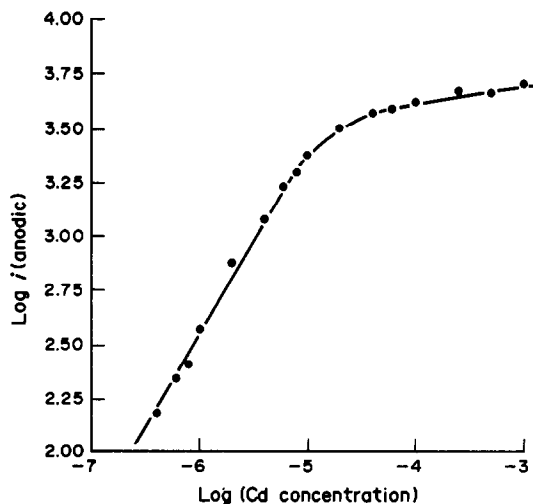


Fig. 4. Variation of anodic peak current with Cd $^{2+}$ concentration ($0.5M$ KCl supporting electrolyte).

RESULTS AND DISCUSSION

In the present study it was noted that at the very beginning of the pseudo-scan resulting from the cathodic potential step, at times less than 0.3 times the cell time constants, the current-time curve showed a brief negative excursion (Fig. 3). In practical terms, this means that the blank (capacitive only) cathodic current during that period was greater than the sample (capacitive + faradaic) current. This suggests that this initial faradaic portion of the current was anodic in nature, leading to a smaller total current, which was otherwise entirely cathodic.

The magnitude of the anodic faradaic peak was found to be linearly related to depolarizer concentration over a limited concentration range (Fig. 4). Moreover, the current depended on the concentration of the supporting electrolyte, increasing in a non-linear fashion (Fig. 5).

The data in Table 1 show that the size of the anodic peak for Cd $^{2+}$ in different supporting electrolytes varied almost linearly with cation mobility. While the data were mostly obtained with chlorides, additional work has shown that potassium nitrate as electrolyte gave similar results. The size and position of the cathodic potential step significantly influenced the anodic peak: it decreased in magnitude with decreasing step size. This was the case when the initial potential was kept constant and the final potential was changed in the anodic direction and also when the initial potential was shifted cathodically and the final potential was left at -1.0 V (Fig. 6).

The addition of 0.0035% Triton X-405 detergent obliterated the entire transient effect,

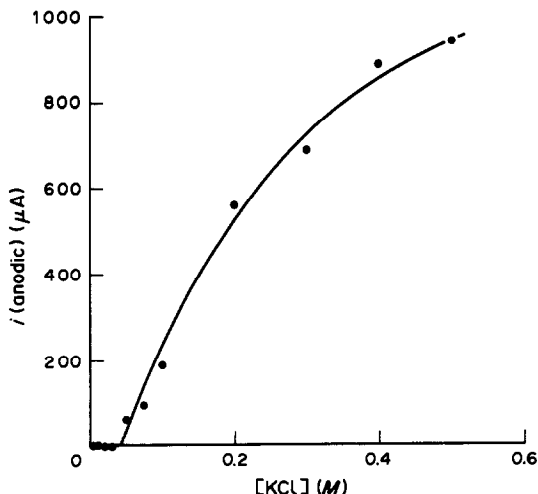


Fig. 5. Variation of anodic peak current of $5.0 \times 10^{-6} M$ Cd^{2+} with KCl concentration.

both anodic and cathodic, in the chronoamperogram. Only at high concentrations of Cd^{2+} ($1.0 \times 10^{-3} M$ and above) were both peaks discernible again.

As pointed out in the procedure section, the electrode was normally left at the initial potential of 0.0 V for 5–10 sec before the potential step was applied. The length of this period was found to have no significant effect—the final chronoamperogram showed no changes even when the initial potential was applied for several minutes.

To find further evidence for the origins of the anodic peak, the influence of cathodic preconcentration was investigated. A potential of -1.0 V vs. SCE was applied to the working electrode for a duration of 100 sec in Cd^{2+} solutions ranging from 5.0×10^{-7} to $1.0 \times 10^{-5} M$. This was followed by the customary 0.0 to -1.0 V potential step. In all cases it was found that the size of the anodic peak increased about fourfold relative to the corresponding situation without preconcentration.

The propagation delay and current settling time of the potentiostatic control circuit were less than 300 nsec, while the relevant electrochemical responses typically extended to approximately 100 msec. This precludes electronic artifacts as the causes of the observed effects and indicates the presence of electrochemical transients, even in the earliest measurements. The most plausible explanation of the phenomenon involves the time-average *resident* (not necessarily adsorbed) depolarizer species at the electrode surface.⁴ It should be noted that existing theory does not specifically address the early

part of the faradaic transient and does not recognize the possibility that the conditions created by the double-layer charging current require a finite time to develop fully. We propose that the slowness of movement of hydrated ions in aqueous solution, relative to the movement of electrons in a metallic conductor, results in a brief “precapacitive” period immediately following the application of the potential step. During this time, the electrode potential is close (or even equal) to the applied potential, since the potential drop due to the charging current has not yet developed. This allows for the momentary reaction of the electroactive species resident at the electrode surface at that instant, provided that the charge transfer is sufficiently fast. This contention is supported by our observation that the capacitive (blank) current initially rises to a maximum, before it decays according to equation (1). The rise typically lasts 6–8 μ sec in our system with 0.5M potassium chloride solution and is resolved into 3 or 4 data points. The faradaic processes that occur during the precapacitive period, *i.e.*, before the capacitive current has risen sufficiently to cause an electrode potential drop below the decomposition potential, are resolved into 1 or 2 data points. The bulk of the precapacitive reduction probably takes place during the first 1–2 μ sec following the potential step and therefore falls outside the time resolution capability of our instrument.

The fast reduction and concurrent amalgamation of cadmium and lead ions renders them amenable to the precapacitive surface reduction described above. The beginning of

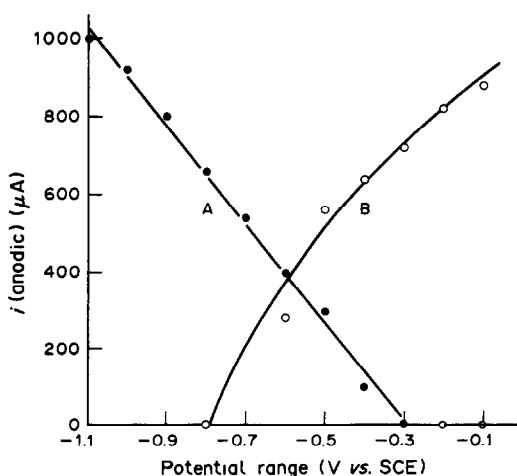


Fig. 6. Variation of the anodic peak current of $10 \times 10^{-5} M$ Cd^{2+} in 0.5M KCl with range of potential step sizes; A, from 0.0 V to final potential and B, from initial potential to -1.0 V.

the capacitive process therefore sees a quantity of amalgam, formed under the influence of the precapacitive full applied potential, in the very surface layer of the mercury drop. The subsequent flow of double-layer charging current shifts the electrode potential in an anodic direction and causes the re-oxidation of this amalgam. The resulting anodic current is effectively subtracted from the capacitive current, which is overwhelmingly "cathodic" in direction. The initially measured cathodic current in a solution containing a reversible depolarizer is, therefore, smaller than the corresponding current in a solution with supporting electrolyte only. The various currents involved in the precapacitive and early capacitive processes are shown in Fig. 7.

The explanation offered here accounts for the observed dependence of the anodic peak on depolarizer concentration. The time-average presence of depolarizer at the electrode surface is essentially a bulk effect and the amount of precapacitive amalgam formed therefore depends directly on the depolarizer concentration. The loss of linearity observed at higher concentrations (Fig. 4) results from surface saturation of the electrode by resident species. The number density of depolarizer ions sufficiently close to the surface to be available for precapacitive reduction has an upper limit dictated by the hydrated radius of the ion. Further increases in concentration beyond this saturation point cannot produce more amalgam for subsequent re-oxidation and the anodic peak current therefore reaches a maximum.

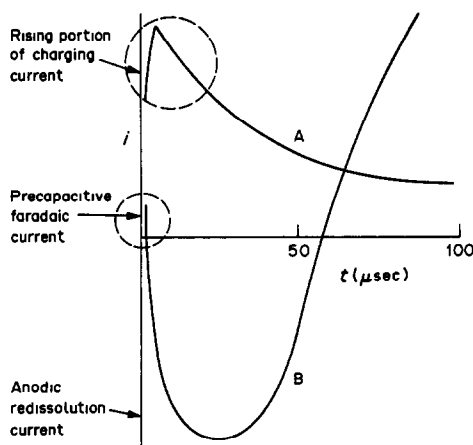


Fig. 7. Magnified view of earliest measurable portions of transient currents. A, double-layer charging current; B, faradaic current. First data point approx. 2 μ sec after potential step.

The enhancement of the anodic peak by an increase in supporting electrolyte concentration and by greater ion mobility provides further evidence for the proposed mechanism. Both result in increased capacitive surges upon double-layer formation and hence lead to increased anodic shifts during the process. This, in turn, gives rise to a higher re-oxidation current.

As mentioned above, a smaller potential step produces a smaller anodic peak, whether the initial potential is more cathodic or the final potential is more anodic. This is also in agreement with the precapacitive mechanism; the smaller step decreases the capacitive surge and hence the anodic potential drop, leading to decreased re-oxidation current. If the size of the potential step is reduced by shifting the final potential anodically, an additional effect is operative: the precapacitive electrode potential is now less cathodic, so the extent of initial amalgamation is decreased. This leads to a yet smaller re-oxidation current.

The observation that the addition of detergent to the solution eliminates both anodic and cathodic transient peaks is expected in view of electrode surface coverage by the detergent and disturbances in the extent and speed of double-layer formation.

Strong evidence for the proposed mechanism is provided by the cathodic preconcentration experiment, especially in contrast with the case where non-electrolytic initial potentials are used. A separate and prolonged reductive accumulation of cadmium and lead in the electrode leads to a greatly enhanced anodic transient, which is no longer dependent on the presence of resident species at the electrode surface. Since the reduction in this case is not limited to the brief precapacitive period and the accumulation is therefore significantly greater, the amount of amalgam available for re-oxidation is increased. The anodic potential drop during the capacitive surge, however, is still effective, and the anodic peak increases in accordance with the amount of preconcentrated depolarizer. For all bulk concentrations considered at the chosen preconcentration time, the anodic peak increased linearly, suggesting that the mechanism can be likened to an ultra-fast anodic stripping procedure. It is worth noting that depolarizer adsorption on the electrode does not appear to play a major role under the conditions of this study, since leaving the electrode at the starting potential (0.0 V vs. SCE)

for relatively long periods did not change the eventual anodic peak current.

CONCLUSIONS

The proposed process, involving a precapacitive period during which species resident at the electrode surface are reduced and re-oxidized during the capacitive surge, accounts for the observed anodic component in an otherwise entirely cathodic process. The mechanism is suggested as a plausible explanation of the experimental findings. The present investigation has dealt with a mercury-drop electrode and amalgam-forming depolarizers and further studies are needed to determine whether similar processes are operative with non-amalgamating depolarizers and at noble metal and carbon electrodes. Interesting possibilities exist for analytical applications of such fast anodic stripping of preconcentrated analytes, with speed of analysis as the prime benefit.

Acknowledgement—The authors gratefully acknowledge support of this work by the University of Idaho Research Council.

REFERENCES

1. L.-H. Lai Miaw and S. P. Perone, *Anal. Chem.*, 1979, **51**, 1645.
2. L.-H. Lai Miaw, *Ph.D. Thesis*, Purdue University, West Lafayette, IN, 1978.
3. S. W. Feldberg, in *Electroanalytical Chemistry*, A. J. Bard (ed.), Vol. 3, p. 199. Dekker, New York, 1966.
4. S. O. Arhunmwunde and R. von Wandruszka, *Anal. Chim. Acta*, 1989, **226**, 337.
5. S. O. Arhunmwunde, *M.S. Thesis*, University of Idaho, Moscow, ID, 1989.
6. H. A. Laitinen and I. M. Kolthoff, *J. Am. Chem. Soc.*, 1939, **61**, 3344.
7. A. J. Bard and L. R. Faulkner, *Electrochemical Methods: Fundamentals and Applications*, p. 214. Wiley, New York, 1980.
8. R. von Wandruszka, *Anal. Instrum.*, 1984, **13**, 193.
9. R. von Wandruszka and M. Maraschin, *Anal. Lett.*, 1981, **14**, 463.
10. S. S. Fratoni, Jr. and S. P. Perone, *Anal. Chem.*, 1976, **48**, 287.

ON-LINE MONITORING OF CHLORAMINE REACTIONS BY MEMBRANE INTRODUCTION MASS SPECTROMETRY

TAPIO KOTIAHO*, ANITA K. LISTER, MARK J. HAYWARD and R. GRAHAM COOKS†
Department of Chemistry, Purdue University, West Lafayette, IN 47907, U.S.A.

(Received 14 June 1990. Revised 16 July 1990. Accepted 25 July 1990)

Summary—Membrane introduction mass spectrometry has been applied to on-line monitoring of the reaction of monochloramine with hydrogen chloride. The detection limit for monochloramine introduced by a sheet-membrane direct-insertion probe and measured by electron impact ionization and selected ion detection was found to be 0.7 mg/l. Formation of dichloramine, trichloramine and molecular chlorine in response to the addition of hydrogen chloride to the monochloramine solution was measured on-line. The flow-through membrane introduction mass spectrometry method for detection of chloramines and characterization of their chemistry has minimal memory effects, high molecular specificity, high speed of analysis owing to fast response times, and low detection limits.

Monochloramine, dichloramine and trichloramine are toxic compounds formed during chlorination of potable and waste water. Monochloramine (typical levels 1 mg/l.) is sometimes used as a disinfectant in drinking water.¹⁻⁶ The standard methods used for measuring these compounds are colorimetric, spectrophotometric and titrimetric,^{1-5,7} and sometimes high-performance liquid chromatography is also used.^{4,8,9} All the methods above are susceptible to interferences, and differentiation between chloramines can be difficult. Savikas *et al.*¹⁰ indicated that membrane introduction mass spectrometry (MIMS) might provide a solution to these problems.

Membrane introduction mass spectrometry is a well-established analytical technique, which has undergone several stages of development¹¹⁻¹⁶ since its introduction by Hoch and Kok in 1963.¹¹ An important recent advance was the introduction of the flow-through concept¹⁴⁻¹⁵ which has since been used by various groups.¹⁶⁻¹⁸ In the flow-through method the sample flows through or across the membrane surface, which is located in the ion source of the mass spectrometer. This procedure minimizes the problems due to analyte dilution, memory effects and slow response times associated with interfaces where the membrane is remote from the ion

source. Membrane introduction mass spectrometry has already proven to have important applications in the analysis of trace organic compounds in aqueous solutions,^{12,13,17} environmental analysis¹⁹⁻²² and the monitoring of biochemical processes.^{23,24}

In the present work, procedures are developed to detect and quantify monochloramine, dichloramine and trichloramine by on-line membrane introduction mass spectrometry. The detection limit for monochloramine has been measured and the chemistry of chloramine interconversion monitored.

EXPERIMENTAL

An instrumental configuration which allows on-line reaction monitoring experiments to be performed with a mass spectrometer interfaced to a membrane introduction system has already been described.¹⁴ The present work employed a modified form of this interface with a sheet direct insertion membrane probe, S-DIMP,¹⁶ instead of a capillary tube interface (Fig. 1). As in previous work, the membrane was a dimethylvinyl silicone polymer (ASTM: VMQ Dow Corning) with a thickness of 0.13 or 0.25 mm. The temperature of the membrane probe, which was controlled independently of that of the ion source, was 70°. The main advantages of the S-DIMP interface are that memory effects sometimes encountered with the capillary tube interface were almost entirely eliminated and response times were decreased

*On leave from Technical Research Center of Finland, Chemical Laboratory, Biologinkuja 7, 02150 Espoo, Finland.

†Author for correspondence.

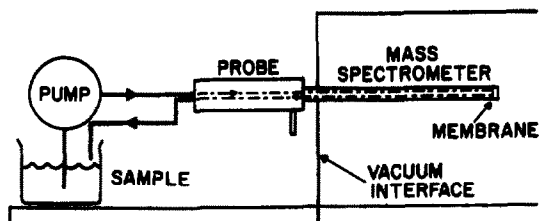


Fig. 1. Instrumentation for on-line monitoring of the reactions of monochloramine with HCl, employing the sheet direct insertion membrane probe and a triple quadrupole mass spectrometer.

through optimization of the membrane temperature. Detection limit data were obtained with the flow-injection analysis apparatus described elsewhere²⁴ with sample sizes of 250 μ l. A water stream was continuously supplied to the probe by an Ismatec multichannel peristaltic pump (Model 7618-30) and aliquots of reaction mixture or standard solution were injected into this stream as needed. A Finnigan 4500 triple quadrupole mass spectrometer equipped with an Incos data system and operated under electron impact (70 eV) ionization conditions was employed. Full mass spectra and selected ion monitoring experiments were performed. When data were recorded as a function of reaction time, the results were manipulated with the data handling system normally used to record chromatography experiments. The identities of the reaction products were confirmed by measuring the spectra of the daughter ions obtained with a collision energy of 20 eV and collision gas (argon) pressure of 1 mtorr, which corresponds to multiple collision conditions.

The monochloramine solutions (540 and 140 ppm) were supplied by the United States Environmental Protection Agency, Cincinnati. Solutions for the detection limit studies were prepared by serial dilution of the stock solutions with distilled water. The on-line reaction monitoring experiments were done either by adding known volumes of 0.1M hydrochloric acid or concentrated hydrochloric acid to a 540 ppm monochloramine solution (15 ml) or by adding calcium hypochlorite (6 ml of 1 mg/ml solution) to an aqueous ammonia solution (50 ml, 0.015M) and then acidifying the mixture by stepwise addition of 0.1M hydrochloric acid or concentrated hydrochloric acid. In the latter procedure, the pH of the reaction mixture was measured with a Corning 130 pH meter and continuously recorded with a chart recorder. The resulting solution was sampled continuously with the apparatus shown in Fig. 1.

RESULTS AND DISCUSSION

Table 1 lists the ions observed in the EI mass spectrum of an aqueous solution (540 ppm) of monochloramine. The mass spectrum of this compound has not previously been reported. The molecular ion, NH_2Cl^+ , constitutes the base peak and is remarkably stable in contrast to the high reactivity and instability of its neutral counterpart.¹ The daughter ion mass spectrum recorded for both isotopic forms of the molecular ion of monochloramine confirms its stability (Table 2). The agreement between these two daughter spectra confirms the assignments made in Table 1. The detection limit ($S/N = 3$) for monochloramine by membrane introduction mass spectrometry is 0.7 mg/l. (Fig. 2). The detection limit was measured by using flow-injection analysis apparatus (250 μ l sample volume), EI and selected ion detection (ions monitored at m/z 51, 53, 55). The detection limits for dichloramine and trichloramine are about the same, as indicated by similar responses in the corresponding experiments. Under steady state conditions still lower detection limits can be reached.

The reactions of monochloramine with hydrogen chloride were studied on-line and they clearly show formation of dichloramine and trichloramine (Fig. 3) as Margerum *et al.*^{2,3} demonstrated earlier by using spectrophotometry. Data presented in Fig. 3 were collected by scanning full EI mass spectra (mass range 33-300) in real time as the reaction, induced by addition of portions of hydrochloric acid, proceeded. The initial rise of the monochloramine signal represents the time during which water was replaced by 540 ppm monochloramine solution. After the first addition of hydrochloric acid (5 ml of 0.1M solution, added after 3.1 min) formation of dichloramine was

Table 1. EI mass spectrum of monochloramine (mass range 33-100)

m/z	% Rel. abund.	Ion species*
35	<0.5	$^{35}\text{Cl}^+$
36	0.6	$\text{H}^{35}\text{Cl}^{++}$
37	<0.5	$^{37}\text{Cl}^+$
38	<0.5	$\text{H}^{37}\text{Cl}^{++}$
49	5	$\text{N}^{35}\text{Cl}^{++}$
50	1	$\text{NH}^{35}\text{Cl}^+$
51	100	$\text{NH}_2^{35}\text{Cl}^+$; $\text{N}^{37}\text{Cl}^{++}\ddagger$
52	2	$\text{NH}_2^{37}\text{Cl}^+$; $\text{NH}^{37}\text{Cl}^+\ddagger$
53	31	$\text{NH}_2^{37}\text{Cl}^+$
54	0.5	$\text{NH}_3^{37}\text{Cl}^+$

*Inferred from isotopic abundance distribution.

†Ca. 1.5%.

‡Ca. 0.3%.

Table 2. Daughter ion spectrum of different isotopic forms of the molecular ion of monochloramine, dichloramine, and trichloramine

Parent ion			Main daughter ions		
<i>m/z</i>	% Rel. abund.	Ion species	<i>m/z</i>	% Rel. abund.	Ion species
Monochloramine					
51	100	NH ₂ ³⁵ Cl ⁺⁺	50	5	NH ³⁵ Cl ⁺
			49	2	N ³⁵ Cl ⁺⁺
			36	9	H ³⁵ Cl ⁺
			35	5	³⁵ Cl ⁺
			16	7	NH ₂ ⁺
15	3	NH ⁺			
53	100	NH ₂ ³⁷ Cl ⁺⁺	52	6	NH ³⁷ Cl ⁺
			51	2	N ³⁷ Cl ⁺⁺
			38	7	H ³⁷ Cl ⁺
			37	7	³⁷ Cl ⁺
			16	8	NH ₂ ⁺
15	4	NH ⁺			
Dichloramine					
85	30	NH ³⁵ Cl ₂ ⁺	50	100	NH ³⁵ Cl ⁺
			49	31	N ³⁵ Cl ⁺⁺
87	63	NH ³⁵ Cl ³⁷ Cl ⁺	52	87	NH ³⁷ Cl ⁺
			51	31	N ³⁷ Cl ⁺⁺
			50	100	NH ³⁵ Cl ⁺
			49	38	N ³⁵ Cl ⁺⁺
Trichloramine					
119	9	N ³⁵ Cl ₃ ⁺	84	100	N ³⁵ Cl ₂ ⁺
			49	16	N ³⁵ Cl ⁺⁺
121	16	N ³⁵ Cl ₂ ³⁷ Cl ⁺	86	100	N ³⁵ Cl ³⁷ Cl ⁺
			84	49	N ³⁵ Cl ₂ ⁺
			51	9	N ³⁷ Cl ⁺⁺
			49	19	N ³⁵ Cl ⁺⁺
123	19	N ³⁵ Cl ³⁷ Cl ₂ ⁺	88	49	N ³⁷ Cl ₂ ⁺
			86	100	N ³⁵ Cl ³⁷ Cl ⁺
			51	18	N ³⁷ Cl ⁺⁺
			49	9	N ³⁵ Cl ⁺⁺

Collision energy 20 eV and collision gas (argon) pressure 1 mtorr.

observed and a short time later small amounts of trichloramine were also detected. The full EI mass spectrum (Fig. 4A) at this point (4.4 min) shows ions characteristic of dichloramine and traces of ions characteristic of trichloramine. The mass spectra of the daughter ions from parents with *m/z* 85 and 87 confirm the production of dichloramine (Table 2). Note that almost all monochloramine has been removed, as demonstrated by the negligible abundance of *m/z* 53, which is the heavy isotopic form of the molecular ion, *m/z* 51, of monochloramine. The peak for *m/z* 51 is due to both the molecular ion of monochloramine, NH₂³⁵Cl⁺⁺, and a fragment ion, N³⁷Cl⁺⁺, of dichloramine and trichloramine. The latter ion is formed by dehydrochlorination of the molecular ion (isotopic form *m/z* 87) of dichloramine or by chlorine loss from the molecular ion (isotopic forms *m/z* 121 and 123) of trichloramine. This is demonstrated by

the measured daughter ion mass spectra (Table 2). For this reason the NH₂³⁷Cl⁺⁺ ion, *m/z* 53, is the appropriate ion for monitoring monochloramine.

The production of trichloramine occurred in good yield after the second addition of hydrochloric acid (1 ml of concentrated acid) at 9.1 min (Fig. 3). It shows up clearly in the mass spectrum taken at this time (Fig. 4B) and is confirmed by its daughter spectra (Table 2). The daughter spectra of the molecular ions of dichloramine and trichloramine both show preferential formation of the ionized bivalent species NHCl⁺ and NCl₂⁺. Note that Fig. 4B demonstrates the generation of molecular chlorine (ions *m/z* 70, ³⁵Cl₂⁺; *m/z* 72, ³⁵Cl³⁷Cl⁺ and *m/z* 74, ³⁷Cl₂⁺) simultaneously with the trichloramine. As shown in Fig. 3, the chlorine produced by the second addition of hydrochloric acid disappears quite rapidly, whereas that produced by

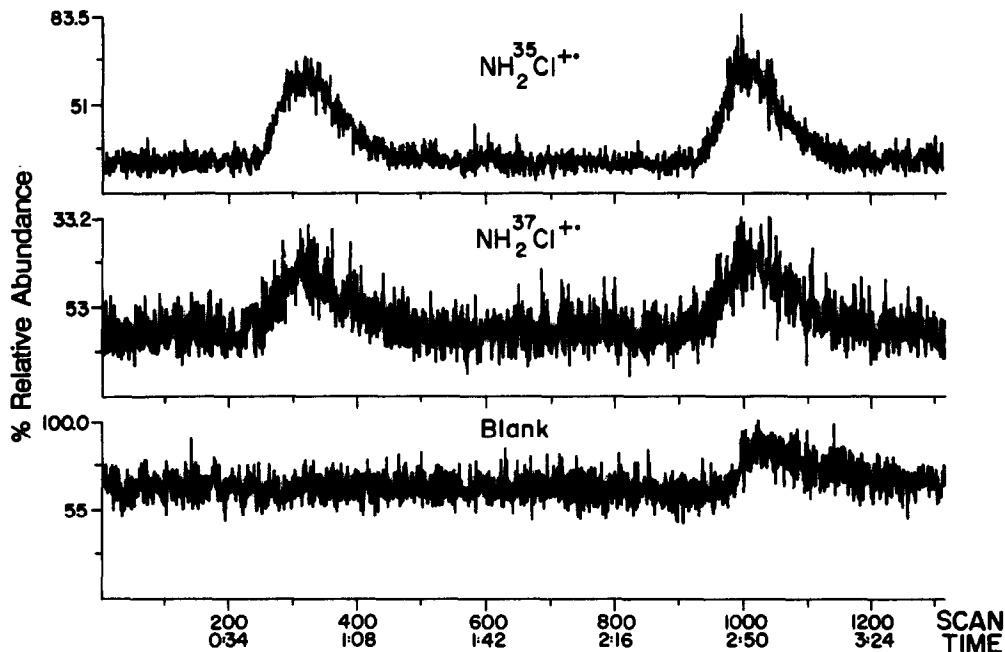


Fig. 2. Two consecutive injections (250 μ l each) of 0.7 mg/l. monochloramine solution, illustrating the detection limit obtained by MIMS. Data were collected by use of EI and the selected ion detection mode. Ions measured were m/z 51 ($\text{NH}_2^{35}\text{Cl}^{+\bullet}$), m/z 53 ($\text{NH}_2^{37}\text{Cl}^{+\bullet}$) and m/z 55 (background ion).

further additions of the acid disappears only slowly.

The reaction sequence above was also carried out with a monochloramine solution which was

generated *in situ* from ammonia and calcium hypochlorite solutions at a pH of 11.7. In the case of this reaction mixture, formation of dichloramine was observed after the pH of the

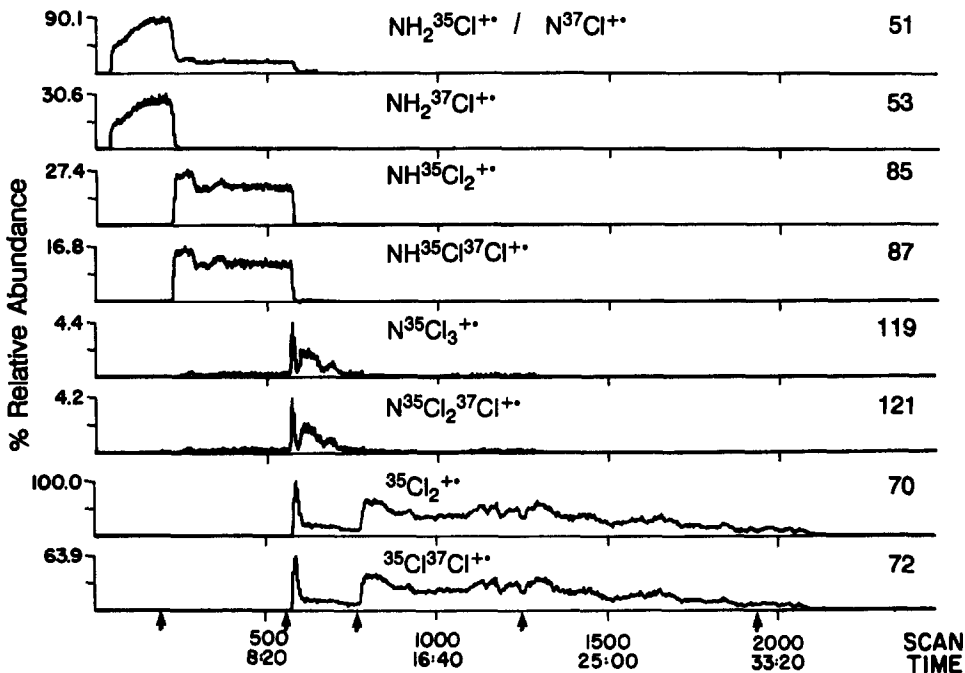


Fig. 3. On-line monitoring of the reactions of monochloramine with HCl. Mass chromatograms presented are m/z 51 ($\text{NH}_2^{35}\text{Cl}^{+\bullet}$) and m/z 53 ($\text{NH}_2^{37}\text{Cl}^{+\bullet}$) for $\text{NH}_2^{35}\text{Cl}$, m/z 70 ($^{35}\text{Cl}_2^{+\bullet}$) and m/z 72 ($^{35}\text{Cl}^{37}\text{Cl}^{+\bullet}$) for chlorine, m/z 85 ($\text{NH}^{35}\text{Cl}_2^{+\bullet}$) and m/z 87 ($\text{NH}^{35}\text{Cl}^{37}\text{Cl}^{+\bullet}$) for NHCl_2 , and m/z 119 ($\text{N}^{35}\text{Cl}_3^{+\bullet}$) and m/z 121 ($\text{N}^{35}\text{Cl}_2^{37}\text{Cl}^{+\bullet}$) for NCl_3 . Additions of HCl were made at the times indicated by the arrows. Data were collected by scanning the full EI mass spectra (m/z 33–300). Note that the ion m/z 51 is due to $\text{NH}_2^{35}\text{Cl}^{+\bullet}$ and $\text{N}^{37}\text{Cl}^{+\bullet}$, in the proportion 4:1.

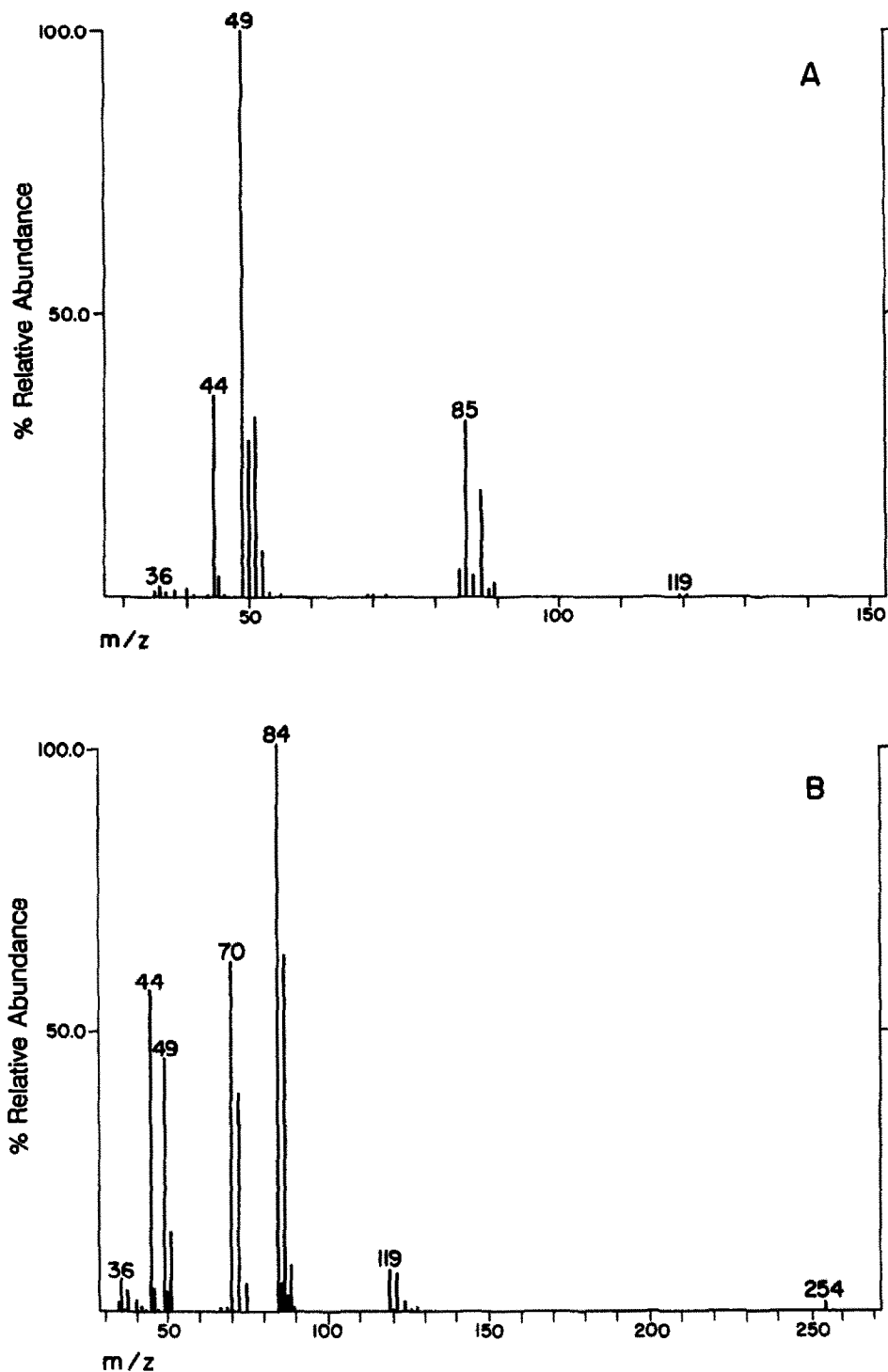


Fig. 4. Representative EI mass spectra for the on-line monitoring experiment (see Fig. 3). A, shows the mass spectrum acquired during scans 266 to 270 (4.4 min) and B, shows the mass spectrum acquired during scans 580 to 585 (9.1 min).

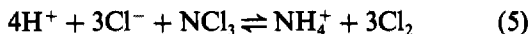
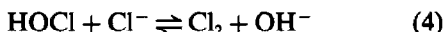
mixture was lowered to 3.3 by addition of hydrochloric acid. Formation of trichloramine required that the pH of the reaction mixture be further lowered to 0.4 by further addition of acid. These results are consistent with the sug-

gestion² that monochloramine, dichloramine, and trichloramine are formed according to the following reactions:





At pH above 9.5 only the formation of monochloramine is observed, and this is in agreement with the suggestion that the only reaction channel available is reaction (1).² When the pH of the reaction mixture is lowered, formation of dichloramine is observed first [reaction (2)] and with further additions of hydrochloric acid conversion of dichloramine into trichloramine is observed [reaction (3)]. The formation of large amounts of chlorine at the same time occurs because, at a pH of 3 or below, the amount of molecular chlorine in equilibrium with hypochlorous acid [HOCl, reaction (4)] is substantial.¹ Chlorine formation could also proceed partly by reaction (5), proposed by Corbett *et al.*,²⁵ since soon after the second hydrochloric acid addition the signal due to trichloramine disappears (Fig. 3). Owing to its high volatility¹ trichloramine may also be partly lost by evaporation.



Other ions of interest observed during the reaction occur at m/z 36, 38, 44, 127 and 254. Ions with m/z 36 and 38 are due to hydrochloric acid, and the ion with m/z 254 is most probably due to molecular iodine, which is liberated from iodide impurities under the strong oxidizing conditions, and m/z 127 is the I^+ fragment. The signal at m/z 44 increases significantly when the solution is acidified and is due to carbon dioxide which is driven out of the solution with decreasing pH, in accordance with the well known bicarbonate (HCO_3^-) and carbonate (CO_3^{2-}) equilibria. The identity of the ion with m/z 44 was confirmed by recording its daughter spectrum (m/z 28, 40%). The signal at m/z 44 decreases slowly after its initial rise and is detected until the end of the experiment (about 30 min).

This study clearly demonstrates the advantages of membrane introduction mass spectrometry for on-line monitoring of the reactions of chloramines and for the determination of chloramines in water down to low ppm levels. The main advantages of MIMS are high specificity for chloramines, high speed of analysis, low detection limits and the ability to automate the sampling process.

Acknowledgements—The authors thank William L. Budde of the US Environmental Protection Agency (Cincinnati, Ohio) for valuable suggestions and H. Paul Ringhand of the

same agency for providing the monochloramine samples. The support of the US Environmental Protection Agency (EPA CR-815749-01-0) is acknowledged. The support provided for T.K. by the Emil Aaltonen Foundation and Suomen Kulttuurirahasto is greatly appreciated.

REFERENCES

1. G. C. White, *The Handbook of Chlorination*, 2nd Ed., Van Nostrand Reinhold, New York, 1986.
2. E. T. Gray, Jr., D. W. Margerum and R. P. Huffman, in *Organometals and Organometalloids: Occurrence and Fate in the Environment*, F. E. Brinckman and J. M. Bellama (eds.), p. 264. ACS, Washington, D. C., 1978.
3. D. W. Margerum, E. T. Gray, Jr. and R. P. Huffman, in *Organometals and Organometalloids: Occurrence and Fate in the Environment*, F. E. Brinckman and J. M. Bellama (eds.), p. 278. ACS, Washington D.C., 1978.
4. V. C. Hand and D. W. Margerum, *Inorg. Chem.*, 1983, **22**, 1449.
5. K. Kumar, R. W. Shinness and D. W. Margerum, *ibid.*, 1987, **26**, 3430.
6. G. R. Helz and L. Kosak-Channing, *Environ. Sci. Technol.*, 1984, **18**, 48A.
7. T. Aoki, *ibid.*, 1989, **23**, 46.
8. F. E. Scully, Jr., J. P. Yang, K. Mazina and F. B. Daniel, *ibid.*, 1984, **18**, 787.
9. M. T. Lukasewycz, C. M. Bleringer, R. J. Liukkonen, M. E. Fitzsimmons, H. F. Corcoran, S. Lin and R. M. Carlson, *ibid.*, 1989, **23**, 196.
10. P. J. Savickas, M. A. Lapack and J. C. Tou, *Anal. Chem.*, 1989, **61**, 2332.
11. G. Hoch and B. Kok, *Arch. Biochem. Biophys.*, 1963, **101**, 160.
12. L. B. Westover, J. C. Tou and J. H. Mark, *Anal. Chem.*, 1974, **46**, 568.
13. J. C. Weaver and J. H. Abrams, *Rev. Sci. Instrum.*, 1979, **50**, 478.
14. J. S. Brodbelt and R. G. Cooks, *Anal. Chem.*, 1985, **57**, 1153.
15. M. E. Bier and R. G. Cooks, *ibid.*, 1987, **59**, 597.
16. M. E. Bier, T. Kotiaho and R. G. Cooks, *Anal. Chim. Acta*, 1990, **231**, 175.
17. S. Dheandhanoo and J. Dulak, *Rapid Comm. Mass Spectrom.*, 1989, **3**, 175.
18. A. Sturaro, L. Doretti, G. Parvoli, F. Cecchinato, G. Frison and P. Traldi, *Biomed. Environ. Mass Spectrom.*, 1989, **18**, 707.
19. B. J. Hartland, P. J. D. Nicholson and E. Gillings, *Wat. Res.*, 1987, **21**, 107.
20. D. Wenhui, C. Kuangnan, L. Jianli and D. Zhenying, *Mass Spectrosc. (Tokyo)*, 1987, **35**, 122.
21. A. K. Lister, K. V. Wood, K. Noon and R. G. Cooks, *Biomed. Environ. Mass Spectrom.*, 1989, **18**, 1063.
22. P. W. Langvardt, K. A. Brzak and P. E. Kastl, *Annual Conference on Mass Spectrometry and Allied Topics*, Cincinnati, 1986.
23. E. Heinzle and M. Reuss, *Mass Spectrometry in Biotechnological Process Analysis and Control*, Plenum Press, New York, 1987.
24. M. J. Hayward, A. K. Lister, T. Kotiaho, R. G. Cooks, G. D. Austin, R. Narayan and G. T. Tsao, *Biotech. Techniq.*, 1989, **3**, 361.
25. R. E. Corbett, W. S. Metcalf and F. G. Soper, *J. Chem. Soc.*, 1953, 1927.

THE RESPONSE OF SOME ORGANIC MICROSENSOR COATINGS TO A VARIETY OF VAPORS

ALAN R. KATRITZKY*, G. PAUL SAVAGE and MARIA PILARSKA

Department of Chemistry, University of Florida, Gainesville, FL 32611, U.S.A.

(Received 12 April 1990. Revised 25 May 1990. Accepted 12 June 1990)

Summary—Six organic compounds were spray-coated onto surface acoustic wave devices which were then exposed to vapors of acetone, diethyl ether, dichloromethane, chlorobenzene, benzene, and acetonitrile. Changes in the resonant frequency of the device or in the resistance of the coating were collected by computer-controlled data acquisition. Different patterns of response to the six vapors were observed for each of the coatings.

We have previously reported the utility of a number of coatings for chemiresistor and surface acoustic wave (SAW) microsensor devices.¹⁻⁴ Chemiresistor devices⁵ record the change in the resistance between the interdigitated electrodes on the surface of the device upon exposure of a thin film of semiconducting coating to a vapor. SAW microsensors^{6,7} record changes in the resonant frequency of the device upon exposure to vapors. The mode of operation of SAW devices has been described in detail elsewhere.^{4,7}

There are two basic aspects in the development of chemical microsensors. One involves the interface or surface problems associated with the effective and reproducible application of the coating materials to small electronic devices, to take maximum advantage of the chemical properties of the coating. The other is the planning, synthesis, and characterization of new coating materials that satisfy requirements such as sensitivity, selectivity, and chemical stability for the expected operational lifetime of the chemical sensor. Although microsensor technology shows great promise, the lack of adequate coating materials currently impedes their successful development and use.

We have already prepared and tested novel organic compounds as coatings for the sensitive and selective detection of chloroethyl ethyl sulfide (CEES) vapor (a mustard gas simulant) and dimethyl methylphosphonate (DMMP) vapor (a nerve agent simulant). Each coating was also tested against water vapor as this would be the main interferent (in the form of ambient

humidity). This investigation has important application for industrial pesticide monitoring and military defense.⁴ We now turn our attention to coatings that may be suitable for the detection of various other vapors of industrial (acetonitrile, acetone, diethyl ether) and environmental (chlorinated hydrocarbons, benzene) importance. In addition, the detection of diethyl ether vapor has an important application in the monitoring of illicit drug manufacture, as it is a common solvent used in the preparation of cocaine.

The compounds we have selected (1-6, Fig. 1) to test against these vapors have previously been tested against CEES, DMMP and, most importantly, water.^{2,8,9} In each case a minimal response to water vapor was observed.

EXPERIMENTAL

The following compounds have been prepared previously by our group, checked for purity and used without further purification: (1) 2'-*tert*-butyl-5,6-dihydro-4-phenylbenzo[*h*]chromenylium tetrafluoroborate, m.p.¹⁰ 212-214°; (2) 4-*tert*-butylphenylmethylphosphoric acid, m.p.¹¹ 193-194°; (3) diethyl 4-cyanophenylphosphonate, m.p.^{12,13} 31-33°; (4) 4-carboxyphenylphosphonic acid, m.p.^{12,14} > 300°; (5) 2,5-bis(octylthio)-1,3,4-thiadiazole, m.p.⁹ 32°; (6) *N,N*-dimethyl-*N*-octyl-*N*-(2-dodecylthio-1,3,4-thiadiazole-5-thioethyl)ammonium bromide, m.p.¹⁵ 96-98°. The structures are shown in Fig. 1.

Simultaneous chemiresistor and SAW measurements were performed while exposing the device (in turn) to acetone, diethyl ether,

*Author for correspondence.

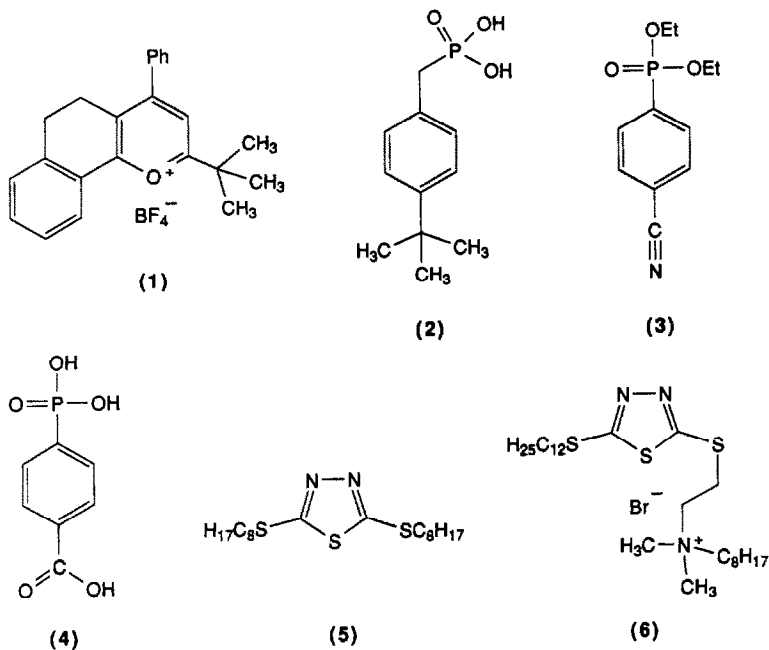


Fig. 1. Structures of compounds investigated.

dichloromethane, chlorobenzene, benzene, and acetonitrile vapors. The dual 52-MHz surface acoustic wave apparatus used (Microsensor Systems, Inc.), has been described in detail previously.^{1,4}

The SAW resonant frequency was monitored with a digital frequency counter, Phillips Model PM 6674 universal frequency counter (550 MHz). Conductivity measurements were made by application of a I-V bias to one of the two remaining electrodes, and measurement of the current. The precision current-to-voltage converter used consisted of an operational amplifier and a switch-selectable feedback resistor.

The coatings were dissolved in a volatile organic solvent, typically spectroscopic grade dichloromethane, and the device was spray-coated with an air brush, with dry nitrogen as the propellant. The coating thickness was monitored by means of the frequency counter, until a frequency shift of *ca.* 50 kHz was obtained. The frequency shifts caused by the coating were recorded as an indication of coating thickness. Test vapors were generated by passing a regulated flow of nitrogen through the pure liquid at 0°, in a vapor bubbler equipped with a gas dispersion tube. The flow-rate over the detector device was controlled with a flowmeter and was found to be 7.5 ml/min by means of a bubble meter. The vapor concentrations were calculated¹ and were as follows: acetone 190 mg/l., dichloromethane 820 mg/l., benzene 126

mg/l., diethyl ether 840 mg/l., chlorobenzene 15 mg/l., and acetonitrile 60 mg/l. The conditions used were kept the same for successive runs.

Initially the system was purged with nitrogen for 5 min to establish a baseline. The device was then exposed to the vapor for 40 min and this was followed by a nitrogen purge for 50–60 min. If a response was irreversible, the SAW device was cleaned and recoated before exposure to the next vapor. The SAW devices used were rinsed with acetone between runs and this was followed by ultrasonic cleaning for 10 min in spectroscopic grade 2-propanol.

RESULTS AND DISCUSSION

The responses obtained are recorded in Table 1. The frequency shifts were calculated by subtracting the lowest frequency recorded during vapor exposure from the initial (baseline) frequency. Resistance changes were calculated by dividing the initial (baseline) resistance by the lowest resistance recorded during exposure to the vapor. Thus, for the resistance factors, a value close to unity essentially denotes no change. Values marked with an asterisk indicate responses that were irreversible. Results were reproducible within $\pm 5\%$.

As can be seen from Table 1, the compounds were generally of little value as chemiresistor coatings. Because of the noise inherent in

Table 1. Response of compounds 1-6† to various vapors

Vapor	Change in frequency, kHz						Change in resistance (factor)					
	1	2	3	4	5	6	1	2	3	4	5	6
Acetone	5.0	1.6	6.3	2.4	0.0	1.0	2.6	1.3	5.8	1.0	1.0	1.0
Diethyl ether	0.0	2.4	1.7	4.5	6.4	2.2	2.2*	1.6	1.3	1.0	1.0	1.0
CH ₂ Cl ₂	14.9	3.6	9.8	5.3	0.0	3.4	2.6	4.8	17.9	1.5	1.0	1.0
Chlorobenzene	1.0	1.5	2.3	4.4	4.7	1.9	1.0	0.6*	2.6	1.0	1.0	1.0
Benzene	0.0	0.0	1.9	4.0	0.0	1.4	2.6	1.0	2.8*	2.0	1.0	1.0
CH ₃ CN	6.1	0.0	3.3	0.0	0.0	0.4	6.8	1.0	9.0	1.0	1.0	10.0*

*Irreversible response.

†Each coating was applied to a thickness that caused a shift of 53 ± 2 kHz in the frequency.

chemiresistor devices, a signal-to-noise ratio of at least 3 is required and a change in resistance of at least 100-fold is desirable. The largest chemiresistor response recorded with these coatings was 17.9-fold (compound 3 with dichloromethane).

In contrast, several of the compounds showed good responses as SAW coatings. SAW devices usually have better signal-to-noise ratios than chemiresistor devices and so even a frequency shift of a few kHz can be easily distinguished as a signal.

Figure 2 shows the SAW adsorption/desorption curves for the six vapors with compound 1 as the coating. With the vapors that caused a response, it can be seen that the response is quite rapid (*ca.* 5 min) and that the return to baseline frequency also occurs reasonably rapidly when exposure to the vapor is stopped (*ca.* 45 min). This adsorption/desorption profile is typical of each of the coatings.

It is immediately apparent from Table 1 that none of the coatings is completely selective. In

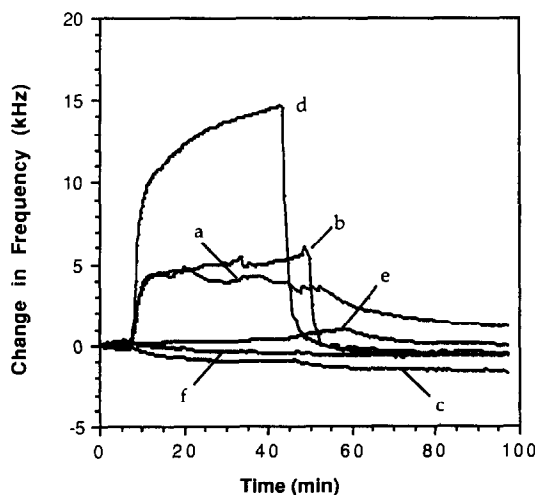


Fig. 2. Plot of change in SAW frequency vs. time for different vapors, with 1 as coating: a, acetone; b, acetonitrile; c, benzene; d, dichloromethane; e, chlorobenzene; f, diethyl ether.

each case a response was observed for at least two different vapors. However, the six coatings gave such different patterns of responses (Fig. 3) that an array of these coatings, coupled with a microprocessor and a pattern-recognition technique,¹⁶⁻²⁰ could easily distinguish between the vapors. Indeed, even the three coatings 1, 2 and 5 together in an array could adequately distinguish between the six vapors.

A clear rationale for the occurrence of these differing responses is not immediately evident. However, compound 1 gave its best responses to the more polar vapors and no response to the less polar vapors (benzene and diethyl ether). This can easily be rationalized in terms of the solubility of the analyte in the coating, and the

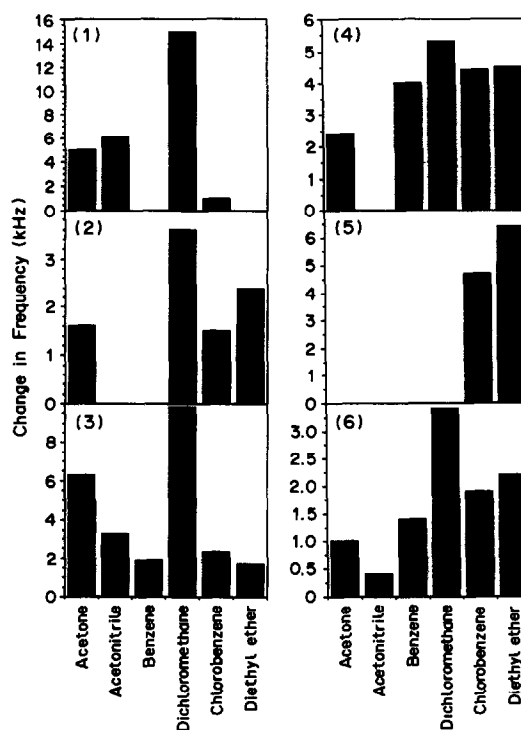


Fig. 3. Patterns of responses of coatings 1-6 to various vapors. The coating is indicated in the top left of each graph.

hydrogen-bond acceptor/donor natures of the analyte and coating. Such interactions in the adsorption of organic compounds have previously been discussed in terms of linear solvation energy relationships.^{21,22}

REFERENCES

1. A. R. Katritzky, R. J. Offerman, J. Aurrecoechea and G. P. Savage, *Talanta*, 1990, **37**, 911.
2. A. R. Katritzky, G. P. Savage, R. J. Offerman and B. Pilarski, *ibid.*, 1990, **37**, 921.
3. A. R. Katritzky, G. P. Savage, J. N. Lam and M. Pilarska, *Chem. Scripta*, 1989, **29**, 197.
4. A. R. Katritzky and R. J. Offerman, *CRC Crit. Rev. Anal. Chem.*, 1989, **21**, 83.
5. H. Wohltjen, W. R. Barger, A. W. Snow and N. L. Jarvis, *IEEE Trans. Elect. Dev.*, 1985, **ED-32**, 1170.
6. R. M. White and F. W. Voltmer, *Appl. Phys. Lett.*, 1965, **7**, 314.
7. H. Wohltjen, *Sens. Actuators*, 1984, **5**, 307.
8. A. R. Katritzky, G. P. Savage, Z. Dega-Szafran and M. Pilarska, *Chem. Scripta*, 1989, **29**, 235.
9. A. R. Katritzky, G. P. Savage and M. Pilarska, *ibid.*, 1989, **29**, 315.
10. A. R. Katritzky, C. M. Marson, S. S. Thind and J. Ellison, *J. Chem. Soc. Perkin Trans. 1*, 1983, 487.
11. A. R. Katritzky, B. Pilarski and J. W. Johnson, *Org. Prep. Proc. Int.*, 1990, **22**, 209.
12. A. R. Katritzky and B. Pilarski, unpublished results.
13. P. Tavs, *Chem. Ber.*, 1970, **103**, 2428.
14. G. O. Doak and L. D. Freedman, *J. Am. Chem. Soc.*, 1951, **73**, 5658.
15. A. R. Katritzky, Z. Wang and R. J. Offerman, *J. Heterocycl. Chem.*, 1990, **27**, 139.
16. W. P. Carey, K. R. Beebe, B. R. Kowalski, D. L. Illman and T. Hirschfield, *Anal. Chem.*, 1986, **58**, 149.
17. W. P. Carey, K. R. Beebe, B. R. Kowalski, D. L. Illman and T. Hirschfield, *Anal. Chem.*, 1986, **58**, 3077.
18. W. P. Carey, K. R. Beebe and B. R. Kowalski, *ibid.*, 1987, **59**, 1529.
19. W. P. Carey and B. R. Kowalski, *ibid.*, 1988, **60**, 541.
20. D. S. Ballantine Jr., S. L. Rose, J. W. Grate and H. Wohltjen, *ibid.*, 1986, **58**, 3058.
21. R. W. Taft, M. H. Abraham, R. M. Doherty and M. J. Kamlet, *J. Am. Chem. Soc.*, 1985, **107**, 3105.
22. R. W. Taft, T. Gramstad and M. J. Kamlet, *J. Org. Chem.*, 1982, **47**, 4557.

SOLUBILITY OF IRON(II) CARBONATE AT TEMPERATURES BETWEEN 30 AND 80°

ROBERT D. BRAUN

Department of Chemistry, University of Southwestern Louisiana, Lafayette, LA 70504-4370, U.S.A.

(Received 19 March 1990. Revised 18 May 1990. Accepted 22 May 1990)

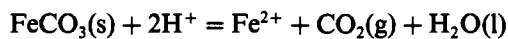
Summary—Measurements were made of the forward rate-constant (k_f) for the dissolution of FeCO_3 at 10° temperature intervals between 30 and 80° and in buffered solutions at pH 4, 5, 6 and 7. The solubility product (K_{sp}) of FeCO_3 was measured at the same six temperatures. The forward rate-constant is related to temperature (T , $^\circ\text{C}$) and pH by $\text{p}k_f = \text{pH} - 0.0350T + 0.695$. The solubility product of FeCO_3 is related to temperature by $\text{p}K_{sp} = 0.0314T + 10.20$. Kinetic data indicate that, under the conditions of the study, the rate-determining step of the dissolution reaction is $\text{FeCO}_3(\text{s}) + \text{H}^+ \rightarrow \text{Fe}^{2+} + \text{HCO}_3^-$.

In carbon dioxide environments, iron(II) carbonate scale often forms in iron and steel pipes. In some cases the scale is protective and retards or prevents corrosion.¹ Carbonate and iron(II) carbonate have been suggested^{2,3} to be important factors in the mechanisms of corrosion of iron. For that reason, it is important to have reliable values of the solubility product and rate of dissolution of iron(II) carbonate, and these can be used to help estimate corrosion rates. In this study measurements have been made between pH 4 and 7, and at 10° temperature intervals between 30 and 80° .

Measurements of the iron(II) carbonate solubility product are complicated by carbonate/bicarbonate equilibria in aqueous solutions, and accurate determinations require accurate values of the equilibrium constants for the several chemical equilibria involved. Furthermore, heterogeneous chemical equilibria between solid minerals such as siderite (FeCO_3) and its ions in solution are often established slowly. It is probably for these reasons that relatively few successful studies of the solubility parameters of iron(II) carbonate have been completed.

Smith⁴ measured the solubility product of iron(II) carbonate in a carbon dioxide environment and found its value to be 3.453×10^{-11} at 25° . Singer and Stumm⁵ later obtained values of 7.6×10^{-11} , 6.1×10^{-11} , 5.8×10^{-11} and 5.6×10^{-11} at temperatures of 17, 22.5, 25 and 30° respectively. Bardy and Pere⁶ reported a value of 4.0×10^{-11} at 20° . Helgeson⁷ used a value of 2.0×10^{-11} at 25° for thermodynamic calculation of values at higher temperatures.

The calculated values are 9.1×10^{-12} , 6.2×10^{-12} , 1.1×10^{-12} , 1.4×10^{-13} , 8.9×10^{-15} , 4.8×10^{-16} and 2.1×10^{-17} at 50, 60, 100, 150, 200, 250 and 300° respectively. In a related study, Reiterer *et al.*⁸ found the equilibrium constant at 50° for the reaction



to be 4.07×10^7 . Apparently no experimental values of K_{sp} for FeCO_3 at temperatures above 30° are available.

EXPERIMENTAL

Iron(II) was measured spectrophotometrically at 508 nm as its 1,10-phenanthroline complex.⁹ Standard and analyte solutions were prepared by adding sufficient 1,10-phenanthroline solution (Aldrich Chemical Co., Gold Label, 2.50 g/l.) to occupy a tenth of the volume (10–500 ml) of the chosen standard flask. A portion (1–5 ml) of the analyte solution was pipetted into the standard flask and the solution was diluted to the mark with demineralized water. After at least 15 min, a portion of the well-mixed solution was placed in a 1-cm cuvet and its absorbance measured at 508 nm. A calibration curve was prepared, covering the range from 5×10^{-6} to $2 \times 10^{-4} M$. Analyte solutions were diluted so that their concentrations were within this range.

Owing to the large number of calculations performed in the study, the calibration graph was stored in either a Commodore 64 or a Heath H89 computer by use of the appropriate

BASIC program, which was also used to calculate analyte concentrations from the readings taken with a Beckman model B spectrophotometer. Programs were also written in BASIC to perform the remainder of the calculations described in the paper. Listings of the programs can be obtained from the author.

Each of the studies was performed at least three times. The buffer solutions used were prepared as described elsewhere.¹⁰ The pH 4 and 7 buffers had accurately known pH values throughout the temperature range used. The pH 4 buffer was 0.0500*M* potassium hydrogen phthalate. The pH 5 buffer was prepared by adding 430.0 ml of 0.1052*M* sodium hydroxide to 1000 ml of 0.1000*M* potassium hydrogen phthalate. The pH 6 solution was prepared by adding 114.0 ml of 0.1052*M* sodium hydroxide to 1000 ml of 0.1000*M* potassium dihydrogen phosphate. The pH 7 buffer was 0.025*M* potassium dihydrogen phosphate/0.025*M* disodium hydrogen phosphate. The pH 4 and 7 buffers were used for adjustment of the pH-meter to the corresponding known pH¹⁰ at each temperature. The pH values of the thermally equilibrated pH 5 and 6 buffers were measured at each temperature with the adjusted pH-meter and a glass indicator electrode. The values are listed in Table 1. The pH of each test solution was measured at the appropriate temperature after each study. The buffer solutions were used to adjust the pH-meter prior to each measurement.

Studies were performed with the reaction systems in constant-temperature baths at 30, 40, 50, 60, 70 and 80°, controlled to ±0.1° for water baths and to ±1° for oil-baths (70 and 80° only).

Test solutions were prepared by adding 100 ml of buffer solution to 2 g of FeCO₃ (Strem Chemicals, Inc., Newbury, MA) in a 250-ml glass reagent bottle; the bottle was immediately placed in the appropriate bath, the time recorded, and the solution deaerated by rapid passage of high-purity nitrogen through it. The

bottle was then tightly sealed with a rubber stopper, and allowed to come to thermal equilibrium.

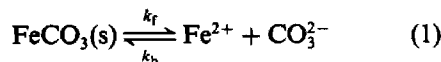
An appropriate portion (1–5 ml) of the supernatant liquid was removed from the bottle by pipet (under an atmosphere of nitrogen) once a day for the first 5 days of each study, and thereafter about once a week until equilibrium was established. The sample was collected at the bath temperature. No correction was applied for volume expansion when taking samples at various temperatures. After removal of each portion, the solution was simultaneously stirred and deaerated by rapid passage of nitrogen through it for about 1 min, and the bottle was then immediately tightly stoppered again. Because the iron carbonate was a finely divided powder, it formed a suspension that typically required a day to settle. Tyndall scattering from suspended particles would interfere with the spectrophotometry so sampling was limited to once each day. Each bottle remained in the constant-temperature bath throughout the entire procedure. The starting time and sampling times were recorded to the nearest minute. Each sample was assayed for iron(II) as described above.

THEORY

The solubility of the iron(II) carbonate in each of the buffers at all six temperatures was measured by monitoring the concentration of iron(II) as a function of time until equilibrium was established, as shown by a constant absorbance for several consecutive samplings. After each final iron(II) determination the pH of the sample mixture was measured.

Forward rate-constant

The dissolution of iron(II) carbonate is shown in equation (1), where k_f is the forward rate-constant and k_b is the reverse (backward) rate-constant:



The carbonate released during the dissolution will be in equilibrium with bicarbonate or carbonic acid:



These two reactions have an effect on the dissolution, shifting the equilibrium in equation (1)

Table 1. The pH values of the buffer solutions at the temperatures of the studies

Temp., °C	Buffer solution			
	4	5	6	7
30	4.02	5.09	6.08	6.85
40	4.04	5.07	6.01	6.84
50	4.06	5.10	6.01	6.83
60	4.09	5.13	6.00	6.84
70	4.13	5.20	6.02	6.85
80	4.16	5.24	6.02	6.86

to the right. More dissolution should occur as the pH is decreased. The rate of dissolution is given by equation (4), where the brackets represent molar concentrations, and t is time:

$$\text{Rate} = d[\text{Fe}^{2+}]/dt = k_f - k_b[\text{Fe}^{2+}][\text{CO}_3^{2-}] \quad (4)$$

Early during the dissolution process, little Fe^{2+} and CO_3^{2-} exist in the solution. The concentration of Fe^{2+} is always greater than that of CO_3^{2-} because of the effect of the reactions shown in equations (2) and (3). If the concentrations of Fe^{2+} and CO_3^{2-} are sufficiently small, then $k_b[\text{Fe}^{2+}][\text{CO}_3^{2-}]$ in equation (4) is negligible relative to k_f , and the equation simplifies to:

$$\text{Rate} = d[\text{Fe}^{2+}]/dt = k_f \quad (5)$$

Integration of equation (5) yields

$$[\text{Fe}^{2+}] = k_f t \quad (6)$$

From this equation it is apparent that in the early course of dissolution a plot of $[\text{Fe}^{2+}]$ vs. t should be linear with a slope of k_f . Plots obtained for dissolution in the pH 4 and 5 buffers are linear for the first five days of study, with regression coefficients >0.92 , and these data were used to calculate k_f .

Typical plots are shown in Fig. 1. At $\text{pH} > 5$, k_f was smaller than at pH 4 or 5. Equilibrium was established more rapidly at higher pH because the equilibrium concentrations were lower. Consequently, the forward rate-constant could be calculated from data obtained during a shorter period (typically one or two days).

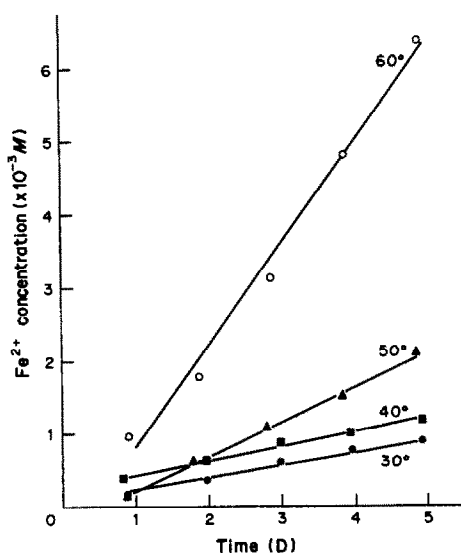


Fig. 1. Typical plots of iron(II) concentration as a function of time for the first 5 days of studies in pH 4 buffered solutions.

Equilibrium calculations

To estimate K_{sp} (the solubility product) for FeCO_3 , a knowledge of the equilibrium constants for reactions (2) and (3) at the temperatures of the studies is required:

$$K_1 = [\text{H}^+][\text{HCO}_3^-]/[\text{H}_2\text{CO}_3] \quad (7)$$

$$K_2 = [\text{H}^+][\text{CO}_3^{2-}]/[\text{HCO}_3^-] \quad (8)$$

K_1 and K_2 are temperature-dependent. It is possible to use the enthalpy changes and equilibrium constants for these reactions at 25° along with the van't Hoff equation to estimate K_1 and K_2 at other temperatures, but this approach assumes that the enthalpies are temperature-independent. A better approach uses the work of Oddo and Tomson,¹¹ who fitted equations to observed values of conditional equilibrium constants at different temperatures and ionic strengths. Those equations were used in this study.

For measurement of the K_{sp} values for FeCO_3 in the various buffers it is necessary for chemical equilibrium to be established. In the pH 4 buffer this required between $3\frac{1}{2}$ and 7 months, whereas in the pH 7 buffer equilibrium was usually established within several days. Intermediate periods were required to establish equilibrium in the pH 5 and 6 systems. Equilibrium was established more rapidly at higher pH, primarily because less FeCO_3 dissolved. During the lengthy equilibrium periods a significant amount of FeCO_3 dissolves (equivalent to $0.01M$ Fe^{2+} or more in the pH 4 buffer). As FeCO_3 dissolves, both the ionic strength and the pH of the test solution are altered. The volume of the test solution also significantly decreases during the lengthier experiments owing to the many samples removed for assay, and some carbon dioxide may escape from the solution at lower pH. Because of the complications associated with these and other experimental problems, the data obtained with the pH 7 buffer were exclusively used to calculate the K_{sp} of FeCO_3 . In the pH 7 solutions, equilibrium was established relatively rapidly, the pH did not change during the study, and escape of CO_2 should have been negligible.

Because FeCO_3 is sparingly soluble at pH 7, the ionic strength (I) of the solution will be governed by the buffer components, and for the pH 7 buffer is $0.100M$. According to Oddo and Tomson,¹¹ the equilibrium constants K_1 and K_2 [equations (7) and (8)] vary with temperature

(τ , °F) as shown in equations (9) and (10), where the superscript indicates a corrected variable:

$$pK_1^T = 6.4093 - 1.5936 \times 10^{-3}\tau + 8.517 \times 10^{-6}\tau^2 \quad (9)$$

$$pK_2^T = 10.6059 - 4.9700 \times 10^{-3}\tau + 13.3080 \times 10^{-6}\tau^2 \quad (10)$$

These equilibrium constants also vary with ionic strength, the combined effect being expressed by

$$pK_1^{I,T} = pK_1^T - 0.4772I^2 + 0.1180I \quad (11)$$

$$pK_2^{I,T} = pK_2^T - 1.1660I^2 + 0.3466I \quad (12)$$

The values used in the present study were obtained by using equations (9)–(12). First pK_1^T and pK_2^T were calculated for each temperature used (after conversion of the temperature units), and then substituted into equations (11) and (12) along with the ionic strength to give $pK_1^{I,T}$ and $pK_2^{I,T}$.

The corresponding values of $K_1^{I,T}$ and $K_2^{I,T}$ were used to calculate K_{sp} of FeCO_3 . The various values for the pH 7 buffer systems are listed in Table 2.

Because the only source of carbonate in each test solution was the FeCO_3 dissolved, the mass-balance equation for carbonate is

$$[\text{Fe}^{2+}] = [\text{H}_2\text{CO}_3] + [\text{HCO}_3^-] + [\text{CO}_3^{2-}] \quad (13)$$

In this and the other equations, $[\text{H}_2\text{CO}_3]$ should be understood to mean the sum of $[\text{H}_2\text{CO}_3(\text{aq})]$ and $[\text{CO}_2(\text{aq})]$. From the values of $K_2^{I,T}$ listed in Table 2, it is apparent that in these studies $[\text{CO}_3^{2-}]$ is negligible compared to $[\text{HCO}_3^-]$, so the mass-balance simplifies to

$$[\text{Fe}^{2+}] = [\text{H}_2\text{CO}_3] + [\text{HCO}_3^-] \quad (14)$$

The values of $K_1^{I,T}$ in Table 2 can be used to obtain an expression for $[\text{H}_2\text{CO}_3]$ in terms of $[\text{HCO}_3^-]$ at each temperature used. Substitution of that expression and the measured equilibrium concentration of iron(II) into equation (14) allows calculation of $[\text{HCO}_3^-]$. The calculated value of $[\text{HCO}_3^-]$ is then used with the

expression for $K_2^{I,T}$ at the appropriate temperature and the equilibrium hydrogen-ion concentration to calculate $[\text{CO}_3^{2-}]$, and hence the solubility product of FeCO_3 at that temperature:

$$K_{sp} = [\text{Fe}^{2+}][\text{CO}_3^{2-}] \quad (15)$$

RESULTS AND DISCUSSION

Forward rate-constant

The forward rate-constant varies as a function of both the temperature and the pH of the solution. The measured values are listed in Table 3. The pK_f values at a particular temperature varied with pH according to

$$pK_f = a\text{pH} + b \quad (16)$$

where a and b are constants at that temperature. The constants and regression coefficients obtained by least-squares fits of the data points are listed in Table 4. An example of a plot of pK_f as a function of pH is shown in Fig. 2.

The slopes (a) were essentially constant, irrespective of temperature, the mean slope for the six plots being 1.02 ± 0.04 (standard deviation). The slope corresponds to the reaction order with respect to H^+ . Hence the dissolution reaction is first order in H^+ throughout the temperature and pH range used, so the rate-determining step in the dissolution is



The intercepts (b) on the pK_f axis varied linearly ($r = 0.993$) with temperature (T , °C):

$$b = -0.0350T + 0.695 \quad (18)$$

A single equation relating pK_f to temperature and pH can be obtained by taking a as unity and substituting b into equation (16):

$$pK_f = \text{pH} - 0.0350T + 0.695 \quad (19)$$

which can be used to estimate the rate constant for the dissolution of FeCO_3 at any pH between 4 and 7, and at any temperature between 30 and 80°.

Table 2. The conditional equilibrium constants for the first and second dissociations of carbonic acid at the temperatures of the study in the pH 7 buffered solutions

Temp., °C	pK_1^T	$pK_1^{I,T}$	$K_1^{I,T}$	pK_2^T	$pK_2^{I,T}$	$K_2^{I,T}$
30	6.3353	6.3423	4.55E-7	10.2769	10.2999	5.01E-11
40	6.3357	6.3427	4.54E-7	10.2329	10.2559	5.55E-11
50	6.3417	6.3487	4.48E-7	10.1977	10.2207	6.02E-11
60	6.3531	6.3601	4.36E-7	10.1709	10.1939	6.40E-11
70	6.3701	6.3771	4.20E-7	10.1528	10.1758	6.67E-11
80	6.3926	6.3996	3.98E-7	10.1434	10.1664	6.82E-11

Table 3. Measured forward rate constants (k_f) for the dissolution of iron(II) carbonate; SD is the standard deviation of the results

Temp., °C	pH	Mean k_f (M/D)	SD	Trials
30	4.02	1.91E-4	0.05E-4	5
	5.09	6.28E-5	0.46E-5	6
	6.08	3.87E-6	2.23E-6	5
	6.85	4.42E-7	0.22E-7	2
40	4.04	2.27E-4	0.12E-4	3
	5.07	5.37E-5	0.06E-5	3
	6.01	6.17E-6	2.21E-6	3
	6.84	2.05E-7	1.43E-7	3
50	6.84	6.13E-7	2.31E-7	3
	4.06	5.19E-4	0.81E-4	6
	5.10	2.52E-4	0.63E-4	3
	6.01	7.41E-6	0.21E-6	5
60	6.83	1.31E-6	0.05E-6	3
	4.09	1.25E-3	0.22E-3	3
	5.13	1.45E-3	0.42E-3	3
	6.00	7.58E-6	0.17E-6	3
70	6.84	1.77E-6	0.14E-6	3
	4.13	3.12E-3	0.08E-3	3
	5.20	2.47E-3	0.05E-3	3
	6.02	1.94E-5	0.26E-5	3
80	6.85	1.40E-5	0.28E-5	3
	4.16	1.81E-3	0.26E-3	6
	5.24	1.32E-3	0.26E-3	5
	6.02	2.85E-5	1.64E-5	6
	6.86	3.95E-6	0.17E-6	3

Several other experimental factors could affect the dissolution rate, such as particle size and stirring rate. The iron(II) carbonate particle size was too small to be measured with the equipment available but was sufficiently small to result in a suspension which took about a day to settle, so it is unlikely that the dissolution rate would have been significantly increased by further decrease in particle size. The stirring rate

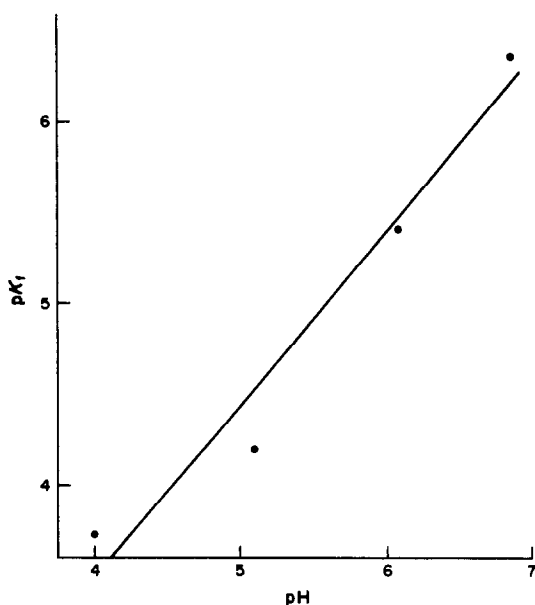


Fig. 2. A plot of pK_f as a function of pH at 30°.

Table 4. Terms in equation (17) as obtained from least squares fits of plotted values of pK_f as a function of pH; r is the correlation coefficient

Temp., °C	a	b	r
30	0.95	-0.316	0.98
40*	1.03	-0.744	0.98
50	1.00	-1.036	0.97
60†	1.06	-1.376	1.00
70	1.00	-1.886	0.90
80	1.06	-2.010	0.94

*All five points from Table 3 were used to calculate these values.

†The anomalous reading at pH 5 was ignored when calculating the values at 60°.

could be important because it could determine the total iron carbonate surface area exposed to the solvent, and because without stirring the dissolution rate is governed by the diffusion coefficients of the ions concerned. In this study the mixture was stirred once each day immediately after removal of the test sample. Although stirring was not extensive, it was sufficient to cause some of the iron carbonate to become suspended. Continuous stirring was not practicable, since the suspension did not completely settle until just before acquisition of the next sample. In any case, it cannot be assumed that the rate constants measured in this study would apply to iron(II) carbonate dissolution when the particle size or mixing rate varied from that used for these measurements.

It was also possible that phosphate or phthalate from the buffer solutions could form complexes with iron(II), thereby increasing the rate of dissolution. Very few studies of iron(II) complexation with phosphate or phthalate have been performed. Lahiri and Aditya¹² proposed

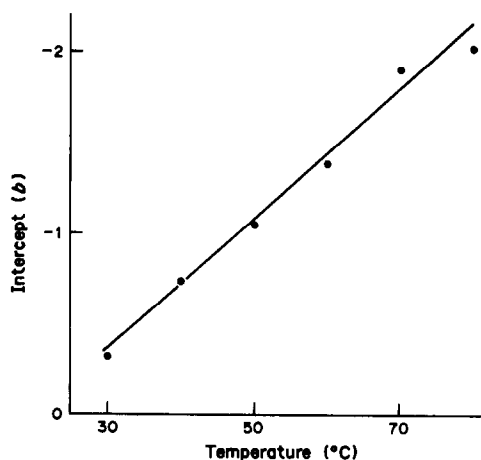


Fig. 3. Variation of the intercepts b (of plots of pK_f as a function of pH) with temperature.

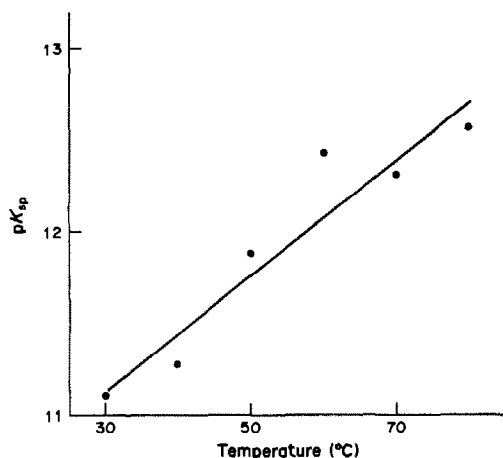


Fig. 4. A plot of pK_{sp} for $FeCO_3$ as a function of temperature.

the existence of an $FeHPO_4$ complex. Their conclusions were based upon potentiometric measurements of solutions containing mixtures of iron(III) and iron(II), but their results are incompatible with the much lower values reported later by Nriagu.¹³ However, the $FeHPO_4$ complex is certainly weak.

Koh and Ryan¹⁴ performed fluorimetric studies of iron dissolved in phthalic acid solutions at pH 4–5. The presence of an iron(II)–phthalate complex was not considered and it is unlikely that such a complex exists. Therefore, the conclusions from the studies performed in the solutions at pH 4 and 5 should not be affected by the use of phthalate buffer solutions.

The presence of an $FeHPO_4$ complex could affect the dissolution kinetics in the pH 6 and pH 7 buffer solutions. The presence of the complex would not have been detectable in the present study. Because 1,10-phenanthroline forms a strong complex with iron(II) ($\log K = 21.3$),¹⁵ the HPO_4^{2-} in any $FeHPO_4$ complex formed would have been displaced by 1,10-phenanthroline during the assay, and this would have caused an erroneously high value for the concentration of dissolved Fe^{2+} , resulting in an erroneously large rate constant for the dissolution.

Solubility product

The solubility product of $FeCO_3$ at each temperature was calculated from the measured values of $[Fe^{2+}]$ at equilibrium in the pH 7 buffer and the conditional equilibrium constants for carbonic acid, as described above. The results are listed in Table 5. The value of K_{sp} decreased with increasing temperature, as observed for a

Table 5. Measured mean solubility products of $FeCO_3$; SD is the standard deviation of the results

Temp., °C	Mean K_{sp}	SD	Trials	pK_{sp}
30	7.85E-12	1.21E-12	3	11.105
40	5.35E-12	1.16E-12	3	11.272
50	1.31E-12	0.48E-12	3	11.883
60	3.68E-13	0.77E-13	3	12.434
70	4.87E-13	0.91E-13	3	12.312
80	2.69E-13	0.95E-13	3	12.571

smaller temperature range by Singer and Stumm,⁵ and as calculated by Helgeson.⁷ The pK_{sp} values varied linearly with temperature, and the equation for the best straight line ($r = 0.947$) was found to be

$$pK_{sp} = 0.0314T + 10.20 \quad (20)$$

for the centigrade temperature range 30–80°.

Extrapolation of this equation yields $K_{sp} = 1.0 \times 10^{-11}$ at 25°, which compares favorably (within the probable accumulated experimental error) with the value of 2.0×10^{-11} used by Helgeson for his calculations. The value obtained at 60° by using equation (21), however, is 8.2×10^{-13} , compared to Helgeson's calculated value of 6.2×10^{-12} at the same temperature. In light of these studies, perhaps some of the results from calculations based upon Helgeson's calculated K_{sp} values should be reconsidered. Comparisons are made with Helgeson's values because those values are widely used in corrosion studies.

A comparison of the literature values of K_{sp} reported in the introduction to this paper, with values calculated by equation (21), is shown in Table 6. In each case the value obtained from equation (21) is less than the literature value. If significant formation of an $FeHPO_4$ complex had occurred, the calculated K_{sp} values should have been erroneously large. Since the actual values are less than the corresponding values obtained by other workers who did not use phosphate buffers, it is unlikely that the use of a phosphate buffer significantly altered the results.

Table 6. A comparison of K_{sp} values of $FeCO_3$ obtained by using equation (21) with literature values

Temp., °C	Equation (21)	Literature	Ref.
17	1.8×10^{-11}	7.6×10^{-11}	4
20	1.5×10^{-11}	4.0×10^{-11}	6
22.5	1.2×10^{-11}	6.1×10^{-11}	5
25	1.0×10^{-11}	5.8×10^{-11}	5
		3.5×10^{-11}	4
30	7.2×10^{-12}	5.6×10^{-11}	5

Acknowledgements—The author gratefully acknowledges the partial financial support of AMOCO Corp., ARCO Oil and Gas, CHEVRON U.S.A., CONOCO Inc., EXXON Chemical Co., Kerr McGee Corp., Petrolite R and D, TENNECO Oil Co., Texaco U.S.A., Baker Performance Chemicals and SOHIO.

REFERENCES

1. J. G. N. Thomas, T. J. Nurse and R. Walker, *Br. Corros. J.*, 1970, **5**, 87.
2. G. I. Ogundele and W. E. White, *Corrosion*, 1986, **42**, 71.
3. R. Jasinski, *ibid.*, 1987, **43**, 214.
4. H. J. Smith, *J. Am. Chem. Soc.*, 1918, **40**, 879.
5. P. C. Singer and W. Stumm, *J. Am. Water Works Assoc.*, 1970, **62**, 198.
6. J. Bardy and C. Pere, *Trib. CEBEDEAU*, 1976, **29**, 75; *Chem. Abstr.*, 1976, **84**, 185526b.
7. H. C. Helgeson, *Am. J. Sci.*, 1969, **267**, 729.
8. F. Reiterer, W. Johannes and H. Gamsjager, *Mikrochim. Acta*, 1981 **I**, 63.
9. R. D. Braun and F. H. Walters, *Applications of Chemical Analysis*, p. 131, McGraw-Hill, New York, 1982.
10. R. C. Weast (ed.), *CRC Handbook of Chemistry and Physics*, 64th Ed., pp. D150–D151, CRC Press, Boca Raton, FL, 1984.
11. J. E. Oddo and M. B. Tomson, *J. Pet. Technol.*, 1982, 1583.
12. S. C. Lahiri and S. Aditya, *J. Indian Chem. Soc.*, 1964, **41**, 517.
13. J. O. Nriagu, *Geochim. Cosmochim. Acta*, 1972, **36**, 459.
14. K. J. Koh and D. E. Ryan, *Anal. Chim. Acta*, 1971, **54**, 303.
15. J. D. Ingle, Jr. and S. R. Crouch, *Spectrochemical Analysis*, p. 388, Prentice-Hall, Englewood Cliffs, NJ, 1988.

DETERMINATION OF LEAD(II) BY ARGENTIMETRY

O. E. S. GODINHO, J. J. R. ROHWEDDER, M. N. EBERLIN,
L. M. ALEIXO and G. DE OLIVEIRA NETO

Instituto de Química, Universidade Estadual de Campinas, C.P. 6154, 130891 Campinas, SP, Brazil

(Received 10 August 1989. Revised 11 July 1990. Accepted 25 July 1990)

Summary—A titrimetric method for determination of lead(II), based on the reaction between plumbite and silver ions, is described. Sodium hydroxide solution is added to the sample until the precipitate of lead hydroxide has redissolved. The solution is then made 0.025M in sodium chloride and titrated with silver nitrate. The titration is monitored with a silver electrode. An error smaller than 0.5% has been obtained for 0.05M lead (II).

The yellow precipitate formed by the reaction between plumbite and silver ions was first described by Wöhler,¹ who gave it the formula $\text{Ag}_2\text{O} \cdot 2\text{PbO}$. Compounds such as $\text{Ag}_2\text{O} \cdot \text{PbO}$, $2\text{Ag}_2\text{O} \cdot \text{PbO}$, $2\text{Ag}_2\text{O} \cdot 3\text{PbO}$ and $2\text{Ag}_2\text{O} \cdot 7\text{PbO}$ have been described by Aston.² Ag_2PbO_2 was first synthesized in the crystalline form by Bullheimer.³ Later Byström and Evers⁴ studied the crystal structure of this compound and found that the other compounds obtained by Aston are actually mixtures of Ag_2PbO_2 and Ag_2O or PbO . Recently Godinho and Eberlin⁵ drew attention to the fact that although known for a long time, this compound is no longer employed for analytical purposes but could be employed, for example, for the identification of lead or silver ions. The present work describes a method for determination of lead(II) by titration of plumbite with silver nitrate, monitored by use of a silver electrode.

EXPERIMENTAL

Reagents

All reagents were of analytical grade. Silver nitrate solutions were standardized by potentiometric titration of sodium chloride in the usual way.⁶ Lead nitrate solutions were standardized by EDTA titration, with Eriochrome Black T as indicator.⁷

Apparatus

A Micronal B375 pH-meter, a silver electrode made in the laboratory, and a Metrohm EA 404 calomel electrode with a salt bridge made with saturated sodium nitrate solution were employed in potentiometric measurements. The silver electrode consisted of a 1-cm length of

1-mm diameter silver wire, but any commercially available silver electrodes may be employed.

Procedure

Pipette 25 ml of 0.05M lead(II) solution into a 100-ml beaker, slowly add 3.0–3.5 ml of 4M sodium hydroxide or alternatively enough sodium hydroxide to dissolve the precipitate. Add 3 ml of 0.25M sodium chloride, immerse the electrodes in the solution and titrate with 0.1M silver nitrate. Read the potential difference after the addition of each aliquot of titrant. By using the titrant volume–potential data-points near the equivalence point, analytically evaluate the end-point by the second derivative method.⁸

During the addition of sodium hydroxide the solution needs to be stirred to avoid the formation of the alkali-insoluble yellow lead(II) oxide. The silver electrode should be conditioned in 0.5M sodium hydroxide solution for about 30 min before beginning the titration.

RESULTS AND DISCUSSIONS

Some examples of titration curves corresponding to the titration of lead(II) in the presence of 0.5M sodium hydroxide with silver nitrate are shown in Fig. 1, which shows a decrease in potential after the inflection corresponding to the equivalence point in the titration performed in the absence of chloride. At this point the precipitate flocculates and acquires a green tone due to the adsorption of silver oxide at the surface of the precipitate. The drop in potential may be explained by considering the formation of a supersaturated solution

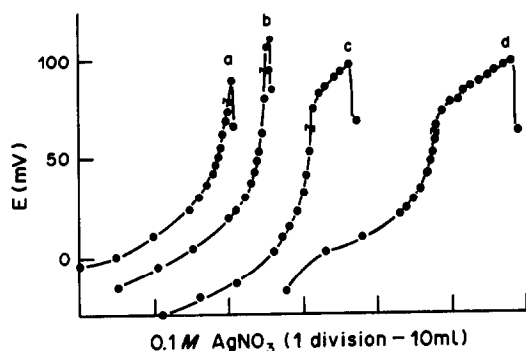


Fig. 1. Titration curves corresponding to the titration of 20.01 ml of solution, 0.0499M in $\text{Pb}(\text{NO}_3)_2$ and 0.5M in NaOH with 0.1005M AgNO_3 : (a) in absence of chloride; (b) in presence of $1.0 \times 10^{-3} \text{M Cl}^-$; (c) $2.5 \times 10^{-2} \text{M Cl}^-$; (d) $5.0 \times 10^{-2} \text{M Cl}^-$. Equivalence volume = 19.88 ml

of silver ions before the adsorption of silver oxide. After this point, following the addition of titrant, the formation of a black precipitate of silver oxide in the supernatant solution is observed. However, in the presence of chloride, there is precipitation of silver chloride after the equivalence point and the fall of potential is retarded.

The results of the study of the influence of concentration of sodium hydroxide on the titration of 0.05M lead(II) in the form of plumbite with silver nitrate are shown in Fig. 2. The most adequate working range of sodium hydroxide concentration is between 0.4 and 1.0M. It was observed for 0.05M lead(II) solutions that if sodium hydroxide solution is added until dissolution of the lead(II) hydroxide, the resulting alkali concentration lies in this favourable range although even in this range a positive systematic error, tends to be observed. This error, which is of the order of +1% for lead(II) concentrations equal to or above 0.05M, tends to increase with decrease in the concentration of lead(II).

Fortunately, for 0.05M lead(II) solutions, this error may be reduced if the titration is performed in the presence of chloride. As may be seen in Table 1, good accuracy was obtained when the titrations were performed in 0.5M

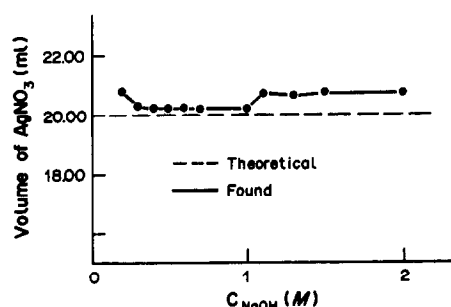


Fig. 2. Influence of the concentration of NaOH on the results of titration of 20.00 ml of 0.0502M $\text{Pb}(\text{NO}_3)_2$ with 0.1000M AgNO_3 , in the absence of chloride.

sodium hydroxide and in the chloride concentration range 0.01–0.05M. Above 0.05M chloride there is a decrease in potential jump at the equivalence point. Thus the presence of 0.025M sodium chloride was included in the procedure.

The range of concentration of lead(II) adequate for the application of the method is between 0.05 and 0.07M. For concentrations of lead(II) above 0.07M the formation of yellow lead(II) oxide, which is difficult to dissolve in excess of alkali, was observed. In the recommended lead(II) concentration range addition of the volume of sodium hydroxide solution just necessary to allow dissolution of the precipitate is adequate for the application of the method.

The results of the study of the effect of some foreign ions on the precision and accuracy of the method are presented in Table 2. The non-interference of carbonate shows that it is not necessary to avoid the influence of carbon dioxide during the titration.

Sulphate, if present at the level of concentration of lead(II), does not interfere, irrespective of the order of addition of sulphate and sodium hydroxide. If sulphate is added first, a precipitate of lead(II) sulphate occurs with subsequent dissolution in sodium hydroxide if this is added immediately. At first, this fact indicates the possibility of previous separation of lead(II) from interfering ions in the form of its sulphate,

Table 1. Determination of lead(II) in the presence and absence of chloride

Concentration of lead(II) taken, M	Chloride present, M	Concentration of lead(II) found,*M	r.s.d., %	Error %
0.0503	—	0.0508	0.2	+1.0
0.0503	0.0100	0.0502	0.4	-0.2
0.0503	0.0250	0.0505	0.4	+0.4
0.0503	0.0425	0.0502	0.4	-0.2

*Average of 6 determinations.

Table 2. Study of the influence of foreign ions: the concentration of all interfering ions is 0.05M and all solutions are also 0.025M in chloride

Ion present	Concentration of lead(II) taken, M	Concentration of lead(II) found, M	Error, %
CO ₃ ²⁻	0.0503	0.0504	+ 0.2
SO ₄ ²⁻	0.0503	0.0505	+ 0.4
Zn(II)	0.0503	0.0500	- 0.6
Cu(II)	0.0503	0.0501	- 0.4
NH ₃	0.0496	0.0513	+ 3.4

with subsequent dissolution of the precipitate with sodium hydroxide followed by titration with silver nitrate. However, it was observed that when the suspension of lead(II) sulphate is submitted to the treatment required⁷ for adequate filtration of the precipitate its quantitative dissolution does not occur.

Zinc(II) and copper(II) ions do not interfere at the concentration level studied, which may be of interest in the application of the method to the determination of lead(II) in some alloys. In the first case, the titration is performed in the presence of tetrahydroxozincate and in the second the titration can be performed even in the presence of the precipitate of copper(II) hydroxide.

However, tin(IV) is not completely dissolved and adequate titration curves are not obtained

in its presence. Therefore, it is necessary to separate tin before the titration of lead. Similarly, the large error observed in the case of ammonia is due to difficulty of location of the end-point of titration in virtue of the formation of the silver diammine complex.

The method is simple and requires only readily available reagents. Its accuracy is comparable to that of some classical titrimetric methods. The method may be employed instead of gravimetric or other titrimetric methods where great accuracy is required.

REFERENCES

1. F. Wöhler, *Ann. Phys. Chem.*, 1837, **41**, 344.
2. E. Aston, *J. Chem. Soc.*, 1891, **59**, 1093.
3. F. Bullnheimer, *Ber.*, 1898, **31**, 1287.
4. A. Byström and L. Evers, *Acta Chem. Scand.*, 1950, **4**, 613.
5. O. E. S. Godinho and M. N. Eberlin, *Quim. Nova*, 1985, **8**, 115.
6. A. I. Vogel, *A Text-book of Quantitative Inorganic Analysis*, 3rd Ed., p. 950. Longman, London, 1961.
7. I. M. Kolthoff and J. P. Elving, *Treatise on Analytical Chemistry*, Part II, Vol. 6, 2nd Ed., p. 155. Interscience, New York, 1964.
8. A. I. Vogel, *A Text-book of Quantitative Inorganic Analysis*, 3rd Ed., p. 930. Longman, London, 1961.

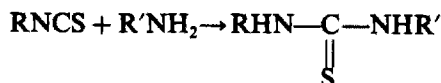
REDOX REACTIONS IN NON-AQUEOUS MEDIA: DETERMINATION OF ORGANIC ISOTHIOCYANATES ALONE, IN FORMULATIONS AND IN IMPORTANT MIXTURES

B. C. VERMA*, S. B. KALIA, V. S. JAMWAL, SUDHIR KUMAR, D. K. SHARMA and ANILA SUD
 Department of Chemistry, Himachal Pradesh University, Summer Hill, Shimla 171005, India

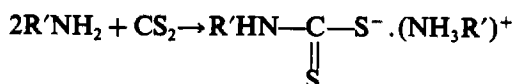
(Received 9 February 1990. Revised 1 June 1990. Accepted 12 June 1990)

Summary—A simple potentiometric method for the determination of organoisothiocyanates is described. The isothiocyanate is treated in acetonitrile medium with an excess of primary amine to convert it into a substituted thiourea and the surplus amine is converted into a dithiocarbamate by addition of carbon disulphide. The solution is then titrated with a copper(II) solution in acetonitrile. The three-step titration curve enables the results to be calculated on the basis of the dithiocarbamate and/or thiourea formed. The method has been successfully applied to the analysis of a commercial insecticide formulation based on isothiocyanate and important mixtures containing isothiocyanates.

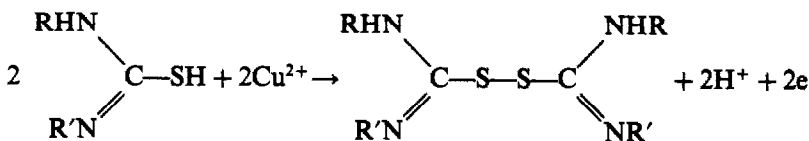
The wide commercial use of organoisothiocyanates necessitates convenient and reliable procedures for their determination. The method described here is based on the following reactions. In acetonitrile medium an excess of primary amine smoothly and quantitatively converts isothiocyanates into the corresponding substituted thioureas:



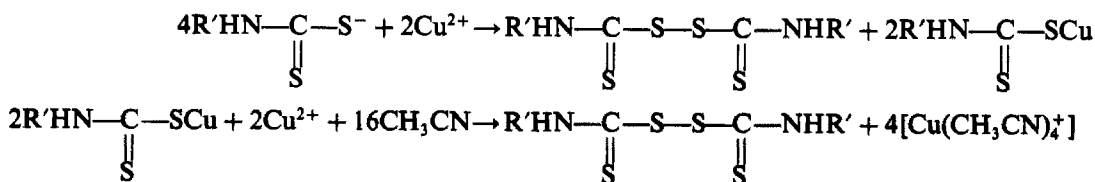
The residual amine can be converted into a dithiocarbamate by treatment with carbon disulphide:



Copper(II) perchlorate in acetonitrile medium oxidizes the thiourea to the corresponding substituted formamidine disulphide¹



and the dithiocarbamate to the corresponding thiuram disulphide² in two well-defined steps:



*Author for correspondence.

The first of these steps results in simultaneous formation of thiuram disulphide and copper(I) dithiocarbamate, the organic moiety of which is then also oxidized to thiuram disulphide.

Potentiometric titration of this system gives a curve with three distinct inflection points. The dithiocarbamate is completely titrated before the potential rises enough to begin the oxidation of the substituted thiourea. This has been confirmed by titration of various mixtures of dithiocarbamates and thioureas.

The method gives the option of calculating the results on the basis of the first and/or second inflection points (corresponding to the amount of dithiocarbamate) or the third inflection point (corresponding to the amount of thiourea formed). The method has been used for analysis of a commercial insecticide formulation (based on methyl isothiocyanate) and analysis of isothiocyanate–isocyanate and isothiocyanate–thiourea mixtures.

Isothiocyanates and isocyanates are similar both in structure and their reactions with ammonia and amines to form substituted thioureas and ureas respectively. Treatment of a mixture (containing one of each species) with an excess of amine and then with carbon disulphide in acetonitrile followed by potentiometric titration with copper(II) could be used to determine both components. The first two steps in the titration curve correspond to the amount of dithiocarbamate (and consequently indirectly to the amount of isothiocyanate and isocyanate present in the mixture) and the third corresponds to the amount of thiourea produced and hence the isothiocyanate content of the mixture. The amount of isocyanate can be found by difference.

The analysis of isothiocyanate–thiourea mixtures is also of importance since isothiocyanates serve as the starting materials for the preparation of thioureas and the method can again be used.

EXPERIMENTAL

Reagents

Acetonitrile (Merck). Distilled twice from phosphorus pentoxide (5 g/l.).

Copper(II) perchlorate standard solution in acetonitrile. Prepared and standardized as described earlier.³

Organoisothiocyanates. Allyl, methyl and phenyl isothiocyanates (Fluka) were distilled

before use. Other alkyl isothiocyanates were prepared by a known method.⁴

Organoisocyanates. *n*-Butyl and α -naphthyl isocyanates (Fluka) were distilled before use. Phenyl isocyanate was prepared by the method of Allen and Bell.⁵

Thioureas. Thiourea (Sarabhai M. Chemicals) was recrystallized before use. Alkyl thioureas were prepared from their corresponding isothiocyanates.⁴

Apparatus

Potentiometric titrations were performed with a bright platinum wire as indicator electrode, a modified calomel electrode (filled with saturated methanolic potassium chloride solution) as reference, and a Toshniwal (India) CL06A type potentiometer.

Potentiometric determination of isothiocyanates with copper(II) perchlorate

Aliquots of isothiocyanate solution in acetonitrile were added with stirring to known volumes of standard (0.02M) *n*-butylamine in acetonitrile, in glass-stoppered vessels and the volumes made up to 20–25 ml with acetonitrile. The vessels were stoppered, swirled to mix the reactants and set aside for 5 min to complete the reaction. Each solution was mixed with 1 or 2 drops of carbon disulphide and titrated at room temperature ($\sim 23^\circ$) with standard (0.2M) copper(II) perchlorate potentiometrically. Figure 1 shows the profile of a typical three-step potentiometric titration. The results calculated on the basis of the first (residual amine) and third (thiourea formed) breaks are given in Table 1.

Analysis of formulations

The experimental details are the same as described above for organoisothiocyanates, the only difference being that aliquots of an acetonitrile solution of the liquid formulation (instead of the isothiocyanate) were added to known volumes of standard *n*-butylamine solution. The profiles of the potentiometric titrations are similar to those obtained for isothiocyanates. The results (Table 2) are compared with those obtained by an independent method.⁶

Analysis of isothiocyanate–isocyanate mixtures

Aliquots of acetonitrile solutions of isothiocyanate and isocyanate in various proportions were analysed by the procedure already given

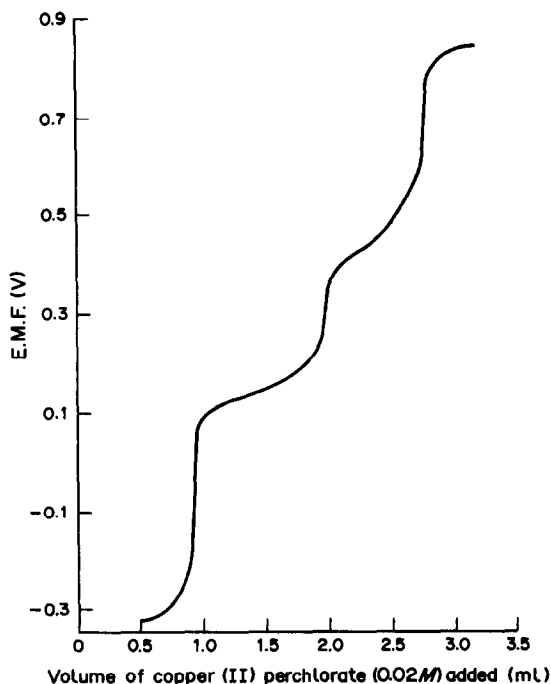


Fig. 1

for isothiocyanates. The results for a mixture of phenyl isothiocyanate and phenyl isocyanate are given in Table 3.

Analysis of isothiocyanate-thiourea mixtures

Aliquots of acetonitrile solutions of isothiocyanates and thioureas in various proportions were also analysed in the same way as isothiocyanate solutions. The results for analysis of a mixture of *n*-butyl isothiocyanate and *n*-butyl thiourea are given in Table 4.

RESULTS AND DISCUSSION

Organoisothiocyanates are quite resistant to oxidation and reduction. However, they react

Table 2. Recovery of methyl isothiocyanate from technical formulation containing 23.5% active ingredient (mean \pm standard deviation of 5 determinations)

Active ingredient taken, mg	Present method		Comparison method ⁶	
	Found, mg	Recovery, %	Found, mg	Recovery, %
2.82	2.78	98.6 \pm 0.36	2.77	98.4 \pm 0.42
5.64	5.58	98.9 \pm 0.68	5.56	98.6 \pm 0.58
8.46	8.39	99.2 \pm 0.52	8.32	98.3 \pm 0.60
11.28	11.09	98.3 \pm 0.48	11.11	98.5 \pm 0.50

with primary amines to form substituted thioureas, which can be easily oxidized. Hence, this reaction could serve as an important tool for the determination of isothiocyanates. Because isothiocyanates are insoluble in water but react with it⁷ and substituted thioureas are sparingly soluble in water, a non-aqueous solvent is required for the transformation of isothiocyanates into thioureas and oxidimetric determination of the latter. Acetonitrile has been chosen as the solvent for the following reasons.

(i) It is a versatile solvent for non-aqueous redox titrations because of its high dielectric constant, resistance to oxidation reduction, convenient liquid range, ready availability, wide electrochemical range and low toxicity.^{8,9}

(ii) A solution of copper(II) perchlorate in acetonitrile is very stable and is a powerful oxidizing agent.^{8,9}

(iii) In this solvent, carbon disulphide converts amines quantitatively into dithiocarbamates, so isothiocyanates can also be determined through measurement of the residual amine from the derivatization reaction.

Table 1. Potentiometric determination of organoisothiocyanates with copper(II) perchlorate (mean \pm standard deviation of 10 determinations)

Isothiocyanates	On the basis of excess of amine as dithiocarbamate		On the basis of thiourea formed	
	Amount found*, mg	Amount found†, mg	Amount found*, mg	Amount found†, mg
Allyl	2.50 \pm 0.021	4.95 \pm 0.040	2.48 \pm 0.021	4.97 \pm 0.046
Methyl	2.48 \pm 0.020	4.96 \pm 0.051	2.47 \pm 0.022	4.95 \pm 0.058
<i>n</i> -Propyl	2.49 \pm 0.030	5.04 \pm 0.052	2.52 \pm 0.034	4.96 \pm 0.061
Isopropyl	2.52 \pm 0.020	4.97 \pm 0.041	2.48 \pm 0.017	5.05 \pm 0.048
<i>n</i> -Butyl	2.51 \pm 0.030	4.96 \pm 0.039	2.49 \pm 0.036	4.95 \pm 0.043
Isobutyl	2.47 \pm 0.020	5.03 \pm 0.030	2.52 \pm 0.022	5.04 \pm 0.038
Phenyl	2.52 \pm 0.015	4.98 \pm 0.050	2.51 \pm 0.018	4.96 \pm 0.056

*Amount taken, 2.5 mg.

†Amount taken, 5.0 mg.

Table 3. Analysis of a mixture containing phenyl isothiocyanate and phenyl isocyanate (mean \pm standard deviation of 10 determinations)

Phenyl isothiocyanate in the mixture		Phenyl isocyanate in the mixture		Ratio of isothiocyanate to isocyanate in the mixture
Taken, mg	Found, mg	Taken, mg	Found, mg	
4.00	4.04 \pm 0.032	4.00	4.04 \pm 0.028	1:1
4.00	4.03 \pm 0.036	8.00	7.96 \pm 0.024	1:2
4.00	3.96 \pm 0.032	12.00	12.06 \pm 0.048	1:3
4.00	4.00 \pm 0.018	16.00	15.92 \pm 0.072	1:4
8.00	7.94 \pm 0.072	4.00	4.05 \pm 0.036	2:1
12.00	11.93 \pm 0.056	4.00	4.04 \pm 0.032	3:1
16.00	16.12 \pm 0.067	4.00	3.97 \pm 0.032	4:1

Copper(II) oxidizes both a dithiocarbamate and a thiourea in a mixture of the two, giving a three-step titration curve (Fig. 1). The redox potentials of thioureas and dithiocarbamates are sufficiently different to permit selective titration [E° for diethyldithiocarbamate-tetraethyl thiuram disulphide is -0.58 V (*vs.* SCE);¹⁰ E° for thiourea-formamidine disulphide is $+0.42$ V (*vs.* SCE)¹¹]. The results in Table 1 show that the overall standard deviations calculated from the pooled data of all the titrations performed with 2.5 and 5 mg of each isothiocyanate are 0.022 and 0.043 mg, respectively (on the basis of the first potential break, for residual amine) and 0.024 and 0.050 mg, respectively (on the basis of the third potential break, for thiourea formed). The recoveries of methyl isothiocyanate in the analysis of the formulation were in the range 98.3–99.2% with standard deviations in the range 0.4–0.7% (Table 2).

The proposed methods for the analysis of isothiocyanate-isocyanate and isothiocyanate-thiourea mixtures, besides being simple, accurate and reliable, have the added advantage that the complete analysis can be conducted with the same sample solution, resulting in a saving of time and effort. A single potentiometric titration with copper(II) perchlorate enables each mixture to be analysed for both

components. The synthetic mixtures of phenyl isothiocyanate and phenyl isocyanate with ratios in the range 1:4–4:1 were analysed with an average standard deviation of 0.7% for phenyl isothiocyanate and 0.6% for phenyl isocyanate (Table 3). The method has been extended to other mixtures such as ethyl isothiocyanate/ethyl isocyanate; n-propyl isothiocyanate/n-propyl isocyanate; isopropyl isothiocyanate/isopropyl isocyanate; n-butyl isothiocyanate/n-butyl isocyanate, with similar performance to that for the model mixture. The method has also been applied to the analysis of mixtures of isothiocyanates and thioureas. The results recorded in Table 4 for the analysis of synthetic mixtures of n-butyl isothiocyanate and n-butylthiourea with ratios in the range 1:4–4:1 have an average standard deviation of 0.6% for both components. The method has been extended to other mixtures such as methyl isothiocyanate/methyl thiourea; ethyl isothiocyanate/ethyl thiourea; n-propyl isothiocyanate n-propyl thiourea; isobutyl isothiocyanate/isobutyl thiourea; pentyl isothiocyanate/pentyl thiourea, with performance similar to that for the model mixtures.

Acknowledgement—The authors thank the Council of Scientific and Industrial Research, New Delhi, for financial assistance.

Table 4. Determination of a mixture containing n-butyl isothiocyanate and n-butylthiourea (mean \pm standard deviation of 10 determinations)

n-Butyl isothiocyanate in the mixture		n-Butyl thiourea in the mixture		Ratio of n-butyl isothiocyanate to n-butylthiourea in the mixture
Taken, mg	Found, mg	Taken, mg	Found, mg	
4.00	4.03 \pm 0.020	4.00	4.04 \pm 0.038	1:1
4.00	3.96 \pm 0.022	8.00	7.95 \pm 0.034	1:2
4.00	4.04 \pm 0.036	12.00	11.94 \pm 0.056	1:3
4.00	3.97 \pm 0.022	16.00	15.94 \pm 0.069	1:4
8.00	7.92 \pm 0.056	4.00	4.00 \pm 0.036	2:1
12.00	11.93 \pm 0.062	4.00	4.03 \pm 0.028	3:1
16.00	16.08 \pm 0.068	4.00	3.96 \pm 0.018	4:1

REFERENCES

1. B. Kratochvil and D. A. Zatzko, *Anal. Chem.*, 1968, **40**, 422.
2. B. C. Verma, S. Chauhan, A. Sood, D. K. Sharma and H. S. Sidhu, *Talanta*, 1985, **32**, 139.
3. P. F. Quirk and B. Kratochvil, *Anal. Chem.*, 1970, **42**, 535.
4. N. L. Drake, *Org. Synth*, 1941, **21**, 81, 83.
5. C. F. H. Allen and A. Bell, *Org. Synth., Collective Vol. III*, 1955, p. 846.
6. M. Ottnad, N. A. Jenny and C.-H. Röder, in G. Zweig (ed.), *Anal. Methods Pestic. Plant Growth Regul.*, 1978, **X**, 563.
7. J. H. Karchmer, *The Analytical Chemistry of Sulphur and its Compounds*, Part II, p. 715. Wiley-Interscience, New York, 1972.
8. B. Kratochvil, *Chem. Canada*, 1968, **20**, 19.
9. *Idem*, *CRC Crit. Rev. Anal. Chem.*, 1971, **1**, 415.
10. P. W. Preisler and L. Berger, *J. Am. Chem. Soc.*, 1947, **69**, 322.
11. E. C. Gregg and W. P. Tyler, *ibid.*, 1950, **72**, 4561.

EXTRACTION AND SEPARATION OF URANIUM AND LEAD WITH LIQUID ANION-EXCHANGERS

N. M. SUNDARAMURTHI and V. M. SHINDE

Analytical Laboratory, Institute of Science, 15 Madam Cama Road, Bombay 400032, India

(Received 24 May 1989. Revised 29 January 1990. Accepted 16 July 1990)

Summary—A method is proposed for the extraction and separation of microgram amounts of uranium(VI) and lead(II) from sodium salicylate solution with high molecular-weight amines such as Aliquat 336, TOA, TIOA, Amberlite LA-1 or Amberlite LA-2 dissolved in xylene. From a critical study of pH, salicylate concentration, amine concentration, diluent and period of equilibration, the optimum conditions were identified. The method permits separation of uranium and lead from binary mixtures with metal ions commonly associated with them, the determination of uranium, and of lead in air samples.

Lead, a toxic and harmful element, is an important constituent of some copper alloys and tin-based white metals. Uranium, an essential element for nuclear energy programmes, is found in association with metals such as copper, iron, cerium, titanium, vanadium, chromium and thorium in ores such as carnotite, torbernite, davidite and brannerite. Estimation of lead at ppm level in environmental samples is also required. There are comparatively few methods for extraction and spectrophotometric determination of uranium(VI) and lead(II). High molecular-weight amines such as trioctylamine (TOA),¹⁻⁵ Aliquat 336,^{6,7} n-dodecylamine,² tri-laurylamine,⁷ Amberlite LA-1,⁷⁻¹¹ Amberlite LA-2,^{12,13} Primene JMT⁷ and tri-iso-octylamine¹⁴ have been used for the extraction of uranium and lead from various aqueous solutions. However, the existing methods suffer from limitations such as the need for strict temperature control,¹⁻⁴ long extraction time^{2,8,12} and emulsification problems.^{2,7} In a few methods^{4,6,10,13,14} the extractions are incomplete. Spectrophotometric determinations at trace level often require pre-concentration of the analyte by extraction, but there has been no systematic study for both uranium and lead, so an attempt has been made to develop a simple method for extraction, separation and spectrophotometric determination of uranium and lead. The method is free from the limitations mentioned above.

EXPERIMENTAL

Apparatus

A Unicam SP 500 spectrophotometer with 1-cm fused-silica cells, a Control Dynamics

digital pH-meter with a combined glass electrode, wrist-action flask shakers and a Varian Techtron AA6 atomic-absorption spectrometer were used.

Reagents

All chemicals used were of analytical grade unless indicated otherwise.

Stock solutions of uranium and lead were prepared by dissolving 1.0 g of uranyl nitrate in 2 ml of concentrated nitric acid, and 0.4 g of lead nitrate in 1 ml of concentrated nitric acid and accurately diluting to 250 ml with distilled water. The solutions were standardized by known methods¹⁵ and diluted as required.

Aliquat 336 (tricaprylylmethylammonium chloride), TOA (trioctylamine), TIOA (tri-iso-octylamine), Amberlite LA-1 (*N*-dodecyltrialkylmethylamine) and Amberlite LA-2 (*N*-lauryltrialkylmethylamine) were used without purification. Solutions of Aliquat 336 (10 mg/ml), TOA, TIOA, Amberlite LA-1 and Amberlite LA-2 (50 mg/ml) in xylene were equilibrated with an equal volume of 1M sodium salicylate before use.

A 1 mg/ml aqueous solution of 4-(2-pyridyl-azo)resorcinol (PAR) was used for spectrophotometric determination of uranium and lead, at 530 and 520 nm respectively.

Sample solution preparation

Add 5 ml of concentrated nitric acid to 0.1 g of leaded copper-base alloys such as gunmetal, brass or bronze and evaporate the solution to dryness. Take up the residue with 4M nitric acid and filter off any metastannic acid, washing it

with 5 ml of hot dilute nitric acid and finally with 10 ml of hot water. Dilute the filtrate to 25 ml with water. Dissolve 0.1 g of tin-base white metal in 5 ml of 47% hydrobromic acid, evaporate the solution to dryness, cool, add 3 ml of 25% v/v sulphuric acid and evaporate the mixture nearly to dryness. Finally dissolve the white mass in 4 ml of concentrated hydrochloric acid and dilute to 25 ml with distilled water.

Heat a suitable weight of calcined bone ash or milk powder with 10 ml of *aqua regia* for 5 min, cool, dilute to about 15 ml, filter, and dilute accurately to 25 ml with water.

For analysis of air-borne particulates, bring the sample into solution by digesting it with a few ml of 25% v/v nitric acid, filter the solution and dilute it accurately to 10 ml.

Extraction of uranium(VI) and lead(II)

To an aliquot of solution containing 1–80 μg of uranium or lead add enough sodium salicylate to give the desired concentration in a final volume of 25 ml. Adjust the pH with dilute hydrochloric acid and sodium hydroxide sodium, transfer the sample into a 125-ml separating-funnel and extract with 5 ml of the selected extraction reagent. Separate the two layers and strip the metal ion from the organic phase with the appropriate stripping agent (see Table 1). Wash the strippings with 5 ml of xylene to remove any dissolved amine and then analyse for the metal ion, either spectrophotometrically or by atomic-absorption spectrometry.

RESULTS AND DISCUSSION

Extraction conditions

Uranium(VI) and lead(II) were extracted over the pH range 3.0–10.0 from sodium salicylate

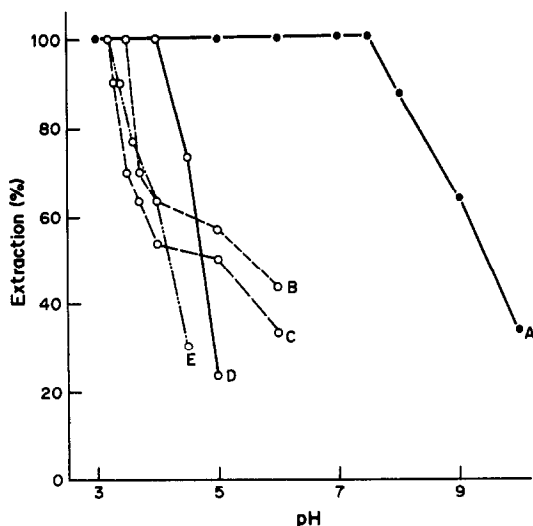


Fig. 1. Extraction behaviour of uranium(VI) as a function of pH. Extraction of uranium from 0.05M sodium salicylate solution with (A) 1% Aliquat 336; (B) 5% Amberlite LA-1; (C) 5% Amberlite LA-2; (D) 5% TOA and (E) 5% TIOA as an extractant.

solutions in the range 0.0025–0.125M, with various concentrations (0.125–5%) of the high molecular-weight amines. The optimum extraction conditions are reported in Table 1 and Figs. 1 and 2. Microgram amounts of lead were determined by atomic-absorption spectrometry and the results compared with those obtained spectrophotometrically. Both methods were sufficiently sensitive. Since Aliquat 336 extracts metal ions over a wider range of pH than the other ions it was used for further studies.

Effects of solvents

The effect of various solvents such as xylene, toluene, benzene, chloroform, carbon tetrachloride, hexane and cyclohexane on the extraction of uranium and lead with Aliquat 336 was studied and it was found that the extraction of uranium was quantitative with xylene, toluene

Table 1. Optimum extraction conditions for uranium(VI) and lead(II)

Metal ion amount	Salicylate concentration, M	Extractant	pH	Extraction period, sec	Stripping agent	Determination procedure
Uranium(VI) 60 μg	0.05	1% Aliquat 336	3.0–7.5	30	0.5M NaOH (2 \times 4 ml)	Spectrophotometry with 0.5 ml of 0.1% 4-(2-pyridylazo)-resorcinol ⁷
		5% TOA	3.0–4.0	60		
		5% Amberlite LA-1	3.0–3.5	60		
		5% Amberlite LA-2	3.0–3.2	60		
		5% TIOA	3.0–3.2	60		
Lead(II) 38 μg	0.025	1% Aliquat 336	3.0–8.0	15	Water (2 \times 8 ml)	Spectrophotometry with 0.5 ml of 0.1% 4-(2-pyridylazo)-resorcinol ¹⁶ or atomic-absorption spectrometry
		5% TOA	5.0–7.0	30		
		5% Amberlite LA-1	5.5–7.0	30		
		5% Amberlite LA-2	5.5–7.0	30		
		5% TIOA	5.0–5.5	30		

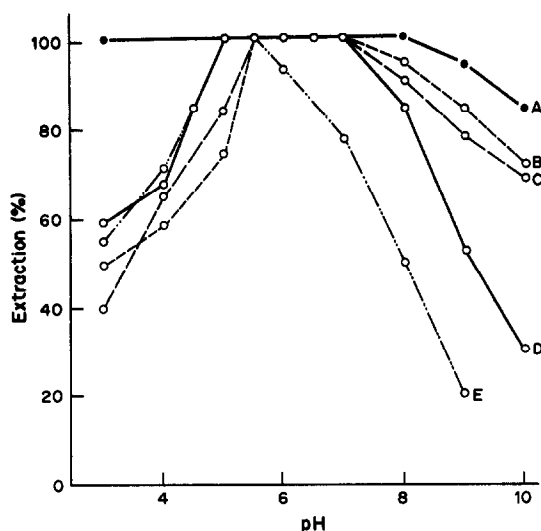


Fig. 2. Extraction behaviour of lead(II) as a function of pH. Extraction of lead from 0.025M sodium salicylate solution with (A) 1% Aliquat 336; (B) 5% Amberlite LA-2; (C) 5% Amberlite LA-1; (D) 5% TOA and (E) 5% TIOA as an extractant.

and benzene whereas extraction of lead is feasible only with xylene and toluene. Aliquat 336 solutions (10 mg/ml) in other solvents such as chloroform, carbon tetrachloride, hexane and cyclohexane gave only 74–96% extraction of lead and uranium.

Shaking time

The shaking time for extraction was varied from 10 to 120 sec. The minimum shaking time required is shown in Table 1; longer shaking has no adverse effect.

Choice of stripping agent

Mineral acids in the concentration range 0.8–1.0M and sodium hydroxide solution (0.5–3.0M) were found to be suitable for stripping uranium, but water does not strip it. The results are shown in Fig. 3. Distilled water

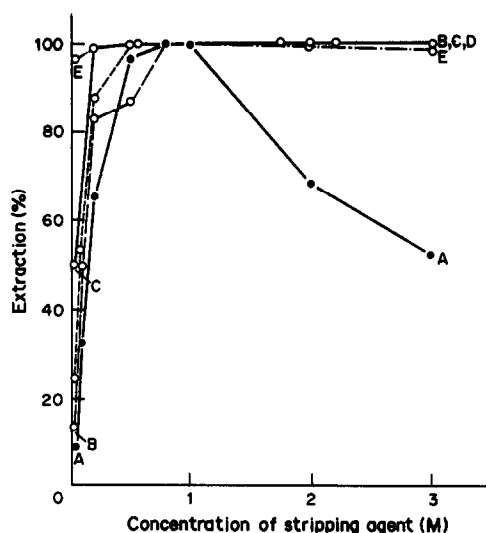


Fig. 3. Effect of different stripping solutions for uranium. (A) Hydrochloric acid; (B) nitric acid; (C) sodium hydroxide, (D) perchloric acid and (E) sulphuric acid.

quantitatively strips lead from the organic phase.

Nature of the extracted species

A log–log plot of distribution ratio *vs.* Aliquat 336 concentration at fixed pH and salicylate concentration or of distribution ratio *vs.* salicylate concentration at fixed pH and Aliquat 336 concentration, showed the molar ratio of both extractant and salicylate to metal ion to be 2:1, for both uranium and lead. Hence the species extracted were thought to be ion-association complexes of probable composition $2R_4N^+ \cdot UO_2Sal_2^-$ and $2R_4N^+ \cdot PbSal_2^-$.

Effect of foreign ions

The effect of various amounts of foreign ions on the extraction and determination of uranium and lead (with Aliquot 336 as extractant) was tested. The tolerance limit was set at the amount of foreign ion required to cause $\pm 2\%$ error in

Table 2. Tolerance limit for added ions

Metal ion	Foreign ion tolerated*
Uranium(VI) (60 μg)	Ca (3000); Ba (3000); Hg (2400); Cr (2400); As (1800); W (1800); Au (1200); Al (1200); Mg (1800); Mo (1200); Zn (1200); Cd (1200); Co (600); Ca (600); Ni (600); Mn (600); Hf (600); Pb (600); Ru (600); Ce (300); Os (300); Bi (300); Ti (300); Zr (180); Fe (180); V (150); thiourea (4800); nitrate (4800); fluoride (4800); iodide (3600); bromide (3600); EDTA (3000); citrate (3000); cyanide (2400); oxalate (2400); thiosulphate (2400); tartrate (2400); phosphate (2400); chloride (1800); sulphate (1200); thiocyanate (600).
Lead(II) (38 μg)	Mg (950); Ba (950); Te (950); As (950); W (950); Bi (760); Cr (760); U (570); Hg (380); Zr (380); Fe (380); Al (380); Ce (380); Pd (380); Au (380); Hf (380); V (190); Ca (190); Mo (115); Sb (115); cyanide (3800); fluoride (3800); thiocyanate (3800); thiourea (3800); sulphate (2850); nitrite (2850); nitrate (2850); chloride (2850); thiosulphate (1900); iodide (1900); tartrate (950); citrate (380); oxalate (190).

*Values in parentheses are in μg .

the recovery of uranium and lead. The results are reported in Table 2. A 180- μg amount of both zirconium(IV) and iron(III) is up to 50% co-extracted but does not interfere in the subsequent spectrophotometric determination of uranium with PAR. However, 150 μg of interface vanadium interferes.

In the extraction of lead, ions such as zirconium(IV), iron(III) and zinc(II) are co-extracted but the interference by zinc can be eliminated by selective masking with thiocyanate. Zirconium and iron, however, do not interfere in the determination of lead with PAR. Copper is co-extracted with uranium and lead, and thus interferes in their determination. However, copper can be separated by the selective stripping technique described in the separation of binary mixtures.

Separation from binary mixtures

The separation of uranium(VI) from binary mixtures containing thorium(IV), titanium(IV), zirconium(IV), hafnium(IV) or cerium(IV) was done by selective stripping of uranium with 8 ml of 0.5M sodium hydroxide. Thorium, titanium, zirconium, hafnium and cerium remained in the organic phase and were subsequently stripped with 0.8M hydrochloric acid, 2M sulphuric acid, 2M hydrochloric acid, 1M perchloric acid and 2M hydrochloric acid, respectively. Separation of uranium from copper(II) and calcium(II) was done by first stripping copper and

calcium with water and then stripping uranium with 0.5M sodium hydroxide. Vanadium(V) and chromium(VI) are not extracted into Aliquat 336, so their separation from uranium is possible. Unextracted vanadium and chromium were determined in the aqueous phase whereas the uranium, in the organic phase, was stripped and determined by the recommended procedure. Separation of uranium and iron was done by stripping iron(III) with 1M hydroxylamine hydrochloride and uranium with 0.5M sodium hydroxide.

Similarly, the binary separation of lead from nickel, copper, cobalt and manganese was attempted by selective stripping of nickel and cobalt with 1M ammonia solution, copper with 0.5M ammonia solution and manganese with hydrogen peroxide in ammonia solution. Lead was not separated with any of these solutions, but was finally removed with distilled water and determined by the recommended procedure. Separation of lead from uranium, iron and titanium was done by stripping lead with water, and uranium, iron and titanium with 0.5M sodium hydroxide, 1M hydrochloric acid and 2M sulphuric acid, respectively. Chromium and vanadium are not extracted and hence their separation from lead was possible. The results of the separations are given in Table 3. The recoveries of uranium(VI), lead(II) and the added ions were $\geq 98.8\%$.

Table 3. Separation of uranium(VI) and lead(II) from binary mixtures

Synthetic mixture, μg	Amount found, μg	Recovery, %	Spectrophotometric procedure for the determination of added ion
U (60)-Th (80)	U, 60; Th, 79.5	U, 100.0; Th, 99.4	Thoron ¹⁷
U (60)-Ti (450)	U, 59.6; Ti, 448	U, 99.3; Ti, 99.6	Hydrogen peroxide ¹⁷
U (60)-Zr (75)	U, 59.6; Zr, 74.3	U, 99.3; Zr, 99.1	Alizarin Red S ¹⁷
U (60)-Hf (25)	U, 60; Hf, 25	U, 100.0; Hf, 100.0	Xylenol Orange ¹⁷
U (60)-Ce (100)	U, 60; Ce, 99.4	U, 100.0; Ce, 99.4	Arsenazo III ²¹
U (60)-Cu (16)	U, 60; Cu, 15.9	U, 100.0; Cu, 99.4	PAN ¹⁸
U (60)-Ca (60)	U, 60; Ca, 60	U, 100.0; Ca, 100.0	Murexide ¹⁷
U (60)-V (120)	U, 59.6; V, 119	U, 99.0; V, 99.2	Phosphotungstovanadic acid ¹⁵
U (60)-Fe (12)	U, 59.8; Fe, 12	U, 99.7; Fe, 100.0	1,10-Phenanthroline ¹⁷
U (60)-Cr (24)	U, 60; Cr, 24	U, 100.0; Cr, 100.0	Diphenylcarbazide ¹⁷
Pb (38)-U (60)	Pb, 38; U, 60	Pb, 100.0; U, 100.0	PAR ⁷
Pb (38)-Ni (40)	Pb, 37.7; Ni, 39.7	Pb, 99.2; Ni, 99.3	Dimethylglyoxime ¹⁷
Pb (38)-Fe (12)	Pb, 38.0; Fe, 12	Pb, 100.0; Fe, 100.0	1,10-Phenanthroline ¹⁷
Pb (38)-V (120)	Pb, 37.7; V, 119	Pb, 99.2; V, 99.2	Phosphotungstovanadic acid ¹⁵
Pb (38)-Ti (150)	Pb, 38; Ti, 150	Pb, 100.0; Ti, 100.0	Hydrogen peroxide ¹⁷
Pb (38)-Co (10)	Pb, 37.7; Co, 9.9	Pb, 99.2; Co, 99.0	PAN ¹⁹
Pb (38)-Cu (10)	Pb, 37.8; Cu, 9.9	Pb, 99.2; Cu, 99.0	PAN ¹⁸
Pb (38)-Mn (50)	Pb, 37.6; Mn, 49.4	Pb, 98.9; Mn, 99.8	PAR ²⁰
Pb (38)-Cr (24)	Pb, 38; Cr, 23.8	Pb, 100.0; Cr, 99.2	Diphenylcarbazide ¹⁷

*Average of six determinations.

Table 4. Analysis of standard samples for lead and uranium

Sample and its composition	Certified value	Amount found, %*	Standard deviation	Coefficient of variation, %
Leaded gunmetal (BCS 183/4) Cu, 84.06; Sn, 7.27; Zn, 3.47; Pb, 3.15; Ni, 1.0; Sb, 0.23; As, 0.13; Fe, 0.056; P, 0.09	3.15% Pb	3.13	0.24	0.76
Tin base white metal (BCS 178/2) Sn, 82.2; Sb, 9.45; Cu, 4.58; Pb, 3.18; Ni, 0.17; Cd, 0.14; Bi, 0.11; Zn, 0.04; Fe, 0.024	3.18% Pb	3.15	0.028	0.90
Leaded brass (BCS 385) Cu, 58.7; Zn, 38.5; Pb, 2.24; Sn, 0.27 Fe, 0.15; Ni, 0.13; Al, 0.005	2.24% Pb	2.21	0.027	1.22
Leaded bronze (BCS 364) Cu, 80.6; Sn, 9.35; Pb, 9.25; Ni, 0.28; Sb, 0.18; Zn, 0.13; P, 0.056	9.25% Pb	9.20	0.015	0.16
Gunmetal (ITA Lab, 4382) Cu, 76.53; Sn, 4.86; Sb, 0.53; Pb, 12.08; Fe, 0.15; Ni, 0.42; Zn, 5.41; P, 0.011	12.08% Pb	12.00	0.018	0.15
Calcined animal bone	0.08% U†	0.08	0.141	0.88
Powdered milk	0.08% U†	0.08	0.189	1.18

*Average of six determinations.

†Uranium added.

Analysis of lead and uranium in 'real' samples

The proposed method was applied to the separation and determination of lead in lead-based alloys such as gunmetal, brass, bronze and tin-base white metal. The results are in good agreement with the certified value (Table 4). The air-borne particles collected from 5 different sites in Bombay by Municipal Corporation Air Quality Monitoring were brought into solution and were extracted as described in the extraction procedure. Results are given in Table 5. Levels of uranium in spiked samples such as calcined animal bone and powdered milk are given in Table 4. The detection limit of lead and uranium was 1–80 $\mu\text{g}/25\text{ ml}$. In environmental samples the detection limit of lead was 0.38 $\mu\text{g}/\text{m}^3$.

Acknowledgement—The authors thank the University Grants Commission, New Delhi for financing the project and the award of a fellowship to N.M.S. Thanks are also due to Mrs. Deshpande, Scientist-in-charge, Municipal Corporation Air Quality Monitoring Bombay for providing air-borne particles.

REFERENCES

1. T. Sato, *J. Inorg. Nucl. Chem.*, 1966, **28**, 1461.
2. *Idem*, *J. Appl. Chem.*, 1966, **16**, 143.
3. *Idem*, *J. Inorg. Nucl. Chem.*, 1964, **26**, 1295.
4. *Idem*, *ibid.*, 1963, **25**, 441.
5. E. R. Schmid and E. Kennler, *Radiochem. Radioanal. Lett.*, 1976, **26**, 259.
6. P. R. Danesi, R. Orlandini and G. Scibona, *J. Inorg. Nucl. Chem.*, 1965, **27**, 449.
7. M. B. Dalvi and S. M. Khopkar, *Talanta*, 1978, **25**, 599.
8. A. Haggag, W. Sanad, E. M. Mikhail and N. Tadros, *Analyst*, 1982, **107**, 916.
9. B. Ya. Spivakov, V. I. Lebedev, V. M. Shkinev, N. P. Krivenkova, T. S. Plotnikova, I. P. Kharlamov and Yu. A. Zolotov, *Zh. Analit. Khim.*, 1976, **31**, 757.
10. G. Nakagawa, *J. Chem. Soc. Japan*, 1960, **81**, 1255.
11. T. Suzuki and T. Sotobayashi, *Bunseki Kagaku*, 1963, **12**, 910.
12. *Idem*, *ibid.*, 1965, **140**, 420.
13. G. Nakagawa, *Bunseki Kagaku*, 1960, **9**, 821.
14. H. T. Delves, G. Shepherd and P. Vinter, *Analyst*, 1971, **96**, 260.
15. A. I. Vogel, *A Textbook of Quantitative Inorganic Analysis*, 3rd Ed., pp. 443, 540, 790. Longmans, London, 1962.
16. A. A. Yadav and S. M. Khopkar, *Talanta*, 1971, **18**, 883.

Table 5. Determination of lead in air samples

Site	Standard value, $\mu\text{g}/\text{m}^3$ *	Lead found, $\mu\text{g}/\text{m}^3$ †
Tilak Nagar	1.26	1.26
Khar	0.38	0.38
Khar	1.40	1.40
Khar	0.83	0.83
Parel	0.42	0.42

*Lead determined by atomic-absorption spectrometry before extraction.

†Lead determined by atomic-absorption spectrometry after extraction.

17. Z. Marczenko, *Spectrophotometric Determination of Elements*, pp. 539, 556, 186, 309, 215, Ellis Horwood, Chichester, 1976.
18. B. F. Pease and M. B. Williams, *Anal. Chem.*, 1959, **31**, 1044.
19. H. Flaschka and J. Garrett, *Talanta*, 1968, **15**, 595.
20. D. Nonova and B. Evtimora, *ibid.*, 1973, **20**, 1347.
21. A. Kosturiak and D. Kalavska, *Chem. Zvesti*, 1981, **35**, 255.

SPECTROPHOTOMETRIC DETERMINATION OF NICKEL IN VEGETABLE OIL WITH AMMONIUM 2-AMINO-1-CYCLOHEXENE-1-DITHIOCARBOATE

A. SAFAVI, A. A. ENSAFI and A. MASSOUMI

Department of Chemistry, Faculty of Sciences, Shiraz University, Shiraz, Iran

(Received 4 January 1990. Revised 8 August 1990. Accepted 24 August 1990)

Summary—The reaction between nickel and ammonium 2-amino-1-cyclohexene-1-dithiocarboate in aqueous acetone medium at pH 3.0–8.0 results in a stable dark red complex. The ratio of reagent to nickel in the complex is 2:1 and the formation constant is $7.38 \pm 0.12 \times 10^{10}$. Beer's law is obeyed up to $4 \mu\text{g/ml}$ nickel at the absorption maximum at 535 nm. The apparent molar absorptivity is $2.8 \times 10^4 \text{ l. mole}^{-1} \cdot \text{cm}^{-1}$, and the detection limit is 10 ng/ml nickel. The method is applied to the determination of nickel in vegetable oil.

Ammonium 2-amino-1-cyclohexene-1-dithiocarboate (AACD) was first synthesized by Takeshima *et al.*¹ To the best of our knowledge, no work on the chelation properties and analytical use of this compound has been reported. An intense dark red complex is formed between AACD and nickel(II). It is soluble in most organic solvents and in an acetone–water mixture. The colour of the complex ($\lambda_{\text{max}} = 535 \text{ nm}$) contrasts well with the yellow reagent solution ($\lambda_{\text{max}} = 388 \text{ nm}$), permitting the visual detection of very small amounts of nickel. 2-Amino-1-cyclopentene-1-dithiocarboic acid, an analogue of AACD, was introduced earlier as an analytical reagent for nickel.²

A review of the existing analytical methods for the determination of nickel in oils and fats shows that there are some drawbacks associated with each of them.^{3–5}

The spectrophotometric procedure described here is a simple and highly sensitive means of determining trace concentrations of nickel. The method is applied to the determination of nickel in different synthetic samples and in vegetable oil.

EXPERIMENTAL

Reagents

A nickel stock solution (1 mg/ml) was prepared in distilled demineralized water from nickel nitrate and diluted further as required. Stock solutions of other elements (10 mg/ml) were prepared by dissolving suitable salts in water or dilute sulphuric or hydrochloric acid.

AACD was prepared and purified according to Takeshima *et al.*¹ and used as an aqueous $1.0 \times 10^{-3} M$ solution.

Apparatus

The spectra were recorded on a Beckman DK-2A spectrophotometer. Absorbances at a fixed wavelength were measured with a Spectronic 70 spectrophotometer.

General procedure

Transfer 2 ml of a nearly neutral solution containing not more than $40 \mu\text{g}$ of nickel into a 10-ml standard flask, add 1 ml of AACD solution ($3 \times 10^{-3} M$) and dilute to the mark with acetone. Measure the absorbance at 535 nm against a reagent blank, in 1-cm path-length cells.

Determination of nickel in vegetable oil

The standard-addition technique is used. For this purpose, transfer 40.0 g of oil into a 100-ml standard flask and dilute to the mark with acetone. Transfer 5-ml aliquots of this solution into 10-ml standard flasks and add appropriate volumes of standard nickel solution containing 0–20 μg of nickel. Then add 1.0 ml of $3.0 \times 10^{-3} M$ AACD in acetone to each flask and dilute the solution to the mark with acetone. Measure the absorbances at 535 nm against the appropriate blank. Plot absorbance *vs.* amount of nickel added and read the intercept on the *x*-axis in the usual way.

RESULTS AND DISCUSSION

In an aqueous solution, nickel and AACD form a sparingly soluble reddish complex. In water-acetone mixtures the complex is formed almost instantaneously and is soluble if the acetone content of the mixture is $\geq 50\%$ v/v. The absorption maximum of the complex is at 535 nm and that of the ligand is at 388 nm. As neither nickel nor the ligand shows any absorption at 535 nm, this wavelength is used for analytical purposes.

The absorption spectrum of the complex in 50% v/v aqueous acetone was examined at various apparent pH values. Formation of the complex was found to be maximal at apparent pH values in the range 3-8.

The complex is quite stable and the calibration graph is linear. Beer's law is obeyed for nickel concentrations up to 4 $\mu\text{g/ml}$. The molar absorptivity is $2.8 \times 10^4 \text{ l. mole}^{-1} \text{ cm}^{-1}$ at 535 nm and the detection limit is 10 ng/ml nickel.

The continuous-variations⁶ and molar-ratio⁷ methods both show that a 2:1 ligand:metal complex is formed.

Because the nickel complex of AACD is only sparingly soluble in water, an organic solvent must be added. Methanol, ethanol, acetone, acetonitrile and dioxan were tried in different proportions. Aqueous acetone and dioxan were found to be the best solvents. The maximum sensitivity was reached when the organic solvent content was 50% v/v or more.

Varying the ionic strength between 1.17×10^{-4} and 2.00 (with sodium perchlorate) did not affect the absorbance.

The formation constant of the complex, calculated by the method of Likussar and Boltz,⁸ is $(7.38 \pm 0.12) \times 10^{10}$.

Interferences

The criterion for interference was taken as a change of $\pm 2\%$ in the absorbance for 10 μg of

Table 1. The tolerance limit for cations in the determination of 1.0 $\mu\text{g/ml}$ nickel

	Concentration, $\mu\text{g/ml}$
Zn(II), Al(III), Hg(I), Zr(IV), Mg(II), Na(I), K(I), Pt(IV), Pd(II), Mo(VI), La(III), Ce(III), Ti(IV), Hf(IV), Sn(II), Sn(IV), Te(IV), Ca(II)	1000*
Fe(II), Mn(II), Co(II)†	200
Fe(III), Cu(II), Bi(III), Ag(I), Cd(II)‡	50

*Maximum concentration examined.

†After treatment for removal.

‡After precipitation with Na_3PO_4 .

nickel, in the presence of a tenfold molar ratio of AACD. No interference results from the presence of 1000-fold weight ratio of chloride, bromide, iodide, sulphate, nitrate, oxalate, citrate, acetate, tartrate, periodate and phthalate. However, carbonate and phosphate interfere when present at 50-fold weight ratio to nickel. These ions can be removed by the addition of barium nitrate to the test solution and filtration of the precipitate prior to the addition of AACD. EDTA is obviously a serious interferent and must be absent.

The tolerance limits for various cations in the determination of 1.0 $\mu\text{g/ml}$ nickel are given in Table 1. Al(III), Zr(IV), Zn(II), Hg(I), La(III), Pd(II), Pt(IV), Ca(II), Mg(II), Hf(IV), Na(I), K(I), Mo(VI), Ce(III), Ti(IV), Te(IV), Sn(II), Sn(IV) at 1 mg/ml concentration did not interfere. Cu(II), Co(III), Fe(II), Fe(III), Mn(II), Bi(III), Ag(I) reacted with the reagent and thus interfered. The effect of these interferents was easily removed by the addition of saturated ammonium thiocyanate to the test solution and separation of any precipitate [Bi(III)] or extraction of the complexes into methyl isobutyl ketone. Under the recommended conditions, thiocyanate does not react with nickel. Pb(II) and Hg(II) can be removed by the addition of sulphate and iodate, respectively, to the test solutions prior to addition of AACD.

Table 2. Analysis of samples by the proposed method

Matrix*	Ni added, μg	Ni found
$\text{Fe}^{2+}(5)$, $\text{Cu}^{2+}(5)$, $\text{Co}^{2+}(5)$	1.0	0.96, 0.98 μg
$\text{Mn}^{2+}(5)$, $\text{Cu}^{2+}(3)$, $\text{Co}^{2+}(3)$, $\text{Fe}^{3+}(3)$	1.0	0.98, 0.98 μg
$\text{Bi}^{3+}(3)$, $\text{Fe}^{3+}(2)$, $\text{Ag}^{+}(2)$, $\text{Mn}^{2+}(5)$	1.0	0.97, 0.96 μg
Vegetable oil† (before post bleaching)‡	—	2.94, 2.98, 2.92 $\mu\text{g/g}$
Vegetable oil (after post bleaching)§	—	0.390, 0.396, 0.387 $\mu\text{g/g}$

*The number in parentheses indicates mg of element in the aliquot taken for analysis.

†Vegetable oils were of soya bean origin.

‡Ni content obtained by atomic-absorption spectrometry = $2.85 \pm 0.06 \mu\text{g/g}$.

§Ni content obtained by atomic-absorption spectrometry = $0.401 \pm 0.010 \mu\text{g/g}$.

Applications

The recommended procedure is highly sensitive for the determination of nickel and sufficiently selective for analysis of some natural samples as well as a variety of nickel-containing alloys. The method is simple and rapid. Its utility is shown by the satisfactory analysis of various synthetic samples and by the determination of nickel in vegetable oil (Table 2).

Acknowledgement—The authors are thankful to Shiraz University Research Council for support of this work.

REFERENCES

1. T. Takeshima, A. Yano, N. Fukada, Y. Hirose and M. Muraoka, *J. Chem. Research (S)*, 1979, 140.
2. M. Yokoyama and T. Takeshima, *Anal. Chem.*, 1968, **40**, 1344.
3. L. V. Cock and C. Van Rede, *Laboratory Handbook for Oil and Fat Analysis*, p. 349. Academic Press, New York, 1966.
4. D. Swern, *Bailey's Industrial Oil and Fat Products*, 4th Ed., Vol. 2, Wiley-Interscience, New York, 1982.
5. *Idem*, *op. cit.*, p. 491.
6. P. Job, *Ann. Chim. (Paris)*, 1928, **9**, 113.
7. J. H. Yoe and A. L. Jones, *Ind. Eng. Chem., Anal. Ed.*, 1944, **16**, 111.
8. W. Likussar and D. F. Boltz, *Anal. Chem.*, 1971, **43**, 1265.

ANALYTICAL DATA

X-RAY POWDER DIFFRACTION DATA FOR NINE ANALGESICS

J. E. KOUNTOURELLIS* and C. K. MARKOPOULOU

School of Pharmacy, 106, Aristotle University, Thessaloniki, 54006, Greece

F. A. UNDERWOOD and B. CHAPMAN

School of Physics, University of Bath, Bath BA2 7AY, England

(Received 22 November 1989. Revised 18 March 1990. Accepted 6 July 1990)

Summary—X-Ray powder diffraction data for nine analgesics have been obtained by using a powder diffractometer. The results obtained by using the McCreery and Byström-Asklund methods of sample loading were averaged and tabulated in terms of the lattice spacings and the relative line intensities. Data from powder camera films were compared with the diffractometer data, and certain discrepancies in the intensities are discussed.

The early work by Hanawalt *et al.*¹ introduced the powder diffraction technique as an instrumental analytical method for the identification of polycrystalline materials. This technique is used here to characterize nine analgesics in terms of interplanar *d* spacings and line intensities relative to the intensity of the strongest line. As the pharmaceutical compounds² examined have not been studied previously by X-ray diffraction and these data are not included in the 1987 Powder Diffraction File,³ the new information may be useful for their identification.

EXPERIMENTAL

Samples

The samples of buprenorphine ($C_{12}H_{17}NO_3$), diclofenac sodium ($C_{14}H_{10}Cl_2NNaO_2$), flufenamic acid ($C_{14}H_{10}F_3NO_2$), mefenamic acid ($C_{15}H_{15}NO_2$), nefopam hydrochloride ($C_{17}H_{19}NO.HCl$) and niflumic acid ($C_{13}H_9F_3N_2O_2$) were purchased from Sigma. Fentiazac acid ($C_{17}H_{12}ClNO_2S$), dipyrone ($C_{13}H_{16}N_3NaO_4S$), (Ercifar S.A. Pharmaceuticals, Athens) and tolmetin ($C_{14}H_{10}F_3NO_2$), (Farmalex S.A. Pharmaceutique, Athens) were kindly donated by the manufacturers.

The samples were at least 99.6% pure and most of them were dried overnight in an oven at 60°. Some samples were suitable as supplied, but

when necessary the particle size was reduced to less than 5 μm by grinding in an agate mortar. The grinding was performed under an infrared lamp to avoid adsorption of atmospheric moisture. Microscopy was used, with the aid of a graticule, to measure the particle size, and the well defined lines on the X-ray diffraction photographs were a strong indication that all the particles were of approximately the same size.

Apparatus and sample preparation

The Debye-Scherrer X-ray photographs were obtained with a Philips 11.4 cm diameter camera (PW 1034/10) with iron-filtered cobalt radiation ($Co K_{\alpha}$ 1.790 Å)

The Philips diffractometer goniometer (PW 1050/25) was used in conjunction with a Xenon proportional counter (PW 1965/30) and a Philips ratemeter/single channel analyser (PW 4620) with output to a chart recorder (PM 8000). Nickel-filtered copper radiation ($Cu K_{\alpha}$ 1.542 Å) was produced by a normal focus tube operated at 40 kV and 20 mA. Samples were scanned at 20° over the 2θ range 5–45° at 1°/min.

In applying this technique, three fundamental methods of packing the sample are possible: (i) loading the powder from the front, (ii) the McCreery method of loading the powder from the back, and (iii) the Byström-Asklund method of loading the powder from the edge.⁴⁻⁷

*Author for correspondence.

Table 1. X-Ray diffraction data in terms of lattice spacings (d , Å) and relative line intensities*

Fentiazac acid		Diclofenac Na		Dipyrrone		Nefopam.HCl		Niflumic acid		Mefenamic acid		Tolmetin		Flufenamic acid		Bufexamac		
d	I/I_1	d	I/I_1	d	I/I_1	d	I/I_1	d	I/I_1	d	I/I_1	d	I/I_1	d	I/I_1	d	I/I_1	
7.69	28	14.0sh	33	8.27	98	11.6	9	10.9	40	14.0	65	15.2	11	12.4	9b	11.9	32	
7.37	13	13.2	100	7.20	2	8.30	4	7.76	16	7.03	3b	12.4	30	6.66	8	7.97	7	
6.76	7	10.3	59	6.97	2	7.25	38					10.4	2					
6.51	6	7.83	35	6.71	4	6.46	69	6.92	87	6.42	67	9.02	13	6.42	2	5.54	10	
5.64	43	6.92	18	6.19	24	5.87sh	4	5.44	72	6.24	60	8.19	2	6.24	11	5.28	100	
5.16	33	6.61	8	5.61	56	5.72	88	4.85	17	5.91	74	7.63	25	6.03	11	4.75	84	
5.04	8	6.19	8	5.22	3	5.31	26	4.72	19	5.61	100	6.24	98	5.91	8	4.62sh	20	
4.93	35	5.83	94	5.10	5	4.96	11	4.27sh	41	5.28	10b	5.72	100	4.98	34	4.51	42	
4.60	43	5.47	16	4.96	16	4.62	38sh					4.90sh	17	4.90sh	17	4.51	40	
4.51	11	5.15	47	4.70sh	28	4.53	100	4.19	100	5.13	5b	5.07	23	4.69	42	4.42	35	
4.44	19	4.98	31	4.67	30	4.27	11	3.85	57	4.96	3b	4.82	88	4.53	54	4.35	30	
4.11	12	4.46	63	4.55	67	4.19	11	3.74	15	4.42	49	4.62	5	4.48sh	30	4.17sh	22	
4.06	10	4.23	10	4.40	35	4.10	12	3.58	77	4.17	96	4.19	82b	4.17	8	4.06	95	
3.95	21	4.13	12	4.11	40	3.88	23	3.47	57	4.00	2b	3.95	28b	4.02	26	4.06	88	
3.85	64	4.08	4	3.99	7	3.79	52	3.40	3b	3.92	2b	3.86	23b	3.77	24	3.99	25	
3.69	100	3.99	8	3.85	11	3.68sh	28	3.29	3b	3.83	2b	3.75	23b	3.65	100	3.62	64	
3.58	24	3.93	13	3.72	13	3.65	72	3.16	3b	3.74	5b	3.53	35b	3.47	2	3.49	12	
3.47	11	3.79	67	3.68	19	3.52	11	3.07	25	3.55	9	3.43	23b	3.33	15	3.41	23	
3.39sh	19	3.72sh	31	3.52	16	3.41	34	2.978	5	3.41	96	3.30	4b	3.25	8	3.34	23	
		3.69sh	15											3.18	12			
3.35	38	3.56	31	3.43	2	3.29	4	2.903	3	3.22	33	3.20	4b	2.903	26	3.25b	6	
3.25	15	3.45	18	3.35	100	3.22	26	2.722	2b	3.10	2b	3.09	4b	2.823	2	3.14b	6	
3.16	8	3.29	47	3.20b	7	3.13b	12	2.621	2b	3.00	2b	2.849	5b	2.726	2	3.06b	18	
3.10	8	3.20	57	3.18b	9	2.831b	4	2.536	2b	2.940	6b	2.706	4b	2.691	2	2.969b	9	
3.05	17	3.09	22	3.09	25	2.714b	4	2.436	12	2.858	8					2.921b	8	
2.849	20	2.90	5	3.06	23	2.629b	4			2.805	8					2.831b	8	
2.823	18	2.903	4	3.00b	4	2.564b	4			2.730	6					2.747b	4	
2.771	4	2.849	3	2.797b	4					2.461	4					2.730sh	16	
2.585	6	2.780	3	2.750	12					2.227	10					2.652sh	8	
				2.637	2											2.629b	10	
				2.564	2											2.495b	3	
				2.455	2											2.455b	3	
				2.368	2											2.368b	3	
				2.276	12												2.368b	3

*sh = shoulder on strong line; b = broad line; the three most intense lines are underlined.

The front-packing method is the least successful way of preparing samples because preferred orientation is not reduced to a minimum. In this case the relative intensities of lines at low angles are distorted and the data may be misleading. Loading methods (ii) and (iii) were therefore employed, and the data in Table 1 are averages of results from the two methods. The diffractometer patterns were recorded by mounting ~2 g of sample in a window in an aluminium specimen holder and then exposing it to the X-ray beam for ~40 min. The calibration of the goniometer was checked with silicon as a standard.

RESULTS AND DISCUSSION

Table 1 shows the data obtained for the nine analgesics in terms of the lattice spacings and the relative line intensities.

The best results, in terms of resolution and separation, were obtained by the powder diffractometer technique. In general the powder camera patterns agreed well with the diffractometer traces, but there were discrepancies in the case of mefenamic acid. Generally, most of the characteristic lines in the diffraction patterns were prominent and sharp, so measurement of the angles and hence of d -values was accurate.

In the diffraction data for the tolmetin the lines occurring at $2\theta > 20^\circ$, although of reasonable intensity, were broad compared to the other lines. In this case the values for the d spacings should be treated with caution.

When the Debye-Scherrer photographic technique was employed for the investigation of mefenamic acid, it was observed that the first two or three lines at low Bragg angles were very intense. The corresponding lines in the patterns obtained by the powder diffractometer, where preferred orientation was reduced to a minimum, were of low or moderate intensity. If these lines at low Bragg angles are ignored, the three most intense lines indicated in Table 1 were the same for both the diffractometer and camera techniques.

Flufenamic acid exhibited the least reproducible diffraction pattern intensities. Some lines in the patterns or in the microdensitometer traces were very intense and prominent in one diffraction pattern or very weak in another under identical conditions of sample loading

and diffractometer operation. Specifically, the lines at 4.69, 4.53, 3.18 and 2.903 Å were sometimes observed to be very intense and at other times rather weak while the lines at 4.98, 4.53 and 3.65 Å were of variable intensity and were either very often split into two lines or had a characteristic shoulder.

In the case of dipyrone, the first line at 8.27 Å is included as one of the three strongest lines because its intensity was not reduced even when the specified alternative methods of packing the sample were used. In some diffraction patterns, the line at 5.61 Å was split into two peaks (5.64, 5.57 Å), and the lines at 4.67 and 3.52 Å had shoulders.

For the remaining compounds, the values of the interatomic d spacings and relative intensities are in agreement for both techniques and both methods of preparing the samples.

CONCLUSION

X-Ray powder diffraction patterns provide a means of identification of crystalline pharmacologically active compounds, but attention to sample preparation is essential. In this study the data presented were obtained by the diffractometer technique, with use of two methods of packing by which random alignment of crystals in the sample is achieved. No fundamental discrepancies in the d spacings were found when comparisons were made with the powder camera results. Some variation between the intensities of the strongest lines in the diffraction patterns obtained by two techniques are explained in terms of preferred orientation in the specimens.

REFERENCES

1. J. D. Hanawalt, H. W. Rinn and L. K. Frevel, *Ind. Eng. Chem., Anal. Ed.*, 1938, **10**, 457.
2. Martindale, *The Extra Pharmacopoeia*, 28th Ed., p. 234. The Pharmaceutical Press, London, 1982.
3. *Powder Diffraction File*, Joint Committee on Powder Diffraction Standards, Swarthmore, PA, 1987.
4. J. E. Kountourellis, F. A. Underwood, P. P. Georgakopoulos and A. Raptouli, *Talanta*, 1986, **33**, 631.
5. J. T. R. Owen, J. E. Kountourellis and F. A. Underwood, *J. Assoc. Off. Anal. Chem.*, 1981, **64**, 1164.
6. A. M. Byström-Asklund, *Am. Mineral.*, 1966, **51**, 1233.
7. L. S. D. Glasser, *Crystallography and Its Applications*, p. 133. Van Nostrand Reinhold, Wokingham, 1977.

CHARACTERIZATION OF RETENTIVITY OF REVERSED PHASE LIQUID CHROMATOGRAPHY COLUMNS

PETER T. YING*

Department of Chemistry, University of Florida, Gainesville, FL 32611, U S A

JOHN G. DORSEY†

Department of Chemistry, University of Cincinnati, Cincinnati, OH 45221-0172, U S A

(Received 17 August 1990. Revised 9 October 1990. Accepted 3 November 1990)

Summary—There are dozens of commercially available reversed phase columns, most marketed as C-8 or C-18 materials, but with no useful way of classifying their retentivity. A useful way of ranking these columns in terms of column “strength” or retentivity is presented. The method utilizes a value for $\ln k'_w$, the estimated retention of a solute from a mobile phase of 100% water, and the slope of the plot of $\ln k'$ vs $E_T(30)$, the solvent polarity. The method is validated with 26 solutes varying in $\ln k'_w$ from about 2 to over 20, on 14 different reversed phase columns. In agreement with previous work, it is found that the phase volume ratio of the column is the most important parameter in determining retentivity. It is strongly suggested that manufacturers adopt a uniform method of calculating this value and that it be made available in advertising, rather than the uninterpretable “% carbon”.

The molecular mechanism of retention for small molecules in reversed phase liquid chromatography is becoming well understood.¹ Dill and co-workers have developed mean-field statistical mechanical theory to account for the interactions of the solute in the mobile phase and in the stationary phase, and have accounted for the variation in chain interactions as a function of the bonding density of alkyl chains on the silica surface.^{2,3} We have been experimentally investigating these theories, and in general, have found excellent agreement.

Theory predicts that two driving forces dominate retention: (i) the free-energy change due to contact interactions of the solute with surrounding molecular neighbors in the stationary and mobile phases, as measured by binary interaction constants, and (ii) the partial ordering of the grafted stationary-phase chains which, at sufficiently high bonding density, leads to an entropic expulsion of solute from the stationary phase relative to that which would be expected in a simpler amorphous oil-phase/water partitioning process. We have tested (i) against an extensive data base of almost 350 sets of experiments and in agreement with theory have found that the mobile-phase contribution to retention

can be described by the binary interaction constants of solutes with solvents.⁴ We have also tested (ii) by synthesizing reversed phase stationary phases over an octadecyl bonding-density range of 1.6–4.1 $\mu\text{mole}/\text{m}^2$, and have found a maximum in the partition coefficient at approximately 3.0 $\mu\text{mole}/\text{m}^2$.⁵ At bonding densities in excess of this value actual partitioning decreases, as the energy required to create a cavity in the stationary phase becomes the dominant force. At low bonding densities retention is driven by enthalpic processes, and at high bonding densities ($> 3.0 \mu\text{mole}/\text{m}^2$), retention is driven by entropic processes. The bonding density of virtually all commercially available reversed phase columns is in the range 2.3–3.0 $\mu\text{mole}/\text{m}^2$.

Whereas partitioning goes through a maximum as a function of bonding density, retention, as measured by the capacity factor, reaches an approximate plateau at a chain-density value of 3.0 $\mu\text{mole}/\text{m}^2$. This apparent anomaly is easily explained. The capacity factor is the product of the partition coefficient and the phase-volume ratio (stationary/mobile) and at high chain densities, while the partition coefficient is decreasing, the volume of the stationary phase is increasing, and the two effects virtually offset each other. This “leveling off” behavior has been reported by others.⁶⁻⁸

*Present address Wesley-Jessen, 400 West Superior Street, Chicago, IL 60610, U S A

†Author for correspondence

While theory has adequately described the partitioning process, there is still a need for a convenient empirical description of retentivity, or column strength. Reversed phase columns are made with a wide variety of functional groups, including C-18, C-8, C-1, phenyl, cyano, and others. Recent studies have compared the retentivity and selectivity of many of these columns, and have shown that even for ostensibly equivalent columns, such as C-18 materials, there are great differences in their properties.⁹⁻¹¹

This variability is due to many factors, including properties of the initial silica such as surface area, pore diameter and volume, and impurities, and also to differences in the bonding reaction used to synthesize the reversed phase material. These variabilities have caused many difficulties for the practicing chromatographer. Choosing the "best" column for a given separation is most often a trial and error process, and methods developed in one laboratory are difficult to use in another unless the brand and manufacturer of the column are the same.

There have been many attempts to classify columns according to their retentivity or selectivity for a particular class of compounds. They include chemometric approaches,¹²⁻¹⁴ the use of compounds from Snyder's solvent selectivity triangle,¹⁵ and others.^{16,17} Smith and Burr have advocated a retention index system based on a series of alkyl aryl ketones to define the retention properties of different columns; a different set of constants for each column is obtained for every different mobile phase composition used, requiring new calibration every time either the mobile phase or stationary phase is changed.^{18,19} Sander and Wise have proposed a series of three polyaromatic hydrocarbons as a probe of the shape-selectivity characteristics of reversed phase materials, and these compounds are now available as a National Institute of Standards and Technology Standard Reference Material (SRM 869).²⁰ Antle and Snyder used gradient elution theory to characterize columns according to their solvophobic retention.^{21,22} They examined columns produced from the same base silica but having different bonded functional groups, such as C-18, C-8, phenyl, C-1 and cyano groups. One unique aspect of their studies was the use of 22 solutes of widely differing chemical properties in the hope that their results would be more widely applicable to everyday separation problems. They combined the phase-volume ratio and the polarity of the stationary phase into an effective "strength"

parameter and ordered the columns in terms of retentivity as C-18 > C-8 > phenyl > C-1 > cyano. They further concluded that the contribution of the polarity of the column to retentivity is small compared to the contribution of the phase-volume ratio. Though their results are useful for other workers, the methodology does not lend itself to characterization of new columns, because of the complexity of the data collection, and the necessity to use both a reference and a standard column.

Here we present a simple method to characterize the retentivity of commercial reversed phase columns, by use of binary mobile phases of water and an organic solvent under isocratic conditions. No reference or standard column is necessary, and solutes of widely varying chemical properties are used to ensure the results will be broadly applicable to everyday separation problems.

EXPERIMENTAL

All retention measurements were obtained either with a Spectra-Physics SP8700 ternary proportioning LC system (Spectra-Physics, San Jose, CA, USA) or with two Spectroflow 400 pumps (ABI Analytical, Kratos Division, Ramsey, NJ, USA). A Valco C6W injection valve (Valco Instrument Company, Houston, TX, USA) and a 20 μ l sample loop were used to inject the solutes. The detection system was either a Spectroflow 783 absorbance detector/gradient controller or a Spectroflow 757 absorbance detector (ABI Analytical) operated at 254 nm. When the two Spectroflow 400 pumps were used, a Rainin Dynamax dual chamber mixer (Rainin Instrument Company, Inc., Woburn, MA, USA) was placed before the injector valve for better mixing of the binary solvents. A Fisher Recordall Series 5000 (Fisher Scientific, Pittsburgh, PA, USA) strip chart recorder was used to record the chromatographic peaks. The solvents used were HPLC grade from Fisher Scientific and the water was treated with a Barnstead Nanopure II system (Barnstead Company, Dubuque, IA, USA) before use.

Chromatographic columns

All DuPont Zorbax columns were purchased from Fisher Scientific; the B&J columns were from Burdick & Jackson Laboratories, Inc. (Baxter Healthcare Corp., Burdick & Jackson Division, Muskegon, MI, USA), and the

Ultrasphere column from Beckman (Beckman Instruments, Inc., Fullerton, CA, USA). The high-density column was synthesized and packed in our laboratories.²³ Some of the properties of these columns, as supplied by the manufacturers, are listed in Table 1.

Chromatographic parameters

The columns were maintained at 30° by a water jacket and a Haake D1 circulator (Fisher Scientific). The 26 solutes used are listed in Table 2. They were from various suppliers and were used without further purification. The solutes were initially injected individually and then, to prevent peak overlap, were grouped into mixtures containing no more than five solutes. Peak assignments were made by comparing both peak area and elution order. The void volume of each column was determined by the injection of water at a mobile phase composition of 75% water and 25% organic modifier. The flow-rate was maintained at 1 ml/min, except for the Burdick & Jackson C-18 column which was used with a flow-rate of 1.5 ml/min. All the retention data were obtained by averaging at least two measurements of a solute. The $E_T(30)$ polarity values for the different mobile phase compositions were calculated from the quadratic relationship between percentage of organic modifier and the $E_T(30)$ values reported by Dorsey and Johnson.²⁴

Regression calculations

The regression calculations were performed with the StatWorks (Heydon and Son Inc., Philadelphia, PA, USA) program on a Macintosh SE (Apple Computer, Inc., Cupertino, CA, USA) microcomputer.

RESULTS AND DISCUSSION

For any given column, the retention is adjusted by changing the strength of the mobile

Table 1 Properties of the RPLC columns as supplied by the manufacturers

Column	Ligand	Surface area, m^2/g	Carbon loading, %
Zorbax ODS	C ₁₈	340	20
Zorbax C-8	C ₈	330	10
Zorbax phenyl	Phenylpropyl	300	5
Zorbax TMS	C ₁	320	5
Zorbax cyano	Cyanopropyl	320	5
B&J C-8	C ₈	250	8
B&J C-18	C ₁₈	250	13
Ultrasphere C-8	C ₈	200	12

Table 2. List of test solutes used in this study

Methyl paraben	Ethyl paraben
Propyl paraben	Butyl paraben
Cortisone	Corticosterone
Toluene	Hexylfluorobenzene
Benzyl alcohol	<i>o</i> -Nitrophenol
Propachlor	1-Methylnaphthalene
Tri- <i>p</i> -tolylphosphate	Methylbenzylamine
Fluorobenzene	Chloropropham
Dimethyl phthalate	Diethyl phthalate
Butyl benzyl phthalate	Dibutyl phthalate
1-Methylphenanthrene	Dioctyl phthalate
<i>p</i> -Terphenyl	Chrysene
1,1,4,4,-Tetraphenyl-1,3-butadiene	Octadecanophenone

phase. Then it is necessary to have an accurate description of mobile-phase strength effects on retention before column retentivity can be explored. It is commonly assumed that a plot of the logarithm of the capacity factor ($\ln k'$) vs. volume fraction of organic modifier will show linear behavior. In fact, it has been known for many years that this is not strictly true. It has been shown both theoretically² and experimentally²⁵ that there is a quadratic dependence of retention on the volume fraction of organic modifier. We have previously shown that the strength of the mobile phase can be conveniently expressed by its $E_T(30)$ solvatochromic solvent polarity.²⁶ With a data set of 332 different retention/volume fraction dependencies, we showed that there is a linear relationship between $\ln k'$ and $E_T(30)$ solvent polarity.²⁶ This relationship can be expressed as

$$\ln k' = mE_T(30) + C \quad (1)$$

where $E_T(30)$ is the polarity value (kcal/mole) of the mobile phase, and m and C are the slope and y -intercept of the linear regression. The slope is then a valid measure of mobile phase strength. Moreover, the slope has also been shown to be directly proportional to the size of the solutes and to the binary interaction constant of water and the organic modifier.⁴ We feel the slope from equation (1) is then a valid descriptor for the mobile-phase contribution to solute retention.

Molecular descriptor approach

The first approach we took was to search for a molecular descriptor of the test solutes that would show the retention effects of the stationary phase and that would be a convenient measure to plot against the slope of equation

Table 3 Regression data for slopes from equation (1) plotted vs van der Waals volume, V_w , of the test solutes

Column	Modifier	Slope $\times 10^3$	y-intercept	r^2
Zorbax ODS	ACN*	4.08	0.845	0.533
Zorbax C-8	ACN	3.82	1.03	0.534
Zorbax phenyl	ACN	4.27	0.593	0.484
Zorbax TMS	ACN	9.25	0.336	0.861
Zorbax cyano	ACN	6.98	0.310	0.472

*Acetonitrile

(1). The slope of this plot should show the retentivity of the column being tested. As cavity creation in the stationary phase is a major contribution to solute retention,¹⁻³ we felt a linear relationship should exist between the slope from equation (1) and a molecular size descriptor. It has previously been reported that a linear dependence exists between $\ln k'$ for some solutes and the van der Waals volume, V_w ,²⁷⁻²⁹ or the molecular connectivity index, χ .^{30,31} Slopes from equation (1) were plotted against both of these descriptors, and the regression results for five Zorbax columns are given in Tables 3 and 4. The V_w and χ values were calculated by the methods given in the papers cited, and Figs. 1 and 2 show the data from the Zorbax TMS column, which gave the "best" results with these descriptors. It is curious that this column gave the best results with these descriptors, as the retention mechanism of a TMS column is probably dominated by "adsorption" effects, meaning that the chain length is too short for penetration of the solute into the bonded stationary phase.

The coefficients of determination, r^2 , of these regressions are all well below 0.9, indicating that there is no significant correlation between the slopes from equation (1) and the two molecular size descriptors chosen. There are several possible reasons for this poor correlation. Both the van der Waals volume and the molecular connectivity index are *estimations* of a solute size; furthermore, they cannot account for other interactions that may occur between the solute and the stationary phase.

Table 4 Regression data for plots of slopes from equation (1) vs molecular connectivity index of the test solutes

Column	Modifier	Slope $\times 10^2$	y-intercept	r^2
Zorbax ODS	ACN*	6.21	0.992	0.401
Zorbax C-8	ACN	6.54	1.14	0.417
Zorbax phenyl	ACN	7.14	0.723	0.379
Zorbax TMS	ACN	16.7	0.563	0.829
Zorbax cyano	ACN	11.5	0.531	0.354

*Acetonitrile.

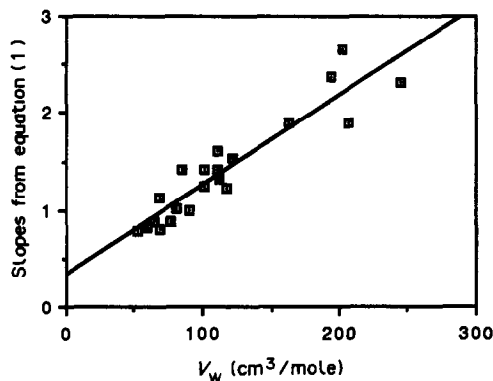


Fig. 1 Slope from equation (1) vs. van der Waals volume for the 26 test solutes, on the Zorbax TMS column.

Approach using $\ln k'_w$

The second approach we took was to seek a parameter which would accurately include all the interactions between the solute and the stationary phase. An *experimental* measure would be best, as no approximations would be necessary. It had been previously shown that the logarithm of the capacity factor of a solute with a mobile phase composition of 100% water, $\ln k'_w$, is highly correlated to the logarithm of the partition coefficient between octanol and water for that solute.³²⁻³⁵ The $\ln k'_w$ value should be ideal for the purposes of assessing stationary phase retentivity, as it is a measure of partitioning between the stationary phase in question and *pure water*, which effectively deconvolutes any contributions from the mobile phase.

One problem with this descriptor is that it is extremely difficult to measure experimentally. Excessively long retention times and poor peak shapes arising from slow mass transfer effectively eliminate experimental determination of this value, and $\ln k'_w$ is most often estimated by extrapolation (to 100% water) of a linear

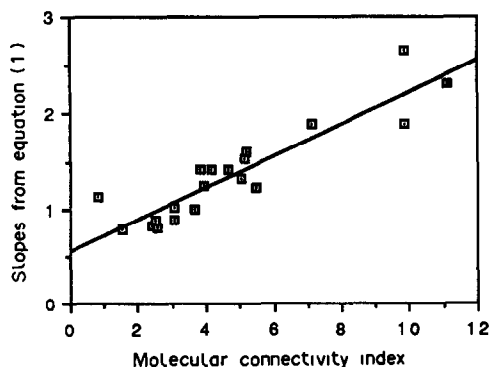


Fig. 2 Slope from equation (1) vs molecular connectivity index for the 26 test solutes, on the Zorbax TMS column

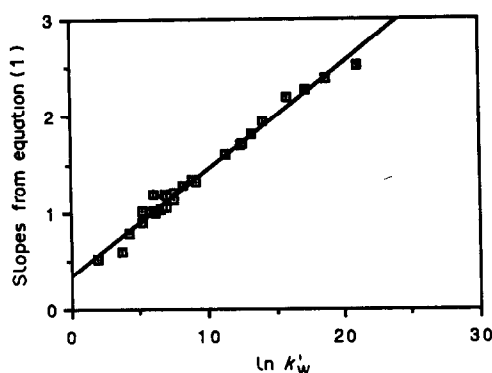


Fig. 3 Slope from equation (1) vs $\ln k'_w$, the capacity factor in 100% water, for the 26 test solutes, on the Zorbax TMS column

regression of $\ln k'$ vs. volume per cent organic modifier.^{32,33,36-38}

$$\ln k'_w = S(\% \text{ organic}) + C'$$

We have recently shown that this extrapolation leads to *different* values for the same solute and column with methanol/water and acetonitrile/water mobile phases.³⁹ However, an extrapolation of $\ln k'$ vs. $E_T(30)$ solvent polarity leads to a common intersection for methanol/water, ethanol/water and acetonitrile/water mobile phases for a given solute/column combination, giving much greater confidence that the extrapolated value is meaningful.^{39,40}

Since the slopes from equation (1) and $\ln k'_w$ of the solute summarize the retention effects due to the mobile phase and any specific solute interactions with the stationary phase, respectively, the slope of a plot of these two parameters for a column should be independent of the two effects and should unveil the retentivity of the column, see Fig. 3. The regression parameters of these

plots for all the columns studied are presented in Table 5. The 95% confidence intervals of the slopes of these regressions have been calculated and are listed in the last column of Table 5. The confidence intervals show that almost all the slopes of the regressions are statistically different from one another. Good linearity between the two parameters is also shown, with $r^2 > 0.9$ for all the columns tested, except for the Zorbax ODS and C-8 columns with acetonitrile as the organic modifier. The high r^2 confirms that the slopes from equation (1) are highly correlated with $\ln k'_w$ for the test solutes.

This type of slope vs. $\ln k'_w$ plot is not new. Hammers *et al.* have shown that plots of the slope S and $\ln k'_w$ from equation (2) are linear.⁴¹ They found that the slopes and y -intercepts of these plots formed two empirical parameters that can be used to classify solutes into different groups, and these solute groups can be used to recommend the use of $\ln k'_w$ for the estimation of $\log P_{o/w}$. Schoenmakers *et al.* found good linearity for equation (2) when methanol is used as the mobile-phase modifier but not with acetonitrile or THF.²⁵ They have shown that when linearity is observed, the slopes of these plots can be used to specify the shape of the gradient program to be employed. Moreover, these slopes can be employed to predict isocratic capacity factors from a simple gradient analysis.²⁵ Baty and Sharp observed good correlation between S and $\ln k'_w$ methanol, acetonitrile and THF, with structurally similar solutes.³⁶ They tried to use the slopes and y -intercepts of these plots to predict the capacity factors of the solutes but found that the slopes and y -intercepts vary with the nature of the organic modifiers and columns. Therefore, the chro-

Table 5 Regression data for plots of slopes from equation (1) vs. $\ln k'_w$ of the test solutes for all the columns

Column	Modifier	Slope	y -intercept	r^2	CI†
Zorbax ODS	ACN*	0.0835	0.525	0.894	±0.004
Zorbax C-8	ACN	0.069	0.727	0.834	±0.035
Zorbax Phenyl	ACN	0.104	0.293	0.98	±0.005
Zorbax TMS	ACN	0.110	0.349	0.982	±0.007
Zorbax Cyano	ACN	0.126	0.241	0.99	±0.005
Zorbax ODS	MeOH	0.120	0.320	0.977	±0.003
Zorbax C-8	MeOH	0.124	0.310	0.987	±0.004
Zorbax Phenyl	MeOH	0.129	0.271	0.993	±0.003
Zorbax TMS	MeOH	0.134	0.346	0.979	±0.006
Zorbax Cyano	MeOH	0.130	0.362	0.96	±0.006
B&J C-8	MeOH	0.134	0.209	0.987	±0.009
B&J C-18	MeOH	0.114	0.326	0.945	±0.012
Ultrasphere C-8	MeOH	0.122	0.307	0.99	±0.004
High density	MeOH	0.115	0.314	0.923	±0.013

*Acetonitrile

†95% confidence interval of the slopes of the regressions

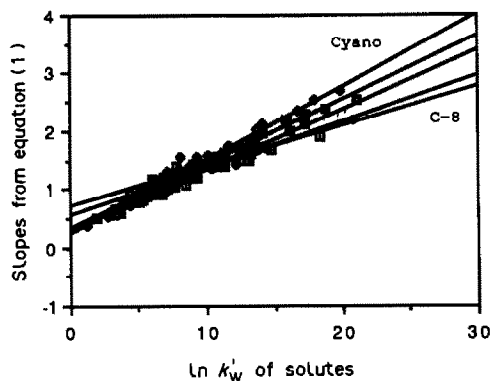


Fig 4 Slope from equation (1) vs $\ln k'_w$ for the 26 test solutes on five Zorbax columns

matographic system and the solute group have to be defined before the capacity factors can be predicted.

For a given organic modifier the general retentivity of the columns in this study is found to be inversely proportional to the slope of a plot of the slopes from equation (1) vs $\ln k'_w$. The usefulness of this relative retentivity scale can be seen by plotting the linear regressions for the five Zorbax columns with acetonitrile as modifier, on one graph, Fig. 4. The slopes from equation (1) are found to be proportional to the size of the cavity created by the solutes;⁴ therefore, at a given solute cavity size, the linear regression having the smallest slope will correspond to the largest $\ln k'_w$ and hence the largest retentivity. From the data shown in Fig. 4, the Zorbax cyano column has the largest slope, followed by the TMS column, phenyl column, ODS column and C-8 column; the retentivity of these columns is in the order C-8 > ODS > phenyl > TMS > cyano. The Zorbax C-8 column seems to have a higher retentivity than the Zorbax ODS column when acetonitrile is used as modifier. However, a careful examination of the confidence interval of these two slopes demonstrates that they actually have no statistical difference. These rankings for the Zorbax columns agree with those found by Walczak *et al.*¹⁴ and Antle *et al.*²² and lend confidence that our approach is valid. The apparently stronger retentivity of the Zorbax cyano column compared to the TMS column with methanol as modifier can be attributed to the hydrogen bonding between the surface silanol groups and the methanol. Cyano columns have been shown to have silanol groups that are more accessible than those of other columns.^{15,42} Since methanol can form hydrogen bonds with these silanol groups,

the surface of cyano columns is significantly modified by the methanol and hence its apparent retentivity is stronger than that of the TMS column. When acetonitrile is used as modifier, its lack of hydrogen-bonding ability results in the retentivity of the TMS column being greater than that of the cyano column. Other commercial columns can be tested by the same procedures and their retentivity compared with that of the Zorbax columns. With methanol as modifier, the B&J C-18 column is found to have greater retentivity than any of the Zorbax columns. The B&J C-8 column is found to have approximately the same retentivity as the Zorbax TMS column, and the Ultrasphere C-8 column is shown to have retentivity between that of the Zorbax ODS and the C-8 columns.

One interesting point raised by many researchers is the importance of the phase ratio of the column on the total retentivity of the column. The significance of the phase ratio for retentivity was also investigated in this study. There is some ambiguity in the calculation of this value. Many methods have been recommended for the measurement of the mobile phase volume.⁴³⁻⁴⁶ Here we use the *maximum* volume of mobile phase as measured by the gravimetric method.⁵ Though this volume includes any organic modifier in the solvation structure of the stationary phase, this still seems the most relevant volume, as there is no energy barrier for diffusion of a solute associated with that organic modifier in the solvation layer, back into the moving mobile phase. The stationary-phase volume was calculated by the method of Sentell and Dorsey and is the volume occupied by the bonded alkyl chains.⁴⁷ The phase ratios of the columns studied were calculated and are listed in Table 6. These values should be viewed with some caution, however, as we used the nominal values for % carbon as supplied by the manufacturer. These values had only one or two significant figures and were probably

Table 6 Phase-volume ratio of the columns in this study

Column	Phase ratio
Zorbax ODS	0.367
Zorbax C-8	0.226
Zorbax phenyl	unknown
Zorbax TMS	0.172
Zorbax cyano	unknown
B&J C-8	0.0619
B&J C-18	0.110
Ultrasphere C-8	0.380
High density	0.465

averages from several production runs. In the case of the phenyl and cyano columns, the density of the ligands was not available and the stationary-phase volume and phase ratio of these columns could not be calculated. With the exception of the two B&J columns, the phase ratio of the columns displays the same order as the relative retentivity of the columns. The high-density column, which has the largest phase ratio, is found to be close to having the highest retentivity. This result points out that the phase ratio of a column indeed makes a vital contribution to the overall retentivity of the column.

CONCLUSIONS

This work demonstrates a simple method for the classification of the retentivity or "strength" of reversed phase columns. In agreement with previous work, we have found that the phase-volume ratio is the dominant parameter in determining retentivity. Carbon content, which is the most often used figure of merit in the advertising of commercial columns, is only useful for predicting retentivity if presented along with surface area of the bare silica, or with the bonding density of the ligands. The two most useful values for the practicing chromatographer are bonding density and phase-volume ratio, and the adoption of these numbers is strongly encouraged.

Acknowledgements—The authors are grateful to NIH GM 33382 for support of this work. They also gratefully acknowledge gifts of columns from N H C Cooke, Beckman Scientific, and Paul Sadek, Burdick & Jackson, and are grateful to Pfizer, Inc., Central Research for continued funding of their research.

REFERENCES

- 1 J G Dorsey and K A Dill, *Chem. Rev.*, 1989, **89**, 331
- 2 K A Dill, *J Phys Chem.*, 1987, **91**, 1980
- 3 K A Dill, J Naghizadeh and J A Marqusee, *Ann Rev Phys Chem.*, 1988, **39**, 425
- 4 P T Ying, J G Dorsey and K A Dill, *Anal Chem.*, 1989, **61**, 2540.
- 5 K B Sentell and J G Dorsey, *ibid.*, 1989, **61**, 930
- 6 S A Tomellini, S-H Hsu, F D Fazio and R A Hartwick, *HRC CC*, 1985, **8**, 337
- 7 M L Miller, R W Linton, S G Bush and J W Jorgenson, *Anal Chem.*, 1984, **56**, 2204
- 8 M C Hennon, C Picard and M Caude, *J Chromatog.*, 1978, **166**, 21
- 9 A P Goldberg, *Anal Chem.*, 1982, **54**, 342
- 10 L C Sander and S A Wise, *HRC CC*, 1988, **11**, 383
- 11 J H Park, P W Carr, M H. Abraham, R W Taft, R M Doherty and M J. Kamlet, *Chromatographia*, 1988, **25**, 373.
- 12 J R Chrétien, B. Walczak, L M Allory, M Dreux and M Lafosse, *J Chromatog.*, 1986, **371**, 253
- 13 M F Delaney, A. N Papas and M J Walters, *ibid.*, 1987, **410**, 31
- 14 B Walczak, L M Allory, M Lafosse, M Dreux and J R Chrétien, *ibid.*, 1987, **395**, 183
- 15 W T Cooper and L.-Y Lin, *Chromatographia*, 1986, **21**, 335
- 16 F M Yamamoto, S Rokushika and H Hatano, *J Chromatog Sci.*, 1989, **27**, 704
- 17 H Engelhardt and M Jungheim, *Chromatographia*, 1990, **29**, 59
- 18 R M Smith and C M Burr, *J Chromatog.*, 1989, **475**, 57
- 19 *Idem*, *ibid.*, 1989, **475**, 75
- 20 L C Sander and S A Wise, *LG-GC*, 1990, **8**, 378
- 21 P E Antle and L R Snyder, *ibid.*, 1985, **2**, 840
- 22 P E Antle, A P Goldberg and L R Snyder, *J Chromatog.*, 1985, **321**, 1
- 23 K B Sentell, K W Barnes and J G Dorsey, *ibid.*, 1988, **455**, 95
- 24 J G Dorsey and B P Johnson, *J Liq Chromatog.*, 1987, **10**, 2695
- 25 P J Schoenmakers, H A H Billiet and L J de Galan, *J Chromatog.*, 1979, **185**, 179
- 26 B P Johnson, M G Khaledi and J G Dorsey, *Anal Chem.*, 1986, **58**, 2354
- 27 R M Smith, *J Chromatog.*, 1981, **209**, 1
- 28 K Jinno and K Kawasaki, *Chromatographia*, 1983, **17**, 337
- 29 T Hanai and J Hubert, *J Chromatog.*, 1984, **290**, 197.
- 30 M J M Wells, C R Clark and R M Patterson, *ibid.*, 1982, **235**, 61
- 31 *Idem*, *Anal Chem.*, 1986, **58**, 1625
- 32 T Braumann, *J Chromatog.*, 1986, **373**, 191
- 33 T Braumann, H Geneser, C Lüllman and B Jastorff, *Chromatographia*, 1987, **24**, 777
- 34 D J Mimick, J J Sabatka and D A Brent, *J Liq Chromatog.*, 1987, **10**, 2565
- 35 K Miyake, N Mizuno and H Terada, *J Chromatog.*, 1988, **439**, 227
- 36 J D Baty and S Sharp, *ibid.*, 1988, **437**, 13
- 37 D Reymond, G N Chung, J M Mayer and B Testa, *ibid.*, 1987, **391**, 97
- 38 P Jandera and J Kabát, *ibid.*, 1990, **500**, 281
- 39 J J Michels and J G Dorsey, *ibid.*, 1988, **457**, 85
- 40 *Idem*, *ibid.*, 1990, **499**, 435
- 41 W E Hammers, G J Meurs and C L Lingy, *ibid.*, 1982, **247**, 1
- 42 R M Smith and S L Miller, *ibid.*, 1989, **464**, 297
- 43 W R Melander, J F Erard and Cs Horváth, *ibid.*, 1983, **282**, 211
- 44 R M Smith, T G Hurdley, R Gill and A C Moffat, *ibid.*, 1986, **351**, 259
- 45 H Engelhardt, H Müller and B Dreyer, *Chromatographia*, 1984, **19**, 240
- 46 M C Hennon and R Rosset, *ibid.*, 1988, **25**, 43
- 47 K B Sentell and J G Dorsey, *J Liq Chromatog.*, 1988, **11**, 1875

DETERMINATION OF AMINOSACCHARIDES BY HIGH-PERFORMANCE ANION-EXCHANGE CHROMATOGRAPHY WITH PULSED AMPEROMETRIC DETECTION

DEAN A. MARTENS and WILLIAM T. FRANKENBERGER, JR

Department of Soil and Environmental Sciences, University of California, Riverside, CA 92521, U S A

(Received 6 June 1990 Revised 14 August 1990 Accepted 18 August 1990)

Summary—High-performance anion-exchange chromatography (HPAC) was used for the determination of aminosaccharides in microbial polymers, chitin, animal waste, sewage sludge, plant residues and soil. The aminosaccharides, galactosamine, mannosamine and glucosamine were separated on a strong anion-exchange column with 10mM sodium hydroxide as the eluent and determined by pulsed amperometric detection (PAD). The HPAC-PAD methodology was compared with high-performance liquid chromatography (HPLC) with refractive index detection (RI) in terms of selectivity and sensitivity for aminosaccharides. The results indicate that HPAC-PAD required less sample preparation, and was more precise and nearly two orders of magnitude more sensitive than HPLC-RI. HPAC-PAD was not subject to matrix interferences and was highly selective for aminosaccharides. More than 3% of the total nitrogen in alfalfa, and 20% of that in straw, was found to be present as aminosaccharides.

Aminosaccharides are widely distributed in nature and have been reported to occur in plants,¹ micro-organisms,² and crustaceans,³ and have recently been found to be an important constituent of the soil nitrogen pool.⁴ They not only serve as a nitrogen source for plant growth, but may also have an important role in the promotion of good soil structure.⁵

It is believed that 5–10% of the total nitrogen in surface soils is present as aminosaccharides.⁴ Chitin is a polymer of *N*-acetylglucosamine frequently found in soil, and is present in the cell walls, structural membranes and skeletal components of insects and fungal mycelia.⁵ Conditions which favor microbial growth and proliferation in soils tend to increase the hexosamine content of soils. Aminosaccharides are somehow protected from decomposition in soils by being incorporated into the humic acid fraction.^{6,7}

Aminosaccharides in soils are normally extracted by hydrolysis with hydrochloric acid and the resulting ammonium ion is determined by the standard colorimetric method of Elson and Morgan⁸ or by alkaline distillation. The Elson and Morgan method is based on the chromogen formed when the aminosaccharide is heated with an alkaline solution of acetylacetone and then an acidic ethanolic solution of *p*-dimethylaminobenzaldehyde. However, many sub-

stances in soils, including iron and amino acids, produce colors which interfere with this determination of aminosaccharides. The alkaline distillation method involves deamination of aminosaccharides by heating with an alkali. The ammonia released through deamination is then determined by steam distillation, collection in boric acid solution,⁹ and titration.

Aminosaccharides have been isolated from soil hydrolysates by both paper chromatography and ion-exchange chromatography. Previous studies have indicated that most of the aminosaccharides occur as D-glucosamine and D-galactosamine, with the former occurring in the greatest amounts.⁵ *N*-Acetylglucosamine has also been found in soils.¹⁰

High-performance liquid chromatography (HPLC) analysis with refractive index (RI) detection is the most common method for quantification of saccharides but has lagged behind in the determination of aminosaccharides because of poor selectivity of the existing stationary phases and insensitivity of the RI detector. The use of high-performance anion-exchange chromatography (HPAC) with pulsed amperometric detection (PAD) has several advantages over RI detection. PAD with a gold electrode is selective only for compounds containing oxidizable functional groups, including hydroxyl, amine and sulfide. Aminosaccharides

are weak acids with pK_a values in the range 9–11 and thus can be separated as anions by control of the pH of the mobile phase.

The objective of this study was to optimize the chromatography in the determination of aminosaccharides in biological materials and to compare HPAC–PAD with HPLC–RI for quantification of aminosaccharides. Chromatographic parameters such as selectivity, resolution and precision were determined for various aminosaccharides to optimize separation and detection.

EXPERIMENTAL

Reagents

All saccharide standards were obtained from Supelco (Bellefonte, PA). Chitin was obtained from Sigma (St. Louis, MO).

Chromatographic instrumentation

HPAC–PAD detection. The HPAC–PAD analysis was performed with a Dionex (Sunnyvale, CA) LC gradient pump module and Model PAD2 detector. Sample injection was by a Dionex autosampler equipped with a 200- μ l sample loop. Aminosaccharides were separated with a CarboPac PA1 pellicular anion-exchange resin (250 \times 4 mm) and a CarboPac PA guard column (25 \times 3 mm) at a flow-rate of 0.8 ml/min at ambient temperature with a 5–200mM sodium hydroxide gradient system. The aminosaccharides were eluted isocratically with 5mM sodium hydroxide for 15 min, then the eluent concentration was ramped to 200mM in 5 min, and then maintained at this level for a further 5 min. With the instrumentation used, this was achieved with three solutions: A was 18-M Ω water filtered through a 0.22- μ m membrane, B was 100mM sodium hydroxide and C 200mM sodium hydroxide. These were combined in the following proportions.

	0–15 min	15–20 min	20–25 min
A, %	95	95 \rightarrow 0	0
B, %	5	5 \rightarrow 0	0
C, %	0	0 \rightarrow 100	100

The 200mM sodium hydroxide was used to elute interfering species that may act as displacing ions and shorten the retention times in subsequent runs. The mobile phase was degassed to prevent sorption of carbon dioxide and subsequent production of carbonate which would act as a displacing ion and shorten retention times. Sodium hydroxide (300mM) was used as

a post-column addition to reduce baseline shifts that occur with the 5–200mM sodium hydroxide gradient and also to increase the PAD sensitivity. Detection was by triple-pulsed amperometry with a gold working electrode.¹¹ The following working pulse potentials and durations were used for detection of aminosaccharides: $E_1 = 0.05$ V ($t_1 = 720$ msec); $E_2 = 0.60$ V ($t_2 = 120$ msec); $E_3 = -0.60$ V ($t_3 = 120$ msec). The CHOH groups are oxidized at E_1 , E_2 removes the reaction products and E_3 cleans the electrode. Cyclic voltammetry was used in selection of the three potentials. The response time of the PAD was set to 1 sec. Chromatographic data were collected and plotted with the Dionex AutoIon 300 software.

HPLC–RI. The HPLC–RI analysis was performed with a Beckman (Fullerton, CA) System Gold™ liquid chromatograph equipped with a Beckman 110B solvent pump and a Rheodyne Model 7000 sample injector (Berkeley, CA) fitted with a 20- μ l stainless-steel injection loop. The system was composed of the following: a Vydac (Separations Group, Hesperia, CA), 1630 anion-exchange column (250 \times 4.1 mm i.d.), a Bio-rad (Richmond, CA) carbohydrate microguard column (30 \times 4.6 mm), a Beckman μ -Spherogel 300 \times 7.5 mm carbohydrate column (300 \times 7.5 mm i.d.), an Eldex Model III (Menlo Park, CA) thermostatic column heater, an Altex (Fullerton, CA) 156 refractive index detector, and a Hewlett–Packard Model 3390A printer–plotter integrator with variable input voltage. The mobile phase was HPLC-grade water (heated to 85°) at a flow-rate of 0.5 ml/min.

Gas chromatography

Samples were reduced and the acetylated derivatives analyzed by gas chromatography¹ with a Hewlett–Packard 5890A gas chromatograph with a flame-ionization detector. The column used was a 0.2-mm i.d. Chrom Q fused silica capillary column (Alltech, Deerfield, IL). The operating conditions with helium as a carrier gas were injection temperature, 250°; detector temperature, 250° and column temperature, 210°; gas flow, 20.0 ml/min.

Soil treatment

Field plots (2 m \times 2 m) were established by incorporating 25 metric tons per hectare levels of straw (*Hordeum vulgare*) [carbon/nitrogen ratio (C/N), 48.0], poultry manure (C/N, 5.0), sewage sludge (C/N, 5.0) (Riverside, CA), and

alfalfa (*Medicago sativa*) (C/N, 7.0) into an Arlington soil (coarse-loamy Haplic Durixeralf) (pH 7.9; C/N, 12.0) at the Citrus Field Station of the University of California, Riverside. The additives were mixed into the upper 15 cm of soil and irrigated (12 cm water/day) once a week for three months. Field-moist soil samples were sieved through a 1-mm mesh sieve to remove large organic debris. The carbon content was determined by a modified Mebius method¹² and the nitrogen content by a micro-Kjeldahl method.¹³

Isolation of bacterial polymers

The bacterial polymers were isolated as described by Anderson *et al.*¹⁴ and Martin and Richards.¹⁵

Aminosaccharide extraction

Samples (1 g) of air-dried soil, 0.5-g samples of sewage sludge and poultry manure, 0.3-g samples of straw and alfalfa, 0.1 g of chitin, and 1 mg of bacterial polymer carbon [*Chromobacterium violaceum*, American Type Culture Collection (ATCC) 9544 and *Hansenula holstii*, ATCC 2448] were treated with 1.25 ml of 12*N* sulfuric acid for 2 hr at room temperature, then after addition of 1.25 ml of water (to give 6*N* sulfuric acid) were heated at 90° under a reflux condenser for 16 hr.⁴ The mixtures were cooled, then treated with 4–5 ml of water and 1 ml of 0.1*M* EDTA, titrated to pH 4 with 5*M* potassium hydroxide, and centrifuged at 10⁴ rpm. The supernatant solution was diluted to 12 ml.

Purification of acidic extracts

A 1-ml aliquot of acid extract of organic additive, microbial polymer or soil was diluted to 5 ml with water and passed through a Supelco™ strong-acid cation-exchanger (3-propylsulfonic acid, H⁺ form) 3-ml solid-phase extraction column (SCX) (Bellefonte, PA). The SCX column was then rinsed with 3 ml of water to elute all non-retained compounds. The aminosaccharides were eluted with 5 ml of 0.3*M* hydrochloric acid. Quantification by HPLC–RI required further purification of the extracts. An aliquot to be analyzed by HPLC–RI and containing 10–25 mg of aminosaccharides was applied to a column of Bio-Gel™ P-2 (100–200 mesh, 12 × 2.8 cm; Bio-Rad, Richmond, CA). The aminosaccharides were eluted with water.

All samples were filtered through GS 0.22- μ m filters (Millipore, Bedford, MA) before analysis.

RESULTS AND DISCUSSION

Extraction

Numerous reports have shown that aminosaccharides can be extracted from biological materials by treatment with hot mineral acids,^{1,4,16} but the use of these acids at 6*N* concentration results in a high salt concentration in the extracts. The high levels of salts and other possible interference present in the 6*N* acid extracts cause few difficulties for the HPAC–PAD analysis, because of the high level of sodium hydroxide (300*mM*) used as a post column treatment. On the other hand, the HPLC–RI method is subject to many interferences in the analysis of plant and soil extracts. The non-saccharide impurities were selectively removed from the extracts. EDTA (disodium salt) was added before neutralization to prevent co-precipitation of the bi- and trivalent cations with the saccharides extracted. Strong-acid cation-exchange columns were used to retain the aminosaccharides, and elution with water removed most of the impurities. Tests conducted with the SCX resins and the aminosaccharide standards galactosamine, mannosamine, glucosamine, acetyl-D-galactosamine, acetyl-D-glucosamine and acetyl-D-mannosamine showed 98–100% recovery. Acid extracts analyzed by HPLC–RI required an additional pretreatment with the Bio-Rad P-2 gel for removal of salts and other neutral low molecular-weight compounds. Tests conducted with the same aminosaccharide standards showed 100% recovery with the gel. HPAC–PAD required only the treatment with SCX resin before the analysis. Neutral (non-ionic) and basic compounds were eluted in the void volume during the HPAC–PAD analysis.

Liquid chromatographic analyses

The chromatographic characteristics, including t_R , k' and number of theoretical plates are listed in Table 1. The retention times of selected aminosaccharides detected by HPLC–RI indicate co-elution problems with galactosamine, mannosamine and glucosamine (6.30–6.50 min) and *N,N'*-diacetylchitobiose, acetylgalactosamine, acetylmannosamine and acetylglucosamine (10.60–10.72 min). Chromatograms of a mixture of 7 aminosaccharides analyzed by HPLC–RI and HPAC–PAD are shown in Figs. 1 and 2, respectively. All 7 aminosaccharides were detected by HPAC–PAD, but only 3 peaks were evident with HPLC–RI. 2-Deoxy-

Table 1 Chromatographic characteristics in detection of aminosaccharides by HPAC-PAD and HPLC-RI*

Aminosaccharide	HPAC-PAD			HPLC-RI		
	t_R , min	k' †	N ‡	t_R , min	k' †	N ‡
D-Galactosamine	11.24	4.50	3300	6.45	1.1	1160
D-Mannosamine	12.44	5.20	2800	6.50	1.1	2601
D-Glucosamine	13.69	5.50	3100	6.30	1.1	2804
<i>N,N'</i> -Diacetylchitobiose	15.01	6.30	5500	10.60	2.6	2978
Acetyl-D-galactosamine	17.65	6.80	5800	10.68	2.6	2873
Acetyl-D-mannosamine	18.67	6.85	6200	10.72	2.7	2468
Acetyl-D-glucosamine	19.90	7.05	6600	10.63	2.6	2970

*HPAC-PAD; CarboPac PA1 (250 × 4.6 mm); eluent, 5mM NaOH for 15 min then ramped to 200mM NaOH in 5 min

HPLC-RI column, Beckman μ -Spherogel (300 × 7.5 mm), eluent, HPLC grade H₂O (85°).

† $k' = (t_R - t_M)/t_M$, where t_R = retention time of solute and t_M = retention time of solvent front

‡ N , number of theoretical plates = $16[t_R/W]^2$ where t_R is the retention time and W the peak width

ribose was used as an internal standard for both analyses. The time of analysis for detection of all 7 solutes by HPAC-PAD was < 20 min.

Column efficiency, expressed as number of theoretical plates (N), ranged from 2800 (D-mannosamine) to 6600 (acetyl-D-glucosamine) for the HPAC-PAD analysis and 1160 (D-galactosamine) to 2978 (*N,N'*-diacetylchitobiose) for the HPLC-RI analysis (Table 1). When the N values were pooled and averaged for all the solutes, the mean N was 4757 for HPAC-PAD and 2550 for HPLC-RI, indicating that the HPAC-PAD analysis was almost twice as efficient for separation of the aminosaccharides.

The precisions and limits of detection (LODs) for HPAC-PAD and HPLC-RI quantification of the selected saccharides are given in Table 2. Precision was determined from the results of ten

200- μ l (HPAC-PAD) or 20- μ l (HPLC-RI) injections of combined standards at 1 mg/l. level for HPAC-PAD and 20 mg/l. for HPLC-RI. The relative standard deviations for detection of various saccharides ranged from 0.1 to 0.25% (HPAC-PAD) and from 0.5 to 0.9% (HPLC-RI). The LODs were examined by spiking extracts with a known amount of the saccharide to be determined. The results show that the LODs for the saccharides tested ranged from 0.15 to 0.35 mg/l. with HPAC-PAD (200- μ l injection), and 30 to 50 mg/l. with HPLC-RI (20- μ l injection), based on a 3-fold signal-to-noise ratio for the baseline ($S/N = 3$). The HPAC-PAD response was linear from the LOD to 5 mg/l. Samples were diluted when necessary. HPAC-PAD gave detection limits nearly two orders of magnitude lower than those given by HPLC-RI. Increasing the injection size beyond 20 μ l in the HPLC-RI analysis

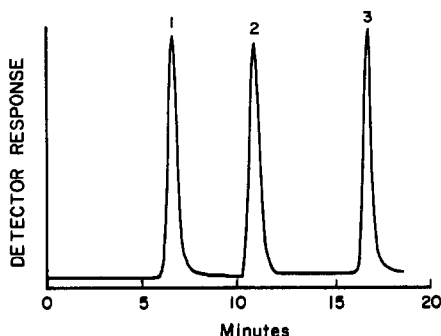


Fig 1 Chromatogram of aminosaccharides detected by HPLC-RI [1 = galactosamine, glucosamine and mannosamine, 2 = *N,N'*-acetylchitobiose, acetylgalactosamine, acetylmannosamine, and acetylglucosamine, 3 = 2-deoxyribose (internal standard)].

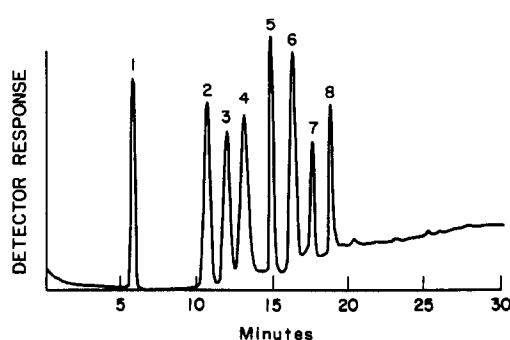


Fig 2 Chromatogram of aminosaccharides detected by HPAC-PAD [1 = 2-deoxyribose (internal standard); 2 = galactosamine, 3 = mannosamine, 4 = glucosamine; 5 = *N,N'*-diacetylchitobiose, 6 = acetylgalactosamine, 7 = acetylmannosamine; 8 = acetylglucosamine].

Table 2 Precision and detection limits of HPAC-PAD and HPLC-RI analyses for selected aminosaccharides*

Aminosaccharide	Relative standard deviation, %†		Detection limit, mg/l.‡	
	HPAC-PAD	HPLC-RI	HPAC-PAD	HPLC-RI
D-Galactosamine	0.15	0.90	0.15	50
D-Mannosamine	0.15	0.70	0.15	50
D-Glucosamine	0.10	0.90	0.20	50
<i>N,N'</i> -Diacetylchitobiose	0.15	0.50	0.35	30
Acetyl-D-galactosamine	0.25	0.60	0.20	35
Acetyl-D-mannosamine	0.20	0.50	0.25	30
Acetyl-D-glucosamine	0.25	0.50	0.30	30

*HPAC-PAD: CarboPac PA1 (250 × 4.6 mm), eluent, 5mM NaOH for 15 min, then ramped to 200mM NaOH in 5 min. HPLC-RI: column, Beckman μ -Spherogel (300 × 7.5 mm); eluent, HPLC grade H₂O (85°)

†Based on ten injections of a standard, concentration 1 mg/l (HPAC-PAD) and 20 mg/l (HPLC-RI).

‡Assumed to be three times the signal-to-noise ratio at the baseline ($S/N = 3$).

resulted in decreased resolution, owing to increased peak distortion and overlap.

Table 3 shows the resolution (R_s) of selected aminosaccharides detected by HPAC-PAD and HPLC-RI. Overall, HPAC-PAD provided much better separation, with R_s values ranging from 1.05 to 6.10, indicating >96% resolution of Gaussian peaks.¹⁷

Detection of aminosaccharides in chitin, plants and soil

Acetyl-D-glucosamine is a major constituent in the hard shells of crustaceans. Crab shell chitin was used to evaluate the hydrolysis procedure, preliminary purification, and detection of aminosaccharides by HPAC-PAD. Figure 3 is a chromatogram showing the detection of D-glucosamine and acetylglucosamine in a 6N sulfuric acid extract of crab shell chitin. Approximately 65% of the chitin sample solubilized by 6N sulfuric acid was recovered as glucosamine and acetylglucosamine.

Figure 4 shows the HPAC-PAD chromatograms of sulfuric acid extracts of alfalfa,

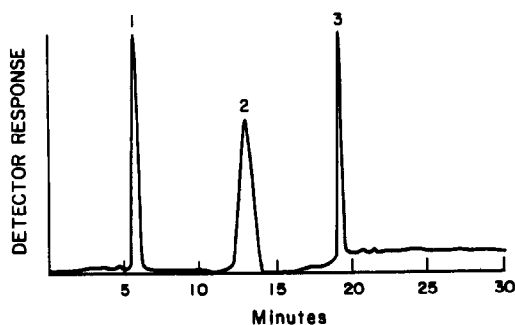


Fig 3 HPAC-PAD chromatogram of an acidic extract of chitin. Chromatographic conditions as described in Table 1 [1 = 2-deoxyribose (internal standard), 2 = glucosamine; 3 = acetylglucosamine]

soil amended with alfalfa (after three months of decomposition), and an unamended soil. In the alfalfa and alfalfa-amended soil, higher levels of galactosamine, mannosamine, glucosamine, *N,N'*-diacetylchitobiose, acetylglucosamine and acetylmannosamine were detected than in the unamended soil. Gas chromatographic analysis confirmed the

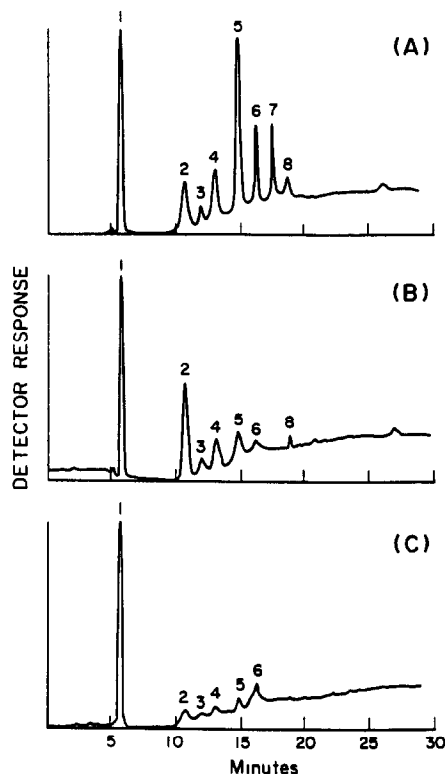


Fig. 4. HPAC-PAD chromatograms of the acidic extracts of (A) alfalfa, (B) alfalfa-amended soil after three months, (C) unamended soil. Chromatographic conditions as described in Table 1 [1 = 2-deoxyribose (internal standard); 2 = galactosamine, 3 = mannosamine; 4 = glucosamine; 5 = *N,N'*-diacetylchitobiose; 6 = acetylglucosamine; 7 = acetylmannosamine, 8 = acetylglucosamine]

Table 3 Resolution (R_s)* of aminosaccharides detected in acid extract† by HPAC-PAD and HPLC-RI

	D- Galactosamine	D- Mannosamine	D- Glucosamine	N,N'-Diacetyl- chitobiose	Acetyl-D- galactosamine	Acetyl-D- mannosamine	Acetyl-D- glucosamine
D-Galactosamine	—	1.30 (0.01)†	2.96 (0.01)	4.33 (3.61)	5.20 (3.60)	5.50 (3.60)	6.10 (3.60)
D-Mannosamine	—	—	1.46 (0.01)	3.00 (3.60)	4.42 (3.60)	5.16 (3.60)	5.72 (3.60)
D-Glucosamine	—	—	—	1.57 (3.60)	3.81 (3.60)	4.52 (3.60)	4.80 (3.60)
N,N'-Diacetylchitobiose	—	—	—	—	1.20 (0.01)	2.00 (0.01)	2.40 (0.01)
Acetyl-D-galactosamine	—	—	—	—	—	1.25 (0.01)	1.80 (0.01)
Acetyl-D-mannosamine	—	—	—	—	—	—	1.05 (0.01)
Acetyl-D-glucosamine	—	—	—	—	—	—	—

* $R_s = 2(\{t_R\}_y - \{t_R\}_x) / (W_x + W_y)$, where x and y denote two solutes and W is the width of the peak at baseline, expressed in time units

†HPAC-PAD column, CarboPac PA1 (250 × 4.5 mm), eluant 5% 100mM NaOH for 15 min, then ramped to 200mM in 5 min, detection pulsed amperometric detection HPLC-RI column, Beckman μ -Spherogel carbohydrate (300 × 7.5 mm), eluant HPLC grade water (85°C), detection refractive index

‡The values in parentheses indicate R_s values for HPLC-RI detection

Table 4 Composition and quantity (mg/kg) of aminosaccharides extracted from chitin, organic amendments, organic-amended soil and microbial polymers

Aminosaccharide	Chitin	Poultry manure (PM)	PM-treated soil		Sewage sludge (SS)		SS-treated soil		Straw (ST)		ST-treated soil		Alfalfa (AL)		AL-treated soil		Check soil		Chromo-bacterium violaceum		Hansenula holstii		
			soil	soil	soil	soil	soil	soil	soil	soil	soil	soil	soil	soil	soil	soil	soil	soil	soil	soil	soil	soil	soil
Galactosamine	ND*	49	4	188	5	141 × 10 ³	5	183 × 10 ³	5	13	1	2.06 × 10 ⁴	1	2.06 × 10 ⁴	1	2.06 × 10 ⁴	1	2.06 × 10 ⁴	1	2.06 × 10 ⁴	1	2.06 × 10 ⁴	ND*
Mannosamine	ND	39	3	90	3	230	3	685	3	2	<1	7.02 × 10 ³	2	7.02 × 10 ³	2	7.02 × 10 ³	2	7.02 × 10 ³	2	7.02 × 10 ³	2	7.02 × 10 ³	ND
Glucosamine	7.15 × 10 ⁴	38	4	115	5	905	5	1.21 × 10 ³	5	34	2	8.63 × 10 ³	5	8.63 × 10 ³	5	8.63 × 10 ³	5	8.63 × 10 ³	5	8.63 × 10 ³	5	8.63 × 10 ³	ND
N,N'-Diacetylchitobiose	ND	187	6	84	3	1.31 × 10 ⁴	3	6.04 × 10 ³	4	5	1	1.27 × 10 ⁴	5	1.27 × 10 ⁴	5	1.27 × 10 ⁴	5	1.27 × 10 ⁴	5	1.27 × 10 ⁴	5	1.27 × 10 ⁴	1.09 × 10 ³
Acetylgalactosamine	ND	18	<1	35	1	149	1	245	13	1	1	2.38 × 10 ³	1	2.38 × 10 ³	1	2.38 × 10 ³	1	2.38 × 10 ³	1	2.38 × 10 ³	1	2.38 × 10 ³	ND
Acetylmannosamine	ND	67	2	73	3	390	3	1.57 × 10 ³	3	0	1	1.96 × 10 ⁴	0	1.96 × 10 ⁴	0	1.96 × 10 ⁴	0	1.96 × 10 ⁴	0	1.96 × 10 ⁴	0	1.96 × 10 ⁴	ND
Acetylglucosamine	1.21 × 10 ⁵	60	3	59	2	968	2	1.95 × 10 ³	3	1	<1	1.23 × 10 ⁴	1	1.23 × 10 ⁴	1	1.23 × 10 ⁴	1	1.23 × 10 ⁴	1	1.23 × 10 ⁴	1	1.23 × 10 ⁴	ND
Total	1.93 × 10 ⁵	458	23	644	22	1.72 × 10 ⁴	22	1.35 × 10 ⁴	36	56	7	8.33 × 10 ⁴	56	8.33 × 10 ⁴	56	8.33 × 10 ⁴	56	8.33 × 10 ⁴	56	8.33 × 10 ⁴	56	8.33 × 10 ⁴	1.09 × 10 ³

*ND, not detected

detection of glucosamine, galactosamine and mannosamine. The concentration of glucosamine detected in the organic-amended soils was comparable with the values obtained in GC analysis of soils by Benzing-Purdie,¹ although the GC analyses did not detect acetyl-aminosaccharides present in the samples. The concentration of the total aminosaccharides directly extracted from the animal wastes and plant residues ranged from 0.46 g/kg (poultry manure) through 0.64 g/kg (sewage sludge) and 13.5 g/kg (alfalfa), to 17.2 g/kg for straw (Table 4). Glucosamine was the predominant aminosaccharide in the plant materials. Previous work suggested that aminosaccharides in soil were of microbial origin and not from plant additions.^{1,18} However, this study indicates that animal and plant residues may make an important contribution to the aminosaccharide pool in soil. The results also indicate that about 3.7% of the total nitrogen in alfalfa and about 20% of that in straw was present as aminosaccharides. The *Chromobacterium violaceum* polymer contained about 8% aminosaccharides, mainly galactosamine, acetylmannosamine, *N,N'*-diacetylchitobiose and acetylglucosamine whereas, the *Hansenula holstii* polymer contained only a low amount of *N,N'*-diacetylchitobiose (Table 4). Upon decomposition of plant residues in soil, aminosugars released may provide energy for the soil organisms or be complexed in the organic matter fraction.^{7,19}

CONCLUSIONS

The HPAC-PAD work described for quantification of aminosaccharides allows separation and analysis of a complex mixture of aminosaccharides in plant materials, chitin and soil. This study shows that minimal sample preparation is needed for HPAC-PAD. The

combination of an anion-exchange column with triple-pulse amperometric detection and SCX purification results in high selectivity for aminosaccharides. HPAC-PAD is much more rapid, precise, sensitive and selective than HPLC-RI for the determination of aminosaccharides.

REFERENCES

- 1 L. Benzing-Purdie, *Soil Sci Soc Am J*, 1981, **45**, 66.
- 2 H. R. Perkins, *Bact Rev*, 1963, **27**, 18
- 3 G. Ledderhose, *Ber*, 1876, **9**, 1200
- 4 J. M. Bremner and K. Shaw, *J Agr Sci*, 1954, **44**, 152
- 5 F. J. Stevenson (ed), *Nitrogen in Agricultural Soils*, p 67 Am Soc. Agron., Madison, WI, 1982
- 6 J. N. Ladd and R. B. Jackson, in *Nitrogen in Agricultural Soils*, F. J. Stevenson (ed), p 173 Am Soc Agron, Madison, WI, 1982
- 7 E. Bondietti, J. P. Martin and K. Haider, *Soil Sci Soc Am Proc*, 1972, **36**, 597.
- 8 L. A. Elson and W. T. J. Morgan, *Biochem J*, 1933, **27**, 1824
- 9 J. M. Bremner, in *Methods of Soil Analysis*, C. A. Black (ed), 1st Ed., Part 2, p. 1148 Am Soc Agron, Madison, WI, 1965
- 10 J. Skujins and A. Pukite, *Soil Sci Biochem*, 1970, **2**, 141
- 11 S. Hughes and D. C. Johnson, *Anal Chim Acta*, 1981, **132**, 11
- 12 D. W. Nelson and L. E. Sommers, in *Methods of Soil Analysis*, A. L. Page, R. H. Miller and D. R. Keeney (eds), 2nd Ed., p 539 Am Soc Agron, Madison, WI, 1982
- 13 J. M. Bremner and C. S. Mulvaney, in *Methods of Soil Analysis*, A. L. Page, R. H. Miller and D. R. Keeney (eds), 2nd Ed., p 610 Am Soc Agron, Madison, WI, 1982
- 14 R. F. Anderson, M. C. Cadmus, R. G. Benedict and M. E. Slodki, *Arch Biochem Biophys*, 1960, **89**, 289
- 15 J. P. Martin and S. J. Richards, *J Bacter*, 1963, **85**, 1288
- 16 J. M. Bremner, *J Sci Food Agr.*, 1958, **9**, 528.
- 17 D. A. Skoog, *Principles of Instrumental Analysis*, 3rd Ed., Saunders College Publ, Philadelphia, 1985
- 18 F. J. Stevenson, *Soil Sci*, 1957, **2**, 99.
- 19 L. Benzing-Purdie, *Soil Sci Soc Am J*, 1984, **48**, 219

DETERMINATION OF METAL IONS BY LIQUID CHROMATOGRAPHIC SEPARATION OF THEIR 2-ACETILPYRIDINE-4-ETHYL-3-THIOSEMICARBAZONE CHELATES

MARK V. MAIN and JAMES S. FRITZ*

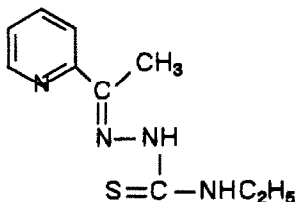
Ames Laboratory and Department of Chemistry, Iowa State University, Ames, IA 50011, U S A

(Received 15 June 1990 Revised 27 July 1990 Accepted 1 August 1990)

Summary—A new thiosemicarbazone was prepared, characterized, and used as a complexing reagent for the chromatographic separation and determination of metal complexes by reverse-phase HPLC. The reagent was sufficiently soluble in methanol-water solutions for metal ions to be complexed in this aqueous organic phase, without need for extraction. Many variables affected the retention times of the metal complexes. Several metals were determined selectively by complexation with the reagent and chromatographic separation of the complexes. Interference effects from other metal ions were also investigated.

Determination of several metal ions in the same test sample is often made possible by adding a complexing agent to the sample and then separating the various metal complexes by liquid chromatography. Several review articles have appeared on this approach.¹⁻⁶ It is most convenient to use reagents that form complexes which are water-soluble but are easily separated from each other by liquid chromatography, such as β -diketones,⁷ methylhydroxamic acids,⁸ and bis-hydrazones of 2,6-diacetylpyridine.^{9,10}

In the present work, 2-acetylpyridine-4-ethyl-3-thiosemicarbazone (abbreviated to Hapet) is used for the determination of metal ions through chromatographic separation of their metal complexes.



Hapet

Thiosemicarbazones derived from 2-formyl- and 2-acetylpyridine have proved useful for chelation of various metal ions both for medicinal use¹¹⁻¹⁶ and analytical application.¹⁷⁻²² However, no chromatographic separation of

metal complexes of this type has yet been proposed for the determination of metal ions.

EXPERIMENTAL

Synthesis and characterization of Hapet

To a 100-ml round-bottomed flask were added 0.027 mole of 2-acetylpyridine (Aldrich) and 0.027 mole of 4-ethyl-3-semicarbazide (Aldrich) in approximately 45 ml of absolute ethanol. The mixture was refluxed for 3 hr and after the reaction mixture had cooled, 25 ml of water were added and approximately 45 ml of the ethanol/water solvent was removed under vacuum, with the temperature kept below 35° at all times. The product, 2-acetylpyridine-4-ethyl-3-thiosemicarbazone, was then collected and washed with 10 ml of a 1:1 v/v mixture of methanol and water. The product, which had a very detectable odor, probably due to the presence of excess of 2-acetylpyridine, was recrystallized from 3:2 v/v methanol-water mixture, yielding white needle-shaped crystals.

The following procedures were used to characterize the product. The infrared spectrum was taken with an IBM IR/98 instrument (KBr pellet). The NMR spectrum was obtained on a Nicolet NT-300 with CDCl₃ as the solvent and TMS as the chemical shift standard. The mass spectrum of the sample was obtained with a Kratos MS-50. Elemental analysis of the crystals gave 54.0% C, 6.4% H, 25.2% N, and 14.7% S; C₁₀H₁₄N₄S requires 54.03% C, 6.35% H, 25.20% N, and 14.42% S.

*Author for correspondence

Liquid chromatography studies

The chromatographic system consisted of an LKB 2156 solvent conditioner, an LKB 2249 HPLC gradient pump (mixing chamber volume 0.5 ml), a Rheodyne 7125 injector (20- μ l injection loop) and a Kratos Spectroflow 783 UV-VIS detector. Critical parts of the pump and injector were made of titanium. The column was a PLRP-S 100-Å, 5- μ m polystyrene-divinylbenzene (15 cm \times 4.6 mm) column from Polymer Laboratories.

Eluents were prepared daily by dissolving the components in mixtures of specified volumes of Fisher HPLC grade acetonitrile and tetrahydrofuran and water purified with a Barnstead Nanopure II system. No corrections were made for non-additivity of volume. Acids, bases and ion-pairing salts were all reagent grade or better. All eluents were prepared with aqueous buffers. Possible changes in apparent pH were ignored, except in the study of the effect of eluent pH on retention times of the metal complexes. Most eluents contained $5 \times 10^{-4}M$ Hapet, 25 mM sodium perchlorate, and 21 mM ammonium acetate (pH = 7), unless stated otherwise. Eluent components were mixed and then filtered with 0.2- μ m Nylon 66 (Rainin) filters before use. The flow-rate was 1.0 ml/min

Preparation of solutions

Stock solutions of the metals were prepared from appropriate salts (chloride, sulfate, nitrate and perchlorate). The gallium solution was a commercial standard purchased from Aldrich.

The UV-VIS spectra of Hapet and its gallium complex in 20 mM formate buffer (pH 4.0) were taken, with the buffer as reference. The Hapet

concentration was 40 μ M, and that of the gallium complex was 10 μ M.

Chromatographic samples were prepared by taking an aliquot of stock metal solution and adding enough Hapet to give a final concentration of 1–3 mM. Metal complexes were formed by adding excess of reagent to a somewhat acidic sample and then adjusting the pH. All sample solutions were buffered at the pH of the eluent, and all adjustments in pH were made with sodium hydroxide solution. The samples for the interference studies were prepared in the same way except that the final Hapet concentration was held constant at 3mM. Analyte and interferent metals were both present before addition of the reagent. Analytes were held constant at $1 \times 10^{-4}M$ concentration throughout the interference study (except for gallium, which was $5 \times 10^{-2}M$). The interference study was conducted with an eluent composed of 60% CH₃CN, 40% H₂O, 25 mM NaClO₄, 0.5 mM Hapet, and 12 mM formate (pH = 4.0).

Hapet is moderately soluble in methanol at room temperature. It is possible to prepare a 5 mM stock solution of the reagent in methanol and dilute it with water to 1 mM Hapet, without precipitation of the reagent. The physical characteristics of Hapet are given in Table 1.

RESULTS AND DISCUSSION

Hapet is similar in chemical structure to the bis-hydrazones of 2,6-diacetylpyridine previously used for chromatographic separation of metal ions.^{9,10} However, replacement of the carbonyl groups in the latter reagent by the thiocarbonyl group in Hapet would be expected to

Table 1 Characterization of Hapet

Melting point, °C	IR maxima, cm ⁻¹	Major mass spectral lines		Proton shift of NMR	
		m/z	Relative intensity	ppm	Integral
127–8	696	222 1	78	8 72	0 36
	756	207 1	8	8 61–8 59	0 36
	906	144 1	9	7 97–7 9	0 38
	1028	134 1	20	7 75–7 6	0 41
	1068	121.1	100	7 32–7 2	0 43
	1373	106 1	28	3 82–3 7	0 63
	1452	79 0	36	2 4	0 88
	1493	78 0	31	2 0	0 09
	1601	60 0	13	1 36–1 3	1
	2850				
	2920				
	3028				
	3061				
	3082				

result in increased complexation of metal ions having an affinity for sulfur, and decreased complexation of metal ions that prefer oxygen. A preliminary survey based on spectral evidence indicated that many metal ions form complexes with Hapet, including (a) Hg^{2+} , Pb^{2+} , Cu^{2+} , Bi^{3+} and several platinum-group metal ions, and (b) Co^{2+} , Ni^{2+} , Zn^{2+} , Cd^{2+} , Fe^{3+} , Ga^{3+} and In^{3+} . Good chromatographic separations were obtained for the group (b) Hapet complexes, but the group (a) complexes produced either chromatographic peaks that were too broad to be useful, or none at all.

Both Hapet and its metal ion complexes are soluble in water containing some methanol or acetonitrile. The metal complexes can be separated on polymeric LC columns and detected spectrophotometrically

Conditions for detection

Hapet and its metal complexes absorb in the ultraviolet region. Most of the complexes also absorb in the visible region and are yellow. The spectra of Hapet and the gallium(III) complex at pH 4 are shown in Fig. 1. Most of the other metal complexes gave spectra similar to the spectrum of the gallium(III) chelate. A bathochromic shift is observed on changing from pH 7 to pH 3.3 or 4.0. Detection wavelengths of 380 and 405 nm for chromatographic separations performed at pH 7 and 4, respectively, were chosen so as to maximize the absorbance of the metal complexes relative to that of the free reagent.

The molar absorptivities of most of the metal complexes at 380 nm were about 10^4

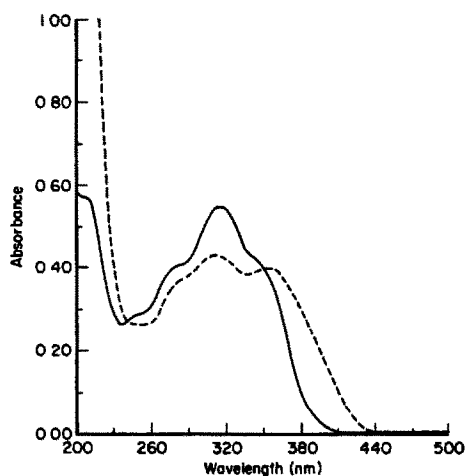


Fig 1 Absorbance spectra of Hapet (—) and gallium complex (---) at pH 4

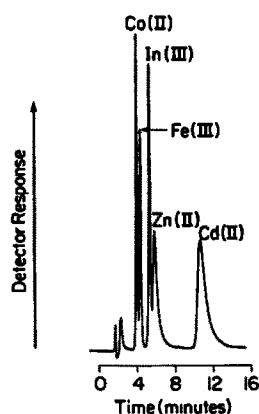


Fig 2 Separation of Co(II), Fe(III), In(III), Zn(II) and Cd(II) Hapet complexes on a PLRP-S column. Eluent conditions: 60% CH_3CN , 40% H_2O , 25 mM NaClO_4 , 0.5 mM Hapet, 21 mM ammonium acetate (pH 7).

$\text{l.mole}^{-1}.\text{cm}^{-1}$ at pH 7, and slightly lower at 405 nm and pH 4, with the exception of the cadmium and zinc complexes, for which they were only 600 and 400 $\text{l.mole}^{-1}.\text{cm}^{-1}$, respectively. The absorbance of free Hapet in the eluent was subtracted electronically.

Eluent

It was necessary to add Hapet to the eluent to prevent partial decomposition of the metal complexes during their chromatographic separation. The retention times of the complexes were not affected by change in the Hapet concentration used, but the chromatographic peaks were considerably broader at very low Hapet concentrations. A concentration of 0.5 mM Hapet gave good peaks (Fig. 2) for 0.1 mM concentrations of the complexed metal ions. The peak at around 2 min appears to be associated with iron in the sample.

Figure 3 shows that as the percentage of acetonitrile in the eluent was increased, the retention times of the complexes were reduced. The slopes of the plots are not parallel, indicating that the elution order can be affected by the percentage of acetonitrile in the eluent.

As the concentration of the ion-pairing reagent (ClO_4^-) in the eluent was increased, the retention time of the Co(II), Fe(III) and In(III) complexes increased, indicating these complexes are positively charged. In contrast, the retention time of the Cd(II) and Zn(II) complexes did not increase with increase in perchlorate concentration in the pH 7 eluent, indicating that the Cd(II) and Zn(II) complexes are neutral. The Zn(II) and Cd(II) complexes were also much more insoluble than the other metal complexes,

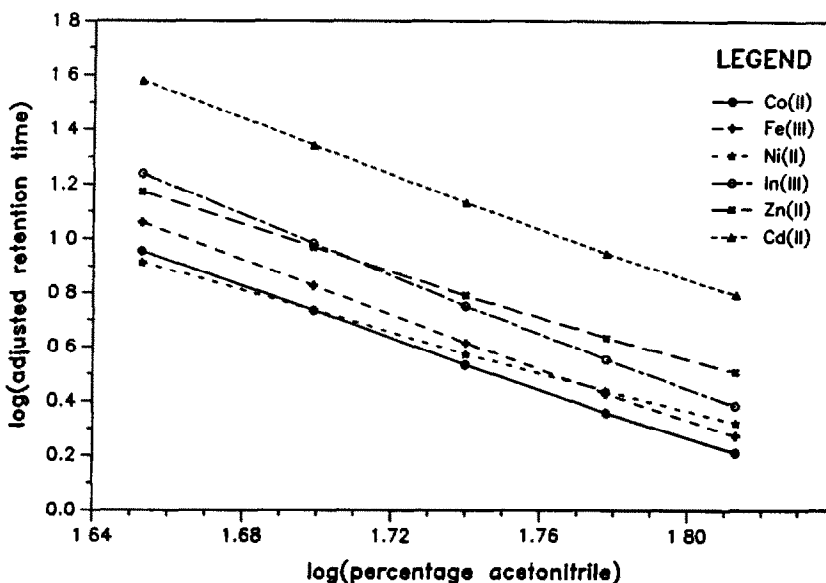


Fig. 3. Dependence of adjusted retention time on the percentage of acetonitrile in the eluent

which would also indicate that they were neutral.

Table 2 shows that the adjusted retention times of the Ga, Co, Fe and In complexes were unaffected by the eluent pH, whereas those of the Zn, Ni and Cd complexes varied greatly. Formation of neutral complexes of these metal ions with Hapet would require the removal of protons, so dependence of their retention time on pH is not surprising. Either the thiol or thione form of the semicarbazone could be involved in chelation of the metal ions, but the exact structure of the metal complexes in solution was not determined.

Chromatographic separation of metal-Hapet complexes

Many of the metal complexes could be separated successfully under both neutral (pH = 7) and acidic (pH = 4) conditions. The Ni(II), Co(II), Fe(III), In(III) and Ga(III) complexes all produced nice chromatographic peaks under both conditions. Figures 4 and 5 show chromatographic separations of the Ni(II), Co(II), Fe(III) and In(III) complexes and the Ga(III) and In(III) complexes,

respectively, under acidic conditions. Almost identical results were obtained under neutral conditions.

Although an excellent separation of complexed gallium(III) and indium(III) was obtained (Fig. 5), the iron(III)-Hapet complex was co-eluted with the gallium complex. It was hoped that reduction of iron from (III) to (II) and complexation with 1,10-phenanthroline would permit the chromatographic determination of gallium without interference from iron, but though this treatment did remove the chromatographic peak due to iron, the gallium peak was also missing from the chromatogram. Attempts were also made to resolve the iron and gallium peaks by replacing some of the acetonitrile in the eluent with tetrahydrofuran, but this only decreased the already poor resolution of the two metal complexes.

Calibration and determination

Calibration graphs were prepared for In(III), Co(II), Zn(II), Ni(II), Ga(III), Fe(III) and Cd(II) under isocratic elution conditions. The elution conditions, linear calibration range, and limits of detection are shown in Table 3. All the

Table 2. Adjusted retention time of metal complexes as a function of eluent pH

Aqueous pH	Apparent pH of eluent	Adjusted retention time, min						
		Ga	Co	Zn	Fe	In	Ni	Cd
7.00	7.49	11.5	9.9	14.4	12.6	19.0	8.2	37.2
5.00	5.93	12.6	10.8	10.0	13.6	20.8	7.6	21.1
4.00	4.82	12.5	10.7	5.3	13.4	20.6	4.9	8.8
3.30	4.08	12.2	10.2	5.6	13.0	19.5	3.6	5.4

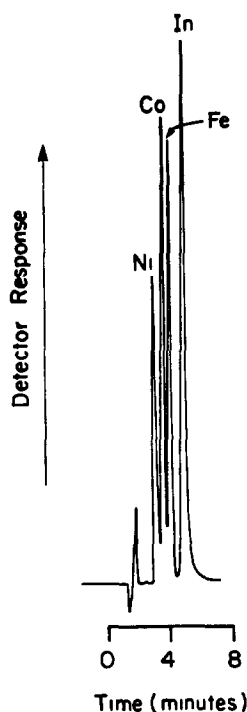


Fig. 4 Separation of Ni(II), Co(II), Fe(III) and In(III) Hapet complexes on a PLRP-S column. Eluent conditions: 60% CH₃CN, 40% H₂O, 25 mM NaClO₄, 0.5 mM Hapet, 12 mM formate (pH 4)

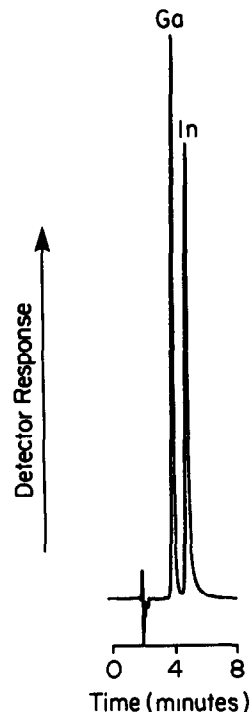


Fig. 5 Separation of the Ga(III), and In(III) Hapet complexes on a PLRP-S column. Eluent conditions: 60% CH₃CN, 40% H₂O, 25 mM NaClO₄, 0.5 mM Hapet, 12 mM formate (pH 4)

metal complexes were eluted at between 3 and 8 min under the conditions used.

Good linear calibration plots were obtained for all the metals over at least 2 orders of magnitude, except for zinc. The lower end of the range for some metal complexes was limited because of co-elution of excess of reagent. The upper end of the range for Zn(II) and Cd(II) at

pH 7 was limited by the solubility of the metal complexes. Although most of the calibration work was performed for neutral pH conditions, it should be noted that In(III) also gave a linear calibration curve from 7×10^{-7} to $1 \times 10^{-3} M$ at pH 4.3. For determination of Ni(II), Co(II), Ga(III), Fe(III) and In(III) a pH of 4 appears to work quite nicely. If Zn(II) or Cd(II) are also

Table 3 Eluent composition for determination of various metals by HPLC with Hapet as the complexing agent

Metal ion	Eluent composition,* % v/v	Linear calibration range, M	Detection limit, M
In(III)	60 CH ₃ CN	4×10^{-7} – 7×10^{-4}	9×10^{-8}
	40 H ₂ O		
Co(II)	60 CH ₃ CN	3×10^{-7} – 6×10^{-4}	1×10^{-7}
	40 H ₂ O		
Zn(II)	60 CH ₃ CN	3×10^{-6} – 2×10^{-4}	1×10^{-6}
	40 H ₂ O		
Ni(II)	60 CH ₃ CN	3×10^{-6} – 7×10^{-4}	4×10^{-7}
	40 H ₂ O		
Ga(III)	60 CH ₃ CN	6×10^{-7} – 3×10^{-4}	3×10^{-7}
	40 H ₂ O		
Fe(III)	60 CH ₃ CN	3×10^{-6} – 7×10^{-4}	6×10^{-7}
	40 H ₂ O		
Cd(II)	70 CH ₃ CN	7×10^{-8} – 3×10^{-5}	2×10^{-8}
	30 H ₂ O		

*For all eluents flow-rate 1.0 ml/min, UV detection at 380 nm, injection volume 10 μ l, 0.5 mM Hapet, 27 mM NaClO₄, 21 mM ammonium acetate (pH = 7.0)

present, however, the pH should be raised to increase their retention times and remove their potential interference.

Interferences

These were tested for by adding various metal ions to sample solutions containing Ni(II), Co(II), Fe(III), Ga(III) and In(III). A foreign ion was considered to interfere if the peak height of the metal complex was changed by more than $\pm 5\%$. A 1000-fold molar ratio (to analyte) of Na^+ and Ca^{2+} , 100-fold molar ratio of Al^{3+} and 10-fold molar ratio of Mn^{2+} , Pb^{2+} , Ce^{3+} and Bi^{3+} gave no interference in the analyses. Hg^{2+} , Cu^{2+} , Zn^{2+} and Cd^{2+} could be tolerated only at equimolar concentrations. It should be noted that although the Zn(II) and Cd(II) complexes interfere in determination of many of the metal complexes at pH 4, this interference can be removed by raising the pH of the eluent.

Acknowledgements—Ames Laboratory is operated for the U S Department of Energy under Contract No W-7405-Eng-82 This work was supported by the Director of Energy Research, Office of Basic Energy Sciences

REFERENCES

- 1 B R Willeford, Jr and H Veening, *J Chromatog*, 1982, **251**, 61
- 2 H Veening and B R Willeford, Jr, *Adv Chromatog*, 1983, **22**, 117
- 3 J W O'Laughlin, *J. Liq. Chromatog*, 1984, **7**, 127
- 4 G Nickless, *J Chromatog*, 1984, **313**, 129
- 5 B Steinbrech, *J Liq. Chromatog*, 1987, **10**, 1
- 6 A R Timerbaev, O M Petrukhin and Yu A Zolotov, *Z Anal. Chem*, 1987, **327**, 87
- 7 M D Palmien and J S Fritz, *Anal Chem*, 1987, **59**, 2226.
- 8 *Idem, ibid.*, 1988, **60**, 2244.
- 9 M V Main and J S Fritz, *ibid*, 1989, **61**, 1272.
- 10 *Idem, Anal Chim Acta*, 1990, **229**, 101
- 11 D L Klayman, J F Barcoserich, T S Griffin, C J Mason and J P Scovill, *J Med Chem*, 1979, **22**, 855
- 12 D L Klayman, J P Scovill, J F Bartoserich and J Bruce, *ibid*, 1983, **26**, 35
- 13 L A Saryan, E Ankel, C Krishnamurti, D H Petering and H Elford, *ibid*, 1979, **22**, 1218
- 14 M Das and S E Livingstone, *Br J Cancer*, 1978, **37**, 463
- 15 S K Jain, B S Garg and Y K Bhoon, *Spectrochim Acta*, 1986, **42A**, 959
- 16 R N Hanson and M A Davis, *Int J Nucl. Med Biol*, 1982, **9**, 97
- 17 J L Gómez Arza, J M Cano Pavón and F Pino, *Talanta*, 1976, **23**, 460
- 18 D J Leggett and B W Buděšínský, *Microchem J*, 1971, **16**, 87
- 19 D J Leggett and W A E McBryde, *Talanta*, 1974, **21**, 1005
- 20 *Idem, ibid*, 1975, **22**, 781
- 21 J L Gómez Arza and J M Cano Pavón, *Anal Lett*, 1976, **9**, 677
- 22 M T Martinez Aguilar, J M Cano Pavón and F Pino, *Anal Chim Acta*, 1977, **90**, 335.

METHODS FOR THE SEPARATION OF RHENIUM, OSMIUM AND MOLYBDENUM APPLICABLE TO ISOTOPE GEOCHEMISTRY

J. W. MORGAN,* D. W. GOLIGHTLY† and A. F. DORRZAPF, JR.
U S Geological Survey, 981 National Center, Reston, VA 22092, U S A

(Received 5 June 1990 Accepted 27 July 1990)

Summary—Effective methods are described for the chemical separation of rhenium, osmium and molybdenum. The methods are based on distillation and anion-exchange chromatography, and have been the basis for rhenium–osmium isotope studies of ore deposits and meteorites. Successful anion-exchange separation of osmium requires both recognition and careful control of the osmium species in solution; thus, distillation of osmium tetroxide from a mixture of sulfuric acid and hydrogen peroxide is preferred to anion-exchange. Distribution coefficients measured for perhenate in sulfuric acid media are sufficiently high ($K_d > 500$) for rhenium to be directly loaded onto an ion-exchange column from a distillation residue and subsequently eluted with nitric acid. Polymerization of molybdenum species during elution is prevented by use of a solution that is 1M in hydrochloric acid and 1M in sodium chloride.

The rhenium-187–osmium-187 decay scheme provides the basis for a powerful geochemical and geochronological tool that has been known for more than 30 years.^{1,2} The widespread application of this isotopic system, however, has been hampered by the lack of suitable mass-spectrometric techniques and appropriate chemical separations. Renewed interest in rhenium–osmium isotopes has been created by the recent demonstration of the ability of secondary ionization mass spectrometry (SIMS) to measure precisely and sensitively isotopes of these two elements.^{3,4} At least four other techniques now may become competitive with SIMS by virtue of sensitivity, speed of measurement, and precision; these techniques are laser microprobe mass analysis, inductively coupled plasma mass spectrometry (ICP-MS), tandem accelerator mass spectrometry, and resonance ionization mass spectrometry (RIMS). Each of these techniques has been applied to measurements of osmium isotopes.⁵⁻⁸

Previous analytical methods reported for the rhenium–osmium isotopic system have generally depended on the acid dissolution of a metal,

sulfide or silicate, followed by distillation of osmium tetroxide from a sulfuric acid medium containing Cr(VI)^{2,3,9} or Ce(IV).⁸ In another approach, fusion with sodium peroxide was used to dissolve Cretaceous–Tertiary boundary material before distillation of osmium tetroxide from perchloric acid.⁶ In a related area, the quantitative distillation of osmium tetroxide from a mixture of sulfuric acid and hydrogen peroxide, after an alkaline fusion,¹⁰ has been used successfully in the carrier-free separation of osmium from platinum metal ore for neutron-activation analysis.¹¹ After osmium separation, rhenium may be recovered by distillation at a higher temperature from a dichromate–sulfuric acid solution^{2,9} or from perchloric acid.¹² In most recent studies, solvent extraction of rhenium has been preferred. Aliquat-336‡ and other quaternary amines are widely favored,^{13,14} but the ease of back-extraction into alkaline or ammoniacal media has made tertiary amines¹⁵ particularly attractive.^{3,8}

Approaches to the separation of rhenium, osmium and molybdenum reported here have formed the basis for the development of effective rapid methods for numerous studies of rhenium–osmium isotope geochemistry and geochronology.¹⁶⁻¹⁹ Materials analyzed contain from less than 1 ng/g to more than 10 µg/g rhenium and osmium and vary widely in place of origin, geological age and bulk composition. Samples include iron meteorites, carbonaceous

*Author for correspondence

†Present address Ross Laboratories, 625 Cleveland Avenue, Columbus, OH 43215, U S A

‡Any use of trade names or trademarks is for descriptive purposes only and does not constitute endorsement by the U S Geological Survey

and enstatite chondrites, chromitites, gold-rich ores and many types of sulfides. Chemically, the sulfides ranged from molybdenite (molybdenum disulfide) to ores containing up to 19% copper and up to 49% nickel. The separations described in detail in this account of research provide data on anion-exchange and chemical species that are applicable to many chemical investigations of rhenium and osmium in rocks, minerals and meteorites.

EXPERIMENTAL

Apparatus

The elution of osmium, rhenium and molybdenum from ion-exchange columns was monitored by inductively coupled plasma atomic emission spectrometry (ICP-AES). Aerosols produced from eluent solutions by a fixed cross-flow nebulizer were injected into an argon plasma sustained by 1.1 kW of forward power from a 27.12-MHz generator. Flows of argon through each of the plasma-torch channels were: injector, 0.64; intermediate, 0; and outer, 17 l./min. A constant flow (0.8 l./min) of each eluent solution to the nebulizer was provided by a peristaltic pump (Gilson Minipuls 2). Background-corrected relative intensities of the Mo(II) 202.030 nm, Os(II) 228.226 nm, and Re(I) 197.313 nm lines were measured at 16-mm observation height with a direct-reading polychromator (Jarrell-Ash model 1160) having a focal length of 0.75 m and a bandpass of 0.036 nm. The polychromator was equipped with a separate 0.5-m Ebert monochromator (bandpass 0.04 nm) that functioned as a tunable channel.²⁰ Measurements for osmium and rhenium were made with the 0.5-m Ebert monochromator, which, unlike the polychromator, has no motor-driven quartz refractor plate at the entrance slit to enable automatic correction of the spectral background. Thus, the signal generated by a blank solution was subtracted from the gross line signal to provide the background correction, which always constituted less than 5% of the gross signal. Concentrations of osmium, rhenium and molybdenum in the eluent solutions were kept well above the detection limits²¹ (by a factor of at least 50) to enable relative standard deviations of less than 1% for four replicate measurements.

Reagents

Osmium Much of the fascination, and most of the exasperation, related to osmium chemistry

lies in the multiplicity of oxidation states and complex species that can exist, and often co-exist, in solution. Thus, preparation of a recognizable single species is an important first step because both the ion-exchange behavior and the response of the ICP-AES are affected by the chemical form of osmium.^{22,23} Three 250-ml stock solutions [Os-1, Os-2 and Os-3] were prepared from 0.25 g each of osmium tetroxide (Fisher purified osmic acid) contained in sealed glass ampules. Each solution was treated so that it contained a species of osmium different from that in the others. Three dilutions of each stock solution were made, and each dilute solution was treated to form or maintain a distinct osmium species. A fourth solution was prepared from ammonium hexachloro-osmate(IV). Details concerning the preparation of these solutions are given below.

Os-1. The osmium tetroxide dissolved rapidly in a solution of 10.5 g of sodium hydroxide in 100 ml of water to give a brown solution of $\text{Na}_2[\text{OsO}_4(\text{OH})_2]$. Ethanol (5 ml) was added, and the solution turned very dark brown. The solution was warmed for 20 min, during which the brown color changed to purple. Another 5 ml of ethanol were then added, and the solution was gently heated to complete the color transformation to purple. This solution was diluted to 250 ml with 1M sodium hydroxide to provide a final concentration of 624 $\mu\text{g/ml}$ Os as $\text{Na}_2[\text{OsO}_2(\text{OH})_4]$. Portions of 30 ml each were treated as follows and diluted to give 100 ml of solution containing 187 $\mu\text{g/ml}$ osmium.

Os-1A. Addition of 2.8 g of sodium hydroxide to a portion of Os-1 solution and subsequent dilution gave a purple solution of $\text{Na}_2[\text{OsO}_2(\text{OH})_4]$ in 1M sodium hydroxide.

Os-1B. Addition of 32.5 ml of 4M nitric acid to a portion of Os-1 solution caused the solution to become opaque black and to appear on the point of precipitating hydrated OsO_2 . The solution became colorless after stirring for 20 min. After dilution, this solution contained OsO_4 in 1M nitric acid.

Os-1C Addition of 11 ml of 12M hydrochloric acid to an Os-1 solution gave, after dilution, a pale brownish-yellow solution (unlike solution Os-2, described later) of $\text{Na}_2(\text{OsO}_2\text{Cl}_4)$ in 1M hydrochloric acid.

Os-2. Osmium tetroxide was dissolved in sodium hydroxide solution and diluted to a final volume of 250 ml to give a solution containing 603 $\mu\text{g/ml}$ osmium as $\text{Na}_2[\text{OsO}_4(\text{OH})_2]$ in 1M sodium hydroxide. Portions of 30 ml were

diluted to 100 ml after the following treatments, to give solutions containing 181 $\mu\text{g/ml}$ osmium.

Os-2A. Addition of 2.8 g of sodium hydroxide to a portion of Os-2 solution gave the same light brown solution as Os-2, which contained $\text{Na}_2[\text{OsO}_4(\text{OH})_2]$ in 1M sodium hydroxide.

Os-2B. Addition of 32.5 ml of 4M nitric acid to a portion of Os-2 solution immediately produced a colorless solution without the intermediate blackening observed previously for Os-1B.

Os-2C. Addition of 11 ml of 12M hydrochloric acid to a portion of Os-2 solution and subsequent dilution immediately gave a colorless solution that contained OsO_4 in 1M hydrochloric acid. The solution gradually became colored, and after one week it was light yellow, presumably because of the presence of $\text{H}_2(\text{OsO}_2\text{Cl}_4)$.

Os-3. Osmium tetroxide was dissolved in 100 ml of 2M nitric acid but went into solution very slowly. The solution was diluted to 200 ml to contain 720 $\mu\text{g/ml}$ osmium as OsO_4 in 1M nitric acid. Portions of 25 ml were treated as described below and diluted to 100 ml each to contain 180 $\mu\text{g/ml}$ osmium.

Os-3A. Addition of 18.8 ml of 4M nitric acid to a portion of Os-3 solution and subsequent dilution gave a colorless solution that contained OsO_4 in 1M nitric acid.

Os-3B. Addition of 5.2 g of sodium hydroxide to a portion of Os-3 solution and subsequent dilution gave the same light-brown solution obtained as Os-2; the resulting solution contained $\text{Na}_2[\text{OsO}_4(\text{OH})_2]$ in 1M sodium hydroxide.

Os-3C. Sodium hydroxide (5.2 g) and 1 ml of ethanol were added to a portion of Os-3 solution. As this mixture was warmed, the dark brown color that developed on addition of ethanol changed to purple, as with Os-1. After dilution with water, the solution contained $\text{Na}_2[\text{OsO}_2(\text{OH})_4]$ in 1M sodium hydroxide.

Os-4. Ammonium hexachloro-osmate $[(\text{NH}_4)_2\text{OsCl}_6]$ was heated to constant weight at 150° and then dissolved in 250 ml of 4M hydrochloric acid to give a reddish-yellow solution containing 320 $\mu\text{g/ml}$ osmium. A 25-ml portion of the resulting solution was diluted to 200 ml in 3M hydrochloric acid to give a solution that contained 40.0 $\mu\text{g/ml}$ osmium.

Rhenium. High-purity rhenium ribbon (H. B. Cross, 0.03-mm thick, 7.6-mm wide) weighing 0.1034 g was dissolved in 10 ml of concentrated nitric acid (J. T. Baker, Ultrex), and the result-

ing colorless solution was diluted to 250 ml to give a solution containing 414 $\mu\text{g/ml}$ rhenium as HReO_4 in 1.4M nitric acid. This solution was used for the elution experiments. In the batch equilibration experiments to determine distribution coefficients in sulfuric acid medium, evaporation of this solution to remove nitric acid gave erratic results, apparently because of incomplete dissolution of the dried residue. A second stock solution was prepared by dissolving KReO_4 in the appropriate concentration of sulfuric acid (0.25–2.5M) to give solutions containing between 194 and 207 $\mu\text{g/ml}$ rhenium.

Molybdenum. Two stock solutions were prepared, one from ammonium heptamolybdate tetrahydrate, $(\text{NH}_4)_6\text{Mo}_7\text{O}_{24}\cdot 4\text{H}_2\text{O}$ and one from sodium molybdate. A 23-g quantity of the heptamolybdate was dissolved in a mixture of 150 ml of water and 20 ml of concentrated ammonia solution, and then diluted to 250 ml to give a solution containing 50 mg/ml molybdenum in 1M ammonia solution. A quantity of 2.52 g of $\text{Na}_2\text{MoO}_4\cdot 2\text{H}_2\text{O}$ was dissolved in H_2O together with 8 g NaOH to give 200 ml a solution containing 5.0 mg/ml molybdenum in 1M sodium hydroxide.

Anion-exchange columns. Anion-exchange resin was supported between plugs of glass wool in Pyrex glass columns that were 1 cm in diameter and 15 cm long. Each column had a 200-ml spherical glass reservoir at the top and a Teflon stopcock at the bottom. The columns were packed with 5.5 g wet weight (equivalent to 3.5 g of dry weight) of BioRad AG 1 \times 8 resin, 200–400 mesh, chloride form, that had been slurried with water, to yield a column 12–13.5 cm long. The columns were washed with 100 ml of water to remove a pink impurity from the resin, and then conditioned with the appropriate acid.

RESULTS AND DISCUSSION

Rhenium

The anion-exchange of ReO_4^- in chloride and nitrate systems is well known^{24–26} and, in principle, provides a ready means to separate rhenium from molybdenum and other contaminants.^{22,27,28} Most osmium distillation procedures leave a residual solution that is 2–4M in sulfuric acid. Rhenium may be recovered from this solution by solvent extraction with a tertiary amine dissolved in chloroform,³ but this procedure can be messy and rhenium recoveries may be inexplicably low. An ion-exchange

procedure that could be applied directly to the residual sulfuric acid solution appeared attractive. Although the strong sorption of rhenium by anion-exchange resin from sulfuric acid medium seems well known,²⁹ this element was not included in the extensive study by Strelow and Bothma³⁰ and apparently has not been systematically studied in a quantitative way elsewhere.

Distribution coefficients (K_d) were determined by taking 1-g (dry weight) batches of resin that had been converted into the sulfate form and then pre-equilibrated for 4 hr with the appropriate concentration of sulfuric acid. The resin was then equilibrated for 4 hr with 25-ml aliquots of sulfuric acid varying in concentration from 0.25 to 2.5M and each containing 200 $\mu\text{g/ml}$ rhenium. Equilibrations at each concentration were conducted in triplicate. The concentration of Re remaining in the solution was determined by ICP-AES; because the K_d values are large (>500), estimation of the amount of rhenium on the resin by difference introduced insignificant error. Results are summarized in Table 1. Over the concentration range studied, rhenium is strongly sorbed by the anionic resin. The variation of $\log K_d$ with \log molality or molarity of sulfuric acid is remarkably linear, particularly above 0.5M (Fig 1). The underlying physicochemical reasons for this linearity are not clear, as it is not observed with hydrochloric, hydrobromic, or nitric acids²⁵ (Fig 2). For a wide range of acid concentration, Re occurs almost entirely as the strong monobasic acid HReO_4 ,³¹ and sorption by the resin depends largely upon competition with the major anionic species. In the resin, the sulfuric acid is present predominantly as HSO_4^- .³² The K_d values for rhenium in the various acids might be expected to follow inversely the trends determined by acid strength [$\text{ClO}_4^- > \text{NO}_3^- > \text{Br}^- > \text{Cl}^- > \text{HSO}_4^-$], so that

Table 1 Distribution coefficients* (K_d) for rhenium in sulfuric acid solution

H ₂ SO ₄		K_d †
Molarity	Molality	
0.25	0.253	4180 ± 150
0.50	0.510	2510 ± 70
1.00	1.04	1300 ± 25
1.50	1.59	866 ± 8
2.00	2.16	677 ± 7
2.50	2.76	523 ± 7

*BioRad AG 1 × 8 resin, 200–400 mesh
†Mean ± standard deviation of triplicate measurements

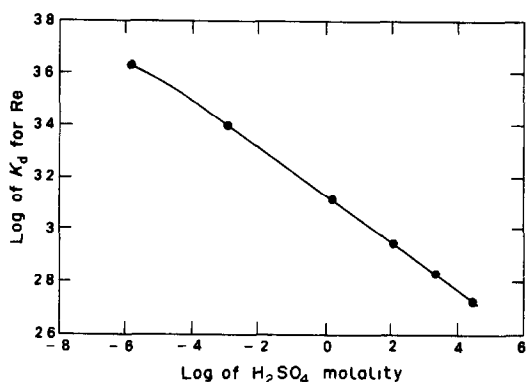


Fig 1 $\log K_d$ for rhenium vs \log (molality of sulfuric acid) BioRad AG 1 × 8 resin, 200–400 mesh

K_d values for the sulfuric acid systems would be larger than those for hydrochloric acid systems, as is the case for solvent extraction with tertiary amines.¹⁵ In fact, the reverse, is true, as can be seen from Figs. 1 and 2, the K_d values for sulfuric acid solutions are uniformly lower than those for hydrochloric acid solutions.

Osmium

Osmium can be reversibly sorbed by anion-exchange resins from dilute hydrochloric acid, apparently as $\text{OsO}_2\text{Cl}_4^{2-}$.^{22,33} This observation was confirmed for 3 ml of solution Os-1, containing 624 $\mu\text{g/ml}$ osmium as the purple $\text{Na}_2[\text{OsO}_2(\text{OH})_4]$. The solution was acidified, diluted to a final volume of 10 ml in 1M hydrochloric acid, and allowed to stand at room temperature for 10 min before it was loaded onto the column, predominantly as $\text{Na}_2(\text{OsO}_2\text{Cl}_4)$. Elution with 0.8M nitric acid appeared to remove osmium from the column, although, for reasons discussed later, the experiment was not quantitative. In a second experiment, the same procedure was followed, except

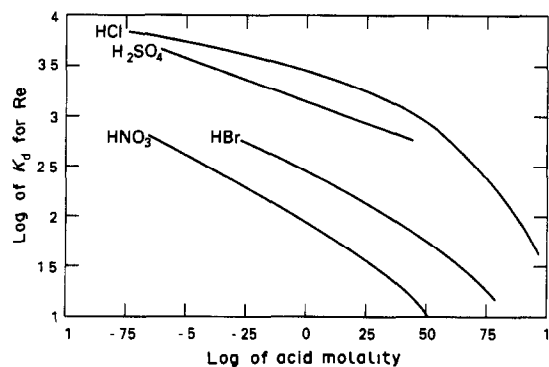


Fig 2 $\log K_d$ rhenium vs \log (molality of hydrochloric, hydrobromic and nitric acids) BioRad AG 1 × 8 resin, 200–400 mesh

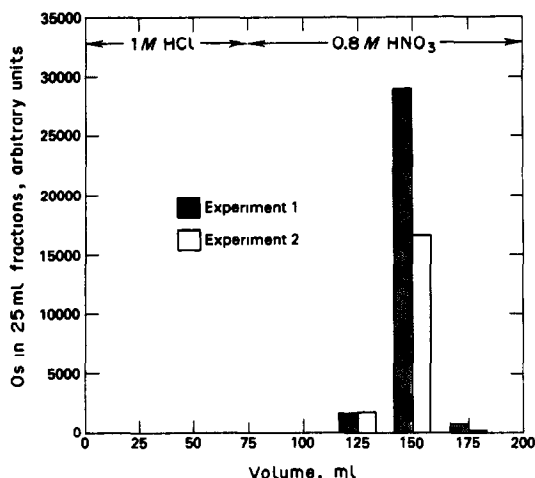


Fig 3 Elution of osmium with 1M hydrochloric acid and 0.8M nitric acid from BioRad AG 1 × 8 resin, 200–400 mesh, chloride form, in a column 10 mm in diameter and 125 mm long

that the solution in 1M hydrochloric acid was gently warmed for 10 min before being cooled quickly in ice and loaded onto the column. This experiment also could not be shown to be quantitative, and the recovery was lower, possibly because of the formation of some Na_2OsCl_6 , which is strongly retained by the resin (Fig. 3). The elution experiments were not continued because the easy sorption of rhenium from the residual liquid from the osmium distillation offered an attractive alternative means of separation. In addition, Wee³³ has confirmed that osmium and rhenium can be separated cleanly and in good yield by elution with nitric acid.

The elution experiments for osmium were not quantitative because of a peculiarity in the determination of this element by ICP–AES. Very large differences in response were observed for the various chemical forms of osmium (Table 2). The results confirm the marked increase of sensitivity for osmium when present as OsO_4 in non-alkaline solution.^{23,34} The signal observed for OsO_4 in hydrochloric acid and

nitric acid solution is approximately 20 times that of corresponding solutions containing Os(VIII) or Os(VI) in sodium hydroxide or Os(VI) and Os(IV) in hydrochloric acid. Mallet *et al.*³⁴ found the sensitivity for Os(VIII) as OsO_4 to be 10 times that for Os(VI) as hexachloro-osmate. Summerhays *et al.*²³ reported an enhancement of a factor of 50 for OsO_4 in water relative to “ OsCl_3 ” in 10% v/v hydrochloric acid, and a 15-fold increase in sensitivity if the “ OsCl_3 ” were oxidized in 9M nitric acid for 4 hr. Given these large variations and the uncertainty concerning the chemical form of osmium (originally present as $\text{OsO}_2\text{Cl}_4^{2-}$) that is eluted with 0.8M nitric acid, accurate standardization was not possible. For osmium, radioactive tracer experiments would clearly be a better choice for quantitative elution studies.

Molybdenum

The anion-exchange behavior of molybdenum has been studied for nitric acid, hydrochloric acid,^{26,35} sulfuric acid³⁰ and sodium hydroxide solutions,³⁶ and also for hydrochloric acid–hydrofluoric acid and hydrochloric acid–ammonium thiocyanate mixtures.^{35,37} The marked minimum in K_d for molybdenum in approximately 1M hydrochloric acid²⁷ should afford an easy separation from rhenium, which has a K_d of 1000,²⁸ or more,²⁵ at this acidity. Most previous studies were made at very low concentrations of molybdenum, however, and many investigators used radioactive tracers. The chemistry of molybdenum is complicated by a tendency towards condensation polymerization reactions that are strongly dependent on molybdenum concentration.³⁸ In an initial experiment, a solution made from ammonium heptamolybdate containing 150 mg of molybdenum in 25 ml of 2.5M hydrochloric acid formed a green band on the resin. The band separated into several components that were difficult to elute cleanly. Suspecting that the problem arose from the

Table 2 Relative sensitivities of ICP–AES for osmium species

Solution	Oxidation state	Species	Medium	Color	Relative sensitivity*
4	IV	OsCl_6^{2-}	3M HCl	Reddish-yellow	110
1A	VI	$\text{OsO}_2(\text{OH})_2^{2-}$	1M NaOH	Purple	110
3C	VI	$\text{OsO}_2(\text{OH})_2^{2-}$	1M NaOH	Purple	90
1C	VI	$\text{OsO}_2\text{Cl}_4^{2-}$	1M HCl	Yellow	120
2A	VIII	$\text{OsO}_4(\text{OH})_2^{2-}$	1M NaOH	Light brown	130
3B	VIII	$\text{OsO}_4(\text{OH})_2^{2-}$	1M NaOH	Light brown	100
1B	VIII	OsO_4	1M HNO ₃	None	1800
2C	VIII	OsO_4	1M HCl	None	2700

*Relative sensitivity for Os is measured for the Os (II) 228 226 nm line, in counts $\text{sec}^{-1} \mu\text{g}^{-1}$

original heptamolybdate form, we fused the salt with sodium hydroxide at 625 K for 1 hr; this fusion produced no significant improvement. The starting material was changed to sodium molybdate, and the elution experiments were repeated at much lower concentration (1.5 mg of Mo in 10 ml of 1M hydrochloric acid loaded onto the column). There was no sign of polymerization, and tailing was insignificant. At higher concentrations, polymerization became more apparent, even with sodium molybdate. Tailing was significant when 15 mg of molybdenum in 10 ml of 1M hydrochloric acid was loaded onto the column; at higher concentrations, polymerization was indicated by the fractionation of colored bands on the resin, and multiple elution peaks. These problems were easily circumvented, however, by replacing the 1M hydrochloric acid medium with a 1M hydrochloric acid–1M sodium chloride mixture. Tailing was reduced to very low levels to give almost symmetrical elution peaks (Fig. 4), and even with a solution containing 150 mg of molybdenum in 50 ml, no polymerization was visible. These results provide a simple means for the study of rhenium and osmium in molybdenite. In this mineral, osmium is entirely radiogenic [^{187}Os formed from the decay of ^{187}Re ($t_{1/2} = 4.23 \times 10^{10}$ years)³⁹]. Even for the oldest molybdenites, the sample size needed is governed by the sensitivity for osmium, because rhenium is present in large excess. For sample sizes up to 500 mg, after sodium hydroxide–sodium peroxide fusion, an aliquot (5 or 10% of total volume) could be taken for the rhenium analysis, and a solution suitable for ICP–MS

or RIMS obtained in a single anion-exchange step. Alternatively, sample sizes of up to 250 mg of molybdenite (containing 150 mg of molybdenum) could be processed by two anion-exchange steps.

CONCLUSIONS

Anion-exchange studies of rhenium, molybdenum and osmium suggest that these elements may be separated from each other. Rhenium is readily held on the column from sulfuric acid of concentration up to 2.5M or hydrochloric acid up to at least 5M, and from dilute (< 1M) nitric acid. Elution by higher nitric acid concentrations (> 3M) is essentially quantitative. The strong sorption from sulfuric acid solution is particularly useful if osmium is first distilled from sulfuric acid–hydrogen peroxide because the residue can then be passed directly through an anion-exchange column for recovery of rhenium. Separation of rhenium from substantial amounts of molybdenum (important because molybdenite is the major rhenium-rich mineral) is possible in one or two steps when polymerization of molybdenum is curtailed by using hydrochloric acid–sodium chloride solution. Osmium can be reversibly sorbed as $\text{OsO}_2\text{Cl}_4^-$ by an anion-exchange resin from dilute hydrochloric acid and eluted with nitric acid, but distillation may be preferable. The sensitivity of determination of osmium by ICP–AES is very dependent on the presence of osmium tetroxide, and for quantitative elution experiments, use of radioactive tracers may be a more useful technique for this element.

REFERENCES

- 1 W Herr and E. Merz, *Z Naturforsch*, 1955, **10a**, 613
- 2 B Hirt, W Herr and W Hoffmeister, *Radioactive Dating*, p 35. IAEA, Vienna, Austria, 1963
- 3 J-M Luck, *Ph.D Dissertation*, University of Paris VII, 1982
- 4 J-M Luck and C J Allegre, *Nature*, 1983, **302**, 130
- 5 M Lindner, D A Leich, R J Borg, G P Russ, J M Bazan, D S Simons and A R. Date, *ibid*, 1986, **320**, 246
- 6 F E Lichte, S M Wilson, R R Brooks, R D Reeves, J Holzbecher and D E Ryan, *ibid*, 1986, **322**, 816
- 7 U Fehn, R Teng, D Elmore and P W Kubik, *ibid*, 1986, **328**, 707
- 8 R J Walker, S B Shrey and O Stecher, *Earth Planet. Sci Lett*, 1988, **87**, 1
- 9 W Herr, W Hoffmeister, B Hirt, J Geiss and F G Houtermans, *Z Naturforsch*, 1961, **16a**, 1053
- 10 K S Chung and F E Beamish, *Talanta*, 1968, **15**, 823
- 11 *Idem*, *Anal Chim Acta*, 1968, **43**, 357

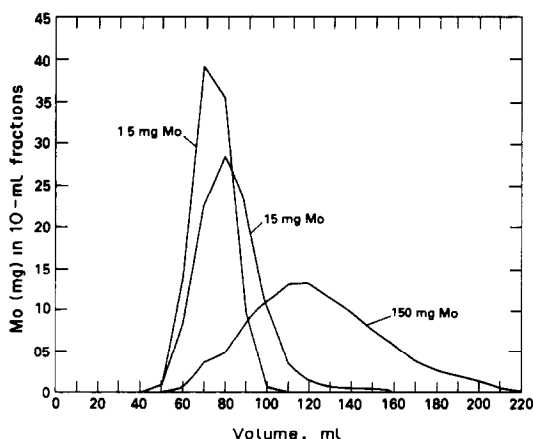


Fig 4 Elution of 1.5, 15 and 150 mg of molybdenum by 1M hydrochloric acid–1M sodium chloride solution from Bio-Rad AG 1 \times 8 resin, 200–400 mesh, chloride form, in a column 10 mm in diameter and 125 mm long

- 12 M W Solt, J S Wahlberg and A. T. Meyer, *Talanta*, 1969, **16**, 37
- 13 W J Maeck, G L Booman, M E Kussy and J E Rein, *Anal. Chem.*, 1961, **33**, 1775
- 14 E V Elhott, K R Stever and H H Heady, *At Abs Newsl*, 1974, 113
- 15 V Yatirajam and L R Kakkar, *Anal Chim Acta*, 1970, **52**, 555
- 16 J W Morgan and R J Walker, *ibid*, 1989, **222**, 291
- 17 R J Walker and J W Morgan, *Science*, 1989, **243**, 519
- 18 D D Lambert, J W Morgan, R J Walker, S B Shurey, R W Carlson, M L Zientek and M S Koski, *Science*, 1989, **244**, 1169
- 19 J W Morgan, R J Walker and J N Grossman, *Lunar Planet Sci*, 1990, **21**, 809
- 20 J J Leary, A E Brooks, A F Dorrzapf and D. W Golightly, *Appl. Spectrosc*, 1982, **36**, 37
- 21 R K. Winge, V A Fassel, V J Peterson and M A Floyd, *Inductively Coupled Plasma Atomic Emission Spectroscopy; An Atlas of Spectral Information*, Elsevier, New York, 1985
22. J W. Morgan, *Ph D. Dissertation*, Australian National University, 1965
- 23 R D Summerhays, P J. Lamothe and T L. Fries, *Appl Spectrosc*, 1983, **37**, 25
- 24 K A Kraus and F Nelson, *Proc First Intern Conf. Peaceful Uses Atomic Energy*, 1955, **7**, 113 United Nations, New York, 1956
- 25 B Chu and R M Diamond, *J Phys Chem*, 1959, **63**, 2021
- 26 J P Faris and R. F. Buchanan, *Anal Chem*, 1964, **36**, 1157.
- 27 V. W Meloche and A. F. Preuss, *ibid*, 1954, **26**, 1911.
- 28 E H Huffman, R L Oswald and L A Williams, *J Inorg. Nucl Chem*, 1956, **3**, 49
- 29 R N Sen Sarma, E Anders and J M Miller, *J Phys Chem*, 1959, **63**, 559
- 30 F W E Strelow and C J C Bothma, *Anal Chem*, 1967, **39**, 559
- 31 J E Early, D Fortnum, A Wojcicki and J E Edwards, *J Am. Chem Soc*, 1959, **81**, 1295
- 32 F Nelson and K A Kraus, *ibid*, 1958, **80**, 4154
- 33 P S -L Wee, *M S Dissertation*, University of Toronto, 1986
34. R. C Mallet, S. J. Royal and T. W Steele, *Anal. Chem.*, 1979, **51**, 1617
35. K. A. Kraus, F. Nelson and G E. Moore, *J Am. Chem. Soc*, 1955, **77**, 3972
36. S. A. Fisher and V. W Meloche, *Anal. Chem*, 1952, **24**, 1100
37. H. Hamaguchi, K. Kawabuchi and R Kuroda, *ibid.*, 1964, **36**, 1654
- 38 A I Busev, *Analytical Chemistry of Molybdenum*, Humphrey Science Publishers, Ann Arbor, 1969
- 39 M Lindner, D A Leich, G P. Russ, J M Bazan and R J Borg, *Geochim Cosmochim Acta*, 1989, **53**, 1597

SORPTION OF NOBLE-METAL IONS ON SILICA WITH CHEMICALLY BONDED NITROGEN-CONTAINING LIGANDS

T. I. TIKHOMIROVA, V. I. FADEEVA, G. V. KUDRYAVTSEV,* P. N. NESTERENKO,
V. M. IVANOV, A. T. SAVITCHEV and N. S. SMIRNOVA

Department of Chemistry, M. V. Lomonosov State University, Moscow 119899, U.S.S.R.

(Received 9 January 1990 Revised 27 July 1990 Accepted 22 August 1990)

Summary—A study has been made of the sorption of Ir(IV), Rh(III), Pt(IV), Ru(IV), Os(VIII), Pd(II) and Au(III) from aqueous solutions by silica chemically modified with nitrogen-containing organic ligands, as a function of hydrochloric acid concentration, time of contact, concentration of the element and the ionic strength. Sorption of noble-metal ions at $\text{pH} > 1$ on a sorbent containing monoamine groups seems to be due to a complexation mechanism, and to an anion-exchange mechanism at $\text{pH} < 1$. With aminopropyl-silica 1000-fold concentration of Ir(IV) and Rh(III) from their 10^{-8} – $10^{-7}M$ solutions was achieved and these metals were subsequently determined on the sorbent surface by X-ray fluorescence. Detection limits were 10–20 ng/ml. There was no interference from 1000-fold quantities of non-ferrous metal ions and Fe(III). With the sorbent containing bonded diethylenetriamine groups, 1000-fold concentration of Au(III) was achieved, and it was then determined on the sorbent surface by an atomic-emission method. Conditions for desorption of Au(III) with pyridine and potassium thiocyanate were developed.

Elucidation of the mechanism of sorption of noble-metal ions and optimization of the sorption conditions are difficult. Despite the great variety of papers devoted to this problem the methods developed for sorption concentration and separation of noble metals do not meet all analytical requirements.

Many different sorbents have been used to extract noble metals from solution, the greatest attention now being paid to complex-forming sorbents. These sorbents are characterized by the higher selectivity and efficiency of sorption of noble metals in the presence of accompanying metals (especially Cu, Fe, Ni, Co, Al and Ca, which are the main components of most natural and industrial samples) that can be attained with ion-exchangers. The functional groups of these polymeric sorbents often contain sulphur¹ and, more frequently, nitrogen atoms; in particular, diethylamine,² ethylenediamine,³ iminodiacetate⁴ and heterocyclic nitrogenous ligands⁵ may be mentioned.

A distinctive feature of platinum metals is their very low rate of ligand exchange, which results in their sorption on complex-forming sorbents taking place only on prolonged heating. This fact, together with the very complex

range of ionic states of platinum metals in aqueous solutions, presents difficulties when sorption procedures are developed.

In recent years, polymeric organic sorbents have been developed, including polymeric tertiary amines of general formula $[(\text{CH}_2)_3\text{N}]_n$,⁶ which are characterized by a rather high rate of sorption of platinum metals at room temperature. Sorption on these sorbents is a two-stage process. First an anion-exchange reaction takes place, with the formation of ion-associates, then, with increasing sorption time and temperature, co-ordinately solvated compounds are formed with the sorbent functional groups.

We are mainly interested in the sorbents based on silica with organic ligands chemically bonded to the surface. These sorbents can be successfully used for concentration and separation of various transition metals,⁷ mainly because of the rapidity of the reactions. However, there have been practically no publications on their use for sorption of platinum metals, probably because of the low rate of sorption as the result of the kinetic inertness of these metals. This means that one of the main merits of the chemically modified silicas is lost, so the change from an organic polymer matrix to a mineral matrix for the sorption is not justified. This view is in general confirmed by the published data for

*Author for correspondence

sorption of platinum metals by silicas chemically modified with cyclopentenedithiocarbonyl groups,⁸ pyrrole-, furan- and thiophenecarbonamides,⁹ formazans,¹⁰ thioaniline¹¹ and 5-methylene-2-(2'-thiazolylazo)anisole.¹² In our view, however, this choice of ligands⁸⁻¹² does not allow the advantages of chemically modified silicas to be utilized. We have used silica bonded with aliphatic amines and polyamines, since the analogous polymeric organic sorbents give the highest rates of interaction with noble metal ions. Preliminary investigations were encouraging, equilibrium for sorption of Pt(IV), Pd(II) and Ir(III) on aminopropyl-silica being attained in 2 min.¹³

The present paper discusses the results of a systematic investigation of the sorption of platinum metal ions and gold(III) on chemically modified silicas. Examples of applications to concentration, separation and determination of these elements are given.

EXPERIMENTAL

Apparatus

Absorbance was measured with an SF-16 spectrophotometer. X-Ray fluorescence determinations of elements in the sorbent matrix were performed with an EGG-ORTEC TEFA-III X-ray fluorescence energy-dispersive analyser equipped with an X-ray tube having a double Mo/W anode. Radiation from ²⁴¹Am (59 keV, activity 2.2×10^{12} dpm, irradiation for 600 sec) was used as an excitation source for samples containing rhodium, ruthenium and palladium. The intensities of the K_{α} -lines for rhodium, ruthenium and palladium and the L_{α} -lines for iridium, osmium and platinum were used as analytical parameters.

An alternating current arc (8 A) was used for atomic-emission analyses. The 267.6-nm line was used for gold. Samples of the sorbent were placed in the carbon electrode channels (2.5 mm depth and 4.5 mm inner diameter). The activity of the solutions was measured with a PPV-8 unit and an MST-17 counter, at constant geometry.

Reagents

Standard solutions of platinum metal salts (concentrations 0.7–5 mg/ml) were prepared by dissolving precise quantities of $K_4[Ru_2OCl_{10}]$, K_2IrCl_6 , $RhCl_3 \cdot 4H_2O$, $PdCl_2$ and $HAuCl_4$ in 2M hydrochloric acid, $H_2PtCl_6 \cdot 6H_2O$ in 1M hydrochloric acid, and $H_2[OsO_4(OH)_2]$ in 0.4M sodium hydroxide, and were standardized

gravimetrically. Less concentrated solutions were obtained by dilution of the initial solutions before use. All reagents used were of analytical reagent grade. Demineralized distilled water was used for dilution.

Sorbents

The sorbents were synthesized with Silochrome S-120 silica (specific surface area 120 m²/g, mean pore diameter 45 nm, particle size 0.1–0.2 mm) as substrate Aminopropyl-silica (sorbent I) was obtained by reaction with γ -aminopropyltriethoxysilane in toluene at 100° (10 hr); sorbents II–V were obtained by modification of the silica with 3-bromopropyltrichlorosilane followed by ethylenediamine (II), diethylenetriamine (III) or tetraethylenepentamine (IV) in ethanol or by reaction with trimethylamine (V) in nitromethane. The surface concentration of the bonded ligands was determined by combustion analysis. For sorbents I–IV potentiometric titration with an acid was also used.

Sorption by the batch method

The required amount of solution containing the metal ions to be studied and a calculated amount of hydrochloric acid or sodium hydroxide solution (to create the necessary acidity) were diluted with water to a fixed volume in a vessel fitted with a glass stopper. For pH > 1, the acidity was measured before and after the sorption. Then 0.1–0.2 g of the sorbent was added and the vessel was shaken on a mechanical vibrator until equilibrium was attained. The sorbent was filtered off and the equilibrium concentrations of metal ions in the aqueous phase were determined by spectrophotometry: Ru with 1,10-phenanthroline, Os with sodium thiocyanate, Pd with 4-(2-pyridylazo)resorcinol, Pt with stannous chloride, Rh with 1-(2-pyridylazo)-2-naphthol, Au with Chrompyrazole I (and radiometrically with ¹⁹⁸Au), and Ir by the luminescence method with 2,2'-bipyridyl. The equilibrium concentration in the sorbent phase was determined as the difference between initial concentration and the equilibrium concentration in the aqueous phase. At pH < 1 the metal content in the sorbent phase was determined by X-ray fluorescence analysis.

To plot the calibration graphs, the required amounts of standard platinum metal solution were added to 0.2-g portions of sorbent and ground with silica in an agate mortar, the total weight being 1.5 g (for Ir, Os, Pt) or 2.0 g (for

Rh, Ru, Pd). The sample for X-ray fluorescence analysis was prepared by pressing the powder thus obtained into tablets (32 mm diameter, pressure 2.5×10^3 kg/cm²). The background radiation was approximated by a cubic polynomial (by the least-squares method) and the maximum background noise was used.¹⁴ The calibration curve of analytical signal *vs.* metal concentration, $I = f(c)$, was obtained by the method of Savitchev and Fogelson.¹⁵ The detection limit for Rh, Ru and Pd is 6 μ g/g, while for Ir, Os and Pt it is 4 μ g/g.

Sorption under dynamic conditions

A 0.2–0.4 g portion of sorbent was packed into a 5-mm bore chromatographic column and washed with hydrochloric acid of the same concentration as that in the test solution. The test solution was then passed through the column at the preselected rate and the column was washed with 5–10 ml of the hydrochloric acid. In the case of the platinum metals, the sorbent was taken out of the column, dried and analysed by X-ray fluorescence. In the case of Au(III), the analyte was desorbed and then determined by spectrophotometry, or was determined directly on the sorbent by atomic-emission analysis.

RESULTS AND DISCUSSION

The commonest oxidation states of the noble metals—Ru(IV), Rh(III), Pd(II), Os(VIII), Ir(IV), Pt(IV) and Au(III)—were examined. Hydrochloric acid medium was used because the metals are generally separated and identified in the form of chloride complexes, and their standard solutions are generally prepared from the chloride complexes.

Silicas chemically modified with (1) aliphatic mono- and polyamines that can act as weak anion-exchangers and complex-formers, and (2) tetra-alkylammonium salts, which are strong anion-exchangers, were used as sorbents (Table 1). They are easily obtained, especially

Table 1 Sorbents investigated

Sorbent	Grafted group	Surface of concentration grafted groups, mmole/g
I	$-(\text{CH}_2)_3\text{NH}_2$	0.36
II	$-(\text{CH}_2)_3\text{NHCH}_2\text{CH}_2\text{NH}_2$	0.40
III	$-(\text{CH}_2)_3\text{NH}(\text{CH}_2\text{CH}_2\text{NH})_2\text{H}$	0.20
IV	$-(\text{CH}_2)_3\text{NH}(\text{CH}_2\text{CH}_2\text{NH})_4\text{H}$	0.30
V	$-(\text{CH}_2)_3\text{N}(\text{CH}_3)_3^+\text{Cl}^-$	0.20

aminopropyl-silica, and can be widely used in the analytical chemistry of noble metals.

The concentration of the grafted ligands is fairly high, and equal to 1–2 molecules per nm² of surface. At the same time, there are still many residual silanol groups on the surface, and in some cases these groups can participate in sorption.¹⁶ To find whether this was the case, an additional study was made of noble metal sorption on the unmodified silica Silochrome S-120.

The main factors influencing the sorption (duration of phase contact, acidity and ionic strength of the solution, metal ion concentration) were studied. All investigations were made at room temperature.

Duration of phase contact

One of the most surprising facts found was the high rate of equilibration, which was similar to that for non-ferrous metals. Under batch conditions a constant degree of sorption was reached for Rh(III), Pd(II), Ir(IV), Pt(IV), Au(III) in 1–5 min, and for Ru(IV) and Os(VIII) in 10 min. Under dynamic conditions the sorption of platinum metals attained a maximum at a flow-rate of 10–20 ml.min⁻¹.cm⁻², and gold was quantitatively extracted at a flow-rate of 60–70 ml.min⁻¹.cm⁻². The sorption rates of Rh(III) and Ir(IV) were almost the same in both strongly acidic and weakly acidic media.

Solution acidity

Figures 1–3 show the effect of solution acidity on the sorption of microquantities of platinum metal ions on sorbent I and silica, and of Au(III) on all the sorbents studied. In the first place it can be concluded that the contribution of the silanol groups to the sorption is negligible

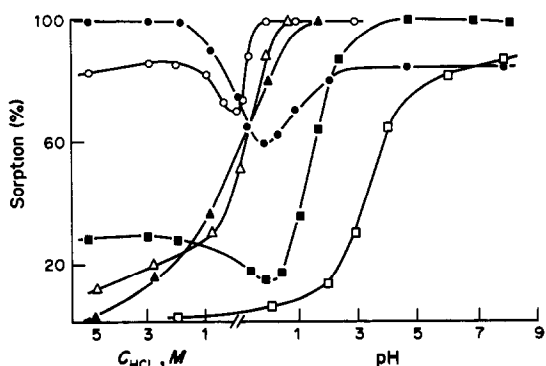


Fig 1 Effect of pH on sorption of Ru(IV) (■), Rh(III) (●), Pd(II) (▲), Os(VIII) (□), Ir(IV) (○) and Pt(IV) (△) on aminopropyl-silica I. $C_{\text{Me}} = 5 \times 10^{-5} \text{M}$, sorbent 0.1 g, solution volume 10 ml, duration of phase contact 30 min.

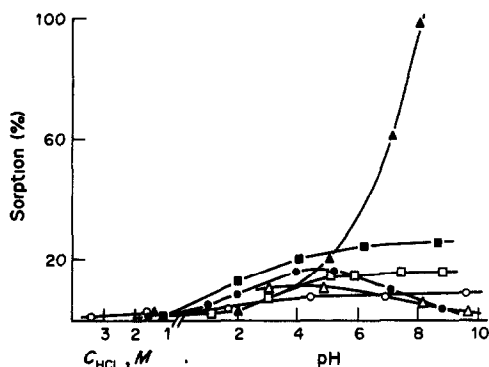


Fig 2 Effect of pH on sorption of Ru(IV) (■), Rh(III) (●), Pd(II) (▲), Os(VIII) (□), Ir(IV) (○) and Pt(IV) (△) on silica. Conditions as for Fig 1

and that the metal ions are bound solely by their interaction with the grafted ligands.

The multiple maxima and minima on the curves for sorption of Au(III) on all sorbents except strong anion-exchanger V were of great interest. The curves obtained were reproduced many times and their form was independent of the sorption mode (batch or dynamic) and the method of analysis (radioactive tracer method or spectrophotometry). The fact that similar maxima and minima are obtained with different sorbents strongly suggests that they arise from changes in the forms of gold in the solution, owing to aquation and hydrolysis,¹⁷ and differences in the strength of binding of the grafted ligands with various Au(III) complexes. Interaction of Au(III) with polyamines in hydrochloric acid solutions also leads to different complexes, depending on the acidity of the

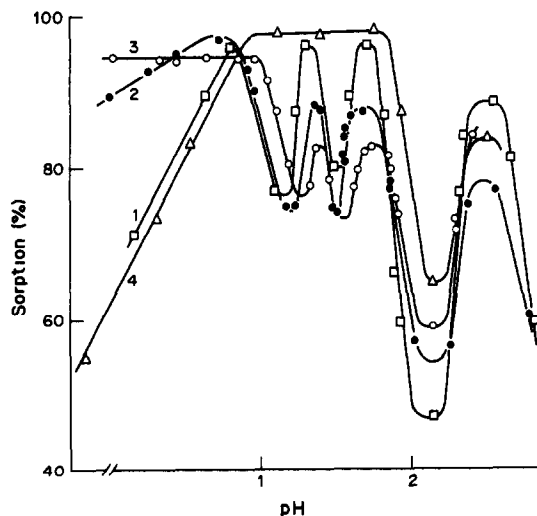


Fig 3 Effect of pH on sorption of Au(III) on sorbents I (1), II (2), IV (3) and V (4). $C_{Au} = 6 \times 10^{-5} M$, $I = 1$ (NaCl), other conditions as for Fig. 1

solution.^{18,19} Similar effects are also found for the platinum metal ions but, as can be seen from Figs. 1 and 2, to a much lesser extent.

In our opinion, the form of the curves for sorption of Ru(IV), Ir(IV) and Rh(III) on aminopropyl-silica is due to changes in the sorption mechanism. We propose that in strongly acidic medium (1–6M hydrochloric acid) these ions are sorbed on the protonated amino groups by an anion-exchange mechanism. Under these conditions, Rh(III) will exist at least partly as the $[RhCl_6]^{3-}$ complex, and the charge of this, being higher than that of the other platinum-metal chloro-complexes, is presumably responsible for the better sorption of Rh(III). With decreasing solution acidity the contribution of complex formation to bonding of the metal ions increases.

Sorption mechanism

There are no direct proofs of insertion of the grafted ligands into the inner co-ordination spheres of the noble metal ions. However, in our opinion the results given below strongly support this hypothesis. As can be seen from Fig. 3, there is a fundamental difference between the sorption of Au(III) on the complex-forming sorbents I–IV and on the strong anion-exchanger V. The decrease in sorption of Au(III) on sorbent V with increasing acidity can be attributed to the aquation reaction, which is very specific for Au(III):



This reaction takes place in strong acid medium and leads to the formation of uncharged species.¹⁷ The sorption on the complex-forming sorbents in strong acid media is significantly higher than that on sorbent V. The decrease in the degree of extraction with increasing acidity is probably due to protonation of the grafted ligands and thus a decrease in the surface concentration of the free complexing ligands. The increase in the denticity of the grafted ligands, in the sorbent sequence $I < II < III < IV$, should enhance the stability of the complexes. This is confirmed by the shift of the sorption curves with increase in acidity (Fig. 3). With increasing concentration of background electrolytes ($NaClO_4$, Li_2SO_4 and $NaCl$) the degree of Au(III) sorption decreases (Fig. 4). The effect of these electrolytes on the sorption is in the order $LiCl > Li_2SO_4 > NaClO_4$. If sorption had taken place by an anion-exchange mechanism, Li_2SO_4 should have had the greatest effect. The fact

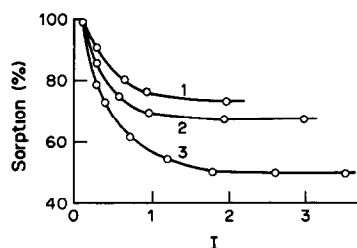


Fig 4 Effect of ionic strength (I) on sorption of Au(III) on sorbent I 1—NaClO₄, 2—Li₂SO₄, 3—NaCl

that lithium chloride has the greatest suppressive effect indicates the existence of two competitive reactions: formation of a complex with the grafted ligand and formation of chloride complexes.

Pt(IV), Ir(IV) and Pd(II) ions have a greater tendency than Ru(IV), Rh(III) and Os(VIII) to form complexes with aliphatic amines. As can be seen from Fig. 1, at pH 0–6 (where the complex-formation reaction is dominant) the sequence of sorption of metal ions on sorbent I, in general, coincides with the stability sequence of the amine complexes. Formation of different complexes during sorption of Ru(IV), Ir(IV) and Rh(III) and correspondingly change in the sorption mechanism with the solution acidity (Fig. 1), is confirmed by mathematical simulation of the equilibria in the system Pd(II)–(HCl, H₂O)–aminopropyl-silica. It has been shown that the predominant forms in the sorbent phase are the complex PdCl₃R (pH 4–1M HCl) and the ion-associate PdCl₃⁻RH⁺ (>1M HCl), where R is the sorbent functional group. Different molecular and ionic forms were taken into consideration: PdCl_x, PdCl_xR_n, PdCl_x(RH), RH (charges are omitted for simplicity).

Effect of metal concentration

As seen from Fig. 5, the sorption capacity of the sorbents for noble metals does not exceed 0.15 mmole/g, much lower than for similar sorbents based on organic polymers. When the metal concentration and degree of surface coverage with metal ions are low, the isotherms are linear. Under optimal sorption conditions, the distribution coefficients are 10⁴ ml/g for Ru(IV), Rh(III), Ir(IV), Pd(II) and Pt(IV), 10³ ml/g for Os(VIII) and 10⁵ ml/g for Au(III).

The modified silicas studied can be recommended for noble metal extraction from dilute solution. In this case the low sorption capacity is not important, but the high distribution coefficients and sorption rates are.

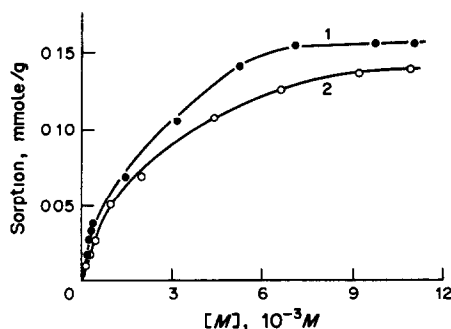


Fig 5 Effect of metal ion concentration on sorption of Rh(III) (1) and Ir(IV) (2) C_{HCl}, 1—3.0M, 2—2.0M; sorbent 0.05 g, solution volume 10 ml, duration of phase contact 1 hr

Desorption

Desorption of Au(III) was studied in detail. Two acids were selected for desorption: hydrochloric because chloride is a complexant for Au(III), and perchloric because it contains a large anion. In addition, different compounds forming stable complexes with Au(III) were used, among them ammonium salts, thiocyanate, thiourea and pyridine. The degree of desorption under the following conditions was used to estimate the elution power of these species: 50 μg of Au sorbed on 0.2 g of sorbent; 5 ml of eluent at a flow-rate of 20 ml·min⁻¹·cm⁻². The degree of desorption was monitored by a radioactive tracer method.

Typical dependences of the desorption on eluent concentration are shown in Fig. 6. Mineral acids are ineffective for eluting Au from sorbents I–IV, but the elution power of hydrochloric acid is higher than that of perchloric acid. Desorption by mineral acids is quantitative only for the strong anion-exchanger V. This difference in the behaviour of sorbents I–IV and V is additional evidence for the formation of

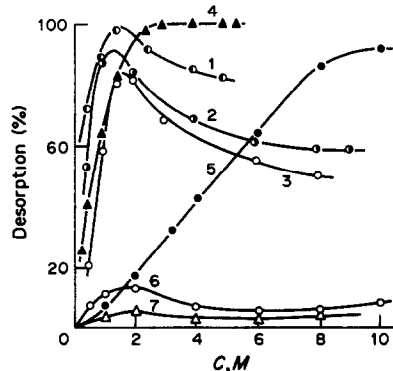


Fig. 6 Desorption of Au(III) with different eluents. 1–3—NH₄SCN; 4—pyridine, 5,6—HCl, 7—HClO₄, Sorbents: II—2,6, III—1,4, IV—3,7, V—5

Au(III) complexes with the amino-groups of sorbents I-IV.

Desorption of Au(III) by an ammonium nitrate solution is also inefficient. Gold is quantitatively desorbed from all sorbents with 0.1M thiourea in 0.1M hydrochloric acid, but this eluent cannot be used for analytical purposes because it causes difficulties in the determination of Au in the eluates. However, it is convenient to use for regeneration of the sorbents. Among the eluents studied, 1-2M potassium thiocyanate²⁰ and 3M pyridine are the best and give quantitative desorption of Au(III) from all the sorbents.

The platinum metals are eluted by acids only under conditions so severe that the sorbent is destroyed. An alternative is the application of strong complexants [as in the case of Au(III)], but the subsequent determination of metals is rather difficult.

Analytical application

There are two trends in application of sorbents in analytical chemistry: (a) ion sorption with subsequent desorption and determination by routine techniques; (b) sorption and direct determination of the sorbed ions in the sorbent phase, by any physical method applicable to solid samples (hybrid methods of analysis²¹). In general, the analyte is both separated from accompanying elements and concentrated at the sorption stage. During elution, the concentration factor decreases because the mass of eluent is larger than that of the sorbent. The detection limits obtained by the hybrid method are then of particular advantage.

Two methods were used to determine the ions in the sorbent phase: X-ray fluorescence for the platinum metals and atomic emission for Au.

The noble metals were first concentrated from the initial solution. Sorbent I was used for Rh(III) and Ir(IV), and sorbent III for Au(III).

The acidity was adjusted to give maximum extraction of the ion and at the same time separation from accompanying transition metal ions or other noble metals. Rh(III) and Ir(IV) were concentrated from 3M hydrochloric acid, and at pH 0.6. The results obtained are presented in Table 2. A systematic negative error (75% extraction) was found for Rh and Ir. This is probably due to a fraction of these metals being in a form with lower reactivity (as a result of competitive equilibria, polymerization, *etc*) which are not sorbed under dynamic conditions. The error can be compensated for by means of a correction factor or applying the whole procedure to the calibration standards.

The detection limit obtained by X-ray fluorescence is 0.01-0.02 $\mu\text{g/ml}$, for concentration from 1 litre of solution with 0.3 g of sorbent. Atomic-emission spectrometry is more sensitive and permits the detection of 0.1 μg of Au(III) on 0.02 g of sorbent, so the detection limit for concentration from 1 litre of solution with 0.1 g of sorbent is 0.5 ng/ml in the initial solution.

Under similar conditions, the noble metals can be separated from large amounts of transition metal ions—Cu, Co, Ni, Mn, Zn, Fe(III), *etc.* (Table 3). These metals are concomitant with noble metals in many natural and technological materials.

Separation of the platinum metals is also of great interest. X-Ray fluorescence permits the detection of pairs of these metals, one from each of the triads (Ru-Rh-Pd and Os-Ir-Pt) in a ratio of 1:10³. For metals in the same triad, however, the analytical lines are so close that determination is difficult. Table 4 shows that sorption of Ir(IV) from 3M hydrochloric acid (dynamic conditions) allows its separation from a 50-fold quantity of Pt(IV) and 1000-fold quantity of Os(VIII). The separation of Ir and Pt can be improved by using lower concentrations of these ions in the test solution. Under the same

Table 2 Results for concentration of Rh(III) and Ir(IV) with sorbent I and of Au(III) with sorbent III under dynamic conditions, initial content of Rh and Ir 100 μg , Au 15 μg ; sorbent 0.3 g, mean \pm standard deviation ($n = 3$)

Solution volume ml	Rh(III)		Ir(IV)		Au(III)	
	Found, %	CF*	Found, %	CF*	Found, %	CF*
10	80 \pm 2	27	90 \pm 4	30	100 \pm 1	33
100	79 \pm 2	2.6 \times 10 ²	77 \pm 4	2.6 \times 10 ²	100 \pm 1	3.3 \times 10 ²
250	76 \pm 3	6.3 \times 10 ²	76 \pm 2	6.3 \times 10 ²	99 \pm 1	8.2 \times 10 ²
500	74 \pm 3	1.2 \times 10 ³	75 \pm 3	1.3 \times 10 ³	98 \pm 2	1.6 \times 10 ³
1000	73 \pm 3	2.5 \times 10 ³	74 \pm 3	2.5 \times 10 ³	98 \pm 2	3.2 \times 10 ³

*CF concentration factor = (concentration in eluate)/(concentration in initial solution)

Table 3 Rh(III), Ir(IV), Au(III) sorption in the presence of accompanying ions, initial content of Rh and Ir—50 µg in 1000 ml of solution, Au—15 µg in 15 ml, means ± standard deviation (n = 3)

Element (E)	Rh(Ir):E	Rh found, %	Ir found, %	Au:E	Au found, %
Co ²⁺	1 · 10 ⁴	99.2 ± 2.0	97.2 ± 1.9	1:10 ³	99.4 ± 1.0
Ni ²⁺	1 · 10 ⁴	99.6 ± 1.0	97.2 ± 1.9	1 · 10 ³	99.9 ± 1.0
Cu ²⁺	1 · 10 ⁴	99.8 ± 2.0	97.2 ± 2.9	1 · 10 ³	99.4 ± 2.0
Fe ³⁺	1 · 10 ⁴	99.6 ± 1.0	97.8 ± 2.9	1 · 10 ³	99.3 ± 2.0
Al ³⁺	1.5 × 10 ⁴	99.3 ± 2.0	97.8 ± 1.0	—	—
Σ Co, Ni, Cu, Fe, Al	1.5 × 10 ⁴	99.2 ± 3.0	97.1 ± 2.9	—	—
Zn ²⁺	—	—	—	1 · 10 ³	98.6 ± 2.0
Cd ²⁺	—	—	—	1 · 10 ³	96.2 ± 2.0

Table 4 Separation of Rh and Ir from the other platinum metals on sorbent I, initial content of Rh and Ir—100 µg; mean ± standard deviation (n = 3)

Element (Me)	Accompanying element (E)	E Me, w/w	Volume of solution, ml	Sorption of Me, %	Sorption of E, %
Rh(III)	Pd(II)	10	500	72 ± 4	1
		50	500	70 ± 4	0.8
	Ru(IV)	1	10	78 ± 2	23
		1	100	71 ± 4	21
	Σ Pt(IV), Os(VIII), Ru(IV), Pd(II), Ir(IV)	1 (for each metal)	10 100	77 ± 3 71 ± 4	Pd—3, Ru—20 Pd—non-detectable, Ru—20
Ir(IV)	Pt(IV)	10	500	75 ± 4	non-detectable
		50	500	70 ± 3	0.3
	Os(VIII)	100	100	77 ± 4	non-detectable
		1000	100	76 ± 3	0.5
	Σ Pt(IV), Os(VIII), Ru(IV), Rh(III), Pd(II)	1 (for each metal)	10 100	84 ± 3 76 ± 4	Os—non-detectable, Pt—82 Pt and Os—non-detectable

conditions Rh(III) can be separated from a 50-fold quantity of Pd(II), but quantitative separation of Rh and Ru is not successful even at 1:1 Rh:Ru ratio.

CONCLUSION

Silicas with chemically grafted aliphatic mono- and polyamines have a high rate of sorption for noble metals. This is attributed to the combined mechanisms of ion-exchange and complex formation. The high strength of binding of the noble metal ions permits their concentration from dilute solutions, with concentration factors of ~10³, as well as their quantitative separation from 10⁴-fold quantities of accompanying metals. Desorption of the noble metal ions from the surface of the modified silicas is complicated, so it is best to determine them directly in the sorbent phase by X-ray fluorescence and atomic emission

REFERENCES

- O M Petrukhin, G I Malofeeva, V I Nefedov, Ya V Salyn, E V Marcheva, V A Shestakov, O A Shryaeva, Yu L Murnov, Yu E Nikitin and Yu A Zolotov, *Zh Analit Khim*, 1983, **38**, 250
- E Káralová and H Špičková, *Sb Vys Sc Chem Technol Praze, Anorg Chem Technol.*, 1982, **B27**, 105
- E Káralová, Z Radová, F Švec and J Káral, *Collection Czech Chem Commun*, 1978, **43**, 604.
- M Knothe, *Isotopenpraxis*, 1982, **18**, 241
- G V Myasoedova, I I Antokol'skaya and S B Savvin, *Talanta*, 1985, **32**, 1105
- N N Kazanova, O M Petrukhin, I I Antipova-Karataeva, G I Malofeeva, E V. Marcheva and Yu. I Murnov, *Koord. Chem*, 1986, **12**, 108.
- I P Almarin, V I Fadeeva, G V Kudryavtsev, I M. Loskutova and T. I Tikhomirova, *Talanta*, 1987, **34**, 103
- T. Seshadri and A Kettrup, *Z. Anal Chem*, 1982, **310**, 1
- K Lechtenborger, H G. Srebny and A Kettrup, *ibid*, 1983, **314**, 135
- M. Grote, A Schwalk and A Kettrup, *ibid.*, 1982, **313**, 297
- T Seshadri and H I Haupt, *Anal Chem*, 1988, **60**, 47
- P Sutthivayakit and A Kettrup, *Anal Chim Acta*, 1985, **169**, 331
- I P Almarin, P N Nesterenko and V M Ivanov, *Dokl Akad Nauk SSSR*, 1983, **271**, 627
- B V L'vov (ed.), *Dostizheniya i problemi prakticheskogo primeneniya spektralnogo analiza*, Nauka, Leningrad, 1985
- A T Savitchev and M S Fogelson, *Izv Akad. Nauk SSSR, Ser Geologiya*, 1987, 103
- T I Tikhomirova, I M Loskutova, V I Fadeeva, I.

- R Zmievskaya and G V Kudryavtsev, *Zh Analit. Khim*, 1984, **39**, 1630
- 17 B I Peshchevitski, V I Belevantsev and S. V Zemskov, *Izv Sib. Otd. Akad. Nauk SSSR, Ser. Khim. Nauk*, 1976, No 2, 24
18. W H Baddley, F Basolo, H. B Gray, C Nolting and J. A. Poe, *Inorg Chem*, 1963, **2**, 921.
19. B P Block and J C Bailar, *J Am Chem Soc*, 1951, **73**, 4722.
- 20 P N Nesterenko, V M. Ivanov, G V. Kudryavtsev and G V Lisichkin, *Zh. Analit. Khim.*, 1982, **39**, 456.
- 21 Yu. A. Zolotov and N M. Kuz'min, *Kontsentrirovaniye Mikroelementov*, Khimiya, Moscow, 1982

OPTIMIZATION OF FLOW-INJECTION SYSTEMS FOR DETERMINATION OF SUBSTRATES BY MEANS OF ENZYME AMPLIFICATION REACTIONS AND CHEMILUMINESCENCE DETECTION

ELO H. HANSEN, LARS NØRGAARD and MIKAEL PEDERSEN

Chemistry Department A, Technical University of Denmark, Building 207, DK-2800 Lyngby, Denmark

(Received 2 July 1990 Revised 25 July 1990 Accepted 31 July 1990)

Summary—A flow-injection system is described that incorporates a small column reactor containing two co-immobilized, synergistically operating oxidoreductases, allowing determination of minute amounts of substrates by means of enzyme amplification and subsequent chemiluminescence detection of the hydrogen peroxide generated in the repeated redox cycling. With lactate oxidase and lactate dehydrogenase, and taking advantage of the fact that the enzymatic degradation step and the ensuing detection step can be individually optimized, the FIA-system has been optimized by factorial experiments to yield an amplification factor of over 140 for each of the two substrates lactate and pyruvate. With a linear calibration range of 0–6 μ M, the limits of detection for the two species were 48 and 103 nM, respectively, and the sampling rate was 50–60/hr. The optimized system has also been employed for assay of glucose by utilizing a column reactor with immobilized glucose oxidase and glucose dehydrogenase, but yielded amplification factors of only 3–4. The large discrepancy in the performance of the two enzyme systems is discussed.

In a previous communication,¹ we reported the determination of minute amounts of substrates by means of enzyme amplification, with two synergistically operating oxidoreductase enzymes co-immobilized on small glass beads in a small column-reactor which was incorporated into a flow-injection analysis (FIA) system.² Because the repeated recyclings consume oxygen and NADH and generate NAD⁺ and hydrogen peroxide (Fig. 1), it was found preferable to base the ultimate detection on a chemiluminescence reaction of the hydrogen peroxide formed. To make the analytical system practical, a preset condition was that the entire analytical cycle could be accomplished within 1–1.5 min, thus facilitating a sampling frequency of at least 40/hr. Preliminary investigations with a model system comprised of lactate oxidase (LOD) and lactate dehydrogenase (LDH) demonstrated that the approach worked satisfactorily, but as the amplification factor was only 38 it was assumed that the system could be further optimized. This paper reports an optimization procedure which has resulted in amplification factors of more than 140. In addition, the optimized FIA system has been used in an attempt to assay glucose with a column-reactor containing

immobilized glucose oxidase and glucose dehydrogenase.

Because the enzymatic step and the detection step in the FIA approach are entirely separate, in contrast to the case for enzyme electrodes, it is feasible to optimize them individually. In concordance with the previously reported work, this optimization was focused on (a) the influence of the relative flow-rates and concentration levels of the reagents used in the chemiluminescence detection of the hydrogen peroxide generated and of the sequence of mixing the reagent and analyte streams (*i.e.*, the detection step) and (b) the molar ratio of the two co-immobilized enzymes and their absolute quantities (*i.e.*, the enzymatic degradation step).

Inherently, the optimized FIA system should be applicable for assay of a variety of substrates provided that suitable oxidoreductase combinations can be found. One such combination is glucose oxidase (GOD) and glucose dehydrogenase (GDH). As seen in Fig. 1, the LOD/LDH and GOD/GDH enzyme systems operate very similarly, but in the glucose system there is a possible side-reaction, *i.e.*, the glucono- δ -lactone formed as an intermediate in the degradation of glucose might be hydrolysed to gluconic acid; if this happens, the cycle will be

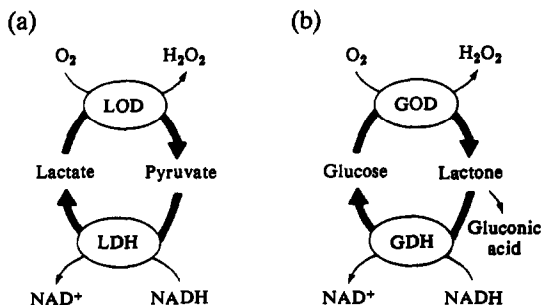


Fig 1 Amplification reactions for (a) pyruvate and lactate by means of lactate oxidase (LOD) and lactate dehydrogenase (LDH) and (b) glucose by means of glucose oxidase (GOD) and glucose dehydrogenase (GDH). In the latter the side-reaction leading to formation of gluconic acid will remove the substrate for the GDH and hence terminate the cycle

terminated. This side-reaction is very fast, and indeed Schubert *et al.*,³ who attempted to use this enzyme combination in a membrane electrode, only managed to obtain amplification factors of 3–8. In a column reactor in a FIA system, where the radial mass transfer is much more intense than in diffusion-controlled membrane, it might be expected that this side-reaction could be minimized, thereby allowing determination of glucose in the sub-micromolar range.

EXPERIMENTAL

Reagents

Distilled demineralized water was used throughout. L-Lactate dehydrogenase [LDH] (EC 1.1.1.27, lyophilized, salt-free powder, 940 U/mg), lactate oxidase [LOD] (EC 1.1.3.2, crystalline, 30 U/mg), L(+) -lactic acid (Li salt) and pyruvic acid were purchased from Sigma. A batch of lactate oxidase (lyophilized, 20 U/mg) was also obtained from Boehringer Mannheim Biochemicals. Glucose dehydrogenase [GDH] (EC 1.1.1.47, lyophilized, 220 U/mg) and D(+) -glucose were from Merck. Glucose oxidase [GOD] (EC 1.1.3.4, lyophilized, 240 U/mg) and NADH were supplied by Serva. Other chemicals used were of analytical reagent quality.

As support for the immobilized enzymes CPG 10 glass beads (diameter 0.75–0.125 mm, pore size 70 nm, Serva) silanized with 3-aminopropyltriethoxysilane in sodium-dried toluene,^{1–4} were used. Approximately 4–5 mg of enzyme mixture was dissolved in 1 ml of phosphate buffer (pH 7.0). For the LOD/LDH pair, the best results were obtained with a

molar enzyme ratio of *ca.* 1:1 (see Results and Discussion).

The enzymes were co-immobilized on 100 mg (250 μ l) of the support by the glutardialdehyde method as detailed previously.^{1,4} For use, the treated glass beads were packed into a column consisting of a piece of polyethylene tubing (i.d. 1.18 mm) furnished with small nylon nets at the ends to retain the glass beads within the reactor during operation. When not in use, the packed column reactors were stored in 0.1M citrate buffer (pH 6.0) in a refrigerator at 4° to minimize microbiological degeneration.

Aqueous lactate, pyruvate, glucose and hydrogen peroxide standards in the range 1–100 μ M were made by sequential dilution of 1.0mM L(+) -lactic acid, pyruvic acid, glucose and hydrogen peroxide stock solutions with distilled water. All solutions were freshly prepared every day. The liquid streams propelled in the FIA system shown in Fig. 2 (which depicts the finally optimized FIA manifold for the LOD/LDH system) were: carrier stream of distilled water; buffer stream of 0.015M phosphate buffer (pH 6.8) containing 1.5mM NADH; 1.5mM luminol (5-amino-2,3-dihydro-1,4-phthalazinedione) in 0.1M potassium carbonate (pH 11.5), and 30mM aqueous potassium hexacyanoferrate(III). For the manifold containing the GOD/GDH enzyme reactor the parameters were the same, except that pH 6.0 phosphate buffer was used.

Apparatus

The FIA manifold (Fig. 2) comprised two peristaltic pumps: P1 (Ventur, variable flow, Alitea, Sweden) for the aqueous carrier stream [into which the sample solution (50 μ l) was injected] and the buffer/NADH stream, and P2 (Mini-S-840, Ismatec, Switzerland) for the

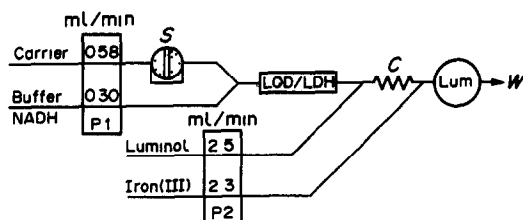


Fig 2 Optimized FIA manifold for the determination of lactate or pyruvate by enzyme amplification with ensuing detection by chemiluminescence (Lum). S, sample injection (50 μ l), LOD/LDH, column reactor (140 μ l) containing the two co-immobilized enzymes (LOD/LDH), C, mixing coil (40 cm) and W, waste. Solutions were propelled by two peristaltic pumps (that for the carrier and buffer/NADH streams allowing variable pumping rates)

reagent streams [luminol and hexacyanoferrate(III)] needed for the chemiluminescence determination of the hydrogen peroxide generated by the enzymatic conversion processes in the packed reactor. The detector consisted of a home-made luminometer with two photodiodes (BPW 34), details of which have been given elsewhere.⁴ All connecting lines in the FIA manifold consisted of 0.5 mm i.d. Microline tubing.

All experiments were executed at room temperature (*ca.* 20°) and to make the apparatus as simple and practical as possible, no attempt was made to operate the FIA manifold at controlled or elevated temperature.

RESULTS AND DISCUSSION

Optimization of the detection system

The optimization was based on that of the previously used FIA manifold,¹ which was rather similar in design to that in Fig. 2, except that the luminol and hexacyanoferrate(III) streams were mixed before joining the combined carrier/buffer stream. The reason for this approach, which has been used extensively in this laboratory, is that a composite solution of these two reagents is not stable, so they have to be mixed immediately before use, which can best be done in the manifold. However, it was found that the signal to noise ratio and the signal amplitudes could be considerably improved with the sequence of addition shown in Fig. 2, which was therefore adopted. This improvement is probably due to more efficient mixing of the strongly alkaline luminol stream and the combined carrier/buffer stream, which has a certain buffering capacity.

The FIA system was first optimized for assaying hydrogen peroxide, in order to obtain as low a detection limit as possible, *i.e.*, the LOD/LDH reactor was not used in these tests. In addition to the preselected condition as to sampling frequency (*i.e.*, a minimum of 40 samples/hr), the following restrictions were imposed.

(a) The injection volume should be maintained at 50 μ l (to allow for situations where sample material might be limited).

(b) The flow velocities of the buffer stream and the carrier stream should be about the same and the combined flow velocity should not exceed 1.0 ml/min (so that in the complete system there would be sufficient residence time for the sample in the enzyme reactor and any risk that tight packing of the column material

might lead to increased back-pressure would be minimized).

(c) The concentration of phosphate in the combined carrier/buffer stream solution should be 0.005M and the pH should be fixed at 7.0. This should secure sufficient buffering capacity to maintain this pH within the enzyme reactor.

(d) The concentration of potassium carbonate in the luminol solution should be maintained at 0.1M, which had previously been found reasonable.⁵

(e) The length of the mixing coil should be 40 cm, which is a judicious compromise between efficient mixing and acceptable dispersion (and hence dilution) of the injected sample solution.

(f) The distance between the last merging point and the chemiluminescence detector should be minimized so that the chemiluminescence (CL) signal (which appears as a rapid pulse) actually recorded would be as large as possible. In this case the distance was 2 cm, the minimum physically allowable length in the detection device used.¹

With these restrictions imposed, six parameters were to be optimized. These were first screened in a fractional factorial experiment, where each parameter was tested at two levels as follows (the values in brackets denote the high and low levels used). (1) The flow velocity of the combined carrier/buffer stream (0.5 and 1.0 ml/min); (2) the flow velocity (1.5 and 2.5 ml/min) and (3) the concentration (10 and 20mM) of the hexacyanoferrate(III) stream; (4) the flow velocity (1.5 and 2.5 ml/min) and (5) the concentration (0.2 and 1.0mM) of the luminol stream; (6) the pH of the luminol solution (10.5 and 11.5) The response function chosen was the peak height from injection of a 30 μ M hydrogen peroxide standard solution, and the screening experiment showed that the parameters should all be used at the high level. Therefore two series of complete 2² factorial experiments were executed to find the interdependence between the two reagent flows, and their combined influence on the response. One series used the flow velocities of the luminol and hexacyanoferrate(III) solutions as parameters, and the other the concentrations of the two reagent solutions as parameters. Because the aim was to minimize the limit of detection, yet maintain high sensitivity and a low blank value, the response function (*RF*) was chosen as $RF = 100 [0.50 PH_5 + 0.25\alpha + 0.25(1 - \beta)]$ where PH_5 is the peak height obtained for injection of a 5 μ M hydrogen peroxide standard

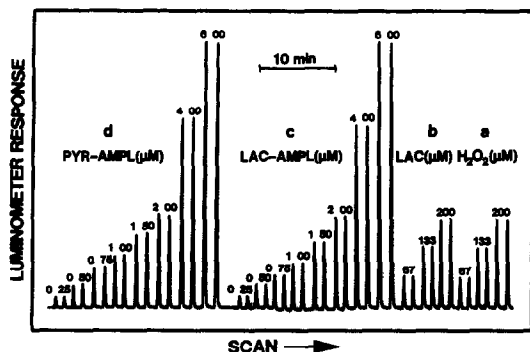


Fig 3 Calibration runs for lactate and pyruvate with the system in Fig 2 (a) Hydrogen peroxide standards in the concentration range 67–200 μM and (b) lactate standards in the same concentration range, with a buffer stream not containing NADH (*i.e.*, non-amplified signals), the peaks indicate that 100% conversion of lactate was obtained under the prevailing conditions (c) Lactate standards and (d) pyruvate standards in the concentration range 0.25–6.00 μM with a carrier/buffer stream containing NADH (*i.e.*, amplified signals), revealing an amplification factor of 100 for both species (*cf.* Fig 4) Note that the residence time for the sample is less than 1 min, allowing a sampling frequency exceeding 60/hr

solution, α the slope of the calibration graph and $(1 - \beta)$ the intercept on the ordinate. Obviously, the three values were weighted 50, 25 and 25%, respectively. All values were normalized, *e.g.*, $PH_5 = (PH_5^{\text{obs}} - PH_5^{\text{min}})/(PH_5^{\text{max}} - PH_5^{\text{min}})$, where the superscript *obs* refers to the observed values in an individual experiment and *min* and *max* to the minimum and maximum values in a series.

This fine-tuning showed that the optimal combinations of flow velocity and concentration for the luminol and hexacyanoferrate(III) solutions were 2.5 ml/min and 1.5 mM and 2.3 ml/min and 30 mM, respectively. Combined with the results of the screening experiment, this resulted in the manifold design depicted in Fig. 2 (except that the LOD/LDH reactor was absent and the carrier and buffer streams were pumped at equal rates, *i.e.*, 0.5 ml/min). The system was calibrated by injection of standards of aqueous hydrogen peroxide, and the detection limit was found to be 0.19 μM . This is *ca.* 10 times lower than that with the non-optimized system¹

Optimization of the FIA enzyme amplification system

The FIA system was next optimized with the LOD/LDH enzyme reactor installed. In these experiments a reactor with 1:1 molar ratio of the two immobilized enzymes (corresponding to

a weight ratio of 2:3) was employed, because the earlier reported experiments indicated that this would be preferable (for further discussion, see below). The manifold was further slightly modified in that the ratio of the carrier to buffer flow-velocity was altered to 2:1 to limit the dispersion and hence dilution of the injected sample, thereby ultimately securing a lower limit of detection. For the same reason, the phosphate concentration in the buffer stream was increased to 0.015 M to give a final concentration of 0.005 M in the combined carrier/buffer stream.

For optimization of the total FIA system, one of the parameters would be the flow-rate of the combined carrier/buffer stream, because this affects the residence time of the sample in the enzyme reactor and thus the amplification. In this context it is important to keep in mind that the detection system was optimized to yield maximum CL response at a fixed flow-rate of the combined carrier/buffer stream (*viz.* 1 ml/min). Because the CL signal is dynamic in nature and appears as a rapidly fading pulse, any change in the flow-rate of the carrier/buffer stream, and hence the flow velocity through the detector, will cause a shift in the portion of response that is actually recorded by the detector. If the conversion of analyte is proportional to the residence time, a lower flow-rate through a given reactor volume should increase the conversion, but would result in a lower CL signal, whereas a higher flow-rate (*i.e.*, close to 1 ml/min), despite the shorter residence time would give a higher signal. With these considerations in mind, the following experiments were executed.

With a packed enzyme column reactor having a volume of 75 μl , the system was subjected to a complete 2³ factorial experiment, where the following parameters were tested (the values in brackets denote the high and low levels used and refer to the conditions immediately prior to, and *in*, the reactor): (1) the pH (7.0 and 7.5); (2) the NADH concentration (0.33 and 0.50 mM), (3) the flow-velocity (0.64 and 0.88 ml/min) of the combined carrier/buffer stream. In all cases, lactate standards in the concentration range 0–6 μM were injected. The response function was selected as $RF = 100[(AF^{\text{obs}} - AF^{\text{min}})/(AF^{\text{max}} - AF^{\text{min}})]$, where *AF* is the amplification factor and the superscripts have the same meanings as above. This response function obviously requires that the efficiency of conversion of lactate by LOD (*i.e.*, without NADH present in

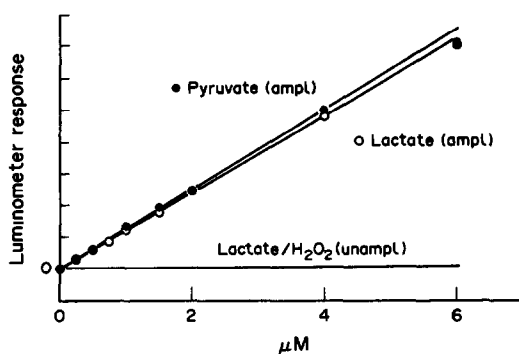


Fig 4 Calibration plots for hydrogen peroxide and lactate (unamplified) together with pyruvate (●) and lactate (○) (both amplified) in the concentration range 0–6 μM (cf Fig 3) For concentrations exceeding *ca* 5–6 μM , the calibration signals for both species start to level off, indicating depletion of reagent (*i.e.*, NADH)

the carrier stream) is 100% and this was found to be the case (Fig. 3). In addition to the amplification experiments, a calibration for hydrogen peroxide was run for each combination of experimental parameters, because it can alter with a change in the pertinent parameters. In particular, the total flow velocity will influence the CL response. The sampling rate was omitted from the factorial design, because all the preliminary tests showed that a rate of 50/hr was possible, which satisfied the requirement of a minimum rate of 40/hr.

The results of this analysis showed that the influence of NADH concentration within the range tested was negligible. However, with the other parameters constant it was found preferable to operate the system at the low flow velocity and low pH levels which yielded an amplification factor of 56. From the literature it is known that the two enzymes in soluble form have maximum activity at pH 6.5 (LOD) and 7.5 (LDH), respectively^{6,7} Although these pH maxima might change when the enzymes are immobilized, they will very likely remain at the same order of magnitude.⁸ A pH of *ca.* 7.0 should therefore be more favourable for the combined system, as corroborated by these experiments. The lower flow velocity implies a longer residence time of the sample within the enzyme reactor (allowing a greater number of redox cycles, leading to increased amplification), but leads to a lower sampling frequency. The lack of influence of the concentration of NADH can be explained by the fact that the LDH is already saturated with the coenzyme when this is present at the lower level.

The length of the reactor might influence the amplification and hence the signal recorded, because a longer reactor should allow more redox cycles (provided that the reagents, oxygen and NADH, are in excess). For that reason, an experiment was conducted with a longer column reactor, of 110- μl volume, and the same enzyme preparation as before (with a flow-rate of 0.64 ml/min for the combined carrier/buffer stream, containing 0.5mM NADH). This system yielded an amplification factor of 82. Further optimization of the pH of the carrier/buffer stream showed that the optimal pH was 6.8, resulting in an amplification factor of 99.5. Hence, this pH was used in all further experiments. The concentration of the phosphate buffer was not altered, because the buffering capacity at this slightly lower pH value is only marginally affected and was sufficiently large.

As stated above, the original detection system was optimized with a combined carrier/buffer flow-rate of 1.0 ml/min, which for the given parameters of the detection system itself yielded the maximum CL response. Hence, with the pumping rate at the high level (0.88 ml/min, which was the closest possible to 1.0 ml/min with the available pump tubes when operating at the carrier:buffer ratio 2:1), it is necessary to use a longer enzyme reactor in order to reach an amplification factor of say, 100. In this case a 140- μl column was required. The FIA manifold of this system is that shown in Fig. 2, and its performance is reproduced in Fig. 3. When the signals for the unamplified lactate and hydrogen peroxide standards are compared, it is seen that the conversion for lactate was 100% and from the unamplified and amplified lactate signals it is seen that the amplification factor was indeed 100. Pyruvate also gave 100% conversion and the amplified pyruvate and lactate signals were virtually identical for similar concentrations. The calibration plots in the recorded range were linear, as shown in Fig. 4, and almost congruent. Therefore, a single calibration graph could be used, but for the highest precision it is preferable to calibrate for the two species individually. At higher concentrations (6 μM and above) the calibration signals start to level off, indicating shortage of reagents. This is not a limitation, however, because at higher concentrations the species can be assayed directly without the need for amplification reactions. The detection limit for this system was found to be 48nM for lactate and 103nM for pyruvate, as calculated from the regression bands (95%

confidence interval) of the calibration plot.⁹ The precision for lactate, determined from estimated response variances for the eight calibration standards ($n = 16$), was 1.9%; for pyruvate it was slightly higher. It was also calculated that for a response equal to the average response of the standards in the range 0–4 μM inclusive, the 95% confidence limits for the corresponding lactate concentration would be $1.20 \pm 0.05 \mu\text{M}$ (expected value 1.25 μM). The sampling frequency was 50–60/hr.

The incorporation of even larger enzyme columns in the FIA system yielded higher amplification factors, but the increase was not proportional to the reactor volume. There was also an increased back-pressure, resulting in variations in performance of the system and impaired precision, and for that reason it was decided not to use columns with a volume larger than *ca.* 140 μl , which already gave amplification factors (of *ca.* 100) which were considered to be very satisfactory. Furthermore, increased amplification would lead to a still narrower calibration range because of depletion of the reagents, particularly NADH. Although the concentration of this species can potentially be increased, it was previously found that this was not advisable because higher concentrations appeared to induce side-reactions with the hydrogen peroxide generated.¹ Furthermore, it has been reported that impurities in high concentrations of NADH can inhibit enzymes.¹⁰ As far as the interplay between the pumping rate of the combined carrier/buffer stream and the length of the enzyme reactor column is concerned, it appears that for given dimensions of the detection system and a required sampling frequency, it is necessary to optimize each system individually.

The results compare very favourably with those of a recent work where the detection limit for lactate was reported to be 119 nM.¹¹ However, in that work an enzyme reactor of 350 μl and a sample volume of 200 μl were used and detection was based on use of a specially constructed flow-cell for amperometric determination of the consumption of oxygen. The largest amplification factor was 70.

Optimization of the packed enzyme column reactor

Previously published results indicated that the molar ratio of the two enzymes should be close to unity.¹ This is intuitively to be expected, because it would mean (provided that the

enzymes are randomly immobilized on the support) there would be a higher probability of contiguous site-fixation of the two enzymes, which should favour the repeated redox cycling of the analyte. To corroborate this, a series of enzyme columns was prepared with molar ratios of LOD/LDH ranging from 1:3 to 4:1. With the same column size (140 μl) and the optimized conditions stated in Fig. 2, the amplification factors varied between 100 and 142 (in the latter case the detection limit for lactate was lowered to 34 nM). These variations were not statistically significant, in view of the inherent lack of absolute control of the immobilization procedure. It was therefore concluded that the molar ratio, contrary to expectation, does not play an important role provided that it approximates to unity. Both crystalline and lyophilized enzyme preparations were tested, but owing to lack of sufficient materials it was not possible to draw any firm conclusion as to the preference for either. These findings are in good agreement with those reported by Asouzu *et al.*,¹¹ although these authors did not elaborate on this theme. The enzyme reactor columns did not reveal any significant decrease in activity over a period of two months.

It is concluded that the increase in amplification, over that in the previously reported procedure, is to be ascribed mainly to the optimized detection system. It is possible that glass beads of pore size other than that used in this investigation and enzymes of improved quality and higher specific activity could influence the amplification, but probably only marginally. However, although higher amplification would give a lower limit of detection, it would be at the expense of a shorter linear calibration range.

Determination of glucose

The optimized FIA system in Fig. 2 was subsequently adapted for assay of glucose by incorporating a 150- μl enzyme column reactor with GOD/GDH mixed in *ca.* 1:1 weight ratio (prepared from one Merck vial of GDH, *i.e.*, *ca.* 250 U, and 2 mg of GOD, corresponding to *ca.* 440 U). With the same NADH carrier/phosphate buffer stream as for lactate (0.005 M NADH, pH 6.8) and glucose standards in the range 10–100 μM , the amplification factor was found to be only 3.5 (for 50 μM glucose). Lowering the pH of the combined carrier/buffer stream enhanced the amplification factor slightly. Thus for a pH of 6.0 it was increased to 4.1, but further decrease in pH lowered it

again (to 3.7 at pH 5.5). Citrate buffers were also tested, but produced no significant change in amplification. Although very disappointing, these results are similar to those of Schubert *et al.*,³ who found an amplification of 3 for 0.1–1.0mM glucose with 1mM NADH, which was increased to 8 by using 0.1M NADH but at the expense of very long response times (several minutes). Scheller *et al.*¹² employed a large column reactor (0.8 ml) of co-immobilized GOD, GDH and catalase, and enthalpimetric quantification, but even with this very sensitive system they only managed to obtain an amplification of 8 for 100 μ M glucose. Thus, although it was hoped that the combination of convection and diffusion in the column reactor of the FIA system would result in much better amplification, it appears that the poor results compared with those of the LOD/LDH-system are due to some fundamental differences, for which there are several possible explanations.

First, the Michaelis–Menten constants (K_M) for the GOD/GDH enzyme systems are almost two orders of magnitude larger than for the LOD/LDH enzymes. The K_M -values for the enzymes are as follows: LOD (lactate) 0.7mM;¹² LDH (pyruvate) 0.14mM;¹² GOD (glucose) 33mM;^{13,14} GDH (glucose) 47mM.¹⁵ Thus although the substrate concentrations in all experiments were well below the K_M -values, ensuring pseudo first-order reaction conditions, the reaction rate of the GOD/GDH system would be considerably lower than that of the LOD/LDH system. This is all the more unfavourable because of the inherent risk of the side-reaction of spontaneous hydrolysis of the primarily formed glucono- δ -lactone. This irreversible reaction, whereby the lactone is removed from the reaction sequence and the cycle terminated, is very fast. Generally, the rate of hydrolysis of lactones decreases at lower pH values. Hence, the slightly enhanced amplification factor at pH 6.0 might be ascribed to this phenomenon, although this pH is not likely to be the optimum for the enzyme pair (pH_{opt} is ca. 8 for GDH,¹⁵ and 5.5 for GOD^{13,16}). It has also been reported that the hydrolysis *per se* is fairly slow, but is catalysed by the enzyme gluconolactonase present as an impurity in the commercial preparations of glucose oxidase.^{17,18} Thus, Hanazato *et al.*¹⁷ found that at pH lower than 6, the spontaneous hydrolysis of glucono- δ -lactone hardly occurred, but its rate increased exponentially with pH at pH > 6, and was greatly accelerated when gluconolactonase was

present. Interestingly, they also found that the activity of gluconolactonase was strongly inhibited by phosphate, and was minimal at pH 5.5. Therefore the use of a phosphate buffer at this pH should ostensibly be preferable to other buffer solutions for the enzyme amplification applications. The results reported here do not appear to support this, however.

A second complication is the potential presence of catalase in the enzyme preparations, because this would result in degradation of the generated hydrogen peroxide and thus exclude it from detection by the luminescence procedure. Catalase is probably the enzyme with the highest known specific activity (4×10^4 U/mg), and therefore even minute amounts of this constituent would have serious effects on the method. Both enzyme preparations were therefore examined for the possible presence of catalase, by making separate column reactors in which approximately similar number of units of the two enzymes were immobilized either individually or together, then injecting hydrogen peroxide standards into the FIA system with and without the enzyme column installed, and comparing the areas under the peaks. For the GOD, which according to the manufacturer's specification contains less than 5 U of catalase per mg (the GOD/catalase ratio being guaranteed to be at least 60), no significant differences in the recorded areas were found, indicating that catalase was not a problem. Furthermore, injection of equimolar standards of hydrogen peroxide and glucose (50 μ M) showed that the peaks were identical, indicating 100% conversion. For the GDH columns, however, injection of hydrogen peroxide standards gave considerably smaller signal areas than those for the "empty" system, irrespective of whether NADH was present. The commercially available GDH enzyme from Merck is reported to have been prepared by chromatography and no mention is made as to the presence of catalase. When NADH is present in the carrier/buffer stream, the decrease in signal could be explained by the previously mentioned side-reaction between hydrogen peroxide and NADH (as catalysed by the enzyme), but the decrease without NADH present is truly surprising. Whether the decrease in signal is due to the presence of catalase remains to be determined, but the observed phenomenon does partly account for the fact that such poor amplification is recorded. In this context it is interesting to note that Schubert *et al.*³ measured the disappearance of oxygen as

the basis for quantification of the amplification. If the initially generated hydrogen peroxide is partly split into oxygen and water, it would explain why these authors found amplification factors of the same order of magnitude as reported here, although their detection method relied only on diffusion (in the electrode assemblies), whereas the present work employed a combination of diffusion and convection in the FIA column-reactor

CONCLUSIONS

Application of the FIA approach for assaying substrate concentrations in the nM – μM range by means of enzyme amplifications, based on the use of co-immobilized enzymes contained within a small column reactor incorporated into an FIA manifold, appears to be very attractive, because it allows the enzymatic degradation step and the ensuing detection of a suitable reaction product to be individually investigated and optimized. The conditions optimized by factorial experiments with co-immobilized LOD and LDH in a molar ratio of 1:1 and chemiluminescence for detection of the hydrogen peroxide formed by the repeated redox cycling yielded an amplification factor of more than 140 in assays of lactate or pyruvate. Since the entire analytical cycle could be accomplished in less than 1 min, thus allowing sampling rates of *ca.* 60/hr, the FIA approach seems to have interesting potential. Inherently, the optimized FIA system should be applicable for assays of a variety of substrates, provided that suitable oxidoreductase combinations can be found. One such combination, glucose oxidase (GOD) and glucose dehydrogenase (GDH), has been tested, but the amplification factor was found to be only about 4. Possible explanations for this low amplification might be the presence of gluconolactonase in the GOD and catalase in the GDH. Gluconolactonase would increase the rate of hydrolysis

of the initially formed glucono- δ -lactone, thereby terminating the cycling procedure, and the presence of catalase would lead to degradation of the concurrently formed hydrogen peroxide and thereby prevent monitoring of the amplification sequence. It is therefore possible that purer enzyme preparations could lead to considerably improved amplification

Acknowledgement—The authors wish to express their appreciation to the Danish Council for Industrial and Scientific Research for partial financial support of this research project.

REFERENCES

- 1 E H Hansen, A Arndal and L Nørgaard, *Anal Lett*, 1990, **23**, 225
- 2 J Růžička and E H. Hansen, *Flow Injection Analysis*, 2nd Ed, Wiley, New York, 1988
- 3 F Schubert, D Kirstein, K L Schroder and F W Scheller, *Anal Chim Acta*, 1985, **169**, 391
- 4 B A Petersson, E H Hansen and J Růžička, *Anal Lett*, 1986, **19**, 649
- 5 C Ridder, E H Hansen and J Růžička, *ibid*, 1982, **15**, 1751
- 6 *Sigma Technical Bulletin*, 1986
- 7 R B McComb, L W Bond, R W Burnett, R C Keech and G N Bowers, *Clin Chem*, 1976, **22**, 141
- 8 H H Weetall, *Anal Chem*, 1974, **46**, 602A
- 9 M A Sharaf, D L Illman and B R Kowalski, *Chemometrics*, New York, 1986
- 10 H U Bergmeyer (ed), *Methods of Enzymatic Analysis*, Vol 1, Verlag Chemie, Weinheim, 1987
- 11 M U Asouzu, W K Nonidez and M H Ho, *Anal Chem*, 1990, **62**, 708
- 12 F Scheller, N Stegbahn, B Danielsson and K Mosbach, *ibid*, 1985, **57**, 1740
- 13 H J Bright and M Appleby, *J Biol Chem*, 1969, **244**, 3625
- 14 G Johansson, L Ögren and B Olsson, *Anal. Chim Acta*, 1983, **145**, 71
- 15 *Merck Biochemica Catalog*, p 24, Merck, Darmstadt, 1989
- 16 D T Bostick and D M Hercules, *Anal Chem*, 1975, **47**, 447
- 17 Y Hanazato, K Inatomi, M. Nakako, S Shiono and M Maeda, *Anal Chim Acta*, 1988, **212**, 49
- 18 Y Hanazato, S Shiono and M. Maeda, *ibid*, 1990, **231**, 213

MANUAL AND FLOW-INJECTION SPECTROPHOTOMETRIC ASSAY OF THIOLS, BASED ON THEIR *S*-NITROSATION

KRISHNA K. VERMA and KENT K. STEWART*

Department of Biochemistry and Nutrition, Virginia Polytechnic Institute and State University,
Blacksburg, VA 24061, U S A

ARCHANA JAIN, DAYASHANKER GUPTA and SUNIL K. SANGHI

Department of Chemistry, Rani Durgavati University, Jabalpur 482001, Madhya Pradesh, India

(Received 16 June 1990 Revised 27 August 1990 Accepted 4 September 1990)

Summary—A general assay procedure for a wide variety of thiols is described. The technique has three steps: (1) formation of *S*-nitrosothiols with nitrous acid, (2) destruction of the excess of nitrous acid, (3) hydrolysis of the *S*-nitrosothiols with mercuric ions and subsequent formation of an azo-dye by means of the nitrous acid liberated. Both manual and flow-injection analysis (FIA) versions of the assay are described. Since the final step of the assay does not depend on the thiol assayed but only on the reaction of nitrous acid to form azo-dyes, the calibration graphs should be identical for all thiols. The manual system is about four times as sensitive as the FIA system, but the latter permits a high sample throughput and shows significantly lower sensitivity to interference by tryptophan. Though this general technique cannot be used for the assay of many sterically hindered thiols, it can be used for the assay of some protein thiol groups.

The assay of thiols is of interest in a broad range of disciplines, including biochemistry, synthetic organic chemistry and environmental monitoring. Accordingly there are many reports of analytical methods for the assay of thiols, based on a variety of techniques, including titrimetry, chromatography, atomic-absorption spectrometry and colorimetry. There have been several recent reviews on the assay of thiols.¹⁻⁶ Though other techniques obviously have their strengths, colorimetric and fluorometric assays are attractive because of their simplicity and ease of automation. The disadvantages of such assays are that some lack specificity, some respond to other functional groups, and many have differential responses to different thiols.¹⁻¹¹ We have been interested in developing methods which retain the simplicity of the colorimetric and fluorometric assays but have greater selectivity than most of them. We have chosen to examine multi-step methods based on the reaction of thiols with nitrous acid to form their stable *S*-nitroso derivatives, destruction of the excess of nitrous acid, metal-catalyzed hydrolysis of

the *S*-nitroso derivatives, and formation of azo-dyes with the nitrous acid released.

Specific methods for the detection and determination of thiols by means of their reaction with nitrous acid have been reviewed by Ashworth.¹² The thiols are mixed with sodium nitrite and ethanol, and then acidified. Primary and secondary thiols yield a red product, whereas tertiary and aromatic thiols produce a short-lived green product which then turns red. These products are the comparatively stable *S*-nitrosothiols, which absorb light strongly in the range 330–344 nm. The reactions are normally quantitative. Examples of this type of assay include the assay of 2-mercaptoethanol in thiodyglycol,¹³ thioglycollic acid in hair-waving solution,^{13,14} glutathione reductase in rat liver,¹⁵ and tertiary thiols.¹⁶ The addition of some metal ions, *e.g.*, magnesium¹⁸ or cobalt,¹⁹ produces a hyperchromic effect. The titration of thiols with sodium nitrite in acid medium has been reported.²⁰

The *S*-nitrosothiols are resistant to hydrolysis,²¹ and normally unaffected by large amounts of various compounds (*e.g.*, ammonium sulfate) which are known to react rapidly with nitrous acid. However, the hydrolysis of

*Author for correspondence

the nitrosothiols is catalyzed by mercury(II), silver(I), and copper(II) salts. The nitrous acid liberated can be detected by reaction with sulfanilamide followed by coupling the resulting diazonium compound with *N*-(1-naphthyl)ethylenediamine to give an azo-dye. The azo-dye can then be determined spectrophotometrically. The sulfhydryl groups of cysteine as the free amino-acid^{22,33} and in proteins^{24,25} have been determined in this manner.

The potential usefulness of the coupling of *S*-nitrosation¹⁷ and azo-dye formation²¹ prompted us to investigate its utility as a general method for assay of thiols. We report the utilization of this method as a batch technique as well as its utilization in FIA systems for the assay of thiols in complex mixtures. The three steps are shown below.

- (1) $\text{RSH} + \text{HNO}_2 \rightarrow \text{RSNO} + \text{H}_2\text{O}$
 $\text{HNO}_2(\text{excess}) + \text{NH}_2\text{SO}_3\text{NH}_4$
 $\rightarrow \text{N}_2 + \text{NH}_4\text{HSO}_4 + \text{H}_2\text{O}$
- (2) $\text{RSNO} + \text{Hg}^{2+} + \text{H}_2\text{O}$
 $\rightarrow \text{RSHg}^+ + \text{HNO}_2 + \text{H}^+$
- (3) $\text{HNO}_2 + \text{sulfanilamide}$
 $+ \text{N}-(1\text{-naphthyl})\text{ethylenediamine} \rightarrow \text{azo-dye}$

EXPERIMENTAL

Reagents

All reagents used were of analytical grade. The stock solutions were 2 mg/ml sodium nitrite in water, 20 mg/ml ammonium sulfamate in water and 0.1M hydrochloric acid. Reagent A was prepared by stirring 2 g of sulfanilamide with 1.5 ml of concentrated hydrochloric acid, diluting the mixture with about 100 ml of water, adding 1 g of mercuric chloride and (after complete dissolution of the solid) diluting the mixture to a final volume of 200 ml. Reagent B was made by dissolving 0.1 g of *N*-(1-naphthyl)ethylenediamine dihydrochloride in 50 ml of water, adding 1 ml of concentrated hydrochloric acid and diluting to a final volume of 100 ml.

Samples

All thiol samples were high-purity chemicals. Solutions of toluene- α -thiol, 4-toluenethiol and benzenethiol were prepared in acetonitrile and standardized by iodimetry.²⁶ An accurately weighed amount of a fresh sample of penicil-

lamine (Sigma) was treated with 1 ml of 0.1M hydrochloric acid, dissolved in water and diluted to a known volume. Solutions of other thiols were made in water and standardized by titration with 2-iodosobenzoate for cysteine hydrochloride, homocysteine and glutathione,²⁷ by reaction with hexacyanoferrate(III) for mercaptosuccinic acid and 3-mercaptopropionic acid,²⁸ by reaction with mercury(II) for 2-mercaptopropionic acid and thioglycolic acid,²⁹ and by iodimetry for 2-mercaptoethanol, 2-diethylaminoethanethiol hydrochloride and 2-mercaptoethylammonium chloride.²⁶ Stock solutions were standardized immediately before use and sequentially diluted to the desired concentration.

Apparatus

A Pye Unicam SP8-100 spectrophotometer (1-cm fused-silica cells) was used for the batch method absorbance measurements.

A schematic of the flow-injection manifold used is shown in Fig. 1. A Rainin model Rabbit miniplus II peristaltic pump (with 1.0 mm bore Tygon pump tubings) was employed to deliver both the reagents and carrier solution. Samples were introduced into the carrier stream through a Valco C14W 6-way injection valve with a 50- μ l loop made of 0.5 mm bore tubing. Teflon tubing (0.5 mm bore) joined with Omnifit high-pressure connectors and Chemnert Milton Roy Tees (Kel-F, 0.79 mm bore) was used for the flow lines. The absorbance of the azo-dye formed was measured at 544 nm in a Gilford 260 spectrophotometer provided with a Hellma 1-cm path-length 8- μ l flow-through cell. An OmniScribe chart recorder operated at 100 mV full scale was used to record the FIA peaks. The peak maximum appeared 11 sec after sample injection.

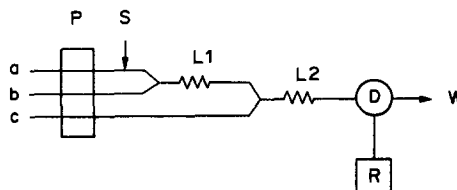


Fig. 1 Schematic of FIA manifold used for thiol determination ($L_1 = 50$ cm, $L_2 = 100$ cm). (a) Hydrochloric acid carrier; (b) reagent A (mercuric chloride and sulfanilamide); (c) reagent B [*N*-(1-naphthyl)ethylenediamine dihydrochloride]. General features: P, peristaltic pump (flow-rate in each channel, 1 ml/min); S, sample injected (50 μ l); D, detector, 1-cm path-length, 8 μ l volume; R, recorder; W, waste, all tubes in contact with the sample were 0.5 mm bore.

Procedures

Batch method. In step (1) known volumes of standard thiol solution (to give 1–35 μM final thiol concentrations) were separately added to 25-ml standard flasks and mixed with 0.5 ml of 2-mg/ml sodium nitrite solution and 1 ml of 1% v/v hydrochloric acid. In step (2) the reaction mixture was allowed to stand for 1 min then the residual nitrous acid was destroyed by the addition of 1 ml of 20-mg/ml ammonium sulfamate solution, shaking the mixture, then letting it stand for 2 min. In step (3) 5 ml each of reagents A and B were added to the reaction mixture, with swirling, and the solution was diluted to the mark with demineralized water. The absorbance of the sample was measured at 544 nm in 1-cm path-length cells. A correction was applied for the reagent blank before the calibration graph was plotted. Samples were analysed in an identical manner.

FIA method. The general procedure for preparation of the calibration graph and analysis of unknown thiol solutions consisted of the manual reactions for *S*-nitroso derivative formation, steps (1) and (2), followed by flow-injection analysis of the product from step (2).

RESULTS AND DISCUSSION

This method of determining thiols by their *S*-nitrosation should be of general applicability to a wide variety of thiols. Since each mole of thiol reacts with one mole of nitrous acid and that nitrous acid is subsequently released by the mercury-catalyzed hydrolysis, all thiol assays utilize the same final reaction (*i.e.*, the azo-dye determination of nitrous acid), so widely differing thiols should all yield the same standard calibration graph.

Although mercury(II), copper(II) and silver(I) all catalyze the hydrolysis of *S*-nitrosothiols, the use of mercuric chloride is recommended since it forms colorless water soluble mercaptides (RSHgCl) in the presence of excess of reagent. Copper mercaptides may be colored³⁰ and these colors can interfere in the measurement of the azo-dye. Many of the silver mercaptides are insoluble and their precipitation could cause interference with the spectrophotometric assay and could also plug the FIA tubing.

The final step of the assay is diazotization of an aromatic primary amine by the liberated nitrous acid and the formation of an azo-dye by coupling to another amine or phenolic

compound. Theoretically, any delay in the addition of amine to the hydrolyzed solution of *S*-nitrosothiol could cause a partial loss of the nitrous acid, owing to a reaction with the ammonium sulfamate present. However, when we used a mixed reagent containing both mercuric chloride and sulfanilamide there was no evidence of a loss of nitrous acid by this side-reaction.

Batch method

With this method, the absorbance (A) of the azo-dye formed was a linear function of concentration (C , μM) of thiol in the final solution; over the range 1–35 μM the observed regression equation was $A = 0.002 + 0.0413C$. The results for assay of fourteen different thiols (Table 1) demonstrate that this method has broad applicability and is precise. The mean molar absorptivity was $4.11 (\pm 0.12) \times 10^4 \text{ l. mole}^{-1} \cdot \text{cm}^{-1}$.

The method has been used for the assay of primary, secondary and tertiary thiols in the presence of other reactive groups such as aliphatic primary amino, tertiary amino, hydroxyl, carboxyl or amide groups. In general, such groups did not cause any interference (see Table 2). Tryptophan was an exception, probably because its indole nucleus reacts with nitrous acid to yield a diazo compound that also couples (though relatively slowly) with *N*-(1-naphthyl)ethylenediamine.^{31,32} Organic sulfides (*e.g.*, methionine) and disulfides (*e.g.*, cystine) do not interfere. Urea, ascorbic acid, hydrazine, ammonium ion, guanine, adenine and 2-aminopyridine do not affect the color reaction but rapidly consume nitrous acid in step (1). A sufficient excess of sodium nitrite should be added in step (1) when these compounds are known to be present. A 10-fold molar ratio of hydrogen sulfite to thiol does not interfere with the reaction. Methanol and ethanol form nitrite esters which are not completely destroyed by the addition of ammonium sulfamate, step (2). The alcohol nitrite esters do decompose under the conditions of step (3), however, and thus at high concentrations they interfere with the thiol assays. Thus we did not use alcohols as solvents for water-insoluble thiols, and used acetonitrile instead.

This assay technique did not give acceptable results for sterically hindered thiols (*e.g.*, triphenylmethane thiol), dithiols (*e.g.*, D,L-dithiothreitol and 2,5-dimercaptopyridic acid), and thiol-thione tautomers (*e.g.*, benzothiazol-2-thiol, benzoxazole-2-thiol, benzimida-

Table 1. Determination of thiols through nitrosation and azo-dye formation

Thiol	Thiol, μM		
	Taken*	Found†	
		Batch method	FIA
Cysteine	1.01	0.98 (0.5)	1.00 (0.3)
	3.25	3.18 (0.4)	3.21 (0.3)
	8.71	8.80	8.75
	11.54	11.47 (0.5)	11.57 (0.4)
	14.79	14.86	14.85
	20.13	20.18 (0.6)	—
	30.24	30.31	—
	35.27	35.16 (0.8)	—
	—	—	—
Glutathione	1.56	1.51 (0.4)	1.52 (0.2)
	3.77	3.68	3.75
	7.55	7.65 (0.5)	7.61 (0.4)
	10.32	10.28	10.39
	15.10	15.19 (0.6)	—
	18.87	18.95	—
Penicillamine	2.86	2.80 (0.5)	2.82 (0.3)
	5.26	5.18	5.22
	8.45	8.52 (0.5)	8.50 (0.4)
	12.33	12.27	12.35
	18.49	18.57	—
	24.46	24.54 (0.6)	—
2-Mercaptoethanol	3.75	3.82 (0.3)	3.75 (0.3)
	6.35	6.41	6.44
	10.11	10.02 (0.4)	10.18 (0.4)
	14.28	14.34	14.24
	22.40	22.49 (0.6)	—
Homocysteine	3.25	3.20 (0.4)	3.27 (0.3)
	6.71	6.79	6.65
	14.84	14.90 (0.5)	14.83 (0.4)
	18.51	18.60	—
Mercaptosuccinic acid	1.85	1.79 (0.5)	1.82 (0.3)
	5.03	5.06	5.08
	11.21	11.25 (0.5)	11.25 (0.4)
	14.15	14.10	14.17
	21.07	21.00 (0.6)	—
	28.26	28.31	—
	35.11	34.97 (0.8)	—
2-Diethylaminoethanol hydrochloride	2.58	2.63	2.56
	5.33	5.36 (0.5)	5.41 (0.3)
	8.64	8.60	8.66
	14.74	14.81 (0.6)	—
2-Mercaptoethylammonium chloride	5.64	5.69 (0.4)	5.62 (0.4)
	8.73	8.76	8.79
	15.02	15.10 (0.7)	15.09 (0.5)
	20.52	20.46	—
	24.83	24.91 (0.8)	—
	—	—	—
Thioglycolic acid	2.03	2.08 (0.5)	2.05 (0.4)
	6.27	6.19	6.24
	12.55	12.61 (0.4)	12.59 (0.4)
	17.88	17.83	—
	23.10	23.04 (0.6)	—
2-Mercaptopropionic acid	3.12	3.08 (0.5)	3.15 (0.3)
	7.02	7.07	7.04
	10.14	10.09 (0.6)	10.11 (0.5)
	16.32	16.28	16.35 (0.7)
	21.71	21.65 (0.6)	—
	28.38	28.42 (0.7)	—
3-Mercaptopropionic acid	2.01	1.98 (0.6)	2.03 (0.4)
	5.34	5.42	5.44
	9.97	10.02 (0.5)	10.05 (0.5)
	11.60	11.54	11.64
	18.54	18.48 (0.6)	18.50 (0.8)
	23.19	23.36	—
	28.98	29.02 (0.6)	—
	33.10	33.19 (0.7)	—

Continued

Table 1—continued

Thiol	Thiol, μM		
	Taken*	Found†	
		Batch method	FIA
Benzenethiol	5 18	5 21 (0.5)	—
	10 35	10 29	—
	15 35	15 58 (0.6)	—
	20 61	20 85	—
	25.63	25 59 (0 6)	—
	31 07	31 16	—
Toluene- α -thiol	7 48	7 52 (0 5)	—
	14 97	15 10	—
	22 45	22 57 (0 6)	—
	29 83	29 99	—
	34 75	34.63 (0 7)	—
	4.85	4 90 (0.4)	—
4-Toluenethiol	9 71	9 66	—
	14 56	14 48 (0 6)	—
	19 42	19 34	—
	24 27	24 12 (0 6)	—
	31 18	31 09	—

*The thiol solutions were standardized as detailed in the text

†Average of 6 determinations, with relative standard deviation (%) in parentheses, — indicates that no determination was done

zole-2-thiol and 1-methylimidazole-2-thiol). The results were not quantitative and the recovery varied with the concentration and structure of the individual thiol. Thus the method described here cannot at present be recommended for the assay of sterically hindered thiols, dithiols, and

thiol–thione tautomers; further studies on the assay of these thiols are needed.

Flow-injection method

Nitrogen is formed during the destruction of nitrous acid, step (2), and gas bubbles cause

Table 2 Determination of thiols in the presence of potentially interfering substances

Thiol	Substance added	Thiol Substance molar ratio	Thiol recovery,* %
Cysteine	Methionine	1 8	100.1 ^a
		1 10	99 8 ^b
		1 10	99 7 ^a
Penicillamine	Tyrosine	1 10	100 0 ^b
		1 6	99.6 ^a
		1 10	99 9 ^b
	Tryptophan	1 1	154 2 ^a
		1 10	100 1 ^b
		1 25	100 5 ^b
Glutathione	Hydrogen sulfite	1 50	101 2 ^b
		1 5	99 7 ^a
		1 10	99 4 ^a
		1 5	99 8 ^b
		1 10	99.8 ^b
		1 15	97 6 ^b
		1 20	95 7 ^b
2-Mercaptoethanol	Glutamic acid	1 10	99 8 ^a
		1 15	100 2 ^b
	Asparagine	1 10	100 3 ^a
		1 10	99 9 ^b
	Homocysteine	1 10	99 7 ^a
		1 10	99 8 ^b
Thioglycolic acid	Urea	1 5	99 6 ^a
		1 8	99 8 ^b
	Cysteine	1 8	98 6 ^b
		1 5	100 1 ^b
	Hydrogen sulfide	1 5	99 6 ^a
		1 7	99 8 ^b

*Relative to amount found in the absence of interfering substance, ^abatch method; ^bFIA

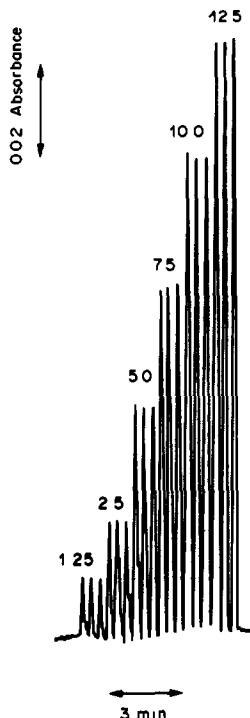


Fig 2 FIA peaks from the triphcate assay of homocysteine samples. The numbers on the peaks correspond to the concentration of the thiol (μM) in the original sample

severe noise in FIA systems.³³ Thus we did not attempt the nitrosation and the destruction of nitrous acid in the flow system, but performed these steps manually.

We made a preliminary optimization of the flow-injection system, varying the parameters in the ranges given below in parentheses. The final configuration of the three-channel FIA manifold (Fig. 1) had a 50-cm hydrolysis coil (L1) (30–150 cm) and a 100-cm coupling coil (L2) (60–200 cm). The flow-rate in each channel was 1 ml/min (1–3 ml/min). Maximum peak absorbances were obtained with the reagent concentrations given in the recommended procedure. Further increases in the reagent concentrations had no effect on the peak heights obtained over the thiol concentration ranges reported. With a 50- μl loop (20–200 μl), the *S*-nitroso derivatives could be assayed with a sample throughput of 180 per hr. Typical calibration peaks for 1.25–12.50 μM homocysteine standards are shown in Fig. 2. The regression equation obtained for the 1–15 μM thiol range was $A = 0.0018 + 0.0104C$. The slope of the FIA system response was about a quarter of that for the batch method. This loss of sensitivity was apparently due to the dispersion of the sample plug. The dispersion coefficient,

D ,³⁴ found for potassium dichromate injected into the flow system described in Fig. 1, was 4.

Generally, the application and limitations of FIA methods parallel those of batch procedures. However, a significant tolerance was found for the presence of as much as 50-fold molar ratio of tryptophan to thiol in the FIA method, whereas even trace amounts caused severe interference in the batch method.

We have also made preliminary studies on the use of the FIA method for the assay of thiol groups in bovine serum albumin (molecular weight 6.6×10^4). The levels of free thiol groups are known to vary from sample to sample, depending on the prior history of the sample. With our FIA assay we found 0.65 (1.1% RSD) thiol groups per albumin "molecule", and 0.68 (1.4% RSD) by use of the Ellman reagent³⁵ when we assayed the sample of bovine serum albumin. We believe that our technique has significant potential for the assay of thiols in proteins and peptides.

REFERENCES

- 1 A Fontana and C Tomiolo, in *Chemistry of the Thiol Group*, Part I, S Patai (ed), p 271 Wiley, London, 1974
- 2 P C Jocelyn, *Methods in Enzymology*, 1987, **143**, 44
- 3 K Imai and T Toyooka, *ibid*, 1987, **143**, 67
- 4 R C Fahey and G L Newton, *ibid*, 1987, **143**, 85
- 5 M W Fariss and D J Reed, *ibid*, 1987, **143**, 101
- 6 E G DeMaster and B Redfern, *ibid*, 1987, **143**, 110
- 7 D B Hunsaker, Jr and G H Schenk, *Talanta*, 1983, **30**, 475
- 8 K V Veksler and G M Trakhnova, *Otkrytiya Izobret*, 1985, **33**, 84
- 9 M K Tummura, B S Reddy and C S P Sastry, *Microchem J*, 1987, **36**, 159
- 10 K Nakashima, H Akimoto, K Nishida, S Nakatsuj and S Akiyama, *Talanta*, 1985, **32**, 167
- 11 T Kamidate, A Katayama and H Watanabe, *Anal Sci*, 1988, **4**, 329
- 12 M R F Ashworth, *The Determination of Sulphur-Containing Groups*, Vol II, p 33 Academic Press, London, 1976
- 13 F N Woodward, *Analyst*, 1949, **74**, 179
- 14 F Hirsch, *Seifen-Ole-Fatte-Wachse*, 1951, **77**, 457
- 15 G T Walker and F M Freeman, *Mfg Chemist*, 1955, **26**, 11
- 16 D E Kizer and B A Howell, *Proc Soc. Exp Biol. Med*, 1963, **112**, 967
- 17 G W Ashworth and R E Keller, *Anal Chem.*, 1967, **39**, 373
- 18 D. V Singh and P. P. Mukherjee, *Indian J Technol.*, 1972, **10**, 469
- 19 A Besada, *Anal. Lett*, 1988, **21**, 435.
- 20 J. P. Danahy and V. J. Eha, *Anal Chem*, 1972, **44**, 1281

- 21 A Wacek and J Smitt-Amundsen, *Monatsh Chem*, 1958, **89**, 110
- 22 B. Saville, *Analyst*, 1958, **83**, 670
- 23 H F Liddell and B Saville, *ibid*, 1959, **84**, 188
- 24 P Todd and M Gronow, *Anal. Biochem*, 1969, **28**, 369.
- 25 M Gronow and P Todd, *ibid.*, 1969, **29**, 540.
- 26 J. W Kimball, R L. Kramer and E E Reid, *J Am. Chem Soc.*, 1921, **43**, 1199
27. K. K. Verma and S Bose, *Analyst*, 1975, **100**, 366.
28. K. K. Verma, *Talanta*, 1979, **26**, 277.
- 29 K K Verma and A K Gulatia, *Anal Chem*, 1982, **54**, 2633
30. S Bose, M P Sahasrabudhey and K. K Verma, *Talanta*, 1976, **23**, 725.
- 31 S M S Basha and R M Roberts, *Anal. Biochem.*, 1977, **77**, 378.
32. K. K. Verma, A Jain and J Gasparič, *Talanta*, 1988, **35**, 35.
- 33 M A. Koupparis and P. I Anagnostopoulou, *Anal. Chim. Acta*, 1988, 204, 271.
34. J. Růžička and E H. Hansen, *Flow Injection Analysis*, 2nd Ed., p. 23. Wiley-Interscience, New York, 1988.
35. M. J F. Diez, D. T. Osuga and R. E. Feeney, *Arch Biochem Biophys*, 1964, **107**, 449

SIMPLE UNSEGMENTED FLOW CONFIGURATIONS FOR SIMULTANEOUS KINETIC DETERMINATIONS

M. ROMERO-SALDANA, A RIOS, M D. LUQUE DE CASTRO and M. VALCARCEL

Department of Analytical Chemistry, Faculty of Sciences, University of Córdoba, Córdoba, Spain

(Received 25 August 1989 Revised 18 April 1990 Accepted 3 September 1990)

Summary—Two unsegmented-flow manifolds were designed for simultaneous determinations based on differences in the kinetic behaviour of two analytes with the same reagent. The determination of Fe(III) and Co(II), based on displacement of Fe(III) and Co(II) from their EGTA complexes by PAR, was used as a model system. The displacement reactions were photometrically monitored at 510 nm

Simultaneous determinations are of interest because they reduce analytical cost and time. In addition a high degree of automation can be achieved by using flow-injection systems.^{1,2} There are three basic ways of implementing simultaneous determinations in flow-injection analysis (FIA) with single-channel configurations.

(a) By using fast scan detectors, when the optical^{3,4} or electroanalytical^{5,6} features of the analytes (or reaction products) are suitable, the detector performing a complete scan at the maximum of the FIA peak.

(b) By using stopped-flow methods,⁵ when the two analytes react with the same reagent to yield similar products, but at different rates (optical detectors are most frequently used for this purpose). Differential kinetic methods can be applied to determine the analyte concentration.

(c) By altering the manifold to obtain more than one signal per injection. Proportional equation methods are normally applied in this case.

The last option is the most interesting from the point of view of economy and design, and offers several possibilities, such as use of a very large sample volume,⁶ use of manifolds with splitting and merging points,⁷ internally coupled valves,⁸ and open-closed configurations.⁹ Additional information about these alternatives can be found in monographs on FIA.^{2,10} In all cases, signals at different reaction times are obtained, which can be used for kinetic determinations.

This paper reports two manifolds which were evaluated by means of the well-known ligand-

displacement reaction between EGTA complexes and PAR, based on the different reaction rates of the EGTA complexes of Fe(III) and Co(II).¹¹ This chemical system was selected because its kinetic features make it suitable for checking the performance of the proposed automated operational modes. The manifolds allow two absorbance signals to be obtained at different reaction times, the values of these forming the basis for the simultaneous determinations.

EXPERIMENTAL

Reagents

The reagents used were aqueous $1 \times 10^{-3} M$ ethyleneglycol bis(β -aminoethyl ether)-*N,N,N',N'*-tetra-acetic acid (EGTA) and 2 mg/ml 4-(2-pyridylazo)resorcinol (PAR) monosodium salt monohydrate solutions. The pH of the EGTA solution was adjusted to 10.1 with sodium hydroxide. Standard stock solutions (1.000 g/l.) of iron(III) and cobalt(II) were also used.

Apparatus

A Pye-Unicam SP-500 single-beam spectrophotometer with a Hellma 178.12-QS flow-cell (inner volume 18 μ l), a Gilson Minipuls peristaltic pump, a Rheodyne 5041 injection valve, a Tecator TM-III chemifold and a Radiometer REC-80 recorder were used. The tubing of the reactor lines had an internal diameter of 0.5 mm.

RESULTS AND DISCUSSION

Manifolds

Both configurations allow the sample solution to react with the reagent for two reaction times.

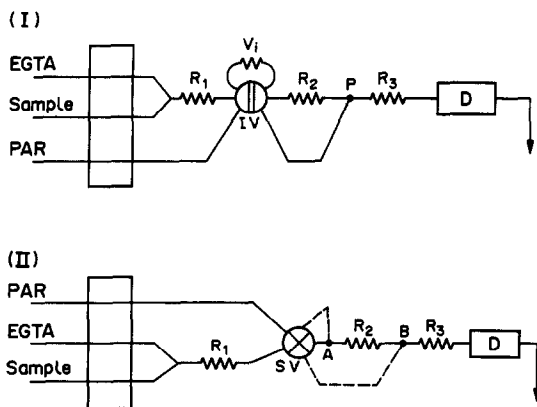


Fig 1 Manifolds designed for the simultaneous determination of Fe(III) and Co(II) (I), With injection valve; (II), with selecting valve

The longer residence time is different for the two manifolds and results in different types of signal, transient for the configuration with the injection valve and a plateau for the configuration with the selecting valve.

Function of the manifold(I) with injection valve and reagent injection. The sample containing both analytes is continuously merged with a $1 \times 10^{-3} M$ EGTA stream (pH 10.1) and mixed within the reactor R_1 [Fig. 1(I)]. When the loop of the injection valve, I.V., is being filled with $7.8 \times 10^{-5} M$ PAR (pH 9.82), the stream is merged with the main channel at a point between R_2 and R_3 . This configuration allows the displacement reaction to take place within R_3 while the injection valve is in the filling position and yields a continuous signal that is the sum of the contributions of both analytes. Switching I.V. to the load position inserts a plug of PAR between R_1 and R_2 , giving a longer duration of the displacement reaction and a corresponding change in the contributions of the two analytes to the total signal provided by the detector, resulting in a sharp peak superimposed on the

continuous signal [Fig. 2(a)]. The difference in the contributions of the two analytes to the continuous and transient signals allows a set of simultaneous equations to be established for the system.

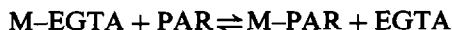
Function of the manifold(II) with a selecting valve. Replacement of the injection valve with a selecting valve, S.V. [Fig. 1(II)] allows the two streams (sample + EGTA, and PAR) to be diverted differently, depending on its position. In one position, the sample-EGTA mixture is selected and PAR inserted at point B (in this case the reaction takes place only in reactor R_3). In the other position, the PAR stream is selected and the sample-EGTA mixture is inserted at point A; the reaction takes place in reactors R_2 and R_3 before detection. The two continuous signals or plateaux obtained [Fig. 2(b)] allow the mixture to be resolved.

There are major differences between the two flow schemes. The simpler configuration I has the following shortcomings: (i) the volume of PAR injected must be large enough ($250 \mu l$) to prevent the degree of reaction from being offset by the high dispersion; (ii) the mixing of the sample with the injected reagent is not very efficient; (iii) the signal is disturbed by the merging of the injected plug of PAR with the continuous PAR stream entering at point P, this disturbance being increased by the large injected volume (this effect is especially important with coloured reagents (e.g., PAR, or with solutions containing organic solvents).

Manifold II eliminates these shortcomings and was therefore selected for developing the analytical method.

Kinetics of the process

The chemical reactions used were the instantaneous formation of the M-EGTA complex [M = Fe(III) or Co(II)] in basic medium and the displacement reaction with PAR:



which occurs at different rates for Fe(III) and Co(II), as shown in Fig. 3. The absorbance-time recordings were obtained with the manifold II, and a very short R_2 (12 cm). The rate constants (k) of these reactions were calculated from plots of $\log(A_\infty - A_t)$ vs. time (A_∞ being the final absorbance and A_t that at a given reaction time), the slopes being $-k/2.303$. The values $k_{Fe} = 5.1 \text{ min}^{-1}$ ($r = 0.9994$) and $K_{Co} = 2.1 \text{ min}^{-1}$ ($r = 0.9988$) show the faster displacement undergone by the Fe(III)-EGTA complex.

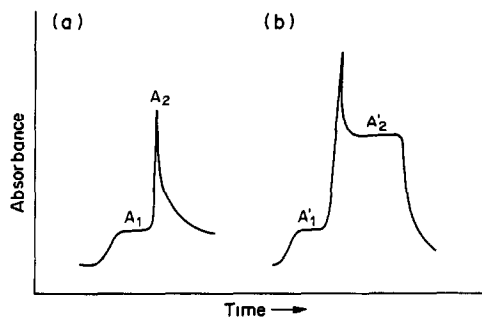


Fig. 2 Recordings obtained with, (a) manifold I, (b) manifold II. A_1 and A_1' are the signals obtained at residence time t_1 , A_2 and A_2' are those obtained at residence time t_2

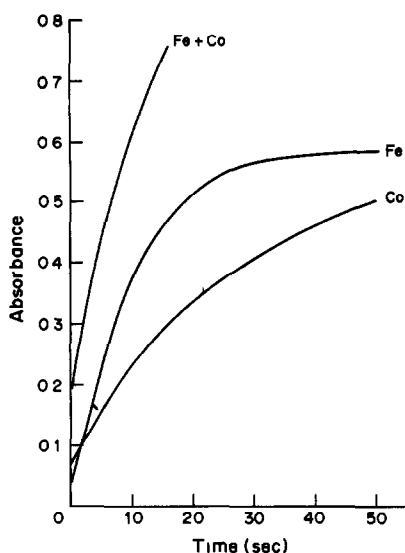


Fig. 3 Absorbance-time curves obtained by stopping the flow immediately after mixing the reactants. Concentration of Fe(III) and Co(II) 2.0 $\mu\text{g/ml}$

Effect of variables

The optimum values found for the chemical variables were those stated in the experimental section. Because of the higher stability of the PAR complexes, the concentration of this reagent was kept lower than that of the EGTA to ensure the maximum possible difference in kinetic behaviour between the two chemical systems.

The optimum injection volume for manifold I was 270 μl . The influence of the flow-rate and reactor lengths was similar for both manifolds. Figure 4a shows the effect of flow-rate on the absorbance difference between the signals at the two residence times. The behaviour of the two analytes was similar and a flow-rate of 1.3 ml/min was found to be optimum. The length of R_1 is not significant, as the formation of the EGTA complexes is instantaneous, so it was fixed at 45 cm. R_3 must be short enough (50 cm) to ensure a short residence time corresponding to the first signal; on the other hand

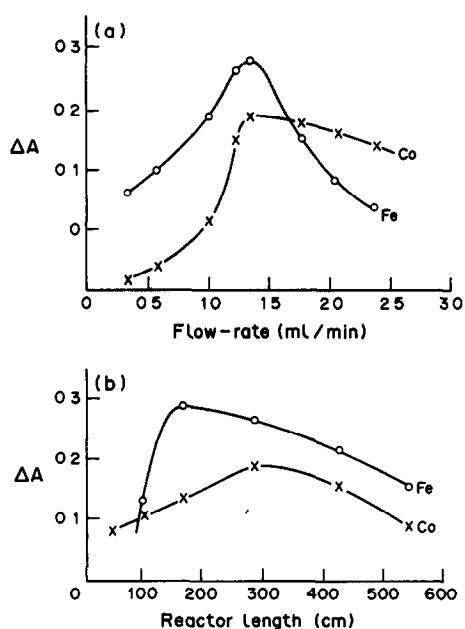


Fig. 4 Influence of (a) the flow-rate and (b) the length of R_2 on the difference (ΔA) between the signals obtained at the two residence times

the length of R_2 is important since it must ensure an adequate difference between the two residence times. Figure 4b shows an optimum length of 150 cm for iron(III) (the faster reaction) and 300 cm for cobalt(II). A compromise of 250 cm was chosen for R_2 .

Calibration curves

Fe(III) and Co(II) (each in the absence of the other) can be determined by measuring (a) the absorbance of the first signal (measured at residence time t_1), (b) the absorbance of the second signal (residence time t_2) or (c) the difference between them.

Table 1 summarizes the features of the calibration curves obtained. As the Fe(III)-EGTA displacement reaction was rather fast, the calibration curve based on method (c) had poor sensitivity [0.010 ($\mu\text{g/ml}$)], and was clearly unsuitable for the determination of this analyte;

Table 1 Features of the individual determination of Fe(III) and Co(II)

Parameter*	Equation†	Regression coefficient	Linear range, $\mu\text{g/ml}$
A_1	$A_1 = 0.2765[\text{Fe}^{3+}] - 0.2047$	0.9998	1.0-5.0
A_1	$A_1 = 0.0375[\text{Co}^{2+}] - 0.0093$	0.9985	1.0-12.0
A_2	$A_2 = 0.2775[\text{Fe}^{3+}] - 0.063$	0.9982	1.0-5.0
A_2	$A_2 = 0.0975[\text{Co}^{2+}] + 0.031$	0.9996	0.5-7.0
ΔA	$\Delta A = 0.060[\text{Co}^{2+}] + 0.040$	0.9951	0.5-8.0

* A_1 = absorbance at residence time t_1

A_2 = absorbance at residence time t_2

$\Delta A = A_2 - A_1$

†Concentrations in $\mu\text{g/ml}$

hence it does not appear in Table 1. This type of measurement was very suitable for Co(II), however, the sensitivity being twice that obtained by method (a).

Effect of other metal ions

The influence of various metal ions on the proposed method was studied. Alkali-metal and alkaline-earth metal ions, Ni(II), Cd(II), Hg(II) and Pb(II) did not interfere, at least in a 1:1:10 (Fe(III): Co(II):foreign ion) ratio. Zn(II), Cu(II), Al(III), MoO_4^{2-} and WO_4^{2-} gave positive and Mn(II), Sn(II) and Cr(III) negative interferences. Mn(II), Cu(II) and Cr(III) were tolerated at a 1:1.1 ratio, while Zn(II), MoO_4^{2-} and WO_4^{2-} gave positive (between 10–20%), and Al(III) and Sn(II) higher negative errors at that ratio.

Simultaneous determination of Fe(III) and Co(II)

When both analytes are present the signals are not linearly additive. To solve this problem, calibration curves for Co(II) were run in the presence of constant amounts of Fe(III).¹² Thus, the general equation for Co(II) measured at residence time t_1 was:

$$A_1 = m[\text{Co}^{2+}] + n$$

where the slope, m , and the intercept, n , are linear functions of the concentration of Fe(III) in the sample.

$$m = 0.0215[\text{Fe}^{3+}] - 0.0123 \quad (r = 0.9965)$$

$$n = 0.1675[\text{Fe}^{3+}] - 0.026 \quad (r = 0.9955)$$

From the signals measured at t_2 , calibration curves for Fe(III) in the presence of constant amounts of Co(II) were constructed. The slopes found were very similar and their average was

$$m' = 0.1612$$

and the intercept was a linear function of the Co(II) concentration:

$$n' = 0.006625[\text{Co}^{2+}] + 0.095 \quad (r = 0.9896)$$

The final set of equations was

$$A_1 = (0.0215[\text{Fe}^{3+}] - 0.0123)[\text{Co}^{2+}]$$

$$+ 0.1675[\text{Fe}^{3+}] - 0.026$$

$$A_2 = 0.1612[\text{Fe}^{3+}] + 0.0662[\text{Co}^{2+}] + 0.095$$

which were solved with the aid of a simple BASIC program which requires input of the

Table 2 Analysis of mixtures of Fe(III) and Co(II)

Added, $\mu\text{g/ml}$		Found, $\mu\text{g/ml}$	
Fe(III)	Co(II)	Fe(III)	Co(II)
3.00	1.00	2.98	1.09
3.00	3.00	3.03	3.18
4.00	1.00	4.00	0.91
4.00	3.00	4.03	2.89
1.00	2.00	1.16	1.91
1.00	4.00	0.95	3.95
2.00	1.00	2.01	1.08
2.00	3.00	2.05	3.12
2.00	4.00	2.03	4.02

coefficients of these equations and the A_1 and A_2 values for each sample.

Table 2 lists the results obtained for some synthetic samples. The precision, expressed as r.s.d., was 2.4% for Fe(III) and 3.6% for Co(II) (for $n = 11$, $P = 0.05$ and $2.0 \mu\text{g/ml}$ of analyte in both cases). The sampling frequency was 25/hr.

CONCLUSIONS

Two novel manifold configurations are proposed for simultaneous determinations based on the different kinetic behaviour of two analytes with a single reagent.

Acknowledgement—The CICyT is thanked for financial support (Grant No PA86-0146).

REFERENCES

- 1 M D Luque de Castro and M Valcárcel, *Analyst*, 1984, **109**, 413
- 2 J Růžicka and E H Hansen, *Flow Injection Analysis*, 2nd Ed, Wiley, New York, 1988
- 3 E A G Zagatto, A O Jacintho, L C R Pessenda, F J Krug, B F Reis and H Bergamin F^o, *Anal. Chim Acta*, 1981, **125**, 37
- 4 W D Basson and J F Van Staden, *Z Anal Chem*, 1980, **302**, 370
- 5 F Lázaro, M D Luque de Castro and M Valcárcel, *Anal Chem*, 1987, **59**, 950
- 6 A Fernández, M D Luque de Castro and M Valcárcel, *Anal Chim Acta*, 1987, **193**, 107
- 7 *Idem*, *Anal Chem*, 1984, **56**, 1146
- 8 A Ríos, M D Luque de Castro and M Valcárcel, *ibid*, 1986, **58**, 663
- 9 *Idem*, *ibid*, 1985, **57**, 1803
- 10 M Valcárcel and M D Luque de Castro, *Flow Injection Analysis Principles and Applications*, Horwood, Chichester, 1988
- 11 M. Tanaka, S Funahashi and K Shirai, *Anal Chim Acta*, 1967, **39**, 437
- 12 A Ríos and M Valcárcel, *Talanta*, 1985, **32**, 851

KINETIC DETERMINATION OF EDTA AND CITRATE BY THE DISPLACEMENT OF FLUORIDE FROM Al³⁺-F⁻ COMPLEXES AND USE OF A FLUORIDE ION-SELECTIVE ELECTRODE

J. G. PENTARI, C. E. EFSTATHIOU* and T. P. HADJIIOANNOU

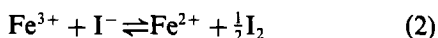
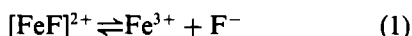
Laboratory of Analytical Chemistry, University of Athens, Panepistimiopolis (Kouponia),
Athens 157 71, Greece

(Received 1 May 1990 Revised 11 July 1990 Accepted 25 July 1990)

Summary—The displacement of fluoride from its aluminium complexes by the action of EDTA, citrate and other ligands is a relatively slow process which can be monitored potentiometrically with a fluoride ion-selective electrode. Some characteristics of these reactions are presented. There is evidence that [AlF]²⁺ reacts with the competitive ligand faster than the simple free (hydrated) Al³⁺ species does. The relative rates of release of fluoride by the action of various aminopolycarboxylic acids have been determined. Potentiometric reaction-rate methods have been developed for the determination of 0.2–1.5 μmole of EDTA and 0.1–1.0 μmole of citric acid, with average relative errors of ~3%.

Aluminium forms a series of complexes with fluoride of the general type [AlF_n(H₂O)_{6-n}]⁽³⁻ⁿ⁾⁺ where *n* = 1–6. For simplicity, water molecules will be omitted from the formulae for the aluminium species shown below. Baumann,¹ using potentiometric data obtained with a fluoride ion-selective electrode (ISE), has calculated the successive formation constants of the lower (*n* = 1–4) Al–F complexes, whereas Agarwal and Moreno,² using the same sensor, have calculated the formation constants of these complexes under a wide range of conditions (at ionic strengths 0.05–0.5, and in the temperature range 25–37°).

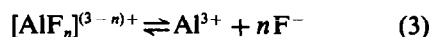
Aluminium ion reacts slowly with almost all ligands, including fluoride and aminopolycarboxylic acids. Srinivasan and Rechnitz³ have investigated the kinetics of the formation of the complexes [FeF]²⁺ and [AlF]²⁺, by using the fluoride ISE. They have also used the electrode for indirectly studying the kinetics of the reaction between Fe(III) and iodide, by monitoring the rate of release of fluoride according to the overall scheme⁴



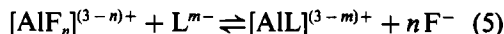
As equilibrium (1) is quickly established and [FeF]²⁺ is inactive towards iodide, monitoring

the rate of release of fluoride provides an indirect, but adequate, means of monitoring reaction (2), since the rate of release of fluoride will be governed by the rate of reaction (2).

In the present study, the fluoride ISE has been used for monitoring the release of fluoride from its complexes with aluminium after the addition of a competitive complexing reagent (an aminopolycarboxylic acid or α-hydroxy-acid) in a buffered (acetate) medium. The overall displacement reaction can be written



Since the equilibria for reactions Al³⁺ and F⁻ are established slowly, the rate of fluoride release cannot be considered as indicative of the rate of reaction (4). Furthermore, the direct displacement reaction



cannot be excluded, and experimental data, presented in this study, reveal that it proceeds faster than the direct complexation of “fluoride-free” aluminium species with L^{m-}.

The overall rate of release of the fluoride, as the result of numerous parallel reactions, has only comparative value and may serve as a measure of the effectiveness of L as a “fluoride demasking reagent”. It should be stressed that

*Author for correspondence

the rate and completeness of the fluoride displacement reaction is of particular importance for the potentiometric determination of total fluoride in samples containing elevated concentrations of aluminium (*e.g.*, tooth-pastes, mineral waters and industrial effluents). The treatment of such samples with solutions containing competitive complexing reagents such as DCTA or tartrate must always precede the measurement step.^{5,6}

In this study, the conditions of the reactions between the Al-F complexes and the complexing reagents were investigated and optimized to obtain potential recordings with a slope ($\Delta E/\Delta t$) proportional to the amount of the complexing reagent. A kinetic procedure based on these displacement reactions was developed and 0.2–1.5 μmole of EDTA was determined with an average relative error of $\sim 3\%$. Other complexing reagents (DCTA, citrates and isocitrates) readily displace fluoride from Al-F complexes, but the initial fast release of fluoride is followed by its slow recombination with the excess of aluminium, resulting in a minimum in the potential-time recordings. It was found that the depth of the minimum can be linearly related to the logarithm of the amount of the complexing reagent. A kinetic procedure based on this observation was developed for the determination of 0.1–1.0 μmole of citrate with an average relative error of $\sim 3\%$.

EXPERIMENTAL

Apparatus

A potentiometric rate measurement system consisting of a digital electrometer (Orion 801 pH-pIon meter) interfaced to a microcomputer (Amstrad CPC-6128) was used. A brief description of the system hardware and the control program KINMOD can be found elsewhere.⁷ Alternatively, the potential of the fluoride ISE can be conventionally recorded.

A combination fluoride electrode (Orion Model 96-09) was used and all measurements were performed in a constant-temperature ($25 \pm 0.2^\circ$) reaction cell with continuous magnetic stirring. The electrode was stored in 1.0M fluoride solution when not in use.

Reagents

All solutions were prepared from analytical grade reagents and demineralized distilled water was used throughout. The following stock solutions were prepared: 0.1000M sodium fluoride

(stored in a polyethylene bottle), 0.0500M aluminium nitrate, 2.50M sodium nitrate and acetate buffer solutions (0.10M total acetate) over the pH range 3.8–5.5.

The following aminopolycarboxylic acid solutions (0.0500M) were used: nitrilotriacetic acid (NTA), ethylenediamine-*N,N,N',N'*-tetra-acetic acid (EDTA), *N*-hydroxyethylethylenediamine-*N,N',N'*-tetra-acetic acid (HEDTA), *trans*-1,2-diaminocyclohexane-*N,N,N',N'*-tetra-acetic acid (DCTA), 2,2'-ethylenedioxybis(ethyliminodiacetic acid) (EGTA), diethylenetriamine-*N,N,N',N'',N''*-penta-acetic acid (DTPA), triethylenetetramine-*N,N,N',N'',N''',N'''*-hexa-acetic acid (TTHA). These solutions were prepared by the addition of small volumes of 5M sodium hydroxide to a vigorously stirred suspension of the free acid, maintaining the pH at 6–7, and diluting to volume after complete dissolution.

Solutions (0.0500M) of the following α -hydroxy-acids or their sodium or potassium salts were used: glycollic, pyruvic, lactic, α -hydroxyisobutyric, mandelic, malic, tartaric, citric and isocitric. These solutions were stored in a refrigerator.

Standard $\text{Al}^{3+}/\text{F}^-$ solutions, at a given pH and ionic strength, were prepared by mixing the appropriate volumes of fluoride stock solution, acetate buffer, and sodium nitrate stock solution in a standard flask, adding the required volume of aluminium stock solution (diluted with almost enough water to make up the total volume needed), with vigorous shaking (to eliminate the possibility of formation of insoluble aluminium salts by local excess of aluminium) and finally diluting to the mark. Standard solution A was 0.625mM $\text{Al}(\text{NO}_3)_3$, 1.00mM NaF, pH 4.1 (total acetate 2.50mM), 0.100M NaNO_3 .

Standard solution B was prepared in the same way as solution A but was 0.750mM in $\text{Al}(\text{NO}_3)_3$. These standard solutions were stored in polyethylene bottles and it was found potentiometrically that their fluoride activities remained stable for at least a week.

Working standard solutions of EDTA (in the range 0.2–1.5mM) and citrate (in the range 0.1–1.0mM) were prepared daily from the stock solutions by dilution with water.

Procedures

General studies. A 10.00-ml volume of standard $\text{Al}^{3+}/\text{F}^-$ solution was transferred into the reaction cell. The stirrer was started and after

the potential had stabilized (20–30 sec) the reaction was initiated by the rapid injection of 10–50 μl of the stock solution of the complexing reagent. The reaction was followed for about 30–60 sec and its course was monitored by the microcomputer. The potential–time ($E-t$) data were stored on magnetic disks for later use. The cell was emptied and washed with two 10-ml portions of the $\text{Al}^{3+}/\text{F}^-$ solution.

Kinetic measurement of EDTA. A 10.00-ml volume of standard solution A was transferred into the reaction cell. The stirrer was started and, after the potential had been stabilized (about 30 sec), the reaction was initiated by the rapid injection of 1.00 ml of working standard or sample solution of EDTA in the concentration range 0.20–1.5mM. The reaction was followed for about 30–60 sec and its progress was monitored by the microcomputer. The analytical signal ($\Delta E/\Delta t$, mV/sec) was automatically calculated by the program by linear regression of the $E-t$ data obtained between 10 and 30 sec after sample injection. The cell was then emptied and washed as above.

Calibration graphs of $\Delta E/\Delta t$ vs. C_{EDTA} were constructed by using standard solutions of EDTA.

Kinetic measurement of citrate. A modified version of the KINMOD program was used to facilitate the measurement of the peak height, ΔE , of the potential–time plot ($\Delta E = E_{\text{eq}} - E_{\text{peak}}$), where E_{peak} was the lowest potential obtained after the addition of the citrate sample, and E_{eq} was the equilibrium potential prior to the addition of the citrate sample.

A 10.00-ml volume of standard solution B was transferred into the reaction cell. The stirrer was started and after the potential had stabilized the reaction was initiated by the rapid injection of 1.00 ml of working standard or sample solution of citrate (Cit) in the concentration range 0.10–1.0mM. The reaction was followed for 60 sec and the analytical signal (ΔE , mV) was automatically calculated by the program. The cell was then emptied and washed as above.

Calibration graphs of ΔE vs. $\log C_{\text{Cit}}$ were constructed by using standard solutions of citrate.

RESULTS AND DISCUSSION

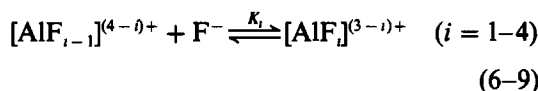
Kinetic characterization of the $\text{Al}^{3+}/\text{F}^-/\text{EDTA}$ system

Although aluminium forms very stable complexes with EDTA ($K_f = 1.3 \times 10^{16}$) and other

aminopolycarboxylic acids, its direct titration with these compounds (except DCTA)⁸ is virtually impossible in the presence of high concentrations of neutral electrolytes.⁹

The influences of parameters such as the analytical concentrations of aluminium (C_{Al}) and fluoride (C_{F}), pH, ionic strength, and temperature were examined. With each set of parameters, the rate of displacement of the fluoride ion from Al–F complexes (expressed in terms of $-\Delta E/\Delta t$) was measured with various amounts of EDTA. In each case the linearity of the recordings obtained was evaluated to establish conditions for reproducible measurement of $\Delta E/\Delta t$. The linearity and slope of the resulting calibration graphs were also examined.

With a constant analytical concentration of fluoride, the concentration of each aluminium species and the concentration of uncomplexed fluoride are dependent on the analytical concentration of aluminium. From the equilibria



and the relevant mass-balance equations for aluminium and fluoride, the following implicit function of $[\text{F}^-]$ is obtained:

$$[\text{F}^-] \left(1 + \frac{[\text{H}^+]}{K_{\text{HF}}} \right) + \frac{\sum_{i=1}^4 \left(i [\text{F}^-]^i \prod_{j=1}^i K_j \right)}{1 + K_h/[\text{H}^+] + \sum_{i=1}^4 \left([\text{F}^-]^i \sum_{j=1}^i K_j \right)} C_{\text{Al}} = C_{\text{F}} \quad (12)$$

Equation (12) is solved numerically for $[\text{F}^-]$ by using the Newton–Raphson iterative procedure.¹⁰ The concentrations of all other species are calculated from their explicit functions obtained from the relevant equilibrium expressions. The mole fractions of all aluminium species, and $\log [\text{F}^-]$, are shown as functions of C_{Al} in Fig. 1.

The successive formation constants (K_i) used for the calculations were $K_1 = 2.8 \times 10^6$, $K_2 = 1.6 \times 10^5$, $K_3 = 6.2 \times 10^3$, $K_4 = 1.5 \times 10^3$ (calculated at 25° and ionic strength 0.1).² The dissociation constant of HF, K_{HF} , and the

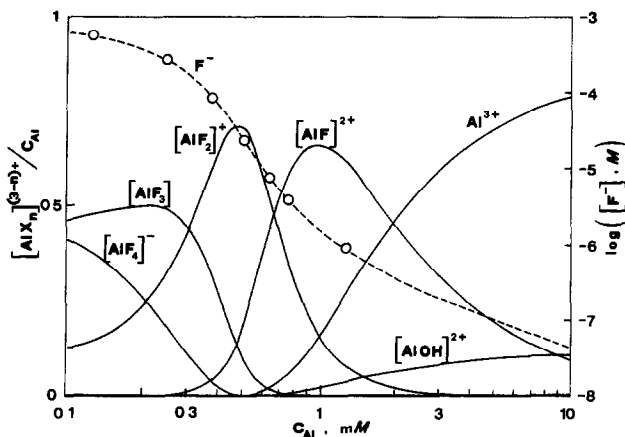


Fig 1 Calculated mole fractions of aluminium species and values of $\log [F^-]$ (dashed line) as functions of C_{Al} , C_F 1.00mM, pH 4.1, ionic strength 0.10, temperature 25°

hydrolysis constant of Al^{3+} , K_h , were taken as 5.9×10^{-4} and 1.1×10^{-5} , respectively.^{2,11}

Standard Al^{3+}/F^- solutions with C_{Al} in the range 0.125–1.25mM and fixed $C_F = 1.00mM$ were prepared. The concentration of free fluoride in each of these solutions was measured potentiometrically and found to be in excellent agreement with the calculated values (the experimental points are shown in Fig. 1). This fact confirms that the acetate (total acetate concentration 2.50mM), added to increase the buffer capacity of the standard Al^{3+}/F^- solutions, does not participate to any great extent in the overall Al–F equilibria.

Calibration graphs, for amounts of EDTA corresponding to final analytical concentrations in the range 0.025–0.125mM, were prepared

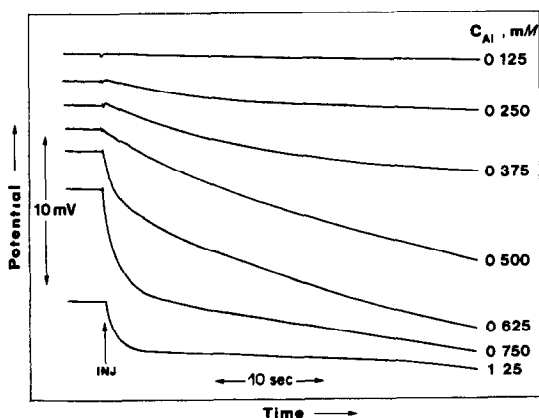


Fig 2 Effect of the analytical concentration of aluminium (C_{Al}) on the recorded curves of the fluoride ISE potential during the reaction of the Al^{3+}/F^- standard solutions with EDTA at $25.0 \pm 0.2^\circ$, C_{Al} as shown on recordings, C_F 1.00mM, C_{EDTA} 0.150mM, pH 4.1 (total acetate 2.50mM), ionic strength 0.10 (NaNO₃), INJ = injection of EDTA solution

with each standard solution and it was found that optimum linearity and sensitivity were obtained at $C_{Al} = 0.625mM$. At this analytical concentration of aluminium, the predominant aluminium species are $[AlF]^{2+}$ and $[AlF_2]^+$, with mole fractions of 0.40 and 0.55, respectively.

Typical curves recorded during the reaction of the Al^{3+}/F^- standard solutions with the same amount of EDTA, are shown in Fig. 2. The recordings obtained with the standard solution with $C_{Al} = 0.625mM$ had an extensive linear portion and the highest (absolute) slope. The initial potential change is especially pronounced for $C_{Al} > 0.625mM$, where the doubly-charged complex $[AlF]^{2+}$ predominates. Probably, $[AlF]^{2+}$ reacts much faster with the negatively charged species of EDTA than the other complexes do, owing to the stronger attractive coulombic forces. Apparently, the solution is quickly depleted of $[AlF]^{2+}$, because of the slow re-establishment of the equilibria among the Al–F complexes.

In an attempt to enhance the sensitivity of the kinetic determination of EDTA, the previous experiments were repeated with C_F fixed at 0.250mM and C_{Al} in the range 0.04–0.40mM. The optimum C_{Al} was found to be $\sim 0.25mM$, but no improvement in sensitivity or linearity of the calibration graph was observed. Furthermore, lower fluoride concentrations resulted in a much slower stabilization of the potential of the fluoride ISE.

For standard solutions with $C_{Al} = 0.625mM$, $C_F = 1.00mM$ and pH values in the range 4.1–5.6, recordings were obtained with various EDTA concentrations as before. It was found that the slope of the initial portion of the potential recordings increased with increasing

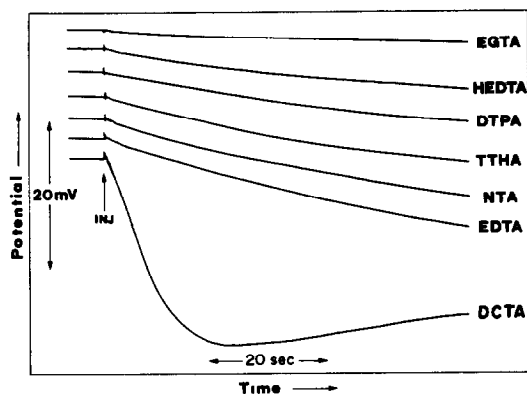


Fig 3 Recorded curves of the fluoride ISE potential during the reaction of the $\text{Al}^{3+}/\text{F}^-$ standard solution with various aminopolycarboxylic acids (L) at $25.0 \pm 0.2^\circ$, C_F 1.00 mM, C_{Al} 0.625 mM, C_L 0.100 mM, pH 4.1 (total acetate 2.50 mM), ionic strength 0.10 (NaNO_3), INJ = injection of aminopolycarboxylic acid solution

pH, but the absence of extended linear portions of these recordings dictated the use of pH 4.1. Replacing acetate by monochloroacetate and repeating the measurements in the pH range 3.5–4.0 resulted in linear potential recordings, but no increase in the slope of the calibration graph was achieved.

The rate of the fluoride displacement by EDTA was examined with standard $\text{Al}^{3+}/\text{F}^-$ solutions with ionic strengths in the range 0.1–1.0 (adjusted with sodium nitrate). The rate of fluoride release decreased when the ionic strength was increased, denoting a rate-determining step between species of opposite charge. It is known that the reaction of aluminium with EDTA is retarded by high ionic strength.⁸ Although the absence of ionic background would result in enhanced sensitivity of the kinetic determination of EDTA, an ionic strength of 0.10 was selected to overcome small variations in the ionic strength of the samples.

The rate of the displacement reaction increased with temperature. From the slopes of the calibration graphs obtained at temperatures in the range 23–32° (normalized for the temperature effect on the pre-logarithmic factor of the Nernst equation), an activation energy of 16.0 ± 0.8 kcal/mole was calculated. However, it should be noted that the consistent curvature observed on the relevant Arrhenius plots denotes that more than one rate-determining reaction step is involved.

Kinetic measurement of EDTA

The EDTA contents of 1.00-ml samples of aqueous solutions containing 0.2–1.5 μmole of

EDTA were measured by the reaction rate method. Calibration graphs were obtained with four standard solutions. A typical calibration graph is described by the equation

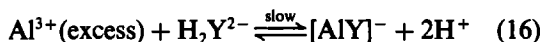
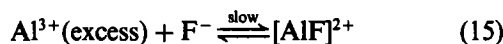
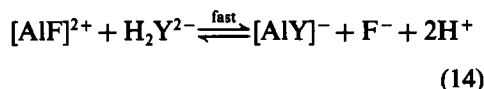
$$-\Delta E/\Delta t (\text{mV/sec}) = -0.014 + 0.232(\text{EDTA}, \mu\text{mole}), \quad r = 0.999 \quad (13)$$

The average absolute and relative errors of the measurement (single measurements) were 0.02 μmole and 3.1%, respectively. The relative standard deviations of repetitive measurements of samples containing 0.40 and 1.20 μmole of EDTA were 3.0 and 2.4%, respectively ($N = 9$).

Comparison of EDTA with other aminopolycarboxylic acids

Other aminopolycarboxylic acids were examined to determine the relative rates of their displacement reactions. Typical recordings are shown in Fig. 3.

DCTA reacts much faster than the others, resulting in a non-monotonic release of fluoride. Probably, the following reactions take place ($\text{H}_4\text{Y} = \text{DCTA}$):



Reaction (16) must be much slower than reaction (14), otherwise a monotonic release of fluoride would occur. Probably, partial complexation of aluminium with fluoride weakens the polymeric structure of hydrated aluminium ions, making them more reactive.

The relative rate of release of fluoride by each of the aminopolycarboxylic acids examined was determined from the slopes of the calibration plots obtained by varying the amount of complexing reagent. The extended reaction curves were used for preparing the calibration plots except in the case of DCTA, where the initial slopes of the recordings were used. The rates for the aminopolycarboxylic acids examined, relative to that for EDTA, are:

DCTA	EDTA	NTA	TTHA	DTPA	HEDTA	EGTA
9.0	1.00	0.75	0.74	0.70	0.33	0.20

These values justify the customary use of DCTA, rather than EDTA, in total ionic

strength adjustment buffer (TISAB) formulations for fluoride ISE applications in the presence of aluminium.

Kinetic characterization of the system $Al^{3+}/F^-/citrate$

Citrate readily replaces fluoride from Al-F complexes. The fluoride ions released recombine with the excess of Al^{3+} , resulting in non-monotonic trough-shaped recordings even sharper than those obtained with DCTA. It soon became apparent that the depth of the minimum of the potential-time recordings could serve as an analytical signal for the determination of small amount of citrate and was a linear function of the logarithm of the amount of citrate added.

The reaction conditions were optimized with regard to high sensitivity and linearity, as described above for EDTA.

Typical recordings obtained with C_F fixed at 1.00mM and C_{Al} in the range 0.25–1.50mM, at pH 4.1 and ionic strength 0.10, are shown in Fig. 4. The sharpest and deepest troughs were obtained at C_{Al} 0.750–1.00mM, a concentration range in which $[AlF]^{2+}$ is the predominant species (Fig. 1).

As in the case of EDTA, the effect of pH was examined by repeating the measurements with $C_{Al} = 0.750mM$ over the pH range 3.5–5.5. Sharp potential troughs appeared at pH 4.1–4.5, whereas at pH > 5.0 only a relatively small potential change was observed. It was found that increasing ionic strength results in a flatter change in potential.

The effect of temperature was examined over the range 25–38° and at various analytical concentrations of citrate. The thermal coefficient was found to be 0.1 mV/deg or less. Therefore, small temperature fluctuations will not have a noticeable effect on the measurements.

Kinetics measurement of citrate

The citrate contents of 1.00-ml samples of aqueous solutions containing 0.1–1.0 μ mole of citrate were measured from the maximum change in potential (ΔE). Calibration graphs were obtained with four standard solutions. A typical calibration graph is described by the equation

$$\Delta E(mV) = 14.70 + 10.04 \log(Cit, \mu\text{mole})$$

$$r = 0.99992 \quad (17)$$

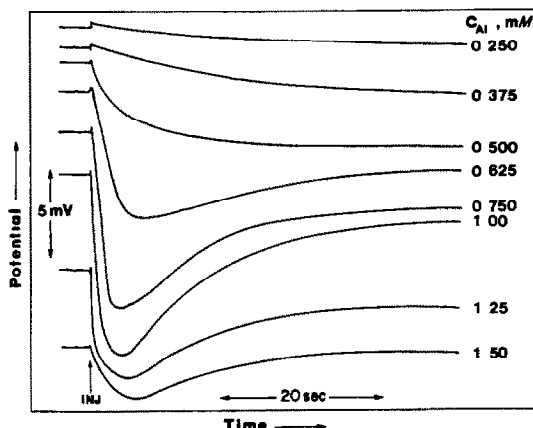


Fig. 4 Effect of the analytical concentration of aluminum (C_{Al}) on the recorded curves of the fluoride ISE potential during the reaction of the Al^{3+}/F^- standard solutions with citrate at $28.0 \pm 0.2^\circ$; C_{Al} as shown on recordings, C_F 1.00mM, C_{Cit} 0.030mM, pH 4.1 (total acetate 2.50mM), ionic strength 0.10 ($NaNO_3$), INJ = injection of citrate solution

The average absolute and relative errors of the measurement (single measurements) were 0.01 μ mole and 2.7%, respectively. The relative standard deviations of repetitive measurements of samples containing 0.10 and 0.75 μ mole of citrate were 2.0 and 1.9%, respectively ($N = 10$).

Comparison of citrate with other α -hydroxy-acids

Other α -hydroxy-acids were similarly examined. It was found that the monocarboxylic acids (glycollic, pyruvic, lactic, α -hydroxyisobutyric and mandelic) did not displace fluoride from its aluminium complexes. The dicarboxylic acids (malic and tartaric) displaced fluoride by an initially fast reaction which quickly subsided. Reaction curves obtained with isocitrate were similar to those obtained with citrate. Taking the analytical sensitivity (slope of the calibration graph) for the determination of citrate as unity the analytical sensitivities of the four reactive α -hydroxy-acids are

Isocitric	Citric	Malic	Tartaric
1.05	1.00	0.38	0.20

CONCLUSIONS

The displacement of fluoride from its complexes with aluminium by the action of EDTA, citrate and other related compounds is relatively slow, and easily monitored potentiometrically. The determination of individual reaction

rate constants is virtually impossible by exclusive monitoring of free fluoride. However, semi-quantitative inspection of the experimental data shows that fluoride is displaced quickly from the $[AlF]^{2+}$ species, and this complex reacts faster with DCTA, citrate and isocitrate than uncomplexed aluminium species do.

The applicability of the described kinetic procedures for the determination of EDTA and citrate is limited owing to the great number of interferents. Some kinetic discrimination may be possible. Ions forming complexes with fluoride, EDTA or citrate that are more stable than those of aluminium, or that form precipitates with fluoride or aluminium, should be considered as potential interferents. However, monitoring of the displacement reaction by means of a fluoride ion-selective electrode may serve as a sufficiently sensitive scheme for the post-column

detection of complexing reagents in LC and FIA systems.

REFERENCES

- 1 E. W. Baumann, *J. Inorg. Nucl. Chem.*, 1969, **31**, 3155.
- 2 R. R. Agarwal and E. C. Moreno, *Talanta*, 1971, **18**, 873.
- 3 K. Srinivasan and G. A. Rechnitz, *Anal. Chem.*, 1968, **40**, 1818.
- 4 *Idem, ibid.*, 1968, **40**, 1955.
- 5 *Instruction Manual: Fluoride Electrodes, Models 94-09 and 96-09*, Orion Research, Inc., Cambridge, MA, 1982.
- 6 Orion Research Inc., *Newsletter*, 1972, IV, No. 3/4.
- 7 H. A. Archontaki, M. A. Koupparis and C. E. Efsthathiou, *Analyst*, 1989, **114**, 591.
- 8 R. Přibil and V. Veselý, *Talanta*, 1962, **9**, 23.
- 9 R. Přibil, *Applied Complexometry*, pp. 171-173. Pergamon Press, Oxford, 1982.
- 10 J. B. Dence, *Mathematical Techniques in Chemistry*, p. 54. Wiley, New York, 1975.
- 11 F. A. Cotton and G. Wilkinson, *Advanced Inorganic Chemistry*, 5th Ed., p. 41. Wiley, New York, 1988.

KINETIC SPECTROPHOTOMETRIC DETERMINATION OF NANOGRAM AMOUNTS OF CYANIDE

A. VELASCO, M. SILVA and M. VALCARCEL

Department of Analytical Chemistry, Faculty of Sciences, University of Córdoba, 14004 Córdoba, Spain

(Received 9 November 1989 Revised 18 September 1990 Accepted 19 September 1990)

Summary—A sensitive kinetic method for determination of nanogram amounts of cyanide is reported. It is based on the measurement of the induction period imposed by cyanide on the copper(II)-catalysed oxidation of 3-hydroxybenzaldehyde azine (3-OHBAA) by potassium peroxydisulphate. Kinetic data are recorded spectrophotometrically at 465 nm, the maximum absorption wavelength of the oxidation product of 3-OHBAA. From the kinetic study and other experimental tests it may be concluded that the cyanide ion undergoes copper(II)-catalysed oxidation during the induction period. The calibration plot is linear in the range 150–600 ng/ml cyanide and the detection limit is 50 ng/ml. The precision of the method, expressed as the relative standard deviation, is 3.2% for 350 ng/ml cyanide. Good recoveries are obtained in applying the method to analysis for cyanide in water samples.

The determination of inorganic anions by their catalytic effect on redox reactions is less common than that of metal ions. Many anions act as inhibitors in metal-catalysed reactions because they can form stable complexes with metal ions, but this facilitates their determination by kinetic or catalytic titration methods.¹

Despite the great ability of cyanide to form stable complexes with transition metal ions, few kinetic methods have been developed for its determination. Two types of method have been used: direct determination of cyanide based on its catalytic effect on redox^{2,3} and decomposition⁴ reactions and indirect determination on the basis of its inhibitory effect on metal-catalysed reactions⁵⁻⁷ and on one uncatalysed reaction.⁸ Catalytic titrations have scarcely been used for cyanide determination.^{9,10}

The kinetic determination of cyanide reported in this paper is based on the copper(II)-catalysed oxidation of 3-hydroxybenzaldehyde azine (3-OHBAA) by potassium peroxydisulphate in ammoniacal medium, an indicator reaction previously used for the kinetic determination of nanogram amounts of copper in a large variety of samples.¹¹ In this reaction, the cyanide interacts with the potassium peroxydisulphate rather than with copper(II), imposing an induction period (proportional to the amount of cyanide present in the sample) in the absorbance vs. time plots recorded at the maximum absorption wavelength of the oxidation product of 3-OHBAA. The proposed method

permits the determination of ng/ml levels of cyanide with appreciable selectivity (*e.g.*, in the presence of large amounts of thiocyanate) and its application to the analysis of water samples with good results.

EXPERIMENTAL

Reagents

All chemicals used were of analytical-reagent grade. A 3-hydroxybenzaldehyde azine solution (3 mg/ml) was prepared in ethanol. The reagent was synthesized according to the procedure of Luque de Castro and Valcárcel.¹² A standard cyanide solution (1.0 mg/ml) was prepared by dissolving 2.5 g of potassium cyanide (equivalent to 1 g of cyanide) in 1 litre of 0.05M sodium hydroxide, and standardized argentometrically.¹³ A standard copper solution (1.000 mg/ml) was made by dissolving 1.000 g of pure electrolytic copper in the minimum volume of nitric acid (1 + 1) and diluting to exactly 1 litre with 1% v/v nitric acid.

Apparatus

All spectrophotometric measurements were made with a Perkin-Elmer Lambda 5 double-beam spectrophotometer furnished with an automatic recorder and a dry thermostat (Peltier system) with 1-cm cells. A Radiometer PHM62 pH-meter furnished with a combined glass-calomel electrode was also used.

Procedure

To a 10-ml standard flask add 2.0 ml of ethanolic 3-OHBA solution, 4.0 ml of ethanol, 1.0 ml of distilled water, 100 μ l of 1.000 μ g/ml copper(II) solution, appropriate volumes of cyanide solution to give a final concentration of cyanide between 150 and 600 ng/ml, 1.0 ml of 0.1M potassium peroxydisulphate and 0.8 ml of concentrated ammonia solution. Make up to volume with distilled water, mix, and after 10 min, transfer a portion to a 1-cm spectrophotometric cell kept at $25 \pm 0.1^\circ$. Wait for 30 sec before starting to record the absorbance (at 465 nm) as a function of time against a blank containing no cyanide or copper (uncatalysed reaction). Calculate the induction period from the kinetic curve; it should be proportional to the concentration of cyanide in the sample.

RESULTS AND DISCUSSION

Copper(II) catalyses the oxidation of 3-hydroxybenzaldehyde azine by potassium peroxydisulphate in ammoniacal solutions. The oxidation product formed gives rise to an intense band centred at 465 nm. In the presence of cyanide this band is again present but there is an induction period in the absorbance *vs.* time plot (Fig. 1). After this delay time, the catalytic reaction exhibits the same kinetic behaviour (initial rate) as in the absence of the cyanide ion. This can be attributed to an interaction between cyanide and potassium peroxydisulphate rather than with the catalyst. In fact, taking into account the experimental results reported in this paper, it appears that the cyanide ion is oxidized

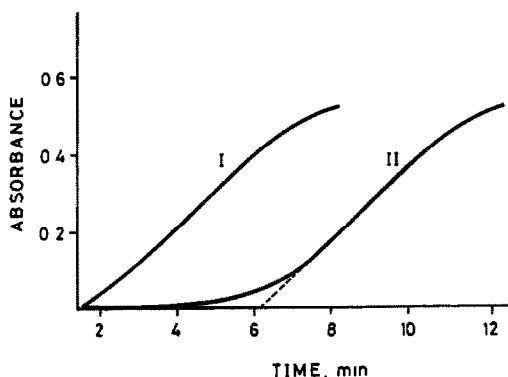


Fig. 1. Modifying effect of cyanide on the copper(II)-catalysed oxidation of 3-OHBA by potassium peroxydisulphate. (I) reaction catalysed by 10 ng/ml copper(II), (II) as for (I), but in the presence of 300 ng/ml cyanide. Reaction conditions as described in "Procedure"

by the potassium peroxydisulphate in a reaction which is also catalysed by copper(II). Thus, the start of the copper(II)-catalysed oxidation of 3-OHBA (once cyanide has been completely oxidized) is marked by an increase in the absorbance at 465 nm (Fig. 1).

Influence of reaction variables

The effect of temperature on the oxidation of cyanide was examined in the range $15\text{--}40^\circ$ (Fig. 2). Although the induction period was longer at low temperatures (giving higher sensitivity in the kinetic determination of cyanide), the initial rate of the 3-OHBA/S₂O₈²⁻/Cu²⁺ system was lower and graphical errors in the determination of the induction period were therefore larger. Thus, the temperature was fixed at 25° (room temperature) for subsequent experiments, taking into account the appreciable extent of the induction period and the ease with which this temperature can be achieved in the spectrophotometer cell compartment.

To optimize the concentration of potassium peroxydisulphate the initial value was varied in the range $3 \times 10^{-3}\text{--}1.3 \times 10^{-2}M$, while keeping the concentrations of the other reactants constant [Fig. 3(a)]. From the results, we established the kinetic dependence of the oxidation of the cyanide ion on the concentration of potassium peroxydisulphate. Thus, if a pseudo first-order dependence was assumed, the corresponding rate equation could be written as

$$-d[\text{CN}^-]/dt = k[\text{S}_2\text{O}_8^{2-}] \quad (1)$$

As the oxidant concentration was in large excess with respect to the cyanide concentration,

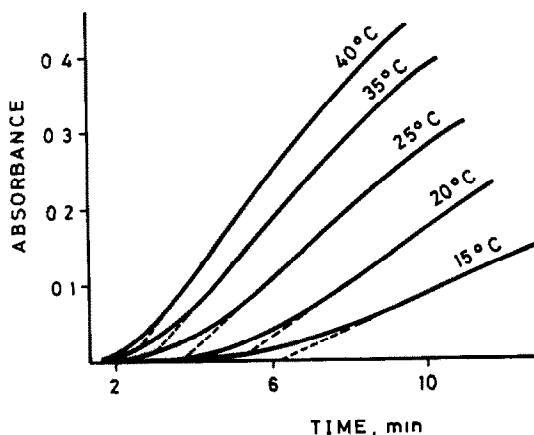


Fig. 2. Absorbance/time curves recorded at different temperatures for the 3-OHBA/S₂O₈²⁻/Cu²⁺ system in the presence of 250 ng/ml cyanide. Other conditions as described in "Procedure"

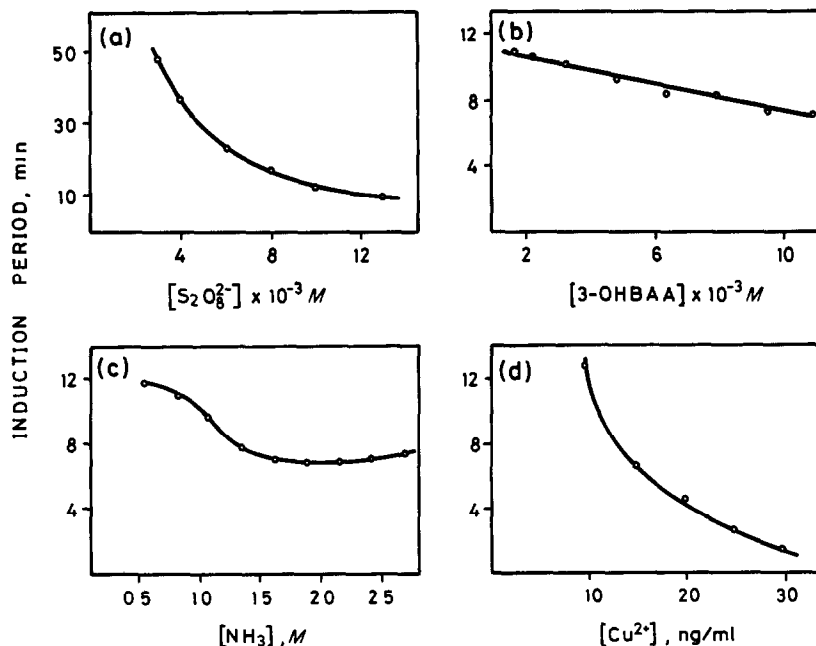


Fig 3 Effect of chemical variables on the kinetic determination of 500 ng/ml cyanide (a) $S_2O_8^{2-}$, (b) 3-OHBAAs, (c) NH_3 ; (d) Cu^{2+}

it could be assumed to be constant, and integration of equation (1) over the limits $[CN^-]_0 - [CN^-]_f$, corresponding to $t = t_0$ (start of the reaction) and $t = t_f$ (end of the cyanide oxidation reaction), would yield:

$$[CN^-]_0 - [CN^-]_f = k[S_2O_8^{2-}](t_f - t_0) \quad (2)$$

which, assuming $t_f - t_0 = IP$ (induction period) and $[CN^-]_f \rightarrow 0$ can be simplified to

$$[CN^-]_0 = k[S_2O_8^{2-}]IP \quad (3)$$

from which, taking into account that $[CN^-]_0$ was constant in all the experiments concerned, equation (3) can be rewritten as:

$$IP = k'/[S_2O_8^{2-}] \quad (4)$$

where $k' = [CN^-]_0/k$.

This theoretical dependence was experimentally confirmed by the straight line ($r = 0.994$, $n = 6$) obtained in the plot of the induction period against the reciprocal of the oxidant concentration. From these studies, the optimum oxidant concentration was taken to be $0.01M$ (corresponding to 1 ml of $0.1M$ potassium peroxydisulphate in the reaction mixture).

The effect of the concentration of 3-OHBAAs on the induction period is reflected in Fig. 3(b). Although the 3-OHBAAs does not take part in the oxidation of cyanide ion, the results suggest that the 3-OHBAAs/ $S_2O_8^{2-}$ / Cu^{2+} system exerts an accelerating effect on this oxidation reaction.

In order to increase the sensitivity we used a 3-OHBAAs concentration of $2.5 \times 10^{-3}M$ (2.0 ml of 3-mg/ml ethanolic solution in 10 ml) in the reaction.

The effect of the ammonia concentration on the length of the induction period was studied by following the proposed procedure and adding between 0.4 and 2.0 ml of concentrated ammonia to a series of 10-ml standard flasks containing cyanide and the other reactants. A $1.08M$ ammonia concentration was chosen as optimal since although lower concentrations would give longer induction periods and use of higher concentrations would be less sensitive to loss of ammonia, in both cases the graphical determination of the induction period proved more troublesome.

The influence of pH was examined at a fixed initial concentration of ammonia ($1.08M$) by adding dilute hydrochloric acid or sodium hydroxide. A zero-order kinetic region was found at pH values of about 10.8–13.2, so a pH of 11.9, which was accomplished by addition of 0.8 ml of concentrated ammonia solution to the reaction mixture, was selected.

The variation of the induction period was studied as a function of the copper(II) concentration in the range 10–30 ng/ml [Fig. 3(d)]. The dependence of the induction period on the concentration of copper was found to be similar to that on the concentration of the oxidant,

which suggests a pseudo first-order dependence of the rate of oxidation of cyanide on the copper(II) concentration:

$$-d[\text{CN}^-]/dt = k_1[\text{Cu}^{2+}] \quad (5)$$

If copper(II) does exert a catalytic effect on this reaction, its concentration must be kept constant during the determinations. Direct dependence between the induction period and the reciprocal of the copper(II) concentration is indicated by integration of equation (5) similarly to equation (1). The straight line obtained ($r = 0.9988$, $n = 6$) for the experimental relationship confirms this dependence and the catalytic effect of copper(II) on the oxidation of cyanide by potassium peroxydisulphate. The copper(II) concentration selected was 10 ng/ml [100 μ l of 1.000 μ g/ml copper(II) solution].

Increase in the ethanol concentration between 20 and 65% v/v linearly increased the length of the induction period by a factor of up to 2.8. Thus, the cyanide oxidation reaction was markedly hindered by increased ethanol contents. According to the Kirkwood equation,¹⁴ the rate of reaction between two ions with the same charge sign increases with increasing dielectric constant of the medium. Therefore, we may assume an interaction of two ions with the same charge sign to be the rate-determining step in the copper(II)-catalysed oxidation of cyanide by potassium peroxydisulphate. From this study, a 60% v/v ethanol concentration was chosen as optimum.

Finally, the length of the induction period was found to increase non-linearly with the cyanide concentration [Fig. 4(a)]. In order to account for this behaviour, we may assume a kinetic dependence of order -1 between the oxidation rate of cyanide and its concentration:

$$-d[\text{CN}^-]/dt = k_0/[\text{CN}^-] \quad (6)$$

Integration of equation (6) between the limits $t_1 = t_0$, $[\text{CN}^-]_1 = [\text{CN}^-]_0$ and $t_2 = t_f$, $[\text{CN}^-]_2 = [\text{CN}^-]_f$ gives

$$[\text{CN}^-]_0^2 - [\text{CN}^-]_f^2 = 2k_0(t_f - t_0) = 2k_0\text{IP} \quad (7)$$

$[\text{CN}^-]_f$ can be neglected and equation (7) can be rewritten as

$$\text{IP} = k'_0[\text{CN}^-]_0^2 \quad (8)$$

where $k'_0 = 1/2k_0$

This relation between the induction period and the cyanide concentration was experimentally confirmed, as shown in Fig. 4(b).

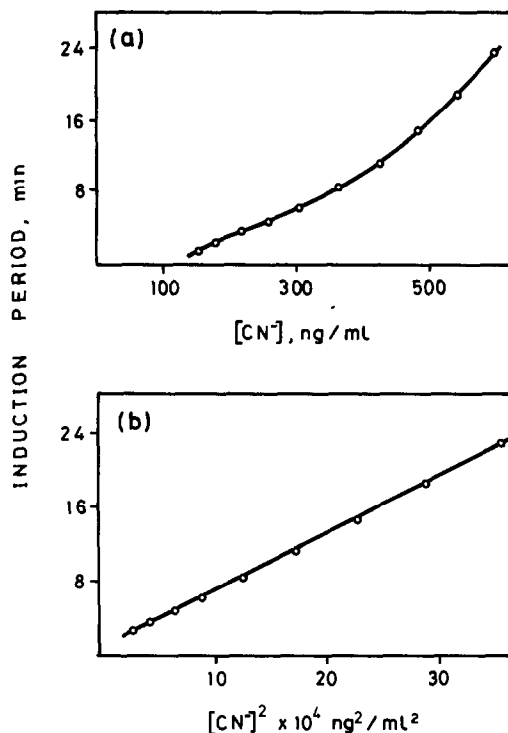


Fig. 4 Kinetic determination of cyanide (a) effect of the cyanide concentration on the induction period, (b) linear calibration function used for the determination of cyanide

In consistence with the study above, the following rate equation is suggested for the copper(II)-catalysed oxidation of cyanide by potassium peroxydisulphate, in which the 3-OHBAAs/S₂O₈²⁻/Cu²⁺ system acts as a "developing reaction":



where K is the rate constant.

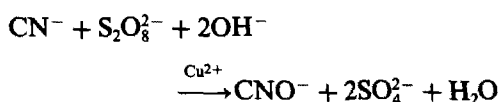
Oxidation of cyanide, and catalytic effect of copper(II)

According to the results found in the kinetic study, we may assume the 3-OHBAAs/S₂O₈²⁻/Cu²⁺ system to be subject to an induction period in the presence of cyanide ion, which is oxidized by potassium peroxydisulphate in a reaction also catalysed by copper(II). Although the kinetic dependence on copper(II) is indicative of its catalytic effect, four further assays were made to confirm this point: (a) oxidation of 3-OHBAAs by potassium peroxydisulphate catalysed by 10 ng/ml copper(II); (b) the same reaction in the presence of 450 ng/ml cyanide; (c) preparation of the sample as in (b) but with the 3-OHBAAs added after 7 min [*i.e.*, once the cyanide had been oxidized by S₂O₈²⁻ in the presence of copper(II) as catalyst]; (d) preparation of the

sample as in (b), but with both the 3-OHBAA and copper(II) added after 7 min.

The results are listed in Table 1. The absence of an induction period in (c) and its occurrence in (d) clearly confirm the catalytic effect of copper(II) on the oxidation of cyanide by potassium peroxydisulphate. The small difference between the induction periods in (b) and (d) can be attributed to slight oxidation of cyanide in the delay time (7 min) before addition of the copper.

In summary, the kinetic curve recorded has two distinct parts: (1) an induction period in which the cyanide is oxidized by potassium peroxydisulphate in a reaction catalysed by copper(II) according to:



and (2) the typical absorbance *vs.* time response, measured at 465 nm, corresponding to the oxidation of 3-OHBAA by potassium peroxydisulphate, also catalysed by copper(II).

Kinetic determination of cyanide

Under the experimental conditions given above, the plot of the induction period against the square of the concentration of cyanide was essentially linear between 150 and 600 ng/ml cyanide. The sensitivity, expressed as the slope of the calibration function, was 62.8 min.ml².ng⁻². The detection limit (50 ng/ml) was evaluated as the concentration corresponding to three times the standard deviation of the induction period for 30 determinations of low analyte concentration¹⁵ (200 ng/ml cyanide). The reproducibility of the method was checked on 11 replicate determination of 350 ng/ml cyanide. The relative standard deviation obtained was 3.2%.

The effect of various anions generally accompanying cyanide was studied at a cyanide concentration of 300 ng/ml. The results obtained

Table 1 Catalytic effect of copper(II) on the oxidation of cyanide

Experiment	Induction period, sec
(a) Cu ²⁺ + 3-OHBAA + S ₂ O ₈ ²⁻	—
(b) 3-OHBAA + Cu ²⁺ + CN ⁻ + S ₂ O ₈ ²⁻	370
(c) Cu ²⁺ + CN ⁻ + S ₂ O ₈ ²⁻ + wait 7 min + 3-OHBAA	—
(d) CN ⁻ + S ₂ O ₈ ²⁻ + wait 7 min + 3-OHBAA + Cu ²⁺	340

Table 2 Influence of foreign anions on the kinetic determination of 0.3 µg/ml cyanide

Anion added	Tolerate ratio, w/w
F ⁻ , Cl ⁻ , Br ⁻ , BrO ₃ ⁻ , SO ₄ ²⁻ , CO ₃ ²⁻ , NO ₃ ⁻ , SCN ⁻ , ClO ₄ ⁻ , PO ₄ ³⁻ , B ₄ O ₇ ²⁻ , acetate, tartrate	100
SO ₃ ²⁻ , AsO ₄ ³⁻ , SeO ₃ ²⁻ , citrate	50
CrO ₄ ²⁻ , I ⁻ , ClO ₃ ⁻ , IO ₃ ⁻ , S ₂ O ₃ ²⁻	20
C ₂ O ₄ ²⁻	10
IO ₄ ⁻	5

are listed in Table 2, in which the tolerated ratio of each foreign anion is the largest amount yielding an error less than ±5% in the induction period. The maximum level tested was 30 µg/ml (tolerated anion to cyanide weight ratio = 100).

The results indicate a good tolerance to common anions such as fluoride, chloride, bromide, bromate, nitrate, sulphate, *etc.*, and especially to thiocyanate, which is a serious interferent in several methods for the determination of cyanide. The effect of common metal ions was also tested. The maximum tolerated ratio of metal ions to cyanide were calcium and magnesium, 100, iron and aluminium, 20; lead, 10; cadmium, 5. Manganese, zinc, silver, mercury, cobalt and nickel interfered when present in 1:1 weight ratio to cyanide, owing to their ability to form strong complexes with it; this behaviour can be exploited for their determination and resolution in mixtures with copper(II)¹⁶

Determination of cyanide in water samples

Cyanide, as a water pollutant, may enter the environment from many sources. Thus, as it is used extensively in many industrial processes, it may be present in wastes and wastewaters as well as in streams receiving uncontrolled and unpurified industrial effluents. Because cyanide is highly toxic even at low concentrations, monitoring of low cyanide levels is required within sewage treatment works in order to improve the quality of the effluent. In this context, and in order to validate the proposed kinetic method, it was applied to analysis for cyanide in water samples.

Water samples were spiked with 0.28–0.50 µg/ml cyanide and analysed directly by the procedure described. As can be seen from the results obtained (Table 3), the recoveries ranged from 97.7 to 100.7%, with an average of 99.5%

Table 3 Recovery of cyanide added to water samples

Sample	Cyanide content, $\mu\text{g/ml}$		Recovery, %
	Added	Found*	
Drinking water	0.300	0.302	100.7
	0.400	0.399	99.7
	0.500	0.491	98.2
River water	0.280	0.276	98.6
	0.350	0.342	97.7
	0.450	0.447	99.5
		Mean	99.1
	Standard deviation	1.2	

*For three separate determinations

for drinking water and 98.6% for river water. The relative standard deviation for the overall procedure was 1.2%. These recoveries show the good performance of the proposed kinetic method in the determination of cyanide in this type of sample.

REFERENCES

- 1 D. Pérez-Bendito and M. Silva, *Kinetic Methods in Analytical Chemistry*, Horwood, Chichester, 1988
- 2 V. G Badding and J L Durney, *Plat Surf Finish*, 1980, **67**, 49
- 3 S. Rubio, A. Gómez-Hens and M Valcárcel, *Talanta*, 1984, **31**, 783.
- 4 M A. Ditzler, F. L Keohan and W F Gutknecht, *Anal Chim Acta*, 1982, **135**, 69.
- 5 H Weisz, S. Pantel and W. Meiners, *ibid.*, 1976, **82**, 145
- 6 J. L. Ferrer, *Doctoral Thesis*, University of Córdoba, 1980
- 7 Z. Gregorowicz, T Suwinska and P Gorka, *Chem Anal. (Warsaw)*, 1974, **19**, 447.
- 8 M Phull, S. N Rai and P. C Nigam, *Indian J. Chem.*, 1983, **22A**, 482.
- 9 N Kiba and M Furosawa, *Anal Chim Acta*, 1978, **98**, 343
- 10 H A Mottola and H Freiser, *Anal Chem*, 1968, **40**, 1266
- 11 A Velasco, M Silva and M Valcárcel, *Anal. Chim. Acta*, 1990, **229**, 107.
- 12 M D Luque de Castro and M Valcárcel, *Afinidad*, 1978, **35**, 243
- 13 I. M Kolthoff and E B Sandell, *Textbook of Quantitative Inorganic Analysis*, 2nd Ed, p 574 Macmillan, New York, 1947
- 14 K. J Laidler, *Chemical Kinetics*, 2nd Ed., p 226 McGraw-Hill, New York, 1965
- 15 J A Glaser, D L Foerst, G D McKee, S. A Quave and W L Budde, *Environ Sci Technol.*, 1981, **15**, 1426
- 16 A Velasco, M Silva and M Valcárcel, *Microchem J*, 1990, **42**, 110

KINETICS OF THE DISSOLUTION OF COPPER METAL IN AQUEOUS SOLUTIONS CONTAINING UNSATURATED ORGANIC LIGANDS AND COPPER(II)

F. REBER BROWN* and QUINTUS FERNANDO

Department of Chemistry, University of Arizona, Tucson, AZ 85721, U S A

TETSUYA OGURA

Departamento de Química, Universidad Autónoma de Guadalajara, Guadalajara, Jalisco, Mexico

(Received 16 July 1990 Revised 27 August 1990 Accepted 5 September 1990)

Summary—The kinetics of the dissolution of copper metal in an aqueous solution containing copper(II) and an unsaturated organic ligand was followed by using an automated flow-injection analysis technique to determine the concentration of copper(I) in solution as a function of time. The results suggest that the rate of dissolution of the copper metal is dependent on electron transfer between the copper(II) and copper atoms on the surface of the copper metal, and on the stabilization of copper(I) by the unsaturated organic ligand in solution.

Copper(I) has long been known to form stable π -complexes with olefinic ligands. This property has been exploited for the determination of copper(I) in the presence of copper(II),¹ for the removal of trace levels of impurities from copper metal,² for the purification of olefins^{3,4} and in an investigation of the kinetics of reduction of copper(II) by copper metal in the presence of allyl alcohol.⁵ In the kinetic study it was found that the rate of oxidation of copper metal was first order with respect to the copper(II) concentration, the pH of the solution and the allyl alcohol concentration. The reaction was followed by periodically withdrawing samples from the reaction vessel with a microsyringe and determining the concentrations of copper(I) and copper(II). This manual sampling was tedious and introduced errors caused by the difficulty in withdrawing samples at reproducible time intervals. An obvious solution to this problem is to automate the sampling procedure.

In the work described in this paper, flow-injection analysis (FIA), was used to automate the sampling process.⁶ FIA has high reproducibility and sample throughput, and is relatively easy to automate. The kinetics of the oxidation

of copper metal to copper(I) in the presence of a variety of unsaturated ligands was investigated by an FIA technique. In these reaction systems, the reaction rates were sufficiently rapid to enable us to obtain adequate kinetic data within minutes.

EXPERIMENTAL

Materials

Copper granules (20–30 mesh) were washed with dilute perchloric acid, rinsed with distilled demineralized water, rinsed with acetone, and dried prior to the experiment. The ethyl alcohol used to make up solutions was refluxed over solid potassium hydroxide and aluminum powder for 8 hr and distilled prior to use. The allyl alcohol and allyl cyanide (Aldrich), acrylamide, propionitrile and butyronitrile (Eastman Kodak), acrylonitrile and acetonitrile (Mallinckrodt), were of reagent grade purity and all were used without further purification.

Apparatus

The apparatus used is shown in Fig. 1. It consisted of a main pump (#1, Buchler Polystaltic), a sample recirculation pump (#2, Cole-Palmer Masterflex #7014), an air-actuated sample-injection valve system with a sample loop volume of $\sim 100 \mu\text{l}$ (Rheodyne 5020 Teflon Rotary Valve, 50-01 Pneumatic Actuator, and 7163 Solenoid), and a Gilford Model 240

*Present address California Public Health Foundation, Hazardous Materials Laboratory, 2151 Berkeley Way, Berkeley, CA 94704, U S A

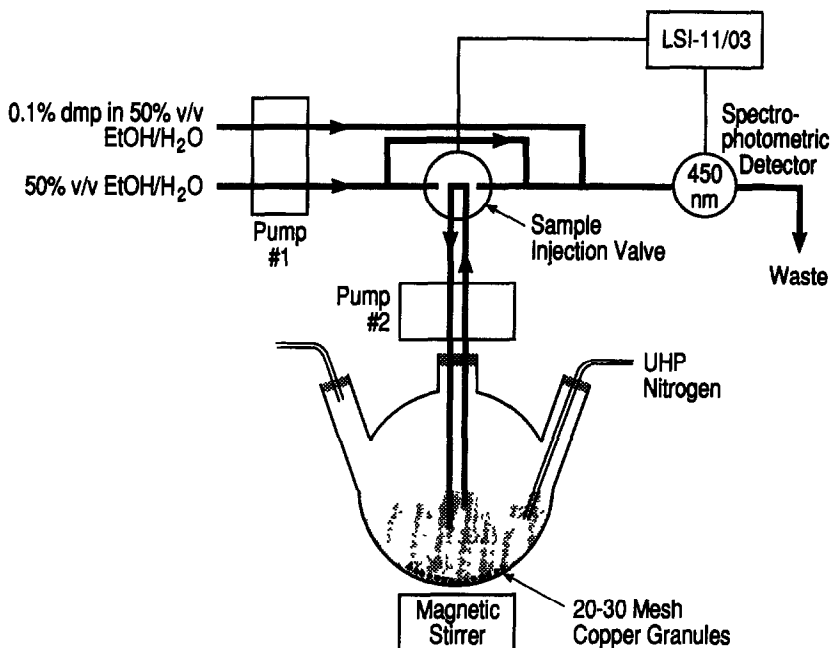


Fig 1 Schematic representation of the flow-injection analysis system for the automated determination of complexed copper(I) in solution

spectrophotometer fitted with a flow-cell (NSG Precision Cells # 513). All tubing was 0.8 mm bore Teflon and the flow-rate in the FIA system was 5.5 ml/min. The temperature of the 300-ml reaction vessel was kept constant at 25°.

An LSI-11 personal computer programmed with Fortran IV was used to perform the data acquisition, open and close the injection valve, and analyse the data. A Data Translation DT2781 was used to perform the analog to digital conversion and to provide digital I/O to toggle the injection valve. The DT2781 provided 12-bit conversion, and was used in the bipolar mode. The range was ± 1 V.

Procedure

The reaction mixture (~35 ml) consisted of 3 ml of copper(II) perchlorate solution, the ligand, and 25 ml of 0.1M sodium perchlorate. The pH of the solution was adjusted with perchloric acid. Dissolved oxygen was removed from the solution by passage of nitrogen which had been freed from traces of oxygen by bubbling through an alkaline pyrogallol solution. The reaction was started by adding 15 g of the copper granules to the reaction mixture, which was recirculated through the sample injection valve, and injected into the carrier stream (50% v/v ethanol-water) at a rate of four injections per minute. The carrier stream was merged with a 0.1% solution of 2,9-dimethyl-

1,10-phenanthroline (dmp) in 50% v/v ethanol-water. The absorbance of the $\text{Cu}(\text{dmp})_2^+$ complex formed was measured at 450 nm.

The effect of various unsaturated ligands on the rate of oxidation of copper metal was determined in a system in which the initial copper(II) concentration, pH and surface area of the copper metal were kept constant and the concentration of the unsaturated ligand was varied. The rate of oxidation of copper metal, expressed as $-\text{d}[\text{Cu}^{2+}]/\text{d}t = \frac{1}{2}\text{d}[\text{Cu}^+]/\text{d}t$ was determined by the initial rate method.

RESULTS

The effect of the initial copper(II) concentration, pH, and allyl alcohol concentration on the rate of oxidation of copper metal was investigated. The effect of the initial copper(II) concentration is shown in Fig. 2. Each experimental point in Fig. 2 was obtained from the average of a large number of measurements of the initial rate. It was found that the reaction was first order with respect to the initial copper(II) concentration up to $2.5 \times 10^{-3}M$, at pH 2.25 and an allyl alcohol concentration of 0.41M.

The effect of pH on the reaction rate is shown in Table 1. The results show that the reaction rate increases by more than a factor of two, with increase in pH from 0.7 to 4.8.

Table 2 shows that the rate of reaction increases linearly with allyl alcohol concentration

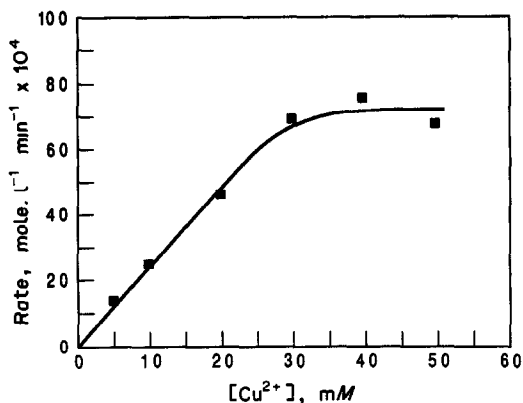


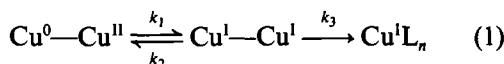
Fig 2 Effect of copper(II) concentration on the reaction rate, at pH 2.25 and 0.41M allyl alcohol concentration

up to about $1.47 \times 10^{-2}M$, and then becomes constant.

The effect of various unsaturated ligands on the reaction rate was investigated and the results are shown in Table 2. As in the case of allyl alcohol, the reaction rates initially increased linearly with ligand concentration and subsequently leveled out.

DISCUSSION

The following sequence of reactions is proposed for the dissolution of copper metal in the presence of an unsaturated ligand, L. Copper(II) ions are adsorbed on the surface of the copper metal and the resultant species is represented as Cu^0-Cu^{II} . This species on the surface of the copper metal is in equilibrium with the species Cu^I-Cu^I , as a consequence of electron transfer. In the presence of the ligand in contact with the surface of the copper metal, the species Cu^IL_n is formed in the solution phase. The rate constants, k_1 , k_2 , k_3 , that are involved in this series of reactions are shown in the reaction scheme.



and are given by the following rate equations:

$$-\frac{d}{dt} [Cu^0-Cu^{II}] = k_1 [Cu^0-Cu^{II}] - k_2 [Cu^I-Cu^I] \quad (2)$$

$$\begin{aligned} \frac{d}{dt} [Cu^I-Cu^I] &= k_1 [Cu^0-Cu^{II}] \\ &- k_2 [Cu^I-Cu^I] \\ &- k_3 [Cu^I-Cu^I][L]^n \quad (3) \end{aligned}$$

Table 1 Effect of initial pH on the rate of reaction at an initial copper(II) concentration of $2 \times 10^{-3}M$ and allyl alcohol concentration of 0.41M

pH	Rate $\times 10^4$, mole. l ⁻¹ min ⁻¹
0.70	2.4
1.01	2.6
1.40	3.0
2.01	3.7
3.01	3.7
3.60	4.0
4.10	4.5
4.75	5.6

$$\frac{d}{dt} [Cu^IL_n] = k_3 [Cu^I-Cu^I][L]^n \quad (4)$$

Since the reaction rates were found to be first order with respect to the ligand L, the value of n in equations (3) and (4) is unity. Under steady-state conditions, when $[Cu^I-Cu^I]$ is constant,

$$\frac{d}{dt} [Cu^I-Cu^I] = 0, \quad (5)$$

$$[Cu^I-Cu^I] = \frac{k_1 [Cu^0-Cu^{II}]}{k_2 + k_3 [L]} \quad (6)$$

Table 2 Effect of the initial concentration of unsaturated ligand on the reaction rate at pH 3.01 and $[Cu(II)] = 1.05 \text{ mM}$

Ligand	Concentration, mM	Rate $\times 10^4$, mole l ⁻¹ min ⁻¹
Allyl alcohol	2.94	1.1
	5.88	1.6
	14.7	2.3
	29.2	2.3
	118	2.2
Acrylamide	1.00	0.34
	4.00	1.2
	10.0	2.1
	20.0	2.9
	60.0	2.8
	120	3.0
	Acrylonitrile	3.04
6.08		0.38
15.2		0.60
30.4		1.3
60.8		1.5
122		21.6
Acetonitrile	3.77	0.24
	19.0	0.33
	38.0	0.59
	75.9	1.8
	152	2.2
	228	2.8
	304	2.7
Allyl cyanide	4.97	0.88
	12.4	1.2
	24.9	1.6
	49.7	1.6
	99.4	1.8

Table 3. Calculated ratios of the rate constants, k_3/k_2 , [equation (10)] from the experimental values of S and C [equations (8) and (9)]

Unsaturated ligand	$S \times 10^2$	$C \times 10^4$	$r \times 10^{-2} = \frac{k_3}{k_2} \times 10^{-2}$
Allyl alcohol	0.40	2.0	2.0
Acrylamide	3.6	3.0	1.2
Allyl cyanide	0.54	2.0	0.27
Acrylonitrile	0.49	1.6	0.31
Acetonitrile	0.15	2.8	0.54
Propionitrile	0.16	2.5	0.62
Butyronitrile	0.18	0.9	0.20

Hence, the rate of the reaction is given by

$$\frac{d}{dt} [\text{Cu}^{\text{I}}\text{L}] = \frac{k_1 k_3 [\text{L}] [\text{Cu}^0 - \text{Cu}^{\text{II}}]}{k_2 + k_3 [\text{L}]} \quad (7)$$

When $k_3[\text{L}] \ll k_2$, the initial slope, S , of a plot of the rate of the reaction *vs.* $[\text{L}]$ is given by

$$S = \frac{k_1 k_3}{k_2} [\text{Cu}^0 - \text{Cu}^{\text{II}}] \quad (8)$$

When $k_2 \ll k_3[\text{L}]$ in equation (7), a plot of the rate of the reaction *vs.* $[\text{L}]$ is a constant, C , given by

$$C = k_1 [\text{Cu}^0 - \text{Cu}^{\text{II}}] \quad (9)$$

The ratio of the rate constants k_3 and k_2 can be calculated from the ratio, r , of the experimental values of S and C :

$$r = \frac{S}{C} = k_3/k_2 \quad (10)$$

The larger the numerical value of r , the greater the tendency for the forward reaction, *i.e.*, dissolution of copper metal, to occur [equation (1)]. Since the total surface area of the copper metal and the concentration of the copper(II) remain constant during the course of an experiment, it may be deduced from equation (9) that the higher the value of C , the greater the value of the rate constant, k_1 . The values of S , C , and r for the various unsaturated ligands investigated are shown in Table 3. The variation in the value of r in the series of ligands reflects the stability of the species $\text{Cu}^{\text{I}}\text{L}$.

Acknowledgement—This work was supported in part by the University of Arizona Center for Advanced Studies in Copper Recovery and Utilization, under Defense National Stockpile Center Grant No DN-004

REFERENCES

1. G Ulibarri, T Ogura, J Tzeng, N Scott and Q Fernando, *Anal Chem*, 1982, **54**, 2307.
2. N Yanagihara, *Ph D Dissertation*, Universidad Autonoma de Guadalajara, Guadalajara, Jalisco, Mexico, 1985
3. E R Gilliland, J E. Seebold, J R Fitzhugh and P S Morgan, *J Am Chem Soc.*, 1939, **61**, 1960.
4. H Tropsch and W J Mattox, *ibid.*, 1935, **57**, 1102
5. N Yanagihara, T Ogura, N Scott and Q Fernando, *Anal Chem*, 1984, **56**, 2830
6. J Růžicka and E H Hansen, *Flow Injection Analysis*, 2nd Ed., Wiley, New York, 1988

HYDROLYSIS OF GADOLINIUM(III) IN LIGHT AND HEAVY WATER

L. GARCIA RODENAS and S J. LIBERMAN

Comisión Nacional de Energía Atómica, Avda del Libertador 8250, Buenos Aires 1429, Argentina

(Received 17 May 1989 Revised 18 July 1990. Accepted 3 September 1990)

Summary—The hydrolysis constants of Gd^{3+} and the solubility products of $Gd(OH)_3$ and $Gd(OD)_3$ in nitrate solutions at 25 and 70° in H_2O and D_2O have been determined because of their importance in nuclear technology. The constants are defined (charges omitted for clarity) as $*K_{11} = a_{GdOH} a_H / a_{Gd}$, $*K_{21} = a_{Gd(OH)_2} a_H^2 / a_{Gd}$, $*K_{30} = a_{Gd} / a_H^3$. The values for the H_2O system were $p*K_{11} = 7.87 \pm 0.02$, $p*K_{21} = 15.16 \pm 0.09$, $p*K_{30} = -19.32 \pm 0.03$ at 25° and $p*K_{11} = 7.55 \pm 0.03$, $p*K_{21} = 13.04 \pm 0.03$, $p*K_{30} = -16.16 \pm 0.04$ at 70°. For the D_2O system they were $p*K_{11}^D = 8.17 \pm 0.01$, $p*K_{21}^D = 16.00 \pm 0.09$, $p*K_{30}^D = -21.18 \pm 0.04$ at 25° and $p*K_{11}^D = 7.84 \pm 0.02$, $p*K_{21}^D = 13.95 \pm 0.02$, $p*K_{30}^D = -17.34 \pm 0.04$ at 70°. The mean enthalpy changes of the reactions were also calculated.

Our interest in the stability of Gd^{3+} species in light and heavy water is due to the use of gadolinium as a neutron-absorber in the control of reactivity in CANDU nuclear reactors. Gadolinium nitrate solution is added to the moderator heavy water circuit, where the temperature is about 70°. The use of this additive requires the heavy water to be kept slightly acidic to avoid hydrolysis, and precipitation of gadolinium deuterioxide.

Calculation of the solubility limit of $Gd(NO_3)_3$ as a function of pD in CANDU nuclear reactors requires not only knowledge of the solubility product of the gadolinium deuterioxide but also of the first and second hydrolysis constants of Gd^{3+} in heavy water at the temperatures of interest in the reactor (25–70°). At present there seems to be no reliable information in the literature. It is also of interest to compare the behaviour in heavy and light water in order to enlarge knowledge of the properties of electrolyte solutions in both media.

Hydrolysis constants of Gd^{3+} in H_2O at 25° have been reported in the literature. The $*\beta_{qp}$ values ($*\beta_{qp} = [Gd_p(OH)_q]^{(3p-q)+} [H^+]^q / [Gd^{3+}]^p$) were determined at different ionic strengths, so to make a comparison between them, we calculated the $*K_{qp}$ values ($*K_{qp} = a_{Gd_p(OH)_q}^+ a_H^q / a_{Gd^{3+}}^p$) listed in Table 1 from the literature data by means of the Pitzer equation.¹

The spread in the $*pK_{11}$ values is considerable, some methods being more reliable than others;⁶ however, the values in the range 7.8–8.0 fit closely with the trends of the hydrolysis

constants for the other lanthanide ions.¹¹ The solubility product in H_2O at 25° has also been determined by several authors under different conditions, for different aging times, and the $p*\beta_{30}$ values ($*\beta_{30} = [Gd^{3+}] / [H^+]^3$) range from -21.7 to -15.1.^{2,6,11-17} In some instances, over-simplifications were made in which hydrolysis was not considered.¹²⁻¹⁵ In Table 1 we list only the $p*\beta_{30}$ values obtained by the best defined experimental and calculation procedures.^{2,6} We also include the $*K_{30}$ value ($*K_{30} = a_{Gd^{3+}} / a_H^3$) from an empirical relation¹¹ derived for aged lanthanide hydroxides.

For polynuclear complex formation, Ngo and Burkov found results compatible with $Gd_2(OH)_4^{2+}$ ($p*\beta_{22} = 14.23$),² and Kragten and Decnop-Weever postulated the existence of the species $Gd_3(OH)_4^{3+}$ ($p*\beta_{43} = 19.0$).⁶ These poly-complexes have not been characterized by other means.

The studies of gadolinium in heavy water solutions are limited; Amaya *et al.*⁹ reported $p*K_{11}^D = 6.82$ at 25°, and Baumann,¹³ disregarding hydrolysis, reported $p*\beta_{30}^D$ to be -19.96 for a precipitate aged for 7 days.

In the present study the hydrolysis constants of Gd^{3+} and the solubility product of $Gd(OH)_3(s)$ or $Gd(OD)_3(s)$ in light or heavy water at 25 and 70° were determined by potentiometric measurements, under experimental conditions reasonably close to those existing in the moderator system in the CANDU nuclear reactor. The thermodynamic parameters of the Gd^{3+} species in both media were also examined.

EXPERIMENTAL

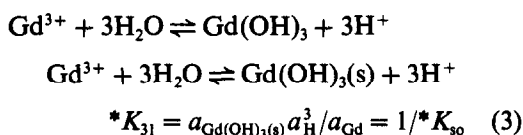
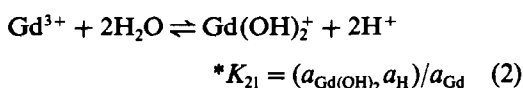
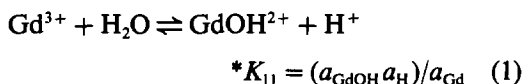
All reagents were analytical grade and the solutions were prepared with triply distilled light or heavy water (99.8% pure). Gadolinium nitrate [$\text{Gd}(\text{NO}_3)_3 \cdot 6\text{H}_2\text{O}$, 99.9% pure], from Nucor Research Chemicals, was used without further purification. Solutions were saturated with nitrogen to eliminate carbon dioxide.

Potentiometric titrations were performed at $25.00 \pm 0.02^\circ$ and $70.00 \pm 0.02^\circ$ with a Metrohm 654 pH-meter provided with a glass combined electrode standardized with standard buffer solutions at pH values (conventional activity scale) of 4.00 ± 0.02 and 7.00 ± 0.02 at 25° and 4.11 ± 0.02 and 6.98 ± 0.02 at 70° . For heavy water solutions, the electrode was standardized with phosphate and carbonate buffers prepared in heavy water. The pD values given by Bates¹⁸ for these solutions are 7.43 ± 0.02 and 10.74 ± 0.02 at 25° and 7.39 ± 0.02 and 10.44 ± 0.02 at 70° .

The titrations were performed with standardized sodium hydroxide solution, and gadolinium nitrate concentrations of $1.00 \times 10^{-2} \text{ M}$ for H_2O at 25 and 70° and 1.00×10^{-2} and $8.00 \times 10^{-3} \text{ M}$ for D_2O at 25 and 70° , respectively, for determination of the hydrolysis constants. For the solubility product measurements the concentrations were 0.920×10^{-3} and $0.732 \times 10^{-3} \text{ M}$ in H_2O and 0.857×10^{-3} and $0.953 \times 10^{-3} \text{ M}$ in D_2O at 25 and 70° respectively. The pH or pD of the solutions reached a constant value within about 5 min after addition of base. No supporting electrolyte was added, so that the conditions would be close to those in the CANDU moderator system.

Evaluation of the thermodynamic constants

For evaluation of the hydrolysis constants $*K_{11}$ and $*K_{21}$ and the solubility product $*K_{s0}$ in aqueous or deuteroaqueous solutions of Gd^{3+} , equations (1)–(3) were considered (charges are omitted in the subscripts, for the sake of clarity):



together with the mass-balance relationships (4) and (5):

$$c = [\text{Gd}^{3+}] + [\text{GdOH}^{2+}] + [\text{Gd}(\text{OH})_2^+] + [\text{Gd}(\text{OH})_3] + n_s / (V_0 + V) \quad (4)$$

$$c_b = (V c_{\text{OH}}) / (V_0 + V) = [\text{GdOH}^{2+}] + 2[\text{Gd}(\text{OH})_2^+] + 3[\text{Gd}(\text{OH})_3] + 3n_s / (V_0 + V) + [\text{OH}^-] \quad (5)$$

where a_i is the activity of species i , $a_{\text{Gd}(\text{OH})_3(\text{s})} = 1$, c , c_{OH} and c_b are the molar concentrations of gadolinium nitrate, sodium hydroxide and base in the solution, n_s is the number of moles of $\text{Gd}(\text{OH})_3$ precipitated and V_0 and V are the volumes (in litres) of the $\text{Gd}(\text{NO}_3)_3$ solution and added base respectively. The slight influence of $\text{Gd}^{3+} - \text{NO}_3^-$ ion-association is discussed below; volume changes due to reaction are negligible at the concentrations used. From these equations, as shown in the Appendix, equations (6) and (7) were derived, in which the constants $*K_{11}$, $*K_{21}$ and $*K_{s0}$ can be evaluated from the experimental results:

$$y = *K_{11}x + *K_{21} \quad (6)$$

where

$$n_s = 0, [\text{Gd}(\text{OH})_3] = 0, c \gg c_b, [\text{OH}^-] \ll c_b,$$

$$y = (c_b / 2c) a_{\text{H}}^2 \gamma_{\text{Gd}(\text{OH})_2} / \gamma_{\text{Gd}}$$

$$x = a_{\text{H}} \gamma_{\text{Gd}(\text{OH})_2} / 2 \gamma_{\text{GdOH}}$$

$$y_s = *K_{s0} x_s \quad (7)$$

where

$$y_s = 3c - c_b, c_b / c < 3$$

$$x_s = 3a_{\text{H}}^3 / \gamma_{\text{Gd}} + 2*K_{11} a_{\text{H}}^2 / \gamma_{\text{GdOH}} + *K_{21} a_{\text{H}} / \gamma_{\text{Gd}(\text{OH})_2}$$

The activity coefficients of species i were calculated at the given ionic strengths by both the Davies equation (8)¹⁹ and equation (9) derived by the mean spherical approximation (MSA) for aqueous electrolyte mixtures:²⁰

$$\log \gamma_i = Az_i^2 \{ [\sqrt{I} / (1 + \sqrt{I})] - 0.30I \} \quad (8)$$

$$\ln \gamma_i = \ln \gamma_i^{\text{elec}} + \ln \gamma_i^{\text{hs}} \quad (9)$$

In (8), z is the charge of species i , I is the ionic strength and A is the Debye–Hückel constant. The A values for H_2O and D_2O are 0.5115 and 0.5155 at 25° and 0.5625 and 0.5691 at 70° . In (9), the first and second terms are the electrostatic and the hard-sphere contributions respectively.

Table 1 Reported stability constants of Gd^{3+} species in light and heavy water at 25°, calculated for zero ionic strength

p^*K_{11}	p^*K_{21}	$p^*\beta_{30}$	$p^*K_{11}^D$	Method	Reference
7.8		-17.5†		potentiometric titration	2
8.0				potentiometric titration	3
7.8				potentiometric titration	4
8.0				empirical relation	5
6.6	13.3	-17.0‡		pGd-pH determination (23°)	6
6.9				solvent extraction	7
6.7				solvent extraction	7
6.8				coulometry and pH	8
			6.8	coulometry and pH	9
8.8				pH determination	10
8.4				pH determination	10
6.9				pH determination	10
	16.4	$p^*K_{30} = -15.6$		empirical relation	11

†3M NaClO₄, aging time 20 min‡NaClO₄, $I = 1.0$, aging time 30 min

The complete sets of explicit equations to calculate these terms are given by Corti.²⁰ The only parameters involved in this calculation are charge, concentration of ionic species and radii of hydrated ions. For the latter we have chosen the following values: Gd^{3+} 0.335, $GdOH^{2+}$ 0.30, $Gd(OH)_2^+$ 0.30, OH^- 0.18, NO_3^- 0.175, Na^+ 0.158 nm.

Equation (6) is valid in a pH or pD range low enough to avoid the presence of $Gd(OH)_3$ and $Gd(OH)_3(s)$ or their deuterated analogues, and equation (7) must be applied at higher pH or pD values when solid is present. This method provides an independent determination of $*K_{11}$ and $*K_{21}$ from $*K_{30}$.

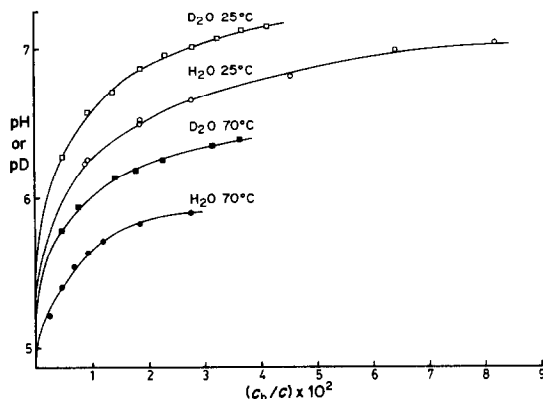


Fig 1 Potentiometric titrations of $Gd(NO_3)_3$ solutions for hydrolysis constant evaluations \circ , \square , \bullet , $c = 1.00 \times 10^{-2}M$, \blacksquare , $c = 8.00 \times 10^{-3}M$. The lines are calculated from the least-squares fit to the experimental data [equation (6)]

RESULTS AND DISCUSSION

Hydrolysis constants

Figure 1 shows the pH and pD measurements in light and heavy water solutions of $Gd(NO_3)_3$, as a function of the fraction of added base, c_b/c , at 25 and 70°. The ionic strength, 0.048M in D₂O solutions at 70° and 0.06M in all the others, was constant within 0.6%. The activity coefficients calculated by the Davies equation and the MSA approximation agree within 0.05%.

Least-squares calculations of the slope and intercept of the linear equation (6) with these experimental results gave the values for $*K_{11}$ and $*K_{21}$ listed in Table 2 (with their standard deviations). The theoretical curves calculated with these values give a good fit to the experimental data, as shown in Fig. 1.

The presence of polynuclear species is not consistent with our results: the species $Gd_2(OH)_2^{4+}$ ($p^*\beta_{22} = 14.23$ at $I = 3M$) postulated by Ngo and Burkov² would be formed at higher Gd^{3+} concentration, and $Gd_3(OH)_4^{5+}$ ($p^*\beta_{43} = 19.00$ at $I = 1M$) postulated by Kragten and Decnop-Weever⁶ does not fit with our data.

From Tables 1 and 2, comparison of our p^*K_{11} values with published data indicates good agreement with the results of Ngo and Burkov,² Usherenko and Skorik,³ Frolova *et al.*⁴ and the empirical correlation of Kumok and Serebrennikov,⁵ but not with those of Kragten and Decnop-Weever,⁶ Guillaumont *et al.*,⁷ Amaya

Table 2 Hydrolysis constants and solubility product for Gd^{3+} in light and heavy water

Temperature, °C	p^*K_{11}	p^*K_{21}	p^*K_{30}	$p^*K_{11}^D$	$p^*K_{21}^D$	$p^*K_{30}^D$
25	7.87 ± 0.02	15.16 ± 0.09	-19.32 ± 0.03	8.17 ± 0.01	16.00 ± 0.09	-21.18 ± 0.04
70	7.55 ± 0.03	13.04 ± 0.03	-16.16 ± 0.04	7.84 ± 0.02	13.95 ± 0.02	-17.34 ± 0.04

et al.,^{8,9} and Moeller.¹⁰ The results obtained by the last three sets of authors are subject to rather large uncertainties: Guillaumont *et al.* used a not too reliable solvent extraction method, Amaya *et al.* reported hydrolysis constants for several lanthanide ions besides Gd^{3+} , all lower than those found in the literature,¹¹ and Moeller gave $*K_{11}$ values which depended on the concentration. The procedure used by Kragten and Decnop-Weever is accurate and gives results coincident with those of the Kumok and Serebrennikov method, as well as with reliable literature data for other lanthanides,^{21,22} but not for Gd^{3+} . We cannot elucidate the discrepancy.

With respect to $*K_{21}$, again our result is lower than that of Kragten and Decnop-Weever,⁶ but not too far away from the prediction made by Baes and Mesmer¹¹ that $p*K_{21}$ is approximately twice the $p*K_{11}$ values, as for most other lanthanides.

With regard to the results for the D_2O system, the values of $*K_{11}^D$ and $*K_{12}^D$ are slightly lower than $*K_{11}$ and $*K_{12}$. This effect is consistent with that found in the literature for other cations.²³ Again, the $p*K_{11}^D$ value reported by Amaya *et al.*⁹ is higher than ours.

The hydrolysis constants increased with temperature for both solvents, as expected.

The constants in Table 2 were calculated by assuming that $[GdNO_3^{2+}]$ was negligible compared with $[Gd^{3+}]$ at $[Gd(NO_3)_3] = 0.01M$; this is true only to a certain extent. The $Gd^{3+}-NO_3^-$ ion-association constants β_1 ($\beta_1 = [GdNO_3^{2+}]/[Gd^{3+}][NO_3^-]$) given in the literature refer to higher concentrations than those in the present study: 2.33 for the $Gd(NO_3)_3$ concentration range 0.23–2.17M,²⁴ and between 6.40 and 2.38 for 0.05–0.35M $Gd(NO_3)_3$.²⁵ These values give an estimate of the extent of the association but are not precise enough to be used in our calculations. Equation (I) in the Appendix shows the corrections to be made to $*K_{11}$ and $*K_{21}$ to allow for the association. If we assume $\beta_1 = 2$, the constants will increase by 6% and $p*K_{11} = 7.84$ and $p*K_{21} = 15.13$ will be obtained. The corresponding corrections for the D_2O system should be similar to these.

Solubility product

Figure 2 shows the pH and pD measurements in light and heavy water solutions of $Gd(NO_3)_3$ at 25 and 70° as a function of c_b/c until hydroxide precipitation occurs.

Least-squares fitting of these results to equation (7) gives the $*K_{30}$ values listed in Table 2.

Because the ionic strength did not remain constant during the titrations, the true activity coefficients of the species were calculated by an iterative procedure until two successive $*K_{30}$ values were the same. The activity coefficients calculated by the Davies equation¹⁹ and the MSA approximation²⁰ agreed within 0.05%. The theoretical curves in Fig. 2, calculated with the $*K_{11}$, $*K_{12}$ and $*K_{30}$ values from Table 2, gave a good fit to the experimental data.

The solubility product of $Gd(OH)_3$ is higher than that of $Gd(OD)_3$, in agreement with Baumann's results for the aged hydroxides.¹³ The solubility products also increase with temperature, which seems to be in contradiction with the results of Meloche and Vrátný¹² over the range 10–40°. However, these authors did not take into account the change in the ionic product of water with temperature. Making the proper corrections to their results, we found not only an increase in the solubility product with temperature for $Gd(OH)_3$, but also the hydroxides of Pr, Nd, Sm and Y.

The $p*K_{30}$ value from our experiments is smaller than any of those listed in Table 1; the difference is even larger at $I = 0$. This discrepancy perhaps should be attributed to the longer aging times used in the earlier work. On the other hand, from the standard free energy of reaction (3), 110.3 kJ/mole, calculated from the $*K_{30}$ value in Table 2 by using the relationship $\Delta G_3^0 = -RT \ln *K_{31}$, and the standard free energies of formation –688 kJ/mole for $Gd^{3+}(aq)$ and –237 kJ/mole for H_2O ,²⁶ the value –1289 kJ/mole is derived for the standard free energy of formation of $Gd(OH)_3(s)$, in close agreement

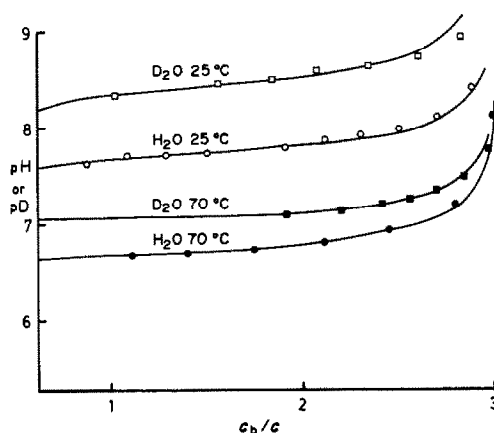


Fig. 2. Potentiometric titrations of $Gd(NO_3)_3$ solutions for solubility product evaluations. \circ , $0.920 \times 10^{-3}M$; \square , $0.857 \times 10^{-3}M$; \bullet , $0.732 \times 10^{-3}M$; \blacksquare , $0.953 \times 10^{-3}M$. The lines are calculated from the least-squares fit to the experimental data [equation (7)]

Table 3 Mean standard enthalpy change of reactions (1)–(3) (kJ/mole)

	ΔH_{11}^0	ΔH_{21}^0	ΔH_{31}^0
H ₂ O	14 ± 2	92 ± 5	138 ± 3
D ₂ O	14 ± 1	89 ± 5	167 ± 4

with the value -1288 kJ/mole reported in the literature.²⁶

The influence of $\text{Gd}^{3+}-\text{NO}_3^-$ ion-association on the $*K_{s0}$ values in Table 2 could be estimated by use of equation(II) in the Appendix. If we consider $\beta_1 = 2$, $*K_{s0}$ will decrease by 5% and a value of $p*K_{s0} = -19.30$ will be obtained. It is clear that the main source of error in the values of the constants given in Table 2 is the lack of information regarding $\text{Gd}^{3+}-\text{NO}_3^-$ association.

From the data in Table 2, thermodynamic functions for the equilibria involved can be derived. Table 3 shows the mean standard enthalpy change $\Delta H_{qp}^0 = RT^2 \ln *K_{qp}/dT$ for reactions (1)–(3) in the temperature range 25–70° in H₂O and D₂O. The values are positive and, within experimental error, identical for both solvents with the exception of ΔH_{31}^0 , which is more endothermic for D₂O medium.

In Fig. 3, the distribution of Gd^{3+} species is plotted as a function of pD at 70° for $10^{-4}M$ Gd^{3+} , the maximum concentration of this "poison" used in the moderator circuit to shut down the reactor. The species distribution at 25°, corresponding to the period during which the reactor is not under operation, is also included. The concentrations in this diagram were calculated by taking into account the changes in the activity coefficients with pD, by application of the iterative procedure used for the $*K_{s0}$ calculation. The vertical lines correspond to the pD for initial precipitation at each temperature

This stability diagram indicates that pD in the CANDU moderator circuit should be kept

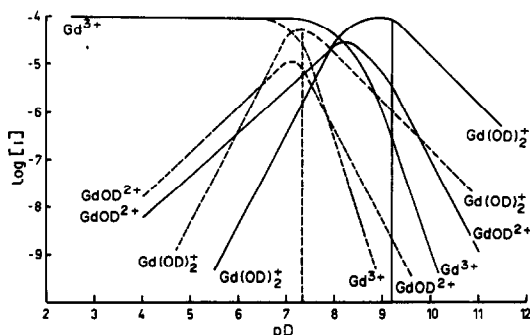


Fig 3 Speciation in $10^{-4}M$ $\text{Gd}(\text{NO}_3)_3$ solution in heavy water, — 25°, ---- 70°

below 7.36 (for safety reasons the pD is much lower) to avoid precipitation of the hydroxide after the liquid shut-down system has operated. When the moderator cools down to room temperature the pD should be below the precipitation value (9.20).

Acknowledgements—We are indebted to Dr H. Corti for his assistance in the application of the MSA method

REFERENCES

- 1 K S Pitzer, *J. Phys. Chem.*, 1973, **77**, 268
- 2 Nguyen Din Ngo and K A Burkov, *Russ J Inorg. Chem.*, 1974, **19**, 680
- 3 L N Usherenko and N. A. Skorik, *ibid.*, 1972, **17**, 1533
- 4 U K. Frolova, V N. Kumok and V. V. Serebrennikov, *Izvest. Vyssh Ucheb Zaved SSSR*, 1966, **9**, 176.
- 5 V. N. Kumok and V V Serebrennikov, *Russ J. Inorg. Chem.*, 1965, **10**, 1095
- 6 J Kragten and L G Decnop-Weever, *Talanta*, 1980, **27**, 1047
- 7 R. Guillaumont, B Désiré and M Galin, *Radiochem Radioanal Lett*, 1971, **8**, 189
- 8 T Amaya, H Kakihana and M Maeda, *Bull Chem Soc Japan*, 1973, **46**, 1720
- 9 *Idem, ibid*, 1973, **46**, 2889
- 10 T Moeller, *J Phys Chem.*, 1946, **50**, 242
- 11 C F Baes, Jr and R E Mesmer, *The Hydrolysis of Cations*, Wiley, New York, 1976
- 12 C C Meloche and F Vrátny, *Anal Chim Acta*, 1959, **20**, 415
- 13 E Baumann, *J Inorg Nucl Chem.*, 1980, **42**, 1705
- 14 T Moeller and H E Kremers, *J Phys Chem.*, 1944, **48**, 395
- 15 T Moeller and N Vogel, *J Am Chem Soc.*, 1951, **73**, 4481
- 16 Z Orhanović, B Pokrc, H Furedi and M Branica, *Croat Chem Acta*, 1966, **38**, 269
- 17 N Aksel'rud, *Zh Neorgan Khim.*, 1963, **8**, 11
- 18 R Bates, *Determination of pH Theory and Practice*, Wiley, New York, 1964
- 19 C Davies, *Ion Association*, Butterworths, London, 1962
- 20 H R Corti, *J Phys Chem.*, 1987, **91**, 686
- 21 J Kragten and L G Decnop-Weever, *Talanta*, 1977, **25**, 147
- 22 *Idem, ibid*, 1979, **26**, 1105
- 23 H Kakihana, T Amaya and M Maeda, *K Tek Hoegsk Handl*, 1972, **49**, 248–296
- 24 A S C Cheung and D E Irish, *J Inorg Nucl Chem.*, 1981, **43**, 1383
- 25 R Garnsey and D W Ebdon, *J Am Chem Soc.*, 1969, **91**, 50
- 26 R C Weast (ed), *Handbook of Chemistry and Physics*, 60th Ed, Chemical Rubber Co, Boca Raton, 1980–81.

APPENDIX

Equation (6) is derived as follows. Equations (4) and (5) are expressed in terms of $[\text{Gd}^{3+}]$ and equated

$$c_b[1 + *K_{11}\gamma_{\text{Gd}}/a_{\text{H}}\gamma_{\text{GdOH}} + *K_{21}\gamma_{\text{Gd}}/a_{\text{H}}^2\gamma_{\text{Gd(OH)}_2}] = c[*K_{11}\gamma_{\text{Gd}}/(a_{\text{H}}\gamma_{\text{GdOH}}) + 2*K_{21}\gamma_{\text{Gd}}/a_{\text{H}}^2\gamma_{\text{Gd(OH)}_2}]$$

Rearrangement gives

$$c_b/c = (1 - c_b/c) * K_{11} \gamma_{Gd} / a_H \gamma_{GdOH} \\ + (2 - c_b/c) * K_{21} \gamma_{Gd} / a_H^2 \gamma_{Gd(OH)_2}$$

If c_b is negligible compared with c , then

$$c_b/c = *K_{11} \gamma_{Gd} / a_H \gamma_{GdOH} + 2 *K_{21} \gamma_{Gd} / a_H^2 \gamma_{Gd(OH)_2}$$

and multiplying by $a_H^2 \gamma_{Gd(OH)_2} / \gamma_{Gd}$ gives

$$(c_b/2c) a_H^2 \gamma_{Gd(OH)_2} / \gamma_{Gd} = *K_{11} a_H \gamma_{Gd(OH)_2} / 2 \gamma_{GdOH} + *K_{21}$$

which is identical to equation (6)

Equation (7) is derived as follows $[Gd(OH)_3]$ and $n_s / (V_0 + V)$ are eliminated by means of equations (4) and (5), to give

$$3c - c_b - [OH^-] = 3[Gd^{3+}] + 2[GdOH^{2+}] + [Gd(OH)_2^+]$$

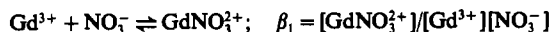
Then $[OH^-]$ is treated as negligible compared with c_b , and $[Gd^{3+}]$, $[GdOH^{2+}]$ and $[Gd(OH)_2^+]$ are replaced by functions

of $*K_{11}$, $*K_{21}$ and $*K_{30}$, giving

$$3c - c_b = *K_{30} [3a_H^3 / \gamma_{Gd} + 2 *K_{11} a_H^2 / \gamma_{GdOH} + *K_{21} a_H / \gamma_{Gd(OH)_2}]$$

which is the same as equation (7).

The $Gd^{3+} - NO_3^-$ ion-association reaction



could be taken into account by including $[GdNO_3^{2+}]$ in the mass balance equation (4). Then, instead of equations (6) and (7), the following equations can be derived by a procedure similar to that above

$$(c_b/2c) a_H^2 \gamma_{Gd(OH)_2} / \gamma_{Gd} \\ = *K_{11} / (1 + \beta_1 [NO_3^-]) a_H \gamma_{Gd(OH)_2} / 2 \gamma_{GdOH} \\ + *K_{21} / (1 + \beta_1 [NO_3^-]) \quad (I)$$

and

$$3c - c_b = *K_{30} (3a_H^3 / \gamma_{Gd} + 2 *K_{11} a_H^2 / \gamma_{GdOH} \\ + *K_{21} a_H / \gamma_{Gd(OH)_2} + \beta_1 [NO_3^-] 3a_H^3 / \gamma_{Gd}) \quad (II)$$

ION FLOTATION OF RHODIUM(III) AND PALLADIUM(II) WITH ANIONIC SURFACTANTS

HE XING-CUN

Department of Chemistry, Guangxi Normal University, Guilin, Guangxi, People's Republic of China

(Received 19 March 1990 Revised 18 August 1990 Accepted 28 August 1990)

Summary—The ion flotation of rhodium(III) and palladium(II) with some anionic surfactants has been investigated. Two flotation procedures are proposed for the separation of some platinum metals, based on differences in the kinetic properties of the chloro-complexes of rhodium(III), palladium(II) and platinum(IV). The first involves the selective flotation of $\text{Rh}(\text{H}_2\text{O})_6^{3+}$ from PdCl_4^{2-} and PtCl_6^{2-} in dilute hydrochloric acid with sodium dodecylbenzenesulfonate (SDBS). After precipitation of the hydroxide and redissolution in dilute acid, the Rh(III) is converted into $\text{Rh}(\text{H}_2\text{O})_6^{3+}$, Pd(II) and Pt(IV) remaining as PdCl_4^{2-} and PtCl_6^{2-} respectively, and separation is achieved by floating the $\text{Rh}(\text{H}_2\text{O})_6^{3+}$ with SDBS. The second is for separation of Pd(II). Prior to flotation, the solution of PdCl_4^{2-} and PtCl_6^{2-} is heated with ammonium acetate to convert PdCl_4^{2-} into $\text{Pd}(\text{NH}_3)_4^{2+}$. The chloro-complex of Pt(IV) is unaffected. The complex cation, $\text{Pd}(\text{NH}_3)_4^{2+}$, is then selectively floated with SDBS. The procedures are fast, simple and do not require expensive reagents and apparatus.

In recent years, there has been considerable interest in ion flotation, leading to the development of a number of methods for separation of numerous cationic and anionic complexes.¹⁻¹¹ The ion flotation properties and separation of the anionic chloro-complexes of some platinum metals have been studied systematically,¹²⁻¹⁷ but no flotation studies of the cationic complexes of platinum metals have been noted in the literature.

The platinum metals have similar chemical properties. In many cases several of these metals are present in the sample, and interferences may occur in determinations. It is important to separate the platinum metals from each other in their determination and purification. The differences in kinetic properties of the platinum group metals in the formation of cationic, anionic and neutral species have been widely used for their separation. Though many studies have indicated considerable success in separation of some platinum metals by ion-exchange and solvent extraction methods, the advantage of the differences in their labile character could be further utilized. In this paper, we describe use of the charge selectivity of surfactants to achieve separation by adjustment of the initial solution conditions so that the complex ions of interest are opposite in charge sign. Our results show that the rapid formation of $\text{Rh}(\text{H}_2\text{O})_6^{3+}$ can be used in the flotation procedure. The aquo-cation of Rh(III) can be obtained by precipitation of

the hydroxide and its redissolution in dilute acid, and can then be floated with sodium dodecylbenzenesulfonate (SDBS) from Pd(II) and Pt(IV) which remain as PdCl_4^{2-} and PtCl_6^{2-} respectively. Our results also indicate that the rate of formation of the cationic ammine-complex of Pd(II) from its chloro-complex is sufficiently different from that of the Pt(IV) complex to permit isolation of the Pd(II) complex by flotation. The complete conversion of PdCl_4^{2-} into $\text{Pd}(\text{NH}_3)_4^{2+}$ can be achieved by heating the solution with ammonium acetate. Pt(IV) does not form an ammine-complex under these conditions. The $\text{Pd}(\text{NH}_3)_4^{2+}$ can then be floated from PtCl_6^{2-} with SDBS. In this paper, the influence of several factors on the flotation is reported, and the optimum ion flotation conditions are presented.

EXPERIMENTAL

Apparatus

The flotation cell is made by joining a G4(3-4 μm nominal pore size) sintered-glass funnel to a glass tube. A hole is drilled in the funnel 1 cm above the sintered glass disc and fitted with a rubber stopper for sample removal. Nitrogen saturated with water is passed through the sintered-glass disc. The flow-rate is controlled by a regulator valve.

A Shimadzu model UV-240 spectrophotometer was used to obtain the spectra of the

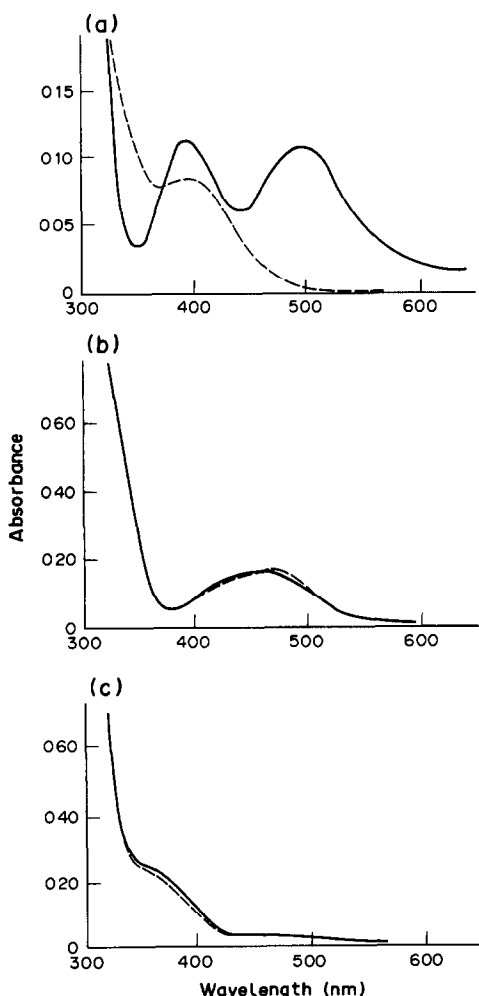


Fig 1 The spectra of Rh(III), Pd(II) and Pt(IV) (a) Rh(III) (b) Pd(II) (c) Pt(IV) The dotted lines mean the spectra after pretreatment

complex ions of Rh(III), Pd(II) and Pt(IV). A model 72 spectrophotometer (Shanghai Analytical Instrument Factory) and a Hitachi model 180/80 atomic-absorption spectrometer were used for determination of the metals.

Reagents

Tetrachloropalladate(II) and hexachloroplatinate(IV) stock solutions were prepared by dissolving high-purity palladium and platinum in *aqua regia*, repeatedly evaporating the solutions to dryness with hydrochloric acid, and making up to known volume in 2M hydrochloric acid. Hexachlororhodate(III) stock solution was prepared by dissolving $\text{Rh}_2\text{O}_3 \cdot 5\text{H}_2\text{O}$ (99.9% pure) in concentrated hydrochloric acid, refluxing the solution for 2 hr to ensure that all the rhodium was present as RhCl_6^{3-} , and making up the final solution in 2M hydrochloric acid. The anionic surfactants sodium dodecyl-

benzenesulfonate (SDBS), sodium dodecyl-sulfonate (SDS) and sodium lauryl sulfate (SLS) were prepared and $5 \times 10^{-3}M$ stock solutions in water were made. All other chemicals used were analytical reagent grade.

Procedures

Sample pretreatment. To convert RhCl_6^{3-} into $\text{Rh}(\text{H}_2\text{O})_6^{3+}$, the sample solution was treated in the following manner. Sodium hydroxide solution was added to the sample solution until Rh(III) hydroxide was completely precipitated. After standing for 2 hr at pH 2, the precipitate was dissolved in 0.5M hydrochloric acid to yield $\text{Rh}(\text{H}_2\text{O})_6^{3+}$. When treated in the same way, Pd(II) and Pt(IV) were reconverted into PdCl_4^{2-} and PtCl_6^{2-} respectively. For the complete conversion of PdCl_4^{2-} into $\text{Pd}(\text{NH}_3)_4^{2+}$ the solution of PdCl_4^{2-} was heated with ammonium acetate until the brownish-red color of PdCl_4^{2-} disappeared; the chloro-complex of Pt(IV) was unaffected.

Flotation experiments. Solutions were prepared for flotation by pipetting sufficient of the pretreated sample solutions into 50-ml standard flasks to give a final metal concentration of $1 \times 10^{-4}M$, followed by addition of 4 ml of surfactant solution and 0.3 ml of absolute ethanol and dilution to volume. The solutions were then mixed for 10 min. Each was then transferred to the flotation cell, and nitrogen saturated with water was passed through it at a controlled flow-rate of 30 ml/min for 25 min.

Measurement techniques. After the maximum flotation was achieved, the foam was collected with a sampling tube described by Mizuike and Hiraide,² and collapsed by addition of a small amount of ethanol. The floated metals were recovered from the sublates by wet ashing with nitric acid, followed by repeated heating to dryness with a few drops of concentrated hydrochloric acid. Finally, the residues were taken up in dilute hydrochloric acid and the amounts recovered were measured by atomic-absorption spectrometry. The progress of the flotation was monitored by measurements on samples removed from the cell at appropriate intervals. Spectrophotometric measurements were also used to supplement the tracer studies. Both palladium and platinum were determined with 2-(5-bromo-2-pyridylazo)-5-diethylamino-phenol in the presence of poly(ethyleneglycol)-octylphenyl ether.¹⁸

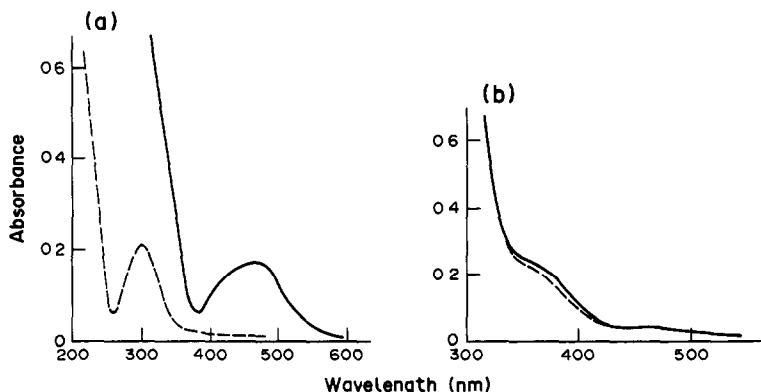


Fig 2 The spectra of (a) Pd(II) and (b) Pt(IV) The dotted lines mean the spectra after pretreatment

RESULTS AND DISCUSSION

Oxidation states of Rh, Pd and Pt after pretreatment

The solutions of Rh, Pd and Pt, after pretreatment as described above, were examined spectrophotometrically and the absorption spectra are given in Fig.1. For comparison, the absorption spectra of RhCl_6^{3-} , PdCl_4^{2-} and PtCl_6^{2-} are also shown. It was observed that after pretreatment the spectra of the Pd(II) and Pt(IV) species were the same as those of PdCl_4^{2-} and PtCl_6^{2-} . This indicated that the Pd(II) and Pt(IV) remained as PdCl_4^{2-} and PtCl_6^{2-} respectively. The case of Rh(III) was different. After the hydrolysis and acidification, the pink color of the solution of Rh(III) changed to a yellowish color. Figure 1(a) shows the change in the spectra. The absorption peak at 396 nm confirmed the presence of $\text{Rh}(\text{H}_2\text{O})_6^{3+}$ (${}^1\text{A}_{1g} - {}^1\text{T}_{1g}$).¹⁹

When the solution of Pd(II) was heated with ammonium acetate, the brownish-red color of PdCl_4^{2-} disappeared, and a colorless ammine-complex of Pd(II) was formed. This colorless ammine-complex of Pd(II) was regarded as $\text{Pd}(\text{NH}_3)_4^{2+}$.^{20,21} The differences in the spectra of PdCl_4^{2-} and $\text{Pd}(\text{NH}_3)_4^{2+}$ are shown in Fig. 2(a). However, the chloro-complex of Pt(IV) was not affected by the presence of ammonium acetate. The color and spectrum [shown in Fig. 2(b)] of the solution of Pt(IV) did not change.

Reactions of $\text{Rh}(\text{H}_2\text{O})_6^{3+}$ and $\text{Pd}(\text{NH}_3)_4^{2+}$ with surfactants

It was found that white precipitates were formed in the bulk solutions when $\text{Rh}(\text{H}_2\text{O})_6^{3+}$ and $\text{Pd}(\text{NH}_3)_4^{2+}$ were mixed with SDBS, SDS or SLS. However, $\text{Rh}(\text{H}_2\text{O})_6^{3+}$ and $\text{Pd}(\text{NH}_3)_4^{2+}$ do not form precipitates with cationic surfactants such as tetradecyldimethylbenzylammonium

chloride, cetylpyridinium chloride and cetyltrimethylammonium bromide. No rhodium or palladium remained in the solutions after the precipitates were filtered off. Thus flotation procedures seem reasonable choices for recovering these elements.

As Rh(III) and Pd(II) formed cationic complexes after pretreatment, anionic surfactants should be used as collectors in the flotation. The flotation curves for $\text{Rh}(\text{H}_2\text{O})_6^{3+}$ and $\text{Pd}(\text{NH}_3)_4^{2+}$ with different surfactants are presented in Fig. 3. It can be seen that SDBS is the most efficient collector. The reason for this may be that SDBS has a longer hydrocarbon chain than SDS and SLS, that stability of the foam layer is proportional to the chain length, and stable foam is necessary to support the sublate. Thus, SDBS was chosen for further experimentation.

Effects of surfactant and metal concentrations

It is important to know whether variations in the initial concentrations of either the surfactant or metal ion result in significant differences in flotation efficiencies. For the first series of experiments, the metal concentration was fixed at $1 \times 10^{-4} \text{M}$ and the surfactant concentration was varied. For the second series, the molar ratio of SDBS to metal ion was held at 4:1, and the metal ion concentration was varied.

As the sublate salt has a stoichiometric ratio of colligend to collector, to obtain complete flotation of bivalent and trivalent ions, the surfactant must be present in at least 2:1 and 3:1 molar ratio respectively, to these ions. The experimental results confirmed that quantitative flotation was obtained only when there was an excess of collector. However, a large excess of collector, which produces a large volume of foam, should be avoided. Suitable molar

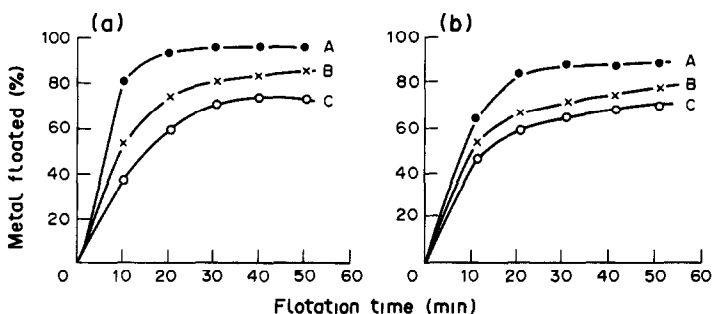


Fig 3 The effects of flotation time and surfactants (a) The flotation curves of $\text{Rh}(\text{H}_2\text{O})_6^{3+}$, (b) The flotation curves of $\text{Pd}(\text{NH}_3)_4^{2+}$. The concentrations of metals and surfactants were 1×10^{-4} and $4 \times 10^{-4}M$, respectively A SDBS B SDS, C SLS

ratios of SDBS to metal ion in the initial solution were found to be 3.5–5.0. The initial concentration of SDBS used in this work was therefore fixed at $4 \times 10^{-4}M$.

The results of the second series of experiments indicated that satisfactory flotation efficiencies with SDBS were obtained if the concentrations of Rh(III) and Pd(II) were in the range 2×10^{-5} – $4 \times 10^{-4}M$. If the concentrations of Rh(III) and Pd(II) were higher than $4 \times 10^{-4}M$, large amounts of SDBS were needed, and flotation was incomplete. The decrease in flotation efficiencies was attributed to the formation of micelles which rendered the substrate hydrophilic.

Effect of ethanol

It was observed in the flotation experiments that addition of a small amount of ethanol increased the flotation efficiencies. The reason for this was that the addition of ethanol reduced the coagulation of gas bubbles and produced a stream of numerous tiny bubbles. Bubbles having diameters below 0.5 mm are easily captured by precipitates, and therefore flotation was more efficient in the presence of a small amount of ethanol. However, it was of importance to control the amount of ethanol added. A large amount should be avoided, since it destroys the foam layer and causes partial redispersion of the substrate into the solution. A suitable amount of

ethanol was found to be 0.1–0.5 ml in 50 ml of sample solution.

Effects of bubbling time and gas flow-rate

Bubbling time and gas flow-rate should be carefully optimized. If the gas flow-rate is too low, it would take a long time to achieve complete flotation. If it is too high, the stability of the foam layer decreases, and moreover some bulk solution will be captured in the foam layer. From the flotation curves shown in Fig. 3, it can be seen that the best flotation efficiencies were obtained by the passage of nitrogen for 20 min at 30 ml/min flow-rate. In the flotation experiments, 25 min and 30 ml/min were chosen as the bubbling time and flow-rate, respectively.

Effect of ammonium ion on the separation of Rh(III) and Pd(III)

It was observed that the presence of ammonium ion in the initial sample interfered with the separation of Rh(III) and Pd(II). When the pH is adjusted for precipitation of the Rh(III), the ammonia will be liberated and form an ammine complex with the Pd(II). This complex is so stable that it is not decomposed by the addition of dilute hydrochloric acid. Since not only $\text{Rh}(\text{H}_2\text{O})_6^{3+}$ but also $\text{Pd}(\text{NH}_3)_4^{2+}$ can be floated by SDBS, if ammonium ion is originally present the separation of Rh(III) and Pd(II) is incomplete and even impossible. Therefore, ammonium ion must be absent from the original sample, or removed from it chemically, e.g., by evaporation to low bulk and heating with concentrated nitric acid.²²

Separation tests

Binary mixtures of the ions were separated. Rh(III) was floated by the first procedure from two binary mixtures under conditions similar to those for Rh(III) alone. Pd(II) was floated by

Table 1 Recovery data for flotation separation of binary mixtures of Rh(III), Pd(II) and Pt(IV) (each 500 μg per 50 ml)

Mixture	Recoveries, %			
	Floated		Not floated	
	Rh	Pd	Pd	Pt
Rh(III)–Pd(II)	94.0		99.8	
Rh(III)–Pt(IV)	91.2			99.1
Pd(II)–Pt(IV)		88.3		99.4

the second procedure from a binary mixture under conditions similar to those for Pd(II) alone. The results presented in Table 1 indicate that binary mixtures of these three platinum metals can be satisfactorily separated.

As osmium and ruthenium are easily converted into their tetroxides, which can be distilled, it was not considered necessary to examine their behavior in the system. Iridium was also not examined, because of its complicated oxidation and complexation behavior.

CONCLUSIONS

(a) The cationic complexes of rhodium(III) and palladium(II) can be floated with SDBS. (b) The differences in the kinetic properties of platinum metals can be used in their separation by ion flotation. (c) Satisfactory separations of binary mixtures of Rh(III), Pd(II) and Pt(IV) can be achieved by the proposed flotation procedures. (d) The proposed flotation procedures are fast, simple and do not require expensive reagents and apparatus. They may be useful for both laboratory and industrial separations of these three platinum metals.

REFERENCES

- 1 A N Clark and D J Wilson, *Sep Purif Methods*, 1978, 7, 55
- 2 A Mizuike and M Hiraide, *Pure Appl. Chem*, 1982, 54, 1556
- 3 R. Lemlich (ed.), *Adsorptive Bubble Separation Techniques*, Academic Press, New York, 1972.
- 4 R B. Grieves, *Chem. Eng. J.*, 1975, 9, 93
- 5 P Somosundaran, *Sep. Sci.*, 1975, 10, 93.
- 6 T Nozaki, K. Dokan, H. Onishi and Y Horiuchi, *Bunseki Kagaku*, 1976, 25, 277.
- 7 T. Nozaki, M Takahashi, T Kaneko, K Matsuoka, K Okamura and Y. Soma, *ibid*, 1982, 31, 353
8. Xu Qi-Heng, *Huaxue Tongbao*, 1981, 11, 43
9. Qi Wen-Bin and Pu Bing-Yin, *Surfactants and Analytical Chemistry (II)*, Chinese Gauge Press, Beijing, 1987
10. K Young Sang and C Hi Sun, *Hwahak Kwa Kongop Ui Chinbo*, 1989, 29, 5
- 11 M Caballero, R Cela and J A. Pérez-Bustamente, *Talanta*, 1990, 37, 275
12. E W Berg and D M Downey, *Anal Chim Acta*, 1980, 120, 237
- 13 *Idem, ibid*, 1980, 121, 239
- 14 *Idem, ibid*, 1981, 123, 1
- 15 E W. Berg, *ibid*, 1982, 134, 313
- 16 D M. Downey and S A Clipper, *ibid*, 1985, 174, 279
- 17 Deng Hua-Ling and Hu Zhi-De, *Talanta*, 1989, 36, 633
- 18 Fang Guozhen and Liu Xin, *Gaodeng Xuxiao Huaxue Xuebao*, 1986, 7, 315
- 19 C K Jørgensen, *Acta Chem Scand*, 1956, 10, 500.
- 20 W M MacNevin and W B Crummett, *Anal Chem*, 1953, 25, 1628
- 21 F V S Toerien and M Levin, *J S Afr Chem. Inst*, 1974, 27, 87
- 22 A. W Groves, *Silicate Analysis*, 2nd Ed, pp 66-67 Allen & Unwin, London, 1951

ELECTROTHERMAL ATOMIC-EMISSION SPECTROMETRIC DETERMINATION OF LITHIUM WITH A METAL-TUBE ATOMIZER AND A MATRIX MODIFIER

KIYOHISA OHTA,* SYN-ICHI ITOH and TAKAYUKI MIZUNO

Department of Industrial Chemistry, Faculty of Engineering, Mie University, Tsu, Mie 514, Japan

(Received 6 June 1990 Revised 12 September 1990 Accepted 20 September 1990)

Summary—Electrothermal atomic-emission spectrometric determination of lithium with use of a tungsten tube has been investigated. Lanthanum nitrate is used as a matrix modifier to eliminate the interference of Al, Ca, Cu, Fe, K, Mg, Na, Pb and Zn. Lithium in biological samples has been determined by the method. The recovery of lithium in the samples was >91%.

Electrothermal atomic-emission spectrometry with graphite furnaces and metal tubes¹⁻¹² is very useful as an analytical method for some elements. However, the high levels of background radiation emitted by graphite furnaces are a drawback. We have found atomic-emission spectrometry with a metal-tube atomizer to be a useful alternative.⁶⁻¹⁰

Lithium is an essential element in the life processes of organisms. Some workers have reported the trace determination of lithium in food as well as somatic and biological samples by electrothermal atomic-absorption spectrometry^{2,11-14} with graphite furnaces but there is severe chemical interference.^{1,2,15,16}

In this paper, we report on the effect of lanthanum as a matrix modifier in lithium emission spectrometry. A relatively simple and sensitive method for trace determination of lithium in biological samples is demonstrated.

EXPERIMENTAL

Instrumentation

The atomic emission was measured with a Nippon-Jarrell Ash Ebert-type monochromator fitted with an R 928 photomultiplier (Hamamatsu Photonics Co.), run at 680 V, a dc amplifier, an oscilloscope (Iwatsu MS-5021), and a microcomputer (Sord M223). The slit-width was chosen so as to give a spectral band-pass of 0.02 nm. The time constant of the detection system was 4 msec. The signal from the computer was recorded with a plotter (Graphtec WX4675). A lithium hollow-cathode

lamp (Hamamatsu Photonics Co.) was used for alignment of the atomic-emission line at 670.78 nm. The small tungsten tube (2-mm internal diameter, 35 mm long and 0.05-mm wall) used as an excitation source was made from high-purity tungsten sheet (99.95%, Goodfellow Metals Ltd.). Two legs for supporting the tube at both ends were made from molybdenum sheets (0.1-mm thickness, 99.95% purity, Rembar Co.). The power for heating the metal tube atomizer was applied by a step-down transformer (TP-Y, Takabayashi Electric Co. Ltd.) and a volt-slider (3 kVA, Yamabishi Co.). The arrangement of the tube atomizer, condensing lenses, light apertures, and detection system was described earlier.¹⁰ The temperature signal from the tube wall, which was preliminarily calibrated with an optical pyrometer (Chino Works), was obtained from a photodiode (S641, Hamamatsu Photonics Co.) and fed to the microcomputer with the simultaneous emission signal. A glass micropipette (1 μ l) with a Teflon tip was calibrated gravimetrically with a microbalance (Mettler H20).

Water used in the study was purified four times by demineralizing and distilling, with an autodistiller (Isuzu Works), a demineralizer (Monopet type, Organo Co.) and a superpurifier (FS-1 type, Fujiwara Works).

Reagents

A standard 1 mg/ml stock solution of lithium was prepared by dissolving lithium carbonate in 0.15M nitric acid. A lanthanum stock solution (10 mg/ml) was prepared by dissolving lanthanum nitrate [La(NO₃)₃·6H₂O] in water.

*Author for correspondence

Matrix solutions were prepared from the metal nitrates. All working solutions were prepared from the stock solutions just before use.

Analytical-reagent grade chemicals were used throughout.

Procedure

Hydrogen at a flow-rate of 20 ml/min was added to the argon purge gas (flow-rate 480 ml/min) to protect the metal tube from oxidation by traces of oxygen in the system. This mixture was selected on the basis of a previous study.⁹ Since lithium may be present at trace levels in glassware and laboratory apparatus, Teflon and plastic ware cleaned with acid and fourfold purified water was used. The voltage supplied to the photomultiplier was 680 V.

A 1 μ l-aliquot (10 pg of Li) of sample solution was placed in the metal tube by micropipette, dried at 360 K for 10 sec, pyrolysed at 570 K for 20 sec and atomized by heating to 2620 K (at a ramp rate of 5.0 K/msec). Molecular emission generated by decomposition or vaporization of concomitant species was characterized by heating the interferent alone and measuring the emission at the lithium atomic resonance line (670.78 nm).

RESULTS AND DISCUSSION

Reproducibility and detection limit

The detection limit (0.02 ng/ml, $S/N = 2$) for plasma-emission determination is poorer than that of flame emission determination (1 pg/ml, $S/N = 2$),¹⁷ because a large fraction of the lithium atoms will be ionized in an inductively coupled plasma having a gas temperature of 9000–10000 K.¹⁸ The detection limit by atomic-fluorescence spectrometry with ICP as an atom cell has been reported as 0.3 ng/ml.¹⁹ The mass detection limit in the graphite-funace emission method is 0.5 pg,^{15,16} corresponding to 0.025 ng/ml. However, the detection limit in our metal-tube atomizer system, defined as the weight of lithium giving an emission signal equal to three times the standard deviation of the background signal, is 0.04 pg (corresponding to 0.004 ng/ml in a 10- μ l injection). Even though the efficiency of the small tube for emission measurements is limited, owing to the short residence time of the atomic vapour, the detection limit is comparable to that of flame emission.

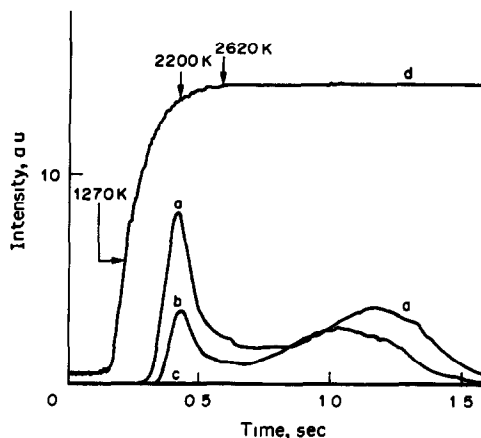


Fig 1 CRT display showing the effect of lead on atomic emission of lithium (a) 10 pg of lithium, (b) 10 pg of lithium and 10 ng of lead, (c) 10 ng of lead, (d) temperature trace, a.u. = arbitrary units

The relative standard deviation (RSD) calculated from 9 measurements of 10 pg of lithium was 8%. The RSD for lithium (10 pg) in the presence of 50 ng of lanthanum was 5% (10 measurements). The RSD in the presence of organic matrix and 50 ng of lanthanum was 18–32% for three replicates.

Interference and matrix modifier study

Biological material, in general, contains large amounts of Al, Ca, Cu, Fe, K, Mg, Na, Pb and Zn (particularly Ca, K and Mg). The effect of these elements on the lithium emission profile was investigated by injection of a mixture of 10 pg of lithium and 10 ng of interferent into the metal atomizer (Table 1). A typical interference is shown in Fig 1. The results show that all these elements except iron caused a reduction in peak height. When the interferences caused by Ca, K and Mg in 100 ng amounts were further investigated, the lithium signals were found to be decreased to 35–40% of the signal in the absence of interferent.

Lanthanum is one of the most popular matrix modifiers for determinations of alkali and alkaline-earth metals by flame and electrothermal atomization atomic-absorption spectrometry.^{20–24} The effect of 50 ng of lanthanum on the lithium emission signal is shown in Fig. 2. It was found that the second peak in the emission signal for lithium alone was suppressed when lanthanum was present, and the lithium signal was slightly depressed and shifted to a lower temperature region. The second peak (in the signal for lithium alone) is thought to be due to molecular emission.

Table 1 Effect of lanthanum on interferences in determination of lithium (10 pg)*

Interfering element (10 ng)	Peak height†		Peak area†	
	Without La	With La	Without La	With La
(Li)	8 08 ± 0 64	6 11 ± 0 31	6700 ± 210	4790 ± 530
Al	6 79 ± 0 12	6 15 ± 0 32	5950 ± 210	4370 ± 130
Ca	5 95 ± 0 31	6.73 ± 0 32	2750 ± 320	7210 ± 1200
Cu	7.17 ± 0 20	6.15 ± 0 37	3509 ± 300	6480 ± 1180
Fe	8 08 ± 0 21	6 22 ± 0 33	9071 ± 1540	6210 ± 780
K	5 54 ± 0.51	6.00 ± 0 13	2440 ± 290	6200 ± 900
Mg	5 30 ± 0 16	6.23 ± 0 66	1880 ± 150	4390 ± 300
Na	6 43 ± 0 54	6 10 ± 0 69	3400 ± 350	7560 ± 960
Pb	3 50 ± 0 26	6 27 ± 0 22	5340 ± 950	9130 ± 570
Zn	6 23 ± 0 75	6 28 ± 0 21	5980 ± 350	5950 ± 1770

*3-10 measurements in each case

†Arbitrary units

The effect of lanthanum as a matrix modifier for suppressing the interferences was investigated. Figure 3 shows the effect of lanthanum (50 ng) on the lithium emission signal in the presence of lead. The emission signal for lead in the presence of lanthanum was negligible, and so was the effect of lead on the signal for lithium. The addition of lanthanum modified the interferences with respect to peak height (Table 1) but all the interferents except potassium, sodium and lead caused the lithium signal to be broader and to shift to a higher temperature region. The appearance temperature of the lithium signal, which is defined as the temperature of the atomizer at the time when an emission signal can first be perceived above the baseline noise, and the temperature for maximum emission were similar in the presence or absence of K, Na or Pb when lanthanum was added as matrix modifier. The presence of 100 ng of Ca, K or Mg lowered the lithium signal by about 25%.

Though lanthanum is known to act as a releasing agent for metal ions by preferential formation of compounds with interfering anions,²⁰⁻²³ and has been used as a radiation buffer in determination of calcium in phosphate rocks,²⁴ the mechanism in the present case is less obvious. It has been reported, however, that when lithium nitrate and lanthanum nitrate are heated together for 10 hr at 800° a compound LiLaO_2 is produced.²⁵ This reaction should proceed much more rapidly at the higher temperatures attained in the tungsten tube, and the modifying effect of the lanthanum may be due to "protection" afforded by formation of this compound.

Determination of lithium in biological materials

Biological samples were dried in an electric oven at 350 K for 4 hr and a 0.1-g sample was weighed and transferred into a Uni-seal vessel; 4 ml of concentrated nitric acid and 1 ml of 30%

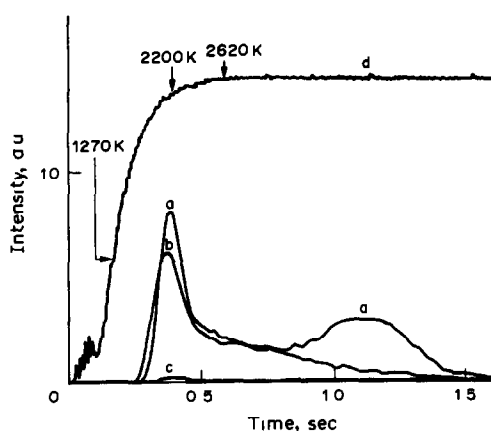


Fig 2 CRT display showing the effect of lanthanum on atomic emission of lithium (a) 10 pg of lithium, (b) 10 pg of lithium and 50 ng of lanthanum, (c) 50 ng of lanthanum, (d) temperature trace, a u = arbitrary units

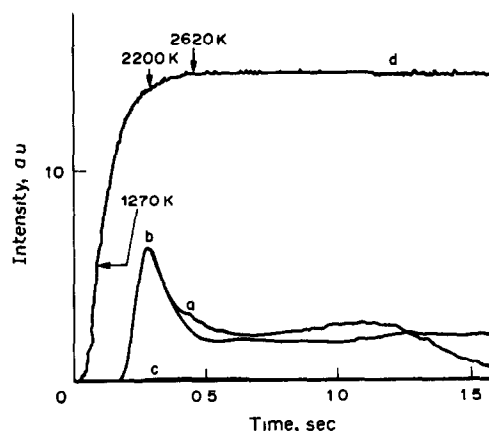


Fig 3 CRT display showing the effect of lanthanum on the interference of lead (a) 10 pg of lithium and 50 ng of lanthanum, (b) 10 pg of lithium and 10 ng of lead with lanthanum, (c) 10 ng of lead and 50 ng of lanthanum, (d) temperature trace, a u = arbitrary units

Table 2 Determination and recovery of lithium in biological samples

Sample	Amount of lithium, $\mu\text{g/g}$	
	Added	Found
Bovine liver*	—	$0.42 \pm 0.07\ddagger$
	5.1	$5.51 \pm 0.8\text{\S}$
Oyster tissue*	—	$2.4 \pm 0.7\ddagger$
	4.8	$6.9 \pm 0.5\text{\S}$
Pepper bush†	—	$0.56 \pm 0.11\ddagger$
	11.3	$10.8 \pm 1.4\text{\S}$
Orchard leaves #	—	$0.60 \pm 0.19\ddagger$

*NIST standard

†NIES standard

‡Three determinations.

§Five determinations

NIST standard, certified value $0.6 \mu\text{g/g}$

hydrogen peroxide were added and the sealed vessel was heated for 3 hr in an electric oven at 390 K. After the digestion, the solution was transferred to a Teflon beaker and evaporated to dryness in a poly(ethylene glycol) bath at 380 K. The residue was dissolved in about 2 ml of 1M nitric acid and the solution was evaporated to dryness. This cycle was repeated, then the residue was taken up in 1 ml of the acid, the requisite amount of matrix modifier was added, and the solution was transferred to a 10-ml standard flask and made up to the mark with water. When necessary the solution was further diluted with water.

For atomic-emission measurements, $1 \mu\text{l}$ of the solution was introduced into the excitation tube by pipette after the addition of lanthanum. The emission signal was measured and a calibration graph was obtained by use of standard solutions (containing lanthanum); it was linear up to 10 pg of lithium.

Some studies with known quantities of lithium added to the samples indicated good recovery (Table 2). A result compared with a certified value is also listed in Table 2 and found to be almost quantitative.

The method presented requires only acid digestion of the biological sample. With lanthanum as matrix modifier, atomic emission spectrometry with a metal tube offers a simple and sensitive technique for the determination of

lithium in biological materials. The main disadvantage at present is the lack of a suitable commercial instrument, and this restricts wider use of the technique, despite its obvious applicability.

Acknowledgements—The authors wish to express their gratitude to Tsutomu Nakagawa and Yasutosi Tajima for their technical assistance. They also thank Dr R. A. Chalmers for valuable comments and suggestions

REFERENCES

- 1 F. Shaw and J. M. Ottaway, *Anal. Lett.*, 1975, **8**, 911
- 2 J. P. Matousek and L. E. Smythe, *Appl. Spectrosc.*, 1978, **32**, 54
- 3 M. S. Epstein, T. C. Rains and T. C. O'Haver, *ibid.*, 1976, **30**, 324
- 4 D. C. Gregoire and C. L. Chakrabarti, *Spectrochim. Acta*, 1982, **37B**, 625.
- 5 L. Bezur, J. Marshall, J. M. Ottaway and R. Fakhrul-Aldeen, *Analyst*, 1983, **108**, 553.
- 6 M. Suzuki and K. Ohta, *Talanta*, 1981, **28**, 177
- 7 M. Suzuki, K. Ohta and T. Yamakita, *Anal. Chem.*, 1981, **53**, 1796
- 8 M. Suzuki and K. Ohta, *Z. Anal. Chem.*, 1982, **313**, 34
- 9 *Idem*, *Anal. Chem.*, 1985, **57**, 26
- 10 K. Ohta, *Z. Anal. Chem.*, 1987, **326**, 132
- 11 K. S. Subramanian, *Prog. Anal. Spectrosc.*, 1986, **9**, 237
- 12 C. Baluja-Santos, A. González-Portal and J. M. Bouzas-Bouzas, *Anal. Chim. Acta*, 1987, **196**, 283
- 13 I. Moynier, E. Bourret, M. Fussellier and L. Bardet, *Analysis*, 1987, **15**, 306
- 14 C. Rios, H. Valero and T. Sanchez, *At. Spectrosc.*, 1987, **8**, 67
- 15 H.-M. Huang and Y.-H. Liu, *Spectrochim. Acta*, 1984, **39B**, 493
- 16 H.-M. Huang, Y.-H. Liu and D.-Y. Lou, *Fenxi Huaxue*, 1985, **13**, 561
- 17 M. L. Parsons, S. Major and A. R. Forster, *Appl. Spectrosc.*, 1983, **37**, 411
- 18 N. Kovacic and R. Barnes, *Z. Anal. Chem.*, 1987, **326**, 49
- 19 B. W. Smith, M. R. Glick, K. N. Spears and J. D. Winefordner, *Appl. Spectrosc.*, 1989, **43**, 376
- 20 J. Yofé, R. Avni and M. Stiller, *Anal. Chim. Acta*, 1963, **28**, 331.
- 21 C. B. Belcher and K. A. Brooks, *ibid.*, 1963, **29**, 202.
- 22 T. V. Ramakrishna, J. W. Robinson and P. W. West, *ibid.*, 1966, **36**, 57
- 23 J. B. Willis, *Spectrochim. Acta*, 1960, **16**, 551.
- 24 L. V. Shikheeva and L. F. Chernozhukova, *Zh. Analit. Khim.*, 1984, **39**, 467, *Chem. Abstr.*, 1984, **101**, 53897h
- 25 N. I. Sevost'yanova, I. A. Murav'eva, L. M. Kovba, L. I. Maetyenko and V. I. Spitsyn, *Dokl. Akad. Nauk SSSR*, 1965, **161**, 1359, *Chem. Abstr.*, 1965, **63**, 6405g

DETERMINATION OF TEN RARE-EARTH ELEMENTS AND YTTRIUM IN SILICATE ROCKS BY ICP-AES WITHOUT SEPARATION AND PRECONCENTRATION

M. S. RATHI, P. P. KHANNA* and PULOK KUMAR MUKHERJEE

Spectra Laboratory, Wadia Institute of Himalayan Geology, 33 General Mahadeo Singh Road,
Dehra Dun 248 001, India

(Received 20 October 1989 Revised 25 July 1990. Accepted 19 September 1990)

Summary—Lanthanum, cerium, neodymium, samarium, europium, gadolinium, dysprosium, erbium, ytterbium, lutetium and yttrium have been determined in 8 international rock standards by inductively coupled plasma atomic emission spectrometry (ICP-AES) without prior ion-exchange separation and preconcentration. The results for La, Ce, Nd, Eu, Dy, Yb and Y were in good agreement with the reported values, whereas those for Sm, Gd, Er and Lu were less accurate. However, the results for Sm, Gd, Er and Lu can also be used for studies of petrogenesis.

Rare-earth element (REE) geochemistry has been established as one of the most powerful tools for petrogenetic studies of rocks. REEs (except for Ce) are comparatively inert towards secondary geological processes, and hence their relative abundances even in altered rocks, give valuable information about the origin of rocks.¹

High-resolution ICP-AES has become a widely used and popular technique for measurement of major and trace elements, including REEs,³⁻⁸ in analytical geochemistry. However, preparation of samples for ICP-AES determination of the REEs in rock samples generally involves separation of REE fractions by cation-exchange, followed by concentration by evaporation.³⁻⁸ This procedure is quite tedious and thus hinders the routine production of REE data.

The aim of the present investigation was to find whether the separation and preconcentration steps can be avoided by calibrating the instrument with standards having a chemical matrix similar to that of the samples.

EXPERIMENTAL

Dried samples (0.5 g) were digested with a hydrofluoric-perchloric acid mixture in open PTFE beakers. The digestion was repeated 5 or 6 times with evaporation to perchloric acid fumes after each, in order to ensure complete dissolution, and the final solution was made up accurately to 50 ml. The instrumentation used

was a Jobin Yvon model JY 70 Plus ICP, with a 1-m focal length Czerny-Turner, holographic grating, 3600 grooves/mm, and a Meinhard concentric glass nebulizer "type C". The RF generator was a 40.68 MHz single-phase unit, with power stable to better than 0.01%. The gas flow-rates (l./min) were: outer (coolant) 12; intermediate (auxiliary) 0; central (carrier + sheath) 0.55.

A set of four rock standards (Syenite STM-1, Quartz latite QLO-1, Diabase W-2, supplied by U.S.G.S. and Granite GS-N, supplied by A.N.R.T., France) and a blank were used for calibration in order to cover a wide compositional range of geological materials. Six rock standards (Basalt BE-N, from A.N.R.T., Basalt BHVO-1, Mica schist SDC-1, Granite G-2, Rhyolite RGM-1 and Granodiorite GSP-1 from U.S.G.S.) were treated as unknown samples and analysed for REE and Y. A validation test was done with a different set of standards for calibration (SDC-1, BE-N, BHVO-1, W-2, and Gabbro MRG-1, supplied by C.C.R.M.P., Canada) and a blank, for measurement of REEs and Y in QLO-1, GS-N, G-2, RGM-1 and GSP-1. The results are summarized in Table 1.

RESULTS AND DISCUSSION

The concentrations of the REEs and Y in the reference rock standards were taken from the latest compilation by Govindaraju.⁹ Some of the REE values for these reference rocks are not

*Author for correspondence

Table 1 Results ($\mu\text{g/g}$) for analysis with (A) STM-1, QLO-1, W-2 and GS-N as calibration standards and (B) SDC-1, BE-N, BHVO-1, W-2 and MRG-1 as calibration standards (recommended values⁹ are given in parentheses)

Element	Line, <i>m</i> m	BE-N		BHVO-1		SDC-1		QLO-1		GS-N		G-2		RGM-1		GSP-1	
		(A)	(B)	(A)	(B)	(A)	(B)	(A)	(B)	(A)	(B)	(A)	(B)	(A)	(B)	(A)	(B)
La	398 852	80 (82)	21.7 (15.8)	42 (42)	30.5 (27)	74.5 (75)	84	93 (89)	25	27 (24)	162	184 (184)					
Ce	413 765	136 (152)	47 (39)	92 (93)	62 (54.6)	148 (135)	155	187 (160)	56	59 (47)	374	457 (399)					
Nd	430.358	64 (70)	32.2 (25.2)	45 (40)	27 (26)	50.5 (50)	54	55 (55)	27	24 (19)	159	188 (196)					
Eu	381 967	3.7 (3.6)	2.37 (2.06)	2.1 (1.71)	1.62 (1.43)	1.9 (1.7)	1.8	1.8 (1.4)	1.1	1.0 (0.66)	3.1	3.1 (2.33)					
Dy	353 171	6.2 (6.4)*	5.5 (5.2)	6.6 (6.7)	4.8 (3.8)	4 (3)*	3.2	3.3 (2.4)	4.5	4.7 (4.8)	6.8	7.1 (5.5)					
Yb	328 937	2.5 (1.8)	2.68 (2.02)	3.3 (4)	2.3 (2.32)	1.4 (1.5)	0.9	0.8 (0.8)	2.4	2.3 (2.6)	1.6	1.5 (1.7)					
Sm	359 260	13 (12)	9.6 (6.2)	12 (8.2)	7 (4.88)	9.2 (7.7)	10.9	10.2 (7.2)	8.3	6.8 (4.3)	28.6	28.4 (26.3)					
Gd	335 048	18.6 (9.5)*	17.8 (6.4)	8 (7.2)	3 (4.7)*	3 (5.2)	4.6	2.6 (4.3)*	3.3	1.7 (3.7)	7.5	4.4 (12.1)					
Er	337 271	2.1 (2.5)*	2.4 (2.4)	3.1 (4.1)*	0.6 (2.3)	0.7 (1.7)*	1.4	0.51 (0.92)*	0.8	0.3 (2.6)	1.9	0.7 (2.7)*					
Lu	261 542	0.4 (0.24)	0.39 (0.29)	0.29 (0.53)*	0.2 (0.37)	0.21 (0.22)	0.12	0.12 (0.11)*	0.14	0.14 (0.41)	0.2	0.2 (0.214)*					
Y	371 030	27 (30)	27.7 (27.6)	30 (40)	32 (24)	22 (19)	10.0	13 (11)	22	31 (25)	23	33 (26)					

Table 2 Comparison of REE and Y concentrations ($\mu\text{g/g}$) in 6 rock standards, measured with and without use of a separation technique [calibration sets as for Table 1, N R means not reported, (C) indicates the results reported in the reference given for use of the separation method, percentage deviations from recommended⁹ values are given in parentheses]

Element	G-2		GS-N		GSP-1		QLO-1		SDC-1		BE-N	
	(A)	(C) ¹⁰	(B)	(C) ⁸	(A)	(C) ⁶	(B)	(C) ⁵	(A)	(C) ⁷	(A)	(C) ¹¹
La	84 (6)	85.5 (4)	74.5 (1)	73 (3)	162 (12)	177 (4)	30.5 (13)	26.4 (2)	42 (0)	41.2 (2)	80 (2)	82.87 (1)
Ce	155 (3)	156 (3)	148 (10)	144 (7)	374 (6)	431 (8)	62 (14)	52.1 (5)	92 (1)	87.6 (6)	136 (11)	152.08 (0)
Nd	54 (2)	53 (4)	50.5 (1)	50.0 (0)	159 (19)	197 (0.5)	27 (4)	21.2 (19)	45 (13)	40.8 (2)	64 (9)	63.21 (10)
Eu	1.8 (29)	1.31 (6)	1.9 (12)	1.66 (2)	3.1 (33)	2.91 (25)	1.62 (13)	1.3 (9)	2.1 (23)	1.65 (4)	3.7 (3)	3.71 (3)
Dy	3.2 (33)	2.22 (8)	4 (33)	3.1 (3)	6.8 (24)	6.17 (12)	4.8 (26)	3.57 (6)	6.6 (2)	6.3 (6)	6.2 (3)	6.27
Yb	0.9 (13)	0.61 (24)	1.4 (7)	1.4 (7)	1.6 (6)	1.33 (22)	2.3 (1)	2.29 (1)	3.3 (18)	3.41 (15)	2.5 (39)	1.77 (2)
Sm	0.9 (51)	7.22 (0.3)	9.2 (20)	6.9 (10)	28.6 (9)	25.8 (2)	7 (46)	4.21 (14)	12 (46)	8.1 (1)	13 (8)	11.85 (1)
Gd	4.6 (7)	4.07 (5)	3 (42)	4.5 (11)	7.5 (38)	11.7 (3)	3 (36)	3.58 (24)	8 (11)	7.4 (3)	18.6 (96)	10.01 (5)
Er	4.4 (52)	N R	0.7 (59)	N R	1.9 (30)	2.56 (5)	0.6 (74)	2.13 (7)	3.1 (24)	3.46 (16)	2.1 (16)	2.49 (0.4)
Lu	0.12 (9)	0.08 (27)	0.21 (5)	0.25 (14)	0.2 (7)	0.17 (21)	0.2 (46)	0.38 (3)	0.29 (45)	0.47 (11)	0.4 (67)	0.26 (8)
Y	10 (9)	N R	22 (16)	N R	23 (12)	23.2 (11)	30 (25)	22.8 (5)	32 (20)	32.3 (19)	27 (10)	30.87 (3)

Table 3 Slopes and intercepts of the calibration graphs obtained with the two sets of standards

Element	Set (A)		Set (B)	
	Slope	Intercept	Slope	Intercept
La	0.093	-9.5	0.023	-6.2
Ce	0.18	-24.4	0.052	-20.2
Nd	0.069	-19.8	0.039	-14.4
Eu	0.0032	-1.2	0.0027	-0.8
Dy	0.0078	-3.3	0.0072	-2.4
Yb	0.0026	-0.5	0.0023	-0.3
Sm	0.017	-10.2	0.012	-6.9
Gd	0.0037	-1.9	0.0076	-0.7
Er	3.6×10^{-6}	0.0	2.3×10^{-5}	0.0
Lu	0.0032	-1.2	0.0027	-0.8
Y	0.0028	0.0	0.0038	-1.2

well characterized and are proposed only for information (they are marked with an asterisk in Table 1).

A comparison of our results (Table 2) with those obtained by use of a separation technique^{6-8,10,11} and also with the consensus values,⁹ shows that those for La, Ce, Nd, Eu, Dy, Yb, and Y are in good agreement. Agreement for Sm, Gd, Er and Lu is rather poor, but most of the differences are within the acceptable limits of error for petrogenetic purposes. Some of our measurements (underlined in Table 2) are in better agreement with the reported values than are those obtained by using a separation technique.

The values found for Er were always lower than the reported values, whereas those for Sm were always high. The accuracy of the results for these two elements was better for basic rocks than for granitic rocks. The reason for this is unclear, but is possibly spectral interference by elements such as Ba, Sr, Zr, etc. which are generally present in granitic

rocks at levels as much 10-100 times those in basic ones.

The cation-exchange methods do not give complete separation of the REEs from the other rock components, some elements, such as Ba, Ca, Sr, Ti and Zr, being incorporated in the REE fraction.^{3,7} In our method, however, rock standards were used instead of salt standards for calibration, and as these are chosen so that their matrices are similar to those of the samples, there is some degree of compensation of chemical and spectral interferences. The results obtained for G-2, RGM-1 and GSP-1 differed, however, according to which set of calibration standards was used. All the calibrations were found to satisfy a first order fit. The slopes and intercepts obtained for both calibration sets are given in Table 3. The major component composition of the standards is given in Table 4.

In summary, it may be concluded that separation and preconcentration of REEs is not essential for their determination in silicate rock

Table 4 Major component composition (%) of the standards used for calibration

Standard	SiO ₂	Al ₂ O ₃	Fe ₂ O ₃	FeO	MnO	MgO	CaO	Na ₂ O	K ₂ O	TiO ₂	P ₂ O ₅
GS-N (Granite)	65.80	14.67	1.92	1.65	0.056	2.30	2.50	3.77	4.63	0.68	0.28
QLO-1 (Quartz latite)	65.55	16.18	1.02	2.97	0.093	1.00	3.17	4.20	3.60	0.624	0.254
STM-1 (Syenite)	59.64	18.39	2.87	2.09	0.22	0.101	1.09	8.94	4.28	0.135	0.158
W-2 (Diabase)	52.44	15.35	1.52	8.31	0.163	6.37	10.87	2.14	0.627	1.06	0.131
SDC-1 (Mica schist)	65.85	15.75	2.62	3.93	0.114	1.69	1.40	2.05	3.28	1.01	0.158
BE-N (Basalt)	38.20	10.07	5.34	6.74	0.20	13.15	13.87	3.18	1.39	2.61	1.05
BHVO-1 (Basalt)	49.94	13.80	2.82	8.58	0.168	7.23	11.40	2.26	0.52	2.71	0.273
MRG-1 (Gabbro)	39.09	8.46	8.36	8.66	0.17	13.55	14.71	0.74	0.18	3.77	0.08

samples. It is difficult to determine Pr, Tb, Ho and Tm by this method, but the rest of the REEs and Y can be measured with reasonable accuracy in a 10-mg/ml rock solution by using high-resolution ICP-AES. The accuracy achieved is sufficient for the purpose of geological interpretation. The results could probably be further improved by using calibration standards that all closely match the samples in chemical composition.

Acknowledgements—The authors are grateful to Dr. V. C. Thakur, Director, W I H.G., for providing all facilities for this study. The Department of Science and Technology (Government of India) is thanked for financial support for procurement of the ICP unit, under the Solid Earth Scheme. Professor A. K. Sinha is thanked for his encouragement throughout the work.

REFERENCES

- 1 P. Henderson (ed.), *Rare Earth Element Geochemistry*, p. 510 Elsevier, Amsterdam, 1984
- 2 S. E. Church, *Geostand. Newsl.*, 1981, **5**, 133.
- 3 J. N. Walsh, F. Buckley and J. Barker, *Chem. Geol.*, 1981, **33**, 141.
- 4 K. Govindaraju and G. Mevelle, *Spectrochim. Acta*, 1983, **38B**, 1447
- 5 I. Jarvis and K. E. Jarvis, *Chem. Geol.*, 1985, **53**, 335
- 6 K. E. Jarvis and I. Jarvis, *Geostand. Newsl.*, 1988, **12**, 1
- 7 J. G. Crock, F. E. Lichte, G. O. Riddle and C. L. Beech, *Talanta*, 1986, **33**, 601
- 8 I. Roelandts and G. Michel, *Geostand. Newsl.*, 1986, **10**, 135.
- 9 K. Govindaraju, *ibid.*, 1989, **13**, 1.
- 10 I. Roelandts, *Chem. Geol.*, 1988, **67**, 171
- 11 K. Govindaraju and G. Mevelle, *J. Anal. At. Spectrom.* 1987, **2**, 615.

COULOMETRIC GENERATION OF H⁺ AND D⁺ IONS IN AQUEOUS MEDIA BY ANODIC OXIDATION OF HYDROGEN AND DEUTERIUM DISSOLVED IN PALLADIUM

RANDJEL P. MIHAJLOVIĆ*

Faculty of Science, Kragujevac, R Domanovića 12, Yugoslavia

VILIM V VAJGAND

Faculty of Science, Belgrade, Yugoslavia

LJILJANA N. JAKŠIĆ

Faculty of Science, Priština, Yugoslavia

(Received 27 May 1989 Revised 28 June 1990 Accepted 10 October 1990)

Summary—Coulometric generation of H⁺ and D⁺ ions in aqueous media by the oxidation of hydrogen and deuterium dissolved in palladium, is described. Hydrogen and deuterium dissolved in palladium were found to be oxidized at more negative potentials than the oxidation potentials of water and other components present. The H⁺ and D⁺ ions generated were used for the titration of tris(hydroxymethyl)aminomethane, piperidine, triethylamine and sodium tetraborate, the end-point being determined potentiometrically with a glass electrode and an SCE. In titrations of 0.001–0.1 M solutions of the bases, the current efficiency was 100%.

In previous work,¹⁻³ we have generated H⁺ ions in non-aqueous media by anodic oxidation of hydrogen dissolved in palladium. Titrations of organic bases with the ions generated in this way showed that the current efficiency in the generation was 100%. Therefore, we considered it interesting to investigate the generation of H⁺ and D⁺ ions in aqueous media by anodic oxidation of hydrogen and deuterium, dissolved in palladium. No data on the coulometric generation of D⁺ ions have hitherto been reported.

EXPERIMENTAL

Reagents

All chemicals used were of analytical reagent grade (Merck and Fluka). Tris(hydroxymethyl)aminomethane⁴ and sodium tetraborate were prepared as primary standard solutions. Piperidine and triethylamine solutions were standardized by potentiometric titration with standard perchloric acid solution. The supporting electrolyte was 1 M sodium perchlorate or sulphate in water. Deuterium oxide (heavy water), 99.8%, was purchased from the Radioisotope Division of IGN Chemicals.

Electrodes

The electrode for generating D⁺ was a palladium plate (1 × 2 × 0.5 cm) saturated with deuterium obtained by electrolysis of heavy water. The other electrodes used, the apparatus and the procedure were as described earlier.³

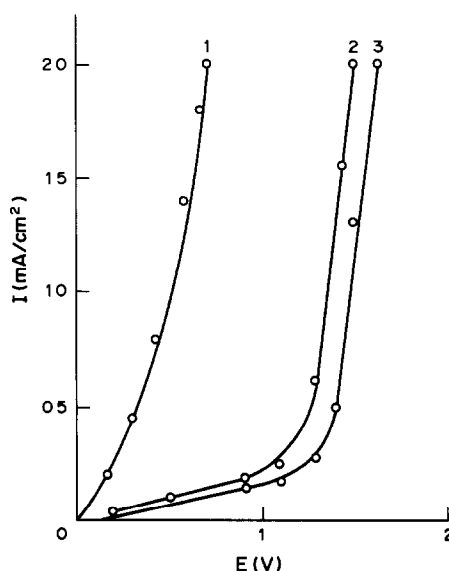


Fig 1 Change in anodic potential with current density (1) H₂ (D₂) dissolved in palladium, (2) THAM, (3) water

*Author for correspondence

Table 1 Current efficiency in the titration of bases in water with H⁺ and D⁺ ions generated by the oxidation of hydrogen and deuterium dissolved in palladium, at 0.015 A

Base titrated	Generator electrode	Taken, mg	Number of determinations	Purity found, %
THAM	H ₂ /Pd	22.48	6	99.9 ± 0.3
THAM	H ₂ /Pd	14.28	4	100.0 ± 0.4
THAM	H ₂ /Pd	22.48	4	100.2 ± 0.3*
THAM	H ₂ /Pd	14.28	5	100.3 ± 0.2*
Piperidine	H ₂ /Pd	4.21	5	99.9 ± 0.7
Triethylamine	H ₂ /Pd	7.44	5	100.0 ± 0.9
Na ₂ B ₄ O ₇	H ₂ /Pd	7.56	7	99.9 ± 0.1
THAM	D ₂ /Pd	6.42	5	99.9 ± 0.5
Na ₂ B ₄ O ₇	D ₂ /Pd	23.59	5	99.8 ± 0.7
Piperidine	D ₂ /Pd	2.12	5	99.7 ± 0.7
Triethylamine	D ₂ /Pd	11.97	5	100.0 ± 0.9

*Supporting electrolyte 1M sodium sulphate

RESULTS AND DISCUSSION

Although hydrogen and deuterium dissolved in palladium have been extensively studied,⁵⁻⁸ no data are reported on their practical application as sources of H⁺ and D⁺ ions for quantitative determination of bases in aqueous media.

Previous direct coulometric titrations of organic bases with H⁺ ions generated by the oxidation of water at a platinum anode were not successful, as the bases titrated were oxidized as well.

By recording the current-potential curves for water, the bases to be titrated, and hydrogen and deuterium dissolved in palladium (Fig. 1) we found that in 1M aqueous solutions of sodium sulphate or perchlorate, hydrogen and deuterium dissolved in palladium were oxidized at potentials more negative (slightly above 0V) than those for oxidation of the bases and water.

In order to establish whether the reactions $H_2/Pd \rightarrow 2H^+ + 2e^-$ and $D_2/Pd \rightarrow 2D^+ + 2e^-$ are quantitative, we titrated solutions of tris(hydroxymethyl)aminomethane (THAM), piperidine, triethylamine and sodium tetraborate, with H⁺ and D⁺ ions obtained by the oxidation of hydrogen and deuterium. The results obtained under the optimum experimental conditions are presented in Table 1. Under the optimum conditions the current efficiency was 100%.

Since the oxidation potentials of hydrogen and deuterium dissolved in palladium are only slightly above 0V, these species can be used for generation of H⁺ and D⁺ for titrimetric determination of organic bases, with 100% current efficiency.

The palladium plate used (1 × 2 × 0.5 cm) can be utilized for the generation of H⁺ (D⁺) ions in water for more than 80 hr at a current of 0.015 A. After consumption of the hydrogen (deuterium) dissolved in the palladium, the electrode can again be saturated with hydrogen (deuterium).

From the results presented in Table 1 it may be concluded that hydrogen and deuterium dissolved in palladium are ideal for the coulometric generation of H⁺ and D⁺ ions in water; their oxidation potentials are low and they can be quantitatively oxidized. Furthermore, their application brings no foreign organic compounds into the solution under investigation.

REFERENCES

- 1 V J Vajgand, R P Mihajlović, R M Džudović and Lj N Jakšić, *Anal Chim Acta*, 1987, **202**, 231
- 2 V J Vajgand, R P Mihajlović and R M Džudović, *Talanta*, 1989, **36**, 1154
- 3 R P Mihajlović, Lj V Mihajlović, V J Vajgand and Lj N Jakšić, *ibid.*, 1989, **36**, 1135
- 4 W C Hoyle, W F Koch and H Diehl, *ibid.*, 1975, **22**, 649
- 5 T Graham, *Phil Trans*, 1866, **156**, 389, *Proc Roy. Soc* 1868-9, **17**, 212*
- 6 G A Moore, *Trans Electrochem Soc.*, 1939, **75**, 237
- 7 F A Lewis, G E Roberts and A R Ubbelohde, *Proc R Soc. A*, 1953, **220**, 279
- 8 F A Lewis and A R Ubbelohde, *J Chem Soc.*, 1954, 1710

*The wrong date for this reference was given in an earlier paper³

INDICATOR CHARACTERISTICS OF BROMOTHYMOLO BLUE DERIVATIVES

J. B. PUSCHETT and B. S. RAO

Department of Medicine, Renal Electrolyte Division, 1191 Scaife Hall, University of Pittsburgh, Pittsburgh, PA 15261, U S A

B. M. KARANDIKAR and K. MATYJASZEWSKI*

Department of Chemistry, Carnegie Mellon University, 4400 Fifth Avenue, Pittsburgh, PA 15213, U S A

(Received 3 January 1990 Revised 5 September 1990 Accepted 10 September 1990)

Summary—Some Bromothymol Blue derivatives with a nitro, amino, isothiocyanato or sulfonamide group substituted on the sulfonated ring of the dibromothymolsulfonephthalein have been studied spectrometrically. All the dyes have two characteristic absorption peaks which can be used to measure pH in the physiological range. The molar absorptivities, wavelengths of maximum absorption and pK_a values have been determined from the absorbances, and are similar for all four dyes.

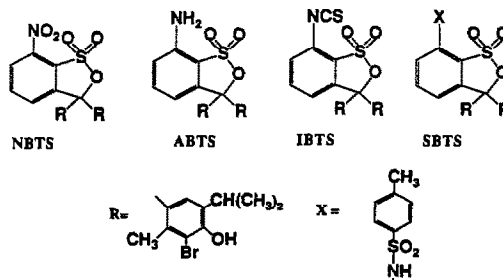
Indicator dyestuffs can be used to measure pH spectrophotometrically, by use of the Henderson-Hasselbalch equation.¹ The scope of this method can be widened by the use of fiber optics in measuring the absorbance of the dyestuff. Light is transmitted by a fiber to a chemically sensitive dye immobilized at the fiber tip. The fraction of the light absorbed by the dye is determined by measuring the absorbance or reflectance by carrying the appropriate radiation through another fiber to a detector. Several pH sensors based on this principle have been reported.²⁻⁷ In these systems, the dye was immobilized on a cross-linked hydrophilic copolymer, attached to glass fibers. One of the disadvantages of these methods is that the reagent is not covalently bound to the fiber and may be leached out. Some applications may require high flexibility of the fibers and high resistance to breakage on bending and twisting. Glass fibers are much more fragile than plastic fibers. It is also difficult to miniaturize some of these devices.

Zemel and co-workers^{8,9} reported the use of a pair of twisted plastic fibers, which gave a high degree of mechanical flexibility combined with very small size and a low cost construction of a disposable probe.

In our work on development of a fiber optic sensor for *in vivo* pH measurements, it was of

interest to prepare flexible plastic optical fibers with dye molecules covalently bound to their surface.¹⁰ For the construction of such a probe, phenolsulfonephthalein and 3,3'-dibromothymolsulfonephthalein (Bromothymol Blue, BTB) are among the most suitable dyes, because they are sensitive to pH in the physiological range.

Attachment of dye molecules to the optical fibers requires the presence of reactive functional groups on the fiber surface as well as on the dye itself. Introduction of groups other than the hydroxyl group into Bromothymol Blue offers a possibility for immobilization of the indicator on a plastic optical fiber. We have therefore prepared derivatives of Bromothymol Blue containing nitro (NBTS), amino (ABTS), isothiocyanato (IBTS) and sulfonamide (SBTS) groups on the sulfonated ring of Bromothymol Blue.



3-Nitro-2-sulfobenzoic anhydride was condensed with thymol in the presence of anhydrous zinc chloride to yield 3-nitrothymolsulfonephthalein (NTS), which was then

*Author for correspondence

brominated in acetic acid to afford 3-nitro-3',3''-dibromothymolsulfonephthalein (NBTS). This compound was catalytically reduced, by using palladium on charcoal, and hydrazine hydrate, to obtain the corresponding 3-amino-3',3''-dibromothymolsulfonephthalein (ABTS), from which the isothiocyanato (IBTS) and *p*-toluenesulfonamide (SBTS) derivatives were prepared.¹⁰ ABTS and IBTS were subsequently covalently attached to plastic fibers with functional groups on their surface, *e.g.*, amino groups on the surface of poly(methylmethacrylate) fiber cladding¹⁰ and sulfonyl chloride groups on the surface of the polystyrene fibers. It is hence important to know how such chemical modification affects the indicator characteristics of the dyes. SBTS was used as a model for predict-

ing the behavior of ABTS attached to chlorosulfonated polystyrene fibers.

The synthesis and characterization of the dyes used are described elsewhere.¹¹

EXPERIMENTAL

An IBM 9430 spectrophotometer and a Fisher Accumet Model 805MP pH meter were used. For each dye, a stock solution of known concentration was prepared in dilute alkali, and divided into several portions. Various small amounts of hydrochloric acid were added to these portions to yield solutions of different pH. The change in volume resulting from addition of the acid was negligible. The spectrum of each solution over the 300–700 nm range was then recorded and the pH was measured.

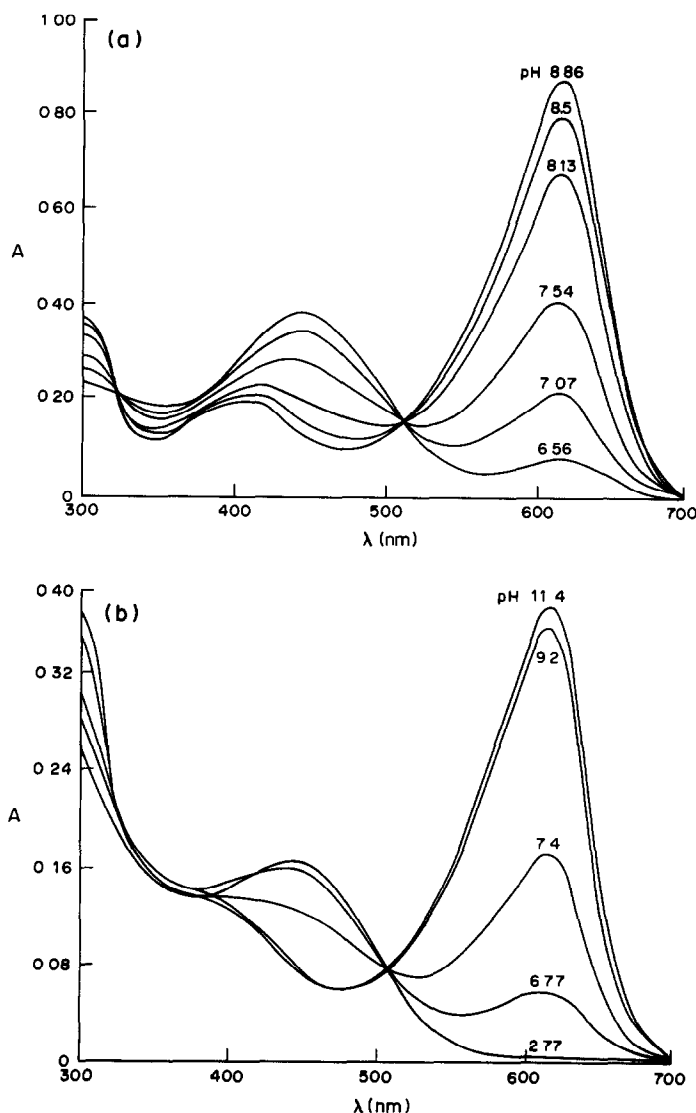
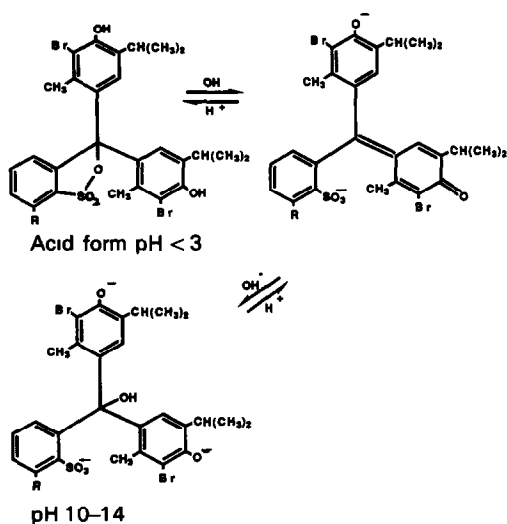


Fig. 1 Spectra at various pH values and 25° for (a) $2.0 \times 10^{-5} M$ IBTS in water, (b) $0.76 \times 10^{-5} M$ SBTS in water

RESULTS AND DISCUSSION

The effect of pH on the spectra of IBTS and SBTS over the 300–700 nm range is shown in Fig. 1. For both dyes, two absorption peaks are seen, the peak at about 600 nm being the more sensitive in the pH range 6.5–8.5. The isosbestic points at ~ 500 nm indicate quantitative transformation without any side products. A similar effect of pH was also observed for NBTS and ABTS. The occurrence of two absorption peaks and the observed effect of pH on the spectrum can be explained on the basis of the work of Blow and Rich,¹² who postulate the following structures for BTB:



At low pH the sultone form exists as a yellow neutral species, which on addition of alkali is ionized to the blue form and its canonical forms, which can be further deprotonated at high pH. The short wavelength peak for the derivatives (Fig. 1) can be attributed to the corresponding yellow form and the long wavelength peak to the quinonoid form. In the pH range of interest, the first equilibrium shifts to the right when alkali is added, resulting in an increase in the

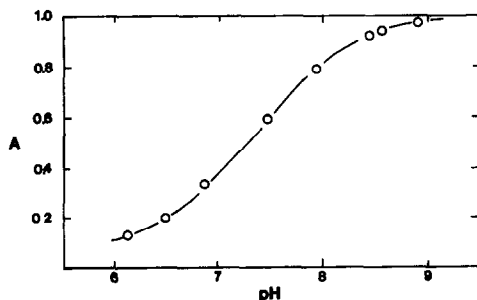


Fig 2 Dependence of the absorbance of $2.0 \times 10^{-5} M$ IBTS at $\lambda_{\max} = 615$ nm (temperature 25°)

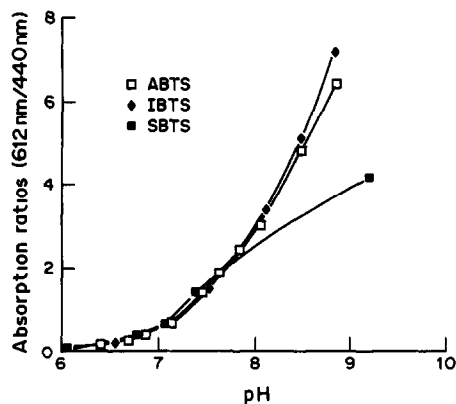


Fig 3. Dependence ratio of the absorbances at the two maxima, on pH, for IBTS, ABTS, and SBTS in water, at 25°

concentration of the phenolate ion (due to neutralization of the phenolic proton). At lower pH the neutral form predominates. It is clearly seen from Fig. 1 that the absorbances of the two peaks, which are proportional to the concentrations of the relevant species, vary with pH. Similar results were observed for NBTS and ABTS.

Since there is a sharp isosbestic point in the spectra (Fig. 1) the ratio of the absorbance at the long wavelength peak to that at the isosbestic point is independent of the dye concentration and is a function of only the pH. Likewise, the ratio of the absorbances at the short and long wavelength peaks will be a function of only pH. For ABTS, IBTS and SBTS, these ratios are plotted against pH in Fig. 2. This property is the basis of the spectrophotometric determination of the pH of solutions.¹³ ABTS and IBTS give almost the same values as each other for the ratio over the pH range examined. For SBTS, however, the ratio is much lower for pH above 8.

The pK_a values were estimated by the Brode procedure.¹³ For each dye, the absorbance at the long wavelength peak was plotted as a function of pH. The abscissa of the point of inflexion gave an estimate of pK_a . A typical plot for IBTS is shown in Fig. 3. The pK_a of IBTS at 25° was estimated as 7.6, in good agreement with the reported value of 7.1 for BTB.

Table 1 lists the pH sensitivity ranges, pK_a values, wavelength maxima, molar absorptivities and color changes for various Bromothymol Blue derivatives, and pertinent literature information on TS and BTB. The molar absorptivities were determined from the absorbances, at the long wavelength maximum, of alkaline

Table 1 Wavelength maxima, pH sensitivity ranges and color changes for various dyes

Dye	pH range	pK _a	λ_{\max} , nm	ϵ^* , 10 ⁴ l mole ⁻¹ .cm ⁻¹	Color change
TS	8.0–9.6	8.9	594	4.6	yellow–blue
NTS	8.0–10.0	9.0	592	2.2	yellow–violet blue
BTB	6.2–7.6	7.1	617	4.9	yellow–blue
NBTS	7.5–9.5	8.5	607	1.6	yellow–blue
ABTS	6.5–8.5	7.6	612	3.5	yellow–blue
IBTS	6.5–8.5	7.6	615	5.4	yellow–blue
SBTS	6.5–8.5	7.7	612	4.2	yellow–blue

*At the longer wavelength maxima and the highest pH

solutions of known concentrations. The pH transition range of 8–10 observed for NTS is in excellent agreement with the pH range 8.2–9.6 reported earlier.¹⁴

From the tabulated data, the effect of substituents on the indicator characteristics can be assessed. Substitution on the sulfonated ring appears to shift the pH transition range to slightly higher values. From comparison of the pK_a values of TS and NTS and of BTB and NBTS, it can be seen that the nitro group, which has a strong electron-withdrawing character, on the sulfonated ring slightly increases the pK_a values. Similar results have been reported for some phenolsulfonephthaleins with halogen substituents on the sulfonated ring.¹⁵ In contrast, the introduction of bromine atoms into the thymol moiety of TS lowers the pK_a from 8.9 for TS to 7.1 for BTB. Thus, the electron-withdrawing group attached to the phenol rings has an opposite and stronger effect on the pK_a value than when it is attached to the sulfonated ring. These apparently anomalous effects can be reconciled by considering entropy effects,¹⁶ by analogy with the chloroacetic acids. When the electron-withdrawing groups are on the sulfonated ring, the effect will be to increase the degree of localization of negative charge on this ring and hence increase the ordering effect on the water solvation shell, which in turn makes the entropy of solvation less positive and hence the free-energy change of ionization more positive, thus increasing pK_a. When the groups are on the phenol ring however, the charge on the anion is more uniformly distributed over the ion, the entropy of solvation is more positive and hence pK_a is reduced. Similar results have been reported for phenolsulfonephthaleins prepared from substituted phenols.¹⁵

In conclusion, the results of the present study indicate that the introduction of a

functional group on the sulfonated ring of BTB or further sulfonamide derivatization does not change the absorption wavelength or the high sensitivity of TS and BTB, which can be conveniently used as spectrophotometric pH probes with the low cost He–Ne laser (wavelength 632 nm). Further work on the surface modification and the covalent attachment of indicator molecules to optical fibers as well as the probe construction and pH sensing by laser optics is under way

REFERENCES

- 1 D J Pietrzyk and C W Frank, *Analytical Chemistry*, 2nd Ed, Academic Press, London, 1979
- 2 J I Peterson, S R Goldstein, R V Fitzgerald and D K Buckhold, *Anal Chem.*, 1980, **52**, 864
- 3 S R Goldstein, J I Peterson and R V Fitzgerald, *J Biomed Eng*, 1980, **102**, 141
- 4 G F Kirkbright, R Narayanaswamy and N A Welti, *Analyst*, 1984, **109**, 15
- 5 *Idem*, *ibid*, 1984, **109**, 1025
- 6 J Růžička and E H Hansen, *Anal Chim Acta*, 1985, **173**, 3
- 7 A M Scheggi and F Baldini, *Optica Acta*, 1986, **33**, 1587
- 8 Z N Zemel, B Keramati, C Spivak and A D Amico, *Sens Actuators*, 1981, **1**, 427
- 9 M El-Sherif and J N Zemel, *Transducers '85, Int Conf Solid-State Sensors and Actuators, Digest of Technical Papers*, p 434 IEEE, New York, 1985
- 10 B. Karandikar, J B Puschett and K Matyjaszewski, *Polym Preprints*, 1989, **30**, 250
- 11 B S Rao, J B Puschett, B M. Karandikar and K Matyjaszewski, *Dyes Pigm.*, accepted for publication
- 12 D M Blow and A Rich, *J Am Chem Soc*, 1960, **82**, 3572
- 13 W R Brode, *ibid*, 1924, **46**, 581
- 14 H A Lubs and S F Acree, *ibid*, 1916, **38**, 2772
- 15 D S Breslow and H Skolnik, *The Chemistry of Heterocyclic Compounds*, A Weissberger (ed). Interscience, New York, 1966
- 16 H J V Tyrell and A E Beezer, *Thermometric Titrimetry*, p. 82 Chapman & Hall, London, 1968

SYNTHESIS AND CHARACTERIZATION OF 2-(3,5-DICHLORO-2-PYRIDYLAZO)-5-DIMETHYLAMINO- PHENOL AS A REAGENT FOR DETERMINATION OF LANTHANUM

LILIANA FERNANDEZ and ROBERTO OLSINA

Department of Analytical Chemistry, Faculty of Chemistry, Biochemistry and Pharmacy,
University of San Luis, Argentina

(Received 16 October 1989 Revised 11 September 1990 Accepted 19 September 1990)

Summary—2-(3,5-Dichloro-2-pyridylazo)-5-dimethylaminophenol (3,5-diCIDMPAP) has been synthesized and its spectral properties, acid-base equilibria, physical constants, and solubility and stability are presented. This reagent is highly promising for the determination of lanthanides. The influence of Triton X-100 on the dissociation constant has been investigated and the association constant between the reagent and the surfactant determined. Analytical data for the 3,5-diCIDMPAP complexes with La(III), Eu(III), Gd(III), Er(III) and Yb(III) are given, La(III) in synthetic samples has been determined with 3,5-diCIDMPAP.

The lanthanides have a wide range of industrial applications, especially in the preparation of catalysts, in alloys and as geochemical tracers, and there has been much interest in development of organic reagents for their determination.¹⁻⁹

The reagents of azo-type, particularly the pyridylazo compounds,⁶⁻⁹ give colored lanthanide complexes that are suitable for spectrophotometric determination. Introduction of halogens into the pyridine ring should considerably increase the sensitivity,¹⁰ so in the present work 2-(3,5-dichloro-2-pyridylazo)-5-dimethylaminophenol (3,5-diCIDMPAP) was examined as a reagent for spectrophotometric determination of some lanthanides. To enhance the sensitivity further, a surfactant was added to the reaction mixture.

EXPERIMENTAL

Apparatus

A Varian 634-UV spectrophotometer was used with 1-cm path-length glass cells. An Orion 701-A pH-meter equipped with a combination glass-calomel electrode was used for pH measurement.

Reagents

Reagents were of analytical quality, except for those used in the synthesis of 3,5-diCIDMPAP, which were purified before use.

Synthesis of reagent

3,5-Dichloro-2-aminopyridine was synthesized by the method of Shibata *et al.*¹¹ A solution of 10 g of the purified product in 150 ml of benzene was placed in a 500-ml glass flask fitted with a reflux condenser and a tube for introduction of a gas. The solution was deaerated by passage of nitrogen through it for 5 min. Sodium amide (3 g) dispersed in benzene that had been deaerated was then introduced, and the mixture was refluxed for about 1 hr under an atmosphere of nitrogen; 15 ml of recently prepared isoamyl nitrate were then added¹² and the mixture was refluxed for 5 hr with continuous passage of nitrogen. The condenser was removed, and the mixture was evaporated to half its volume, then cooled. The light yellow precipitate of diazotate was filtered off by gentle suction and washed with small portions of diethyl ether. A solution of 12 g of diazotate in 70 ml of distilled water and a solution of 5 g of recently purified 3-dimethylaminophenol in 30 ml of ethanol were placed in a 500-ml glass flask fitted with a reflux condenser and bubbler tube, and the mixture was refluxed at a temperature not above 65° for 5 hr, with passage of a slow stream of carbon dioxide. When the solution was cooled, a dark red product was obtained, and filtered off with a sintered glass filter.

The product was purified by repeated recrystallization from chloroform. Analysis gave C 50.1%, H 4.0%, N 17.9%; $C_{13}H_{12}N_4OCl_2$ requires C 50.18%, H 3.99% and N 18.01%. The melting point was 191° .

RESULTS AND DISCUSSION

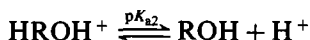
Spectral studies

The mass spectrum was taken and had a peak at $m/z = 310$, for the ^{35}Cl isotopic compound. The proton NMR spectrum was in agreement with that reported by Nakamura *et al.*¹³

The reagent should exhibit three acid-base equilibria. Starting with the species present in very acid solution, these equilibria are



corresponding to deprotonation of the pyridinium ring, followed by



for deprotonation of the quaternary ammonium group, and finally



An absorptometric method was used to evaluate the constants.¹⁴ In all cases the solvent used was 15% v/v ethanol and the ionic strength was kept constant at 0.1M.

Azo-reagents are widely applied in the determination of metal ions. Solvent mixtures such as ethanol-water are frequently used to dissolve the reagent and the complexes formed. Additives such as surfactants are also used to stabilize and/or solubilize the complexes and increase the sensitivity of the method. Triton X-100, a non-ionic poly(ethylene oxide) surfactant, was used in the present work.

The acidity constants in the presence of the surfactant were determined in conditions analogous to those described above, with the concentration of Triton X-100 kept constant at 0.4% v/v ($\approx 7 \times 10^{-3}M$), which permits the existence of micelles (the cmc is $2 \times 10^{-4}M$). Table 1 shows the values obtained in the presence and absence of Triton X-100

The presence of the surfactant slightly changes the absorption spectra of the various reagent forms. In the case of the ROH species, there is a red shift of 5 nm and an absorbance decrease of 19%. This is related to changes in the probability of the transitions of the π -electrons present in the chromophores^{15,16}

Table 1 Acidity constants of 3,5-diCIDMPAP

Constant	Conditions	Value
pK_{a1}	15% v/v ethanol	-1.2
pK_{a2}	15% v/v ethanol	1.7
	0.4% v/v Triton X-100,	
	15% v/v ethanol	0.9
pK_{a3}	15% v/v ethanol	11.6
	0.4% v/v Triton X-100,	
	15% v/v ethanol	11.8

Association constant of the reagent with Triton X-100

The acid-base properties of 3,5-diCIDMPAP are strongly modified by the presence of micellar additives. The lanthanide complexes of the reagent are generally formed at $pH > 7$, so the reagent form generally involved is ROH. The variation of pK_{a3} with Triton X-100 concentration was studied in the absence of ethanol. To determine the association constant the expression¹⁵

$$1/K_{a(app)} = 1/K_{a(H_2O)} + C_D D_{HA}/K_{a(H_2O)}$$

was used, where $K_{a(app)}$ is the dissociation constant of the phenolic OH group in the presence of the surfactant, $K_{a(H_2O)}$ is the same constant for aqueous medium, K_{HA} is the constant for association of the reagent anion and the micelles, and C_D is the concentration of surfactant present in micellar form.

$$(C_D = C_T - cmc)$$

Figure 1 shows the results obtained. The value of K_{HA} is 6.1×10^{-3} .

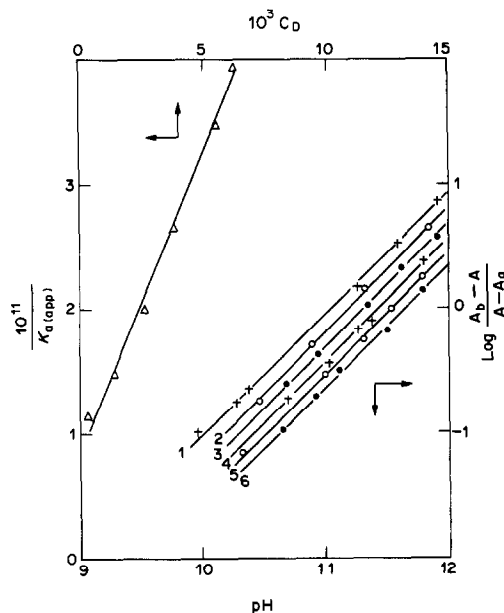


Fig 1 Determination of the association constant C_T (M) 1, 2×10^{-4} , 2, 1.5×10^{-3} , 3, 2.8×10^{-3} , 4, 3.6×10^{-3} , 5, 6.3×10^{-3} , 6, 1.7×10^{-2}

Table 2 Spectrophotometric measurement of rare-earth elements with 3,5-diCIDMPAP

Ion	Molar absorptivity, $10^5 \text{ l mole}^{-1} \text{ cm}^{-1}$	pH	$\Delta\lambda$, nm	Other conditions*
La(III)	1.45	9.8	135	1
Eu(III)	1.40	7.7	145	1
Eu(III)	1.96	8.5	80	2
Gd(III)	3.10	8.2	145	1
Gd(III)	1.95	8.3	80	2
Er(III)	2.00	10.4	112	1
Er(III)	1.80	10.5	82	2
Yb(III)	1.84	6.6	140	1
Yb(III)	1.55	10.0	110	2

*1, 0.4% v/v Triton X-100, [reagent]/[lanthanide] = 15.2, Extraction from benzene; [reagent]/[lanthanide] = 20

Determination of lanthanides

Table 2 presents some experimental conditions for the spectrophotometric determination of lanthanides with 3,5-diCIDMPAP, and the molar absorptivities obtained.

The main advantage of the reagent, however, is that all its lanthanide complexes except that with lanthanum can be extracted into benzene. Thus if the lanthanides can be separated from the elements accompanying them in rocks, etc., 3,5-diCIDMPAP can be used to determine lanthanum in the aqueous phase after extraction of its complexes with the other lanthanides. Methods such as that of Crock *et al.*¹⁷ can be

Table 3 Determination of La(III) in synthetic samples

Sample	Composition, %	La(III) found,* %
La(III)	40.0	40.2 ± 0.6
Other REE	60.0	CL = 40.0 ± 0.4
La(III)	3.0	3.03 ± 0.07
Other REE	97.0	CL = 3.03 ± 0.06
La(III)	90.0	89.7 ± 0.6
Other REE	10.0	CL = 89.7 ± 0.05

*Mean ± standard deviation of σ determinations, and 95% confidence limits (CL _{$\alpha=0.05$})

used for the initial separation of the lanthanides from the matrix elements.

The method has a sensitivity equal to that of atomic-absorption spectrometry with electrothermal atomization and four orders of magnitude better than that of flame atomic-absorption spectrometry.

Table 3 shows some results for analysis of synthetic mixtures of lanthanides.

Acknowledgements—The authors wish to thank CONICET, UNSL and SECYT for financial support

REFERENCES

- 1 I. K. Guseinov and D. N. Askerov, *Azerb. Khim. Zh.*, 1983, 84
- 2 Sh. U. Islamov and F. Yu. Mirbabaeva, *Neorgan. Soedin. sintez i Svoistva Baku*, 1983, 85
- 3 D. Liu, R. Cai, X. Yu and W. Zeng, *Kexue Tongbao*, 1983, 78, 1207
- 4 M. Guo and Y. Bei, *Fenxi Huaxue*, 1983, 11, 775
- 5 P. K. Spitsyn, *Zavodsk. Lab.*, 1982, 48, No. 8, 16
- 6 X. Wang, *Huaxue Shiji*, 1982, 23, 362
- 7 B. Kuznik, *J. Inorg. Nucl. Chem.*, 1981, 43, 3363
- 8 J. Hernandez Mendez, B. Moreno Cordero and J. L. Perez Pavon, *Talanta*, 1988, 35, 293
- 9 L. Fernandez and R. Olsina, in the press
- 10 E. B. Sandell and H. Orishi, *Photometric Determination of Traces of Metals*, 4th Ed., Part I, Wiley, New York, 1978
- 11 S. Shibata, M. Furukawa, Y. Ishiguro and S. Sasaki, *Anal. Chim. Acta*, 1971, 55, 231
- 12 W. A. Noyes, *J. Am. Chem. Soc.*, 1933, 55, 3888
- 13 M. Nakamura, Y. Sakanashi, H. Chikushi, F. Kai, S. Sato, T. Sato and S. Uchikawa, *Talanta*, 1987, 34, 369
- 14 E. King, *Equilibrium Properties of Electrolyte Solutions*, Pergamon Press, Oxford, 1965
- 15 E. Pramauro, C. Minero and E. Pelizzetti, in *Ordered Media in Chemical Separations*, W. L. Hinze and D. W. Armstrong (eds.), p. 152, ACS, Washington, D.C., 1987
- 16 S. B. Savvin, *CRC Crit. Rev. Anal. Chem.*, 1979, 8, 69
- 17 J. C. Crock, F. E. Lichte, G. O. Riddle and C. L. Beech, *Talanta*, 1986, 33, 601

SPECTROPHOTOMETRIC DETERMINATION OF ANTIMONY WITH VANILLYLFLUORONE IN THE PRESENCE OF POLY(VINYL ALCOHOL)

ITSUO MORI,* YOSHIKAZU FUJITA, MINAKO TOYODA, KEIJI KATO,
KAZUMI FUJITA and YUJI OKAZAKI

Osaka University of Pharmaceutical Sciences, Matsubara-shi, Osaka 580, Japan

(Received 12 June 1989 Revised 26 January 1990 Accepted 30 August 1990)

Summary—Antimony in the range up to 2.5 $\mu\text{g/ml}$ in the final solution is determined spectrophotometrically with vanillylfluorone in the presence of poly(vinyl alcohol) in acidic media. The method is compared with that using *o*-hydroxyhydroquinonephthalein (Qnph). It is simple, rapid and sensitive, without need for heating or solvent extraction, and the apparent molar absorptivity (ϵ) is $5.0 \times 10^4 \text{ l mole}^{-1} \text{ cm}^{-1}$ at 545 nm, for the Qnph method ϵ is $2.8 \times 10^4 \text{ l mole}^{-1} \text{ cm}^{-1}$ at 520 nm. Tests with an artificial wastewater gave 99–103% recovery.

High-purity antimony is used in the manufacture of semiconductors, and the antimony levels in the urine of workers in the factories should be monitored.¹

Numerous xanthene and triphenylmethane dyes such as phenylfluorone and its derivatives,²⁻⁴ Gallein,^{5,6} Bromopyrogallol Red⁷ and Brilliant Green,^{8,9} have been used for spectrophotometric determination of antimony, and the effect of surfactants on some of these methods has been examined.^{5,7,10-12} However, the purity of commercial phenylfluorones is variable and their solutions in methanol are not always stable.

Vanillylfluorone (2,6,7-trihydroxy-9-vanillylxanthene-3-one, Vfl), is reported to be superior in ease of purification and stability in organic solvents.¹³

In this paper, the colour reaction of Vfl with antimony in the presence and absence of dispersion agents is compared with the corresponding reaction with *o*-hydroxyhydroquinonephthalein (Qnph), which is also recommended^{14,15} as superior to phenylfluorone. A simple, rapid and sensitive spectrophotometric method for the assay of antimony with Vfl in the presence of poly(vinyl alcohol), PVA, is proposed and compared with the corresponding method employing Qnph.

EXPERIMENTAL

Reagents

A $1.0 \times 10^{-3} \text{ M}$ Vfl solution in methanol was prepared, and a Qnph solution as described earlier.^{14,15} Antimony stock solution ($1.0 \times 10^{-2} \text{ M}$) was prepared by dissolving antimony metal (Mitsuwa Chemical Co., Ltd., 99.999% pure) in concentrated sulphuric acid, cooling and diluting with water to give 20% v/v sulphuric acid in the final solution. A $5.0 \times 10^{-4} \text{ M}$ antimony working solution was prepared by dilution of the stock solution with 20% v/v sulphuric acid.¹⁶ A 1.0% solution of PVA ($n = 500$, Kishida Chemical Co., Ltd.) in water was prepared, and 20% v/v sulphuric acid was used for adjustment of acidity. All reagents and materials were of analytical-reagent grade. Demineralized water was used throughout.

Spectrophotometric procedure

Pipette various volumes of standard antimony solution, to give up to 25 μg of antimony, into a series of 10-ml standard flasks. Add 1.5–3.0 ml of 20% v/v sulphuric acid, 2.0 ml of 1.0% PVA solution and 1.5 ml of $1.0 \times 10^{-3} \text{ M}$ Vfl solution. Mix thoroughly and dilute to the mark with water. After about 10 min measure the absorbance at 545 nm against a reagent blank prepared in the same way. Analyse sample solutions similarly.

A similar procedure can be used with Qnph, with measurement at 520 nm.

*Author for correspondence

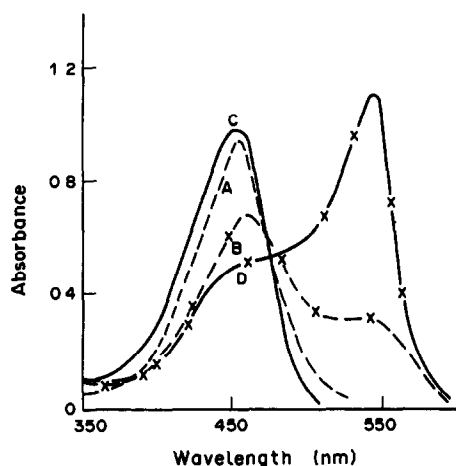


Fig 1 Absorption spectra of Qnph, Vfl, and their antimony complexes in the presence of PVA. Antimony $5.0 \times 10^{-5}M$, Qnph or Vfl $5.0 \times 10^{-5}M$, PVA 0.2%, reference water. A, Qnph solution, B, Vfl solution, C, Qnph-antimony solution, D, Vfl-antimony solution

RESULTS AND DISCUSSION

Of the reagents Pyrogallol Red, Bromopyrogallol Red, phenylfluorone derivatives, Gallein, Xylenol Orange and Vfl, the last was best in terms of sensitivity, stability and reproducibility. Though Vfl gave good colour development in the presence of a cationic surfactant such as hexadecylpyridinium chloride, the product was somewhat lacking in stability and gradually precipitated. However, the colour developed in the presence of PVA (as a dispersion or stabilizing agent) was more stable and reproducible than that in its absence. Figure 1 shows the absorption spectra of the Vfl-antimony and Qnph-antimony complexes and of Vfl and Qnph, and shows the greater sensitivity of the Vfl system.

Maximal and constant absorbance was obtained at 4–8% v/v final sulphuric acid concentration for the Vfl-antimony complex, and at pH 1.1–1.5 (obtained with 0.5–3.0 ml of 1.0% v/v sulphuric acid, for the Qnph-antimony complex.

A final PVA concentration of 0.1% was optimal, and PVA was superior to Triton X-100, Brij 35, poly(*N*-vinyl-2-pyrrolidone) and gelatine for the purpose. Maximal absorbance for a fixed amount of antimony was obtained with 1.4–3.0 ml of $1.0 \times 10^{-3}M$ Vfl, so final concentrations of $2.8 \times 10^{-4}M$ Vfl and 0.1% PVA were selected for use. Beer's law holds over the concentration range 0–2.5 $\mu\text{g/ml}$ antimony in the final solution with Vfl and 0–6.0 $\mu\text{g/ml}$ with Qnph. The apparent molar absorptivity was $5.0 \times 10^4 \text{ l.mole}^{-1}.\text{cm}^{-1}$ for Vfl, and $2.8 \times 10^4 \text{ l.mole}^{-1}.\text{cm}^{-1}$ for Qnph. The relative standard deviation was 0.5% for 1.05 $\mu\text{g/ml}$ antimony (5 replicates).

Interferences

Tin(IV) interfered seriously in the assay of antimony with Vfl, giving a positive error, and thorium and bismuth gave negative errors. Other cations tested, such as aluminium, cobalt(II), indium, tantalum, manganese(II), iron(III), did not interfere, nor did anions such as iodide, fluoride and cyanide, at 100-fold molar ratio to antimony, but thiosulphate caused interference.

Table 1 shows the tolerance levels for these ions. The Vfl method is less prone to interference than the Qnph method, and is more sensitive than the phenylfluorone, Bromopyrogallol Red, Gallein and Brilliant Green methods.³⁻⁹

Table 1. Effect of foreign ions on determination of 1.22 $\mu\text{g/ml}$ antimony

Ion	Added, $\mu\text{g/ml}$	Molar ratio (ion/antimony)	Absorbance at 520 nm	Tolerance ratio for Vfl method relative to Qnph method
—	—	—	0.500	
Sn(IV)	0.3	0.25	0.499	10
Bi(III)	20.9	10	0.488	10
Th(IV)	23.2	10	0.459	20
Al(III)	80.9	300	0.501	10
In(III)	34.3	300	0.505	20
Fe(III)	55.8	100	0.514	1000
Mn(II)	54.9	100	0.510	10
Cu(II)	63.6	100	0.490	2
Co(II)	176.8	300	0.500	5
Ni(II)	176.1	300	0.495	10
$\text{S}_2\text{O}_3^{2-}$	5.6	5	0.485	5
F^-	38.0	100	0.498	10
Tartrate	1200	1000	0.496	10
NTA	1711	1000	0.491	5

The reaction between Vfl and antimony can be prevented by masking the antimony with tartrate, but the reaction with tin(IV) is not affected, so Vfl can be used for the determination of tin in the presence of antimony. The composition of the Vfl-antimony complex in the presence of PVA was found to be 1:1 by the continuous-variation and molar-ratio methods. The molar ratio of Vfl to PVA was not investigated. The recovery of antimony from an artificial wastewater containing antimony, cobalt(II), aluminium, magnesium, iron(III), was found to be 99–103%.

REFERENCES

1. S Costantini, R Giordano, M Rizzica and F Benedetti, *Analyst*, 1985, **110**, 1355
2. O. G Koch, *Z Anal Chem.*, 1973, **265**, 29
3. V P Antonovich, E M. Nevskaya, E N Suvorova and V A Nazarenko, *Zh Analit. Khim*, 1978, **33**, 458
4. E Asmus and K Brandt, *Z Anal Chem*, 1965, **208**, 189
5. W Cai, Y Ouyang, L. He and J. Xu, *Fenxi Huaxue*, 1987, **15**, 828; *Anal. Abstr.*, 1988, **50**, 4B106
6. L. Naruskevicius, R Kazlauskas and J Skadauskas, *Liet TSR Aukst. Mokyklu Mokslo Darb.*, *Chem. Technol.*, 1979, **21**, 13, *Anal. Abstr.*, 1980, **39**, 4B115
7. D H Christopher and T S West, *Talanta*, 1966, **13**, 507
8. L A. Soldatova, Z G Kilina and G A. Kataev, *Zh Analit. Khim*, 1964, **19**, 1267
9. A G Fogg, J. Jillings, D. R Marriott and D T Burns, *Analyst*, 1969, **94**, 768.
10. V. P Antonovich, E N. Suvorova and E L. Shelikhina, *Zh. Analit. Khim.*, 1982, **37**, 429
11. H. Li, Q Pan, Q Rong and D. Tan, *Ceshi Tongao Fenxi*, 1986, **5**, No 6, 6; *Chem. Abstr*, 1987, **107**, 69819u.
12. X Wu and H. Ding, *Fenxi Shiyanshi*, 1986, **5**, No. 11, 34; *Anal. Abstr.*, 1987, **49**, 10B132.
13. W. Lin and M. Chen, *Fenxi Huasue*, 1988, **16**, 202; *Chem. Abstr.*, 1989, **110**, 87560u
14. I. Mori, Y Fujita, Y. Kamada and T. Enoki, *Bunseki Kagaku*, 1976, **25**, 388.
15. I. Mori, Y. Fujita, K. Fujita, A. Usami, H. Kawabe, Y Koshuyama and T. Tanaka, *Bull. Chem Soc. Japan*, 1986, **59**, 1623.
16. I Mori, *Yakugaku Zasshi*, 1969, **89**, 475

DETERMINATION OF SOME SULPHUR COMPOUNDS WITH *N*-BROMOIMIDES

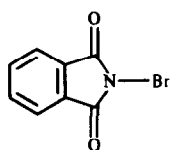
C MOHANA DAS

Department of Chemistry, St Joseph's College, Bangalore 560001, India

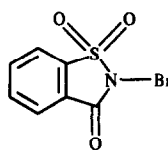
(Received 12 January 1990 Revised 1 August 1990 Accepted 7 September 1990)

Summary—Two stable oxidants, *N*-bromophthalimide and *N*-bromosaccharin are proposed as reagents for the visual and potentiometric titrimetric of thioureas, isothiocyanates, xanthates, dithiocarbamates, thiols, sulphur, thiosulphate, thiocyanate and thiocarbonate. The results are precise within 0.1–0.3%.

The *N*-haloimides have evoked interest as sources of halonium cations, hypohalite species and imide anions, and some have been used as redox titrants,^{1–11} but their instability is a disadvantage. Recently *N*-bromophthalimide and *N*-bromosaccharin (abbreviated to NBP and NBSA) have been developed as oxidimetric titrants and are reported to be more stable than most of the related *N*-halo compounds.^{7,11–13} These two compounds have been used for the determination of a wide range of compounds,^{14–18} but only a few sulphur compounds. This paper extends the range of sulphur compounds examined.

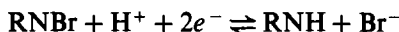


N-Bromophthalimide
(NBP)



N-Bromosaccharin
(NBSA)

The half-cell for these oxidants (denoted by RNBr) is:



EXPERIMENTAL

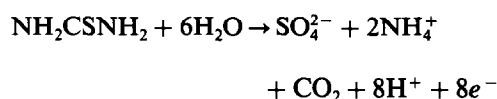
Reagents

NBP and NBSA were prepared by bromination of phthalimide and saccharin, respectively, as reported earlier.¹⁵ They are fairly soluble in glacial acetic acid and the stock solutions were prepared by dissolving 11.3 g of NBP (or 13.1 g of NBSA) in 1 litre of anhydrous acetic acid and were kept in amber bottles. The solutions were standardized iodimetrically as for dichloramine-T.¹

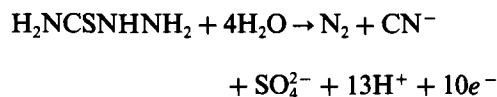
Xanthates were prepared by reaction of the corresponding sodium alkoxides with carbon disulphide. The products were dissolved in acetone, the solutions were filtered, and the compounds precipitated by addition of petroleum ether (b.p. 60–80°).¹⁹ Sodium diethyldithiocarbamate was a commercial product and the other dithiocarbamates were prepared by the usual methods.^{20–22} Amines, commercial grade, were distilled before use. All other chemicals used were of reagent grade. The sulphur compounds were standardized by established methods.

Procedure for thioureas

Thioureas are quantitatively oxidized to sulphate:



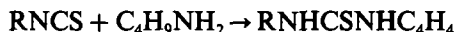
Thiosemicarbazide reacts as follows



A known volume of the test solution is taken in a 100-ml beaker and 1 g of sodium acetate and 2 or 3 drops of Quinoline Yellow indicator are added. If a sample is dissolved in an organic solvent, enough water is added to make the initial organic solvent concentration 50–60% v/v. The sample is titrated with 0.025*M* oxidant until the yellow colour disappears. For potentiometric titrations the apparatus described earlier³ was used.

Procedure for isothiocyanates

Organic isothiocyanates are quantitatively converted into thioureas with n-butylamine in dimethylformamide at room temperature:



A known volume of a solution of organic isothiocyanate in dimethylformamide is taken in a 100-ml beaker and 3 ml of n-butylamine are added. The solution is diluted to 10 ml with dimethylformamide and after 15 min for completion of the reaction, is titrated in the same way as for thioureas.

Procedure for dithiocarbamates and xanthates

In acetonitrile medium dithiocarbamates and xanthates are quantitatively oxidized according to:



A known volume of the sample solution is dissolved in 20 ml of acetonitrile. About 30 ml of methanol and 50 mg of potassium iodide are added and the mixture is titrated until the colour of iodine appears. The concentration of the organic solvent should be 60–70% v/v.

Procedure for thiols and thiosulphate

Thiols and thiosulphates are quantitatively oxidized to the disulphides and tetrathionate, respectively, according to:



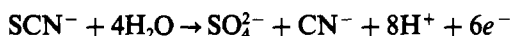
A known volume of sample solution is taken in a 100-ml beaker and diluted with water to make the concentration of organic solvent < 50% v/v; about 50 mg of potassium iodide is added and the analyte is titrated. For visual titrations, the appearance of a pale yellow colour is taken as the end-point

Procedure for elemental sulphur

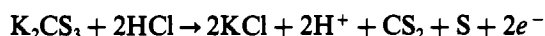
Elemental sulphur (3–20 mg) is first converted into thiosulphate by dissolving it completely in chloroform or n-heptane (3–5 ml), and adding 5 ml of 1M sodium sulphite. Ethanol is added in small quantities, with shaking of the mixture, until a homogeneous liquid is obtained. The thiosulphate produced is titrated as above, after the addition of 10 ml of 40% formaldehyde solution to mask the excess of sulphite.

Procedure for thiocyanate

An aliquot of sample solution is taken in a beaker, 5 ml of concentrated hydrochloric acid are added and the mixture is titrated. For visual titration 2 or 3 drops of Methyl Orange indicator are added; the indicator is decolorized at the end-point. Oxidation takes place according to:

*Procedure for thiocarbonate*

Thiocarbonate is oxidized to sulphur in the presence of hydrochloric acid and iodide:



A known volume of sample solution is diluted with acetic acid (75% v/v) and 10 ml of 10% v/v hydrochloric acid are added along with 50 mg of potassium iodide. The solution is titrated to appearance of a pale yellow colour.

Procedure for sulphite

Sulphite is oxidized to sulphate according to the equation:



Excess of oxidant is added to a sample of the reductant solution and the surplus is determined by titration with thiosulphate after the addition of 10 ml of 10% potassium iodide solution.

RESULTS AND DISCUSSION

Results of the determinations are given in Table 1. The coefficients of variation show all the methods are precise, but problems arise with certain compounds. In the case of phenyl thiourea, the results were high (but so was the result obtained by the reference method). Allyl thiourea does not react stoichiometrically. Dithiocarbamates and xanthates react with NBP and NBSA in aqueous organic medium, but the reactions are sluggish and the stoichiometry variable. If iodide is present, however, the reaction is rapid and stoichiometric. The apparently low value obtained for diethyldithiocarbamate is presumably due to low purity of the starting material, since the comparison method gave a correspondingly low value. The results for thiols show that the use of aqueous organic media gives sufficiently accurate results, but 3-mercaptopropionic and mercaptosuccinic acid are oxidized beyond the disulphide stage in an unaccountable fashion, and the method is

Table 1 Determination of some sulphur compounds with *N*-bromocompounds

Compound	Range studied, mmole	Recovery,*		Mean recovery by comparison method,† %
		<i>N</i> -Bromophthalimide	<i>N</i> -Bromosaccharin	
Thiourea	0.13–0.26	99.9 ± 0.2	99.7 ± 0.3	99.9 ^a
Thiosemicarbazide	0.12–0.25	99.7 ± 0.3	99.8 ± 0.2	99.9 ^a
<i>n</i> -Amyl thiourea	0.28–0.55	99.5 ± 0.3	100.2 ± 0.2	99.8 ^b
<i>n</i> -Butyl thiourea	0.24–0.48	99.2 ± 0.2	99.3 ± 0.2	99.1 ^c
<i>m</i> -Bromophenyl thiourea	0.29–0.57	96.5 ± 0.3	97.2 ± 0.3	97.0 ^d
<i>m</i> -Chlorophenyl thiourea	0.32–0.64	101.8 ± 0.2	102.1 ± 0.1	101.6 ^e
Methyl thiourea	0.19–0.35	99.2 ± 0.2	98.7 ± 0.2	99.1 ^f
Phenyl thiourea	0.24–0.49	104.1 ± 0.2	105.1 ± 0.3	104.3 ^f
Methyl isothiocyanate	0.18–0.37	100.1 ± 0.2	100.2 ± 0.1	99.8 ^g
Ethyl isothiocyanate	0.14–0.28	100.0 ± 0.2	100.1 ± 0.2	99.9 ^g
Propyl isothiocyanate	0.24–0.48	100.2 ± 0.2	100.3 ± 0.2	100.2 ^g
Isopropyl isothiocyanate	0.22–0.41	100.1 ± 0.3	100.2 ± 0.1	101.1 ^g
<i>n</i> -Butyl isothiocyanate	0.21–0.42	99.2 ± 0.2	99.4 ± 0.1	99.8 ^g
Isobutyl isothiocyanate	0.42–0.81	99.6 ± 0.2	99.8 ± 0.1	99.9 ^g
Ethyl xanthate	0.24–0.48	90.2 ± 0.1	90.4 ± 0.2	90.6 ^h
1-Propyl xanthate	0.12–0.21	98.2 ± 0.1	98.4 ± 0.2	98.5 ^h
1-Butyl xanthate	0.28–0.45	95.8 ± 0.3	95.2 ± 0.1	95.5 ^h
Isoamyl xanthate	0.11–0.24	96.2 ± 0.3	96.2 ± 0.2	96.5 ^h
Diethylthiocarbamate	0.22–0.41	78.0 ± 0.2	77.9 ± 0.2	78.2 ⁱ
Di- <i>n</i> -butyldithiocarbamate	0.12–0.24	91.2 ± 0.3	92.2 ± 0.2	91.8 ⁱ
Diamyldithiocarbamate	0.13–0.24	92.1 ± 0.3	92.3 ± 0.2	92.5 ⁱ
Di-isopropyldithiocarbamate	0.15–0.30	88.4 ± 0.2	88.3 ± 0.2	88.0 ⁱ
Ethane thiol	0.16–0.32	100.1 ± 0.1	99.8 ± 0.1	100.4 ^j
Glutathione	0.18–0.36	99.2 ± 0.2	98.9 ± 0.2	99.1 ^k
<i>p</i> -Toluene thiol	0.28–0.56	98.4 ± 0.2	98.2 ± 0.2	98.5 ^l
1-Propane thiol	0.33–0.65	95.2 ± 0.2	95.6 ± 0.2	95.2 ^m
1-Butane thiol	0.24–0.47	90.3 ± 0.3	90.8 ± 0.3	90.5 ⁿ
2-Butane thiol	0.22–0.44	97.5 ± 0.3	97.2 ± 0.3	97.8 ^m
Sulphite	0.21–0.42	99.9 ± 0.1	99.9 ± 0.1	100.0 ^o
Sulphur	0.30–0.40	99.2 ± 0.3	99.7 ± 0.3	99.0 ^o
Thiosulphate	0.92–1.76	100.0 ± 0.2	99.9 ± 0.1	101.1 ^p
Thiocyanate	0.32–0.64	96.7 ± 0.2	96.2 ± 0.2	97.1 ^q
Thiocarbonate	0.88–1.76	92.8 ± 0.2	92.2 ± 0.2	92.0 ^q

*Average ± standard deviation of ten replicates

†Average of duplicates: the methods used were ^aiodimetry,²³ ^biodine trichloride,²⁴ ^chypiodite,²³ ^dcerimetry,²⁵ ^enon-aqueous cerimetry,²⁶ ^fbromimetry,²⁷ ^gelemental analysis for sulphur, ^hAg⁺ titration,²⁸ ⁱiodimetry,²⁹ ^jiodimetry,³⁰ ^kiodimetry,³¹ ^lCu²⁺ titration,³² ^malkalimetry,³³ ⁿacetylation,³⁴ ^ohydrogen sulphide,³⁵ ^pdichromate titration,³⁶ ^q*N*-bromohydantoin³⁷

not recommended for these compounds. Thio-sulphate reacts quantitatively with NBP or NBSA only in presence of iodide. Elemental sulphur can be determined after conversion into thiosulphate. Thiocyanate can be determined only in the presence of hydrochloric acid, and thiocarbonate is oxidized quantitatively in the presence of hydrochloric acid and iodide. For sulphite no auxiliary agent is needed, but in the direct titration, the results may be low owing to aerial oxidation, so a back-titration procedure is recommended. As is generally the case for oxidants, the selectivity of the methods is largely governed by the redox potentials of the analytes and there is typical interference from Fe(II), As(III), Sb(III), ascorbic acid, hydrazine, semicarbazide and isoniazid.

Acknowledgements—The author is thankful to Professors C G R Nair and P Indrasenan for their helpful suggestions

REFERENCES

- 1 T J Jacob and C G R Nair, *Talanta*, 1972, **19**, 347
- 2 J M. Bechawat, N S Ramegowda, A. K. Kovi, C. K. Narang and N K Mathur, *Indian J Chem*, 1973, **11**, 614
- 3 C. G R Nair and P Indrasenan, *Talanta*, 1976, **23**, 239
- 4 R Prakash and I C Shukla, *Proc. Indian Natl. Sci. Acad.*, 1979, **45A**, 383
- 5 D S Mahadevappa and M. S Ahmed, *Talanta*, 1979, **26**, 590
- 6 H. S. Y Rajan, D S Mahadevappa and Rangaswamy, *ibid*, 1980, **27**, 52.
- 7 A Abou Ouf, M I Walash, M. El-Kerdaway and S El-Ashry, *J. Drug Res*, 1980, **12**, 77.
- 8 M P Radhamma and P Indrasenan, *Talanta*, 1983, **30**, 49.
- 9 *Idem*, *Indian J. Chem*, 1983, **22A**, 729.
- 10 N. Jayashree and P. Indrasenan, *Talanta*, 1985, **32**, 1067
- 11 R. Prakash and I. C Shukla, *Proc. Indian. Natl. Sci. Acad.*, 1979, **45A**, 383

- 12 C M. Das and P. Indrasenan, *Indian J Chem*, 1984, **23A**, 869.
- 13 *Idem, ibid*, 1987, **25A**, 55
- 14 *Idem, ibid.*, 1987, **26A**, 717
- 15 *Idem, Int J Food Sci Technol*, 1987, **22**, 339
- 16 A Abou Ouf, M. I. Walash and F B. Salem, *Analyst*, 1981, **106**, 949
- 17 K G Kumar, C M Das and P Indrasenan, *Talanta*, 1988, **35**, 651.
- 18 S. C Shukla, V N Pathak and I C Shukla, *Indian J Pharm Sci*, 1985, **47**, 204.
- 19 A. I Vogel, *A Text-book of Practical Organic Chemistry*, p 499 ELBS, London, 1968
- 20 H L Klopping and G J M Vanderkerk, *Rec Trav Chim*, 1951, **70**, 917
- 21 J Issoire and L Musso, *Mem. Poudres*, 1960, **42**, 427
- 22 J P. Fackler, Jr and D C Ouvanis, *J Am Chem Soc*, 1966, **88**, 3913
- 23 I M Kolthoff, R Belcher, V A. Stenger and G Matsuyama, *Volumetric Analysis*, Vol III p 387 Interscience, New York, 1957
- 24 B Singh B C Verma and M S. Saran, *J Indian Chem Soc*, 1962, **39**, 490
- 25 B Singh and B. C Verma, *ibid*, 1963, **40**, 39
- 26 B C. Verma and S Kumar, *Talanta*, 1973, **20**, 916
- 27 P C Gupta, *Analyst*, 1963, **83**, 986
- 28 R F Makens, *J Am Chem Soc.*, 1935, **57**, 405
- 29 A L Linch, *Anal Chem*, 1951, **23**, 293
- 30 J W Kimball, R L Kramer and B E Reid, *J Am Chem. Soc.*, 1921, **43**, 1199
31. J W Patterson and A Lazarow, *Methods of Biochemical Analysis*, Vol II, pp 63, 267 Interscience, New York, 1961
- 32 G R Bond, *Ind Eng Chem., Anal. Ed*, 1933, **5**, 257
- 33 J. S. Fritz and N M Lisiki, *Anal Chem*, 1951, **23**, 588
- 34 G H Schenk and J S Fritz, *ibid*, 1960, **32**, 987
- 35 A R V Murthy, V R Narayan and M R A Rao, *Analyst*, 1956, **81**, 373
- 36 A I. Vogel, *A Text Book of Quantitative Inorganic Analysis*, 3rd Ed, p 350 Longmans, London, 1969
- 37 M P Radhamma, *Ph D Thesis*, University of Kerala, India, 1983

BOOK REVIEWS

Thermal Analysis: Proceedings of the Fourth European Symposium on Thermal Analysis and Calorimetry, Jena, GDR, 23-28 August 1987 (2 volumes). D SCHULTZE, (editor), Wiley, Chichester, and Akadémiai Kiadó, Budapest, 1988. Pages 1297 \$60 00

These two volumes of the Proceedings of ESTAC 4 contain, bound together in hard covers, the material in the four issues of Vol 33 of the *Journal of Thermal Analysis* devoted to the lectures and papers presented at the symposium. As such, it is in a convenient form for libraries, and others, who may wish to keep Conference Proceedings together and separate from normal journal issues or who do not receive the relevant journal but wish to have a complete set of Proceedings. In addition to reproducing plenary (14) and award (2) lectures, the volumes have sections devoted to papers on theory (17), instrumentation (16), earth sciences and materials (8), solid-state reactions (18), inorganic chemistry, glass, ceramics (55), pharmacy, biology, medicine (34) and final section devoted to assessments (6) of some of the advances recorded. The texts of the plenary and award lectures are given in full and the lengths of the other papers range from 4 to 8 pages, 6 being the most common. All the papers are in English and, being typeset rather than the more common offset from typescript, are very easy to read: the diagrams, too, are very clearly reproduced. However, the paper used in some parts of the volumes is of rather poor quality, with the result that some of the half-tones are not as clear as they might be. An unusual feature is that each plenary lecture is accompanied by a photograph of the lecturer, taken during its delivery—an innovation that, to this reviewer, makes the volumes much less formal and conveys the spirit of friendliness always found among thermal analysts and calorimetrists. It would be invidious to select any of the papers for comment here: suffice it to say that many new ideas and novel approaches are proposed, although, as is usual at conferences, not all papers are of the same scientific standard. Having already been published as parts of a journal, abstracts of all the papers have already appeared in the relevant abstract journals. The quality of the English expression is generally high throughout, indicating careful editing. Moreover, the two volumes have very useful author and subject indexes. Disappointingly, however, the title of the books appears nowhere on the cloth board covers, even on the spine, with the result that once the dust covers are worn or removed, the volumes will be incognizable. Despite this, these two very useful volumes are likely to appear on the bookshelves of many more thermal analysts and calorimetrists than the original parts of the journal, especially so in view of the very moderate cost.

R C MACKENZIE

Thin-Layer Chromatography—Reagents and Detection Methods, Volume 1a: H JORK, W FUNK, W FISCHER and H WIMMER, VCH, Weinheim, 1990. Pages xv + 464. DM148 00

This is an ideal laboratory handbook of reagents and detection methods currently available for use in thin-layer chromatography (TLC). In the first part of the book the theory and methodology of spectrophotometric and, in particular, spectrofluorimetric methods of detection and their use in both qualitative and quantitative analysis are given. The presentation here, which is also characteristic of the rest of the book is clear, simple, logical and easy to follow and understand. *In situ* Pre-chromatographic derivatization techniques such as reactions involving oxidation, reduction, halogenation and danylation are summarized in tabular form. This has enabled the authors to put a large number of illustrative examples into a few pages. Each example quoted is referenced and a brief description of the method, reagent and end-products is given. The judicious selection of examples means that the wide range of applications covered should cater for all interests. In the section on post-chromatographic detection techniques attention is rightly focused on the advantages and disadvantages of the various ways of processing the chromatograms and on the possible errors involved. The concluding section on documentation is essential reading for those involved with, in particular, quality control.

The second part of the book gives in alphabetical order a list of the most commonly used chemical detecting reagents. For each reagent its preparation, the compounds with which it reacts, the reaction, and the method of use are all given. Particularly commendable is the fact that the authors have tested every procedure in their laboratories and have included the results of their tests in full. A good index means that it is relatively easy to find the appropriate reagent for a particular compound or class of compound.

All chapters in both parts of the book are very well referenced. This very up-to-date compact book contains a wealth of readily accessible information which will be of value to any experimentalist involved in TLC.

R R MOODY

Chemical Sensors and Microinstrumentation: R W MURRAY, R E DESSY, W R HEINEMAN, J JANATA and W R SEITZ (editors), ACS, Washington, DC, 1990. Pages xii + 410. \$89 95

In considering a book such as this, that is, one devoted to a rapidly advancing field and compiled from the reports of work in progress submitted at a Symposium, (the 196th Meeting of the American Chemical Society, Los Angeles, California,

BOOK REVIEWS

Thermal Analysis: Proceedings of the Fourth European Symposium on Thermal Analysis and Calorimetry, Jena, GDR, 23-28 August 1987 (2 volumes). D SCHULTZE, (editor), Wiley, Chichester, and Akadémiai Kiadó, Budapest, 1988. Pages 1297 \$60 00

These two volumes of the Proceedings of ESTAC 4 contain, bound together in hard covers, the material in the four issues of Vol 33 of the *Journal of Thermal Analysis* devoted to the lectures and papers presented at the symposium. As such, it is in a convenient form for libraries, and others, who may wish to keep Conference Proceedings together and separate from normal journal issues or who do not receive the relevant journal but wish to have a complete set of Proceedings. In addition to reproducing plenary (14) and award (2) lectures, the volumes have sections devoted to papers on theory (17), instrumentation (16), earth sciences and materials (8), solid-state reactions (18), inorganic chemistry, glass, ceramics (55), pharmacy, biology, medicine (34) and final section devoted to assessments (6) of some of the advances recorded. The texts of the plenary and award lectures are given in full and the lengths of the other papers range from 4 to 8 pages, 6 being the most common. All the papers are in English and, being typeset rather than the more common offset from typescript, are very easy to read: the diagrams, too, are very clearly reproduced. However, the paper used in some parts of the volumes is of rather poor quality, with the result that some of the half-tones are not as clear as they might be. An unusual feature is that each plenary lecture is accompanied by a photograph of the lecturer, taken during its delivery—an innovation that, to this reviewer, makes the volumes much less formal and conveys the spirit of friendliness always found among thermal analysts and calorimetrists. It would be invidious to select any of the papers for comment here: suffice it to say that many new ideas and novel approaches are proposed, although, as is usual at conferences, not all papers are of the same scientific standard. Having already been published as parts of a journal, abstracts of all the papers have already appeared in the relevant abstract journals. The quality of the English expression is generally high throughout, indicating careful editing. Moreover, the two volumes have very useful author and subject indexes. Disappointingly, however, the title of the books appears nowhere on the cloth board covers, even on the spine, with the result that once the dust covers are worn or removed, the volumes will be incognizable. Despite this, these two very useful volumes are likely to appear on the bookshelves of many more thermal analysts and calorimetrists than the original parts of the journal, especially so in view of the very moderate cost.

R C MACKENZIE

Thin-Layer Chromatography—Reagents and Detection Methods, Volume 1a: H JORK, W FUNK, W FISCHER and H WIMMER, VCH, Weinheim, 1990. Pages xv + 464. DM148 00

This is an ideal laboratory handbook of reagents and detection methods currently available for use in thin-layer chromatography (TLC). In the first part of the book the theory and methodology of spectrophotometric and, in particular, spectrofluorimetric methods of detection and their use in both qualitative and quantitative analysis are given. The presentation here, which is also characteristic of the rest of the book, is clear, simple, logical and easy to follow and understand. *In situ* Pre-chromatographic derivatization techniques such as reactions involving oxidation, reduction, halogenation and danylation are summarized in tabular form. This has enabled the authors to put a large number of illustrative examples into a few pages. Each example quoted is referenced and a brief description of the method, reagent and end-products is given. The judicious selection of examples means that the wide range of applications covered should cater for all interests. In the section on post-chromatographic detection techniques attention is rightly focused on the advantages and disadvantages of the various ways of processing the chromatograms and on the possible errors involved. The concluding section on documentation is essential reading for those involved with, in particular, quality control.

The second part of the book gives in alphabetical order a list of the most commonly used chemical detecting reagents. For each reagent its preparation, the compounds with which it reacts, the reaction, and the method of use are all given. Particularly commendable is the fact that the authors have tested every procedure in their laboratories and have included the results of their tests in full. A good index means that it is relatively easy to find the appropriate reagent for a particular compound or class of compound.

All chapters in both parts of the book are very well referenced. This very up-to-date compact book contains a wealth of readily accessible information which will be of value to any experimentalist involved in TLC.

R R MOODY

Chemical Sensors and Microinstrumentation: R W MURRAY, R E DESSY, W R HEINEMAN, J JANATA and W R SEITZ (editors), ACS, Washington, DC, 1990. Pages xii + 410. \$89 95

In considering a book such as this, that is, one devoted to a rapidly advancing field and compiled from the reports of work in progress submitted at a Symposium, (the 196th Meeting of the American Chemical Society, Los Angeles, California,

1988) it is salutary to refer back to accounts of earlier Symposia. If the International Meeting on Chemical Sensors held in Fukuoka, Japan, 1983 is selected for this purpose it can be seen that most of the fundamental concepts were well known at that time, but there have been considerable advances in the technology of construction and instrumentation. Indeed, the papers collected in the present work may be said to be based on three well established techniques, those based on electrochemical measurements, those utilizing piezoelectric crystal oscillators and those using conventional spectrophotometric techniques combined with the use of optical fibres. The most significant developments reported are concerned with the microminiaturization of probes, and so successful have been the attempts to produce microelectrodes that spatial resolutions of the order of $1\ \mu\text{m}$ have been achieved. With such equipment it has been possible to study the concentration gradients in solutions such as those encountered in flow analysis. A further advance has been in the combination of biochemical systems, such as enzymes and polymers, with electrodes so as to produce electrical signals from biologically active molecules, and there have been similar developments in probes based on optical signals. Probably the most interesting research dealt with in the present volume is the modification of piezoelectric devices so as to optimize their response to a particular chemical vapour by stimulating the production of surface acoustic waves. The value of such devices in environmental monitoring is self-evident, one paper reports such an application and it is to be expected that there will be many more. The book is recommended to all practising analytical chemists who may find their work in the future increasingly dependent on the use of chemical sensors.

J. R. MAJER

Instrumental Effects in Homodyne Electron Paramagnetic Resonance Spectrometers: R. CZOCH and A. FRANCIK, Horwood, Chichester, 1989. Pages 395 £45.00

Several factors are contributing to a growth in the usage of EPR spectrometers. These include diagnosis of certain cancers, characterization and quantification of irradiation dosages in foods, and the development of EPR imaging. The appearance of a new book on practical aspects of the technique will therefore arouse considerable interest. Most commercial EPR spectrometers are of the homodyne type and this book is devoted to an examination of the instrumental errors and distortions which can affect the resonance signals. The first three chapters introduce the basic theory and technique and catalogue the main types of random and systematic instrumental effects. Chapters 4–8 deal in detail with particular effects such as those due to saturation and modulation. The heart of the book is a particularly thorough treatment of adsorption and dispersion including sample control distortions from the AFC system. Microwave detection errors, e.g., delay effects, errors of digital processing and truncation errors, background effects and inhomogeneity are also analysed in these chapters. The final part of the book in chapters 9 and 10 describes methods of optimizing instrumental variables and testing the resolution, sensitivity and reproducibility of spectra.

The book has been well translated and provides access to the literature from Russian and Polish sources. It contains an interesting description of an EPR spectrometer produced commercially by the Institute of Telecommunication and Acoustics of the Technical University of Wrocław, which few in the West will have had the opportunity to see. Some of the facts mentioned in this book are quite enlightening. For example, the wings of a Lorentzian line are truncated by random noise and this can lead to errors in the double integral as great as 19% even for S/N ratios of 250! A useful table for the estimation and correction of this error is given.

The authors present detailed mathematical analysis of many of the distortions but, sadly for the non-specialist, few references to computer algorithms are given. This book will appeal to technically minded EPR exponents and should be a useful reference text for those engaged in quantitative analysis by EPR.

J. C. WALTON

Data Analysis in the Chemical Industry: Volume 1, Basic Techniques: R. CAULCUTT, Horwood, Chichester, 1989. Pages 231 £45.00

This book is the first of a series based on the author's manuals for his short courses on applied statistics for industry. However, it has been redesigned as a self-study text, and the author states that he believes many people will learn more by studying the book than they would by attending a four- or five-day course.

The book offers a completely practical approach to statistics, with the use of diagrams and worked examples to explain the aims of the tests described. It is ideal for a chemist who feels intimidated by the equations in a normal statistical text.

The topics covered included quality assessment (mean, standard deviation, confidence limits, confidence interval, tolerance limits), comparisons (combined standard deviation, confidence interval for the difference between two population means), regression, significance testing (t -tests, normal probability plots, outliers, Dixon's test, Wilcoxon's matched pairs test, non-parametric tests), more significance tests and confidence intervals (Wilcoxon's rank sum test, Tukey's quick test, chi-squared test, one-sided and two-sided significance tests), and detecting sudden changes (cusum analysis). All the necessary statistical tests are included.

I recommend this book as an excellent introduction to the practical application of statistics in the chemical industry, and I look forward to the rest of the Series.

MARY MASSON

1988) it is salutary to refer back to accounts of earlier Symposia. If the International Meeting on Chemical Sensors held in Fukuoka, Japan, 1983 is selected for this purpose it can be seen that most of the fundamental concepts were well known at that time, but there have been considerable advances in the technology of construction and instrumentation. Indeed, the papers collected in the present work may be said to be based on three well established techniques, those based on electrochemical measurements, those utilizing piezoelectric crystal oscillators and those using conventional spectrophotometric techniques combined with the use of optical fibres. The most significant developments reported are concerned with the microminiaturization of probes, and so successful have been the attempts to produce microelectrodes that spatial resolutions of the order of $1\ \mu\text{m}$ have been achieved. With such equipment it has been possible to study the concentration gradients in solutions such as those encountered in flow analysis. A further advance has been in the combination of biochemical systems, such as enzymes and polymers, with electrodes so as to produce electrical signals from biologically active molecules, and there have been similar developments in probes based on optical signals. Probably the most interesting research dealt with in the present volume is the modification of piezoelectric devices so as to optimize their response to a particular chemical vapour by stimulating the production of surface acoustic waves. The value of such devices in environmental monitoring is self-evident, one paper reports such an application and it is to be expected that there will be many more. The book is recommended to all practising analytical chemists who may find their work in the future increasingly dependent on the use of chemical sensors.

J. R. MAJER

Instrumental Effects in Homodyne Electron Paramagnetic Resonance Spectrometers: R. CZOCH and A. FRANCIK, Horwood, Chichester, 1989. Pages 395 £45.00

Several factors are contributing to a growth in the usage of EPR spectrometers. These include diagnosis of certain cancers, characterization and quantification of irradiation dosages in foods, and the development of EPR imaging. The appearance of a new book on practical aspects of the technique will therefore arouse considerable interest. Most commercial EPR spectrometers are of the homodyne type and this book is devoted to an examination of the instrumental errors and distortions which can affect the resonance signals. The first three chapters introduce the basic theory and technique and catalogue the main types of random and systematic instrumental effects. Chapters 4–8 deal in detail with particular effects such as those due to saturation and modulation. The heart of the book is a particularly thorough treatment of adsorption and dispersion including sample control distortions from the AFC system. Microwave detection errors, e.g., delay effects, errors of digital processing and truncation errors, background effects and inhomogeneity are also analysed in these chapters. The final part of the book in chapters 9 and 10 describes methods of optimizing instrumental variables and testing the resolution, sensitivity and reproducibility of spectra.

The book has been well translated and provides access to the literature from Russian and Polish sources. It contains an interesting description of an EPR spectrometer produced commercially by the Institute of Telecommunication and Acoustics of the Technical University of Wrocław, which few in the West will have had the opportunity to see. Some of the facts mentioned in this book are quite enlightening. For example, the wings of a Lorentzian line are truncated by random noise and this can lead to errors in the double integral as great as 19% even for S/N ratios of 250! A useful table for the estimation and correction of this error is given.

The authors present detailed mathematical analysis of many of the distortions but, sadly for the non-specialist, few references to computer algorithms are given. This book will appeal to technically minded EPR exponents and should be a useful reference text for those engaged in quantitative analysis by EPR.

J. C. WALTON

Data Analysis in the Chemical Industry: Volume 1, Basic Techniques: R. CAULCUTT, Horwood, Chichester, 1989. Pages 231 £45.00

This book is the first of a series based on the author's manuals for his short courses on applied statistics for industry. However, it has been redesigned as a self-study text, and the author states that he believes many people will learn more by studying the book than they would by attending a four- or five-day course.

The book offers a completely practical approach to statistics, with the use of diagrams and worked examples to explain the aims of the tests described. It is ideal for a chemist who feels intimidated by the equations in a normal statistical text.

The topics covered included quality assessment (mean, standard deviation, confidence limits, confidence interval, tolerance limits), comparisons (combined standard deviation, confidence interval for the difference between two population means), regression, significance testing (t -tests, normal probability plots, outliers, Dixon's test, Wilcoxon's matched pairs test, non-parametric tests), more significance tests and confidence intervals (Wilcoxon's rank sum test, Tukey's quick test, chi-squared test, one-sided and two-sided significance tests), and detecting sudden changes (cusum analysis). All the necessary statistical tests are included.

I recommend this book as an excellent introduction to the practical application of statistics in the chemical industry, and I look forward to the rest of the Series.

MARY MASSON

Ion-Selective Electrodes, 5: E PUNGOR, (editor), Pergamon Press, Oxford, 1989. Pages xv + 675. £85 00, \$135 00

This volume includes the invited lectures, the papers, and an account of all the (sometimes very lively) discussions from the Fifth Symposium on Ion-Selective Electrodes held at Matrafured, Hungary, 9–13 October 1988. The papers, which cover a very wide range of interesting topics, are reproduced from camera-ready copy. The author list includes most of the well known names in the field of ion-selective electrodes. Also included are a tribute to Professor Ernő Pungor, on the occasion of his 65th birthday, by H. Malissa, and some Reflections of the History of Analytical Chemistry in Hungary, by the Historian of Analytical Chemistry, F Szabadváry.

MARY MASSON

Spectrometric Titrations: J POLSTER and H LACHMANN, VCH, Weinheim, Germany, 1989. Pages xvi + 433. DM196.0, £66 00

The title "Spectrometric Titrations" conveyed the wrong message to me about the subject matter of this monograph, however, the sub-title "Analysis of Chemical Equilibria" clarifies matters. The authors choose to distinguish between a photometric titration, in which a spectrophotometer is used to locate the end-point of what we would normally consider to be a titration, and a spectrophotometric titration, which aims to investigate, for the example, the pH-dependence of an absorption spectrum, in order to obtain information about the number and type of dissociable groups in a substance, or establish the corresponding dissociation constants. The authors admit that their use of the word titration is inconsistent with the IUPAC definition, and give their own definition as "controlled displacement of a chemical equilibrium by means of a titration reagent (R), the titrant". My personal opinion is that analytical chemists would be happier without re-definition of well accepted terms such as "titration".

The actual subject matter of the book is a very mathematical treatment of the analysis of the various chemical equilibria that can be studied by making spectrophotometric measurements of a solution at each step in a "titration". The material is nicely presented, with many clear diagrams, aided sometimes by the use of a second colour. There are three main parts, a brief introduction on "The Theoretical and Methodological Basis of Spectrophotometric Titration", a major second one on "The Formal Treatment and Evaluation of Titration Systems", and a shorter final one on the "Instrumental Methods" that can be used to provide the data. Listings of two computer programs for use in data analysis are also included.

MARY MASSON

Fuel Science and Technology Handbook: J G SPEIGHT (editor), Dekker, New York, 1990. Pages xii + 1193. \$195 00 (U S A & Canada), \$234 00 (rest of the world)

Any reader new to this topic cannot fail to be impressed by its breadth, and all readers will undoubtedly be impressed by the huge amount of information, much of it very recent, which Dr Speight and his team of eight other writers have assembled together in one volume. There are five major sections, dealing with Petroleum (315 pages), Tar sands (119), Coal (355), Oil shale (358) and Natural gas (113). Each section deals with Origin, occurrence and recovery, Terminology and classification, Composition and properties, and Chemicals from each source. Much of the material will be of interest to chemical engineers, but there are substantial sections relevant to pure chemists and also to analytical chemists.

One of the big hurdles for a writer in this field to surmount is that it is impossible to generalize time and again we read "may be as big as, or as little as" as each writer struggles to present an impression of the magnitude of a problem in production, the minimum economic scale for a process or a well, or the estimated-size of known resources. The reader will have to be patient—there is no simple answer to these questions, and likewise, to each simple question there will be as many answers as there are questioners. The authors usually try to give illustrative examples, as in the chapter on natural gas, with typical compositions of "wet" and "dry" gas as a guide and no more.

I found the chapters light on the chemical aspects of production, certainly of gas and oil where there is a lot of chemistry and a widespread use of chemicals in the production processes, but perhaps this was compensated for by the detail in the technology for processing and converting the fuels—gasification and liquefaction of coals, retorting of shales and so on—and also, as in the chapters on natural gas and on petroleum, on the compilation of methods (API and ASTM) for characterizing the materials and measuring their properties. Interesting references are made to the Fischer retorting method for shales, and the extent to which industrial processes can often obtain higher yields than this "standard" analytical method.

Sections on processing tend to have rather many line diagrams which are not particularly informative for most readers, and on pages 52 and 123 we find the same figure for the constituents of petroleum reproduced. While the book is generally well referenced, it is annoying, especially in the introductory chapter, to find frequent reference to earlier works by the editor, rather than to original sources.

A large book, at a large price, and a "mine" of information for engineers in fuel technology, it will be helpful to the analytical chemist first encountering problems in the fuel industries, because it will create a background awareness of the processes and the terminology. For the analytical methods themselves the reader will have to look elsewhere.

I L MARR

Analytical Artifacts GC, MS, HPLC, TLC and PC: B. C. MIDDLEDITCH, Elsevier, Amsterdam, 1989. Pages xxiv + 1033. \$241.50, Dfl 495.00

This catalogue is Volume 44 in the Elsevier Journal of Chromatography Library and contains information on impurities, by-products, contaminants and other artifacts that the analytical chemist may encounter.

Each substance or topic is covered in alphabetical order in an individual monograph. The general format of each substance monograph is common name, nominal mass, mass spectrum, structure, Chemical Abstracts Service name and registry number, Merck Index reference number, synonyms, occurrence of artifact, mass spectra of derivatives and cross-references. Not all substances are given equal treatment and the information can range from a few lines to a few pages of text. A retention index for most toxicologically relevant substances is given pertaining to retention on SE-30 or OV-1 chromatography columns.

Interdispersed between the substance monographs are very useful topics related to general areas of consideration. Examples of contaminants from plastic wash bottles, parafilm, Pasteur pipettes, grease, resins, syringes, filter paper, etc., are mentioned. Cautionary tales of, *e.g.*, changes in trade-names, unusual chromatography results (rat peaks, ghost peaks, pink beards), handling of lunar samples, blood collection devices and turpentine poisoning are mentioned.

It is hoped that the information in this reference work will help prevent publication of analytical reports that draw the wrong conclusions.

For example, an article once claimed to have identified the pheromone emitted by bitches in season to attract male dogs. However, this was later shown to be only a widely used antimicrobial agent.

Some monographs in the text are limited in their content but the excellent indexes and full literature citations make this a very useful compilation—especially for those involved with trace analysis and GC-MS.

P. J. Cox

KINETIC FLUOROMETRIC FIA DETERMINATION OF TOTAL ASCORBIC ACID, BASED ON USE OF TWO SERIAL INJECTION VALVES

H. K. CHUNG and J. D. INGLE, JR.*

Department of Chemistry, Oregon State University, Gilbert Hall 153, Corvallis, OR 97331-4003, U.S.A.

(Received 30 August 1990. Accepted 27 October 1990)

Summary—The kinetic determination of total ascorbic acid with a flow-injection analysis system is described. The sample is loaded into two serial sample injection valves and injected into a carrier system containing mercuric chloride and *o*-phenylenediamine. The formation of a fluorescent product is monitored. The single-point and double-point kinetic methods are compared by using both peak height and peak area as the analytical signal. A detection limit of 0.1 $\mu\text{g/ml}$ for vitamin C was achieved with a sample throughput rate of 30 per hour.

Several methods have been proposed to use flow-injection analysis (FIA) for analytical kinetic measurements of relatively slow reactions. These methods include the single-point methods in which the peak height or area is taken as proportional to the amount of product formed in a fixed time period,^{1,2} a two-point kinetic assay based on the difference in signals from two flow-through detector cells,³ the stopped-flow technique in which the dispersed sample zone is stopped for a predetermined period when it reaches the detection cell, during which the reaction-rate measurement is performed,⁴ a two-point kinetic method based on the simultaneous injection of the sample with two serial injection valves into one reagent carrier stream,⁵ and a multiple-point method based on an array of detectors along an observation tube.⁶ The single-point kinetic method does not provide the advantages of a true kinetic method because an absolute signal rather than a change in signal is measured. Also, if the sample contains a non-reacting species which contributes to the detector response, an error will result.

Fernandez *et al.*⁷ demonstrated that kinetic information can be obtained in a single-line manifold by injecting a relatively large sample volume (*e.g.*, 1000 μl) into the reagent stream. Two reaction zones and two peaks are produced, because little or no reagent/sample mixing occurs in the middle of the sample zone. The kinetic determinations are based on the

difference in peak heights or areas. Chung and Ingle⁸ proposed a kinetic method also based on injection of a relatively large volume of sample into a single-line manifold, the FIA profile being normalized with respect to sample dispersion. Under proper conditions, the normalized signal increases from the center to the edge of the profile and rate information can be extracted.

Most of the FIA techniques suggested^{1,2,9,10} for determination of ascorbic acid (AA) are single-point methods with electrochemical or spectrophotometric detection.

The purposes of this paper are to demonstrate that a fluorometric kinetic procedure developed for the determination of total ascorbic acid in a conventional fluorometric cell¹¹ is adaptable to FIA measurements, and also to compare kinetic FIA measurements made with the single-point method and a two-point method based on two serial injection valves. The effects of non-reacting interferences and peak height *vs.* peak area measurements are also considered.

EXPERIMENTAL

Instrumentation

All measurements were performed with a microcomputer-controlled single-line FIA manifold and a fluorescence detection system that have already been described.¹² The FIA manifold consists of a valveless positive-displacement carrier-stream pump, two sample-loop injection valves separated by a reaction coil of 400-cm length, and a flow cell (20- μl volume,

*Author for correspondence.

1-mm path-length) for fluorescence measurement. Another pump is used to aspirate sample solutions into the sample loops from the sample reservoir. All connecting tubing in the main line is 0.5-mm i.d. Teflon tubing. The length of tubing between the second injector and the flow cell was approximately 50 cm.

The microcomputer controls the pumps and load/injection position of the sample-injection valves, and the data acquisition, after which it calculates and reports the heights and areas for both peaks and the differences in these quantities. For both valves, the sample-loop volume was 30 μ l, and both sample loops were filled with the same test solution and switched to the injection position simultaneously under microcomputer control. Two FIA peaks are obtained. If a slow reaction occurs between the analyte and reagent carrier stream, the second peak is larger because the sample plug is in contact with the reagent stream for a longer period of time (*i.e.*, there is longer reaction time) and the system can be used to obtain kinetic information.

Solutions and measurement conditions

This FIA system was evaluated for the determination of AA by means of a fluorescence reaction developed for use in a conventional sample cell.¹¹ This reaction involves the rapid oxidation of AA by mercuric chloride to dehydro-*l*-ascorbic acid, which then reacts with *o*-phenylenediamine (OPDA) over a period of several minutes to form a fluorescent quinoxaline. A carrier solution of 1mM mercuric chloride and 50mM OPDA in pH-4.75 acetate buffer was used. Calibration data were obtained from 3 repetitive injections for each standard. A 1- μ g/ml quinine sulfate solution in 0.05M sul-

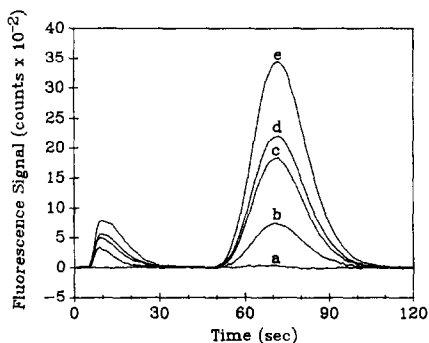


Fig. 1. Baseline-corrected FIA peaks for the ascorbic acid standards: (a) blank, (b) 1 μ g/ml, (c) 5 μ g/ml, (d) 6.25 μ g/ml, (e) 10 μ g/ml. Injected sample, 30 μ l; flow-rate, 1 ml/min.

Table 1. Calibration data for the determination of ascorbic acid

Quantity*	Magnitude \dagger , counts	Slope \dagger , counts . ml . μ g ⁻¹	Intercept \S , counts
$(S_2)_m$	6995 (0.7)	343 (6.9)	71.7 (40)
A_2	81207 (1.8)	8055 (98)	596 (560)
ΔS_m	2703 (1.5)	284 (5.0)	-134 (29)
ΔA	71014 (1.7)	7150 (70)	-519 (400)

* $(S_2)_m$ = maximum signal for second peak; A_2 = area of second peak; $\Delta S_m = (S_2)_m - (S_1)_m$; $\Delta A = A_2 - A_1$.

\dagger For 10- μ g/ml AA; RSD (%) in parentheses.

\dagger The standard error of the slope is given in parentheses.

\S The standard error of the intercept is given in parentheses.

furic acid was used for calibrating the loop volumes. For measurements of AA, the excitation wavelength was 366 nm (17-nm spectral bandpass) and the emission wavelength was 435 nm (21-nm spectral bandpass). Quinine sulfate (QS) measurements were made under the same conditions except that the emission wavelength was 460 nm.

RESULTS AND DISCUSSION

Figure 1 shows the baseline-corrected FIA peaks. Calibration data are summarized in Table 1 for the second peak (single-point kinetic method) and as rates calculated from the difference in peak heights and peak areas. The calibration plots are linear up to at least 10 μ g/ml AA. Typically, RSD values are 1–2%. The detection limits for AA estimated for all four methods are not significantly different and range between 0.05 and 0.1 μ g/ml. The proposed FIA method provides a simple means to determine vitamin C that should be applicable to pharmaceutical samples. The sample throughput with the present manifold is about 30 samples per hour.

It is important to note that if the sample already contains a fluorophore that does not react in the system but gives a signal under the excitation and emission conditions used, the single-point methods based on peak height or peak area will not discriminate between this signal and the one from the AA reaction. However, the two-point kinetic method does provide partial or complete discrimination against such interferents, depending on the situation. If the volumes of the two sample loops could be made exactly equal, the areas of the two peaks for a non-reacting fluorophore would be identical. This assumption was tested with 1- μ g/ml QS solution. The ratio of the peak areas ($r_A = A_2/A_1$) was 1.012. For the sample loop

volumes used, such a species would contribute only 1.2% of its signal to the ΔA signal for AA. Complete discrimination can be achieved by calculating a corrected difference in area ($\Delta A'$) based on $\Delta A' = A_2/r_A - A_1$.

The effect of non-reacting interferents on the difference in peak heights is much more serious as it depends on the difference in the sample loop volumes and in the dispersion for the two peaks. From the peaks obtained by injecting the 1- $\mu\text{g/ml}$ QS standard, the ratio of the baseline-corrected peak heights (r_p) was 0.342. The dispersion coefficients at the peak maximum are 2.95 and 8.50 for the first and second peaks, respectively. Hence a non-reacting interferent, yielding a maximum signal of S_2 for the second peak, would contribute a signal equal to $-1.92S_2$ to the peak height difference (ΔS_m) for AA. A compensated value ($\Delta S'_m$) can be obtained by calculating from $\Delta S'_m = (S_2)_m / r_p - (S_1)_m$. This possibility was not realized in the original work on the dual-injection kinetic method.⁷

REFERENCES

1. J. Růžička and E. H. Hansen, *Flow Injection Analysis*, 2nd Ed., Wiley, New York, 1989.
2. M. Valcárcel and M. D. Luque de Castro, *Flow Injection Analysis: Principles and Applications*, Horwood, Chichester, 1987.
3. E. H. Hansen, J. Růžička and B. Rietz, *Anal. Chim. Acta*, 1977, **89**, 241.
4. J. Růžička and E. H. Hansen, *ibid.*, 1979, **106**, 207.
5. A. Fernández, M. D. Luque de Castro and M. Valcárcel, *Analyst*, 1987, **112**, 803.
6. D. J. Hooley and R. E. Dessy, *Anal. Chem.*, 1983, **55**, 313.
7. A. Fernandez, M. D. Luque de Castro and M. Valcárcel, *Anal. Chim. Acta*, 1987, **193**, 107.
8. H. K. Chung and J. D. Ingle, Jr., *Anal. Chem.*, 1990, **62**, 2547.
9. F. Lázaro, A. Rios, M. D. Luque de Castro and M. Valcárcel, *Analyst*, 1986, **111**, 163.
10. J. Hernández-Méndez, A. Alonso Mateos, M. J. Almendral Parra and C. García de María, *Anal. Chim. Acta*, 1986, **184**, 243.
11. H. K. Chung and J. D. Ingle, Jr., *Anal. Chim. Acta*, in the press.
12. *Idem*, *Anal. Chem.*, 1990, **62**, 2541.

KINETIC DETERMINATION OF ZINEB IN AGRICULTURAL SAMPLES BY CONTINUOUS ADDITION OF REAGENT

M. C. QUINTERO, M. SILVA and D. PEREZ-BENDITO

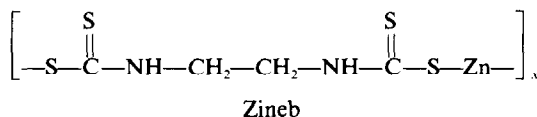
Department of Analytical Chemistry, Faculty of Sciences, University of Córdoba, 14004 Córdoba, Spain

(Received 16 January 1990. Revised 2 November 1990. Accepted 3 November 1990)

Summary—The technique of automatic continuous addition of reagent has been applied for the determination of zineb in pesticides. The method is based on photometric monitoring of the fast complexation reaction between zinc(II) and Zincon. The special feature of the technique is the direct kinetic measurement, which provides a highly selective determination of zineb at $\mu\text{g/ml}$ levels. The sampling rate of 140 samples/hr makes the method very useful in routine analysis for this pesticide in vine and olive leaves.

The degree of automation achieved in mixing of reagents and samples, and in acquisition and processing of data, has roused increasing interest in kinetic methods of analysis.^{1,2} In this context, the continuous addition of reagent (CAR) technique permits direct rate measurements to be made for systems having half-reaction times in the millisecond region. The theoretical and practical aspects of this technique have recently been discussed.³ It permits continuous recording of the signal as a function of time, and thus provides a kinetic curve. It is a useful alternative to the stopped-flow technique inasmuch as it requires very much simpler (and readily available) instrumentation and is particularly suitable for routine analysis. The feasibility of this approach has been shown for photometric³ and fluorimetric⁴ methods, and has been applied to determination of sulphonamides in pharmaceuticals.⁵

In this work we extend the technique to the determination of zineb, a dithiocarbamate-type pesticide and fungicide used for treatment of fruit and vegetables. In the EEC and U.S.A., tolerance levels are set for dithiocarbamate fungicides, and methods for their determination are important.



Most methods for the determination of zineb are based on its decomposition by digestion with hot acid, and determination of the carbon

disulphide released. Photometric,⁶⁻⁹ gas chromatographic,¹⁰⁻¹² and precipitation titrimetric¹³ methods have been used for the final determination, but these methods are non-specific since any dithiocarbamate pesticide (such as maneb, mancozeb, nabam and amoban) yields carbon disulphide on acid decomposition. Methods based on the determination of the organic component of the pesticide, such as that based on the conversion of zineb into the molybdenum ethylenedithiocarbamate complex,¹⁴ are subject to various interferences. The methods based on analysis for zinc generally use dithizone as the chromogenic reagent, either in homogeneous medium¹⁵ or with liquid-liquid extraction,¹⁶ but will be subject to interference by other heavy-metal dithiocarbamate pesticides such as maneb and mancozeb.

The proposed kinetic method for the determination of zineb is based on acid decomposition of the pesticide and complexation of the liberated zinc with Zincon (2-carboxy-2'-hydroxy-5'-sulphoformazylbenzene), monitored by the CAR technique. It gives a sensitive (dynamic linear range 0.25–3.0 $\mu\text{g/ml}$) and selective determination of zineb that is applicable to commercial formulations and their residues on vegetables. This method is not specific for zineb, as there is interference by other Zn-containing fungicides, such as propineb and ziram, which can be similarly determined. It can be used, of course, to determine the sum of any Zn-containing fungicides present. The potential interference of maneb [since manganese(II) is also complexed by Zincon] is avoided owing to the

special features of the CAR technique, which can be used for the simultaneous kinetic determination of both pesticides, as will be shown in a future report.

EXPERIMENTAL

Reagents

All chemicals were of analytical-reagent grade. All dilute solutions were prepared immediately prior to use. Zineb (Chem. Service Inc., West Chester, PA) was used as supplied. A 250 mg/l. standard solution was prepared by dissolving 25 mg of the pesticide in 2.0 ml of concentrated nitric acid, heating until dissolution was complete and diluting to volume with distilled water in a 100-ml standard flask. The zinc content of this solution was determined by EDTA titration. A stock solution of Zincon ($2.95 \times 10^{-3}M$) was prepared by dissolving 130.0 mg of the chemical in 2.0 ml of 0.1M sodium hydroxide and diluting to 100 ml with distilled water. A 0.1M sodium borate/boric acid buffer of pH 9.0 was also prepared.

Apparatus

The instrumental arrangement has already been described.³ A Radiometer PHM62 pH-meter equipped with a combined glass-calomel electrode was used for pH measurements.

Procedures

Determination of zineb. To the reaction vessel of the CAR system were added a known volume of the standard zineb solution, containing between 15 and 180 μg of the pesticide, and 5.0 ml of 0.1M sodium borate/boric acid buffer of pH 9.0, followed by accurate dilution to 60 ml with distilled water. Then $7.4 \times 10^{-4}M$ Zincon was continuously added at 35 ml/min, with stirring at 200 rpm. The absorbance at 620 nm was monitored. The computer system recorded the full absorbance *vs.* time curve and calculated the initial rate (over a period of about 1 sec) and the zineb concentration.

Analysis of formulations. About 400 mg of sample was weighed accurately into a beaker, 8 ml of concentrated nitric acid were added, and when the brisk evolution of brown fumes had ceased, the solution was heated gently to complete the dissolution, then cooled and diluted to volume with distilled water in a 1-litre standard flask. Suitable volumes were analysed as above.

Analysis of plant residues. Known volumes (0.25–3.0 ml) of ZZ-azul triple micro-formu-

lation suspension (400 mg/l.) were added to vine and olive leaves. The leaves were then dried in the sun and later in the shade. Each sample was extracted with two 25-ml portions of chloroform; the combined extracts were evaporated to dryness and the residue was treated with 2 ml of concentrated nitric acid. When the brisk effervescence of nitrogen dioxide had ceased, the solution was evaporated to low bulk to remove nitrous fumes and most of the acid, diluted to 40 ml with water, adjusted to pH 6–8, placed in the reaction vessel and after addition of 5.0 ml of the pH 9.0 buffer was diluted to 60 ml and analysed as above.

RESULTS AND DISCUSSION

Zineb was determined through its metal constituent, by formation of the complex between zinc(II) and Zincon, which has been widely used for the photometric determination of zinc(II) in a variety of samples.¹⁷ Its application to the determination of zineb requires mineralization of the pesticide, which can easily be done with concentrated nitric acid.

The formation of the Zn-Zincon complex is so fast that its pseudo first-order reaction rate constant could not be determined even by the stopped-flow technique. This accounts for the fact that zinc(II) has not hitherto been determined kinetically by direct complexation with this ligand, but only by ligand-exchange reactions.¹⁸ The singular feature of the CAR technique that allows the kinetic determination of zinc(II) with Zincon is that the reaction then conforms to pseudo second-order kinetics³ and hence the reaction rate is somewhat slower.

The method involves continuous addition of Zincon solution at constant rate to a stirred zinc(II) solution and monitoring of the absorbance of the complex as a function of time, to produce a kinetic curve. The kinetic data thus generated are acquired by the computer at a collection rate of 20 points per second. The slope of the initial linear portion of the curve (initial rate method) is proportional to the analyte concentration and is used as the measurement parameter. Figure 1 shows a typical curve. The slight increase in absorbance at longer reaction times (≥ 3 sec) is due to absorption of light by the excess of ligand. The contribution of Zincon to the initial absorbance changes is negligible.

As the method is based on the reaction of Zincon with free zinc ions, it is necessary to

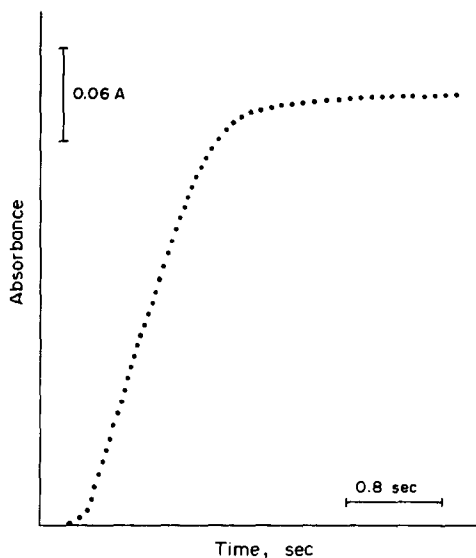


Fig. 1. Typical absorbance vs. time plot for the determination of zineb ($3.0 \mu\text{g/ml}$) with Zincon. Experimental conditions as described in the text.

mineralize the sample, and preliminary experiments showed that this could best be done by treatment with concentrated nitric acid, which was found to be quantitative.

Effect of variables

The influence of both chemical and instrumental variables on the determination of zineb was evaluated by examining plots of initial rate as a function of the variable. All concentrations quoted are the initial concentration in the autoburette or in the reaction vessel; the effects of dilution were considered small enough to be ignored.

The effect of rate of addition of the Zincon solution was examined over the range 5–45 ml/min. As expected from the theory of the method,³ the initial rate increased linearly with the rate of addition. A rate of 25 ml/min, giving an initial rate midway along the linear portion of the plot, was selected for use, but as the effect of this variable is closely related to that of the Zincon concentration used, both were re-optimized later. The stirring rate is another critical variable. The maximum precision of the initial rate was achieved with a stirring speed of 200 rpm, which gave adequate mixing and avoided eddies (which could result in spurious signals). The effect of the initial volume of sample solution in the cell was studied over the range 60–100 ml. As the amount of zinc taken in the reaction vessel was the same in all the experiments, the initial rate decreased with in-

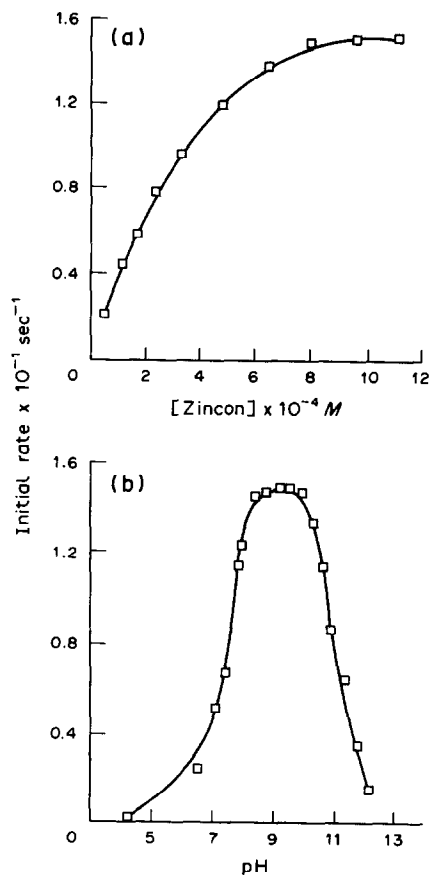


Fig. 2. Dependence of the initial rate on (a) the Zincon concentration and (b) the pH. [Zineb] = $3.0 \mu\text{g/ml}$. Experimental conditions as described in the text.

creasing initial volume. An initial volume of 60 ml was selected as a compromise between that needed to give the maximum initial rate and that needed to accommodate the stirrer and the optical probe so that no bubbles or eddies were produced by the stirring, and the light-path of the probe was filled with solution.

The effect of chemical variables such as the Zincon concentration, the sample pH and the analyte concentration were also examined. Figure 2(a) shows the results obtained by varying the Zincon concentration between 2.95×10^{-5} and $1.03 \times 10^{-3} M$. The initial rate increased with the Zincon concentration up to about $7.5 \times 10^{-4} M$, and then remained constant. A concentration of $7.4 \times 10^{-4} M$, which resulted in the maximum reliability and sensitivity and yielded the best reagent mixing throughout the reaction vessel, was selected. With this reagent concentration, use of an addition rate of 35 ml/min improved the sensitivity. The effect of pH on the initial rate was studied over the range 4–12 and Fig. 2(b) shows that the initial rate

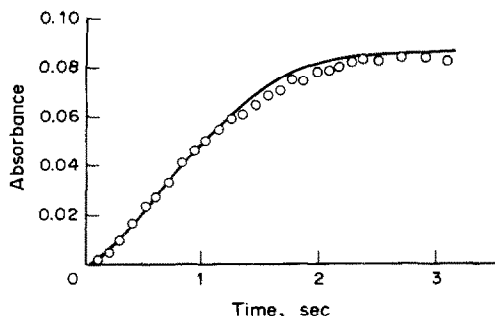


Fig. 3. Experimental (○) and simulated (—) curves for the zinc(II)-Zincon system.

was almost unchanged in the pH range 8.5–9.6. A pH of 9.0 was selected, and was obtained by inclusion of 5.0 ml of 0.1M boric acid/sodium borate buffer (pH 9.0) in the final volume of 60 ml.

Under the optimal conditions thus established, the initial rate was found to be linearly related to the zineb concentration over the range 0.25–3.0 $\mu\text{g/ml}$.

Determination of the pseudo second-order rate constant

The pseudo second-order rate constant of the complexation reaction between zinc(II) and Zincon was determined by using the integrated rate equation governing the method.³ The average value obtained was $k = (9.9 \pm 0.5) \times 10^4 \text{ l. mole}^{-1} \text{ sec}^{-1}$ for use of $7.4 \times 10^{-4} \text{ M}$ Zincon, an addition rate of 35 ml/min and an initial sample volume of 60 ml. To check the validity of the proposed equation a simulated kinetic curve was constructed by using the integrated rate equation and the experimental k value and gave good agreement with the experimental kinetic curve (Fig. 3).

Analytical figures of merit

The initial rate method was applied to absorbance *vs.* time plots recorded for different zinc (or equivalent zineb) concentrations. The features of the analytical method are summarized in Table 1. The sensitivity was taken as the slope of the calibration graph, the detection

limit was calculated according to IUPAC¹⁹ and the precision was determined from analysis of 11 samples each containing 1.0 $\mu\text{g/ml}$ zineb. The throughput was calculated from the time required for three replicate analyses, including the period needed to refill the reaction vessel, and was very high because the kinetic curve is rapidly computed.

The dynamic linear range for determination of zinc(II) was found to be 0.06–0.72 $\mu\text{g/ml}$, which is narrower than that for the conventional photometric determination of zinc(II) with Zincon²⁰ (0.1–2.4 $\mu\text{g/ml}$), but has a lower determination limit.

Interferences

As the pesticide sample is decomposed to release its metal content, pesticides containing no metal ion cannot cause interference and only maneb and copper(II) were tested as interferences, as they often accompany zineb in commercial formulations. Solutions of zineb and maneb (both mineralized with nitric acid) or of copper(II) were mixed to obtain samples containing the equivalent of 1 $\mu\text{g/ml}$ zineb and up to 100 $\mu\text{g/ml}$ interferent. The tolerance ratio of interferent to zineb was taken as the largest giving an error of less than $\pm 3.0\%$ in the initial rate for 1.0 $\mu\text{g/ml}$ zineb. For maneb the ratio was 50, but the CAR technique can be adapted for simultaneous determination of zineb and maneb (to be reported later). For copper(II) (added as the oxychloride) the ratio was 2 but could be increased to 4 by addition of 5 $\mu\text{g/ml}$ cyanide, which is adequate to allow the determination of zineb in commercial formulations containing copper oxychloride. Analysis of samples containing free zinc(II) as well as zineb requires extraction of the fungicide into an organic solvent as described below.

Analysis of commercial formulations and agricultural samples

Zineb, like other dithiocarbamate fungicides, is widely used in agriculture, and is an active ingredient of various formulations used to control leaf diseases in vegetables. The present procedure was applied to the routine determination of zineb in formulations and in vine and olive leaves.

To avoid interference by any free zinc(II) present in the samples, the zineb was extracted into chloroform, and the organic phase was then treated as described above for analysis of plant residues. It was confirmed that all the

Table 1. Analytical features of the determination of zineb (or equivalent zinc) by the CAR technique

Feature	Zineb	Zinc
Dynamic linear range, $\mu\text{g/ml}$	0.25–3.0	0.06–0.72
Sensitivity, $\mu\text{g/ml}$	0.054	0.014
Detection limit, $\mu\text{g/ml}$	0.04	0.01
Precision (RSD), %	1	1.8
Sample throughput, samples/hr	140	140

Table 2. Recovery of zineb in its determination in ZZ-azul triple micro formulations

Aliquot, ml	Found,* µg/ml	Added, µg/ml	Recovery	
			µg/ml	%
2.0	2.04			
1.0	1.02	1.00	2.04	101.0
0.5	0.52	1.50	2.05	101.5

*In the presence of 0.5 µg/ml cyanide.

Table 3. Recovery of zineb added as ZZ-azul triple micro to leaf samples

Type of leaf	Zineb added, µg	Zineb found,* µg	Recovery, %
Vine	60	61.9	103.1
		58.1	96.8
		58.3	97.1
Olive	60	55.8	93.0
		61.3	102.1
		58.9	98.2
		Average	98.4
	Standard deviation	3.8	

*Determination in presence of 0.5 µg/ml cyanide.

free zinc(II) remained in the aqueous phase (the average recovery of zineb in the organic phase was 98.3%).

The method was applied to determination of zineb in a commercial formulation, namely ZZ-azul triple micro (dust, 15% zineb, 20% maneb and 15% copper as oxychloride). Recoveries close to 100% for added zineb were obtained (Table 2). The zineb content in the formulation was found to be $15.4 \pm 0.1\%$, in good agreement with the nominal value given by the manufacturers.

For determination of zineb on vine and olive leaves treated with this pesticide we tested the recoveries from leaves treated with known amounts of ZZ-azul triple micro, and found them to be close to 100% (Table 3).

From the limit of determination by the method (0.25 µg/ml zineb), the initial sample volume in the reaction cell (60 ml) and the mean weight of one vine leaf (0.350 g) or three olive leaves (0.250 g), the limit of determination of

zineb can be estimated as 43 and 60 mg/kg for vine and olive leaves, respectively.

CONCLUSIONS

Zineb concentrations at mM level can be determined by the CAR technique and direct complexation of zinc(II) (released from zineb by nitric acid treatment) with Zincon. The blue complex is rapidly formed and its absorbance can be readily monitored by this new approach, which affords direct rate measurements on the msec time scale. The suitability of the technique for routine determination of zineb in agricultural samples has been demonstrated.

Acknowledgement—The authors gratefully acknowledge financial support from the CICyT (Project No. PB87-0821).

REFERENCES

1. D. Pérez-Bendito and M. Silva, *Kinetic Methods in Analytical Chemistry*, Horwood, Chichester, 1988.
2. D. Pérez-Bendito, M. Silva and A. Gómez-Hens, *Trends Anal. Chem.*, 1989, **8**, 302.
3. M. Márquez, M. Silva and D. Pérez-Bendito, *Analyst*, 1988, **113**, 1733.
4. *Idem*, *Anal. Lett.*, 1989, **22**, 2485.
5. *Idem*, *Anal. Chim. Acta*, 1990, **237**, 353.
6. T. E. Cullen, *Anal. Chem.*, 1964, **36**, 221.
7. G. E. Keppel, *J. Assoc. Off. Anal. Chem.*, 1971, **54**, 528.
8. B. W. Simpson, *Pestic. Sci.*, 1971, **2**, 127.
9. J. Piechocka, *Rocz. Panstw. Zakl. Hig.*, 1984, **35**, 83.
10. H. A. McLeod and K. A. McCully, *J. Assoc. Off. Anal. Chem.*, 1969, **52**, 1226.
11. K. Makino, N. Kashihiro, K. Kirita and Y. Watanabe, *Bunseki Kagaku*, 1982, **31**, 417.
12. *Analyst*, 1981, **106**, 782.
13. M. Mingot, *An. Inst. Nac. Invest. Agron.*, 1970, **19**, 83.
14. A. L. J. Rao and N. Verma, *Talanta*, 1989, **36**, 1041.
15. V. G. Atabekyan and V. P. Pal'mova, *Gig. Sanit.*, 1981, **8**, 68.
16. E. B. Muzhanovskii, A. F. Fartushnyi and A. I. Sedov, *Sud-Med. Ekspert.*, 1982, **25**, 42.
17. Z. Marczenko, *Spectrophotometric Determination of Elements*, Horwood, Chichester, 1976.
18. G. M. Ridder and D. W. Margerum, *Anal. Chem.*, 1977, **49**, 2090.
19. G. L. Long and J. D. Winefordner, *ibid.*, 1983, **55**, 712A.
20. F. D. Snell, *Photometric and Fluorimetric Methods of Analysis, Metals, Part 2*, Wiley, New York, 1979.

QUANTIFICATION OF VOLATILE SOLVENTS IN BLOOD BY STATIC HEADSPACE ANALYSIS

RUSSELL L. DILLS,* STUART D. KENT, HARVEY CHECKOWAY and DAVID A. KALMAN

Department of Environmental Health, School of Public Health and Community Medicine, University of Washington, Seattle, WA 98195, U.S.A.

(Received 8 August 1990. Revised 19 September 1990. Accepted 5 October 1990)

Summary—A static headspace method for determination of volatile solvents in blood was developed. The solvents determined were 1,1,1-trichloroethane, toluene, xylene (*o*-, *m*- and *p*-), ethylbenzene, styrene, α -methylstyrene and 4-methylstyrene at concentrations ranging from 0.01 to 1 $\mu\text{g/ml}$. Internal standard calibration was used. Parameters affecting sensitivity and precision were determined and optimized.

Volatile organic solvents are common contaminants in the environment and work place. Recent human exposure to these contaminants is most accurately assessed by monitoring the concentration of individual solvents in the blood. One method of quantifying solvent concentration in blood is headspace analysis, in which analytes dissolved in blood are partitioned between the blood and air in a closed system and the concentrations of analytes in the airspace (headspace) over the blood are determined. The concentrations of analytes in the headspace are proportional to their concentrations in the blood.¹

As part of our research in monitoring exposures to environmental and work place contaminants, we wanted a general screening method for blood that could detect low levels of common solvents. The desired quantification limit was approximately the level expected in an average human exposed to a concentration equal to 1% of the occupational guideline suggested by the American Conference of Governmental Industrial Hygienists. Ramsey *et al.*^{2,3} have developed a method for screening volatile organic compounds in blood by headspace analysis. Their method was created for diagnostic use in high-exposure situations occurring with solvent abuse and acute poisoning. They used low-resolution (packed-column) gas chromatography (GC) and did not automate the method. We have therefore developed and validated an automated method for headspace analysis of blood from humans with low-level exposure to solvents.

The method described in this report differs from previously published analyses in that: (a) the quantification limit is lower (as low as 0.01 $\mu\text{g/ml}$ in blood); (b) the system is fully automated, permitting up to 20 hr of unattended operation; (c) the range of volatility for analytes is wide (b.p. 12–170°); and (d) high-resolution gas chromatography is used, permitting discrimination between xenobiotics and background agents.

EXPERIMENTAL

Materials

“Nanograde” toluene was obtained from Mallinckrodt (St Louis, MO). 1,1-Difluoro-1,2,2-trichloroethane was purchased from PCR (Gainesville, FL). 1,1,1-Trichloroethane (TCE), ethylbenzene, *p*-xylene (gold label; inhibited with 10–15 ppm 4-*tert*-butylcatechol), *m*-xylene, *o*-xylene (HPLC grade), styrene (gold label; inhibited with 10–15 ppm 4-*tert*-butylcatechol), 4-chlorofluorobenzene, α -methylstyrene (inhibited with 15 ppm 4-*tert*-butylcatechol), and 4-methylstyrene (inhibited with 0.1% by weight hydroquinone) were bought from Aldrich Chemical Company (Milwaukee, WI). Dimethylsulfoxide (DMSO) was obtained from Burdick and Jackson (Muskegon, MI). Analytical-reagent grade chemicals were used unless otherwise indicated. The styrenes and 1,1-difluoro-1,2,2-trichloroethane were kept refrigerated because of their tendency for slow degradation. The chemicals used for standards were analyzed by gas chromatography/mass spectrometry (GC/MS) for impurities. We noticed some variation of purity in the chemicals,

*Author for correspondence.

depending on source and lot. The sources and grades indicated above were satisfactory.

Gas chromatography

A capillary gas chromatograph with a flame ionization detector (Hewlett-Packard model 5880A; Avondale, PA) was used. The nitrogen make-up gas flow to the detector was approximately 30 ml/min. The detector temperature was 250°. Liquid carbon dioxide was the coolant for sub-ambient temperature programming and was controlled by the sub-ambient temperature control-option available for the 5880A gas chromatograph. The oven temperature control was turned off for the duration of the analyte transfer (5 min), by commands in the run table.

The multi-ramp oven temperature program was as follows: -10° for 5.2 min initial temperature; heating to 40° at 15°/min followed by an 8-min isothermal period; heating to 65° at 4°/min; ballistic heating to 220° followed by a 6-min isothermal period (for post-analysis column conditioning).

A DB-WAX capillary column (30 m × 0.32 mm i.d., 0.25 mm film thickness; J&W Scientific, Folsom, CA) was directly connected to the transfer line of the headspace sampler with a zero dead-volume union (ZU.5TJ with graphite ferrules; Valco Instruments Company, Inc., Houston, TX). If the union became cooled, during sub-ambient temperature programming, for example, split peaks were observed in the chromatogram. To prevent this, the union was placed inside the heated zone of the capillary injector, ensuring that the union remained at 150°. The linear velocity of the helium carrier gas was 20 cm/sec at 150°.

Headspace sampler

A Hewlett-Packard 19395A headspace sampler was used with an 18906A constant heating-time accessory. The headspace sampler hardware and operation have been described by Wylie,⁴ as has the constant heating-time apparatus.⁵ In brief, the headspace sampler maintained samples at a constant temperature for a preselected period prior to sampling. To sample the headspace, the sample vial was first pressurized with helium admitted through a needle piercing the septum of the vial. The vial was then vented, whereby a positive-pressure transfer of the helium/headspace mixture was made to a volumetric injection loop (1 ml). When the loop had been filled, it was switched into the

carrier gas stream and its contents swept into the gas chromatographic column. Operational parameters for analyses with the headspace sampler are shown in Table 1.

Cryotrap

The cryotrap was a brass tube (13 × 0.635 cm o.d.) suspended in the gas chromatograph oven. The gas chromatographic column was centered in the brass tube with graphite ferrules swaged onto the tube ends. When there was a tight seal between the column and the ferrules, multiple split peaks were observed in the chromatogram. We attributed this phenomenon to the existence of cold spots where the column contacted the ferrules. To avoid this phenomenon, the holes drilled in the ferrules were oversized.

Liquid nitrogen was the coolant for the cryotrap and entered it counter-current to the gas chromatographic column carrier-gas flow. The liquid-nitrogen supply was controlled by a solenoid valve that was activated when the headspace sampler probe descended. The cryotrap was cooled for 7 min and then warmed by compressed air until the trap temperature reached approximately 40°. The compressed air was controlled by a solenoid valve activated through the run table.

The coolant flow was regulated to maintain a temperature of -120° (temperature controller, Model 310; Omega Engineering, Stamford, CT). The thermocouple (type J) was attached to a brass screw opposite the liquid-nitrogen inlet. A second thermocouple (type K) was used to monitor the outer surface temperature of the trap. This thermocouple was wired to the "auxiliary temperature 2" sensor input on the 5880A gas chromatograph.

Sample preparation

The recommendations of the Centers for Disease Control for the handling of blood were

Table 1. Operational parameters for headspace analyses

Parameter	Value
Sample heating time	74 min
Sample temperature	60°C
Sampling valve temperature	65°C
Analysis time	37 min
Vial overpressure	1.2 bar*
Carrier gas pressure	1.4 bar*
Sample loop size	1 ml
Vial pressurization duration	1 min
Vial venting duration	2 sec
Injection duration	5 min

*Above atmospheric pressure.

followed.⁶ Blood samples were taken in "vacutainers" containing sodium citrate as an anti-coagulant. Samples were kept at approximately 4° until sample preparation. The "vacutainers" were filled as completely as possible, to minimize the headspace above the blood sample.

To prepare a sample for analysis, 2 ml of water containing 2 mg of sodium azide were placed in a 10-ml crimp-top vial (23 mm o.d., 47 mm in height; Alltech Associates, Deerfield, IL) and frozen. When the ice in the vial began to thaw slightly, 1 ml of blood was pipetted onto the ice with an Eppendorf Combitips pipettor (Brinkman Instruments, Westbury, NY) and an 18-gauge needle. A Teflon-lined butyl rubber septum (Hewlett-Packard, part no. 9301-0976) and an aluminum seal (20-mm o.d. seal without centers; Alltech Associates) were immediately placed on the vial and the seal was crimped. We found that these septa are the most resistant to gas leakage. Once sealed, the vials were stored at 4° until analysis.

Immediately prior to analysis, 10 μ l of an internal standard (a solution of 61 μ g of 4-chlorofluorobenzene and 78 μ g of 1,1-difluoro-1,2,2-trichloroethane per ml in DMSO) were added to the prepared blood sample. The internal standard solution was carefully injected under the surface of the blood-water mixture with a 500- μ l syringe (gas-tight, Luer tip; Hamilton Company, Reno, NV), a PB-600 repeating dispenser (Hamilton), and a 26-gauge needle. The final concentrations of internal standards in the blood were 0.61 μ g of 4-chlorofluorobenzene and 0.77 μ g of 1,1-difluoro-1,2,2-trichloroethane per ml.

Standard preparation

For method validation experiments, standard curves and blanks, out-of-date human blood was used as the matrix. Out-of-date blood was obtained from a local blood bank and was one or two days past its expiry date. The blood was not hemolyzed or septic.

With each set of samples, a set of spiked blood standards was analyzed and a standard curve constructed. The blood was spiked by the same procedure as described for the addition of internal standard to samples. The concentrations of each analyte in the spiking solutions were approximately 1.0, 5.0, 10, 50 and 100 μ g/ml which gave, respectively, concentrations of 0.01, 0.05, 0.1, 0.5 and 1.0 μ g/ml in the blood. Along with the spiked blood standards, a blood

sample containing only internal standard was analyzed as a blank. The result from this blank analysis was used as the zero point in the standard curve.

Standard curves

Standard curves were prepared daily. Peak-area ratios (of analyte to internal standard) were computed. Weighted least-squares linear regression of blood concentration of analyte *vs.* area ratios yielded the slopes and intercepts. When non-weighted linear regression was used, the highest concentration data points had undue influence, causing poor fits of the regression lines at the lower concentration data points. The square-root of the reciprocal of the concentration was used as the weighting factor. Heteroscedasticity was reduced by this weighting scheme. Regressions were performed with the MGLH module of Systat (Systat, Inc., Evanston, IL).

RESULTS AND DISCUSSION

GC parameters

The choice of satisfactory columns was limited. Our primary criterion for chromatographic separation was resolution of the xylene isomers and ethylbenzene. Only columns with a polyethylene glycol stationary phase achieved resolution of these solvents. Columns of 0.25 mm i.d. occasionally became blocked with ice, a problem that was avoided by using 0.32 mm i.d. columns (as had been reported by others^{4,7}). A film thickness of 0.25 μ m was chosen to maximize resolution between the xylenes. Though a DB-wax column afforded resolution of the solvents tested, it did not resolve the most volatile components (Fig. 1).

The connection of the transfer line from the headspace sampler to the gas chromatographic column had considerable influence on the sensitivity and precision of the headspace analysis. When the transfer line was inserted into the split/splitless injector port through the septum, and the injector was operated in the split mode as recommended in the headspace sampler manual,⁸ the sensitivity was not sufficient for our needs. As the split ratio was decreased, the sensitivity increased. However, the precision decreased, and at a split ratio of 10 the coefficient of variation was approximately 20–30%. When the injector was used in the splitless mode, no increase in sensitivity was

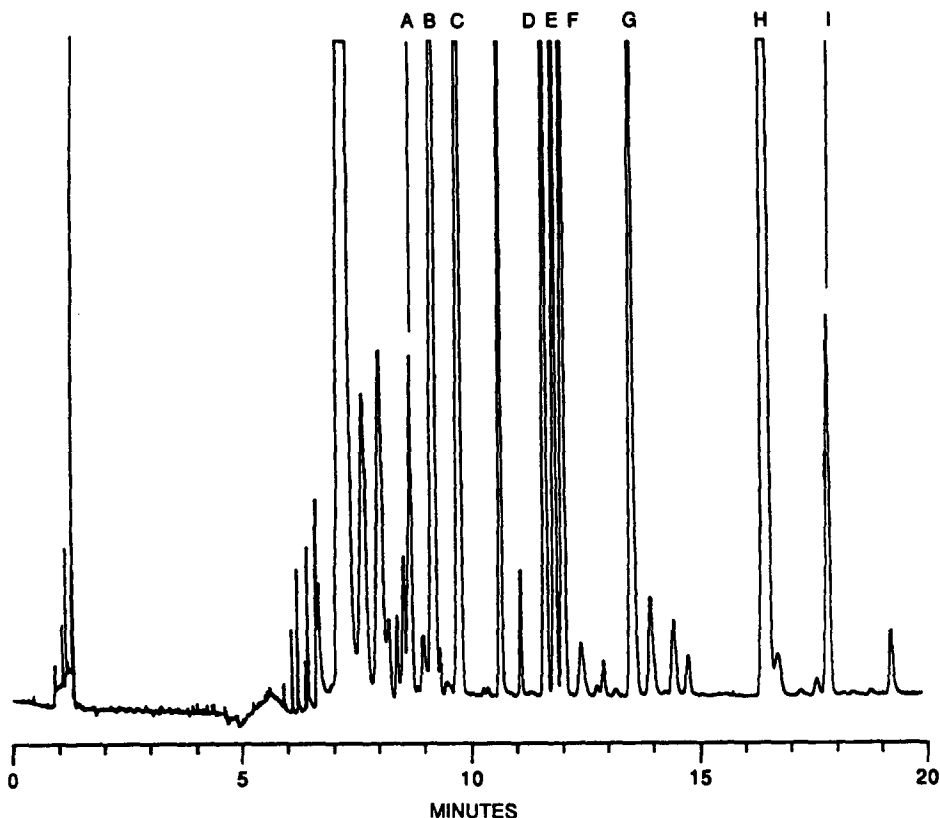


Fig. 1. Chromatogram of a spiked blood sample. The concentration of the analytes was approximately $0.1 \mu\text{g/ml}$. Transfer of analytes to the gas chromatographic column was between 0 and 5.7 min. A = 1,1,1-trichloroethane; B = 1,1-difluoro-1,2,2-trichloroethane; C = toluene; D = ethylbenzene; E = *p*-xylene; F = *m*-xylene; G = *o*-xylene; H = 4-chlorofluorobenzene; I = styrene. The methylstyrenes were eluted between 20 and 25 min. 1,1-Difluoro-1,2,2-trichloroethane and 4-chlorofluorobenzene were used as internal standards.

gained, because slow transfer of the analytes from the large volume injector into the capillary column caused gross tailing and distortion of the chromatographic peaks. The solution to the sensitivity and precision problem was to connect the column and transfer line directly. This increased the sensitivity while maintaining the precision at acceptable levels (coefficient of variation $< 10\%$).

Because the gas chromatograph inlet was bypassed by direct connection of the gas chromatographic column to the transfer line, the headspace sampler supplied the gas chromatograph with carrier gas. Assuming continuous and instantaneous mixing of the contents of the 1 ml sample loop with carrier gas incoming at a flow-rate of 1.0 ml/min, the time required for transfer of 99% of the analytes to the column (4.6 min) was calculated by use of a gas dilution equation.⁹ This calculation neglected the small dead volume of the transfer line (0.13 ml). Therefore, the transfer time (injection time) was set at 5 min.

Cryotrap

Because of the 5 min transfer of the headspace mixture, a cryotrap was necessary to focus the analytes that were more volatile than *m*-xylene into a narrow region of the gas chromatographic column. Without the cryotrap, *p*-xylene, *m*-xylene and ethylbenzene were poorly resolved, toluene was not resolved from endogenous volatile compounds in blood, and TCE was not detectable.

The optimum arrangement of coolant flow and heating-air flow was determined. Peak width was minimized when the coolant flow was counter-current to the carrier-gas flow and heating-air flow. Kolb *et al.*⁷ noted that this configuration formed a temperature gradient in the column and reduced the peak width.

Occasionally analytes escaped collection in the cryotrap. This was typically caused by coolant supply problems and was evidenced by breakthrough of the untrapped compounds during the sample transfer. Compounds re-

tained on the column at room temperature, such as styrene, were unaffected by trap failure.

Headspace sampler parameters

The optimum conditions for headspace sampling were determined in a series of experiments with either blood or water as the sample matrix. Blood was used as the matrix when the matrix was likely to influence the optimization. Both response and precision were evaluated during the optimization. The parameters optimized were heating time, sample temperature, the method used to fill the sample loop, equilibration time for headspace vial pressurization, the overpressure and pressurization time.

The sensitivity of headspace analyses has been improved by heating the sample matrix, which increases the concentration of analytes in the gas phase.¹ To determine the effect of sample temperature on the sensitivity and precision, vials containing either 3 ml of water or 1 ml of blood and 2 ml of water were spiked and the headspace concentrations of the analytes were determined. Sample temperature had different effects upon the response for analytes in blood or water as matrix (Fig. 2). For water, the response increased with temperature over the range 40–90° while for blood, the response was maximal at 60°. At higher temperatures, blood coagulated prior to sampling. The partitioning of analyte from a solid (coagulated blood) to air was less efficient than from a liquid to air. The precision, in all cases, was inversely proportional to the response.

To evaluate the effect of sample heating time on the response and precision, replicate headspace vials containing toluene, the xylenes, internal standard and styrene in a water matrix

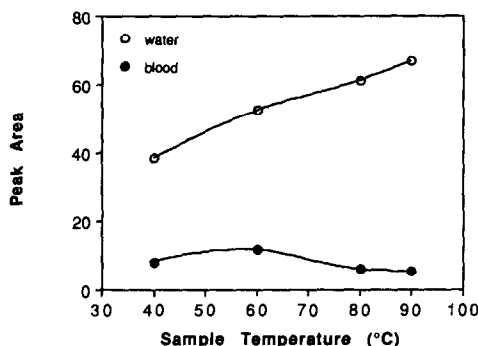


Fig. 2. The effect of sample temperature on the response for styrene. Headspace samples were equilibrated for 80 min prior to analysis. Two different sample matrices, water and a 1:2 mixture of blood and water, were examined in this experiment. Similar results for other analytes were observed in these two matrices.

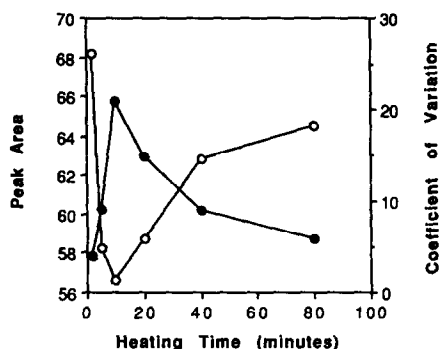


Fig. 3. The effect of heating time on response and precision for styrene. Headspace samples were prepared at room temperature and then heated. The heating time is the length of time the sample remained at 60° prior to analysis. Thermal equilibrium was achieved in approximately 5 min. Three replicate analyses were performed for each heating time. Other analytes exhibited similar trends in response and precision. (●) Coefficient of variation; (○) peak area.

were prepared and analyzed with the headspace sampler. As the headspace vials warmed to 60°, a new equilibrium concentration of analyte vapor in the headspace was approached. The vials reached thermal equilibrium in approximately 5 min. However, the concentration of analyte vapor in the headspace continued to rise for at least 80 min (Fig. 3). The coefficient of variation was inversely proportional to the concentration of analyte vapor (Fig. 3). Experiments with blood as matrix showed similar behavior. Thus, the optimum heating time for a sample would be at least 80 min.

Because of the mechanics of the constant heating-time apparatus, the heating time was required to be some multiple of the run time. Each sample was heated for two runs (74 min). Although a longer heating time would have allowed the analytes to reach equilibrium, the next allowable duration (111 min) would have significantly decreased the number of samples analyzed per day. Even though the analytes in the headspace vial were not in complete thermodynamic equilibrium between the phases, reproducible measurements could be made with the constant heating-time apparatus, because the heating period before sampling of the headspace was the same for each vial.⁵

A hyperbolic relationship between response and overpressure was derived from the basic gas laws. Response was proportional to the concentration in the headspace sample (C_s), in this case,

$$C_s = C_i \left(\frac{P_i}{P_i + P_a} \right) \quad (1)$$

where C_i is the concentration of analyte in the headspace prior to pressurization, P_i the initial headspace pressure (atmospheric), and P_a the overpressure (pressurization above atmospheric). This relationship was confirmed experimentally (data not shown). In order to deliver at least 1 ml of helium/headspace mixture to the sample loop, P_a had to be greater than approximately 0.2 bar. There was no discernible relationship between the precision and overpressure.

We confirmed that more analyte was contained in the sample loop when the loop and vial were not completely depressurized as indicated in the instrument manual.⁸ Therefore, the duration of sample venting was set to 2 sec, an insufficient time for complete depressurization. However, we noted that better reproducibility was achieved if P_a was 0.8–1.2 bar, which was higher than the overpressure optimum for sensitivity.

The optimum duration for pressurization and the time allowed for pressure equilibration in the sample vial were determined by replicate analysis of water spiked with analytes. Pressurization required at least 30 sec; shorter times resulted in poor precision and reduced sensitivity. Equilibration time did not affect the sensitivity. However, precision was highest with equilibration times greater than 30 sec.

Sample preparation

For valid measurements, the septum sealing the headspace vial must not allow analyte to escape. By pressurizing the vial and then submerging it under water, we evaluated the integrity of the septum seal, for silicone rubber–Teflon and butyl rubber–Teflon composite septa. Silicone rubber septa leaked after a single puncture with the 26-gauge needle used to add internal standard to the sample. Furthermore, this type of septum did not always form an air-tight seal. However, the butyl rubber–Teflon septa performed excellently and did not leak under 3 bar pressure even after the vial had been punctured five times. Gill *et al.*³ studied the loss of analytes from headspace vials and concluded that either Teflon- or aluminum-lined septa offered the best stability.

The effect of sample volume on response was determined experimentally. Blood (10 ml) was spiked with toluene, ethylbenzene, the xylenes, styrene, α -methylstyrene, and 4-methylstyrene, and a series of headspace vials was prepared, with different volumes of spiked blood. The

samples were then analyzed according to the standard procedure.

The response changed with blood volume as expected, but the magnitude of the change and the optimum volume were dependent on the analyte (Fig. 4). Apparently the compounds that are partitioned to the greatest extent into the air were most affected by the blood volume. Small variations in the blood volume dispensed would be more likely to affect the precision for compounds with a lower affinity for blood.

The relationship between blood volume and response was derived from the mass balance equation describing the partitioning of analyte between the two phases in the headspace vial. The mass balance equation is:

$$V_b C_i = V_b C_b + V_a C_a \quad (2)$$

where V_b is the volume of blood and water mixture in the headspace vial, C_i the concentration of analyte in the blood before partitioning, C_b the concentration of analyte in the blood after partitioning, V_a the volume of air (gas phase) in the headspace vial and C_a the concentration of analyte in the gas phase of the headspace vial after partitioning. By definition the partition coefficient between the blood and water mixture and air ($k_{b/a}$) is given by $k_{b/a} = C_b/C_a$, and the total vial volume is $V_i = V_b + V_a$; substituting these variables in equation (2) and solving for C_a gives:

$$C_a = \frac{V_b C_i}{V_b(k_{b/a} - 1) + V_i} \quad (3)$$

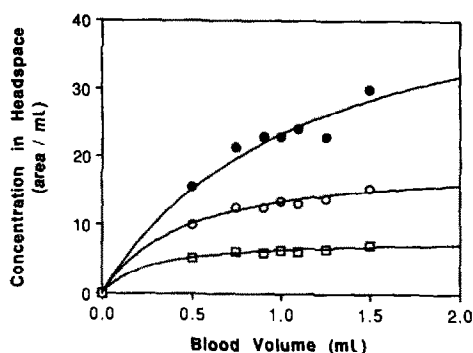


Fig. 4. The effect of sample volume on response. The blood was spiked with a solvent mixture (0.1 $\mu\text{g/ml}$) and various volumes were analyzed according to the procedure described. The standard volume of blood analyzed was 1 ml, to which 2 ml of water were added. The relationship between the blood volume and response is given by equation (3), but as $k_{b/a}$ was not known, least-squares non-linear regression was used to fit an equation of the form $C_a = V_b/(aV_b + b)$, where a and b are constants, to the results. The lines are the regression lines. Similar relationships held for all compounds analyzed. (●) Toluene; (○) styrene; (□) 4-methylstyrene.

The liquid phase is the blood-water mixture.

The sensitivity in headspace analyses can be increased by adding compounds that increase partitioning of the analyte into air. Inorganic salts have greatly increased the sensitivity of analyses for polar chemicals, such as alcohols^{1,10-12} and water-miscible ketones and aldehydes.¹ However, there is very little effect, if any, with non-polar chemicals.^{1,13,14} We have examined several additives which alter the physico-chemical structure of blood. In these experiments, 1 ml of blood was placed in a headspace vial with 2 ml of an additive. Additives were 0.9% saline water, 8M urea, 1M aluminum sulfate and 1 ml of water followed by 1 ml of 4.0M ammonium sulfate. Unadulterated blood (1 ml) was analyzed as a control. Three replicates were analyzed for each additive and control.

The additives which caused the blood to coagulate, ammonium sulfate and aluminum sulfate, increased the variability (Table 2). The importance of preventing blood from coagulating was noted previously, but without explanation.¹⁵ The additives which lysed the blood cells, *i.e.*, water and 8M urea, decreased the variability, as did saline which, in essence, thinned the blood. The response was increased most by addition of water to the blood. The concentrations of chloroform, toluene and styrene in the headspace were previously shown to be increased by hemolysis of blood by water.¹⁶ Hemolysis probably increased the response because it retarded coagulation of the blood. Solid-gas phase partitioning of analytes is less efficient than liquid-gas phase partitioning. In addition, hemolysis probably increased the availability of analytes from the blood cells,

which apparently contain higher concentrations of solvents than the surrounding plasma does.^{17,18}

The effect of sample storage upon response was evaluated. Replicate samples of spiked blood were prepared according to the standard procedure and stored at 4°. Sets of samples were analyzed on the day of preparation, and then 24 and 72 hr later. The response did not decrease during 72 hr of storage. Gill *et al.*³ showed that samples stored without headspace in bottles with Teflon-lined caps did not lose analyte during storage for 30 days.

Standard preparation

Four methods have previously been used to spike blood: direct addition of neat analyte to blood, addition of an aqueous solution of analyte to blood, addition of a blood solution of analyte to blood and addition of analyte in a water-miscible vehicle to blood. The primary goals in preparing standards for headspace analysis were quantitative transfer of the analyte into the liquid phase and rapid achievement of physicochemical equilibrium. Not all these methods could achieve these objectives.

Equilibrium was reached slowly (>24 hr) when immiscible liquids were mixed to prepare standards of halogenated hydrocarbons^{19,20} and aromatic hydrocarbons²⁰ in water. Furthermore, Radzikowska-Kintzi and Jakubowski¹⁵ indicated that introduction of μl volumes of undissolved hydrocarbons into blood samples caused problems with precise dosage. Formation of a micro-emulsion of immiscible solute dispersed in aqueous solution was discussed by Sanemasa *et al.*²¹ Solutions of analytes in blood have been used to spike samples.^{3,15} This ap-

Table 2. The effect of additives to the headspace blood sample on response and precision

Compound	Additive											
	None		Saline		Water		$(\text{NH}_4)_2\text{SO}_4$		$\text{Al}_2(\text{SO}_4)_3$		Urea	
	Mean	CV, %	Mean	CV, %	Mean	CV, %	Mean	CV, %	Mean	CV, %	Mean	CV, %
Toluene	113	22	129	4	146	6	72	16	128	21	119	4
Ethylbenzene	89	17	102	3	116	7	62	17	113	28	103	5
<i>p</i> -Xylene	88	16	105	2	113	7	61	19	111	31	97	5
<i>m</i> -Xylene	88	16	104	3	115	7	62	20	108	29	96	5
<i>o</i> -Xylene	84	14	100	2	107	6	62	23	115	29	83	4
4-Chloro- fluorobenzene	75	13	83	4	97	6	50	20	79	26	71	3
Styrene	66	9	68	3	76	5	47	28	32	80	41	2
α -Methylstyrene	51	7	61	2	70	6	47	32	29	87	38	3
4-Methylstyrene	33	10	49	5	42	5	33	34	23	86	26	3

Response was the mean peak area from three replicate analyses. Two ml of additive were added to 1 ml of blood prior to the analyses, except for $(\text{NH}_4)_2\text{SO}_4$ [where 1 ml of water was added, followed by 1 ml of $(\text{NH}_4)_2\text{SO}_4$ solution]. Aqueous solutions were: 0.9% saline, 4.0M $(\text{NH}_4)_2\text{SO}_4$, 1.0M $\text{Al}_2(\text{SO}_4)_3$, and 8M urea. CV is the coefficient of variation.

proach appeared to give good results, with a reported stability of 3 weeks for solutions of aromatic hydrocarbons and TCE. However, storage of blood solutions is problematic for some solvents, because of blood-induced degradation, for example, of esters²² and ethanol.¹¹ Furthermore, blood deteriorates during storage and this is accelerated by sepsis.

We prefer to use a spiking solution made with a water-miscible vehicle. Addition of a second solute to water, in this case the vehicle, has been shown to change the solute-vapor equilibrium constant.^{21,23} These secondary solutes have an influence only when their mole fraction is greater than 5×10^{-3} .²³ For this reason, we used 10 μ l of vehicle, which corresponded to a DMSO mole fraction of 1.5×10^{-3} in the aqueous phase of the headspace vial.

We initially used methanol as the vehicle but found it unsatisfactory because it was eluted early in the chromatogram and interfered with the quantification of TCE and toluene. Therefore, we evaluated several water-miscible solvents as substitutes, namely formamide, DMSO, dimethylformamide, 3,3'-oxydipropionitrile, hexamethylphosphoramide and propylene glycol. Formamide and dimethylformamide contained impurities and the solutions were not stable. A major peak, possibly for a contaminant in the solvent, appeared early in the chromatogram when 3,3'-oxydipropionitrile was used. Their high viscosity made it difficult to transfer solutions in propylene glycol. Hexamethylphosphoramide caused baseline disturbances on the chromatogram and posed additional handling problems because of its toxicity.

DMSO proved satisfactory as the vehicle. It was eluted very late in the chromatogram and did not interfere with any of the analytes. Solutions of the analytes in DMSO were stable when stored frozen at 4°. Freezing and thawing of DMSO solutions of analytes did not affect the analyte concentration. The DMSO solutions used contained only minor (<0.1%) impurities or decomposition products which were eluted before TCE. The impurities were identified by GC/MS as dimethylsulfide and methylsulfide.

Because the internal standard was used to correct for recoveries of analytes, it had to behave similarly to the analytes. We found that one potential internal standard, 4-chlorofluorobenzene, behaved similarly to all the aromatic analytes in method development experiments, but TCE and 4-chlorofluoroben-

zene exhibited different recovery and response as the experimental parameters were changed. To find an internal standard for TCE we therefore examined compounds structurally related to it. Few compounds satisfied the constraint of being chromatographically resolvable from the analytes and common blood components and not being present as an environmental or work place contaminant. 1,1-Difluoro-1,2,2-trichloroethane satisfied these constraints but was not ideal, owing to its slow degradation in aqueous solution at elevated temperatures (60°).

Analytical performance

Standard curves were obtained for six levels of analyte in spiked samples of human blood: 1, 0.5, 0.1, 0.05, 0.01 and 0 μ g/ml. Over this range the standard curve was linear (Table 3). TCE was not reliably quantified below 0.1 μ g/ml because of interference from the peaks of endogenous blood substances. Styrene and toluene had measurable background concentrations; these concentrations fluctuated, depending on the batch of blood used for standard preparation, but were less than 0.1 μ g/ml. The precision of response was calculated for each calibration point (Table 4). The coefficient of variation was generally less than 5%.

CONCLUSIONS

Static headspace analysis is an accurate and useful method for quantifying solvents in blood. Studies performed during development of the method showed that the headspace methodology must be optimized specifically for blood, rather than by use of parameters derived from headspace experiments with aqueous media. For example, procedures used to increase sensitivity in water analyses, such as salting-out, decreased the sensitivity for blood analyses because of their coagulative effects on blood.

Table 3. Linearity of the calibration curves [peak-area ratio, analyte to internal standard, plotted *vs.* concentration (μ g/ml)]

Compound	Intercept*	Slope*	r^2
TCE	0.014 \pm 0.004	0.41 \pm 0.01	0.981
Toluene	-0.034 \pm 0.001	0.36 \pm 0.005	0.998
Ethylbenzene	0.000 \pm 0.002	0.45 \pm 0.01	0.993
<i>p</i> -Xylene	-0.002 \pm 0.002	0.45 \pm 0.01	0.996
<i>m</i> -Xylene	-0.011 \pm 0.002	0.48 \pm 0.01	0.996
<i>o</i> -Xylene	-0.006 \pm 0.002	0.44 \pm 0.01	0.996
Styrene	-0.062 \pm 0.003	0.85 \pm 0.01	0.995

*Estimated value \pm standard error. Weighted least-squares linear regression (weight = $1/\sqrt{\text{concentration}}$).

Table 4. Precision of the method estimated from three replicates measurements of peak-area ratio for analyte/internal standard (ND = not detected)

Concentration in blood, $\mu\text{g/ml}$	TCE		Toluene		Ethylbenzene		p-Xylene		m-Xylene		o-Xylene		Styrene	
	Mean	CV, %	Mean	CV, %	Mean	CV, %	Mean	CV, %	Mean	CV, %	Mean	CV, %	Mean	CV, %
1.00	2.49	3.0	2.86	1.5	2.22	1.2	2.24	1.5	2.11	1.8	2.29	1.64	1.28	0.8
0.50	1.07	3.1	1.45	3.5	1.14	5.2	1.11	1.3	1.05	1.2	1.12	4.87	0.64	1.3
0.10	0.19	6.9	0.40	4.6	0.18	11.6	0.19	3.4	0.22	4.5	0.23	1.20	0.18	2.9
0.05	ND		0.25	2.9	0.07	3.8	0.09	4.3	0.11	1.1	0.10	16.5	0.12	3.2
0.01	ND		0.12	7.0	0.03	1.9	0.03	2.6	0.05	3.6	0.04	5.79	0.09	3.6
0.00	ND		0.09	3.2	ND		ND		ND		ND		0.08	3.2

For optimum sensitivity and precision, standards and samples must be prepared and manipulated in a way that minimizes loss of the volatile analytes. For valid quantification with the internal standard method of calibration, the physicochemical properties of the internal standard must be closely matched to those of the analytes; an internal standard that would be adequate for all the compounds investigated could not be found.

Acknowledgements—This research was supported by grants from the National Institute of Environmental Health Sciences (NIEHS ES 04696) and the National Institute of Occupational Safety and Health (NIOSH OH-02629). Support was also provided by the Workmen's Compensation Fund of the State of Washington, which is administered by the Washington Department of Labor and Industries. We thank P. L. Wylie (Hewlett-Packard) for his helpful suggestion on interfacing the headspace sampler to the gas chromatographic column.

REFERENCES

1. B. V. Ioffe and A. G. Vitenberg, *Headspace Analysis and Related Methods in Gas Chromatography*, Wiley-Interscience, New York, 1982.
2. J. D. Ramsey and R. J. Flanagan, *J. Chromatog.*, 1982, **240**, 423.
3. R. Gill, S. E. Hatchett, M. D. Osselton, H. K. Wilson and J. D. Ramsey, *J. Anal. Toxicol.*, 1988, **12**, 141.
4. P. L. Wylie, *Chromatographia*, 1986, **21**, 251.
5. *Idem*, *Headspace Analysis with Constant Sample Heating Time*, Application Note 228-58, Hewlett-Packard, Avondale, PA, 1988.
6. *Centers for Disease Control*, *MMWR*, 1987, **36**, Sup. 2S, 1.
7. B. Kolb, B. Liebhardt and L. S. Ettre, *Chromatographia*, 1986, **21**, 305.
8. *Operating and Service Manual for the HP 19395A Headspace Sampler*, Hewlett-Packard, Avondale, PA, 1988.
9. G. O. Nelson, *Controlled Test Atmospheres*, p. 100. Ann Arbor Science, Ann Arbor, MI, 1971.
10. M. Termonia, A. De Meyer, M. Wybauw and H. Jacobs, *J. HRC. & CC*, 1982, **5**, 377.
11. D. S. Christmore, R. C. Kelly and L. A. Doshier, *J. Forensic Sci.*, 1984, **29**, 1038.
12. M. Pelletier, M. Martin and W. Haerdi, *Mitt. Geb. Lebensmittelunters. Hyg.*, 1983, **74**, 339.
13. H. Kersting and H. Heberer, *Z. Gesamte Hyg. Ihre Grenzgeb.*, 1986, **32**, 552.
14. P. L. Wylie, *Trace Analysis of Volatile Compounds in Water*, Using the HP 19395A Headspace Sampler, Application Note 228-40, Hewlett-Packard, Avondale, PA, 1985.
15. H. Radzikowska-Kintzi and M. Jakubowski, *Int. Arch. Occup. Environ. Health*, 1981, **49**, 115.
16. M. Jakubowski, H. Radzikowska-Kintzi and G. Meszka, *Bromatol. Chem. Toksykol.*, 1980, **13**, 263.
17. D. D. Davies, R. B. Douglas and S. Ling, *Br. J. Anaesth.*, 1986, **58**, 1440.
18. M. J. Kamlet, R. M. Doherty, J. M. Abboud, M. H. Abraham and R. W. Taft, *Chemtech*, 1986, **16**, 566.

19. L. K. Jansen, *Determination and Use of Solute/Vapor Equilibrium Constants for Chlorinated Hydrocarbons, with Application to Industrial Hygiene Practice, Master's Thesis*, University of Washington, 1987.
20. M. E. McNally and R. L. Grob, *J. Chromatog.*, 1984, **284**, 105.
21. I. Sanemasa, Y. Miyazaki, S. Arakawa, M. Kumamaru and T. Deguchi, *Bull. Chem. Soc. Japan*, 1987, **60**, 517.
22. P. Pfäffli and N. Suartling, *J. Chromatog.*, 1985, **345**, 386.
23. C. Munz and P. V. Roberts, *Environ. Sci. Technol.*, 1986, **20**, 830.

ELECTRODEPOSITION ON PYROLYTIC GRAPHITE PLATFORMS FOR ELECTROTHERMAL ATOMIC-ABSORPTION SPECTROSCOPIC DETERMINATION OF LABILE LEAD IN SALINE WATER

JUWADEE SHIOWATANA

Department of Chemistry, Mahidol University, Bangkok 10400, Thailand

JAROSLAV P. MATOUSEK*

Department of Analytical Chemistry, The University of New South Wales, P.O. Box 1,
Kensington, N.S.W. 2033, Australia

(Received 31 October 1989. Revised 25 July 1990. Accepted 3 August 1990)

Summary—A technique for the determination of labile Pb in sea-water has been developed which uses co-deposition with mercury on 6–14-mg pyrolytic graphite platforms, followed by electrothermal atomization of the deposit. Optimization of the applied voltage, pH and sodium chloride concentration with respect to the deposition efficiency yielded a detection limit of 0.15 $\mu\text{g/l}$. Pb for 120-sec depositions with a single platform. As the amount of deposit increases linearly with deposition time up to 5 min and the simultaneous use of two platforms increases the analytical signal by a factor of 1.73, a further improvement is possible. Near-shore sea-water and estuarine water samples containing lead in the concentration range 0.4–1.3 $\mu\text{g/l}$. were analysed with an RSD better than 10%. Background correction was not required as the technique eliminates spectral interferences due to molecular absorption.

Although various techniques can be used for removing or suppressing interferences in electrothermal atomic-absorption spectrometry (ETAAS) methods, there are always limitations to their use, especially when dealing with high-salt matrices. Selective volatilization to remove the interferents prior to atomization is applicable when there is sufficient difference between the volatilities of the analyte and the interferents.¹ For determination of some elements, Zeeman background correction (with platform atomization), chemical modification, selective volatilization and use of peak integration are some of the possibilities for dealing with high-salt matrices.^{2–4} The modification of furnace design has also shown some potential for solving the problems arising from high-salt matrices. However, without separation of the salts from the analyte before the introduction of samples into the furnace, salt build-up at the cool ends of the furnace by condensation can occur rapidly after a few firings.⁵ Moreover, when very low concentrations, close to the detection limit, are involved, which is most

likely for trace metals in sea-water, preconcentration is often necessary.

Of the many preconcentration methods available, those which also separate the analyte from the matrix, such as solvent-extraction, sorption methods and electrodeposition, are more desirable for combination with ETAAS techniques.

Electrodeposition has many advantages in terms of sample size required, concentration factor, simplicity and freedom from contamination. The use of preconcentration by electrodeposition coupled with AAS methods was reported as early as 1967 by Brandenberger and Bader, who concentrated mercury from urine on a copper spiral electrode which was subsequently transferred to the absorption tube for atomization of the deposited mercury.^{6,7} They later extended the technique to determine Cd, Zn, Pb, Tl, Cu, Ag, Au and Pt, using tungsten or platinum wires⁸ in the same manner. Fairless and Bard have successfully used hanging mercury drop electrodes⁹ for electrodeposition and subsequent atomization. The hanging mercury drop electrode was not easy to handle and the mercury drop could not be reproducibly positioned in the graphite furnace, although its

*Author for correspondence.

transfer to a carbon filament was satisfactory. Jensen *et al.* overcame the problem by using a graphite boat to keep the drop in position.¹⁰ The wire methods, which were often followed by electrical heating in a cool inert atmosphere for atomization,^{6-8,11-15} suffer, like the wire loop¹⁶ and carbon rod¹⁷ methods, from recombination and condensation, which reduce the atomic population and cause background absorption. In addition, the residence time of the atoms in the light-path is often very short and spatial inhomogeneity of the atomic population makes selection of the measuring zone critical.¹⁸ Heating the wire (with deposit) in the hot reducing environment of a hydrogen flame^{15,19,20} or a graphite furnace²¹ overcame these problems. Czobik and Matousek²¹ deposited lead from sea-water or a blood digest on a thin tungsten wire, which was then inserted vertically into the centre of a graphite furnace for atomization. This approach combined the advantages of the graphite furnace technique with preconcentration and separation by electrodeposition. However, only a very thin wire was employed, in order to maximize the heating rate and minimize light-loss; the wire had a surface area of 0.012 cm². Thomassen *et al.*²² employed exhaustive electrolysis on a graphite rod, which was then ground and placed in the graphite furnace for atomization. This approach has the advantage of determination of several elements in the ground sample, but is time-consuming and prone to contamination from the several steps involved.

A more elegant development is direct deposition from a recirculated sample onto the inner surface of a graphite furnace tube, as proposed by Batley and Matousek²³ and Volland *et al.*²⁴ This technique was later applied to chemical speciation of chromium in natural water²⁵ and also served as a sampling technique²⁶ by *in situ* deposition of lead and cadmium from sea-water. After the deposition, the graphite tubes can be transported to the laboratory for immediate measurement or stored for later investigation, without any change in the amount of deposit. The efficiency of deposition on the graphite tube inner wall was improved threefold when a nylon insert was used to produce a thin layer flow-through cell configuration, as reported by Frick and Tallman,²⁷ who employed an HGA-2100 graphite tube for the determination of mercury in water samples. The improvement in sensitivity was explained by the increased linear velocity of the solution passing through the

electrode, which resulted in reduced thickness of the hydrodynamic diffusion layer. Toris *et al.*²⁸ designed a flow system for *in situ* deposition on a glassy-carbon furnace cup in the same manner. Only a very narrow linear range (up to 0.02 absorbance) was reported.

In this work, electrodeposition of labile lead from sea-water on a thin pyrolytic graphite platform has been examined. The electrodeposition step was followed by ETAAS determination in a tubular graphite furnace. This approach obviates the need to remove and replace the furnace tube for each determination. Since selectivity is not a problem in the ETAAS method, a simple two-electrode electrochemical system with a fixed applied voltage was used (rather than electrolysis at a cathodic potential controlled with a potentiostat). The effects of electrolysis conditions and atomization parameters have been studied, as well as the possibility of using more than one platform, to increase the sensitivity.

EXPERIMENTAL

Apparatus

A Varian Techtron AA-5 atomic-absorption spectrometer fitted with a Varian Techtron model 90 CRA furnace was used. For time-resolved measurements, the signal from the photomultiplier was processed by a simple current amplifier with an *RC* time constant of 10 msec, and was fed into a Tracor Northern TN-1505 signal averager.

The standard pyrolytic graphite-coated tubular furnaces were positioned between the support rods so that the sample injection hole was blocked by one of the rods to reduce diffusional loss of atoms. Thin platforms with dimensions 6.5 × 2.3 × 0.18 and 6.5 × 2.3 × 0.43 mm were machined from a solid pyrolytic graphite block (Ringsdorff). The finished platforms weighed approximately 6 and 14 mg, respectively.

Electrodeposition

Electrodepositions were done with a regulated d.c. supply with a voltage range of 0–12 V. A Perspex cell equipped with a magnetic stirrer (Fig. 1) was used. The electrode holder (Fig. 2) was machined from Teflon and a nylon screw was used to hold the platform. The platinum wire anode and cathode were inserted through holes drilled through the Teflon holder.

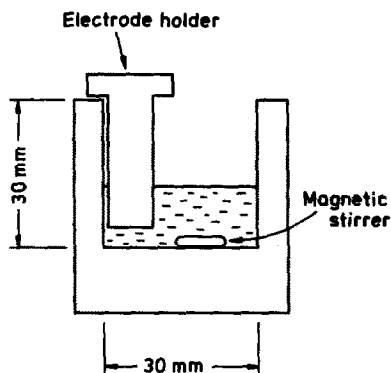


Fig. 1. Perspex cell for electrodeposition.

Reagents

Acetate buffer solutions and mercury(II) nitrate solutions were prepared from Merck "Suprapur" grade chemicals. Isopiastically distilled nitric acid and doubly distilled Milli-Q filtered water (referred to as Milli-Q water) were used throughout. A standard lead solution was prepared from analytical-grade chemicals and diluted with Milli-Q water when needed.

Samples of near-shore sea-water (Sydney) and estuarine water (Port Stephens) were collected in acid-washed polyethylene bottles, filtered through 0.45- μm membrane filters and stored at 4° until analysed.

Procedure

The cell, electrode holder and all glassware were soaked overnight in 1.0M nitric acid and cleaned with distilled and Milli-Q water before use.

A 10-ml sea-water sample was pipetted into the cell, followed by 0.10 ml of $1.5 \times 10^{-2}M$

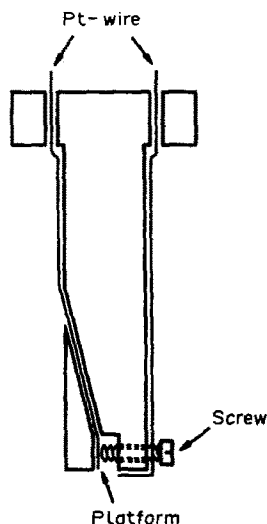


Fig. 2. Electrode holder.

mercury(II) nitrate solution and 0.05 ml of 1M acetic acid/2M sodium acetate buffer. With Teflon-tipped tweezers, one or two platforms were placed in position in the electrode holder and the nylon screw was tightened. The voltage supply was then switched on and the electrode holder (with platforms) submerged in the stirred solution for the required time. On completion of electrolysis, the assembly was quickly transferred into a beaker containing Milli-Q water, without disconnection of the electrical circuit, and was left there for 15 sec. The platforms were then detached, gently touched with filter paper to remove adhering water, and transferred to the furnace for atomization.

RESULTS AND DISCUSSION

Effect of electrode washing on AA signals

Electrodeposition in the presence of mercury(II) results in formation of a very thin film of mercury with trace metals co-deposited. The thin film is not very stable and can be removed by strong rubbing with a filter paper or by dissolution in acid solution, as confirmed by ETAAS determination of mercury before and after such treatment (Fig. 3). The mercury deposit was virtually unaffected when washed in water, with or without disconnection of the circuit, but traces of sodium chloride remained on the platform, as indicated by the second

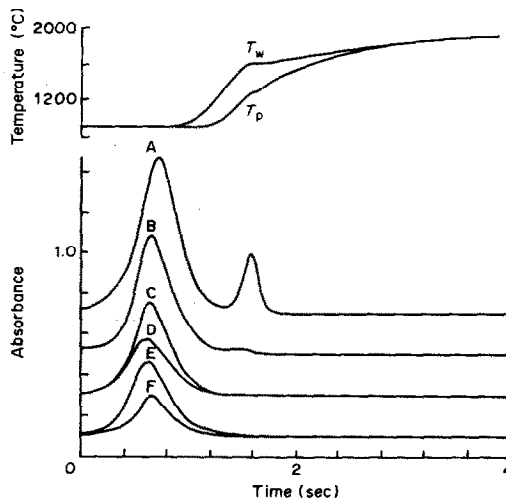


Fig. 3. Stability of the thin mercury film, monitored by AA at 253.6 nm. Platform with deposit washed with: A; Milli-Q water; B; Milli-Q water (and then rubbed with filter paper); C; 0.1% HNO_3 ; D; 0.1% HNO_3 , circuit disconnected; E; 1.0% HNO_3 ; F; 1.0% HNO_3 , circuit disconnected. Traces T_w and T_p represent the atomizer wall and platform temperatures, respectively, as measured with a radiational thermometer.

(sodium chloride molecular absorption) peak in trace A.

The effect of acid leaching was confirmed by the results for lead determination after different treatments, as shown in Fig. 4. Pure metallic lead could not be obtained, even with thorough washing of the deposit obtained from sodium chloride solution, because a small amount of sodium chloride was always found to be present on the platform, as manifested by the shift of appearance of the lead peak. For this reason, the peak for metallic lead (trace A in Fig. 4) was obtained by depositing lead from 25 $\mu\text{g/l}$. lead solution in 0.01% nitric acid without any other reagents added, and the platform washed with water thoroughly after deposition. The peak for metallic lead appeared to slightly precede the peak for lead in nitric acid solution, in agreement with the results of Czobik and Matousek.²¹

Figure 4 indicates that treatment with acid reduces the lead signals considerably. The shift to low temperature of the peak in trace B in Fig. 4 is due to residual sodium chloride, since the peak coincided with the lead peak originating from lead nitrate in the sodium chloride matrix (trace D). According to the procedure, the electrode is transferred to the wash solution with approximately 0.05 ml of sample solution

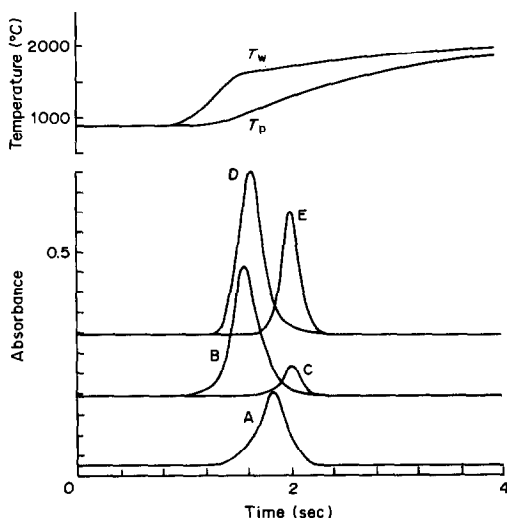


Fig. 4. AA peak appearance for Pb in various forms, measured at 217.0 nm with use of a 14-mg platform. Lead atomized from: A; metallic form; B; deposit following the proposed procedure; C; as for B, but washed with 1.0% HNO_3 ; D; 1 ml of 0.24 mg/l. Pb aqueous standard solution in 100 mg/l. NaCl; E; 1 μl of 0.10 mg/l. Pb in 1.0% HNO_3 . T_w and T_p represent atomizer wall and platform temperatures, respectively, as measured with a radiational thermometer.

adhering to the holder, which is diluted to about 100 mg/l. sodium chloride concentration in the 20 ml of wash water. Attempts to wash the platforms more thoroughly, with running water, to leave only the lead amalgam (which should give a peak appearing at the same temperature as in trace A) were unsuccessful, resulting in poor reproducibility, reduction of the peak height, and inconsistent peak appearances and shapes. Washing by immersion in Milli-Q water was therefore considered suitable, not only for these reasons, but also because of the freedom from contamination.

Effect of pH and applied voltage

The pH of the sample solution and the applied voltage have an important effect on the deposition efficiency in that they influence the degree of hydrogen evolution. Hydrogen evolution could increase the deposition efficiency of lead by contributing to the stirring action, thus reducing the diffusion layer thickness and improving the efficiency, but could also decrease the efficiency by reducing the surface available for lead deposition. In addition, the pH of the sample solution determines the amount of labile lead in the sea-water sample and thus affects the deposition efficiency.

The influence of applied voltage on electro-deposition efficiency was investigated over a wide pH range (Fig. 5). The results showed a sharp increase in the response at above 1.5 V, followed by an equally sharp decrease at above 3.5 V, which may have been caused by hydrogen covering the electrode, as hydrogen bubbles were clearly visible at this stage. The results showed that the optimum signals were obtained at between 2.0 and 3.0 V and these limits were used for the remainder of the experiments. At these applied voltages, the AA signals were only slightly affected by variations of pH between 3.0 and 6.1. The downward shift of the curves for pH 6.8 and 7.5 resulted from the lower availability of labile lead species at these pH values.

Metals in natural systems can occur in various forms, both labile and non-labile, depending on the pH. Batley and Florence have developed an anodic stripping voltammetry (ASV) speciation scheme for heavy metals in natural waters,^{29,30} with a pH of 4.8 as a boundary for labile form discrimination. For this reason, the same pH was used for electro-deposition in order to deposit the metals from their labile forms.

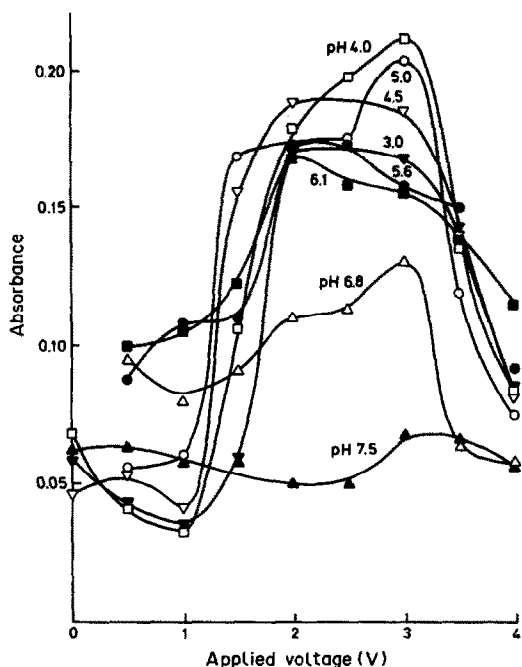


Fig. 5. The effects of applied voltage and pH on Pb AA signals measured at 217.0 nm. Sea-water pH was adjusted by adding μl amounts of 10% v/v HNO_3 , and 10-ml samples were electrolysed in the presence of $1.5 \times 10^{-4} \text{M}$ $\text{Hg}(\text{NO}_3)_2$ for 30 sec.

Effect of mercury(II) nitrate concentration

Mercury-plated electrodes have been shown to improve sensitivity and resolution in ASV analysis,^{31,32} and have found practical use in the determination of amalgam-forming elements by analytical methods employing preliminary electrodeposition, such as voltammetry and chronopotentiometry,³³ ASV³⁴ and a.c. voltammetry.³⁵ The advantage of mercury-plated over unplated electrodes (made of the same material) arises from the increased rate of the electrode processes, owing to amalgam formation. Florence³⁶ obtained the same advantage, for ASV analysis, by simultaneous deposition of mercury and trace metals from sample solutions to which mercury(II) nitrate had been added.

As co-deposited mercury causes no apparent interference in ETAAS analysis, mercury(II) nitrate was added to the sample solution to

maximize the efficiency of electrodeposition. The optimum amount of mercury(II) nitrate was investigated; a $1.5 \times 10^{-4} \text{M}$ concentration was considered to be sufficient for obtaining maximum signals with the present experimental arrangement.

Standard-addition technique with sea-water

Sea-water and estuarine water samples were analysed for lead by the standard-addition technique. The standard-addition plot was linear up to 0.2 absorbance and then only slightly curved up to 0.3 absorbance. The reagent blank was checked by doubling the concentrations of the added reagents and was found to be negligible.

To evaluate the accuracy of the proposed method, the samples were also analysed by ASV (Table 1). The two approaches gave comparable results, considering the ultratrace levels and the difficult matrix. As in some earlier work^{23,26} however, the electrodeposition-ETAAS technique appears to yield consistently higher results. The fact that the ASV analyses were performed under clean-room conditions and this facility was unavailable for the ETAAS work, could be a contributing factor.

It was pointed out by Florence and Batley³⁷ that the recovery of the trace metals added to natural waters cannot be determined by measuring the recovery of an ionic spike unless the water has first been treated to convert all forms of the metal into the free metal ions. It is unlikely that lead will be adsorbed on inorganic colloids at pH 6.0,^{38,39} but lead in sea-water can be adsorbed on organic colloids at the pH employed. For this reason, the standard-addition technique was also applied for lead in 3.5% sodium chloride solution for comparison with the standard-addition plot for sea-water. The slopes in both cases were the same within experimental error, which indicated that the lead added to the sea-water was present in the labile form. In practical terms, this means that analyses can be done with lead standards prepared in 3.5% sodium chloride solution instead of by the more time-consuming standard-addition technique.

Table 1. Results of Pb determination in saline water

Sample	Pb content, $\mu\text{g/l}$.	
	This method*	ASV†
Sea-water (Coojee Bay, Sydney)	0.44 ± 0.05	0.38 ± 0.03
Estuarine water 1 (Port Stephens)	0.65 ± 0.08	0.62 ± 0.05
Estuarine water 2 (Port Stephens)	1.32 ± 0.14	1.20 ± 0.10

*Deposition for 120-sec at 2.0 V, performed in triplicate.

†ASV at pH 4.8 performed in triplicate by G. E. Batley.

However, sea-water from different sources may contain colloidal organic matter which could strongly bind, adsorb or occlude the added lead at the pH used. Accordingly, it is important to realize that the proposed method is limited to the determination of labile lead. Total lead can be determined by digesting the sea-water samples with nitric acid, adjusting the pH and following the method described.

Deposition efficiency

Under certain electrolysis conditions the electrochemical properties of the electrolyte are related to the electrolysis time and the ratio of the original and final concentrations of the analyte, according to equation (1):^{40,41}

$$\log\left(\frac{C_0}{C_t}\right) = \frac{0.43 DA t}{V\Delta} \quad (1)$$

where D is the diffusion coefficient (cm^2/sec) of the species being reduced, A the electrode area (cm^2), Δ the diffusion layer thickness (cm), t the electrolysis time (sec), V the electrolyte volume (ml) and C_0 and C_t the original and final (at time t) concentrations, respectively.

Equation (1) can be rearranged to give

$$\frac{C_0}{C_t} = \exp(DAt/V\Delta)$$

$$\frac{(C_0 - C_t)V}{C_0V} = 1 - \exp(Kt/V) \quad (2)$$

where $K = DA/\Delta$.

In this equation the term $(C_0 - C_t)V$ represents the amount of metal deposited, and the term C_0V signifies the original amount of the analyte metal. It follows that the amount of metal deposited will be proportional to the original amount as long as Kt/V is kept constant. This means that not only exhaustive electrolysis but also substoichiometric electrolysis can be employed.

To increase the deposition efficiency, some of the parameters above were investigated. The diffusion layer thickness was minimized by vigorous mechanical stirring of the electrolyte in the deposition step, and slow stirring during washing of the platform helped to minimize any possible deposition from the wash solution and to protect the deposited film.

Use of a small volume of electrolyte increases the relative concentration factor (C_0/C_t) when the other parameters are kept constant. This alters the concentration of the remaining sol-

ution (C_t) considerably, so repeated deposition from the same sample solution is not feasible. Furthermore, the use of small sample volumes for deposition causes non-linearity in the dependence of deposited amount on time, as can be seen below.

From equation (2)

$$\frac{C_0 - C_t}{C_0} = \frac{Kt}{V} - \frac{K^2t^2}{2V^2} + \dots \quad (3)$$

From the relationship $C_0/C_t = \exp(Kt/V)$, $Kt/V \rightarrow 0$ when C_0/C_t is ~ 1 , so

$$\frac{C_0 - C_t}{C_0} = \frac{Kt}{V} \quad (4)$$

This result implies that the amount deposited is a linear function of time when C_0/C_t is close to unity. This is true for larger volumes of electrolyte. On the other hand, if V is small, C_0/C_t will be greater than unity and the terms following Kt/V in equation (3) cannot be neglected. Under these circumstances, the graph of amount deposited *vs.* time becomes non-linear.

It can be concluded from the reasoning above that although any constant V and t can be employed for preconcentration by electrodeposition, a wider linear relationship between the amount of deposit and time is obtained with larger sample volumes. In addition, repeated depositions can be made from the same solution.

To determine the fraction of lead deposited on the platform when 10 ml of sample solution was electrolysed for 60 sec, the result from direct injection of 1 μl of 0.24 mg/l. lead (0.24 ng) in 100 mg/l. sodium chloride solution onto the platform was compared with the signal obtained by the electrodeposition procedure. On this basis, it was established that under the experimental conditions employed the amount electrodeposited was 0.3% of the total lead content of the sample.

Effect of deposition time

The sensitivity of the electrodeposition-ETAAS method can be increased by extending the deposition period. Theoretically, the amount of metal deposited increases linearly with time when C_0/C_t is close to unity [equation (4)]. This was confirmed experimentally, as a linear relationship was obtained for deposition times of up to 5 min. A longer period of time was not tested, because of the practical consideration of limiting the analysis time, but C_0/C_t can

be calculated from equation (1) to predict whether C_0/C_t will be a non-linear function of t at any deposition time. For example, for 30-min deposition, the fraction deposited will be 8.6% compared with the 0.3% for 1-min deposition, giving a 4.2% deviation from linearity at 30 min in the plot of amount of deposit *vs.* time. The characteristic concentration found for the determination of lead in sea-water with deposition for 120 sec was $0.04 \mu\text{g/l}$.

Effect of sodium chloride concentration

As the sodium chloride concentration influences both the diffusion coefficient (D) and the diffusion layer thickness (Δ) in equation (1), its effect on the slope of the standard-addition plots was investigated. The results (Fig. 6) showed a decrease in the slope with decreasing sodium chloride concentration. These changes are apparently due to the composite effect of D and Δ . The thickness of the diffusion layer decreases with decreasing viscosity. Changes in the sodium chloride concentration can influence speciation of the analyte, and thus the concentration, nature and size of the diffusing species, which alter the value of D . Lead, at the pH employed for sea-water analysis, is present mostly in the form of chloro-complexes.⁴² The lead species in the absence of sodium chloride are likely to be aquo-complexes or free ions. From the results presented in Fig. 6, it is evident that the chloro-complexes have larger diffusion coefficients. This result agrees with the observations of Meites,⁴³ who reported the diffusion current constant (proportional to $D^{1/2}$) to be

greater for lead in 1M hydrochloric acid than in 1M nitric acid.

There are some additional factors influencing D and Δ , such as temperature, but it is not the purpose of this work to examine these aspects in detail. However, the samples to be electrolysed were always brought to room temperature to minimize effects due to temperature variations.

Enhancement of sensitivity with multiple platforms

As the electrodeposition efficiency depends on the surface area of the platform used, the sensitivity of the method can be enhanced either by increasing the surface area of one platform or by atomization of deposits from several platforms. In this work, a two-platform system was investigated. The result obtained by the standard-addition technique with two platforms used simultaneously, agreed with that of the single-platform approach, as shown in Fig. 7. There would be the disadvantage of light-loss by use of more platforms, owing to the obstruction of the light-path, and also difficulty in handling. It was observed in this experiment that light-losses of 3 and 9% occurred for use of two and three platforms, respectively, whereas one platform caused no perceptible loss. The sensitivity achieved with the two-platform system was 1.73 times better than that with a single platform. This is less than the theoretical value of 2, because the heating rate of the two platforms is lower than that of the single platform at the same furnace-temperature setting.

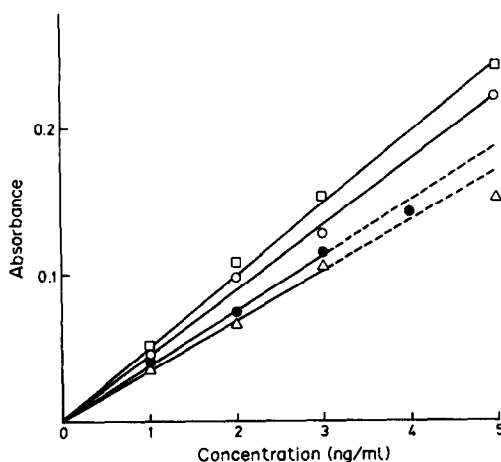


Fig. 6. Effect of NaCl concentration on the slope of standard-addition plots. Sea-water was diluted to various degrees: (□) 100%, (○) 60%, (●) 30%, (△) 0% sea-water. Sea-water (10 ml) containing $1.5 \times 10^{-4}M$ $\text{Hg}(\text{NO}_3)_2$ and acetate buffer (pH 4.8) was electrolysed at 2.0 V for 60 sec.

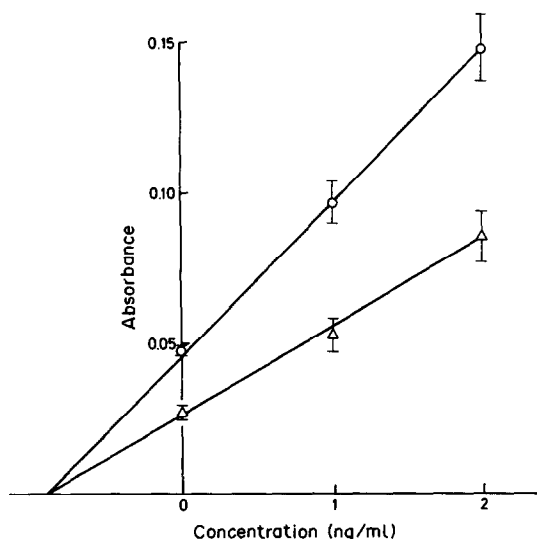


Fig. 7. Comparison of standard-addition plots for (△) single-platform and (○) two-platform atomization. Experimental conditions are the same as for Fig. 6, except for use of 30-sec deposition time.

Interference effects

Interference effects in this method can originate from both the electrodeposition and atomization steps. In the atomization step, under optimum experimental conditions no molecular absorption was observed, as confirmed by the use of a hydrogen lamp, and, therefore, background correction was not required. However, the small amount of sodium chloride remaining on the platform, though causing no spectral interference, did shift the appearance of the peak to lower temperatures, as seen in Fig. 4. Good reproducibility of peak-height measurements confirmed that a small variation in the amount of sodium chloride adhering to the platform before atomization did not influence the ETAAS determinations. The co-deposited mercury should not cause any interference in the atomization of lead, since it evaporates and atomizes at a temperature well below the appearance temperature of lead. Other metals likely to be co-deposited along with lead from sea-water include Bi, Cu, Cd, Zn, Tl, In, Sb, Mn and Ag. Thomassen *et al.*²² found no interference effect on 50 $\mu\text{g/l}$. lead in the presence of a thousandfold ratio of Cd, Mg, Fe, Mn, Zn or Ni, with exhaustive electrolysis on a carbon rod.

By analogy with the deposition step in thin-film ASV techniques, interference with electrodeposition in this method can occur as a result of competitive reduction of other elements co-existing in the sample solution. Florence⁴⁴ has examined such effects on each of eight species [Bi, Sb(III), Cu, Pb, In, Cd, Tl and Zn] in the presence of all the others plus Ni, Mn and Fe, at 10 times their normal concentration levels in sea-water. He found that the stripping current for Zn was depressed by Cu and Ni as a result of the formation of intermetallic compounds, but no other interferences were observed for ASV of the remaining elements.

Table 2. Reproducibility of the electrodeposition-ETAAS method

Pb concentration in sea-water, $\mu\text{g/l}$.	Mean absorbance (10 replicates)	RSD, %
0.65	0.075	5.7
1.40	0.146	9.3

These observations appear to be confirmed by the present work, as the results for standard addition of lead showed a linear plot and identical slopes for sea-water samples and 3.5% sodium chloride solution.

Reproducibility and detection limit

The reproducibility of the electrodeposition-ETAAS method was evaluated by obtaining the standard deviations for 10 determinations at two different concentration levels (Table 2). The detection limit, defined as the concentration that gives a reading equal to three times the standard deviation of a series of 10 determinations at or near blank level, was calculated to be 0.15 $\mu\text{g/l}$. for 120-sec deposition and use of a single platform. This detection limit is adequate only for the determination of lead in estuarine or near-shore sea-water from polluted areas. For the determination of open-ocean sea-water with lower lead concentration levels, a double-platform system combined with an extension of the deposition time would be necessary.

CONCLUSIONS

This work uses electrodeposition for preconcentration and separation of lead onto thin pyrolytic graphite substrates and then platform atomization for detection by atomic-absorption spectrometry.

Table 3 compares the sensitivity of several methods which use electrodeposition and graphite furnace atomization. The normalized

Table 3. Comparison of characteristic concentrations and electrode surface areas for some electrodeposition-furnace AAS techniques

Technique	Estimated electrode surface area, cm^2	Characteristic concentration, with 5 min deposition, $\mu\text{g/l}$.	Normalized characteristic concentration, $\mu\text{g/l}$.
W wire ²¹	0.012	0.15	0.002
Pyrolytic graphite-coated tube ²³	0.85	0.02	0.017
Glassy-carbon cup ²⁸	0.35	0.06	0.021
Present work			
(one platform)	0.30	0.016	0.0050
(two platforms)	0.60	0.009	0.0054

*Normalized for 1 cm^2 surface area of electrode.

sensitivity was obtained by assuming linear relationships between the amount of deposit and time, and the amount of deposit and surface area. This assumption was justified in this case, as can be seen from equation (1). The normalized sensitivities for the pyrolytic graphite coated tube and the glassy-carbon cup methods show comparable values, whereas the platform method increased the sensitivity by a factor of about four. This improvement could originate from variations in many factors, such as atomization of lead from different compounds and under different electrodeposition conditions (effects of temperature and electrolyte mobilization). Furthermore, in direct deposition on the furnace tube and cup,^{29,33} the metals are distributed evenly along the furnace length or cup depth, which results in reduced residence time in the light-path for the atoms deposited at the furnace ends. In addition, the cup configuration gives a different pattern of atom loss during atomization.

The tungsten wire method²¹ appears to offer the highest sensitivity. The faster heating rate due to the small mass of the wire and possibly to the high thermal conductivity of tungsten is considered to play an important role in this context. Therefore, for elements with low atomization temperatures, deposition on a tungsten platform followed by atomization in a graphite furnace could give improved results.

Acknowledgements—The authors wish to express gratitude to Dr. G. E. Batley for ASV analyses and valuable discussions and to Dr. H. K. J. Powell for helpful comments.

REFERENCES

1. C. L. Chakrabarti, C. C. Wan and W. C. Li, *Spectrochim. Acta*, 1980, **35B**, 93.
2. G. R. Carnrick, W. Slavin and D. C. Manning, *ibid.*, 1981, **53**, 1866.
3. E. Pruszkowska, G. R. Carnrick and W. Slavin, *Anal. Chem.*, 1983, **55**, 182.
4. Z. Grobowski, R. Lehman, B. Radziuk and U. Völlkopf, *At. Spectrosc.*, 1984, **5**, 87.
5. Discussion Session following the lecture by W. Slavin, held at the School of Chemistry, UNSW, April 1985.
6. H. Brandenberger and H. Bader, *Helv. Chim. Acta*, 1967, **50**, 1409; *At. Abs. Newsl.*, 1967, **6**, 101.
7. *Idem, ibid.*, 1968, **7**, 53.
8. H. Brandenberger, *Chimia*, 1968, **22**, 449.
9. C. Fairless and A. J. Bard, *Anal. Chem.*, 1973, **45**, 2289.
10. F. O. Jensen, J. Doležal and F. J. Langmyhr, *Anal. Chim. Acta*, 1974, **72**, 245.
11. W. Lund and B. V. Larsen, *ibid.*, 1974, **70**, 299.
12. *Idem, ibid.*, 1974, **72**, 57.
13. W. Lund, B. V. Larsen and N. Gundersen, *ibid.*, 1976, **81**, 319.
14. V. I. Rigin, *J. Anal. Chem. USSR*, 1979, **34**, 1782.
15. M. P. Newton and D. G. Davis, *Anal. Chem.*, 1975, **47**, 2003.
16. M. H. West, J. F. Molina, C. L. Yuan, D. G. Davis and J. V. Chauvin, *ibid.*, 1979, **51**, 2370.
17. C. Fairless and A. J. Bard, *Anal. Lett.*, 1972, **5**, 433.
18. M. D. Amos, P. A. Bennett, K. G. Brodie, P. W. Y. Lung and J. P. Matousek, *Anal. Chem.*, 1971, **43**, 211.
19. B. Holen, R. Bye and W. Lund, *Anal. Chim. Acta*, 1981, **130**, 257.
20. *Idem, ibid.*, 1981, **131**, 37.
21. E. J. Czobik and J. P. Matousek, *Spectrochim. Acta*, 1980, **35B**, 741.
22. Y. Thomassen, B. V. Larsen, F. J. Langmyhr and W. J. Lund, *Anal. Chim. Acta*, 1976, **83**, 103.
23. G. E. Batley and J. P. Matousek, *Anal. Chem.*, 1977, **49**, 2031.
24. G. Volland, P. Tschöpel and G. Tölg, *Anal. Chim. Acta*, 1977, **90**, 15.
25. G. E. Batley and J. P. Matousek, *Anal. Chem.*, 1980, **52**, 1570.
26. G. E. Batley, *Anal. Chim. Acta*, 1981, **124**, 121.
27. D. A. Frick and D. E. Tallmann, *Anal. Chem.*, 1982, **54**, 1217.
28. G. Torsi, E. Desimoni, F. Palmisano and L. Sabbatini, *Anal. Chim. Acta*, 1981, **124**, 143.
29. G. E. Batley and T. M. Florence, *Mar. Chem.*, 1976, **4**, 347.
30. *Idem, Anal. Lett.*, 1976, **9**, 379.
31. D. K. Roe and J. E. A. Toni, *Anal. Chem.*, 1965, **37**, 1503.
32. W. R. Matson, D. K. Roe and D. E. Carritt, *ibid.*, 1965, **37**, 1594.
33. S. P. Perone and K. K. Davenport, *J. Electroanal. Chem.*, 1966, **12**, 269.
34. S. P. Perone and A. Brumfield, *ibid.*, 1967, **13**, 124.
35. E. M. Roizenblat, L. F. Levchenko and G. N. Veretina, *J. Anal. Chem. USSR*, 1973, **28**, 25.
36. T. M. Florence, *J. Electroanal. Chem.*, 1970, **27**, 273.
37. T. M. Florence and G. E. Batley, *CRC Crit. Rev. Anal. Chem.*, 1980, **9**, 219.
38. R. R. Gadde and H. A. Laitinen, *Anal. Chem.*, 1964, **46**, 2022.
39. T. M. Florence, *Water Res.*, 1977, **11**, 681.
40. J. J. Lingane, *J. Am. Chem. Soc.*, 1945, **67**, 1916.
41. *Idem, Electroanalytical Chemistry*, Interscience, New York, 1953.
42. T. M. Florence and G. E. Batley, *Talanta*, 1976, **23**, 179.
43. L. Meites, *Polarographic Techniques*, Interscience, New York, 1955.
44. T. M. Florence, *J. Electroanal. Chem.*, 1972, **35**, 237.

DETERMINATION OF LEAD IN HOUSEHOLD REFUSE FLY-ASH BY X-RAY FLUORESCENCE SPECTROMETRY AND A MODIFIED STANDARD-ADDITION TECHNIQUE

MARIT ANDERSSON and ÅKE OLIN*

Department of Analytical Chemistry, Uppsala University, P.O. Box 531, S-751 21 Uppsala, Sweden

(Received 26 April 1990. Accepted 9 October 1990)

Summary—Lead in fly-ash from a garbage incinerator has been determined by X-ray fluorescence spectrometry (XRFS) and a modified standard-addition method. To keep the attenuation properties of the spiked samples constant, decreasing amounts of an attenuation modifier [mercury (II) acetate] were added together with increasing amounts of the standard (lead nitrate). Linearity between fluorescence intensity and amount of lead was thus obtained, so the amount of lead in the sample could be evaluated by linear regression. The amount of modifier needed could be calculated from a simple expression. The method was validated by comparison with the results obtained by applying atomic-absorption spectrometry (AAS) to solutions made by leaching the fly-ash with strong acid. For 8 fly-ash samples, containing between 0.8 and 1.35% lead, the largest absolute difference between the two sets of results was 0.03%. Theoretical calculations based on a simplified version of the Sherman equation were performed to confirm the linearity of the modified standard-addition curves.

The standard-addition method is often used in analysis by instrumental methods when the matrix affects the sensitivity. For most instrumental techniques the relationship between the analytical signal and the amount, or concentration, of the analyte is linear or can be made linear by a simple transformation. The standard-addition function, *i.e.*, the relationship between the analytical signal and the standard addition, can then be evaluated by linear regression to yield the analytical result.

The relationship between line intensity and concentration is non-linear in X-ray fluorescence spectrometry (XRFS).¹ At low analyte concentrations, however, the relationship approaches linearity and the standard-addition method can be used.^{2,3} The concentration range in which linearity can be expected depends on the properties of the analyte as well as on those of the matrix.⁴ The heavier the analyte and the lighter the matrix, the more restricted will the linear range be.

A non-linear variant of the standard-addition function was used previously for the determination of lead in fly-ash from a garbage incinerator.⁵ This analysis represents the case of a heavy absorber in a light matrix. A three-parameter standard-addition function was used

to evaluate the lead concentration from the measurements. The results agreed well with those found by atomic-absorption spectrometry (AAS) applied to solutions obtained by digestion of the samples with strong acid. The method is time-consuming, however, since an increased number of standard additions must be made, owing to the increased number of parameters. Also, the result seemed to be sensitive to small experimental errors, but this was not more closely investigated. We have, therefore, been looking for a method which yields a linear standard-addition plot. The results of this investigation are presented here.

THEORY

In the standard-addition method, additions, b_i , of a standard (B) are made to portions, a_i , of the analytical sample (A) where $i = 1, 2, \dots, N$ is the running number of a portion. The weights of A and B taken can be denoted by a_i and b_i , respectively.

In the "normal" standard-addition method, as applied, for instance, to an AAS analysis of an aqueous sample, the sample portions are of equal size. The portion of sample plus the added standard is diluted to a fixed volume in order to guarantee that the concentrations of the interferences are equal in all solutions used to generate the standard-addition curve. In the standard-

*Author for correspondence.

addition method proposed here for XRFs, such restrictions are unnecessary. Since solid samples are analysed in XRFs, it would be inconvenient to have to weigh out exactly equal amounts of sample. The variation in sample size is allowed for by using the weight taken (a_i) in the derivation of the equations used for the method. The only restrictions on a_i are that the weights can be determined with acceptable accuracy and that the amount is sufficient to make a disk for the fluorescence measurement.

For a heavy element in a light matrix there is no enhancement of the XRF signal and the line intensity, I , can be written as⁶

$$I_i = Q(C_x + y_i C_0) \int_{\lambda_0}^{\lambda_{edge}} \frac{\mu_x(\lambda) J(\lambda) d\lambda}{\mu_A^*(\lambda) + y_i \mu_B^*(\lambda)} \quad (1)$$

where Q is a constant of proportionality, $\mu_x(\lambda)$ the mass-attenuation coefficient of the analyte, $\mu_A^*(\lambda)$ and $\mu_B^*(\lambda)$ are the effective mass-attenuation coefficients of the sample and standard, $J(\lambda)$ is the intensity of the tube spectrum and y_i the ratio b_i/a_i . The integral is taken from the short-wavelength end of the spectrum to the absorption edge of the analytical line.

When the analyte is present at low concentration in the sample, the concept of an equivalent wavelength, λ_e , that is largely independent of small changes in the sample composition, may be applied.⁷ Equation (1) can then be written as

$$I_i = \frac{Q'(C_x + y_i C_0) \mu_x(\lambda_e)}{\mu_A^*(\lambda_e) [1 + y_i \mu_B^*(\lambda_e) / \mu_A^*(\lambda_e)]} \quad (2)$$

where Q' now includes the constant intensity of the excitation radiation. The equation contains three unknown parameters [$Q' \mu_x(\lambda_e) / \mu_A^*(\lambda_e)$; $\mu_B^*(\lambda_e) / \mu_A^*(\lambda_e)$; C_x] and was used in the previous method for the determination of lead in household fly-ash.⁵ The non-linearity of the standard-addition function $I = f(y)$, is caused by the term $y \mu_B^* / \mu_A^*$ in the denominator. Only when this term is small compared to unity, will the function be linear. By dilution of the sample with a diluent, and use of the same size of a_i , y can be made smaller, since smaller standard additions are required. However, for many samples, the addition of a diluent also diminishes μ_A^* , so $y \mu_B^* / \mu_A^*$ might then still inflict a curvature on the standard-addition line.

If additions to the sample can be made so that the denominator of the integrand in equation (1) remains constant, the curvature would be removed. This might be achieved by adding not only the standard but also a second compound,

called the (absorption) modifier. The modifier will be denoted by M and it does not contain the analyte. Equation (1) would then read

$$I_i = Q \left(C_x + \frac{b_i}{a_i} C_0 \right) \times \int_{\lambda_0}^{\lambda_{edge}} \frac{\mu_x(\lambda) J(\lambda) d\lambda}{\mu_A^*(\lambda) + \frac{b_i}{a_i} \mu_B^*(\lambda) + \frac{m_i}{a_i} \mu_M^*(\lambda)} \quad (3)$$

Proportionality between I and the factor involving concentrations will be obtained if the value of the integral can be made constant, *i.e.*, independent of b_i , by a suitable choice of m_i . This would be the case if, for each excitation wavelength, the quantity $z_i(\lambda)$ given by

$$z_i(\lambda) = \frac{\mu_x(\lambda)}{\mu_A^*(\lambda) + \frac{b_i}{a_i} \mu_B^*(\lambda) + \frac{m_i}{a_i} \mu_M^*(\lambda)} = \frac{\mu_x(\lambda)}{\mu_i^*(\lambda)} \quad (4)$$

can be made independent of b_i .

The largest addition of standard, b_N , is usually chosen so that the analyte concentration is increased by a factor of 2–4. This addition will give the denominator of equation (4) its greatest value, $\mu_N^*(\lambda)$, and no modifier is added ($m_N = 0$). The modifier should be added to the other sample mixtures so that $\mu_i^*(\lambda)$ equals $\mu_N^*(\lambda)$. Thus

$$\begin{aligned} \mu_A^*(\lambda) + \frac{b_i}{a_i} \mu_B^*(\lambda) + \frac{m_i}{a_i} \mu_M^*(\lambda) \\ = \mu_A^*(\lambda) + \frac{b_N}{a_N} \mu_B^*(\lambda) \end{aligned} \quad (5)$$

or

$$\begin{aligned} m_i(\lambda) = \frac{\mu_B^*(\lambda)}{\mu_M^*(\lambda)} \left(\frac{a_i b_N}{a_N} - b_i \right) \\ = r(\lambda) \left(\frac{a_i b_N}{a_N} - b_i \right) \end{aligned} \quad (6)$$

For the amount of modifier to be independent of the exciting wavelength, the quotient $\mu_B^*(\lambda) / \mu_M^*(\lambda)$ must be independent of λ . The quotient can be written

$$r(\lambda) = \frac{\mu_B^*(\lambda)}{\mu_M^*(\lambda)} = \frac{\mu_B(\lambda) + G \mu_B(\lambda_f)}{\mu_M(\lambda) + G \mu_M(\lambda_f)} \quad (7)$$

where λ_f is the fluorescence wavelength and G a constant. An approximately constant value of $r(\lambda)$ can be expected only if $\mu_B(\lambda) / \mu_M(\lambda) \sim \mu_B(\lambda_f) / \mu_M(\lambda_f)$. Hence, the modifier and the analyte must absorb the exciting radiation between absorption edges of the same notation. This must also be the case for the analytical line.

Therefore the analyte and the modifier elements in general must be close together in the same period of the periodic table, with the atomic number of the modifier lower than that of the analyte. The factor $\mu_x(\lambda)J(\lambda)$ in the integrand of equation (3) determines the wavelength range in the tube spectrum that is of importance for excitation. In certain cases, only a limited range need be considered and in the limit the exciting spectrum can be replaced by a narrow wavelength range centred around λ_c . In this case $r(\lambda)$ will be given by

$$r(\lambda_c) = \frac{\mu_B(\lambda_c) + G\mu_B(\lambda_r)}{\mu_M(\lambda_c) + G\mu_M(\lambda_r)} \quad (8)$$

and the previous restrictions on the modifier can be slackened.

The value of $r(\lambda)$ can be calculated from equation (7) without knowledge of the composition of the sample. It should also be noted that the modifying element may be present in the original sample. These attributes follow from the additivity of absorption. Once a tentative value of $r(\lambda)$ has been calculated from equation (7) or (8), equation (3) can be used to test by theoretical calculations whether proportionality between I and amount of analyte is indeed achieved.

The value of $r(\lambda)$ is obtained by calculation and an error in $r(\lambda)$ will lead to a systematic error in C_x . The values of the mass attenuation coefficients may vary by up to 10% between different sources. Fortunately, quotients between coefficients, as needed here, are more consistent. An estimate of the error caused in the analytical result by an uncertainty in $r(\lambda)$ is needed. It will be developed for the case when only a single standard addition is made. Excitation by monochromatic radiation will be assumed, in order to simplify the equations. The intensity will then be

$$I_1 = \frac{Q''C_x}{\mu_A^* + rb_2\mu_M^*/a_2} \quad (9)$$

Index 1 refers to the portion to which only modifier is added, and index 2 to the portion to which only the standard is added. The calculated value of $r(\lambda)$ is denoted by r .

In a two-point standard addition, C_x is calculated from

$$C_x = \frac{I_1 \Delta C}{I_2 - I_1} \quad (10)$$

where ΔC is b_2C_0/a_2 , equation (3).

From equations (9) and (10) we obtain

$$\frac{dC_x}{dr} = \frac{dI_1 dC_x}{dr dI_1} = -\frac{C_x I_2 \alpha}{(I_2 - I_1)(1 + \alpha r)} \quad (11)$$

where $\alpha = b_2\mu_M^*/a_2\mu_A^*$. The relative error in C_x , $\Delta C_{x,rel}$, is

$$\Delta C_{x,rel} = -\frac{I_2 \alpha r \Delta r_{rel}}{(I_2 - I_1)(1 + \alpha r)} \quad (12)$$

The influence of moderate values of Δr_{rel} on I_1 is small and the first factor in equation (12) may be regarded as constant. Hence the relative error in C_x is largely determined by, and diminishes with, αr . From equation (7) and the definition of α we find $\alpha r \sim b_2\mu_B^*/a_2\mu_A^*$. This suggests that the standard addition should be kept as small as possible after due consideration of the error in C_x introduced by the uncertainties in the measurement of I_1 and I_2 .

EXPERIMENTAL

Fly-ash samples

The fly-ash samples were obtained from the garbage incinerator in Uppsala, Sweden. The samples, which contained about 1% lead, were homogenized in a mixer. Nitric acid digests of the samples⁵ were used for the AAS determinations.

Reagents

The lead standards were prepared from lead nitrate and contained 80.0 or 40.0 g/l. lead. Solid mercury(II) acetate was used as the modifier. The reagents were of *p.a.* quality.

Apparatus

The X-ray measurements were made with a Philips PW 1410 X-ray spectrometer equipped with a PW 1710 processor. The PbL_α and PbL_β lines and the backgrounds on both sides of a line were measured by use of a scandium/molybdenum dual-anode X-ray tube operated at 60 kV/45 mA, a lithium fluoride crystal (200) and a scintillation detector. The counting time was 5 sec for each line and background measurement. The measurement sequence of background 1, peak, background 2 was repeated three times. Unless spurious peaks appeared, the average from the three repetitions was used to calculate the net intensity.

Sample preparation

Standard additions of lead were made by pipetting 0–2 ml of an aqueous lead standard onto about 4 g of the sample in a Teflon container, drying in a microwave oven, and adding the calculated amount of solid mercury(II) acetate as modifier. Then two steel balls were added and the container was shaken mechanically for 3 min. The disks for the X-ray measurements were prepared as described earlier.⁵ The pressure on the die was 130 MPa and not 11 MPa as erroneously reported previously.

Calculations

The theoretical calculation of the integral in equation (3) and of related quantities was performed as described in a previous communication.⁸

RESULTS AND DISCUSSION

Figure 1 shows the intensities from a fly-ash sample to which standard additions of lead (as the nitrate) had been made. The curvature of the standard-addition graph is clearly visible. An attempt to determine the lead content of the fly-ash by linear regression leads to a gross error. As described earlier,⁵ the lead concentration can be obtained by fitting equation (2) to the data by non-linear regression. This method, however, is sensitive to small experimental errors. It also requires an inconveniently large number of standard additions since three parameters are involved in the regression. Experimental linearization of the standard-addition function as described above was therefore tested.

Mercury, added as the acetate, was chosen as the modifying element. The value of $r(\lambda)$ in equation (7) is 1.07 for the PbL_α line when calculated from the attenuation coefficient

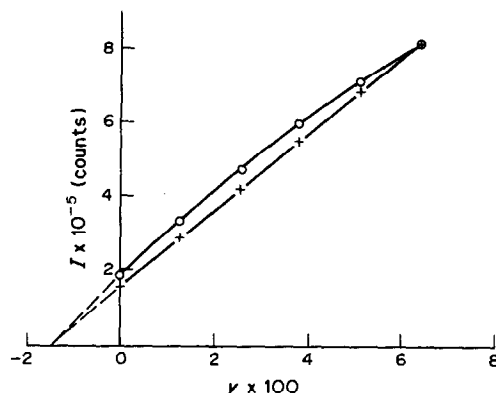


Fig. 1. Line intensity, I , as a function of the ratio between the weights of added lead nitrate and sample, y ; \circ , without modifier; $+$, with modifier.

expression given by Thinh and Leroux.⁹ It is almost independent of the exciting wavelength between the K and L_{III} absorption edges. For the PbL_β line, $r(\lambda)$ varies with the excitation wavelength since this line is absorbed by mercury between the K and L edges but not between the L and M edges (as the PbL_α line is). Hence PbL_α was chosen as the analytical line. Figure 1 also shows the effect of the modifier; the same standard additions were made as in the experiment without modifier. The amount of modifier was calculated from equation (6). A straight line was fitted to the points and the analytical result thus obtained differed by 2% from the result obtained by non-linear regression. In this and similar experiments the correlation coefficient was 0.9999 or better.

A number of experiments were performed to test the concordance of the results obtained with the technique. In one set of experiments the concentration interval of the standard additions was decreased from 4 to 2% but the standard procedure with five additions was maintained.

Table 1. Analytical results obtained with different standard-addition schemes applied to the same specimen of fly-ash; in all experiments mercury(II) acetate was added as an absorption modifier

Experiment	No. of additions	Lead added, %	Analyte found, %	Range, %
1	5	0–4	0.775	0.770–0.776
2*	5	0–4	0.768	—
3	5	0–2	0.760	0.751–0.768
4	1	0.8	0.764	0.760–0.767
5	1	1.6	0.769	0.763–0.777
6	1	2.4	0.768	0.765–0.769
7	1	3.2	0.770	0.760–0.785
8	1	4.0	0.771	0.768–0.773
			mean 0.768 ± 0.005	

*An extra 50 mg of mercury(II) acetate was added to each aliquot of fly-ash.

In another set the performance with single standard additions was studied. The results are summarized in Table 1. Ranges rather than relative standard deviations are presented since there were only four replicates. The results demonstrate that the precision of the method is good; the largest deviation from the mean is about 2%. There is no significant difference in results between the various addition modes. The decrease in precision expected for use of small additions (experiments 4–8) does not show up.

The imprecision of a single intensity measurement can be estimated from the primary data to be about 0.5% and seems to be largely independent of the size of the standard addition. It probably arises from the preparation of the disks and their presentation to the spectrometer. The contribution from counting statistics to the imprecision is small, considering that the average of three measurements on each disk was used in the calculation. A calculation of error on the assumption of a constant relative imprecision of 0.5% in the intensity measurement yields an estimated imprecision in the analytical result amounting to 2% for the smallest and 1% for the largest standard addition.

Experiment 2 shows that presence of the modifier in the original sample does not affect the analytical result.

The accuracy of the results was estimated by determination of lead in 8 fly-ash samples, by the single-addition variant, with an addition of 3% of lead. A comparison was made with the results from AAS measurements. The lead con-

tent of the samples varied from 0.8 to 1.35%. The mean absolute difference between the XRFS and AAS results was 0.016% and the largest difference 0.03%. This indicates that the accuracy of the method is good. The results from the XRFS measurements were systematically higher, which might indicate that a small fraction of the lead could have been left behind in the digestion step of the AAS procedure, but this was not further investigated.

The influence of an error in the quantity of modifier was tested, by the single standard-addition variant. To portions of fly-ash (4.00 g) amounts of mercury(II) acetate were added that corresponded to an error of 0, ± 5 , ± 10 , ± 20 , and $\pm 25\%$ in $r(\lambda)$. The intensities from these samples correspond to I_1 in equation (9). These intensities were then combined with measurements, I_2 , on similar samples to which 0.256 g of lead nitrate had been added. The apparent lead concentration of the sample was evaluated from equation (10). The relative error in the result was calculated on the premise that the result obtained with the theoretical r -value was correct. The errors are presented in Table 2 together with the estimates from equation (12). The ratio μ_B^*/μ_A^* needed for the calculation of these estimates was obtained experimentally. Equation (2) was fitted to standard-addition measurements made without modifier, and the parameter μ_B^*/μ_A^* was found to be 2.7 by non-linear regression. The central value of αr is thus 0.17. The agreement between the experimentally determined and estimated errors is fairly good, and most important, the data indicate that the accuracy of the analytical result is not very sensitive to errors in r .

As previously mentioned, $r(\lambda)$ is not constant for the PbL_β line. A computer simulation showed, however, that the exciting radiation is centred around the MoK_α line (0.71 Å), which is close to the absorption edges for lead. The r -value for this wavelength, calculated from equation (8), is 0.55. Calculations indicated that this value of $r(\lambda)$ should yield a linear standard-addition function. This was confirmed by experiment. A linear standard-addition plot (corr. coeff. = 0.9999) was obtained for five additions of lead in the range 1–4%. The lead concentration found from linear regression was 0.775%, which differs by 0.008% (1% relative) from the result obtained with the PbL_α line ($r = 1.07$). As expected, the standard-addition graph for PbL_α was slightly curved for $r = 0.55$. The analytical result from linear regression was in error by about 15%.

Table 2. Relative error ($\Delta C_{x,rel}$) in the analytical result, caused by a relative error (Δr_{rel}) in the value of $r(\lambda)$ used to calculate the amount of absorption modifier from equation (6); the true value of $r(\lambda)$ ($\Delta r_{rel} = 0$; $\Delta C_{x,rel} = 0$) is assumed to be 1.07, as calculated from equation (7) for lead nitrate as standard and mercury(II) acetate as modifier; the experimental conditions are given in the text and C_x was calculated from equation (10) and the estimated relative error in C_x from equation (12)

Δr , %	C_x , %	$\Delta C_{x,rel}$, %	
		Experimental	Estimated
25	0.761	-2.8	-5.1
20	0.759	-3.1	-4.0
10	0.770	-1.7	-2.0
5	0.778	-0.6	-1.0
0	0.783	0	0
-5	0.794	1.4	1.0
-10	0.803	2.6	2.0
-20	0.819	4.6	4.0
-25	0.831	6.1	5.1
-100*	0.957	22.2	—

*No modifier added.

CONCLUSIONS

This study indicates that this modified standard-addition method can be used to obtain a linear standard-addition function in XRFS for matrices and analyte concentrations that otherwise would yield a non-linear function. The results also show that good precision is achieved with only one standard addition at an analyte level of about 1%. Compared to dilution techniques, the method suffers only a small reduction in line intensity, which is a distinct advantage.

Acknowledgement—Thanks are due to Pertti Knuutila for performing the XRFS measurements

REFERENCES

1. J. Sherman, *Spectrochim. Acta*, 1955, **7**, 283.
2. W. J. Campbell and H. F. Carl, *Anal. Chem.*, 1954, **26**, 800.
3. N. Pind, *Talanta*, 1984, **31**, 1118.
4. R. Tertian and F. Claisse, *Principles of Quantitative X-Ray Fluorescence Analysis*, p. 216. Heyden, London, 1982.
5. M. Andersson, C. Ericzon and Å. Olin, *Talanta*, 1988, **35**, 337.
6. R. Tertian and F. Claisse, *op. cit.*, p. 59.
7. *Idem*, *op. cit.*, p. 84.
8. M. Andersson and Å. Olin, *Talanta*, 1990, **37**, 185.
9. T. P. Thinh and J. Leroux, *X-Ray Spectrom.*, 1979, **8**, 85.

ADSORPTIVE VOLTAMMETRIC BEHAVIOUR OF IMMUNOGLOBULIN M

JOSE M. FERNANDEZ ALVAREZ¹, MALCOLM R. SMYTH^{1,*} and RICHARD O'KENNEDY²

¹School of Chemical Sciences and ²School of Biological Sciences, Dublin City University, Dublin 9, Ireland

(Received 26 January 1990. Revised 28 May 1990. Accepted 19 September 1990)

Summary—The adsorptive voltammetric behaviour of immunoglobulin M (IgM) has been investigated at the static mercury drop electrode. The stripping process yields an analytically useful signal and the detection limit is $1.2 \times 10^{-10} M$. The adsorptive voltammetric behaviour of IgM has been compared with that of IgG and streptavidin.

Immunoglobulin M (IgM) is a macroglobulin with an approximate molecular weight of 9×10^5 and it accounts for about 10% of the serum immunoglobulin pool.¹ Electron microscope studies of IgM proteins from various species have led to the accepted structure of IgM as a circular pentameric molecule stabilized by disulphide linkages and the presence of an additional peptide J (joining) chain which is thought to assist the process of polymerization prior to secretion by the antibody-producing cell.² Monomeric IgM also exists in low concentrations in normal serum, but can occur in higher concentrations in certain disease states (e.g., systemic lupus erythematosus and Waldenstrom's macroglobulinaemia). Although IgG is by far the predominant antibody produced in most *secondary* antibody responses, IgM is the major class of antibody secreted into the blood in the early stages of a *primary* antibody response.

Adsorptive stripping voltammetry has received much attention in recent years for the determination of a variety of inorganic and organic species which can undergo adsorptive accumulation at electrode surfaces, either directly or following a suitable complexation reaction.^{3,4} We have reported on the adsorptive voltammetric behaviour of a series of proteins^{5–11} and have made use of this technique to monitor different immunological reactions^{5–7} and to assess the stability of chemically modified enzymes.¹⁰ We now present the adsorptive voltammetric behaviour of bovine IgM

and compare it with the behaviour of the monomeric Y-shaped IgG and the globular protein streptavidin.

EXPERIMENTAL

Apparatus

Voltammetric experiments were performed with a Princeton Applied Research Corporation (PARC) Model 303A Static Mercury Drop Electrode (SMDE) (drop area 0.025 cm^2) coupled to a PARC Model 264A Polarographic Analyser and a PARC Model 305 Magnetic Stirrer. Voltamperograms were recorded on a Houston Instruments Model 2000 X–Y Recorder. A platinum wire was used as auxiliary electrode and all potentials were measured *vs.* an Ag/AgCl/satd. KCl reference electrode.

Reagents

Bovine IgM, purified by precipitation and gel filtration, was obtained from Sigma as a 1.1 mg/ml stock solution in 0.05M Tris–HCl, 0.15M NaCl, 0.01M glycine medium with 0.1% sodium azide as preservative. A 0.025M phosphate buffer (pH 7.4) was used as background electrolyte and distilled water was purified using a Waters Milli-Q water purification system. All chemicals used were of analytical reagent grade.

Procedure

Before each voltammetric experiment the electrolyte was purged with oxygen-free nitrogen for 15 min. After addition of the sample the solution was purged for a further 30 sec. The potential was then set at the required accumu-

*Author for correspondence.

lation potential, E_{acc} , for the required accumulation time, t_{acc} , with stirring at 400 rpm. The stirring was stopped automatically and, after a 15 sec equilibrium time, the potential was scanned in the differential pulse (DP) mode in the cathodic direction, with a pulse amplitude of 50 mV, and a scan-rate of 10 mV/sec. A scan-rate of 100 mV/sec was used for linear sweep voltammetry (LSV) and cyclic voltammetric (CV) experiments.

RESULTS AND DISCUSSION

The cyclic voltammetric behaviour of 55 mg/l. IgM at the static mercury drop electrode (SMDE) is shown in Fig. 1. A potential scan performed under solution-phase conditions ($t_{acc} = 0$ sec) gave rise to a very small response, the magnitude of which is close to that of curve *c* in Fig. 1. On the other hand, a symmetrical and well defined peak was obtained when a preconcentration step preceded the potential scan, proving that the substance could be accumulated at the SMDE. The peak potential, E_p , was -0.58 V and the width at half height, $W_{1/2}$, was 60 mV. It can also be seen that the process is irreversible in nature and the peak current

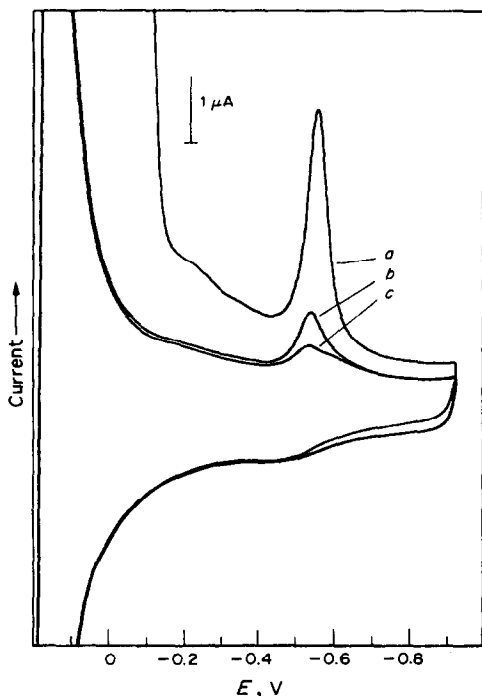


Fig. 1. Multicyclic voltamperograms for a 52.4 mg/l. solution of bovine IgM. Curve *a* was obtained after a t_{acc} of 300 sec; curves *b* and *c* are successive scans at the same drop. Scan-rate 100 mV/sec.

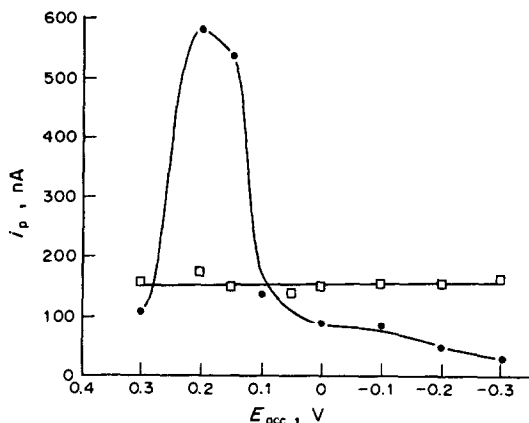


Fig. 2. Effect of the accumulation potential, E_{acc} , (●) and of the starting potential (□) (accumulation at open circuit) on the DP voltammetric responses for a 5.5 mg/l. solution of IgM; t_{acc} 180 sec.

decreases on repetitive scanning at the same drop.

Stripping peaks obtained for a 26.8 mg/l. solution of IgM with accumulation for 120 sec and increasing scan-rates showed the existence of a linear relationship between the current intensity, i_p , and the scan-rate, v , in the range 5–100 mV/sec ($r = 0.9998$; $n = 5$), as expected for an adsorption-controlled process.

Different preconcentration schemes and potential scan modes were examined. Differential pulse voltammetry (DPV) provided analytical signals that were twice as sensitive as those achieved by linear sweep voltammetry (LSV). Accordingly, the DPV mode was selected for the rest of the study. Preconcentration experiments performed under both electrolytic and open-circuit conditions revealed that in both instances IgM was adsorbed at the SMDE.

The influence of the accumulation potential, E_{acc} , on the peak intensity is shown in Fig. 2, where the influence of the starting potential for open-circuit preconcentration experiments is also shown. The use of an E_{acc} of +0.2 V provided the optimum signals, with respect to both the peak intensity and the peak morphology. Under these conditions well defined and symmetrical peaks ($W_{1/2} = 90$ mV) were obtained, whereas for other values of E_{acc} the peaks were broader and somewhat distorted.

It is worth emphasizing that the pattern exhibited by i_p as a function of E_{acc} is closely resembled, but in an inverse way, by the graph of $W_{1/2}$ vs. E_{acc} (Fig. 3). Moreover, when the preconcentration step is performed at open circuit, the peak intensity remains approximately

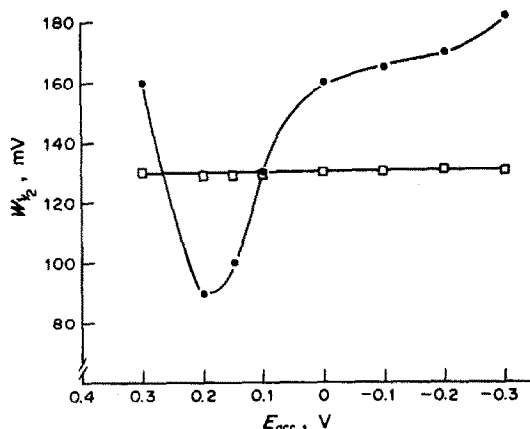


Fig. 3. Effect of the accumulation potential, E_{acc} , (●) and of the starting potential (□) (accumulation at open circuit) on the peak width at half height, $W_{1/2}$, of the DP voltammetric responses for IgM. Conditions as for Fig. 2.

constant regardless of the potential value at which the scan is started. The magnitude of this peak equals that obtained with electrolytic pre-concentration at $E_{acc} = +0.1$ V, and again the widths of these two peaks are practically the same (Fig. 3).

The range of pH values within which immunoglobulins are active is very limited and, accordingly, the effect of pH on the adsorptive behaviour of IgM was restricted to the range from 7.0 to 8.0. Although there was not a dramatic effect on the peak intensity, a trend to increasing current response with increasing pH was observed. Furthermore, the optimum E_{acc} values were seen to decrease as the pH was lowered and the best analytical signals were obtained for an E_{acc} of +0.15 V at pH 7.4 and for an E_{acc} of +0.05 V at pH 7.0. The pI (isoelectric point) values for immunoglobulins are not known precisely, but they lie in the range 8–9. Besides the hydrophobicity of certain regions of the molecule, the adsorption onto the electrode involves electrostatic interactions,¹² and when the pH is increased towards the pI value, the overall positive charge on the molecule is reduced. In other words, as the pH approaches pI, more of the negatively polarized portions of the molecule become available, favouring adsorption onto an increasingly positively charged electrode.

As expected, the use of increasing pulse amplitudes and larger drop sizes gave rise to an increase in the current. However, larger background currents accompanied the use of higher pulse amplitudes, and optimum operational conditions were established as a trade-off be-

tween sensitivity and signal discrimination. As a consequence, a pulse amplitude of 50 mV and a large drop size were used for further studies.

The effect of increasing accumulation times on the peak currents obtained for increasing concentrations of IgM are shown for three cases in Fig. 4(a). As expected, i_p showed a steady increase with t_{acc} for each concentration until monolayer saturation of the electrode was reached. In addition, there was a linear relationship between the slopes of the accumulation curves and the corresponding concentration, as shown in Fig. 4(b). It is interesting to note that monolayer coverage of the electrode is reached for the pentameric IgM structure at a t_{acc} of ~ 300 sec [Fig. 4(a), curve 3], in contrast to the linear increase of current response up to $t_{acc} = 900$ sec obtained for a similar concentration of IgG.⁶ On the other hand, the first peak observed for IgG⁶ is clearer than that for IgM, indicative of different conformations of the molecules in the adsorbed state, and consequently a different availability of certain regions of each protein to the electrode surface. The fact that the accumulation curves have different intercepts indicates that the adsorption of IgM at the SMDE does not proceed according to a simple Langmuir isotherm. Indeed, a recent paper by Lin *et al.*¹³ has shown that the adsorption of IgG at a clean mica surface occurs through a co-operative process, depending on the formation of aggregates. These workers further demonstrated that isolated molecules are rapidly desorbed from the surface, that ridges of adsorbed molecules are formed during the formation of a monolayer, and that for-

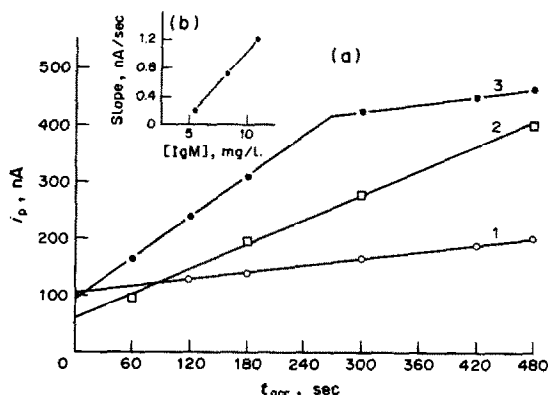


Fig. 4. (a) Effect of the accumulation time, t_{acc} , on the DP voltammetric current for (○) 5.50 mg/l., (□) 8.25 mg/l. and (●) 11.00 mg/l. solutions of IgM. (b) Variation of the slope of the accumulation curves in a with the concentration of IgM. $E_{acc} = +0.1$ V.

mation of subsequent layers does not take place until monolayer formation is nearly complete.

By preconcentrating IgM at the SMDE for 300 sec at the optimum E_{acc} (+0.2 V), and subsequently stripping the adsorbate in the DPV mode under the optimized experimental conditions, a detection limit of 0.11 mg/l. ($1.2 \times 10^{-10} M$) was obtained. The calibration graph was linear between 0.28 and 6.60 mg/l. (3.1×10^{-10} and $7.3 \times 10^{-9} M$) ($r = 0.9996$; $n = 9$) with a slope of 150 ng.l.mg^{-1} . Typical calibration voltamperograms are shown in Fig. 5.

The larger number of disulphide linkages existing in the molecule of IgM^{1,2} could account for the detection limit being lower than that for IgG, even when a shorter t_{acc} was used. However, the linear span of the calibration is one order of magnitude for both molecules, and,

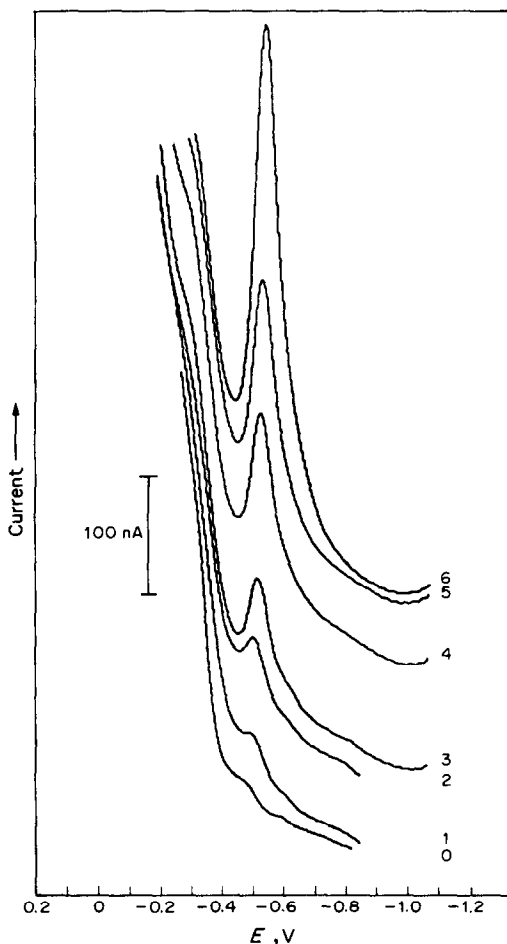


Fig. 5. Effect of concentration on the DP voltammetric current for IgM: 0, blank; 1, 0.11 mg/l. (limit of detection); 2, 0.28 mg/l.; 3, 0.55 mg/l.; 4, 0.83 mg/l.; 5, 1.10 mg/l.; 6, 2.20 mg/l. $E_{acc} + 0.2 \text{ V}$; t_{acc} 300 sec.

which is more important, the slopes of the calibration plots are very similar (150 and 160 nA.l.mg^{-1} for IgM and IgG, respectively) implying that the current produced per unit of concentration is the same.

In conclusion, it is difficult to agree with the assumption usually made in the literature¹⁴⁻¹⁶ that reduction of the disulphide linkages is the only process responsible for the electrochemistry of this type of protein. Recently, we have reported on the electrochemistry of streptavidin, a globular protein which is completely devoid of sulphur-containing amino-acid residues^{17,18} but still undergoes an electrode process at the same potential as the disulphide-containing proteins.¹¹ Emons *et al.*¹⁹ have recently suggested that the voltammetric signal for IgG is due to an interfacial process connected with reversible protein re-orientations in the adsorbed layer and, possibly, with fast faradaic reactions of both adsorbed redox states of the immunoglobulin. It is clear that much more work is required to elucidate the origin of the voltammetric response produced by these proteins.

Acknowledgement—José M. Fernández Alvarez wishes to thank the Spanish Ministry of Education and Science for the award of a postdoctoral scholarship.

REFERENCES

1. I. Roitt, J. Brostoff and D. Male, *Immunology*, Chapter 5, Churchill Livingstone, Edinburgh, 1985.
2. M. W. Steward, *Antibodies: Their Structure and Function*, p. 75. Chapman and Hall, London, 1984.
3. J. Wang, *Stripping Analysis: Principles, Instrumentation and Analysis*, VCH, Deerfield Beach, Florida, 1985.
4. W. F. Smyth, in M. R. Smyth and J. G. Vos (eds.) *Electrochemistry, Sensors and Analysis*, pp. 29–36. Elsevier, Amsterdam, 1986.
5. J. Rodríguez Flores and M. R. Smyth, *J. Electroanal. Chem.*, 1987, **235**, 317.
6. M. R. Smyth, E. Buckley, J. Rodríguez Flores and R. O'Kennedy, *Analyst*, 1988, **113**, 31.
7. J. Rodríguez Flores, R. O'Kennedy and M. R. Smyth, *ibid.*, 1988, **113**, 525.
8. E. Buckley, P. Reilly, J. Rodríguez Flores, R. O'Kennedy and M. R. Smyth, *J. Pharm. Biomed. Anal.*, 1989, **7**, 543.
9. P. Carty, R. O'Kennedy, E. Lorenzo Abad, J. M. Fernández Alvarez, J. Rodríguez Flores, M. R. Smyth and K. Tipton, *Analyst*, 1990, **115**, 617.
10. J. M. Fernández Alvarez, C. O'Fagain, R. O'Kennedy, C. G. Kilty and M. R. Smyth, *Anal. Chem.*, 1990, **62**, 1022.
11. E. Buckley, J. M. Fernández Alvarez, M. R. Smyth and R. O'Kennedy, *Electroanalysis*, in the press.

12. J. D. Andrade (ed.), *Surface and Interfacial Aspects of Biomedical Polymers*, Vol. 2, p. 1. Plenum Press, New York, 1982.
13. J. N. Lin, B. Drake, A. S. Lea, P. K. Hansma and J. D. Andrade, *Langmuir*, 1990, **6**, 509
14. B. Breyer and F. J. Radcliff, *Nature*, 1951 **167**, 79.
15. R. Cecil and P. D. J. Weitzman, *Biochem. J.*, 1964, **93**, 1.
16. U. Forsman, *Anal. Chim. Acta*, 1984, **166**, 141.
17. N. M. Green, in M. L. Anson and J. T. Edsell (eds.), *Advances in Protein Chemistry*, Academic Press, New York, 1975.
18. A. Pähler, W. A. Hendrickson, M. A. Gawinowicz Kolks, C. E. Argaraña and C. R. Cantor, *J. Biol. Chem.*, 1987, **262**, 13933.
19. H. Emons, G. Werner and W. R. Heineman, *Analyst*, 1990, **115**, 405.

ACCURACY IN THE PRECISE COULOMETRIC TITRATION OF AMMONIA AND AMMONIUM ION WITH ELECTROGENERATED HYPOBROMITE

AKIHARU HIOKI,* MASAOKI KUBOTA and AKIRA KAWASE

National Chemical Laboratory for Industry, 1-1, Higashi, Tsukuba-shi, Ibaraki 305, Japan

(Received 20 December 1989. Revised 26 October 1990. Accepted 31 October 1990)

Summary—A precise and accurate method in which ammonia and ammonium ions are coulometrically titrated with electrogenerated hypobromite was studied. Through the measurement of the current efficiency for generating hypobromite and the dependencies of titration results on electrolysis current and delay time between sampling and starting electrolysis, precision and accuracy of 0.01 and 0.02%, respectively, were obtained. The accuracy of the titration was compared with that of acidimetric coulometric titration of ammonia.

Since ammonia or ammonium ions can be formed from many nitrogen compounds¹⁻⁵ and water or hydrogen in various materials,^{6,7} the present study is important as a basis of wide application. Coulometric titration is an absolute method, based on Faraday's law, and can yield high precision and accuracy, without the need for a reference material.⁸⁻¹³

Ammonia or ammonium ions react with hypobromite in weakly alkaline solution¹⁴⁻¹⁶ to give nitrogen and bromide, and this reaction has been used in coulometric titration of ammonium ions with electrogenerated hypobromite,¹⁷⁻²¹ which has been applied to determination of some nitrogen compounds.^{20,22-24} The best precision reported¹⁷ was 0.1% for 230 μg of ammonia.

In the present study the dependence of the current efficiency of hypobromite generation on the current density was measured, and the loss of ammonia or ammonium ions, during both the electrolysis and the delay time after sampling, was estimated, and corrections for these factors allowed the total ammonia concentration to be measured with high precision and accuracy. To validate the accuracy, a solution of ammonia in excess of sulphuric acid was prepared, and its oxidimetric coulometric titration was compared with a coulometric acidimetric titration. The coulometric oxidative titration was also used to determine the purity of high-grade ammonium chloride.

EXPERIMENTAL

Reagents

Demineralized water was further purified by isopiestic distillation. Reagent-grade chemicals were used unless otherwise stated. Analytical-reagent grade ammonia solution and ultrapure sulphuric acid were used.

Approximately $2.54 \times 10^{-2} m$ ($m \equiv$ mole per kg of solution) sulphuric acid was used for preparing a solution of ammonia (*ca.* $5.9 \times 10^{-3} m$) in *ca.* $1.27 \times 10^{-2} m$ sulphuric acid. Ammonium chloride was dried for 6 hr at 50° under reduced pressure. An ammonium chloride solution (*ca.* $6.68 \times 10^{-3} m$) was prepared by diluting a solution containing *ca.* 7.16 g of the dried ammonium chloride in 1 kg of water. Each sample solution was kept in a Teflon-PFA bottle. Buoyancy corrections were always applied.

Apparatus

The constant-current source was a model 220 type (Keithley, Cleveland). The electrolysis currents were determined by measuring the voltage drop across a standard resistor (10 or 100 Ω , Type 2792, Yokogawa, Tokyo) in series with the source. The voltage drop was read with a digital voltmeter (Model 8800A, John Fluke, Seattle) calibrated against an unsaturated Weston standard cell (Type 2749, Yokogawa). The linearity of the voltmeter response was confirmed by the fact that ten times the ratio of the voltage drop across the 10- Ω resistor to that across the 100- Ω resistor was unity at different currents. The

*Author for correspondence.

current measurements were accurate to within 0.01% with no dummy load and the error in measuring the electrolysis time was less than 0.001%. The density of the solutions was determined to within 0.00005 g/ml with a DA-101B densimeter (Kyoto Electronics, Kyoto).

The coulometric titration cell (Fig. 1) was equipped with silicone rubber stoppers and a bubble trap to exclude air. The temperature of the solutions was $25 \pm 3^\circ$. Pure nitrogen was

always passed through the solution in the counter-electrode chamber to remove dissolved oxygen.

For the oxidimetry the cell shown in Fig. 1(a) was used. The generation medium was 120 ml of 1M sodium bromide containing 10 g/l. borax and was adjusted to pH 8.5^{17,19}. The solution in the counter-electrode chamber was 80 ml of 10 g/l. borax solution at pH 9.0. The end-point was detected by dead-stop titration with a dual

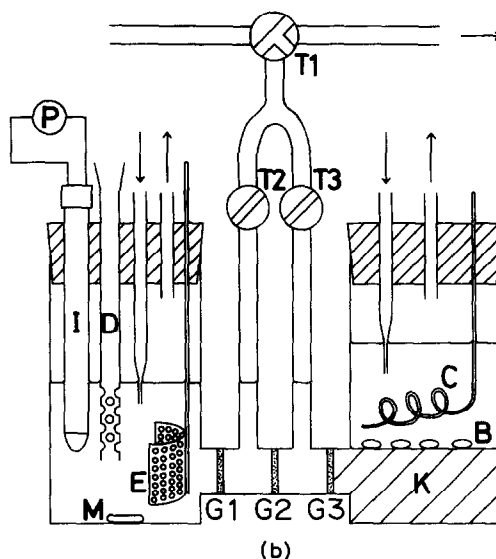
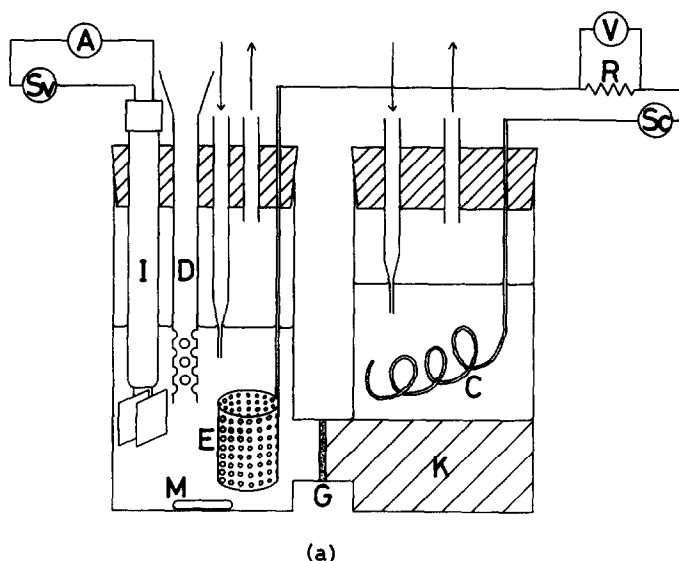


Fig. 1. (a) Electrolysis cell for hypobromite generation: A, ammeter; Sv, constant voltage source; V, voltmeter; R, standard resistor; Sc, constant current source; I, platinum indicator electrode; C, platinum wire counter-electrode; K, agar gel (3 g of agar-agar in 100 ml of 30-mg/ml sodium sulphate solution); G, porosity-4 sintered-glass disk; M, stirring bar; E, platinum generating electrode (20 cm² area each side); D, glass tube for introduction of sample solution; the arrows show the flow of nitrogen. (b) Electrolysis cell for hydroxide-ion generation: I, combination glass electrode; K, agar gel (3 g of agar-agar in 100 ml of 1M potassium chloride); E, platinum generating electrode (10 cm² area each side); P, pH-meter; B, solid barium carbonate; T1, T2 and T3, stopcocks; C, M and D as in Fig. 1(a); G₁ and G₂, porosity-3 sintered-glass disks; G₃, porosity-4 sintered-glass disk.

platinum-plate electrode. The voltage impressed across the two plates [each of surface area *ca.* 2 cm² (one side)] was 150 mV supplied by a d.c. voltage source (E-150A, TOA, Tokyo). The indicator current was obtained as the output of a μ A meter (TR-8641, Takeda Riken, Tokyo), averaged for 5 sec with a digital integrator (RD-202, Tokyo Kagaku, Tokyo) to improve the precision of end-point detection.

For the acidimetry a cell with two centre compartments²⁵ [Fig. 1(b)] was used. The generating chamber contained 100 ml of 1M potassium chloride and the counter-electrode chamber contained 90 ml of 1M potassium chloride and some solid barium carbonate.²⁶ Use of this electrolysis cell eliminates loss of ammonium ions into the counter-electrode chamber.²⁵ The indicator electrode was a combination pH electrode (GST-5211C, TOA), used with a D-150A pH-meter (TOA).

Oxidimetric coulometric titration with hypobromite

Pure nitrogen was passed through the generation medium for 30 min, then the solution, stirred at constant rate, was electrolysed until the indicator current was *ca.* 4 μ A (a stable current was attained in 1–2 min). A 5-g portion of sample solution (weighed to 0.1 mg) was introduced from a gravimetric burette through the sample-inlet tube, which was then rinsed with 5.0 ml of water added dropwise from a transfer pipette. The solution was electrolysed with a continuous current until just before the end-point, and then with successive 1-sec pulses of 10 mA until the indicator current was *ca.* 4 μ A. The generating efficiency of the pulses was $\geq 99.7\%$ of that of the continuous current, and this slight difference caused only a negligible error. A stable indicator current was attained after 1–2 min. The indicator current exhibited slight upward curvature just before the end-point and the intersection of extrapolations of the linear portions was used as the end-point. Five successive measurements were made in the same batch of generation medium, resulting in successive decreases in the sodium bromide concentration from (12/13)M for the first titration to (12/17)M for the last. The Faraday was taken as 96485 C/equivalent.^{27–29} Any systematic error in the end-point determination was regarded as self-cancelling in this method.^{17,19,30,31} By treating the first of the five measurements as a pretitration, the effect of impurities in the generation medium was minimized.³¹ Formation of hypo-

bromite from bromide by oxygen is negligible, so any oxygen produced in the generation medium during electrolysis or present dissolved in the sample solution could be ignored. The time elapsed between the addition of sample solution and the start of electrolysis was recorded.

Acidimetric coulometric titration

The inflexion point on the titration plot can be regarded as the equivalence point in this case.^{32,33} For sulphuric acid, the end-point was taken as being indicated by a pH of 7.00, which was sufficiently close to the inflexion point. Pure nitrogen was continuously passed through the generation medium at pH 5.2, and after 1 hr the electrolysis was conducted with 1-sec pulses of 10 mA until the pH rose to *ca.* 8. A stable pH value was obtained in 2 min. A 25-g portion of the sample solution was then introduced through the sample-inlet tube, which was rinsed with 5.0 ml of water. The solution was electrolysed with a continuous current of 50 mA until the pH reached 5.4, corresponding to *ca.* 99.7% completion of the titration, nitrogen being continuously passed over the solution. Nitrogen was passed through the solution for a further hour, and the titration was then completed with 1-sec pulses of 10 mA. The efficiency of the pulse was 99.7% of that of the continuous current and this difference could be neglected. The generation medium was used for only one measurement. For titration of a solution of ammonia in excess of sulphuric acid, the inflexion point was used to locate the second end-point.

RESULTS AND DISCUSSION

Current efficiency

According to Bishop,³⁴ the efficiency of coulometric generation of hypobromite is close to 100%. Current density and electrode potential measurements have been utilized to ascertain the efficiency of coulometric generation.^{35–37} The relation between the anode potential measured with respect to an SCE (HC-205C, TOA) and the current was determined. A Luggin capillary filled with agar gel (30 mg/ml agar in 4M potassium chloride) was used as a liquid junction and kept *ca.* 2 mm from the anode surface. The potential was measured in the region where the anode was closest to the sintered glass disk.

When five successive additions of 5 g of $6.68 \times 10^{-3}m$ ammonium chloride and 5.0 ml of

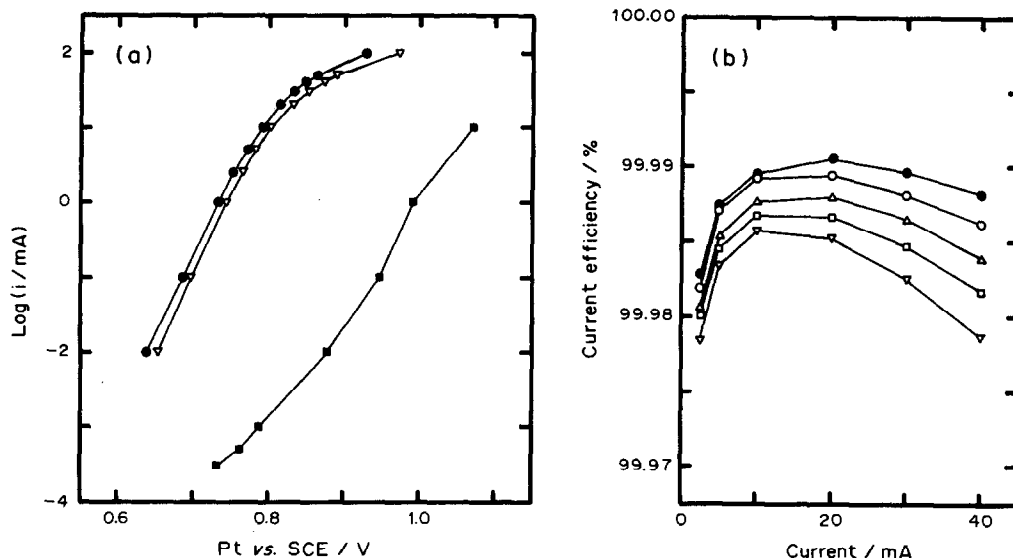


Fig. 2. (a) Relation between current and electrode potential. (b) Dependence of the current efficiency on the current. ●: $[\text{NaBr}] = (12/13)M$; ○: $[\text{NaBr}] = (12/14)M$; △: $[\text{NaBr}] = (12/15)M$; □: $[\text{NaBr}] = (12/16)M$; ▽: $[\text{NaBr}] = (12/17)M$; ■: $[\text{NaBr}] = 0$. Anode area (one side), 20 cm^2 .

water were made to the 120 ml of generation solution containing sodium bromide, the anode potential [Fig. 2(a)] and the solution pH were practically unaffected by the degree of dilution. The anode potential in the 10 g/l. borax solution, (adjusted to the same pH, 8.5, as that in the presence of sodium bromide) was also independent of dilution with water, but the pH decreased to 8.4 after addition of 50 ml of water. The efficiency of hypobromite generation can be calculated from the ratio between the currents in the presence and absence of sodium bromide at a given anode potential.³⁷ Figure 2(b) shows the dependence of the generation efficiency on both the current and the dilution. Corrections were applied on the basis of Fig. 2(b).

Oxidimetry of ammonium ions in sulphuric acid medium

Figure 3(a) shows the effect of the generation current on the oxidation of ammonium ions in sulphuric acid medium, when the delay time was 5 min. The ordinate represents the concentration found relative to the mean value ($5.86089 \times 10^{-3}M$) found by electrolysis at 20 mA. There is a maximum variation of about 0.06% for replicate determinations at a given degree of dilution of the sodium bromide solution. The repeatability of 7 determinations [electrolysis current 20 mA, delay time 5 min, and sodium bromide concentration $(12/14)M$] corresponding to the maximum variation gives an sd of 0.019%. Since the values shown in

Fig. 3(a) decrease approximately linearly with the time needed for electrolysis [Fig. 3(b)], it is thought that the values obtained at the lower currents might be smaller owing to loss of ammonia by volatilization or diffusion into the counter-electrode chamber. If ionic migration of ammonium ions were the cause of the lower values in Fig. 3(a), the loss should depend only on the total quantity of electricity and be independent of the time needed for the electrolysis. The ionic migration of the ammonium ion should depend on its ability to transfer charge during the electrolysis, *i.e.*, it depends on the ionic mobility³⁸ of sodium, bromide and ammonium ions, and on the concentration ratio between the ammonium ion and sodium bromide. The error caused by ionic migration was estimated as less than 0.005%, in terms of loss of ammonia during the electrolysis.

The parameters for the individual regressions [Fig. 3(b)] are as follows: numbers of data, slopes (%/min) and intercepts (%) for the dilution steps 2, 3, 4 and 5 are 11, -2.15×10^{-3} (0.29×10^{-3}) and 100.013 (0.008), 8, -1.52×10^{-3} (0.32×10^{-3}) and 100.005 (0.007), 9, -1.63×10^{-3} (0.24×10^{-3}) and 100.026 (0.006), and 8, -1.26×10^{-3} (0.32×10^{-3}) and 100.000 (0.012), respectively, where values in parentheses are the corresponding standard deviations. Since the intercepts did not differ significantly, the regression lines in Fig. 3(b) were recalculated on the basis of a common intercept (100.011%, s.d. 0.004%) for the

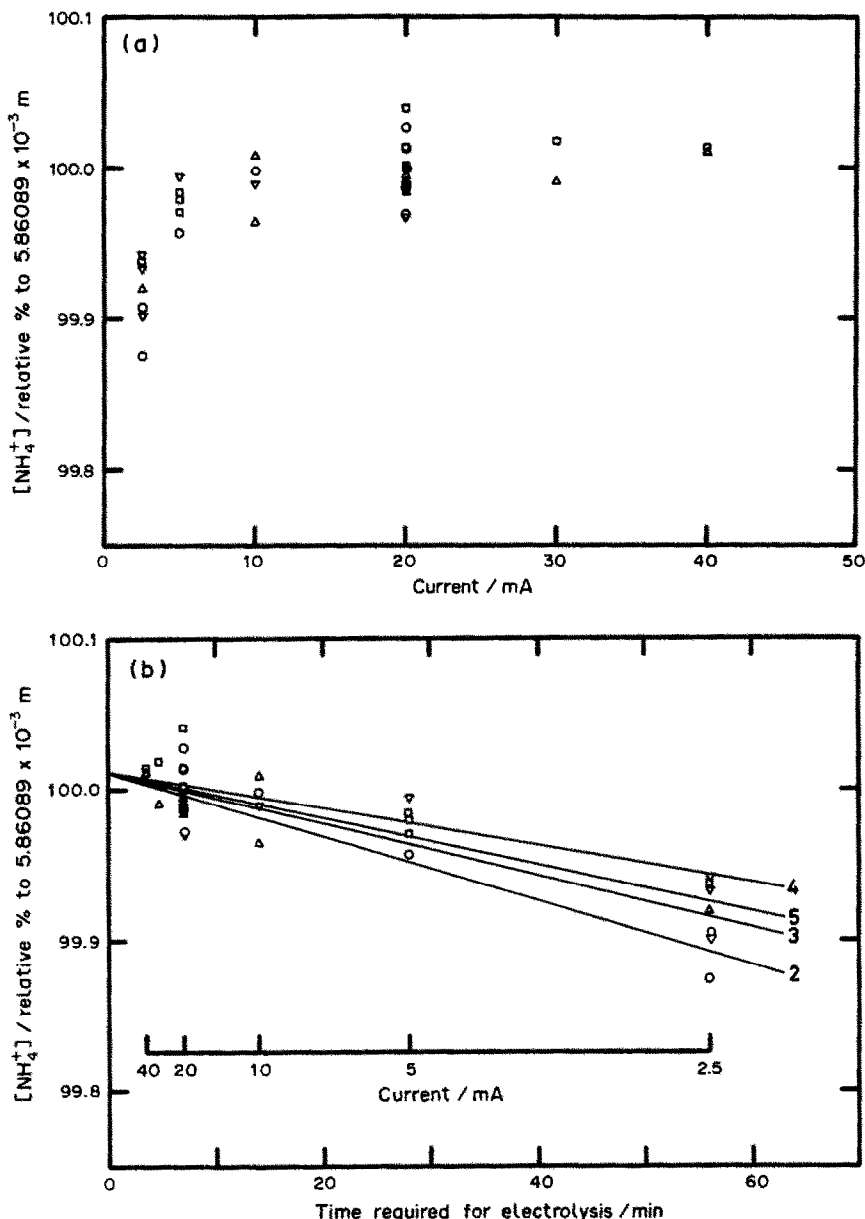


Fig. 3. Dependence of the results for the solution of ammonia in sulphuric acid, obtained by coulometric titration with hypobromite ions, on (a) the electrolysis current and (b) the time required for electrolysis. \circ : $[\text{NaBr}] = (12/14)M$; \triangle : $[\text{NaBr}] = (12/15)M$; \square : $[\text{NaBr}] = (12/16)M$; ∇ : $[\text{NaBr}] = (12/17)M$ [corresponding to 2, 3, 4 and 5, respectively, on the calculated lines in Fig. 3(b)]. Delay time before starting electrolysis, 5 min.

data of the four steps of dilution, and the slopes (%/min) for the dilution steps 2, 3, 4 and 5 became -2.11×10^{-3} (0.23×10^{-3}), -1.71×10^{-3} (0.31×10^{-3}), -1.21×10^{-3} (0.26×10^{-3}) and -1.52×10^{-3} (0.19×10^{-3}), respectively. At currents > 10 mA, there is little difference among the results obtained for the successive runs.

Figure 4 represents the effect of the delay time on the results obtained for the sulphuric acid solution of ammonia, with electrolysis at 20

mA. The loss of ammonium ions was directly proportional to delay time.

The parameters for the regressions were calculated as for Fig. 3(b): the numbers of data, slopes (%/min) and intercepts (%) for the dilution steps 2, 3, 4 and 5 are 11, -6.68×10^{-3} (0.71×10^{-3}) and 100.022 (0.009), 8, -6.41×10^{-3} (0.77×10^{-3}) and 100.019 (0.012), 8, -7.56×10^{-3} (0.57×10^{-3}) and 100.048 (0.009), and 8, -5.60×10^{-3} (0.75×10^{-3}) and 100.016 (0.014), respectively.

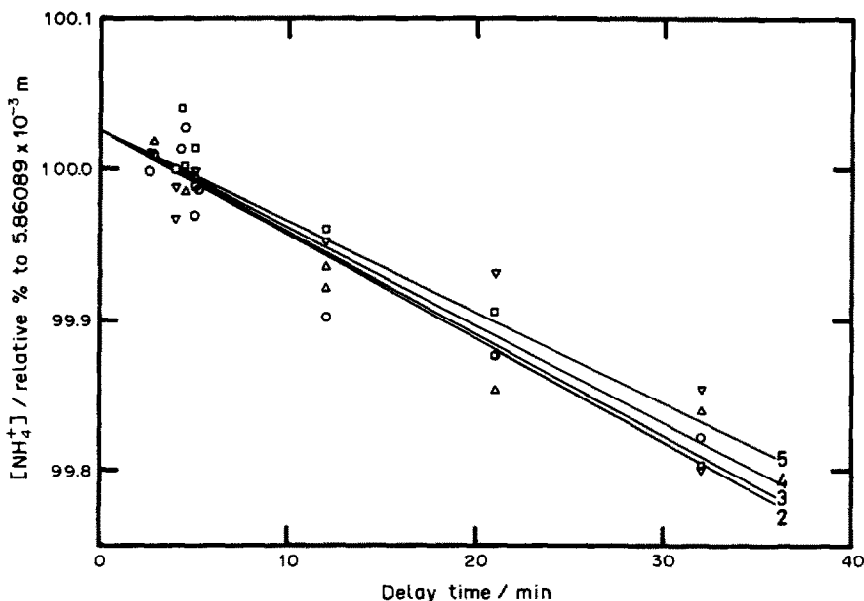


Fig. 4. Dependence of the results for the ammonia solution in sulphuric acid, obtained by coulometric titration with hypobromite ions, on the delay time before starting the electrolysis. Electrolysis current, 20 mA. Symbols *etc.* as for Fig. 3.

The regression lines in Fig. 4 were calculated on the basis of a common intercept (100.025%, s.d. 0.006%) for the data of the four steps of dilution, and the slopes (%/min) for the dilution steps 2, 3, 4 and 5 are -6.87×10^{-3} (0.60×10^{-3}), -6.75×10^{-3} (0.58×10^{-3}), -6.45×10^{-3} (0.54×10^{-3}) and -5.99×10^{-3} (0.47×10^{-3}), respectively.

The total concentration of ammonia was obtained by correcting the intercept for the loss of 0.011% occurring during the electrolysis at 20 mA, and found to be $(5.8630 \pm 0.0008) \times 10^{-3}m$. The accuracy was estimated from the sd (0.0056%) of the intercept in Fig. 4, the sd (0.003%) of the loss at 20 mA, estimated from Fig. 3(b), the error (less than 0.005%) of measuring the 20-mA current, and the negative error (less than 0.005%) due to ionic migration. The addition of the sample solution caused little change of pH, and the indicator current was scarcely changed by the presence of free sulphuric acid. The slope of the plot of indicator current *vs.* time, after the end-point, was decreased in approximately the same proportion as the degree of dilution.¹⁹

Acidimetric coulometric titration

Since the titration of the sulphuric acid solution of ammonia is the reverse of the titration of a monoacidic base with a strong acid, the change in the hydrogen-ion concentration near

the equivalence point is expressed by equation (1),^{32,33}

$$a = 1 - p_1/[H] + p_2[H] \quad (1)$$

where p_1 and p_2 are constants and a is the degree of titration defined as

$$a = (t_0 + t_i - t)/t_0 \quad (2)$$

where t is an arbitrary electrolysis time at a certain current, t_i is the electrolysis time needed to reach the equivalence point, and t_0 is the time interval corresponding to neutralization of one equivalent of the base. Equation (3) is derived from equations (1) and (2):

$$t = t_i + p_1 t_0 \gamma_H 10^{\text{pH}} - p_2 t_0 \gamma_H^{-1} 10^{-\text{pH}} \quad (3)$$

where γ_H is the hydrogen-ion activity coefficient. It is believed that γ_H is constant during the course of the coulometric titration. The value of t_i is derived from the experimental data (pH *vs.* t) by a non-linear least-squares method^{39,40} applied to the three parameters t_i , $p_1 t_0 \gamma_H$ and $p_2 t_0 \gamma_H^{-1}$ in equation (3).

From titrations of the sulphuric acid solution of ammonia and the sulphuric acid solution alone (four determinations for each) the total concentration of ammonia in the former was estimated as $(5.8620 \pm 0.0019) \times 10^{-3}m$. The error was estimated from the sd values of both sets of results for the same solutions. The difference from the concentration obtained by oxidimetry is *ca.* 0.02%, which is within the

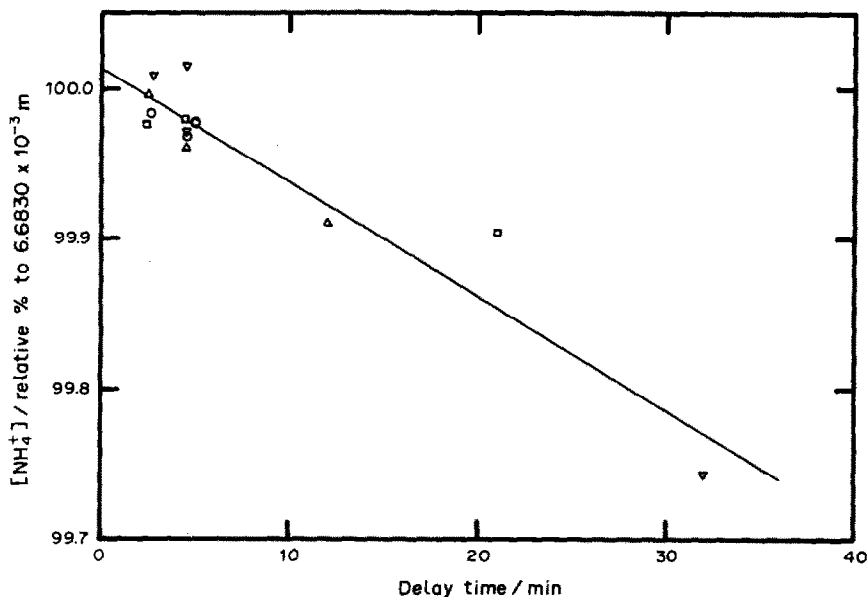


Fig. 5. Dependence of the results for the ammonium chloride solution, obtained by coulometric titration with hypobromite ions, on the delay time before starting the electrolysis. Electrolysis current, 20 mA. Symbols as for Fig. 3.

estimated precision. Thus the accuracy of oxidimetry by hypobromite generation was further established.

Ammonium chloride solution

Figure 5 shows the dependence of the oxidimetric results obtained for the ammonium chloride solution (*ca.* $6.68 \times 10^{-3}m$) on the delay time, when the current used was 20 mA. The ordinate represents the concentration found titrimetrically, relative to that based on the weight of ammonium chloride used. The uncertainty in the chemical formula weight (53.4910 ± 0.0009) is less than 0.002%.⁴¹ As it was expected from Fig. 4 that hardly any difference would be made by the four dilution steps, all the data in Fig. 5 were used for extrapolation. The number of data, slope (%/min) and intercept (%) are 14, -7.63×10^{-3} (0.72×10^{-3}) and 100.014 (0.008), respectively. As the ammonium chloride concentration is similar to the total ammonia concentration in the sulphuric acid solution of ammonia and the slope in Fig. 5 is reasonably close to that in Fig. 4, the exact concentration of ammonium chloride, $(6.6847 \pm 0.0010) \times 10^{-3}m$, was obtained by correcting for the loss during the course of the electrolysis (0.011% at 20 mA) estimated from Fig. 3. This concentration is 100.02%, relative to that based on the weight taken, and its inaccuracy was estimated as 0.02% at most, from the s.d. (0.0084%) of the

intercept in Fig. 5, the s.d. of the loss during the course of electrolysis at 20 mA, the accuracy of determining the 20-mA current, the negative error due to ionic migration, and the uncertainty in the formula weight of ammonium chloride.

In the oxidimetric coulometric titration of ammonium ions presented in this paper, high accuracy will be obtained if the current efficiency and the loss of the sample are taken into consideration. The determination of ammonium ions by this method can be utilized for determining the purity of reference materials. The method should also be useful for determination of nitrogen as ammonia or ammonium ions after pretreatment such as Kjeldahl digestion.⁴²

REFERENCES

1. A. J. Clear and M. Roth, in I. M. Kolthoff and P. J. Elving (eds.), *Treatise on Analytical Chemistry*, Part II, Vol. 5, p. 281. Interscience, New York, 1961.
2. H. D. Drew, in C. A. Streuli and P. R. Averell, *The Analytical Chemistry of Nitrogen and Its Compounds*, Part I, pp. 3–13. Wiley, New York, 1970.
3. F. W. Allerton, *Analyst*, 1947, **72**, 349.
4. Y. Morita, *Bull. Chem. Soc. Japan*, 1968, **41**, 2029.
5. L. A. Fabbro, L. A. Filachek, R. L. Iannacone, R. T. Moore, R. J. Joyce, Y. Takahashi and M. E. Riddle, *Anal. Chem.*, 1971 **43**, 1671.
6. T. Yoshimori and S. Ishiwari, *Bull. Chem. Soc. Japan*, 1969, **42**, 1282.
7. *Idem*, *Talanta*, 1970, **17**, 349.
8. J. K. Taylor and S. W. Smith, *Science*, 1956, **124**, 940.

9. S. W. Smith and J. K. Taylor, *J. Res. Natl. Bur. Stds.*, 1959, **63C**, 65.
10. G. Marinenko and J. K. Taylor, *ibid.*, 1963, **67A**, 31, 453.
11. T. Yoshimori, *Talanta*, 1975, **22**, 827.
12. *Idem*, *Bunseki*, 1975, 551.
13. E. Bishop, *Coulometric Analysis*, in C. L. Wilson and D. W. Wilson (eds.), *Comprehensive Analytical Chemistry*, Vol. IID, p. 24. Elsevier, Amsterdam, 1975.
14. H. H. Willard and W. E. Cake, *J. Am. Chem. Soc.*, 1920, **42**, 2646.
15. I. M. Kolthoff and V. A. Stenger, *Ind. Eng. Chem., Anal. Ed.*, 1935, **7**, 79.
16. D. Kőszegi and É. Salgó, *Z. Anal. Chem.*, 1954, **143**, 423.
17. G. M. Arcand and E. H. Swift, *Anal. Chem.*, 1956, **28**, 440.
18. A. F. Krivis, G. R. Supp and E. S. Gazda, *ibid.*, 1963, **35**, 2216.
19. G. D. Christian, E. C. Knoblock and W. C. Purdy, *ibid.*, 1963, **35**, 2217.
20. N. L. Kovalenko, N. V. Grizan, L. A. Temerbaeva, G. D. Mal'chikov and N. A. Shestakova, *Zh. Analit. Khim.*, 1988, **43**, 1443.
21. U. Spohn, M. Hahn, H. Matschiner, G. Ehlers and H. Berge, *Z. Anal. Chem.*, 1989, **332**, 849.
22. W. Werner and G. Tőlg, *ibid.*, 1975, **276**, 103.
23. U. Schilbach and E. M. Kirmse, *Chem. Anal. (Warsaw)*, 1978, **23**, 1025.
24. E. A. Bondarevskaya, T. V. Kirillova, E. V. Buyanova and O. P. Sakovets, *Zh. Analit. Khim.*, 1980, **35**, 755.
25. J. K. Taylor and S. W. Smith, *J. Res. Natl. Bur. Stds.*, 1959, **63A**, 153.
26. T. Yoshimori and I. Hikawa, *Bunseki Kagaku*, 1967, **16**, 927.
27. E. R. Cohen and B. N. Taylor, *J. Phys. Chem. Ref. Data*, 1973, **2**, 663.
28. T. Arikawa and H. Hirakawa, *Kagaku Sosetsu*, 10, p. 153. Chemical Society of Japan, University of Tokyo Press, Tokyo, 1976.
29. H. Diehl, *Anal. Chem.*, 1979, **51**, 318A.
30. G. W. Ewing, *Instrumental Methods of Chemical Analysis*, 4th Ed., p. 333. McGraw-Hill, New York, 1975.
31. p. 159 in ref. 13.
32. D. Rosenthal and P. Zuman, in I. M. Kolthoff and P. J. Elving, *Treatise on Analytical Chemistry*, 2nd Ed., Part I, Vol. 2, pp. 217-221. Wiley, New York, 1979.
33. M. Tanaka and G. Nakagawa, *Anal. Chim. Acta*, 1965, **33**, 543.
34. p. 503 in ref. 13.
35. J. J. Lingane and J. H. Kennedy, *Anal. Chim. Acta*, 1956, **15**, 465.
36. J. J. Lingane, C. H. Langford and F. C. Anson, *ibid.*, 1957, **16**, 165.
37. G. Marinenko and J. K. Taylor, *Anal. Chem.*, 1967, **39**, 1568.
38. *CRC Handbook of Chemistry and Physics*, 67th Ed., 1986-1987, R. C. Weast (ed.), p. D-167. CRC Press, Boca Raton, 1986.
39. T. R. McCalla, *Introduction to Numerical Methods and FORTRAN Programming*, Wiley, New York, 1967.
40. T. Nakagawa and Y. Oyanagi, *SALS Programme*, UP Applied Mathematics Series, Vol. 7, University of Tokyo Press, Tokyo, 1982.
41. *Pure Appl. Chem.*, 1988, **60**, 841.
42. G. D. Christian and P. D. Jung, *J. Assoc. Off. Anal. Chem.*, 1966, **49**, 865.

MASS SPECTROMETRIC APPROACHES IN STRUCTURAL IDENTIFICATION OF THE REACTION PRODUCTS ARISING FROM THE INTERACTION BETWEEN GLUCOSE AND LYSINE

A. LAPOLLA, C. GERHARDINGER, G. CREPALDI and D. FEDELE

Instituto di Medicina Interna, Patologia Medica I, Policlinico Università di Padova, Italy

M. PALUMBO and D. DALZOPPO

Dipartimento di Chimica Organica, Università di Padova, Italy

C. J. PORTER

VG Analytical, Altrincham, England

E. GHEZZO, R. SERAGLIA and P. TRALDI

Consiglio Nazionale delle Ricerche, Area di Ricerca, Padova, Italy

(Received 9 October 1990. Accepted 15 November 1990)

Summary—The products arising from the reaction of α -protected lysine with glucose have been studied by different techniques, *viz.* high-performance liquid chromatography (HPLC) with UV detection, fast atom bombardment (FAB) mass spectrometry (MS), and HPLC/MS. Most of the analytical data were obtained by the last approach and allowed identification of many molecular species for a thorough knowledge of possible reaction pathways or structural data already available in the literature.

Accumulation of brown advanced glycation products in proteins has been proposed as relevant to the development of long-term complications of diabetes mellitus.^{1,2} In the past, the structure of these products has been studied, starting from glycated proteins, by means of chemical and enzymatic hydrolysis and other separative and analytical techniques.³⁻⁵ New information has been added to that already known by Njoroge *et al.*, who demonstrated that chemical hydrolysis can lead to artifacts.⁶ In a recent study⁷ we compared data from chemical and enzymatic hydrolysis and were able to confirm these earlier⁶ findings.

However, since the structure of the brown products in the complex hydrolysis mixture is difficult to determine by those techniques, we decided to take a different approach, namely to study the products of the chemical reaction of glucose and protected lysine. This approach is expected to provide useful information about the mechanism of this reaction and form a promising starting point for future studies *in vivo*.

EXPERIMENTAL

Synthesis of N- α -acetyl-L-lysine methyl ester

N- α -Acetyl-L-lysine methyl ester was prepared and purified according to Irving and Gutmann.⁸ It was a dense yellow oil. The protected lysine (100 mg) and D-glucose (5 g) were dissolved in 5 ml of sodium phosphate buffer (pH 7.5, 0.05M Na) and the solution was incubated for 28 days at 37°, and then was lyophilized.

HPLC separation

A Perkin-Elmer series 3B liquid chromatograph connected to an LC-75 spectrophotometric detector was used. The detector wavelength was set at 320 nm. A μ -Bondapak C-18 reverse phase column was used for the separation. Each sample was diluted tenfold with distilled water before injection. Gradient elution at a flow-rate of 2 ml/min was used, with a mixture of acetonitrile and water in ratio progressively changed from 1:99 to 20:80 in 30 min.

Mass spectrometric measurements

Fast atom bombardment (FAB) measurements were made with a VGZAB 2F mass spectrometer.⁹ Glycerol solutions of the sample were bombarded with 8 keV Xe atoms. GC/MS was performed on a Finnigan ITD 800 system operating in electron ionization mode (100 eV, 100 μ A), with a fused-silica capillary column (25 m long, i.d. 0.32 mm) coated with a 0.4- μ m layer of SE54. The temperature was programmed to rise from 70 to 250° at 7°/min. HPLC/MS measurements were performed with a VG ZAB-VE instrument operating under plasma-spray conditions with a probe temperature of 250° and a source temperature of 240°. The HPLC conditions were as described above.

RESULTS AND DISCUSSION

The HPLC chromatogram of the reaction of protected lysine and glucose is shown in Fig. 1. There are three main peaks, with retention times of 6, 11 and 12 min respectively. GC/MS analysis of each peak led to unsatisfactory results, possibly owing to the high polarity of the compounds investigated. However, FAB MS of the whole reaction mixture, shown in Fig. 2a, gave a spectrum which differed from that of the pure protected lysine (Fig. 2b). For the mixture, ions at m/z 285 and 263 were detectable (with a

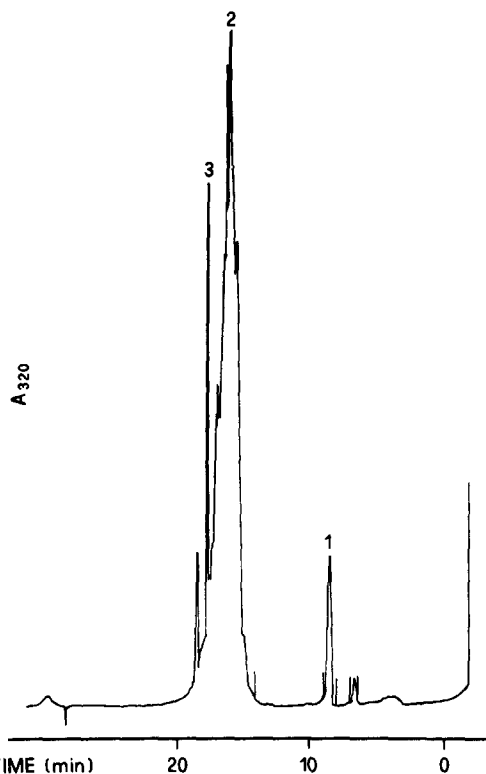


Fig. 1. HPLC chromatogram obtained by detection at 320 nm.

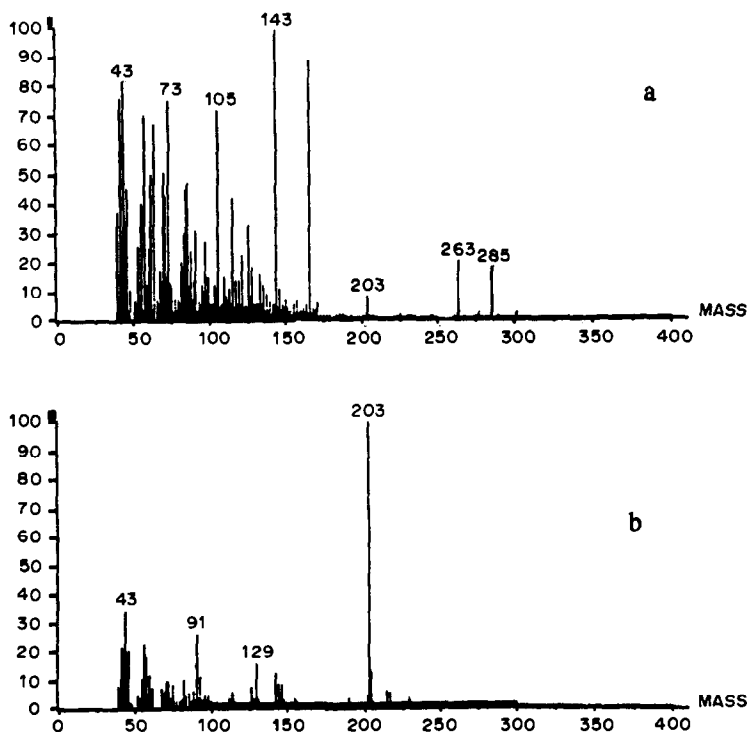


Fig. 2. FAB mass spectra of (a) whole reaction mixture; (b) α -protected lysine.

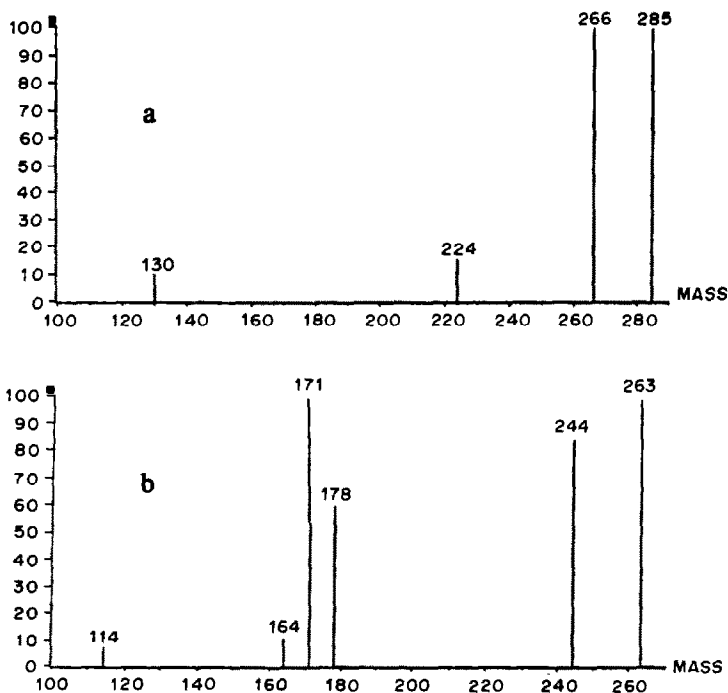
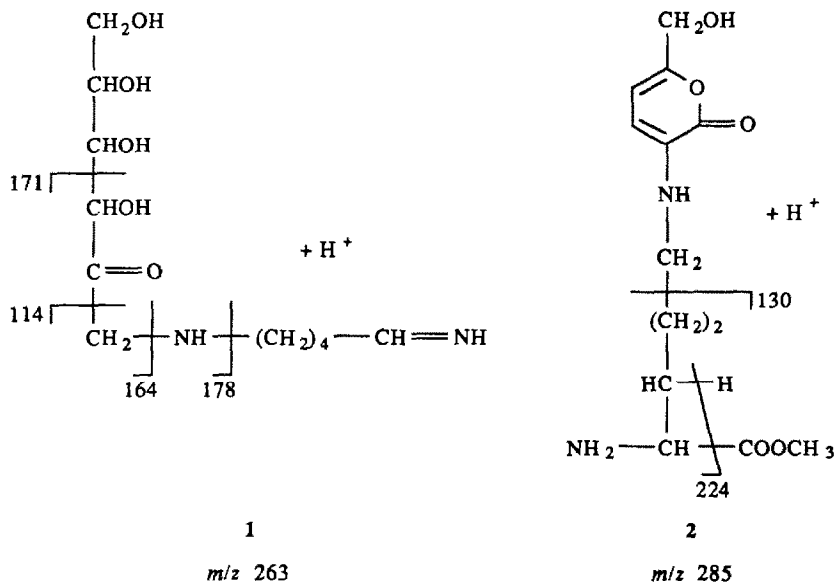


Fig. 3. Daughter ion spectra: (a) ion at m/z 285; (b) ion at m/z 263.

signal/chemical background ratio of about 20). Daughter ion spectra (Fig. 3) suggested that these species had structures 1 and 2 respectively (Scheme 1).

The very high chemical noise observed under the FAB conditions suggests the presence of many other molecular species. For this reason, HPLC/MS measurement was the method of choice. The reconstructed total ion chromatogram

obtained under the same HPLC conditions is shown in Fig. 4. Practically no chromatographic resolution was obtained. However, mass spectra obtained at different elution times led to an effective description of the molecular species present in the complex mixture. Figure 5 shows the spectra obtained for scans 18, 25 and 37. In the first, many different ionic species are easily detected in the range m/z



Scheme 1

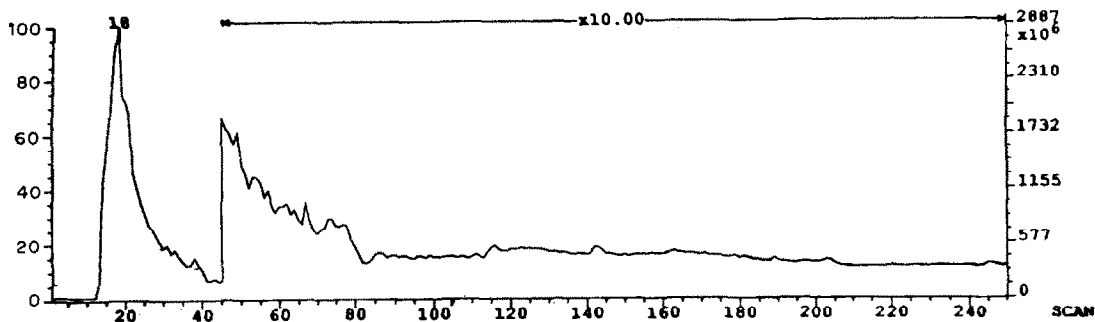


Fig. 4. Reconstructed ion chromatogram for HPLC/MS analysis of reaction mixture under plasma-spray conditions.

150–500, and in the third new molecular species becomes detectable at m/z 324.

Neither GC/MS analysis of every component obtained by preparative HPLC runs, nor mass spectrometric analysis of the whole mixture by FAB was satisfactory. No compound related to the Amadori reaction could be detected by GC/MS, possibly because of the high polarity of such molecules. The FAB mass spectrum of the whole reaction mixture differed from that of protected lysine (Fig. 2b), mainly by the presence of ions at m/z 285 and 263 (Fig. 2), but it must be stressed that this spectrum is quite unsatisfactory. Ionic species are present at every m/z

value. Also the ions of interest have a signal/chemical background ratio of about 20, which suggests many other molecular species may be present but are concealed by the chemical background. For the ions at m/z 285 and 263, the daughter ion spectra (Fig. 3) suggest the structures 1 and 2 (in Scheme 1) which could originate from lysine and glucose (Schiff's base) with subsequent Amadori rearrangement and decarboxylation. Both compounds 1 and 2 show the formal loss of H_3O^+ (possibly from sequential losses of H^+ and H_2O) in the daughter spectra, leading to ions at m/z 244 and 266 respectively.

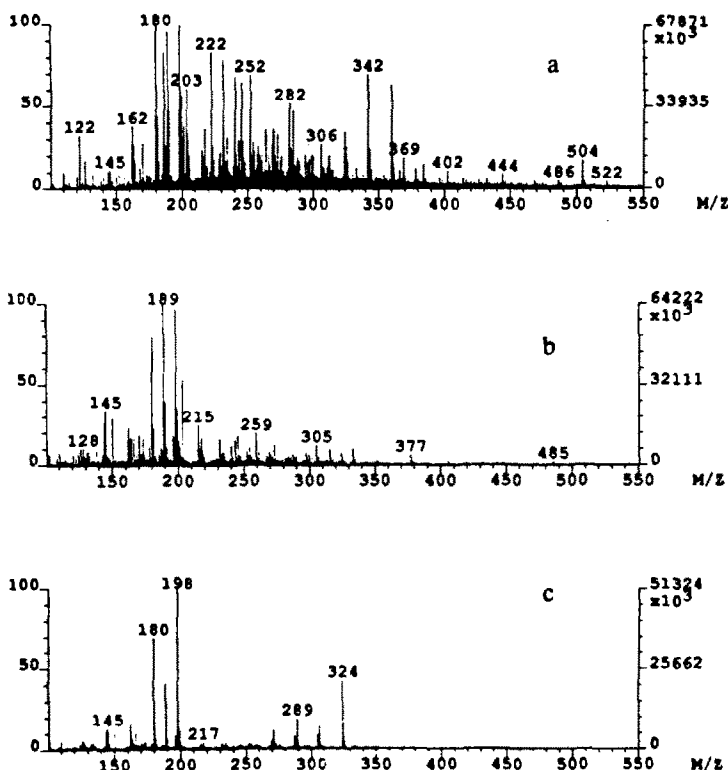
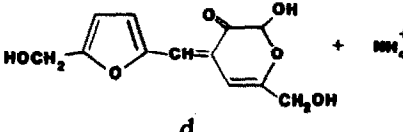
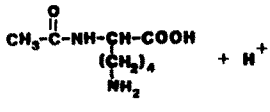
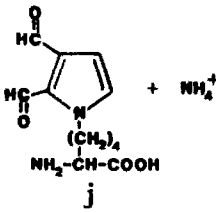
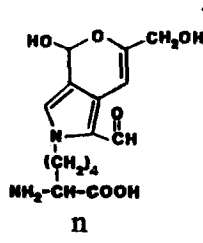

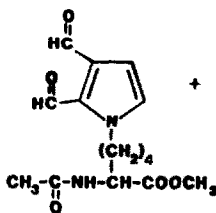
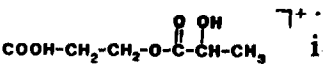
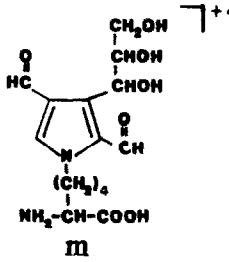
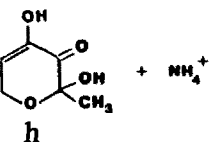
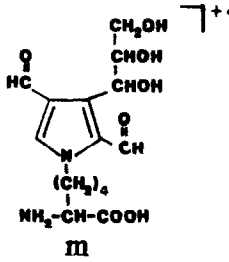
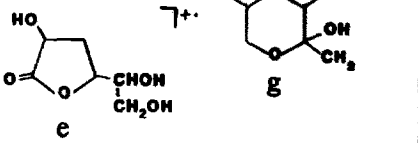
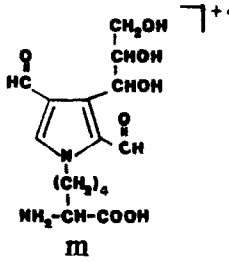
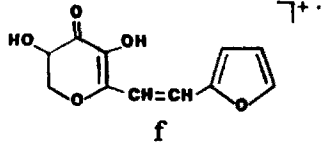
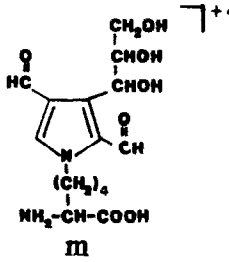
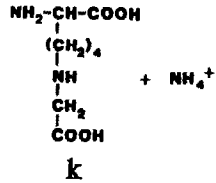
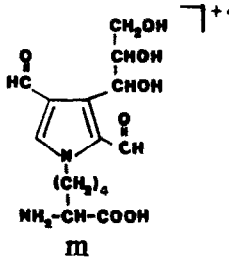


Fig. 5. Mass spectra obtained at different elution times by HPLC/MS analysis: (a) mass spectrum of scan No. 18, (b) mass spectrum of scan No. 25, (c) mass spectrum of scan No. 37.

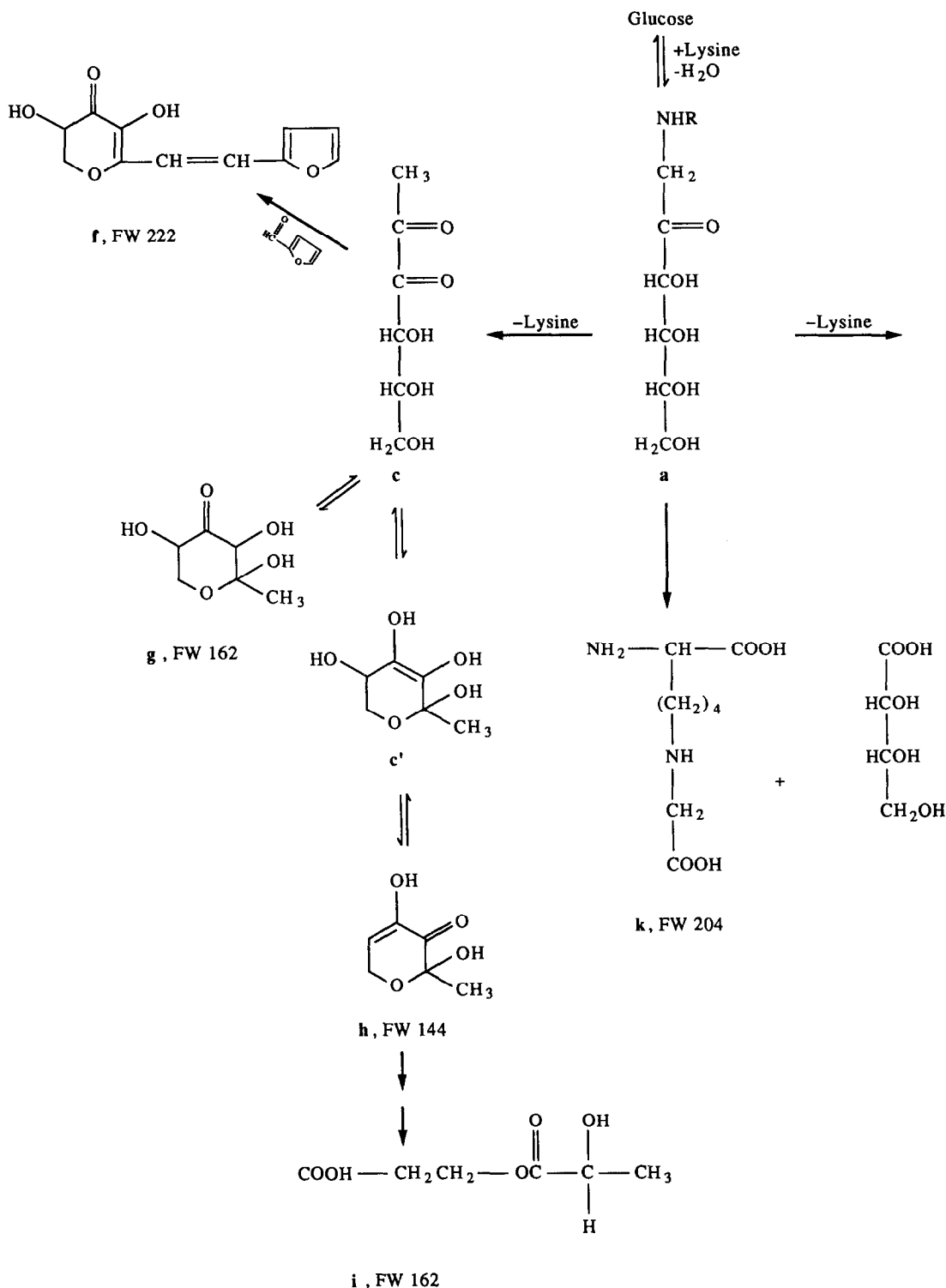
To obtain more satisfactory results, we performed a series of HPLC/MS measurements. Under the HPLC conditions described we obtained the total ion chromatogram reported in Fig. 4. The practically complete loss of resolution in comparison with UV detection

Table 1. Possible structures detected by plasma-spray HPLC/MS

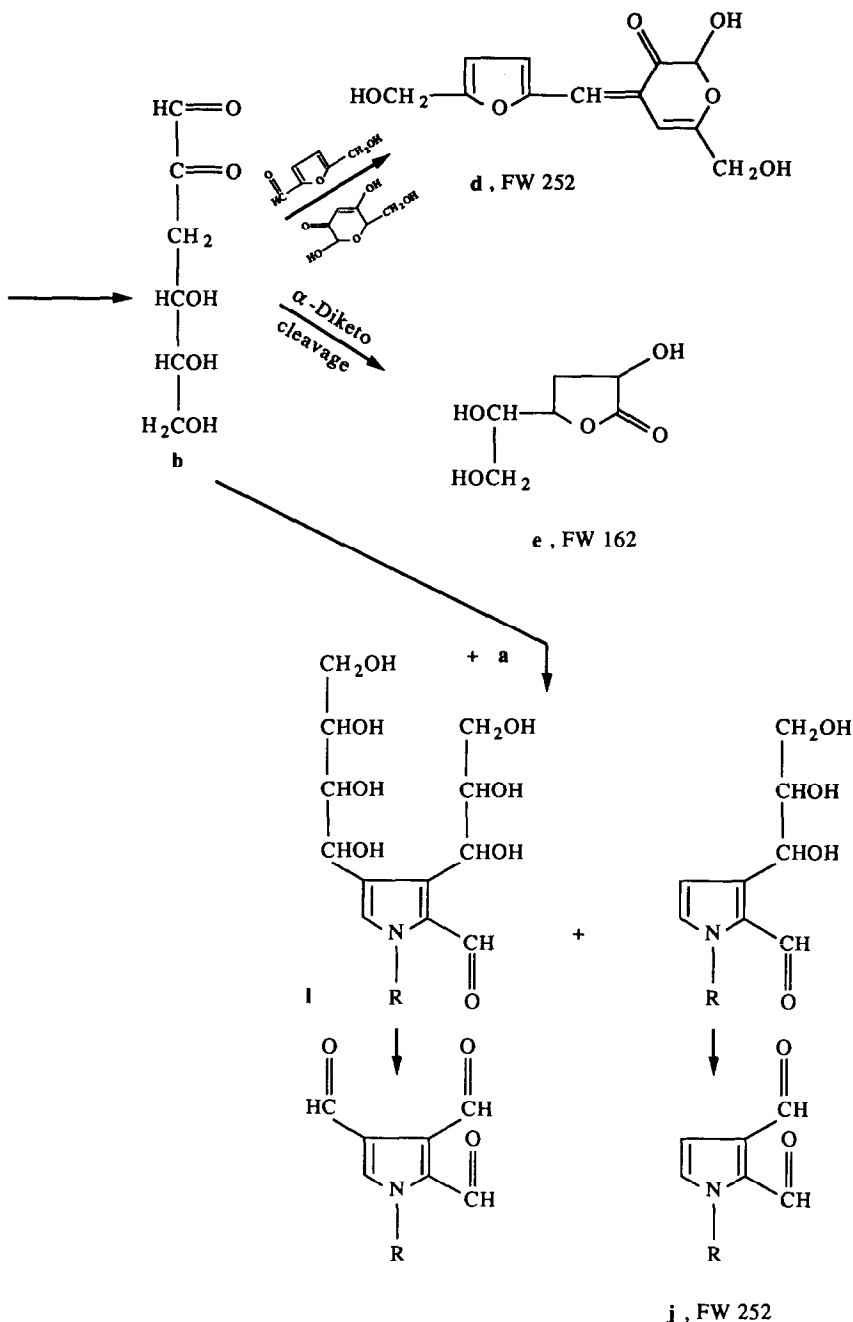
<i>m/z</i>	Structures	<i>m/z</i>	Structures
180	Glucose γ^+	270	 d
189	 + H ⁺	 + NH ₄ ⁺ j	
198	Glucose + NH ₄ ⁺	324	 n
162	 b	326	 + NH ₄ ⁺ o
	 i	342	 m
	 h	342	 m
	 e	342	 m
222	 f	360	 m
	 + NH ₄ ⁺ k	360	 m
240	f + NH ₄ ⁺	360	m + NH ₄ ⁺

shows that the latter is artificially selective, in that it can detect those components containing the chromophoric moiety but not describe the real composition of the mixture. In contrast, the mass spectra obtained at different elution times

can give an effective description of the molecular species in the complex mixture (*e.g.*, Fig. 5). The spectrum for scan 18 corresponding to the maximum of the reconstructed total ion current (Fig. 4) shows many different ionic species in the



Scheme 2, Part 1.



Scheme 2, Part 2.

Scheme 2. Possible pathways leading to structures compatible with the molecular weight found in HPLC/MS analysis, where $\text{R} = -(\text{CH}_2)_4-\text{CH}(\text{NH})-\text{COOH}$.

range m/z 150–500. Though some of them are easily attributable to molecules present in the reaction mixture (as for example m/z 180 and 198 corresponding to $\text{M}^{+\cdot}$ and $[\text{M} + \text{NH}_4]^+$ for glucose, respectively), others are rather difficult to account for, since their structure is inferred only from their molecular weight. For these reasons we propose for them isobaric structures already suggested and/or described in the

literature, as intermediate and final glycation products. At longer retention times most of the ionic species shown in scan No. 18 disappear, but new molecular species at m/z 324 become detectable.

In recent years many efforts have been made to obtain a general view of the possible patterns related to the Maillard reaction. Some useful results have been obtained either from theoretic-

cal or experimental approaches. The structures deduced from HPLC/MS data were proposed on the basis of studies of the Maillard reaction under physiological conditions. Our own opinion is that structure assignment based solely on molecular weight can sometimes give misleading results, but at this stage of the present research, reliable information on the molecular weights of the Maillard products is important.

Possible pathways leading to structures compatible with the molecular weights found by HPLC/MS are reported in Scheme 2. Loss of lysine from the Schiff's base arising from the reaction of glucose and lysine (Scheme 2, structure *a* proposed by Paulsen and Pflughaupt³) can lead at first to two different structures (*b* and *c* in Scheme 2). Such behaviour was already proposed by Anet,¹⁰ Kato¹¹ and Beck *et al.*,¹² and, considering the reaction conditions seems more than reasonable. Both structures *b* and *c* undergo further rearrangements with losses of neutral moieties such as furan-2-aldehyde and analogous products. By this pathway structures *d*, *e* and *f* are obtained; they have been well described by Ledl and co-workers^{4,13,14} and Sengl.¹⁵ It is significant that several ions, at *m/z* 252 (*d*), 222 (*f*) and 162 (*e*) are present in the mass spectrum reported in Fig. 5a. The further rearrangement of compound *c* to *c'*, favoured from a thermodynamic point of view, accounts for the formation of both compounds *g* and *h* (molecular weights 162 and 144 respectively). The latter, in aqueous solution, readily adds water to yield the compound with molecular weight 162. The pathways described above, leading to compounds *c'*, *g*, *h* and *i*, have already been described by Ledl and Severin,⁵ Sengl¹⁵ and Mills *et al.*¹⁶

The right-hand part of Scheme 2 shows the reaction of compound *b* with *a* through condensation and further cleavage of the polyol chain, followed by oxidation. This process leads to compound *j*, the molecular ion of which is still present in the spectrum in Fig. 5a at *m/z* 252. The formation of such a compound has already been proposed by Krönig.¹⁷ Also the formation of carboxymethyl-lysine (compound *k*), described by Ahmed *et al.*,¹⁸ cannot be excluded. In fact, the ion at *m/z* 222, shown in Fig. 5a, could be due to the cationization of compound *k* with NH_4^+ , as often observed under plasma-spray conditions. All these findings are shown in Table 1, where the possible structures related to the most abundant ionic species in the spectra shown in Fig. 5 are proposed.

In addition to the ionic species which can be attributed to the structures described above and already reported in the literature, we detected some other molecular ions of unknown structure. Thus, the ions at *m/z* 342 and 360 can be attributed to structures *m* and *m* + NH_4^+ respectively (Table 1). These structures easily originate from selective oxidation of the side alcohol chain of molecule *l* (Scheme 2).¹⁹⁻²¹ The ions at *m/z* 324 are not so easily identified. Structure *n* in Table 1 can be tentatively proposed.

In conclusion, by comparing HPLC, GC/MS, FAB and HPLC/MS data for the products arising from the interaction of glucose and protected lysine we were able to identify many different molecular species, most of which have the same molecular weight as the products described in the literature. Other compounds, not reported in the literature, were assigned a structure on a mechanistic basis.

REFERENCES

1. M. Brownlee, H. Vlassara and A. Cerami, *Ann. Int. Med.*, 1984, **101**, 527.
2. V. M. Monnier and A. Cerami, *Clin. Endocrinol. Metab.*, 1982, **11**, 431.
3. H. Paulsen and K. W. Pflughaupt, in *Carbohydrates*, Vol. 1B, W. Pigman and D. Horton (eds.), pp. 881-927. Academic Press, New York, 1980.
4. F. Ledl and T. Severin, *Z. Lebensm. Unters. Forsch.*, 1982, **175**, 262.
5. *Idem*, *ibid.*, 1979, **169**, 173.
6. F. G. Njoroge, A. A. Fernandes and V. M. Monnier, *J. Biol. Chem.*, 1988, **263**, 10646.
7. C. Gerhardinger, A. Lapolla, E. Ghezzi, P. Traldi, G. Crepaldi and D. Fedele, submitted to *Chim. Clin. Acta*.
8. C. C. Irving and H. R. Gutmann, *J. Org. Chem.*, 1959, **24**, 1979.
9. M. Barber, R. S. Bordoli, R. D. Sedgwick and A. N. Tyler, *Nature*, 1981, **293**, 270.
10. E. F. L. J. Anet, *Aust. J. Chem.*, 1960, **13**, 396.
11. H. Kato, *Bull. Agr. Chem. Soc. Japan*, 1960, **24**, 1.
12. J. Beck, F. Ledl and T. Severin, *Carbohydr. Res.*, 1988, **178**, 240.
13. F. Ledl, J. Hiebl and T. Severin, *Z. Lebensm. Unters. Forsch.*, 1983, **177**, 353.
14. J. Beck, F. Ledl and T. Severin, *ibid.*, in the press.
15. M. Sengl, *Dissertation*, University of Munich, 1988.
16. F. D. Mills, D. Weisleder and J. E. Hodge, *Tetrahedron Lett.*, 1970, 1243.
17. U. Krönig, *Dissertation*, University of Munich, 1974.
18. M. U. Ahmed, S. R. Thorpe and J. Baynes, *Fed. Proc.*, 1985, **44**, 1621.
19. J. G. Farmer, P. C. Ulrich and A. Cerami, *J. Org. Chem.*, 1988, **53**, 2346.
20. F. G. Njoroge, L. M. Sayre and V. M. Monnier, *Carbohydr. Res.*, 1987, **167**, 211.
21. T. Severin and U. Krönig, *Z. Lebensm. Unters. Forsch.*, 1973, **152**, 42.

THE RATE OF REDUCTION OF SELENIUM(VI) TO SELENIUM(IV) IN HYDROCHLORIC ACID

JEAN PETTERSSON* and ÅKE OLIN

Department of Analytical Chemistry, Uppsala University, P.O. Box 531, S-751 21 Uppsala, Sweden

(Received 9 February 1990. Revised 9 May 1990. Accepted 1 October 1990)

Summary—The reduction of selenium(VI) to selenium(IV) in 4, 5 and 6M hydrochloric acid was studied at temperatures between 50 and 95°. The reaction rate was determined by measurement of the selenium(IV) formed, by continuous-flow hydride-generation atomic-absorption spectrometry. The most notable feature of the reaction is the strong increase in rate with increasing hydrogen-ion concentration and temperature. The rate increases initially with chloride concentration at constant acidity (mixtures of hydrochloric and perchloric acid) but levels off to an almost constant value at high chloride concentrations.

A number of methods are available for the determination of selenium at trace level. Those most frequently used determine only the selenium(IV) present in the final sample. This applies to procedures that are based on the formation of piaszelenols (molecular fluorescence and gas chromatography), hydrogen selenide (atomic spectroscopy), or selenides (stripping voltammetry). Any selenium(VI) present in the original sample or formed during pretreatment of the sample must therefore be transformed into the quadrivalent state if determination of total selenium is required. Reduction by chloride in strongly acidic medium,¹⁻³ photolysis in slightly alkaline medium,⁴ and reduction to elemental selenium and subsequent reoxidation to selenium(IV) by a bromine/bromide buffer⁵ have been used for the conversion of selenium(VI) into selenium(IV).

Reduction by 4–6M hydrochloric acid at elevated temperatures is by far the most commonly used method. A number of recommendations, sometimes conflicting, for performing the reaction can be found in the literature. This prompted Bye and Lund⁶ to investigate the rate of the reaction between selenate and hydrochloric acid. They determined the time necessary for complete reduction at various temperatures and concentrations of acid. Their results indicated that the reaction is first-order with respect to selenium(VI) and that the activation energy is 83 kJ/mole. They pointed out that the reaction rate may be matrix-dependent, and that the

conflicting results reported may be due to matrix effects.

This paper presents the results from a study of the kinetics of selenate reduction in hydrochloric acid, a flow-injection technique being used for sampling. The reaction can be followed more efficiently in this way than by the batch technique used previously.⁶ Rate constants at various temperatures and the activation energy have been determined. The influence of chloride on the reaction rate was also investigated.

EXPERIMENTAL

Reagents

All chemicals used were of analytical grade. Standard solutions of selenium(VI) and (IV) were prepared as described earlier.⁷

Apparatus

The hydride-generation atomic-absorption spectrometry (HG-AAS) equipment has been described elsewhere.⁸ The signal from the AAS instrument was evaluated with an integrator (Shimadzu C-R3A).

The kinetic experiments were done with the sample in a beaker covered by a Teflon lid and fitted into a central boring in an aluminium cylinder provided with an aluminium lid. The cylinder was heated on a hot-plate and the temperature controlled to $\pm 0.2^\circ$ by a resistance thermometer fitted through the lid. Holes were also drilled for addition of reagents and for tubing to collect samples. The reaction mixture was stirred with a magnetic bar. Sampling was

*Author for correspondence.

generally done by continuously pumping the reaction mixture from the beaker through Teflon tubing (i.d. 0.7 mm) to the sample loop (0.5 ml) of the HG-AAS apparatus. Just after emerging from the thermostat the tubing passed through a cooling device, which lowered the temperature to 17° in less than 10 sec. At this temperature the reaction rate is negligible.

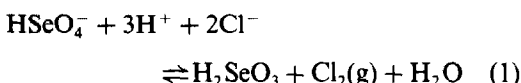
Procedure

Hydrochloric acid (200 ml) of the appropriate concentration was transferred to the beaker. When the desired reaction temperature had been reached and had stabilized, 1 ml of selenium(VI) solution in hydrochloric acid was added to yield a concentration of about 5 ng/ml in the reaction mixture. At the instant of mixing, the pump and a timer were started. The timer controlled the injection valve of the HG-AAS apparatus and a measurement was generally made every 30 sec. Calibrations were performed with standard solutions of selenium(IV) before, during and after the kinetic run.

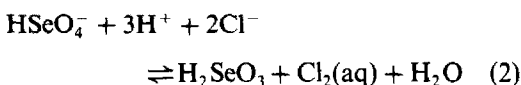
At low reaction rates, sampling and analysis were controlled manually. The interval between samplings was increased as the reaction progressed. Standards were run between determinations, to allow a correction to be made for changes in the sensitivity of the HG-AAS apparatus.

RESULTS AND DISCUSSION

The equilibrium constant of the reaction



has been found⁹ to be $K_1 = 7.1 \times 10^{-10}$ atm.kg⁵.mole⁻⁵. The reduction of selenate at trace level by chloride is more appropriately written as



The equilibrium constant of reaction (2) can be found by combining K_1 with the constant for $\text{Cl}_2(\text{g}) \rightleftharpoons \text{Cl}_2(\text{aq})$. This constant was estimated from the solubility of chlorine in water¹⁰ to be 0.1 mole.kg⁻¹.atm⁻¹. The constant for reaction (2) is then $K_2 = 7.1 \times 10^{-11}$ kg⁴/mole⁴. A calculation of K_2 from standard potentials¹¹ yields $K_2 = 4.9 \times 10^{-11}$ l.⁴/mole⁴. The standard enthalpy change for reaction (2) was calculated to be 110 kJ/mole.¹² The value of K_2 at 80°, an average

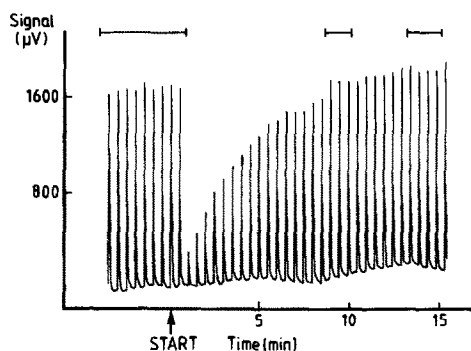


Fig. 1. Recorder tracing of a kinetic run of 5 µg/l. selenate in 5M hydrochloric acid at 85°. —|—| Calibrations.

temperature for the kinetic experiments, can then be estimated to be 6×10^{-8} l.⁴/mole⁴. The conditional constant in 4–6M hydrochloric acid can be estimated to be larger by a factor of 10–500. The estimate of K_2 indicates that reaction (2) would be quantitative at a selenium(VI) concentration of 1×10^{-7} M (8 ng/ml). The reverse reaction can therefore be neglected in our experiments.

Kinetic measurements were made for 4, 5 and 6M hydrochloric acid media in the temperature range 50–95°, depending on the medium. Figure 1 shows the recorder trace for a kinetic run. The data were evaluated on the assumption that the formation of selenium(IV) at constant hydrochloric acid concentration followed a rate law which was first-order with respect to selenium(VI), *i.e.*,

$$C = C_0(1 - e^{-kt}) \quad (3)$$

where C is the concentration of selenium(IV), C_0 the concentration of selenium(VI) at $t = 0$, and k is the pseudo first-order rate constant. The value of k was obtained by fitting the function

$$C = A - Be^{-kt} \quad (4)$$

to the data by non-linear regression. The reason for using a more general function is due to some complications introduced by the experimental set-up: (i) a delay between sampling and time of analysis; (ii) an uncontrolled period at the start of the reaction before the reaction mixture is homogeneous; (iii) continued progress of the reaction in the cooler; (iv) the fact that the analytical result is an average concentration for the time interval during which the sampling loop is filled. Provided that the pumping rate and the temperature profile in the cooler remain constant during an experiment and that plug flow can be assumed, it can be shown that equation (4) should be valid.

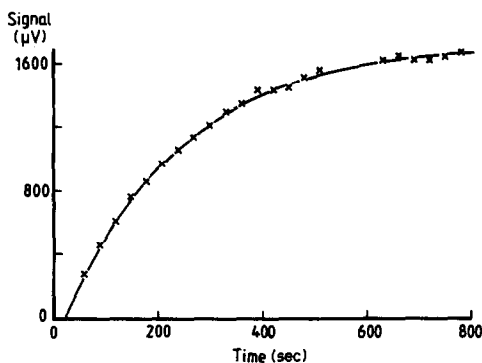


Fig. 2. Fit of the equation $C = A - Be^{-kt}$ to the data in Fig. 1.

A comparison of equations (3) and (4) shows that A should be equal to C_0 , which also should be the value of C at $t = \infty$, C_∞ . This was checked now and then by letting the reaction go to completion. A and C_∞ generally agreed within 5%. The intercept on the t -axis of the fitted function formally corresponds to a delay time, which was usually less than 15 sec. The fit of equation (4) to the data in Fig. 1 is shown in Fig. 2.

From a practical point of view, the most pronounced feature of the reduction of selenium(VI) by hydrochloric acid is the marked dependence of the rate on temperature and acidity. This is demonstrated in Fig. 3 where $\ln k$ is shown as a function of $1/T$. Reasonably straight lines can be drawn for each concentration of the acid, and the mean of the activation energy, E_A , is 126 ± 10 kJ/mole. The observed half-lives (min), $t_{1/2}$, can be reproduced by the empirical relationship

$$t_{1/2} = 2.8 \times 10^{-14} \{\text{HCl}\}^{-3.73} e^{126000/RT} \quad (5)$$

where $\{\text{HCl}\}$ is the mean molar activity of the hydrochloric acid medium at 25° .¹³ The ratio of the half-lives calculated from equation (5) to the observed values was 0.97 ± 0.15 . The tempera-

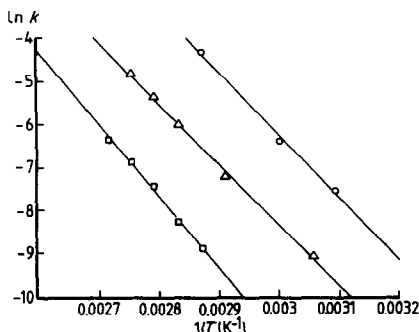


Fig. 3. Values of $\ln k$ as a function of $1/T$ for \square , $4M$; \triangle , $5M$; \circ , $6M$ hydrochloric acid media.

tures needed to reach 99.9% reduction in about 30 min are 105 , 85 and 65° for 4 , 5 and $6M$ hydrochloric acid, respectively. This result agrees with the findings by Bye and Lund.⁶ Their value of E_A is, however, 40 kJ/mole less than ours.

The difference in activation energy could be a medium effect, since Bye and Lund measured the rate in 10:1 v/v mixtures of hydrochloric acid (2 – $10M$) and concentrated perchloric acid. The reported value of E_A was determined from experiments with a medium made up from $4M$ hydrochloric acid. A measurement in this medium with our equipment at 80° yielded a value of $1.04 \times 10^{-3} \text{ sec}^{-1}$ for k . Bye and Lund reported $3.3 \times 10^{-4} \text{ sec}^{-1}$. To find whether this difference in the rate constant was due to our experimental technique, the determination was repeated in the batch mode. A 110-ml volume of the medium was heated to 80° and then selenium(VI) was added at temperature equilibrium. The reaction mixture was sampled at intervals and the samples were treated as described earlier.⁶ The value of k obtained was $1.08 \times 10^{-3} \text{ sec}^{-1}$. The two experimental techniques thus resulted in closely agreeing values for the rate constant.

We next repeated the measurement by the procedure described in detail by Bye and Lund.⁶ When the water-bath was set at 80° a smaller value of k was obtained ($4.7 \times 10^{-4} \text{ sec}^{-1}$). It was noted, however, that the reaction mixture attained its final temperature about 15 min after the start of an experiment and this temperature was about 4° below that of the water-bath. When the temperature of the water-bath was increased so that the temperature of the medium was 80° and the selenium(VI) was not added until temperature equilibrium was reached, the experiment yielded $k = 1.05 \times 10^{-3} \text{ sec}^{-1}$, in agreement with the previous values.

The medium investigated was a $3.6M$ hydrochloric/1.1M perchloric acid mixture. It will be demonstrated later that exchange of chloride for perchlorate at high chloride concentrations and constant acidity will have only a minor effect on the rate constant. If we therefore assume that the medium behaves like $4.7M$ hydrochloric acid, k is estimated from equation (5) to be $1.3 \times 10^{-3} \text{ sec}^{-1}$, in fair agreement with our experimental result. The value of k obtained at 60° differed only by 20% from the value obtained by Bye and Lund. We are therefore inclined to believe that the difference in E_A is mainly due to uncertainties in temperature rather than to a difference in medium.

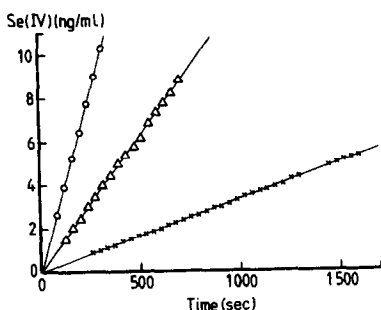


Fig. 4. The selenium(IV) signal as a function of time at three chloride concentrations in mixtures of hydrochloric and perchloric acid. The total acid concentration was $5M$ and the temperature 54° . The rate was determined by linear regression. $[Cl^-]$: \times , 0.2 ; \triangle , 0.4 ; \circ , $0.8M$.

A strongly acid digest containing no chloride ions is obtained when the analytical sample is decomposed with mixtures of strong acids. It is therefore of interest to study the influence of the chloride concentration on the reaction rate. Such a study was performed at 54° with mixtures of hydrochloric and perchloric acid; the sum of the acid concentrations was kept constant at $5M$. The chloride concentration was varied from 0.05 to $5M$. The measurements were made at a high (usually 1000 ng/ml) initial concentration of selenium(VI), C_0 . The rate constant was evaluated from the initial rate of the reaction R .

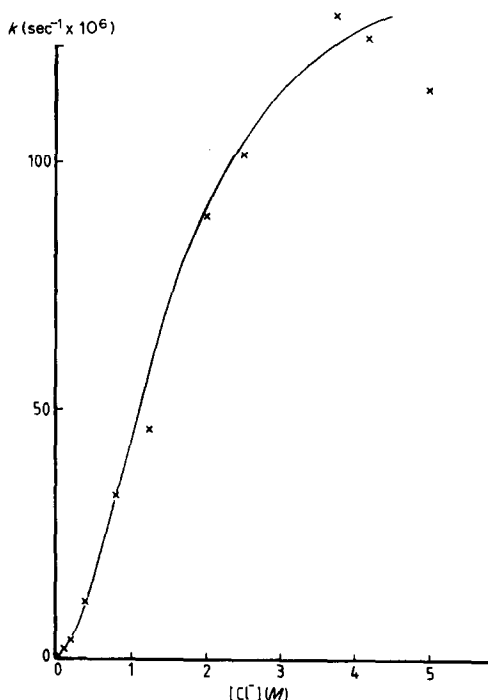


Fig. 5. The rate constant as a function of the chloride concentration, determined by use of equation (6). The curve corresponds to equation (7).

$$R = \frac{d[Se(IV)]}{dt} = kC_0 \quad (6)$$

R was obtained from the slope of a plot of selenium(IV) concentration vs. time.

Figure 4 shows the results of some experiments and Fig. 5 the variation of k with the chloride concentration. The rate increases rapidly with chloride concentration up to about $2.5M$, then levels off. The maximum in k at high chloride concentration is not unique to the $5M$ medium. It was observed in similar measurements with a total acidity of $4M$. A plot of $\log k$ vs. $\log [Cl^-]$ for $[Cl^-] < 0.8M$ indicated a reaction order of 1.75 . The observed rate constant (sec^{-1}) roughly follows the relationship

$$k = \frac{6.85 \times 10^{-5} [Cl^-]^{1.75}}{1 + 0.45 [Cl^-]^{1.75}} \quad (7)$$

which indicates a multi-step reaction.

The weak dependence of the rate on chloride concentration above $\sim 3M$ is not peculiar to a total acid concentration of $5M$. Experiments with mixtures of hydrochloric and perchloric acid, with lithium chloride, and lithium perchlorate to keep the ionic strength constant at $5M$, also yielded rates at 80° that were almost independent of the concentration of chloride in the ranges $2M < [Cl^-] < 5M$; $3M < [H^+] < 5M$. From a practical point of view these results indicate that the addition of chloride to an acid digest should be limited to give a concentration of about $2.5M$.

The dependence of the reaction rate on the hydrogen-ion concentration is very marked. The reaction order was almost 5 at constant chloride concentration (5 or $4M$) and a constant ionic strength of $5M$. The high order is in agreement with results reported by Brimmer *et al.*¹⁴ The order of reaction is thus greater than the stoichiometric coefficient for H^+ in reaction (2). The high dependence of the reaction rate on acidity indicates that some kind of selenate-proton cluster might be formed before the selenium atom is attacked by chloride.

REFERENCES

1. G. A. Cutter, *Anal. Chim. Acta*, 1978, **98**, 59.
2. H. Robberecht and R. Van Grieken, *Talanta*, 1982, **29**, 823.
3. V. Krivan, K. Petrick, B. Welz and M. Melcher, *Anal. Chem.*, 1985, **57**, 1703.
4. C. I. Measures and J. D. Burton, *Anal. Chim. Acta*, 1980, **120**, 177.
5. Y. Shimoishi and K. Tôei, *ibid.*, 1978, **100**, 65.

6. R. Bye and W. Lund, *Z. Anal. Chem.*, 1988, **332**, 242.
7. L. Hansson, J. Pettersson and Å. Olin, *Talanta*, 1987, **34**, 829.
8. J. Pettersson, L. Hansson and Å. Olin, *ibid.*, 1986, **33**, 249.
9. M. S. Sherill and E. F. Izard, *J. Am. Chem. Soc.*, 1928, **50**, 1665.
10. G. Hägg, *General and Inorganic Chemistry*, p. 468. Wiley, New York, 1969.
11. A. E. Martell and L. G. Sillén, *Stability Constants of Metal-Ion Complexes*, Special Publication No. 17. The Chemical Society, London, 1964.
12. W. M. Latimer, *Oxidation Potentials*, 2nd Ed., Prentice-Hall, New York, 1952.
13. R. A. Robinson and R. H. Stokes, *Electrolyte Solutions*, p. 491, Butterworths, London, 1959.
14. S. P. Brimmer, W. R. Fawcett and K. A. Kulhavy, *Anal. Chem.*, 1987, **59**, 1470.

EFFECT OF pH ON THE REACTION OF TRIS(2,2'-BIPYRIDYL)RUTHENIUM(III) WITH AMINO-ACIDS: IMPLICATIONS FOR THEIR DETECTION

STEPHEN N. BRUNE and DONALD R. BOBBITT*

Department of Chemistry and Biochemistry, University of Arkansas, Fayetteville, AR 72701, U.S.A.

(Received 18 June 1990. Revised 10 July 1990. Accepted 26 July 1990)

Summary—A new technique for the detection of amino-acids is described, which is based on their chemiluminescence reaction with tris(2,2'-bipyridyl)ruthenium(III). The pH-dependence of this reaction has been investigated and found to be the key experimental parameter in application of this reaction as a detection technique. The chemiluminescence emission obtained is maximal at pH values higher than the N-terminal amino group pK_a of the amino-acid. The background reaction between the ruthenium reagent and hydroxide ion does not occur with the same efficiency as the amino-acid reaction and the optimum signal to noise ratio is obtained at pH 10. A limit of detection of 30 picomole was found for valine and the response was shown to be linear over two orders of magnitude.

New advances in protein sequencing and amino-acid analysis are critical for the continued development and future progress of a variety of emerging biomedical technologies, including those involving recombinant DNA procedures and gene cloning.¹ Most modern techniques for amino-acid analysis require either pre- or post-column derivatization to enhance detection. These methods involve reaction of the amino-acid with ninhydrin,² dansyl chloride,³ *o*-phthal-aldehyde,⁴ 1-fluoro-2,4-dinitrobenzene,² or dimethylaminoazobenzenesulfonyl chloride,⁵ followed by detection of the derivative by conventional ultraviolet or fluorescence spectrometry. Derivatization techniques can suffer from poor sensitivity as a result of incomplete reaction. Derivatization also adds complexity to the technique and may become time and labor intensive. Further, the derivative may not be stable and must therefore be determined immediately. Finally, derivatization limits the separation/detection procedure in that it must be based on the characteristics of the derivative rather than those of the free amino-acid. Frequently, the reagent moiety added to the analyte dominates the chromatographic properties of the derivative, thereby affecting separation efficiency and resolution.

One way to circumvent these limitations inherent in derivatization techniques would be to use a chemiluminescence reaction to detect

amino-acids directly. Chemiluminescence techniques offer many advantages over techniques based on fluorescence and ultraviolet absorption. Further, chemiluminescence detection requires no excitation source and the reaction is usually fairly selective. In addition, the theoretically zero background expected in the absence of analyte suggests that chemiluminescence techniques would be extremely sensitive.

There have been several recent reports which deal with the chemiluminescence (CL) detection of amino-acids.⁶⁻¹¹ Many of the CL techniques have detection limits in the femtomole range.^{6,8,11} However, most of these techniques require precolumn derivatization, which can result in increased analysis time. Of the techniques that do not require derivatization, the reaction of l-amino-acids with l-amino-acid oxidase provides a response for only eight of the amino-acids.⁷ The amperometric method described by Kok *et al.*¹² and the chemiluminescence method presented by Koerner and Nieman⁹ both involve the complexation of amino-acids with copper(II) ions and have detection limits in the picomole range.

It can be postulated that the ideal chemiluminescence detection system would possess the following characteristics: (1) fast reaction kinetics to facilitate miniaturization of the detection system; (2) high reaction efficiency to enhance selectivity; (3) the capability to generate the reagent at the site of reaction, to avoid the need for precolumn chemistry. The methods

*Author for correspondence.

discussed above do not detect the free amino-acid directly but rather through some property of a reagent such as copper(II) or a specific derivatizing agent. Therefore, one way to improve the detection limits for amino-acids would be to find a chemiluminescence reagent capable of reacting directly with the amino-acid. One reagent which might satisfy these requirements and undergo a direct chemiluminescence reaction with amino-acids is tris(2,2'-bipyridyl)ruthenium(III), $\text{Ru}(\text{bpy})_3^{3+}$. Electro-generated $\text{Ru}(\text{bpy})_3^{3+}$ has been observed by Rubinstein *et al.*¹³ to produce CL upon reaction with a variety of molecules, including oxalate ions. Similarly, Noffsinger and Danielson¹⁴ observed CL when electrogenerated $\text{Ru}(\text{bpy})_3^{3+}$ was reacted with primary, secondary and tertiary amines. Detection limits of 0.28 and 2.4 picomole were found for tripropylamine and oxalic acid, respectively. The method was found to be 60 times more sensitive for tertiary than for primary amines and this was attributed to differences in the first ionization potentials of the different classes of compounds. The mechanism for this reaction has been outlined for the oxalate system¹³ and it is believed that the amines react by a similar mechanism. Both Rubinstein *et al.*¹³ and Hoffinger and Danielson¹⁴ found that the ruthenium-based CL reaction was dependent upon the pH of the reaction mixture. In both studies maximum chemiluminescence was obtained between pH 4 and 6, although pH values above 7 were not investigated because hydroxide ions are known to produce CL with $\text{Ru}(\text{bpy})_3^{3+}$. No chemical or theoretical explanation was given for this pH response. From the reported correlation of chemiluminescence intensity with the ionization potential of the first non-bonding orbital (*i.e.*, the lone pair of electrons on a nitrogen atom) it would be expected that a neutral amine group would be more easily ionized than a protonated one. Thus, it would appear that the maximum CL signal should occur at a pH at which the NH_3^+ group is substantially deprotonated (*i.e.*, $\text{pH} > \text{pK}_a$). However, the relative CL intensities produced by reaction with primary, secondary, and tertiary amines should still be controlled by their ionization potentials.

In the present work, the pH-dependence of the reaction of $\text{Ru}(\text{bpy})_3^{3+}$ with amino-acids was investigated. It was found that the maximum CL signal for amino-acids occurs at pH values above 7. The generality of this technique was found to hold for amines as well as amino-acids

and the implications of this for detection in HPLC or FIA will be discussed.

EXPERIMENTAL

Apparatus

$\text{Ru}(\text{bpy})_3^{3+}$ was generated by using a PAR (Princeton, NJ) model 363 Potentiostat/Galvanostat with a standard three-electrode arrangement consisting of a platinum gauze working electrode, a silver-wire quasi-reference electrode, and a platinum-wire auxiliary electrode. The auxiliary electrode was separated from the $\text{Ru}(\text{bpy})_3^{3+}$ solution by a glass frit to prevent formation of ruthenium metal at the electrode surface. A 1.5mM $\text{Ru}(\text{bpy})_3(\text{ClO}_4)_2$ solution (in 0.4M sodium sulfate as supporting electrolyte) was used for all studies. The potential at the working electrode was set at 1.10 V *vs.* the Ag wire. The electrolysis was run for 20 min per 50 ml of ruthenium solution. When the electrolysis had run to completion the ruthenium solution had changed in color from orange to a clear green, corresponding to the formation of $\text{Ru}(\text{bpy})_3^{3+}$. The $\text{Ru}(\text{bpy})_3^{3+}$ was then pumped to the detection cell by means of a Gilson (Middleton, WI) Minipuls 3 peristaltic pump. To keep the volume in the electrolysis cell constant, $\text{Ru}(\text{bpy})_3^{3+}$ was pumped into the electrolysis cell at the same rate at which $\text{Ru}(\text{bpy})_3^{3+}$ was removed. The electrolysis was operated continuously, to provide a constant concentration of $\text{Ru}(\text{bpy})_3^{3+}$ to the detection cell. Tests with a standard sample over a period of 1 hr showed that there was less than 5% variation in the measured signal, confirming that a steady-state concentration of $\text{Ru}(\text{bpy})_3^{3+}$ was produced. The detection cell consisted of a small coil of clear poly(vinyl chloride) tubing (*i.d.* 0.76 mm) positioned in front of a Hamamatsu (Hamilton, NJ) R928 photomultiplier tube. An ISCO (Lincoln, NE) LC-5000 syringe pump was coupled to the detector through a Rheodyne (Cotati, CA) 7010 injector fitted with either a 20 or a 750 μl loop.

The PMT current was monitored with a Keithley (Cleveland, OH) 485 picoammeter, the output of which was sent to a personal computer through an IEEE-488 interface (Model PC-2A; National Instruments, Austin, TX). The experimental configuration is shown schematically in Fig. 1.

Reagents

All amino-acids were purchased from Sigma (St. Louis, MO) and used without further purifi-

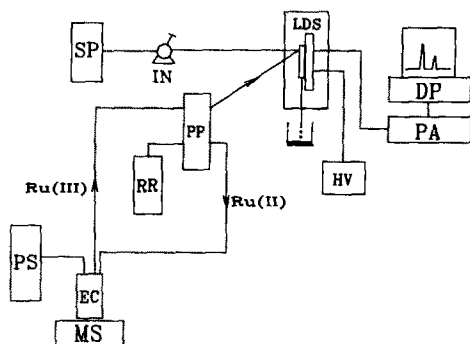


Fig. 1. Experimental arrangement for the chemiluminescence detection of underivatized amino-acids. SP, syringe pump; IN, injection system; LDS, light detection system (detection cell coupled to a photomultiplier tube); HV, photomultiplier power supply; PA, picoammeter; DP, data procurement and display; PP, peristaltic pump; RR, ruthenium(II) reservoir; MS, magnetic stirrer; EC, electrochemical cell; PS, potentiostat.

cation. $\text{Ru}(\text{bpy})_3\text{Cl}_2$ was purchased from Aldrich (Milwaukee, WI) and converted into the perchlorate before use. All other chemicals were reagent grade and used as received.

Amino-acid solutions were analyzed within 3 days after preparation. The buffers used were 0.05M KH_2PO_4 at pH 6, 7 and 8, 0.05M H_3BO_3 at pH 9 and 10, and 0.025M K_2HPO_4 at pH 11 and 12.

Procedure

The pH studies were performed by injecting a 750 μl plug of buffer followed by either the amino-acid or amine buffered at the same pH. The carrier stream containing the sample plug was merged with the $\text{Ru}(\text{bpy})_3^{3+}$ stream at the detection cell. Since the efficiency of transport of the $\text{Ru}(\text{bpy})_3^{3+}$ was not determined, all pH studies were conducted with at least a 10:1 mole ratio of $\text{Ru}(\text{bpy})_3^{3+}$ to amine or amino-acid to ensure that an excess of ruthenium reagent was available. The flow-rates of the $\text{Ru}(\text{bpy})_3^{3+}$ and the amino-acid solutions were 0.6 and 0.5 ml/min, respectively.

RESULTS AND DISCUSSION

As already mentioned, the development of techniques for the detection of underivatized amino-acids is an important area of investigation. Previous studies by Bard and co-workers have shown that $\text{Ru}(\text{bpy})_3^{3+}$ will react with a variety of compounds including oxalate¹³ and other organic acids,¹⁵ to yield chemiluminescence. From its reactivity, as determined from these studies, it appeared that $\text{Ru}(\text{bpy})_3^{3+}$ might

be capable of reacting with a variety of amino-acids to yield chemiluminescence and serve for their sensitive detection. However, the technique appeared to have limited analytical utility as initial studies had shown that the reaction does not occur with great efficiency under the usual conditions suggested for $\text{Ru}(\text{bpy})_3^{3+}$ studies (*i.e.*, at $\text{pH} \leq 7$).

A previous study¹⁶ of the oxidation of amino-acids by hexacyanoferrate(III) suggested that the reactive species was the anion of the amino-acid. If the reaction mechanism is similar with $\text{Ru}(\text{bpy})_3^{3+}$, the reaction should be faster at pH values equal to or greater than the pK_a of the N-terminal amine of the amino-acid, but a complication is that hydroxide ion also reacts with $\text{Ru}(\text{bpy})_3^{3+}$ to yield chemiluminescence. However, this approach would still have analytical merit if the reaction of the ruthenium complex with an amino-acid occurred with greater efficiency than that with hydroxide ion. The pH-dependence of the $\text{Ru}(\text{bpy})_3^{3+}$ /amino-acid reaction was therefore investigated to test this hypothesis.

Table 1 contains a summary of the pH-dependence of the reaction of $\text{Ru}(\text{bpy})_3^{3+}$ with glutamic acid. It is clear that at $\text{pH} < \text{pK}_a$ for glutamic acid (9.2), the amino-acid reaction does not produce sufficient chemiluminescence to be distinguishable from the buffer blank. However, at $\text{pH} > 8$, the reaction of $\text{Ru}(\text{bpy})_3^{3+}$ with the amino-acid occurs with greater facility than that with hydroxide. The chemiluminescence increases dramatically over the pH range 9–11. Besides glutamic acid (GLU, carboxylic acid side-chain), valine (VAL, hydrocarbon side-chain) and triethylamine (TEA) were tested in the pH range 6–11; pH values > 11 were not investigated because at pH 12 the hydroxide ion concentration was larger than the $\text{Ru}(\text{bpy})_3^{3+}$ concentration. The tertiary amine was chosen in order to compare the results of this study with a previous study of the reaction of amines with

Table 1. Luminescence signal vs. pH

pH	Luminescence signal		
	GLU	VAL	TEA
6	0.00	0.00	0.00
7	0.00	0.00	0.19
8	0.01	0.02	0.74
9	0.22	0.21	1.0
10	0.75	0.84	0.80
11	1.0	1.0	0.79

*Corrected for background and normalized to largest signal within a given data set.

$\text{Ru}(\text{bpy})_3^{3+}$.¹⁴ The results are summarized in Table 1.

From the data in Table 1 it is clear that pH is an important experimental variable in the amino-acid/ $\text{Ru}(\text{bpy})_3^{3+}$ reaction. Figure 2 clearly illustrates this. In Fig. 2, the signal for glutamic acid (a) is plotted along with the signal (b) for the buffer blank at each pH tested. It is evident that the amino-acid response is much greater than the signal from the hydroxide reaction. From the noise measured on the background signal, the signal-to-noise ratio (SNR) at each pH was determined and normalized, and is also plotted in Fig. 2c. The highest SNR, which corresponds to the optimum detectability, occurs at approximately pH 10, corresponding to the pH at which the nitrogen site in the amino-acid is appreciably deprotonated. The apparent slight decrease in the SNR at pH 11 is indicative of the fact that most (86%) of the amino-acid is deprotonated at pH 10. Thus, in going from pH 10 to 11, a substantial increase in the background signal is observed because the hydroxide ion concentration increases from 10^{-4} to $10^{-3}M$. At the same time, the fraction of amino-acid in the deprotonated form increases only from 86 to 98%. However, the background noise increased in proportion to the background signal with increase in pH, resulting in a decrease in SNR at pH values $> \sim 10$.

The pH-dependence of the reaction of $\text{Ru}(\text{bpy})_3^{3+}$ with amino-acids should also hold for the reaction with amines, but this would contradict a previous study¹⁴ which suggested that $\text{Ru}(\text{bpy})_3^{3+}$ reacts optimally with amines at between pH 4.5 and 6.0. To determine the origin of this discrepancy, the pH-dependence of the reaction of triethylamine with $\text{Ru}(\text{bpy})_3^{3+}$ was

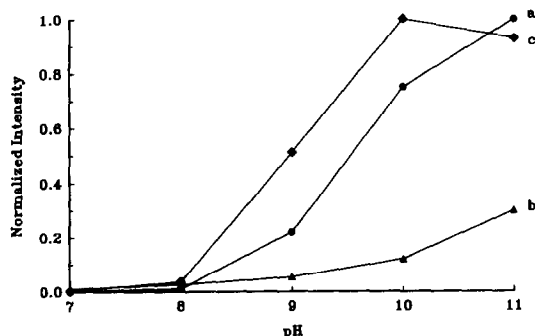
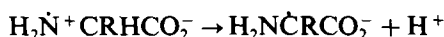
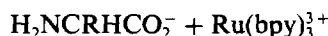


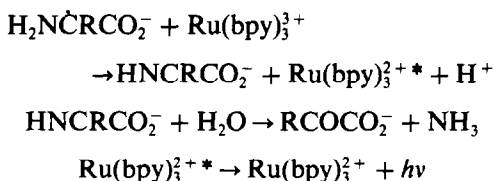
Fig. 2. Effect of pH on the chemiluminescence of glutamic acid. (a) Background-corrected glutamic acid signal; (b) background signal from OH^- reaction; (c) SNR obtained from (a) and the noise measured on (b), at each pH. Concentration of $\text{Ru}(\text{bpy})_3^{3+}$ was $1.5mM$ in $0.4M$ Na_2SO_4 supporting electrolyte.

studied. In the previous study¹⁴ maximum chemiluminescence occurred at pH 6, whereas in the present work (Table 1) it was obtained at pH 9. A possible explanation is that in the previous study both the $\text{Ru}(\text{bpy})_3^{3+}$ and the amine solutions were buffered at the pH to be tested. Bard¹³ has shown that $\text{Ru}(\text{bpy})_3^{3+}$ solutions are most stable at $\text{pH} < 6$. Therefore, as the pH is increased to 7, some decomposition of the $\text{Ru}(\text{bpy})_3^{3+}$ solution would be expected, resulting in a diminished amount of the reagent available for the chemiluminescence reaction. In the previous study¹⁴ the results would be very sensitive to the amount of $\text{Ru}(\text{bpy})_3^{3+}$ available, since an approximately 10:1 molar ratio of amine to $\text{Ru}(\text{bpy})_3^{3+}$ was used. The optimum pH measured under such conditions would therefore represent a trade-off between the availability of the analyte in its most reactive form and the stability of the $\text{Ru}(\text{bpy})_3^{3+}$ reagent.

To avoid this problem, we used an unbuffered $\text{Ru}(\text{bpy})_3^{3+}$ solution and buffered only the amine or amino-acid to be tested. In addition, the $\text{Ru}(\text{bpy})_3^{3+}$ was used in at least 10-fold molar ratio to the amine or amino-acid. By measuring the pH of the solution after the reaction had occurred, it was ascertained that no significant pH change occurred as a result of either the dilution or the reaction.

Noffsinger and Danielson¹⁴ related the observed chemiluminescence for the reaction of $\text{Ru}(\text{bpy})_3^{3+}$ with amines to the first ionization potential of the non-bonding orbital of the nitrogen atom. In such a model, the observed chemiluminescence results from the formation of an amine radical by reaction of the amine with $\text{Ru}(\text{bpy})_3^{3+}$. The radical then reacts with a second $\text{Ru}(\text{bpy})_3^{3+}$ ion, producing an excited $\text{Ru}(\text{bpy})_3^{2+*}$, which subsequently decays to the ground state with the emission of a photon. Support for this model has been offered by Laloo and Mahanti¹⁶ who investigated the reaction of hexacyanoferrate(III) with amino-acids. By consideration of these studies, a mechanism can be offered for the reaction of $\text{Ru}(\text{bpy})_3^{3+}$ with amino-acids. The sequence is outlined below. It should be noted that in this mechanism, the deprotonation at the amine site is very important.





Therefore, on the basis of the $\text{p}K_a$ values alone, the normalized CL should be at a maximum at pH values slightly above the $\text{p}K_a$ of the protonated amine group. Thus, for the amino-acids, the optimum signal would be expected at $\text{pH} > 9$, and for triethylamine at $\text{pH} > 11$. Only the amino-acids showed the expected pH-dependence, however, triethylamine giving an optimal signal at a pH of approximately 9, well below its $\text{p}K_a$ value of 11.

A possible explanation for this requires consideration of the ionization potentials of amines and amino-acids. In general, it would be expected that the higher the ionization potential of the nitrogen site, the more important is the state of protonation at that site, in terms of the ability of the nitrogen atom to donate an electron. Thus donation of an electron by triethylamine, a tertiary amine with an ionization potential of only 8.0 eV,¹⁷ would be expected to be less dependent on the state of protonation than would be the case for the amino-acids, which are primary amines with ionization potentials of approximately 9.5 eV for the non-bonding electron on the nitrogen atom.¹⁸ This would result in a less straightforward dependence of the chemiluminescence reaction on pH. In support of this, for the reaction of $\text{Ru}(\text{bpy})_3^{3+}$ with ethylamine, $\text{p}K_a$ 11 and ionization potential 9.5 eV,¹⁹ it was found that the optimum signal was obtained at a pH of approximately 11 (highest pH tested), lending credence to the idea that the pH-dependence is related to the ionization potential of the nitrogen site.

The analytical capabilities of the $\text{Ru}(\text{bpy})_3^{3+}$ chemiluminescence technique were investigated by using a flow-injection system. Figure 3 shows the reproducibility of multiple injections of methionine over an order of magnitude range of injected mass. For multiple injections of the same standard, the reproducibility was better than 5%. A plot of normalized peak height *vs.* normalized mass of amino-acid injected was a straight line with a slope of 0.98 ± 0.04 , an intercept of 0.03 ± 0.03 and a correlation coefficient of 0.998 (5 points). For valine, a linear response was obtained from 1×10^{-10} to 100×10^{-10} mole. Linear plots were also obtained for arginine, glutamic acid and methion-

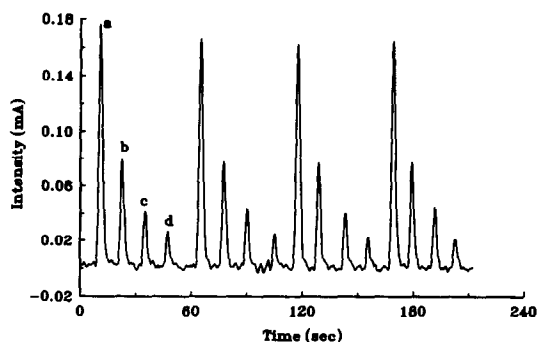


Fig. 3. Chemiluminescence response *vs.* methionine concentration. Multiple 20 μl injections of (a) 0.5, (b) 0.2, (c) 0.1 and (d) 0.05M methionine buffered at pH 10. $\text{Ru}(\text{bpy})_3^{3+}$ flow-rate 0.6 ml/min; pH 10 (borate, 0.05M) buffer flow-rate 0.5 ml/min. Ruthenium concentration as for Fig. 2.

ine over the range from 1.5×10^{-10} to 100×10^{-10} mole. After system optimization an injection of 1×10^{-10} mole of valine buffered at pH 10 gave a signal of 5.3 μA , and the root mean square noise in the buffer blank was found to be 0.50 μA . From these values, the minimum measurable injected quantity for the $\text{Ru}(\text{bpy})_3^{3+}$ system was calculated to be 3×10^{-11} mole of amino-acid ($3\sigma_{\text{blank}}$ criterion). The system was found to be stable for periods of several hours, as determined by repeated injections of the same standard.

To investigate the generality of this approach, eight different amino-acids were tested, representing the different side-chains found in the naturally occurring amino-acids. The results are summarized in Table 2. It is interesting that tryptophan, a secondary amine, gave no more chemiluminescence than the primary amine amino-acids, whereas secondary amines would be expected¹⁴ to give greater chemiluminescence than primary amines. It is possible that the aromatic ring in tryptophan may provide some delocalization of the electrons on the nitrogen atom, thereby diminishing the chemiluminescence.

Table 2. Relative luminescence for eight different amino-acids

Amino-acid	Side-chain type	Relative* luminescence
VAL	Hydrocarbon	1.00
MET	Sulfur-containing	0.79
PHE	Aromatic	0.71
GLU	Carboxylic acid	0.57
TRP	Aromatic amine	0.35
ARG	Basic/amine	0.28
GLY	Hydrogen	0.06
THR	Alcohol	0.04

*Normalized to valine.

As is evident, the $\text{Ru}(\text{bpy})_3^{3+}$ system provides an extremely sensitive way to detect amino-acids without derivatization. The relative response for the different amino-acids varies widely, but even in the least sensitive case (threonine), the limit of detection is estimated to be approximately 0.9 nmole of injected amino-acid. The optical system was not optimized, since the reaction chemistry was the primary reason for the investigation. With the pH-dependence resolved, optical optimization may provide significant improvements in the detectability. For example, visual observation of the reaction coil has shown that the amino-acid emission is localized in a region smaller than that sampled by the present detection system, but the background emission arising from the reaction with hydroxide ion occurs in a much larger region of the detection coil. Thus, more of the background signal than necessary is being sampled and optical imaging may help to isolate the analyte emission region while excluding regions of emission due only to the background hydroxide reaction.

In summary, the pH-dependence of the reaction of amino-acids with $\text{Ru}(\text{bpy})_3^{3+}$ has been investigated in terms of its implications for the detection of underivatized amino-acids separated by HPLC or introduced into a flow-injection system. It has been shown that the optimum chemiluminescence emission for amino-acids is observed at a pH between 10 and 11, which corresponds to the pH at which a significant percentage of the amino-acid exists in the anionic form. A background reaction between the $\text{Ru}(\text{bpy})_3^{3+}$ reagent and hydroxide ion has been observed to be less pH-dependent and it does not limit the technique. The method gives a linear response to amino-acid over a range of two orders of magnitude, and a minimum measurable quantity of 30 pmole of valine has been attained with a flow-injection system. These limits are already significant, considering that they were obtained with underivatized

amino-acid, but improvements are expected from optimization of the optical system. Studies to identify the relative importance of various parameters in the reaction chemistry are currently under investigation, including the role of the α -hydrogen atom on the reaction efficiency, and the importance of steric considerations at the nitrogen site.

Acknowledgement—D. R. B. acknowledges the support of the Camille and Henry Dreyfus Foundation through a teacher-scholar fellowship.

REFERENCES

1. L. M. Smith, *Anal. Chem.*, 1988, **60**, 381A.
2. J. D. Rawn, *Biochemistry*, Harper & Row, New York, 1983.
3. K. Imai, Y. Matsunaga, Y. Tsukamoto and A. Nishitani, *J. Chromatog.*, 1987, **400**, 169.
4. P. Lindroth and K. Mopper, *Anal. Chem.*, 1979, **51**, 1667.
5. J. Y. Chang, R. Knecht and D. G. Braun, *Methods Enzymol.*, 1983, **91**, 41.
6. S. Spurlin and M. M. Cooper, *Anal. Lett.*, 1986, **19**, 2277.
7. H. Jansen, U. A. Th. Brinkman and R. W. Frei, *J. Chromatog.*, 1988, **440**, 217.
8. K. Miyaguchi, K. Honda and K. Imai, *ibid.*, 1984, **316**, 501.
9. P. J. Koerner, Jr. and T. A. Nieman, *Mikrochim. Acta*, 1987 **II**, 79.
10. T. G. Curtis and W. R. Seitz, *J. Chromatog.*, 1977, **134**, 343.
11. S. Kobayashi and K. Imai, *Anal. Chem.*, 1980, **52**, 424.
12. W. Th. Kok, U. A. Th. Brinkman and R. W. Frei, *J. Chromatog.*, 1983, **256**, 17.
13. I. Rubinstein, C. R. Martin and A. J. Bard, *Anal. Chem.*, 1983, **55**, 1580.
14. J. B. Noffsinger and N. D. Danielson, *ibid.*, 1987, **59**, 865.
15. I. Rubinstein and A. J. Bard, *J. Am. Chem. Soc.*, 1981, **103**, 512.
16. D. Laloo and M. Mahanti, *J. Chem. Soc., Dalton Trans.*, 1990, 311.
17. S. F. Nelsen, *J. Org. Chem.*, 1984, **49**, 1891.
18. P. H. Cannington and N. S. Ham, *J. Electron Spectrosc. Relat. Phenom.*, 1983, **32**, 139.
19. S. Katsumata, T. Iwai and K. Kimura, *Bull. Chem. Soc. Japan*, 1973, **46**, 3391.

EQUILIBRIUM CONSTANTS AND ASSAY OF BASES IN ACETONITRILE

JOSE BARBOSA, VICTORIA SANZ-NEBOT and ELENA TORRERO

Department of Analytical Chemistry, University of Barcelona, 08028 Barcelona, Spain

(Received 14 February 1990. Revised 3 July 1990. Accepted 24 October 1990)

Summary—The acid–base equilibria of a series of bases of pharmaceutical interest have been studied in acetonitrile medium and used to investigate the possibility of the use of this solvent to determine basic substances with complex and diverse structure. The pK_{HB} values of a series of cardiovascular compounds have been determined. From these values, simple potentiometric and visual titrations in acetonitrile media are proposed for the assay of bases in pharmaceutical formulations.

Acetonitrile is one of the most important dipolar aprotic solvents. It is used extensively as a reaction medium in synthesis and for mechanistic studies, as well as in electrochemistry, spectrophotometry and liquid chromatography. It owes its manifold applications in such diverse fields to a combination of physical properties,¹ particularly its high polarity ($\pi^* = 0.75$)² accompanied by only modest “chemical” solvating power towards many polar and ionic solutes. In common with all other dipolar aprotic solvents,³ acetonitrile typically behaves as a very weak electrophile. It is a much weaker hydrogen-bond donor than water ($\alpha = 0.19$)² but unlike protophilic dipolar aprotic solvents,³ it is also a weak hydrogen-bond acceptor ($\beta = 0.31$).² In consequence, many solutes have high and strongly differentiated reactivities (both kinetically and thermodynamically) in acetonitrile.

Acetonitrile is a much more differentiating solvent than water, reflected by its much smaller autoprotolysis constant⁴ ($pK_{ap} = 33.6$). Nevertheless, the dielectric constant of acetonitrile is high enough ($\epsilon = 36.0$) to allow extensive electrolytic dissociation of ionic solutes. However, many of the potential benefits of acetonitrile as a reaction medium are not fully realized because in the majority of cases the selection of this solvent was largely based on trial and error, as little information was available about the exact nature of the various solute species present and their interactions in this solvent.

The acid–base equilibria of a series of benzodiazepines in acetonitrile have previously been studied.⁴ In the present work, the dissociation constants of the protonated bases in another

series of cardiovascular compounds, the β -blockers, have been determined.

β -Adrenergic blocking agents are widely used in the treatment of cardiac arrhythmias, hypertension, angina and thyrotoxicosis and, because they are also used as doping agents in sport, these substances have been added to the list of substances forbidden by the International Olympic Committee (I.O.C.).

Although methods for the determination of β -adrenergic blocking drugs in urine or other biological fluids are of importance,⁵ rapid and simple quality-control methods for their assay in pharmaceutical formulations are also of interest.

This paper discusses acid–base equilibria in acetonitrile and proposes simple potentiometric and visual titrations for the assay of bases in pharmaceutical preparations.

EXPERIMENTAL

Apparatus

For potentiometric titrations, a Crison Digilab 517 pH-meter equipped with a Radiometer G202C glass electrode and the Pleskov (Ag/0.01M AgNO₃ in acetonitrile) reference electrode, with 0.1M tetraethylammonium perchlorate in acetonitrile as salt bridge, was used.⁶ This perchlorate was used on the assumption that the liquid-junction potential introduced would remain essentially constant.⁷ The titrant was added with a Metrohm 655 Multi-Dosimat automatic burette with a 2-ml exchangeable unit. Sample solutions were titrated in a double-walled vessel maintained at $25.0 \pm 0.1^\circ$ by circulating water, with magnetic stirring, under a continuous flow of nitrogen.

Reagents

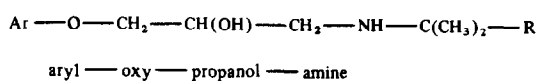
Acetonitrile (Merck, for chromatography); nitromethane (Fluka, analytical grade); perchloric acid (Carlo Erba, RPE-ACS grade), 0.1M solution in nitromethane; picric acid (Doesder, analytical grade, vacuum-dried); tetraethylammonium perchlorate (Carlo Erba, RS grade) and tetrabutylammonium hydroxide (TBAH), 0.1M solution in propan-2-ol (Carlo Erba, RPE grade).

All β -blocker drugs were purified materials kindly supplied by Lab. Esteve (propranolol and metoprolol), Almirall (atenolol), Fides (alprenolol and sotalol), Squibb Ind. Farm, (nadolol), Ciba-Geigy (oxprenolol), Hoechst (penbutolol) and Rhône-Poulenc (acebutolol), pharmaceutical laboratories from Barcelona and Madrid.

Structure and nomenclature

Most β -adrenergic blocking agents can be structurally generalized by the formula shown in Fig. 1(a); they are oxypropanolamines which

(a)



(b)

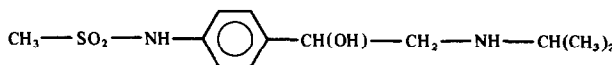


Fig. 1. (a) General structure of β -adrenergic blocking agents. (b) Structure of sotalol, *N*-(4-[1-hydroxy-2-[(1-methylethyl)amino]ethyl]phenyl)methanesulphonamide.

differ in polarity because of the different aryl groups. Among the β -blockers studied, sotalol differs from the general structure and is shown in Fig. 1(b). The substituents at key positions of the compounds studied may be found in Table 1.

Determination of the dissociation constants

The dissociation constants were determined by potentiometry at $25.0 \pm 0.1^\circ$.

From the dissociation constant value of 10^{-11} found for picric acid in a careful study by

Table 1. Structure of β -adrenergic blocking agents

Substance	Ar	R	Systematic name
Acebutolol	$\text{CH}_3 - \text{CH}_2 - \text{CH}_2 - \text{CO} - \text{NH} - \text{C}_6\text{H}_4 - \text{CO} - \text{CH}_3$	—H	<i>N</i> -[3-Acetyl-4-(2-hydroxy-3-[(1-methylethyl)amino]propoxy)phenyl]butanamide
Alprenolol	$\text{CH}_2 = \text{CH} - \text{CH}_2 - \text{C}_6\text{H}_4$	—H	1-[(1-Methylethyl)amino]-3-[2-(2-propenyl)phenoxy]-2-propanol
Atenolol	$\text{NH}_2 - \text{CO} - \text{CH}_2 - \text{C}_6\text{H}_4$	—H	4-(2-Hydroxy-3-[(1-methylethyl)amino]-propoxy)benzeneacetamide
Metoprolol	$\text{CH}_3 - \text{O} - \text{CH}_2 - \text{CH}_2 - \text{C}_6\text{H}_4$	—H	1-[4-(2-Methoxyethyl)phenoxy]-3-[(1-methylethyl)amino]-2-propanol
Nadolol		—CH ₃	5-(3-[(1,1-Dimethylethyl)amino]-2-hydroxypropoxy)-1,2,3,4-tetrahydro-2,3-naphthalenediol
Oxprenolol	$\text{CH}_2 = \text{CH} - \text{CH}_2 - \text{O} - \text{C}_6\text{H}_4$	—H	1-[(1-Methylethyl)amino]-3-[2-(2-propenyloxy)phenoxy]-2-propanol
Penbutolol		—CH ₃	1-(2-Cyclopentylphenoxy)-3-[(1,1-dimethylethyl)amino]-2-propanol
Propranolol		—H	1-[(1-Methylethyl)amino]-3-(1-naphthyl)oxy)-2-propanol

Kolthoff and Chantooni,⁸ the standard potential of the cell was determined by titration of $5 \times 10^{-5} M$ picric acid in acetonitrile with TBAH, and the computer program ACETERISO⁹ was used to calculate the autoprotolysis constant of the medium as reported previously.^{6,10} In picrate-picric acid solutions in acetonitrile, water and alcohols up to $0.5 M$ have no effect on the pH,³ because the picrate ion has practically no hydrogen-bond acceptor properties.

The dissociation constants of the bases were determined by potentiometric titration of their $5 \times 10^{-3} M$ solutions in acetonitrile with $0.1 M$ perchloric acid in nitromethane. For atenolol, propranolol and sotalol, the constants were also determined in acetonitrile-water solutions (water approximately 0.025 and $0.05 M$). The electrode came to equilibrium very quickly after each addition of titrant.

The dissociation constant, K_{HB^+} , of the protonated base is given by

$$K_{HB^+} = a_{HS^+} \frac{[B]y_B}{[HB^+]y_{HB^+}} \quad (1)$$

where a represents activity and y the molar activity coefficient.

From the standard potential of the cell, a_{HS^+} can be calculated from the Nernst equation and the pH is defined by $pH = -\log a_{HS^+} \cdot [HB^+]$ and $[B]$ are computed from the analytical concentration of the base; y_B is assumed to be 1 and the activity coefficient of HB^+ is calculated from the "reduced" Debye-Hückel equation⁷

$$\log y_{HB^+} = -355z_i^2 \epsilon^{3/2} I^{1/2}$$

where z_i is the ionic charge, ϵ the dielectric constant and I the ionic strength. With these values, the pK_{HB^+} of the base is computed from each point of the titration.⁶

RESULTS AND DISCUSSION

Equation (1) was used in the manner described earlier⁴ to determine the pK_{HB^+} values of β -adrenergic blocking agents in acetonitrile. The results are shown in Table 2, together with literature data for the other bases. We estimate

Table 2. Equilibrium constants of bases: dissociation constants (pK_{HB^+}) and effective acidities (pK'_{HB^+}) in acetonitrile; formation constant of perchlorate salt ($\log K_{f,HA_c}^{BHClO_4}$) in acetic acid and dissociation constants (pK_{H_2O}) in water

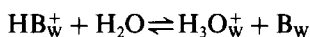
Substance	pK_{HB^+}	pK'_{HB^+}	$\log K_{f,HA_c}^{BHClO_4}$	pK_{H_2O}	ΔpK_{AN-H_2O}
1. n-Butylamine	18.26 ^a	10.16	8.65 ^b	10.59	7.67
2. Diethylamine	18.75 ^a	10.65	8.62 ^b	10.98	7.77
3. Triethylamine	18.46 ^a	10.36	8.39 ^b	10.65	7.81
4. <i>tert</i> -Butylamine	18.14 ^a	10.04	8.77 ^b	10.45	7.69
5. Isobutylamine	17.92 ^a	9.82	8.79 ^b	10.43	7.49
6. Benzylamine	16.76 ^a	8.66	8.64 ^b	9.34	7.42
7. 1,3-Diphenylguanidine	18.34 ^c	10.24	8.35 ^c	10.00	8.34
8. Urea	8.52 ^c	0.42	4.88 ^c	0.20	8.32
9. Trimethoprim	16.12 ^c	8.02	9.11 ^c	6.60	9.52
10. Pyridine	12.57 ^c	4.47	9.18 ^c	5.17	7.40
11. Nicotinamide	10.93 ^c	2.83	8.26 ^c	3.30	7.63
12. Pyridinolcarbamate	10.42 ^c	2.32	8.26 ^c		
13. Sulphamethoxazole	7.19 ^c	-0.81	6.48 ^c		
14. 2-Ph-1,1,3,3-TMG	20.60 ^d	12.50		12.18	8.42
15. Medazepam	14.34 ^e	6.24	9.17 ^f	6.25	8.09
16. Chlordiazepoxide	12.83 ^e	4.73	9.27 ^f	4.90	7.93
17. Clotiazepam	12.06 ^e	3.96	8.67 ^f		
18. Bromazepam	11.10 ^e	3.00	7.83 ^f	2.90	8.20
19. Diazepam	10.90 ^e	2.80	7.98 ^f	3.30	7.60
20. Nitrazepam	10.25 ^e	2.15	7.45 ^f	3.20	7.05
21. Flunitrazepam	9.11 ^e	1.01	6.73 ^f	1.80	7.31
22. Oxazepam	9.07 ^e	0.97	6.12 ^f	1.70	7.37
23. Clonazepam	8.71 ^e	0.61	5.80 ^f	1.50	7.21
24. Lormetazepam	7.58 ^e	-0.42	4.03 ^f	1.30	6.28
25. Acebutolol	17.89	9.79	8.63 ^g	9.40	8.49
26. Alprenolol	17.66	9.56	8.22 ^g	9.50	8.16
27. Atenolol	17.59	9.49	8.74 ^g	9.60	7.99
28. Metoprolol	17.62	9.52	8.47 ^g	9.70	7.92
29. Nadolol	17.73	9.63	8.81 ^g	9.67	8.03
30. Oxprenolol	17.85	9.75	8.28 ^g	9.50	8.35
31. Penbutolol	17.59	9.49	8.26 ^g	9.30	8.29
32. Propranolol	17.52	9.42	8.72 ^g	9.50	8.02
33. Sotalol	17.46	9.36	8.36 ^g	9.80	7.66

^aReference (11), ^bcalculated from reference (12), ^creference (6), ^dreference (13), ^ereference (4), ^freference (14), ^greference (15).

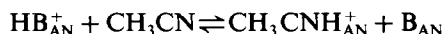
that the pK_{HB^+} values in Table 2 should be accurate to better than ± 0.10 . This table includes only bases for which pK_{HB^+} and the formation constant of the perchlorate salt in acetic acid medium, $K_{\text{f,HAc}}^{\text{BHCIO}_4}$,^{14,15} are known, but additional data are available.^{4,6,11-15}

In solvents of relatively high dielectric constant, such as acetonitrile, in which perchlorate salts can be considered to be completely dissociated, the pH at 50% neutralization, pH_{HNP} , is equal to pK_{HB^+} if activity coefficients are neglected, even though homoconjugated species are present.³ In our work, however, activity coefficients are taken into consideration, *e.g.*, for sotalol the potential $E_{\text{HNP}} = -385.2$ mV, which corresponds to $\text{pH}_{\text{HNP}} = 17.55$ compared with $pK_{\text{HB}^+} = 17.46$.

All the protonated bases studied are much weaker acids in acetonitrile than in water. The factors contributing to the $\Delta pK_{\text{AN-H}_2\text{O}}$ values in Table 2 are illustrated by comparing the following equilibria:



and



where the subscripts indicate solvation by water (W) or acetonitrile (AN). Although the influence of the solvent is complex, taking into account the ability of acetonitrile to solvate cations but not anions, the dominant factor must be the much lower proton-acceptor power of acetonitrile compared with that of water.

In a study of the K_{HB^+} values of a large number of base cations in acetonitrile and water, Coetzee and Padmanabhan¹¹ found that ΔpK for aliphatic amines, pyridine, pyrrolidine and piperidine varied between 7.2 and 8.3, the average being 7.6. For the aromatic amines aniline and *p*-toluidine they found a difference of about 6 (Table 2). Similarly, Leffek *et al.*¹³ found that for a series of 30 phenyl-substituted derivatives of 2-phenyl-1,1,3,3-tetramethylguanidine (PhTMG) the mean value of ΔpK was 8.1 ± 0.5 the same as we find for β -blockers. The values reported⁴ for the benzodiazepines are in line with these results, with an average ΔpK value of 7.6.

The difference in pK_{HB^+} between acetonitrile and water in terms of transfer activity coefficients is expressed¹⁶ by equation (2):

$$\begin{aligned} {}^{\text{AN}}\Delta^{\text{W}}pK_{\text{HB}^+} &= (pK_{\text{HB}^+})_{\text{AN}} - (pK_{\text{HB}^+})_{\text{W}} \\ &= p\gamma_{\text{W} \rightarrow \text{AN}}^{\text{t}}(\text{HB}^+) - p\gamma_{\text{W} \rightarrow \text{AN}}^{\text{t}}(\text{H}^+) \\ &\quad - p\gamma_{\text{W} \rightarrow \text{AN}}^{\text{t}}(\text{B}) \end{aligned} \quad (2)$$

in which $\gamma_{\text{W} \rightarrow \text{AN}}^{\text{t}}(i)$ is the transfer activity coefficient from water to acetonitrile for species *i*. The symbol $\gamma_{\text{W} \rightarrow \text{AN}}^{\text{t}}$ is preferred here to the alternative one, ${}^{\text{AN}}\gamma_i^{\text{O}}$, approved by IUPAC.¹⁷

The transfer activity coefficient is closely related to $\Delta G_{\text{W} \rightarrow \text{AN}}^{\text{t}}(i)$, the standard free energy of transfer of 1 mole of species *i* from water to acetonitrile.

$$\log \gamma_{\text{W} \rightarrow \text{AN}}^{\text{t}}(i) = [\Delta G_{\text{W} \rightarrow \text{AN}}^{\text{t}}(i)]/2.303RT$$

A recent review¹⁸ discussed the various extrathermodynamic assumptions made in finding transfer activity coefficients. In the present work the $\log \gamma_{\text{W} \rightarrow \text{AN}}^{\text{t}}(\text{H}^+)$ value of 8.1 reported by Kolthoff and Chantooni¹⁹ is used, based on the "Parker" (or "tetraphenylborate") assumption that $\gamma^{\text{t}}(\text{AsPh}_4^+) = \gamma^{\text{t}}(\text{BPh}_4^-)$, which appears to yield more accurate $\gamma_{\text{W} \rightarrow \text{AN}}^{\text{t}}(i)$ values than any other assumption.²⁰ There is no uniform agreement on the sign convention. In this work a value of $\log \gamma_{\text{W} \rightarrow \text{AN}}^{\text{t}}(\text{H}^+)$ of 8.1 means that a solute giving a hydrogen-ion activity of 1 in acetonitrile would give an activity of $10^{-8.1}$ in water. Therefore, positive values of $\log \gamma^{\text{t}}$ indicate that the solvent-solute interactions are greater for the solute in water than in the solvent.

Taking into account that the $\Delta pK_{\text{AN-H}_2\text{O}}$ values determined are close to 8.1 (Table 2), the influence of the proton-transfer activity coefficient value on the difference in pK_{HB^+} values could be important [equation (2)].

Even though acetonitrile is much more inert than water, it still solvates ammonium ions significantly, since in acetonitrile, as in water, tertiary ammonium ions are generally stronger acids than the corresponding secondary or primary ammonium ions.

Aromatic ammonium ions (anilinium and *p*-toluidinium ions) are considerably stronger acids in acetonitrile than would be predicted from the strength of protonated aliphatic amines. This fact indicates probably either decreased solvation of aromatic amines or increased solvation of aromatic ammonium ions by water.^{11,21}

On the other hand, in the case of derivatives of the PhTMG bases¹³ there is no hydrogen bonding to stabilize the base and consequently $\Delta pK_{\text{AN-W}}$ is practically equal to $\log \gamma_{\text{W} \rightarrow \text{AN}}^{\text{t}}(\text{H}^+)$.

Even in solvents with very poor hydrogen-bonding donor ability, such as acetonitrile,² hydrogen-bonding with acids is strong enough to make dimerization of the acids very small and

virtually negligible in dilute solution.³ However, particularly in protophobic solvents such as acetonitrile, hydrogen-bonding between an anion and its conjugate acid (homoconjugation) has a large effect on the slope of the titration curve and makes acetonitrile not very suitable for successive titrations of acids in mixtures, although it is a solvent with good resolving power for acids.³ The corresponding complexes AHA^- formed between Brønstad acids and their anions are more stable than the BHB^+ complexes.¹¹ This difference reflects the fact that the solvation of cations rather than anions is more marked for acetonitrile than for water.²² The formation constants of hydrogen-bonded complexes between free and protonated bases, BHB^+ , in acetonitrile have been determined and their values in general are very small.^{4,11} In this paper the formation constants of the BHB^+ homoconjugated complexes for the β -blockers are evaluated by the method of Coetzee *et al.*²² from plots of $(E^0 - E) - g \log y_{\text{HB}^+}$ vs. $\log (c_b/c_s)$, where E^0 and E are the standard potential and the potential of the cell respectively, $g = 2.303RT/F$ and c_b and c_s are the analytical concentrations of the base and salt, respectively. Plots for several β -blockers are shown in Fig. 2.

It follows from the Nernst equation that a plot of $(E^0 - E) - g \log y_{\text{HB}^+}$ vs. $\log ([\text{B}]/[\text{HB}^+])$ will be linear with a slope of 59 mV/decade at 25°. If no complexation occurs between B and HB^+ , $[\text{B}]$ and $[\text{HB}^+]$ are given by c_b and c_s respectively, but otherwise the plot will deviate from linearity, increasing the slope.

Figure 2 shows no evidence for formation of BHB^+ complexes for β -blockers under

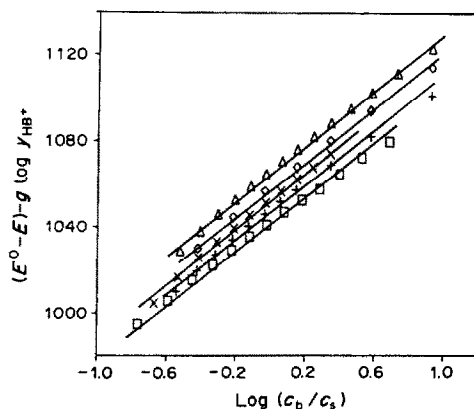


Fig. 2. Plot of $(E^0 - E) - g \log y_{\text{HB}^+}$ vs. $\log (c_b/c_s)$ for several β -blockers. \square , Sotalol; \triangle , oxprenolol; \diamond , nadolol; \times , atenolol; $+$ propranolol.

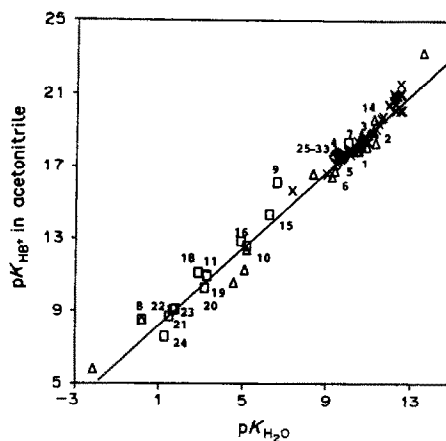


Fig. 3. Plot of pK_{HB^+} in acetonitrile vs. $pK_{\text{H}_2\text{O}}$ for bases numbered as in Table 2. \square , From references (4) and (6); \triangle , from reference (11); \times , from reference (13); \diamond , β -blockers.

the experimental conditions used, since in all cases linear plots with slopes close to 59 mV/decade were obtained. The curves for the neutralization of β -blockers with perchloric acid in acetonitrile can therefore be calculated in the same way as for aqueous media, since homoconjugation is negligible in dilute solutions, as is usually the case for bases.²³

In order to study the effects of hydrogen-bond donors such as water on the pK_{HB^+} values of β -blockers in acetonitrile, the representative β -blockers atenolol, propranolol and sotalol were also studied in acetonitrile containing low concentrations of water (up to 0.05M). The results were not significantly different from those in Table 2, which can be explained by these bases having very low homoconjugation constants.³

Analytically, resolution of acid strength in dipolar aprotic solvents is very important. For acids of a given class, HB^+ , the resolution R in acetonitrile is given by the relationship

$$(pK_{\text{HB}_2^+} - pK_{\text{HB}^+})_{\text{AN}} = R(pK_{\text{HB}_2^+} - pK_{\text{HB}^+})_{\text{W}}$$

in which the left-hand side is the difference in pK_{HB^+} values in acetonitrile, and the right-hand side is the difference in water, multiplied by R .³

For the substituted benzoic acids and for non-*ortho*-substituted phenols, the values of R in acetonitrile were 2.60 and 2.24, respectively.³ However, a plot of pK_{HB^+} values of bases in acetonitrile vs. the pK_{HB^+} values in water is roughly linear, as shown in Fig. 3, with a slope of 1.06. Figure 3 also shows all the pK_{HB^+} literature data from references 4, 6, 11 and 13.

This low value of R is in agreement with the observation that aprotic solvents do not much improve the resolution of acid strength of cationic acids, in contrast to the case for uncharged acids.³

From equation (2), the difference between ${}^{\text{AN}}\Delta^{\text{w}}\text{p}K_{\text{HB}_2^+}$ and ${}^{\text{AN}}\Delta^{\text{w}}\text{p}K_{\text{HB}_1^+}$, (${}^{\text{AN}}\Delta\Delta^{\text{w}}\text{p}K_{\text{HB}_2^+}^{\text{HB}_1^+}$), can be expressed in terms of the transfer activity coefficients:³

$$\begin{aligned} {}^{\text{AN}}\Delta\Delta^{\text{w}}\text{p}K_{\text{HB}_2^+}^{\text{HB}_1^+} &= [\text{p}\gamma_{\text{W}\rightarrow\text{AN}}^{\text{HB}_2^+}] \\ &\quad - \text{p}\gamma_{\text{W}\rightarrow\text{AN}}^{\text{HB}_1^+}] \\ &\quad - [\text{p}\gamma_{\text{W}\rightarrow\text{AN}}^{\text{B}_2}] \\ &\quad - \text{p}\gamma_{\text{W}\rightarrow\text{AN}}^{\text{B}_1}] \end{aligned}$$

From this expression, it appears that the resolution R is independent of the proton transfer activity coefficient.

In the case of uncharged acids, the main reason for the resolution obtained could be that the capacity of acetonitrile to solvate anions is very weak.³ Acetonitrile has practically no hydrogen-bond donor capacity, whereas water has a high hydrogen-bonding donor capacity with a solvatochromic parameter of 1.17.² Thus, acids such as carbon acids, the anions of which are not hydrogen-bonded in hydrogen-bond donating solvents, do not exhibit resolution of acid strength between amphiprotic and aprotic solvents³ and no difference was found in the resolution of acid strength between non-hydrogen-bond donor solvents such as acetonitrile, *N,N*-dimethylformamide and dimethylsulphoxide.²⁴

The difference in hydrogen-bond accepting capacity between acetonitrile ($\beta = 0.31$)² and water ($\beta = 0.47$)²⁵ is much smaller, however, than the difference in their hydrogen-bond donor capacities, and acetonitrile solvates HB^+ cations much better than A^- anions. This explains why the resolution of acid strengths of cationic acids HB^+ is very much smaller than for uncharged acids HA .

Traditional $\text{p}K$ measurements reflect the degree of dissociation of a species in a given solvent, but do not provide a valid measure of the relative proton activity.²⁶ One of the main purposes of studies dealing with the influence of solvents on acid–base equilibria is to obtain a solvent-independent acidity or basicity scale. By referring the acid–base character of non-aqueous solvents to the same aqueous standard state, an “absolute” pH' scale is obtained which allows the acidity and

basicity of aqueous solutions to be compared directly:²⁷

$$\text{pH}' = \text{pH} + \text{p}\gamma_{\text{W}\rightarrow\text{S}}^{\text{H}^+}$$

The transfer activity coefficient represents the acid end of the solvent-independent pH' scale in each distinct solvent S , with ultimate reference to the familiar aqueous pH scale and physical comparability with the latter. The basic limit of the pH' scale in any solvent is conventionally defined by its autoprotolysis constant.²⁸

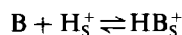
For an aprotic solvent such as acetonitrile, the dissociation constants are translated into the absolute scale by the equation

$$\text{p}K'_{\text{HB}^+} = \text{p}K_{\text{HB}^+} + \text{p}\gamma_{\text{W}\rightarrow\text{AN}}^{\text{H}^+}$$

The effective acidity ($\text{p}K'_{\text{HB}^+}$) provides a measure of both the proton activity in non-aqueous media and the ability to catalyse proton-induced reactions.²⁹ The values of $\text{p}K'_{\text{HB}^+}$ shown in Table 2 provide a measure of the effective acidity of the protonated bases, irrespective of the medium.

On the other hand, the autoprotolysis constant defines the normal range of pH in the solvent and also has important bearings on acid–base titrations in non-aqueous media, where the “ pH jump” at the equivalence point is larger, the greater the $\text{p}K_{\text{ap}}$ value. This value is a composite function of the intrinsic acidic and basic strengths of the solvent and its relative permittivity.³⁰

Then, in the titration of a base



where H_5^+ denotes the solvated proton, the weaker the solvent is as a base and as an acid, the further to the right the equilibrium lies and the larger the “ pH jump” at the equivalence point. For these reasons, very weak bases such as urea and lormetazepam^{4,6} are titrated in acetonitrile, because the formation constant of HB^+ increases and K_{HB^+} decreases with decreasing acid–base strength of the solvent.

Although acetic acid has been a popular solvent for the titration of bases,^{1,14,15,31} the formation constants of HB^+ are much larger in acetonitrile [$K_{\text{f}}(\text{HB}^+) = 1/K_{\text{HB}^+}$] than in acetic acid ($K_{\text{f},\text{HAc}}^{\text{BHClO}_4}$),¹⁴ as shown in Table 2. Hence the break in pH at the end-point is much greater for titration in acetonitrile than in acetic acid. Titration in acetonitrile extends the potential range at the basic end to several hundred mV below that for acetic acid.⁴ The difference in the

"pH jump" is approximately equal to the difference between pK_{HB^+} and $\log K_{f,HAc}^{BHClO_4}$.

Furthermore, for the differentiating titration of two or more bases of different strengths, it is frequently necessary to avoid the levelling effect of acetic acid. This may be done by titration in a non-levelling solvent such as acetonitrile, with perchloric acid dissolved in nitromethane.^{4,6}

The usefulness of acetonitrile for the titration of mixtures of bases was tested in this work and earlier^{4,6} and we conclude that binary mixtures of bases differing in pK_{HB^+} by ≥ 2.5 can be successfully titrated with perchloric acid in nitromethane with potentiometric detection of the end-point. Some mixtures are of great pharmaceutical interest, *e.g.*, trimethoprim and sulfa-methoxazole, potentiometric titration provides a differentiating assay with errors of less than 2%.

$K_{f,HAc}^{BHClO_4}$ values¹⁵ are plotted against the respective dissociation constants of the protonated bases in acetonitrile in Fig. 4. Most of the bases investigated, despite their marked structural differences and the fact that their equilibrium constants were estimated under different experimental conditions, fall into one of two groups, each with reasonable linearity. Only sulphamethoxazole seems not to conform.

The vertical straight line can certainly be attributed to the levelling properties of anhydrous acetic acid. Thus, bases with a pK_{HB^+} value in acetonitrile greater than ~ 12.5 or a pK_{H_2O} value greater than ~ 5 are levelled in acetic acid medium.¹⁵ In contrast, levelling of the strongest bases does not occur in acetonitrile, as this solvent is too weak an acid.¹¹

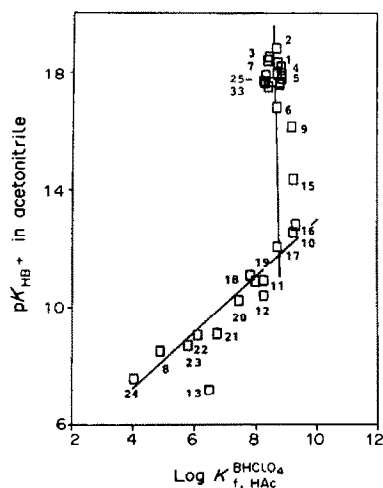


Fig. 4. Plot of pK_{HB^+} values in acetonitrile vs. $\log K_{f,HAc}^{BHClO_4}$ for bases, numbered as in Table 2.

It is of interest that for bases that are not levelled in acetic acid medium, there is a negative correlation between the formation constants, $\log K_f(HB^+)$, in acetonitrile, acetic acid and water and their solvatochromic parameters E_T^N ,³² if their pK_{H_2O} values are greater than 1.5.

The intrinsic acidic and basic strengths of the solvent and its relative permittivity have an influence on $K_f(HB^+)$, *i.e.*, on the pH change at the end-point of a titration.^{29,30} Acetonitrile, acetic acid and water are similar in basic strength, since their β values are not very different.^{2,25} However, they are very different in polarity and acidic strength. The correlation of $\log K_f(HB^+)$ and E_T^N for these three solvents can be explained by the fact that the E_T^N parameter is a measure of the polarity-polarizability of the solvent and its hydrogen-bond donor acidity.³²

The answer to how strong a base must be to give a satisfactory potentiometric titration end-point in acetonitrile is that pK_{HB^+} must be approximately 6 or greater. This theoretical principle has been tested.

Hence, titration graphs with sharp and reproducible inflection points, and $< 2\%$ error were obtained in acetonitrile for all the bases investigated (Table 2), even for the extremely weak bases urea and lormetazepam, which cannot be titrated potentiometrically in acetic acid medium with any degree of accuracy.

On the other hand, those organic bases employed in pharmaceutical preparations and which show a sharp break in the titration curve, may be determined by the more rapid indicator method with the same accuracy and precision as by the potentiometric method.

The change in pH near the equivalence point can be calculated from the dissociation constant of the protonated base, so it is possible to predict which indicators (I) will give sharp colour changes in the equivalence range, since the pK_{HI^+} values and the quality of colour change in acetonitrile are known.^{10,33} The β -blockers were visually titrated with errors $< 2\%$, the indicator selected on the basis of pK_{HI^+} and the quality of colour change being Tropaeolin 00. For visual titrations of bases in acetonitrile we suggest the use of the previously reported series of indicators for the acid-base scale in acetonitrile,¹⁰ from which it is easy to select the best indicator for a specific titration.^{10,33}

Acknowledgement—The financial support of the Comissió Interdepartamental de Recerca i Innovació Tecnològica of the Catalan Government is gratefully acknowledged.

REFERENCES

1. I. M. Kolthoff and P. J. Elving (eds.), *Treatise on Analytical Chemistry*, 2nd Ed., Part 1, Vol. 2, Wiley-Interscience, New York, 1979.
2. M. J. Kamlet, J.-L. M. Abboud, M. H. Abraham and R. W. Taft, *J. Org. Chem.*, 1983, **48**, 2877.
3. I. M. Kolthoff, *Anal. Chem.*, 1974, **46**, 1992.
4. J. Barbosa and V. Sanz-Nebot, *Talanta*, 1989, **36**, 837.
5. M. Ahnoff, M. Ervik, P. Lagerström, B. Persson and J. Vessman, *J. Chromatog.*, 1985, **340**, 73.
6. J. Barbosa, D. Barrón, J. E. Beneyto and V. Sanz-Nebot, *J. Pharm. Biomed. Anal.*, 1988, **6**, 709.
7. J. F. Coetzee and G. R. Padmanabhan, *J. Phys. Chem.*, 1962, **66**, 1708.
8. I. M. Kolthoff and M. K. Chantooni, Jr., *J. Am. Chem. Soc.*, 1965, **87**, 4428.
9. M. Rosés, *Colloquium Chemiometricum Mediterraneum*, Barcelona, 1987.
10. J. Barbosa, M. Rosés and V. Sanz-Nebot, *Talanta*, 1988, **35**, 1013.
11. J. F. Coetzee and G. R. Padmanabhan, *J. Am. Chem. Soc.*, 1965, **87**, 5005.
12. O. W. Kolling, *Anal. Chem.*, 1968, **40**, 956.
13. K. T. Leffek, P. Pruszyński and K. Thanapaalasingham, *Can. J. Chem.*, 1989, **67**, 590.
14. J. Barbosa and D. Barrón, *Analyst*, 1989, **114**, 471.
15. J. Barbosa, D. Barrón and M. E. Torrero, *Analisis*, in the press.
16. I. M. Kolthoff and M. K. Chantooni, Jr., *J. Am. Chem. Soc.*, 1973, **95**, 8539.
17. B. Trémillon and J. F. Coetzee, *Pure Appl. Chem.*, 1978, **50**, 587.
18. Y. Marcus, *ibid.*, 1986, **58**, 1721.
19. I. M. Kolthoff and M. K. Chantooni, Jr., *J. Phys. Chem.*, 1972, **76**, 2024.
20. Y. Marcus, *Pure Appl. Chem.*, 1983, **55**, 977.
21. J. F. Coetzee and D. K. McGuire, *J. Phys. Chem.*, 1963, **67**, 1810.
22. J. F. Coetzee, G. R. Padmanabhan and G. P. Cunningham, *Talanta*, 1964, **11**, 93.
23. I. M. Kolthoff, M. K. Chantooni, Jr. and S. Bhowmik, *Anal. Chem.*, 1967, **39**, 1627.
24. M. K. Chantooni, Jr. and I. M. Kolthoff, *J. Phys. Chem.*, 1973, **77**, 527.
25. Y. Marcus, M. J. Kamlet and R. W. Taft, *ibid.*, 1988, **92**, 3613.
26. O. Popovych, *Anal. Chem.*, 1974, **46**, 2009.
27. P. Ugo, S. Daniele, G.-A. Mazzocchin and G. Bontempelli, *Anal. Chim. Acta*, 1988, **208**, 207.
28. T. Mussini and F. Mazza, *Electrochim. Acta*, 1987, **32**, 855.
29. W. C. Barrette, Jr., H. W. Johnson, Jr. and D. T. Sawyer, *Anal. Chem.*, 1984, **56**, 1890.
30. S. Rondinini, P. Longhi, P. R. Mussini and T. Mussini, *Pure Appl. Chem.*, 1987, **59**, 1693.
31. A. Pietrogrande, A. Guerrato, B. Bortoletti and G. Dalla Fini, *Analyst*, 1984, **109**, 1541.
32. C. Reichardt, *Solvents and Solvent Effects in Organic Chemistry*, VCH, Weinheim, 1988.
33. J. Barbosa, E. Bosch and M. Rosés, *Analisis*, in the press.

STUDIES ON METAL CARBONATE EQUILIBRIA—PART 21* STUDY OF THE U(VI)–H₂O–CO₂(g) SYSTEM BY THERMAL LENSING SPECTROPHOTOMETRY

G. BIDOGLIO, P. CAVALLI, I. GRENTHE,† N. OMENETTO,‡ PAN QI§ and G. TANET

Commission of the European Communities Joint Research Centre, Ispra Establishment,
21020 Ispra (Va), Italy

(Received 29 January 1990. Revised 18 June 1990. Accepted 30 October 1990)

Summary—Equilibria in the U(VI)–H₂O–CO₂(g) system in 0.5M sodium perchlorate medium at 25° have been studied. By using thermal lensing spectrophotometry (TLS) and a very low total concentration of U(VI) ($4 \times 10^{-6}M$) information could be obtained on equilibria involving $UO_2(CO_3)_2^{2-}$ without complications due to formation of the trimer $(UO_2)_3(CO_3)_6^{6-}$. The experimental data allowed a precise determination of the equilibrium constant $\log K_3 = 6.35 \pm 0.05$ for the reaction $UO_2(CO_3)_2^{2-} + CO_3^{2-} \rightleftharpoons UO_2(CO_3)_3^{4-}$. The interpretation of TLS data is briefly discussed, as well as the potential use of this technique for studies of the speciation of trace elements in natural water systems.

Uranium(VI) forms strong complexes with the carbonate ion. The following species have been identified:¹ UO_2^{2+} , $UO_2CO_3(aq)$, $UO_2(CO_3)_2^{2-}$, $UO_2(CO_3)_3^{4-}$, and the trimer $(UO_2)_3(CO_3)_6^{6-}$. $UO_2(CO_3)_3^{4-}$ is the limiting complex, *i.e.*, it contains the maximum number of co-ordinated carbonate ions per UO_2^{2+} ion. The trimer is very stable and the equilibrium constant for the reaction



in 0.5M sodium perchlorate medium is $\sim 10^{7.6}$. As a result, the concentration of the trimer is much larger than that of the monomer $UO_2(CO_3)_2^{2-}$, except at a very low total concentration of U(VI), *i.e.*, $10^{-5}M$ or lower. Special experimental methods must be used to detect and study the properties of $UO_2(CO_3)_2^{2-}$. Solubility experiments may give the desired information provided that the solubility of the solid phase is sufficiently low. This is the case for $UO_2CO_3(s)$.¹ Conventional spectrophotometry was used by Scanlan² to study the equilibrium between $UO_2(CO_3)_3^{4-}$ and $UO_2(CO_3)_2^{2-}$. Despite the low total concentration of U(VI) used,

$10^{-4}M$, the concentration of $(UO_2)_3(CO_3)_6^{6-}$ was not negligible.

Thermal lensing spectrophotometry (TLS)³ has many of the characteristics of conventional spectrophotometry but much higher sensitivity. In previous communications^{4,5} we have outlined how this method may be used for the quantitative study of equilibria in solution.

Spectrophotometry is a quick and reliable experimental method, but its use in equilibrium analysis is complicated by the need to determine the equilibrium constants *and* the molar absorptivities for the various complexes, *cf.* Rossotti and Rossotti.⁶ There are many reports on the use of graphical⁶ and numerical methods^{7,8} for the evaluation of spectrophotometric equilibrium data. To establish a unique chemical model it is generally necessary to rely on experimental data of high precision and to vary the concentrations of the reactants over as large a concentration range as possible. When this is not possible there will invariably be ambiguities in the interpretation.

TLS and laser-induced photoacoustic spectroscopy (LIPAS) have been proposed as possible tools for the determination of the chemical form of trace elements (speciation) in ground water systems.⁹⁻¹³ Both methods have the required high sensitivity but, as will be outlined in this work, this is in general not sufficient to determine the speciation of a trace element in a multiligand system such as ground water.

*Part 20: J. Bruno, I. Grenthe and P. Robouch, *Inorg. Chim. Acta*, 1989, **158**, 221.

†On leave from the Royal Institute of Technology, Department of Inorganic Chemistry, Stockholm, Sweden.

‡Author for correspondence.

§On leave from the Institute of Mechanics, Chinese Academy of Sciences, Beijing, People's Republic of China.

This communication describes the experimental technique used to obtain TLS data, and their chemical interpretation. Some remarks on the use of TLS (which can also be applicable to other laser techniques) for the study of speciation of trace elements in ground waters will also be made.

EXPERIMENTAL

Chemicals

All chemicals used were of reagent grade. The various stock solutions of HClO_4 , NaClO_4 , NaHCO_3 and $\text{UO}_2(\text{ClO}_4)_2$ were prepared and analysed as described before.¹⁴ Carbon dioxide (100%) and a 10.33% CO_2/N_2 gas mixture were obtained from SIO, Milan, and analysed by them.

TLS equipment

The excimer laser and the dye laser systems were the same as described before.¹⁵ The measurements were made at 448 nm, obtained by using Coumarin 450 dissolved in spectroscopically pure methanol. The total concentration of U(VI) was $4 \times 10^{-6} \text{M}$. The overall efficiency of the system was only about 40% of that obtained in our previous studies,^{4,5} mainly because of the lower performance of the excimer laser. The maximum energy available from the dye was $\sim 1 \text{ mJ/pulse}$. The TLS signals, obtained by boxcar averaging of 30 laser firings, were displayed on a chart recorder. These signals were then normalized by means of an

external reference solution (a dilute aqueous solution of potassium dichromate) which was measured immediately before and after the test solutions. This procedure allowed correction for unavoidable random drifts and variations in the efficiency of the system, which were not simply due to fluctuations in the laser power, which was constantly monitored with a pyroelectric detector. For each test solution, the measuring sequence was external standard, test solution, external standard. The experimental results obtained at 25° are collected in Table 1, together with their estimated random error.

Carbonate concentrations from 10^{-9} to 10^{-4}M must be studied to cover the entire complex-formation range in the U(VI)- H_2O - $\text{CO}_2(\text{g})$ system. It is advantageous to use a titration technique as described previously.⁵ This system was modified slightly by the addition of a gas trap after the filter, to prevent the gas-bubbles released by the pressure drop over the filter from reaching the cuvette. This device worked quite well, although some gas-bubbles occasionally entered the cuvette and caused extensive random deflections of the probe laser beam. When this happened the measurements were repeated.

The carbonate concentration was varied by titrating an initial solution of composition 20.00mM NaHCO_3 , 0.480M NaClO_4 , $4 \times 10^{-6} \text{M}$ U(VI) with a solution of composition 200.0mM HClO_4 , 0.300M NaClO_4 , $4 \times 10^{-6} \text{M}$ U(VI). The total concentration of U(VI) was thus kept constant, throughout the

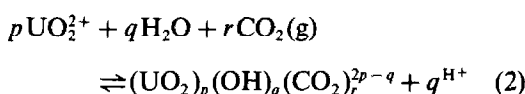
Table 1. Experimental TLS data for the UO_2^{2+} - H_2O - $\text{CO}_2(\text{g})$ system in 0.5M NaClO_4 at 25°; the experimental data in each series are given as $\log(P_{\text{CO}_2}/[\text{H}^+]^2)$, S^*/BS_3 ; the random error in individual S^*/BS_3 values is given in parentheses, and is the absolute variation in the last one or two decimal places in the value given

SERIES 1 (100% CO_2):	11.812, 0.923 (2); 11.650, 0.879 (12); 11.521, 0.824 (8); 11.393, 0.813 (12); 11.237, 0.763 (13); 11.055, 0.733 (21).
SERIES 2 (100% CO_2):	11.822, 0.938 (2); 11.812, 0.923 (2); 11.717, 0.919 (2); 11.586, 0.894; 11.406, 0.869; 11.241, 0.798; 11.024, 0.715; 10.781, 0.558; 10.629, 0.482; 10.422, 0.397.
SERIES 3 (100% CO_2):	11.812, 0.923 (2); 11.653, 0.873 (13); 11.535, 0.857 (12); 11.376, 0.810 (9).
SERIES 4 (100% CO_2):	11.812, 0.923 (2); 11.518, 0.855 (11); 11.342, 0.839 (14); 11.197, 0.760 (8); 11.095, 0.691 (17); 10.984, 0.655 (7); 10.892, 0.602 (17); 10.750, 0.486 (7); 10.622, 0.414 (10); 10.463, 0.345 (8); 10.098, 0.246 (7); 9.469, 0.205 (9).
SERIES 5 (100% CO_2):	11.812, 0.923 (1); 11.785, 0.903 (17); 11.460, 0.834 (14); 11.322, 0.811 (10); 10.815, 0.472 (6); 10.379, 0.293 (9); 10.280, 0.258 (7); 10.037, 0.205 (13); 9.888, 0.184 (7); 9.706, 0.162 (7); 9.331, 0.154 (7); 9.158, 0.144 (5); 8.681, 0.110 (6).
SERIES 6 (10.33% CO_2):	12.798, 0.959 (10); 12.311, 0.952 (4); 12.088, 0.947 (11); 11.953, 0.928 (13); 11.814, 0.923 (1).
SERIES 7 (100% CO_2):	11.812, 0.923 (1); 11.322, 0.792 (9); 10.916, 0.547 (12); 10.686, 0.428 (9); 10.500, 0.345 (7); 10.362, 0.289 (10); 10.314, 0.273 (11); 10.200, 0.258 (18); 10.362, 0.289 (10); 10.314, 0.273 (11); 10.200, 0.258 (18); 10.104, 0.238 (7); 9.993, 0.233 (9); 9.915, 0.229 (11); 9.780, 0.212 (18); 9.611, 0.188 (7); 9.496, 0.185 (11); 8.942, 0.152 (6); 8.661, 0.115 (10).

titration and $[H^+]$ and $[CO_3^{2-}]$ varied. The partial pressure of $CO_2(g)$ was kept constant throughout the titrations by bubbling CO_2 through the test solutions. The hydrogen-ion concentration was measured with a glass electrode, calibrated by means of the known hydrogen-ion concentration in the initial solution, which was calculated from the known value of $\log K_{a1} = -7.607$, the equilibrium constant for the reaction $CO_2(g) + H_2O \rightleftharpoons H^+ + HCO_3^-$ in the given ionic medium and at the temperature used.²⁰ The titrant was added by use of calibrated Eppendorf pipettes. The experimental results are given in Table 1 and in Fig. 1.

Interpretation of data

The chemical equilibria in the U(VI)- H_2O - $CO_2(g)$ system can be described by



where $(OH)CO_2^-$ represents HCO_3^- and $(OH)_2CO_2^{2-}$ represents CO_3^{2-} .

From previous work¹ it is known that the complexes formed under the conditions used in this study are mononuclear and contain only CO_3^{2-} as the ligand (the latter point being verified by the fact that the data in Fig. 1 were independent of P_{CO_2}). It follows that equation (2) can be written as

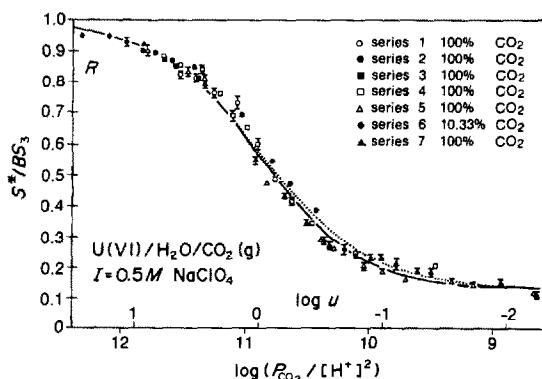


Fig. 1. Experimental TLS data points for S^*/BS_3 vs. $\log(P_{CO_2}/[H^+]^2)$ and normalized curves for R vs. $\log u$. The full line is the best normalized curve, shown in the position of best fit (obtained by using $S_2/S_3 = 0.2$, $S_1/S_3 = 0.15$, $S_0/S_3 = 0.1$, $L = 0.15$, $M = 10^{-3}$). The dotted line was similarly calculated but with $L = 0.10$. From the position of best fit we obtain (for $\log u = 0$):

$$\log K_3 = 17.25 - \left(\log \frac{P_{CO_2}}{[H^+]^2} \right)_{\log u = 0} = 6.35 \pm 0.05$$

The TLS signal (S^*) corrected for the effect of the solvent is given by

$$S^* = S - S_{\text{solv}} = B \left(\frac{S_3 \beta_3 a^3 + S_2 \beta_2 a^2 + S_1 \beta_1 a + S_0}{\beta_3 a^3 + \beta_2 a^2 + \beta_1 a + 1} \right) \quad (4)$$

where S and S_{solv} are the TLS signals for the test solution and the solvent, respectively, B is total concentration of U(VI), S_n is the molar value of the TLS signal for $UO_2(CO_3)_n^{2-2n}$ (S_n is analogous to the molar absorptivity), β_n is the equilibrium constant for reaction (3), and a is the free carbonate concentration. By introducing the normalized variables $1/u = \beta_2/\beta_3 a$; $L = \beta_1 \beta_3 / \beta_2^2$ and $M = \beta_3^2 / \beta_2^3$ we can transform equation (4) into

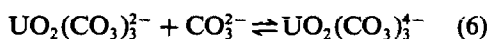
$$S^* = BS_3 \left[\frac{1 + (S_2/u + S_1 L/u^2 + S_0 M/u^3)/S_3}{1 + 1/u + L/u^2 + M/u^3} \right] \equiv BS_3 R \quad (5)$$

From equation (4) it is obvious that $S^*/BS_3 \rightarrow 1$ with increasing a . In Fig. 1 we have plotted the experimental data S^*/BS_3 as a function of $\log(P_{CO_2}/[H^+]^2)$ (the latter quantity is proportional to $\log a$).

The experimental data can be compared with model functions $R(u, L, M, S_n)$ where the function R is as defined in equation (5). The shape of the model function depends on L , M and S_n . By comparing graphs of R vs. u with the experimental plots for S^*/BS_3 vs. $\log(P_{CO_2}/[H^+]^2)$ (or $\log a$), we can, in principle, determine the parameters in equation (4). At the position of best fit, we obtain (at $\log u = 0$)

$$\log \frac{\beta_3}{\beta_2} = \log K_3 = 17.25 - \left(\log \frac{P_{CO_2}}{[H^+]^2} \right)_{\log u = 0}$$

where $17.25 = -\log K_{a2}$.²⁰ For further details refer to the literature.^{5,16-18} From Fig. 1 it is obvious that the largest variations in the experimental quantity occur in the region where the complexes $UO_2(CO_3)_3^{4-}$ and $UO_2(CO_3)_2^{2-}$ are predominant. The variations are much smaller in the range where UO_2^{2+} and $UO_2CO_3(aq)$ are present. Hence, we should be able to obtain the most precise information for the reaction



with equilibrium constant $K_3 = \beta_3/\beta_2$, as is indeed the case.

The value of S_3 is obtained from the initial solution in the absence of $CO_2(g)$. The carbon-

ate concentration is then so high that all U(VI) is present as $\text{UO}_2(\text{CO}_3)_3^{4-}$.

RESULTS AND DISCUSSION

As seen from Table 1, the precision in the individual determinations of S^*/BS_3 was fairly good, but repeating the experiments gave a much larger scatter in the results (*cf.* Fig. 1). An uncertainty of ± 0.02 in S^*/BS_3 therefore seems to be a better estimate than the values obtained for the individual test solutions. In the present experiment the absolute error obtained was the same for all the solutions investigated. The large relative error in S^*/BS_3 in the range where UO_2^{2+} and $\text{UO}_2\text{CO}_3(\text{aq})$ predominate means that we can only determine the equilibrium constants β_1 and β_2 with a low degree of accuracy.

The experimental data can be described quite well with just equilibrium reaction (6). A least-squares refinement gave $\log K_3 = 6.42$ and $S_2/S_3 = 0.11$. However, from previous experiments it is known that $\text{UO}_2\text{CO}_3(\text{aq})$ and UO_2^{2+} will be present in non-negligible amounts in some of the test solutions at the lower values of $-\log [\text{H}^+]$. Hence, we preferred to make the curve-fitting by using the complete equation (5), but with S_1/S_3 and S_0/S_3 as fixed parameters estimated as described below. The variables L and M were also assigned a fixed value. By comparing the experimental data with plots for different model functions R *vs.* $\log u$, we obtained, in the position of best fit, $\log K_3 = 6.35 \pm 0.05$ by using a curve with $S_2/S_3 = 0.20 \pm 0.05$; $S_1/S_3 = 0.15$; $S_0/S_3 = 0.1$; $L = 0.15 \pm 0.05$; $M = 10^{-3}$.

The value of $\log K_3$ is not very sensitive to the values of the other parameters, with the exception of S_2/S_3 . The full line in Fig. 1 is the normalized curve in the position of best fit. The dotted line was obtained by using $L = 0.1$, with the other parameters the same as for the full line. By comparing the two curves we estimate the error in L to be ± 0.05 .

The ratio S_0/S_3 was estimated from the experimental curve to be approximately 0.1 at low values of $\log(P_{\text{CO}_2}/[\text{H}^+]^2)$. From the experimental data we observe that S^*/BS_3 increases as UO_2^{2+} is transformed into $\text{UO}_2\text{CO}_3(\text{aq})$. Hence the value of S_1/S_3 should be larger than the value of S_0/S_3 (*i.e.*, > 0.1) but smaller than S_2/S_3 (*i.e.*, < 0.2), so we have chosen $S_1/S_3 = 0.15$.

We can now compare the results obtained in this TLS investigation with previous results, *cf.*

Table 2. The agreement between the equilibrium constants is satisfactory. The ratio S_2/S_3 can also be calculated from the spectra given by Bidoglio *et al.*⁴ In that case, in the solution denoted " $\text{UO}_2(\text{CO}_3)_3^{4-}$ ", about 90% of the uranium was present as $\text{UO}_2(\text{CO}_3)_3^{4-}$, and the rest as $\text{UO}_2(\text{CO}_3)_2^{2-}$; the solution denoted " $\text{UO}_2(\text{CO}_3)_2^{2-}$ " contained approximately equal concentrations of $\text{UO}_2(\text{CO}_3)_3^{4-}$ and $\text{UO}_2(\text{CO}_3)_2^{2-}$. Using this information and the TLS signals reported in the previous study,⁴ we obtain $S_2/S_3 \sim 0.2$, in good agreement with our result.

To calculate the various β_n values we need information not only on K_3 and L but also on M . The latter quantity can only be obtained from the data at the lower end of the S^*/BS_3 *vs.* $\log a$ curve, where the experimental errors are the largest. Hence, no precise value can be obtained for M in this study; a model with $M = 0$ and $S_2/S_3 = 0.12$ will fit the experimental data as well as the one proposed. However, even this model gives $\log K_3 = 6.35$ and $S_1/S_3 = 0.2$. Other mononuclear models do not give a satisfactory fit. If noticeable quantities of $(\text{UO}_2)_3(\text{CO}_3)_6^{6-}$ had been formed, the experimental (and model) curve would have been much steeper.¹⁹ Thus, at the level of precision attained in this study, we can safely exclude the formation of quantities of the oligomer $(\text{UO}_2)_3(\text{CO}_3)_6^{6-}$ larger than 5%, but not smaller quantities of this or other complexes than those postulated. The limitations just discussed are not characteristic for the TLS method, but for *any* solution chemical method.

Information about the speciation of trace elements in natural water systems is of interest for several reasons. The chemical form of the trace metal may influence its toxicity or its beneficial effects. The chemical form may also influence the rate of transport of the trace elements, *e.g.*, by affecting their sorption on the solid phases encountered along the transport path. The speciation is often derived indirectly

Table 2. Comparison between equilibrium data and spectroscopic information obtained in this study with some literature data

$\log K_3$	L	S_2/S_3	References
$6.20 \pm 0.11^*$	0.10 ± 0.02	—	1, 20
6.35 ± 0.06	0.15 ± 0.05	0.2 ± 0.05	This study
—	—	$\sim 0.2^\dagger$	4

*This value was recalculated²⁰ from the original data published¹ earlier.

†Calculated from the TLS spectra⁴ as discussed in the text.

by calculating the species distribution from known analytical data for the water (*e.g.*, pH, redox potential, total concentration of ligands and concentrations of the major cations), and a suitable thermodynamic database for the elements in question. The quality of the calculation is no better than the quality of the database. TLS and other laser techniques, such as LIPAS, are important experimental tools because they allow us to study chemical equilibria in the laboratory at concentrations closer to those found in nature. This is particularly important for elements which may form polynuclear complexes when "ordinary" experimental methods (which in general require total concentrations of $10^{-4}M$ or larger) are used, but form mononuclear complexes at the very low total concentrations usually encountered in surface and ground water systems. One example is the hydrolysis of metal ions,⁵ another is the oligomerization of $UO_2(CO_3)_2^{2-}$, as discussed in this communication. The laser methods thus make it possible to improve the databases used for equilibrium ("speciation") calculations.

The laser techniques may also be useful for on-line investigations of trace elements, either at a fixed wavelength or at several different wavelengths. In order to obtain information on speciation in systems containing more than one ligand it is necessary to have rather large differences in the spectra of the complexes. This is rarely the case for inorganic ligands. However, elements such as the actinides have quite different spectra in each oxidation state. The laser techniques then offer a convenient way to obtain information on the oxidation states, as exemplified by the work of Pollard *et al.*¹³

Acknowledgements—Many useful discussions with Dr. G. Rossi are gratefully acknowledged. I. G. gratefully acknowledges the financial support of the Joint Research Centre and the Swedish Nuclear Fuel Supply Co.

REFERENCES

1. I. Grenthe, D. Ferri, F. Salvatore and G. Riccio, *J. Chem. Soc. Dalton Trans.*, 1984, 2439.
2. J. P. Scanlan, *J. Inorg. Nucl. Chem.*, 1977, **39**, 635.
3. N. Dovichi, *CRC Crit. Rev. Anal. Chem.*, 1987, **17**, 357.
4. G. Bidoglio, G. Tanet, P. Cavalli and N. Omenetto, *Inorg. Chim. Acta*, 1987, **140**, 293.
5. I. Grenthe, G. Bidoglio and N. Omenetto, *Inorg. Chem.*, 1989, **28**, 71.
6. F. J. C. Rossotti and H. S. Rossotti, *The Determination of Stability Constants, and other Equilibrium Constants in Solution*, McGraw-Hill, New York, 1961.
7. L. G. Sillén and B. Warnqvist, *Ark. Kemi*, 1969, **31**, 377.
8. G. Carta and G. Crisponi, *J. Chem. Soc. Perkin Trans. II*, 1986, 371.
9. J. V. Beitz and J. P. Hessler, *Nucl. Technol.*, 1980, **51**, 169.
10. P. M. Pollard, *U.K. At. Energy Res. Establ., Rept., AERE-R, 1985, AERE R11496*.
11. R. Stumpe, J. I. Kim, K. Schrepp and H. Walther, *Appl. Phys. B*, 1984, **B34**, 203.
12. M. M. Doxtader, V. A. Maroni, J. V. Beitz and M. Heaven, *Mat. Res. Soc. Symp. Proc.*, 1987, **84**, 173.
13. P. M. Pollard, M. Liezers, J. W. McMillan, G. Phillips, H. P. Thomason and F. T. Ewart, *Radiochim. Acta*, 1988, **44/45**, 95.
14. L. Ciavatta, D. Ferri, I. Grenthe and F. Salvatore, *Inorg. Chem.*, 1981, **20**, 463.
15. N. Omenetto, P. Cavalli, G. Rossi, G. Bidoglio and G. C. Turk, *J. Anal. Atom. Spectrom.*, 1987, **2**, 579.
16. L. G. Sillén, *Acta Chem. Scand.*, 1956, **10**, 803.
17. G. Biedermann and L. G. Sillén, *ibid.*, 1956, **10**, 1011.
18. D. Ferri, I. Grenthe and F. Salvatore, *ibid.*, 1981, **A35**, 165.
19. I. Grenthe, C. Riglet and P. Vitorge, *Inorg. Chem.*, 1986, **25**, 1679.
20. I. Grenthe, J. Fuger, R. J. Lemire, A. B. Muller, C. Nguyen-Trung and H. Wanner, *Chemical Thermodynamics of Uranium*, OECD/NEA, in the press.

STUDIES OF POLYFUNCTIONAL *O*-LIGANDS: FORMATION AND STABILITY OF Mg^{2+} AND Ca^{2+} COMPLEXES OF 1,2,4,5-BENZENETETRACARBOXYLIC ACID IN AQUEOUS SOLUTION AT 25°

ALESSANDRO DE ROBERTIS and CONCETTA DE STEFANO

Istituto di Chimica Analitica dell'Università, Salita Sperone 31, P.O. Box 30,
I-98166 S. Agata di Messina, Messina, Italy

(Received 21 February 1990. Revised 5 November 1990. Accepted 9 November 1990)

Summary—The stabilities of the Ca^{2+} and Mg^{2+} complexes with 1,2,4,5-benzenetetracarboxylic acid (pyromellitic acid) were studied potentiometrically, at 25°. The species ML , MHL , MH_2L , and M_2L [L = pyromellitate⁴⁻; M = Ca^{2+} , Mg^{2+}] were found to be present in solution (for Mg^{2+} the species MH_3L was also found). The dependence of the formation constants on ionic strength, and the stability trends of the Ca^{2+} and Mg^{2+} complexes with carboxylate ligands, are discussed.

Magnesium and calcium cations form not very strong complexes with carboxylate ligands.¹⁻⁹ As an example, monocarboxylate ligands form CaL^+ complexes (L = acetate, phenoxyacetate, salicylate) with a mean stability constant $\log K = 0.9$ ($I = 0M$, $T = 25^\circ$)^{4,6,8} and dicarboxylate ligands form CaL complexes (L = malonate, maleate, succinate and phthalate) with a mean stability constant $\log K = 2.4$ ($I = 0M$, $T = 25^\circ$).^{5,6} Increasing the number of carboxylate groups rapidly enhances the stability of the Mg^{2+} and Ca^{2+} complexes [citrate, $\log K = 4.9$ ($I = 0M$, $T = 25^\circ$) and 4.7 ($I = 0M$, $T = 25^\circ$) for calcium and magnesium, respectively⁹].

Since polycarboxylate ligand complexes represent the first step for understanding the complexing ability of several polyelectrolytes and natural ligands (such as humic and fulvic acids), we have studied previously the formation of the alkali-metal complexes of 1,2,4,5-benzenetetracarboxylic acid (H_4L , pyromellitic acid);¹⁰ the solubility and thermal stability of the alkali-metal and alkaline-earth metal salts of pyromellitic acid;¹¹ and the stabilities at different temperatures and ionic strength of alkali-metal and alkaline-earth metal ion complexes with citrate.^{12,13}

Here we report a potentiometric determination of the stability of Mg^{2+} and Ca^{2+} pyromellitate complexes at 25°, in aqueous solution.

EXPERIMENTAL

Materials

Tetraethylammonium iodide (Et_4NI , Fluka) and tetramethylammonium hydroxide (Me_4NOH , Fluka) were recrystallized as described by Perrin *et al.*;¹⁴ Me_4NOH was standardized against potassium hydrogen phthalate, and hydrochloric acid (C. Erba, concentrate ampoules) against sodium carbonate. The solutions of calcium and magnesium chlorides were prepared from the analytical-grade reagents (Fluka) and standardized with EDTA.¹⁵ Lithium chloride solution was prepared from the analytical-grade salt (Fluka), dried under vacuum. All the solutions were prepared by using doubly distilled water and grade A glassware.

Potentiometric equipment and procedure

The free hydrogen-ion concentration was measured with a potentiometer (Metrohm E600) connected to a Ross combination pH electrode model 8102, supplied by Orion. The titrant was delivered by an Amel model 882 dispenser, readable to 1 μl . The measurement cell was maintained at $25 \pm 0.2^\circ$; a magnetic stirrer was employed, and purified nitrogen was bubbled through the solution during the titration.

Table 1. Experimental conditions for the potentiometric titrations of the system $H^+-Mg^{2+}-Cl^- - L^{4-}$ (L^{4-} = pyromellitate), at 25°

Titration	$[H_4L]$, M	$[MgCl_2]$, M	pH	I^* , M	n^\dagger
1	0.00502	0.00506	2.1-5.3	0.03	69
2	0.00502	0.00998	1.9-5.9	0.05	67
3	0.00502	0.02026	1.9-5.8	0.07	69
4	0.00502	0.03992	1.9-5.9	0.13	70
5	0.00502	0.07983	1.8-6.0	0.24	72
6	0.00502	0.1603	1.8-5.6	0.47	76
7	0.01795	0.00506	1.6-4.9	0.06	52
8	0.01795	0.00998	1.6-5.4	0.07	58
9	0.01795	0.02026	1.6-5.6	0.09	60
10	0.01795	0.03992	1.6-5.5	0.14	59
11	0.01795	0.07993	1.5-5.2	0.24	60
12	0.01795	0.01049	1.5-5.3	0.32	58

770

*Mean ionic strength. The ionic strength varies throughout the titration, and this was taken into account by the computer program STACO.

†Number of points in the titration.

The test solutions (see Tables 1 and 2) containing the ligand and magnesium chloride or calcium chloride were titrated with standard 0.4M Me_4NOH . The E° value for all the solutions was calculated from separate titrations of 0.010M hydrochloric acid at the same ionic strength as the solution under study. For the solutions containing Mg^{2+} the self-medium method was used, whereas for those containing Ca^{2+} the titrations were done in the presence of 1M lithium chloride. Protonation constants and Li^+ complex formation constants were obtained from titrations of the pyromellitic acid in the presence of $LiCl$ and Et_4NI , by a method already reported for studying weak complexes.⁶ We used Me_4NOH as titrant in order to avoid the formation of other complex species with Na^+ and K^+ , and because Me_4N^+ ions do not form complex species with carboxylate ligands.⁶

Calculations

Protonation constants and the ligand purity were calculated by the computer program ESAB.^{16,17} Formation constants of the Mg^{2+} and Ca^{2+} complexes were calculated by the computer program STACO.¹⁸ The formation constants of weak Li^+ complexes were calculated by using the computer program ES2WC.^{6,19} All these programs are based on non-linear least-squares methods. In the calculations, the association of Mg^{2+} and Ca^{2+} with Cl^- was taken into account, by using the formation constants reported previously.²⁰ Distribution diagrams were calculated by using the computer program ES4EC.²¹⁻²³

The dependence of the protonation and complex formation constants on ionic strength was taken into account by using the equation^{6,24}

$$\log \beta = \log^T \beta - z^*[\sqrt{I}/(2 + 3\sqrt{I}) + 0.1I^{3/2}] + CI \quad (1)$$

Table 2. Experimental conditions for the potentiometric titrations of the system $H^+-Li^+-Ca^{2+}-Cl^- - L^{4-}$ (L^{4-} = pyromellitate), at 25° and $I = 1M(LiCl)$

Titration	$[H_4L]$, M	$[CaCl_2]$, M	pH	n^*
1	0.00790	0.00293	2.1-5.3	44
2	0.00790	0.00601	2.1-5.4	44
3	0.00790	0.00894	2.1-5.5	44
4	0.00790	0.01848	2.1-5.6	44
5	0.00790	0.03587	2.1-3.1	22
6	0.00491	0.00498	2.3-5.4	44
7	0.00491	0.00601	2.3-5.8	45
8	0.00491	0.00806	2.3-5.7	44
9	0.00491	0.00996	2.3-5.4	44
10	0.00999	0.00498	2.0-4.9	60
11	0.00951	0.00586	2.1-5.3	45

480

*Number of points in the titration.

Table 3. Protonation constants of pyromellitic acid and formation constants of Li^+ complexes, at 25°

pqr^*	$\log \beta_{pqr}^\dagger$ ($I = 1M$)	$\log \beta_{pqr}^\dagger$ ($I = 0.1M$) ¹⁰	C^\ddagger
011	5.70 ± 0.02	5.435	2.03
012	10.13 ± 0.02	9.69	3.52
013	12.96 ± 0.03	12.34	4.65
014	14.83 ± 0.05	14.08	5.20
110	1.70 ± 0.03		
111	6.85 ± 0.03		
112	10.76 ± 0.04		
113	13.00 ± 0.06		
210	2.50 ± 0.04		
211	6.87 ± 0.10		

*Indices refer to the reaction $pLi^+ + qL^{4-} + rH^+ = Li_pL_rH_r^{(p+r-4q)}$.

†Mean ± 3 standard deviations.

‡Empirical parameter of equation (1).

Table 4. Formation constants of Mg^{2+} -pyromellitate complexes, at 25° and $0.03 \leq I \leq 0.5M$ (self-medium)*

pqr^\dagger	$\log \beta_{pqr}^\ddagger$ ($I = 0.1M$)	C^\S
110	2.63 ± 0.05	4.57 ± 0.06
111	7.41 ± 0.04	5.40 ± 0.08
112	10.92 ± 0.06	6.08 ± 0.10
113	13.07 ± 0.10	5.92 ± 0.15
210	3.72 ± 0.07	5.62 ± 0.09

*Calculations performed with the formation of species $MgCl^+$ considered.

†Indices refer to the reaction $pMg^{2+} + qL^{4-} + rH^+ = Mg_pL_qH_r^{(2p+r-4q)}$.

‡Mean ± 3 standard deviations.

§Empirical parameter of equation (1).

where ${}^T\beta$ is the overall formation constant at infinite dilution,

$$z^* = \Sigma(\text{charge})_{\text{reactants}}^2 - \Sigma(\text{charge})_{\text{products}}^2,$$

and C is an empirical parameter. The program STACO is able to calculate C in addition to the formation constants.

The protonation constants of pyromellitic acid and the formation constants of the Li^+ complexes, reported in Table 3, are in agreement with previous findings.⁴⁰

RESULTS AND DISCUSSION

The analysis of the potentiometric data indicates the formation of the species MgL^{2-} , $MgHL^-$, MgH_2L , MgH_3L^+ and Mg_2L . In the calculations, the formation of the $MgCl^+$ species was also considered. In Table 4, we report the formation constants calculated by the program STACO, together with the empirical parameter C [equation (1)], which accounts for the dependence of $\log \beta$ on ionic strength. In Fig. 1 we show the distribution of Mg^{2+} -pyromellitate species *vs.* pH. The stability of the Mg^{2+} -pyromellitate complexes is quite high: at $pH \geq 6.5$, the fraction of pyromellitate present as MgL^{2-} and Mg_2L in the solution (in the conditions of Fig. 1) is over 90%.

For the determination of the stability of Ca^{2+} -pyromellitate complexes it was not possible to use the self-medium method, because of the low solubility of Ca_2L and CaH_2L ($pK_{s0} = 11.85$ and 17.71 , respectively).¹¹ Therefore, we decided to use a constant medium with

Table 5. Formation constants (mean ± 3 standard deviations) of Ca^{2+} -pyromellitate complexes, at 25° and $I = 1M$ (LiCl)

pqr^*	$\log \beta_{pqr}^\ddagger$	$\log \beta_{pq}^\ddagger$
110	3.86 ± 0.04	4.16 ± 0.04
111	8.20 ± 0.03	8.63 ± 0.03
112	11.47 ± 0.04	12.00 ± 0.04
210	5.59 ± 0.08	6.47 ± 0.07

*Indices refer to the reaction $pCa^{2+} + qL^{4-} + rH^+ = Ca_pL_qH_r^{(2p+r-4q)}$.

†Calculations did not consider the formation of species $CaCl^+$.

‡Calculations did consider the formation of species $CaCl^+$.¹⁰

$I = 1M$ (LiCl). Lithium chloride was chosen as background for two reasons: (i) Li^+ and Cl^- do not interact significantly²⁵ (and therefore the calculated ionic strength is, in practice, the effective ionic strength); (ii) Li^+ forms quite well-defined complexes with pyromellitate. The analysis of the potentiometric data indicates the formation of the species CaL^{2-} , $CaHL^-$, CaH_2L and Ca_2L (Table 5). It was impossible to find the species CaH_3L , in contrast to the Mg^{2+} system, owing to the lower metal concentrations. The chloride complex $CaCl^+$ was also taken into consideration. In Fig. 2 we show the distribution of Ca^{2+} -pyromellitate species *vs.* pH. Apparently, the degrees of formation of Ca^{2+} -pyromellitate complexes are lower than those for the corresponding complexes of Mg^{2+} (Fig. 1), but this apparent difference is due to the presence of $1M Li^+$ which forms complexes having a stability that is unusual for alkali-metal complexes. Attempts to find mixed Li^+ - Ca^{2+} pyromellitate complexes were unsuccessful*.

On comparing the stability of the complexes studied here with those of citrate^{9,13} [$\log K(ML)$

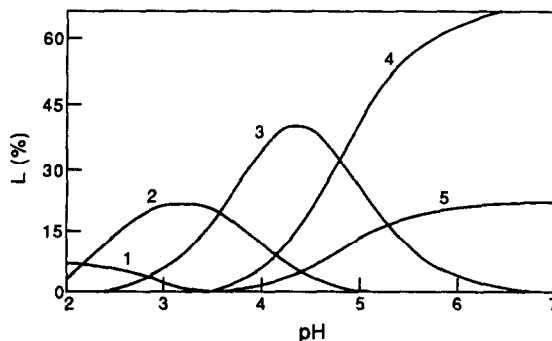


Fig. 1. Distribution of the Mg^{2+} -L ($L = \text{pyromellitate}^{4-}$) complex species *vs.* pH, at 25°, $I = 0.1M$ ($MgCl_2$). In this diagram, only Mg^{2+} species are reported. $C_{Mg} = 0.033M$; $C_L = 0.005M$. Species: 1, $MgLH_3$; 2, $MgLH_2$; 3, $MgLH$; 4, MgL ; 5, Mg_2L .

*Varying the LiCl concentration in the experiments might allow the species $LiCaL^-$ to be found, so the formation constants of Table 5 must be regarded as conditional ones, *i.e.*, valid only in $1M$ LiCl medium.

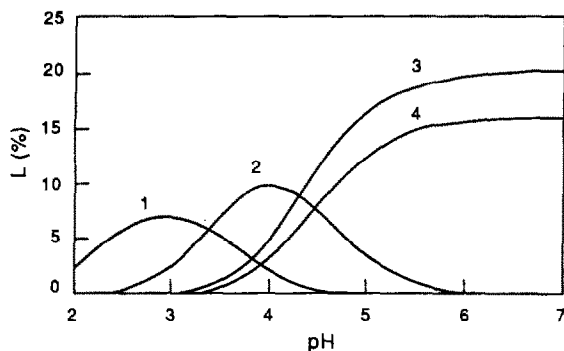


Fig. 2. Distribution of the Ca^{2+} -L ($L = \text{pyromellitate}^{4-}$) complex species vs. pH, at 25° , $I = 1M(\text{LiCl})$. In this diagram, only Ca^{2+} species are reported. $C_{\text{Ca}} = 0.02M$; $C_L = 0.005M$. Species: 1, CaLH_2 ; 2, CaLH ; 3, Ca_2L ; 4, CaL .

$= 4.7$ ($I = 0M$, $T = 25^\circ$), 4.9 ($I = 0M$, $T = 25^\circ$) and $\log K(\text{MHL}) = 2.4$ ($I = 0M$, $T = 25^\circ$), 2.8 ($I = 0M$, $T = 25^\circ$) for magnesium and calcium, respectively] we observe that with citrate the unprotonated complexes are more stable than the monoprotated complexes, whereas the reverse is the case with pyromellitate. This behaviour can be explained, for pyromellitate unprotonated complexes by the simultaneous presence of the binuclear M_2L species, and for the monoprotated complexes by the presence of a residual negative charge on the ligand. Nevertheless, these comparisons, though widely used in the literature, can often be misleading, in particular when dealing with polyfunctional ligands.

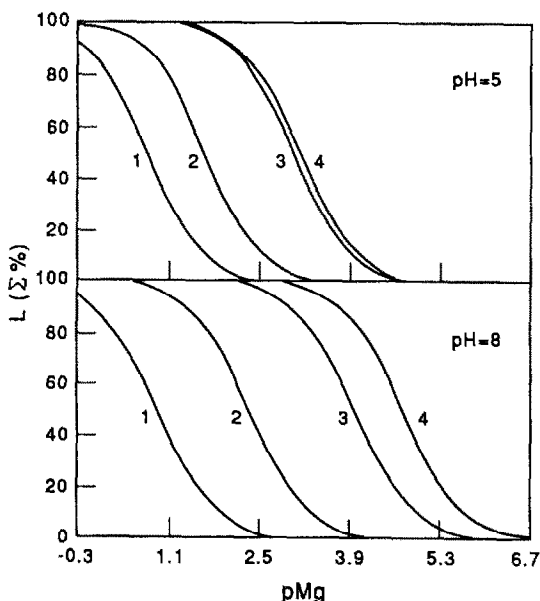


Fig. 3. Fraction of Mg^{2+} in complexed form, $(\Sigma\%)_L$, vs. $p\text{Mg}$. Ligands (L): 1, acetate; 2, malonate; 3, pyromellitate; 4, citrate.

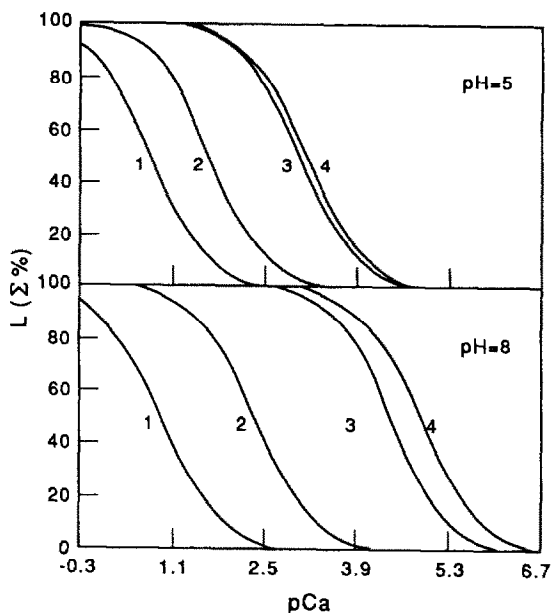


Fig. 4. Fraction of Ca^{2+} in complex form, $(\Sigma\%)_L$, vs. $p\text{Ca}$. Ligands (L): 1, acetate; 2, malonate; 3, pyromellitate; 4, citrate.

Stability constants for a metal-ligand system can be of interest in several fields of chemistry, one of which, related to the speciation of multi-component fluids, is the analytical study of the sequestering ability of a series of ligands for a particular metal ion. In this case the fraction of metal present in the form of complexes in solution (as the sum of the fractions for the individual complexes) is the best parameter for comparing the stabilities of different systems. As an example, in Figs. 3 and 4 we report the sum of percentages of Mg^{2+} and Ca^{2+} complexes of acetate, malonate, citrate and pyromellitate, as a function of the total metal concentration pM ($= -\log [\text{Mg}]$ or $-\log [\text{Ca}]$), at pH 5 and 8. The curves indicate clearly (and quantitatively) the stability of each metal-ligand system, with a parameter independent of the type of species formed. Moreover, calculations performed at different pH values show how the differences in the sequestering ability of ligands for a metal ion are dependent on pH. As can be seen in Figs. 3 and 4, the sharp difference at pH 8 between the Mg^{2+} and Ca^{2+} citrate complexes, (compared with the corresponding pyromellitate complexes) disappears in practice at pH 5.

In the introduction we stated that increasing the number of carboxylate groups rapidly enhances the stability of Mg^{2+} and Ca^{2+} complexes. This is not true for the unprotonated citrate and pyromellitate complexes. Therefore,

Table 6. Constants of Ca²⁺ and Mg²⁺ pyromellitate complex formation at different ionic strengths, at 25°

pqr	Metal	logβ _{pqr}					
		I = 0	I = 0.1	I = 0.25	I = 0.5	I = 0.75	I = 1.0
011	—	6.12†	5.44†	5.38†	5.48†	5.61†	5.70
012	—	10.89	9.69	9.59	9.75	9.98	10.13
013	—	13.86	12.34	12.23	12.46	12.79	12.96
014	—	15.77	14.08	13.96	14.23	14.60	14.83
110	Mg ²⁺	3.94‡	2.63	2.60	2.91	3.31‡	
111	Mg ²⁺	9.08	7.41	7.32	7.64	8.06	
112	Mg ²⁺	12.73	10.92	10.84	11.23	11.73	
113	Mg ²⁺	14.9	13.1	13.0	13.3	13.8	
210	Mg ²⁺	5.81	3.72	3.48	3.65	3.94	
110	Ca ²⁺	4.39§	3.08§	3.05§	3.36§	3.77§	4.16
111	Ca ²⁺	9.23	7.56	7.47	7.79	8.21	8.63
112	Ca ²⁺	12.5	10.7	10.6	11.0	11.5	12.0
210	Ca ²⁺	8.05	5.96	5.73	5.89	6.19	6.47

*Indices refer to the reaction $pM^{2+} + qL^{4-} + rH^+ = M_pL_qH^{(2p+r-4q)}$.

†From Daniele *et al.*¹⁰

‡Extrapolated values.

§Values calculated by using, for the ionic strength dependence of formation constants, the parameters determined for the system Mg²⁺-pyromellitate.

the statement must be revised. In fact, we can say that the stability increases with the number of carboxylate groups only if they are effective in the co-ordination, and this is not true for pyromellitate. This ligand can be considered to be similar to phthalate, with additional groups that are not involved in the co-ordination. Additional alkaline-earth metal-carboxylate ligand systems are being studied in this laboratory, to provide information for a model of the stability of the complexes formed in such systems.

The dependence of the Mg²⁺ complex formation constants on ionic strength (Table 4) is in good agreement with previous findings for several complex systems.^{6,24} In Table 6 we report the formation constants of Mg²⁺ and Ca²⁺ complexes at different ionic strengths for the Ca²⁺ complexes; the C values [equation (1)] found for the Mg²⁺ complexes were used.

Acknowledgements—This work was supported by the Ministero dell'Università e della Ricerca Scientifica e Tecnologica and by the Consiglio Nazionale delle Ricerche, Rome. We thank Professor S. Sammartano for helpful discussion.

REFERENCES

- L. G. Sillén and A. E. Martell, *Stability Constants*, Special Publications Nos. 17 and 25, Chemical Society, London, 1964 and 1971.
- D. D. Perrin, *Stability Constants, Organic Ligands*, Pergamon Press, Oxford, 1979.
- A. E. Martell and R. M. Smith, *Critical Stability Constants*, Vol. 3, Plenum Press, New York, 1977.
- A. De Robertis, C. De Stefano, C. Rigano, S. Sammartano and R. Scarcella, *J. Chem. Res.*, 1985 (S) 42, (M) 629.
- A. De Robertis, C. De Stefano, R. Scarcella and C. Rigano, *Thermochim. Acta*, 1984, **80**, 197.
- P. G. Daniele, A. De Robertis, C. De Stefano, S. Sammartano and C. Rigano, *J. Chem. Soc., Dalton Trans.*, 1985, 2353.
- A. De Robertis and C. De Stefano, *Thermochim. Acta*, 1987, **117**, 317.
- A. Casale, A. De Robertis and C. De Stefano, *ibid.*, 1988, **128**, 261.
- P. Amico, P. G. Daniele, C. Rigano and S. Sammartano, *Ann. Chim. (Rome)*, 1982, **72**, 1.
- P. G. Daniele, A. De Robertis, C. De Stefano and S. Sammartano, *ibid.*, 1990, **80**, 177.
- R. Curini, G. D'Ascenzo, A. De Robertis, C. De Stefano and S. Sammartano, *Thermochim. Acta*, in the press.
- P. G. Daniele, A. De Robertis, C. De Stefano, A. Gianguzza and S. Sammartano, *J. Chem. Res.*, 1990 (S) 300, (M) 2316.
- S. Sammartano, work in preparation.
- D. D. Perrin, W. L. F. Armorego and D. R. Perrin, *Purification of Laboratory Chemicals*, Pergamon Press, Oxford, 1966.
- H. A. Flaschka, *EDTA Titrations*, Pergamon Press, Oxford, 1959.
- C. Rigano, M. Grasso and S. Sammartano, *Ann. Chim. (Rome)*, 1984, **74**, 537.
- C. De Stefano, P. Princi, C. Rigano and S. Sammartano, *ibid.*, 1987, **77**, 643.
- A. De Robertis, C. De Stefano, C. Rigano and S. Sammartano, *Colloquium Chemiometricum Mediterraneum, Abstracts*, p. 87. Barcelona, Spain, 1987.
- A. De Robertis, C. De Stefano, S. Sammartano and C. Rigano, *Talanta*, 1987, **34**, 933.
- A. De Robertis, C. Rigano, S. Sammartano and O. Zerbiniati, *Thermochim. Acta*, 1987, **115**, 241.

21. A. De Robertis, C. De Stefano, S. Sammartano and C. Rigano, *Anal. Chim. Acta*, 1986, **191**, 385.
22. C. De Stefano, P. Princi, C. Rigano and S. Sammartano, *Comput. Chem.*, 1989, **13**, 343.
23. C. De Stefano, P. Princi and C. Rigano, *Ann. Chim. (Rome)*, 1988, **78**, 671.
24. A. Casale, P. G. Daniele, A. De Robertis and S. Sammartano, *ibid.*, 1988, **78**, 249.
25. E. Högfel'dt, *Stability Constants of Metal-Ion Complexes, Part A: Inorganic Ligands*, Pergamon Press, Oxford, 1982.

EVALUATION OF VARIOUS N-PHENYLTHIOSEMICARBAZONES AS CHROMOGENIC REAGENTS IN SPECTROPHOTOMETRIC ANALYSIS

E. CRISTOFOL, F. SANCHEZ ROJAS and J. M. CANO-PAVON

Department of Analytical Chemistry, Faculty of Sciences and Polytechnic School, University of Málaga,
29071 Málaga, Spain

(Received 14 August 1989. Revised 30 May 1990. Accepted 9 October 1990)

Summary—The synthesis, physicochemical properties and interactions with metal ions of three new reagents of the *N*-phenylthiosemicarbazone family, namely pyridoxal phenylthiosemicarbazone, 3-hydroxypyridine-2-aldehyde phenylthiosemicarbazone and 2,6-diacetylpyridine bis(phenylthiosemicarbazone), as well as their ionization constants and the spectral features of their complexes with transition-element cations are reported. A photometric determination of cobalt with pyridoxal phenylthiosemicarbazone in perchloric acid medium is proposed and has been used in analysis of steels.

Thiosemicarbazones and phenylthiosemicarbazones generally react as chelating ligands with transition metal ions by bonding through the sulphur and hydrazine nitrogen atoms,^{1,2} but occasionally behave as terdentate ligands and bond through an additional co-ordinating group. As a rule, phenylthiosemicarbazones are more advantageous than thiosemicarbazones, as their complexes have much higher absorptivities.³

So far, pyridine-2-aldehyde,^{4,5} 2-acetylpyridine,⁶ 2-benzoylpyridine⁷ and di-2-pyridyl ketone phenylthiosemicarbazones⁸ as well as diacetyl⁹ and dipyridylglyoxal diphenylthiosemicarbazones¹⁰ have been used as spectrophotometric reagents. Likewise, the diphenylthiosemicarbazones of 1,2-cyclohexanedione and its 2-methyl and 5,5'-dimethyl derivatives have been used in the non-catalytic kinetic determination of copper(II).¹¹⁻¹³

This paper reports on the synthesis, physicochemical properties and analytical behaviour of three new phenylthiosemicarbazones, *viz.* pyridoxal (PPT), 3-hydroxypyridine-2-aldehyde (3-OH-PAT) and 2,6-diacetylpyridine bis(4-phenylthiosemicarbazone) (2,6-DAPT). These compounds, not studied so far, feature quite different structures and properties. We have made a comprehensive photometric study of the complexes they form with a variety of transition metal ions, to evaluate and compare their potential analytical applications.

EXPERIMENTAL

Reagents

The chelation study was made with 0.05 and 0.1% solutions of the compounds in question in dimethylformamide (DMF). Analytical reagent grade chemicals were used throughout. All metal ion solutions were standardized.

Synthesis of the compounds

PPT. 1 g of pyridoxal hydrochloride was dissolved in 15 ml of water and mixed in a flask with 0.8 g of 4-phenylthiosemicarbazide dissolved in 50 ml of ethanol. The resulting solution was neutralized with sodium acetate and heated under reflux for 30 min. It was allowed to stand at room temperature until yellow crystals were formed; these were then recrystallized from ethanol. The melting point of the product obtained was 150° (decomposition).

3-OH-PAPT. A solution of 1.5 g of 3-hydroxy-2-hydroxymethylpyridine hydrochloride in 150 ml of water was heated together with 0.8 g of manganese dioxide and 200 ml of chloroform at 60° under reflux for 30 min, after which 50 ml of 0.3M sulphuric acid were added dropwise to the mixture. After 10 min of further heating, the solution was cooled gently and the layers formed were decanted. The chloroform solution was dried over sodium sulphate and then evaporated in a rotating film evaporator at

30–40°. The remaining white solid, 3-hydroxypicolinaldehyde, was dissolved in 30 ml of ethanol and added to a solution containing 1 g of 4-phenylthiosemicarbazide in 50 ml of ethanol. The mixture was heated under reflux for 6 hr and then allowed to cool to room temperature. The yellow crystals obtained were recrystallized from methanol. Their melting point was 155° (decomposition).

2,6-DAPT. A 1.1 g amount of 2,6-di-acetylpyridine was dissolved in the minimum volume of absolute ethanol and mixed in a round-bottomed flask with 2.2 g of 4-phenylthiosemicarbazide in ethanol. The mixture was heated under reflux for 3 hr and then allowed to stand at room temperature for 12 hr. The crystals obtained were filtered off, washed with several portions of cold ethanol and then recrystallized from ethanol. Their melting point was 152°.

The purity of the products obtained was confirmed by elemental analysis.

Chelation study

The solutions used in this study were prepared in 25-ml standard flasks with different concentrations of the metal ions, 5 ml of a solution of the reagent in question in DMF, 10 ml of buffer and dilution with distilled water to the mark.

Absorbances were measured against a reagent blank.

Determination of cobalt with PPT in perchloric acid medium

To 3 ml of 0.5 mg/ml PPT solution in dimethylformamide in a 25-ml standard flask, add a known volume of cobalt solution containing between 12.5 and 100 µg of cobalt, 2 ml of dimethylformamide, 0.05 g of ascorbic acid and 5 ml of 60% perchloric acid, and dilute to volume with water. Measure the absorbance at

430 nm against a reagent blank prepared at the same time as the sample. Construct calibration graphs with standard solutions treated in the same way.

Determination of cobalt in steels

Dissolve 0.1–1.0 g of steel in 20–50 ml of *aqua regia* under reflux. Remove the excess of acid by heating. Dilute the solution to 100 ml in a standard flask with distilled water. Analyse an aliquot of this solution by the procedure described above. Any silica or tungstic acid precipitated should be filtered off.

RESULTS AND DISCUSSION

We recorded the infrared spectra of the three compounds by the potassium bromide pellet technique and assigned the corresponding bands to —NH—, C=N and C=S stretching vibrations. We also obtained the ¹H NMR spectra of solutions of the compounds in a mixture of CHCl₃-d₁, DMSO-d₆ and MeOH-d₄. The mass spectra were also recorded and the molecular peaks were found to be consistent with the expected molecular weights. Spectral data are summarized in Table 1.

The ultraviolet spectra of the reagents in various solvents showed intense *n* → *π** bands between 250 and 360 nm, as expected for these systems. The wavelengths of the bands decreased (blue shift) with an increase in the solvent polarity.¹⁴

Acid–base behaviour

The reagents PPT and 3-OH-PAPT both have one protonation constant and two dissociation constants, which, on comparison with those of similar compounds, can be assigned to the protonation of the pyridine nitrogen atom (*K*₁), release of the proton of the hydroxyl group (*K*₂), and release of the proton of the —SH group,

Table 1. Physicochemical properties of the ligands

Property	PPT	3-OH-PAPT	2,6-DAPT
Solubility in ethanol, g/l.	3.20	1.60	0.13
Solubility in water, g/l.	0.40	0.20	0.04
Solubility in dimethylformamide, g/l.	18.50	25.40	1.04
C=N frequency (stretch), cm ⁻¹	1600 m	1600 s	1590 s
C=S frequency (stretch), cm ⁻¹	1040 s	1070 s	1080 m
Aromatic —CH— protons (NMR), ppm	7.1–7.8	7.1–8.2	7.1–8.5
CH ₃ protons, ppm	2.4		2.7–2.9
Imine proton, ppm	8.5	8.5	
Molecular peak (mass spectrum) <i>m/z</i>	316	272	
p <i>K</i> ₁ (protonation of pyridine N atom)	3.25	3.25	1.80
p <i>K</i> ₂ (OH group)	7.75	7.70	—
p <i>K</i> ₃ (SH group)	10.50	11.85	10.50

(which is in tautomeric equilibrium with the C=S group) (K_1); this last process is typical of all thiosemicarbazones and phenylthiosemicarbazones. On the other hand, besides its protonation constant 2,6-DAPT has only one dissociation constant although it has two phenylthiosemicarbazide chains; presumably, as with other dithiosemicarbazones,⁹⁻¹¹ this arises because of the long distance between the two —SH groups, which may make their dissociations spectrophotometrically indistinguishable. The protonation constants (Table 1) were calculated by plotting the absorbance values as a function of pH and applying the customary Stenström and Goldsmith¹⁵ and Sommer¹⁶ methods. As can be seen, pK_1 for 2,6-DAPT is smaller than that for the other two compounds and also smaller than the usual value for pyridine compounds; this is also the case with pyridine 2,6-dialdehyde dithiosemicarbazone,¹⁷ and probably arises from the steric hindrance exerted by the two chains at positions 2 and 6 which block access of protons to the pyridine nitrogen atom through the so-called "face strain effect".

Reaction with metal ions

We studied the reactivity of the three reagents towards 40 cations at concentrations up to 100 ppm and at different pH values. As(III) and (V), Sn(II) and (IV), Al, Cr(III), Be, U(VI), Th, La, Ce(III), W(VI), Mo(VI), alkali-metal and alkaline-earth metal ions did not react with any of the three to an appreciable extent. The most sensitive reactions were with Co(II), Fe(II) and (III), Ni, Cu(II), Zn(II) and Cd(II).

We made a spectrophotometric study of the complexes formed and determined their optimum pH ranges and molar absorptivities, which are listed in Table 2. As can be seen, the values obtained for DAPT were lower than those for the other two compounds; hence its potential analytical interest is smaller.

One of the most outstanding features of these reagents is the high stability of their Co(II) complexes, which are formed even in perchloric acid media, unlike other complexes. This allows their use in the selective determination of traces of cobalt in acid media as the products show no appreciable tendency to decompose in such acidic media. The best results were obtained with PPT, which was therefore chosen for the selective photometric determination of cobalt.

Table 2. Photometric properties of complexes

Ligand	Metal ion	λ , nm	Optimum pH	$\epsilon \times 10^4$ l.mole ⁻¹ .cm ⁻¹
PPT	Co(II)	430	1	1.35
	Co(II)	450	4.5-6.5	1.40
	Ni(II)	430	4-6	1.90
	Cu(II)	440	2.5-5.5	2.17
	Zn(II)	430	5-6	1.62
	Cd(II)	405	4.5-5.5	8.60
	Fe(II)	440	4-6	2.45
	Fe(III)	420	3-5.5	2.40
3-OH-PAPT	Co(II)	435	1-2	2.75
	Co(II)	450	8.5-11	2.60
	Ni(II)	440	8.5-11.5	3.45
	Cu(II)	450	7.5-9	2.10
	Zn(II)	430	10-12	3.83
	Cd(II)	435	5.5-8.5	3.56
	Fe(II)	440	2-3.5	2.12
	Fe(III)	470	8-10	2.57
2,6-DAPT	Co(II)	400	2.5-5	1.93
	Ni(II)	390	4.5-7.5	1.66
	Cu(II)	380	5-10	1.44
	Zn(II)	385	4-9	1.85
	Cd(II)	380	6-10.5	1.60
	Fe(II)	380	4-8	2.97
	Fe(III)	385	3.5-8.5	3.48

Study of the cobalt(II)-PPT complex

The Co(II)-PPT complex was found to have 1:2 stoichiometry. We studied its formation in a perchloric acid medium and found the absorbance did not vary significantly up to an acid concentration of 1.2M. To avoid precipitation of the reagent the DMF content of the final solution must not be below 20%. The optimum order of addition is cobalt-reagent-DMF-ascorbic acid-perchloric acid.

Determination of cobalt

A method for the determination of cobalt with PPT in perchloric acid medium has been developed. Beer's law is obeyed over the range 0.5-4.0 ppm, with a molar absorptivity of 1.35×10^4 l.mole⁻¹.cm⁻¹ at 430 nm. The minimum error zone in a Ringbom graph was between 1.2 and 3.6 ppm.

The method was subject to few interferences as the complexes of most of the potential interferences are either not formed or are decomposed in the strongly acidic medium used. The tolerated levels of the different species tested are listed in Table 3.

The technique described above has been applied to the determination of cobalt in steels. Standard steels were supplied by CENIM. The compositions of these steels were as follows, Steels 1, 2 and 3: Ni, 3.878-3.893%; Mo, 0.490-0.492%; Mn, 0.580-0.583%; Cr, 1.046-1.048%; C, 0.158-0.159%; Si, 0.290-0.291%; S, 0.01%;

Table 3. Interference of foreign ions in the determination of cobalt with PPT

Ion	Tolerance ratio, w/w
Ni(II), Cd(II), Zn(II), Pb(II), Mn(II), Bi(III), Hg(I), Zr(IV), Sb(III), Ca(II), Sr(II), Be(II), Mg(II), Ba(II), Li(I), Tl(I), K(I), Na(I), Fe(II) or (III) (in the presence of ascorbic acid), sulphite, sulphate, phosphate, bromide, thiocyanate, nitrite, oxalate, iodide, chloride, ascorbic acid	> 100
V(V), Hg(II)	40
Iodate	20
Fe(III), Cu(II), Ag(I), Mo(VI), W(VI), arsenate, tartrate, citrate, borate, bromate	10
Cr(III), Al(III)	5

Table 4. Determination of cobalt in steels (mean \pm standard deviation)

Sample	Co present, %	Co found, %
1	0.10	0.10 \pm 0.002
2	0.29	0.30 \pm 0.005
3	0.49	0.49 \pm 0.003
4	4.90	5.19 \pm 0.09
5	4.75	4.56 \pm 0.05
6	9.50	9.22 \pm 0.06

P, 0.014%; Co, 0.10, 0.29 and 0.49%, respectively. Steel 4: W, 18.63%; V, 1.077%; Mo, 0.0953%; Cr, 4.223%; Mn, 0.290%; C, 0.755%; Si, 0.316%; P, 0.016%; S, 0.009%; Co, 4.90%. Steels 5 and 6: Cr, 4.30 and 4.52%, respectively; W, 18.90 and 18.95%; Ni, 0.21 and 0.16%; Mo, 1.06 and 1.12%; V, 1.70 and 1.88%; Cr, 4.30 and 4.52%; Cu, 0.10 and 0.08%; Mn, 0.26 and

0.27%; C, 0.90 and 0.98%; Si, 0.29 and 0.26%; P, 0.022 and 0.029%; S, 0.009 and 0.013%; Co, 4.75 and 9.50%. The results are shown in Table 4 (averages of three determinations). In general, the procedure devised can be applied to a wide variety of steels, except those with an appreciable content of chromium and tungsten.

REFERENCES

1. M. J. M. Campbell, *Coord. Chem. Rev.*, 1975, **15**, 279.
2. R. B. Singh, B. S. Garg and R. P. Singh, *Talanta*, 1978, **25**, 619.
3. J. M. Cano-Pavón, *Microchem. J.*, 1981, **26**, 155.
4. J. L. Gómez Ariza, J. M. Cano-Pavón and F. Pino, *Talanta*, 1976, **23**, 460.
5. J. L. Gómez Ariza and J. M. Cano-Pavón, *Anal. Lett.*, 1976, **9**, 677.
6. M. T. Martínez Aguilar, J. M. Cano-Pavón and F. Pino, *Anal. Chim. Acta*, 1977, **90**, 335.
7. M. T. Martínez Aguilar and J. M. Cano-Pavón, *Mikrochim. Acta*, 1977 **11**, 631.
8. *Idem*, *Anal. Lett.*, 1978, **11**, 373.
9. A. G. Asuero and J. M. Cano-Pavón, *Analyst*, 1978, **103**, 140.
10. M. González Balairón, J. M. Cano-Pavón and F. Pino, *Talanta*, 1978, **26**, 71.
11. J. Rodríguez, A. García de Torres and J. M. Cano-Pavón, *ibid.*, 1981, **28**, 131.
12. *Idem*, *Anal. Chim. Acta*, 1984, **156**, 319.
13. *Idem*, *Mikrochim. Acta*, 1985 **1**, 69.
14. H. McConnell, *J. Chem. Phys.*, 1952, **20**, 700.
15. W. Stenström and N. Goldsmith, *J. Phys. Chem.*, 1926, **30**, 1683.
16. L. Sommer, *Folia Fac. Sci. Nat. Univ. Purkynianae Brun.*, 1964, **5**, 1.
17. F. Castañeda, A. García de Torres and J. M. Cano-Pavón, *Microchem. J.*, 1983, **28**, 556.

ANALYTICAL DATA

PROTONATION AND COMPLEX FORMATION CONSTANTS OF 3-AMINO-1,2,4-TRIAZOLE IN NaCl AND CaCl₂ MEDIA AT DIFFERENT TEMPERATURES AND IONIC STRENGTHS

LORENZO ABATE, RICCARDO MAGGIORE and CARMELO RIGANO

Dipartimento di Scienze Chimiche dell'Università, Viale A. Doria 6, 95125 Catania, Italy

CONCETTA DE STEFANO

Istituto di Chimica Analitica dell'Università, Salita Sperone 31, 98166 S. Agata di Messina, Italy

(Received 1 February 1990. Revised 27 June 1990. Accepted 31 October 1990)

Summary—The protonation of 3-amino-1,2,4-triazole was studied potentiometrically (glass electrode) in sodium chloride and calcium chloride solutions, $0.13 \leq I \leq 0.92M$, at 10, 25, 37 and 45°. The effect of the background electrolyte on the protonation constants is explained by a complex formation model. The species CaL^+ , $CaHL^{2+}$ and H_2LCl ($HL = 3\text{-amino-1,2,4-triazole}$) are proposed. Stability constants, together with their dependence on temperature (ΔH°) and on ionic strength, are reported for the protonated and complex species.

The speciation of natural fluids, *i.e.*, the determination of all the species present in the fluid (free metal ions and ligands, hydrolytic species, stable and weak complexes), requires knowledge of accurate thermodynamic parameters for the metal-ligand interactions. Since pesticides are often involved in complexation reactions, the study of the thermodynamics of formation of pesticide complexes would be highly desirable, particularly for the speciation of ground waters. Moreover, transport and plant uptake of pesticides can be favoured by complexation with cations present in the ground, and therefore the knowledge of the stability of these complexes is important also for pesticide transport and uptake models.

As a further contribution to our studies on complexing ability of pesticides and related compounds,¹⁻⁴ we chose, as an interesting nitrogen-containing ligand, the herbicide 3-amino-1,2,4-aminotriazole (AmitroleTM). Here we report a potentiometric study of the protonation of this ligand in sodium chloride and calcium chloride aqueous solution, at different temperatures and ionic strengths. Salt effects are tentatively explained by a complex formation model.

EXPERIMENTAL

Materials

3-Amino-1,2,4-triazole (Aldrich) of >99.5% purity (standardized by acidimetric titration); sodium chloride (Carlo Erba RPE, standardized by argentometric titration) and calcium chloride dihydrate (Carlo Erba RPE, standardized by EDTA titration), were used without further purification.

Potassium hydroxide and hydrochloric acid stock solutions were prepared by diluting the contents of Merck or Carlo Erba ampoules of concentrates, and standardized against potassium hydrogen phthalate and sodium carbonate respectively.

Apparatus

Potentiometric measurements were performed with a Metrohm 654 pH-meter coupled with Orion glass-saturated calomel electrodes, with an instrumental resolution of ± 0.1 mV. The titrant solution (potassium hydroxide) was delivered by a Metrohm model 654 dispenser (minimum reading 0.01 ml). An IBM PC XT and a Honeywell printer were coupled with the pH-meter and the dispenser in order to add

Table 1. Protonation constants of 3-amino-1,2,4-triazole in aqueous NaCl and CaCl₂ solutions* (two independent experiments, first and second row)

I, M	T, °C	NaCl		CaCl ₂	
		log K ₁ ^{H'}	log K ₂ ^{H'}	log K ₁ ^{H'}	log K ₂ ^{H'}
0.13	10	10.671	4.383	10.606	4.389
		10.696	4.400	10.605	4.393
	25	10.406	4.172	10.294	4.168
		10.416	4.180	10.293	4.169
	37	10.204	4.029	10.079	4.014
		10.205	4.031	10.071	4.022
45	10.069	3.940	9.945	3.937	
	10.068	3.939	9.947	3.932	
0.48	10	10.663	4.475	10.488	4.428
		10.661	4.473	10.489	4.430
	25	10.396	4.253	10.208	4.211
		10.394	4.255	10.203	4.212
	37	10.177	4.101	9.991	4.063
		10.177	4.087	10.007	4.065
45	10.032	4.009	9.871	3.977	
	10.023	4.009	9.888	3.979	
0.92	10	10.686	4.562	10.464	4.473
		10.693	4.565	10.453	4.473
	25	10.431	4.341	10.145	4.251
		10.429	4.339	10.146	4.253
	37	10.197	4.182	9.964	4.116
		10.201	4.185	9.982	4.115
45	10.059	4.090	9.866	4.037	
	10.040	4.088	9.857	4.033	

*3σ(log K₁^{H'}) = 0.005–0.02; 3σ(log K₂^{H'}) = 0.003–0.01.

preselected volumes of titrant and to print out the corresponding e.m.f. values. The measurement cells (25 ml) were kept within 0.2° of the required temperature. All titrations were done with magnetic stirring, and purified nitrogen passed through the solution.

Procedure

Each solution to be investigated was prepared by mixing, in a 250-ml standard flask, ~1M hydrochloric acid, a weighed amount of 3-amino-1,2,4-triazole and a suitable volume of ~5M sodium chloride or ~1.7M calcium chloride, so that the concentration of organic ligand was approximately 10mM, that of hydrochloric acid 20mM and the ionic strength about

0.1, 0.5 or 1.0M according to the added amount of salt. The solution obtained was titrated with standard potassium hydroxide solution. The electrode couple was standardized, in terms of pH = -log[H⁺], by titrating 10mM hydrochloric acid containing the same sodium chloride or calcium chloride concentration as the solution under study. The excess of hydrochloric acid allowed the internal E° and the liquid-junction potential⁵ to be determined.

Calculations

Calculations of protonation constants and ligand purity were performed by the non-linear least-squares computer program ESAB2M.^{5,6} The dependence of the protonation constants on temperature and ionic strength was calculated by the REGIS⁷ program. Weak complex formation constants, and their dependence on temperature and ionic strength, were calculated by the non-linear least-squares program ES2WC⁸ and distribution diagrams were calculated by the ES4EC program.^{9,10} Previously reported pK_w values¹¹ for different temperatures and ionic strengths were used in the calculations. Protonation constants were expressed as

$$K_j^H = [H_j L] / ([H][H_{j-1} L])$$

(primes will be used to indicate conditional protonation constants, see results).

Concentrations, and hence the thermodynamic parameters, were always expressed on the molarity scale. Throughout the paper, uncertainties are given as three times the standard deviation.

RESULTS AND DISCUSSION

Protonation constants calculated without allowing for weak interactions are given in Table 1. The dependence of the formation

Table 2. Ionic strength dependence of protonation constants [see equation (1)] of 3-amino-1,2,4-triazole in NaCl and CaCl₂ media (I = 0.1–0.9M)*

Medium	B'	C'	(∂C'/∂T) × 10 ³	D'	(∂D'/∂T) × 10 ³
First protonation step					
NaCl	1.5	0.55	-0.51	-0.315	0
CaCl ₂	1	0.098	0.54	0	0
Second protonation step					
NaCl	—	0.219	-1.95	-0.0153	1.11
CaCl ₂	—	0.163	-2.34	-0.0466	2.75

*The primes indicate that the parameters are apparent quantities, calculated without allowing for any weak-complex formation.

Table 3. Thermodynamic parameters* ($\pm 3 \times$ std. devn.) for the protonation of 3-amino-1,2,4-triazole at $I = 0M$

$T, ^\circ C$	$\log {}^T K_1^H$	$\log {}^T K_2^H$
10	10.84 ± 0.03	4.364 ± 0.015
25	10.57 ± 0.03	4.150 ± 0.005
37	10.35 ± 0.04	4.003 ± 0.004
45	10.22 ± 0.05	3.917 ± 0.006
	ΔH_1°	ΔH_2°
25	-30.6 ± 1.1	-22.2 ± 0.2
		ΔC_p°
		120 ± 30

* ΔH° in kJ/mole, ΔC_p° in J.mole $^{-1}$.K $^{-1}$.

constants on ionic strength can be taken into account by using the equation¹²⁻¹⁴

$$\log \beta = \log {}^T \beta - z^* A \sqrt{I} / (1 + B \sqrt{I}) + CI + DI^{3/2} \quad (1)$$

where

- β = generic formation constant;
- ${}^T \beta$ = formation constant extrapolated to zero ionic strength;
- $z^* = \Sigma (\text{charge})_{\text{reactants}}^2 - \Sigma (\text{charge})_{\text{products}}^2$;
- $A = 0.5115 + 9.123 \times 10^{-4} (T - 25) + 4.93 \times 10^{-6} (T - 25)^2$;
- $B = 1.5$ or 1^\dagger .

A and B are the parameters of the Debye-Hückel equation, C and D are empirical parameters, and T is the centigrade temperature.

In Table 2 we report the numerical values of the empirical parameters together with their dependence on ionic strength. Extrapolation to

\dagger The parameter B assumes the value 1.5 when the dimensional parameter a in the Debye-Hückel equation is $\sim 5 \text{ \AA}$. In some cases, particularly when weak interactions are neglected, it is better to use $B = 1$. This is the case for the protonation constants of aminotriazole determined in CaCl_2 medium (see below).

\ddagger When dealing with systems where weak interactions are studied, the association of the background electrolyte has to be considered, in our opinion, since small differences in the assumptions made in deriving formation constants may drastically change the picture of the solution under study. On the other hand, high uncertainties affect the association constants for the background, as in our case for the species NaCl and CaCl^+ . In any case, it is of great importance to give clearly in the paper all the information that allows the reader to know exactly the assumptions under which thermodynamic parameters are calculated.

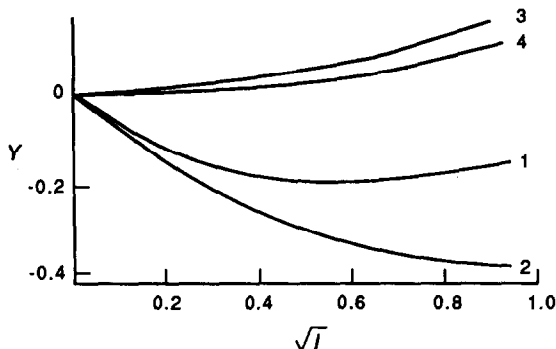


Fig. 1. Dependence of protonation constants on ionic strength, calculated without allowing for weak-complex formation. $y = \log K^H (I=0) - \log K^{H'} (I)$. 1, $\log K_1^{H'}$ (NaCl); 2, $\log K_1^{H'}$ (CaCl_2); 3, $\log K_2^{H'}$ (NaCl); 4, $\log K_2^{H'}$ (CaCl_2).

zero ionic strength gave the thermodynamic parameters, reported in Table 3, together with ΔH° and ΔC_p° values obtained from the dependence of the protonation constants on temperature, (by using the equation of Clarke and Glew¹⁵). Figure 1 shows the function $\log K^{H'}$ vs. I .

When analysing salt effects on the protonation of 3-amino-1,2,4-triazole, we must consider (i) the complex formation between the protonated form H_3L and Cl^- , as for similar systems,¹⁶⁻¹⁸ and (ii) the formation of weak complexes with Ca^{2+} , as suggested by the fact that the protonation constants in calcium chloride medium are significantly lower than those in sodium chloride medium (see Fig. 1). By making the same assumption as in preceding papers on salt effects on the protonation of amines,^{16,20} and by using calculation procedures for weak complexes,^{8,12} we found the formation of the species H_2LCl , CaL^+ and CaHL^{2+} ($\text{HL} = 3\text{-amino-1,2,4-triazole}$), the formation constants of which, extrapolated to zero ionic strength, are reported in Table 4. To calculate the dependence of the formation constants of these species on ionic strength, it is necessary to decide whether association of the background electrolyte should be considered. \ddagger

We performed the relative calculations with and without considering the association of background (for the species NaCl and CaCl_2 we

Table 4. Formation constants ($\pm 3 \times$ std. devn.) of 3-amino-1,2,4-triazole- Ca^{2+} and Cl^- complexes at $I = 0M$ ($\text{HL} = \text{aminotriazole}$)

Reaction	$T, ^\circ C$	$\log K$			
		10	25	37	45
$\text{H}_2\text{L}^+ + \text{Cl}^- = \text{H}_2\text{LCl}$		-0.42 ± 0.15	-0.27 ± 0.10	-0.17 ± 0.12	-0.12 ± 0.15
$\text{Ca}^{2+} + \text{L}^- = \text{CaL}^+$		1.14 ± 0.15	1.08 ± 0.08	1.00 ± 0.11	0.95 ± 0.15
$\text{Ca}^{2+} + \text{HL} = \text{CaHL}^{2+}$		-0.3 ± 0.2	-0.3 ± 0.2	-0.5 ± 0.3	-0.5 ± 0.3

Table 5. Formation constants of the species formed in the system 3-amino-1,2,4-triazole-Ca²⁺-Cl⁻ at $I = 0.75M$

Reaction	$T, ^\circ C$	$\log K_{(e)}^*$	$C_{(e)}^{*\dagger}$	$D_{(e)}^{*\dagger}$	$\log K$	C^\dagger	D^\dagger
$L^- + H^+ = HL$	10	10.69	0.55	-0.30	10.68	0.54	-0.30
	25	10.43	0.54	-0.24	10.42	0.52	-0.24
	37	10.20	0.47	-0.19	10.19	0.45	-0.19
	45	10.05	0.42	-0.16	10.04	0.40	-0.16
$L^- + 2H^+ = H_2L^+$	10	15.17	0.70	-0.30	15.17	0.69	-0.30
	25	14.66	0.64	-0.24	14.65	0.62	-0.24
	37	14.25	0.53	-0.19	14.24	0.51	-0.19
	45	13.99	0.45	-0.16	13.98	0.43	-0.16
$L^- + 2H^+ + Cl^- = H_2LCl$	10	14.60	1.25	-0.60	14.34	1.23	-0.60
	25	14.24	1.18	-0.48	14.04	1.14	-0.48
	37	13.92	1.00	-0.38	13.78	0.96	-0.38
	45	13.73	0.87	-0.31	13.62	0.84	-0.31
$Ca^{2+} + L^- = CaL^+$	10	0.71	0.95	-0.60	0.58	0.93	-0.60
	25	0.77	0.97	-0.48	0.64	0.93	-0.48
	37	0.67	0.88	-0.38	0.49	0.85	-0.38
	45	0.57	0.81	-0.31	0.41	0.78	-0.31
$Ca^{2+} + L^- + H^+ = CaHL^{2+}$	10	10.6	0.70	-0.30	10.5	0.69	-0.30
	25	10.1	0.64	-0.24	10.1	0.62	-0.24
	37	9.7	0.53	-0.19	9.6	0.53	-0.19
	45	9.5	0.45	-0.16	9.4	0.43	-0.16

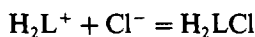
*The subscript (e) indicates parameters calculated by considering effective free concentrations of all components, *i.e.*, by allowing for both ligand-background interactions and background electrolyte association.

†For parameters for the ionic strength dependence of formation constants, see equation (1).

used formation constants obtained in previous work⁷), and in Table 5 we report the results. At $I = 0.75M$, in the case of the H_2LCl and CaL^+ species, quite different results are obtained with the two types of calculations.

In Fig. 2 we report the distribution diagram of the system $Ca^{2+}-Cl^-$ -3-amino-1,2,4-triazole. Errors in formation percentages, arising from errors in formation constants,^{9,10} are compatible with correct speciation. For example, at $I = 0.75M$, $C_{Ca} = 0.25M$, $C_{Cl} = 0.5M$ and $C_L = 0.005M$, the maximum percentages are: H_2LCl $21 \pm 4\%$, at pH 2; CaL^+ $50 \pm 6\%$, at pH 11; $CaHL^{2+}$ $11 \pm 6\%$, at pH 7.

Complex-formation constants are slightly dependent on temperature, and we calculated for the chloride complexation:



$$\Delta H^\circ = 15 \pm 7 \text{ kJ/mole}$$

and for calcium complexation:



$$\Delta H^\circ = -9 \pm 5 \text{ kJ/mole.}$$

No comparison can be made with the literature for the thermodynamic parameters reported in this work, but in Table 6 we report some formation constants found for Ca^{2+} and Cl^- complexes with pyridine,^{16,19} imidazole,¹⁷

ethylenediamine²⁰ and other amines.¹⁸ The stability of these complexes (similar reactions for different ligands are taken into account) is quite close, indicating similar side-reactions. The conditions of the distribution diagram in Fig. 2 were chosen to show a hypothetical system where all the interactions are significant. Concentrations in natural (irrigation) waters are much lower²¹⁻²³ (average values $0.45mM$, $0.82mM$ and $5.4\mu M$ for Cl^- , Ca^{2+} and amino-triazole, respectively; $I \sim 3mM$). In these conditions, as reported in Fig. 3, the only important species is HL . On the other hand, in some particular situations, the concentrations may be

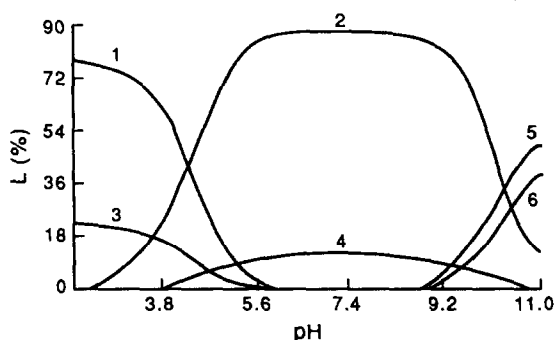


Fig. 2. Distribution of the species vs. pH in the system $Ca^{2+}-Cl^-$ -aminotriazole (L^-). Percentages are calculated with respect to the ligand. $C_L = 0.01M$, $C_{Ca} = 0.25M$, $C_{Cl} = 0.5M$ ($I = 0.75M$). 1, H_2L^+ ; 2, HL ; 3, H_2LCl ; 4, $CaHL^{2+}$; 5, CaL^+ ; 6, L^- .

Table 6. Formation constants of some *N*-ligands at 25° and *I* = 0*M*

Reaction	Ligand*	log <i>K</i>	Reference
$H_2L^+ + Cl^- = H_2LCl$	py (<i>i</i> = 1)	-0.1	19
	im (<i>i</i> = 1)	-0.27	17
	en (<i>i</i> = 1)	-0.1	20
	am (<i>i</i> = 1)	-0.24	18
	at (<i>i</i> = 2)	-0.27	this work
	mean	-0.2 ± 0.15	
$Ca^{2+} + H_2L = CaHL_2^{2+}$	py (<i>i</i> = 0)	-0.48	19
	im (<i>i</i> = 0)	-0.2	17
	at (<i>i</i> = 1)	-0.3	this work
	mean	-0.3 ± 0.2	

*py = pyridine, im = imidazole, en = ethylenediamine, am = generic amine, at = 3-amino-1,2,4-triazole.

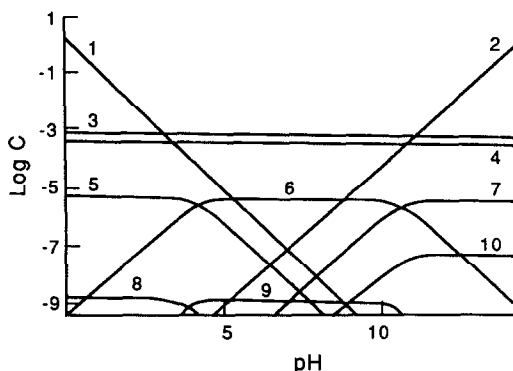


Fig. 3. Logarithms of the concentrations of the species vs. pH, in the system Ca^{2+} - Cl^- -aminotriazole (L^-) under natural water (irrigation water) conditions. $C_L = 5.4 \mu M$; $C_{Cl^-} = 0.45 mM$; $C_{Ca^{2+}} = 0.82 mM$. 1, H^+ ; 2, OH^- ; 3, Ca^{2+} ; 4, Cl^- ; 5, H_2L^+ ; 6, HL ; 7, L^- ; 8, H_2LCl ; 9, $CaHL_2^{2+}$; 10, CaL^+ .

higher, and the formation constants reported here for different temperatures and ionic strengths allow the speciation of aminotriazole in the presence of Ca^{2+} and Cl^- , under a wide range of conditions. Furthermore, interactions between amines and Mg^{2+} , SO_4^{2-} and other cations and organic anions should be considered, and are under study in our laboratories.

Acknowledgements—This work was partially supported by Ministero della Pubblica Istruzione and C.N.R. (Rome). We thank Professor Silvio Sammartano for helpful discussions, and one of the referees for valuable suggestions.

REFERENCES

- A. Casale, A. De Robertis and S. Sammartano, *Thermochim. Acta*, 1985, **95**, 15.
- A. Casale, A. De Robertis and C. De Stefano, *ibid.*, 1988, **128**, 261.
- L. Abate, C. De Stefano, R. Maggiore and C. Rigano, *ibid.*, 1989, **199**, 149.
- Idem*, *ibid.*, 1990, **162**, 449.
- C. Rigano, M. Grasso and S. Sammartano, *Ann. Chim. (Rome)*, 1984, **74**, 537.
- C. De Stefano, P. Princi, C. Rigano and S. Sammartano, *ibid.*, 1987, **77**, 643.
- A. De Robertis, C. Rigano, S. Sammartano and O. Zerbinati, *Thermochim. Acta*, 1987, **115**, 241.
- A. De Robertis, C. De Stefano, S. Sammartano and C. Rigano, *Talanta*, 1987, **34**, 933.
- Idem*, *Anal. Chim. Acta*, 1986, **191**, 385.
- C. De Stefano, P. Princi, C. Rigano and S. Sammartano, *Comput. Chem.*, 1989, **13**, 343.
- A. De Robertis, S. Sammartano and C. Rigano, *Thermochim. Acta*, 1984, **74**, 343.
- P. G. Daniele, A. De Robertis, C. De Stefano, S. Sammartano and C. Rigano, *J. Chem. Soc. Dalton Trans.*, 1985, 2353.
- P. G. Daniele, C. Rigano and S. Sammartano, *Anal. Chem.*, 1985, **57**, 2956.
- P. G. Daniele, A. De Robertis, C. De Stefano and S. Sammartano, from a book in honour of Prof. Enric Casassas, in the press.
- E. C. W. Clarke and D. N. Glew, *Trans. Faraday Soc.*, 1966, **62**, 539.
- S. Capone, A. Casale, A. Curró, A. De Robertis, C. De Stefano, S. Sammartano and R. Scarcella, *Ann. Chim. (Rome)*, 1986, **76**, 441.
- P. G. Daniele, A. De Robertis, C. De Stefano and S. Sammartano, *J. Solution Chem.*, 1989, **18**, 23.
- A. Casale, C. De Stefano, S. Sammartano and P. G. Daniele, *Talanta*, 1989, **36**, 903.
- A. Casale, A. De Robertis and F. Licastro, *Thermochim. Acta*, 1989, **143**, 289.
- A. Casale, A. De Robertis, F. Licastro and C. Rigano, *J. Chem. Res.*, 1990, (S) 204, (M) 1601-1620.
- R. J. Demint, P. A. Frank and R. D. Comes, *Weed Sci.*, 1978, **18**, 439.
- J. R. Thoman, *Persistence of Amitrole in Water*, Dept. of Health, Education and Welfare, Report, 13 Nov. 1963.
- W. Stumm and J. J. Morgan, *Aquatic Chemistry*, 2nd Ed., Wiley, New York, 1981.

ANALYTICAL DATA

POTENTIOMETRIC DETERMINATION OF THE PROTONATION CONSTANTS OF 1,3-PROPANEDIAMINE- *N,N'*-DIACETATE-*N,N'*-DI-3-PROPIONATE

PREDRAG DJURDJEVIĆ* and DUSAN RADANOVIĆ

Faculty of Science, P.O. Box 60, 34000 Kragujevac, Yugoslavia

MILICA CVIJOVIĆ

Faculty of Agriculture, Tenjska bb., 54000 Osijek, Yugoslavia

DRAGAN VESELINOVIĆ

Faculty of Chemistry, Physical Chemistry Department, P.O. Box 550, 11000 Beograd, Yugoslavia

(Received 18 December 1989. Revised 29 October 1990. Accepted 31 October 1990)

Summary—The protonation constants of 1,3-propanediamine-*N,N'*-diacetate-*N,N'*-di-3-propionate (1,3-pddadp) were determined in sodium nitrate solution of various concentrations and in 0.1M potassium nitrate medium. The values of the thermodynamic functions (ΔG , ΔH and ΔS) for the successive protonation equilibria, in 0.1M (Na)NO₃ medium, at 25°, are also reported.

In the recent past, attention has been paid to aminopolycarboxylic acids structurally related to ethylenediaminetetra-acetic acid (EDTA), owing to their importance in chemistry,¹⁻³ medicine⁴ etc.

Aminopolycarboxylic acids form strong complexes with many metal ions;⁵ the high values of the stability constants of such complexes may be attributed to the presence of the basic secondary or tertiary amino groups, the large negative charge of the acid anion, and the formation of five- or six-membered chelate rings.¹

To investigate the effect of chelate ring size on the stability of metal complexes in solution, numerous substituted and structurally related EDTA-type ligands have been tested,^{1,2}

The ligand studied here (abbreviated as 1,3-pddadp or simply pddadp) is a newly synthesized aminopolycarboxylic acid^{6,7} capable of forming three six-membered (one diamine and two 3-propionate) chelate rings and two five-membered (glycinate) rings with metal ions. Its protonation constants have not previously been reported in the literature. In this work, they

have been determined in (Na)NO₃† and K(NO₃) medium at 15, 20, 25, 30 and 35° from potentiometric measurements with the glass electrode.

Reagents

The 1,3-pddadp was prepared by condensation of 1,3-propanediamine-*N,N'*-diacetic acid with 3-chloropropionic acid in aqueous potassium hydroxide solution as described previously.⁶⁻⁸ Elemental analysis gave C 45.6%, H 6.2%, N 8.5%; C₁₃H₂₂O₈N₂ requires C 46.70%, H 6.63%, N 8.38%. A stock solution was prepared by dissolving a weighed amount of the acid, previously dried at 80° for 3 hr and stored in a desiccator, in doubly distilled water. A stock solution of nitric acid, 'Suprapur' (Merck) was standardized against tris(hydroxymethyl)aminomethane. Carbonate-free sodium hydroxide and potassium hydroxide p.a. (Merck) were standardized against potassium hydrogen phthalate, by using a Gran plot. Stock solutions of sodium nitrate p.a. (Merck) and potassium nitrate p.a. (Fluka) were prepared by dissolving the doubly recrystallized salt in doubly distilled water. The salt content was determined by evaporation of a known volume of solution to dryness at 150° and weighing the residue.

*Author for correspondence.

†Notation of the medium is in accordance with Sillén and Martell.⁵

Apparatus

Potentiometric measurements were made on solutions in a double-walled glass vessel at 15.00, 20.00, 25.00, 30.00 and $35.00 \pm 0.02^\circ$, with a commercial Beckman (39501 B8U) combined electrode. The emf was measured with a Beckman model 4500 digital pH-meter with a precision of ± 0.1 mV. The temperature was controlled by circulation of water through the jacket, from a VEB model E3E ultrathermostat bath and maintained within $\pm 0.02^\circ$. Purified nitrogen was bubbled through the solution in order to maintain an inert atmosphere. Efficient stirring of the solution was achieved with a magnetic stirrer. All test solutions (TS) were prepared in a constant ionic medium, 0.1, 0.5, 1.0M (Na)NO₃ or 0.1M (K)NO₃ by mixing the appropriate amounts of ligand, nitric acid, and sodium nitrate (or potassium nitrate) solutions. The concentration of hydrogen ion was decreased by the addition of sodium hydroxide (or potassium hydroxide), prepared in the ionic medium used for the test solution. At each medium concentration, at least 6 titrations with various concentration ratios of H₄-1,3-pddadp to nitric acid (1.0–5.0mM pddadp and 10.0–20.0mM HNO₃) were performed, over the pH range 1.0–11.0. Approximately 150 points were collected in each titration.

The concentration of free hydrogen ion, h , at each point of the titration was calculated from the measured emf, E , of the cell RE/TS/GE (RE and GE denote the reference and glass electrode, respectively) from the Nernst equation:

$$E = E_0 + Q \log h \quad (1)$$

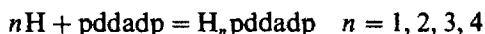
where E_0 is a constant which includes the standard potential of the glass electrode, and Q is the slope of the glass electrode response. The value of E_0 for the electrode was determined from a separate titration of nitric acid with sodium hydroxide, both of known concentration, under the same temperature and medium conditions as for the test solution titration. The data so obtained were analysed by the program MAGEC.⁹ During the MAGEC calculation the auto-protolysis constant of water, K_w , was refined until the best value for Q was obtained. The values of Q at various temperatures were found to be: at 15°, 57.0 mV; 20°, 58.1 mV; 25°, 59.0 mV; 30°, 60.1 mV; 35, 61.0 mV. The results obtained indicate the reversible Nernstian response of the glass electrode used.

These values were employed in all subsequent calculations. The E_0 values obtained from strong acid–strong base titrations were used in conjunction with the data obtained for titration of H₄-1,3-pddadp with strong base, in the program SUPERQUAD¹⁰ for refining the values of the protonation constants of the ligand. In the SUPERQUAD calculation, the total ligand, total proton and strong base concentrations were kept constant and E_0 and the protonation constants of the ligand were varied. When the resulting statistics and standard deviations were acceptable, the refined values of E_0 did not deviate by more than 1% from the initial values. When the statistics and residuals were unacceptable, the total proton concentration was also refined, which mostly led to a much improved set of statistics and a reasonably good scatter of residuals. However, the results were accepted only if the changes in E_0 and total proton concentration did not exceed 1% of the initial values. Otherwise, the titration was rejected. Standard deviations of protonation constants obtained from SUPERQUAD calculations reflect the random errors inherent in experiments. The errors which may arise from temperature variations, standardization of reagents, electrode calibration and sample weighing and dilutions were estimated from the corresponding instrumental precision, and used in the calculation of the total absolute errors of the protonation constants. It was found that the total absolute errors of the protonation constants corresponded to an error of < 0.05 in $\log K$.

Proton magnetic resonance spectra of 1,3-pddadp solutions were recorded on a Varian FT-80A High Resolution Spectrometer operating at 80 MHz, with samples kept at $30.0 \pm 0.5^\circ$. All solutions were made in D₂O in order to provide an internal lock signal. Chemical shifts are reported in ppm and measured relative to sodium-3-(trimethylsilyl)-1-propanesulphonate (tms*). Typically 50–100 transients were accumulated.

RESULTS AND DISCUSSION

The protonation equilibria of 1,3-pddadp may be represented by



(where charges are omitted for simplicity). The successive protonation constants, K_n ,

of the various protonated forms are defined as

$$K_n = \frac{[H_n L]}{[H][H_{n-1} L]} \quad L = 1, 3\text{-pddadp}$$

The constants were calculated by minimizing the error-square sum, U , of the potentials:

$$U = \sum w_i (E_{\text{obs}} - E_{\text{calc}})^2 \quad (2)$$

where E_{obs} and E_{calc} refer to the measured potential and that calculated from equation (1). The weighting factor w_i is defined as the reciprocal of the estimated variance of measurement:

$$w_i = 1/\sigma^2 = 1/[\sigma_E^2 + (\delta E/\delta V)\sigma_V^2]$$

where σ_E^2 and σ_V^2 are the estimated variances of the potential and volume readings, respectively. The minimization in equation (2) was performed with the aid of SUPERQUAD.¹⁰ The quality of fit was judged by the values of the sample standard deviation, s , and the goodness of fit, χ^2 , (Pearson's test). At $\sigma_E = 0.1$ mV and $\sigma_V = 0.005$ ml, the values of s in different sets of titrations were between 1.0 and 1.8, and χ^2 was between 12.0 and 13.0. The scatter of residuals ($E_{\text{obs}} - E_{\text{calc}}$) vs. pH was reasonably random, without any significant systematic trends, thus indicating a good fit of the experimental data.

The calculated values of the protonation constants in various concentrations of the (Na)NO₃ medium at 25° are shown in Table 1. It can be seen that the influence of the medium on the protonation constants of 1,3-pddadp is not very pronounced and is much lower than in the case of EDTA.¹¹ Variations of $\log K_n$ with the medium concentration may be attributed to changes in only the activity coefficients. That is, it appears that any complexation of 1,3-pddadp with Na⁺ can be neglected. A distribution diagram of the various protonated forms of 1,3-pddadp, calculated by using the SPECIES¹² program indicates that the formation of the 1,3-pddadp⁴⁻ anion starts at pH ~ 9.0 and sharply increases with increasing pH.

In Table 2 the protonation constants of ethylenediaminetetra-acetate (EDTA) ethylene-

Table 2. Protonation constants of some EDTA-type ligands in 0.1M (K)NO₃ medium

	EDTA ^a	edtp ^a	eddadp ^a	pdta ^b	pddadp ^c	pddadp ^d
log K_1	10.26	9.60	9.83	10.46	10.11	10.21
log K_2	6.13	6.77	5.98	8.02	8.11	8.30
log K_3	2.67	3.43	3.79	2.47	3.75	3.76
log K_4	2.00	3.00	3.00	1.88	2.85	2.79

^aAt 30°. ¹³

^bAt 20°. ¹⁴

^cAt 30°, this work.

^dAt 20°, this work.

diaminetetra-3-propionate (edtp), ethylenediamine - *N,N'*-diacetate - *N,N'*-dipropionate (eddadp), 1,3-propanediaminetetra-acetate (pdta) and 1,3-pddadp, in the same media, are presented together.

The values for the first and second protonation constants, $\log K_1$ and $\log K_2$ respectively, of 1,3-pddadp are similar to the corresponding constants of pdta and are quite close to the protonation constants of 1,3-propanediamine ($\log K_1 = 10.62$, $\log K_2 = 8.64$).¹⁵ This suggests that the two constants, K_1 and K_2 , refer to protonation of the nitrogen atoms. The constants for the third and fourth protonation steps of 1,3-pddadp, $\log K_3$ and $\log K_4$ respectively, differ very little from the corresponding constants for eddadp and edtp, so they may be ascribed to protonation of the propionic carboxylate groups.

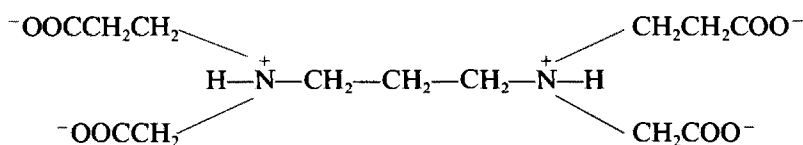
The increase in the values of $\log K_1$ for the series edtp, eddadp, pddadp and EDTA arises from the increasing concentration of negative charge on the basic nitrogen atoms, leading to an increase in the binding energy for H⁺ ions. The second protonation constant ($\log K_2$) of pddadp is approximately two units higher than the corresponding value for eddadp, and the difference between these two values roughly corresponds to the difference between the $\log K_2$ values of 1,3-propanediamine and 1,2-ethylenediamine¹⁵ (1.65). Comparison of the $\log K_3$ values of pdta and pddadp (2.47 and 3.75) shows that their difference is approximately equivalent to the difference between the $\log K_2$ values of 3-aminopropionic and 2-aminoacetic acid¹⁵ (1.19). Bearing in mind the structures of the chelating agents involved, the explanation of the differences discussed may be found in the greater electrostatic inductive effect of the =N—H group on the second nitrogen atom in eddadp or the acetate carboxyl group in pdta, in comparison with the same groups in pddadp. From the electrostatic point of view, the stabilization of the groups where the electropositive

Table 1. Protonation constants for 1,3-pddadp in various concentrations of (Na)NO₃ medium at 25°

	0.1M	0.5M	1.0M
log K_1	10.06	9.95	9.92
log K_2	8.24	8.07	7.84
log K_3	3.73	3.55	3.41
log K_4	2.98	2.79	2.87

nitrogen atom is separated by two carbon atoms from the group to be protonated is higher than in the case where the separation is by three carbon atoms. Therefore, in eddadp and pdta the second nitrogen atom and the acetic carboxyl group respectively, are more acidic than in pddadp.

The existence of protonated nitrogen atoms in the molecule of 1,3-pddadp indicates that it has a zwitterionic structure:



That the ion has this structure in solution is also indicated by the values of the protonation constants obtained in a 50% v/v water-ethanol mixture, and given in Table 3.

Comparing the values of the protonation constants of 1,3-pddadp in 0.1M (K)NO₃ water solution (Table 2) and at the same salt concentration but in mixed water-ethanol solution (Table 3) it can be seen that in ethanolic solution the values of the protonation constants remain the same (log K_1 and log K_2) or are only slightly raised (log K_3 and log K_4) compared with those for aqueous medium. Such behaviour is common for amino-acids¹⁵ and characterizes dipolar ions.¹⁶

The data presented in Table 3 can conveniently be discussed in terms of $\Delta G_{(\text{ion.})}$ defined as $2.303RT (\log K^{(w)} - \log K^{(s)})$, *i.e.*, the difference between the standard free energies of ionization in the mixed solvent and in water.¹⁶ The ionization process can be represented by the general equation:



where S denotes a molecule of solvent. Since the solutes involved in the ionization are charged,

Table 3. Protonation constants for 1,3-pddadp in 50% v/v mixed water-ethanol solvent containing 0.1M (K)NO₃ as ionic medium

	20°	30°
log K_1	10.56	10.30
log K_2	8.41	8.16
log K_3	4.09	4.03
log K_4	3.06	3.05

then of the two basic steps in solute-solvent interactions, *i.e.*, charge transfer and charge separation,¹⁶ only the first will be dominant. Therefore, although the difference in dielectric constant between pure water and the water-ethanol mixture is appreciable (78.3 *vs.* 49.0 at 25°), it will have little effect on the protonation constants of the solutes. Also, the solvation in mixed ethanol-water as solvent should not differ much from that in water, since

the structures of the two solvents are similar. Consequently the two effects will result in relatively small values of $\Delta G_{(\text{ion.})}$.

In order to confirm the zwitterionic structure of 1,3-pddadp in solution, the proton nmr spectrum, at various pH values of the ligand were recorded. The nmr spectrum of 1,3-pddadp over the pH range 2.7-13.0 consists of a sharp singlet for the acetate methylenic protons, a triplet-like pattern for the protons of the two nitrogen-bound methylenic groups of the propanediamine part of the ligand (2.45 ppm, pH 12) a broad quintet-like pattern for the protons of the central methylenic group of the propanediamine part of the ligand (1.85 ppm, pH 12) and a complex multiplet for the protons from the two propionate groups (2.95 ppm, pH 12). The chemical shifts of all resonances of the ligand are pH-dependent, as illustrated by the chemical shift data for the acetate methylenic protons in Table 4.

On the basis of the chemical shifts of structurally related protons in other aminopolycarboxylic acids¹⁷⁻²⁰ it can be concluded that the two nitrogen atoms in 1,3-pddadp are protonated first, followed by protonation of the propionate groups.

The values obtained for the thermodynamic functions ΔG^0 , ΔH^0 , and ΔS^0 associated with the protonation reactions investigated are pre-

Table 4. The pH-dependence of the chemical shifts of the acetate methylenic protons in 1,3-pddadp

pH	2.80	6.00	12.00	13.00
δ , ppm	3.85	3.75	3.35	3.10

Table 5. Thermodynamic quantities, $\log K_n$, ΔG_n^0 (kcal/mole), ΔH_n^0 (kcal/mole) and ΔS_n^0 (cal. mole⁻¹. K⁻¹) for the stepwise protonation reaction $nH + L = H_nL$ (L = pddadp, EDTA, pdta, ida)

	1,3-pddadp [0.1M (Na)NO ₃ medium]					ΔG_{298}^0	ΔH^0	ΔS_{298}^0
	15°	20°	25°	30°	35°			
$\log K_1$	10.16	10.12	10.06	10.00	9.93	-13.7	-4.5	31
$\log K_2$	8.34	8.27	8.24	8.17	8.13	-11.2	-4.1	24
$\log K_3$	3.69	3.72	3.73	3.77	3.79	-5.1	+1.7	23
$\log K_4$	2.94	2.97	2.98	3.01	3.00	-4.1	+0.1	14
EDTA (0.1M KNO ₃) ²¹								
$\log K_1$			10.19			-13.9	-5.6	27.9
$\log K_2$			6.13			-8.4	-4.2	14.1
$\log K_3$			2.69			-3.7	+1.4	17.1
$\log K_4$			1.99			-2.7	+0.3	10.1
pdta (0.1M KNO ₃) ²²								
$\log K_1$		10.46				-14.02	-5.16	30.2
$\log K_2$		8.02				-10.75	-4.43	21.6
ida (0.1M KNO ₃) ²²								
$\log K_1$		9.45				-12.67	-8.15	15.4

sented in Table 5 for 1,3-pddadp and some other complexones.

Within experimental error the values of ΔH^0 for all the protonation steps are reasonably constant over the entire temperature range from 15 to 35°. Thermodynamic quantities were calculated from the equation²³

$$\ln K = -\frac{\Delta H^0}{RT} + \frac{\Delta C_p}{R} \ln T + \frac{\Delta S_0 - \Delta C_p}{R}$$

by plotting $\log K$ against $1/T$ and taking $\Delta C_p = 0$ over the temperature range used.

From Table 5 it can be seen that the heat of the first protonation step decreases in the order ida, EDTA, pdta, pddadp. Since for the protonation of ammonia,²³ $\Delta H^0 = -12.4$ kcal/mole it may be concluded that increasing the substitution on the nitrogen atom causes the binding energy for H⁺ to decrease.

Values of ΔH^0 for pdta, EDTA and pddadp are about half of those for glycine and β -alanine (~ 10 kcal/mole).⁵ Such lowered values may

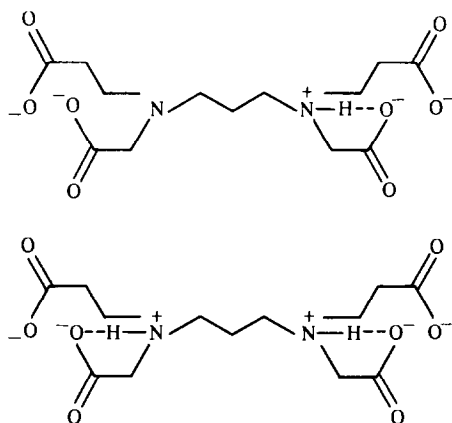
partly arise from the formation of a hydrogen bond between the proton from the =N—H group and the nearest negatively charged oxygen atom from the carboxyl group, resulting in weakening of the bond between the nitrogen atom and the proton. Owing to steric hindrance in pddadp, hydrogen bonds may be formed only with the negatively charged oxygen atoms in the acetate groups (Scheme 1).

The entropy change of the first protonation step for all ligands in Table 5 is large and may be attributed to the decrease in the negative charge of the ligands and consequent redistribution of water molecules in the first solvation sphere.

Acknowledgements—This work was supported by the U.S.–Yugoslav Joint Fund for Scientific and Technological Corporation in co-operation with the National Science Foundation under Grant No. 8818818. Acknowledgement is also made to the Serbian Research Fund for part of the financial support.

REFERENCES

1. G. Anderegg, *Complexones*, in G. Wilkinson (ed.), *Comprehensive Coordination Chemistry*, Vol. 2, Pergamon Press, Oxford, 1987.
2. D. J. Radanović, *Coord. Chem. Rev.*, 1984, **54**, 159.
3. H. Ogino and M. Shimura, *Adv. Inorg. Bioinorg. Mech.*, 1986, **4**, 107.
4. R. A. Bulman, *Structure, Bonding (Berlin)*, 1987, **67**, 91.
5. L. G. Sillén and A. E. Martell, *Stability Constants of Metal-Ion Complexes*, Special Publication No. 25, The Chemical Society, London, 1971.
6. D. J. Radanović, S. R. Trifunović, C. Maricondi and B. E. Douglas, *Inorg. Chem.*, 1988, **27**, 764.
7. S. Kaizaki, M. Byakuno, M. Hayashi, J. I. Legg, K. Umakoski and S. Ooi, *ibid.*, 1987, **26**, 2395.



Scheme 1

8. D. J. Radanović, S. R. Trifunović, M. Cvijović and B. E. Douglas, unpublished results.
9. P. M. May and D. R. Williams, in D. J. Leggett (ed.), *Computational Methods for the Determination of Formation Constants*, pp. 37–70. Plenum Press, New York, 1985.
10. P. Gans, A. Sabatini and A. Vacca, *J. Chem. Soc. Dalton Trans.*, 1985, 1195.
11. G. Anderegg, *Critical Survey of Stability Constants of EDTA Complexes*, Pergamon Press, Oxford, 1977.
12. L. Pettit (University of Leeds), personal communication.
13. R. C. Courtney, S. Chabarek and A. E. Martell, *J. Am. Chem. Soc.*, 1953, **75**, 4814.
14. D. D. Perrin, *Stability Constants of Metal Ion Complexes, Part B: Organic Ligands*, Pergamon Press, Oxford, 1979.
15. A. Albert and E. P. Serjeant, *The Determination of Ionization Constants*, Chapman & Hall, London, 1971.
16. J. E. Gordon, *The Organic Chemistry of Electrolyte Solutions*, Wiley, New York, 1975.
17. W. Byers and B. E. Douglas, *Inorg. Chem.*, 1972, **11**, 1470.
18. B. J. Fuhr and D. L. Rabenstein, *ibid.*, 1973, **12**, 1868.
19. J. L. Sudmeier and C. N. Reilley, *Anal. Chem.*, 1964, **36**, 1698, 1707.
20. L. A. Fedorov and A. N. Ermakov, *Spektroskopiya YAMR v Neorganicheskom Analize*, pp. 112–121. Nauka, Moscow, 1989.
21. A. E. Martell and R. J. Motekaitis, *Determination and Use of Stability Constants*, VCH, Weinheim, 1988.
22. G. Anderegg, *Helv. Chim. Acta*, 1964, **47**, 1801.
23. R. P. Bell, *The Proton in Chemistry*, 2nd Ed., p. 72. Chapman & Hall, London, 1973.

BOOK REVIEWS

Physical Chemistry: P. W. ATKINS, 4th Edition, OUP, Oxford, 1990. Pages xii + 995. £40.00 (hardback), £19.50 (softback).

The author of this very popular textbook is now producing a new edition every four years and the many chemists who have contributed material will be pleased with this current tome.

The arrangement of topics is very similar to that in previous editions, with the three major divisions, equilibrium, structure and change, encompassing 30 chapters. Many excellent diagrams are included in the text and each chapter is prefixed by a check-list of key ideas and concluded with a bibliography for further reading. The number of worked examples in the text has been increased and this is to be welcomed. The student can quickly grasp concepts through such exercises, provided of course that the workings are correct. Additional exercises—the simpler ones—plus additional problems are also grouped together at the end of each chapter. As with previous editions a separate solutions manual is available.

In Part 1 the concepts of thermodynamics are covered comprehensively and applied to changes of state. Where the student may find the mathematics difficult, help is provided by careful explanations and—where deemed necessary—by reverting to basics, as with partial derivatives. In this sense a gentle but firm guide through the mathematics is provided. Ideal and real solutions, phase diagrams and electrochemical cells are included in this section.

Whereas the equilibrium section is dominated by thermodynamics, the more extensive structure section is dealt with from the viewpoint of quantum mechanics. Again, theoretical aspects are treated very clearly and comprehensively even to the point of straying into what some might call inorganic chemistry. The author's own interests are evident here, as he has also produced the well received text *Molecular Quantum Mechanics*. Applied diffraction methods, spectroscopy (the discussions of magnetic resonance and the use of lasers have both been extended), statistical thermodynamics and electrical and magnetic properties of molecules are also covered in this section.

Part 3 is concerned with change and hence chemical kinetics, dynamic electrochemistry and surface processes are much in evidence. Here, as in Part 2, thermodynamics is included where appropriate.

All in all, the book is a comprehensive account of physical chemistry with the emphasis on the theory rather than the applied nature of the subject. The suggestions for further reading should suffice for those who consider their own special interests scantily served. Academics will now have to remember to change the edition number associated with this textbook, on their lists of recommended books for students of chemistry.

P. J. COX

Mass Spectrometry of Biological Materials: C. N. MCEWEN and B. S. LARSEN (eds.), Dekker, New York, 1990. Pages xiii + 515. \$125.00 (U.S. and Canada), \$150.00 (elsewhere).

The large number of books and other publications relating to mass spectrometry is indicative of the necessity to gain information on the structure of chemical compounds. Included among these compounds are biologically active molecules and this book deals with the use of mass spectrometry in the structural elucidation and analyses of such molecules.

The book is comprised essentially of two sections, the first dealing with the use of mass spectrometry in the analysis of proteins (including protein sequencing), glycoproteins, and peptides. The second section is dedicated to mass spectrometry of biological materials such as lipids, steroids, bile acids, pesticides and nitrogen-containing compounds, including amines, indoles and their metabolites.

Although the contributors assume that the reader has a reasonably detailed knowledge of the ionization techniques used in mass spectrometry, it is gratifying to note that descriptions are given of the theories and practicalities of techniques such as fast atom bombardment, plasma desorption, desorption chemical ionization and other innovations in ionization methods. In addition, clear explanations are given of the principles and use of tandem mass spectrometry, linked scanning, Fourier-transform techniques, and gas chromatography and liquid chromatography linked to mass spectrometry.

In most of the chapters, methods are described for the isolation, extraction and derivatization of compounds prior to mass spectrometry, and this aspect will be of considerable benefit to those who require a general reference guide for application to their own work.

The contributors and editors are to be congratulated for the manner in which the chapters are written and presented in clear, unequivocal terms. The book is designed primarily as a working manual rather than as a review of various topics and it will be an extremely useful addition to the laboratories (in addition to libraries) of those who are actually engaged in the use of mass spectrometry in the analysis of biological compounds in the course of their work.

A. SMITH

Spectroscopy of Biological Molecules—New Advances: E. D. SCHMID, F. W. SCHNEIDER and F. SIEBERT (eds.), Wiley, Chichester, 1988. Pages xvii + 509. £52.50.

This book is compiled from the proceedings of the Second European Conference on the Spectroscopy of Biological Molecules, Freiburg, Germany, 1987, covering the applications of vibrational spectroscopy to this field.

BOOK REVIEWS

Physical Chemistry: P. W. ATKINS, 4th Edition, OUP, Oxford, 1990. Pages xii + 995. £40.00 (hardback), £19.50 (softback).

The author of this very popular textbook is now producing a new edition every four years and the many chemists who have contributed material will be pleased with this current tome.

The arrangement of topics is very similar to that in previous editions, with the three major divisions, equilibrium, structure and change, encompassing 30 chapters. Many excellent diagrams are included in the text and each chapter is prefixed by a check-list of key ideas and concluded with a bibliography for further reading. The number of worked examples in the text has been increased and this is to be welcomed. The student can quickly grasp concepts through such exercises, provided of course that the workings are correct. Additional exercises—the simpler ones—plus additional problems are also grouped together at the end of each chapter. As with previous editions a separate solutions manual is available.

In Part 1 the concepts of thermodynamics are covered comprehensively and applied to changes of state. Where the student may find the mathematics difficult, help is provided by careful explanations and—where deemed necessary—by reverting to basics, as with partial derivatives. In this sense a gentle but firm guide through the mathematics is provided. Ideal and real solutions, phase diagrams and electrochemical cells are included in this section.

Whereas the equilibrium section is dominated by thermodynamics, the more extensive structure section is dealt with from the viewpoint of quantum mechanics. Again, theoretical aspects are treated very clearly and comprehensively even to the point of straying into what some might call inorganic chemistry. The author's own interests are evident here, as he has also produced the well received text *Molecular Quantum Mechanics*. Applied diffraction methods, spectroscopy (the discussions of magnetic resonance and the use of lasers have both been extended), statistical thermodynamics and electrical and magnetic properties of molecules are also covered in this section.

Part 3 is concerned with change and hence chemical kinetics, dynamic electrochemistry and surface processes are much in evidence. Here, as in Part 2, thermodynamics is included where appropriate.

All in all, the book is a comprehensive account of physical chemistry with the emphasis on the theory rather than the applied nature of the subject. The suggestions for further reading should suffice for those who consider their own special interests scantily served. Academics will now have to remember to change the edition number associated with this textbook, on their lists of recommended books for students of chemistry.

P. J. COX

Mass Spectrometry of Biological Materials: C. N. MCEWEN and B. S. LARSEN (eds.), Dekker, New York, 1990. Pages xiii + 515. \$125.00 (U.S. and Canada), \$150.00 (elsewhere).

The large number of books and other publications relating to mass spectrometry is indicative of the necessity to gain information on the structure of chemical compounds. Included among these compounds are biologically active molecules and this book deals with the use of mass spectrometry in the structural elucidation and analyses of such molecules.

The book is comprised essentially of two sections, the first dealing with the use of mass spectrometry in the analysis of proteins (including protein sequencing), glycoproteins, and peptides. The second section is dedicated to mass spectrometry of biological materials such as lipids, steroids, bile acids, pesticides and nitrogen-containing compounds, including amines, indoles and their metabolites.

Although the contributors assume that the reader has a reasonably detailed knowledge of the ionization techniques used in mass spectrometry, it is gratifying to note that descriptions are given of the theories and practicalities of techniques such as fast atom bombardment, plasma desorption, desorption chemical ionization and other innovations in ionization methods. In addition, clear explanations are given of the principles and use of tandem mass spectrometry, linked scanning, Fourier-transform techniques, and gas chromatography and liquid chromatography linked to mass spectrometry.

In most of the chapters, methods are described for the isolation, extraction and derivatization of compounds prior to mass spectrometry, and this aspect will be of considerable benefit to those who require a general reference guide for application to their own work.

The contributors and editors are to be congratulated for the manner in which the chapters are written and presented in clear, unequivocal terms. The book is designed primarily as a working manual rather than as a review of various topics and it will be an extremely useful addition to the laboratories (in addition to libraries) of those who are actually engaged in the use of mass spectrometry in the analysis of biological compounds in the course of their work.

A. SMITH

Spectroscopy of Biological Molecules—New Advances: E. D. SCHMID, F. W. SCHNEIDER and F. SIEBERT (eds.), Wiley, Chichester, 1988. Pages xvii + 509. £52.50.

This book is compiled from the proceedings of the Second European Conference on the Spectroscopy of Biological Molecules, Freiburg, Germany, 1987, covering the applications of vibrational spectroscopy to this field.

The book commences with a very useful review section on recent advances and then continues to look at applications of several techniques to study of protein structure, biomembranes, chromophore-containing systems, and nucleic acids, and is completed by a most informative section on the medical and pharmaceutical applications, including *in vivo* studies.

Each paper is reproduced in its original form, and as a reference text for those working in this field the book will prove most valuable.

S. M. MACMANUS

Liquid Chromatography/Mass Spectrometry—Applications in Agricultural, Pharmaceutical and Environmental Chemistry: M. A. BROWN (ed.), ACS, Washington, D.C., 1990. Pages xii + 298. \$64.95.

The ACS Symposium Series No. 420 provides a useful monograph on applications of LC/MS and contains papers on agricultural, pharmaceutical and environmental chemistry which are in camera-ready form and reviewed under the supervision of the editor, Mark Brown, with the assistance of the Series Advisory Board. Unfortunately, there is a wide variation in the standard of presentation in this format which detracts somewhat from the overall quality of the book.

Eighteen papers formed into chapters deal progressively with agrochemicals, pesticide metabolism and degradation (2–7), pharmaceuticals and metabolism (8–12), and environmental analysis (13–18). These applications of LC/MS are preceded by Chapter 1, a short review of the development of LC/MS techniques by Cairns and Siegmund. This paper highlights the advantages of LC/MS over GC/MS in the analysis of molecules that are either thermally labile, or of low volatility or high polarity. Although not an in-depth review, it does form a useful, limited introduction and deals with the practicalities, advantages and disadvantages of the various LC/MS interfaces that have been developed.

Because of the stereotyped format, there is some inevitable overlap and repetition in description and practical aspects from paper to paper. However, the applications provide a good indication of the wide use of LC/MS techniques in these fields.

The first category of papers describes techniques for enhancing structural information, confirmation of pesticide residues by LC/Tandem MS, the use of solvent ions to confirm structure of selected herbicides with thermospray (TSP), chlorinated herbicide analysis by LC/MS, multi-residue analysis of thermally labile sulphonylurea herbicides in crops, and the application of negative-ion MS in studies of herbicide metabolism.

The second category considers structural elucidation of xenobiotic conjugates obtained from either biological fluids or from enzymatic/chemical synthesis by positive-ion TSP, LC/MS and LC/MS/MS; exploratory qualitative analysis of novel pharmaceuticals, nemadectins and tetracyclines in fermentation broths by TSP/LC/MS; quantification of components of human plasma, endogenous retinoic acid, by LC/NCI-MS at picogram levels; LC/MS in bioanalysis dealing with three aspects, namely, optimization strategy for TSP, and two applications (i) confirmatory evidence for aminotrazepam in blood, involving TSP LC/MS and MS/MS and (ii) analysis after chiral separation of metoprolol enantiomers with a phase system switching approach and MB/LC/MS; monitoring of *in vivo* cyclic acetylation and deacetylation of anticonvulsants by TSP/LC/MS.

The third section highlights aspects of applications in environmental analysis. Two papers deal with target and non-target pollutants in hazardous wastes and phenols, and their sulphates and conjugates utilizing particle beam MS. Vestal, a leader in the development of TSP, describes a combination ion source for the detection of environmentally important compounds. DLI and FAB LC/MS are applied to the analysis of metabolites of benzo(a)pyrene. The use of ion-exchange TSP tandem MS for polar urinary metabolites and use of LSIMS (caesium ion) for structural studies of *in vitro* alkylation of haemoglobin by electrophilic methods, *viz.* with styrene-7,8-oxide, are also presented. The latter paper highlights the powerful application of a four sector (EBEB) MS/MS instrument for the sequencing of tryptic peptides isolated from human globins.

In conclusion, this monograph provides valuable and exemplary information on the wide use of a range of LC/MS techniques for qualitative, quantitative and structural analyses and is a useful addition to the literature dealing with this important subject.

P. J. BAUGH

Inorganic Chemistry: D. F. SHRIVER, P. W. ATKINS and C. H. LANGFORD (eds.), OUP, Oxford, 1990. Pages xiii + 706. £40.00 (hardback), £16.50 (softback).

A single text dealing with inorganic chemistry must be extensive, as the discipline covers over a hundred elements and extends into many other branches of science. Inevitably this new work will be compared with *Advanced Inorganic Chemistry* by Cotton and Wilkinson and *Chemistry of the Elements* by Greenwood and Earnshaw. It is aimed at the undergraduate student and is keenly priced.

The approach adopted by the authors is selective and interpretative rather than comprehensive. The 19 chapters of the book are arranged under five section headings: structure, reactions, *s*- and *p*-block elements, *d*- and *f*-block elements and interdisciplinary topics (which comprise catalysis, structure and properties of solids and bioinorganic chemistry). Not all chapters are strictly sequential and it would be possible to move directly from say Chapter 3 on *d*-metal complexes to Chapter 14 on bonding and spectra of complexes. There are several worked examples together with additional problems, and short answers are supplied to all exercises; these will be useful to both teacher and student. A separate publication, *Guide to Solutions*, by Prof. S. Strauss accompanies the text but has not been seen by this reviewer. Suggestions for further reading (supplementary books) are given at the end of each chapter. In the text the columns in the periodic table are numbered from 1 to 18 and (for the main groups) from I to VIII, so that the oxygen group is Group VI/16 and the chromium group is Group 6.

The book commences with a very useful review section on recent advances and then continues to look at applications of several techniques to study of protein structure, biomembranes, chromophore-containing systems, and nucleic acids, and is completed by a most informative section on the medical and pharmaceutical applications, including *in vivo* studies.

Each paper is reproduced in its original form, and as a reference text for those working in this field the book will prove most valuable.

S. M. MACMANUS

Liquid Chromatography/Mass Spectrometry—Applications in Agricultural, Pharmaceutical and Environmental Chemistry: M. A. BROWN (ed.), ACS, Washington, D.C., 1990. Pages xii + 298. \$64.95.

The ACS Symposium Series No. 420 provides a useful monograph on applications of LC/MS and contains papers on agricultural, pharmaceutical and environmental chemistry which are in camera-ready form and reviewed under the supervision of the editor, Mark Brown, with the assistance of the Series Advisory Board. Unfortunately, there is a wide variation in the standard of presentation in this format which detracts somewhat from the overall quality of the book.

Eighteen papers formed into chapters deal progressively with agrochemicals, pesticide metabolism and degradation (2–7), pharmaceuticals and metabolism (8–12), and environmental analysis (13–18). These applications of LC/MS are preceded by Chapter 1, a short review of the development of LC/MS techniques by Cairns and Siegmund. This paper highlights the advantages of LC/MS over GC/MS in the analysis of molecules that are either thermally labile, or of low volatility or high polarity. Although not an in-depth review, it does form a useful, limited introduction and deals with the practicalities, advantages and disadvantages of the various LC/MS interfaces that have been developed.

Because of the stereotyped format, there is some inevitable overlap and repetition in description and practical aspects from paper to paper. However, the applications provide a good indication of the wide use of LC/MS techniques in these fields.

The first category of papers describes techniques for enhancing structural information, confirmation of pesticide residues by LC/Tandem MS, the use of solvent ions to confirm structure of selected herbicides with thermospray (TSP), chlorinated herbicide analysis by LC/MS, multi-residue analysis of thermally labile sulphonylurea herbicides in crops, and the application of negative-ion MS in studies of herbicide metabolism.

The second category considers structural elucidation of xenobiotic conjugates obtained from either biological fluids or from enzymatic/chemical synthesis by positive-ion TSP, LC/MS and LC/MS/MS; exploratory qualitative analysis of novel pharmaceuticals, nemadectins and tetracyclines in fermentation broths by TSP/LC/MS; quantification of components of human plasma, endogenous retinoic acid, by LC/NCI-MS at picogram levels; LC/MS in bioanalysis dealing with three aspects, namely, optimization strategy for TSP, and two applications (i) confirmatory evidence for aminotrazepam in blood, involving TSP LC/MS and MS/MS and (ii) analysis after chiral separation of metoprolol enantiomers with a phase system switching approach and MB/LC/MS; monitoring of *in vivo* cyclic acetylation and deacetylation of anticonvulsants by TSP/LC/MS.

The third section highlights aspects of applications in environmental analysis. Two papers deal with target and non-target pollutants in hazardous wastes and phenols, and their sulphates and conjugates utilizing particle beam MS. Vestal, a leader in the development of TSP, describes a combination ion source for the detection of environmentally important compounds. DLI and FAB LC/MS are applied to the analysis of metabolites of benzo(a)pyrene. The use of ion-exchange TSP tandem MS for polar urinary metabolites and use of LSIMS (caesium ion) for structural studies of *in vitro* alkylation of haemoglobin by electrophilic methods, *viz.* with styrene-7,8-oxide, are also presented. The latter paper highlights the powerful application of a four sector (EBEB) MS/MS instrument for the sequencing of tryptic peptides isolated from human globins.

In conclusion, this monograph provides valuable and exemplary information on the wide use of a range of LC/MS techniques for qualitative, quantitative and structural analyses and is a useful addition to the literature dealing with this important subject.

P. J. BAUGH

Inorganic Chemistry: D. F. SHRIVER, P. W. ATKINS and C. H. LANGFORD (eds.), OUP, Oxford, 1990. Pages xiii + 706. £40.00 (hardback), £16.50 (softback).

A single text dealing with inorganic chemistry must be extensive, as the discipline covers over a hundred elements and extends into many other branches of science. Inevitably this new work will be compared with *Advanced Inorganic Chemistry* by Cotton and Wilkinson and *Chemistry of the Elements* by Greenwood and Earnshaw. It is aimed at the undergraduate student and is keenly priced.

The approach adopted by the authors is selective and interpretative rather than comprehensive. The 19 chapters of the book are arranged under five section headings: structure, reactions, *s*- and *p*-block elements, *d*- and *f*-block elements and interdisciplinary topics (which comprise catalysis, structure and properties of solids and bioinorganic chemistry). Not all chapters are strictly sequential and it would be possible to move directly from say Chapter 3 on *d*-metal complexes to Chapter 14 on bonding and spectra of complexes. There are several worked examples together with additional problems, and short answers are supplied to all exercises; these will be useful to both teacher and student. A separate publication, *Guide to Solutions*, by Prof. S. Strauss accompanies the text but has not been seen by this reviewer. Suggestions for further reading (supplementary books) are given at the end of each chapter. In the text the columns in the periodic table are numbered from 1 to 18 and (for the main groups) from I to VIII, so that the oxygen group is Group VI/16 and the chromium group is Group 6.

The book commences with a very useful review section on recent advances and then continues to look at applications of several techniques to study of protein structure, biomembranes, chromophore-containing systems, and nucleic acids, and is completed by a most informative section on the medical and pharmaceutical applications, including *in vivo* studies.

Each paper is reproduced in its original form, and as a reference text for those working in this field the book will prove most valuable.

S. M. MACMANUS

Liquid Chromatography/Mass Spectrometry—Applications in Agricultural, Pharmaceutical and Environmental Chemistry: M. A. BROWN (ed.), ACS, Washington, D.C., 1990. Pages xii + 298. \$64.95.

The ACS Symposium Series No. 420 provides a useful monograph on applications of LC/MS and contains papers on agricultural, pharmaceutical and environmental chemistry which are in camera-ready form and reviewed under the supervision of the editor, Mark Brown, with the assistance of the Series Advisory Board. Unfortunately, there is a wide variation in the standard of presentation in this format which detracts somewhat from the overall quality of the book.

Eighteen papers formed into chapters deal progressively with agrochemicals, pesticide metabolism and degradation (2–7), pharmaceuticals and metabolism (8–12), and environmental analysis (13–18). These applications of LC/MS are preceded by Chapter 1, a short review of the development of LC/MS techniques by Cairns and Siegmund. This paper highlights the advantages of LC/MS over GC/MS in the analysis of molecules that are either thermally labile, or of low volatility or high polarity. Although not an in-depth review, it does form a useful, limited introduction and deals with the practicalities, advantages and disadvantages of the various LC/MS interfaces that have been developed.

Because of the stereotyped format, there is some inevitable overlap and repetition in description and practical aspects from paper to paper. However, the applications provide a good indication of the wide use of LC/MS techniques in these fields.

The first category of papers describes techniques for enhancing structural information, confirmation of pesticide residues by LC/Tandem MS, the use of solvent ions to confirm structure of selected herbicides with thermospray (TSP), chlorinated herbicide analysis by LC/MS, multi-residue analysis of thermally labile sulphonylurea herbicides in crops, and the application of negative-ion MS in studies of herbicide metabolism.

The second category considers structural elucidation of xenobiotic conjugates obtained from either biological fluids or from enzymatic/chemical synthesis by positive-ion TSP, LC/MS and LC/MS/MS; exploratory qualitative analysis of novel pharmaceuticals, nemadectins and tetracyclines in fermentation broths by TSP/LC/MS; quantification of components of human plasma, endogenous retinoic acid, by LC/NCI-MS at picogram levels; LC/MS in bioanalysis dealing with three aspects, namely, optimization strategy for TSP, and two applications (i) confirmatory evidence for aminotrazepam in blood, involving TSP LC/MS and MS/MS and (ii) analysis after chiral separation of metoprolol enantiomers with a phase system switching approach and MB/LC/MS; monitoring of *in vivo* cyclic acetylation and deacetylation of anticonvulsants by TSP/LC/MS.

The third section highlights aspects of applications in environmental analysis. Two papers deal with target and non-target pollutants in hazardous wastes and phenols, and their sulphates and conjugates utilizing particle beam MS. Vestal, a leader in the development of TSP, describes a combination ion source for the detection of environmentally important compounds. DLI and FAB LC/MS are applied to the analysis of metabolites of benzo(a)pyrene. The use of ion-exchange TSP tandem MS for polar urinary metabolites and use of LSIMS (caesium ion) for structural studies of *in vitro* alkylation of haemoglobin by electrophilic methods, *viz.* with styrene-7,8-oxide, are also presented. The latter paper highlights the powerful application of a four sector (EBEB) MS/MS instrument for the sequencing of tryptic peptides isolated from human globins.

In conclusion, this monograph provides valuable and exemplary information on the wide use of a range of LC/MS techniques for qualitative, quantitative and structural analyses and is a useful addition to the literature dealing with this important subject.

P. J. BAUGH

Inorganic Chemistry: D. F. SHRIVER, P. W. ATKINS and C. H. LANGFORD (eds.), OUP, Oxford, 1990. Pages xiii + 706. £40.00 (hardback), £16.50 (softback).

A single text dealing with inorganic chemistry must be extensive, as the discipline covers over a hundred elements and extends into many other branches of science. Inevitably this new work will be compared with *Advanced Inorganic Chemistry* by Cotton and Wilkinson and *Chemistry of the Elements* by Greenwood and Earnshaw. It is aimed at the undergraduate student and is keenly priced.

The approach adopted by the authors is selective and interpretative rather than comprehensive. The 19 chapters of the book are arranged under five section headings: structure, reactions, *s*- and *p*-block elements, *d*- and *f*-block elements and interdisciplinary topics (which comprise catalysis, structure and properties of solids and bioinorganic chemistry). Not all chapters are strictly sequential and it would be possible to move directly from say Chapter 3 on *d*-metal complexes to Chapter 14 on bonding and spectra of complexes. There are several worked examples together with additional problems, and short answers are supplied to all exercises; these will be useful to both teacher and student. A separate publication, *Guide to Solutions*, by Prof. S. Strauss accompanies the text but has not been seen by this reviewer. Suggestions for further reading (supplementary books) are given at the end of each chapter. In the text the columns in the periodic table are numbered from 1 to 18 and (for the main groups) from I to VIII, so that the oxygen group is Group VI/16 and the chromium group is Group 6.

The book is extremely well produced, with wide margins which contain many excellent diagrams. In particular there are numerous structures which emphasize the three-dimensional nature of the subject. However, I did notice that one structure of tin referred to in the formula index was actually a polymer of sulphur (S_n). Bonding and mechanistic models are explained clearly and co-ordination chemistry is well surveyed. Periodic trends rather than isolated treatments of elements are emphasized, *e.g.*, the inorganic chemistry of phosphorus is mentioned in various chapters, *viz.* those on the nitrogen and oxygen groups, the structures of solids, molecular structure, Brønsted acids and bases, Lewis acids and bases, oxidation and reduction, hydrogen and its compounds, main group organometallics, and *d*- and *f*-block organometallics. Also, uranium is not mentioned in the general index but some uranium chemistry is scattered here and there in the text. The terms "*d*-orbital splitting" and "crystal field theory" are also absent but "ligand field splitting" and "ligand field theory" are present, along with "frontier orbital energy level" diagrams.

As a general introductory text with a structural bias it certainly succeeds in its interpretative approach.

P. J. COX

Dictionary of Drugs—Chemical Data, Structures and Bibliographies: J. ELKS and G. R. GANELLIN (eds.), Chapman & Hall, London, 1989. £675.

This 2-volume work provides a concise up-to-date reference source on structures, physical properties and pharmacological properties of more than 6000 drugs of current interest. The compilation brings together essential data that are otherwise difficult to retrieve, and together with additional references allows a rapid access to original data.

The main work is clearly presented in the style of the *Dictionary of Organic Compounds* with extensive cross-referenced indexing. The Structure Index, however, though providing a source of rapid scanning for structural recognition, is confusingly condensed.

This will be a key source for scientists of many disciplines working with pharmaceuticals as well as for the industry itself. The editors are to be commended on their labours, but not surprisingly for such a specialized publication the cost is high. It will be of interest to see whether the high standard of these volumes is to be maintained in subsequent additions.

D. G. DURHAM

The book is extremely well produced, with wide margins which contain many excellent diagrams. In particular there are numerous structures which emphasize the three-dimensional nature of the subject. However, I did notice that one structure of tin referred to in the formula index was actually a polymer of sulphur (S_n). Bonding and mechanistic models are explained clearly and co-ordination chemistry is well surveyed. Periodic trends rather than isolated treatments of elements are emphasized, *e.g.*, the inorganic chemistry of phosphorus is mentioned in various chapters, *viz.* those on the nitrogen and oxygen groups, the structures of solids, molecular structure, Brønsted acids and bases, Lewis acids and bases, oxidation and reduction, hydrogen and its compounds, main group organometallics, and *d*- and *f*-block organometallics. Also, uranium is not mentioned in the general index but some uranium chemistry is scattered here and there in the text. The terms “*d*-orbital splitting” and “crystal field theory” are also absent but “ligand field splitting” and “ligand field theory” are present, along with “frontier orbital energy level” diagrams.

As a general introductory text with a structural bias it certainly succeeds in its interpretative approach.

P. J. COX

Dictionary of Drugs—Chemical Data, Structures and Bibliographies: J. ELKS and G. R. GANELLIN (eds.), Chapman & Hall, London, 1989. £675.

This 2-volume work provides a concise up-to-date reference source on structures, physical properties and pharmacological properties of more than 6000 drugs of current interest. The compilation brings together essential data that are otherwise difficult to retrieve, and together with additional references allows a rapid access to original data.

The main work is clearly presented in the style of the *Dictionary of Organic Compounds* with extensive cross-referenced indexing. The Structure Index, however, though providing a source of rapid scanning for structural recognition, is confusingly condensed.

This will be a key source for scientists of many disciplines working with pharmaceuticals as well as for the industry itself. The editors are to be commended on their labours, but not surprisingly for such a specialized publication the cost is high. It will be of interest to see whether the high standard of these volumes is to be maintained in subsequent additions.

D. G. DURHAM

HIGH-PERFORMANCE LIQUID CHROMATOGRAPHY OF METAL CHELATES: ENVIRONMENTAL AND INDUSTRIAL TRACE METAL CONTROL

A. R. TIMERBAEV* and O. M. PETRUKHIN

D. I. Mendeleev Moscow Institute of Chemical Technology, 125190 Moscow, USSR

I. P. ALIMARIN✠ and T. A. BOL'SHOVA

Department of Chemistry, M. V. Lomonosov Moscow State University, 117234 Moscow, USSR

(Received 20 July 1989. Revised 30 November 1990. Accepted 14 December 1990)

Summary—The methodological aspects of the use of HPLC in determination of metals in the form of their chelates are discussed. Rational schemes for the analysis of complex environmental and industrial samples are presented, including choice of chelating reagent, chelate preparation, metal concentration, separation method and detection method. Examples of the application of HPLC of metal chelates to environmental, production and quality control are presented.

To ensure ecological safety and improve production processes, special attention should be paid to determination of heavy metals in environmental and technological samples. Automated HPLC systems can serve this purpose because of their speed, throughput, reproducibility and repeatability, and, ease of automation. In combination with computer systems, they are almost ideal sensors for environmental monitoring and process control.

When metals are determined in the form of chelates,¹ another advantage of HPLC is the diversity of possible separation methods, and hence of approaches for solving the analytical problem.

The present paper is devoted to developing the chemical fundamentals and methodology of the HPLC of metal chelates, and their use for the analysis of environmental and industrial samples.

EXPERIMENTAL

Instrumentation

The work was done with high-performance liquid chromatographs manufactured in the USSR (Milikhrom, Tsvet 306 and 3006, KhZh 1305) and equipped with spectrophotometric detectors. Steel columns of standard size and microcolumns (2 mm i.d.) packed with appropriate sorbents were used. Preconcentration

was performed in glass columns (usually 5 × 100 mm) filled with Teflon FT-4 (0.10–0.25 μm) treated with an organic solvent or a solution of a chelating reagent (extraction–chromatographic preconcentration), or in steel columns (4 × 50 mm) packed with silanized silica gel or a high-capacity ion-exchanger (sorption and ion-exchange preconcentration, respectively).

Reagents

Standard metal solutions were prepared from salts or the metals (analytical-reagent grade) and standardized by conventional methods. Chelating reagents (sodium diethyldithiocarbamate, potassium dibutyldithiophosphate, 8-hydroxyquinoline (Fluka), 4-(2-pyridylazo)resorcinol and 1-(2-pyridylazo)-2-naphthol (Reanal, Hungary) were purified by recrystallization, sublimation or extraction,¹⁻³ and used as aqueous or ethanol solutions or in solid form.

The chelates were obtained by mixing the aqueous analyte solution with the reagent, by extraction or by extraction chromatography.

Other chemicals were of analytical-reagent grade. Doubly distilled or demineralized water was used.

The organic solvents (hexane, chloroform, dichloromethane, benzene, toluene, acetone, 2-propanol, acetonitrile, etc.) of “pure for chromatography” or analytical-reagent grade were used without further treatment.

*Author for correspondence.

RESULTS AND DISCUSSION

Types of chelates used in HPLC

Depending on the electronic structure of the analyte metal M, the type of chelating reagent HL, and the complex formation conditions, different types of complexes can be formed, including (1) neutral chelates ML_n ; (2) cationic ML_n^+ or anionic ML_n^- chelates; (3) mixed-ligand chelates ML_mX_{n-m} (X = a singly charged unidentate or bidentate ligand). In the presence of hydrophobic ions of opposite charge, charged complexes can form ion-associates, *e.g.*, $ML_n^- B^+$.

All these forms of complexes have been used in metal determination by HPLC, and the separation method used is determined by the type of metal chelate (Table 1).

Selection of the chelating reagent

In general, reagents designed for separation and determination of metals by HPLC should fulfil the following requirements.

(1) Neutral or charged complex formation with a large number of metals (*i.e.*, the reagent should have a sufficiently mobile electronic or geometric structure).

(2) Formation of a single well defined co-ordinatively saturated complex under the conditions used, with high stability in the chromatographic system and sufficient solubility in the mobile phase.

(3) Comparatively low hydrophobicity.

These properties can be achieved by tailoring the reagent molecule by varying the chelating

group structure, insertion of substituents with different numbers of carbon atoms, and different electronic and steric effects, insertion of electron-acceptor atoms and ionogenic groups, and by optimizing the complex formation conditions and the mobile phase composition.

The following should also be taken into account.

(1) The kinetics of complex formation (especially during the chromatographic process or post-column detection).

(2) The stability of the reagent under the conditions of complex formation.

(3) The possibility of metal preconcentration and removal of reagent excess.

(4) Adequate sensitivity (*e.g.*, high molar absorptivity) and difference in the characteristics of the complexes and the reagent.

(5) Ready availability and/or simplicity of synthesis.

(6) Specificity for the analytical problem being solved.

(7) Material and labour costs.

Chelate preparation

Several techniques are used for formation of metal chelates for analysis by HPLC.^{4,5}

(1) Complex formation in aqueous medium, followed by extraction with an organic solvent, or extraction of metals from an aqueous solution with a solution of the chelating reagent in an organic solvent.

(2) Complex formation in aqueous medium, followed by sorption on a column of an inert

Table 1. Determination of metals in the form of different types of chelates

Type of chelate	Example	Method of preparation (concentration)	Chromatographic variant	Species determined
ML_n	$Cu(DEDTC)_2$ $Co(Ox)_3$	Extraction, extraction chromatography, sorption	Normal- or reversed-phase adsorption	Cu, Ni, Co, Zn, Cd, Hg, Fe, Pb <i>etc.</i> Co(III), Cr(III), Mo(VI), W(VI), platinum metals
$ML_{n-m}X_m$	$Pt(PAN)Cl$	Extraction, extraction chromatography	Normal- or reversed-phase adsorption	Pt, Pd, Rh Cu, Ni, Co
ML_n^+	$Fe(DAM)_3^+$	Extraction, extraction chromatography	Normal-phase adsorption	Fe, Ti, Zr, rare-earth elements
ML_n^- $ML_n B_m$	$Zn(PAR)_2^-$ $Ni(PAR)_2(R_4N)_2$	Direct mixing, ion-exchange Direct mixing, extraction, extraction chromatography	Ion-exchange Ion-pair	Co, Cu, Ni, Zn, Fe <i>etc.</i> Fe, Co, Ni, Cu, Zn, Ga <i>etc.</i>

*DEDTC = diethyldithiocarbamate; Ox = 8-hydroxyquinoline; DAM = diantipyrylmethane; PAN = 1-(2-pyridylazo)-2-naphthol; PAR = 4-(2-pyridylazo)resorcinol; R_4N = quaternary ammonium ion.

support coated with an organic solvent, or passage of the sample solution through a column of an inert support coated with a solution of the chelating reagent in an organic solvent.

(3) Chelate formation in aqueous medium with subsequent sorption on a column of a hydrophobic sorbent, a polymeric support or a high-capacity anion-exchanger.

(4) Formation of the chelates by passing the sample through a precolumn of silica gel coated with octadecylsilane and loaded with the reagent.

(5) Direct injection of the chelate mixture in aqueous or homogeneous water-organic medium into the analytical column.

(6) Precolumn on-line formation by injection of the sample into an eluent containing the chelating reagent.

(7) On-column formation with the sample injected directly into the column, the reagent being present in the mobile phase.

Only the first four variants permit simultaneous concentration of the metals, and are to be preferred. In a number of cases, however, a simpler and faster formation of the complexes can be achieved by direct mixing of the metal and reagent solutions or by on-column formation (see below). The choice of chelate preparation technique is partly dependent on the nature of the metals to be determined. For example complexes of kinetically inert metals can only be obtained under static conditions.

Concentration

As a rule, preconcentration is necessary in the determination of traces of metals by HPLC.⁶

Liquid-liquid extraction, the most widely used group separation method in inorganic analysis (including HPLC),⁴ also offers the possibility of relative concentration of metals. This makes concentration by extraction indispensable in the determination of trace elements in the presence of large amounts of matrix components. However, the concentration factors achieved rarely exceed 100.

Extraction chromatography (the dynamic mode of extraction) can give a degree of concentration that is about twice that attainable in static (batch) extraction. Further, performance of the concentration stage in a closed system practically eliminates the risk of metal losses and contamination. The same advantages are inherent in sorption concentration, and the

capacity of columns of hydrophobic sorbents is substantially higher, which allows separation of larger amounts of metals, at a higher flow-rate.

In general, extraction and extraction chromatographic concentration are better combined with normal-phase chromatography, whereas sorption concentration is more suitable for reversed-phase and ion-pair chromatography.

Ion-exchange concentration of metals is conducted on a small precolumn (which may have a back-flush facility) or directly on a separation column. The latter possibility is due to the low elution power of water, as a result of which much greater sample volumes can be used in ion-exchange chromatography than in the other HPLC methods (up to 500 μl or, on average, larger by a factor of 50).

The choice of concentration technique is determined not only by the chromatographic mode and the concentration of the analyte, but also by the nature of the sample. For instance, in sorption concentration of samples with a high salt background the matrix components are partially eluted by the polar solvent (acetonitrile or methanol) used to elute the concentrate from the column. Therefore, for analysis of mineral salts, extraction concentration is recommended, but for solutions which contain a large amount of low-polarity organic compounds, sorption concentration is preferable.

Chelate separation mechanism

As mentioned above, the choice of HPLC method and therefore the separation mechanism is primarily determined by the type of metal chelate (see Table 1).

The retention mechanism of neutral chelates ML_n in adsorption chromatography has been comprehensively discussed by Timerbaev and Petrukhin.⁴ In the case of co-ordinatively saturated chelates (the complexes of choice) retention is determined by the formation of hydrogen bonds with the surface hydroxyl groups (normal-phase variant) or with the mobile phase polar molecules (reversed-phase variant). The energy of these interactions is proportional to the total electronegativity of the ligand donor atoms: the higher the electronegativity the stronger the adsorption on specific sorbents and the weaker on non-polar sorbents. In turn, the effective charge on the donor atoms is proportional to the effective charge on the metal ion. In reversed-phase chromatography the contribution of non-specific chelate-sorbent interactions and, especially, the solvophobic

effect caused by disordering of the water structure, can become appreciable.⁷

The same features are observed for the cationic chelates ML_n^+ . However, a distinguishing feature of their chromatographic behaviour is the influence of the nature of the counter-ion B^- on the retention of different chelates of the same metal. In mixed-ligand chelates $ML_{n-m}X_m$, if X^- is a unidentate ligand it can affect the electron density distribution in the chelate ring and thereby the proton-acceptor ability of the donor atoms. As a consequence, the ability of such compounds to participate in specific intermolecular interactions also depends on the anionic composition of the medium. Anionic chelates ML_n^- can be retained in ion-pair HPLC by both ion-exchange and adsorption. The relative contributions of these mechanisms then strongly depend on the mobile phase composition (mainly on the eluting strength and concentration of the organic modifier), and under certain conditions a mixed retention mechanism may occur. This is why the elution sequence of complexes can vary considerably and even be completely reversed.

When separation is performed on organic anion-exchangers, anionic chelates, because of their rather high hydrophobicity, are retained simultaneously by ion-exchange and hydrophobic adsorption.

Detection

Since most metal chelates are highly coloured, spectrophotometric detection is generally used.⁴ For consecutive determination of all the components, with comparable sensitivity, close similarity of the spectral characteristics of the metal chelates (wavelength of absorption maxima, and molar absorptivity) is desirable. On the other hand, if there is sufficient difference in the chelate absorption spectra, there is a possibility of determining one metal in the presence of large amounts of another.⁸ Thus the selectivity can be increased, and interferences eliminated by appropriately changing the detection wavelength.

Detectors of the other types (electrochemical, atomic-emission, atomic-absorption, fluorescence) have various drawbacks, compared with spectrophotometric detectors, and are rarely used.⁴

Sample analysis

The advantages of HPLC as a multielement method are manifested in the analysis of multi-

component mixtures in which the analytes are present at comparable concentrations. The method is particularly useful for complex water samples containing traces of metals (natural water, treated waste water). Moreover, since only a comparatively short time is required for the treatment of such samples, another advantage of HPLC—speed of analysis—becomes prominent.

A number of analytical problems, however, require selective determination of one or several metals in the presence of large amounts of macrocomponents. Characteristic examples are the determination of trace platinum metals in the presence of non-ferrous metals,^{3,8} determination of cobalt in nickel salts,⁸ or analysis of waste water from wash tanks in electroplating works.⁹

The selectivity of HPLC determination of metals can be increased in several ways.

- (1) By choice of chelating reagent.
- (2) By choice of chelate preparation conditions (pH control, use of masking agents, kinetic effects *etc.*).
- (3) By varying the separation conditions, utilizing the differences in the chromatographic stability of the complexes, and changing the separation mechanism.
- (4) By changing the spectrophotometric detection conditions or using a selective detection method (atomic-emission spectrometry, atomic-absorption spectrometry, *etc.*)⁴

PRACTICAL APPLICATIONS

Some examples of applications to various analytical problems will now be given, with an outline of the methods used, and some typical results (Table 2).

Environmental samples

To demonstrate the possibilities of HPLC in environmental control, natural samples of three different types have been chosen: mineral (ground) waters, surface (lake) waters, and soils.

*Mineral waters.*¹⁰ To determine heavy metals, the sample (up to 500 ml) was made 0.1M in hydrochloric acid and 0.3M in sodium chloride, and 20–70 mg of potassium dibuthyldithiophosphate was added. The complexes formed were concentrated on a glass column containing 2 g of FT-4 impregnated with 1 ml of toluene, and then eluted with toluene (the total volume eluate is 3 ml). A 10- μ l portion of the eluate was analysed on a column (62 \times 2 mm) of 5- μ m

Table 2. Results for metal determination in different samples

Reagent	HPLC variant†	Concentration technique	Detection limit, ng	Linear range, ng/ml	Metals determined	Found	
						Present method‡	Certified value
DBDTP*	NP	Extraction chromatography	<i>Mineral waters (2 samples)</i>				
			1-10	10-5000	Cu	31 ± 1 µg/ml	30
					Pb	160 ± 5	—
					Cu	240 ± 5	250
				Pb	250 ± 5	—	
Ox	NP	Extraction	<i>Surface waters (2 samples)</i>				
			0.5-0.6	1-35	Mo	1.3 ± 0.1 ng/ml	—
					W	5.3 ± 0.2	—
					Mo	1.6 ± 0.1	—
				W	8.9 ± 0.9	—	
DBDTP	NP	Extraction chromatography	<i>Soils</i>				
			1-10	10-5000	Cu	0.78 ± 0.05 µg/ml	0.71
DEDTC	RP	Sorption			Pb	0.19 ± 0.02	—
					Cu	0.75 ± 0.05	0.71
				Mn	132 ± 4	135	
DBDTP	NP	Extraction chromatography	<i>Waste waters (5 samples)</i>				
			1	6-2000	Cu	1.25 ± 0.05 µg/ml	—
DEDTC	RP	Sorption			Cu	1.31 ± 0.07 µg/ml	1.5
			2-10	50-2500	Ni	0.46 ± 0.02	0.5
				Fe	5.1 ± 0.6	5.0	
				Cd	0.28 ± 0.03	0.2	
				Pb	0.53 ± 0.07	0.5	
PAR	IP	—	3-16	5 × 10 ² -5 × 10 ⁴	Cu	6.8 ± 0.3 µg/ml	7
					Fe	14.9 ± 0.3	15
			1.2-15	5 × 10 ² -5 × 10 ⁴	Cu	80 ± 3 µg/ml	70
				Ni	40 ± 2	40	
PAR	IE	—	1.8-6	10 ² -5 × 10 ⁴	Cu	0.51 ± 0.03 µg/ml	0.5
					Ni	0.37 ± 0.02 µg/ml	0.4
					Zn	0.82 ± 0.05 µg/ml	0.8
PAR	IP	—	<i>Steel</i>				
			3-16	5 × 10 ² -5 × 10 ⁴	Fe	53.1 ± 1.1%	—
					Co	17.8 ± 0.2	17.7
				Ni	29.6 ± 1.2	29.0	
PAR	IP	—	<i>Metallic nickel</i>				
			7.5	5 × 10 ² -5 × 10 ⁴	Fe	0.71 ± 0.02%	0.75
PAN	RP NP	Extraction chromatography	<i>Copper alloy</i>				
			1-7	10-1000	Pd	0.28 ± 0.01 µg/ml	0.28
					Pt	0.49 ± 0.03	0.50
				Rh	1.05 ± 0.10	1.07	
Ox	NP	Extraction	<i>Catalysts (2 samples)</i>				
			3	10 ³ -6 × 10 ⁴	Pt	2.40 ± 0.10%	2.64-2.80
				Pt	3.53 ± 0.18	3.52-3.80	
Ox	NP	Extraction	<i>Salts (NaCl, NaNO₃)</i>				
			0.6	2 × 10 ² -6 × 10 ³	Co	1.22 ± 0.23 µg/ml	—
Ox	NP	Extraction	<i>Technological solutions (4 samples)</i>				
			0.5-0.7	2 × 10 ² -7 × 10 ³	Mo	0.81 ± 0.05 mg/ml	0.98
					W	12.1 ± 0.2	—
					Mo	0.15 ± 0.03	0.1
					W	1.90 ± 0.06	1.8
					Mo	17.2 ± 2 µg/ml	—
					W	43 ± 7	—
					Co	57 ± 8	—
					Cr	110 ± 17	—
DBDTP	NP	Extraction chromatography	1	10-5000	Cu	7 ± 1 µg/ml	7

*DBDTP = dibutylthiophosphate.

†NP = normal-phase; RP = reversed-phase; IP = ion-pair; IE = ion-exchange.

‡Mean ± standard deviation of 4-9 determinations.

Silasorb-600 (Lachema) with toluene-hexane (70:30 v/v) mixture (flow-rate 1 ml/min), followed by spectrophotometric detection at 300 nm.

Surface waters.⁸ To determine molybdenum and tungsten, a 70–100 ml sample of lake water was adjusted to pH 4 with 0.1M hydrochloric acid, 30 mg of crystalline 8-hydroxyquinoline were added and the mixture was left to stand overnight. It was then passed through a glass column (100 × 3 mm) containing 0.2 g of FT-4 treated with 1M 8-hydroxyquinoline solution in chloroform, at a flow-rate of 0.5 ml/min. The concentrate was eluted with 0.5 ml of chloroform and the eluate was washed with 0.1M hydrochloric acid [to remove the excess of reagent and eliminate interferences by Fe(III), Al(III), Cu(II) and other ions]. A 10- μ l aliquot was chromatographed on the same Silasorb column with a dichloromethane-isopropyl alcohol (95:5 v/v) mixture as the mobile phase, and spectrophotometric detection at 254 nm was used.

Soils.⁹ A finely ground sample (5 g) was stirred with 50 ml of acetate buffer (pH 4.8) for 1 hr. The suspension was filtered (filter paper) and after adjustment to pH 8 with 1M ammonia solution was treated with 4 mg of sodium diethyldithiocarbamate. The mixture was passed through a glass column filled with 2 g of FT-4, the concentrate was eluted with 3 ml of acetonitrile, and a 4- μ l aliquot of the eluate was analysed on a column (64 × 2 mm) of 10- μ m Separon C₁₈ (Chemapol) by elution with acetonitrile-water-chloroform (70:28:2 v/v) at a flow-rate of 100 μ l/min. The absorbance of the eluate at 280 nm was measured.

Waste waters

Waste waters from electroplating plants are a potential source of environmental pollution with toxic heavy metals. This type of waste water is analysed before and after purification. In this case the analysis data allow simultaneous control of the ecological safety of a given production process and the efficiency of the purification systems.

Four procedures have been developed,^{2,9–11} based on (a) combination of extraction-chromatographic concentration by normal-phase HPLC of metal dibutyldithiophosphates, (b) sorption concentration and reversed-phase HPLC of metal diethyldithiocarbamates, (c) ion-pair HPLC and (d) anion-exchange HPLC of metal pyridylazoresorcinol (PAR) complexes.

Purified waters. In procedure (a) the metals were determined as dibutyldithiophosphates by the procedure used for analysis of mineral waters.¹⁰

In method (b) the sample (100–400 ml) was adjusted to pH 8 with 1M ammonia solution, 10 mg of sodium diethyldithiocarbamate were added, and the mixture was passed through a column of 2 g of FT-4 or C₁₆-phase. The concentrated complexes were desorbed with 5 ml of acetone, the eluate was evaporated to dryness, and the residue was dissolved in 1 ml of acetonitrile. A 2- μ l aliquot of this solution was chromatographed on the Separon column with acetonitrile-water-chloroform (70:29:1 v/v) as mobile phase (flow-rate 100 μ l/min), followed by detection at 280 nm. Figure 1 shows chromatograms of waste water samples before and after four stages of electroflotation treatment.¹²

Untreated waters. Analysis of waste water from electroplating wash tanks can be performed without preconcentration.

Ion-pair HPLC was used in two different ways. In the first, 1 ml of acetate buffer (pH 5), 1 ml of acetonitrile and 0.6 ml of 5 × 10⁻³M PAR were added to a known volume of sample, and a 10- μ l aliquot of the mixture was analysed on a column (62 × 2 mm) of Nucleosil RP-18 (Merck), with a mobile phase consisting of

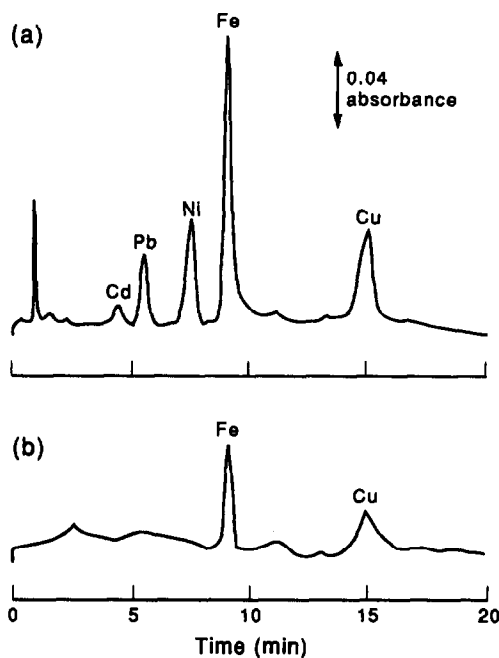


Fig. 1. Chromatograms of waste water samples: (a) before treatment, (b) after purification. For chromatographic conditions see text.

40:60 v/v acetonitrile–acetate buffer (pH 5) mixture containing 0.01M cetyltrimethylammonium bromide, at a flow-rate of 100 μ l/min. In the second, 10 ml of 2×10^{-3} M PAR were added to the sample and 50 μ l of this mixture were injected into a column (100 \times 6 mm) of 10- μ m Silasorb-600 C₁₈, and the analytes were eluted with acetonitrile–water (20:80 v/v) or acetone–water (30:70 v/v) containing 6×10^{-3} M tetrabutylammonium hydroxide and 0.1M sodium carbonate (pH 11.5) (flow-rate 1.5 ml/min).

In the anion-exchange HPLC, a corresponding excess of 1×10^{-3} M PAR was added to the sample, and 100 μ l of the mixture were chromatographed on a column (200 \times 6 mm) of the low-capacity surface-modified resin-based anion-exchanger XIKS-1 (USSR), with a mixture (40:60 v/v) of acetone and 0.04M sodium carbonate (pH 12) as eluent (flow-rate 2 ml/min), followed by spectrophotometric detection at 500 nm (Fig. 2).

When the iron content was high [e.g., in the purification of effluents by co-precipitation of metals with hydrous iron(III) oxide], modification of the anion-exchange chromatography by on-column formation of the metal PAR complexes proved to be effective. In contrast to other metals, the iron(III) does not form a complex under these conditions, probably for kinetic reasons,¹³ and does not interfere.

Industrial samples

There are two objectives with this type of sample: quality control in metallurgical and other industries (analysis of steels, alloys, metals, etc.) and monitoring of technological

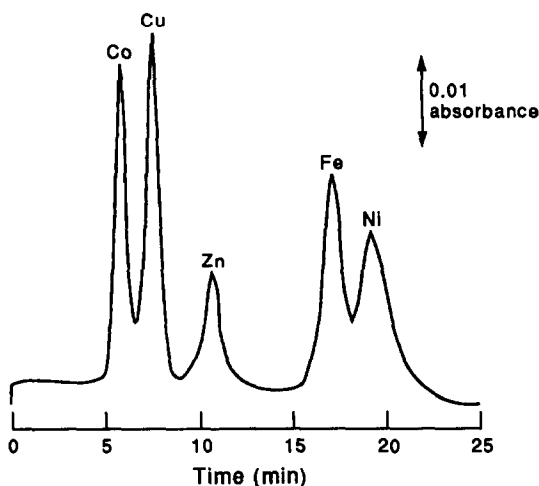


Fig. 2. Anion-exchange separation of metal PAR chelates. For chromatographic conditions see text.

solutions and intermediate products to control or improve the technological process.

Steels, metals.² A sample (0.1 g) of steel or metallic nickel was dissolved by heating with *aqua regia* and the solution was evaporated to a moist residue, which was dissolved in 0.1M hydrochloric acid and accurately diluted with water to 250 ml. A 0.1–0.5 ml portion was adjusted to pH 5, and the determination was performed as in the analysis of waste waters (ion-pair variant).

Alloys, catalysts.^{3,8} These samples may contain traces of platinum metals.

To determine palladium(II), platinum(II) and rhodium(III) in a copper alloy (0.01% of platinum metals), the sample (0.5 g) was dissolved by heating with 10 ml of *aqua regia*. The solution was carefully evaporated to minimum volume, then diluted with concentrated hydrochloric acid and again evaporated. This operation was repeated until destruction of nitroso compounds was complete and all the metals were present as their chlorides. The precipitate of silver chloride was filtered off on paper, and washed with 10-mg/ml sodium chloride solution. The filtrate and washings were diluted to 25 ml, 5 g of sodium sulphate and 5–7 ml of 6M sulphuric acid were added and the mixture was boiled until dissolution of metal hydroxo- and oxo-chlorides was complete, then cooled and diluted accurately to 20 ml with 0.1M sulphuric acid. A 10-ml aliquot was buffered with 4M sodium acetate and 1M sulphuric acid to pH 3, one drop of 1-(2-pyridylazo)-2-naphthol solution (PAN, 1 mg/ml solution in dimethylformamide) was added and then 0.25M EDTA saturated with isopentanol, until copper was completely masked (colour change from violet to green). The solution obtained was heated to 85° and passed through a steel column (140 \times 5 mm) packed with FT-4 (1 g) impregnated with PAN solution in isopentanol and kept at 85° (flow-rate 0.25 ml/min). The column was washed with 2 ml of 0.01M EDTA and cooled, then the concentrate was eluted with 2 ml of chloroform–isopropyl alcohol mixture (2:1 v/v) and 10 μ l of the eluate was analysed on a column (200 \times 2 mm) 5- μ m Spherisorb CN (Merck) or (250 \times 4.6 mm) 5- μ m Silasorb-600 with a mobile phase of acetonitrile–0.1M sodium perchlorate (40:60 v/v, pH 4) or benzene–isopropyl alcohol (90:10 v/v), respectively, followed by spectrophotometric detection at 440 nm (Fig. 3).

A 10–20 mg sample of carbon fibre-based catalyst was dissolved in 3 ml of

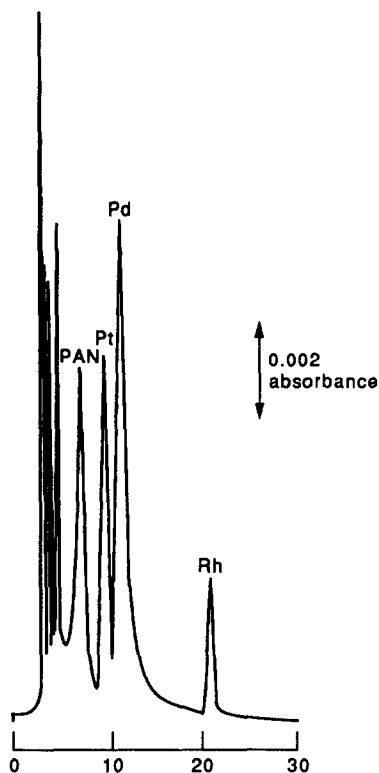


Fig. 3. Chromatogram of a mixture of palladium, platinum and rhodium PAN chelates. Chromatographic conditions: column, 5- μ m Spherisorb CN, 200 \times 2 mm; mobile phase, acetonitrile/0.1M sodium perchlorate, pH 4, (40:60 v/v); flow-rate, 1 ml/min; detection at 440 nm.

concentrated sulphuric acid and 1 ml of 3% hydrogen peroxide solution, heated till the solution became colourless, and then cooled. One ml of *aqua regia* was added and the solution was heated until sulphur trioxide fumes appeared. The solution was cooled, and to remove nitrogen oxides 1 ml of concentrated hydrochloric acid was added and evaporated to a moist residue, this operation being repeated three times. After cooling, the residue was dissolved in water and diluted to 25 ml. One ml of 50 mg/ml ascorbic acid solution was added to 1–2 ml of this solution (accurately measured) and the pH was adjusted to 4.8 with acetate buffer. Then 8-hydroxyquinoline (30 mg; was added, followed by heating on a boiling water-bath for 2 hr. After cooling, the platinum metal chelates were extracted with 2 ml of chloroform. The extract was washed with 0.1M sodium hydroxide (to remove the reagent excess), and a 10- μ l aliquot was sorbed on a Silasorb column and the chelates were eluted with dichloromethane-isopropyl alcohol mixture (97:3 v/v) at a flow-rate of 100 μ l/min (Fig. 4). Under these conditions it is possible to determine all the

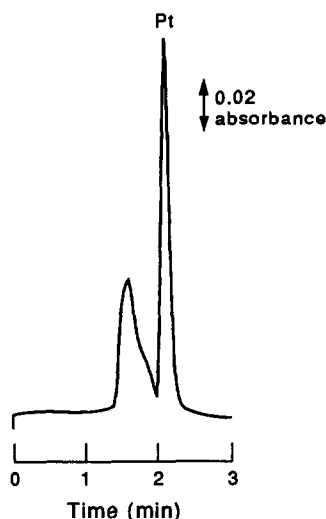


Fig. 4. Determination of platinum in carbon fibre-based catalyst as 8-hydroxyquinolate. Detection at 254 nm. For chromatographic conditions see text.

platinum metals in the sample in less than 12 min.¹⁴

Salts.⁸ The content of colour-producing metals, such as cobalt and chromium, in raw materials (alkali metal salts) should be controlled in the production of optical glasses.

A 10-g sample of sodium chloride or nitrate was dissolved in 30 ml of acetic buffer (pH 4.5) and 8-hydroxyquinoline (30 mg) was added. After heating on a boiling water-bath for 30 min the mixture was cooled and then shaken with 5 ml of chloroform for 5 min. The extract was washed twice with 0.1M hydrochloric acid, then evaporated to dryness. The residue was dissolved in 0.1 ml of the eluent to be used (95:5 v/v dichloromethane-isopropyl alcohol) and a 5 or 10 μ l aliquot was chromatographed on a Silasorb column.

Technological solutions.¹⁵ For determination of molybdenum, tungsten, cobalt and chromium in

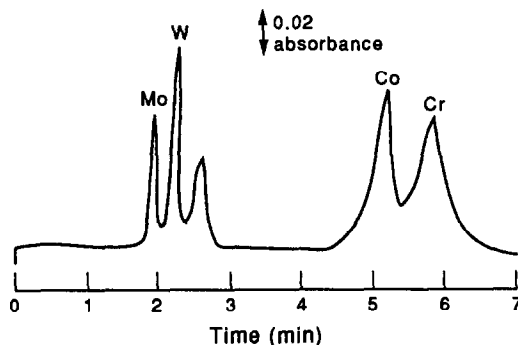


Fig. 5. Chromatogram of technological solution sample. Mobile phase, dichloromethane/isopropyl alcohol (95:5 v/v). Other conditions as for Fig. 4.

the leaching solutions from oxidized and sulphide copper ores (Fig. 5), the same procedure was used as for salt analysis. Mo and W in the technological solutions of ore processing were determined under the same chromatographic conditions. The sample was heated with 10 ml of concentrated sulphuric acid and 6 ml of concentrated nitric acid on a sand-bath and the solution was then evaporated to dryness. The residue was dissolved in 2% v/v nitric acid and diluted accurately to 100 ml with water. A 1–5 μ l portion of this solution was taken for HPLC analysis.

Copper was determined in the technological solutions of plastics production by a procedure similar to the one described above for analysis of mineral waters. Non-ionic surfactants present in considerable amounts in the sample did not interfere.

Comparison of different HPLC methods

The data in Table 2 and other metrological and analytical characteristics can be used to compare the analytical possibilities provided by the HPLC methods reported above for analysis of metal chelates.

The detection limits for the metals are on average about 1 ng. With a 10- μ l volume of sample injected this corresponds to 0.1 μ g/ml in the final test solution. With preconcentration the detection limit will be about 1 ng/ml, which for many metals is comparable with the sensitivity of such instrumental methods as atomic-absorption, X-ray fluorescence and X-ray emission spectrometry, and others.

The sensitivity depends on the molar absorptivity of the metal chelates and on the separation efficiency. The dispersion of the chromatographic zones, under conditions of comparable sorbent characteristics, flow-rates and sorbate molecular size, is determined by the nature of the mobile phase. Because of this, the lowest detection limits are observed in normal-phase HPLC, where less viscous eluents are used.

The linear calibration range covers 2–3 orders of magnitude, and the absolute determination limit primarily depends on the degree of metal concentration.

Reproducibility (in terms of relative standard deviation) varies on the average from 3 to 7% for trace and environmental analysis but can be somewhat worse when multicomponent mixtures are analysed (owing to peak overlap)

or when the sample has a complex composition (soils, technological solutions).

The accuracy of the results, provided separation of the reagent excess is complete (at the sample treatment or the chromatographic stage), is sufficiently high. The separation time usually does not exceed 10–15 min.

Nevertheless, each chromatographic variant has its own analytical peculiarities.

The HPLC of neutral chelates, which is at present better developed both theoretically and methodologically, is characterized by higher selectivity. However, adsorption chromatography has the disadvantage of the more strict requirements for the stability and kinetic inertness of metal chelates.¹⁶ The dissociation of low-stability and labile complexes in the mobile and stationary phases leads to a decrease in the number of metals that can be determined and worsens the metrological characteristics of the determination.

Ion-pair and ion-exchange HPLC are distinguished by the ability to use spectrophotometric reagents (dyes, metallochromic indicators) which form highly coloured chelates with numerous metals, as well as to vary the separation selectivity within wide limits by changing the mobile phase composition. Moreover, the metal chelates formed by this type of multi-dentate reagent are rather stable in the chromatographic process. The increased sensitivity often makes the metal preconcentration stage unnecessary, which speeds up and simplifies the analysis. The somewhat lower sensitivity of ion chromatography (because of the lower efficiency of the available ion-exchangers) is compensated by the higher sample volumes that can be used.

Thus, at present the different HPLC modifications do not compete but complement each other.

With regard to the competitiveness of HPLC of metal chelates as a whole, we should note that its advantages over the other analytical methods follow from (a) the possibility of multi-element determination, (b) consecutive determination of metals in different oxidation states and in different chemical forms, as well as non-metals (anions, including metal oxo-anions) and organic compounds (both neutral and charged); (c) the possibility of being combined with various metal preconcentration methods; (d) low dependence of the analysis results on sample treatment; (e) good technical equipment.

CONCLUSIONS

High-performance liquid chromatography as a method of inorganic analysis came into being in the middle 1970s. In metal analysis an important role is played by the HPLC of metal chelates, the progress of which is connected with the development of its main field of practical application—the analysis of complex water samples. At present, however, there is rapid development of other chromatographic techniques in which complex formation is utilized to a greater or lesser extent. These are cation-exchange HPLC with post-column reaction detection, ion chromatography of metal cyanide complexes and HPLC on chelating bonded phases. The future will show which chromatographic variants will become the most competitive, and when.

Acknowledgements—The authors express their gratitude to their colleagues Drs. E. N. Shapovalova, E. M. Basova, N. B. Morozova, A. Yu. Malykhin, I. G. Tsoii and other staff members of the Departments of Analytical Chemistry at Moscow State University and Moscow Institute of Chemical Technology for their assistance.

REFERENCES

1. A. R. Timerbaev and O. M. Petrukhin, *Anal. Chim. Acta*, 1984, **159**, 229.
2. I. P. Alimarin, E. N. Shapovalova, E. M. Basova and T. A. Bol'shova, *Zavodsk. Lab.*, 1990, **56**, No. 5, 11.
3. Yu. S. Nikitin, N. B. Morozova, S. N. Lanin, T. A. Bol'shova, V. M. Ivanov and E. M. Basova, *Talanta*, 1987, **34**, 223.
4. A. R. Timerbaev and O. M. Petrukhin, *Liquid Adsorption Chromatography of Metal Chelates*, Nauka, Moscow, 1989 (in Russian).
5. A. R. Timerbaev, O. M. Petrukhin and Yu. A. Zolotov, *Zh. Analit. Khim.*, 1981, **36**, 1160.
6. *Idem*, *Z. Anal. Chem.*, 1987, **327**, 87.
7. A. R. Timerbaev, I. G. Tsoy and O. M. Petrukhin, *J. Chromatog.*, 1990, **498**, 337.
8. A. Yu. Malykhin, *Ph.D. Thesis*, Moscow, 1989.
9. I. G. Tsoy, *Ph.D. Thesis*, Moscow, 1990.
10. A. R. Timerbaev, E. N. Shapovalova, T. A. Bol'shova, O. M. Petrukhin, I. G. Tsoii and V. V. Tsoii, *Zh. Analit. Khim.*, 1990, **45**, 390.
11. A. A. Aratskova, V. I. Orlov, A. R. Timerbaev and O. M. Petrukhin, *ibid.*, 1989, **44**, 2090.
12. N. N. Pulev, V. A. Kolesnikov and E. A. Shalyt, *Khim. Technol. Vody*, 1990, **12**, 216.
13. V. I. Orlov, *Ph.D. Thesis*, Moscow, 1990.
14. I. P. Alimarin, E. M. Basova, A. Yu. Malykhin and T. A. Bol'shova, *Talanta*, 1990, **37**, 485.
15. T. A. Bol'shova, A. Yu. Malykhin and E. M. Basova, *Vestn. MGU, Khimiya*, 1989, **30**, 172.
16. A. R. Timerbaev and O. M. Petrukhin, *Zh. Analit. Khim.*, 1989, **44**, 1424.

LIQUID-LIQUID DISTRIBUTION OF ION-ASSOCIATES OF ACIDIC DYES WITH QUATERNARY AMMONIUM COUNTER-IONS

KOICHI YAMAMOTO

Department of Industrial Chemistry, Yonago National College of Technology 4448, Hikona-cho,
Yonago-shi, Tottori 683, Japan

SHOJI MOTOMIZU

Department of Chemistry, Faculty of Science, Okayama University, 3-1-1, Tsushima-naka, Okayama-shi,
Okayama 700, Japan

(Received 24 July 1990. Revised 19 October 1990. Accepted 3 November 1990)

Summary—Diprotic acid dyes [H_2A : Bromophenol Blue (BPB), Bromochlorophenol Blue (BCPB), Bromocresol Purple (BCP), Bromocresol Green (BCG), Bromothymol Blue (BTB)] can be extracted as 1:1 ion-associates Q^+HA^- and 1:2 ion-associates $(Q^+)_2A^{2-}$ with quaternary ammonium cations (Q^+) into chloroform. The extraction constants ($\log K_{ex}$) of the 1:1 and 1:2 ion-associates have been determined. Linear relationships between $\log K_{ex}$ and the number of methylene groups in the quaternary ammonium ions were observed; from the slope of the line, the contribution of a methylene group to $\log K_{ex}$ was found to be $\sim 0.43-0.65$. The extractability with alkyltrimethylammonium cations was larger than that with symmetrical tetra-alkylammonium cations, for both the 1:1 and 1:2 ion-associates. From the extraction constants obtained, the extractability of acidic dyes was in the order $BTB > BCG > BPB > BCPB > BCP$.

The extraction behaviour of ion-associates of triphenylmethane dyes such as Methylene Blue, Ethyl Violet and Crystal Violet, with various monovalent anions has been widely studied.¹⁻³ Although acidic dyes, such as Bromophenol Blue, Bromocresol Purple and Bromocresol Green, have frequently been used for the extraction-spectrophotometric determination of amines and quaternary ammonium compounds,⁴⁻⁶ the extraction behaviour of the acidic dyes themselves has not been examined in detail. In the present work, the extraction constants for the ion-associates of five acidic dyes [Bromophenol Blue (BPB), Bromochlorophenol Blue (BCB), Bromocresol Purple (BCP), Bromocresol Green (BCG) and Bromothymol Blue (BTG)] with quaternary ammonium counter-ions distributed between an aqueous phase and chloroform were determined and correlated with the numbers of carbon atoms in the counter-ions. A parameter related to the extractability of the acidic dyes was determined from the extraction constants obtained. Such a parameter will be useful for prediction of the extractability of ion-associates with the acidic dyes and the design of new extraction systems.

EXPERIMENTAL

Apparatus

Absorbances were measured with a Japan Spectroscopic Uvidec-430 spectrophotometer with fused-silica cells of 10-mm path-length. The pH values were measured with a Hitachi-Horiba Model F-8 dp pH meter. An Iwaki Model V-SX type KM shaker was used for horizontal shaking of the 25-ml stoppered test-tubes used for the extractions.

Reagents

Acidic dye solutions were prepared by dissolving the appropriate amounts of dyes (see Fig. 1) in 0.01M sodium hydroxide and diluting to 200 ml with distilled water.

Stock solutions of quaternary ammonium ions were prepared by dissolving accurately weighed amounts of the chlorides listed in Table 1, in distilled water. Working solutions were prepared by diluting the stock solutions before use.

Sulphuric acid, acetic acid, acetate buffer solution, phosphate buffer solution, ammoniacal buffer solution and sodium hydroxide solution

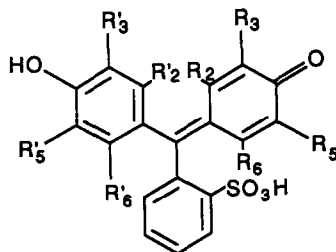


Fig. 1. Structural formulae of acidic dyes.

Acidic dye	R ₂ = R' ₂	R ₃ = R' ₃	R ₅ = R' ₅	R ₆ = R' ₆	Abbreviation
Bromophenol Blue	H	Br	Br	H	BPB
Bromochlorophenol Blue	H	Br	Cl	H	BCPB
Bromocresol Purple	H	Br	CH ₃	H	BCP
Bromocresol Green	H	Br	Br	CH ₃	BCG
Bromothymol Blue	CH ₃	CH(CH ₃) ₂	Br	H	BTB

(0.05M) were used to adjust the pH of the solutions to 2.3–12.5.

A 0.33M sodium sulphate solution was used to adjust the ionic strength of the aqueous solution to a final value of $\mu = 0.2$.

Chloroform was used without further purification, and was saturated with distilled water before use.

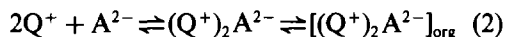
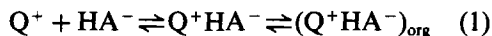
All reagents were of analytical-reagent grade and were used without further purification.

Procedure for the determination of extraction constants

A 5-ml volume of an aqueous solution containing $1.2 \times 10^{-5}M$ acidic dye, 0.01M buffer solution, sodium sulphate solution and an appropriate amount of aqueous quaternary ammonium salt solution ($\mu = 0.2$) was mechanically shaken with 5 ml of chloroform for a fixed time at 25.0°. After phase separation, the absorbance of the organic phase was measured at the wavelength of the absorption maximum of the ion-associate.

Calculation of the extraction constants

A diprotic acid dye (H_2A) dissociates protons to form two kinds of anion, HA^- and A^{2-} . An extraction system in which a quaternary ammonium cation (Q^+) reacts with HA^- and A^{2-} to form the ion-associates Q^+HA^- and $(Q^+)_2A^{2-}$ respectively, in the aqueous phase, involves the following equilibria, provided that the extracted ion-associates do not dissociate or aggregate:



where the subscript org refers to the organic phase and the aqueous phase is unmarked. The extraction constants, K_{ex1} and K_{ex2} , for equations (1) and (2) are given by:

$$K_{ex1} = [Q^+HA^-]_{org} / [Q^+][HA^-] \quad (3)$$

$$K_{ex2} = [(Q^+)_2A^{2-}]_{org} / [Q^+]^2[A^{2-}] \quad (4)$$

Table 1. Salts of quaternary ammonium cations examined

Salt	Abbreviation	Supplier*	Purity, %
Group I			
Octyltrimethylammonium chloride	OTMA	A	>98
Decyltrimethylammonium chloride	DTMA	A	>95
Dodecyltrimethylammonium chloride	DDTMA	A	
Tetradecyltrimethylammonium chloride	TDTMA	A	>98
Group II			
Tetraethylammonium chloride	TEA	A	>98
Tetrapropylammonium chloride	TPA	B	>90
Tetrabutylammonium chloride	TBA	A	>98
Tetraamylammonium chloride	TAA	B	>95

*A—Tokyo Kasei Co., Ltd.; B—Wako Pure Chemicals Inc.

Table 2. Analytical parameters for determination of the extraction constants

Ion-associate (ratio of anion:cation)	Dye	pK ₂	Experimental conditions			
			pH (α _{HA⁻})*	Shaking time, † min	Ion associate λ _{max} , nm	ε ‡
1:1	BPB	3.8	2.6	5-20 (10)	416	2.5
			(1.06)			
1:2	BCPB	4.1	7.1	10-20 (12)	608	9.4
1:1			(1.03)	2.6	5-20 (10)	413
1:2	BCP	6.3	6.9	10-20 (12)	606	8.4
1:1			(1.03)	2.6	5-20 (10)	410
1:2	BCG	4.6	10.7	10-20 (12)	605	7.9
1:1			(1.03)	2.6	5-20 (10)	419
1:2	BTB	6.8	11.7	20-30 (25)	634	5.9
1:1			(1.03)	3.9	5-20 (10)	416

*The figures in parentheses are the values of α_{HA⁻} in equation (8).

†The figures in parentheses are the shaking times used for the determination of the extraction constants.

‡Molar absorptivity, 10⁴ l. mole⁻¹. cm⁻¹.

The concentration of the ion-associate in the organic phase was calculated from equation (5)

$$A_{X(o)} = \epsilon_{X(o)} C_{X(o)} \quad (5)$$

where $A_{X(o)}$, $\epsilon_{X(o)}$ and $C_{X(o)}$ are the absorbance, molar absorptivity and concentration of the ion-associate (X) in the organic phase, respectively. In application of equation (5), the $\epsilon_{Q^+HA^-(o)}$ and $\epsilon_{(Q^+)_2A^{2-}(o)}$ values obtained by using TDTMA or TAA as a counter-cation were used. The distribution ratios of HA⁻ and A²⁻, D_{HA^-} and $D_{A^{2-}}$, are given by the following equations:

$$D_{HA^-} = [Q^+HA^-]_{org}/[HA^-] = K_{ex1}[Q^+] \quad (6)$$

$$D_{A^{2-}} = [(Q^+)_2A^{2-}]_{org}/[A^{2-}] = K_{ex2}[Q^+]^2 \quad (7)$$

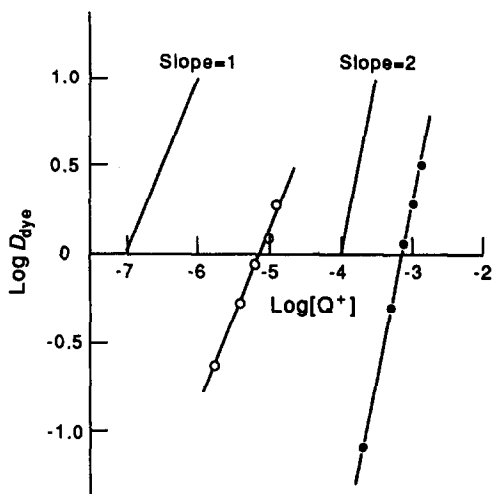


Fig. 2. Plots of log D_{dye} vs. log $[Q^+]$. Dye, BCP; Q^+ , DTMA; \circ , 1:1 ion-associate; \bullet , 1:2 ion-associate. The pH values are those in Table 2.

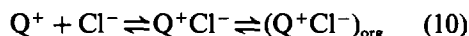
The side-reaction coefficient for HA⁻, α_{HA⁻}, is given by

$$\begin{aligned} \alpha_{HA^-} &= [HA^-]/[HA^-] \\ &= ([HA^-] + [A^{2-}])/[HA^-] \\ &= 1 + [A^{2-}]/[HA^-] \\ &= 1 + K_2/[H^+] \end{aligned} \quad (8)$$

where $[HA^-]$ is the total concentration of dye anion that is not bound in ion-associates with Q^+ , and K_2 is the apparent second dissociation constant of a diprotic acid dye (see Table 2). $[HA^-]$ can be calculated from the α_{HA⁻} values in Table 2 and the following equation:

$$[HA^-] = [HA^-]/\alpha_{HA^-} \quad (9)$$

The side-reaction of quaternary ammonium ions shown in equation (10) does not occur.



This was confirmed by the calculation with the extraction constant⁷ for the quaternary ammonium ion with chloride ion.

RESULTS AND DISCUSSION

Effect of shaking time

The effect of the shaking time on the extraction of the ion-associate was examined by varying the time from 1 to 20 min (30 min for the 1:2 ion-associate of BCG). The shaking times required to reach extraction equilibrium are summarized in Table 2. The wavelengths of maximum absorption and the molar absorptivities of the ion-associates in the organic phase are also given in Table 2.

Table 3. Extraction constants for 1:1 and 1:2 ion-associates

Cation	Anion	log K_{ex} †	Cation	Anion	log K_{ex} †
OTMA	HBTB ⁻	5.69 ± 0.02 (3)	TEA	HBTB ⁻	3.76 ± 0.02 (4)
OTMA	HBCG ⁻	5.64 ± 0.08 (3)	TEA	HBCG ⁻	3.69 ± 0.02 (3)
OTMA	HBPB ⁻	4.95 ± 0.03 (3)	TEA	HBPB ⁻	3.06 ± 0.08 (4)
OTMA	HBCPB ⁻	4.62 ± 0.02 (3)	TEA	HBCPB ⁻	2.62 ± 0.04 (2)
OTMA	HBCP ⁻	3.84 ± 0.06 (3)	TEA	HBCP ⁻	1.99 ± 0.06 (2)
OTMA	BCG ²⁻	5.16 ± 0.06 (3)	TPA	HBTB ⁻	5.19 ± 0.01 (2)
OTMA	BPB ²⁻	4.98 ± 0.10 (3)	TPA	HBCG ⁻	5.30 ± 0.03 (2)
OTMA	BCPB ²⁻	4.14 ± 0.03 (2)	TPA	HBPB ⁻	4.64 ± 0.05 (4)
OTMA	BCP ²⁻	3.45 ± 0.18 (2)	TPA	HBCPB ⁻	4.26 ± 0.01 (3)
DTMA	HBCG ⁻	6.78 ± 0.02 (2)	TPA	HBCP ⁻	3.42 ± 0.05 (5)
DTMA	HBPB ⁻	6.12 ± 0.12 (3)	TPA	BCG ²⁻	4.29 ± 0.07 (2)
DTMA	HBCPB ⁻	5.92 ± 0.11 (2)	TPA	BPB ²⁻	4.21 ± 0.01 (2)
DTMA	HBCP ⁻	5.14 ± 0.04 (5)	TBA	HBPB ⁻	6.68 ± 0.16 (3)
DTMA	BCG ²⁻	7.83 ± 0.20 (3)	TBA	HBCPB ⁻	6.37 ± 0.09 (2)
DTMA	BPB ²⁻	7.69 ± 0.09 (3)	TBA	HBCP ⁻	5.67 ± 0.09 (2)
DTMA	BCPB ²⁻	7.14 ± 0.02 (2)	TBA	BCG ²⁻	8.66 ± 0.10 (5)
DTMA	BCP ²⁻	6.29 ± 0.03 (3)	TBA	BPB ²⁻	8.52 ± 0.05 (4)
DDTMA	HBCP ⁻	5.92 ± 0.12 (3)	TBA	BCPB ²⁻	7.95 ± 0.10 (3)
DDTMA	BCG ²⁻	10.15 ± 0.10 (3)	TBA	BCP ²⁻	6.54 ± 0.02 (3)
DDTMA	BPB ²⁻	9.99 ± 0.09 (3)	TAA	BCG ²⁻	12.81 ± 0.45 (2)
DDTMA	BCPB ²⁻	9.48 ± 0.07 (3)	TAA	BPB ²⁻	12.47 ± 0.34 (2)
DDTMA	BCP ²⁻	8.87 ± 0.10 (4)	TAA	BCPB ²⁻	12.07 ± 0.42 (2)
			TAA	BCP ²⁻	10.60 ± 0.17 (2)

† Mean value. The figures in parentheses are the numbers of measurements.

Determination of the extraction constants

The plots of $\log D_{HA^-}$ and $\log D_{A^{2-}}$ against $\log [Q^+]$ for the extraction system with DTMA and BCP are shown in Fig. 2. As expected from equations (6) and (7), straight lines with a slope of +1 for 1:1 ion-associates and +2 for 1:2 ion-associates were obtained. This result supports the extraction equilibria shown in equations (1) and (2).

The five acidic dye anions in Fig. 1 and the seven quaternary ammonium cations in Table 1 (other than TDTMA) were examined, and the extraction constants were calculated from equations (3) and (4): the results obtained are summarized in Table 3.

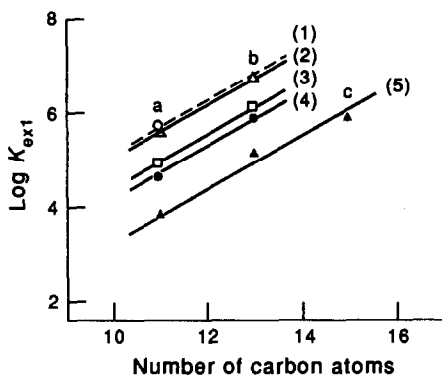


Fig. 3. Relationship between $\log K_{ex1}$ and the number of carbon atoms in the alkyltrimethylammonium ions. Counter-anion: (1) HBTB⁻, (2) HBCG⁻, (3) HBPB⁻, (4) HBCPB⁻, (5) HBCP⁻. Q⁺: (a) OTMA, (b) DTMA, (c) DDTMA (see group I in Table 1).

Relationship between the extraction constants and number of carbon atoms in the quaternary ammonium ion

As shown in Figs. 3–6, for the same carbon number the extractability with long-chain alkyltrimethylammonium ions (group I) is larger than that with tetra-alkylammonium ions (group II). This indicates that the cations of group I, with their longer alkyl chains, make the ion-associates more hydrophobic and more soluble in chloroform. The plots of $\log K_{ex}$ vs. number of carbon atoms in the quaternary ammonium ion are linear; the slopes are listed in Table 4. The contribution of a methylene group to the extraction constant ($\log K_{ex}$) was

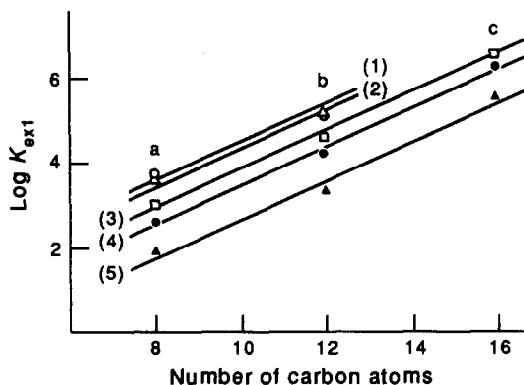


Fig. 4. Relationship between $\log K_{ex1}$ and the number of carbon atoms in the tetra-alkylammonium ions. Counter-anion: (1) HBTB⁻, (2) HBCG⁻, (3) HBPB⁻, (4) HBCPB⁻, (5) HBCP⁻. Q⁺: (a) TEA, (b) TPA, (c) TBA (see group II in Table 1).

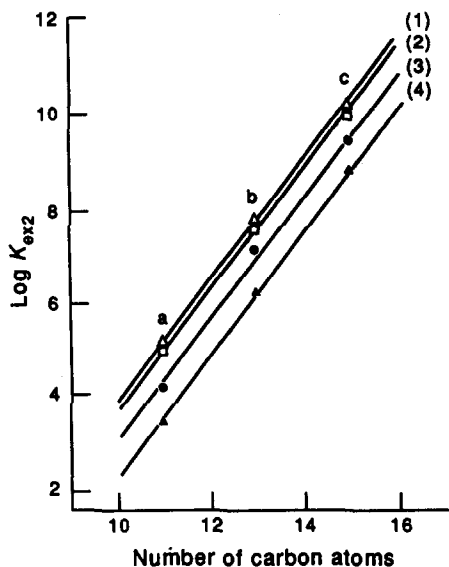


Fig. 5. Relationship between $\log K_{ex}$ and the number of carbon atoms in the alkyltrimethylammonium ions. Counter-anion: (1) BCG^{2-} , (2) BPB^{2-} , (3) $BCPB^{2-}$, (4) BCP^{2-} . Q^+ : (a) OTMA, (b) DTMA, (c) DDTMA (see group I in Table 1).

characterized as the value of the slope for the 1:1 ion-associates, and as half the value of the slope for the 1:2 ion-associates: the magnitude is about 0.58 for group I ions and about 0.43 for group II ions in the 1:1 ion-associates, and about 0.65 for group I and about 0.52 for group II ions in the 1:2 ion-associates. These values are in close agreement with those previously reported.⁸⁻¹²

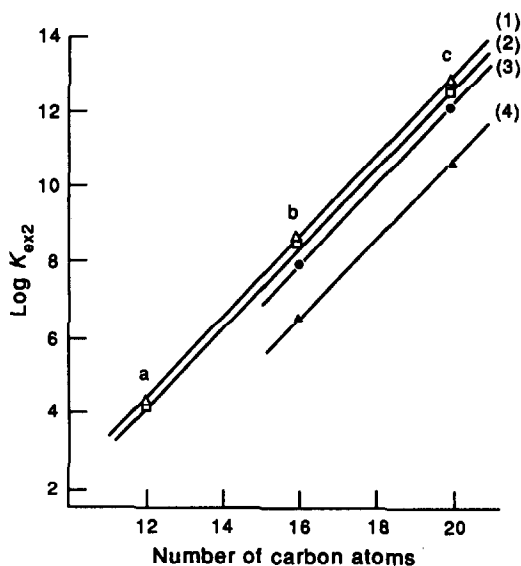


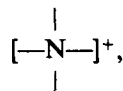
Fig. 6. Relationship between $\log K_{ex}$ and the number of carbon atoms in the tetra-alkylammonium ions. Counter-anion: (1) BCG^{2-} , (2) BPB^{2-} , (3) $BCPB^{2-}$, (4) BCP^{2-} . Q^+ : (a) TPA, (b) TBA, (c) TAA (see group II in Table 1).

Table 4. Slopes of the plots of $\log K_{ex}$ vs. carbon number of the quaternary ammonium ion

Cation	Anion	Slope
<i>1:1 ion-associates</i>		
Group I	HBCG ⁻	0.57
	HBPB ⁻	0.59
	HBCPB ⁻	0.65
	HBCP ⁻	0.52
	Mean	0.58
Group II	HBTB ⁻	0.36
	HBCG ⁻	0.40
	HBPB ⁻	0.45
	HBCPB ⁻	0.47
	HBCP ⁻	0.46
Mean	0.43	
<i>1:2 ion-associates</i>		
Group I	BCG ²⁻	1.24
	BPB ²⁻	1.26
	BCPB ²⁻	1.34
	BCP ²⁻	1.36
	Mean	1.30
Group II	BCG ²⁻	1.06
	BPB ²⁻	1.04
	BCPB ²⁻	1.04
	BCP ²⁻	1.02
	Mean	1.04

Extractability of acidic dyes

The possibility of estimating an extraction constant has been examined.^{7,13} The intercepts on the ordinate, obtained by extrapolating the straight lines in Fig. 3 to zero carbon atoms in the alkyltrimethylammonium cation, can be used to give a parameter (A) related to the extractability of an anion. To obtain a parameter, C , related to the extractability of a cation, the hypothetical cation,



an alkyltrimethylammonium cation with no alkyl groups, was assigned the value $C = 0$. Therefore C values for any alkyltrimethylammonium cation in 1:1 ion-associates can be calculated from equation (11):

$$C = 0.58n \quad (11)$$

where n is the number of carbon atoms in Q^+ and 0.58 is the contribution of a methylene group to the extraction constant (π_{CH_2}). The value of $\log K_{ex}$ for 1:1 ion-associates was considered to be the sum of two quantities, C and A :

$$\log K_{ex} = C + A \quad (12)$$

Values of A for each univalent dye anion, calculated from $\log K_{ex}$ in Table 3, and equations (11) and (12) are listed in Table 5.

Table 5. Values of A for dye anions

Anion	A^*
HBTB ⁻	-0.69
HBCG ⁻	-0.75 ± 0.01 (2)
HBPB ⁻	-1.43 ± 0.01 (2)
HBCPB ⁻	-1.69 ± 0.07 (2)
HBCP ⁻	-2.57 ± 0.19 (3)
BCG ²⁻	-9.19 ± 0.14 (3)
BPB ²⁻	-9.35 ± 0.15 (3)
BCPB ²⁻	-9.98 ± 0.20 (3)
BCP ²⁻	-10.70 ± 0.12 (3)

*Mean value. The figures in parentheses are the numbers of measurements.

From the plots of $\log K_{\text{ex}}$ vs. n in Fig. 4, we can say that the C values for tetra-alkylammonium cations in 1:1 ion-associates are given by equation (13):

$$C = 0.43n + a \quad (13)$$

where 0.43 is π_{CH_2} and a is a constant for a cation, 0.99, which was determined from $\log K_{\text{ex}}$ in Table 3, the A values in Table 5, and equations (12) and (13). From the finding that the slope of the plot of $\log K_{\text{ex}}$ vs. n for 1:2 ion-associates is about twice that for 1:1 ion-associates for both the alkyltrimethylammonium and the tetra-alkylammonium cations in Table 4, the value of $\log K_{\text{ex}}$ for 1:2 ion-associates can be expressed as equation (14).

$$\log K_{\text{ex}} = 2C + A \quad (14)$$

The C and A values in equation (14) were estimated similarly to those for equation (12). The C values for alkyltrimethylammonium and tetra-alkylammonium cations in 1:2 ion-associates can be calculated from equations (15) and (16), respectively:

$$C = 0.65n \quad (15)$$

$$C = 0.52n + 0.59 \quad (16)$$

where 0.65 in equation (15) and 0.52 in equation (16) are π_{CH_2} ; and 0.59 in equation (16) was determined from $\log K_{\text{ex}}$ (except for BCP) in Table 3, A values in Table 5 and equation (14). The A values for each bivalent dye anion, calculated from $\log K_{\text{ex}}$ in Table 3 and equations (14) and (15), are listed in Table 5.

From the A values obtained, it was found that the extractability of the acidic dyes was in the order BTB > BCG > BPB > BCPB > BCP in both the 1:1 and 1:2 ion-associates. This order in the extractability of the dyes may be explained as due to two factors: the increase of the hydrophobic effect on introduction of alkyl groups, and the effective distribution of the electrons in dye molecules, caused by the introduction of an electron-attracting halogen group.

REFERENCES

1. S. Motomizu and K. Tōei, *Anal. Chim. Acta*, 1980, **120**, 267.
2. S. Motomizu, S. Fujiwara and K. Tōei, *ibid.*, 1981, **128**, 185.
3. *Idem*, *Bunseki Kagaku*, 1983, **32**, 91.
4. N. Ohno and T. Sakai, *ibid.*, 1985, **34**, 695.
5. T. Sakai, S. Ojima, E. Saeki and M. Tanaka, *ibid.*, 1986, **35**, 177.
6. T. Sakai, Y. Ohsugi, T. Kamoto, N. Ohno and H. Sasaki, *ibid.*, 1988, **37**, 174.
7. S. Motomizu, *ibid.*, 1984, **33**, 31.
8. S. Motomizu, S. Hamada and K. Tōei, *ibid.*, 1983, **32**, 648.
9. R. Modin and G. Schill, *Acta Pharm. Suecica*, 1970, **7**, 585.
10. G. Schill, *ibid.*, 1965, **2**, 13.
11. K. O. Borg and D. Westerlund, *Z. Anal. Chem.*, 1970, **252**, 275.
12. B.-A. Persson and S. Eksborg, *Acta Pharm. Suecica*, 1970, **7**, 353.
13. S. Motomizu, *Bunseki Kagaku*, 1989, **38**, 147.

EXTRACTION OF PALLADIUM WITH TRI-ISOBUTYLPHOSPHINE SULPHIDE (CYANEX 471) IN TOLUENE FROM CHLORIDE SOLUTIONS CONTAINING THIOCYANATE

M. HIDALGO, A. MASANA and V. SALVADO

Unitat de Química, Col·legi Universitari de Girona, U.A.B., 17071 Girona, Spain

M. MUÑOZ and M. VALIENTE*

Química Analítica, U.A.B., 08193, Bellaterra, Barcelona, Spain

(Received 21 April 1989. Revised 24 October 1990. Accepted 16 November 1990)

Summary—The extraction of Pd(II) by tri-isobutylphosphine sulphide, TIBPS (Cyanex 471x), in toluene from aqueous chloride solutions (containing small amounts of thiocyanate) has been investigated. The extraction is enhanced by the presence of thiocyanate, owing to formation of mixed-ligand Pd(II)-Cl⁻-SCN⁻-TIBPS complexes. Analysis of the metal distribution suggests the formation of PdCl(SCN)·TIBPS, PdCl(SCN)₂·2TIBPS, Pd(SCN)₂·TIBPS and Pd(SCN)₂·2TIBPS in the organic phase. The equilibrium constants are logK₁₁₁ = 9.56, logK₁₁₂ = 12.70, logK₁₂₁ = 14.73 and logK₁₂₂ = 17.17, respectively. The ultraviolet absorption spectra of the organic phase support the hypothesis of formation of mixed-ligand complexes.

Solvent extraction has been widely used for the separation of palladium,¹ especially with sulphur-containing extractants, which are known to be highly selective for extraction of metals classified as "soft acids".

Cyanex 471x is a phosphine sulphide reagent, the active component of which is tri-isobutylphosphine sulphide (TIBPS). It has been reported as effective for extraction of Pd(II),²⁻⁵ Ag(I)⁶ and Hg(II)⁷ and the separation of Pd(II)-Pt(IV) mixtures. However, the slow rate of the extraction of Pd(II) is one of the major problems in the separation of the platinum group metals.⁸

Al-Bazi and Freiser⁹ reported a large increase in the rate of extraction of Pd(II) by Kelex 100 [7-(1-vinyl-3,3,5,5-tetramethylhexyl)-8-quinolinol] when sodium thiocyanate was present in the aqueous phase, and regarded this as due to the *trans*-effect in Pd(SCN)₃Cl²⁻ produced in the aqueous phase.

The aim of the present work was to investigate the effect of thiocyanate on the Pd(II)-Cl-TIBPS system and to explain the role of thiocyanate in enhancement of the extraction rate.

EXPERIMENTAL

Reagents

Tri-isobutylphosphine sulphide, TIBPS, was obtained from Cyanex 471x (kindly supplied by the American Cyanamid Co.) by recrystallization from an ethanol-water mixture,³ and used to prepare a stock 1 × 10⁻³M solution in toluene (Merck p.a.) which had been successively washed with 0.5M sodium hydroxide, distilled water, 0.5M hydrochloric acid and doubly distilled water before use. Sodium chloride (Merck p.a.) was purified as previously described.¹⁰ Sodium thiocyanate solutions were standardized by titration with silver nitrate, iron(III) ammonium sulphate being used as indicator.

A stock solution of Pd(II) (3 × 10⁻³M, pH = 1) was prepared by dissolving the required amount of the chloride (Spanish Society of Precious Metals) in 0.1M hydrochloric acid, and was standardized gravimetrically with dimethylglyoxime.¹¹

In the aqueous phases the total concentrations of Pd(II) used were 3 × 10⁻⁵, 1.2 × 10⁻⁴ and 2.3 × 10⁻⁴M. The total thiocyanate concentration was varied between 2.5 × 10⁻⁵ and 1 × 10⁻³M. The pH was kept constant at 2.5 to avoid hydrolysis of palladium. The total chloride concentration was 1M.

*Author for correspondence.

The total TIBPS concentration was varied in the range from 2×10^{-4} to $1 \times 10^{-3}M$.

Apparatus

A Bausch and Lomb Spectronic 2000 spectrophotometer was used.

Procedure

Aqueous solutions with a total chloride concentration of $1.0M$ and various concentrations of palladium and thiocyanate were prepared. Equal volumes (10 ml) of the organic and aqueous phases were mixed in stoppered glass tubes and shaken for 90 min on a rack rotating at 40 rpm and kept at $22 \pm 1^\circ$. Preliminary work had shown that shaking for 90 min was adequate for equilibrium to be reached (Fig. 1).

The mixture was then centrifuged and the phases were separated. Excess of thiocyanate was added to the aqueous phase and the absorbance at 310 nm was measured to determine the palladium.¹² For several sets of conditions the Pd(II) mass balance was checked by stripping the palladium from the organic phase with $0.1M$ sodium thiocyanate and measuring the absorbance of the resulting aqueous phase.

RESULTS AND DISCUSSION

The palladium distribution coefficient, D , is given by

$$D = \frac{[\text{Pd(II)}]_{\text{org}}}{[\text{Pd(II)}]_{\text{aq}}} \quad (1)$$

where $[\text{Pd(II)}]_{\text{org}}$ and $[\text{Pd(II)}]_{\text{aq}}$ are the total palladium concentrations in the organic and aqueous phase, respectively.

Figure 2 gives the palladium distribution coefficient as a function of the total TIBPS concentration for total Pd(II) concentrations of 3.2,

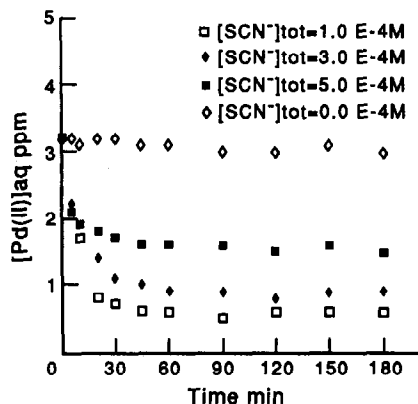


Fig. 1. Palladium concentration in the aqueous phase, plotted against time, for different SCN^- concentrations. $[\text{Pd(II)}]_{\text{tot}} = 3.0 \times 10^{-5}M$; $[\text{TIBPS}]_{\text{tot}} = 7.0 \times 10^{-4}M$.

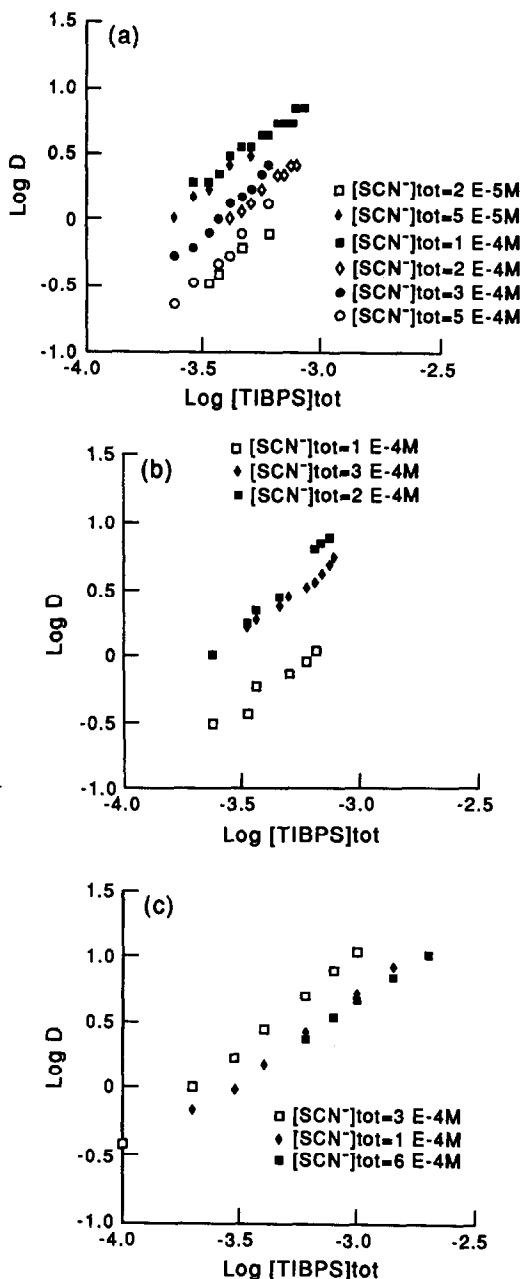


Fig. 2. Experimental distribution data, $\log D$ vs. $\log [\text{TIBPS}]_{\text{tot}}$ at different SCN^- levels. $[\text{Pd(II)}]_{\text{tot}}$: (a) $3.0 \times 10^{-5}M$; (b) $1.2 \times 10^{-4}M$; (c) $2.3 \times 10^{-4}M$.

12.8 and 24.8 ppm and different thiocyanate concentrations and Fig. 3 shows the data in the form $\log D$ vs. $\log [\text{SCN}^-]_{\text{tot}}$.

Taking into account that in our case ($[\text{Cl}^-] = 1.0M$), in the absence of SCN^- the Pd(II) in the aqueous phase will be present as the PdCl_4^{2-} complex, equation (1) can be expressed as:

$$D = \frac{[\text{Pd(II)}]_{\text{org}}}{[\text{PdCl}_4^{2-}](1 + \sum K_i [\text{SCN}^-]^i / [\text{Cl}^-]^i)} \quad (2)$$

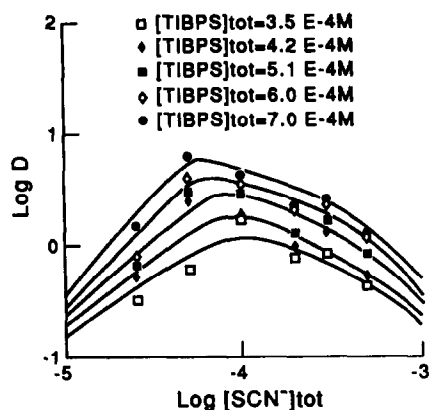


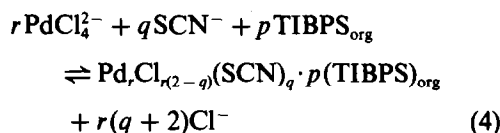
Fig. 3. Experimental distribution data, $\log D$, plotted against $\log [\text{SCN}^-]_{\text{tot}}$. $[\text{Pd(II)}]_{\text{tot}} = 3.0 \times 10^{-5} \text{M}$. Solid lines are the calculated curves based on the proposed model.

where the K_i values are the equilibrium constants of the reactions



with $i = 1, 2, 3$ and 4 . The values of K_i obtained from the literature¹³ were $\log K_1 = 6.03$, $\log K_2 = 10.93$, $\log K_3 = 14.52$ and $\log K_4 = 17.55$.

Likewise, the general extraction reaction when SCN^- is added could be expressed as:



where $q = 0-2$. The equilibrium constant can be termed K_{exp} . Since TIBPS is a neutral extractant,⁵ it follows that its role in the extraction is solely solvation of the palladium complex extracted, which itself must therefore be neutral.

The solubility of TIBPS in aqueous solution was determined by equilibrating hydrochloric acid with a solution of TIBPS in toluene, and analysing the aqueous phase for TIBPS by ICP spectrometry and HPLC. The solubility of TIBPS in aqueous solution was found to be $< 1.10 \times 10^{-6} \text{M}$.

To evaluate the composition of the extracted species as well as the corresponding formation constants, the experimental data were analysed numerically with the LETAGROP-DISTR program,¹⁴ which is based on minimization of the error-square sum, U :

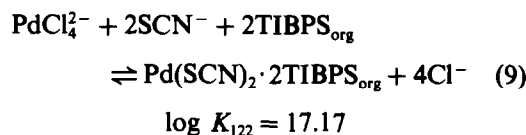
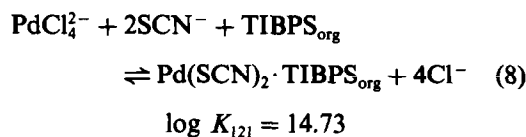
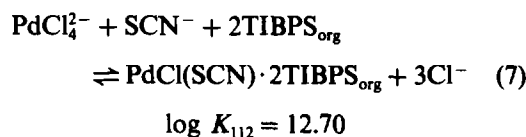
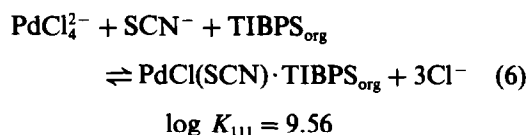
$$U = \sum_N (\log D_{\text{cal}} - \log D_{\text{exp}})^2 \quad (5)$$

where D_{exp} are the experimental values of the distribution coefficient and D_{cal} are the corresponding values calculated from the relevant

mass-balance equations for a proposed model: N is the total number of experimental points.

Our proposed models include the mixed-ligand complexes present in the aqueous phase [equation (3)] and protonation of thiocyanate as a constant set in all calculations. The results of the LETAGROP-DISTR calculations for different models tested, based on equation (4), are summarized in Table 1. Polynuclear species of Pd(II) were also tested but were always rejected. It is interesting that the results obtained for extraction of PdCl_2 solvated with TIBPS, model I, are far from agreement with the experimental data, and when mixed species are included in the model (e.g., VII), the PdCl_2 species is rejected. A binuclear species is also rejected in the calculations (models VI and IX).

As seen from Table 1, model X, consisting of the species $\text{PdCl}(\text{SCN}) \cdot \text{TIBPS}$, $\text{PdCl}(\text{SCN}) \cdot 2\text{TIBPS}$, $\text{Pd}(\text{SCN})_2 \cdot \text{TIBPS}$ and $\text{Pd}(\text{SCN})_2 \cdot 2\text{TIBPS}$ formed in the organic phase gives the best fit to the experimental data. Thus, the chemical reactions regarded as responsible for the extraction seem to be



Figures 4 and 5 show the distributions of the species proposed in this model, as a function of the total TIBPS and thiocyanate concentrations, respectively. As seen, the species containing $\text{Pd}(\text{SCN})_2$ predominate under most conditions, and although $\text{Pd}(\text{SCN})_2 \cdot \text{TIBPS}$ is predominant in the range of extractant concentrations studied, $\text{Pd}(\text{SCN})_2 \cdot 2\text{TIBPS}$ becomes more important as the concentration of TIBPS increases (as might be expected).

In additional experiments the ultraviolet absorption spectra of the organic phases obtained

Table 1. Results of numerical calculations for the species $\text{PdCl}_{r(2-q)}(\text{SCN})_q \cdot p\text{TIBPS}$ [equation (4)] by the program LETAGROP-DISTR; n (number of experimental points) = 89

Model	Species		$\log K_{rqp}$	$\sigma(\log D)$	U	Remarks
	r, q, p					
I	1,0,2	10.27; 10.51		0.76	0.45E2	
II	1,1,2	14.21 \pm 0.19		0.42	0.16E2	
III	1,1,1	10.83 \pm 0.20		0.42	0.17E2	
IV	1,1,1	9.90; 10.55		0.42	0.15E2	
	1,1,2	14.15; 14.38				
V	1,1,1	9.74 \pm 0.17		0.20	0.35E1	
	1,2,1	14.79 \pm 0.09				
VI	1,1,1	9.00; 9.68		0.19	0.33E1	
	1,2,1	14.82 \pm 0.08				
	2,2,2	—				rejected
VII	1,1,1	9.70 \pm 0.20		0.20	0.34E1	
	1,2,1	14.80 \pm 0.09				
VIII	1,0,2	—				rejected
	1,1,1	9.51; 9.80		0.17	0.27E1	
	1,1,2	12.76; 13.20				
IX	1,2,1	14.79 \pm 0.10				
	1,1,1	9.60; 9.90		0.18	0.28E1	
	1,1,2	12.68; 13.21				
	1,2,1	14.81 \pm 0.09				
X	2,2,2	—				rejected
	1,1,1	9.56; 9.86		0.16	0.20E1	
	1,1,2	12.70; 13.17				
	1,2,1	14.73 \pm 0.23				
	1,2,2	17.17; 17.83				

The standard deviation $\sigma(\log D)$ is defined as $\sigma(\log D) = (U/(N - N_k))^{1/2}$ where N_k is the number of constants to be adjusted. The error in the constants vs is given as $\pm 3\sigma(\log K)$ but for $\sigma(K) > 0.2K$, the "best" value of $\log K$ and the maximum value $[\log(K + 3\sigma(K))]$ are given.

by extraction of aqueous Pd(II) solutions (in the presence and absence of thiocyanate) with a toluene solution of TIBPS were recorded. For the extraction without thiocyanate present the shaking time was extended to a week to ensure that equilibrium was reached. The spectra are shown in Fig. 6(a). As seen, there is a blue-shift of the absorbance maximum when the extraction is done with thiocyanate present in the

aqueous phase, whereas there is a red-shift in the spectrum of the initial aqueous phases when thiocyanate is added, Fig. 6(b). The blue-shift seems to be a consequence of the change in medium as well as the ligand-exchange (and is analogous to the spectral differences between palladium thiocyanate species in aqueous medium and in molten salts¹²) and the red-shift

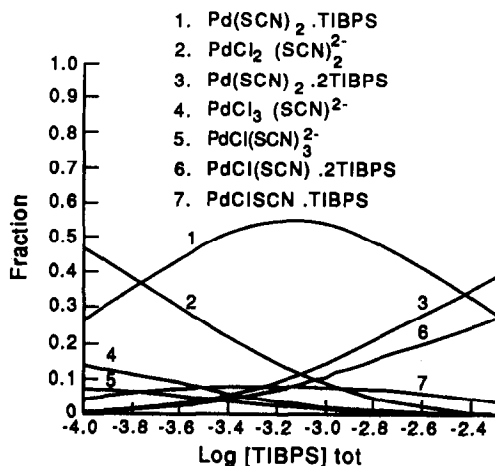


Fig. 4. Distribution diagram of metal species vs. $[\text{TIBPS}]_{\text{tot}}$. $[\text{Pd(II)}]_{\text{tot}} = 3.0 \times 10^{-5}M$; $[\text{SCN}^-]_{\text{tot}} = 1.0 \times 10^{-4}M$.

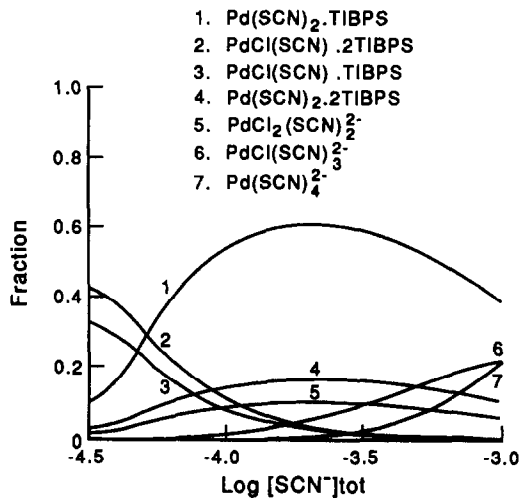


Fig. 5. Distribution diagram of palladium-containing species vs. aqueous $[\text{SCN}^-]_{\text{tot}}$. $[\text{Pd(II)}]_{\text{tot}} = 3.0 \times 10^{-5}M$; $[\text{TIBPS}]_{\text{tot}} = 1.0 \times 10^{-3}M$.

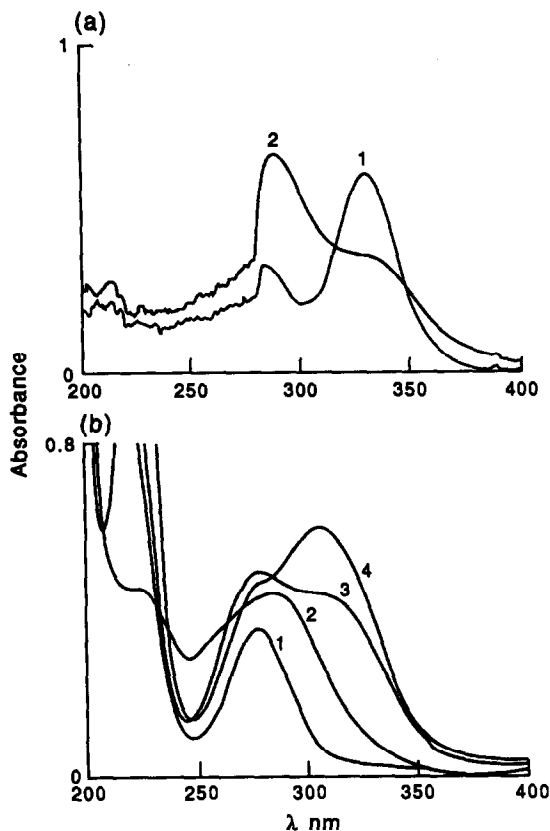


Fig. 6. (a) Ultraviolet spectra of organic species: $[\text{Pd(II)}]_{\text{tot}} = 3.0 \times 10^{-5} M$. 1, No SCN^- present in the aqueous phase; 2, $[\text{SCN}^-]_{\text{tot}} = 5.0 \times 10^{-5} M$. (b) Ultraviolet spectra of aqueous complexes: $[\text{Pd(II)}]_{\text{tot}} = 3.0 \times 10^{-5} M$. 1, No SCN^- present; 2, $[\text{SCN}^-]_{\text{tot}} = 5.0 \times 10^{-5} M$; 3, $[\text{SCN}^-]_{\text{tot}} = 5.0 \times 10^{-4} M$; 4, $[\text{SCN}^-]_{\text{tot}} = 1.0 \times 10^{-3} M$.

a consequence of ligand-exchange in aqueous medium.^{15,16}

A comparison of these results with those reported by Walker and Bautista² and by Inoue and co-workers³⁻⁵ leads to conclusions different from theirs. Walker and Bautista,² explain the extraction of Pd(II) by TIBPS in xylene, in the absence of thiocyanate, as due to formation of Pd(TIBPS)_2 species in the organic phase, and Inoue and co-workers consider that a binuclear 2:2 complex also contributes to the extraction into toluene. In both systems metal extraction is assumed to occur by a solvating mechanism. Neither Walker and Bautista nor Inoue and co-workers give values for the reaction constants. The main difference from our results is related to the formation of the binuclear species reported by Inoue and co-workers, and this may be due to the different ranges of Pd(II) concentration used, which in our case were limited by the solubility of Pd(II) in aqueous solutions containing thiocyanate. Furthermore, thio-

cyanate provides a different chemical environment, which may result in a different speciation.

Species with 1:2 metal:extractant stoichiometry are also found when triphenylphosphine in 1,2-dichloroethane is used as the extractant (in the absence of thiocyanate).¹⁷ Our results also partially agree with those reported in the literature for the extraction of different metals with Cyanex 471x, e.g., Ag(I) is extracted from nitrate solutions as $\text{AgNO}_3 \cdot 2\text{TIBPS}$,⁶ and Hg(II) from chloride media as $\text{HgCl}_2 \cdot 2\text{TIBPS}$,⁷ and a recent study concerning Au(III) extraction from hydrochloric acid media with Cyanex 471x showed that the species $\text{AuCl}_3 \cdot \text{TIBPS}$ and $\text{AuCl}_3 \cdot 2\text{TIBPS}$ are responsible for the gold extraction.¹⁸

In our study the effect of thiocyanate on the extraction of Pd(II) from chloride solutions has been shown to be related to the formation of mixed-ligand complexes $\text{PdCl}_{4-i}\text{SCN}_i^{2-}$ in the aqueous phase, which react more rapidly than the corresponding tetrachloro-complex PdCl_4^{2-} . As a result an increase in the rate of Pd(II) extraction is obtained (see Fig. 1). The trends observed at the different thiocyanate concentrations may be related to the similar trend in the relative concentrations of the species $\text{PdCl}_2(\text{SCN})_2^{2-}$ and $\text{PdCl}(\text{SCN})_3^{2-}$ under the corresponding experimental conditions.

Such behaviour has previously been explained as a catalytic process based on a *trans*-ligand effect.⁹ However, taking into account our findings that thiocyanate is present in the extracted metal species, the effect of the thiocyanate should now be considered as a particular case of synergism rather than catalysis, although a *trans*-effect of the thiocyanate in the mixed-ligand aqueous complexes may well be important in formation of the metal species finally extracted.

Acknowledgements—The present work is part of the CAICYT project MAT88-752. M. H. also thanks the Catalan Institution CIRIT for its financial contribution towards the equipment needed to carry out this work.

REFERENCES

1. F. E. Beamish, *The Analytical Chemistry of the Noble Metals*, Pergamon Press, London, 1966.
2. R. D. Walker and R. Bautista, *Proc. Int. Solv. Ext. Conf., ISEC⁸⁶*, Munich, 1986, Paper II-107.
3. K. Inoue and Y. Baba, *ibid.*, Paper II-263.
4. Y. Baba, M. Ohshima and K. Inoue, *Bull. Chem. Soc. Japan*, 1986, **59**, 3829.
5. Y. Baba and K. Inoue, *Ind. Eng. Chem. Res.*, 1988, **27**, 1613.

6. K. Inoue, Y. Baba and M. Tagaki, *Proc. Int. Solv. Ext. Cond., ISEC '86*, Munich, 1986. Paper II-65.
7. Y. Baba, Y. Umezaki and K. Inoue, *Solv. Ext. Ion Exch.*, 1986, **4**, 15.
8. S. J. Al-Bazi and A. Chow, *Talanta*, 1986, **31**, 815.
9. S. J. Al-Bazi and H. Freiser, *Solv. Ext. Ion Exch.*, 1986, **4**, 1121.
10. *Some Laboratory Methods, Inorganic Chemistry*, The Royal Institute of Technology (KTH), Stockholm, 1959.
11. A. I. Vogel, *Textbook of Quantitative Inorganic Analysis*, 4th Ed., Longmans, London, 1978.
12. K. S. De Haas, *J. Inorg. Nucl. Chem.*, 1973, **35**, 3231.
13. A. A. Biryukou and V. I. Shlenskaya, *Russ. J. Inorg. Chem.*, 1967, **12**, 1362.
14. D. H. Liem, *Acta Chem. Scand.*, 1971, **25**, 1521.
15. L. I. Elding, *Inorg. Chim. Acta*, 1972, **6**, 647.
16. A. K. Sundaram and E. B. Sandell, *J. Am. Chem. Soc.*, 1955, **77**, 855.
17. M. Mojski, *Talanta*, 1980, **27**, 7.
18. V. Salvadó, M. Hidalgo, A. Masana, M. Muñoz, M. Valiente and M. Muhammed, *Solv. Ext. Ion Exch.*, 1990, **8**, 491.

TRACE MEASUREMENTS OF RHODIUM BY ADSORPTIVE STRIPPING VOLTAMMETRY

JOSEPH WANG and ZIAD TAHA

Department of Chemistry, New Mexico State University, Las Cruces, NM 88003, U.S.A.

(Received 14 August 1990. Revised 12 September 1990. Accepted 21 September 1990)

Summary—A sensitive stripping voltammetric procedure for quantifying rhodium is described. The complex of rhodium with chloride ions is adsorbed on the hanging mercury drop electrode, and the reduction current of the accumulated complex is measured during a negative-going scan. Cyclic voltammetry is used to characterize the interfacial and redox behaviors. The effect of pH, chloride concentration, accumulation potential and other variables is discussed. The detection limit is $1 \times 10^{-8} M$ (~ 1 ng/ml) with 5-min accumulation. A linear current-concentration relationship is observed up to $7 \times 10^{-7} M$ and the relative standard deviation (at the $2 \times 10^{-7} M$ level) is 3.0%. Possible interferences by co-existing metals are investigated.

Because of the importance of rhodium, a sensitive method is required for its reliable measurement. In particular, the quantification of rhodium at trace levels is desired for geological surveys, catalytic applications and materials science. Spectroscopic procedures have been proposed for measuring low levels of rhodium, after solvent extraction,¹ liquid chromatography² or preferential complexation.³ Such schemes, however, are time-consuming and costly.

The present paper describes a sensitive stripping voltammetric procedure for trace measurement of rhodium. The polarographic behavior of rhodium has been explored by different groups.⁴⁻⁷ These studies elucidated the redox mechanism of rhodium in the presence of various complexing agents. The quantification of rhodium by coulometry⁶ or catalytic polarography⁷ has also been reported. However, the utility of stripping analysis (the most sensitive electrochemical technique⁸) for rhodium has not been reported. The combination of the voltammetric activity of rhodium chloro-complexes with their surface-active properties results in an effective adsorptive stripping procedure, the characteristics of which are described in this paper.

EXPERIMENTAL

Apparatus

A PAR Model 264 voltammetric analyzer was used with a PAR Model 303 static mercury drop electrode.

Reagents

All solutions were prepared with doubly distilled water. A 1000 mg/l. rhodium stock solution (atomic absorption standard; Aldrich) was diluted as required for standard additions. Potassium chloride solutions were prepared by dissolving the reagent in water and adjusting the pH with hydrochloric acid or sodium hydroxide solution.

Procedure

Potassium chloride solution (10 ml, pH 1.3) was pipetted into the polarographic cell and purged with nitrogen for 4 min. The preconcentration potential (-0.20 V) was applied to a fresh mercury drop while the solution was stirred. After the preconcentration, the stirring was stopped and 15 sec later the background voltamperogram obtained by applying a negative-going scan terminating at -0.60 V. A known volume of rhodium standard was then added and the adsorptive and stripping cycle was repeated with a new mercury drop.

RESULTS AND DISCUSSION

Repetitive cyclic voltamperograms for 50 ng/ml rhodium in 2.5M potassium chloride (pH 1.3) were used to evaluate the interfacial and redox behavior (Fig. 1). In the absence of prior accumulation only a small peak from the reduction of the rhodium chloro-complex was observed, at -0.52 V (Fig. 1, B). When the

experiment was repeated with a 120-sec stirring period (at -0.20 V) a large peak was observed at -0.52 V in the first negative-going scan. Subsequent scans gave a much smaller peak (of approximately constant height), indicating desorption of the product from the surface (Fig. 1, A). According to the work of Van Loon and Page,⁶ the complex adsorbed under these experimental conditions should be mainly RhCl_2^- .

Figure 2 shows that for a 20 ng/ml rhodium solution, the longer the preconcentration time, the more metal complex is adsorbed on the surface, and the larger is the peak current. For example, with 120-sec preconcentration (Fig. 2, e) there is a fivefold enhancement of the peak current relative to that obtained without preconcentration (Fig. 2, a). As a result, excellent signal-to-background characteristics are obtained which permit measurements at nanomolar concentration levels. Also shown in Fig. 2 (inset) are plots of peak current *vs.* preconcentration time at two levels of rhodium [(A) 20 and (B) 40 ng/ml]. In both cases the current increases linearly with time. The slopes are 9.6 nA/sec (A) and 26.2 nA/sec (B) (correlation coefficients, 0.999 and 0.996, respectively).

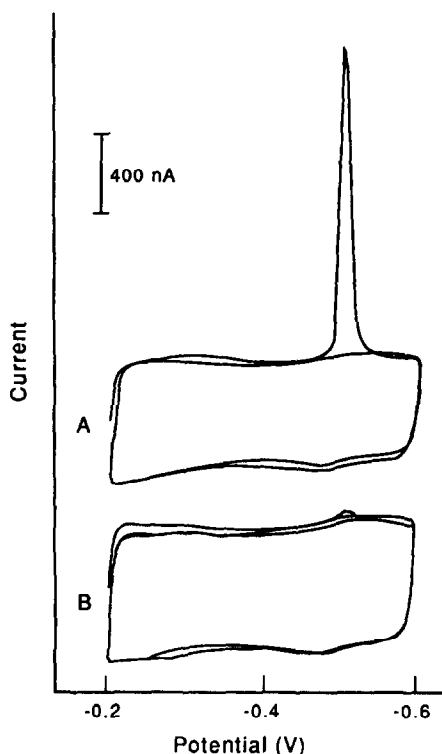


Fig. 1. Repetitive cyclic voltamperograms for 50 ng/ml rhodium, in 2.5M KCl (pH 1.3) solution, (A) with and (B) without 120-sec preconcentration (at -0.20 V), with 400 rpm stirring; scan-rate, 50 mV/sec.

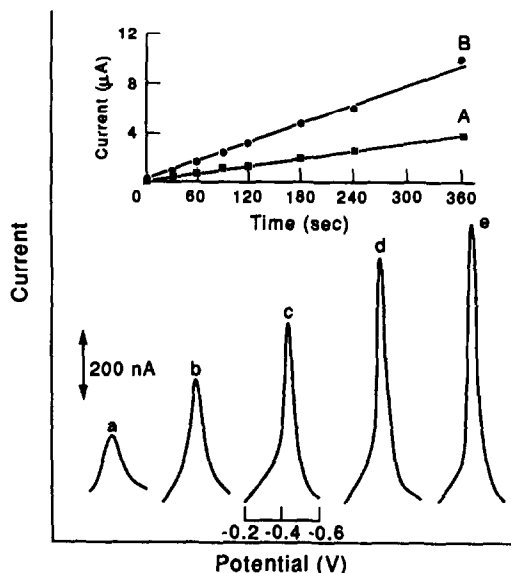


Fig. 2. Differential pulse voltamperograms for 20 ng/ml rhodium after different preconcentration times: (a) 0, (b) 30, (c) 60, (d) 90, (e) 120 sec, and 400 rpm stirring. Inset are current *vs.* preconcentration time plots for (A) 20 ng/ml and (B) 40 ng/ml Rh. Conditions: 2.5M KCl (pH 1.3); accumulation at -0.20 V; scan-rate 10 mV/sec; pulse amplitude, 25 mV.

The stripping current depends strongly on the solution pH (Fig. 3A). Increasing the pH from 3 to 7 results in a sharp decrease in peak height. This could be explained by the affinity of Rh^{3+} for hydroxide ions at high pH.⁶ A similar pH-current profile was obtained for polarographic work. A sharp increase in the peak width was observed as the pH was increased from 4 to 7 (Fig. 3B). The effect of convection mass transport was also evaluated.

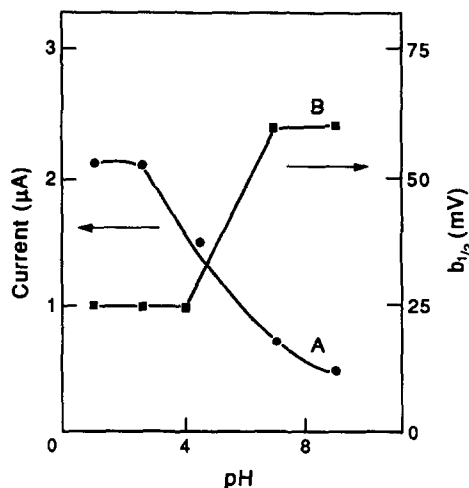


Fig. 3. Effect of pH on the adsorptive stripping current (A) and the peak half-width (B): 50 ng/ml Rh; preconcentration time, 60 sec; other conditions as for Fig. 2.

Accumulation of rhodium chloro-complexes from a stirred solution gave rise to a peak current 2.2 times as large as that obtained with the quiescent solutions.

The chloride ion concentration has a pronounced effect on the stripping current (Fig. 4A). The stripping peak for 50 ng/ml rhodium increases linearly with increasing potassium chloride concentration between 1 and 2.5M, and then decreases. As the chloride concentration increases, the mole fraction of RhCl_6^{3-} increases, giving rise to a higher signal. According to the work of Shlenskaya *et al.*,⁹ this increase is almost linear between 1.5 and 2.5M potassium chloride, in agreement with the signal trend shown in Fig. 4A. At low chloride concentration aquo-chloro mixed-ligand complexes are formed.^{4,6} The dependence of the stripping current on the preconcentration potential over the range from +0.10 to -0.40 V was examined (Fig. 4B). The response increased sharply between 0.00 and -0.20 V and then decreased at more negative potentials. The optimal conditions for rhodium measurements are there-

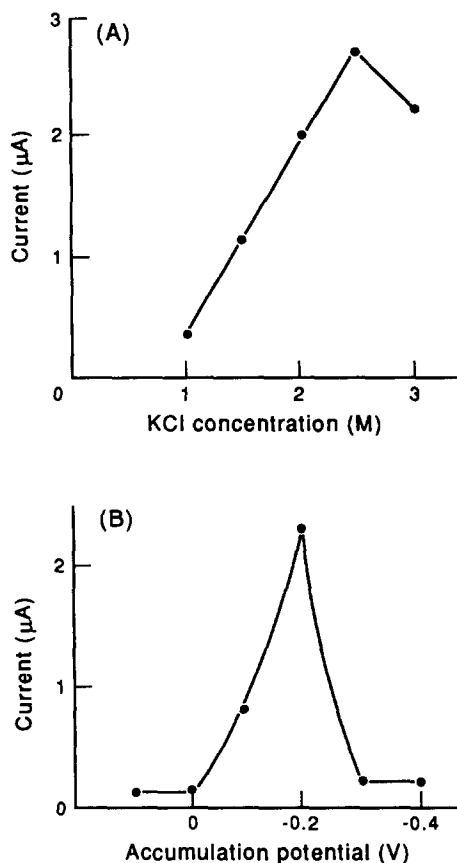


Fig. 4. Dependence of the adsorptive stripping current on (A) the KCl concentration and (B) the accumulation potential: 50 ng/ml Rh; other conditions as for Fig. 2.

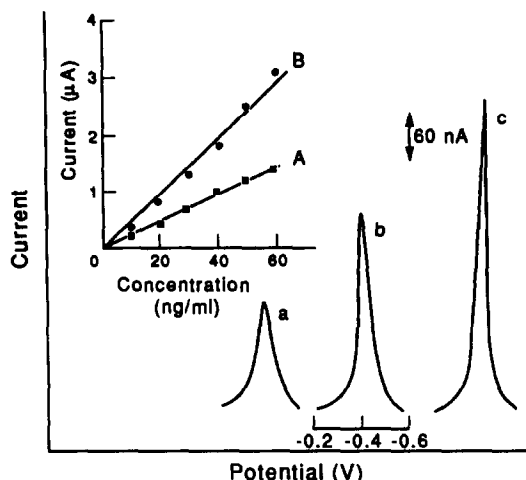


Fig. 5. Stripping voltamperograms obtained for solutions of increasing rhodium concentration over the range 10–30 ng/ml (a–c). Preconcentration for 45 sec; other conditions as for Fig. 2. Inset are calibration plots for different accumulation times: (A) 45 and (B) 90 sec.

fore 2.5M potassium chloride as supporting electrolyte (pH 1.3) and a preconcentration potential of -0.20 V.

Figure 5 shows stripping voltamperograms obtained for 10–30 ng/ml rhodium solutions after a 45-sec preconcentration time. Calibration plots over a wider concentration range (10–60 ng/ml), obtained by using different preconcentration times, are also shown in Fig. 5 (inset). The response is linear over this range [slopes, (A) 24.7 and (B) 54.8 nA.ml.ng⁻¹, both with correlation coefficients of 0.997]. The detection limit was estimated to be 10nM (1 ng/ml) with a 5-min accumulation ($S/N = 3$). The precision was estimated from eight successive measurements of 50 ng/ml rhodium solution (90-sec preconcentration); the mean peak current was 1426 nA (range 1360–1470 nA and relative standard deviation 3.0%).

The following metal ions (20 ng/ml) were tested and found not to affect the 20 ng/ml rhodium peak: Ag(I), Ni(II), Zn(II), Co(II), Pd(II), Au(III), Ti(IV), Fe(II), Fe(III), Pb(II) and Cu(II). A decrease in the rhodium stripping peak was observed in the presence of Mn(II) and Sn(II). Hence, a separation step would be required in the presence of these metals. The effects of several anions were also examined. No interference was observed in the presence of 2mM nitrate or bromide. An additional peak was observed in the presence of 2mM iodide, at ca. 140 mV negative to the peak of interest, but did not affect the determination of rhodium.

In conclusion, the method described provides a simple approach for the determination of trace levels of rhodium. The interfacial accumulation results in a substantial enhancement of the voltammetric response, permitting convenient quantification at the ng/ml level. Depending on the sample matrix, a separation step may be required to isolate rhodium from interfering metals.

REFERENCES

1. Y. Shijo, K. Nakaji and T. Shimizu, *Analyst*, 1988, **113**, 519.
2. B. J. Mueller and R. J. Lovett, *Anal. Chem.*, 1985, **57**, 2693.
3. A. L. J. Rao, U. Gupta and B. K. Puri, *Analyst*, 1986, **111**, 1401.
4. D. Cozzi and F. Pantani, *J. Inorg. Nucl. Chem.*, 1958, **8**, 385.
5. J. B. Willis, *J. Am. Chem. Soc.*, 1944, **66**, 1067.
6. G. Van Loon and J. A. Page, *Talanta*, 1965, **12**, 227.
7. P. W. Alexander and G. L. Orth, *J. Electroanal. Chem.*, 1971, **31**, App. 3.
8. J. Wang, *Stripping Analysis: Principles, Instrumentation and Applications*, VCH, Deerfield Beach, 1985.
9. V. I. Shlenskaya, O. A. Efremenko, S. V. Oleinikova and I. P. Alimarin, *Bull. Acad. Sci. USSR, Chem. Sci.*, 1969, **18**, 1525.

THE SYNTHESIS OF SOME LIPOPHILIC TETRA-ARYLBORATES FOR USE IN MEMBRANE ELECTRODE PREPARATION

AGNES YOO and CARL E. MOORE
Loyola University, Chicago, Illinois 60626

(Received 24 July 1990. Revised 19 October 1990. Accepted 3 November 1990)

Summary—Synthetic methods for preparing four lipophilic tetra-arylborates considered suitable candidates for use in membrane electrodes are described. Qualitative precipitation tests were performed with several cations. The sodium salts of the four tetra-arylborates were found to have limited stability but the cesium salts were relatively stable.

The tetrakis-*p*-chlorophenylborate anion, first reported in 1965,^{1,2} has found use in the fabrication of membrane electrodes^{3,4} suitable for sensing certain large cations. It seems likely that the activity of tetrakis-*p*-chlorophenylborate as the active agent in membrane electrodes is due in large part to the lipophilic character of the *p*-chlorophenyl moiety. Private communications with workers in the field of membrane electrodes have revealed an interest in, and a need for, additional tetra-arylborate ionophores suitable for the formulation of cation-sensing membranes.

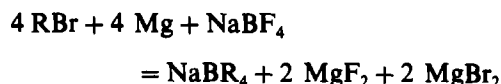
We have attempted to meet this need by the synthesis of a number of tetra-aryl borates which have an unbranched aliphatic chain in the position *meta* to the carbon atom bonded to the boron atom. The study required the preparation of several new compounds as well as the resynthesis of a few compounds previously prepared in this laboratory. Our choice of the *meta*-position for the alkyl-substituent was predicated on our experience—and that of others⁵⁻⁹—with other tetra-arylborates that alkyl-substituents placed in the *para*-position relative to the carbon-boron bond yield compounds of lower stability than their *meta*-substituted analogs.

The following salts were prepared and supplied to other laboratories for membrane electrode studies.

1. Cesium tetrakis(*m*-methylphenyl)borate
2. Cesium tetrakis(*m*-ethylphenyl)borate
3. Cesium tetrakis(*m*-propylphenyl)borate
4. Cesium tetrakis(*m*-butylphenyl)borate

Synthesis of sodium tetrakis(m-alkylphenyl)borates

The *in situ* synthetic procedure of Vandenberg¹⁰ was used, which proceeds according to the equation:



As in all Grignard syntheses, the apparatus and reagents must be completely free from water. To achieve this, the *m*-alkylphenyl halide was dried over anhydrous CaSO₄ overnight, anhydrous diethyl ether was dried over sodium metal overnight, magnesium turnings were dried at 120°, and sodium tetrafluoroborate was dried at 120° overnight.

All apparatus was dried overnight at 120°. A 500-ml three-necked round-bottomed flask was fitted with a magnetic stirring bar, a reflux condenser, a 60-ml dropping funnel, and a glass tube and stopcock for introduction of nitrogen. The dropping funnel was stoppered, a drying tube attached to the condenser and the cooling water turned on. Nitrogen was passed through the flask and the flame of a Bunsen burner swept over the flask until there was no visible condensation of moisture in the condenser. An additional dropping funnel can be added (with a suitable adapter) for the addition of diethyl ether.

The following procedure is scaled for the use of 0.1 mole of alkylphenyl halide starting material.

Weigh 2.8 g of sodium tetrafluoroborate into the reaction flask. To expose a fresh metal

surface, grind 2.5 g of magnesium turnings with a dry mortar and pestle. Add the magnesium to the flask, then just sufficient anhydrous diethyl ether to cover the solid reagents. Dissolve 0.1 mole of the alkylphenyl halide in approximately 20 ml of anhydrous diethyl ether and introduce it into the dropping funnel. Add about 5 ml of the alkylphenylhalide solution to the reaction flask, from the dropping funnel. Stir the solution while gently warming it with a heating mantle. The appearance of turbidity signifies the beginning of the reaction. The reaction mixture bubbles vigorously, and turns yellow, green or brown. When the reaction has started, add sufficient anhydrous diethyl ether to the flask to bring the volume to approximately 200 ml. Let the remaining alkylphenyl halide solution drip into the flask. The Grignard reaction usually takes from 5 to 45 min to start. Addition of the alkylphenyl halide solution requires approximately an hour. The drop rate must be regulated throughout, to avoid an excessively vigorous reaction. If the reaction becomes too energetic, the flask should be immersed in an ice-water bath. After all the alkylphenylhalide has been added, stir for an additional 3 hr with sufficient heating to maintain a gentle reflux. During the reaction there will be a considerable loss of ether by evaporation.

Work-up of the product

The tetra-arylborates are easily decomposed by acids and by the free radicals produced by ether hydroperoxides. The use of basic solutions and peroxide-free ether in the work-up will minimize these problems.

Prepare 200 ml of ice-water and make it slightly basic with dilute sodium hydroxide solution. Pour the reaction mixture into the ice-water, with stirring. Add 0.5 g of anhydrous sodium carbonate and stir. Wash the reaction flask with peroxide-free diethyl ether and add the washings to the aqueous mixture. Separate the ether layer, which contains the crude sodium salt of the tetrakis (*m*-alkylphenyl)borate. Saturate the aqueous layer with sodium chloride and extract it with three 30-ml portions of peroxide-free ether.

Preparation of cesium tetrakis-alkylphenylborates

The reaction proceeds as follows:



Add the combined ether extracts of the

sodium salts dropwise to about 600 ml of 1% cesium chloride solution containing $10^{-4}M$ aluminum sulfate to promote coagulation of the precipitate. Heat the solution to about 40° and stir it vigorously during the addition. When the addition is complete, continue the stirring for 1 hr. Then chill the precipitate and supernatant liquid in an ice-water bath for 1 hr, filter and wash the product twice with chilled demineralized water.

Suspend the product in 100 ml of xylene and filter. Repeat this step, then air-dry the product. Dissolve it in 0.7–1.5 l. of redistilled acetone containing 5% v/v demineralized water. Warm the solution slightly (maximum 30°) and filter to remove foreign particles. Evaporate with a rotary evaporator in a 35–40° water-bath, to a volume of 100–200 ml. Chill the solution and filter. Dry the precipitate under vacuum for 12 hr.

RESULTS AND DISCUSSION

Study of properties of the sodium salts

Qualitative precipitation tests. One ml of 0.1M aqueous cation solution was mixed with 10–15 drops of the ether solution of the reagent (sodium salt). The cations tested were Li^+ , K^+ , Rb^+ , Cs^+ , Tl^+ , NH_4^+ , $(\text{CH}_3)_3\text{NH}^+$, $(\text{CH}_3)_4\text{N}^+$, Ba^{2+} , Sr^{2+} , Pb^{2+} , Cd^{2+} , Mn^{2+} , Zn^{2+} , Ni^{2+} and Ca^{2+} . The reactions of interest are summarized in Table 1.

Stability tests. A portion of the combined ether extracts from the work-up step was stored in a stoppered test-tube at 5–10°. A second portion was purged with nitrogen before similar storage in the refrigerator. A third portion in a stoppered test-tube was left at room temperature. Each was tested at intervals by qualitative precipitation with rubidium. Failure to produce a precipitate indicated that an appreciable amount of decomposition had occurred during storage.

The ether solution of the sodium salts was found to be stable for about two days. No significant differences in stability were observed between ether solutions kept under nitrogen and in air. Use of ether that had been redistilled in the presence of lithium aluminum hydride appeared to increase the stability of the reagent.

Because the pure sodium salts were not stable in solid form, attempts to obtain them were unsuccessful. The cesium salts are considerably more stable, however, and could be easily pre-

Table 1. Precipitation profile

Cation	Tetrakis(<i>m</i> -alkylphenyl)borate			
	Methyl	Ethyl	Propyl	Butyl
K ⁺	+++ (I)	—	—	—
Rb ⁺	+++ (I)	+++ (I)	+++ (I)	++ (I)*
Cs ⁺	+++ (I)	+++ (I)	+++ (I)	+++ (S)†
Tl ⁺	+++ (I)	+++ (I)	++ (I)	+ (S)
NH ₄ ⁺	+++ (I)	+++ (S)	T (S)	T (S)
(CH ₃) ₃ NH ⁺	+++ (I)	+ (S)	T (S)	—
(CH ₃) ₄ N ⁺	+++ (I)	+ (S)	T (S)	T (S)
Sr ²⁺	—	T (S)	nd	nd
Ba ²⁺	—	+ (S)	+++ (I)	nd
Pb ²⁺	T (S)	++ (S)	—	nd

+++ heavy precipitate.

++ medium precipitate.

+ slight precipitate.

T trace precipitate.

— no reaction.

(I) precipitates immediately.

(S) precipitates slowly.

nd not tested for.

*more concentrated ether solution gave +++ (I).

†dilute ether solution precipitates Cs⁺ faster than Rb⁺.

pared. Their infrared and NMR spectra were consistent with the structures expected for the compounds, and analysis for carbon, hydrogen and boron gave results in agreement with those expected (Table 2). The compounds were found to be soluble in dimethylsulfoxide (DMSO). Saturated solutions of the salts were prepared in acetone, acetonitrile, and water by warming for 30 min, in a warm water-bath, in glassware washed and rinsed with demineralized water, DMSO, and acetone. The resulting solutions were allowed to equilibrate for two days at room temperature. Measured volumes were taken, the solvent was evaporated, and the residue was dried at 120° and cooled in a desiccator. The molar solubilities were determined by dissolving the residue in a 90/10 v/v DMSO–water mixture and analysis for boron by DC-plasma emission spectrometry.¹¹ The results are given in Table 3.

The solubility of cesium tetraphenylborate in water was found to be more than an order of magnitude higher than the value previously reported.¹² An intriguing zig-zag pattern occurred in a plot of solubility *vs.* chain length of

the alkyl group. The solubilities were lower for the odd-numbered alkyl side-chain derivatives than for the even-numbered alkyl side-chain compounds. Within each group (odd or even number of carbon atoms) the compounds with longer alkyl chains were more soluble than those with shorter chains.

Three of the tetra-arylborates synthesized are new compounds, the *m*-methyl analog, prepared for comparative purposes, having been previously described. Increasing the length of aliphatic chains is known to enhance the lipophilicity of ionophores. The degree of lipophilicity of the reagent that is incorporated into the PVC matrix, in addition to whatever effects it may have on the selectivity and solubility, is of paramount importance in the preparation of ion-sensing membrane electrodes, because it controls the amount of reagent that leaches out of the membrane.

The sodium salts of the *m*-ethyl, *m*-*n*-propyl, *m*-*n*-butyl, and *m*-methyl compounds were found to be of limited stability in aqueous solution. In peroxide-free diethyl ether solution the period of stability increased to 2–3 days.

Table 2. Elemental analysis of the cesium tetrakis(*m*-alkylphenyl)borates

Alkyl	Found, %			Theory, %		
	C	H	B	C	H	B
None	63.5	4.48	2.44	63.76	4.46	2.39
Methyl	66.0	5.59	2.18	66.17	5.55	2.13
Ethyl	68.5	6.53	1.87	68.10	6.43	1.92
Propyl	70.1	7.25	1.79	69.69	7.15	1.74
Butyl	71.3	7.71	1.62	71.05	7.70	1.60

Table 3. Solubilities of cesium tetrakis(*m*-alkylphenyl)borates at room temperature

Alkyl	Acetone,	Acetonitrile,	Water,*
	10 ⁻² M	10 ⁻² M	10 ⁻⁴ M
None	2.7	1.5	4
Methyl	0.2	0.2	3
Ethyl	2.4	0.9	5
Propyl	1.3	0.6	2
Butyl	2.2	1.2	4

These sodium salts, because of their solubility in ether, can be incorporated into PVC membrane electrodes, where they may have sufficient stability in the PVC matrix to warrant further study.

Generally, the longer the alkyl chain, the greater the selectivity of the anion toward the larger cations. For example, tetrakis(*m*-*n*-butylphenyl)borate formed heavy precipitates only with cesium and rubidium. Cesium can be separated from rubidium by precipitation with tetrakis(*m*-*n*-butylphenyl)borate if the concentration of the reagent solution is suitably adjusted (*cf.* Table 1).

REFERENCES

1. F. P. Cassaretto, J. J. McLafferty and C. E. Moore, *Anal. Chim. Acta*, 1965, **32**, 376.
2. H. Holzapfel, O. Wildner and P. Nenning, *Z. Chem.*, 1965, **5**, 275.
3. W. E. Morf, G. Kahr and W. Simon, *Anal. Lett.*, 1974, **7**, 9.
4. G. Baum and M. Lynn, *Anal. Chim. Acta*, 1973, **65**, 393.
5. G. Wittig and W. Herwig, *Chem. Ber.*, 1955, **88**, 962.
6. V. A. Sazonova and V. N. Leonov, *Zh. Analit. Khim.*, 1959, **14**, 483.
7. J. L. R. Williams, J. C. Doty, P. J. Grisdale, R. Searle, T. H. Regan, G. P. Happ and D. P. Maier, *J. Am. Chem. Soc.*, 1967, **89**, 5153.
8. J. L. R. Williams, J. C. Doty, P. J. Grisdale, T. H. Regan, G. P. Happ and D. P. Maier, *ibid.*, 1968, **90**, 53.
9. W. S. Murphy, Jr., *M.S. Thesis*, Loyola University of Chicago, 1961.
10. J. T. Vandeberg, *Ph.D. Dissertation*, Loyola University of Chicago, 1969.
11. A. L. Yoo, C. E. Moore, R. Jones and A. Synstebly, *Appl. Spectrosc.*, 1986, **40**, 1073.
12. C. E. Moore and J. T. Vandeberg, *C.R.C. Crit. Rev. Anal. Chem.*, 1971, **2**, 1.

NUCLEATION IN PREMICELLAR AGGREGATION

CHRISTOPHER P. LORAN and RAY VON WANDRUSZKA*

Department of Chemistry, University of Idaho, Moscow, ID 83843, U.S.A.

(Received 13 August 1990. Revised 17 October 1990. Accepted 3 November 1990)

Summary—The role of a nucleating agent (cholesterol) in the premicellar aggregation of sodium lauryl sulfate (SLS), cetyltrimethylammonium bromide, Triton X-405 and Brij 35 has been investigated. The I_1/I_3 ratios of pyrene in the solutions indicate that SLS is strongly nucleated by cholesterol, but the other detergents appear to be so to a lesser extent. However, quenching studies show that premicellar Brij 35 also forms nucleated aggregates that protect the probe from the quencher. Energy transfer data with Triton X-405 suggest that such aggregates have a more open structure than self-assembling ones and are more accessible to water.

The formation of surfactant aggregates at concentrations below the critical micelle concentration (cmc) has been reported.¹⁻³ It can be deduced from fluorescence measurements involving probes associated with these aggregates. Specific methods suitable for these investigations include the assessment of polarity from spectral features, fluorescence quenching and energy transfer. In the present study all three are used to evaluate the role of nucleation of detergent by a relatively hydrophobic species (cholesterol) in the premicellar aggregation process.

Relative band intensities in the vibronic structure of the fluorescence emission spectrum of pyrene have previously been used to assess the polarity of the environment of the fluorophore in premicellar and micellar media.⁴⁻⁹ The ratio of the peak heights of the first and third emission bands (I_1/I_3) is a sensitive gauge of the nature of the immediate surroundings of the probe. The higher the ratio the greater is the polarity of the microenvironment and this in turn indicates the association of the probe with nonpolar entities in aqueous solution and hence the existence of such aggregates.

The fluorescence of polyaromatic hydrocarbons is quenched by some anionic species¹⁰⁻¹⁴ if the quenching species can come into direct physical contact with the fluorophore. The quenching mechanism may be collisional (dynamic quenching) or involve ground-state complex formation (static quenching). Either may be prevented by isolation of the fluorophore from the quenching species and this may be achieved by association of the fluorophore with detergent aggregates. Protection arising from hydrophobic interactions between probe and

detergent is especially effective against hydrophilic ionic quenchers such as bromide. This shielding effect leads to a notable increase in fluorescence intensity.¹⁵

Rothenberger *et al.* have shown that micellar systems allow for efficient energy transfer if the donor and acceptor species are sufficiently close to each other.¹⁶ The donor and acceptor may both be extraneous species that have penetrated the nonpolar micellar interior, or, as in this study, the donor may be the species forming the micelle. Kalyanasundaram and Thomas have studied the transfer of excitation energy from the phenyl groups of micellar Igepal C-630 to solubilized molecules of pyrene,¹⁷ and efficient energy transfer has been shown to occur between sodium phenylundecanoate micelles and naphthalene.¹⁸ Previous work in our laboratory has demonstrated micellar sensitization in the benzyltrimethylhexadecylammonium chloride (BDCH)/naphthacene, Triton X-405 (TX-405)/pyrene and TX-405/Brij 35 systems.¹⁹

EXPERIMENTAL

Pyrene (98% pure) (Sigma) was recrystallized twice from absolute ethanol and sublimed onto a cold finger. TX-405 (70% aqueous solution), sodium lauryl sulfate (98% pure), Brij 35 and cholesterol (Sigma) were used without further purification. Potassium bromide (analytical grade, J. T. Baker) was used as supplied. The water used in all solutions was distilled and treated with a 0.22- μ m Millipore filter system to give 18 M Ω .cm resistivity.

An aqueous stock solution of pyrene was prepared by adding a 4- μ l aliquot of a

5.1-mg/ml ethanolic solution to a dry 1000-ml standard flask. The solvent was then evaporated and about 800 ml of water was added. After sonication for 4 hr the flask was filled to the mark to make a $1.0 \times 10^{-7} M$ pyrene solution. Stock solutions with the surfactants [SLS, Brij 35, CTAB (cetyltrimethylammonium bromide) and TX-405] were prepared from the pyrene solution in a similar manner, with surfactant concentrations ranging from 1.00×10^{-7} to $0.01 M$. Cholesterol solutions were all saturated ($5.16 \times 10^{-6} M$). Fluorescence spectra were recorded with a Perkin-Elmer MPF 66 spectrofluorimeter equipped with a temperature-controlled sample compartment. This instrument gives corrected excitation and emission spectra through the use of a built-in Rhodamine 101 quantum counter. Excitation and emission slit-widths were set for 5 and 2 nm bandpass, respectively, and all measurements were corrected for a blank. The fluorescence intensity values reported are the averages of triplicate measurements. Unless otherwise stated, readings were taken at 24° .

RESULTS AND DISCUSSION

Polarity effects

When small amounts of cholesterol are added to SLS solutions containing pyrene, the conductivity and surface tension values measured are not affected. These techniques lack the sensitivity necessary to record relatively subtle alterations in the solution environment. The I_1/I_3 ratio of the pyrene emission spectrum can be effectively used to monitor the polarity of the immediate environment of the fluorophore.¹⁹ A direct relationship exists between the ratio and the polarity. In Fig. 1, for the solution free from cholesterol the critical micelle concentration

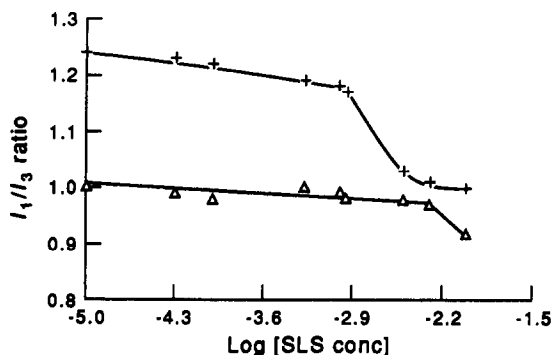


Fig. 1. Variation of I_1/I_3 ratio of pyrene emission with SLS concentration with (Δ) and without (+) cholesterol ($5.16 \times 10^{-6} M$) present.

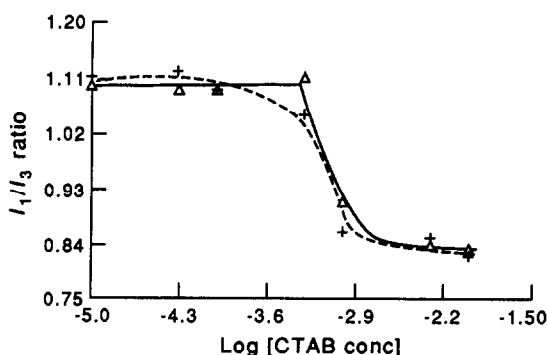


Fig. 2. Variation of I_1/I_3 ratio of pyrene emission with CTAB concentration with (---) and without (—) cholesterol present.

(cmc) is reached at about $10^{-3} M$ SLS, the concentration at which the I_1/I_3 ratio begins to decrease sharply. In the presence of cholesterol, a lower ratio persists at SLS concentrations up to about $5 \times 10^{-3} M$, indicating that the microenvironment of pyrene is considerably less polar in this case. This effect is not observed when cholesterol and pyrene are together in a solution without surfactant, suggesting that SLS associates with dissolved cholesterol even at very low detergent concentrations, and that pyrene exists in a relatively nonpolar environment within these aggregates.

A similar study with CTAB gave very different results. Figure 2 shows the variation of the I_1/I_3 ratio with CTAB concentration. Cholesterol had a negligible effect on the measured values. A similar lack of preaggregation was observed when Brij 35 was used as the detergent.

Aggregates of SLS that have formed around a nucleus of cholesterol are notably more sensitive to temperature than those of pure SLS (Fig. 3). In the presence of cholesterol the I_1/I_3 ratio of pyrene is consistently greater at the higher temperature, indicating that the cholesterol/SLS aggregate is thermally disturbed in the warmer solution. The values of the ratio at different temperatures are relatively close together at the extremities of the graph: at very low SLS concentrations the extent of aggregation is small, and so temperature change has less effect; at high SLS concentrations micelles are formed which have less thermal lability than the premicellar aggregates. The temperature effects are minimal in the absence of cholesterol.

Bromide quenching

Micellar aggregates afford protection from fluorescence quenching by species such as

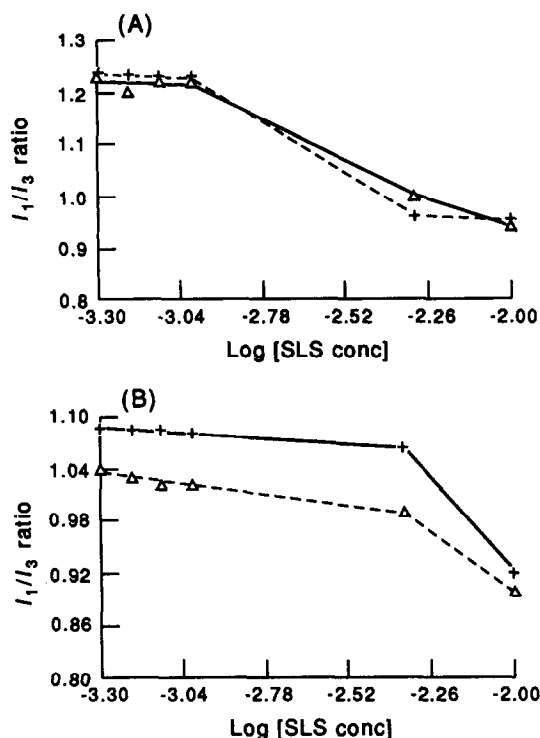


Fig. 3. Variation of I_1/I_3 ratio of pyrene emission with SLS concentration at different temperatures: (---) 22.2°; (—) 58.0°. (A) Without cholesterol; (B) with $5.16 \times 10^{-5} M$ cholesterol present.

bromide ions, by providing the probe with a hydrophobic environment that is inaccessible to the hydrophilic quencher. The assessment of fluorescence quenching can expose surfactant aggregation behavior that may not be evident from the I_1/I_3 ratio measurements.

The successive addition of $2\text{-}\mu\text{l}$ increments of $0.01 M$ potassium bromide to $10^{-7} M$ pyrene solution with and without $5.16 \times 10^{-5} M$ cholesterol present gives a steady decrease in the ratio of quenched to unquenched intensity (I_q/I_0), as shown in Fig. 4, A. The effect of cholesterol is small when no detergent is present and in the presence of CTAB and SLS. However, for Brij 35 a consistently higher I_q/I_0 ratio is observed in the presence of cholesterol, Fig. 4, B–D.

The data indicate various degrees of protection of the fluorophore by premicellar detergents in the presence of cholesterol. Though cholesterol enhances protection in all cases, the effect is minor with the cationic surfactant CTAB present. This may be partially due to the attraction of a "halo" of bromide by this detergent, as reported before from this laboratory.³ However, the observation that the I_1/I_3 ratio is not affected by CTAB suggests that the detergent does not form extensive premicellar

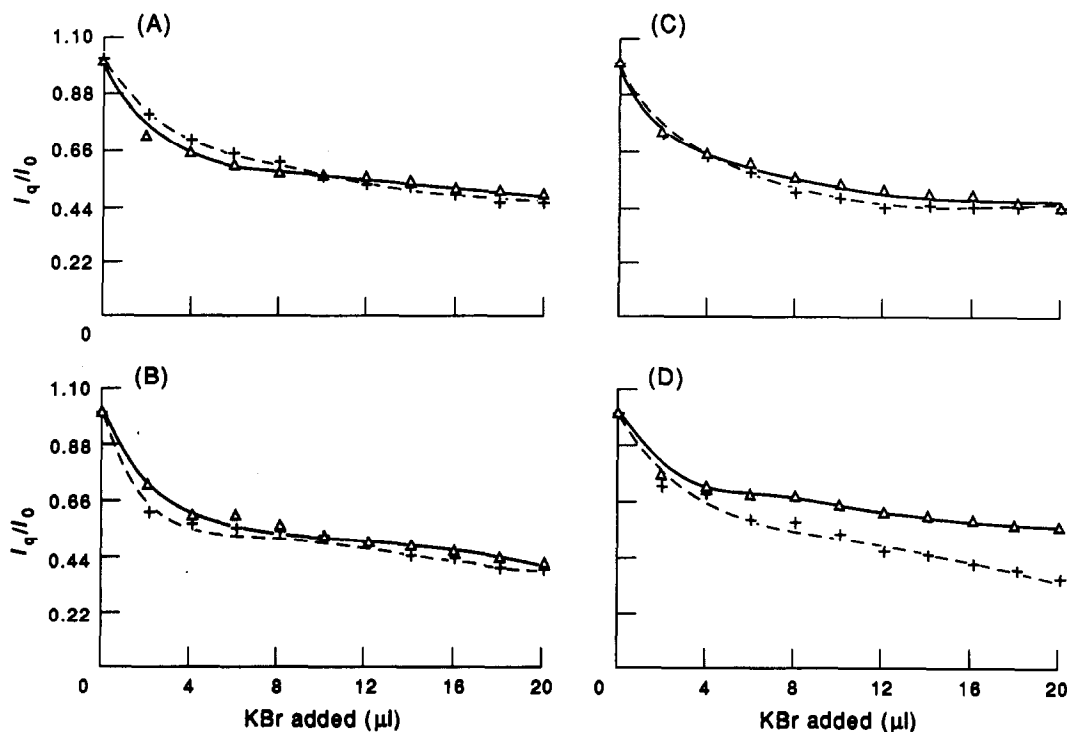


Fig. 4. Variation of the ratio of quenched to unquenched fluorescence intensity (I_q/I_0) in detergent solutions with added ($0.01 M$) KBr with (—) and without (---) cholesterol present. (A) No detergent; (B) $1 \times 10^{-3} M$ CTAB; (C) $1 \times 10^{-4} M$ SLS; (D) $5 \times 10^{-6} M$ Brij 35.

aggregates with dissolved cholesterol as nucleus. In the case of SLS it can be concluded from both the I_1/I_3 ratio data and the quenching measurements that such nucleation takes place to a significant extent. Brij 35 presents an interesting case since the I_1/I_3 ratio measurements suggest no nucleated premicellar aggregation, but the quenching measurements indicate strong protection. This apparent dichotomy may be ascribed to the nature of the Brij molecule. It consists of two relatively long linked chains: one is a hydrocarbon (the "dry" portion), and the other a polyoxyethylene ether (the "wet" portion). It has been reported that the latter is distended with water even in Brij micelles.¹⁹ A loose premicellar association between Brij 35 and dissolved cholesterol can provide a protective environment for pyrene with regard to bromide, especially for dynamic (collisional) quenching. If the probe is close to the polar portion of the detergent moiety, its I_1/I_3 ratio may not be significantly lowered.

Energy transfer

Energy transfer from TX-405 to pyrene has been shown to occur in micellar solutions of the detergent.¹⁹ The phenyl group of TX-405 is excited at 292 nm, and the characteristic pyrene emission at 373 nm is monitored. Most of the observed emission is due to energy transfer, and only a small fraction is caused by direct excitation (and this can be effectively eliminated by spectral subtraction of the emission from pyrene excited at 292 nm).

The I_1/I_3 ratio can again be used to monitor the polarity of the microenvironments of the sensitized fluorophore. In this case emission is observed only from pyrene molecules that are located sufficiently close to the aromatic center of TX-405 to allow for energy transfer. Fluorescence was observed from sensitized pyrene in premicellar solutions of both TX-405 alone and TX-405 with cholesterol. Figure 5 shows that the I_1/I_3 ratio in the latter case was higher up to a detergent concentration of about $2.9 \times 10^{-4} M$, at which the ratios became the same as those corresponding to the cmc.

To interpret these results it should first be noted that excitation energy transfer takes place in premicellar TX-405, as reported in an earlier communication from this laboratory.¹ The presence of cholesterol appears to create a more polar environment for pyrene associated with these aggregates. It may be postulated that this is due to the size of the nucleated aggregates and

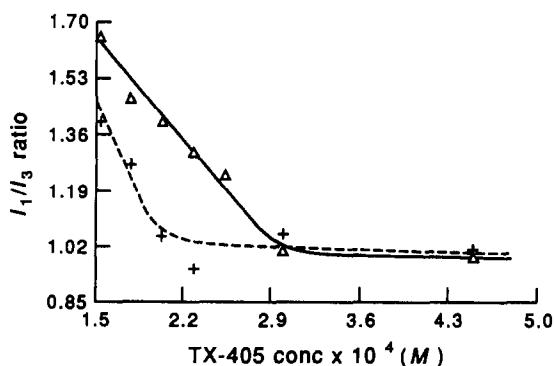


Fig. 5. Variation of I_1/I_3 ratio of sensitized pyrene with TX-405 concentration, with (—) and without (---) cholesterol present.

their accessibility to water compared to the self-assembling ones. In order to make sensitization feasible, the pyrene must be located in a similar position relative to the detergent phenyl group, in both types of aggregates. This rules out greater proximity of the polyoxyethylene ether portion of the TX-405 agglomerate as the cause of the higher I_1/I_3 ratio. Detergent aggregation around a cholesterol molecule as nucleus may, however, form a larger, more open structure, with a greater amount of associated water. Thus the pyrene experiences a more polar environment, as reflected in an increase in the I_1/I_3 ratio. When the cmc is reached, the aggregate contracts while forming the micelle, squeezing out the water and reducing the polarity around the pyrene probe. The I_1/I_3 ratios in the two types of aggregate therefore become the same at the cmc, as shown by the convergence of the plots in Fig. 5.

CONCLUSIONS

While it may be expected that detergents attach themselves to hydrophobic species in aqueous solution in the process of solubilizing them, the fluorescence data presented here indicate that this type of nucleated premicellization occurs to varying degrees. In some cases it provides a hydrophobic environment for the probe at very low detergent concentrations. However, the nucleated aggregates have a relatively open structure, probably with detergent chains somewhat separated around a central cholesterol core, with water penetrating between them. The formation of premicellar aggregates appears to be generally promoted by the presence of a nucleating species.

REFERENCES

1. T. T. Ndou and R. Von Wandruszka, *J. Lumin.*, 1990, **46**, 33.
2. M. E. Díaz García and A. Sanz-Medel, *Talanta*, 1986, **33**, 255.
3. T. T. Ndou and R. Von Wandruszka, *Anal. Lett.*, 1988, **21**, 2091.
4. A. Nakajima, *Bull. Chem. Soc. Japan*, 1971, **44**, 3272.
5. *Idem*, *J. Lumin.*, 1974, **8**, 266.
6. *Idem*, *Spectrochim. Acta*, 1974, **30A**, 860.
7. K. Kalyanasundaram and J. K. Thomas, *J. Am. Chem. Soc.*, 1977, **99**, 2039.
8. R. Waris, W. E. Acree, Jr. and K. W. Street, Jr., *Analyst*, 1988, **113**, 1465.
9. T. T. Ndou and R. Von Wandruszka, *Abstract*, Idaho Academy of Science Annual Meeting, 1989.
10. J. C. Dederen, M. van der Auweraer and F. C. de Schryver, *Chem. Phys. Lett.*, 1979, **68**, 451.
11. H. D. Burrows, S. J. Formosinho, M. Fernanda and J. R. Paiva, *J. Photochem.*, 1980, **12**, 285.
12. F. Grieser and R. Tausch-Treml, *J. Am. Chem. Soc.*, 1980, **102**, 7258.
13. T. Nakamura, A. Kira and M. Imanura, *J. Phys. Chem.*, 1982, **86**, 3359.
14. H. D. Burrows, S. J. Formosinho, M. F. J. R. Paiva and J. Rasburn, *J. Chem. Soc. Faraday Trans.*, 1980, **76**, 685.
15. W. L. Hinze, H. N. Singh, Y. Baba and N. G. Harvey, *Trends Anal. Chem.*, 1984, **3**, 193.
16. G. Rothenberger, P. P. Infelta and M. Grätzel, *J. Phys. Chem.*, 1979, **83**, 1871.
17. K. Kalyanasundaram and J. K. Thomas, in *Micellization, Solubilization and Microemulsions*, K. L. Mittal, (ed.), p. 569. Vol. 2, Plenum Press, New York, 1977.
18. M. Almgren, *Photochem. Photobiol.*, 1972, **15**, 297.
19. T. T. Ndou and R. Von Wandruszka, *ibid.*, 1989, **50**, 547.

PRECONCENTRATION OF NICKEL AND COBALT ON ALGAE AND DETERMINATION BY SLURRY GRAPHITE-FURNACE ATOMIC-ABSORPTION SPECTROMETRY

MO SHENGJUN* and JAMES A. HOLCOMBE†

Department of Chemistry and Biochemistry, The University of Texas at Austin, Austin, TX 78712, U.S.A.

(Received 28 August 1990. Revised 20 November 1990. Accepted 10 December 1990)

Summary—Unicellular green algae have been utilized to preconcentrate Ni²⁺ and Co²⁺ ions from sea-water and riverine water samples. Studies have shown that rinsing the algae with 0.12M hydrochloric acid improves the adsorption of nickel and cobalt, and the optimum range of pH of extraction is wide. The maximum extraction efficiencies were 84 and 73% for Ni and Co, respectively, at ng/ml levels. The sea-water matrix and relatively small amounts of many impurities reduce the adsorption efficiency for both nickel and cobalt. The preconcentration is achieved by mixing 6 mg of algae with 50–100 ml of sample, and subsequently isolating the algae by centrifugation. The pellet of algae is then resuspended in 1 ml of 0.08M nitric acid, and analyzed as a slurry by graphite-furnace atomic-absorption spectrometry. The values found for nickel and cobalt in riverine (SLRS-1) and sea-water (CASS-1) standard reference materials are within the limits of certification.

Graphite-furnace atomic-absorption spectrometry (GFAAS) is in routine use for the determination of ultratrace amounts of nickel and cobalt. However, considerable difficulty can be encountered in the direct determination of nickel and cobalt in complex samples owing to matrix interferences, and because the concentrations are at or below the limits of detection. Chelation and solvent extraction or immobilized-ligand separation combined with GFAAS have been used to determine nickel and cobalt in such samples, but poor selectivity and time-consuming procedures are inherent in many of these approaches.

Biological organisms have the potential ability to adsorb selectively specific elements without preconcentrating the matrix.^{1–6} Unicellular green algae have been used successfully to separate and preconcentrate copper from a sea-water sample,⁶ but no reports consider the preconcentration of nickel and cobalt by algae. Mahan *et al.*¹ have studied the ability of three unicellular algae strains to adsorb thirteen elements, including nickel and cobalt. The possibility of preconcentrating nickel and cobalt from dilute

solutions was indicated. However, the concentrations in this study were in the µg/ml range and no attempt was made to preconcentrate the metals from complex samples.¹ In the present work, the conditions for preconcentration of nickel and cobalt by the algae have been studied and the method has been applied to the analysis of riverine and sea-water samples. The results show that when the algae are not washed with 0.12M hydrochloric acid, the recovery is critically dependent on the pH of the solutions, especially for cobalt extraction. However, if the algae are washed initially in 0.12M hydrochloric acid, adsorption of nickel and cobalt by the algae is nearly constant between pH 6 and pH 9, with extraction efficiencies for Ni and Co of 84 and 73%, respectively. When the concentration of the metal ion is between 1 and 16 ng/ml, the uptake efficiency on the algae is independent of the concentration of metal. The sea-water matrix and relatively small amounts of many impurities reduce the adsorption efficiency. Therefore, for complex samples it was necessary either to prepare a calibration curve after determining the extraction efficiencies from matrix-matched standards, or to use standard-addition methods with the unknown samples.

Although there have been several studies of metal uptake by algae, little is known regarding the binding mechanism. Christ *et al.*⁷ have

*On leave from the Department of Chemistry, South China Normal University, Guangzhou, People's Republic of China.

†Author for correspondence.

considered the functional groups that may be available for ion-exchange or metal binding. These included amine and carboxyl groups from both amino-acids and polysaccharides, although no experimental verification was made. Majidi and co-workers⁸ have presented direct evidence of binding of Cd^{2+} by using ^{113}Cd NMR as a probe, and concluded that the site for cadmium binding was probably a carboxyl group. Mahan and co-workers^{1,9} have shown through Langmuir plots that multiple binding sites probably exist. Similar non-Langmuirian adsorption isotherms can be inferred from similar studies by other researchers.

In short, there have been few studies that elucidate the binding mechanism or the chemical nature of the exterior cell wall. Certainly, a polysaccharide structure is known to exist, but there are also several protein groups. Of course, it is not known which of these might be present on the surface under the conditions in which the algae are grown.

EXPERIMENTAL

Preparation of algae

The algae used in this study were a form of unicellular green *Chlorella*. Preparation and cultivation of the algae have been described previously.⁶ Before use, 6 mg of algae were added to 10 ml of 0.12M hydrochloric acid (Mallinckrodt, analytical reagent grade), then the mixture was agitated, centrifuged, and the supernatant decanted and discarded. The pellet of algae was then washed with 5 ml of demineralized water and centrifuged again. After discard of the rinse solution, the algae were ready for use.

Apparatus

All experiments utilized an AA-875 spectrophotometer equipped with a GTA-95 graphite-furnace atomizer (Varian Techtron). The operational conditions and temperature programs for the determination of nickel and cobalt are listed in Table 1. The analytical wavelengths

used for nickel and cobalt were 232.0 and 240.7 nm, respectively. The spectral bandpass of the monochromator was 0.2 nm. All studies were performed with deuterium-lamp background correction and wall atomization, with a 10- μl aliquot of the slurry suspension or supernatant. All data were recorded as peak areas. The algae did not represent a complex matrix, even though the original solution composition might have contained a high concentration of dissolved salts. As a result, simple wall atomization was adequate for matrix-free analysis and no platform was employed.

Procedure

The sample was prepared by adding 6 mg of algae to 10 ml of a solution containing nickel or cobalt. The pH of each solution was adjusted to between 6 and 8 by dropwise addition of hydrochloric acid or sodium hydroxide solution. The mixture was agitated for 20 min and centrifuged. The supernatant was decanted and the pellet of algae was resuspended in 2 ml of 0.08M nitric acid. This slurry was then transferred to an autosampler sampling vial for analysis. Three replicates were run for each experiment, and a distilled water blank was run through the extraction and analysis for all experiments. When a significant blank value was detected, it was subtracted from the corresponding sample signal. Typical blank values are shown later in the paper.

After the algae had been washed with hydrochloric acid, the procedure required about 40 min for the preconcentration of six samples. All reported extraction efficiencies are based on concentrations derived from calibration graphs prepared for simple aqueous cobalt and nickel standards in 0.08M nitric acid.

RESULTS AND DISCUSSION

Dependence of adsorption on pH

Nickel and cobalt were present as trace minerals in the growth medium and might be

Table 1. Furnace operating conditions

Step No.	Temperature, °C	Ramp time, sec	Hold time, sec	Argon flow, l./min	Read
1	75	5		3	
2	90	40		3	
3	130	10	40	3	
4	1400	10	40	3	
5	1400		5	0	
6	2400	1.1	3	0	*
7	2400		3	3	

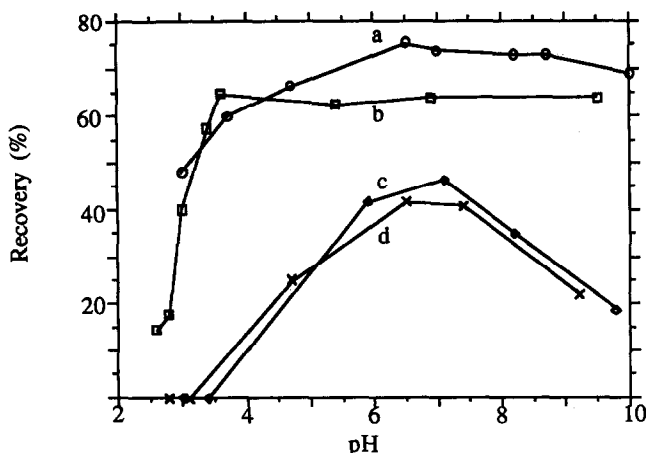


Fig. 1. The effect of pH on adsorption of cobalt by algae. Before use, the algae were either washed in $0.12M$ hydrochloric acid (curves a, b) or not washed (c, d). Both $\text{Co(NO}_3)_2$ (b, d) and CoCl_2 (a, c) were tested in the analytical solution. The cobalt concentration was 5 ng/ml for all starting solutions, and all final suspensions were $0.08M$ in nitric acid.

contained within the intercellular material or adsorbed on the cell wall. In an attempt to minimize the blank, the algae were washed in dilute acid ($0.12M$ hydrochloric acid). In previous studies with copper, a difference in the metal uptake efficiency had been found to occur as a result of an acid wash.⁶ Figures 1 and 2 show similar effects for nickel and cobalt and also display the uptake efficiencies as a function of solution pH.

The mechanism of removal of metal by the acid wash could be as simple as a displacement process at ion-exchange sites on the surface, or as complicated as a partial denaturation of complex proteins that bind with these metals.

In the two figures, curves a and b denote the algae that were washed with $0.12M$ hydrochloric acid; curves c and d represent the algae that were not washed. Both NiCl_2 and CoCl_2 (curves a and c) and $\text{Ni(NO}_3)_2$ and $\text{Co(NO}_3)_2$ (curves b and d) were tested in the analytical solutions. The pH was adjusted by dropwise addition of sodium hydroxide or acid. When acid was added, either hydrochloric or nitric acid was used, depending on the anion of the analyte salt being studied. Nickel and cobalt concentrations were 10 and 5 ng/ml , respectively, for these test solutions. The final biomass pellet was suspended in $2.0 \pm 0.1 \text{ ml}$ of $0.08M$ nitric acid.

Figures 1 and 2 clearly demonstrate the importance of the preliminary wash with hydro-

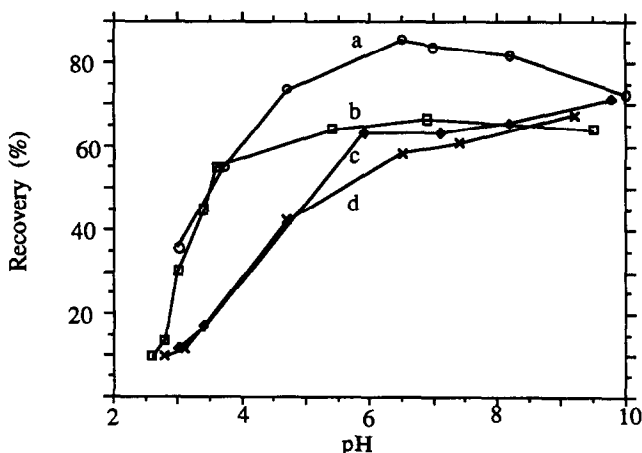


Fig. 2. The effect of pH on adsorption of nickel by algae. Before use, algae were either washed in $0.12M$ hydrochloric acid (curves a, b) or not washed (c, d). Both $\text{Ni(NO}_3)_2$ (b, d) and CoCl_2 (a, c) were tested in the analytical solution. The nickel concentration was 10 ng/ml for all starting solutions, and all final suspensions were $0.08M$ in nitric acid.

Table 2. The effect of various salts common to a sea-water matrix on adsorption of nickel by algae*

Matrix and concentration, mg/ml	Concentration added, ng/ml	Concentration found, ng/ml	Recovery, %	Relative change in recovery†, %	
No matrix	10.0	8.40 ± 0.39	84.0 ± 3.9	0.0	
NaCl	30	16.0	9.50 ± 0.46	59.4 ± 2.9	-29.3
	10	10.0	6.37 ± 0.05	63.7 ± 0.5	-24.2
	5	10.0	7.43 ± 0.42	74.3 ± 4.2	-11.6
	1	10.0	8.12 ± 0.45	81.2 ± 4.5	-3.3
	0.5	10.0	8.44 ± 0.13	84.4 ± 1.3	+0.5
KCl	1	16.6	10.3 ± 0.4	64.4 ± 2.5	-23.3
	0.5	16.0	11.6 ± 1.5	72.5 ± 9.4	-13.7
Ca(NO ₃) ₂	2	16.0	10.2 ± 0.2	63.8 ± 1.3	-24.0
	0.5	16.0	11.8 ± 1.2	73.8 ± 7.5	-12.1
MgCl ₂	6	16.0	12.6 ± 0.2	78.8 ± 1.3	-6.2
	1	16.0	12.7 ± 0.3	79.4 ± 1.9	-5.5
NaCl‡	10	16.0	11.9 ± 0.8	74.4 ± 5.0	-11.4
KCl	0.5				
Ca(NO ₃) ₂	0.5				
MgCl ₂	1				
NaCl‡	30	16.0	11.9 ± 0.2	74.4 ± 1.3	-11.4
KCl	1				
Ca(NO ₃) ₂	2				
MgCl ₂	6				

*Approximate sea-water concentrations of NaCl, KCl, Ca(NO₃)₂ and MgCl₂ are 26.7, 0.72, 1.64 and 5.34 mg/ml.

†Relative to the recovery in the absence of added matrix.

‡Composite matrix.

chloric acid. When the algae were not washed with acid, the efficiency of adsorption showed a stronger dependence on pH. Figure 1 shows that adsorption of cobalt by the unwashed algae increases gradually up to pH 7, then decreases gradually. However, nickel adsorption by the unwashed algae increases continuously with pH (Fig. 2, curves c and d). After the acid wash, the efficiency of adsorption is relatively constant between pH 6 and 9.

The data also show that the acid wash especially improves the efficiency of adsorption when the chlorides of the analytes are present. The maximum extraction efficiencies are 84.0% for NiCl₂, 66.4% for Ni(NO₃)₂, 73.0% for CoCl₂, and 64.8% for Co(NO₃)₂, in contrast to 65.6%, 60.8% and 46.5%, 41.6%, respectively, for samples without acid washing. These results are similar to those reported previously for Cu.⁶

Effect of sea-water matrix

The data in Tables 2 and 3 show that adsorption of nickel and cobalt, in contrast to that of lead and copper,^{6,10} is more sensitive to the presence of concomitants in the solution. However, the adsorption appears to be less affected by the common alkali-metal and alkaline-earth metal salts than indicated by previous reports for zinc and cadmium.^{2,10} Zinc adsorption was shown to be negligible in the presence of 0.2M

sodium chloride or magnesium nitrate in the solution,¹⁰ and cadmium adsorption was dramatically decreased by the sea-water matrix so that the attempted preconcentration of cadmium from sea-water was not successful.² Table 2 shows that even with a 2×10^6 -fold ratio of sodium chloride present, a 59% recovery of nickel was still obtained. A 4×10^6 -fold ratio of the same salt yielded a 56% recovery for cobalt, which is 23% less than that obtained in the absence of a matrix. Though it is thought that this might be due to competitive binding of matrix cations at the algae sites, the data do not preclude possible influence by complexation with the matrix anion, e.g., Cl⁻ or NO₃⁻. It is also interesting that the interference from mixed matrices was not significantly more than that observed when a single matrix salt was used, which confirms that the interference is not a simple cumulative effect.

The interference by the sea-water matrix on nickel adsorption was generally less than that for cobalt. For example, when the concentration of potassium chloride was 1 and 0.5 mg/ml, the relative decrease in the nickel adsorption was 2 and 14% whereas the corresponding decrease for cobalt was 30 and 21%. Concentrations of sodium chloride less than 1 mg/ml gave no effect on nickel adsorption by the algae, but the effect on cobalt adsorption was obvious.

Table 3. The effect of various salts common to a sea-water matrix on adsorption of cobalt by algae

Matrix and concentration, mg/ml	Concentration added, ng/ml	Concentration found, ng/ml	Recovery, %	Relative change in recovery*, %
No matrix	5.0	3.65 ± 0.14	73.0 ± 0.2	0.0
NaCl 30	8.0	4.49 ± 0.29	56.1 ± 3.6	-23.2
10	5.0	2.89 ± 0.35	57.8 ± 7.0	-20.8
5	5.0	2.82 ± 0.20	56.4 ± 4.0	-22.7
1	5.0	3.30 ± 0.17	66.0 ± 3.4	-9.6
0.5	5.0	3.32 ± 0.16	66.4 ± 3.2	-9.0
KCl 1	8.0	4.09 ± 0.09	51.1 ± 1.1	-30.0
0.5	8.0	4.63 ± 0.54	57.9 ± 6.7	-20.7
Ca(NO ₃) ₂ 2	8.0	4.16 ± 0.42	52.0 ± 5.3	-28.8
0.5	8.0	3.59 ± 0.40	44.9 ± 5.0	-38.5
MgCl ₂ 6	8.0	4.84 ± 0.48	60.5 ± 6.0	-17.1
1	8.0	4.06 ± 0.44	50.8 ± 5.5	-30.4
NaCl† 10	8.0	4.30 ± 0.86	53.8 ± 10.8	-26.3
KCl 0.5				
Ca(NO ₃) ₂ 0.5				
MgCl ₂ 1				
NaCl† 30	8.0	4.95 ± 0.07	61.8 ± 0.09	-15.3
KCl 1				
Ca(NO ₃) ₂ 2				
MgCl ₂				

*Relative to the recovery in the absence of added matrix.

†Composite matrix.

The effect of combinations of agents

The effects of two organic ligands and one ionic surfactant on nickel and cobalt adsorption were considered. The adsorption was inhibited entirely by the presence of either 0.2% sodium citrate or 0.1% ethylenediaminetetra-acetic acid (EDTA). Dodecyl sodium sulfate (0.01%) decreased the nickel and cobalt adsorption by 38 and 30%, respectively, relative to that observed for simple aqueous solutions; this behavior is unlike the results obtained previously for copper, where little effect was observed.⁶ The stability of the analyte complex may play an important role in some instances, since the EDTA complexes are very stable: Ni-EDTA ($K_f = 4.16 \times 10^{18}$), Co-EDTA ($K_f = 2.04 \times 10^{16}$). The citrates are less stable, with typical K_f values of ca. 10^5 .

The effects of impurities

Several elements which may be capable of displacing nickel or cobalt (by competitive binding at the algae adsorption sites) were also considered. They are Pb²⁺, Cu²⁺, Cd²⁺, Mn²⁺ and V³⁺. The results shown in Tables 4 and 5 indicate that the effects on the adsorption are variable and complicated. For example, adsorption of Pb²⁺ by algae was shown previously to be stronger than adsorption of V³⁺,¹ but the impact of Pb²⁺ on Ni²⁺ and Co²⁺ adsorption is less than that of V³⁺. From previous studies, the

strength of Cu²⁺ and Mn²⁺ adsorption by the algae should be between that for Pb²⁺ and V³⁺, but the effect of 1000 ng/ml Cu²⁺ and Mn²⁺ on nickel and cobalt adsorption is larger than that of the other elements tested.

Explanation of the observed effects of these sets of elements at different concentrations is complicated. The situation for each element appears to be different. For example, the effect of 100 ng/ml manganese appears to be negligible, but a lower concentration of Mn (10 ng/ml) measurably reduces both nickel and cobalt adsorption. The reason for differences in the effects of 10–1000 ng/ml cadmium on cobalt adsorption is not obvious. The situation is even more complicated, because of the presence of other trace elements in the sample solution. With the exception of Pb²⁺ as a concomitant, the general effect of added metal salts was similar for both nickel and cobalt.

Concentration by uptake of nickel and cobalt

A series of nickel and cobalt solutions (1–16 ng/ml) was prepared, and a 10-ml aliquot of each was used to prepare 1 ml of preconcentrated slurry. The concentrations of nickel and cobalt in these concentrates were then determined from a working curve prepared from aqueous standards. In these experiments the extraction efficiencies for nickel and cobalt were $84 \pm 5\%$ and $73 \pm 5\%$, respectively. There

Table 4. The effect of added solution impurities on adsorption of nickel by algae

Impurities and concentration, ng/ml	Concentration added, ng/ml	Concentration found, ng/ml	Recovery, %	Relative change in recovery, %
None	10.0	8.40 ± 0.39	84.0 ± 3.9	0.0
Pb ²⁺ (as PbCl ₂)				
1000	16.0	11.1 ± 0.2	69.4 ± 1.3	-17.4
250	16.0	10.3 ± 0.9	64.4 ± 5.6	-23.3
100	16.0	12.3 ± 1.1	76.9 ± 6.9	-8.9
10	16.0	12.4 ± 0.8	77.5 ± 5.0	-8.1
Cd ²⁺ [as Cd(NO ₃) ₂]				
1000	16.0	9.96 ± 0.28	62.2 ± 1.8	-25.9
250	16.0	8.82 ± 0.78	51.4 ± 4.9	-39.5
100	16.0	9.44 ± 1.44	59.0 ± 9.0	-29.8
10	16.0	9.04 ± 0.64	56.5 ± 4.0	-32.7
Cu ²⁺ (as CuCl ₂)				
1000	16.0	1.24 ± 0.28	7.8 ± 1.8	-90.7
250	16.0	12.0 ± 0.4	75.0 ± 2.5	-10.7
100	16.0	10.6 ± 0.6	66.3 ± 3.8	-21.1
10	16.0	7.4 ± 0.3	46.3 ± 1.9	-44.9
Mn ²⁺ (as MnCl ₂)				
1000	16.0	0.92 ± 0.04	5.8 ± 0.04	-93.1
250	16.0	4.16 ± 0.72	26.0 ± 4.5	-69.0
100	16.0	13.1 ± 0.1	81.9 ± 0.6	-2.56
10	16.0	9.74 ± 0.82	60.9 ± 5.1	-27.5
V ³⁺ [as V(NO ₃) ₃]				
1000	16.0	8.16 ± 0.80	51.0 ± 5.0	-39.3
250	16.0	7.88 ± 0.12	49.2 ± 1.3	-41.4
100	16.0	9.32 ± 0.44	58.2 ± 2.8	-30.7
10	16.0	12.0 ± 0.7	75.0 ± 4.4	-10.7

Table 5. The effect of added solution impurities on adsorption of cobalt by algae

Impurities and concentration, ng/ml	Concentration added, ng/ml	Concentration found, ng/ml	Recovery, %	Relative change in recovery, %
None	5.0	3.65 ± 0.14	73.0 ± 0.3	0.0
Pb ²⁺ (as PbCl ₂)				
1000	8.0	4.38 ± 0.16	54.8 ± 2.0	-22.2
250	8.0	3.80 ± 0.24	47.5 ± 3.0	-34.9
100	8.0	4.32 ± 0.08	54.0 ± 1.0	-26.0
10	8.0	5.00 ± 0.28	62.5 ± 3.5	-14.4
Cd ²⁺ [as Cd(NO ₃) ₂]				
1000	8.0	4.02 ± 0.10	50.2 ± 1.2	-31.2
250	8.0	3.48 ± 0.08	43.5	-40.1
100	8.0	3.82 ± 0.30	47.8 ± 3.8	-34.5
10	8.0	3.70 ± 1.0	46.2 ± 1.2	-36.7
Cu ²⁺ (as CuCl ₂)				
1000	8.0	0.64 ± 0.05	8.0 ± 0.6	-89.0
250	8.0	5.02 ± 0.12	62.8 ± 1.5	-14.0
100	8.0	4.51 ± 0.27	56.4 ± 3.4	-22.7
10	8.0	3.68 ± 0.08	46.0 ± 1.0	-37.0
Mn ²⁺ (as MnCl ₂)				
1000	8.0	1.12 ± 0.32	14.0 ± 4.0	-80.8
250	8.0	2.28 ± 0.36	28.5 ± 4.5	-61.0
100	8.0	5.68	71.0 ± 7.0	-2.8
10	8.0	4.28 ± 0.64	53.5 ± 8.0	-26.7
V ³⁺ [as V(NO ₃) ₃]				
1000	8.0	3.70 ± 0.06	46.2 ± 0.8	-36.7
250	8.0	3.48 ± 0.12	43.5 ± 1.5	-40.4
100	8.0	3.88 ± 0.08	48.5 ± 1.0	-33.6
10	8.0	4.82 ± 0.18	60.2 ± 2.2	-17.5

Table 6. The effect of sample volume on adsorption of nickel and cobalt by algae

Element	Initial sample volume, ml	Final slurry volume, ml	Concentration factor	Recovery, %	Average, %
Ni	10	2	5	84.0	82.8
	50	1	50	78.7	
	100	1	100	85.6	
Co	10	2	5	73.0	72.3
	50	1	50	70.4	
	100	1	100	73.4	

does not appear to be any consistent trend with changing concentration; the variations probably reflect uncertainty in the method. The results show that adsorption of nickel and cobalt on the algae does not depend on their initial solution concentrations.

Preconcentration factor and sampling volume

One of the potential advantages of extracting nickel and cobalt from sample solutions is the improvement of analytical sensitivity as well as reduction of interference by the original sample matrix. Although the magnitude of the preconcentration is independent of the nickel and cobalt concentrations in the original sample, it remains to be determined whether some variation in extraction efficiency is caused by the preconcentration factor, *i.e.*, the ratio of initial to final volume.

To evaluate the effect of sample volume on extraction efficiency, 6 mg of algae were added to 20, 50 and 100 ml of solution containing a total of 160 ng of nickel and 80 ng of cobalt. The solutions were preconcentrated to a final volume of either 1.0 or 2.0 ml. The extraction efficiency results given in Table 7 represent a range of preconcentration factors from 5 to 100. The results show that with different sample volumes and different preconcentration factors, the recoveries of nickel and cobalt remain nearly constant, with no obvious dependence on the initial sample volume.

Riverine and sea-water analysis

To study the capability of these algae for

Table 7. Concentration of nickel and cobalt in the riverine and sea-water reference samples

Sample	Element determined	Values found, ng/ml	Certified values, ng/ml
CASS-1	Ni	0.21, 0.27*	0.290 ± 0.031
	Co	0.026, 0.030*	0.023 ± 0.004
SLRS-1	Ni	0.94, 1.02†	1.07 ± 0.06
	Co	0.038, 0.042†	0.043 ± 0.010

*Calibration graph method.

†Standard-addition method necessary.

preconcentrating nickel and cobalt in environmental samples, two standard reference solutions were preconcentrated and analyzed: near-shore sea-water (CASS-1) and riverine water (SLRS-1) (National Research Council of Canada). The algae were acid-washed in batches by the procedure described previously. Before preconcentration, the samples were neutralized by dropwise addition of sodium hydroxide solution to raise the pH to 7 ± 1 . The sample volumes were 100 ml for CASS-1 and 50 ml for SLRS-1, so the preconcentration factors were 100 and 50, respectively, with a final solution volume of 1.0 ml. A blank solution was carried through the same procedure and the signal obtained was subtracted from the corresponding sample signal. Typical metal concentrations in the algae suspensions and a 100-ml blank solution were 3.7 ± 0.2 ng/ml nickel and 3.3 ± 0.5 ng/ml cobalt. The source of the metal is not the algae but most likely impurities in the sodium hydroxide.

The calibration graph method was used to analyze the sea-water sample. The method of standard additions was used for analysis of SLRS-1 to compensate for sample-dependent variations in extraction efficiency rather than to correct for interferences in the GFAA analysis. The concentrations in the riverine water were obtained from the value found by the standard addition method, by dividing it by the preconcentration factor. Table 7 shows the results obtained for the SLRS-1 riverine water, and these were in good agreement with the certified values. The concentrations found for nickel and cobalt in SLRS-1 were both low if a simple calibration curve prepared from aqueous standards was used, and a previously determined extraction efficiency was assumed.

In sea-water the main matrix components are sodium, potassium, magnesium and calcium chlorides. The uptake efficiency (75 and 62% for nickel and cobalt) in the presence of the synthetic sea-water matrix was used, in conjunction with a calibration graph prepared with aqueous

standards. This approach is simpler, faster and conserves sample. The concentration read from the calibration graph was divided by the preconcentration factor and the extraction efficiency to yield the results listed in Table 7, which are within the limits of the certified values. The standard-addition method was also tried for the sea-water sample, but only one sample was used owing to a shortage of the reference material. The results were 0.26 ng/ml for nickel and 0.022 mg/ml for cobalt.

CONCLUSION

This study has demonstrated that unicellular green *Chlorella* algae can be used to separate and preconcentrate nickel and cobalt from sea-water and riverine water samples. The extraction efficiencies for nickel and cobalt from aqueous solutions are 84 and 73%, respectively, and appear relatively insensitive to solution pH in the range 6–9 (if the algae have been washed with 0.12M hydrochloric acid) and to the ratio of solution volume to mass of algae, at least in the range 0.8–16 ml per mg. However,

the extraction efficiency appears sensitive to the presence of high concentrations of the alkali and alkaline-earth metal salts, and to low concentrations of many accompanying impurities.

REFERENCES

1. C. A. Mahan, V. Majidi and J. A. Holcombe, *Anal. Chem.*, 1989, **61**, 624.
2. V. Majidi and J. A. Holcombe, *J. Anal. At. Spectrom.*, 1989, **4**, 439.
3. V. Majidi and J. A. Holcombe, *Spectrochim. Acta*, 1988, **43B**, 1423.
4. A. Nakajima and T. Sakaguchi, *Appl. Microbiol. Biotechnol.*, 1986, **24**, 59.
5. T. Sakaguchi, T. Tsuji, A. Makajima and T. Horikoshi, *J. Appl. Microbiol. Biotechnol.*, 1979, **41**, 207.
6. M. Shengjun and J. A. Holcombe, *Anal. Chem.*, 1990, **62**, 1994.
7. R. H. Christ, K. Oberholser, N. Shank and M. Nguyen, *Environ. Sci. Technol.*, 1981, **15**, 1212.
8. V. Majidi, D. A. Laude, Jr. and J. A. Holcombe, *Environ. Sci. Technol.*, 1990, **24**, 1309.
9. V. Majidi, C. Mahan and J. A. Holcombe, 'Biological Organisms for Preconcentration and Speciation at the Sub-ppb Level,' presented at 1989 Pittsburgh Conference and Exposition, Atlanta, GA, 6–10 March 1989.
10. J. Ferguson and B. Bubela, *Chem. Geology*, 1974, **13**, 163.

INDIRECT SPECTROPHOTOMETRIC DETERMINATION OF TRACE CYANIDE WITH CATIONIC PORPHYRINS

HAJIME ISHII* and KATSUNORI KOHATA

Chemical Research Institute of Non-Aqueous Solutions, Tohoku University, Katahira, Aoba-ku, Sendai, 980 Japan

(Received 13 July 1990. Revised 25 October 1990. Accepted 20 November 1990)

Summary—Three highly sensitive methods for the determination of cyanide have been developed, based on the fact that the complexation of silver ions with three cationic porphyrins, 5,10,15,20-tetrakis(1-methyl-2-pyridinio)porphine [T(2-MPy)P], 5,10,15,20-tetrakis(1-methyl-3-pyridinio)porphine [T(3-MPy)P] and 5,10,15,20-tetrakis(1-methyl-4-pyridinio)porphine [T(4-MPy)P], in alkaline media is inhibited by cyanide and the decrease in absorbance of the silver(II) complex is proportional to the cyanide concentration. Sensitivities of the procedures developed are 0.133, 0.126 and 0.234 ng/cm², respectively for an absorbance of 0.001. Cadmium(II), copper(II), mercury(II), zinc(II), iodide and sulfide interfere with the cyanide determination. One of the proposed methods was applied to the determination of cyanide in waste-water samples, with satisfactory results.

It has been reported¹ that three cationic porphyrins, 5,10,15,20-tetrakis(1-methyl-2-pyridinio)porphine [T(2-MPy)P], 5,10,15,20-tetrakis(1-methyl-3-pyridinio)porphine [T(3-MPy)P] and 5,10,15,20-tetrakis(1-methyl-4-pyridinio)porphine [T(4-MPy)P], react rapidly with silver(I) at pH 9.6–12.0 to form yellow complexes which are oxidized by dissolved oxygen to the corresponding stable red silver(II) complexes within several minutes at room temperature. These complexation reactions are applicable to the spectrophotometric determination of trace amounts of silver. It was also reported that the reactions are strongly inhibited by cyanide, the decrease in absorbance of the silver(II) complexes being directly related to the cyanide concentration, which suggests the possibility of the indirect spectrophotometric determination of micro-amounts of cyanide.

In the present work, the fundamental conditions for the determination of cyanide in this way have been investigated and three highly sensitive methods for cyanide determination have been developed.

EXPERIMENTAL

Reagents

All reagents used were of analytical-reagent grade unless stated otherwise. All solutions were prepared with distilled, demineralized water.

T(2-MPy)P, *T(3-MPy)P* and *T(4-MPy)P* solutions, 1.6×10^{-4} M. Prepared by dissolving the required weight of porphyrin tosylate in water. The tosylates were synthesized and purified by a method described in the literature.^{2,3}

Standard cyanide solution, 0.5 mg/ml. Potassium cyanide (0.125 g) was dissolved in 100 ml of water and the solution was stored in a polyethylene bottle. This solution was unstable, and was therefore prepared every second day and standardized titrimetrically with silver nitrate.⁴ Working solutions were prepared just before use, by diluting this solution with water.

Standard silver(I) solution, 1.0×10^{-2} M. Prepared by dissolving 170 mg of silver nitrate (dried at 110°) in 50 ml of 0.1M nitric acid and diluting to 100 ml with water. Working solutions were prepared by dilution of this solution with water and addition of enough aqueous ammonia solution to give an ammonia concentration of 0.5M. The solutions thus obtained were stable for more than one month, when stored in amber bottles.

Lead(II) solution, 5×10^{-4} M. Prepared by dissolving 0.17 g of lead nitrate in 1 litre of water and adding sufficient nitric acid to give a pH of about 2.

Procedures

Procedure A, with T(3-MPy)P. To a known volume of sample containing up to 3.2 µg (0.12 µmole) of cyanide ion, in a 25-ml standard flask, add 1 ml of 1.9×10^{-4} M silver(I) solution

*Author for correspondence.

with ammonia concentration adjusted to 0.5*M*, a sufficient amount of 0.1*M* sodium hydroxide or 0.1*M* nitric acid to adjust the pH to about 12, and 2 ml of 1.6×10^{-4} *M* T(3-MPy)P solution. After allowing to stand for about 10 min, add 1 ml of 5×10^{-4} *M* lead(II) and 3 ml of 2*M* sodium nitrate, and dilute to the mark with water. Measure the difference in absorbance (ΔA) at 427 nm (10-mm path-length cells) between the resultant colored solution and a reagent blank solution similarly prepared.

Procedure B, with T(2-MPy)P. Prepare the colored solution as in procedure A, but adjusting the pH to about 10.6 and using 2 ml of 1.6×10^{-4} *M* T(2-MPy)P solution instead of T(3-MPy)P solution. Measure ΔA at 423.5 nm.

Procedure C, with T(4-MPy)P. Take an aliquot containing up to 5.8 μg (2.2×10^{-7} mole), of cyanide ion and prepare the colored solution as in procedure A, but adjust the pH to about 11.4 and use 2 ml of 1.6×10^{-4} *M* T(4-MPy)P solution instead of T(3-MPy)P solution. Measure ΔA at 431 nm.

RESULTS AND DISCUSSION

Absorption spectra

The complexation of silver ions with porphyrins in alkaline media is suppressed by cyanide, the decrease in absorbance of silver(II)–porphyrin complexes being proportional to the cyanide concentration. As has been reported,¹ whichever porphyrin is used, the Soret band of the silver(II)–porphyrin complex considerably overlaps that of the porphyrin itself in alkaline media, whereas the Soret band of the lead(II)–porphyrin complex is well separated from that of the porphyrin and its silver(II) complex. Hence, the absorbance of the silver(II) complex should be measured after any free porphyrin has been converted into its lead(II) complex.

Figure 1 shows the spectral change in the Soret region of the T(3-MPy)P–silver(II)–cyanide–lead(II) system when the cyanide concentration is increased. The absorbance of the silver(II)–T(3-MPy)P complex at 427 nm decreases and that of the lead(II)–T(3-MPy)P complex at 471 nm increases. The reason is that with increasing cyanide concentration, the amount of the silver(II)–T(3-MPy)P complex formed decreases, so that the amount of T(3-MPy)P available to form the complex with lead(II) increases. It can also be seen that the difference between the absorbances of a solution

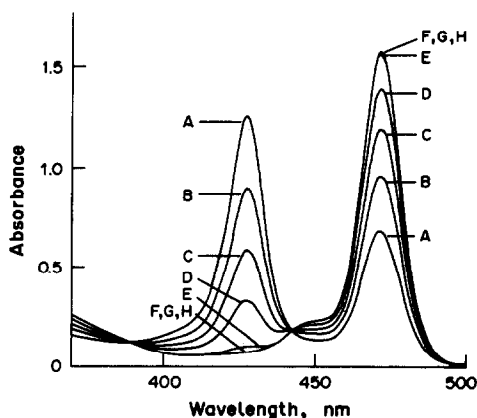


Fig. 1. Spectral change of the T(3-MPy)P–silver(II)–cyanide–lead(II) system with increasing cyanide concentration. T(3-MPy)P, 6.4×10^{-6} *M*; Ag(I), 3.0×10^{-6} *M*; Pb(II), 9.3×10^{-6} *M*; NaNO₃, 0.24*M*; pH, 12.0; reference, water. CN⁻/Ag(I)—A, 0.00; B, 0.56; C, 1.12; D, 1.68; E, 2.41; F, 3.35; G, 4.50; H, 6.50.

containing cyanide and of those containing no cyanide (and hence the sensitivity is higher) is larger at 427 nm than at 471 nm. Similar spectral changes were observed when T(2-MPy)P and T(4-MPy)P were used instead of T(3-MPy)P.

The effect of pH on the cyanide determination is shown in Fig. 2. The optimum pH and wavelength for absorbance measurements in each procedure are shown in Table 1.

Effect of ammonia concentration

Usually, to avoid interference by various ions in the determination of cyanide, hydrogen cyanide is distilled from acidified sample solution and trapped in a sodium hydroxide solution, which is then analysed.⁴ If silver ions are added to this alkaline solution, they are hydrolysed, so it is better to add the silver as its

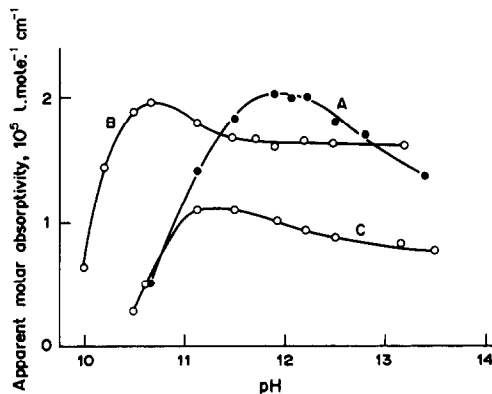


Fig. 2. Effect of pH on the cyanide determination. Wavelength (nm)—A, 427; B, 423.5; C, 431. A, B and C correspond to procedures A, B and C, respectively.

Table 1. Optimum pH values, wavelengths for absorbance measurements, calibration equations and apparent molar absorptivities (ϵ)

Procedure	Porphyrin to be used	Optimum pH	Wavelength, nm	Calibration equation	ϵ , l.mole ⁻¹ .cm ⁻¹
A	T(3-MPy)P	12.0	427	CN ⁻ (ng/ml) = 126 ΔA	2.04×10^5
B	T(2-MPy)P	10.6	423.5	CN ⁻ (ng/ml) = 133 ΔA	1.95×10^5
C	T(4-MPy)P	11.4	431	CN ⁻ (ng/ml) = 234 ΔA	1.11×10^5

ammine complex, which undergoes ligand substitution by cyanide. Figure 3 shows the effect of the ammonia concentration on this ligand substitution in the cyanide determination with T(3-MPy)P. At ammonia concentrations $<0.02M$ in the final solution ΔA decreases, presumably because hydrolysis of the silver ions increases, and at concentrations $>0.02M$ the ammonia binds the surplus silver ions more strongly and interferes with the porphyrin reaction. At a final ammonia concentration of about $0.02M$ the influence of both effects is minimal.

Effect of other variables

The effects of the concentrations of silver(I), porphyrin and lead(II) were examined. The results revealed that a constant and maximum ΔA value is obtained in all three procedures provided that more than an equimolar ratio of silver(I) to cyanide, more than 1.5-fold molar excess of the porphyrin relative to silver(I), and more than 1.5-fold molar excess of lead(II) relative to the porphyrin are added.

Under the recommended conditions, the formation of the silver(I) ammine and porphyrin complexes was instantaneous and that of the lead(II)-porphyrin complexes rapid, but formation of the stable silver(II)-porphyrin complexes took about 10 min at room temperature.

Adsorption of the porphyrins and their silver(II) complexes on the inner surface of the

glassware could be suppressed almost completely by the presence of at least $0.2M$ sodium nitrate in the final solution.

Composition of the silver(I)-cyanide complex

A computer calculation of the distribution of species in the cyanide-silver(I)-ammonia system showed that the 1:2 complex $Ag(CN)_2^-$ should be formed irrespective of the molar ratio of silver to cyanide present, and the surplus silver will be present as the $Ag(NH_3)_2^+$ complex under the conditions for the determination of cyanide. A plot of the absorbances at 427 and 471 nm, as a function of the concentration ratio of cyanide to silver (Fig. 4) confirmed this point.

Calibration graph and precision

Calibration graphs for the cyanide determination were prepared for all three procedures and gave straight lines which conformed to Beer's law. The regression equations and the apparent molar absorptivities calculated from them are summarized in Table 1. Of the methods developed, procedure A has the highest sensitivity, but procedure B is almost as sensitive.

Seven standard solutions containing 44.4 ng/ml cyanide were analysed by procedure A. The results had a relative standard deviation of 1.6%.

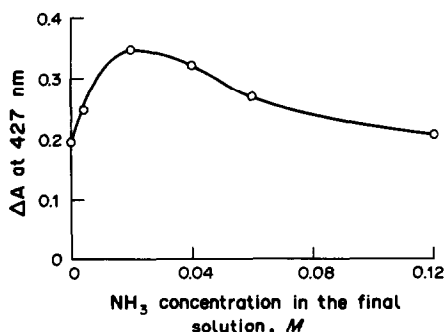


Fig. 3. Effect of the ammonia concentration in procedure A. CN⁻, 44.4 ng/ml; T(3-MPy)P, $5.1 \times 10^{-6}M$; Ag(I), $3.0 \times 10^{-6}M$; Pb(II), $9.3 \times 10^{-6}M$; NaNO₃, $0.24M$; pH, 12.0; wavelength, 427 nm.

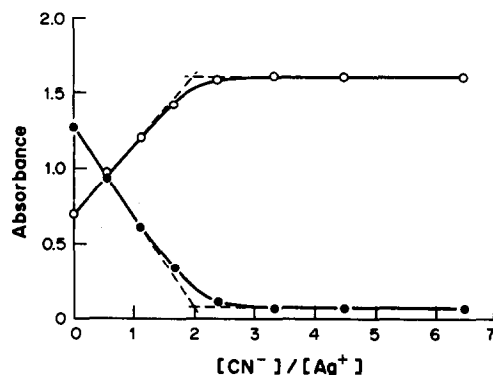


Fig. 4. Confirmation of the composition of the silver(I)-cyanide complex by the mole-ratio method. Experimental conditions as for Fig. 1. Wavelength (nm)—● 427; ○ 471.

Table 2. Tolerance limits for various ions in the determination of 38.4 ng/ml CN⁻ by procedure A with T(3-MPy)P

Ion	Tolerance limits
Cl ⁻	600 µg/ml
Br ⁻	0.6 µg/ml
I ⁻	Strong interference
SCN ⁻	4.5 µg/ml
S ²⁻	Strong interference
NO ₃ ⁻	31000 µg/ml*
SO ₄ ²⁻	48000 µg/ml*
Mg(II)	800 ng/ml
Ca(II)	280 ng/ml
Fe(III)	170 ng/ml
Cu(II)	Strong interference
Zn(II)	Strong interference
Cd(II)	Strong interference
Hg(II)	Strong interference

*Maximum tested.

Interferences

Interferences were studied by preparing solutions containing a fixed amount of cyanide and various amounts of other ions and applying the procedures developed. An error of $\pm 3\%$ in the absorbance reading was considered tolerable. Table 2 shows the influence of other ions on procedure A. Similar results were obtained with the other two porphyrins. Cadmium(II), copper(II), mercury(II), zinc(II), iodide and sulphide interfered seriously with the cyanide determination because of reaction with the porphyrin or silver(I). The tolerance limits for bromide and thiocyanate are also not high. However, as already mentioned, cyanide is usually determined after it has been separated from interfering ions by distillation, so these interferences should not arise.

Table 3. Determination of cyanide in wastewater samples

Sample	Cyanide added, Cyanide found,	
	ng/ml	ng/ml
A	0.0	0.0
	44.4	44.8
	88.8	88.3
B	0.0	0.2
	44.4	44.1
	88.8	88.4

Application to real samples

Cyanide in wastewater samples was determined by procedure A, after isolating it from co-existing ions by distillation.⁴ The results are given in Table 3.

Comparison with other methods

The proposed methods for the determination of cyanide are rapid and simple. The sensitivities of the methods are higher than those of any current spectrophotometric methods for cyanide.⁴⁻⁷

REFERENCES

1. H. Ishii, Y. Satoh and K. Satoh, *Anal. Sci.*, 1989, **5**, 713.
2. P. Hambright, T. Gore and M. Burton, *Inorg. Chem.*, 1976, **15**, 2314.
3. R. F. Pasternack, P. R. Huber, P. Boyd, G. Engasser, L. Francesconi, E. Gibbs, P. Fasella, G. C. Ventura and L. deC. Hinds, *J. Am. Chem. Soc.*, 1972, **94**, 4511.
4. *Japanese Industrial Standard (JIS)*, K 0102-1981, p. 112.
5. Wei Fu-sheng, Han Bai and Shen Nai-kui, *Analyst*, 1984, **109**, 167.
6. T. Pal and A. Ganguly, *ibid.*, 1987, **112**, 1327.
7. P. Kaur, S. Upadhyay and V. K. Gupta, *ibid.*, 1987, **112**, 1681.

RAPID DISSOLUTION OF CHROMITE WITH SULPHURIC ACID-LITHIUM SULPHATE MIXTURE CONTAINING CERIC SULPHATE, MANGANESE DIOXIDE OR PERIODATE, AND SPECTROPHOTOMETRIC DETERMINATION OF CHROMIUM

NOBUTAKA YOSHIKUNI

Laboratory for Analytical Chemistry, Faculty of Engineering, Chiba University, Yayoi-cho, Chiba, Japan

(Received 7 July 1989. Revised 7 December 1990. Accepted 14 December 1990)

Summary—Cr₂O₃ and chromite ore can be dissolved in H₂SO₄-Li₂SO₄-Ce(SO₄)₂ (20/10/1 v/w/w), H₂SO₄-Li₂SO₄-MnO₂ (20/10/1 v/w/w) and H₂SO₄-Li₂SO₄-KIO₄ (20/10/2 v/w/w) mixtures. The turbid solution produced can be clarified by treatment with H₂O₂ or solvent extraction and the chromium determined spectrophotometrically at 614 nm.

The chief ore of chromium is chromite, which is one of the most refractory minerals with respect to chemical dissolution. The chromite can be fused with alkali metal borate but dissolution of the cooled melt in mineral acid is slow (and impossible if boron trioxide is used as the fusion flux).¹ Previous studies² have shown that a sulphuric acid-lithium sulphate mixture can easily dissolve refractory oxides such as hafnium oxide, titanium dioxide and zirconium oxide but not the more refractory chromium(III) oxide. However, if a strong oxidizing reagent such as ceric sulphate, manganese dioxide, potassium permanganate or potassium periodate is added to the sulphuric acid-lithium sulphate mixture, chromium(III) oxide can be dissolved. This paper demonstrates the dissolution of chromium(III) oxide and chromite in this way and that the chromium in the resultant solution is present as chromium(III) and chromium(VI). The chromium(VI) can then be reduced to chromium(III) with hydrogen peroxide in sulphuric acid medium and the chromium(III) determined spectrophotometrically.

EXPERIMENTAL

Reagents

Chromium(III) oxide, ceric sulphate tetrahydrate, 30% hydrogen peroxide, manganese dioxide, sulphuric acid, lithium sulphate monohydrate, potassium periodate, potassium permanganate and potassium dichromate were Wako Pure Chemical Co. analytical grade. All

other reagents were also of analytical grade. Demineralized distilled water was used throughout. A chromium stock solution was prepared by dissolving 0.9527 g of potassium dichromate in 150 ml of 6.0M sulphuric acid in a beaker, transferring the solution into a 200-ml standard flask, and rinsing the beaker and diluting to the mark with 6.0M sulphuric acid.

Chromite sample

Chromite ore was obtained from Steelport, Transvaal, Republic of South Africa, and ground with a mortar and pestle.

Dissolution procedures

Dissolution of chromium(III) oxide and chromite with H₂SO₄-Li₂SO₄-Ce(SO₄)₂ mixture. Accurately weigh approximately 100 mg of Cr₂O₃ or 50 mg of very finely powdered chromite and transfer it into a dry 100-ml Kjeldahl flask. Weigh out roughly 10 g of Li₂SO₄·H₂O and 1 g of Ce(SO₄)₂·4H₂O, and add them to the flask. Add 20 ml of concentrated sulphuric acid to the flask in such a way that any solid caught in the neck is washed down. Place a small short-stemmed funnel in the neck of the flask and heat the flask with a Bunsen burner in a well-ventilated fume-hood, with the flask at 45° from the vertical. Start with a strong flame, rapidly increasing the temperature until the acid begins to fume. Rotate and shake the flask, and continue the heating until a clear brown solution is obtained. Let the flask stand for about 5 min, then cautiously add

about 50 ml of water little by little, and then 30% hydrogen peroxide until reduction of the ceric sulphate is complete. Cool, filter through a glass microfibre filter (e.g., Whatman GF/A, 7.0 cm diameter) into a 100-ml standard flask and dilute to the mark with water.

For 100 mg of chromite double the quantity of lithium sulphate and ceric sulphate should be used, with 20 ml of concentrated sulphuric acid. This mixture can easily dissolve 100 mg of chromite.

Dissolution with H_2SO_4 - Li_2SO_4 - MnO_2 mixture. The procedure is the same as that described above, but with 1 g of manganese dioxide instead of the ceric sulphate, and with 20 ml of concentrated sulphuric acid and 10 g of $Li_2SO_4 \cdot H_2O$ for 100 mg of sample. The fuming is continued for only 3–4 min.

Dissolution with H_2SO_4 - Li_2SO_4 - KIO_4 mixture. For 100–200 mg of Cr_2O_3 or chromite (in a 100-ml Kjeldahl flask) use 20 ml of concentrated sulphuric acid, 10 g of $Li_2SO_4 \cdot H_2O$ and 2 g of potassium periodate, and gently heat for 5 min with a Bunsen burner. Increase the temperature until the acid fumes, rotate and shake the flask, and continue the heating for 10–15 min. After cooling, add 50 ml of water, transfer the solution to a 200-ml separatory funnel, add 50 ml of carbon tetrachloride and shake the funnel for 1 min to extract the iodine produced. Discard the organic phase. Filter the aqueous phase into a 100-ml standard flask and dilute to the mark with water.

*Decomposition of chromite by fusion with NaOH and Na_2O_2 .*³ Accurately weigh 100–250 mg of finely powdered chromite into a nickel crucible, add 3 g of sodium hydroxide and 3 g of sodium peroxide, fuse the mixture for 20 min, cool, dissolve the product in 3.6*M* sulphuric acid, transfer the solution into a 100-ml standard flask and dilute to the mark with 3.6*M* sulphuric acid.

Spectrophotometric determination of chromium

Take 1–10 ml portions (accurately measured) of chromium standard solution or the sample solution and evaporate them to dryness in beakers on a hot-plate and dissolve the residues with 15 ml of 11.5*M* sulphuric acid. Then add 1 ml of 30% hydrogen peroxide to each, cover the beakers, and heat them on a hot-plate. Repeat the addition of peroxide three times. If potassium periodate was used, continue addition of hydrogen peroxide until all the periodate has been decomposed, and evaporate the

solution to about 15 ml. When the colour has changed from the blue of the sample solutions or the orange of the standard solutions to deep green, cool, and transfer the solutions into 25-ml standard flasks. Add 6.0 ml of concentrated sulphuric acid to each and dilute to the mark with water. Measure the absorbance at 614 nm against a reagent blank prepared under the same conditions.

RESULTS AND DISCUSSION

Dissolution of chromium(III) oxide and chromite

Chromite is one of the most refractory minerals with respect to chemical dissolution. However, if a strong oxidizing reagent such as potassium permanganate is used in conjunction with concentrated sulphuric acid or its mixture with lithium sulphate, chromite and chromium(III) oxide can easily be decomposed, but such mixtures can be explosive when heated.

The effect of other powerful oxidizing reagents, such as ceric sulphate, manganese dioxide, potassium periodate, nitric acid, potassium bromate and potassium peroxodisulphate, in sulphuric acid and sulphuric acid–lithium sulphate media, on the dissolution time of chromium(III) oxide has therefore been examined (Table 1).

Chromium(III) oxide (100 mg) can be dissolved in a few minutes by heating with 20 ml of concentrated sulphuric acid and 1 g of ceric sulphate in a Kjeldahl flask, but the cerium(III) products (the oxide or oxysulphate) cannot be completely dissolved on addition of water.

However, if lithium sulphate (10 g) is also present, the decomposition is complete in 1 min or less, and the cerium(III) is in a form that is readily soluble in water. The colour of the solution is changed from brown to clear blue by the addition of 1 ml of 30% hydrogen peroxide.

Chromium(III) oxide (100 mg) can be completely dissolved by heating for a few minutes with H_2SO_4 - KIO_4 (20 ml, 2 g) or H_2SO_4 - Li_2SO_4 - KIO_4 (20 ml, 10 g, 2 g) mixture in a Kjeldahl flask. For chromite, only the H_2SO_4 - Li_2SO_4 - KIO_4 mixture is efficient, but heating for 15–20 min is required. Iodine is generated in this method, and if it is not completely volatilized during the heating, must be removed by extraction with carbon tetrachloride, to prevent its interference in the chromium(III) determination. Silica and silicates are not decomposed and must be filtered off (glass microfibre filter). MnO_2^{4-6} or manganese ore⁴ can

Table 1. Dissolution time of Cr_2O_3 (0.1 g) in various media

Dissolution media*	Reagent ratio†	Dissolution time, ‡ min	Vessel
$\text{H}_2\text{SO}_4\text{-Ce}(\text{SO}_4)_2$	20/1 (v/w)	not clarify	Kjeldahl flask
$\text{H}_2\text{SO}_4\text{-Li}_2\text{SO}_4\text{-Ce}(\text{SO}_4)_2$	20/10/1 (v/w/w)	≤ 1	Kjeldahl flask
$\text{H}_2\text{SO}_4\text{-KIO}_4$	20/2 (v/w)	< 5	Kjeldahl flask
$\text{H}_2\text{SO}_4\text{-Li}_2\text{SO}_4\text{-KIO}_4$	20/10/2 (v/w/w)	< 3	Kjeldahl flask
$\text{H}_2\text{SO}_4\text{-MnO}_2$	20/1 (v/w)	> 5	Kjeldahl flask
$\text{H}_2\text{SO}_4\text{-Li}_2\text{SO}_4\text{-MnO}_2$	20/10/1 (v/w/w)	≤ 1	Kjeldahl flask
$\text{H}_2\text{SO}_4\text{-H}_2\text{O-MnO}_2$	25/25/0.2 (v/v/w)	> 5	Kjeldahl flask
$\text{H}_2\text{SO}_4\text{-H}_2\text{O-MnO}_2$	25/25/0.2 (v/v/w)	> 15	Beaker§
$\text{H}_2\text{SO}_4\text{-KMnO}_4$	20/2 (v/w)	explosion	Kjeldahl flask
$\text{H}_2\text{SO}_4\text{-Li}_2\text{SO}_4\text{-KMnO}_4$	20/10/2 (v/w/w)	explosion	Kjeldahl flask
$\text{H}_2\text{SO}_4\text{-H}_2\text{O-KMnO}_4$	20/10/2 (v/w/w)	explosion	Kjeldahl flask
$\text{H}_2\text{SO}_4\text{-Li}_2\text{SO}_4\text{-HNO}_3$	20/10/5 (v/w/v)	N.C.D.	Kjeldahl flask
$\text{H}_2\text{SO}_4\text{-Li}_2\text{SO}_4\text{-HNO}_3$	10/20/5 (v/w/v)	N.C.D.	Kjeldahl flask
$\text{H}_2\text{SO}_4\text{-H}_3\text{PO}_4\text{-HNO}_3$	20/10/5 (v/v/v)	N.C.D.	Kjeldahl flask
$\text{H}_2\text{SO}_4\text{-H}_3\text{PO}_4\text{-HNO}_3$	10/20/5 (v/v/v)	N.C.D.	Kjeldahl flask
$\text{H}_2\text{SO}_4\text{-H}_3\text{PO}_4\text{-HNO}_3$	10/20/5 (v/v/v)	> 30	Beaker

* Li_2SO_4 as monohydrate, $\text{Ce}(\text{SO}_4)_2$ as tetrahydrate.

†v in ml, w in g.

‡N.C.D. = not completely dissolved unless more HNO_3 was added.

§Method of Mandal *et al.*⁴.

quantitatively oxidize chromium(III) in the presence of sulphuric acid, but the reaction is slow (Table 1). The $\text{H}_2\text{SO}_4\text{-H}_2\text{O-MnO}_2$ system also gives only slow reaction. In contrast, the $\text{H}_2\text{SO}_4\text{-Li}_2\text{SO}_4\text{-MnO}_2$ mixture gives very rapid

decomposition and the diluted solution is readily clarified with 1 ml of 30% hydrogen peroxide. There is no risk of explosion. Chromium(III) oxide is virtually insoluble in the $\text{H}_2\text{SO}_4\text{-Li}_2\text{SO}_4\text{-HNO}_3$ system. The $\text{H}_2\text{SO}_4\text{-}$

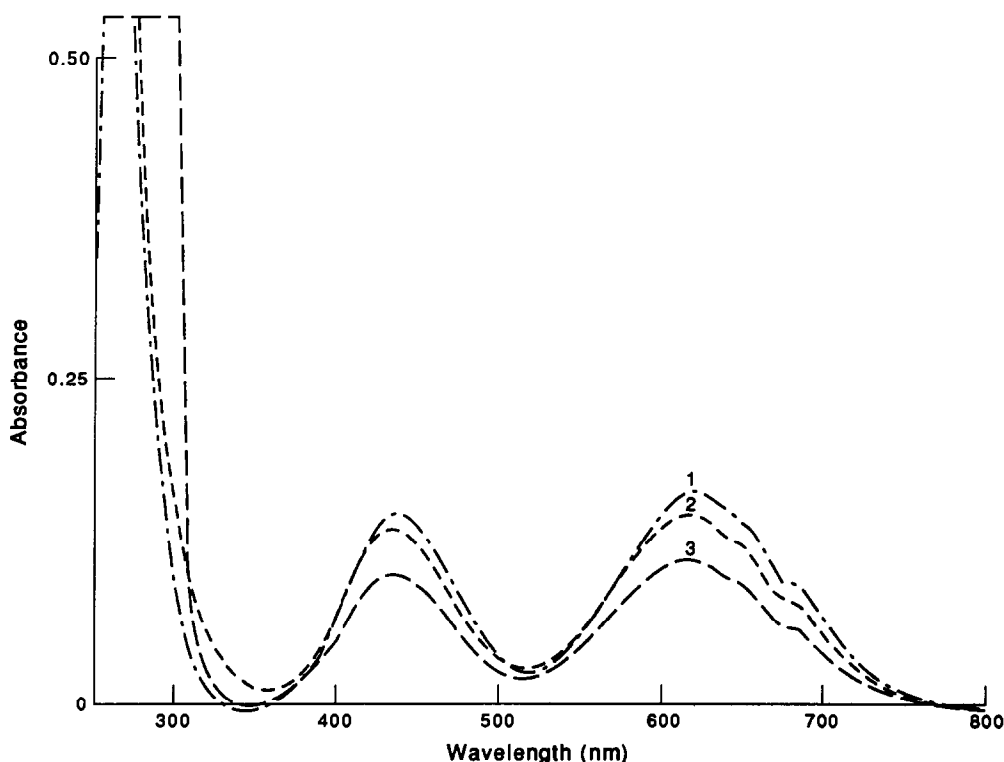


Fig. 1. Absorption spectra of chromium solutions: 1, $\text{K}_2\text{Cr}_2\text{O}_7$ dissolved in 11.5M H_2SO_4 and treated with H_2O_2 (Cr 406 $\mu\text{g/ml}$); 2, Cr_2O_3 dissolved with $\text{H}_2\text{SO}_4\text{-Li}_2\text{SO}_4\text{-MnO}_2$ (20/10/2, v/w/w), followed by dilution to 11.5M H_2SO_4 and treatment with H_2O_2 (Cr 358 $\mu\text{g/ml}$); 3, Cr_2O_3 dissolved with $\text{H}_2\text{SO}_4\text{-Li}_2\text{SO}_4\text{-Ce}(\text{SO}_4)_2$ (20/10/1, v/w/w), followed by dilution to 11.5M H_2SO_4 and treatment with H_2O_2 (Cr 275 $\mu\text{g/ml}$).

Table 2. Determination of chromium in Cr_2O_3 (contains 68.4% Cr) and chromite ore

Dissolution and decomposition systems	Sample	Sample weight, mg	Cr found		Dissolution time, min
			mg	%	
$\text{H}_2\text{SO}_4\text{-Li}_2\text{SO}_4\text{-Ce}(\text{SO}_4)_2$ (20/10/1, v/w/w)	Cr_2O_3	119.9	83.0	69.2	5
			81.0	67.6	
	Chromite	48.5	13.7	28.2	10
			13.9	28.7	
	Chromite	50.1	14.5	28.9	12
			13.6	27.1	
	Chromite	53.7	15.5	28.9	10
			14.9	27.7	
$\text{H}_2\text{SO}_4\text{-Li}_2\text{SO}_4\text{-Ce}(\text{SO}_4)_2$ (20/20/2, v/w/w)	Cr_2O_3	164.4	112.4	68.4	5
			26.9	28.3	
	Chromite	95.2	27.0	28.4	12
			30.4	27.5	
	Chromite	110.6	31.0	28.0	12
			30.8	27.3	
	Chromite	112.9	33.2	29.4	14
$\text{H}_2\text{SO}_4\text{-MnO}_2$ (20/1, v/w)	Cr_2O_3	103.5	64.0	61.8	5
			62.4	60.3	
$\text{H}_2\text{SO}_4\text{-Li}_2\text{SO}_4\text{-MnO}_2$ (20/10/1, v/w/w)	Cr_2O_3	121.6	84.2	69.2	5
			83.0	68.3	
	Chromite	100.6	29.6	29.4	5
			28.0	27.8	
	Chromite	102.8	29.3	28.5	5
			28.2	27.4	
	Chromite	122.6	35.9	29.4	5
			35.1	28.6	
$\text{H}_2\text{SO}_4\text{-Li}_2\text{SO}_4\text{-KIO}_4$ (20/10/2, v/w/w)	Cr_2O_3	101.3	69.0	68.2	5
			67.0	67.0	
	Chromite	251.5	30.0	29.3	15 ~ 20
			32.2	29.7	
	Chromite	102.4	41.0	27.9	15 ~ 20
			42.2	28.2	
	Chromite	146.9	41.2*	27.5	15 ~ 20
			60.3	29.7	
	Chromite	203.0	58.0*	28.6	15 ~ 20
			58.4	28.2	
	Chromite	207.1	56.0*	27.0	15 ~ 20
$\text{NaOH-Na}_2\text{O}_2$ (3/3, w/w)	Chromite	100.2	27.6	27.5	
			28.0	27.9	
	Chromite	164.9	27.6	27.5	
			28.1*	28.0	
	Chromite	164.9	47.0	28.5	
			50.0	30.3	
	Chromite	245.4	45.2*	27.4	
			69.5	28.3	
	Chromite	245.4	70.0	28.5	
			72.0	29.3	

*Spectrophotometric determination after removal of iron.

$\text{H}_3\text{PO}_4\text{-HNO}_3$ system, though successful when used in a beaker, proved unsuitable when used in a Kjeldahl flask, unless more nitric acid was added from time to time. Chromium(III) oxide cannot be dissolved in $\text{H}_2\text{SO}_4\text{-Li}_2\text{SO}_4$ mixture with the aid of other oxidizing agents such as potassium bromate or potassium peroxodisulphate.

In the dissolution with the $\text{H}_2\text{SO}_4\text{-Li}_2\text{SO}_4\text{-Ce}(\text{SO}_4)_2$ system, the iron(II) in the chromite ore reduces some of the cerium(IV) and it is necessary either to use a smaller sample (50 mg) or double the amounts of lithium sulphate and ceric sulphate if a 100-mg sample is used. The $\text{H}_2\text{SO}_4\text{-Li}_2\text{SO}_4\text{-Ce}(\text{SO}_4)_2$ system can be heated rapidly to a high temperature and chromite can

be decomposed in a few minutes, but other metal oxides such as iron oxide dissolve more slowly (10–15 min).

After heating for 10–15 min, the colour of the $\text{H}_2\text{SO}_4\text{--Li}_2\text{SO}_4\text{--Ce}(\text{SO}_4)_2$ system is changed from the initial turbid yellow to a clear yellowish brown, and to a clear brown if heated with chromite. After dilution with water the chromium(VI) in the solution is readily reduced by addition of 1 ml of 30% hydrogen peroxide. In this mixed system the ratio of lithium sulphate to ceric sulphate is of importance because the lithium sulphate appears to prevent the formation of insoluble cerium oxide or oxysulphate. Any silica or silicate present in the chromite ore cannot be dissolved by this method and has to be filtered off, with a glass microfibre filter.

Heating with the $\text{H}_2\text{SO}_4\text{--Li}_2\text{SO}_4\text{--MnO}_2$ (20 ml, 10 g, 1 g) system decomposes 100 mg of chromite in about 5 min. The turbid solution is black or deep violet, and is readily changed to sky blue by the addition of a few drops of 30% hydrogen peroxide. Any silica or silicate is left undissolved and must be removed (glass microfibre filter).

Spectrophotometric determination of chromium

The chromate and diphenylcarbazide methods^{7,8} are widely used for spectrophotometric determination of chromium. The atomic-absorption photometric determination of trace and moderate amounts of chromium in ores, rocks and other materials was studied by Donaldson.^{8,9} However, these methods are unsuitable for determination of chromium in chromite ores because they are highly sensitive and the samples must be extensively diluted. To overcome this drawback the possibility of using the less sensitive absorbance measurement of chromium(III) in a high concentration of sulphuric acid was examined. In 11.5M sulphuric acid, Cr(III) exhibits absorption peaks at 432 and 614 nm (Fig. 1). Iron(III) interferes with the measurement at 432 nm, so the 614 nm peak is used for chromite analysis. The calibration graph obeys Beer's law from 10 to 500 $\mu\text{g/ml}$ Cr(III). In reduction of chromium(VI) by treatment with hydrogen peroxide the sulphuric acid

concentration must be kept in the range 10.5–12.5M because there is a slight red-shift of the chromium absorption spectrum with increase in sulphuric acid concentration.

Determination of chromium in chromium(III) oxide and chromite

Table 2 gives the results obtained for analysis of Cr_2O_3 and chromite ore under the recommended conditions. The dissolution of Cr_2O_3 with the $\text{H}_2\text{SO}_4\text{--Li}_2\text{SO}_4\text{--Ce}(\text{SO}_4)_2$, $\text{H}_2\text{SO}_4\text{--Li}_2\text{SO}_4\text{--MnO}_2$ and $\text{H}_2\text{SO}_4\text{--Li}_2\text{SO}_4\text{--KIO}_4$ systems is complete and the procedure can be recommended for determination of chromium. Decomposition with $\text{H}_2\text{SO}_4\text{--MnO}_2$ mixture gave low results.

For chromite, analysis after fusion of the sample with $\text{NaOH--Na}_2\text{O}_2$, gave 28.3% chromium (standard deviation 0.9%), which is comparable to the results obtained (grand average 28.4%, standard deviation 0.8%) by using the dissolution method with $\text{H}_2\text{SO}_4\text{--Li}_2\text{SO}_4$ mixture containing one of the oxidizing agents $\text{Ce}(\text{SO}_4)_2$, MnO_2 or KIO_4 (see Table 2).

This is a very easy and rapid dissolution method for chromium oxide and chromite ore under atmospheric conditions, and a very simple method for determination of chromium. It seems particularly useful for rapid evaluation of the quality of chromium ores.

Acknowledgement—The author wishes to thank Professor Rokuro Kuroda, Chiba University, for warm encouragement and his kind interest in this manuscript.

REFERENCES

1. E. Kiss, *Anal. Chim. Acta*, 1987, **193**, 315.
2. N. Yoshikuni, *Talanta*, 1989, **36**, 709.
3. R. Bock, *A Handbook of Decomposition Methods in Analytical Chemistry*, International Textbook Company, Glasgow, 1979.
4. S. K. Mandal, S. B. Rao and B. R. Sant, *Talanta*, 1979, **26**, 135.
5. *Idem, ibid.*, 1981, **28**, 771.
6. J. C. Stauter and R. T. Um, *U.S. Patent* 4,029,734, 14 June 1977.
7. E. B. Sandell, *Colorimetric Determination of Traces of Metals*, 3rd Ed., Interscience, New York, 1959.
8. E. M. Donaldson, *Methods for The Analysis of Ores, Rocks, and Related Minerals*, 2nd Ed., CANMET Monograph 881, 1982.
9. *Idem, Talanta*, 1980, **27**, 779.

THE INFLUENCE OF HYDROGEN PEROXIDE AND pH ON THE MOHR TITRATION

REIKO FUJITA

Department of Chemistry, School of Liberal Arts and Sciences, Iwate Medical University,
Honcho-dori 3-16-1 Morioka, Japan 020

(Received 6 November 1989. Revised 26 November 1990. Accepted 14 December 1990)

Summary—The official Japanese method for determination of chloride in hot-spring waters requires any H_2S present to be oxidized with hydrogen peroxide in ammoniacal medium. When this was done, and the solution was titrated with silver nitrate at pH 9.7, the indicator colour changed from yellow to brownish grey, owing to reduction of silver ions to the metal by hydrogen peroxide. The effect can be eliminated by adjusting the pH to 7.0–7.5 before the titration.

Almost all hot-spring waters contain dissolved H_2S , and this interferes with the determination of chloride by various analytical methods, including the Mohr titration. This interference is due to the formation of Ag_2S , which causes a positive error for chloride. The official Japanese *Analytical Methods of Mineral Spring Water*,¹ therefore specifies oxidation of the sulphide by treatment with hydrogen peroxide in ammoniacal medium.

However, it is known that in the presence of ammonium salts a positive error arises from formation of $Ag(NH_3)_2^+$ unless the pH is sufficiently low.²⁻⁵ Moreover, hydrogen peroxide reduces Ag_2O to silver in alkaline medium. Therefore, to develop an accurate method for titration of chloride in hot-spring water containing soluble H_2S , it was felt necessary to study the interaction between pH, Ag^+ , and H_2O_2 to elucidate potential interference in the titration.

The goals of the present work were to elucidate the interference mechanisms in titration of chloride with silver nitrate and find a satisfactory modification of the pretreatment in which soluble H_2S is removed by oxidation with hydrogen peroxide.

EXPERIMENTAL

Reagents

A 0.36M stock chloride solution was prepared by dissolving 2.1038 g of sodium chloride in 100 ml of distilled water, and working solutions (approximately 320 $\mu g/ml$ chloride) were prepared from it by dilution. Hydrogen peroxide solution were prepared as required, by addition of a 30% stock solution. H_2S -water

was prepared by saturating distilled water with H_2S , and the solution was standardized.⁶

Determination of Cl^- by the Mohr method

Potassium chromate indicator (0.25M) was added to 20 ml of chloride solution, which was then titrated with 0.1M silver nitrate (with stirring by magnetic stirrer). A blank solution was similarly titrated and a correction applied for the value obtained.

Relationship between the concentration of H_2O_2 and the oxidation of H_2S

Kunimi hot-spring water (20 ml) with and without H_2S -water (20 ml) was mixed with hydrogen peroxide in a flask to give a range of peroxide concentrations from 0.42mM to 1.8M. After 10 min the residual H_2S was determined as follows.⁶

Acetic acid was added to the sample solution, containing 3–4 mg of sulphide, until the pH was lowered to about 2, then 5–10 ml of 50 mg/ml cadmium acetate solution were added. The flask was sealed and shaken, then the precipitate was filtered off, washed with 1% v/v acetic acid and dissolved in 3M hydrochloric acid. The solution was accurately diluted to 50 ml and a 5–20 ml portion was heated at 60–80° for 10 min, then cooled. The pH was adjusted to 10 by addition of 3M ammonia solution, Cu–PAN indicator was added, and the cadmium present (which corresponded to the sulphide in the original solution) was titrated with 0.01M EDTA.

Modified method for the oxidation of sulphide

The pH of a sample solution (50 ml) containing 0–150 ppm H_2S was adjusted to 10–11 by

the addition of 1M sodium hydroxide. This solution was oxidized by the addition of 30% v/v hydrogen peroxide (1 ml), and then boiled for 10 min. After cooling, the pH of the solution was lowered to 7.0–7.5 by the addition of sulphuric acid (with monitoring by pH-meter). Leakage of chloride from the reference electrode was found to correspond to less than 1 ppm in the test solution, in 5 min.

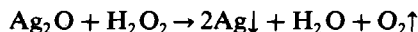
RESULTS AND DISCUSSION

The Japan official method for removing soluble H_2S consists of oxidation with hydrogen peroxide in ammoniacal medium.¹ When, in the present work, the method was applied to two kinds of hot-spring water containing 83–151 ppm H_2S , before their titration with silver nitrate to determine chloride, detection of the end-point was difficult, and accurate determination of the chloride impossible. The colour changes at the end-point were as follows. The yellow of the chromate solution changed to a turbid brownish green immediately after each addition of titrant and also just before the end-point. In addition, many bubbles occurred at the same time that the colour changed. If these solutions were filtered after the production of bubbles ceased, a greyish black precipitate was collected and a clear yellow solution obtained. The absorption spectrum of this solution was the same as that of potassium chromate. Since Ag_2S is black, the colour change was thought to be due to precipitation of Ag_2S formed from Ag^+ and residual H_2S . Hence, the relationship between the concentration of H_2O_2 used and the oxidation of sulphide was investigated, with the result shown in Fig. 1. No sulphide could be detected in either Kunimi

hot-spring water or H_2S -water when the peroxide concentration used was $\geq 18mM$, which was lower than the concentration specified in the standard method. This suggested that all the sulphide had been oxidized and that the precipitate was not Ag_2S . In fact, qualitative analysis showed that the precipitate was metallic silver. Since it was found that precipitation of silver did not occur if the solution was adjusted to a neutral pH after oxidation with peroxide, the relationship between $[Ag^+]$, $[H_2O_2]$ and pH was further studied. It was found that the excess of peroxide did not influence titrations done at pH 7.0–7.4.

The effect of H_2O_2 over the pH-range 6.9–11.3 [adjusted with sodium hydroxide instead of ammonia, to avoid formation of $Ag(NH_3)_2^+$] was investigated. In the presence of peroxide at pH > 10.0, chloride could not be determined by the Mohr method, since gas was evolved when silver nitrate was added, and the colour of the solution changed to greyish black because a precipitate of metallic silver was formed.

It is known that hydrogen peroxide reacts with Ag_2O but not with Ag^+ , and acts as a reductant:



According to calculations based on the relevant constants, a precipitate of Ag_2O should not form at pH < 11.0 under the conditions of the Mohr method. However, Ag was formed even at pH 10.0, which is lower than the upper pH limit (10.5) recommended for use of the Mohr method. This is presumably due to the non-equilibrium conditions existing at the point of entry of the titrant into the chloride solution, where the resulting local concentration of Ag^+ could be high enough to produce a small amount of Ag_2O , which would react with the peroxide and perhaps induce the well-known Haber–Weisz chain reaction for decomposition of peroxide.

It follows that if peroxide is present, it is essential to keep the pH sufficiently low to prevent localized formation of Ag_2O . The requirement for oxidation of sulphide with peroxide at relatively high pH and titration at lower pH can be met by first adjusting the pH to 10–11 with sodium hydroxide for the oxidation reaction, and then lowering the pH to 7–7.5 by addition of sulphuric acid. The Mohr titration can then be applied.

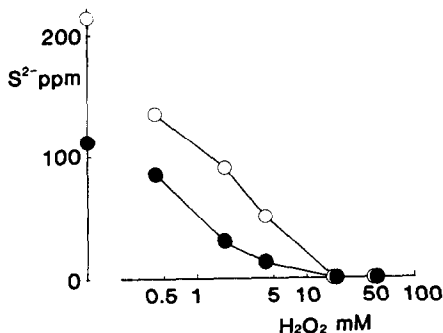


Fig. 1. Influence of the concentration of H_2O_2 on the oxidation of S^{2-} : plots of residual S^{2-} vs. peroxide concentration used. ●, Kunimi Hot Spring water; ○, H_2S -water.

Table 1. Determination of chloride after removal of H₂S

Sample	S ²⁻ , μg/ml	Cl ⁻ found,* μg/ml	Total Cl ⁻ found,* μg/ml	Recovery of added Cl ⁻ , %
Kunimi Hot Spring (Ishizuka Ryokan)	127	291 ± 2	491 ± 1†	98
Narugo Hot Spring (Yusa-Ya)	93	171 ± 1	376 ± 0†	100
H ₂ S-water	102	0	161 ± 1‡	101

*Mean ± standard deviation (5 replicates).

†Added chloride: 205 μg/ml.

‡Added chloride: 160 μg/ml.

Application of the Mohr method

The following experiment was planned to confirm the effectiveness of the modified method of oxidation of H₂S. The samples used were H₂S-water and two kinds of hot-spring water, each containing chloride. A known amount of sodium chloride solution was added to the hot-spring water, and the results for these solutions were compared with those for hot-spring water to which no chloride had been added. The experiment was repeated five times with the same samples, and the results are shown in Table 1. The determination of the added Cl⁻ was acceptably accurate (98–101% recovery). The modified method was evidently suitable for the determination of chloride in hot-spring water containing substantial amounts of H₂S.

Acknowledgements—The author is deeply grateful to Professor M. Rikimaru of Iwate Medical University for this kind support. Thanks are also due to Professor K. Nakadate and especially to Miss I. Katsura, Miss M. Ishibane, Miss K. Takahashi and Mr. K. Matsuda for their kind encouragement. The author also thanks Dr. P. Langman for his help with English.

REFERENCES

1. *Guide Book to Analysis of Mineral Spring Water*, Revised Ed., p. 53. Society of Engineers for Mineral Springs, Tokyo, 1978 (in Japanese).
2. I. M. Kolthoff, E. B. Sandell, E. J. Meehan and S. Bruckenstein, *Quantitative Chemical Analysis*, 4th Ed., p. 796. Macmillan, Toronto, 1969.
3. R. Belcher, A. M. G. Macdonald and E. Parry, *Anal. Chim. Acta*, 1957, **16**, 524.
4. J. Block and O. B. Waters, Jr., *Talanta*, 1967, **14**, 1130.
5. T. Anfalt and D. Jagner, *ibid.*, 1969, **16**, 555.
6. E. Minami and K. Watanuki, *Bunseki Kagaku*, 1960, **9**, 958 (in Japanese).

A RAPID TURBIDIMETRIC METHOD FOR THE DETERMINATION OF TOTAL SULPHUR IN ZINC CONCENTRATE

R. RAGHAVAN

R.A. Mines, Hindustan Zinc Limited, Agucha, 311029, India

SUBHIR RAHA

Zinc Smelter, Hindustan Zinc Limited, Udaipur, 313024, India

(Received 13 November 1989. Revised 9 November 1990. Accepted 19 November 1990)

Summary—A rapid, simple and reliable routine method for the determination of total sulphur in zinc concentrates, roasted products and leached residues from zinc smelters is described. The method involves the fusion of the sample with sodium peroxide and sodium carbonate or routine acid decomposition and dissolution to give soluble compounds. The absorbance of the barium sulphate suspension produced by the addition of barium chloride powder to a dilute hydrochloric acid solution of the sample, containing cetyltrimethylammonium bromide solution as a dispersing agent, is measured at 420 nm. The results obtained for some zinc concentrates and other products are compared with those obtained by the conventional gravimetric barium sulphate method. Results for a reference zinc concentrate and other samples with various matrices and the results obtained with standard additions to the samples are good.

Sulphur is present mostly as sulphide in zinc concentrates and during roasting is converted into sulphur dioxide, which is used to manufacture sulphuric acid in most "roast-leach-electro-win" hydrometallurgical plants. The roasted product and leached residues contain unreacted sulphides and sulphates in amounts which depend on the roasting conditions, and this severely affects the leaching efficiency, precious-metal recovery, sulphate balance and recovery efficiency of the plant operations, so their analytical control is essential at all levels.

The total sulphur content in zinc plant samples varies from 2 to 32%. Our laboratory uses a uniform method for the determination of sulphur by the usual nitric acid decomposition in the presence of potassium bromate and a solution of bromine in carbon tetrachloride to form soluble sulphate, followed by the conventional gravimetric method.¹⁻³ Titrimetric, potentiometric and polarographic methods have been reported in the literature for the determination of sulphate in certain samples, but these methods are not suitable for zinc concentrates and other residues, owing to the complexity of the samples.

For simpler and more rapid determination of total sulphur, modification of the decomposition technique for converting all the sulphur

compounds into soluble sulphates is needed and the gravimetric barium sulphate method must be replaced. The universal technique proposed by Bhargava *et al.*⁴ for rapid dissolution of materials encountered in the steel industry has not hitherto been tried for these types of zinc plant samples, though it seems well suited for the purpose. For determination of low levels of sulphate the use of nephelometry^{5,6} or turbidimetry⁷ has been found advantageous. Hence it seemed to us that combination of the alkaline fusion technique with turbidimetric determination would provide a rapid and useful method for use in production control.

In the proposed method, the sample is fused with sodium peroxide and sodium carbonate in a nickel crucible, and the cooled fusion cake is leached with water and dissolved completely in hydrochloric acid, the sulphur species in the sample all being in soluble sulphate form. Powdered barium chloride is added to the solution, the barium sulphate suspension produced being stabilized by cetyltrimethylammonium bromide. The absorbance is measured at 420 nm.

This method is simple, rapid and reliable, and the results are comparable with those of the standard gravimetric method. The decomposition brings the major and minor constituents into solution, providing in a single operation a sample solution suitable for complete analysis.

EXPERIMENTAL

Reagents

All reagents used were of analytical grade.

Standard sulphate solution (2 mg/ml). Dissolve 2.958 g of anhydrous sodium sulphate in sulphate-free demineralized water and dilute the solution exactly to 1000 ml.

Cetyltrimethylammonium bromide (CTAB) solution. Dissolve 2.00 g of CTAB in 100 ml of 6M hydrochloric acid. Dilute 2 ml of this stock solution to 1000 ml with demineralized water.

Bromine solution in carbon tetrachloride. Mix 20 ml of bromine and 30 ml of carbon tetrachloride in an amber glass-stoppered bottle.

Barium chloride powder. Grind the reagent and sieve it, collecting the fraction (< 300 μ m particle size) passing through a BSS 52-mesh sieve.

Apparatus

A JASCO double-beam UVIDEK 430 spectrophotometer, a magnetic stirrer with built-in speed regulator, and Teflon-coated stirrer bars (10 mm diameter, 25 mm length) were used.

Sample preparation

Acid decomposition. To 1.000 g of powdered (100-mesh) sample in a dry 400-ml beaker add 3–4 g of potassium bromate. Cover the beaker with a dry watch-glass, and swirl it to mix the sample with the potassium bromate. Add 8–10 ml of the carbon tetrachloride solution of bromine and let stand for 15 min. Add 10 ml of concentrated nitric acid and stand the beaker on an asbestos pad on a hot-plate, for slow reaction and evaporation. Remove the cover and evaporate the solution to dryness. Cool, add 10–15 ml of concentrated hydrochloric acid, evaporate to

dryness and slightly bake the residue. Repeat this acid treatment twice to decompose the sample completely. To the baked sample add 2–3 g of sodium chloride and disperse it over the sample. Add 50 ml of 6M hydrochloric acid and heat to dissolve the soluble salts. Filter (Whatman 12.5-cm No. 1 filter paper) and wash the residue with 6M hydrochloric acid, collecting the filtrate and washings in a 250-ml standard flask. Make up to the mark with 6M hydrochloric acid.

Alkaline fusion. Cover 1.000 g of powdered sample in a 50-ml zirconium or nickel crucible with 8 g of sodium peroxide and 2 g of sodium carbonate. Fuse the mixture over a Méker burner or in a muffle furnace at 700° until the melt is cherry red and clear. Cool. Extract with the minimum (10 ml) of water. After the effervescence has ceased, empty the crucible into a beaker, add 10 ml of concentrated hydrochloric acid to the crucible and empty it into the beaker. Rinse the crucible with the minimum amount of water, collecting the washings in the beaker. Boil the solution for 5 min, then let it cool. If any residue is found, filter (Whatman 12.5-cm No. 1 filter paper) and wash the residue with 6M hydrochloric acid. Transfer the solution into a 250-ml standard flask and dilute to volume with 6M hydrochloric acid.

Turbidimetric determination

Pipette a volume of sample solution containing up to 2.5 mg of sulphate into a 100-ml standard flask, and dilute to volume with CTAB solution. Transfer the solution to a 150-ml beaker, add a stirrer bar and place the beaker on the magnetic stirrer. Stir the solution at constant speed (500–700 rpm). Add 0.25 g of barium chloride powder and continue stirring for 1 min.

Table 1. Results obtained for total sulphur in various process samples by the standard gravimetric method and the proposed method (dissolution by both acid and alkali decomposition techniques)

Sample	% S (gravimetric)*			% S (turbidimetric)†			% S (gravimetric)‡			% S (turbidimetric)‡		
	Mean	Min	Max	Mean	Min	Max	Mean	Min	Max	Mean	Min	Max
Zinc Concentrate§ (Canmet CZN-1)	30.2	29.9	30.4	30.0	29.2	30.1	30.2	30.0	30.5	30.2	29.8	30.3
Zinc concentrate I	29.6	29.5	29.8	29.3	29.2	29.6	29.7	29.6	29.9	29.5	29.2	29.7
Zinc concentrate II	28.0	27.8	28.0	27.6	27.5	27.8	28.0	27.6	28.4	27.8	27.4	28.6
Zinc concentrate III	29.3	29.2	29.4	29.2	29.1	29.3	29.3	29.2	29.6	29.3	29.1	29.3
Calcine	3.61	3.59	3.62	3.61	3.57	3.62	3.61	3.58	3.68	3.61	3.58	3.62
Leached residue	10.09	10.08	10.10	10.08	10.06	10.10	10.12	10.09	10.28	10.10	10.05	10.12
Jarosite	6.13	6.03	6.20	6.13	6.05	6.18	6.12	6.00	6.28	6.14	6.02	6.25

*Averages of 5 replicate analyses. The general composition of the samples is given in Table 3.

†Acid decomposition technique.

‡Alkaline decomposition technique.

§Certified value of CZN-1: 30.20 \pm 0.2%.

Table 2. Results for recovery of original plus added sulphate by the proposed method

Sample	Acid decomposition			Alkaline decomposition		
	Added, mg	Found, mg	Recovery, %	Added, mg	Found, mg	Recovery, %
Zinc concentrate	—	0.900	—	—	0.905	—
(CANMET CZN-1)	0.500	1.380	98.6	0.500	1.389	98.9
	1.000	1.870	98.4	1.000	1.882	98.8
Zinc concentrate I	—	0.880	—	—	0.886	—
	0.500	1.346	97.5	0.500	1.361	98.2
	1.000	1.824	97.0	1.000	1.849	98.0
Zinc concentrate II	—	0.828	—	—	0.835	—
	0.500	1.279	97.0	0.500	1.308	98.0
	1.000	1.770	97.4	1.000	1.789	97.5
Zinc concentrate III	—	0.875	—	—	0.878	—
	0.500	1.334	97.0	0.500	1.353	98.2
	1.000	1.800	96.0	1.000	1.844	98.2
Calcine	—	1.083	—	—	1.083	—
	0.500	1.580	99.8	0.500	1.583	100.0
	1.000	2.080	99.8	1.000	2.075	99.6
Leached residue	—	1.210	—	—	1.210	—
	0.500	1.710	100.0	0.500	1.710	100.0
	1.000	2.205	99.8	1.000	2.190	99.1
Jarosite	—	0.920	—	—	0.921	—
	0.500	1.406	99.0	0.500	1.418	99.8
	1.000	1.907	99.3	1.000	1.919	99.9

Immediately transfer some of the suspension into a 10-mm path-length cell and measure the absorbance at 420 nm against a blank similarly prepared. Prepare a calibration graph, with standards prepared in the same way, covering the range up to 3.0 mg of sulphate per 100 ml.

RESULTS AND DISCUSSION

The method was validated by analysing various samples generated at the zinc smelter, as well as a certified zinc concentrate reference sample (Tables 1 and 2). Various amounts of sulphate were added at the measurement stage to determine the efficiency of dispersion under the experimental conditions for different matrices and the results obtained are reported as % recovery in Table 2.

The results obtained for total sulphur in solutions prepared by the two decomposition methods and analysed by both methods (gravimetric and turbidimetric) were in good agreement. Both methods of determination were applied to each sample solution. The alkaline fusion decomposition method was found to be

more effective and much faster than the acid decomposition. Although silica is also brought into solution in the alkaline fusion decomposition, there is no effect on the sulphur values obtained.

Since the sample solution is also used for determination of various major and minor constituents, especially lead and silver, to save time in these determinations a 6M hydrochloric acid concentration is used.

The reagent blanks must be run through the entire procedure, including the decomposition step, because the minor constituents are determined by atomic-absorption spectrophotometry, and contamination from the crucible used for the fusion must be allowed for. With zirconium crucibles no difficulty has been encountered.

The proposed method is very simple, rapid and accurate for zinc plant samples of various types and is a useful alternative to the standard gravimetric method, which is long and tedious.

Barium sulphate suspensions prepared in CTAB solution were found to have maximum absorbance at 420 nm. The calibration graph

Table 3. Composition of the samples

Sample	Zn, %	Fe, %	Pb, %	Cu, %	Cd, %	Ag, %	Mn, %	Mg, %
Zinc concentrate I (Zawar)	48.5	10.2	3.05	0.13	0.186	0.021	0.043	0.50
Zinc concentrate II (Dariba)	51.0	7.1	0.92	0.114	0.365	0.025	0.100	0.12
Zinc concentrate III (Feed)	50.7	8.6	2.73	0.126	0.268	0.023	0.243	0.37
Calcine (roasted product)	58.38	10.70	3.46	0.144	0.348	0.028	0.44	0.54
Feed to flotation (leached residue)	17.93	19.8	5.38	0.154	0.183	0.035	1.49	0.75
Jarosite (final leached residue)	5.20	15.40	4.61	0.098	0.106	0.0287	0.31	0.38

was linear up to 2.5 mg of sulphate in 100 ml of solution.

Copper, cadmium, zinc, iron and chloride cause practically no interference.

The barium chloride should be thoroughly ground to pass a 52-mesh sieve, to provide uniform particle size, and this has been found effective for producing the barium sulphate dispersion in CTAB solution. The amount added is based on the practical requirement of reaction with all the sulphate present, without leaving undissolved reagent dispersed in the solution; 0.25 g in 100 ml of solution was found satisfactory. Equal amounts of the barium chloride powder, with uniform particle size, must be used for all samples, standards and blanks, since turbidimetric methods require production of reproducible particle size distributions.

Dilute CTAB solution is used as the stabilizer to keep the barium sulphate in suspension. Too high a CTAB concentration causes frothing, however. Another conditioning agent, glycerol in hydrochloric acid,⁸ was also tried as the stabilizer but did not give satisfactory results. Toennies and Bakay used an ethanol-dipropylene glycol mixture as stabilizer⁶ but its efficacy was not tested in the present work.

The absorbance measurement should be made immediately after a constant time has elapsed after addition of the barium chloride. Generally 1 or 2 min is sufficient to attain a uniform suspension of barium sulphate in the CTAB solution.

Acknowledgements—We thank the management of Hindustan Zinc Limited for their kind permission to publish the work, as well as Om P. Bhargava of Stelco Steel, Ontario, Canada, for his valuable suggestion for improving the decomposition technique.

REFERENCES

1. W. F. Hillebrand, G. E. F. Lundell, H. A. Bright and J. I. Hoffmann, *Applied Inorganic Analysis*, 2nd Ed., p. 711. Wiley, New York, 1953.
2. N. H. Furman, *Standard Methods of Chemical Analysis*, 6th Ed., p. 1003. Van Nostrand, Princeton, 1962.
3. E. M. Donaldson, *Methods for the Analysis of Ores, Rocks and Related Materials*, 2nd Ed., p. 354. Energy, Mines and Resources, Ottawa, Canada, 1982.
4. O. P. Bhargava, M. Gmitro and W. G. Hines, *Talanta*, 1980, **27**, 263.
5. H. J. Keily and L. B. Rogers, *Anal. Chem.*, 1955, **27**, 263.
6. G. Toennies and B. Bakay, *ibid.*, 1953, **25**, 160.
7. A. Steinbergs, *Analyst*, 1953, **78**, 47.
8. H. Bechhold and F. Hebler, *Kolloid Z.*, 1922, **31**, 70.

A FIBER-OPTIC CYCLODEXTRIN-BASED SENSOR

J. P. ALARIE and T. VO-DINH*

Advanced Monitoring Development Group, Health and Safety Research Division, Oak Ridge National Laboratory, Oak Ridge, TN 37831-6101, U.S.A.

(Received 29 August 1990. Revised 14 November 1990. Accepted 24 November 1990)

Summary—This paper describes the development of a fiber-optic cyclodextrin-based (FCD) sensor. The device uses laser excitation and fluorescence detection with β -cyclodextrin as the reagent phase, immobilized at the tip of an optical fiber. The sensitivity of the FCD sensor is 14 times as great as that of a bare optical fiber when measurements are made with the fiber immersed in a buffer after a 10-min incubation period. The selectivity of the sensor is illustrated with pyrene as the model compound and 5,6-benzoquinoline as the interferent. An interference study with a contaminated environmental ground water sample is used to illustrate the usefulness of the FCD device.

An important class of fiber-optic chemical sensors relies on the interaction of the analyte with a reagent phase immobilized at the sensing end of the optical fiber to produce a spectroscopic signal. Antibodies and enzymes are often used as the reagent phases in fiber-optic sensors because of their high specificity toward the analyte of interest.¹⁻⁵ Cyclodextrins (CDs) have lower specificity than antibodies and enzymes but because of their ability to form complexes with various molecules have been utilized in chromatographic separation of organic and inorganic compounds.⁶

Cyclodextrins are sugar molecules having the structure of a hollow truncated cone with a hydrophobic cavity. Their complexation ability has been attributed to four factors.⁷ (1) Van der Waals interaction, (2) hydrogen-bonding, (3) displacement of high-energy water molecules from the cavity, and (4) release of the strain energy of the CD on inclusion of the guest molecule. The hydrophobicity of the guest molecule also plays a key role in the stability of the complex. The stoichiometry of the complexes is not necessarily 1:1; instances of 2:1 and 1:2 complexes are known.^{7,8} Complexation with cyclodextrins also enhances the fluorescence⁹ and phosphorescence of certain analytes¹⁰⁻¹⁴ and for this purpose CDs have been used on immobilized quartz plates in a fiber-optic probe.¹⁵

This work involves the development of a CD-based fiber-optic chemical sensor with β -

CD immobilized at the distal face of an optical fiber, that combines the selectivity of the CD with enhancement of the fluorescence of the complexed molecule. The polynuclear aromatic hydrocarbon (PAH) pyrene is used as the model compound. The complexation ratio for pyrene has been shown to be 1:1 for concentrations below $10^{-6}M$,^{8,16} which is the case for all pyrene solutions used in this work. The performance of the FCD sensor (analytical curve and response time) is described, and its selectivity has been investigated by using 5,6-benzoquinoline as an interferent, together with a ground water spiked with pyrene, and containing other PAHs as contamination.

EXPERIMENTAL

Materials

β -Cyclodextrin, glycidoxypropyltrimethoxysilane (GOPS), sodium hydride, pyrene and 5,6-benzoquinoline were obtained from Aldrich (Milwaukee, WI). Toluene, *N,N*-dimethylformamide (DMF), methanol and ethanol were obtained from EM Science (Cherry Hill, NJ). Phosphate-buffered saline (PBS) was obtained from Sigma (St. Louis, MO). The optical fiber was a multimode fused-silica 600- μ m diameter fiber purchased from General Fiber Optics (Cedar Grove, NJ). Fluorescence spectra were obtained with a Perkin-Elmer model MPF-43A spectrofluorimeter.

Procedures

β -CD was immobilized on the optical fiber by a method described previously.⁶ In this study, a

*Author for correspondence.

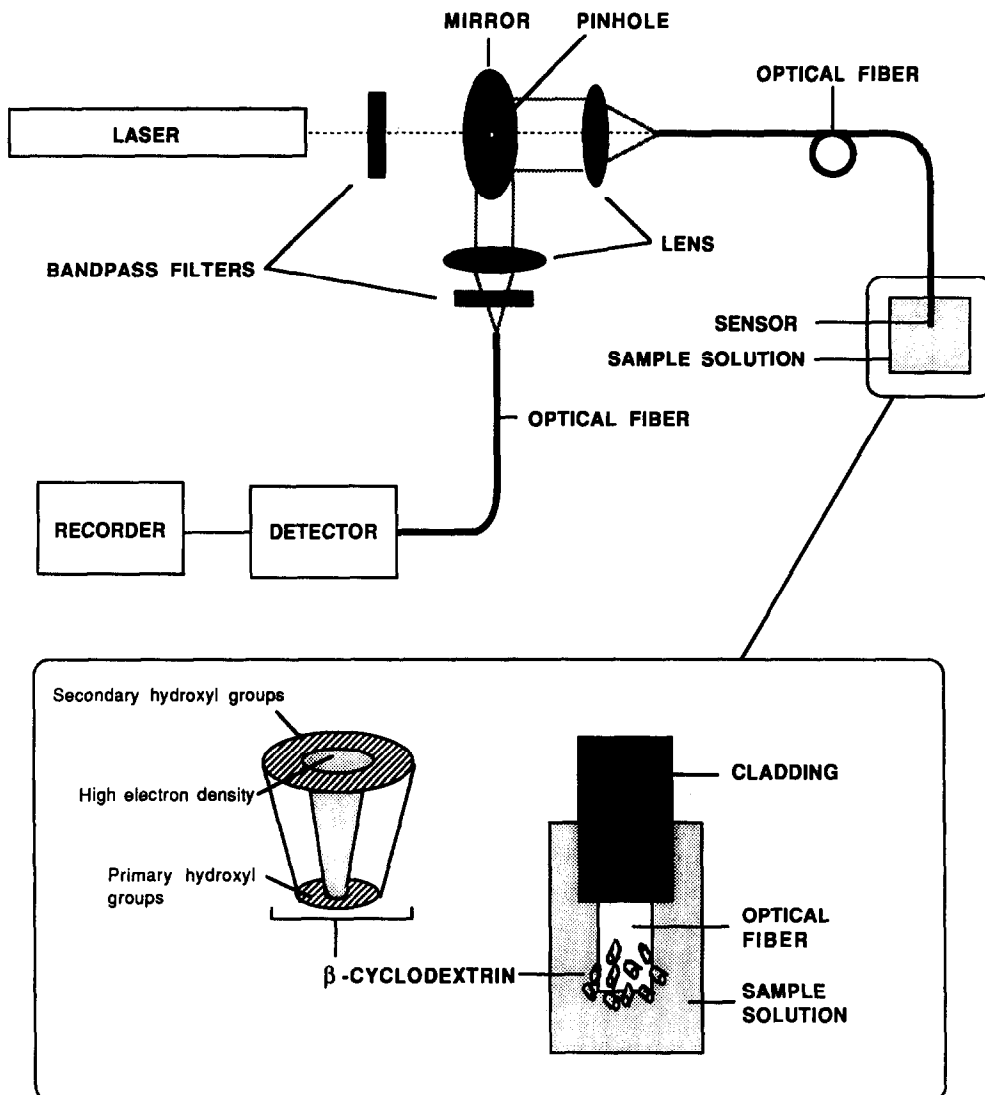


Fig. 1. Schematic diagram of the fiber-optic cyclodextrin (FCD) based sensor.

1-cm length of cladding was stripped from the fiber end and the fiber was heated overnight at 100°. The stripped tips (of several fibers) were then modified by immersing them in a 10% v/v GOPS solution in toluene, which was then refluxed for 3 hr.

The distal ends were washed with toluene and then methanol, and the fibers were heated overnight at 100°. Under an atmosphere of nitrogen, 500 mg of β -CD (heated overnight at 60°) was dissolved in 30 ml of DMF, sodium hydride (125 mg) was added, and the mixture was allowed to react for 15 min. The excess of sodium hydride was filtered off (still under a nitrogen atmosphere) and the solution refluxed for 2 hr with the fiber tips immersed in it. The fiber tips were then washed with DMF, methanol, toluene,

water and methanol in succession and heated overnight at 60°. They were then ready for use.

Apparatus

The optical configuration of the FCD sensor is straightforward and is shown schematically in Fig. 1. A brief description of the instrumental system is as follows. The 325-nm line of an He-Cd laser (Omnichrome, Chino, CA) was focused onto the untreated end of the optical fiber after passing through a beam-splitter consisting of a mirror with a 2-mm pinhole through its center. The fluorescence emitted by the sensor/analyte system was transmitted back through the fiber, reflected by the mirror and focused onto a collection fiber after passing through a 380–420 nm bandpass filter. The

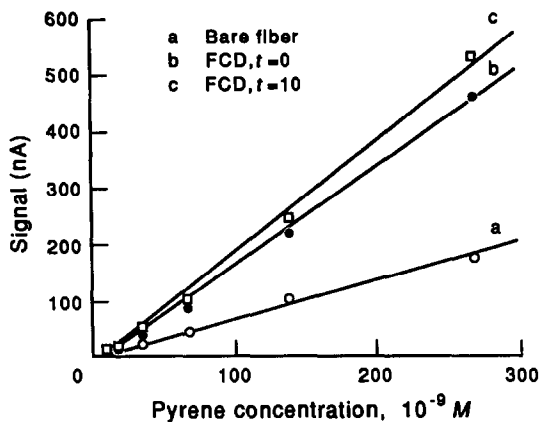


Fig. 2. Response curves for: a, bare fiber; b, FCD at $t = 0$ and c, FCD at $t = 10$ min.

collection fiber was connected to a photomultiplier (Hamamatsu, model R760), the current from which was processed by a Keithley model 485 autoranging picoammeter.

Measurements

All measurements were performed as follows. The samples were pyrene solutions for calibration and a pyrene/5,6-benzoquinoline mixture for the interference study. The sensor end of the fiber was immersed in the sample solution for a 10-min incubation period, then transferred into a fresh PBS solution. Measurements were taken when the fiber was first placed in the sample solution ($t = 0$), after 10 min (*i.e.*; immediately prior to removal ($t = 10$), and immediately it was placed in the PBS solution ($t = \text{post-incubation}$). The fiber could be reused after rinsing with a 60:40 v/v methanol/water mixture until the baseline signal was restored (generally in less than 1 min). In the interference study, the solutions were stirred.

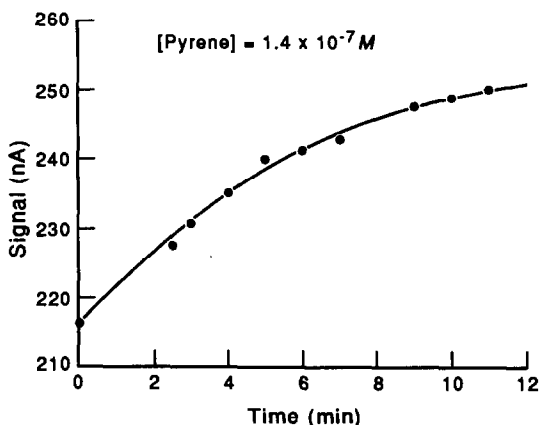


Fig. 3. Temporal response of the FCD sensor.

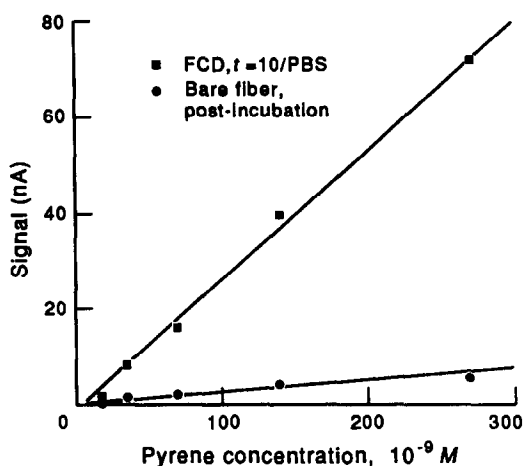


Fig. 4. Response curves for bare fiber, post-incubation, and FCD, post-incubation.

RESULTS AND DISCUSSION

Direct measurements in sample solutions

The performance of the β -CD derivatized fibers was evaluated by establishing response graphs for a pyrene concentration range of 8.5×10^{-9} – $2.7 \times 10^{-7} M$. Four response plots were obtained to characterize the β -CD fibers. The first was for the response of an underivatized optical fiber, *i.e.*, a blank (Fig. 2, curve a). The second and third lines (b and c in Fig. 2) were for the response of the β -CD fibers at incubation times $t = 0$ and $t = 10$ min. The linearity of these three response plots was excellent over the concentration range investigated, with correlation coefficients of (a) 0.9986, (b) 0.9986 and (c) 0.9980. However, the β -CD fibers are much more sensitive than the underivatized fiber, owing to the fluorescence enhancement obtained when pyrene molecules are complexed by β -CD. The measurement at $t = 0$ produces an enhancement factor of 2.7 and that at $t = 10$ min improves the factor to 3.1. Further improvement by measurement after incubation for more than 10 min would be minimal, as the response of the FCD levels off after about 10 min (Fig. 3).

The fourth response plot was for the post-incubation measurements and is shown in Fig. 4. This would be the actual working calibration plot since only the pyrene molecules complexed by the β -CD would be measured, which was not the case for the measurements at $t = 0$ and $t = 10$ min (Fig. 2), because the optical fiber, when in the analyte solution, "saw" beyond the β -CD layer and therefore non-complexed pyrene molecules in the solution as well as any interferents were also measured.

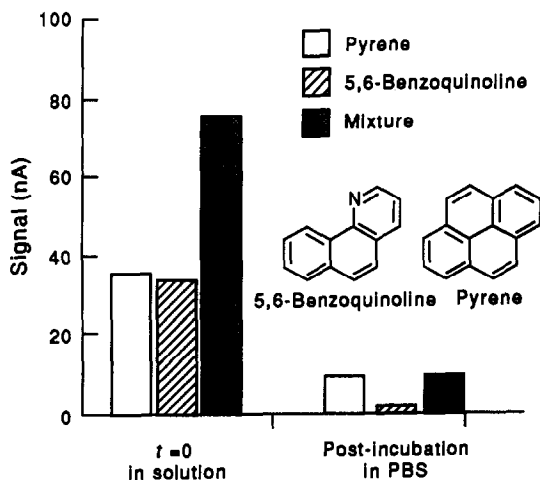


Fig. 5. Interference study. Detection of pyrene in the presence of 5,6-benzoquinoline.

When the fiber is removed from the sample solution and placed in the PBS solution, however, only molecules (of analyte or interferent) bound by the β -CD are measured. Figure 4 also shows the result of leaving (for 10 min) a bare fiber in pyrene solutions of the same concentrations as those used with the β -CD fibers, and measuring the post-incubation signal. This indicates that some of the signal from the FCD may be due to non-specific adsorption. With the limit of detection (LOD) defined as the concentration of pyrene which yields an S/N ratio of 4 (noise = 0.8 nA), the LOD for the FCD is

$1.9 \times 10^{-8} M$ pyrene. The LOD may be extended to lower concentrations by increasing the amount of β -CD immobilized on the optical fiber, therefore allowing a longer incubation period without saturation of the β -CD.

The sensitivity of the FCD post-incubation measurements is 14 times that of the bare fiber post-incubation measurements. This enhancement occurs because more pyrene molecules are complexed by the FCD than are adsorbed by the bare optical fiber. The enhancement is also larger than that achieved by the solution measurements (at $t = 0$ and $t = 10$ min) as only complexed pyrene molecules (and no free pyrene molecules in solution) are being measured.

Reproducibility

The reproducibility was investigated by repetitive measurements of $6.8 \times 10^{-8} M$ pyrene solutions. For a total of 10 measurements ($t = 0$ signal), an average signal of $46.2 \pm 3.4 \mu A$ was obtained, producing a relative standard deviation (RSD) of 7.3%. This RSD value may include variations due to incomplete rinsing (with 60:40 methanol/water mixture) between measurements, as well as to fluctuations in the pyrene concentration in the field of view of the optical fiber. When signal variations from fiber to fiber are also taken into account the RSD is estimated to be 15%.

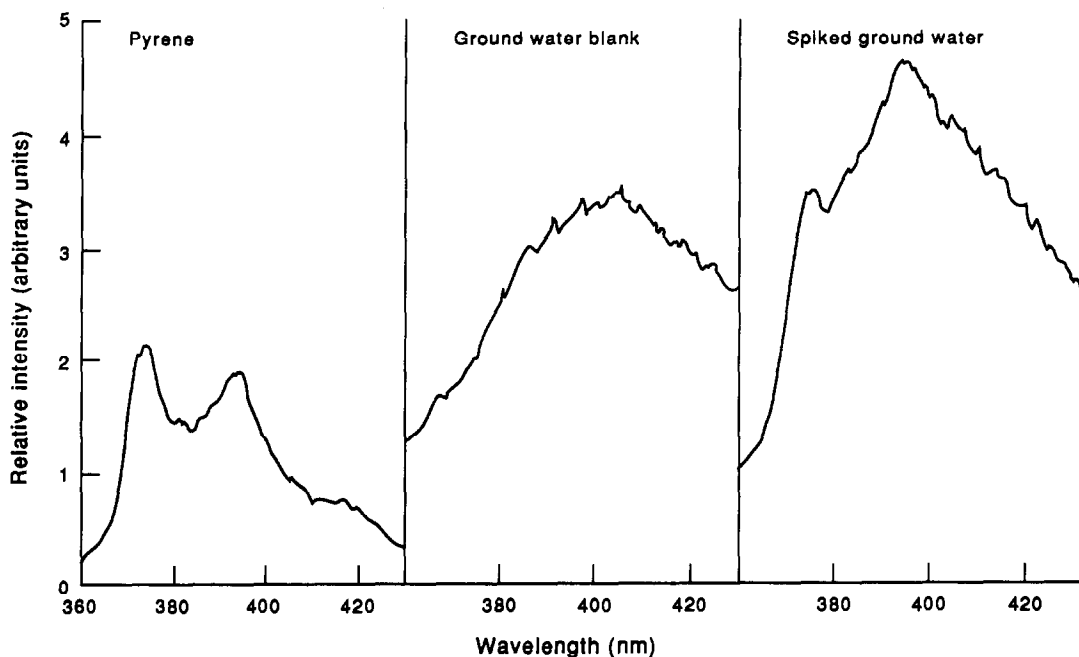


Fig. 6. Fluorescence emission spectra of pyrene, a ground water blank, and the ground water sample spiked with pyrene.

Interference studies

An interference study was performed with pyrene as the model compound and 5,6-benzoquinoline as the interferent. Owing to the hydrophobic nature of the internal cavity of the β -CD, 5,6-benzoquinoline, which contains a nitrogen atom (see Fig. 5), is not expected to form stable complexes with β -CD, as homocyclic pyrene does. The concentration of the 5,6-benzoquinoline was $1.3 \times 10^{-7} M$ and the pyrene concentration was $3.4 \times 10^{-8} M$. Figure 5 shows the signals for the individual pyrene and 5,6-benzoquinoline solutions and for a mixture of the two compounds, at $t = 0$ and post-incubation (following a 10-min incubation period). When they are determined individually, at $t = 0$, the pyrene and 5,6-benzoquinoline samples yield similar fluorescence signals, which are approximately additive for a mixture. However, when the FCD is used in post-incubation mode, the 5,6-benzoquinoline signal is practically zero whereas the signal for pyrene and the mixture are 8.5 and 8.7 nA respectively. The result illustrates the selectivity of the FCD sensor in the presence of non-complexing or weakly complexing interferents. The selectivity in this case is based on the reduced ability of 5,6-benzoquinoline to form stable complexes inside the β -CD cavity. Pyrene, which forms stable complexes in the hydrophobic cavity, can be measured by the FCD sensor in the presence of a 4-fold molar ratio of 5,6-benzoquinoline.

The selectivity of the FCD was also analyzed by using a ground water sample spiked with pyrene. This ground water sample was known from synchronous luminescence measurements

to have PAH contamination.¹⁷ The extent of contamination was not further examined either qualitatively or quantitatively. Figure 6 shows the fluorescence emission spectra of pyrene ($1.4 \times 10^{-7} M$), a ground water blank, and a ground water sample spiked with pyrene, excitation at 325 nm. The results of analysis with the FCD are shown in Fig. 7. For measurement at $t = 0$, the ground water blank signal is higher than the pyrene signal, and that for the spiked ground water signal is approximately the sum of the signals from the individual samples. For the post-incubation measurements, the ground water blank signal is almost negligible and the pyrene and spiked ground water sample yield practically identical signals. This indicates that there are no other interferents present in the ground water sample which can be complexed by β -CD. This also illustrates the ability of the FCD to measure pyrene selectively in a complex mixture.

CONCLUSION

The analytical properties of a simple fiber-optic chemical sensor utilizing the selectivity of immobilized β -CD have been described. Besides being used to detect analytes in an unknown mixture, the FCD may also be utilized to study the complexation of cyclodextrins with select fluorophors. Other uses might include further studies of the fluorescence enhancement effect, along with determination of formation constants and other bonding characteristics.

Acknowledgements—This work was sponsored by the Office of Health and Environmental Research, U.S. Department of Energy, under Contract Number DE-AC05-84OR21400 with Martin Marietta Energy Systems, Inc.

REFERENCES

1. T. Vo Dinh, B. J. Tromberg, G. D. Griffin, K. R. Ambrose, M. J. Sepaniak and E. M. Gardenhire, *Appl. Spectrosc.*, 1987, **41**, 735.
2. B. J. Tromberg, M. J. Sepaniak, T. Vo-Dinh and G. D. Griffin, *Anal. Chem.*, 1987, **59**, 1226.
3. T. Vo-Dinh, T. Nolan, Y. F. Cheng, G. D. Griffin, M. J. Sepaniak and J. P. Alarie, *Appl. Spectrosc.*, 1990, **44**, 128.
4. J. P. Alarie, M. J. Sepaniak and T. Vo-Dinh, *Anal. Chim. Acta*, 1990, **229**, 169.
5. T. Vo-Dinh, G. D. Griffin and K. R. Ambrose, *Appl. Spectrosc.*, 1986, **40**, 696.
6. D. W. Armstrong, *U.S. Patent 4,539,399*, 3 September 1985; *Chem. Abstr.*, 1985, **103**, 226754f.
7. J. Szejtli, *Cyclodextrins and Their Inclusion Complexes*, Akadémiai Kiadó, Budapest, 1982.
8. L. A. Blyshak, K. Y. Dodson, G. Patonay, I. M. Warner and W. E. May, *Anal. Chem.*, 1989, **61**, 955.

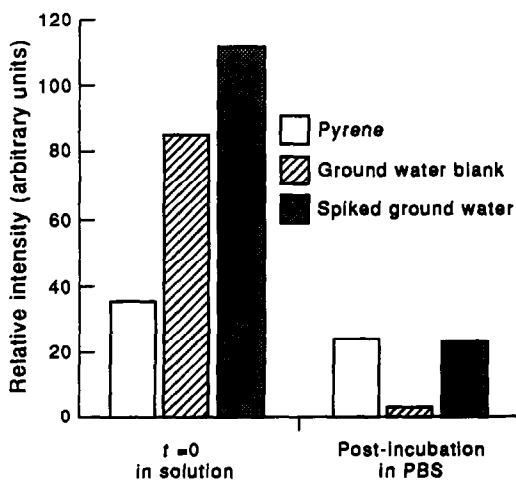


Fig. 7. Interference study. Detection of pyrene in contaminated ground water.

9. A. M. Alak, E. Heiweil, W. L. Hinze, H. Oh, and D. W. Armstrong, *J. Liq. Chromatog.*, 1984, **7**, 1273.
10. F. J. DeLuccia, and L. J. Cline Love, *Anal. Chem.*, 1984, **56**, 2811.
11. J. Bello and R. J. Hurtubise, *Appl. Spectrosc.*, 1986, **40**, 790.
12. T. Vo-Dinh and A. M. Alak, *ibid.*, 1987, **41**, 963.
13. A. M. Alak and T. Vo-Dinh, *Anal. Chem.*, 1988, **60**, 596.
14. A. M. Alak, N. Contolini and T. Vo-Dinh, *Anal. Chim. Acta*, 1989, **217**, 171.
15. K. S. Litwiler, G. C. Catena and F. V. Bright, *ibid.*, 1990, **237**, 485.
16. A. Nakajima, *Spectrochim. Acta*, 1983, **39A**, 913.
17. G. H. Miller, and T. Vo-Dinh. Oak Ridge National Laboratory, Internal communication.

SYNTHESIS OF NEW MICROSENSOR COATINGS AND THEIR RESPONSE TO TEST VAPORS

2,4,6-TRISUBSTITUTED-1,3,5-TRIAZINE DERIVATIVES

ALAN R. KATRITZKY,* JAMSHED N. LAM and HASSAN M. FAID-ALLAH

Department of Chemistry, University of Florida, Gainesville, FL 32611-2046, U.S.A.

(Received 6 June 1990. Revised 30 October 1990. Accepted 3 November 1990)

Summary—Novel 1,3,5-triazine derivatives were spray-coated onto surface acoustic wave (SAW) devices and exposed to vapors of dimethyl methylphosphonate (DMMP), chloroethyl ethyl sulfide (CEES) and water. Changes in chemiresistor and SAW responses were monitored and recorded by computer-controlled data-acquisition techniques. All the derivatives tested showed little or no chemiresistor or SAW responses to water vapor. The largest reversible chemiresistor response to DMMP vapor was observed with the dicarboxylic acid derivative. The largest SAW response to DMMP was with the dithione, and the dichloro-octylthio derivative showed the largest response to CEES.

The need to design instruments to detect airborne contaminants has increased rapidly in recent years. The need to detect contaminants in parts per million (ppm) concentrations for gas leaks, chemical warfare (CW) agents and illicit drug manufacture makes the use of GC/MS (which has been used for the detection of atmospheric pollutants) and other large monitoring devices impractical.

Microelectronics and computer design have been used in the fabrication of selective and sensitive vapor detectors which are small in size and are applicable to military, industrial and environmental use. These devices include chemiresistor,^{1,2} surface acoustic wave (SAW)³⁻⁵ and bulk-wave piezoelectric quartz crystal sensors.⁶ The chemiresistor and SAW devices are both manufactured from piezoelectric quartz with an interdigitated electrode array (usually gold) lithographically deposited on the surface of the quartz crystal.¹ It is this similarity between the two devices that allows resistance (chemiresistor) and frequency (SAW) measurements to be made simultaneously.⁷ The principles of operation of SAW devices^{3,8} as well as those of chemiresistors¹ have already been described in detail. Details of the system used in our laboratory and its modes of operation have been published in two reviews by our group^{9,10} and will not be discussed here. The work described in this report is part of a project involving rapid

preliminary screening of heterocyclic derivatives and the behavior of various classes of compounds in an attempt to utilize these microsensors to their full potential. Heterocyclic systems tested so far include benzimidazole,¹¹ pyridine and pyrylium,¹² thiadiazole,¹³ nicotinamide,¹⁴ acridinium betaine,¹⁵ and phosphorus¹⁶ derivatives. It is hoped that acquisition of such data will provide valuable insight into the vapor/coating interactions and afford a better understanding of the effects of various functional groups on the device responses. In this paper, we report the responses of a variety of trisubstituted-1,3,5-triazines to DMMP (a nerve-agent simulant), CEES (a sulfur mustard-gas simulant) and water (an interferent).

EXPERIMENTAL

Simultaneous chemiresistor and SAW measurements were performed while exposing the device to water, CEES and DMMP vapors in turn. The results were usually reproducible to within 5%. The dual 52-MHz surface acoustic wave apparatus used (Microsensor Systems, Inc.), has been described in detail previously.^{9,11,15}

The resonant frequency was monitored with a digital frequency counter, Phillips Model PM 6674 universal frequency counter (550 MHz). The conductivity measurements were made by the application of a 1-V bias to either of the two remaining electrodes, and measurement of the current with a precision current-to-voltage

*Author for correspondence.

converter consisting of an operational amplifier and a switch-selectable feedback resistor.

SAW and chemiresistor data-acquisition was controlled by an Apple II computer with an IEEE-488 interface, connected to the frequency counter and an electrometer (Keithley 617 Programmable Electrometer).

The coatings were dissolved in a volatile organic solvent, typically spectroscopic grade chloroform, and the device was spray-coated with an air brush, with dry nitrogen as the propellant. The coating thickness was monitored with the frequency counter until a frequency shift of *ca.* 50 kHz was obtained. The frequency shifts caused by the coating were recorded as an indication of coating thickness. Test vapors were generated by passing a regulated flow of nitrogen through the neat liquid at 0°, in a vapor bubbler equipped with a gas dispersion tube. The flow-rate over the device was controlled with a flowmeter and was found to be 7.5 ml/min by use of a bubble meter. The absolute concentrations of the test vapors were calculated by methods described previously.¹⁵ Thus at 0°, the vapor pressures of DMMP, CEES and water afforded concentrations of 5.2, 30.7 and 4.8 g/m³ respectively.

Initially the system was purged with nitrogen for 5 min to establish a baseline curve. The device was then exposed to the vapor for 40 min, followed by a nitrogen purge for 50–60 min. If a response was irreversible, the SAW device was cleaned and recoated before exposure to the next test vapor.

The SAW devices used were rinsed with acetone between runs, followed by ultrasonic cleaning for 15 min in spectroscopic grade 2-propanol.

Melting points were determined on a Thomas-Hoover capillary melting point apparatus, and were uncorrected. ¹H NMR spectra were recorded on a Varian Model EM 360L spectrometer with tetramethylsilane (TMS) as the internal standard. ¹³C NMR spectra were recorded at 25 MHz on a JEOL Model JNM-FX 100, with solvent peaks (CDCl₃, δ77.0 or (CD₃)₂SO δ39.5) as internal references.

Synthesis of coating materials

2,4-Dichloro-6-octylthio-1,3,5-triazine (5), b.p. 140–145°/5 mmHg, literature value¹⁷ 146–148°/0.4 mmHg, and 2,4-dichloro-6-dodecylthio-1,3,5-triazine (8), literature value¹⁷ m.p. 23–26° (see Tables 1 and 2) were prepared by known literature procedures.

Preparation of 2,4-dioctylamino-6-octylthio-1,3,5-triazine (2). A solution of 2,4-dichloro-6-octylthio-1,3,5-triazine (15.0 g, 50 mmole) in acetone (50 ml) and water (20 ml) was cooled to 0–5°. Octylamine (13.1 g, 110 mmole) was added dropwise while the temperature was maintained at 0–5°. Cooling was continued as aqueous sodium hydroxide solution (2*M*, 50 ml) was slowly added. The mixture was then stirred for 24 hr at ambient temperature and the precipitate was filtered off, washed with water and dried. Crystallization from dilute methanol resulted in colorless plates (22.5 g, 93%), m.p. 56° (see Tables 1 and 2).

*Preparation of 2-octylthio-1,3,5-triazine-4(3*H*),6(5*H*)-dithione (3).* A solution of 2,4-dichloro-6-octylthio-1,3,5-triazine (8.0 g, 27 mmole) and thiourea (4.0 g, 54 mmole) in acetone (100 ml) was heated under reflux for 1 hr. The reaction mixture was then cooled to 0° and aqueous sodium carbonate solution (0.5*M*, 200 ml) was added slowly, with the temperature kept below 5°. The mixture was then stirred at room temperature overnight, the precipitate filtered off and the filtrate neutralized with 5% v/v hydrochloric acid. The product was filtered off, washed with water and dried (see Tables 1 and 2).

Preparation of 2,4-di(carboxymethylthio)-6-octylthio- (6) and 2,4-di(carboxymethylthio)-6-dodecylthio- (9) 1,3,5-triazines. A solution of (5) or (8) (50 mmole) in acetone (100 ml) was cooled to 0–5°. Mercaptoacetic acid (9.3 g, 100 mmole) and then collidine (13.5 g, 110 mmole) were added dropwise while the temperature was maintained at 0–5°. The mixture was stirred for 24 hr at ambient temperature, poured into water (100 ml) and extracted with diethyl ether (3 × 75 ml). The ethereal solution was dried over anhydrous sodium sulfate and evaporated under reduced pressure to yield the products, as white solids (see Tables 1 and 2).

General procedure for the synthesis of tris(dialkylaminoethylthioethoxy)-1,3,5-triazines (7a–c)

The appropriate dialkylaminoethanethiol hydrochloride (140 mmole) was added to a solution of cyanuric chloride (4) (8.7 g, 47 mmole) in acetone (100 ml). The mixture was cooled to 0–5° and aqueous sodium hydroxide solution (2*M*, 140 ml) was added slowly so that the temperature remained at 0–5°. After the addition was complete, the reaction mixture was stirred for 24 hr at ambient temperature, poured into water (75 ml), and extracted with diethyl

ether (3×50 ml). The combined ether extracts were washed with water (25 ml) and dried over anhydrous sodium sulfate. Removal of the ether under reduced pressure gave the triazine derivatives (**7a-c**) as sticky oils which were then converted into the picrates and characterized. Each picrate was then dissolved in dichloromethane and washed with aqueous sodium hydroxide solution to afford the pure product (see Tables 1 and 2).

RESULTS AND DISCUSSION

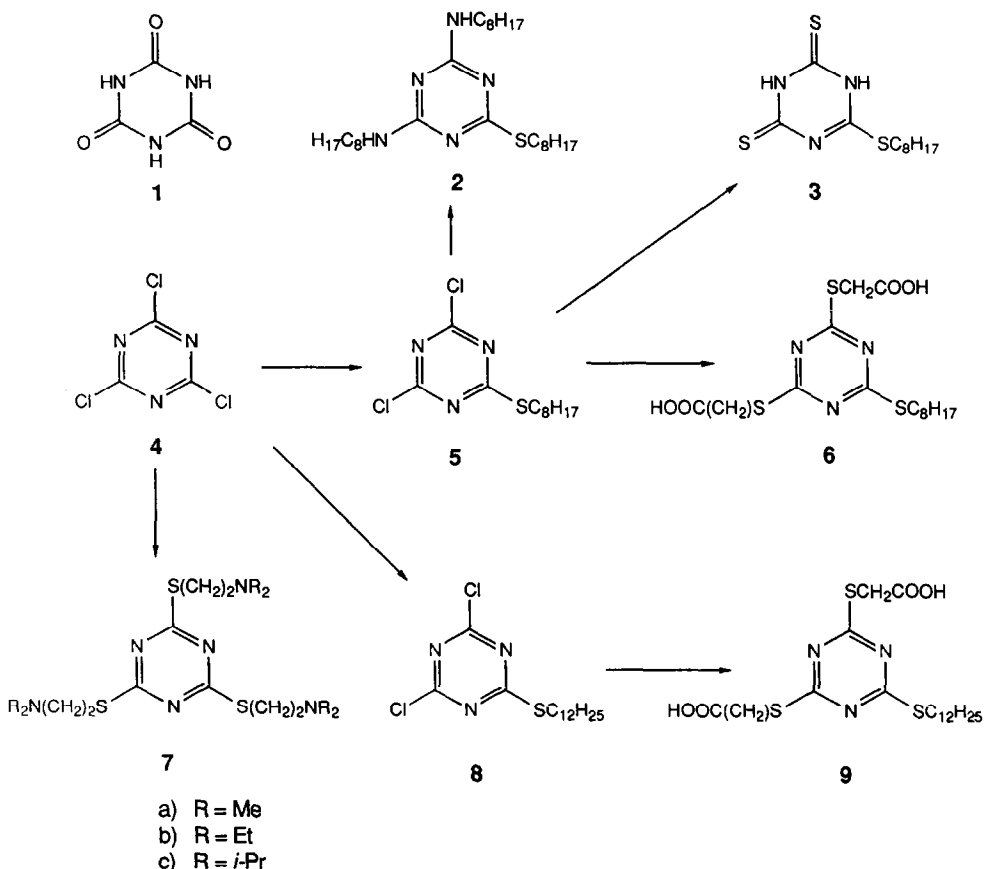
Derivatives of the 1,3,5-triazines, such as cyanuric acid (**1**), were discovered as early as 1776,¹⁸ although the parent compound 1,3,5-triazine was identified only much more recently by Grundmann and Kreutzberger.¹⁹

The most important precursor for the synthesis of 1,3,5-triazine derivatives is cyanuric chloride (**4**), the substituents in which can be displaced readily by nucleophiles to afford trisubstituted-1,3,5-triazines. Thus symmetrical tri(alkylthio)- and tri(arylthio)-triazines have

been prepared by the reaction of sodium mercaptides with (**4**).²⁰

We have now found that treatment of (**4**) with various dialkylaminoethanathiols at 0° in the presence of sodium hydroxide gives the trithioethers (**7**) in yields of 83–90%. The compounds were characterized by elemental analysis and their characteristic NMR spectra. In all three cases, the single aromatic carbon signal appeared between 178.7 and 179.4 ppm. The aliphatic $N-C_\alpha$ carbon atom in NCH_2CH_2S showed an upfield shift of about 6.7 ppm as the dialkylamino substituent was changed from methyl to ethyl to isopropyl. The $N-C_\beta$ carbon atom of the isopropyl substituent (**7c**) gave a shift 3 ppm downfield from the signal for the dimethyl (**7a**) and diethyl (**7b**) derivatives.

Previous workers found that the use of a weaker base such as collidine¹⁷ or pyridine²¹ and equimolar amounts of cyanuric chloride and a thiol or an alcohol, led to the displacement of a single chlorine atom to give monosubstituted adducts, which with other nucleophiles, formed unsymmetrical trisubstituted triazines.



Scheme 1

Table 1. Preparation of 2,4,6-trisubstituted-1,3,5-triazines

Compound No.	Yield, %	M.P., °C	Crystal form	Recryst. solvent	Molecular formula	Found (Theory), %		
						C	H	N
2	93	56	Plates	dil. MeOH	C ₂₇ H ₃₃ N ₅ S·H ₂ O	65.5 (65.21)	11.0 (10.80)	14.1 (14.11)
3	63	155	Microcrystals	H ₂ O	C ₁₁ H ₁₉ N ₃ S ₃	45.7 (45.67)	6.6 (6.62)	14.5 (14.53)
5	93	Oil	—	—	C ₁₁ H ₁₇ Cl ₂ N ₃ S	—	—	—
6	89	163	Needles	dil. MeOH	C ₁₅ H ₂₃ N ₃ O ₄ S·H ₂ O	42.4 (42.55)	5.6 (5.91)	9.9 (9.91)
7a	83	Oil*	—	—	C ₁₅ H ₃₀ N ₆ S ₃ ·2Pic	38.0 (38.20)	4.2 (4.27)	19.6 (19.80)
7b	87	Oil†	—	—	C ₂₁ H ₄₂ N ₆ S ₃ ·Pic	44.9 (44.93)	6.1 (6.51)	17.8 (17.47)
7c	90	Oil‡	—	—	C ₂₇ H ₅₄ N ₆ S ₃ ·Pic	49.0 (49.19)	7.1 (7.30)	15.9 (15.70)
8	92	Oil	—	—	C ₁₅ H ₂₅ Cl ₂ N ₃ S	—	—	—
9	79	152–153	Needles	C ₆ H ₆ /MeOH	C ₁₉ H ₃₁ N ₃ O ₄ S ₃	49.2 (49.43)	6.7 (6.77)	9.0 (9.10)

*M.P. of picrate 205°. †M.P. of picrate 76°. ‡M.P. of picrate 162°.

As expected, reaction of cyanuric chloride with equimolar amounts of octanethiol or dodecylthiol in the presence of collidine afforded the monosubstituted thioethers (5) and (8) respectively. The remaining two chlorine atoms in (5) were readily displaced by octylamine in the presence of sodium hydroxide to give 4,6-di-(octylamino)-2-octylthiotriazine (2). Reaction of (5) and (8) with mercaptoacetic acid, with collidine as the base, formed (6) and (9) in yields of 89 and 79% respectively. With two equivalents of thiourea, (5) gave the dithione derivative (3).

Compounds 2, 3 and 5–9 were then tested as microsensors coatings by exposure to DMMP, CEES and water vapors (Table 3). The frequency shifts were calculated by subtracting the lowest frequency recorded during vapor exposure from the initial (baseline) frequency. Resistance changes were the ratios of the initial

resistance to the lowest resistance recorded over the same period (thus, a value close to unity denotes no change). The low signal to noise ratio in the SAW device enables small frequency changes to be detected quite readily. Typically, for an SAW delay line operating in the frequency range of 30–300 MHz, mass changes of the order of 10⁻⁹ g can be detected. However, for chemiresistor devices, a 100-fold change is required for a compound to be considered a good coating.

A large reversible resistance change (351-fold) on exposure to DMMP was observed with 2,4-dicarboxymethylthio-6-octylthio-1,3,5-triazine (6) as the coating. The dodecylthio analog (9) showed a comparable change (283-fold). This large resistance change is not surprising since the presence of two carboxylic acid groups would be expected to result in some interaction with an ester group. What is surprising though

Table 2. ¹H and ¹³C NMR data for 2,4,6-trisubstituted-*s*-triazines

Compound No.	¹ H	¹³ C
2	5.26(2H, bs), 3.3(6H, m), 1.33(36H, bs), 0.9(9H, t, J = 7Hz)	164.5, 164.1, 41.2, 40.6, 31.8, 30.5, 29.7, 29.2, 26.9, 22.6 and 14.0.
3	9.50(2H, bs), 3.25(2H, t, J = 7Hz), 1.15(12H, m), 0.75(3H, t, J = 7Hz)	177.3, 164.6, 31.3, 30.0, 28.5, 28.3, 28.0, 27.1 and 14.0.
5	3.20(2H, t, J = 7Hz), 1.3(12H, bs), 0.90(3H, t, J = 7Hz)	186.3, 169.7, 31.5, 30.9, 28.8, 28.7, 28.4, 28.2, 22.4 and 13.8.
6	6.7(2H, bs), 3.90(4H, s), 3.15(2H, t, J = 7Hz), 1.30(12H, bs), 0.92(3H, t, J = Hz)	179.0, 178.6, 169.8, 33.5, 31.2, 29.6, 28.6, 28.0, 22.1 and 13.9
7a	3.29(6H, t, J = 7Hz), 2.60(6H, t, J = 7Hz), 2.30(18H, s)	179.2, 58.0, 45.1 and 27.9.
7b	3.3–2.3(24H, m), 1.05(18H, t, J = 7Hz)	178.8, 51.2, 46.4, 27.5 and 11.5.
7c	2.95(18H, bs), 1.05(36H, t, J = 7Hz)	179.4, 48.6, 44.5, 31.3 and 20.7.
8	3.2(2H, m), 1.75(2H, m), 1.25(18H, bs), 0.85(3H, t, J = 7Hz)	186.5, 169.9, 31.8, 31.1, 29.5, 29.3, 29.0, 28.9, 28.7, 28.6, 28.3, 22.6 and 14.0.
9	8.3(2H, bs), 3.95(4H, s), 3.15(2H, t, J = Hz), 1.2(20H, m), 0.85(3H, t, J = 7Hz)	179.2, 178.4, 169.4, 33.1, 31.3, 29.7 29.1, 28.9, 28.6, 28.1, 22.1 and 13.8

Table 3. Response of 2,4,6-trisubstituted-1,3,5-triazines to test vapors

Compound No.	Coating mass, * kHz	Resistance change factor			Frequency shift, kHz		
		DMMP	CEES	H ₂ O	DMMP	CEES	H ₂ O
2	55	1.0	1.0	1.1	2.5	1.9	0.3
3	56	126.9	3.9	1.0	52.6	2.8	2.8
5	52	37.0	34.0	1.0	4.1	18.1	0.3
6	47	351.0	11.9	8.5	27.2	2.7	1.0
7a	48	1.0	1.0	1.4	2.6	9.6	2.2
7b	54	15.0	6.4	2.0	2.0	6.0	0.1
7c	53	20.8	22.3	1.8	2.1	11.4	0.8
8	50	5.2	37.4	1.0	4.1	4.9	0.3
9	55	283.0	2.4	8.0	17.4	1.3	0.7

*Frequency change equivalent to the mass.

is the fact that both these coatings showed a comparatively low response to water vapor (Fig. 1). Furthermore, both displayed good frequency responses to DMMP (27.2 and 17.4 kHz, respectively) indicating that there was a mass loading (absorption) effect. A large resistance change with a low frequency change would have implied a surface effect.

The largest resistance change (37.4-fold) for CEES vapor was observed with 2,4-dichloro-6-dodecylthio-1,3,5-triazine (8). The octylthio compound (5) also gave a high response (34.0-fold) to CEES and a similar response (37-fold) to DMMP vapor. Compound 8, however, did not show a comparable response to the DMMP vapor. The highest responses to water vapor were from the dicarboxylic acids (6) and (9), but these were still low, so these derivatives would make good chemiresistor coatings for the detection of DMMP vapors.

The greatest SAW frequency response was with the dithione (3), which displayed a frequency shift of 52.6 kHz for DMMP and

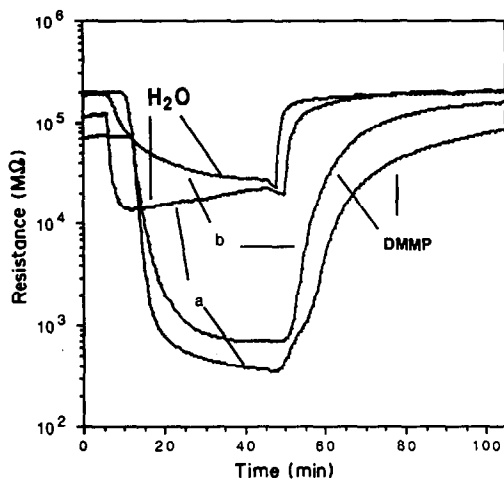


Fig. 1. Chemiresistor response of: a, compound 6 and; b, compound 9 vs. time, for exposure to DMMP and water vapor.

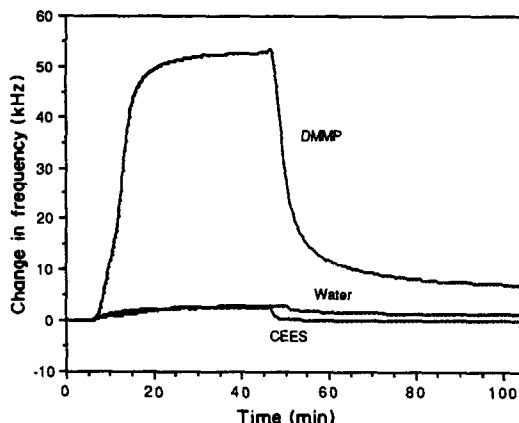


Fig. 2. Frequency response of 2-octylthio-1,3,5-triazine-4(3H),6(5H)-dithione (3) vs. time, for exposure to vapor.

had good discrimination, shown by its small response to CEES and water vapors (Fig. 2). Furthermore, it was 90% reversible. Consequently, this makes it a very good coating for an SAW device in the detection of DMMP in the presence of CEES and water vapors. A sharp change in frequency when the vapor is turned on and off is shown in Fig. 3. After purging of the

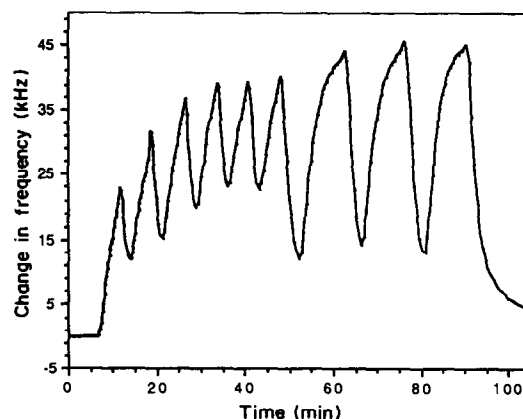


Fig. 3. Frequency response of 2-octylthio-1,3,5-triazine-4(3H),6(5H)-dithione (3) vs. time for periodic vapor exposure to DMMP (on/off time interval 5/2 min until $t = 48$ min, then 10/4 min until $t = 90$ min).

system with nitrogen for 5 min the vapor was repeatedly turned on for 5 min and then off for 2 min over a period of 40 min. The on/off times were then changed to 10 and 4 min respectively for a further 60 min. Analysis of the results shows that for both absorption and desorption the change in frequency is a quadratic function of time (with correlation factors of 0.992 and 0.997 respectively). The dicarboxylic acids (6) and (9) also showed good selectivity, displaying a large response only to DMMP vapor. For CEES vapor, the largest response was with the dichloro-octylthio compound (5) with low responses towards DMMP and water, thus displaying potential as a coating for the detection of CEES vapors. However, the dodecyl derivative (8) showed poor responses to all three vapors.

Previous work in our group¹³ has shown that within series of dimethyl-, diethyl- and di-isopropyl-amino derivatives, the frequency response to CEES decreases, indicating that steric hindrance around the amino group is an important factor for interaction with CEES vapor. Interestingly, in the present case, the tris(*N,N*-di-isopropylamino) analog (7c) showed the greatest response of the three. This further highlights the fact that there is still a lack of understanding of the precise interactions between coatings and vapors.

In all cases when a high response to DMMP or CEES vapor occurred, there was a low response to water vapor, indicating a low interference by humidity. The moderate to good solubility of these triazine derivatives in chloroform caused no difficulties in the spraying of these coatings. The relatively low volatility (as indicated by a baseline drift of *ca.* 1 kHz/hr, which is normal in a laboratory environment without temperature control), indicated a negligible tendency of the coating to vaporize when exposed to air, and hence the possibility of a reasonable lifetime, since the responses were reversible.

The coating thicknesses were much the same for all the triazines tested. Although a thicker coating would display a larger response, owing to the greater number of sorption sites, there are other factors such as shear modulus and film mass-density that come into play. The

vapor diffusion rate and device response times are closely related,³ and very close packing (high mass-density) of the coating would hinder easy diffusion of the analyte and the corresponding response time would be greater. It is for this reason that we have chosen not to study the relation between coating thickness and response times.

Acknowledgement—We thank G. Paul Savage for his helpful advice in this work and his suggestions in the preparation of this manuscript.

REFERENCES

1. H. Wohltjen, W. R. Barger, A. W. Snow and N. L. Jarvis, *IEEE Trans. Electron Devices*, 1985, **ED-32**(7), 1170.
2. T. E. Edmonds and T. S. West, *Anal. Chim. Acta*, 1980, **117**, 147.
3. H. Wohltjen, *Sens. Actuators*, 1984, **5**, 307.
4. C. T. Chuang, R. M. White and J. J. Bernstein, *IEEE Electron Device Lett.*, 1982, **EDL-3**(6), 145.
5. A. Venema, E. Nieuwkoop, M. J. Vellekoop, M. S. Nieuwenhuizen and A. W. Barendsz, *Sens. Actuators*, 1986, **10**, 47.
6. W. H. King, Jr., *Anal. Chem.*, 1964, **36**, 1735.
7. A. W. Snow, W. R. Barger, M. Klusty, H. Wohltjen and N. L. Jarvis, *Langmuir*, 1986, **2**, 513.
8. M. S. Nieuwenhuizen and A. W. Barendsz, *Sens. Actuators*, 1987, **11**, 45.
9. A. R. Katritzky and R. J. Offerman, *Crit. Rev. Anal. Chem.*, 1989, **2**, 83.
10. A. R. Katritzky and G. P. Savage, *Rev. Heteroatom Chem.*, 1990, **3**, 160.
11. A. R. Katritzky, G. P. Savage, J. N. Lam and M. Pilarska, *Chem. Scr.*, 1989, **29**, 197.
12. A. R. Katritzky, G. P. Savage, M. Pilarska and Z. Dega-Szafran, *ibid.*, 1989, **29**, 235.
13. A. R. Katritzky, G. P. Savage and M. Pilarska, *ibid.*, 1989, **29**, 317.
14. A. R. Katritzky, G. P. Savage, M. Pilarska, N. S. Bodor and M. E. Brewster, *ibid.*, 1989, **29**, 319.
15. A. R. Katritzky, R. J. Offerman, J. M. Aurrecoechea and G. P. Savage, *Talanta*, 1990, **37**, 911.
16. A. R. Katritzky, G. P. Savage, R. J. Offerman and B. Pilarski, *ibid.*, 1990, **37**, 921.
17. H. Koopman, J. H. Uhlenbroek, H. H. Haeck, J. Daams and M. J. Koopmans, *Rec. Trav. Chim. Pays-Bas*, 1959, **78**, 967.
18. E. M. Smolin and L. Rapoport, in *s-Triazines and Derivatives*, A. Weissberger (ed.), Interscience, New York, 1959.
19. C. Grundmann and A. Kreutzberger, *J. Am. Chem. Soc.*, 1954, **76**, 632.
20. P. Klason, *J. Prakt. Chem.*, 1886, **33**, 116.
21. J. R. Geigy A.-G., *Brit. Patent*, 977, 589, Dec. 9, 1964; U.S. Appl. April 12, Aug. 3, 1960, and Feb. 21, 1961; *Chem. Abstr.*, 1965, **62**, 11834d.

PIEZOELECTRIC CRYSTAL SENSOR FOR THE DETERMINATION OF FORMALDEHYDE IN AIR

ORLANDO FATIBELLO-FILHO*, AHMAD A. SULEIMAN and GEORGE G. GUILBAULT†

Department of Chemistry, University of New Orleans, New Orleans, Louisiana 70148, U.S.A. and
Universal Sensors, P.O. Box 736, New Orleans, Louisiana 70148, U.S.A.

(Received 4 April 1990. Revised 19 July 1990. Accepted 26 July 1990)

Summary—Formaldehyde in air was detected and assayed with a piezoelectric quartz crystal coated with a 7,10-dioxa-3,4-diaza-1,5,12,16-hexadecatetrol/chromotropic acid solution. Water vapor and several gaseous interferences were removed by passing the sampling stream through a column of anhydrous magnesium perchlorate. The response curves were linear in the concentration ranges 0.4–4.5 and 0.4–3.6 ppm v/v CH₂O with and without the scrubber column, respectively. A single coating was used for 12 days (500 assays) without significant loss in sensitivity. With a single-point daily recalibration, the useful lifetime of the coating is about 2 months.

Formaldehyde is a major air contaminant in residential and industrial occupational environments.¹⁻³ Its effects on the health of humans^{1,4} and animals⁵⁻⁷ have generated great interest in developing techniques to control and monitor this compound.

OSHA and NIOSH have set the acceptable levels of formaldehyde exposures in the industrial atmosphere at 3 and 1 ppm v/v respectively,^{8,9} while AGCIH has recommended a voluntary standard of 0.1 ppm v/v in residential areas.¹⁰

Several methods have been developed for the determination of formaldehyde in air,^{2,11-20} but many are laborious or time-consuming.

Guilbault²¹ has developed an enzyme-coated piezoelectric crystal formaldehyde detector by immobilization of formaldehyde dehydrogenase together with both co-factors (reduced glutathione and nicotinamide adenine dinucleotide) on both sides of silver-plated metal electrodes, but this sensor has a lifetime of only 3 days.

In this paper, a new piezoelectric sensor for the detection and determination of formaldehyde in air is described, which can be portable, simple, of low cost and with fast response.

The theory and general application of the piezoelectric crystal sensors have been well reviewed²²⁻²⁴ and sensors for several atmospheric pollutants have been reported. The principle of

the sensor is that the frequency of vibration of an oscillating crystal is decreased by the selective adsorption of a target gaseous pollutant on the crystal surface. The linear relationship between the mass added onto the crystal surface and the change in its frequency can be derived from the Sauerbrey^{25,26} equation

$$\Delta F = -2.3 \times 10^6 F \Delta M / A$$

where ΔF is the frequency change (Hz), F is the basic frequency of the quartz crystal (MHz), ΔM is the mass of the deposited material (g), and A is the surface area of the quartz crystal (cm²).

Several compounds were evaluated as coating substrates for the detection of formaldehyde. Among these, a 2:1 v/v mixture of saturated solutions of 7,10-dioxa-3,4-diaza-1,5,12,16-hexadecatetrol and chromotropic acid in chloroform showed good sensitivity, response time, recovery time and stability. The effect of many potential interferences, flow-rate, temperature and amount of coating on the response of this sensor was also examined.

EXPERIMENTAL

Figure 1 shows a schematic diagram of the experimental manifold used, which is a modification of that used in previous work.²⁷ The 10-MHz piezoelectric crystals were AT-cut quartz crystals with gold-plated electrodes that were mounted in an HC6/U holder (Bliley, Erie, PA). The instrumentation utilized was a PZ 101 gas phase detector (Universal Sensors, New

*On leave from Universidade Federal de São Carlos, Departamento de Química, P.O. Box 676, 13560 São Carlos, S.P. Brazil.

†Author for correspondence.

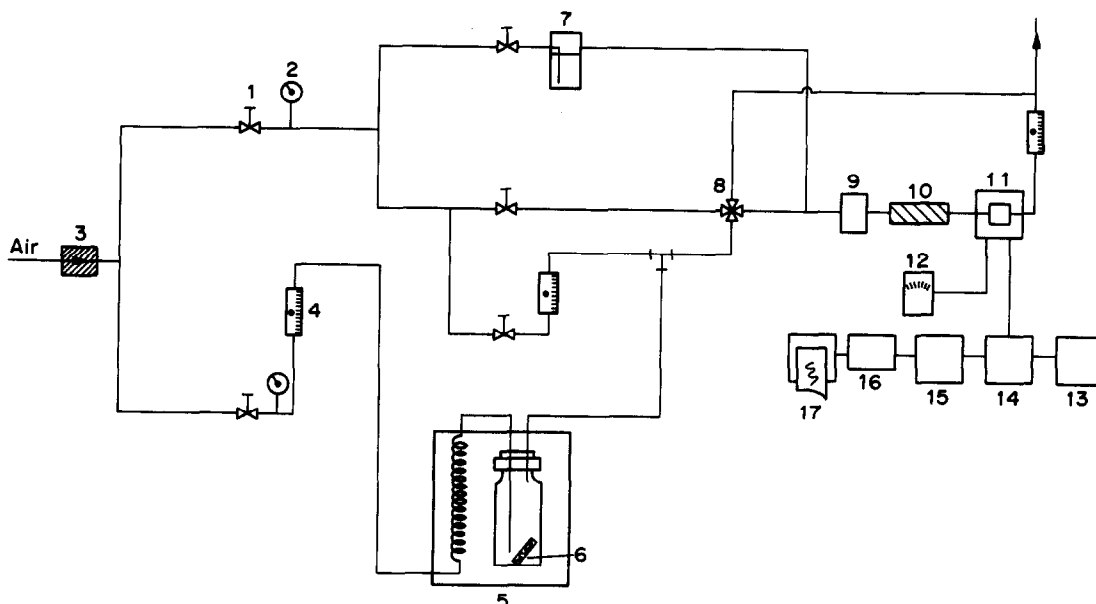


Fig. 1. Schematic representation of the experimental manifold: 1, control valve; 2, pressure gauge; 3, silica gel column; 4, flowmeter; 5, precision calibration system; 6, permeation tube; 7, humidity source; 8, four-way valve; 9, hygrometer; 10, $\text{Mg}(\text{ClO}_4)_2$ column; 11, test cell; 12, temperature control; 13, power supply; 14, oscillator; 15, frequency counter; 16, digital-to-analog converter; 17, recorder.

Orleans, LA), which is equipped with oscillator circuitry, frequency counter and dual-crystal chamber and can be interfaced to a recorder or a computer. The response was determined by monitoring the difference in frequency changes between reference (uncoated) and sensor (coated) crystals and was read from either the counter or recorder. Temperature monitoring was done with a thermistor (Thermometrics, Edison, NJ) connected to a multimeter (Honeywell Digitest, Model 33R).

Air (Air Products and Chemicals, Inc., Allentown, PA) was passed through a water bubbler in the humidity study and the relative humidity was monitored with a digital hygrometer (model HI8064, Cole-Parmer Ind. Co., Chicago, IL). The various concentrations of formaldehyde were prepared by the permeation method. A certified formaldehyde permeation tube 5.0 cm long (type HE, VICI Metronics, Santa Clara, CA) with a permeation rate of $250 \text{ ng} \cdot \text{min}^{-1} \cdot \text{cm}^{-1}$, generating 10 ppm v/v formaldehyde at a flow-rate of 100 ml/min, and a calibration system (model 570, Kin-Tek Laboratories, Texas City, TX) were used. Different formaldehyde concentrations were generated by dilution with nitrogen.

The 7,10-dioxa-3,4-diaza-1,5,12,16-hexadecatetrol was synthesized as described by Jordan.²⁸ All other reagents used were of analytical grade.

Preparation of coating

The best coating material was prepared by mixing saturated solutions of 7,10-dioxa-3,4-diaza-1,5,12,16-hexadecatetrol and chromotropic acid (in chloroform), in 2:1 v/v ratio.

The crystals were coated onto both gold electrodes of the piezoelectric crystal by addition of known volumes of the mixed solution with a microsyringe and spreading the solution with a glass rod. The coated crystal was placed in an oven at 85° for 2 hr to evaporate the chloroform, leaving a thin film of coating on the surface. The amount of coating applied to the crystal was calculated from the Sauerbrey equation and by monitoring the frequency change due to the coating.

RESULTS AND DISCUSSION

Choice of coating material

Table 1 contains a list of some of the substances tested as coatings for adsorption of formaldehyde. The results indicate that 7,10-dioxa-3,4-diaza-1,5,12,16-hexadecatetrol/chromotropic acid (2:1 v/v) mixture gives the most sensitive and reproducible coating. The use of a mixture improved the sensor response and performance. None of the other mixtures tested gave a synergic effect, and this coating was therefore used for all subsequent work.

Table 1. Initial evaluation of possible coatings for detection of formaldehyde at 10 ppm v/v levels with 10 MHz crystals*

Coating	$\Delta F, \dagger$ Hz
7,10-Dioxa-3,4-diaza-1,5,12,16-hexadecatetrol/ chromotropic acid (2:1 v/v)	190
7,10-Dioxa-3,4-diaza-1,5,12,16-hexadecatetrol	100
7,10-Dioxa-3,4-diaza-1,5,12,16-hexadecatetrol/ Girard T reagent (2:1 v/v)	80
7,10-Dioxa-3,4-diaza-1,5,12,16-hexadecatetrol/ <i>N</i> -benzylethanolamine	65
Diphenylamine	60
<i>N,N</i> -bis(2-hydroxyethyl)ethylenediamine	45
Armeen 25	45
Silicone gum rubber SE-30	18
SGP-386 (PDEAS)	15
Chromotropic acid	15
GP 58D Ethofat	12
2,3-Diaminonaphthalene	11
1,10-Diaminodecane	10
Girard T reagent	0
<i>N</i> -Benzylethanolamine	0
3-Methyl-2-benzotriazolinone	0

*Flow-rate 100 ml/min; temperature 25°; sampling time 1 min.

†Average for $n = 5$.

Amount of coating

It is evident from Fig. 2 that the frequency change (ΔF) increases as the amount of coating applied to the crystal increases, and this is due either to a decrease in the rate of saturation of the coating or to an increased probability of interaction between the coating material and the CH₂O molecules. The response levels off at 30–35 μg ($\Delta F = 13000\text{--}16000$ Hz) of coating, indicating saturation of the surface contact area with formaldehyde. Higher coating levels overloaded the crystal and impaired vibration.

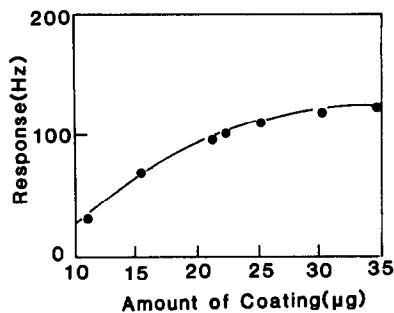


Fig. 2. Effect of coating on sensitivity: [CH₂O], 3.4 ppm v/v; temperature, 25°; flow-rate, 100 ml/min; sampling time, 2 min.

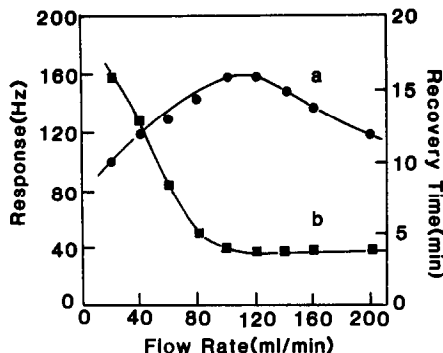


Fig. 3. Effect of flow-rate on (a) sensitivity and (b) recovery time: [CH₂O], 10.0 ppm v/v; temperature, 25°; amount of coating, 35 μg ; sampling time, 2 min.

Therefore, 30–35 μg of coating is sufficient for good response and reproducibility.

Flow-rate and reversibility

The effect of flow-rate on the sensitivity and recovery time of the formaldehyde sensor is shown in Fig. 3. The results indicate that the highest response was obtained in the flow-rate range 95–120 ml/min. In subsequent studies, a flow-rate of 100 ml/min was used for convenience in dilution. The recovery time was longer when lower flow-rates were used. Complete reversibility was obtained in 4 min at a flow-rate of 100 ml/min with sampling times of 2 min for a 3.4 ppm v/v CH₂O sample, and varied from 3 to 6 min over the formaldehyde concentration range 0.4–4.5 ppm v/v.

Effect of cell temperature

Figure 4 shows the effect of temperature on the sensor response. The response decreased

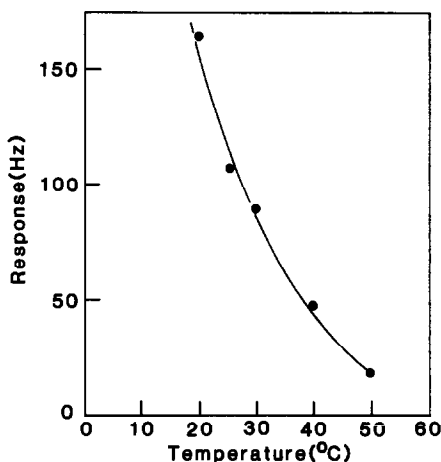


Fig. 4. Effect of temperature on the response: [CH₂O], 3.4 ppm v/v; flow-rate, 100 ml/min; amount of coating, 35 μg ; sampling time, 2 min.

drastically as the temperature rose from 20 to 50°, indicating that the adsorption of CH₂O by the coating decreases with increase in temperature, which seriously affects the sensitivity of the sensor. Recovery times of 4 and 3 min were obtained for a sample of 3.4 ppm v/v CH₂O at 25 and 40°, respectively. Although shorter recovery times can be achieved at higher temperatures, this improvement is not worth the sacrifice in sensitivity, so 25° is chosen as the optimum temperature.

For practical applications it is recommended that the temperature is controlled or the sensor recalibrated to minimize effects of temperature variations.

Effect of interferences

Several potential inorganic and organic interferences which would be expected to exist in the atmosphere were tested at their TLV (threshold limit values). The effect of moisture was studied by a continuous process, while other gases, including NH₃, H₂S, CO, SO₂, NO₂, COCl₂, HCl, chloroform, carbon tetrachloride, methanol, acetone, ethanol, toluene, xylene, and propionaldehyde were studied by the syringe dilution method. This study showed that NH₃, chloroform, carbon tetrachloride, methanol, acetone, ethanol, toluene, xylene and water caused high frequency changes in comparison with a sample of 3.4 ppm v/v formaldehyde.

Several approaches to elimination of these interferences were tested, with use of several desiccants, hydrophobic membranes, and molecular sieves.

Table 2. Effect of other substances on the assay of formaldehyde at TLV concentrations

Interferent	Concentration, ppm v/v	Interference, † %
NH ₃	50	0
H ₂ S	20	0
CO	50	0
NO ₂	5	0
COCl ₂	0.1	0
Chloroform	50	85
Methanol	200	0
Acetone	1000	7
Ethanol	1000	3
Toluene	200	8
Xylene	100	6
Water		0‡
Propionaldehyde	10	0
Carbon tetrachloride	10	85

*The Mg(ClO₄)₂ scrubber was used.

†Average for *n* = 5.

‡Relative humidity levels of 8–80%.

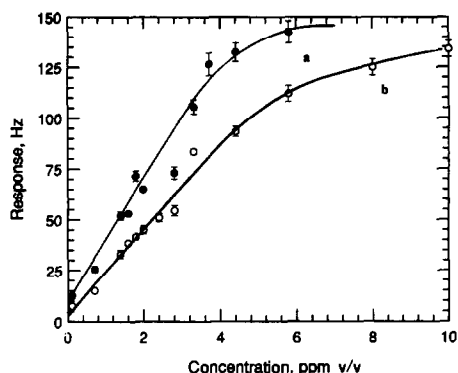


Fig. 5. Response of the sensor to CH₂O under two different conditions: (a) without column, (b) with Mg(ClO₄)₂ column; temperature, 25°, flow-rate, 100 ml/min; amount of coating, 35 µg; sampling time, 2 min. The error bars represent the spread of five measurements.

All of these interferences, except those of high levels of chloroform and carbon tetrachloride, were completely eliminated by passing the sampling stream through a column of anhydrous magnesium perchlorate (Table 2). Although about 24% of the CH₂O was also absorbed by the column, a calibration curve with adequate sensitivity for the determination of CH₂O could be constructed.

Calibration curves, lifetime and precision

The effect of sampling times (0.5–4 min) on the response of the CH₂O sensor was initially studied in the concentration range 0.4–8.0 ppm v/v formaldehyde. Figure 5 shows representative calibration curves obtained with a sampling time of 2 min. Curve a was obtained for dry gas without use of the Mg(ClO₄)₂ scrubber, and curve b was obtained with use of the scrubber. Curves a and b were linear over the concentration ranges 0.4–3.6 and 0.4–4.5 ppm v/v CH₂O, respectively. The good linearities (*r* = 0.987 for a and 0.988 for b) and the sensitivities of 29.0 and 22.1 Hz/µg, respectively, show that use of the scrubber does not affect the determination of CH₂O.

A single coating was used for 12 days (500 assays) without significant loss in sensitivity. With a daily single-point recalibration, a coated crystal can be used for 2 months with good results, the response decreasing by only 15% during this time. The proposed sensor is more stable than that reported earlier,²¹ and has the advantage that real applications are possible.

The reproducibility of the coating preparation was checked for 5 crystals. The performance of each crystal was evaluated under the optimum

conditions found [sampling time 2 min, flow-rate 100 ml/min, concentration of CH₂O 3.4 ppm v/v, (Mg(ClO₄)₂) scrubber used, temperature 25°]. The average $\Delta F \pm$ standard deviation found was 81 ± 3 Hz.

CONCLUSIONS

The piezoelectric sensor coated with 7,10-dioxa-3,4-diaza-1,5,12,16-hexadecatrol/chromotropic acid mixture possesses good selectivity, sensitivity and reproducibility for the detection and determination of CH₂O in air. The sensor is useful in the ranges corresponding to the acceptable levels set by several regulatory agencies, portable, simple, of low cost and with fast response.

Acknowledgements—The financial support of the National Institute of Environmental Health Sciences in the form of an SBIR Grant (IR43 ES048 19-01) is gratefully acknowledged. The scholarships furnished by CNPq (Conselho Nacional de Desenvolvimento Científico e Tecnológico, Processo No. 20.0749/86-QU-2) and FAPESP (Fundação de Amparo à Pesquisa do Estado de São Paulo, Processo No. 86/2196-0) to the Brazilian author are gratefully acknowledged.

REFERENCES

1. P. W. Preuss, R. L. Dailey and E. S. Lehman, in *Formaldehyde—Analytical Chemistry and Toxicology*, pp. 247–259. V. Turoski (ed.), ACS, Washington, 1985.
2. P. A. Stewart, D. A. Cubit, A. Blair and R. Spirtas, *Appl. Ind. Hyg.*, 1987, **2**, 61.
3. E. Priha and I. Ahonen, *Anal. Chem.*, 1986, **58**, 1195.
4. R. B. Hayes, J. W. Raatgever, A. de Bruyn and M. Gerin, *Intern. J. Cancer*, 1986, **37**, 487.
5. M. T. O'Berg, in *Formaldehyde—Analytical Chemistry and Toxicology*, V. Turoski, (ed.), pp. 289–295, ACS, Washington, 1985.
6. F. Perera and C. Petito, *Science*, 1982, **216**, 1285.
7. *NIOSH Current Intelligence Bulletin*, No. 34, 15 April 1981.
8. *General Industry Safety and Health Standards*; Table 21, p. 506. U.S. Department of Labor Occupational Safety and Health Administration OSHA 2206 (29 CFR 1910). Revised January 1976.
9. I. Turiel, *Indoor Air Quality and Human Health*, pp. 18–19. Stanford University Press, Stanford, 1985.
10. T. Godish, *Air Quality*, p. 313. Lewis, Chelsea, MI, 1985.
11. T. G. Matthews and T. C. Howell, *Anal. Chem.*, 1982, **54**, 1495.
12. L. J. Papa and L. P. Turner, *Chromatog. Sci.*, 1972, **10**, 744.
13. R. K. Beasley, C. E. Hoffman, M. L. Rueppel and J. W. Worley, *Anal. Chem.*, 1980, **52**, 1110.
14. J. C. Septon and J. C. Ku, *Am. Ind. Hyg. Assoc. J.*, 1982, **43**, 845.
15. E. R. Kennedy, D. L. Smith and C. L. Geraci, Jr., in *Formaldehyde—Analytical Chemistry and Toxicology*, V. Turoski (ed.), pp. 151–159. ACS, Washington, 1985.
16. T. G. Matthews, *Am. Ind. Hyg. Assoc. J.*, 1982, **43**, 547.
17. A. D. Eckmann, K. A. Dally, L. D. Hanrahan and H. A. A. Anderson, *Environ. Int.*, 1982, **41**, 334.
18. W. S. Kim, C. L. Geraci and R. E. Kupel, *Am. Ind. Hyg. Assoc. J.*, 1980, **41**, 334.
19. D. L. Daggett and T. H. Stock, *ibid.*, 1985, **46**, 497.
20. D. L. Smith, M. Bolyard and E. R. Kennedy, *ibid.*, 1983, **44**, 97.
21. G. G. Guilbault, *Anal. Chem.*, 1983, **55**, 1682.
22. *Idem*, *Ion-Sel. Electrode Rev.*, 1980, **2**, 3.
23. J. F. Alder and J. J. McCallum, *Analyst*, 1983, **108**, 1169.
24. G. G. Guilbault and J. M. Jordan, *CRC Crit. Rev. Anal. Chem.*, 1988, **19**, 1.
25. G. Z. Sauerbrey, *Z. Phys.*, 1959, **155**, 206.
26. *Idem*, *ibid.*, 1964, **178**, 457.
27. F. Filho-Fatibello, J. F. de Andrade, A. A. Suleiman and G. G. Guilbault, *Anal. Chem.*, 1989, **61**, 746.
28. J. M. Jordan, *M. Sc. Thesis*, University of New Orleans, New Orleans, LA, 1985.

LIQUID CHROMATOGRAPHY AMPEROMETRIC DETECTION OF CARBOXYLIC ACIDS AND PHENOLIC ACIDS WITH A COPPER-BASED CHEMICALLY-MODIFIED ELECTRODE

JIANXUN ZHOU and ERKANG WANG*

Laboratory of Electroanalytical Chemistry, Changchun Institute of Applied Chemistry, Chinese Academy of Sciences, Changchun, Jilin 130022, People's Republic of China

(Received 15 October 1990. Accepted 20 November 1990)

Summary—A copper-based chemically-modified electrode has been constructed and characterized by various experimental parameters in flow-through amperometric detection of carboxylic acids and phenolic acids. Novel hydrodynamic voltamperograms were first obtained in flow-through amperometric detection with the Cu-based CME and subsequently negative and positive peaks were observed in a single chromatogram. This unique and flexible potential dependence could be of great benefit in chromatographic speciation and quantification. These observations suggest that the detector response was governed by the complexation reaction of copper ions with the solutes.

The development of detection methods for aliphatic compounds, including carbohydrates, amino-acids and organic acids in liquid chromatography (LC) has presented an analytical challenge of major proportions. The absence of a strongly absorbing chromophore in simple aliphatic compounds restricts the use of direct UV-visible detection to wavelengths in the range 180–250 nm and thereby makes the usual spectrophotometric techniques largely unsuitable or insensitive. Consequently, the approaches most commonly employed for these analytes, especially for carbohydrates, have relied on either refractive-index detection (with its characteristically poor sensitivity) or chemical derivatization to produce sense adducts with better spectral characteristics.¹

Simple and sensitive direct detection in LC will always be preferred, when available. Historically, however, researchers have agreed that aliphatic compounds are not amenable to direct amperometric detection.² This difficulty encountered in LC electrochemical detection (LCEC) for direct sensing of aliphatic compounds at trace levels has been solved by several approaches. The first was pulsed amperometric detection (PAD), developed by Johnson and LaCourse³ platinum⁴⁻⁶ or gold^{7,8} electrodes. In the most typical applications, the method provides quantification at 100–500 ng levels.

However, because of the surface cleaning and regeneration steps necessary to obtain stable and reproducible responses, triple-pulsed potential wave-forms are required for acceptable long-term use of these electrodes. PAD systems are more expensive than the usual constant-potential detectors, and less sensitive for flow-through analysis applications, because of the accompanying charging current.

In the second approach, catalytic electrodes with oxidizable metals such as nickel,⁹ copper¹⁰ and silver¹⁰ have been developed and characterized mainly for the catalytic oxidation of carbohydrates. Detectability of 1 ng for glucose has been found with the Ni electrode. Strongly alkaline conditions were essential for these catalytic electrodes, as well as for the PAD methods with Pt and Au electrodes in the first approach, and this largely restricted the selection of chromatographic separation systems.

For the third approach, copper electrodes were used as either potentiometric¹¹⁻¹³ or amperometric¹⁴⁻¹⁷ LCEC sensors, for the detection of aliphatic compounds, including amino-acids and aliphatic and aromatic carboxylic acids. The detector response was inferred to be governed by the complexation reaction between the solutes and the cupric ion in neutral or alkaline media.

Recently, copper-based chemically-modified electrodes (CMEs) have been developed and characterized¹⁸⁻²⁰ for the catalytic LCEC

*Author for correspondence.

detection of polyhydroxy compounds, including carbohydrates, amino sugars, alditols and sugar-acids. The lowest detection limit of 0.1 ng for ribitol by FIA with such a CME was obtained at a typical catalytic oxidation potential of +0.50 V *vs.* Ag/AgCl.

This paper describes a copper-based chemically-modified electrode constructed by a method similar to that of Prabhu and Baldwin¹⁹ and used in flow-through systems (FIA and HPLC) for the detection of carboxylic and phenolic acids. The dependence of the detector response for these analytes on various experimental conditions, such as the pH and flow-rate of the mobile phases and the working potential applied, was investigated. Novel hydrodynamic voltamperograms for the solutes of interest were first obtained with the modified electrode. Subsequently, both negative and positive peaks were observed for the first time in the same LCEC chromatogram. On the basis of all the observations, it is suggested that the detector response in flow-stream measurement resulted from the difference in solubility of the cupric or cuprous species formed by the components of the mobile phase and the analyte ligands at the electrode surface.

EXPERIMENTAL

Reagents

Cupric chloride (analytical reagent grade) was purchased from the Beijing Chemical Co.; analytical-grade carboxylic acids (oxalic, citric, malic, tartaric and glyceric) were from Merck; 3,4-dihydroxyphenylacetic acid was from Fluka; vanillic and benzoic acids were from Shanghai 1st Chemical Co. and gallic acid was from Zunyi 2nd Chemical Co. (Zunyi, China). All were used as received. Other chemicals were of analytical grade. Doubly-distilled water was used for the preparation of all solutions. Phenolic acid stock solutions were kept under purified nitrogen at 4° in the dark. The mobile phase was 0.025M phosphate buffer (pH 7.0), thoroughly degassed in an ultrasonic bath before use.

Electrode

The working electrode was modified by a procedure similar to that of Prabhu and Baldwin.¹⁹ A freshly polished thin-layer glassy-carbon electrode was immersed in 0.15M sodium hydroxide for about 10 min, then rinsed thoroughly with water and immersed face-up in an aqueous 0.05M solution of copper(II) chlor-

ide, together with a small slice of metallic copper, for about 20 min, whereupon a uniform white deposit appeared on the glassy-carbon surface. At this point, the electrode was removed from the chloride solution and rinsed with water, and was ready for use. A fresh glassy-carbon surface could be obtained, whenever necessary, by immersion of the Cu-based electrode surface in 1M hydrochloric acid for 1 min.

Apparatus

Cyclic voltammetry was performed with a home-made potentiostat employing a conventional three-electrode cell, with a 3-mm diameter glassy-carbon working electrode (modified or unmodified), an Ag/AgCl (saturated KCl) reference electrode and a platinum-wire counter-electrode. Flow-injection and chromatographic experiments were performed with a JASCO-350 pump, a home-made injection valve with a 10- μ l loop and a TL-5A electrochemical detector (Bioanalytical Systems). A laboratory-made bipotentiostat was used to control the detector. The column was 7 μ m Nucleosil C₁₈ (200 \times 4 mm i.d.). The chromatograms were obtained at room temperature (20 \pm 2°). In these experiments the reference electrode was of the saturated calomel type.

RESULTS AND DISCUSSION

Electrochemistry

Cyclic voltamperograms (CVs) for the Cu-coated electrode in 0.15M sodium hydroxide and pH 7.0 phosphate buffer, respectively, are shown in Fig. 1. In 0.15M sodium hydroxide, curve A(1), a broad oxidation wave and another small one at peak potentials of +0.55 and +0.70 V *vs.* Ag/AgCl, respectively, were observed on the initial scan. In subsequent scans, these two waves decreased in magnitude and rapidly disappeared, curve A(2). This behaviour was consistent with that in an earlier study.¹⁸ Several views on the electrode surface species and the electrode mechanism of the oxidation process described by Fig. 1A have been advanced,¹⁸⁻²⁰ but considerable uncertainty remains. However, such an inactive electrode surface did catalyse glucose oxidation, with a peak potential of +0.58 V *vs.* Ag/AgCl, curve A(2), as already reported.¹⁸ CVs obtained in neutral phosphate buffer (Fig. 1B) were quite different from those in 0.15M sodium hydroxide. A rather broad oxidation wave with a peak

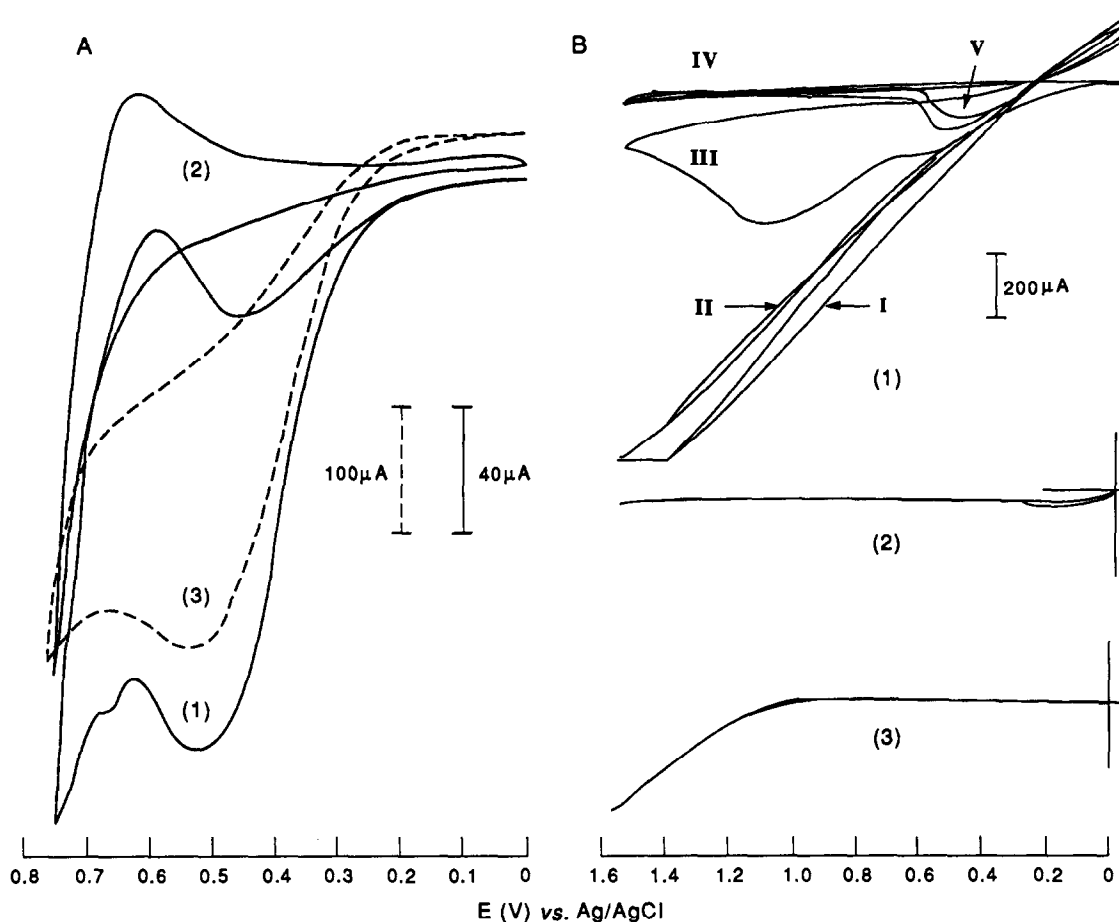


Fig. 1. Cyclic voltamperograms of the Cu-based CME in (A) 0.15M NaOH: (1), initial scan; (2), fourth scan; (3), (2) plus 10mM glucose; (B) pH 7.0 phosphate buffer: (1), initial to fifth scans; (2), tenth scan; (3), (2) plus 10mM tartaric acid. Scan-rate, 20 mV/sec.

potential of +1.10 V *vs.* Ag/AgCl was clearly observed only on the third scan, but it then decreased in magnitude and rapidly disappeared, curve B(2); a reduction wave on the reverse scan, as observed in alkaline solution, curve A(2), could no longer be observed. Furthermore, such an inactive electrode surface did not catalyse the oxidation of tartaric acid in neutral buffer solution, curve B(3), although this exhibited a catalytic oxidation wave with an E_p of +0.60 V *vs.* Ag/AgCl at such a Cu-based CME in strongly alkaline media.¹⁹

The white deposit, as suggested previously,^{19,20} is most probably crystalline CuCl resulting from the interaction of the Cu(II) solution with metallic copper to form the Cu(I) salt, the subsequent reactions of which account well for the colour of the Cu-based CME at various stages in its usage: light-coloured initially and then green on exposure to air, CuCl; yellow after exposure to neutral buffer, Cu₂O; black after exposure to oxidizing potentials,

CuO. Accordingly, the broad oxidation waves in Fig. 1 should correspond to the Cu(I)/Cu(II) oxidation process.

Once the modification was accomplished and the electrode reassembled into the thin-layer cell, the initial background current (lasting about 20 sec) on exposure to oxidizing potentials (0.0–0.15 V *vs.* SCE) in a flowing stream with pH 7.0 phosphate buffer as the mobile phase was so large that it could not be compensated instrumentally. After about 40 sec, this large background current gradually decreased until, after about 10 min, it reached a steady level which could easily be compensated instrumentally. The larger the initial oxidizing potential applied, the longer the time necessary to stabilize the background current. The function of this step for passivation of the electrode surface is similar to that for metallic copper electrodes by polarization with negative and positive potentials applied alternately.^{15,17}

Flow-through system detection

Applied potential. It seemed unclear whether or not the facile amperometric detection of carboxylic and phenolic acids in a flow-through system could be done with the copper-based electrode at modest positive potentials in neutral media, in view of the fact that no significant oxidation current was observed in the CVs of tartaric and other carboxylic acids, as shown in curve B(3) of Fig. 1. This doubt, however, was removed by making serial injections of 1mM oxalic acid and applying FIA-EC at +0.15 V *vs.* SCE (Fig. 2). Reproducible current responses were obtained, as illustrated in Fig. 2. After 40 injections, the peak response was still nearly 97% of its initial value, with a relative standard deviation of only 2.4%.

Novel hydrodynamic voltamperograms (HDVs) for carboxylic and phenolic acids were obtained with the Cu-based CME and are shown in Figs 3 and 4, respectively. These responses were different from both the *S*-shaped ones obtained on metallic copper electrodes for amino-acids in neutral buffer solution^{15,17} and the peaks obtained on a similar Cu-CME for glucose catalysis in strongly alkaline media.¹⁸

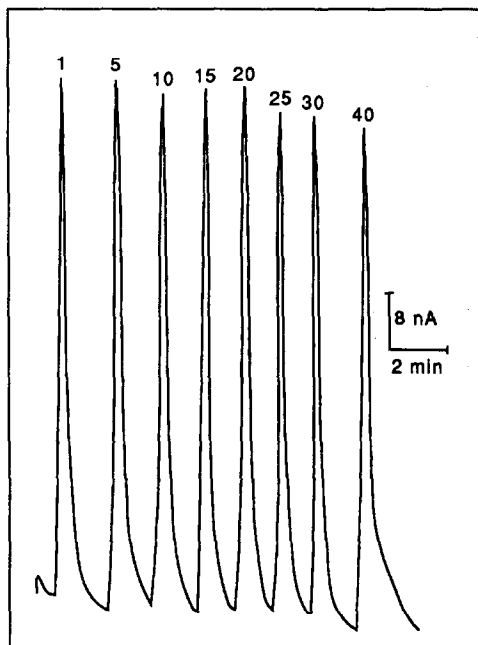


Fig. 2. FIA response obtained at the Cu-CME for a series of injections of 1mM oxalic acid: potential, +0.15 V *vs.* SCE; mobile phase, pH 7.0, 0.025M phosphate buffer; flow-rate, 0.5 ml/min. The serial number is given at the top of the peak, and recording was stopped during the other injections.

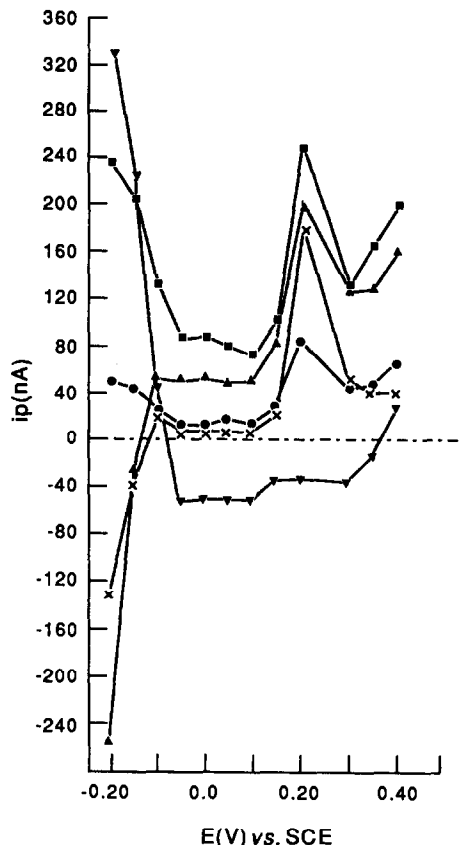


Fig. 3. Hydrodynamic voltamperograms for 1mM citric acid (■), oxalic acid (▲), tartaric acid (●), malic acid (×), glyceric acid (∇), at the Cu-CME. Flow conditions as for Fig. 2.

Figure 3 shows HDVs for some carboxylic acids. In the potential range more negative than -0.10 V *vs.* SCE, glyceric acid exhibited an anodic current that decreased as the potential became more positive; when the potential was more positive than -0.05 V, a cathodic current appeared, which gradually decreased with more positive potentials. Oxalic and malic acids behaved oppositely to glyceric acid. In the potential range more negative than -0.10 V, they exhibited cathodic currents, which decreased sharply at more positive potentials, and anodic currents appeared at potentials more positive than -0.10 V, slightly decreasing with more positive potentials. Citric and tartaric acids possessed similar HDV behaviour, always giving sharply decreasing anodic currents in the potential range investigated (from -0.20 to 0.50 V *vs.* SCE), then a peak-shaped curve up to $+0.30$ V; after that the response increased with more positive potentials. All these carboxylic acids, except glyceric acid, produced similar HDVs in the potential range from -0.50 to 0.40

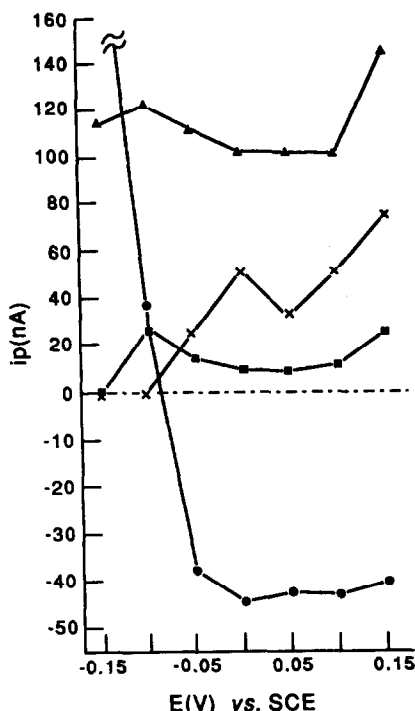


Fig. 4. Hydrodynamic voltamperograms for 0.24mM gallic acid (▲), 50mM 3,4-dihydroxyphenylacetic acid (▲), 10mM vanillic acid (●), 50mM benzoic acid (×). Experimental conditions as for Fig. 2.

V vs. SCE, exhibiting curves with identical peak potentials of +0.20 V.

Among the phenolic acids (Fig. 4), vanillic acid exhibited HDV behaviour similar to that of glyceric acid, giving anodic currents at poten-

tials more negative than -0.10 V vs. SCE, which decreased very rapidly as potentials became more positive, and then reached a nearly steady level in the potential range from -0.05 to 0.15 V. Gallic acid and 3,4-dihydroxyphenylacetic acid had similar HDV behaviour, exhibiting identical peak potentials -0.10 V, whereas benzoic acid had a peak potential of 0.0 V. The anodic currents of gallic, 3,4-dihydroxyphenylacetic and benzoic acids increased again (at different rates) in the potential range 0.05 – 0.15 V.

Negative peaks would be expected for either a single analyte at different applied potentials or a mixture of analytes at one fixed potential properly selected for flow-through LC detection according to the observed HDVs of the carboxylic and phenolic acids. This unique feature was obtained with the Cu-CME and is shown in Figs. 5–8.

The identification of the actual mechanism for the appearance of negative peaks in flow-through amperometric detection still proved difficult, however. There is no possibility of a catalytic electrode mechanism such as was reported for the detection of polyhydroxy compounds with a Cu-CME in strongly alkaline media,¹⁹ as has been proved by CV experiments [Fig. 1, curve B(3)]. It is worth noting that similar negative peaks were obtained in LC potentiometric detection for organic acids with a metallic copper electrode and neutral phosphate

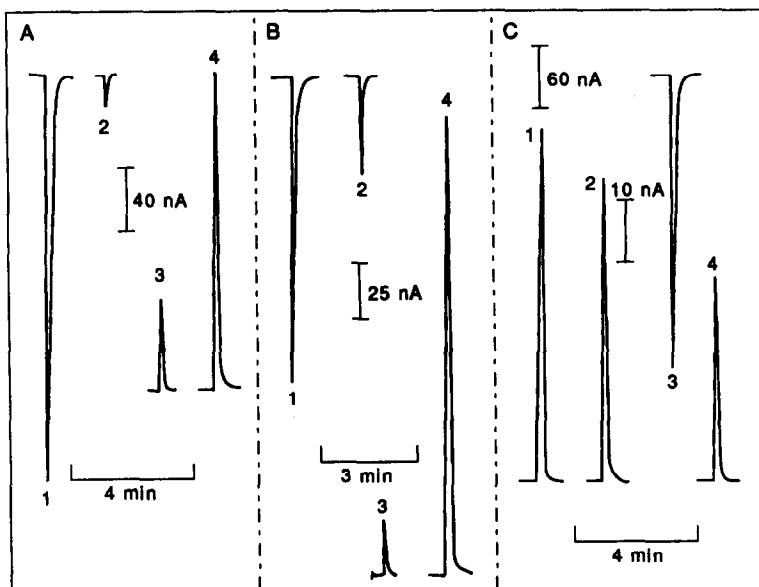


Fig. 5. FIA response for 1mM oxalic acid (A), malic acid (B), glyceric acid (C). Applied potential (A) 1, -0.20 ; 2, -0.15 ; 3, -0.10 ; 4, $+0.20$; (B) 1, -0.20 ; 2, -0.15 ; 3, -0.10 ; 4, $+0.20$; (C) 1, -0.20 ; 2, -0.10 ; 3, 0.0 ; 4, $+0.40$ V vs. SCE. Other experimental conditions as for Fig. 2.

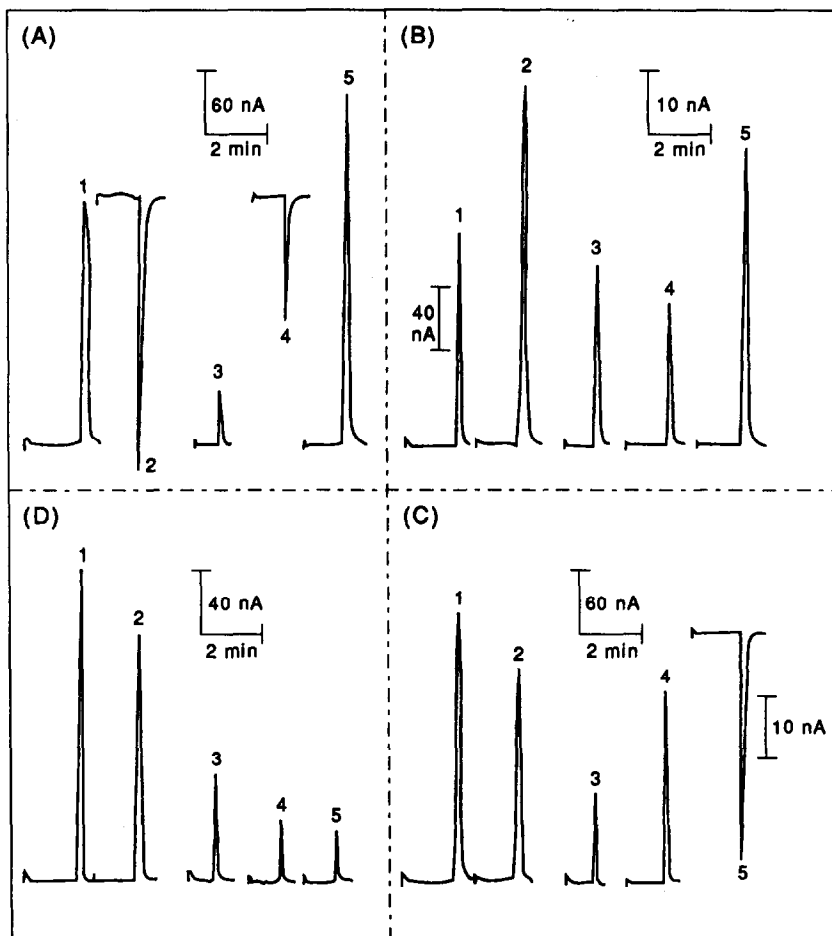


Fig. 6. Chromatograms of citric acid (1), oxalic acid (2), tartaric acid (3), malic acid (4), glyceric acid (5), each 1mM, at the Cu-CME with applied potentials of -0.20 (A), -0.10 (B), $+0.20$ (C) $+0.40$ (D) V vs. SCE. Column, Nucleosil C_{18} ($7 \mu\text{m}$) 200×4 mm i.d. Other parameters as for Fig. 2.

buffer as mobile phase.¹¹ That response was explained as resulting from the difference in complexation strength between compounds in the mobile phase and the analytes injected. Eluted species may form stronger or weaker copper complexes than do the ligands in the mobile phase, resulting in either an increase or a decrease in the observed electrode potential, hence both positive and negative peaks could be expected. The explanation was based theoretically on the Nernstian relationship between the copper electrode potential and the total ligand concentration under conditions where formation of a single complex species of copper with the analyte ligand predominated. Any explanation based on the Nernstian relationship is not applicable to the detector response in flow-through amperometric detection. Alternatively, there is a possibility that the response of a Cu-CME in flow-through amperometric detection resulted from the difference in the solubility

of compounds formed between the components in the mobile phase or the analyte ligands present in the injected sample with Cu(I) or Cu(II) (depending on the applied potential) produced at the electrode surface. Eluted species may form more or less water-soluble copper complexes than do the components of the eluent, increasing or decreasing the copper concentration at the electrode surface and, thereby, the current observed for copper oxidation, resulting in amperometrically negative or positive peaks.

The flexible dependence of the detector response on the operating potential could be a unique and critical characteristic of the Cu-based CME in flow-through amperometric detection for carboxylic and phenolic acids and, if properly utilized, could be of great benefit in LCEC detection both qualitatively and quantitatively. In the case where a single compound is concerned, oxalic acid for example, different working potentials can serve different purposes

(Fig. 5A): $+0.20$ V *vs.* SCE is obviously the proper selection for conventional LCEC detection of the carboxylic acids, with high sensitivity. If oxalic acid is the compound of interest, the selection of -0.20 V, at which there is a distinct negative peak, would enable it to be distinguished from other eluted species (Fig. 6A), making chromatographic speciation and quantification easier. If oxalic acid is regarded as an interfering species, however, it is advantageous to operate the LCEC detection at -0.15 V *vs.* SCE if possible. For mixtures of the five analytes, operating at -0.10 V *vs.* SCE results in conventional chromatograms with amperometric detection. When glyceric acid is the species of interest, it could be clearly recognized at a working potential of $+0.20$ V (Fig. 6C).

It is worth noting that the higher applied potential did not necessarily increase the current response with a Cu-CME for LCEC detection of organic acids, unlike the case for amino-acids with metallic copper electrodes.^{15,17} In some cases, for example, the LCEC detection of carboxylic acids at modest positive potentials, $+0.40$ V (Fig. 6B), resulted only in a decrease in detector response, except for citric acid, compared with that obtained at -0.10 V (Fig. 6D), as well as an increased background current.

This flexible dependence, on electrode potential, of the detector response for phenolic acids,

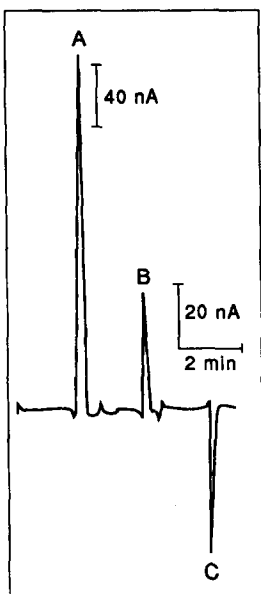


Fig. 7. Chromatograms of 10mM vanillic acid at the Cu-CME with applied potential of -0.15 (A), -0.10 (B), 0.0 (C) V *vs.* SCE. Chromatographic conditions as for Fig. 6.

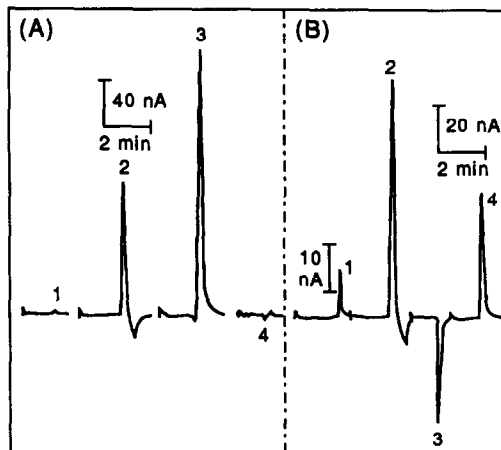


Fig. 8. Chromatograms of 0.24mM gallic acid (1), 50mM 3,4-dihydroxyphenyl acetic acid (2), 10mM vanillic acid (3), 50mM benzilic acid (4) at the Cu-CME with applied potentials of -0.15 (A) and 0.0 (B) V *vs.* SCE. Flow conditions as for Fig. 6.

which are conventionally electroactive at oxidation potentials above 0.60 V *vs.* SCE in neutral media and electro-inactive in the potential range investigated (from -0.15 to $+0.15$ V *vs.* SCE) on a bare glassy-carbon electrode, could be used in different ways for various requirements. As can be seen from Fig. 8, selective detection of 3,4-dihydroxyphenylacetic and vanillic acids in the presence of gallic and benzilic acids could be realized by employing a working potential of -0.15 V *vs.* SCE (Fig. 8A); the selection of 0.0 V enables vanillic acid to be distinguished from the others, making the facile chromatographic speciation and quantification of vanillic acid practical. It should be noted that this unique feature would never be observed in conventional LCEC sensing of phenolic acids with a bare glassy-carbon electrode.

Flow-rate dependence. The dependence of the detector response on the flow-rate of the mobile phase was studied for oxalic and other organic acids and is shown in Fig. 9 (for oxalic acid at $+0.15$ V *vs.* SCE). It is clear that the response always decreased with increasing flow-rate, contrasting sharply with conventional LCEC detection with unmodified electrodes.^{21,22} This suggests that the detector response is controlled entirely by the kinetics of the reaction with copper ions. In conventional LC systems, the choice of flow-rate involves a compromise between the detector sensitivity and the sample throughput. In this work, for example, a typical flow-rate of 0.5 ml/min was used throughout. This flow-rate dependence is especially

advantageous for compatibility with microbore HPLC, high sensitivity being attained at rather low flow-rates of the mobile phase.

Dependence on pH. It was found that the Cu-based CME could perform effectively in neutral and alkaline media (pH 7.0–11) for LCEC detection of carboxylic and phenolic acids. Lowering the pH of the mobile phase made the detector less efficient. As shown in Fig. 10, the detector gave smaller and broader current responses at pH 6.0 (except for glyceric acid) than those obtained at pH 7.0.

This pH-dependence, similar to that of metallic copper electrodes for organic acids,^{14–17} turned out to be somewhat less limiting than that previously observed with Pt and Au electrodes in PAD mode^{4–8} and Cu-based CMEs for the catalytic detection of polyhydroxy compounds,^{18,19} which functioned well only down to 0.001 M hydroxide concentration. The ability of the Cu-based CME constructed in this work to function at much lower pH values was important because it allowed greater freedom for the selection of an effective chromatographic system.

Difference between pH values for separation and detection. Although the pH-dependence of the Cu-based CME was found less limiting there was still a difference between the pH values for optimal reversed-phase chromatographic separation and amperometric detection of the organic acids studied: the former required low pH values (typically 2.0–3.0) and the latter pH > 6.0. With a pH 7.0 mobile phase in reversed-phase LC systems with ODS columns carboxylic acids were eluted with nearly identical retention times of *ca.* 1.5 min and the phenolic acids were eluted close together in the range 2–2.5 min. A possible means of resolution might be the use of ion-pairing to suppress the ionization of the

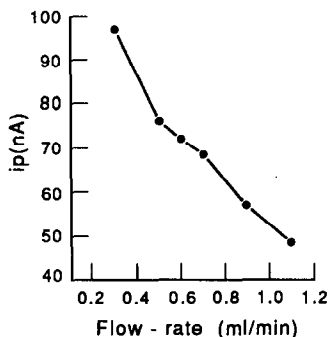


Fig. 9. Effect of the mobile-phase flow-rate on the FIA response for 1mM oxalic acid at the Cu-CME. Experimental conditions as for Fig. 2.

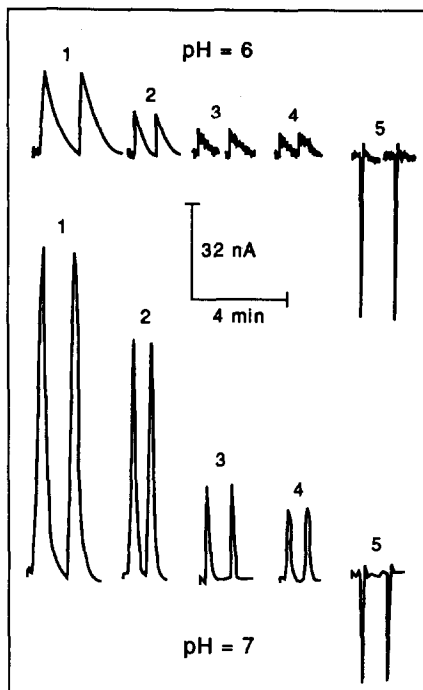


Fig. 10. The dependence of the FIA response on mobile phase pH for 1mM citric acid (1), oxalic acid (2), tartaric acid (3), malic acid (4), glyceric acid (5). Experimental parameters as for Fig. 2.

analytes in neutral media. The first pairing ion tested was TBA⁺ (as tetrabutylammonium perchlorate), which had little effect on the retention of these organic acids under the chromatographic conditions employed throughout this work, with the mobile phase pH > 7.0. Other, more hydrophobic, pairing ions, such as HTA⁺ (as hexadecyltrimethylammonium bromide), increased the retention of these analytes, under the conditions above, but the detector performance was much poorer, which might have resulted from poisoning of the electrode by bromide, as has been reported for a metallic copper electrode.¹⁴

CONCLUSIONS

A copper-based CME has been constructed and used in flow-through amperometric detection of carboxylic and phenolic acids. The dependence of the detector response on the operating potential, the pH and flow-rate of the mobile phase was systematically investigated. A unique potential-peak current relationship in flowing streams was obtained and its potential for analytical applications has been demonstrated. On the basis of all the observations, it is suggested that the detector response is

governed by the reaction of copper ions with the solutes. There is still a difference between the pH values required for optimum separation and detection of these organic acids in reversed phase LC with amperometric detection employing Cu-based CMEs.

Acknowledgement—The support of the National Natural Science Foundation of China is gratefully appreciated.

REFERENCES

1. R. W. Frei and J. F. Lawrence (eds.), *Chemical Derivatization in Analytical Chemistry: Chromatography*, Vol. 1, Plenum Press, New York, 1981.
2. R. N. Adams, *Electrochemistry at Solid Electrodes*, Dekker, New York, 1969.
3. D. C. Johnson and W. R. LaCourse, *Anal. Chem.*, 1990, **62**, 589A.
4. S. Hughes and D. C. Johnson, *Anal. Chim. Acta*, 1981, **132**, 11.
5. *Idem*, *J. Agric. Food Chem.*, 1982, **30**, 712.
6. *Idem*, *Anal. Chim. Acta*, 1983, **149**, 1.
7. G. G. Neuburger and D. C. Johnson, *Anal. Chem.*, 1987, **59**, 203.
8. *Idem, ibid.*, 1987, **59**, 150.
9. R. E. Reim and R. M. Van Effen, *ibid.*, 1986, **58**, 3203.
10. Yu. B. Vassilyev, O. K. Khazova and N. N. Nikolaeva, *J. Electroanal. Chem.*, 1985, **196**, 127.
11. P. R. Haddad, P. W. Alexander and M. Trojanowicz, *J. Chromatog.*, 1984, **315**, 261.
12. P. W. Alexander, P. R. Haddad and M. Trojanowicz, *Chromatographia*, 1985, **20**, 179.
13. P. R. Haddad, P. W. Alexander, M. Y. Croft and D. F. Hilton, *ibid.*, 1987, **24**, 487.
14. W. Th. Kok, G. Groenendijk, U. A. Th. Brinkman and R. W. Frei, *J. Chromatog.*, 1984, **315**, 271.
15. K. Štulík, V. Pacáková, M. Weingart and M. Podolák, *ibid.*, 1986, **367**, 311.
16. W. Th. Kok, H. B. Hanekamp, P. Bos and R. W. Frei, *Anal. Chim. Acta*, 1982, **142**, 31.
17. W. Th. Kok, U. A. Th. Brinkman and R. W. Frei, *J. Chromatog.*, 1983, **256**, 17.
18. S. V. Prabhu and R. P. Baldwin, *Anal. Chem.*, 1989, **61**, 852.
19. *Idem, ibid.*, 1989, **61**, 2258.
20. P. Lou, S. V. Prabhu and R. P. Baldwin, *ibid.*, 1990, **62**, 752.
21. P. L. Meschi and D. C. Johnson, *Anal. Chim. Acta*, 1981, **124**, 303.
22. S. Prabhu and J. L. Anderson, *Anal. Chem.*, 1987, **59**, 157.

A GLASSY-CARBON ELECTRODE MODIFIED BY DISPERSED α -ALUMINA AS AN ENHANCED ELECTROCHEMICAL DETECTOR IN LIQUID CHROMATOGRAPHY FOR CYSTEINE AND GLUTATHIONE

WEIYING HOU and ERKANG WANG*

Laboratory of Electroanalytical Chemistry, Changchun Institute of Applied Chemistry, Chinese Academy
of Sciences, Changchun, Jilin 130022, People's Republic of China

(Received 15 October 1990. Accepted 17 November 1990)

Summary—The dispersion of alumina particles on a glassy-carbon surface serving as a modified electrode significantly enhances the amperometric detection of cysteine and glutathione following liquid chromatography. With an applied potential of 0.8 V *vs.* SCE, the detection limits were 1.2 ng for cysteine and 8 ng for glutathione and the electrode response was linear up to 600 ng for cysteine and 1.8 μ g for glutathione. The modified electrode displayed high sensitivity and stability and was easy and inexpensive to prepare.

Since Zak and Kuwana¹ found that dispersions of alumina particles on glassy-carbon surfaces had electrocatalytic properties for the oxidation of ascorbic acid, catechol, hydroquinone and oxalic acid, few papers²⁻⁶ have dealt with the α -alumina modified electrode. Wang and Freiha⁶ have detected ascorbic acid, epinephrine and oxalic acid at the α -alumina-modified glassy-carbon electrode (α -Al₂O₃/GC) following liquid chromatography and obtained high sensitivity, selectivity and stability.

At most conventional electrodes, cysteine (Cys) and glutathione (GSH) exhibit irreversible oxidation, at extreme positive potentials. Consequently, electrochemical detection of these species following liquid chromatography (LC) is usually performed at mercury⁷⁻¹⁰ or metal amalgam^{11,12} electrodes at which the mercury sulfide species formed can be oxidized at comparatively low applied potentials. Use of mercury electrodes may be undesirable because of their possible toxicity and instability. Carbon electrodes require undesirably large working potentials of the order of 1.0 V *vs.* Ag/AgCl (or higher).¹³ Halbert and Baldwin^{14,15} have developed carbon-paste electrodes containing cobalt phthalocyanine for the determination of Cys and GSH in LC with electrochemical detection (LCEC) at 0.75 V *vs.* Ag/AgCl. Recently, Wring *et al.*^{16,17} have developed a carbon-epoxy resin

composite electrode chemically modified with cobalt phthalocyanine for determination of GSH with LCEC at 0.45 V *vs.* Ag/AgCl.

In this paper we report that the α -Al₂O₃/GC electrode enhances the oxidation of Cys and GSH, giving responses of high sensitivity and stability. The principal advantages of the electrode are its ease of preparation and its stability. The electrode can be used as an inexpensive enhanced LCEC detector.

EXPERIMENTAL

Apparatus

A laboratory-built cyclic voltammetric analyser was used. A three-electrode cell system with either a glassy-carbon (GC) or an α -Al₂O₃/GC working electrode, a silver chloride (saturated potassium chloride) reference electrode and a platinum auxiliary electrode was employed in the conventional electrochemical arrangement.

The LC system consisted of a model 510 pump and a U6K injection valve from Waters Associates. The injection volume was 20 μ l. A Nucleosil C₁₈ (20 cm \times 4 mm i.d.; 7 μ m) column (packed by the Dalian Institute of Chemical Physics, Dalian, China) was used, together with a Model TL-5A thin-layer electrochemical cell (Bioanalytical Systems Inc.). A laboratory-built bipotentiostat was used for the amperometric detection.¹⁸ A saturated calomel reference electrode (SCE) was used.

*Author for correspondence.

Reagents

All chemicals were of analytical-reagent grade, except the following, which were biochemical-reagent grade. Glutathione (reduced form) was from the Shanghai Institute of Biochemistry, Chinese Academy of Sciences. DL-Cysteine was obtained from the Chemical Factory of Caoyang Second Middle School (Shanghai).

Procedure

All solutions were prepared in doubly distilled water, unless stated otherwise. Immediately before LCEC analysis, DL-cysteine and glutathione were dissolved separately in potassium hydroxide solution, and these solutions were diluted to 5 mg/ml with water and protected from light. Portions of these solutions were diluted to the appropriate concentrations with the mobile phase, 0.2M potassium dihydrogen phosphate (containing 50 μ M EDTA) adjusted to pH 3.0 with phosphoric acid. The flow-rate was 1.0 ml/min.

Electrodes

The α -Al₂O₃/GC electrode was prepared by polishing the GC surface with an aqueous slurry of 0.3- μ M α -alumina on a polishing cloth. The electrode was then rinsed several times with doubly distilled water and used immediately. An ordinary bare GC electrode was obtained by cleaning the polished surface in an ultrasonic bath for 30 min, with frequent changes of doubly distilled water in the bath.

RESULTS AND DISCUSSION

Electrochemical behaviour of Cys and GSH

The electrochemical behaviour of Cys and GSH was studied at GC and α -Al₂O₃/GC working electrodes. The cyclic voltamperograms for the oxidation of Cys and GSH on the GC and α -Al₂O₃/GC electrodes in a conventional electrochemical cell are shown in Figs. 1 and 2, respectively. Each yields irreversible oxidation waves. It is apparent that the response was enhanced, with a slight increase of background current, by use of the α -Al₂O₃/GC electrode. The oxidation waves of Cys and GSH on the α -Al₂O₃/GC electrode showed no obvious peaks.

Liquid chromatography with electrochemical detection (LCEC)

Good separation of the Cys and GSH was achieved with a mobile phase of 0.2M potass-

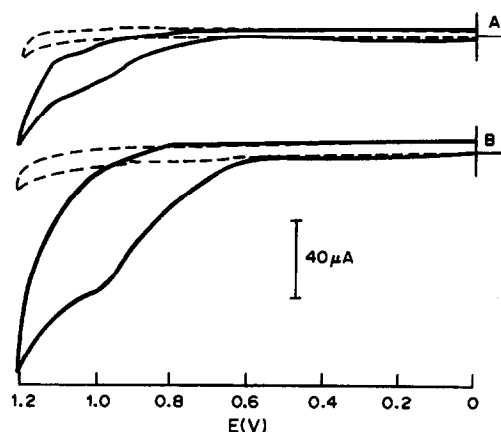


Fig. 1. Cyclic voltamperograms of cysteine at GC (A) and α -Al₂O₃/GC (B) electrodes. Electrolyte solution, 0.2M KH₂PO₄ (pH 3.0); scan rate, 50 mV/sec; broken line, blank solution; solid line, 1mM cysteine.

ium dihydrogen phosphate (containing 50 μ M EDTA) at pH 3.0 with a flow-rate of 1 ml/min (Fig. 3).

Hydrodynamic voltamperograms (HDVs) were obtained for Cys and GSH at both the GC and α -Al₂O₃/GC electrodes by injecting fixed volumes of the standard solutions and varying the potential between 0.5 and 1.0 V in the electrochemical detection (Fig. 4). At the GC electrode, no response to Cys or GSH was obtained at applied potentials less than 0.7 V. Significant responses were obtained only in high potential regions, and were subject to considerably larger background currents and a greater likelihood of interference. At the α -Al₂O₃/GC electrode, enhanced responses to Cys and GSH were obtained compared with those at the GC electrode. When the applied potential exceeded 0.5 V the oxidation currents of Cys and GSH

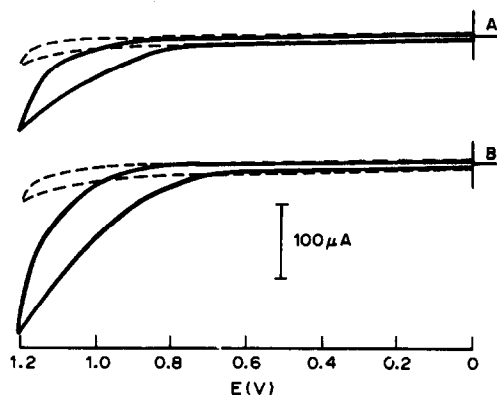


Fig. 2. Cyclic voltamperograms of glutathione at GC (A) and α -Al₂O₃/GC (B) electrodes. Electrolyte solution, 0.2M KH₂PO₄ (pH 3.0); scan rate, 50 mV/sec; broken line, blank solution; solid line, 6mM glutathione.

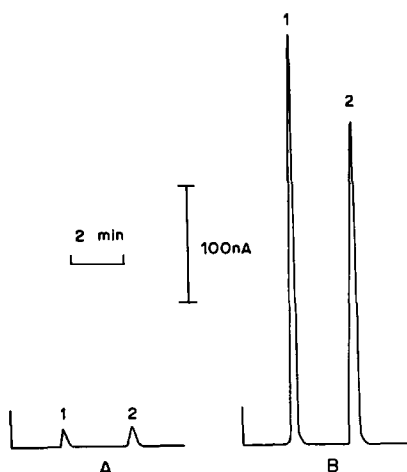


Fig. 3. Chromatograms for 40 $\mu\text{g/ml}$ cysteine (1) and 200 $\mu\text{g/ml}$ glutathione (2), with GC (A) and $\alpha\text{-Al}_2\text{O}_3/\text{GC}$ (B) electrodes as detectors, $E = 0.80\text{ V}$; same mobile phase and flow-rate as for Fig. 4.

were produced. However, the HDVs obtained do not show plateau currents, which is consistent with their cyclic voltamperograms not showing peaks. Operation at high potentials would be disadvantageous for LCEC, because of the higher background current, so a potential of 0.8 V was selected for the detection of Cys and GSH at the $\alpha\text{-Al}_2\text{O}_3/\text{GC}$ electrode. Figure 3 compares chromatograms for a mixture of 40 $\mu\text{g/ml}$ Cys (1) and 200 $\mu\text{g/ml}$ GSH (2) obtained with GC (A) and $\alpha\text{-Al}_2\text{O}_3/\text{GC}$ (B) detectors. It can be seen that the response peaks obtained at the $\alpha\text{-Al}_2\text{O}_3/\text{GC}$ electrode were 14 and 11 times larger for Cys and GSH, respectively, than at the GC electrode at the same potential. At the same time, equal noise levels (peak-to-trough amplitude of about 80 pA) were obtained at the GC and $\alpha\text{-Al}_2\text{O}_3/\text{GC}$ electrodes (not shown).

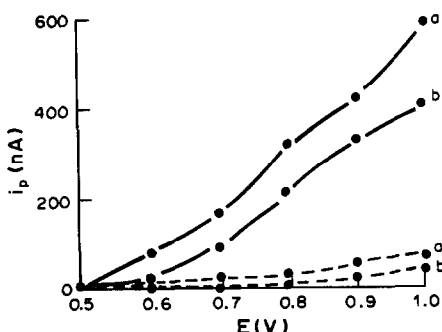


Fig. 4. Hydrodynamic voltamperograms of 40 $\mu\text{g/ml}$ cysteine (a) and 200 $\mu\text{g/ml}$ glutathione (b) at GC (---) and $\alpha\text{-Al}_2\text{O}_3/\text{GC}$ (—) electrodes. Mobile phase, 0.2M KH_2PO_4 (containing 50 μM EDTA) at pH 3.0; flow-rate, 1 ml/min.

The stability of the $\alpha\text{-Al}_2\text{O}_3/\text{GC}$ electrode was examined by comparing peak currents over a period of operation. The results indicate that the peak currents decreased substantially in the very early stages of the experiment, perhaps because some "loose" particles were washed off by the mobile phase.¹⁶ After about four injections, however, the peak currents became stable. The electrode was washed with doubly-distilled water each day after the LCEC experiments and then stored in water overnight. The peak current was 45% greater than the last on the previous day for Cys and 67% larger for GSH when the electrode was used again, and the peak currents again decreased substantially over four successive injections. We therefore think that the non-oxidizable products of the Cys and GSH oxidations may be adsorbed on the surface of the electrode and poison it. Poisoning was more obvious in the very early stages of each day's experiments and resulted in substantial decrease of the peak currents. The first four injections each day were therefore routinely disregarded. Eight replicate injections of the standard solution containing 10 $\mu\text{g/ml}$ Cys and 50 $\mu\text{g/ml}$ GSH were made over 50 min; the coefficients of variation for the peak currents were 1.6% for Cys and 2.1% for GSH. The stability of the response for eight measurements of 10 $\mu\text{g/ml}$ Cys and 50 $\mu\text{g/ml}$ GSH during an unbroken period of 3 hr at a flow-rate of 1 ml/min was examined: the coefficients of variation for the peak currents were 4% for Cys and 6.1% for GSH. When the $\alpha\text{-Al}_2\text{O}_3/\text{GC}$ electrode was used for three days, the LCEC system being washed with water after each day's experiments, no obvious decrease of activity was observed. These results indicate that the alumina particles remaining at the electrode surface maintain their activity over long periods of time, despite the vigorous hydrodynamic conditions prevailing in the narrow channel.

Calibration graphs were linear for injected amounts of Cys from 600 ng down to 1.2 ng (9.9 pmole) and of GSH from 1.8 μg down to 8 ng (26 pmole). The lowest amounts cited yielded S/N ratios of approximately 3 and thus represented the detection limits. The correlation coefficients were 0.9999 for Cys and 0.9994 for GSH and the slopes of the calibration graphs were 172 pA/ng for Cys and 28 pA/ng for GSH.

In conclusion, the experiments described above clearly indicate that the α -alumina-modified glassy-carbon electrode is very promising for use in LCEC of Cys and GSH and

performs with high sensitivity and selectivity. The main advantage of the alumina-modified electrode over the usual CMEs formed by adsorption, covalent attachment, polymer coating *etc.* is that it is easy to prepare, inexpensive, and very stable. In addition, it is apparent that the use of CMEs offers the possibility of extending LCEC techniques to Cys and GSH, which otherwise are poorly suited to electroanalysis.

Acknowledgement—The support of the National Natural Science Foundation of China is gratefully acknowledged.

REFERENCES

1. J. Zak and T. Kuwana, *J. Am. Chem. Soc.*, 1982, **104**, 5514.
2. *Idem*, *J. Electroanal. Chem.*, 1983, **150**, 645.
3. S. Dong and T. Kuwana, *J. Electrochem. Soc.*, 1984, **131**, 813.
4. *Idem*, *Yingyong Huaxue*, 1985, **2**, No. 1, 34.
5. *Idem*, *Huaxue Xuebao*, 1985, **43**, 712.
6. J. Wang and B. Freiha, *Anal. Chem.*, 1984, **56**, 2266.
7. D. L. Rabenstein and R. Saetre, *ibid.*, 1977, **49**, 1036.
8. R. Saetre and D. L. Rabenstein, *ibid.*, 1978, **50**, 276.
9. *Idem*, *Anal. Biochem.*, 1978, **90**, 684.
10. D. L. Rabenstein and R. Saetre, *Clin. Chem.*, 1978, **24**, 1140.
11. R. F. Bergstrom, D. R. Kay and J. G. Wagner, *J. Chromatog.*, 1981, **222**, 415.
12. L. A. Alison and R. E. Shoup, *Anal. Chem.*, 1983, **55**, 8.
13. I. Mefford and R. N. Adams, *Life Sci.*, 1978, **23**, 1167.
14. M. K. Halbert and R. P. Baldwin, *Anal. Chem.*, 1985, **57**, 591.
15. *Idem*, *J. Chromatog.*, 1985, **345**, 43.
16. S. A. Wring, J. P. Hart and B. J. Birch, *Analyst*, 1989, **114**, 1563.
17. *Idem*, *ibid.*, 1989, **114**, 1571.
18. H. Ji and E. Wang, *Fenxi Huaxue*, in press.

NITRON TETRACHLOROAUROATE(III) ELECTRODES WITH POLY(VINYL CHLORIDE) AND LIQUID MEMBRANES FOR THE SELECTIVE DETERMINATION OF GOLD

SAAD S. M. HASSAN*

Department of Chemistry, Faculty of Science, Ain Shams University, Cairo, Egypt

EMAN M. ELNEMMA and MARAWAN A. HAMADA

Department of Chemistry, Faculty of Science, Qatar University, Doha, Qatar

(Received 14 November 1989. Revised 9 July 1990. Accepted 26 October 1990)

Summary—PVC matrix and liquid membrane electrodes have been developed for direct potentiometric determination of gold(III). The membranes incorporate nitron tetrachloroaurate(III) as electroactive material. Fast response for gold(III) over the concentration range 10^{-5} – $0.1M$, with response slopes of 52.8–55.2 mV/decade is obtained. The electrodes show good selectivity for gold(III) at pH 2–5 in the presence of many anions and cations. The PVC membrane electrode offers the advantages of greater selectivity (except for Cr^{3+} , Mn^{2+} and ClO_4^-) and higher thermal stability. The liquid membrane electrode gives a higher response slope and faster time of response than the PVC membrane electrode. Determination of $AuCl_4^-$ over the range 2 $\mu g/ml$ –2 mg/ml shows an average recovery of 98.5% and a mean standard deviation of 1.0%. Determination of gold in some gold alloys (58.3–99.9% Au) and pharmaceutical preparations gave an average recovery of 99.4% and a mean standard deviation of 0.7%, which are comparable with the performance obtained with the spectrophotometric Malachite Green and gravimetric U.S. Pharmacopeia methods.

Membrane electrodes responsive to gold(III) have been based on the ion-association complexes of dicyanoaurate(I),^{1,5} and tetrachloroaurate(III)^{3,5-13} with trinonyloctadecylammonium,^{1,2} Methylene Blue,⁵ Malachite Green,⁵ Butylrhodamine B,^{6,7} tetradecylphosphonium,³ tetraphenylarsonium,^{3,4,8,9} hexadecylpyridinium,¹⁰ tetraphenylpyridinium,¹¹ benzyldimethyloctadecylammonium,¹² and hexadecyltrioctylammonium¹³ cations, as electroactive materials dispersed in lipophilic solvents^{1,2,4,5} and polymeric matrices.^{3,6-13} All but one of these reports, however, were originally published in Russian and Chinese, which makes it difficult to obtain detailed information about the performance characteristics of these sensors. It appears, however, that some of these electrodes have long response time, or are inapplicable for monitoring gold(III) concentrations below $10^{-4}M$,^{3,5} or suffer from serious interference by Ag^+ , Bi^{3+} , Tl^{3+} , ClO_4^- , I^- and PO_4^{3-} ions.^{1,2,5,11,12}

Membrane electrodes for SCN^- ,¹⁴ ReO_4^- ,¹⁵ ClO_4^- ,¹⁶ and BF_4^- ,¹⁷ based on the use of nitron as a counter-cation in the electroactive materials, have some significant advantages for the determination of these ions in terms of fast response, and high stability and selectivity.

In the present investigation the nitron-tetrachloroaurate(III) ion-pair complex was prepared and characterized. The high stability of this complex and its extractability into lipophilic solvents, as well as its good selectivity, suggested its use as an electroactive material in liquid and poly(vinyl chloride) matrix membrane electrodes. The performance characteristics of these electrode systems have been evaluated according to IUPAC recommendations¹⁸ and compared. Both electrodes display fast linear response for 10^{-5} – $0.1M$ gold(III) over the pH range 2–5 without interference by many anions and cations. The membranes of these electrodes show remarkable stability towards high temperatures and γ -radiation. Determination of gold in some pharmaceuticals and alloys by the electrodes gave results in fairly good agreement with those obtained by the standard methods.

EXPERIMENTAL

Apparatus

Potentials were measured with an Orion pH/mV meter (Model SA 720) and a nitron tetrachloroaurate(III) liquid or poly(vinyl chloride) membrane electrode in conjunction with an Orion Ag/AgCl double-junction reference

*Author for correspondence.

electrode (Model 90-02) with its outer chamber filled with 100-mg/ml potassium nitrate solution. All measurements were made at $25 \pm 1^\circ$ unless otherwise specified. All pH adjustments were monitored with an Orion combination pH electrode (Model 91-02). The conductivity of nitron tetrachloroaurate(III) solution in nitrobenzene was measured with a Tacussel conductivity cell (Type CM 0.05/G) and Prolabo conductivity meter (Type CD 6N). A gamma cell 220 (Atomic Energy of Canada Ltd.) was used for irradiation of the PVC membranes. The infrared spectra were taken with a Pye Unicam SP 3-100 infrared spectrometer.

Reagents

Wherever possible, analytical-reagent grade chemicals and doubly distilled demineralized water were used. Nitrobenzene, tetrahydrofuran, dioctyl phthalate, chloroauric acid and poly(vinyl chloride) were obtained from B.D.H. Chemicals Ltd. (Poole, England). Nitron was purchased from Pfaltz and Bauer (Waterbury, CT, U.S.A.). A 0.1M gold(III) solution was prepared from chloroauric acid in $10^{-3}M$ hydrochloric acid and standardized iodometrically by the standard method.¹⁹ Dilute solutions (10^{-6} – $10^{-2}M$) were prepared by appropriate dilutions with $10^{-3}M$ hydrochloric acid. *Aqua regia* was prepared by mixing concentrated nitric and hydrochloric acids in 1:3 ratio, and diluted with an equal volume of demineralized water. Certified gold alloys were used.

Nitron-tetrachloroaurate(III) ion-pair complex

Twenty ml of $10^{-2}M$ nitron solution in 20% acetic acid and 10 ml of $10^{-2}M$ chloroauric acid were mixed and stirred for 15 min. The brown precipitate was filtered off with a porosity-3 sintered-glass crucible, washed with demineralized distilled water, dried at room temperature and ground (melting point 153°). The elemental analysis agreed with the composition $[C_{20}H_{17}N_4^+][AuCl_4^-]$.

Nitron tetrachloroaurate(III) PVC membrane electrode

PVC (0.35 g), 0.86 g of dioctyl phthalate and 0.023 g of nitron tetrachloroaurate(III) were dissolved in about 7 ml of tetrahydrofuran. The mixture was poured into a Petri-dish (~ 7.5 cm diameter), covered with a filter paper and allowed to stand overnight. Sections of the resulting membrane were cut out with a cork borer and used as described by others.^{20,21} A platinum

wire (~ 0.5 mm diameter) soldered on to a shielded cable was used as an internal reference electrode. A solution (pH 3–4) containing chloroauric acid and sodium chloride, each at a concentration of $10^{-3}M$, was used as an internal reference solution.

Nitron tetrachloroaurate(III) liquid membrane electrode

An Orion liquid membrane electrode body (Model 92) was used in conjunction with an Orion porous membrane (92-81-04). The internal Ag/AgCl reference electrode was replaced by a platinum wire (~ 0.5 mm diameter) soldered on to a shielded cable. The internal reference solution was a mixture of equal volumes of $2 \times 10^{-3}M$ sodium chloride and $2 \times 10^{-3}M$ $AuCl_4^-$, at pH 3–4. The liquid membrane was $10^{-2}M$ nitron tetrachloroaurate(III) solution in nitrobenzene.

Performance of the electrode systems

The electrodes were conditioned by soaking for 24 hr in approximately $10^{-3}M$ $AuCl_4^-$ and stored in the same solution when not in use. They were washed thoroughly with doubly distilled demineralized water between measurements. Calibration was done by measuring the potential yielded by 10^{-6} – $0.1M$ $AuCl_4^-$ solutions (pH 3–4) when the readings were stable within ± 1 mV.

The selectivity coefficients ($k_{Au, B}^{pot}$) were evaluated by the separate solution method^{18–20} with $10^{-2}M$ solutions of the interferent and $AuCl_4^-$ at pH 3–4. For cationic interference studies the metal chlorides were used (except for silver and lead, used as their nitrates). For anionic interference studies, sodium or potassium salts were used. All potential measurements for response curves and selectivity coefficients were made in triplicate.

The response times were taken as the times required for the electrodes to reach values within 1 mV of the final equilibrium potential when transferred from one tetrachloroaurate(III) solution to another differing from it in concentration by a factor of 10.

The detection limit was evaluated as the concentration giving an emf differing by 18 mV from the extrapolation of the linear section of the calibration graph.

Determination of gold in alloys

A 0.1–0.2 g sample was heated with ~ 3 ml of *aqua regia* in a 50-ml beaker, covered with a

watch-glass, until the evolution of nitrogen oxides ceased. The solution was evaporated almost to dryness. The residue was dissolved with ~25 ml of $10^{-3}M$ hydrochloric acid. The solution was adjusted to pH 3–4, transferred to a 50-ml standard flask and made up to the mark with $10^{-3}M$ hydrochloric acid, and 5 ml of this solution was diluted to volume with $10^{-3}M$ hydrochloric acid in another 50-ml standard flask (alternatively the original residue solution could be diluted directly to 500 ml). The potential given by the solution was measured with the nitron tetrachloroaurate(III) PVC matrix membrane electrode in conjunction with the double-junction Ag/AgCl electrode and the gold concentration was read from a calibration graph covering the range 10^{-4} – $10^{-2}M$. The spiking technique²¹ was used, the potential of the gold test solution being measured before and after addition of 0.50 ml of standard $0.1M$ $AuCl_4^-$ solution.

Determination of gold in pharmaceutical preparations

The contents of three ampoules of gold-containing pharmaceutical preparations were diluted to 10.0 ml with doubly distilled water and filtered. A 2-ml aliquot of the filtrate was transferred to a 50-ml Kjeldahl flask and treated with ~5 ml of concentrated nitric acid, followed by slow addition of 5 ml of concentrated sulphuric acid. The solution was gently heated on a hot plate until evolution of sulphur trioxide fumes. The flask was allowed to cool to room temperature, and the residue was dissolved in ~5 ml of *aqua regia* and heated again almost to dryness. The residue was dissolved in ~25 ml of $10^{-3}M$ hydrochloric acid and adjusted to pH 3–4. The solution was then transferred to a 50-ml standard flask and diluted to the mark with $10^{-3}M$ hydrochloric acid. The potential of the solution was measured with the PVC membrane electrode as described above.

RESULTS AND DISCUSSION

Response characteristics of the electrodes

The liquid membrane had electrical resistance of $7 \times 10^3 \Omega$ and an equivalent conductivity (Λ) of $1.95 \text{ ohm}^{-1} \cdot \text{mole}^{-1} \cdot \text{cm}^2$. The PVC membrane was prepared by using a casting solution of the composition 28:2:70 w/w PVC, nitron-tetrachloroaurate(III) complex and dioctyl phthalate plasticizer, respectively. Table 1 summarizes the response characteristics of both

Table 1. General performance characteristics of nitron tetrachloroaurate(III) liquid and PVC membrane electrodes

Parameter	Liquid membrane	PVC membrane
Slope, <i>mV/decade</i>	55.2 ± 0.4	52.8 ± 0.5
Intercept, <i>mV</i>	550.4	690.5
Correlation coefficient, <i>r</i>	0.998	0.998
Lower limit of linear range, <i>M</i>	10^{-5}	10^{-5}
Lower detection limit, <i>M</i>	8×10^{-6}	8×10^{-6}
Response time for $10^{-3}M$, <i>sec</i>	20	30
Working acidity range, <i>pH</i>	1.5–5	1.5–5

electrode systems, from data collected over a period of 2 months for 4 different electrode assemblies. Similar results, but with the potential values 5 mV less negative were obtained with standard $AuCl_4^-$ solutions prepared in hydrochloric acid (pH 3–4) containing $0.1M$ sodium chloride.

Response time and stability

The response times of both electrodes were 10–30 sec for $\geq 10^{-3}M$ $AuCl_4^-$ and 20–60 sec for $\leq 10^{-4}M$. The steady-state potentials were attained 10–20 sec more quickly with the liquid membrane electrode than the PVC matrix membrane. For both electrodes the average change in potential for five consecutive measurements of standard 10^{-5} – $10^{-1}M$ $AuCl_4^-$ solutions during 2 hr was not more than 1.8 mV. Changes in the calibration slopes did not exceed ± 0.5 mV/decade. The long term reproducibility and stability of the potentials were evaluated by preparing 10 calibration graphs for both electrodes over a period of 2 weeks. During this period, the electrodes were stored and conditioned in $10^{-3}M$ $AuCl_4^-$ solution and washed with doubly distilled demineralized water between measurements. Although the absolute potentials of the electrodes became more positive by 4–8 mV, the slopes of the calibration graphs remained practically constant within ± 1 mV/decade over this period. No significant changes in the detection limit, selectivity coefficients and response time were observed.

Effect of pH

Standard 10^{-3} and $10^{-4}M$ $AuCl_4^-$ aqueous solutions were prepared and adjusted to various pH values in the range 0–10 with dilute hydrochloric acid and sodium hydroxide solution. Figure 1 revealed that within the working pH range 2–5, the potential given by both electrodes did not vary by more than ± 1 mV. The negative shift of the potential at pH below 1.5 is due to a change in the boundary phase of

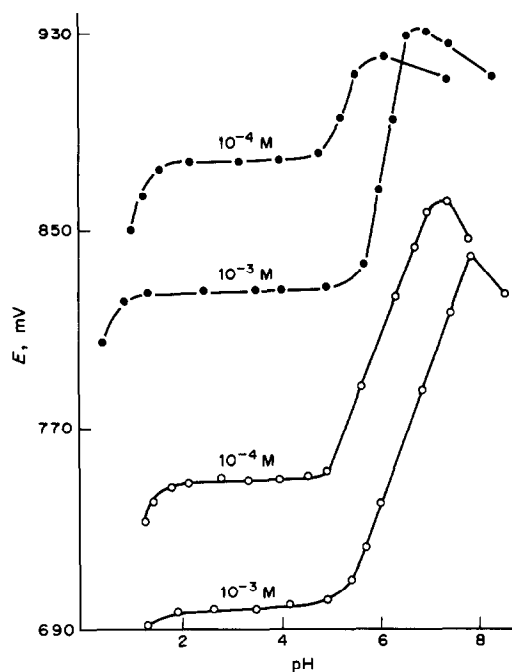


Fig. 1. Effect of pH on the potential response of nitron tetrachloroaurate(III) electrodes: ●, PVC membrane; ○, liquid membrane.

the membrane caused by the increased acid concentration at the membrane surface. The sharp increase of potential at pH above 5 is due to the decrease in AuCl_4^- concentration and formation of AuCl_3 followed by $\text{Au}(\text{OH})_3$.²² These species are not sensed by the anionic membrane sensors. At pH above 8, the membrane behaviour is influenced by the hydroxide concentration, a phenomenon observed with all membranes containing nitron as counter-cation.¹⁴⁻¹⁷ It is therefore necessary to adjust the gold test solution to pH 3-4 with hydrochloric acid before measurement of the potential.

Effect of foreign ions

The responses of the electrodes to 21 different cations and anions were studied by measuring the selectivity coefficients ($k_{\text{Au}, \text{B}}^{\text{pot}}$) by the separate solutions method,^{20,21} with fixed concentration of the interferent (10^{-2}M), at pH 3-4. The selectivity coefficients are shown in Table 2. The selectivity of the liquid membrane electrode for AuCl_4^- is generally lower than that of the PVC matrix membrane electrode, but it shows better selectivity than the PVC membrane electrode in the presence of Cr^{3+} , Mn^{2+} and ClO_4^- ions.

The selectivity coefficient data for most of the previously described electrode systems have not been reported, so it is difficult to make quanti-

Table 2. Potentiometric selectivity coefficients for nitron tetrachloroaurate(III) liquid and PVC membrane electrodes

Interferent, B	$K_{\text{Au}, \text{B}}^{\text{pot}}$	
	PVC membrane	Liquid membrane
Cu^{2+}	1.1×10^{-2}	1.6×10^{-2}
Ni^{2+}	5.0×10^{-3}	2.6×10^{-2}
Cd^{2+}	3.2×10^{-3}	4.2×10^{-3}
Co^{2+}	3.5×10^{-3}	3.3×10^{-2}
Cr^{3+}	6.3×10^{-3}	2.2×10^{-3}
Fe^{3+}	5.0×10^{-3}	2.0×10^{-2}
Mg^{2+}	5.2×10^{-3}	3.2×10^{-2}
Zn^{2+}	7.1×10^{-3}	2.0×10^{-2}
Mn^{2+}	1.1×10^{-2}	2.9×10^{-3}
Hg^{2+}	8.9×10^{-3}	1.2×10^{-2}
Pt^{2+}	7.1×10^{-3}	2.0×10^{-2}
Pb^{2+}	4.8×10^{-3}	3.9×10^{-2}
Ti^{3+}	7.9×10^{-3}	3.5×10^{-2}
Pd^{2+}	7.6×10^{-3}	1.1×10^{-2}
Ag^+	3.3×10^{-3}	1.6×10^{-2}
NO_3^-	6.0×10^{-3}	1.8×10^{-2}
SCN^-	3.2×10^{-2}	5.0×10^{-2}
Br^-	1.1×10^{-2}	1.3×10^{-2}
PO_4^{3-}	5.6×10^{-3}	1.6×10^{-2}
ClO_4^-	1.0×10^{-2}	5.5×10^{-3}

tative comparisons with the present data. It should be noted, however, that Fe^{3+} , Hg^{2+} , Cu^{2+} , Ni^{2+} , Cr^{3+} , Ag^+ , Ti^{3+} and ClO_4^- ions which are major and serious interferences even at low concentrations in many of the standard spectrophotometric,²³ potentiometric,^{1,2,5,11,12} and anodic stripping voltammetric²⁴ procedures, have little influence on the response of the present electrode systems. The concentrations of these ions must be at least 100 times that of the gold before significant interference is observed. Separate studies for determination of 10^{-2}M AuCl_4^- in the presence of up to 100-fold concentrations of some cations of alloying elements commonly associated with gold, such as Ag^+ ,

Table 3. Direct potentiometric determination of gold in chloroauric acid with the PVC membrane electrode

Au added, $\mu\text{g/ml}$	Recovery,* %
2.0	95.0 ± 1.3
10.0	98.0 ± 1.2
20.0	98.5 ± 1.2
50.0	98.4 ± 1.1
100.0	98.5 ± 1.1
200.0	99.3 ± 1.0
300.0	99.1 ± 0.8
1000	99.7 ± 0.9
1500	99.3 ± 0.8
2000	99.6 ± 0.8

*Average \pm standard deviation of 3 measurements.

Table 4. Determination of gold in some alloys by direct potentiometry with the PVC membrane electrode and spectrophotometrically by the Malachite Green method

Gold alloy	Certified Au, %	Electrode method		Spectrophotometry	
		Au found, %	Recovery,* %	Au found, %	Recovery,* %
24 carat	99.9	99.8 ± 0.5	99.9	99.6 ± 0.9	99.7
21 carat	87.5	87.0 ± 0.6	99.4	86.8 ± 1.1	99.2
18 carat	75.0	74.6 ± 0.9	99.5	74.3 ± 1.2	99.1
14 carat	58.3	57.6 ± 0.9	98.8	57.4 ± 1.3	98.5

*Average ± standard deviation of 5 measurements.

Cu²⁺ and Cd²⁺, showed minimal interferences. The average recovery of gold ranged from 96 to 102% with a standard deviation of 2% ($n = 5$).

Effect of temperature and γ -radiation

A gradual increase in the potential values was observed as the temperature was increased from 20 to 50°, but there was no significant variation in the limit of detection, response time, and slope of the calibration graph. The temperature coefficients of the potential were 0.25 and 0.5 mV/deg for the PVC and liquid membranes, respectively.

Electrodes incorporating PVC matrix membranes that had been exposed to 10³, 10⁵ and 10⁷ rad doses of cobalt-60 γ -rays gave essentially the same slope and linear response range as those made with the non-irradiated membranes, but gave faster response times. A shift of the response curve by +5 mV was observed for membranes irradiated with a dose of 10⁷ rad. The infrared spectrum of a pure sample of solid nitron-tetrachloroaurate(III) complex was almost the same before and after irradiation with up to 10⁸ rad, indicating high stability of the electroactive material.

Determination of gold in alloys

The accuracy and reliability of the results obtained with the electrodes were tested by measuring the concentrations of 2–2000 $\mu\text{g/ml}$ standard AuCl₄⁻ solutions by the standard-

addition (spiking) technique.²¹ The average recovery (Table 3) was 98.5% and the mean standard deviation 1.0%. The method was also applied to determination of gold in some certified gold-base alloys. Table 4 presents the results.

The average recovery was 99.4% of the certified value and the mean standard deviation was 0.7% ($n = 5$). For the same alloys the spectrophotometric Malachite Green method gave an average recovery of 99.1% and a mean standard deviation of 1.1% ($n = 5$) which agreed fairly well with the results obtained by the electrode method.

Determination of gold in pharmaceutical preparations

Gold in some pharmaceuticals commonly used in the treatment of rheumatoid arthritis was determined as described above. The results obtained (Table 5) show an average recovery of 99.8% of the nominal gold content and a mean standard deviation of 0.6%, in agreement with results obtained by the gravimetric method recommended by the U.S. Pharmacopeia²⁵ (average recovery 99.7%, mean standard deviation 0.6%).

In conclusion, the present electrode systems offer at least three main advantages over many of those previously reported, which suffered from a higher limit of detection,^{3,5} or slower response time and lower selectivity,^{1,2,5,11,12} Of

Table 5. Determination of gold in some pharmaceutical preparations by potentiometry with the PVC membrane electrode and gravimetrically by the U.S. Pharmacopeia method

Sample, trade name and source	Nominal content, mg/ampoule	Recovery,* %	
		Electrode method	USP method
Sodium aurothiomalate	10	99.5 ± 0.6	99.8 ± 0.5
Myocrisin (May & Baker, U.K.)	50	99.8 ± 0.5	99.7 ± 0.4
Sodium aurothiosulphate	50	99.8 ± 0.7	99.5 ± 0.8
Sanocrysin (Ferrosan, Denmark)	100	100.1 ± 0.6	99.9 ± 0.7

*Average ± standard deviation of 5 measurements.

the present electrodes, the liquid membrane electrode has the advantages of higher calibration slope and shorter response time, but the PVC membrane electrode displays higher selectivity (except in the presence of Cr^{3+} , Mn^{2+} and ClO_4^-) and higher thermal stability.

REFERENCES

1. E. S. Borovskii, E. M. Rakhman'ko, G. L. Starobinets and N. P. Labetskaya, *Zavodsk. Lab.*, 1982, **48**, No. 20, *Anal. Abstr.*, 1983, **45**, 1J191.
2. E. M. Rakhman'ko, E. S. Borovskii, G. L. Starobinets and N. P. Labetskaya, *Zh. Analit. Khim.*, 1982, **37**, 1966; *Anal. Abstr.*, 1983, **45**, 2J169.
3. E. N. Avdeeva, Yu. V. Shavnaya and O. M. Petrukhin, *ibid.*, 1982, **37**, 1434; *Anal. Abstr.*, 1983, **44**, 5J126.
4. A. S. Bychkov, O. M. Petrukhin, V. A. Zarinskii, Yu. A. Zolotov, L. V. Bakhtinova and G. G. Shanina, *ibid.*, 1976, **31**, 2114; *Anal. Abstr.*, 1977, **32**, 5J103.
5. V. N. Golubev and S. K. Timofeeva, *ibid.*, 1983, **38**, 1998; *Anal. Abstr.*, 1984, **46**, 9J128.
6. D. Dan, P. Xu and L. Liu, *Fenxi Huaxue*, 1987, **15**, 706; *Anal. Abstr.*, 1988, **50**, 3J155.
7. L. Cai, S. Lu and Z. Lu, *Huaxue Tongbao*, 1983, **12**, 23; *Anal. Abstr.*, 1984, **46**, 10J133.
8. H. Hua, M. Cao, Q. Zhou and G. Wei, *Fenxi Huaxue*, 1982, **10**, 65; *Anal. Abstr.*, 1982, **43**, 2J114.
9. Z. Xi, B. Tian, Z. Ceng and D. Zhang, *Lihua Jianya, Huaxue Fence*, 1987, **23**, 231; *Anal. Abstr.*, 1988, **50**, 3J154.
10. X. Tan, G. Lai and Z. Peng, *Fenxi Huaxue*, 1984, **12**, 479; *Anal. Abstr.*, 1985, **47**, 2J138.
11. J. A. Ortuno, T. P. Ruiz and C. S. Pedreno, *Anal. Chim. Acta*, 1986, **185**, 351.
12. W. Zhang, Y. Du, F. Zou, H. Hua, Y. Ni, Q. Tang and J. Zhou, *Fenxi Huaxue*, 1987, **15**, 565; *Anal. Abstr.*, 1988, **50**, 2J123.
13. H. Chen, *Fenxi Shiyanshi*, 1987, **6**, 14; *Anal. Abstr.*, 1988, **50**, 4J128.
14. S. S. M. Hassan and M. A. M. F. Elmosalamy, *Analyst*, 1987, **112**, 1709.
15. S. S. M. Hassan and M. A. Hamada, *Talanta*, 1988, **35**, 361.
16. S. S. M. Hassan and M. A. Elsaied, *ibid.*, 1986, **33**, 679.
17. S. S. M. Hassan and M. A. Elmosalamy, *Z. Anal. Chem.*, 1986, **325**, 178.
18. *Pure Appl. Chem.*, 1976, **48**, 127.
19. F. E. Beamish, *The Analytical Chemistry of the Noble Metals*, Pergamon Press, Oxford, 1966.
20. A. Craggs, G. J. Moody and J. D. R. Thomas, *J. Chem. Ed.*, 1974, **51**, 541.
21. T. S. Ma and S. S. M. Hassan, *Organic Analysis Using Ion Selective Electrodes*, Academic Press, London, 1982.
22. J. C. Bailar, Jr., H. J. Emeléus, R. Nyholm and A. F. T. Dickenson, *Comprehensive Inorganic Chemistry*, Volume 3, pp. 129–186. Pergamon Press, Oxford, 1975.
23. Z. Marczenko, *Spectrophotometric Determination of Elements*, pp. 281–287. Horwood, Chichester, 1986.
24. M. Lintern, A. Mann and D. Longman, *Anal. Chim. Acta*, 1988, **209**, 193.
25. *United States Pharmacopeia XXI, National Formulary XVI*, pp. 468–9. United States Pharmacopeial Convention, Rockville, MD, 1984.

BOOK REVIEWS

Multielement Detection Systems for Spectrochemical Analysis: K. W. BUSCH and M. A. BUSCH, Wiley, New York, 1990. Pages xxi + 688. £70.00

This book should be of interest to analytical scientists involved with the design, development or operation of multi-channel spectrometers. Most texts on spectrochemical analysis concentrate on applications of the techniques and give little coverage to the fundamental design of the instruments. With this in mind, Ken and Marianna Busch have endeavoured to produce a textbook which considers, in some detail, the principles of the optical systems and detectors employed in a variety of multi-channel instruments operated primarily in the UV-visible wavelength region. The book is intended for graduate students in analytical spectroscopy and researchers in other disciplines who use optical spectroscopy for chemical analysis. The authors have tried to simplify the mathematical explanation of fundamental optical principles (*e.g.*, in Chapters 2 and 3), but I think that they are being somewhat optimistic when they suggest that the mathematical level "should be comprehensible to readers with an undergraduate background in chemistry or related science". Perhaps chemistry graduates in the USA are required to know more mathematics than students taking equivalent courses in some UK and European universities!

The book has essentially three parts. Chapters 1-7 deal with optical principles, Chapters 8-11 cover various types of detection systems and Chapters 12-15 discuss how optical systems and detectors can be combined to produce multi-channel spectrometers for chemical analysis. I believe that Chapters 2-11 will prove most useful to the majority of readers. Chapter 3 provides a rigorous treatment of the principles of diffraction. Important mathematical derivations and relationships are clearly explained and comprehension is assisted through liberal use of helpful diagrams and optical figures. Anyone who has struggled with the basic principles of transform spectroscopy will find Chapters 5-7 extremely useful. Chapter 5 includes sections on multiplexing and Hadamard transform spectroscopy, Chapter 6 is devoted to the principles of interference and Chapter 7 provides an overview of Fourier transform spectroscopy. Introductions to photoelectronic detection (Chapter 9) and image detectors (Chapter 10) are followed by a discussion of the attributes of solid-state detectors, such as the photodiode array and charge transfer devices, in Chapter 11. This is an area of rapid change, so it is not too surprising that some of the more recent advances in solid-state detectors have not been included in the authors' literature survey, which covers publication up to 1987.

The book has very few weaknesses. Although Chapter 13 provides only a superficial introduction to analytical atomic spectrometry, it contains excellent sections on the role of noise in spectroscopic systems, and the benefits of modulation. In the latter part of the book, some of the tables of analytical data do not indicate the techniques used to obtain the information and this might be considered a minor irritation by some readers. As might be expected, the literature quoted is heavily biased towards US publications or the work of US authors reported in European journals. There is no doubt that many important developments in multi-channel systems have emanated from the USA, but scientists from other locations have also made important contributions and might have expected recognition in such a text. For example, in Chapter 14, devoted to a survey of transform spectrometric systems, the work of Canadian and American scientists in FT-UV spectrometry is discussed in some detail, but there is no mention of equally important research performed by Thorne and colleagues at Imperial College, London.

In general, the authors have been reasonably successful in their attempts to produce a textbook which covers fundamental physical principles and the philosophy of instrument design in multi-element detection systems. For this reason, the book should be a valuable addition to the libraries of analytical chemists, physicists, engineers and anyone concerned with the use of optical spectroscopy in spectrochemical analysis.

D. LITTLEJOHN

Bioluminescence and Chemiluminescence—Studies and Applications in Biology and Medicine: M. PAZZAGLI, E. CADENAS, L. J. KRICKA, A. RODA and P. E. STANLEY (eds.), Wiley, Chichester, 1989. Pages 646. £92.00.

This book represents the Proceedings of the Fifth International Symposium on Bioluminescence and Chemiluminescence held in Bologna, 25-29 September 1988, and is a reprint from Volume 4, 1989, of the Journal of Bioluminescence and Chemiluminescence. The contents of the book are organized into nine main sections covering such topics as bioluminescence in biosystems: detection of low-level chemiluminescence; chemiluminescence associated with phagocytosing leucocytes; instrumentation, biosensors and natural bioluminescence; luminescence assays, including immunoassays, used in measurements of enzyme activity, and their use in the fields of genetic engineering and nucleic acid hybridization. The sections devoted to the use of luminescence assays in the detection and quantification of biomolecules is very topical and coincides with the advent of luminescent procedures which are gradually replacing radiometric methods, particularly in automated assays. The final section of the book is devoted to the proceedings of a variety of workshops on the diverse clinical applications of chemiluminescence techniques.

BOOK REVIEWS

Multielement Detection Systems for Spectrochemical Analysis: K. W. BUSCH and M. A. BUSCH, Wiley, New York, 1990. Pages xxi + 688. £70.00

This book should be of interest to analytical scientists involved with the design, development or operation of multi-channel spectrometers. Most texts on spectrochemical analysis concentrate on applications of the techniques and give little coverage to the fundamental design of the instruments. With this in mind, Ken and Marianna Busch have endeavoured to produce a textbook which considers, in some detail, the principles of the optical systems and detectors employed in a variety of multi-channel instruments operated primarily in the UV-visible wavelength region. The book is intended for graduate students in analytical spectroscopy and researchers in other disciplines who use optical spectroscopy for chemical analysis. The authors have tried to simplify the mathematical explanation of fundamental optical principles (*e.g.*, in Chapters 2 and 3), but I think that they are being somewhat optimistic when they suggest that the mathematical level "should be comprehensible to readers with an undergraduate background in chemistry or related science". Perhaps chemistry graduates in the USA are required to know more mathematics than students taking equivalent courses in some UK and European universities!

The book has essentially three parts. Chapters 1-7 deal with optical principles, Chapters 8-11 cover various types of detection systems and Chapters 12-15 discuss how optical systems and detectors can be combined to produce multi-channel spectrometers for chemical analysis. I believe that Chapters 2-11 will prove most useful to the majority of readers. Chapter 3 provides a rigorous treatment of the principles of diffraction. Important mathematical derivations and relationships are clearly explained and comprehension is assisted through liberal use of helpful diagrams and optical figures. Anyone who has struggled with the basic principles of transform spectroscopy will find Chapters 5-7 extremely useful. Chapter 5 includes sections on multiplexing and Hadamard transform spectroscopy, Chapter 6 is devoted to the principles of interference and Chapter 7 provides an overview of Fourier transform spectroscopy. Introductions to photoelectronic detection (Chapter 9) and image detectors (Chapter 10) are followed by a discussion of the attributes of solid-state detectors, such as the photodiode array and charge transfer devices, in Chapter 11. This is an area of rapid change, so it is not too surprising that some of the more recent advances in solid-state detectors have not been included in the authors' literature survey, which covers publication up to 1987.

The book has very few weaknesses. Although Chapter 13 provides only a superficial introduction to analytical atomic spectrometry, it contains excellent sections on the role of noise in spectroscopic systems, and the benefits of modulation. In the latter part of the book, some of the tables of analytical data do not indicate the techniques used to obtain the information and this might be considered a minor irritation by some readers. As might be expected, the literature quoted is heavily biased towards US publications or the work of US authors reported in European journals. There is no doubt that many important developments in multi-channel systems have emanated from the USA, but scientists from other locations have also made important contributions and might have expected recognition in such a text. For example, in Chapter 14, devoted to a survey of transform spectrometric systems, the work of Canadian and American scientists in FT-UV spectrometry is discussed in some detail, but there is no mention of equally important research performed by Thorne and colleagues at Imperial College, London.

In general, the authors have been reasonably successful in their attempts to produce a textbook which covers fundamental physical principles and the philosophy of instrument design in multi-element detection systems. For this reason, the book should be a valuable addition to the libraries of analytical chemists, physicists, engineers and anyone concerned with the use of optical spectroscopy in spectrochemical analysis.

D. LITTLEJOHN

Bioluminescence and Chemiluminescence—Studies and Applications in Biology and Medicine: M. PAZZAGLI, E. CADENAS, L. J. KRICKA, A. RODA and P. E. STANLEY (eds.), Wiley, Chichester, 1989. Pages 646. £92.00.

This book represents the Proceedings of the Fifth International Symposium on Bioluminescence and Chemiluminescence held in Bologna, 25-29 September 1988, and is a reprint from Volume 4, 1989, of the Journal of Bioluminescence and Chemiluminescence. The contents of the book are organized into nine main sections covering such topics as bioluminescence in biosystems: detection of low-level chemiluminescence; chemiluminescence associated with phagocytosing leucocytes; instrumentation, biosensors and natural bioluminescence; luminescence assays, including immunoassays, used in measurements of enzyme activity, and their use in the fields of genetic engineering and nucleic acid hybridization. The sections devoted to the use of luminescence assays in the detection and quantification of biomolecules is very topical and coincides with the advent of luminescent procedures which are gradually replacing radiometric methods, particularly in automated assays. The final section of the book is devoted to the proceedings of a variety of workshops on the diverse clinical applications of chemiluminescence techniques.

This book is a very timely overview of the mechanisms of chemiluminescence and their use in bioassays, and there is more than ample material within the numerous papers to satisfy the appetites of chemists and biologists alike who have common research interest in this exciting field. As a leucocyte biologist, who monitors the activities of these cells in normal and pathological situations by using luminescent assays, I found this book very stimulating, not only for the section on leucocyte bioluminescence, but also for the extremely interesting papers on the mechanisms of chemiluminescence and the instrumentation and assays used in measurement, all of which are very lucidly written.

The editors are to be congratulated for their endeavours in assembling the Proceedings into this handsome volume which serves not only to honour Professor William McElroy, whom many consider to be the father of bioluminescence, but also as a very fitting dedication to the memory of Marlene DeLuca who, along with Professor McElroy, has been an important contributor to our understanding of the biochemistry of bioluminescence reactions. I am confident this book will enjoy wide readership among senior undergraduates, postgraduates and active scientific and clinical researchers in the field of bioluminescence and chemiluminescence. Only the price will limit the number of purchasers, but all good scientific and clinical libraries should stock this book.

R. G. P. PUGH-HUMPHREYS

HPLC of Biological Macromolecules—Methods and Applications: K. M. GOODING and F. E. REGNIER (eds.), Dekker, New York, 1990. Pages xiii + 676. \$150.00 (U.S. and Canada), \$180.00 (elsewhere).

Before I opened this book I had expected from the title a balance between sections on experimental methods and the applications of HPLC to proteins, polynucleotides and carbohydrates. However, on examining the contents pages I was struck immediately by the fact that it is heavily biased towards proteins. I suppose it is a reflection of both the variety and importance of this particular class of macromolecule that proteins take first place in this book.

The book is divided into three parts. Part 1 (nine chapters) deals with the technique of HPLC, Part 2 (thirteen chapters) with polypeptides and Part 3 (1 chapter) with polynucleotides. I should add that carbohydrates are not completely left out in the cold, because Chapter 21 deals with glycoproteins, *i.e.*, proteins with covalently bound sugars.

In Chapter 1 various properties of silica as a support are examined. Chapter 2 is a description of various forms of organic supports while Chapter 3, which deals with size exclusion chromatography (SEC) begins by considering the confusion which has arisen in the literature by the use of the alternative terms "gel filtration" and "gel permeation chromatography." A useful chapter on ion-exchange chromatography—mainly for protein separation—is followed by one on hydrophobic interaction chromatography (HIC) with a nice balance of theoretical and practical aspects. Chapter 6, a well referenced chapter, deals with reverse-phase chromatography with a section on tryptic maps.

Metal interaction chromatography is the subject of Chapter 7. In this technique retention and separation of sample components are achieved largely by interaction with chelated metal ions. Sample preparation is the topic of the next chapter, and Chapter 9 rounds off Part 1 by dealing with the principles of gradient elution separations. Chapter 10 looks at the application of HPLC to amino-acid analysis and protein-sequence analysis.

Because enzyme purification is of immense importance to biochemists it is fitting to find a chapter on preparative enzyme purification by HPLC. Judging by the number of publications in this field in recent years the method promises to be of central importance in the near future.

In a chapter describing ribosomal protein separation, computer simulation is detailed, which allows separation patterns in complex chromatograms to be predicted, thus enabling the design of multistep gradients to maintain high resolution.

When it is realized that HPLC can cut down the time required for antibody purification from several weeks to a few hours it is not surprising that there is growing interest in this particular application. This is reflected in a chapter on the HPLC of antibodies, which is well referenced. Another chapter focuses on the application of size exclusion chromatography to the study of molecular interactions; methods for both ligand-protein and protein-protein binding are considered.

Part 2 concludes with a chapter on the application of HPLC to the assay of enzymatic activities; to date nearly one hundred enzymatic activities have been assayed by this method. Part 3 is concerned with the resolution of oligonucleotides and transfer RNAs where the advantages of speed and resolution, compared with those of the still widely used conventional methods, are amply demonstrated. Topics covered by other chapters include the HPLC of peptides, isoenzymes, membrane proteins, human haemoglobin variants, cereal endosperm storage proteins, histone and glycoproteins.

The book has well over a thousand references, about forty tables and is well illustrated with over two hundred figures. The chapters complement each other admirably. It is a source of up-to-date information on techniques and applications which will serve as an invaluable practical guide to anyone who is engaged in the HPLC of biological macromolecules.

A. K. DAVIES

Dictionary of Chemistry and Chemical Technology (English-German): H. GROSS, W. BORS DORF and J. KNEPPER, 4th Ed., Elsevier, Amsterdam, 1989. Pages 752. US\$ 146.50, Dfl. 300.00.

The fact that it has been deemed necessary to produce four editions of the dictionary in the space of six years testifies to the proliferation of technical terms and jargon within that period. This new edition is 40 pages longer than the first edition (which appeared in 1984) and contains about 5000 more terms. Stated so baldly, that does not sound much to have achieved, but some 12,500 new terms have been added since the third edition, room being made for them by elimination of certain terms that are either seldom used or already universally understood (and available in the earlier editions or in standard

This book is a very timely overview of the mechanisms of chemiluminescence and their use in bioassays, and there is more than ample material within the numerous papers to satisfy the appetites of chemists and biologists alike who have common research interest in this exciting field. As a leucocyte biologist, who monitors the activities of these cells in normal and pathological situations by using luminescent assays, I found this book very stimulating, not only for the section on leucocyte bioluminescence, but also for the extremely interesting papers on the mechanisms of chemiluminescence and the instrumentation and assays used in measurement, all of which are very lucidly written.

The editors are to be congratulated for their endeavours in assembling the Proceedings into this handsome volume which serves not only to honour Professor William McElroy, whom many consider to be the father of bioluminescence, but also as a very fitting dedication to the memory of Marlene DeLuca who, along with Professor McElroy, has been an important contributor to our understanding of the biochemistry of bioluminescence reactions. I am confident this book will enjoy wide readership among senior undergraduates, postgraduates and active scientific and clinical researchers in the field of bioluminescence and chemiluminescence. Only the price will limit the number of purchasers, but all good scientific and clinical libraries should stock this book.

R. G. P. PUGH-HUMPHREYS

HPLC of Biological Macromolecules—Methods and Applications: K. M. GOODING and F. E. REGNIER (eds.), Dekker, New York, 1990. Pages xiii + 676. \$150.00 (U.S. and Canada), \$180.00 (elsewhere).

Before I opened this book I had expected from the title a balance between sections on experimental methods and the applications of HPLC to proteins, polynucleotides and carbohydrates. However, on examining the contents pages I was struck immediately by the fact that it is heavily biased towards proteins. I suppose it is a reflection of both the variety and importance of this particular class of macromolecule that proteins take first place in this book.

The book is divided into three parts. Part 1 (nine chapters) deals with the technique of HPLC, Part 2 (thirteen chapters) with polypeptides and Part 3 (1 chapter) with polynucleotides. I should add that carbohydrates are not completely left out in the cold, because Chapter 21 deals with glycoproteins, *i.e.*, proteins with covalently bound sugars.

In Chapter 1 various properties of silica as a support are examined. Chapter 2 is a description of various forms of organic supports while Chapter 3, which deals with size exclusion chromatography (SEC) begins by considering the confusion which has arisen in the literature by the use of the alternative terms "gel filtration" and "gel permeation chromatography." A useful chapter on ion-exchange chromatography—mainly for protein separation—is followed by one on hydrophobic interaction chromatography (HIC) with a nice balance of theoretical and practical aspects. Chapter 6, a well referenced chapter, deals with reverse-phase chromatography with a section on tryptic maps.

Metal interaction chromatography is the subject of Chapter 7. In this technique retention and separation of sample components are achieved largely by interaction with chelated metal ions. Sample preparation is the topic of the next chapter, and Chapter 9 rounds off Part 1 by dealing with the principles of gradient elution separations. Chapter 10 looks at the application of HPLC to amino-acid analysis and protein-sequence analysis.

Because enzyme purification is of immense importance to biochemists it is fitting to find a chapter on preparative enzyme purification by HPLC. Judging by the number of publications in this field in recent years the method promises to be of central importance in the near future.

In a chapter describing ribosomal protein separation, computer simulation is detailed, which allows separation patterns in complex chromatograms to be predicted, thus enabling the design of multistep gradients to maintain high resolution.

When it is realized that HPLC can cut down the time required for antibody purification from several weeks to a few hours it is not surprising that there is growing interest in this particular application. This is reflected in a chapter on the HPLC of antibodies, which is well referenced. Another chapter focuses on the application of size exclusion chromatography to the study of molecular interactions; methods for both ligand-protein and protein-protein binding are considered.

Part 2 concludes with a chapter on the application of HPLC to the assay of enzymatic activities; to date nearly one hundred enzymatic activities have been assayed by this method. Part 3 is concerned with the resolution of oligonucleotides and transfer RNAs where the advantages of speed and resolution, compared with those of the still widely used conventional methods, are amply demonstrated. Topics covered by other chapters include the HPLC of peptides, isoenzymes, membrane proteins, human haemoglobin variants, cereal endosperm storage proteins, histone and glycoproteins.

The book has well over a thousand references, about forty tables and is well illustrated with over two hundred figures. The chapters complement each other admirably. It is a source of up-to-date information on techniques and applications which will serve as an invaluable practical guide to anyone who is engaged in the HPLC of biological macromolecules.

A. K. DAVIES

Dictionary of Chemistry and Chemical Technology (English-German): H. GROSS, W. BORS DORF and J. KNEPPER, 4th Ed., Elsevier, Amsterdam, 1989. Pages 752. US\$ 146.50, Dfl. 300.00.

The fact that it has been deemed necessary to produce four editions of the dictionary in the space of six years testifies to the proliferation of technical terms and jargon within that period. This new edition is 40 pages longer than the first edition (which appeared in 1984) and contains about 5000 more terms. Stated so baldly, that does not sound much to have achieved, but some 12,500 new terms have been added since the third edition, room being made for them by elimination of certain terms that are either seldom used or already universally understood (and available in the earlier editions or in standard

This book is a very timely overview of the mechanisms of chemiluminescence and their use in bioassays, and there is more than ample material within the numerous papers to satisfy the appetites of chemists and biologists alike who have common research interest in this exciting field. As a leucocyte biologist, who monitors the activities of these cells in normal and pathological situations by using luminescent assays, I found this book very stimulating, not only for the section on leucocyte bioluminescence, but also for the extremely interesting papers on the mechanisms of chemiluminescence and the instrumentation and assays used in measurement, all of which are very lucidly written.

The editors are to be congratulated for their endeavours in assembling the Proceedings into this handsome volume which serves not only to honour Professor William McElroy, whom many consider to be the father of bioluminescence, but also as a very fitting dedication to the memory of Marlene DeLuca who, along with Professor McElroy, has been an important contributor to our understanding of the biochemistry of bioluminescence reactions. I am confident this book will enjoy wide readership among senior undergraduates, postgraduates and active scientific and clinical researchers in the field of bioluminescence and chemiluminescence. Only the price will limit the number of purchasers, but all good scientific and clinical libraries should stock this book.

R. G. P. PUGH-HUMPHREYS

HPLC of Biological Macromolecules—Methods and Applications: K. M. GOODING and F. E. REGNIER (eds.), Dekker, New York, 1990. Pages xiii + 676. \$150.00 (U.S. and Canada), \$180.00 (elsewhere).

Before I opened this book I had expected from the title a balance between sections on experimental methods and the applications of HPLC to proteins, polynucleotides and carbohydrates. However, on examining the contents pages I was struck immediately by the fact that it is heavily biased towards proteins. I suppose it is a reflection of both the variety and importance of this particular class of macromolecule that proteins take first place in this book.

The book is divided into three parts. Part 1 (nine chapters) deals with the technique of HPLC, Part 2 (thirteen chapters) with polypeptides and Part 3 (1 chapter) with polynucleotides. I should add that carbohydrates are not completely left out in the cold, because Chapter 21 deals with glycoproteins, *i.e.*, proteins with covalently bound sugars.

In Chapter 1 various properties of silica as a support are examined. Chapter 2 is a description of various forms of organic supports while Chapter 3, which deals with size exclusion chromatography (SEC) begins by considering the confusion which has arisen in the literature by the use of the alternative terms "gel filtration" and "gel permeation chromatography." A useful chapter on ion-exchange chromatography—mainly for protein separation—is followed by one on hydrophobic interaction chromatography (HIC) with a nice balance of theoretical and practical aspects. Chapter 6, a well referenced chapter, deals with reverse-phase chromatography with a section on tryptic maps.

Metal interaction chromatography is the subject of Chapter 7. In this technique retention and separation of sample components are achieved largely by interaction with chelated metal ions. Sample preparation is the topic of the next chapter, and Chapter 9 rounds off Part 1 by dealing with the principles of gradient elution separations. Chapter 10 looks at the application of HPLC to amino-acid analysis and protein-sequence analysis.

Because enzyme purification is of immense importance to biochemists it is fitting to find a chapter on preparative enzyme purification by HPLC. Judging by the number of publications in this field in recent years the method promises to be of central importance in the near future.

In a chapter describing ribosomal protein separation, computer simulation is detailed, which allows separation patterns in complex chromatograms to be predicted, thus enabling the design of multistep gradients to maintain high resolution.

When it is realized that HPLC can cut down the time required for antibody purification from several weeks to a few hours it is not surprising that there is growing interest in this particular application. This is reflected in a chapter on the HPLC of antibodies, which is well referenced. Another chapter focuses on the application of size exclusion chromatography to the study of molecular interactions; methods for both ligand-protein and protein-protein binding are considered.

Part 2 concludes with a chapter on the application of HPLC to the assay of enzymatic activities; to date nearly one hundred enzymatic activities have been assayed by this method. Part 3 is concerned with the resolution of oligonucleotides and transfer RNAs where the advantages of speed and resolution, compared with those of the still widely used conventional methods, are amply demonstrated. Topics covered by other chapters include the HPLC of peptides, isoenzymes, membrane proteins, human haemoglobin variants, cereal endosperm storage proteins, histone and glycoproteins.

The book has well over a thousand references, about forty tables and is well illustrated with over two hundred figures. The chapters complement each other admirably. It is a source of up-to-date information on techniques and applications which will serve as an invaluable practical guide to anyone who is engaged in the HPLC of biological macromolecules.

A. K. DAVIES

Dictionary of Chemistry and Chemical Technology (English-German): H. GROSS, W. BORS DORF and J. KNEPPER, 4th Ed., Elsevier, Amsterdam, 1989. Pages 752. US\$ 146.50, Dfl. 300.00.

The fact that it has been deemed necessary to produce four editions of the dictionary in the space of six years testifies to the proliferation of technical terms and jargon within that period. This new edition is 40 pages longer than the first edition (which appeared in 1984) and contains about 5000 more terms. Stated so baldly, that does not sound much to have achieved, but some 12,500 new terms have been added since the third edition, room being made for them by elimination of certain terms that are either seldom used or already universally understood (and available in the earlier editions or in standard

dictionaries). Though the main purpose is obviously the provision of accurate German equivalents of English terms, a minor benefit may be the opportunity afforded for checking translation of German neologisms or author-constructed terms into English, by back-translation into German with the aid of this dictionary, and consequent avoidance of translation errors such as the legendary English–Swahili dictionary rendering of “out of sight, out of mind” as “invisible idiot”. It is to be hoped that a new edition of the corresponding German–English Dictionary of Chemistry and Chemical Technology will soon be available.

R. A. CHALMERS

Pore Size Engineering in Zeolites: E. F. VANSANT, Wiley, Chichester, 1990. Pages xi + 145. £24.95.

Separation science has benefited greatly from the application of zeolites. Zeolites are crystalline aluminosilicates, the open architecture of which gives rise to regularly repeated internal spaces or pores which serve as molecular sieves. The diffusion pathways giving access to these pores normally increase in size in steps. However, chemists have learned to fine-tune the entry size by a variety of methods, and these are the subject of the title of the book. Amongst the methods described are modification of the framework itself, by silanation, boronation, ion-exchange, implantation, and pre-adsorption of polar molecules.

The author is well-qualified to write this book; he and his group have been leaders in the field. However, it is necessary to express some reservations about the content, level and physical production of the book. The contents read like a collection of research papers strung together; specialists might as well read the originals and beginners will gain little appreciation of the subject. The references are inadequate; excluding the historical and standard reference books, they number less than 30. The book production is sub-standard; the text seems not to have been properly edited or proofread. Although the type face is legible, it is difficult to read because the spacing between words varies widely: indeed it is often non-existent.

F. P. GLASSER

dictionaries). Though the main purpose is obviously the provision of accurate German equivalents of English terms, a minor benefit may be the opportunity afforded for checking translation of German neologisms or author-constructed terms into English, by back-translation into German with the aid of this dictionary, and consequent avoidance of translation errors such as the legendary English–Swahili dictionary rendering of “out of sight, out of mind” as “invisible idiot”. It is to be hoped that a new edition of the corresponding German–English Dictionary of Chemistry and Chemical Technology will soon be available.

R. A. CHALMERS

Pore Size Engineering in Zeolites: E. F. VANSANT, Wiley, Chichester, 1990. Pages xi + 145. £24.95.

Separation science has benefited greatly from the application of zeolites. Zeolites are crystalline aluminosilicates, the open architecture of which gives rise to regularly repeated internal spaces or pores which serve as molecular sieves. The diffusion pathways giving access to these pores normally increase in size in steps. However, chemists have learned to fine-tune the entry size by a variety of methods, and these are the subject of the title of the book. Amongst the methods described are modification of the framework itself, by silanation, boronation, ion-exchange, implantation, and pre-adsorption of polar molecules.

The author is well-qualified to write this book; he and his group have been leaders in the field. However, it is necessary to express some reservations about the content, level and physical production of the book. The contents read like a collection of research papers strung together; specialists might as well read the originals and beginners will gain little appreciation of the subject. The references are inadequate; excluding the historical and standard reference books, they number less than 30. The book production is sub-standard; the text seems not to have been properly edited or proofread. Although the type face is legible, it is difficult to read because the spacing between words varies widely: indeed it is often non-existent.

F. P. GLASSER

ANALYTICAL APPLICATIONS OF 1,10-ANTHRAQUINONES: A REVIEW

AURORA NAVAS DIAZ

Department of Analytical Chemistry, Faculty of Sciences, University of Málaga, 29071-Málaga, Spain

(Received 7 March 1988 Revised 19 November 1990 Accepted 24 January 1991)

Summary—Analytical aspects of the chemistry in solution of 1,10-anthraquinone (AQ) derivatives is reviewed. The information about photometric and fluorimetric determination of inorganic species has been condensed and presented in tabular form.

Although technological advances in instrumentation have shifted the emphasis of analytical research towards improvement of methods by means of new and more powerful instruments or by modification of the instrumental configuration, the principle of chemical analysis still remains chemical reaction between the substance to be determined and an auxiliary substance to be added, the reagent. The extensive but widely dispersed amount of information on reaction chemistry makes a comprehensive and sufficiently critical review of great value for choosing a reagent for a particular application.

This review deals with anthraquinone (AQ) derivatives, a group of reagents widely used in analytical chemistry, but not hitherto surveyed.

The chemistry of anthraquinones has received much attention¹⁻⁵ because of its relevance to some important technological processes. Anthraquinone derivatives have also been widely used in analytical chemistry, mainly as strong chelating agents and chromophores. The major focus of this paper is on their optical properties, which are extensively used in analytical practice, mainly photometry and fluorimetry, and in the study of acid-base, redox, complexation and photochemical reactions. These compounds also display interesting electrochemical behaviour but its analytical use is more limited.

The basic chemical structure of anthraquinones is shown in Fig 1, with the position and nomenclature of the substituents. The trade names used by the dyestuff manufacturers can be obtained from the Colour Index⁶ and the chemical structures and properties can be found in the book by Venkataraman.¹

In dyes obtained by chemical synthesis, only substances which have formed during manufac-

ture, together with small amounts of electrolytes obtained during neutralization, will appear. In the commercial dyes different types of impurities may be present.⁷ Separation of anthraquinone dyes has been discussed¹ and various chromatographic procedures are available for analytical⁷⁻¹² and preparative scale^{13,14} separations.

The properties of anthraquinone and its derivatives that are of main interest in analytical chemistry are related to their spectral features. Theoretical and experimental studies of the absorption¹⁵⁻²⁵ and emission²⁵⁻³⁰ electronic spectra have been reported. The spectral characteristics of AQ compounds are related to the molecular structure and to the nature and relative positions of the electronic states. AQ is characterized by the electronic states S_0 , T_{n,π^*} , T_{π,π^*} , S_{n,π^*} , S_{π,π^*} . The weak long-wavelength absorption is due to the S_{n,π^*} transition. Phosphorescence occurs from the T_{π,π^*} transition. Both transitions are mainly due to the carbonyl group, which ensures minimum energy difference between the lowest excited and ground (S_0) electronic levels.³¹ S_{π,π^*} transitions are responsible for the intense short-wavelength absorptions.^{22,31}

The optical properties of AQ derivatives are modified by various factors: the nature and positions of the substituents, the formation of hydrogen bonds, and other intermolecular and intramolecular interactions. The spectral, photochemical and photophysical properties of the AQs have recently been reviewed.³²

ACID-BASE PROPERTIES

Studies have been made of the effect of pH on the spectra of AQ derivatives, in terms of the acid-base equilibria,³³⁻³⁶ which depend on the nature, number and position of the substituents.

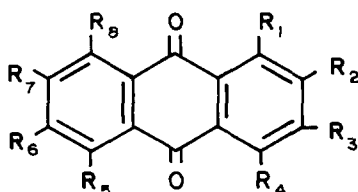


Fig 1 Basic chemical structure of 1,10-anthraquinone

Although the agreement between the various reports of pK_a values is generally quite good, there are some discrepancies, which may be attributed to differences in the solvent system and the method of calculation.

In strong acid media, the nitrogen atom of 1- and 2-aminoanthraquinone is protonated³⁷ and in sufficiently acidic media so are the sulphonic groups in 1,5- and 1,8-dihydroxyanthraquinone-disulphonic acid ($pK_{A_r(SO_3H)H^+} = -6.03$ and -3.90 respectively).³⁸ At $pH < 4-6$ the imino-nitrogen atom in arylaminoanthraquinones is protonated³³

The acidity of a derivative depends on the electron-donor or acceptor nature of the substituent and on the conjugation effects involved

Generally, the pK value for the amino group is higher for the non-sulphonated compounds than the corresponding sulphonated derivatives^{33,34,39-41} This is usually attributed to the inductive effect of the sulphonate group leading to easier ionization of the amino group.

1,4-Diaminoanthraquinone and 1,4-dihydroxyanthraquinone have higher pK_a values than those for the imine groups of Quinizarin Green and its non-sulphonated derivative. For the diaminoanthraquinone this is attributed to the greater electron-donor power of the aryl-amino substituents in the latter compounds, and for the dihydroxyanthraquinones to the effect of intramolecular hydrogen bonding³³ The effect of different substituents can be observed in the pK value of the amino group for some 1-aminoanthraquinone derivatives: for 1-aminoanthraquinone-2-sulphonic acid $pK_a = 3.79$, for 1-aminoanthraquinone-2-carboxylic acid $pK_a = 5.74$, for 1-amino-4-hydroxyanthraquinone $pK_a = 9.10$, and for 1-amino-2-bromo-4-hydroxyanthraquinone $pK_a = 9.93$ ²³

Changes in the position of substitution can affect the pK values. For example, the values for 1-hydroxyanthraquinone are about two units greater than those for the 2-hydroxy compound,³⁵ but the dissociation constants of 1,2-dihydroxyanthraquinone are similar to those of the 2,3-dihydroxy derivative⁴²

Intramolecular hydrogen bonding also affects the acidity of AQ derivatives The markedly higher pK values of the 2- than the 1-derivatives have been attributed to intramolecular hydrogen bonding.¹⁷ Taking as examples alizarin (1,2-dihydroxyanthraquinone) and quinalizarin (1,2,5,8-tetrahydroxyanthraquinone), the hydrogen bond of the 8-hydroxyl group with the carbonyl group should affect the stability of the hydrogen bond of the 1-hydroxyl group with the same carbonyl group, this reduces the basicity of the 1-hydroxyl group.⁴³

In methanol, the amino- and *N*-substituted 2-aminoanthraquinones are markedly more basic than the corresponding 1-amino derivatives. Hydroxyanthraquinones show a similar effect.¹⁷ The basic strength of 1-dimethylaminoanthraquinone is higher than that of either amino- or methylaminoanthraquinone, because in the former the amino group is out of the plane of the aromatic nucleus, so the conjugation is reduced and the group tends to exert its normal basicity.¹⁷

The pK values measured in pure aqueous solutions are mostly higher than those obtained in mixed solvents ($< 40\%$ v/v water/organic solvent), the latter leading to increased ionization,^{33,34,37,44} but pK values have been reported for 1,4-dihydroxyanthraquinone,⁴² 1,8-dihydroxyanthraquinone⁴⁵ and 1,2,7-trihydroxyanthraquinone⁴⁶ in water which are greater than those obtained in mixed solvents ($> 30\%$ v/v water/ethanol).

The ionization of AQ derivatives is influenced by the nature and concentration of the solvent system. The changes in pK_a with organic solvent concentration, though mainly governed by the dielectric constant, are also affected by the solvent basicities^{33,34}

The pK of AQ derivatives increases as the dielectric constant of the medium decreases, e.g., in the presence of high proportions of alcohols,^{33,34,46} acetone^{33,34} or dioxan^{33,47} but decreases with increase in amount of ethylene glycol or glycerol. This is explained on the basis that the latter solvents act as proton-acceptors rather than donors, leading to easier dissociation.^{33,34}

The acidity constants of hydroxy- and aminoanthraquinones in 1.2 v/v dioxan-water are always higher for the excited singlet^{37,48} and triplet⁴⁹ states than for the ground state, but the triplet state constant lies much closer to the ground state value than does that for the singlet state

Some AQ derivatives, mainly the hydroxy-anthraquinones, change colour with pH and have been used as acid–base indicators. For analytical purposes the most suitable transition of HAQs is that between yellow and red. Quinizarin (1,4-dihydroxyanthraquinone) and Alizarin S (1,2-dihydroxyanthraquinone sulphonate) are very good indicators with a colour change quality similar to that of Bromocresol Green; alizarin is also a good indicator but with slightly lower colour change quality, and the colour change of quinizarin (1,2,5,8-tetrahydroxyanthraquinone) is still poorer.⁵⁰

Diaminoanthraquinones, which do not show such marked colour changes with pH as do various aminohydroxyanthraquinones in aqueous medium, have been used as indicators in the titration of weak bases such as urea and sodium acetate, benzoate or salicylate with perchloric acid in glacial acetic acid alone^{51–55} and mixed with other solvents,^{56,57} but are not applicable in the titration of weaker bases with perchloric acid.⁵²

COMPLEXATION REACTIONS

Anthraquinones have long been used as analytical reagents and particularly as chromogenic and fluorogenic ligands for various metal ions.

The co-ordination reactions of AQ derivatives characteristically display moderate selectivity and large absorbance changes.⁵⁸ The absorption and emission properties of these compounds and their complexes give great fluorimetric potential, but the relatively high blank signal and the comparatively small spectral shifts due to complexation impair the analytical performance.⁵⁸

The optical characteristics of the anthraquinone co-ordination compounds are due to intraligand transitions, so the complexation results in modification of only the position of the absorption and emission maxima, and non-fluorescent derivatives do not generate fluorescent complexes. It has been shown that, depending on the acidity, the solvent and the metal ion, the same reagent may give either excellent or poor analytical response.⁵⁹

When a more highly acidic reagent, such as Quinizarin Green in comparison with 1,4-dihydroxyanthraquinone,⁶⁰ is used, the stability of the complexes of the more acidic reagent will be lower than that of the complexes of the less acidic compound, and also the formation of its

complexes should be affected less by the pH of the solution.⁶⁰

When the colour contrast is due to differences in the positions of the absorption band maxima of the various acid–base forms, to make full use⁶¹ of the contrast it is essential to adjust the acidity or choose a solvent so that the free reagent will be in its molecular form, but the anionic form will be present in the metal complex.

As regards the influence of the solvent in the complexation, it has been shown⁴⁶ that it is necessary to consider the influence of the dielectric constant of the medium. An increase in the dielectric constant causes⁶² a decrease in the relative fluorescence intensity in both reagent and complex. The absorption maxima of both the reagent and the complex are shifted to longer wavelengths with increasing solvent polarity. The pH for maximum difference in absorbance between 1,2,7-trihydroxyanthraquinone and its Cu(II) complex as a function of the dielectric constant of the medium, shifts in parallel to the corresponding pK value for the reagent.⁴⁶

The nature of the metal, its position in the Periodic Table, the ionic charge, radius and potential, cation-field energies *etc.*, all affect the properties of the complexes.

It has been shown⁴³ that the molar absorptivity and luminescence intensity of alizarin and its complexes with group IIIa and IIIb elements are inversely related to the cation-field energy. The higher the field energy of the cation introduced into the complex, the higher the degree of localization of the n -electrons of the heteroatom, and the greater the electron-density deficiency in the ring. This affects the optical properties of the molecules. Hence reagents such as alizarin have been recommended⁴³ for determination of elements with cations which have a lower cation-field energy or ionic potential, *i.e.*, cations with large radius and small charge.

Mixed-ligand complexes of elements of subgroup IIIb with hydroxyanthraquinones and auxiliary ligands have been widely studied. The auxiliary ligands include 8-hydroxyquinoline,^{63,64} ethylenediamine,^{64,65} phenazone,^{66,67} benzoic acid,⁶⁸ *N*-phenylbenzohydroxamic acid⁶⁹ and sulphosalicylic acid.⁷⁰ It has been shown that auxiliary ligands containing nitrogen donor atoms form the most stable ternary complexes.⁷⁰ The order of stability of the ternary Th(IV) complexes of 3-amino-1,2-dihydroxyanthraquinone is as follows, for the auxiliary ligands

named: 1,10-phenanthroline > 2,2'-bipyridyl > salicylic acid > 5-sulphosalicylic acid = 5-nitrosalicylic acid. This order is explained⁷⁰ as due to interaction between the π -systems of the two ligands bound to Th(IV). These ternary complexes are more stable than the binary complex.

For the mixed-ligand complexes of the rare-earth metals with 1,2,5,8,-tetrahydroxyanthraquinone and 8-hydroxyquinoline the molar absorptivity depends directly on the ionic potential (cation-field energy)⁴³. Addition of boric acid to the system increases the linear range.⁶³

The reported complexation reactions of AQ derivatives generally show moderate sensitivity and selectivity, but in some cases the variables were not optimized for modern instrumentation. Also, recent approaches^{62,71-73} have improved the general performance of the analytical methods, especially sensitivity and selectivity. For example, a significant improvement in sensitivity and selectivity in the determination of Be(II) is achieved by use of its inclusion complex in cyclodextrins.⁵⁸ Again, developments in the treatment of spectral signals allow analysis of mixtures of lanthanides at trace levels, which is otherwise difficult because of interelement interferences.^{71,73}

The most important information on the use of anthraquinones in determination of elements by complexation reactions is given in Table 1 at the end of the paper. The most widely used reagents and their types of co-ordination are summarized below.

Hydroxy-, polyhydroxy- and carboxyanthraquinones have two oxygen donor-atoms, some typical configurations are shown in Fig. 2. Thus chelation by the quinonoid oxygen atom and the hydroxy group occurs in the Alizarin S complexes with Th(IV), Hf(IV) and Cr(III), and chelation by the two hydroxyl groups of the same reagent occurs with Pb(II), V(V), W(VI), UO₂(II)⁷⁴ and with Zr(IV).⁷⁵

It has been reported that with 1-hydroxyanthraquinone an ML₂ chelate is formed with Mg(II) whereas with 1,4-dihydroxyanthra-

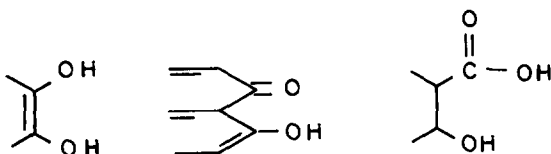


Fig. 2 Configurations of (a) hydroxy-, (b) polyhydroxy- and (c) carboxyanthraquinones

quinone a 1:1 complex is formed.⁷⁶ The latter was reported to be polymeric.

Some complexes are polymers. For example, the fluorescent product formed between 1,2,4-trihydroxyanthraquinone-3-carboxylic acid and Cu(II) is said to have a polymeric complex structure.⁷⁷ Polymeric characteristics have also been assigned⁷⁸ to the lakes that are often formed by AQ derivatives and metal ions (Fig. 3).

The alizarin-Co(II)-Co(III) complex shows a similar structure, with participation of the 2-hydroxy group in the polymerization.⁷⁹ It has been reported that chain co-ordination polymers of 1,4-dihydroxyanthraquinone and bivalent metal ions with co-ordination number 4 can be formed from the metal acetylacetonates.⁷⁶ Alcohol solutions of *o*-hydroxyanthraquinones form internal complex salts when treated with magnesium acetate.⁸⁰ Because of its polarity, *N,N*-dimethylformamide is very often used as the medium for obtaining polymers.^{77,81}

The formation of insoluble hydroxyanthraquinone complexes of ion metals has long been used in qualitative analysis. Thus, Al(III) is identified by means of the red lake formed with alizarin in basic medium. Quinalizarin is used for the identification of magnesium and various bi-, ter- and quadrivalent cations by means of lake formation.

Amino-, polyamino- and aminohydroxyanthraquinones are compounds with *N,N* or *O,N* donor-atom configurations, as shown in Fig. 4

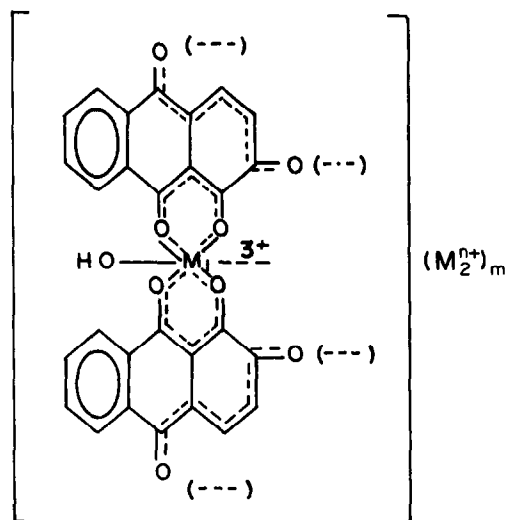


Fig. 3 Schematic formula of the lakes in which M₂ⁿ⁺ is a trivalent metal and M₂ is hydrogen, or a univalent, bivalent or quadrivalent metal

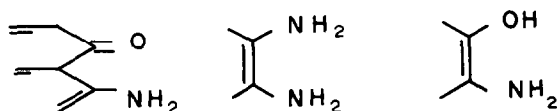


Fig 4 Configurations of (a) amino-, (b) polyamino- and (c) aminohydroxyanthraquinones

The co-ordination sites of the complexes of these AQ derivatives may be the carbonyl and amino groups, but the structure of the chelates may be due not only to the donor character of the carbonyl group and the displacement of a proton from the amino group by a metal but also to the donor character of the amino nitrogen atom. Furthermore, several of the reactions with metal ions may be attributed to redox processes.

Aminoanthraquinones, in contrast to the "broad spectrum" reactivity of the hydroxyanthraquinones, exhibit selectivity in their reactions, particularly in ethanolic medium.⁸² This selectivity is decreased in sulphuric acid medium, however.^{83,84} Thus in ethanolic media aminoanthraquinones react with the transition metal ions Pd(II), Cu(II) and Co(II), which tend to prefer nitrogen donor atoms. The Cu(II) complex with 1,2-diaminoanthraquinone has been used as a metallochromic indicator in the complexometric titration of calcium and strontium.⁸⁵

In contrast, in concentrated sulphuric acid medium, aminoanthraquinones co-ordinate with Se(IV), boric acid, calcium, strontium and barium. Selenium(IV) reacts with aromatic compounds containing amino and carbonyl groups. Of the monoamino anthraquinones only the 1-isomer reacts to form the dimer (Se)₂(1-AAQ)₂.⁸⁶ Similarly, 4,5-diamino-1,8-dihydroxyanthraquinone has an amino group adjacent to the quinone oxygen and reacts with Se(IV) to give both an SeL and an SeL₂ complex.⁸⁷

Aminohydroxyanthraquinones form metal co-ordination compounds which have the characteristics of both the amino- and hydroxyanthraquinone complexes. With metals such as Be, Th and the lanthanides they react in a similar manner to the hydroxyanthraquinones, and with Pd and Cu similarly to aminoanthraquinones. The stability constant of the 1:1 complexes of some rare-earth metals with 1-amino-4-hydroxyanthraquinone are very similar, increasing as the size of the cation decreases.⁸⁸

The anthraquinone-complexan reagents are derivatives which possess an iminodiacetic group, and have been applied for the photometric determination of several ions and as complexometric indicators.^{89,90} Alizarin Complexan (Alizarin Fluorine Blue) forms red complexes with Ce(III), La(III) and Pr(III). When fluoride is present it replaces a molecule of water in the co-ordination sphere of the metal ion and a blue ternary complex is formed (Fig. 5).⁸⁹⁻⁹²

Other anthraquinone derivatives used in complexation reactions are nitroanthraquinones and arylaminoanthraquinones. It has been reported⁵⁹ that the reaction between Ti(IV) and nitroalizarin gives a colour contrast comparable with that of the reaction of Al(III) and alizarin. 1,4-Diamino-5-nitroanthraquinone is not itself fluorescent, but gives an orange fluorescence with ions such as Au(III) and V(V).⁹³ The complexation equilibria of La(III)⁹⁴ and Y(III)⁶⁰ with 1,4-bis(4'-methylamino)anthraquinone (Quinizarin Green) have been studied spectrophotometrically.

Among the coloured chelates of anthraquinone derivatives and transition metal ions, the most widely studied and used is that of Zr with Alizarin Red S in strong acid medium. This reaction has been applied in the photometric determination of Zr in various materials, such as plutonium-uranium fission alloys^{95,96} and other alloys^{97,98} and minerals.^{99,100}

The most widely studied of the reactions of Aqs with subgroup IIIa elements are those of aluminium with Alizarin Red S, which is suitable for determination of aluminium in various materials,¹⁰¹⁻¹⁰³ and those of boron with carminic acid¹⁰⁴⁻¹¹⁰ and quinalizarin.^{104,111-114}

The reaction between fluoride and Alizarin Complexan⁸⁹⁻⁹² is one of the few colour reactions of the fluoride ion. It has been widely studied and applied.¹¹⁴⁻¹²⁰

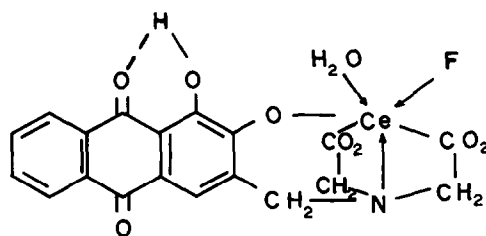


Fig 5 Chemical structure of the ternary complex Alizarin Complexan-Ce(III)-F⁻

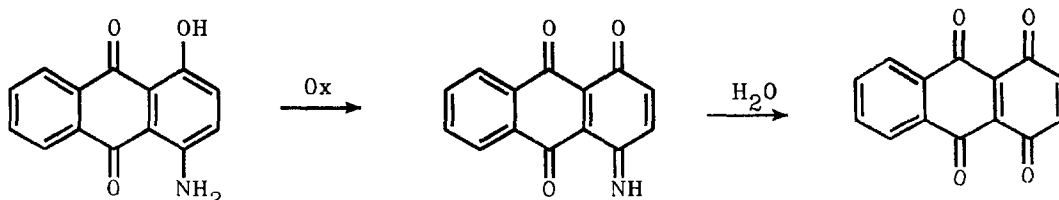


Fig 6 Oxidation reaction of *p*-aminohydroxyanthraquinone

REDOX REACTIONS

Chemical oxidation

Anthraquinone derivatives readily undergo reduction-oxidation reactions under proper conditions of acidity. Amino-, hydroxy- and aminohydroxyanthraquinones are capable of further oxidation to a variety of anion radicals, quinones and quinone-imines. Oxidation of *o*- or *p*-amino- and aminohydroxyanthraquinone results in the corresponding *o*- or *p*-quinone through the intermediate imino- or di-iminoquinone^{121,122} (e.g., Fig 6)

The colour or fluorescence change accompanying their oxidation facilitates the use of a number of these AQ derivatives as redox indicators in titration of reducing agents such as ascorbic acid,^{121,123-127} phenazone,¹²¹ arsenic(III),^{121,123-127} hydrazine sulphate,¹²⁵ Fe(II),¹²⁷ but the reagents decompose in the presence of an excess of oxidizing agent and hence cannot be used¹²⁸ in titrations of oxidants.

There appear to be two stages of oxidation,¹²⁸ the first (perhaps a one-electron oxidation to an anion radical) producing a hypsochromic shift, and the second (perhaps a further one-electron oxidation to give the quinone) producing a bathochromic shift to restore the original colour

The redox reactions of AQ derivatives have been used for kinetic determination of the oxidant, the reductant or a catalyst. Catalytic methods give very high sensitivity¹²⁹⁻¹³³. Their mechanisms have been reviewed by Bontchev.¹³⁴

AQ derivatives provide good indicator reactions for kinetic photometric and fluorimetric methods of analysis, because they give pronounced colour^{129,134} and fluorescence^{122,134-137} changes in their redox transformation, and extremely low concentrations of the species involved can be determined.

Kinetic determinations based on the redox reactions of AQ derivatives show a greater selectivity^{122,130-132,134,136,137} than those based on the complexation reactions.

Various AQ derivatives have been used in indicator reactions. Thus, *o*-dihydroxyanthraquinones are oxidized by hydrogen peroxide in the presence of traces of cobalt,^{133,138-140} in borate buffer. The alizarin-hydrogen peroxide indicator reaction¹⁴⁰ permits the determination of cobalt in a range of about 1-7 ng/ml, Zn, Cd and Ni interfere.

The quinalizarin-H₂O₂ (or sodium perborate) reaction is quoted as an indicator reaction with which the sensitivity for Co at 100° is 20 and 0.2 pg/ml with H₂O₂ and NaBO₃ respectively as oxidizing agents.¹³⁸ After a detailed optimization study¹³³ the same reaction has been used at 25° to determine Co (sensitivity 0.5 ng/ml). A mechanism similar to that for enzymatic reactions was postulated to explain the optimal conditions found. Tartrate, citrate and oxalate have an inhibiting effect.

The reaction between 1-amino-4-hydroxyanthraquinone and V(V)¹³⁶ to yield an oxidation product of the reagent allows a sensitive (100-530 ng/ml) and selective [only Ce(IV) interferes seriously] kinetic fluorimetric determination of V(V).

Fluorimetric¹⁴¹ and kinetic-fluorimetric¹³⁷ methods have been proposed for the determination of Fe(II) and Ti(III), based on the intense green fluorescence that appears when these cations react with 1,4-diamino-2,3-dihydroanthraquinone. The fluorescence is due to the oxidative transformation of the reagent in the presence of these cations.

The blue non-fluorescent reagent 4,8-diamino-1,5-dihydroxyanthraquinone-2,6-disulphonic acid is transformed into a pink, highly fluorescent, product by oxidation in acid medium. This reaction is slow, but in the presence of certain inorganic oxidants it is accelerated and completed in about 30 min. This allows the kinetic determination of V(V),¹²² Fe(III),¹⁴² Ce(IV),¹⁴³ Au(III)¹³² and Mn(II).¹³⁵ The combined action of Fe(III) and V(V) notably increases the sensitivity of either or both determinations, and concentrations as low as

1 ng/ml V(V)¹³⁰ and 2 ng/ml Fe(III)¹³¹ can be determined

Oxidation of 1,2,4-trihydroxyanthraquinone-3-carboxylic acid by bromate¹⁴⁴ or iodate¹⁴⁵ in hydrochloric acid medium has served as the basis for their spectrophotometric determination and for a fluorimetric method for iodate¹³⁴ which is more selective and 10 times more sensitive than the spectrophotometric method.

Electrochemical reduction

Polarographic studies of analytically important anthraquinones have been made, to investigate their redox characteristics.³⁹ Because of their quinonoid structure, anthraquinones display interesting electrochemical behaviour.³⁹ When reduced¹⁴⁶ by taking up a single electron, they form semiquinones, and the uptake of a further electron results in the formation of hydroquinones. In all the redox processes of AQs these three oxidation states are expected to be involved. Whether under given experimental circumstances a single two-electron polarographic wave or two one-electron waves will be observed, depends on the stability of the semiquinone. Additionally, each oxidation state can involve different degrees of protonation.³⁹

The polarographic behaviour of anthraquinones depends as much on the nature of the derivative^{39,146-158} as on the pH,^{39,146,147,150,152,157,158} the solvent^{39,148,149,153} and the supporting electrolyte solution

For the complexes of Alizarin Red S with Be and Al information has been obtained on the structure of the complexes by polarographic reduction of the ligand.¹⁵⁹ Similarly, from voltametric and spectrophotometric studies it has been deduced that the two adjacent hydroxyl groups are involved in formation of the highly stable Zr-Alizarin Red S complex.⁷⁵

It has also been established¹⁶⁰ that the half-wave potential for the polarographic reduction of some AAQs is correlated with the wavelength of maximum absorption in the visible region and also with the polarizability of the carbonyl groups. Each AAQ can be determined in the range 0.1–0.5 mg/ml.

Redox photochemical properties

The excited states of some AQ derivatives are very reactive chemical species. The photochemical reactions involving these species can compete with luminescence for deactivation of the excited electronic states. The photo-

chemistry of AQs has been useful in analytical chemistry, from the point of view of photo-reaction and of deactivation of excited states. The absorption and fluorescence spectra of some AQs have been studied in relation to the photochemical properties.^{2,161,162}

The photochemical oxidation of anthraquinones is confined to oxidation of the side-chain, which is characteristic of *p*-quinones.³

Photochemical reduction is the simplest photochemical reaction of anthraquinones. It involves^{3,4,31} the addition of an electron or a hydrogen atom to the oxygen atom of the carbonyl group under conditions where the analogous dark reactions are impossible. The facile reduction of AQs to anthrahydroquinones under the influence of light has long been recognized⁴ as one of the major causes of the photoinstability and photoreactivity of these dyes.

The photochemical reactivity of an AQ derivative depends critically upon the nature of the lowest excited electronic state. Anthraquinones in which this lowest state is n,π^* are associated^{3,4,31,163} with high photochemical activity, because in that state the oxygen atom of the carbonyl group is electron-deficient, which renders it⁴ extremely reactive towards the hydrogen atom or electron abstraction. In the case of π,π^* states, and more particularly charge-transfer (C-T) states, photoexcitation causes an electron shift towards the oxygen atom, which lessens its affinity for the hydrogen atom and electron abstraction. Anthraquinones which possess low-lying π,π^* or C-T states are therefore comparatively unreactive.

Anthraquinone derivatives vary widely in their photochemical reactivity. They are divided into "strong" and "weak" sensitizers^{2,163,164} in the oxidation of the environment. The former give phosphorescence emission and semiquinone radical formation, while the latter give only fluorescence emission.¹⁶⁴

AQ and its derivatives with electron-accepting substituents ($-\text{HSO}_3$, $-\text{NO}_2$, halogens) are very photochemically reactive, but the position of the substituents can have a profound effect on their photochemical behaviour.^{4,163} Sodium anthraquinone-2-sulphonate, and 2,6- and 2,7-disulphonates are more active sensitizers than the 1- and 1,5-sulphonates, and the 1,8-disulphonate is inactive.^{163,165}

Powerful electron-donating groups ($-\text{OH}$, $-\text{NH}_2$, $-\text{NRR}'$) diminish the sensitizing power of AQs in the photochemical process,^{1,3,163} a substituent in the 1-position gener-

Table 1 Photometric and fluorimetric methods for determination of inorganic species with anthraquinone derivatives

Ion	Reagent	Type of method	Conditions	Range	Interferences, remarks	Reference
Al(III)	1,2DHAQ-3S	c/Ph	pH 4.8, λ 490 nm	0.08-0.76 ng/ml	Mn, Fe, Ca	171
	1,4DHAQ-2S	c/Ph	MeOH, λ 560 nm	<1.7 μ g/ml	Be, Sc, Th, Ti, Y, Zr, F ⁻ , PO ₄ ³⁻ , lanthanides	172
	1,2,4THAQ-3S	c/F	pH 4.76, λ_{ex} 500, λ_{em} 558 nm	11-54 ng/ml		173
	1,2,7THAQ	c/Ph	pH 5.5, λ 580 nm	0.5-3 μ g/ml		174
	Alizarin Complexan	c/Ph	λ 500 nm, standing time 2.4 hr pH 4.1-4.3, heat at 70°, standing	0-2 μ g/ml 1-12 μ g/ml	Detn in presence of Fe and Ti	175
Au(III)	1,4DAAQ-2,3DS	c/Ph	pH 9, λ 425 nm	5-30 μ g/ml	Many ions	177
	4,8DA-1,5DHAQ-2,6DS	k/F	0.15M HCl, λ_{ex} 525, λ_{em} 585 nm	4.6-26.5 μ g	Fe, Ce, V	132
B(III)	1,4DHAQ	c/F	91-96% H ₂ SO ₄ , λ_{ex} 365, λ_{em} 595 nm	4 \times 10 ⁻⁶ -8 \times 10 ⁻⁵ M	I ⁻ , ClO ₃ ⁻ , Sb, Fe	178
	1,4DHAQ-2S	c/F	conc H ₂ SO ₄ , λ_{ex} 522, λ_{em} 578 nm, standing time > 15 min	25-250 ng/ml	NO ₃ ⁻ , F ⁻	179
	1,8DHAQ	c/Ph	conc H ₂ SO ₄ , λ 580 nm	0.1-3 μ g/ml	Fe, Ni, Co, Cr	180
	1,2,5,8TTTHAQ	c/Ph	93% H ₂ SO ₄ , λ 615 nm	0.01-0.1%	Ge, As, F ⁻	111
	Carmic acid	c/Ph	92-94% H ₂ SO ₄ , λ 610 nm	0.15-1.6 μ g/ml		105
	1,8DA-4,5DHAQ	c/Ph	96% H ₂ SO ₄ , λ 525 nm	2-7 μ g	Oxidant anions, F ⁻ , Ti	181
	1,5DH-4,8DAAQ	c/Ph	96% H ₂ SO ₄ , λ 600 nm	2-10 μ g		182
Be(II)	1,2DHAQ-3S	c/Ph	pH 5.4-5.6, λ 180 nm	0.2-4.7 μ g/ml	Pb, Zn, Cu, Ce, Co, Ni, V(V), Mo	183
	1,4DHAQ-2S	c/Ph	pH 6, λ 575 nm	1-20 μ g	PO ₄ ³⁻ , F ⁻ , Al	184
	1,4DHAQ-2,6DS	c/F	8 \times 10 ⁻³ M HAc, λ_{ex} 475, λ_{em} 575 nm	1-7 ng/ml	Large amts of Cu and small amts of Al and Fe interfere	186
		c/Ph	pH 7, λ 530 nm, 7% Na ₂ S ₂ O ₃ , heat 5 min at 60-70°	0.1 μ g/ml		
	1A-4HAQ	c/F	0.02M NaOH, λ_{ex} 540, λ_{em} 620 nm	0.2 μ g/ml	Li, Cr(VI)	187
	1H-2CAQ	c/F	pH 10.2, 10 ⁻³ M β -cyclodextrin	10-70 ng/ml	Mg, AsO ₃ ⁻	58
		c/Ph	4 \times 10 ⁻³ M NaOH, λ 470-480 nm	0.4-1.2 μ g/ml		
	4,8DA-1,5DHAQ-2,6DS	c/F	λ_{ex} 470, λ_{em} 580 nm	30-130 ng/ml	Zn, Al, Y	188
		c/Ph	0.02M NaOH, λ 645 nm	0.4-1.13 μ g/ml	Cu, Cr, Co, V(V), Ag, Ge, Al, Ni	190
	Carmic acid	c/Ph	pH 4, λ 580 nm	0.4-1.6 μ g/ml	Several ions	191
c/Ph		pH 7.2, λ 480 nm, extn with Adogen soln in toluene	0.09-0.36 μ g/ml			
Alizarin Complexan	c/Ph	pH 6, λ 550 nm	5-35 μ g	Several ions	192	
Be(II)/Mg(II)	1H-2CAQ	c/Ph	50% EtOH, pH 11, λ 463 nm for Mg λ 492 nm for Be	0.1-1.5 μ g/ml Mg	Be up to 0.4 μ g/ml Mg up to 1.5 μ g/ml	194
				0.04-0.4 μ g/ml Be		194
BrO ₃ ⁻	1,2,4THAQ-3C	rx/Ph	1.92M HCl, λ 520 nm	1-8 μ g/ml	Oxidants and other ions	144

Ca(II)	1,2DHAQ-3S 1,8DHAQ 1,2,4THAQ-3S 1,2,3THAQ 1,2,7THAQ 1,4DAAQ	c/Ph c/F c/Ph c/Ph c/Ph c/Ph	pH 10.2, λ 509 nm 0.01M NH ₃ , λ_{ex} 485, λ_{em} 615 nm pH 11 pH 10.5, 80% DMF EtOH, λ 560 nm 50% H ₂ SO ₄ , λ 400 nm	<0.15 mg/ml 50-550 ng/ml 0.5-4.5 μ g/ml 2-12 μ g/ml 1-6 μ g/ml 1.4-3.5 μ g/ml	Several ions Many ions No interference by Mg, Sr, Ba, PO ₄ ³⁻ , EDTA	195 196 197 198 199 200
	Alizarin Complexan Anthrapurpurn Complexan	c/F c/Ph c/Ph	50% H ₂ SO ₄ , λ_{ex} 410, λ_{em} 580 nm pH 10.31, λ 610 nm pH 10.58, λ 580 nm	150-400 ng/ml 2-10 μ g/ml 2-10 μ g/ml	Ba, Sr cause positive errors	201 202 203
Cd(II)	Alizarin Complexan	c/Ph	pH 8, λ 620 nm, standing time 30 min	2-11 μ g/ml		204
Ce(IV)	1,2DHAQ-3S 4,8DA-1,5DHAQ-2,6DS	c/Ph k/F	pH 9.9-10.10, λ 500 nm 0.2M H ₂ SO ₄ , λ_{ex} 525, λ_{em} 585 nm	0.07-0.15% 0.02-0.37 μ g/ml	Impurities can be extracted at pH 4-5 with oxine in chloroform Hg, V, Cr(VI)	205 143
Co(II)	1,2DHAQ 1,2DHAQ-3S 1,2,5,8,11THAQ	k/Ph k/Ph k/Ph	pH 9.4, 0.035M H ₂ O ₂ , λ 510 nm pH 12, λ 565 nm, 25° H ₂ O ₂ , 100°, Na ₂ BO ₃ , 100°, Na ₂ BO ₃	2×10^{-3} - 2×10^{-4} μ g/ml 0.05 ng/ml 1×10^{-6} - 2×10^{-7} M <20 pg/ml <0.2 pg/ml 0-2.5 μ g/ml 1-3 μ g/ml 0.95-3.8 μ g/ml	Zn, Cd, Ni CN ⁻ , tartrate, citrate, C ₂ O ₄ ²⁻	140 206 133 138 138 207 208 209
	1,2,4THAQ-3S 1,2DAAQ 1,2DAAQ-3S	c/Ph c/Ph c/Ph	pH 5.38, λ 590 nm 0.32M NaOH, λ 690 nm pH 7.8, λ 580 nm, standing 15 min		Ni Stabilized with poly(vinyl alcohol)	
Cr(III)	1,2DHAQ-3S	c/Ph	pH 3-6, λ 525 nm	0.2-10.4 μ g/ml		210
Cu(II)	1,2,7THAQ 1,2,4THAQ-3C 1,2DAAQ 4,8DA-1,5DHAQ-2,6DS Anthrapurpurn Complexan	c/Ph c/Ph c/F c/Ph c/Ph c/Ph	pH 8, λ 520 nm, extn with isoamyl alcohol 0.02M NaOH, λ 750 nm 0.01M NaOH, 80% DMF, λ_{em} 515 nm 0.32M NaOH, λ 650 nm pH 7.13, λ 690 nm pH 4.6, λ 515 nm	0-7 μ g/ml 0.1-1.0 μ g/ml 50-250 ng/ml 1-7 μ g/ml 3-9 μ g/ml 1-20 μ g/ml	Many ions Stabilized with poly(vinyl alcohol)	211 212 213 214 215 216
F ⁻	1,2DHAQ-3S 1,2DHAQ-3S + Th 1,4DHAQ-3S + Zr 1,2,3,5,6,7THAQ + Zr Alizarin Complexan	c/Ph ic/Ph ic/Ph ic/Ph c/Ph	pH 2.9-3.0, λ 415 nm, F ⁻ titrated with 0.01M Zr(IV) 1% NH ₂ OH HCl, λ 525 nm, λ 525 nm 0.1M HCl, λ 545 nm 1M HCl, λ 560 nm pH 4.6, λ 574 nm, Na dodecyl sulphate	1.14-1.90 mg/g 0.05-1 μ g/ml 0.4-4 μ g/ml 0.3-5 μ g/ml 0-7 μ g/ml 0.08-1.2 mg/l	Al, SO ₄ ²⁻ Differential method <25 μ g/ml SO ₄ ²⁻ Flow-injection determination	217 218 219 220 221

Table 1—continued

Ion	Reagent	Type of method	Conditions	Range	Interferences, remarks	Reference
F ⁻	Alizarin Complexan + La	tc/Ph	La complex immobilized on Amberlite CG-400 or IRA-938	950 µg	NH ₄ ⁺ , Mg, Ca, Al, Fe(III)	222
	Alizarin Complexan-5S + La	tc/Ph	La complex immobilized on Amberlite CG-400 or IRA-938	0.003–1 µg/ml		223
	Alizarin Complexan + Ce(IV) or La	tc/Ph	pH 5.0–5.2, λ 610–620 nm	0–60 µg	Al, Fe, Sn, Ca, Mg PO ₄ ³⁻ , SO ₄ ²⁻ , C ₂ O ₄ ²⁻ , oxidants	59–61, 224
	1,2DHAQ-3S	c/Ph	pH > 4.2, λ 570 nm, extn with Aliquat 336 soln in CHCl ₃	0.02–1.5 µg/ml		225
Fe(III)	1,2,4THAQ-F ⁻	c/Ph	pH 8.1, λ 595 nm, extn into MIBK	0.025–0.250 µg/ml	Masked with CN ⁻	226
	1,4DA-2,3DHyaAQ	rx/F	pH 4.9	0.28–0.6 µg/ml	Au, Ti, Ce, Pt	141
	4,8DA-1,5DHAQ-2,6DS	k/F	pH 3.4, λ _{ex} 400, λ _{em} 470 nm	0.05–0.6 µg/ml	Au, Ti, Ce, Pt, V(V)	137
		k/F	0.012M HCl, λ _{ex} 525, λ _{em} 585 nm	2.5–25 µg	Au, Ce, V(V), Th, F ⁻	142
		k/F	25 µg V(V)	1.5–25 µg	BrO ₃ ⁻ , Th	131
	1,2DHAQ-3S	c/Ph	pH 3–5, λ 490 nm	0.55–14 µg/ml		227
	1,2DHAQ-3S	c/Ph	pH 3.3, 20% EtOH, λ 505 nm, 0.04M hexadecylpyridinium bromide	0.28 µg/ml	No interference by Al, Cu, In, Sb, Ti, Ce, Zn	228
	1,2,5,8TTTHAQ	c/Ph	pH 5, NH ₄ OAc, NaF, heat at 80°	0.1–10 µg	Many ions	229
	1,2DHAQ-3S	c/Ph	pH 7, λ 470 nm, extn into CCl ₄	5–40 µg		230
	1,2,3THAQ	c/Ph	90% MeOH, 4 × 10 ⁻⁴ M, λ 490 nm	1–5 µg/ml		231
1,2,4THAQ	c/Ph	40% EtOH, pH 1–4, λ 490 nm	0.4–12.7 µg/ml	BO ₂ ⁻ , SO ₄ ²⁻ , NO ₃ ⁻ , OAc ⁻ , PO ₄ ³⁻ do not interfere	232	
1,2,7THAQ	c/Ph	conc H ₂ SO ₄	0.4–15 µg/ml		233	
Alizarin Complexan	c/Ph	90% EtOH, 4 × 10 ⁻⁴ M NH ₃ , λ 470 nm	0.5–4 µg/ml	4.1 (R Ge) complex formed	234	
	c/Ph	pH 7, λ 445	0.2–4 µg/ml GeO ₂		235	
	c/Ph	pH 8, λ 450 nm	0.5–6 µg/ml Ge	4.1 (R Ge) complex formed	236	
Alizarin Complexan + Rhodamine 6G	tc/Ph	pH 5–6, λ 520 nm	0.02–1 µg/ml GeO ₂	Cl ⁻ , Br ⁻ , I ⁻ , NO ₃ ⁻ , ClO ₄ ⁻	237	
Alizarin Red S (II) + DPhG (I)	tc/F	λ _{em} 543 nm	2–100 ng/ml GeO ₂		238	
	tc/Ph	pH 4, λ 475 nm, extn into CHCl ₃ , acetone (1:4) at pH 7–8	0.013–0.63 µg/ml	Ion assoc with Ge (I) (II) ratio 1:2:2	238	
Quinalizarin + DPhG	tc/Ph	pH 4, λ 500 nm, extn with CHCl ₃	0.1–2 µg/ml		239	
Hf(IV)	1,2DHAQ-3S	c/Ph		0.80 mg/l HfO ₂		240
In(III)	1,2DHAQ-3S	c/Ph	pH 3.8–4.5, λ 530 nm	0.23–27 µg/ml		241
	Alizarin Complexan	c/Ph	pH 4.3, λ 520 nm	1–9 µg/ml	Several ions	242
	1,2-DHAQ-3S + DPhG	tc/Ph	pH 5.3–5.9, λ 525 nm, extn into CHCl ₃	0.3–2.8 µg/ml		243

IO ₃ ⁻	1,2,4THAQ-2C	rx/Ph rx/F	70% EtOH, 1.56M HCl, λ 520 nm 1.20M HCl, λ_{ex} 515, λ_{em} 625 nm	50-350 μ g 5-50 μ g	Oxidants and other ions Oxidants and other ions	145 244
	La(III)					
La(I)	IHAQ-2C	c/Ph	pH 4.9, 80% EtOH, λ_{ex} 465, λ_{em} 520 nm	0.1-1 μ g/ml	Several ions	45
	1,2DHAQ-3S	c/Ph	pH 3.5-6.5, λ 520 nm	0.42-10 μ g/ml	Many ions	246
	1,2,5,8TTTHAQ	c/Ph	pH 6-8, λ 570 nm	0.08-1.6 μ g/ml	In presence of boric acid	247
	1,2DHAQ-3S + phenazone	tc/Ph	pH 5, λ 540 nm, extrn into butanol or isobutyl alcohol	1-6 μ M		66
	1,2DHAQ-3S + 8-hydroxyquinoline	tc/Ph	λ 530 nm, extrn into butanol	30-50 μ g		64
	QG	c/Ph	pH 7.6, 40% DMF, λ 600 nm	2×10^{-5} - 3×10^{-4} M		94
	1,8DHAQ	c/F	90% EtOH, λ_{ex} 495, λ_{em} 625 nm	100-700 ng/ml	Separation of L ₁ is recommended	248
		c/F	90% acetone, 2.5×10^{-4} M NaOH, λ_{ex} 525, λ_{em} 615 nm	50-450 ng/ml		
	1,4DHAQ	c/F	90% MeOH, pH 4.5, λ 560 nm for Lu, λ 564 for Pr	1-100 mg	Lu Pr tolerance from 1.5 to 5 l	71
	Mg(II)					
1,4DHAQ-2S	c/F	pH 10, 60% EtOH, λ_{ex} 545, λ_{em} 610 nm	20-200 ng/ml	Fe(II), Be	249	
1,5DHAQ	c/F	pH 9.1-9.6, λ_{ex} 490, λ_{em} 610 nm	10-100 ng/ml	Many ions	250	
1,8DHAQ	c/Ph	90% EtOH, 8×10^{-3} M NH ₃ , λ 510 nm	0.25-2.00 μ g/ml	Many ions	251	
1,2,7THAQ	c/Ph	40% EtOH, 4×10^{-3} M NaOH, λ 540 nm	1-6 μ g/ml	Many ions	252	
IH-2CAQ	c/Ph	90% EtOH, 0.04M NH ₃ , λ 530 nm	9-45 μ g/ml	Mn, Zn, Co, Ca	253	
Mn(II)						
Alizarin Complexan	c/Ph	pH 11.1-11.6, λ 570 nm	1-8 μ g/ml		254	
Anthrapurpurin Complexan	c/Ph	pH 11.4-11.8, λ 550 nm	1-7 μ g/ml		255	
4,8-DA-1,5DHAQ-2,6DS	k/Ph	0.016M NaOH, 0.16M HCl, λ 518 or 560 nm	3-11 μ g	Oxdrn, redn and complexing agent	135	
	k/F	λ_{ex} 525, λ_{em} 585 nm	0.16-0.54 μ g			
Mo(VI)						
1,2DHAQ-3S	c/Ph	pH 5, λ 525 nm, extrn with 1,2-dichloroethane	0.2-6.5 μ g/ml	F ⁻ and EDTA added to mask Co, Zn, Cu, Th, U(VI)	256	
1,2,5,8TTTHAQ	c/Ph	pH 5, λ 540 nm	1-10 μ g/ml	UO ₂ ²⁺	257	
Carmine acid	c/Ph	pH 4-5, λ 336 nm, λ 565 nm	4-11 μ g/ml 1.5-8 μ g/ml		258	
	c/F	pH 5.2, λ_{ex} 560, λ_{em} 590 nm	0.1-0.9 μ g/ml	Previous separation is recommended	259	
Nb(V)						
1,2DHAQ-3S	c/Ph	2M H ₂ SO ₄ , λ_{ex} 499, λ_{em} 562 nm, hexadecyltrimethylammonium bromide, standing time 2 hr	<32 μ g		260	
Ni(II)						
1,2,4THAQ	c/Ph	pH 8.5, λ 525 nm, extrn into MIBK	0-25 μ g	Many ions	261	
1,2,4THAQ-3S	c/Ph	pH 8.1, λ 520 nm	0-3 μ g/ml	Co	205	

Table 1—continued

Ion	Reagent	Type of method	Conditions	Range	Interferences, remarks	Reference
Ni(II)	1H-2CAQ	c/Ph	50% EtOH, $8 \times 10^{-3} M$ NH ₃	2.6–6.6 $\mu\text{g/ml}$	Several ions	262
	Alzann Complexan + La	c/Ph	pH 4.5, λ 550 nm	$0-10^{-5} M$	Co, Cu, Zn, Th, Ce, Fe	263
Pd(II)	1,2DHAQ-3S	c/Ph	pH 4, λ 450 nm	0.4–11 $\mu\text{g/ml}$		264
	1,2,4THAQ-3C	c/Ph	80% EtOH, λ 670 nm	0.30–2.40 $\mu\text{g/ml}$	Many ions	265
	1,5DAAQ-2,6DS	c/Ph	pH 2.5, λ 650 nm	4–20 $\mu\text{g/ml}$	Many ions	266
	4,8DA-1,5DHAQ-2,6DS	c/Ph	pH 10.5, λ 720 nm	4.8–18.2 $\mu\text{g/ml}$		267
	1,4DA-5NAQ	c/Ph	0.64M NaOH, λ 640 nm	2–10 $\mu\text{g/ml}$	Stabilized with poly(vinyl alcohol)	268
	Carmine acid	c/F	pH 5.3, acetone, λ_{ex} 546, λ_{em} 580 nm	0.1–1 μg	Interferences removed by pptn of Pd	269
	1,2DAAQ-phenylhydrazone	c/Ph	0.4M NH ₃ , λ 675 nm	0.5–2 $\mu\text{g/ml}$		270
Rh(III)	1,2DHAQ-3S	c/Ph	pH 4, λ 450 nm, heat at 100° for 1.5 hr	1.5–8.6 $\mu\text{g/ml}$	Pd, Cu, Ru	271
Se(III)	1,5DHAQ-2,6DS	c/Ph	pH 3.5–5.1, λ 495 nm	0.3–4 $\mu\text{g/ml}$		272
	1,4DHAQ	c/F	0.02M NaOH, λ_{ex} 545, λ_{em} 600 nm, $10^{-2} M$ β -cyclodextrin	3–4 μg	Only Be interferes seriously	72
Se(IV)	1,2,7THAQ	c/F	DMF, λ_{ex} 485, λ_{em} 563 nm	12–225 ng/ml		62
	4.5DA-1,8DHAQ	c/Ph	99.8–100% H ₂ SO ₄ , λ 610 nm, heat at 90° for 21 hr	0–4.3 $\mu\text{g/ml}$		87
Sr(II)	3A-1,2DHAQ + eosin	tc/Ph	pH 6.5–7.2, λ 560 nm	0.16–2.0 $\mu\text{g/ml}$	Al, CN ⁻ Add EDTA to mask Al	273
	Alzann Complexan	c/Ph	pH 10.9, λ 610 nm	2–12 $\mu\text{g/ml}$	Many ions	274
Th(IV)	1,2DHAQ-3S	c/Ph	pH 3.2–8	0.23–16.7 $\mu\text{g/ml}$		256
	1,2,7THAQ	c/Ph	EtOH, λ 540 nm, standing time 2 hr	7–21 $\mu\text{g/ml}$		275
	1,2,5,8TTTHAQ	c/Ph	λ 570 nm	2.5–25.0 μg		276
	1,2,3,5,6,7HHAQ	c/Ph	λ 530 nm, 10M HCl	5–12 $\mu\text{g/ml}$		277
	4,8DA-1,5DHAQ-2,6DS	c/Ph	pH 3.5, λ 685 nm	7.5–22.5 $\mu\text{g/ml}$	As, Au, Al, Fe, Cr, Zn	278
	BMArAQ	c/Ph	pH 4.6, 40% DMF, λ 620 nm	4.7–18.5 $\mu\text{g/ml}$	UO ₂ ²⁺ , Ba F ⁻	279
Ti(IV)	3A-1,2DHAQ + 5-sulphosalicylic acid	tc/Ph	pH 4.6–5.5, λ 580 nm, 20% EtOH	60–560 μg	CN ⁻ , NO ₂ ⁻ , HPO ₄ ²⁻ , F ⁻	70
	1,2DHAQ-3S	c/Ph	λ 660 nm	10–100 μg		280
	1,2DHAQ-3S	c/Ph	pH 3.5, λ 515 nm, standing time 15 min, hexadecyltrimethylammonium bromide	<24 μg		260
Ti(III)	1,4DA-2,3DHyaQ	k/F	pH 3.4, λ_{ex} 400, λ_{em} 470 nm	0.05–0.4 $\mu\text{g/ml}$	Au, Fe, Ce	137
		rx/F	pH 3.6, standing 90 min	0.1–3 $\mu\text{g/ml}$	Au, Fe, Ce, V	141

Tm(III)/Nd(III)	c/f	MeOH, pH 4.5, λ 557 nm for Nd λ 559 nm for Tm	0.4-1.20 μ g/ml Tm 0.4-1.20 μ g/ml Nd	Tm Nd tolerance from 2.5 1 to 1 2.5	73
1,4DHAQ	c/f				
U(VI)					
1,2DHAQ-3S	c/Ph	pH 4.5-5.5, λ 550 nm	40-250 μ g/ml	Cl ⁻ , NO ₃ ⁻ , SO ₄ ²⁻	281
1,4DHAQ-3S	c/Ph	λ 550-590 nm	50 μ g	Ce and Th must be absent	282
1,2,5,8THAQ	c/Ph	pH 5.5, λ 630-660 nm	3.5-21 μ g/ml	Mo and others	257, 283
V(V)					
1,2DHAQ-3S	c/Ph	pH 3.5-5.8, λ 455 nm	0.1-3.67 μ g/ml	Various ions	284
1A-4HAQ	k/f	0.5M HCl, λ_{ex} 480, λ_{em} 575 nm	0.1-0.5 μ g/ml	Ce	136
1,4DA-5NAQ	c/f	2M HCl, λ_{ex} 475, λ_{em} 550 nm	100-800 ng/ml		93
4,8DA-1,5DHAQ-2,6DS	k/f	0.4M HCl, λ_{ex} 524, λ_{em} 582 nm	0.04-0.5 μ g/ml	Ce, Fe, I ⁻	122
4,8DA-1,5DHAQ-2,6DS	k/f	0.4M HCl, λ_{ex} 524, λ_{em} 582 nm 5 μ g/ml Fe(III)	1-10 ng/ml	Ce, Fe(II), I ⁻	130
W(VI)					
1,2DHAQ-3S	c/Ph	pH 3.5-5.8, λ 470 nm	0.4-13.3 μ g/ml	Many ions	285
1,2DHAQ-3S	c/f	pH 4.8-6.2	0.5-4 μ g/ml	Al must be absent	286
Carmine acid	c/f	pH 4, λ 483 nm, at 30°, hexadecyltrimethylammonium	<10 μ g/ml		
Y(III)					
QG	c/f	pH 4.6, λ_{ex} 515, λ_{em} 585 nm	0.04-0.36 μ g/ml	Previous separation is recommended	259
Zn(II)					
Alzann Complexan	c/Ph	pH 7.7, 40% DMF	7.12-28.5 μ g/ml		60
Zr(IV)					
Alzann Complexan	c/Ph	pH 4.3, λ 500 nm, standing time 30 min	0.13-0.5 μ g/ml		287
1A-4HAQ	c/Ph	pH 3.5, λ 600 nm	24-113 μ g	Interferents masked with CN ⁻	288
4,8DA-1,5DHAQ-2,6DS	c/Ph	0.17M HCl, λ 700 nm	20-200 μ g	PO ₄ ³⁻ , F ⁻ , BrO ₃ ⁻ , H ₂ PO ₄ ⁻ , EDTA, Fe, C ₂ O ₄ ²⁻	289
1,2DHAQ-F ⁻	tc/Ph	pH 8.9, λ 556 nm, MIBK	<20 μ g	Interferents masked with EDTA	290
1,2DHAQ-3S	c/Ph	0.1M HCl, λ 510 nm	0-10.3 mg		75, 97
1,2,4-THAQ-3S	c/Ph	pH 0.75-0.93, λ 600 nm	0-80 mg/l ZrO ₂		240
1,2,3,5,6,7THAQ	c/Ph	1M HCl, λ 560 nm	0-7 μ g/ml		207
1,2,3,5,6,7THAQ	c/Ph		3-9 μ g/ml		220
Abbreviations used Alizarin Complexan, [(3,4-dihydroxy-2-anthraquinyloxy)methyl]iminoacetic acid, Anthrapurpurin Complexan, [(1,2,7-trihydroxy-3-anthraquinyloxy)methyl]imino- diacetic acid, 3A-1,2DHAQ, 3-amino-1,2-dihydroxyanthraquinone, 1A-4HAQ, 1-amino-4-hydroxyanthraquinone, BMAAQ, 1,4-Bis(4-methylamino)anthraquinone, c, complex formation, Carmine acid, 7- α -D-glucopyranosyl-3,5,6,8-tetrahydroxy-1-methylanthraquinone-2-carboxylic acid, 1,2DAAQ, 1,2-diaminoanthraquinone, 1,2DAAQ-phenylhydrazine, 1,2-diaminoanthraquinone phenylhydrazine, 1,2DAAQ-3S, 1,2-diaminoanthraquinone-3-sulphonic acid, 1,4DA-2,3DS, 1,4-diaminoanthraquinone-2,3-disulphonic acid, 1,5DAAQ-2,6DS, 1,5-diaminoanthraquinone-2,6-disulphonic acid, 1,4DA-2,3DHAQ, 1,4-diamino-2,3-dihydroanthraquinone, 1,8DA-4,5DHAQ, 1,8-diamino-4,5-dihydroxy- anthraquinone, 4,8DA-1,5DHAQ-2,6DS, 4,8-diamino-1,5-dihydroxyanthraquinone-2,6-disulphonic acid, 1,4DA-5NAQ, 1,4-diamino-5-nitroanthraquinone, df, differential method, 1,2DHAQ, 1,2-dihydroxyanthraquinone, 1,4DHQ-2,6DS, 1,4-dihydroxyanthraquinone-2,6-disulphonic acid, 1,2DHAQ-3S, 1,2-dihydroxyanthraquinone-3-sulphonic acid, 1,4DHQ-2S, 1,4-dihydroxyanthraquinone-2-sulphonic acid, 1,5DH-4,8 DAAQ, 1,5-dihydroxy-4,8-diaminoanthraquinone, DPhG, diphenylguanidium, F, fluorimetric method, IH-2CAQ, 1-hydroxy-2-carboxyanthraquinone, 1,2,3,5,6,7THAQ, 1,2,3,5,6-hexahydroxyanthraquinone, ic, indirect method, k, kinetic method, Ph, photometric method, PhQz-DS, 2-phenoxymizarin-3,4-disulphonic acid, QG, 1,4-bis-(2-sulpho-4-methylamino)anthraquinone, Quinalizarin, 1,4,5,8-tetrahydroxyanthraquinone, rx, redox reaction, tc, ternary complex, 1,2,3THAQ, 1,2,3-trihydroxyanthraquinone, 1,2,4THAQ-2C, 1,2,4-trihydroxy-2-carboxyanthraquinone, 1,2,4THAQ-3S, 1,2,4-trihydroxyanthraquinone-3-sulphonic acid, 1,2,5,8THAQ, 1,2,5,8-tetrahydroxyanthraquinone					

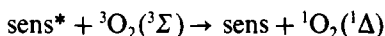
ally having a much more pronounced effect than one in the 2-position.^{1,4}

In the absence of a hydrogen donor, photoexcited AQs can undergo photoreduction by the abstraction of an electron. Aminoanthraquinones that are relatively unreactive towards hydrogen-atom abstraction, because of the C-T character of the lowest excited state, can undergo photoreduction by electron transfer¹⁶² from hydroxide ions in solutions of high pH.

The photochemistry of anthraquinone-2-sulphonate and anthraquinone-2,6-disulphonate has received much attention,²⁻⁵ and various reaction mechanisms have been proposed. These photoreactions have been used in liquid chromatography to detect compounds¹⁶⁶⁻¹⁶⁸ that do not absorb ultraviolet-visible radiation at all. An anthraquinone-sensitized photo-oxygenation reaction produces hydrogen peroxide during the oxidation of the analytes (alcohols, aldehydes, ethers and saccharides) by hydrogen-atom abstraction. Once formed, the hydrogen peroxide is measured by a chemiluminescence reaction. The photoreduction of anthraquinone-2,6-disulphonate to dihydroxyanthracene-2,6-disulphonate has been used for the determination of several herbicides.¹⁷⁰

Anthraquinone-2-sulphonates which have been reduced photochemically can serve as electron donors, and thus can behave as sensitizers of the reduction of electron acceptors.¹³

Another aspect of the photochemistry of anthraquinones is concerned with the generation of singlet oxygen. Energy transfer between the triplet state of a dye and molecular oxygen occurs as follows



Anthraquinones which possess relatively long-lived triplet states are likely candidates as sensitizers for the formation of singlet oxygen. 1-Amino-4-hydroxyanthraquinone and its 2-methoxy derivative are extremely efficient sensitizers of singlet oxygen production. Seven of the components of the dye C.I. Disperse Blue 35 are efficient producers of singlet oxygen under the influence of light, the most photoactive component being 1,8-diamino-4,5-dihydroxyanthraquinone.⁴

CONCLUSION

The anthraquinones are very versatile reagents. A summary of their principal analytical applications is given in Table 1.

Acknowledgement—The Comisión Asesora de Investigación Científica y Técnica is thanked for supporting this study (Project 3007/83 C02-02)

REFERENCES

- 1 K Venkataraman, *The Chemistry of Synthetic Dyes*, Vol II, Academic Press, New York, 1952
- 2 J F McKellar, *Radiat Res Rev*, 1971, **3**, 141
- 3 A V El'tsov, O P Studzinski and U M Grebenkina, *Russ Chem Rev*, 1977, **46**, 93
- 4 I H Leaver, in *Photochemistry of Dyed and Pigmented Polymers*, N S Allen and J F McKellar (eds), Applied Science Publishers, Barking, 1980
- 5 J M Bruce, in *The Chemistry of Quinoid Compounds*, S Patai (ed), Wiley, New York, 1974
- 6 *Colour Index*, Society of Dyers and Colourists, and American Association of Textile Chemists and Colorists, Bradford, 2nd Ed., 1956
- 7 G S Egerton, J M Gleade and N N Uffindell, *J Chromatog*, 1967, **26**, 62
- 8 A M Arsov, B K Mesrob and A B Gateva, *ibid*, 1973, **81**, 181
- 9 P P Rai and T D Turner, *ibid*, 1975, **104**, 196
- 10 J Franc and M Hájková, *ibid*, 1964, **16**, 345
- 11 P Wollenweber, *ibid*, 1962, **7**, 557
- 12 R J Passaraelli and E S Jacobs, *J Chromatog Sci*, 1975, **13**, 153
- 13 I B Rubin, M V Buchanan and G Olerich, *Anal Chim Acta*, 1982, **135**, 111
- 14 I B Rubin and M V Buchanan, *ibid*, 1982, **135**, 121
- 15 H Labhart, *Helv Chim Acta*, 1957, **40**, 1410
- 16 R A Morton and W T Earlam, *J Chem Soc*, 1941, 159
- 17 R H Peters and H H Sumner, *ibid*, 1953, 2101
- 18 Z Yoshida and F Takabayashi, *Tetrahedron*, 1968, **24**, 913
- 19 G S Egerton and A G Roach, *J Soc Dyers Colourists*, 1958, **74**, 401
- 20 H Hartmann and E Lorenz, *Z Naturforsch*, 1952, **7a**, 360
- 21 M S El-Ezaby, T M Salem, A H Zewail and R Issa, *J Chem Soc B*, 1970, 1293
- 22 A Novák, M Titz and M Nepřaš, *Collection Czech Chem Commun*, 1974, **39**, 1532
- 23 S H Etaiw, M M Abou Sekkina, G B El-Hefnawey and S S Assar, *Can J Chem*, 1982, **60**, 304
- 24 H Inoue, M Hoshi, J Yoshina and Y Tanizaki, *Bull Chem Soc Japan*, 1972, **45**, 1018
- 25 N A Shcheglova, D N Shigorin and N S Dokunikhin, *Russ J Phys Chem*, 1964, **38**, 1067
- 26 *Idem*, *Zh Fiz Khim*, 1968, **2**, 2724
- 27 N A Shcheglova, D N Shigorin, R A Nezhel'skaya, L V Galitsina and N S Dokunikhin, *Russ J Phys Chem*, 1974, **48**, 163
- 28 N A Shcheglova, R A Nezhel'skaya, D N Shigorin, L V Galitsina and N S Dokunikhin, *ibid*, 1974, **48**, 166
- 29 M Nepřaš, J Fabian, M Titz and B Gaš, *Collection Czech Chem Commun*, 1982, **47**, 2569
- 30 K R Popov, N V Platonova and L V Smirnov, *Opt Spektrosk*, 1972, **32**, 1097
- 31 D N Shigorin, *Russ J Phys Chem*, 1970, **44**, 1527
- 32 A Navas Díaz, *J Photochem Photobiol A, Chem*, 1990, **53**, 141

- 33 K A Idriss and M M Seleim, *Indian J Chem*, 1980, **19A**, 771
- 34 I M Issa, R M Issa, K A Idriss and A M Hamman, *ibid*, 1976, **14B**, 117
- 35 K A Idriss, I M Issa and M M Seleim, *Rev Roum Chim*, 1979, **24**, 555
- 36 K A Idriss, A Awad, M M Seleim and M S Abu-Bakr, *Bull Soc Chim Fr*, 1981, I-180
- 37 H H Richtol and B R Fitch, *Anal Chem*, 1974, **46**, 1749
- 38 J Horyna, *Collection Czech Chem Commun*, 1959, **24**, 2637
- 39 G Ali Qureshi, G Svehla and M A Leonard, *Analyst*, 1979, **104**, 705
- 40 C K Laird and M A Leonard, *Talanta*, 1970, **17**, 173
- 41 M A Leonard, *Analyst*, 1975, **100**, 275
- 42 M Román, A Fernández Gutierrez and C Marín, *Afinidad*, 1977, **34**, 481
- 43 A V Karyakin, T S Sorokina, V M Ivanov, T G Akimova, N A Lebedeva and A A Karyakin, *Zh Analit Khim*, 1982, **37**, 1171
- 44 R M Issa, M S El-Ezaby and A H Zewail, *Z Phys Chem*, Leipzig, 1970, **244**, 155
- 45 M Román, A Fernández Gutierrez and M C Mahedero, *An Quim*, 1978, **74**, 439
- 46 D V González García, A Arrebola Ramirez and M Román Ceba, *J Inorg Nucl Chem*, 1980, **42**, 1453
- 47 H Gillet and J Ch Pariaud, *Bull Soc Chim Fr*, 1966, 2624
- 48 F Salinas, A Muñoz de la Peña and J A Murillo, *Talanta*, 1986, **33**, 923
- 49 H H Richtol and B R Fitch, *Anal Chem*, 1974, **46**, 1860
- 50 J Barbosa, E Bosch and R Carrera, *Talanta*, 1985, **32**, 1077
- 51 F Capitán, E de Manuel and F Salinas, *Quim Anal*, 1974, **28**, 153
- 52 F Capitán, E de Manuel and M J Ruedas, *ibid*, 1975, **29**, 27
- 53 F Capitán, F García Sánchez and A Gómez Hens, *Bol Soc Chil Quim*, 1978, **23**, No 2, 16
- 54 F García Sánchez and A Navas Díaz, *Afinidad*, 1979, **36**, 133
- 55 F Capitán, F García Sánchez and A Gómez Hens, *Quim Anal (Barcelona)*, 1982, **1**, 178
- 56 I Krausz and A E Havas, *Magy Kem Foly*, 1967, **73**, 135
- 57 I Krausz, A E Havas, M Kaldy and E Fodor, *Ann Univ Sci Budapest, Rolando Eotvos Nominatae, Sect Chim*, 1968, **10**, 77
- 58 F García Sánchez, M Hernández López and A Heredia, *Anal Chim Acta*, 1986, **187**, 147
- 59 A T Pilipenko and L I Savranskii, *Zh Analit Khim*, 1977, **32**, 421
- 60 K A Idriss, M K Hassan, M S Abu-Bakr and H Sedaira, *Analyst*, 1984, **109**, 1389
- 61 A T Pilipenko and L I Savranskii, *Izv Vyssh Ucheb Zaved*, *Khim Khim Tekhnol*, 1973, **16**, No 1, 32
- 62 F García Sánchez, C Cruces Blanco and A Heredia Bayona, *Talanta*, 1987, **34**, 345
- 63 M K Akhmedli, P B Granovskaya and R A Neimatova, *Zh Analit Khim*, 1976, **31**, 298
- 64 L S Serdyuk and S M Lazorina, *ibid*, 1966, **21**, 561
- 65 L S Serdyuk and L I Avramenko, *ibid*, 1972, **27**, 464
- 66 L S Serdyuk, V F Silich and U S Smirnaya, *Tr Komis po Analit Khim*, *Akad Nauk SSSR, Inst Geokhim i Analit Khim*, 1963, **14**, 271
- 67 M K Akhmedli, A A Melikov, *Uch Zap Azerb Gos Univ*, *Ser Khim Nauk*, 1968, No 1, 18
- 68 N S Poluektov, O P Makrenko, A I Kirillov and R S Lauer, *Zh Analit Khim*, 1973, **28**, 285
- 69 N S Poluektov, L A Ovchar, S F Potapova and R S Lauer, *ibid*, 1975, **30**, 235
- 70 K A Idriss, M M Seleim, M K Hassan, M S Abu-Bakr and H Sedaira, *Analyst*, 1985, **110**, 705
- 71 F García Sánchez, M Hernández López and J C Márquez Gómez, *Talanta*, 1987, **34**, 639
- 72 *Idem*, *Analyst*, 1987, **112**, 1037
- 73 F García Sánchez, M Hernandez, J C Márquez, A L Ramos, C Cruces and C Carnero, *Inorg Chim Acta*, 1987, **140**, 249
- 74 A K Dey and S K Banerji, *Proc Symp Chem Coord Compounds, Agra, India*, 1959, Part 2, 198
- 75 H E Zittel and T M Florence, *Anal Chem*, 1967, **39**, 321
- 76 R Suemitsu, *Agr Biol Chem*, 1963, **27**, 1
- 77 M Román, A Fernández Gutierrez and A Muñoz de la Peña, *An Quim*, 1983, **79B**, 128
- 78 E G Kiel and P M Heertjes, *J Soc Dyers Colourists*, 1963, **79**, 363
- 79 J Laszlovszky, *Acta Chim Acad Sci Hung*, 1964, **41**, 133
- 80 S Shibata, M Takito and O Tanaka, *J Am Chem Soc*, 1950, **72**, 2789
- 81 V V Korshak, S V Vinogradova, V S Artemova, *Vysokomolekulyarnye Soedineniya*, 1960, **2**, 492
- 82 F Capitán, M Román and F García Sánchez, *Inf Quim Anal*, 1973, **27**, 7
- 83 M Román, A Fernández Gutierrez and F Cárdenas, *An Quim*, 1980, **76B**, 442
- 84 K Emi, K Toei and K Harada, *Nippon Kagaku Zasshi*, 1957, **78**, 1299
- 85 M Román, F García Sánchez and L F Capitán Vallvey, *Bol Soc Quim Peru*, 1976, **42**, 192
- 86 I Dahl and J A Myrstad, *Acta Chem Scand*, 1966, **20**, 1758
- 87 R S Brown, *Anal Chim Acta*, 1975, **74**, 441
- 88 A K Jain, V P Aggarwala, P Chand and S P Garg, *Talanta*, 1972, **19**, 1481
- 89 R Belcher, M A Leonard and T S West, *J Chem Soc*, 1958, 2390
- 90 M A Leonard and T S West, *ibid*, 1960, 4477
- 91 R Belcher, M A Leonard and T S West, *ibid*, 1959, 3577
- 92 *Idem*, *Talanta*, 1959, **2**, 92
- 93 M Román, F García Sánchez and A Gómez Hens, *Quim Anal*, 1974, **28**, 191
- 94 K A Idriss, A A Harfoush, A S El-Shahawy and H Sedaira, *Analyst*, 1985, **110**, 709
- 95 R F Buchanan, J P Hughes and C A A Bloomquist, *Talanta*, 1960, **6**, 100
- 96 H B Evans, A M Hrobar and J H Patterson, *Anal Chem*, 1960, **32**, 481
- 97 G B Wengert, *ibid*, 1952, **24**, 1449
- 98 D F Wood and R H McKenna, *Analyst*, 1962, **87**, 880
- 99 N B Stanton, *ibid*, 1968, **93**, 802
- 100 H Degenhardt, *Z Anal Chem*, 1956, **153**, 327

- 101 J A Corbett and B D Guerin, *Analyst*, 1966, **91**, 490
- 102 H G C King and G Pruden, *ibid*, 1968, **93**, 601
- 103 L A Lancaster and R Balasubramaniam, *J Sci Food Agr*, 1974, **25**, 381
- 104 G W Goward and V R Wiederkehr, *Anal Chem*, 1963, **35**, 1542
- 105 D L Callicoat and J D Wolzon, *ibid*, 1959, **31**, 1434
- 106 D G Higgs, *Analyst*, 1960, **85**, 897
- 107 F Ráb, *Collection Czech Chem Commun*, 1959, **24**, 3654
- 108 R S Brown, *Anal Chim Acta*, 1970, **50**, 157
- 109 J T Hatcher and L V Wilcox, *Anal Chem*, 1950, **22**, 567
- 110 E N Pollock and L P Zopatti, *Talanta*, 1963, **10**, 118
- 111 K C Berger and E Truog, *Ind Eng Chem, Anal Ed*, 1939, **11**, 540
- 112 A H Jones, *Anal Chem*, 1957, **29**, 1101
- 113 F J Langmyhr and A Holme, *Anal Chim Acta*, 1966, **35**, 220
- 114 H K L Gupta and D F Boltz, *Mikrochim Acta*, 1971, 577
- 115 R Greenhalgh and J P Riley, *Anal Chim Acta*, 1961, **25**, 179
- 116 S S Yamamura, M A Wade and J H Sikes, *Anal Chem*, 1962, **34**, 1308
- 117 M Hanocq and L Molle, *Anal Chim Acta*, 1968, **40**, 13
- 118 H Kubota, *Microchem J*, 1967, **12**, 525
- 119 H N S Schafer, *Anal Chem*, 1963, **35**, 53
- 120 J P S Haarsma and J Agterdenbos, *Talanta*, 1971, **18**, 747
- 121 I Krausz and A Endroi-Havas, *Proc S A C Conference*, Nottingham, 1965, p 568
- 122 F García Sánchez, A Navas Díaz, M Santiago and F Grases, *Talanta*, 1981, **28**, 833
- 123 F Capitán, M Román and F García Sánchez, *Inf Quim Anal*, 1973, **27**, 1
- 124 F Capitán, F García Sánchez and A Gómez Hens, *Afinidad*, 1977, **34**, 755
- 125 *Idem*, *An Quim*, 1978, **74**, 272
- 126 F García Sánchez and A Navas Díaz, *Rev Soc Quim Mex*, 1982, **26**, No 2, 80
- 127 F Salinas, F García Sánchez and C Genestar, *Afinidad*, 1982, **39**, 261
- 128 E Bishop (ed), *Indicators*, Pergamon Press, Oxford, 1972
- 129 K B Yatsimirskii, *Kinetic Methods of Analysis*, Pergamon Press, Oxford, 1966
- 130 A Navas Díaz, M Santiago, F Grases, J J Laserna and F García Sánchez, *Talanta*, 1982, **29**, 615
- 131 A Navas Díaz and F Sánchez Rojas, *Analyst*, 1984, **109**, 1435
- 132 A Navas Díaz and F Sánchez Rojas, *Quim Anal (Barcelona)*, 1983, **2**, 112
- 133 Gh Ionescu, Al Duca and F Matei, *Mikrochim Acta*, 1980 **I**, 329
- 134 P R Bontchev, *Talanta*, 1970, **17**, 499
- 135 A Navas Díaz and F Sánchez Rojas, *ibid*, 1984, **31**, 437
- 136 F Salinas, F García Sánchez, F Grases and C Genestar, *Anal Lett*, 1980, **13**, 473
- 137 F Salinas, C Genestar and F Grases, *Anal Chim Acta*, 1981, **130**, 337
- 138 J Bognár and O Jellinek, *Mag Kem Foly*, 1961, **67**, 147
- 139 J Bognár, *Mikrochim Acta*, 1961, 901
- 140 N V Parkhomenko, G A Prik and K B Yatsimirskii, *Zh Analit Khim*, 1961, **16**, 599
- 141 F Salinas, F García Sánchez and C Genestar, *Anal Lett*, 1982, **15**, 747
- 142 A Navas Díaz and F Sánchez Rojas, *Microchem J*, 1985, **31**, 50
- 143 A Navas Díaz and F Sánchez Rojas, *Mikrochim Acta*, 1982 **I**, 175
- 144 M Román, A Fernández Gutierrez and A Muñoz de la Peña, *Microchem J*, 1984, **29**, 19
- 145 *Idem*, *An Quim*, 1984, **80**, 332
- 146 N H Furman and K G Stone, *J Am Chem Soc*, 1948, **70**, 3055
- 147 F Capitán, A Guiraum, J L Vilchez and J F Arenas, *Can J Chem*, 1979, **57**, 3243
- 148 L A Wiles, *J Chem Soc*, 1952, 1358
- 149 R Jones and T McL Spotswood, *Aust J Chem*, 1962, **15**, 492
- 150 F Capitán, E Alvarez Manzaneda and J L Vilchez, *Proc Indian Acad Sci, (Chem Sci)*, 1984, **93**, 59
- 151 M Román Ceba, A Sánchez Misiego, A Fernández Gutierrez and A Muñoz de la Peña, *Ann Chim Roma*, 1984, **74**, 837
- 152 R Gill and H I Stonehill, *J Chem Soc*, 1952, 1845
- 153 V D Bezuglyi, V A Shapovalov and V Ya Fain, *Zh Obshch Khim*, 1976, **46**, 696
- 154 A D Broadbent and R J Melanson, *Can J Chem*, 1975, **53**, 3757
- 155 A D Broadbent and E F Sommermann, *J Chem Soc, B*, 1967, 376
- 156 *Idem*, *ibid*, 1968, 519
- 157 F Capitán, J L Vilchez and A Navalón, *Analyst*, 1982, **107**, 953
- 158 F Capitán, A Guiraum and J L Vilchez, *Can J Chem*, 1981, **59**, 1201
- 159 F Umland, *Zh Analit Khim*, 1978, **33**, 612
- 160 S D Popescu and E Barbacaru, *Anal Lett*, 1985, **18**, 947
- 161 N S Allen, P Bentley and J F McKellar, *J Photochem*, 1976, **5**, 225
- 162 A K Davies, J F McKellar and G O Phillips, *Proc Roy Soc Ser A*, 1971, **323**, 69
- 163 F Wilkinson, *J Phys Chem*, 1962, **66**, 2569
- 164 H H Dearman and A Chan, *J Chem Phys*, 1966, **44**, 416
- 165 H R Cooper, *Trans Faraday Soc*, 1966, **62**, 2865
- 166 M S Gandelman and J W Birks, *J Chromatog*, 1982, **242**, 21
- 167 *Idem*, *Anal Chem*, 1982, **54**, 2131
- 168 J R Poulsen and J W Birks, *ibid*, 1989, **61**, 2267
- 169 *Idem*, *ibid*, 1990, **62**, 1242
- 170 S Traore and J J Aaron, *Anal Lett*, 1987, **20**, 1995
- 171 W Oelschlager, *Z Anal Chem*, 1957, **154**, 321
- 172 E G Owens and J H Yoe, *Anal Chem*, 1959, **31**, 384
- 173 F Capitán, M Román and A Guiraum, *An Quim*, 1974, **70**, 508
- 174 F Capitán-García, M Román and E Alvarez Manzaneda, *Bol Soc Quim Peru*, 1973, **39**, 125
- 175 F Capitán and M Román, *Rev Univ Ind Santander*, 1967, **9**, No 3/4, 17
- 176 F Ingman, *Talanta*, 1973, **20**, 999
- 177 F Capitán, F García Sánchez and A Gómez Hens, *Afinidad*, 1977, **34**, 467
- 178 A Holme, *Acta Chem Scand*, 1967, **21**, 1679

- 179 F Salinas, A Muñoz de la Peña, J A Murillo and J C Jiménez Sánchez, *Analyst*, 1987, **112**, 913
- 180 R Ruggieri, *Anal Chim Acta*, 1961, **25**, 145
- 181 E C Cogbill and J H Yoe, *Anal Chem*, 1957, **29**, 1251
- 182 G Wunsch, *Z Anal Chem*, 1972, **258**, 30
- 183 P K Govil and S K Banerji, *J Inst Chem, Calcutta*, 1972, **44**, 128
- 184 M W Cucci, W F Neuman and B J Mulryan, *Anal Chem*, 1949, **21**, 1358
- 185 A Guiraum and J L Vilchez, *Quim Anal*, 1975, **29**, 265
- 186 L O Matveev and I S Mustafin, *Tr Komis po Analit Khim, Akad Nauk SSSR, Inst Geokhimi Anal Khim*, 1960, **11**, 217
- 187 M H Fletcher, C E White and M S Sheftel, *Ind Eng Chem, Anal Ed*, 1946, **18**, 179
- 188 F Capitán, F Salinas and L M Franquelo, *An Quim*, 1976, **72**, 529
- 189 *Idem*, *Anal Lett*, 1975, **8**, 753
- 190 A Navas Díaz and F García Sánchez, *An Quim*, 1979, **75**, 514
- 191 P Kaur and V K Gupta, *Z Anal Chem*, 1989, **334**, 447
- 192 F Salinas, J J Berzas Nevado, A Espinosa Mancilla and T Román Galán, *Bull Soc Chim Belg*, 1987, **96**, 71
- 193 E G Owens and J H Yoe, *Anal Chem*, 1960, **32**, 1345
- 194 F Salinas, A Muñoz de la Peña and J A Murillo, *ibid*, 1987, **112**, 1391
- 195 H V Connerty and A R Briggs, *Clin Chem*, 1965, **11**, 716
- 196 M C Mahedero, M Román Ceba and A Fernández Gutierrez, *Anal Lett*, 1986, **19**, 1725
- 197 M Román, A Fernández Gutierrez and F Cárdenas, *Rev Soc Quim Mex*, 1977, **21**, No 3, 89
- 198 *Idem*, *Bol Soc Chil Quim* 1980, **25**, No 1, 1
- 199 F Capitán and M Román, *Inf Quim Anal*, 1968, **22**, 134, *Ars Pharm*, 1968, **9**, 65
- 200 M Román, A Fernández Gutierrez and F Cárdenas, *Afinidad*, 1981, **38**, 253
- 201 *Idem*, *Microchem J*, 1980, **25**, 576
- 202 F Capitán, A Guiraum and J Bullejos, *Afinidad*, 1975, **32**, 461
- 203 F Capitán, M Román and A Guiraum, *An Quim*, 1972, **68**, 989
- 204 F Capitán, M Román and A Fernández Gutierrez, *Bol Soc Chil Quim*, 1971, **17**, No 2, 29
- 205 E Illner, *Z Chem, Leipzig*, 1965, **5**, 389
- 206 V I Vershinin, V T Chuiko and B E Reznik, *Zh Analit Khim*, 1971, **26**, 1710
- 207 M Román and E Alvarez Manzaneda, *Quim Anal*, 1975, **29**, 253
- 208 F Capitán, M Román and F García Sánchez, *Rev Univ Ind Santander*, 1978, **8**, No 8, 43
- 209 F García Sanchez, F Bosch Reig and J M Estela, *An Quim*, 1980, **76B**, 273
- 210 S P Sangal, *Chim Anal, Paris*, 1964, **46**, 492
- 211 M Román, A Arrebola and F Perera, *Afinidad*, 1979, **36**, 27
- 212 M Román, A Fernández Gutierrez and A Muñoz de la Peña, *ibid*, 1983, **40**, 355
- 213 *Idem*, *An Quim*, 1983, **79B**, 128
- 214 F Capitán, M Román and F García Sánchez, *Inf Quim Anal*, 1973, **27**, 179
- 215 A Navas and F García Sánchez, *An Quim*, 1979, **75**, 506
- 216 F Capitán, A Guiraum and J L Vilchez, *Afinidad*, 1980, **37**, 129
- 217 R I Spirina and K V Lyakhova, *Zavodsk Lab*, 1989, **55**, No 4, 6
- 218 J M Icken and B M Blank, *Anal Chem*, 1953, **25**, 1741
- 219 F Capitán and A Guiraum, *Ars Pharm*, 1971, **12**, 397
- 220 F Capitán, F Salinas and J Cobo, *Rev Soc Venez Quim* 1972, **8**, No 4/5, 163
- 221 M E León Gonzalez, M J Santos-Delgado and L M Polo Diez, *Anal Chim Acta*, 1989, **219**, 329
- 222 M Chikuma, Y Okabayashi, T Nakagawa, A Inoue and H Tanaka, *Chem Pharm Bull*, 1987, **35**, 3734
- 223 Y Okabayashi, R Oh, T Nakagawa, H Tanaka and M Chikuma, *Analyst*, 1988, **113**, 829
- 224 M M Ferris, B Bingham and M A Leonard, *Anal Proc*, 1988, **25**, 58
- 225 S Przeszlakowski, *Chem Anal, Warsaw*, 1988, **33**, 617
- 226 M Román Ceba, A Arrebola Ramirez and J J Berzas Nevado, *Talanta*, 1982, **29**, 142
- 227 Ch D Dwivedi, K N Munshi and A K Dey, *Microchem J*, 1965, **9**, 218
- 228 A T Plipenko and E G Maksimyuk, *Ukr Khim Zh*, 1987, **53**, 58
- 229 O Engel and S Král, *Hutn Listy*, 1970, **25**, 432
- 230 M K Akhmedli, D G Gasanov and R A Alieva, *Azerb Khim Zh*, 1965, No 4, 92
- 231 M Román and A Fernández Gutierrez, *Bol Soc Quim Peru*, 1975, **41**, No 1, 1
- 232 M Finkel'shteinaite and J Garjonyte, *Zh Vses Khim Obshch*, 1968, **13**, 593
- 233 M Finkel'shteinaite, J Garjonyte and V Skominaitė, *Liet TSR Aukst Mokykhu Mkslo Darb Chem Chem Technol*, 1970, **11**, 69
- 234 M Román and A Fernández Gutierrez, *Quim Anal*, 1975, **29**, 203
- 235 V A Nazarenko, G V Flyantikova, L I Korolenko and Yu N Anisimov, *Zh Analit Khim*, 1975, **30**, 1354
- 236 M Román and A Fernández Gutierrez, *Quim Anal*, 1975, **29**, 281
- 237 G V Flyantikova and L I Korolenko, *Zh Analit Khim*, 1975, **30**, 1349
- 238 D I Zul'fugarly, I K Guseinov and Kh N Kulieva, *Azerb Khim Zh*, 1972, No 2, 173
- 239 G V Flyantikova, V A Nazarenko and I G Kostenko, *Zh Analit Khim*, 1975, **30**, 814
- 240 E Crepaz, L Marchesina and G Mazzolini, *Met Ital*, 1962, **54**, 373
- 241 M Otomo and K Tonosaki, *Talanta*, 1971, **18**, 438
- 242 M Román, A Fernández Gutierrez, M C Mahedero and A Muñoz de la Peña, *Rev Port Quim*, 1983, **25**, 41
- 243 E A Biryuk and V A Nazarenko, *Zh Analit Khim*, 1975, **30**, 1720
- 244 A Fernández Gutierrez, A Muñoz de la Peña and J A Murillo, *Anal Lett*, 1983, **16**, 759
- 245 F Salinas, A Muñoz de la Peña and J A Murillo, *Microchem J*, 1987, **36**, 79
- 246 L S Serdyuk and U F Silich, *Izv Vyssh Ucheb Zaved, Khim Khim Tekhnol*, 1962, **5**, 38

- 247 K C Srivastava and S K Banerji, *J Prakt Chem*, 1968, **38**, 327
- 248 M Román Ceba, A Fernández Gutierrez and M C Mahedero, *Anal Lett*, 1981, **14**, 1579
- 249 F Salinas, A Muñoz de la Peña and F Muñoz de la Peña, *Mikrochim Acta*, 1985 **III**, 361
- 250 M Román Ceba, A Fernández Gutierrez and C Marín Sánchez, *Anal Lett*, 1982, **15**, 1621
- 251 *Idem*, *Microchem J*, 1982, **27**, 339
- 252 M Román Ceba, A Fernández Gutierrez and A Palomera, *Anal Lett*, 1977, **10**, 907
- 253 F Capitán, F Salinas and L M Franquelo, *Quim Anal*, 1977, **31**, 275
- 254 F Capitán, M Román and A Guiraum, *Quim Ind*, 1971, **17**, 15
- 255 *Idem*, *An Quim*, 1971, **67**, 147
- 256 S N Sinha and A K Dey, *Z Anal Chem*, 1963, **195**, 416
- 257 S Rami and S K Banerji, *Microchem J*, 1973, **18**, 636
- 258 A Lee and D F Boltz, *ibid*, 1972, **17**, 380
- 259 G K Kirkbright, T S West and C Woodward, *Talanta*, 1966, **13**, 1637
- 260 E Blanco González, J I García Alonso, M E Díaz and A Sanz-Medel, *Quim Anal (Barcelona)*, 1986, **5**, 428
- 261 T Román Galán, A Arrebola Ramírez and M Román Ceba, *Microchem J*, 1982, **27**, 210
- 262 F Salinas and L M Franquelo, *Quim Anal*, 1975, **29**, 319
- 263 M A Leonard and F I Nagi, *Talanta*, 1969, **16**, 1104
- 264 S P Sangal, *Chim Anal*, Paris, 1968, **50**, 131
- 265 M Román, A Fernández Gutierrez and A Muñoz de la Peña, *Microchem J*, 1984, **29**, 275
- 266 F Capitán, F García Sánchez and A Gómez Hens, *Bol Soc Chil Quim*, 1979, **24**, No 1, 1
- 267 A Navas and F García Sánchez, *Afinidad*, 1979, **36**, 161
- 268 M Román, F García Sánchez and A Gómez Hens, *ibid*, 1977, **34**, 118
- 269 A T Pilipenko, T L Shevchenko, *Zh Analit Khim*, 1989, **44**, 1262
- 270 F García Sánchez, F Bosch Reig and J M Estela, *Afinidad*, 1979, **36**, 156
- 271 K K Saxena and B V Agarwala, *Indian J Chem*, 1976, **14A**, 634
- 272 J C MacDonald and J H Yoe, *Anal Chim Acta*, 1963, **28**, 264
- 273 K A Idriss, M M Seleim, M S Abu-Bakr and M S Saleh, *Analyst*, 1982, **107**, 12
- 274 M Román Ceba, A Fernández Gutierrez and F Cárdenas, *An Quim*, 1980, **76B**, 447
- 275 F Capitán and M Román, *Ars Pharm*, 1967, **8**, 7
- 276 T Barra and B Seeger, *Rev Real Acad Cienc Exactas, Fis Natur Madrid*, 1967, **61**, 827
- 277 F Capitán, F Salinas and J Cobo, *Rev Soc Venez Quim* 1971, **8**, No 1, 33
- 278 A Navas Díaz and F García Sánchez, *An Quim*, 1979, **75**, 511
- 279 M M Seleim, K A Idriss, M S Abu-Bakr and M S Saleh, *An Quim*, B, 1988, **84**, 168
- 280 V I Kuznetsov and A I Zabelin, *Zh Analit Khim*, 1962, **17**, 318
- 281 A K Mukherji and A K Dey, *Z Anal Chem*, 1958, **160**, 98
- 282 I M Issa, R M Issa and Y Z Ahmed, *Microchem J*, 1973, **18**, 569
- 283 J M Ramirez de Verger and F Pino Pérez, *Inf Quim Anal*, 1963, **17**, 39
- 284 S N Sinha and A K Dey, *J Prakt Chem*, 1963, **20**, 225
- 285 *Idem*, *Z Anal Chem*, 1961, **183**, 182
- 286 T Pérez Ruiz, C Martínez Lozano and A Cánovas García, *Afinidad*, 1987, **44**, 273
- 287 F Burriel Martí, A Cabrera Martín and C Fuentes Gutierrez, *Inf Quim Anal*, 1965, **19**, 165
- 288 K A Idriss, M M Seleim, M S Saleh, M S Abu-Bakr and H Sedaira, *Analyst*, 1988, **113**, 1643
- 289 F Sánchez Rojas, *Afinidad*, 1988, **45**, 222
- 290 R López Nuñez, M Callejón Monchón and A Guiraum Pérez, *Anal Chim Acta*, 1987, **192**, 119

DESIGN AND PERFORMANCE OF A DIRECT-READING, MULTICHANNEL SPECTROMETER FOR THE DETERMINATION OF CHLORINATED PURGEABLE ORGANIC COMPOUNDS BY FLAME INFRARED-EMISSION SPECTROMETRY

S WAYNE KUBALA, DAVID C. TILOTTA, MARIANNA A. BUSCH and KENNETH W. BUSCH*
The Department of Chemistry, P. O. Box 97348, Baylor University, Waco, TX 76798-7348, U S A

(Received 26 September 1990 Revised 5 December 1990 Accepted 10 December 1990)

Summary—The feasibility of determining chlorinated, purgeable organic compounds (POCs) in aqueous samples by flame infrared-emission (FIRE) spectrometry was evaluated with a specially designed, multichannel, dispersive spectrometer having sufficient resolving power to prevent interference from large amounts of non-halogenated POCs that could also be present in the sample. The polychromator was based on a Czerny–Turner optical mounting with a 0.15-m focal length, a nominal focal ratio of $f/3$, and a reciprocal linear dispersion of $0.15 \mu\text{m}/\text{mm}$ in the first order. The HCl and CO_2 infrared emission bands (3.77 and $4.42 \mu\text{m}$, respectively) were monitored in two analytical channels, while a third reference channel, used for background subtraction, monitored the H_2O background emission at $2.8 \mu\text{m}$. Instrumental performance was evaluated with dichloromethane, trichloromethane, trichloroethylene, 1,1,2,2-tetrachloroethane and monochlorobenzene as test compounds, and parameters such as the linear dynamic range, reproducibility, detection limit and signal-to-noise ratio, and extent of spectral crosstalk between channels were determined. The feasibility of performing a quantitative analysis of a two-component mixture of dichloromethane and trichloromethane at trace levels was demonstrated.

Flame/furnace infrared-emission (FIRE) spectrometry is a relatively new laboratory technique that shows considerable promise in a number of important analytical areas.¹ The FIRE detector monitors well-defined infrared emission bands resulting from vibrationally excited molecules, such as CO_2 , H_2O , HCl and HF, that are produced when organic compounds containing C, H, Cl and F are combusted in a low-background hydrogen/air flame.² Alternatively, an electrically heated furnace can be used to produce infrared emission from vibrationally excited analyte molecules, without decomposition.³

Because FIRE spectrometry is a relatively new analytical technique, most of the initial studies have focused on exploring potential applications^{4–9} and improving instrumental performance.¹⁰ To date, FIRE spectrometry has been used for element-selective detection (of C, Cl and F) in gas and liquid chromatography,^{4–7} for determination of total inorganic carbon (TIC) in environmental water samples,⁸ for de-

termination of chloride and available chlorine in aqueous samples⁹ and for determination of ethanol in gasohol.³

In almost all previous FIRE applications,^{3,6–9} the infrared emission band was detected by using a simple filter radiometer consisting of transfer optics, a chopper, a commercially available optical notch filter for wavelength isolation, and a lead selenide photoconductivity detector. Although use of an optical notch filter to isolate the analytical emission band from the source background has the advantage of being simple, not subject to misadjustment, and capable of high optical throughput, commercially available stock interference filters were found to have a number of disadvantages. First, commercial filters were not always available for the optimum analytical wavelength,⁹ and the band-pass of the filter was sometimes too wide or too narrow for the infrared emission band of interest.⁹ Moreover, in some applications, combinations of filters were required to reduce spectral interference from intense background and concomitant emission bands.⁷ Finally, filter selection often required a compromise involving

*Author for correspondence

signal intensity, adequate background rejection and removal of spectral interference from other emission bands.^{7,9}

Because the FIRE system can detect chlorine-containing species that form HCl in the flame,^{2,7,9} one important application for FIRE spectrometry could be the determination of purgeable chlorinated organic compounds in aqueous samples.¹ Chlorinated organics are a type of environmental contaminant resulting from the improper disposal of such widely used industrial products as dry-cleaning agents, degreasing agents, and pesticides,¹¹ and from the chlorination of drinking water.¹² Many chlorinated compounds are either carcinogenic or have other associated health risks,¹¹ and their maximum contaminant level in drinking water is strictly regulated.¹²⁻¹⁴ Because water utilities must monitor chlorinated organics on a regular basis, FIRE might serve either as a method for the determination of purgeable total organic halides (purgeable TOXs) or as a rapid inexpensive screening procedure to determine whether an environmental sample required more extensive analysis by gas chromatography-mass spectrometry (GC-MS).

The FIRE analytical system developed for TIC determinations⁸ has been shown to be potentially useful for the determination of purgeable organic compounds (POCs) in water samples¹ when the detector is operated in the carbon-selective mode. Problems were encountered, however, when the FIRE system was used for the determination of chlorinated POCs¹⁵ in the chlorine-selective mode. Because the transmission characteristics of the 3.8- μm optical notch filter used to monitor the emission from HCl⁹ had a 0.1% transmittance in the vicinity of the 4.42- μm CO₂ infrared emission band, significant optical leakage of this band through the chlorine filter was observed whenever large amounts of CO₂-producing materials were also present in the flame. Filter bleed was not a serious obstacle in the chlorine-specific detection of compounds in gas chromatography⁷ because prior separation of the mixture always ensured that the amount of CO₂ present in the flame was relatively low. In the determination of chlorinated POCs, however, significant amounts of volatile, non-chlorinated organics presented a serious problem,¹⁵ requiring an improved wavelength isolation system.

The ideal wavelength isolation system for FIRE spectrometry would have a high luminosity-resolving power product,¹⁶ be capable of

producing the highest possible analyte-band-to-background ratio, have a variable spectral bandwidth, be tuneable for different wavelengths and permit selective wavelength monitoring of desired emission bands on a continuous basis. Wavelength isolation systems based on Fourier transform¹⁷ or Hadamard transform spectroscopy¹⁸ offer no multiplex or luminosity advantage¹⁶ in the case of FIRE spectrometry because the FIRE system appears to be flame-noise limited rather than detector-noise limited.^{6,7} Moreover, acquiring the complete infrared spectrum from an initial wavelength to a final wavelength is completely unnecessary, since only very specific regions of the infrared spectrum are of interest from a quantitative analytical standpoint.¹ Therefore, a non-transform approach involving a dispersive, multichannel spectrometer could be beneficial for FIRE spectrometry provided an optically fast system could be employed.

This paper reports the development of a direct-reading, multichannel spectrometer specifically designed for the determination of chlorinated POCs by flame/furnace infrared emission spectrometry. To evaluate the analytical performance of this newly developed FIRE spectrometer, the determination of five chlorinated POCs in aqueous samples was studied.

EXPERIMENTAL

FIRE detection system

The multichannel FIRE detector, shown schematically in Fig. 1, consists of an optical section and an electronic signal-processing section. The optical system collects, disperses and focuses the infrared radiation from the flame onto the infrared detector array which is located at the exit focal plane of the polychromator. The components were mounted on a 30.5 \times 53.3 \times 1.0-cm aluminum plate and consisted of a miniature capillary-head, hydrogen/entrained-air burner, external light collection optics, a polychromator, and three PbSe infrared detectors arranged in an array. As shown in Fig. 1, one of the detectors provides a reference signal, while the other two detectors provide analytical signals.

The miniature capillary-head burner was fabricated from an aluminum block and has been described previously.^{1,5} The burner head consists of a circular array of six capillaries surrounding a seventh, central capillary used for sample introduction into the flame. The

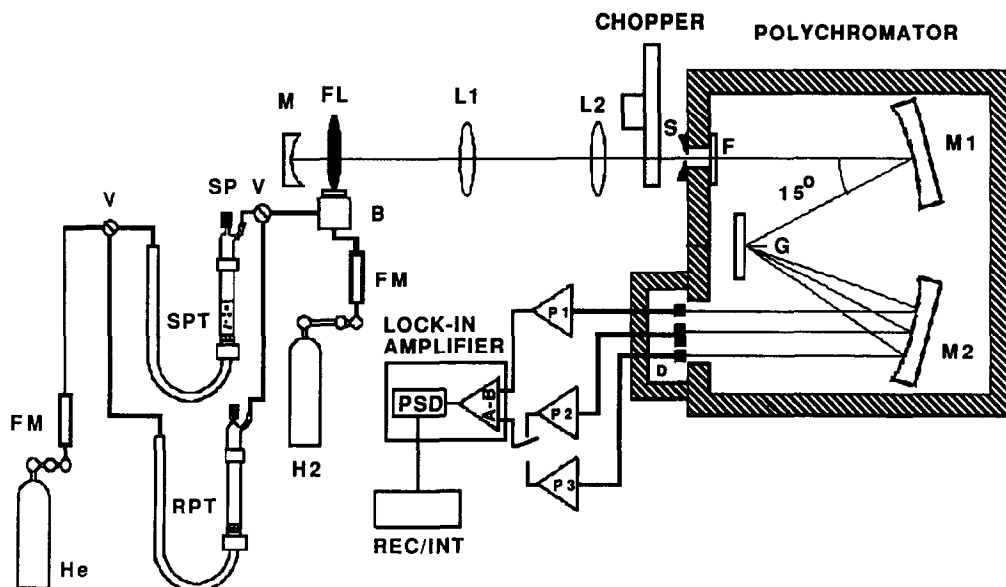


Fig 1 Schematic diagram of the direct-reading, multichannel FIRE spectrometer M, back-collection mirror, FL, hydrogen/entrained-air flame, B, capillary burner, L₁, collimating lens, L₂, focusing lens, S, slit, F, long-pass filter, M₁, collimating mirror, M₂, focusing mirror, G, grating, FM, flow meters, H₂, hydrogen cylinder, He, helium cylinder, V, three-way switching valves, SPT, sample purge tube, RPT, reference purge tube, SP, septum for sample introduction, D, detectors, P₁, preamplifier for H₂O reference channel, P₂, preamplifier for HCl analytical channel, P₃, preamplifier for CO₂ analytical channel, A-B, lock-in amplifier input, PSD, phase-sensitive detector, REC/INT, recorder-integrator

optimum flow-rate of hydrogen to the burner was 324 ml/min, with combustion supported only by entrained air. The hydrogen supply pressure was regulated at 0.75 atm with triple-stage regulation. The burner was enclosed in an aluminum shield and chimney assembly to minimize temperature fluctuations resulting from air drafts and other environmental effects.

The infrared emission from the flame was collected and focused onto the entrance slit of the polychromator by a back-collection mirror and two lenses. An $f/1$, 2.5-cm focal length, concave back-collection mirror (Model 44341, Oriel Corp., Stratford, CT) was positioned at the $2f$ point behind the flame to focus a 1:1 image of the flame onto itself. An $f/2$, 5-cm focal length CaF₂ lens (Model 43150, Oriel Corp.) was used to collect and collimate the flame infrared emission onto a second, identical CaF₂ lens that focused this radiation onto the entrance slit of the polychromator. A laboratory-constructed chopper, placed between the focusing lens and the entrance slit, modulated the infrared radiation at 530 Hz.

The polychromator, fabricated in the laboratory, was based on the symmetrical Czerny-Turner design.¹⁶ The optical components and adjustable optical mounts utilized in the polychromator were mounted in a

19.0 × 18.1 × 13.3-cm light-tight box constructed from aluminum sheet. The inside of the box was painted flat black to reduce reflections. The entrance slit of the polychromator was constructed by splitting a two-edged razor blade in half and placing the sharp edges over a 5-mm diameter hole drilled in the front plate of the polychromator. The two portions of the razor blade were held in place by screws in the front plate of the polychromator and could be adjusted to form any desired slit width. In this study, the slit width was fixed at 2 mm for all experiments.

The infrared radiation passing through the entrance slit of the polychromator was collimated and directed onto a grating by an $f/3$, 15-cm focal length, concave mirror. The mirror was placed at an angle of 15° to the entrance optical axis (Fig. 1). The 5 × 5-cm plane diffraction grating was ruled at 40.96 grooves/mm and was blazed for 3.2 μm (Model 35-63-06-811, Milton Roy Co., Rochester, NY). The dispersed infrared radiation from the grating was focused onto the PbSe detectors by a second, $f/3$, 15-cm focal length concave mirror. A long-pass filter with a cut-on wavelength of 3.0 μm at 5% absolute transmittance (Part R1-3000F, Corion, Holliston, MA) was placed over the entrance slit as an order-sorting filter.

Three infrared emission bands were detected with three PbSe infrared detectors located in the exit focal plane of the spectrometer (Fig 1). Two 1 × 1-mm detectors (Part #BF1, Cal-Sensors, Inc, Santa Rosa, CA) were used to detect portions of the emission bands due to CO₂ and H₂O. A 2 × 2-mm PbSe detector (Part #BR2, Cal-Sensors, Inc) was used to detect a portion of the P-branch of the HCl stretching vibration. The overall detector dimensions were 3.0 × 1.5 × 0.64 mm and 4.5 × 2.5 × 0.64 mm for the 1 × 1-mm and 2 × 2-mm response areas, respectively. Segments of tinned copper wire (0.76 mm diameter × 25.4 mm long) were soldered to the detector leads and served as the electrical connection.

The PbSe infrared detectors were placed in a detector carriage (Fig. 2) fabricated from a 2.54 × 3.81 × 1.25-cm block of plexiglas[®]. A slot in the plexiglas[®] block (Fig 2) allowed the detectors to be adjusted for maximum signal response. The detectors were glued to plexiglas[®] mounts with silicone sealant. The detector mounts were placed in the slot of the detector carriage, and holes (1.0-mm diameter) for each detector lead were drilled approximately 0.8 cm from the top and bottom of the detector carriage. Segments of standard, solid-core, electrical wire (1-mm diameter, 2-cm long) were positioned in these holes, flush with the front of the detector carriage. The leads of the detectors were soldered onto the wire segments (allowing some movement of the detectors in the detector carriage), and the surplus lead was removed. The connections to the preamplifier circuits were made from the ends of the wire segments

that protruded from the back of the detector carriage.

The detector carriage with the detectors placed inside was mounted over a 2.54 × 2.54-cm opening in the front plate of the polychromator at the exit focal plane. In this study, the 1 × 1-mm detectors monitored a portion of the flame water-emission band centered at 2.9 μm (detector D₁, Fig. 2) and the asymmetric stretching vibration of CO₂ centred at 4.42 μm (detector D₃, Fig. 2). A portion of the P-branch of the HCl stretching vibration centered at 3.77 μm was detected with the 2 × 2-mm detector (detector D₂, Fig. 2).

The electronics associated with the FIRE detector include an optical chopper, lock-in amplifier (LIA), detector and operational amplifier power supplies, preamplifier circuits and a recorder/integrator. The preamplifier circuits used with the PbSe detectors have been described previously.⁶ The three circuits were placed on a single breadboard and located in close proximity (approximately 4 cm) to the detector carriage. A 9.5 × 5.8 × 8.3-cm aluminum housing, mounted on the front plate of the polychromator, was used to enclose the detectors, detector carriage, and preamplifier circuits.

The detectors were operated at room temperature and powered from a common split source consisting of a 122 V battery supply. The bias voltage for each PbSe detector was independently controlled by a separate potentiometer in series with the common power supply. For this study, the bias voltage (*i.e.*, the actual voltages across the detector itself) for the 2 × 2-mm HCl detector was fixed at 66 V, and

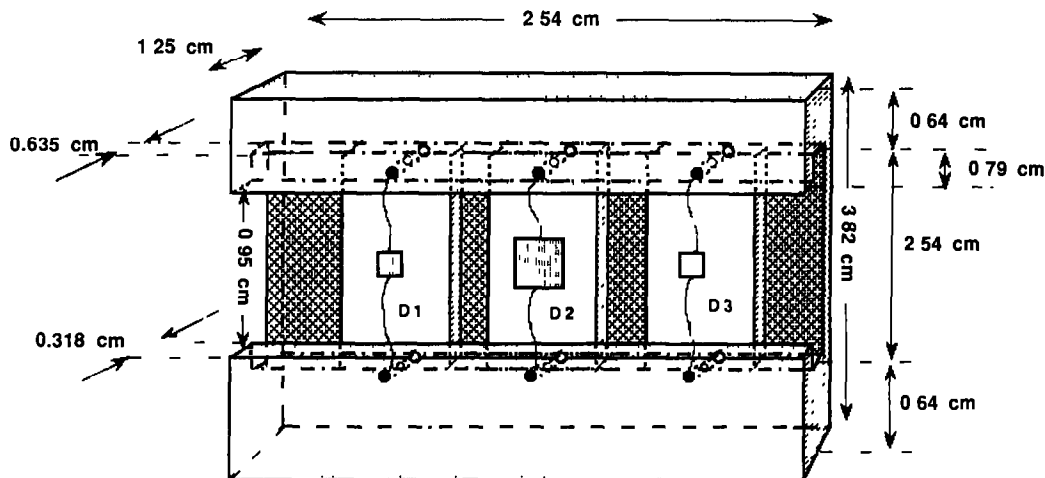


Fig 2 Schematic diagram and dimensions for the plexiglas[®] detector carriage. D₁, detector for H₂O reference channel, D₂, detector for HCl analytical channel, D₃, detector for CO₂ analytical channel, ●, holes for detector leads

the bias voltages of the 1×1 -mm H_2O and CO_2 detectors were adjusted with the potentiometers as described below. The operational amplifiers (Part #TLO71, Texas Instruments, Dallas, TX) employed in the preamplifier circuit were powered at ± 15 V from a regulated bipolar power supply (Part #2718, Heath Co., Benton Harbor, MI). The amplifier output signals from the preamplifier circuits were demodulated by a lock-in amplifier (Model #3962, Ithaco, Ithaca, NY) operated in the differential input (*i.e.*, subtracted) mode. A 1-sec time constant was used for all measurements. The signal was recorded on a recorder/integrator (Model #3394A, Hewlett-Packard Corp., North Hollywood, CA).

Purging apparatus

The purging apparatus has been described previously^{8,9} and consists of two 5-ml demountable purge tubes connected in parallel by polyethylene tubing and two three-way switching valves (Fig. 1). One of the purge tubes serves as the sample chamber and the second as the reference chamber. An opening located at the top of each purge tube was fitted with a rubber septum to allow samples to be introduced by a syringe (Model 1001, Hamilton Co., Reno, NV). Each purge tube can be disconnected easily for removal of the spent aqueous sample and for cleaning.

The volatile components in the aqueous samples were purged into the flame of the FIRE detector with helium maintained at a flow-rate of 100 ml/min with a rotameter (Model 1110-05F1A1A, Brooks Instrument Div., Emerson Electric Co., Hatfield, PA). The supply pressure of the helium was regulated at 0.75 atm with triple-stage regulation.⁸

Reagents

All chemicals were reagent grade and used without further purification. Dichloromethane was obtained from Mallinckrodt, Inc. (St Louis, MO), trichloromethane from Sargent-Welch Scientific Co. (Skokie, IL), trichloroethylene from Aldrich Chemical Co., Inc. (Milwaukee, WI), monochlorobenzene from J. T. Baker Chemical Co. (Phillipsburg, NJ), and 1,1,2,2-tetrachloroethane from Fisher Scientific Co. (Fair Lawn, NJ). Aqueous standard solutions having concentrations of 5, 10, 20, 40, 60, 80, and 100 ppm v/v were prepared in standard flasks by measuring the appropriate volume of the compound with a μl syringe (Model 701,

Hamilton Co.) and diluting it to volume with demineralized water.

Procedure

Before use, the multichannel FIRE detection system was allowed to warm up for approximately 1 hr. During this initial stabilization period, the switching valves were set so that the helium purge gas was directed through the dry reference purge tube (Fig. 1) and into the flame. When the instrument had stabilized, the phase angle of the LIA was set in the unsubtracted mode of operation^{6,7} by using the background signal from the HCl detector. Once the phase angle was set, the LIA was returned to the subtracted mode of operation. The bias voltage of the H_2O detector was then adjusted until the reading of the LIA fluctuated around 0.0 mV. After this adjustment, the HCl analytical channel was disconnected from the LIA, and the CO_2 analytical channel was connected. In a similar manner, the bias voltage of the CO_2 detector was adjusted until the output of the LIA fluctuated around 0.0 mV. Sample determinations in either analytical channel could then be made by connection of the appropriate detector output to the LIA, or by employing two LIAs and two chart recorders.

After the initial establishment of the operating conditions of the LIA, the helium purge gas was redirected through the sample purge tube and after about 30 sec a 1.0-ml aliquot of the sample containing a chlorinated POC was injected through the septum located at the top of the purge tube. The volatile components in the aqueous sample were purged from solution and carried into the flame for combustion and vibrational excitation of the CO_2 and HCl. After the peak profiles had been acquired, the helium purge gas was redirected to the reference purge tube. The sample purge tube was then disconnected from the purge device and rinsed with demineralized water to remove the spent aqueous sample. Calibration graphs of peak height *vs* concentration for each individual compound were prepared by repeating the procedure with the other chlorinated POC standards.

All data reported in the CO_2 analytical channel were corrected for spectral crosstalk between the channels by subtracting 1.35% of the peak-height signal recorded in the HCl channel from the peak-height signal in the CO_2 channel. No corrections were required for data obtained in the HCl channel.

RESULTS AND DISCUSSION

Optical design

Although a dispersive optical system is expected to provide superior wavelength isolation compared with a filter instrument, the luminosity¹⁶ of the dispersive system is expected to be much less. If luminosity is sufficiently reduced, no signal will be detected. As a result, the light throughput of the optical system was an important consideration in the design of the polychromator used in this study. An initial attempt to design an $f/2$ polychromator was not successful because a large off-axis incident angle (approximately 50°) was required to fill the grating with light. Because of coma and astigmatism,¹⁶ this large mirror angle severely distorted the entrance-slit images that were formed at the exit focal plane of the polychromator. As a result, the direct-reading, multichannel, infrared spectrometer ultimately employed in this study was based on a Czerny–Turner optical configuration with a 0.15-m focal length and an $f/3$ nominal focal ratio.

In order to maximize the light throughput of the polychromator, the collimating mirror should be completely filled with light. Since an $f/3$ lens was not available, a dual-lens system (Fig. 1), consisting of two CaF_2 lenses that formed a 1:1 image of the flame on the entrance slit of the polychromator, was employed to maximize the light throughput. Although the dual-lens arrangement overfilled the collimating mirror of the polychromator, no significant problems from stray light were observed. The light-collection efficiency of the optical system was increased by an additional factor of two by placing a back-collection mirror behind the burner at twice the focal length of the mirror so as to form a 1:1 image of the flame on itself.

Optical alignment of the system

The detector carriage (Fig. 2) was designed to allow detectors to be easily positioned in the vertical and horizontal directions of the exit focal plane. A slot, machined in the carriage, allowed the detector mounts (with the detectors glued onto them) to move freely in the horizontal direction, and yet be held firmly enough to stay in position in the exit focal plane. (Vertical adjustment could be attained by raising or lowering the entire carriage.) Thus, different wavelength regions within the exit focal plane of the polychromator could be monitored by the appropriate positioning of detectors. In ad-

dition to providing a convenient means of detector positioning, the plastic detector carriage also prevented contact of the detector leads with the aluminum polychromator housing.

From previous work,^{2,7} the combustion of chlorinated organic compounds in a hydrogen/air flame was known to produce infrared emission bands from HCl as well as from CO_2 and H_2O . The spectra shown in Fig. 3 were obtained with a Fourier transform infrared spectrometer (appropriately reconfigured for emission²) and illustrate the regions where the infrared emission from CO_2 , H_2O and HCl occurs. As shown in Fig. 3B, the CO_2 emission band is centered at $4.42 \mu\text{m}$, while the R- and P-branches of the HCl emission band (Fig. 3C) occur in the $3.17\text{--}4.55 \mu\text{m}$ wavelength region. Although the R-branch of the HCl emission is completely free from spectral overlap with the CO_2 emission band, a small amount of spectral overlap does occur between the P-branch of the HCl emission and the emission from CO_2 . The corresponding flame background spectrum due

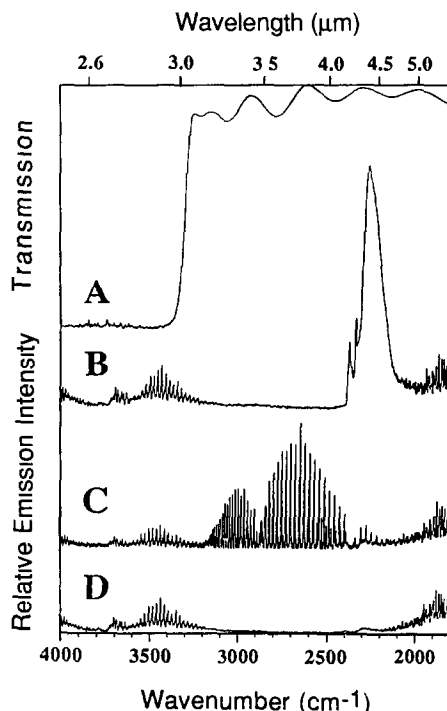


Fig. 3 Fourier-transform infrared emission spectra (A) Transmission spectrum of the long-pass filter used in the multichannel FIRE detector (maximum T, 75%, cut-on wavelength of $3.0 \mu\text{m}$ at 5% T, <0.10% T elsewhere), (B) FIRE spectrum from a hydrogen/entrained-air flame containing CO_2 , (C) FIRE spectrum from a hydrogen/entrained-air flame containing HCl, (D) background emission from a hydrogen/entrained-air flame in the absence of CO_2 and HCl.

to water emission bands is shown for comparison in Fig. 3D. Figure 3A shows the spectrum of the 3.0- μm long-pass filter used for order sorting and attenuation of the water reference band for subtraction, as discussed in the following section

The width of the spectral observation window selected for this study, although adjustable, was determined by the need to monitor simultaneously the emission bands from H_2O and CO_2 , centered at 2.9 μm and 4.42 μm , respectively. Since the more intense portion of the P-branch of the HCl stretching vibration (centered at 3.77 μm) was approximately at the center of the spectral region of interest, the alignment of the polychromator was performed for this wavelength by positioning the HCl detector in the middle of the detector carriage. The wavelength axis of the polychromator was set by replacing the 3.0- μm long-pass filter with a 3.7- μm band-pass filter⁹ (full width at half-maximum transmission, FWHM, of 0.11 μm) and rotating the grating until the maximum signal due to background water emission was detected in the HCl analytical channel

The optimum locations of the CO_2 and H_2O detectors in the exit focal plane were determined in a manner similar to that used to optimize the HCl analytical channel. To set the position of the CO_2 detector, a 4.4- μm band-pass filter⁸ (FWHM 0.15 μm) that isolated the CO_2 emission band was placed in front of the entrance slit of the polychromator. The CO_2 detector was then moved horizontally along the detector carriage until the maximum signal due to background water emission was found.

Finally, a 3.0- μm band-pass filter⁶ (FWHM 0.12 μm) was placed in front of the entrance slit, and the H_2O detector was moved horizontally along the detector carriage until the signal from the water background emission was maximized. After this horizontal alignment with the 3.0- μm filter, the H_2O detector was moved approximately 1 mm toward the short-wavelength side of the detector carriage. This slight adjustment reduced spectral overlap from the R-branch of the HCl stretching vibration and placed the detector in a region of the spectrum that was attenuated by the 3.0- μm long-pass filter. Partial attenuation of the water emission intensity was found to be beneficial because it reduced the magnitude of the water background signal to a level more closely matching that experienced by the HCl and CO_2 detectors

All detectors were maintained at the same vertical height in the detector carriage. This ensured that each detector sampled the same vertical portion of the flame.

Detector dimensions

Once the detector is properly positioned in the focal plane of the polychromator, increasing the width of the detector causes a larger spectral band-pass to be monitored. An increase in spectral band-pass may cause an increase in detector noise (due to increased detector area¹⁹), an increase in background noise (due to flame water emission), and, for analytical signals which are broader than the band-pass of the instrument, an increase in signal from the analyte

In the case of FIRE, the increase in detector noise will not be significant because detector noise is much less than flame background noise^{6,7}. Thus, as long as the signal from the analyte increases faster than the flame background noise, an increase in spectral band-pass will result in an improvement in signal-to-noise ratio (SNR). This situation will be encountered in cases where the detector monitors a region of the spectrum in which the analytical signal is relatively diffuse and the flame water bands are relatively weak

In the case of HCl emission, the rotational fine structure spreads the analytical signal out over a large wavelength region, which is mostly free from intense flame water background emission. Thus, increasing the width of the detector is expected to improve the SNR in the HCl channel, as long as the system remains flame-background limited. For spectral bands such as that of CO_2 , however, the analytical signal is relatively dense, and the water background emission is more intense (Fig. 3). Thus, increasing the spectral band-pass (detector area) does not substantially increase the percentage of the CO_2 emission band sampled, compared with the increase in background, and the SNR is not improved.¹⁹ For these reasons, the HCl detector was able to utilize an area which was four times larger (2 \times 2 mm) than that employed by the detector in the CO_2 channel (1 \times 1 mm)

Reciprocal linear dispersion

The theoretical reciprocal linear dispersion of the multichannel FIRE polychromator may be calculated¹⁶ from equation (1)

$$R_d = \frac{d \cos \theta}{fm} \quad (1)$$

where R_d is the reciprocal linear dispersion, θ is the angle of diffraction, f is the focal length of the system, m is the order, and d is the grating constant. From equation (1), the reciprocal linear dispersion for the FIRE polychromator was found to be $0.16 \mu\text{m}/\text{mm}$ in the first order for a 15° angle of diffraction. From this value of R_d and the width of the detectors, the spectral band-pass of each detector could be calculated. The $2 \times 2\text{-mm}$ detector in the HCl channel sampled a wavelength region of $0.32 \mu\text{m}$, centered at $3.7 \mu\text{m}$. The $1 \times 1\text{-mm}$ detectors in the H_2O reference channel and the CO_2 analytical channel each sampled a bandwidth of $0.16 \mu\text{m}$, centered at 2.8 and $4.4 \mu\text{m}$, respectively.

For comparison purposes, the value of R_d for the polychromator was determined experimentally by measuring the distance between the centers of the HCl and CO_2 detectors. From the measured distance and the known wavelength interval between the HCl and CO_2 detectors, an R_d of $0.15 \mu\text{m}/\text{mm}$ was obtained—in good agreement (6%) with the theoretically expected value ($0.16 \mu\text{m}/\text{mm}$). From the experimental R_d , the center wavelength sampled by the H_2O detector was calculated from the measured distance (center-to-center) between the HCl detector and the H_2O detector and found to be $2.8 \mu\text{m}$.

Spectral overlap in the polychromator system

Spectral overlap by a portion of the HCl emission band (Fig. 3) results in a spectral interference that increases the signal level in the CO_2 analytical channel whenever a chlorinated organic compound is combusted. In order to determine the extent to which this spectral overlap affects the performance of the instrument, the signal intensities due to the combustion of Cl_2 gas in the flame were recorded in both the HCl and CO_2 channels under identical conditions. The Cl_2 gas was produced by oxidation of a 10 mM sodium chloride solution with permanganate/sulfuric acid mixture as described earlier.⁹ From this experiment, it was found that the ratio of the peak-height signal in the CO_2 channel (due to HCl) to the peak-height signal in the HCl channel was 1.74 , and that the signal recorded in the HCl channel would contribute 1.35% of its total intensity to the signal in the CO_2 channel. To compensate for this spectral overlap (channel crosstalk), all measured peak-height signals for the CO_2 channel were corrected by subtracting 1.35% of the peak-height signal recorded in the HCl channel

The effect of spectral overlap by a portion of the CO_2 emission band on the signal observed in the HCl channel was also investigated. This was accomplished by injecting 0.1-ml aliquots of CO_2 gas into the sample purge tube (Fig. 1) and recording the peak-height signals in both analytical channels. (This amount of CO_2 is equivalent to that obtained by purging 1 ml of an aqueous sample containing 64.3 mg/l of pentane.) Since no signal was observed in the HCl channel upon injection of the CO_2 gas sample, it was assumed that any signal that might have been present had a peak height between zero and one-half of the background peak-to-peak noise ($N_{\text{p-p}}$) in the HCl channel. Using one-half $N_{\text{p-p}}$ in the HCl channel as an estimate of the worst possible situation, the *minimum* ratio of the intensity in the HCl channel to that in the CO_2 channel was calculated to be 1.3192 . This result indicates that for the sample concentrations used in this study, the wavelength region monitored by the HCl detector is relatively free from interfering effects due to CO_2 emission. Therefore, no correction for CO_2 -producing species was applied to the signal measured in the HCl channel.

Background subtraction

Under flame-noise limited conditions, background subtraction has proven to be an effective means of increasing the signal-to-noise ratio (SNR) obtained with the FIRE detector.^{6,7} For background subtraction to be successful, however, certain prerequisites must be satisfied. (1) Background fluctuations in the analytical channel must be sampled independently of the analytical signal. (2) Background fluctuations must be additive with respect to the analytical signal. (3) Background fluctuations in the reference and analytical channels must be temporally correlated. Background subtraction will not compensate for detector noise, because detector noise (excluding such common-mode noise as power supply ripple) in each channel is independent (*ie*, not temporally correlated). In fact, whenever a detector-noise limited situation is encountered, subtraction of the signal in the reference channel from that in the analytical channel can actually increase the noise and degrade the SNR through a combination of the two independent noise sources¹⁶ according to

$$N_t = \sqrt{N_a^2 + N_r^2} \quad (2)$$

where N_a is the detector noise in the analytical channel, N_r is the detector noise in the reference

channel, and N_t is the total detector noise resulting from background subtraction

In previous work employing background subtraction as a means of noise reduction,^{6,7} a dual-channel system was formed by using a beam splitter to divide the radiation from the flame into two spatially separated beams. Although the beam-splitter approach is convenient when filters are used as the means of wavelength isolation, a beam splitter also reduces the intensity of available radiation in the analytical channel. In the polychromator system, no beam splitter is needed, and the three optical channels are separated spatially by means of the diffraction grating. As a result, more of the radiation from the source can be made available for detection.

With the polychromator system, two detector signals were fed into the LIA, which was capable of subtracting the signal in the reference channel (*i.e.*, the flame background) from the signal in the analytical channel (*i.e.*, the analytical signal plus the flame background). As in previous work,^{6,7} the background signal in the HCl channel was used in the unsubtracted mode of operation to set the phase angle automatically

After phase-angle adjustment, the amplifier was returned to the subtracted mode, and the output from the LIA was then adjusted to zero by equalizing the background signal levels in each channel. In the dual-channel, filter, FIRE detector, equalization was accomplished opti-

cally by means of an iris diaphragm.^{6,7} With the polychromator system, this approach cannot be used, and equalization was accomplished by adjusting the bias voltage of the reference detector (approximately 27 V) until the background level from the reference detector matched that from the HCl detector. The bias voltage for the HCl detector was set at 66 V, which was the highest obtainable with the 122 V power supply. (In the preamplifier circuit, the load resistor was in series with the detector, so the circuit behaved as a voltage divider.) In a similar manner, the bias voltage to the CO₂ detector was subsequently adjusted to approximately 32 V with the potentiometer to match the background level in the CO₂ analytical channel with that in the H₂O reference channel. (The magnitude of this voltage adjustment could be experimentally determined. When the background levels were properly equalized, blocking the entrance slit of the polychromator did not change the subtracted output of the LIA.)

To demonstrate the correlation of the noise fluctuations in the three channels (H₂O, HCl, CO₂), background noise profiles as a function of time were obtained simultaneously in the unsubtracted mode of operation (Fig 4A) by using three lock-in amplifiers and three recorders. Figure 4A shows that the noise in the single-channel FIRE mode of operation is comparable for all three channels, even though the HCl detector area is four times that of the other two detectors—behavior characterizing a

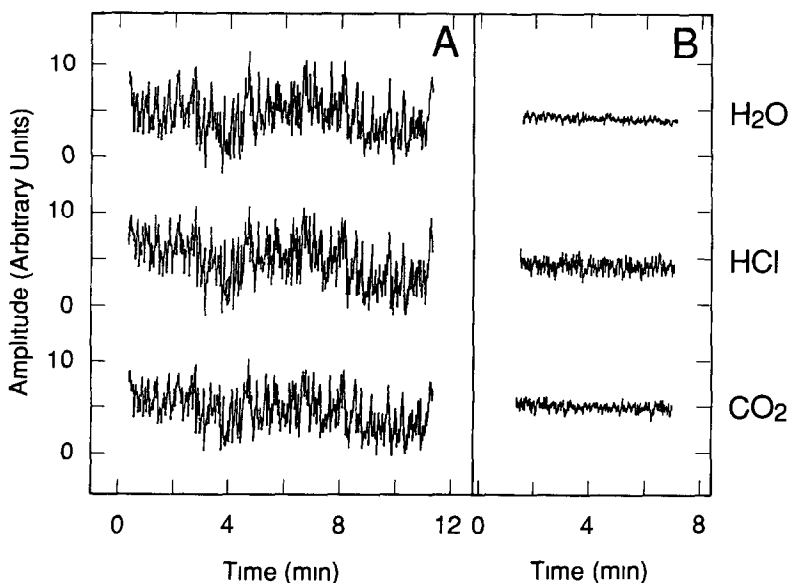


Fig 4 Comparison of (A) flame background and (B) detector noise fluctuations for the three FIRE polychromator channels

flame-noise limited situation.¹⁹ Figure 4A also shows that the fluctuations in the two analytical channels (HCl and CO₂) are temporally correlated with the background fluctuations in the H₂O reference channel. Thus, real-time subtraction of the flame background in the reference channel from the background in the analytical channels should result in a lower noise level.

Deviations from perfect noise correlation in Fig 4A are most probably due to uncorrelated detector noise. Detector noise profiles (Fig. 4B) were obtained by blocking the entrance slit of the polychromator and recording the associated noise under the conditions used to obtain the background noise profiles (Fig. 4A). In a detector-noise limited situation, the root-mean-square (rms) noise is often proportional to the square root of the detector area,¹⁹ and, as expected, the noise in the HCl channel (Fig. 4B) is approximately twice that observed in either the H₂O or CO₂ channel.

The effect of the background subtraction procedure was studied by recording the peak-to-peak noise (N_{pp}) in the subtracted signal as a function of the magnitude of the subtracted output. Figure 5 shows a plot of the rms noise (taken as 1/5 of the measured N_{pp}) as a function

of different levels of background compensation from undercompensated ($A - B > 0$) to overcompensated ($A - B < 0$). In Fig. 5A, background water emission in the reference channel is being subtracted from the background water emission present in the HCl analytical channel. In Fig. 5B, background water emission in the reference channel is being subtracted from the background water emission present in the CO₂ analytical channel. It is readily apparent from Fig. 5 that the minimum rms noise in both analytical channels occurs when the magnitude of the subtracted output from the lock-in amplifier is zero. This indicates that the flame-background noise in all channels is correlated in magnitude as well as in time.

Subtraction of the H₂O background reduced the noise by factors of 3.2 and 3.5 for the HCl and CO₂ analytical channels, respectively. From equation (2) and the noise profiles in Fig 4, it can be readily determined that the residual noise in the subtracted output can be almost entirely accounted for by summing the detector noise in the reference and analytical channels [equation (2)]. This indicates that the majority of the flame noise has been removed by the subtraction process, and that the dual-channel FIRE system is nearly detector-noise limited.

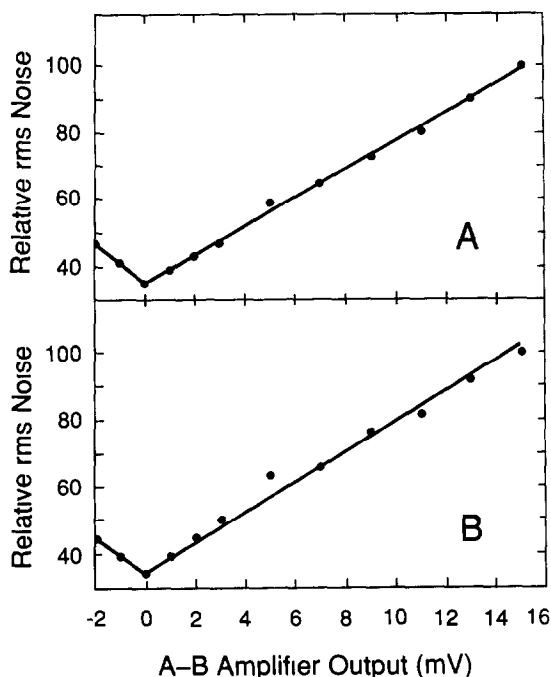


Fig 5 Relative rms noise in the HCl (A) and CO₂ (B) analytical channels, plotted as a function of amplifier output resulting from subtraction of different levels of background compensation

Selection of analytical conditions

In single-component determinations, the instrumental operating conditions are optimized for the particular component of interest. However, in simultaneous multicomponent determinations a compromise must be reached for all components, since the operating conditions cannot be optimized for each component individually.²⁰ Since the HCl emission intensity that occurs from the combustion of a chlorinated organic compound is lower than the corresponding CO₂ emission intensity,² the multi-channel FIRE detection system was optimized to produce the highest possible SNR in the HCl analytical channel.

For these studies, a 50 ppm v/v aqueous standard solution of trichloromethane was used to determine the effect of helium purge gas flow-rate and flame fuel-to-oxidant ratio on the SNR in the HCl analytical channel. As observed in previous studies,^{7,9} the hydrogen/entrained-air flame produced SNRs for chlorine that were approximately 8.5 times greater than those obtained under fuel-lean flame conditions.

Analytical performance of the multichannel FIRE detector

The performance of the multichannel, dispersive FIRE spectrometer was evaluated by injecting aqueous solutions of five chlorinated POCs into the sample purge device according to the procedure outlined in the experimental section. Dichloromethane, trichloromethane (trihalomethane or THM), trichloroethylene, monochlorobenzene and 1,1,2,2-tetrachloroethane were selected for study because of their potential importance in environmental monitoring.

Figure 6 shows typical peak profiles obtained in the HCl and CO₂ analytical channels (CO₂ shown at one-eighth actual height) by purging the five volatile compounds (40 ppm v/v) into the hydrogen/entrained-air flame. The differences in the trailing edges of the peak profiles obtained for each compound are undoubtedly due to differences in the purging efficiencies for the individual compounds. The purging efficiency determines the rate at which a compound is released from solution and is a function of a number of factors such as volatility, boiling point and solubility of the compound in water.²¹⁻²³

Small negative signals were observed in the leading edge of the peaks obtained in the HCl channel. These negative pen deflections, which may result in part from the difference in size of the HCl and H₂O detectors, have been observed in previous work⁹ and do not affect the analytical results.

The total time required for signal acquisition from a chlorinated POC standard was approximately 3 min (from sample injection to purge-tube disconnection and clean-up). Maintaining

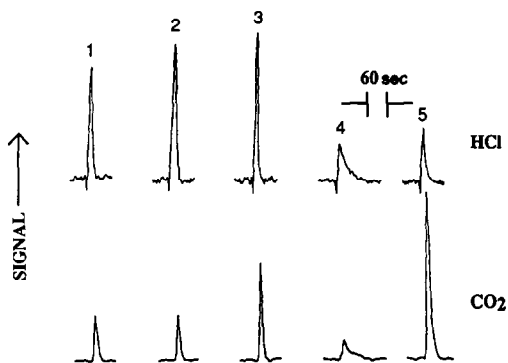


Fig. 6. Peak profiles obtained with the multichannel FIRE detector. Signals obtained from 1.0-ml injections of 40 ppm v/v aqueous standards: (1) Dichloromethane, (2) trichloromethane, (3) trichloroethylene; (4) 1,1,2,2-tetrachloroethane, (5) monochlorobenzene. Peaks shown for CO₂ channel are 1/8 of actual height.

a flow of dry helium through the reference purge device (Fig. 1) to the flame between sample determinations was found to be beneficial in reducing baseline drift and removing residual moisture on the inside walls of the sample introduction capillary.

Reproducibility The precision of the signals obtained by the FIRE technique was studied by recording the peak-height signals from eight injections of 20 ppm v/v standard solutions of the five chlorinated POCs. Peak heights were measured from the baseline and negative pen deflections observed for the HCl channel were ignored. The results are shown in Table 1.

For the five compounds studied, the average relative standard deviation (RSD) of the peak-height measurements was 3.8% and 3.4% for the HCl and CO₂ analytical channels, respectively. The poorest reproducibilities were obtained for 1,1,2,2-tetrachloroethane and chlorobenzene—compounds with relatively high boiling points (146 and 132°, respectively). Since broad peak profiles were observed in both the HCl and CO₂ channels for 1,1,2,2-tetrachloroethane (Fig. 6), poorer purging efficiency most probably accounts for the poorer reproducibility of the peak-height measurements. In the case of chlorobenzene, however, the peak profile obtained in the CO₂ channel indicates relatively good purging efficiency. In this case, poorer reproducibility for peak-height measurements in the HCl channel may simply reflect the relatively small amount of chlorine present in the standard solution.

Calibration graphs Calibration plots for each compound were prepared by purging 1-ml injections of 5–100 ppm v/v standard solutions according to the experimental procedure. The correlation coefficients (Table 1), based on only concentrations within the linear dynamic range of the system, indicate that the overall linearity of the individual curves is reasonably good.

The slopes of the individual calibration lines for the HCl and CO₂ channels are reported in Table 1 as mm/μmole Cl and C, respectively. If the combustion and purging efficiencies for each compound were the same, the slopes obtained within each channel for the five different compounds would be equal. It is clear from Table 1 that this is not the case. The smallest slopes are observed for 1,1,2,2-tetrachloroethane in both the HCl and CO₂ channels, again suggesting poor purging and possibly poor combustion efficiency for this compound. The lack of agreement in the slopes means that the FIRE system,

Table 1 Summary of analytical data

Sample	HCl channel				CO ₂ channel #			
	Slope* (y-intercept)†	r ‡	Detection limit§	RSD, ¶ %	Slope* (y-intercept)	r ‡	Detection limit§	RSD, ¶ %
Dichloromethane	38.4 (-0.051)	0.9985	1.5	2.2	214 (3.83)	0.9993	0.073	3.6
Trichloromethane	45.7 (-0.227)	0.9993	1.2	2.5	298 (0.796)	0.9994	0.063	3.3
Trichloroethylene	49.6 (0.632)	0.9999	1.0	2.3	371 (0.794)**	0.9999**	0.052	2.9
1,1,2,2-Tetrachloroethane	10.4 (0.488)	0.9996	4.8	6.8	68.4 (-0.451)	0.9998	0.28	4.8
Monochlorobenzene	68.2 (-0.054)**	0.9999**	0.76	5.1	262 (6.80)**	0.9996**	0.072	2.1

*mm/μmole Cl (HCl channel), mm/μmole C (CO₂ channel)

†mm

‡Correlation coefficient

§mg/l Cl at 2 rms noise (HCl channel), mg/l C at 2 rms noise (CO₂ channel)

¶RSD of peak heights for 8 repetitive injections of 20 ppm v/v standard

All data corrected for contribution from HCl emission

**60, 80, and 100 ppm v/v standards not included in regression analysis

as currently configured, cannot be used for the determination of total organic halide (TOX) in unknown aqueous multicomponent mixtures of chlorinated hydrocarbons without prior separation of the mixture

Detection limits The detection limits for the five compounds, defined as twice the rms noise, are given in Table 1 for both the HCl and CO₂ channels. Although the detection limits in the HCl channel with the present system are all in the low ppm range, they are too high by a factor of about 100 to be useful for screening drinking water samples. The sample size used in this study (1 ml), however, is less than that generally employed in such analyses (5–10 ml volumes are more typical²⁴) Lower detection limits could be obtained by purging a larger volume of sample, by increasing the efficiency of the purging process by heating the sample, and by employing existing purge-and-trap technology.²⁴

Two-component mixture analysis. Although it is not possible to analyze a mixture of several unknown components directly with the information available in a single channel, because the calibration curves are different for different compounds, analysis of a mixture of two known components should be possible by use of information available from two analytical channels. To demonstrate the feasibility of using the system in the determination of individual component concentrations in a two-component mixture, three dichloromethane/trichloromethane mixtures in water were prepared and analyzed. The concentrations of dichloromethane and trichloromethane in the aqueous samples were 10/10, 20/10, and 10/20 ppm v/v, respectively. The peak-height emission signals from each mixture were recorded simultaneously in both the HCl and CO₂ analytical channels, according to the procedure outlined in the experimental section. The slopes of previously prepared calibrations graphs for dichloromethane and trichloromethane in the HCl and CO₂ channels were used to perform the necessary calculations.

Since the total emission intensity recorded for each channel should be equal to the sum of the individual emission intensities due to dichloromethane and trichloromethane, their individual concentrations in the mixture may be found by solving the following matrix equation

$$\begin{bmatrix} I_T^{\text{HCl}} \\ I_T^{\text{CO}_2} \end{bmatrix} = \begin{bmatrix} m_{\text{dichloro}}^{\text{HCl}} & m_{\text{trichloro}}^{\text{HCl}} \\ m_{\text{dichloro}}^{\text{CO}_2} & m_{\text{trichloro}}^{\text{CO}_2} \end{bmatrix} \begin{bmatrix} C_{\text{dichloro}} \\ C_{\text{trichloro}} \end{bmatrix} \quad (3)$$

where I_T represents the total intensity in the given channel, m is the slope of the calibration

curve for the given component in a given channel, and C is the concentration of the given component. Solving equation (3) for the individual concentrations of the two components gives

$$\begin{bmatrix} C_{\text{dichloro}} \\ C_{\text{trichloro}} \end{bmatrix} = \begin{bmatrix} m_{\text{dichloro}}^{\text{HCl}} & m_{\text{trichloro}}^{\text{HCl}} \\ m_{\text{dichloro}}^{\text{CO}_2} & m_{\text{trichloro}}^{\text{CO}_2} \end{bmatrix}^{-1} \begin{bmatrix} I_{\text{T}}^{\text{HCl}} \\ I_{\text{T}}^{\text{CO}_2} \end{bmatrix} \quad (4)$$

Table 2 compares the actual and experimentally determined concentrations of dichloromethane and trichloromethane in the three synthetic two-component mixtures. The results obtained with the FIRE detector were based on the average peak-height signals for four replicate injections of 1-ml aliquots of the synthetic mixture. As shown in the table, the average relative error between the results obtained with the FIRE detector and the nominal concentrations in the synthetic mixture was of the order of 12%—a reasonable value from a trace analytical standpoint.

CONCLUSIONS

The feasibility of fabricating a multichannel, dispersive spectrometer with sufficiently high optical throughput for use in flame infrared emission spectrometry was demonstrated. Because of spectral overlap of the HCl emission band with the CO₂ emission band, signals in the HCl channel were found to contribute 1.35% of their intensity to those in the CO₂ channel. The wavelength region isolated by the HCl detector was found to be free from measurable interfering effects from CO₂ emission. Therefore, this instrument could be useful for the determination of chlorinated POCs in aqueous samples, even in the presence of significant amounts of volatile, non-chlorinated, CO₂-producing contaminants.

The feasibility of using the specially designed polychromator to determine chlorinated POCs in aqueous samples by flame infrared emission spectrometry was demonstrated with dichloromethane, trichloromethane, trichloroethylene, 1,1,2,2-tetrachloroethane and chlorobenzene as test compounds. With a 1-ml aqueous sample,

detection limits for Cl were found to be in the 0.76–4.8 mg/l range. Analytical plots of peak height *vs.* concentration were linear up to 100 ppm v/v for dichloromethane, trichloromethane, trichloroethylene, and 1,1,2,2-tetrachloroethane, and 40 ppm v/v for chlorobenzene.

The signal obtained in the CO₂ analytical channel gives the FIRE detector an alternative way of determining halogenated POCs as well as the potential for determining non-halogenated POCs. With the CO₂ analytical channel and a 1-ml aqueous sample size, detection limits for C in the five compounds were found to be in the 52–280 µg/l. range. Plots of peak height *vs.* concentration were linear up to 100 ppm v/v for dichloromethane, trichloromethane and 1,1,2,2-tetrachloroethane, and about 40 ppm v/v for trichloroethylene and chlorobenzene.

It was shown that a two-component mixture of dichloromethane and trichloromethane at trace levels could be analysed quantitatively with precisions that were reasonable for trace analysis levels (about 12%). Because the slopes of the calibration graphs for the two compounds were not identical, the determination required data from both the HCl and CO₂ analytical channels. Extension of the method to mixtures containing a larger number of components is theoretically feasible, if additional analytical channels can be employed (the HF channel,⁷ for example).

Although the detection limits obtained with the present FIRE system in the chlorine mode for the chlorinated hydrocarbons in aqueous samples are too high by a factor of 10–100 for routine environmental screening applications,^{12–14} the sample size used in this feasibility study was quite small. Lower detection limits should be easily achievable through a number of improvements, however, such as purging a larger sample volume, heating the purge device to increase purge efficiency, and/or using conventional purge-and-trap technology to preconcentrate the sample prior to discharge into the flame.²⁴ Even at its present stage of development, the FIRE polychromator may still

Table 2 Analysis of a two-component mixture containing dichloromethane and trichloromethane

Sample	CH ₂ Cl ₂			CHCl ₃		
	Expected, ppm v/v	Found, ppm v/v	Relative error, %	Expected, ppm v/v	Found, ppm v/v	Relative error, %
1	10	9.6	-4	10	11	+10
2	20	22	+10	10	10	0
3	10	14	+40	20	19	-5

be useful for certain process applications, where a limited number of identifiable compounds are present at concentrations appropriate for the FIRE detection limits.

Acknowledgements—This work was supported by Baylor University Research Grant 0100-032-1510 Infrared Emission Research. The authors would like to express their appreciation to Milton Luedke of the Baylor Chemistry/Physics Machine Shop for fabricating specialized parts for the instrument. This work was taken from the Ph D dissertation of S Wayne Kubala.

REFERENCES

- 1 K W Busch, M A Busch, D C Tilotta, S W Kubala, C K Y Lam and R Srinivasan, *Spectroscopy*, 1989, **4**, No 8, 22
- 2 D C Tilotta, K W Busch and M A Busch, *Appl Spectrosc*, 1989, **43**, 704
- 3 D C Tilotta, M A Busch and K W Busch, *ibid*, 1991, **45**, 178
- 4 M K Hudson and K W Busch, *Anal Chem*, 1987, **59**, 2603
- 5 *Idem*, *ibid*, 1988, **60**, 2110
- 6 S Ravishankar, D C Tilotta, S W Kubala, M A Busch and K W Busch, *ibid*, 1990, **62**, 1604
- 7 S Ravishankar, D C Tilotta, K W Busch and M A Busch, *Appl Spectrosc*, 1990, **44**, 1247
- 8 S W Kubala, D C Tilotta, M A Busch and K W Busch, *Anal Chem*, 1989, **61**, 1841
- 9 *Idem*, *ibid*, 1989, **61**, 2785
- 10 C K Y Lam, D C Tilotta, K W Busch and M A Busch, *Appl Spectrosc*, 1990, **44**, 318
- 11 M A Busch, *Encyclopedia of Physical Science and Technology*, Vol 6, p 409 Academic Press, New York, 1987
- 12 S J Randtke, *J Am Water Works Assoc*, 1988, **80**, No 5, 40
- 13 B W Lykins, Jr, R M Clark and J Q Adams, *ibid*, 1988, **80**, No 5, 85
- 14 Safe Drinking Water Act (U S Public Law 93-523), 16 December 1974, amended (U S Public Law 99-339), 19 June 1986
- 15 S W Kubala, *Ph D Dissertation*, Baylor University, Waco TX, 1990
- 16 K W Busch and M A Busch, *Multielement Detection Systems for Spectrochemical Analysis*, Wiley, New York, 1990
- 17 P R Griffiths and J A de Haseth, *Fourier Transform Infrared Spectrometry*, Wiley, New York, 1986
- 18 M Harwit and N J A Sloane, *Hadamard Transform Optics*, Academic Press, New York, 1979
- 19 R H Kingston, *Detection of Optical and Infrared Radiation*, Springer-Verlag, Berlin, 1978
- 20 D F Brost, B B Malloy and K W Busch, *Anal Chem*, 1977, **49**, 2280
- 21 J W Graydon, K Grob, F Zuercher and W Giger, *J Chromatog*, 1984, **285**, 307
- 22 J Urban, *Adv Instrum*, 1987, **42**, 539
- 23 P K Kuo, E S K Chian, F B DeWalle and J H Kim, *Anal Chem*, 1977, **49**, 1023
- 24, A E Greenberg, J J Connors and D Jenkins, *Standard Methods for the Examination of Water and Wastewater*, 15th Ed, p 538 American Public Health Association, Washington, DC, 1981

AN ELECTROLYTIC DEVICE FOR PREPARATION OF HYDROGEN AND OXYGEN FROM WATER FOR ISOTOPIC ANALYSIS

MOHAMMAD S. IQBAL*, FAROOQ RASHID and NAIMAT A JAVED

Nuclear Chemistry Division, Pakistan Institute of Nuclear Science and Technology, P O Nilore,
Islamabad, Pakistan

(Received 14 April 1990 Revised 15 August 1990 Accepted 21 September 1990)

Summary—An electrolytic device for decomposition of water has been developed which readily gives hydrogen and oxygen for isotopic measurement with a mass spectrometer. A 20- μ l sample can be decomposed quantitatively in 10 min with good reproducibility. The results produced are comparable with those obtained by reduction with uranium.

Production of hydrogen from water is vital in the mass spectrometric analysis of water for isotopic ratio determinations. The methods available in the literature¹ are: (a) reduction with heated metals such as uranium and zinc, (b) reduction on heated filaments, (c) reduction by compounds such as calcium hydride and lithium aluminium hydride, (d) equilibration of water with hydrogen of known composition and (e) electrolysis. The first method is usually used for routine work. The other methods are less frequently used owing to their lower efficiency or greater fractionation problems. All these methods except electrolysis involve the interaction of water with some other reagent, which may be a source of fractionation or memory effects to a variable degree. Electrolysis appears to be a neat method; the fractionation problems associated with it may be overcome if the sample is completely electrolysed. In the electrolysis of water, the electrolytic fractionation factor with respect to the ¹⁶O/¹⁸O isotopes is only about 1.01–1.03. Thus, electrolysing only 90% of the water introduces a maximum error of only 0.6% in oxygen isotope analysis. However, the fractionation factor with respect to the ¹H/²H isotopes has been reported to range from 3 to 10.¹ It can be shown that even with a fractionation factor of only 3, electrolysing 99.72% of a sample of natural water will result in a deuterium concentration in the gas that is 14% too low and even electrolysing all but 0.0085% of the

water will result in a 4% negative error in the deuterium determination.¹

Wright² developed a method in which water was fed continuously into a V-shaped electrolytic cell operated under constant volume, temperature and current conditions. At equilibrium, which was reached within seven days, the number of moles of deuterium put into the cell as feed water was equal to the number of moles of deuterium leaving the cell as electrolysed gas and water vapour. The average deviation from the mean was 0.0002 mole%. If we could avoid the long equilibration time and electrolyse water quantitatively the electrolytic method would be advantageous in that it provides oxygen for ¹⁸O and ¹⁷O analysis in the same sample without any additional work. In the present work we report an electrolytic device by which small amounts of water can be quantitatively electrolysed in about ten minutes, making this method rapid, efficient and hence acceptable for routine work.

EXPERIMENTAL

Construction of the electrolytic device

The device is shown in Figs. 1 and 2. The upper part is made of Perspex and consists of an injection port and one nozzle for connection to a vacuum line through a valve by the use of Swagelok fittings (with Teflon ferrules). The injection port is provided with a rubber septum capped with a screw-on nut. The lower part (called the cell) consists of two stainless-steel (SS 316L) blocks (28 × 15 × 15 mm) held together by two bolts. A thin (0.2 mm) sheet of Teflon is placed between the blocks for insulation. The

*Author for correspondence. Present address: Pakistan Atomic Energy Commission, DNFM, P O Box 1114, Islamabad, Pakistan

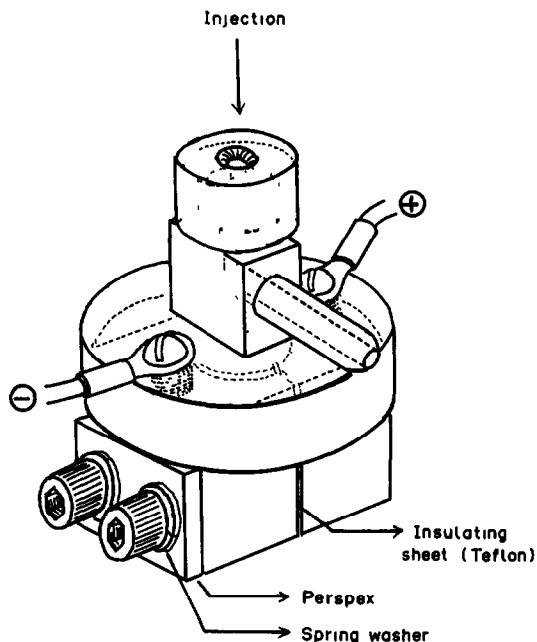


Fig 1 Perspective view of the electrolytic device

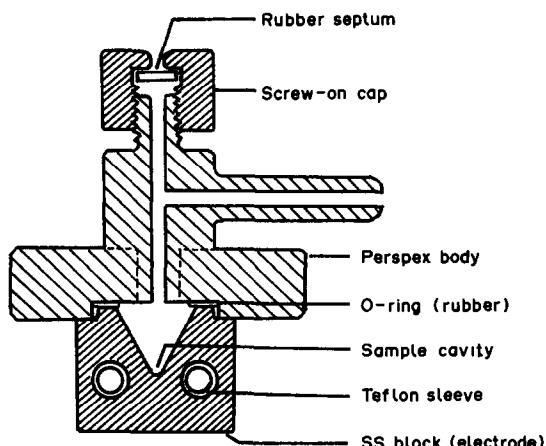


Fig 2 Cross-sectional view

bolts run through Teflon sleeves in one block (for insulation) and screw into the other. A Perspex sheet is provided between the heads of the bolts and the block for insulation. When joined together the blocks are well insulated and measure $30 \times 28 \times 15$ mm. One of the two 30×28 -mm surfaces of this piece, taken as the top, is machined to provide a 2-mm high circular platform about 20 mm in diameter. Each of the two blocks is machined at the top so that when they are joined together there is a conical cavity (about 5 mm deep and 8 mm in diameter) where the sample is placed for electrolysis. The injection port and the cell, with a rubber O-ring between them, are held together by two screws which also serve as connectors to a 6-V 10-A d.c. supply (or an ordinary car battery). Thus the two steel blocks act as the electrodes of the cell. A sample placed in the cavity is readily quantitatively electrolysed. The device is dismantled for cleaning by unscrewing the two screws joining the two parts. The dimensions are arbitrary and not critical except that the insulating Teflon sheet between the electrodes should be as thin as practicable to ensure contact of the liquid with both electrodes right up to the end, so that the maximum amount of water is electrolysed.

Sampling procedures

The device is connected to the inlet of the mass spectrometer by a Swagelok system and evacuated, after which the inlet valve is closed

and the metallic part of the device is immersed in liquid nitrogen so that the water vapour derived by evaporation of the sample into the evacuated system is condensed. When the sample is placed in the device it is put directly into the cavity, which is colder than the upper part. The water sample (around $20 \mu\text{l}$) is injected with a microsyringe through the rubber septum into the cavity. A small bead of a solid polymeric electrolyte (Nafion type, du Pont de Nemours), with a radius similar to that of the curvature at the bottom of the cone, is placed in the cavity, and no other electrolyte is required for the electrolysis. The liquid nitrogen bath is removed and as soon as defrosting at the outer surface starts, current is passed for about 10 min for electrolysis of a $15\text{--}20 \mu\text{l}$ sample. After this time the electrodes are again immersed in liquid nitrogen, with the current kept on so that any unelectrolysed water is trapped and electrolysed. Our experience indicates that 10 min is sufficient for complete electrolysis of $20 \mu\text{l}$ of water. The cell is allowed to warm to near ambient temperature and the valve to the inlet is opened to introduce the hydrogen-oxygen mixture thus obtained into the inlet for mass spectrometric measurements.

Analysis of tap water

A tap water sample ($20 \mu\text{l}$) was injected into the device and electrolysed for 10 min. The gaseous product was transferred to the "sample"

port of a Delta E (Finnigan MAT) mass spectrometer, which has a dual inlet system. The inlet is designed so that the gas enters pre-evacuated (5×10^{-5} bar) reservoirs of variable size (capacity 2–20 ml) through stainless-steel tubes (i.d. 3 mm, length 90 mm) on the “standard” and “sample” sides. Here the gas is kept for at least 1 min for equilibration, as the total volume of the system (reservoir cell and lines) is about 40 ml, the risk of overpressure and fractionation in the lines is covered. From the reservoir the gas is introduced into the mass spectrometer through capillaries by the use of pneumatically controlled valves. A working standard (20 μ l) is similarly electrolysed with the same device and transferred to the “standard” port of the mass spectrometer. Three sets of mass spectrometric measurements of the gaseous electrolysis product, each set consisting of twelve measurements for $\delta D/H$, were obtained with background measurement before and after each set. The $\delta D/H$ ratio is defined as:

$$\delta D/H = \frac{(D/H)_{\text{sample}} - (D/H)_{\text{std}}}{(D/H)_{\text{std}}} \times 1000\text{‰}$$

The mass spectrometer instrumental error thus evaluated was less than 0.2‰. The same procedure was repeated by taking ten more aliquots of the sample and the standard to determine the reproducibility of the electrolysis method. To compare the results with another method, ten aliquots of the sample and the standard were reduced over heated uranium according to the standard procedure^{3,4} and subjected to mass spectrometric analysis as before.

RESULTS AND DISCUSSION

The $\delta D/H$ values obtained for the tap water sample by the electrolytic and uranium-reduction techniques are listed in Table 1. The reproducibility of the electrolytic method is quite good (S.D. 0.135‰) and the results obtained by the two techniques are very close. In another experiment to demonstrate the “completeness” of electrolysis, the sample and the standard were taken from the same source, one being treated by electrolysis and the other by uranium-reduction. The mean $\delta D/H$ thus obtained was $-0.0258 \pm 0.005\text{‰}$ (see Table 2). The mean $\delta D/H$ value obtained by the uranium-reduction method in the experiment was $-0.0261 \pm 0.004\text{‰}$. Both values are statistically equivalent to zero and very close to each other, suggesting that the electrolysis is complete to

Table 1 Mean $\delta D/H$ values for 10 aliquots of tap water analysed by the electrolytic and uranium-reduction methods

Aliquot	Mean $\delta D/H$ (from three sets of 12 measurements each) \pm standard deviation, ‰	
	Electrolysis	Uranium-reduction
1	$-2\ 163 \pm 0\ 182$	$-2\ 256 \pm 0\ 191$
2	$-2\ 104 \pm 0\ 164$	$-2\ 531 \pm 0\ 135$
3	$-2\ 235 \pm 0\ 158$	$-2\ 467 \pm 0\ 177$
4	$-2\ 201 \pm 0\ 136$	$-2\ 438 \pm 0\ 160$
5	$-2\ 451 \pm 0\ 152$	$-2\ 300 \pm 0\ 163$
6	$-2\ 536 \pm 0\ 143$	$-2\ 315 \pm 0\ 158$
7	$-2\ 312 \pm 0\ 135$	$-2\ 281 \pm 0\ 131$
8	$-2\ 205 \pm 0\ 132$	$-2\ 320 \pm 0\ 152$
9	$-2\ 361 \pm 0\ 140$	$-2\ 256 \pm 0\ 141$
10	$-2\ 223 \pm 0\ 138$	$-2\ 111 \pm 0\ 125$
Mean \pm SD	$-2\ 279 \pm 0\ 135$	$-2\ 327 \pm 0\ 122$

Table 2 $\delta D/H$ values obtained by treating the sample by electrolysis and the standard by uranium-reduction, and by treating both by uranium-reduction

Aliquot	$\delta D/H$ (electrolysis and uranium- reduction), ‰	$\delta D/H$ (only uranium- reduction), ‰
	1	-0.032
2	-0.029	-0.032
3	-0.021	-0.025
4	-0.024	-0.023
5	-0.028	-0.030
6	-0.022	-0.031
7	-0.033	-0.027
8	-0.019	-0.021
9	-0.024	-0.025
10	-0.026	-0.027
Mean \pm SD	-0.0258 ± 0.005	-0.0261 ± 0.004

an acceptable extent. The sample preparation time for the uranium-reduction method was 20–30 min, which is about 2–3 times more than that for the electrolytic device. The new electrolytic device reported here therefore provides a rapid, efficient and precise decomposition method for water for subsequent mass spectrometric measurements.

REFERENCES

- 1 I Kirshenbaum *Physical Properties and Analysis of Heavy Water*, Chapter 4 McGraw-Hill, New York, 1951
- 2 M M Wright, *Trail Report 63, SAM Report 100XR-6097*, August 28, 1944, The Consolidated Mining & Smelting Company of Canada Ltd, Chemical and Fertilizer Department, Trail, British Columbia, Canada (taken from Ref 1)
- 3 J Bigeleisen, M L Perlman and H C Prosser, *Anal Chem*, 1952, **24**, 1356
- 4 I Friedman and R L Smith, *Geochim Cosmochim Acta*, 1958, **15**, 218

HPLC COUPLED WITH IN-LINE PHOTOLYSIS, HYDRIDE GENERATION AND FLAME ATOMIC-ABSORPTION SPECTROMETRY FOR THE SPECIATION OF TIN IN NATURAL WATERS

LES EBDON, STEVE J HILL and PHILIP JONES

Plymouth Analytical Chemistry Research Unit, Department of Environmental Sciences,
Polytechnic South West, Drake Circus, Plymouth, Devon PL4 8AA, England

(Received 28 October 1989 Revised 22 November 1990 Accepted 6 December 1990)

Summary—The use of an in-line photolysis coil in a continuous-flow system of high-performance liquid chromatography coupled with hydride generation and flame atomic-absorption spectrometry for the speciation of tin in natural waters is described. Irradiation with ultraviolet light is shown to convert tributyltin into organic tin(IV), from which a volatile hydride can be produced in the conventional way. The effect of various conditions on the analytical performance is discussed. A detection limit of 2 ng for tin was obtained, and the tin species could be completely separated within 6 min. Use of the technique for quantification of tributyltin compounds in local coastal waters is described.

Investigation of the forms in which a trace metal occurs, so-called "speciation", is now recognized as vitally important in determining the toxicity and environmental fate of the metal. This has stimulated interest in new techniques for trace metal speciation. One approach which appears to be particularly successful is chromatographic separation coupled with detection by atomic spectrometry.^{1,2} The specificity of detection allows use of less than optimum chromatographic separation from other metals, with a consequent saving in time for sample clean-up and analysis.

The demand for sensitive techniques for speciation of organotin compounds has markedly increased in recent years. The presence of butyltin³ and methyltin⁴ species at concentrations in the ng/l range in a variety of natural waters has been reported. More recently, however, particular attention has been paid to the organotin compounds used in the formulation of anti-fouling paints, *e.g.*, bis(tributyltin)oxide and tributyltin fluoride.⁵ Such paints, containing about 12% tributyltin (TBT) in the dry paint film, were introduced in the late 1960s and became widely used in the 1970s. However, following initial studies into the decline of the shellfish industry in parts of France,⁶ and more recent detailed studies on the effects on shellfish in the U.K.,^{7,8} the governments of both countries have now banned the use of organotin-based paints and waxes on boats under 25 m

in length, and also on various structures, including fish cages, in both freshwater and marine environments. Obviously, concern remains over the levels of TBT already in the environment,⁹ particularly since the new legislation excludes larger vessels, the effect of which has already been reported.¹⁰

In a previous paper,¹¹ we described a simple yet effective coupling of high-performance liquid chromatography (HPLC) with flame atomic-absorption spectrometry (FAAS), utilizing pulsed nebulization and a slotted-tube atom-trap for the speciation of tin. The detection limit for this system was 200 ng of Sn; preconcentration allowed detection of the 20 ng/l tributyltin concentration taken by the U.K. Department of the Environment (DoE) as the limit for TBT in water. In later work,¹² tributyltin ions were determined by HPLC and fluorimetric detection with morin in a micellar solution. The sample was preconcentrated on an ODS column to give a detection limit of 16 ng of Sn. Here we present a further development of the HPLC-FAAS technique utilizing hydride generation to improve the sensitivity still further and allow the determination of tributyltin at well below the DoE target of 20 ng/l (7.3 ng/l Sn) in ambient waters.

In recent years the hydride-generation method for the determination of certain metalloid elements, notably arsenic and selenium, has proved extremely popular. The hydride is

generated by chemical reduction, entrained in a current of inert gas, and led into the observation zone, where it is decomposed by heat to form the atomic vapour. Several methods have been based on this principle, but differ in the means of reduction and atomization¹³

The use of hydride generation after separation by HPLC has been reported by several groups of workers. For example, arsenite, arsenate and the mono- and dimethylarsenic species, may be separated by reversed-phase HPLC on an ion-exchange column and then pumped with sodium tetrahydroborate solution and hydrochloric acid into a gas/liquid separator. The hydrides produced may then be swept into an atom cell for flame atomic-absorption spectrometry, flame atomic-fluorescence spectrometry or inductively coupled plasma atomic-emission spectrometry¹⁴. Unfortunately such a simple approach is not applicable to tributyltin ions, because tributyltin hydride is a liquid at room temperature. Thus this approach to the speciation of solutions containing tributyltin requires further investigation. In one such study¹⁵ it was found that hydride generation coupled with electrothermal atomization atomic-absorption spectrometry readily allows the determination of tin in organotin compounds after mineralization, and has the advantage over gas-liquid chromatographic systems for the methyltin series that no redistribution reactions take place¹⁶. For tetramethyl- and tetraethyltin the response was similar to, but not

identical with, that for inorganic tin, but the response for other tin compounds, although linearly related to concentration, was a function of the thermal stability and volatility of the hydrides produced.

The tributyltin ion is extremely stable and is only decomposed under vigorous mineralization conditions, which are considered unsuitable for in-line operation owing to problems of dilution, contamination, and disintegration of pump tubing. However, in-line ultraviolet photolysis of organic matter is an established technique for the decomposition of organic species¹⁷ and was selected for the present work to convert the tributyltin compounds into inorganic tin(IV) species, and thus allow a continuous-flow hydride-generator to be used for the determination of both the inorganic and organic tin species present.

EXPERIMENTAL

Apparatus

The continuous-flow hydride-generation system and atom cell are shown in Fig 1. Two small peristaltic pumps (Minipump, Schuco Scientific) were used to pump the sodium tetrahydroborate and sample solutions through a 6-turn mixing coil into the gas/liquid separator. The separator was fitted with a constant-head device. The hydrides were swept by a slow flow of nitrogen to the base of the burner, where they were mixed with a slow flow of hydrogen prior to decomposition in the flame. Full details of this continuous-flow system are given elsewhere¹⁸.

The burner consisted of a borosilicate glass tube (8.5 mm i.d., 100 mm long) with inverted "V" side-arms to act as gas inlets. It was positioned vertically in the spectrometer, replacing the conventional burner/nebulizer assembly. The atomic-absorption spectrometer (Pye Unicam model SP192), was fitted with a tin hollow-cathode lamp and the 286.3-nm tin line was used. The observation height was 10 mm above the burner top. The output from the spectrometer was displayed on a chart recorder (Pye Unicam model AR25).

The tin species were separated by use of a solvent delivery system (Pye Unicam model PU4010) equipped with an injector (Waters Associates, model U6K) with either a 1-ml or 100- μ l sample loop, and connected to a Whatman Partisil-10-SCX analytical column (10 μ m particle size, 25 cm \times 4.6 mm). Samples

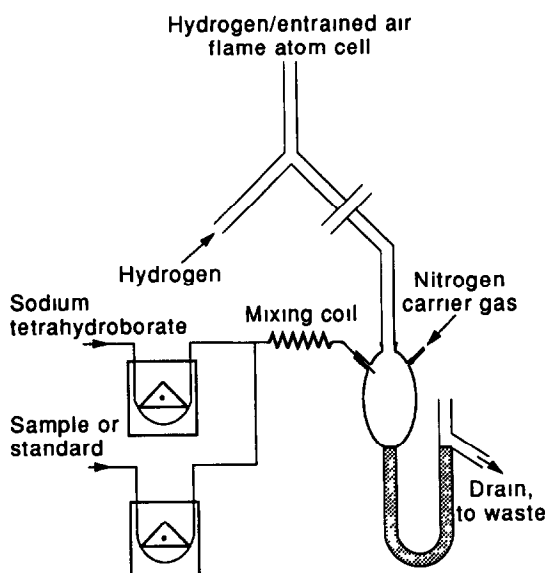


Fig 1 Continuous-flow system for the generation of gaseous hydrides

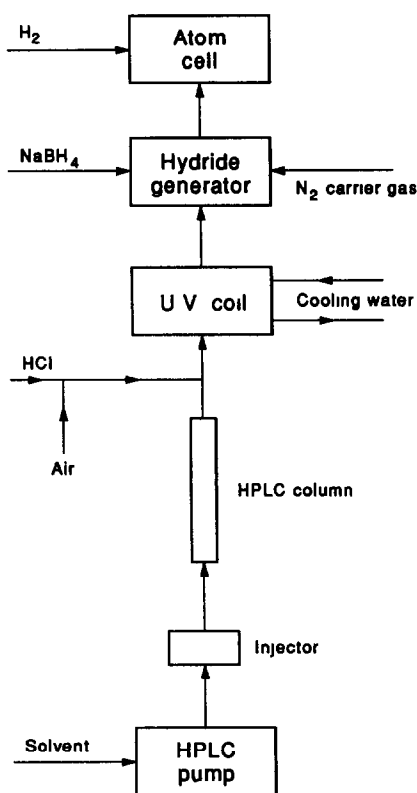


Fig 2 Schematic diagram of the analytical system

were injected directly into the column with a 100- μ l syringe (Scientific Glass Engineering).

Reagents

Unless otherwise stated, all reagents were of analytical reagent grade.

A solution of 1 g of sodium tetrahydroborate (G.P.R., Fisons Scientific) in 100 ml of 0.1M sodium hydroxide was used as the reductant; it was usable for 2–3 days.

A standard tin(IV) stock solution (100 μ g/ml Sn) was prepared by dissolving granulated tin in concentrated sulphuric acid and diluting the solution appropriately.¹⁹ Working standard solutions were prepared daily from the stock solution.

Tributyltin chloride (TBTC, Aldrich) was used as a solution in methanol.

Preservation of standards

It has been shown²⁰ that tin(IV) ions are rapidly adsorbed onto glass surfaces but not onto polyethylene. The reverse is true for organotin compounds, especially the R_3SnX compounds, solutions of which are stable for up to 1 year when stored in borosilicate glass.²¹ All

standards were therefore stored in the appropriate type of container.

Ultraviolet photolysis system

Tributyltin was decomposed in an in-line irradiation coil of the type used in an automatic dissolved organic carbon analyser.¹⁷ A 25-m long coil (of fused-silica capillary) (1.5 mm i.d.) was wound on a glass former with a diameter large enough for an ultraviolet lamp (Engelhard Hanovia) to be inserted in the centre of the coil. One end of the coil was connected to the outlet of the HPLC column, and the other to the inlet of the hydride generator, thus allowing continuous-flow operation. A schematic diagram is shown in Fig 2.

RESULTS AND DISCUSSION

Initial studies showed that though the system would convert tributyltin into a form of tin suitable for producing a volatile hydride, it needed various modifications for optimal performance. One of the main problems resulted from the wide bore (1.5 mm) of the fused-silica coil, which allowed back-diffusion of the sample. This was overcome by segmenting the flow through the coil with air bubbles in a manner similar to that proposed by Skeggs.²² It was found, however, that the size of the bubbles was also important: if too large they tended to break up, and if too small they left pockets of solution behind and hence allowed mixing. A bubble with a length 2–3 times the bore of the tubing appeared to be ideal.

To optimize the system the HPLC instrument was disconnected and the sample was supplied to the rest of the apparatus by means of a peristaltic pump. The optimum conditions found by varying the acid and sodium tetrahydroborate solution flow-rates to the hydride generator, the flow-rate of nitrogen carrier gas, and the pH for decomposition of tributyltin in the coil, are summarized in Table 1.

Table 1 shows that the optimum pH for the irradiation step is lower than the pH that would be achieved by mixing the acid and reductant streams recommended as optimal for efficiency of hydride generation. It has been reported²³ that the response for tin decreases if the acid concentration in the hydride generator exceeds 0.7M. However, from the kinetic curve plotted to find the efficiency of decomposition in the coil (Fig. 3) it was noted that the signal for tin originally present as TBT^+ in a solution at pH 1

Table 1 Optimum conditions for the hydride-generation determination of tributyltin ions after photolysis

<i>Hydride generator</i>	
Acid	0.2 M HCl
Flow-rate	1.5 ml/min
Reductant	1% solution of NaBH ₄ in 0.1 M NaOH
Flow-rate	1.8 ml/min
Carrier-gas flow-rate	120 ml/min
<i>Photolysis of sample</i>	
pH < 1 for maximum yield	

was only 84% of that for the same amount of inorganic tin(IV) at the same pH. The possible use of pH adjustment for further improvement was considered, but not incorporated into the system, because it was thought likely that the resulting sample dilution would counteract any increase of the 84% conversion already obtained. To ensure maximum conversion in 20 min it was essential to keep the inside of the fused-silica coil clean by occasionally flushing it with concentrated hydrochloric acid to remove any deposits of SnO₂, which would impair the irradiation process (they would also account for at least part of the incompleteness of conversion)

The optimum pH for the decomposition in the irradiated coil reflects the variation in the forms of tin in solution, as shown in Fig. 4. The soluble forms would be expected to be Sn⁴⁺ species at low pH, and stannate ions at high pH. In the neutral region, less soluble tin species such as Sn(OH)₄ will exist. Thus the efficiency of the photolysis will probably depend on the solubility of the tin species present, so acidic conditions were maintained in all later work.

Once these parameters had been optimized, the chromatograph was reconnected. Ideally a completely aqueous elution system would be employed to minimize absorption in the ultra-

violet region by the organic solvent. However, the HPLC system we have reported previously for tin speciation,¹¹ consisting of a cation-exchange column and a mobile phase of 80:20 v/v methanol/0.1 M ammonium acetate, was found to give acceptable results. A detection limit of 20 ng of tin was obtained with this system, *i.e.*, two orders of magnitude better than before. A typical chromatogram (100 μl injection of a solution containing 500 μg/ml Sn⁴⁺ and 250 μg/ml TBTC) is shown in Fig. 5. It should be noted that the chromatography takes only 6 min for the separation, the extra time needed for the complete chromatogram to be obtained being due to the time the sample spends in the photolysis coil. However when a series of samples is to be analysed, injections may be made in the conventional way, *i.e.*, every 6 min, the results from each injection following consecutively on the chromatographic record.

Finally the technique was tested for the determination of tin species in a sample of harbour water. The organotin compounds were quantitatively extracted from 1 litre of sample into chloroform,¹¹ and after evaporation of the chloroform, were redissolved in 10 ml of methanol for injection into the HPLC column. This procedure gives a concentration factor of 100. The results obtained are shown in Fig. 6. The peaks for Sn⁴⁺ and TBT⁺ were identified by co-injection of appropriate spikes, and the level

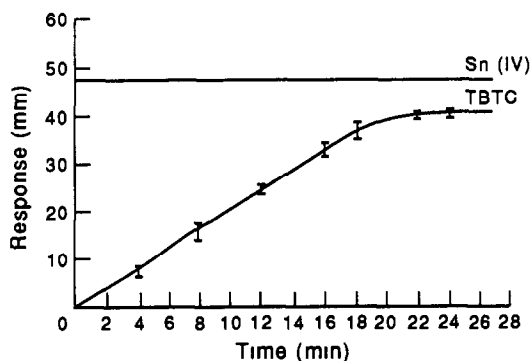


Fig. 3 Photolysis of TBTC as a function of time, for a 100-ng/ml (as Sn) solution at pH 1. The Sn(IV) signal corresponds to 100-ng/ml Sn standard solution

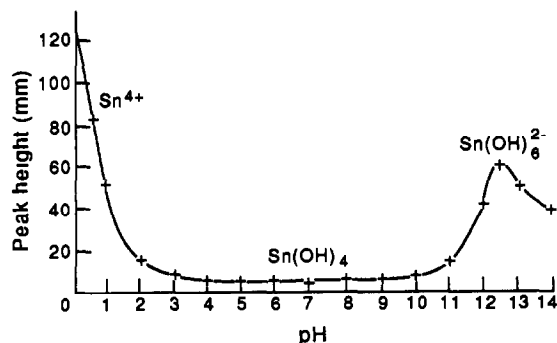


Fig. 4 Effect of sample pH on the signal for a TBTC solution passed through the pyrolysis coil

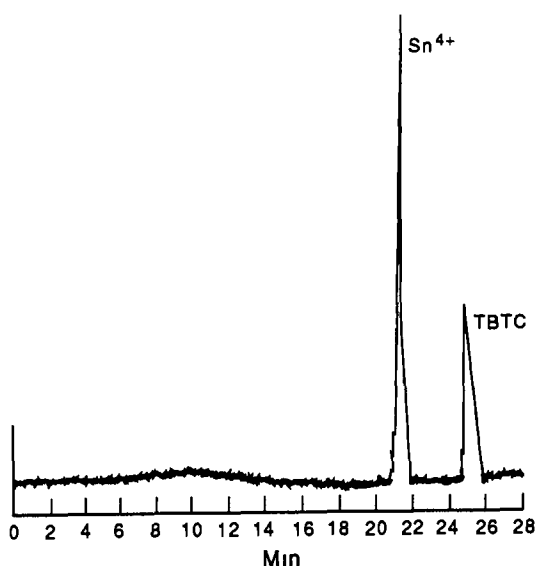


Fig 5 Typical chromatogram obtained by use of hydride generation after photolysis, injection of 100 μ l of solution containing 500 μ g/l Sn^{4+} and 250 μ g/l TBT^+

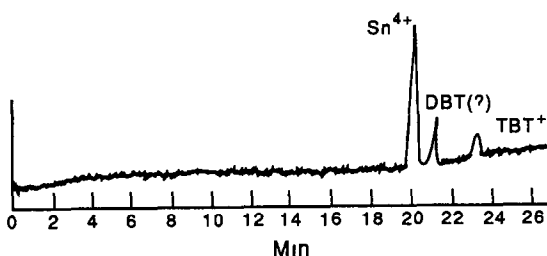


Fig 6 Chromatogram obtained from injection of 100 μ l of methanol solution derived by 100-fold pre-concentration from 1 litre of harbour water

of TBT^+ was found to be 0.20 μ g/l. in the original sample. The third species was not identified at the time, but later work indicated that it was probably dibutyltin.

CONCLUSIONS

The use of a photolysis coil has been shown to enable the sensitive technique of in-line hydride generation to be extended to the determination of species (such as tributyltin) that do not themselves form volatile hydrides

The chromatograms obtained have well defined peaks, indicating good resolution and the absence of carry-over between samples. The detection limit of 2 ng of Sn is the lowest yet

reported for the determination of tin species by directly coupled HPLC-AAS. The technique has been applied here for the determination of organotin compounds, but it is obviously potentially useful for many other hydride-forming elements, such as arsenic, which can occur in forms which do not readily yield volatile hydrides.

Acknowledgements—The authors thank Dr R F C Mantoura of IMER, Plymouth, for the loan of the fused-silica coil, and the SERC for provision of a studentship (to S J H)

REFERENCES

- 1 L Ebdon, S J Hill and R W Ward, *Analyst*, 1986, **111**, 1113
- 2 *Idem, ibid* 1987, **112**, 1
- 3 V F Hodge, S L Seidel and E D Goldberg, *Anal Chem*, 1974, **51**, 1256
- 4 R J Maguire, Y K Chau, G A Bengert, E J Hale, P T S Wong and O Kramar, *Environ Sci Technol*, 1982, **16**, 698
- 5 J C Evans and P J Smith, *J Oil Colour Chem Assoc*, 1975, **58**, 160
- 6 C Y Alzieu, M H Thibaud and B Boutier, *Rev Trav Inst Peches Marit*, 1980, **44**, 301
- 7 A R Beaumont and M D Budd, *Mar Pollut Bull*, 1984, **15**, 402
- 8 M J Waldock and J E Thain, *ibid*, 1983, **14**, 411
- 9 L Ebdon, K Evans and S Hill, *Sci Total Environ*, 1988, **68**, 207
- 10 S K Bailey and I M Davies, *Environ Pollut* 1989, **55**, 161
- 11 L Ebdon, S J Hill and P Jones, *Analyst*, 1985, **110**, 515
- 12 L Ebdon and J I Garcia Alonso, *ibid*, 1987, **112**, 1551
- 13 R G Godden and D R Thomerson, *ibid*, 1980, **105**, 1137
- 14 L Ebdon, S Hill, A P Walton and R W Ward, *ibid*, *Analyst*, 1988, **113**, 1159
- 15 D T Burns, F Glockling and M Harnott, *ibid*, 1981, **106**, 921
- 16 *Idem, J Chromatog*, 1980, **200**, 305
- 17 R F C Mantoura and F M S Woodward, *Geochim Cosmochim Acta*, 1983, **47**, 1293
- 18 L Ebdon, J R Wilkinson and K W Jackson, *Anal Chim Acta*, 1982, **136**, 191
- 19 A Ashton, A G Fogg and D T Burns, *Analyst*, 1973, **98**, 202
- 20 H A Meinema, T Burger-Wiersma, G Versluis-de Haan and E Ch Gevers, *Environ Sci Technol*, 1978, **12**, 288
- 21 K L Jewett and F E Brinckman, *J Chromatog Sci*, 1981, **19**, 583
- 22 L T Skeggs, *Am J Clin Pathol*, 1957, **28**, 3111
- 23 K C Thompson and D R Thomerson, *Analyst*, 1974, **99**, 595

DETERMINATION OF CADMIUM, LEAD AND COPPER IN WATER SAMPLES BY FLAME ATOMIC-ABSORPTION SPECTROMETRY WITH PRECONCENTRATION BY FLOW-INJECTION ON-LINE SORBENT EXTRACTION

ZHAOLUN FANG*, TIEZHENG GUO† and BERNARD WELZ‡

Department of Applied Research, Bodenseewerk Perkin-Elmer GmbH, D-7770 Überlingen,
Federal Republic of Germany

(Received 3 March 1990 Revised 7 September 1990 Accepted 7 December 1990)

Summary—Cadmium, lead and copper were determined in synthetic sea-water, drinking water and the NBS 1643b Trace Elements in Water standard reference material at $\mu\text{g/l}$ levels by flame atomic-absorption spectrometry after on-line preconcentration by sorbent extraction with a flow-injection system Bonded silica with octadecyl functional groups packed in a micro column of 100 μl capacity was used to collect diethylammonium diethyldithiocarbamate complexes of the heavy metals in the aqueous samples The sample loading time was 20 sec at a flow-rate of 3.3 ml/min Ethanol or methanol was used to elute the adsorbed analytes into the spectrometer The sample loading rate, elution rate and pH were optimized Enrichment factors of 19–25 for Cd, Pb and Cu were achieved at sampling frequencies of 120/hr with precisions of 1.4, 1.0 and 1.3% *rsd* ($n = 11$), respectively The detection limits (3σ) for Cd, Pb and Cu were 0.3, 3 and 0.2 $\mu\text{g/l}$, respectively Determination of Cd, Pb and Cu in NBS SRM 1643b showed good agreement with the certified values Recoveries of Cd and Pb added to sea-water were 95 and 102%, respectively

On-line separation and preconcentration have evolved into two of the most prominent contributions of the flow-injection (FI) technique to atomic spectrometry Conventional procedures for separation and preconcentration, including ion-exchange, adsorption, solvent extraction, precipitation *etc*, although effective, are often extremely tedious, consume large quantities of sample and reagent, and are vulnerable to contamination. The FI approach, in contrast, can offer a highly efficient and economical technique which is capable of separating interfering matrices, producing 20–30-fold enhancement in sensitivity, with about 1 ml of sample, at sampling frequencies of 120 samples/hr in flame-atomic absorption spectrometry (FAAS).^{1,2} The majority of work conducted in this area has been associated with preconcentration on packed columns either by ion-exchange or by adsorption. Solvent extraction on-line preconcentration for FAAS has also been shown to be

very efficient.^{3,4} Its rather limited popularity might be due to the more complicated experimental set-up, the relatively short lifetime of the separation membranes and the need for stricter control of experimental parameters than for column techniques. Recent publications by Karlberg⁵ and Ruzicka and Arndal⁶ have shown that sorbent extraction may be used as an alternative to solvent extraction in FI systems. Sorbent extraction can be performed on packed columns, analogously to procedures established for ion-exchange preconcentration, with all the specificity of well accepted solvent extraction separation procedures. Sorbent extraction is achieved with a hydrophobic sorbent solid phase which collects analyte complexes formed in the aqueous phase. The metal complexes are later eluted by an organic solvent which is not necessarily immiscible with water, thus providing more flexibility to the technique Ruzicka and Arndal⁶ have demonstrated the outstanding versatility of preconcentration by on-line sorbent extraction for FAAS, and predicted a promising future for this combination. Of the three chelating systems they studied, the one based on diethyldithiocarbamate (DDC) appears to be the most broadly applicable to heavy metals in various sample matrices. The

*On leave from Flow Injection Analysis Research Centre, Institute of Applied Ecology, Academia Sinica, Shenyang, China

†On leave from Institute of Rock and Mineral Analysis, Beijing, China

‡Author for correspondence

DDC complexes have been studied thoroughly, and detailed information on their behaviour is readily accessible in the literature.^{9,10} Ruzicka and Arndal used a bonded silica sorbent with octadecyl functional groups (C_{18}) to collect the complexes, followed by elution with ethanol or methanol.⁶ A $10\text{-}\mu\text{g/l}$ detection limit was reported for Pb with 80 sec preconcentration, and an estimated sampling frequency of 20–30/hr.

In the work reported here, the performance of the DDC- C_{18} -ethanol scheme of sorbent extraction preconcentration for FAAS was further improved by using an efficient on-line column preconcentration system reported previously^{1,2} for ion-exchange preconcentration by FAAS. The method was applied successfully to the determination of Cd, Pb and Cu in various water samples

EXPERIMENTAL

Perkin-Elmer models 3030 and 2100 atomic-absorption spectrometers equipped with deuterium-arc background correction were used throughout. Hollow-cathode lamps were used for the determination of lead, cadmium and copper at their primary resonance lines at 283.3, 228.8 and 324.7 nm respectively. Flame conditions slightly leaner than recommended were chosen, to compensate for the effect of the organic solvents which were introduced during elution and acted as an additional fuel. Flow spoilers were used in the spray chambers, for all measurements

With the 3030 instrument, the graphite-furnace mode was used in order to study the FI peak with high time-resolution. Peaks were recorded by a Perkin-Elmer model 56 strip-chart recorder and printed by a model PR-100 printer. The time constant for peak-height evaluation was 0.2 sec, with a measuring time of 10 sec initiated by the actuation of the injector for column elution.

The 2100 instrument was operated in the FI mode. Peaks, peak heights and statistical data were printed by an Epson EX-800 printer.

Two FI systems were used. The first, used with the 3030 instrument, was a Bifok 8410 modular FI system with two 4-channel 40 rpm peristaltic pumps. Tygon tubes were used for sample loading and for propelling the complexing reagent. A Perkin-Elmer Series 2 HPLC pump was used to propel the ethanol eluent. A modified Bifok/Tecator V-100 sample injector described previously,⁷ with its by-passes

blocked but with three additional ports on the rotor instead of two, was used throughout. The second system was a prototype of the Perkin-Elmer model FIAS-200 FI unit for atomic spectrometry, which was coupled to the 2100 instrument, and employed the same sample injector as the first system. Silicone rubber tubes were used for propelling ethanol and methanol, and Tygon tubes were used for all other solutions. The FI on-line column preconcentration manifold used is illustrated in Fig. 1. The micro sorbent-extraction columns were made from sections of plastic Eppendorf pipette tips with 5 mm i.d. at the top end and 4 mm i.d. at the other, and packed tightly over a length of 5 mm with C_{18} -bonded silica, 40–63- μm particle size (J. T. Baker, "Bakerbond"). The packing was kept in place by small plugs of plastic foam. The upper end of the column was sealed by a small section of silicone rubber tubing pushed into the column. To minimize dispersion, the column was arranged in the manifold so that the sample and reagent stream flowed from the narrower end of the column to the broader, and the eluent flowed through it in the reverse direction. The column was connected to the injector, and the injector to the nebulizer, with 0.35 mm i.d. PTFE tubing. A 10 cm length of straight tubing or a 25 cm length of three-dimensionally disoriented knotted reactor (made as described previously¹) was used for the latter connection. Similar sensitivities were obtained with both

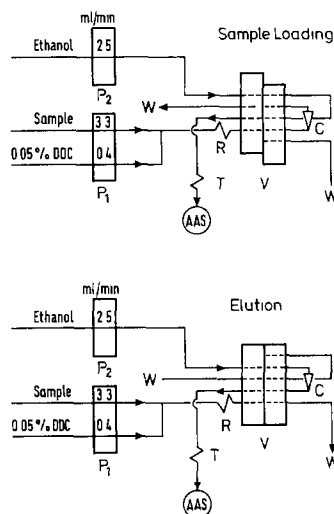


Fig. 1 FI manifold for on-line sorbent extraction column preconcentration. P₁, P₂—pumps, V—injector valve, C—conical column packed with C_{18} sorbent, W—waste, R—reaction coil, 0.5 mm i.d., 4 cm long, T—transport conduit, 0.35 mm i.d., 25 cm long knotted reactor, AAS—flame atomic-absorption spectrometer

but the knotted reactor connection gave slightly better precision. The FI instruments were programmed for a 20 sec loading period and a 10 sec elution period. The sample loading rate was 3.3 ml/min. DDC solution (0.5 mg/ml) was introduced at 0.4 ml/min and mixed with the acidified sample (pH 2) at a confluence point on a "chemifold" (integrated connector block). The optimum elution rate was found to be 2.5 ml/min. At first the solvent used for elution (ethanol or methanol) was continuously pumped into the nebulizer to maintain constant flame conditions. Later it was found that stopping the organic solvent flow during the sample loading period had no detrimental effect on the overall performance. The pump for the solvent was therefore programmed to stop after the elution period and to resume action 5 sec before the next elution. All elutions were done with a free nebulizer uptake rate optimized for the analyte in alcoholic solution (corresponding to 7.2 ml/min for aqueous solutions). Identical results were obtained for the two FI systems, with the same manifold.

All reagents were of analytical-reagent grade and demineralized water was used throughout. The diethylammonium diethyldithiocarbamate (Merck) solution (0.5 mg/ml) was prepared by dissolving the reagent in an aqueous 0.01M acetic acid/0.02M ammonia mixture (pH 9.2). Standard solutions of cadmium, lead and copper were prepared by diluting 1000 mg/ml. stock solutions (Merck, Titrisol) and acidified to pH 2 with nitric acid. A synthetic sea-water matrix containing 35000 mg/l. sodium chloride, 1300 mg/l. magnesium, 400 mg/l., calcium was prepared (with magnesium chloride and calcium nitrate) and acidified to pH 2 after spiking with the analytes. Ethanol and methanol (Merck) were degassed before use to prevent the formation of air bubbles in the stream during elution, which would degrade the precision.

RESULTS AND DISCUSSION

Optimization of the on-line preconcentration system

The design of the on-line sorbent extraction preconcentration system was based on that of a high-efficiency, low sample-consumption on-line ion-exchange preconcentration FAAS system which had provided good performance for the determination of trace metals in water.^{1,2} The system was modified as described in the experimental section, to meet the special

requirements and conditions of the sorbent extraction approach

First, the intermittent introduction of water between elutions (which was previously used to remove the acid eluate from the spray chamber in order to minimize corrosion) was no longer necessary. Instead, it was found beneficial to precondition the flame before the elution, by introducing the organic solvent during the sample loading phase, for at least 5 sec prior to initiation of the readout. The organic solvent flow may be discontinued for the preceding part of the loading phase in order to save reagent. An extra channel was drilled in the rotor of the injector to provide this capability (see Fig. 1).

Secondly, the column design had to be modified because of the smaller particle size (40–63 μm) of the sorbent material used in this study. When the C_{18} sorbent was packed in a conical column identical to the 65- μl column described by Fang and Welz,¹ excessive pressure developed in the system at the normal flow-rates used for sample loading, causing leakages at the connections. It was also difficult to increase the sample loading rate above 1 ml/min because of limitations in the peristaltic pumps, which are designed for relatively low-pressure systems. The diameter of the column was therefore increased by using a wider section of the Eppendorf pipette tip, and a packing thickness of only 5 mm. This modification has proved to permit trouble-free operation at a 3.3 ml/min sample loading rate for over 500 repeated injections. Such modifications may not be necessary if larger particle sizes of the C_{18} sorbent, as used by Ruzicka and Arndal⁶ (150 μm), are employed. However, the smaller particle size may favour more efficient sorption and elution of the metal chelates and may be one of the reasons for the better performance obtained in this study, in spite of the larger dispersion effects in the larger columns. It should be noted that the sample loading rate of 3.3 ml/min in this study, which was limited by the column packing, was considerably lower than that of 4.8 ml/min used for ion-exchange preconcentration.¹ This was one of the reasons for the lower concentration efficiency of the present system compared to that of ion-exchange systems (see following sections). Larger particle sizes will lead to higher flow-rates and may be expected to more than compensate for the loss in enrichment factor associated with their less favorable kinetic properties.

Table 1 The effects of reaction coil configuration and length on the enrichment factor for Cd (10 $\mu\text{g/l}$), Pb (200 $\mu\text{g/l}$) and Cu (50 $\mu\text{g/l}$), PTFE tubing (0.5 mm i.d.) was used throughout

Configuration	Reaction coil Length, cm	Enrichment factor		
		Cd	Pb	Cu
Straight	4	25	20	19
Straight	24	22	18	18
Knotted	24	18.5	16	16.5

Thirdly, the dimensions and configuration of the reaction coil between the confluence point of the sample and reagent solutions and the injector which incorporated the sorbent column were found to have a significant effect on the enrichment factor for analytes such as lead and cadmium (see Table 1). This is a phenomenon which has not been observed in ion-exchange preconcentration and may be associated with kinetic aspects of the adsorption of the metal chelates on the sorbent. The shortest connection (4 cm, 0.5 mm i.d.) with the shortest residence time produced the highest enrichment factor. The differences in results for the straight 24 cm, 0.5 mm i.d. reaction conduit and the knotted^{1,8} reactor made from the same tubing imply that, as well as the reaction time, the mixing conditions have a substantial influence on the enrichment factor. It seemed quite surprising that the more complete radial mixing in the knotted reactor should lead to inferior results. The phenomenon seems to favour the assumption that the metal chelates should be formed shortly before their sorption and that sample and reagent should not be allowed to be in contact for any longer period of time. However, the studies conducted thus far are not sufficient to provide a satisfactory explanation and more work will be necessary for the elucidation of

this phenomenon. Nevertheless, the confluence point for sample and reagent was placed as close as possible to the injector in order to achieve the best enrichment factors.

The exclusion of a washing step between sample loading and elution has been proved to be beneficial in on-line preconcentration with ion-exchange columns.¹¹ This procedure was equally effective in this work with the sorbent extraction preconcentration system. The application of the method to the determination of trace elements in sea-water (as representative of a concentrated and complex matrix) was quite successful (see section on performance).

Effects of experimental parameters on the performance of sorbent extraction preconcentration

The effect of eluent flow-rate on peak absorbance and precision for the measurements of 50 $\mu\text{g/l}$ Cu are shown in Fig. 2. It can be seen that, as was the case with on-line ion-exchange preconcentration, the peak absorbance remained essentially constant for eluent flow-rates ranging from 1.3 to 4 ml/min, implying higher elution and nebulization efficiencies at the lower flow-rates, but the precision was considerably degraded at elution flow-rates below 1.6 ml/min. Another unfavourable aspect of the lower flow-rates was that the elution peak was broader, which meant that it took longer to complete the elution, thus reducing the sampling frequency and concentration efficiency CE (enrichment factor \times samples per min). An elution flow-rate of 2.5 ml/min was selected as optimal with respect to overall performance and economy of reagents.

DDC reagents have been reported to form chelates with metals at high acidities.^{9,10} As the water samples used in this work are always acidified during collection to a pH of 2 or even lower, a study on the effects of acidity on the preconcentration was undertaken to assess its limits and to investigate the necessity for buffering the sample solutions. Concentrations of 6 $\mu\text{g/l}$ Cd, 200 $\mu\text{g/l}$ Pb and 50 $\mu\text{g/l}$ Cu acidified to different degrees with nitric acid were analyzed and the peak absorbances compared to those obtained at pH 3. The peak signals for lead and copper were not influenced at all by the acidity, even by 1M nitric acid (pH 0), whereas a 10% lower signal was obtained for cadmium under these conditions. The acidity limit for cadmium was found to be approximately 0.8M nitric acid (pH 0.1), which is well above the acidity of normal water samples. It was

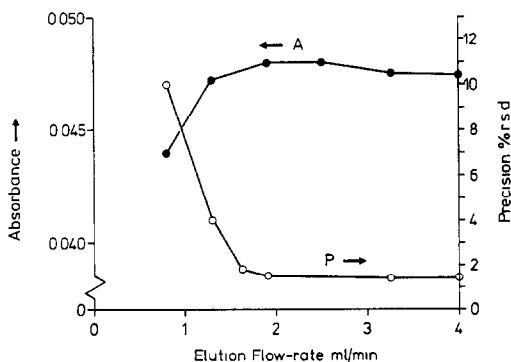


Fig. 2 Effect of elution flow-rate on peak absorbance (A) and precision (P) for on-line sorbent extraction preconcentration of copper (50 $\mu\text{g/l}$) with the FI manifold in Fig. 1, loading period 20 sec

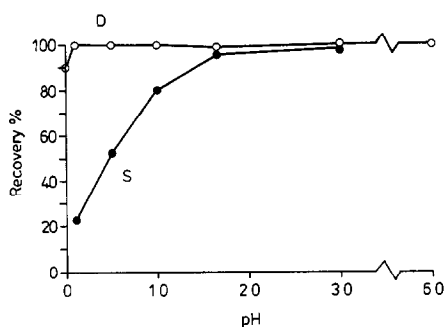


Fig 3 Effect of sample acidity on the recovery of 6 µg/l cadmium in demineralized water (D) and sea-water (S) with the manifold in Fig 1, loading period 20 sec

therefore considered unnecessary to buffer the samples during complexation. The buffer solution in the DDC reagent was added only for the purpose of stabilizing the reagent, which decomposes much faster at lower pH. For sea-water, however, in contrast to the observations for simple aqueous standards, when the pH of the sample was lower than 1.5 the recovery for cadmium gradually deteriorated to about 20% at 0.8M nitric acid (Fig. 3). The difference in behaviour in the sea-water matrix might be due to the higher ionic strength. The acidity limit for determination of cadmium in sea-water was therefore considered to be pH 2. The eluents, ethanol and methanol, were found to be quite similar in performance. Ethanol was used in most of the experiments because of its lower toxicity. Longer chain alcohols such as *n*-butanol were also tested as eluents but were found to give much lower enrichment factors.

Performance of the on-line sorbent extraction preconcentration system

The enrichment factors, detection limits, precisions and sampling frequencies for Cd, Pb and Cu, as well as their recoveries in synthetic sea-water and tap water by use of the optimized on-line sorbent extraction system with FAAS, are shown in Table 2. The enrichment factors (EF) and sampling frequencies show that the CE values of the system, which are the products of the two parameters, are in the range 38–50 EF/min, somewhat lower than those achieved by preconcentration with a column packed with CPG-8Q (8-quinolinol immobilized on porous glass) ion-exchanger.^{1,2} In addition, it should not be overlooked that organic solvent effects in the flame produced a signal enhancement factor of about 2.2 in the case of sorbent extraction, so the actual increase in concentration at the peak maximum would be less than 12-fold at

Table 2 Performance of the on-line sorbent extraction preconcentration FAAS system sampling frequency 120/hr, sample volume 1.4 ml

	Cd	Pb	Cu
Concentration, µg/l	6	200	50
Enrichment factor	25	20	19
CE, EF/min*	50	40	38
RSD, % (n = 11)	1.4	1.0	1.3
Detection limit (3σ), µg/l	0.3	3	0.2
Recovery from sea-water†, %	94–96	98–102	—
Recovery from tap water‡, %	97–102	97–101	—

*Concentration efficiency = enrichment factor (EF) × samples per min

†Spiked with 20 µg/l Pb and 10 µg/l Cd

‡Spiked with 30 µg/l Pb and 3 µg/l Cd

sampling frequencies of 120 hr, corresponding to a CE value of only 17–23 EF/min. The lower CE is due to the slower release of the complexed metals from the sorbent into the organic solvent, compared to the elution of complexed heavy metals by strong acids from chelating ion-exchange columns. Nevertheless, the detection limits obtained for the two techniques were quite similar. Recovery studies in sea-water and tap water for the analytes Cd and Pb, which may be susceptible to interferences also show a better tolerance of interferences, with the sorbent extraction approach. This is best illustrated by the recoveries of cadmium in a sea-water matrix. With on-line ion-exchange preconcentration with CPG-8Q columns no satisfactory recoveries could be obtained, owing to competition in complex formation by the relatively high concentration of magnesium. The best recovery obtained was 73%. Only after a 1.2 dilution of the sea-water sample was it possible to come close to 90% recovery.¹ The Cd-DDC complex shows much higher stability even at very low pH, and DDC does not form stable chelates with the alkaline and alkaline-earth metals even at low acidity, hence excluding the possibility of their interference. However, the competition for adsorption sites on the sorbent by other heavy metals in the sample, which also form stable DDC chelates, has to be considered more carefully.

The tolerance for co-existing heavy metals was examined by adding relatively high concentrations of Pb and Cu to 100 µg/l Cd. Interferences begin to be significant (84% recovery) in a solution containing 4 mg/l each of Pb and Cu, which is not likely to be encountered except in waste water samples, and 96% recovery was obtained at half these interferent concentrations. The interference effects could be partially or completely overcome by using larger

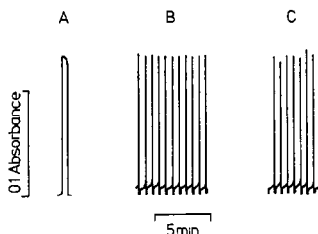


Fig 4 Recorder traces for on-line sorbent extraction pre-concentration of 0.1 $\mu\text{g/l}$ Cd standard solution (B) and 0.1 mg/l Cd in synthetic sea-water (C) with the FI manifold in Fig 1, compared to the trace for 2 mg/l Cd standard solution with conventional aspiration (A). Sample uptake rate 7.2 ml/min. Preconcentration (loading) period 20 sec.

columns, at the expense of lower enrichment factors, as is also the case for ion-exchange preconcentration.¹¹ Alternatively, masking agents could be used to form stronger complexes with the interfering ions. However, these were not found to be necessary for the water samples studied. A recorder trace obtained with the 3030 instrument in the determination of 0.1 mg/l cadmium in sea-water by on-line sorbent extraction preconcentration FAAS is compared in Fig. 4 with the signals for 0.1 mg/l Cd in a simple aqueous standard and a signal obtained by conventional aspiration of a 2 mg/l Cd solution.

The performance of the on-line sorbent extraction preconcentration system was further tested by analysing NBS standard reference material 1643b, Trace Elements in Water. The normal sample loading period of 20 sec was sufficient for the determination of cadmium and copper but a longer loading period of 60 sec was required to achieve consistent results for lead. The results are shown in Table 3 and the time-resolved elution curves are depicted in Fig. 5. Substantial background absorbance was observed in the cadmium and lead determinations. This was caused by the change in flame conditions when a small amount of sample matrix, remaining in the column at the end of the sample loading period, was flushed into the flame by the organic solvent. This had no effect

Table 3 Analytical results for determination of Cd, Pb and Cu in NBS SRM 1643b, Trace Elements in Water

Element	Measured value,* $\mu\text{g/l}$	Certified value, $\mu\text{g/l}$
Cd	19 ± 0.3	20 ± 1
Pb	$23 \pm 0.3 \dagger$	20.7 ± 0.7
Cu	22.0 ± 0.4	22.3 ± 0.4

*Average of triplicate determinations

†60 sec preconcentration period

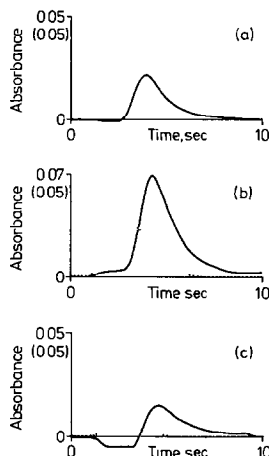


Fig 5 Elution curves and background absorbance (dotted line) for (a) copper, (b) cadmium and (c) lead in NBS SRM 1643b, Trace Elements in Water. The absorbances in parentheses give the scale for the background.

on the peak-height measurements, particularly when background correction was used. In the case of lead (Fig 5c) a significant distortion of the elution curve was clearly visible. This was most probably caused by an over-correction of the background, owing to strong hydroxyl bands in the flame, which exhibit a fine structure at the wavelength used (283.3 nm). This phenomenon disappeared when a different wavelength (217.0 nm) was used. However, the signal distortion was found to have no effect on the peak-height absorbance, so the determination could be done at 283.3 nm, the wavelength with the best signal to noise ratio.

No contamination problems were encountered in this study, mainly because a closed preconcentration system was used. Owing to the small amount of reagent introduced during the sample loading, reagent blanks were absent or close to the detection limit. The reagent grade organic solvent used for elution never produced any noticeable blank values, because the contamination therein (if any) did not undergo preconcentration.

CONCLUSIONS

The on-line sorbent extraction column preconcentration system described in the present study has proved to be an extremely efficient and versatile means of improving the sensitivity and selectivity of FAAS. Detection limits for cadmium, lead and copper were improved by a factor of 20, with sampling frequencies and sample volumes matching those of conventional FAAS analysis.

The precision and recovery obtained in the analysis of sea-water, and the good agreement of the analytical results with the recommended values for the standard reference material 1643b show the reliability and accuracy of the method. The good recovery obtained for cadmium in the sea-water sample was particularly outstanding, because hitherto it has been rather difficult to obtain acceptable recoveries for this element with on-line ion-exchange preconcentration.^{1,11} Further work is in progress to extend the method to the analysis of other samples with more complex matrices. The detection limits achieved for the analytes studied show that the on-line sorbent extraction preconcentration FAAS system may be used for the control of water quality for environmental purposes, which until now could only be accomplished by graphite-furnace AAS.

Acknowledgements—The authors wish to express their thanks to M Sperling and B Radziuk for inspiring discussions

REFERENCES

- 1 Z Fang and B Welz, *J Anal At Spectrom*, 1989, **4**, 543
- 2 *Idem*, *Proc XXVI Colloquium Spectroscopicum Internationale*, Vol VI, p 53
- 3 L Nord and B Karlberg, *Anal Chim Acta*, 1980, **118**, 285
- 4 Z Fang, Z Zhu, S Zhang, S Xu, L Guo and L Sun, *ibid*, 1988, **214**, 41
- 5 B Karlberg, *ibid*, 1988, **214**, 29
- 6 J Ruzicka and A Arndal, *ibid*, 1989, **216**, 243
- 7 Z Fang and B Welz, *J Anal At Spectrom*, 1989, **4**, 83
- 8 H Engelhardt and U D Neue, *Chromatographia*, 1982, **15**, 403
- 9 A Hulanicki, *Talanta*, 1967, **14**, 1371
- 10 G H Morrison and H Freiser, *Solvent Extraction in Analytical Chemistry*, Wiley, New York, 1957
- 11 Z Fang, S Xu and S Zhang, *Anal Chim Acta*, 1987, **200**, 35

CATALYTIC DETERMINATION OF ULTRATRACE AMOUNTS OF RUTHENIUM WITH OSCILLOPOLAROGRAPHIC DETECTION

JIANG ZHI-LIANG

Laboratory of Instrumental Analysis, Department of Chemistry, Guangxi Normal University,
Gulin, People's Republic of China

(Received 29 May 1990 Revised 10 November 1990 Accepted 6 December 1990)

Summary—The oscillopolarographic behaviour of Methyl Red in sodium hydroxide medium has been studied, and the results show that the wave at -0.79 V is an irreversible two-electron adsorption wave. A very sensitive and selective catalytic reaction—oscillopolarographic method for the determination of Ru down to 3 ng/l is described, based on the Ru(III)-catalysed redox reaction of Methyl Red and potassium periodate in hydrochloric acid medium. Potassium thiocyanate is used to quench the reaction and the oscillopolarography is then performed with sodium hydroxide as the supporting electrolyte. The influence of 41 foreign ions has been examined. Ruthenium in ore samples has been determined by the method, with satisfactory results.

Several polarographic methods have been reported for the determination of trace amounts of ruthenium,¹⁻⁹ but their sensitivity or selectivity is not very satisfactory. Many catalytic reaction systems¹⁰⁻¹⁵ have been proposed for determining trace amounts of Ru by spectrophotometric, potentiometric and thermometric methods, but no catalytic method with oscillopolarographic detection has yet been published for Ru. To develop such a method, some of the catalytic reaction systems of Ru were examined. The results demonstrate that some of the Ru-KIO₄-azo-compound systems can be utilized. In the present work, we investigated the Ru(III)-KIO₄-Methyl Red system in detail. A very sensitive and selective catalytic oscillopolarographic method for Ru was developed, with a detection limit of 3 ng/l. and a determination range of $8-220$ ng/l. by the fixed-time method.

EXPERIMENTAL

Apparatus

A model JP-2 single-sweep oscillopolarograph (Chendu Instrumental Factory) with a three-electrode system [dropping mercury electrode (DME), SCE and platinum electrode], was used. A thermostat was used to control the temperature.

Reagents

A standard solution of Ru(III) (100 μ g/ml in 2.4 M hydrochloric acid) was prepared with NH₄RuCl₄. Working solutions were prepared by dilution of the standard solution shortly before use, and also by the procedure used to prepare the sample. Solutions of potassium periodate (9.0×10^{-3} M, usable for a week) and Methyl Red (MR, 5.00×10^{-5} M) were used.

Procedure

Into a 25-ml graduated test-tube fitted with a glass stopper, a known volume of solution containing between 0.2 and 5.5 ng of Ru was transferred, 2.0 ml of 1 M hydrochloric acid and 0.40 ml of 9.0×10^{-3} M potassium periodate were added, and the solution was diluted accurately to 10 ml with doubly distilled water. The tube was placed in the thermostat (at $55 \pm 0.1^\circ$) and after about 5 min, 0.50 ml of 5.00×10^{-5} M MR was added, and the stop-watch was started while the tube was shaken vigorously to mix the solution. The tube was kept in the thermostat for 10 min, then the reaction was stopped by addition of 1.0 ml of 0.01 M potassium thiocyanate. The tube was cooled, 7.0 ml of 1 M sodium hydroxide were added and the solution was diluted accurately to 25 ml with water. A portion of the solution was transferred into a polarographic cell and the second derivative

peak current, $I''_{p,cs}$, was measured with scanning from -0.40 V in the positive direction. $I''_{p,uncat}$ for the uncatalysed reaction was measured in a similar manner. The $\log(I''_{p,uncat}/I''_{p,cs})$ values for a range of Ru concentrations were plotted as a function of Ru concentration to prepare a calibration graph.

Preparation of ore sample¹⁶

A 1.0 g sample of ore was weighed accurately into a nickel crucible and mixed with 5 g of sodium peroxide. The mixture was heated at 700° for about 25 min, cooled, and extracted with water. The solution was transferred into a distillation flask, acidified with 10M sulphuric acid, and treated with 10 ml of saturated potassium permanganate solution and 0.20 ml of 200 mg/ml sodium chloride solution. Ruthenium tetroxide was distilled, and absorbed in 10 ml of 0.1M sodium hydroxide. This solution was transferred to a 100-ml beaker, treated with about 5 ml of 12M hydrochloric acid, then evaporated almost to dryness, and cooled. About 40 ml of water and 5 ml of 12M hydrochloric acid were added, and the mixture was boiled for about 2 min, then cooled and transferred to a 500-ml standard flask and diluted to the mark with water. A suitable aliquot, further diluted if necessary, was analysed.

RESULTS AND DISCUSSION

Oscillopolarographic behaviour of MR

Tachi^{17,18} reported that MR in acid or base medium exhibits a d.c. polarographic wave, and Pittoni¹⁹ reported $E_{1/2}$ for Methyl Red, but the oscillopolarographic behaviour of MR does not seem to have been reported. Our experiments show that oscillopolarography is more sensitive for MR in sodium hydroxide medium than in hydrochloric acid medium. The influence of periodate, iodate, chloride and thiocyanate on oscillopolarographic measurement of MR in sodium hydroxide medium was examined at 25° , and no effect was observed. I''_p is maximal and constant when the sodium hydroxide concentration is 0.05–0.7M, and proportional to the MR concentration between 1.0×10^{-8} and $2.5 \times 10^{-5}M$. The electrocapillary curve is lower in the presence of $1.0 \times 10^{-6}M$ MR than in its absence, owing to adsorption of MR on the surface of the DME changing the surface tension of the mercury drop. The anodic and cathodic waves are

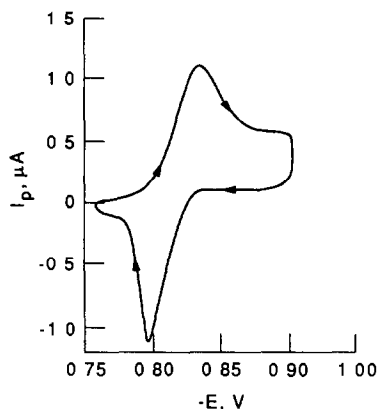


Fig 1 Cathodic and anodic waves for $5.00 \times 10^{-6}M$ MR in $-0.2M$ NaOH

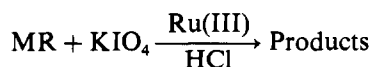
shown in Fig 1, from which $-I_{pc}/I_{pa} = 0.77$ and $\Delta E_p = 40$ mV, so from ΔE (mV, 25°) = $58/n$, $n = 1.45$. The mean temperature coefficient is $-1.9\%/deg$ in the range $20-40^\circ$. The wave disappears when the surfactants polyvinyl alcohol, cetyltrimethylammonium bromide, TX-10 and TX-100 are added.

These results verify that the wave is a 2-electron irreversible adsorption wave.

Ru(III)-KIO₄-MR catalytic reaction system

Rysev *et al.*¹⁰ first found that Ru(IV) catalysed the decolorization reaction of MR and potassium periodate, and used it for the spectrophotometric determination of Ru from 2.0×10^{-4} to 3.0×10^{-3} $\mu g/ml$. In the present work, the system was adapted to oscillopolarographic analysis and based on the catalytic effect of Ru(III) on the reaction. Because thiocyanate can reduce periodate quickly in hydrochloric acid medium and MR exhibits a very sensitive oscillopolarographic wave in sodium hydroxide medium, potassium thiocyanate and sodium hydroxide were selected as the quenching reagent and the supporting electrolyte, respectively. $I''_{p,cs}$ and $I''_{p,uncat}$ remain constant for 60 min after addition of 1.0 ml of 0.01M potassium thiocyanate.

The overall reaction may be expressed as



Under the chosen conditions, the periodate concentration is greater than the MR concentration, and it is presumed that a pseudo first-order reaction (with respect to MR) occurs. Since the catalytic and uncatalysed reactions

occur simultaneously in the analytical system, the rate equation of the overall reaction is

$$V_{cs} = -d[MR]/dt = k_c[MR][Ru] + k_{un}[MR] \quad (1)$$

$$-d[MR]/[MR] = (k_c[Ru] + k_{un}) dt \quad (2)$$

where k_c and k_{un} are the rate constants of the catalytic and uncatalysed reactions, respectively, for use of a fixed concentration of periodate and hydrochloric acid. Integration of equation (2) gives

$$-\log[MR]_{t,cs} = (k_c[Ru] + k_{un})t + \log B \quad (3)$$

where $B = [MR]_{0,cs}$, the initial concentration of MR in the catalytic reaction solution. When $[Ru] = 0$, only the uncatalysed reaction takes place, and equation (3) has the form

$$-\log[MR]_{t,un} = k_{un,t} + \log B \quad (4)$$

where $[MR]_{t,un}$ is the concentration of MR in the uncatalysed-reaction solution at time t . Combining (3) and (4), we obtain

$$\log([MR]_{t,un}/[MR]_{t,cs}) = k_c[Ru]t \quad (5)$$

Since $I_p'' = k'[MR]$, where k' is a constant equation (5) may be rewritten as

$$\log([I_p'']_{t,un}/[I_p'']_{t,cs}) = k_c[Ru]t \quad (6)$$

Equation (6) suggests that the best method of calibration is to plot the logarithmic term against the ruthenium concentration, with the other variables and the reaction time and temperature held constant for the given system.

Effects of variables

The effect of the concentrations of periodate, MR and hydrochloric acid, and the reaction

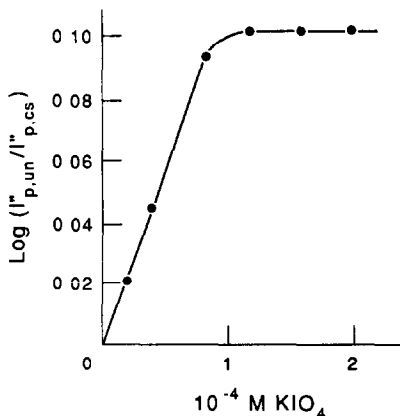


Fig 2 Effect of KIO_4 concentration on the log term. Other conditions as in the procedure

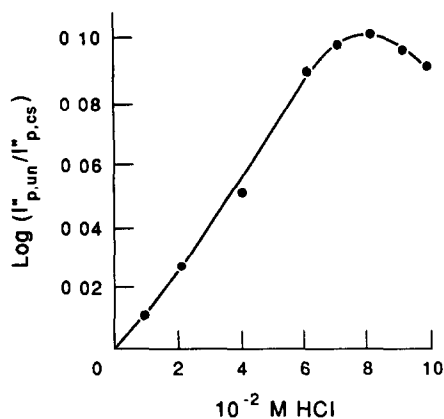


Fig 3 Effect of HCl concentration on the log term

time and temperature on the rate (expressed as the logarithmic term) of the indicator reaction was studied. The logarithmic term increases with time up to 20 min. A fixed reaction time of 10 min was chosen for use, giving a good compromise between high sensitivity and short analysis time. Figures 2-5 show that $1.4 \times 10^{-4} \text{ M}$ periodate, 0.08 M hydrochloric acid and $1.00 \times 10^{-6} \text{ M}$ MR in the final solution and a reaction temperature of 55° are best, so these values were chosen as optimal

Effect of foreign ions

The influence of 41 foreign ions on the system was examined with $4.0 \times 10^{-5} \mu\text{g/ml}$ Ru. The results are summarized in Table 1, and show that the catalytic-reaction oscillopolarographic method has high selectivity. The tolerance limit is that giving not more than $\pm 5\%$ error.

Calibration graph

The two types of working solution gave very similar calibration plots. The relationship

Table 1 Influence of foreign ions on determination of 40 ng/l Ru

Tolerance ratio [Ion]/[Ru]	Ion added
4×10^6	SO_4^{2-}, ClO_4^-
4×10^5	$IO_3^-, ClO_3^-, NO_3^-, PO_4^{3-}$
1×10^5	$I^-, Br^-, Ni(II), Zn(II), Se(IV), Mo(VI), W(VI), Ca(II), Mg(II), Ba(II), Pb(II), La(III), Sb(III)$
7×10^3	$Cr(VI), Si(IV)$
4×10^3	$Fe(III), Co(II)$
3×10^3	$Hg(II), Te(IV), As(III), Cu(II)$
1×10^3	$Ti(IV), Ag(I), Tl(I), Mn(II), Bi(III), Sn(IV), Cd(II)$
5×10^2	$V(V), Os(IV), Pt(IV), Pd(II), Au(III)$
1×10^2	$Rh(III)$
40	$Ir(IV)$

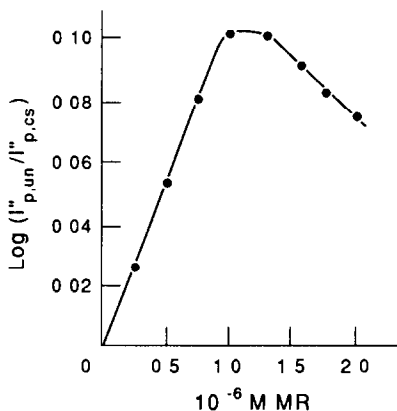


Fig 4 Effect of MR concentration on the log term

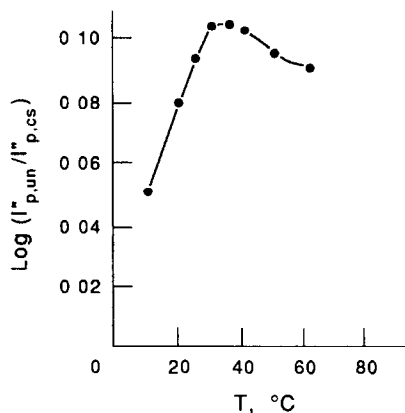


Fig 5 Influence of temperature on the log term

Table 2 Analysis results and recovery

Sample	Ru added, ng	Ru found, ng	Recovery, %	Content (%)	
				This method	Reference method ²⁰
Ore I	—	1.25	—	0.00625	
	—	1.28	—	0.00640	0.0064
	—	1.28	—	0.00640	
	1	2.18	90		
	2	3.06	89.5		
Ore II	3	4.15	96		
	—	0.51	—	0.00255	
	—	0.55	—	0.00275	0.0031
	—	0.56	—	0.00280	
	0.5	1.00	92		
	1	1.50	96		
	2	2.48	97		

between $\log(I''_{p,un}/I''_{p,cs})$ and Ru concentration in the final solution is linear from 8.0×10^{-6} to 2.20×10^{-4} $\mu\text{g/ml}$. The relative standard deviation for 4.0×10^{-5} $\mu\text{g/ml}$ Ru was 4.7% (10 replicates). The detection limit was 3×10^{-6} $\mu\text{g/ml}$.

Analysis of samples

The method was applied to analysis of ore samples, which were also analysed by the catalytic Ru-Ce(IV)-As(III) spectrophotometric method.²⁰ Recovery of standard additions of Ru to the sample was also determined. The results are given in Table 2.

CONCLUSION

With respect to sensitivity, working range and selectivity, the method is superior to the catalytic spectrophotometric method¹⁰. The method is the most sensitive oscillopolarographic method for Ru and also one of the most sensitive catalytic methods at present.

REFERENCES

- 1 M. A. El Guebely, *Anal. Chim. Acta*, 1956, **15**, 580
- 2 D. L. Love and A. E. Greendale, *Anal. Chem.*, 1960, **32**, 780
- 3 Erkang Wang and Huichun Song, *Hua Hsueh Hsueh Pao*, 1965, **31**, 384
- 4 J. Hojman, A. Stefanović, B. Stanković and P. Zuman, *J. Electroanal. Chem.*, 1971, **30**, 469
- 5 J. P. Buckley, *Anal. Chim. Acta*, 1970, **52**, 379
- 6 D. T. Sawyer, R. J. Kula and A. L. Budd, *J. Electroanal. Chem.*, 1962, **4**, 242
- 7 M. Wagnerová, *Collection Czech. Chem. Commun.*, 1962, **27**, 1130
- 8 E. P. Medyantseva, N. A. Ulaklovich, O. N. Romanova and G. K. Budnikov, *Zh. Analit. Khim.*, 1989, **44**, 695
- 9 E. P. Medyantseva, G. K. Budnikov, O. N. Romanova and I. V. Zhivolup, *ibid.*, 1987, **42**, 1846
- 10 A. P. Rysev, I. I. Alekseeva, S. F. Koryavova, L. P. Zhitlenko and A. I. Hakshunskii, *ibid.*, 1976, **31**, 508
- 11 A. P. Rysev, L. P. Zhitlenko and I. I. Alekseeva, *ibid.*, 1979, **34**, 1132
- 12 Chen Si-Zhen, *Fenxi Huaxue*, 1978, **6**, 42
- 13 K. B. Yatsimirskii and L. P. Tikhonova, *Talanta*, 1987, **34**, 69
- 14 P. Viñas, M. Hernández Córdoba and C. Sánchez-Pedreño, *Analyst*, 1987, **112**, 1019

- 15 A P Gumenyuk, V V Aleshina and S P Mushtakova, *Zh Analit Khim*, 1986, **41**, 1400
- 16 Shu-xing Cai and Chao Huang, *Gui Jin Shu Fen Xi*, p 166 Yejin gongye Publ House, Beijing, 1984
- 17 I Tachi, *Mem Coll Agr, Kyoto Imp Unw*, 1937, **40**, 11
- 18 *Idem, ibid*, 1938, **42**, 1
- 19 A Pittoni, *Ricerca Sci Ricostruz*, 1947, **17**, 1396, *Chem Abstr*, 1949, **43**, 7368h
- 20 C Surasiti and E B Sandell, *Anal Chim Acta*, 1960, **22**, 261

CATALYTIC KINETIC DETERMINATION OF ULTRATRACE AMOUNTS OF RUTHENIUM(III) BASED ON THE OXIDATION OF BENZYLAMINE BY ALKALINE HEXACYANOFERRATE(III)

SURENDRA PRASAD* and PREM C NIGAM

Department of Chemistry, Indian Institute of Technology, Kanpur 208016, India

(Received 19 July 1989 Revised 31 December 1990 Accepted 16 January 1991)

Summary—A kinetic method is proposed for the determination of ruthenium(III) by means of its catalytic effect on the oxidation of benzylamine by hexacyanoferrate(III) in alkaline medium. The reaction is followed spectrophotometrically by measuring the decrease in the absorbance of hexacyanoferrate(III) at 420 nm. Under the optimum experimental conditions ruthenium(III) can be determined in the range 10–121 ng/ml with an average error of 1.7% and maximum relative standard deviation of 1.3%. The influence of many potential interferents has been examined and the method has been tested for determination of ruthenium(III) in synthetic mixtures. The method is convenient, reliable and rapid.

Ruthenium and its chloro-complexes, particularly in the tervalent oxidation state, have become of interest in recent years because of their use in homogeneous and heterogeneous catalysis of the oxidation of a wide range of organic substrates.¹⁻⁴ Despite the large number of reactions which are catalysed by ruthenium,⁵ only a few have been used for determining traces of ruthenium, mostly in its higher oxidation states, because of their poor selectivity. Ruthenium(VIII) has been determined by Worthington and Pardue⁶ by its catalytic effect on the Ce(IV)–As(III) reaction. The catalytic effect of Ru(III) on the oxidation of Indigo Carmine by iodate has been used for the determination of ruthenium in synthetic mixtures.³ Viñas *et al.*⁷ were the first to propose the use of an activator, *viz.* iodide, in the selective determination of Ru(III) by its catalytic effect on the *p*-ethoxy-chrysoidine-periodate reaction, but for high sensitivity the reaction has to be performed at 45°.

In the present paper we report a rapid and simple kinetic method for the determination of Ru(III), based on its catalysis of the oxidation of benzylamine by alkaline hexacyanoferrate(III). The method permits the determination of Ru(III) concentrations down to 10 ng/ml with good accuracy and reproducibility. We have tested the method for the

determination of Ru(III) in synthetic mixtures and shown it to be sensitive and selective.

EXPERIMENTAL

Reagents

Redistilled water was used throughout for preparation of solutions. A 0.04M stock solution of benzylamine (analytical grade, Sigma) that had been purified by distillation under reduced pressure was prepared. A 0.04M stock solution of potassium hexacyanoferrate(III) (analytical grade, S.D.S.) was prepared, and standardized iodometrically,⁸ it was stored in dark amber-coloured bottles and diluted to the required concentration just before use. Sodium hydroxide and perchloric acid were used to adjust the pH to the desired value. Standard B.D.H. buffers were used for standardization of the pH-meter. Sodium perchlorate (*purum*, Fluka) was used to maintain the ionic strength at 0.5M. A stock solution of ruthenium(III) ($5 \times 10^{-3}M$) was prepared by dissolving the appropriate amount of ruthenium trichloride ($RuCl_3 \cdot 3H_2O$, Johnson Matthey) in 1M hydrochloric acid,⁹ working solutions were prepared immediately before use, by dilution as required. All other reagents used were of certified analytical-reagent grade.

Instrumentation

A Shimadzu double-beam spectrophotometer, model UV-240, equipped with 1-cm

*Author for correspondence

path-length fused-silica cells and an automatic digital recorder, was used for recording spectral changes and absorbances. The cell compartment was kept at a constant temperature of $35.0 \pm 0.1^\circ$ by circulation of water from a Remi Ultra Cryostat model C-702 thermostatic bath. All pH measurements were made on an Elico digital pH-meter, model LI-120, fitted with an Elico CL-51 combined glass and saturated calomel electrode. The glassware used was scrupulously cleaned to eliminate any traces of metal ions from the glass surface. The cells were cleaned after use, by immersion in nitric acid (1 + 1) for 15 min to remove traces of ruthenium adsorbed on their walls.

Procedure

Adjust all the sample solutions to pH 10.5 ± 0.1 and bring them to the same temperature by immersion in a thermostat at $35.0 \pm 0.1^\circ$ for 30 min.

To a 10-ml glass-stoppered standard flask (kept in the thermostat) add 2.0 ml each of $2.0 \times 10^{-3}M$ potassium hexacyanoferrate(III) and $4 \times 10^{-2}M$ sodium hydroxide in that order, followed by 2.0 ml of 4×10^{-7} – $4.8 \times 10^{-6}M$ ruthenium(III) immediately before the run, to avoid any possible interaction between these reagents. Initiate the reaction by injecting 2.0 ml of $4 \times 10^{-3}M$ benzylamine solution. Shake the mixture and transfer a portion to a 1-cm

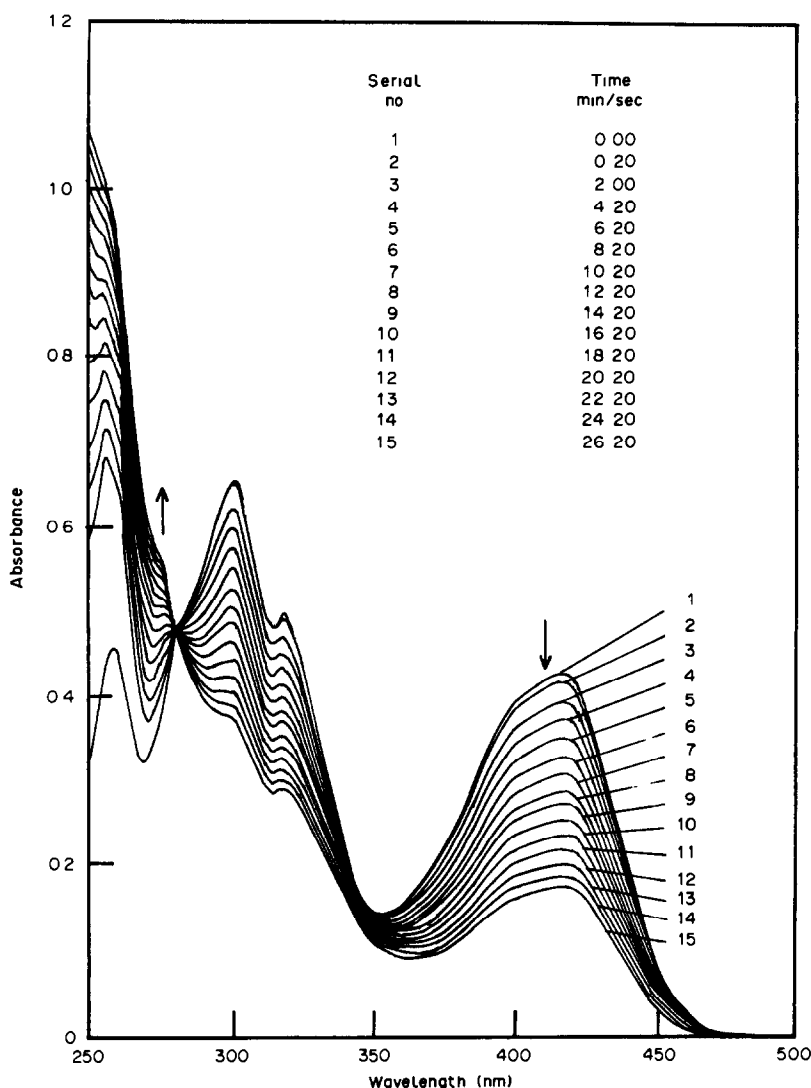


Fig 1 Repetitive scan of the reaction mixture during a typical kinetic run $[\text{Fe}(\text{CN})_6^{3-}] = 4 \times 10^{-4}M$, $[\text{benzylamine}] = 1 \times 10^{-3}M$, $[\text{Ru}^{3+}] = 1 \times 10^{-6}M$, $[\text{NaOH}] = 1 \times 10^{-2}M$, $\text{pH} = 10.5 \pm 0.1$, $I = 0.5M$ (NaClO_4), $\text{temp} = 35.0 \pm 0.1^\circ$

path-length cell in a temperature-controlled cell-compartment at $35.0 \pm 0.1^\circ$. Measure the change in the hexacyanoferrate(III) absorbance at 420 nm ($\epsilon = 1020 \text{ l.mole}^{-1}.\text{cm}^{-1}$) after exactly 5 min. Plot the change in absorbance vs. Ru(III) concentration. Analyse samples similarly.

RESULTS AND DISCUSSION

The calibration obtained by the fixed-time method (with a 5-min reaction time) is linear between 10 and 121 ng/ml Ru(III), and non-linear at higher concentrations. Linear plots can also be obtained with fixed-time intervals longer or shorter than 5 min, but the relative errors are larger.

The oxidation of benzylamine by alkaline hexacyanoferrate(III) is slow but is catalysed by ruthenium(III). The kinetics and mechanism of this reaction have been reported by Nath and Singh¹⁰ After some valid approximations the rate expression for the catalysed reaction was reported as

$$\frac{d[\text{Fe}(\text{CN})_6^{3-}]}{dt} = \frac{kK_1K_2[\text{Substrate}][\text{Ru}^{3+}]}{1 + K_1[\text{OH}^-]} \quad (1)$$

where k is the rate constant for formation of the benzylamine oxidation product from the intermediate Ru-benzylamine complex, and K_1 and K_2 are the stability constants of the reactive Ru species and of the intermediate Ru-benzylamine complex, respectively

Thus with other conditions fixed, the rate of disappearance of hexacyanoferrate(III) is linearly related to the Ru(III) concentration. The spectral changes occurring during a typical kinetic run are shown in Fig 1, and confirm the coexistence of $[\text{Fe}(\text{CN})_6^{3-}]$ and $[\text{Fe}(\text{CN})_6^{4-}]$ during the reaction, and formation of the latter as assumed in the proposed mechanism¹⁰

The detection limit was evaluated according to the method of Tanaka¹¹ by using the expression

$$X_D = \bar{X}_{B1} + tS_{B1}\sqrt{2} \quad (2)$$

where \bar{X}_{B1} is the average and S_{B1} the standard deviation of the blank values, and t is a constant, S_{B1} is taken as R/d_2 , $1/d_2$ being the factor for obtaining S from the range R Tanaka recommends using $t = 3$; $1/d_2$ is 0.59 when the range of three blank measurements is used. The sensitivity, expressed as the slope of the calibration function, was sufficiently high ($1.98 \times 10^5 \text{ l mole}$), and it can be improved by

Table 1 Effect of diverse ions on the determination of $7 \times 10^{-7}M$ ruthenium(III)

Ions added	Limiting molar concentration ratio, ((Interfering ion)/[Ru(III)])
NO_3^- , SO_4^{2-} , acetate, tartrate, oxalate, citrate, $\text{S}_2\text{O}_3^{2-}$, ClO_4^- , Cr(III), La(III), Br(III), Mg(II), K(I), Mo(VI)	1200*
Cu(II), Co(II), Ni(II), Cd(II), Zn(II), Mn(II), Hg(II), Pd(II)	570
Fe(III), Ce(III), Rh(III), Pt(IV)	200
Br^- , BrO_3^- , CN^-	50
Ce(IV), Ag(I)	20
EDTA(Na_2 salt), Os(VIII), Ir(III), I^-	10

*Maximum ratio tested

increasing the time interval to 7 minutes or more, but loss in precision. The relative standard deviation for triplicate determination ranges from 0.1 to 1.3% and the error from -4 to +1.7% in the ruthenium concentration range 10-121 ng/ml

The selectivity was tested by studying possible interferences in the kinetic determination of $7 \times 10^{-7}M$ ruthenium(III). Table 1 shows the tolerance ratios to ruthenium. The tolerance limit is taken as the concentration which causes an error of no more than $\pm 4\%$ in ruthenium determination. Surasiti and Sandell¹² have described methods for conversion of osmium into Os(VIII) with retention of ruthenium as Ru(III)

Application to determination of ruthenium(III) in synthetic mixtures

To establish the reliability and applicability of the proposed method, recovery experiments were performed on laboratory mixtures con-

Table 2 Application of the method to synthetic mixtures

Sample	Composition of the synthetic mixture, ng/ml	Ruthenium found, ng/ml
1	Ru(III) 15.2, Mo(VI) 7580, Pd(II) 303, Rh(III) 758	15.8
2	Ru(III) 20.2, Rh(III) 2020, Fe(III) 1000, Os(VIII) 101	21.0
3	Ru(III) 30.2, Ir(III) 151, Ag(I) 241, Os(VIII) 151, Rh(III) 1027	31.1
4	Ru(III) 80.9, Os(VIII) 243, Ir(III) 243, Pd(II) 404, Rh(III) 1617	84.9

taining other metals. This was done because authentic samples containing trace amounts of ruthenium were not available. The results are shown in Table 2.

Acknowledgement—The authors are indebted to the Department of Environment and Forest, Government of India, for sanction of a research project No J.12017/58/83-ENV I

REFERENCES

- 1 M M T Khan and R S Shukla *J Mol Catal*, 1985, **34**, 19
- 2 M P Singh, H S Singh and M K Verma, *J Phys Chem*, 1980, **84**, 256
- 3 G K Muthakia and S B Jonnalagadda, *Int J Chem Kinetics*, 1989, **21**, 519
- 4 R K Dwivedi, M Verma, P Kumar and K Behari, *Tetrahedron*, 1983, **39**, 815
- 5 V E Kalina and K B Yatsimirskii, *Problems in Kinetics and Catalysis* (in Russian), p 43 Ivanova, 1974
- 6 J B Worthington and H L Pardue, *Anal Chem*, 1970, **42**, 1157
- 7 P Viñas, M H Córdoba and C Sánchez-Pedreño, *Analyst*, 1987, **112**, 1019
- 8 J Bassett, *Vogel's Text Book of Quantitative Inorganic Analysis*, 4th Ed, p 463 Longmans, London, 1978
- 9 H H Caddy and R E Connick *J Am Chem Soc*, 1958, **80**, 2646
- 10 N Nath and L P Singh *J Indian Chem Soc*, 1985, **62**, 108
- 11 N Tanaka, *Kyoto-fu Eisei Kogai Kenkyusho Nempo*, 1977, **22**, 121, *Chem Abstr*, 1979, **90**, 114401V
- 12 C Surasiti and E B Sandell, *Anal Chim Acta*, 1960, **22**, 261

SOME NEW ACRIDINIUM TRIFLUOROMETHANESULFONATES AS SPECTROPHOTOMETRIC DERIVATIZATION REAGENTS FOR AROMATIC AND ALIPHATIC PRIMARY AMINES

JAMES W. DUNNING JR and JAMES T STEWART*

Department of Medicinal Chemistry and Pharmacognosy, College of Pharmacy, University of Georgia,
Athens, GA 30602, U S A

(Received 17 July 1990 Revised 27 November 1990 Accepted 10 December 1990)

Summary—Some new 9-substituted 10-methylacridinium trifluoromethanesulfonate (triflate) salts have been synthesized and shown to react in methanol with the model aromatic and aliphatic amines, aniline and n-butylamine, to form derivatives which absorb strongly at 445 and 439 nm, respectively. The color development is affected by heat and heating time and by the quantity of acridinium triflate used. A 10–50-fold molar excess of the triflate should be used and the solution heated at 60° for 30 min. The linearity and reproducibility of the assay are improved by the presence of pyridine (for aniline) and triethylamine (for n-butylamine) in the reaction mixture. Beer's law is obeyed over the range 0–1860 ng/ml for aniline and 0–1440 ng/ml for n-butylamine, with each of the new reagents. The relative error and the precision of determination depends on the acridinium triflate used.

9-Chloroacridine has been demonstrated by Stewart and co-workers to have a number of useful applications as an analytical derivatization reagent for the determination of primary aromatic amines, both by colorimetry^{1,2} and by fluorescence quenching.³ It has also been shown that 9-methoxyacridine is of comparable value as an analytical reagent for primary aliphatic amines.⁴

These assay methods generally involved heating the analytical solution for various time periods with excess of acridine reagent in order to achieve reproducible results. Investigation of ways to further enhance the reactivity of the 9-position of the acridine ring toward nucleophiles such as amines, and thus make these acridine reagents significantly more useful as derivatization agents, has led us to synthesize some new 9-substituted 10-methylacridinium trifluoromethanesulfonate (triflate) salts (Table 1).

The goal of this study was to investigate the reaction of these new 9-substituted 10-methylacridinium salts, featuring highly labile leaving groups at C-9, with aniline and n-butylamine as model aromatic and aliphatic primary amines. Spectrophotometric applications of these reactions are reported here.

EXPERIMENTAL

Materials

9-Chloroacridine and triethylamine were obtained from Eastman Kodak, Rochester, NY. 6,9-Dichloro-2-methoxyacridine, methyl trifluoromethanesulfonate (methyl triflate), aniline, and n-butylamine were purchased from Aldrich Chemical Co., Milwaukee, WI. 9-Methoxy and 9-ethoxy acridines were prepared from 9-chloroacridine by a reported method.⁵ Aniline and n-butylamine were distilled prior to use. Absolute methanol and acetonitrile were supplied by J. T. Baker Chemical Co., Phillipsburg, NJ. All other chemicals were obtained commercially and used as received.

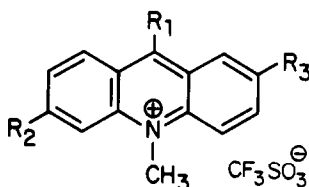
Apparatus

Ultraviolet spectra and single-wavelength measurements were recorded with a Beckman Model DU-7 UV/VIS spectrophotometer interfaced to a PE Model 7500 computer equipped with a Hewlett-Packard 2-pen plotter.

Melting points were determined in open capillary tubes with a Hoover Uni-melt apparatus, and were uncorrected. Proton NMR spectra were obtained with a JEOL FX90-Q spectrometer. Infrared spectra (KBr discs) were recorded with a Perkin-Elmer Model 684 IR Spectrophotometer also interfaced with the PE

*Author for correspondence

Table 1 9-Substituted 10-Methylacridinium trifluoromethanesulfonates (triflates)



Compound	R ¹	R ²	R ³	Formula*	m p, °C	Yield, %
1	—Cl	—H	—H	C ₁₅ H ₁₁ ClF ₃ NO ₃ S	227–9	94
2	—Cl	—Cl	—OCH ₃	C ₁₆ H ₁₂ Cl ₂ F ₃ NO ₄ S	238–41	62
3	—OCH ₃	—H	—H	C ₁₆ H ₁₄ F ₃ NO ₄ S	193–5	46
4	—OCH ₂ CH ₃	—H	—H	C ₁₇ H ₁₆ F ₃ NO ₄ S	125–7	61

*The microanalysis results were within $\pm 0.2\%$ of the calculated values for C, H, N

7500 computer. Microanalyses were performed by Atlantic Microlab, Inc., Atlanta, GA.

Syntheses of acridinium triflates

9-Chloro-10-methylacridinium triflate (1). In an oven-dried flask, 9-chloroacridine (6.07 g) was dissolved in 60 ml of dichloromethane with stirring, at ambient temperature. After the addition of 10 ml of methyl triflate, a dark turbidity appeared, instantaneously followed by a copious, bright yellow precipitate. After continued stirring at ambient temperature for 3 hr, the reaction mixture was filtered and the crystals were washed with cold dichloromethane and dried under vacuum.

6,9-Dichloro-2-methoxy-10-methylacridinium triflate (2) 6,9-Dichloro-2-methoxyacridine (5.0 g) was dissolved in 150 ml of dichloromethane with stirring in an oven-dried flask at ambient temperature, and 2.5 ml of methyl triflate was added. The mixture was stirred for 30 min and the fine yellow crystalline deposit produced was then collected by filtration. The mother liquor was further concentrated under reduced pressure and a second crop of crystals was collected. The two lots of crystals were combined, washed with cold dichloromethane and dried under vacuum.

9-Methoxy-10-methylacridinium triflate (3). In an oven-dried flask, 9-methoxyacridine (2.0 g) was dissolved in 40 ml of dichloromethane and 2.5 ml of methyl triflate were added. Precipitation took place after stirring of the reaction mixture for 4–5 hr at ambient temperature. The reaction mixture was filtered and the brilliant yellow crystals collected were washed with cold, dried tetrahydrofuran. The mother liquor was further concentrated by mild heating (45°) to yield additional crystals.

9-Ethoxy-10-methylacridinium triflate (4). 9-Ethoxyacridine (2.0 g) was dissolved in 20 ml of

dichloromethane and methyl triflate (1.5 ml) was added. The reaction mixture was stirred at ambient temperature for 2 hr, an additional 1.5 ml of methyl triflate were added, and the mixture was refluxed for another hour. The reaction mixture was filtered and the brilliant yellow crystals were washed with cold tetrahydrofuran and dried under vacuum.

Preparation of stock solutions

Stock solutions were prepared by dissolving weighed quantities of each acridinium triflate in absolute methanol. Final concentrations of $10^{-2}M$ for **1**, $2 \times 10^{-2}M$ for **2**, $5 \times 10^{-2}M$ for **3**, and $3 \times 10^{-2}M$ for **4** were obtained. Prior to dilution to volume with methanol, pyridine (for aniline assay) or triethylamine (for n-butylamine assay) was added to give a concentration of 50 μ l/ml in the stock solution. Stock solutions ($10^{-3}M$) of aniline and n-butylamine were also prepared in absolute methanol.

Preparation of calibration graphs

Into 1-ml standard flasks equipped with ground-glass stoppers were placed 200- μ l aliquots of acridinium triflate/pyridine or acridinium triflate/triethylamine stock solution, 0, 25, 50, 100 and 200 μ l of aniline or n-butylamine stock solution (as appropriate) were added and the solutions were mixed on a Vortex mixer for 30 sec. Enough methanol was added to give a total volume of about 400 μ l in each flask. The flasks were tightly stoppered, and placed in a shaking water-bath at 60° for 30 min. After cooling, the mixtures were transferred quantitatively to 10-ml standard flasks and diluted to volume with absolute methanol, and their absorbances were read at 445 nm for the aniline mixtures and 439 nm for the n-butylamine mixtures.

Assay procedure

A 200- μ l aliquot of approximately $10^{-3}M$ amine solution was mixed with 200 μ l of the appropriate acridinium triflate/pyridine or acridinium triflate/triethylamine stock solution in a 1-ml standard flask, shaken on the Vortex shaker for 30 sec, then heated *etc.* as described above. The concentration of amine was calculated from the absorbance and the calibration data

RESULTS AND DISCUSSION

The acridinium triflates were prepared by adding a slight excess of methyl triflate to a solution of the substituted acridine in dichloromethane and stirring for various time periods. One of the triflates (compound 4) also required refluxing of the dichloromethane solution. Table 2 presents a summary of selected spectral properties of these new compounds.

Aromatic nucleophilic substitution is enhanced in structures which contain an electronegative heteroatom,⁶ and is further enhanced when the heteroatom is rendered quaternary by alkylation.⁷ This ease of nucleophilic substitution can be harnessed for the purposes of analytical chemistry when the 9-position of the

acridine ring bears a facile leaving group. The reactions of aniline and n-butylamine with each of the acridinium triflates were observed to be more spontaneous than the corresponding reaction with tertiary acridines previously reported by this laboratory.¹⁻⁴ Absorption spectra of the reaction products of aniline and n-butylamine with 9-chloro-10-methylacridinium triflate are shown in Fig. 1, along with the reagent blank spectra. The reaction conditions were optimized by a series of univariate experiments designed to select the best ratio of acridinium triflate to analyte, reaction temperature and of reaction time, in that order.

Up to 50-fold excess of each acridinium triflate was reacted with aniline and n-butylamine at ambient temperature, the absorbance being measured at 30-min intervals. It was found that different molar excesses of the various acridinium triflates were needed for the aniline assay, but a 30-fold excess of each reagent was suitable for the n-butylamine determination. For aniline, a 10-fold excess of compound 1, 20-fold excess of compound 2, 50-fold excess of compound 3, and a 30-fold excess of compound 4 were necessary for best results.

Next, reaction temperatures of 25, 40, 50 and 60° were investigated with the optimized excess

Table 2 Selected spectral properties of 9-substituted 10-methylacridinium trifluoromethanesulfonates

Compound	Ultraviolet λ_{max} , <i>nm</i>	Infrared band, <i>cm</i> ⁻¹	NMR
1	426 (4.05×10^3)	3105 (NR ₄ ⁺)	4.79 (3H,s,NCH ₃)
	401 (5.77×10^3)	1605 (arom)	8.16 (2H,m,arom)
	363 (1.61×10^4)	1571 (arom)	8.51 (4H,m,arom)
	261 (9.52×10^4)	1378 (C-F)	8.91 (2H,m,arom)
		1190 (sulfonate)	
		1030 (sulfonate)	
		767 (C-Cl)	
2	418 (6.02×10^3)	3104 (NR ₄ ⁺)	4.12 (3H,s,NCH ₃)
	377 (1.50×10^4)	1621 (arom)	4.69 (3H,s,OCH ₃)
	277 (7.09×10^4)	1574 (arom)	8.05 (3H,m,arom)
		1380 (C-F)	8.61 (3H,m,arom)
		1287 (OCH ₃)	
		1162 (sulfonate)	
		632 (C-Cl)	
3	398 (6.50×10^3)	3110 (NR ₄ ⁺)	4.62 (3H,s,NCH ₃)
	352 (9.18×10^3)	1615 (arom)	4.64 (3H,s,OCH ₃)
	260 (8.61×10^4)	1582 (arom)	7.91 (2H,m,arom)
		1373 (C-F)	8.40 (4H,m,arom)
		1260 (OCH ₃)	8.75 (2H,m,arom)
		1157 (sulfonate)	
4	399 (7.12×10^3)	3120 (NR ₄ ⁺)	1.69 (3H,t,CH ₃)
	351 (8.60×10^3)	1610 (arom)	4.73 (3H,s,NCH ₃)
	260 (8.21×10^4)	1579 (arom)	4.90 (2H,m,OCH ₂)
		1384 (C-F)	7.85 (2H,m,arom)
		1267 (OCH ₃)	8.40 (6H,m,arom)
		1150 (sulfonate)	

*Molar absorptivity ($l \text{ mole}^{-1} \text{ cm}^{-1}$) in parentheses

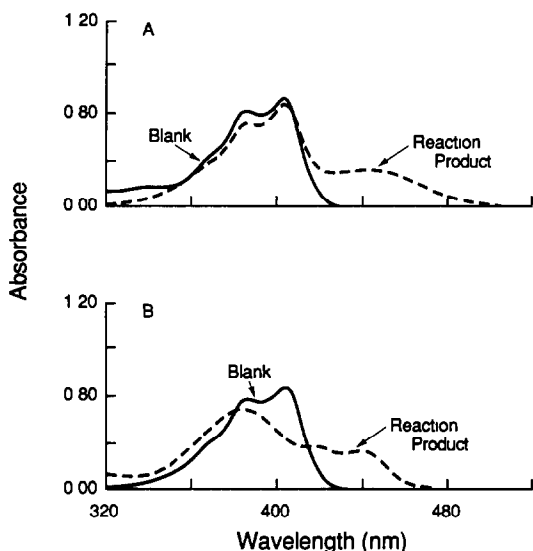


Fig 1 Typical absorption spectra of the product of reaction of $10^{-3}M$ aniline (A) and $10^{-3}M$ n-butylamine (B) with $10^{-2}M$ 9-chloro-10-methylacridinium triflate, and of the reagent blank

of reagent, and 60° was found to give the best precision and accuracy. Finally, samples with optimum reagent composition were heated at 60° for 0, 2.5, 5, 10, 15, 30, 45, and 60 min and heating for 30 min was found to give not only maximum absorbance but also the best linearity of calibration.

It was interesting that though the maximum absorbance was obtained within minutes after preparation of the analytical solution, the linearity and reproducibility were poor until the solution had been heated at 60° for 30 min.

It appears necessary to degrade the excess of acridinium triflate by heating for a sufficient time, to minimize its interference.

It was found that addition of the tertiary amines, pyridine and triethylamine, to the acridinium triflate stock solutions aided in improving the linearity. It was hypothesized that the reaction of triflates 1 and 2 with amines released free protons into the reaction solution, which probably prevented the nucleophilic addition product from being quickly formed, and that a proton-scavenger such as pyridine or triethylamine might be useful to force the reaction to proceed at a faster rate. What was discovered, however, was that their addition dramatically improved the linearity even for those reagents (*i.e.*, the 9-alkoxy triflates) with which no free protons would be formed in the reaction. The exact mechanism of the effect of the tertiary amines in the acridinium triflate-amine reaction remains unknown. Nucleophilic addition of the tertiary amine at the 9-position of the acridinium salt, resulting in *in situ* generation of a 9-quaternary ammonium intermediate, is an interesting possibility. Table 3 gives the results of a study comparing the absorbance at 445 nm for an analytical sample containing triflate 1, aniline, and pyridine, with that of a solution containing only triflate 1 and aniline. Linearity of the calibration plot is clearly superior when pyridine is present. Similar results were obtained with triethylamine for n-butylamine and triflate 1. The other triflates follow the same pattern with both amines.

Table 3 Effect of pyridine as an additive in the 9-chloroacridinium triflate procedure for aniline determination (heating at 60° for 30 min)

[Aniline], ng/ml	Absorbance at 445 nm		Linear regression data	
	Pyridine present	Pyridine absent	Pyridine present	Pyridine absent
0	0.000	0.000	slope 0.00024	slope 0.000065
230	0.124	0.050	intercept 0.029	intercept 0.013
930	0.236	0.095	$r = 0.9888$	$r = 0.9536$
1860	0.469	0.137		

Table 4 Linear regression data for calibration graphs prepared for aniline with each acridinium triflate*

Acridinium triflate	Slope	Intercept	Correlation coefficient ($n = 4$)
1	0.00021	0.015	0.9864
2	0.00025	-0.006	0.9995
3	0.00027	-0.010	0.9995
4	0.00019	-0.002	0.9959

*Concentration of triflate compounds was in the range $1-5 \times 10^{-2}M$, concentration range of aniline was 0-1860 ng/ml

Table 5 Analysis of spiked aniline samples with each acridinium triflate

Acridinium triflate	Aniline added, ng/ml	Aniline found, ng/ml*	Error, %
1	370	387 ± 20	+4.6
	1400	1380 ± 110	-1.4
2	370	354 ± 39	-4.3
	1400	1312 ± 54	-6.3
3	370	371 ± 57	+0.3
	1400	1310 ± 81	-6.4
4	370	446 ± 82	+20.5
	1400	1586 ± 95	+13.3

*Mean ± standard deviation, (n = 3)

Table 6 Linear regression data for calibration graphs prepared for n-butylamine with each triflate*

Acridinium triflate	Slope	Intercept	Correlation coefficient
1	0.00107	0.063	0.9992
2	0.00071	0.015	0.9988
3	0.00067	0.005	0.9993
4	0.00012	0.052	0.9952

*Concentration of triflate compounds was in the range $1-5 \times 10^{-2}M$, concentration range of n-butylamine was 0-1440 ng/ml

Table 7 Analysis of spiked n-butylamine samples with each acridinium triflate

Acridinium triflate	n-Butylamine added, ng/ml	n-Butylamine found, ng/ml*	Error, %
1	290	253 ± 20	-12.8
	1080	1027 ± 36	-4.9
2	290	279 ± 7	-3.8
	1080	1048 ± 26	-3.0
3	290	286 ± 40	-1.4
	1080	1058 ± 11	-2.0
4	290	225 ± 25	-22.4
	1080	1089 ± 260	+0.8

*Mean ± standard deviation, (n = 3)

Despite their high reactivity, the acridinium triflates are chemically stable for up to 18 months when stored in tightly sealed bottles at ambient temperature. However, methanolic solutions of the compounds rapidly degenerate and must be prepared not more than 10 min before use.

Tables 4 and 6 show the linear regression data obtained for the acridinium triflates 1-4 when each is reacted with aniline and n-butylamine at 60° for 30 min and the absorbances are measured at 445 and 439 nm, respectively. Tables 5 and 7 give the relative error (*i.e.*, the

accuracy) and precision data (RSD) for spiked samples of aniline and n-butylamine, respectively, assayed by the method described, with each triflate. All the triflates except 4 provide reasonable accuracy and precision in the determination of these model amines. Triflates 1 and 2 appear to provide the best overall accuracy and precision. In this laboratory, triflate 1 has recently been shown to be applicable for the determination of some primary aromatic amine type drugs in an on-line HPLC procedure where the triflate is added to the flowing stream post-column and derivatization is achieved in a mixing coil before the detector. In another example, triflate 1 was reacted with cycloserine in an HPLC pre-column method in which the resulting cycloserine-acridinium triflate product was separated from the rest of the reaction matrix by a silica HPLC column and was quantified by measurement of its fluorescence intensity.

Even though compound 4 possesses the strongest native absorbance in the 439-445 nm range, interference from the excess of reagent is most formidable, even after lengthy heating of the analytical solution. It may be that this interference can only be minimized by use of a flowing stream system such as HPLC, where reagent and product can potentially be separated.

Acknowledgements—The authors thank Professors C D Blanton, R K Hill and P C Ruenitz for their helpful contributions to the syntheses.

REFERENCES

- 1 J T Stewart, T D Shaw and A B Ray, *Anal Chem*, 1969, **41**, 360
- 2 J T Stewart and D M Lotti, *J Pharm Sci*, 1970, **59**, 838
- 3 J T Stewart and R E Wilkin, *ibid*, 1972, **61**, 432.
- 4 J. T. Stewart, Unpublished results.
- 5 A. Albert, *The Acridines: Their Preparation, Physical, Chemical, and Biological Properties and Uses*, p 281 Arnold, London, 1966
- 6 E F V Scriven, in A R Katritzky and C W Rees (eds), *Comprehensive Heterocyclic Chemistry*, Vol 2, p 166 Pergamon Press, Oxford, 1984
- 7 F A Carey and R J Sundberg, *Advanced Organic Chemistry, Part A: Structure and Mechanisms*, p 212 Plenum Press, New York, 1977

EXTRACTION SPECTROPHOTOMETRIC METHOD FOR THE DETERMINATION OF ASCORBIC ACID IN PHARMACEUTICAL PREPARATIONS, URINE AND FRUIT JUICES WITH POTASSIUM IODATE

SAIDUL ZAFAR QURESHI, AHSAN SAEED, SEEMA HAQUE and MUBEEN AHMAD KHAN

Analytical and Environmental Research Laboratories, Department of Chemistry,
Aligarh Muslim University, Aligarh-202 002, India

(Received 22 March 1989 Revised 7 December 1990 Accepted 28 January 1991)

Summary—An indirect determination of ascorbic acid is based on extraction of the iodine produced by reduction of potassium iodate. Beer's law is obeyed over the range 0.02–0.36 mg/ml ascorbic acid.

The detection and determination of ascorbic acid has been reviewed.¹ It has been determined spectrophotometrically with the Folin phenol reagent,² chloranil,³ sulphonated ferrozine⁴ and a new ferriox type reagent.⁵ The 2,4-dinitrophenylhydrazine and phosphotungstic acid methods for spectrophotometric determination of ascorbic acid have been compared.⁶ It has been determined spectrophotometrically by reaction with tetrazolium chloride derivatives⁷ and by first-derivative direct spectrophotometry.⁸ The silver-gelatin complex has been used in a reductive spectrophotometric method.⁹ Oxidation with bromine has been applied kinetically, spectrophotometrically and titrimetrically.¹⁰ The colour reaction with ferricinium trichloroacetate has been used for extraction spectrophotometry.¹¹ Ascorbic acid has been titrated with chloranil in the presence of hexamethylenetetramine in acetone-water mixture.¹² Heating an ascorbic acid solution with acidified ammonium vanadate yields a green product which can be measured at 680 nm.¹³ Other spectrophotometric methods are based on reduction of iron(III) in presence of dimethylglyoxime and of the iron(III)-EDTA complex in the presence of 2,2'-bipyridyl.¹⁵ In our studies, ascorbic acid has been found to react with potassium iodate in presence of hydrochloric acid to produce a yellow product, which on extraction with carbon tetrachloride gives a pink solution which can be used for spectrophotometric determination.

EXPERIMENTAL

Reagents

A 10 mg/ml ascorbic acid solution, a 0.1M potassium iodate solution and 0.01M hydro-

chloric acid were prepared with conductivity water.

Procedure

To a known volume of solution containing 0.1–1.8 mg of ascorbic acid add 1 ml of 0.1M potassium iodate followed by 1 ml of 0.01M hydrochloric acid. Shake the solution with 5 ml of carbon tetrachloride for a few minutes and separate the organic layer. Dry it over anhydrous sodium sulphate and measure its absorbance at 520 nm against carbon tetrachloride.

Analysis of formulations

Weigh several tablets individually, grind them to a powder and mix it. Similarly weigh and mix the contents of several capsules. Weigh an amount of sample equivalent to about 50 mg of ascorbic acid, stir it with 30 ml of conductivity water, let stand for 15 min, filter off the residue on a Whatman No. 42 paper and wash it with water. Dilute the filtrate and washings to volume in a 50-ml standard flask and proceed as above.

Determination of ascorbic acid in urine

To 40 ml of urine sample add 10 ml of 20% metaphosphoric acid and analyse for ascorbic acid by the procedure above.

Determination of ascorbic acid in fruit juices

Squeeze the juice from the fruit, add 50 ml of 20% trichloroacetic acid solution to a known volume of the juice to prevent oxidation of the ascorbic acid, centrifuge, and mix the supernatant liquid with 10 ml of 3% metaphosphoric acid solution and filter. Dilute the filtrate to a

suitable total volume and analyse a 1-ml aliquot as above.

RESULTS AND DISCUSSION

Determination of ascorbic acid

The absorption spectrum of the yellow extract in carbon tetrachloride has a maximum at 520 nm. In an optimization study it was found that

1 ml of 0.1M potassium iodate and 1 ml of 0.01M hydrochloric acid are adequate for the determination. Beer's law is obeyed over the range 0.1–1.8 mg of ascorbic acid in the organic phase

Results for the determination of ascorbic acid in pharmaceutical preparations, urine and fruit juices are given in Tables 1 and 2 and are compared with those obtained by reference

Table 1 Results for determination of ascorbic acid in pharmaceutical preparations

Drug	Nominal composition, mg	Present	C V, †%	Comparison	Reference
		method,* mg		method, mg	
Livogen	75 ascorbic acid	76	0.3	71	18
	1.50 folic acid				
	150 ferrous fumarate				
	10 vitamin B ₁₂				
	5 vitamin B ₁				
	5 vitamin B ₂				
	1.50 vitamin B ₆				
	5.0 calcium pantothenate				
	45 nicotinamide				
	25.0 dried yeast				
Hematrin	25 ascorbic acid	23	0.4	20	18
	0.5 folic acid				
	100 ferrous succinate				
	2.5 vitamin B ₁₂				
Sukcee	15 nicotinamide	498	0.1	493	12
	500 ascorbic acid				
	0.3 folic acid				
	ferrous calcium				
	500 citrate complex				
Rarical	2 vitamin B ₁	34	0.5	—	—
	1 vitamin B ₆				
	1 vitamin B ₁₂				
	35 ascorbic acid				
	500 ferrous cal cit				
	2 calcium pantothenate				
	1.5 vitamin B ₁				
	1 vitamin B ₂				
	2 vitamin B ₆				
	10 nicotinamide				
Chewcee	0.3 folic acid	497	0.1	510	12
	2000 IU vitamin A				
	150 IU vitamin D ₃				
	vitamin B ₁₂				
	500 ascorbic acid				
	300 ascorbic acid				
	10 vitamin B ₁				
	10 vitamin B ₂				
	2 vitamin B ₆				
	100 niacinamide				
Besiton	50 calcium pantothenate	315	0.1	318	12
	1.5 folic acid				
	4 µg vitamin B ₁₂				
	300 ascorbic acid				
	10 vitamin B ₁				
	10 vitamin B ₂				
	3 vitamin B ₆				
	5 µg vitamin B ₁₂				
	50 niacinamide				
	12.5 calcium pantothenate				
Becosules	1.0 folic acid	306	0.1	310	12
	150 ascorbic acid				
	10 vitamin B ₁				
	10 vitamin B ₂				
	3 vitamin B ₆				
	5 µg vitamin B ₁₂				
	50 niacinamide				
	12.5 calcium pantothenate				
	1.0 folic acid				
	150 ascorbic acid				
Cilatn	10 sodium hydrogen sulfite	144	0.2	142	12
	10 sodium hydrogen sulfite				

*Average of six determinations

†Coefficient of variation

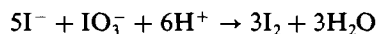
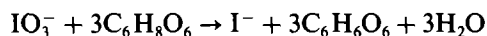
Table 2 Determination of ascorbic acid in urine and fruit juices

Sample	Ascorbic acid found,* mg/100 ml		
	Aliquot, ml	Present method	Comparison method
Urine	2	19.5	19
Tomato	1	105	103
Lemon	1	150	151
Orange	1	114	115

*Average of three determinations

methods. Species such as folic acid, ferrous fumarate, vitamins B₁, B₂, B₆, B₁₂, nicotinamide and calcium pantothenate, that are commonly present in the pharmaceutical preparations, do not affect the results.

Hurka gave an early review of organic compounds which can be determined by oxidation with potassium iodate,¹⁶ and Erdey *et al.*¹⁷ have reported that iodate oxidizes ascorbic acid in moderately acidic medium and if present in excess is reduced to iodine, which can be extracted into carbon tetrachloride. The reaction may be regarded as the composite result of reduction to iodide, followed by the well known iodide/iodate reaction to yield iodine.



REFERENCES

- 1 L A Pachla, D L Reynolds and P T Kissinger, *J Assoc Off Anal Chem*, 1985, **68**, 1
- 2 S K Jagota and H M Dani, *Anal Biochem*, 1982, **127**, 178
- 3 N K Pandey, *Anal Chem*, 1982, **54**, 763
- 4 E L McGown, M G Rusnak, C M Lewis and J A Tillotson, *Anal Biochem*, 1982, **119**, 55
- 5 A A Schilt and M R Di Tusa, *Talanta*, 1982, **29**, 129
- 6 A Castelli, G E Martorana, A M Frasca and E Meucci, *Acta Vitaminol Enzymol*, 1981, **3**, 103
- 7 P Wassileva-Alexandrova and A Nejtšcheva, *Mikrochim Acta*, 1982 **1**, 387
- 8 M E Abdel-Hamid, M H Barary, E M Hassan and M A Elsayed, *Analyst*, 1985, **110**, 831
- 9 T Pal and D S Maity, *Anal Lett*, 1985, **18**, 1131
- 10 M A Abdel-Salam, M E Abdel-Hamid and M A H Elsayed, *Sci Pharm*, 1982, **50**, 11
- 11 M M Aly, M K Hassan and R M Souliman, *J Chem Technol Biotechnol*, 1980, **30**, 435
- 12 K K Verma, A Jain and R Rawat, *J Assoc Off Anal Chem*, 1984, **67**, 262
- 13 V N Pathak, A L Singh and I C Shukla, *J Indian Chem Soc*, 1984, **65**, 652
- 14 I Z Al-Zamil, M A Al-Hajjaji, S A Al-Tamrah, A M Aziz-Alrahman and S M Sultan, *Orient J Chem*, 1986, **2**, 6
- 15 D Nagahama, *Rinsho Byori*, 1983, **31**, 331
- 16 W Hurka, *Mikrochemie*, 1944, **31**, 83
- 17 L Erdey, E Bodor and I Buzás, *Z Anal Chem*, 1951, **134**, 22
- 18 *Official Methods of Analysis*, 12th Ed, p 829 AOAC, Arlington, 1975

COMPARISON OF THREE COLORIMETRIC METHODS FOR THE DETERMINATION OF MANGANESE IN FRESHWATERS

B CHISWELL and K R O'HALLORAN

Department of Chemistry, The University of Queensland, Brisbane, QLD 4072 Australia

(Received 6 February 1989 Revised 21 January 1991 Accepted 28 January 1991)

Summary—Three colorimetric methods for the determination of manganese in freshwaters have been investigated and compared with the atomic-absorption spectrometry (AAS) method. Two of the methods, viz the formaldoxime (FAD) and pyridylazonaphthol (PAN) methods were found to yield poor calibration curves upon standardization, and to have high average errors for the estimation of manganese concentrations in standard solutions. The FAD method, when applied to freshwater samples, was found to be subject to an interfering UV absorbance which could not be negated successfully by a reagent blank, the method thus tended to give high estimations at low concentrations of manganese, but the results obtained also appear to be very sensitive to the nature of the freshwater matrix. On the other hand the PAN method was found to give very high estimations for the concentration of manganese, in both standard solutions and in freshwater samples, owing to the nature of the absorbance of the ligand used for manganese determination. This method also appears to be affected by the freshwater matrix, leading to gross overestimation of manganese levels. A third method, based on a porphyrin ligand [T-(4-CP)P], was found to give results comparable with those of the AAS method in estimating the soluble manganese content in freshwaters.

Standard Methods for the Analysis of Water and Wastewater describes only one colorimetric method for the determination of manganese in water.¹ This method is based on the persulphate oxidation of lower oxidation states of manganese to the purple permanganate ion. However, the molar absorptivity of MnO_4^- is only about $2.4 \times 10^3 \text{ l. mole}^{-1} \cdot \text{cm}^{-1}$, and even with the use of 5-cm spectrophotometric cells, the lower level of manganese detectable by this method is only approximately 40 $\mu\text{g/l.}$

Although World Health Organization limits for manganese in potable water have been put at 100 $\mu\text{g/l.}$, many water authorities find that manganese levels in excess of 50 $\mu\text{g/l.}$ in reticulation systems can lead to problems associated with black deposits in pipes and, consequently, black water from taps.

The two colorimetric methods that have found wide usage for the determination of manganese in freshwater, down to a concentration of 15 $\mu\text{g/l.}$, are those employing either formaldoxime (FAD) or 1-(2'-pyridylazo)-2-naphthol (PAN) as reagent. Both techniques have a minimum detectable concentration of manganese of roughly 15 $\mu\text{g/l.}$, but the work reported here indicates that both methods have

difficulties in yielding accurate results for manganese in dam waters.

In an earlier paper² we reported upon the development of a very successful colorimetric method for the determination of manganese, based on the use of the reagent $\alpha, \beta, \gamma, \delta$ -tetrakis(4-carboxyphenyl)porphine [T(4-CP)P], which we have comprehensively tested for down to 10 $\mu\text{g/l.}$ manganese in dam waters, and which can be used either for batch analysis in the laboratory, or in an autoanalyser unit.

The work here reported demonstrates the clear superiority of the T(4-CP)P method over both the FAD and PAN methods of manganese determination, and demonstrates how well its results correlate with those obtained by atomic-absorption spectrometry (AAS), for manganese determination in freshwaters.

EXPERIMENTAL

Sampling and sample pretreatment

Dam waters were sampled by use of a portable double-ended PVC cylindrical depth-sampler manufactured by Research Instruments MFG of Canada. Samples were transferred into polythene bottles which had been previously twice washed with 2M nitric acid and then

thoroughly washed with reagent-grade water. It should be noted that although samples for AAS analysis were stored at pH < 2 prior to analysis, samples to be analysed by other techniques were not necessarily acidified upon collection, unless the sample was to be analysed for total manganese.

Immediately after collection, samples were filtered through 0.45- μ m cellulose acetate membranes (Sartorius) with a Sartorius polycarbonate SM16510 filter holder and a Nalgene Mityvac (Newark, U.S.A.) hand vacuum pump.

The reproducibility of the filtration technique was found to be approximately 4% in terms of manganese concentration found in the filtrates and the residues retained.³ On two different days, ten replicate samples were drawn from the depth samples, filtered, and analysed for manganese by AAS, with the results shown in Table 1.

Colorimetric methods

All reagents used were of analytical grade unless otherwise specified. All distilled water was further purified by passage through a "Milli-Q" purification unit (Waters), this is hereafter termed reagent-grade water. A Hewlett-Packard HP8540 spectrometer was used for taking spectra and measuring absorbances.

Formaldehyde (FAD) method. The FAD reagent was prepared by mixing hydroxylamine hydrochloride (8.0 g) in reagent-grade water (50 ml) with formaldehyde solution (30% w/w, 4 ml) and making up to 100 ml with reagent-grade water. The EDTA reagent was prepared by dissolving the disodium salt (9.3 g) in reagent-grade water (100 ml).

To 20 ml of water sample (in a 25-ml standard flask) were added FAD reagent (1 ml) and ammonia solution (15% w/w, 1 ml). After mix-

ing and being allowed to stand for 2 min, the sample solution was treated with EDTA reagent (1 ml) and hydroxylamine hydrochloride solution (10% w/w, 2 ml). The absorbance of the red-brown solution was measured at 450 nm after 10 min, against a reagent blank.

Pyridylazonaphthol (PAN) method. A buffer solution of pH 9.2 was prepared by mixing 2M ammonia solution (30 ml) and 2M ammonium chloride solution (70 ml) and diluting to 1 litre with reagent-grade water.

To 10 ml of water sample (in a 25-ml standard flask) were added sodium ascorbate (10 mg), triethanolamine solution (20% v/v, 1 ml), buffer solution (1 ml), Triton X-100 solution (20% v/v, 1 ml), potassium cyanide solution (5% w/w, 0.5 ml) and PAN solution (10 mg/ml in methanol, ml), with mixing after each addition. The mixture was made up to volume with reagent-grade water and the absorbance of the red-orange solution was measured at 562 nm against a reagent blank.

Porphyrin [T-(4-CP)P] method. T-(4-CP)P was prepared by refluxing a propionic acid solution of 4-carboxybenzaldehyde and pyrrole (both 0.24M) for 6 hr. Upon cooling, purple crystals of T-(4-CP)P separated out; these were recrystallized by dissolution in warm methanol followed by filtration under gravity, cooling, and initiation of crystallization by addition of the minimum amount of chloroform needed. The 2×10^{-4} M reagent solution was prepared by dissolving the porphyrin (79.1 mg) in 0.1M sodium hydroxide (5 ml) and diluting to 500 ml with reagent-grade water and storing in an amber glass bottle. Cadmium chloride solution, 6×10^{-4} M, was prepared by dissolving 0.0505 g of CdCl₂ in 500 ml of reagent-grade water. A buffer solution of pH 8.0, which was 0.15M with respect to imidazole, was prepared by adding successively 0.025M sodium tetraborate (50 ml), 0.1M hydrochloric acid (20 ml) and imidazole (1.02 g in 25 ml of water), the pH, adjusted to 8.0 by addition of 0.1M hydrochloric acid, and diluting to volume in a 100-ml standard flask.

To the water sample (20 ml for 0–100 μ g/l manganese) in a 25-ml standard flask with its outside painted black (except for the area around the graduation mark), were successively added cadmium chloride solution (1 ml), buffer (1 ml) and T-(4-CP)P solution (3 ml). The mixture was made up to volume with reagent-grade water, and the absorbance of the green-brown solution measured at 468 nm after 5 min, against a reagent blank.

Table 1. Reproducibility of the effect of 0.45- μ m filtration on ten duplicate samples drawn from dam water on two different days, as evidenced by manganese analyses performed by AAS.

	Mean, ng/ml	Standard deviation, ng/ml	Relative standard deviation, %
Day 1			
Filterable Mn	965	25	2.6
Residual Mn	360	9	2.4
Total Mn	1325	19	1.4
Day 2			
Filterable Mn	714	2	0.3
Residual Mn	565	3	0.5
Total Mn	1279	5	0.4

Atomic-absorption spectrometry

Water samples for analysis were always acidified to $\text{pH} < 2$ by dropwise addition of concentrated hydrochloric acid. Analysis measurements were done on a Varian AA875 spectrometer at wavelengths of either 279.5 or 403.1 nm, using an oxidizing air/acetylene flame. Manganese standards up to 1000 $\mu\text{g/l}$ were prepared by suitable dilution of an Aldrich 1000 mg/l atomic-absorption standard solution. As the range of concentrations was large, two calibration graphs were prepared, covering the ranges 0–100 and 100–1000 $\mu\text{g/l}$, their correlation coefficients are given in Table 2.

RESULTS AND DISCUSSION

Formaldehyde (FAD) method

The method widely used is that described by Abdullah,⁴ which includes the addition of ascorbic acid to remove iron interference. We have found that at the 450 nm wavelength used, the rate of decrease in absorbance with time introduces a large error when batch analyses are undertaken in which there are variable times between mixing of reagents and the taking of spectrophotometric readings (see Fig. 1). We believe that the instability of the Mn–FAD complex, in the presence of ascorbic acid, is due to the reducing nature of the latter. The Mn–FAD complex is reported to be a six-coordinate Mn(IV) compound,⁵ which would be amenable to reductive decomposition, resulting in destruction of the complex and decrease in the absorbance at 450 nm.

The method of Goto *et al.*⁶ was used in the work described here, as the colour developed in this method is relatively stable with time (see Fig. 1). The method of Henriksen,⁷ which in-

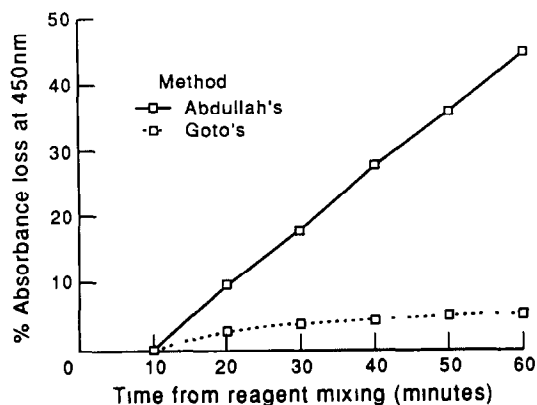


Fig. 1 Comparison of colour stability for the two methods of manganese determination by the formaldehyde method

volves the addition of iron(II) to assist in removal of the Fe–FAD interference by use of an EDTA–hydroxylamine mixture, gave no improvement in results for the range of manganese concentrations studied.

The value of both the Goto *et al.* and Henriksen methods may, of course, depend on the level of iron present in the sample under analysis. Iron concentrations in the dam waters sampled were of the same order of magnitude as those of manganese, *i.e.*, from $< 10 \mu\text{g/l}$ to 1 mg/l.

A guide to the precision of any colorimetric method can be found in the correlation coefficients, which represent the adherence to the Beer–Lambert law over a given analyte concentration range. The accuracy can be best judged by comparing experimentally determined results either with known values, or with the results obtained by a reference technique, which in this case was the AAS method. Table 2 gives a comparison of the correlation coefficients and average absolute errors for the three colorimetric techniques and the AAS method, over two analyte concentration ranges.

For the 0–100 $\mu\text{g/l}$ range the FAD method shows poor linearity. Over this range the average error for an unknown manganese concentration is 11%. However, for the 100–1000 $\mu\text{g/l}$ range the average error improves significantly to 3.8%. It is reasonable to conclude that the accuracy of the FAD method is doubtful over the 0–100 $\mu\text{g/l}$ range, without any additional sources of interference associated with real sample analysis.

Based on results obtained over a twelve-month period for filtered (0.45 μm membranes) water samples collected from two dams in south-east Queensland, it was found that the FAD method gave higher results than AAS for manganese concentrations $< 100 \mu\text{g/l}$, but lower results than AAS for manganese concentrations $> 100 \mu\text{g/l}$. We believe that these differences are related to both the nature of the dam water matrix and the changes in manganese speciation with time and depth of sampling. The possibility that the (variable) presence of iron in the samples analysed could lead to the discrepancies in the results obtained by the two analytical methods could not be substantiated, no correlation could be observed between iron concentration and discrepancy.

Figure 2 shows a typical spectrum obtained with the FAD method for a dam water sample. For this sample the manganese concentration found by AAS was below the AAS detection

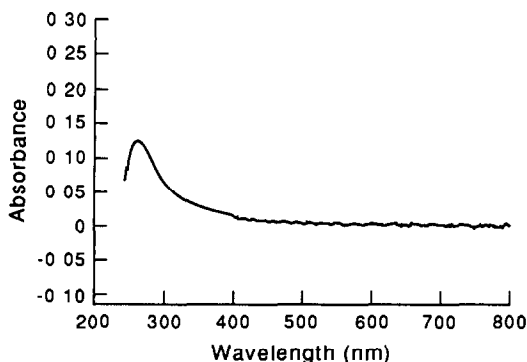


Fig 2 Spectrum obtained when a North Pine Dam water sample, containing no AAS-determinable manganese, is analysed by the FAD method, with a reagent blank in the reference beam

limit for manganese quoted by the instrument manufacturers,⁸ the FAD method gave 13 $\mu\text{g/l}$. The feature to note is the prominent peak at 260 nm. Its cause is not known, but it occurs in all spectra for dam water samples, varying both in wavelength of absorption maximum and in absorbance. We believe that the peak is probably associated with humic materials in the dam water matrix, which, depending on their chemical nature, absorb in the 250–300 nm region.⁹

Humic material varies, both in concentration and nature, with dam water depth, which accounts for the variability in wavelength and absorbance values between samples. This high absorbance in the ultraviolet region greatly increases the apparent manganese concentration determined by the FAD method. We conclude that for natural water samples containing humic matter (especially in cases of low concentration of manganese) the FAD method, which lacks sensitivity, will tend to overestimate the manganese concentration significantly.

To provide a reagent blank which successfully negates the ultraviolet absorbance of the humic material, thereby removing the interference in the manganese determination in the visible region, would require the preparation of different blanks, constituted from the raw water being analysed, for each analysis, as the dam water matrix constitution changes with depth. Such an approach is impractical for a large number of samples and the method is not amenable to automation.

The reason why the FAD method underestimates manganese concentrations above 100 $\mu\text{g/l}$ is not known.

Pyridylazonaphthol (PAN) method

The complex formed between manganese and PAN is not soluble in aqueous solution, so various methods of extraction into organic phases prior to spectrophotometric reading have been proposed.^{10,11} The method used in this work avoided this tiresome step by adaptation of the method of Goto *et al.*,¹² which uses a synthetic surfactant, Triton X-100, to avoid the need for extraction. Although these workers propose the use of sodium ascorbate to keep the manganese complex in the bivalent state, which stops discoloration of the complex, we have found that the Mn–(PAN) colour is stable for at least 2 hr and that the use of sodium ascorbate is not necessary in analysis of the waters studied here.

Table 2 indicates that the precision and accuracy of the PAN method in the present work were poor over the manganese concentration range 0–100 $\mu\text{g/l}$., with an average error of 11% for a set of 10 samples containing a known manganese concentration. The plot of absorbance against manganese concentration was markedly non-linear, with an obvious scatter of points (see Fig 3). This suggests that the method is useless for low manganese concentrations. For the 100–1000 $\mu\text{g/l}$ range better linearity was observed, the average error for known manganese concentrations being 7.2%, but even at these concentrations such a large error makes the PAN method unacceptable.

The major failure of the method arose from the nature of the spectrum close to the peak (at 562 nm) used for manganese determination. Figure 4 shows the spectrum of PAN in reagent-grade water, measured against a reagent-grade

Table 2 Correlation coefficients of calibration curves and average percentage errors for the four analysis methods used to determine manganese in standard solutions

Method	[Mn], 0–100 $\mu\text{g/l}$		[Mn], 100–1000 $\mu\text{g/l}$	
	Linear correlation coefficient	Average error, %	Linear correlation coefficient	Average error,* %
FAD	0.9882	11	0.9983	3.8
PAN	0.9844	11	0.9931	7.2
T-(4-CP)P	0.9996	2.0	0.9999	0.4
AAS	0.9999	1.5	0.9999	0.5

*Average error (%) in Mn determination was obtained by preparing a set of 10 samples containing known amounts of manganese and determining the concentration by using previously prepared calibration curves for both the colorimetric and AAS methods. The average errors in these analyses were than calculated.

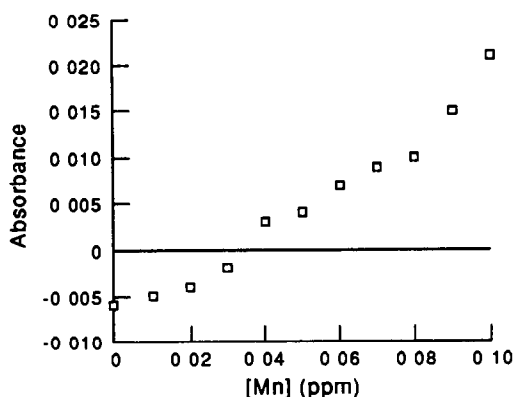
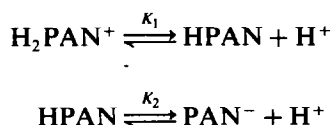


Fig 3 Plot of absorbance against manganese concentration, for standard solutions (0.0–0.1 mg/l) analysed by the PAN method (with a reagent blank in the reference beam), showing the non-linearity of the calibration data

water blank at pH 9.2; two main features are discernible (a large peak at about 470 nm and a shoulder at about 400 nm) but no peak is seen at 562 nm.

Absorption bands at 440, 470 and 495 nm are said to arise from the successive dissociations of the ligand.¹³



where $\text{p}K_1$ for dissociation of a proton from the pyridinium group in the protonated reagent is 2.9, and $\text{p}K_2$ for dissociation of the phenol proton is 11.6. H_2PAN^+ gives a broad band at 400–450 nm, HPAN a band at about 470 nm with a shoulder at 400 nm, and PAN^- gives a peak at 495 nm.

When manganese is added to a PAN solution at pH 9.2 a peak at 562 nm appears (Fig. 5),

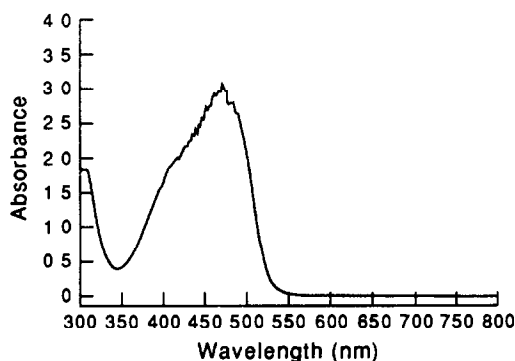


Fig 4 Spectrum of PAN ligand solution at a concentration equivalent to that of a reagent blank, with reagent-grade water in the reference beam

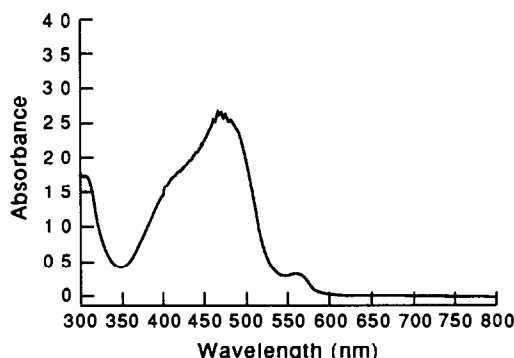


Fig 5 Spectrum of a PAN ligand solution at a concentration equivalent to that of a reagent blank, to which has been added 10 ml of 1 mg/l Mn^{2+} solution, with reagent-grade water in the reference beam

presumably by the formation of $[\text{Mn}(\text{PAN})_2]$, in which both PAN moieties have lost their dissociable protons.

If the reagent-grade water reference used to obtain Fig 5 was replaced by the reagent blank (containing PAN) described in the experimental section, the peak at 562 nm became much more easily distinguishable from the shorter wavelength peaks (Fig 6), as the reagent blank then cancelled out the peaks due to the uncomplexed ligand. However, a further peak was apparent at about 525 nm, and its amplitude indicated that it was associated with the Mn–PAN complex and thus was not negated by the reagent blank. A similar double peak appears in the spectrum of Mn–PAN in ether solution.^{14,15} It seems likely that this strong peak at 525 nm may affect the Mn–PAN absorbance measured at 562 nm, which is used to determine the manganese concentration

The problem is exemplified by reference to Fig 7, in which the PAN signal at 562 nm (for

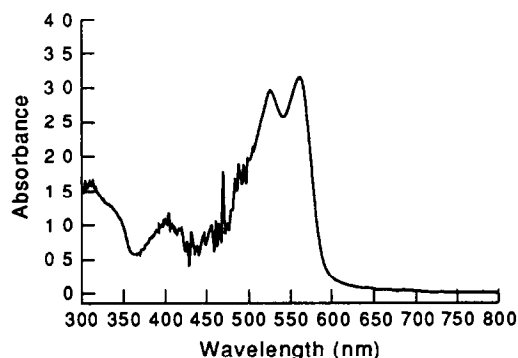


Fig 6 Spectrum of a PAN ligand solution at a concentration equivalent to that of a reagent blank, to which has been added 10 ml of 1 mg/l Mn^{2+} solution, with a reagent blank in the reference beam

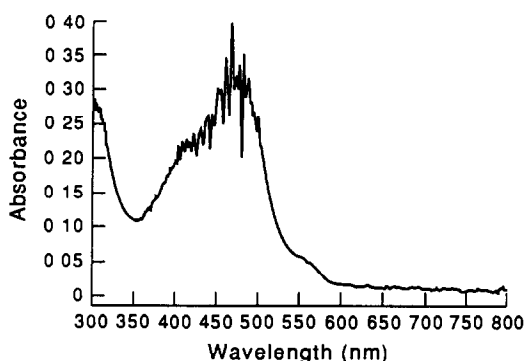


Fig 7 Spectrum obtained when a North Pine Dam sample, containing $62 \mu\text{g/l}$ AAS-determinable manganese, is analysed by the PAN method with a reagent blank in the reference beam

a sample of filtered North Pine Dam water (taken at the 9-m level) appears only as a shoulder and gives a manganese result of $220 \mu\text{g/l}$, whereas the value found by AAS was only $62 \mu\text{g/l}$. Such a large error cannot be entirely attributed to the poor calibration curve associated with the PAN method. It would appear that the water matrix is affecting the PAN ligand, resulting in a greatly overestimated manganese concentration.

Two sets of analyses of ten samples collected on two different days, at 3-m intervals from the surface down to 21 m (including samples at 10 and 11 m) showed that the PAN method consistently gave higher results than the AAS method. On average, the PAN results were about three times those obtained by AAS, with the largest relative errors at the lowest manganese values.

The PAN method is not amenable to automation, as the insoluble nature of the Mn-PAN complex results in significant build-up on the walls of the flow-through cells often used in Auto-Analyser or FIA systems.

Porphyrin [T-(4-CP)P] method

The method used was that of Ishii *et al.*, who used the porphyrin ligand to determine manganese in tea leaves¹⁶. The porphyrin, being a macrocyclic ligand, gives complexes of high stability and appears to be more selective than either FAD or PAN, as no masking agents are required when it is used. Furthermore, the water-soluble nature of the Mn-[T-(4-CP)P] complex results in a method which is simple, rapid, inexpensive and amenable to Auto-Analyser operation.² The selectivity of the T-(4-CP)P ligand is no doubt linked to the process by which the manganese complex is formed. At pH

8, Cd^{2+} is complexed by the porphyrin ligand in preference to Mn^{2+} , presumably for kinetic reasons. However, the higher stability constant of the Mn-[T-(4-CP)P] complex results in exchange of the Cd^{2+} for Mn^{2+} , although the exchange reaction is very slow. Imidazole is employed as a catalyst, allowing the exchange reaction to go to completion within 5 min. The Mn(II) complex formed is oxidized to an Mn(III) complex by dissolved oxygen.¹⁶ The result is a very selective method for determining Mn^{2+} in solution.

A further advantage of the method is that the molar absorptivity of the Mn-[T-(4-CP)P] complex is $7.6 \times 10^4 \text{ l mole}^{-1} \cdot \text{cm}^{-1}$, greater than that of either the Mn-PAN ($4.6 \times 10^4 \text{ l mole}^{-1} \cdot \text{cm}^{-1}$) or Mn-FAD complex ($1.6 \times 10^4 \text{ l mole}^{-1} \cdot \text{cm}^{-1}$). The sensitivity of the porphyrin method is thus superior to that of either of the other two methods, and the peak used for manganese determination is far less prone to dam water matrix interference, such as that found with the FAD method.

Figure 8 shows the spectra obtained during the exchange process. The significant feature is the large bathochromic shift between the Soret bands of the T-(4-CP)P ligand, the Cd(II)-[T-(4-CP)P] complex and the Mn(III)-[T-(4-CP)P] complex, which allows measurement of the Mn(III)-[T-(4-CP)P] band without possible interference from neighbouring absorbance peaks, which was found to be a major drawback of the PAN method.

Table 2 illustrates the precision and accuracy of the T-(4-CP)P method for both manganese concentration ranges studied. It can be seen that

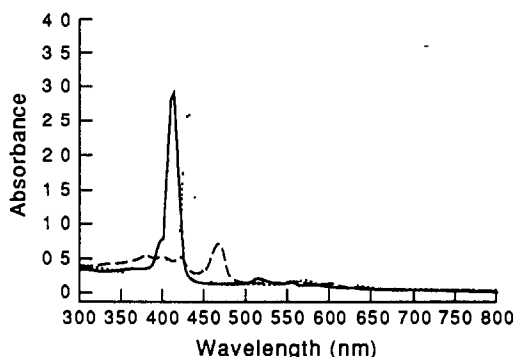


Fig 8 — Spectrum of a T-(4-CP)P ligand solution at a concentration equivalent to that of a reagent blank. Spectrum of the same solution to which has been added 1 ml of $6 \times 10^{-4} \text{ M Cd}^{2+}$ ---- Spectrum of the ligand/ Cd^{2+} solution to which has been added 10 ml of 1 mg/l Mn^{2+} solution. Reagent-grade water is used in the reference beam throughout.

Table 3 Results for manganese determinations by the three colorimetric methods and AAS for filtered water samples from North Pine Dam

Sample depth, <i>m</i>	Manganese concentration, $\mu\text{g/l}$			
	FAD	PAN	T-(4-CP)P	AAS
0	0.06	0.20	0.047	0.056
3	0.02	0.03	0.014	0.016
6	0.01	0.02	<0.010	<0.003
8	0	0.03	<0.010	0.007
9	0.04	0.16	0.024	0.034
10	0.02	0.03	0.017	0.016
11	0.02	0.03	<0.010	0.012
15	0.08	0.20	0.071	0.065
18	0.09	0.24	0.100	0.105
21	0.12	0.26	0.126	0.127

the correlation coefficients and average errors in manganese determination by the T-(4-CP)P method are very similar to those for the AAS method

CONCLUSIONS

The results in Table 3 allow comparison of the three colorimetric methods with each other and with the AAS method for filtered dam water samples. It is clear that the T-(4-CP)P and AAS results are in excellent agreement though with a general tendency of the former results to be lower. The FAD method also gives results in relatively good agreement with AAS. On the other hand the discrepancy between results ob-

tained by the PAN method and those of the three other analytical techniques is only too obvious; the use of this ligand gives gross over-estimation of the manganese present in dam water samples

REFERENCES

- 1 *Standard Methods for the Examination of Water and Wastewater*, 16th Ed., M A M Franson, A E Greenberg, R R Trussell and L S Clesceri (eds), pp 229-232 APHA, Washington, D C, 1985
- 2 P Aldridge, B Chiswell, M K Leigh, K R O'Halloran and M Pascoe, *Water*, 1989, **15**, 35
- 3 M B Mokhtar, *Ph D Thesis*, University of Queensland, 1987
- 4 M I Abdullah, *Anal Chim Acta*, 1968, **40**, 526
- 5 Z Marczenko, *ibid*, 1964, **31**, 224
- 6 K Goto, T Omatsu and T Furukama, *ibid*, 1962, **27**, 331
- 7 A Henriksen, *Analyst*, 1966, **91**, 647
- 8 *Water Analysis by Atomic Absorption Spectroscopy*, C R Parker, Varian Techtron, 1972
- 9 R A Dobbs, R H Wise and R B Dean, *Water Res*, 1972, **6**, 1173
- 10 T Yotsuyanagi, K Goto, M Nagayama and K Aomura, *Bunseki Kagaku*, 1969, **8**, 478
- 11 E M Donaldson and W R Inman, *Talanta*, 1966, **13**, 489
- 12 K Goto, S Taguchi, Y Fukue, K Ohta and H Watanabe, *ibid*, 1977, **24**, 752
- 13 B F Pease and M B Williams, *Anal Chem*, 1959, **31**, 1044
- 14 S Shibata, *Anal Chim Acta*, 1960, **23**, 367
- 15 *Idem*, *ibid*, 1961, **25**, 348
- 16 H Ishii, H Koh and K Satoh, *ibid*, 1982, **136**, 347

ION-EXCHANGE SEPARATION AND SPECTROPHOTOMETRIC DETERMINATION OF VANADIUM IN ENVIRONMENTAL SAMPLES

NEESHA SHAH and M. N. DESAI

Department of Chemistry, University School of Sciences, Gujarat University, Ahmedabad-380 009, India

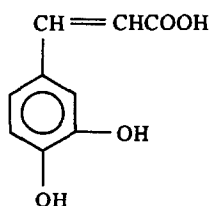
S K MENON and Y K AGRAWAL

Analytical Laboratory, Pharmacy Department, Faculty of Technology and Engineering, M S University of Baroda, Kalabhavan, Baroda, India

(Received 17 January 1989 Revised 31 December 1990 Accepted 11 January 1991)

Summary—A selective and sensitive method for the extraction and spectrophotometric determination of vanadium(V) in microgram quantities is described. The molar absorptivity of the yellow vanadium(V)—caffeic acid—Aliquat 336 extract is $1.3 \times 10^4 \text{ l mole}^{-1} \text{ cm}^{-1}$ at 370 nm. The method is compared with the atomic-absorption spectrometric method and applied to the trace determination of vanadium in steel, alloys, a rock and environmental samples.

Caffeic acid (I) is a versatile reagent used in organic, inorganic and pharmaceutical analysis.¹⁻³ In acidic medium it forms a stable yellow complex with vanadium(V) which can be extracted with isoamyl alcohol. This paper describes the extraction of the vanadium(V)—caffeic acid complex with the liquid ion-exchanger Aliquat 336, which can be applied to the determination of microgram amounts of the metal. The spectrophotometric method developed has been compared with the AAS method



EXPERIMENTAL

Reagents

All chemicals used were of guaranteed reagent (Merck) or AnalaR (BDH) grade. Vanadium(V) stock solution was prepared by dissolving 0.0585 g of ammonium metavanadate in 500 ml of doubly distilled water and standardized spectrophotometrically.⁴ It was further diluted as required. A 1 mg/ml caffeic acid solution was prepared in methanol

Buffer solutions in the pH range 2.0–6.0 were prepared from mixtures of 0.1 M sodium citrate and 0.1 M hydrochloric acid, or 0.2 M sodium acetate and 0.2 M acetic acid.⁵

Amberlite LA-1 (*N*-dodecyltrialkylamine, Rohm and Hass, Philadelphia), Aliquat 336 (tricaprylmethylammonium chloride, Fluka) and trioctylamine (Fluka) were dissolved in suitable diluents in various proportions.

Apparatus

A VSU 2 P spectrophotometer (Carl Zeiss, Jena) with matched fused-silica cells was used for spectral measurements. A GBC 901 atomic-absorption spectrometer equipped with a vanadium hollow-cathode lamp was used. The 318.4 nm vanadium line and a nitrous oxide–acetylene flame were used.

Dissolution of samples

General analytical procedures⁶⁻⁸ for bringing the samples into solution were followed. In all cases, complete oxidation to vanadium(V) was ensured by adding 0.05 M potassium permanganate dropwise to the solution until a light pink colour persisted for 1–2 min.

Rock samples. A 0.5-g sample was transferred into a 100-ml Teflon beaker and a mixture of concentrated hydrofluoric acid (10 ml), sulphuric acid (15 ml) and nitric acid (5 ml) was added. The mixture was then digested on a

steam-bath for 2–3 hr, diluted with water and filtered. The residue was washed and the filtrate and washings were finally diluted to volume in a 100-ml standard flask with distilled water.

Steel samples. A 1.0-g sample was transferred into a 150-ml borosilicate glass beaker and 25 ml of concentrated hydrochloric acid were added, followed by digestion on a sand-bath for 1 hr and evaporation to dryness. The residue was dissolved in 10–15 ml of concentrated hydrochloric acid along with 0.5 g of ammonium persulphate. The solution was diluted and filtered, and finally diluted to volume in a 100-ml standard flask with distilled water.

Plant samples. A known weight of sample (~100 g) was ashed, and 10 g of the ash was transferred into a 250-ml borosilicate glass beaker and digested on a sand-bath with 100 ml of concentrated hydrochloric acid and 20 ml of concentrated nitric acid for about 1 hr. The hot solution was centrifuged, and the supernatant liquid was decanted from any siliceous matter. The residue was washed with 10 ml of 0.1M hydrochloric acid and the combined solution was evaporated to dryness. The residue was taken up in 0.1M hydrochloric acid and accurately diluted to 100 ml with distilled water.

Soil samples. A 1–2 g sample of the dried soil was digested with 50 ml of concentrated hydrochloric acid and 10 ml of concentrated nitric acid for 1 hr on a sand-bath, then the solution was evaporated to dryness. The residue was boiled with 50 ml of 0.1M hydrochloric acid and filtered, then the filtrate and washings were evaporated to dryness and the residue was taken up and the solution diluted accurately to 100 ml with 0.1M hydrochloric acid.

Blood samples. A 2-ml blood sample was digested with 20 ml of concentrated hydrochloric acid and 0.25 g of ammonium persulphate for 1 hr, then the mixture was diluted and filtered. The filtrate and washings were evaporated to dryness and the residue was taken up and the solution diluted to volume in a 25-ml standard flask with 0.1M hydrochloric acid.

Water samples. A known volume of sample was evaporated to dryness and the residue was treated in the same way as plant ash.

Dissolution of Nb₂O₅ and Ta₂O₅

Niobium. Niobium oxide (1.79 g) was fused with 10.0 g of potassium bisulphate and the cooled melt was dissolved in 1M tartaric acid; the solution was diluted to 500 ml. The final

Table 1 Effect of pH on the extraction of 49 µg of vanadium(V) with caffeic acid and Aliquat 336 (conditions as in procedure)

pH	Absorbance	Extraction, %
3.0	0.060	12.0
3.2	0.180	36.0
3.5	0.360	72.0
3.9	0.500	99.9
4.0	0.550	99.9
4.2	0.500	99.9
4.5	0.250	49.9
5.0	0.050	10.0
6.0	0.020	4.0

concentration (2.5 mg/ml) of niobium was determined spectrophotometrically.⁹

Tantalum. Tantalum oxide (2.99 g) was fused with 10.0 g of potassium bisulphate and the cooled melt was dissolved in 1M ammonium oxalate; the solution was diluted to 250 ml. The final concentration of tantalum (9.8 mg/ml) was determined gravimetrically.¹⁰

Procedure

A suitable aliquot of sample solution containing 2.5–125 µg of vanadium was transferred into a 60-ml separatory funnel, 5 ml of 1-mg/ml caffeic acid solution were added and the pH was adjusted initially with alkali and finally with buffer to 4.0. The mixture was shaken gently with 5 ml of a 10-mg/ml solution of Aliquat 336 in isoamyl alcohol for about 1 min. The organic extract was collected and dried over anhydrous sodium sulphate and finally diluted to volume with isoamyl alcohol in a 25-ml standard flask. The absorbance was measured at 370 nm against a reagent blank.

For AAS measurements, the same extraction procedure was applied and the extracts were analysed by the EPA method¹¹ either directly or after back-extraction of the vanadium into 0.01M nitric acid.

Table 2 Effect of various diluents on the extraction of 49 µg of vanadium(V) at pH 4 with 5 ml of 1-mg/ml caffeic acid solution and 5 ml of Aliquat 336 solution (concentration A, 10 mg/ml, B, 20 mg/ml, C, 30 mg/ml)

Diluent	Extraction, %		
	A	B	C
Isoamyl alcohol	99.9	99.9	99.9
Benzene	10.2	10.0	10.2
Toluene	2.0	2.0	2.0
Hexane	1.5	1.5	1.5
Chloroform	0.5	0.5	0.5
Isobutyl methyl ketone	30.0	30.0	30.0

Table 3 Effect of different liquid anion-exchangers on the extraction of 49 μg of vanadium(V) at pH 4 with 5 ml of 1-mg/ml caffeic acid solution and 5 ml of 10-mg/ml exchanger solution

Liquid anion-exchanger	Diluent	Extraction, %
Aliquat 336	Isoamyl alcohol	99.9
	Benzene	10.2
Amberlite LA-1	Isoamyl alcohol	60.5
	Benzene	6.6
Trioctylamine	Isoamyl alcohol	48.9
	Benzene	3.5

RESULTS AND DISCUSSION

The yellow vanadium(V)-caffeic acid complex is readily extracted into a 10-mg/ml solution of Aliquat 336 in isoamyl alcohol from an aqueous medium of pH 4.0. The species extracted has maximum absorbance at 370 nm. The reagent blank does not show appreciable absorbance at this wavelength. The molar absorptivity is $1.3 \times 10^4 \text{ l mole}^{-1} \text{ cm}^{-1}$. The system obeys Beer's law in the range 0.1–5.0 ppm vanadium at 370 nm and the optimum range (Ringbom plot) is 0.1–4.8 ppm.

Effect of experimental variables

The vanadium(V) complex was found to be completely extracted into isoamyl alcohol over the pH range 3.9–4.2 (Table 1) and 5 ml of 1-mg/ml caffeic acid solution was found to be sufficient for complex formation. A larger excess of reagent has no adverse effect.

The optimum concentration of Aliquat 336 was studied by varying the concentration from 10 to 60 mg/ml in isoamyl alcohol. The extraction was quantitative over this range and 5 ml of 10-mg/ml solution was adopted for use. Various solvents for the Aliquat 336 were tested (Table 2). Isoamyl alcohol was found to be the most suitable. Aliquat 336 was selected as the liquid-anion exchanger, since it was found that of the three reagents tested (Table 3) it was the only one that gave complete extraction. It

Table 4 Determination of vanadium in NBS and BCS standard samples

No	Sample	Certified vanadium value, %	Vanadium found by present method,* %
67	Manganese steel (NBS)	0.17–0.19	0.185 \pm 0.010
117	Ferrotitanium (NBS)	0.05–0.08	0.062 \pm 0.020
132	Steel	1.60–1.68	1.69 \pm 0.02
224	Cr–V Steel (BCS)	0.240	0.24 \pm 0.01
241/1	High Speed Steel (BCS)	1.570	1.57 \pm 0.02

*Mean \pm standard deviation (8 determinations)

Table 5 Vanadium in natural materials

Sample	Vanadium found,* ppm	No of determinations	AAS, ppm
Potato sample 1	5.72 \pm 0.05	10	5.74
Potato sample 2	6.82 \pm 0.09	8	6.84
Onion sample 1	7.45 \pm 0.05	10	7.43
Onion sample 2	6.83 \pm 0.02	10	6.82
Carrots	3.55 \pm 0.02	8	3.55
Spinach	6.35 \pm 0.02	8	6.33
Cabbage	5.75 \pm 0.02	10	5.76
Unripe mango skin	1.54 \pm 0.03	9	1.55
Ripe mango skin	3.55 \pm 0.01	10	3.55
Tobacco	2.05 \pm 0.01	9	2.04
Corn leaves	1.10 \pm 0.01	9	1.10
Tomato	1.55 \pm 0.01	9	1.55
Rice	1.00 \pm 0.01	10	1.01
Peas (leaves)	0.75 \pm 0.02	12	0.77
Affluent I†	1.20 \pm 0.04	8	1.18
Affluent II†	0.08 \pm 0.02	10	0.07
Blood sample‡	0.022 \pm 0.02	10	0.021
MS-I§	330 \pm 0.2	8	332
DV-I§	320 \pm 0.2	8	318
DV-III§	330 \pm 0.1	8	333
Soil†	0.08 \pm 0.02	20	0.07

*Mean \pm standard deviation

†Samples from Nandesari Industrial Area of Baroda

‡Whole blood samples from adult males

§Samples from Mussories phosphate deposits

was found that a second extraction was not necessary.

Effects of diverse ions

Solutions containing a fixed concentration (1.32 ppm) of vanadium(V) and various amounts of a potentially interfering ion were extracted as described in the procedure. Barium, cadmium, calcium, cobalt(II), copper(II), nickel, titanium(IV) and tungstate can be tolerated up to 40 mg in the determination of 33 μg of vanadium. Mercury(II) and manganese(II) can be tolerated up to 50 mg, aluminium, lead and uranyl ion up to 60 mg. Tantalum and molybdenum interfere at 200 μg , and niobium at 225 μg , but in the presence of oxalate and tartrate as masking agents can be tolerated in amounts up to 40 mg, and so can zirconium. However, molybdenum interfered in the atomic-absorption determination of 33 μg of vanadium in the presence of 40 mg of Na, Ca, Mg, Cu, Ni, Zn, Pb, Cr, Al, Bi, Mo or Sb.

Determination of vanadium in various samples

The present method was compared with an AAS method with a reported detection limit of 0.2 ppm for vanadium.¹² Chromium(VI), iron(III), tin(IV) and molybdenum(VI) suppressed the absorption seriously for the direct determination but they did not interfere after extraction

of vanadium with the caffeic acid and Aliquat 336.

The results for the analysis of standard samples for vanadium are given in Table 4, and for rock, soil, blood samples *etc* in Table 5. The values are in good agreement with those obtained by AAS.

Acknowledgement—The authors are thankful to Dr R. A. Chalmers for his keen interest, valuable suggestions and criticism

REFERENCES

- 1 J C Somogyi, *J Vitaminol*, 1971, **17**, 165
- 2 R K Ibrahim, *J Chromatog*, 1969, **42**, 544
- 3 C F Timberlake, *J Chem Soc*, 1959, 2795
- 4 Y K Agrawal, *Anal Chem*, 1975, **47**, 940
- 5 D D Perrin and B Dempsey, *Buffers for pH and Metal Ion Control*, Chapman & Hall, London, 1974
- 6 I M Kolthoff, E B Sandell, E J Meehan and S Bruckenstein, *Quantitative Chemical Analysis*, 4th Ed., pp 1119–1139 Macmillan, London, 1969
- 7 *Comprehensive Analytical Chemistry*, C L Wilson and D N Wilson (eds), Vol IC, pp 560–563 Elsevier, Amsterdam, 1962
- 8 F J Welcher (ed), *Standard Methods of Chemical Analysis*, 6th Ed., Vol IIA, pp 691, 693, 694, 701, 702 Van Nostrand, Princeton, 1963
- 9 R Villarreal and S A Barker, *Anal Chem*, 1969, **41**, 611
- 10 F J Langmyhr and T Hongslo, *Anal Chim Acta*, 1960, **22**, 301
- 11 *Methods for Chemical Analysis of Water and Wastes*, EPA-600-4-79-020, U S Environmental Protection Agency, Ohio, 1979
- 12 A E Greenberg, J J Connors and D Jenkins (eds), *Standard Methods for Examination of Water and Waste Water*, 15th Ed., pp 141–146 American Public Health Association, Washington, 1980

PRECIPITATION AND EXTRACTION OF SOME BIVALENT METAL IONS WITH BIS(DIPHENYLPHOSPHINYL)METHANE AND PERCHLORATE

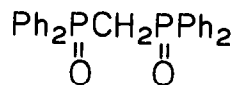
SHIGEO UMETANI,* NAOKI SHIGEMURA,† SORIN KIHARA and MASAKAZU MATSUI
Institute for Chemical Research, Kyoto University, Uji, Kyoto 611, Japan

(Received 1 August 1989 Revised 22 January 1991 Accepted 1 February 1991)

Summary—The solvent extraction of alkaline-earth and some bivalent transition metal ions such as Co^{2+} , Ni^{2+} , Cu^{2+} , Zn^{2+} and Cd^{2+} with the bidentate phosphine oxide compound, bis(diphenylphosphinyl)methane (BDPPM), and perchlorate into 1,2-dichloroethane has been investigated. When benzene is used as the solvent, the complexes consisting of metal ion, BDPPM and perchlorate are not extracted but are precipitated at the liquid-liquid interface. The precipitates have been isolated and their compositions determined.

The specificity of the adduct formation reactions of the bidentate neutral ligands, bis(diphenylphosphinyl)methane (BDPPM) and its ethane analogue, has been examined by investigation of the synergistic extraction of alkaline-earth,¹ rare-earth² and some bivalent³ metal ions. In the synergistic extraction of alkaline-earth metal ions with acylpyrazolone derivatives and BDPPM into benzene,¹ it was found that when sodium perchlorate was present, a precipitate appeared at the benzene-water interface, and the metal ions were not detectable in either the organic or the aqueous phase. A similar reaction was observed in the synergistic extraction of some bivalent metals into benzene with 1-phenyl-3-methyl-4-benzoyl-5-pyrazolone and BDPPM.³ These precipitation reactions suggest that ion-association complexes consisting of metal ion, BDPPM and perchlorate are formed, and precipitated because of their low solubility in both the benzene and water phases. This suggests that the complexes might be extractable into a more polar organic solvent. The possible use of BDPPM as a solvating extractant is interesting, since BDPPM is expected to be a more powerful ligand than 1,10-phenanthroline (phen),⁴ trioctylphosphine oxide (TOPO)⁵ and tributyl phosphate (TBP),⁶ owing to its strong

complex-formation ability and the high hydrophobicity.⁷⁻¹⁰ This possibility was examined in the present work.



BDPPM

EXPERIMENTAL

Reagents

BDPPM^{11,12} was prepared by oxidation of bis(diphenylphosphino)methane (Aldrich) with dilute hydrogen peroxide solution and purified by recrystallization from toluene. All other reagents were reagent-grade and used without further purification.

Apparatus

Metal-ion concentrations were measured with a Hitachi 180-70 polarized Zeeman atomic-absorption spectrophotometer and a Japan Jarrel Ash ICAP-500 inductively coupled argon-plasma emission spectrophotometer. A Shimadzu UV-180 double-beam spectrophotometer was used for spectrophotometric measurements. Infrared spectra were taken with a Hitachi 260-50 infrared spectrophotometer. The pH measurements were performed with a Hitachi-Horiba F-7ss pH-meter, equipped with a combination glass electrode.

*Author for correspondence

†Present address: Kimoto Electric Co., Ltd., 3-1 Funahashi-cho, Tennoji-ku, Osaka 543, Japan

Extraction of perchloric acid

A 5-ml portion of 1M perchloric acid was equilibrated at $25 \pm 1^\circ\text{C}$ in a 30-ml centrifuge tube with an equal volume of an organic solvent containing the required amount of BDPPM, for 1 hr. The acid concentration in the aqueous phase was measured by titration with sodium hydroxide. The acid content in the organic phase was measured by titration after back-extraction into water. The sum of the perchlorate concentrations in the two phases agreed well with the initial concentration.

Precipitation reaction

The precipitation reaction was examined in a similar way. A 10-ml portion of an aqueous phase containing the metal ion and sodium perchlorate was shaken with an equal volume of 0.01M BDPPM solution in benzene, at $25 \pm 1^\circ\text{C}$ for 1 hr. The pH of the aqueous phase was adjusted to *ca.* 2.0 with hydrochloric acid. The aqueous phase was filtered and the concentration of metal ion in it was measured by atomic-absorption spectrometry or ICP atomic-emission spectrometry. The amount of metal ion in the precipitate was obtained by subtracting the metal concentration found in the aqueous phase from that initially taken.

Determination of composition of the precipitates

The precipitates were collected by filtration, washed with water and dried under reduced pressure. A dichloroethane (DCE) solution of the precipitate was shaken with dilute hydrochloric acid and the amount of metal ion extracted into the aqueous phase was measured. The amount of BDPPM in the DCE solution was measured spectrophotometrically, and so was the amount of perchlorate in the aqueous solution, after extraction into chlorobenzene with Crystal Violet.¹³

Extraction of metal ions

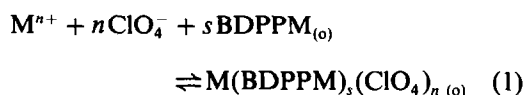
A 5-ml portion of 0.01M hydrochloric acid (pH 2.0) containing $1-2 \times 10^{-5}\text{M}$ metal ion and the required amount of sodium perchlorate was equilibrated with an equal volume of 0.01M BDPPM solution in DCE for 1 hr at $25 \pm 1^\circ\text{C}$. The ionic strength was adjusted by addition of sodium nitrate to the aqueous phase to keep the sum of $[\text{NaClO}_4]$ and $[\text{NaNO}_3]$ at 0.1M. After phase separation, the concentration of the metal ion in the aqueous phase was measured. The concentration of metal ion in the organic phase was determined in the same way after stripping

with dilute hydrochloric acid. The sum of the metal concentrations in the two phases agreed well with the initial concentration.

RESULTS AND DISCUSSION

Extraction of perchloric acid

The equilibrium for extraction of a metal ion (M^{n+}) or perchloric acid ($\text{M}^{n+} = \text{H}^+$) and the extraction constant, K_{ex} , can be expressed as



$$K_{\text{ex}} = \frac{[\text{M}(\text{BDPPM})_s(\text{ClO}_4)_n]_{(\text{o})}}{[\text{M}^{n+}][\text{ClO}_4^-]^n[\text{BDPPM}]_{(\text{o})}^s} \quad (2)$$

where subscript (o) denotes a species in the organic phase and s is the number of BDPPM molecules in one "molecule" of the extracted species. The distribution of perchloric acid is shown in Fig. 1, as a function of $\log [\text{BDPPM}]_{(\text{o})}$. The slopes of the straight portion of the plots is found to be very close to 2, indicating that two moles of BDPPM react with one mole of perchloric acid to form an $\text{H}(\text{BDPPM})_2(\text{ClO}_4)$ ion-pair. The extraction constants were calculated by use of equation (2). The values of $\log K_{\text{ex}}$ are 2.27 for DCE, 1.90 for benzene and 0.20 for chloroform. A similar trend in the effect of the organic solvent on the K_{ex} value has been reported for the extraction of some acids with TOPO.^{14,15} The poor extraction

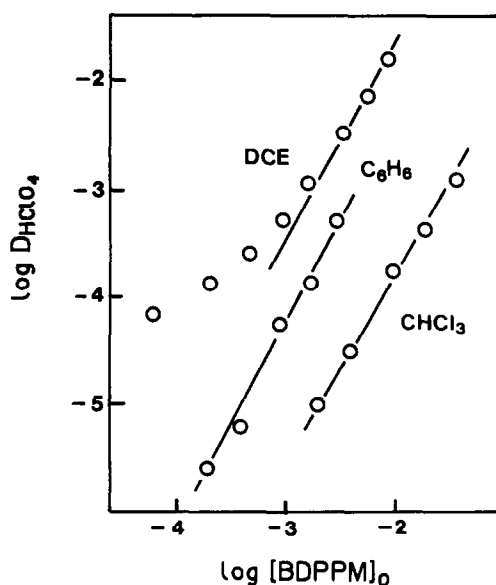
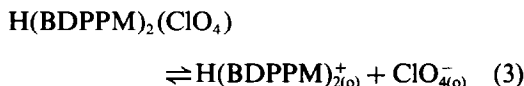


Fig. 1 Extraction of perchloric acid into various organic solvents, as a function of $\log [\text{BDPPM}]_{(\text{o})}$.

into chloroform suggests a strong hydrogen-bonding interaction of chloroform and the extractant, as suggested in the literature^{14,15} The deviation from the straight line at lower $[\text{BDPPM}]_{(o)}$ in the DCE system might be due to dissociation of the complex, because the dielectric constant of DCE is fairly large (10.36 at 25°), and in such conditions dissociation of the ion-pair could be considered dominant, especially when both the cation and the anion are singly charged and bulky, and the concentration is low¹⁶ The dissociation would be regarded as



Alternatively, the deviation could be the result of extraction of $\text{H}(\text{BDPPM})(\text{ClO}_4)$ when the BDPPM concentration is very low

Precipitation

The precipitation reactions of metal ions with BDPPM and perchlorate are illustrated in Figs 2 and 3, as a function of $\log [\text{ClO}_4]$ The precipitation reaction sets in suddenly when the perchlorate concentration exceeds a certain value, and the metal complexes are then precipitated completely. As $[\text{ClO}_4]$ increases, the alkaline-earth metal ions are precipitated in the order Ba^{2+} , Sr^{2+} , Ca^{2+} , Mg^{2+} , *i.e.*, the largest ion first and the smallest last. The bivalent transition metal ions are precipitated in the order Cd^{2+} , Zn^{2+} , Co^{2+} , Cu^{2+} , Ni^{2+} .

The compositions of the precipitates isolated are summarized in Table 1. The infrared absorption spectra of the complexes were measured by the KBr method and the characteristic bands

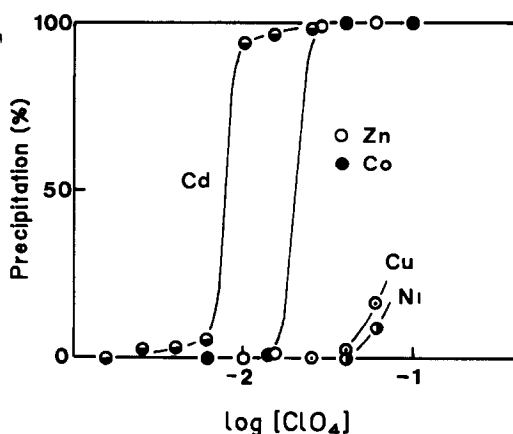


Fig 2 Precipitation of bivalent transition metals with BDPPM, as a function of $\log [\text{ClO}_4]$ BDPPM 0.01M in benzene, pH ca 2.0

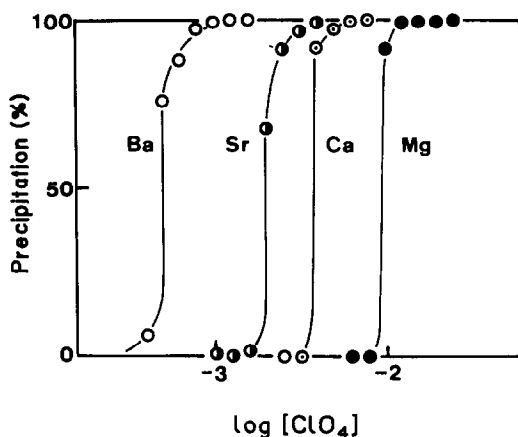


Fig 3 Precipitation of alkaline-earth metals with BDPPM, as a function of $\log [\text{ClO}_4]$ BDPPM 0.01M in benzene, pH ca 2.0

attributed to the $\text{P}=\text{O}$ group are also given in Table 1. The mole ratios for $\text{M}:\text{BDPPM}:\text{ClO}_4$ were found to be close to 1.4:2 for strontium and barium, and 1.3:2 for the other metals. The composition of the magnesium complex could not be expressed as the ratio of small whole numbers. The "theoretical" carbon and hydrogen contents were calculated from the proposed molecular formulae. The calculated values exhibit satisfactory agreement with the values found except for the Cd complex. The values found for the Mg complex are close to those for a 1:3:2 complex. The apparent deviation from simple stoichiometry is probably due in part to impurity in the precipitates, since no attempt was made to purify them.

Extraction of metal ions

Various organic solvents were examined. The metal ions examined are extractable into 1,2-dichloroethane (DCE) with BDPPM and perchlorate and can be stripped into water. Although the precipitates consisting of BDPPM, the metal ion and perchlorate are soluble in chloroform, no extraction into chloroform was observed under the conditions used. The complexes are completely extracted into nitrobenzene, but the metal ions cannot be back-extracted into water. A precipitate was observed at the benzene-water interface when the phases were separated by centrifugation. This precipitate dissolved if the aqueous phase was removed and the benzene phase replaced by the same volume of 0.01M hydrochloric acid and the phases were shaken; this occurred because equilibrium (1) is shifted to the left in the absence of perchlorate in the aqueous phase

Table 1 Composition of the metal complexes

M	BDPPM	ClO ₄	Found, %		Calcd, %		P=O band, cm ⁻¹
			C	H	C	H	
Mg	—	—	60.3	4.45	61.18*	4.52*	1175
Ca	1.292	1.94	60.4	4.41	60.53	4.47	1175
Sr	1.408	2.10	61.6	4.50	61.53	4.54	1190
Ba	1.418	2.04	59.6	4.46	60.00	4.43	1190
Co	1.305	1.97	59.6	4.51	59.78	4.41	1165
Ni	1.312	1.71	59.3	4.39	59.79	4.42	1165
Cu	1.327	2.04	59.1	4.38	59.59	4.40	1150
Zn	1.322	1.99	59.0	4.34	59.52	4.40	1170
Cd	1.313	1.98	56.9	4.42	57.73	4.26	1160

*Values for 1:3:2 complex

The same amount of metal ion as added initially was found in this new aqueous phase. Hydrocarbons such as cyclohexane are not suitable for use with BDPPM because of its low solubility in them. Accordingly, DCE was selected as the organic phase in the investigation of solvent extraction.

The extraction of metal ions into DCE with BDPPM, as a function of [ClO₄], is illustrated in Figs 4 and 5. The orders of efficiency of extraction of metal ions are Cd²⁺ > Zn²⁺ > Co²⁺ > Cu²⁺ > Ni²⁺ and Ca²⁺ > Ba²⁺, Mg²⁺ > Sr²⁺. The extraction order in Fig. 4 is the same as that of precipitation shown in Fig. 2. The order of precipitation of alkaline-earth metal ions (Fig. 3) is also the order in which their ionic radii decrease, but not the order of extraction shown in Fig. 5. This could be considered to indicate that the extractability of these metals is

not simply governed by formation of a complex cation with BDPPM and distribution of the ion-pair with perchlorate into the organic phase. As can be seen in Table 1, the characteristic bands attributed to the P=O group in the complexes are observed at 1150–1190 cm⁻¹. The decrease in wave number from that of BDPPM (1200 cm⁻¹) could be considered to correspond to the stability of the BDPPM complex. However, the order of the extraction and precipitation reactions (Figs. 2–5) cannot be accounted for only in terms of the stability of the complex (as derived from Table 1). For example, Cu²⁺ forms very stable complexes with many chelating reagents and these are readily extracted into an organic phase. Its BDPPM complex absorbs at 1150 cm⁻¹ (Table 1) suggesting that this complex is the most stable of those examined. In practice, however, of the transition metals tested, copper is one of the most difficult to extract or precipitate in this system as also is

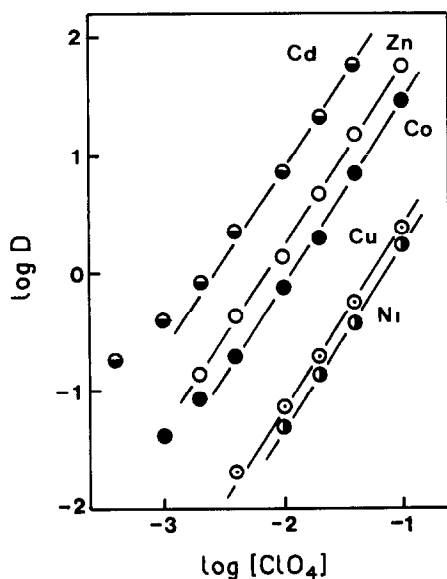


Fig. 4 Extraction of bivalent transition metals with BDPPM, as a function of log [ClO₄]. BDPPM 0.01M in DCE, [NaClO₄] + [NaNO₃] = 0.1M, pH ca 2.0

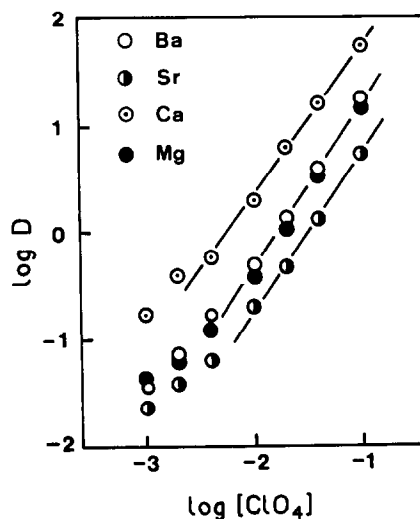
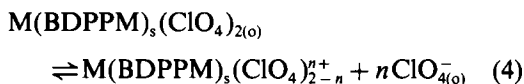


Fig. 5 Extraction of alkaline-earth metals with BDPPM, as a function of log [ClO₄]. BDPPM 0.01M in DCE, [NaClO₄] + [NaNO₃] = 0.1M, pH ca 2.0

nickel. This suggests that the copper and nickel complexes may differ from the others in structure.

It is difficult to explain the extraction behavior of the alkaline-earth metals. As suggested by the wave numbers for the P=O bands (Table 1), the stability of the complexes increases as the ionic radii of the metals decrease, as expected, but the extraction order is not that of the stabilities or of the ionic radii. In any event, it is notable that the alkaline-earth metals, which are among the least extractable bivalent elements, are readily and quantitatively extracted.

The slopes of the straight portion of the plots in Figs 4 and 5 are found to be 1.5–1.8. If the extraction equilibrium is truly described by equation (1), a logarithmic plot of the distribution ratio of the metal ions, $\log D$, vs $\log [\text{ClO}_4^-]$, for $[\text{BDPPM}]_0$ constant, should be a straight line with slope of 2. Any decrease in perchlorate concentration in the aqueous phase (owing to extraction with BDPPM) is negligible, since the extraction constant is not large enough for the degree of extraction to be significant under the conditions set in Figs. 4 and 5. An experiment on the extraction of sodium with BDPPM and perchlorate indicated that decrease in the concentration of perchlorate and BDPPM, caused by the extraction of sodium, is negligible. The lower value of the slope is again attributable to dissociation in the organic phase



The metal ions studied in the present work were not extracted with TOPO, a monodentate neutral ligand, under the same conditions as for BDPPM. This greater extractability with BDPPM could be attributed to its chelating ability and the highly hydrophobic nature of the ion-pair formed with perchlorate.

BDPPM has some advantages over *N,N*-bidentate ligands such as 1,10-phenanthroline (phen) or 2,2'-bipyridyl, as follows. The extraction of "hard metals", such as the alkaline-earth and rare-earth metals, as ion-pairs of their complexes with phen, is not satisfactory, prob-

ably owing to the very low stability of the chelates. Further, such extraction with phen is impossible in acidic media, because of protonation of the nitrogen atoms in phen. In contrast, the extraction of alkaline-earth metals (and others) with BDPPM and perchlorate is satisfactory, and the distribution of BDPPM does not depend on the pH, unlike that of phen or 2,2'-bipyridyl. It is therefore possible to use the BDPPM system at increased acidity provided that this is not so high that extraction of $\text{H}(\text{BDPPM})_2\text{ClO}_4$ takes place and decreases the concentration of free BDPPM. This type of extraction system could be considered to be analogous to that employing phenanthroline or crown ethers, namely extraction with a solvating reagent. It is expected that the BDPPM could be more widely applied, owing to its strong co-ordinating ability and hydrophobic nature. It may also be expected to give greater selectivity than that of conventional extraction systems.

REFERENCES

- 1 S Umetani, S Kihara and M Matsui, *Chem Lett*, 1986, 1545
- 2 S Umetani and H Freiser, *Inorg Chem*, 1987, **26**, 3179
- 3 S Umetani, S Kihara and M Matsui, *Anal Chim Acta*, 1990, **232**, 293
- 4 A A Schilt, R L Abraham and J E Martin, *Anal Chem*, 1973, **45**, 1808
- 5 S Kusakabe and T Sekine, *Bull Chem Soc Japan*, 1981, **54**, 2930
- 6 S Kalyanaraman and S M Khopkar, *Anal Chem*, 1975, **47**, 2041
- 7 T H Siddall III, *J Inorg Nucl Chem*, 1964, **26**, 1991
- 8 J W O'Laughlin and D F Jensen, *Anal Chem*, 1969, **41**, 2010
- 9 N E Kochetkova, M K Chmutova and B F Myasoe-dov, *Radiokhimiya*, 1983, **25**, 599
- 10 Y Yamashoji, T Matsushita and T Shono, *Anal Sci*, 1987, **3**, 327
- 11 M A Carey and C V Banks, *J Inorg Nucl Chem*, 1969, **31**, 533
- 12 T Aoki, E Deguchi, M Matsui and T Shigematsu, *Bull Inst Chem Res, Kyoto Univ*, 1971, **49**, 307
- 13 S Uchikawa, *Bull Chem Soc Japan*, 1967, **40**, 798
- 14 J J Bucher, M Zirin, R C Laugen and R M Diamond, *J Inorg Nucl Chem*, 1971, **33**, 3869
- 15 M Nitsui and T Sekine, *ibid*, 1975, **37**, 1054
- 16 M H Abraham and A F Danil de Namor, *J Chem Soc Faraday Trans 1*, 1976, **72**, 955

ON THE APPLICATION OF THE DUMAS TECHNIQUE FOR THE DETERMINATION OF NITROGEN IN REFRACTORY NITRIDES

WALTER LENGAUER

Institute for Chemical Technology of Inorganic Materials, Technical University of Vienna,
Getreidemarkt 9, A-1060 Vienna, Austria

(Received 30 November 1990 Accepted 29 January 1991)

Summary—The classical Dumas apparatus has been modified. The generally recommended oxidants CuO and V₂O₅ were found to give relatively high blank values and were therefore replaced by Cu₂O. The preparation of the Cu₂O is described. It is an exceptionally suitable oxidant for the Dumas analysis of the Group Va nitrides as well as manganese nitrides and molybdenum nitrides because it does not release oxygen into the gas phase. The reaction of the Group IVa nitrides as well as of CrN with CuO and Cu₂O is, however, not completely quantitative at 1000–1150° in reasonable reaction times. The results of the Dumas analysis of a Group IVa nitride should be corrected by measuring the nitrogen content of the residue (*e.g.*, by hot extraction). The relative standard deviations do not exceed 0.38%. The nitrogen contents (% w/w) of the residues range from <0.001% for Mo₂N + MoN to 0.54% for Cr₂N + CrN. BN, Si₃N₄ and AlN could not be decomposed with copper oxides under the conditions used. AlN could be analysed by adding V₂O₅, but the *rsd* was 0.55% and the nitrogen content in the residue was 0.52% w/w. Neither BN nor Si₃N₄ could be analysed by addition of V₂O₅.

Transition-metal (mono)nitrides exist over an extended range of homogeneity of up to 10–30 atom% N¹. In this homogeneity region the solid-state properties (*e.g.*, lattice parameter, superconduction transition temperature, micro-hardness) show a substantial dependence on the chemical composition. An accurate chemical analysis for the main constituents as well as the impurities is therefore not only of considerable interest in itself, but is essential if the variation of physical properties with composition within the homogeneity region is to be studied.

In the Dumas analysis the sample is oxidized and the nitrogen evolved is measured volumetrically. It is one of the methods with the greatest accuracy and precision. In recent years improved equipment has been constructed which permits determination of nitrogen by gas chromatography (GC) with an error not exceeding about 1 atom%. This Dumas–GC technique appears to be the most accurate technique that is suitable for automation.^{2,3} The conditions for automatic Dumas–GC analysis of refractory transition-metal nitrides have been studied only recently,⁴ and the main disadvantages are the low sample loads and the relatively low decomposition temperatures that can be used. In addition, this technique needs well characterized standards.

The most accurate modification of the Dumas technique at present still appears to be the method described by Kern and Brauer.⁵ These authors heated titanium, niobium and tantalum nitrides in a stream of pure CO₂ with CuO or CuO + Cu₂O (for niobium nitrides) as the oxidant. They obtained excellent accuracy. Their method, however, has several experimental disadvantages such as low measured volumes of nitrogen (and thus low sample loads) as well as complicated CO₂ storage, sample heating and temperature control, making the apparatus difficult to handle.

Several modifications have been suggested for the oxidation or decomposition of the sample in the Dumas analysis,^{6–12} but all have given generally less precise results. However, no studies have been made of the nitrogen contents of the residues (reacted nitride + copper oxides) to determine whether or not the reaction is quantitative.

The present study was performed in order to update the classical technique described by Kern and Brauer⁵ and to investigate whether the combustion procedure is quantitative. For the latter purpose the reaction products were analysed by hot extraction. An improved technique for the Dumas analysis was also used. The apparatus allowed easier and faster handling

and produced data with an accuracy of the same order of magnitude as that given by the Kern and Brauer method, when corrected for the nitrogen contents of the residues (determined by hot extraction).

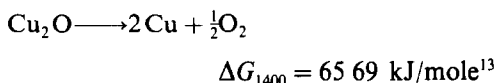
EXPERIMENTAL

Oxidant requirements and preparation of Cu₂O

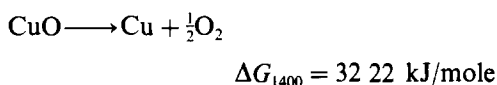
It has been stated that there is no need for an additional oxidant, since CO₂ reacts with all transition-metal nitrides quantitatively, setting free all combined nitrogen.¹⁰⁻¹² This reaction, however, leads to the conversion of CO₂ into CO, the removal of which would complicate the experimental arrangements and present an additional source of error.

CuO and V₂O₅ have been recommended as oxidants. We have tested them, and found that both substances gave such high blank values that they led to unreliable results. Therefore we also performed blank tests with Cu₂O and investigated the reaction of this compound during analysis. Cu₂O is an excellent oxidant which gives a blank value below the nitrometer's determination limit of 0.005 ml.

The replacement of CuO by Cu₂O does not significantly alter the conditions of thermodynamic equilibrium. During the analysis Cu₂O is reduced according to



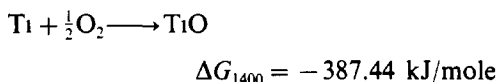
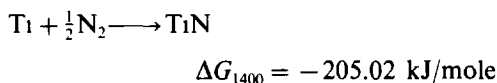
and CuO according to



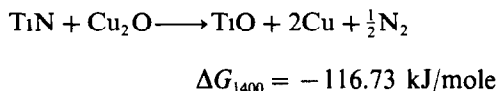
where ΔG_{1400} is the free-energy change at 1400 K.

In order to decide whether an admixed nitride can be oxidized by reaction with copper oxide, it is necessary to check whether the free energy of the reaction products is lower than the free energy of the nitride-copper oxide mixture. Only in the latter case will the reaction proceed (negative free-energy change) as required for the Dumas analysis.

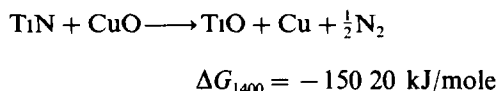
The stabilities of the nitride and the oxide (TiO is chosen as the least stable titanium oxide) are



Hence, the free-energy change of the oxidation reaction with Cu₂O is



and of that with CuO



It is obvious that the free-energy change of the total reaction is largely influenced by the difference between the free-energy changes of the nitridation and oxidation reactions. Hence the oxidation reaction should proceed completely to the right irrespective of the oxidation state of the copper in the oxide used. Since the nitrides are all thermochemically less stable than the oxides, these considerations are valid for any compound with respect to the Dumas analysis.

Some of the oxides and nitrides (e.g., TiO and TiN) form solid solutions. Therefore a thermochemical model which introduces the partial molar free-energy values would more nearly represent the true situation, especially when the nitrogen contents in the reaction products are of interest. However, the pertinent data are not available for the oxynitride systems and—as discussed below—the amount of residual nitrogen is influenced more by kinetic effects (oxygen diffusion) than by equilibrium conditions.

For use in the Dumas analysis Cu₂O was prepared in the following way. A porcelain boat containing CuO was placed in a fused-silica tube, one end of which had been sealed and the other connected to a rotary pump. The silica tube was then evacuated and the end with the boat was heated to 900° for 2 hr, after which the internal oxygen pressure had dropped to 6×10^{-2} mbar. The silica tube with the sample was then allowed to cool to room temperature outside the furnace but still under vacuum. The product so obtained was purple and consisted of single-phase Cu₂O (as shown by X-ray diffraction). The composition was checked by weighing before and after vacuum heating as well as by reduction of Cu₂O to Cu by heating in hydrogen.

Apparatus and procedure

The apparatus and the procedure are essentially the same as described by Kern and Brauer,⁵ but with a few modifications in the

construction of the apparatus.

1. Instead of two separate heated nets of Cu and CuO, one partially oxidized "Cu-Cu₂O" net was used
2. The high-purity CO₂ was supplied from a cylinder so that the flow-rate could be easily adjusted.
3. An electric furnace with three independently adjustable heating zones was used.
4. A water-jacketed nitrometer was used to keep the measured nitrogen at constant temperature. The maximum nitrogen volume which could be determined was increased to 10 ml
5. Pirani- and Bourdon-type manometers were introduced

The entire apparatus was made of glass or metal lines and joints. The leakage rate could be kept very low. In several trial runs for test purposes a vacuum of better than 10⁻² mbar could be maintained over a period of several days. The apparatus is illustrated in Fig. 1

RESULTS AND DISCUSSION

Table 1 lists the nitrogen contents of the nitrides analysed with a 3-10-fold amount of

Cu₂O. The temperatures applied for the analyses are also given. It can be seen that in several cases excellent precision was obtained. To check the completeness of the reaction between the nitride and copper(I)oxide the nitrogen contents of the residues from the nitrogen analyses (reacted nitride + Cu₂O) were determined by hot extraction. These contents, which refer to the amount of nitride, are also listed in Table 1. Since the compounds are in most cases not stoichiometric, the corresponding theoretical nitrogen contents are not listed. Obviously the Group Va and molybdenum nitrides react quantitatively. The nitrogen contents of these residues were very low. In contrast, the nitrogen values of the residues of the Group IVa metal nitrides are somewhat higher. The lengths of the reaction times (and analysis times) for the latter are also longer. This can be attributed to the substantial influence of kinetic parameters (diffusion rate of oxygen) on the oxidation reaction and to a minor extent to the greater stability of Group IVa nitrides as compared to Group Va nitrides. It is clear that the melting process occurring during the reaction of both VN and NbN with Cu₂O as well as the sublimation of MoO₃ during the reaction of MoN or Mo₂N with Cu₂O

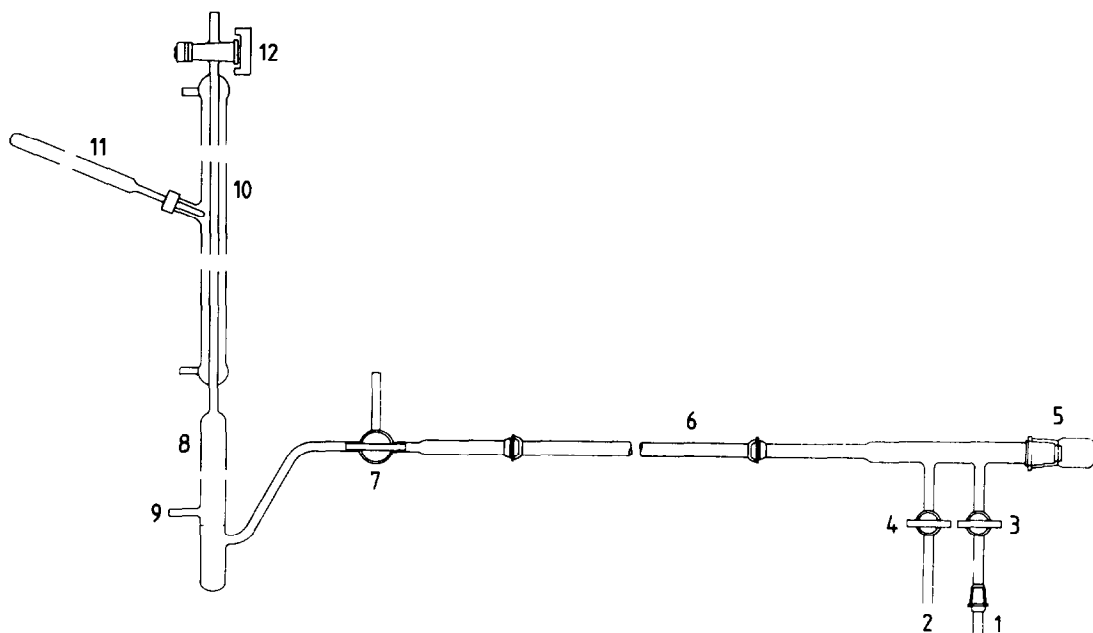


Fig. 1 Design of a modified Dumas apparatus for the analysis of transition metal nitrides. 1, Cu line for CO₂ (Pirani and Bourdon manometers not shown), 2, line to the pump, 3, stopcock, open during flushing and analysis, 4, stopcock, open during evacuation, 5, cap, for loading and unloading the sample, 6, fused-silica tube (tube furnace not shown), 7, two-way stopcock, 8, nitrometer (---- mercury level), 9, connection to levelling bottle, 10, water-jacket on nitrometer, 11, thermometer, 12, stopcock, open for renewing the KOH solution

Table I Analysis conditions and results for the samples investigated

Sample*	Weight per analysis, mg	Heating temperature, °C	Time for analysis, min	N found†, % w/w	Relative std devn, %	N in residue‡, % w/w	Total N, % w/w	Total relative std devn, %
TiN	20-30	1050	40	22.11	0.2 ₈	0.12 (1)	22.33	0.3 ₁
ZrN	50-70	1050	40	11.93	0.1 ₉	0.16 (2)	12.09	0.3 ₆
HfN	90-120	1050	40	7.23	0.3 ₀	0.18 (1)	7.41	0.4 ₄
VN	20-30	1000	25	17.28	0.1 ₀	<0.001 (1)	17.28	0.1 ₀
NbN	50-70	1000	25	12.03	0.2 ₀	0.005 (1)	12.04	0.2 ₁
TaN	90-120	1050	30	7.00	0.2 ₇	0.015 (3)	7.02	0.3 ₁
CrN	30-40	1150	180	11.87	0.3 ₀	0.54 (1)	12.41	0.3 ₈
MoN	60-80	800	15	9.76	0.1 ₀	<0.001 (1)	9.76	0.1 ₁
MnN	30-40	1000	25	9.13	0.1 ₁	0.09 (1)	9.22	0.2 ₂
AlN§	10-15	1100	60	33.3	0.5 ₅	0.52 (2)	33.8	0.6 ₁

*TiN NbN, δ -MeN_{1-x}, TaN, ϵ -TaN, CrN, Cr₂N + δ -CrN, MoN, Mo₂N + MoN, MnN, Mn₂N_{1-x}

†Values obtained from 5-7 determinations

‡Refers to the nitride, content can be directly added to the Dumas value, standard deviation in parentheses (value obtained from 3 determinations) refers to last digit

§Analysed by use of 150 mg of V₂O₅

increases the rate of the oxidative attack. However, TaN and Mn₂N_{1-x} (no occurrence of a liquid phase during the analysis) also react faster than the Group IVa nitrides. The latter are known to form dense oxide layers which protect them from further oxidation.

The role of oxygen diffusion within the solid-solid reaction mixture becomes more obvious in the case of CrN. Because of the formation of a dense chromium oxide layer on the particle surfaces, CrN cannot be quantitatively decomposed at temperatures up to 1150° within reasonable reaction times. For higher reaction temperatures the fused-silica tube must be replaced by a fully dense ceramic tube.

The nitrides AlN, Si₃N₄ and BN react even more sluggishly with copper oxides. Replacement of Cu₂O by V₂O₅ (which is liquid at the reaction temperatures) brought some improvement, but only for AlN. The nitrogen content of the residue was 0.52% by weight (relative to AlN).

As observed from a comparison between the behaviour of Cu₂O and V₂O₅, the entire oxygen content from copper(I)oxide is available for the oxidation whereas only a small part of that in vanadium(V)oxide (probably about one mole of oxygen per mole of oxide, depending on the temperature) is available under the conditions prevailing for the Dumas analysis performed here. Because of the sometimes violent reaction of vanadium(V)oxide with transition-metal nitrides (e.g., with HfN, but not with ZrN) a blank value for V₂O₅ cannot be given with the desired accuracy. Also, with different amounts and kinds of samples, different maximum reaction temperatures are reached, which influence the amount of oxygen released into the CO₂ atmosphere.

In order to obtain figures for the accuracy of the Dumas modification applied here, the nitrides would have to be measured by other methods of nitrogen determination. We observed that the vanadium content of VN_{1-x}, determined by oxidation as well as by titration,¹⁴ together with the nitrogen value from the present Dumas analysis adds up to 100 ± 0.1%. Similar results were obtained for TiN, when the nitrogen content of the residue was taken into consideration. Thus it can be concluded that in such cases, where the decomposition is practically quantitative, the error is of the same order of magnitude as the precision. For the Group IVa nitrides the nitrogen content in the residue must be added to the Dumas value (Table I).

CONCLUSIONS

In the present study an improved technique for the Dumas analysis was used. The apparatus allowed more convenient handling and produced data with an accuracy of the same order of magnitude as that reported by Kern and Brauer.⁵ It is recommended as a reference apparatus for use with determination techniques which require well-characterized standards (Dumas-GC, hot extraction). However, as can be seen from the analysis of the reaction products, attention must be paid to the fact that in certain cases a small, but certainly quantifiable, nitrogen content remains, which has not hitherto been taken into consideration in the literature.

Acknowledgements—The author would like to thank Professor Peter Eitmayer for his continued interest. Thanks are also due to Mrs Cathryn Jelinek for her help during preparation of the manuscript.

REFERENCES

- 1 P Ettmayer and W Lengauer, *Nitrides*, in *Ullmann's Encyclopedia of Industrial Chemistry*, Vol. A17, in the press
- 2 B Colombo and G Giazzi, *Int Lab*, 1982, Sept, 76
- 3 W J Kirsten and G U Hesselius, *Microchem J*, 1983, 28, 529
- 4 R Taubler, M Groschner, W Lengauer and P Ettmayer, *Proc DGM-Meeting "Nichtmetalle in Metallen"*, Munster, FRG, D Hirschfeld (ed.), p 101 DGM-Informationsges Verlag, 1990.
- 5 W Kern and G Brauer, *Talanta*, 1964, 11, 1177
- 6 R J Hynek and J A Nelen, *Anal Chem*, 1963, 35, 1655
- 7 A Tolk, J C Plakman, W A Lingerak and A Kout, *Anal. Chim Acta*, 1969, 47, 373
- 8 L P Morgenthaler and R P Menichelli, *Anal Chem*, 1965, 37, 570
- 9 R A Meyer, E P Parry and J H Davies, *ibid.*, 1967, 39, 1321
- 10 J Rottman and H Nickel, *Z Anal Chem*, 1969, 247, 208
- 11 A Naomidis, H Nickel, J Rottmann and H J Stocker, *ibid*, 1967, 226, 175
- 12 A W Dupraw and H J O'Neill, *Anal Chem*, 1959, 31, 1104
- 13 J F Elliott and M Gleiser, *Thermochemistry for Steel-making*, Addison-Wesley, Reading, 1960
- 14 W Lengauer, *Fres Z Anal Chem*, 1985, 322, 23

NON-AQUEOUS CERIMETRIC DETERMINATION OF DITHIOCARBAMATES AND ITS APPLICATION TO THE DETERMINATION OF AMINES

D K SHARMA* and R D SHARMA

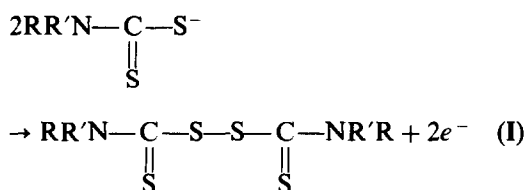
Department of Chemistry, Himachal Pradesh University, Summer Hill, Shimla-171005, India

(Received 22 May 1990, Revised 14 November 1990 Accepted 21 November 1990)

Summary—A non-aqueous titrimetric method for determination of dithiocarbamates with cerium(IV), is described. The compounds are titrated at room temperature, with visual and potentiometric end-point detection. In visual titrations, the reagent serves as self-indicator and turns the solution yellow at the end-point. Methyl Red can also be used as the indicator. The method has been applied to the determination of amines after their quantitative conversion into dithiocarbamates by reaction with carbon disulphide. The proposed method is accurate to $\pm 0.8\%$ with a relative standard deviation of $\pm 0.7\%$.

Non-aqueous redox methods are frequently used for determination of organic compounds which are insoluble in water, or react with it through hydrolysis or redox reactions. The scope of these methods can be further extended to the determination of compounds which tend to react with the media of aqueous redox titrations or yield products which interfere with determinations in aqueous media.

Dithiocarbamates find extensive use as agricultural fungicides and as vulcanization accelerators in the rubber industry. These compounds are easily oxidized to the corresponding thiram disulphides (I), but conventional oxidimetric methods cannot be used for their determination, owing to their tendency to undergo decomposition with acids^{1,2} (which serve as the media for a variety of redox titrations) and also to interference by their water-insoluble oxidation products^{3,4} (II) in neutral aqueous media. These problems can be overcome if non-aqueous redox methods are used for the determination



Ammonium hexanitratocerate(IV) is a suitable oxidimetric reagent in acetonitrile media.

It has a standard potential of 0.755 V vs. an Ag/AgNO₃ reference electrode.⁵ Rao and Murthy⁶ found the solution of the oxidant to be relatively stable, no decrease in titre being observed over several days. The present work uses this reagent (in acetonitrile) for titration of dithiocarbamates in acetonitrile-dimethylformamide media, with visual or potentiometric end-point detection. The acetonitrile solution of the reagent is orange-red and imparts a distinct yellow colour to the solution at the end-point. Alternatively, Methyl Red may be used as an indicator. The potentiometric titrations are performed with a platinum and modified calomel electrode assembly.

The ease with which carbon disulphide quantitatively transforms primary and secondary amines into the corresponding monoalkylammonium monoalkyl dithiocarbamates (II) and dialkylammonium dialkyldithiocarbamates⁷ (III), respectively, in acetonitrile medium, and



the simplicity and reliability of the titration of dithiocarbamates with ammonium hexanitratocerate(IV) in acetonitrile-dimethylformamide, prompted us to extend the method to the determination of amines. Excess of carbon disulphide does not interfere in any way. The amount of parent amine is stoichiometrically related to the amount of dithiocarbamate produced. The proposed methods have significant advantages over the acidimetric methods commonly

*Author for correspondence

employed for the determination of amines. First, the amines can be determined in the presence of basic compounds that might interfere in an acidimetric determination. Secondly, as tertiary amines cannot react with carbon disulphide, the methods can be extended to the determination of primary or secondary amines in the presence of tertiary amines.

EXPERIMENTAL

Apparatus

Potentiometric titrations were performed with a Toshniwal CLO6A type potentiometer with a bright platinum wire as indicator electrode and a modified calomel electrode (saturated methanolic potassium chloride solution) as reference.

Reagents

Acetonitrile. Purified by distilling twice from phosphorus pentoxide (5 g/l.).

Dimethylformamide. Purified by storing over anhydrous analytical grade sodium carbonate for 2 days, decanting and distilling. The fraction distilled at 148.5–149.5° was collected in coloured bottles

Carbon disulphide. The Baker analysed product, estimated chromatographically to be 100% pure, was used as received.

Ammonium hexanitratocerate(IV), 0.04M solution in acetonitrile Prepared by dissolving a little more than the calculated amount of the oxidant (Fluka) in acetonitrile and standardized by titration with standard ferrous ammonium sulphate solution in the presence of dilute sulphuric acid, with ferroin as indicator.

Methyl Red. A 1-mg/ml solution in dimethylformamide

Dithiocarbamates. Sodium diethyldithiocarbamate was recrystallized before use. The sodium salts of methyl, ethyl, n-propyl, n-butyl, isobutyl, dimethyl, di-n-propyl, di-n-butyl, and dibenzyl dithiocarbamic acids were prepared and purified by known methods.⁸⁻¹¹ Alkylammonium alkyl dithiocarbamates were prepared by the method of Anschutz^{12,13} by mixing the primary or secondary amines with carbon disulphide in dry diethyl ether. Monoalkylammonium monoalkyl dithiocarbamates, $\text{RHN} \cdot \text{CS} \cdot \text{S}^- \cdot (\text{NH}_3\text{R})^+$ with R = methyl, ethyl, n-propyl, n-butyl and n-pentyl, and dialkylammonium dialkyl dithiocarbamates, $\text{R}_2\text{N} \cdot \text{CS} \cdot \text{S}^- \cdot (\text{NH}_2\text{R}_2)^+$, with R = methyl, ethyl, n-propyl and n-butyl, were prepared and

kept in a vacuum desiccator. The purity of each dithiocarbamate was checked by non-aqueous titration with iodine monobromide¹⁴

Amines. Methylamine (40% aqueous solution), ethylamine (50% aqueous solution), dimethylamine (40% aqueous solution) and diethylamine (60% aqueous solution) were used as received. n-Propylamine, n-butylamine, n-pentylamine, di-n-propylamine, di-n-butylamine, dibenzylamine and isobutylamine (Fluka) were distilled before use

Procedures

Determination of dithiocarbamates. Dissolve a known weight of the dithiocarbamate in an accurately known volume of acetonitrile, and transfer a known volume (containing 5–10 mg of the dithiocarbamate) into a titration vessel, dilute to 10 ml with acetonitrile and add 20 ml of dimethylformamide. Titrate the solution at room temperature ($\sim 23^\circ$) with the ammonium hexanitratocerate(IV) solution (in acetonitrile). In visual titrations, the end-point is shown by a pale yellow colour imparted to the solution by the first drop of the oxidant added in excess. The colour is stable for about 1 min. Alternatively use 3 drops of Methyl Red indicator, the red solution turns yellow at the end-point. In potentiometric titrations, sharp jumps in potential are obtained at the equivalence point. Typical results are given in Table 1. The results obtained in visual titrations with or without indicator

Table 1 Determination of dithiocarbamates

Dithiocarbamates	Amount found*, mg	
	Visual method	Potentiometric method
<i>Sodium salts</i>		
Methyl	7.94 ± 0.035	7.95 ± 0.032
Ethyl	8.05 ± 0.042	7.96 ± 0.028
n-Propyl	8.08 ± 0.051	8.06 ± 0.048
n-Butyl	7.92 ± 0.040	8.05 ± 0.030
Isobutyl	7.94 ± 0.038	7.95 ± 0.032
Dimethyl	8.06 ± 0.048	8.03 ± 0.039
Diethyl	7.95 ± 0.052	8.02 ± 0.050
Di-n-propyl	7.93 ± 0.042	7.96 ± 0.029
Di-n-butyl	8.07 ± 0.038	7.95 ± 0.032
Dibenzyl	7.96 ± 0.052	8.05 ± 0.041
<i>Mono/dialkylammonium salts</i>		
Methyl	8.06 ± 0.048	7.96 ± 0.036
Ethyl	7.94 ± 0.052	8.05 ± 0.037
n-Propyl	7.95 ± 0.037	7.96 ± 0.037
n-Butyl	8.05 ± 0.036	7.95 ± 0.030
Dimethyl	7.92 ± 0.050	8.04 ± 0.048
Diethyl	8.08 ± 0.038	7.94 ± 0.028
Di-n-propyl	8.06 ± 0.044	8.05 ± 0.040
Di-n-butyl	7.92 ± 0.048	7.95 ± 0.032

*Mean ± standard deviation of 10 replicates, each containing 8.00 mg of sample

Table 2 Determination of amines

Amine	Amount found*, mg	
	Visual method	Potentiometric method
Methyl	5.94 ± 0.032	6.05 ± 0.028
Ethyl	6.06 ± 0.040	5.96 ± 0.037
n-Propyl	6.04 ± 0.038	5.95 ± 0.032
n-Butyl	5.94 ± 0.048	5.96 ± 0.028
n-Pentyl	5.95 ± 0.042	6.04 ± 0.039
n-Hexyl	6.06 ± 0.047	5.95 ± 0.037
Dimethyl	5.94 ± 0.050	5.97 ± 0.042
Diethyl	5.96 ± 0.044	5.97 ± 0.042
Di-n-propyl	5.97 ± 0.040	6.04 ± 0.032
Di-n-butyl	6.05 ± 0.050	6.03 ± 0.036

*Mean ± standard deviation of 10 replicates, each containing 6.00 mg of amine

agreed so well that only results obtained without indicator are given

Determination of amines

Prepare a solution of a known weight of amine in a known volume of acetonitrile, transfer a suitable fraction (containing 6–8 mg of amine) into a titration vessel, add one drop of carbon disulphide and dilute to 10 ml with acetonitrile. Add 20 ml of dimethylformamide and titrate as for dithiocarbamates. Typical results are given in Table 2

RESULTS AND DISCUSSION

The method commonly employed for the determination of dithiocarbamates involves hydrolysing them with hot mineral acids to the corresponding amines and carbon disulphide, either of which may be determined. Usually carbon disulphide is selected and measured by the xanthate method,¹⁵ i.e., the gas is absorbed in alcoholic potassium hydroxide solution and the resulting xanthate titrated with iodine in neutral solution. The hydrolysis method is quite laborious and time-consuming. Special appar-

Table 4 Results of single titrations of ten independent samples of a secondary amine (di-n-propylamine)

Amount taken, mg	Amount found, mg	
	Visual method	Potentiometric method
5.2	5.25	5.20
6.5	6.45	6.54
7.8	7.86	7.75
9.1	9.18	9.02
11.7	11.61	11.78
13.0	13.10	13.06
15.6	15.48	15.72
16.9	16.75	16.98
18.2	18.32	18.10
19.5	19.32	19.62

atus is required, and the experimental conditions must be closely adhered to for the evolution of carbon disulphide to be quantitative. Hence there is a need for methods which are accurate, precise, simple and rapid. The oxidimetric method described here meets these requirements and has been found useful for the determination of dithiocarbamates. The overall standard deviations calculated from the pooled results of all the visual and potentiometric titrations performed with 8-mg samples of each dithiocarbamate were 0.044 and 0.066 mg, respectively and the corresponding values for 20-mg samples were 0.036 and 0.057 mg, only the results for the 8-mg samples are given in Table 1. The scope of the method was extended to determination of amines, and the overall standard deviations for all the visual and potentiometric titrations performed with 6-mg samples of each primary and secondary amine were 0.043 and 0.065 mg, respectively, the values for 18-mg samples being 0.035 and 0.056 mg; only the results for the 6-mg samples are given, in Table 2.

The replicate samples of each amine were not weighed individually, but were aliquots from a bulk solution. Acidimetric titrations were also performed to confirm that the aliquots contained the same amount of amine. The quantitative nature of the reaction with carbon disulphide was verified by use of different amine sample sizes. The results are given in Tables 3 and 4.

Acknowledgement—The authors are indebted to Professor B. C. Verma, Himachal Pradesh University, for his guidance and advice

REFERENCES

- 1 M. L. Shankaranarayana and C. C. Patel, *Anal. Chem.*, 1961, **33**, 1398
- 2 A. Hulanicki and L. Shishkova, *Talanta*, 1965, **12**, 485

Table 3 Results of single titrations of ten independent samples of a primary amine (n-butylamine)

Amount taken, mg	Amount found, mg	
	Visual method	Potentiometric method
6.0	5.94	5.96
7.2	7.14	7.15
8.4	8.46	8.32
9.6	9.65	9.64
10.8	10.80	10.86
12.0	11.90	11.92
14.4	14.30	14.52
15.6	15.75	15.72
16.8	16.64	16.70
18.0	18.12	17.90

- 3 M L Shankaranarayana and C. C. Patel, *Z. Anal Chem*, 1961, **179**, 263
- 4 R C. Paul, N C. Sharma, R K Chauhan and R Parkash, *Indian J Chem.*, 1972, **10**, 227
- 5 G P Rao and A R. V Murthy, *J Phys Chem*, 1964, **68**, 1573
- 6 *Idem*, *Z. Anal Chem*, 1960, **177**, 86
- 7 E E Reid, *Organic Chemistry of Bivalent Sulphur*, Vol IV, p 211 Chemical Publishing Co, New York, 1962
- 8 H L Klopping and G J M van der Kerk, *Rec Trav Chim*, 1951, **70**, 917
- 9 J Issoire and L Musso, *Mem Poudres*, 1960, **42**, 427
- 10 E J Kupchik and P J Calabretta, *J Inorg Chem*, 1965, **4**, 973
- 11 D J Halls, A. Townshend and P Zuman, *Anal Chim Acta*, 1968, **40**, 459, 1968, **41**, 51
- 12 R Anschutz, *Ann*, 1908, **359**, 202, 1910, **371**, 201
- 13 *Idem*, *Chem Zig*, 1910, **34**, 89
- 14 B C Verma and S Kumar, *Mikrochim Acta*, 1976 I, 209
- 15 J H Karchmer, *The Analytical Chemistry of Sulfur and its Compounds*, Part II, pp 629, 652 Wiley-Interscience, New York, 1972

REVERSED-PHASE HPLC DETERMINATION OF SOME NOBLE METALS AS THEIR THIAZOLYLAZORESORCINOL CHELATES

LIU QIPING, ZHANG HUASHAN and CHENG JIEKE*

Department of Chemistry, Wuhan University, Wuhan 430072, People's Republic of China

(Received 30 October 1989 Revised 1 December 1990 Accepted 16 January 1991)

Summary—The first use of 4-(2-thiazolylazo)resorcinol (TAR) as a chelating reagent in the reversed-phase HPLC separation and determination of Os, Rh and Ru is reported. A precolumn derivatization method is used, followed by separation on an octadecyl-bonded silica stationary phase with a methanol–water mobile phase. The coloured complexes of Os, Rh, and Ru are completely separated within 8 min with a 60:40 v/v methanol–water mixture (pH 4.0, tetrabutylammonium as counter-ion). The detection limits for Rh, Ru and Os at 550 nm are 5, 6 and 17 ng/ml respectively. Recoveries of 94–102% have been obtained for these trace noble metals in analysis of anode slime.

The application of HPLC to the separation and determination of metal ions has increased rapidly in recent years. The development of inorganic HPLC has involved many organic chromogenic chromatographic reagents, and increased the use of many organic chelating agents, such as PAR,¹ PAN,² dithizone,³ dithiocarbamates,^{4,5} diacetyldioxime,⁶ β -diketones,⁷ and porphyrins.⁸ However, there is no reported use of thiazolylazo reagents in HPLC separations.

The determination of noble metals has long been an active field in analytical chemistry. The development of HPLC has made it possible to separate and determine them in a rapid, sensitive and effective way. The reversed-phase ion-chromatography method originated from the separation of Ru–bipyridyl complexes.⁹ The use of PAN¹⁰ and PAR¹¹ as precolumn derivatization agents for separation of platinum group metals has been reported. Mueller and Lovett¹² separated Rh and Pd with diethyldithiocarbamate. Gurira and Carr¹³ separated Co, Be, Rh, Cr(III), Pb, Pt and Ru as acetylacetone and benzoylacetone complexes. Ebina *et al.*¹⁴ separated Pt(II) and Pd(II) with dimercaptomaleonitrile.

Much attention has been paid to the HPLC separation and determination of Pt and Pd, but fewer reports on Os, Rh, Ru, and Ir have appeared. Although other instrumental or chemical methods have been utilized for deter-

mination of Os, Rh and Ru, a simple and rapid method for analysis of their mixtures has never been developed.

In this work, a thiazolylazo reagent was used for the first time as a chelating agent for the separation and determination of noble metals by a precolumn derivatization method. The complexes of Os, Rh and Ru were completely separated within 8 min on a YQG-C₁₈ column with methanol–water mixture as the mobile phase. The method was rapid and simple. The detection limits were 5, 6 and 17 ng/ml for Rh, Ru, and Os, respectively, with measurement at 550 nm.

EXPERIMENTAL

Apparatus

LC-10 HPLC equipment (Japan Analytical Ind.) was used with a YQG-C₁₈H₃₇ (ODS) column (5 μ m particle diameter, 150 \times 4.6 mm) and an S-3702 UV-VIS detector (AJC, Japan).

Reagents

Stock solutions of Os(IV), Rh(III) and Ru(III) in 1M hydrochloric acid were prepared from (NH₄)₂OsCl₆, RhCl₃ and RuCl₃. 4-(2-Thiazolylazo)resorcinol (TAR) was synthesized according to Hovind¹⁵ and a 0.5 mg/ml solution was prepared by dissolving it in absolute alcohol. Tetrabutylammonium bromide (TBABr) (analytical grade, Shanghai Chemical Co., Shanghai), was used as the ion-pairing reagent. Doubly distilled water was used for all solution

*Author for correspondence

preparation. The mobile phase was a 60.40 v/v methanol-water mixture containing 10mM TBABr and 10mM acetate buffer (pH 4.0).

Procedure

A 5.0-ml portion of 1.0M acetate buffer (pH 6.0) and 2.0 ml of 0.5 mg/ml TAR solution were mixed with a known volume of the sample solution, and the mixture was diluted to 25.00 ml with water, heated in boiling water for 1 hr, then cooled to room temperature before HPLC analysis.

Separation of the complexes and reagent

For the HPLC analysis, the ODS column was equilibrated with methanol-water (60.40 v/v, containing 10mM TBABr and 10mM acetate buffer, pH 4.0). A 20- μ l aliquot of the prepared test solution was injected into the ODS column and the complexes were eluted at a flow-rate of 1.0 ml/min. The detection wavelength was 550 nm, and the sensitivity was set at 0.02 absorbance for full scale deflection. The peak areas were measured

RESULTS AND DISCUSSION

Hovind has reported that Os(IV), Rh(III) and Ru(III) can be complexed with TAR at pH 6.0 and 100°. At room temperature, Ga(III),

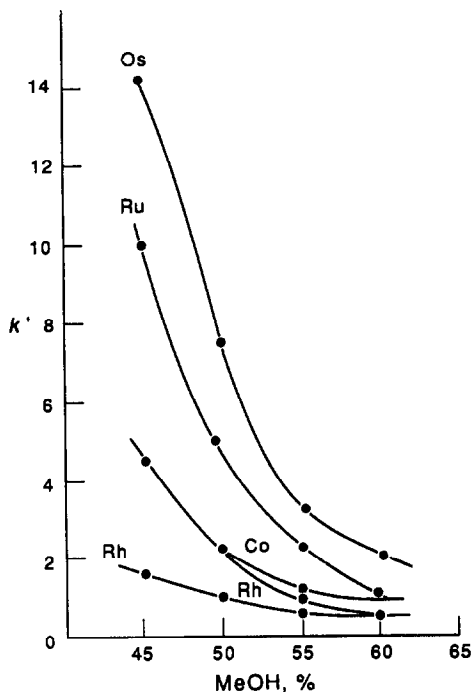


Fig 1 Effect of MeOH concentration on k' 10mM pH 3.19 buffer, 10mM TBABr

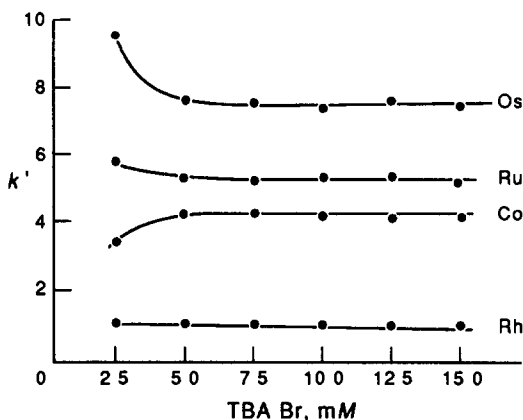


Fig 2 Effect of TBABr concentration on k' MeOH H₂O = 50:50 v/v, 10mM pH 3.19 buffer

In(III) and V(V) form chelates with TAR at pH 5.0, whereas Cu(II), Fe(III), Ni(II) and Co(II) react with it at pH 6.0. Our experiments showed that the Os, Rh, Ru, Cu, Fe, Ni and Co complexes are all stable at 100°, but those of Ga, In and V are not. The wavelengths of the absorption maxima of the Os, Rh, Ru, Co, Cu, Ni and Fe complexes range from 540 to 560 nm (Os 560, Rh and Ru 550, Co, Cu, Ni and Fe 540 nm). The molar absorptivities (ϵ) range from 0.93×10^4 to 4.4×10^4 l. mole⁻¹. cm⁻¹. A wavelength of 550 nm was chosen for the determinations.

Separation of the Os, Rh and Ru complexes

The effects of methanol, acetone and acetonitrile on the separation of Os, Rh and Ru, were investigated. It was found that aqueous methanol was most suitable as the mobile phase. Figure 1 shows the effect of the methanol concentration on the capacity factors (k'). Two curves were found for Rh, and this may be due

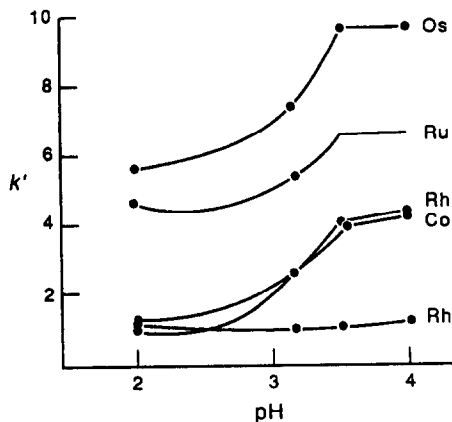


Fig 3 Effect of pH on k' MeOH H₂O = 50:50 v/v, 10mM TBABr

to different oxidation states or species. The two curves coincide when the ratio of methanol to water is >57.43 v/v. When the ratio was 60:40, Rh gave only one peak on the chromatogram, so this eluent composition was selected.

Tailing of the peaks occurred in the absence of TBABr, but the presence of >5 mM TBABr resulted in peaks that were sharp and symmetric, and in stable k' values, as shown in Fig. 2. A TBABr concentration of 10 mM was chosen. Figure 3 shows that Rh should give a single peak at about pH 2–2.5, but two peaks at pH >3 . Variation of the buffer concentration in the range 5–30 mM had no effect on the results, and 10 mM buffer was chosen.

All three complexes could be separated and determined in 8 min. Linear calibration plots were obtained for Os, Rh and Ru, in the ranges 0.14–2.28, 0.02–1.00 and 0.05–0.39 $\mu\text{g}/\text{ml}$ respectively.

Effect of foreign ions

The potential interference of numerous ions was examined by determination of 5.0 μg of Os,

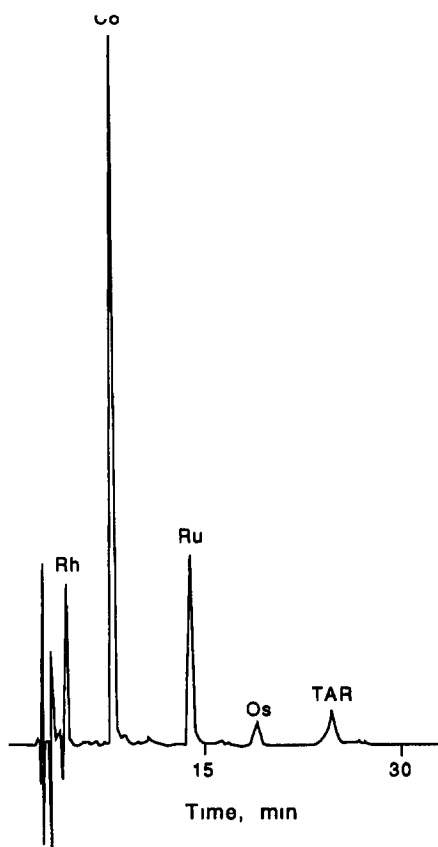


Fig. 4 Separation of Os, Rh, Ru, and Co TAR complexes by HPLC MeOH:H₂O = 50:50 v/v, 10 mM pH 3.19 buffer, 10 mM TBABr

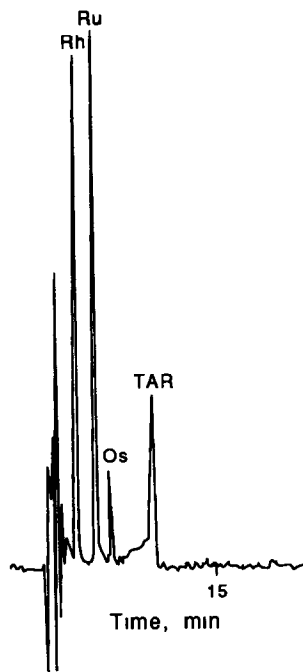


Fig. 5 Separation of Os, Rh, and Ru TAR complexes by HPLC MeOH:H₂O = 60:40 v/v, 10 mM pH 4.0 buffer, 10 mM TBABr

Rh or Ru in the presence of each foreign ion. The amounts (μg) found to be tolerable were as follows. V(V), V(IV), Cr(III), Cr(VI), Mn(II), Nb, Ta, W, Ga, In, Al, Bi, 100; Zn, Pb, Hg(II), Cd, Ag, Pt(II), Pd(II), Au(I), Ir(VI), 60; Fe(III), Co(II), Ni, Cu(II), 20.

The behaviour of cobalt was particularly interesting. Figures 1 and 3 show that the peak for elution of cobalt will coincide with one or both of the rhodium peaks under certain conditions, but at pH 4.0, with 50:50 v/v methanol–water mobile phase one of the rhodium peaks will be usable for analysis, though with lower sensitivity. Figures 4 and 5 show separations obtained (under optimum conditions) in the presence and absence of cobalt.

Analysis of an anode slime

An anode slime from electrolytic refining of copper was spiked with Os, Rh and Ru and analysed for these three metals. The slime sample was ground to 100-mesh particle size

Table 1 Reproducibility of retention times

Complex	Retention time, min				
	1	2	3	4	5
Os-TAR	7.60	7.60	7.56	7.60	7.62
Rh-TAR	4.96	4.96	4.96	4.96	5.00
Ru-TAR	6.38	6.38	6.38	6.37	6.37

Table 2 Reproducibility of peak areas (arbitrary units)

Complex	1	2	3	4	5
Os-TAR	1 08	1 05	1 03	1 07	1 09
Rh-TAR	10 89	11 01	10 67	10 89	10 50
Ru-TAR	4 96	4 94	4 97	5 02	4 96

Table 3 Results of slime analyses

Added, μg			Found, μg		
Os	Rh	Ru	Os	Rh	Ru
7 13	4 88	4 00	7 23	4 65	3 91
14 25			13 72		
	4 88			4 93	
		8 00			7 52

and dried at 110° for 2 hr. A 5.0 g sample was gently heated with 40 ml of nitric acid (1 + 1), and then filtered. The residue was heated with concentrated hydrochloric-nitric acid mixture (1 : 1 v/v) until it had all dissolved. The solution was cooled, 1 ml of 100 mg/ml sodium chloride solution was added, and the mixture was evaporated nearly to dryness, then washed into a 100-ml standard flask, and diluted to the mark with water. A 10 ml portion was analysed as above. The results are shown in Table 3.

Acknowledgement—This investigation was supported by the National Science Foundation of China.

REFERENCES

- 1 H Yamada and T Hattori, *J Chromatog*, 1986, **361**, 331
- 2 H Wade, S Neza, T Ozawa and G Nakagawa, *ibid*, 1984, **295**, 413
- 3 M Lohmuller, P Heizmann and K Ballschmiter, *ibid*, 1971, **137**, 165
- 4 A M Bond, R W Knight, J B Reust, D J Tucker and G G Wallace, *Anal Chim Acta*, 1986, **182**, 47
- 5 S R Hutchins, P R Haddad and S Dilli, *J Chromatog*, 1982, **252**, 185
- 6 P C Uden and F H Walters, *Anal Chim Acta*, 1975, **79**, 175
- 7 J F K Huber, J C Kraak and H Veening, *Anal Chem*, 1972, **44**, 1554
- 8 M Kohayashi, K Saitoh and N Suzuki, *Chromatographia*, 1985, **20**, 72
- 9 S J Valenty and P E Behnken, *Anal Chem*, 1978, **50**, 834
- 10 Yu S Nikitin, N B Morozova, S N Lamin, T A Bol'shova, V M Ivanov and E M Basova, *Talanta*, 1987, **34**, 223
- 11 Y Feng, Z Hu and P Zhu, *Huaxue Shiji*, 1986, **8**, 328
- 12 B J Mueller and R J Lovette, *Anal Chem*, 1985, **57**, 2693
- 13 R C Gurra and P W Carr, *J Chromatog Sci*, 1982, **20**, 461
- 14 T Ebina, H Suzuki and T Yotsuyanagi, *Bunseki Kagaku*, 1983, **32**, 575
- 15 H R Hovind, *Analyst*, 1975, **100**, 769

THE APPLICATION OF DEUTERIUM-PALLADIUM ELECTRODES IN THE COULOMETRIC-POTENTIOMETRIC DETERMINATION OF BASES IN KETONE MEDIA

R P MIHAJLOVIĆ

Faculty of Science, University of Kragujevac, Kragujevac, Yugoslavia

V J VAJGAND and R M DŽUDOVIĆ

Faculty of Science, University of Belgrade, Belgrade, Yugoslavia

(Received 9 November 1990 Accepted 10 January 1991)

Summary—The application of deuterium-palladium electrodes as generator, indicator and reference electrodes for the determination of organic bases in acetone and methyl ethyl ketone has been investigated. Deuterium dissolved in palladium is oxidized at a potential that is close to the oxidation potential of hydrogen in palladium and more negative than the oxidation potentials of the bases titrated, indicator, and the solvents used. The anodic oxidation of deuterium dissolved in palladium proceeds with 100% current efficiency in the solvents investigated. The relative errors for the determination of $5 \times 10^{-4} M$ solutions of bases are less than 1%.

Palladium-hydrogen electrodes at which the hydrogen is continually generated have been used for pH measurements¹ and in acid-base titrations in water and non-aqueous solvents.² Palladium wires previously saturated with hydrogen by electrolysis of water have been used as indicator and reference electrodes in the titration of bases³ and phenol⁴ in non-aqueous solvents and as generator electrodes in coulometric-potentiometric titrations in water and non-aqueous solvents.⁵⁻⁷ Recent work by Fleischmann and Pons⁸ prompted interest in the deuterium-palladium electrode and this paper describes its applications as generator, indicator and reference electrodes in the coulometric titration of bases in acetone and methyl ethyl ketone.

EXPERIMENTAL

Reagents

Analytical-reagent grade chemicals (Merck or Fluka) were used, but acetone and methyl ethyl ketone were further purified.⁹ Solutions of bases were standardized by titration with hydrogen ions generated at an H_2/Pd anode with potentiometric end-point detection by means of the couples glass electrode-SCE and H_2/Pd_{ind} -SCE. The supporting electrolyte was 0.1 M sodium perchlorate in the appropriate solvent. A 1 mg/ml solution of Methyl Red in acetone was used as the indicator for visual end-point

detection. Deuterium oxide (99.8% pure, ZGN Chemical Radioisotope Division) was used for the generation of deuterium.

Apparatus

The apparatus for titrations with visual end-points has been described elsewhere.⁷ That for titrations with potentiometric end-points is essentially the same as that used before,⁷ except that (a) D_2/Pd electrodes were used, (b) the cathode compartment (a glass tube with a porosity-4 glass sinter at the end) was inserted through the top of the cell instead of being integral with it, and (c) the reference electrode was a D_2 -saturated Pd wire in a 0.1 M sodium perchlorate solution in the appropriate solvent. The reference electrode was contained in a tube similar to the cathode compartment. The volumes of anolyte and catholyte solution were 50 and 10 ml respectively.

Procedures

Visual end-point detection. The procedure was the same as for titration with protons,⁷ except for the use of a D_2/Pd anode giving deuterium ions. Two or three drops of indicator and 0.6-1 ml of base solution were added to the anolyte solution (ca 5 ml) for titration.

Potentiometric end-point detection. The procedure was the same as for titration with protons,⁷ except that deuterium ions were generated

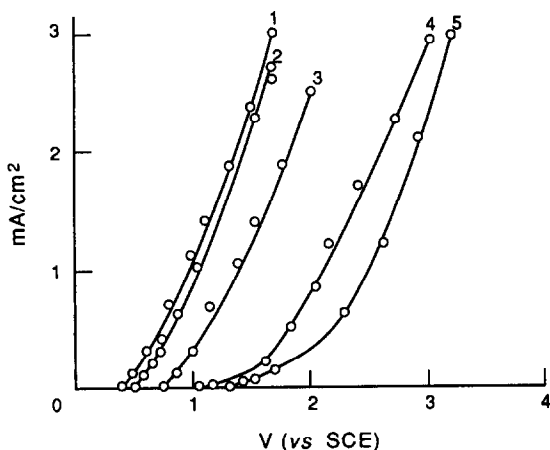


Fig 1 Changes of current density with anodic potential (relative to the reference SCE) in acetone/sodium perchlorate media (1) H_2 in palladium, (2) D_2 in palladium, (3) N,N -diphenylguanidine, (4) Methyl Red, (5) solvent

from the D_2/Pd anode. End-points were calculated from the second derivative curve

RESULTS AND DISCUSSION

The D_2/Pd electrode as the generator electrode

To check whether deuterium dissolved in palladium can be used as a source of deuterium ions for the coulometric determination of bases in ketones, we have recorded current-potential curves for the solvent, indicator, titrated bases, hydrogen in palladium and deuterium in palladium. Figure 1 shows the current-potential curves for acetone, Methyl Red, N,N -diphenylguanidine, hydrogen dissolved in palladium, and deuterium dissolved in palladium. From Fig. 1 it is seen that deuterium dissolved in palladium is oxidized at a potential which is very close to the oxidation potential of hydrogen in palladium and much more negative than the oxidation potentials of the other components in the solution. Similar current-potential curves were obtained with methyl ethyl ketone as the medium.

The deuterium ions obtained by oxidation of deuterium dissolved in palladium were used for the titration of N,N -diphenylguanidine and brucine in acetone and methyl ethyl ketone, respectively, with visual and potentiometric end-point detection. The results obtained (Table 1) show that the oxidation of deuterium is quantitative and proceeds with 100% current efficiency.

The results obtained by the application of the D_2/Pd electrode as the generator electrode are consistent with the results obtained with H_2/Pd

generator electrodes. Therefore, further investigations on the behaviour of the D_2/Pd electrode as reference and indicator electrodes in the potentiometric determination of bases were made, with H_2/Pd generator electrodes

D_2/Pd indicator and reference electrodes

To investigate the application of D_2/Pd indicator and reference electrodes, we first followed their changes in potential in 0.1M sodium perchlorate solutions in the solvents investigated, at 25.0°. When the D_2/Pd electrode was used, relative to a modified SCE as the indicator electrode, the potential changed by 5–8 mV in 8 hr, but when it was the reference electrode the potential changed by only 2–3 mV over the same time period. Since one titration lasts 30 min at the most, these changes in potential can be neglected

The behaviour of the D_2/Pd electrode as the indicator and reference electrodes in acetone and methyl ethyl ketone media was checked by titrating several bases of different strengths. The titration curves obtained are shown in Fig 2. The potentials in the course of the titration and at the equivalence point were rapidly established. The titration curves obtained with the D_2/Pd electrode have shapes similar to those obtained with glass and H_2/Pd indicator electrodes. The largest jump at the end-point was obtained with the glass electrode, a somewhat

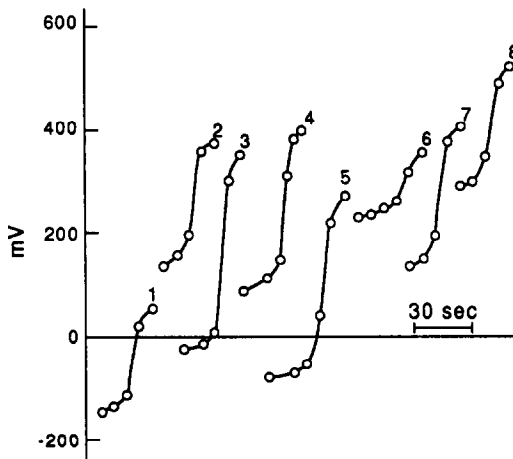


Fig 2 Coulometric titration curves for bases in acetone (1–4) and methyl ethyl ketone (5–8) with D_2/Pd indicator and reference electrodes (1) N,N -diphenylguanidine ($D_2/Pd_{ind}-SCE$), (2) N,N -diphenylguanidine ($D_2/Pd_{ind}-D_2/Pd_{ref}$), (3) 1,1,3,3-tetramethylguanidine ($D_2/Pd_{ind}-SCE$), (4) brucine ($D_2/Pd_{ind}-SCE$), (5) N,N -diphenylguanidine ($D_2/Pd_{ind}-SCE$), (6) aminopyrrene ($D_2/Pd_{ind}-SCE$), (7) brucine ($D_2/Pd_{ind}-SCE$) and (8) brucine ($D_2/Pd_{ind}-D_2/Pd_{ref}$)

Table 1 Coulometric titrations of bases by the application of the D_2/Pd electrode with visual and potentiometric end-point detection (supporting electrolyte, 0.1M sodium perchlorate, generation current 5 mA)

Solvent	Base titrated	Taken, μg	Found*, %	End-point detection
Acetone	Brucine	6 895	100.1 \pm 0.2 (7)†	Methyl Red
Acetone	Brucine	13 895	100.0 \pm 0.5 (4)†	Glass electrode-SCE
Acetone	Brucine	14 711	100.1 \pm 0.1 (3)‡	D_2/Pd_{ind} -SCE
Acetone	<i>N,N</i> -Diphenylguanidine	5 900	99.8 \pm 0.2 (7)‡	D_2/Pd_{ind} -SCE
Acetone	<i>N,N</i> -Diphenylguanidine	5 900	100.1 \pm 0.1 (4)‡	D_2/Pd_{ind} - D_2/Pd_{ref}
Acetone	Tetramethylguanidine	3 428	100.2 \pm 0.7 (5)‡	D_2/Pd_{ind} -SCE
Methyl ethyl ketone	<i>N,N</i> -Diphenylguanidine	3 025	99.9 \pm 0.5 (8)†	Methyl Red
Methyl ethyl ketone	<i>N,N</i> -Diphenylguanidine	6 074	100.0 \pm 0.4 (5)†	Glass electrode-SCE
Methyl ethyl ketone	<i>N,N</i> -Diphenylguanidine	5 918	100.5 \pm 0.5 (5)‡	D_2/Pd_{ind} -SCE
Methyl ethyl ketone	Aminopyrine	7 557	100.1 \pm 0.4 (5)‡	D_2/Pd_{ind} -SCE
Methyl ethyl ketone	Brucine	14 711	100.2 \pm 0.6 (5)‡	D_2/Pd_{ind} -SCE
Methyl ethyl ketone	Brucine	14 711	99.8 \pm 0.4 (3)‡	D_2/Pd_{ind} - D_2/Pd_{ref}

*Mean standard deviation for the number of titrations given in brackets

† H_2/Pd generator electrode

‡ D_2/Pd generator electrode

smaller jump was obtained with the D_2/Pd electrode and the smallest jump was given by the H_2/Pd electrode. Thus, in the titration of $5 \times 10^{-4}M$ *N,N*-diphenylguanidine in methyl ethyl ketone, the potential change at the end-point was about 350 mV with the glass electrode, 250 mV with the D_2/Pd electrode and about 120 mV with the H_2/Pd electrode. The results obtained in coulometric titrations of bases in 0.1M sodium perchlorate media in acetone and methyl ethyl ketone are listed in Table 1.

On the basis of these results it may be concluded that the deuterium-palladium electrode can be successfully applied as the generator, indicator and reference electrode in the coulometric-potentiometric determination of bases in acetone and methyl ethyl ketone

REFERENCES

- 1 J P Schwing and L B Rogers, *Anal Chim Acta*, 1956, **15**, 379
- 2 J T Stock, W C Purdy and T R Williams, *ibid*, 1959, **20**, 73
- 3 V J Vajgand and R P Mihajlović, *Bull Soc Chem Belgrade*, 1975, **40**, 96
- 4 S Kaufman, *Anal Chem*, 1975, **47**, 494
- 5 R P Mihajlović, *Doctoral Dissertation*, Belgrade, 1978
- 6 V J Vajgand, R P Mihajlović, R M Džudović and Lj N Jakšić, *Anal Chim Acta*, 1987, **202**, 231
- 7 R P Mihajlović, Lj V Mihajlović, V J Vajgand and Lj N Jakšić, *Talanta*, 1989, **36**, 1135
- 8 M Fleischmann and S Pons, *J Electroanal Chem*, 1989, **261**, 301
- 9 A P Kreshkov, L N Bykova and N A Kazaryan, *Kislотно-osnovnoe Titrovanie v Nevodnikh Rastvorakh*, Khimya, Moscow, 1967

KINETIC DETERMINATION OF SELENIUM, BASED ON INHIBITION OF THE Pd(II)-CATALYSED REACTION BETWEEN PYRONINE G AND HYPOPHOSPHITE

C SANCHEZ-PEDREÑO, M I ALBERO, M S GARCIA and A SAEZ

Department of Analytical Chemistry, Faculty of Sciences, University of Murcia, Murcia, Spain

(Received 27 November 1989 Revised 22 November 1990, Accepted 21 January 1991)

Summary—A new kinetic method for determination of selenium is based on its inhibitory effect on the Pd(II)-catalysed reaction between Pyronine G and hypophosphite. Under the optimum experimental conditions ($6 \times 10^{-5} M$ Pyronine G, $0.4 M$ hypophosphite, $0.4 \mu\text{g/ml}$ Pd(II), pH 2.8, temperature $22.0 \pm 0.2^\circ$), Se can be determined in the concentration range 0.033 – $0.50 \mu\text{g/ml}$. The method suffers from numerous interferences and is thus limited in application. It has been applied to the determination of selenium in spring waters and pharmaceutical preparations.

In an earlier paper we reported on use of the Pd(II)-catalysed reduction of Pyronine G by hypophosphite for kinetic determination of palladium.¹ We found that several ions strongly inhibit this system, and have used this to develop sensitive kinetic methods for the indirect determination of Ag(I), I^- and As(III).^{1,2} We now report a similar application for determination of selenium.

The toxicological and physiological significance of selenium^{3,4} necessitates its determination, which is most often achieved by spectrophotometric or fluorimetric measurement of the piarselenol formed by the reaction with an aromatic *o*-diamine.^{5,6}

Selenium can also be determined by catalytic methods, such as those based on its catalysis of the sulphide reduction of some organic substrates such as Methylene Blue,⁷⁻¹¹ Tolidine Blue¹² and picrate.^{13,14}

Kawashima and Tanaka¹⁵ have determined selenium by its catalysis of the reduction of 1,4,6,11-tetra-azanaphthacene with hypophosphorous acid, but this method suffers from non-linear calibration. A method based on the Landolt reaction, *viz* the chlorate–chloride–hydrazine sulphate system, has been reported¹⁶ and methods based on the oxidative coupling of *p*-hydrazinobenzenesulphonic acid with 1-naphthylamine or *m*-phenylenediamine have been proposed.^{17,18} The catalytic effect of selenium on the reduction of the tetranitro blue

tetrazolium ion by dithiothreitol has also been used.¹⁹

EXPERIMENTAL

Apparatus

Absorbance *vs.* time (*A*–*t*) curves were recorded with a Perkin–Elmer 550SE spectrophotometer furnished with 1-cm path-length cells kept at constant temperature by an MCIII Minicyostat. The pH-measurements were made with a Radiometer PHM63 pH-meter.

Reagents

Pyronine G. An aqueous $6 \times 10^{-4} M$ solution (0.1816 g/l.) was prepared from 3,6-bis(dimethylamino)xanthene hydrochloride (C.I. 45005).

Sodium hypophosphite solution (3M). This should be freshly prepared.

Palladium chloride solution. Prepared [100 mg/l. PdCl_2 , which corresponds to $60 \mu\text{g/ml Pd(II)}$] with $2 \times 10^{-2} M$ hydrochloric acid.

Selenite stock solution. This contained $500 \mu\text{g/ml}$ selenium and was prepared by dissolving previously dried $\text{Na}_2\text{SeO}_3 \cdot 5\text{H}_2\text{O}$ (Merck) in water. Working standards were prepared by dilution with water.

Britton–Robinson buffers. These were prepared for pH values between 1.7 and 4.4.

Solutions of various metal nitrates and the sodium salts of different acids were prepared for the study of interferences.

All solutions were made from analytical-grade reagents and doubly distilled water, and diluted as required

Recommended procedure for calibration

In a dry spectrophotometer cell place 0.30 ml of $6 \times 10^{-4} M$ Pyronine G, 0.50 ml of pH 2.80 buffer, 0.20 ml of 6.00 $\mu\text{g/ml}$ Pd(II) solution and an accurately measured volume (0.10, 0.15, 0.20–1.50 ml) of standard Se(IV) solution containing 1.00 $\mu\text{g/ml}$ selenium. Dilute the mixture to 2.60 ml with distilled water and place the cell in a thermostat at $22.0 \pm 0.2^\circ$ for 10 min. Then add 0.40 ml of 3M sodium hypophosphite and start the spectrophotometer recorder. Homogenize the solution by stirring, dry the faces of the cell, place it in the spectrophotometer compartment and record the absorbance at 548 nm as a function of total elapsed time. Repeat for volumes of selenium solution corresponding to final concentrations of 0.033–0.50 $\mu\text{g/ml}$. Plot the reciprocal of the time required for the initial absorbance to decrease by 0.100, against the selenium concentration

Determination of selenium in pharmaceuticals

Heat the sample (0.25–0.50 g) with concentrated hydrochloric acid and evaporate the mixture almost to dryness. Add some concentrated nitric acid, heat and again evaporate the mixture almost to dryness. Cool, take up the residue in water, filter, and adjust the pH to between 6 and 8 with 1M sodium hydroxide. All the selenium is then present as selenite. Dilute this solution to volume with water in a 250-ml standard flask and determine the selenium in 50- μl aliquots, as described for calibration

Determination of selenium in spring waters

Remove metal ions from the sample by treatment with Amberlite IR-120 ion-exchange resin. Use the standard-addition method by use of 1-ml aliquots of sample plus 0.3, 0.4 or 0.5 ml of 1.14 $\mu\text{g/ml}$ selenium(IV) and application of the calibration procedure

RESULTS AND DISCUSSION

Previous work had demonstrated that over a wide pH range hypophosphite does not reduce Pyronine G at an appreciable rate, but that Pd(II) is an efficient catalyst for this process. We have found that selenite has no effect on the H_2PO_2^- -Pyronine G system, but a strong inhibi-

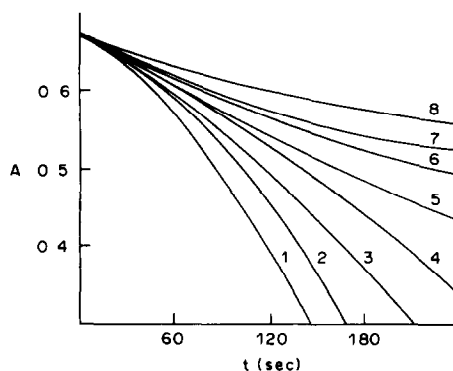


Fig. 1 $A-t$ curves run in the presence of 0.40 $\mu\text{g/ml}$ Pd(II) [Pyronine G] = $6 \times 10^{-5} M$, $[\text{H}_2\text{PO}_2^-] = 0.4 M$, pH 2.8, $22.0 \pm 0.2^\circ$, Se(IV) concentration (1) 0, (2) 0.04, (3) 0.12, (4) 0.20, (5) 0.27, (6) 0.34, (7) 0.42, (8) 0.57 $\mu\text{g/ml}$

tory effect on the Pd(II)-catalysed reaction. For a fixed amount of Pd(II) in the medium, the rate of the catalysed process is proportional to the Se(IV) concentration. The process is monitored spectrophotometrically at 548 nm by measuring the decrease in the absorbance of Pyronine G, and the reciprocal of the time required for the absorbance to decrease by 0.100 is plotted against the selenium concentration. Figure 1 shows that the rate of the process decreases with increase in the Se(IV) concentration, even at very low concentrations of this ion

Influence of pH

The influence of pH on the reaction rate was studied over the range 1.7–4.4, with Britton-Robinson buffers. Figure 2 shows that the rate of the process remained virtually constant over the pH range 2.5–3.6, the difference between the rate of the catalysed and the inhibited reaction being maximum in the range 2.3–3.2. We chose a pH of 2.8 for all subsequent experiments. The Pyronine G has an absorption maximum at 548 nm at this pH

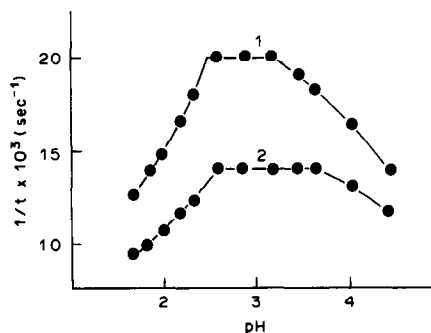


Fig. 2 Influence of pH on the reaction rate [Pyronine G] = 6×10^{-5} , $[\text{H}_2\text{PO}_2^-] = 0.4 M$, (1) 0.40 $\mu\text{g/ml}$ Pd(II), (2) 0.40 $\mu\text{g/ml}$ Pd(II) plus 0.20 $\mu\text{g/ml}$ Se(IV)

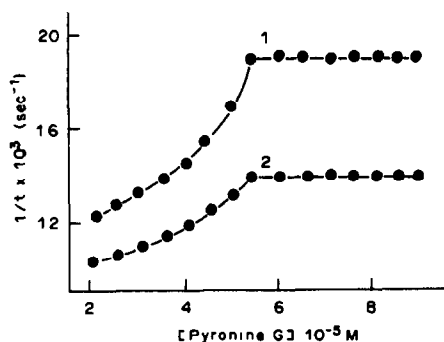


Fig 3 Influence of the Pyronine G concentration on the reaction rate $[H_2PO_2^-] = 0.4M$, pH 2.8, (1) $0.40 \mu\text{g/ml}$ Pd(II), (2) $0.40 \mu\text{g/ml}$ Pd(II) plus $0.20 \mu\text{g/ml}$ Se(IV)

Influence of other variables

The influence of the other variables was studied by varying them one at a time, with the other conditions kept constant. Figure 3 shows that the rate of both the catalysed and the inhibited reaction increased with the concentration of Pyronine G up to $5.5 \times 10^{-5}M$, above which it remained constant and the rate difference was maximal. A $6 \times 10^{-5}M$ concentration of Pyronine G, which yielded suitable absorbances, was selected.

The rates of the catalysed and inhibited reactions increased with increasing hypophosphite concentration up to $0.7M$, above which they remained virtually constant. Figure 4 shows that the difference between the two rates was maximal and constant for hypophosphite concentrations between 0.3 and $0.6M$ and we chose $0.4M$ for further experiments.

Influence of temperature; activation energy

Figure 5 shows the influence of temperature on the rate of the catalysed and inhibited reac-

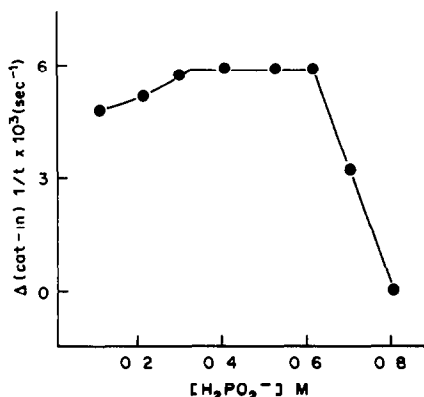


Fig 4 Influence of the hypophosphite concentration on the inhibitory effect of selenium.

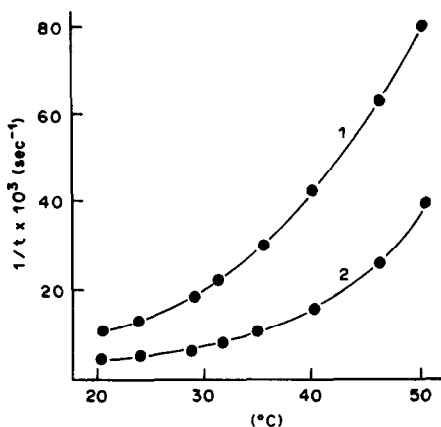


Fig 5 Influence of temperature on the reaction rate $[Pyronine\ G] = 6 \times 10^{-5}M$, $[H_2PO_2^-] = 0.4M$, pH 2.8, (1) $0.40 \mu\text{g/ml}$ Pd(II); (2) $0.40 \mu\text{g/ml}$ Pd(II) plus $0.42 \mu\text{g/ml}$ Se(IV)

tions, and we chose a temperature of $22.0 \pm 0.2^\circ$ as optimum

The activation energies found for the Pd(II)-catalysed reaction in the absence of Se(IV) and for the inhibited reaction in its presence were 14.0 and 15.3 kcal/mole respectively

Influence of the Pd(II) concentration

At constant Se(IV) concentration, the rate of the process increased linearly with the catalyst concentration up to a constant value at Pd(II) concentrations between 0.2 and $1.9 \mu\text{g/ml}$. The study was finished by assaying two series of samples at the selected pH, temperature, and

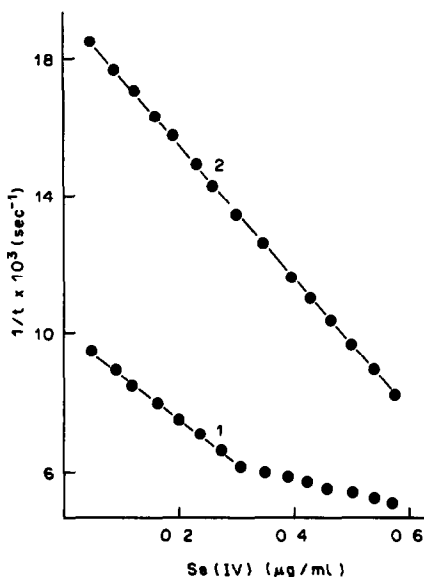


Fig 6. Influence of Pd(II) concentration. $[Pyronine\ G] = 6 \times 10^{-5}M$; $[H_2PO_2^-] = 0.4M$, pH 2.8, $22.0 \pm 0.2^\circ$, (1) 0.20 , (2) $0.40 \mu\text{g/ml}$ Pd(II)

Table 1 Effect of various foreign ions on the determination of Se(IV)

Foreign ion (FI)	Maximum tolerated [FI]/[Se(IV)] molar ratio
Ni(II)*	10 ⁴
Co(II)*	4 × 10 ³
HPO ₄ ²⁻ *	7 × 10 ²
Zn(II)†	4 × 10 ²
F ⁻ *, Cl ⁻ †	2 × 10 ²
Mn(II)*, ClO ₄ ⁻ *	40
Pb(II)*, Mg(II)*	10
SO ₃ ²⁻ *, WO ₄ ²⁻ †	1
Ag(I)*, U(VI)*, Cu(II)*, MoO ₄ ²⁻ *	0.5
Cd(II)*, As(III)*, Hg(II)*, Fe(III)†	0.1
Ru(III)*, Te(IV)*, Br ⁻ †, S ²⁺ *, V(V)*	
SCN ⁻ *, S ₂ O ₃ ²⁻ *	
Au(III)†, Bi(III)*, I ⁻ *, Cr(VI)*	
SO ₄ ²⁻ , NO ₃ ⁻ , Ca(II), Na(I), K(I), Se(IV)	No interference

*Positive error

†Negative error

Pyronine G and hypophosphite concentrations, plus 0.20 (Fig. 6, curve 1) or 0.40 µg/ml Pd(II) (curve 2) and varied concentrations of Se(IV) Curve 2, which corresponds to higher [Pd(II)]/[Se(IV)] ratios, has a steeper slope and wider linear range than curve 1. Hence, we chose a Pd(II) concentration of 0.40 µg/ml

Calibration graph and rate equation

Under the selected experimental conditions (6 × 10⁻⁵ M Pyronine G, 0.4 M H₂PO₂⁻, 0.40 µg/ml Pd(II), pH 2.8, 22.0 ± 0.2°), the rate of the process was linearly related to the Se(IV) concentration over the range 0.033–0.50 µg/ml.

The regression equation found was $y = 0.0191 - 0.0194x$, with correlation coefficient $r = 0.9989$. The limit of detection and the limit of quantification calculated according to the IUPAC recommendations²⁰ were 0.012 and 0.030 µg/ml Se(IV) respectively. The coefficients of variation for 10 determinations of 0.19 and

Table 2 Determination of selenium in pharmaceutical preparations

Sample* (source)	Selenium content found†, mg/g	
	Proposed method	Piazselenol method
Sebum selen (Llorente)	13.8 ± 0.6	13.2 ± 0.7
Abbotselsum (Abbot)	13.6 ± 0.3	13.5 ± 0.3
Caspiselenium (Kin)	13.9 ± 0.3	13.7 ± 0.2

*Sebum selen selenium sulphide 0.025 g, benzalkonium chloride 0.003 g, excipient up to 1 g (nominal Se content 13.8 mg/g) Abbotselsum selenium sulphide 0.025 g, excipient up to 1 g (nominal Se content 13.8 mg/g) Caspiselenium selenium sulphide 0.025 g, excipient up to 1 g (nominal Se content 13.8 mg/g)

†Average of three determinations ± SD

Table 3 Recoveries of selenium added to pharmaceutical preparations

Pharmaceutical	Se content, mg/g	Se added, mg/g	Recovery,* %
Sebum selen	13.2	10.0	99.3 ± 0.7
Abbotselsum	13.5	10.0	98.9 ± 0.7
Caspiselenium	13.7	10.0	100.0 ± 0.4

*Average of three determinations ± SD

0.34 µg/ml Se(IV) were 3.4 and 1.8%, respectively, and the relative errors were ±2.5 and ±1.3% respectively.

Under the recommended experimental conditions, the kinetic equation representative of the process is

$$-d[\text{Pyronine G}]/dt = k[\text{H}_2\text{PO}_2^-][\text{Pd(II)}]/[\text{Se(IV)}]$$

and the apparent rate constant, k , between 20 and 50°, ranges between 0.0157 and 0.23 min⁻¹.

Interferences

The interference of foreign ions with the proposed procedure was studied in experiments with 0.20 µg/ml of Se(IV) and various concentrations of the ion in question. The results are listed in Table 1, which also states the type of error caused. A given ion was considered to interfere when its presence resulted in an error larger than ±3% in the determination of Se(IV).

Applications

Because of the serious interference of numerous common ions, the proposed method is limited in its applications but has been satisfactorily applied to the determination of selenium in some pharmaceuticals, in which selenium is found as selenium sulphide (SeS₂). The results obtained by the proposed method and with a

Table 4 Recoveries of selenium added to spring waters

Sample	Se added, µg/ml	Se found,* µg/ml
1	0.190	0.192
	0.152	0.150
	0.114	0.111
2	0.190	0.186
	0.152	0.150
	0.114	0.115
3	0.190	0.191
	0.152	0.149
	0.114	0.113

*Average of three determinations

piaszelenol method²¹ that uses *o*-phenylenediamine are given in Table 2. The results compare well but the method proposed in this paper is considerably quicker than the piaszelenol method. The results of some recovery experiments by the standard addition method are shown in Table 3.

The method has also been tested for its applicability to determination of selenium in some spring waters. As the natural selenium content was below the limit of detection, some recovery experiments were done with added selenium. The results obtained with three bottled spring waters (chloride content 8.4, 7.1 and 6.2 $\mu\text{g/ml}$, respectively) are summarized in Table 4.

REFERENCES

- 1 C Sánchez-Pedreño, M I Albero and M S García, *Quim Anal*, 1985, **4**, 168
- 2 M S García, A Garre, M I Albero and C Sánchez-Pedreño, *An Quim*, 1988, **84B**, 247
- 3 H Robberecht and R Van Grieken, *Talanta*, 1982, **29**, 823
- 4 H Robberecht and H Deelstra, *ibid*, 1984, **31**, 497
- 5 J Hoste and J Gillis, *Anal Chim Acta*, 1958, **2**, 402
- 6 C A Parker and L G Harvey, *Analyst*, 1962, **87**, 558
- 7 F Feigl and P W West, *Anal Chem*, 1947, **19**, 351
- 8 H Goto, T Hirayama and S Ikeda, *Nippon Kagaku Zasshi*, 1952, **73**, 652
- 9 P W West and T V Ramakrishna, *Anal Chem*, 1968, **40**, 966
- 10 B B Mesman and H Doppelmayr, *ibid*, 1971, **43**, 1346
- 11 F Grases, G Genestar and R Forteza, *Int Environ Anal Chem*, 1986, **23**, 321
- 12 T Pérez Ruiz, C Martínez Lozano and M Hernández, *An Univ Murcia*, 1982, **39**, 213
- 13 E P Diamandis and T P Hadjioannou, *Anal Chim Acta*, 1981, **123**, 143
- 14 J M Hwang, T S Wei and Y M Chen, *J Chin Chem Soc*, 1986, **33**, 109
- 15 T Kawashima and M Tanaka, *Anal Chim Acta*, 1968, **40**, 137
- 16 J Bognár and S Sarosi, *Mikrochim Acta*, 1969, 361
- 17 T Kawashima, S Nakano and M Tanaka, *Anal Chim Acta*, 1970, **49**, 443
- 18 T Kawashima, J Kai and S Takashima, *ibid*, 1977, **89**, 65
- 19 W Hawkes, *ibid*, 1986, **183**, 197
- 20 G L Long and J D Winefordner, *Anal Chem*, 1983, **55**, 712A
- 21 F Snell, *Photometric and Fluorometric Methods of Analysis*, p 514 Wiley-Interscience, New York, 1981

FLUORIMETRIC DETERMINATION OF HYDROGEN PEROXIDE BY USE OF THE FLUORESCENCE REACTION BETWEEN *N*-(4'-HYDROXYPHENYL)-*N*-(4-METHYLQUINOLINYL)AMINE AND COBALT(II) IN THE PRESENCE OF TRIMETHYLSTEARYLAMMONIUM CHLORIDE*

ITSUO MORI,† YOSHIKAZU FUJITA, MINAKO TOYODA, KEIJI KATO,
NAOMI YOSHIDA and MASAO AKAGI

Osaka University of Pharmaceutical Sciences, Matsubara-shi, Osaka 580, Japan

(Received 19 November 1990 Revised 16 January 1991 Accepted 23 January 1991)

Summary—The fluorimetric determination of hydrogen peroxide by using the fluorescence reaction between *N*-(4'-hydroxyphenyl)-*N*-(4-methylquinolinyl)amine (HPMQ), cobalt(II) and hydrogen peroxide in the presence of trimethylstearylammmonium chloride (STAC) as a cationic surfactant was proposed. The calibration graph was linear in the range 0–2500 ng of hydrogen peroxide per 10 ml of solution at an emission wavelength of 522 nm with excitation at 410 nm. The recovery tests in foods were good.

Hydrogen peroxide has been used as a bleaching agent, as a disinfectant for medicine, and in food additives. Its carcinogenicity has raised interest in recent years and, therefore, a rapid and simple method for its microlevel determination is needed. In previous papers,^{1,2} we have discussed the fluorescence formation reaction between diarylamine compounds such as *N*-(4'-hydroxyphenyl)-*N*-(4-methylquinolinyl)amine (HPMQ) or *N*-(4'-hydroxy-3'-carboxyphenyl)-*N*-(4-methylquinolinyl)amine (MQAS) with cobalt(II) and hydrogen peroxide. In this paper, a simple and sensitive fluorimetric determination of hydrogen peroxide by using the fluorescence reaction of HPMQ or MQAS, cobalt(II) and hydrogen peroxide in the presence of the cationic surfactant trimethylstearylammmonium chloride (STAC) was systematically investigated.

EXPERIMENTAL

Apparatus and reagents

Spectrofluorophotometric measurements were performed on a Hitachi model 3000 spectrofluorophotometer with 10-mm silica cells and a 150-W Xenon arc source. A Hitachi-Horiba F-8 pH meter was used for all pH measurements.

Analytical-reagent grade chemicals were used throughout. Solutions of $1.0 \times 10^{-2} M$ cobalt(II), $1.0 \times 10^{-3} M$ HPMQ, methanol and STAC solutions were prepared according to previous reports.^{1,2} A solution of hydrogen peroxide was prepared by dilution of a 30% hydrogen peroxide solution (Mitsubishi gas Chemical Co., Ltd) and corrected by permanganimetry. Demineralized water was used throughout.

Recommended procedure

To a solution containing 2500 ng of hydrogen peroxide in a 10-ml standard flask were added 3.0 ml of borax buffer solution (pH 10.0), 2.0 ml of $5.0 \times 10^{-3} M$ STAC, 1.0 ml of $5.0 \times 10^{-5} M$ cobalt(II) and 0.75 ml of $1.0 \times 10^{-4} M$ HPMQ. The mixture was diluted to volume with water, kept at 50° for 20 min and cooled to room temperature (10–25°) (solution A). The difference between the relative fluorescence intensities (R.f.Int.) of solution A and a blank (solution B) prepared without hydrogen peroxide, was measured at an emission wavelength of 522 nm with excitation at 410 nm.

RESULTS AND DISCUSSION

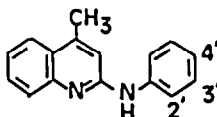
Fluorescence reaction between hydrogen peroxide and anilinoquinoline derivatives

The fluorescence formation reactions between the *N*-(phenyl)-*N*-(4-methylquinolinyl)amine

*The application of diarylamine compounds in analytical chemistry, Part III

†Author for correspondence

Table 1 Fluorescence reaction of anilinoquinoline derivatives, hydrogen peroxide and cobalt(II)



No	Anilinoquinolines(R)	Em R fl Int, %		
		nm	R	R-H ₂ O ₂
I	(phenyl)-	395	1.1	2.3
II	(2'-hydroxyphenyl)-	395	1.4	24.0
III	(3'-hydroxyphenyl)-	395	1.0	4.3
IV	(4'-hydroxyphenyl)-(HPMQ)	460	7.6	49.6
V	(3'-hydroxy-4'-carboxyphenyl)-(MQAS)	395	1.0	14.3

I-V $1.0 \times 10^{-5}M$, cobalt(II) $1.0 \times 10^{-6}M$, hydrogen peroxide $2.0 \times 10^{-4}M$, pH 10.0, Ex 320 nm

derivatives: *N*-(phenyl)-, *N*-(2'-hydroxyphenyl)-, *N*-(3'-hydroxyphenyl)-, *N*-(4'-hydroxyphenyl)-*N*-(4-methylquinolinyl)amines and MQAS and hydrogen peroxide and cobalt(II) were systematically investigated in weakly basic media (pH 10) in the absence of STAC. As shown in Table 1 HPMQ was the optimum and gave a strong fluorescence

Fluorescence spectra

As shown in Fig. 1, the fluorescence product of HPMQ-cobalt(II)-hydrogen peroxide in the presence of STAC has a maximum emission wavelength (*Em*) at 522 nm with an excitation wavelength (*Ex*) at 410 nm (Fig 2). In the absence of STAC a maximum emission occurred at 460 nm with *Ex* at 240 nm *Ex*

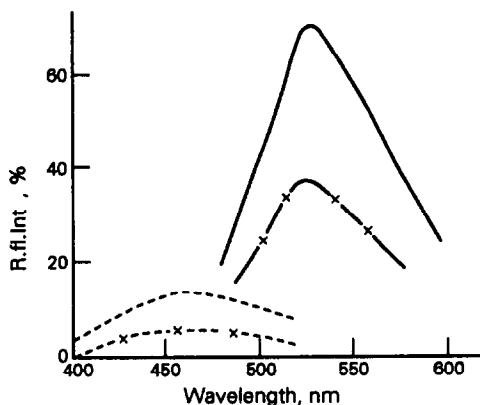


Fig 1 Emission spectra of HPMQ-cobalt(II) and HPMQ-cobalt(II)-hydrogen peroxide in the presence and absence of STAC HPMQ $1.5 \times 10^{-5}M$, cobalt(II) $5.0 \times 10^{-6}M$, hydrogen peroxide $5.0 \times 10^{-6}M$, STAC $1.0 \times 10^{-3}M$, pH 10 ----- HPMQ-cobalt(II)-hydrogen peroxide (*Ex* 360 nm) --x-- HPMQ-cobalt(II) (*Ex* 360 nm) — HPMQ-cobalt(II)-hydrogen peroxide-STAC, (*Ex* 410 nm) —x— HPMQ-cobalt(II)-STAC (*Ex* 410 nm)

at 410 nm was chosen for considering the effect of emission wavelength for further investigation. The difference of R.fl.Int (ΔF) at *Em* 522 nm with *Ex* 410 nm between HPMQ-cobalt(II)-hydrogen peroxide-STAC (solution A) and HPMQ-cobalt(II)-STAC solutions (solution B) was proportional to the concentration of hydrogen peroxide

Effect of pH

A maximum and constant ΔF value at 522 nm was obtained in the limited range of pH 9.3-10.8 by addition of 2.0-3.0 ml of $2.0 \times 10^{-2}M$ Sørensen borax buffer in 10 ml of solution.

Effect of metal ions

Table 2 shows the relative effects of different metal ions on the fluorescence signal in the

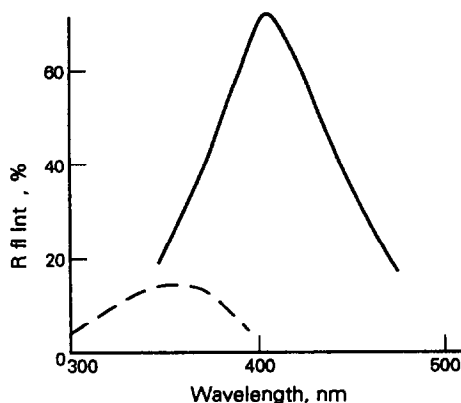


Fig 2 Excitation spectra of HPMQ-cobalt(II)-hydrogen peroxide solution in the presence or absence of STAC HPMQ $1.5 \times 10^{-5}M$, cobalt(II) $5.0 \times 10^{-6}M$, hydrogen peroxide $5.0 \times 10^{-6}M$, STAC $1.0 \times 10^{-3}M$, — HPMQ-cobalt(II)-hydrogen peroxide-STAC solution (*Em* 522 nm), — HPMQ-cobalt(II)-hydrogen peroxide solution (*Em* 460 nm)

Table 2 Effect of metal ions

Metal ion	R fl Int at 522 nm, %	
	HPMQ-metal ion	HPMQ-metal ion-hydrogen peroxide
—	30.8	33.0
Cobalt(II)	38.0	55.3
Nickel(II)	24.9	25.6
Copper(II)	282.4	282.4
Manganese(II)	257.5	261.7
Iron(II)	25.7	29.8
Palladium(II)	7.6	7.6
Molybdenum(VI)	48.1	48.1

Hydrogen peroxide 850 ng/10 ml, STAC $1.0 \times 10^{-3}M$, Metal ions $5.0 \times 10^{-6}M$, HPMQ $1.5 \times 10^{-5}M$, pH 10.0, Ex 410 nm

presence of hydrogen peroxide. Cobalt(II) caused the greatest fluorescence intensity enhancement and its optimum concentration, at a hydrogen peroxide concentration of $1.0 \times 10^{-5}M$, was $5.0 \times 10^{-6}M$. Accordingly, $5.0 \times 10^{-6}M$ cobalt(II) was used for further investigation.

Effects of surfactant and HPMQ concentration

As recognized in previous reports,^{1,2} the fluorescence reaction between HPMQ, hydrogen peroxide and cobalt(II) was remarkably enhanced by the coexistence of cationic surfactants such as STAC. Anionic surfactants such as sodium dodecylsulphate (SDS), and non-ionic surfactants such as Tween 20, were not effective. Table 3 summarizes the results of the effects of different surfactants. Although the ΔF in the presence of STAC was relatively small in comparison to that in its absence, the R.fl.Int. of solutions A and B in the presence of STAC, out of the tested cationic surfactants

STAC, *N*-hexadecylpyridinium chloride (HPC), hexadecyltrimethylammonium chloride (HTAC), benzyldimethyl-tetradecylammonium chloride (Zephiramine, Zp), gave the more stable and reproducible fluorescence. Its presence was therefore most effective and its optimum concentration was $1.0 \times 10^{-3}M$.

Effects of temperature and time

The optimal reaction conditions of temperature and time were investigated for the assay of hydrogen peroxide and a standard procedure was established—standing for 20 min at 50°—when considering the stability and reproducibility of maximum ΔF and the simplicity of the procedure.

Calibration graph and reproducibility

A linear calibration graph was produced over the range 0–2500 ng of hydrogen peroxide per 10 ml. For 850 ng of hydrogen peroxide, the coefficient of variation (C.V.) estimated for 5 replicates was 2.4%. Thus, the proposed method was relatively sensitive, with good reproducibility in comparison to other methods e.g., the titanium,³⁻⁶ vanadium(V)–Xylenol Orange⁷ and chemical luminescence methods.^{8,9}

Effects of diverse ions

The influence of diverse ions on the determination of 85 ng of hydrogen peroxide per millilitre was examined, and the tolerance limits were taken as the amounts that caused about $\pm 3\%$ error in R.fl.Int. The coexistence of copper(II) and manganese(II) gave positive errors at concentrations 1/5-th that of hydrogen peroxide, and iron(III) gave a negative error at a concentration 1/50-th that of hydrogen peroxide

Table 3 Effect of surfactants

Surfactant	R fl Int at max Em, %			
	Ex, nm	Em, nm	HPMQ	HPMQ-hydrogen peroxide
—	360	460	4.9	13.2
STAC	410	522	38.0	71.8
HTAC	410	522	30.2	59.2
HPC	360	485	0.8	1.4
Zp	360	460	4.4	12.6
SDS	360	460	7.4	12.9
Brij 35	360	455	30.5	51.8
Tween 20	360	455	45.6	60.6

Cationic surfactants—STAC, hexadecyltrimethylammonium chloride (HTAC), *N*-hexadecylpyridinium chloride (HPC), benzyldimethyltetradecylammonium chloride (Zephiramine, Zp) $1.0 \times 10^{-3}M$, anionic surfactant—SDS, non-ionic surfactant—Brij 35, Tween 20 0.1%, HPMQ $1.5 \times 10^{-5}M$, pH 10.0, hydrogen peroxide $5.0 \times 10^{-6}M$

Table 4 Effect of foreign ions

Foreign ions	Added			ΔF, %
	as	μg/10 ml	molar ratio	
—	—	—	—	17.3
Cu(II)	sulphate	0.03	1/50	17.2
Ni(II)	nitrate	0.03	1/50	16.5
		0.29	1/5	11.8
Mn(II)	chloride	0.03	1/50	16.9
Fe(III)	sulphate	0.03	1/50	16.4
Mo(VI)	molybdate	4.80	2	17.0
Ca(II)	chloride	200.40	200	17.0
Mg(II)	oxide	24.30	40	17.0
NO ₂ ⁻	sodium	46.01	40	16.7
BrO ₃ ⁻	potassium	1279.02	400	16.9
Citrate	sodium	192.4	40	17.3
Tartrate	sodium	600.45	200	16.8
Oxalate	sodium	88.00	40	17.2
L-Ascorbate	—	440.03	100	15.1
Glucose	—	180.16	40	16.8
Albumin	—	20.00	—	14.0

Hydrogen peroxide taken 850 ng/10 ml, HPMQ $1.5 \times 10^{-5}M$, cobalt(II) $5.0 \times 10^{-6}M$, STAC $1.0 \times 10^{-3}M$, pH 10.0, Ex 410 nm

(see Table 4). However, the coexistences of calcium(II), magnesium(II), phosphate, chloride, tartrate and citrate ions did not interfere, and albumin was tolerated up to 20 μg per 10 ml. In addition, the proposed method did not suffer from interference by other oxidizing agents such as bromate, iodate and nitrate ions.

Application

The proposed method was applied to the assay and recovery of hydrogen peroxide in different foods such as vermicelli, noodles and fish galantine. The detection reaction by the proposed method was negative in these samples—addition of hydrogen peroxide in these foodstuffs was forbidden and the recovery test was good (99.4%) in comparison with other methods (4-aminoantipyrine-modified method¹⁰ was 92.0–86.3%).

REFERENCES

- 1 I. Mori, Y. Fujita, K. Kato, M. Toyoda and M. Akagi, *Bull. Chem. Soc. Japan*, 1990, **63**, 359
- 2 *Idem*, *Anal. Lett.*, 1990, **23**, 2107
- 3 A. C. Egerton, A. J. Everett, G. J. Minkoff, S. Rudrakanchana and K. C. Salooja, *Anal. Chim. Acta*, 1954, **10**, 422
- 4 H. Pobiner, *Anal. Chem.*, 1961, **33**, 1423
- 5 C. Matsubara and K. Takamura, *Bunseki Kagaku*, 1980, **29**, 759
- 6 *Idem*, *ibid.*, 1981, **30**, 682
- 7 M. Veber and L. J. Csányi, *Microchem. J.*, 1977, **22**, 238.
- 8 P. van Zoonen, D. A. Kammenga, C. Gooijer, N. H. Velthorst and R. W. Frei, *Anal. Chim. Acta*, 1985, **167**, 249
- 9 V. Patrovský, *Talanta*, 1976, **23**, 533
- 10 Y. Ito, *Syokuhinsei Kenkyu*, 1981, **31**, 15
- 11 M. Iwaido, Y. Ito, Y. Tonogai, H. Suzuki, S. Ogawa, H. Hasegawa, K. Tanaka, M. Kondo and M. Fujii, *Nippon Nokeikagaku Kaishi*, 1981, **55**, 483

BOOK REVIEWS

Aquatic Chemical Kinetics: W STUMM (editor), Wiley, Chichester, 1990 Pages xiii + 545 £70 50

This book consists of 18 chapters by different U S and European authorities. Rather more than half is concerned with homogeneous reactions in water, including complexation of metal ions, catalysis, photo-oxidation, enzyme reactions and the fate of organic pollutants. The remainder covers reactions at mineral surfaces, including adsorption, dissolution, redox reactions, weathering and colloids, and thus more than usual emphasis is given to this aspect of chemistry in natural waters. The basic principles are introduced and much useful matter is covered for the graduate student or working environmental chemist or geochemist. For the general analytical chemist, it is very much background reading, but this should not be discounted when speciation increasingly forms part of the analytical task and an understanding of the processes in solution is particularly helpful. The sub-title stresses natural waters, but how many such waters are completely unaffected by industrial or agricultural discharges, and what about acid rain? Some attention is paid to these problems, but those concerned with pollution might have wished for extra chapters. This well-produced volume is nevertheless a welcome addition to a valuable series which one hopes to see further extended.

D MIDGLEY

Flavour Science and Technology: Y BESSIERE and A F THOMAS (editors), Wiley, Chichester, 1990 Pages xii + 369 £60 00

This book contains (according to the editors) most of the papers presented at the 6th Weurman Symposium held in May 1990 in Geneva, Switzerland. Flavour science encompasses the chemistry and sensory properties of flavorful materials, but the organizers of the Symposium selected as its main topics the chemistry of flavours, energy applications and food flavour systems, and instrumentation and data treatment. Hence there are few articles on sensory assessment of flavour. About half of the 60 or so contributions should be of interest to readers of *Talanta* in that they deal with aspects of composition and analysis. Both separation and extraction of flavorful volatiles—often present in food at less than 10 ppm in total—from the matrix are covered. It is a feature of the organoleptic properties of a flavorful chemical that often both intensity and character differ quite markedly between enantiomers. Hence chiral analytical methods are becoming increasingly important in flavour research and several papers are directed to this topic.

Individual articles are short, no more than 4 pages, but the book as a whole gives a good overview of current interests in flavour chemistry. The book has been produced from authors' typescripts by photographic methods, but reproduction of both text and figures is clear.

P HOWGATE

X-Ray Absorption Principles, Applications, Techniques of EXAFS, SEXAFS and XANES: Edited by D C KONINGSBERGER and R PRINS, Wiley, New York, 1988 Pages xii + 673 £77 50

Extended X-ray absorption fine-structure methods are powerful tools for the determination of atomic arrangements and chemical bonding in both crystalline and amorphous substances. This book is aimed at the growing numbers of EXAFS users and is a collection of 11 chapters, divided into three parts, contributed by distinguished workers in the field. Part A comprises two chapters dealing with the theory of EXAFS and XANES in a particularly lucid manner, although h and \hbar are occasionally confused, this should not upset the alert reader unduly. The simplifying assumptions made in the derivation of the EXAFS equation are discussed at some length and appropriate corrections are given. Part B, 4 chapters, describes instrumentation, experimental design and data analysis. The use of both synchrotron and laboratory sources is described and their relative merits are compared. X-Ray optics are also treated. The remaining five chapters, Part C, deal with applications to biochemistry, catalysis and amorphous and liquid systems, and with SEXAFS (with a somewhat predictable, jokey title) and XANES.

The real usefulness of this book lies in its combination of rigorous theoretical treatment with practical advice and insights into the problems and pitfalls that may be encountered. Chapters 3-5 will be particularly useful for those wishing to set up their own instruments. Similarly, Chapter 6, which deals with data processing and analysis, gives much practical advice on such topics as the elimination of problems caused by various aspects of the instrumentation, the estimation and removal of background signals, and the effects of disorder. The interpretation of Fourier transforms is also discussed in this chapter.

The chapters on applications, which make up Part C, maintain the standards of the previous chapters. Additional theoretical treatment is given where necessary along with practical considerations before published results are detailed. A critical review of the literature is given rather than a simple regurgitation.

The book is well illustrated with diagrams and figures, and there is a comprehensive bibliography. It is certainly a vital text for anyone wishing to embark upon a career in X-ray absorption.

ERIC LACHOWSKI

Phosphorimetry—Theory, Instrumentation, and Applications: R J HURTUBISE, VCH, Cambridge, 1990 Pages xii + 370 DM 114 00, £70 50

This book is a well done introduction to phosphorimetry. It is written for the beginner as well as the user of phosphorimetric techniques. The writing is extremely good and the book is fun to read. Chapter 2 on photophysical aspects of luminescence is primarily directed towards the quantification aspects of luminescence rather than structure-spectra relationships. Chapter 3 on instrumentation is an excellent review of the principles, operation and use of various instrumental components in phosphorimeters. I would like to have seen a more thorough discussion of spectral correction for instrumental parameters. Chapter 4 on important analytical considerations concerns relationships between phosphorescence intensity or signal and concentration, and signal-to-noise ratio aspects, including limits of detection. Chapters 4 and 5 are primarily tutorial and are very useful for those students and researchers who are beginning work involving phosphorimetric measurements.

Chapter 5 on low-temperature phosphorimetry and Chapter 6 on solid-surface room-temperature phosphorimetry are both extremely well done. These chapters are very useful to both the beginner and the advanced researcher. Chapter 7 on physicochemical interactions in solid-surface phosphorescence gives a detailed and well done discussion of the important physical-chemical interactions in solid-surface RTP, and is the most extensive chapter in the book. Chapter 8, applications in solid-surface RTP, Chapter 9, sensitized and quenched phosphorescence in solution at room temperature, Chapter 10 on micelle-stabilized, cyclodextrin, and colloidal/microcrystalline RTP, Chapter 11 on phosphorescence of proteins, polypeptides, and peptides, and Chapter 12 on structural characterization of polymers are all well done and of considerable interest to anyone interested in the use of phosphorimetry in scientific applications. Chapter 13 on final comments and future trends is very short and not too useful.

Overall, this book is well worth having in your personal library. It is a well written book for analytical chemists as well as those scientists who use or could use phosphorimetry. The numerous tables, figures, and references are extremely useful for anyone working in the area of phosphorimetry. Dr. Hurtubise should be congratulated on this fine publication.

J D WINEFORDNER

PIXE—A Novel Technique for Elemental Analysis: S A E JOHANSSON and J L CAMPBELL, Wiley, Chichester, 1988 Pages xii + 347 £42 50

As a comprehensive introduction to a novel analysis technique, this is an admirable effort. The first half of the book is somewhat dry, of necessity in a discussion of the technical and mathematical basis of the PIXE technique, but the breadth of applications covered later compensates well for this. PIXE, Particle (or Proton) Induced X-Ray Emission, is competing in a difficult field, surrounded by something of a plethora of alternative techniques. That it has made such an impact, as represented in this book, is a consequence of the significant advantages inherent in the technique. These are primarily speed of analysis, extremely high sensitivity and the facility for simultaneous multielemental analysis. The fact that PIXE has "come of age some 15 years after its first demonstration" is testament to its capabilities as a high-speed technique with high absolute sensitivity. As with most new techniques, the development of significant new data-analysis techniques has been required and the importance of this is emphasised in this book. It appears, however, that at its present state of development, PIXE is the best elemental analysis technique in terms of absolute sensitivity for trace quantities.

A casual, or semi-casual, reader—that is, one who is not a PIXE expert—would be well advised to approach the book with the order of the halves reversed. The second half, dealing with applications, is far more likely to stimulate further reading and investigation into the method, dealing as it does with the manifold applications of the PIXE technique. These range from quasi real-time monitoring of the composition of acid rain, through analysis of geological samples and works of art, to the determination of the minute concentrations of life-sustaining trace elements in the various organs of the body. In addition, some of the more prosaic aspects are covered, such as where PIXE can be performed, how much it costs, how rapid it is, *etc*. Having read the book in order, I approached the last chapters asking three questions, and was somewhat relieved to find the answers therein.

With the invitation to further investigation supported by a comprehensive bibliography facilitating this, the book seems ideal even for those on the periphery of interest in the subject, and should help increase general awareness of the technique. In spite of being no expert in the field, I felt that the comprehensive coverage of the fundamentals of PIXE in the first half of the book also appeared to offer useful material for those with a deeper understanding of, and interest in, this obviously expanding technique.

C C WILSON

FLOW-INJECTION STOPPED-FLOW KINETIC SPECTROPHOTOMETRIC DETERMINATION OF DRUGS, BASED ON MICELLAR-CATALYSED REACTION WITH 1-FLUORO-2,4-DINITROBENZENE

CONSTANTINOS A. GEORGIU, MICHAEL A. KOUPPARIS*
and THEMISTOCLES P. HADJIIOANNOU

Laboratory of Analytical Chemistry, Department of Chemistry, University of Athens, Panepistimiopolis,
Kouponia, Athens 15771, Greece

(Received 10 October 1990. Accepted 18 December 1990)

Summary—A flow-injection stopped-flow kinetic spectrophotometric method for the determination of hydrazines, hydrazides, amines and amino-acids, based on the cetyltrimethylammonium bromide catalysed reaction with 1-fluoro-2,4-dinitrobenzene is described. With the proposed method dihydralazine, isoniazid, levodopa and aspartame can be determined at concentrations of $0.1-6 \times 10^{-4}M$. The calibration ranges can be varied by adjusting the pH and surfactant concentration. The determination of amphetamine, cysteine, *s*-carboxymethylcysteine, cephalixin, tobramycin and gentamicin is also feasible. The method has been applied to the determination of levodopa, isoniazid and aspartame in commercial pharmaceutical formulations. The determination of isoniazid in formulations containing the highly coloured antibiotic rifamycin, and of aspartame in coloured beverages was also accomplished. The results were in good agreement with those obtained by reference methods and the throughput was 40 measurements per hour with 0.4-3.9% RSD.

1-Fluoro-2,4-dinitrobenzene (FDNB), the so-called Sanger reagent, has been used as a chromogenic reagent for the spectrophotometric determination of amino-acids and primary and secondary amines,¹⁻⁷ amino-acid nitrogen in plasma and urine (Goodwin's method),^{8,9} isoniazid,¹⁰ various aminoglycoside antibiotics (gentamicin, tobramycin, amikacin),¹¹ phenols,¹² and the enzyme amidase.¹³ It has also been used in high-performance liquid chromatography for the determination of amines and aminoglycosides and in thin-layer chromatography.¹⁴⁻¹⁶

These methods have inherent disadvantages, however, *e.g.*, a long reaction time is needed, or heating to speed up the reaction, and additional steps for hydrolysis of the excess of FDNB and extraction of the dinitrobenzene product for measurement. The methods cannot be applied to coloured samples. Kinetic methods overcome such problems associated with equilibrium methods. Recently a kinetic potentiometric method has been developed for the determination of amines,¹⁷ amino-acids,¹⁸ hydrazines, hydrazides and azides¹⁹ and phenols,²⁰ in which

the reaction with FDNB is monitored with a fluoride-selective electrode.

The suitability of FDNB as a general reagent for routine determinations, especially in pharmaceutical analysis, renders automation of the kinetic procedures using FDNB highly desirable. This is more imperative since the FDNB reagent is rather difficult to handle and use (it is vesicatory and hydrolyses in alkaline solutions). Flow-injection (FI) is a very attractive technique for automated manipulation of reagent and sample solutions, with data collection during measurements. The classical FI technique is a kinetic one-point (fixed time) procedure, and can be used with FDNB methods, provided that the reaction rate is adequate. Multipoint kinetic procedures can also be achieved by using the combination of flow injection and stopped flow (FI-SF).²¹ This approach provides more precise kinetic measurements and is suitable for use with coloured sample solutions.

Kinetic studies of FDNB reactions in aqueous media have shown that they can be accelerated considerably by micellar catalysis, with various surfactants. This catalytic action has been used to speed up equilibrium spectrophotometric^{22,23} and kinetic potentiometric methods.^{20,24}

*Author for correspondence.

The development of an automated FI-SF kinetic method, described in this work, increases the measurement throughput and the precision of the determinations (multipoint measurements), allows reduction of the number of steps before measurement (in-line pH adjustment and reagent addition, no need to extract the final dinitrobenzene product), provides safe manipulation of the FDNB reagent, and permits the analysis of coloured sample solutions (background signals do not interfere in the FI-SF technique).²⁵

EXPERIMENTAL

Apparatus

A laboratory made automated FI-SF spectrophotometric analyser was used. It consists of a remote controlled multichannel pump (Ismatec MPN-8), an injection valve (Rheodyne 5001) equipped with a pneumatic actuator controlled by the microcomputer through solenoid valves, Teflon mixing coils (0.8 mm i.d.), a spectrophotometer (Bausch & Lomb, Spectronic 21) equipped with an 18- μ l flow-through cell (Hellma), an AIM 65 microcomputer (Rockwell) with the appropriate home-made control interface and a 12-bit ADC card (Rockwell RM65-5302E). It provides automated sampling, mixing with reagent and buffer solutions, stopping the reaction mixture in the cell, multipoint reaction rate (absorbance) measurement, and data reduction and evaluation. The data-logging routine, written in assembly, permits fast (up to 7.5 kHz) data acquisition and is called by the SLOP.BAS program that is used for routine assays. Two other utility programs were developed for use during the development of a new FI-SF method. The PEAK.BAS program determines the residence time in the FI manifold and the INVQ.BAS program determines the linear segment of the reaction curve for each standard. These parameters are then used by the SLOP.BAS program in routine measurements.

The FI manifold designed and optimized for the proposed method is shown in Fig. 1. A stable acidified aqueous ethanolic solution of FDNB reagent is premixed with an alkaline micellar solution at the optimum pH and then merged with the injected sample zone. After adequate mixing, the reaction mixture is stopped in the flow cell for the reaction rate measurement.

The preliminary spectrophotometric study of the reaction was performed with a double-beam spectrophotometer capable of successive scans (Perkin-Elmer Lambda 7).

Reagents

All reagents were of analytical reagent grade and demineralized distilled water was used throughout.

The FDNB stock solution (0.168M) was prepared by dissolving 3.13 g of FDNB (Sigma) in acetone and dilution to 100.0 ml. This solution was stored in a sealed amber glass vial in the refrigerator and was opened only when used. It should be handled carefully as it is vesicatory. The FDNB working solution ($8.40 \times 10^{-3}M$) was prepared daily by 20-fold dilution of the stock solution with 0.001M hydrochloric acid in 20% v/v ethanol solution in water.

Borate buffer (0.10M adjusted to pH 9.5) was prepared according to usual practice, and contained cetyltrimethylammonium bromide (CTAB, Sigma) at a concentration of $3.5 \times 10^{-3}M$ (for isoniazid and dihydralazine) or $1.5 \times 10^{-3}M$ (for levodopa and aspartame). During the optimization studies, the following buffers were used: (a) pH 8.0 and 8.5 (TRIS 0.10M), (b) pH 9.0 and 9.5 (boric acid 0.10M) and (c) pH 10.0 and 10.5 (borate 0.060M), containing various (0.00, 0.75, 1.50, 3.50, 5.50 and 7.50mM) concentrations of CTAB.

Stock $1.000 \times 10^{-2}M$ solutions of isoniazid, levodopa and aspartame and a $2.000 \times 10^{-3}M$ solution of dihydralazine hydrochloride were prepared from the pure substances (Sigma), the purity of which was determined by the U.S. Pharmacopeia (USP) XXI and National

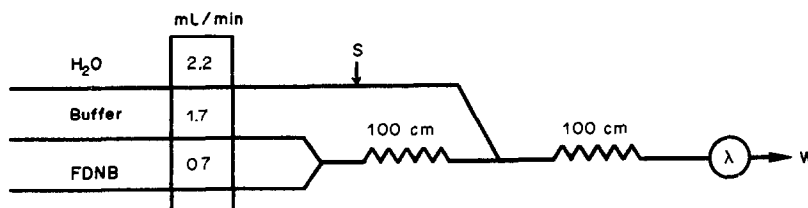


Fig. 1. Manifold used in the automated kinetic determinations. Sample volume 200 μ l.

Formulary (NF) XVI methods. Working standard solutions in the ranges shown later in Table 3, were prepared by appropriate dilution of the stock solutions. Other substances tested for possible determination by the method were amphetamine, cysteine, cystine, *s*-carboxymethylcysteine, cephalixin, tobramycin, gentamicin, propranolol, isoxsuprine, amoxicillin and acetaminophen (paracetamol).

Kinetic study of the reaction

Appropriate volumes of a working solution of each substance studied, the FDNB reagent and the borate buffer (pH 9–10) were mixed and transferred into the observation cell of the scanning spectrophotometer. Successive scans were made (at 1 scan/min) with a scanning rate of 980 nm/min in the range 300–600 nm. From the spectra obtained the λ_{\max} values for the 2,4-dinitrobenzene derivatives were found.

Measurements with the FI-SF analyser

The spectrophotometer of the FI-SF analyser was set at the λ_{\max} of the corresponding 2,4-dinitrobenzene derivative (428 nm for isoniazid and dihydralazine, 342 nm for aspartame and 352 nm for levodopa), then the residence time and the time interval (measurement time) during which the $A = f(t)$ reaction curve is linear were determined by using the working standard solutions of the substance and the appropriate investigative program (PEAK.BAS and INVQ.BAS, respectively). Subsequently, the SLOP.BAS program was loaded and the timing parameters for the determination and information for the number of standards, samples and runs per standard and sample were provided to the program.

When the optimized manifold (Fig. 1) was used with 200 μ l of sample or standard, the flow was stopped for 16 sec (residence time), followed by a time interval of 2 sec for mechanical equilibration of the stopped mixture, then multiple (40–256) absorbance readings, equally spaced on the time axis, were taken during a measurement time of 15–40 sec, as estimated by the INVQ.BAS program for each determination. The pump was then restarted and a time interval of 40 sec was allowed for washing the measured sample from the manifold and loading the next sample into the sample loop. Subsequently, the experimental reaction rate ($\Delta A/\Delta t$) was calculated by linear regression of the absorbance readings, and was used for construction of the calibration curve or

determination of the analyte concentration in the samples.

Sample preparation

For solid formulations the official USP sampling procedures were followed. From the final fine powder an accurately weighed portion was dissolved in water, so that the concentration of the drug was in the range of the corresponding calibration curve (Table 3). An ultrasonic bath or a mechanical shaker was used to ensure complete disintegration of the powder, and any insoluble matter was allowed to settle or was filtered off or centrifuged. For the analysis of beverages containing aspartame, carbon dioxide was expelled by purging with nitrogen and the sample was diluted tenfold with the buffer used.

All measurements were performed in an air-conditioned laboratory maintained at a nominal temperature of about 25°.

RESULTS AND DISCUSSION

Preliminary kinetic investigation

To find λ_{\max} for the coloured 2,4-dinitrobenzene (DNB) derivative of each analyte and obtain a rough estimate of the reaction rate, a kinetic spectrophotometric study was performed as described above. Figure 2 shows successive spectra obtained from the reaction of FDNB with isoniazid. The DNB-isoniazid derivative, with $\lambda_{\max} = 428$ nm, is formed rather slowly, so the reaction must be accelerated for use in an FI-SF method with sufficient sensitivity and short analysis time. Micellar catalysis with CTAB was chosen to accelerate the reaction. The λ_{\max} values for the DNB derivatives of the other substances studied were 346 nm for amphetamine, 342 nm for aspartame, 352 nm for levodopa, 340 nm for cysteine, 342 nm for cephalixin, 344 nm for tobramycin, and 350 nm for gentamicin and *s*-carboxymethylcysteine. Several substances (phenols and cystine) form water-insoluble DNB derivatives which render spectrophotometric measurements impossible because of the cloudy solutions obtained.

The λ_{\max} of FDNB is 240 nm, that of its ethanolysis product is 283 nm and that of its hydrolysis product (2,4-dinitrophenol) is 360 nm.

Design and optimization of the FI-SF method

In an FI procedure using FDNB, the problem of stabilizing the reagent solution has to be solved. FDNB is only slightly soluble in water, and undergoes base-catalysed solvolysis

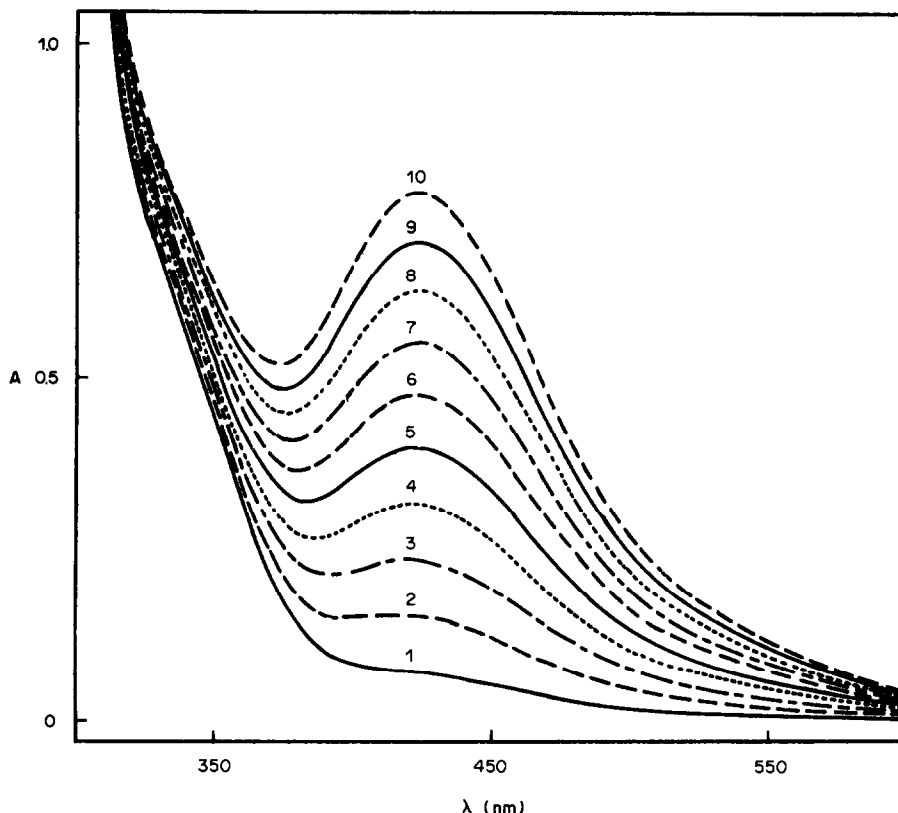


Fig. 2. Kinetic study of the FDNB-isoniazid reaction. [Isoniazid] $1.25 \times 10^{-4} M$, [FDNB] $1.4 \times 10^{-3} M$, in $0.33 M$ borate buffer adjusted to pH 9.5. Ten successive scans at 1 scan/min.

in solvents that contain active hydrogen atoms, such as ethanol and water. A very stable FDNB stock solution can be prepared in acetone, but solutions containing more than 5% v/v acetone cannot be pumped through the conventional silicone rubber tubing used in peristaltic pumps. Therefore, the working FDNB solution was prepared daily in 20% v/v ethanol solution acidified with hydrochloric acid. A spectrophotometric stability study of working FDNB solution containing ethanol at concentrations of 20, 30, 40 and 50% v/v revealed 4, 6.5, 8 and 8% solvolysis of FDNB, respectively in a period of

8 hr. Therefore, a 20% content of ethanol in the working FDNB solution provides a reagent stable enough for an 8-hr routine operation of the analyser.

The effect of pH and surfactant concentration on the analytical reaction was studied. Table 1 shows the characteristics of the calibration curves for isoniazid, constructed by measuring the reaction rate of standards over the pH range 9.0–10.5. The sensitivity increases with pH but so does the blank value (due to base-catalysed FDNB solvolysis), whereas the linear concentration range decreases. A pH of 9.5 was chosen

Table 1. Effect of pH on the calibration graph for isoniazid ([CTAB] $1.5 \times 10^{-3} M$)

pH	Slope, $mA \cdot sec^{-1} \cdot l. \cdot mole^{-1}$	Intercept, $mA \cdot sec^{-1}$	DL*, $10^{-3} M$	r	Range, $10^{-4} M$	Blank $\pm SD (n = 6),$ $mA \cdot sec^{-1}$
9.0	$(2.73_6 \pm 0.02_7) \times 10^3$	0.03 ± 0.03	19	0.9996	2–50	0.06 ± 0.17
9.5	$(5.70_0 \pm 0.063) \times 10^3$	0.18 ± 0.06	9.5	0.9995	1–40	0.11 ± 0.18
10.0	$(2.18_5 \pm 0.025) \times 10^4$	0.50 ± 0.10	3.3	0.9993	1–8	0.37 ± 0.24
10.5	$(3.82 \pm 0.14) \times 10^4$	1.3 ± 0.3	0.08	0.999	1–6	0.49 ± 0.01

*Detection limit: concentration corresponding to a net analytical signal equal to three times the standard deviation of the blank.

as a compromise between sufficient sensitivity, wide linear response range, low blank value, good linearity and precision. The effect of the surfactant concentration on the characteristics of the calibration curve for isoniazid is shown in Table 2. The sensitivity and the blank value increase with the surfactant concentration, but the linear concentration range decreases at $[CTAB] \geq 0.0015M$. A CTAB concentration of $0.0035M$ was chosen as a compromise between sensitivity and low blank value. The same optimum pH and CTAB concentration were found for dihydralazine, while for the determination of aspartame and levodopa the optimum CTAB concentration was $0.0015M$. The linear range and the sensitivity of the determinations can be varied by changing the reaction pH and/or the CTAB concentration.

Evaluation of the method

Typical calibration data for aspartame, levodopa, dihydralazine hydrochloride and isoniazid under the optimized conditions are shown in Table 3. The linearity of calibration was excellent and the precision (relative standard deviation, RSD) of the measurements

Table 4. Recovery for isoniazid ($4 \times 10^{-4}M$) in mixed solutions with excipients and rifamycin

Interferent	Interferent: isoniazid ratio, w/w	Recovery, %
Talc	10	99.7
Gelatin	10	97.0
Cellulose acetate	10	86.3
hydrogen phthalate	5	95.2
	1	97.8
Lactose	10	98.6
Magnesium stearate	10	99.4
Starch	10	99.6
Sodium lauryl sulphate	10	45.6
	5	75.9
	1	95.9
Carboxypolymethylene (carbopol)	10	59.0
	5	84.8
	1	93.9
Galactose	10	90.7
	5	95.6
	1	100.0
Sorbitol	10	93.6
	5	95.6
	1	100.6
Rifamycin	10	94.0
	5	97.4
	1	97.7

ranged from 0.4 to 3.9% ($n = 6$). The analytical concentration ranges were suitable for drug assays in pharmaceutical preparations.

Table 2. Effect of [CTAB] on the calibration graph for isoniazid (pH 9.5)

[CTAB], $10^{-3}M$	Slope, $mA \cdot sec^{-1} \cdot l. \cdot mole^{-1}$	Intercept, $mA \cdot sec^{-1}$	DL* $10^{-5}M$	r	Range, $10^{-4}M$	Blank $\pm SD$ ($n = 6$), $mA \cdot sec^{-1}$
0.0	870 ± 9	0.054 ± 0.021	10	0.9998	8-40	0.082 ± 0.029
0.75	959 ± 9	0.007 ± 0.02	9.4	0.9997	4-40	0.091 ± 0.030
1.5	$(5.77 \pm 0.07) \times 10^3$	0.27 ± 0.07	0.9	0.9994	1-40	0.114 ± 0.018
3.5	$(2.46_7 \pm 0.02_3) \times 10^4$	0.55 ± 0.05	0.09	0.9997	0.1-6	0.4640 ± 0.0070
5.5	$(3.19_5 \pm 0.04) \times 10^4$	0.84 ± 0.10	0.20	0.9993	0.1-6	0.658 ± 0.021
7.5	$(3.56 \pm 0.05) \times 10^4$	1.03 ± 0.08	0.57	0.9993	0.1-4	0.772 ± 0.067

*Detection limit: concentration corresponding to a net analytical signal equal to three times the standard deviation of the blank.

Table 3. Typical calibration data for (a) aspartame, (b) levodopa, (c) dihydralazine hydrochloride and (d) isoniazid. pH = 9.5, [CTAB] = $1.5 \times 10^{-3}M$ (a and b) or $3.5 \times 10^{-3}M$ (c and d)

	Slope, $mA \cdot sec^{-1} \cdot l. \cdot mole^{-1}$	Intercept, $mA \cdot sec^{-1}$	DL* $10^{-5}M$	r	Range $10^{-4}M$	Blank $\pm SD$ ($n = 6$), $mA \cdot sec^{-1}$
(a)	$(1.20_5 \pm 0.02) \times 10^4$	0.780 ± 0.006	2.0	0.9993	0.6-6	0.632 ± 0.081
(b)	$(4.32 \pm 0.05) \times 10^4$	0.452 ± 0.020	0.63	0.9996	0.1-2	0.861 ± 0.090
(c)	$(1.62_7 \pm 0.066) \times 10^4$	2.620 ± 0.030	1.8	0.997	0.5-6	2.20 ± 0.10
(d)	$(2.46_7 \pm 0.023) \times 10^4$	0.55 ± 0.05	0.09	0.9997	0.1-6	0.4640 ± 0.0070

*Detection limit: concentration corresponding to a net analytical signal equal to three times the standard deviation of the blank.

Table 5. Determination of isoniazid, aspartame and levodopa in commercial formulations (tablets) by FI-SF and reference methods

Formulation	Drug content, mg/tablet			
	Nominal	Found \pm SD*		<i>t</i> -test†
		FI-SF	Reference method†	
<i>Isoniazid</i>				
Dianicotyl	100	100.7 \pm 0.4	102 \pm 1	2.091
Rimactazid	100§	100.0 \pm 0.5	98 \pm 2	1.680
Rimactazid	150	154 \pm 2	152 \pm 2	1.225
<i>Aspartame</i>				
Canderel	18	18.1 \pm 0.7	17.8 \pm 0.9	0.456
<i>Levodopa</i>				
Madopar	50	51.0 \pm 0.7	52.0 \pm 0.7	1.750

*Average \pm standard deviation for three samples each measured in triplicate.

†Reference methods (USP XXI): isoniazid, bipotentiometric titration with bromine in strong acid solution after extraction of rifamycin with chloroform; levodopa, spectrophotometric method; aspartame, HPLC method.²⁶

‡Theoretical *t*-value for 95% confidence level and 3 + 3 measurements, 2.776.

§Contains 150 mg of rifamycin.

||Contains 300 mg of rifamycin.

To examine the applicability of the proposed FI-SF method to routine pharmaceutical analyses, the effect of various excipients and the antibiotic rifamycin, which is present in mixed formulations with isoniazid, was studied. Recovery results for mixed solutions of isoniazid and the substances studied are shown in Table 4. Common excipients do not interfere, except sodium lauryl sulphate and carboxypolyethylene (carbopol), which give negative errors (possibly by formation of mixed micellar solutions or partial saturation of the surfactant micelles, and a consequent change in catalytic

action). Experiments with these two excipients and a surfactant-free buffer solution gave recoveries of 97.2–101.4%, so formulations containing these two excipients can be analysed by use of a surfactant-free buffer but with lower sensitivity and decreased measurement throughput. This also applies to mixed isoniazid–rifamycin formulations.

Applications

The proposed FI-SF method was applied to the determination of isoniazid, aspartame and levodopa in commercial formulations and of

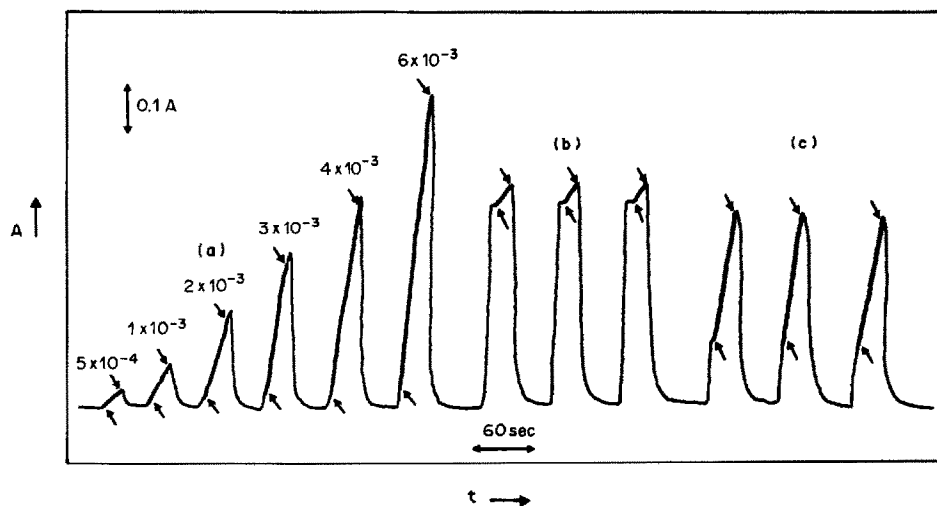


Fig. 3. FI-SF recordings for the determination of isoniazid (INH) in (a) standard solutions and in tablet solutions containing (b) 300 mg and (c) 150 mg of rifamycin per tablet. [INH] $\sim 6 \times 10^{-4} M$ in (b) and $3 \times 10^{-3} M$ in (c). The analytical parameter is the slope of the line between arrows.

Table 6. Results for the determination of aspartame in beverages by FI-SF method and comparison with reference method

Beverage	Aspartame, mg/ml		
	Nominal	Found \pm SD	
		FI-SF*	Reference method†
Sprite	0.50	0.43 ± 0.01	0.41
Coca Cola	0.50	0.51 ± 0.02	0.48

*Three samples each measured in triplicate.

†HPLC method.²⁶

aspartame in diet ("light") beverages. It compares favourably with reference methods (Table 5) and permits the determination of isoniazid in mixed isoniazid-rifamycin formulations. Typical FI-SF recordings for this otherwise tedious determination are given in Fig. 3. The FI-SF technique is based on measurement of the slope of the rising part of the curve, eliminating interferences due to coloured substances in the sample.

For the determination of aspartame in beverages (Table 6), the results obtained by the proposed FI-SF method were higher than those obtained by the HPLC²⁶ reference method. This may be due to small amounts of amino-compounds or phenols present in the beverages. The time required for a single measurement with the HPLC method is 15–20 min, discouraging its use in routine analysis, whereas the FI-SF method requires only 1.5 min per measurement, allowing a high sample throughput in routine analysis. Typical FI-SF recordings for aspartame determinations are shown in Fig. 4. The

advantage of the FI-SF methods of avoiding interferences due to background signals is utilized in the determination of aspartame in Coca Cola, which contains highly coloured caramel colouring.

The method can also be applied for the determination of other substances which give soluble 2,4-dinitrobenzene derivatives, such as cephalixin, tobramycin and gentamicin.

CONCLUSIONS

The proposed FI-SF kinetic method overcomes problems associated with (a) incompleteness of analytical reactions which require high temperatures and long reaction times when used in equilibrium spectrophotometric methods, and (b) the need to hydrolyse the surplus reagent and then extract the reaction product from the mixture. The method permits analysis in highly coloured samples and features a measurement throughput of 40 per hour. As stated above, the proposed method (with spectrophotometric detection) is not suitable for the determination of phenols. The applicability of the method can be extended to phenols of pharmaceutical interest by use of a fluoride-selective flow-through electrode as detector in the FI-SF system.

Acknowledgements—We gratefully acknowledge support from the Ministry of Industry, Energy and Technology, General Secretariat of Research and Technology of Greece, the Greek State Scholarships Foundation and the Greek National Drug Organization.

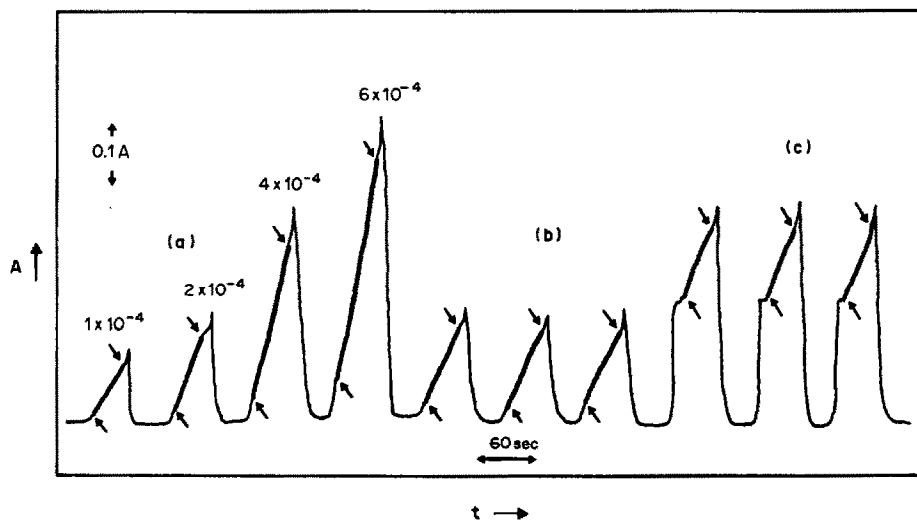


Fig. 4. FI-SF recordings for the determination of aspartame in (a) standard solutions, (b) Sprite and (c) Coca Cola. The analytical parameter is the slope of the line between arrows.

REFERENCES

1. F. C. McIntire, L. M. Clements and M. Sproull, *Anal. Chem.*, 1953, **25**, 1757.
2. O. H. Lowry, H. T. Graham, F. B. Harris, M. K. Priebat, A. R. Marks and V. R. Bregman, *J. Pharmacol. Exptl. Therap.*, 1954, **112**, 116.
3. S. M. Rosenthal and C. W. Tabor, *ibid.*, 1956, **116**, 131.
4. M. J. Kolbezen, J. W. Eckert and B. F. Bretschneider, *Anal. Chem.*, 1962, **34**, 583.
5. D. T. Dubin, *J. Biol. Chem.*, 1960, **235**, 783.
6. J. R. Couch, *J. Assoc. Off. Anal. Chem.*, 1975, **58**, 599.
7. J. D. Weber, *J. Pharm. Sci.*, 1976, **65**, 105.
8. J. F. Goodwin, *Clin. Chim. Acta*, 1968, **21**, 231.
9. *Idem*, *Clin. Chem.*, 1968, **14**, 1080.
10. N. F. Poole and A. E. Meyer, *Proc. Soc. Exp. Biol. Med.*, 1958, **98**, 375.
11. J. A. Ryan, *J. Pharm. Sci.*, 1984, **73**, 1301.
12. P. A. Lehmann F., *Anal. Chim. Acta*, 1971, **54**, 321.
13. P. R. Chen and W. C. Dauterman, *Anal. Biochem.*, 1970, **38**, 224.
14. J. F. Lawrence and R. W. Frei, *Chemical Derivatization in Liquid Chromatography*, Elsevier, Amsterdam, 1976.
15. D. M. Barends, J. S. Blauw, C. W. Mijnsbergen, C. J. L. R. Govers and A. Hulshoff, *J. Chromatog.*, 1985, **322**, 321.
16. W. Sadee and G. C. M. Beelen, *Drug Level Monitoring*, Wiley, New York, 1980.
17. E. Athanasiou-Malaki, M. A. Koupparis and T. P. Hadjiioannou, *Anal. Chem.*, 1989, **61**, 1358.
18. E. Athanasiou-Malaki and M. A. Koupparis, *Analyst*, 1987, **112**, 757.
19. *Idem*, *Talanta*, 1989, **36**, 431.
20. H. A. Archontaki, M. A. Koupparis and C. E. Efstathiou, *Analyst*, 1989, **114**, 591.
21. J. Růžička and E. H. Hansen, *Flow Injection Analysis*, 2nd Ed., p. 79. Wiley, New York, 1988.
22. K. A. Connors and M. P. Wong, *J. Pharm. Sci.*, 1979, **68**, 1470.
23. M. P. Wong and K. A. Connors, *ibid.*, 1983, **72**, 146.
24. E. Athanasiou-Malaki and M. A. Koupparis, *Anal. Chim. Acta*, 1989, **219**, 295.
25. P. J. Worsfold, J. Růžička and E. H. Hansen, *Analyst*, 1981, **106**, 1309.
26. N. G. Webb and D. D. Beckman, *J. Assoc. Off. Anal. Chem.*, 1984, **67**, 510.

MACROSCOPIC AND MICROSCOPIC ACID DISSOCIATION CONSTANTS OF DIPROTIC ACIDS—A POTENTIOMETRIC AND SPECTROPHOTOMETRIC STUDY

PAOLO UGUAGLIATI* and LUCIANO CANOVESE

Dipartimento di Chimica, Facoltà di Scienze, Università di Venezia, S. Marta, Venezia, Italy

(Received 1 October 1990. Accepted 24 January 1991)

Summary—A state-of-the-art survey of the determination of acid dissociation microconstants of diprotic acids is presented. It is shown that potentiometric and spectrophotometric titration data can yield *macroscopic* constants but are not sufficient to completely resolve the *microconstant* system unless some sort of assumption is made, which may not always be warranted. Such an estimative deduction procedure is applied to 2,6-di(methylthiomethyl)-3-hydroxypyridine chloride.

The acid dissociation equilibria of polyprotic acids are characterized by the so-called *macroscopic* constants which are unrelated to the specific protonation sites of the various species present in solution. Such macroscopic constants are a composite of the *microscopic* constants which are related to the dissociation equilibria of the individual species. As will be shown in this report, potentiometric or spectrophotometric techniques can only provide the values of macroscopic constants. Assessment of the microscopic constants is based on further assumptions which may not always be justified.

A wealth of research efforts have been devoted to determining microconstants by a variety of spectral methods.^{1,2} The aim of the present paper is to outline the state-of-the-art of the subject in order to clarify matters and describe the application of potentiometric and spectrophotometric techniques to a novel 3-hydroxypyridine derivative to be studied as a chelating ligand for transition metal complexes.

Theory

Consider the diprotic acid derived from a substituted 3-hydroxypyridine (I; Scheme 1).

The macroscopic constants K_2 and K_1 , which can be determined by titration of I with a strong base, are related to the microscopic ones by the equations:

$$K_2 = K_{12} + K_{13}$$

$$K_1 = K_{24} \cdot K_{34} / (K_{24} + K_{34})$$

$$= K_{12} \cdot K_{24} / (K_{12} + K_{13})$$

$$K_2 \cdot K_1 = K_{12} \cdot K_{24} = K_{13} \cdot K_{34}$$

$$K_{23} = K_{13} / K_{12} = K_{24} / K_{34} \quad (1)$$

Only three equations relate the four microconstants K_{12} , K_{13} , K_{24} and K_{34} , so that at least one piece of additional information is required for a complete determination.

Let's now express the concentrations of species involved in the above equilibria in terms of pH and system variables.

Let:

$$S = K_{12} + K_{13}; \quad pS = -\log S \quad (2)$$

$$P = K_{12} \cdot K_{24}; \quad pP = -\log P \quad (3)$$

so that

$$pK_2 = pS$$

$$pK_1 = pP - pS$$

If a volume V_0 of a solution of I at analytical concentration $c_0 M$ is titrated with a volume V of a solution of strong base at concentration c , we have from equation (1):

$$V_T = V_0 + V$$

$$a_0 = 1 / (1 + 10^{pP - pS - pH} + 10^{pP - 2pH})$$

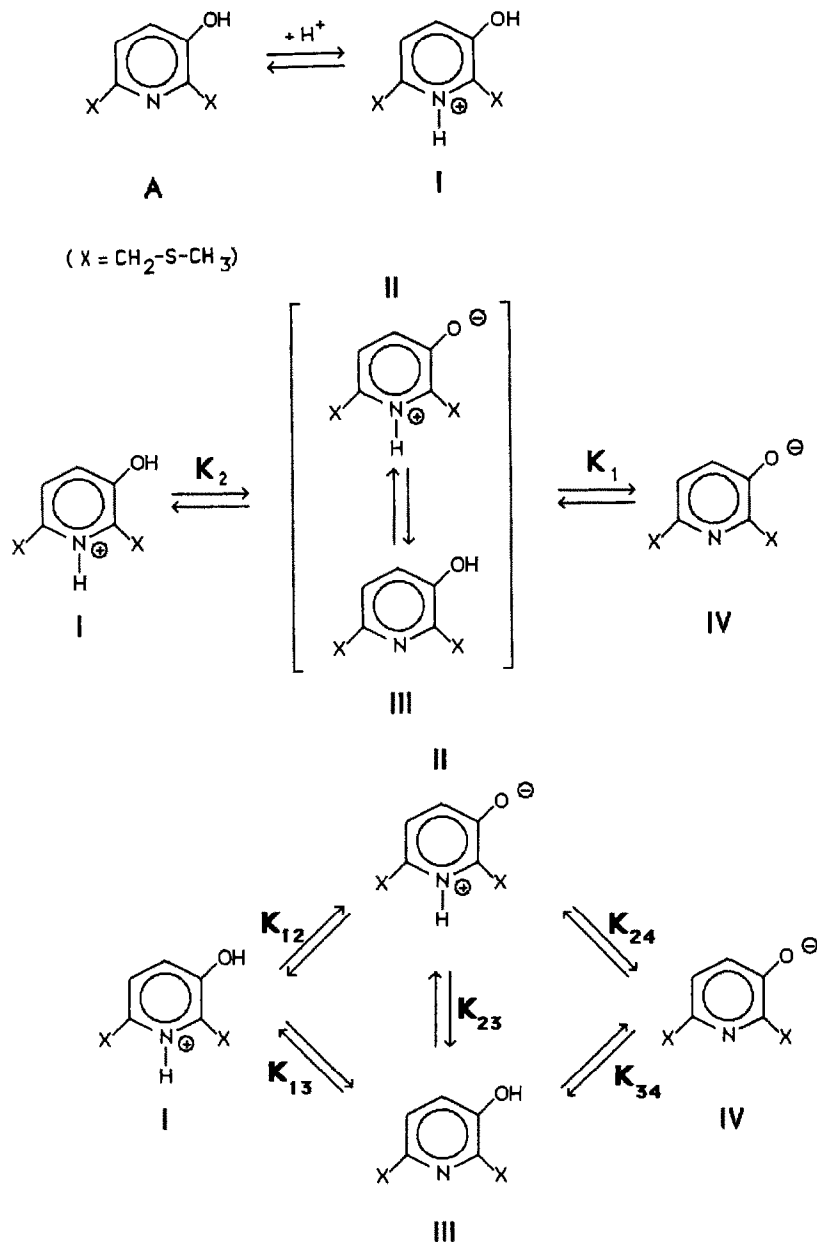
$$[\text{I}] = (c_0 V_0 / V_T) a_0 10^{pP - 2pH}$$

$$[\text{II}] = (c_0 V_0 / V_T) a_0 10^{pK_{24} - pH}$$

$$[\text{III}] = (c_0 V_0 / V_T) a_0 K_{23} 10^{pK_{24} - pH}$$

$$[\text{IV}] = (c_0 V_0 / V_T) a_0 \quad (4)$$

*Author for correspondence.



The electroneutrality equation is:

$$[\text{H}^+] - [\text{OH}^-] + cV/V_T - (c_0 V_0/V_T) a_0 (2 + 10^{pP - pS - \text{pH}}) = 0 \quad (5)$$

and contains only pP and pS as refinable parameters. Non-linear regression of pH vs. V data will only yield values for $P = K_{12} \cdot K_{24}$ and $S = K_{12} + K_{13}$. There is no way of getting the values of individual microconstants without further assumptions.

Equation (4) can be rewritten as:

$$\begin{aligned} \text{[I]} &= H \cdot R \\ \text{[II]} &= K_{12} \cdot R \end{aligned}$$

$$\text{[III]} = (S - K_{12})R = K_{13} \cdot R$$

$$\text{[IV]} = (P/H)R$$

where

$$H = [\text{H}^+]$$

$$R = (c_0 V_0/V_T)/(H + S + P/H) \quad (6)$$

It is evident that if it were possible to measure the sum $\text{[I]} + \text{[III]}$ (or $\text{[II]} + \text{[IV]}$) then non-linear fitting of such sums to pH data would open the way to S , P and K_{13} (or K_{12}) and thus to the complete microconstant set according to equations 1, 2 and 3.

Equation (5) can be recast as

$$V = V_0[c_0(R' - 1) + H - OH]/(OH - H - c) \quad (7)$$

where

$$H = [H^+]$$

$$OH = [OH^-]$$

$$R' = (H/K_{13} - K_{34}/H)/(1 + H/K_{13} + 1/K_{23} + K_{34}/H)$$

from which, again, only R' values can be obtained. These, combined with equations (2) and (3), are still one equation less than the four independent ones that are required to solve for the four unknowns K_{12} , K_{24} , K_{13} and K_{34} . Now, one way out of the circle would be the knowledge of the constant for the equilibrium between the zwitterion II and the neutral species III ($K_{23} = [III]/[II]$), which is not affected by changes in pH.

If we resort to spectrophotometric titrations, then the absorbance of a solution of I at concentration c_0 vs. pH is expressed by

$$\begin{aligned} A_{\lambda, \text{pH}} &= c_0 R [H\epsilon_1 + K_{12}\epsilon_{II} \\ &\quad + K_{13}\epsilon_{III} + (P/H)\epsilon_{IV}] \\ &= c_0 R [H\epsilon_1 + \Sigma_K + (P/H)\epsilon_{IV}] \end{aligned} \quad (8)$$

where

$$R = 1/(H + S + P/H)$$

$$\Sigma_K = K_{12}\epsilon_{II} + K_{13}\epsilon_{III}$$

The apparent extinction coefficient of monoprotonated species is therefore the sum of constant fractions of the extinction coefficients of II and III, so that the latter behave spectrally as though they were one single component. Thus, the condition for observing a global isobestic point is

$$\epsilon_1 = \epsilon_{IV} = \Sigma_K/S$$

Fulfillment of such a condition can be expected to be rather uncommon. In the pH range where one of the species does not contribute to the absorbance, partial isobestic points may be observed. However, their presence cannot be exploited to deduce the presence of only two spectral components.

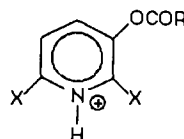
Non-linear regression of absorbance vs. pH [equation (8)] will only give the parameters S and P , and the sum Σ_K , from which the single microconstants K_{12} and K_{13} could be extracted if

both extinction coefficients ϵ_{II} and ϵ_{III} were known independently; this again requires additional pieces of information not available from the titration data alone (the extinction coefficients of I and IV can be deduced from limiting absorbance data taken at low and high pH, respectively, or allowed to float in the optimization process as further parameters to be refined while S and P can be taken from the potentiometric titration or included in the refinement for consistency).

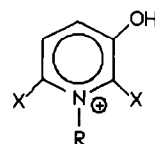
Summing up, fitting models corresponding to equations (5), (7) and (8) are overparameterized and attempts at refining (in the least-squares sense) all microconstants imbedded in the models, will eventually lead to singular normal equations, extremely sluggish convergence rates and parameter partial correlation coefficients with absolute values virtually equal to unity. All these symptoms indicate the need for reducing the dimensionality of parameter space by only refining proper combinations of some of the parameters, as we have shown above.^{3,4}

The mathematical formulation and the arguments outlined so far can be easily extended, without loss of generality, to acid-base equilibria involving other polyprotic systems, such as aminoacids, catecholamines, catechols, aminophenols, etc.^{1,2}

The earliest attempts at determining microscopic constants in equilibria of the type of **Scheme 1** were based on the assumption that blocking one of the active groups (e.g., by esterification or alkylation) would leave the acid-base properties of the other unaltered.^{1,2,5-7} For instance, if one assumes that K_{13} in **Scheme 1** is virtually identical to the acid dissociation constant for the ester



then it is possible to resolve the whole microconstant equilibrium system. In an analogous way, N -alkylation in the pyridinium derivative



would provide a breakthrough to the K_{12} value. Such an assumption may be justified for specific systems, depending on the particular molecular

structure of the species involved, but its generalized use is not warranted.⁸

Another approach is based on the fact that, if the two acidic groups can be associated with characteristic spectral features, then dissociation of one group can be followed independently of the other. In other words, it is assumed that the spectral properties of one group are independent of whether the other group is protonated or not. In this way, it is possible to assess the microconstants from the fractional deprotonation of one of the two groups as a function of pH. This approach, earlier introduced by Edsall *et al.*,⁷ allows the experimental measurement of the sums [II + IV] or [I + III] in equation (6), from which K_{12} or K_{13} can be evaluated, respectively. In practice, it is assumed that in equation (8) $\epsilon_I \cong \epsilon_{III}$ and $\epsilon_{II} \cong \epsilon_{IV}$ at suitable wavelengths, so that the absorbance data can be successfully fitted in terms of parameters S , P and K_{12} (or K_{13}).^{5,9-13}

A similar approach has been adopted for IR¹⁴ and Raman¹⁵ spectral data pertaining to related systems. However, the validity of results is often limited by lack of precision.

Nuclear magnetic resonance spectrometry has also been widely employed for the determination of microconstants, based on the calculation of the fractional deprotonation of one of the acidic groups as a function of pH from the chemical shift of a unique resonance, on the premise that the substrate contains an NMR-active nucleus whose chemical shift effects depend on dissociation of only one dissociable group.¹⁶⁻¹⁹ However, in some cases reliable values of microconstants cannot be obtained due to the high correlation between the parameters and the poor conditioning of equations involved.

Summing up, all the methods devised so far entail some sort of assumption that may not always be warranted. As a consequence, the results from different experimental approaches often disagree seriously.¹³ Any attempt at determining all microconstants from spectral data based on the equation²⁰

$$\alpha_{OH} = H \cdot S / (H^2 + H \cdot S + P)$$

(where α_{OH} is the mole fraction of singly dissociated phenolate anions in catechol derivatives) through subsequent mathematical reworking is an exercise in self-delusion.

EXPERIMENTAL

The substrates **A** and **B** ($X = \text{CH}_2\text{SCH}_3$) were prepared by a route to be described in a forth-

coming paper. All other chemicals were of reagent grade purity.

Potentiometric titrations

Potentiometric titrations were carried out with a Metrohm 654 pH-meter at 25° under a nitrogen stream. The glass electrode was calibrated with the standard Metrohm buffer (pH 4 and 7). A 50-ml volume of a 0.001M solution of the chlorhydrate $A \cdot \text{HCl}$ (prepared *in situ* by adding the stoichiometric amount of standard hydrochloric acid to a weighted amount of **A**) was titrated with a freshly prepared CO₂-free solution of 0.01M sodium hydroxide. The ionic strength was maintained by using a 0.1M solution of sodium chloride in doubly distilled and degassed water as the solvent for all solutions.

Spectrophotometric titrations

These were carried out with a Perkin-Elmer Lambda 5 spectrophotometer equipped with a cell compartment kept at 25° at constant ionic strength (0.1M sodium chloride) in doubly distilled and degassed water. To 5-ml aliquots of a 5.01×10^{-4} M solution of **A** were added 5-ml aliquots of standard hydrochloric acid or sodium hydroxide solutions. The pH (1-13) and the UV-VIS spectra (220-380 nm) of the resulting solutions were recorded.

Data analysis

Mathematical and statistical analysis and graphical display of experimental titration data were carried out on an IBM PS/2 70 personal computer equipped with an Intel 80387 maths coprocessor by use of locally adapted non-linear regression and plotting algorithms written in TurboBasic (Borland).

RESULTS AND DISCUSSION

Potentiometric titrations

Potentiometric titration data for the system in **Scheme 1** ($X = \text{CH}_2\text{SCH}_3$) were analysed according to models in equations (4-6) to determine the *macroscopic* dissociation constants K_2 and K_1 [equation (1)] in the following way. A weighted non-linear least-squares fitting of pH *vs.* V data was carried out by use of Marquardt's algorithm^{21,22} with pS and pP as the refinable parameters. During each iterative cycle, equation (5) was solved numerically for pH at each data point by a modified iterative bisection equation solver.^{23,24} Partial derivatives of the object function with respect to the parameters

were approximated by a numerically efficient forward differentiation scheme.²⁵ The function minimized was $\sum w_i (\text{pH}_{\text{obs}} - \text{pH}_{\text{calcd}})^2$ with the weighting scheme²⁶ $w_i = 1/(\text{pH}_{i+1} - \text{pH}_{i-1})^2$ to avoid lending too much influence to the less accurate pH values in the steeply-rising portion of the titration curve. Convergence to the optimized parameter vector was rapidly reached to yield the values of $\text{p}S = 3.90 \pm 0.02$ and $\text{p}P = 12.30 \pm 0.02$. Uncertainties quoted throughout are one standard error of estimate from the inverse covariance matrix. The parameter correlation coefficient was 0.79. At convergence, the experimental pH values agreed with those calculated from equations (4–5) and the optimized parameters to within 0.06 of a pH unit (weighted standard error of fit = 1.3). Residuals were randomly scattered and approximated a normal distribution.

The macroscopic dissociation constants are therefore $\text{p}K_2 = 3.90 \pm 0.02$ and $\text{p}K_1 = 8.40 \pm 0.04$. These values are sufficiently far apart to allow the mixture of monoprotinated species II + III to be predominant around pH 6.

Spectrophotometric titrations

The dependence of the absorbance of solutions of A on wavelength and pH from spectrophotometric titration is shown in Fig. 1. in which spectra at some selected experimental pH values were omitted for the sake of clarity.

An *a priori* parameter identifiability analysis of the model in equation (8) indicated that only *three* parameters could be uniquely determined by non-linear regression, *i.e.*, S , P and Σ_K .²⁷ The extinction coefficients ϵ_I and ϵ_{IV} were determined

directly from absorbances at low and high pH, respectively. Further, the parameter vector in equation (8) could be reduced to the single parameter Σ_K by fixing S and P at the values derived from potentiometric analysis (see earlier). This may serve to check the consistency of data and the overall experimental layout.

Non-linear least-squares fits of absorbance to pH for the 3-parameter model at different wavelengths gave S and P values virtually independent of wavelength and in very good agreement with those determined potentiometrically ($\text{p}S = 3.97 \pm 0.05$, $\text{p}P = 12.31 \pm 0.03$ as averages of values at five selected wavelengths). The standard error of estimate was about 5 absorbance units. Parameter correlation coefficients are fairly high (0.7–0.9, in absolute value), probably due to an intrinsic feature of the model and of the instrumental method. Figure 2 shows a 3-D representation of the 2-variable function $A_{\lambda, \text{pH}}$ in equation (8), using the optimized parameters.

As can be seen from Figs. 1 and 2, a global isosbestic point is present at 339 nm, where the condition $\epsilon_I = \epsilon_{IV} = \Sigma_K/S$ appears to be verified. Figures 3(a) and (b) show the results of spectrophotometric titration at two wavelengths and the corresponding contributions of the species I, II + III, IV to the observed overall absorbance as a function of pH.

Up to this point, all the information we could gather is embodied in the following 4-unknown 2-equation system:

$$\begin{cases} K_{12} \cdot \epsilon_{II} + K_{13} \cdot \epsilon_{III} = \Sigma_K \\ K_{12} + K_{13} = S \end{cases} \quad (9)$$

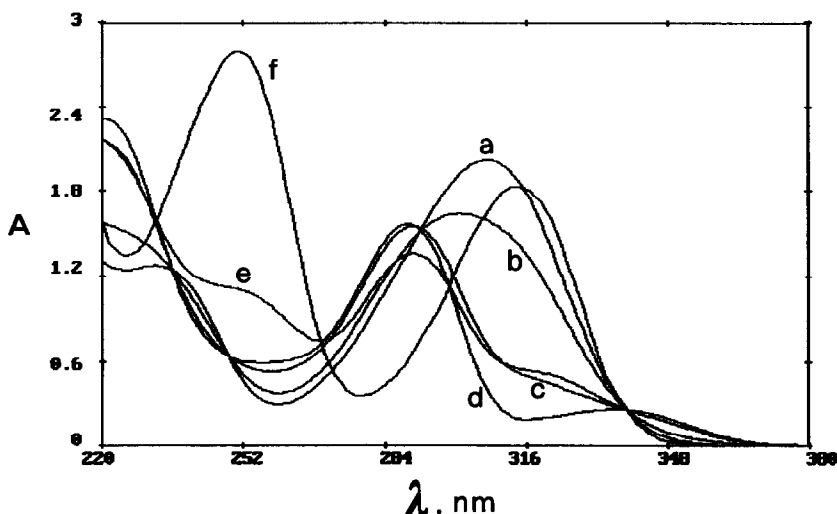


Fig. 1. Spectra of a $2.505 \times 10^{-4} M$ solution of A as a function of pH. (a) pH 1.05; (b) 3.65; (c) 4.79; (d) 6.12; (e) 7.72; (f) 12.71.

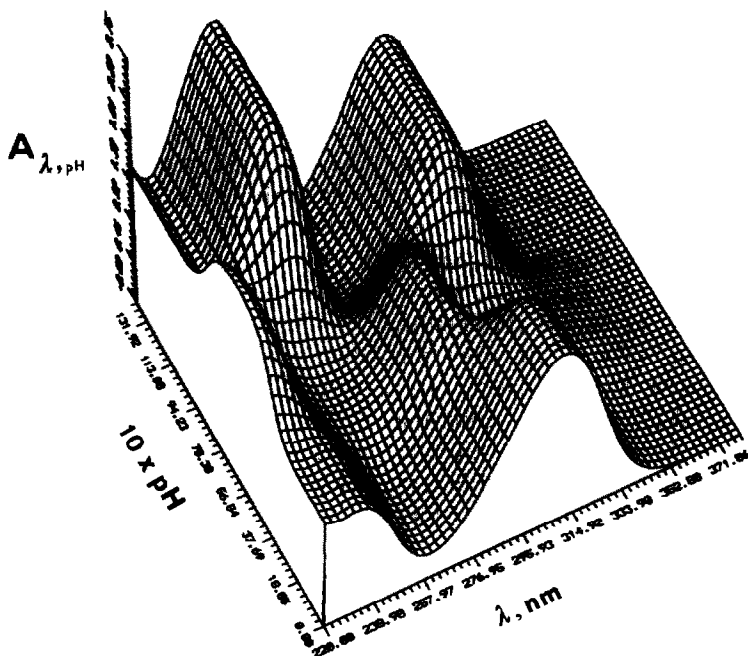


Fig. 2. 3-D representation of the dependence of absorbance of a $2.505 \times 10^{-4}M$ solution of A on pH and wavelength as in equation (8).

(the equations $P = K_{12} \cdot K_{24} = K_{13} \cdot K_{34}$ would introduce the additional unknowns K_{24} and K_{34} , respectively). Our inadequacy in solving system (9) stems from the fact that we ignore both the individual concentration of II and III and their extinction coefficients. Therefore, we have squeezed the last drop of information from all combined experimental data at hand. From now on, we must resort to some kind of assumption or approximation if we are to completely resolve the microconstant scheme.

The microconstant system

As noted earlier, there may be a wavelength range in the spectra of Fig. 1 in which it may be justifiable to make the assumptions

$$\epsilon_1 \cong \epsilon_{III}; \quad \epsilon_{II} \cong \epsilon_{IV} \quad (10)$$

Let's now surmise that equations (10) apply to the spectra around 260 nm, which is tantamount to assuming that loss of the proton from the nitrogen group does not affect the spectrum of the ionized phenolic group. Analogous assumptions were first advocated by Edsall *et al.*⁷ in their pioneering studies of protonation equilibria of related polyprotic systems. Then equation (8) becomes

$$A = c_0 R [(H + S)\epsilon_1 + K_{12}(\epsilon_{IV} - \epsilon_1) + (P/H)\epsilon_{IV}] \quad (11)$$

A least-squares fit of absorbance to pH data in equation (11) at 260 nm with S and P fixed at the potentiometric values yields $pK_{12} = 4.71$, from which the whole set of microconstants is calculated as:

$$pK_{12} = 4.71; \quad pK_{13} = 3.97$$

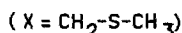
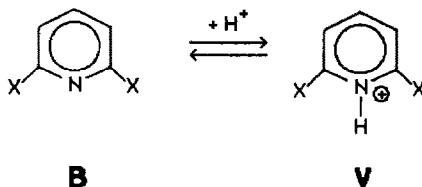
$$pK_{34} = 8.33; \quad pK_{24} = 7.59$$

$$pK_{23} = -0.74 \quad \text{whence} \quad [II]/[III] = 0.18$$

The same results are of course arrived at if system (9) is solved with the aid of equation (10) and the Σ_K value corresponding to the appropriate wavelength.

Attempts at applying equations (10) and (11) outside the range 260–270 nm will lead to absurd (negative) values for either K_{12} or K_{13} .

Support for this approach can be gathered from the pK_A value for compound V as the chloride,



which we established to be 4.04 ± 0.02 by potentiometric and spectrophotometric titrations. The higher acidity of the NH^+ group in I and

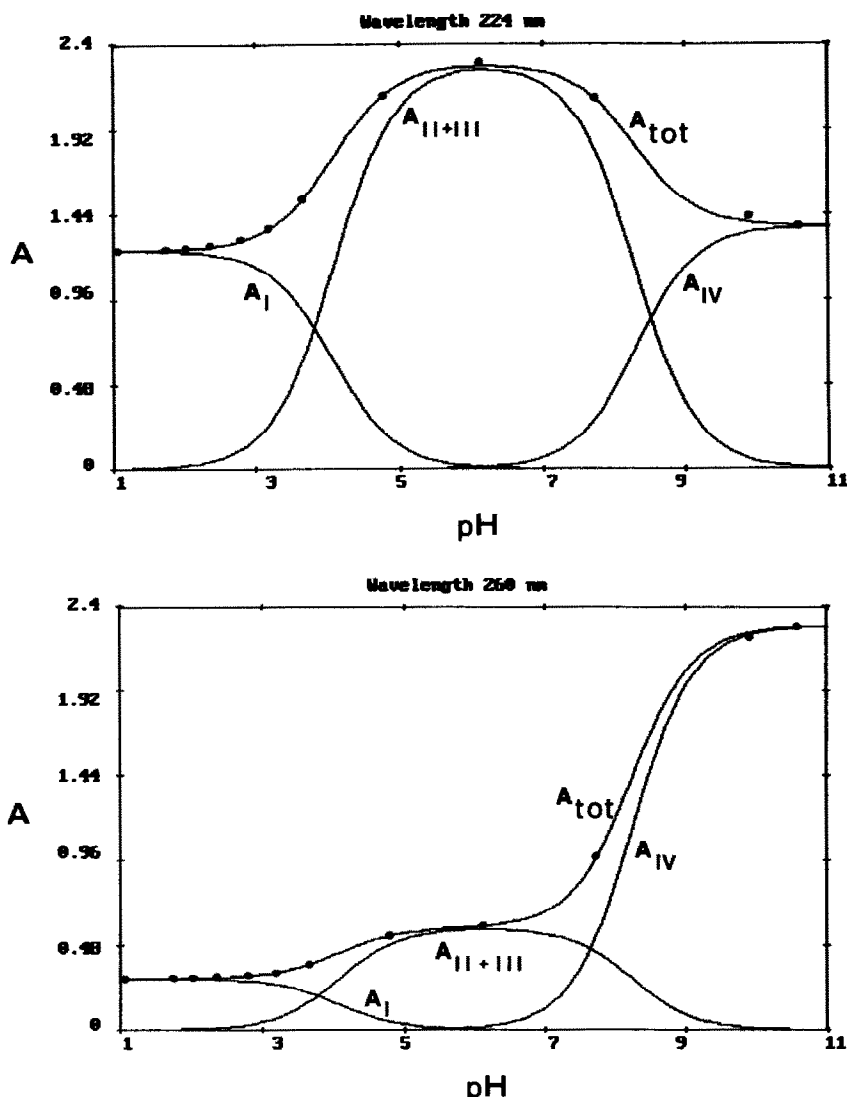


Fig. 3. Spectrophotometric titration of A at (a) 224 nm and (b) 260 nm. Solid line A_{tot} is the fitting curve of equation (8). The circles are observed data points ($c_0 = 2.505 \times 10^{-4} M$). Solid lines A_I , A_{II+III} , and A_{IV} are the relative contributions of I, (II + III), and IV, respectively, to the total absorbance as a function of pH from equation (8).

V as compared to that in pyridinium ion (pK_A 5.25) is likely to be caused by the presence of the two electron-withdrawing methylthiomethyl (CH_2SCH_3) substituents [the electron-attracting character of these groups is reflected by the pK_A value of 4.64 for 2-(methylthiomethyl)pyridine²⁸]. The higher acidity of the OH group in III relative to phenol is comparable to that in *m*-nitrophenol (pK_{34} 8.33 *vs.* pK_A 8.38) and stems from the presence of the heterocyclic nitrogen which has been suggested to be roughly equivalent to a nitro-group.⁵ This is consistent with the very large increase in acidity of the phenolic proton relative to phenol in I (pK_{12} 4.71 *vs.* pK_A 9.9), due to the presence of

the additional positive charge (*cf.* pK_A 4.96 for *N*-methyl-3-hydroxypyridinium iodide²⁹). Finally, the negative charge of the phenolate group in zwitterion II renders its NH^+ proton much less acidic than its counterpart in the cationic phenol I (pK_{24} 7.59 *vs.* pK_{13} 3.97).

It appears from our scheme that the neutral hydroxypyridine III predominates over the phenolate-pyridinium zwitterion II. This is in contrast with Lunn and Morton's assumption about related 3-hydroxypyridines for which the zwitterion was claimed to be the only monoprotonated species present in the pH range midway between the two macroscopic pK_2 and pK_1 values.³⁰ Based on the analysis of the problem

that we have presented in this paper and on the spectral changes reported,³⁰ we cannot see how such a claim could be sustained.

Acknowledgement—The Italian Ministry for University and Scientific Research is gratefully acknowledged for the grant of a research fund (MPI 60%).

REFERENCES

1. A. E. Martell and R. J. Motekaitis, *The Determination and Use of Stability Constants*, Chap. 7, VCH, New York, 1988.
2. J. Polster and H. Lachmann, *Spectrometric Titrations*, Chap. 12, VCH, New York, 1989.
3. G. A. F. Seber and C. J. Wild, *Nonlinear Regression*, Wiley, New York, 1989.
4. D. M. Bates and D. G. Watts, *Nonlinear Regression Analysis and its Applications*, Wiley, New York, 1988.
5. D. E. Metzler and E. E. Snell, *J. Am. Chem. Soc.*, 1955, **77**, 2431.
6. M. A. Grafius and J. B. Neilands, *ibid.*, 1955, **77**, 3389.
7. J. T. Edsall, R. B. Martin and B. R. Hollingworth, *Proc. Natl. Acad. Sci.*, 1958, **44**, 505.
8. A. Bryson, N. R. Davies and E. P. Serjeant, *J. Am. Chem. Soc.*, 1963, **85**, 1933.
9. E. Coates, P. G. Gardam and B. Rigg, *Trans. Faraday Soc.*, 1966, **62**, 2577.
10. E. Coates, C. G. Marsden and B. Rigg, *ibid.*, 1969, **65**, 3032.
11. R. B. Martin, *J. Phys. Chem.*, 1971, **75**, 2657.
12. H.-L. Fung and L. Cheng, *J. Chem. Ed.*, 1974, **51**, 106.
13. A. G. Splittgerber and L. L. Chinander, *ibid.*, 1988, **65**, 167.
14. F. J. Anderson and A. E. Martell, *J. Am. Chem. Soc.*, 1964, **86**, 715.
15. D. Garfinkel and J. T. Edsall, *ibid.*, 1958, **80**, 3823.
16. D. L. Rabenstein and T. L. Sayer, *Anal. Chem.*, 1976, **48**, 1141.
17. T. L. Sayer and D. L. Rabenstein, *Can. J. Chem.*, 1976, **54**, 3392.
18. R. F. Jameson, G. Hunter and T. Kiss, *J. Chem. Soc. Perkin II*, 1980, 1105.
19. T. Kiss and B. Tóth, *Talanta*, 1982, **29**, 539.
20. T. Ishimitsu, S. Hirose and H. Sakurai, *ibid.*, 1977, **24**, 555.
21. D. W. Marquardt, *S.I.A.M. J. Appl. Math.*, 1963, **11**, 431.
22. P. Valkó and S. Vajda, *Advanced Scientific Computing in BASIC*, Chap. 3, Elsevier, Amsterdam, 1989.
23. A. C. Norris, *Computational Chemistry: An Introduction to Numerical Methods*, Chap. 4, Wiley, New York, 1981.
24. M. D. Johnson, Jr., *Computational Chemistry*, Chap. 6, Elsevier, Amsterdam, 1988.
25. J. C. Nash and M. Walker-Smith, *Nonlinear Parameter Estimation*, Chap. 3, Dekker, New York, 1987.
26. Ref. 1, Chap. 4.
27. J. V. Beck and K. J. Arnold, *Parameter Estimation in Engineering and Science*, Chap. 1 and Appendix A, Wiley, New York, 1977.
28. K. Kahmann, H. Sigel and H. Erlenmeyer, *Helv. Chim. Acta*, 1964, **47**, 1754.
29. A. Albert, *Heterocyclic Chemistry*, pp. 43–62, Essential Books, Fair Lawn, NJ., 1956.
30. A. K. Lunn and R. A. Morton, *The Analyst*, 1952, **77**, 718.

SPECTROPHOTOMETRIC EXAMINATION OF REDOX EQUILIBRIA BY USE OF LOGARITHMIC TRANSFORMATIONS

S. KOCH and G. ACKERMANN

Bergakademie Freiberg, Sektion Chemie, Freiberg-9200, Germany

(Received 12 February 1990. Accepted 21 January 1991)

Summary—For the spectrophotometric characterization of redox reactions, a logarithmic transformation is proposed by which it is possible to analyse indirectly the functions $E = f(\text{pH})$ and $E = f(C)$ derived from experimental data. Besides the mechanism of the reaction the equilibrium constant can also be calculated. The method is generally usable for equimolar redox systems and also for non-equimolar ones if a single equilibrium exists in the range under examination. References to the evaluation are given and the practicability is demonstrated with the system $\text{Fe}^{3+}/\text{SO}_3^{2-}$.

Spectrophotometric methods of examining redox equilibria are rarely published because the potentials of the half-cells are known and therefore the reactions can be formulated. In the examination of unknown redox reactions, however, experimental methods must be used. When the components are coloured, spectrophotometric methods are applicable, such as Job's method¹ or the molar ratio method.² In the case of equimolar systems it is disadvantageous that these methods give only the possibility of finding the relative molar coefficients (m/n). It is not always possible to characterize complicated redox systems unequivocally with these coefficients. Moreover, with these methods only reactions with high equilibrium constants can be tested. By applying special kinds of transformations containing the equilibrium constants, the absolute coefficients (m, n) can be determined. The transformation proposed by Ceba *et al.*³ can be used for the determination of the molar coefficients and equilibrium constants, but a statement of the number of protons exchanged is not possible.

This paper reports a generally applicable logarithmic transformation with which it is possible to find the stoichiometry of the reaction, including the number of protons exchanged and the equilibrium constant.

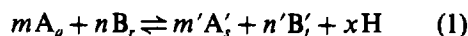
EXPERIMENTAL

The spectrophotometric measurements were made with a Beckman DU spectrophotometer and 1-cm cells. All samples were prepared by

adding the reagents in the following sequence: iron solution, perchloric acid, sodium sulphite and sodium chloride. Measurements were made immediately after mixing (pH curve) or after 2 months (C_R curve). The iron(III) standard solution was prepared by dissolving the sulphate in 0.1M sulphuric acid. The concentration of the sodium sulphite solution was determined iodometrically.

General aspects

A general redox reaction between A_q and B_r to yield A'_s and B'_t can formally be written, including polynuclear species, as



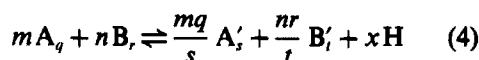
where charges are omitted for simplicity. At equilibrium

$$mq = m's \quad (2)$$

and

$$nr = n't \quad (3)$$

Equation (1) can therefore be written as



The species A'_s and B'_t are in this case in the stoichiometric relation

$$[A'_s]:[B'_t] = m':n' = \frac{mq}{s} : \frac{nr}{t} \quad (5)$$

Also, the total concentrations of A and B (C_A and C_B) are given by

$$C_A = q[A_q] + s[A'_s] \quad (6)$$

$$C_B = r[B_r] + t[B'_t] \quad (7)$$

If the ionic strength (I) is practically constant, the law of mass action is valid, and

$$K^* = \frac{[A'_s]^{m'} [B'_t]^{n'} [H]^x}{[A_q]^m [B_r]^n} \quad (8)$$

$(m, n, m', n') = 1, 2, \dots; x = 0, \pm 1, \pm 2, \dots$

For proton-free equilibria, the corresponding constant K , resulting from (8) with $x = 0$, is

$$K = \frac{[A'_s]^{m'} [B'_t]^{n'}}{[A_q]^m [B_r]^n} \quad (9)$$

Fundamentals of the transformation

As extended examination has shown, because of the exponential form of (8) and (9), linear relationships can only be established if logarithmic functions are used. From equation (8),

$$\log \frac{[A'_s]^{m'} [B'_t]^{n'}}{[A_q]^m [B_r]^n} = x\text{pH} + \log K^* \quad (10)$$

If the concentration term is called Z then

$$\log Z = x\text{pH} + \log K^* \quad (11)$$

which is the equation of a straight line with slope x and intercept $\log K^*$. An indirect analysis with a simple assumption of linearity cannot be performed, since because of the use of a logarithmic function linearity would result even if x , m or n' were wrong. In the case of the true molar coefficients a straight line results:

$$\log Z = f(x\text{pH})_{(K^* = \text{const.})} \quad (12)$$

and x is the value of the slope in the correct mathematical equation. The calculation of the equilibrium constant is first demonstrated for a general model with coloured components. For further convenience, A_q , B_r , etc. are simplified and written as A, B, ...

According to the Lambert-Beer law, for a path-length d , the absorbance A is given by

$$A/d = \epsilon_A[A] + \epsilon_{A'}[A'] + \epsilon_B[B] + \epsilon_{B'}[B'] \quad (13)$$

By combination of equations (5), (6) and (7), the values of the concentrations are

$$[A'] = \frac{m'(qrA/d - r\epsilon_A C_A - q\epsilon_B C_B)}{m'r(q\epsilon_{A'} - s\epsilon_A) + n'q(r\epsilon_{B'} - t\epsilon_B)} \quad (14)$$

$$[B'] = \frac{n'[A']}{m'} \quad (15)$$

$$[A] = \frac{C_A - s[A']}{q} \quad (16)$$

$$[B] = \frac{C_B - t[B']}{r} \quad (17)$$

Since $m' = mq/s$ and $n' = nr/t$, m' and n' can be replaced in the logarithmic function (10) to give

$$\log Z = \frac{mq}{s} \log [A'] + \frac{nr}{t} \log [B'] - m \log [A] - n \log [B] \quad (18)$$

Equilibria involving protons

To solve this problem it is necessary to analyse the curve $A = f(\text{pH})$ resulting from experiments with constant C_A , C_B , I and λ , after use of transformation (11), equations (14)–(17) or (18) and a plot of the results. The parameters (x, m, n) used are only the correct values if the straight line function $\log Z = f(x\text{pH})$ meets the criterion

$$\frac{\Delta \log Z}{\Delta(x\text{pH})} = x \quad (19)$$

Both m and n can have only a positive sign, but the values of x can be either positive or negative, positive for systems in which protons are released.

Extrapolation of the straight line resulting from use of the correct values of the molar coefficients gives $\log K^*$ from the intercept on the ordinate: since this results from extrapolation to $x = 0$ or $\text{pH} = 0$, all values of x give the correct value for the equilibrium constant.

Proton-free equilibria

Redox equilibria that are independent of pH are relatively few. For systems with $A = f(\text{pH}) = \text{constant}$, the function $A = f(C_B)$ is obtained from a set of experiments with C_A , I and λ all constant. For the evaluation, equations (18) and (14)–(17) with varying (m, n) , are again used.

For the correct parameters, the criterion $\log Z(C_B) = \text{const.}$ must be fulfilled. By applying this formulation with C_A , pH, I and λ constant, equilibria involving protons can also be handled. In this case, only (m, n) results. An apparent constant $K' = K^*/[H]^x$ is obtained, defined by

$$\log K' = \log Z \quad (20)$$

Table 1. Transformation $Z = f(\text{pH}, C)$; absorption by only one component

Condition	Concentration [A']
$\epsilon_A > 0$	$\frac{\epsilon_A C_A - qA/d}{s\epsilon_A}$
$\epsilon_A' > 0$	$A/d\epsilon_A'$
$\epsilon_B > 0$	$\frac{m'(\epsilon_B C_B - rA/d)}{n'\epsilon_B}$
$\epsilon_B' > 0$	$m'A/dn'\epsilon_B'$

In the case of proton-free equilibria, the equilibrium constant K for expression (9) is easily obtained with correct coefficients from $\log K = \log Z$.

Application of the transformations

The logarithmic transformations give the possibility of analysing the functions $A = f(\text{pH})$ and $A = f(C)$ resulting from spectrophotometric measurements. Before starting the experiments it must be known that the mechanism and species involved will always be the same. Only under these conditions will the transformations work.

For application of the mathematical equations, the molar absorptivities ϵ_A , ϵ_B , etc., must be known. Generally, a wavelength can be found at which only some of the components absorb. If 1, 2 or 3 of the species are coloured, equation (14) will give [A']. As equations (15), (16) and (17) show, the functions for [B'], [A] and [B] are not affected. The necessary relationships are compiled in Tables 1, 2 and 3.

To characterize colourless systems, it is necessary either to use the ultraviolet region or to change one component into a coloured compound. In the latter case, this derivatization must not noticeably influence the primary redox

Table 2. Transformation $\log Z = f(\text{pH}, C)$ (absorption by two components)

Condition	Concentration [A']
$(\epsilon_A, \epsilon_A') > 0$	$\frac{qA/d - \epsilon_A C_A}{q\epsilon_A' - s\epsilon_A}$
$(\epsilon_A, \epsilon_B') > 0$	$\frac{m'(qA/d - \epsilon_A C_A)}{n'q\epsilon_B' - m's\epsilon_A}$
$(\epsilon_A', \epsilon_B') > 0$	$\frac{m'A}{d(m'\epsilon_A' + n'\epsilon_B')}$
$(\epsilon_B, \epsilon_A) > 0$	$\frac{m'(r\epsilon_A C_A + q\epsilon_B C_B - qrA/d)}{m'rs\epsilon_A + n'q\epsilon_B}$
$(\epsilon_B, \epsilon_A') > 0$	$\frac{m'(rA/d - \epsilon_B C_B)}{m'r\epsilon_A' - m'\epsilon_B}$
$(\epsilon_B, \epsilon_B') > 0$	$\frac{m'(rA/d - \epsilon_B C_B)}{n'(r\epsilon_B' - t\epsilon_B)}$

Table 3. Transformation $\log Z = f(\text{pH}, C)$ (absorption by three components)

Condition	Concentration [A']
$(\epsilon_A, \epsilon_A', \epsilon_B') > 0$	$\frac{m'(qA/d - \epsilon_A C_A)}{m'(q\epsilon_A' - s\epsilon_A) + n'q\epsilon_B'}$
$(\epsilon_A, \epsilon_A', \epsilon_B) > 0$	$\frac{m'(qrA/d - r\epsilon_A C_A - q\epsilon_B C_B)}{m'r(q\epsilon_A' - s\epsilon_A) - n'q\epsilon_B}$
$(\epsilon_A, \epsilon_B, \epsilon_B') > 0$	$\frac{m'(r\epsilon_A C_A + q\epsilon_B C_B - qrA/d)}{m'rs\epsilon_A - n'q(r\epsilon_B' - t\epsilon_B)}$
$(\epsilon_A', \epsilon_B, \epsilon_B') > 0$	$\frac{m'(rA/d - \epsilon_B C_B)}{m'r\epsilon_A' + n'(r\epsilon_B' - t\epsilon_B)}$

mechanism. It is therefore best to use a reaction in which weak co-ordination complexes are formed. In this case it is not recommended to determine the equilibrium constant.

In performing the experiments, there are some conditions which must be kept constant by using a suitable salt. Because of side-reactions, buffer solutions are not recommended. The timing of the procedure must be very carefully regulated, in case kinetic effects interfere. Besides this, it has to be taken into account that the equilibrium must not be fully shifted to the right, since the mathematical model would then not be valid, because $[A_r] \rightarrow 0$ and $[B_r] \rightarrow 0$. Partial reaction can often be achieved by suitable selection of the pH and reactant concentrations. It is advantageous that there are no approximations in the transformation, i.e., that there is no restriction concerning the total concentrations C_A and C_B .

Though it is not possible to give general instructions for application of this transformation, some remarks can be made.

It can first be supposed that the quantities q , r , s and t are known. Otherwise, besides

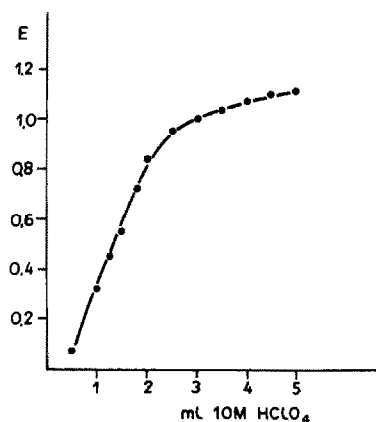


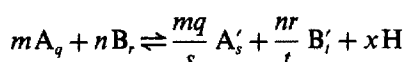
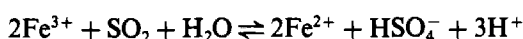
Fig. 1. pH function of the system $\text{Fe}^{3+}/\text{SO}_3^{2-}$ ($C_{\text{Fe}} = 2 \times 10^{-3} M$, $C_{\text{SO}_2} = 2 \times 10^{-2} M$, $1 M \text{ NaCl}$, $\lambda = 380 \text{ nm}$).

variation of x , m and n , the variation of s and/or t is also necessary. The criteria $\log Z(C_B) = \text{constant } \Delta \log Z / \Delta(x\text{pH}) = x$ are also valid in this case. In this connection the relative molar coefficients $V = n/m$ (determined by the Job method or photometric or potentiometric titration) are valuable, since by using these quantities it becomes possible to predict m and n .

Thereafter the reaction processes can be formulated. In the case of oxyanion oxidants the role of water must be considered. Here, an exact assignment of the general and particular equations of the reactions is of importance.

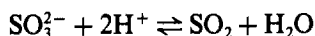
Example

We have examined the stoichiometry of the system $\text{Fe}^{3+}/\text{SO}_3^{2-}$ in a strong acid medium. From the properties of SO_2 and SO_4^{2-} the following reaction can be formulated:



Comparison of the general and particular reactions shows that the reaction equation is unequivocally determined by x , m and n . The shape of the function $A = f(\text{pH})$ (Fig. 1) indicates a positive number of protons is involved.

Iron(III) is measured as its chloro-complex, for which the Lambert-Beer law, with $\epsilon_{\text{Fe(III)}} = 550 \text{ l. mole}^{-1} \cdot \text{cm}^{-1}$ holds in the pH range from 0.18 to 0.58. The pH values used for the evaluation are given by the concentration of perchloric acid used, with due regard to the reaction



For evaluation under the conditions $\epsilon_A > 0$ and $q = r = s = t = 1$, the cases to be applied (Table 1) are

$$[A'] = \frac{\epsilon_A C_A - A/d}{\epsilon_A}$$

$$[B'] = \frac{n}{m} [A']$$

$$[A] = C_A - [A']$$

$$[B] = C_B - [B']$$

$$\log Z = m \log [A'] + n \log [B']$$

$$-m \log [A] - n \log [B].$$

By use of these equations, transformations according to equation (11) are possible. From

Table 4. Indirect logarithmic analysis of molar coefficients in the system $\text{Fe}^{3+}/\text{SO}_3^{2-}$ (pH 0.18–0.58)

m	n	x	Slope
2	1	1	8.33
2	1	2	4.17
2	1	3	2.93
2	1	4	2.08
2	1	5	1.67
3	1	1	11.91
3	1	2	5.95
3	1	3	3.91
3	1	4	2.98
3	1	5	2.38
1	2	1	8.13
1	2	2	4.06
1	2	3	2.62
1	2	4	2.03
1	2	5	1.63
1	3	1	11.25
1	3	2	5.71
1	3	3	3.66
1	3	4	2.74
1	3	5	2.20
1	1	1	5.45
1	1	2	2.72
1	1	3	1.82
1	1	4	1.36
1	1	5	1.09

a graph of $\log Z$ vs. $x\text{pH}$ the value of x can be found. The results are compiled in Table 4. The coefficients $m = 2$, $n = 1$ and $x = 3$ necessary for $\Delta \log Z / \Delta(x\text{pH}) = x$ to be fulfilled, are in agreement with the known equation. This example shows the value of the proposed method. Finally, in Fig. 2 some typical straight lines for $m = 2$, $n = 1$ and $x = 1 \dots 5$ are shown. The straight line with $x = 3$ represents the case with the correct parameters.

The mechanism is confirmed by the analysis of a C_B -function with $\epsilon_{\text{Fe(III)}} = 820$, over the

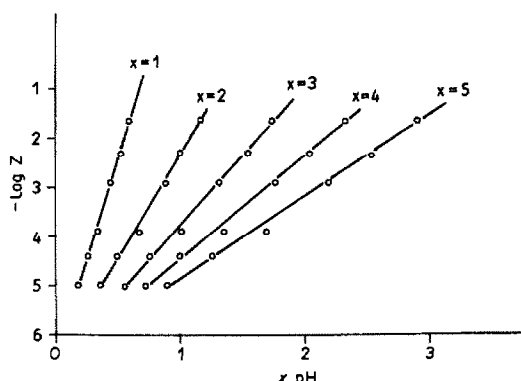


Fig. 2. Linear transformation $\log Z = f(x\text{pH})$ of the system $\text{Fe}^{3+}/\text{SO}_3^{2-}$ ($m = 2$, $n = 1$).

sulphite concentration range from 0.08 to 0.18M. The following values were obtained for $\log Z$: -0.954, -0.927, -0.931, -0.958, with $m = 2$, $n = 1$. Only in the case of $m = 2$ and $n = 1$ is the criterion $\log Z(C_B) = \text{constant}$ fulfilled.

REFERENCES

1. D. Svobodová and J. Gasparič, *Mikrochim. Acta*, 1975 II, 529.
2. S. Koch and G. Ackermann, *Z. Chem.*, 1988, **28**, 376.
3. M. Román Ceba, J. A. Muñoz Leyva and J. J. Berzas Nevado, *Anal. Chim. Acta*, 1981, **130**, 183.

DIRECT SPECTROPHOTOMETRIC DETERMINATION OF Nd IN MIXED RARE EARTHS WITH SEMI-XYLENOL ORANGE AND CETYLPYRIDINIUM CHLORIDE

NAI-XING WANG

Department of Chemistry, Shandong University, Jinan, Shandong, 250100, People's Republic of China

(Received 17 August 1990. Revised 20 November 1990. Accepted 14 December 1990)

Summary—The derivative absorption spectra of the neodymium complex with Semi-Xylenol Orange and cetylpyridinium chloride has been investigated. The characteristic absorption of the complex is ~ 350 times that of neodymium chloride. The fourth-order derivative spectrum has been used to eliminate the interference of the other lanthanides, and to increase the sensitivity by a further factor of 6. Beer's law is obeyed for 0–7.5 μg of Nd in 25 ml of solution. The relative standard deviation for 7 determinations of 1.8 $\mu\text{g}/25$ ml neodymium was 1.3%. The detection limits were 5.8 ng/ml in the absence of lanthanum and 11.2 ng/ml in the presence of 44 ng/ml lanthanum (or 36 ng/ml yttrium). The method has been used for the determination of neodymium in mixed rare earths, with satisfactory results.

There has always been interest in determination of individual lanthanides in their mixtures, on the basis of the absorption bands of their 4f electron transitions.¹⁻⁷ Various complexing agent/surfactant systems have been reported for determination of the lanthanides but few of them are useful for the determination of individual elements in the group.⁸⁻¹⁰

Semi-Xylenol Orange has been used in the presence of cetylpyridinium bromide for the spectrophotometric determination of the lanthanides¹¹ and we have now found that use of cetylpyridinium chloride as the surfactant, and the fourth-order derivative spectra, eliminates the interference of the other lanthanides in the determination of neodymium and increases the sensitivity, with Semi-Xylenol Orange as the chromophore.

EXPERIMENTAL

Apparatus

A Shimadzu UV-3000 double-beam spectrophotometer with 4.0-cm path-length cells was used.

Reagents

Standard solutions of the lanthanides were prepared from the pure oxides (Johnson Matthey), ignited before use.

Standard solutions of Semi-Xylenol Orange (SXO, $5.00 \times 10^{-4}M$) and cetylpyridinium chloride (CPC, $2.00 \times 10^{-2}M$) were prepared by

dissolving 0.1369 g of SXO (Shanghai Reagent Three Plant, China) in 500 ml of water and 1.790 g of CPC (Fluka) in 250 ml of water, respectively.

Buffer solutions were prepared by mixing 1.0M hexamine solution with suitable volumes of 0.1M hydrochloric acid or 0.1M sodium hydroxide. Analytical-reagent grade chemicals were used wherever possible.

Procedure

Transfer a known volume of lanthanide solution to a 25-ml standard flask, add 0.75 ml of $5.00 \times 10^{-4}M$ SXO, 5.0 ml of pH-8.2 hexamine buffer solution and 1.0 ml of $2.00 \times 10^{-2}M$ CPC. Dilute to the mark with distilled water and after 15 min record the fourth-order derivative spectrum against a reagent blank (or suitable amounts of a corresponding lanthanum complex solution) as reference, using 4.0-cm cells.

RESULTS AND DISCUSSION

Absorption spectra

The absorption spectra of the neodymium and representative lanthanide complexes and of the neodymium ion are shown in Fig. 1.

From Fig. 1a it is evident that the absorption maximum for all the lanthanide-SXO-CPC complexes is in the region of 585–607 nm, so it is not possible to determine neodymium directly in the presence of other lanthanides, especially

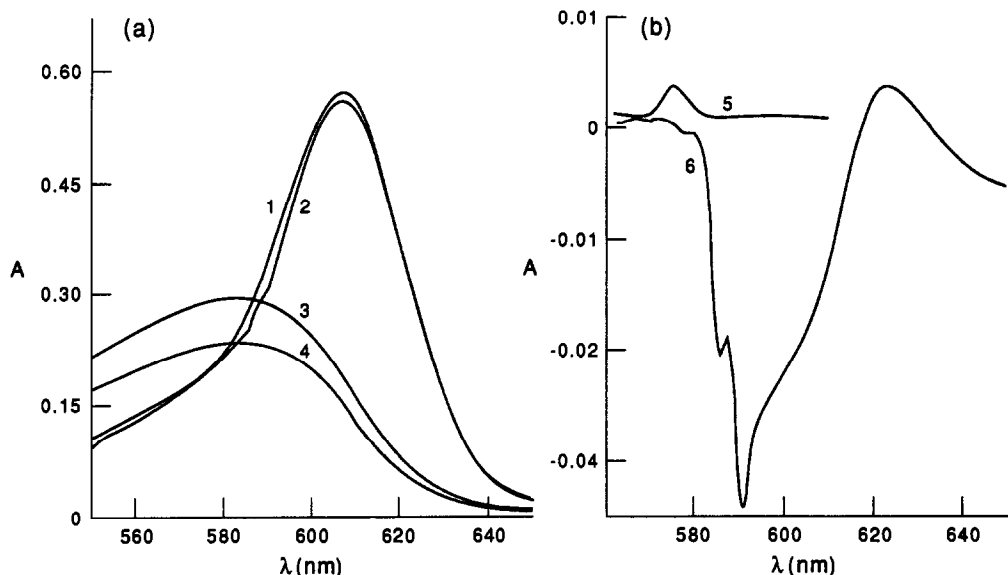


Fig. 1. Absorption spectra of neodymium and lanthanide (Ln) complexes. (a): $[Ln] = 1.0 \times 10^{-6} M$; $[SXO] = 1.5 \times 10^{-5} M$; $[CPC] = 8.0 \times 10^{-4} M$; pH = 8.2; 4.0-cm cells; 1, La; 2, Nd; 3, Y; 4, Ho. Reagent blank as reference. (b): 5, Nd^{3+} ($[Nd] = 1.0 \times 10^{-4} M$) against water as reference; 6, Nd-SXO-CPC against La-SXO-CPC as reference. Other conditions as for (a).

lanthanum, which has almost the same absorption pattern. However, there is a slight difference at 586 nm between the absorption spectra of the neodymium complex and the other lanthanide complexes. The absorption spectrum of the neodymium complex, measured against the lanthanum complex as reference is shown in Fig. 1b, along with that of neodymium measured against water. It is clear that the amplitude of the neodymium absorption band is red-shifted and remarkably increased by the complexation. The molar absorptivity calculated for the neodymium complex was $2.3 \times 10^3 \text{ l. mole}^{-1} \cdot \text{cm}^{-1}$, which is ~ 350 times that for neodymium chloride.

To eliminate the interference of the other lanthanides in the determination of neodymium, we investigated the 1st–4th order derivative spectra of the complexes. The optimal conditions proved to be use of the fourth-order derivative with $\Delta\lambda = 1.8 \text{ nm}$, band-pass = 1.0 nm and scan rate = 50 nm/min. Figure 2 shows the fourth-order derivative spectra of the lanthanide complexes, from which it is clear that the derivative spectrum of the neodymium complex is very different from the spectra of the other complexes. The amplitudes at 585 and 587 nm are significant for neodymium, and negligible for the other lanthanides.

Optimization of reaction conditions

The pH and the concentrations of SXO and CPC were optimized by varying one of

them at a time (Figs. 3–5), and the values selected are those given in the procedure. To allow for consumption of the reagents by other lanthanides present in analysis of mixtures, the amounts recommended in the procedure are about 10 times greater for SXO and 650 times greater for CPC than necessary for the sum of the lanthanides present.

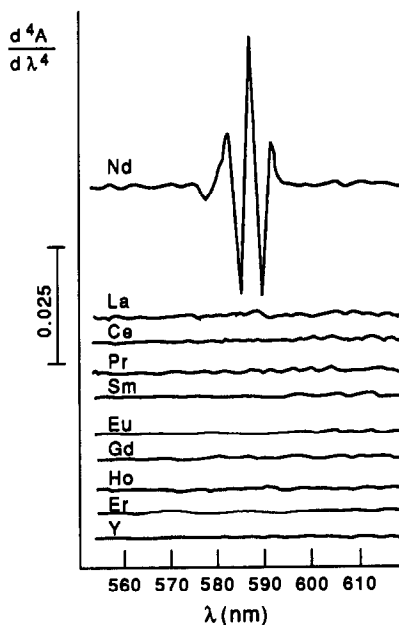


Fig. 2. Fourth-order derivative spectra of lanthanide complexes. $\Delta\lambda = 1.8 \text{ nm}$; band-pass = 1.0 nm; scan-rate = 50 nm/min. Other conditions as for Fig. 1(a).

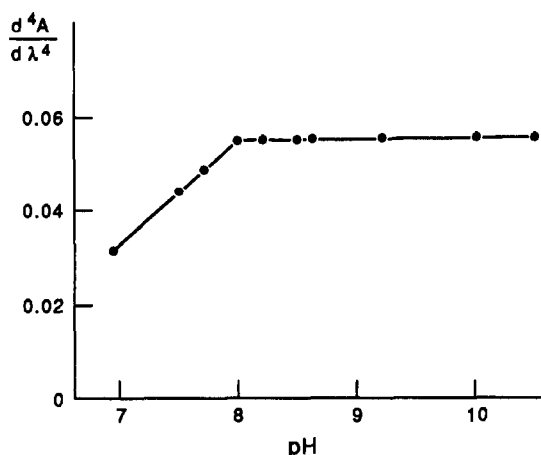


Fig. 3. Effect of pH on the fourth derivative absorption of the neodymium complex. $[\text{Nd}] = 1.0 \times 10^{-6} \text{ M}$; $[\text{SXO}] = 1.5 \times 10^{-3} \text{ M}$; $[\text{CPC}] = 8.0 \times 10^{-4} \text{ M}$; 4.0-cm cells; $\Delta\lambda = 1.8 \text{ nm}$; band-pass = 1.0 nm; scan-rate = 50 nm/min; peak to trough amplitude at 585 and 587 nm.

The complex takes 15 min to form completely and is stable for at least 24 hr.

Calibration graph and detection limits

A linear calibration graph was obtained by plotting the peak to trough amplitudes at 585 and 587 nm for neodymium in the concentration range 0–7.5 $\mu\text{g}/25 \text{ ml}$ and the derivative molar absorptivity was found to be $1.38 \times 10^4 \text{ l. mole}^{-1} \cdot \text{cm}^{-1}$, ~ 2000 times greater than for neodymium chloride. The calibration spectra are shown in Fig. 6. The relative standard deviation for 7 determinations of 1.8 $\mu\text{g}/25 \text{ ml}$ neodymium was 1.3%. The detection limits were 5.8 ng/ml in absence of lanthanum and 11.2 ng/ml in the presence of 44 ng/ml lanthanum (or 36 ng/ml yttrium).

To test the utility of the method, a synthetic lanthanide sample was prepared with composition (%) La_2O_3 24.10, CeO_2 52.30, Pr_6O_{11} 5.28, Nd_2O_3 15.32, Sm_2O_3 1.12, Eu_2O_3 0.15, Gd_2O_3 0.10, Ho_2O_3 0.20, Er_2O_3 0.20, Y_2O_3

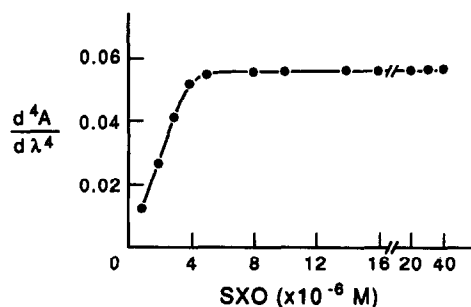


Fig. 4. Effect of $[\text{SXO}]$ on the fourth derivative absorption of the neodymium complex: pH = 8.2; other conditions as for Fig. 3, except for $[\text{SXO}]$.

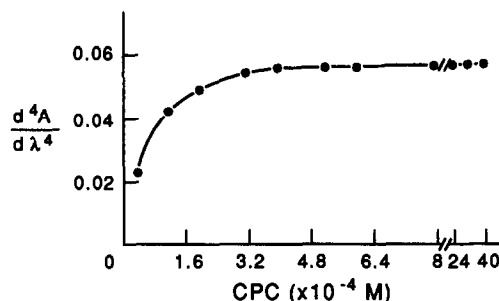


Fig. 5. Effect of $[\text{CPC}]$ on the fourth derivative absorption of the neodymium complex: pH = 8.2; other conditions as for Fig. 3, except for $[\text{CPC}]$.

1.23. The result obtained for Nd_2O_3 was 15.62% (relative error 2.0%). The relative standard deviation (6 determinations) was 1.8%. In addition, the amount of neodymium in a reference

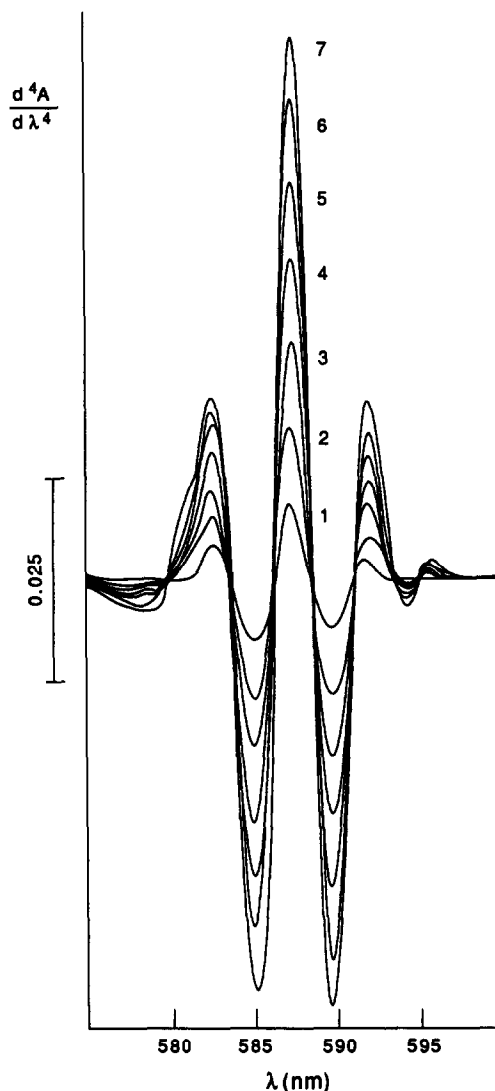


Fig. 6. Calibration spectra. $[\text{Nd}]$ ($\mu\text{g}/25 \text{ ml}$): 1, 1.08; 2, 2.16; 3, 3.24; 4, 4.32; 5, 5.40; 6, 6.48; 7, 7.56; pH 8.2, $\Delta\lambda = 1.8 \text{ nm}$; band-pass 1.0 nm; scan-rate 50 nm/min.

material* was determined. The value found was 17.05% and the certified value was 16.75% (relative error 1.8%). The relative standard deviation (5 determinations) was 1.7%. This shows that the accuracy and precision of the method are quite satisfactory.

REFERENCES

1. T. Taketatsu and C. V. Banks, *Anal. Chem.*, 1966, **38**, 1524.
2. L. I. Kononenko and T. P. Piontkovskaya, *Zh. Analit. Khim.*, 1969, **24**, 379.
3. Z.-X. Yang, *Fenxi Huaxue*, 1975, **3**, 133.
4. M. T. M. Zaki, A. F. Shouky and M. B. Hafez, *Analyst*, 1983, **108**, 531.
5. J.-W. Kang, R.-Y. Chen and G.-B. Bei, *Acta Chim. Sin.*, 1984, **42**, 921.
6. S.-F. Zhou and N.-X. Wang, *Fenxi Huaxue*, 1987, **11**, 1041.
7. S.-F. Zhou and Z. Li, *Talanta*, 1990, **3**, 341.
8. P. Qi and N.-X. Wang, *Fenxi Huaxue*, 1989, **12**, 1125.
9. S.-F. Zhou and N.-X. Wang, *Talanta*, 1990, **3**, 337.
10. N.-X. Wang, *Chinese Chem. Lett.*, in the press.
11. Beijing Rare Earths Academy, *Xitu Yingyong*, 1977, **2**, 24.

*From Baotou Rare Earths Academy, China. The composition is CeO₂ 49.21%, La₂O₃ 27.11%, Pr₆O₁₁ 5.18%, Nd₂O₃ 16.75%, Sm₂O₃ 1.29%, heavier rare earth and yttrium oxides 1.09%.

A PC-BASED GENERAL PROGRAM FOR THE SIMULATION AND ANALYSIS OF CYCLIC VOLTAMMETRIC EXPERIMENTS

DAVID K. GOSSER JR.* and FENG ZHANG

Department of Chemistry, The City College of the City University of New York, New York, NY 10031 U.S.A.

(Received 19 September 1990. Revised 9 January 1991. Accepted 15 January 1991)

Summary—A PC-based program, a General Program for Simulation of Cyclic Voltammetric Experiments (GPS-CV), is described. GPS-CV, written in Turbo Pascal 5.5, utilizes advances in simulation methodology that increase efficiency, allow for generality of mechanism, and include *IR* drop and capacitive current effects. An accessible user interface is used, and a graphical analysis program is provided. Cyclic voltammograms for nearly any mechanism can be simulated by the user. A companion program, CVFIT, combines the GPS-CV program with a least-squares fit by simplex minimization to give the best-fit parameters, with error estimates. The use of CVFIT is demonstrated with a three-parameter fit of experimental cyclic voltammograms.

Computer simulation by the explicit finite difference method has proven to be a powerful tool for the analysis of cyclic voltammetric experiments. The shape of a cyclic voltammetric curve reflects both electron transfer at the electrode and the solution chemical reactions that are coupled to the electron transfer. Thus, through a cyclic voltammetric study, a great deal of information can often be deduced regarding electrode processes and chemical reactions in solution that are initiated by electron transfer at the electrode. Simulations are often helpful in the preliminary stages of a cyclic voltammetric study, assisting in predicting mechanism(s) that can give rise to the cyclic voltammograms observed. Once a particular mechanism is decided upon, experimental results can be compared with successive simulations in order to extract rate and equilibrium parameters of the chosen mechanism. Because of the recognized importance of simulation, much attention has been focused on improving the original method proposed by Feldberg.¹ Among notable advances are the description of an expanding space grid to save computation time,² the inclusion of the mutually interrelated effects of *IR* drop and capacitive current,³ and the development of general methods for treatment of solution chemical reactions in the context of the explicit finite difference method.^{4,5}

This work describes a PC-based program which enables the experimentalist to simulate the cyclic voltammetry (CV) for almost any desired mechanism, and compare the result with experiment. The desired mechanism is entered in a simple manner with a full screen display, with options for varying the diffusion coefficients of individual species. In addition, the fitting program which is included finds a best fit for the experimental data. The value of such an approach lies in the elimination of the need to solve by analytical or numerical means the partial differential equation that models each new mechanism. Thus, more time is available for the consideration of problems of a chemical nature, and a large amount of repetitious work is avoided. In addition, the increased computational power now available in personal computers has meant that a generalized program can be an accessible tool for the mechanistic analysis of cyclic voltammograms.

Five main objectives were considered in the construction of a generalized program.

1. Mechanistic generality. The program uses a modular structure with a general solution of the homogeneous chemical kinetics. This means that virtually any electrochemical mechanism that can be formulated as a combination of electron transfers at the electrode and homogeneous chemical reactions can be simulated.

2. Speed of computation. An expanding space grid is used to minimize computation time. In

*Author for correspondence.

addition, the program is written in Turbo Pascal 5.5, which can take advantage of the gain in speed offered by the 8087, 80287 or 80387 math co-processors commonly used in personal computers.

3. Ease of use. A full screen display for input of mechanistic and experimental parameters, with options for corrections and changes, is utilized. The parameters are entered for the most part in common experimental units, not in dimensionless units. A graphic analysis program is provided for on-screen view of simulated or experimental files. Input is "error corrected"; that is, if a "fatal" error is made in the input (such as entry of a real number instead of an integer), the program will re-request the information.

4. Inclusion of non-ideal factors. A recently described method³ for including the effects of *IR* drop and capacitive current is incorporated in the simulation.

5. Quantitative comparison of experimental and simulated data. A simplex routine is used to optimize the fit between experimental and simulated cyclic voltammograms.

IMPLEMENTATION OF THE PROGRAM

The partial differential equation for linear diffusion and solution chemical kinetics is:

$$\frac{\partial C_q}{\partial t} = D_q \frac{\partial^2 C_q}{\partial x^2} \pm \sum k_g C_{g,1} C_{g,2} \quad (1)$$

where C = concentration, D = diffusion coefficient, x = distance, t = time, k = chemical rate constant, q = species subscript, and g = reaction subscript.

A discrete form of the diffusion term on the right-hand side of equation (1) is:

$$C_{i,j+1} = C_{i,j} + \frac{D\Delta t}{\Delta x^2} [C_{i-1,j} - 2C_{i,j} + C_{i+1,j}] \quad (2)$$

where i is a spatial subscript and j is a time subscript.

Equation (2) is equivalent to the creation of a space and time grid (see Fig. 1). Computation time can be decreased by utilizing an expanding space grid or an expanding space-time grid. Here, an expanding spatial grid was utilized: an expanding time grid can cause inaccurate calculations of the solution chemical kinetics.⁵ The expanding grid was constructed with the spatial increment doubled in size every fourth grid-point, after the method of Seeber and Stefani.⁶

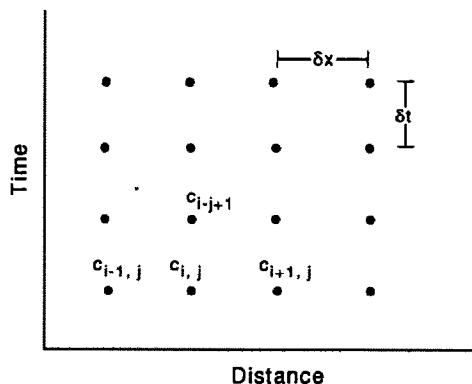


Fig. 1. A time and space grid utilized by the finite difference method. The program described in this work uses an expanding spatial grid to save computation time.

Near to the electrode, the concentrations will be determined by the potential (*i.e.*, through the equations of electrochemical kinetics) and diffusion, and at "infinite" distance the concentrations will be the same as the initial conditions. These facts constitute the boundary conditions for equation (1). In this work, the flux at the electrode was calculated according to a previously described method, which takes into account the flux of species at the surface of the electrode due to both the heterogeneous kinetics as described by the Butler-Volmer equation [equation (3)] and diffusion.⁷ The potential, E , in the Butler-Volmer equation can be corrected for *IR* drop in a number of ways. In this work, following the method of Boyer *et al.*,³ the *IR* term is included by reading an experimental current file and using a measured (or estimated) resistance to calculate *IR*.

$$\frac{i}{nFa} = k^0 [C_{ox} e^{-\alpha nF[E - E^0]} - C_{red} e^{(1-\alpha)nF[E - E^0]}] \quad (3)$$

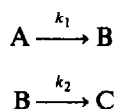
The capacitive current is also calculated as in Boyer *et al.*,³ by using the potential corrected for *IR* drop in calculating the capacitive charging current at each time step in the simulation.

Although diffusion and chemical reaction are concurrent processes, in the explicit finite difference method they are calculated separately. This procedure, which is valid if the time increments are small enough, leads to the possibility of very general treatments of the chemical kinetic term in equation (1). In particular, it has been shown that simple numerical methods such as an iterative modified Euler method⁵ or a Runge-Kutta method⁴ can be used to provide general solutions for the differential equations that model chemical kinetics. Thus, a simple algorithm

based on equation (4) has been used to solve chemical reaction kinetics:

$$C_{q,n} = C_{q,0} + \frac{\Delta t}{2} \left[\frac{\Delta C_{q,0}}{\Delta t} + \frac{\Delta C_{q,n-1}}{\Delta t} \right] \quad (4)$$

where the changes in concentrations are obtained from a differential approximation for the kinetics, based on the initial concentration and the n th concentration. For example, for the kinetic scheme



the n th concentrations $C_{a,n}$ and $C_{b,n}$ for A and B respectively are calculated as:

$$C_{a,n} \equiv C_{a,0} - \frac{k_1 \Delta t}{2} [C_{a,0} + C_{a,n-1}] \quad (5)$$

$$C_{b,n} \equiv C_{b,0} + \frac{k_1 \Delta t}{2} [C_{a,0} + C_{a,n-1}] - \frac{k_2 \Delta t}{2} [C_{a,0} + C_{b,n-1}] \quad (6)$$

The inclusion of all of these features in a General Program for Simulation of Cyclic Voltammetric experiments (GPS-CV) results in a rather complex program structure. Index numbers are assigned to each species in the mechanism, to each electrode reaction, and to each solution chemical reaction. Program loops are used to include all reactions for all species within the usual scheme for simulation by explicit finite differences. This is illustrated by Table 1.

The use of the GPS-CV program is nearly self-evident for those familiar with cyclic voltammetry. However, to give a clear idea of its capabilities and the conventions utilized, a brief summary of the interactive input procedure follows.

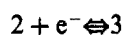
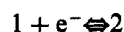
Input/output for GPS-CV

Number of species in the mechanism. An integer equal to the total number of species in the mechanism is entered. Although the screen input is designed for up to 8 species more can be entered if necessary.

Concentrations of the species. The initial concentration of each species is entered in normalized units. That is, the concentration of each species is divided by a chosen normalizing concentration (C_{norm}), typically that of the primary

electroactive species. Each species is now associated with an integer, in the order of entry. Later entries, which describe electrode reactions and chemical reactions, utilize these number identifications.

Redox couples. The integer indexes of the oxidized and reduced forms of each redox couple are entered, followed by the reduction potential (in volts), the heterogeneous rate constant (in cm/sec), and the transfer coefficient. For an electron transfer that is considered to be reversible, a value of 10 cm/sec will ensure reversibility under most circumstances. If a two-electron transfer (where one of the redox species is shared by two couples) is among the electrode reactions, these should be entered in sequence when written as reductions. For instance:



Solution chemical reactions. Each chemical reaction (first- or second-order) is described by entering two indexes for the reactants and two for the products (if the reaction is first order, 0 is entered in the space reserved for the second species of a second order reaction). First-order rate constants are entered in units of sec^{-1} . Second-order rate constants are entered in units of $1. \text{mole}^{-1} \cdot \text{sec}^{-1} \times C_{\text{norm}}$.

Experimental parameters. The number of half cycles (1, 2 or 3), the initial potential, switching potential(s), final potential (V) and scan rate (V/sec) are entered. Asymmetric potential waveforms, which are often useful, are possible in this scheme.

Changes in input. At this point, the user can inspect the entire input screen and change selected parameters. It is also possible to change the default temperature (298.15°) or the default diffusion coefficient for each species ($1.00 \times 10^{-5} \text{ cm}^2/\text{sec}$). The diffusion coefficients are changed by entering a multiplier of the default value (for instance, enter 0.5 for a diffusion coefficient of $5.00 \times 10^{-6} \text{ cm}^2/\text{sec}$). If it is desired to simulate a mechanism with a diffusion coefficient larger than the default coefficient, the default diffusion coefficient must be changed in the source code.

Option for capacitive current. If it is desired to include a capacitive current in the simulation, then the electrode area (cm^2), double-layer capacitance ($\mu\text{F}/\text{cm}^2$), solution resistance ($\text{k}\Omega$), and the normalizing concentration ($\text{mole}/\text{l.}$) are requested.

Option for IR drop. The effect of the IR drop can also be included. It is necessary to provide an experimental data file of current-potential values (1 point per mV), and to enter the resistance, area, and normalizing concentration. The experimental current is read and the simulation potentials are corrected accordingly.

Names of data and graphic output files. The user selects the names of the output files which are to contain the simulated current and potential values. The graphics file contains data to be used in the graphics routine, and the data file contains the simulation data and record of parameters. The data file can also be used as input for commercial graphics programs for high-quality print output.

Stimulated current. The simulated current and potential values are displayed on the

screen during the simulation so that progress can be monitored. The simulated current (I_{sim}) displayed and saved in the output files is related to the actual current (I_{amps}) according to $I_{sim} = I_{amps} / (Area \times C_{norm} \times 100 \times \nu)$, where $Area$ = electrode area and C_{norm} = the normalizing concentration, and ν = scan rate. Generally, the program sets the time increments used in the simulation so as to achieve less than 0.1% error.

If the option for capacitive current and/or IR drop was selected, then the simulation current is output directly in amperes.

Graphics. An on-screen graphics representation of the simulation output can be obtained for CGA or Hercules graphics screens. The initial and final potentials of the desired graph are input, a scale factor for the y (current) axis is selected, and the name of the graphics file is

Table 1. Skeleton of Pascal program (GPS-CV)*

VARIABLE DECLARATIONS {DECLARE ALL VARIABLES} PROCEDURE SETUP

READ THE FOLLOWING INPUT INFORMATION

1. NUMBER OF SPECIES {NSPEC} AND CONCENTRATIONS OF EACH
2. NUMBER OF ELECTRODE COUPLES {NCOUP} AND THERMODYNAMIC AND KINETIC PARAMETERS FOR EACH COUPLE
3. NUMBER OF CHEMICAL REACTIONS {NREACT} AND FORWARD AND REVERSE RATE CONSTANTS FOR EACH REACTION
4. EXPERIMENTAL PARAMETERS {SCAN RANGES AND SCAN RATE}

CALCULATE: FROM MAXIMUM CHEMICAL RATE CONSTANT AND EXPERIMENTAL PARAMETERS THE NUMBER OF TIME INCREMENTS {NT} AND NUMBER OF SPACE INCREMENTS {NS}

OPTION: CHANGE 1, 2, 3 OR 4 OR DEFAULT PARAMETERS {TEMPERATURE OR DIFFUSION COEFFICIENT}

OPTION: READ PARAMETERS NECESSARY TO INCLUDE IR DROP OR CAPACITIVE CURRENT {RESISTANCE, AREA, AND CURRENT}

PROCEDURE ELECTRODE

FOR I = 1 TO NCOUP DO {LOOP OVER ELECTRODE COUPLES}

 CALCULATE THE CURRENT FOR EACH ELECTRODE REACTION

 OPTION: CALCULATE CAPACITIVE CURRENT

 CALCULATE TOTAL CURRENT

 OUTPUT POTENTIAL/CURRENT VALUES TO SCREEN AND TO DATA FILES

PROCEDURE DIFFUSION

FOR I = 1 TO NSPEC DO {LOOP OVER SPECIES}

 FOR J = 1 TO NS DO {LOOP OVER SPATIAL INCREMENTS}

 CALCULATE CONCENTRATION CHANGE DUE TO DIFFUSION FOR SPECIES I

PROCEDURE CHEMREACT

 FOR J = 1 TO NS DO {LOOP OVER SPATIAL INCREMENTS}

 USE MODIFIED EULER METHOD TO CALCULATE CONCENTRATION CHANGES DUE TO SOLUTION CHEMICAL REACTIONS.

{***** MAIN PROGRAM *****}

SETUP,

 FOR I = 1 TO NT {LOOP OVER TIME INCREMENTS}

 INCREMENT THE ELECTRODE POTENTIAL ACCORDING TO SCAN RANGE, SCAN RATE AND AS OPTION CURRENT AND RESISTANCE {IR DROP}

 ELECTRODE;

 DIFFUSION;

 CHEMREACT;

 WRITE OUT SIMULATION PARAMETERS TO DATA FILE

 ANOTHER SIMULATION?

 YES—GOTO SETUP

 NO {FINISH SIMULATION}

*For those interested in the detailed program structure, the source code is available, as described at the end of this paper.


```

[1] 1: 1.0 2: 0.0 3: 1.00 4: 0.0 5: 0.0 6: 0.0
[2] Ox    Red    E    Khet  alpha  Temp=298
     1+e- <=> 2 -0.20 10.0   0.5   Icap?:N
     5+e- <=> 6 -0.35 10.0   0.5   IR drop?:N
[3] Rx1 Rx2  Pr1  Pr2  Kf  Kr
     2   3 <=> 4   5 100.0 25.0
[4] Scan Rate: 1.0          Change #: 0
     Init Pot  : 0.0        0=Continue
     Switch Pot: -0.5       5=Temp
     Final Pot : 0.0        6=Diff Coeff

Save Graph File as: Gdata.pas
Save Graph File as: Data.pas

```

Fig. 2. The appearance of the screen after the input procedure for the following mechanism and experimental parameters. Six chemical species with the following initial concentrations (in normalized units): 1.0, 0.0, 1.0, 0.0, 0.0, 0.0; two redox reactions: $1 + e \rightleftharpoons 2$, $E^0 = -0.20$ V, $k = 10.0$ cm sec⁻¹, $\alpha = 0.5$; $5 + e \rightleftharpoons 6$, $E^0 = -0.35$ V, $k = 10$ cm sec⁻¹, $\alpha = 0.5$; one chemical reaction: $2 + 3 \rightleftharpoons 4 + 5$, $k_1 = 1.00$ sec⁻¹/Cnorm, $k_{-1} = 25$ sec⁻¹/Cnorm; experimental parameters: scan rate = 1 V/sec, initial potential = 0.0 V, switching potential = -0.5 V, final potential = 0.0 V.

requested. A cursor is scrolled across the screen by pressing of arrow keys and the corresponding current/potential values are shown.

Sample input and graphics. The appearance of the input screen for the simulation of a specified mechanism is shown in Fig. 2. It is difficult to indicate the nature of the input procedure, since the input is highly interactive, and the final input screen does not fairly represent the "friendliness" of the program. A hardcopy of the screen graphics for the same simulation is shown in Fig. 3 and that with a capacitive current contribution in Fig. 4.

Sample computation times for fast chemical reactions

Typical computation times for the simulation of an EC mechanism for an experiment (scan rate, 1 V/sec; scan range, 1 V, with increasing values of the rate constant (k) on a Gateway 386 PC (20 MHz) with an 80387 math co-processor are as follows: 1 min ($k = 100$ sec⁻¹), 15 min ($k = 10,000$ sec⁻¹), 2.5 hr ($k = 100,000$ sec⁻¹). Simulations on a 286 PC (with co-processor) took about 4 times as long. Because second-order rate constants are entered as k in $l \cdot mole^{-1} \cdot sec^{-1} \times C_{norm}$, mechanisms involving rates that are nearly diffusion-controlled can be simulated in a reasonable amount of time. In digital simulation, since the computation time is related to the total time of the experiment, the simulation times will be much shorter for

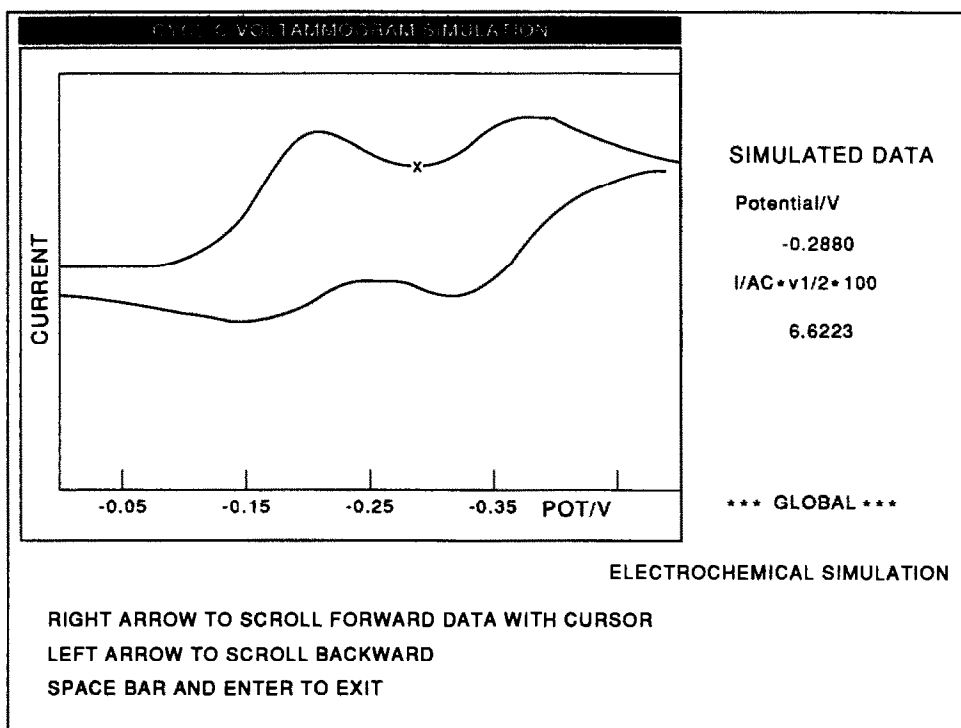


Fig. 3. Screen plot for the simulation of the mechanism described in Fig. 2. Simulated current is given in the units described in the text.

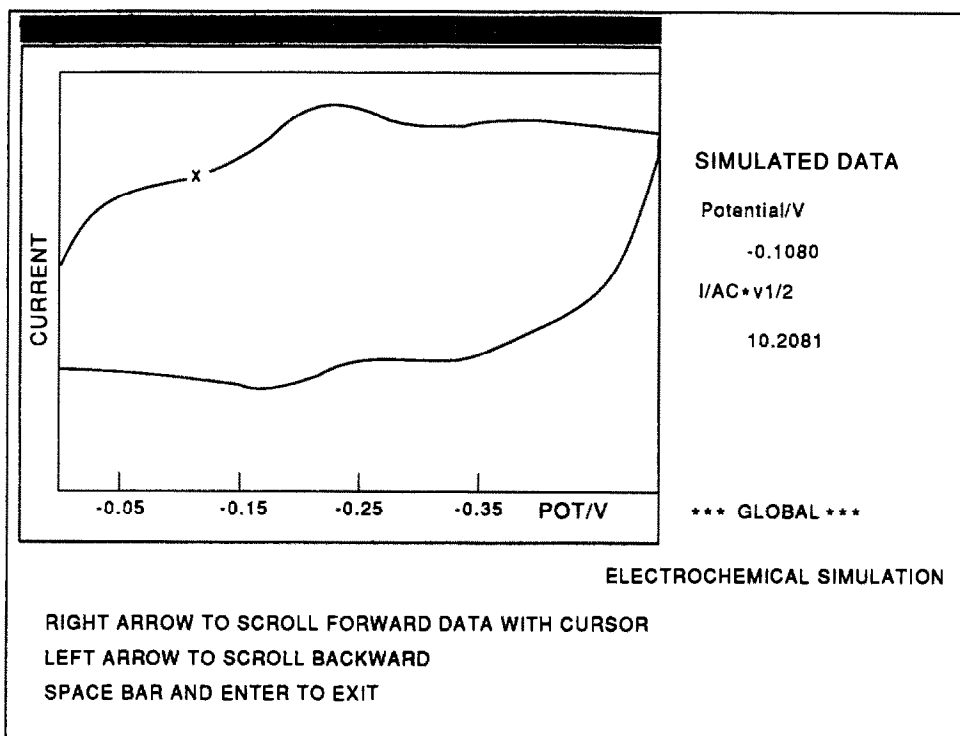


Fig. 4. Screen plot for the same mechanism as in Fig. 3, but with a capacitive current contribution according to the following parameters. Scan rate = 20.0 V/sec, electrode area = 0.02 cm², double layer capacitance = 50 μ F/cm², solution resistance = 3 k Ω .

experiments with faster scan rates, such as might be employed when ultramicroelectrodes are used. For instance, the simulation of the mechanism with $k = 100,000 \text{ sec}^{-1}$ and scan rate = 1000 V/sec is equivalent to the simulation where $k = 100 \text{ sec}^{-1}$ and scan rate = 1 V/sec, and takes only one minute.

CVFIT: GPS-CV WITH SIMPLEX OPTIMIZATION

In order to exploit the power of digital simulation fully for the analysis of cyclic voltammograms, it is necessary to have a quantitative method for comparison of experimental and simulated results. A method that lends itself to a general treatment is nonlinear least-squares fitting,⁸ in which the parameters of interest (*e.g.*, reduction potentials, heterogenous or homogeneous rate constants) are varied in a systematic way until a simulation is found that minimizes the least-squares difference between the experimental result and the simulation. Here, we have utilized the simplex method, a robust algorithm for function minimization.⁹ In curve fitting by least squares, it is desirable to obtain an estimate of the errors in the fitted parameters. We use the procedure of Phillips

and Eyring,¹⁰ in which the error estimate is obtained from a quadratic approximation of the error surface obtained from a simplex minimization. The program CVFIT is a program which couples a simplex fitting routine to the GPS-CV program. The CVFIT program calls the interactive GPS-CV once at the beginning, so that the user can provide a first guess for the simulation parameters. The initial simplex is based on a uniform random distribution centered on the input guesses. It subsequently repeatedly calls an automated version of GPS-CV with new guesses that are provided from the simplex until a best fit is reached within a set tolerance. For the operation of CVFIT it is necessary to identify the parameters to be fitted in the source code. Thus, for the operation of CVFIT, it is necessary to have a Turbo-Pascal Compiler (version 5.5 or higher).

APPLICATION OF CVFIT TO THE ANALYSIS OF THE CYCLIC VOLTAMMETRIC DATA

Experiments were performed with a BAS-100A electrochemical analyzer. The data sets were transferred to a fixed disk on an IBM-compatible computer. The electrochemical cell

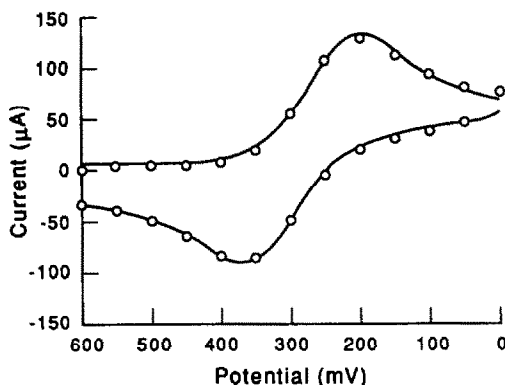


Fig. 5. The best fit simulation (line) compared with selected experimental data (circles) for cyclic voltammetry of ferricyanide at 5 V/sec.

utilized a 3-mm diameter glassy-carbon working electrode and a silver/silver chloride reference electrode. Solutions were 1.5mM ferricyanide with 0.10M potassium chloride, adjusted to a pH of 2.0. The uncompensated resistance was estimated to be 115 Ω with the BAS-100A. The BAS-100A does this by assuming an $R_u C_{dl}$ circuit (where R_u stands for uncompensated resistance and C_{dl} for double-layer capacitance) and the zero-time current for a potential step is extrapolated for the current decay.

As a preliminary test of the efficacy of the overall approach, CVFIT was used to optimize the formal reduction potential (E^0), and the heterogeneous rate parameters (k^0 and α) to give the best fit to cyclic voltammograms of $\text{Fe}(\text{CN})_6^{3-}$ at scan rates of 5.0 and 10.0 V/sec. Literature values¹¹ for the diffusion coefficients of ferricyanide ($7.6 \times 10^{-6} \text{ cm}^2/\text{sec}$) and ferrocyanide ($6.3 \times 10^{-6} \text{ cm}^2/\text{sec}$) were used in the simulation. A linearly extrapolated faradaic background current was subtracted before the

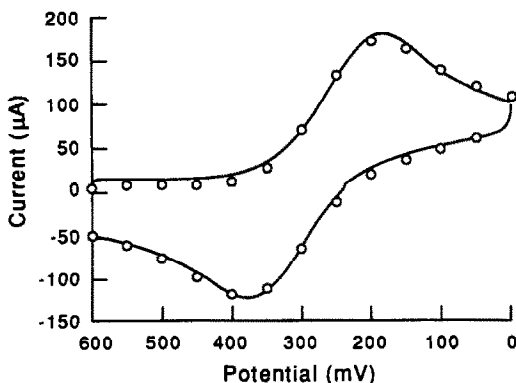


Fig. 6. The best fit simulation (line) compared with selected experimental data (circles) cyclic voltammetry of ferricyanide at 10 V/sec.

Table 2. Summary of best-fit parameters found by the CVFIT program, with and without inclusion of correction for the IR drop

With IR drop simulation		
v , V/sec	5	10
E^0 , V	0.3020 ± 0.0025	0.3035 ± 0.0005
k^0 , cm/sec	0.0115 ± 0.0021	0.0124 ± 0.0013
α	0.5425 ± 0.0022	0.5448 ± 0.0032
Without IR drop simulation		
v , V/sec	5	10
E^0 , V	0.2941 ± 0.0005	0.2925 ± 0.0026
k^0 , cm/sec	0.0114 ± 0.0011	0.0125 ± 0.0012
α	0.4851 ± 0.0022	0.4851 ± 0.0026

fitting procedure. The double-layer capacitance was estimated to be 17 $\mu\text{F}/\text{cm}^2$ by using a preliminary four-parameter fit. The best-fit simulations are compared with experimental data in Figs. 5 and 6, and the best fits with and without inclusion of the IR drop calculation are summarized in Table 2. When IR drop is included, the results are in line with previous estimates of k^0 and α .¹² Our results indicate that IR drop has more effect on the value determined for α than on that for k^0 . Also, as expected, IR drop causes systematic errors in determinations of the reduction potential. The total time for each three-parameter fit was about 1 hr on the Gateway 386 PC.

Work is underway on the application of CVFIT to analysis of electrode mechanisms involving coupled chemical reactions.

Availability of the program—The compiled and source code of the programs GPS-CV and CVFIT (with detailed instructions) are available on request. If possible, please include \$15 to cover the cost of disks, mailing, and to receive upgrades of the programs. The GPS-CV program is a revised and extended version of another program written in FORTRAN and designed for mainframe use. This program is also available by computer mail (Gosser@CCNY).

Acknowledgements—This research was supported in part by grant number 669270 from the PSC-CUNY Research Award Program of the City University of New York. We thank Dr. Edward M. Eyring for kindly providing us with the FORTRAN source code of the error-estimation procedure.

REFERENCES

1. S. W. Feldberg, *Electroanal. Chem.*, 1969, **3**, 199.
2. T. Joslin and D. Pletcher, *J. Electroanal. Chem.*, 1974, **49**, 171.
3. W. J. Boyer, E. E. Engleman and D. H. Evans, *ibid.*, 1989, **67**, 262.
4. M. F. Nielsen, K. Almadal, O. Hammerich and V. D. Parker, *Acta Chem. Scand.*, 1987, **A41**, 423.
5. D. K. Gosser and P. H. Rieger, *Anal. Chem.*, 1988, **60**, 1159.

6. R. Seeber and S. Stefani, *ibid.*, 1981, **53**, 1011.
7. S. W. Feldberg, *J. Electroanal. Chem.*, 1981, **127**, 1.
8. J. F. Rusling, *CRC Crit. Rev. Anal. Chem.*, 1989, **21**, 49.
9. W. H. Press, B. P. Flannery, S. A. Teukolsky and W. T. Vetterling, *Numerical Recipes*, Cambridge University Press, Cambridge, 1985.
10. G. R. Phillips and E. M. Eyring, *Anal. Chem.*, 1988, **60**, 738.
11. R. N. Adams, *Electrochemistry at Solid Electrodes*, p. 219. Dekker, New York, 1969.
12. B. B. Damaskin, *The Principles of Current Methods for the Study of Electrochemical Reactions*, McGraw-Hill, New York, 1967.

THE SEPARATION OF OVERLAPPING PEAKS IN CYCLIC VOLTAMMETRY BY MEANS OF SEMI-DIFFERENTIAL TRANSFORMATION

MARCIN PAŁYS,* TOMAS KORBA, MARTINUS BOS and WILLEM E. VAN DER LINDEN

Laboratory of Chemical Analysis, Department of Chemical Technology, Twente University of Technology, P.O. Box 217, 7500AE Enschede, The Netherlands

(Received 1 October 1990. Accepted 22 January 1991)

Summary—A method for extracting single peaks from complex linear sweep and cyclic voltamperograms is presented. Voltamperograms are transformed by means of semidifferentiation, then all undesired peaks are removed from the semiderivative curve and replaced by calculated baselines. The resulting curve is semiintegrated back, giving a voltamperogram with one peak only. Baselines in the semiderivative domain are determined by the least-squares curve-fitting of datapoints from peak border regions, using the equation that describes the semiderivative peak of a reversible electrode process. With this procedure peaks can be removed without assumptions about the mechanism of the underlying electrode reaction. Due to its design, the algorithm presented is suitable for the fully automatic processing of cyclic and linear sweep voltamperograms. Performance of the procedure was checked with generated reversible voltamperograms as well as in real experiments with both reversible and irreversible systems. The smallest distance between two peaks of equal height, for which the described method can yield correct results, has been found to be 110 mV for a reversible one-electron process at 298 K. This procedure can also be applied to the elimination of the cathodic current from the cyclic voltamperogram of a single component in order to get a pure anodic current value, free from cathodic contribution, or vice versa.

Linear sweep voltammetry (LSV) and cyclic voltammetry (CV) are simple and relatively fast electroanalytical techniques used mainly for qualitative studies. Their experimental simplicity and well-established theoretical background also make them attractive for automated electrochemical investigations to be implemented in an expert system for the elucidation of electrode mechanisms, and this is under study. However, applicability of LSV and CV to quantitative studies is restricted by the shape of the signal: a broad, asymmetric, "tailing" peak. As a consequence of this feature, in composite voltamperograms peaks often overlap and measurement of their parameters (peak current and peak potential) is significantly hindered. Influence of the cathodic current on the anodic part of the voltamperogram makes measurement of the anodic peak current difficult, or even impossible if several cathodic peaks exist. Therefore, a good method for the separation of overlapping peaks is desired, if one wants to use these techniques to obtain quantitative results. For

our purposes, we would demand the method to have additional features: the ability to separate peaks without any special assumptions about the electrode reaction mechanism and the capability to resolve peaks originating from a multistep reaction of one compound as well as from signals obtained from the mixture of the electroactive species.

The separation of cyclic voltammetric peaks has been an objective of extensive studies.¹⁻⁴ However, most popular methods have some restrictions: direct curve fitting of overlapping peaks¹ requires parameters describing the peak shapes before fitting can start, knowledge of what excludes its application to unknown (or unidentified) mixtures and to peaks resulting from multistep reactions. The deviation-pattern recognition method² needs knowledge about the underlying electrode reaction mechanism. The approach of Perone *et al.*³ works only under supervision of the experimenter, relying on his decision. Interrupt-scan method, as proposed by Boudreau and Perone,⁴ while profitable for qualitative measurements, according to the authors doesn't give satisfactory quantitative results for staircase voltammetry. An extension of work¹ with another, more general approxi-

*On leave from University of Warsaw, Chemistry Department. Author for correspondence.

mate function⁴ to fit overlapping peaks retains the restrictions of the original work, *i.e.*, the necessity of delivering peak-shape parameters prior to the fitting; moreover, the paper⁴ presents results of this method for square-wave voltammetry only.

Problems with overlapping peaks can be partially overcome by combining LSV with a mathematical transformation like semidifferentiation or semiintegration.^{5,6} The transformed voltamperograms reveal attractive features for both analytical and mechanistic studies, such as the independence of the signal on the potential change function,⁷ higher symmetry and small peak widths,^{5,8} a linear relationship between semiintegrated current and the surface concentration of the reactant at the electrode⁹⁻¹¹ and simpler analytical equations describing the peak shapes.

The increasing number of applications of semidifferentiation and semiintegration coupled to linear sweep voltammetry (also called semi-differential/semiintegral electroanalysis or convolution potential sweep voltammetry) is reflected by the fact, that recently commercially available instrumentation is equipped with these possibilities (*e.g.*, Bioanalytical Systems Inc, PARC EG & G Corp.). However, the number of electrode processes, for which a full theoretical description of the signals is available is rather small. As far as semiintegration is concerned, Saveant and co-workers published a series of papers,¹²⁻¹⁷ in which a number of equations has been derived. These equations, employing both current and its semiintegral cannot be used, however, for the direct interpretation of semiintegrated curves. For semidifferentiated voltamperograms, Goto and Ishii⁵ reported an equation describing the peak of the reversible process, while Dalrymple-Alford *et al.*^{6,18} gave the result for the irreversible case. Goto and Ishii⁸ also investigated the influence of the use of staircase instead of linear sweep voltammetry.

In contrast to semiderivative voltammetry, the theory of cyclic voltammetry is well developed. For mechanistic investigations, voltammetric curves can be studied according to the standard procedures if the necessary parameters are available. These procedures, most employing variations of peak potential, E_p , peak current, i_p , and anodic to cathodic current ratio with scan rate and concentration, often require values of currents which cannot always be directly measured from the recorded curve.

In this paper an approach is proposed, which combines the benefits of the easy interpretation of voltamperograms and the enhanced resolution characteristics of semidifferentiated linear sweep and cyclic voltammetry curves. This goal is achieved by semidifferentiation of a complex voltamperogram, separation of the semiderivative signals, removal of the undesired peaks by replacing them with the appropriate fragments of the baseline and semiintegration back to the $i(E)$ form, that will now contain peaks of interest only. Moreover, the proposed method is relatively universal and can be applied to electrochemical processes with different kinetics.

THEORY

The current in a linear sweep voltamperogram with two overlapping peaks can be described as the sum of two independent current functions, $i(t) = i_1(t) + i_2(t)$. Due to the linear and homogeneous character of the semidifferential operator,^{9,19} this additivity remains valid also in the semiderivative domain:

$$\frac{d^{1/2}}{dt^{1/2}} i(t) = \frac{d^{1/2}}{dt^{1/2}} i_1(t) + \frac{d^{1/2}}{dt^{1/2}} i_2(t) \quad (1)$$

After subtracting the contribution of one of the components from the total semidifferentiated signal, the remaining curve can be semiintegrated yielding the original current peak of this component due to the relationship:

$$\frac{d^{-1/2}}{dt^{-1/2}} \left(\frac{d^{1/2}}{dt^{1/2}} i(t) \right) = i(t) \quad (2)$$

Semidifferentiation and semiintegration can easily be performed with standard algorithms. The problem of removing unwanted peaks from a semiderivative curve and reconstruction of the baseline in these regions must be solved now. Voltammetric peaks which are not very close to each other are sometimes fully separated in the semiderivative domain. This results from the fact that semiderivative peaks are much narrower than voltammetric ones and that the value of the semiderivative drops rapidly to zero at the descending part of the peak, in contrast to the long "diffusional tail" of the original signal (see for example^{20,21}). This case is shown in Fig. 1A. To remove peak 1, baseline values at points marked A and B must be estimated. Then all datapoints between A and B are replaced by new values calculated under the assumption, that the baseline is linear in this range. Additionally, for the purpose explained later it is

assumed, that its slope is fairly small. These assumptions are generally valid, if the original voltamperogram is background-corrected.

The situation is more complicated when the semiderivative peaks also overlap (Fig. 1B). The dashed line marks the baseline for peak 1. The part marked as B is a sum of two contributions: a linear one, corresponding to what was previously called baseline and a non-linear one, being the descending branch of peak 0 in the region where peaks overlap. To be able to remove peak 1, the curve between C and A must be replaced by the sum of these two components, so it is necessary to estimate both of them separately.

The equation that describes the semiderivative peak of a reversible process is:^{5,18}

$$\frac{d^{1/2}}{dt^{1/2}} i = (n^2 F^2 A \nu c D^{1/2} / 4RT) \cosh^{-2} \times [(nF/2RT)(E - E_{1/2})] \quad (3)$$

and it was found, that it can be used for fitting data from irreversible electrode processes,^{22,23} too. For the present purpose, it is also assumed that a function of this type can describe the part of the peak far away from its top, irrespective of the reaction mechanism.

In the considered fragment of the semiderivative voltamperogram, equation (3) can be rewritten in the simplified form

$$\frac{d^{1/2}}{dt^{1/2}} i = h \cosh^{-2} [k(E - E_p)] \quad (4)$$

where h , k and E_p denote parameters related to the peak height, to peak width and to the

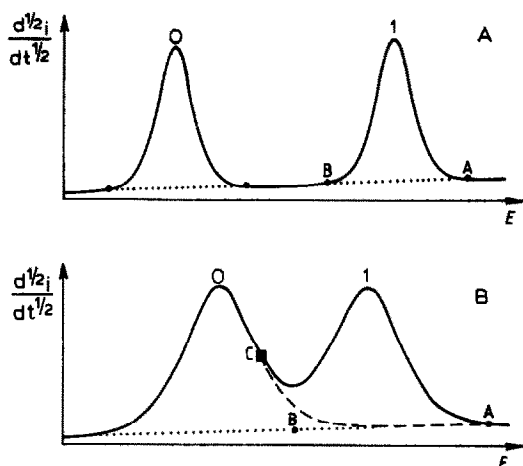


Fig. 1. A—two non-overlapping semiderivative peaks. Small filled circles mark peak borders. B—two overlapping semiderivative peaks.

position of peak top, respectively. It must be noted that the above parameters need not necessarily describe the whole peak, but only the relevant fragment.

To characterize the shape of the non-linear component of the baseline, h , k , and E_p must be found by curve fitting. Additionally, if datapoints used for fitting are selected from a rather small part of the curve lying, for example, around point B in Fig. 1B, the linear component can be considered constant there. It allows for a reduction in the number of parameters and for the equation for the complete baseline to be written as follows:

$$y = y_B + h_0 \cosh^{-2} [k_0(E - E_{p0})] \quad (5)$$

where the first term represents the value of the linear component at point B and the second one the descending branch of peak 0. It should be noted that the slope of the linear component determines the range over which equation (5) is valid.

The overall semi-differentiated signal in the range of selected datapoints can be finally written by adding the function describing the ascending branch of peak 1 to equation (4) resulting in:

$$y = y_B + h_0 \cosh^{-2} [k_0(E - E_{p0})] + h_1 \cosh^{-2} [k_1(E - E_{p1})] \quad (6)$$

from which the parameters required have to be obtained by curve fitting (indexes indicate peak number). Once y_B is found, the linear component of the baseline fragment necessary for the replacement of peak 1 can be obtained by using the value of y_A at the point A. Calculation of the y_A value at the free end of the overlapping peak can be done in the same manner as calculations at the border points of the non-overlapping peak from Fig. 1A. For these purposes, however, another procedure was used. The method often used of taking the datapoint(s) value(s) at an arbitrary distance from the peak top (far enough to ensure, that the peak contribution is zero) was not employed, because it is subjective and can give wrong results in the case where noise or another peak appears in that region. Instead, an approach was used based on the fitting of datapoints around the peak border point to equation (5) (border point is selected on the basis of peak derivative). In this situation, however, the interpretation of the parameters in equation (5) is slightly different: now y_B denotes the wanted value of the baseline at the peak

border, while the second term is a contribution of the residual of the peak branch. Again, if datapoints are chosen in a narrow range, or if the baseline slope is small, the method yields the baseline value at the border point even if the position of this point was selected not very precisely.

When all necessary baseline parameters are calculated at both peak borders, the unwanted peak can be removed. In case of non-overlapping peaks, it is done just by drawing the straight line between points A and B in Fig. 1A. If the peak overlaps, then the dashed line from Fig. 1B is calculated with the equation

$$y = y_0 + sE + h_0 \cosh^{-2}[k_0(E - E_{p0})] \quad (7)$$

in which y_0 and s are terms describing the offset and the slope of the linear baseline component (obtained from values of y_A and y_B) and the third term is identical to the second term on equation (5), *i.e.*, the descending branch of peak 0. The procedure proposed can also be used for removing peak 1 instead of peak 0. In this case, h_0 , k_0 and E_{p0} in equations (5) and (7) have to be replaced by h_1 , k_1 and E_{p1} , respectively.

EXPERIMENTAL

Reagents

Solutions (0.1M) of In^{3+} , Tl^+ , Co^{2+} and Zn^{2+} were prepared from indium nitrate, thallium sulphate, cobalt perchlorate (Merck, *p.a.*) and zinc sulphate (Fluka, *p.a.*). Potassium chloride (1M) (Suprapur, Merck) was used as the supporting electrolyte in all experiments. All substances were dissolved in demineralized water filtered through a Millipore Q-II installation. Oxygen was expelled with specially pure (polarographic grade) nitrogen (Hoekloos).

Equipment

Experiments were carried out with the Autolab-100 fully computer-controlled electrochemical system (Eco Chemie, Utrecht, The Netherlands) connected to a Metrohm 663 VA static mercury drop electrode. An Ag/AgCl electrode (3M potassium chloride) was used as the reference electrode. In all experiments. All calculations were done with an Olivetti M24 personal computer (IBM PC/XT compatible).

Recording procedure

Voltamperograms were recorded with 50 ml of supporting electrolyte. The solution was deaerated for 15–20 min before the experiments.

Two series of measurements for each pair of A and B compounds were done. In the first series, a blank voltamperogram, a voltamperogram of A and a voltamperogram of A + B were recorded by subsequently adding solutions of the respective ions into the cell. The peak of compound A, obtained via processing of the A + B voltamperogram were compared to the original voltamperogram of A. In the second series, the order of additions was reversed: voltamperograms of a blank, of B and of B + A were recorded. The peak of B separated from the voltamperogram of B + A was compared to the peak of B alone. No correction for the volume change was made, because the total volume change did not exceed 0.2%.

All voltamperograms were stored on disk before further calculations.

Procedure

The whole procedure for peak separation was implemented in the form of a menu-driven program written in C (Microsoft-C version). In the development of the program, standard assembler routines from the Autolab-100 analyzer package were used for experimental set-up control.

General scheme. Depending on the kind of studies, voltamperograms were recorded or generated (see below). After completing this step, semidifferentiation was carried out, and baselines of all semiderivative peaks were calculated by curve fitting. All undesired peaks were then removed and replaced by their baselines. The cycle was completed by semiintegration of the processed semiderivative curves yielding the voltamperogram that contains only the peaks(s) of interest.

Data acquisition. Voltamperograms were recorded by varying the potential according to a staircase function and measuring the current in the last 20% of each step (but no longer than 20 msec). To reduce the noise, voltamperograms were digitally filtered (Savitzky–Golay procedure²⁴) or several voltamperograms recorded at subsequent mercury drops were averaged. In the standard procedure, background voltamperograms were always subtracted.

Data generation for simulation purposes. Voltamperograms of reversible systems were generated by use of equation (3). First, the semiderivative peaks for the cathodic and the anodic part were generated, then the whole curve was semiintegrated giving the artificial reversible voltamperogram. Different peak com-

binations were obtained by changing heights and potentials. The program was capable of generating them for different temperature values as well.

Semidifferentiation/semiintegration. A Grünwald definition of these operations (discrete differintegration)²⁵ was used in a modified first-order algorithm (G0 according to Oldham²⁶). This algorithm possesses very attractive features: it is fast, simple and can be used for both semidifferentiation and semiintegration (details can be found in the Appendix). There was no significant change in results when the higher order (G1) algorithm was used. In the implementation presented here, the operation on a curve containing 400 data points took approx. 2.8 sec (IBM PC/XT 8 MHz with coprocessor).

Detection of peak overlapping. The program recognized overlapping and non-overlapping peaks automatically. Test for peak overlapping was based on the check, whether two ranges of datapoints for fitting, as calculated for non-overlapping peaks (see below), overlap or not.

Fitting of non-overlapping peak border zones. This procedure was used at the free (non-overlapping) ends of peaks. Datapoints for fitting to equation (5) were selected around the peak border within a distance equal to 1/6 of the distance between peak border and peak top. The border of a peak, used in datapoints range selection, was defined as a point, in which the derivative is equal to 0.1% of its maximal value in the corresponding inflection point. The derivative calculations were carried out with Savitzky-Golay's "smooth derivative" method;²⁴ this enables typical noise enhancement caused by differentiation to be overridden. This definition of peak border has several advantages. It is independent of the presence of a baseline with a constant value; due to the very low value of the derivative (practically equal to zero in most situations), if peaks overlap, the border point is placed in the minimum at the curve between them. In case of real voltamperograms containing noise, the border point is selected at the place where noise becomes comparable to the signal. The situation, when the method doesn't give good results is a combination of a very low noise level and a baseline with a large slope.

As initial guesses of the parameters to be fitted, the peak height measured from the curve was used for h_0 , 0.1% of this value as y_B , E_{p0} was set to the value of the peak potential read from the curve and k_0 was calculated from the

datapoint with highest absolute value, using equation (5).

Fitting of data in the overlap zone. All datapoints constituting the middle 1/3 of the range between peak tops (minimum of 15 points) were fitted to equation (6). This choice was a compromise between requirements of the curve fitting (large number of points spread over the range) and assumptions, under which equation (6) was derived (small range covered by datapoints). Five parameters in this equation (y_B , h_0 , k_0 , h_1 and k_1) were fitted, while the other two (E_{p0} and E_{p1}) were directly estimated from the curve by using simple correction because their changes due to overlapping are relatively small. In the first generation of initial guesses, peak potentials (as read from the curve) were used for E_{p0} and E_{p1} , for h_0 and h_1 —directly measured peak heights, y_B was set to 0.1% of the highest value of h_0 or h_1 and k_0 and k_1 were calculated from the last datapoints at borders of the fitting range assuming, that curve there follows a pure \cosh^{-2} function. In the next step, the appropriate corrections for the positions of peak tops, due to overlapping, were calculated with guesses from the first generation. The second generation was then created consisting of corrected E_{p0} and E_{p1} values and new k_0 and k_1 values re-evaluated with new peak potentials. Finally, y_B , h_0 , k_0 , h_1 and k_1 were used in the curve-fitting procedure for refinement, while E_{p0} and E_{p1} were not corrected further.

The procedure used for curve-fitting was a least-squares one according to Wentworth.²⁷ Fitting was performed until corrections to h_0 , h_1 , k_0 and k_1 were smaller than 0.1%.

Removal of undesired peaks. After calculating all the necessary parameters, the baseline was drawn as a straight line, or, baseline points were calculated by using equation (7), depending on whether the removed peak overlaps or not. This procedure covered all points, for which the difference between the original and the new value exceeded 3%.

RESULTS AND DISCUSSION

The method presented can be applied to the separation of voltammetric peaks in two situations. The first one occurs when both overlapping peaks are present in the same branch, either cathodic or anodic, and the second one occurs when they lie in different branches of the voltamperogram. This latter application deals with the separation of cathodic and anodic

peaks. It is well known, that in studies of reduction of substances, the anodic peak appears at the "tail" of the cathodic one and consequently the measured anodic current is a sum of the cathodic and anodic contributions (this can easily be seen when the voltamperogram is plotted in $i-t$ coordinates instead of $i-E$). From the point of view of peak separation, this situation is similar to the first case, where the latter cathodic peak rises from the "tail" of the previous one. Application of the presented method allows the anodic peak current (an important parameter in mechanistic investigations) to be read directly from the processed voltamperogram.

In the practical part both applications were checked with generated voltammetric curves. To check if the shape of the remaining peak is not influenced by the procedure, four peak parameters were tested: peak potential, peak current and potentials of inflection points. Inflection points were chosen for characterization, because in contrast to the half-peak potentials, their positions are not influenced by a constant or linearly varying background. In order to check the method in reality, two experiments with real electrochemical systems were also performed.

The developed program worked relatively fast: a separation of the voltamperogram of two systems took typically 20–80 sec, depending on the noise (which slowed down curvefitting) and the total number of points (increasing differentiation time). In comparison to the method described by Perone *et al.*,³ a high number of decisions is done by the program, so no special skill, experience or extensive knowledge about the algorithm principles is demanded from the operator.

Calculations with generated data

For artificially generated cyclic voltamperograms two series of tests were carried out. In the first, a pair of peaks (cathodic and anodic), simulated for a reversible electrode reaction was separated giving the anodic peak. Because in the process of semidifferentiation only points preceding the investigated one are included in calculations of the semiderivative value, removal of the anodic peak does not influence the cathodic one. The error in the peak current (i_{pa}) in separated voltamperograms can be expected to depend on the difference between the peak potential and the potential of the turning point ($E_{pc}-E_{turn}$).

An example of this separation is shown in Fig. 2. Errors in the anodic peak current, i_{pa} , and the anodic peak potential, E_{pa} , as a function of the difference between cathodic peak potential (E_{pc}), and the potential turning point (E_{turn}) are collected in Table 1. It can be seen, that for $E_{pc}-E_{turn} > \sim 75$ mV, the error in peak current was less than 1%, but for very small distances it grew rapidly.

As far as the potential of the anodic peak is concerned, its shift was less than 1 mV if the distance, $E_{pc}-E_{turn}$, was 80 mV or more (data points were generated with an interval of 0.98 mV). It is not clear, why two values of errors in E_{pa} , for $E_{pc}-E_{turn}$ in range of 200–300 mV, deviate from the general trend.

The second test with generated data was carried out in order to find a separation limit for peaks occurring in one branch of the voltamperogram and to study errors in their parameters obtained with the proposed procedure. For this purpose, artificial voltamperograms of two reversible systems were first added up and then separated (heights of cathodic peaks were equal). The parameters obtained were compared with their initial values (an example of the results is presented in Fig. 3, where the voltamperogram containing 2 anodic and 2 cathodic peaks is drawn together with the results obtained—two separated voltamperograms of each system). All results of this test (errors in i_p , E_p and potentials of inflection points, E_{asc}^{inf} and E_{desc}^{inf}) for all four peaks are collected in Tables 2–5. It can be seen, that errors are small and have a random character with increasing absolute values for smaller peak distances. Single values deviating from the general trend are due to the discontinuities of the peak function at points where replacement stops. If such discontinuity appears very close to, for example, the inflection point, the obtained respective parameter will be influenced more strongly. The limit of separation, 110 mV for a one-electron process, was determined by the convergence of the curve-fitting. Below this value, real potentials of semiderivative peaks differ significantly from values estimated from the overlapped curve, and fitting doesn't converge. This separation limit appears to be smaller than the one presented in a comparable method.³

Experimental data

The method was checked with real electrochemical systems as well. In two series, a couple of reversible + reversible systems and a couple

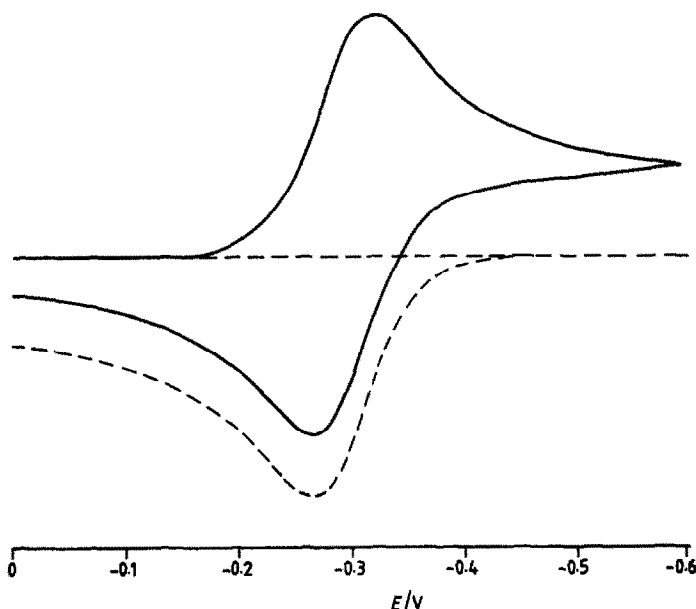


Fig. 2. Generated voltamperogram of one-electron reversible system. Peak potential $E_{pc} = -0.329$ V, potential of turning point $E_{turn} \approx -0.6$ V, scan rate 0.1 V/sec, potential step 4 mV, temperature 298 K (solid line) and result of removing the cathodic peak (dashed line).

of non-reversible + non-reversible systems were separated. As an example of the first case, a solution of $\text{In}^{3+} + \text{Tl}^{+}$ ions (ΔE^0 approx. 115 mV) was prepared with concentrations of 2×10^{-5} and $6 \times 10^{-5} M$, respectively (voltammetric peaks with approximately equal heights). Voltamperograms were recorded with a scan rate of 0.66 V/sec with a potential step of 1.6 mV. Figure 4 presents one of these voltamperograms and two curves obtained as a result of the processing. From the procedure outlined above it could be expected that no baseline remains. However, for the In^{3+} peak a small potential-dependent baseline is observed, which

can be attributed to the small number of points. This number is determined by the lowest potential step height that can be realized with the 12-bits D/A converter of the measuring system.

In the second experiment, a mixture of Zn^{2+} and Co^{2+} ions (both concentrations $10^{-4} M$) in 1M potassium chloride was examined with a scan rate of 1.0 V and a potential step of 3.6 mV. Results of the experiments and experimental conditions are collected in Tables 6 and 7.

In both cases, only cathodic peaks are reported, because with the experimental set-up (relatively small mercury drop) and the potential sweep rate limited by keeping potential step height small, a strong accumulation effect for $\text{In}^{3+} + \text{Tl}^{+}$ couple occurred, significantly changing the shape of anodic peaks. This change was large enough to set the convergence limit of curve-fitting above 115 mV. In case of the reduction of Co^{2+} ions, no anodic peak was observed.

All voltamperograms had to be smoothed before processing, because in case of a high S/N ratio, the determination of the peaks borders as described and the curve fitting do not give good results. However, in the authors' experience problem of high noise was encountered very seldom and it was always possible to overcome it by the averaging of several voltamperograms. It should be noted that background subtraction is very important for good performance of the

Table 1. Errors in the anodic peak potential (E_{pa}) and the current (i_p) as a function of the difference between cathodic peak potential (E_{pc}) and turning point potential (E_{turn}) for the generated reversible voltamperogram of one system (absolute values). Conditions: $n = 1$, $D_{ox} = D_{red}$, $T = 298$ K, potential step 0.98 mV

$E_{pc} - E_{turn}$, V	$\Delta i_p / i_p$, %	ΔE_p , mV
0.041	3.69	4.5
0.051	2.52	4.3
0.071	1.11	3.3
0.096	0.4	2.6
0.121	0.17	1.6
0.171	0.08	0.4
0.221	0.04	1.7
0.271	0.05	1.3
0.321	0.02	0.2
0.421	0.09	0.3

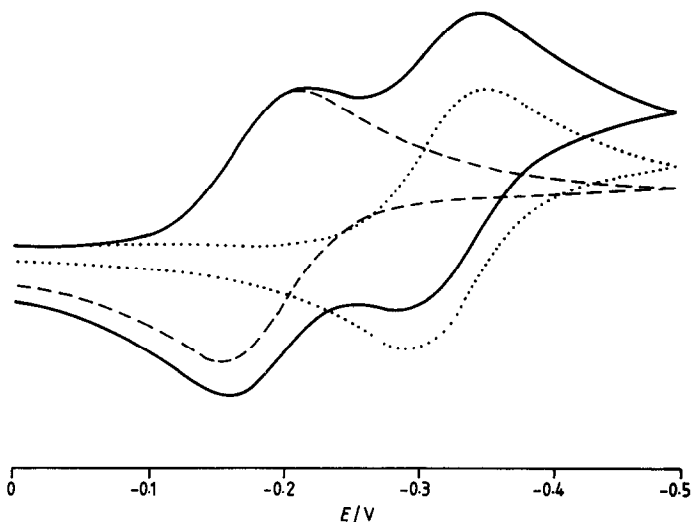


Fig. 3. Solid line: generated voltamperogram of the mixture of two one-electron reversible systems: $E_{pc1} = -0.219$ V, $E_{pc2} = -0.359$ V, $E_{turn} = -0.5$ V, scan rate 0.1 V/sec, potential step 2 mV; dashed line: result of removing of the contribution of the second system; dotted line: result of removing of the contribution of the first system.

routine because semidifferentiation changes a constant or a linear background of the voltamperograms into baselines of complicated shapes²¹ in the semiderivative domain and assumptions about a linear form of the background become invalid.

Table 2. Errors in peak potentials obtained as a result of separation of single systems from the generated voltamperogram of two reversible systems in dependence on formal potentials (E^0) difference (absolute values). Conditions: equal concentrations, $n_1 = n_2 = 1$, all diffusion coefficients equal, $T = 298$ K, potential step 0.98 mV. C1 and A1 refer to peaks of system 1 (easier reducible), C2 and A2 refer to system 2

$\Delta E^0, V$	$\Delta E_{pc1}, mV$	$\Delta E_{pa1}, mV$	$\Delta E_{pc2}, mV$	$\Delta E_{pa2}, mV$
0.110	0.5	0.2	1.2	0.3
0.115	0.4	0.4	0.8	0.9
0.120	0.0	0.3	0.1	0.1
0.125	0.6	0.5	0.2	0.8
0.130	0.6	0.3	0.7	0.3
0.140	0.5	3.0	0.2	1.1
0.150	2.1	0.4	0.4	2.0
0.160	1.5	0.4	0.4	2.0
0.170	0.4	0.4	0.4	1.6

Table 3. Errors in peak currents obtained as a result of separation of single systems from the generated voltamperogram of two reversible systems in dependence on formal potentials (E^0) difference (absolute values). Conditions: equal concentrations, $n_1 = n_2 = 1$, all diffusion coefficients equal, $T = 298$ K, potential step 0.98 mV. C1 and A1 refer to peaks of system 1 (easier reducible), C2 and A2 refer to system 2

$\Delta E^0, V$	$\Delta i_{pc1}/i_{pc1}, \%$	$\Delta i_{pa1}/i_{pa1}, \%$	$\Delta i_{pc2}/i_{pc2}, \%$	$\Delta i_{pa1}/i_{pa1}, \%$
0.110	0.59	1.39	0.78	1.09
0.115	1.23	3.19	3.17	1.55
0.120	0.57	1.13	1.44	0.17
0.125	1.10	1.51	1.67	0.43
0.130	0.5	0.82	0.11	0.28
0.140	0.24	1.84	0.56	0.47
0.150	0.26	0.61	0.81	0.81
0.160	0.56	0.57	0.74	1.23
0.170	0.11	0.56	0.76	0.70

Table 4. Errors in potentials of inflection points on ascending branches of peaks obtained as a result of separation of single systems from the generated voltamperogram of two reversible systems in dependence on formal potentials (E^0) difference (absolute values). Conditions: equal concentrations, $n_1 = n_2 = 1$, all diffusion coefficients equal, $T = 298$ K, potential step 0.98 mV. C1 and A1 refer to peaks of system 1 (easier reducible), C2 and A2 refer to system 2

$\Delta E^0, V$	$\Delta E_{pc1}^{infl,asc}, mV$	$\Delta E_{pa1}^{infl,asc}, mV$	$\Delta E_{pc2}^{infl,asc}, mV$	$\Delta E_{pa2}^{infl,asc}, mV$
0.110	3.5	0.2	0.0	0.2
0.115	1.4	0.1	0.3	1.4
0.120	0.1	0.9	0.8	0.3
0.125	0.7	0.5	0.5	0.8
0.130	0.4	0.9	0.4	0.4
0.140	0.9	0.3	3.2	0.0
0.150	0.3	0.5	0.6	0.7
0.160	0.5	3.8	4.4	0.4
0.170	0.7	0.0	0.1	0.3

Table 5. Errors in potentials of inflection points on descending branches of peaks obtained as a result of separation of single systems from the generated voltamperogram of two reversible systems in dependent on formal potentials (E^0) difference (absolute values). Conditions: equal concentrations, $n_1 = n_2 = 1$, all diffusion coefficients equal, $T = 298$ K, potential step 0.98 mV. C1 and A1 refer to peaks of system 1 (easier reducible), C2 and A2 refer to system 2

$\Delta E^0, V$	$\Delta E_{pc1}^{infl,desc}, mV$	$\Delta E_{pa1}^{infl,desc}, mV$	$\Delta E_{pc2}^{infl,desc}, mV$	$\Delta E_{pa2}^{infl,desc}, mV$
0.110	0.2	0.4	0.0	1.1
0.115	0.5	0.7	0.7	0.6
0.120	0.4	0.5	0.3	0.5
0.125	0.6	0.5	0.3	0.4
0.130	0.4	0.4	0.1	0.4
0.140	0.5	0.3	0.2	0.6
0.150	0.7	0.7	0.3	0.8
0.160	0.4	0.7	0.3	0.3
0.170	2.1	1.1	0.3	0.9

CONCLUSIONS

The method presented here can be applied to the resolution of overlapping LSV or CV peaks originating from both reversible and non-reversible systems with reliable results. When used for the separation of peaks in one branch (cathodic or anodic), a resolution limit of 110 mV (reversible case, one electron transfers) could be obtained.

When resolving peaks lying in different branches of the cyclic voltammetric curve, the anodic and cathodic peak of the investigated system, free from a cathodic or anodic peak influence, respectively, can be obtained. Precision of the calculated peak parameters depends in this case on the distance between peak top and the turning point of the voltamperogram.

Accumulation in the mercury drop influences the shape of the semiderivative peaks in the anodic segment and increases the minimal distance between the two peaks that can be resolved. When two voltammetric peaks strongly

overlap and the accumulation effect occurs, the anodic part of the voltamperogram sometimes cannot be separated even though the cathodic part can.

The algorithm needs hardly any decisions by the operator, which is an attractive feature when

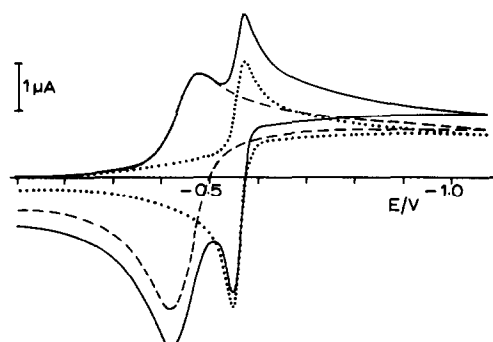


Fig. 4. Experimental cyclic voltamperogram of the $Tl^+ + In^{3+}$ mixture (experimental conditions as in Table 6) (solid line) and the individual contributions calculated by the procedure described: dashed line— Tl^+ ion contribution, dotted line— In^{3+} contribution.

Table 6. Errors in parameters of the cathodic peak obtained by the separation of peak of interest from a voltamperogram of two reversible systems—experimental data. Experimental conditions: solution $\text{In}^{3+} + \text{Tl}^+$ ($2 \times 10^{-5}M + 6 \times 10^{-5}M$ in $1M$ KCl, ΔE^0 115 mV), scan rate: 0.66 V/sec, potential step: 1.6 mV

System	$\Delta i_p/i_p$, %	ΔE_p , mV	ΔE_{asc}^{inf} , mV	ΔE_{desc}^{inf} , mV
Tl ⁺ /Tl	-0.31	-2.3	-0.7	-2.8
In ³⁺ /In	-0.31	-1.8	-0.4	-1.5

Table 7. Errors in parameters of the cathodic peak obtained by separation of the peak of interest from a voltamperogram of two irreversible systems—experimental data. Experimental conditions: solution $\text{Zn}^{2+} + \text{Co}^{2+}$ ($10^{-4}M + 10^{-4}M$ in $1M$ KCl, ΔE_p 440 mV), scan rate: 1.0 V/sec, potential step: 3.6 mV

System	$\Delta i_p/i_p$, %	ΔE_p , mV	ΔE_{asc}^{inf} , mV	ΔE_{desc}^{inf} , mV
Zn ²⁺ /Zn	+1.6	-1	-5	+1.2
Co ²⁺ /Co	+5.8	-2	-3	-9

the automatic processing of voltamperograms is concerned. This implies that the program can be used by personnel having little experience in using electrochemical methods.

APPENDIX

The Grünwald definition of discrete differintegration is:

$$\frac{d^u f(t_j)}{dt^u} = \lim_{N \rightarrow \infty} \left[\frac{(N/t')^u}{\Gamma(-u)} \sum_{j=1}^N \frac{\Gamma(N-j-u)}{\Gamma(N-j+1)} f(t_j) \right]$$

where $f(t_j)$ is a value of the function to be differintegrated at time t_j , N is the number of evenly spaced points preceding the point t_j , t' is the time interval between points, u is the instance of differintegration (1/2 for semidifferentiation and -1/2 for semiintegration). This equation can be rewritten in the convolutional form

$$\begin{aligned} \frac{d^u f(t_j)}{dt^u} &= \lim_{N \rightarrow \infty} \left[(N/t')^u \sum_{j=1}^N \frac{\Gamma(N-j-u)}{\Gamma(-u)\Gamma(N-j+1)} f(t_j) \right] \\ &= \lim_{N \rightarrow \infty} \left[(N/t')^u \sum_{j=1}^N w_j f(t_j) \right] \end{aligned}$$

where w_j are values of a weighting function depending only on u and N . This reformulation gives an approach equivalent to the G0 algorithm described by Oldham.²⁶

Inspection of the last w_j values gives:

$$W_N = \frac{\Gamma(N-N-u)}{\Gamma(-u)\Gamma(N-N+1)} = 1$$

$$w_{N-k} = \frac{\Gamma(N-N+k-u)}{\Gamma(-u)\Gamma(N-N+k+1)} = \frac{\Gamma(k-u)}{\Gamma(-u)\Gamma(k+1)}$$

$$\begin{aligned} W_{N-k-1} &= \frac{\Gamma(N-N+k+1-u)}{\Gamma(-u)\Gamma(N-N+k+2)} \\ &= \frac{(k-u)\Gamma(k-u)}{(k+1)\Gamma(-u)\Gamma(k+1)} = \frac{k-u}{k+1} W_{N-k} \end{aligned}$$

and leads to the general recursive formula

$$W_j = \frac{k-u}{k+1} W_{j+1}, \quad W_N = 1$$

where k is an index counting from the end, $k = N - j - 1$.

This definition makes the weighting function independent of the value of N . It can be found, that for differintegration of a set of N points it is enough to calculate the set of N weights only once at the beginning and then differintegration becomes a summation of weighted point values. This approach allows one to make a very compact and simple algorithm for differintegration, in which, after calculation of weights, only n multiplications and $n-1$ additions (plus one multiplication by a normalizing factor) are to be done in order to calculate the differintegral value in j -th point.

GLOSSARY

A	electrode surface area
c	concentration
D	diffusion coefficient
E	actual electrode potential
$E_{1/2}$	potential of polarographic halfwave of the compound
E_{p0}, E_{p1}	parameters related to potential at which semiderivative peak # 0 and # 1 appear
F	Faraday constant
h	semiderivative peak height
h_0, h_1	parameters related to height of respectively semiderivative peak # 0 and # 1
$i, i(t)$	current
k	parameter describing width of the semiderivative peak
k_0, k_1	parameters related to width of respectively semiderivative peak # 0 and # 1
n	number of electrons involved in electrode process
N	actual number of the point, counting from the lower limit of the semiderivative
s	slope of the baseline in semiderivative domain
T	absolute temperature

t'	time interval between two subsequent points
u	instance of differintegration
v	scan rate
w_j	weight for point j
y	value of semiderivative of the current in respect to time
y_A, y_B	baseline value at semiderivative peak border
y_0	constant term in linear baseline equation, obtained from combination of baseline values at both peak borders.

REFERENCES

1. W. F. Gutknecht and S. P. Perone, *Anal. Chem.* 1970, **42**, 906.
2. J. F. Rusling and T. F. Connors, *ibid.*, 1983, **55**, 776.
3. S. P. Perone, J. W. Frazer and A. Kray, *ibid.*, 1971, **43**, 1485.
4. P. A. Boudreau and S. P. Perone, *ibid.*, 1979, **51**, 811.
5. M. Goto and D. Ishii, *J. Electroanal. Chem.* 1975, **61**, 361.
6. P. Dalrymple-Alford, M. Goto and K. B. Oldham, *Anal. Chem.* 1977, **49**, 1390.
7. K. B. Oldham, *ibid.*, 1972, **44**, 196.
8. M. Goto and D. Ishii, *J. Electroanal. Chem.* 1979, **102**, 49.
9. K. B. Oldham and J. Spanier, *ibid.*, 1970, **26**, 331.
10. C. P. Andrieux, L. Nadjo and J. M. Savéant, *ibid.*, 1970, **26**, 147.
11. J. C. Myland, K. B. Oldham and C. G. Zoski, *ibid.*, 1985, **193**, 3.
12. J. C. Imbeaux and J. M. Savéant, *ibid.*, 1973, **44**, 169.
13. F. Ammar and J. M. Savéant, *ibid.*, 1973, **47**, 215.
14. L. Nadjo, J. M. Savéant and D. Tessier, *ibid.*, 1974, **52**, 403.
15. J. M. Savéant and D. Tessier, *ibid.*, 1975, **61**, 251.
16. *Idem*, *ibid.*, 1975, **65**, 57.
17. *Idem*, *ibid.*, 1977, **77**, 225.
18. P. Dalrymple-Alford, M. Goto and K. B. Oldham, *ibid.*, 1977, **85**, 1.
19. K. B. Oldham, *S.I.A.M. J. Math. Anal.* 1983, **14**, 974.
20. D. E. Smith, *Anal. Chem.* 1976, **48**, 517A.
21. K. B. Oldham and C. G. Zoski, *J. Electroanal. Chem.* 1983, **145**, 265.
22. J. J. Toman and S. D. Brown, *Anal. Chem.* 1981, **53**, 1497.
23. D. M. Caster, J. J. Toman and S. D. Brown, *ibid.*, 1983, **55**, 2143.
24. A. Savitzky and M. J. E. Golay, *ibid.*, 1964, **36**, 1627.
25. K. B. Oldham and J. Spanier, *The Fractional Calculus*, Academic Press: New York, London, 1974.
26. K. B. Oldham, *J. Electroanal. Chem.* 1981, **121**, 341.
27. W. E. Wentworth, *J. Chem. Ed.* 1965, **42**, 96.

ELIMINATION OF THE COPPER-ZINC INTERFERENCE IN ANODIC STRIPPING VOLTAMMETRY BY ADDITION OF A COMPLEXING AGENT

ALDALEA LOPES BRANDES MARQUES (Dep. Tecnologia Quimica/UFMA) and
GILBERTO ORIVALDO CHIERICE* (IFQSC/USP/Sao Carlos)
Caixa Postal 369, CEP 13560, Sao Carlos/SP, Brazil

(Received 24 September 1990. Revised 22 December 1990. Accepted 14 January 1991)

Summary—The addition of cyanide and Triton X-100 suppress the formation of the Cu-Zn intermetallic compound in ASV making it possible to determine traces of zinc(II) in the presence of an excess of copper ions. The precision of the method (5%) and the accuracy (error of 1.4%) in sea water are satisfactory.

The formation of Cu-Zn intermetallic compounds causes interferences in the analysis of either element by anodic stripping voltammetry (ASV), particularly when working with a mercury film electrode (MFE).¹ The addition of gallium can successfully displace copper to form a much more stable copper-gallium compound.² However, the method does not give good recovery for solutions in which the copper content is higher than that of zinc.³ Other methods which may be used include the use of a twin-electrode thin-layer cell in which copper and zinc are deposited at two different working electrodes⁴ and a method where the generalized standard addition technique is applied to eliminate the interference.⁵ However, neither of these methods is simple or universally applicable.

Although a complexing agent to eliminate the Cu-Zn interference in ASV has not yet been suggested, the use of such reagents to solve other metallic interferences in ASV has been studied.⁶⁻⁸ The present work investigates the possibility of using the known reaction between cyanide and the cupric ion to prevent the formation of Cu-Zn intermetallic compounds in ASV. The strong $\text{Cu}(\text{CN})_4^{2-}$ complex does not show a d.c. polarographic reduction wave because its half-wave potential is very negative.⁹ On this basis we have extended the use of cyanide as a masking agent for copper in a supporting electrolyte in the determination of zinc by ASV. The results obtained show a recovery of 100% for the zinc peak in the presence of an excess of copper. A procedure is

described for the determination of zinc in standard solutions and sea water samples.

EXPERIMENTAL

Apparatus

Voltammetric measurements were made with a hanging mercury drop electrode (HMDE) and a MFE in a PAR Model 174A polarographic analyser connected with a PAR model 303 electrode and a PAR model 0089 X-Y recorder. A 0.6-cm diameter glassy-carbon disk electrode was used as a substrate for the mercury film. The MFE was adapted to a PAR system model 303 (Fig. 1). The glassy-carbon disk was inserted into a Pyrex glass tube, which was attached to the glass capillary tube of the HMDE. The electric contact was obtained with the mercury inside the glass tube and the mercury from the capillary. Such a system is very easily constructed and can be extended to other solid electrodes.

The electrode was polished with 0.3 μm of alumina powder each day. Preformed MFE was plated with mercury in a 40-mg/l. $\text{Hg}(\text{II})$ -1M sodium nitrate solution at pH 2, acidified with nitric acid.

All glassware, plastic containers, utensils, etc., were soaked for several days in 7M nitric acid and then rinsed with Millipore Milli-Q water before use. The addition of reagents and the dilutions were done with automatic micropipettes.

Reagents

The metals standard solutions were prepared by diluting A.A.S. standard (1000 mg/l.). Nitric

*Author for correspondence.

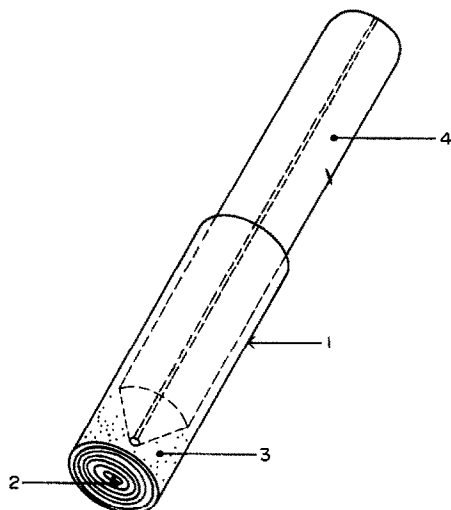


Fig. 1. Adaptation scheme of the glassy-carbon electrode to PAR model 303 electrode. (1) pyrex tube (\varnothing , 6 mm); (2) glassy-carbon disk (\varnothing , 5 mm); (3) compartment filled with mercury; (4) glass capillary referent to the hanging mercury drop electrode.

acid was of suprapure grade (Merck). All the solutions were prepared with Millipore Milli-Q water. Super dry nitrogen was used to remove dissolved oxygen.

The sodium perchlorate and phosphate buffer solutions were purified with liquid-liquid extraction with sodium diethyldithiocarbamate in tetrachloride media. A sea water sample was collected, filtered (0.45- μm pore size) and stored naturally and in acidic media (nitric acid) at 1°.

Procedures

After the electrode^{1,3} was prepared it was removed from the plating solution, rinsed carefully with ultrapure water and then transferred to the cell for measurements. A freshly prepared deposit was used in each experiment.

The measurements were performed in a cell, with a suitable aliquot (limited to 10 ml) of standard or sample solution. The pH was adjusted to 8.5 with 100 μl of a 1M phosphate buffer. In this medium, Triton X-100 (10⁻⁴% *v/v*) and cyanide were added for the copper complexation reaction. The solution was then purged with nitrogen for 20 min. The preconcentration potential was applied to the working electrode in the stirred solution and after a 30-sec rest period a positive-going scan was initiated and the resulting voltamperogram recorded. Aliquots of the zinc(II) standard solution were then added and the precon-

centration/oxidation cycle was repeated with a MFE or a new mercury drop.

For the determination of zinc the $\text{CN}^-/\text{Cu(II)}$ ratio must be high to eliminate the copper peak. The zinc peak, in a solution containing 40 $\mu\text{g/l}$. zinc ions and 40 $\mu\text{g/l}$. copper ions, has previously been found to tolerate a large excess of cyanide, up to 4.600 $\mu\text{g/l}$., but here a different response was evident. A decrease in the slope of the calibration curve was observed leading to an increase in the recovery from 96 to 150%. A $\text{CN}^-/\text{Cu(II)}$ ratio between 20 and 50 alters the background curve but does not change the slope; ratio values close to 20 are generally sufficient. On the other hand, the $\text{CN}^-/\text{Cu(II)}$ ratio also depends on the $\text{Cu(II)}/\text{Zn(II)}$ ratio. Therefore, a $\text{CN}^-/\text{Cu(II)}$ ratio range of 15–50 was considered ideal.

The polarographic parameters were as follows: accumulation potential (E_a), -0.9V or -1.3V; scan direction, positive; pre-electrolysis time, 1–10 min; rest time, 30 sec; DPASV/HMDE: scan rate, 5 mV/sec; pulse amplitude, 50 mV; drop time, 0.5 sec; DCASV/MFE: scan rate, 20 or 50 mV/sec.

RESULTS AND DISCUSSION

Copper-zinc interference

Previous reports have described that inter-metallic interferences are more pronounced at MFE's, which has been detected whenever the MFE has been used, regardless of the experimental conditions.^{1,3} To provide a direct observation of the severity of the problem the MFE was used for this study.

To establish the effect of the Cu-Zn interference on stripping voltammetry zinc ions from a 200 $\mu\text{g/l}$. solution were deposited at a preformed MFE for 2 min at -1.3V and stripped with the subsequent positive scan which produced a well defined zinc wave (Fig. 2, curve 2). When the same experiment was repeated with 100 $\mu\text{g/l}$. Cu(II) in the sample, a 50% depressed zinc wave was recorded along with an enhanced copper wave (Fig. 2, curve 3). Curve 4 shows the same experiment but the electrode was plated at -0.9V (where zinc is not reduced) and the copper wave is smaller. This fact provides evidence that the Cu-Zn compound is oxidized at the same potential as copper inducing two errors, positive and negative, for both copper and zinc respectively, when the electrode is plated at -1.3V.

Elimination of Cu-Zn interference

Five different complexing agents were tested, based on the stability of the formed complex, disodium ethylenediaminetetracetate, azide, thiocyanate, diethanoldithiocarbamate and cyanide; the last presented the best applicability and experimental results. This is confirmed by the stability constants of the $\text{Cu}^{\text{I}}(\text{CN})_4^{3-}$ ($\log \beta_4 = 30$) and $\text{Zn}^{\text{II}}(\text{CN})_4^{2-}$ ($\log \beta_4 = 19$) complexes.¹⁰

The magnitude of the error due to Cu-Zn interference and its elimination by cyanide addition on the working electrolyte is illustrated in Fig. 3. Curve 1 shows a zinc peak depression due to the addition of copper and curve 2 shows the zinc peak recovery in the same sample, obtained by addition of cyanide at pH 8.5.

Figure 4 shows the zinc(II) calibration curves between 20 and 210 $\mu\text{g}/\text{l}$. in a solution containing 20 $\mu\text{g}/\text{l}$. Cu(II) in the absence (curve 1) and presence (curve 2) of cyanide. Curve 1 is not linear while the curve 2 is linear in the 20–170 $\mu\text{g}/\text{l}$. concentration range. This suggests that in the absence of cyanide there is a formation of successive complexes of Cu-Zn intermetallic compounds.

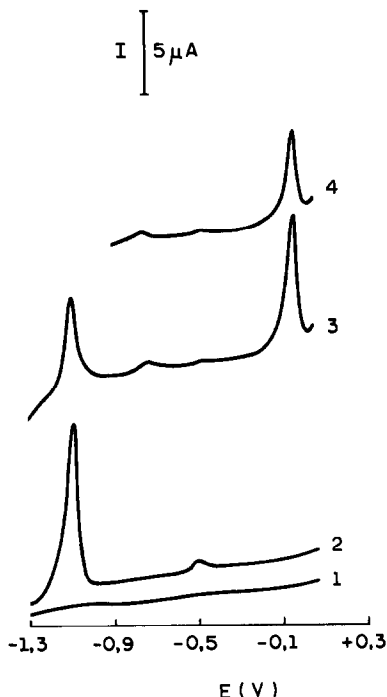


Fig. 2. Effect of the Cu-Zn interference on stripping voltammetry. Deposition potential of (1–3), -1.3 V; (4), -0.9 V; deposition time, 2 min. Scan (1), $0.02M$ NaClO_4 ; scan (2), (1) + 200 $\mu\text{g}/\text{l}$. $\text{Zn}(\text{II})$; scan (3), (2) + 100 $\mu\text{g}/\text{l}$. $\text{Cu}(\text{II})$; scan (4), replicate scan (3).

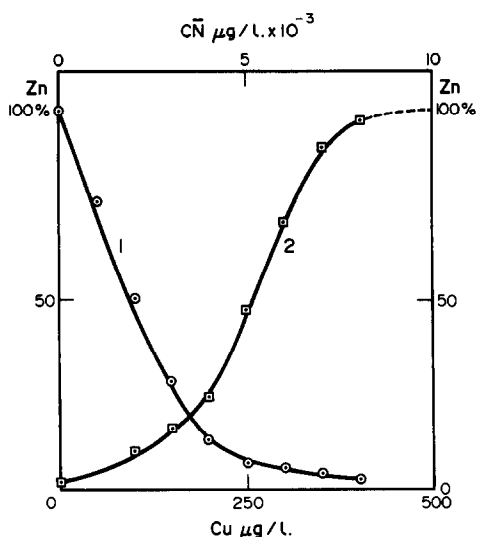


Fig. 3. Occurrence and elimination of Cu-Zn interference. Deposition potential, -1.3 V; deposition time, 1 min; pH 8.5; $0.02M$ NaClO_4 ; 200 $\mu\text{g}/\text{l}$. $\text{Zn}(\text{II})$. Curve 1, zinc peak depression (current, %) vs. copper(II) concentration; Curve 2, zinc peak recovery (current, %) vs. cyanide concentration.

These satisfactory results obtained when the copper concentration in the solution is higher than that of zinc (Fig. 3) confirm the applicability of the proposed method, in contrast to the gallium addition method where, under the same conditions, the magnitude of interference is only lowered.³

The observed behaviour can be explained by the fact that the strong complexation of copper(I) by cyanide shifts its reduction potential to a more cathodic region than that where zinc(II) reduction occurs. In fact, the calculated potential shift is about $-0.94V$ for the $\text{Cu}(\text{I})/\text{Cu}(\text{Hg})$

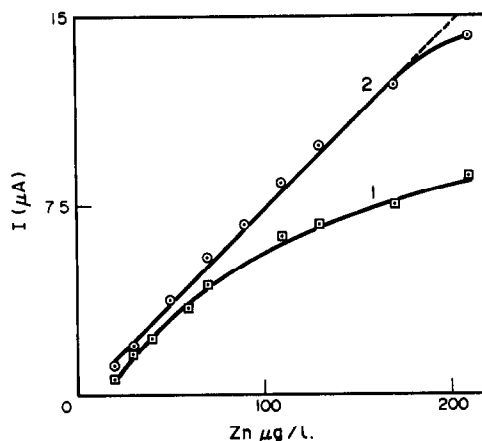


Fig. 4. Calibration curves of zinc(II) in the absence (Curve 1) and presence (Curve 2) of cyanide. Deposition potential, -1.3 V; deposition time, 2 min; pH 8.5; $0.02M$ NaClO_4 ; 20 $\mu\text{g}/\text{l}$. $\text{Cu}(\text{II})$; 400 $\mu\text{g}/\text{l}$. CN^- .

system and only -0.15V for the Zn(II)/Zn(Hg) system:

$$\Delta E_{\text{Cu(II)}}^0 = -0.059 \log \beta_4[\text{CN}^-]^4 = -0.94\text{V}$$

$$\Delta E_{\text{Zn(II)}}^0 = -0.029 \log \beta_4[\text{CN}^-]^4 = -0.15\text{V}$$

It has been found that the presence of $10^{-4}\%$ (v/v) of Triton X-100, as suggested in the literature,^{6,7} gave a better definition of the anodic peak of zinc. Thus all working solutions contain this non-ionic surfactant.

Influence of pH

The effect of pH was studied by measurement at a fixed concentration of $50 \mu\text{g/l}$. zinc(II), $25 \mu\text{g/l}$. copper(II) and $500 \mu\text{g/l}$. CN^- over the pH range 7–10. The experiments showed that zinc peak height was affected by pH variations in the presence of phosphate buffer and that the peak-height for zinc was greatest at pH 8–9.

Practical application

Voltammetric methods are most suitable for the analysis of saline water because it is an ideal electrolyte for voltammetry.¹¹

The proposed method was tested by zinc determination in a standard solution and a sea water sample. The determination of zinc in the presence of copper in standard solution, showed good recovery (95%) at low concentrations ($2 \mu\text{g/l}$), which indicates that the method can be used in sea water. The same procedure was applied in a sea water sample (Fig. 5): Curves 1–2, in Fig. 2, shows the occurrence of the interference, in sea water; Curve (3), its elimination; Curves (4–6), the reproducibility of the measurements and curves (7–9), the standard additions of zinc(II). Before, copper was determined at -0.9V (where the zinc is not deposited) and the necessary cyanide concentration was calculated according to copper concentration. After, an aliquot with a 10-fold excess of cyanide over copper was added to mask copper (curve 3). In this way zinc was determined at -1.3V with a collection period of 10 min. In both cases the two metals were determined by the standard addition method without prior decomposition of the organic matter because in preliminary tests it had been found that wave form was not influenced by dissolved organic matter. This means that the determination corresponds only to the free zinc species.

A comparison of the zinc content found by DPASV/HMDE and DCASV/MFE was used

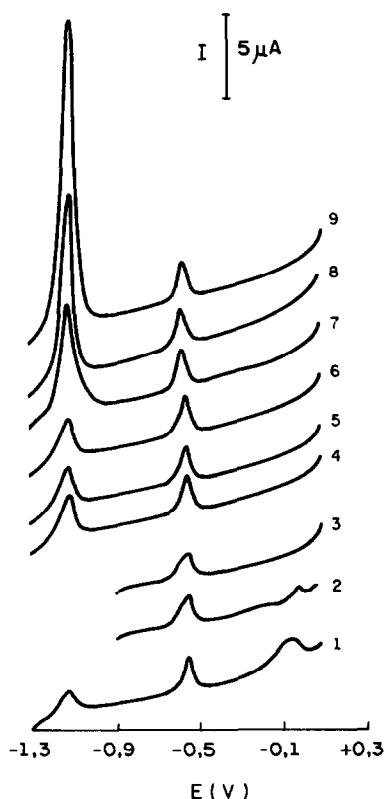


Fig. 5. DCASV/MFE scans of sea water after 10 min collection. Scan rate, 20 mV/sec ; pH 8.5; deposition potentials of (1) and (4–9), -1.3 V ; (2–3), -0.9 V ; scans (1–2), sea water; scan (3), (2) + $100 \mu\text{g/l}$. CN^- ; scans (4–6), 3 replicates of the scan (3); scan (7), (6) + $19.42 \mu\text{g/l}$. Zn(II) ; scan (8), (6) + $38.83 \mu\text{g/l}$. Zn(II) ; scan (9), (6) + $58.25 \mu\text{g/l}$. Zn(II) .

to evaluate the relative accuracy of the proposed method, based on the fact that the copper–zinc interference was not observed in the HMDE at this concentration. A sea water sample was analysed 3 times in succession and the results showed good agreement between the obtained results by DCASV/MFE [$7.1 \mu\text{g/l}$. Zn(II)] and DPASV/HMDE [$7.2 \mu\text{g/l}$. Zn(II)].

The precision was evaluated by means of 3 replicate analysis of a sea water sample. The relative standard deviation for zinc, when CN^- ions were present, was 5%.

CONCLUSION

The present work shows a new manner to eliminate the interference of copper on the determination of zinc by ASV. The method involves additions of cyanide, which avoid the formation of the Cu–Zn intermetallic compounds because the $\text{Cu}^{(II)}(\text{CN})_4^{3-}$ complex is not reduced, consequently there is no diffusion of copper ions to the drop.

Acknowledgement—The authors are grateful to Professor Eduardo A. Neves and Professor Auro A. Tanaka for their suggestions and comments on the manuscript.

This work was supported by the "Coordenadoria de Capacitação e Aperfeiçoamento do Pessoal de Ensino Superior—CAPES".

REFERENCES

1. J. A. Wise, D. A. Roston and W. R. Heineman, *Anal. Chim. Acta*, 1983, **154**, 95.
2. T. R. Copeland, R. A. Osteryoung and R. K. Skogerboe, *Anal. Chem.*, 1974, **46**, 2093.
3. J. Obiols, R. Devesa and A. Malet, *Analyst*, 1988, **113**, 1529.
4. D. A. Roston, E. E. Brooks and W. R. Heineman, *Anal. Chem.*, 1979, **51**, 1728.
5. R. W. Gerlach and B. R. Kowalski, *Anal. Chim. Acta*, 1982, **134**, 119.
6. J. Opydo, *Mikrochim. Acta*, 1989, **II**, 15.
7. S. Tanaka, Y. Morimoto, M. Taga and H. Yoshida, *Talanta*, 1983, **30**, 867.
8. J. Hernández-Méndez, R. Carabias-Martínez and J. I. García-García, *Anal. Chim. Acta*, 1981, **132**, 59.
10. Ju. Lurie, *Handbook of Analytical Chemistry*, p. 293. Mir. Publishers, Moscow, 1975.
11. J. Wang, *Stripping Analysis*, p. 110. VCH Publishers Inc., Florida, 1985.

VOLTAMMETRIC MEASUREMENT OF HALOPERIDOL FOLLOWING ADSORPTIVE ACCUMULATION AT GLASSY-CARBON ELECTRODES

PENG TUZHI,* YANG ZHONGPING and LU RONGSHAN

Department of Chemistry, Hangzhou University, Hangzhou 310028, People's Republic of China

(Received 17 October 1990. Revised 9 December 1990. Accepted 31 December 1990)

Summary—A sensitive stripping voltammetric method is reported for trace measurement of the psychotherapeutic drug haloperidol. The method is based on adsorptive preconcentration of haloperidol on the glassy-carbon electrode in an open circuit, followed by medium exchange and voltammetric determination of surface species. Cyclic voltammetry was used to explore the adsorptive behaviour and the results obtained suggest that the adsorption of haloperidol corresponds to the Frumkin-type isotherm. The adsorptive stripping response was evaluated with respect to stripping mode, electrolyte, pH, preconcentration time, concentration dependence, possible interference and other variables. The detection limit was $1.3 \times 10^{-9}M$ (10 min preconcentration) and the response was linear. The relative standard deviation (at the $1.3 \times 10^{-6}M$ level) was 2.3%. Applicability to a patient's urine sample is illustrated.

Haloperidol is an important psychotherapeutic drug and has been widely used as a tranquiliser in recent years. This long-acting neuroleptic is particularly useful in the treatment of schizophrenia and in the prevention of psychotic relapse. Usually, UV spectrophotometry¹ is used for routine analysis of the drug although other methods, such as GC,² TLC,³ fluorimetry⁴ and radioimmunoassay,⁵ have been reported. The sensitivities for most of these methods are not high and more sensitive techniques are required for assaying the drug in body fluids after therapeutic doses.

Bishop and Hussein⁶ studied anodic voltammetry of butyrophenone neuroleptics at platinum and gold electrodes and found that haloperidol shows neither anodic nor cathodic activity in 0.1M sulphuric acid.

The present study reports an extremely sensitive stripping voltammetric procedure for measuring trace amounts of haloperidol. The drug can be adsorbed on the surface of glassy-carbon electrodes, and then shows anodic activity in linear scan voltammetry. The adsorptive characteristic, which usually prevents voltammetry from being a useful analytical method, is exploited for obtaining effective preconcentration. It is demonstrated that immersing the glassy-carbon electrode in the haloperidol solution for short time periods allows convenient

measurements at the $10^{-8}M$ concentration level. Cyclic voltammetry is employed to examine adsorptive and electrochemical behaviour on the electrode surface. The scheme of open circuit accumulation/medium exchange/stripping voltammetry⁷ is used to minimize interference resulting from macro solution constituents. Trace amounts of haloperidol in urine have been measured without pre-isolation.

EXPERIMENTAL

Apparatus and reagents

Stripping and cyclic voltammetric data were collected with a BAS-100A electrochemical analyzer. The working electrode was a BAS glassy-carbon voltammetry electrode. The 10-ml sample cell was fitted with an Ag/AgCl reference electrode (BAS RE-1B) and a platinum wire auxiliary electrode, on the BAS C-1A cell stand which provided magnetic stirring during preconcentration. A BAS PL-10 digital plotter was used for obtaining voltamperograms.

Pure haloperidol was supplied by Shanghai No. 19 pharmaceutical laboratory; a stock solution ($2.7 \times 10^{-3}M$) was prepared by dissolving appropriate weights in ethanol. All other solutions were prepared with demineralized water and analytical grade reagents. Unless specified otherwise, the supporting electrolyte was Britton-Robinson buffer (pH 9.0). Urine samples were obtained from patients in Hangzhou No. 7 hospital.

*Author for correspondence.

Procedure

A fresh working electrode surface was utilized for each experiment. The surface was hand-polished for 30 sec with 0.05 μm of alumina slurry (BAS PK-3). The electrode was then rinsed with demineralized water to remove residual polishing material from the surface. The polished electrode was immersed into a sample solution, and adsorptive accumulation was begun in an open circuit for a selected time, while the solution was stirred at 400 rpm. Following this, the electrode was transferred into a "clean" supporting electrolyte solution. The linear scan or differential pulse voltamperograms were recorded by applying a positive-going potential. The scan was initiated at +0.4 V, terminated at +0.9 V. No nitrogen was needed to remove oxygen during the experiment.

RESULTS AND DISCUSSION

Figure 1 shows repetitive cyclic voltamperograms for $4.3 \times 10^{-7} M$ haloperidol at the glassy-carbon electrode in Britton-Robinson buffer (pH 9.0). Stirring the solution for 2 min in an open circuit resulted in a large anodic peak in the first scan (designated as 1), with a peak potential of 0.53 V. No peaks were observed in the cathodic branch. Subsequent repetitive scans yielded significantly smaller peaks, indicating rapid desorption of the product from the electrode surface or formation of a non-electroactive product. Repetitive scans without prior preconcentration did not yield any peak. There were no peaks obtained at platinum and gold electrodes for $1 \times 10^{-4} M$ concentration with 2 min preconcentration (not shown), meaning no adsorption on these metallic surfaces. It is obvi-

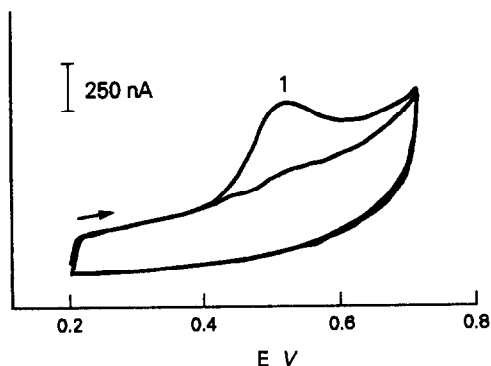


Fig. 1. Repetitive cyclic voltamperograms for $4.3 \times 10^{-7} M$ haloperidol in a Britton-Robinson buffer solution (pH 9.0), after 2 min stirring (400 rpm in an open circuit). Scan rate 25 mV/sec.

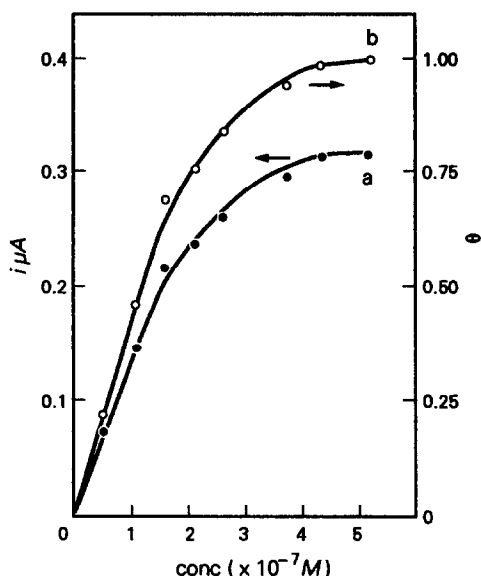


Fig. 2. Influence of the concentration on the linear scan stripping peak current (a) and on the fraction of covered surface (b) for haloperidol after an 8-min accumulation period. Other conditions as in Fig. 1.

ous that the anodic peak is caused by adsorptive haloperidol on the glassy-carbon surface.

Adsorption of haloperidol at glassy-carbon electrodes can be estimated by using linear scan voltammetry. The fraction of covered surface (θ) can be obtained from the ratio of peak area to maximum peak area. Logarithm forms for Langmuir and Frumkin adsorption isotherms are expressed as follows:

$$\log \frac{\theta}{(1-\theta)C} = \log \beta \quad (1)$$

$$\log \frac{\theta}{(1-\theta)C} = 2\alpha\theta \log e + \log \beta \quad (2)$$

If $\log[\theta/(1-\theta)C]$ is a constant [equation (1)], or a function of θ [equation (2)], the adsorption obeys the Langmuir or Frumkin isotherm respectively.⁸ Figure 2 shows the influence of the concentration (8 min accumulation time) on the peak current and the fraction of covered surface (θ). The plots are linear up to $1.5 \times 10^{-7} M$, and then they level off, indicating the electrode surface is saturated subsequently. The relationship of $\log[\theta/(1-\theta)C]$ and θ can be obtained from the data of Fig. 2 (see Fig. 3). The plot is linear (slope 0.95, intercept 6.48 and correlation coefficient 0.991) indicating that haloperidol adsorption on the glassy-carbon surface corresponds to the Frumkin isotherm. On the basis of the plot, the adsorption coefficient (β) is determined as 3.0×10^6 l./mole, and the attraction factor (α) is 1.09.

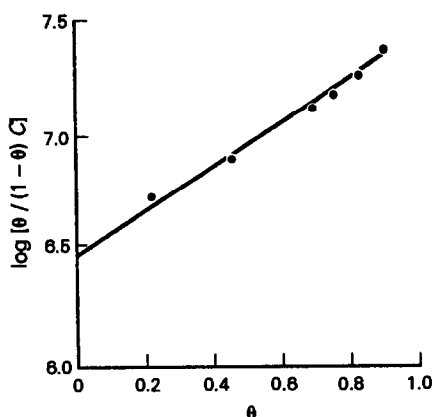


Fig. 3. Plot of $\log [\theta / (1 - \theta) C]$ vs. θ for haloperidol adsorption. All data are from Fig. 2.

The adsorbed haloperidol can be measured by using different voltammetric waveforms. Well-defined peaks after accumulation were obtained by both linear scan (Fig. 1) and differential pulse voltammetry (Fig. 4). The latter technique was preferred because it is almost three times more sensitive than linear scan voltammetry, *e.g.*, for $1.3 \times 10^{-6} M$ haloperidol after a 1-min accumulation time, the peak current in differential pulse voltammetry (scan rate 10 mV/sec, pulse amplitude 50 mV and pulse period 0.5 sec) is 2.3 times higher than that obtained in linear scan voltammetry (scan rate 25 mV/sec).

The adsorption properties of the drug can vary with the composition of the supporting electrolyte. Various electrolytes *e.g.*, phosphate buffer, borate buffer, ammonium acetate buffer and Britton–Robinson buffer, were evaluated as suitable media for the adsorptive stripping measurement of haloperidol. Best results (with

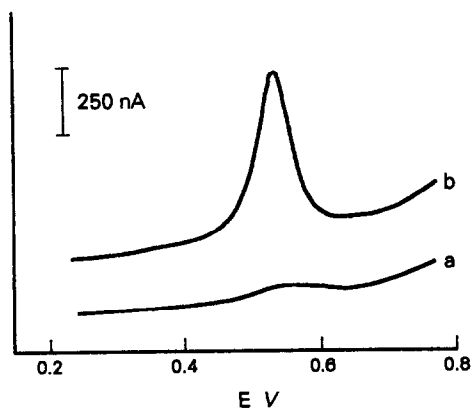


Fig. 4. Differential pulse stripping voltamperograms for $1.3 \times 10^{-6} M$ haloperidol after different accumulation periods: a, 0; b, 1 min. Scan rate, 10 mV/sec; pulse amplitude, 50 mV; pulse period, 0.5 sec. Other conditions as in Fig. 1.

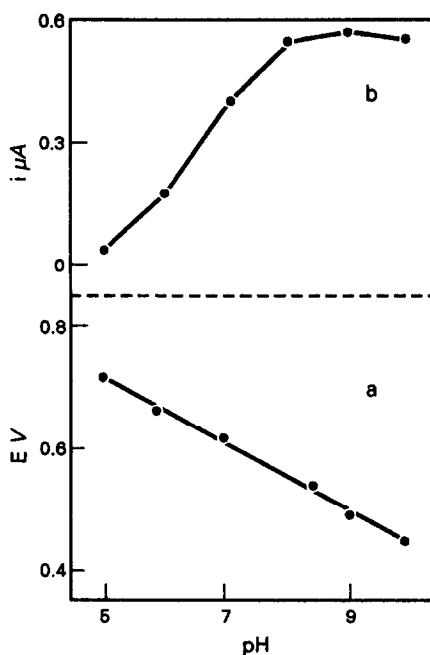


Fig. 5. Influence of the solution pH on the stripping peak potential (a) and on the peak current (b). Other conditions as in Fig. 4.

respect to signal enhancement and peak shape) were obtained with the Britton–Robinson buffer and therefore this electrolyte solution was used. The adsorptive stripping signal of haloperidol depends on the buffer pH. Figure 5(b) shows the dependence of the peak enhancement on the solution acidity. Almost no response to haloperidol was observed in solutions more acidic than pH 5.0. Increasing the pH from 5.0 to 9.0 resulted in a rapid increase in peak enhancement. The peak current decreased at higher pH. Accordingly pH 9.0 was used throughout to satisfy the sensitivity. The effect of the solution pH on the peak potential was also evaluated [Fig. 5(a)]. The peak potential shifted negatively, from 0.73 to 0.45 V, upon increasing pH from 5 to 10. The plot of peak potential vs. the solution pH was linear, with a slope of 53 mV per pH unit and a correlation coefficient of 0.998.

The effect of instrument conditions on the haloperidol adsorptive stripping response is examined. As expected, the peak height increased rapidly upon increasing the scan rate. However, as both the peak current and background current must be considered, more than a 10 mV/sec scan rate is not recommended. The stripping current also increased with both pulse amplitude and period. But increasing these two pulse parameters increased peak width and background current. In order to obtain an adequate analytical

response, the following parameters were chosen: pulse amplitude 50 mV and pulse period 0.5 sec.

It is difficult to obtain good reproducibility for the adsorptive stripping response of haloperidol on the glassy-carbon surface. Repetitive measurements on the same electrode surface caused the peak current to decrease rapidly. In order to obtain a reproducible surface, polishing with alumina for 30 sec was employed. The precision of this method was estimated by nine repeated measurements of $1.3 \times 10^{-6} M$ haloperidol (conditions as in Fig. 4). The mean peak current was 585 nA with a range of 570–595 nA and a relative standard deviation of 2.3%. It is obvious that the reproducibility of the results is attributed to the use of a fresh electrode surface in each run.

The adsorptive behaviour of haloperidol is affected by the mass-transport conditions during the preconcentration step. For example, a stirring rate of 400 rpm resulted in a 6-fold enhancement of the response, compared to that obtained in a quiescent solution ($1.3 \times 10^{-6} M$ haloperidol, 1 min preconcentration). Figure 6 shows the dependence of the adsorptive stripping peak current on the preconcentration time at two concentration levels. It is clear that the adsorptive accumulation is effective. The longer the preconcentration time, the more haloperidol adsorbed and the larger the peak current. Delahay and Fike⁹ have shown that for diffusing-controlled adsorption, the quantity of adsorbed material is proportional to the square root of the adsorption time, on the condition that the fraction of the surface covered is far from its equilibrium value. For haloperidol adsorption, the peak current is almost linear with the accumulation time. The deviation from linearity is observed only for solution of higher concentra-

tions. Similar results were reported for adsorptive stripping measurements of *cis*-dichlorodiammineplatinum(II).¹⁰ Such behaviour indicates that the adsorption is not controlled solely by the diffusion toward the surface.

The adsorptive stripping current increased with the concentration of haloperidol. The response was linear over 5.3×10^{-9} – $2.6 \times 10^{-8} M$ concentration range with 5 min accumulation (slope 4.2 nA/ $10^{-9} M$, correlation coefficient 0.999), and over 5.3×10^{-8} – $2.6 \times 10^{-7} M$ concentration range with 2 min accumulation (slope 10 nA/ $10^{-8} M$, correlation coefficient 0.998). The detectability was estimated from measurements of $5 \times 10^{-9} M$ haloperidol after 10 min preconcentration. The limit of detection, calculated from 3 times the noise, was found to be $1.3 \times 10^{-9} M$.

Because of open circuit accumulation and medium exchange in this method, most of the common metal ions did not interfere during the measurements. The following metal ions were tested at the 100 ppm level and found not to affect the $1.3 \times 10^{-6} M$ haloperidol peaks: Cu(II), Pb(II), Ni(II), Zn(II), Cd(II) and Fe(III). However, the stripping measurements based on adsorption are subject to interference from organic surfactants, which may also compete with haloperidol for space on the electrode surface. It is important to demonstrate susceptibility of this procedure to the presence of these materials for the direct voltammetric measurements of haloperidol in biological samples. Ascorbic acid and uric acid (100 ppm) did not affect the haloperidol peaks ($1.3 \times 10^{-6} M$, 1 min accumulation) but 100 ppm glucose, 40 ppm cholesterol and 5 ppm gelatin resulted in depression of the peak current to 11, 12 and 14% respectively.

In complex samples, such as body fluids, the advantages of the open circuit adsorption preconcentration/medium exchange/stripping voltammetric measurement are apparent. Such samples contain lots of chemicals, some at major component concentration; direct voltammetric measurements of analytes in such samples at trace levels are often impossible. Figure 7 shows the determination of haloperidol in a patient's urine sample (20 mg per day) diluted (1:10) with Britton–Robinson buffer. The drug peak in the voltamperogram was observed at +0.5 V [Fig. 7(a)]. A standard addition of $2.7 \times 10^{-7} M$ haloperidol caused this peak to rise [Fig. 7(b)]. A haloperidol concentration of $2.4 \times 10^{-6} M$ was found in the patient's urine. The

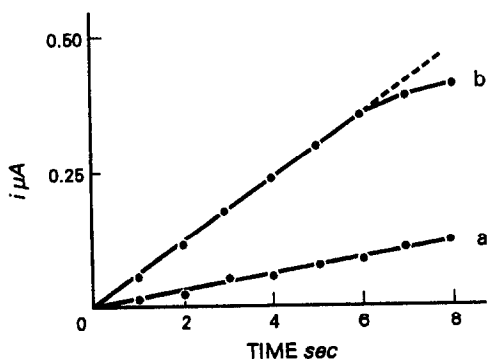


Fig. 6. Influence of accumulation time on different concentrations of haloperidol: a, $1.3 \times 10^{-8} M$; b, $1.3 \times 10^{-7} M$. Other conditions as in Fig. 4.

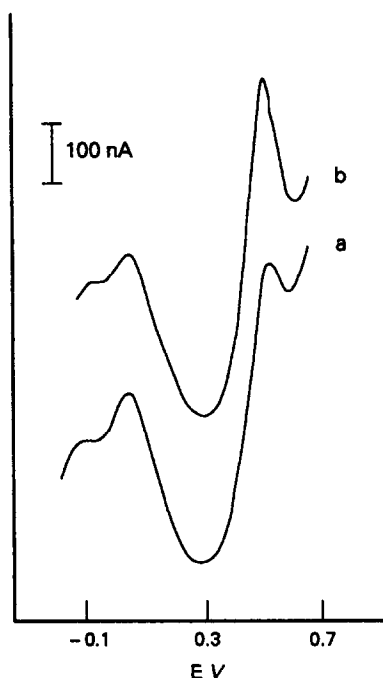


Fig. 7. Voltamperograms for the diluted (1:10) patient's urine sample with Britton-Robinson buffer solution (a), and the sample solution spiked with $2.7 \times 10^{-7}M$ haloperidol (b). Other conditions as in Fig. 4.

measurement is simple and convenient. No sample pretreatment was used other than 1:10 dilution with supporting electrolyte.

In conclusion, haloperidol does not show electroactivity at platinum and gold electrodes; the oxidation takes place only after adsorption at glassy-carbon electrodes which means that adsorption plays an important role in electrode reactions and may be the cause of reaction to some degree. Thus, a study of some non-electroactive organic compounds by use of adsorptive stripping voltammetry is expected.

REFERENCES

1. *Pharmacopeia of the People's Republic of China*, p. 355. The Commission of the Pharmacopeia of P.R.C., Beijing, 1977.
2. G. Bianchetti and P. L. Morselli, *J. Chromatog.*, 1978, **153**, 203.
3. A. Pluym, *J. Pharm. Sci.*, 1978, **68**, 1050.
4. W. Baeyens, P. De Moerloose and L. De Taeye, *ibid.*, 1977, **66**, 1787.
5. B. R. Clark, B. B. Tower and R. T. Rubin, *Life Sci.*, 1977, **20**, 319.
6. E. Bishop and W. Hussein, *Analyst*, 1984, **109**, 139.
7. J. Wang and B. A. Freiha, *Anal. Chim. Acta*, 1983, **148**, 79.
8. L. Hernandez, A. Zapardiel, J. A. P. Lopez and E. Bermejo, *J. Electroanal. Chem.*, 1988, **255**, 85.
9. P. Delahay and C. Fike, *J. Am. Chem. Soc.*, 1958, **80**, 2628.
10. J. Wang, T. Peng and M.-S. Lin, *J. Electroanal. Chem.*, 1986, **212**, 395.

DETERMINATION OF MOLYBDENUM BY ATOMIC-ABSORPTION SPECTROMETRY AFTER SEPARATION BY 5,5'-METHYLENEDISALICYLOHYDROXAMIC ACID EXTRACTION AND FURTHER REACTION WITH THIOCYANATE AND TIN (II)

MERCEDES SANCHEZ,* DOMINGO GAZQUEZ and PALOMA GARCIA

Department of Analytical Chemistry, Faculty of Sciences, University of Granada, Granada, Spain

(Received 24 November 1989. Revised 31 January 1991. Accepted 7 February 1991)

Summary—A method is described for the determination of molybdenum down to the microgram level, in samples of soil, steels, fertilizers and pharmaceuticals. After attack with acids, this element is separated from matrix elements by extraction of its 5,5'-methylenedisalicylohydroxamic acid (MEDSHA) complex from 4*M* hydrochloric acid, into methyl isobutyl ketone. Molybdenum is determined by atomic-absorption spectrometry (AAS), after conversion of the Mo-MEDSHA complex into the Mo-SCN⁻ complex in the organic phase. The detection limit is 0.03 µg/ml, with a relative standard deviation not exceeding 1.5% at a level of 2 µg/ml. The method is highly selective and suffers only from interference by tungsten.

Application of flame atomic-absorption spectrometry (AAS) for determination of molybdenum has been studied by many workers. Because the determination is subject to many interferences and low sensitivity,¹⁻³ preconcentration of very small amounts of molybdenum, as in geological samples or biological materials, is necessary before its AAS determination. The analytical aspects of the most commonly used extraction methods are summarized in Table 1.

α -Benzoinoxime is very widely used for extraction of molybdenum into various solvents,^{7,10,11} and Aliquat 336 has been used for the extraction of Mo together with Sb, As, Bi, Cd, Cu, Pb, Ag and Zn.^{12,13}

Hydroxamic acids such as *N*-benzoyl-*N*-phenylhydroxylamine¹⁶ and benzohydroxamic acid¹⁸ have also been utilized. The chelate formed with the first is extracted into toluene, while the benzohydroxamate complex is extracted into ethyl acetate as an ion-pair with Adogen 464.

The reaction between molybdenum(VI), SCN⁻ and Sn(II) in hydrochloric acid medium is probably the most used system. Kim and co-workers have described several methods in which the thiocyanate complex is extracted into methyl isobutyl ketone (MIBK)⁵ or as an

ion-pair with Amberlite LA1⁶ or Aliquat 336⁸ into chloroform. Aliquat 336 gives a very selective procedure but before the AAS measurement the chloroform must be evaporated and the residue dissolved in MIBK.

This paper describes the successful determination of Mo in several steels, a soil, a fertilizer and a pharmaceutical, based on extraction into MIBK with MEDSHA, followed by change of the Mo-MEDSHA complex into the Mo-SCN⁻ species. The method presents high sensitivity and satisfactory precision, and is practically free from interferences, so we think that it is more advantageous than the direct Mo-SCN⁻ extraction procedure.⁵

EXPERIMENTAL

Reagents

Stock molybdenum solution, 1000 µg/ml. Prepared by dissolving 1.84 g of analytical grade ammonium heptamolybdate tetrahydrate in distilled water and diluting to 1000 ml. Working solutions were prepared from this stock solution by appropriate dilution.

Stannous chloride solution, ~100 g/l. Prepared by warming analytical grade SnCl₂·2H₂O (20 g) and a small piece of analytical grade tin metal in 10*M* hydrochloric acid (20 ml), until a clear solution was obtained. After cooling, the

*Author for correspondence.

Table 1. Methods of determination of molybdenum by solvent extraction and flame AAS

Extraction system*	Extraction conditions	Performance characteristics	Observations and applications	Reference
MIBK-APDC	pH 1-1.4	RSD 1% (0.8 µg/ml)	Cu, Ca and P interfere† Hard dental tissues of rats	4
MIBK-SCN ⁻ -Sn(II)	1M HCl	Range 1-500 µg/ml RSD from 0.7% (100 µg/ml) to 8% (~1 µg/ml) DL 0.100 µg/ml	20 ions do not interfere Soils and geological samples	5
CHCl ₃ -SCN ⁻ -Sn(II)-Amberlite LA-1	2M HCl	Range 0.1-1 µg/ml DL 0.02 µg/ml	W and Re interfere†	6
CHCl ₃ -α-benzoinoxime	1.75M HCl 0.13M tartaric acid	—	Intended for reference work, W and Pd interfere Iron, steels and ores	7
CHCl ₃ -SCN ⁻ -Sn(II)-Aliquat 336	1M HCl	RSD <5% (1 g of sample) Range 0.1-1.25 µg/ml in organic phase	Re interferes Soils, sediments and natural waters	8
Isoamyl alcohol-BMPP	pH 1-3	—	Fe, Cr and V interfere Sea-water	9
MIBK-α-benzoinoxime	pH 1.3-3 (HClO ₄)	Range up to 10 µg/ml RSD 2.3%	Iron and steels	10
CH ₂ Cl ₂ -α-benzoinoxime	—	DL 0.5 µg/ml	Flotation tailings	11
MIBK-Aliquat 336	6M HCl 30% ascorbic acid 15% KI	—	Geological materials	12, 13
Acetylacetone-acetone	pH 2.6	Range up to 1 µg/ml DL 0.021 µg/ml RSD 2.2% (0.5 µg/ml)	Ti and V interfere†	14
MIBK-TOPO	15% v/v HCl	DL 0.5 µg/ml RSD <50% for geological samples	Fe interferes† Geological samples	15
Toluene-BPHA	8-9N H ₂ SO ₄	RSD 6%	Ti, W, Nb, Sn, Ta and V do not interfere Geological samples	16
MIBK-SCN ⁻ -Sn(II)	1M HCl	RSD 2.0%	Fe and Al interfere† Clay-supported catalysts	17
Ethyl acetate-benzohydroxamic acid-Adogen	pH 4.6 acetate buffer	Range up to 0.8 µg/ml RSD 1.2% (0.8 µg/ml)	25 elements do not interfere Rat organs	18
MIBK-3,4-dithiol	pH 0.6-0.8	Range up to 30 µg/ml DL 0.045 µg/ml RSD 0.8%	— —	19

*APDC = ammonium pyrrolidinedithiocarbamate; Aliquat 336 = methyltricaprylammonium chloride; BMPP = 4-benzoyl-3-methyl-1-phenylpyrazolin-5-one; TOPO = trioctylphosphine oxide; BPHA = *N*-benzoyl-*N*-phenylhydroxylamine; Adogen = methyltrioctylammonium.

†Limited study of interferences.

solution was diluted to 200 ml with distilled water and a small piece of tin metal was placed in it.

Potassium thiocyanate solution, ~100 g/l.

5,5'-Methylenedisalicylohydroxamic acid. The synthesis has been reported previously.²⁰ A 0.02M solution was prepared by dissolving 0.6360 g of MEDSHA in 100 ml of dilute ammonia solution.

All other reagents and organic solvents used were of analytical grade.

Instrumentation

A Perkin-Elmer 2380 atomic-absorption spectrometer with a nitrous oxide-acetylene (6-5) cm single-slot burner head (N₂O flow-rate 12 l./min, C₂H₂ flow-rate 3.9 l./min) and a molybdenum hollow-cathode lamp were used. The 313.3 nm line was used with a 0.7-nm spectral band-pass. The burner was positioned so that the light-beam was about 0.8 cm above the slot.

Procedure

Transfer a measured sample containing less than 50 µg of molybdenum into a 100-ml separating funnel. Add 7.1 ml of concentrated hydrochloric acid (to provide an acid concentration of 4M), 5 ml of MEDSHA solution and distilled water to 20 ml. Shake for 1 min with 5 ml of methyl isobutyl ketone (MIBK). Discard the aqueous phase and add to the organic phase 1.8 ml of concentrated hydrochloric acid, 1 ml of thiocyanate solution, 2 ml of tin chloride solution and distilled water to 20 ml. Shake for 2 min and let the phases separate. Centrifuge the organic phase and aspirate it into the flame. A blank is prepared in the same way. In the analysis of samples containing titanium and tungsten, add enough sodium fluoride to give a 1M concentration in the sample solution to mask these ions.

Preparation of sample solutions

Steel samples. Dissolve a suitable weight of steel sample in 12M hydrochloric acid in a 50-ml Kjeldahl flask by warming gently until the whole reaction has ceased, adding more acid if necessary. Add concentrated nitric acid dropwise to oxidize iron(II) and carbides. Evaporate the solution to dryness, dissolve the residue in 12M hydrochloric acid and dilute to volume in a standard flask of suitable size.

Fertilizers. Place 50 ml of fertilizer in a 250-ml beaker and add 40 ml of 20% v/v hydrochloric acid. Heat for 30 min, reducing the volume to

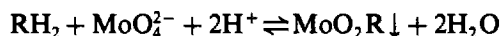
about 20 ml. Add 50 ml of distilled water, heat to boiling, cool and filter the solution (Whatman No. 40 paper) into a 100-ml standard flask. Wash down the sides of the beaker with water and filter into the flask, diluting to volume with water. The composition of the liquid fertilizer analysed was: total nitrogen 6%, P₂O₅ 4%, K₂O 6%, Mg 0.5%, Mn 0.05%, B 0.029%, Zn 0.05%, Mo 0.0006% and Co 0.0006% (values given by the manufacturer).

Soils.⁵ Moisten 1 g of soil sample with water in a 100-ml Teflon beaker, add 4 ml of 70% perchloric acid and 10 ml of concentrated hydrofluoric acid. Evaporate the solution on a hot-plate at about 200° until white fumes of perchloric acid appear, add another 10 ml of hydrofluoric acid and evaporate to dryness. Wash down the walls of the beaker with 4M hydrochloric acid and add about 20 ml more, cover with a watch-glass and boil gently for a short time to dissolve the residue. Cool and transfer the solution into a 100-ml separating funnel, washing the cover and the beaker with 4M hydrochloric acid to give a final volume of 40-50 ml.

Pharmaceuticals. Weigh 2 ml of sample, e.g., a vitamin complex, into a 100-ml beaker, add 10 ml of concentrated nitric acid and heat, with care to avoid a violent reaction, until a tranquil solution is produced. Cool it, slowly add 5 ml of 60-70% perchloric acid, and heat until brown fumes of nitrogen dioxide appear. If the solution has a dark colour, add 2 ml of concentrated nitric acid and continue the heating until white fumes of perchloric acid appear. Cool the solution and dilute to a final volume of 50 ml with 2M hydrochloric acid. The composition of the liquid vitamin complex analysed was (per ml): vitamin A 8333 IU, vitamin D 1667 IU, thiamine hydrochloride 2.5 mg, riboflavin 2 mg, pyridoxine hydrochloride 0.83 mg, nicotinamide 16.67 mg, ascorbic acid 83.33 mg, MnSO₄ 1.53 mg, K₂SO₄ 5.58 mg, ZnSO₄·7H₂O, 1.75 mg, Na₂MoO₄·2H₂O 0.63 mg, Fe 3.33 mg, saccharin 1.05 mg.

RESULTS AND DISCUSSION

In acidic media molybdenum forms an insoluble yellow complex with MEDSHA (RH₂) according to the reaction²¹⁻²³



The precipitate formed, the composition of which is MoO₂(C₁₅H₁₂N₂O₆)·3H₂O, is fairly

easily extracted into MIBK. Several experimental factors influencing the efficiency of extraction were investigated in detail.

Effects of the acidity and reagent concentration

Figure 1 shows the absorbance values for Mo, after a single extraction of its MEDSHA complex with 10 ml of MIBK from various concentrations of hydrochloric acid and between pH 1 and 8. When the concentration of hydrochloric acid is increased the volume of the organic phase decreases because of the solubility of MIBK in the aqueous phase. For that reason a volume-change correction has been made for the organic phase, taking as reference a volume of 10 ml.

It can be seen that the absorbance of the organic phase is constant in the range from 5M hydrochloric acid to pH 2, although it is lower than expected, and that at pH above 2 it diminishes gradually as the pH is increased. The increase in absorbance of the aqueous phase at pH above 5 indicates a decrease of the extraction efficiency. On the other hand, the absorbance of both the aqueous and organic phases increases when the hydrochloric acid concentration is higher than 5M. This effect may be due to destruction of the Mo-MEDSHA complex and the formation of a chloride complex which is partially extractable into MIBK.²⁴ The logical conclusion, confirmed later, is that the Mo-MEDSHA complex precludes complete atomization of molybdenum in the flame.

The results obtained for the effect of the reagent concentration on the extraction efficiency from 4M and 2M hydrochloric acid and on the molybdenum absorbance are shown in Fig. 2. The extraction percentages have been calculated from measurement of the

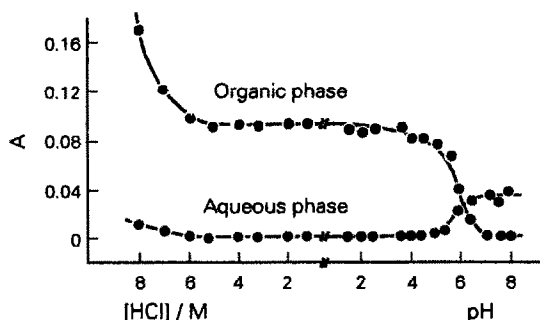


Fig. 1. Extraction of molybdenum with MEDSHA into MIBK, as a function of hydrochloric acid concentration and pH. Molybdenum(VI) 10 $\mu\text{g}/\text{ml}$; MEDSHA, $1.0 \times 10^{-3}\text{M}$; MIBK, 10 ml. The absorbances of the organic phases were corrected for volume change (see text).

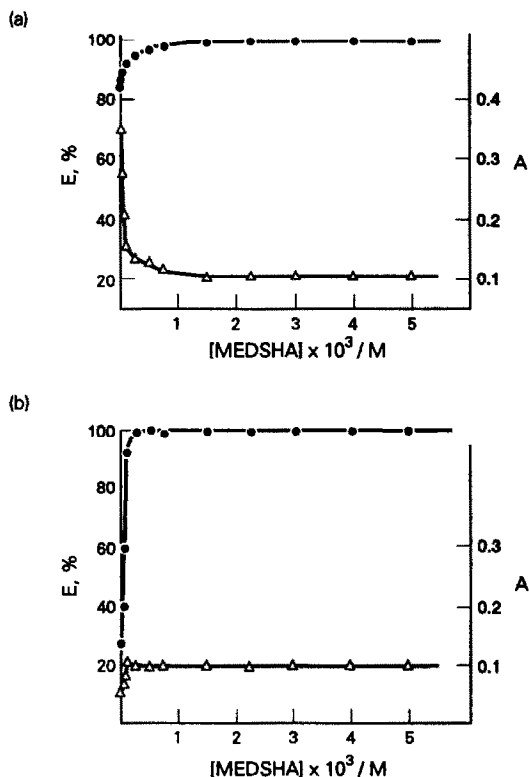


Fig. 2. Dependence of absorbance (Δ) and degree of extraction (\bullet) of molybdenum(VI), on the concentration of MEDSHA in the aqueous phase. Molybdenum(VI), 0.2 mg/20 ml; MIBK, 10 ml; [HCl], (a) 4M, (b) 2M.

molybdenum that remains in the aqueous phase, by the method of Kim *et al.*⁵

It is observed that at both acidities the extraction efficiency improves when the reagent concentration is increased. With a reagent concentration of 5×10^{-4} and $1.5 \times 10^{-3}\text{M}$, for the 2 and 4M hydrochloric acid media respectively, the extraction is quantitative and the absorbance does not change.

The large decrease of the absorbance in the 4M hydrochloric acid phase as the reagent concentration is increased, suggests that at low MEDSHA concentrations a chloride complex of molybdenum is extracted, which is confirmed by the absence of this phenomenon for the 2M hydrochloric acid medium, where the degree of formation and extraction of the chloride complex is lower.

These facts, together with the results obtained in the study of the effect of acidity, show that the atomization efficiency of Mo in the flame, when present as the Mo-MEDSHA complex, is low. Several experiments were done on transformation of that species, after its extraction from 4M hydrochloric acid (this medium was selected in order to obtain as selective a procedure as

Table 2. Comparison of the calibration graphs corresponding to extraction of molybdenum into MIBK by the SCN^- -Sn(II) method and by MEDSHA and further reaction with SCN^- -Sn(II)

Mo, $\mu\text{g/ml}$	Absorbances of organic phases*	
	SCN^- -Sn(II) extraction†	MEDSHA extraction and SCN^- -Sn(II) reaction‡
1	0.117	0.114
2	0.227	0.224
3	0.337	0.338
4	0.437	0.435

*Aqueous phase 20 ml; organic phase 5 ml.

†HCl, 1M; KSCN, 0.05M; SnCl_2 , 0.045M.

‡MEDSHA, 0.003M; HCl, 4M.

possible), into a non-refractory one. The best results were obtained by shaking the organic phase (containing the Mo-MEDSHA complex) for 2 min with a fresh solution of 0.05M potassium thiocyanate and 0.045M stannous chloride in 1M hydrochloric acid.⁵ In this way the Mo-MEDSHA complex is quantitatively transformed into an Mo- SCN^- species, which remains in the organic phase. This fact was checked by preparing two calibration curves for a molybdenum concentration range from 1 to 4 $\mu\text{g/ml}$, the first corresponding to extraction with the SCN^- -Sn(II) system and the second to the MEDSHA extraction and further transformation with SCN^- and Sn(II). The results summarized in Table 2 make evident the effectiveness of the reaction.

Effect of other variables

Shaking for 30 sec is enough to complete the extraction of the Mo-MEDSHA complex under the conditions described.

The effect of the volume ratio of the aqueous and organic phases in the next step was studied, with 10 ml of MIBK for the extraction of molybdenum from various volumes of aqueous phase containing between 10 and 40 μg of

Table 3. Effect of foreign elements

Ion	Tolerance ratio (ion/Mo w/w)
Cs(I), Rb(I), Li(I), Tl(I), Ag(I), Zn(II), Ca(II), Co(II), Mg(II), Ba(II), Be(II), Ni(II), Mn(II), Pb(II), Sr(II), Cu(II), Cd(II), Hg(II), Pd(II), Sb(III), Ce(III), As(III), Cr(III), Al(III), Y(III), La(III), Bi(III), In(III), Tl(III), Fe(III), Sn(IV), Se(IV), Zr(IV), Ce(IV), As(V), U(VI), BO_2^- , I^- , Br^- , F^- , SO_4^{2-} , $\text{C}_2\text{O}_4^{2-}$, SCN^- , PO_4^{3-} , citrate, acetate, tartrate	1000*
Ti(IV)†	800
Th(IV)	400
V(V)	300
W(VI)†	10

*Maximum amount tested, except for F^- (tolerance ratio 1.9×10^4).

†In the presence of 1M sodium fluoride.

molybdenum. Linear calibration graphs were obtained even when the aqueous phase volume was increased to 200 ml, which shows that 50 $\mu\text{g/l}$ molybdenum can be determined.

Calibration graph

The atomic-absorption signal was linear up to 6 $\mu\text{g/ml}$ molybdenum in the aqueous solution, and the equation for the calibration graph was $A = 0.104C + 0.006$, for C in $\mu\text{g/ml}$, with $r^2 = 0.9998$. A detection limit of 0.03 $\mu\text{g/ml}$ molybdenum was obtained^{25,28} (from ten blanks measured against MIBK), and the precision (RSD) for seven replicate determinations of 2 $\mu\text{g/ml}$ molybdenum was 1.1%.

Interference studies

A detailed study of interference effects was made for cations and anions, in amounts ranging up to $2 \times 10^4 \mu\text{g}$, with 20 μg of molybdenum. Ions were considered as not interfering, if they produced an error in absorbance

Table 4. Determination of molybdenum in different samples

Sample	Proposed method		Sn- SCN^- method	Certified or supplier's value
	Found*	RSD*%		
BCS 451/1 steel	0.040%	2.63	—	0.039%
NBS-SRM 33e steel	0.227%	1.84	—	0.224%
NBS-SRM 364 steel	0.492%	0.98	—	0.490%
Fertilizer	6.6 $\mu\text{g/ml}$	0.57	6.8 $\mu\text{g/ml}$	6.0 $\mu\text{g/ml}$ †
Vitamin complex	243 $\mu\text{g/ml}$	2.24	238 $\mu\text{g/ml}$	249 $\mu\text{g/ml}$ ‡
Morocco soil	1.62 $\mu\text{g/g}$	2.21	1.51 $\mu\text{g/g}$	—

*Results of seven replicate determinations.

†Value given by BASF Española, S.A.

‡Value given by Abbot Laboratories, S.A.

of less than twice the coefficient of variation. The tolerance limits are summarized in Table 3.

Among the ions tested, the only major interferences were from Ti(IV) and W(VI), which form bulky precipitates that adsorb or occlude the molybdenum(VI) complex. However, these interferences can be eliminated or minimized, respectively, by adding sodium fluoride before the MEDSHA.

Applications

The proposed method was applied to the determination of the molybdenum content of three certified reference steel samples and a molybdenum-deficient soil. It was also applied to the analysis of a pharmaceutical preparation and a liquid fertilizer, for which approximate molybdenum values were available.

In the samples with a molybdenum content that was not exactly known, the results were compared with those obtained by the direct Sn-SCN⁻ method.

As shown in Table 4, the proposed method shows reasonably good agreement with other values and its accuracy (certified samples) and precision are satisfactory.

CONCLUSIONS

Among the different solvent extraction methods that have been proposed for the determination of molybdenum by flame atomic-absorption spectrometry, the one based on the extraction of this element into MIBK with SCN⁻ and Sn(II),⁵ from hydrochloric acid medium, is perhaps the most useful. We propose a method that makes indirect use of this system and offers some advantages over it: it has a lower detection limit and suffers interference only from W(VI).

Acknowledgement—The authors wish to express their gratitude to Dr R. A. Chalmers for his suggestions about the paper.

REFERENCES

1. D. J. David, *Analyst*, 1961, **86**, 730.
2. *Idem, ibid.*, 1968, **93**, 79.
3. A. Purushottam, P. P. Naidu and S. S. Lal, *Talanta*, 1972, **19**, 1193.
4. C. A. Helsby, *ibid.*, 1973, **20**, 779.
5. C. H. Kim, C. M. Owens and L. E. Smythe, *ibid.*, 1974, **21**, 445.
6. C. H. Kim, P. W. Alexander and L. E. Smythe, *ibid.*, 1975, **22**, 739.
7. E. M. Donaldson, *ibid.*, 1980, **27**, 79.
8. C. H. Kim, P. W. Alexander and L. E. Smythe, *ibid.*, 1976, **23**, 229.
9. Y. Akama, T. Nakai and F. Kawamura, *Nippon Kaisui Gakkaishi*, 1979, **33**, 180.
10. J. R. Castillo, M. A. Bellarra and J. Aznarez, *At. Spectrosc.*, 1982, **3**, 58.
11. K. Ise, *Bunseki Kagaku*, 1981, **30**, 629.
12. J. G. Viets, R. M. O'Leary and J. R. Clark, *Analyst*, 1984, **109**, 1589.
13. R. M. O'Leary and J. G. Viets, *At. Spectrosc.*, 1986, **7**, 4.
14. A. M. Ghe, D. Carati and C. Stefanelli, *Ann. Chim. (Rome)*, 1983, **73**, 705.
15. E. P. Welsch, *Talanta*, 1985, **32**, 996.
16. N. K. Roy, A. K. Das and C. K. Ganguli, *At. Spectrosc.*, 1986, **7**, 177.
17. N. Carrión, A. Llanos, Z. Benzo and R. Fraile, *ibid.*, 1986, **7**, 52.
18. J. G. March, R. Forteza and F. Grases, *Microchem. J.*, 1986, **33**, 39.
19. L. H. J. Lajunen and A. Kubin, *Talanta*, 1986, **33**, 265.
20. L. F. Capitán-Vallvey, F. Salinas and D. Gázquez, *Proc. Indian Acad. Sci., Chem. Sci.*, 1982, **91**, 399.
21. D. Gázquez, L. F. Capitán-Vallvey and F. Salinas, *Quim. Anal. Barcelona*, 1986, **5**, 216.
22. L. F. Capitán-Vallvey, D. Gázquez and F. Salinas, *Thermochim. Acta*, 1982, **56**, 15.
23. L. F. Capitán-Vallvey, D. Gázquez and F. Salinas, *An. Quim.*, 1987, **83B**, 298.
24. G. R. Waterbury and C. E. Bricker, *Anal. Chem.*, 1957, **29**, 129.
25. *Spectrochim. Acta*, 1978, **33B**, 242.
28. G. L. Long and J. D. Winefordner, *Anal. Chem.*, 1983, **55**, 713A.

DETERMINATION OF COPPER AT ng LEVELS BY IN-LINE PRECONCENTRATION AND FLOW-INJECTION ANALYSIS COUPLED WITH FLAME ATOMIC-ABSORPTION SPECTROMETRY

RAJESH PUROHIT and SUREKHA DEVI*

Department of Chemistry, Faculty of Science, M.S. University of Baroda, Baroda 390002, India

(Received 2 May 1989. Revised 19 December 1990. Accepted 7 February 1991)

Summary—Oxine/formaldehyde/resorcinol and oxine/formaldehyde/hydroquinone resins have been synthesized and their physicochemical properties studied. Conditions were optimized for the preconcentration of copper by batch extraction and column chromatography with the resins. A flow-injection analysis (FIA) manifold was constructed for the determination of copper at ng levels by preconcentration on microcolumns containing the resins, stripping, and atomic-absorption spectrometry. For batch preconcentration a pH of about 2.5–3 was optimal whereas in the FIA system a broader pH range (~2–3.5) could be used. Separations of binary mixtures of Cu(II) with Ni(II) or Pb(II) at $\mu\text{g/ml}$ level did not show any cross-contamination. In the FIA, a 2 cm long column and 2 ml/min flow-rate were adequate for quantitative uptake of copper; 50 μl of 0.1M hydrochloric acid quantitatively eluted the copper.

There is a need for improved automatic/semiautomatic methods for the determination of heavy metal ions in water. Flame atomic-absorption spectrometry (AAS) lacks sensitivity in detection at $\mu\text{g/l}$. levels. Electrothermal-atomization and hydride-generation AAS *etc.* are sensitive but suffer from matrix interferences. Flow-injection analysis (FIA) has contributed¹⁻⁵ to the development of several semiautomatic methods of preconcentration and determination of metal ions. These have employed activated alumina,⁴ oxine immobilized on silica gel,^{3,6,7} Chelex 100,^{2,5} resin 122,⁶ and tri(pyridylmethyl)ethylenediamine.⁸

Chelating resins containing oxine groups are synthesized either from oxine, formaldehyde and resorcinol by condensation^{9,10} or by diazotization of a poly(aminostyrene) resin followed by coupling to oxine.¹¹ The resins have low metal-exchange capacities and slow exchange rates. Their properties were improved by Pennington and Williams¹² and by Parrish and Stevenson¹³ by controlling the water regain and the curing conditions, but the samples required storage in moist conditions. Vernon and Nyo,¹⁴ and Parrish,¹⁵ have reported that the resins are unstable in $>2M$ hydrochloric acid at room temperature. We have attempted to improve the

kinetics of metal exchange and the stabilities of the oxine-containing resins by using hydroquinone in place of resorcinol in the condensation reaction. A new synthetic route has also been established for the synthesis of oxine/resorcinol/formaldehyde resins. Both resins are useful in the semiautomatic FIA method for the determination of copper at ng levels. Conditions have been optimized for determination of copper by (i) flow injection, (ii) a batch method and (iii) column chromatography.

EXPERIMENTAL

Synthesis of resins

Oxine/formaldehyde/resorcinol (8HOQFR) resin was made by refluxing 0.1 mole of oxine in 50 ml of dimethylformamide (DMF) with 0.25 mole of formaldehyde for 20 min. A further 0.1 mole of resorcinol in 50 ml of DMF was added to the refluxing mixture. A reddish gel was formed within 10 min. Refluxing was continued for a further 30 min. The gel was collected, washed with DMF and methanol, and cured at 80° (open cure). The resin to be used for further studies was ground to 60–80 mesh size. Oxine/formaldehyde/hydroquinone (8HOQFHQ) resin could not be synthesized by this method, so a base-catalysed process was used instead. Oxine (0.1 mole) in finely powdered form was stirred into 20 ml of 2M sodium hydroxide. To this

*Author for correspondence.

suspension, 0.25 mole of formaldehyde was added with stirring and heating in a water-bath. Hydroquinone (0.1 mole) in 20 ml of 2M sodium hydroxide was added to the oxine-formaldehyde mixture with stirring. The condensation reaction was continued until a black gel was formed, and this was open cured at 80°. The 60–80 mesh resin was washed thoroughly with water, converted into H⁺-form and used for further studies.

The resins were characterized, and used for batch and column chromatographic studies of copper exchange. The optimal pH for copper uptake was found by following the literature procedure¹⁶ and the copper left in solution was determined complexometrically.¹⁷ The copper taken up by the resin was eluted and similarly determined. The rate constant and activation energy for formation of the chelate were obtained by observing the exchange kinetics at various temperatures. The mode of diffusion of metal ions through the solution towards the resin was determined by the interruption test^{16,18} and was confirmed by the method reported by Nativ *et al.*¹⁹ During the kinetics study by the interruption test the resin beads were removed from the solution for a brief period of time (10 min) and were then re-immersed. The plots of % exchange *vs.* time give the nature of diffusion of the ions.¹⁶ The efficiency of the eluents was tested by the batch method.

Chromatographic separations

Chromatographic columns, 19 cm long, i.d. 7 mm, were prepared with the synthesized resins. Binary and ternary mixtures (25 ml) of copper, cobalt, lead and nickel (each 400 µg/ml) were passed through columns of 8HOQFR and 8HOQFHQ at pH 2 or 3 and a flow-rate of 1 ml/min, followed by washing with water. The

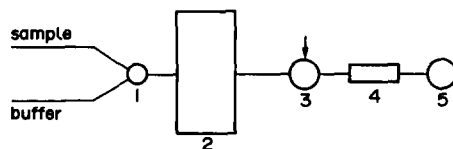


Fig. 1. FIA manifold: 1, two-way stopcock; 2, peristaltic pump; 3, injection valve; 4, column containing resin; 5, detector (AAS).

metal ions were eluted with 3M hydrochloric acid, 0.1M hydrochloric acid, 1M acetic acid and 0.1M hydrochloric acid respectively.

Characterization of the columns

The void volume of the columns was determined by the method given by Helfferich.¹⁶ The break-through capacities and column capacities were determined as described by Inczedy.²⁰

Determination of copper at ng level

A Varian model AA 775 atomic-absorption spectrometer with a chart recorder was used for determination of copper at 324.8 nm. The operating conditions were monochromator band-pass 1 nm, lamp current 2.5 mA, sample uptake rate 1 ml/min, air pressure 39 psig, acetylene pressure 9.8 psig.

The FIA manifold was constructed as shown in Fig. 1. A Gilson Minipuls peristaltic pump was used along with a rotary injection valve (Rheodyne RH 5020). Microcolumns (4 cm long, 2 mm bore) containing an oxine resin were connected in the manifold with 0.5 mm bore Teflon tubing. Acetate solutions (0.2M) adjusted to pH 2 and 3 with a small amount of hydrochloric acid were used as carrier streams. Standard copper solutions were passed through the column at 1 ml/min flow-rate. Copper was eluted from the column by injection of 50 µl of 0.5M hydrochloric acid and determined by flame AAS. The column was further washed

Table 1. Physicochemical properties of the resins

Properties	8HOQFR	8HOQFHQ
Moisture content, %	3	8
Density, g/cm ³	1.4	1.5
Mesh size	60–80	60–80
Sodium exchange capacity, mmole/g	4.6	5.0
$t_{1/2}^*$ for sodium, min	7	40
$t_{1/2}$ for copper, min	15	30
$t_{1/2}$ for nickel, min	5	8
$t_{1/2}$ for lead, min	15	10
$t_{1/2}$ for zinc, min	120	8
K_d for nickel (pH 6)	7.33	8.25
K_d for copper (pH 3)	19.30	19.27
K_d for lead (pH 4)	15.55	12.69
k_d for zinc (pH 6)	13.62	9.98

* $t_{1/2}$ = time required for 50% exchange of the metal ion.

Table 2. Comparison of resin properties

Property	8HOQFR	8HOQFHQ	Reference
Stability towards acid (maximum acidity)	5M	5M	Present work
	4M	—	14
	2M	—	15
Copper capacity, mmole/g	0.7*	—	14
	2.32*	—	15
	1.72†	1.74†	Present work
$t_{1/2}$ for sodium	6 hr	—	14
	7 min	40 min	Present work

*At pH 5.

†At pH 3.

with two 50 μ l injections of acid and passage of buffer solution through the system. A three-way stopcock was used to control the flow of standard solution and buffer.

RESULTS AND DISCUSSION

The physicochemical properties of the resins synthesized (8HOQFHQ and 8HOQFR) are listed in Table 1. The resins are insoluble in most organic solvents, and in acids and alkalis of higher concentrations. They are thermally stable up to 300°. The infrared spectra show a broad band at 3400–3200 cm^{-1} for polymeric —OH stretching, a sharp but weak band for the aromatic tertiary C—N vibration at 1370 cm^{-1} , a methylene group bending vibration at 1400 cm^{-1} and a stretch at 1500 cm^{-1} indicating aromaticity. A weak band at 1600 cm^{-1} indicates the presence of C=N stretching. Unlike the resins reported earlier,^{14,15} our 8HOQFR resin did not show instability in 2–4M acids, and although it had the same resorcinol/oxine/formaldehyde ratio as the earlier resins, its

water content was lower. The exchange capacity for copper was higher (1.72 mmole/g at pH 3, against¹⁴ 0.7 at pH 5). The copper capacity of our 8HOQFHQ was also high, 1.74 mmole/g at pH 3.

The $t_{1/2}$ values for exchange of Cu(II), Ni(II), Zn(II) and Pb(II) are quite low, except for Zn(II) on 8HOQFR (Table 1). Our resins also showed greater stability towards acids and faster equilibration rates than the resins reported earlier (Table 2). The interruption test¹⁶ indicated that the exchange of metal ions with these resins is governed by diffusion within the particles. The interruption gives time for the concentration gradients in the beads to level out, and in particle-controlled diffusion, the rate immediately after re-immersion is greater than that prior to the interruption. In film-controlled diffusion, there is no concentration gradient within the bead, and the diffusion rate depends on the concentration gradient in the film. The interruption does not affect the gradient and hence has no effect on the rate.

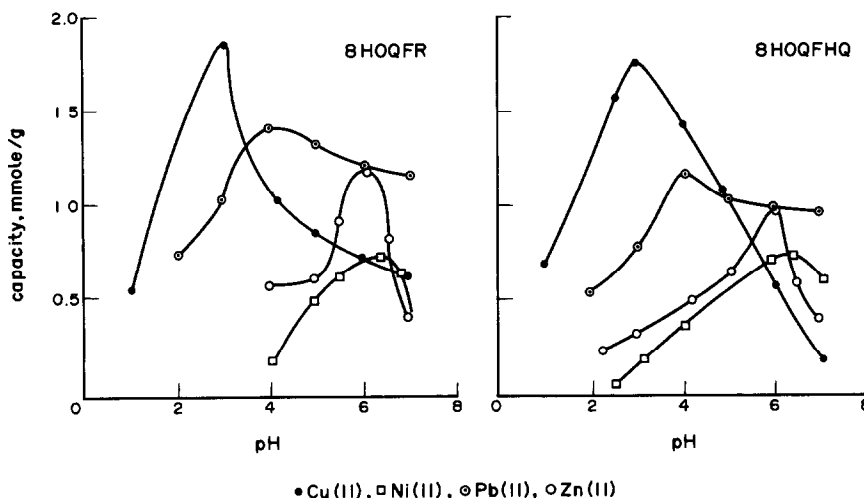


Fig. 2. Effect of pH on metal exchange (batch method): ● Cu(II), □ Ni(II), ○ Pb(II), ○ Zn(II); 0.1M metal ion.

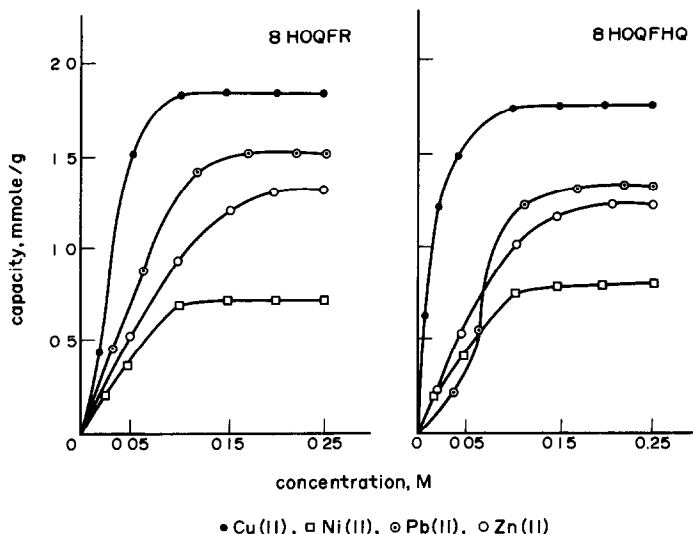


Fig. 3. Effect of metal ion concentration on exchange capacity: ● Cu(II), □ Ni(II), ○ Pb(II), ○ Zn(II).

The effect of pH on the metal exchange capacities is shown in Fig. 2. The selectivity, based on the distribution coefficients, was observed to be $\text{Cu} > \text{Zn} > \text{Ni} > \text{Pb}$ at 0.1M metal concentration, for both the resins. The uptake of metal ions by the resins increases (Fig. 3) and the distribution coefficient decreases with increasing metal ion concentration.

For elution of the chelated metal ions, 0.1–5M acids, sodium chloride, sodium citrate, sodium tartrate, potassium thiocyanate, thiourea and 5–50% w/w perchloric acid were tested. Copper, zinc and nickel were quantitatively eluted with 3, 0.2 and 0.1M hydrochloric acid respectively, and Pb(II) with 1M acetic acid. Conditions for separations of Cu–Ni, Cu–Pb, and Cu–Ni–Co can be predicted from the pH and elution studies.

Column chromatographic separations

Mixtures (25 ml) of Cu–Ni, Cu–Pb and Cu–Ni–Co in 1:1 and 1:1:1 proportions, prepared from 400 $\mu\text{g}/\text{ml}$ metal ion solutions and adjusted to pH 3, were passed through the column at a flow-rate of 1 ml/min. The column was washed with water, then the metal ions were eluted with appropriate reagents. As shown in Fig. 4, separation of copper from nickel with 8HOQFR is incomplete, but is satisfactory with 8HOQFHQ. The kinetics in column processes is faster than for the batch process, because the resin surface is constantly coming into contact with fresh mobile phase. This also indicates that the mechanism of the column process is different from that of the batch process.

When the ternary mixture of Cu–Ni–Co is adjusted to pH 2 and passed through the column, nickel and cobalt are detected in the effluent, but copper is retained, and can then be eluted with 3M hydrochloric acid. However, if the mixture is at pH 3, the cobalt and part of the nickel pass through the column; the copper and the rest of nickel are retained on the column and can then be eluted by gradient elution. The separation shows cross-contamination to some extent. Lead and copper can be completely separated by consecutive elution with 2M acetic acid and 3M hydrochloric acid respectively.

Thermodynamics and rate of copper exchange

The rates for uptake of copper by the resins at three different temperatures were calculated from the equations for a first order reaction

$$-\frac{dc}{dt} = kc; \quad -\log(a-f) = \frac{kt}{2.303}$$

where a is the initial concentration of metal ion and f is the concentration left in solution after time t . Therefore $(a-f)$ gives the uptake of metal ion by the resin. A plot of $\log(a-f)$ vs. t gave straight lines passing through the origin, for 8HOQFR, the slopes giving the values of k . However, the plots for 8HOQFHQ were not linear, and a mirror method^{21,22} was used. The rate constant was calculated from the initial rate of the reaction, the appropriate part of the plot being identified by placing a mirror normal to the curve, and moving it until the reflection was a smooth continuation of the plot. The tangent was then drawn perpendicular to the mirror and

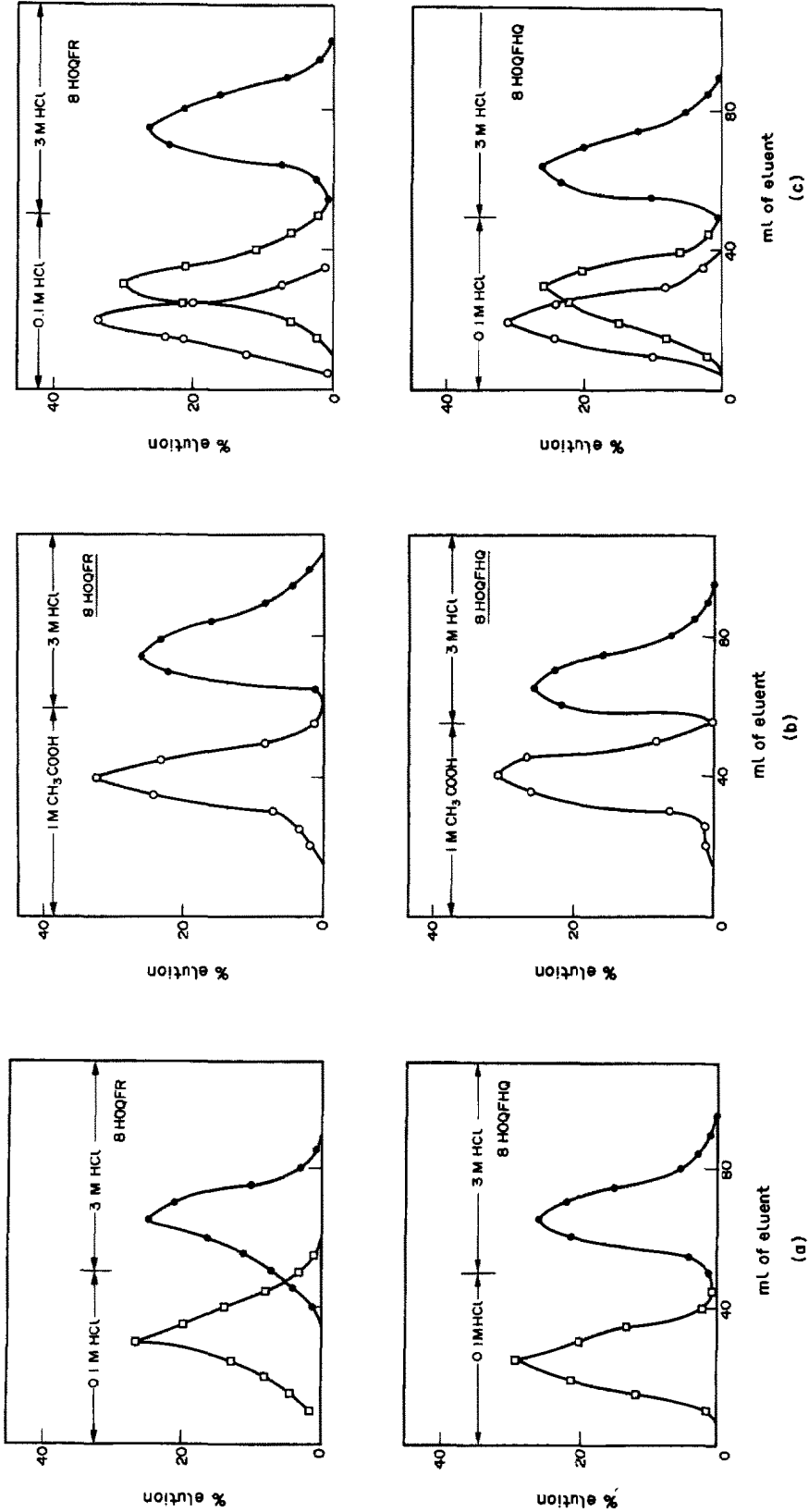


Fig. 4. Chromatographic separations. (a) ● Cu(II) and □ Ni(II), (b) ● Cu(II) and ○ Pb(II), (c) ● Cu(II), □ Ni(II) and ○ Co(II). Concentration of each metal ion in mixture, 400 μg/ml, flow-rate 1 ml/min, pH 3, total volume of mixture 25 ml.

Table 3. Rate constant and activation energy data

Temperature °C	Rate constant k , sec^{-1}	
	8HOQFR	8HOQFHQ
30	1.8	1.2
40	2.8	2.0
50	4.6	3.6
Activation energy, kcal/mole	9.15	9.86

from the slope of the line the rate constant (k) was calculated. The activation energy of complex formation was determined by using the Arrhenius equation

$$k = Ae^{-\Delta E/RT}$$

and a plot of $\log k$ vs. $1/T$ is given in Table 3. The activation energy is higher for 8HOQFHQ than for 8HOQFR, which indicates a slower exchange rate for copper on the former and is in agreement with the $t_{1/2}$ values (Table 1).

Flow-injection system

Copper at ng level was determined with the FIA manifold shown in Fig. 1. When copper was preconcentrated on the chelating-resin microcolumn by passage of 5 ml of $1 \times 10^{-7}M$ copper solution, the column effluent did not show the presence of copper when continuously analysed by AAS, indicating quantitative chelation of copper on the microcolumn. The column was then washed with buffer, and the chelated copper was eluted by injection of 50 μl of 0.5M hydrochloric acid to ensure quantitative elution. The dispersion due to the FIA system was calculated from the AAS signals for direct nebulization of a 50 $\mu\text{g}/\text{ml}$ copper solution and for 50 μl of the same solution injected into the FIA system, with and without introduction of the present microcolumn. It was found that use of the microcolumn did not affect the peak height.

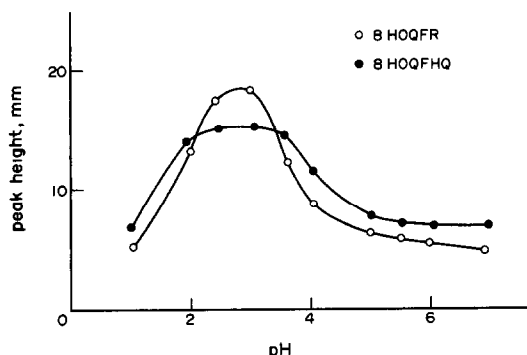


Fig. 5. Effect of pH in FIA method: flow-rate 2 ml/min, column length 2 cm, Cu(II) 5 ml, $10^{-7}M$.

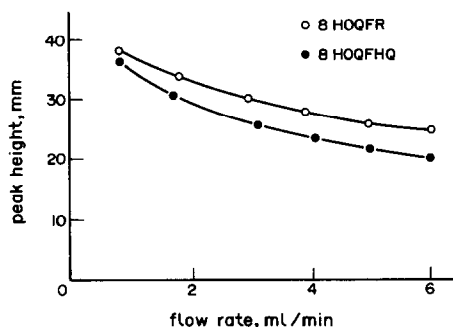


Fig. 6. Effect of flow-rate in FIA analysis: pH 3, column length 2 cm, Cu(II) 5 ml, $10^{-6}M$.

The dispersion was found to be 1.5. The sharp peak for the elution of copper from the microcolumn indicates faster kinetics. Continuous elution of copper with 0.5M hydrochloric acid also gives a narrow peak, of comparable height, indicating that the analyte is concentrated in a relatively narrow zone of the eluent. The dispersion of the system depends on the volume of sample injected. Conventional flame AAS gives $\mu\text{g}/\text{ml}$ detection levels whereas the FIA system with a microcolumn for preconcentration gives ng/ml levels.

The FIA system was optimized by varying the pH of the copper solution (Fig. 5). The optimum pH was lower than that for the batch system (Fig. 2). Tris, phosphate and acetate

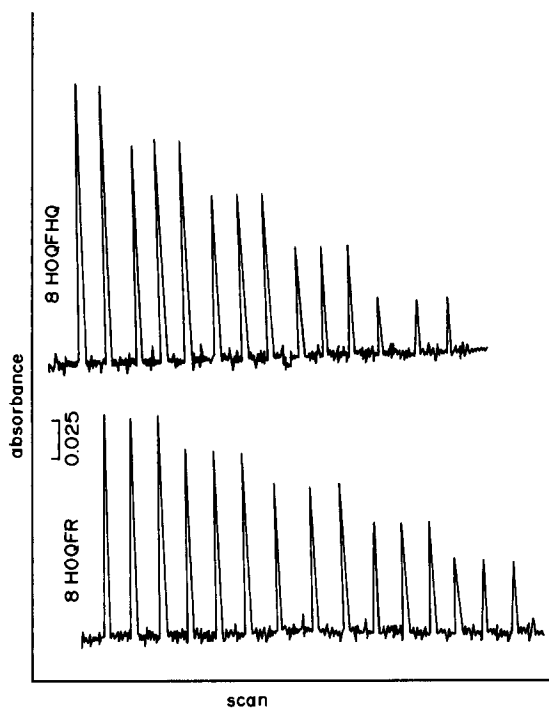


Fig. 7. Calibration peaks: 10 ml of 20, 40, 60, 80 and 100 ng/ml Cu solution, 20 μl of 0.5M HCl injected.

buffers (0.2M) were tested as carriers in the FIA system. With phosphate buffer the system was less critically sensitive to variation in pH.

The effect of column length was studied with a carrier stream flow-rate of 2 ml/min. A 2 cm column (i.d. 2 mm) is sufficient for preconcentration. A column length greater than 6 cm increases the dispersion coefficient to ~15%. Increasing the flow-rate decreases the peak height and broadens the width of the peak (Fig. 6). A 2 ml/min flow-rate is recommended.

Elution of copper was quantitative with 20 μ l of $\geq 0.1M$ hydrochloric acid, but lower concentrations gave only 20–30% elution. To ensure complete elution 50 μ l of 0.5M acid is recommended.

A calibration graph for copper was obtained by passing 10 ml of each standard solution through the FI system and eluting the copper with 50 μ l of 0.5M hydrochloric acid. Each data point was measured in triplicate. The regression coefficients for the 8HOQFR and 8HOQFHQ plots were 0.9917 and 0.9940 respectively. The lower limit of detection, based on the copper concentration equivalent to three times the standard deviation of the blank signal for the carrier stream, was 5 ng/ml with preconcentration from 15 ml of solution.

REFERENCES

1. J. Růžička and E. H. Hansen, *Flow Injection Analysis*, 1st Ed., Wiley-Interscience, New York, 1981.
2. S. Olsen, L. C. R. Pessenda, J. Růžička and E. H. Hansen, *Analyst*, 1983, **108**, 905.
3. F. Malamas, M. Bengtsson and G. Johansson, *Anal. Chim. Acta*, 1984, **160**, 1.
4. Y. Zhang, P. Riby, A. G. Cox, C. W. McLeod, A. R. Date and Y. Y. Cheung, *Analyst*, 1988, **113**, 125.
5. S. D. Hartenstein, J. Růžička and G. D. Christian, *Anal. Chem.*, 1985, **57**, 21.
6. Z. Fang, S. Xu and S. Zhang, *Anal. Chim. Acta*, 1984, **164**, 41.
7. M. A. Marshall and H. A. Mottola, *Anal. Chem.*, 1985, **57**, 729.
8. M. Bengtsson, F. Malamas, A. Torstensson, O. Regnell and G. Johansson, *Mikrochim. Acta*, 1985 **III**, 209.
9. H. Lillin, *Angew. Chem.*, 1954, **66**, 649.
10. J. R. Parrish, *Chem. Ind.*, 1955, 386.
11. *Idem, ibid.*, 1956, 137.
12. L. D. Pennington and M. B. Williams, *Ind. Eng. Chem.*, 1959, **51**, 759.
13. J. R. Parrish and R. Stevenson, *Anal. Chim. Acta*, 1974, **70**, 189.
14. F. Vernon and K. M. Nyo, *ibid.*, 1977, **93**, 203.
15. J. R. Parrish, *Anal. Chem.*, 1982, **54**, 1890.
16. F. Helfferich, *Ion Exchange*, p. 256, McGraw-Hill, New York, 1962.
17. A. I. Vogel, *Text Book of Quantitative Inorganic Analysis*, 3rd Ed., pp. 435, 441. ELBS, London, 1978.
18. Y. R. E. Kressman and J. A. Kitchener, *Disc. Faraday Soc.*, 1949, **7**, 90.
19. M. Nativ, S. Goldstein and G. Schmuckler, *J. Inorg. Nucl. Chem.*, 1975, **37**, 1951.
20. J. Inczédy, *Analytical Applications of Ion Exchangers*, Pergamon Press, London, 1966.
21. A. A. Frost and R. G. Pearson, *Kinetics and Mechanism*, p. 46. Wiley, New York, 1961.
22. H. Diehl, *Talanta*, 1989, **36**, 799.

ASCORBIC ACID AS A MATRIX MODIFIER FOR DETERMINATION OF TIN IN CONCENTRATED BORIC ACID SOLUTIONS BY ELECTROTHERMAL ATOMIC-ABSORPTION SPECTROMETRY

ANATOLY B. VOLYNSKY,* EVELINE M. SEDYKH and LIDIYA N. BANNYKH

V. I. Vernadsky Institute of Geochemistry and Analytical Chemistry, USSR Academy of Sciences, Moscow, 117975, USSR

(Received 26 February 1990. Revised 27 October 1990. Accepted 21 January 1991)

Summary—It has been found that the atomic-absorption signal for tin is reduced in the presence of 5 μ l of 0.05–0.30M boric acid at STPF-conditions. It has been proposed that the reason for the boron interferences is the formation of SnB(g) at the atomization stage. In the presence of palladium chloride the interferences from 0.2M boric acid are reduced by a factor of 1.3. The interferences are reduced most effectively when the sample is atomized from a polycrystalline graphite platform or in the presence of ascorbic acid. The interference of up to 0.2M boric acid can be suppressed and the area of the tin signal doubled. It is proposed that the observed phenomenon is connected with the bonding of boron as non-volatile B₄C. Ascorbic acid is the most effective matrix modifier for the determination of different trace elements in boron compounds.

Boron compounds at high concentrations are reported to reduce the atomic-absorption signals for Cr, Fe, Ga and other elements.^{1,2} To diminish or compensate for this, the volatilization of boron as boric acid esters,³ the method of standard additions¹ and addition of boric acid to the standard solutions² have been used. For the determination of tin in solutions prepared by fusing geological reference materials with lithium metaborate and dissolution in acid, various matrix modifiers have been used, such as an ascorbic acid/iron(III) nitrate mixture, ammonia solution, and diammonium hydrogen phosphate.⁴

To elucidate the mechanism of formation of tin ore deposits, the solubility of cassiterite in boric acid solutions at high temperatures and pressures has been studied.⁵ In development of the method of analysis of the solutions obtained, the influence of high concentrations of boric acid (up to 0.3M) on the tin determination was investigated. It was shown that ascorbic acid is the most effective matrix modifier, and a mechanism for its action has been postulated.

EXPERIMENTAL

Reagents

Analytical-grade reagents and distilled water were used. A standard tin solution was prepared by dissolving 100 mg of tin in 2.5 ml of a 1:3 v/v mixture of concentrated hydrochloric and nitric acids. The solution was diluted to 100 ml with 3M hydrochloric acid. To obtain boron and silicon solutions appropriate weights of boric acid and sodium metasilicate nonahydrate were dissolved in demineralized water. Only freshly made ascorbic acid solutions in water were used.

Apparatus

A Perkin-Elmer Zeeman/3030 atomic-absorption spectrophotometer equipped with an HGA-600 electrothermal atomizer and "Intensitron" hollow-cathode lamps was used. The analytical lines used were 286.3 nm (band-width 0.7 nm) for tin, 249.7 nm (band-width 0.7 nm) for boron and 251.6 nm (band-width 0.2 nm) for silicon. The sample solutions (5 or 10 μ l) were injected manually. Pyrolytic graphite platforms (Perkin-Elmer) and platforms home-made from polycrystalline graphite MPG-6 (USSR) were used. Graphite tubes without pyrolytic graphite coating were used as a rule.

*Present address: Laboratory of Organic Analysis, Department of Chemistry, Moscow State University, 119899, Moscow, USSR.

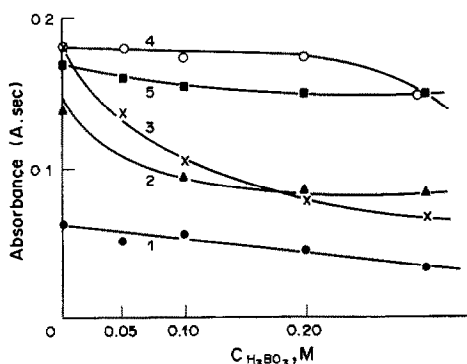


Fig. 1. Effect of boric acid on tin determination in the graphite tube with pyrolytic graphite coating (1) and without coating (2-5). 1, 2, Evaporation from the wall; 3, evaporation from the pyrolytic graphite platform; 4, evaporation from the pyrolytic graphite platform in the presence of 50 mg/ml solution of ascorbic acid; 5, evaporation from the polycrystalline graphite platform.

Procedure

For study of the matrix interferences 10 μ l of 0.15 μ g/ml tin solution in 0.5M hydrochloric acid, and 5 μ l of boric acid solution and/or modifier solution were successively injected into the atomizer. The temperature/time programme optimized for tin determination in the presence of 0.2M boric acid (atomization from the pyrolytic graphite platform) was: drying, temperature 120°/ramp time 5 sec/hold time 25 sec; ashing, 750°/5 sec/15 sec; atomization, 2200°/0

sec/3 sec (gas-stop mode); cleaning, 2600°/1 sec/2 sec. The same temperature/time programme was used for tin determination without the graphite platform, and for the determination of silicon. The temperature/time programme for boron determination (atomization from the wall of a graphite tube with pyrolytic graphite coating) was: drying, 110°/5 sec/25 sec; ashing, 400°/5 sec/12 sec; atomization, 2750°/0 sec/3 sec (gas-stop mode); cleaning, 2800°/1 sec/2 sec.

RESULTS AND DISCUSSION

Tin determination in pure solutions

The lowest response in tin determination in 0.5M hydrochloric acid is observed for atomization of the sample from the wall of a graphite tube with pyrolytic graphite coating. A higher signal is obtained with the graphite tube without coating (Fig. 1), since the partial pressure of free oxygen (p_{O_2}) in the atomizer gas phase is lower because the chemical activity of the polycrystalline graphite is higher than that of the pyrolytic graphite.^{6,7}

The signal is also increased when the sample is atomized from the platform (Fig. 1), owing to the shift of the signal to higher temperatures, where p_{O_2} is minimal. The platform material influences the tin signal area negligibly, but markedly affects the shapes of the signals (Fig. 2a). When

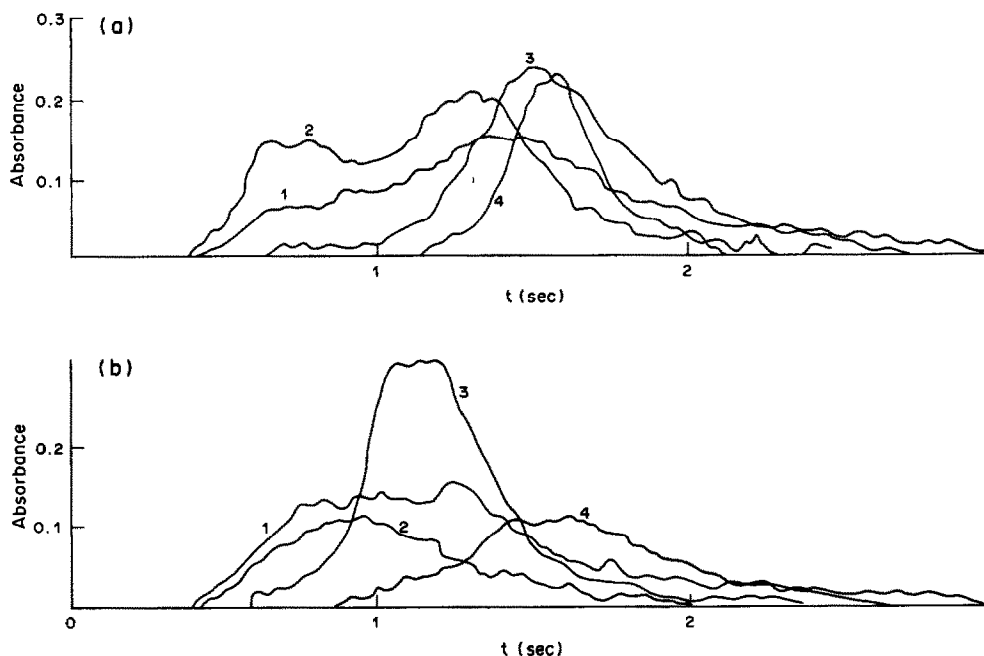


Fig. 2. Signals for tin (1.5 ng) in the absence of the matrix (a) and in the presence of 0.2M H_3BO_3 (b). 1, Evaporation from the polycrystalline graphite platform; 2-4, evaporation from the pyrolytic graphite platform; 3, in the presence of 50 mg/ml solution of ascorbic acid; 4, in the presence of 1 μ g of palladium.

the polycrystalline graphite platform is used, the tin signal appears at higher temperatures. The reason for this is that the tendency of tin to form lamellar compounds with graphite⁸ is reduced when pyrolytic graphite is used, owing to the relatively low chemical activity and smaller specific surface area of this material.

When tin is atomized from the pyrolytic graphite platform in the presence of ascorbic acid the appearance time of the signal significantly increases (Fig. 2). In this case the amorphous carbon formed as a result of thermal decomposition of the ascorbic acid may favour formation of the lamellar compounds. According to the signal shapes (Fig. 2a) the thermal stability of these compounds is lower than that of palladium-tin alloys and the corresponding intermetallic compounds formed when palladium is used as the matrix modifier.⁹

Tin determination in the presence of boric acid

The mutual solubility of tin oxides and boron oxides is very low; the corresponding chemical compounds are not formed.¹⁰ In our experiments the shape of the curves for tin signal *vs.* ashing temperature (Fig. 3) and *vs.* atomization temperature is not changed significantly by the presence of boric acid, and boric acid also does not greatly influence the appearance times of the tin signals (Fig. 2b). Hence atomization of the tin depends only slightly on the interaction of boric acid and tin compounds on the atomizer surface. The most likely causes of suppression of the tin signals in the presence of boric acid are the gas-phase processes. This assumption is corroborated by the decrease in interference when the sample is atomized from the graphite

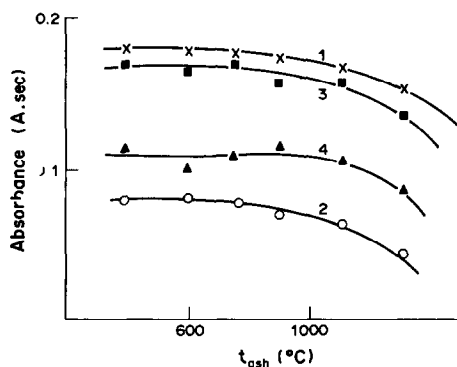


Fig. 3. Effect of the ashing temperature on signal for tin (1.5 ng); evaporation from the pyrolytic graphite platform. 1, Tin solution in 0.5M HCl; 2-4, determination in the presence of 0.2M H₃BO₃; 3, in the presence of 50 mg/ml solution of ascorbic acid; 4, in the presence of 1 μg of palladium.

platform. The dissociation of the molecules in the gas phase is more complete in this atomizer.¹¹

The interferences from boric acid are lower if the analyte is atomized from the polycrystalline graphite platform (Fig. 1), but such platforms are not commercially produced and have relatively short lifetimes. All other experiments were done with the pyrolytic graphite platforms. Atomization of the sample from these platforms in the absence of the matrix modifier does not effectively suppress the influence of boric acid (Fig. 1).

According to Havezov¹² the molecular absorption lines for BO are split in the magnetic field and may overlap with the analytical lines of tin, but in our experiments (atomization from the graphite platform, $\lambda = 286.3$ nm, bandwidth 0.7 nm) the signals from solutions of boric acid did not differ from the background.

Comparison of different matrix modifiers

The influence of the atomization temperature on the tin signal in the presence of 0.2M boric acid and 1 μg of palladium was studied. Increase in the atomization temperature to >2200° increases the peak height but has practically no effect on the peak area, so an atomization temperature of 2200° is recommended when palladium is used as matrix modifier. For the maximal effectivity of this matrix modifier the palladium solution is added to the platform, then dried and ashed at 750° for 15 sec. The temperature/time programme is then interrupted, the solutions of tin and boron are added to the atomizer, and the programme is restarted.¹³ We do not use a mixture of the solutions of ascorbic acid and palladium as was used previously,¹³ since in that case a significant complication of the processes in the graphite furnace is possible because of the interaction of the reductant and/or its thermal decomposition products with the analyte.

In the presence of boric acid and palladium the maximum ashing temperature is increased and the tin signal shifts to higher temperature (Figs. 2b and 3). Hence boric acid does not interfere in the formation of the tin-palladium compounds⁹ on the atomizer surface, but palladium does not eliminate the boron interferences completely (Fig. 3).

Some water-soluble organic compounds have also been studied as matrix modifiers. When 5 μl of 0.2M boric acid is used, the tin peak area is increased by 20, 20 or 10% if 5 μl of a 50

mg/ml solution of glucose, oxalic or citric acids respectively is also used. Under these conditions the presence of ascorbic acid (5 μ l of a 50 mg/ml solution) more than doubles the tin peak area. This quantity of ascorbic acid is optimal: increasing the concentration and/or the volume used causes rapid build-up of carbon-rich residue on the platform, which sharply decreases the reproducibility of the determination. The relative standard deviation of tin determination (10 μ l of a 0.15 μ g/ml solution) in the presence of 5 μ l of 0.2M boric acid solution is 7.8% ($n = 8$, $P = 0.95$). In the presence of ascorbic acid the reproducibility is improved to 5.0% ($n = 7$, $P = 0.95$). The corresponding value for a pure tin solution is 4.3%. This method was used for the determination of 0.005–0.100 μ g/ml tin in 0.002–0.2M boric acid solutions.⁵

Proposed mechanism of ascorbic acid action

The most probable reason for the decrease of the tin signal in the presence of boron compounds is the formation of SnB(g). The equilibrium $\text{Sn(g)} + \text{B(g)} \rightleftharpoons \text{SnB(g)}$ is defined partly by the quantity of boron in the graphite furnace and partly by the degree of boron atomization at the atomization stage.

It is known that in the presence of ascorbic acid the concentrations of carbon monoxide and hydrogen significantly increase in the ETA gas phase at 100–1200 $^{\circ}$,¹⁴ but the formation of boranes B_xH_y ,¹⁵ which would remove boron from the graphite furnace at the ashing step, is also slightly possible under such conditions. The sensitivity of boron determination is increased

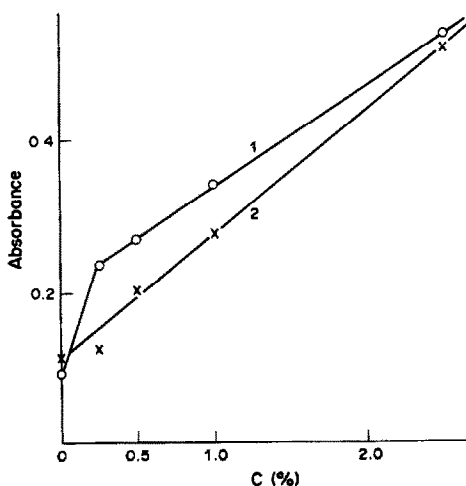


Fig. 4. Effect of 10 μ l of ascorbic acid solution on the signal for boron (1 μ g). 1, Integrated signal, absorbance·sec; 2, absorbance.

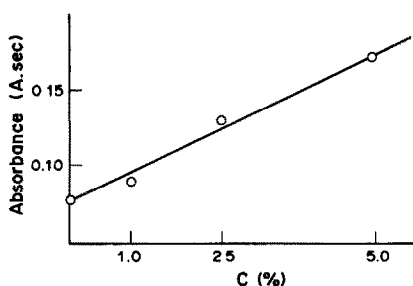


Fig. 5. Effect of ascorbic acid on determination of tin (1.5 ng) in the presence of 0.2M H_3BO_3 .

in the presence of ascorbic acid (Fig. 4), which confirms the data of Goyal *et al.*¹⁶ It is known that the concentration of B(g) increases with decrease in the free oxygen concentration in the gas phase of the graphite furnace.¹⁷ In the presence of ascorbic acid p_{O_2} decreases as a result of the interaction of oxygen with amorphous carbon.⁷

At a relatively low tin atomization temperature (2200 $^{\circ}$) boron may exist in the graphite furnace as $\text{B}_4\text{C(s)}$ and B(g); formation of BO(g) is also possible.¹⁷ Evidently, the formation of $\text{B}_4\text{C(s)}$ will favour reduction of the negative boron interferences. The tin signal obtained in the presence of boric acid increases in proportion to the ascorbic acid concentration in the solution (Fig. 5). Apparently, in the presence of the chemically active carbon formed as a result of the thermal decomposition of ascorbic acid, the kinetics of $\text{B}_4\text{C(s)}$ formation is improved. When the polycrystalline graphite platform is used, boron is more effectively bound as $\text{B}_4\text{C(s)}$ because the chemical activity of this graphite is higher than that of pyrolytic graphite.

We could not check experimentally the hypothesis concerning the decrease of B(g) concentration in the presence of ascorbic acid at the atomization temperature of tin (2200 $^{\circ}$), because of the low sensitivity of boron determination at this temperature. However, it is well-known that the behaviour of silicon in the graphite furnace is to a large extent analogous to the behaviour of boron. At high temperatures silicon is also susceptible to the formation of carbide $\text{SiC}_2\text{(g)}$ and oxide SiO(g) .¹⁸ The sensitivity of silicon determination by ETAAS is significantly higher than that for boron. Under the conditions of tin determination the silicon signal decreases with increasing ascorbic acid concentration (Fig. 6). We propose that the concentration of free boron atoms in the gas phase in the graphite tube at 2200 $^{\circ}$ also decreases in the presence of ascorbic

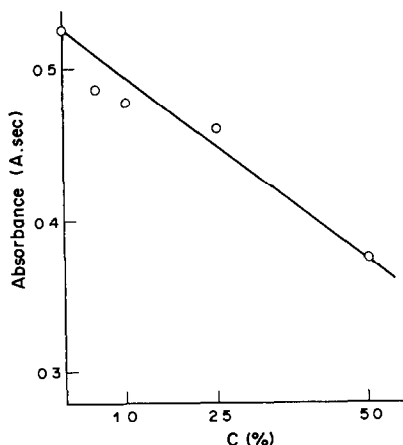


Fig. 6. Effect of 10 μ l of ascorbic acid solution on the signal for silicon (40 ng); evaporation from the pyrolytic graphite platform.

acid. Silicon by itself, up to a concentration of 0.2M, does not influence the tin signal.

CONCLUSION

The most effective matrix modifier for the ETAAS determination of tin in the presence of high concentrations of boric acid is ascorbic acid. The amorphous carbon formed as a result of thermal destruction of ascorbic acid favours the bonding of boron in $B_4C(s)$, which is rather stable at the atomization temperature of tin (2200°). On the basis of the data obtained, ascorbic acid may be recommended as matrix modifier for the determination of other elements as impurities in the presence of high concentrations of boron compounds. Palladium chloride is less effective as the modifier in this case.

Acknowledgements—The authors express their gratitude to Ivan Havezov (Bulgarian Academy of Sciences) and Elena K. Wulfson for helpful discussions.

REFERENCES

1. H. J. Rath, *Z. Anal. Chem.*, 1980, **302**, 275.
2. K. Smolander, R. Järnström and A. Sajalinna, *ibid.*, 1989, **335**, 392.
3. Z. Yu, Z. Zhang and S. Liu, *Huaxue Shiji*, 1983, **5**, 315.
4. E. Lundberg and B. Bergmark, *Anal. Chim. Acta*, 1986, **188**, 111.
5. N. I. Kovalenko, B. N. Ryuzhenko, V. A. Dorofeeva, A. G. Volosov and L. N. Bannykh, *Geokhimiya*, in the press.
6. B. V. L'vov and G. N. Ryabchuk, *Spectrochim. Acta*, 1982, **37B**, 673.
7. A. B. Volynsky, E. M. Sedykh, B. Ya. Spivakov and I. Havezov, *Anal. Chim. Acta*, 1985, **174**, 173.
8. C.-H. Chung, E. Iwamoto and Y. Yamamoto, *Talanta*, 1987, **34**, 927.
9. E. M. Savitsky, V. P. Polyakova and M. A. Tylkina, *Palladium Alloys*, Nauka, Moscow, 1967 (in Russian).
10. H. Bitterer (ed.), *Gmelin Handbuch der Anorganischen Chemie*, Zinn, Teil C2, p. 215. Springer-Verlag, Berlin, 1975.
11. B. V. L'vov, L. A. Pelieva and A. I. Sharnopolsky, *Zh. Prikl. Spektrosk.*, 1977, **27**, 395.
12. I. Havezov, private communication.
13. L. M. Voth-Beach and D. E. Shrader, *J. Anal. Atom. Spectrom.*, 1987, **2**, 45.
14. G. F. R. Gilchrist, C. L. Chakrabarti and J. P. Byrne, *ibid.*, 1989, **4**, 533.
15. E. Wiberg, *Angew. Chem.*, 1953, **65**, 16.
16. N. Goyal, A. R. Dhobale, B. M. Patel and M. D. Sastry, *Anal. Chim. Acta*, 1986, **182**, 225.
17. W. Frech, A. Cedergren and E. Lundberg, *Analytik-treffen: Atomspektroskop. Fortschr. Anal. Anwend., Hauptvortr.* 1982, p. 102, Karl-Marx-University, Leipzig; *Chem. Abstr.*, 1982, **102**, 89081x.
18. W. Frech, E. Lundberg and A. Cedergren, *Prog. Anal. Atom. Spectrosc.*, 1985, **8**, 257.

DETERMINATION OF NITRIC ACID CONCENTRATION BY USING EUROPIUM ION FLUORESCENCE

J. C. CORIA-GARCIA and T. M. NIEMCZYK*

Department of Chemistry, University of New Mexico, Albuquerque, NM 87131, USA

(Received 8 January 1991. Accepted 14 January 1991)

Summary—A method is presented for the determination of 2–10M nitric acid based on the fact that the presence of high nitric acid concentration causes an enhancement of the intensity of some bands in the fluorescence spectra of rare earth ions in solution. The 616-nm band of Eu^{3+} shows the most dramatic intensity enhancement with increasing nitric acid concentration. The present method, based on the measurement of the ratio of Eu^{3+} fluorescent band intensities is shown to be independent of Eu^{3+} concentration and relatively free of interference. This robust method allows the presence of an interferent to be determined from the experimental data.

There are a number of processing environments that require a high nitric acid concentration for proper operation. Perhaps the most significant of these is in nuclear fuel reprocessing where the free acid content must be determined to ensure that the fuel samples are appropriately decontaminated or that loss of recoverable fuel is minimized.¹⁻³ Further, the free acid content must be known to enable the waste solutions to be appropriately neutralized before disposal.

In a review of the methods which may be used to measure nitric acid concentrations, Gallagher and Johnson⁴ presented the requirements for a successful measurement technique and critiqued the potential methods. The requirements for successful determination of the mineral acid concentration of nuclear processing streams are rather severe. First, the method has to measure acid concentrations with a precision of $\pm 5\%$ over the concentration range 1–10M. The method must be able to operate in the presence of heavy metal salts, and the processing environment can be rather harsh. This is especially true of a nuclear fuel reprocessing environment where corrosivity and high levels of radiation must be expected. Thus, any method that can operate with all major pieces of equipment and all electronic components remote to the actual measurement site will be desirable. Spectroscopic methods have the potential of utilizing optical fibers to enable isolation of all instrumentation from the measurement site and are thus worthy of investigation.

We propose here a method of measurement of high nitric acid concentrations based on a fluorescence process. The measurement depends on the enhancement of a hypersensitive transition of Eu^{3+} owing to the formation of an inner-sphere co-ordination complex with nitrate ion in highly acidic solutions. This method potentially meets all the requirements of a method capable of determining nitric acid concentration over the concentration range of interest in a harsh processing environment. The Eu^{3+} probe must be present or added to the solution but the Eu^{3+} concentration does not affect the measurement.

EXPERIMENTAL

Instrumentation

Fluorescence measurements were carried out with an LS-5 Luminescence Spectrometer (Perkin-Elmer) with quartz cells (1 cm, Fisher). Instrument settings and data acquisition were carried out through an RS-232C interface between the LS-5 and a Zenith 159 microcomputer. Fluorescence spectra and intensity *vs.* concentration data were acquired with software developed in-house for these experiments. Fluorescence spectra were obtained with the following instrument parameters: excitation/emission slit apertures set to nominal 10/5 nm bandpass; scan speed, 120 nm/min; RC filter response, 4; excitation wavelengths (5–7), $\text{Eu}^{3+}/392$ nm, $\text{Sm}^{3+}/402$ nm, $\text{Dy}^{3+}/350$ nm and $\text{Tb}^{3+}/372$ nm. Spectral data were acquired every 0.5 nm. Intensity *vs.* concentration data were obtained at the

*Author for correspondence.

same excitation wavelengths. In these experiments, excitation/emission slits were set at a nominal 10-nm bandpass, and the RC filter response had a value of 4. Software used in these experiments acquired 250 data points at fixed emission/excitation wavelengths, the data were averaged, and the standard deviation was obtained. Final intensity data were obtained by subtracting the blank from the analyte signal, and the standard deviation was determined by error propagation.⁸

Chemicals and solutions

All reagents (ACS reagent grade) were used as obtained. Lanthanum(III) oxides and the disodium salt of EDTA were purchased from Alfa Products. Acetic acid, sodium acetate, nitric acid, sulfuric acid and hydrochloric acid were obtained from Fisher. Xylenol Orange (95% dye) and sodium carbonate were purchased from Aldrich.

All solutions were prepared from triply-distilled water passed through cation exchange, anion exchange and activated carbon columns. Lanthanum(III) 0.01M stock solutions were prepared by dissolving the corresponding oxide in the minimum amount of 20% (v/v) hydrochloric acid. Excess of acid was removed by evaporation and the remaining chloride salt was then dissolved in the required amount of water. Lanthanum(III) stock solutions were standardized versus EDTA (0.01M) in an acetate buffer medium with Xylenol Orange as indicator.⁹ Stock solutions of acid (12.5M) were prepared by diluting the appropriate amount of con-

centrated acid to one liter with water. Fresh solutions were made weekly. Nitric acid stock solutions were standardized by titration against sodium carbonate with Bromocresol Green as indicator.

Procedure

Blank solutions consisted of purified water for all measurements. The solutions of different Ln^{3+} /acid ratios were prepared by mixing appropriate amounts of the corresponding stock solutions and diluting to a volume of 50 ml with water. All solutions were allowed to stand for a period of at least one hour to reach room temperature and ensure complexation, and were then filtered through a sintered glass filter prior to use. The quartz cell was always kept in place inside the cell container of the LS-5 to avoid any errors caused by changing the cell walls facing the emission and/or excitation monochromators. Before any new solution was placed in the cell, the cell was thoroughly rinsed with water and the new solution with a micropipette.

RESULTS AND DISCUSSION

There are several bands in the fluorescence spectrum of aqueous Eu^{3+} when the solution is excited at 394 nm. Of these, the most intense bands are those observed at 591, 616 and 694 nm.^{5,6} The emission bands at 616 nm ($^5\text{D}_0 \rightarrow ^7\text{F}_2$, $\Delta J = 2$) and 694 nm ($^5\text{D}_0 \rightarrow ^7\text{F}_4$, $\Delta J = 4$) are "forbidden" according to the Laporte selection rule. This accounts for their low emission intensity when compared to that of

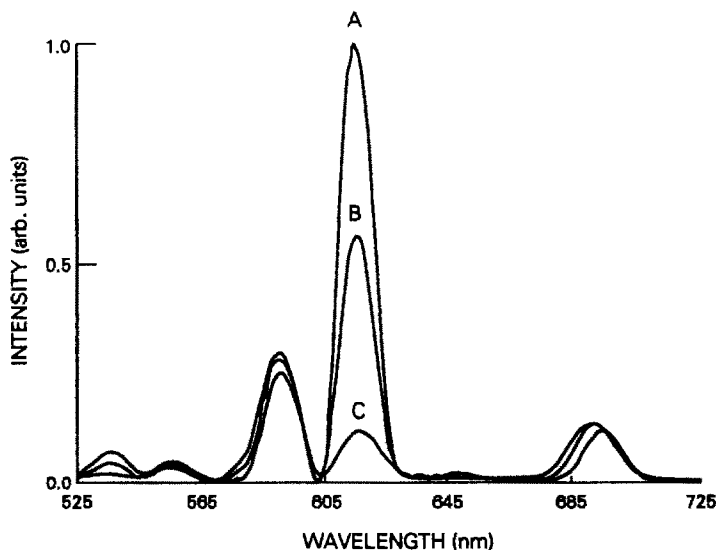


Fig. 1. Fluorescence spectra of Eu^{3+} ions in solutions of varying nitric acid concentration. A: 10M HNO_3 . B: 5.0M HNO_3 . C: Triply distilled water.

the "allowed" 591 nm ($^5D_0 \rightarrow ^7F_1$, $\Delta J = 1$) band.¹⁰ The 616 nm band has been designated as a "Hypersensitive Transition" (HT).⁶ This term conveys the effect of the environment surrounding the ion has on the emission intensity of this band.¹⁰ HT or $\Delta J = 2$ transitions have also been observed in the fluorescence emission spectra of other lanthanides in aqueous media such as Sm^{3+} (640 nm, $^4G_{5/2} \rightarrow ^6H_{9/2}$), Tb^{3+} (491 nm, $^5D_4 \rightarrow ^7F_6$) and Dy^{3+} (577 nm, $^4F_{9/2} \rightarrow ^6H_{13/2}$).⁵

Shown in Fig. 1 are the fluorescence emission spectra of aqueous Eu^{3+} ions in water (C), 5M nitric acid (B) and 10M nitric acid (A). The HT at 616 nm shows a six-fold increase when the solvent is changed from water to 10M nitric acid. This enhancement has been extensively discussed in the literature¹⁰⁻¹⁵ and is generally attributed to the inner sphere complexation of the nitrate ion with Eu^{3+} . In a study of the fluorescence behavior of the $\text{Eu}^{3+}/\text{HNO}_3$ system, Piriou and Svoronos¹³ suggested that the composition of the aquanitrate complex of Eu^{3+} has the formula $[\text{Eu}(\text{NO}_3)_m(\text{H}_2\text{O})_n]^{(3-m)+}$ where the value of m is dependent upon the concentration of nitric acid. This dependence might suggest that the intensity of the HT is a direct function of the number of NO_3^- ions complexed with Eu^{3+} . When compared to the HT transition, the other Eu^{3+} transitions do not show dramatic intensity shifts with changes in nitric acid concentration. The 591 and 694 nm bands show only a slight increase in intensity *ca.* 5%, when the solvent changes from water to 10M nitric acid. This slight intensity change was previously reported by Gallagher¹⁰ and is attributed to a near-linear increase in the observed fluorescence lifetime of the 5D_0 state due to $\text{Eu}^{3+}/\text{NO}_3^-$ complexation. Although a small shift in the wavelength of maximum intensity is observed in the band between 680 and 705 nm, the strongest emission remains at 694 ± 2 nm in nitric acid concentrations above 2M.

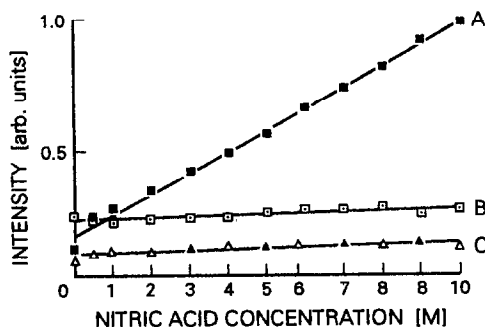


Fig. 2. Intensity of the Eu^{3+} ion bands as a function of nitric acid concentration. A: 616 nm. B: 591 nm. C: 694 nm.

As mentioned above, the fluorescence emission spectra of Sm^{3+} , Tb^{3+} and Dy^{3+} also contain HT bands. Complementary fluorescence studies of these ions in the 1–10M nitric acid range have shown that, like Eu^{3+} , an increase in the intensity of the respective HT is observed. However, unlike Eu^{3+} , the $\Delta J = 1$ bands of these ions (Sm^{3+} , 596 nm; Tb^{3+} , 479 nm and Dy^{3+} , 479 nm) show a considerable increase in intensity as well. The fact that the $\Delta J = 1$ transition of Eu^{3+} stays relatively constant presents the possibility of using it as an "internal standard."

A plot of emission intensity versus nitric acid concentration of the 591, 616 and 694-nm Eu^{3+} bands is shown in Fig. 2. The intensity of the 616-nm band increases linearly with nitric acid concentration over the range 2–10M. As discussed above, the bands at 591 and 694 nm increase only slightly with nitric acid concentration, $\sim 5\%$. All three plots in Fig. 2 are linear at nitric acid concentrations above 2M. The features illustrated in Fig. 2 allow for the development of a technique to measure high nitric acid concentrations based on Eu^{3+} ion fluorescence. We have used various spectral features to investigate the calibration of nitric acid concentration: (I) the intensity of the band at 616 nm; (II) the ratio of the intensity of the band at 616 nm to the intensity of the band at 591 nm; (III) the ratio of the intensity of the band at 616 nm to the intensity of the band at 694 nm and (IV) the ratio of the intensity of the band at 616 nm band to the intensity of the band at 591 nm minus the intensity of the band at 694 nm.

For the method to be useful, the measurement should not depend upon the concentration of Eu^{3+} and should be insensitive to the presence of potential interferents. As would be expected, the intensity of any individual band is directly proportional to the Eu^{3+} concentration. The use of a ratio of intensities should result in a measurement that does not depend upon the Eu^{3+} concentration. This is analogous to the use of an internal standard. Further, many potential interferents would be expected to affect the entire Eu^{3+} spectrum, thus the ratio of peak intensities should be constant. The various calibration procedures have been tested under varying conditions, and the results of these tests are outlined below.

Although the intensity of the Eu^{3+} band at 616 nm varies dramatically with the nitric acid concentration, results obtained by using the

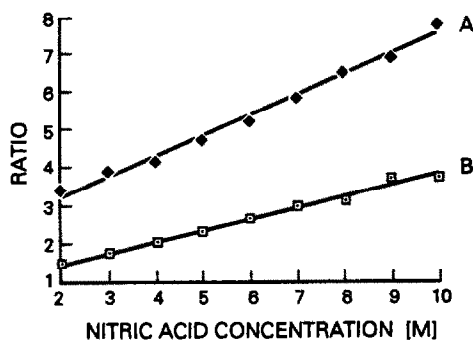


Fig. 3. Intensity ratios as a function of nitric acid concentration. A. I_{616}/I_{694} . B. I_{616}/I_{591} .

intensity of this band as a measure of nitric acid concentration proved highly unreliable. The band intensity varies significantly with excitation intensity fluctuations, the presence of particulate matter and the presence of other metals. The use of ratios of Eu^{3+} band intensities results in freedom from most of these effects (Fig. 3). All three ratios produce linear plots over the range 2–10M nitric acid. The plots of $I_{616}/(I_{591} - I_{694})$ and I_{616}/I_{694} vs. nitric acid concentration are nearly identical and somewhat more sensitive than that of I_{616}/I_{591} vs. nitric acid concentration. All data discussed above were obtained with a Eu^{3+} concentration of 150 ppm. Figure 4 shows the plots of the I_{616}/I_{694} intensity ratios at 0, 2.5, 5.0, 7.5 and 10M nitric acid as a function of Eu^{3+} concentration over the range 50–250 ppm. The ratio remains constant between 100 and 250 ppm Eu^{3+} . Europium(III) concentrations below 100 ppm show a slight decrease in the intensity ratio. Although not shown here, the plot of I_{616}/I_{591} vs. Eu^{3+} concentration follows the same trend as that of Fig. 4. These data suggest that the concentration of the Eu^{3+} ion employed in the fluorescence determination of nitric acid can be in the range 150–250 ppm Eu^{3+} , but the exact concentration of Eu^{3+} is not important.

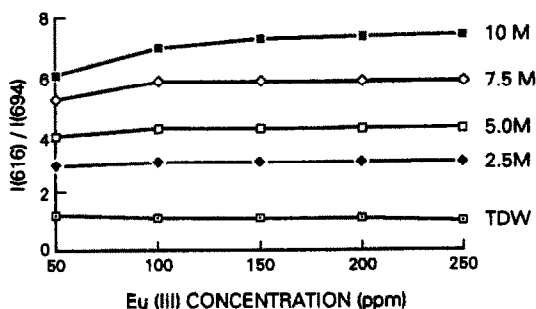


Fig. 4. Plot of the intensity ratio, I_{616}/I_{694} , versus Eu^{3+} concentration for various nitric acid concentrations.

Table 1. Concentration of nitric acid as determined from the Eu^{3+} probe fluorescence. The nitric acid concentration was 6.20M in all solutions. The concomitants were all present at 150 ppm, except as noted

Solution	Nitric acid concentration, M		
	I_{616}	I_{616}/I_{591}	I_{616}/I_{694}
Water	6.26 ± 0.07	6.06 ± 0.03	6.26 ± 0.06
SM	6.33 ± 0.07	5.78 ± 0.03	6.09 ± 0.07
Tb	6.23 ± 0.07	6.30 ± 0.03	6.13 ± 0.07
Dy	6.25 ± 0.07	6.01 ± 0.03	6.08 ± 0.08
SM/Tb/Dy	6.40 ± 0.07	5.57 ± 0.03	6.10 ± 0.08
Al	6.28 ± 0.07	6.33 ± 0.03	6.20 ± 0.08
Fe (50 ppm)	4.32 ± 0.11	6.55 ± 0.03	6.62 ± 0.06
Fe	2.15 ± 0.19	6.39 ± 0.03	6.77 ± 0.06
Al/Fe	2.15 ± 0.19	6.44 ± 0.03	6.00 ± 0.06
UO_2^{2+} (560 ppm)	6.41 ± 0.03	4.92 ± 0.02	6.05 ± 0.03
Ru (Satd. RuCl_3)	1.09 ± 0.02	6.62 ± 0.02	5.93 ± 0.03

As stated above the method must be relatively insensitive to the presence of other metals to be generally useful. This point was tested by preparing a set of test solutions containing 150 ppm Eu^{3+} , 6.20M nitric acid and a selection of potential interferents. The rare earth ions were tested because they have fluorescent properties similar to Eu^{3+} , their fluorescence spectra are affected by nitric acid and they are present in raffinate solutions.¹⁶ Iron(III) and Al^{3+} have been found to interfere in other nitric acid determinations due to hydrolysis,^{2,3} but the interference is only noted at concentrations higher than those typically found in raffinate solutions.

The results of the interference studies are summarized in Table 1. All determinations are made by comparing the data obtained in these studies to calibration data obtained in pure water (i.e., the data presented in Fig. 3). The standard deviations included in the Table are the result of three or more independent determinations of each solution. The differences in the results for pure water and the expected results represent day-to-day variations and changing the cell.

As can be seen from the data presented in Table 1, the most significant interference appears to be the presence of Fe^{3+} in the sample solution. The Eu^{3+} fluorescence is quenched by Fe^{3+} , hence the large error in the nitric acid measurement based solely on the intensity of the band at 616 nm. However, the Eu^{3+} fluorescence is uniformly quenched, and the results based on ratio determinations remain fairly accurate. Using a desired accuracy of 5% (the ratio of determinations), suitable results are produced when Fe^{3+} is present when using the intensity of the band at 616 nm divided by the

intensity of the band at 591 nm. The alternative ratio, I_{616}/I_{694} , produces results that are approximately 9% high when Fe^{3+} is present.

The presence of both UO_2^{2+} and Ru^{3+} had an effect on the measurement. When present at 150 ppm UO_2^{2+} caused little interference but at 560 ppm (selected as this was a concentration measured in a raffinate solution¹⁶) it did affect the I_{616}/I_{591} ratio. Ru^{3+} causes a significant baseline shift. A baseline subtraction (linear baseline) yielded the results in Table 1.

The data in Table 1 show that there is obviously some interference due to Sm^{3+} . We believe this to be a spectral interference as Sm^{3+} has a broad excitation peak centered at 402 nm. This peak certainly overlaps the excitation band, centered at 396 nm used to excite the Eu^{3+} fluorescence. Samarium(III) has an emission band at 596 nm that is enhanced by high nitric acid concentration. This band contributes some intensity to the measurement made at 591 nm, and the I_{616}/I_{591} ratio is lowered. Thus, the result of the nitric acid determination with I_{616}/I_{591} is 6.7% too low. There is no Sm^{3+} emission near the Eu^{3+} band at 694 nm and thus the ratio I_{616}/I_{694} produces acceptable results when Sm^{3+} is present.

In one set of experiments, the solutions were run without filtering. A new set of plastic bottles were used to store the solutions, and the bottles were either not washed properly or the high nitric acid concentrations contributed to some reaction with the vessel walls, so that the solutions had significant particle concentrations. The particle suspensions were easily visible and caused a noticeable increase in scattering. The fluorescence spectra of these solutions were measured and compared to the calibration data. The scattering produced by these solutions were manifest by an increase in background signal, especially at low wavelengths. At the low wavelength end, 525 nm, the background signal was increased by 50% compared to filtered solutions, whereas the high wavelength end was increased only slightly. The nitric acid concentrations, as determined from the I_{616}/I_{591} ratio, were identical to those determined with filtered solutions within the deviations seen in Table 1. The I_{616}/I_{694} ratio produced results that were consistently low, ~10%, when compared to the filtered results. The fact that the I_{616}/I_{591} ratio is unaffected by the presence of particulates is explained by the observation that the background increases nearly identically at 616 nm and 591 nm when particulates are present. Thus,

the method can be used without interference from particulate matter when the I_{616}/I_{591} ratio is used.

CONCLUSION

The Eu^{3+} probe method presented here produces results (<5% error) for the determination of high nitric acid concentrations for most situations tested. The method is not ideal in that the probe, the Eu^{3+} , must be added or be present in the analyte solution. While the addition of a reagent is easily accomplished in a laboratory setting, it might not be so straightforward in a processing environment. However, the fact that the Eu^{3+} concentration can vary significantly and not affect the measurement accuracy somewhat alleviates this constraint. Further, the fact that the measurement can be made with a fiber optic system to separate the measurement instrumentation from the sample site might be a real advantage in some situations.

A totally interference-free measurement would be highly desirable. The results presented here were based on the measurement of the fluorescent intensity at three fixed wavelengths. In the case of the Sm^{3+} interference (*i.e.*, one that is spectral), it is highly likely that the interference could be allowed for by utilizing more of the spectral information available. This would be accomplished at some expense in instrumentation relative to the simplest systems envisioned for a fixed three wavelength measurement.

The data in Table 1 clearly shows that the use of an internal standard, *i.e.*, the Eu^{3+} fluorescence at 591 or 694 nm, makes the measurement much less susceptible to interferents. The I_{616}/I_{694} ratio in general produces somewhat better results than does the I_{616}/I_{591} data. The only significant deviation is produced by high Fe^{3+} concentration, a 9.1% error. Again, use of more of the spectral data might diminish the effects of Fe^{3+} on the measurement.

An important point that can be seen in the data presented here is that an interference is noted when the three measurement results do not agree. Thus, the method produces the correct result, or in the situation where an interferent is present, the potential failure of the method is indicated by the lack of agreement of the various calibration methods.

It might be possible to immobilize the Eu^{3+} probe in a manner that would still allow the

required nitrate ion interaction to produce the intensity enhancement of the band at 616 nm. If this were possible, the complication of adding the probe ion to the analyte solution would be eliminated. The measurement could then be accomplished by placing a fiber optic probe with the immobilized reagent into the process stream or sample whose nitric acid concentration was to be determined.

Acknowledgement—This research was sponsored in part by Los Alamos National Laboratory under contract No. 9-X3D-16076-1 and, in part, by the U.S. Department of Energy, through the Waste-Management Education and Research Consortium (WERC).

REFERENCES

1. J. E. Strain, *U.S. Department of Energy Report TM-6800*, Oak Ridge, TN, May 1979.
2. E. W. Baumann and B. H. Torrey, *Anal. Chem.*, 1984, **56**, 682.
3. E. W. Baumann, *U.S. Department of Energy Report DP-MS-81-82*, Aiken, SC, October 1981.
4. K. Y. Gallagher and C. M. Johnson, U.S. Department of Energy Report *RFP-2986*, Golden, CO, October 1980.
5. M. Elbanowski, S. Lis, B. Mąkowska and J. Konarski, *Monatsh. Chem.*, 1985, **116**, 901.
6. M. Elbanowski, B. Mąkowska and S. Lis, *ibid.*, 1982, **113**, 907.
7. M. Elbanowski, S. Lis and B. Mąkowska, *ibid.*, 1983, **114**, 185.
8. D. A. Skoog in *Principles of Instrumental Analysis*, pp. 14–15. Saunders College Publishing, New York, 1985.
9. J. B. Headridge, *Photometric Titrations*, p. 83. Pergamon Press, New York, 1961.
10. P. K. Gallagher, *J. Chem. Phys.*, 1964, **41**, 3061.
11. J. P. Breen and W. DeW. Horrocks, Jr., *Inorg. Chem.*, 1983, **22**, 536.
12. J.-C. G. Bünzli and J. R. Yersin, *ibid.*, 1979, **18**, 605.
13. B. Piriou and D.-R. Svoronos, *J. Less-Comm. Metals*, 1985, **112**, 275.
14. G. R. Choppin, *ibid.*, 1985, **112**, 193.
15. I. Abrahamer and Y. Marcus, *Inorg. Chem.*, 1967, **6**, 2103.
16. T. Matsui, H. Fujimori and K. Suzuki, *J. Nuc. Sci. Tech.*, 1988, **25**, 868.

COMPARISONS OF INTEGRATION *vs.* RATE MEASUREMENTS FOR OXIDASE ENZYMATIC ANALYSES

LAWRENCE C. THOMAS* and RASHID AL OTHMAN

Department of Chemistry, Seattle University, Seattle, Washington 98122, U.S.A.

(Received 6 June 1990. Revised 31 October 1990. Accepted 4 November 1990)

Summary—Results obtained by integration of net indicator-substance signals during the progress of a reaction are compared to those concurrently achieved by rate estimation with the time *vs.* signal data, for glucose oxidase assays and enzymatic glucose determinations. Computer-simulated integration results typically exhibit data quality superior to that of rate measurements, for the entire very wide ranges of oxidase activities and concentrations studied. Only at extreme instrument-noise levels and low analyte values did any of the rate procedures (the variable-time method) show some advantage over integration. The data quality, expressed as relative uncertainties, of the simulated results obtained by use of the integration method was typically up to 120 times better than that obtained by rate methods, with greater enhancement at higher enzyme activities or substrate concentrations. Experimental results spanning physiological concentrations showed similar trends, but the advantage was not as great as that shown in the simulations.

Integration of the net indicator-substance response over a specified time interval can be used for kinetic analyses.¹⁻⁷ Other methods of kinetic analysis include rate-estimation⁸⁻¹⁰ and curve-fitting.¹⁰⁻¹³ Some of the rate-estimation methods employ integration of signals over two time intervals, which can be consecutive¹⁴⁻¹⁶ or separated by a delay interval.¹⁴ The difference between the two integrals (which are equivalent to time-averaged responses) can then be used to mimic the two-point differential methods. The curve-fitting methods calculate the "best-fit" to response *vs.* data. The curve is then either compared with a well-known set of data to establish analytical results,¹⁰⁻¹² or is extrapolated to predict a value such as an equilibrium concentration.^{10,13}

Integration over an interval has distinct advantages over the methods based on rate estimation by the fixed-time, variable-time and continuous derivative methods.⁸ Often, a limiting requirement for rate measurements is that changes in transducer response should be directly proportional to time during the measurement interval. Differential methods are usually used with zero-order, first-order or pseudo first-order reactions, but only seldom with second- and higher-order reactions, and may sometimes be mistakenly used in cases for which their theoretical basis is not met

or is otherwise invalid. Thus, rate-estimating methods are sometimes beset with difficulties which cause determinate errors or excessive uncertainties,^{9,14-16} or are restricted to only a narrow range of conditions.

The integration method sums a large number of data over a fairly long period and thereby reduces the relative noise, by signal averaging. This may result in better detection limits, sensitivity, precision and accuracy.⁷ Also, the integration method may often be used for complicated reactions for which rate estimates may fail, *e.g.*, those showing maxima, minima or inflections.^{3,7} Moreover, it does not require well-known kinetic data^{1,3} nor does it require calculations to be made after the experimental run is completed.⁷

In this study, the integration method is directly compared with the fixed-time, variable-time and continuous derivative methods, by use of identical time *vs.* response data from oxygen-consuming enzymatic reactions. Replicate results for the various methods are collected for many variations of the main parameters. These data are characterized statistically as relative uncertainties and compared for the variations explored.

EXPERIMENTAL

Reagents

For laboratory comparisons, enzyme solutions were made from glucose oxidase (130

*Author for correspondence.

I.U./mg) purchased from Sigma Biochemical Co. Buffered solutions (0.1M phosphate, pH 5.5) were prepared with reagent grade chemicals, including *d*-glucose. Distilled water was used for all dilutions.

mole l⁻¹.min⁻¹. No oxygen-consuming or oxygen-depleting interferences were considered in this theoretical work. The enzymatic rate of reaction was assumed to be directly proportional to the concentration of glucose:

$$\left(\frac{dC_{O_2}}{dt}\right)_{\text{overall}} = \frac{-\text{const. [G.O.A.][Glucose]}(1 - 10^3 [H_2O_2])(C_{O_2,eq} - C_{O_2,t})}{C_{O_2,eq}}$$

Instrumentation

The amperometry cell for reactions was an open 30-ml beaker with a 1-cm Teflon-coated magnetic stirring bar and an immersed Beckman oxygen sensor. The electrode system was monitored by a Princeton Applied Research (PAR) 174 potentiostat with the working electrode maintained at -0.55 V *vs.* an Ag/AgCl reference electrode. A typical current from the sensor was 16 nA for solution at equilibrium with air, with white noise approximating 0.15 nA. The beaker was set on a 2-cm thick styrofoam insulator above a magnetic stirring motor.

For theoretical mathematical modeling, an Epon Equity II+ computer was used. Computer programs were written with Microsoft's QuickBasic 4.0 (listings available from the senior author on request).

Procedures

Theoretically-derived current *vs.* time relations were calculated with mathematical models and kinetic data from other work.¹⁶⁻¹⁸ The sensitivity of the amperometric response to oxygen was assumed to be 10⁵ nA.l.mole⁻¹, yielding a current of 25 nA at 2.5 × 10⁻⁴M equilibrium oxygen concentration when a stirred analysis solution with a volume of 1.0 ml was used. On the basis of the oxygen-electrode performance, the constant white noise was assigned a standard deviation of 0.01 nA and the proportional white noise a standard deviation of 0.001*i*_t*n* where *i*_t is the measured current (in nA) and *n* is selected from the set *n* = 1.00, 1.78, 3.16, 5.624, 10, 17.8, 32.6, 56.24 and 100.

Inhibition by peroxide was assumed to diminish the initial glucose oxidase activity (G.O.A.) by 0.1*x*% where *x* is the hydrogen peroxide concentration in μmole/l. Incorporation of oxygen from the atmosphere by the stirring and diffusion (SD) was assumed to be proportional to the degree of oxygen depletion of the test solution,³ and its rate was taken as (dC_{O₂}/d*t*)_{SD} = 0.01 (C_{O₂,eq} - C_{O₂,t})/(C_{O₂,eq})

where [H₂O₂] is in μmole/l. and the constant includes the factor 0.01 from the equation for the rate of incorporation of oxygen from the atmosphere.

For glucose determinations, the G.O.A. concentration used was 10⁻¹¹ I.U./l. and added glucose concentrations were varied between 0 and 0.075M in eight steps (1.00, 1.335, 1.78, 2.372, 3.16, 4.217, 5.624 and 7.5) within each decade. For glucose oxidase assays, the initial concentration of glucose was set at 10⁻³M, consistent with the values used in routine work.^{3,6} The added glucose oxidase activity was either zero or varied in eight steps (again 1.00, 1.335, 1.78, 2.372, 3.16, 4.217, 5.624 and 7.5) within each decade from 10⁻¹³ to 10⁻⁹ I.U./l.

For optimizations, 10⁻¹¹ I.U./l. glucose oxidase was used, with glucose spanning the concentration ranges specified above. Integration time increments of 0.1, 0.25, 0.5, 1.0 and 2.5 sec were used for each entire set of glucose concentrations. The calculations described below were done with 25 replications for each combination. The relative precisions were compared, to select the optimal integration time increment, integration duration and fixed-time intervals used for subsequent studies of relative precisions.

After optimization for each replication within a set of conditions, the time *vs.* oxygen concentration relation was simulated with 0.1-sec time increments and the time-dependent rates for that set of conditions. The corresponding current *vs.* time relations were also generated concurrently with rate estimates and integrations performed continuously as the *i*_t *vs.* time relations developed. Fixed-time estimates were calculated as the difference between the current at 10 sec after addition of the analyte, and the average (over 30 sec) of that at equilibrium before initiation of the catalytic reaction; this procedure is consistent with that typically used for fixed-time measurements.⁸ Variable-time estimates were calculated similarly by using the time required to change *i*_t by 0.3 nA from its equilibrium value; the effects of time-averaging of the non-equilibrium data used for fixed-time

and variable-time measurements are being evaluated in other work, and the results should help to improve data quality for those methods. Maximum rates of change of i_t with respect to time were estimated as the greatest value of $\Delta i/\Delta t$ for any 1-sec time interval. Integrations were summed as shown in Fig. 1(c).

For each set of 25 replications for each variation in conditions, the average (\bar{x}) and standard deviation (s) were calculated. The data quality was defined as \bar{x}/s , for each set, and the values obtained were used in log-log plots against variations in conditions spanning several orders of magnitude.

RESULTS AND DISCUSSION

Results from simulations

Short time increments, e.g., 0.1 sec, produced the best relative uncertainty (s/\bar{x}) values for the procedures investigated. Overall, the data quality for integrations was best with 90-sec integrations, and somewhat inferior for 15-, 30-, 60- and 120-sec integrations, but each integration time gave superior precision for some particular enzymatic activity range. The fixed-

time method had its best overall precision for a measurement time of 10 sec. Consequently, data discussed below are for 10-sec fixed-time intervals, 90-sec integration duration and 0.1-sec data intervals, i.e., 10 Hz sampling frequency.

The current vs. time relations were similar to those found for routine analyses and other research (see Fig. 1).^{3,6} Averaged results changed as expected, with the variable-time method showing high values at low catalysis rates and low values at high rates, the reverse of the behavior of other rate estimates and the integrations. At higher noise levels, all the results exhibit worse precision, as evidenced by less consistent averages (Fig. 2) and lower \bar{x}/s values (Figs. 3 and 4).

The relative uncertainties for glucose oxidase assays by the integration procedure were much better than those obtained with any of the rate-estimating methods, over all catalytic rates when the noise levels were low to moderate, as would be expected for good to poor current-measuring instruments. Similarly, the integration method was substantially better than the fixed-time and continuous derivative methods over all catalytic rates and noise levels

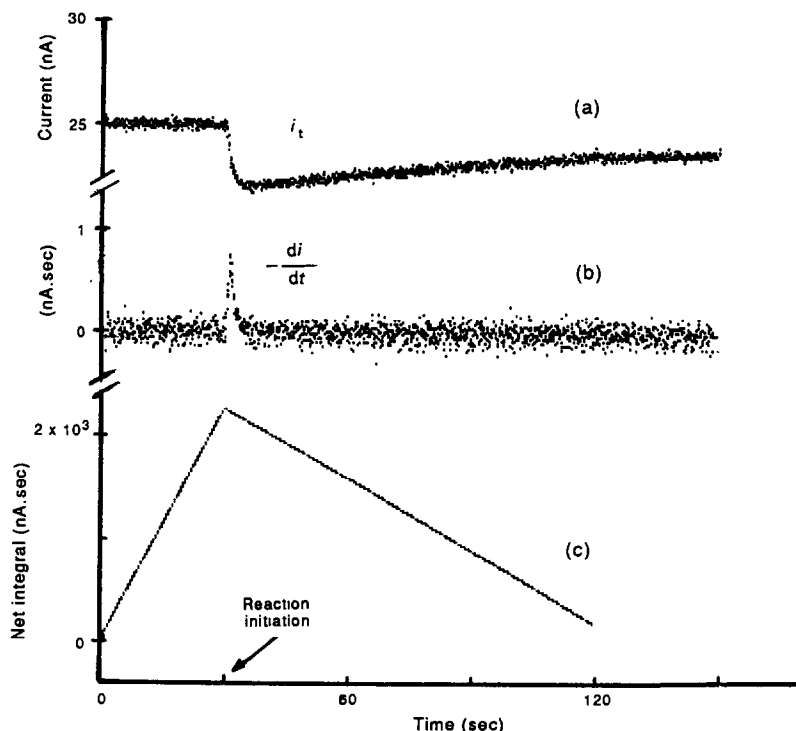


Fig. 1. Time-dependence of (a) response-current for oxygen (i_t), (b) $-di/dt$, and (c) integration data, for 10^{-11} I.U./l. glucose oxidase activity = $3.16 \times 10^{-3} M$ glucose and $\sigma_{\text{noise}} = (0.0056i + 0.01)$ nA. The integration data were obtained by summing the pre-reaction current (multiplied by 3) at 0.1-sec intervals for 30 sec, then subtracting the reaction current at 0.1-sec intervals over the next 90 sec.

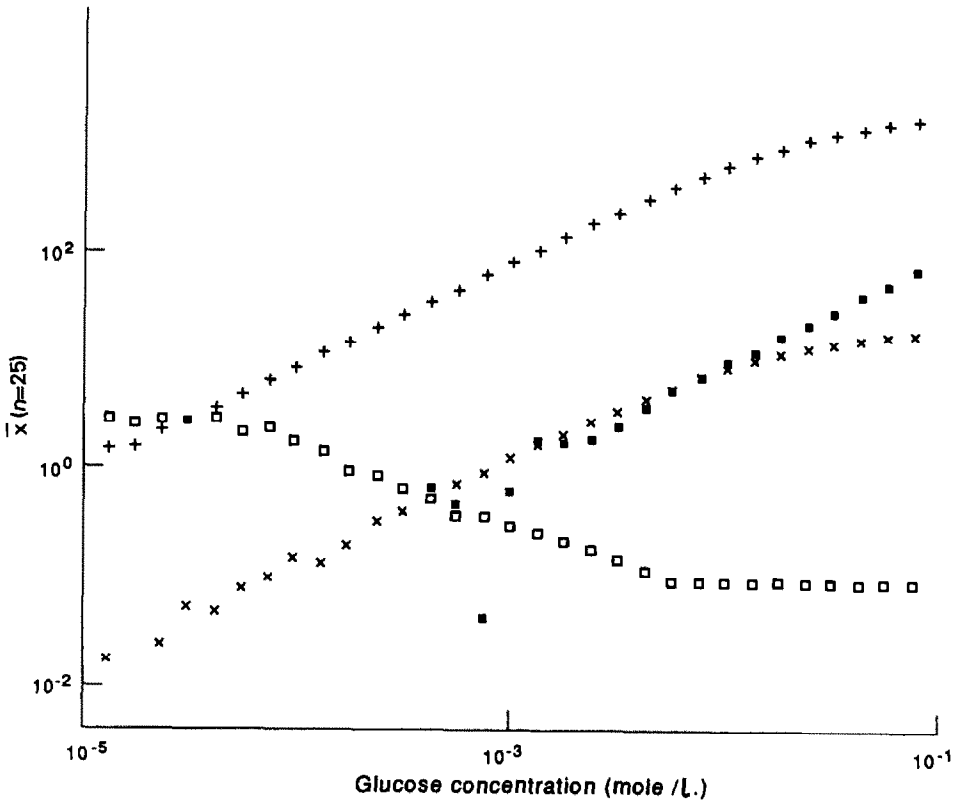


Fig. 2. Average results ($n = 25$) vs. C_{glucose} for integrations (+), variable-time (\square), fixed-time (\times) and maximum continuous derivatives (\blacksquare) for glucose oxidase activity of 10^{-11} I.U./l. and $\sigma_{\text{noise}} = (0.00316i + 0.01)$ nA.

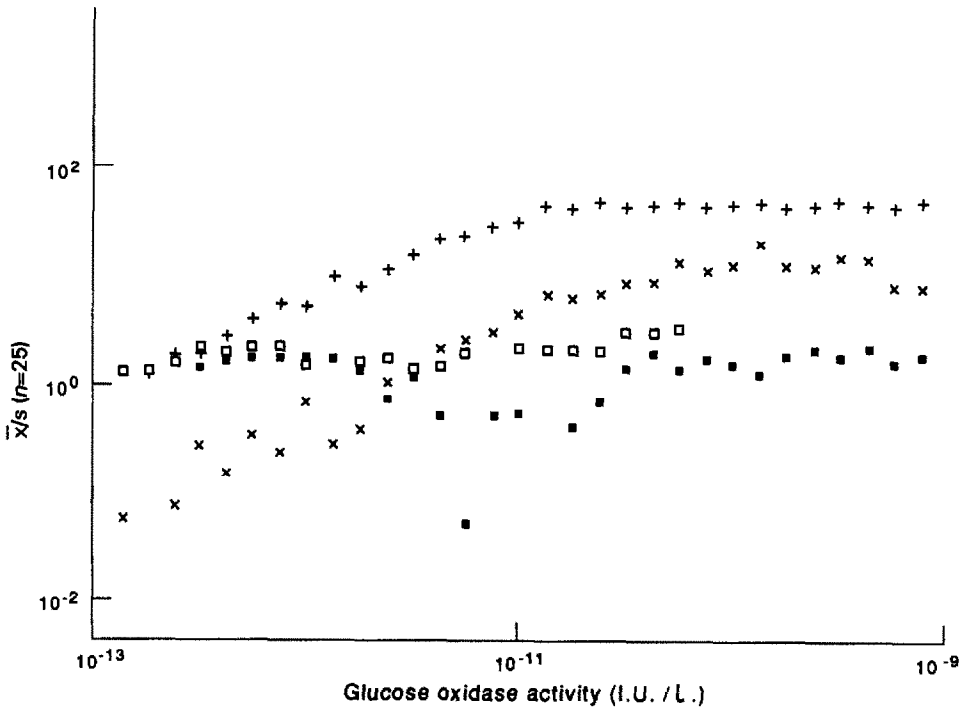


Fig. 3. Data quality estimates ($n = 25$) vs. glucose oxidase analyte activity for integrations (+), variable-time (\square), fixed-time (\times) and maximum continuous derivatives (\blacksquare) for $10^{-3}M = C_{\text{glucose}}$ and $\sigma_{\text{noise}} = (0.0056i + 0.01)$ nA.

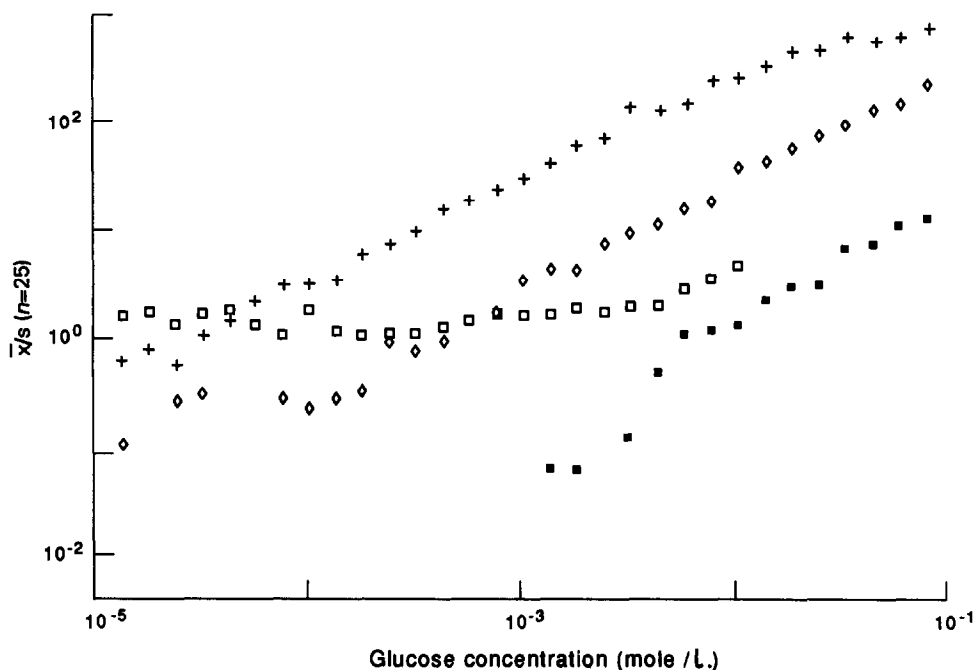


Fig. 4. Data quality estimates ($n = 25$) vs. glucose concentrations for integrations (+), variable-time (\square), fixed-time (\diamond) and maximum continuous derivatives (\blacksquare) for glucose oxidase activity of 10^{-11} I.U./l. and $\sigma_{\text{noise}} = (0.0178i + 0.01)$ nA.

evaluated. However, at very high current uncertainties [$> \pm(0.0056i + 0.01)$ nA], its variable-time data quality was not degraded as dramatically as that of the other methods, showing higher x/s values at low catalytic rates than did other rate-measuring procedures. Also, with extreme noise levels, e.g., ± 10 nA for 15–25 nA total current, the integration method gave better results than all the other methods at all catalytic rates investigated.

Enzymatic determinations of glucose by monitoring the current in glucose oxidase reaction systems showed overall results similar to those achieved for oxidase assays (Fig. 4). For low to moderate noise levels, $< \pm(0.0316i + 0.01)$ nA, the integration method gave higher x/s values than did any of the rate-estimating methods, for all glucose concentrations used, which spanned a much wider range than that of typical routine analyses. However, as observed for the G.O.A. assays, at high and extreme noise levels the variable-time method had better relative uncertainties than did the integration method, for low concentrations of glucose. For high glucose concentrations, however, the integrations showed better data quality than the rate-estimates, over all the noise levels explored.

Experimental results

Determinations of glucose concentrations between 0.0025 and 0.010M (0.46–1.86 mg/ml) were done concurrently by the three rate-estimate methods and the integration method. Within this narrow range of physiological concentrations, the integration data quality (x/s for $n = 10$) was better by a factor of 2–10 than the variable-time results and 2–50 than the fixed-time and continuous derivative methods. This superiority of data quality was slightly lower than that predicted by theory (see Fig. 4). Extreme concentrations and noise levels were not examined in these laboratory experiments.

Relative calculations, of x/s , indicated that the integration method generally, but not always, gave better results than concurrently made rate-estimates did. Comparisons between integration and fixed-time results typically showed 5–10-fold enhancement of x/s when integration was used for glucose determinations and 2–20-fold enhancement for oxidase assays. Integration gave up to 120-fold improvement in x/s in comparison with the maximum continuous-derivative method. In comparison with variable-time results, integration was usually several times better at normal noise levels, but at very high noise levels the variable-time data quality

was nearly the same as that for integration, and sometimes somewhat better.

CONCLUSIONS

Overall, the integration method gives much better results than do rate-estimation procedures, over broad variations of oxidase reaction conditions, for both simulated and experimental data. This is evident even when minima occur in the current *vs.* time relations during the integration period. The improved data quality offered by integration may therefore improve the reliability of measurements made on non-equilibrium systems during progress of the reaction.

REFERENCES

1. L. C. Thomas and G. D. Christian, *Anal. Chim. Acta*, 1975, **77**, 153.
2. L. C. Thomas, G. D. Christian and J. D. S. Danielson, *ibid.*, 1975, **77**, 163.
3. G. E. Radke and L. C. Thomas, *ibid.*, 1984, **161**, 91.
4. L. C. Thomas, G. E. Radke and A. J. Charter, *Anal. Lett.*, 1985, **18**, 1321.
5. L. C. Thomas and G. D. Christian, *Anal. Chim. Acta*, 1975, **78**, 271.
6. *Idem*, *ibid.*, 1977, **89**, 83.
7. L. C. Thomas, A. Dorizas and E. Mech, *Anal. Lett.*, 1989, **22**, 989.
8. H. A. Mottola and H. B. Mark, Jr., in *Instrumental Analysis*, 2nd Ed., G. D. Christian and J. E. O'Reilly (eds.), pp. 560-591. Allyn and Bacon, Boston, MA, 1986.
9. P. D. Wentzell and S. R. Crouch, *Anal. Chem.*, 1986, **58**, 2855.
10. H. L. Pardue, *Anal. Chim. Acta*, 1989, **216**, 69.
11. S. D. Hamilton and H. L. Pardue, *Clin. Chem.*, 1982, **28**, 2359.
12. J. A. Larsson and H. L. Pardue, *Anal. Chem.*, 1989, **61**, 1949.
13. *Idem*, *Anal. Chim. Acta*, 1989, **224**, 289.
14. E. M. Cordos, S. R. Crouch and H. V. Malmstadt, *Anal. Chem.*, 1968, **40**, 1812.
15. J. D. Ingle, Jr. and S. R. Crouch, *ibid.*, 1970, **42**, 1055.
16. G. P. Hicks, A. A. Eggert and E. C. Toren, Jr., *ibid.*, 1970, **42**, 729.
17. F. R. Duke, M. Weibel, D. S. Page, V. G. Bulgrin and J. Luthy, *J. Am. Chem. Soc.*, 1969, **91**, 3904.
18. V. Bloomfield, L. Peller and R. A. Alberty, *ibid.*, 1962, **84**, 4367.

URICASE-LIKE CATALYTIC ACTIVITY OF ION-EXCHANGE RESINS MODIFIED WITH METALLOPORPHYRINS

MASAKI MIFUNE, JUNICHI ODO, AKIMASA IWADO and YUTAKA SAITO*

Faculty of Pharmaceutical Sciences, Okayama University, 1-1-1 Tsushima-Naka, Okayama 700, Japan

NORIKO MOTOHASHI

Kobe Women's College of Pharmacy, 4-19-1 Motoyamakita-Machi, Higashi-Ku, Kobe 658, Japan

MASAHIKO CHIKUMA

Osaka University of Pharmaceutical Sciences, 2-10-65 Kawai, Matsubara-city 580, Japan

HISASHI TANAKA

Kyoto Pharmaceutical University, 5 Nakauchi-cho, Misasagi, Yamashina-Ku, Kyoto 607, Japan

(Received 17 October 1990. Revised 19 November 1990. Accepted 27 December 1990)

Summary—The uricase-like catalytic activity of the ion-exchange resins modified with metalloporphyrins has been investigated through the oxidation of uric acid. The anion-exchange resins modified with Mn^{3+} -tetrakis(sulfophenyl)porphine and the cation-exchange resin modified with Mn^{3+} -tetrakis(1-methylpyridinium-4-yl)porphine exhibited the highest uricase-like activity among the modified resins tested. The fact that these resins accelerated the oxidation of uric acid even after ten cycles of use indicates that the modified resins act as catalysts in the reaction catalyzed by uricase. Some of the modified resins may be effectively used for the determination of uric acid in place of uricase.

Previously, we have demonstrated that the ion-exchange resins modified with metalloporphyrins (M-P_r) exhibit catalase-like^{1,2} and peroxidase-like^{3,4} activities, and are useful for the determination of hydrogen peroxide in clinical assays as a mimesis of the enzymes.^{5,6} We have reported briefly that some M-P_r exhibit enzyme-like catalytic activity in the oxidation of uric acid.⁷ As uricase is one of the important enzymes in the clinical analysis,⁸ the development of its effective artificial mimesis has been attempted. In this paper, we deal with the results of a detailed study on the uricase-like catalytic activity of M-P_r, and its application to the determination of uric acid.

EXPERIMENTAL

Materials

Tetrakis(sulfophenyl)porphine (H₂-TPPS), tetrakis(4-carboxyphenyl)porphine (H₂-TCPP), protoporphyrin (H₂-PP) and tetrakis-

(1-methylpyridinium-4-yl)porphine (H₂-TMPyP) were purchased from Tokyo Kasei Company and Dojin Chemical Laboratories, and were used without further purification for the preparation of metalloporphyrins. Other reagents were of analytical or reagent grade.

Preparation of the modified resins

Aqueous solutions of metalloporphyrins were prepared and used to modify an anion-exchange resin (Amberlite IRA 900, 24-42 mesh) and a cation-exchange resin (Dowex MSC-1, 20-50 mesh) as described previously.¹⁻⁴ The absorption spectra of the solutions of metalloporphyrins agreed with those reported in the literature.^{9,10} All the modified resins contained 25 μmoles of metalloporphyrin per 1 g (dry resin).

Apparatus

Absorption spectra and absorbances were measured on a Shimadzu UV-180 double-beam spectrophotometer and a Shimadzu UV-100 spectrophotometer, respectively, with a 10-mm fused-silica cell.

*Author for correspondence.

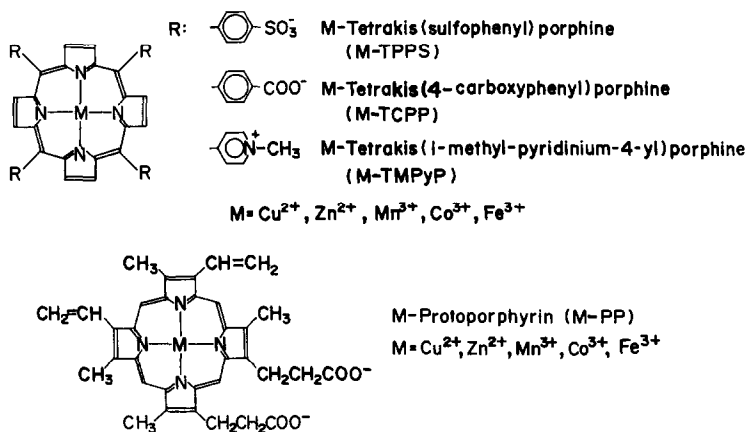


Fig. 1. Structures of metalloporphyrins.

Aqueous solution of uric acid

A 100-mg amount of uric acid (Sigma Co., No. 21F-5062) was dissolved in about 80 ml of water containing 60 mg of lithium carbonate and the solution was diluted to exactly 100 ml with water. This stock solution (1 mg/ml) was diluted to the desired concentration with water.

Evaluation of the uricase-like activity

A modified resin (100 mg) was added to a mixture of the uric acid solution (300 $\mu\text{g}/\text{ml}$, 0.5 ml) and 0.05M borate buffer (pH 8.0, 4.0 ml), and the mixture was incubated at 35° for 30 min. The absorbance of the supernatant was measured at 293 nm against water and the control absorbance was obtained by using IRA 900 in place of the modified resin. The activities of the resins were evaluated by the decrease in absorbance of the control. In the case of M-TMPyP, 0.2M carbonate buffer (pH 11.0) and the cation-exchange resin MSC-1 were used as the buffer and the control, respectively.

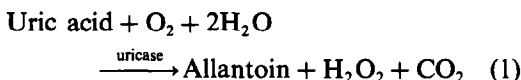
RESULTS AND DISCUSSION

Metalloporphyrins

The metalloporphyrins used in this study are shown in Fig. 1. All of them are water-soluble. The complexes were immobilized easily and firmly on the ion-exchange resins as discussed previously, by ion-exchange reaction and physical adsorption.¹⁻⁴

Reaction catalyzed by the modified resins

Uricase catalyzes the following reaction (1), and uric acid is oxidized to allantoin.



To confirm that M-P, catalyzed reaction (1), the formation of allantoin and hydrogen peroxide were investigated by using Mn^{3+} -TPPS. To detect allantoin, the supernatant of the reaction mixture was dried and the residue obtained gave relatively strong IR bands around 1770, 1650, 1515, 1180, 810 and 754 cm^{-1} , coinciding with those of standard allantoin, and gave mass peaks (FAB⁺) in glycerol matrix at 159 and 251, which could be attributed to [allantoin + H]⁺ and [allantoin + glycerol + H]⁺, respectively. However, only trace amounts of hydrogen peroxide were detected in the reaction mixture by the colour reaction with peroxidase, phenol and 4-aminoantipyrine.¹¹ Hydrogen peroxide formed from uric acid was decomposed immediately by the catalase-like activity of Mn^{3+} -TPPS, which has been reported previously. When air was replaced by nitrogen, the reaction hardly proceeded even in the presence of catalysis. We concluded from these results that the modified resins catalyze reaction (1).

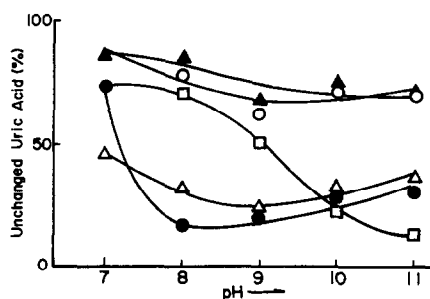


Fig. 2. Effect of pH (1) in borate buffer. \circ Zn^{2+} -TPPS; \bullet Mn^{3+} -TPPS; \triangle Co^{3+} -TPPS; \blacktriangle Cu^{2+} -TPPS; \square Fe^{3+} -TPPS.

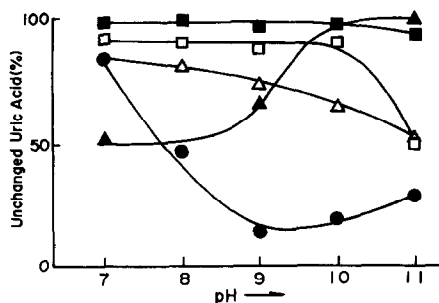


Fig. 3. Effect of pH (2) in borate buffer. ● Mn^{3+} -TCPP; Δ Co^{3+} -TCPP; \blacktriangle Co^{3+} -PP; \square Fe^{3+} -TCPP; \blacksquare Fe^{3+} -PP; \bullet H_2 -PP.

Reaction conditions

The following examinations were carried out to obtain optimum conditions. A considerable amount of uric acid is adsorbed by the anion-exchange resin. Accordingly, the control by the use of IRA 900 should be referred to in each examination, except for the cases of M-TMPyP_r.

Effect of pH. The amount of unchanged uric acid (%) in reaction mixtures of various pH values are presented in Figs. 2-4. As seen in Fig. 4, Mn^{3+} -TMPyP_r decomposed most of the uric acid at pH 11, but not when the pH was below 9.

On the other hand, the adsorption of uric acid by the anion-exchange resin IRA 900 increases at higher pH. Accordingly, we chose pH 8 for the resins prepared from IRA 900 and pH 11 for the resins prepared from MSC-1.

Effect of buffer. The decomposition of uric acid was found to be affected by the composition of the buffer solutions such as 0.05M borate, 0.2M borate, 0.2M phosphate, 0.033M phosphate and 0.2M tris buffers. Among these buffers used, 0.05M borate, 0.033M phosphate and 0.2M tris buffers give good results. This effect may be attributed to the coordination of a component of the buffer to metalloporphyrins as an axial ligand. However, in the case of

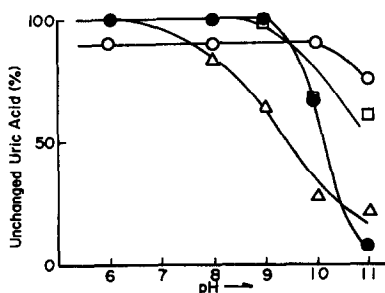


Fig. 4. Effect of pH (3) in acetate (pH 6) and borate (pH 7-11) buffer. ○ Fe^{3+} -TMPyP; ● Mn^{3+} -TMPyP; Δ Co^{3+} -TMPyP; \square Zn^{2+} -TMPyP.

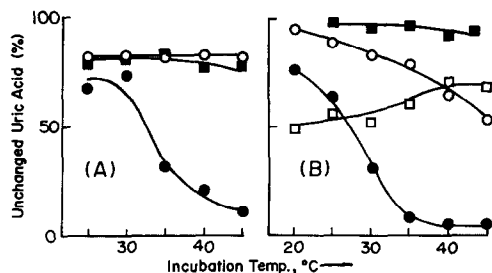


Fig. 5. Effect of incubation temperature. (A): ○ Cu^{2+} -TPPS; ● Mn^{3+} -TPPS; \blacksquare H_2 -TPPS. (B): ○ Fe^{3+} -TMPyP; ● Mn^{3+} -TMPyP; \square Zn^{2+} -TMPyP; \blacksquare H_2 -TMPyP.

M-TMPyP_r, 0.2M carbonate and 0.05M borate buffers (pH 11) gave almost the same result. In this study, we used 0.2M carbonate buffer (pH 11) for M-TMPyP_r and 0.05M borate buffer (pH 8) for other modified resins.

Effect of temperature. Unchanged uric acid (%) decreased with increasing incubation temperature in all cases of M-P_r tested, except for Zn^{2+} -TMPyP_r. (Fig. 5). In particular, for Mn^{3+} -TPPS_r and Mn^{3+} -TMPyP_r, the increase in activity with increasing temperature was remarkable and the maximum activity was observed above 35°. In the case of Mn^{3+} -TMPyP_r, the resin crumbled to pieces at 45°. H_2 -TMPyP_r and H_2 -TPPS_r, which contain no metal, decomposed uric acid only slightly in all the temperature ranges tested, indicating that the central metal is essential for the activity.

Time courses

A 30-min incubation period was sufficient as shown in Figs. 6 and 7. It is of interest that the time needed to attain equilibrium depended on the type of central metal in M-P_r, which indicates that the metal influences not only the activity but also the reaction rate. For example, in the case of Co^{3+} -TPPS_r, the reaction came to equilibrium after about 10 min of reaction. However, the reaction by Fe^{3+} -TMPyP_r was

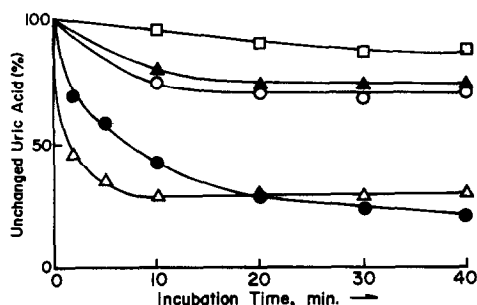


Fig. 6. Time courses (1). ○ Zn^{2+} -TPPS; ● Mn^{3+} -TPPS; Δ Co^{3+} -TPPS; \blacktriangle Cu^{2+} -TPPS; \square Fe^{3+} -TPPS.

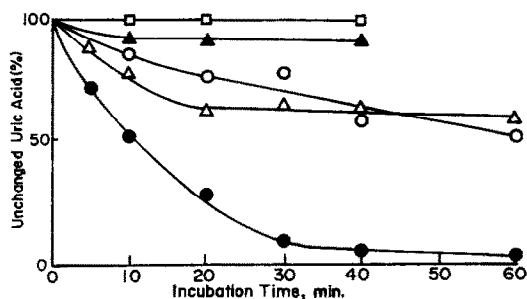


Fig. 7. Time courses (2). ○ Fe³⁺-TMPyP_r; ○ Mn³⁺-TMPyP_r; △ Zn²⁺-TMPyP_r; ▲ Fe³⁺-TCPP_r; □ Zn²⁺-PP_r.

found to be slow and equilibrium was attained after 1 hour of the reaction. As far as the reaction rate is concerned, Co³⁺-TPPS_r gives the best catalysis. For the evaluation of the activity, incubation was carried out for 30 min.

Uricase-like activity

Table 1 shows the unchanged uric acid (%) after treatment with the modified resins. Some of the resins modified with manganese complexes gave relatively high uricase-like activity compared to the other resins tested, similar to peroxidase- and catalase-like activities.¹⁻⁴ It is of interest that Mn³⁺-TMPyP_r, which did not show both the peroxidase- and catalase-like activities,^{2,4} exhibited the highest uricase-like activity among the modified resins tested. The resins modified with Co³⁺-porphyrins showed less activity than Mn³⁺-complexes. These results indicate that the enzyme-like activities of the modified resins depend not only on the kind of porphyrins but also the central metals.

Repeated uses

The effect of repeated use on the activity was examined to confirm its catalytic nature. The results are shown in Fig. 8. Mn³⁺-TMPyP_r and Mn³⁺-TPPS_r maintained their uricase-like activity even after ten cycles of use, although a slight decrease in the activity was observed. The activity of Co³⁺-TPPS_r

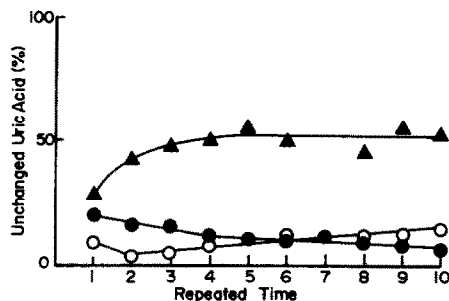


Fig. 8. Effect of repeated uses. ○ Mn³⁺-TMPyP_r (pH 11); ● Mn³⁺-TPPS_r (pH 8); ▲ Co³⁺-TCPP_r (pH 8).

decreased when used a second time. This result indicates that Mn³⁺-TMPyP_r and Mn³⁺-TPPS_r are superior to Co³⁺-TPPS_r as a mimesis of uricase.

Analytical application

The reaction (1), catalyzed by uricase, has been used for the clinical assay of uric acid,⁸ by measuring the decrease of absorbance at 293 nm, where uric acid has an absorption maximum. For the application of the modified resins in place of uricase to the determination of uric acid, Mn³⁺-TMPyP_r is more suitable than Mn³⁺-TPPS_r, because the adsorption of uric acid upon the ion-exchange resin does not take place for Mn³⁺-TMPyP_r, which is prepared from the cation-exchange resin. According to the procedure described above, the decrease of absorbance at 293 nm was measured. The calibration curve obtained with the standard solutions gave good linearity in the range 25–300 μg of uric acid. The sensitivity was comparable to that of the method with uricase. This result indicates that Mn³⁺-TMPyP_r can be used in place of uricase for the determination of uric acid.

In conclusion, some of the ion-exchange resins modified with metalloporphyrins exhibit uricase-like activity. In particular, Mn³⁺-TMPyP_r is useful for the determination of uric acid as an artificial mimesis of uricase.

Table 1. Unchanged uric acid (%)*

M =	Mn ³⁺	Co ³⁺	Fe ³⁺	Cu ²⁺	Zn ²⁺	H ₂
M-TPPS _r	16.6	32.6	70.6	84.0	77.9	84.5
M-TCPP _r	46.9	80.9	91.4	93.5	94.8	—†
M-PP _r	100.0	47.1‡	100.0	75.6	100.0	100.0
M-TMPyP _r	8.0	28.2‡	78.0‡	76.3‡	60.5‡	97.5

*In borate buffer (pH 8) at 35, except for M-TMPyP_r pH 11 carbonate buffer.

†Not tested.

‡Small amount of M-porphyrin was eluted.

Acknowledgements—The authors thank Miss Atsuko Taguchi for her technical assistance. This work was supported in part by a Grant-in-Aid for Scientific Research from the Ministry of Education, Science and Culture, Japan.

REFERENCES

1. Y. Saito, M. Mifune, J. Odo, Y. Tanaka, M. Chikuma and H. Tanaka, *Reactive Polymers*, 1986, **4**, 243.
2. Y. Saito, M. Mifune, T. Kawaguchi, J. Odo, Y. Tanaka, M. Chikuma and H. Tanaka, *Chem. Pharm. Bull.*, 1986, **34**, 2885.
3. Y. Saito, M. Mifune, S. Nakashima, Y. Tanaka, M. Chikuma and H. Tanaka, *ibid.*, 1986, **34**, 5016.
4. Y. Saito, M. Mifune, S. Nakashima, H. Nakayama, J. Odo, Y. Tanaka, M. Chikuma and H. Tanaka, *ibid.*, 1987, **35**, 869.
5. Y. Saito, M. Satouchi, M. Mifune, T. Tai, J. Odo, Y. Tanaka, M. Chikuma and H. Tanaka, *Bull. Chem. Soc. Jpn.*, 1987, **60**, 2227.
6. Y. Saito, M. Mifune, S. Nakashima, J. Odo, Y. Tanaka, M. Chikuma and H. Tanaka, *Anal. Sci.*, 1987, **3**, 171.
7. Y. Saito, M. Mifune, T. Karasudani, A. Taguchi, Y. Tanaka, M. Chikuma and H. Tanaka, *J. Pharmacobio-Dyn.*, 1987, **10**, s-16.
8. Y. Nakagiri and T. Yamamoto, *Nippon Eiseikensa*, 1971, **20**, 751; *Chem. Abstr.*, 1972, **76**, 69586g.
9. R. F. Pasternack, L. Francesconi, D. Raff and E. Spiro, *Inorg. Chem.* 1973, **12**, 2606.
10. R. F. Pasternack, P. R. Huber, P. Boyd, G. Engasser, L. Francesconi, E. Gibbs, P. Fasella, G. C. Venturo and L. dec. Hinds, *J. Am. Chem. Soc.*, 1972, **94**, 4511.
11. P. Kabasakalian, S. Kalliney and A. Westcott, *Clin. Chem.*, 1974, **20**, 606.

INDIRECT DETERMINATION OF TRACES OF THIOSULPHATE BY DIFFERENTIAL-PULSE POLAROGRAPHY

K. BRODERSEN and U. WERNER

Institut für Anorganische Chemie I der Universität Erlangen-Nürnberg, Egerlandstr. 1, D-8520 Erlangen,
Germany

Y. A. GAWARGIOUS*

National Research Centre, Dokki, Cairo, Egypt

S. HUANG

Shanxi University, Taiyuan, Shanxi, People's Republic of China

(Received 31 August 1990. Revised 27 January 1991. Accepted 4 February 1991)

Summary—Two methods are reported for the indirect determination of thiosulphate down to *ca.* 0.02 $\mu\text{g/ml}$ by differential-pulse polarography. Both methods involve prior oxidation of thiosulphate with iodine, either in acidic medium to tetrathionate or in alkaline medium to sulphate, whereby ultimately one and eight equivalents of iodate are obtained, respectively. The concentration of iodate in the resulting solution is then measured by differential-pulse polarography under optimum conditions. The average recovery for each method amounted to 100.1%, and the relative standard deviations were 1.3 and 1.4% for the two methods.

Thiosulphate is used as a fixing salt in photography, as a detoxicating agent (through thiocyanate formation) in treatment of cyanide poisoning, and as a titrant of universal application in various methods involving iodine. However, like other sulphur compounds,² thiosulphate is considered an environmental pollutant, being susceptible to bacterial attack³ yielding sulphuric acid, which is known to cause serious damage in many industries, particularly corrosion of concrete sewers. Most of the conventional methods for thiosulphate determination, *e.g.*, volumetric, amperometric, coulometric and potentiometric titrations⁴⁻⁶ are designed for macro- or micro-scale levels. Use of 6-fold,⁷ 48-fold^{7,8} and 24-fold⁹ iodometric amplification methods has succeeded in the determination of micro and submicro amounts of thiosulphate, down to about 4.5 μg .⁸

With the advent of modern polarographic and voltammetric techniques,¹⁰ the reducing and complex-forming properties of thiosulphate have been exploited in developing more sensitive and selective methods.^{1-3,11-13} Knittel *et al.*³ developed a differential-pulse anodic stripping

voltammetric method specific for thiosulphate determination from 5 ng/ml to 3 $\mu\text{g/ml}$ in aqueous media, though the calibration graph reported (0-5 $\mu\text{g/ml}$) was linear only from 1.5 to 5 $\mu\text{g/ml}$.

The present work offers an alternative method for the indirect determination of traces of thiosulphate by differential-pulse polarography (DPP), enabling accurate measurement down to *ca.* 0.02 $\mu\text{g/ml}$ in aqueous media.

EXPERIMENTAL

Apparatus

All differential-pulse polarograms were obtained with a Princeton Applied Research (PAR) Model 264A Polarographic Analyzer/Stripping Voltammeter equipped with a PAR Model 303A three-electrode system composed of a static mercury dropping electrode (SMDE) as the working electrode, a silver/silver chloride (0.1M KCl) reference electrode,[†] and a platinum wire as counter-electrode, a 10-ml electrode cell, a Model RE0089 X-Y recorder, and a Model 305 stirrer.

A "WTW" microprocessor pH-meter Model 95 (Germany), having a combined glass electrode with integral temperature sensor and

*Author for correspondence.

†The potential differs by +0.049 V from that *vs.* SCE (*cf.* Henze and Neeb,¹⁰ p. 152).

precise to ± 0.01 , was used and calibrated for the pH range 2–8.

An Eppendorf microlitre pipette accurate to $\pm 0.1 \mu\text{l}$ was used to measure 10–100 μl volumes and a Brand (Germany) microlitre pipette accurate to $\pm 0.5 \mu\text{l}$ for volumes of 200–1000 μl .

Reagents

Except where otherwise mentioned, all reagents were of high analytical grade (Merck Titrisol and Suprapur) and doubly-distilled demineralized water was always used.

Sodium thiosulphate. A $2 \times 10^{-3} M$ solution was prepared and stabilized by addition of 0.02 g of sodium carbonate per 200 ml. This solution was stable for two weeks and was frequently standardized against potassium iodate solution.

Potassium iodate. A 0.1N solution was prepared from standard ampoules and diluted to 0.01 or 0.001N as required for standardization and for the polarographic calibration curves.

Other reagents were a 1.2 mg/ml iodine solution in chloroform, 2M sodium acetate, 50% v/v formic acid solution, saturated bromine water, 1 and 5M sodium hydroxide and 2M sulphuric acid.

Procedures

Tetrathionate procedure. Transfer an aliquot of test solution containing between 3.5 and 60 μg of thiosulphate into a 100-ml separating funnel, add 0.4 ml of the iodine solution, dilute to ca. 5 ml with water and add 5 ml of chloroform. Shake well for 2 min and allow to stand for 1 min.

Discard the chloroform layer and remove the last minute traces of iodine suspended in the aqueous layer, by extraction with five 5-ml portions of chloroform, with vigorous shaking for 1 min each time. Transfer the aqueous layer quantitatively into a 100-ml conical flask, add 1.5 ml of 2M sodium acetate, 1 ml of saturated bromine water and stir the mixture for 3 min. Destroy the excess of bromine by dropwise addition of formic acid (0.25 ml) and adjust the pH to 3.5. Transfer into a 25-ml standard flask and dilute with water to the mark.

Rinse the electrodes and the clean cell with a few ml of the test solution, then pipette ca. 10 ml of it into the electrode cell. Deaerate by passage of pure nitrogen for 4 min and record the differential-pulse polarogram of the iodate at room temperature, using a drop time of 1 sec, a pulse amplitude of 50 mV, a potential scan-rate of 2 mV/sec within the potential range

from -0.20 to -0.75 V, and 20 μA full-scale deflection.

Prepare a calibration curve for 4.0–96 μg of by applying the same procedure, plotting peak current (μA) vs. weight (μg) of iodate or thiosulphate (100 μg of $\text{IO}_3^- \equiv 64.1 \mu\text{g}$ of $\text{S}_2\text{O}_3^{2-}$).

Sulphate procedure. Mix 5 ml of 1M sodium hydroxide and 0.5 ml of iodine solution in a 100-ml separating funnel, add an aliquot of the test solution containing between 2.8 and 45 μg of thiosulphate and shake well for 2 min. After 5 min, add 3.5 ml of 2M sulphuric acid and 8.5 ml of chloroform, shake for 1 min and leave standing for 1 min more to allow separation.

Discard the chloroform layer and remove the remaining traces of iodine by extraction with five 8.5-ml portions of chloroform, shaking vigorously for 1 min each time. Transfer the aqueous layer quantitatively into a 100-ml conical flask, add 1.5 ml of 5N sodium hydroxide followed by 3 ml of 2M sodium acetate to give a pH of about 8. Add 1 ml of saturated bromine water and stir the mixture for 5 min. Add formic acid (0.8 ml) dropwise to destroy the excess of bromine and to adjust the solution to pH 3.5. Transfer the solution quantitatively into a 100 ml-standard flask and dilute with water to the mark.

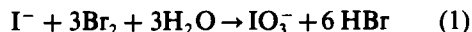
Record the differential-pulse polarogram of the iodate under the conditions given for the tetrathionate procedure, but use a lower sensitivity of 100 μA full-scale deflection.

Prepare a calibration curve for 30–600 μg of iodate by the same procedure, plotting peak current (μA) vs. weight of iodate (μg) (100 μg of $\text{IO}_3^- \equiv 8.02 \mu\text{g}$ of $\text{S}_2\text{O}_3^{2-}$).

RESULTS AND DISCUSSION

The tetrathionate procedure

This method makes use of the iodine–thiosulphate reaction yielding tetrathionate and iodide, which is then quantitatively oxidized with bromine water to iodate:



In earlier work,⁷ the Leipter reaction was applied to the iodate, but despite the 6-fold amplification, less than 0.1 mg of thiosulphate could not be determined. When the iodate was measured by d.c. polarography, by means of the irreversible cathodic reduction of iodate at the dropping mercury electrode: $\text{IO}_3^- + 6\text{H}^+ + 6e^- \rightarrow \text{I}^- + 3\text{H}_2\text{O}$, only mg amounts of thiosulphate could be determined.¹⁴ However, d.c.

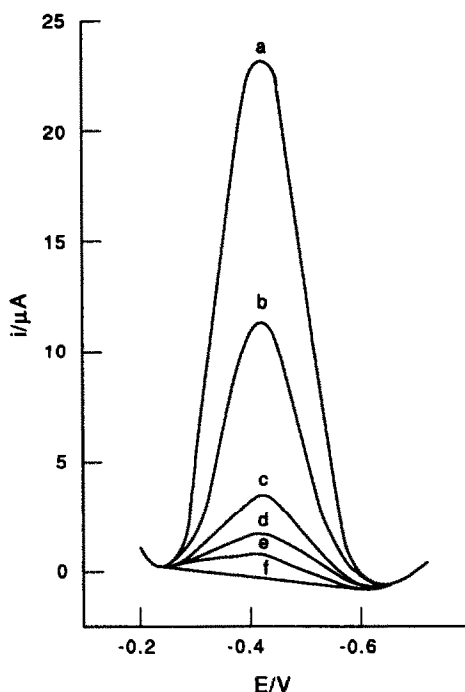


Fig. 1. Representative DP polarograms for the iodate calibration graph (tetrathionate method). Iodate ($\mu\text{g}/25\text{ ml}$): a, 96; b, 48; c, 16; d, 8; e, 4; f, blank.

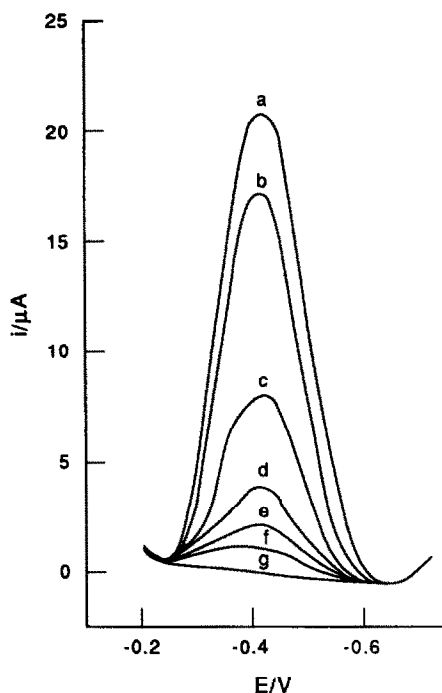


Fig. 2. Representative DP polarograms for the thiosulphate calibration graph (tetrathionate method). Thiosulphate ($\mu\text{g}/25\text{ ml}$): a, 56.5; b, 42.6; c, 21.3; d, 10.6; e, 7.04; f, 3.52; g, blank.

polarography has been reported¹⁵ to enable determination of inorganic ions only down to $10^{-4}M$, whereas the more sensitive DPP technique has been reported¹⁶ to measure iodate concentrations down to *ca.* $2.4 \times 10^{-6}M$ at pH 3.

Accordingly, the present work is based on combination of the iodometric oxidation of thiosulphate to yield ultimately an equivalent amount of iodate, with measurement of the iodate by DPP.

Since the half-wave potential and the peak height of the iodate wave are pH-dependent,^{14,16} differential pulse polarograms were initially recorded for a solution containing $10\ \mu\text{g}$ of iodate and at pH 2–4, with different polarographic settings. The most precise results were those obtained at pH 3.5, with the peak maximum occurring at -0.42 V .

Experiments were then performed with the tetrathionate procedure cited elsewhere⁷ until a

modified scaled-down version has been developed and proved suitable for the quantitative oxidation of thiosulphate in amounts ranging between 3.5 and $60\ \mu\text{g}$ in a final volume of 25 ml. At first, recoveries consistently high by about 2–3% were obtained, which was thought to be due to contamination from one or more of the reagents used. A series of blank determinations revealed that 5-fold extraction with chloroform, instead of the 3-fold extraction prescribed earlier,⁷ is necessary to eliminate the last traces of iodine completely, and this procedure gave correct results. The tetrathionate produced has no effect on the results, and calibration graphs for iodate standards and thiosulphate standards were identical. Representative differential pulse polarograms from both sets are shown in Figs. 1 and 2.

Excellent results were achieved for 3.5–56.5 μg of thiosulphate (Table 1).

Table 1. Results obtained by the tetrathionate method

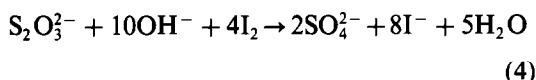
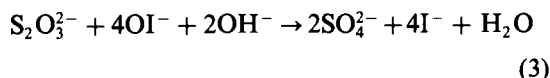
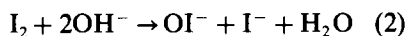
	Taken	3.52	7.04	10.6	21.3	42.6	56.5
	Found (8 replicates)	3.45–3.60	6.91–7.20	10.4–10.8	21.0–21.7	41.2–43.1	55.8–56.9
	Average	3.53	7.03	10.6	21.3	42.5	56.5
Thiosulphate, μg							
Theoretical iodate equivalent, μg		5.49	11.0	16.5	33.2	66.4	88.1
Peak current of iodate, μA		1.2	2.4	3.8	8.0	17.2	21.2
Relative standard deviation, %		1.5	1.4	1.3	1.4	1.4	0.7

Table 2. Results obtained by the sulphate method

	Taken	2.83	5.61	11.2	22.4	37.0	44.9
	Found (8 replicates)	2.77–2.90	5.52–5.70	11.0–11.4	21.8–22.9	36.3–37.8	43.6–46.2
Thiosulphate, μg	Average	2.82	5.61	11.2	22.4	37.0	45.2
Theoretical iodate equivalent, μg		35.3	70.0	140	280	462	560
Peak height of iodate, μA		3.8	7.5	15	30	50	60
Relative standard deviation, %		1.5	1.1	1.2	1.6	1.3	1.8

The sulphate method

The sulphate method depends upon the disproportionation of iodine in strongly alkaline medium (pH 12) to form equimolar amounts of hypoiodite and iodide [reaction (2)]. Thiosulphate is oxidized to sulphate by hypoiodite [reaction (3)] which is itself reduced to iodide, leading to an overall stoichiometry [reaction (4)] of one mole of thiosulphate being equivalent to eight moles of iodide and to eight moles of iodate on oxidation with bromine water [reaction (1)].



Thus slight modifications of the iodometric procedures described in previous works,^{7,8} and adjustment of the pH of the iodate-containing solution to 3.5 as before but dilution to a larger final volume of 100 ml, allowed DPP measurement of the resulting iodate by use of the lowest sensitivity value of 100 μA full-scale deflection under polarographic conditions otherwise the same as for the tetrathionate method. The iodate peak maximum again occurred at -0.42 V, as expected.

The lowest sensitivity and the dilution to 100 ml final volume were selected to compensate for the 8-fold amplification in the sulphate method, as only in this way could the complete DPP peak be recorded on the chart (which was 25 cm wide).

Amounts of thiosulphate in the range 2.8–45 μg were determined and quite reproducible results (Table 2) were obtained.

Unfortunately the instability of lower concentrations of thiosulphate and/or their non-stoichiometric oxidation resulted in inconsistent and erroneous values. However, thiosulphate concentrations as low as 0.14 and 0.02 $\mu\text{g}/\text{ml}$ could be accurately determined by the two indirect methods developed, corresponding to 0.22 and 0.35 $\mu\text{g}/\text{ml}$ iodate, which compares

favourably with the 0.42 $\mu\text{g}/\text{ml}$ limit reported for pure iodate solution.¹⁶

The calibration graphs prepared with thiosulphate and iodate standards were again identical.

All anions and cations that undergo redox reactions with iodine, liberating iodide, interfere in the determination (*cf.* Belcher *et al.*⁸) but sulphate (the reaction product in this variant) does not interfere. The pulse polarograms for the reagent blank showed slight curvature above the baseline, corresponding to not more than 0.04 μg of iodate or 0.025 μg of thiosulphate, which is within acceptable limits; all results were corrected accordingly.

Acknowledgements—Y. A. Gawargious forwards thanks to DAAD, Alexander-von-Humboldt-Stiftung, and DFG, Bonn, for the financial support that enabled him to participate in this work.

REFERENCES

1. K. Wienhold and H. Sohr, *Z. Chem.*, 1980, **7**, 265.
2. J. J. Renard, G. Kubes and H. I. Bolker, *Anal. Chem.*, 1975, **47**, 1347.
3. D. Knittel, P. Valenta, M. Aydin and W. A. König, *Z. Anal. Chem.*, 1985, **322**, 581.
4. A. I. Vogel, *A Text Book of Quantitative Inorganic Analysis*, 3rd Ed., Longmans, London, 1961.
5. J. J. Lingane, *Electroanalytical Chemistry*, Interscience, New York, London, 1958.
6. C. L. Wilson and D. W. Wilson, *Comprehensive Analytical Chemistry*, Vol. IIA, p. 128. Elsevier, Amsterdam, 1964.
7. S. K. Tobia, Y. A. Gawargious, A. Besada and S. Y. Kareem, *Z. Anal. Chem.*, 1975, **277**, 376.
8. R. Belcher, S. S. Liao and A. Townshend, *Talanta*, 1976, **23**, 541.
9. A. Besada, *Z. Anal. Chem.*, 1984, **317**, 132.
10. G. Henze and R. Neeb, *Elektrochemische Analytik*, Springer-Verlag, Heidelberg, 1986.
11. Y. Zemu and W. Erkang, *Fenxi Huaxue*, 1984, **12**, 174; *Chem. Abstr.*, 1984, **101**, 182819h.
12. G. S. Vorob'eva and V. I. Gorokhovskaya, *Zh. Analit. Khim.*, 1984, **39**, 2137; *Chem. Abstr.*, 1984, **102**, 89220s.
13. A. P. Pnevva and V. V. Pnev, *Otkrytiya Izobret*, 1986, **21**, 178; *Chem. Abstr.*, 1986, **105**, 164160g.
14. G. M. Habashy, Y. A. Gawargious and B. N. Faltaos, *Talanta*, 1968, **15**, 403.
15. I. M. Kolthoff and J. J. Lingane, *J. Am. Chem. Soc.*, 1939, **61**, 825.
16. Y. M. Temerk, M. E. Ahmed and M. M. Kamal, *Z. Anal. Chem.*, 1980, **301**, 414.

EXTRACTIVE-CHROMATOGRAPHIC SEPARATION OF BISMUTH WITH ALIQUAT 336S FROM CITRATE SOLUTIONS

S. K. SAHOO

Department of Metallurgical Engineering, Indian Institute of Technology,
Bombay 400 076, India

(Received 7 August 1990. Revised 14 January 1991. Accepted 1 February 1991)

Summary—Bismuth is extracted from 0.01M citric acid at pH 3.0 with Aliquat 336S coated on a silica gel column, by extraction chromatography. It was then stripped with 0.1M sulphuric acid and determined spectrophotometrically at 460 nm as the iodide complex. Bismuth was effectively separated from binary as well as ternary mixtures by taking advantage of the difference in the stability of the citrate complexes with metal ions in mineral acids. The method was extended to the analysis of bismuth from low fusible alloys.

The extractive-chromatographic methods for the separation of bismuth involve use of solvating solvents and liquid ion exchangers as the stationary phase. The separation of bismuth from mineral acid media, using liquid anion exchangers has been studied, but such studies from organic acid media are few. Tributylphosphate was used for the extractive-chromatographic separation of bismuth from lead, thallium and silver.^{1,2} Bismuth was separated from transition elements with trioctylphosphine oxide³ and bis(2-ethylhexyl)phosphoric acid⁴ as the stationary phase. The separation of bismuth from silver, cadmium and zinc by extraction chromatography was done with trioctylamine.^{5,6} However, these methods failed to separate bismuth from elements which are associated with fission products.

This paper described the systematic investigation of the extractive-chromatographic studies of bismuth with Aliquat 336S from citric acid solutions. Novel methods are developed to separate bismuth from associated elements. The method is applied to the determination of bismuth in low fusible alloys.

EXPERIMENTAL

Apparatus

A GS 866C spectrophotometer (ECIL, India), provided with corex glass cuvettes with an optical path length of 10 mm and a LI 120 pH meter (ELICO, India) were used.

Reagents

Aliquat 336S (methyltri-n-alkylammonium chloride) (Fluka AG, Switzerland) was used without further purification.

A stock solution of bismuth was prepared by dissolving 2.94 g of bismuth nitrate pentahydrate in 250 ml of distilled water containing 1% nitric acid. The solution was standardized complexometrically.⁷ It contained 4.7 mg/ml of bismuth. A diluted solution containing 100 µg/ml was prepared by appropriate dilution.

The silica gel (100–200 mesh) was dried at 120° for 2 hr and then packed into a U-tube. A stream of dry nitrogen was passed for 2–3 hr through a small Drechsel bottle containing 25 ml of dimethyldichlorosilane, and then through a U-tube containing the silica gel to convert the surface silanol groups to silyl ether groups. The silica gel was then washed with anhydrous methanol to convert the unreacted hydroxyl groups to methoxy groups, as well as to remove hydrochloric acid from the silica gel. The treated silica gel was then dried at 100°. In routine work 1 ml of dimethyldichlorosilane is adequate to render 10 g of silica gel hydrophobic.

A solution containing 1 ml of Aliquat 336S in benzene was prepared and transferred into a flask containing 4 g of the hydrophobic silica gel. The benzene was slowly removed from the suspension with a rotary vacuum evaporator until dry silica gel was obtained; a low vacuum was applied to remove air from the micropores

and to accelerate evaporation of benzene. The silica gel coated with Aliquat 336S was then slurried with citric acid solution and poured into a column (10×0.8 cm). A 4-g amount of the coated silica gel was sufficient to give a bed height of 8 cm and was used for the column studies.⁸

General procedure

An aliquot of solution containing $100 \mu\text{g}$ of bismuth was mixed with 5 ml of $0.01M$ citric acid. The pH of the solution was adjusted to 3.0 with $0.01M$ citric acid or $0.01M$ sodium hydroxide. The solution was passed through the column and bismuth was extracted with Aliquat 336S as the stationary phase. Bismuth was stripped with various mineral acids. Ten 5-ml fractions were collected and bismuth from each fraction was determined spectrophotometrically as the iodide complex at 460 nm .⁹

RESULTS AND DISCUSSION

Effect of pH

The extraction studies of bismuth as a function of pH were carried out in the pH range 1.0–6.0. The extraction commenced at pH 1.0 (45.4%) and it was quantitative from pH 3.0 to 5.0. On increasing the pH further, there was a decrease in the extraction of bismuth, this may be due to hydrolytic precipitation of bismuth. The optimum pH for the quantitative extraction of bismuth was 3.0 (Fig. 1).

Effect of citric acid concentration

The extraction of bismuth was carried out by varying the concentration of citric acid from 1×10^{-4} to $1 \times 10^{-1}M$. The optimum concentration for complete extraction was $1 \times 10^{-2}M$.

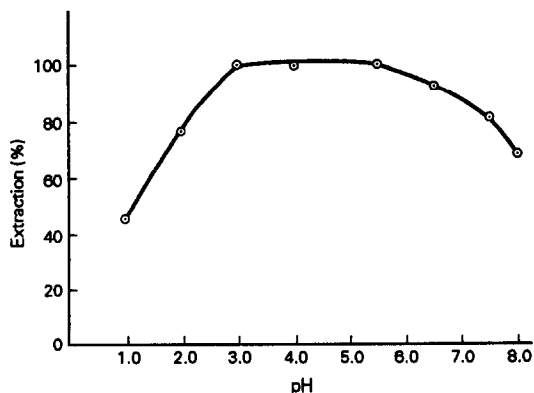


Fig. 1. Effect of pH on extraction of bismuth from citric acid.

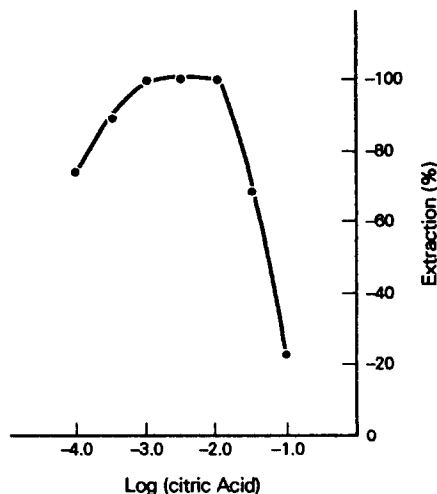


Fig. 2. Effect of citric acid concentration on extraction of bismuth.

At higher concentration there was a decrease in extraction perhaps because of competitive equilibria between the anionic bismuth citrate complex and the citrate anion itself, for the liquid anion exchanger. At lower citric acid concentration, however, there was a decrease in extraction and an increase in turbidity due to the formation of bismuth oxysalt (Fig. 2).

Effect of stripping agent

The stripping of bismuth was affected by various mineral acids (Table 1). The stripping was quantitative with $4M$ hydrochloric, $0.1M$ sulphuric or $2M$ nitric acid. It was interesting to note that at lower concentration *i.e.*, less than

Table 1. Effect of stripping agents

Stripping agents	Concentration, M	Recovery, %
HCl	0.25	39.1
	0.5	54.2
	1.0	69.7
	1.5	76.4
	2.0	85.4
	2.5	89.2
	3.0	90.1
	3.5	94.5
HNO ₃	4.0	100.0
	0.5	71.4
	1.0	96.2
	1.5	98.4
	2.0	100.0
	2.5	100.1
H ₂ SO ₄	3.0	99.8
	0.025	74.2
	0.05	98.4
	0.1	100.5
	0.5	100.0
	1.0	100.0
	2.0	99.8
3.0	100.0	

2M hydrochloric acid, stripping was not quantitative as bismuth formed an anionic chloro complex, which in turn was re-extracted by Aliquat 336S on the column. Similarly, less than 2M nitric acid could not strip effectively. Alkali hydroxides were not useful as they caused either precipitation or solid phase formation. The lower concentrations of sulphuric acid were preferred because of the formation of sulphato complexes. Thus, for all practical purposes, 0.1M sulphuric acid was utilised as the stripping agent for bismuth.

Separation of bismuth from binary mixtures

Bismuth was separated from several elements in binary mixtures by making use of the differences in their ability to form anionic complexes (Table 2). Thus, since alkali and alkaline earths, iron(II), zinc, cadmium, lead, cobalt, aluminium and manganese could not form anionic citrate complexes, they were not extracted and hence

Table 2. Separation of bismuth from other elements in binary mixtures (Bi added, 100 µg)

Foreign ion	Added as	Amount, µg	Recovery of Bi, %
Li ⁺	Li ₂ (SO ₄)·H ₂ O	4600	99.8
Na ⁺	NaCl	5500	99.5
K ⁺	KCl	6000	100.0
Rb ⁺	RbCl	1000	99.8
Be ²⁺	Be(NO ₃) ₂ ·3H ₂ O	2200	99.4
Mg ²⁺	MgSO ₄ ·7H ₂ O	1800	99.8
Ca ²⁺	Ca(NO ₃) ₂	2100	99.6
Sr ²⁺	Sr(NO ₃) ₂ ·2H ₂ O	1900	99.2
Ba ²⁺	Ba(NO ₃) ₂ ·2H ₂ O	2000	99.6
Fe ²⁺	FeSO ₄ ·7H ₂ O	300	99.5
Ag ⁺	AgNO ₃	350	99.4
As ³⁺	AsCl ₃	250	98.8
Y ³⁺	Y(NO ₃) ₃ ·2H ₂ O	500	99.2
Zn ²⁺	ZnSO ₄ ·7H ₂ O	250	100.0
Cd ²⁺	Cd(NO ₃) ₂ ·4H ₂ O	350	99.8
Ni ²⁺	Ni(NO ₃) ₂ ·6H ₂ O	400	100.0
Cu ²⁺	CuSO ₄ ·5H ₂ O	200	99.7
Co ²⁺	Co(NO ₃) ₂ ·6H ₂ O	250	99.6
Al ³⁺	Al(NO ₃) ₃ ·9H ₂ O	400	99.6
Pb ²⁺	Pb(NO ₃) ₂	250	100.0
Mn ²⁺	MnSO ₄ ·7H ₂ O	150	99.2
Ti ³⁺	TiCl ₃	250	99.7
Sb ³⁺	SbCl ₃ ·3H ₂ O	250	98.2
Au ³⁺	AuCl ₃	200	98.5
Fe ³⁺	Fe ₂ (SO ₄) ₃ ·7H ₂ O	250	99.4
Ga ³⁺	GaCl ₃	100	100.0
Sc ³⁺	Sc(NO ₃) ₃	100	99.2
V ⁴⁺	VOSO ₄	100	98.5
Zr ⁴⁺	Zr(NO ₃) ₄ ·5H ₂ O	150	99.0
Th ⁴⁺	Th(NO ₃) ₄ ·4H ₂ O	250	100.2
UO ₂ ²⁺	UO ₂ (NO ₃) ₂ ·6H ₂ O	200	99.0
SeO ₃ ²⁻	Na ₂ SeO ₃	100	98.5
WO ₄ ²⁻	Na ₂ WO ₄	150	99.2
Mo ₇ O ₂₄ ⁶⁻	(NH ₄) ₂ Mo ₇ O ₂₄ ·4H ₂ O	100	100.0
SiO ₃ ²⁻	Na ₂ SiO ₃	200	98.2
CN ⁻	KCN	150	99.0

were separated from bismuth. The differences in stability of citrato complexes of various elements were exploited to devise some separations. Zirconium, thorium, uranium and molybdenum formed relatively stable citrato complexes in comparison with the citrato complex of bismuth. Therefore, bismuth was first stripped with 0.1M sulphuric acid and subsequently all those elements which formed stable complexes were stripped with 2M sulphuric acid.

Separation of bismuth from multicomponent mixtures

A mixture of lead/nickel, bismuth and tin(IV) were passed on the column at pH 3.0 and citrato complexes of bismuth and tin(IV) were extracted while lead/nickel passed through the column unextracted. Then bismuth was stripped with 4M hydrochloric acid and finally tin(IV) was stripped with 1M sulphuric acid.

Arsenic, bismuth and antimony were separated by passing the mixture on the column; arsenic was not extracted and was washed with water. Then bismuth was stripped with 4M hydrochloric acid and antimony with 1M nitric acid.

The separation of zinc, bismuth, thorium and zirconium was carried out by passing the mixture through the column; zinc passed through, as it did not form an extractable citrato complex, while the extracted bismuth was stripped with 0.1M sulphuric acid, thorium with 0.25M

Table 3. Separation of bismuth from multicomponent mixtures

Mixture	Amount taken, µg	Recovery, %	Stripping agents, M	Standard deviation
Pb/Ni	100	100.0	H ₂ O	0.305
Bi	100	101.0	4 HCl	0.321
Sn(IV)	96	96.4	1 H ₂ SO ₄	0.435
As(III)	50	98.0	H ₂ O	0.529
Bi	100	101.0	4 HCl	0.321
Sb	75	98.1	1 HNO ₃	0.585
Zn	100	100.0	H ₂ O	0.057
Bi	100	100.0	0.1 H ₂ SO ₄	0.264
Th	110	101.0	0.25 H ₂ SO ₄	0.435
Zr	100	99.0	2 HCl	0.152
Pb	100	100.0	H ₂ O	0.305
Bi	100	100.0	0.1 H ₂ SO ₄	0.264
Th	110	98.0	0.25 H ₂ SO ₄	0.611
Mo	70	101.4	2 HNO ₃	0.435
Al	90	100.0	H ₂ O	0.305
Bi	100	102.0	0.1 H ₂ SO ₄	0.435
Fe(III)	100	99.0	0.25 HCl	0.416
Tl(III)	150.0	99.8	1 HClO ₄	0.305

Table 4. Analysis of various bismuth alloys

Alloy	Bi, %		Sn, %		Pb, %		Sb, %	
	Found	Actual	Found	Actual	Found	Actual	Found	Actual
White Metal	0.09	0.11	—	—	—	—	—	—
SD*	0.503							
Sealing Alloy	57.20	58.00	—	—	35.8	36.0	5.8	6.0
SD	0.603				0.836		0.251	
Bismuth Solder	26.60	27.50	44.9	45.0	28.0	27.5	—	—
SD	0.458		0.321		0.153			

*SD—Standard deviation.

sulphuric acid and zirconium with 2M hydrochloric acid.

The separation of lead, bismuth, thorium and molybdenum was effected by washing lead with water, bismuth was stripped with 0.1M sulphuric acid, thorium with 0.25M sulphuric acid and molybdenum with 2M nitric acid.

Aluminium, bismuth, iron(III) and thallium(III) were separated by passing the mixture on the column when aluminium was not extracted; extracted bismuth was stripped with 4M hydrochloric acid, iron(III) with 0.25M hydrochloric acid and thallium with 1M perchloric acid. These analyses were carried out in triplicate and standard deviations are shown in Table 3. In all these cases, the elements were determined spectrophotometrically by the use of appropriate chromogenic ligands.

Determination of bismuth from bismuth based alloys

The method was extended to the separation of bismuth from white metal, sealing alloys and bismuth solder.

About 0.1 g of an alloy was dissolved in *aqua regia*. The filtrate was evaporated to dryness, to remove excess acid, and then leached with dilute hydrochloric acid and made up to a known volume. An aliquot of solution containing lead, bismuth, antimony and tin was passed on the column from 0.01M citric acid buffered at pH 3.0 when all elements except

lead were extracted. Then bismuth was stripped with 4M hydrochloric acid, tin with 1M sulphuric acid and antimony with 1M nitric acid (Table 4).

The separation of bismuth from zinc, lead, tin, antimony, aluminium and thallium was important as they are associated in various low fusible alloys and the separation of bismuth from zirconium, molybdenum and thorium was significant as these are associated in fission products. The proposed method is simple, rapid with the time required less than 2 hr.

Acknowledgements—I am thankful to Prof. S. M. Khopkar, Department of Chemistry for his guidance and encouragement and to Prof. T. R. Ramamohan, Department of Metallurgical Engineering for providing the necessary facilities.

REFERENCES

1. I. Stronski, *Radiochimica Acta*, 1966, **6**, 163.
2. T. Braun and A. B. Farag, *Anal. Chim. Acta*, 1972, **62**, 476.
3. R. B. Heddur and S. M. Khopkar, *Bull. Bismuth Institute*, 1982, **38**, 6.
4. Y. Y. Vin and S. M. Khopkar, *ibid.*, 1989, **57**, 5.
5. I. Akaza, T. Tajima and T. Kiba, *Bull. Chem. Soc. Japan*, 1973, **46**, 1199.
6. T. Honjo, S. Ushijima and T. Kiba, *ibid.*, 1973, **46**, 3764.
7. A. I. Vogel, *A Text Book of Quantitative Inorganic Analysis*, p. 442. Longmans Green, London, 1964.
8. S. K. Sahoo and S. M. Khopkar, *Anal. Lett.* 1989, **22**, 1033.
9. F. D. Snell, *Photometric and Fluorometric Methods of Analysis*, Wiley & Sons, New York, 1978.

SPECIFICATION OF COLOUR CHANGES OF METALLOCHROMIC INDICATORS IN THE TITRATION OF BISMUTH WITH EDTA

K. M. M. KRISHNA PRASAD* and S. RAHEEM

School of Chemistry, Andhra University, Visakhapatnam 530 003, India

(Received 4 September 1990. Revised 9 January 1991. Accepted 25 January 1991)

Summary—The quality of the colour changes at the end-point in the complexometric titration of bismuth(III) with EDTA, using the indicators Hemotoxylin, PAN [1-(2-Pyridylazo)-Naphthol-2], PAR [4-(2-Pyridylazo)-Resorcinol], Xylenol Orange and Thoran is studied by means of the CIE 1931 trichromatic system, using specific colour discrimination (SCD) and colour difference (ΔE^*). The indicators are arranged in order of colour change quality. Of the indicators studied, Hemotoxylin is recommended as the most suitable for this titration.

The detection of the end-point in a titration is based on the colour transition of the indicator at the equivalence point of the reaction between titrant and titrand. Evaluation of this colour transition, by tristimulus colorimetry,¹ allows determination of the most adequate indicator for a specific determination.

Reilley and co-workers^{2,3} stated that for specification of the colour transition of visual indicators, the logical choice is to employ the chromaticity values of the International Commission on Illumination which suggested the use of absorbance values instead of transmittance values in conventional tristimulus colorimetry calculations to determine complementary chromaticity co-ordinates. An expression was derived to relate these co-ordinates to the true colour coordinates by the following expression

$$P_r = G_r - J(Q_r - G_r) - J^2(Q_r - G_r + Q_r^d)$$

where P_r is the true colour point, G_r the grey point, Q_r the complementary colour point, J the colour concentration and Q_r^d the dichromatistic deviation. Breckenridge and Schaub⁴ proposed RUCS (rectangular uniform chromaticity scale) co-ordinates, U and V , for representing the colour, where equidistant colour points represent an equal colour discrimination which are calculated from the

following equations:

$$U = 0.075 - \frac{0.823(x + y - 1)}{x - 7.05336y - 1.64023}$$

$$V = \frac{3.697 - 5.07713y - 1.36896}{x - 7.05336y - 1.64023} - 0.5$$

where (x, y) is the colour point on the chromaticity diagram for a given colour. Using the values of (U, V) , Bhuchar *et al.*⁵ determined a parameter, the specific colour discrimination (SCD), which is a measure of the quality of colour change and is given by,

$$\text{SCD} = \frac{1}{2}(1000) \frac{\Delta\sigma}{\Delta(C_L/C_M)}$$

where $\Delta\sigma = [(U_2 - U_1)^2 + (V_2 - V_1)^2]^{1/2}$, (C_L/C_M) is the ratio of the concentration of ligand to that of the metal ion.

In 1976, the CIE committee on colorimetry recommended the chromaticity co-ordinates L^* , a^* and b^* for the specification of colours.^{6,7} The equations for calculation of these parameters are presented as

$$L^* = 116 \left(\frac{Y}{Y_n} \right)^{1/3} - 16$$

$$a^* = 500 \left[\left(\frac{X}{X_n} \right)^{1/3} - \left(\frac{Y}{Y_n} \right)^{1/3} \right]$$

$$b^* = 200 \left[\left(\frac{Y}{Y_n} \right)^{1/3} - \left(\frac{Z}{Z_n} \right)^{1/3} \right]$$

*Author for correspondence.

where $X_n = 98041$, $Y_n = 100,000$ and $Z_n = 118,103$ are colour stimuli for white light for a light source C , where X , Y and Z are tristimuli for an indicator solution.

The chromaticity difference between two colours is given by the equation,

$$\Delta E^* = [(\Delta L^*)^2 + (\Delta a^*)^2 + (\Delta b^*)^2]^{1/2}$$

Cacho *et al.*⁸ proposed a parameter

$$\Delta J / \Delta(C_L / C_M)$$

to assess the quality of colour change. But Calatayud *et al.*¹ who stated that values of ΔJ show a non-uniform behaviour, preferred the parameter ΔS , standard deviation of colour matching, given by

$$\Delta S = g_{11} \Delta x^2 + 2g_{12} \Delta x \Delta y + g_{22} \Delta y^2$$

where Δx and Δy are changes in CIE coordinates and g_{11} , g_{12} and g_{22} are the values of constants of MacAdam⁹ ellipses corresponding to colour points.

Kotrly and Vytras¹⁰ studied the suitability of six indicators in the titration of Pb(II) with EDTA. Calatayud *et al.*¹¹ carried out investigations on Arsenazo(III) as indicator in the titrations of Ca(II), Pb(II), Bi(III), Fe(III) and La(III) with EDTA. Similar studies have been carried out in the complexometric titrations of the metal ions Pb(II),¹² Ca(II)^{12,13} and Zn(II).¹⁴

In this paper, the results of a detailed investigation of the specification of colour changes of indicators in the titration of bismuth(III) with EDTA are presented and a screened indicator is proposed to improve the quality of colour change.

EXPERIMENTAL

A Shimadzu U.V. Visible double-beam recording spectrophotometer with temperature control attachment was used. An OMC OMEGA-58000 minicomputer was used for calculating the parameters, by running the program in FORTRAN-77 for the weighted ordinate algorithm.

Reagents

Appropriate amounts of bismuth nitrate and the sodium salt of ethylenediaminetetraacetic acid, both analytical-reagent grade from Sarabai M. Chemicals, were dissolved in triply distilled water to give 0.01M solutions.

Indicators

Solutions ($1 \times 10^{-5}M$) of the indicators Hemotoxylin (Sigma), PAN (BDH-LR) and Xylenol Orange (BDH-LR) in ethanol, PAR (BDH-LR) and Thorn (BDH-LR) in water, were prepared.

Determination of chromatic parameters

A 10-ml portion of 0.01M Bi(III) solution and 0.1 ml of indicator solution are taken in a clean, dry beaker and the total volume is adjusted to 50 ml with varying volumes of EDTA and water after adjusting the pH with dilute ammonia.

The spectrum in each case is recorded on a Shimadzu spectrophotometer in the wavelength range 380–770 nm at 10 nm intervals. The absorbance values are treated with a computer program written in FORTRAN-77 and compiled on an OMEGA-58000 computer system. The algorithm adapted for the calculation of chromaticity parameters is the weighted ordinate method with $\Delta\lambda = 10$ nm, using the coefficients of the standard illuminant C and "10° standard observer".¹⁵

RESULTS AND DISCUSSION

The pH of the solution at the beginning of the titration, when using Hemotoxylin as indicator, is adjusted to 1.5 with dilute ammonia solution, while for the other indicators the pH is adjusted to the following ranges for each indicator: PAN: 1–3; PAR: 1–2; Xylenol Orange: 1–3 and Thoran: 2–3.

From the spectra of the indicators at different values of (C_L / C_M) (Fig. 1a–e), the tristimulus values X , Y and Z are determined by using the expressions:

$$X = \sum \bar{x} E T \Delta\lambda$$

$$Y = \sum \bar{y} E T \Delta\lambda$$

$$Z = \sum \bar{z} E T \Delta\lambda$$

where $\bar{x}E$, $\bar{y}E$ and $\bar{z}E$ (the product of the energy distribution values and tristimulus of pure spectrum colours) are values at different wavelengths in the range 380–770 nm with intervals of 10 nm, and are taken for standard illuminant C , where T is transmittance. The true colour co-ordinates of any coloured solution are given by

$$x = \frac{X}{X + Y + Z} \quad \text{and} \quad y = \frac{Y}{X + Y + Z}$$

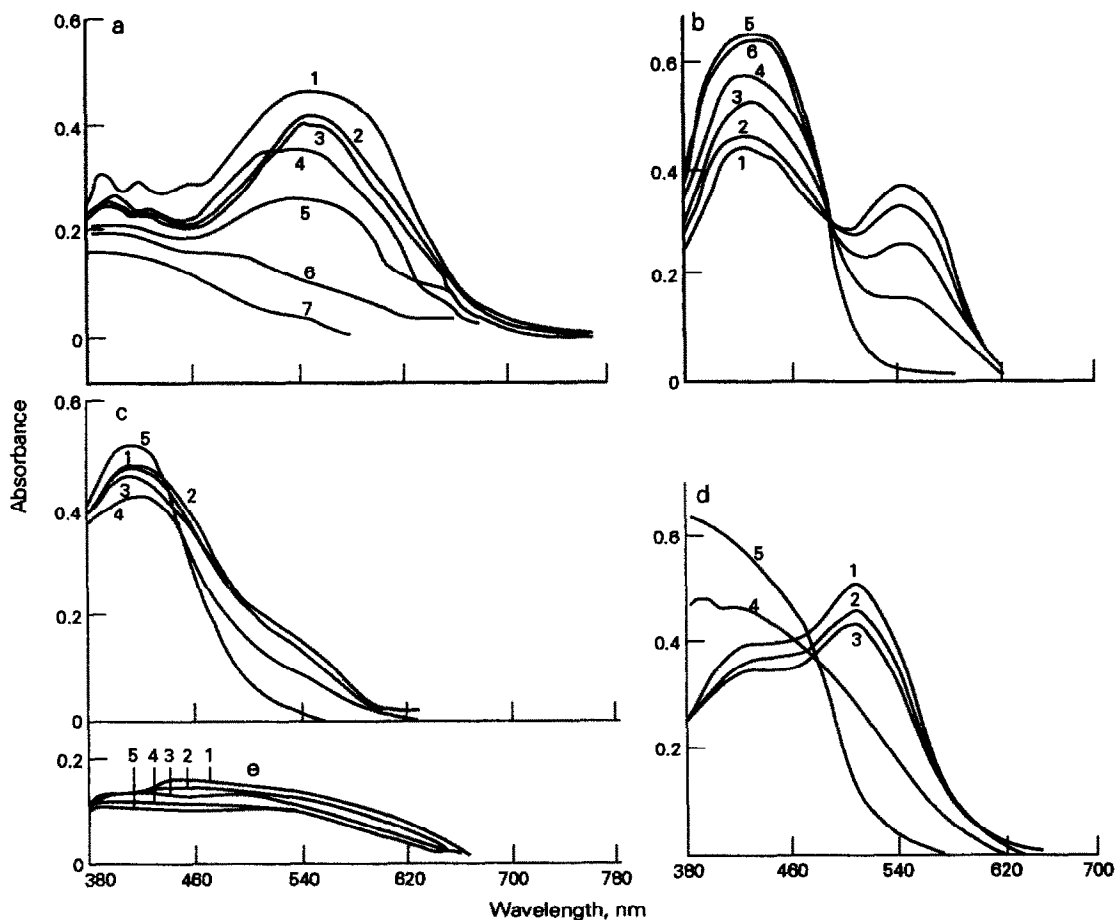


Fig. 1. Spectra of different indicators at different (C_L/C_M) ratios. (a) Hemotoxylin; (1) 0.92, (2) 0.94, (3) 0.96, (4) 0.98, (5) 1.0, (6) 1.02, (7) 1.04. (b) PAN; (1) 0.92, (2) 0.94, (3) 0.96, (4) 0.98, (5) 1.0, (6) 1.02. (c) Xylenol Orange; (1) 0.914, (2) 0.936, (3) 0.957, (4) 0.978, (5) 1.00. (d) PAR; (1) 0.92, (2) 0.94, (3) 0.96, (4) 0.98, (5) 1.0. (e) Thoran; (1) 0.92, (2) 0.94, (3) 0.96, (4) 0.98, (5) 1.0.

These values for all the studied indicators during the course of transition are tabulated in Table 1, along with the complementary colour co-ordinates (Q_x, Q_y) which are calculated by using absorbance values instead of transmittance values. The tristimulus value, Y , represents the brightness of the colour of the solution, whereas the purity of the colour of the solution is the ratio of the distance between the sample point and the illuminant point to the distance between the corresponding pure spectrum point and illuminant point. These two values, along with dominant wavelength (λ_d), which is the wavelength of the pure spectrum colour to be mixed with standard illuminant C to achieve the colour of the solution, are also included in Table 1, since these three parameters correspond closely to the three psychological attributes, brilliance (Y), saturation (pe) and hue (λ_d). The parameter J ,

known as the colour concentration, calculated from the expression

$$J = \frac{X + Y + Z}{X_n + Y_n + Z_n}$$

enables calculation of the volume ratio of the indicator with one or two inert dyes to obtain a screened indicator involving a colour transition at the end-point between complementary colours through greyness (colourlessness), and thereby enhance the quality of colour change.

The colour transition curves of all the indicators studied in the titration of bismuth(III) with EDTA are presented in Fig. 2. According to Reilley *et al.*,^{2,3} in comparing the quality of colour changes of different indicators at the equivalence point, apart from the fact that the distance between the colour points at the equivalence point should be large, the location of the

Table 1. Chromaticity co-ordinates for the colour changes of some metallochromic indicators for bismuth

	C_L/C_M	J	Y	x	y	Q_x	Q_y	λd	pe
Hemotoxylin	0.92	0.6531	55932.9	0.2904	0.2709	0.3579	0.4205	566.97	0.3717
	0.94	0.6698	58438.5	0.2760	0.2941	0.3587	0.4088	566.00	0.3192
	0.96	0.6357	56623.7	0.3028	0.2817	0.3275	0.3932	560.23	0.2492
	0.98	0.7741	73749.1	0.3134	0.3014	0.2980	0.3758	537.28	0.0836
	1.00	0.7088	72331.0	0.2125	0.3288	0.1505	0.1409	631.77	0.1201
	1.02	0.6753	65689.6	0.1881	0.3077	0.1454	0.1059	607.90	0.2131
	1.04	0.6102	55551.0	0.1672	0.2879	0.1443	0.1356	598.76	0.6033
	1.06	0.5730	46533.0	0.1491	0.2569	0.1404	0.1174	591.10	0.9521
PAN	0.92	0.4530	49438.4	0.3144	0.3452	0.2148	0.2805	557.90	0.1659
	0.94	0.5126	56944.7	0.3557	0.3515	0.2120	0.2604	580.21	0.2876
	0.96	0.5200	62100.6	0.3630	0.3777	0.1994	0.2147	575.69	0.0503
	0.98	0.5354	69840.4	0.3546	0.4126	0.1769	0.1524	567.32	0.0490
	1.00	0.4398	67467.4	0.2556	0.4852	0.1465	0.0563	528.61	0.0557
	1.02	0.4346	66824.3	0.2564	0.4864	0.1467	0.0595	530.14	0.5760
	1.04	0.4375	67406.5	0.2567	0.4874	0.1460	0.0565	530.41	0.5787
	1.06	0.4340	66728.7	0.2553	0.4863	0.1477	0.0598	522.63	0.5747
Xylenol Orange	0.893	0.6123	75473.2266	0.3434	0.3899	0.1643	0.1548	567.4328	0.4219
	0.914	0.5972	74106.6484	0.3459	0.3925	0.1665	0.1577	567.8650	0.4366
	0.936	0.6084	75534.7813	0.3458	0.3927	0.1624	0.1515	567.8000	0.5372
	0.957	0.6059	75127.8672	0.3446	0.3922	0.1653	0.1530	567.4850	0.4326
	0.978	0.5382	67799.7891	0.2653	0.3984	0.1594	0.1303	515.0720	0.3376
	1.000	0.3685	43032.1680	0.1495	0.3694	0.1501	0.0522	494.9290	0.6199
	1.021	0.4226	53135.5391	0.1753	0.3977	0.1508	0.0504	498.3110	0.5647
	1.042	0.4636	61134.3320	0.2052	0.4171	0.1520	0.0583	503.0109	0.4878
	1.063	0.4153	52806.8711	0.1760	0.4022	0.1506	0.0518	504.0200	0.4762
	PAR	0.92	0.5491	57673.9063	0.3981	0.3322	0.1877	0.2932	599.8058
0.94		0.5706	60013.5820	0.3908	0.3327	0.1886	0.2914	598.5100	0.2966
0.96		0.5873	62164.2617	0.3879	0.3348	0.1860	0.2852	596.7093	0.2992
0.98		0.5844	70922.7969	0.3706	0.3839	0.1656	0.1867	576.0660	0.4594
1.00		0.6381	86075.3906	0.3648	0.4267	0.1514	0.0803	568.4752	0.5875
1.02		0.6326	87046.3281	0.3694	0.4353	0.1481	0.0711	568.4350	0.6214
0.92		0.6865	70231.4922	0.2432	0.3236	0.1573	0.2720	658.1666	0.3060
0.94		0.5919	55079.8711	0.1940	0.2943	0.1431	0.3049	599.2882	0.8345
Thoran	0.96	0.5895	54618.8633	0.1941	0.2931	0.1434	0.3112	598.6868	0.4820
	0.98	0.5761	54872.6758	0.1969	0.3013	0.1368	0.2744	602.8720	0.4108
	1.00	0.4602	41098.8867	0.1546	0.2825	0.1299	0.1385	597.7512	0.6884
	1.02	0.4609	41281.9688	0.1547	0.2833	0.1295	0.1358	598.0109	0.6805
	1.04	0.4439	40468.4531	0.1549	0.2884	0.1314	0.1352	599.8580	0.6352
	1.06	0.4455	40072.5781	0.1534	0.2845	0.1349	0.1430	598.5274	0.6738

points and their relative positioning with regard to greyness (illuminant point) are also important. The colour transition curve of Hemotoxylin shows a long separation between the colour points at the equivalence point, and the curve passes very near to that of the illuminant point, clearly showing that this indicator is exhibiting the qualities of a good indicator. In the case of PAN and PAR, the colour transition curves show similar behaviour with comparable distances, and are present in the same location of the colour diagram. Even though Thoran has a longer distance between the points at the equivalence point, the colour change is not sharp and a gradual decrease in saturation of the colour is observed.

Since the co-ordinates of the colour diagram are non-uniform, CIE has recommended new parameters defined by CIE $L^*a^*b^*$ 1976.^{6,7} The curves drawn (Fig. 3) between a^* and b^* exhibit clearly the superiority of the indicator Hemo-

toxylin over all the other indicators studied, since its (a^* , b^*) curve passes very near to the grey point and requires no further screening.

PAN and PAR exhibit behaviour similar to each other, whereas Xylenol Orange and Thoran have a colour transition in a single quadrant of the (a^* , b^*) graph which indicates a decrease in saturation as the colour changes at the equivalence point.

A more quantitative method for the measurement of the quality of colour change of chemical indicators in visual titrations is suggested by Bhuchar *et al.*,⁵ and involves the calculation of the average number of colour discrimination steps for one (C_L/C_M) unit, which is known as the 'specific colour discrimination' (SCD). The SCD *vs.* (C_L/C_M) curves represented in Fig. 4 clearly show that Hemotoxylin, the indicator with the maximum SCD value, is the most suitable indicator in this titration among the indicators studied. The half band-width pertains-

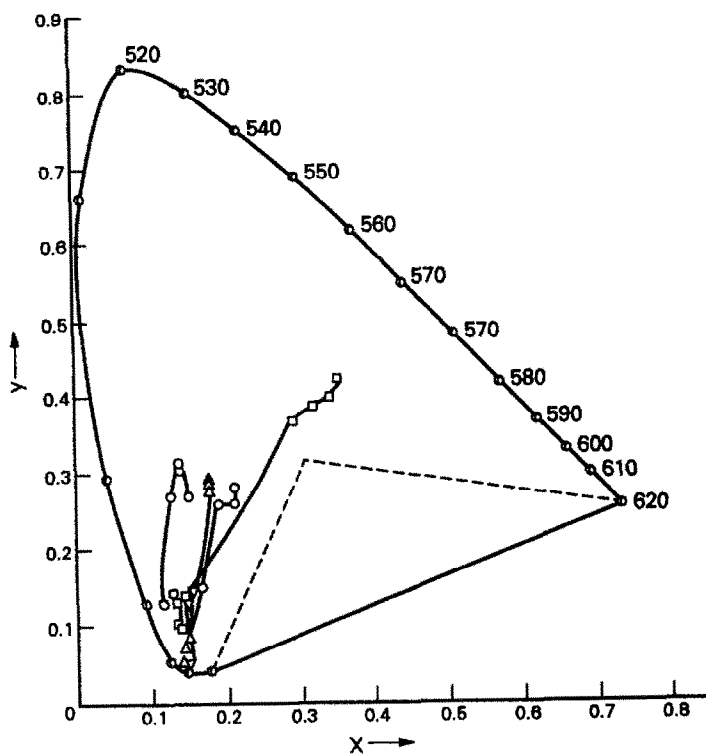


Fig. 2. Colour transition curves of \square — \square Hemotoxylin, \circ — \circ PAN, ∇ — ∇ Xylenol Orange, \triangle — \triangle PAR, \otimes — \otimes Thoran.

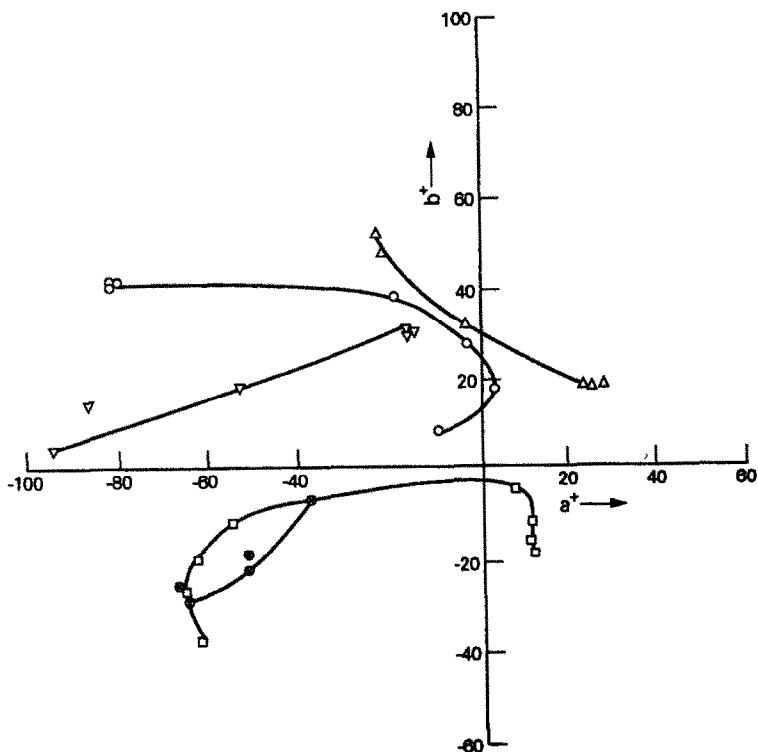


Fig. 3. Change of colour co-ordinates a^* and b^* (Index as in Fig. 2).

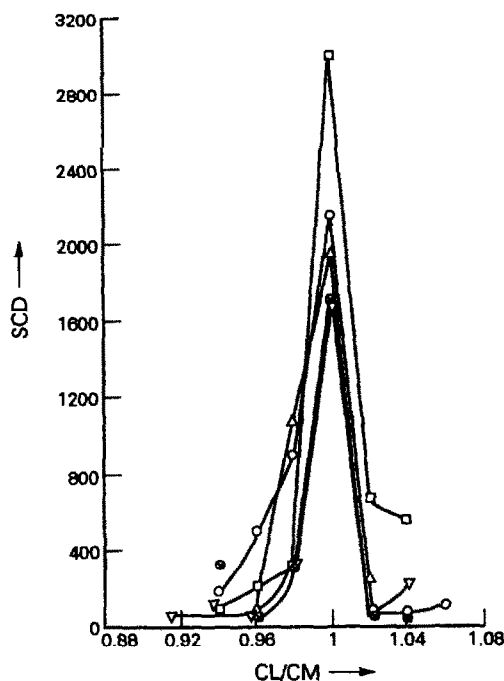


Fig. 4. Specific colour discrimination versus (C_L/C_M) (Index as in Fig. 2).

ing to this indicator is very low, which indicates the higher rapidity of colour change. (The rapidity of colour change is inversely proportional to the half band-width of (SCD) *vs.* (C_L/C_M) peak.) From the absolute values of SCD at $C_L/C_M = 1.0$ (Table 2), the order of increasing quality of colour change of the studied indicators is:

Thoran < Xylenol Orange < PAR
< PAN < Hemotoxylin

Even though the value of the half band-width of the SCD curve of Xylenol Orange indicates that this indicator has a better rapidity of colour change in comparison with PAR, the colour change of the former indicator at the end-point consists of only a decrease of intensity and hence the latter is considered to be the superior of the two. The absolute values of SCD shown in Table 2 also support this argument. A large number of visual titrations with all these indi-

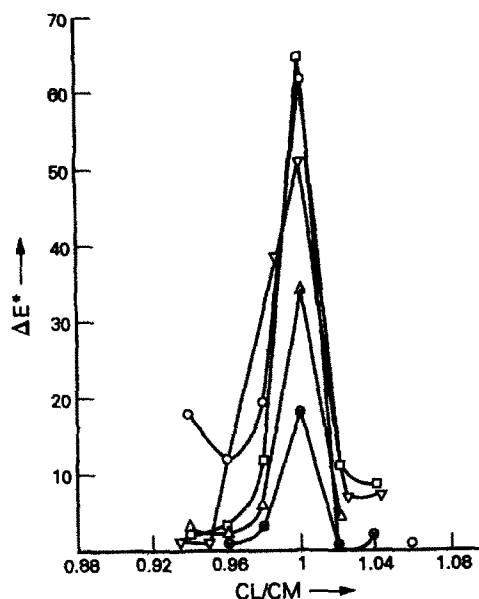


Fig. 5. E^* versus (C_L/C_M) (Index as in Fig. 2).

cators confirms the above mentioned order of quality of colour change.

In their search for the most uniform parameter (against ΔS) for evaluation of the colour break point of the chemical indicators, Calatayud *et al.*¹ reported that the 'total colour difference', ΔE^* , is the most suitable parameter in this regard. The total colour difference values calculated for these indicators also exhibit the same order of decrease as observed in the case of SCD values (Table 2), indicating ΔE^* is also a good parameter. The curves of ΔE^* *vs.* (C_L/C_M) (Fig. 5) confirm the adequacy of the parameter ΔE^* in evaluating the quality of colour change of chemical indicators.

Screening

The quality of colour change of the indicator PAN in this titration is improved by mixing this indicator with Methylene Blue in the concentration ratio of 6:1. The colour change at the equivalence point for the screened indicator is found to be from violet to green through grey-ness ($a^* = -0.06$; $b^* = -0.25$ at equivalence point). The results obtained with screened and

Table 2. SCD values, ΔE^* colour difference at maximum colour change of some metallochromic indicators for bismuth

Indicator	SCD at max. colour change	Half band width of SCD	ΔE^* at max. colour change
Hematoxylin	3001.1	1.7	65.21
PAN	2161.1	2.6	62.99
Xylenol Orange	1677.9	2.5	51.33
PAR	1958.3	3.4	34.09
Thoran	1669.5	2.4	18.42

Table 3. Results obtained with PAN (single) as indicator and PAN + Methylene Blue (6:1) screened indicator in the titration of Bi(III) with EDTA

Bi(III) taken, mg		Bi(III) found, mg	Relative standard deviation, %	Relative error, %
2.42	Single	2.48	0.66	2.48
	Screened	2.44	0.41	0.82
4.85	Single	4.93	0.16	1.64
	Screened	4.88	0.20	0.61
7.27	Single	7.35	0.13	1.10
	Screened	7.31	0.12	0.55
9.70	Single	9.77	0.10	0.72
	Screened	9.73	0.09	0.31
12.12	Single	12.21	0.07	0.74
	Screened	12.14	0.09	0.16

unscreened indicators, presented in Table 3, shows the higher accuracy achievable while using the screened indicator due to the distinctive colour change at the end-point which passes through colourlessness.

CONCLUSION

The quality of colour change of the indicators in the titration of bismuth(III) with EDTA is measured quantitatively with the help of tri-chromatic colorimetry, using the parameters SCD (specific colour discrimination) and ΔE^* (total colour difference) and it is found that Hemotoxylin is the best indicator out of those

studied in this titration. The application of the screened indicator PAN–Methylene Blue (6:1) yields improved accuracy over that using just PAN in this titrimetric determination.

REFERENCES

1. J. M. Calatayud, M. C. Pascual Martí and P. Campins Falco, *Anal. Chem.*, 1986, **58**, 200.
2. C. N. Reilley, H. A. Flaschka, S. Laurent and B. Laurent, *ibid.*, 1960, **32**, 1218.
3. C. N. Reilley and E. M. Smith, *ibid.*, 1960, **32**, 1233.
4. F. C. Breckenridge and W. R. Schaub, *J. Opt. Soc. Am.*, 1939, **29**, 370.
5. V. M. Bhuchar, V. P. Kukreja and S. R. Das, *Anal. Chem.*, 1971, **43**, 1847.
6. C.I.E. Colorimetry Committee, *J. Opt. Soc. Am.*, 1974, **64**, 896.
7. H. Pauli, *ibid.*, 1976, **66**, 866.
8. J. Cacho, C. Nerín, L. Ruberte and E. Rivas, *Anal. Chem.*, 1982, **54**, 1446.
9. D. L. MacAdam, *J. Opt. Soc. Am.*, 1943, **33**, 18.
10. S. Kotrlý and K. Vytřas, *Sb. Ved. Praci, Vys. Sk. Chem. Technol., Pardubice*, 1969, **19**, 21.
11. J. M. Calatayud, M. C. Pascual Martí and R. M. Marin Saez, *Anal. Chem.*, 1986, **14**, 508.
12. J. M. Calatayud, M. C. Pascual Martí and S. Sagrado Vives, *ibid.*, 1985, **13**, 87.
13. J. Cacho, A. Garnica and C. Nerín, *Anal. Chim. Acta*, 1983, **162**, 113.
14. K. Vytřas, J. Vytřasová and S. Kotrlý, *Talanta*, 1975, **22**, 529.
15. D. B. Judd, *J. Opt. Soc. Am.*, 1933, **23**, 359.

A HIGHLY SENSITIVE COLOUR REACTION FOR CHROMIUM(VI) WITH THE IODIDE-BASIC XANTHENE DYE-PVA SYSTEM

LIU SHAOPU and WANG FUCHANG

Department of Chemistry, South West China Normal University, Beibei, Chongqing, Sichuan, People's Republic of China

(Received 28 June 1990. Revised 26 November 1990. Accepted 14 December 1991)

Summary—A highly sensitive spectrophotometric method has been developed for determination of chromium(VI), based on oxidation of I^- to I_3^- in acid medium, then formation of a 1:1 ion-association compound of I_3^- with a basic xanthene dye in the presence of poly(vinyl alcohol). The molar absorptivity is 1.79×10^5 l.mole $^{-1}$.cm $^{-1}$ at 600 nm for the Rhodamine B system, 1.56×10^5 l.mole $^{-1}$.cm $^{-1}$ at 600 nm with Ethylrhodamine B, 1.56×10^5 l.mole $^{-1}$.cm $^{-1}$ at 570 nm with Rhodamine 6G and 2.01×10^5 l.mole $^{-1}$.cm $^{-1}$ at 590 nm with Butylrhodamine B, respectively. Preconcentration of chromium(VI) by an improved trioctylamine extraction procedure greatly increases the selectivity of the method and can be applied in the spectrophotometric determination of trace amounts of chromium(VI) in tap water, hot-spring water and river water.

For the spectrophotometric determination of chromium(VI), the diphenylcarbazide (DPC) method is most commonly used.¹ The method has good selectivity, but the sensitivity is not very high, the molar absorptivity being only 4.3×10^4 l.mole $^{-1}$.cm $^{-1}$.

In recent years, some highly sensitive spectrophotometric methods for determination of chromium(VI) have been developed, for example, the *o*-hydroxyhydroquinone-phthalein-cetyltrimethylammonium chloride,² *o*-nitrophenylfluorone-cetyltrimethylammonium bromide³ and *p*-chlorophenylfluorone-CTAB-sodium laurylsulphonate method,⁴ with molar absorptivities of about 1×10^5 l.mole $^{-1}$.cm $^{-1}$, but lengthy heating is needed and the selectivity is rather poor.

Spectrophotometric determination of selenium(VI) by its oxidation of iodide to triiodide, and extraction of the tri-iodide ion-association complex with a basic dye in the presence of a surfactant has been reported,⁵ and the same principle is now applied for determination of chromium(VI). Poly(vinyl alcohol), PVA, is used as the surfactant and Rhodamine B (RhB), Rhodamine 6G (Rh6G), and the ethyl and butyl esters of Rhodamine B (ERhB and BRhB respectively) are used as the counter-ion. The colour reactions have high sensitivities, with molar absorptivities between 1.56×10^5 and 2.01×10^5 l.mole $^{-1}$.cm $^{-1}$.

EXPERIMENTAL

Reagents

Standard chromium(VI) solution. A stock solution containing 100 μ g/ml chromium was prepared by dissolving 282.9 mg of pure potassium dichromate in 1000 ml of distilled water, and diluted further as required.

Phosphoric acid, 4M.

Potassium iodide solution, 100 mg/ml.

PVA solution, 1%,

RhB solution, 0.2 mg/ml.

ERhB solution, 0.2 mg/ml.

BRhB solution, 0.1 mg/ml.

Rh6G solution, 0.1 mg/ml.

Trioctylamine (TOA) solution, 5% in chloroform.

Saturated sodium sulphate solution.

Saturated sodium chloride solution.

Apparatus

A Hitachi U-3400 spectrophotometer and a 721 spectrophotometer were employed for absorbance measurement.

Procedure

Place a sample (≤ 5 ml) containing up to 5 μ g of chromium(VI) in a 25-ml standard flask, add 1 ml of 4M phosphoric acid and 2 ml of potassium iodide solution and dilute to 10 ml with water. Set aside for 5 min, then add 5 ml

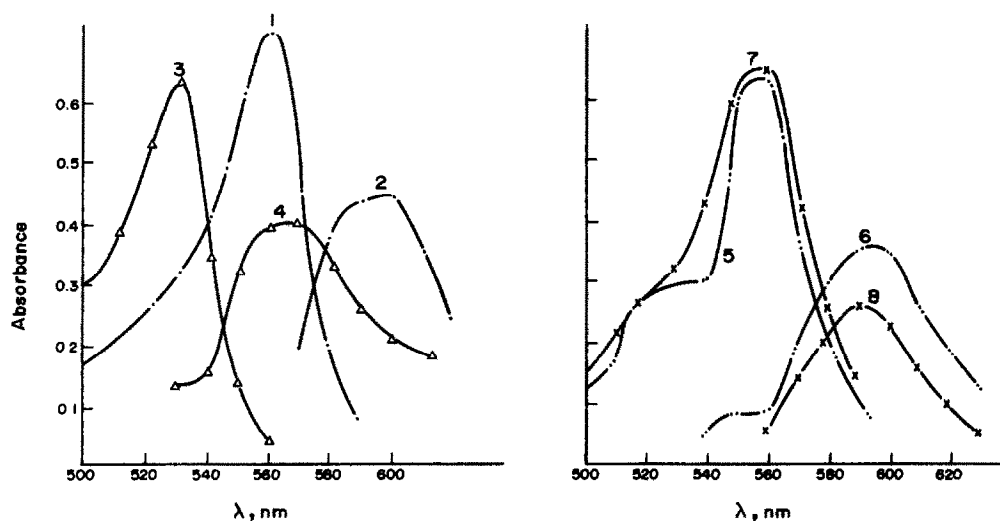


Fig. 1. Absorption spectra of the ion-associates: 1, RhB *vs.* water; 2, Cr(VI)-KI-RhB *vs.* RhB [Cr(VI), 4 μ g]; 3, Rh6G *vs.* water; 4, Cr(VI)-KI-Rh6G *vs.* Rh6G [Cr(VI) 3 μ g]; 5, ERhB *vs.* water; 6, Cr(VI)-KI-ERhB *vs.* ERhB [Cr(VI) 3 μ g]; 7, BRhB *vs.* water; 8, Cr(VI)-KI-BRhB *vs.* BRhB [Cr(VI) 2 μ g].

of basic dye solution and 2 ml of PVA solution. Dilute to the mark with water and mix. Measure the absorbance in a 1-cm cell at the wave-length of maximum absorbance against a reagent blank.

RESULTS AND DISCUSSION

Absorption spectra

Figure 1 shows the absorption spectra of the ion-associates of the I_3^- ion with four basic xanthene dyes. The absorption maxima are at 600 nm for the RhB and ERhB systems, 570 nm for the Rh6G system and 590 nm for the BRhB system; a bathochromic shift of 20–40 nm from the absorption maxima of the reagent blanks.

Effect of acidity

Figure 2 shows the dependence of the absorbance of the ion-associate on acidity. All the reactions are carried out in dilute phosphoric acid medium, but the optimum acidity ranges vary according to the system.

Effect of reagent concentrations

The optimum concentrations of potassium iodide are 0.024–0.048M for the RhB and BRhB systems, 0.036–0.060M for the Rh6G system, and 0.048–0.072M for the ERhB system, respectively.

The optimum concentrations of the basic dyes are as follows: $(0.76\text{--}1.35) \times 10^{-4}$ M RhB, $(0.84\text{--}1.01) \times 10^{-4}$ M Rh6G, $(0.70\text{--}0.94) \times 10^{-4}$ M ERhB and $(0.76\text{--}1.06) \times 10^{-4}$ M BRhB.

Effect of PVA and β -cyclodextrin

In the presence of PVA or β -cyclodextrin (β -CD), the solution remains clear and the absorbance has good stability. The optimum amounts of 10 mg/ml PVA or β -CD solution are between 0.5 and 4.0 ml. With PVA the absorbance is stable for 60 min for the RhB, Rh6G and ERhB systems, and 30 min for the BRhB system. In the absence of PVA or β -CD, the ion-associates are precipitated and the solutions are turbid.

Composition of the ion-associates

The reacting ratio of chromium(VI) to RhB was found to be 2:3 by the Job method and the

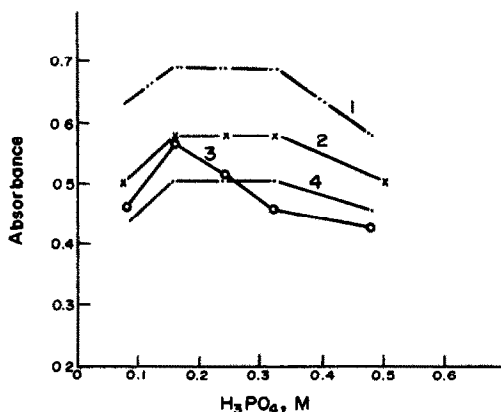
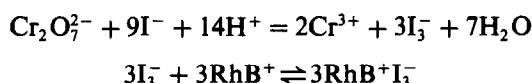


Fig. 2. Effect of acidity on determination of 5 μ g of Cr(VI): 1, Cr(VI)-KI-RhB system; 2, Cr(VI)-KI-ERhB system; 3, Cr(VI)-KI-Rh6G system; 4, Cr(VI)-KI-BRhB system.

Table 1. Interference of foreign ions in the determination of 5 μg of chromium(VI) with the RhB system

Ion	Amount added, μg	Cr(VI) found, μg	Ion	Amount added, μg	Cr(VI) found, μg
Ca^{2+}	10000	5.0	Br^-	10000	4.7
Zn^{2+}	10000	4.7	HCO_3^-	10000	5.0
Ni^{2+}	10000	4.8	F^-	5000	5.0
Mn^{2+}	10000	5.2	Ac^-	5000	5.0
Mg^{2+}	5000	5.0	NO_3^-	5000	5.2
Al^{3+}	20	5.2	BO_3^-	5000	5.0
Cu^{2+}	10	5.1	ClO_4^-	500	5.3
Hg^{2+}	10	4.8	AsO_4^-	500	5.2
Co^{2+}	10	4.8	$\text{S}_2\text{O}_3^{2-}$	5	5.0
Sb(V)	5	5.1	HSO_3^-	5	5.0
Fe^{3+}	5	5.0	NO_2^-	1	5.0
Pb^{2+}	5	4.8		1	5.1
Cd^{2+}	2	5.2			
Ag^+	2	5.0			

equilibrium shift method, indicating that the colour system is based on the equations



Sensitivity and selectivity

The molar absorptivities were found to be $2.01 \times 10^5 \text{ l. mole}^{-1} \cdot \text{cm}^{-1}$ for the BRhB system, $1.79 \times 10^5 \text{ l. mole}^{-1} \cdot \text{cm}^{-1}$ with RhB, and $1.56 \times 10^5 \text{ l. mole}^{-1} \cdot \text{cm}^{-1}$ with Rh6G and ERhB. Beer's law is obeyed over the range 0–0.2 $\mu\text{g/ml}$ chromium (but 0–0.08 $\mu\text{g/ml}$ for the BRhB system).

The selectivity of the RhB system was investigated in the determination of 5 μg of chromium(VI) in the presence of a series of other ions. Table 1 shows the results. The main interfering ions are Hg(II), Pb(II), Sb(III, V), Fe(III), Ag(I), Cu(II), Se(VI) and some strong oxidants

or reductants. Se(IV) interferes when present in amounts $> 2 \mu\text{g}$.

The interference of MnO_4^- can be eliminated by added dropwise suitable amounts of sodium nitrite solution, and the effect of nitrite can be eliminated by adding urea.

Adam and Přibil⁶ have reported a procedure for extraction of chromium(VI) with trioctylamine, which very effectively separates it from large amounts of iron, aluminium, copper, cobalt, zinc, uranium, vanadium, *etc.* We have improved the procedure, extracting chromium(VI) with a chloroform solution of trioctylamine from 0.1–0.2M sulphuric acid, then stripping the chromium(VI) with 0.3M sodium hydroxide. The chromium(VI) is then determined as already described. The interference of many common metal ions and strong oxidants or reductants is eliminated. Thus the method has very high sensitivity and selectivity, and can be applied to the spectrophotometric determination of trace amounts of chromium(VI) in environmental water samples *etc.* Se(IV) can then be tolerated in amounts up to 5 μg .

Extraction of Cr(VI)

Concentrate 250 ml of water sample to 25 ml by heating, add 1 ml of saturated sodium sulphate solution, 10 ml of saturated sodium chloride solution. 10 ml of 1M sulphuric acid and dilute with water to about 50 ml. Shake with 5 ml of TOA solution in chloroform for 2 min, and discard the aqueous layer. Add 5 ml of 0.3M sodium hydroxide to the organic layer, shake the mixture for 2 min, and transfer the aqueous layer to a 25-ml standard flask. Complete the determination as above.

Table 2. Determination of chromium(VI) in synthetic water samples

No.	Cr(VI) added, mg/l.	Sample composition, mg/l.	Cr(VI) found, mg/l.
1	0.200	Fe^{3+} 200, Al^{3+} 200, Ca^{2+} 200, Zn^{2+} 200, Cu^{2+} 200, Co^{2+} 20, U(VI) 20, V(V) 20, Ti(VI) 10, Mo(VI) 10	0.210
2	0.120	Fe^{3+} 200, Al^{3+} 200, Ca^{2+} 200, Zn^{2+} 200, Cu^{2+} 200, Co^{2+} 20, U(VI) 20, V(V) 20, Ti(IV) 10, Mo(VI) 10, Pb^{2+} 0.2, Hg^{2+} 0.4, Sb(V) 0.2, Ag^+ 0.08, Cd^{2+} 0.08	0.114

Table 3. Determination of chromium(VI) in water samples

Name of samples	Cr(VI) found, mg/l.	Cr(VI) added, mg/l.	Cr(VI) found, mg/l.	Recoveries, %
North hot spring water	0.000	0.0500	0.0490	98
Campus lake water	0.000	0.0200	0.0195	97
Jialing water 1	0.006	0.0200	0.0258	99
Jialing water 2	0.006	0.0240	0.0288	95

Application

The method was applied to the determination of chromium(VI) in natural water and synthetic water samples; the results are shown in Tables 2 and 3.

Acknowledgement—The project was supported by the National Natural Science Foundation of China.

REFERENCES

1. Z. Marczenko, *Separation and Spectrophotometric Determination of Elements*, p. 237. Horwood, Chichester, 1986.
2. I. Mori, Y. Fujita and T. Enoki, *Bunseki Kagaku*, 1979, **28**, 707.
3. Wen-Bin Qi and Li-Zhong Zhu, *Talanta*, 1986, **33**, 694.
4. Tong-Sheng Chen and Guan-Yu Shang, *Huanjin Huaxue*, 1988, **7**, No. 5, 58.
5. S. Liu, G. Zhou and Z. Huang, *Talanta*, 1990, **37**, 749.
6. J. Adam and R. Pffibil, *ibid.*, 1971, **18**, 91.

ANNOTATION

IS NITRATE REALLY AN INERT ELECTROLYTE?

A BRIEF REVIEW

MADELEINE ŠTULÍKOVÁ

Lečkova 1521, 149 00 Prague 4, Czechoslovakia

(Received 16 November 1990. Accepted 5 February 1991)

Summary—It has been common practice to use sodium or potassium nitrate as a supposedly inert background electrolyte or for adjustment of ionic strength, but nitrate forms sufficiently stable complexes with many metals for its use to result in erroneous values for stability constants. This note surveys the effects.

It is generally accepted that voltammetric, and indeed all, electrochemical methods for determining low concentrations of a test substance (ion) must be applied in the presence of a large excess of a supporting (background) electrolyte, *i.e.*, that a constant and fairly high ionic strength (I) must be maintained in the test solution. The reasons for this requirement are so well known that it is not necessary to examine this subject here. It is obvious that this supporting electrolyte should in no way affect the test system or the electrode and hence the results obtained.

Fifteen or twenty or even more years ago, when the nature of electrochemical processes was not fully understood, considerable effort was expended to elucidate the mechanisms of electrochemical reactions. Consequently, the supporting electrolyte and other components of the solution were not taken for granted and consequently ignored in investigation of the main reaction of interest, as has often happened in more recent work, but were considered as potential participants in the overall electrochemical processes. As will be seen below, considerable information has been obtained on the role that the supporting electrolyte can play in these reactions. In recent years, the shift of interest away from theoretical study of voltammetric and polarographic processes and greater concern with the applications of these methods has led to a tendency to ignore the literature on the potential participation of "inert" electrolytes in electrode processes. There is a general

impression that perchlorates are always "inert" as background electrolytes and that nitrates are very similar, and that no great error is incurred in assuming them to have no effect on electrochemical processes occurring in the solution. These assumptions ignore the fact that the supporting electrolyte solution always contains ions that can interact in some manner with the test ions and/or the electrode surface and thus affect the reactions (properties) being studied. Unless there is a fairly detailed understanding of the types and magnitudes of these interactions, no assumptions can be made about the degree of inertness of a given electrolyte, and when these assumptions are made blindly, there is a very real danger (as will be pointed out below) that the whole set of measured data may be seriously in error. These considerations hold for all types of supporting electrolytes and buffer solutions, but only the case of nitrates in this context will be examined more closely here, as they provide particularly good example of the pitfalls in wait for the unwary.

The possible interactions of nitrates with the electrode/electrolyte/test substance system fall into a number of categories. These will be considered separately, but of course more than one type may be operative (and not necessarily independently) in a particular system. The cation in the supporting electrolyte will be neglected, not because it is not also a potential participant, but as being beyond the scope of this discussion.

Complex formation

The likelihood of formation of complexes of the test ion (usually a metal cation) with nitrate¹⁻⁵ is by far the greatest danger in the use of nitrates as "inert" electrolytes, but tends to be frequently ignored. In addition, mixed complexes can be formed with the participation of other anions or cations present in the solution.^{6,7} Neglecting such complexes can lead to serious errors when stability constants of weak complexes are measured, especially when the metal ion is present in excess and the change in free ligand is measured. A high nitrate concentration can then significantly decrease the concentration of free metal ion. When mixed nitrate/test anion/test cation complexes are formed, the results can be even more misleading. A large number of original papers on nitrate complexes have been published, and the stability constants have been tabulated in various compilations. Although this danger has been repeatedly pointed out in the literature,^{4,5} subsequent papers have consistently ignored earlier warnings, although it is obvious that doing so can at the very least lead to doubt as to the reliability of the results obtained. For example, nitrate was employed as the supporting electrolyte anion¹⁴ in a study of the stability constants of fluoride and chloride complexes of a number of metal ions, although an earlier work⁵ had specifically pointed out that this approach must necessarily lead to errors in these results.

The tendency for mixed complexes, including nitrate ions from the supporting electrolyte, to be formed and the effect that this can have on electrochemical studies have been discussed in a number of papers. For example, mixed cadmium–azide–nitrate complexes can be formed and their formation constants have been determined.⁶ The effect of these complexes on the electrochemical behaviour led the authors to suggest perchlorate as a replacement for nitrate in these systems, although this exchange may not be without its own dangers; a detailed discussion was given of the effect of mixed complexes on the electrochemical system.⁶ No attempt will be made here to give a detailed survey of the determination of the stability constants of nitrate complexes with various ions (see, for example, references 1–13) or of papers that have consistently ignored this danger. Rather, it will be pointed out that this factor should always be considered when employing nitrate and mixed electrolytes and that a careful

literature survey is the only basis for reliable results.

Electrode effects

So far, we have considered only the effects that can arise from interactions in the electrolyte solution. However, the effect that the solution components can have on the processes occurring at the electrode surface is obviously a factor that cannot (or at least should not) be ignored.

Nitrate ions can affect the electrode surface and reactions in a number of ways. For example, it has been found for certain solutions (where there was no evidence for complex formation between the test ion and nitrate) that nitrate ions were nonetheless specifically adsorbed on the electrode surface.¹⁵ This adsorption hindered the charge-transfer reaction of interest and was especially pronounced for the Cu^+/Cu reaction at mercury electrodes.¹⁵ In an apparently far more complicated interaction, nitrate has been found to enhance the adsorption of 2,2'-bipyridyl cadmium(II) complexes, through a complex equilibrium.¹⁶ A number of other papers have been published considering these specific adsorption effects (*e.g.*, by Fawcett and Solomon,¹⁷ and by Cachet *et al.*¹⁸). The effect of adsorption on the stability constants determined by polarographic methods of complexes of metal ions with adsorbable ligands was considered in a comprehensive work some twenty years ago.¹⁹

The effect of the adsorption of electrolyte species on the electrode surface is not, of course, limited to simple physical occupation of active electrode sites. These species must also necessarily affect the properties of the electrode double layer, as was pointed out a quarter of a century ago²⁰ but is now often forgotten. Double-layer effects in the absence of specific adsorption can also be significant (see, for example, references 21–23).

An effect that is not often considered is the catalytic influence that the test ion can have on reduction of nitrate. Such processes can lead to electrode responses that would be absent in the base electrolyte alone and could erroneously be attributed to the electrode reaction(s) of the test ion(s). For example, lanthanum has been found to catalyse nitrate reduction through the formation of at least two types of complexes,²⁴ which also affect the concentration of lanthanum available for electrode reactions. The underpotential deposition of cadmium has also been found to catalyse the reduction of nitrate

ions^{25,26} and lead reduced on the surface of a gold electrode has a similar effect.²⁷ Studies have been carried out (see, for example, references 28–30) to elucidate the mechanisms of these effects, which have even been utilized in the development of methods for nitrate determination, for example by Boese *et al.*³¹ and by Gómez-Nieto *et al.*³²

CONCLUSIONS

The list of ways in which the electrolyte ions can affect the test ions (through complexation, changes in the hydration,¹¹ solubility effects,³³ changes in the diffusion coefficients and solution viscosity³⁴) and the electrode surface^{35,36} (double-layer effects, changes in the number and type of active sites, specific adsorption of simple and complex ions, changes in the zero-charge potentials,³⁷ effects on the electrode kinetics³⁸) is far longer than is generally acknowledged in most practical applications (and even in some theoretical studies). Obviously, a detailed description of these effects for all types of test systems is more suited to a book than to such a short review. Here, it will only be emphasized again that a thorough literature survey including all the pertinent papers (*e.g.*, for possible effects on the determination of stability constants³⁹ and formation constants^{40,41}) is essential before beginning any experimental work with an "inert" electrolyte.

Acknowledgements—The author wishes to thank Dr. R. A. Chalmers of the University of Aberdeen for suggesting the subject of this review and for stimulating discussions, and the University of Aberdeen, Scotland, for providing facilities.

REFERENCES

- L. G. Sillén and A. E. Martell (eds.), *Stability Constants of Metal-Ion Complexes*, The Chemical Society, London, Special Publications No. 17 (1964) and No. 25 (1971).
- A. M. Bond and G. T. Hefter, *Critical Survey of Stability Constants and Related Thermodynamic Data of Fluoride Complexes in Aqueous Solution*, Pergamon Press, Oxford, 1980.
- S. Kotrlý and L. Šúcha, *Handbook of Chemical Equilibria in Analytical Chemistry*, Horwood, Chichester, 1985.
- G. T. Hefter, C. B. Chan and N. H. Tioh, *Anal. Chem.*, 1984, **56**, 749.
- A. M. Bond and T. A. O'Donnell, *J. Electroanal. Chem. Interfacial Electrochem.*, 1970, **26**, 137.
- D. W. Franco, E. A. Neves and P. Senise, *ibid.*, 1975, **60**, 341.
- A. Hannisdal and K. H. Schröder, *ibid.*, 1989, **263**, 23.
- Š. Komorsky-Lovrić, M. Lovrić and M. Branica, *ibid.*, 1986, **214**, 37.
- G. A. Bottomley and L. G. Glossop, *ibid.*, 1981, **118**, 433.
- Š. Komorsky-Lovrić and M. Branica, *ibid.*, 1987, **226**, 253.
- R. E. Hester and R. A. Plane, *Inorg. Chem.*, 1964, **3**, 769.
- Idem*, *J. Chem. Phys.*, 1964, **40**, 411.
- K. Momoki, H. Ogawa and H. State, *Anal. Chem.*, 1969, **41**, 1826.
- V. Majer and K. Štulík, *Talanta*, 1982, **29**, 145.
- A. W. M. Verkroost, M. Sluyters-Rehbach and J. H. Sluyters, *J. Electroanal. Chem. Interfacial Electrochem.*, 1973, **47**, 323.
- E. A. Neves and F. C. Anson, *ibid.*, 1973, **43**, 71.
- W. R. Fawcett and P. H. Solomon, *ibid.*, 1988, **251**, 183.
- C. Cachet, M. Fromet, F. Wenger and R. Wiart, *ibid.*, 1975, **61**, 121.
- A. M. Bond and G. T. Hefter, *ibid.*, 1971, **31**, 477.
- G. G. Susbilles, P. Delahay and E. Solon, *J. Phys. Chem.*, 1966, **70**, 2601.
- J. L. Anderson and I. Shain, *Anal. Chem.*, 1978, **50**, 163.
- W. S. Go, J. J. O'Dea and J. Osteryoung, *J. Electroanal. Chem. Interfacial Electrochem.*, 1988, **255**, 21.
- H. L. Jindall, K. Matsude and R. Tamamushi, *ibid.*, 1978, **90**, 185.
- J. Knoeck, *Anal. Chem.*, 1969, **41**, 2069.
- X. K. Xing and D. A. Scherson, *J. Electroanal. Chem. Interfacial Electrochem.*, 1986, **199**, 485.
- Idem*, *Anal. Chem.*, 1987, **59**, 962.
- J. Garcia-Domenech, M. A. Climent, A. Aldaz, J. L. Vazquez and J. Clavilier, *J. Electroanal. Chem. Interfacial Electrochem.*, 1983, **159**, 223.
- H. Hemmi, K. Hasebe, K. Ohzeki and T. Kambara, *Talanta*, 1984, **31**, 319.
- P. Ostapczuk and Z. Kublik, *J. Electroanal. Chem. Interfacial Electrochem.*, 1976, **68**, 193.
- N. Kato and K. Aoki, *ibid.*, 1989, **261**, 309.
- S. W. Boese, V. S. Archer and J. W. O'Laughlin, *Anal. Chem.*, 1977, **49**, 479.
- M. A. Gómez-Nieto, M. D. Luque de Castro and M. Valcárcel, *J. Electroanal. Chem. Interfacial Electrochem.*, 1983, **153**, 201.
- F. M. Abd El Wahad, M. G. A. Khedr and A. M. Shams El Din, *ibid.*, 1978, **86**, 383.
- J. A. Bolzen, *ibid.* 1975, **59**, 303.
- Z. Stojek and J. Osteryoung, *Anal. Chem.*, 1988, **60**, 131.
- D. G. Peters and W. D. Schults, *J. Electroanal. Chem. Interfacial Electrochem.*, 1964, **8**, 200.
- L. Campanella, *ibid.*, 1970, **28**, 228.
- P. Kulesza, T. Jędral and Z. Galus, *ibid.* 1980, **109**, 141.
- H. S. Rossotti, *Talanta*, 1974, **21**, 809.
- K. Momoki and H. Ogawa, *Anal. Chem.*, 1971, **43**, 1664.
- D. J. Leggett, *Talanta*, 1980, **27**, 787.

BOOK REVIEWS

Advances in Spectroscopy, Volume 18—Time Resolved Spectroscopy: R.J.H. CLARK and R. E. HESTER (editors), Wiley, Chichester, 1989. Pages xxi + 406. £100.00.

It is only fairly recently that experimental techniques and fundamental theory have progressed sufficiently to allow the probing of a rate process directly at the microscopic, molecular level. This achievement has required a major international scientific effort in the development of time-resolved spectroscopic methods to monitor both reaction kinetics and the molecular dynamic changes which occur during chemical and biological reactions. This book is, therefore, a timely contribution to the considerable progress made in this field and provides a detailed account of the state of some optically based techniques at the time of publication. A series of nine chapters by an international team of authors from the U.S.A., U.S.S.R., Canada, France and Japan provides a comprehensive review of the field, with all chapters quoting references up to 1988 and most up to 1989. The book is technique-based and all chapters provide a basic outline of the theoretical principles underlying a specific technique, a detailed experimental description and, finally, a discussion of some chemical systems to illustrate the type of information generated. A valuable feature of all the articles is the summary outline, by the authors, of future applications and development.

Chapter 1 introduces the novel technique of picosecond transient-phase grating spectroscopy which derives information on non-radiative energy relaxation processes in optically excited molecules by monitoring the changes in the index of refraction induced in the material by these processes. A substantial part of the book (Chapters 2, 3, 4, 6 and 7) is dedicated to developments in time-resolved Raman spectroscopy. Chapter 2 discusses the use of resonance rotational Raman spectroscopy to yield sub-picosecond dephasing of resonant electronic states of gases with rotational and vibrational specificity, and Chapter 3 discusses the monitoring of sub-picosecond vibrational dephasing in the condensed phase by coherent Raman scattering and libration relaxation by degenerate four-wave mixing using temporally incoherent light. Time-resolved resonance Raman spectroscopy is reviewed in Chapter 4, with a focus on transient radical intermediates produced in radiation and photochemical reactions in solution. A valuable discussion on time-resolved Fourier-transform infrared spectroscopy is given in Chapter 5, demonstrating the use of continuous-scan and step-and-sample (SAS) techniques to overcome a natural disadvantage of Fourier transform instruments, namely the requirement of a complete scan of the moving mirror in the Michelson interferometer to generate an interferogram from which spectral information is obtained. At the time of publication, microsecond time resolution had been achieved, with new instruments being developed capable of nanosecond time resolution. The application of time-resolved spectroscopy to biochemical systems is tackled in Chapters 6, 7 and 8 which demonstrate the use of resonance Raman and FTIR spectroscopy in obtaining vibrational information on the transient states in photosynthetic bacterial reaction centres and in obtaining sub-picosecond resonance Raman spectra of heme proteins. The final chapter in the book provides an exciting review of the current state-of-the-art in the generation of ultrashort optical pulses to realize femtosecond time-resolved spectroscopy.

This text represents another excellent addition to the "Advances in Infrared and Raman Spectroscopy" series and is an extremely worthwhile contribution to the field of time-resolved spectroscopy.

R. RAVAL

Electroanalysis of Biologically Important Compounds: J. P. HART, Ellis Horwood, Chichester, 1990. Pages 213. £42.50.

This book surveys amperometric electrochemical methods of estimating clinical and biochemical analytes. The techniques covered are voltammetry, polarography, stripping voltammetry and the use of amperometric detectors in liquid chromatography.

After a brief chapter on theory which serves to survey the various techniques, there follows the bulk of the book, which reviews recent work on a wide variety of analytes. There are separate chapters on pyrimidines and purines, amino-acids, peptides and proteins, vitamins, and coenzymes. Each chapter has sections on electroanalysis and liquid chromatography. New apparatus and techniques, and improvements to old methods, are all included. There is a very useful index of chemical substances and a rather short general index.

The book contains a great deal of useful information about the electrochemistry of the analytes discussed and experimental detail about possible methods of estimation. This information should be useful to an analytical expert when deciding which techniques are applicable to the solution of a particular problem.

This is an excellent book for an expert in either electrochemistry or biochemical or clinical analysis, but is not suitable for the novice, as it assumes considerable background knowledge and experience.

B. G. COOKSEY

Field Desorption Mass Spectrometry, L. PROKAI, Dekker, New York, 1990, Pages vi + 291. \$99.75 (U.S.A. and Canada), \$119.50 (elsewhere).

The aim of this volume 9 in the "Practical Spectroscopy Series" is a relatively complete description of fundamentals, recent developments in instrumentation and experimental techniques. The text is written for specialists working in the field of organic mass spectrometry. The book contains four chapters, each with 100–150 references.

The first part discusses the mechanisms of ion formation. The fundamentals of field desorption and ionization are treated only briefly but there is an excellent book by Beckey on this subject. Consequently, attention is directed primarily to the description of ion emission from the analyte on the emitter. Aspects such as transport along the emitter, the volatility of sample, and field-included extraction from electrolytic solutions and salts are dealt with.

The second chapter is devoted to experimental techniques and represents a major strength of the book. The different approaches for preparation and activation of the emitters are extensively treated, with many practical details and illustrations, showing the experimental set-up as well as micrographs of the resulting emitters. The operational procedures (*e.g.*, temperature selection) are discussed. Concerning instrumentation, many data and observations are packed into rather long sections. A better structure with more headings would have improved the readability of this part of the book. Additional topics such as high resolution, negative ions, tandem instruments and kinetics of the FD method are included. The chapter fulfils the two objectives of the book: an excellent source for practice and a valuable starting point for further reading.

A major part of the third chapter concentrates on the chemistry at the emitter surface. The principal processes and the possibilities to exploit additives and matrices are highlighted in a concise and very accessible way. A good coverage of typical fragmentations and their use for structural analysis is given. The problems related to quantification, and the precautions required, are presented with abundant references. Finally, field desorption is evaluated within the context of other methods for the analysis of thermolabile, high molecular-weight compounds and polymers. The discussion is primarily based on a table of representative papers. It would have been desirable to extend this section substantially and to give more adequate comments on the respective advantages and disadvantages of the techniques mentioned. The selection of the most appropriate technique for a practical problem remains the most important and frequently encountered task of a modern chemist and the specialists should share all their expertise on this aspect.

Part of this criticism is answered indirectly by the last chapter, dealing with selected applications in the field of pharmaceutical research and biosciences, environmental studies, characterization of fossil fuel and petrochemicals, study of inorganic and organometallic compounds and polymer applications. These topics give a well balanced view of the merits of field desorption for qualitative purposes as well as for quantification. Sometimes, the use of other techniques is mentioned, but little comparison is made.

In conclusion, this book provides excellent coverage of the practical aspects and fulfils its scope as a starting point for further reading on most aspects of the method. The major criticisms concerns the somewhat long sections, which could be better structured, and the lack of comparative discussion of field desorption in relation to other recent ionization techniques in organic mass spectrometry.

R. GIJBELS

Principles and Practice of Analytical Chemistry, 3rd Edition: F. W. FIFIELD and D. KEALEY, Blackie, Glasgow, 1990. Pages xii + 521. £19.95 (softback only).

The fact that this is the third edition of this book indicates both the success of earlier editions and the changing nature of the broad subject area, which necessitates frequent updating of material.

Following a short introduction which incorporates a glossary of terms, there is a short but useful chapter on the assessment of analytical data. The labelling of Fig. 2 can be construed as being deliberately vague as the section heading is "The Nature and Origin of Errors". A few worked examples on statistics are included but in general the problem exercises in the text are, unfortunately, not supplied with answers. Chapter 3 covers pH, complexation and solubility equilibria. These topics are dealt with at a very basic level, requiring no previous knowledge in these subject areas.

The amount of space devoted to each analytical technique is based upon its application in industry and Chapter 4 on separation techniques is the largest in the book. Solvent extraction, chromatography and zone electrophoresis are covered. More detail on HPLC instrumentation has been included and GC-mass spectrometry and GC-IR are mentioned. Chapter 5 introduces titrimetry and gravimetry and Chapter 6 covers electrochemical techniques.

Analytical spectrometry is introduced in Chapter 7 and dealt with at the atomic level (absorption and emission) and at the molecular level in subsequent chapters. Both qualitative and quantitative aspects of analysis are covered. Mass fragmentation analysis (strictly not a spectroscopic technique), NMR and IR are included along with visible and ultraviolet spectrometry. I would like to have seen some mention of spectrofluorimetry in this section.

A separate chapter on radiochemical methods is very basic and attempts to cover this entire field in less than thirty pages. The chapter on thermal methods (new for the 3rd edition) is an essential addition for a general text on analytical chemistry.

The penultimate chapter includes very useful examples of real analytical problems and discusses how the analyst selects relevant procedures to determine analytes present in a sample. The excellent examples could be supplemented with one involving the use of HPLC. The book concludes with a very competent chapter on the role of computers in analytical chemistry.

Overall this book is to be recommended for the undergraduate student because all the important analytical techniques are covered at an elementary level. It is also a very useful book for the analyst to have in the laboratory as a convenient

Field Desorption Mass Spectrometry, L. PROKAI, Dekker, New York, 1990, Pages vi + 291. \$99.75 (U.S.A. and Canada), \$119.50 (elsewhere).

The aim of this volume 9 in the "Practical Spectroscopy Series" is a relatively complete description of fundamentals, recent developments in instrumentation and experimental techniques. The text is written for specialists working in the field of organic mass spectrometry. The book contains four chapters, each with 100–150 references.

The first part discusses the mechanisms of ion formation. The fundamentals of field desorption and ionization are treated only briefly but there is an excellent book by Beckey on this subject. Consequently, attention is directed primarily to the description of ion emission from the analyte on the emitter. Aspects such as transport along the emitter, the volatility of sample, and field-included extraction from electrolytic solutions and salts are dealt with.

The second chapter is devoted to experimental techniques and represents a major strength of the book. The different approaches for preparation and activation of the emitters are extensively treated, with many practical details and illustrations, showing the experimental set-up as well as micrographs of the resulting emitters. The operational procedures (*e.g.*, temperature selection) are discussed. Concerning instrumentation, many data and observations are packed into rather long sections. A better structure with more headings would have improved the readability of this part of the book. Additional topics such as high resolution, negative ions, tandem instruments and kinetics of the FD method are included. The chapter fulfils the two objectives of the book: an excellent source for practice and a valuable starting point for further reading.

A major part of the third chapter concentrates on the chemistry at the emitter surface. The principal processes and the possibilities to exploit additives and matrices are highlighted in a concise and very accessible way. A good coverage of typical fragmentations and their use for structural analysis is given. The problems related to quantification, and the precautions required, are presented with abundant references. Finally, field desorption is evaluated within the context of other methods for the analysis of thermolabile, high molecular-weight compounds and polymers. The discussion is primarily based on a table of representative papers. It would have been desirable to extend this section substantially and to give more adequate comments on the respective advantages and disadvantages of the techniques mentioned. The selection of the most appropriate technique for a practical problem remains the most important and frequently encountered task of a modern chemist and the specialists should share all their expertise on this aspect.

Part of this criticism is answered indirectly by the last chapter, dealing with selected applications in the field of pharmaceutical research and biosciences, environmental studies, characterization of fossil fuel and petrochemicals, study of inorganic and organometallic compounds and polymer applications. These topics give a well balanced view of the merits of field desorption for qualitative purposes as well as for quantification. Sometimes, the use of other techniques is mentioned, but little comparison is made.

In conclusion, this book provides excellent coverage of the practical aspects and fulfils its scope as a starting point for further reading on most aspects of the method. The major criticisms concerns the somewhat long sections, which could be better structured, and the lack of comparative discussion of field desorption in relation to other recent ionization techniques in organic mass spectrometry.

R. GIJBELS

Principles and Practice of Analytical Chemistry, 3rd Edition: F. W. FIFIELD and D. KEALEY, Blackie, Glasgow, 1990. Pages xii + 521. £19.95 (softback only).

The fact that this is the third edition of this book indicates both the success of earlier editions and the changing nature of the broad subject area, which necessitates frequent updating of material.

Following a short introduction which incorporates a glossary of terms, there is a short but useful chapter on the assessment of analytical data. The labelling of Fig. 2 can be construed as being deliberately vague as the section heading is "The Nature and Origin of Errors". A few worked examples on statistics are included but in general the problem exercises in the text are, unfortunately, not supplied with answers. Chapter 3 covers pH, complexation and solubility equilibria. These topics are dealt with at a very basic level, requiring no previous knowledge in these subject areas.

The amount of space devoted to each analytical technique is based upon its application in industry and Chapter 4 on separation techniques is the largest in the book. Solvent extraction, chromatography and zone electrophoresis are covered. More detail on HPLC instrumentation has been included and GC–mass spectrometry and GC–IR are mentioned. Chapter 5 introduces titrimetry and gravimetry and Chapter 6 covers electrochemical techniques.

Analytical spectrometry is introduced in Chapter 7 and dealt with at the atomic level (absorption and emission) and at the molecular level in subsequent chapters. Both qualitative and quantitative aspects of analysis are covered. Mass fragmentation analysis (strictly not a spectroscopic technique), NMR and IR are included along with visible and ultraviolet spectrometry. I would like to have seen some mention of spectrofluorimetry in this section.

A separate chapter on radiochemical methods is very basic and attempts to cover this entire field in less than thirty pages. The chapter on thermal methods (new for the 3rd edition) is an essential addition for a general text on analytical chemistry.

The penultimate chapter includes very useful examples of real analytical problems and discusses how the analyst selects relevant procedures to determine analytes present in a sample. The excellent examples could be supplemented with one involving the use of HPLC. The book concludes with a very competent chapter on the role of computers in analytical chemistry.

Overall this book is to be recommended for the undergraduate student because all the important analytical techniques are covered at an elementary level. It is also a very useful book for the analyst to have in the laboratory as a convenient

reference source for most available techniques. (Some minor techniques are omitted and others such as flow-injection analysis are mentioned only briefly.) If more detail of techniques is required the reader can refer to the lists of recommended books, which are given at the end of each chapter. The book compares favourably with "Fundamentals of Analytical Chemistry" by Skoog and West.

P. J. COX

TrAC—Trends in Analytical Chemistry, Reference Edition Vol. 7: Elsevier, Amsterdam, 1988, Pages xii + 404. US\$200.0, Dfl. 380.00.

This book is the current volume in a series presenting a compilation of the archival material reprinted from the regular monthly edition of Trends in Analytical Chemistry (TrAC) 1988.

The regular monthly topics of *feature, trends, computer corner, interface, meeting reports, book reviews* and *in the news* are all reprinted. The page numbers are common to both editions.

The stated scope of TrAC is to provide broadly-based, easy-to-read scientific reviews of current developments in the analytical sciences, backed up by news and other features of interest to analytical chemists. Particular attention is paid to the impact of computers and biotechnology on analytical chemistry.

In all of the articles this remit has been fulfilled: the items are relatively short and very readable. However, there are only two items listed under biotechnology focus: chemiluminescence immunoassays and flow-through microfluorometry of immobilized enzymes—more might have been hoped for. The effect of computers is much more evident, with a regular monthly article *computer corner* and the four articles on interfacing; some of the trend items are also computer-orientated.

This book is well produced but at \$200 (£100 +) it is costly.

W. BRYCE

Silent Spring Revisited: G. J. MARCO, R. M. HOLLINGWORTH and W. DURHAM (editors), ACS, Washington, 1987. Pages xxiii + 214. U.S.A. and Canada: \$17.95 (softback), \$29.95 (hardback). Elsewhere: \$21.95 (softback), \$35.95 (hardback).

The focal point of *Silent Spring Revisited*, Rachel Carson's *Silent Spring*, has always been a seminal work. This 12-chapter symposium is an appraisal of recent knowledge and thinking on the application of pesticides in relation to the 1962 publication. As such it is difficult to categorize, but it would seem to have a role as a general and specialized source. The two main sections, Regulations and Overviews, include areas of concern which have been expanded since Carson, particularly the contamination of ground water, its effect on aquatics and also the analysis of toxic residues. If Carson's major contribution was to alert the authorities to the dangers of organochlorine insecticides, which resulted in their withdrawal in the U.S.A., then the preoccupation of the nineties may well be whether the replacement organophosphates and carbamates are really safe. The controversial question of carcinogenesis is also discussed. Some useful tables of data illustrate the effects of pesticides on both wildlife and human populations. Each chapter includes references and a glossary, but there are some overlaps and slightly confusing synonyms. A comprehensive index helps to weld together a rather disparate work.

H. J. FLETCHER

Fourier Transforms in N.M.R., Optical and Mass Spectrometry, A User's Handbook: A. G. MARSHALL and F. R. VERDUN, Elsevier, Amsterdam, 1990. Pages xvi + 450. U.S. \$107.25, Dfl. 220.00 (hardback), U.S. \$46.25, Dfl. 95.00 (softback).

The commercial availability of computer-controlled, pulsed, generating and detecting equipment is presently stimulating a renaissance in nearly all branches of spectroscopy. Applications of pulse techniques are continuously being developed and extended, and not only are they causing enormous changes in physics, chemistry, biochemistry, biology and medicine, they are also enormously influencing the training of spectroscopists. It is now crucially important that spectroscopists understand Fourier transform methods and be able to apply them.

This very interesting book has arrived at just the right time. It provides a self-contained unified mathematical treatment of Fourier transform methods and their applications to several branches of spectroscopy. It is aimed at practising spectroscopists, so non-ideal effects are treated in some detail. Noise, non-linear response, limits to spectrometer performance arising from finite detection periods, finite data size, misphasing, etc., are all considered. The use of complex variables to represent physically real quantities, the interpretation of negative-frequency signals, chirping, on-resonance vs. off-resonance responses, Hadamard codes, multiplex advantages and disadvantages, are just examples of topics that are explained.

The fundamental line shapes that are encountered in all branches of spectroscopy are introduced in Chapter 1. Chapters 2 and 3 summarize the basic mathematics of continuous (analogue) and discrete (digital) Fourier transforms, and their practical implications. Chapter 4 discusses common experimental aspects of *signals* encountered in spectroscopy. Chapter 5 similarly discusses *noise*. In Chapter 6, non-Fourier transform methods, including autoregression and maximum entropy methods, are introduced and critically compared with Fourier transform techniques. Chapters 7 and 8 discuss aspects of Fourier transform spectroscopy that are unique to ion cyclotron mass spectroscopy and nuclear magnetic resonance

reference source for most available techniques. (Some minor techniques are omitted and others such as flow-injection analysis are mentioned only briefly.) If more detail of techniques is required the reader can refer to the lists of recommended books, which are given at the end of each chapter. The book compares favourably with "Fundamentals of Analytical Chemistry" by Skoog and West.

P. J. COX

TrAC—Trends in Analytical Chemistry, Reference Edition Vol. 7: Elsevier, Amsterdam, 1988, Pages xii + 404. US\$200.0, Dfl. 380.00.

This book is the current volume in a series presenting a compilation of the archival material reprinted from the regular monthly edition of Trends in Analytical Chemistry (TrAC) 1988.

The regular monthly topics of *feature, trends, computer corner, interface, meeting reports, book reviews* and *in the news* are all reprinted. The page numbers are common to both editions.

The stated scope of TrAC is to provide broadly-based, easy-to-read scientific reviews of current developments in the analytical sciences, backed up by news and other features of interest to analytical chemists. Particular attention is paid to the impact of computers and biotechnology on analytical chemistry.

In all of the articles this remit has been fulfilled: the items are relatively short and very readable. However, there are only two items listed under biotechnology focus: chemiluminescence immunoassays and flow-through microfluorometry of immobilized enzymes—more might have been hoped for. The effect of computers is much more evident, with a regular monthly article *computer corner* and the four articles on interfacing; some of the trend items are also computer-orientated.

This book is well produced but at \$200 (£100 +) it is costly.

W. BRYCE

Silent Spring Revisited: G. J. MARCO, R. M. HOLLINGWORTH and W. DURHAM (editors), ACS, Washington, 1987. Pages xxiii + 214. U.S.A. and Canada: \$17.95 (softback), \$29.95 (hardback). Elsewhere: \$21.95 (softback), \$35.95 (hardback).

The focal point of *Silent Spring Revisited*, Rachel Carson's *Silent Spring*, has always been a seminal work. This 12-chapter symposium is an appraisal of recent knowledge and thinking on the application of pesticides in relation to the 1962 publication. As such it is difficult to categorize, but it would seem to have a role as a general and specialized source. The two main sections, Regulations and Overviews, include areas of concern which have been expanded since Carson, particularly the contamination of ground water, its effect on aquatics and also the analysis of toxic residues. If Carson's major contribution was to alert the authorities to the dangers of organochlorine insecticides, which resulted in their withdrawal in the U.S.A., then the preoccupation of the nineties may well be whether the replacement organophosphates and carbamates are really safe. The controversial question of carcinogenesis is also discussed. Some useful tables of data illustrate the effects of pesticides on both wildlife and human populations. Each chapter includes references and a glossary, but there are some overlaps and slightly confusing synonyms. A comprehensive index helps to weld together a rather disparate work.

H. J. FLETCHER

Fourier Transforms in N.M.R., Optical and Mass Spectrometry, A User's Handbook: A. G. MARSHALL and F. R. VERDUN, Elsevier, Amsterdam, 1990. Pages xvi + 450. U.S. \$107.25, Dfl. 220.00 (hardback), U.S. \$46.25, Dfl. 95.00 (softback).

The commercial availability of computer-controlled, pulsed, generating and detecting equipment is presently stimulating a renaissance in nearly all branches of spectroscopy. Applications of pulse techniques are continuously being developed and extended, and not only are they causing enormous changes in physics, chemistry, biochemistry, biology and medicine, they are also enormously influencing the training of spectroscopists. It is now crucially important that spectroscopists understand Fourier transform methods and be able to apply them.

This very interesting book has arrived at just the right time. It provides a self-contained unified mathematical treatment of Fourier transform methods and their applications to several branches of spectroscopy. It is aimed at practising spectroscopists, so non-ideal effects are treated in some detail. Noise, non-linear response, limits to spectrometer performance arising from finite detection periods, finite data size, misphasing, etc., are all considered. The use of complex variables to represent physically real quantities, the interpretation of negative-frequency signals, chirping, on-resonance vs. off-resonance responses, Hadamard codes, multiplex advantages and disadvantages, are just examples of topics that are explained.

The fundamental line shapes that are encountered in all branches of spectroscopy are introduced in Chapter 1. Chapters 2 and 3 summarize the basic mathematics of continuous (analogue) and discrete (digital) Fourier transforms, and their practical implications. Chapter 4 discusses common experimental aspects of *signals* encountered in spectroscopy. Chapter 5 similarly discusses *noise*. In Chapter 6, non-Fourier transform methods, including autoregression and maximum entropy methods, are introduced and critically compared with Fourier transform techniques. Chapters 7 and 8 discuss aspects of Fourier transform spectroscopy that are unique to ion cyclotron mass spectroscopy and nuclear magnetic resonance

reference source for most available techniques. (Some minor techniques are omitted and others such as flow-injection analysis are mentioned only briefly.) If more detail of techniques is required the reader can refer to the lists of recommended books, which are given at the end of each chapter. The book compares favourably with "Fundamentals of Analytical Chemistry" by Skoog and West.

P. J. COX

TrAC—Trends in Analytical Chemistry, Reference Edition Vol. 7: Elsevier, Amsterdam, 1988, Pages xii + 404. US\$200.0, Dfl. 380.00.

This book is the current volume in a series presenting a compilation of the archival material reprinted from the regular monthly edition of Trends in Analytical Chemistry (TrAC) 1988.

The regular monthly topics of *feature, trends, computer corner, interface, meeting reports, book reviews* and *in the news* are all reprinted. The page numbers are common to both editions.

The stated scope of TrAC is to provide broadly-based, easy-to-read scientific reviews of current developments in the analytical sciences, backed up by news and other features of interest to analytical chemists. Particular attention is paid to the impact of computers and biotechnology on analytical chemistry.

In all of the articles this remit has been fulfilled: the items are relatively short and very readable. However, there are only two items listed under biotechnology focus: chemiluminescence immunoassays and flow-through microfluorometry of immobilized enzymes—more might have been hoped for. The effect of computers is much more evident, with a regular monthly article *computer corner* and the four articles on interfacing; some of the trend items are also computer-orientated.

This book is well produced but at \$200 (£100 +) it is costly.

W. BRYCE

Silent Spring Revisited: G. J. MARCO, R. M. HOLLINGWORTH and W. DURHAM (editors), ACS, Washington, 1987. Pages xxiii + 214. U.S.A. and Canada: \$17.95 (softback), \$29.95 (hardback). Elsewhere: \$21.95 (softback), \$35.95 (hardback).

The focal point of *Silent Spring Revisited*, Rachel Carson's *Silent Spring*, has always been a seminal work. This 12-chapter symposium is an appraisal of recent knowledge and thinking on the application of pesticides in relation to the 1962 publication. As such it is difficult to categorize, but it would seem to have a role as a general and specialized source. The two main sections, Regulations and Overviews, include areas of concern which have been expanded since Carson, particularly the contamination of ground water, its effect on aquatics and also the analysis of toxic residues. If Carson's major contribution was to alert the authorities to the dangers of organochlorine insecticides, which resulted in their withdrawal in the U.S.A., then the preoccupation of the nineties may well be whether the replacement organophosphates and carbamates are really safe. The controversial question of carcinogenesis is also discussed. Some useful tables of data illustrate the effects of pesticides on both wildlife and human populations. Each chapter includes references and a glossary, but there are some overlaps and slightly confusing synonyms. A comprehensive index helps to weld together a rather disparate work.

H. J. FLETCHER

Fourier Transforms in N.M.R., Optical and Mass Spectrometry, A User's Handbook: A. G. MARSHALL and F. R. VERDUN, Elsevier, Amsterdam, 1990. Pages xvi + 450. U.S. \$107.25, Dfl. 220.00 (hardback), U.S. \$46.25, Dfl. 95.00 (softback).

The commercial availability of computer-controlled, pulsed, generating and detecting equipment is presently stimulating a renaissance in nearly all branches of spectroscopy. Applications of pulse techniques are continuously being developed and extended, and not only are they causing enormous changes in physics, chemistry, biochemistry, biology and medicine, they are also enormously influencing the training of spectroscopists. It is now crucially important that spectroscopists understand Fourier transform methods and be able to apply them.

This very interesting book has arrived at just the right time. It provides a self-contained unified mathematical treatment of Fourier transform methods and their applications to several branches of spectroscopy. It is aimed at practising spectroscopists, so non-ideal effects are treated in some detail. Noise, non-linear response, limits to spectrometer performance arising from finite detection periods, finite data size, misphasing, etc., are all considered. The use of complex variables to represent physically real quantities, the interpretation of negative-frequency signals, chirping, on-resonance vs. off-resonance responses, Hadamard codes, multiplex advantages and disadvantages, are just examples of topics that are explained.

The fundamental line shapes that are encountered in all branches of spectroscopy are introduced in Chapter 1. Chapters 2 and 3 summarize the basic mathematics of continuous (analogue) and discrete (digital) Fourier transforms, and their practical implications. Chapter 4 discusses common experimental aspects of *signals* encountered in spectroscopy. Chapter 5 similarly discusses *noise*. In Chapter 6, non-Fourier transform methods, including autoregression and maximum entropy methods, are introduced and critically compared with Fourier transform techniques. Chapters 7 and 8 discuss aspects of Fourier transform spectroscopy that are unique to ion cyclotron mass spectroscopy and nuclear magnetic resonance

spectroscopy. Chapter 9 briefly considers Fourier transform/interferometry applications in other regions of the spectrum, particularly in infrared and Raman spectroscopy.

This is a timely, well-written, well-indexed book. Each chapter has a set of well-constructed examples, and their solutions. The lists of references include historically important key articles and reviews. The appendices include integrals and theorems for Fourier transform applications, Fast Fourier Transform program listings in both Fortran and Basic, and a pictorial atlas of Fourier transform pairs.

This is a book that deserves to be carefully read by all modern serious spectroscopists, of all kinds.

A. L. PORTE

An Introduction to Surface Analysis by Electron Spectroscopy: J. F. WATTS, OUP, Oxford, 1990. Pages x + 85. £9.95 (softback).

This book provides a short but excellent and comprehensive overview of the theory, practice, and application of X-ray photoelectron and Auger electron spectroscopy in surface analysis. The basic concepts, spectrometer design, and interpretation of spectra are described in clear and simple terms with an ample supply of illustrations. The sections on compositional depth profiling, applications to material science, and comparisons with other analytical techniques indicate clearly that this is now one of the principal methods of qualitative and quantitative analysis, and potential users of this and related techniques will find this book to be one of the best on the subject and exceedingly good value for money.

J. B. CRAIG

Practical Surface Analysis, Volume 1—Auger and X-Ray Photoelectron Spectroscopy: D. BRIGGS and M. P. SEAH (editors), 2nd Edition, Wiley, Chichester, 1990. Pages xiv + 657. £85.00.

The first edition of this book was published in 1983 and quickly achieved a very high reputation among surface spectroscopists. As in other fields, information and developments have expanded to such an extent that a new edition became necessary.

The book opens with a perspective by the principal authors on the analysis of surfaces and interfaces: this is followed by chapters on instrumentation, spectral interpretation, and depth profiling and quantification by Auger electron and X-ray photoelectron spectroscopy. The remaining chapters deal with the applications of AES in microelectronics, metallurgy, and heterogeneous catalysis, with the application of XPS in polymer technology, and with the applications of both techniques in corrosion science. There are nine appendices dealing comprehensively with scale calibration, charge referencing techniques, data analysis, chemical shifts, photoelectron and Auger energies, sensitivity factors, line positions, and kinetic energies.

Each chapter is well written, well illustrated and well documented, and the book is remarkably inexpensive; the reviewer has no hesitation in recommending this edition to practical and theoretical surface spectroscopists and to those in industry who desire better qualitative and quantitative surface characterization of their products. It is to be hoped that the covers of this edition are strong enough to withstand the constant usage that it is likely to encounter.

J. B. CRAIG

Understanding Insulin Action—Principles and Molecular Mechanisms: J. ESPINAL, Ellis Horwood, Chichester, 1989. Pages 129. £26.00.

There is a large amount of work currently published annually on insulin and this compact text presents primarily the recent facts and ideas. Details of metabolism and its control are only included when they relate directly to insulin, and relevant background knowledge is required.

The initial chapter attempts to convey the significance of the discovery of insulin by outlining the history of diabetes mellitus. This brief review covers the period from the description of the disease in the first century AD to the production of genetically engineered insulin in 1979. This is followed by a chapter on the chemistry, synthesis and secretion of insulin, and incorporates a section on the insulin gene. A chapter on the pathophysiology of insulin covers the effect of the hormone on muscle, adipose tissue and the liver. The metabolism of these tissues is examined in relation to the action of insulin and within this limitation it provides a useful review of the control of carbohydrate and fat metabolism. The latter part of this chapter discusses diabetes mellitus, its classification, diagnosis, symptoms, aetiology, complications and treatment. Under the heading of molecular mechanisms involved in insulin action consideration is given to the effects of insulin on proteins through enzyme phosphorylation/dephosphorylation and the movement of target proteins within the cell. Further chapters consider the insulin receptor and a number of compounds which have been proposed as possible secondary messengers within the cell. Finally the author attempts to summarize the data and provide a current molecular mechanism for the mode of action of insulin.

As a user of such texts I found this book valuable and a good source of references to review articles on insulin and related topics.

J. E. ATKINSON

spectroscopy. Chapter 9 briefly considers Fourier transform/interferometry applications in other regions of the spectrum, particularly in infrared and Raman spectroscopy.

This is a timely, well-written, well-indexed book. Each chapter has a set of well-constructed examples, and their solutions. The lists of references include historically important key articles and reviews. The appendices include integrals and theorems for Fourier transform applications, Fast Fourier Transform program listings in both Fortran and Basic, and a pictorial atlas of Fourier transform pairs.

This is a book that deserves to be carefully read by all modern serious spectroscopists, of all kinds.

A. L. PORTE

An Introduction to Surface Analysis by Electron Spectroscopy: J. F. WATTS, OUP, Oxford, 1990. Pages x + 85. £9.95 (softback).

This book provides a short but excellent and comprehensive overview of the theory, practice, and application of X-ray photoelectron and Auger electron spectroscopy in surface analysis. The basic concepts, spectrometer design, and interpretation of spectra are described in clear and simple terms with an ample supply of illustrations. The sections on compositional depth profiling, applications to material science, and comparisons with other analytical techniques indicate clearly that this is now one of the principal methods of qualitative and quantitative analysis, and potential users of this and related techniques will find this book to be one of the best on the subject and exceedingly good value for money.

J. B. CRAIG

Practical Surface Analysis, Volume 1—Auger and X-Ray Photoelectron Spectroscopy: D. BRIGGS and M. P. SEAH (editors), 2nd Edition, Wiley, Chichester, 1990. Pages xiv + 657. £85.00.

The first edition of this book was published in 1983 and quickly achieved a very high reputation among surface spectroscopists. As in other fields, information and developments have expanded to such an extent that a new edition became necessary.

The book opens with a perspective by the principal authors on the analysis of surfaces and interfaces: this is followed by chapters on instrumentation, spectral interpretation, and depth profiling and quantification by Auger electron and X-ray photoelectron spectroscopy. The remaining chapters deal with the applications of AES in microelectronics, metallurgy, and heterogeneous catalysis, with the application of XPS in polymer technology, and with the applications of both techniques in corrosion science. There are nine appendices dealing comprehensively with scale calibration, charge referencing techniques, data analysis, chemical shifts, photoelectron and Auger energies, sensitivity factors, line positions, and kinetic energies.

Each chapter is well written, well illustrated and well documented, and the book is remarkably inexpensive; the reviewer has no hesitation in recommending this edition to practical and theoretical surface spectroscopists and to those in industry who desire better qualitative and quantitative surface characterization of their products. It is to be hoped that the covers of this edition are strong enough to withstand the constant usage that it is likely to encounter.

J. B. CRAIG

Understanding Insulin Action—Principles and Molecular Mechanisms: J. ESPINAL, Ellis Horwood, Chichester, 1989. Pages 129. £26.00.

There is a large amount of work currently published annually on insulin and this compact text presents primarily the recent facts and ideas. Details of metabolism and its control are only included when they relate directly to insulin, and relevant background knowledge is required.

The initial chapter attempts to convey the significance of the discovery of insulin by outlining the history of diabetes mellitus. This brief review covers the period from the description of the disease in the first century AD to the production of genetically engineered insulin in 1979. This is followed by a chapter on the chemistry, synthesis and secretion of insulin, and incorporates a section on the insulin gene. A chapter on the pathophysiology of insulin covers the effect of the hormone on muscle, adipose tissue and the liver. The metabolism of these tissues is examined in relation to the action of insulin and within this limitation it provides a useful review of the control of carbohydrate and fat metabolism. The latter part of this chapter discusses diabetes mellitus, its classification, diagnosis, symptoms, aetiology, complications and treatment. Under the heading of molecular mechanisms involved in insulin action consideration is given to the effects of insulin on proteins through enzyme phosphorylation/dephosphorylation and the movement of target proteins within the cell. Further chapters consider the insulin receptor and a number of compounds which have been proposed as possible secondary messengers within the cell. Finally the author attempts to summarize the data and provide a current molecular mechanism for the mode of action of insulin.

As a user of such texts I found this book valuable and a good source of references to review articles on insulin and related topics.

J. E. ATKINSON

Chiral Separations by HPLC—Applications to Pharmaceutical Compounds: A. M. KRSTULOVIĆ (editor), Ellis Horwood, Chichester, 1989. Pages 548. £78.45.

This book fully achieves the aim set out by the editor in the preface, namely to present the state of the art in chiral HPLC separations. The editor is to be complimented on achieving a consistently high standard of content and presentation from many different international experts.

Part I consists of four chapters dealing with chirality in nature, the unacceptability of data on racemates, enzymes, and enantiomer separation by crystallization. To some extent, Part I is remote from the main thrust of the book but Chapters 2 and 3 do serve to point out forcefully (and accurately) the limitations of drug investigations which ignore the existence of chirality. Part II covers, in three chapters, the main types of mobile phase additives; metal ions, chiral counter-ions; and the cyclodextrins. Part III forms the majority of the volume and begins with two chapters which give an introduction to the use of chromatography for chiral separations, and some pharmacokinetic and metabolism applications. Subsequent chapters deal with the diverse types of chiral stationary phases in current use. All of the chapters in Parts I and II incorporate good coverage of the principles of interaction and examples of separations achieved.

The content of the book as a whole is broad enough to provide the reader with a useful overview. Each chapter, however, is sufficiently detailed and well enough referenced to be useful to chromatographers practically engaged in chiral separation and analysis.

R. B. TAYLOR

Flow Injection Atomic Spectroscopy: J. L. BURGUERA (editor), Dekker, New York, 1989. Pages xii + 353. \$125 (U.S.A. and Canada), \$150 (elsewhere).

The development of flow injection analysis (FIA) has seen probably the most remarkable increase in research activity, as evidenced by publications, of any of the recent advances in instrumental analytical chemistry. This text breaks new ground in that it is the first on FIA to deal with a specific aspect, FIA as a sample introduction system for atomic spectrometry. The various aspects of the subject are covered, including theoretical aspects, instrumentation, applications and current trends. There are a large number of contributors, which leads to a certain amount of repetition and even conflicting view-points so the book is stimulating in this regard. It is thus not a text book presenting material in a logical sequence of steps but rather it sets out to serve both as a practical handbook on experimental aspects and also to bring the reader up to date with recent developments. It certainly succeeds with the latter objective, being a most comprehensive account of the state of the subject. I would criticize the book in that FIA is essentially a practical subject and more information could have been given on building systems from standard laboratory components. Much is left vague, requiring consultation with the literature to investigate whether any more detailed experimental information is available, particularly with regard to the flow-injection-spectrometer interface. In this regard the book is insufficient to let experimenters see for themselves the potential of such systems prior to purchasing commercial equipment. This book will be of most use to those analytical chemists who need to be rapidly acquainted with potential applications of FIA-atomic spectrometry or those who are already users and wish to extend the application to new samples.

A. R. MORRISON

Atomic Spectroscopy: J. W. ROBINSON, Dekker, New York, 1990. Pages vi + 299. \$55.00 (on orders of 5 or more copies, for classroom use only). \$99.75 (U.S.A. and Canada). \$119.50 (all other countries).

There are some good points about this book, but overall I was disappointed by Professor Robinson's introductory text on atomic spectroscopy.

Chapter 1 provides a brief but comprehensive background to the subject with useful sections on atomic structure and atomic spectra. Those new to the subject (*e.g.*, undergraduates) will find the comments on significant figures, reliability of results and sampling of particular interest. Chapter 2 is devoted to atomic-absorption spectrometry (AAS). The basics of AAS instrumentation are described, but there is little information on atomization and interference mechanisms in both flame and electrothermal atomization (ETA). Indeed, of the fourteen pages on ETA, only two pages describe modern developments. Unfortunately, Chapter 2 is dated in many respects. Most commercial AAS instruments only permit operation with premixed air/acetylene and nitrous oxide/acetylene flames, so details about total consumption burners and the use of air/hydrogen or air/coal gas flames are unnecessary. Contrary to the author's comments, oxy-acetylene and oxy-hydrogen flames are not routinely used in AAS.

Chapter 3 covers the basics of atomic-fluorescence spectrometry (AFS) and gives balanced comments on the advantages and limitations of the technique. Unfortunately, little information is given about the main commercial AFS system, which uses an inductively coupled plasma (ICP) as the atomizer. Also, there is no mention of the benefits of laser AFS with an electrothermal atomizer.

I am not sure why a separate chapter was devoted to flame atomic-emission spectrometry (FAES), or Flame Photometry as Chapter 4 is titled, as few analysts now use this technique. I suppose the table of FAES wavelengths will be useful to some readers who may perform occasional analyses by FAES, with commercial FAAS instruments.

Chiral Separations by HPLC—Applications to Pharmaceutical Compounds: A. M. KRSTULOVIĆ (editor), Ellis Horwood, Chichester, 1989. Pages 548. £78.45.

This book fully achieves the aim set out by the editor in the preface, namely to present the state of the art in chiral HPLC separations. The editor is to be complimented on achieving a consistently high standard of content and presentation from many different international experts.

Part I consists of four chapters dealing with chirality in nature, the unacceptability of data on racemates, enzymes, and enantiomer separation by crystallization. To some extent, Part I is remote from the main thrust of the book but Chapters 2 and 3 do serve to point out forcefully (and accurately) the limitations of drug investigations which ignore the existence of chirality. Part II covers, in three chapters, the main types of mobile phase additives; metal ions, chiral counter-ions; and the cyclodextrins. Part III forms the majority of the volume and begins with two chapters which give an introduction to the use of chromatography for chiral separations, and some pharmacokinetic and metabolism applications. Subsequent chapters deal with the diverse types of chiral stationary phases in current use. All of the chapters in Parts I and II incorporate good coverage of the principles of interaction and examples of separations achieved.

The content of the book as a whole is broad enough to provide the reader with a useful overview. Each chapter, however, is sufficiently detailed and well enough referenced to be useful to chromatographers practically engaged in chiral separation and analysis.

R. B. TAYLOR

Flow Injection Atomic Spectroscopy: J. L. BURGUERA (editor), Dekker, New York, 1989. Pages xii + 353. \$125 (U.S.A. and Canada), \$150 (elsewhere).

The development of flow injection analysis (FIA) has seen probably the most remarkable increase in research activity, as evidenced by publications, of any of the recent advances in instrumental analytical chemistry. This text breaks new ground in that it is the first on FIA to deal with a specific aspect, FIA as a sample introduction system for atomic spectrometry. The various aspects of the subject are covered, including theoretical aspects, instrumentation, applications and current trends. There are a large number of contributors, which leads to a certain amount of repetition and even conflicting view-points so the book is stimulating in this regard. It is thus not a text book presenting material in a logical sequence of steps but rather it sets out to serve both as a practical handbook on experimental aspects and also to bring the reader up to date with recent developments. It certainly succeeds with the latter objective, being a most comprehensive account of the state of the subject. I would criticize the book in that FIA is essentially a practical subject and more information could have been given on building systems from standard laboratory components. Much is left vague, requiring consultation with the literature to investigate whether any more detailed experimental information is available, particularly with regard to the flow-injection-spectrometer interface. In this regard the book is insufficient to let experimenters see for themselves the potential of such systems prior to purchasing commercial equipment. This book will be of most use to those analytical chemists who need to be rapidly acquainted with potential applications of FIA-atomic spectrometry or those who are already users and wish to extend the application to new samples.

A. R. MORRISON

Atomic Spectroscopy: J. W. ROBINSON, Dekker, New York, 1990. Pages vi + 299. \$55.00 (on orders of 5 or more copies, for classroom use only). \$99.75 (U.S.A. and Canada). \$119.50 (all other countries).

There are some good points about this book, but overall I was disappointed by Professor Robinson's introductory text on atomic spectroscopy.

Chapter 1 provides a brief but comprehensive background to the subject with useful sections on atomic structure and atomic spectra. Those new to the subject (*e.g.*, undergraduates) will find the comments on significant figures, reliability of results and sampling of particular interest. Chapter 2 is devoted to atomic-absorption spectrometry (AAS). The basics of AAS instrumentation are described, but there is little information on atomization and interference mechanisms in both flame and electrothermal atomization (ETA). Indeed, of the fourteen pages on ETA, only two pages describe modern developments. Unfortunately, Chapter 2 is dated in many respects. Most commercial AAS instruments only permit operation with premixed air/acetylene and nitrous oxide/acetylene flames, so details about total consumption burners and the use of air/hydrogen or air/coal gas flames are unnecessary. Contrary to the author's comments, oxy-acetylene and oxy-hydrogen flames are not routinely used in AAS.

Chapter 3 covers the basics of atomic-fluorescence spectrometry (AFS) and gives balanced comments on the advantages and limitations of the technique. Unfortunately, little information is given about the main commercial AFS system, which uses an inductively coupled plasma (ICP) as the atomizer. Also, there is no mention of the benefits of laser AFS with an electrothermal atomizer.

I am not sure why a separate chapter was devoted to flame atomic-emission spectrometry (FAES), or Flame Photometry as Chapter 4 is titled, as few analysts now use this technique. I suppose the table of FAES wavelengths will be useful to some readers who may perform occasional analyses by FAES, with commercial FAAS instruments.

Chapter 5 provides an introduction to arc and spark atomic-emission spectrometry. The latter technique is still widely used in the metallurgical industry, but arc AES is rarely used in modern laboratories. The chapter has an instrumental bias and is of historical interest. The tables of arc and spark detection limits provide a good basis for comparison of the techniques.

Chapter 6 describes the newer developments in emission spectrometry, with emphasis on inductively coupled plasma (ICP) and direct current plasma (DCP) sources. The instrumentation required for both techniques is discussed but the fundamental processes of plasma spectroscopy are not covered in any detail. A few pages on ICP-mass spectrometry are included at the end of the chapter.

At the reduced bulk purchase price, this book may be an attractive introductory text for undergraduate courses on atomic spectrometry, but it would need to be supplemented by more detailed information on recent developments if such a course was to be truly up-to-date. Its most useful features are the tables of wavelengths for AAS, AFS and AES, the comparative data on detection limits and the information on instrumental systems. However, at the full-cost price, I suspect that the book will not be considered great value by analytical chemists looking for a fundamental text or an up-to-date reference text on analytical methodology.

D. LITTLEJOHN

Chemometrics—Applications of Mathematics and Statistics to Laboratory Systems: R. G. BRERETON, Ellis Horwood, Chichester, 1990. Pages 307. £45.00.

Chemometrics (the design and analysis of laboratory experiments) is of undoubted importance—it does not need much more than a brief scan through the scientific literature to see how poorly many experiments are planned, and how inadequately their data are processed. In many ways the wide availability of the laboratory microcomputer-controlled experiment makes the need for a good understanding of design even more important, yet it is scarcely even mentioned at undergraduate level. Richard Brereton's book will help: it gives good explanations, is readily understood with a minimum of mathematics and covers a wide range of topics. It is very much a "how to do it" publication, although necessarily within the confines of 307 pages the detail may not always be sufficient to enable readers to carry out such procedures for themselves without further information. However, the background obtained from this book will be invaluable when moving to more advanced references.

The topics include factorial design, principal component analysis, univariate and multivariate analysis, and pattern recognition. Interestingly, the maximum entropy method is included with an example involving NMR spectroscopy.

I have one criticism. In its natural handling of prior knowledge and its modification through experiment, Bayesian statistics is the obvious way to proceed in chemometrics rather than use of classical, frequentist statistics. Throughout the book the author uses the language of Bayesian statistics; his approach is also Bayesian. Why then is his mathematical formalism based on classical approaches with not even a mention of the Bayes theorem?

Nonetheless, this is a book to be welcomed—I know I shall be using it.

C. J. GILMORE

Chapter 5 provides an introduction to arc and spark atomic-emission spectrometry. The latter technique is still widely used in the metallurgical industry, but arc AES is rarely used in modern laboratories. The chapter has an instrumental bias and is of historical interest. The tables of arc and spark detection limits provide a good basis for comparison of the techniques.

Chapter 6 describes the newer developments in emission spectrometry, with emphasis on inductively coupled plasma (ICP) and direct current plasma (DCP) sources. The instrumentation required for both techniques is discussed but the fundamental processes of plasma spectroscopy are not covered in any detail. A few pages on ICP-mass spectrometry are included at the end of the chapter.

At the reduced bulk purchase price, this book may be an attractive introductory text for undergraduate courses on atomic spectrometry, but it would need to be supplemented by more detailed information on recent developments if such a course was to be truly up-to-date. Its most useful features are the tables of wavelengths for AAS, AFS and AES, the comparative data on detection limits and the information on instrumental systems. However, at the full-cost price, I suspect that the book will not be considered great value by analytical chemists looking for a fundamental text or an up-to-date reference text on analytical methodology.

D. LITTLEJOHN

Chemometrics—Applications of Mathematics and Statistics to Laboratory Systems: R. G. BRERETON, Ellis Horwood, Chichester, 1990. Pages 307. £45.00.

Chemometrics (the design and analysis of laboratory experiments) is of undoubted importance—it does not need much more than a brief scan through the scientific literature to see how poorly many experiments are planned, and how inadequately their data are processed. In many ways the wide availability of the laboratory microcomputer-controlled experiment makes the need for a good understanding of design even more important, yet it is scarcely even mentioned at undergraduate level. Richard Brereton's book will help: it gives good explanations, is readily understood with a minimum of mathematics and covers a wide range of topics. It is very much a "how to do it" publication, although necessarily within the confines of 307 pages the detail may not always be sufficient to enable readers to carry out such procedures for themselves without further information. However, the background obtained from this book will be invaluable when moving to more advanced references.

The topics include factorial design, principal component analysis, univariate and multivariate analysis, and pattern recognition. Interestingly, the maximum entropy method is included with an example involving NMR spectroscopy.

I have one criticism. In its natural handling of prior knowledge and its modification through experiment, Bayesian statistics is the obvious way to proceed in chemometrics rather than use of classical, frequentist statistics. Throughout the book the author uses the language of Bayesian statistics; his approach is also Bayesian. Why then is his mathematical formalism based on classical approaches with not even a mention of the Bayes theorem?

Nonetheless, this is a book to be welcomed—I know I shall be using it.

C. J. GILMORE

REVIEW: POLYANILINE—A NOVEL POLYMERIC MATERIAL

AKHEEL A. SYED* and MARAVATTICKAL K. DINESAN

Department of Studies in Chemistry, University of Mysore, Mysore, 570 006, India

(Received 23 July 1990. Revised 13 December 1990. Accepted 14 January 1991)

Summary—Polyaniline synthesis by chemical and electrochemical methods is reviewed. The considerable progress which has been made in characterizing and understanding the properties of polyaniline derived from aniline is discussed. Finally, the progress towards technological applications is evaluated.

The evolution of conducting polymers began in 1975, with the discovery that polysulphur nitride, [(SN)_x], becomes superconducting at low temperatures.¹ Two years later, a linear, conjugated organic polymer, polyacetylene, was shown to have metallic properties.^{2,3} This gave rise to a surge of activity directed towards the exploration, synthesis and characterization of the members of this class of material. Polyaniline is one such organic polymer, which has been rediscovered as a result of this exploration.⁴

Polyaniline (PANI) is now establishing itself as a novel material in the field of conducting polymers. The proposed and anticipated technological potential of PANI is due to its remarkable stability and processibility.

The variety and complexity of the behaviour of PANI—which is assumed to be a reflection of its complicated structure—is clearly manifested in the literature, wherein divergent views have been put forth by different schools of research working on several basic aspects, such as polymerization and redox mechanisms, electronic and ionic conductance, role of protons and water, importance of capacity effects and electrostatic interactions, and stability and solubility, to mention just a few. Therefore, it is not surprising that much of the work on PANI has been, up until now, rudimentary and exploratory in nature. The purpose of this article is to provide an overview of the status and understanding of this complex and interesting polymer.

HISTORICAL BACKGROUND

Polyaniline was first known in 1835 as "aniline black", a term used for any product obtained by the oxidation of aniline. A few years later,

Fritzche^{5,6} carried out the tentative analysis of the products obtained by the chemical oxidation of this aromatic amine. Thereafter, Letheby⁷ discovered that the final product of anodic oxidation of aniline at a platinum electrode, in aqueous sulphuric acid solution, is a dark brown precipitate. Subsequent investigators⁸⁻¹¹ have verified these results, and similar observations have been made during the oxidation of aqueous hydrochloric acid solutions of aniline.¹² Bucherer^{13,14} proposed a phenazene type structure which is more complex, contrary to the present day understanding. Green and co-workers¹⁵⁻²⁰ proposed a linear octameric structure, of the quinone-imine type in the *para*-position, for the product obtained by the chemical oxidation of aniline. The base of the octamer is leuco-emeraldine which exhibits four distinct states of oxidation. They are: protoemeraldine, emeraldine, nigraniline and pernigraniline (Fig. 1). In 1935, Yasui²¹ suggested a reaction scheme for the anodic oxidation of aniline at a carbon electrode. No further research was carried out until the middle of this century when Khomutov and Gorbachev^{22,23} re-examined the results of Yasui, and verified Letheby's original observation about the green precipitate. In addition, on the basis of current-time curves, two different mechanisms for the electrode reaction were proposed. It seems that pursuit of the earlier lines of research on oxidative condensation of aniline, will help us obtain a better understanding of aniline polymerization and the structure of PANI which are currently of interest.

CONSTITUTION AND NOMENCLATURE

Since the resurgence of PANI, there has been considerable confusion regarding its constitution. Studies since then have resulted in the

*Author for correspondence.

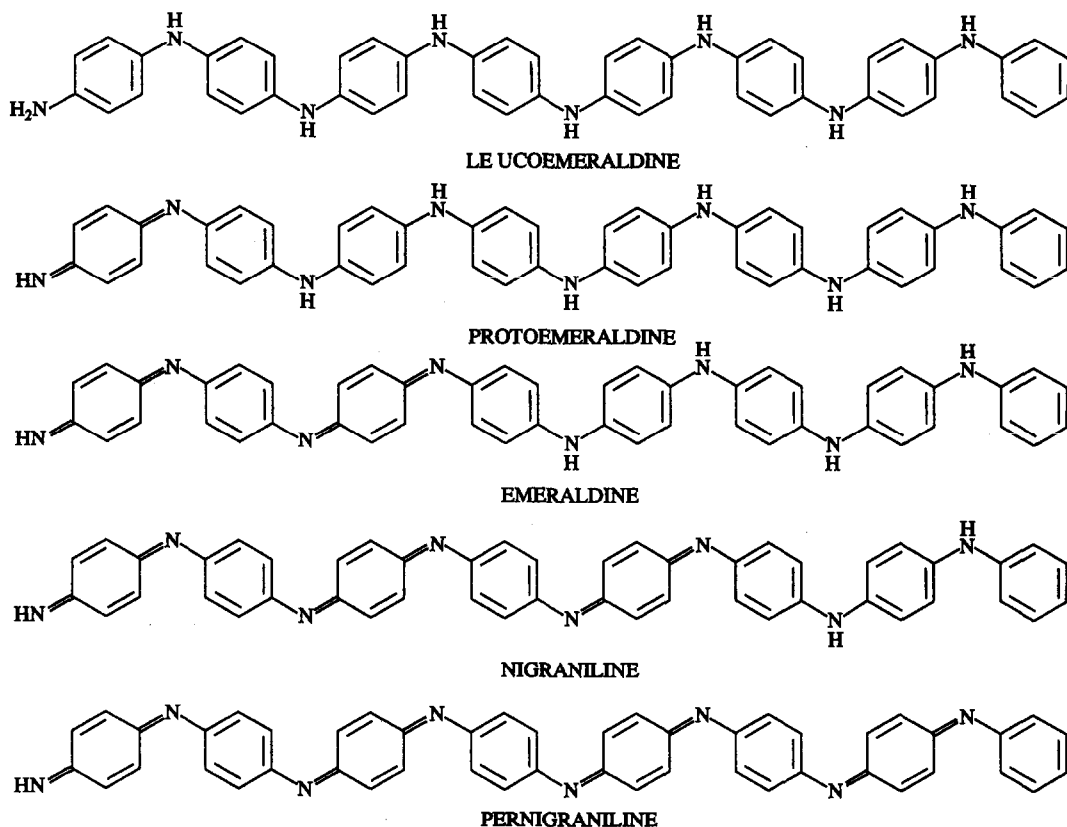


Fig. 1. Four oxidation states of leucoemeraldine.

formulation of a proposed structure for the polyanilines, together with a modification of the nomenclature based on the older concepts. As mentioned earlier, Green and Woodhead¹⁵ gave various trivial names to PANI, but they did not know the structure of the polymer at that time, believing it to be an octameric molecule.

PANI may be described as a combination of any desired relative ratio of the idealized repeating units depending on the experimental conditions to which the polymer is subjected. Different names have been proposed in the literature. For the sake of simplicity, we may summarize them as follows. PANI contains two

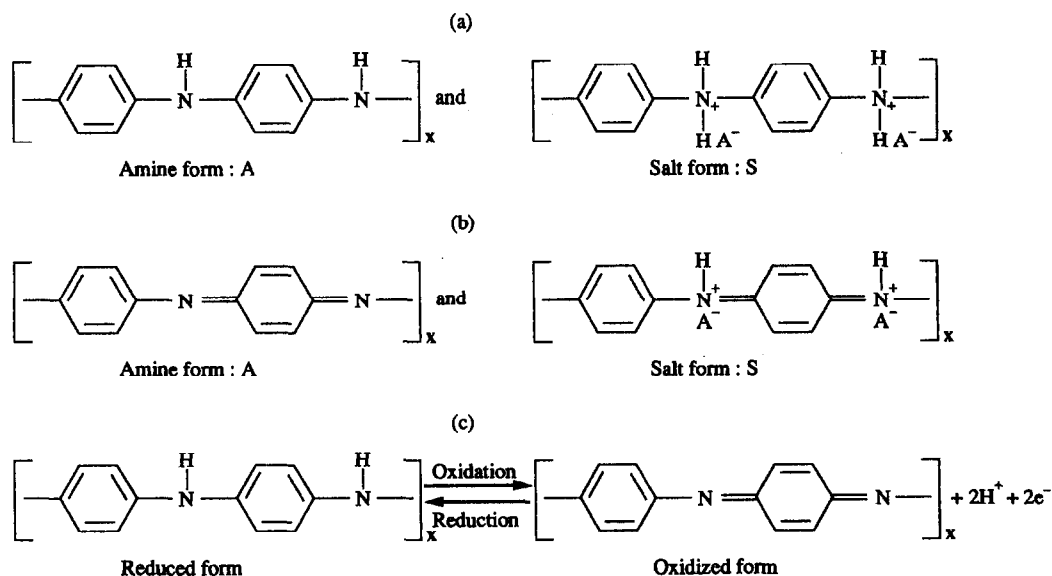


Fig. 2. Chemical structures of polyaniline.

principal units: (i) the completely reduced form of a repeat unit containing two benzenoid rings (Fig. 2a) and (ii) the completely oxidized form of a repeat unit containing one benzenoid ring and one quinonoid ring (Fig. 2b). In both cases, either one or both, of the nitrogen atoms in a repeat unit may be protonated, depending on the pH of the solution to which the polymer has been exposed. The base and protonated forms are referred to as the amine (A) and the salt (S) forms respectively²⁴ (Figs 2a and 2b). Proto-emeraldine, emeraldine and nigaraniline are the intermediate oxidation states of the above mentioned forms of PANI. Older nomenclature is also still in use; the only difference now being that 'poly' is prefixed to the earlier names. For example, the older term, 'emeraldine', is now replaced by 'polyemeraldine'. However, it is interesting to note that the smallest number of reduced and/or oxidized repeat units which can be used, and which will permit interconversion between the above five compositions, is eight—a finding which is in full agreement with the structure proposed by Green and co-workers¹⁵⁻²⁰ for polyaniline. The conversion of the completely reduced form to the completely oxidized state involves a loss of electrons and protons, as illustrated in Fig. 2c. The reversibility of the reaction opens up technological applications which will be discussed later.

Of the five oxidation states of PANI, polyemeraldine, with the structure shown in Fig. 1 has been most widely studied. For the convenience of readers, the term 'emeraldine' or 'polyemeraldine' will henceforth be used for the emeraldine oxidation state of polyaniline, and the term 'polyaniline' (PANI) for the polymer skeleton containing any one or more oxidation states of polyaniline.

SYNTHESIS

Polyaniline may be synthesized by two principal methods: the direct oxidation of aniline by chemical oxidants, or by anodic oxidation on an inert electrode. (Henceforth, the term PANIC will be used to represent chemically synthesized polyaniline, and PANIE for electrochemically polymerized polyanilines.)

Chemical synthesis

PANIC is a precipitated product from an aqueous solution containing typical reagents: ammonium peroxydisulphate (persulphate),

acids like hydrochloric, sulphuric, nitric or perchloric, and aniline. This direct route represents the classical approach to polyaniline synthesis in which, aniline, the monomer, is converted directly to a conjugated polymer by a condensation process. One of the disadvantages of this direct approach stems from the experimental observation that an excess of the oxidant and higher ionic strength of the medium lead to materials^{25,26,27} that are essentially intractable.

It is not possible to polymerize the *ortho*- and *meta*-substituted aniline derivatives, due to the steric and weak inductance effects of the substituents. The *para*-position should be kept free for radical coupling. During oxidative condensation of aniline, the solution progressively becomes coloured and yields a black precipitate. The colouration of the solvent is probably due to the soluble oligomers. The intensity of colouration depends on the nature of the medium and the concentration of the oxidant.

Many variations of the synthesis of PANIC have appeared in the literature. Four major parameters affect the course of the reaction, and the nature of the final product. These are: (1) nature of the medium, (2) concentration of the oxidant, (3) duration of the reaction and (4) temperature of the medium. Besides these, we have studied the combined effect of the concentration of ammonium persulphate (oxidant), and of duration of the polymerization reaction on the percentage yield of insoluble precipitate (polyaniline). The results are displayed in a three-dimensional diagram (Fig. 3).

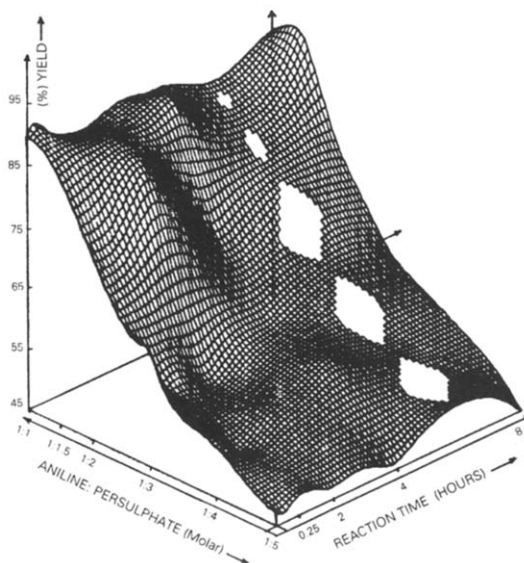


Fig. 3. Chemical synthesis of polyaniline. Three-dimensional diagram.

Medium. While choosing a medium for the synthesis of PANIC the following factors have to be kept in mind to obtain desirable results: (1) low ionic strength, (2) volatility and (3) non-corrosive nature of the medium. No medium satisfies all of the above requirements. Sulphuric acid is dependable, but due to low volatility, a thin film of acid is left on the polyaniline powder after drying (to remove water) under dynamic vacuum. Hydrochloric acid and a novel anhydrous medium²⁷—a eutectic mixture of HF and NH_4F with an average formula of $\text{NH}_4\text{F} \cdot 2.3\text{HF}$ (henceforth referred to as NF) are both corrosive, even though they are more volatile than sulphuric acid. The demonstrated advantage of the NF medium is that the percentage yield of PANIC is maximum, when compared to any other medium.²⁷ Thus, the oligomers formed in the reaction are at a minimum, and one can expect an ordered material. We have employed²⁷ sulphuric acid containing 0.5M sodium sulphate (pH = 1) as a medium for the synthesis of PANIC. A low sulphuric acid concentration avoids undesirable cations^{25,26} While the presence of appreciable amounts of sulphate ions enhances the growth rate of the polymer chain.²⁸ It is generally admitted that the faster growth rate of nucleation yields better results. The unwanted thin film of sulphuric acid remaining on the particles of the powder could be eliminated by simple equilibration of the powder with 1M HCl.²⁹ This treatment imposes the chloride ions on the polymer, and eliminates sulphate ions. This has been demonstrated in many polyanilines prepared under various conditions, and thus, can be regarded as a general feature of polyanilines. Elimination of sulphate ions assumes importance if PANI is used as a battery material in non-aqueous solvents such as propylene carbonate—1M lithium perchlorate medium, because the presence of sulphate ions in the polymer matrix leads to undesirable precipitation of lithium sulphate.²⁹ The use of salts, such as sodium sulphate or sodium chloride, in sulphuric or hydrochloric acid, may probably contribute to the buffer effect and conductivity of the medium. Thus, the net effect results in augmentation of percentage yield of the insoluble precipitate, and of the 'quality' of the polymer obtained.

Concentration of the oxidant. Ammonium persulphate, potassium dichromate, ceric sulphate, sodium vanadate, potassium ferricyanide, potassium iodate and hydrogen peroxide have been employed as oxidants for the polymerization of aniline in acidic media. Ammonium persulphate

is most extensively used and the yield, elemental composition, conductivity and degree of oxidation of the resulting polymer are essentially independent of the value of the initial aniline/persulphate mole ratio (r), when $r \leq 1.15$.^{30,31} However, an $r > 1.15$ results in over-oxidation of the polyaniline, with a concomitant decrease in the conductivity³¹ and yield of the polymer.³² A marked change in morphology is also observed.³² In the case of higher concentrations ($r > 1.15$) of the oxidants, such as cerium(IV) sulphate, potassium dichromate, sodium vanadate and potassium ferricyanide, a complexation reaction probably occurs which results in products containing a large percentage of the metal,³² as is indicated by elemental composition data. This supposition may be further confirmed by igniting the sample, and analyzing the residue which must indicate the presence of the metal.³²

Duration of the reaction. The percentage yield of the polyaniline increases with time (0–2 hr), when $r \leq 1.15$. Thereafter, the duration of the reaction has only a limited influence on the yield, conductivity and elemental composition of the polymer.^{31,32}

Effect of temperature. The process of chemical oxidation of aniline consists of a slow endothermic step, which is dependent on the pH, temperature and the concentration of the reactants, and in which the dissolved oxygen in the solvent does not have any influence (in contrast to oxidation–reduction reagents which reduce the induction time); and a fast exothermic step which depends on the temperature and varies with the concentration of the oxidant. Furthermore, the rate of the polymerization reaction varies with temperature in the range 0–80°, whereas, the total enthalpy of the reaction ($H = 372$ kJ/mole) remains almost constant.³³

Apart from the major parameters discussed above, we have studied the effect of the standard reduction potential (SRP) of the chemical oxidant on the nature and yield of the final product, the polyaniline. The results of our preliminary studies along with the conclusions drawn by Pron *et al.*³⁴ are summarized below:

We have employed^{27,32} five oxidants, namely: ammonium persulphate, cerium(IV) sulphate, potassium dichromate, sodium vanadate and potassium ferricyanide. These oxidants have their SRP in the range 2.01–0.36 V *vs.* NHE. Pron *et al.*³⁴ have employed potassium iodate and hydrogen peroxide, as well as ammonium persulphate and potassium dichromate. The major conclusions we draw from these studies

Table 1. Chemical synthesis of PANI using different oxidants and varied reaction conditions

Oxidant	Time of reaction, hr	Temperature, °C	Reaction medium	Normalized aniline/oxidant ratio	Yield, %
*KIO ₃	15	Zero	2M HCl	0.61	100.0
*KIO ₃	3	Zero	2M HCl	0.61	48.5
*(NH ₄) ₂ S ₂ O ₈	1.5	Zero	2M HCl	0.61	82.4
*H ₂ O ₂	15	Room temp.	4M HCl	0.61	60.0
(NH ₄) ₂ S ₂ O ₈	1	Room temp.	1M H ₂ SO ₄	1.00	99.0
Ce(SO ₄) ₂	1	Room temp.	1M H ₂ SO ₄	1.00	75.4
K ₂ Cr ₂ O ₇	1	Room temp.	1M H ₂ SO ₄	1.00	96.0
Na VO ₃	1	Room temp.	1M H ₂ SO ₂	1.00	94.4
K ₃ [Fe(CN) ₆]	1	Room temp.	1M H ₂ SO ₄	1.00	2.1

*Data from Pron *et al.*³⁴

are: (1) the SRP of the oxidant greatly affects the yield of polyaniline and (2) ammonium persulphate is a better oxidant for the polymerization of aniline, because of (i) high SRP, (ii) non-metallic oxidizing species and (iii) non-interference of the reduction product, namely the sulphate ion. On the other hand, Pron *et al.* are of the opinion that: (1) the process of polymerization of aniline is probably much less dependent on the redox potential than on the degradation process; (2) degradation is significantly slowed down in the case of chemical preparation; (3) hydrogen peroxide is ruled out as a reagent in the synthesis of PANIC; and (4) potassium iodate is the most convenient, since it gives good quality samples in a wide range of synthesis parameters. However, it is desirable to mention that the latter employed different temperatures and reaction times for different oxidizing agents (Table 1). Hence, the conclusion drawn that potassium iodate is a better oxidant for the synthesis of PANIC appears to be arbitrary. Nevertheless, another recent communication reports³⁵ that potassium iodate has been used as the oxidant for the preparation of colloidal polyaniline.

Summing up the procedure, one may state that polyaniline was obtained as an insoluble residue during the oxidative condensation of aniline; it was then separated by filtration, washed with a copious amount of the acidic solution of desired ionic strength to remove oligomers, and dried under dynamic vacuum for *ca.* 48 hr. The resulting dark powder was generally transferred to a soxhlet apparatus to remove low-molecular-weight species, and extracted with CH₃CN until the extract was colourless. The material was dried under dynamic vacuum.

Chemical synthesis of emeraldine hydrochloride and emeraldine base

The method³⁶ used for the synthesis of emer-

aldine hydrochloride is summarized as follows. An aqueous solution of ammonium persulphate was added slowly to a solution of aniline in 1.0 mole/dm³ aqueous hydrochloric acid (both solutions precooled to 1°). The reaction mixture was stirred for about an hour (~5°). The precipitate formed was removed by filtration, and washed repeatedly with 1.0M hydrochloric acid, and dried under dynamic vacuum for 48 hr. The material thus obtained was identified as emeraldine hydrochloride.²⁴

The moist emeraldine hydrochloride precipitate cake was suspended in ammonium hydroxide solution for ~15 hr. The separated powder was washed and dried under dynamic vacuum, as described earlier. The powder obtained was analyzed as emeraldine base.³⁷ In conclusion, the chemical preparation of polyaniline is a good method, and at present, electrochemical methods also provide a satisfactory route.

Electrochemical polymerization

There is at present a two-fold interest in the electrochemical polymerization (ECP) process. First, ECP reactions provide a new method of polymerization with a fine control of the initiation and termination steps. Second, ECP have technological potential. Besides, one of the important features found in ECP reactions of conducting polymers is that they proceed with electrochemical stoichiometry. This is because electrochemical reactions are often much cleaner, with respect to possible pollutants, than chemical reactions. Moreover, electrons, as a reagent, are inherently pollution-free, at least, at the point of use.

Electrochemical methods generally employed for ECP of aniline are: (1) constant current or galvanostatic; (2) constant potential or potentiostatic and (3) potential scanning/cycling or sweeping methods. The first essentially consists of a two-electrode assembly dipped in an electro-

lyte solution containing the monomer. Passing a current density of *ca.* 1 mA/cm² will lead to the deposition of a PANIE film on the surface of a platinum foil electrode. Polymerization of aniline at constant potential produces a powder which adheres poorly to the electrode.⁴ On the other hand, electrooxidation of aniline by continuous cycling between the predetermined potentials produces an even polymeric film which adheres strongly to the electrode surface.^{4,38-40} This thin film can be cycled between oxidized and reduced states which are conducting. Thicker films can be produced and can be peeled off from the electrode surface to yield a free-standing, electrically conducting film. As these films are in the oxidized state, they represent polyaniline cations, and their overall charge balance is achieved by incorporation of counter anions from the electrolyte of the solution. The counter anions reported in the literature are F⁻,³⁸⁻⁴⁰ Cl⁻,²⁴ ClO₄⁻,²⁸ SO₄²⁻,^{28,29} and BF₄⁻.^{24,41}

The anodic oxidation of aniline is generally carried out on an inert electrode. Though the usual anode material would be platinum, or conducting glass, many metals such as Fe,⁴²⁻⁴⁴ Cu⁴⁵ and Au⁴⁶ have been employed. Graphite,⁴⁷ vitreous carbon,^{48,49} stainless steel³² and n-type silicon⁵⁰ have been used. Metals such as Ag or Al, which get oxidized more readily than aniline monomer, would obviously not be a good choice for the anode. Until recently, it was believed that PANIE deposited from aprotic solutions such as CH₃CN is electro-inactive, and, therefore, it was thought that electroactive polyaniline could be formed only from acidic aqueous solutions. However, it has been demonstrated that electroactive polyaniline can be synthesized in an aprotic solvent, such as a propylene carbonate solution containing an organic acid (CF₃COOH) and an electrolyte, lithium perchlorate.⁵¹

The ECP of aniline is described as a bimolecular reaction involving a radical cation intermediate. The reaction has a ΔH equal to 121 kJ/mole⁻³, αn equal to 1.2-1.3,⁵² where $n = 2$.⁵³ Here, n is the number of electrons consumed during the electrochemical polymerization and α is the transfer coefficient. The values reported in the literature for the number of electrons (n) consumed during ECP of aniline are 2.60-2.70,^{39,40} 2.16,⁴ and 2.25-2.29.²⁸ In summary, electrochemical methods have definite advantages over chemical methods of synthesis of polyaniline, mostly because of the reliability of the techniques. Moreover, the results show that the stoichiometric electropolymerization reaction

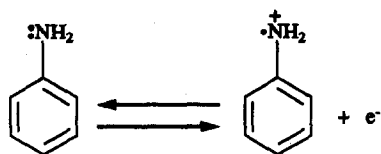
can be a general procedure for the preparation of organic polymer films, with electroactive properties and good electrode behaviour, polyaniline is one such example.

MECHANISMS OF POLYANILINE FORMATION

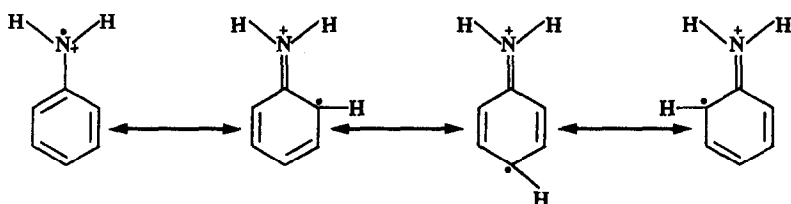
The numerous methods employed to synthesize PANI have produced several products which differ in their nature and properties and must represent the results of a multitude of polymerization mechanisms of aniline. In general, polymerization proceeds via the radical cation of the monomer, which then reacts with a second radical cation of the monomer to give a dimer by eliminating two protons. At the potential required to oxidize the monomer, the dimer or higher oligomer would also be oxidized, and thus could react further with the radical cation of the monomer to build up the aniline chain.

Mohilner *et al.*,⁵² Breitenbach and Heckner,⁵⁴⁻⁵⁶ Hand and Nelson,^{48,49} and Genies and co-workers^{38,39} have proposed mechanisms for electropolymerization of aniline. The point of agreement in the proposed mechanisms is the first step of oxidation of aniline, *i.e.*, formation of the radical cation. This radical cation gives three different resonance forms as shown in Fig. 4. Two mechanisms for the anodic oxidation of aniline in acidic and alkaline media have been reported.^{52,54-56} The mechanism in acidic media was proposed by Mohilner *et al.*⁵² based upon measurement of the kinetic parameters for the initial charge transfer step, and upon direct comparison of the properties, including infrared studies of the precipitate formed on the anode. On the basis of their experimental evidence, it was suggested that *p*-aminodiphenylamine is one of the intermediates in the electrochemical oxidation of aniline. They also demonstrated *p*-aminodiphenylamine undergoing electrochemical oxidation with greater facility than aniline. The mechanism of polymerization of aniline in a basic medium, like acetonitrile-pyridine, proceeds in a way essentially similar to that proposed earlier in the acid medium.

The anodic oxidation of aniline stipulates only the dimerization process.^{48,49} The formation of oligomers with the n value > 2 is ruled out in case the resulting product is a linear chain. Furthermore, it was concluded that the electrolysis product of aniline earlier characterized as "aniline black", emeraldine, *etc.*, is largely, if



FORMATION OF ANILINE RADICAL CATION



RESONANCE FORMS OF ANILINE RADICAL CATION

Fig. 4. Formation of aniline radical cation. Resonance forms of aniline radical cation.

not completely, composed of quinone–hydroquinone mixtures with a small amount of benzdine salt, and composition contingent upon the parent molecule. This is contradictory to our present understanding where the n value determined by gel permeation studies is shown to be greater than 800 repeat units.³⁸

The mechanism proposed by Genies and

co-workers^{38,39} for the electropolymerization of aniline in acidic media is based on detailed studies.^{57–59} Nevertheless, the results concerning the chronoamperometric plots during potential scanning, and potential step methods of electrodeposition of PANI have been taken into account.^{38–40} The mechanism is displayed in Fig. 5.

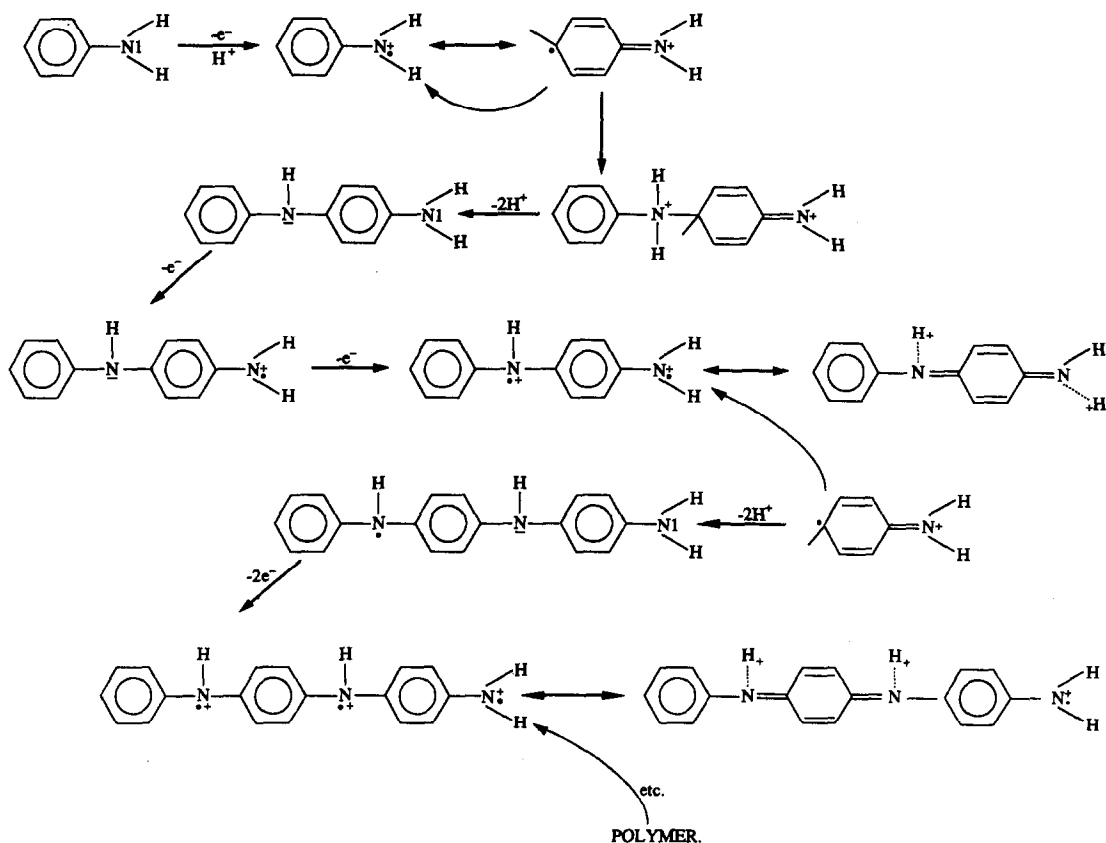


Fig. 5. Mechanism of formation of conducting polyaniline.³⁸ Reprinted with permission of Gordon and Breach, U.S.A.

CHARACTERIZATION

General considerations of "Doping" in conjugated polymers

The treatment of a conjugated polymer with ionizing agents (charge-transfer agents) leads to a concomitant increase in conductivity. This process was named "doping", by analogy with the treatment of silicon with such elements as arsenic, boron and phosphorus. In crystalline silicon, which is tetravalent, the tri- or penta-valent element replaces silicon at a lattice site to produce a "hole" or "electron", respectively. These dopants as they are called are only added at ppm level as the mobility of the carriers is so high, whereas, the charge carriers of the polymers under discussion have lower mobility. Hence, the dopant concentration is increased considerably to attain desired mobility. The polymers derived from organic compounds, with π -electron conjugation and high "dopant" concentration, are termed conducting organic polymers. The nature of the dopant decides the type of conduction in the resulting conducting polymer chain. For example, positive charge carriers in an acceptor-doped polymer results in p-type conduction, while, negative charge carriers in a donor-doped polymer show n-type conduction.

The name "doping" has raised some controversy among scientists for the following reasons: (1) the presence of the "dopant" in conducting polymers is to balance the charge created either by electron removal or addition in the polymer chain, by a redox process unlike that in inorganic semiconductors; (2) the dopants are added at ppm levels to an inorganic material to make it semiconducting, while the amount of counterions in conducting polymers are in the range 10–50% by weight of the material composition; and (3) in inorganic semiconductors the dopants are metals, whereas in organic polymers they are generally non-metallic species. However, the word "doping" is still in use, probably because: (1) it helps to demonstrate similarities between conducting polymers and inorganic semiconductors; (2) in both cases doping changes the state of oxidation without changing the structure (in conducting polymers, doping changes only packing order, whereas the 1-dimensional properties exhibit only along the chains); and (3) the higher concentration of dopants in conducting polymers is to attain desired mobility of the charge carriers on par with inorganic semiconductors. For intrinsic conductivity the carrier concentration decreases exponentially with increasing band gap

(roughly equivalent to the optical absorption threshold), whereas, in conjugated polymers, due to relatively large band gaps, (the conductivity is not intrinsic) the concentration of free carriers is very low at normal temperatures. Therefore, even though conjugated polymers have backbone structures well suited to conduction (*i.e.*, high carrier mobilities), the low carrier concentration results in negligible conductivity. The other question, which remains unclear, is whether doping of polymers is also at random, as it is in a classical semiconductor. Here it is assumed that the dopant "dissolves" in the polymer matrix, unless the doping level exceeds a certain limit of solubility, which is perhaps in the vicinity of a few per cent. This assumption does not contradict the available structural data and is supported by the experimental results on the temperature-dependence of the electrical conductivity in the low doping regime.

Doping in polyaniline: A new concept

The novelty of the polyaniline is that it has a symmetrical conjugated structure, having extensive charge delocalization, resulting from a new type of doping of an organic-polymer salt formation rather than oxidation which occurs in the p-doping of all other conducting polymer systems. PANI differs from earlier studied conducting polymers such as polyacetylene and polypyrrole in that the electronic state of PANI can be controlled through both variation in the number of electrons and in the number of protons per repeat unit (Fig. 6).

The redox activity of PANI is pH-dependent in aqueous medium. It has been established that the electroactivity of PANI ceases in aqueous media of $\text{pH} > 4$.^{27,28} On the other hand, the electrochemical behaviour of PANI, investigated in an aprotic solvent, such as propylene carbonate, in the presence of 1M lithium perchlorate as supporting electrolyte demonstrates two purely electronic processes.²⁹ However, these redox processes also vanish, if a small amount of 2,4,6-trimethyl pyridine (a strong base) is added to the system.^{39,40} Furthermore, the dramatic effect of conductivity of PANI upon variation of pH (changing pH from 0 to 6 decreases electrical conductivity, σ , by six orders of magnitude)⁶⁰ clearly demonstrates that besides, the dopants (counterions), the presence of protons invariably has a pronounced effect on the conductivity. In a recent study,⁶¹ evidence is provided which proves that the emeraldine base form of polyaniline is doped by protonic acids to the metallic

conducting regime by a process involving neither oxidation nor reduction of the polymer, thereby introducing a new concept of doping to the conducting polymer field. In brief, proton-induced conductivity in polyaniline is a remarkable physical phenomenon demanding explanation.

Conductivity measurements

The electrical conductivity (σ) of a polymer may be defined as the ratio of net charge motion, J (or current density), brought about by an electric field, E .

$$\sigma = J/E$$

Poor solubility of polyaniline in commonly known solvents is the prime factor for the solid-state conductivity measurements. Both DC and AC conductivity experiments on polyaniline are reported in the literature. In DC conductivity studies, only the net charge which traverses the entire polymer is measured. In contrast, for AC

conductivity experiments, the electrical conductivity is measured as a function of the frequency of an alternating electric field.

The DC conductivity measurements of chemically synthesized polyaniline were first carried out by French scientists.^{25,26,62,63} A thin 13-mm diameter pellet previously compressed was placed between two mercury conductors and its conductivity was measured. The technique that is generally used now for measuring the solid-state conductivity of pressed pellets, or films of polyaniline, was developed by van der Pauw.⁶⁴ Here, four points of contact, almost equally spaced on the periphery of the sample, are made with a conductive paste such as electrodag. Alternatively, four wires can be embedded into the periphery of the sample. Current (i) is passed through two adjacent contacts while the voltage drop (V) is measured across the other two as shown in Fig. 7. The van der Pauw technique takes into account the sample thickness (d) and thus it must be measured along with the current-voltage characteristics of the sample. The formula employed for the measurement of conductivity, σ , is:

$$\sigma = \frac{\ln 2}{\pi d} \frac{i}{V}$$

A configuration based on the models of Fan *et al.*⁶⁵ and Paul *et al.*⁶⁶ for the *in situ* resistance measurement of polyaniline is reported in the literature.⁶⁶ The authors claim that this configuration is simpler than the one used earlier. The problems usually encountered in conductivity measurements are degradation of the physical form of the polyaniline pellet or film, such as cracking, exfoliation, and loss of electrical contact, to mention just a few. In summary, the electrical conductivity measured by any of

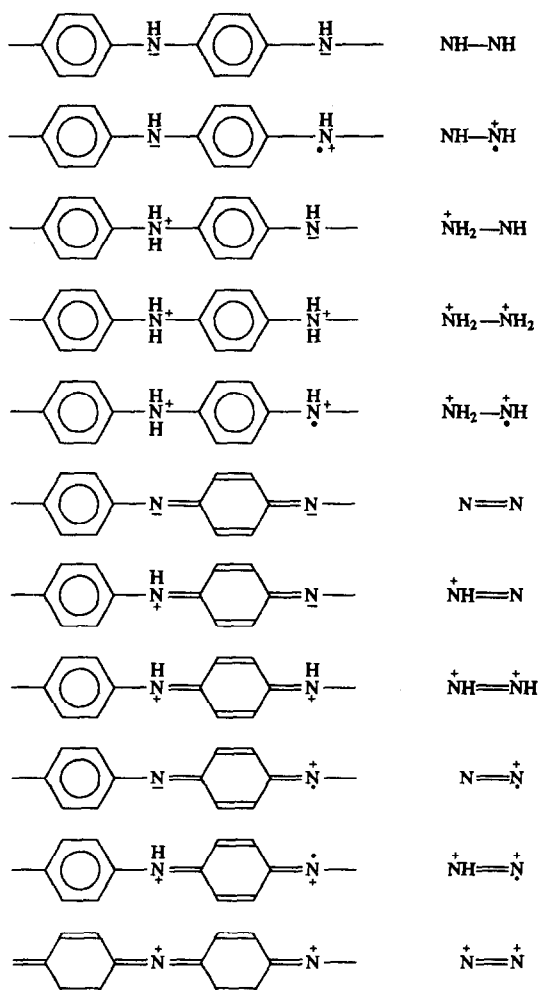


Fig. 6. Electroactive molecular structures in polyaniline.

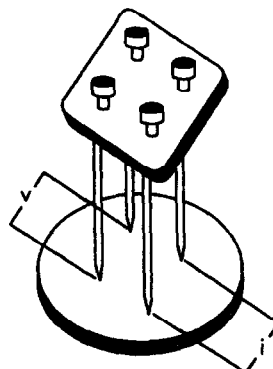


Fig. 7. van der Pauw configuration for the measurement of conductivity.

the above techniques represents a lower limit for the inherent doped polyaniline.

Factors affecting the conductivity of polyaniline

The DC conductivity (henceforth referred to as conductivity) of chemically and electrochemically synthesized PANI is dependent on a number of parameters. For example, temperature,^{60,67-69} protonation/pH,^{41,60,61,70-79} humidity,^{70,71,79-81} oxidation state^{70,74,75,78,82-84} and counterion⁷⁰ exert major influences on the conductivity of PANI. Besides, temperature of synthesis,⁸⁵ pressure, and duration of compression of PANI powders^{25,26,30,32} also have a considerable influence on the conductivity of PANI.

Temperature. It is well known that the effect of temperature on the conductivity of metallic conductors and on semiconductors is quite different. In metals, or metal-like substances an increase in temperature causes a gradual decrease in conductivity, while the heating of a semiconductor results in a sharp increase in conductivity. The conductivity of PANI has been studied over a wide range of temperatures, *viz.* 5–300 K,⁶⁰ 20–340 K⁶⁸ and 80–300 K.⁶⁷ The data reveal the metallic character of the polymer. Besides temperature dependence, thermopower⁷² and wide range frequency (dc, 10^1 – 10^5 Hz, 6.5×10^9 Hz)⁶⁸ the effect on conductivity has also been reported in the literature. The temperature dependence of the dielectric constant indicates an increase of the coherence length with increasing temperature.⁶⁸ The details are beyond the scope of this article. Hence, the readers are requested to refer to the original papers cited under reference.

Protonation. Insulator-to-metal transition in polyaniline, effected via protonation, was first reported in 1985.^{41,60} Since then, extensive investigations have been carried out to establish proton induced insulator-to-metal transition phenomenon through magnetic,^{69,73,77} optical,^{83,86-90} photoinduced optical,^{91,92} transport,^{60,68,73} thermopower⁶⁰ and ESR studies.⁹³ The earlier studies led to the proposal that the electronic structure of insulator polyaniline (also referred to as emeraldine base) is transformed to that of a granular polaron metal upon protonation (also referred to as emeraldine salt form). Recent studies on protonic acid doping of the emeraldine salt form of polyaniline lend support to the idea that the distribution of protons between polymer and bathing solution is in thermodynamic equilibrium.⁹⁴

In brief, the conductivity of polyaniline is a function of protonation. The proton induced insulator-to-metal ($\sigma \cong 10^{-10}$ ohm⁻¹ cm⁻¹– $\sim 10^0$ ohm⁻¹ cm⁻¹) transition is an interesting phenomenon in polyaniline. This is not observed in other conducting polymers such as polythiophene and polypyrrole. This unique behaviour of polyaniline is due to three important causes. First of all, polyaniline does not have symmetric charge conjugation. That is, the Fermi level and band gap are not formed in the centre of the band, so that valence and conduction bands are quite asymmetric. Secondly, both carbon rings and nitrogen atoms lie within the conjugation path. This configuration differs, for example, from polypyrrole, whose heteroatoms do not contribute significantly to the π -band formation. Thirdly, the electronic state of the polymer can be changed through variation of either the number of electrons or the number of protons.

Humidity. This is an important parameter which greatly affects the conductivity of polyaniline. As indicated earlier, it was reported in 1971^{62,63} which led to the important conclusion that electronic conductivity is associated with the ionic state of the polymer. This information has aroused a great deal of interest. Extensive studies in recent years have demonstrated the importance of moisture content in understanding the behaviour and conduction mechanism of polyaniline. The details will be discussed later. In brief, the conductivity of polyaniline increases extremely rapidly upon exposure to water vapour in contrast to the slow decrease in conductivity under dynamic vacuum.⁸⁰

Oxidation state. PANI exists in many forms classified as follows: fully reduced and neutralized PANI (NH); the protonated species (NH₂⁺); the first oxidized, neutral and/or protonated forms, N= and NH⁺; and the fully oxidized state, N⁺. These forms are in thermodynamic relation to each other according to a classical "square scheme". Based on the hypothesis concerning the relative thermodynamic potential and pK-values for electron transfer, some interesting potential *vs.* pH diagrams are reported in the literature.^{74,75,78} These diagrams have contributed to a better understanding of that fact that quinonic imine is more basic than the corresponding aromatic amine in the polymer chain. These particulars are in conformity with the earlier observations.

A novel method of representing "state" of polyaniline in a three dimensional diagram was first reported by Salaneck *et al.*⁷⁴ Later Genies

and Vieil⁷⁸ proposed a three-dimensional surface diagram for the charge and conductivity to enable convenient and unambiguous description of the electrically conducting state of polyaniline-based polymers. These diagrams are useful, for example, in battery applications and electromagnetic interference (EMI) shielding.⁷⁸

Counterion. The dependence of resistivity of electrochemically synthesized polyaniline (PANIE) on the nature of the counterion was first observed by Paul, Ricco and Wrighton.⁴⁶ This resistivity shows typical U-type functional dependence on the electrochemical potential. The experiment was repeated by Fock and co-workers^{70,71} who used different anions [hydron buffer, paratoluene sulphonate ($\text{CH}_3\text{-C}_6\text{H}_4\text{-SO}_3^-$), tetrafluoroborate (BF_4^-), trifluoroacetate (CF_3COO^-) and chloride (Cl^-)] at pH 2. They also observed a similar U-type functional dependence.

In summary, proton assisted doping-induced conductivity in PANI is a remarkable physical phenomenon, greatly in need of explanation.

CONDUCTION MECHANISMS

The charge transfer in the "emeraldine" form of polyaniline has become the subject of increased study because of the interesting discovery of insulator-to-metal transition as a function of protonation. The proposal of the transition from the electronic structure for insulator PANI (base form of emeraldine) to a polaronic, metal-electronic structure of PANI (salt form of emeraldine) upon protonation is supported by a series of optical, magnetic and band structure studies (references cited in the preceding section). Much of the work on conduction mechanisms of polyaniline is centred around French^{81,95,96} and American^{68,70,71,79} groups. The only point of agreement between the two groups is that the conductivity of the metallic emeraldine salt polymer is sensitive to environmental humidity. The French group of researchers have proposed the presence of a conduction mechanism based on electron hopping between localized states, with a proton-exchange-assisted conduction of electrons, which they enthusiastically refer to

as PEACE. On the other hand, the American group, after extensive studies, have concluded that a charging-energy-limited-tunneling theory is most suitable for the explanation of transport phenomena in the emeraldine form of polyaniline.

The PEACE mechanism⁸¹ is based on room temperature studies of the frequency dependence of conductivity in the range 10^1 Hz– 10^{10} Hz. The French scientists' observation is that the conduction of protonated emeraldine is independent of frequency in this range. But an American group has disputed the choice of this range, and maintained that the measurement should have been conducted at frequencies above and below the aforesaid range also. Their argument is that the hopping mechanism proposed by the French group is not the most suitable for the transport phenomena in the usually existing emeraldine form of PANI.

The American group has carried out an extensive set of optical, photoinduced optical, magnetic, transport, electrochemical and mechanical studies on the polyaniline systems. Their study focuses on the essential role of molecular excitons* and polarons†. Photoexcitation of the exciton absorption in the insulator form leads to the occurrence of polaron absorption features. Insulator-to-metal transition causes a transformation of the electronic structure of the chain into a polaron lattice. These results are in agreement with the charging-energy-limited tunnelling theory. The presence of metallic islands of about 100–200 Å size and average charging energy, E , of about 20 meV and the presence of structural defects, broken bonds, chain links, excess protonation *etc.*, is responsible for sizable barriers between metallic islands. For want of space, this description must necessarily remain incomplete; the reader is requested to refer to the cited original papers, for a more detailed analysis.

In summary, the broad range of optical, magnetic and transport studies show that polyaniline is a system with physics substantially different from polyacetylene and polypyrrole. The present theories certainly account for conduction mechanisms which are interesting, but not conclusive. There is great need to further elucidate the various phenomena in this novel conducting polymer.

ELECTROCHEMICAL STUDIES

As indicated in the preceding sections, polymerization of aniline can be effected by electro-

*An exciton is a non-conduction, non-localized, excited electron state as in a semiconductor.

†A polaron is an excitation in a solid consisting of polar molecules, resulting from the interaction between an electron and its strain field. The presence of a polaron can be detected by irregularities in the shape of the conduction band.

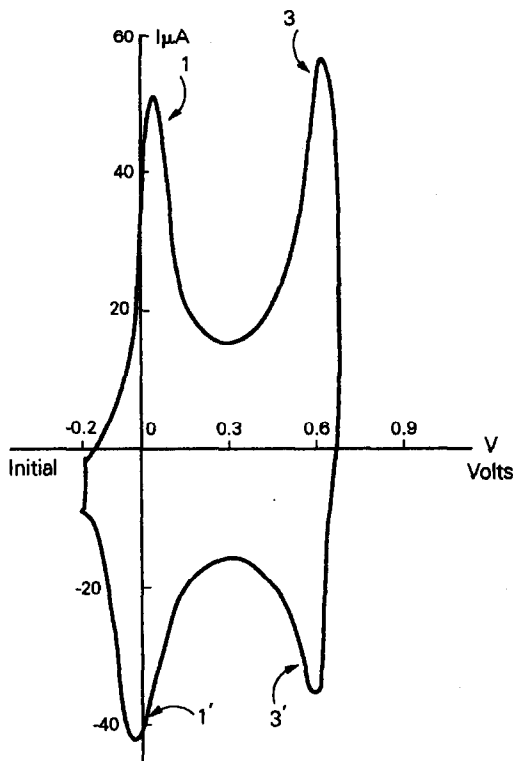


Fig. 8. Electrochemical behaviour of PANI showing two redox systems.

chemical and chemical methods. In the former case, by choosing a suitable medium, polyaniline is obtained which adheres strongly to the electrode. In certain cases a regular growth with almost 100% polymerization yield is seen.³⁸⁻⁴⁰ The strong adherence to the inert electrode has been the basis of detailed electrochemical studies. In contrast, the polyaniline obtained by chemical methods is a dark green, violet, or black amorphous powder which does not adhere to any electrode material. This property has been a serious limitation for extensive electrochemical investigations.

Polyaniline deposited on an inert electrode is conducting in both anodic and cathodic regions. The observations on the electrochemical behaviour of PANI suggest a redox mechanism.³⁸⁻⁴⁰ Notably, the cyclic voltamperogram shows well-defined electroactive regions with at least two rapidly reversible and clearly defined electrochemical systems (Fig. 8).

Electrochemical synthesis of polyaniline

Effect of anodic potential. The cyclic voltamperograms recorded during the electropolymerization of aniline are shown in Fig. 9. At the first cycle, a distant peak corresponding to

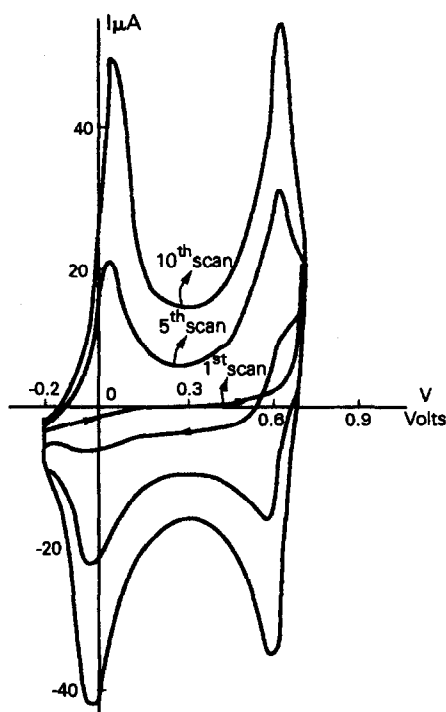


Fig. 9. Cyclic voltamperograms showing the growth of polyaniline film.

the oxidation of aniline is observed at 0.7 V vs. $\text{Ag}/\text{Ag}^+ 10^{-2}M$ ($\text{Ag}/\text{Ag}^+ 10^{-2}M$ refers to silver wire dipped in $10^{-2}M$ silver nitrate solution).

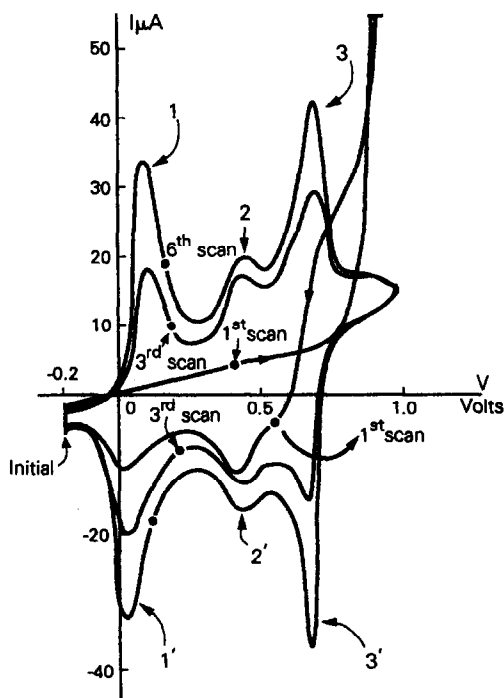


Fig. 10. Cyclic voltamperograms showing the appearance of the third redox system 2,2', when the anodic potential is increased.

New peaks, which are ascribed to the electrochemical response of PANI deposits formed during the oxidation process of aniline, appear after the first cycle. The following cycles indicate a regular growth of polymer deposits. In Fig. 8 the polyaniline shows two redox systems. If the higher potential is applied (up to 0.9 V), the third redox system, 2,2' having its redox potential between 1,1' and 3,3' is seen (Fig. 10). The shape, the redox potentials and the electrochemical behaviour of systems 1,1' and 3,3' remain identical in the presence and in the absence of system 2,2'. Therefore, it is suggested that system 2,2' which shows a redox mechanism independent of the mechanism attributed to system 1,1' and 3,3', probably corresponds to a different polymeric structure.^{39,40} Genies *et al.* in their recent study have attributed the redox system 2,2' to the presence of a polymer containing phenazine rings, which is correlated to the formation of cross-linked polyaniline chains by a direct reaction of nitrenium aniline cation ($C_6H_5NH^+$) and the nitrenium of the polyaniline polymer ($-C_6H_4N^+$).⁹⁷ We²⁷ have carried out similar studies on chemically synthesized polyanilines, and drawn some different conclusions which will be discussed later.

If the anodic potential exceeds a certain limit, degradation of the polyaniline results. This

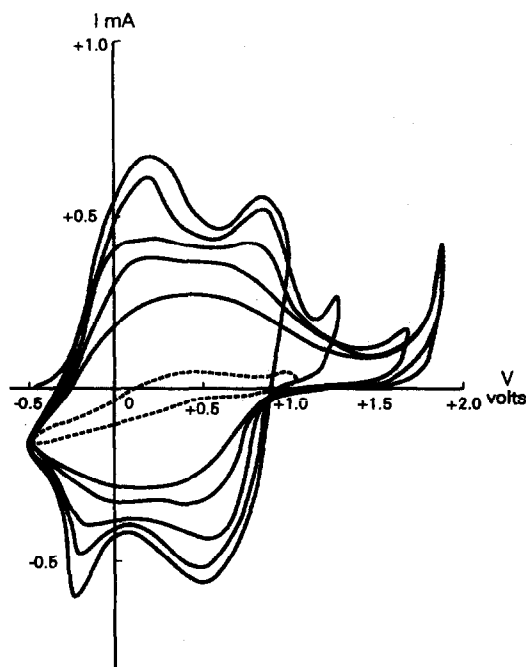


Fig. 11. Cyclic voltamperograms showing the loss of electroactive sites, as the anodic potential is increased after a certain limit (----) cyclic voltamperogram recorded after deterioration of the PANI film.

behaviour has been observed by a number of researchers.^{27,39,40,48,49,52,82,98-102} The degradation products of the polymer depend on the applied anodic potential during electropolymerization, and thereafter. Oxidative degradation of polyaniline refers to the loss of electroactive sites as illustrated in Fig. 11. In most of the cases, degradation occurs in two steps: (1) broadening of the peaks and (2) gradual disappearance of the electroactive sites (redox peaks). High potentials *ca.* 1.8 V in CH_3CN medium, or 1.9 V in aqueous medium, result in the cracking of the film. This is more likely in the case of aqueous media.³² However, it is reported that the redox potential of the 3,3' redox peak is sufficient for the degradation of polyaniline. Quinone and hydroquinone are generally believed to be the products of the oxidative degradation of polyaniline.⁹⁸⁻¹⁰⁰ the mechanism of which has been reported in the literature.⁹⁸⁻¹⁰⁰

Effect of anions. It has been indicated in the preceding section that anions have a limited influence on the conductivity of polyaniline. In contrast, the counterions derived from the supporting electrolyte have considerable influence on the rate of polymerization of aniline, and on the properties of the resulting products.^{28,103,104} The growth rate of a PANI film is 2.7–2.8 times faster in sulphuric acid than in perchloric, nitric, or hydrochloric acids.²⁸ This behaviour has been shown to be due to porous and granular structures of PANI, when synthesized in a sulphuric acid medium, as against smooth morphology of PANI synthesized in hydrochloric or perchloric acid medium.^{103,104} This property is explained on the assumption that the polymerization process proceeds in two stages. The first stage is the polymerization on the bare platinum electrode, or partially blocked electrode, by polyaniline. The second stage is polymerization on the platinum electrode completely covered by polyaniline. In the first stage the Pt-electrode surface is expected to be one of the determining factors of the polymerization rate. When the deposited polyaniline film blocks the platinum electrode surface, the aniline polymerization becomes more difficult, so the polymerization rate decreases. Consequently, further polymerization of aniline (second stage), would depend to some extent, on the morphology of films formed. At this juncture, a pore-rich structure is preferable to a smooth one. Hence, the growth-rate of polyaniline is more pronounced in sulphuric acid solution than in hydrochloric or perchloric acid solution. Similarly, use of HBF_4 , H_3PO_4 or HF results in

net morphological structure. This morphology like granular or porous structure helps for "higher rate", of polymerization of aniline than perchloric or hydrochloric acid medium.^{103,104}

In an interesting study, it is demonstrated that polyaniline has a selectivity for high molecular weight dopants.¹⁰⁵ The electrochemical polymerization of aniline was done in an aqueous solution containing 1M perchloric acid and 1×10^{-2} M sodium salt of polystyrene sulphonic acid, or polyvinyl sulphonic acids, or poly-(2-acrylamide-2-methyl-1-propane) sulphonic acid. The resulting PANI film was subjected to wide-scan electron spectroscopy which revealed the association of polymer electrolyte with the PANI chain. Although, the concentration of polymer electrolyte was one hundredth to that of perchloric acid, it is surprising that polymer electrolyte was selectively incorporated into the polyaniline matrix. This incorporation is explained in terms of a polymer effect, whereby incorporation proceeds just like the closing of a zipper.¹⁰⁵

Effect of the solvent and pH. The solvent has a pronounced effect on the shape of the cyclic voltamperogram of PANI. Discrete and well-defined peaks are observed in the case when polyaniline is synthesized in a eutectic mixture of HF and NH_3 ,^{39,40} while in the case of other media, comparatively broader peaks are observed. Furthermore, the electroactivity of polyaniline is not seen in solvents such as DMF, DMSO, methanol and ethanol. This probably results from the increase in nucleophilicity of the solvent. This conclusion is further supported by the fact that polyaniline does not exhibit electroactivity in a solution with pH greater than 4.²⁸

Electroanalytical techniques

Chronoamperometry and chronocoulometry methods have also been employed for the characterization of PANI. The former technique necessarily derives from the potential step, and the response is measured in terms of $I = f(t)$. From the type of curves, it is possible to distinguish the "quality" of the PANI synthesized in different media and supporting electrolytes. For example, it is shown that polyaniline synthesized in a eutectic mixture of NH_3 and HF medium has better utility for rechargeable batteries than that synthesized in other media.³⁸ The latter technique, also known as potential step chronocoulometric method (PSE), has been employed to determine the number of electrons involved in the redox mechanism of PANI.³⁸⁻⁴⁰ It has

been shown that the number of electrons in the redox mechanism is independent of the thickness of the PANI layer, but is influenced by anions in the solution.^{39,40}

Investigations on the conducting properties and the charge transfer during the redox process of PANI, and measurement of the electron transfer reaction rate at the polymer/solution interface have been carried out with Levich's direct and inverse criteria.¹⁰⁶ This technique is generally used for the study of electrochemical behaviour of the polymer-coated electrodes. The method consists of following the evolution of the current potential curves, corresponding to the electrolysis of redox species in solution, with respect to the rotation rate of the rotating disk electrode (RDE).¹⁰⁷ The evolution of these curves, during the reactions on naked platinum and Pt/PANI RDE allows us to estimate the conducting properties of PANI and helps in the measurement of the electron transfer rate at the polymer/solution interface.¹⁰⁷ It is reported that the charge transfer is a rapid phenomenon^{39,40} at the polymer/solution interface, and in the polymeric bulk.

Cyclic voltammetry studies of chemically synthesized polyaniline

Electrochemical characterization of chemically synthesized polyanilines presents a real challenge, because of their insolubility in solvents commonly employed for electrochemical investigations. Furthermore, they do not adhere to any electrode material, which makes electrochemical investigations extremely difficult. Nevertheless, four methods for the cyclic voltammetric (CV) study of chemically synthesized polyanilines have been reported in the literature. Two of the four methods were developed by American scientists,²⁴ and the other two by ourselves.^{27,29} The details of the first two methods are as follows: (1) The polymer was ground to a fine powder and ca. 1 mg was impregnated into glass filter paper (ca. 1 cm²), either with a spatula or a finger covered with a rubber glove. The filter paper was then shaken to remove the excess of polyaniline powder and placed on a platinum mesh which was folded so as to encase the filter paper on both sides. (2) Finely ground polyaniline powder was suspended in acetone or chloroform, and a few drops of suspension were poured on to a platinum foil (ca. 1 cm²) electrode and allowed to dry in air. The authors claim that these methods yield identical cyclic voltamperograms. However, a preconditioning of chemically prepared polyaniline is necessary to obtain reproducible results.

The methods developed by us are as follows: (1) 2–3 mg of chemically synthesized PANI were pressed on a thin inox grid which acts as a working electrode; an aluminum disc was used as counter electrode, and Ag/Ag^+ $10^{-2}M$ in propylene carbonate as reference electrode. The specially designed electrochemical cell was developed by French scientists.¹⁰⁸ The diagram and details of the components are published elsewhere.¹⁰⁹ The working electrode is mechanically maintained between the current collector and a plastic grid. On most occasions, $1M$ lithium perchlorate in propylene carbonate was used as electrolyte. One of the limitations of the above method is that the cell is unsuitable for use in aqueous media such as $1M$ hydrochloric or sulphuric acid. (2) In the other method,²⁷ we employed a mixture of chemically synthesized polyaniline (an amorphous powder), furnace black (a non-electroactive conductor), and polyvinylidene fluoride, $(-\text{CH}_2\text{CF}_2-)_n$ (slightly ionic conductor and binder) in the ratio 2:5:5 by weight. The mixture was made into a paste by the addition of one or two drops of DMSO solvent. The previously washed platinum wire (area 0.03 cm^2) of the Taccussel electrode was pushed back into the teflon. The paste was smeared and the excess of the DMSO solvent was evaporated by placing the electrode in a vacuum desiccator for about 15 min. This procedure leaves a thin layer adhering to the platinum. The advantage of this method is that the modified electrode can be employed in aqueous and non-aqueous media. Both methods yield encouraging results. We have studied²⁷ the influence of sweep rate on the i_{pa} and i_{pc} values, using our above-mentioned methods. The values rise linearly with the sweep rate as is expected for the redox reaction involving surface attached species. This experiment demonstrates the validity and dependency of our proposed methods. All the four methods involve permeation of electrolyte into the polymer powder particles.

A great deal of information concerning the reversibility and the nature of electron transfer steps can be obtained from cyclic voltamperograms. The characteristics of each scan, in most cases, can be determined by the way peak current and potentials vary with sweep rate. In our studies on PANIC, we have found the values of the slope of $\log i_p$ vs. $\log \nu$ curves for the two anodic and cathodic waves in the range 0.9–1.0. These values demonstrate that i_p tends to be proportional to ν for anodic and cathodic waves.²⁷

Voltammetric peak currents are proportional to ν in the case of thin-layer geometries only when electron-transfer is rapid (“reversible” systems). When electron-transfer begins to exert rate control, the dependence of peak current on ν becomes less than one. Currents observed at polymer-modified electrodes which are first-order in ν are indicative of rapid interfacial electron transfer as well as of facile charge transport through the film.

We²⁹ have demonstrated a very large capacitance background “current” associated with the cyclic voltamperogram of chemically synthesized PANI. From our results we have shown that 40% of the total charge stored in the polymer is the “capacitive” charge which is not related to any chemical redox reactions. The “non-capacitive” currents, representing the current due to the charges involved in the redox process, are too slow to follow, and thus contribute to the a.c. signal. Thus, two kinds of doping sites which are characterized by a long relaxation time ($T_1 > 1000$ sec) and a short relaxation ($T_2 > 10$ sec) are present in polyanilines. The total “capacitive” and “non-capacitive” charges can be deduced by integration of the voltamperograms. They are of the same order of magnitude, and represent about 40 and 60%, respectively, of the total charge stored in the polymer.

Another interesting feature associated with chemically synthesized polyanilines is reported by us. From our cyclic voltammetric studies we have shown that chemically synthesized PANI are 1-dimensional conducting polymers. The first scan of the CV of PANI reveals two well-defined redox systems 1,1' and 3,3'. Subsequent increase in the anodic potential, and/or repeated cycling, results in the 2,2' redox system which is an outcome of a higher oxidation level of PANI than that for the system 1,1' and 3,3'. Supporting evidence has come from solid-state ^{13}C NMR studies of PANI.^{110,111} The spectra obtained for PANI synthesized at a higher anodic potential is quite complex, which reveals the possibility of *ortho*-coupling, or a 3-dimensional matrix.³²

In summary, electroanalytical techniques such as chronoamperometry, chronocoulometry and cyclic voltammetry have been used for the characterization of polyaniline. The latter has played a yeoman role in solving some bewildering problems, such as effect of pH, ionic and electronic processes, *ortho*-coupling and cross linking, capacitance effects and degradation phenomena, to mention a few. Though CV is fundamentally a characterization technique, it does provide a

procedure for the polymerization of aniline-like monomers. Today it is also employed as a powerful electroanalytical tool by scientists working on "conducting polymers".

SOLUBILITY AND MOLECULAR WEIGHT DETERMINATION

The solubilization of polyaniline is of paramount importance, both scientifically and commercially. Scientifically, it provides a medium more conducive to the production of well-resolved analytical data, especially in the determination of molecular weight which helps in elucidating molecular configuration and structure in the conducting and insulator states. In commercial applications, polyaniline solutions would provide a form more amenable to conventional plastics processing technology.

There are conflicting reports on the solubility of polyaniline, contradictory views being advanced as early as 1910. Willstatter and Dorgi^{112,113} reported that an oligomeric (eight-monomer chain compound) aniline was largely insoluble. Green and Woodhead¹⁵ repeated their experiments and claimed solubility of this material in 80% acetic acid, 60% formic acid, pyridine and concentrated sulphuric acid. Later DMF was added to the list of solvents for electrochemically synthesized polyaniline.⁵² Partial solubility of polyanilines in its emeraldine base form in N-methylpyrrolidone,⁸⁰ THF,^{114,115} benzene, DMSO,¹¹⁶⁻¹²¹ chloroform,^{80,114,119,120} and methanol^{119,120} was also reported. As a result, it has become common practice to remove insoluble material⁸⁰ and use the soluble, possibly lower-molecular-weight, fraction for the preparations of films. Such cast films are predominantly amorphous and, generally, they have been categorized as intractable and amorphous material.

Routes towards soluble polyaniline include the preparation of graft polymers,¹²¹ copolymers¹²² and polyaniline derivatives.¹¹⁴ Unfortunately these species invariably show significantly reduced conductivities in comparison with the unmodified homopolymer. In a recent communication,¹²³ the feasibility of solution processing of crystalline, electrically conductive, polyaniline fibres and films was demonstrated. The authors claim that dissolution in sulphuric acid provides a simple means of processing polyaniline into films, fibre *etc.* In a separate communication, solubility of conducting polymers in organic acids (polar solvents) has been attributed to

hydrogen-bonding.¹¹⁸ In brief, solubility data of polyanilines makes possible systematic studies directed towards the understanding of this interesting polymer.

A preliminary investigation on the molecular weight of the soluble fraction of PANI in DMF was first reported in 1985.³⁸ An interesting facet of the reported data, pertinent to the present discussion, is that polyaniline is a macromolecule, and not an octomer, as believed earlier.^{15-20,52} These results were further confirmed by different workers. It is claimed¹¹⁵ that electrochemically synthesized polyaniline has a fraction whose molecular weight is at least 9000. Yet, another report mentions the molecular weight of 4300, measured by the GPC method.¹¹⁷ The viscosity measurements of polyaniline solution in sulphuric acid give an estimate of 12,000 molecular weight (rigid chain limit) and 40,000 molecular weight (flexible chain limit).¹²³ Since the conformation of polyaniline in the liquid state is not yet established, the viscosity data appear to be more of an approximation.

The procedure of dissolving polyaniline and determining its molecular weight has generated much activity among those interested in the commercialization of this novel material. Many new studies have been made in recent years, and continued research will undoubtedly lead to new discoveries and technology.

SPECTROSCOPIC STUDIES

Structural characterization of polyaniline with spectroscopic techniques presents a real challenge. Because of the amorphous nature of this material, information obtained from X-ray and neutron diffraction is quite limited, while its limited solubility restricts the use of standard characterization techniques for classical polymers. (Only recently was polyaniline, in the form of its emeraldine salt, recovered in crystalline form from a solution in sulphuric acid, by precipitation with water or methanol.)¹²³ Furthermore, the optical properties of PANI vary considerably, when it is doped, and when its state of oxidation is altered. New spectroscopic transitions induced by doping offer clues on the identity of the charged species: Spectroelectrochemical,^{1,37,74,75,85,87,88,124-129} UV-visible,^{69,89,116,130-136,139} IR,^{37,90,91,92,116,131-135,137,138,140,141} Raman,^{86,87,88,142-144} ESR,^{91-93,126,127,145} and XPS¹⁴⁶⁻¹⁴⁹ methods have been employed to this end. Solid-state NMR spectroscopy^{110,111,150,151,155,156} is found useful for the characterization of

insulator forms of PANI. The results of these studies are summarized briefly below.

Electrochemical spectroscopy

Spectroelectrochemical techniques are the combination of optical and electrochemical techniques. These techniques are a convenient means for obtaining the spectra and electrochemical potentials, and for observing subsequent chemical reactions during polymerization of aniline, and the doping/undoping of the resultant polymer. UV-visible-, IR-,³⁷ ESR-^{126,127} and Raman-spectroelectrochemical^{87,88} techniques have been employed to this end. Some of the salient features of the studies are: (1) doping/undoping of the polymer has a profound influence on the chromatic behaviour of PANI; (2) using the aforesaid techniques, four forms of PANI can be distinguished;^{74,75} (3) existence of two polaron-bipolaron states in the polymer has been established¹²⁷ and (4) presence of more quinonoid rings in the oxidized state of PANI has been demonstrated.^{87,88}

UV-visible spectroscopy

UV-visible absorption spectra of the electrochemically deposited polyaniline on substrates, such as (i) polyester plastic film coated with a thin layer of gold,¹²⁸ (ii) ITO-covered glass slides,^{87,88} and (iii) gold sputtered on a glass substrate,^{87,88} have been reported in the literature. Attempts have also been made to record spectra of thin free standing film but with limited success,³² probably due to strong absorptions in the optical range. Of late, most of the UV-visible studies are centred around a soluble emeraldine base.¹³⁹ The data derived from the studies demonstrate a red shift in both 2.0 eV and 3.8 eV absorption peaks, comparable to the shifts observed for emeraldine films and powders. The narrow strong absorption peak without the free electron absorption tail was explained as due to strong localization of polarons in solution form.

Infrared spectroscopy

Infrared spectra can yield valuable evidence concerning the electronic structure (and thus the geometry) of the PANI. A systematic IR study of chemically synthesized polyaniline powders, and of the anode precipitate prepared by constant potential electrolysis of aniline in sulphuric acid with platinum anode was first reported by Mohilner *et al.*⁵² The data from the IR spectra indicated the structural similarity of the anodic

precipitate with the chemically synthesized emeraldine and even more so with nigraniline (polyemeraldine and polynigraniline are the names commonly used in the present day literature). The fact that the spectrum of the anodic precipitate is not identical in every detail with either of the chemically synthesized compounds may imply that the electrochemically produced material is not a single substance, but rather a mixture of nigraniline and emeraldine.⁵² The marked similarities in the other properties of the anode precipitate and emeraldine—in particular, solubility in 80% acetic acid—strongly support the hypothesis that the anodically formed material is principally emeraldine. These results were confirmed by Ohira *et al.*¹⁴⁰ However, they note that polyaniline produced by the electrochemical method in neutral or basic media, essentially have 1- and 3-substituted benzene structures which are electroinactive even in acidic solutions. Fourier transform infrared studies on polyaniline analogues such as phenyl-capped octaaniline,¹³¹ aniline oligomers ($n = 2-4$),¹⁴¹ the electropolymerization product of *para*-amino diphenylamine⁵⁷⁻⁵⁹ and polyaniline/zeolite hybrids¹³³ are also reported in the literature.

Resonance Raman spectroscopy

The Resonance Raman Scattering (RRS) of PANI offers valuable information on the structure of the polymers. Moreover, it provides definite structural characterization because of the characteristic dependence of the Raman spectral pattern on the disposition of the ring substituents of aromatic compounds.¹⁴² Furthermore, one of the distinct advantages of RRS over other optical techniques is the possibility of studying the optical transitions even of powdered material. The first study of RRS on PANI powders was carried out by us⁸⁶ and the results are in full agreement with the optical absorption studies of electrochemically synthesized PANI films. Resonance raman scattering studies with electrochemically synthesized PANI¹⁴⁰ and its derivatives,¹⁴³ and with polyaniline-metalloporphyrin¹⁴⁴ are also to be found in the literature. Nevertheless, *in situ* Raman-spectroelectrochemical experiments appear to have resolved the complicated behaviour of the spectra for the various forms of PANI.^{87,88} In brief, RRS is useful in the structural study of complex multichromophore materials like PANI. Information on each chromophore can be obtained separately by a proper choice of exciting wavelength. The results indicate that: (1) the chemically, or

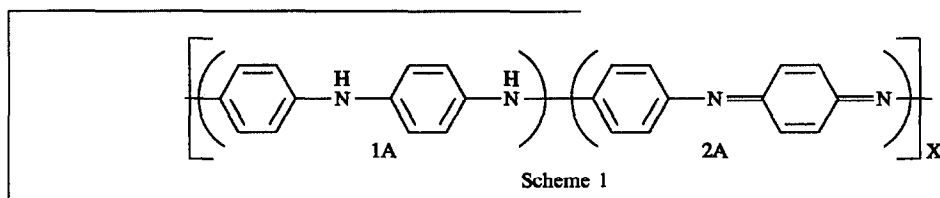
electrochemically, synthesized PANI chain consists of a mixture of benzenoid and quinonoid rings, the relative proportions of which depend on the reduced or oxidized state of the polymer; (2) *para*-substituted benzene and quinone diimine moieties are present in the base form of emeraldine; and (3) there is some evidence in favour of head-to-tail polymerization of aniline, with no *ortho* incorporation of phenylene diimine groups,¹⁴³ especially when combined with other evidence from IR studies.

X-ray photoelectron spectroscopy (XPS)

X-ray photoelectron spectroscopy (XPS) is capable of providing information with respect to the surface elemental composition and dopant level in PANI¹⁴⁶⁻¹⁴⁹ and its derivatives.^{150,151} The data regarding binding energies and surface composition offer some clues on the identity of a desired element present in a complex chemical environment. This information is particularly important in the determination of surface ele-

for this are: (1) compositional defects; (2) a distribution of torsion angles between adjacent rings; (3) variations in *syn* and *anticonformational* arrangements about the benzenoid rings, or *cis* and *trans* configurations about the quinonoid rings; (4) variation in the sequencing of benzenoid and quinonoid units; (5) thermally induced molecular motions; (6) the possibility of rotations or flips of benzenoid rings about their 1,4 axes and (7) a non-uniform charge, and/or spin distribution, for the conducting salts.

Despite broad lines, ¹³C crosspolarization magic angle spinning nuclear magnetic resonance (CPMAS NMR) spectra of deprotonated PANI (insulator form) resolve localized benzenoid and quinonoid ring structures, indicating that extensive electron delocalization along the backbone does not occur.¹⁵²⁻¹⁵⁴ Recent ¹³C NMR studies^{110,111,155,156} have determined that the emeraldine base consists primarily of a well-defined microstructure of alternating 1A and 2A units as shown below:



mental stoichiometry. Interestingly, XPS data of Cl-doped PANI has indicated the presence of covalent chlorine along with the two different ionic chlorine environments in PANI.¹⁴⁹ The relative contribution to the total chlorine signal was observed to be dependent on the applied potential.¹⁴⁹

¹³C NMR spectroscopy

The exact nature of the oxidized form of polyaniline is still unclear. As discussed earlier, the chemical and electrochemical evidence suggests that increasing the oxidation level of polyaniline results in creation of an increasing number of quinone-imine or other type of oxidized polymer sub-units. It is not yet known whether the perturbation in the polymer π -system, induced by an oxidized site, is localized or extensively delocalized.

The chemical shift data of PANI, derived from solid-state ¹³C NMR spectroscopy provides valuable information on the chemical structure of the polymer¹⁵²⁻¹⁵⁷ and its derivatives.¹⁵⁷ However, sequence distributions and chain conformations result in low spectroscopic resolutions, because of broad line-width. Possible reasons

The ¹³C NMR spectra of polyaniline in non-aqueous solvents are also reported in the literature.^{141,145} Recently solid-state ¹⁵N NMR spectroscopy has been utilized as a structural probe for the emeraldine base forms of PANI.¹⁵⁸

MORPHOLOGY

Studies on morphology of chemically and electrochemically synthesized PANI are important for investigating the intrinsic characteristics of the polymer. Many of the studies^{24,103,104,159-162} conducted up till now are rudimentary and exploratory in nature. The dependence of morphology upon variables such as different anions employed in the synthesis, the nature of the electrodes, and/or differences in chemical and electrochemical procedures need to be investigated in detail.

APPLICATIONS

Rechargeable batteries

For the last few years intense activity has been generated in the construction of a polyaniline-metal battery. This is because polyaniline has

certain advantages over other conducting polymers, such as simplicity and rapidity of preparation of the polymer by the chemical or electrochemical method, and chemical durability against aerial oxidation and moisture. Furthermore, the ability of polyaniline to store a considerable charge through the redox process has led to proposals for both non-aqueous^{38,163-167} and aqueous batteries.^{25,26,168-171}

In a non-aqueous medium, lithium is usually employed as the anode material in rechargeable batteries. But the use of a non-aqueous solvent in polyaniline-lithium batteries is beset with a serious problem: on charging, there is a tendency for dendrites to form when lithium is plated on the lithium electrodes, particularly at high charging rates. These dendrites can grow to considerable lengths, and shortcircuit a cell internally. Also, the high cathodic potential of the Li/Li⁺ couple often causes decomposition of the solvent, the mechanism of which has not yet been fully elucidated.¹⁷⁰

The use of polyaniline as cathode material, in conjunction with lithium-doped aluminium as anode material, in propylene carbonate containing 1M lithium perchlorate, results in an open circuit voltage of 3.7 V.³⁸ The massic capacity of 145 Ah/kg, and the self discharge (with separator) rate of about 8% after 90 days make the polyaniline-lithium battery more attractive for new types of technological applications.

In a recent communication,¹⁶⁷ PANIE was shown to have a maximum discharge capacity of 164 Ah/kg, a low rate of self-discharge, and a long life, as a positive active material in a secondary lithium battery. The larger massic capacity of PANIE is attributed to its fibrous structure which is produced galvanostatically, in an aqueous 1M perchloric acid solution containing 0.5M aniline at room temperature, when using the current density of 5 mA/cm². In our experiments, we have observed that PANI synthesized in sulphuric acid media has a granular structure, which is in accordance with the observation made by the aforesaid authors.¹⁶⁷ Propylene carbonate is a good electrolyte solvent, extensively employed in secondary lithium batteries, to ensure longer life and lower self-discharge for PANI. Further research efforts are required to find a new electrolyte system that is compatible with lithium and PANI.

The development of a practical Li/PANI battery is not a simple task. Apart from the technical shortcomings mentioned earlier, there remains the problem of 'safety' from the stand-

point of pollution. As Li is evidently a serious pollutant, it seems realistic to exploit aqueous batteries rather than non-aqueous Li-PANI cells. Also, the use of a water-based electrolyte in rechargeable batteries has certain advantages—an important one being that the ionic conductivity of aqueous electrolytes is greater than that of non-aqueous electrolytes; and hence, other factors being equal, cells employing aqueous electrolytes might be expected to deliver a higher output current.

French scientists^{25,26} were the first to employ two different oxidation states of PANI (now commonly known as 1S and 2S forms) as anode and cathode in a rechargeable battery cell in aqueous 1N sulphuric acid. These cells exhibited an open circuit voltage of ~0.40 volts. Very few data are available concerning the recyclability of either the anode material or the cathode material, in any aqueous electrolyte.

There were renewed efforts to employ polyaniline in conjunction with zinc¹⁶⁸⁻¹⁷¹ or lead oxide^{170,171} as the counter electrode. Polyaniline acts as the negative pole when combined with zinc, while it acts as the positive pole when combined with lead oxide. A difficulty, experienced with zinc as the counter electrode, is its spontaneous dissolution in acidic media, while polyaniline is electroactive only in the lower pH region. An advantage of using lead oxide as counter electrode is that no special caution is needed to avoid over-charging.

In brief, polyaniline is a promising material for both aqueous and non-aqueous storage batteries.

The question whether non-aqueous or aqueous electrolytes would be preferable for a specific purpose cannot be answered until much more information has become available. The use of aqueous electrolytes will, in general, be accepted to result in cells having a smaller potential, and hence, a smaller energy density than batteries employing a non-aqueous electrolyte. Real long-term advances in the field can only be accomplished by detailed studies on chemical and electrochemical reactions, occurring during storage and recycling, under a wide variety of experimental conditions.

Electrochromic devices

The optical characteristics of the PANI films undergo changes with the corresponding changes in the conductivity.^{98-100,172-174} In the oxidized state, PANI films are coloured and highly conductive; while in the reduced state, they are

optically transparent with low conductivity. In fact, colouration and conductivity are associated with the doping of the films.

Kobayashi *et al.*⁹⁸⁻¹⁰⁰ were the first to report the mechanism of the electrochromic reactions of PANI films and its applications to practical electrochromic display devices with liquid electrolytes. The colour of PANI films is reversibly changed to green by oxidation; and to transparent yellow by reduction in 1M hydrochloric acid, in the potential range from -0.2 V to $+0.6$ V *vs.* SCE. The reversibility of the colour change can be observed more than 10^6 times in the aforesaid potential range, with rapid response of less than 100 msec. However, Akhtar *et al.*¹⁷² are of the opinion that the problems of longrange stability, and of encapsulating devices with liquid electrolytes are many, so that the use of a solid-state electrolyte appears to be an attractive alternative. The advantages claimed in their report are protection from atmospheric oxidation and easy control of solid-state electrolyte composition.

In an interesting study, it has been demonstrated that the surface of an oxidized PANI electrochromic film, in contact with pure water, is more hydrophilic than that of a reduced surface. Furthermore, hydrophilicity is directly related to the conductivity of the film: the higher the conductivity, the greater the hydrophilicity of the surface.¹⁷³

Photoelectrochemical cells

The conversion of solar energy to chemical or electrical energy by photoelectrochemical cells (PECs) has attracted considerable attention during the last decade.^{175,176} This is because of their inherent simplicity of manufacture and consequently reduced cost. However, the susceptibility of narrow band-gap semiconductors to photodegradation has been a serious limitation on its wide popularity.

Two applications of PANI in PECs have been studied to date: protection against photo-corrosion of inorganic semiconductors,³⁰ and photoresponse of junction PANI film.¹⁷⁷ In the former case, the polyaniline-coated semiconducting electrodes (Cd-chalcogenides, Si, GaAs, GaP) exhibited enhanced stability of the photocurrent when compared to the current of the naked electrodes; while in the latter case, the photocurrent is induced when visible light from a 500 W xenon lamp is allowed to fall on a PANI film coated on platinum.¹⁷⁷ The authors mention a slow current photo-response of the order of

minutes for PANI in aqueous solution. Subsequent development in this field has resulted in a fast photoresponse of junction polyaniline film.¹⁷⁸

Electronic devices

A large change in electronic conductivity of PANI with a change in electrochemical potential is the basis for the development of PANI-based electronic devices. In practice, PANI deposited on to a gold microelectrode array has been shown to behave like electronic devices such as a diode and a transistor.⁴⁶ These polymer-based, transistor-like devices can be turned 'on' and 'off' by electrical or chemical signals that oxidize and reduce the polymer. For example, redox reagents such as $\text{Fe}(\text{CN})_6^{3-}$ and $\text{Ru}(\text{NH}_3)_6^{3+}$ can be used to turn a polyaniline-based transistor⁴⁶ on and off. In a separate communication, the design and operation of a PANI-transistor sensitive to moisture have been described.¹⁷⁹

Catalysis

Polyaniline and modified polyaniline have been shown to exhibit catalytic activity.^{180, 183} During oxidation of formic acid, using polyaniline-coated electrodes,¹⁸⁰ it was observed that oxidation rates of polyaniline electrodes are comparable to the oxidation rate at a platinumized platinum electrode at low overpotentials. This behaviour is the basis for evaluation of modified PANI as a fuel cell electrode.¹⁸⁰ The electrolytic reduction of oxygen and protons with modified polyaniline films has been reported in the literature.¹⁸²

In an interesting study, electrodeposition of platinum microparticles onto polyaniline film has been demonstrated.¹⁸³ The resultant film exhibits catalytic activity for hydrogen evolution and methanol oxidation. In another communication, polyaniline-nafion composite films have been shown to display better reversibility than the polyaniline alone.¹⁸¹ In brief, catalytic and electrocatalytic activity of polyaniline is of great importance and further research will certainly lead to newer technological applications of polyaniline.

Indicators

The multiple colour changes of polyaniline films^{145,184} on electrodes and chromatic reactions of polyaniline solutions in different pH ranges¹¹⁷ are the bases for development of PANI as an indicator. Recently, Jiang and Dong¹⁸⁴ have developed a PANI/Pt electrode as a redox

colour indicator in the titration of iron(II) with cerium(IV) solution. We¹⁸⁵ have developed soluble polyaniline solution as an acid–base indicator in the titration of 0.05–0.5M sodium hydroxide × sulphuric, hydrochloric, perchloric or nitric acid. The use of polyaniline solution as redox indicator is also investigated.³²

Ion exchange chromatography

Unlike other conducting polymers such as polypyrrole and polythiophene, PANI has a unique feature that the equilibration by acid solution imposes the anion in the polymer. This has been the basis for the use of PANI as an anion exchange polymer.¹⁸⁵ We¹⁸⁵ have shown that mixtures of halide ions can be separated on polyaniline.

CONCLUSIONS

The rediscovered polymer, the polyaniline, in less than a decade's time has travelled the arduous route from laboratory benches to commercial markets. This concise review has attempted to describe the synthesis and the physicochemical properties of polyaniline and to point out its potential in technology. The possibilities disclosed by its unique characteristics are, nevertheless, challenging. The newer applications of polyaniline in diversified technologies will attract increasing attention and interest from industrial and academic laboratories.

Acknowledgements—The authors thank Mr. K. M. Dastur, formerly in C.F.T.R.I., Mysore for his valuable suggestions and encouragement in preparing this review article. MKD gratefully acknowledges the University Grants Commission for the award of Senior Research Fellowship.

REFERENCES

1. R. L. Greene, G. B. Street and L. J. Suter, *Phys. Rev. Lett.*, 1975, **34**, 577.
2. H. Shirakawa, E. J. Louis, A. G. MacDiarmid, C. K. Chiang and A. J. Heeger, *J. Chem. Soc. Chem. Commun.*, 1977, 578.
3. C. K. Chiang, C. R. Fincher, Jr., Y. W. Park, A. J. Heeger, H. Shirakawa, E. J. Louis, S. C. Gau and A. G. MacDiarmid, *Phys. Rev. Lett.*, 1977, **39**, 1098.
4. A. F. Diaz and J. A. Logan, *J. Electroanal. Chem.*, 1980, **111**, 111.
5. J. Fritsche, *J. Prakt. Chem.*, 1840, **20**, 453.
6. *Idem, ibid.*, 1843, **28**, 198.
7. H. Letheby, *J. Chem. Soc.*, 1862, **15**, 161.
8. J.-J. Coquillon, *Compt. rend.* 1875, **81**, 408.
9. *Idem, ibid.*, 1876, **82**, 228.
10. A. Rosenstiehl, *ibid.*, 1875, **81**, 1257.
11. F. Goppelsroeder, *Compt. rend.*, 1876, **82**, 331, 1392.
12. L. Gilchrist, *J. Phys. Chem.*, 1904, **8**, 539.
13. H. T. Bucherer, *Ber*, 1907, **40**, 3412.
14. *Idem, ibid.*, 1909, **42**, 2931.
15. A. G. Green and A. E. Woodhead, *J. Chem. Soc.*, 1910, **97**, 2388.
16. *Idem, ibid.*, 1912, **101**, 1117.
17. A. G. Green and W. Johnson, *Ber.*, 1913, **46**, 3769.
18. A. G. Green and S. Wolff, *ibid.*, 1911, **44**, 2570.
19. *Idem, ibid.*, 1913, **46**, 33.
20. *Idem, J. Soc. Dyers Colorists*, 1913, **29**, 105.
21. T. Yasui, *Bull. Chem. Soc. Jpn.*, 1935, **10**, 305.
22. N. E. Khomutov and S. V. Gorbachev, *Zh. Fiz. Khim.*, 1950, **24**, 1101.
23. *Idem, Sovetsk. Elektrokhim.*, 1950, p. 579. Izdat. Akad. Nauk SSSR, Moscow, 1953.
24. W.-S. Huang, B. D. Humphrey and A. G. MacDiarmid, *J. Chem. Soc., Faraday Trans. I*, 1986, **82**, 2385.
25. R. de Surville, M. Jozefowicz, L. T. Yu, J. Perichon and R. Buvet, *Electrochimica Acta*, 1968, **13**, 1451.
26. M. Jozefowicz, J. H. Perichon, L. T. Yu and R. Buvet, *Br. Patent*, 1970, No. 1216569.
27. A. A. Syed, M. K. Dinesan and E. M. Geniès, *Bull. Electrochem.*, 1988, **4**, 737.
28. A. Kitani, J. Izumi, J. Yano, Y. Hiromoto and K. Sasaki, *Bull. Chem. Soc. Jpn.*, 1984, **57**, 2254.
29. N. Mermilliod, J. Tanguy, M. Hoclet and A. A. Syed, *Synth. Met.*, 1987, **18**, 359.
30. R. de Surville, Thèse Doctorat zème Cycle, Université de Paris, 1967.
31. S. P. Armes and J. F. Miller, *Synth. Met.*, 1988, **22**, 385.
32. A. A. Syed and M. K. Dinesan, unpublished results.
33. L. T. Yu, M. S. Borredon, M. Jozefowicz, G. Belorgey and R. Buvet, *J. Polym. Sci., Part C, Polymer Symposia*, 1967, No. 16, 2931.
34. A. Pron, F. Genoud, C. Menardo and M. Nechtschein, *Synth. Met.*, 1988, **24**, 193.
35. S. P. Armes and M. Aldissi, *J. Chem. Soc. Chem. Commun.*, 1989, 88.
36. J. C. Chiang and A. G. MacDiarmid, *Synth. Met.*, 1986, **13**, 193.
37. J. C. Chiang, *Ph. D. Thesis*, University of Pennsylvania, 1987.
38. E. M. Geniès, A. A. Syed and C. Tsintavis, *Mol. Cryst. Liq. Cryst.*, 1985, **121**, 181.
39. E. M. Geniès and C. Tsintavis, *J. Electroanal. Chem.*, 1985, **195**, 109.
40. *Idem, ibid.*, 1986, **200**, 127.
41. A. G. MacDiarmid, J. C. Chiang, M. Halpern, W. S. Huang, S. L. Mu, N. L. D. Somasiri, W. Wu and S. I. Yaniger, *Mol. Cryst. Liq. Cryst.*, 1985, **121**, 173.
42. G. Mengoli, M. T. Munari, P. Bianco and M. M. Musiani, *J. Appl. Polym. Sci.*, 1981, **26**, 4247.
43. M. M. Musiani, G. Mengoli and F. Furlanetto, *ibid.*, 1984, **29**, 4433.
44. D. W. DeBerry, *J. Electrochem. Soc.*, 1985, **132**, 1022.
45. G. Mengoli, M.-T. Munari and C. Folonari, *J. Electroanal. Chem.*, 1981, **124**, 237.
46. E. W. Paul, A. J. Ricco and M. S. Wrighton, *J. Phys. Chem.*, 1985, **89**, 1441.
47. N. Oyama, Y. Ohnuki, K. Chiba and T. Ohsaka, *Chem. Lett.*, 1983, 1759.
48. R. L. Hand and R. F. Nelson, *J. Am. Chem. Soc.*, 1974, **96**, 850.
49. *Idem, J. Electrochem. Soc.*, 1978, **125**, 1059.
50. R. Noufi, A. J. Nozik, J. White and L. F. Warren, *ibid.*, 1982, **129**, 2261.
51. T. Osaka, S. Ogano and K. Naoui, *ibid.*, 1988, **135**, 539.
52. D. M. Mohilner, R. N. Adams and W. J. Argersinger, Jr., *J. Am. Chem. Soc.*, 1962, **84**, 3618.

53. J. Bacon and R. N. Adams, *J. Am. Chem. Soc.*, 1968, **90**, 6596.
54. M. Breitenbach and K.-H. Heckner, *J. Electroanal. Chem.*, 1971, **29**, 309.
55. *Idem, ibid.*, 1971, **33**, 45.
56. *Idem, ibid.*, 1973, **43**, 267.
57. *Organic electrochemistry*, M. M. Baizer and H. Lund (eds.), Chap. 15, Dekker, New York, 1983.
58. E. M. Geniès, J. F. Penneau and M. Lapkowski, *J. Electroanal. Chem.*, 1989, **260**, 145.
59. E. M. Geniès, J. F. Penneau, M. Lapkowski and A. Boyle, *ibid.*, 1989, **269**, 63.
60. J. P. Travers, J. Chroboczek, F. Devreux, F. Genoud, M. Nechtschein, A. A. Syed, E. M. Geniès and C. Tsintavis, *Mol. Cryst., Liq. Cryst.*, 1985, **121**, 195.
61. W.-S. Huang, A. G. MacDiarmid and A. J. Epstein, *J. Chem. Soc. Chem. Commun.*, 1987, 1784.
62. L. T. Yu and M. Josefowicz, *Rev. Gen. Elec.*, 1966, **75**, 1014.
63. M. Doriomedoff, F. H. Cristofini, R. de Surville, M. Josefowicz, L. T. Yu and R. Buvet, *J. Chim. Phys.*, 1971, **68**, 1055.
64. L. J. van der Pauw, *Philips Tech. Rev.*, 1958/59, **20**, 220.
65. F.-R. F. Fan, T. V. Shea and A. J. Bard, *J. Electrochem. Soc.*, 1984, **131**, 828.
66. M. Gholamian, T. N. S. Kumar and A. Q. Contractor, *Proc. Indian Acad. Sci., Chem. Sci.*, 1986, **97**, 457.
67. B. Lundberg, W. R. Salaneck and I. Lundstrøm, *Synth. Met.*, 1987, **21**, 143.
68. H. H. S. Javadi, F. Zuo, K. R. Cromack, M. Angelopoulos, A. G. MacDiarmid and A. J. Epstein, *ibid.*, 1989, **29**, E409.
69. A. J. Epstein, J.-M. Ginder, F. Zuo, R. W. Bigelow, H.-S. Woo, D. B. Tanner, A. F. Richter, W. S. Huang and A. G. MacDiarmid *ibid.*, 1987, **18**, 303.
70. W. W. Focke, G. E. Wnek and Y. Wei, *J. Phys. Chem.*, 1987, **91**, 5813.
71. W. W. Focke and G. E. Wnek, *J. Electroanal. Chem.*, 1988, **256**, 343.
72. Y. W. Park, Y. S. Lee, C. Park, L. W. Shacklette and R. H. Baughman, *Solid State Commun.*, 1987, **63**, 1063.
73. A. J. Epstein, J.-M. Ginder, F. Zuo, H.-S. Woo, D. B. Tanner, A. F. Richter, M. Angelopoulos, W. S. Huang and A. G. MacDiarmid, *Synth. Met.*, 1987, **21**, 63.
74. W. R. Salaneck, I. Lundstrøm, W. S. Huang and A. G. MacDiarmid, *ibid.*, 1986, **13**, 291.
75. R. J. Cushman, P. M. McManus and S. C. Yang, *J. Electroanal. Chem.*, 1986, **291**, 335.
76. A. G. MacDiarmid, J. C. Chiang, A. F. Richter and A. J. Epstein, *Synth. Met.*, 1987, **18**, 285.
77. J. M. Ginder, A. F. Richter, A. G. MacDiarmid and A. J. Epstein, *Solid State Commun.*, 1987, **63**, 97.
78. E. M. Geniès and E. Vieil, *Synth. Met.*, 1987, **20**, 97.
79. H. H. S. Javadi, M. Angelopoulos, A. G. MacDiarmid and A. J. Epstein, *ibid.*, 1988, **26**, 1.
80. M. Angelopoulos, A. Ray, A. G. MacDiarmid and A. J. Epstein, *ibid.*, 1987, **21**, 21.
81. J. P. Travers and M. Nechtschein, *ibid.*, 1987, **21**, 135.
82. A. Kitani, M. Kaya, J. Yano, K. Yoshikawa and K. Sasaki, *ibid.*, 1987, **18**, 341.
83. H. Kuzmany, N. S. Sariciftci, H. Neugebauer and A. Neckel, *Phys. Rev. Lett.*, 1988, **60**, 212.
84. A. Ray, G. E. Asturias, D. L. Kershner, A. F. Richter, A. G. MacDiarmid and A. J. Epstein, *Synth. Met.*, 1989, **29**, E141.
85. M. Gholamian and A. Q. Contractor, *J. Electroanal. Chem.*, 1988, **252**, 291.
86. H. Kuzmany, E. M. Geniès and A. A. Syed, 63, *Electronic Properties of Polymers and Related Compounds*, H. Kuzmany, M. Mehring and S. Roth (eds.), pp. 223–226. Springer-Verlag, Berlin, 1985.
87. H. Kuzmany and N. S. Sariciftci, *Synth. Met.*, 1987, **18**, 353.
88. N. S. Sariciftci and H. Kuzmany, *ibid.*, 1987, **21**, 157.
89. D. Bloor and A. Monkman, *ibid.*, 1987, **21**, 175.
90. T. Ohsaka, Y. Ohnuki, N. Oyama, G. Katagii and K. Kamisako, *J. Electroanal. Chem.*, 1984, **161**, 399.
91. M. G. Roe, J. M. Ginder, R. P. McCall, K. R. Cromack, A. J. Epstein, T. L. Gustafson, M. Angelopoulos and A. G. MacDiarmid, *Synth. Met.*, 1989, **29**, E425.
92. R. P. McCall, M. G. Roe, J. M. Ginder, T. Kusumoto, A. J. Epstein, G. E. Asturias, E. M. Scherr and A. G. MacDiarmid, *ibid.*, 1989, **29**, E433.
93. H. H. S. Javadi, R. Laversanne, A. J. Epstein, R. K. Kohli, E. M. Scherr and A. G. MacDiarmid, *ibid.*, 1989, **29**, E439.
94. H. Reiss, *J. Phys. Chem.*, 1988, **92**, 3657.
95. M. Nechtschein and C. Santier, *J. Phys. Paris*, 1986, **47**, 935.
96. M. Nechtschein, C. Santier, J. P. Travers, J. Chroboczek, A. Alix and M. Ripert, *Synth. Met.*, 1987, **18**, 311.
97. E. M. Geniès, M. Lapkowski and J. F. Penneau, *J. Electroanal. Chem.*, 1988, **249**, 97.
98. T. Kobayashi, H. Yoneyama and H. Tamura, *ibid.*, 1984, **161**, 419.
99. *Idem, ibid.*, 1984, **177**, 281.
100. *Idem, ibid.*, 1984, **177**, 293.
101. A. Kabumoto, K. Shinozaki, K. Watanabe and N. Nishikawa, *Synth. Met.*, 1988, **26**, 349.
102. D. E. Stilwell and S.-M. Park, *J. Electrochem. Soc.*, 1988, **135**, 2497.
103. B. Wang, J. Tang and F. Wang, *Synth. Met.*, 1986, **13**, 329.
104. *Idem, ibid.*, 1987, **18**, 323.
105. K. Hyodo and M. Nozaki, *Electrochimica Acta*, 1988, **33**, 165.
106. A. J. Bard and L. R. Faulkner, *Electrochemical Methods*, Chap. 8, Wiley, New York, 1980.
107. T. Ikeda, C. R. Leidner and R. W. Murray, *J. Electroanal. Chem.*, 1982, **138**, 343.
108. E. M. Geniès and C. Santier, *French Patent No. 85 16865*.
109. N. Mermilliod, J. Tanguy and F. Petiot, *J. Electrochem. Soc.*, 1986, **133**, 1073.
110. A. A. Syed, M. K. Dinesan and K. N. Somasekharan, *Indian J. Chem.*, 1988, **27A**, 279.
111. A. A. Syed and M. K. Dinesan, *Solid-State Ionic Devices*, B. V. R. Chowdari and S. Radhakrishna, (eds.) pp. 481–487 World Scientific Publ. Co., 1988.
112. R. Willstätter and S. Dorogi, *Ber.*, 1909, **42**, 2147.
113. *Idem, ibid.*, 1909, **42**, 4118.
114. S. Wang, F. Wang and X. Ge, *Synth. Met.*, 1986, **16**, 99.
115. A. Watanabe, K. Mori, Y. Iwasaki and Y. Nakamura, *J. Chem. Soc. Chem. Commun.*, 1987, 3.
116. M. Inoue, R. E. Navarro and M. B. Inoue, *Synth. Met.*, 1989, **30**, 199.
117. R. Jiang and S. Dong, *ibid.*, 1988, **24**, 255.
118. S. K. Dhawan, D. C. Trivedi and K. I. Vasu, *Bull. Electrochem.*, 1989, **5**, 208.

119. S. K. Dhawan and D. C. Trivedi, *ibid.*, 1988, **4**, 729.
120. *Idem*, *Bull. Mater. Sci.*, 1989, **12**, 153.
121. S. Li, Y. Cao and Z. Xue, *Synth. Met.*, 1987, **20**, 141.
122. S. Li, H. Dong and Y. Cao, *ibid.*, 1989, **29**, E329.
123. A. Andreatta, Y. Cao, J. C. Chiang, A. J. Heeger and P. Smith, *ibid.*, 1988, **26**, 383.
124. E. M. Geniès and M. Lapkowski, *J. Electroanal. Chem.*, 1987, **220**, 67.
125. *Idem*, *ibid.*, 1987, **236**, 189.
126. *Idem*, *Synth. Met.*, 1987, **21**, 117.
127. *Idem*, *J. Electroanal. Chem.*, 1987, **236**, 199.
128. E. M. Geniès, J. M. Pernaut, C. Santier, A. A. Syed and C. Tsintavis, in *Electronic Properties of Polymers and Related Compounds*, H. Kuzmany, M. Mehring and S. Roth (eds), pp. 211–217. Springer Verlag, Berlin, 1985.
129. T. Hirai, S. Kuwabata and H. Yoneyama, *J. Chem. Soc., Faraday Trans. 1.*, 1989, **85**, 969.
130. P. M. McManus, S. C. Yang and R. J. Cushman, *J. Chem. Soc. Chem. Commun.*, 1985, 1556.
131. F.-L. Lu, F. Wudl, M. Nowak and A. J. Heeger, *J. Am. Chem. Soc.*, 1986, **108**, 8311.
132. G. E. Asturias, A. G. MacDiarmid, R. P. McCall and A. J. Epstein, *Synth. Met.*, 1989, **29**, E157.
133. P. Enzel and T. Bein, *J. Phys. Chem.*, 1989, **93**, 6270.
134. L. W. Shacklette, J. F. Wolf, S. Gould and R. H. Baughman, *J. Chem. Phys.*, 1988, **88**, 3955.
135. F. Wudl, R. O. Angus, Jr., F. L. Lu, P. M. Allemand, D. J. Vachon, M. Nowak, Z. X. Liu and A. J. Heeger, *J. Am. Chem. Soc.*, 1987, **109**, 3677.
136. W. R. Salaneck, I. Lundstrøm, B. Liedberg, M. A. Hasan, R. Erlandsson, P. Konradsson, A. G. MacDiarmid and N. L. D. Somasiri, in *Electronic Properties of Polymers and Related Compounds*, H. Kuzmany, M. Mehring and S. Roth, (eds.), 1985, pp. 218–222. Springer-Verlag, Berlin.
137. J. Tang, X. Jing, B. Wang and F. Wang, *Synth. Met.*, 1988, **24**, 231.
138. Y. H. Kim, C. Foster, J. Chiang and A. J. Heeger, *ibid.*, 1988, **26**, 49.
139. F. Zuo, R. P. MacCall, J. M. Ginder, M. G. Roe, J. M. Leng, A. J. Epstein, G. E. Asturias, S. P. Ermer, A. Ray and A. G. MacDiarmid, *ibid.*, 1989, **29**, E445.
140. M. Ohira, T. Sakai, M. Takeuchi, Y. Kobayashi and M. Tsuji, *ibid.*, 1987, **18**, 347.
141. Y. Cao, S. Li, Z. Xue and D. Guo, *ibid.*, 1986, **16**, 305.
142. F. R. Dollish, W. G. Fately and F. F. Bentley, *Characteristic Raman Frequencies of Organic Compounds*, Chap. 13. Wiley-Interscience, New York, 1974.
143. Y. Furukawa, T. Hara, Y. Hyodo and I. Harada, *Synth. Met.*, 1986, **16**, 189.
144. K. A. Macor, Y. O. Su, L. A. Miller and T. G. Spiro, *Inorg. Chem.*, 1987, **26**, 2594.
145. R. Jiang, S. Dong and S. Song, *J. Chem. Soc. Faraday Trans. 1.*, 1989, **85**, 1575.
146. A. Volkov, G. Tourillon, P.-C. Lacaze and J.-E. Dubois, *J. Electroanal. Chem.*, 1980, **115**, 279.
147. W. R. Salaneck, I. Lundstrøm, T. Hjertberg, C. B. Duke, E. M. Conwell, A. Paton, A. G. MacDiarmid, N. L. D. Somasiri, W. S. Huang and A. F. Richter, *Synth. Met.*, 1987, **18**, 291.
148. A. P. Monkman, D. Bloor, G. C. Stevens and J. C. H. Stevens, *J. Phys. D: Appl. Phys.*, 1987, **20**, 1337.
149. S. R. Mirrezaei, H. S. Munro and D. Parker, *Synth. Met.*, 1988, **26**, 169.
150. P. Snauwaert, R. Lazzaroni, J. Riga and J. J. Verbist, *ibid.*, 1987, **18**, 335.
151. *Idem*, *ibid.*, 1987, **21**, 181.
152. F. Devreux, G. Bidan, A. A. Syed and C. Tsintavis, *J. Phys. Paris*, 1985, **46**, 1595.
153. T. Hjertberg, W. R. Salaneck, I. Lundstrøm, N. L. D. Somasiri and A. G. MacDiarmid, *J. Polym. Sci. Polym. Lett. Ed.*, 1985, **23**, 503.
154. T. Hjertberg, M. Sandberg, O. Wennerstrøm and I. Lagerstedt, *Synth. Met.*, 1987, **21**, 31.
155. S. Kaplan, E. M. Conwell, A. F. Richter and A. G. MacDiarmid, *J. Am. Chem. Soc.*, 1988, **110**, 7647.
156. *Idem*, *Macromolecules*, 1989, **22**, 1669.
157. P. Hany, E. M. Geniès and C. Santier, *Synth. Met.*, 1989, **31**, 369.
158. A. F. Richter, A. Ray, K. V. Ramanathan, S. K. Manohar, G. T. Furst, S. J. Opella, A. G. MacDiarmid and A. J. Epstein, *ibid.*, 1989, **29**, E243.
159. S.-A. Chen and T.-S. Lee, *J. Polym. Sci., Polym. Lett., Ed.*, 1987, **25**, 455.
160. S. M. Yang and T. S. Lin, *J. Chin. Chem. Soc. (Taipei)*, 1988, **35**, 351.
161. A. Kitani, M. Kaya, S.-I. Tsujioka and K. Sasaki, *J. Polym. Sci., Part A: Polym. Chem.*, 1988, **26**, 1531.
162. Y. Lu, J. Li and W. Wu, *Synth. Met.*, 1989, **30**, 87.
163. E. M. Geniès, M. Lapkowski, C. Santier and E. Vieil, *ibid.*, 1987, **18**, 631.
164. A. G. MacDiarmid, L. S. Yang, W. S. Huang and B. D. Humphrey, *ibid.*, 1987, **18**, 393.
165. K. Okabayashi, F. Goto, K. Abe and T. Yoshida, *ibid.*, 1987, **18**, 365.
166. F. Goto, K. Abe, K. Okabayashi, T. Yoshida and H. Morimoto, *J. Power Sources*, 1987, **20**, 243.
167. S. Taguchi and T. Tanaka, *J. Power Sources*, 1987, **20**, 249.
168. G. Mengoli, M. M. Musiani, D. Pletcher and S. Valcher, *J. Appl. Electrochem.*, 1987, **17**, 515.
169. G. Mengoli, M. M. Musiani, D. Pletcher and S. Valcher, *J. Appl. Electrochem.*, 1987, **17**, 525.
170. A. Kitani, M. Kaya and S. Sasaki, *J. Electrochem. Soc.*, 1986, **133**, 1069.
171. A. G. MacDiarmid, S. L. Mu, N. L. D. Somasiri and W. Wu, *Mol. Cryst. Liq. Cryst.*, 1985, **121**, 187.
172. M. Akhtar, H. A. Weakliem, R. M. Paiste and K. Gaughan, *Synth. Met.*, 1988, **26**, 203.
173. M. A. Habib, *Langmuir*, 1988, **4**, 1302.
174. S. Gottesfeld, A. Redondo and S. W. Feldberg, *J. Electrochem. Soc.*, 1987, **134**, 271.
175. A. J. Nozik, *Annual Rev. Phys. Chem.*, 1978, **29**, 189.
176. S. Chandra and R. K. Pandey, *Phys. Stat. Sol. A*, 1982, **72**, 415.
177. M. Kaneko and H. Nakamura, *J. Chem. Soc. Chem. Commun.*, 1985, 346.
178. E. M. Geniès and M. Lapkowski, *Synth. Met.*, in press.
179. S. Chao and M. S. Wrighton, *J. Am. Chem. Soc.*, 1987, **109**, 6627.
180. M. Gholamian, J. Sundaram and A. Q. Contractor, *Langmuir*, 1987, **3**, 741.
181. T. Hirai, S. Kuwabata and H. Yoneyama, *J. Electrochem. Soc.: Electrochem. Sci. Technol.*, 1988, **135**, 1132.
182. G. Bidan, E. M. Geniès and M. Lapkowski, *J. Chem. Soc. Chem. Commun.*, 1988, 533.
183. K. M. Kost, D. E. Bartak, B. Kazee and T. Kuwana, *Anal. Chem.*, 1988, **60**, 2379.
184. R. Jiang and S. Dong, *J. Chem. Soc. Faraday Trans. 1.*, 1989, **85**, 1585.
185. A. A. Syed and M. K. Dinesan, *Synth. Met.*, 1990, **36**, 209.

QUANTITATIVE INVESTIGATION OF MATRICES FOR DIFFUSE REFLECTANCE INFRARED FOURIER TRANSFORM SPECTROMETRY

MOLLIE L. E. TEVRUCHT

Department of Chemistry, University of Alaska, Anchorage, AK

PETER R. GRIFFITHS*

Department of Chemistry, University of Idaho, Moscow, ID 83843, USSR

(Received 5 December 1990. Revised 11 February 1991. Accepted 19 February 1991)

Summary—Five materials were investigated for use as diluent matrices for diffuse reflectance infrared Fourier transform (DRIFT) spectrometry of powdered samples. DRIFT spectra of powdered carbazole dispersed in germanium, silicon, diamond, potassium chloride and a chalcogenide glass were compared. Three particle size ranges were investigated for five concentrations of carbazole ranging from 0.1–10%. The effects of particle size and refractive index of the matrix are discussed.

Diffuse reflectance infrared Fourier transform (DRIFT) spectrometry has been used to study such varied samples as coals,^{1,2} polymers,³⁻⁵ silanes in glass fibers,^{6,7} silicon dioxide in silicon carbide⁸ and silanes in silica gel.⁹ DRIFT spectra have been acquired of neat, unground samples,^{4,6} of neat, ground samples,^{1,2} of samples with a thin potassium chloride overlayer,^{3,7} and of samples abraded onto silicon-carbide-coated paper.⁵ As most commonly practiced, however, the analyte is dispersed in a non-absorbing matrix and the diffusely reflected radiation is collected to obtain the spectrum.⁸⁻¹¹ DRIFT spectra of samples prepared in this manner most closely resemble transmission spectra of samples pressed in alkali halide pellets.¹² The diluent matrix for DR spectrometry is often an alkali halide such as potassium chloride, favored because of its transparency throughout the mid-infrared, its ease of grinding and its non-toxicity. Drawbacks include its hydrophilicity and ionic nature. Water adsorbs quickly and tenaciously on potassium chloride and the resulting bands in the DRIFT spectra can interfere with the absorptions due to the analyte. Analyte spectra can also be altered by ionic exchange between the analyte and the alkali halide matrix.¹³ A further complication arises when alkali halides are left in a powdered state for several hours before use, as they show a proclivity to adsorb air-borne organic compounds leading to the

appearance of bands around 3000–2800 cm⁻¹.

It would be advantageous to employ a matrix which was non-absorbing, non-hygroscopic, non-reactive, non-toxic and easily ground. Kaihara *et al.*¹¹ proposed a matrix composed of a mixture of cesium iodide and potassium bromide but such a matrix has no advantage over potassium bromide or potassium chloride alone.¹⁴ Azarraga and co-workers investigated several possible matrices,¹⁵ including calcium and magnesium fluoride, sulfur and silver halides. The spectra of calcium fluoride and magnesium fluoride have too many bands that would interfere with the bands in the DRIFT spectrum of the analyte at long wavelengths. Sulfur suffered the same problem and was deemed too reactive for use in some situations, while the silver halides were too soft to grind well. Diamond powder appeared to be the most promising material of those studied. However, the specific effect of a change in matrix on the infrared spectrum of a sample was not studied.

An important application of DRIFT spectroscopy has been for detection and identification in high-performance liquid chromatography (HPLC)¹⁶⁻¹⁸ and thin layer chromatography (TLC).^{19,20} With a direct deposition interface, the chromatographic effluent is sprayed onto the diluent matrix. The presence of water in the effluent can be disastrous if a water-soluble matrix such as an alkali halide is used.¹⁸ A TLC/DRIFT interface, originally developed in our laboratory²¹ and now marketed

*Author for correspondence.

commercially by Laser Precision Analytical (Irvine, CA) uses a chalcogenide glass²² for the matrix. This interface is currently used in our laboratory to study the extracts of coals separated with TLC.²⁰ The chalcogenide glass possesses many of the properties of an ideal matrix: it is nonhygroscopic, inert, easily ground and insoluble in common chromatographic solvents. It is composed of germanium, antimony and selenium with the approximate formula $\text{Ge}_{28}\text{Sb}_{12}\text{Se}_{60}$, and has a refractive index of 2.7. How the spectra obtained with the chalcogenide matrix differ from those acquired with a potassium chloride matrix or a diluent of higher refractive index has never been reported.

Silicon^{12,13} and germanium^{12,13,24} have also been suggested for use as matrix materials. Like the chalcogenide glass, both elements are hydrophobic, easy to grind, have relatively featureless infrared spectra, and are inert. They possess rather high refractive indices of 3.4 and 4.0, respectively. The refractive index of potassium chloride in comparison, is only 1.5 while that of diamond is 2.4. Most organic compounds have refractive indices of around 1.5. It is known that a high refractive index matrix reduces the intensity of the analyte bands,¹² but the effect of the matrix on band intensities and linearity with respect to concentration is unknown. A matrix with a higher refractive index will have higher front surface reflection, which should lead to more scattering. Since the scattering coefficient varies with wavenumber, the effect will not be uniform over the entire spectrum. Also, the penetration depth of the infrared radiation decreases dramatically as the scattering coefficient is increased,²⁵ which would lead to less intense bands. The decrease in effective penetration depth has been postulated to explain the significantly decreased band intensities in spectra of compounds diluted in matrices of high refractive index.^{12,25,26}

A second parameter which should affect band intensities in DRIFT spectra is the particle size of the matrix. With potassium chloride as the matrix, it has been shown^{9,10,12,14,24} that bands become stronger and sharper with decreasing particle size. In one study, particles 5–10 μm in diameter were found to give spectra of higher contrast than larger particles,¹⁰ although another report showed little difference in the spectra of weakly absorbing compounds as long as the particles were less than 75 μm in size.¹² For diamond powder, the optimal particle diameter was reported to be 6 μm .¹⁵ However,

whether this size is appropriate for matrices with a higher refractive index has not been studied. Since the scattering properties of a powder are dependent upon both particle size and refractive index, it is difficult to determine the ideal particle size for germanium and silicon *a priori*.

The effective penetration depth of radiation into a powdered sample is controlled by several factors. For a given matrix and concentration of analyte, the particle sizes of the analyte^{12,26,27} and its diluent matrix govern the effective penetration depth. As the particle size of the sample increases, the beam is increasingly attenuated on transmission through a sample particle. It can be calculated that the absorbance of most fundamentals in the transmission spectrum of a carbazole particle 20 μm in diameter would exceed 2.0 for all but the weakest bands, and particles over 50 μm would completely attenuate the radiation across essentially all spectral features. Assuming some of the radiation reaching the detector has not passed through one analyte particle, the result will be an apparent broadening of all bands in the spectrum.

The effect of particle size can be counteracted through a change in the refractive index of the surrounding matrix. Depending on how the sample is packed prior to spectral acquisition, bands in the DR spectrum of carbazole diluted in potassium chloride can be up to two orders of magnitude greater in intensity than those of carbazole in silicon.¹² When the single beam spectrum of germanium powder is ratioed against that of potassium chloride, the resulting reflectance is less than 50%. The single beam spectra of all four matrices were ratioed against that of potassium chloride, and the resulting reflectance spectra are shown in Fig. 1(A–D). Reflectance spectra of small (5–10 μm diameter) particles of diamond, chalcogenide glass, silicon and germanium are shown in Fig. 1(A), (B), (C) and (D), respectively. Upward-going features in the four spectra arise from the uncompensated bands in the reference spectrum due to adsorbates on the potassium chloride. The inverted bands at 3400 and 1640 cm^{-1} result from the presence of water in the potassium chloride, while that at 2900 cm^{-1} is due to adsorbed organic compounds. The small, sharp feature at 1390 cm^{-1} is from a nitrate contaminant in the potassium chloride. The Si-O stretching band seen in Fig. 1(C) occurs around 1200 cm^{-1} , while the Ge-O stretching band of crystalline Ge is found near 900 cm^{-1} in Fig. 1(D). The broad,

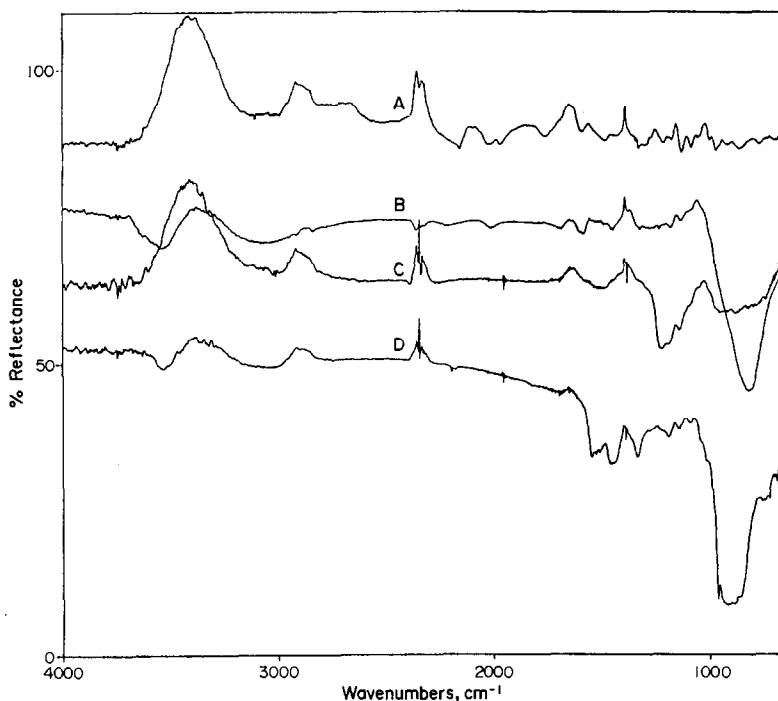


Fig. 1. The single beam spectra of (A) diamond, (B) chalcogenide glass, (C) silicon and (D) germanium ratioed against that of potassium chloride. None of the spectra have been offset, and all are plotted from 0–110% transmittance.

downward-going band near 810 cm^{-1} in Fig. 1(B) is presumably attributable to the stretching mode of Ge-O, shifted by the presence of Se and Sb in the glass.

For a non-absorbing material, the dependence of the reflectance, R , upon the refractive index, n , is described by the Fresnel equations. When the matrix is changed from potassium chloride to germanium, the refractive index increases from 1.5 to 4.0, and the front surface reflectance increases from 0.04 to 0.36 at normal incidence. The increased reflectance of the Ge matrix increases the scattering coefficient and therefore prevents radiation from penetrating into the sample. A significant fraction of the incident radiation does not interrogate analyte particles located more than a few micrometers below the surface.²⁵ The competing effects of refractive index and particle size control the effective penetration depth for DRIFT spectrometry.

In this paper we report the qualitative and quantitative effects of different refractive index and particle size matrices and DRIFT spectra. Spectra obtained with diluent matrices of silicon, germanium, diamond powder, a chalcogenide glass and potassium chloride were analyzed with a typical organic compound, carbazole, as the test analyte. Carbazole has an

infrared spectrum with a number of isolated bands of different intensities, and strong bands at both high and low frequencies. The effect of the matrix on both weak and strong bands can be analyzed, along with the effect of scattering of the radiation by the matrix. Three particle size ranges of carbazole and each matrix were used, as well as a range of concentrations of carbazole in each matrix.

EXPERIMENTAL

Diamond powder (Graves Co., Pompano Beach, FL) was obtained in three particle sizes: $6\text{ }\mu\text{m}$, $30\text{ }\mu\text{m}$ and $45\text{ }\mu\text{m}$. Germanium and silicon (-325 mesh; Alfa Products, Danvers, MA) were ground separately in a stainless steel capsule in a Wig-L-Bug ball-mill grinder (Crescent Manufacturing Company, Lyons, IL). The chalcogenide glass ($\text{Ge}_{28}\text{Sb}_{12}\text{Se}_{60}$, TI Glass No. 1173, Texas Instruments, Dallas, TX) and potassium chloride ("random cuttings", Harshaw, Solon, OH) were broken into small chunks with a mortar and pestle, then ground in the same way as the silicon and germanium. Except for diamond, each matrix was sieved to three particle size ranges in a Sonic Sifter (ATM Corporation, Milwaukee, WI). Carbazole (Eastman Kodak Co., Rochester,

NY) was ground and sieved in a similar manner. The particle size ranges used were 5–10 μm , 20–30 μm and 53–75 μm . These particle sizes were chosen to be approximately equal to the wavelength, slightly larger than the wavelength and several times larger than the wavelength of mid-infrared radiation (2.5–15 μm), respectively.

After the required particle size range had been obtained, carbazole was diluted in each matrix to concentrations of 0.1%, 0.33%, 1.0%, 3.3% and 10% (by weight). The carbazole and matrix material were mixed without further grinding, and were packed into 4.5-mm diameter, 5-mm deep sample cups with a modified Parr pellet press (Moline, IL).²⁸ Although each matrix exhibited very distinct packing characteristics, the amount of sample and the duration and amount of pressure were controlled to achieve consistent and reproducible packing for each sample. Since some materials (KCl, $\text{Ge}_{28}\text{Sb}_{17}\text{Se}_{60}$) were more easily compressed for all particle size ranges than others, samples diluted in them were pressed more compactly than those in the other matrices.

Spectra were measured at 4 cm^{-1} resolution with a Digilab Model FTS-20 spectrometer (Bio-Rad, Digilab Division, Cambridge, MA) equipped with diffuse reflectance optics of the type described by Fuller and Griffiths¹⁰ and an intermediate-range mercury-cadmium-telluride (MCT) detector (Infrared Associated, New Brunswick, NJ). Typically, 256 scans were co-added for each spectrum, and the reference spectrum for each sample was that of its pure matrix. Each experiment was performed three times, and the results averaged.

After taking the ratio of the single beam spectrum of each sample and the appropriate reference spectrum, the reflectance spectrum was converted to $\log(1/R)$, baseline-corrected, converted back to reflectance and then to the Kubelka–Munk format. Baseline correction was required when the pure matrix reflected less radiation than the diluted carbazole, leading to reflectance values greater than 100% in the ratioed spectrum. The baseline correction fitted line segments between four points of the spectrum, then leveled them and added to or subtracted for the flattened baseline to bring it to a $\log(1/R)$ value of zero across the spectrum. The four points selected (3700, 2700, 2100 and 660 cm^{-1}) fell in baseline regions. All spectral manipulations were performed with Spectra-Calc software (Galactic Industries, Salem, NH).

Transmission spectra of 1 wt. % carbazole pressed in a potassium bromide (Harshaw, Solon, OH) pellet were acquired on a Nicolet 740 spectrometer (Nicolet Instrument Company, Madison, WI) equipped with an MCT detector and operated under conditions where the response is linear. Compressed pellets ranged in thickness from 130–280 μm . The spectra were taken at 4 cm^{-1} resolution, and 256 scans were co-added.

RESULTS AND DISCUSSION

The transmission spectrum of 1% carbazole compressed in a potassium bromide pellet of 280 μm thickness is shown in Fig. 2, along with the structure of carbazole. DRIFT spectra of carbazole diluted to 1 weight percent in potassium chloride, diamond, the chalcogenide glass, silicon and germanium of 5–10 μm particle size are shown in Fig. 3(A), (B), (C), (D) and (E). The spectra are plotted in Kubelka–Munk units, and all have been ordinate-expanded to full-scale. Several differences in relative band intensities between the six spectra in Figs. 2 and 3 are readily apparent. The broad feature near 900 cm^{-1} in the germanium spectrum arises from incomplete compensation of a Ge-O band, shown in Fig. 1(D), present in both the sample and the reference spectra. As shown in Fig. 1(C), the spectrum of pure silicon ratioed against that of potassium chloride has bands near 1200 cm^{-1} attributable to Si-O stretching modes, but they are not visible in the spectrum of carbazole diluted in silicon.

The transmission spectrum of the potassium bromide disk most closely matches that of carbazole diluted in silicon or germanium. As the refractive index of the diluent matrix increases, so do the relative intensities of the bands above 3000 cm^{-1} , attributable to the N-H (3420 cm^{-1}) and C-H (3050 cm^{-1}) stretching absorptions of carbazole. In the transmission spectrum, the intensities of the N-H stretching band at 3420 cm^{-1} and the C-H out-of-plane deformation bands between 775 and 700 cm^{-1} have roughly the same intensity, whereas in the potassium chloride DRIFT spectrum the low frequency bands are much more intense. Since both the N-H and C-H stretching modes exhibit the same trends, and since no such suppression is seen in the potassium bromide pellet transmission spectrum, the effect cannot be ascribed to the formation of an amine salt. The spectral features below 2000 cm^{-1} exhibit less dramatic

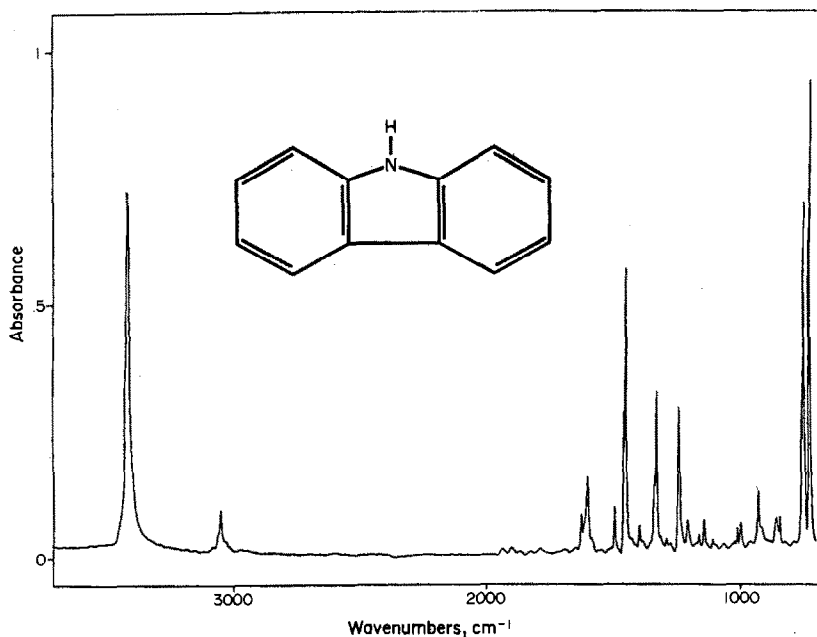


Fig. 2. Transmission spectrum of 1 wt. % carbazole pressed in a potassium bromide pellet. The structure of carbazole is given above the spectrum.

differences. In this region, as the refractive index of the matrix is increased from 1.5 (KCl) to 4.0 (Ge) the analyte bands become sharper and better resolved. This is especially obvious for the C-H out-of-plane deformation bands, as well as the doublet at 1625/1602 cm^{-1} due to C=C

aromatic ring breathing modes. One possible cause for the broadening of the bands in the spectra of carbazole in potassium chloride, diamond, the $\text{Ge}_{28}\text{Sb}_{12}\text{Se}_{60}$ glass is attenuated total reflectance in the matrix particles. When the refractive indices of the sample and the matrix

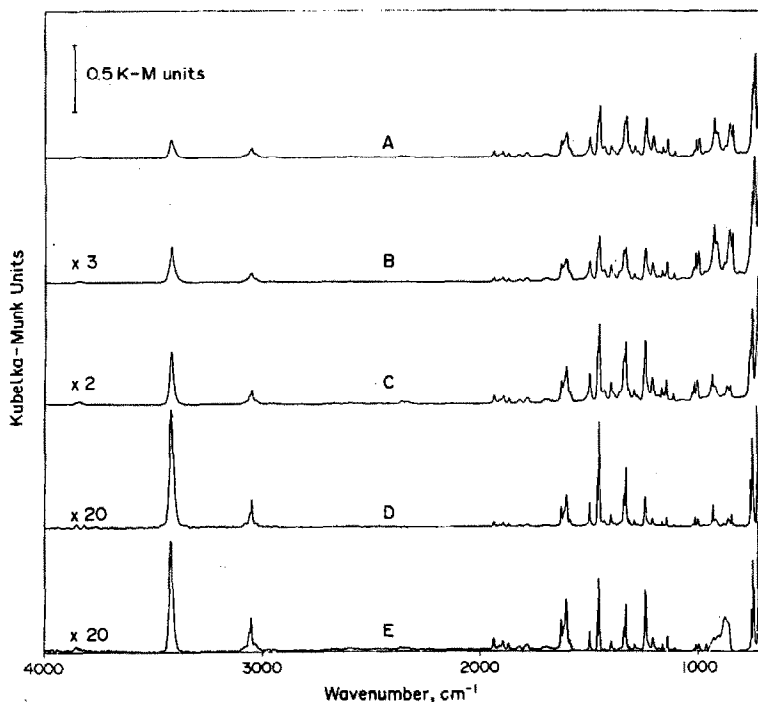


Fig. 3. DRIFT spectra of 1 wt. % carbazole in (A) potassium chloride, (B) diamond, (C) chalcogenide glass, (D) silicon, and (E) germanium. Particles of carbazole and all matrices were between 5 and 10 μm in size. Scale expansions for B through E are indicated on the spectra.

Table 1. Bands in carbazole spectrum chosen for analysis

Frequency, cm^{-1}	Assignment	Absorption coefficient, cm^{-1}
3419	N—H stretching mode	12200
3051	C—H stretching mode	2050
1602	C=C aromatic ring breathing mode	3300
1450	C—C bending mode	10500
1240	C—N stretching mode	5650
727	C—H out-of-plane deformation mode	18200

are similar, there is increased penetration into the analyte particles from adjacent matrix particles. This could result in increased absorption of the impinging radiation and saturation-like effects in the spectrum. Although this explanation is not very plausible, no other causes are evident at this time.

To compare the spectra of carbazole in each of the five matrices quantitatively, the six bands listed in Table 1 were analyzed. The assignment and absorption coefficient calculated from the transmission spectrum of carbazole pressed in a potassium bromide pellet are also listed. The Kubelka–Munk function, $f(R_\infty)$, gives the ratio of the absorption coefficient, k , to the scattering coefficient, s .²⁹ The absorption coefficient was calculated from the potassium bromide disk spectrum as

$$k = \frac{\ln T}{cx} \quad [1]$$

where T is the transmittance of a given band, c is the weight percent concentration of carbazole in the pellet (weight:weight) and x is the pellet thickness in cm.

The selected six bands encompass both high and low frequency absorptions and range from medium-weak to strong intensities. The values for these six bands for small (5–10 μm), medium (20–30 μm) and large (53–75 μm) particle sizes are plotted against weight percent carbazole in potassium chloride, diamond, $\text{Ge}_{28}\text{Sb}_{12}\text{Se}_{60}$, silicon and germanium in Figs. 4–8, respectively. At least three variables control the differences in the spectra, since particle size, index of refraction and packing density all affect the intensities of bands in a given spectrum. Increased pressure applied to the sample results in more intense bands in the resulting spectrum.³⁰

The variation in band intensities with particle size for each matrix will be considered first. The particle sizes of both analyte and diluent were the same for every mixture of carbazole in each matrix. As shown in Fig. 4, for both the small (5–10 μm) and medium (20–30 μm) particle sizes of carbazole dispersed in potassium chlor-

ide ($\text{C}_{12}\text{H}_9\text{N}:\text{KCl}$) the intensities of corresponding bands are roughly equal. The band intensities in the DRIFT spectrum of carbazole diluted in the large (53–74 μm) particles of potassium chloride are weaker; this is particularly evident for the strong feature at 727 cm^{-1} .

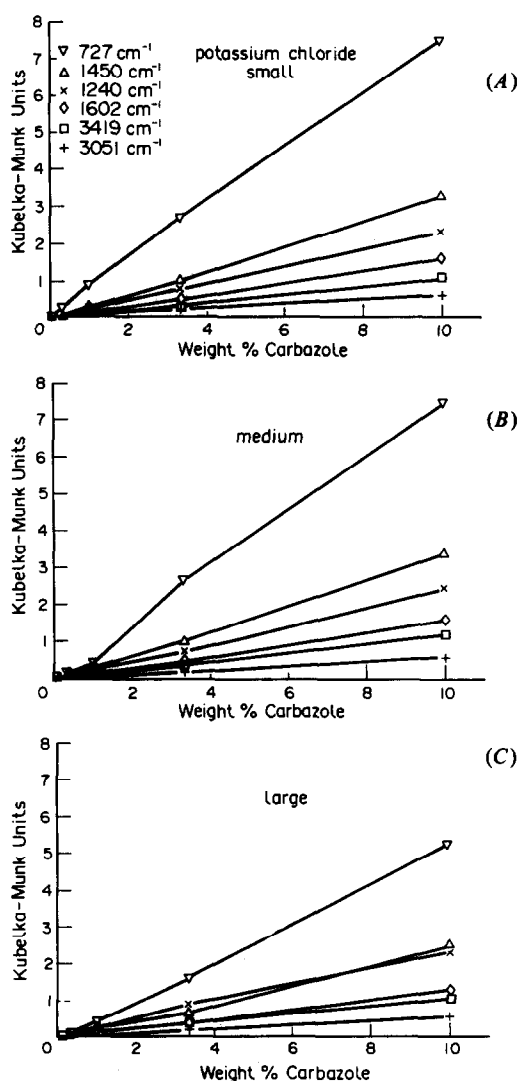


Fig. 4. The Kubelka–Munk intensity of six bands in the DRIFT spectrum of carbazole diluted in potassium chloride. Particles of carbazole and potassium chloride were (A) between 5 and 10 μm , (B) between 20 and 30 μm , and (C) between 53 and 75 μm in size. The key for all three graphs is given in (A).

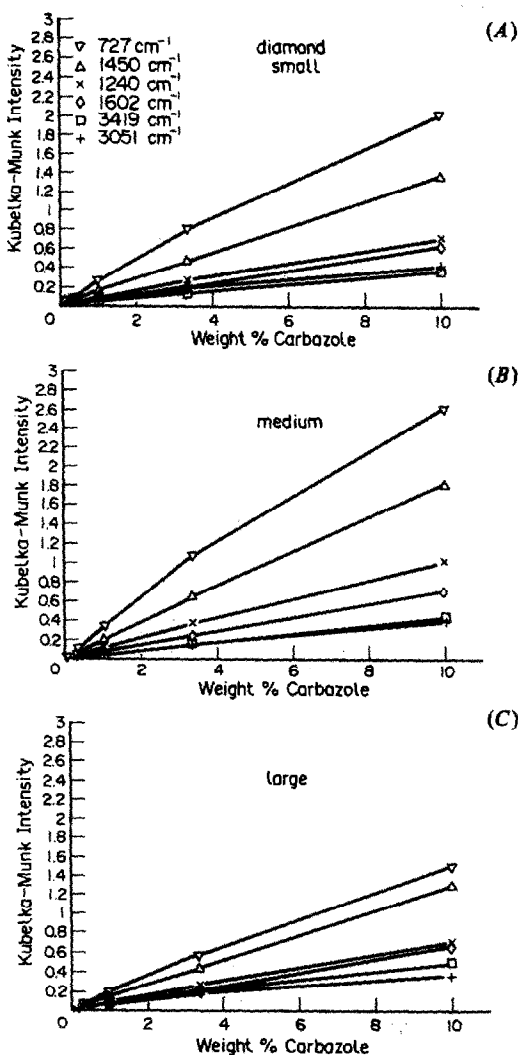


Fig. 5. The Kubelka-Munk intensity of six bands in the DRIFT spectrum of carbazole diluted in diamond powder. Particles of carbazole and diamond were (A) between 5 and 10 μm , (B) between 20 and 30 μm , and (C) between 53 and 75 μm in size. The key for all three graphs is given in (A).

These results are in accord with other published results,^{12,24} and are easily explained since in the Kubelka-Munk equation, $f(R_\infty)$ increases as s decreases. Thus, larger particles, with their lower scattering coefficient, would give rise to more intense spectral features. This will hold only in the absence of front-surface reflection leading to anomalous dispersion or *reststrahlen* features in the spectrum. Chalmers *et al.*²⁴ have demonstrated that for an increase in particle diameter from 2 to 5 to 10 μm , the Kubelka-Munk band intensity increases with increasing particle diameter for all but the strongest bands in the spectrum. The same workers²⁴ showed that for silica spheres dispersed in potassium bromide there is an increase

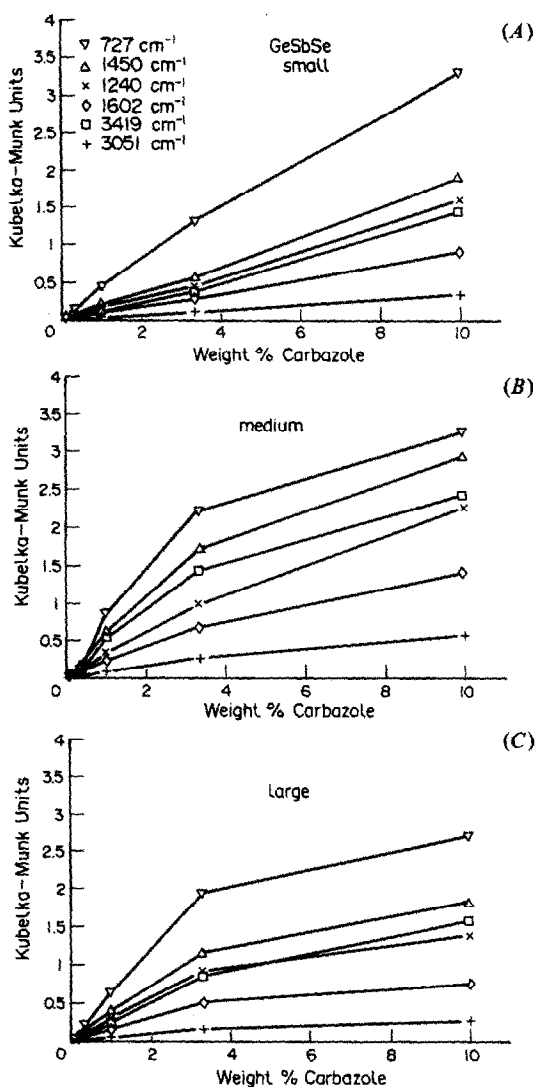


Fig. 6. The Kubelka-Munk intensity of six bands in the DRIFT spectrum of carbazole diluted in $\text{Ge}_{28}\text{Sb}_{12}\text{Se}_{60}$. Particles of carbazole and $\text{Ge}_{28}\text{Sb}_{12}\text{Se}_{60}$ were (A) between 5 and 10 μm , (B) between 20 and 30 μm , and (C) between 53 and 75 μm in size. The key for all three graphs is given in (A).

in bandwidth and decrease in intensity as the diameter of the spheres is increased from 2 to 32 μm . They state that the bands decrease in intensity because the "absorption constants" decrease as the particle diameter increases, but the cause of this effect is not discussed. The particle size dependence of both the scattering and absorption coefficients means that for weak bands, or very small particles, the intensity of bands will increase with increasing particle size. In the DRIFT spectra of an analyte, *reststrahlen* effects will be observed first with very strong bands. Thus, larger particles of analyte or strongly absorbing analytes, the spectra of

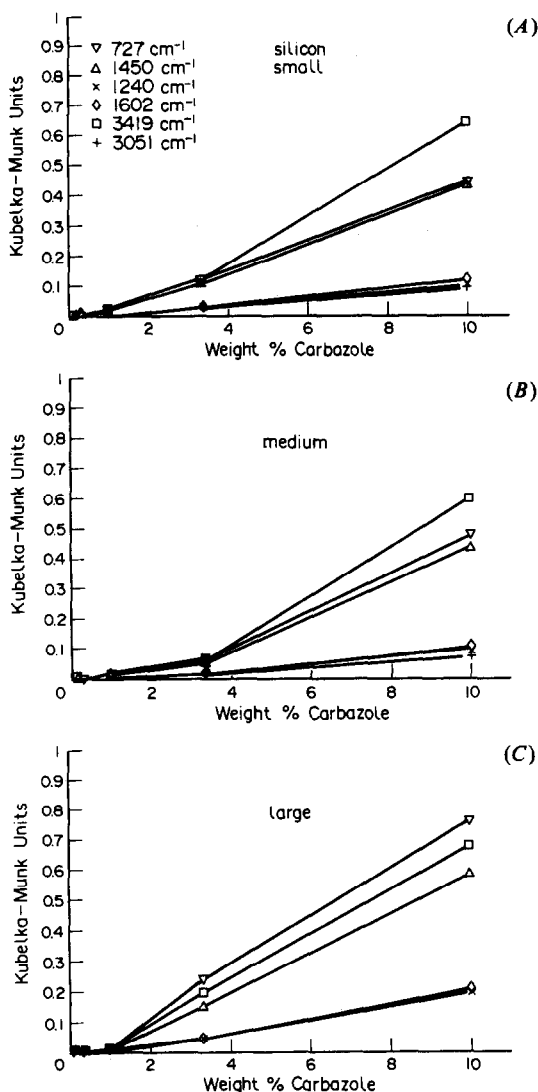


Fig. 7. The Kubelka-Munk intensity of six bands in the DRIFT spectrum of carbazole diluted in silicon. Particles of carbazole and silicon were (A) between 5 and 10 μm , (B) between 20 and 30 μm , and (C) between 53 and 75 μm in size. The key for all three graphs is given in (A).

which would contain relatively strong bands, would be more prone to anomalous dispersion and its attendant diminution of strong spectral features. Chalmers and MacKenzie caution that, since the particle diameter at which the changeover occurs will be different for bands of different intensity, ratios of weak and strong bands will not remain constant as the particle size is altered. Thus, for $\text{C}_{12}\text{H}_9\text{H}:\text{KCl}$ the largest particles give rise to weaker bands than the smaller two particle size ranges of the same mixture; this is most evident for the strongest bands in the spectrum, which as mentioned above are the most susceptible to *reststrahlen* effects.

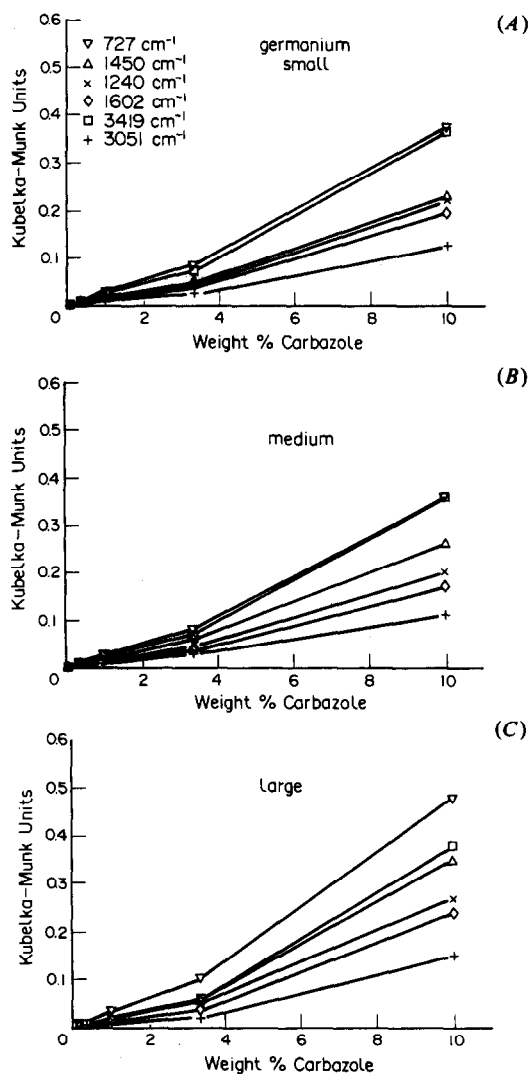


Fig. 8. The Kubelka-Munk intensity of six bands in the DRIFT spectrum of carbazole diluted in germanium. Particles of carbazole and germanium were (A) between 5 and 10 μm , (B) between 20 and 30 μm and (C) between 53 and 75 μm in size. The key for all three graphs is given in (A).

Plots of intensity with respect to the concentration of carbazole in potassium chloride are fairly linear. To measure the linearity of the data, the log of the intensity was plotted against the log of the concentration of carbazole. If the relationship between $f(R_\infty)$ and c were perfectly linear, the slope of the log-log plot would be 1, and for all matrices other than silicon the slope is within 5% of this value, independent of the particle size. The resulting slopes of the log of the intensity *vs.* the log of the weight percent of carbazole in all five matrices are given in Table 2 and shown schematically in Fig. 9.

The slopes of such plots in the small particle size range of potassium chloride for the six

Table 2. Slopes of plot of log(intensity) *vs.* log(concentration)

Matrix	Particle size	Band position, cm^{-1}					
		3419	3051	1602	1450	1240	727
Potassium chloride	5–10 μm	1.04	1.13	1.00	1.05	1.00	1.02
	20–30 μm	1.00	1.12	1.02	1.06	0.96	1.09
	53–75 μm	1.01	0.97	1.05	1.00	0.98	1.07
Diamond	5–10 μm	0.92	0.91	1.03	0.95	0.94	0.96
	20–30 μm	0.99	1.07	0.99	1.01	1.02	0.96
	53–75 μm	1.03	1.05	1.03	0.99	1.04	0.95
$Ge_{28}Sb_{12}Se_{60}$	5–10 μm	1.01	1.00	0.94	0.94	0.95	0.95
	20–30 μm	1.04	0.83	0.86	0.86	0.89	1.05
	53–75 μm	1.33	0.85	0.92	0.98	0.95	1.17
Silicon	5–10 μm	1.44	1.42	1.38	1.51	1.30	1.64
	20–30 μm	1.43	1.29	1.27	1.46	1.35	1.54
	53–75 μm	1.42	1.49	1.59	1.33	1.31	1.17
Germanium	5–10 μm	1.02	1.06	1.06	0.99	1.12	0.97
	20–30 μm	1.11	0.99	1.05	1.07	1.06	0.97
	53–75 μm	1.11	1.09	1.08	1.00	1.12	1.14

bands of carbazole listed in Table 1 ranged from 1.00 to 1.13; for the medium and large particle size potassium chloride corresponding ranges are 0.96 to 1.09 and 0.97 to 1.07, respectively. Overall, the slopes indicate a minor positive deviation from linearity, but the more intense bands display slight negative non-linearity due to saturation at the higher concentrations of carbazole. For carbazole mixed with diamond, which has a refractive index of 2.4, the graphs of band intensity *vs.* concentration are shown in Fig. 5. The difference in the maximum ordinate of the plots in Figs. 4 and 5 immediately indicates that the analyte bands are more than twice as weak when diamond is used as a matrix instead of potassium chloride. The medium sized particles yield slightly more intense bands than the small ones, with the large particles giving the weakest absorptions.

The same trend is shown in Fig. 6 for the data with $Ge_{28}Sb_{12}Se_{60}$ as the diluent matrix. For the chalcogenide glass diluent, there is a pronounced negative deviation in the plot of intensity *vs.* concentration, exceeding that seen for any other matrix used in this study. For the smaller particle size range, linearity is maintained quite well for all bands. For the larger two particle size ranges however, significant non-linearity is shown for concentrations of carbazole of 3 wt. % and above. The $Ge_{28}Sb_{12}Se_{60}$ glass is exceedingly brittle, and it is possible that sample morphology effects are the cause of this non-linearity.

The corresponding plots for carbazole diluted in silicon and germanium are shown in Figs. 7 and 8, respectively. The band intensities are

approximately equal for all particle sizes for both matrices. Unlike the three matrices of lower refractive index, the intensity of bands in the spectra deviate strongly in a positive direction with increasing concentration. The stronger bands exhibit an increased intensity with increasing particle size, probably because of the effect of anomalous dispersion. As the fraction of carbazole grows, the overall refractive index of the sample decreases. By the time the concentration of carbazole is 10 weight percent, there are enough analyte particles on the surface of the sample that a significant fraction of the incident radiation will penetrate into the sample, and hence be absorbed more strongly by the analyte. With a greater proportion of carbazole particles in the sample, there is a greatly increased probability of the infrared radiation interacting with a carbazole particle rather than being reflected out of the sample by a germanium or silicon particle. This effect is important for concentrations of carbazole as low as 3 weight percent for particle diameters between 53 and 75 μm .

Band intensities of carbazole in four of the five matrices decrease with increasing refractive index of the matrix. The exception to this trend is diamond, for which the band intensities are between that of $Ge_{28}Sb_{12}Se_{60}$ and silicon. The anomaly is best explained by considering the packing characteristics of potassium chloride, diamond and $Ge_{28}Sb_{12}Se_{60}$. Unlike diamond, both potassium chloride and $Ge_{28}Sb_{12}Se_{60}$ compress easily and compactly, forming a cohesive mass in the sample cup. Diamond particles show little affinity for one another, and do not

pack well; this is especially true for the medium and large particle size ranges used in this study. Yeboah *et al.* have demonstrated that increased compactness of DRIFT sample leads to increased band intensities in the resulting spectrum.³⁰ Since both potassium chloride and $\text{Ge}_{28}\text{Sb}_{12}\text{Se}_{60}$ are so easily compressed, carbazole dispersed in these materials will be at a higher packing density, leading to more intense bands for those two matrices. Thus, the effect on the scattering coefficient of the decrease in refractive index from $\text{Ge}_{28}\text{Sb}_{12}\text{Se}_{60}$ to diamond is offset by the result of a greater packing density.

CONCLUSION

The choice of the ideal matrix for use in diffuse reflectance infrared Fourier transform spectroscopic measurements depends upon the samples to be studied. If samples can be made with the analyte at concentrations of about 1 weight percent, or if only qualitative information is sought, all five matrices can yield good results. If the analyte is only weakly absorbing or if the concentration is too low, the use of silicon and germanium should be avoided since band intensities may fall below the level of noise in the spectrum. For working over a wide range of concentrations of analyte, potassium chloride, diamond or chalcogenide glass of small particle size is the best selection. From concentrations of 0.1 to 10 weight percent of carbazole in these three matrices of small particle size, the intensity of all but the strongest bands increased linearly with increasing concentration. If potassium chloride is employed as a diluent, small particles (less than 30 μm in diameter) yield optimal spectra, but particles up to 75 μm in diameter provide acceptable results. Diamond of only the smallest particle size range is suitable for use, since the larger particle sizes are extremely difficult to pack reproducibly. Large particles of chalcogenide glass are not recommended because of the highly non-linear relationship between concentration and intensity for particles greater than 20 μm in diameter. If a wide range of analyte particle sizes will be encountered, the choice is narrowed to powdered alkali halides, such as potassium chloride. Band intensity changes between the three different particle size ranges of carbazole and diamond preclude the use of diamond as a matrix. The chalcogenide glass is a suitable matrix for use in the TLC/DRIFT accessory since analyte bands are not severely attenuated in comparison

to spectra acquired with potassium chloride as the matrix, band intensities vary linearly with the low concentrations encountered in such an application, and the material is nonhygroscopic.

Acknowledgement—We thank the Department of Energy for support under Grant No. DE-FG22-87PC79907.

REFERENCES

1. M. P. Fuller, I. M. Hamadeh, P. R. Griffiths and D. E. Lowenhaupt, *Fuel*, 1982, **61**, 529.
2. M. L. E. TeVrucht and P. R. Griffiths, *Energy and Fuels*, 1989, **3**, 522.
3. S. R. Culler, M. T. McKenzie, L. J. Fina, H. Ishida and J. L. Koenig, *Appl. Spectrosc.*, 1984, **38**, 791.
4. F. J. Bergin, *ibid.*, 1989, **43**, 511.
5. R. A. Spragg, *Anal. Chem.*, 1984, **38**, 604.
6. R. T. Graf, J. L. Koenig and H. Ishida, *ibid.*, 1984, **56**, 773.
7. M. T. McKenzie, S. R. Culler and J. L. Koenig, *Appl. Spectrosc.*, 1986, **38**, 786.
8. A. Tsuge, Y. Uwamino and T. Ishizuka, *ibid.*, 1986, **40**, 310.
9. R. S. Shreedhara and D. E. Leyden, *Anal. Chem.*, 1986, **58**, 1228.
10. M. P. Fuller and P. R. Griffiths, *ibid.*, 1978, **50**, 1906.
11. M. Kaihara, H. Mametsuka, N. Gunji, H. Iwata and Y. Gohshi, *Appl. Spectrosc.*, 1989, **43**, 477.
12. P. R. Griffiths and M. P. Fuller, in *Advances in Infrared and Raman Spectroscopy*, Vol. 9, R. J. H. Clark and R. E. Hester (eds.), pp. 75, 76, 81, 82. Heyden & Son, London, 1982.
13. T. Iwaoka, S.-H. Wang and P. R. Griffiths, *Spectrochim. Acta*, 1985, **41A**, 37.
14. M. L. E. TeVrucht and P. R. Griffiths, *Appl. Spectrosc.*, 1989, **43**, 1293.
15. J. M. Brackett, L. V. Azarraga, M. A. Castles and L. B. Rogers, *Anal. Chem.*, 1984, **56**, 2007.
16. D. Kuehl and P. R. Griffiths, *J. Chromatogr. Sci.*, 1979, **17**, 471.
17. D. T. Kuehl and P. R. Griffiths, *Anal. Chem.*, 1980, **52**, 1934.
18. P. R. Griffiths and C. M. Conroy, *Adv. Chromatogr.*, 1986, **25**, 105.
19. S. G. Bush and A. J. Breaux, *Mikrochim. Acta*, 1987 **1**, 17.
20. P. R. Griffiths, M. L. E. TeVrucht and F. Bet-Pera, in *Advances in Coal Spectroscopy*, H.L.C. Meuzelaar (ed.), Plenum Publishing Co., New York, 1991.
21. K. H. Shafer, P. R. Griffiths and W. Shu-Qin, *Anal. Chem.*, 1986, **58**, 2708.
22. P. Klocek, M. Roth and D. Rock, *SPIE Proc.*, 1985, **572**.
23. R. N. Ibbett, *Ph.D. dissertation*, University of East Anglia, 1988.
24. J. M. Chalmers and M. W. Chalmers and M. W. MacKenzie, in *Advances in Applied Fourier Transform Infrared Spectroscopy*, M. W. MacKenzie (ed.), pp. 145–150. Elsevier, Wiley and Sons, Chichester, 1988.
25. D. J. J. Fraser and P. R. Griffiths, *Appl. Spectrosc.*, 1990 **44**, 193.

26. D. J. J. Fraser, K. L. Norton and P. R. Griffiths, *Anal. Chem.*, 1990, **62**, 308.
27. J. M. Olinger, Ph.D. dissertation. University of California, Riverside, 1989.
28. M. L. E. TeVrucht and P. R. Griffiths, *Appl. Spectrosc.*, 1989, **43**, 1492.
29. G. Kortum, *Reflectance Spectroscopy: Principles, Methods, Applications*, p. 111. Springer-Verlag, New York, 1969.
30. S. A. Yeboah, S.-H. Wang and Peter R. Griffiths, *Appl. Spectrosc.*, 1984, **38**, 259.

DETERMINATION OF TRACE AMOUNTS OF A PROTEOLYTIC ENZYME BY FIA WITH A STOPPED-FLOW AND AN ON-LINE PRECONCENTRATION TECHNIQUE

THOMAS GÜBELI,* JAROMIR RŮŽIČKA† and GARY D. CHRISTIAN

Department of Chemistry, BG-10, University of Washington, Seattle, Washington 98195, U.S.A.

(Received 9 January 1991. Revised 19 February 1991. Accepted 20 February 1991)

Summary—An automated method for the determination of small amounts of proteolytic enzymes has been developed, by combining a stopped-flow and an on-line preconcentration technique, using sorbent extraction. It is based on the hydrolysis of a synthetic chromogenic substrate during the stopped-flow period, yielding *p*-nitroaniline, which is then preconcentrated on a C-18 column. The *p*-nitroaniline is then eluted from the column to the spectrophotometer flow cell with methanol. In operation, the substrate solution (500 μ l) is injected into 0.1M tris-HCl buffer carrier and merged with the sample stream. The mixed plug is stopped in a waterbath, kept at constant temperature, for reaction. The operation of the manifold, including data acquisition, is controlled by a personal computer. Optimal parameters were 40°C, pH 8.3, a substrate concentration of 5 mM and wavelength 400 nm. The detection limit, using a 30 min stopped-flow reaction time, is 0.1 μ U protease/ml. The method is intended to be used in combination with portable low volume air samplers for monitoring workplace enzyme dusts in the detergent industry.

Proteolytic enzymes are widely used in the detergent industry. They are added to washing products to remove protein-based stains. These enzymes belong to the group of the subtilisins that are alkaline serine proteases originating from various strains of *Bacillus*.¹ Today only detergent enzyme granulates with a very low enzyme dust content are marketed and it is essential that sensitive analytical methods are developed to control the low enzyme dust levels under operating conditions. The American Conference of Governmental Industrial Hygienists (ACGIH) has established a ceiling limit of 0.06 μ g/m³ for pure airborne enzyme dust,² a level presently not satisfactorily measured by any analytical method. The aim of this work was to develop a flow-injection preconcentration technique for the enhancement of an existing spectrophotometric method applicable for monitoring enzyme dust at the workplace.

The described method is sensitive enough to allow the use of low air sampling volumes and short sampling times. The investigated enzyme is an endoproteinase of the serine type (Savinase™, Novo-Nordisk, Denmark). The

method relies on the proteolytic hydrolysis of a *p*-nitroanilide substrate (N-succinyl-L-alanyl-L-alanyl-L-propyl-L-phenylalanyl-*p*-nitroanilide), yielding the yellow chromophore *p*-nitroaniline (Fig. 1). This substrate has already been used for the determination of various enzymes such as chymotrypsin,³ human leukocyte elastase and cathepsin G,⁴ and detergent enzymes.⁵ The last report proved the suitability of the substrate for the analysis of small quantities of detergent proteases in the presence of high levels of surfactants. In order to achieve the highest sensitivity in the present study, important parameters such as temperature, pH, kinetic constants and wavelength were studied and optimized.

Flow-injection analysis (FIA) has proved its versatility and suitability for automation since its development by Růžička and Hansen in the mid-1970s in several hundred publications.⁶ The novel manifold described here is based on reversed FIA, stopped-flow and preconcentration by means of sorbent extraction; the substrate solution is injected into a buffer carrier solution and then merged with the sample stream. The flow is stopped for 5–30 min to allow reaction, and then the *p*-nitroaniline product is preconcentrated on a C-18 column. It is eluted with methanol to a spectrophotometric detector. The control of all devices by a computer allows

*Department of Pharmacy, University of Bern, Baltzerstr. 5, CH-3012 Bern, Switzerland.

†Author for correspondence.

N-Succ-L-Ala-L-Ala-L-Pro-L-Phe-pNA

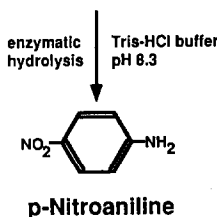


Fig. 1. Schematic diagram of the proteolytic reaction of the enzyme with the substrate yielding the yellow chromophore *p*-nitroaniline.

automated performance of the analysis. Column preconcentration techniques have been used for the analysis of trace amounts of metals^{7,8} as well as anionic species.⁹

EXPERIMENTAL

Reagents

All chemicals were of analytical-reagent grade and demineralized water was used throughout. Methanol (HPLC grade), calcium chloride dihydrate and dimethylsulfoxide were obtained from Baker, Phillipsburg, NJ. N-Succinyl-L-alanyl-L-alanyl-L-propyl-L-phenylalanyl-*p*-nitroanilide, *p*-nitroaniline, and tris[hydroxymethyl]aminomethane were obtained from the Sigma Chemical Company, St Louis, MO. The protease (SavinaseTM), with an activity of 3.46 U/g, was provided by Novo-Nordisk, Denmark. The activity units are Novo internal units (kilo Novo protease unit) expressed as units per gram of enzyme powder and are measured relative to a Novo-Nordisk enzyme standard by a procedure with N,N-dimethylcasein (DMC) substrate and trinitrobenzenesulfonic acid (TNBSA) reagent that reacts with the product.^{10,11} The enzyme powder contained 1% of pure active enzyme.

All FIA and other assays were conducted by using a Tris buffer solution containing 0.1M Tris in 0.01M calcium chloride, adjusted to pH 8.3 at room temperature with 1N hydrochloric acid, unless otherwise stated. The sample, the carrier stream and the substrate solution were prepared in the same buffer and filtered through a Whatman filter No. 5 (2.7- μ m pore size) prior to use. A 12.5mM stock solution of the substrate was prepared by dissolving it in DMSO. Substrate working solutions were produced by appropriate dilution of the stock solution with Tris-hydrochloric acid buffer. Enzyme solutions in the range 0.1–10 μ U/ml were prepared by a two-step dilution of a 5-mU/ml buffered stock

solution, using Tris-HCl buffer for dilution. All solutions were stored at 4° when not in use.

Apparatus

A schematic diagram of the flow-injection manifold is shown in Fig. 2(a). The peristaltic pumps, model C-6V (P1, P2), were obtained from Alitea USA, Medina, WA, and were equipped with PVC pump tubing (0.89 mm i.d., Cole-Parmer, Chicago, IL). Teflon tubing (0.81 mm i.d.) was used for the rest of the system. All streams (sample, carrier and eluent) were propelled at 1 ml/min. Fittings were purchased from Upchurch Scientific (Oak Harbor, WA). The valves (V1, V2) were integrated into a single unit by using an electrically actuated 10-port rotary valve (Valco Instruments, Houston, TX) configured as shown in Fig. 2(b). A Milton-Roy Mini 20 spectrophotometer (Cole-Parmer, Chicago, IL) was used as the detector. The pumps and the valve were controlled by an IBM Data Acquisition and Control Adapter and an IBM PC/AT compatible computer with EGA graphics. The analog signal of the photometer was amplified from 500 mV to 5 V full scale and

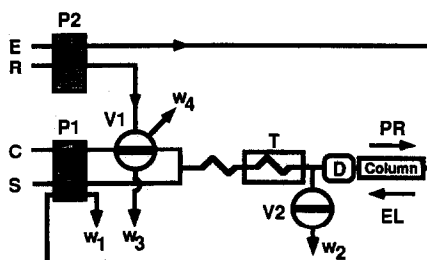


Fig. 2(a). Manifold for the enzyme determination in the inject and preconcentrate position. C, carrier (demineralized water), D, detector, 400 nm, E, eluent (methanol); EL, elution; P1 and P2, peristaltic pumps; PR, preconcentration; R, reagent (substrate); S, sample (enzyme); T, waterbath; V1, V2, injection valves; W1, W2, S3, W4, waste lines.

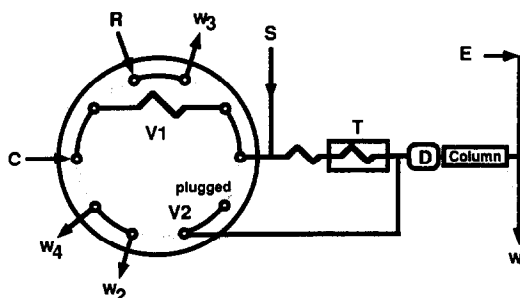


Fig. 2(b). Schematic presentation of the 10-port injection valve in the inject position. The valve comprises the two valves V1 and V2 of the manifold. To go to the load position, the valve is turned clockwise to the position of the dotted lines.

digitized with a 12 bit A/D converter of the IBM board. A menu-driven program written in house based on Microsoft Fortran version 4.1 and 5.0 and Microsoft Macro Assembler version 5.1 allowed the precise control of the pumps and valve, and the collection and treatment of data.¹² Batch spectrophotometric and spectral measurements were made with a Hewlett-Packard 8452A Diode Array Detector.

Procedures

Enzyme activity determination. Batch enzymatic reactions for determining activities were initiated by adding 0.25 ml of substrate working solution to 1 ml of buffered enzyme solution with thorough mixing. Relative reaction rates under different operating conditions for a fixed concentration of enzyme are simply expressed as absorbance units per minute (AU/min) at a pathlength of 10 mm. The absorbance of the *p*-nitroaniline produced was measured continuously, except where otherwise noted.

Temperature influence. A 1.5- μ U/ml enzyme solution in the Tris-HCl buffer, pH 8.0 was used for temperature studies. The reaction rate was determined by recording the absorbance between 1 and 30 min. At 44°, a three point measurement was made (10, 20 and 30 min).

Wavelength and pH value dependence. Absorbance spectra at different pH values were obtained with the diode array detector. Readings were taken at two minute intervals from 2.5 to 28.5 min.

Kinetic constants. The determination of the Michaelis constant, K_m , was conducted at 30° and pH 8.3, with duplicate measurements of the initial reaction velocity at four different substrate levels between 0.25 and 2mM, using a conventional batch technique. The concentration of the enzyme solution was 1 μ U/ml.

Preconcentration of *p*-nitroaniline. A manifold with a peristaltic pump operated at a flow-rate of 1 ml/min, a Perspex column (7 mm \times 2 mm i.d.) filled with 10 mg of C-18 material (40 μ m particle size, Analytichem International, Harbor City, CA) and the diode array detector were used to measure the retention efficiency. Prior to the loading of the *p*-nitroaniline solution (2.5 μ g/ml in Tris-HCl buffer, pH 8.3) the column was activated with approximately 200 μ l of methanol and rinsed with the same volume of Tris-HCl buffer. The *p*-nitroaniline solution was pumped continuously and the unretained amount was measured as it passed through the detector. Absorbance data acquisition was

started 19 seconds after the *p*-nitroaniline solution reached the column.

Operation of the FIA system. The FIA system employed is shown in Fig. 2(a). It has the following functions: inject, mix, incubate, pre-concentrate, elute and monitor. Two peristaltic pumps (P1 and P2) were used to propel the sample (S), buffer (C) and methanol (E) streams as well as to fill the injection loop of valve V1 with reagent (R). The reagent (500 μ l, 5mM substrate) was injected into a carrier stream (Tris-hydrochloric acid buffer), merged with the sample stream (enzyme solution), mixed in a knotted reactor (100 cm \times 0.81 mm i.d.) and subsequently propelled into a reaction coil (240 cm \times 0.81 mm i.d.) placed in a waterbath (T) held at 40°. The mixed zone was stopped there for an incubation time of 5–30 min. Next, the pump (P1) was started again, the hydrolysis product (*p*-nitroaniline) was initially monitored while passing through the detector D (peak A, Fig. 3), and then it was retained on the column packed with C-18. The spent stream left the system through waste line W1. When the retention step (PR) was completed, pump P1 was stopped, and the valve (V1) turned to the load position [see Fig. 2(b)], thereby also opening valve V2 and the waste line W2. Pump P2 was activated and the preconcentrated *p*-nitroaniline eluted (EL) with methanol in a countercurrent mode and subsequently detected (peak B, Fig. 3), leaving at W2. Simultaneous with the elution, the reagent loop was filled again.

Construction of the column and the detector flow cell is shown in Fig. 4. The C-18 cartridges as designed for the Varian Advanced Auto-

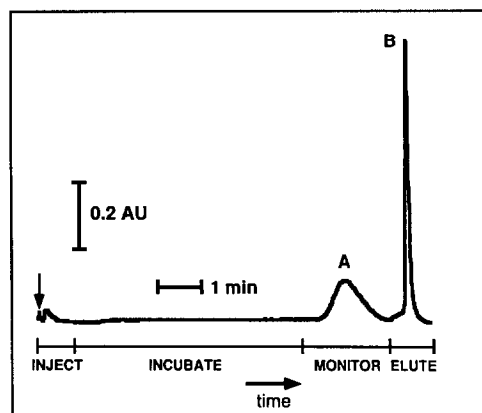


Fig. 3. Typical readout of an assay with an enzyme activity of 5 μ U/ml. Injection volume was 500 μ l (5mM substrate solution). A, monitored signal prior to preconcentration; B, signal of eluted *p*-nitroaniline following preconcentration (reverse flow).

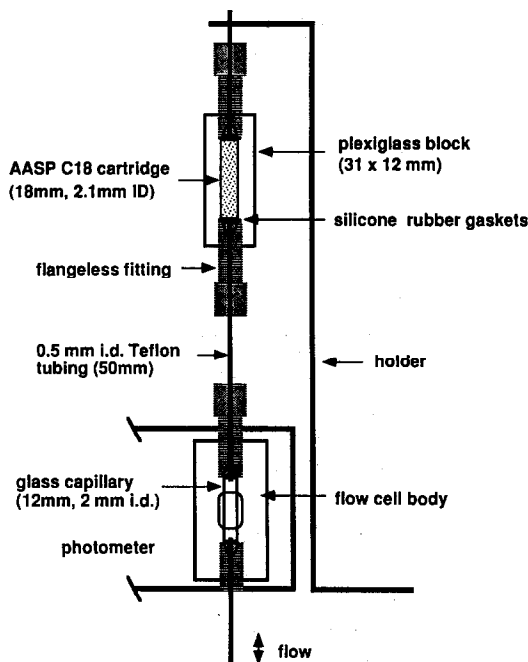


Fig. 4. Preconcentration and detection components.

mated Sample Processor [AASP (13)] cleanup system are available as cassettes consisting of 10 items. For the present use, an individual cartridge was cut off this assembly and mounted in the flow-injection system as shown in Fig. 4.

RESULTS AND DISCUSSION

In order to achieve the required sensitivity for the method, the most important parameters influencing the proteolytic activity were investigated and optimized. The effect of temperature is shown in Fig. 5. At a reaction time of 30 min the reaction rate, expressed in absorbance units per minute, was increased by a factor of 1.44

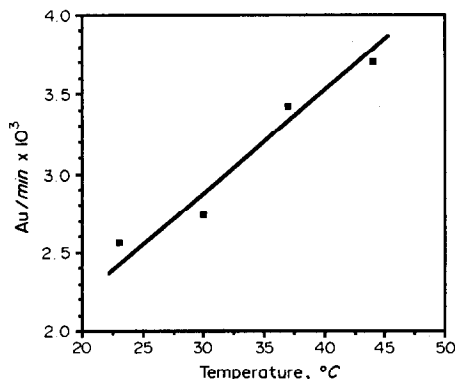


Fig. 5. Effect of temperature on the activity of the proteolytic enzyme. The reaction rate, expressed in absorbance units per minute (AU/min) is based on a reaction time of 30 minutes and an enzyme activity of $1.5 \mu\text{U/ml}$.

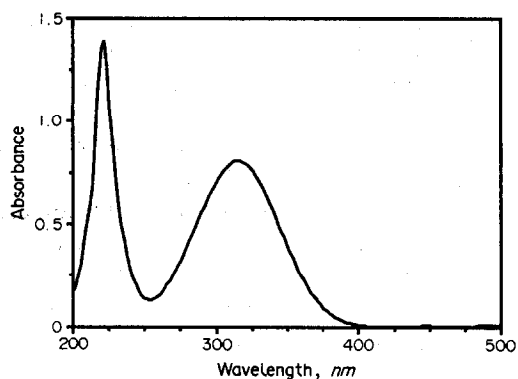


Fig. 6(a). Spectrum of the substrate at pH 8.3. Absorbance maximum is at 315 nm.

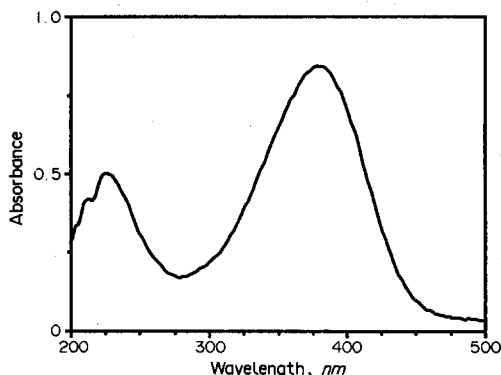


Fig. 6(b). Spectrum of *p*-nitroaniline at pH 8.3. Absorbance maximum is at 382 nm.

when the temperature was changed from 23 to 44° . Higher temperatures can be chosen with this enzyme but this increases the probability of building air bubbles in the FIA-system.

Absorption maxima for the substrate and the *p*-nitroaniline at pH 8.3 are at 315 nm and 382 nm, respectively, as seen in Fig. 6. The dependence of the reaction rates on pH is shown in Fig. 7. From this (curve fitted) figure it can be

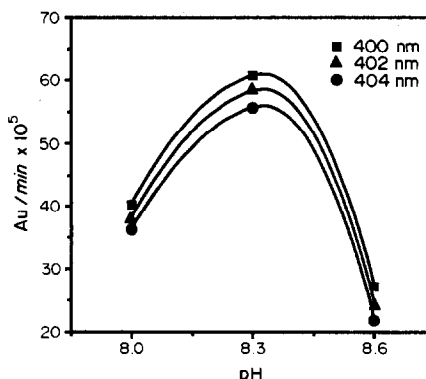


Fig. 7. Wavelength and pH value dependence of the measured reaction rate (AU/min) of a $1 \mu\text{U/ml}$ enzyme solution at 22°C . Readings were taken every two minutes during a reaction time of 28.5 minutes.

seen that the optimum pH is near 8.3 and a wavelength of 400 nm is superior to higher wavelengths while still having sufficiently low blank values [see Fig. 6(a)]. The molar absorptivity of *p*-nitroaniline at 400 nm was determined to be 1.18×10^4 l. mole⁻¹ cm⁻¹ ($n = 3$, pH 8.3). The significant changes of the apparent reaction rates with pH are due to changes in enzyme activity and changes in the molar absorptivity of *p*-nitroaniline. The absorptivity increases by 1.2% from pH 8.0 to 8.3 and by 3.5% from pH 8.3 to 8.6.

The determination of the Michaelis constant K_m was performed at 4 different substrate levels. Using a Lineweaver-Burk plot, K_m was calculated to be 0.53 mM and V_{max} (maximum reaction velocity) for a $1\text{-}\mu\text{U/ml}$ enzyme activity to be 5.2×10^{-3} AU/min ($R = 0.992$). Since the substrate has a limited solubility of approximately 10 mM in Tris-hydrochloric acid buffer³ and the blank value (see Fig. 8) from overlap with the *p*-nitroaniline spectrum should be as low as possible, a concentration of 5 mM was chosen for the experiments.

The preconcentration experiment (Fig. 9) showed that the capacity of C-18 for *p*-nitroaniline is about 0.5 μg (3.6 nmol) for a sorbent mass of 10 mg, with a loss of $<2\%$. However, the retention efficiency diminishes at higher quantities of *p*-nitroaniline, which results in a non-linear calibration curve (Fig. 8). The capacity for the co-retained substrate is about 475 nmole for a loss of $<2\%$. The retention of the *p*-nitroaniline did not appear to be affected by the presence of the substrate.

A typical recording using the described manifold with an incubation time of 5 minutes is shown in Fig. 3. The peak obtained with preconcentration (peak B) is much narrower and more

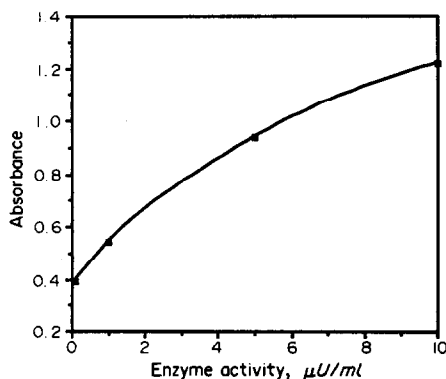


Fig. 8. Plot of the peak height of the preconcentrated reaction products vs. enzyme activity. Stop time: 5 min at 40° .

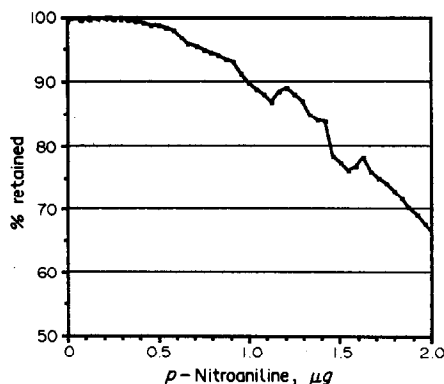


Fig. 9. Retention efficiency of a C-18 column (10 mg, 7×2 mm i.d.) for *p*-nitroaniline. The flowrate was 1 ml/min and the pNA concentration 2.5 $\mu\text{g/ml}$ (Tris-HCl buffer pH 8.3).

than a factor of seven higher than the peak obtained without preconcentration (peak A), thus yielding a sensitivity increase of at least the same magnitude. As seen from this recording, obtained with an enzyme activity of 5 $\mu\text{U/ml}$, a direct measurement without preconcentration would be sufficient. For low activities of 0.1 $\mu\text{U/ml}$, corresponding to the desired sensitivity, a preconcentration step is necessary to achieve a satisfactory signal-to-noise ratio. The calibration graph (Fig. 8) shows that the response curve is not linear. However, by increasing the amount of C-18 to increase the retention capacity, an extended linear relationship can be obtained if desired. Relative standard deviations of net sample signals of the typical two to three repetitive injections were 2.8 – 17% . The sampling frequency is dependent upon the selected incubation time and ranges from 1.7 to 6 samples/hr (incubation time: 5 to 30 min). More than 60 injections were performed without having to change the pump tubings or the column. The detection limit for the protease, with a reaction time of 30 min (40°), is about 0.1 $\mu\text{U/ml}$. Since the Novo-Nordisk protease standard used in this work has an activity of 3.46 U/g and contains 1% of pure active enzyme, this value corresponds to 0.29 ng enzyme/ml. Therefore to achieve the ACGIH limit of 0.06 μg pure enzyme/ m^3 air, the enzyme dust contained in 4.8 litres of air has to be trapped quantitatively in 1 ml of aqueous solution. Battery operated low volume air samplers with Midget impingers¹⁴ may fulfill this purpose.

CONCLUSIONS

The proposed method allows an automated and sensitive determination of extremely low

activities of detergent proteases in solution, and has the potential for continuous monitoring of enzyme dust in the industrial environment. Future work is intended to enhance the performance of the system by implementing double injection and syringe based pumps^{15,16} which will allow interrupted operation of the flow injection system for several thousands of measurements. However, the low sampling frequency of the method will be difficult to overcome due to the necessity of long incubation times. To circumvent this problem and to enhance the sensitivity of the method even more, studies will be made to preconcentrate not only the products of the enzymatic reaction but the enzyme as well on a suitable solid support.

Acknowledgements—The authors express their gratitude to Novo-Nordisk, Denmark, for supporting the project and T.G. thanks the National Science Foundation of Switzerland for a research grant during his visit to the University of Washington.

REFERENCES

1. M. Ottesen and I. Svendsen, in *Methods of Enzymatic Analysis*, H. U. Bergmeyer, J. Bergmeyer and M. Grassl (eds.), 3rd Ed., Vol. 5, p. 159. Chemie, Weinheim, 1984.
2. American Conference of Governmental Industrial Hygienists, *Threshold Limit Values and Biological Exposure Indices*, Cincinnati, OH, 1988.
3. E. G. DelMar, C. Largman, J. W. Brodrick and M. C. Geokas, *Anal. Biochem.*, 1979, **99**, 316.
4. K. Nakajima, J. C. Powers, B. M. Ashe and M. Zimmerman, *J. Biol. Chem.*, 1979, **254**, 4027.
5. T. M. Rothgeb, B. D. Goodlander, P. H. Garrison and L. A. Smith, *J. Am. Oil. Chem. Soc.*, 1988, **65**, 806.
6. J. Růžička and E. Hansen, *Flow-Injection Analysis*, 2nd Ed., Wiley, New York, 1988.
7. S. D. Hartenstein, J. Růžička and G. D. Christian, *Anal. Chem.*, 1985, **57**, 21.
8. S. D. Hartenstein, G. D. Christian and J. Růžička, *Can. J. Spectrosc.*, 1985, **30**, 144.
9. N. Lacy, J. Růžička and G. D. Christian, *Anal. Chem.*, 1990, **62**, 1482.
10. E. Dunn and R. Brotherton, *Analyst*, 1971, **96**, 159.
11. Novo-Nordisk, Denmark, *Internal Rep. No. AF 220/1-GB*.
12. G. D. Clark, G. D. Christian, J. Růžička, G. F. Anderson and J. A. van Zee, *J. Anal. Instrumentation*, 1989, **18**, 1.
13. V. Berry, *CRC Crit. Rev. Anal. Chem.* 1989, **21**, 115.
14. R. M. Harrison and R. Perry, *Handbook of Air Pollution Analysis*, 2nd Ed., Chapman & Hall, New York, 1986.
15. J. Růžička and G. D. Marshall, *Anal. Chim. Acta*, 1990, **227**, 329.
16. J. Růžička, G. D. Marshall and G. D. Christian, *Anal. Chem.*, 1990, **62**, 1861.

INDIRECT DETERMINATION OF THE PESTICIDE DIMETHOXYDITHIOPHOSPHATE IN AN FIA-AAS SYSTEM WITH LIQUID-LIQUID BACK-EXTRACTION

ORONCIO JIMENEZ DE BLAS, JOSE LUIS PEREDA DE PAZ and JESUS HERNANDEZ MENDEZ
Department of Analytical Chemistry, Nutrition and Food Science, University of Salamanca,
37008 Salamanca, Spain

(Received 14 November 1989. Revised 14 February 1991. Accepted 19 February 1991)

Summary—A method has been developed for the determination of dimethoxydithiophosphate (DDTP) by liquid-liquid extraction in a flow-injection analysis (FIA) system with detection by atomic-absorption spectrometry (AAS). It is based on the formation of the Cu(DDTP)_2 complex and its extraction into chloroform, and back-extraction of the copper with an ammonia buffer (pH 10). The method uses small amounts of samples, avoids handling errors and is fast and highly reproducible. It features a detection limit of 0.39 ppm DDTP ($2.45 \times 10^{-6} M$ in the organic phase) and a relative standard deviation of 1.6%. The method has been applied to the determination of the organophosphorus pesticide malathion in an agricultural formulation.

The development of sensitive, selective and fast methods for the determination of pesticides is mandatory nowadays on account of the broad use of these compounds. A major group consists of the organophosphorus pesticides derived from dimethoxydithiophosphate (DDTP). The methods developed for determination of DDTP can equally be applied to the determination of these pesticides once the optimum hydrolysis conditions for yielding DDTP from them have been found. There are several methods in the literature for the determination of DDTP, including titrimetric,¹ chromatographic,²⁻⁴ spectrophotometric⁵⁻¹¹ and atomic-absorption spectrometric techniques.^{12,13}

The spectrophotometric method reported by Norris *et al.*¹⁴ is imprecise owing to the instability of the Cu(DDTP)_2 complex. An internal reaction occurs, resulting in a reversible equilibrium with colourless copper(I) dimethyldithiophosphate and bis(dimethoxyphosphothiorone) disulphide.¹⁵ Extracting the complex increases its stability and this was exploited in earlier work for the indirect determination of DDTP. However, the extract had to be mineralized¹⁶ or the copper back-extracted into an aqueous phase.¹⁷

This paper reports the use of a continuous extraction FIA-AAS system for determination of DDTP, on the basis of the earlier work mentioned above. The use of back-extraction offers substantial advantages over the batch-

extraction and mineralization methods, namely ease of operation, limited need for laboratory ware, lower sample consumption, good stability in time, immediate phase separation, possibility of automation and avoidance of kinetic problems and various manipulative errors, *etc.*

EXPERIMENTAL

Apparatus

A Varian Techtron AA 1475 atomic-absorption spectrometer furnished with a conventional copper hollow-cathode lamp was used.

Reagents

All reagents were of analytical grade and doubly distilled water was used for dilutions. Methanol solutions of DDTP were prepared from the technical liquid product (82.8% pure). The standard copper solutions were prepared from a 0.020M solution made with electrolytic copper.

Malathion was determined in the agricultural formulation Exathion-4, a spraying powder from Cónдор S.A. Standard malathion solutions in methanol were made from the technical liquid product (91.3% pure) and titrated after alcoholic hydrolysis.¹⁶

FIA-AAS ancillary equipment

The manifolds used are depicted schematically in Fig. 1. The ancillary equipment used

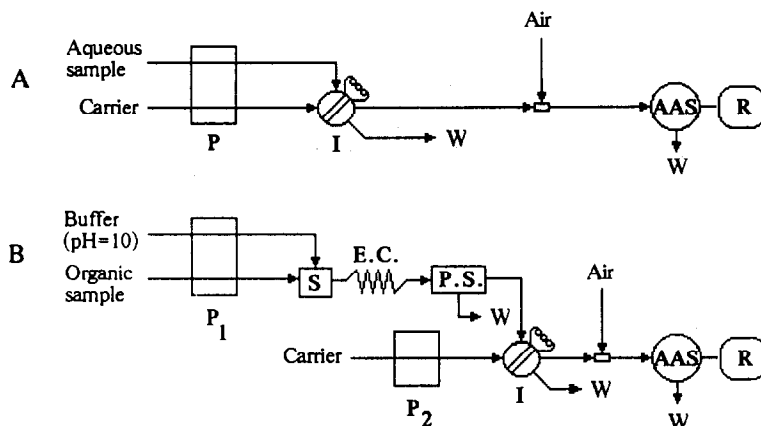


Fig. 1. Flow-injection manifolds used in (A) the determination of copper, and (B) its back-extraction. P, P₁ and P₂, peristaltic pumps; I, injection valve; W, waste; S, segmenter; E.C., extraction coil; P.S., phase separator; R, recorder. Air denotes air compensation.

comprised the following elements; Gilson Minipuls-2 (HP-4) peristaltic pumps fitted with PVC tubes of 0.89 mm i.d. for aqueous phases and Isoversinic fluorinated-plastic tubes of 1 mm i.d. for the organic phase; a Rheodyne 2050 injection valve; a Teflon segmenter, designed and constructed by the authors according to a model reported by Cantwell and Sweileh;¹⁸ a nylon membrane phase-separator, also home-made (Fig. 2); a Millipore HA hydrophilic membrane (0.45 μm pore size).

Measurement of copper standards in the FIA-AAS system

Measurements were made with the manifold depicted in Fig. 1A. Aqueous copper solutions were injected into a carrier stream of doubly distilled water, and the copper was determined by AAS under suitable instrumental conditions. The flow-rate of the carrier and the aspiration rate of the nebulizer of the atomic-absorption spectrometer were air-compensated.^{19,20}

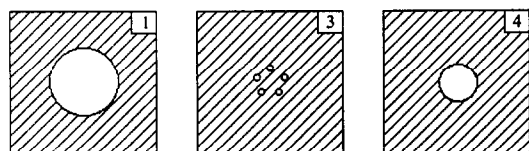
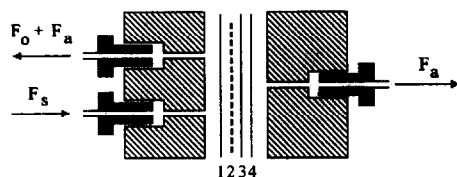


Fig. 2. Detailed view of the phase separator. F_s, segmented flow; F_o, organic stream; F_a, aqueous stream. 1, 3 and 4, Teflon membranes; 2 hydrophilic membrane of 0.45 μm pore size (Millipore HA).

Continuous extraction in the FIA-AAS system

This was studied with the aid of the manifold shown in Fig. 1B. The samples were prepared by extracting the Cu(DDTP)₂ complex into chloroform according to a procedure reported elsewhere.¹⁶ The continuous back-extraction was accomplished with 0.2M NH₄⁺/NH₃ buffer solution (pH 10).¹⁷ The sample and buffer were propelled to the segmenter (S) by a peristaltic pump. The segmented flow was then driven to the extraction coil (EC), where mass transfer took place, and then on to the phase separator (PS). The aqueous phase from the separator filled the injection loop (I), the contents of which were subsequently inserted into a carrier stream (doubly distilled water) which was led to the AA spectrometer nebulizer. The injection of previously separated samples offers the advantage of decreasing their dispersion and hence increasing the sensitivity, notwithstanding the somewhat larger sample volumes required.

The instrumental conditions for the AAS measurements of copper were the same in every case, *viz.* wavelength 324.8 nm, band-pass 0.5 nm, lamp current 3 mA, observation height 11 mm above the burner, air flow-rate 12 l./min and acetylene flow-rate 1.7 l./min.

Procedure

An appropriate amount of DDTP, 3.0 ml of 0.01M nitric acid, 4 ml of chloroform and a small stoichiometric excess of copper were placed in a separatory funnel, which was then shaken for 2 min, and the organic extract was decanted. A further two extractions with 3 ml of chloroform were made.¹⁶ The copper was back-extracted with the 0.2M NH₄⁺/NH₃ buffer

from the samples thus obtained, in the manifold shown in Fig. 1B.¹⁷ The extraction flow-rate was 2 ml/min and a 100-cm knotted reactor was used. The injected volume was 160 μ l and the carrier flow-rate 5 ml/min. The copper was determined under the instrumental conditions described.

RESULTS AND DISCUSSION

Optimization of the measurement of copper in the FIA-AAS system

The FIA-AAS combination is somewhat peculiar as regards dispersion,²¹ as a result of the effect of the nebulizer parameters on the amount of sample aspirated. The flow-rate and the injected volume are the variables which most significantly affect the dispersion;^{22,23} the length and inner diameter of the tubing are less influential, and are frequently overlooked in this type of work. On the other hand, the flow-rates commonly used in continuous extractions (≈ 1 ml/min)²⁴⁻²⁶ must be compatible with the aspiration rates required in atomic-absorption work (5-6 ml/min).

To study the influence of the injected volume on the dispersion volumes of 40, 160 and 245 μ l were used (void volumes not considered). The dispersion decreased with increasing injection volume from 40 to 160 μ l, above which it remained virtually constant. A volume of 160 μ l was therefore chosen for all subsequent experiments.

The influence of the carrier flow-rate on absorbance is illustrated in Fig. 3. The sensitivity

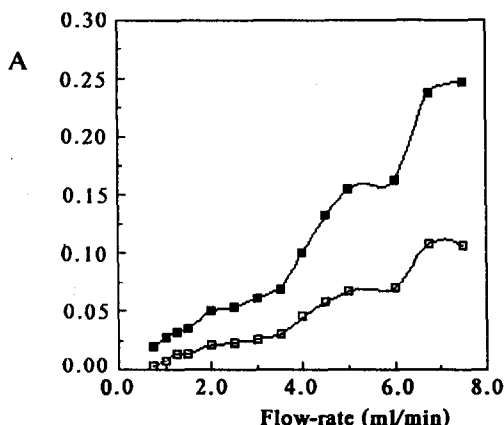


Fig. 3. Influence of the carrier flow-rate on the absorbance of copper: (□) 1.27 ppm Cu (0.125 A with conventional aspiration); (■) 2.54 ppm, Cu (0.256 A with conventional aspiration). The injected volume was 160 μ l in all instances. One carrier stream was used up to 2.75 ml/min, two between 2.75 and 5.0 ml/min, and three between 5.0 and 7.75 ml/min.

Table 1. Influence of the carrier flow-rate on the precision of the measurement of copper in the FIA-AAS system

Flow-rate, ml/min	4.0*	5.0*	6.0†	7.5†
Precision, s, % ($n = 8$, [Cu] = 2.54 ppm)	0.9	0.9	2.2	4.4

*Two carrier lines.

†Three carrier lines.

increases with increasing flow-rate, although rates above 5 ml/min result in pulse problems arising from the peristaltic pump. Table 1 reflects these problems derived from the use of three carrier lines and also shows the variation of the precision with the flow-rate. The carrier flow-rate used to avoid these problems and ensure good precision was 5 ml/min (Fig. 3 and Table 1).

Optimization of the continuous extraction in the FIA-AAS system

The study of the extraction process involved three variables: the type and length of the extraction reactor and the flow-rate. Coiled and knotted reactors were used, and as can be seen in Fig. 4, the extraction yield increased with increasing reactor length. In addition, for a given reactor length, the knotted reactor proved to be more efficient than its coiled counterpart. These results are accounted for by the greater turbulence within knotted reactors, which favours contact between the phases and therefore gives rise to greater mass transfer. Also, the flow-rate appears to affect only the shorter reactors, particularly the 50-cm long coiled reactor. The 100-cm knotted reactor was chosen because although the 300-cm coiled reactor provided higher sensitivity, this did not compensate for the disadvantages of larger amounts of sample and longer determination times

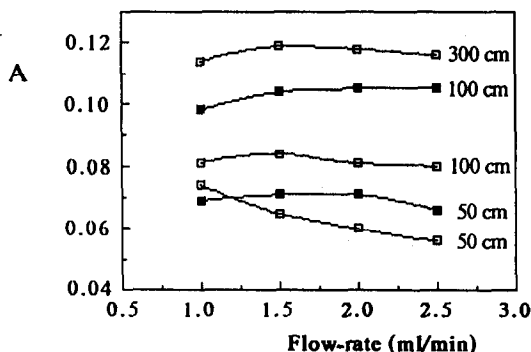


Fig. 4. Influence of the type and length of extraction coil and the flow-rate on the extraction yield: (□) coiled; (■) knotted. The injected volume was 160 μ l and the carrier flow-rate was 4 ml/min in all instances.

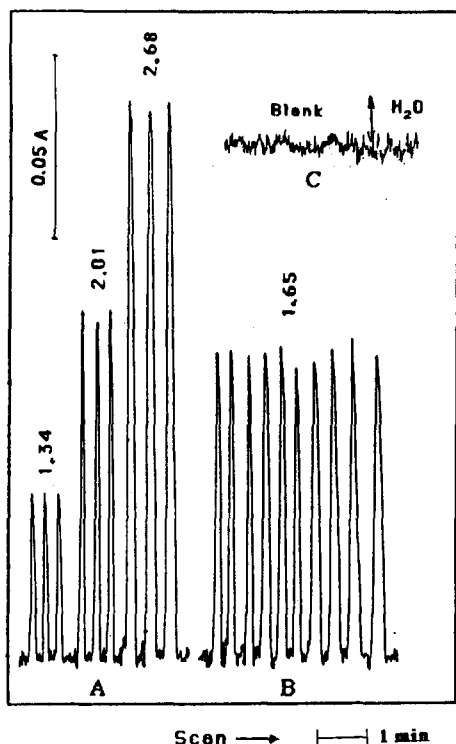


Fig. 5. Calibration peaks obtained upon triplicate injections of three DDTP standards (A) and duplicate injection of one DDTP standard (B), and blank signal (C). The numbers above the peaks denote μmole of DDTP extracted into 25.0 ml of CHCl_3 .

required. The flow-rate selected, 2 ml/min, resulted in a good sampling rate.

Analytical features

By use of the proposed procedure a calibration graph for DDTP was prepared. Figure 5 shows a typical FIA recording obtained from

three injections of each standard. The study of the precision involved 9 injections of a sample obtained by extracting 1.65 μmole of DDTP into 25.0 ml of chloroform ($8.0 \times 10^{-5} M$ in the chloroform solution). The relative standard deviation (rsd) was 1.6%. The detection limit, obtained by applying the 3 s/m criterion,²⁷ was 0.39 ppm DDTP, equivalent to a concentration of $2.45 \times 10^{-6} M$ in the chloroform solution. Table 2 compares the results obtained by the proposed method with those provided by other methods for determination of DDTP^{14,16,17} on the basis of the $\text{Cu}(\text{DDTP})_2$ complex. The proposed method has better analytical features than the standard procedure¹⁴ and although its precision is poorer than that of the back-extraction procedure,¹⁷ the FIA-AAS method is much faster and requires smaller amounts of sample.

Interferences

In previous work¹⁷ interferences with the extraction of the $\text{Cu}(\text{DDTP})_2$ complex were studied. The first group of species considered consisted of some metal ions [$\text{Zn}(\text{II})$, $\text{Fe}(\text{III})$, $\text{Pb}(\text{II})$, $\text{Cu}(\text{II})$ and $\text{Bi}(\text{III})$] which form complexes with DDTP. The serious interference from iron and bismuth can be overcome, although addition of an excess of copper is required.

The second group of species considered comprised certain organophosphorus compounds from different groups of pesticides. Malathion, belonging to the DDTP group, does not interfere as it is not hydrolysed in the acidic medium from which the extraction takes place and hence

Table 2. Analytical features of the determination of DDTP and comparison of methods

Method	Standard (UV-VIS)	Mineralization (AAS)	Back-extraction (AAS)	FIA-AAS
Determination range				
μmole	0.37-7.92	0.01-5.10	0.10-1.80	1.34-2.68
ppm	5.8-125*	0.1-32†	1.6-28†	8.5-17‡
Detection limit				
μmole	0.14	0.006	0.004	0.061
ppm	2.2*	0.04†	0.06†	0.39‡
Precision s_r , %	3.3 ($n = 10$)	1.8 ($n = 10$)	0.8 ($n = 10$)	1.6 ($n = 9$)
DDTP found, μmole §	1.925	1.523	1.530	1.546
S_{n-1} , μmole	0.0635	0.0274	0.0122	0.0251
$F_{\text{experimental}}$ #	6.40	1.19	4.23	
$F_{\text{table}} (95\%)$	3.39	3.39	3.23	
$t_{\text{A}}^{\text{experimental}}$ #	17.42	1.80	1.74	
Degrees of freedom	13	17	14	

*In the final organic solution.

†In the final aqueous solution.

‡In the sample (after extraction into CHCl_3).

§DDTP added, 1.65 μmole in all cases.

Comparison with FIA-AAS method.²⁸

Table 3. Determination of malathion in the agricultural formulation Exathion-4 (4% malathion) ($n = 3$)

Method	Standard (UV-VIS)	Mineralization (AAS)	Back-extraction (AAS)	FIA-AAS
Malathion, %	4.02 \pm 0.18	3.77 \pm 0.07	3.56 \pm 0.03	3.84 \pm 0.12

does not yield DDTP. Some thiophosphate pesticides interfere negatively, which may be due to interferences in the extraction of the complex.¹⁶

Applications

The proposed procedure was applied to the determination of malathion in an agricultural formulation. The optimum hydrolysis conditions to yield DDTP had already been studied,¹⁶ and it was clear that other DDTP group pesticides would interfere with the extraction.¹⁶ The C3ndor S.A. formulation Exathion-4 was used, with a malathion content of about 4%. As preliminary treatment, the active matter was separated by dispersing a known weight (a few grams) of the sample in methanol, filtering, and making up to a given volume with the same solvent. The FIA recordings provided by the malathion standards and the sample are shown in Fig. 6. The results were compared with those obtained by the procedures mentioned above (Table 3). As can be seen, the more precise procedures give malathion contents slightly lower than that stated by the manufacturer. The standard procedure is apparently more accurate, although is not very representative because of its imprecision.

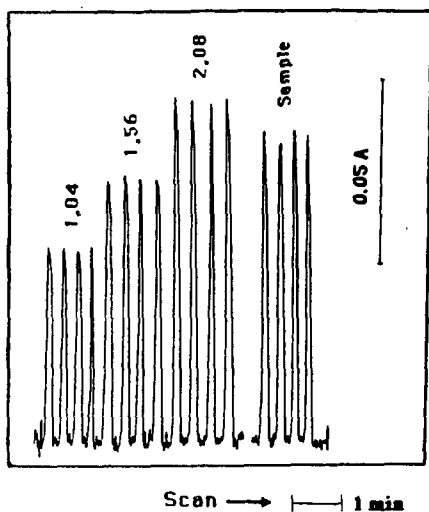


Fig. 6. Recordings obtained for malathion standards and sample. The numbers above the peaks have the same meaning as in Fig. 5.

Acknowledgement—The authors are grateful to Dr. Victor Rodríguez Martín and to Angel Lozano García, for their help in designing and constructing the ancillary equipment used in the continuous extraction FIA-AAS system.

REFERENCES

1. A. C. Hill, M. Akhtar, M. Mumtaz and J. A. Osmani, *Analyst*, 1967, **92**, 496.
2. T. H. Handley and J. A. Dean, *Anal. Chem.*, 1962, **34**, 1312.
3. F. Hirase, G. Saito, M. Nagata and K. Nakamura, *Tokyo Joshi Ika Daigaku Zasshi*, 1979, **49**, 640.
4. C. M. Deshpande and S. S. Bhende, *Indian J. Environ. Prot.*, 1982, **2**, 145.
5. K. Visweswariah and M. Jarayam, *Agric. Biol. Chem.*, 1974, **38**, 2031.
6. M. Syoyama and S. Miyachiki, *Bunseki Kagaku*, 1976, **25**, 179.
7. R. T. Sane and S. S. Kamat, *J. Assoc. Off. Anal. Chem.*, 1982, **65**, 40.
8. N. W. Hanson, *Official, Standardised and Recommended Methods of Analysis*, Society for Analytical Chemistry, London, 1973.
9. E. R. Clark and I. A. Qazi, *Analyst*, 1979, **104**, 1129.
10. *Idem, ibid.*, 1980, **105**, 564.
11. *Idem, Water Res.*, 1980, **14**, 1037.
12. M. H. Jones and J. T. Woodcock, *Anal. Chim. Acta*, 1976, **87**, 463.
13. F. Sánchez Rasero, *J. Assoc. Off. Anal. Chem.*, 1981, **64**, 75.
14. M. V. Norris, W. A. Vail and P. R. Averell, *J. Agric. Food Chem.*, 1954, **2**, 570.
15. A. C. Hill, *J. Sci. Food Agr.*, 1969, **20**, 4.
16. J. Hernández Méndez, O. Jiménez de Blas, V. Rodríguez Martín and E. Sánchez López, *Anal. Lett.*, 1985, **18**, 2069.
17. O. Jiménez de Blas, J. L. Pereda de Paz and J. Hernández Méndez, *Analyst*, 1989, **114**, 1675.
18. F. F. Cantwell and J. A. Sweileh, *Anal. Chem.*, 1985, **57**, 329.
19. N. Yoza, Y. Aoyagi, S. Ohashi and A. Takeda, *Anal. Chim. Acta*, 1979, **111**, 163.
20. I. López García, M. Hernández Córdoba and C. Sánchez Pedreño, *Analyst*, 1987, **112**, 271.
21. J. F. Tyson, *ibid.*, 1985, **110**, 419.
22. W. R. Wolf and K. K. Stewart, *Anal. Chem.*, 1979, **51**, 1201.
23. J. F. Tyson, *Anal. Proc.*, 1981, **18**, 542.
24. L. Nord and B. Karlberg, *Anal. Chim. Acta*, 1983, **145**, 151.
25. M. Gallego and M. Valcárcel, *ibid.*, 1985, **169**, 161.
26. M. Gallego, M. D. Luque de Castro and M. Valcárcel, *At. Spectrosc.*, 1985, **6**, 16.
27. A. Navas and F. Sánchez, *Analyst*, 1984, **109**, 1435.
28. J. C. Miller and J. N. Miller, *ibid.*, 1988, **113**, 1351.

COMPARATIVE STUDY OF A BEENAKKER CAVITY AND A SURFATRON IN COMBINATION WITH ELECTROTHERMAL EVAPORATION FROM A TUNGSTEN COIL FOR MICROWAVE PLASMA OPTICAL EMISSION SPECTROMETRY (MIP-AES)

U. RICHTS

Institut für Spektrochemie und angewandte Spektroskopie** (ISAS), Postfach 10 13 52 D-4600
Dortmund 1, FRG

J. A. C. BROEKAERT*

Universität Dortmund, Fachbereich Chemie, Postfach 50 05 00 D-4600 Dortmund 50, F.R.G.

P. TSCHÖPEL and G. TÖLG**

Laboratorium für Reinststoffanalytik, Max-Planck Institut für Metallforschung, Stuttgart**,
Postfach 12 26 52, D 4600 Dortmund 1, FRG

(Received 20 December 1990. Accepted 12 February 1991)

Summary—Microwave induced plasmas, sustained in a Beenakker resonator and a surfatron, respectively, are used to excite vapours released by electrothermal evaporation of solutions from a tungsten coil. The analytical figures of merit of AES for two easily volatilized elements (Cu, Cd) are compared for argon MIP operated in the two resonators under optimized conditions. In the Beenakker resonator a 1-filament plasma was produced at an argon flow of 0.45 l./min and a forward power of 50 W. In the surfatron a 2-filament plasma with 2.44 l./min argon and a forward power of 130 W was used. The detection limits for Cu and Cd with the surfatron are lower than those obtained with the Beenakker resonator and are in the range 10–20 ng/ml. Also interferences arising from an easily ionized element such as Na are lower with the surfatron than with the Beenakker resonator. The linear dynamic ranges in the case of the surfatron are also superior and extend over three decades of concentration.

Microwave induced plasmas (MIPs) are prominent sources for performing optical emission spectrometric multielement determinations. They are produced without electrodes in a resonator where the microwave energy is coupled to a gas (argon or helium) flowing in a quartz capillary. Microwave induced plasmas for atomic spectrometry were first operated in resonators at reduced pressure, as in the case of the so-called Evenson $\frac{1}{4} \lambda$ resonator.¹ They became of real interest for atomic spectrometric analysis since it was possible to operate them at atmospheric pressure. This could be realized with the TM₀₁₀ resonator, developed by Beenakker² and later improved by van Dalen *et al.*³ In addition, other microwave cavities for use at atmospheric pressure have become available during the last few years. The so-called surfatron⁴ is operated

at atmospheric pressure and was described by Hubert *et al.*⁵ Spectroscopic investigations of argon plasmas⁶ and investigations of the working parameters by use of helium or argon plasmas operated in a surfatron followed.⁷

Since the MIPs are operated at low power, as compared to the inductively coupled plasma (ICP), restrictions for the introduction of samples in MIPs exist. Generally large amounts of matter cannot be brought into MIPs without disturbing their discharge stability. Also, due to the low gas kinetic temperatures⁸ matrix effects are high.

Various methods of sample introduction have been used in combination with MIPs. Pneumatic nebulization of solutions, as it is known from ICP spectrometry, is hampered by the low power of the MIP. Nevertheless, Kollotzek *et al.*^{9,10} could produce a toroidal plasma, into which wet aerosols produced by a Meinhard nebulizer could be taken up. They used a quartz

*Author for correspondence.

capillary with 4 mm i.d. in a TM_{010} resonator and 150 W forward power. Yet a desolvation of a wet aerosol improves the analytical performance.¹¹

Further electrothermal evaporation (ETV) of dry solution residues can be used. Here, solution aliquots are brought into a graphite furnace or put on a metal filament, dried, and subsequently the analyte is released as vapour during a heating stage.¹² The advantage of this approach is the separation of evaporation and excitation. The sample is volatilized in the graphite furnace or on the metal filament, so that the whole energy of the plasma is used for the excitation.

In the case of the MIP, Aziz *et al.*¹³ used a graphite furnace. The sample was evaporated and the solvent vapour was removed through the sampling aperture by an argon flow entering from both sides of the furnace so as to avoid condensation in the treatment line. Heltai *et al.*¹⁴ showed that the toroidal argon MIP could be operated also reliably in combination with electrothermal evaporation.

The use of a metal filament was described by Runnels and Gibson.¹⁵ They used a 0.4-mm platinum filament placed in an evaporation chamber and an argon-MIP for the determination of volatile metal chelates. Other papers on the application of metal filaments included the use of tungsten and tantalum filaments. Aldous *et al.*¹⁶ employed platinum and tungsten filaments, on which a reproducible amount of sample could be collected as a surface film by dipping them into the solution. When using a rapid electronic amplifier/integrator, a linear dynamic range of three decades for Cd was achieved. Kawaguchi *et al.* determined picograms of metals in metal enzymes by using evaporation from a tantalum filament and excitation in a helium-MIP under reduced pressure.¹⁷ They also investigated the interelement effects and the mechanism of excitation of the He-MIP.¹⁸

Van Dalen *et al.*¹⁹ determined halogen and sulphur by using a tantalum filament and a He-plasma produced in a TM_{010} resonator at atmospheric pressure. A special sampling unit which uses a tungsten filament has been described by Brooks and Timmins.²⁰

The aim of this work is to compare under optimized conditions the analytical performance of a Beenakker resonator and a surfatron, respectively, in MIP-AES in combination with the same electrothermal evaporation unit. An objective evaluation of both plasmas is obtained

as the same signal recording equipment is used.

In both cases, a tungsten coil, as described by Berndt *et al.*²¹ for AAS, is employed for analyte evaporation. The detection limits and the linear dynamic ranges for a volatile element (Cd) and a less volatile element (Cu), are determined. Also the influence of an easily ionized element such as Na on the Cd and Cu signals is studied.

EXPERIMENTAL

MIP equipment

For the measurements with the Beenakker resonator a 200 W microwave generator (EMS, Mikroton 200 Mark III) was used. In the case of the surfatron, which requires a higher forward power, a generator with 300 W maximal forward power (AF, GMW 24-301 DR) was used. The TM_{010} resonator used in this work is a modified version² of that described by Beenakker.¹ The surfatron was built after a description given by Selby and Hieftje⁷ (Fig. 1).

Evaporation unit

The tungsten coils used for electrothermal evaporation were produced for halogen lamps (Osram GmbH, Munich, FRG). They consist of 12 turns with dimensions of 3 mm × 7 mm × 1 mm and can be used up to a voltage of 24 V and a power of 250 W. The high melting point of tungsten (3410°) permits it to achieve the temperature of up to 2000° required for the sample volatilization by applying a voltage of 9 V.

For drying sample aliquots of 20–50 μ l within 1 min, a voltage of 0.35 V was selected. Then the coil did not glow at the end of the evaporation time, by which a loss of volatile elements and compounds was prevented. The water vapour produced during the solvent evaporation was released through the side-arm of a three-way valve, placed between the quartz evaporation unit and the argon flow 2 inlet. A PTFE plug was used, which makes greasing superfluous and prevents contaminations. The experimental facilities and operating conditions are given in Table 1.

Measurement

For analysis 20 μ l of the solution was dispensed on the coil with the aid of a micropipette and during this procedure the MIP was operated with the argon flow 2 only. After closing the sample aperture, the sample was dried and

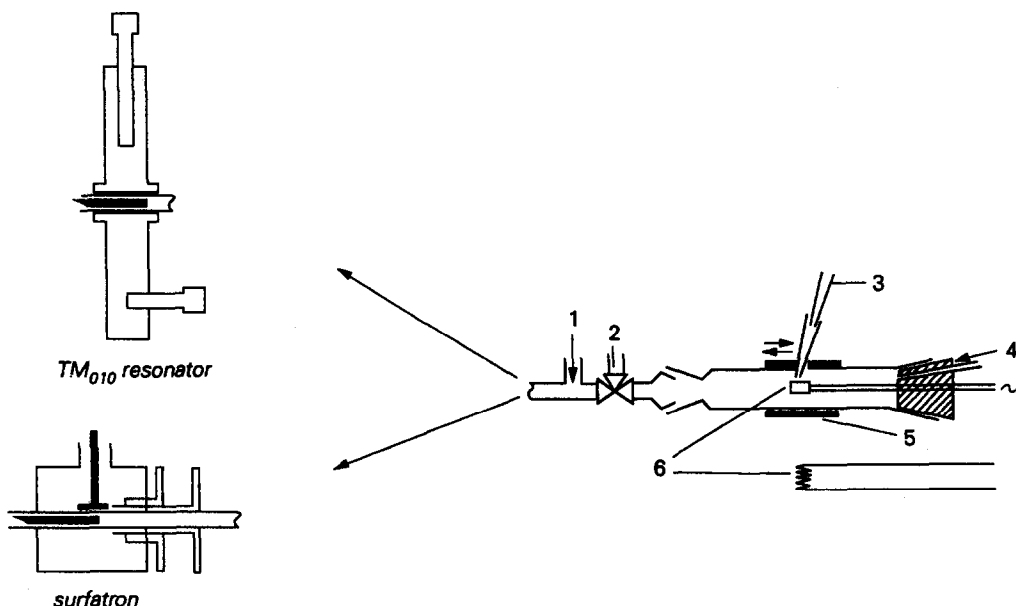


Fig. 1. MIP resonators and evaporation system.

Table 1. Instrumental parameter

Microwave equipment	
Beenakker resonator	
Microwave generator	EMS, Mikroton 200 Mark III frequency: 2.45 GHz; maximal forward power: 200 W
Resonator	water cooled TM_{010} resonator
Capillary	quartz capillary with 1 mm i.d., 5 mm o.d.
Illumination	2 × magnified image on the entrance slit: $f = 52$ mm lens (distance to plasma: 70 mm; distance to entrance slit: 280 mm)
Surfatron	
Microwave generator	AF, GMW 24-301 DR, frequency: 2.45 GHz maximal forward power: 300 Watt
Resonator	water cooled surfatron
Capillary	quartz capillary with 4 mm i.d., 6 mm o.d.
Illumination	2 × magnified image on the entrance slit: $f = 76$ mm lens (distance to plasma: 116 mm; distance to entrance slit: 234 mm)
Tungsten coil	tungsten coil with 12 turns maximal voltage: 24 V
Spectrometer	
Monochromator	0.75-m Ebert monochromator grating: 1800 lines/mm dimensions: 52 mm × 52 mm entrance slit width: 10 μ m exit slit width: 25 μ m
Photomultiplier	1P28
Oscilloscope	Hemeg Digital Storage Scope HM 208
Potentiomet recorder	Linseis; model LS 44

the analyte solvent vapour was released through the three-way valve.

Subsequent to the drying stage, the argon flow was switched from 2 to argon flow 1. After waiting 30 sec for stabilization, the sample was evaporated and transported into the plasma. After recording the signal, the flow was switched back to argon flow 2 and the next sample could be brought onto the coil.

This procedure was used both with the Beenakker resonator and with the surfatron. In the case of the latter we partly worked with argon flow 1 and argon flow 2 together (see Table 2). In all other experiments the argon flow 2 was turned off prior to the analyte evaporation stage.

RESULTS AND DISCUSSION

Measurements with the Beenakker resonator

Stability area of the MIP. In the TM_{010} resonator a 1-filament plasma can be produced by using a clamping device with 4 narrow cuts. The capillaries used may have diameters from 1 to several mm. In the case of a capillary with an internal diameter of 2 mm, the plasma cannot be ignited reproducibly as it changes its burning position. This effect could not be completely eliminated by asymmetrically positioning the capillary in the resonator. As the reproducibility of the signals finally was insufficient, the 2-mm capillary was not used for analytical measurements.

Table 2. Optimal working conditions for the different plasma forms obtained in a surfatron

Plasma form	Chamber depth, mm	Gap length, mm	Forward power, W	Refl. power, W	Argon flow 1, l./min	Argon flow 2, l./min	Signal to background ratio for 3 µg/ml Cu
tor. I	45.5	14.6	100	2.4	0.35	—	18
tor. II	44.4	12.3*	130	2.5	0.38	—	20
1-filament	37.3	10.0	110	1.7	0.90	0.38	22
2-filament	43.0	13.0*	130	2.6	2.44†	—	110

*As low as possible.

†As high as possible.

With a capillary diameter of 1.5 mm and 1 mm, respectively, the plasma filament lied stable at one position and was not disturbed when the coil was heated for evaporating the sample. With gas flows below 0.6 l./min Ar, the signals were found to be reproducible. All further determinations, therefore, were performed with a quartz capillary having an internal diameter of 1 mm.

For a one-filament MIP in a quartz capillary with 1-mm inner diameter the microwave forward power, the gas flow and the selection of the observation zone of the plasma were optimized (Table 3). It was found that a forward power of 50 W and an argon flow 1 of 0.46 l./min gave optimum line to background ratios for the elements studied.

Calibration curves. The linear dynamic ranges for Cd and Cu are different but, as shown for Cd, they also depend on the analyte species present (Fig. 2).

The evaporation temperatures *e.g.* of cadmium chloride and cadmium sulphate are very different, namely 490° and *ca.* 1000°, respectively. The calibration curve of the cadmium chloride bends off at low concentrations, which might be related to the higher volatility as compared to cadmium sulphate where no losses were observed. Therefore, all further measurements are performed with cadmium sulphate.

When measuring peak heights, the linear range of the calibration of Cu is limited. This is due to an increase of the signal duration, which was found to be proportional to the concentration. With Cd the linear dynamic range is

Table 3. Optimized working parameters for the 1-filament plasma in the TM₀₁₀ resonator

Parameter	Range	Optimum
Forward power	40–60 W	50 W†
Position observed*	0–0.5 mm	0.35 mm
Gas flow	0.3–0.6 l./min	0.46 l./min

*0 mm means the edge of the capillary and 0.5 mm is the center of the plasma.

†As low as possible for a stable plasma.

higher than with Cu. It is only limited by a decrease of the temperature and the stability of the plasma with an increase of the amount of analyte introduced. The increase of the signal duration in the case of Cu can be due to effects in the plasma and/or during the evaporation.

The addition of Na generally leads to an increase of the Cu and Cd signals (Fig. 3 and Table 4), which is proportional to the Na concentration. This can be explained by a shift in the ionization equilibrium or by an increased excitation of the low energy Cu and Cd levels at the lower plasma temperature resulting from ionization of the Na added.

Measurements with the surfatron

Stability area of different types of MIPs. After adjusting the coupling plunger until a minimum of reflected power was obtained, various plasma forms could be produced depending on the gap length, the chamber depth, the gas flows and also on the axial position of the capillary in the surfatron. As a result of variations of these parameters four different plasma forms were found, namely, a 1-filament plasma, a 2-filament plasma and two toroidal plasmas, marked as I and II. The latter mainly differ by the conditions under which they were achieved, but also by their stability area and performance (Table 3).

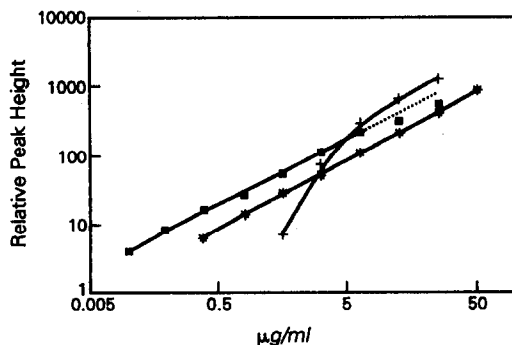


Fig. 2. Calibration curves: 50 W forward power and 0.46 l./min argon. Cd (line Cd I 228.8 nm): + CdCl₂; *CdSO₄, Cu (line Cu I 324.8 nm): ■ CuCl₂.

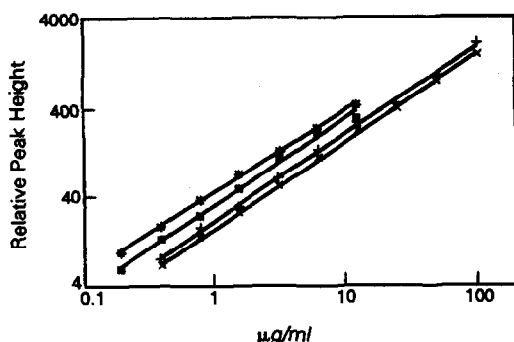


Fig. 3. Influence of Na on the determination of Cd and Cu with MIP-AES using a Beenakker resonator and ETV. \times Cd; \square Cu; \bullet Cd + 20 $\mu\text{g/ml}$ Na (line Cd I 228.8 nm); \circ Cu + 10 $\mu\text{g/ml}$ Na (line Cu I 324.8 nm).

All plasma forms were produced in a capillary with an internal diameter of 4 mm and an outer diameter of 6 mm. Experiments with a capillary having 2 mm i.d. and 6 mm o.d. did not lead to a stable plasma. At the conditions investigated only an unstable 1-filament plasma was obtained.

The toroidal plasma I was obtained at a gas flow between 0.3 and 0.5 l./min and a forward power of 90–120 W. Its reflected power depends on the chamber depth and the gap length [Fig. 4(a) and (b)]. The capillary should not protrude out of the surfatron. At this position the reflected power was minimum (2.4 W).

The toroidal plasma II could be operated stably at a forward power of 130–160 W and a gas flow of 0.3–0.6 l./min. In contrast to the toroidal plasma I, the reflected power here was minimal, when the capillary protruded 10 mm out of the surfatron. The values of the chamber depth and the gap length for minimal reflected power are given in Table 3.

A 1-filament plasma could be obtained at a forward power of 105–115 W and a gas flow between ca. 0.5 and 1.5 l./min. Thus the plasma was stable only within a small range of forward power, whereas the gas flow could be largely

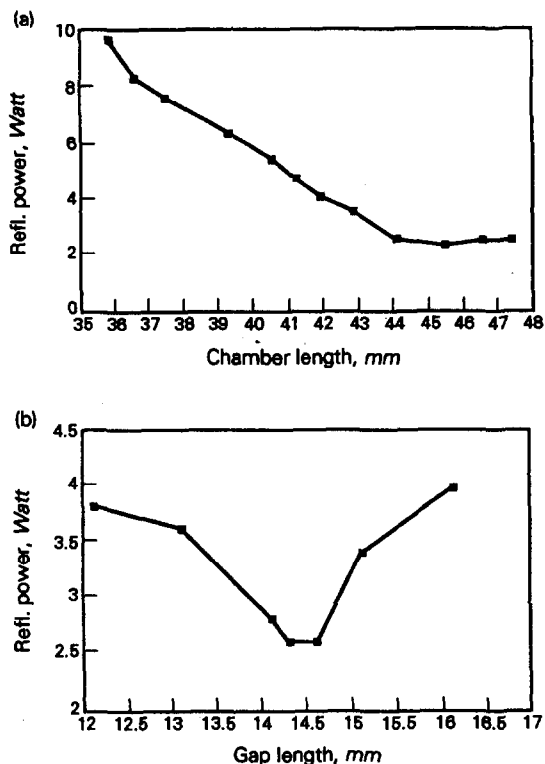


Fig. 4. Optimization of the chamber depth (a) and the gap length (b) of the surfatron (toroidal plasma I). Forward power: 100 W; argon flow 1: 0.35 l./min; (a) with gap length: 14.6 mm; (b) with chamber depth: 45.5 mm.

variated. The reflected power was at a minimum, when the capillary protruded ca. 20 mm out of the surfatron. A 2-filament plasma could be produced at a gas flow of 1.8–2.5 l./min and a forward power of 120–170 W, provided the capillary does not protrude out of the surfatron. Both plasma filaments came together in front of the surfatron and outside the capillary. The position of the two plasma filaments depended on the gas rate. At an argon flow > 2.3 l./min the plasma filaments lay stably above each other. At a gas flow < 2 l./min they lay horizontally side by side, whereas at gas flows between these values the filaments were not stable in either of these positions over a longer time.

The gas flows and the microwave forward powers for the four plasma forms described above were optimized with regard to their analytical performance. The observed region was selected in the center of the capillary, as for all plasma forms the best signal to underground ratio was found here (Table 1).

Calibration curves. Of the four plasmas the 2-filament plasma was selected, because for the elements determined (Cd and Cu) the signal to

Table 4. Influence of different amounts of Na on the signal of Cu and Cd solutions, respectively

Na, $\mu\text{g/ml}$	Matrix effect, %*			
	For 0.8 $\mu\text{g/ml}$ Cu		For 3 $\mu\text{g/ml}$ Cd	
	Beenakker	Surfatron	Beenakker	Surfatron
1	9 \pm 4	—	—	—
2	—	6 \pm 5	—	—
5	13 \pm 6	3 \pm 5	5 \pm 5	10 \pm 6
10	42 \pm 10	12 \pm 8	14 \pm 8	15 \pm 8
20	—	—	25 \pm 10	21 \pm 10

*Numbers behind \pm correspond to a 1 σ confidence level.

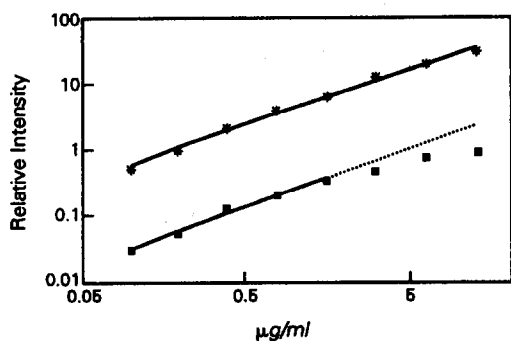


Fig. 5. Calibration curve for Cu (line Cu I 324.8 nm), using a surfatron (2-filament plasma). ■ measuring peak heights; * measuring peak areas.

background ratios and the linear dynamic ranges are superior. Already at low concentrations the calibration curve of Cu tails off when peak heights were measured. The effect, however, is stronger in the case of the surfatron as compared to the TM_{010} resonator. When using peak areas the linear dynamic range increased (Fig. 5). In the case of Cd this has hardly any effect, as the signal duration is not spread out, as already discussed in the case of the Beenakker resonator.

When adding different amounts of Na to the Cu and Cd solutions and measuring peak areas, the calibration curves shift. At lower concentrations the curves with added Na were found to lie above the pure solutions (Fig. 6).

CONCLUSIONS

In this work a 1-filament MIP obtained in a Beenakker resonator and the optimized 2-filament plasma in the surfatron have been studied. The latter plasma form is the most stable. Its detection limits (Table 5), based on the 3σ concept, are in the range 10–20 ng/ml

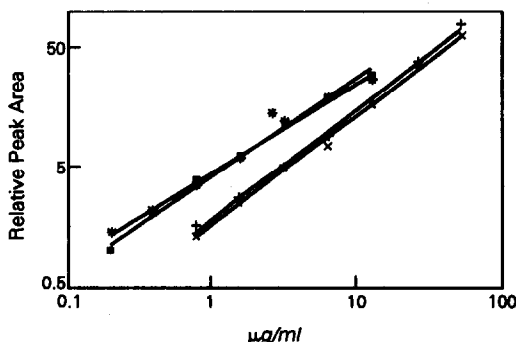


Fig. 6. Influence of Na on the determination of Cd and Cu by MIP-AES, using a surfatron and ETV. × Cd; + Cd + 10 µg/ml Na (line Cd I 228.8 nm). ■ Cu; * Cu + 10 µg/ml Na (line Cu I 324.8 nm).

Table 5. Comparison of the linear dynamic ranges and detection limits

	Beenakker 50 W 1-filament 0.46 l./min		Surfatron 130 W 2-filament 2.44 l./min	
	Cu	Cd	Cu	Cd
Dynamic range	$2 \cdot 10^2$	$1 \cdot 10^3$	$1 \cdot 10^3$	$2 \cdot 10^3$
Detection limit µg/ml (20 µl sample aliquot)	0.05	0.09	0.01	0.02

and thereby come near to those of ETV-ICP spectrometry. They are lower by a factor of 4 to 5 than those obtained with the 1-filament MIP in the Beenakker resonator.

The linear dynamic ranges for Cu and Cd with the surfatron and with peak area are considerably larger than those of the Beenakker resonator (Table 5).

In MIP-AES the matrix effects are higher than those of ICP spectrometry. This is due to the small amounts of material which can be taken up by the plasma without disturbing it and to the influence of elements such as Na. With the surfatron, the influence of Na on the signals of Cu and Cd is lower than with the Beenakker resonator, where especially for the case of Cu the effect is high (see Table 4). This comparison between both resonators is difficult to interpret, because in the case of the surfatron the calibration curves with added Na are not parallel to those of the pure solutions. Due to the high matrix effects, ETV/MIP-AES especially is of use in multistage procedures, where the matrix is separated from the elements to be determined.

Within the linear range the relative standard deviation (RSD) is 3–5% with both resonators. It is similar to the one obtained with graphite furnace AAS or MIP-AES using graphite furnace evaporation.¹³ The RSDs increase as the Na content goes up.

In the case of the 2-filament plasma a side-on observation at the point before the plasma filaments come together, *e.g.*, with an optical fiber, could improve the signal to background ratio, considerably.

Acknowledgement—The work has been supported by the "Ministerium für Wissenschaft und Forschung des Landes Nordrhein-Westfalen" and by the "Bundesministerium für Forschung und Technologie".

REFERENCES

1. R. K. Skogerboe and G. N. Coleman, *Anal. Chem.*, 1976, **48**, 611A.

2. C. I. M. Beenakker, *Spectrochim. Acta*, 1976, **31B**, 483.
3. J. P. J. van Dalen, P. A. de Lezenne Coulander and L. de Galan, *Spectrochim. Acta*, 1978, **33B**, 545.
4. M. Moisan, C. Beaudry and P. Leprince, *IEEE Trans. Plasma Sci.*, 1975, **PS-3**, 55.
5. J. Hubert, M. Moisan and A. Richard, *Spectrochim. Acta*, 1979, **33B**, 1.
6. P. S. Moussanda, P. Ranson and J. Mermet, *ibid.*, 1985, **40B**, 641.
7. M. Selby and G. M. Hieftje, *ibid.*, 1987, **42B**, 285.
8. Gy. Heltai, J. A. C. Broekaert, F. Leis and G. Tölg, *ibid.*, 1990, **45B**, 301.
9. D. Kollotzek, P. Tschöpel and G. Tölg, *ibid.*, 1982, **37B**, 91.
10. *Idem*, *ibid.*, 1984, **39B**, 625.
11. M. H. Abdallah, S. Coulombe, J. M. Mermet and J. Hubert, *ibid.*, 1982, **37B**, 583.
12. H. Matusiewicz, *Spectrochimica Acta Rev.*, 1990, **13**, No. 1, 47.
13. A. Aziz, J. A. C. Broekaert and F. Leis, *Spectrochim. Acta*, 1982, **37B**, 381.
14. Gy. Heltai, J. A. C. Broekaert, P. Burba, F. Leis, P. Tschöpel and G. Tölg, *ibid.*, 1990, **45B**, 857.
15. J. H. Runnels and J. H. Gibson, *Anal. Chem.*, 1967, **39**, 1398.
16. K. M. Aldous, R. M. Dagnall, B. L. Sharp and T. S. West, *Anal. Chim. Acta*, 1971, **54**, 233.
17. H. Kawaguchi and B. L. Vallee, *Anal. Chem.*, 1975, **47**, 1029.
18. H. Kawaguchi, I. Atsuya and B. L. Vallee, *ibid.*, 1977, **49**, 266.
19. H. P. J. Van Dalen, B. G. Kwee and L. de Galan, *Anal. Chim. Acta*, 1982, **142**, 159.
20. E. I. Brooks and K. J. Timmins, *Analyst*, 1985, **110**, 557.
21. H. Berndt and G. Schaldach, *J. Anal. Atom. Spectr.*, 1988, **3**, 709.

ELECTROTHERMAL ATOMIZATION ATOMIC ABSORPTION SPECTROMETRY OF CADMIUM WITH A PLATINUM TUBE ATOMIZER

KIYOHISA OHTA,* SYN-ICHI ITOH and TAKAYUKI MIZUNO

Department of Chemistry for Materials, Faculty of Engineering, Mie University, Mie, Tsu, 514, Japan

(Received 4 January 1991. Revised 18 February 1991. Accepted 26 February 1991)

Summary—The determination of cadmium by electrothermal atomization atomic absorption spectrometry with a platinum tube atomizer in the presence of air has been investigated. The detection limit of cadmium was 0.09 pg (9 pg/ml for a 10- μ l volume). The relative standard deviation of the measurement was 2.9%. For 2.5 pg of cadmium, Cu, Pb, Zn, Al, Ca, Fe, K, Mg and Na (10^4 – 10^5 -fold) did not interfere with the absorption signal. The method has been applied to the determination of cadmium in some biological materials. The average analytical value found for the standards lay within the limits of the certified values. The remarkable merits of the platinum atomizer are its stability in air and long life-time (able to withstand more than 1000 heating cycles in air).

The toxic effects of cadmium are now well recognized and many researchers have reported the determination of cadmium in biological materials by electrothermal atomization atomic absorption spectrometry (ETA–AAS).^{1–9} However, in most cases there is the problem of matrix interference and pre-separation techniques and matrix modifier methods have therefore been performed before analysis.^{1–9}

Metal tubes and wires^{10–14} have recently been developed as atomizers in ETA–AAS and have been found to be excellent in comparison with graphite atomizers. However, there is a limitation for routine *in situ* analysis. For protection from oxidation, both graphite and metal atomizers need a purge gas in a large cylinder, which occupies a relatively large space. The purge gas disturbs the design of a compact AA system with routine analysis. Maeda *et al.* reported that oxygen gas came into play as a stabilizer and background reducer in the determination of cadmium in biological samples by graphite furnace AAS.⁷ In view of these points, platinum metal is the most suitable atomizer. An ETA–AAS system with a platinum wire in an argon atmosphere has been reported.¹² The sensitivities and detection limits were improved over those obtained from conventional flame measurements. Fragale and Bruno¹⁵ described a simple flame emission device for use in teaching laboratories which incorporates a platinum wire

atomizer. Berndt and co-workers^{16–18} reviewed the utilization of metal loops (Pt, Pt/Ir or Ir) for discrete sample introduction into flames. They have reported the benefits of using platinum wires in flames. There is, however, no report of ETA–AAS with a platinum tube atomizer.

In this study, we report the determination of cadmium in biological materials by ETA–AAS with a novel platinum tube atomizer in air. Interference studies with the atomizer were performed. A simple, precise and convenient method for determination of cadmium is shown.

EXPERIMENTAL

Apparatus

The platinum tube atomizer (33 mm long, 2.0 mm i.d. and 0.03 mm wall) was made from a high purity platinum foil (99.98% Koch Chemicals Ltd.). A 0.3-mm diameter hole was drilled at the midpoint of the tube to inject a sample. The atomizer was hung from two electrodes modified from conventional style electrodes, as shown in Fig. 1. The electric power for the atomizer was supplied with a transformer (YAMABISHI, S-130-5, Cap. 500 VA). Two pinhole apertures were placed in front of and in the rear of the atomizer to provide a narrow beam of light about 1.0 mm in diameter and to remove background emission from the atomizer surface. A monochromator (Nippon Jarrell-Ash 0.5 m Ebert-type), an amplifier, a memoriscope (Iwatsu MS-5021),

*Author for correspondence.

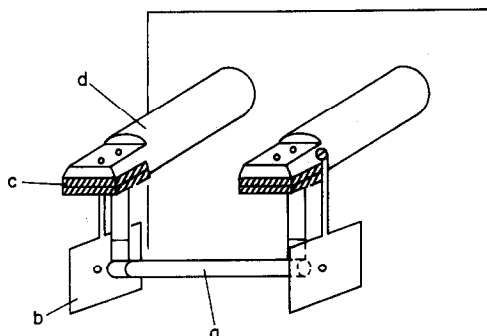


Fig. 1. Platinum tube atomizer: (a) platinum tube (33 mm long, 2.0 mm i.d., 0.03 mm wall), (b) aperture, (c) graphite plate, (d) copper electrode.

and a microcomputer (Sord M223) were used for the atomic-absorption measurements in this study. The light source was a hollow cathode lamp (Hamamatsu photonics Co.) with a Cd-resonance line of 228.8 nm. Background molecular absorption was checked with a deuterium lamp (Original Hanau D200F). The absorption signal from the amplifier and the output signal from a photodiode for the measurement of atomizer temperatures were simultaneously fed into the microcomputer. The calibration of the temperature of the atomizer was done against the photodiode voltage with an optical pyrometer (Chino Works).

Reagents

A standard stock solution (1 mg/ml) of cadmium was prepared as the nitrate by dissolving high purity metal (optical grade) in 7M nitric acid and diluting the solution with demineralized distilled water. Solutions of the matrix compounds for the interference study were prepared as nitrates or chlorides in 0.1–6M acid. The working solutions for measuring atomic-absorption were diluted from the stock solutions with water just before use. All chemicals used were of analytical grade purity.

Procedures

For the interference study, a 1- μ l aliquot of the sample solution containing Cd (2.5 ng/ml) and interferent (25–250 μ g/ml) was pipetted into the platinum tube atomizer. The sample was dried at 350 K for 10 sec and heated to atomization at 1720 K for 3 sec in air. The atomizing temperature corresponded to 1.0 K/msec heating rate. After the atomization of cadmium, the suspended atomizer was immersed into 6M hydrochloric acid in a

small beaker and washed with demineralized distilled water for the removal of the matrix residue.

An accurately weighed biological sample (about 0.1 g) was digested with 8 ml of 14M nitric acid and 2 ml of hydrogen peroxide (30%) in a Uni-seal decomposition vessel by placing it into a preheated 390 K electric oven for 3 hr. After digestion, the solution was transferred to a Teflon beaker and evaporated to dryness in a polyethylene glycol bath (380 K). The residue was dissolved in about 2 ml of 1M nitric acid. The solution was transferred into a 10 ml standard flask and made up to volume with water. The prepared solution was further diluted with demineralized distilled water if required. The ETA-AAS measurement was performed in the same manner as described for the interference studies.

RESULTS AND DISCUSSION

For a sensitive analysis of cadmium with the platinum tube atomizer by ETA-AAS, it is important to investigate the effect of the atomization rate on the cadmium-AA profile. Accordingly, the signal was measured at various heating rates of the atomizer in air. A heating rate greater than 1.24 K/msec was impossible because of the low melting point (2047 K) of platinum metal. Therefore, the following measurements were consequently carried out at 1.0 K/msec heating rate.

Interference study

In general, biological materials contain large amounts of Al, Ca, Fe, K, Mg, Na and Zn. Accordingly, the effects of these elements and of Cu and Pb (of which interferent effects are known¹⁹) on the cadmium (2.5 μ g) absorption signal (peak height and peak area) were investigated with the platinum tube atomizer under the experimental conditions. The use of the peak area was not suitable for the study as shown in Table 1. A typical atomization profile is shown in Fig. 2.

Aluminum, iron, potassium, magnesium and sodium (250 ng) did not interfere with the cadmium signal, as shown in Table 1. However, interferences of 250 ng of copper, lead and zinc on the cadmium were observed; copper particularly depressed the cadmium signal. However, as illustrated in Fig. 2, 25 ng of copper did not influence the cadmium signal, and similar results were found for lead and zinc

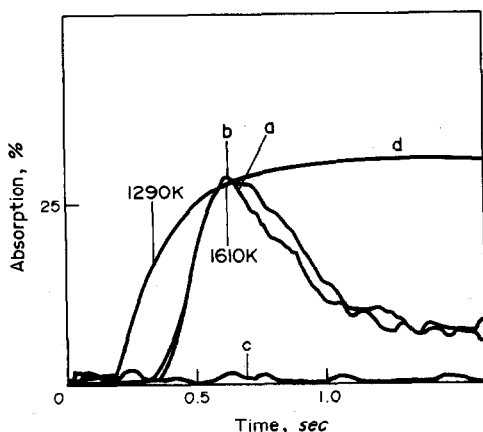


Fig. 2. Atomic absorption signals in the platinum tube atomizer in air: (a) 2.5 pg of cadmium, (b) Cd and 25 ng of copper (c) 25 ng of copper, (d) temperature trace.

as well. The cadmium signal in the presence of 2500 ng of calcium was also investigated, because calcium is one of the most abundant elements in biological materials. Although the cadmium signal was depressed by this amount of calcium, a 250 ng amount did not affect the signal.

In air, as can be seen from the above results, the normal amounts of the matrix elements did not influence the cadmium signal. Maeda *et al.*⁷ reported that the addition of oxygen gas to the graphite furnace in the determination of cadmium greatly decreased the background absorption arising from sample matrices such as milk, orange juice and blood, and that the addition of oxygen gas prevented the cadmium signal depression. These samples contain large amounts of Al, Ca, Fe, K, Mg, Na and Zn, which were also studied by the use of the platinum tube atomizer. The results support the use of oxygen as a matrix modifier in the platinum tube atomizer.

Detection limit, characteristic mass and reproducibility

The detection limit, which was the weight of analyte which gave an atomic-absorption signal equal to three times the standard deviation of the background (obtained from the measurement of a solution blank), was calculated from the height of the cadmium absorption signal. The detection limit of cadmium by use of the platinum tube atomizer was 0.09 pg (corresponding to 9 pg/ml, if 10 μ l is used). The value was better than for carbon atomizers.²⁰

The characteristic mass of cadmium, which was defined as the mass of element giving an absorption of 1% (0.0044 abs), by the atomizer was 0.099 pg, which is comparable to that for carbon atomizers.²⁰

The reproducibility by the use of the platinum atomizer was estimated. The r.s.d. for 2.5 pg of cadmium was 2.9% for 7 measurements. Furthermore, the atomizer could withstand more than 1000 heating cycles in air.

Determination of cadmium

In order to test the applicability of the proposed method to the analysis of real samples, some reference biological materials were analyzed. The biological materials in this study were digested with an acid mixture of concentrated nitric acid and hydrogen peroxide.⁴ The dynamic range of the calibration curve was 0–15 pg. Table 2 shows the results obtained for some biological materials, compared with certified values. The relative standard deviations for the method were 3.7–27% at 3 or 4 replicate analyses. The average value found for the standards lies within the limits of the certified values. The method can be considered satisfactory for the determination of cadmium in biological materials.

Table 1. Interferences on the atomic absorption signal of cadmium

Interferent added, ng	Peak height/Abs	Peak area/rel. Abs*Time	Number of measurements
(Cd 2.5 pg)	0.144 \pm 0.007	21.5 \pm 1.6	5
Al 250	0.141 \pm 0.007	17.8 \pm 0.6	3
Ca 2500	0.118 \pm 0.009	18.9 \pm 1.9	4
250	0.144 \pm 0.004	20.6 \pm 1.8	5
Cu 250	0.085 \pm 0.007	14.6 \pm 0.9	4
25	0.146 \pm 0.005	22.1 \pm 1.2	5
Fe 250	0.144 \pm 0.004	16.1 \pm 2.1	4
K 250	0.140 \pm 0.005	20.5 \pm 1.3	5
Mg 250	0.144 \pm 0.009	13.4 \pm 1.5	5
Na 250	0.148 \pm 0.010	17.7 \pm 1.4	5
Pb 250	0.119 \pm 0.010	20.4 \pm 2.1	4
25	0.140 \pm 0.007	23.1 \pm 1.6	5
Zn 250	0.115 \pm 0.005	18.8 \pm 1.6	5
25	0.144 \pm 0.008	22.3 \pm 1.8	5

Table 2. Determination of cadmium in biological materials

Sample	Amount of cadmium, $\mu\text{g/g}$	
	Found	Certified value
Citrus leaves*SRM1572	0.027 ± 0.001 ($n = 4$)	0.03 ± 0.01
Orchard leaves*SRM1571	0.11 ± 0.03 ($n = 3$)	0.11 ± 0.01
Oyster tissue*SRM1566a	3.6 ± 0.2 ($n = 3$)	3.5 ± 0.4

*NIST standard.

Number of analyses in parentheses.

As described above, the large benefit of the platinum atomizer is inertia and long lifetime in air. In addition, most elements (10^4 – 10^5 -fold for cadmium) did not affect the cadmium absorption signal. These remarkable performance characteristics of the platinum tube served for an accurate determination of cadmium in biological materials. The disadvantages of the use of a platinum atomizer are the low melting point of the metal and a clean-out step. However, the platinum tube atomizer can be used with simple, "low-tec" electrothermal atomization atomic-absorption spectrometry. The atomizer may serve as a tool for the accurate determination of other volatile elements at low cost.

Acknowledgement—This work was supported financially by the Ministry of Education, Science and Culture of Japan and Okasan katou bunka sinkou zaidan.

REFERENCES

1. K. R. Sperling, *Z. Anal. Chem.*, 1988, **332**, 565.
2. H. Han, X. Le and Z. Ni, *Fenxi Huaxue*, 1988, **16**, 220; *Chem. Abstr.*, 1988, **109**, 162504p.
3. T. W. Brueggemeyer and C. A. Bonnin, *Anal. Chem.*, 1988, **60**, 761.
4. K. Ohta, W. Aoki and T. Mizuno, *Talanta*, 1988, **35**, 831.
5. S. Chen and L. Song, *Fenxi Ceshi Tongbao*, 1988, **7**, 56; *Chem. Abstr.*, 1988, **109**, 185031w.
6. P. Dube, C. Krause and L. Windmuller, *Analyst*, 1989, **114**, 1249.
7. T. Maeda, M. Nakatani and Y. Tanimoto, *Bunseki Kagaku*, 1989, **38**, 734.
8. K. Akatsuka and I. Atsuya, *Anal. Chem.*, 1989, **61**, 216.
9. Z. A. De Benzo and R. Fraile, *Anal. Chim. Acta*, 1990, **231**, 283.
10. M. Suzuki and K. Ohta, *Prog. Anal. At. Spectrosc.*, 1983, **6**, 49.
11. K. Ohta and S. Su, *Anal. Chem.*, 1987, **59**, 539.
12. H. Brandenberger, *Chimica*, 1968, **22**, 449; *Chem. Abstr.* 1969, **70**, 63991.
13. H. Berndt and G. Schaldach, *J. Anal. At. Spectrom.*, 1988, **3**, 709.
14. I. Havesov, E. Ivanova, H. Berndt and G. Schaldach, *Z. Anal. Chem.*, 1990, **336**, 484.
15. C. Fragale and P. Bruno, *J. Chem. Educ.*, 1976, **53**, 734.
16. H. Berndt and J. Messerschmidt, *Atomspektrom. Spurenanal., Vortr. Kolloq.*, 1981, 411; *Chem. Abstr.*, 1983, **98**, 226970b.
17. H. Berndt, S. Guecer and J. Messerschmidt, *J. Clin. Chem. Clin. Biochem.*, 1982, **20**, 85; *Chem. Abstr.*, 1982, **96**, 137248p.
18. H. Berndt and J. Messerschmidt, *Anal. Chim. Acta*, 1982, **136**, 407; *Chem. Abstr.*, 1982, **97**, 32754t.
19. M. Suzuki and K. Ohta, *Anal. Chem.*, 1982, **54**, 1686.
20. M. L. Parsons, S. Major and A. R. Foster, *Appl. Spectrosc.*, 1983, **37**, 411.

THE RAMESES ALGORITHM FOR MULTIPLE EQUILIBRIA—IV. STRATEGIES FOR IMPROVEMENT (RAMESES III)

B. W. DARVELL and V. W.-H. LEUNG

Dental Materials Science Unit, University of Hong Kong, Prince Philip Dental Hospital,
34 Hospital Road, Hong Kong

(Received 22 May 1990. Revised 28 January 1991. Accepted 6 February 1991)

Summary—The algorithm RAMESES has been enhanced by the improvement of the forward extrapolation procedure to give more accurate estimates with a smoothed polynomial function in a dynamically adaptive scheme, ADEPT. A class of problems exhibiting chaotic behaviour due to exaggerated feedback has been controlled by limiting the correction factors. Improved execution speed has also been obtained through indirect addressing of sparse array elements. Some illustrative examples are given.

Previously, the principal structure of an efficient algorithm for solving the equations of multiple equilibria,¹ some developments of the programming thereof,² and a modification which led to a substantial increase in the execution speed³ have been reported.* Some further improvements are now presented which (i) reduce execution time (ii) increase the precision of forward extrapolation and (iii) enable the handling of a class of problems previously not anticipated. Some illustrative test results are presented.

NEWTON-RAPHSON

A number of other reported procedures have employed Newton-Raphson (NR) methods of solution, some of which have been acknowledged (principally by their authors) to have limitations,^{1,4} although these are of known origin.⁴ It might be thought that such NR methods ought to be applicable in RAMESES as well and this was explored. The adaptive procedures for adjusting the estimates in RAMESES work through the gain matrix, G [equation (2.4)]. The sensitivity of the system to perturbation of component estimates is allowed for here to some extent. Theoretically,^{5,6} however, it might be thought better to express these procedures in NR terms (with the previous notation^{1,3}), *i.e.*,

$$\mathbf{P}_{A(n+1)} = \mathbf{P}_{A(n)} + (\mathbf{M}^T \mathbf{X}^D \mathbf{M})^{-1} (\mathbf{T} - \mathbf{S}) \quad (1)$$

$$\mathbf{X}_{A(n+1)} = \mathbf{X}_{A(n)} + (\mathbf{M}^T \mathbf{X}^D \mathbf{M})^{-1} \mathbf{X}_{A(n)}^D (\mathbf{T} - \mathbf{S}) \quad (2)$$

*In referring to the earlier reports, equation numbers will be identified by prefix, *e.g.*, 1.5 refers to equation (5) in reference 1.

depending on whether the corrections were to be in concentration or logarithmic concentration. (The superscript D is used here to mean the 'diagonalized' vector, *i.e.*,

$$X_{ii}^D = X_i; \quad X_{ij}^D = 0, \quad i \neq j \quad (3)$$

in order that the algebra be correct.)

Despite the neatness of such statements, and the formal principle upon which they are based (in theory, taking into account all contributions to the sensitivity of the sums, S^j), in attempts to implement either of them [*i.e.*, equations (1) and (2)] we failed to achieve convergence in any of a number of test systems previously used.² That this is a common problem is illustrated by the sophisticated protection against divergence employed in SUPERQUAD,⁷ which can only handle four components,⁷ and itself one of a series of successors to MINQUAD,⁸ developed to overcome deficiencies in that program.^{5,7} The explanation was found to be that in general the multidimensional response surface is not monotonic over a sufficiently large region, and the gross simplification represented by the differentiation implicit in equations (1) and (2) fails to recognise this. The problem is exacerbated by increasing the number of components and equations. The system becomes chaotic, showing extreme sensitivity to changes in values. The attempt was therefore abandoned. Evidently, under limited conditions and convoluted protection procedures, or modified approaches, the NR approach can be made to work.^{1,4,5,7} However, NR and related methods depend on the inversion of $(\mathbf{M}^T \mathbf{X}^D \mathbf{M})$, or some

similar matrix, at each iteration to generate the next vector of concentration shifts.^{5,6} This is itself very time-consuming, but it also involves a considerably greater number of arithmetic operations to form that matrix than the procedure represented by equation (2.4). All of this suggested that little benefit over existing (NR and similar) procedures was likely to be obtained from pursuing the approach now, in view of the considerable developments that have already been made in this area, but especially since the existing RAMESES algorithm appears to be quite efficient.² It is nevertheless pertinent to observe that the difficulties arise simply from the inappropriateness of NR to this general class of problem. One known and serious limitation is that initial estimates must be "sufficiently close" or within the "convergence range", for which no useful measure exists before the event.⁴ In addition, there are recognized difficulties with inverting such matrices in this context, such as loss of precision and the risk of singularities or near-singularities arising. RAMESES cannot ever suffer from singularity in any sense as this term has no relevance in the context of its algebra, there being only the one inversion of the coefficient matrix C_b [equation (1.7)], and this cannot be singular if formed correctly.

FORWARD EXTRAPOLATION

In an earlier paper, we discussed the use of polynomial estimation of the elements of the input vector X_A based on the previous points of a scan.² The coefficients then were derived directly and represented the exact fitting of the polynomial curve of degree $b - 1$ to b points; b was termed the order of the extrapolation.

Noticing that, at each point in the scan, each X_{Ai} has an associated error of a maximum size given by the calculation tolerance, ϵ , some improvement in the accuracy of the prediction might be obtained by smoothing over more points, that is, for a given degree of polynomial, $d < b - 1$. In other words, by fitting a polynomial curve in the least-squares sense, the standard error of the prediction for the next point may be reduced. The direct implementation of this idea would involve much further calculation, including the inversion of the matrix of sums of squares and cross-products of rank $d + 1$ for each of the species' concentrations to be predicted, and for each degree that was to be tested in searching for a 'best fit', a very time consuming procedure. However, for

uniformly spaced points in the independent (scanning) variable, considerable computational simplification is possible, and the weights previously given² emerge as the special case when the degrees of freedom for the curve fit are zero.

The coefficients and theory of such curve fitting are well worked out,^{9,10} and the coefficients have integral values when an overall 'weight' division is taken out.^{9,10} The values of the coefficients and weights for the next point in a series have been tabulated for degrees 1-5, and for up to 25 points in the known sequence, along with the standard errors (σ) of predicted points.⁹ These errors are summarised in Fig. 1. It can be seen that, for a given degree, the values of σ are asymptotically proportional to $b^{-0.5}$, as would ordinarily be expected. More importantly, the error increases substantially with an increase in d . However, one or two points more than the minimum are expected to reduce the error to near that expected for the next lower degree, *i.e.*, the loss of accuracy arising from the use of a higher degree polynomial may be offset by using more points in the prediction.

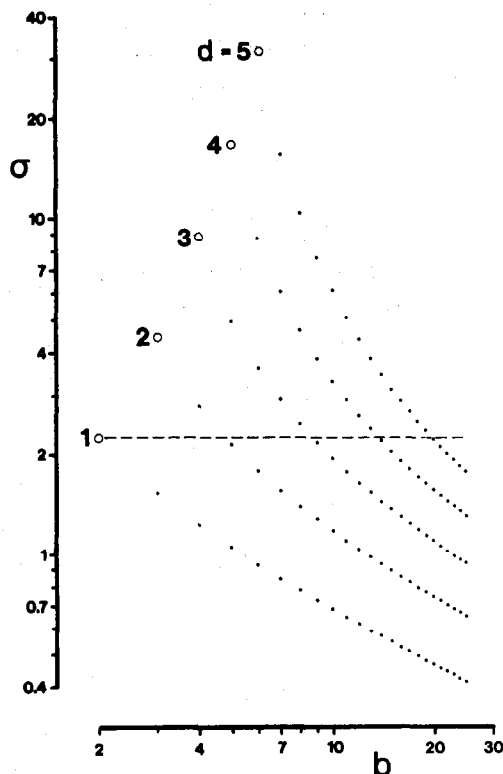


Fig. 1. Log-log plot of the standard error (σ) of polynomial extrapolation to the next evenly-spaced point in a series as a function of the number of points (b) used in the fitted curve, for polynomial degree (d) 1-5. The circled points are for minimum $b (= d + 1)$; the dashed line shows b for each d at near-constant σ . Data taken from reference 10.

The number of extra points so required increases rapidly as b is increased. The questions then arise as to whether any practical predictive improvement can be obtained with $b > d + 1$ and, if so, how far this idea can be taken. Given the many degree and number of points combinations possible, a good many strategies are conceivable. To avoid a too detailed description of the route, the conclusion only of an extensive series of comparisons over several test systems (see EXAMPLES Section) will be given.

The optimum performance, on average, was obtained by the conditions giving as near uniform an expected error, σ , in the predicted point as possible. The number of points to be used can be read off as corresponding to the points nearest below the horizontal dashed line of Fig. 1, viz $b = 2, 5, 9, 14$ and 20 for degrees 1–5, respectively. This expected nearly constant error is on the supposition that the true curve is of the same degree as the line fitted. As the species' log(concentrations) are not polynomial functions in the present sense; there remains the need for a search for the degree of curve giving a 'best fit'. The method used as most effective was in part based on the fact that n , the number of points available for the curve fitting, ranges from zero at the start to an indefinitely large value (depending on the range of the scan and the step interval, h). There is thus constraint initially as $d \leq b - 1$ must hold. Table 1 shows the variation in b used for each d as the number of fitted points increases. After the first point, there is no (real) choice but to use this as the next guess (using $b = 0$ is, on average, rather worse than any reasonable approximation). With two points, no test is possible, but $d = 1$ is on average by far the best choice and was used by default. At $n = 3$, a choice of $d = 1$ and $d = 2$ is possible, and $d = 3$ is not so clearly advantageous in general. After that, the scheme is straightforward, with b increasing towards the general optimum for each d as n increases, and then stopping at that value. The coefficients c , and associated weights, w , used are given in Table 2, and their use is summarized in the following equation, where, to minimize subscripts, we write p_{-j} to represent the log(concentration) for the (i)th species of interest in P_{Ai} at the j th prior point:

$$\hat{P}_{Ai}(d) = \sum_{j=1}^b p_{-j} c_{-j}(d, b) / w(d, b) \quad (4)$$

There is at present no known simple function which can be used to generate these coefficients,

Table 1. Number of points used in the extrapolation procedure ADEPT according to the number of data points available and the degree of the curve to be used

Number, n , of known points	Degree, d					
	0	1	2	3	4	5
1	1	—	—	—	—	—
2	—	2	—	—	—	—
3	1	2	—	—	—	—
4	1	2	3	—	—	—
5	1	2	4	4	—	—
6	1	2	5	5	5	—
7	1	2	5	6	6	6
8	1	2	5	7	7	7
9	1	2	5	8	8	8
10	1	2	5	9	9	9
11	1	2	5	9	10	10
⋮	⋮	⋮	⋮	⋮	⋮	⋮
16	1	2	5	9	14	15
⋮	⋮	⋮	⋮	⋮	⋮	⋮
21	1	2	5	9	14	20
⋮	⋮	⋮	⋮	⋮	⋮	⋮

and the most effective way of using them in a program is entered as a set of DATA statements to be read into an array as required.

Knowledge about the goodness of fit of a given degree of curve can only be based on a test of the immediately prior point. That is, to decide how best to predict p_0 , the goodness of prediction of p_{-1} must be tested with p_{-2}, p_{-3}, \dots . Thus, in equation (4), p_{-j} is replaced by p_{-j-1} . Then, given the expectation of continuity that no jump in best fit d of greater than ± 1 will be required, at most only three values need be tested: $d_i - 1, d_i, d_i + 1$, where d_i is the last chosen degree, subject to $0 \leq d \leq 5$. The test is then of the magnitude of the error of prediction of the previous point:

$$\text{error}(d) = |P_{Ai} - \hat{P}_{Ai}(d)| \quad (5)$$

where the circumflex implies the estimate at degree d , although (of course) P_{Ai} itself has error, the maximum of which is equal to ϵ . The optimisation of the degree of curve used is done for each independent species, independently. The more stable concentrations thus engender less calculation than do the more rapidly varying ones.

When the previous guess is 'exact' to the required tolerance, i.e., requiring zero iterations for a solution, the entire search procedure is skipped, the last prevailing d being used until iteration occurs again.

The Adaptive Extrapolation Procedure written to embody the above ideas is now termed ADEPT for convenience. In the tests described below, this will be described as either

on or off, depending on whether it is invoked or not; the latter case corresponds to $b = 0$ under RAMESES II.²

OSCILLATION

Despite earlier optimism concerning the assuredness of convergence,¹ and the pattern-breaking introduced to cause convergence when a certain kind of oscillation occurred, exploration of the behaviour of the algorithm and its implementation has revealed a class of problems that fails to give convergence for the general worst case of no prior information.²

To reiterate, the initial guesses (that is, for the first point of a scan or with $b = 0$) for the concentrations of the independent species will in general be far removed from the actual solution

values; RAMESES adopts a very low initial concentration for all such species as this is, on average, better than other possible starting points.² Further, the algebra of the problem permits (in principle) any meaningful subset of the species present to be defined as the independent species.^{1,3} For simplicity, this subset may be chosen to represent the 'minimal' notional building blocks required to form every species with only positive coefficients. However, this necessarily results in highly charged independent species when, for example, polybasic acids or high oxidation state metals are present. If one of these is used as the 'free' species, that is the one being used to adjust for charge balance, then the feedback may be so extreme that the system oscillates wildly and uncontrollably, especially when that species is present in very

Table 2. Coefficients and weights, $w(d, b)$, for the polynomial extrapolation functions of ADEPT for each degree up to 5 and the number of points used, b . The coefficients, $c(d, b, -j)$, are given in order of distance from the point to be predicted, and correspond to p_{-1}, p_{-2}, \dots [see equation (4)]

b	w	coefficients, $c_{-1}, c_{-2}, \dots, c_{-b}$
Degree: 1		
2	1	2 -1
Degree: 2		
3	1	3 -3 1
4	4	9 -3 -5 3
5	5	9 0 -4 -3 3
Degree: 3		
4	1	4 -6 4 -1
5	5	16 -14 -4 -4
6	3	8 -4 -4 1 4 -2
7	7	16 -4 -8 -3 4 6 -4
8	14	28 -2 -12 -9 0 8 8 -7
9	126	224 14 -76 -81 -36 24 64 49 -56
Degree: 4		
5	1	5 -10 10 -5 1
6	6	25 -35 10 20 -19 5
7	7	25 -25 -5 15 7 -15 5
8	56	175 -125 -75 45 81 5 -85 35
9	18	50 -25 -25 0 18 15 -5 -20 10
10	12	30 -10 -15 -5 6 10 5 -5 -10 6
11	33	75 -15 -35 -20 4 20 20 5 -15 -21 15
12	396	825 -75 -345 -265 -52 140 220 160 -5 -177 -195 165
13	143	275 0 -100 -95 -41 20 60 65 35 -16 -60 -55 55
14	2002	3575 275 -1100 -1250 -749 -45 540 810 695 251 -340 -770 -605 715
Degree: 5		
6	1	6 -15 20 -15 6 -1
7	7	36 -69 50 15 -48 29 -6
8	4	18 -27 8 15 -6 -13 12 -3
9	12	48 -57 -2 33 12 -23 -18 27 -8
10	15	54 -51 -16 24 24 -4 -24 -9 26 -9
11	33	108 -81 -46 24 48 20 -24 -39 -4 45 -18
12	22	66 139 -32 3 24 20 0 -18 -18 3 24 -11
13	286	792 -363 -398 -69 204 260 120 -90 -216 -153 78 253 -132
14	1001	2574 -891 -1276 -471 390 775 600 75 -450 -639 -324 341 726 -429
15	715	1716 -429 -814 -429 96 425 450 225 -100 -345 -366 -121 264 429 -286
16	104	234 -39 -104 -69 -6 43 60 45 10 -27 -48 -41 -6 39 52 -39
17	1768	3744 -351 -1534 -1209 -348 443 858 825 440 -99 -558 -733 -516 39 650 741 -624
18	1326	2652 -78 -988 -897 -390 149 504 594 440 132 -204 -439 -747 -273 104 468 468 -442
19	1938	3672 102 -1228 -1263 -696 -1 534 774 704 396 -24 -409 -624 -579 -262 228 648 578 -612
20	19380	34884 2754 -10336 -11946 -7746 -1747 3468 6513 6968 5148 1872 -1768 -4638 -5793 -4708 -1509 2796 6086 4896 -5814

low concentration. This lack of control arises essentially from the nature of the oscillation in that it has a period of greater than two iterations, which the adaptive gain procedure² was not designed to handle. In fact, it turns out to be rather difficult to identify oscillation of that kind reliably, so that corrective action can be taken, without severely compromising the present efficiency for other systems. The problem could be avoided by choosing a low charge number (complexed) free species, but this would seriously weaken the principle upon which RAMESES has been designed, namely, to handle any starting conditions reliably without the use of prior knowledge or exploration. Accordingly, a procedure has been designed to handle such situations.

Previously,² no upper limit was found necessary for the elements of F , the (diagonal) matrix of correction factors; this enables rapid convergence in many cases, as does the setting of a rather small lower limit.² It was found, however, that in cases of the uncontrolled oscillation, setting much closer limits permitted the commencement of a convergent series of iterations. Thus, a limit should be adjusted towards unity whenever a calculated F_{ii} lies outside that bound. However, very great changes in the value of F_{ii} may occur under ordinary circumstances in the early iterations (indeed, this is one reason for the algorithm's usual efficiency), and the limit adjustment needs to be held off until it is likely that uncontrolled oscillation is the cause. A slight relaxation of the limits can also be used during convergence to prevent untoward constraint arising spuriously.

A possible implementation of the procedure in BASIC is given in the Appendix as the procedure FLIMIT. After testing the effects of this procedure it was found that the best balance was obtained with the following values for the relevant constants:

- switch%: 4
- dec #: there is a shallow optimum in the region 0.3–0.6; 0.5 was chosen.
- inc #: 1.1; this value is not critical.
- limit #: 25; this was found to be best matched to the factor used in setting the initial guesses for the vector X_A ,² as this then ensured little influence, if any, on the more well-behaved systems. Thus a at equation (2.15) is now 10^{-25} .

INDEXING

Even though RAMESES II achieved lower storage requirements and execution time by eliminating a sparse matrix multiplication, there are still multiplications of matrices containing a large number of zeros, *viz*: at equation (1.12) and (3.6), and other calculations that might be considered redundant. In this latter group are all operations involving components with zero concentration² and fixed partial pressures. There are two main strategies that may be employed in these circumstances: testing for the presence of the zero before doing the multiplication or using an address matrix to indicate the non-zero elements. There is necessarily some execution time required for such schemes, and their benefits must outweigh that loss of speed for them to be worthwhile implementing. Effectively, the trade-off to be considered is the difference in the time to execute an "IF $x = 0$ THEN . . ." test as compared to a location index assignment such as " $i = A(j)$ ", both with respect also to " $y = x * 0$ ". A number of trials served to show that an address matrix was the more efficient, becoming more so as the size of the system increased, particularly the numbers of components, r . Thus, considering as an example the indexing of the matrix C'_A [equation (3.17)] for the calculation of equation (3.6), the zeros are eliminated by row. A BASIC procedure, ROWINDEX, to achieve this is given in the Appendix, as is the code for the implementation of the addressing procedure used in the evaluation of equation (3.6), EQUATION36.

Further indexing for the processing of the independent vector, X_A , to skip zero concentrations, fixed partial pressures and the like, is trivial and need not be elaborated upon.

LOWER BOUND

A potential problem, although as yet not encountered in practice, is that of an independent species' concentration falling below that value corresponding to the smallest positive machine number, EPS, or perhaps more to the point, to less than $\epsilon^{-1} \cdot \text{EPS}$. In contrast to the previously discussed handling of zero or vanishing calculated concentration,² no default condition can be employed. This type of fault is not related to the algorithm employed for solution, but to the system under study, the choice of independent species, and the dynamic range of the machine/language combination in use.

As, again, reliance on prior knowledge is inappropriate, a test for this condition can be built into the tolerance test subroutine. For example, if

$$P_{Ai} < \log_{10}(\text{EPS}/\text{TOL}) \quad (6)$$

holds, at any time after (say) 10 iterations, where $\text{TOL} = \epsilon$, the program should branch to an error handling routine. This could indicate the nature of the problem, permit the choice of a substitute independent species, and then proceed with the column exchange between C_A and C_B , and the corresponding element exchanges between X_A and X_B , and within Q [equation (2.12)], before proceeding to the inversion of the replacement C_B and the second attempt at a solution. This violates the principle of the RAMESES design in that user-intervention is required, but in view of the fact that it is a simple choice and also that the problem has yet to arise, it may not be too much of a burden, and the violation is not considered too serious. Equally, this is essentially a machine-dependent problem and so must apply to any algorithm dealing with this kind of system.

It is worth pointing out at this juncture that, even if a calculated concentration falls well below N_0^{-1} , the 'Avogadro dilution', both the algebraic solution of the system of equations and the existence of the species, in the statistical sense of only rarely occurring for a (very) short duration, remain valid, as does the model. The chemical implications of such species are a matter for a different forum; non-existence depends on interpretation.

EXAMPLES

The program incorporating ADEPT, the extreme oscillatory control and the indexing

refinements is referred to as RAMESES III. The opportunity has been taken to fix up some bugs and inefficiencies that have been found in the code. The testing was done in the same language and on the same machine as before.² RAMESES graphics screen images were printed directly on a dot-matrix printer (P5, NEC Corporation, Tokyo, Japan) with an EGA Screen Dump program (P5DUMP, Imago Software, Sydney, Australia).

The direct comparison of RAMESES II ($b = 0$) and III (ADEPT off), is shown in the left hand part of Table 3. Regardless of other considerations, such a test is essential to ensure freedom from starting-condition constraints.² The test systems that were previously employed were used (despite some doubts about their usefulness otherwise²) to allow ready comparison with previous results. We now refer to the artificial system called ESTIME as System V. Some substantial improvement in all except Systems I and III were obtained. Even in System III, despite nearly doubling the mean iterations (due to detuning, *v.i.*), the indexing gave a net decrease in execution time. The deterioration in System I is proportionately large, but in real terms quite irrelevant. This illustrates essentially the overhead in execution time due to indexing in a very small system.

With ADEPT on the results (Table 3) show an entirely satisfactory improvement in performance. In particular, the number of 'zero iteration' points is a very large proportion of the total for Systems I and IV, and not insignificant in Systems II and III. Only System V proved resistant under these conditions, but even here the minimum number of iterations is, for each set of starting conditions, equal to one.

Table 3. Some illustrative results for the test systems to show the effect on timing of the current implementation of RAMESES III (pH 0–14, $h = 0.25$ [57 points]; $-\log \epsilon = 3$)

System		RAMESES II $b = 0$				RAMESES III				ADEPT on				
		iterations				iterations				iterations				
		τ, sec	max	min	mean	τ, sec	max	min	mean	τ, sec	max	min	mean	zeros
I	a	10	8	1	2.0	13	4	2	3.0	7	3	0	0.6	31
	b	10	8	1	2.0	13	4	2	3.0	6	3	0	0.6	31
	c	17	4	3	2.0	13	4	2	3.0	7	2	0	0.6	25
II		354	110	4	71.7	245	79	4	53.1	35	47	4	6.2	11
III		183	7	4	6.4	176	14	4	11.6	42	4	0	1.5	9
IV		51	4	4	4.0	32	4	2	3.0	16	4	0	0.6	31
V	a	429	131	3	58.0	344	99	4	44.8	86	52	1	10.1	0
	b	578	170	4	78.2	431	127	4	56.2	132	119	1	16.9	0
	c	687	205	4	92.4	485	140	4	65.5	120	81	1	14.3	0
	d	434	120	4	58.2	352	112	4	47.4	87	68	1	10.6	0
	e	742	230	4	100.9	588	178	4	79.7	99	58	1	11.8	0

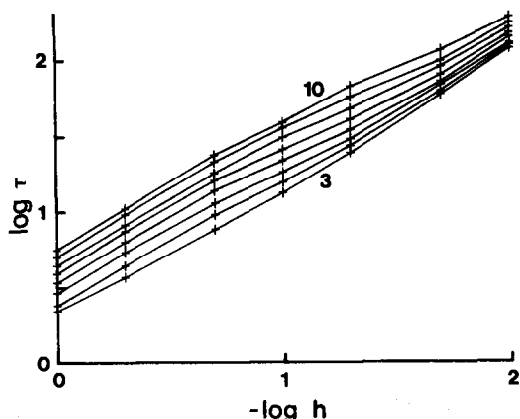


Fig. 2. Log(τ) vs. $-\log(h)$ for System I for $-\log \epsilon = 3-10$.

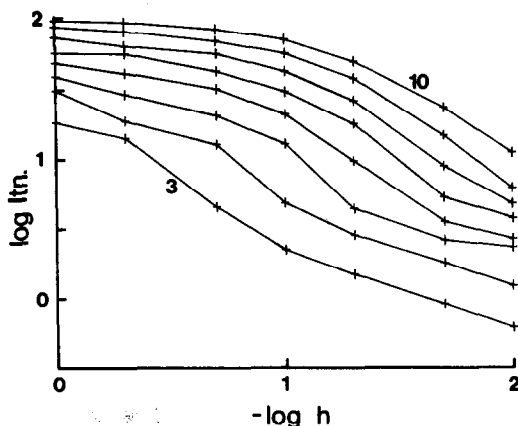


Fig. 4. Log(total Itn.) vs. $-\log(h)$ for System II for $-\log \epsilon = 3-10$.

The 'zero' iterations should perhaps be explained. If the elements of S , the component total vector [equation (1.12)], are each within tolerance with only the extrapolated values of X_A to find X_B , then no refinement of X_A whatsoever is necessary, and the routine skips to the calculation for the next point. Thus no iteration with equation (2.4) has been performed, and the iteration number recorded is zero. The number of zero iterations is therefore a further measure of the effectiveness of the extrapolation, because no calculation beyond that of the polynomial was required. Previously, iterations were counted on entry to the core routine, but this gives a false picture of what the algorithm has actually done. Earlier reported iteration values² (maximum, minimum and mean) should therefore each be reduced by one for proper interpretation (the iteration values for RAMESES II in Table 3 have been so adjusted). This definition of the number of iterations also accounts for the mean falling below one in some case in the present report.

An interaction was expected between the stepping interval and the accuracy of forward extrapolation, depending on the tolerance permitted and the preselected degree of the fitted polynomial under RAMESES II.² Although the latter factor is irrelevant in ADEPT, the interrelationships of run-time (τ), total number of iterations and number of zeros with tolerance (ϵ) and step size (h) were examined for all five test systems for a scan over the range pH 0-14; $h = 1, 0.5, 0.2, 0.1, 0.05, 0.02, 0.01$; $-\log \epsilon = 3-10$. Some representative results are given in Figs. 2-10.

For the simple Systems, I, III and IV, $\log \tau$ increased in fairly uniform steps with $-\log \epsilon$, and was also more or less linearly dependent on the number of steps taken (Fig. 2). For Systems II and V the picture is more complicated (Fig. 3), showing local optima, presumably due to some tuning effect, which optima shifted to smaller h at tighter tolerances.

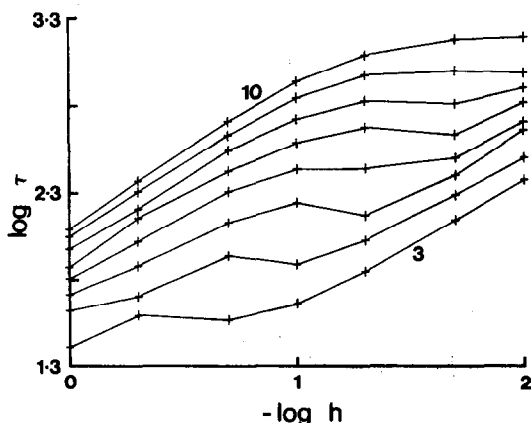


Fig. 3. Log(τ) vs. $-\log(h)$ for System II for $-\log \epsilon = 3-10$.

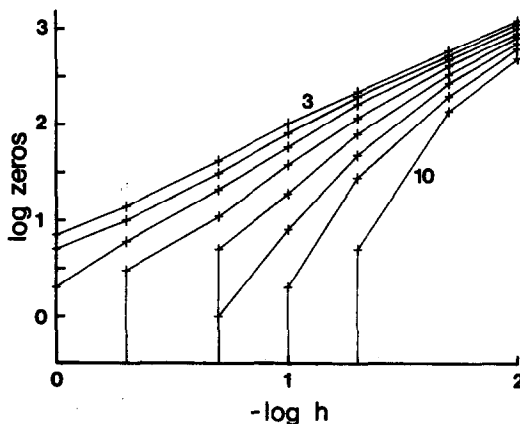


Fig. 5. Log(no. of zero iterations) vs. $-\log(h)$ for System IV for $-\log \epsilon = 3-10$. The vertical line segments indicate zero iteration steps.

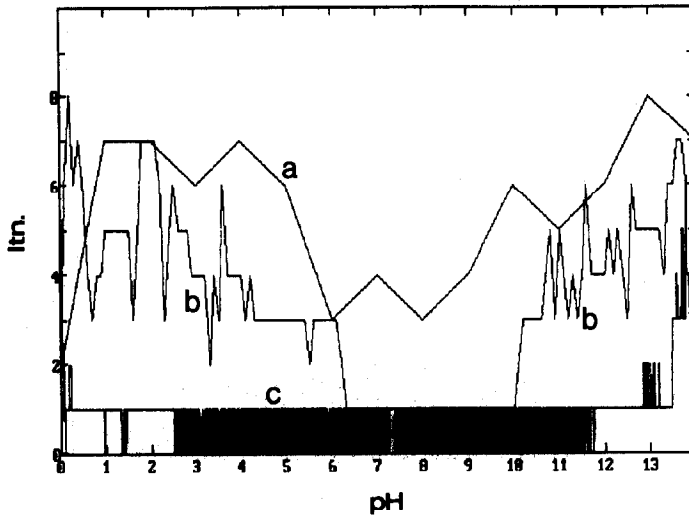


Fig. 6. Number of iterations vs. pH for System I (all conditions) under RAMESES III with ADEPT, $-\log \epsilon = 10$. pH step sizes a : 1, b : 0.1, c : 0.01.

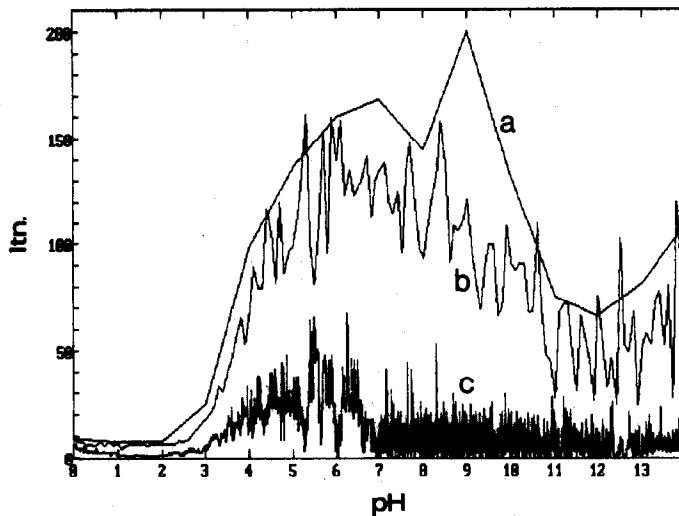


Fig. 7. Number of iterations vs. pH for System II under RAMESES III with ADEPT, $-\log \epsilon = 10$. pH step sizes a : 1, b : 0.1, c : 0.01.

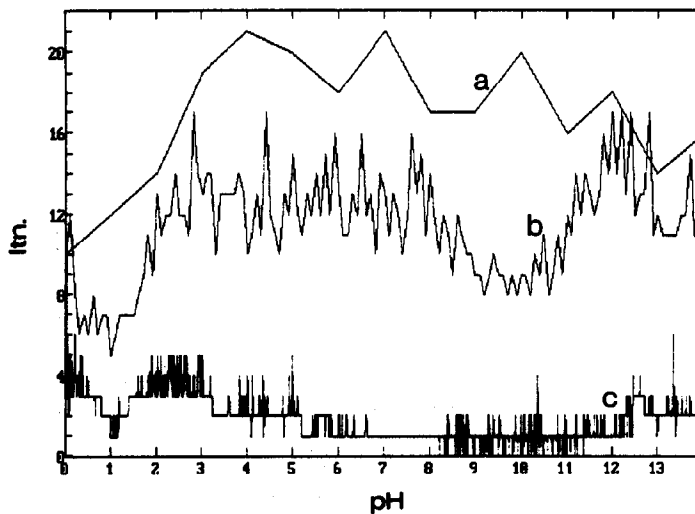


Fig. 8. Number of iterations vs. pH for System III under RAMESES III with ADEPT, $-\log \epsilon = 10$. pH step sizes a : 1, b : 0.1, c : 0.01.

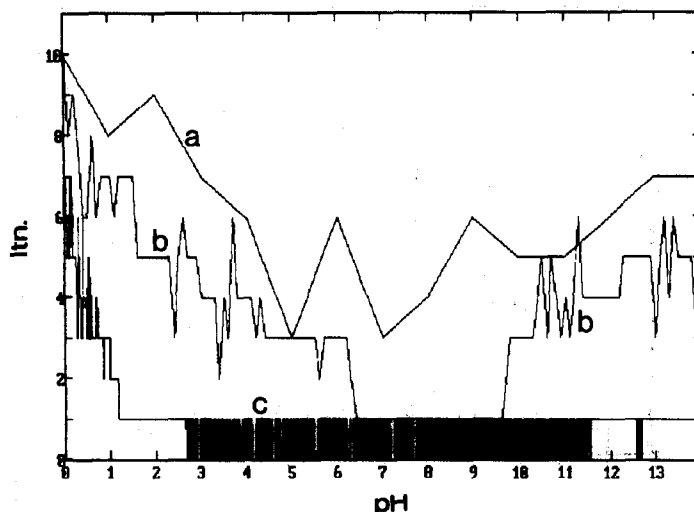


Fig. 9. Number of iterations *vs.* pH for System IV under RAMESES III with ADEPT, $-\log \epsilon = 10$. pH step sizes *a*: 1, *b*: 0.1, *c*: 0.01.

The only differences between plots within these groups were essentially of the scale factors applied to the ordinate. These effects are mirrored in the number of iterations (Fig. 4), more or less uniformly for all systems. The relative differences arise only because of the overhead arising from the size of the system rather than variation in the behaviour of the system or the algorithm. The number of zeros observed increased steadily with a decrease in h , the absolute slope of the log-log plot approaching unity once zeros become possible (Fig. 5). It is nevertheless more difficult to be accurate at tighter tolerances.

We have argued² that, because of condition-sensitivity, algorithm performance should be

demonstrated in part by the variation in number of iterations per point over a scan. Thus, for the five test systems used, we give some such results for the above pH scans for three values of h , namely 1 (*a*), 0.1 (*b*) and 0.01 pH (*c*) (Figs. 6–10). The tolerance was set to 10^{-10} in order to avoid the plots having large and overlapping sections running along the abscissa, *i.e.*, zero iterations, but also to show more clearly the relative effects of changing h and pH. For example, System I at $\epsilon = 10^{-3}$ has respectively 7/15, 105/141 and 1226/1401 (zeros/no. of points) for the three step sizes.

For Systems II and V the difficulty of solution increases markedly for $\text{pH} \geq 3$. It is speculated that 'difficulty' is a property of the system and

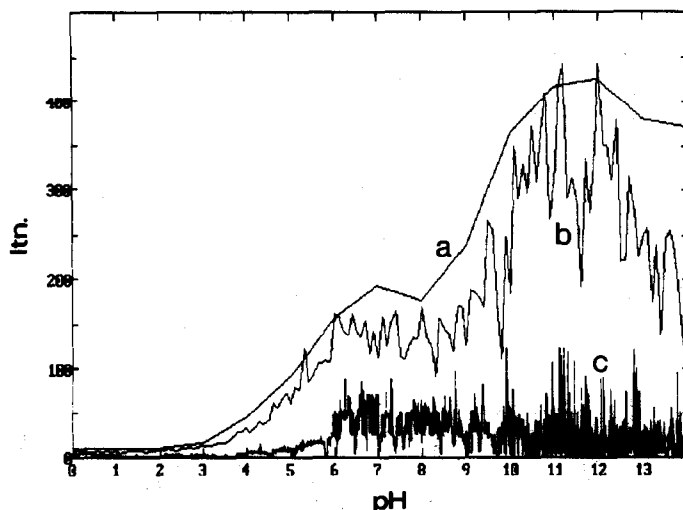


Fig. 10. Number of iterations *vs.* pH for System V (condition *d*) under RAMESES III with ADEPT, $-\log \epsilon = 10$. pH step sizes *a*: 1, *b*: 0.1, *c*: 0.01.

Table 4. Some run results for the system H_3PO_4 in water, using the stated ion as the free (charge balance) species, employing the procedure FLIMIT in RAMESES III (pH 2–6.9, $h = 0.1$ [50 points]; $-\log \epsilon = 3$)

Free Species	ADEPT off iterations				ADEPT on iterations				zeros
	τ , sec	max	min	mean	τ , sec	max	min	mean	
$H_2PO_4^-$	4.8	3	1	2.06	4.6	3	0	0.60	31
HPO_4^{2-}	32.5	30	3	23.60	4.1	23	0	0.46	49
PO_4^{3-}	33.6	28	20	24.30	5.9	64	0	1.78	48

conditions, and not the algorithm, as the same pattern appeared under all the many strategies investigated.

One curiosity that may be detected by inspection of Figs. 6–10, most easily for the lines (b) corresponding to $h = 0.1$ pH, is of an oscillation in the number of iterations taken from point to point superimposed on the general trend. The period is generally equal to 2 or a little greater. Close inspection of the elements of the error matrix E [equation (1.15)] showed the following general explanation. When a solution is delayed because a small number of the X_{Ai} have not settled, the remaining elements of X_A necessarily continue to improve in precision, sometimes to many digits better than the preset tolerance would suggest. This means that the estimates for the next point are good and fewer iterations are required to achieve the required precision because the error of prediction is proportionately smaller. However, in that time, the stable elements will not have achieved the same high precision. This continues for a small number of points but eventually the accumulated errors become large enough to require more iterations. As can be seen, the effect is not large enough to cause concern, but the amplitude is in some sense a measure of the perturbation sensitivity of the system. The larger oscillations occur in regions of greater difficulty, as measured by the (local) average number of iterations.

Phosphoric acid in water provides a good example of the kind of uncontrolled oscillatory behaviour occurring during attempted solution. For a scan in pH from 2 to 7, using either HPO_4^{2-} or PO_4^{3-} as the free species, the calculation fails ever to converge, although for $H_2PO_4^-$ the solution is obtained very rapidly.

Introducing the FLIMIT procedure, all three free species choices can be used successfully in satisfactorily short calculation times and few iterations even with ADEPT off (Table 4). The entry for $H_2PO_4^-$ (ADEPT off) is unaffected by the use of FLIMIT. With ADEPT on, the results were somewhat improved (Table 4). In the case HPO_4^{2-} , only the first point of the 50 in the scan is calculated iteratively, because this species has a constant concentration, while for PO_4^{3-} only the first two points are found by iteration as its $\log(\text{concentration})$ changes linearly.

An example has been given of a system (now labelled System VI) that fails in an established program, GEOCHEM, and of a method of avoiding that difficulty.⁴ It was reported that at pH 7.3 the revised produce took 82 iterations to $\epsilon = 10^{-6}$ (their definition of tolerance appears to be similar to that of RAMESES): no timing was given.⁴ Using the published information (which has some errors*) and adding a background 'NaCl' for charge balance, and scanning over pH 0–14, $h = 0.1$, the results shown in Figs. 11 and 12 and Table 5 were obtained. It can be seen that while there is some more difficulty in the pH range 5–9, RAMESES encountered no particular problem, even with ADEPT off: at pH 7.3, the single calculation required 45 iterations for $\epsilon = 10^{-6}$.

DISCUSSION

The use of smoothing polynomial functions to provide the independent species' concentration estimates for the calculation of the next

Table 5. Some run results for System VI with RAMESES III; pH 0–14, $h = 0.1$. (Dashes under 'zeros' mean 'not applicable'.)

ADEPT	$-\log \epsilon$	τ , sec	Iterations			
			max	min	mean	zeros
off	3	240	40	5	21.5	—
on	3	28	5	0	1.2	33
off	6	325	50	9	29.5	—
on	6	83	13	1	6.1	0

*We have dealt with the typographical errors in the report⁴ as follows: corrected the sign of the $\log(\text{formation constants})$; assumed that (a) total concentrations are given as $-\log(\text{conc.})$, not $\log(\text{conc.})$; (b) "DTPA" complexes are "CaDTPA"; (c) the second "CaDTPA" complex with stoichiometry "110" is in fact "210". The carbonate said to be present, but not defined, was ignored.

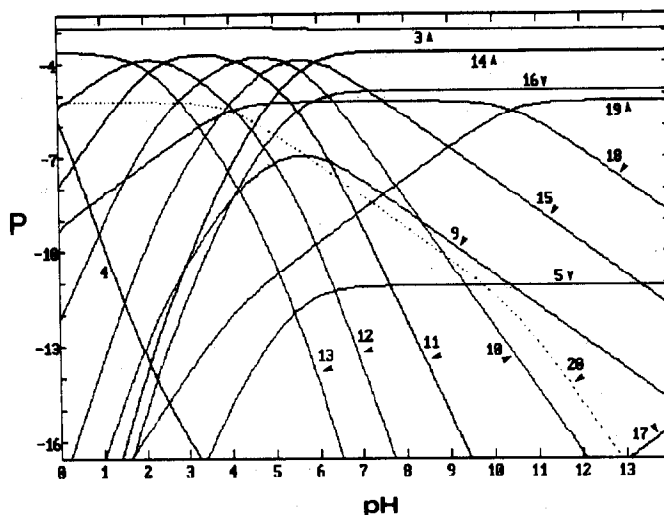


Fig. 11. Distribution diagram for System VI. Species: 3 Ca^{2+} , 4 Fe^{3+} , 5 H_5DTPA^- , 9 DTPA^{5-} , 10 HDTPA^{4-} , 11 $\text{H}_2\text{DTPA}^{3-}$, 12 $\text{H}_3\text{DTPA}^{2-}$, 13 H_4DTPA^- , 14 CaDTPA^{3-} , 15 CaHDTPA^{2-} , 16 Ca_2DTPA^- , 17 CaOH^+ , 18 FeDTPA^{2-} , 19 FeHDTPA^{2-} , 20 FeOHDTPA^{3-} . The 'background' species are omitted, and the Fe-OH species are at very low concentrations.

point in a scan provides the most efficient use of the information available at prior points, given that these functions are approximations. The rapid deterioration of prediction accuracy with degree for the minimum number of points (Fig. 1) can be seen to provide a limitation to the effectiveness of the simple procedure suggested earlier,² but of course then the choice of degree was arbitrary.

It is unfortunate that direct comparison of these results with the theoretically attractive⁵ analytical differentiation for extrapolation, as used for example in PSEQUAD,¹¹ cannot presently be made as no documented examples

are known. We speculate however that since it is essentially based on a form like equation (1), the method will be successful in systems or regions with many straight lines in the plots of $\log(\text{concentration})$ vs. pH for example (such as are seen in Systems II and III, Figs. 7 and 10 in Reference 2). But in more complex regions, such as typifies System V (Fig. 1²), we would expect less efficiency. ADEPT is more flexible.

With the incorporation of ADEPT, any further substantial improvement in speed or efficiency seems unlikely. This remark needs qualification. In the tests that have been done, many combinations of strategies and values for

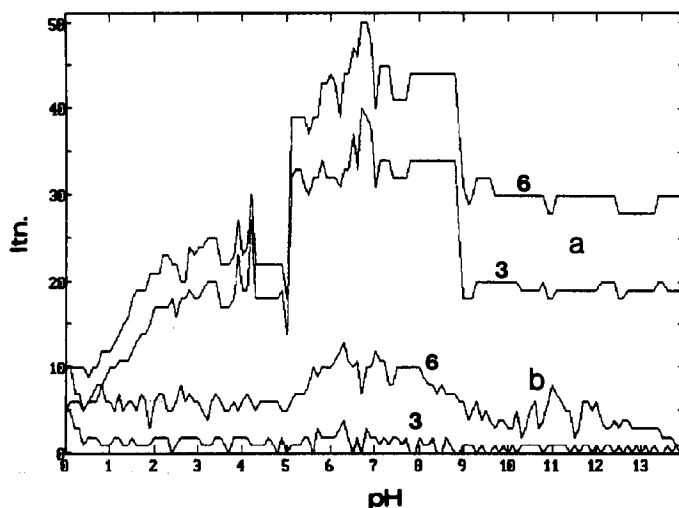


Fig. 12. Number of iterations vs. pH for System VI under RAMESES III with ADEPT (a) off, (b) on; $-\log \epsilon = 3, 6$; $h = 0.1$.

the few arbitrary factors used exist, and for some systems and conditions quite remarkable results can be obtained. However, this has been found to be to the detriment of performance with other systems or conditions, sometimes badly so. Some consequences of this kind of effect are to be seen in the results for Systems I and III (Table 3). Quite clearly, there can be no universal optimum strategy. So, relying on the principle that we have taken as a guide the development of RAMESES, *i.e.*, that prior knowledge should not be needed, we are obliged to concede that the results presented are not by any means the best possible for each system, because we avoid the provision of user-adjustable parameters or switches. Simply put, the user should not need to be concerned with tuning before starting work. In this sense, the production of dedicated programs for particular problems,¹² or more elaborate but still limited generalised solutions to a class of problems,¹³ has required system-specific analysis. But, although this serves immediate purposes, it does not help other users who must tailor such programs to their individual needs. These other approaches are therefore redundant in the face of the existence of algorithms such as RAMESES. We believe that we have come close to an overall optimum tuning of the present program, and that it will be of wide applicability. We shall therefore turn our attention to

handling other aspects of the general problem within the framework of RAMESES. Whether it is the fastest possible program is another matter and is a question we see no point in attempting to address. A speed claim has been made for another program,¹⁴ but this is with a routine that relies on a weak tolerance test.² Such claims are dangerous and not very helpful. Even so, RAMESES III can be seen to compare at least favourably despite the handicap of a rigorous tolerance test.

The oscillation problem now handled represents the same kind of difficulty as defeats some NR techniques inasmuch as the initial estimates are outside of the region of convergence.⁴ However, whether it is capable of being controlled as easily as at present in the NR context cannot be said as, on the one hand, we are unaware of any other treatment of this type of problem, and, on the other, charge balance itself is rarely considered.² It remains noteworthy that the revised algorithm for the NR method only had an "increased" convergence range, *i.e.*, of input estimate values that would lead to a solution; RAMESES only requires each $X_i > 0$, with no sensible upper bound.

Experience to date leads to the confidence that RAMESES can continue to be developed as a robust, efficient algorithm with effective implementation. It is hoped to make the program available for testing shortly.

APPENDIX

Possible BASIC implementations of the procedures described in the text.

FLIMIT:

FOR j% = 1 TO ncom%

IF itm% > switch% THEN

IF F#(j%) > = Ful#(j%) THEN

IF Fulc%(j%) < 2 THEN

Fulc%(j%) = Fulc%(j%) + 1

Flimit#(j%) = Flimit#(j%)*dec#

ELSE

Flimit#(j%) = MIN(Flimit#(j%)*inc#, limit#)

END IF

Fllc%(j%) = 0

END IF

IF F#(j%) < = Fll#(j%) THEN

IF Fllc%(j%) < THEN

Fllc%(j%) = Fllc%(j%) + 1

Flimit#(j%) = Flimit#(j%)*dec#

ELSE

Flimit#(j%) = MIN(Flimit#(j%)*inc#, limit#)

END IF

Fulc%(j%) = 0

END IF

IF F#(j%) > Fll#(j%) AND F#(j%) < Ful#(j%) THEN

Fulc%(j%) = 0

Fllc%(j%) = 0

'procedure to control correction factor limits

'range = no. of components

ELSE

Ful#(j%) = 10 Flimit#(j%)

Fill#(j%) = 10 - Flimit#(j%)

G#(j%) = 1#

END IF

END IF

F#(j%) = MIN(MAX(G#(j%)*(F#(j%) - 1#) + 1#, F11#(j%)), Ful#(j%))

NEXT j%

% indicates an integer; # indicates double precision, floating point.

The arrays have the following interpretations:

F#(): concentration correction factors, F

Ful#(): upper limits for the elements of F#()

Fill#(): lower limits for the elements of F#()

Flimit#(): exponents for calculation Ful#(), Fill#()

Fulc%(): counters for attempted crossings of upper limit

Fill%(): counters for attempted crossings of lower limit

G#(): sensitivity factors²

The constants are:

j%: component index

ncom%: number of components

itn%: iteration counter

switch%: hold off

dec#: decrement factor for absolute value of limit exponent

inc#: increment factor for absolute value of limit exponent (relaxation)

limit#: overall limit for absolute value of limit exponent

ROWINDEX:

'procedure to index non-zero element of
'coefficient matrix CA' = Ca2#()

maxoccr% = 0

FOR i% = 1 to neq%

rocc% = 0

FOR j% = 1 to ncom%

IF Ca2#(i%, j%) THEN rocc% = rocc% + 1

NEXT j%

maxoccr% = MAX(maxoccr%, rocc%)

NEXT i%

maxoccr% = max occhr% + 1

REDIM Ca2ndxr%(neq%, maxoccr%)

'address matrix for rows

FOR i% = 1 to neq%

k% = 0

'initialise counter

FOR j% = 1 to ncom%

IF Ca2#(i%, j%) THEN

i% = k% + 1

'find non-zero element

Ca2ndxr%(i%, k%) = j%

'count non-zero elements

NEXT j%

'store address

Ca2ndxr%(i%, maxoccr%) = k%

'store no. of non-zero elements

NEXT i%

EQUATIONS36:

'procedure using indexed multiplication, eqn 3.6

FOR i% = 1 to neq%

FOR j% = 1 to Ca2ndxr%(i%, maxoccr%)

k% = Ca2ndxr%(i%, j%)

'extract address

Xb#(i%) = Xb#(i%) - Ca2#(i%, k%)*Pa#(k%)

NEXT j%

REFERENCES

1. V. W.-H. Leung, B. W. Darvell and A. P.-C. Chan, *Talanta*, 1988, **35**, 713.
2. B. W. Darvell and V. W.-H. Leung, *ibid.*, 1990, **37**, 413.
3. V. W.-H. Leung and B. W. Darvell, *ibid.*, 1990, **37**, 425.
4. L. M. Dudley and C. S. Coray, *Environ. Sci. Technol.*, 1989, **23**, 245.
5. D. J. Leggett, *Computational Methods for the Determination of Formation Constants*, Chap. 1, Plenum, New York, 1985.
6. P. Gans, *Coord. Chem. Rev.*, 1976, **19**, 99.
7. P. Gans, A. Sabatini and A. Vacca, *J. Chem. Soc., Dalton Trans.*, 1985, 1195.
8. A. Vacca and A. Sabatini, in *Computational Methods for the Determination of Formation Constants*, D. J. Leggett (ed.), Chap. 5, Plenum, New York, 1985.

9. D. J. Cowden, *Weights for fitting polynomial secular trends*, Technical Paper 4, School of Business Administration, University of North Carolina, 1962.
10. M. Kendall and A. Stuart, *The Advanced Theory of Statistics*, Vol. 3, 3rd ed., Chap. 46, Griffin, London, 1976.
11. L. Zekany and I. Nagypal, in *Computational Methods for the Determination of Formation Constants*, D. J. Leggett (ed.), Chap. 8, Plenum, New York, 1985.
12. R. P. Shellis, *Computer Applications Biosciences*, 1988, **4**, 373.
13. I. J. McNaught and G. D. Peckham, *S. Afr. J. Sci.* 1989, **85**, 386.
14. C. De Stefano, P. Princi, C. Rigano and S. Sammartano, *Computers Chem.*, 1989, **13**, 343.

A COMPUTER MODEL OF STRUVITE SOLUTION CHEMISTRY

W. D. SCOTT, T. J. WRIGLEY and K. M. WEBB

Environmental Science, School of Biological and Environmental Sciences, Murdoch University,
Murdoch 6150, Western Australia

(Received 9 March 1990. Revised 18 February 1991. Accepted 26 February 1991)

Summary—A computer model is developed to describe struvite solution chemistry; this includes the electroneutrality equation and allows greater variability in the input components. Relationships between the major ions are retained without approximation. The model results fit data derived both in our laboratory and from the literature. Equilibrium constants which markedly affect the output are identified and solubility constants are derived. Applications of the model include studies of waste-water treatment and of the formation of kidney stones.

The solubility product (K_{sp}) for struvite ($MgNH_4PO_4 \cdot 6H_2O$) has been derived by several authors (e.g., Johnson,¹ Taylor *et al.*,² and Burns and Finlayson³). However, these solubility product values are based on only some of the complex ionic equilibria and various approximations are made which limit their applicability. For instance, Linder and Little⁴ developed a computer model for equilibrium speciation of urine. Good predictions were obtained for the precipitation of calcium oxalate monohydrate, dicalcium phosphate dihydrate, calcium hydroxyapatite and uric acid, but not for struvite.

A more complete understanding of struvite solution chemistry is necessary to solve applied problems such as its formation in waste-water treatment systems and in urinary and kidney stones (uroliths). In the removal of phosphorus in waste-water treatment systems struvite deposition has attracted considerable attention, and is a major precursor of the eutrophication of water bodies.⁵⁻⁷ Struvite is the most common type of urolith deposited in cats and dogs, and forms 15% of all uroliths found in humans. All these depositions occur as a result of increased concentrations of less soluble crystallites at raised pH.⁶⁻¹⁰ Also struvite formation is important after the application of phosphate fertilizers to soils¹¹ and after the canning of seafoods.¹²

There is a need for an algorithm that treats the general problem of struvite equilibria. The aim of this study is to specify mathematically the solubility of struvite, by using the known ionic equilibria. The intention is to compare theoretical solubility data derived from the

model with available data and provide a basis for the development of a predictive model for use in waste-water treatment and medical research.

Chemical equilibria

The appropriate literature values of the solubility constants and dissociation constants are listed in Table 1. The equilibria listed in the first column include only the simplest forms and are presented in the way they are used in the final algorithm (Table 2). The constants in Table 1 are for a standard temperature of 25° and were used to form Figs. 1(a) and 1(b). The second column shows a range of pK values from the references as noted; the third column consists of selected values as used. Note that the literature values are derived from experiments and are dependent on the model used to interpret the experimental results.

The model was developed to understand the optimal conditions for struvite formation and is limited to the range of minimum solubility. It allows for variations of components formed from ammonia, phosphate, magnesium and water. A separate term may be included to account for the addition of an excess of non-reacting ions.

Three assumptions are made, as follows:

(1) No species are present other than those derived from the independently variable components, water, magnesium, ammonia and phosphate. Ionic and molecular species included are Mg^{2+} , $Mg(OH)^+$, NH_3 , NH_4^+ , PO_4^{3-} ,

Table 1. Equilibrium solubility constants relevant to struvite formation

	Range of log <i>K</i> values from literature ^{13,14}	Value of log <i>K</i> used in calculations ¹⁵
$H^+ + NH_3 = NH_4^+$	9.2–9.3 ^{a,b}	9.3
$H^+ + H_2PO_4^- = H_3PO_4$	2.1–2.2 ^{c,d}	2.1
$H^+ + HPO_4^{2-} = H_2PO_4^-$	7.1–7.2 ^{e,f}	7.2
$H^+ + PO_4^{3-} = HPO_4^{2-}$	12.0–12.4 ^g	12.0
$Mg^{2+} + OH^- = MgOH^+$	2.6 ^{h,i}	2.6
$Mg^{2+} + 2OH^- + 6H_2O = Mg(OH)_2 \cdot 6H_2O$	10.5–11.3 ^j	10.9
$Mg^{2+} + HPO_4^{2-} = MgHPO_4$	5.8 ^{k,l}	5.8
$Mg^{2+} + PO_4^{3-} + 8H_2O = Mg_3(PO_4)_2 \cdot 8H_2O$	25.2 ^{k,l}	25.2
$Mg^{2+} + PO_4^{3-} + 22H_2O = Mg_3(PO_4)_2 \cdot 22H_2O$	23.1 ^{k,l}	23.1
$Mg^{2+} + NH_4^+ + PO_4^{3-} + 6H_2O = MgNH_4PO_4 \cdot 6H_2O$	13.2 ^{k,l}	13.2
$H^+ + OH^- = H_2O$	13.9–14.0 ^{m,n}	14.0

^aH. S. Harned and B. B. Owen, *J. Am. Chem. Soc.*, 1930, **52**, 5079.

^bG. N. Lewis and P. W. Schutz, *ibid.*, 1934, **56**, 1913.

^cR. G. Bates, *J. Res. Natl. Bur. Stds.*, 1951, **47**, 127.

^dH. C. Helgeson, *J. Phys. Chem.*, 1967, **71**, 3121.

^eR. C. Phillips, P. George and R. J. Rutman, *Biochemistry*, 1963, **2**, 501.

^fP. Papoff, G. Torsi and P. G. Zamboni, *Gazzetta*, 1965, **95**, 1031.

^gJ. Beukenkamp, W. Riemann III and S. Lindenbaum, *Anal. Chem.*, 1954, **26**, 505.

^hD. I. Stock and C. W. Davies, *Trans. Faraday Soc.*, 1948, **44**, 856.

ⁱP. B. Hostetler, *Am. J. Sci.*, 1963, **261**, 238.

^jR. Nasänen, *Z. Phys. Chem.*, 1941, **188**, 272.

^kA. W. Taylor, A. W. Frazier and E. L. Gurney, *Trans. Faraday Soc.*, 1963, **59**, 1580.

^lA. W. Taylor, A. W. Frazier, E. L. Gurney and J. P. Smith, *ibid.*, 1963, **59**, 1585.

^mR. Lorenz and A. Böhl, *Z. Phys. Chem.*, 1909, **66**, 733.

ⁿG. N. Lewis and M. Randall, *Thermodynamics*, p. 487. McGraw-Hill, New York, 1923.

HPO_4^{2-} , $H_2PO_4^-$, H_3PO_4 , OH^- , H^+ , H_2O and an excess of non-reactive positive and negative ions. In contrast to the work of Verplaetse *et al.*¹⁶ and Stumm and Morgan,¹⁷ this assumption considers the possibility of an excess of acid, ammonium or magnesium ions; it not only applies to the case of dissolution of pure struvite but allows for formation of struvite from its pure components when these are in non-stoichiometric portions.

(2) The effects of ionic strength on activity coefficients can be neglected; it is assumed that the activities of individual ions are equivalent to their concentrations. Currently we have assumed the ionic strength of around 0.1 to be relevant to urine and waste-water treatment. Note that it is possible by repeated calculations to estimate activity coefficients by using the Debye-Hückel or Davies approximations. These calculations are more time-consuming and are to be considered in a follow-up paper. This approximation is already widely used and is unlikely to change the structure of the results.

(3) Only one insoluble solid phase is formed and the mole fractions in the solid are identical to the component activities.

Computational methods

Extensive calculations were made with version 4.2 of the Maple symbolic manipulator¹⁸

run on a Commodore Amiga 2000 with a 20 Mbyte hard disc and 3 Mbytes of RAM. Initially a series of equations describing the variations of the species in the system were found. These equations are derived from the equations of conservation of mass and conservation of charge in solution as presented below. The network of equations is expressed as an input file to Maple in Table 2. This algorithm presents assignments for the equilibria and the equations in a structured form that produces outputs in Fortran code.

First to be considered are the mass-balance equations:

$$Plqd = [H_3PO_4] + [H_2PO_4^-] + HPO_4^{2-}] \\ + [PO_4^{3-}]$$

$$Nlqd = [NH_4^+] + [NH_3]$$

$$Mlqd = [Mg^{2+}] + [MgOH^+]$$

where each is simply a total sum of molarities and where square brackets represent molar concentrations.

Secondly, we recognize the equation of electrical neutrality:

$$[H^+] + [NH_4^+] + 2[Mg^{2+}] + [MgOH^+] \\ = [OH^-] + [H_2PO_4^-] + 2[HPO_4^{2-}] + 3[PO_4^{3-}]$$

Table 2. File input to Maple

MNP:=K1*Mg*NH4*PO4;	# Struvite
NH4:=K2*NH3*H;	# Ammonium
H3P:=K3*H2P*H;	# Phosphoric acid
H2P:=K4*HP*H;	# Dihydrogen phosphate
HP:=K5*PO4*H;	# Hydrogen phosphate
MP8:=K6*Mg^3*PO4^2;	# Magnesium phosphate with 8 H2O
MP22:=K7*Mg^3*PO4^2;	# Magnesium phosphate with 22 H ₂ O
MgOH:=K8*Mg*OH;	# Magnesium hydroxide ion
MgOH2:=K9*Mg*OH^2;	# Magnesium hydroxide
MHP:=K10*Mg*HP;	# Magnesium hydrogen phosphate
OH:=K11/H;	# Water dissociation
f1:=PO4 + HP + H3P + H2P-PLQD;	# Phosphorus balance in the liquid
PO4:=solve(f1,PO4);	
readlib(fortran);	# Activates the fortran conversion library
fortran(PO4,optimized,filename = 'df1:PO4.for');	# produces fortran codes in file
f2:=NH4 + NH3-NLQD;	# Nitrogen balance in the liquid
NH3:=solve(f2,NH3);	
fortran(NH3, optimized, filename = 'df1:NH3.for');	# produces fortran codes in file
f3:=Mg + MgOH-MLQD;	# Magnesium balance in the liquid
Mg:=solve(f3,Mg);	
fortran(Mg,optimized,filename = 'df1:Mg.for');	# produces fortran codes in file
ffff:=H + NH4 + 2*Mg + MgOH-OH-3*PO4-2*HP-H2P;	
# The electroneutrality equation, add Exions to care for added ions	
fff:=normal(ffff);	
ff:=op(1,fff);	
f:=collect(ff,H);	
gggg:=MNP + MP8 + MP22 + MHP + MgOH2-1;	# Overall balance in solid phase
ggg:=normal(gggg);	
gg:=op(2,ggg);	
g:=collect(gg,H);	
fNLQD:=solve(f,NLQD);	
gNLQD:=solve(g,NLQD);	
hhhh:=fNLQD-gNLQD;	# New equation without NLQD
hhh:=normal(hhhh);	
hh:=op(1,hhh);	
h:=collect(hh,PLQD)	
a:=coeff(h,PLQD,2);	
b:=coeff(h,PLQD,1);	
c:=coeff(h,PLQD,0);	
fortran(a,optimized,filename = 'df1:a.for');	
fortran(b,optimized,filename = 'df1:b.for');	
fortran(c,optimized,filename = 'df1:c.for');	

Notes

:= signifies an assignment; # separates out comments and ^ signifies a power. Other operations should be self-evident with special functions, e.g., "solve" being used to perform operations.¹⁸

Extra terms for the excess of non-reactive ions are added as appropriate. Lastly we include an overall mass balance of the constituents in the solid phase (see Table 2).

Two input variables are specified in the input Maple file, namely the total molar concentration of magnesium in the liquid phase (Mlqd) and the concentration of hydrogen ions in solution (H). It is necessary in this fully flexible system to specify two concentrations to determine the equilibria. These degrees of freedom are expected from the Gibbs phase rule¹⁹ for the case of four independently variable components and two phases. The temperature is held constant at 25° and the pressure is 1 atmosphere; two degrees of freedom remain, which we

choose conveniently as the pH and the total molar concentration of magnesium in the liquid (Mlqd). The output from Maple is a series of Fortran codes, which are algebraic and relate all variables to the equilibrium constants; these algebraic expressions fill several pages.

The technique produces an 11th order polynomial in H, so H is used as an argument, one of the input variables. The other argument, Mlqd, then gives an explicit quadratic equation for the total molar concentration of phosphorus in solution (Plqd). The output algebraic code is integrated into a Fortran program which solves for Plqd, then back-substitutes to obtain values for the other 18 variables, producing a data file containing the values of all 20 variables. From

these data, groups of variables are selected for graphical presentation and numerical comparisons.

EXPERIMENTAL

Solutions of the salts magnesium chloride, potassium dihydrogen phosphate and ammonium chloride in distilled water were made up in 200-ml lots in 250-ml Erlenmeyer flasks, and were initially adjusted in pH with 0.4M sodium hydroxide for use in experiments at approximate pH values of 6.5, 7.2, 7.5 and 8.1. Sets of four flasks were prepared for each pH value. The initial flask concentration of magnesium was 7.0mM, of phosphorus 3.1mM and ammonium 130.6mM. The flasks were sealed with parafilm, then placed in a water-bath set at 30°, and rotated at 70 cycles/min. Each flask contained 1 g of borosilicate glass grindings for enhanced nucleation of crystals from solution. Sampling took place at approximately 0.5, 2, 40, 60 and 200 hr. The total number of data points collected was 66.

Samples (5 ml) were drawn from the solutions with a syringe. Each sample was drawn through a Whatman glass fibre filter paper and a 0.45 μm membrane filter to remove solid and glass particles. Magnesium, ammonia and phosphorus were measured according to APHA methods;²⁰ pH was measured in the flask just prior to sample extraction.

RESULTS AND DISCUSSION

Calculated concentration contours

The structure of the system at equilibrium, as derived from the theory above, is presented in Figs. 1(a) and 1(b). These represent three-dimensional surfaces for dissolved phosphorus [Fig. 1(a)] and nitrogen [Fig. 1(b)] in the solution. These calculated concentrations are for a temperature of 25° and are total values at equilibrium in the presence of a precipitate. Figure 1(a) presents contours at constant values of total dissolved phosphorus; Fig. 1(b) gives contours at constant values of total dissolved ammonia (or nitrogen species). The equilibrium constants used are estimated from Högfeldt¹⁵ and are listed in Table 1, column 3.

The contours in Fig. 1(a) indicate that at a given total magnesium concentration in solution, the total phosphorus in solution decreases with increasing pH, *e.g.*, at $10^{-5}M$ magnesium, phosphorus decreases from $10^{-0.5}M$ at

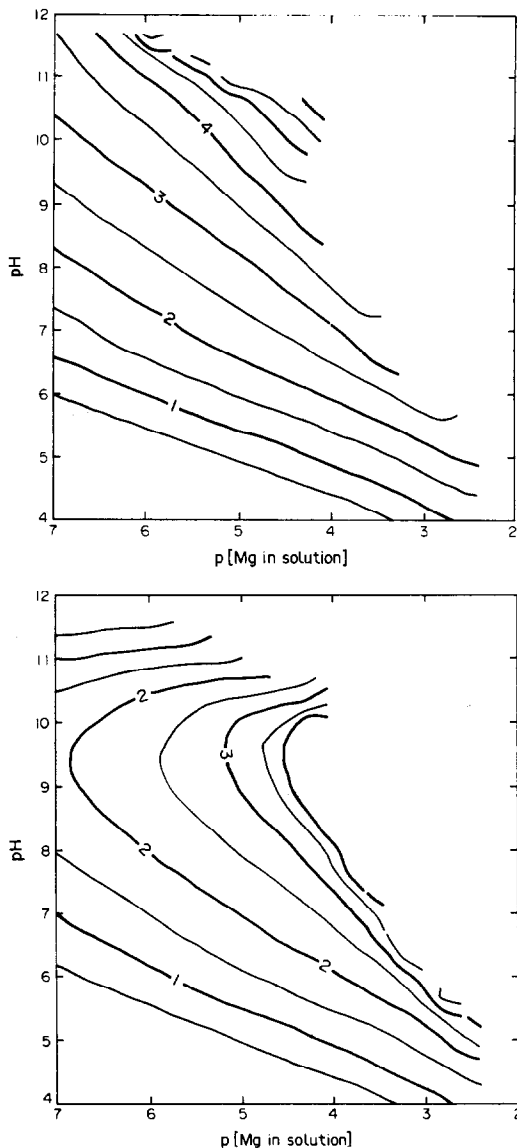


Fig. 1. Plots relating concentration of (a) phosphorus species in solution and (b) nitrogen species in solution to pH and p (magnesium in solution). The numbers on the contours are $-\log[\text{species in solution}]$, at 25°C.

approximately pH 5 to $10^{-4.3}M$ at pH 10. Similarly, in Fig. 1(b) the concentration curve for the solubility of nitrogen at a fixed magnesium value of $10^{-5}M$ indicates that nitrogen in solution decreases from $10^{-0.5}M$ at pH 5 to a minimum concentration of $10^{-3.2}M$ at pH 9.5, then increases in concentration to $10^{-1.5}M$ at pH 11.

The concentration of phosphorus in solution decreases rapidly with an increase in either magnesium or pH; the nitrogen in solution decreases with a increase in magnesium with the smallest rate of change occurring at pH near to 9 [Figs. 1(a) and 1(b)].

Note that these curves have 2 degrees of freedom and require contours to simulate the three-dimensional nature of the equilibria. In contrast, Verplaetse *et al.*¹⁶ show the system as being only a function of pH, a single independent variable. It is clear that their calculations do not require two degrees of freedom. Careful examination of their algorithm shows that they have not directly considered the necessity to consider electrical neutrality. This means that some form of internal adjustment must be expected to bring the system to an electrically neutral state. Perhaps this can be attributed to the complexing agents, but in the general case this is unrealistic.

Our results are difficult to compare with those of Verplaetse *et al.*¹⁶ as their formulation is for the dissolution of struvite in its entirety. That means that if $M_{lqd} = P_{lqd} = N_{lqd}$ our calculated results should be similar to theirs. From Figs. 1(a) and 1(b), $M_{lqd} = P_{lqd} = N_{lqd} = 10^{-3.5} M$ at about pH 7 at 25°. The data of Verplaetse *et al.*¹⁶ indicate that at 37° and pH 7 the corresponding concentrations would be about $10^{-2.5} M$. This is satisfactory agreement, considering the restricted nature of the calculations. The salient point is that though Verplaetse *et al.* used the activity coefficients, they seem to have ignored the electroneutrality equation, so the Gibbs phase rule would have been violated except in special cases.

Our model incorporates all the mass balances as well as the electroneutrality equation. The plots in Fig. 1 are just two examples of contours out of at least 400 curves which can be derived from the model.

Comparison of theoretical model predictions with laboratory and literature data

Laboratory data. Figure 2(a) presents a comparison between the measured and calculated phosphorus concentrations (P_{lqd}); which are significantly correlated ($r^2 = 0.77$ with 66 data points from equilibration times up to 200 hr). For data points derived from times greater than 50 hr this correlation increases in significance [$r^2 = 0.91$, $n = 32$, Figure 2(b)]. The measured nitrogen (N_{lqd}) values are correlated with model-derived values for equilibration times up to 200 hr ($r^2 = 0.85$, $n = 66$) and even more so for times greater than 50 hr ($r^2 = 0.97$, $n = 32$). Note that the nitrogen is in excess and has a limited range in concentration, and that the statistics are not very useful. Figures 3(a) and 3(b) show that the correlation of the P_s values

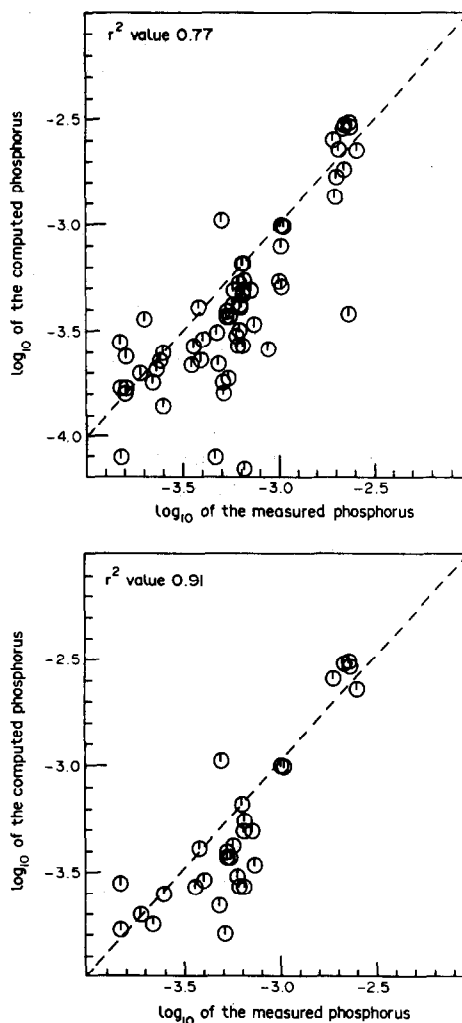


Fig. 2. Phosphorus concentrations in solution at 30°C calculated by the model, compared with laboratory results (a) 0–200 hr and (b) 50–200 hr equilibration.

derived from the model and laboratory data is significant for times up to 200 hr ($r^2 = 0.72$, $n = 66$) and much more so for times greater than 50 hr ($r^2 = 0.96$, $n = 32$); P_s is the conditional solubility product, which is both concentration- and pH-dependent.

Two major conclusions drawn from the comparison of the model data with the laboratory data are (1) the model is successful in predicting struvite solution chemistry and (2) improved correlations are found for equilibration times greater than 50 hr. It appears that true equilibrium exists after 50 hr, in agreement with Taylor *et al.*²

Literature data. A correlation ($r^2 = 0.46$, $n = 20$) exists (Fig. 4) between the model P_{lqd} values and the only other data set available² for an equilibrium struvite solution, that completely specifies the mass and charge balances. The

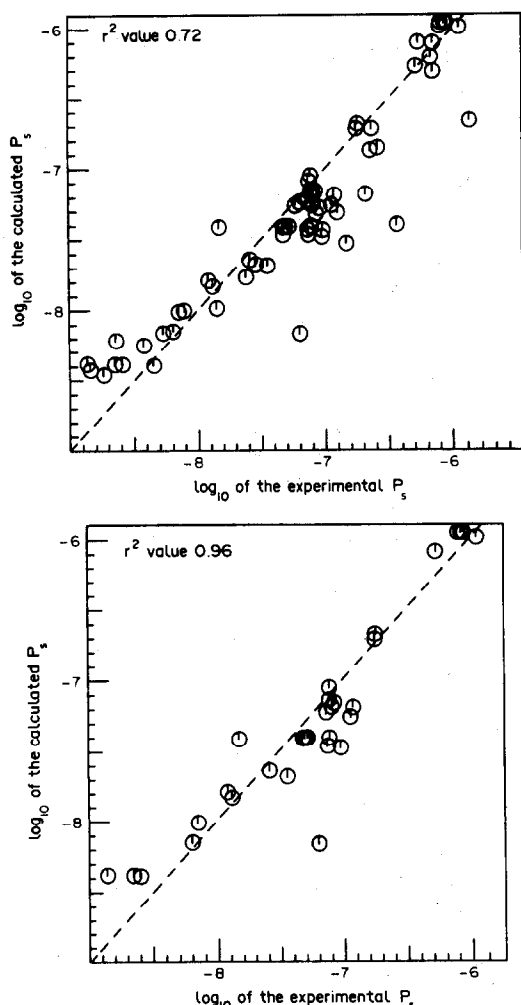


Fig. 3. P_5 values at 30°C calculated by the model, compared with laboratory results for (a) 0–200 hr and (b) 50–200 hr equilibration.

correlation improves if the two outlying points are removed ($r^2 = 0.85$, $n = 18$). These authors used combinations of specific chemicals and

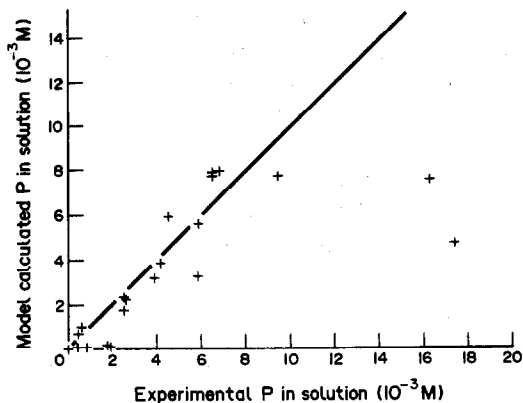


Fig. 4. Phosphorus concentrations in solution at 25°C calculated by the model, compared with the experimental data of Taylor *et al.*² The line has a slope of 1.

have specified the amount of excess ions. The scatter of points may be partly due to a disparity between their quoted values and our estimates of their excess ion values. The relationship between NIqd generated from the model and that derived from the data of Taylor *et al.*² is not highly significant. We believe a major factor in this discrepancy may be difficulty in measuring the nitrogen concentrations.

Derivation of best-fit solubility constants. Literature values of solubility constants have inherent limitations because they have been derived by using approximate solution equilibria. Hence, K values were derived from the present model by applying a least-squares program to laboratory and literature data. This enabled modification of the solubility constants to yield the best fit, as well as allowing an estimate of some of the constants. The second column of Table 3 shows the values derived for the experimental temperature of 30° from some literature values. Six solubility constants

Table 3. A comparison of literature solubility constants with values derived for ionic equilibrium during model calibration

Equilibrium	K fitted from laboratory data (30°C)	K fitted from literature ² (25°C)
$H^+ + NH_3 = NH_4^+$	$1.0 \times 10^{9*}$	$2.0 \times 10^{9†}$
$H^+ + H_2PO_4^- = H_3PO_4$	1.5×10^2	1.4×10^7
$H^+ + HPO_4^{2-} = H_2PO_4^-$	5.0×10^7	1.3×10^8
$H^+ + PO_4^{3-} = HPO_4^{2-}$	1.8×10^{12}	2.2×10^{12}
$3Mg^{2+} + 2PO_4^{3-} + 8H_2O = Mg_3(PO_4)_2 \cdot 8H_2O$	1.2×10^{22}	2.0×10^{24}
$Mg^{2+} + OH^- = Mg(OH)^+$	1.0×10^3	2.4×10^7
$Mg^{2+} + 2OH^- = Mg(OH)_2$	5.0×10^{10}	4.3×10^{14}
$Mg^{2+} + HPO_4^{2-} = MgHPO_4$	1.1×10^5	2.9×10^6
$Mg^{2+} + NH_4^+ + PO_4^{3-} = MgNH_4PO_4$	1.1×10^{13}	1.8×10^{14}
$H^+ + OH^- = H_2O$	$7.1 \times 10^{13‡}$	1.0×10^{14}

*Selected 30°C value—Sillén and Martell¹³ quote $\log K$ 9.08, but Högfeldt¹⁵ quotes 8.38.

†Literature value from Table 1.

‡Selected 30°C value—Sillén and Martell¹³ quote $\log K$ 13.833, but Högfeldt¹⁵ quotes 13.851.

listed in Table 3 were found to have a marked effect on the least-squares comparison. The literature K values often vary by more than one order of magnitude and some of this disparity may be resolved with more information about species. The standard values given by Högfeldt¹⁵ are usually used, but these constants do not take account of all interfering species. We think the present algorithms allow for all known species and should give a "best" set of equilibrium constants.

In conclusion, we have developed a model which considers the known reactions for the formation of a mixed precipitate in a pure solution. The model of struvite formation considers ionic reactions in the solution and reactions in the solid precipitate, without the need for bold approximations. The model allows for all combinations of the three chemical components as well as extra ionic species. Previous workers have only considered the solution of struvite directly, or with specific chemicals added to form known combinations of species. The model has been validated with both laboratory and literature data and several equilibrium constants have been redetermined.

The model still has some deficiencies, in that it does not use activity coefficients, or include other dissolved species, e.g., dissolved MgHPO_4 , MgPO_4^- and $\text{MgH}_2\text{PO}_4^+$, and the effects of organic complexing agents. This work is continuing and a following paper will address some of these points.

The model in its present form is primarily qualitative. That is, the curves simply present the structure of the equilibria and the various deficiencies of the model do not allow precise interpretation. Its real use is in the design of systems that allow a known amount of struvite to be precipitated. When all the appropriate constants are known, this is an inversion problem and not easily solved analytically. Consider the problem of calculating the precipitation of struvite in waste-water, knowing the amounts of ammonia, phosphate and magnesium in the input stream. The present algorithm produces a table of struvite concentrations in the solid for various pH values and amounts of magnesium.

One way of completing the inversion is simply to interpolate in this table while maintaining the appropriate concentrations and amounts of the three inputs. The final outcome is the amount of struvite in the total mix, expressed in g/l., in the stream.

Acknowledgement—We gratefully acknowledge the excellent positive review of our paper by Dr R. A. Chalmers. His efforts have greatly improved the quality of the manuscript.

REFERENCES

1. R. G. Johnson, *J. Urol.*, 1959, **81**, 681.
2. A. W. Taylor, A. W. Frazier and E. L. Gurney, *Trans. Faraday Soc.*, 1963, **59**, 1580.
3. J. R. Burns and B. Finlayson, *J. Urol.*, 1982, **128**, 426.
4. P. W. Linder and J. C. Little, *Inorg. Chim. Acta*, 1986, **123**, 137.
5. L. Liberti, A. Lopez and R. Passino, *Stud. Environ. Sci.*, 1984, **23**, 513.
6. L. Liberti, N. Limoni, A. Lopez, R. Passino and G. Boari, *Water Res.*, 1986, **20**, 735.
7. M. L. Salutsky, M. G. Dunseth, K. M. Ries and J. J. Shapiro, *Eff. Water Treat. J.*, 1972, 505.
8. L. Liberti, A. Lopez and R. Passino, in *Management Strategies for Phosphorus in the Environment*, Lisbon, pp. 136–141. Selper, London, 1985.
9. D. P. Griffith, *Kidney Int.*, 1978, **13**, 372.
10. C. A. Osborne, D. J. Polzin, S. U. Abdullahi, J. R. Leininger, C. W. Clinton and D. P. Griffith, *Advan. Vet. Sci. Comp. Med.*, 1985, **29**, 1.
11. S. S. Prabhudesai and S. B. Kadrekar, *J. Maharashtra Agric. Univ.*, 1982, **7**, 111.
12. R. Jones, *Fish. Ind. Res.*, 1968, **4**, 83.
13. L. G. Sillén and A. E. Martell, *Stability Constants of Metal-Ion Complexes*, Spec. Publ. No. 17, Chemical Society, London, 1964.
14. *Idem*, op. cit. *Supplement No. 1*, Spec. Publ. No. 25, Chemical Society, London, 1971.
15. E. Högfeldt, *Stability Constants of Metal-Ion Complexes, Part A: Inorganic Ligands*, Pergamon Press, Oxford, 1982.
16. H. S. Verplaetse, R. M. H. Verbeeck, H. Minnaert and W. Oosterlinck, *Eur. Urol.*, 1985, **11**, 44.
17. W. Stumm and J. J. Morgan, *Aquatic Chemistry*, Wiley-Interscience, New York, 1981.
18. B. W. Char, K. O. Geddes, G. H. Gonnet, M. B. Monogan and S. M. Watt, *Maple, Maple Reference Library*, 5th Ed., WATCOM, Waterloo, Canada, 1988.
19. J. W. Gibbs, *The Scientific Papers of J. Willard Gibbs*, Vol. 1, *Thermodynamics*, Dover, New York, 1961.
20. *Standard Methods for the Examination of Water and Waste-Water*, American Public Health Association, Washington D.C., 1985.

COMPUTER-ASSISTED ^{13}C NMR SPECTROSCOPIC IDENTIFICATION AND DETERMINATION OF CHLOROHYDRINS IN REACTION MIXTURES FORMED DURING MANUFACTURE OF GLYCEROL

SAJID HUSAIN*, M. KIFAYATULLAH and R. NAGESWARA RAO

Analytical Chemistry Division, Indian Institute of Chemical Technology, Hyderabad 500 007, India

(Received 17 August 1990. Revised 5 November 1990. Accepted 17 December 1990)

Summary—A novel computer-assisted ^{13}C NMR spectroscopic method for the identification and determination of chlorohydrins in reaction mixtures formed during the manufacture of glycerol, is described. It utilizes the unique features of quantitative and edited ^{13}C NMR spectrometry and avoids chromatographic separation for identification and quantification of the mixture components. It is simple, specific and quicker than the GC-MS and GC-IR methods.

1,2,3-Trihydroxypropane (glycerol) is an important intermediate in the manufacture of alkyd resins, ester gums, urethane foams, drugs, cosmetics and toothpastes. It is synthetically produced in large quantities.¹⁻³ The product generally contains chlorohydrins, glycerol, glycidol and their hydrolysis products in different proportions, and complete analysis of the mixture is of great importance not only to determine the extent of reaction but also to optimize the processing conditions. Several methods based on chromatography, spectroscopy and combined techniques such as GC-MS and GC-IR have been reported.⁴⁻¹¹ These methods generally involve a two-step procedure involving isolation of the components, followed by identification and quantification, but they suffer from a number of shortcomings due to lack of selectivity in chromatographic separation.

The present paper describes a simple, specific and single-step procedure using computer-assisted ^{13}C NMR spectrometry. It is based on comparing edited ^{13}C NMR spectra with multiplicity data derived directly from the chemical structures. It does not require a chromatographic separation. The results obtained are comparable with those obtained by GC-MS.

EXPERIMENTAL

Apparatus

A JNM Model FX-90Q FT-NMR spectrometer (JEOL, Tokyo) with a C/H dual probe

containing a quadrature detection system was used.

Reagents

All reagents were of analytical grade unless otherwise specified. Deuterium oxide (minimum isotope purity 99.8%) was obtained from Stohler Isotope Chemicals, U.S.A. Reaction mixtures containing chlorohydrins, glycerol and glycidol were obtained from pilot plants in our laboratory.

Procedures

Determination of quantitative ^{13}C NMR data. Quantitative ^{13}C NMR spectra were obtained by a gated decoupling pulse technique to ensure suppression of the nuclear overhauser effect (NOE). Spin-lattice relaxation was shortened by addition of chromium triacetylacetonate [$\text{Cr}(\text{acac})_3$] at 0.05M concentration. A recycle time of 10 sec between scans was found suitable for quantitative measurements. The spectrometer was operated at a resonance frequency of 22.5 MHz with 8 K (8192) data points and the probe temperature was maintained at 27°. The spectral width was 5 kHz and the pulse width was 28 μsec which was a 90° pulse for the spectrometer. About 100 pulses were needed to obtain a spectrum with a good signal to noise (S/N) ratio. Chemical shifts were measured with TMS as internal reference. The samples were undiluted and were examined in 10 mm o.d. tubes. The internal lock was maintained by means of D_2O in a capillary concentric with the NMR tube.

*Author for correspondence.

Table 1. Simulated ^{13}C NMR data base containing probable components of the reaction mixtures

No.	Compound	No. of peaks	Chemical shift			Multiplicity*		
			CH_3	CH_2	CH	CH_3	CH_2	CH
1	Propylene	3	18.7	115.9	136.2	1	1 ^d	1 ^d
2	Propane	2	15.4	15.9	—	2	1	0
3	1-Hydroxypropane	3	10.0	25.8 63.8	—	1	1.1 ⁺	0
4	2-Hydroxypropane	2	25.1	—	63.4	2	0	1 ⁺
5	1-Chloro-2-hydroxypropane	3	45.6	63.2	71.5	1	1 [×]	1 ⁺
6	2-Chloro-1-hydroxypropane	3	20.9	73.2	58.1	1	1 ⁺	1 [×]
7	1,2-Dichloro-3-hydroxypropane	3	—	53.8	69.3	0	1 [×] , 1 ⁺	1 [×]
8	1,3-Dichloro-2-hydroxypropane	2	—	45.6	70.5	0	2 [×]	1 ⁺
9	1,2,3-Trihydroxypropane	2	—	63.2	72.1	0	2 ⁺	1 ⁺
10	1-Chloro-2,3-epoxypropane	3	—	44.9 52.2	51.2	0	1 [°] , 1 [×]	1 [°]
11	1,2-Epoxy-3-hydroxypropane	3	—	43.9 52.2	61.9	0	1 [°] , 1 ⁺	1 [°]
12	3-Chloro-1-propene	3	—	117.5 48.7	133.7	0	1 ^d , 1 [×]	1 ^d
13	3-Hydroxy-1-propene	3	—	114.9 63.4	137.5	0	1 ^d , 1 ⁺	1 ^d
14	1-Chloro-2,3-dihydroxypropane	3	—	93.6 58.2	81.5	0	1 [×] , 1 ⁺	1 ⁺
15	2-Chloro-1,3-dihydroxypropane	2	—	68.5	68.1	0	2 ⁺	1 [×]

*Gives the number of carbon atoms of type $-\text{CH}_3$, $-\text{CH}_2$ and $-\text{CH}$ contributing to a particular resonance for each compound.

[×], ⁺ and [°] indicate carbon atoms bonded to Cl, OH and O respectively, and ^d indicates a double bond.

Determination of edited ^{13}C NMR data. Multiplicity data were obtained from edited spectra acquired by the distortionless enhanced polarization transfer pulse technique (DEPT) at $\theta = 3\pi/4$ and $\pi/2$. At $\theta = 3\pi/4$, the CH_3 and CH resonance signals are positive, those for CH_2 are negative and those for quaternary carbon atoms are suppressed. At $\theta = \pi/2$, all resonances except those of CH are suppressed. Assignments were based on coincidence of appearance of signals in both the quantitative and edited ^{13}C NMR spectra.

RESULTS AND DISCUSSION

Optimization of operating conditions for quantitative ^{13}C NMR spectrometry

^{13}C NMR spectrometry is used for obtaining both qualitative and reliable¹²⁻¹⁴ quantitative information, but requires close attention to be paid to many experimental parameters.^{15,16} These were considered during design of the present experiments. The spin-lattice relaxation times (T_1) of all the carbon resonances of the compounds to be found in the reaction mixtures were measured by the inversion recovery technique¹⁷ and were used for selecting appropriate recycling times between pulses.

Generally, three methods have been employed in efforts to obtain quantitative results by ^{13}C NMR spectrometry. They are based on

use of long pulse delays ($5T_1$), gated decoupling, and the addition of paramagnetic relaxation reagents such as $\text{Cr}(\text{acac})_3$ and $\text{Fe}(\text{acac})_3$. Shoolery,¹⁵ and Levy and Edlund,¹⁸ studied extensively the limitations and problems associated with use of the relaxation reagents and pointed out that the use of $\text{Cr}(\text{acac})_3$ alone will not ensure complete suppression of the NOE that is due to ^{13}C - ^1H dipole-dipole interaction. They suggested that the NOE may be quenched more effectively by using $\text{Cr}(\text{acac})_3$ and a gated decoupling technique simultaneously, and this approach was therefore used in the present investigation to ensure complete suppression of the NOE in order to obtain reproducible results.

Simulated data base

A data base containing chemical shifts, multiplicities, degeneracy and type of bonding was derived from the molecular structures of all the components to be found in the reaction mixtures. It is presented in Table 1. The multiplicity data for each compound are described effectively by using line notation ($\text{CH}_3/\text{CH}_2/\text{CH}$) and distinguishing the bond-types appropriately. They give the actual number of methyl, methylene and methine group carbon atoms contributing to a particular resonance. These data are used in identifying reaction mixture components by a reverse search procedure¹⁹.

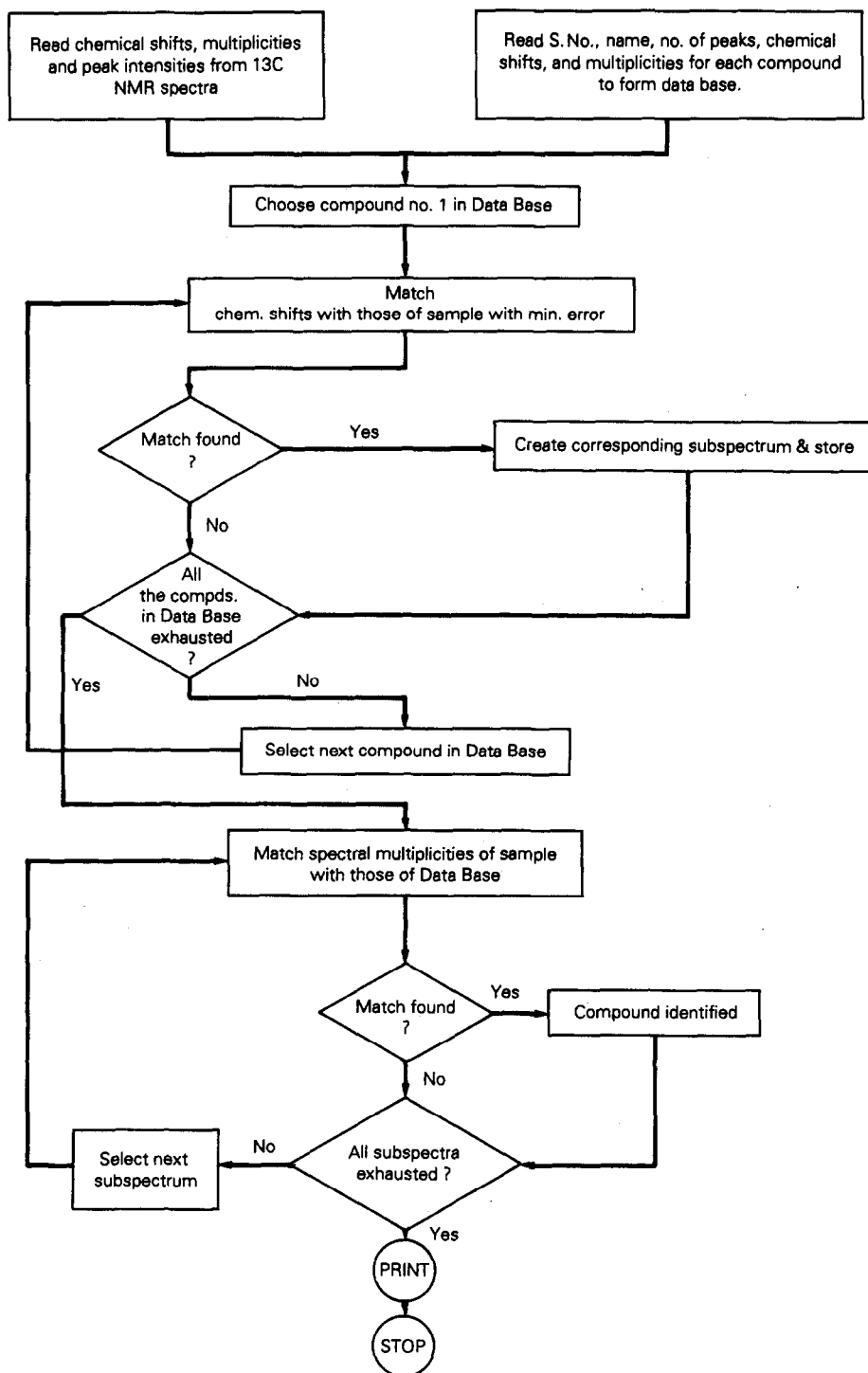


Fig. 1. Flow chart of logic for ^{13}C NMR analysis of reaction mixtures formed in the manufacture of glycerol.

Search algorithm

A flow chart for ^{13}C NMR analysis of a reaction mixture is given in Fig. 1. It involves the processing of quantitative and edited ^{13}C

NMR data to determine relative peak areas and multiplicities arising from hydrogen coupling. In the first step separation of carbon resonances by compound is performed by using chemical shift data. In the second step the simulated

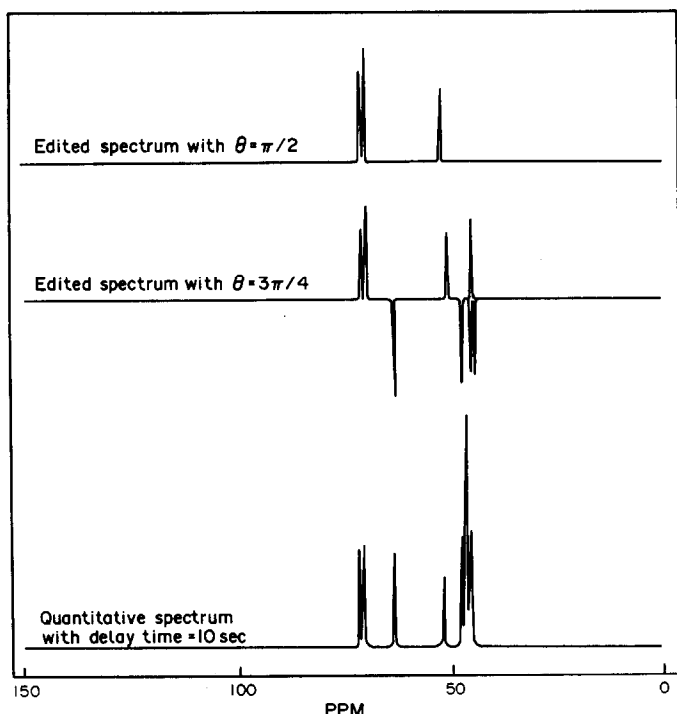


Fig. 2. Quantitative and edited ^{13}C NMR spectra of a three-component mixture containing MCH, DCH and ECH.

library is subjected to a reverse search procedure in which all possible subsets of the library multiplicity data matching with spectral multiplicities are determined. If a suitable match is not found, the tolerance limit is increased and the process is repeated. Thus a unique group of compounds is found in the simulated library, that matches the quantitative and multiplicity data of the reaction mixtures.

Standard mixtures

The method was evaluated by determining the content of a three-component mixture containing 25% monochlorohydrin (MCH), 34% dichlorohydrin (DCH) and 41% epichlorohydrin (ECH), compounds 5, 8 and 10 in

Table 1. The quantitative and edited ^{13}C NMR spectra are shown in Fig. 2. The quantitative spectrum contains a total of 7 resonances, including 1 methyl, 5 methylene and 3 methine carbon atoms. It can be seen from the edited spectrum with $\theta = 3\pi/4$ (Fig. 2) that the peak at 45.57 ppm is actually due to overlap of the two resonances of methyl and methylene carbons. The positive and negative signals at this resonance not only confirm this but also give the relative contributions to the resonance calculated by the distortionless enhanced polarization transfer technique. Table 2 summarizes these results along with the allocations of the resonances in accordance with the algorithm described in Fig. 1.

Table 2. Computer-assisted ^{13}C NMR analysis of a three-component mixture containing 25% MCH, 34% DCH and 41% ECH

Peak no.	Chemical shift, ppm	Multiplicity	Peak area range*	Subset of peak nos.	Compound identified	Found, %
1	44.92	CH_2	135–140			
2	45.57	CH_2, CH_3	252–256			
3	46.65	CH_2	130–139			
4	51.20	CH	137–142	1, 3, 4	ECH	41.0
5	63.23	CH_2	81–90			
6	70.54	CH	170–174	2, 6	DCH	34.0
7	71.46	CH	80–85	2, 5, 7	MCH	25.1

*Arbitrary units; an average of three integrations was fed to the computer.

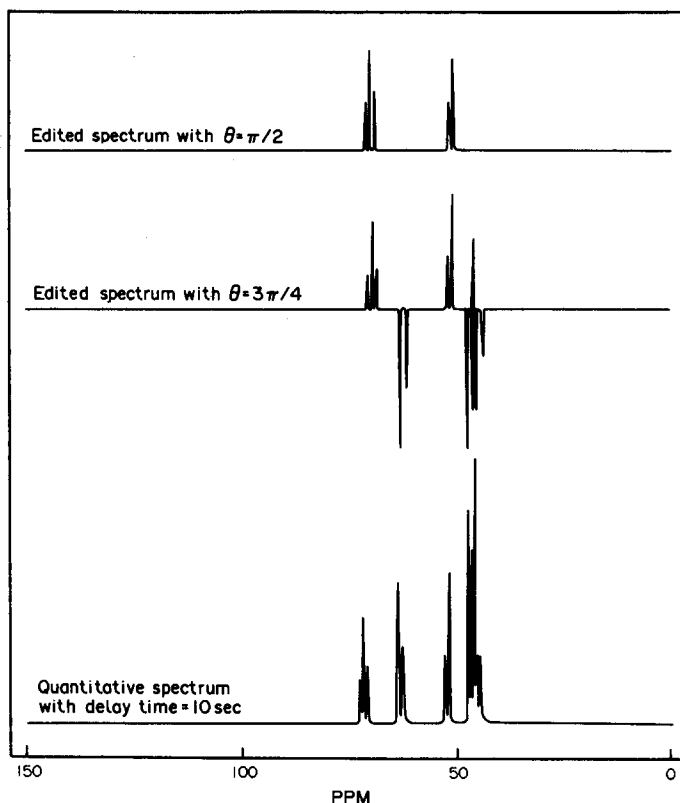


Fig. 3. Typical ^{13}C NMR spectra of reaction mixture from the manufacture of glycerol.

Reaction mixtures

Typical ^{13}C NMR spectra for the reaction mixtures under investigation are shown in Fig. 3. Table 3 gives the computer analysis of ^{13}C NMR data obtained for a typical reaction mixture in the process of manufacturing glycerol. Five compounds, *viz.* glycerol, glycidol, monochlorohydrin, dichlorohydrin and epichlorohydrin are identified in the reaction mixtures. The quantitative ^{13}C NMR spectrum contains a total of 10 resonances. For example the peaks 1, 3 and 4 in Table 3 are initially

matched and identified as belonging to ECH, by use of chemical shift and multiplicity data respectively. The ECH content is subsequently determined from the peak areas. Similarly, the content of each compound is determined by using the areas of the corresponding peaks matched for identification. Three different reaction mixtures were then analysed by the proposed method. Table 4 gives a comparison of these results with those obtained by GC-MS. The time required to complete an analysis was 1 hr by NMR and $\frac{1}{2}$ hr by GC-MS. The results show that the ^{13}C NMR method is not only

Table 3. Computer-assisted ^{13}C NMR analysis of reaction mixtures for the manufacture of glycerol

Peak no.	Chemical shift	Multiplicity	Peak area range*	Subset of peak nos.	Compound identified	Found, %
1	43.9	CH_2	188-195			
2	44.9	CH_2	357-362			
3	45.6	CH_2, CH_3	355-360			
4	46.7	CH_2	365-370			
5	51.2	CH	362-366	2, 4, 5	ECH	33.5
6	52.2	CH	187-192			
7	61.9	CH_2	185-190	1, 6, 7	GDL	20.6
8	63.2	CH_2	245-250			
9	70.5	CH	251-255	3, 9	DCH	18.2
10	71.4	CH	107-112	3, 8, 10	MCH	11.9
11	72.1	CH	134-138	8, 11	GCL	9.8

*Arbitrary units; an average of three integrations was fed to the computer.

Table 4. Comparison of quantitative data obtained by ^{13}C NMR and GC-MS

Reaction mixture	Component	Found (range)		Coefficient of variation, %	
		^{13}C NMR	GC-MS	^{13}C NMR	GC-MS
1	MCH	17.7-18.0	18.5-18.9	0.7	1.2
	DCH	14.7-15.0	13.9-14.3	1.4	1.5
	ECH	53.3-54.8	52.5-54.1	1.5	1.5
	GCL	7.9-8.2	8.3-8.7	1.8	2.0
	GDL	5.0-5.1	5.0-5.2	0.5	2.1
2	MCH	4.0-4.1	4.2-4.4	0.8	1.4
	DCH	7.1-7.3	7.7-8.0	1.5	2.0
	ECH	31.9-32.6	33.3-34.5	1.1	1.7
	GCL	49.6-57.6	45.9-48.4	1.9	2.6
	GDL	5.4-5.5	6.1-6.2	0.8	1.0
3	MCH	17.8-18.3	18.5-18.9	1.4	1.5
	DCH	37.4-38.7	38.3-39.8	1.8	2.0
	ECH	33.6-34.2	31.8-32.7	2.0	1.3
	GCL	7.3-7.6	7.9-8.3	2.1	2.6
	GDL	2.3-3.4	1.8-1.9	2.9	1.1

simple and rapid but also reasonably accurate and precise.

CONCLUSION

A simple, specific and rapid method for identification and determination of chlorohydrins in reaction mixtures formed during the manufacture of glycerol has been developed, based on use of computer-assisted ^{13}C NMR spectroscopy. The lowest limit of detection for any of the components in the reaction mixture was 50 $\mu\text{g/g}$, but this could be improved by increasing the number of quantitative spectra collected.

Acknowledgement—The authors wish to thank Dr. P. J. Reddy, Head, Computer Centre, ICT, Hyderabad, India for valuable discussions.

REFERENCES

- J. C. Kern, in *Encyclopedia of Chemical Technology*, 3rd Ed., p. 923. Interscience, New York, 1980.
- J. E. Going, *Encyclopedia of Industrial Chemical Analysis*, F. D. Snell and L. S. Ettre (eds.) Vol. 13, p. 494. Interscience, New York, 1971.
- K. Yamagishi and O. Kageyama, *Hydrocarbon Processing*, 1976, **55**, 139.
- G. S. Sharifov, R. A. Dzhabiev, I. I. Vyshnepo'skaya and N. M. Sarkisova, *Metody Anal. Kontrolya Kach. Prod. Khim. Prom-sti.*, 1978, No. 14, 19.
- F. L. Zubatova, M. A. Babaev and R. L. Zubaty, *Avtom. Nauchn. Issled. Khim. Khim. Tekhnol. Mater. Vses. Shk. 9th*, A. G. Abilov (ed.), p. 330. Izd. "Elm", Baku 1977.
- F. L. Zubatova, T. D. Ageava, R. L. Zubaty and F. F. Muganlinskii, *Azerb. Khim. Zh.*, 1975, No. 14, 24.
- B. M. Golova, L. V. Motoyilyak, S. F. Politanskii, M. V. Stepanov and V. T. Chelyadin, *Zavodsk. Lab.*, 1974, **40**, 1192.
- P. Adámek and V. Peterka, *Analyst*, 1971, **96**, 807.
- M. R. F. Ashworth, *Analytical Methods for Glycerol*, p. 220. Academic Press, London, 1979.
- D. S. Hirano, J. Geigert and T. D. Lee, *J. High Resolut. Chromatog. Chromatog. Commun.*, 1983, **6**, 38.
- L. V. Gurenko, O. N. Narizhnaya and A. N. Daragan, *Khim. Prom-sti., Ser: Metody Anal. Kontrolya Kach. Prod. Khim. Prom-sti.*, 1980, No. 5, 3.
- S. Husain, M. Kifayatullah and R. N. Rao, *Indian J. Technol.*, 1986, **24**, 130.
- H.-C. Chiang and L.-J. Lin, *Org. Magn. Reson.*, 1979, **12**, 260.
- P. E. Pfeffer, F. E. Luddy, J. Unruh and J. N. Shoolery, *J. Am. Oil. Chem. Soc.*, 1977, **54**, 380.
- J. N. Shoolery, *Prog. Nucl. Magn. Reson. Spectrosc.*, 1977, **11**, Part 2, 79.
- T. H. Mareci and K. N. Scott, *Anal. Chem.*, 1977, **49**, 2130.
- R. L. Vold, J. S. Waugh, M. P. Klein and D. E. Phelps, *J. Chem. Phys.* 1968, **48**, 3831.
- G. C. Levy and U. Edlund, *J. Am. Chem. Soc.*, 1975, **97**, 4489.
- D. A. Laude and C. L. Wilkins, *Anal. Chem.*, 1986, **58**, 2820.

FUNCTIONAL GROUP EFFECTS IN LASER-EXCITED MULTI-PHOTON PHOTOIONIZATION OF ORGANICS IN LIQUID SOLUTIONS

P. A. SNYDER* and E. VOIGTMAN†

Department of Chemistry, University of Massachusetts at Amherst, Amherst,
Massachusetts, 01003, U.S.A.

(Received 8 January 1991. Revised 13 February 1991. Accepted 21 February 1991)

Summary—Of the organic compounds examined for possible two-photon photoionization behavior, 43% were found to yield analytically useful photoionization with excitation at 308 nm. Fifty-five per cent produced greater photoionization responses than aniline, the *de facto* photoionization standard. Additionally, 16 of the surveyed compounds were more *photoionization efficient* (i.e., exhibit higher photoionization per unit absorption cross-section) than aniline. It was found that photoionization is relatively easily achieved with primary amines, anilines and diamines. Less readily photoionized were primary and tertiary amides, esters, alkyl ethers, and most halogenated compounds, the main exceptions being the halogenated anilines. Tertiary amines and fluorinated compounds gave poor photoionization results.

Photoionization occurs when a molecule absorbs one or more photons, causing ejection of an electron. The direct photoionization of a molecule from the ground state generally requires ultraviolet (UV) light.¹ Photoionization (PI) techniques have been used, with considerable effectiveness and high sensitivity, for the gas phase detection of both molecules and atoms. Consecutive multiphoton photoionization (MPPI) of molecules may also be carried out in solution.² The photoionization process is much more complex in the condensed phase than in the gas phase because photoionization produces a cation and either an electron in a solvent cage or an anionic species. Molecular MPPI is analytically useful, in the condensed phase, because the ionization potential is lower due to the solvation stabilization of the photo-generated charge carriers.

In the gas phase, organic molecules typically have ionization potentials of ≈ 9 eV. In solutions, effective ionization potentials are as much as several electron volts less than those observed in the gas phase. Although gas phase photoionization can be an extremely sensitive and practical technique, high energy sources are necessary to photoionize molecules in the gas phase.³ Condensed phase photoionization does

not need as energetic a source due to the lower ionization potentials.

Several studies of photoionization of solutions have been conducted in the past two decades. The photoionization of pyrene has been studied in detail.^{2,4-7} The quantitative determination of aromatic molecules has also been achieved.⁸⁻¹¹ The compounds that have been studied thus far consist mainly of polycyclic aromatic hydrocarbons (PAHs). There is almost no information available on the photoionization of the majority of organic compounds. Langhorst's studies of PI detection of organic compounds in the gas phase suggested that PI sensitivity depends upon carbon number, functional group, and bond type.¹² A survey of several organic compounds in the liquid phase was therefore conducted to determine if correlations between functional group and ease of photoionization could be made as has been done in the gas phase.

EXPERIMENTAL

The experimental instrumentation is illustrated in Fig. 1. Two-photon photoionization was induced by a Questek 2210 xenon chloride excimer laser. Its wavelength of emission was 308 nm (4.03 eV) and the laser was operated at a 20-Hz repetition rate. A windowless flow cell, shown in Fig. 2, was utilized. A -900 V bias voltage was applied to a stainless steel solution

*Present Address: Merck & Co., P.O. Box 2000, RY 71-22,
Rahway, N.J., 07065, U.S.A.

†Author for correspondence.

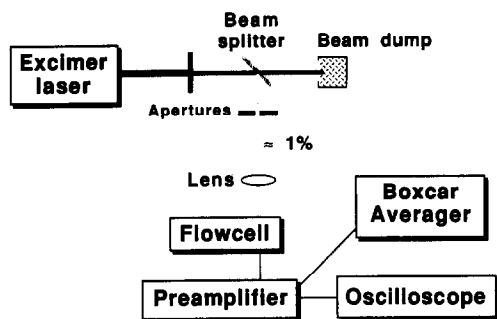


Fig. 1. The experimental apparatus for a laser induced photoionization study.

reservoir. The (negative) photocurrent produced upon two-photon photoionization was detected at the stainless steel pedestal. A voltage-mode preamplifier, capacitively coupled (50 nF, 1600 WV, silvermica) was utilized to convert the photocurrent to a voltage. The gain of the preamplifier was $\sim 3.0 \times 10^6$ V/A. A Tektronix 2465A 350-MHz oscilloscope was used to observe and monitor the waveform magnitude. The SR250 Gated Integrator and Boxcar Averager (Stanford Research Systems) was used to acquire the PI signal from the preamplifier. The oscilloscope was used to monitor setting of the gate width and delay of the boxcar system. The optimum gate width was $\sim 1 \mu\text{sec}$ and the optimum delay $\sim 3\text{--}4 \mu\text{sec}$ after the laser firing. The SR265 software package, for the SR250 Boxcar, was used to select a non-time scan and collect and average four runs of 1024 points. The SR265 program was also used to calculate the average signal and standard deviation, in volts.

Stock solutions of the organic compounds, each at 120 $\mu\text{g/ml}$, were prepared in HPLC-grade methanol (Fisher). Methanol was used because most organic compounds, of preliminary interest, were at least sparingly soluble in it. The purity of the compounds was checked, by melting point determinations, and were found to be in agreement with literature values. Ten-fold methanol dilutions of the stock solutions resulted in 12 $\mu\text{g/ml}$ solutions which were used for the PI detection survey. This concentration is approximately the upper limit concentration for photoionization studies. For several compounds, further dilutions were necessary to avoid saturation of the preamplifier output.

The mean blank (methanol) signal was subtracted from the PI signal produced by each organic compound. The standard deviation of the methanol blank was 23 nA. The blank-subtracted PI signal voltage was divided by 3×10^6

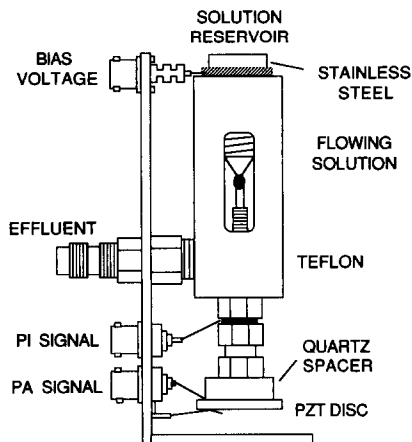


Fig. 2. Schematic of the three mode windowless flow cell.

V/A to produce a nominal photocurrent signal, in nA. The molar absorptivity of each compound, in methanol solution at $\sim 12 \mu\text{g/ml}$, 1.00-cm pathlength and 308 nm, was measured with the Perkin—Elmer Lambda 3B UV-Visible spectrometer.

RESULTS AND DISCUSSION

The tabular results of the photoionization studies are given in Tables 1 and 2, which list the 111 organic compounds examined in this survey. The photocurrent magnitude (I_{ph}) and molar absorptivity at 308 nm (ϵ) are also listed for each compound in Table 2. The 63 compounds in Table 1 either exhibit negligible absorbance at 308 nm, thereby precluding MPPI at the excimer laser wavelength, or they produce photocurrents less than three standard deviations of the blank, *i.e.*, less than ~ 70 nA. Thus, the test solutions were already at or below the detection limit.

Analysis of the results in Tables 1 and 2 indicate that 48 of 111 compounds (43%) yield useful PI detection response with 308-nm excitation. Aniline, which is readily photoionized, may serve as a *de facto* 'photoionization standard', rather like quinine in molecular fluorescence studies and sodium vapor in atomic fluorescence studies. It is seen that 34 of 47 compounds (72%) in Table 2 absorb 308-nm light more strongly than aniline does, while 26 of 47 (55%) produce higher PI signals than aniline, *ceteris paribus*. Accordingly, more than half of the compounds listed in Table 2 should yield lower detection limits than aniline does.

To demonstrate the sensitivity and linearity of MPPI detection, consider the detection limit determination of 1,5-diaminonaphthalene, the

Table 1. Compounds exhibiting negligible absorbance at 308 nm or poor photoionization behavior

<i>m</i> -Nitroaniline	<i>m</i> -Chlorophenol	2,2-Dimethoxypropane
<i>o</i> -Chloroaniline	<i>p</i> -Chlorophenol	Butyl acetate
<i>o</i> -Bromoaniline	3,4,5-Trichlorophenol	Amyl acetate
Dibutylamine	<i>o</i> -Bromophenol	Methyl- <i>p</i> -bromobenzoate
Tributylamine	<i>m</i> -Bromophenol	Methyl- <i>p</i> -iodobenzoate
Nonylamine	<i>p</i> -Bromophenol	Chlorohexadecane
1,2-Diamino-2-methylpropane	<i>m</i> -Iodophenol	Chlorobenzene
1,9-Diaminononane	<i>p</i> -Iodophenol	<i>m</i> -Dichlorobenzene
Tetraethylenepentamine	<i>o</i> -Fluorophenol	<i>p</i> -Dichlorobenzene
<i>n</i> -Butyldodecylamine	<i>m</i> -Fluorophenol	1-Chloro-2-iodobenzene
<i>n,n,n',n'</i> -Tetramethyl-ethylenediamine	3,4-Dimethylphenol	Iodobenzene
Acetamide	3,5-Dimethylphenol	Fluorobenzene
<i>n</i> -Butylamide	2,3,6-Trimethylphenol	Iodobutane
Acrylamide	2,3,5-Trimethylphenol	1-Bromopropane
Carbanilide	2-Amino-4-nitrophenol	2-Bromopropane
<i>n,n</i> -Dimethylformamide	4-Amino-2-nitrophenol	1,4-Dibromobutane
<i>n,n</i> -Diethyl- <i>m</i> -toluamide	Anisole	Phthalic anhydride
Benzonitrile	<i>o</i> -Nitroanisole	Hexamethylenetetramine
3-Cyanobenzaldehyde	<i>p</i> -Iodoanisole	Benzophenonehydrazone
<i>o</i> -Nitrophenol	Ethyleneglycol monomethylether	Azobenzene
<i>o</i> -Chlorophenol	Ethyleneglycol monobutylether	Dansylchloride

second most readily photoionized compound listed in Table 2. A methanol stock solution of 15 $\mu\text{g/ml}$ of 1,5-diaminonaphthalene was prepared. Thirteen binary serial dilutions, in methanol, were performed, with the most dilute solution having a concentration of 1.8 ng/ml. Solutions more concentrated than 1.8 $\mu\text{g/ml}$ produced photoionization signals too large for the boxcar to process. The photoionization signals of the remaining solutions were measured and a log-log plot of photocurrent versus concentration is illustrated in Fig. 3.

The limit of detection ($S/N \equiv 3$) for 1,5-diaminonaphthalene in methanol was found to be 7 ng/ml. This is an extremely good detection limit taking into consideration the noise produced by polar solvents.¹³ Note that detection limits in non-polar solvents are as much as 1000 times better.¹³ The slope of the log-log calibration curve is 0.9989, indicating excellent linearity.

Returning to the analysis, Table 2 also shows the photocurrent magnitudes normalized by respective molar absorptivities. The results are therefore corrected for absorption cross-section. It was found that 16 of 47 (34%) of the surveyed compounds yield normalized photoionization responses that exceed that of aniline. Accordingly, $\sim 1/3$ of the surveyed compounds are more photoionization efficient than aniline.

Photoionization ease

Analysis of the results for compounds in Tables 1 and 2 suggest that photoionization is relatively easily achieved with primary amines, anilines and diamines. Polycyclic aromatic hy-

drocarbons also tend to work well, especially in non-polar solvents. Less readily photoionized, under present experimental conditions, are primary and tertiary amides, esters, alkyl ethers, and most halogenated compounds, the main exceptions being the halogenated anilines. Compounds which exhibit poor photoionization include tertiary amines and fluorinated compounds. Notice that 1,9-diaminononane gives poor PI detection even though it is a diamine. It was hoped that it would yield good performance so that its use as a possible photoionization tag could be explored. The goal was to attach the diamine by utilizing one of its amino groups for bonding to a desired moiety, leaving the other 'end' free for PI detection. Unfortunately, this appears out of the question with 1,9-diaminononane, and the lower molecular weight homologs of it, *e.g.*, cadaverine and putrescine, are too noisome to utilize in this manner.

Photoionization efficiency

Many of the surveyed compounds are readily detected by transmittance measurements, particularly with excitation wavelengths more optimally chosen than 308 nm. Evidently, the best application for laser-excited MPPI is for compounds that are weak absorbers but produce large photoionization signals. These compounds may not be readily detected by transmittance measurements, but are easily detected by MPPI.

Compounds with large ϵ 's and/or small PI signals will have small I_{ph}/ϵ values. Small ϵ 's and/or large PI signals will yield large I_{ph}/ϵ values, so these latter are the compounds best

Table 2. Compounds exhibiting photoionization with 308-nm excitation

Compound	Photocurrent	Molar	I_{ph}/ϵ $nA M cm$
	magnitude, I_{ph} nA	absorptivity, ϵ , $l \cdot mole^{-1} \cdot cm^{-1}$	
3,3'-Diaminobenzidine	71000	15000	4.7
1,5-Diaminonaphthalene	40000	9800	4.1
2,7-Diaminofluorene	27000	2300	1.2
<i>p</i> -Nitrophenol	2300	11000	0.21
<i>n</i> -Phenyldiethanolamine	1700	1700	1.0
<i>p</i> -Chloroaniline	1500	1400	1.1
1-Naphthylamine	1500	6000	0.25
<i>o</i> -Phenylenediamine	1400	1800	0.78
Aminophenol	1100	2500	0.44
2,4-Dimethylaniline	900	350	2.6
Methylaniline	830	2300	0.36
7,8-Benzoquinoline	800	1300	0.62
1,4-Diaminoanthraquinone	630	5200	0.12
<i>m</i> -Iodoaniline	570	1700	0.34
Phenanthrene	500	290	1.7
<i>m</i> -Nitrophenol	500	1700	0.29
Isobutylamine	500	10	50
2-Naphthylacetate	500	1800	0.28
Naphthalene	430	170	2.5
Phthalimide	400	490	0.82
Anthracene	400	1500	0.27
<i>p</i> -Bromoaniline	370	1200	0.31
<i>n</i> -Butylamine	370	20	19
Vanillin	330	10000	0.03
<i>p</i> -Iodoaniline	300	1900	0.16
<i>p</i> -Anisaldehyde	300	870	0.34
Aniline	300	380	0.79
<i>m</i> -Bromoaniline	280	1400	0.20
Hydroquinone	200	1200	0.17
<i>p</i> -Acetamidobenzaldehyde	180	12000	0.02
<i>p</i> -Nitroaniline	170	3200	0.05
<i>p</i> -Hydroxybenzaldehyde	170	2400	0.07
<i>o</i> -Iodoaniline	140	2500	0.06
Benzamide	140	1	140
2-Amino-3-nitrophenol	140	5500	0.03
2,5-Dichlorophenol	140	60	2.3
Phenylhydrazine	130	240	0.54
Ethyleneiodide	130	20	6.5
Benzanilide	110	1600	0.07
3,4-Dichloroaniline	110	2000	0.06
<i>o</i> -Nitrobenzotrile	100	1500	0.07
2,3,4,6-Tetramethylphenol	90	1400	0.06
<i>o</i> -Nitroaniline	80	730	0.11
Maleimide	80	190	0.42
2,4-Dinitrophenylhydrazine	80	3500	0.02
<i>o</i> -Iodophenol	70	60	1.2
Carbohydrazide	70	2	35
2-Ethylphenol	70	20	3.5

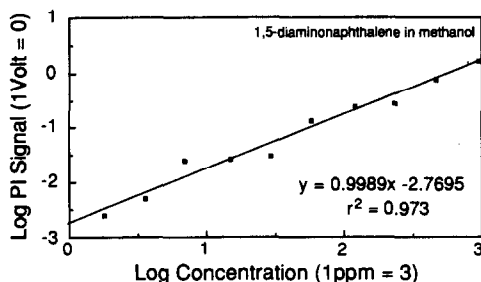


Fig. 3. A log-log plot of photoionization: signal vs. concentration for the 1,5-diaminonaphthalene limit of detection study.

suiting for PI detection. Examined in this light, the most efficient photoionization is achieved with amines, diamines, anilines and amides.

Functional group dependence

Functional group dependence is difficult to evaluate. In the gas phase, the effects of functional group dependence are considerably better understood, though far from complete. Jaffé¹⁴ comprehensively examined the effects of substituents on the ' σ ' substituent constant in the Hammett equation. Crable and Kearns¹⁵ measured ionization potentials of numerous

substituted benzenes and found linear correlation between measured ionization potentials and the ' σ^+ ' values (similar to the Hammett ' σ ' values) of Brown and Okamoto.¹⁶ More recently, Tembreull *et al.*¹⁷ have examined the effect of functional group type and ring location on the ionization potentials of a variety of substituted benzenes, including halogenated benzenes and substituted anilines. They found that ionization is facilitated by electron releasing groups (*e.g.*, $-\text{NH}_2$, $-\text{OH}$, $-\text{CH}_3$), hindered by electron withdrawing groups (*e.g.*, $-\text{NO}_2$, $-\text{CN}$, $-\text{COOH}$) and helped or hindered by halogen substitution, depending on the substitution pattern and other factors. As an example, dichlorinated aniline exhibits a substantial ionization potential lowering only when the chloro groups are in the *meta* and *para* positions.

For photoionization in liquid solutions, the same general observations are likely to be relevant, but great caution must be exercised in extrapolating from the gas phase. The lowered ionization potentials for analyte moieties in solutions are largely unknown and are strongly dependent on numerous solvent system parameters. Furthermore, the quantitative relationship between the measured photoionization currents in solutions and the actual ionization potentials in the solution environments has not been determined. Accordingly, no attempt will be made, at present, to definitively address the matter, since available data are insufficient to the task.

Of the 11 aniline derivatives in Table 2, 10 have higher molar absorptivities at 308 nm than does aniline, yet only 2 of the derivatives are more PI efficient. Several additional aniline derivatives, listed in Table 1, produced PI signals too small to be considered reliable. It appears that substitution generally degrades PI efficiency (in solution), though detection limits should be comparable to that of aniline because photocurrent magnitudes are not much changed by functional group substitution. Roughly speaking, ring activation, especially in the *para* position, appears to enhance the photoionization of substituted aniline. Similarly, *ortho* substitution,

especially with a ring deactivator, tends to decrease photoionization efficiency. These results are in general agreement with the results of Langhorst¹² and Tembreull *et al.*¹⁷

CONCLUSION

Despite the limited number of surveyed compounds and other experimental limitations (*e.g.*, 308-nm excitation and methanol solvent system), the survey of organic compounds illustrated that there is a definite correlation between functional group and ease of photoionization in solution. Compounds similar to those studied, in structure and/or functional groups, should produce similar photoionization results. The photoionization tag studies are potentially very important and are presently in the planning stage.

REFERENCES

1. V. Letokhov, *Laser Photoionization Spectroscopy*, Academic Press, NY, 1987.
2. S. Yamada and T. Ogawa, *Prog. Analyt. Spectrosc.*, 1986, **9**, 429.
3. D. C. Locke, B. S. Dhingra and A. D. Baker, *Anal. Chem.*, 1982, **54**, 447.
4. J. T. Richards, G. West and J. K. Thomas, *J. Phys. Chem.*, 1970, **74**, 4137.
5. E. Voigtman, A. Jurgensen and J. D. Winefordner, *Anal. Chem.*, 1981, **53**, 1921.
6. S. Yamada, K. Kano and T. Ogawa, *Bunseki Kagaku*, 1982, **31**, E247.
7. S. Yamada, A. Hino, K. Kano and T. Ogawa, *Anal. Chem.*, 1983, **55**, 1914.
8. G. Beck and J. K. Thomas, *Chem. Phys. Lett.*, 1972, **13**, 295.
9. *Idem.*, *J. Chrom. Phys.*, 1972, **57**, 3649.
10. L. V. Luken, A. V. Tolmachev and B. S. Yakovlev, *Chem. Phys. Lett.*, 1981, **81**, 595.
11. E. Voigtman and J. D. Winefordner, *Anal. Chem.*, 1982, **54**, 1834.
12. M. L. Langhorst, *J. Chrom. Sci.*, 1981, **19**, 98.
13. E. Voigtman and P. A. Snyder, *Anal. Instrum.*, 1990, **19**, 1.
14. H. H. Jaffé, *Chemical Reviews*, 1953, **53**, 191.
15. G. F. Crable and G. L. Kearns, *J. Phys. Chem.*, 1962, **66**, 436.
16. H. C. Brown and Y. Okamoto, *J. Am. Chem. Soc.*, 1958, **30**, 4979.
17. R. Tembreull, C. H. Sin, P. Li, H. M. Pang and D. M. Lubman, *Anal. Chem.*, 1985, **57**, 1186.

COLOUR REACTION OF PLATINUM(II) WITH 5-(4-NITROPHENYLAZO)-8-(*p*-TOLUENESULPHONAMIDO)- QUINOLINE AND ITS ANALYTICAL APPLICATIONS

ZHAO JIANWEI and XU QIHENG*

Department of Chemistry, Yunnan University, Kunming, 650091, People's Republic of China

(Received 30 May 1990. Revised 22 January 1991. Accepted 9 February 1991)

Summary—A simple, rapid and sensitive spectrophotometric method has been developed for the determination of platinum. 5-(4-Nitrophenylazo)-8-(*p*-toluenesulphonamido)quinoline (NPTSQ) reacts with platinum(II) almost instantaneously in alkaline solution to form a violet-red 1:2 complex with an absorption maximum at 640 nm. Beer's law is obeyed over the concentration range 0–1 $\mu\text{g/ml}$ platinum. The molar absorptivity is $1.37 \times 10^5 \text{ l. mole}^{-1} \cdot \text{cm}^{-1}$. The method has been used for the determination of microamounts of platinum in catalysts and anode slime.

Many spectrophotometric methods have been reported for the determination of platinum.^{1–4} Several^{5–14} involve either heating the solution or allowing it to stand for a long time for maximum colour development. Some reagents^{15–17} cannot tolerate interference by heavy-metal or other ions. Recently, several new organic reagents^{18–23} have been suggested for the determination of platinum and have good sensitivity and selectivity. In this paper, we report the colour reaction of platinum(II) with a new reagent, 5-(4-nitrophenylazo)-8-(*p*-toluenesulphonamido)quinoline (NPTSQ),²⁴ and a method for the rapid spectrophotometric determination of microamounts of platinum. The major advantages of this method over existing ones are that maximum colour intensity is attained almost instantaneously at room temperature and the sensitivity is higher than that of other methods.

EXPERIMENTAL

Apparatus

A spectrophotometer (Model 721, Third Analytical Instrument Factory, Shanghai) with stoppered cells of 1-cm optical path was used for all absorbance measurements.

Reagents

Platinum(II) standard solution. Prepared with pure K_2PtCl_4 to give a stock solution containing 100 $\mu\text{g/ml}$ platinum. Diluted further as required.

NPTSQ solution, $2.0 \times 10^{-4}\text{M}$, in 95% ethanol.

NaOH–KCl solution. Dissolve 4.0 g of sodium hydroxide and 7.5 g of potassium chloride in 30 ml of water, and dilute to 500 ml with water.

Tween-80 solution, 20 mg/ml.

All other reagents were of analytical grade.

Procedures

Determination of microamounts of platinum. Take a known volume of solution containing up to 25 μg of platinum(II), in a 25-ml standard flask, add 2.0 ml of NPTSQ solution, 3.0 ml of Tween-80 solution and 3.0 ml of NaOH–KCl solution, dilute to the mark with distilled water, shake and measure the absorbance at 640 nm against a reagent blank prepared in the same manner.

Determination of platinum in anode slime. Dissolve an accurately weighed sample (0.5–1.5 g) of anode slime by heating with 20 ml of *aqua regia*, evaporate the solution to incipient dryness, add 5 ml of concentrated hydrochloric acid and evaporate until nitrogen dioxide ceases to evolve. Let cool to room temperature (18–25°), add 2.5 ml of 3.0M hydrochloric acid to dissolve soluble salts, filter off the residue and wash it with ~20 ml of distilled water, dilute the combined filtrate and washings to ~25 ml, saturate the solution with sodium chloride and extract with two 10-ml portions of tributyl phosphate (TBP). Strip platinum from the organic phase with three 20-ml portions of 25% v/v nitric acid saturated with sodium nitrate. Evaporate the

*Author for correspondence.

combined nitric acid extracts to incipient dryness in a small beaker, and dissolve the soluble salts in 0.3M hydrochloric acid. Transfer the solution to a 25-ml standard flask and dilute to the mark with distilled water. Take 2.0 or 5.0 ml of the solution in a 25-ml standard flask, add 0.5 ml of 20% potassium iodide solution, then 5 min later add a drop of 5.0% ascorbic acid solution,²² adjust to nearly neutral with 0.2M sodium hydroxide, and complete the determination as above.

Determination of platinum in a catalyst. Weigh accurately about 1.0 g of Pt-Al₂O₃ catalyst and dissolve it in 10 ml of *aqua regia*. Evaporate the solution to incipient dryness, add 5 ml of concentrated hydrochloric acid and evaporate until no more nitrogen dioxide is evolved, then let cool to room temperature. Dissolve the soluble salts with distilled water, filter off the residue and wash it with distilled water, collecting the filtrate and washings in a 50-ml standard flask, and dilute to the mark with distilled water. Take 1.0 ml of the solution in a 25-ml standard flask and add 0.5 ml of 20% potassium iodide solution, then 5 min later add a drop of 5.0% ascorbic acid, 0.5 ml of 2.0% sodium fluoride solution, and complete the determination as above.

RESULTS AND DISCUSSION

Absorption spectra

Under the conditions used, platinum(II) forms a violet-red complex with NPTSQ, as

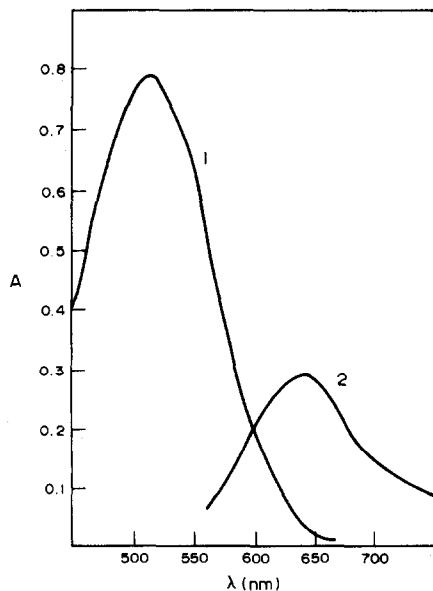


Fig. 1. Absorption spectra of NPTSQ and its platinum(II) complex. (1), NPTSQ (against water as reference); (2), NPTSQ-Pt(II) complex (against reagent blank as reference).

Table 1. Tolerance limits in the determination of 10 μg of platinum(II) with NPTSQ

Ion added	Amount tolerated, μg
I ⁻ , acetate, ascorbate	1000
F ⁻ , Zn(II)	500
Ga(IV)	400
Ca(II), Hg(II), Mo(VI), Ir(III), W(VI)	200
Mg(II), Th(IV), V(V), Cr(VI), Al(III), Os(VIII)	100
Os(IV)	80
Pb(II), Mn(II), phosphate	50
Ag(I), Ge(IV)	40
Fe(III), Cd(II), Ce(IV), Sn(IV), Fe(II)	25
Bi(III)	15
Ni(II)	10
Au(III), Rh(III)	5
Cu(II)	2
Co(II), Ru(III)	1
Pd(II)	0.5

does platinum(IV), but the molar absorptivity of the platinum(IV) complex is very low. The platinum(II) complex exhibits maximum absorption at 640 nm, whereas that of the reagent is at 515 nm. The absorption spectra of NPTSQ and its platinum(II) complex are shown in Fig. 1.

Reaction conditions

The optimum pH for the NPTSQ-Pt(II)-Tween-80 system is in the strongly alkaline region and addition of 2.0–5.0 ml of the NaOH-KCl solution to an approximately neutral test solution was found to give essentially the same absorbance; addition of 3.0 ml is recommended.

In the absence of surfactant or in the presence of an ionic surfactant a precipitate forms in the colour system, but the presence of a non-ionic surfactant, such as the emulsifying agent OP, poly(vinyl alcohol), Triton X-100 or Tween increases the solubility. Tween-80 was found to be the best additive, 1.0–5.0 ml of 2% Tween-80 solution giving good results; 3.0 ml is recommended.

Maximum and stable absorbance was attained with 1.0–3.0 ml of 2×10^{-4} M NPTSQ, and use of 2.0 ml is selected as optimal.

At room temperature, platinum(II) reacts nearly instantaneously with NPTSQ. The

Table 2. Determination of platinum in a catalyst and an anode slime

Sample	Standard content, %	Pt found,* %
Catalyst	0.0419	0.0402 ± 0.0008
Anode slime	0.0020	0.0019 ± 0.0008

*Mean ± standard deviation of five replicates.

Table 3. Comparison of the main characteristics of spectrophotometric determination of platinum with several organic reagents

Reagent	Molar absorptivity, $l. mole^{-1}. cm^{-1}$	Experimental conditions	Interferings ions	Reference
PTK	7.3×10^3	Extract, heat, pH 3-4.5	Fe, Ni, Co, Mn(II) Pb, Cu(II)	5
6-Aminoquinoxaline-2,3-dithiol	7.8×10^4	Extract, pH 0.7	Fe, Cr, Rh, Ir(III) Cu, Co, Ni(II) Fe, Rh(III) Os(VI)	7
MPM	1.71×10^4	30-Fold excess of MPM	Ag(I), Pd(II), I ⁻	18
BDPTK	1.29×10^5	Heating for 15 min, pH 3-4	Au, Ru, Os(III), W(VI) Pb, Co, Hg, Pd, Ni(II)	21
3,5-DiBr-PADAT	7.3×10^4	Heat at 70° for 25 min, pH 6.5	Au, Ru, Rh(III), Ag(I) Os(VIII), Cl ⁻ , NO ₃ ⁻	22
5-Br-PADAP	2.7×10^4	Heat at 100° for 60 min, pH 3.8	Hg, Fe, Sn, Pd, Ni(II) Ru, Ir(III) Os(VIII)	23
NPTSQ	1.37×10^5	Tween-80 pH 12-13	Ni, Co, Cu, Mn, Sn(II) Pd(II), Ag(I) Ru, Rh(III), Ir(IV) Cu, Co, Pd(II) Au, Rh, Ru(III)	This work

chelate is stable in solution for at least 24 hr. The order of addition of reagents seriously affects the system, however. Addition in the order Pt(II), NaOH-KCl solution, Tween-80 solution, NPTSQ solution gives the worst results, whereas the order Pt(II), NPTSQ, Tween-80, NaOH-KCl solution gives the best.

Analytical characteristics

A calibration graph was prepared by the procedure described for determination of microamounts of platinum. Beer's law was obeyed over the concentration range 0-25 μg of platinum in 25 ml of final solution; the linear regression equation obtained was

$$A = 0.0282C + 0.00102 \quad (r = 0.998)$$

where C is expressed as $\mu\text{g}/25$ ml. From this equation, the molar absorptivity was calculated to be 1.37×10^5 $l. mole^{-1}. cm^{-1}$.

The composition of the complex was determined by the molar-ratio and continuous-variation methods, and found to be 1:2 (metal:ligand).

Interferences

The influence of 36 diverse ions on the determination was examined. The ions to be tested were added individually to a solution containing 10 μg of platinum. The tolerance limits (error < 2%) listed in Table 1 showed that platinum could be determined in the presence of many foreign ions, but the interference of Ru(III), Co(II), Pd(II) and Cu(II) was serious. Hence, extraction with TBP^{25,26} was used in the

analysis of samples containing these species. The interference of Al(III) was eliminated by masking with sodium fluoride.

Applications

The method has been applied to the determination of microamounts of platinum in a catalyst and an anode slime. The results are shown in Table 2, along with the values found by a reference method.

Conclusion

The comparison (in Table 3) of the NPTSQ method with others shows that NPTSQ is a highly sensitive spectrophotometric reagent for platinum, and that the method is simple and rapid, more selective and with higher sensitivity. It may be used to determine microamounts of platinum in small samples.

Acknowledgements—The authors wish to thank engineer Zeng Zuo-Tao for his valuable advice and generous help.

REFERENCES

1. F. E. Beamish and J. C. Van Loon, *Recent Advances in the Analytical Chemistry of the Noble Metals*, p. 357. Pergamon Press, Oxford, 1972.
2. Z. Marczenko, *Spectrophotometric Determination of Elements*, Horwood, Chichester, 1976.
3. A. V. Radushev and G. Ackermann, *Zavodsk. Lab.*, 1977, **43**, 516.
4. S. Kallman, *Talanta*, 1987, **34**, 677.
5. P. W. Beaupré and W. J. Holland, *Mikrochim. Acta*, 1983 **I**, 203.
6. R. M. Uttarwar and A. P. Joshi, *Z. Anal. Chem.*, 1977, **287**, 317.

7. C. K. Bhaskare and R. G. Pawashe, *Analyst*, 1981, **106**, 1005.
8. P. W. Beaupré, W. J. Holland and H. R. Notenboom, *Mikrochim. Acta*, 1979 **I**, 303.
9. S. P. Bag and B. K. Chakrabarti, *Talanta*, 1977, **24**, 128.
10. M. Guzman-Chozas, D. Pérez-Bendito and F. Pino, *An. Quim.*, 1974, **70**, 828.
11. P. K. Gangopadhyay, H. R. Das and S. C. Shome, *Anal. Chim. Acta*, 1973, **66**, 460.
12. V. M. Ivanov and G. N. Gorbunova, *Zh. Analit. Khim.*, 1980, **35**, 3363.
13. S. B. Gawali and V. M. Shinde, *Z. Anal. Chem.*, 1976, **280**, 29.
14. Gowda H. S. and K. A. Padmaji, *Microchem. J.*, 1980, **25**, 396.
15. E. D. Golla and G. H. Ayres, *Talanta*, 1973, **20**, 199.
16. S. Gangopadhyay, P. K. Gangopadhyay and S. C. Shome, *Z. Anal. Chem.*, 1976, **281**, 143.
17. G. N. Gorbunova and V. M. Ivanov, *Zh. Analit. Khim.* 1982, **37**, 880.
18. A. Thimmegowda, H. Sankegowda and N. M. Gowda, *Anal. Chem.*, 1984, **56**, 358.
19. S. B. Savvin, R. F. Gur'eva, L. M. Trutneva and N. N. Chalisova, *Zh. Analit. Khim.*, 1983, **38**, 132.
20. D.-S. Zhang, *Fenxi Shiyanshi*, 1985, **4**, No. 8, 45.
21. W.-B. Chang, Y.-W. Qian and Y.-X. Ci, *Fenxi Huaxue*, 1987, **15**, 397.
22. H.-F. Cheng; Z.-M. Dong and Q.-X. Rong, *Fenxi Ceshi Tongbao*, 1989, **8**, No. 3, 42.
23. Y.-Z. Fan, W. Ping and Z.-D. Fu, *Yejin Fenxi*, 1983, **3**, 157.
24. Z.-T. Zeng and Q.-H. Xu, *Fenxi Huaxue*, 1990, **18**, 983.
25. S. J. Al-Bazi and A. Chow, *Talanta*, 1984, **31**, 815.
26. S.-X. Cai and H. Chao, *Analysis of the Noble Metals*, (in Chinese), p. 147. Publishing House of Metallurgical Industry, 1984.

POSTCOLUMN FORMATION OF FLUOROPHORES FROM NITROGENOUS PESTICIDES BY UV PHOTOLYSIS

BHAGWANDAS M. PATEL and H. ANSON MOYE*

Pesticide Research Laboratory, Food Science and Human Nutrition Department, University of Florida, Gainesville, FL 32611-0531, U.S.A.

ROBERT WEINBERGER

Applied Biosystems, Inc., 170 Williams Drive Ramsey, NJ 07446, U.S.A.

(Received 6 July 1990. Revised 18 December 1990. Accepted 27 December 1990)

Summary—The ultraviolet (UV) photolysis of several classes of nitrogenous pesticides was examined with a view to photo-induced fluorescence detection in flow-injection analysis (FIA) and liquid chromatography. The solvents evaluated as typical reversed-phase mobile phases included water, methanol, and 1:1 mixtures of methanol/water and acetonitrile/water, and methanol/acetonitrile/water mixtures. Acetone, acetophenone, the surfactant Triton X-100, and the photocatalyst titanium dioxide were assessed as photosensitizers to enhance the UV photolysis and fluorescence responses. FIA and liquid chromatographic separations of several pesticides were followed by post-column UV photolysis for the fluorescence detection. Ultraviolet photolysis produces some fluorescent products. The type of photolytic solvent seems to play a significant role. The presence of photosensitizers also affects the fluorescence response of some pesticides. The photochemical transformation products of some of the pesticides are suggested. Analytical figures of merit were evaluated for determination of several pesticides in ground water. The post-column UV photolysis approach for fluorescence detection in liquid chromatography was assessed for several nitrogenous pesticides in ground water samples at ng/g concentrations.

A variety of detectors have been developed for liquid chromatographic and gas chromatographic determination of trace levels of pesticides.¹ Although liquid chromatography (LC) with ultraviolet (UV) detection is sensitive for many organic compounds, it lacks selectivity, especially for complex matrices. Fluorometric²⁻⁴ and electrochemical^{5,6} detectors are more selective than UV detection but intrinsically fluorescent and electroactive compounds are relatively few. Recently, it has been shown that the introduction of a UV lamp in-line induces photochemical reactions in several compounds, leading to the formation of active species that respond to electrochemical^{7,8} or fluorescence detection.⁹⁻¹¹

The photochemistry of several classes of pesticides has been reviewed by Crosby,¹² and more recently by Marcheterre *et al.*¹³ Plimmer¹⁴ has summarized the photochemistry of the halogenated pesticides in the light of present knowledge of the mechanism of photochemical loss of chlorine from aromatic systems. A large number of pesticides contain aromatic structures that absorb strongly at some of the shorter wavelengths, resulting in bond fission; intermolecular energy transfer may also occur from

a sensitizer.¹⁵ The effect of UV light on dinitrophenols, phenyl esters, and esters of nitrophenols and pentachlorophenols has been well documented.¹² In the presence of a sensitizer, several compounds that are otherwise inert may undergo photolytic degradation reactions. Addition of acetone as a sensitizer was reported to result in the rapid disappearance of ethylenethiourea under both natural and artificial light.¹⁶ Photolysis was sensitized also by riboflavin, Rhodamine B or Methylene Blue. The production of radicals by photolytic or other homolytic processes may also be an important factor in the biological action of a pesticide.¹⁴

We have constructed a post-column photolysis/fluorescence detector^{10,11} and extensively examined several classes of nitrogenous pesticides for the fluorescence induced by UV photolysis in LC and FIA. Typical reversed-phase mobile phases (methanol, 1:1 mixtures of methanol/water and acetonitrile/water) were evaluated as the photolytic solvents. Acetone, acetophenone, the surfactant Triton X-100 and the photocatalyst titanium dioxide were assessed as potential photosensitizers to enhance photolysis and fluorescence responses. Both flow-injection analysis and liquid chromatographic techniques were employed.

*Author for correspondence.

EXPERIMENTAL

Apparatus

The instrumental system described earlier^{10,11} for LC postcolumn UV photolysis fluorescence detection was used in this work. A schematic diagram of the system is shown in Fig. 1. Briefly, it consisted of a Perkin-Elmer Series 4 liquid chromatograph solvent-delivery system, a Perkin-Elmer ISS-100 autosampler, Milton Roy minipumps, a UV mercury lamp surrounded by an open tubular knitted photolytic reactor, a Kratos FS 970 fluorometer and a Perkin-Elmer LCI-100 laboratory computing integrator. A Kratos Spectroflow 980 programmable fluorescence detector replaced the FS 970 in the later part of the studies. A Tracor Model 965 photoconductivity detector was used with a Soltec Model 261 chart recorder.

Perkin-Elmer 3 × 3 (0.46 × 3.3 cm; 3 μm) and Waters Resolve (0.46 × 15 cm; 5 μm) C18 columns (room temperature) and linear acetonitrile/methanol/water gradients were used for all LC separations. To detect nanogram amounts of pesticides in water, the volume of sample injected in the column was 400 μl, and the solvent program was optimized for the separation of several pesticides in 27 min, as follows: flow-rate 1.0 ml/min; linear gradient from 60:35:5 to 20:55:25 water/acetonitrile/methanol in 11 min; linear gradient to 30:14:56 water/acetonitrile/methanol in 6 min; hold at 30:14:56 for 4 min; linear gradient to 60:35:5 water/acetonitrile/methanol in 4 min; equilibrate for 2 min.

All initial photolysis studies were performed by flow-injection analysis (FIA) to allow rapid screening and to eliminate chromatographic problems. The solvent flow-rate used was 1 ml/min for all solvent/photosensitizer systems.

Fluorescence was measured at wavelengths longer than 418 nm after excitation at 235 nm with a deuterium source. This setting provided maximum response for several pesticides that produced fluorescent species upon photolysis, and had emission and excitation maxima at these wavelengths, but was a compromise for several other analytes. The fluorescence signals were integrated by the LCI-100 and printed on thermal paper. Fluorescence signals were also printed on the Soltec strip-chart recorder. Experimental conditions were optimized by a single univariate optimization method in the following sequence. The Teflon irradiation reactor designs (coiled, or knitted differently in three dimensions), flow-rates through the reactor, residence times, mobile-phase effects on responses, and concentrations were examined and adjusted to provide maximum responses and minimal band broadening on the chromatograms for pesticides.

Reagents

Acetonitrile, acetone and water (all LC grade), methanol (Optima® grade) and Triton X-100 were obtained from Fisher Scientific Company.

Chlorsulfuron, chlorimuron ethyl, metsulfuron methyl and sulfometuron methyl were obtained from Du Pont (Wilmington, DE), and fenoxycarb was from Maag Agrochemicals (Vero Beach, FL). All the other pesticide standards

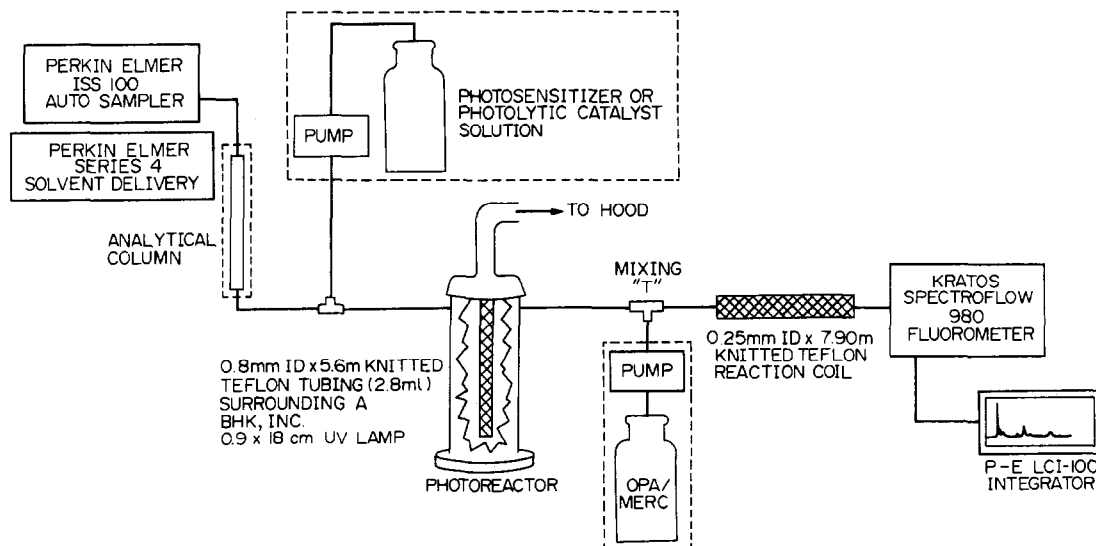
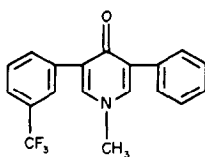
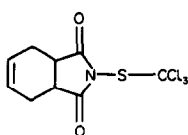


Fig. 1. Schematic diagram of the instrumental system.

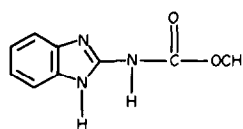
FLURIDONE



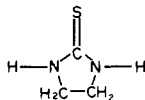
CAPTAN



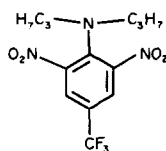
CARBENDAZIM



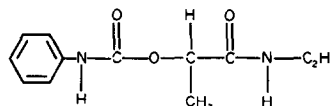
ETHYLENE THIO UREA



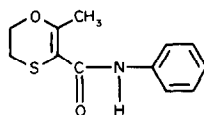
TRIFLURALIN



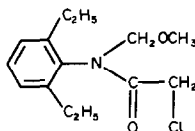
CARBETAMIDE



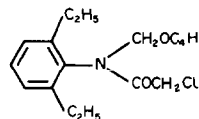
CARBOXIN



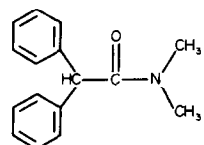
ALACHLOR



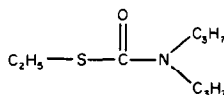
BUTACHLOR



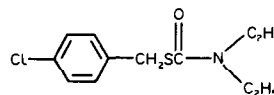
DIPHENAMID



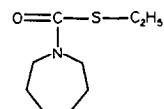
EPTC



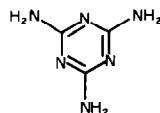
THIOBENCARB



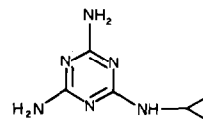
MOLINATE



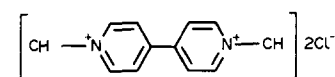
MELAMINE



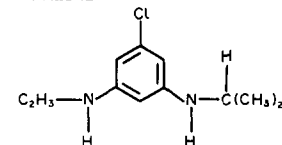
CYROMAZINE



PARAQUAT



ATRAZINE



CHLORAMBEN

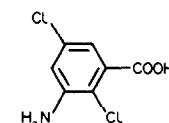
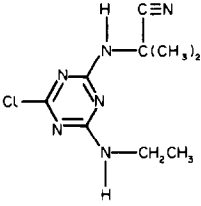
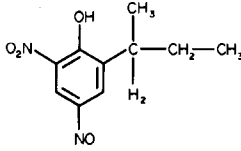


Fig. 2. Chemical structures of the pesticide chemicals.

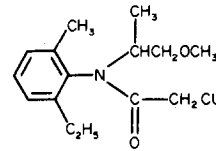
CYANAZINE



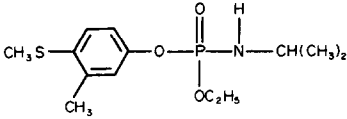
DINOSEB



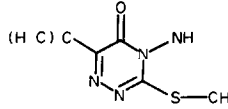
METOLACHLOR



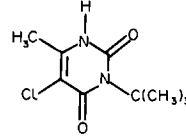
FENAMIPHOS



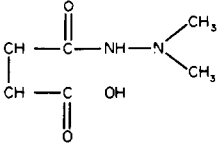
METRIBUZIN



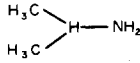
TERBACIL



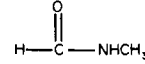
DAMINOZIDE



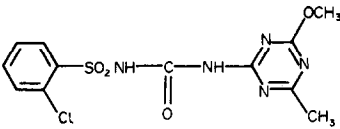
1,1-DIMETHYLHYDRAZINE



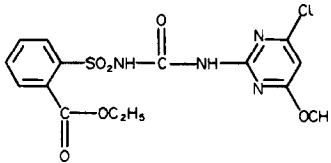
N-METHYL FORMAMIDE



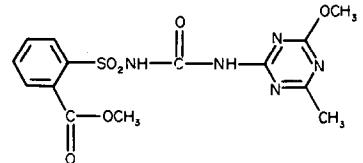
CHLORSULFURON



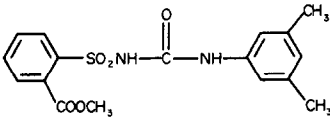
CHLORIMURON ETHYL



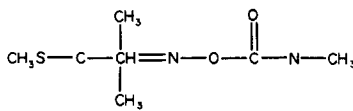
METSULFURON METHYL



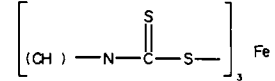
SULFOMETURON METHYL



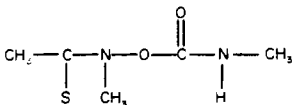
ALDICARB



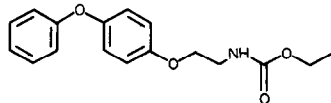
FERBAM



METHOMYL



FENOXYCARB



CHLORPYRIFOS

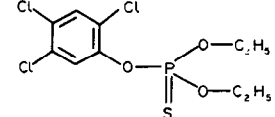


Fig. 3. Chemical structures of the pesticide chemicals.

came from the U.S. Environmental Protection Agency, Pesticides and Industrial Chemicals Repository (Research Triangle Park, NC). The purities ranged from 95 to 100%. The chemical structures of these pesticides (except for avermectin) are shown in Figs. 2 and 3. Solutions of each pesticide (1 mg/ml) were prepared in methanol or water and diluted so that a 1- μ l injection contained between 0.1 and 10 nmole. Injections of 1 μ l were made to minimize the effects of the pesticide solution solvent on the photolysis/fluorescence responses.

Measurement procedure

Relative fluorescence response measurements were initially made without an LC column in place, by FIA for rapid screening. The solvent systems (water, methanol, and 1:1 mixtures of methanol/water and acetonitrile/water) were evaluated for fluorescence response and for use as mobile phases. The solvent systems evaluated with the photosensitizers were water, 1:1 v/v mixtures of methanol/water and acetonitrile/water, each with 0.5% v/v acetone; 1:1 v/v mixtures of methanol/water each with 0.5% v/v acetophenone, 0.02% v/v Triton X-100 or 0.2 mg/ml titanium dioxide. Each of the 37 nitrogenous pesticide solutions (1 μ l) was examined in each of these solvent systems. The fluorescence measurements were performed in two modes of operation: (1) UV lamp off (native fluorescence) and (2) UV lamp on (photo-induced fluorescence). Replicate measurements (at least 3) were made, to evaluate the reproducibility for each analyte. Relative fluorescence intensities, normalized to that of an equimolar amount of quinine sulfate standard, were evaluated after the UV photolysis of each analyte/solvent system combination. The analyte fluorescence response is the difference between the mean of 3–5 measurements (RSD = 5%) with the UV lamp on and the UV lamp off. Fluorescence improvement factors (ratio of fluorescence intensity of photolyzed chemical to fluorescence intensity of untreated chemical) were also evaluated for each analyte. Reversed-phase LC separations were performed and postcolumn UV photolysis and fluorescence measurements were performed for several of those analytes that showed high fluorescence responses in the FIA mode. Analytical figures of merit and recoveries from ground water samples fortified with the analytes at 25–500 ng/ml concentrations were evaluated for several pesticides.

The photosensitizers acetone, acetophenone and Triton X-100 were added directly to the solvents to produce photosensitization, thus eliminating the need for an additional FIA pump.

RESULTS AND DISCUSSION

Fluorescence detection of pesticides

All 37 nitrogenous pesticide chemicals, representing several classes of compounds (see structures in Figs. 2 and 3), were evaluated for fluorescence improvement after UV irradiation and phototransformation. Some of these pesticides are from the EPA Pilot Groundwater Study list because of increasing interest in them.¹⁷ Each of the 9 solvents and photosensitizer systems was employed for screening fluorescence responses and fluorescence improvement following photolysis of each pesticide. The highest fluorescence responses obtained for each compound are listed in Table 1. Also included are the fluorescence improvement factors and the solvent system that produced the highest improvement factor. These results indicate that about 70% of the compounds screened show significant fluorescence improvements upon UV photolysis, with relative fluorescence greater than 1% and/or fluorescence improvement factors larger than 3. It may be noted that the solvent system giving the highest fluorescence response varied from compound to compound. Further, solvent type significantly influenced photolysis efficiencies, fluorescence intensities and relative fluorescences. Scholten *et al.*¹⁸ have reported similar observations. All the compounds in Table 1, except chloramben, gave significant fluorescence responses only after irradiation with UV light, indicating that this fluorescence resulted from some of the phototransformation products. Further, all of these compounds contained an aromatic grouping, suggesting that this fluorescence most likely resulted from phototransformation of this moiety.

Addition of acetone, a photosensitizer, to the 1:1 water/acetonitrile solvent system enhanced the UV photolysis reaction and increased relative fluorescences for the analytes carbetamide, metribuzin, cyromazine and terbacil. These analytes showed lower fluorescence responses in the absence of acetone.

Of all the compounds studied, only two, fluridone and chloramben, showed significant native fluorescence intensity without UV photolysis under the present experimental conditions, and this varied significantly with various solvent

Table 1. Most intense fluorescences obtained by UV photolysis with several solvent/photosensitizer systems for nitrogenous pesticides

Name	Relative fluorescence signal for 1 µg of analyte		Fluorescence response per nmole*	Relative fluorescence†	Solvent/system	Fluorescence improvement‡
	UV-induced (UV on)	Native (UV off)				
Ethylenthiourea (ETU)	0.175	0.080	0.026	0.007	1:1 H ₂ O/CH ₃ CN	3.2
Trifluralin (Treflan)	3.167	0.017	1.056	0.293	1:1 H ₂ O/CH ₃ CN	186.3
Captan	0.069	0.008	0.018	0.005	1:1 H ₂ O/CH ₃ CN	8.6
Carbendazim (Derosal)	0.474	0.023	0.173	0.052	1:1 H ₂ O/CH ₃ OH	20.6
Carbetamide (Legurame)	1.051	0.027	0.242	0.105	1:1 H ₂ O/CH ₃ CN +0.5% acetone	38.9
Carboxin (Vitavax)	2.062	0.005	0.484	0.145	1:1 H ₂ O/CH ₃ OH	412.4
Alachlor (Lasso)	1.276	0.005	0.343	0.081	100% CH ₃ OH	255.2
Butachlor (Machete)	1.100	0.009	0.340	0.080	100% CH ₃ OH	122.2
Avermectin	0.136	0.012	0.108	0.032	1:1 H ₂ O/CH ₃ OH	11.3
Paraquat (Gramoxone)	1.950	0.017	0.497	0.149	1:1 H ₂ O/CH ₃ OH	114.7
Chloramben (Amiben)	8.765	0.105	1.784	0.536	1:1 H ₂ O/CH ₃ OH	83.5
Fenamiphos (Nemacur)	0.652	0.021	0.191	0.058	1:1 H ₂ O/CH ₃ OH	31.0
Metolachlor (Dual)	0.722	0.014	0.201	0.047	100% CH ₃ OH	51.6
Melamine	0.099	0.024	0.01	0.002	100% CH ₃ OH	4.1
Atrazine (Aatrex)	0.15	0.035	0.025	0.006	100% CH ₃ OH	4.3
Metribuzin (Lexone)	0.234	0.035	0.058	0.025	1:1 H ₂ O/CH ₃ CN +0.5% acetone	6.7
N-Methylformamide	0.192	0.012	0.011	0.005	1:1 H ₂ O/CH ₃ CN +0.5% acetone	17.0
Cyromazine	0.159	0.019	0.030	0.013	1:1 H ₂ O/CH ₃ CN +0.5% acetone	9.4
Terbacil (Sinbar)	0.268	0.030	0.052	0.022	1:1 H ₂ O/CH ₃ CN +0.5% acetone	9.9
Cyanazine (Bladex)	0.078	0.022	0.014	0.004	1:1 H ₂ O/CH ₃ CN	3.5
Dinoseb (DNBP)	0.918	0.043	0.23	0.064	1:1 H ₂ O/CH ₃ CN	22.3
Chlorsulfuron	0.074	0.020	0.019	0.009	100% H ₂ O	3.7
Sulfometuron methyl	0.202	0.038	0.12	0.014	1:1 H ₂ O/CH ₃ OH	5.3
Chlorimuron ethyl	0.145	0.003	0.061	0.027	100% H ₂ O	48.3
Metsulfuron methyl§	0.108	0.003	0.08	0.036	100% H ₂ O	36.0
Fenoxycarb	1.695	0.049	0.496	0.019	1:1 H ₂ O/CH ₃ OH	34.6

*Difference between average of measurements with UV lamp on the UV lamp off.

†Ratio of the fluorescence response of pesticide to that of an equimolar amount of quinine sulfate.

‡Fluorescence improvement = Fluorescence intensity of photolyzed chemical/Fluorescence intensity of untreated chemical. §0.5 µg.

systems. The most intense native fluorescence and the optimal solvent systems for these two pesticides are given in Table 2. It is interesting that the native fluorescence intensity of chloramben is 10.5 times greater in 100% methanol than in 1:1 water/methanol (see Table 1). Further, UV photolysis enhanced the fluorescence intensity of chloramben and produced a high fluorescence improvement (83.5; see Table 1).

For several pesticides the relative fluorescence improvement was very dependent upon the solvents used, indicating that the solute environ-

ment was important in the photolysis mechanism. It has been reported that the presence and/or absence of oxygen affects the rates of photolysis and products formed from some pesticides.^{19,20} Even though the solvents used in this investigation were purged with helium to avoid bubble formation during chromatography, the oxygen permeability of Teflon prevented deoxygenation from being achieved during photolysis. Therefore, the role of oxygen, if any, in the photolysis of these pesticides is not known. Further, it has been reported that UV irradiation of Teflon

Table 2. Most intense fluorescences observed without UV photolysis (native fluorescence) for nitrogenous pesticides in several solvent/photosensitizer systems

Name	Relative fluorescence signal for 1 µg of analyte (native fluorescence, no UV)	Fluorescence response per nmole	Relative fluorescence*	Solvent/photosensitizer system
Fluridone (Sonar)	3.595	1.184	0.356	1:1 H ₂ O/CH ₃ OH
Chloramben (Amiben)	1.140	0.235	0.055	100% CH ₃ OH

*Ratio of fluorescence response of pesticide to that of an equimolar amount of quinine sulfate.

Table 3. Photosensitizer-enhanced UV-photolysis and improvement of fluorescence of nitrogenous pesticides

Name	Relative fluorescence signal for 1 µg of analyte		Fluorescence response per nmole*	Relative fluorescence†	Solvent/ photosensitizer system	Fluorescence improvement‡
	UV-induced (UV on)	Native (UV off)				
Trifluralin (Treflan)	0.087	0.015	0.024	0.007	1:1 H ₂ O/CH ₃ OH	5.8
Trifluralin (Treflan)	2.121	0.040	0.698	0.169	1:1 H ₂ O/CH ₃ OH +0.5% acetone	53
Thiobencarb (Bolero)	0.050	0.019	0.008	0.002	1:1 H ₂ O/CH ₃ OH	2.6
Thiobencarb (Bolero)	1.144	0.026	0.288	0.037	1:1 H ₂ O/CH ₃ OH +0.02% Triton X-100	44
Cyromazine	0.032	0.03	0.0003	0.0001	1:1 H ₂ O/CH ₃ CN	1.1
Cyromazine	0.159	0.019	0.030	0.013	1:1 H ₂ O/CH ₃ CN +0.5% acetone	9.4
Dinoseb (DNBP)	0.024	0.028	0.001	0.0003	1:1 H ₂ O/CH ₃ OH	0.9
Dinoseb (DNBP)	0.125	0.031	0.038	0.01	1:1 H ₂ O/CH ₃ OH +0.5% acetone	5
Metribuzin (Lexone)	0.018	0.015	0.0006	0.0002	1:1 H ₂ O/CH ₃ CN	1.2
Metribuzin (Lexone)	0.234	0.035	0.058	0.025	1:1 H ₂ O/CH ₃ CN +0.5% acetone	6.7
Terbacil (Sinbar)	0.014	0.011	0.0007	0.0002	1:1 H ₂ O/CH ₃ CN	1.3
Terbacil (Sinbar)	0.268	0.030	0.052	0.022	1:1 H ₂ O/CH ₃ CN +0.5% acetone	9.9
Daminozide (Alar)	0.015	0.014	0.0003	0.0001	1:1 H ₂ O/CH ₃ CN	1.1
Daminozide (Alar)	0.20	0.011	0.03	0.013	1:1 H ₂ O/CH ₃ CN +0.5% acetone	19.2
N-Methylformamide	0.018	0.015	0.0002	0.00005	1:1 H ₂ O/CH ₃ CN	1.2
N-Methylformamide	0.192	0.012	0.011	0.005	1:1 H ₂ O/CH ₃ CN +0.5% acetone	17
1,1-Dimethylhydrazine	0.029	0.016	0.0008	0.0002	1:1 H ₂ O/CH ₃ CN	1.8
1,1-Dimethylhydrazine	0.126	0.043	0.005	0.002	1:1 H ₂ O/CH ₃ CN +0.5% acetone	2.9

*Difference between average of measurements with UV lamp on the UV lamp off.

†Ratio of fluorescence response of pesticide to that of an equimolar amount of quinine sulfate.

‡Fluorescence improvement = Fluorescence intensity of photolyzed chemical/Fluorescence intensity of untreated chemical.

Table 4. Fluorescence improvements observed upon UV photolysis of several pesticides in various solvent systems

Name	Fluorescence improvement*								
	H ₂ O	CH ₃ OH	1:1 H ₂ O + CH ₃ OH	1:1 H ₂ O + CH ₃ CN	H ₂ O +0.5% acetone	1:1 H ₂ O + CH ₃ OH +0.5% acetone	1:1 H ₂ O + CH ₃ CN +0.02% acetone	1:1 H ₂ O + CH ₃ OH +0.02% Triton X-100	1:1 H ₂ O + CH ₃ OH +0.5% aceto- phenone
Trifluralin	2.6	2.2	5.8	186.3	3	53	41.1	4	3.8
Carbendazim	3.7	9.9	20.6	15.5	0.8	3.8	6.2	10.3	1.3
Carbetamide	0.4	12.8	6.2	11	1	4	38.9	3.9	0.6
Carboxin	34	161	412.4	173.3	1.3	33.5	47.4	91.1	1.3
Alachlor	21.5	255.2	104.3	23.2	0.8	3.7	4.1	54.8	0.7
Butachlor	10.9	122.2	37.1	22.8	1.9	3.5	5.6	44.3	12
Avermectin	1.1	13.6	11.3	2.5	1.7	3.7	7.6	4.7	1.6
Paraquat	6	57.8	114.7	10.1	1.4	1	17.1	44.6	1.9
Chloramben	16.3	2.9	83.5	46.8	2.5	42.9	56.9	55.1	5.3
Fenamiphos	6.5	5.6	31	5.6	1.2	4.8	1.2	13.4	0.7
Metolachlor	11.1	51.6	19	16.5	1.1	3.6	2.8	35.8	1
Metribuzin	0.6	0.5	0.6	1.2	0.8	0.3	6.7	1.3	0.8
Cyanazine	3.9	1.3	2.2	3.5	0.9	1.4	3.5	3	1.2
Terbacil	1.4	6.4	1.1	1.3	1.3	1.1	8.9	2.7	1
Cyromazine	0.4	1.4	0.7	1.1	1.7	2.6	9.4	0.8	0.9
Dinoseb	1.9	1.7	0.9	22.3	0.4	5	9.6	0.4	1.6
Daminozide	1.3	1	0.8	0.9	2.2	1.7	19.2	0.5	1
Molinate	1.4	1.1	1	2.2	1	1.6	10.1	1.6	7
Thiobencarb	2.9	2.3	2.6	9.9	1	0.7	4.9	44	1.6
EPTC	1.4	0.8	1.2	2.3	1.1	0.7	16.3	1.8	1.7
Diphenamid	10.3	8.3	26.9	14	1.1	1.2	2.5	8.9	2

*Fluorescence improvement = Fluorescence intensity of photolyzed chemical/Fluorescence intensity of untreated chemical.

produces protons and fluoride ions, which may also affect photolytic pathways.²¹

The effect of the photosensitizers was evaluated by adding them prior to UV photolysis. Table 3 lists acetone photosensitizer-enhanced UV photolysis and fluorescence response for several compounds. No one solvent system produced the highest fluorescence responses for all the pesticides. Fluorescence responses without acetone are also included for comparison. The presence of acetone enhanced the UV photolysis, giving fluorescence improvement factors 5–15 times higher for all the pesticides except 1,1-dimethylhydrazine. In other instances, however, the presence of acetone in the solvent system produced diminished fluorescence signals. The fluorescence improvements are summarized in Table 4.

The use of the photocatalyst titanium dioxide as a photosensitizer was evaluated by using an aqueous suspension. Initial studies were carried out with 0.2 mg/ml titanium dioxide dispersed in LC grade water. This suspension was constantly stirred and dispensed at a flow-rate of 0.5 ml/min into a 1:1 water/methanol solvent system. The five pesticides showing no significant fluorescence responses with UV photolysis and without a photosensitizer were: ethylenethiourea, trifluralin, thiobencarb, dinoseb and chlorsulfuron. Three of these compounds upon UV photolysis in the presence of titanium dioxide gave a relative fluorescence response greater than 1%. The relative fluorescence (photolysis efficiency) values for three pesticides were: dinoseb (1%), thiobencarb (1.3%), and trifluralin (11%). Further work is needed to evaluate the effect of the photocatalyst titanium dioxide on other pesticides.

Photoconductivity and programmed wavelength fluorescence detection

A preliminary study was done with the photoconductivity detector for measurement of responses of several pesticides following UV photolysis. There was very little difference in photolytic efficiency between the UV sources, when used with either the LC fluorescence instrumentation or the photoconductivity detector. The peaks measured with the photoconductivity detector were somewhat broader, probably because of the open tubular design of the reactor. The limits of detection were within an order of magnitude of each other. All subsequent measurements were made by optical detection, because of the selectivity advantage conferred

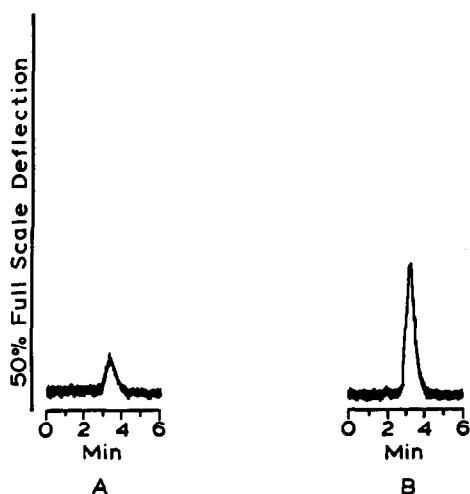


Fig. 4. Typical FIA traces of the LC-integrator output. A = 0.2 ng of diphenamid; B = 1 ng of diphenamid.

by changing the fluorescence excitation and emission wavelengths.

A new programmable fluorescence detector, an ABI Analytical Kratos Division Spectroflow 980 model, was obtained to replace the Kratos model FS 970 detector and a comparative performance study was carried out for several analytes. The fluorescence signal intensities with the Spectroflow 980 detector were 3–4 times higher for equal amounts of analytes than those with the FS 970 detector. The fluorescence responses for several analytes were more than four times as great when measured with the new detector. Typical traces of the fluorescence signals for diphenamid are shown in Fig. 4.

Analytical figures of merit

Analytical figures of merit for determination of some of the more responsive compounds were evaluated by LC, employing UV photolysis for the generation of fluorophores. Several classes of pesticides in ground water were determined by this approach. Aqueous standard solutions of various pesticides (covering a range of concentrations) were examined individually and as mixtures. LC separation of the analytes was achieved in the reversed-phase mode in 27 min with the water/acetonitrile/methanol gradient solvent program mentioned in the experimental section, on a C18 column at room temperature. The chromatographically separated pesticides were UV photolyzed and their fluorescence responses were measured. Typical LC chromatograms are shown in Fig. 5 for a multi-component pesticide mixture. Analytical figures of merit for determination of several

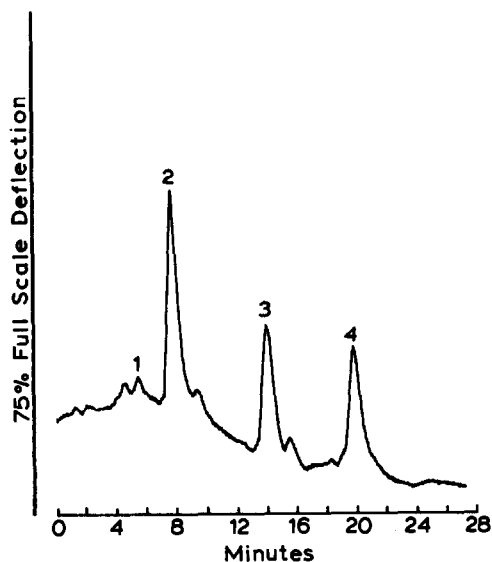


Fig. 5. Chromatograms of multi-component pesticides in water, obtained by the reversed-phase LC and postcolumn UV photolysis and fluorescence detection technique. Column, Waters Resolve C18 (0.46 × 15 cm; 5 μm); sample injection volume, 400 μl; amount of each pesticide, 50 ng. 1, Carbetamide, retention time 5.45 min; 2, carboxin, retention time 7.77 min; 3, alachlor, retention time 14.09 min; 4, butachlor, retention time 19.80 min.

pesticides are given in Table 5. These analytical figures were determined from at least 6–10 measurements of various concentrations. The calibration equation was calculated by a least-squares program with Lotus software. The limit of detection for the analyte was evaluated from 6 or more fluorescence measurements of the lower concentrations. The standard deviation of measurements was within the range 3–5% RSD. Fluorescence signal peak heights, background noise (peak-to-peak) and blank measurements were recorded and detection limits were evaluated from the lower concentrations for a signal-to-noise ratio of 3. The limits of detection for the pesticides with this technique are in the lower μg/kg range. Typical analytical curves for these analytes were linear over an analyte mass

Table 6. Determination of pesticides in ground water samples*

Pesticide	Concentration, μg/kg		Mean recovery, %
	Added†	Found‡	
Alachlor	25	26 ± 1	105
	100	105 ± 4	105
	250	263 ± 8	105
	500	500 ± 15	100
Butachlor	25	28 ± 1	110
	125	130 ± 5	104
	250	243 ± 7	97
Carbetamide	50	58 ± 3	115
	250	275 ± 8	110
	500	475 ± 14	95
Carboxin	25	28 ± 1	110
	50	54 ± 2	108
	250	250 ± 8	100
	500	475 ± 12	95

*The concentration of the analytes in the ground water samples was below the limit of detection.

†To a 400-μl sample injection into the LC column.

‡Mean ± standard deviation of four replicates.

range of 2–3 orders of magnitude with the low end of the curves in the range of lower nanogram amounts.

Analytical applications

LC postcolumn UV photolysis followed by fluorescence detection was applied to the determination of pesticides in ground water samples. The samples were then fortified with pesticides at various levels and the pesticides were determined again in the same way (four replicates). Least-squares and regression analyses of the data are shown in Table 6. The mean recoveries ranged from 95 to 115% at the lower μg/kg concentrations.

CONCLUSIONS

The postcolumn UV photolysis of 37 pesticide chemicals, followed photoinduced fluorescence detection by FIA and LC, with nine solvent-photosensitizer combinations showed that more

Table 5. Analytical figures of merit for the HPLC–UV photolysis fluorescence determination of pesticides in ground water

Pesticide	Range of analyte amount studied, ng	Analyte concentration range, μg/kg	Limit of detection,* μg/kg	Regression equation†	Correlation coefficient, r
Alachlor	4–200	10–500	5	$y = 4.32 + 1.42x$	0.9986
Butachlor	10–200	25–500	12	$y = -2.41 + 1.74x$	0.9985
Carbetamide	20–400	50–1000	38	$y = 1.56 + 1.02x$	0.9999
Carboxin	4–200	10–500	5	$y = -3.78 + 1.22x$	0.9996
Diphenamid	50–200	125–500	50	$y = -3.50 + 2.65x$	0.9973
Fenoxycarb	10–50	25–125	5	$y = 4.68 + 1.15x$	0.9935

*Limit of detection from signal peak-height, blank, and background peak-to-peak noise, for $S/N = 3$.

† y = relative fluorescence, x = analyte concentration (μg/l).

than two-thirds of these compounds produce high fluorescence responses upon UV photolysis. These analytes showed no fluorescence improvement without photolysis, indicating that the fluorescence improvement resulted from some of the phototransformation products. The relative fluorescence response of most analytes was very dependent on the solvent environment and on the presence or absence of photosensitizing agents. Fluorescence response measurements of the analytes after photolysis produced limits of detection in the lower nanogram range. Several pesticides were determined in ground water samples at $\mu\text{g}/\text{kg}$ concentrations with this LC postcolumn UV photolysis fluorescence detection technique. The recoveries for various analytes ranged from 95 to 115% at the lower $\mu\text{g}/\text{kg}$ concentrations.

Acknowledgement—This research was sponsored by the U.S. Department of Interior, Grant no. 14-08-0001-G1722.

REFERENCES

1. L. Muszkat and N. Aharonson, *Anal. Methods Pestic. Plant Growth Regul.*, 1986, **14**, 95.
2. A. Hulshoff and H. Lingeman, *Molecular Luminescence Spectroscopy Methods and Applications*, Part 1, p. 621. Wiley, New York, 1985.
3. R. W. Frei, in R. W. Frei and J. F. Lawrence (eds.), *Chemical Derivatization in Analytical Chemistry*, Vol. 1: *Chromatography*, Plenum Press, New York, 1981.
4. P. Froehlich, *BioChromatography*, 1987, **2**, 144.
5. D. C. Johnson, S. G. Weber, A. M. Bond, R. M. Wightman, R. E. Shoup and I. S. Krull, *Anal. Chim. Acta*, 1986, **180**, 187.
6. K. Štulík and V. Pacáková, *Prog. HPLC*, 1987, **2**, 131.
7. I. S. Krull and W. R. LaCourse, in I. S. Krull (ed.) *Reaction Detection in Liquid Chromatography*, p. 303. Dekker, New York, 1986.
8. X. D. Ding and I. S. Krull, *J. Agric. Food Chem.*, 1984, **32**, 622.
9. R. G. Luchtefeld, *J. Chromatog. Sci.*, 1985, **23**, 516.
10. C. J. Miles and H. A. Moye, *Anal. Chem.*, 1988, **60**, 220.
11. B. M. Patel, H. A. Moye and R. Weinberger, *J. Agric. Food Chem.*, 1990, **38**, 126.
12. D. G. Crosby, in P. C. Kearney and D. D. Kaufman (eds.) *Herbicides: Chemistry, Degradation and Mode of Action*, Vol. 2, 2nd Ed., p. 835. Dekker, New York, 1976.
13. L. Marcheterre, G. G. Choudhry and G. R. B. Webster, *Rev. Environ. Contam. Toxicol.*, 1988, **103**, 61.
14. J. R. Plimmer, *Residue Rev.*, 1971, **33**, 47.
15. R. G. Zepp and D. M. Cline, *Environ. Sci. Technol.*, 1977, **11**, 359.
16. R. D. Ross and D. G. Crosby, *J. Agric. Food Chem.*, 1973, **21**, 335.
17. *Pesticide and Toxic Chemicals News*, 11 February 1987, p. 19.
18. A. H. M. T. Scholten, U. A. Th. Brinkman and R. W. Frei, *Anal. Chim. Acta*, 1980, **114**, 137.
19. P. K. Freeman and K. D. McCarthy, *J. Agric. Food Chem.*, 1984, **32**, 873.
20. P. K. Freeman and E. M. N. Ndip, *ibid.*, 1984, **32**, 877.
21. G. E. Batley, *Anal. Chem.*, 1984, **56**, 2261.

SEPARATION OF TRACES AND LARGER AMOUNTS OF BISMUTH FROM GRAM AMOUNTS OF THALLIUM, MERCURY, GOLD AND PLATINUM BY CATION-EXCHANGE CHROMATOGRAPHY ON A MACROPOROUS RESIN

F. W. E. STRELOW

Division of Processing and Chemical Manufacturing Technology, C.S.I.R., P.O. Box 395, Pretoria 0001, South Africa

(Received 11 July 1989. Revised 27 August 1990. Accepted 26 February 1991)

Summary—Traces and larger amounts of bismuth (up to 50 mg) can be separated from gram amounts of thallium, mercury, gold and platinum (up to 5 g) by sorption from a mixture of 0.1M hydrochloric acid and 0.4M nitric acid on a column containing just 3 g (8.1 ml) of AGMP-50, a macroporous cation-exchange resin. This resin retains bismuth much more strongly than does the usual microporous resin (styrene-DVB with 8% cross-linkage). Other elements are eluted with the same acid mixture as that used for sorption, and bismuth is finally eluted with 1.0M hydrochloric acid. Separations of bismuth are sharp and recoveries quantitative. Only microgram amounts of the other elements remain in the bismuth fraction. Amounts of bismuth as little as 5 μ g have been separated from 5 g of thallium, and determined (r.s.d. = 2%) by flame atomic-absorption. Only 100- μ g amounts of bismuth have been separated from gram amounts of mercury, gold, and platinum, but there is no reason to believe that smaller or larger amounts of bismuth cannot be separated from these elements and recovered with the same accuracy as that for the separation from thallium. The lower limit of the method is determination of 0.4 μ g of bismuth in 10 ml of solution (0.004 absorbance). An elution curve, the relevant distribution coefficients and the results of analysis of synthetic mixtures and two practical samples [thallium metal and mercury(II) nitrate] are presented.

The separation of bismuth from other elements by ion-exchange chromatography has received considerable attention during the past few decades. Probably the first selective method described was that of Lur'e and Filipova who found that bismuth was eluted by 0.05M sulphuric acid, containing 10 mg/ml potassium iodide, from a cation-exchange column, while copper and lead were retained.¹ Many other elements should also be retained.

One of the most selective and generally applicable methods available originates from the work of Nelson and Kraus² who showed that bismuth is retained by strongly basic anion-exchange resins from hydrochloric acid media over practically the whole acid concentration range. Lead can be eluted with 8M hydrochloric acid, followed by elution of iron(III) and most other elements with 0.5M hydrochloric acid. Bismuth is retained and can be eluted with 1M sulphuric acid. Cadmium, zinc and indium are only partially eluted and thallium(III), mercury(II), gold(III), platinum(IV) and palladium(II) are not eluted at all with 0.5M

hydrochloric acid. They accompany bismuth either partially or completely. Numerous variations of this method have appeared in the literature.

Even more selective is anion-exchange in nitric-hydrobromic acid mixtures.³ As much as gram amounts of cadmium can be separated from traces of bismuth by eluting cadmium with 0.03M hydrobromic acid in 2M nitric acid, from a quite small column. This separation is not possible by anion-exchange in pure hydrochloric or hydrobromic acid (or iodide) media, because both elements are strongly retained even at low acid concentrations and show only minor differences in their anion-exchange behaviour in pure halide solutions.

Some species, such as thallium(III), gold(III), mercury(II) and platinum metals, which form very stable chloride or halide complexes, are retained together with bismuth by anion-exchange resins from halide-containing solutions over practically the whole concentration range. Separations of these elements from bismuth by anion-exchange procedures in

halide solutions are therefore difficult or impossible.

It has been shown that bismuth can be sorbed selectively from 8M ammonium nitrate,² or from nitric acid-methanol mixtures,⁴ but the large salt concentrations in the first case could cause problems, and mercury(II), gold(III) and palladium(II) are also sorbed from nitrate or nitric acid-methanol solutions.

A different approach for separation of bismuth from large amounts of thallium has been described recently.⁵ The bismuth is retained from dilute nitric acid by a cation-exchange resin with a low degree of cross-linkage (Bio-Rad AG50W-X4) and thallium, as Tl(I), is eluted with 0.6M nitric acid. As much as 2 g of thallium can be separated. Unfortunately, mercury(II) is also retained and cannot be cleanly separated from bismuth by this method. Large amounts of gold or platinum could cause problems in chloride-free solutions of dilute nitric acid because such solutions tend to become unstable (with respect to reduction to the metal) when the last traces of chloride are removed by repeated evaporations with nitric acid.

Recent publications^{6,7} indicate that macroporous cation-exchange resins such as Bio-Rad AG MP-50 retain bismuth much more strongly from dilute hydrochloric acid solutions than the usual gel-type resin with 8% divinylbenzene (DVB) cross-linkage does, whereas the sorption of mercury(II), gold(III), thallium(III) and platinum(IV) does not change significantly. This seemed to offer good prospects for the separation of traces and also larger amounts of bismuth from large amounts of these species.

Also, because bismuth forms an oxychloride that is quite insoluble in very dilute hydrochloric acid, but becomes more soluble with increase in chloride as well as hydrogen-ion concentration, and distribution coefficients for bismuth are much larger in nitric than in hydrochloric acid,⁷ the use of nitric-hydrochloric acid mixtures as eluting agents seemed to offer possibilities for separating larger amounts of bismuth and for achieving separations on relatively small columns. Distribution coefficients have been determined for bismuth on a gel-type 8% cross-linked resin in the mixed acids,⁸ but such information does not exist for macroporous resins. This paper therefore presents distribution coefficients for bismuth(III) on a macroporous resin in nitric-hydrochloric acid mixtures. The results are used to develop a method for the quantitative separation of traces and larger

amounts of bismuth from thallium(III), gold(III), mercury(II) and platinum(IV).

EXPERIMENTAL

Reagents

Reagents were of analytical grade purity unless stated otherwise, and distilled water was further purified by passage through an Elgastat demineralizer. A standard solution of bismuth was prepared by dissolving 2.000 g of bismuth metal (99.98% pure) in nitric acid, evaporating to dryness on a water-bath, and making up to 1000 ml with 0.50M nitric acid. Solutions containing lower concentrations of bismuth were prepared by dilution as required. Solutions of thallium(III), gold(III) and platinum(IV) were prepared by dissolving the pure metals in *aqua regia*. After evaporation to dryness on the water-bath, the remaining salts were dissolved in hydrochloric acid and the solutions were diluted to the required volume in 0.1M acid (for thallium) or 0.5M acid (for gold and platinum). The gold(III) solutions contained 40 mg/ml of the metal, platinum(IV) solutions 20 mg/ml, and thallium (III) solutions 100 mg/ml. The thallium solution also contained some free chlorine to ensure that thallium was in the +3 oxidation state. Before the final dilution to volume the solutions were purified from traces of bismuth by passing them (in about 0.1M hydrochloric acid) through columns containing 5 g of AGMP-50 resin, washing with 0.1M hydrochloric acid and making up to volume with the same acid (thallium) or adding the concentrated acid to give a final acid concentration of 0.5M (gold, platinum).

The resin was the Bio-Rad AG MP-50 macroporous sulphonated polystyrene cation-exchanger, 100-200 mesh.

Apparatus

Borosilicate glass tubes of 11.8 mm i.d. and 150 mm length, fitted with a No. 1 porosity sintered-glass plate and a burette tap at the bottom, served as columns. The top was connected to an additional piece of wider tube (20 mm i.d., 100 mm long) fitted with a B19 joint to take a separating funnel as reservoir.

The columns were filled with a slurry of AG MP-50 (100-200 mesh) resin in the hydrogen form until the settled resin reached the 8.1 ml mark (3 g of dry resin). The resulting resin column was 74 mm long in water. Because the resin, as received, was found to contain appreci-

able amounts of calcium (about 1 mg per g of dry resin), it was purified by passage of about 200 ml of 5*M* nitric acid followed by 50 ml of demineralized water.

A Varian-Techtron AAS instrument was used for atomic-absorption spectrometry (AAS) with an air-acetylene flame, for all elements. For the smallest amounts of bismuth (20 and 5 μg) a slotted tube made of transparent fused silica, similar in construction to the slotted stainless-steel tube described by Watling,⁹ and Watling and de Villiers¹⁰ was used. The use of the slotted tube enhanced the absorbance signal by a factor of about 3, stabilized the signal, and made it possible to obtain an absorbance of about 0.2 for 2 ppm of bismuth with only moderate scale expansion ($\times 2$).

Distribution coefficients in nitric acid-hydrochloric acid mixtures

Portions (2.500 g) of AG MP-50 resin (dried at 110°) were equilibrated in a mechanical shaker for 24 hr at 20° with 250 ml of a solution containing 10 mg of bismuth and the concentrations of nitric and hydrochloric acid shown in Table 1 and Fig. 1. After equilibration, the resin was separated from the aqueous phase by filtration through a glass column that was 200 mm long and 23 mm wide (i.d.), with a No. 1 porosity sintered-glass plate at the bottom. The resin was transferred into the columns and washed with demineralized water, and the aqueous phase was retained. The sorbed bismuth was then eluted with $\sim 1M$ hydrochloric acid and also retained. The amounts of bismuth in the two phases were determined by flame atomic-absorption after suitable dilution, and the distribution coefficients calculated from the analytical results. The coefficients are presented in Table 1 and Fig. 1.

Elution curves

A solution containing 5.00 g of thallium(III) and 30 mg of bismuth in about 250 ml of 0.10*M* hydrochloric acid containing 0.40*M* nitric acid

Table 1. Distribution coefficients for bismuth(III) in HCl-HNO₃ mixtures with a macroporous resin (AG MP-50)

[HNO ₃], M	[HCl], 0.1 <i>M</i>	[HCl], 0.2 <i>M</i>
0.2	4860	243
0.3	1720	120
0.4	790	67
0.5	385	41.0
1.0	41.1	7.6
2.0	3.8	1.7

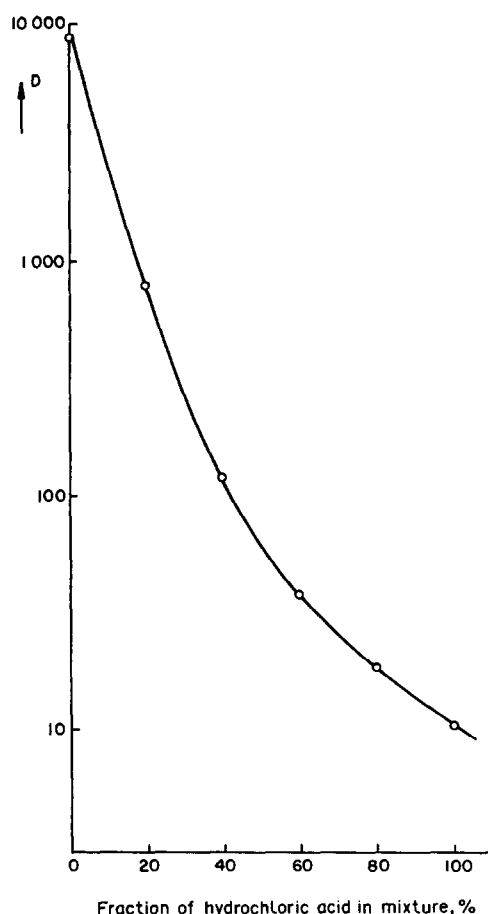


Fig. 1. Distribution coefficients for bismuth in hydrochloric/nitric acid mixtures, 0.50*M* total acid concentration.

was passed through a clean column of 8.1 ml (3 g) of AG MP-50 resin as described above. The column had been conditioned by passage of about 20 ml of a mixture of 0.10*M* hydrochloric and 0.40*M* nitric acid. The solution was washed onto the resin with a few small portions of the acid mixture, which was also used to elute thallium at a flow-rate of 2.0 ± 0.3 ml/min, a total of 100 ml being used. Finally bismuth was eluted with 1.0*M* hydrochloric acid at the same flow-rate. Ten-ml fractions were collected from the beginning of the sorption step, with an automatic fraction collector. The concentrations of thallium and bismuth in the fractions were determined, after suitable dilution, by flame AAS (standard conditions). The experimental elution curve is shown in Fig. 2.

In another experiment, the elution of thallium was continued to establish how strongly 30 mg of bismuth was retained; no bismuth appeared in the first 500 ml of effluent. Elution curves for Au(III), Hg(II) and Pt(IV) were very similar to the curve shown for thallium in Fig. 2.

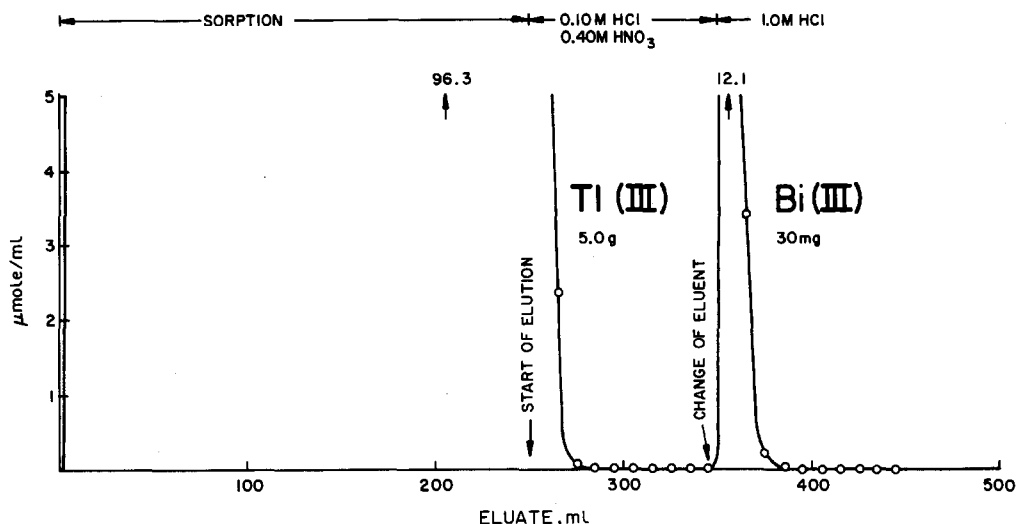


Fig. 2. Elution curve for Tl(III)-Bi(III) mixture, sorbed from 0.10M HCl + 0.40M HNO₃ on 8.1 ml (3 g) of AG MP-50 resin (100-200 mesh). Flow-rate 2.0 ± 0.3 ml/min.

Quantitative separation of synthetic mixtures

Five-ml volumes of a standard solution containing 1.00 μg/ml bismuth in 0.5M nitric acid were added to five bismuth-free solutions, each containing 5.00 g of thallium. Enough 1M hydrochloric and 5M nitric acid were added to give 0.1 and 0.4M concentrations, respectively, when the solutions were diluted to 250 ml. The solutions were then passed through columns containing 3 g of AG MP-50 resin as described earlier. Each was washed onto the resin quantitatively with a few small portions of a mixture of 0.10M hydrochloric and 0.40M nitric acid, then the thallium was eluted with 100 ml of the same reagent at a flow-rate of 2.0 ± 0.3 ml/min. Finally bismuth was eluted with 80 ml of 1.0M hydrochloric acid at the same flow-rate. The bismuth fractions were evaporated to about 1 ml, finally in a 25-ml beaker, and then transferred into 10-ml standard flasks. Triplicate blanks were treated in the same way.

Bismuth was determined in both samples and blanks by flame AAS with the slotted transparent fused-silica tube as already described. The mean blank value was used to correct the recoveries obtained for the synthetic mixtures. The amounts of thallium remaining in the bismuth fraction were also determined by AAS. The experiment was repeated with 20 μg, 100 μg, 500 μg, 2000 μg, 20.00 mg and 50.0 mg amounts of bismuth, more concentrated standard solutions being used for the larger amounts.

The 20-μg amounts were determined by flame AAS with the slotted tube, but direct AAS

without the tube was used for the 100-μg, 500-μg and 2.000-mg amounts. The 500-μg amounts were determined in a volume of 25 ml and the 2.000-mg amounts in 100 ml. The 20.00 and 50.00-mg amounts were determined by titration with EDTA, (Xylenol Orange as indicator). Next, the separation was tried for 100-μg amounts of bismuth and 5.00-g amounts of mercury(II). Then the same amounts of bismuth were separated from 2.00 g of gold(III) and from 1.00 g of platinum by the same procedure.

Determination of bismuth in thallium metal and mercury(II) nitrate

Thallium metal (5 g) and mercury(II) nitrate (8.09 g ≡ 5.00 g of mercury) were separately weighed out accurately into 400-ml beakers. The thallium was dissolved in *aqua regia* and the solution was evaporated to dryness on the water-bath, after some chlorine water had been added. The dry thallium salts were dissolved in about 250 ml of a mixture of 0.10M hydrochloric and 0.40M nitric acid, again with addition of some chlorine water. The mercury(II) nitrate was dissolved in 250 ml of the acid mixture. The separation was performed as described above for the synthetic mixtures. Three blanks were taken through the whole procedure. Finally the bismuth fractions of the samples and blanks were evaporated to ~1 ml, then accurately made up to 10.0 ml and analysed for bismuth by flame AAS with the slotted silica tube and scale expansion.

Table 2. Determination of bismuth in synthetic mixtures

Bismuth taken	Other element taken	Bismuth found	Amount of other element in Bi fraction
5.00 μg	5.00 g Tl	$5.0 \pm 0.1 \mu\text{g}$	60–125 μg
20.0 μg	5.00 g Tl	$19.9 \pm 0.1 \mu\text{g}$	54–111 μg
100.0 μg	5.00 g Tl	$100.1 \pm 0.4 \mu\text{g}$	80–211 μg
500 μg	5.00 g Tl	$500 \pm 2 \mu\text{g}$	49–109 μg
2000 μg	5.00 g Tl	$1998 \pm 7 \mu\text{g}$	51–116 μg
20.00 mg	5.00 g Tl	$20.00 \pm 0.01 \text{mg}\dagger$	n.d.
50.00 mg	5.00 g Tl	$50.02 \pm 0.03 \text{mg}\dagger$	n.d.
100.0 μg	5.00 g Hg	$99.9 \pm 0.3 \mu\text{g}$	7–21 μg
100.0 μg	2.00 g Au	$99.9 \pm 0.3 \mu\text{g}$	6–11 μg
100.0 μg	1.00 g Pt	$100.1 \pm 0.4 \mu\text{g}$	1.8–6.2 μg

*Mean \pm standard deviation of 5 analyses.

\dagger Complexometric titrations.

n.d. = Not determined.

RESULTS AND DISCUSSION

The results for the analysis of synthetic mixtures are presented in Table 2 and those for the analysis of two practical samples in Table 3. These show that the method provides a sharp and quantitative separation of bismuth from gram amounts of thallium, mercury, gold and platinum. As much as 50 mg of bismuth can be separated from 5 g of thallium, mercury, gold or platinum on a column containing just 3 g of AG MP-50 resin. Such a separation is not possible on a similar column of gel-type AG 50W-X8 resin. The distribution coefficient in 0.10M hydrochloric/0.40M nitric acid mixture is 790 (Table 1) for the macroporous resin, compared with 51 for the microporous resin. A much larger column, with 20 g of resin, would therefore be required if a gel-type resin were used. At lower acid concentrations the coefficients for the gel-type resin do increase, but then the solubility of bismuth oxychloride decreases very sharply. Nevertheless, both resins can be used to separate traces of bismuth from large amounts of the other elements named above. However, at the lower acid concentrations which have to be used, the gel-type resin tends to retain considerably larger amounts of the other element together with bismuth (up to several milligrams out of some grams). As little as 5 μg of bismuth has been separated from 5 g amounts of the

other elements and determined in synthetic and practical samples (Tables 2 and 3) with a coefficient of variation of about 2% for 5- μg amounts and better than 1% for 20- μg amounts, and is much smaller for the largest amounts tested. Only microgram amounts of the other elements, which do not interfere, remain in the bismuth fraction. The lower limit of the method, based on the amount of bismuth in 10 ml of solution that will give an absorbance of 0.004 is about 0.4 μg , or 0.08 ppm in a 5-g sample.

Blank runs gave values which were uncertain and at the limit of detectability, about 0.1 μg or less. Obviously considerably smaller amounts and concentrations of bismuth could be separated and determined with use of electrothermal (furnace) AAS for the determination. This could not be investigated because the instrumentation, though available, was not operational.

It may be of interest that a considerably smaller fraction of the gold is retained by the macroporous resin from the hydrochloric-nitric acid mixture used for this work (7–11 μg out of a total of 2.00 g) than that retained by a gel-type resin, such as AG 50 W-X8, from 0.10M hydrochloric acid (8–17 μg out of a total of 50 mg).¹¹ Also, the relatively large amounts of thallium (about 0.1 mg) and the amounts of the other elements that accompany bismuth can be reduced to a few μg , when required, by use of 0.20M hydrochloric acid/0.30M nitric acid mixture as the sample medium and eluent, even though the distribution coefficient for bismuth is only 120 under these conditions and somewhat larger columns (5 or 6 g of resin) have to be used when the sample volume is 250 ml.

Though palladium, rhodium and iridium have not been investigated, these elements

Table 3. Determination of bismuth in practical samples

Sample	Sample weight, g	Bi found,* ppm
Thallium metal (Fluka, <i>puriss.</i>)	5.00	2.34 ± 0.05
Mercury(II) nitrate (Merck, <i>p.a.</i>)	8.09 (\equiv 5.00 g Hg)	0.18 ± 0.03

*Mean and standard deviation of five analyses.

should also be separated by the method. Some low-level tailing could occur, so it is possible that traces of these elements might remain in the bismuth fraction.

REFERENCES

1. Yu. Yu. Lur'e and N. A. Filipova, *Zavodsk. Lab.*, 1948, **14**, 159; *Chem. Abstr.* 1948, **42**, 8696.
2. F. Nelson and K. A. Kraus, *J. Am. Chem. Soc.*, 1954, **76**, 5916.
3. F. W. E. Strelow and T. N. van der Walt, *Anal. Chem.*, 1981, **53**, 1637.
4. S. S. Ahluwalia and J. Korkisch, *Z. Anal. Chem.*, 1965, **208**, 414.
5. E. Meintjies, F. W. E. Strelow and A. H. Victor, *Talanta*, 1987, **34**, 401.
6. F. W. E. Strelow, *ibid.*, 1988, **35**, 385.
7. *Idem*, *Solvent Extr. Ion Exch.*, submitted for publication.
9. R. J. Watling, *Anal. Chim. Acta*, 1987, **97**, 395.
10. R. J. Watling and D. J. De Villiers, *Special Report No. 108*, NPRL, Pretoria, 1977.
11. F. W. E. Strelow, A. H. Victor, J. Steyn and H. H. Lachmann, *Talanta*, 1976, **23**, 173.

USE OF ETHYLENE-VINYL-ACETATE AS A NEW MEMBRANE MATRIX FOR CALCIUM ION-SELECTIVE ELECTRODE PREPARATION

A. EL-JAMMAL, A. A. BOUKLOUZE and G. J. PATRIARCHE

Institut de Pharmacie, CP 205/6, Universite Libre de Bruxelles, Boulevard du Triomphe,
1050 Bruxelles, Belgium

G. D. CHRISTIAN*

Department of Chemistry, BG-10, University of Washington, Seattle, WA 98195, USA

(Received 28 November 1990. Revised 12 February 1991. Accepted 20 February 1991)

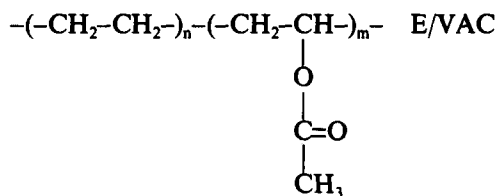
Summary—A new polymer matrix based membrane electrode with an ion-exchanger responding to calcium was constructed by dissolving the copolymer ethylene-vinyl-acetate together with the ion-exchanger in chloroform in the presence of a mixture of dioctylphthalate-nitrobenzene as plasticizer. The ion-exchanger used as the electroactive component was calcium didecyl phosphate in di-(*n*-octylphenyl) phosphonate (Orion). This electrode exhibited near-Nernstian response over the concentration range 10^{-1} – 4×10^{-6} M calcium. The pH did not affect the electrode performance within the range 8–11. Response time varied from 15 to 120 sec and the lifetime exceeded six months. The membrane is subject to static charge buildup, but this is avoided by controlling the level of dryness of the membrane. Selectivity coefficients determined for both monovalent and divalent cations showed negligible interference by most of these ions. The electrode was applied successfully to the determination of calcium in commercial mineral waters.

The use of ion-selective membrane electrodes is finding increasing application in pharmaceutical analysis.¹⁻³ The development of sensors that are easy to use and maintain, fast-responding, with low cost materials have boosted the use of potentiometric methods. Traditional methods for analysis utilizing spectrophotometry,⁴ polarography,⁵ chromatography⁶ and enzymatic measurements⁷ that may be characterized in some cases by low detection limits and high selectivity may possess limitations such as toxicity of reagents, high cost and complexity of the apparatus or the procedure.

Ion-selective polymer-membrane electrodes based on ion-pair or chelating ligand complexes entrapped in the polymer, suffer from problems such as interferences and leaching of the active component and the plasticizer⁸⁻¹⁰ from the polymer matrix. The leaching, which causes the deterioration of the response of the electrodes and leads to limited electrode lifetime, depends primarily on the nature (the lipophilicity) of the softener and the membrane active component.¹¹ In order to minimize the problems of interference, the use of alternatives

to poly(vinyl chloride) (PVC) as the polymer matrix have been suggested.⁸ However, depending on the polymer used, the electrodes may exhibit poorer performance. Hence, the use of VAGH copolymer (hydrolyzed vinyl chloride/vinyl acetate) for calcium electrodes offers no advantages,⁸ while poly(vinyl isobutyl ether) exhibits the same behavior as a PVC electrode containing the same sensing ingredients.¹²

In this paper, we describe the use of ethylene-vinyl-acetate copolymer (E/VAC) as the matrix membrane for construction of ion-selective polymer-membrane electrodes. The use of this copolymer in an ISE has not previously been reported. The structure is as follows:



A new method for the assembly of this electrode was developed. This new membrane has been characterized for use in construction of a calcium ion-selective electrode. The proposed electrode exhibits high selectivity for calcium

*Author for correspondence.

over many cations. The main advantages and disadvantages of the electrode are compared with the ISE, previously developed for the determination of calcium.

EXPERIMENTAL

Reagents

All reagents were of analytical-reagent grade and were used without further purification. E/VAC, 40% weight of the vinyl acetate monomer in the copolymer, (LEVAPREN 400, $m < n$) Bayer was kindly supplied by Professor G. Geuskens (ULB). Sources of all other reagents were as follows: tetrahydrofuran, chloroform and dioctyl phthalate from Janssen and nitrobenzene from Merck. All solutions were prepared in Milli-Q water. Stock solutions, $10^{-1}M$, were stored at room temperature and standard solutions were prepared from stock solutions by sequential dilution with Milli-Q water.

Preparation of the electrode

A commercially available solution of Orion 92-20-02 calcium didecyl phosphatate in di-(*n*-octylphenyl) phosphonate was used as the electroactive material for the calcium ISE. Membranes were prepared by dissolving the electroactive material ($100 \mu\text{l}$) and about 350 mg of E/VAC in 4 ml of an appropriate solvent (chloroform) at about 60° in a water bath. To this solution is added 1 ml of both dioctyl phthalate and nitrobenzene as plasticizer and the mixture was exposed to ultrasound to insure good dispersion of electroactive material in the matrix.

Ag/AgCl	$10^{-1}M$ CaCl ₂	Membrane E/VAC	Sample solution Ca ²⁺ (xM), pH (y)	Buffer bridge	KCl saturated	Hg ₂ Cl ₂ /Hg
---------	------------------------------	-------------------	--	------------------	------------------	-------------------------------------

A simplified scheme of the electrode is shown in Fig. 1. A micropipette tip was used as the electrode body. The end of the tip was dipped in the polymer mixture for a few seconds and then it was left in air for three hours. Longer drying times should not be used, in order to minimize static electricity build up. Calcium chloride solution, $10^{-1}M$, was used as the internal reference solution, and the internal reference electrode was an Ag-AgCl electrode. The electrode was activated before use by soaking it overnight in a $10^{-1}M$ solution of calcium chloride and it was stored in the same solution when not in use.

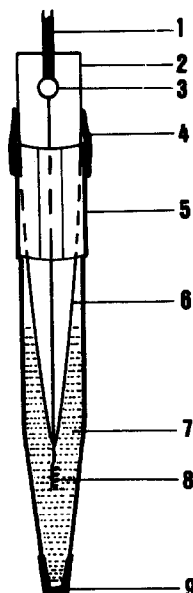


Fig. 1. Schematic diagram of the electrode: (1) coaxial cable; (2) glass tube; (3) cable junction; (4) parafilm; (5) micropipette tip; (6) glass tube; (7) $10^{-1}M$ CaCl₂; (8) Ag/AgCl; (9) E/VAC membrane.

Potential measurements

Potentiometric measurements were carried out at room temperature with a Tacussel Ion processor II. A Tacussel 6000 pH-meter with a Tacussel glass electrode was used to measure pH. A saturated calomel electrode was employed as the reference electrode in both measurements. Electrode response was examined by immersing the membrane electrode in 10 ml of buffered solution together with the double junction saturated calomel reference electrode. The cell used to investigate the characteristics of the electrode may be represented as follows:

The calibration curves were generated by addition of a 0.1-ml aliquot of 10^{-6} – $10^{-1}M$ aqueous primary ion solution to 10 ml of the stirred solution. The potential was recorded when the reading became stable (± 0.1 mV/10 sec) after each addition. The data were plotted as observed potential *vs.* the logarithm of the concentration of the primary ion. Concentration of calcium in commercial mineral water were then determined in a similar manner by means of a calibration graph, and the values obtained were checked by standard addition.

RESULTS AND DISCUSSION

Membrane materials

It has been suggested that polymers with low glass transition temperatures (T_g) are suitable matrices for polymer membrane electrodes.¹³ Our results agree with this hypothesis since polystyrene ($T_g = 100^\circ$) tested in our laboratory resulted in electrodes with no response, while good results have been found for the measurement of both organic (methixene, promethazine and some local anesthetics) and inorganic (calcium) cations by using E/VAC matrix whose glass transition temperature is below room temperature ($T_g = -50^\circ$). This study reports the results for the measurement of calcium ions. An advantage of E/VAC is the wide range of solvents that can be used to dissolve it, which allowed the use of alternatives to tetrahydrofuran and cyclohexanone commonly used with PVC. Six solvents are able to dissolve E/VAC: carbon tetrachloride, chloroform, dichloromethane, *p*-xylene, tetrahydrofuran and toluene. From a response-stability point of view, the use of E/VAC instead of PVC causes an excessive susceptibility of the electrode to static electricity if allowed to become too hard, but this problem can be avoided by controlling the level of dryness of the membrane. Excellent potential stability could be achieved by limiting the dryness to an extent that provides for minimum mechanical strength of the membrane in the ISE, accomplished by allowing to air dry for three hours only.

The technique described for the assembly of the electrode, in which the sensor is inserted into the end of a micropipette tip, demonstrates the use of a simple and inexpensive material for the body of the electrode and insures good protection of the sensor against solution turbulence.

Response characteristics of the electrode

Several parameters were investigated for optimal performance of the electrode. Typical calibration curves obtained for electrodes containing different amounts of calcium ion-exchanger, after one night of conditioning in 0.1M calcium chloride are shown in Fig. 2. The optimal tested amount of the Orion sensor reagent appears to be 0.1 ml per 6 ml of polymer mixture, for maximum potential response to calcium ion. The electrode demonstrates, under these conditions, a linear response in the 10^{-1} – 10^{-5} M range, with a useful range extended to 5×10^{-6} M, a slope of about 26 mV per concen-

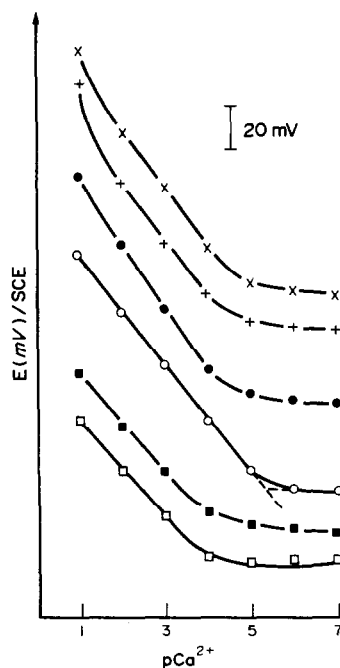


Fig. 2. Dependence of the Ca^{2+} E/VAC membrane electrode response on the calcium ion-exchanger content per 6 ml of polymer mixture. (\square) 20 μl (\blacksquare) 50 μl (\circ) 100 μl (\bullet) 200 μl (+) 500 μl (\times) 1 ml. pH 9.4, Beckman Buffer.

tration decade and a correlation coefficient of 0.9996. The range of linear response for the first three electrodes (Orion sensor reagent > 0.1 ml) can be extended to 10^{-1} M by a much longer period of activation or after several uses of the electrode.

An electrode prepared under the condition of 100 μl of sensor reagent without any other softener gives no response at all. Therefore, we selected the mixture dioctylphthalate nitrobenzene as plasticizer for our calcium ISE. The performance of the electrode with time (Fig. 3)

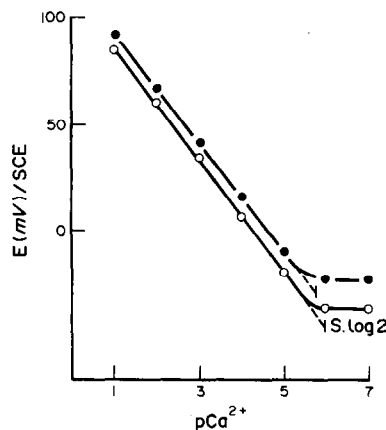


Fig. 3. Calibration plots for Ca^{2+} E/VAC membrane electrodes in buffered solution, pH 9.4. (\bullet) electrode one week old. (\circ) electrode six months old.

Table 1. Characteristics of polymer membrane Ca^{2+} electrodes based on Orion 92-20-02 sensor

	Electrode type		
	E/VAC electrode (this study)	PVC electrode* (this study)	PVC electrode (reported)
Lower limit of response (M)	4×10^{-6}	3×10^{-6}	$5 \times 10^{-5}\ddagger, \parallel; 2 \times 10^{-5}\S$
Detection limit	$1 \times 10^{-6}\dagger$	$2 \times 10^{-6}\dagger$	$5 \times 10^{-6}\S$
Slope (mv/decade)	26	24	30 \ddagger, \parallel
pH range	ca. 8–11	ca. 8–11	7.5–10 \S ; 5–9.5 \parallel

*Electrode prepared with the following composition: to 300 mg PVC dissolved in 4 ml THF is added 100 μl Orion sensor, 1 ml DOP, and 1 ml nitrobenzene.

\dagger Determined by $S \log 2$.

\ddagger Griffiths *et al.*¹⁴

\S Lima and Machado.¹⁵

\parallel Moody and Thomas.¹⁶

was evaluated from calibration curves obtained over six months. In fact, measurements with this electrode prior to any activation step showed a short range of linear response and long response time. Figure 3 was evaluated from calibration curves obtained over six months. During the first week of conditioning, a large variation in the potential was observed. However, after this stage of stabilization, the change in the potential was about 9 mV over six months of use (Fig. 3, linear portions). After six months of use, the lower limit of linear response was $4 \times 10^{-6}M$. And the detection limit (Fig. 3, lowest curve), taken as the calcium concentration at which the potential deviated by $S \log 2$ from the extrapolation of the linear portions of the calibration curve, was $10^{-6}M$.

The major effect of conditioning was to lower the response time of the electrode. The response time depended on the concentration of the test solution. For electrodes conditioned for one week, fast response (ca. 15 sec for 95% response) was observed with solutions $> 10^{-3}M$ while in more dilute solutions, as much as 2 min or more were required for 95% response.

Table 1 summarizes the characteristics of the E/VAC membrane calcium electrode compared with those of a PVC membrane electrode of similar composition prepared in our laboratory and those reported for PVC membrane calcium electrodes based on the same ion-exchanger. The E/VAC membrane electrode shows more-or-less the same performance as the PVC electrode prepared in this study. The limit of linear response is lower than that of other reported PVC electrodes. The slope found here is less than that reported for PVC based electrodes.^{14–16} While we cannot assume a lifetime as long as the eighteen months of the conventional electrode,¹⁶ the calibration parameters found for our electrode after six months of continuous use

indicate a long durability of this electrode. It is evident from Table 1, when comparison is made between E/VAC and PVC electrodes prepared under the same conditions, that E/VAC is as useful as a PVC like matrix membrane for ion-selective electrode construction.

Effect of pH and foreign cations

The pH dependence of the electrode potential was tested over the range 4–11 for 10^{-4} – $10^{-1}M$ calcium chloride (Fig. 4). The pH values of the solutions, prepared in a Beckman buffer at pH 4.9, were adjusted by addition of small volumes of 10M sodium hydroxide solution. The well known dip in the potential–pH curves which characterizes calcium ISEs based on calcium bis-dialkylphosphate type sensor^{17,18} appears for the present membrane below pH 7. The plots in Fig. 4 indicate that at pH 8–11, the potentials are constant. Potentiometric measurements were therefore done at pH about 9.4. We note that at this pH, the electrode exhibits the same

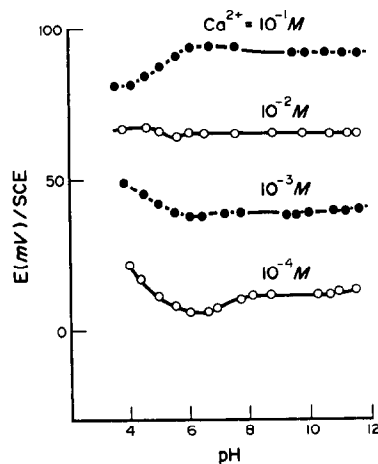


Fig. 4. pH-effect on the Ca^{2+} E/VAC membrane electrode response at four different concentrations of calcium chloride.

characteristics by changing the buffer from a Beckmann buffer to an acetate buffer.

In order to investigate the selectivity of this new membrane, the response of the electrode was examined in the presence of various foreign cations. Potentiometric selectivity coefficients $K_{Ca^{2+}, X^{z+}}$ given in Table 1 were evaluated by both the separate solution method and the mixed solution method following the equation

$$K_{Ca^{2+}, X^{z+}} = [Ca^{2+}]/[X^{z+}]^{2/z}$$

where z is the charge on the foreign ion, $[X^{z+}]$ is its concentration and $[Ca^{2+}]$ is the concentration of calcium that provides equal response to that of the interfering ion under investigation. According to the separate solution method, the electrode potentials were measured for solutions containing only interfering ion. Then the calcium ion concentration that produced the same potential as the foreign ion at $[X^{z+}]$ was determined graphically from the calibration curve established in the absence of any foreign ion. In the mixed solution case, calibration curves were established by measuring potentials of the solutions containing a constant concentration of interfering ion and varying the concentration of calcium from 10^{-6} – $10^{-1}M$. The concentration at which the potential deviates by S log 2 from the extrapolation of the linear

portion of the curve was considered as $[Ca^{2+}]$. If such deviation caused by the presence of the interfering ion did not begin at a concentration of calcium above $4 \times 10^{-6}M$ for the E/VAC electrode and $3 \times 10^{-6}M$ for the PVC electrode, which are the Nernstian limits in a pure solution of calcium, we have considered $K_{Ca^{2+}, X^{z+}}$ as $<10^{-4}$. The cations investigated with the concentrations stated in Table 2 are completely soluble in water at the working pH (9.4) of the electrode.

The selectivity coefficients listed in Table 2 show that the E/VAC membrane calcium electrode has a high selectivity for calcium over many cations, especially relative to Na^+ , K^+ and Mg^{2+} , which are usually present in real samples. Only Mn^{2+} ions interfere significantly. Despite the small selectivity coefficient for Hg^{2+} , the calibration curve obtained in the presence of $10^{-3}M$ Hg^{2+} shows a strong deviation from linearity between 10^{-1} and $10^{-2}M$ calcium. However, the electrode is not affected by immersing it in a solution of Hg^{2+} since complete recovery of the calcium response is observed after washing the electrode, without a need for reconditioning. Generally speaking there is good agreement between the selectivity coefficient values of our E/VAC electrode and those published¹⁴⁻¹⁷ for PVC electrodes, especially when the mixed solution method was applied.

Table 2. Selectivity coefficients for E/VAC membrane Ca^{2+} electrode based on Orion 92-20-02 sensor reagent, compared with PVC membrane electrodes

Interferent specie (X) [*]	$K_{Ca^{2+}, X^{z+}}$ (mixed solution method)			$K_{Ca^{2+}, X^{z+}}$ (separate solution method)		
	Present study		Reported values [†]	Present study		Reported values [†]
	E/VAC	PVC	PVC	E/VAC	PVC	PVC
Li ⁺	$<10^{-4}$	—	1.2 [‡]	$<10^{-4}$	—	—
Na ⁺	$<10^{-4}$	$<10^{-4}$	$1.6 \times 10^{-3}\S$; $6.7 \times 10^{-3}\ $	$<10^{-4}$	$<10^{-4}$	$6.1 \times 10^{-3}\ $
K ⁺	$<10^{-4}$	6×10^{-3}	$5.1 \times 10^{-3}\S$; $2.2 \times 10^{-3}\ $	$<10^{-4}$	$<10^{-4}$	$5.5 \times 10^{-3}\ $
Fe ²⁺	$<10^{-4}$	—	—	$<10^{-4}$	—	—
Hg ²⁺	6.5×10^{-3}	1×10^{-2}	—	5×10^{-3}	3×10^{-1}	—
Cu ²⁺	2×10^{-2}	10	0.21 [#]	4×10^{-3}	—	—
Ni ²⁺	2.5×10^{-2}	—	$5.7 \times 10^{-2}\#$	8×10^{-3}	—	$2.1 \times 10^{-3}\S$
Pb ²⁺	2.5×10^{-2}	—	—	7×10^{-4}	—	—
Co ²⁺	3.1×10^{-2}	—	—	5×10^{-3}	—	—
Sn ²⁺	3.2×10^{-2}	—	—	$<10^{-4}$	—	—
Zn ²⁺	3.5×10^{-2}	4×10^{-2}	$6.5 \times 10^{-2}\ $	2.5×10^{-2}	3.5×10^{-2}	$5.6 \times 10^{-3}\ $; $8 \times 10^{-3}\S$
Mg ²⁺	4.4×10^{-2}	2.5×10^{-2}	$2.2 \times 10^{-1}\ $; $5.2 \times 10^{-2}\#$	2×10^{-2}	10^{-3}	$8 \times 10^{-3}\S$; $4.5 \times 10^{-3}\ $
Ba ²⁺	4.5×10^{-1}	—	$4 \times 10^{-2}\#$; $1.3 \times 10^{-2}\ $	3×10^{-2}	—	$4 \times 10^{-4}\S$; $2.3 \times 10^{-3}\ $
Sr ²⁺	4.5×10^{-2}	—	$3.1 \times 10^{-2}\#$	5×10^{-3}	—	$4.6 \times 10^{-3}\S$
Cd ²⁺	5×10^{-2}	—	—	1×10^{-3}	—	—
Mn ²⁺	3×10^{-1}	2×10^{-1}	—	2.7×10^{-1}	4×10^{-1}	—

*Concentrations of interfering ions were $10^{-3}M$, except for Fe, Pb, Sn and Cd, which were $10^{-4}M$.

[†]Values obtained under similar conditions of interfering ion concentration and calculation procedure as used in this study.

[‡]Griffiths *et al.*¹⁴

[§]Lima and Machado.¹⁵

^{||}Moody and Thomas.¹⁶

[#]Moody and Thomas.¹⁷

Table 3. Potentiometric determination of Ca^{2+} in commercially available mineral water

Sample No.	Mg^{2+} , mg/l.	Ca^{2+} , mg/l.		
	Nominal	Nominal	Found \pm S.D. (n = 5)	Percent accuracy
1	1.3	3.5	3.62 ± 0.07	103
2	0	20	20.2 ± 0.8	101
3	22	23	22.9 ± 0.4	99.6
4	18	65	68 ± 2	105
5	24	78	78 ± 1	100
6	4.2	101	102 ± 4	101
7	36	202	201 ± 2	99.5
8	84	467	468 ± 9	100.2

The comparison is significant here since selectivity coefficients were each determined by the same procedure and under the same conditions. The main difference occurs with Cu^{2+} and Zn^{2+} ions. In contrast to the reported PVC membrane Ca^{2+} electrodes,^{15,16} the presence of Zn^{2+} ions does not alter the response characteristics of the E/VAC membrane towards Ca^{2+} . On the other hand, Cu^{2+} ions cause greater interference with the PVC electrode. Extending this comparison between the E/VAC and reported PVC membrane electrodes to the same membrane composition based PVC membrane electrode prepared in our laboratory allowed us to attribute the improvement of the E/VAC Ca^{2+} electrode parameters concerning interferences with Zn^{2+} and Cu^{2+} to the polymer E/VAC itself. In fact a PVC electrode plasticized with the mixture dioctylphthalate-nitrobenzene exhibits the same behavior in the presence of Zn^{2+} and Cu^{2+} ions as conventional PVC membrane electrodes plasticized with di-(*n*-octylphenyl)phosphonate.

Analytical application

With $10^{-6}M$ detection limit, the electrode described can be used for the determination of calcium in various samples by direct potentiometry. To investigate the applicability of this electrode, the calcium content of samples from different sources of commercially available mineral water was determined by simple immersion of the electrode in the diluted or undiluted sample adjusted to pH 9.4 by addition of a small quantity of concentrated acetate buffer. The potentiometric data listed in Table 3 are in good agreement with the nominal values listed on the bottle containers by the manufacturers. It is possible to determine calcium in the range 3–500 p.p.m. The presence of magnesium, even with a concentration equal to that of calcium in the investigated samples, did not affect the measurement. Recovery of calcium between 99 and 104% by standard addition indicates the feasi-

bility of using the E/VAC membrane Ca^{2+} electrode in analytical applications. A mean standard deviation of 2.4% demonstrates the precision of the method.

CONCLUSION

The use of E/VAC copolymer offers promise as an alternative to PVC in polymer membrane electrodes. The proposed calcium ISE is simple to prepare, inexpensive, easy to use and has a long lifetime. In general, the performance of this electrode is similar to that of PVC electrodes but its particular value lies in its stability toward zinc and other foreign inorganic cations. It exhibits improved selectivity for calcium with respect to copper and the alkali metals. This electrode was applied successfully for the potentiometric determination of calcium in mineral water. The new membrane has been successfully applied to construction of electrodes for the measurement of local anesthetic compounds (Tetracaine, Lidocaine and Procaine) based on ion-pair complexes.¹⁹

Acknowledgements—The authors are grateful to Professor G. Gueskens (ULB) for a generous gift of E/VAC. Thanks are also expressed to the "Fonds National de la Recherche Scientifique" (FNRS Belgium) for support to one of us (G.J.P.), and to the SPPS (Belgium Politic Research, ARC), Contract No. 86/91-89.

REFERENCES

1. E. P. Diamandi and T. K. Christopoulos, *Anal. Chim. Acta*, 1983, **152**, 281.
2. Z. R. Zhang and V. V. Coşofret, *Ion-Sel. Electrode Rev.*, 1990, **12**, 35.
3. J. Koryta, *Anal. Chim. Acta*, 1984, **159**, 1.
4. F. İ Sengün and İ. Fedai, *Talanta*, 1986, **33**, 366.
5. D. A. Hall, D. M. Berry and C. J. Schneider, *J. Electroanal. Chem.*, 1977, **80**, 155.
6. K. D. R. Setchell and A. Matsui, *Clin. Chim. Acta*, 1983, **127**, 1.
7. P. Talalay, *Methods Biochem. Anal.*, 1960, **8**, 119.

8. J. D. R. Thomas, *Anal. Chim. Acta*, 1986, **180**, 289.
9. R. S. Lawton and A. M. Yacynych, *ibid.*, 1984, **160**, 149.
10. J. D. R. Thomas, *J. Chem. Soc., Faraday Trans.*, 1986, **82**, 1135.
11. U. Oesch and W. Simon, *Anal. Chem.*, 1980, **52**, 692.
12. O. F. Schäfer, *Anal. Chim. Acta*, 1976, **87**, 495.
13. U. Fiedler and J. Růžička, *ibid.*, 1973, **67**, 179.
14. G. H. Griffiths, G. J. Moody and J. D. R. Thomas, *Analyst*, 1972, **97**, 420.
15. J. L. F. C. Lima and A. A. S. C. Machado, *ibid.*, 1986, **111**, 799.
16. G. J. Moody, R. B. Oke and J. D. R. Thomas, *ibid.*, 1970, **95**, 910.
17. G. J. Moody and J. D. R. Thomas, in *Chemical Sensors*, T. E. Edmonds (ed.), p. 83. London, 1988.
18. P. L. Bailey, *Analysis with Ion-Selective Electrodes*, 2nd Ed., p. 124. Heyden, London, 1980.
19. A. A. Bouklouze, A. El-Jammal, G. J. Patriarche and G. D. Christian, *unpublished work*.

THALLIMETRIC OXIDATIONS—VI

TITRIMETRIC AND SPECTROPHOTOMETRIC METHODS FOR THE DETERMINATION OF PHOSPHITE AND ANALYSIS OF BINARY MIXTURES OF PHOSPHITE AND OXALATE

M. S. PRASADA RAO, A. RAMA MOHAN RAO, KARRI V. RAMANA and S. R. SAGI
Inorganic Chemistry Laboratories, Andhra University, Waltair 530003, India

(Received 21 June 1990. Revised 29 November 1990. Accepted 14 December 1990)

Summary—Titrimetric and spectrophotometric methods have been developed for the estimation of phosphite at mmole and μ mole levels, respectively. Thallium(III) is used as an oxidant and the thallium(I) produced is determined either oxidimetrically with potassium bromate or by measurement of the absorbance of thallium(III) at 260 nm in the presence of 0.1M hydrochloric acid and 1M perchloric acid. Based on the fact that phosphite and oxalate are oxidized under different conditions, methods are described for the analysis of binary mixtures of phosphite and oxalate. A method is also described for estimation of thallium(III) with phosphite as reductant, and is applied for analysis of mixtures of thallium(I) and thallium(III).

Few redox methods are available for the estimation of phosphite. Rupp and Kroll¹ determined it by treatment with excess of potassium bromate for 1 hr at room temperature or heating at 60° for 30 min in a sulphuric acid medium followed by iodometric titration of the excess. Bernhart² has described a method in which phosphite is oxidized quantitatively to phosphate by heating with cerium(IV) in sulphuric acid solution at 80–100° for 15 min, the excess of cerium(IV) being titrated with iron(II) solution, with ferroin as indicator. Boyer³ developed a method in which excess of iodine slowly oxidizes phosphite to phosphate in bicarbonate solution. The excess of iodine is back-titrated with 0.05M arsenite. Rao and Gowda⁴ oxidized phosphite by heating with vanadate for 20 min in a boiling water-bath in the presence of silver as catalyst, cooling, and titrating the surplus vanadate with 0.05M ammonium iron(II) sulphate with *N*-phenylanthranilic acid as indicator.

There are virtually no methods available for the estimation of phosphite in the μ mole range. We have therefore examined the reaction between thallium(III) and phosphite, and have developed convenient methods for the determination of phosphite in μ mole–mmole amounts.

It has been suggested⁵ that oxalate is likely to occur along with hypophosphite and/or phosphite and must be tested for whenever the purity of these chemicals is determined. We

therefore also examined analysis for phosphite and oxalate in mixtures on the basis of earlier work on the thallium(III)–oxalate system⁶ and the results of the present study.

Most of the thallium(III) complexes with reducing ligands are prone to redox decomposition, at least partially, at relatively high temperatures or in the presence of diffused light, even in the solid state, and some thallium(I) is always found to be present along with thallium(III).⁷ There is a need to analyse such samples and also certain complexes of thallium in mixed oxidation states.⁸ Methods for this have already been developed,^{9,10} and the thallium(III)–phosphite reaction can also be used.

EXPERIMENTAL

Reagents

Thallium(III) solutions in perchloric acid and sulphuric acid were prepared and standardized as reported earlier^{9,11} and their concentrations verified by other methods. An aqueous solution of disodium hydrogen phosphite, (B.D.H. analytical grade) was prepared and standardized by the method of Bernhart.² All other reagents were of analytical grade.

Apparatus

Although the photochemical reactions described take place much faster in direct sunlight,

this has variable intensity, so all the work was done with a Philips high-pressure mercury vapour lamp (200/250 V, 125 W) as the light source, placed 15 cm above the test solutions, which were contained in colourless uncovered glass vessels.

A Shimadzu UV-260 recording spectrophotometer with silica cells of 1-cm path-length was used for the absorbance measurements.

Titrimetric determination of phosphite (mmole range)

Thermal method. To an aliquot of samples containing 0.05–0.5 mmole of phosphite in a 250-ml round-bottomed flask add 20 ml of 5M perchloric acid and 1.5 mmole of thallium(III) and dilute to 100 ml. Reflux for 40 min. Add 15 ml of concentrated hydrochloric acid and cool to 60°. Add 0.1 ml of 1-mg/ml Methyl Orange indicator and titrate the thallium(I) with 0.05N potassium bromate (1.392 g/l.) until the indicator is destroyed. The method is also applicable in sulphuric acid medium.

Photochemical method. To an aliquot of sample, containing 0.05–0.5 mmole of phosphite, in a 200-ml beaker, add 20 ml of 5M perchloric acid, 0.075 mmole of bromide and 1.5 mmole of thallium(III), and dilute to 100 ml. Stir the solution and expose it to the radiation from the high-pressure mercury vapour lamp for 4 hr. Add 15 ml of concentrated hydrochloric acid, 0.1 ml of 0.1 mg/ml Methyl Orange indicator, heat to 60° and titrate with 0.05N potassium bromate (1.392 g/l.) until the indicator is destroyed. The method is also applicable in sulphuric acid medium. Although the method requires prolonged exposure to the mercury vapour lamp, it is useful for the determination of phosphite when heating has to be avoided.

Spectrophotometric determination of phosphite (μ mole range)

To an aliquot of sample, containing 0.5–1.25 μ mole of phosphite, add 1 ml of 5M perchloric acid and 5 ml of 5×10^{-4} M thallium(III). Reflux for 40 min. Transfer the solution to a 25-ml standard flask, add 2.00 ml of 11.6M perchloric acid and 2.5 ml of 1M sodium chloride and dilute to volume (solution I). Prepare a corresponding solution without phosphite (solution II). Mix well, and after 60 min measure the absorbance of solution II against solution I as reference, at 260 nm. The absorbance corresponds to the thallium(III) that has reacted.

Prepare a calibration graph by the same procedure. The amount of phosphite is in 1:1 molar ratio to the amount of thallium(III) that has reacted.

Photochemical method. To an aliquot of sample, containing 0.5–1.25 μ mole of phosphite, add 1 ml of 5M perchloric acid, 0.5 μ mole of sodium bromide, 5 ml of 5×10^{-4} M thallium(III) and expose the solution to the radiation from the mercury vapour lamp for 4 hr. Transfer the solution to a 25-ml standard flask, and complete the determination as above, measuring the absorbance of a reagent blank against the test solution as reference.

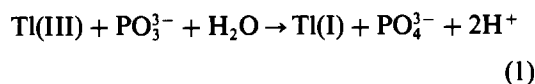
Determination of thallium(III) (mmole range)

The methods are the same as for determination of phosphite in the mmole range but a sample containing 0.05–0.5 mmole of thallium(III) is used with 1.5 mmole of phosphite.

RESULTS AND DISCUSSION

The reaction between thallium(III) and phosphite is slow, but is catalysed by light and is also considerably faster at elevated temperature. Separate studies had shown that phosphite does not interfere in the titration of thallium(I) with bromate, with Methyl Orange as indicator, so the reaction was used to monitor the progress of all the reactions described here. The reactions were carried out in sulphuric or perchloric acid medium.

The molar reacting ratio of thallium(III) and phosphite was found to be 1:1, as shown by the equation



A minimum of threefold molar ratio of thallium(III) to phosphite is required for rapid reaction, but higher ratios do not appear to increase the reaction rate very much. The use of halides to catalyse thallimetric oxidations has been reported,^{6,9,10,12–14} so bromide and chloride were tested as catalysts.

It was found that at high temperatures bromide itself reduces thallium(III) to thallium(I), so its effect on the thermal reaction between thallium(III) and phosphite could not be determined. It was found that the photochemical reaction is fastest when the thallium(III) to bromide ratio is in the range between 4:1 and 1:1. Under these conditions, thallium(III) is likely to be present as TlBr^{2+} (by analogy

with the chloride system¹⁵) and to be photochemically active. Chloride, even at low concentrations, retards both the photochemical and thermal reactions between thallium(III) and phosphite.

An increase in acid concentration up to 1*M* accelerates the rate of the photochemical reaction, but higher concentrations have no noticeable effect. Increase in acid concentration up to 3*M* also increases the rate of the thermal reaction, but with acid concentrations above 4*M* the detection of the end-point in the bromatometric titration becomes difficult. The results of these experiments led to development of the procedures described for titrimetric determination of phosphite. The recovery data in Table 1 show that the methods are satisfactory and accurate.

The absorption spectra¹⁶ of thallium(I) and thallium(III) in 1*M* perchloric acid/0.1*M* hydrochloric acid medium show that thallium(III) has considerable absorption at 260 nm (molar absorptivity 9.15×10^3 l.mole⁻¹.cm⁻¹) but thallium(I) does not absorb. The presence of phosphite and phosphate does not affect the absorption spectrum of thallium(III) under these conditions, and the thallium(III) species obeys Beer's law at 260 nm. In the spectrophotometric method for phosphite an excess of thallium(III) is allowed to react with phosphite either photochemically (with bromide as catalyst) or by heating. The amount of phosphite in the test sample corresponds to the amount of thallium(III) reduced to thallium(I), which can be read from the calibration curve. The method is quite accurate (Table 2).

Analysis of binary mixtures of PO_3^{3-} and $C_2O_4^{2-}$

Chloride and bromide ions in small concentrations catalyse the photochemical oxidation of oxalate by thallium(III).⁶ The photochemical reaction between thallium(III) and phosphite is extremely slow and inhibited by the presence of chloride. Hence oxalate can be selectively deter-

Table 2. Spectrophotometric determination of phosphite

Taken, μ mole	Found, μ mole	
	Thermal	Photochemical
0.450	0.445	0.450
0.550	0.553	0.552
0.650	0.650	0.649
0.750	0.751	0.750
0.850	0.849	0.851
0.950	0.960	0.950

mined in the presence of phosphite by titrating bromatometrically the thallium(I) produced.

In the presence of sufficient bromide, both oxalate and phosphite are completely oxidized by thallium(III) either photochemically or by heating. In both cases, the thallium(I) formed can be determined bromatometrically. Hence the phosphite in a mixture with oxalate can be determined by difference. Typical results are shown in Table 3.

Determination of thallium(III)

It was also found that a threefold molar ratio of phosphite to thallium(III) would give a rapid reaction and that higher ratios do not appreciably alter the rate of reaction. The effect of acidity, chloride and bromide was then examined. The photochemical reaction was found to be reasonably rapid when the Tl(III):Br⁻ molar ratio was between 4:1 and 1:3 in 1*M* perchloric or sulphuric acid medium.

The method could therefore be applied to analysis of mixtures of thallium(I) and thallium(III) with two identical aliquots of sample. The first is titrated with potassium bromate (Methyl Orange as indicator). The second is mixed with phosphite and perchloric acid and either refluxed for 30 min or, in the presence of sufficient bromide, exposed to radiation from a mercury vapour lamp for 4 hr, and then titrated with bromate. The first titration gives the

Table 1. Titrimetric determination of phosphite

Taken, mmole	Found, mmole	
	Thermal	Photochemical
0.050	0.049	0.050
0.060	0.060	0.061
0.070	0.070	0.070
0.100	0.100	0.101
0.200	0.200	0.200
0.300	0.302	0.300
0.400	0.400	0.403

Table 3. Analysis of mixtures of phosphite and oxalate

Oxalate, mmole		Phosphite, mmole	
Taken	Found	Taken	Found
0.050	0.050	0.050	0.050
0.050	0.049	0.150	0.150
0.150	0.149	0.050	0.051
0.100	0.100	0.100	0.100
0.150	0.150	0.150	0.150
0.250	0.250	0.150	0.150
0.150	0.155	0.250	0.240

Table 4. Determination of thallium

Taken, mmole		Found, mmole	
Tl(III)	Tl(I)	Tl(III)	Tl(I)
0.060	—	0.060	—
0.125	—	0.125	—
0.200	0.200	0.200	0.200
0.250	0.250	0.251	0.250
0.400	—	0.401	—
0.450	0.050	0.450	0.050
0.500	0.125	0.505	0.120

amount of thallium(I) and the second gives the total amount of thallium, so the amount of thallium(III) is obtained by difference. Table 4 shows that satisfactory results are obtained.

Interferences

Cd(II), Zn(II), Ru(III), Co(II), Ni(II), Hg(II), Al(III), Pb(II), NH_4^+ , Na^+ , K^+ , Ca^{2+} , Ba^{2+} , SO_4^{2-} , CH_3COO^- , PO_4^{3-} , 2,2'-bipyridyl and 1,10-phenanthroline do not interfere even if present in 100-fold molar ratio to phosphite, but even traces of oxalate or hypophosphite interfere by reducing thallium(III) to thallium(I). Arsenite interferes with the bromatometric titration method itself. Cu(II) up to 0.05M and Fe(III) up to 0.01M do not interfere, but at higher concentrations their colours interfere with detection of the end-point in the bromatometric titration. Even traces of chloride retard the reaction, the effect increasing with chloride concentration. Though bromide catalyses the

reaction at concentrations up to a Tl(III):Br⁻ molar ratio of 1:1, further increase in bromide concentration retards the rate of the reaction.

Acknowledgement—One of the authors (A. Rama Mohan Rao) thanks the C.S.I.R., New Delhi, for the award of a Senior Research Fellowship.

REFERENCES

1. E. Rupp and Kroll, *Arch. Pharm.*, 1911, **249**, 493.
2. D. N. Bernhart, *Anal. Chem.*, 1954, **26**, 1798.
3. Boyer and J. Bauzil, *Pharm. Chim.*, 1918, **18**, 321.
4. G. G. Rao and H. S. Gowda, *Z. anal. Chem.*, 1955, **146**, 167.
5. M. L. Schroff, *Pharmaceutical Chemistry*, Part II, *Inorganic*, 1st Ed., p. 968. National Book Centre, Calcutta, India, 1969.
6. S. R. Sagi, K. A. Rao and M. S. P. Rao, *Can. J. Chem.*, 1983, **61**, 2795.
7. R. C. Aggarwal and A. K. Srivastava, *Indian J. Chem.*, 1965, **3**, 494.
8. S. R. Sagi, M. S. P. Rao and K. V. Ramana, *J. Thermal Anal.*, 1981, **20**, 93.
9. S. R. Sagi, G. S. P. Raju, K. A. Rao and M. S. P. Rao, *Talanta*, 1982, **29**, 413.
10. A. R. M. Rao, M. S. P. Rao, K. V. Ramana and S. R. Sagi, *ibid.*, 1989, **36**, 686.
11. S. R. Sagi and K. V. Ramana, *ibid.*, 1969, **16**, 1217.
12. S. R. Sagi, K. A. Rao and M. S. P. Rao, *ibid.*, 1983, **30**, 282.
13. *Idem*, *Analyst*, 1984, **109**, 53.
14. M. S. P. Rao, A. R. M. Rao, K. V. Ramana and S. R. Sagi, *Talanta*, 1990, **37**, 753.
15. T. G. Spiro, *Inorg. Chem.*, 1965, **4**, 731.
16. L. B. Mønsted, O. Mønsted and G. Nord, *Trans. Faraday Soc.*, 1970, **66**, 936.

SPECTROPHOTOMETRIC DETERMINATION OF ZIRAM, FERBAM AND ZINEB WITH DIPHENYLCARBAZONE

ASHOK KUMAR MALIK and A. L. J. RAO

Department of Chemistry, Punjabi University, Patiala 147002, India

(Received 9 August 1990. Revised 8 February 1991. Accepted 20 February 1991)

Summary—A procedure has been developed for the determination of ziram (zinc dimethyldithiocarbamate), ferbam (ferric dimethyldithiocarbamate) and zineb (zinc ethylenebisdithiocarbamate) after their decomposition and extraction of the diphenylcarbazone complexes of the zinc or iron into isobutyl methyl ketone. These complexes absorb strongly at 520 nm. The method is rapid, sensitive and selective and can be used for the determination of these dithiocarbamates in commercial and synthetic mixtures.

Dithiocarbamates have found a variety of applications in agriculture as pesticides and in the rubber industry as vulcanization accelerators and anti-oxidants. The toxicity of the dithiocarbamates is increased when they are in the form of heavy metal salts. The dithiocarbamates are generally determined on the basis of their decomposition by hot mineral acid to the amine and carbon disulphide. Most of the analytical methods for their determination are based on the Clarke method¹ in which the dithiocarbamate is decomposed in acidic solution to give carbon disulphide, which is then absorbed in methanolic potassium hydroxide solution, and the potassium methyl xanthate so formed is titrated iodimetrically. Various modifications of this method are reported in the literature.²⁻¹³ Dithiocarbamates have also been determined in vegetables by high-pressure liquid chromatography,¹⁴ titrimetry¹⁵ and extraction voltammetry.¹⁸ Ziram, ferbam and zineb have also been determined by converting these into copper^{17,18} or molybdenum¹⁹ complexes in acidic medium. The extraction of the molybdenum complexes is not rapid; for example, the molybdenum ethylenebisdithiocarbamate complex is extractable only after heating for 5 min. Here we present a new, simple, rapid, sensitive and selective method based on the determination of the zinc(II) and iron(III) present in ziram, zineb and ferbam, respectively, by converting them into diphenylcarbazone complexes.

EXPERIMENTAL

Equipment

A digital ECIL pH-meter and an SP-20 Spectronic spectrophotometer were used.

Reagents

All solvents and reagents were of analytical reagent grade.

Ziram, ferbam and zineb solutions, 1 mg/ml. Pure ziram and zineb were obtained from Wilson Laboratories, Bombay. Ferbam was prepared in the laboratory by the method given in the literature.²⁰ The purity of these samples was checked by elemental analysis and by determining their zinc and iron content by EDTA titrations, with Eriochrome Black T and Xylenol Orange, respectively, as indicators.²¹ Stock solutions of ziram and zineb were prepared by dissolving 0.100 g in 100 ml of 0.1M and 0.5M sodium hydroxide, respectively, and of ferbam by dissolving 0.100 g in 100 ml of acetonitrile. These solutions were standardized²¹ and further diluted with sodium hydroxide solution or acetonitrile as required.

Diphenylcarbazone solution, 3 mg/ml. Diphenylcarbazone (0.300 g) was dissolved in 100 ml of absolute ethanol.

Pyridine solution, 50 mg/ml. Pyridine (5.0 g) was dissolved in 100 ml of water.

Buffer solution. Boric acid and potassium chloride solutions (0.2M, 100 ml of each) were mixed, adjusted to pH 9.0 with 0.2M sodium hydroxide, and diluted to 500 ml.

Other solutions. Stock solutions for interference studies were prepared by dissolving suitable salts in water. Synthetic samples were prepared by mixing solutions of suitable salts to give the required composition.

Isobutyl methyl ketone. The purity of the isobutyl methyl ketone was checked spectrophotometrically before use.

Procedure

To aliquots of sample solutions containing 0.12–1.90 $\mu\text{g/ml}$ ziram, 0.11–1.70 $\mu\text{g/ml}$ zineb or 0.35–4.80 $\mu\text{g/ml}$ ferbam add 2.0 ml of pyridine solution to ziram and zineb samples (but not to ferbam samples), and 3.0 ml of buffer solution, so that the pH after dilution to 25 ml is 9.0. Transfer into separating funnels, and add diphenylcarbazone solution (1.0 ml for ziram and zineb and 1.5 ml for ferbam) and 25 ml of isobutyl methyl ketone. Shake the mixtures for 5 min, separate the organic layers and measure the absorbances at 520 nm, against reagent blanks prepared under similar conditions.

RESULTS AND DISCUSSION

The absorption spectra of the zinc(II)–diphenylcarbazone–pyridine and iron(III)–diphenylcarbazone complexes were recorded against reagent blanks. The complexes absorb strongly at 520 nm. The maximum absorbance was observed when the pH of the aqueous phase was 9.0–10.0 for ziram and zineb, and 9.0–11.0 for ferbam, and when 0.8–1.0 ml of 3 mg/ml diphenylcarbazone solution was used for ziram and zineb, and 1.0–1.5 ml for ferbam. Smaller amounts of diphenylcarbazone gave incomplete complex formation, but larger amounts did not increase the absorbance. Therefore use of 1.0 ml for ziram and zineb and 1.5 ml for ferbam is recommended. The binary zinc–diphenylcarbazone complex is not completely extracted into isobutyl methyl ketone,²² but it has been observed that the complex is completely extractable in one step into isobutyl methyl ketone in the presence of 1–100 mg/ml pyridine in the aqueous phase; the extraction of the iron–diphenylcarbazone complex is unaffected by the presence or absence of pyridine.

Various organic solvents were examined for the extraction of the complexes in the presence of pyridine. Chou *et al.*²³ reported that pyridine enhances the extraction of zinc complexes through adduct formation. We have found that in the presence of pyridine the zinc–diphenyl-

carbazone complex is not extractable into diethyl ether and carbon disulphide but is extracted by benzene, n-butyl acetate, acetylacetone, n-amyl alcohol, n-amyl acetate, chloroform, carbon tetrachloride, toluene, isobutyl methyl ketone and ethyl acetate. Of these isobutyl methyl ketone and ethyl acetate were found to be the most effective. The extraction into isobutyl methyl ketone is slower than that into ethyl acetate, but because of the solubility of water in ethyl acetate isobutyl methyl ketone was selected for use. In isobutyl methyl ketone the complexes are stable for more than 8 hr.

The Job, mole-ratio and logarithmic methods indicated the formation of the 1:2:2 (M:L:Py) complex in the case of zinc and 1:3 (M:L) complex in the case of iron(III).

Analytical characteristics

The calibration curves, for measurement at 520 nm, were linear over wide concentration ranges, given in Table 1 along with other performance characteristics. The limit of detection was calculated by the IUPAC recommended procedure.²⁴

Interferences

Various foreign ions were examined for interference in the determination of 40 μg of ziram and zineb, and 100 μg of ferbam. Of the anions examined, the amounts (mg) shown in parentheses are tolerable: acetate (80), bromide (80), chloride (50), tartrate (50), thiosulphate (5); 100 mg of citrate, nitrate, oxalate, sulphate, sulphite or thiourea did not interfere, but metabisulphite and EDTA interfered strongly. Fluoride up to 100 mg is tolerable in the case of ziram and zineb, but only 2 mg in the determination of ferbam.

Of the cations examined, Cu(II) and Hg(II) interfered but could be masked with 1.0 ml of 50 mg/ml thiourea and potassium iodide solutions, respectively. Pb(II), Sn(IV), As(III), Ca(II), Cr(VI), Mo(VI) and Sb(III) are tolerable up to 1.0 mg and Hg(II), Bi(III) and Mn(II) up to 0.1 mg. Interference by free Zn(II) or Fe(III) is

Table 1. Analytical characteristics of the determination of ziram, ferbam and zineb with diphenylcarbazone at 520 nm

Characteristics	Ziram/zineb	Ferbam
Linear range, $\mu\text{g/ml}$	0.12–1.9/0.1–1.7	0.35–4.8
Detection limit, $\mu\text{g/ml}$	0.08	0.18
Molar absorptivity, $l.\text{mole}^{-1}.\text{cm}^{-1}$	8.36×10^4	5.3×10^4
Precision, RSD, %	0.9	1.0

avoided by prior extraction of ziram, zineb or ferbam into chloroform, followed by evaporation of the organic phase to dryness.

The mutual interference of ziram, zineb and ferbam was studied, along with the interference of some common pesticides such as thiram (tetramethylthiuram disulphide), nabam (disodium ethylenebisdithiocarbamate), maneb (manganese ethylenebisdithiocarbamate), vapam (sodium *N*-methylthiocarbamate) and dibam (sodium dimethylthiocarbamate). Pesticides containing no metal ion did not interfere in the determination of ziram, ferbam and zineb. Determination of ziram and zineb in the presence of ferbam and maneb was possible after masking with 2.0 ml of 50 mg/ml sodium fluoride and sodium citrate solutions, respectively. Ferbam in the presence of maneb was determined in the presence of 2.0 ml of 50 mg/ml sodium citrate solution. Ziram and zineb interfere in the determination of each other.

Simultaneous determination of ziram and ferbam, or zineb and ferbam

Ziram and ferbam or zineb and ferbam were taken in various proportions and dissolved in acetonitrile. Equal aliquots of the solution were analysed in the presence and absence of 2.0 ml of 50 mg/ml sodium fluoride solution. The difference in absorbance corresponded to the amount of ferbam.

Applications

The method is one of the most sensitive available for the determination of ziram, ferbam and zineb. Five dilutions of stock solutions prepared from "Ziram 27% S.C." and "Dithane Z-78" were analysed, with pure samples of ziram and zineb as references, and in all cases the recoveries were between 98 and 100% with a relative standard deviation of 2–3%.

Determination of ziram, ferbam and zineb in grain

The procedure was applied to the determination of ziram, ferbam and zineb in grain. A known amount of ziram, ferbam and zineb was crushed with 20 g of grain and the mixture was shaken mechanically with 100 ml of chloroform for an hour. The mixtures were filtered and the residues were washed with three 10-ml portions of chloroform. The extracts were evaporated to 2.0 ml in a current of dry air at room temperature. The ziram and zineb residues were dissolved in 0.1*M* and 0.5*M* sodium hydroxide,

Table 2. Recovery of ziram, ferbam and zineb from grain

Dithiocarbamate added	Dithiocarbamate*		
	Taken, μg	Found, μg	Recovery, %
Ziram	40	38.9	97.5
	50	49.0	98
Ferbam	40	38.0	95
	50	49.5	99
Zineb	20	19.0	95
	40	39.0	97.5

*Mean of three determinations.

respectively, and the ferbam in acetonitrile, and analysed by the general procedure. Untreated samples were taken as reference. The results are given in Table 2.

Comparison of sensitivity

The sensitivity of the present method is better than that of the methods of Lowen,¹² Cullen²⁵ and Chmiel,²⁶ which are based on the determination of liberated CS₂. It is also more sensitive than the direct methods reported by Rao *et al.*^{19,28} (5 and 2 $\mu\text{g}/\text{ml}$ ziram and zineb), Rangaswamy *et al.*^{17,18} (1 $\mu\text{g}/\text{ml}$ zineb and 0.8 $\mu\text{g}/\text{ml}$ ziram and ferbam) and Verma *et al.*²⁷ (0.6 $\mu\text{g}/\text{ml}$ ferbam). By the present method it is possible to estimate 0.12, 0.35 and 0.11 $\mu\text{g}/\text{ml}$ ziram, ferbam and zineb, respectively.

Acknowledgement—The authors thank the Bureau of Police Research and Development, New Delhi (India) for financial assistance to one of them (AKM).

REFERENCES

1. D. G. Clarke, H. Baum, E. L. Stanley and W. E. Hester, *Anal. Chem.*, 1951, **23**, 1842.
2. T. Callan and N. J. Strafford, *J. Soc. Chem. Ind.*, 1924, **43**, 1T.
3. C. H. Hall, *J. Assoc. Off. Agr. Chem.*, 1960, **43**, 371.
4. J. Rosenthal, R. L. Carlsen and E. L. Stanley, *ibid.*, 1953, **36**, 1170.
5. H. Roth and W. Beck, *Mikrochim. Acta*, 1957, 844.
6. N. Yu. Frushevskaya in *Tr. Vses. Soveshch. Issled. Ostatkov Pestits. Profil, Zagryaz, Imi Prod. Pitan., Kormov Vnesh, Sredy, 2nd*, 1970, O. M. Tamm (ed.), p. 276; *Chem. Abstr.*, 1973, **79**, 135377e.
7. W. R. Bontoyan, *J. Assoc. Off. Agr. Chem.*, 1965, **48**, 562.
8. C. Reinhard, *Mitteilunsbl. ADCh-Fachgruppe Lebensmittelchem. Gerichtl. Chem.*, 1971, **25**, No. 1, 1.
9. B. W. Simpson, *Pestic. Sci.*, 1971, **2**, 127.
10. C. L. Hilton and J. E. Newell, Paper presented to Pittsburgh Conf. Anal. Chem. & Appl. Spectroscopy; abstract in *Anal. Chem.*, 1953, **25**, 530.
11. J. Piechocka, *Rocz. Panstw. Zakl. Hig.*, 1984, **35**, 83.
12. W. K. Lowen, *J. Assoc. Off. Agr. Chem.*, 1953, **36**, 484.
13. S. Petrascu, *Rev. Chim. (Bucharest)*, 1966, **17**, 687.
14. K. H. Gustafsson and C. H. Falhgren, *J. Agric. Food Chem.*, 1983, **31**, 461.

15. B. C. Verma, H. S. Sidhu and R. K. Sood, *Talanta*, 1982, **29**, 703.
16. N. A. Ulakhovich, E. P. Medyantseva, V. F. Frolova and O. N. Romanova, *Zh. Analit. Khim.*, 1983, **38**, 1963.
17. J. R. Rangaswamy, P. Poornima and S. K. Majunder, *J. Assoc. Off. Anal. Chem.*, 1971, **54**, 1120.
18. *Idem*, *ibid.*, 1970, **53**, 1043.
19. A. L. J. Rao and N. Verma, *Talanta*, 1989, **36**, 1041.
20. Monsanto Chemical Co., *British Pat.*, 692063, 27 May 1953.
21. A. I. Vogel, *A Text Book of Quantitative Inorganic Analysis*, 3rd Ed., Longmans, London, 1969.
22. H. Einaga and H. Ishii, *Analyst*, 1973, **98**, 802.
23. F. C. Chou, Q. Fernando and H. Freiser, *Anal. Chem.*, 1965, **37**, 361.
24. G. L. Long and J. D. Winefordner, *ibid.*, 1983, **55**, 712A.
25. T. E. Cullen, *ibid.*, 1964, **36**, 221.
26. Z. Chmiel, *Chem. Anal. (Warsaw)*, 1979, **24**, 505.
27. B. C. Verma, R. K. Sood, A. Sood, S. Chauhan and D. K. Sharma, *Proc. Indian Natl. Sci. Acad. A*, 1986, **52**, 662.
28. A. L. J. Rao and N. Verma, *J. Inst. Chemists (India)*, 1988, **60**, 5.

SPECTROPHOTOMETRIC DETERMINATION OF THALLIUM AFTER ITS EXTRACTION AS AN ION-PAIR OF THE CHLORO-COMPLEX AND PYRONINE G

K. KRISHNAN NAMBOOTHIRI, N. BALASUBRAMANIAN and T. V. RAMAKRISHNA*

Department of Chemistry, Indian Institute of Technology, Madras 600 036, India

(Received 21 September 1990. Revised 4 December 1990. Accepted 22 January 1991)

Summary—A sensitive and selective procedure for the spectrophotometric determination of thallium is described. The method is based on the formation of an ion-pair between $[TlCl_4]^-$ and the pyronine G cation in chloride-containing acid media. The ion-pair is extracted into benzene and permits the determination of as low as 0.3 μg of thallium in a final volume of 25 ml at 530 nm. The system obeys Beer's law in the concentration range 1–14 μg of thallium in a final volume of 25 ml. Potassium iodate was found to be highly effective for the oxidation of Tl(I) to Tl(III) and the presence of excess oxidant does not interfere. The method can be used for the determination of thallium in high purity cadmium, cadmium sponge and rock samples.

Numerous methods have been proposed for the spectrophotometric determination of thallium,¹ but the most sensitive ones are based on the ability of the anionic chloro- or bromo-complex of thallium(III) to interact with cationic dyes to form ion association complexes. Methods have been described based on the extraction of the ion-pair formed between the anionic bromo-complex and Brilliant Green² or Crystal Violet,³ and the chloro-complex and Methyl Violet,⁴ Rhodamine B⁵ Methylene Blue⁶ or Methylene Green.⁷ Thallium(I), if present, was oxidized to the trivalent state with Ce(IV),² bromine,^{3,5} hydrogen peroxide⁴ or sodium nitrite.⁶ As the presence of excess of oxidants destroyed the cationic dye, they were removed by boiling the solution (for hydrogen peroxide or bromine) or adding hydroxylammonium chloride [for Ce(IV)] or urea (for NO_2^-). Fogg *et al.*⁸ reviewed the methods which used basic dyes for the determination of thallium and other elements and indicated that problems can arise due to the incomplete oxidation of thallium(I) in the determination.

Our studies on the spectrophotometric determination of thallium(I) revealed that potassium iodate in acid medium is highly effective for its oxidation and the resulting thallium(III), as an anionic chloro-complex, can be made to interact with pyronine G and extracted into benzene. The blank absorbance was almost negligible and

was unaffected by the presence of unused potassium iodate. The method was found to be suitable for the determination of thallium(I) down to 0.3 μg in a final volume of 25 ml.

EXPERIMENTAL

Apparatus

A Carl-zeiss PMQ II spectrophotometer was used with 10-mm quartz cells.

Reagents

All reagents were of analytical grade.

Standard thallium (I) solution, 1000 ppm. Dissolve 1.303 g of thallium nitrate in 1 litre of distilled water containing 2 ml of concentrated nitric acid. Dilute an appropriate volume of this stock solution with water to provide a 2 $\mu\text{g}/\text{ml}$ solution.

Pyronine G, 0.025%. Dissolve 0.25 g of pyronine G in 1 litre of distilled water.

Potassium iodate, 0.025%. Dissolve 0.25 g of potassium iodate in 1 litre of distilled water.

Sulphuric acid, 10N.

Sodium chloride, 5%.

Potassium iodide, 2.5%.

Sodium nitrite, 0.5M.

Sulphamic acid, 5%.

Benzene (thiophene free). Used for extraction.

Procedure

Transfer the sample solution containing not more than 14 μg of thallium into a 60-ml separating funnel and add, while mixing, 1 ml

*Author for correspondence.

each of 10*N* sulphuric acid and 2.5% potassium iodide solution to reduce the thallium(III), if any, to thallium(I). Then, add 1 ml of 0.5*M* sodium nitrite solution and extract off the liberated iodine by equilibrating with 5 ml of benzene. Repeat the extraction if necessary and discard the organic layer.

Transfer the aqueous layer containing thallium(I) into a 25-ml standard flask and treat with 2 ml of a 5% solution of sulphamic acid. Add, with mixing, 5 ml of 10*N* sulphuric acid followed by 2 ml each of 5% sodium chloride, 0.025% pyronine G and 0.025% potassium iodate solutions and dilute to the mark with water. Mix well and allow the solution to stand for 20 min. Transfer the solution into a 60-ml separating funnel and equilibrate with 10 ml of benzene for 2 min. Separate the organic layer and treat with 0.5 g of anhydrous sodium sulphate. Measure the absorbance of the benzene extract at 530 nm with 10-mm cells against a reagent blank. Establish the concentration of thallium by reference to a calibration graph prepared for 1–14 μg of thallium, following the procedure described.

RESULTS AND DISCUSSION

Preliminary experiments were carried out in 2*N* sulphuric acid medium containing 10 μg of thallium(I) and 2 ml each of 5% sodium chloride, 0.025% pyronine G and 0.025% potassium iodate in a final volume of 25 ml. The solutions were equilibrated for 5 min with 10 ml of benzene. The results indicated that the extraction of the ion-pair into benzene was selective as the absorbance of the blank at 530 nm, where the ion-pair absorbed maximally, was found to be negligible. The presence or absence of iodate in the medium had no effect on the blank and the intensity of the absorbance of the sample extract was found to increase in

direct proportion to the amount of thallium(I) present.

The effect of various experimental parameters on the thallium(I) reaction was therefore examined in detail. The results are summarized in Table 1. Except for the study of the effect of acidity, the overall acidity was maintained at 2*N* in a final volume of 25 ml. Extractions were conducted with 10 ml of benzene and the absorbances of the extracts were measured at 530 nm in 10-mm cells.

A reaction time of 20 min was found necessary before extracting into benzene. Equilibration of the phases for about 2 min was found to be sufficient for the quantitative extraction of the ion-pair into the organic phase. The intensity of the extract was found to remain stable for at least 3 hr. The order of addition of reagents had no effect on the absorbance of the extract. Similarly the variation of aqueous phase volume from 25–100 ml had no effect provided the overall concentrations of the reactants in the solution were maintained at the optimum level.

Table 2 gives the data on the extraction behaviour of various solvents tested for the extraction of the ion-pair. Benzene gave maximum extraction of the ion-pair and the blank was very low in this solvent. The presence of chloride in excess of 0.08*M* caused an increase in the blank absorbance although the net absorbance of thallium remained unaffected.

The calibration graph was linear in the concentration range 1–14 μg of thallium(I) in a final volume of 25-ml and the molar absorptivity was $1.2 \times 10^5 \text{ l. mole}^{-1} \text{ cm}^{-1}$. The Sandell sensitivity was found to be 0.0007 $\mu\text{g/cm}^2$. The precision of the proposed procedure was checked by establishing the concentration of 10 samples each containing 10 μg of thallium(I). The mean recovery was 10.08 μg and the coefficient of variation was found to be 1.4%.

Table 1. Effect of different parameters* on thallium(I) determination ($\text{Tl}^+ = 10 \mu\text{g}$)

Acidity									
H ₂ SO ₄ , <i>N</i>	0.25	0.5	0.75	1	1.5	2	2.5	3	3.5
Absorbance	0.340	0.400	0.465	0.505	0.570	0.580	0.580	0.585	0.580
Sodium chloride, 2% solution, ml	1	2	3	4	5	6	7		
Absorbance	0.440	0.510	0.580	0.585	0.575	0.580	0.580		
Pyronine G, 0.01% solution, ml	1	2	3	4	5	6	7		
Absorbance	0.380	0.540	0.580	0.575	0.580	0.585	0.580		
KIO ₃ , 0.01% solution, ml	1	2	3	4	5	6	7		
Absorbance	0.340	0.475	0.580	0.585	0.580	0.590	0.580		

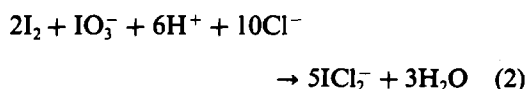
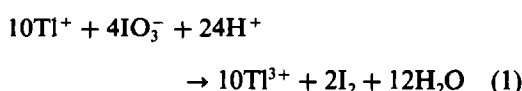
*Except for the variable under study the following concentrations were maintained in a final volume of 25 ml. 5 ml of 10*N* H₂SO₄, 2 ml of 5% NaCl, 2 ml each of 0.025% pyronine G and 0.025% potassium iodate.

Table 2. Extractability of the ion-pair into various solvents (Tl⁺ = 10 μg)

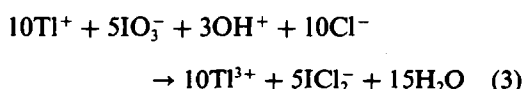
Solvent	Absorbance		
	Blank	Sample	Sample vs. blank
Benzene	0.050	0.635	0.585
Toluene	0.090	0.595	0.505
Xylene	0.090	0.520	0.430
Chloroform	0.180	0.590	0.410
Carbontetrachloride	0.160	0.635	0.475
Iso-propyl ether	0.150	0.575	0.425

Composition of the complex

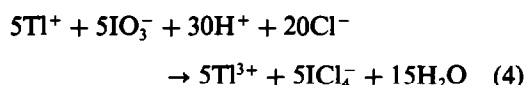
Since treatment of thallium(I) with iodate resulted in the formation of thallium(III), the composition of the extracted complex was established with thallium(III) by Job's continuous variation and molar ratio methods. Both methods indicated that the mole ratio of Tl(III):Cl⁻:Pyronine G in the complex was 1:4:1. However, when identical amounts of thallium(I) and thallium(III) were subjected to extraction under conditions optimal for thallium(I), the absorbances obtained were widely different. Thus for solutions containing 10 μg, the absorbance was found to be 0.580 for thallium(I) and 0.400 for thallium(III). The enhancement observed in the case of Tl(I) determination may be attributed to the formation of an additional ion-pair formed between pyronine G and the anionic species ICl₂⁻ or ICl₄⁻. The formation of ICl₂⁻ species can be explained on the basis of the oxidation of iodine by excess iodate⁹ present in the acidic chloride containing medium in accordance with:



The net reaction being



The species ICl₄⁻, on the other hand, can result from the reduction of iodate by Tl(I) in accordance with the net reaction:



It is evident from the above equations that twice the amount of Tl(I) would be required to produce ICl₂⁻ species equivalent to ICl₄⁻ resulting from the reduction of iodate.

To confirm the nature of the species causing enhancement in the determination of Tl(I), experiments with varying amounts of iodine in benzene were carried out under conditions optimal for Tl(I). Though this experiment would not give direct evidence for the formation of ICl₄⁻, it would provide indirect evidence whether or not the formation of ICl₂⁻ was responsible for the observed enhancement. Experiments with iodine solution showed a linear relationship with increasing amount of iodine and the absorbance produced (0.18) by 2.5 μg of I₂ was identical to the enhancement observed for 10 μg of Tl(I) over Tl(III). Since in accordance with equation (1), 2.48 μg of I₂ would result from 10 μg of Tl(I), it was felt reasonable to conclude that the ICl₂⁻ species [equation (2)] was responsible for the observed enhancement in the case of Tl(I). If ICl₄⁻ had been the species, as evident from equation (4), 5 μg of thallium(I) would have been adequate to cause the observed enhancement.

Interference studies

The interferences of milligram amounts of several ions on the determination of Tl(I) were individually studied and the results are summarised in Table 3.

Iodide, as expected, enhanced the apparent recovery of Tl(I) due to formation of ICl₂⁻ species, but the interference could be overcome by treating the sample with 2 ml of 0.5% sodium nitrite solution and extracting the liberated iodine into benzene. The determination in this instance was completed after adding sulphamic

Table 3. Interference studies

Interferents (1 mg)	Remarks
PO ₄ ³⁻ , ClO ₃ ⁻ , F ⁻ , SO ₄ ²⁻ , C ₂ O ₄ ²⁻ , HCO ₃ ⁻ , CO ₃ ²⁻ , tartrate, Mg ²⁺ , Be ²⁺ , Pb ²⁺ , Ag ⁺ , Al ³⁺ , Li ⁺ , Th ⁴⁺ , Ce ³⁺ , UO ₂ ²⁺ , Zn ²⁺ , Cu ²⁺ , Co ²⁺ , Mn ²⁺ , Ni ²⁺ , Fe ³⁺ , Cd ²⁺ , As ⁵⁺ , Sr ²⁺ , In ³⁺ , Sb ³⁺ and Sn ⁴⁺	No interference
Fe ²⁺ , Sb ³⁺ , As ³⁺ , Sn ²⁺ , Bi ³⁺ , I ⁻ , Hg ²⁺ and NO ₃ ⁻ (>3 mg)	Enhanced the absorbance
WO ₄ ²⁻ , MoO ₄ ²⁻ and Pd ²⁺	Precipitated as an adduct with the dye
Ce ⁴⁺ , NO ₂ ⁻	Interfered by bleaching the dye

Table 4. Application studies

Sample	Weight, g	Tl added, µg/g	Tl found, µg/g	Tl, (recovery) %	Reported value, µg/g
High Purity Cadmium†	—	—	30*	100	—
Cadmium sponge‡	1	—	97*	—	90
	1	100	198	101	—
	1	200	296	99.5	—
<i>Rock samples</i>					
Andesite (AGV.1)	2	—	1.9*	—	1.6
	2	2.5	4.3	96	—
	2	5.0	6.6	94	—
Granodiorite (GSP-1)	2	—	1.5*	—	1.3
	2	2.5	4.05	102	—
	2	5.0	6.4	98	—
Granite (G-2)	2	—	1.5*	—	1.2
	2	2.5	3.9	96	—
	2	5.0	6.4	98	—

*Average value of three determinations with a relative standard deviation of 1.5%.

†Synthetic high purity Cd solution. Cd: 99.90%, Zn: 0.025%, Cu: 0.025%, Pb: 0.025%, Sb: 0.01%, Tl: 0.003%, Ag: 0.010%, As: 0.003%, Sn: 0.01%.

‡Cadmium sponge. Cu: 0.289%, Cd: 37.5%, Ni: 0.388%, Co: 0.414%.

acid to destroy the unreacted nitrite. The interference of Ce(IV) was overcome by reduction with iodide and determination after removing the excess iodide as described above.

Citrate effectively overcame the interference of WO_4^{2-} , MoO_4^{2-} , Pd^{2+} and Bi^{3+} . The influence of Hg(II) and Sb(III) on the reaction was overcome by displacing them from solution with copper foil.¹⁰

Since nitric acid was found to be totally ineffective in oxidizing Tl(I) to Tl(III), it was used to overcome the interferences due to AsO_3^{3-} , Sn^{2+} , Sb^{3+} and Fe^{2+} in Tl(I) determination. In this instance, the excess nitric acid was fumed off with sulphuric acid before subjecting to determination.

Application

The method developed was applied to the analysis of thallium in cadmium sponge, rock samples and a synthetic solution of high purity cadmium. The rock samples were opened out by repeatedly heating 2 g of the finely ground material with concentrated nitric acid and hydrogen fluoride.¹¹ The mixture was treated with 2 ml of 10N sulphuric acid and evaporated to fumes of sulphur trioxide. Cadmium sponge was brought into solution by heating 1 g of the sample with 20 ml of dilute sulphuric acid (1:9) in the presence of 5 ml of concentrated nitric acid and evaporating the solution almost to dryness.¹¹ As no authentic sample of high purity

cadmium was available, a synthetic mixture containing the various metal ions in appropriate proportions¹² corresponding to 1 g of the sample was made. The mixture was treated with 5 ml of concentrated nitric acid and 2 ml of 10N sulphuric acid and evaporated to fumes of sulphur trioxide. The residue in each instance was dissolved in a minimum volume of water, filtered (rock samples and cadmium sponge) and made up to 100 ml (cadmium sponge and high purity cadmium). The entire filtrate (rock samples) or suitable aliquots of the made-up solution were treated with a copper foil on a hot plate for 10 min. The solutions were allowed to cool, treated with 2 ml of 5% citrate solution and the determination was carried out as described. The results of this along with those obtained from samples spiked with thallium(I) are shown in Table 4. The data show that the method works satisfactorily.

REFERENCES

1. M. Sager and G. Tölg, *Mikrochim. Acta*, 1982 II, 231.
2. A. G. Fogg, C. Burgess and D. T. Burns, *Analyst*, 1973, **98**, 347.
3. P. A. Chainani, P. Murugaiyan and Ch. Venkateswarlu, *Anal. Chim. Acta*, 1971, **57**, 67.
4. N. I. Vashilova and T. V. Khomutova, *Zh. Analit. Khim.*, 1969, **24**, 999.
5. Z. Marczenko, *Spectrophotometric Determination of the Elements*, Horwood, Chichester, 1976.
6. V. M. Tarayan, E. N. Ovsepyan and V. Zh. Artsruni, *Zavoedsk. Lab.*, 1969, **35**, 1435.

7. *Idem*, *Dokl-Akad. Nauk Arm. SSR*, 1968, **47**, 27; *Anal. Abstr.*, 1969, **17**, 2634.
8. A. G. Fogg, C. Burgess and D. T Burns, *Talanta*, 1971, **18**, 1175.
9. A. I. Vogel, *A Text Book of Quantitative Inorganic Analysis*, 3rd Ed., p. 374. ELBS, London, 1964.
10. F. Feigl, V. Gentil and D. Goldstein, *Anal. Chim. Acta*, 1953, **9**, 393.
11. F. D. Snell, *Photometric and Fluorimetric Methods of Analysis, Metals, Part I*, pp. 50–52. Wiley, New York, 1978.
12. *Chemical Analysis of Metals and Metal Bearing Ores*, Annual Book of ASTM Standards, 1980.

DETERMINATION OF BUTYLTIN, METHYLTIN AND TETRAALKYLTIN IN MARINE FOOD PRODUCTS WITH GAS CHROMATOGRAPHY-ATOMIC ABSORPTION SPECTROMETRY

D S. FORSYTH and C CLEROUX

Food Research Division, Bureau of Chemical Safety, Food Directorate, Health Protection Branch, Health and Welfare Canada, Ottawa, Ontario K1A 0L2, Canada

(Received 15 January 1991 Revised 5 April 1991 Accepted 17 April 1991)

Summary—Extraction methods were developed for the determination of butyltin, methyltin and tetraalkyltin in marine food products. Alkyltins were complexed with either diphenylthiocarbazone (dithizone) or tropolone from enzymatically hydrolyzed samples. Tetraalkyltins were extracted with hexane. Butyl or methyl derivatives of the alkyltins were made by Grignard reaction for analysis by gas chromatography-atomic absorption spectrometry. Many of the examined marine food products contained ppb levels of alkyltins. Tetramethyltin and tetraethyltin levels were less than the method detection limits of 0.8 and 0.7 ng/g (as Sn), respectively.

Organotin compounds are used in a number of commercial applications including biocide formulations, poly(vinyl) chloride stabilizers and homogenous catalysts.¹

Organotins enter the marine environment through various routes. Tributyltin has been extensively used in antifouling ship paint formulations. Tributyltin released from the paint has been found to adversely affect many non-target organisms, particularly molluscs.²⁻⁴ As a result, some countries, beginning with France in 1982, have banned or restricted the use of tin-based antifouling paints.

Methyltin can be produced from the biomethylation of inorganic tin in the presence of estuarine microorganisms^{5,6} and naturally occurring iodomethane.⁷ Methyltin compounds have been isolated from water,^{8,9} sediments^{8,10} and fish.⁹

Previous methods for the analysis of organotins in biological samples include: (a) the extraction of butyltins by solvent¹¹⁻¹³ or tropolone-solvent^{14,15} followed by gas chromatography of the pentyl,^{14,15} ethyl,^{11,13} methyl¹⁶ or hydride¹² derivatives and (b) the formation of methyltin hydrides^{9,17} from tissue homogenates.

The purpose of this study was to evaluate both the efficacy of alkyllead extraction methods developed by our group¹⁸ for butyl- and methyltins and tetraalkyltins in marine food products and to examine current alkyltin levels in these products. Dual element extraction

methods offer the advantages of less sample preparation time per element and greater sample throughput. The methods reported in this paper use a lipase/protease hydrolysis (to prevent acid induced breakdown of organolead analytes and enhance extraction) and require no sample cleanup prior to analysis by gas chromatography coupled to atomic-absorption spectrometry.

EXPERIMENTAL

Reagents

Me₃SnCl, Me₂SnCl₂, Me₄Sn and Et₄Sn were used as received from Alfa Products, Johnson Matthey, Ward Hill, MA, USA. The Bu₃SnBr contained approx. 20% Bu₂SnBr₂ which was removed by crystallization from a methanol solution. The isolated Bu₂SnBr₂ contained no other tin compounds. The remaining Bu₃SnBr was 97% pure.

Butylmethyltins (BuMe₃Sn, Bu₂Me₂Sn and Bu₃MeSn) were synthesized and isolated as previously described¹⁹ with the exception that Bu₃MeSn was prepared from the corresponding butyltin by reaction with methylmagnesium chloride (3.0M in THF, Aldrich Chem. Co., Milwaukee, USA). Distilled-in-glass grade solvents (Caledon Laboratories Ltd., Georgetown, Ontario) and American Chemical Society reagent chemicals were used. Diphenylthiocarbazone (dithizone) was purchased from BDH Inc.

(Toronto, Ontario). Tropolone was obtained from Aldrich Chemical Co., Inc. (Milwaukee, Wisconsin, USA). Lipase (Type VII) and protease (Type XIV) were purchased from Sigma Chemical Co. (St. Louis, USA).

Instrumentation

The gas chromatograph (GC)-atomic absorption spectrometer (AAS) system used was described previously.¹⁸ The GC was fitted with a glass column (2.1 m × 6 mm o.d., 2 mm i.d.) packed with 3% OV-73 on Chromosorb WHP 100/120 mesh (Chromatographic Specialties Ltd.) Operating conditions were: carrier gas, helium, 30 ml/min; transfer line temperature, 225°; injector temperature, 175° (tetraalkyltins), 200° (butylmethyltin); temperature program (tetraalkyltins) 35° initially (1-min hold) with a linear increase (1.0°/min) to 37° (no hold) followed by a linear increase (20°/min) to 175° (1 min hold); temperature program (butylmethyltins), 40° initially (1-min hold) with a linear increase (15°/min) to 275° (2-min hold).

Operating conditions for the AAS were: bandpass, 0.5 nm; Photron Super Sn hollow cathode lamp (Photron Pty., Victoria, Australia) current, 15 mA; boost current 25 mA, wavelength 224.6 nm. Deuterium background correction was used during tetraalkyltin determination.

A VG Analytical 7070EQ interfaced with a Varian VISTA 6000 was used for GC-MS confirmation. The system (conventional magnetic sector only) was operated in the electron impact mode at 30 eV (to conserve high molecular weight ions) and with a mass resolution of 1000. Gas chromatography operating conditions were: column, J&W DB-5 capillary column (30 m × 0.25 mm i.d., 0.25- μ m film); carrier gas, helium (15 psi); injector temperature

program (on column), 80° initially (0.5-min hold) with a linear increase (80°/min) to 250°; column temperature program, 70° initially (1.5-min hold) with a linear increase (5°/min) to 85° (no hold) followed by a linear increase (15°/min) to 200° (no hold) and a final linear increase (20°/min) to 260°.

Selected ion monitoring (m/z 203, 205 and 207 for Me₃BuSn, 245, 247 and 249 for Me₂Bu₂Sn and 287, 289 and 291 for MeBu₃Sn) was conducted on both samples and standards run under the same GC-MS conditions. All MS analyses were qualitative for confirmation of GC-AAS results.

Sample preparation

Consumer marine food items were purchased from local supermarkets and specialty shops. Fish fillet homogenates were prepared with a meat grinder (Moulinex, Model 244) whereas the shellfish and mollusc samples were prepared with a Polytron tissue homogenizer (Brinkmann Instruments). All samples were stored at -20° until analysis.

Extraction procedure

Methyltin. The methyltins were isolated with the same procedure as reported for alkylleads.¹⁸ The samples were enzymatically hydrolyzed for 24 hr, extracted with 0.05% (w/v) dithizone in 20% dichloromethane/hexane and back extracted into dilute nitric acid (removing most coextractives). The nitric acid extract was re-basified and then extracted three times with the dithizone solution. The pooled dithizone extract was reduced to 1 ml and butylated by adding butylmagnesium chloride.

The method detection limits (Table 1), based on a 5-g sample size, were 0.2 and 0.5 ng Sn/g for Me₃BuSn and Me₂Bu₂Sn respectively

Table 1 Method Detection Limit (MDL)

Analyte	Mean	$N_{SD}, mV\ddagger$	Response		
	$N_{p-p}, mV\ddagger$		factor§	LOD	MDL#
BuMe ₃ Sn	0.0107	0.0036	221.3	4.8	0.2
Bu ₂ Me ₂ Sn	0.0079	0.0025	732.1	11.3	0.5
Bu ₃ MeSn	0.011	0.0052	488.2	12.9	0.5
Me ₄ Sn	0.020	0.011	260.5	13.8	0.8
Et ₄ Sn	0.0139	0.0058	364.9	11.4	0.7

*Of 20 measurements

†Mean peak to peak baseline noise

‡Standard deviation of N_{p-p}

§Inverse of slope from linear regression (pg Sn/mV)

||Limit of Detection, (mean $N_{p-p} + 3N_{SD}$) × response factor (pg Sn)

#Method Detection Limit, [(LOD/mj vol) × extract vol]/sample wgt] × 10⁻³ (ng Sn/g)

Butyltin. Method 1. The samples (5 g) were enzymatically hydrolyzed for 24 hr.¹⁸ The pH was adjusted to 9 and the samples were extracted (rotary tumbled) once (65 rpm, 5 min) with 10 ml of hexane. The hexane was collected after centrifugation (3000 rpm, 5 min) which hastened phase separation. The samples were then extracted once with 0.05% (w/v) dithizone (10 ml) in 20% dichloromethane/hexane. The pooled organic extracts were derivatized as described in Method 4.

Method 2. Samples (5 g) were extracted with the method described by Ohhira and Matsui¹⁵ with the only difference being that the 0.05% tropolone solution was made up in hexane rather than benzene. The samples were processed with a Polytron homogenizer, 1.5 g of sodium chloride and hydrochloric acid were added (to pH 0.5) followed by two extractions (65 rpm, 20 min) with 0.05% (w/v) tropolone (10 ml) in hexane. The pooled organic extracts were reduced in volume to 1 ml at 40° in precalibrated tubes under a nitrogen stream. Derivatization was as per method 4.

Method 3. The samples (5 g) were enzymatically hydrolyzed for 24 hr.¹⁸ The resulting hydrolysates were then extracted as described in Method 2 (minus the homogenization step) and derivatized as described in method 4.

Method 4. The samples (5 g) were enzymatically hydrolyzed for 24 hr¹⁸ and 500 mg of sodium sulphite were added after the enzymes just prior to incubation. The hydrolysates were extracted as described in method 2 (minus the homogenization step). Derivatization was carried out as follows: tetrahydrofuran (1.0 ml) and methylmagnesium chloride (0.8 ml, 3.0M in THF) were added to the dithizone extract. The sample tube was capped under nitrogen, vortexed for approx. 10 sec and rotary tumbled (25 rpm) for 10 min. The samples were cooled in an ice bath and the volume adjusted to 10 ml with prechilled 0.5M nitric acid, which should be added dropwise initially. Isooctane (0.7 ml) was added, and the sample tumbled (25 rpm) for 2 min. Centrifugation (2000 rpm, 5 min) hastened phase separation. The nitric acid layer was discarded, and the organic phase extracted (25 rpm, 2 min) with 8 ml of distilled water. Sample volume was adjusted to 2.0 ml, dried over sodium sulfate (approx. 50 mg) and stored in an autoinjector vial. The method detection limit (Table 1) was 0.5 ng Sn/g for Bu₃MeSn and Bu₂Me₂Sn.

Tetraalkyltins. The samples were processed as previously reported for tetraalkylleads.¹⁸ Homogenized samples (5 g) were enzymatically hydrolyzed for 48 hr with 2 ml of hexane present. The hydrolysates were cooled, extracted for 10 min and then centrifuged. The organic layer was collected and the sample reextracted once with hexane (1 ml). The pooled extracts were made up to 3.0 ml, dried over sodium sulfate and then stored in an autoinjector vial.

The method detection limits (Table 1) for Me₄Sn and Et₄Sn were 0.8 and 0.7 ng Sn/g respectively.

Recovery experiments

Samples of fresh/frozen marine fish fillet, shellfish and mollusc (5.0 g) were spiked prior to hydrolysis with a mixture containing either two butyltins, methyltins or tetraalkyltins. The percentage recovery of each compound was determined by comparing the mean peak area of the recovered compound with the mean peak area of the compound in a blank hydrolysate extract spiked just prior to alkylation (alkyltins) or by comparing the mean peak area of the recovered compound with the mean peak area of the compound in a spiked blank hydrolysate extract diluted to the expected concentration (tetraalkyltins). Marine food samples were quantitated by comparison of peak area to external standards. Reagent blanks were run concurrently with each set of samples.

RESULTS AND DISCUSSION

All of the alkyltin recoveries were 75% or better, with the majority exceeding 90% (Table 2). Methyltins and tetraalkyltins therefore, can be isolated effectively with extraction procedures originally developed for alkyllead compounds.¹⁸ Initial work, however, indicated that the butyltins were not extracted into the acidic back extraction of the method reported for marine fish fillets¹⁸ so a modified procedure (method 1) was developed.

With method 1, tributyltin was extracted with hexane but recovery of dibutyltin required an additional extraction with 0.05% dithizone solution. Dibutyltin and tributyltin recoveries from a mollusc matrix (Table 2) were 41 and 108% respectively. As recoveries from buffer solutions were high, matrix interference was suspected. The addition of potassium cyanide and/or sodium chloride improved recoveries slightly,

but not enough to make the method practical for mollusc matrices.

Method 2, using tropolone-solvent extraction, was based on the work of Ohhira and Matsui.¹⁵ Hexane was substituted for benzene which was considered an unnecessary health hazard. After preliminary work no difference in extraction efficiency between hexane and benzene was observed. Dibutyltin and tributyltin recoveries from oyster were 87 and 62%, respectively (Table 2). Method 2, therefore, recovered more dibutyltin but less tributyltin than method 1. The differences between the extraction efficiencies of methods 1 and 2 were reflected in the butyltin levels found in contaminated fresh clams (Table 3) but not in the canned oyster and mussel.

Enzymatic hydrolysis was included in method 3 as a technique to decrease matrix interferences. Dibutyltin and tributyltin recoveries were 47 and 95% respectively (Table 2). Tributyltin recoveries therefore, were improved by the enzymatic hydrolysis. The dibutyltin, however,

appeared to be partially converted to monobutyltin, which was detected in the GC-AAS chromatograms of recovery samples but not in the blank hydrolysate extracts spiked just prior to methylation. Tributyltin levels in both the fresh and canned contaminated marine food products (Table 3) increased from those reported for method 2. However, there was no conversion of dibutyltin to monobutyltin in the contaminated marine foods analyzed by method 3, resulting in the dibutyltin levels remaining similar to or greater than those determined with method 2 (Table 3). The higher butyltin levels found with method 3 (Table 3) suggest that there was a bound unextractable form in the sample homogenate prior to enzymatic hydrolysis. Other authors have expressed concern over matrix interferences,^{11,13,17} some of which were irreversible. The enzyme hydrolysis used in methods 3 and 4 appears to be effective in reducing matrix interferences and releasing organotin analytes (Table 3) from a variety of marine food matrices.

Table 2 Mean recoveries of organotin compounds from marine food products

Analyte	N*	Method†	Matrix	Spiking Level, ng/g‡	Mean Recovery, % ± SD
Me ₃ SnCl	4	—	clam	12	87 ± 9
	4	—	clam	64	87 ± 5
	4	—	cod	12	78 ± 3
Me ₂ SnBr ₂	4	—	clam	14	99 ± 6
	4	—	clam	70	97 ± 8
	4	—	cod	14	100 ± 12
Me ₄ Sn	6	—	clam	5	100 ± 4
	4	—	clam	75	92 ± 3
	4	—	turbot	5	98 ± 3
Et ₄ Sn	6	—	clam	4	72 ± 4
	4	—	clam	60	84 ± 4
	4	—	turbot	5	100 ± 2
Bu ₂ SnCl ₂	4	1	oyster	60	41 ± 6
	4	2	oyster	60	87 ± 5
	4	3	oyster	60	47 ± 3
	4	3	cod	60	93 ± 2
	6	4	cod	60	100 ± 6
	4	4	clam	60	86 ± 4
	4	4	lobster	60	100 ± 1
Bu ₃ SnBr	4	1	oyster	35	108 ± 12
	4	2	oyster	35	62 ± 3
	4	3	oyster	35	95 ± 6
	4	3	cod	35	69 ± 3
	6	4	cod	35	75 ± 4
	4	4	clam	35	87 ± 1
	4	4	lobster	35	99 ± 3

*N = number of samples

†Method 1 dithizone/solvent extraction Method 2 Ohhira and Matsui¹⁵
Method 3 modified after Ohhira and Matsui¹⁵ Method 4 modified
after Ohhira and Matsui¹⁵ + Na₂SO₃

‡As Sn

Table 3 Effect of extraction technique on butyltin levels* in contaminated marine food products

Samples	N†	Method‡	Analyte concentration, (ng/g wet wt)		
			BuSn ³⁺ §	Bu ₂ Sn ²⁺	Bu ₃ Sn ⁺
Clams, fresh	4	1	—	27 ± 0.2	307 ± 1.0
	4	2	—	43 ± 0.7	184 ± 3.2
	4	3	—	44 ± 0.4	401 ± 1.9
	1	4	—	3.1	42.9
Oyster, canned	4	1	—	44 ± 1.1	563 ± 3.3
	4	2	—	140 ± 0.9	1006 ± 5.2
	4	3	—	176 ± 0.9	1355 ± 9.1
	3	4	14 ± 0.2	136 ± 1.7	1558 ± 12.4
Mussels, canned	1	1	—	8.3	48.4
	1	3	—	51.2	86.1
	1	4	5.9	46.7	152.3
Boston blue fish	1	1	—	<1.0	1.4
	1	4	—	<1.0	2.4
Ocean perch	1	1	—	1.8	2.5
	1	4	—	<1.0	2.2

*Uncorrected for recovery

†N = number of samples

‡Method 1 dithizone/solvent extraction Method 2 Ohhira and Matsui¹⁵ Method 3 modified after Ohhira and Matsui¹⁵ Method 4 modified after Ohhira and Matsui¹⁵ + Na₂SO₃

§No recovery data obtained

The addition of sodium sulphite to the homogenate prior to hydrolysis (method 4) was found to prevent partial dealkylation of dibutyltin to monobutyltin in cod, clam and lobster during recovery trials. Dibutyl- and tributyltin recoveries averaged 95 and 87% respectively (Table 2). In the contaminated marine foods (Table 3), tributyltin levels in the fresh clam remained similar to those obtained with method 3 (Table 3) but increased considerably in the canned oyster and mussels. Dibutyltin levels dropped slightly with low levels of monobutyltin present in the contaminated canned marine foods (Table 3).

Method 4 was adopted for the analysis of marine food products reported in Table 4 since the butyltin recoveries were consistently high and the dealkylation of dibutyltin was suppressed. Method development should be investigated further as: (a) butyltin levels in the contaminated canned marine food products behaved somewhat differently than predicted from recovery experiments with fresh/frozen products and (b) although the appearance of low monobutyltin levels in the canned marine foods with method 4 probably resulted from increased analyte extractability (as found with tributyltin), artifact formation remains a possibility.

Many of the marine food products contained alkyltins (Table 4). Several of the marine fish

fillets contained low levels (<1.2–2.4 ng/g) of tributyltin. Trimethyltin was found in a turbot sample. Dibutyltin was not detected in any of the fish samples.

Both fresh and canned molluscs contained higher levels of butyltin compounds (ranging from <1.0 to 155.8 ng/g) than the marine fish fillets (Table 4). Tributyltin was the predominant species (Table 4) with much lower levels of dibutyltin and possibly monobutyltin present. Trimethyltin was also found, at a low level (0.7 ng/g) in one of the mollusc samples (Table 4). Tetraalkyltin levels in all samples were less than the reported method detection limits (Table 1).

The presence of alkyltin was confirmed in three samples by comparison with standards, using GC-MS. The canned mussel sample (Fig. 1) contained BuMe₃Sn (*m/z* 207 [M-CH₃]⁺), Bu₂Me₂Sn (*m/z* 249 [M-CH₃]⁺) and Bu₃MeSn (*m/z* 291 [M-CH₃]⁺).

The predominance of tributyltin in the marine food products clearly indicates contamination from commercial usage of butyltin based products. Similar levels (69–170 ng/g) of tributyltin have been found previously in aquacultured salmonids²⁰ exposed to tributyltin treated sea pens. Ishizaka *et al.*¹¹ found Bu₂Sn²⁺ and Bu₃Sn⁺ at levels of 0.02–0.05 and 0.02–1.49 ug/g respectively in purchased marine food products.

Table 4 Alkyltin levels* in consumer marine food products

Samples	Analyte concentration, (ng/g wet wt)		
	BuSn ³⁺	Bu ₂ Sn ²⁺	Bu ₃ Sn ⁺
Cod	—	<1.0	<1.2
Boston blue fish	—	<1.0	2.4
Haddock	—	<1.0	<1.2
Ocean perch	—	<1.0	2.2
Trout	—	<1.0	<1.2
Turbot	—	<1.0	<1.2
Clams, fresh	—	3.1	42.9
Baby clams, canned supplier A	—	<1.0	<1.2
Baby clams, canned supplier B	—	<1.0	<1.2
Baby clams, canned supplier C	—	<1.0	<1.2
Clams, fresh	1.2	4.8	94.5
Mussels, fresh	—	<1.0	<1.2
Mussels, fresh	—	<1.0	<1.2
Mussels, canned supplier D	—	3.9	11.6
Mussels, canned supplier E	5.9	46.7	152.3
Cockles, welded can, supplier E	—	5.3	12.4
Cockles, soldered can, supplier E	—	3.1	19.7
Crab meat, canned, supplier F	—	<1.0	<1.2
Crab meat, canned, supplier G	—	<1.0	<1.2
Crab meat, canned, supplier H	—	<1.0	2.9
Lobster, fresh, claw + tail	—	<1.0	<1.2
Lobster, pâté, supplier I	—	<1.0	<1.2
Oyster, fresh	—	<1.0	8.1
Oyster, canned, supplier G	1.4	13.6	155.8
Scallops, frozen, supplier H	—	<1.0	<1.2
Scallops, fresh	—	<1.0	<1.2
Cod liver, canned, supplier E	—	<1.0	<1.2

Me₃Sn⁺ Cockles, welded can 0.7 ng/g, turbot, 2.8 ng/g

*Uncorrected for recovery

The methyltin may originate from environmental methylation of inorganic tin or the use of dimethyl- and monomethyltin compounds as heat and light stabilizers in PVC plastics. Tugrul *et al.*⁹ also found low (0.8–27 ng/g, dry weight basis) levels of methyltin compounds in several marine fish species. Current trends of alkyltin levels in marine food can be assessed only after further analyses are completed.

CONCLUSIONS

Extraction methods originally developed for alkyllead determination can be used to efficiently extract methyltin and tetraalkyltin compounds from marine food products with no or few modifications. A tropolone-solvent extraction procedure proved more effective for butyltin determination than the organolead methods. Recovered butyltin levels in contaminated marine foods increased after enzyme hydrolysis. Many of the consumer marine food items examined contain parts per billion levels of butyltin compounds. Several samples contained low levels of methyltin. The predominance of tributyltin indicates contamination of the marine food supply by commercial

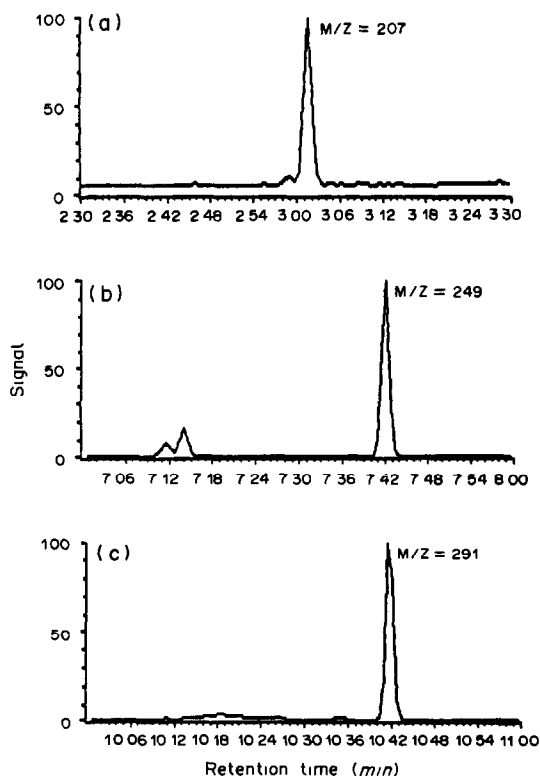


Fig. 1 Selected ion GC-MS of mussel containing (a) BuMe₃Sn, (b) Bu₂Me₂Sn and (c) Bu₃MeSn

usage of the compound in antifouling paint formulations. No tetraalkyltin compounds were detected.

Acknowledgements—The authors thank D Weber, Food Research Division, HPB for carrying out the GC-MS confirmation and R Dabeka and R Morumer for helpful discussions during the preparation of the manuscript

REFERENCES

- 1 C J Evans and S Karpel (eds), *Organotin Compounds in Modern Technology*, Elsevier, Amsterdam, 1985
- 2 S C U'Ren, *Mar Poll Bull*, 1983, **14**, 303
- 3 A R Beaumont and M D Budd, *ibid*, 1984, **15**, 402
- 4 D Minchin, C B Duggan and W King, *ibid*, 1987, **18**, 604
- 5 L E Hallas, J C Means and J J Cooney, *Science*, 1982, **215**, 1505
- 6 J A A Jackson, W R Blair, F E Brinckman and W P Iverson, *Environ Sci Technol*, 1982, **16**, 110
- 7 P J Craig and S Rapsomanikis, *J Chem Soc , Chem Commun*, 1982, 114
- 8 R. J Maguire, R J Tkacz, Y K Chau, G. A Bengert and P T S Wong, *Chemosphere*, 1986, **15**, 253
- 9 S Tugrul, T I Balkas and E D Goldberg, *Mar Poll. Bull*, 1983, **14**, 297
- 10 C C Gilmour, J H Tuttle and J C Means, *Anal Chem*, 1986, **58**, 1848
- 11 T Ishizaka, S Nemoto, K Sasaki, T Suzuki and Y Saito, *J Agric Food Chem*, 1989, **37**, 1523
- 12 T Tsuda, H Nakanishi, T Morita and J Takebayashi, *J Assoc Off Anal Chem*, 1986, **69**, 981
- 13 K Sasaki, T Suzuki and Y Saito, *Bull Environ Contam Toxicol*, 1988, **41**, 888
- 14 A D Uhler, T H Coogan, K S Davis, G S Durell, W G Steinhauer, S Y Freitas and P D Boehm, *Environ Toxicol Chem*, 1989, **8**, 971
- 15 S Ohhira and H Matsui, *J Chromatog*, 1990, **525**, 105
- 16 K Sasaki, T Ishizaka, T Suzuki and Y Saito, *J Assoc Off Anal Chem*, 1988, **71**, 360
- 17 J S Han and J H Weber, *Anal Chem*, 1988, **60**, 316
- 18 D S Forsyth and J R Iyengar, *Appl Organomet Chem*, 1989, **3**, 211
- 19 D S Forsyth, *Sci Total Environ*, 1989, **89**, 299
- 20 J W Short, *Bull Environ Contam Toxicol* 1987, **39**, 412

ATOMIC-ABSORPTION SPECTROMETRIC DETERMINATION OF CALCIUM, MAGNESIUM AND POTASSIUM IN LEAF SAMPLES AFTER DECOMPOSITION WITH MOLTEN SODIUM HYDROXIDE

J. V. GIMENO ADELANTADO, V. PERIS MARTINEZ, A. PASTOR GARCIA
and F. BOSCH REIG

Department of Analytical Chemistry, Faculty of Chemistry, University of Valencia,
46100 Burjasot (Valencia), Spain

(Received 23 June 1989, Revised 1 March 1991, Accepted 11 March 1991)

Summary—The decomposition of standard leaf samples of varied origin and nature by fusion with sodium hydroxide in an open system has been studied. The use of sodium nitrate as an auxiliary agent facilitated the mineralization of most of the samples. The solutions obtained were analysed for calcium, magnesium and potassium by flame atomic-absorption spectrometry. The method is fast and quite precise, with absolute standard deviations of 0.04–0.13, 0.002–0.03 and 0.04–0.12% for calcium, magnesium and potassium contents of 0.8–5.0, 0.13–0.48 and 0.36–2.2% respectively. The limits of detection ($\mu\text{g/ml}$) in the determination step were 0.10 for calcium, 0.011 for magnesium, and 0.09 for potassium.

Calcium, magnesium and potassium are three major mineral components of plants, their contents in which depend on the particular vegetable species and the soil in which these are grown. Deficiencies of these essential elements can cause serious defects in plants.

Although instrumental measurements are occasionally made directly on such samples without prior destruction of the organic matrix,^{1,2} a prior mineralization is generally used, in which case the risk of losses, contamination and interference effects must be considered.

The AOAC³ recommends dry ashing for the mineralization; this approach has several variants, with different ashing temperatures and subsequent treatment and analysis of the ash.^{4–6} The ashing temperature and the mass of analyte present are factors to be taken into account to avoid losses of these three elements at above 450°. Laser ashing⁸ has also been used for this type of sample.

Wet ashing procedures can be divided according to whether they are implemented in an open or a closed system. Open systems have been used for decomposition with various acids or their mixtures.^{9–15} Mixtures of nitric acid and hydrogen peroxide have been used for decomposition with heating in a microwave oven.¹⁷ Closed systems seem to be less prone to result in analyte losses through volatilization during the heating,^{18,19} and use has been made

not only of concentrated acids, but also of hydrogen peroxide in Teflon pressure vessels to reduce the risk of contamination and acid corrosion.²⁰ Rapid destruction of plant material with nitric acid vapour has also been employed in determination of trace elements.²¹

Fusion with sodium hydroxide can be a useful alternative to the wet and dry methods, but has been relatively little exploited in analysis of organic matrices; in fact, it has only been employed in the determination of F⁻,²² As and Sb,²³ P,²⁴ and S,²⁵ with fusion in open systems, and of Ge with fusion in a closed system.²⁶ Earlier problems such as lack of purity of the reagents have now been overcome with the introduction of commercial reagents with very low metal contents. The hygroscopic nature of alkali-metal hydroxides can sometimes be advantageous, in favouring homogenization between the sample and the flux (we have even found it of use to start the attack by adding a few drops of water).²⁵

Once the organic matrix has been decomposed, calcium, magnesium and potassium are usually determined in plant material by AAS^{2,3,5,13} and ICP.^{12,14–16,27}

Here we report the decomposition of leaf samples by fusion with sodium hydroxide in a silver crucible at comparatively low temperature (350°). The results for calcium, magnesium and potassium in standard samples are in agreement with the certified values.²⁸

EXPERIMENTAL

Apparatus

A Perkin-Elmer model 5000 atomic-absorption spectrophotometer was used with the instrumental parameters recommended in the instrument manual. A flow spoiler was employed as impactor.

A Barnstad II water purifier was used.

Reagents

A 0.2M solution of La(III) was prepared from Probus Analytical grade $\text{LaCl}_3 \cdot 7\text{H}_2\text{O}$. Merck *p.a.* grade sodium hydroxide, sodium chloride and hydrochloric acid were used.

Standard samples

The standard leaf samples were those prepared and certified by the Comité Inter-Institute d'Etude des Techniques Analytiques de Diagnostic Foliaire (C.I.I.)²⁸ Their homogeneity was tested by the laboratory which prepared the standards (Centre de Recherches Rhône-Progil), by the CETAMA method.²⁹

The mineralization procedure used in the intercalibration⁵ involved calcination of 2 g of sample at 450° for 2 hr, and subsequent acid treatment of the ashes. The residue was collected on filter paper, ashed at 550° and treated with hydrofluoric acid. The residue from this was dissolved with concentrated hydrochloric acid. Calcium (in the presence of 30 mg/ml lanthanum chloride) and magnesium were then determined in the combined solution by flame atomic-absorption spectrometry (FAAS) and potassium by flame-emission spectrometry.³⁰

The results were subjected to a full statistical analysis³¹

Alkaline fusion

In a 50-ml silver crucible fuse 4 g of sodium hydroxide and swirl the crucible during cooling until the alkali has solidified on the bottom and walls. Weigh 0.1 g of sample, previously dried at 70–80° for 16 hr, into the crucible and add 0.5–1 ml of water to wet the sample and the alkali. Warm gently in the burner flame and swirl the crucible vigorously to obtain a homogeneous mixture of the alkali and organic matter at a relatively low temperature. Keep warming and swirling the crucible until all the moisture has evaporated. Gradually increase the temperature, with continued swirling, until the mixture has fused. Then heat strongly until all organic matter has been destroyed. If a

charred residue is left (as is usually the case), keep heating and add a small amount of sodium nitrate, not more than 0.1–0.2 g, as auxiliary oxidant and continue heating until oxidation is complete and a transparent melt has been formed.

Once cold, the fusion product can be readily dissolved with successive small volumes of hot water (not more than 5 ml at a time). Combine these extracts in a 250-ml beaker, and acidify by dropwise addition of 3M hydrochloric acid with vigorous stirring to help remove the CO_2 released. Boil the clear solution for a few minutes and then transfer it to a 50-ml standard flask, dilute to the mark and mix.

Prepare blank solutions similarly, including the fusion.

Determination

Pipette 1, 2 or 3 ml of the sample solution (depending on the analyte to be assayed and its content in the sample) into a 25-ml standard flask, add 2 ml of the lanthanum solution, dilute to the mark, mix, and measure by FAAS. Run a corresponding volume of blank solution in the same way, and apply the resulting correction.

RESULTS AND DISCUSSION

First we studied the decomposition of various leaf samples with molten sodium hydroxide. Maize was easily mineralized, leaving no carbon residue, and not needing use of the auxiliary oxidant. Golden apple leaves gave the strongest carbonization, necessitating use of the largest amount of auxiliary agent (about 0.2 g). All the other samples behaved similarly to each other and required less than 0.1 g of sodium nitrate. These small differences can be related to the different texture of the samples, and hence their varying composition. The mineralization was accomplished satisfactorily within 5 min in every case. The highest absorbances yielded by the blanks were 0.011, 0.005 and 0.016 for Ca, Mg and K respectively.

Calibration

We ran three calibrations for standards containing lanthanum chloride and the same amounts of sodium chloride as the unknown samples (0.08, 0.16 or 0.24M, corresponding to 1, 2 or 3 ml subsamples from an overall volume of 25 ml) and covering six analyte concentrations in the ranges 0–4 $\mu\text{g/ml}$ Ca,

0–0.5 $\mu\text{g/ml}$ Mg and 0–2 $\mu\text{g/ml}$ K. The experimental results were fitted by linear regression; Table 1 gives the equations and correlation coefficients. As can be seen, the sensitivity decreased with increasing sodium chloride concentration (*i.e.*, the slope decreased). At the

sodium chloride and lanthanum concentrations used in the calibrations, the sample uptake (flow-rate at the nebulizer) was decreased by a factor similar to that for the decrease in sensitivity in the case of potassium and a slightly larger factor for calcium and magnesium, which may be accounted for by the interaction with Cl^- , Na^+ and La^{3+} ions in the flame.³² The high sodium content (1840–5520 $\mu\text{g/ml}$) acted as an ionization buffer for potassium. The detection limits³³ achieved were 0.10, 0.011 and 0.09 $\mu\text{g/ml}$ for Ca, Mg and K respectively.

Table 1 Calibration data (mean \pm standard deviation, 5 data points)

Element	Medium, [NaCl], M	$A = X + YC^*$		
		$X (\times 10^3)$	$Y (\times 10^3)$	r
Ca	0.08	10 \pm 3	51.2 \pm 1.1	0.9993
	0.16	9 \pm 2	46.6 \pm 1.0	0.9993
	0.24	9 \pm 2	42.6 \pm 0.9	0.9993
Mg	0.08	4 \pm 3	475 \pm 9	0.9992
	0.16	3.9 \pm 1	436 \pm 4	0.9998
	0.24	6.5 \pm 1	418 \pm 4	0.9998
K	0.08	5.7 \pm 0.4	93.3 \pm 0.3	0.99998
	0.16	9 \pm 1	91.8 \pm 0.9	0.9998
	0.24	15 \pm 2	87.6 \pm 1.5	0.9994

*C = concentration in $\mu\text{g/ml}$

Analysis of leaf samples

Tables 2–4 list the results obtained, which were analysed statistically (significance level, 95%),³⁴ together with the certified values.

As a rule, the precision of the results obtained by the proposed method was comparable with that of the certified values. The most precise determination was that of Mg, followed by

Table 2 Determination of calcium

Sample	Ca, %				
	Certificate value ²⁸			Found†	
	\bar{x}	s	x_R	\bar{x}	s
Maize	1.122	0.057	1.12	1.13	0.06
Palm	0.800	0.034	0.80	0.78	0.04
Eucalyptus	1.571	0.113	1.56	1.59	0.10
Cotton	3.079	0.195	3.10	2.98	0.05
Peach	2.162	0.109	2.15	2.20	0.11
Codia discolor	0.831	0.037	0.83	0.84	0.04
Hevea	1.0675	0.081	1.08	1.05	0.08
Vine	2.583	0.142	2.55	2.58	0.13
Orange	4.886	0.173	4.91	4.98	0.13
Olive	2.605	0.135	2.59	2.58	0.13
Golden apple	1.279	0.079	1.27	1.29	0.08
Cox's Orange apple	2.137	0.078	2.14	2.14	0.08

* x_R , recommended value

†Five separate decompositions

Table 3 Determination of magnesium

Sample	Mg, %				
	Certificate value ²⁸			Found†	
	\bar{x}	s	x_R	\bar{x}	s
Maize	0.363	0.012	0.36	0.357	0.012
Palm	0.296	0.0132	0.295	0.280	0.028
Eucalyptus	0.207	0.017	0.21	0.208	0.011
Cotton	0.413	0.017	0.41	0.399	0.014
Peach	0.4725	0.024	0.475	0.476	0.019
Codia discolor	0.285	0.0125	0.28	0.284	0.011
Hevea	0.331	0.024	0.33	0.335	0.014
Vine	0.280	0.017	0.28	0.276	0.016
Orange	0.318	0.0225	0.32	0.314	0.012
Olive	0.131	0.007	0.13	0.133	0.002
Golden apple	0.286	0.017	0.29	0.282	0.007
Cox's Orange apple	0.295	0.016	0.29	0.293	0.005

* x_R , recommended value

†Five separate decompositions

Table 4 Determination of potassium

Sample	K, %				
	Certificate value ²⁸			Found†	
	\bar{x}	s	x_R	\bar{x}	s
Maize	1 898	0 110	1 94	1 87	0 06
Palm	0 877	0 062	0 885	0 85	0 05
Eucalyptus	0 694	0 065	0 68	0 67	0 06
Cotton	1 824	0 068	1 84	1 88	0 12
Peach	2 182	0 1255	2 185	2 20	0 12
Codia discolor	0 3665	0 033	0 37	0 36	0 04
Hevea	0.937	0 051	0 93	0 93	0 05
Vine	1 2265	0.073	1 23	1 23	0 07
Orange	1 539	0 1323	1 51	1 54	0 12
Olive	0 511	0 067	0 506	0 52	0 06
Golden apple	1 441	0 0745	1 45	1 46	0 06
Cox's Orange apple	1 037	0 088	1 04	1 07	0 09

* x_R , recommended value

†Five separate decompositions

that of K; the lower precision for Ca could be attributed to the well-known tendency of calcium to form refractory compounds. The average values yielded by the proposed method are statistically comparable with the recommended values.

The accuracy of the proposed method was statistically satisfactory and the confidence ranges were encompassed by the standard selection ranges established by the C.I.I., except for the determination of Ca in cotton, where neither the average certified value nor the recommended value was within the confidence range obtained by the proposed method at the 95% probability level, though they would at the 99.9% level. This exception is due to the small standard deviation ($s = 0.045$) of the results and the high Ca content (2.98%) found, which combine to give a very narrow confidence interval. However, the value found lies within the selected range established for the certified sample (2.884–3.274%).²⁸ Therefore, the proposed method has no systematic error at the stated confidence level.

Conclusions

The proposed method is quite accurate and precise for the analysis of leaf samples. This testifies to the efficiency of alkaline fusion with sodium hydroxide for decomposing organic matter, which has so far been little exploited, probably because of formerly serious drawbacks such as reagent impurities and crucible contamination, which have by now been overcome.

Acknowledgements—The authors are grateful to Dr M Pinta, Research Director and Chief of the Spectrography Department O R S T O M (France), for kindly supplying the leaf standards used in this work

REFERENCES

- 1 M Abdullah and H Haraguchi, *Anal Chem*, 1985, **57**, 2059
- 2 F J Langmyhr and G Wibetoe, *Prog Anal Atom Spectrosc*, 1985, **8**, 193
- 3 Association of Official Analytical Chemists, *Official Methods of Analysis*, 14th Ed., Sections 3001–3016, pp 38–40, AOAC, Arlington, 1984
- 4 A D Hill, K Y Patterson, C Veillon and E R Morris, *Anal Chem*, 1986, **58**, 2340
- 5 M Pinta and C I I, *Oléagineux*, 1973, **28**, 87
- 6 R A Isaac and W C Johnson, *J Assoc Off Anal Chem*, 1985, **68**, 499
- 7 T T Gorsuch, *The Destruction of Organic Matter*, pp 57, 58, 71 Pergamon Press, Oxford, 1970
- 8 M Ahlgren, A Kontkanen, K Vatulainen and H Vehvilainen, *Analyst*, 1988, **113**, 285
- 9 M Miyazawa, M A Pavan and M F M Bloch, *Cienc Cult (Sao Paulo)*, 1984, **36**, 1953
- 10 K L Sahrawat, *Commun Soil Sci Plant Anal*, 1980, **11**, 753
- 11 J Hunt, *ibid.*, 1982, **13**, 49
- 12 D M Kumina, I F Grbovskaya and A V Karyakin, *Zh Analit Khim*, 1985, **40**, 1184
- 13 N Carrion, Z A de Benzo, E J Eljuri, F Ippoliti and D Flores, *J Anal Atom Spectrom*, 1987, **2**, 813
- 14 M Miyazawa, M A Pavan and M F M Block, *Commun Soil Sci Plant Anal*, 1984, **15**, 141
- 15 D J Lyons, K P Spann and R L Roofayel, *Analyst*, 1985, **110**, 955
- 16 C Y L Huang and E E Schulte, *Commun Soil Sci Plant Anal*, 1985, **16**, 943
- 17 R T White, Jr and A E Douthit, *J Assoc Off Anal Chem*, 1985, **68**, 766
- 18 B Bernas, *Anal Chem*, 1968, **40**, 1682
- 19 F J Langmyhr and P E Paus, *Anal Chim Acta*, 1986, **43**, 397
- 20 H Matusiewicz and R M Barnes, *Anal Chem*, 1985, **57**, 406
- 21 A D Thomas and L E Smythe, *Talanta*, 1973, **20**, 469
- 22 R L Baker, *Anal Chem*, 1972, **44**, 1326
- 23 F Bosch Reig and J V Gimeno Adelantado, *Talanta*, 1983, **30**, 437
- 24 J V Gimeno Adelantado, F Bosch Reig, A Pastor Garcia and V Peris Martinez, *ibid.*, 1983, **30**, 974

- 25 J V Gimeno Adelantado and F Bosch Reig, *ibid*, 1986, **33**, 757
- 26 V A Klimova and M D Vitalna, *Zh Analit Khim*, 1964, **19**, 1254
27. T. Liese *Z Anal Chem.*, 1985, **321**, 37
- 28 M. Pinta and C I I, *Analisis*, 1975, **3**, 345
- 29 Commissariat à l'Energie Atomique, *Méthodes statistiques en chimie analytique*, Vol VI, CETAMA, Dunod, Paris, 1962
- 30 M Pinta and C. I I, *Oléagineux*, 1969, **24**, 497
- 31 H de la Roche and K Govindaraju, *Analisis*, 1973, **2**, 59
- 32 M. Pinta, *Spectrometrie d'absorption atomique*, Vol 1, pp 122-123, Masson, Paris, 1978
33. IUPAC, *Compendium of Analytical Nomenclature*, p 117, Pergamon Press, Oxford, 1978
- 34 Y Lacroix, *Analyse chimique. interprétation des résultats par le calcul statistique*, Masson, Paris, 1973.

UNIVERSAL ON-LINE DETECTOR FOR HIGH-PERFORMANCE LIQUID CHROMATOGRAPHY VIA MAGNETO-OPTICAL ROTATION

HIROFUMI KAWAZUMI, HIDEKI NISHIMURA, YUKIAKI OTSUBO and TEICHIRO OGAWA
Department of Molecular Science and Technology, Kyushu University, Kasuga 816, Japan

(Received 8 March 1991 Accepted 4 April 1991)

Summary—Detecting changes in magneto-optical rotation is useful as a universal on-line detector for high-performance liquid chromatography. Such apparatus is similar to a polarimeter except for the external magnetic field on a flow cell. Two modulation modes suitable for the magneto-optical rotation detector are discussed. Use of a semiconductor laser provides better sensitivity than a He-Ne laser. The detection limit is 0.006% (w/w) for polyethylene glycol 20000 in a 20- μ l injection.

Many laser-based analytical systems have been developed. Some of them have been applied to a flow detector for high-performance liquid chromatography (HPLC) and flow-injection analysis.¹ They are classified by their principle of operation, sensitivity, universality, convenience, detector dimensions and cell volume. A refractive index (RI) detector is popular because of its universality. The detectability of the conventional RI detector is in the order of 10^{-7} RI units which corresponds to μ g-sub- μ g hydrocarbon levels. A refractive index gradient detector based on interferometry could improve the detectability to 4×10^{-9} RI units and sub-ng levels.² Recently, the indirect photometric method has been developed and provides the universal sensitivity with absorption,³ fluorescence⁴ and thermal lens⁵ detection. The detection limit of 10^{-2} – 10^{-3} % (w/w) depends on the displacement scheme. This method can improve the mass detectability in the order of 10 ng with small-volume detection, using lasers. In a previous paper,⁶ we demonstrated another universal flow detector based on magneto-optical rotation (MOR).

Magneto-optical rotation, the so-called Faraday effect, is a general optical property of substances in a magnetic field. When the linearly polarized light propagates through a medium in a magnetic field parallel to the direction of the light beam, the polarized plane of the light rotates.⁷ The rotation angle is proportional to the strength of the magnetic field and the optical path length. The proportionality factor is known as the Verdet constant. A change in composition of a solution modifies its rotatory

power. A small change of MOR can be measured with a technique similar to sensitive polarimetry.⁸⁻¹² In a previous paper,⁶ we used external magnetic field modulation and a He-Ne laser for sensitive detection.

In this paper, we evaluate the modulation modes suitable for the MOR detection and describe the utility of a semiconductor laser. It provides very stable light intensity and allows simple replacement with a He-Ne laser for better sensitivity. The semiconductor laser is the most compact and convenient source of laser light. This feature allows versatility in instrumentation designs.

EXPERIMENTAL

Instrumentation

The experimental set-up is shown in Fig. 1. It is basically similar to the laser-based polarimeter reported by Yeung *et al.*⁸ The light source was a He-Ne laser (Uniphase 1101P; 1 mW of light at 633 nm) or a semiconductor laser (Sharp LT023MC; 3 mW of light at 784 nm). The semiconductor laser was operated in the power control mode with an integrated circuit (Sharp IR3C02N) as specified by the manufacturer. The beam of the He-Ne or semiconductor laser was focused with a 20-cm focal length lens or a 3-lens collimator (Sakai Glass), respectively. Careful optical adjustment is important because the light scattering on the cell wall induces depolarization. A pair of Glan-Thompson prisms served as the polarizer and the analyzer, respectively, and provided an extinction ratio of 10^{-6} .

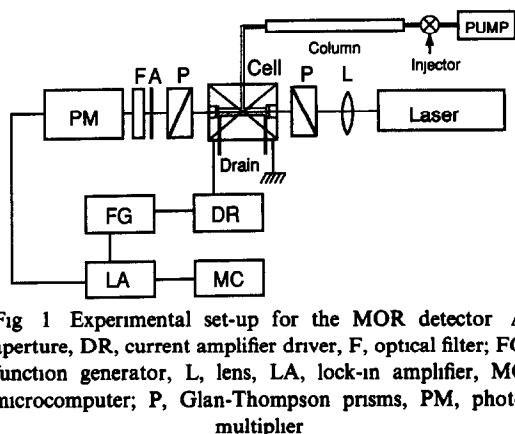


Fig 1 Experimental set-up for the MOR detector A, aperture, DR, current amplifier driver, F, optical filter; FG, function generator, L, lens, LA, lock-in amplifier, MC, microcomputer; P, Glan-Thompson prisms, PM, photomultiplier

The flow cell was made of aluminum with $8\text{-}\mu\text{l}$ volume bores (10-mm long and 1-mm in diameter) and had a central inlet and two side outlets.¹³ This design provided more linear analytical curves than the conventional one with a Z-type inlet and outlet because the laser beam deflection from RI change was small. A coil of 500 turns of 0.8-mm diameter wire was wound round the cell as the modulator of the magnetic field. A 2-A dc current produced a magnetic field strength of 300 G at the flow region. Experiments were carried out at room temperature with no temperature control.

A photomultiplier (Hamamatsu R1333) detected the light traversing the polarizers and an optical filter. The photomultiplier was connected to a lock-in amplifier (NF Circuit 5610B) through a current amplifier (NF Circuit LI-76). The strength of the magnetic field in the flow cell was modulated to a square wave by a bipolar power supply (Metronix BPA182A). A function generator (Kenwood FG273) provided a reference oscillation to the lock-in amplifier and the bipolar power supply. The recovering MOR signal was displayed on a chart recorder. For frequency distribution measurements we calculated fast Fourier transformation (FFT) of the output of the current amplifier with a 12-bit A/D converter (Canopus ANALOG-PRO) and a microcomputer (NEC PC9801).

Chromatography

The chromatography system consisted of an injector with a $20\text{-}\mu\text{l}$ loop (Rheodyne 7413) and a pump (JASCO 880-PU) operated at a flow-rate of 0.5 ml/min. Gel chromatography of polyethylene glycol (PEG) was performed on a 10-cm \times 0.76-cm column (Asahipak GS-310M) with distilled water as the eluent. For part of the measurements the sample was injected directly

into the flow system without a column to eliminate the dilution. All chemicals were of analytical reagent grade.

RESULTS AND DISCUSSION

Modern polarimetry uses an AC modulation technique to improve the signal to noise ratio (S/N).^{8,12} Three typical polarization modulation modes are shown in Fig. 2. The plane of the linearly polarized light is modulated by an angle, α , which is produced through MOR of the solvent itself for the simple and sensitive instrumentation. The amount and direction of the modulation angle, α , can be controlled by the current fed to the coil around the cell. The angle β is MOR due to the solute. Transmitted light intensity is the square of the projection amplitude of an electric vector and is proportional to the square of a rotating angle at $\sin(\text{angle}) \ll 1$. Mode A in Fig. 2 illustrates the simplest operation; the polarization modulates by equal negative and positive angles ($-\alpha$ and $+\alpha$) from the polarizer-analyzer cross alignment. This mode is generally used in optical activity measurements.¹⁰ However, in MOR detection this operation compensates for a MOR change of the solution in the output of the lock-in amplifier. Therefore modes B and C in

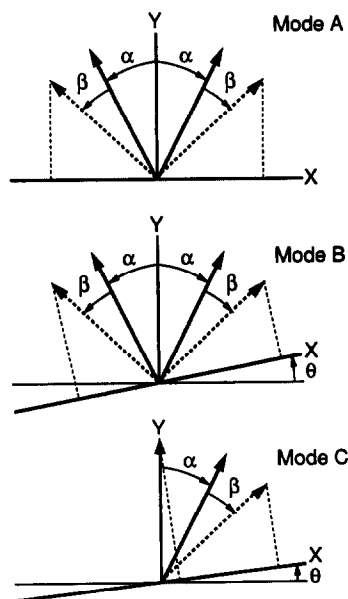


Fig. 2 Three typical polarization modulation diagrams for the MOR detector. Solid and dashed vector represents an electric field of polarized light when a sample is present and absent, respectively. α , modulation angle produced through MOR of the solvent itself; β , MOR due to the solute, θ , offset angle. The X and Y axes correspond to polarization planes of the analyzer and polarizer, respectively

Fig. 2 would be more suitable for the MOR detection. In mode B, the polarization modulates in the same manner as in mode A. In addition, an offset angle, θ , is applied; θ is the angle of the analyzer away from the polarizer-analyzer cross alignment. In mode C, the polarization modulates by the positive angle, $+\alpha$, with the offset angle, θ .

The intensity of light transmitted through the optical system, I_T , is given by¹⁴

$$I_T(\theta, \omega) = I_0[\epsilon \cos^2(\theta + \omega) + (1 + \epsilon^2/4) \sin^2(\theta + \omega)] \quad (1)$$

where ϵ is the extinction ratio of the polarizer and analyzer and ω is the amount of rotation caused by a sample. At a low concentration, ω is a simple sum of MOR's due to the solvent and solute.⁶ Fluctuations of I_T determine noise in the MOR measurement. The S/N ratio of the modulation modes B and C may be described by

$$\frac{S/N_{\text{mode B}}}{=} \frac{[I_T(\theta, \alpha + \beta) - I_T(\theta, \alpha)] - [I_T(\theta, -\alpha - \beta) - I_T(\theta, -\alpha)]}{f_{dc} I_T(\theta, 0) + f_{ac} [I_T(\theta, \alpha) - I_T(\theta, -\alpha)]} \quad (2)$$

and

$$\frac{S/N_{\text{mode C}}}{=} \frac{I_T(\theta, \alpha + \beta) - I_T(\theta, \alpha)}{f_{dc} I_T(\theta, 0) + f_{ac} [I_T(\theta, \alpha) - I_T(\theta, 0)]} \quad (3)$$

respectively, where f_{dc} and f_{ac} are the fluctuation of the dc and ac components, respectively, at the detection frequency of the lock-in amplifier. We can calculate S/N for various combinations of ϵ , θ , f_{dc} and f_{ac} .

Figure 3 shows dependencies of S/N on the offset angle and the extinction ratio (10^{-6} and 10^{-9}) for a 0.1% (w/w) phenol solution in modes B and C. Lines are calculated with equations (1)–(3). The dependencies of S/N are determined by the balance between the increases in the signal component, $\sin(\beta + \theta)$ and the leak of light with θ . The fluctuations, f_{dc} and f_{ac} , are parameters for fitting the observed values. Observed values were obtained in direct injection operation with the He-Ne laser and the modulation of the magnetic field at 100 Hz and 300 G. The 0.1% (w/w) phenol aqueous solution provides $\alpha = 0.065^\circ$ and $\beta = 1.5 \times 10^{-4}$ at the optical length of 10 mm and with a magnetic field intensity of 300 G. The Verdet constant of water and phenol is 2.2×10^{-4} and 5.3×10^{-4} deg/G cm,¹⁵ respectively. The opti-

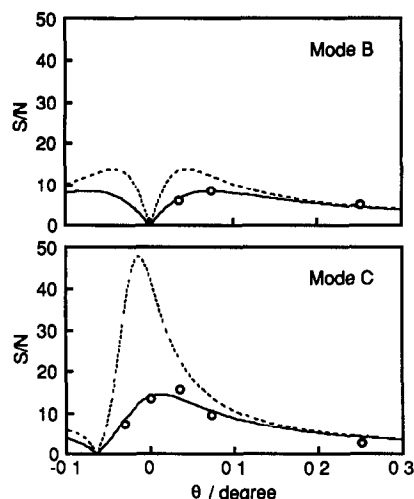


Fig. 3 Dependence of S/N on the offset angle and the extinction ratio for a 0.1% (w/w) phenol solution \circ , observed in mode B and C, respectively, solid line calculated with $\epsilon = 10^{-6}$, dashed line calculated with $\epsilon = 10^{-9}$

imum f_{dc} and f_{ac} is 2.8×10^{-4} and 1.1×10^{-4} , respectively. Both observed and calculated dependencies of S/N on θ agree with each other. The mode B with a modulation by $-\alpha$ and $+\alpha$ requires a certain offset angle to avoid the disappearance of the MOR signal. In mode C, S/N is the largest around the polarizer-analyzer cross alignment ($\theta = 0$). The S/N ratio with the extinction ratio of 10^{-9} is a few times larger than that with 10^{-6} , as shown with dashed lines in Fig. 3. A pair of Glan-Thompson prisms, that serve as the polarizer and analyzer, respectively, with a better extinction ratio should improve the sensitivity. At any conditions, strengthening of the magnetic field increases S/N in a straightforward manner. Since mode C provides a larger S/N at any offset angle than mode B, the following chromatographic measurements were carried out in mode C with an offset angle of 0–0.03°.

The output stability of the light source is important since the fluctuations, f_{dc} and f_{ac} , affect S/N linearly. The frequency distribution of the light intensity fluctuation has been measured to evaluate the optimum modulation frequency, as shown in Fig. 4. Figure 4(a) shows the noise without the laser light and the strength of the magnetic field calibrated by the MOR signal of water in the cell. Peaks at 60 Hz correspond to line noise in the electronics. In Fig. 4(b) and (c), a peak around 300 Hz indicates a MOR signal of water of 0.04° . The longitudinal axis at 0 dB corresponds to the DC component of the light transmitted through the

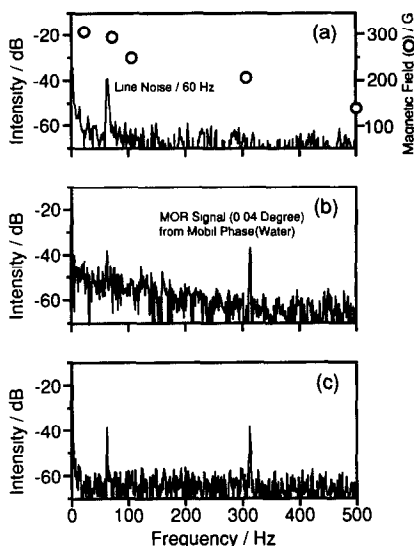


Fig 4 Frequency distribution of intensity fluctuation of light transmitted through the optical system, (a) no laser, (b) He-Ne laser, (c) semiconductor laser. No offset angle is applied

polarizer and analyzer. The strength of the magnetic field decreases with increasing modulation frequency due to the induction effect of the coil. The noise level of the He-Ne laser is higher than that of the semiconductor laser, especially at less than 200 Hz. Gas discharge lasers such as He-Ne or Ar ion ones have larger noise, a typical drift and flicker component is about 1–5% and 0.1–1%, respectively. On the other hand, the output of the semiconductor laser is very stable, because direct conversion of the electronic energy to light can easily control the output with a simple electronic feedback circuit. Both drift and flicker noise of the semiconductor laser can be reduced by the order of 10^{-5} ^{12,16}. We have chosen a modulation frequency of 300 Hz at which the conflict between the increase in noise and the decrease in the strength of the magnetic field is small.

Figure 5 presents the MOR signal of 0.03% (w/w) and 0.015% (w/w) PEG 20000 (average molecular weight: 18000–25000) aqueous solution with the He-Ne laser and the semiconductor laser, respectively. The 20- μ l sample was injected directly into the flow system. The strength of the magnetic field, the modulation frequency and the time constant of the lock-in amplifier are 200 G, 300 Hz and 300 msec, respectively. The background low frequency noise, the so-called drift, improves dramatically by about one order of magnitude when employing the semiconductor laser, even without temperature stabilization. This corresponds to a

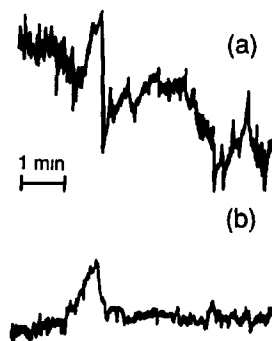


Fig 5 MOR signal from polyethylene glycol 20000 aqueous solution in the flow system; (a) 0.03% (w/w) conc with He-Ne laser, (b) 0.015% (w/w) conc with semiconductor laser. Offset angle is 0.03°.

good S/N of the semiconductor laser at low frequency in the fluctuation distribution measurements; the noise intensity of the semiconductor laser is 15 dB (about 5 times) smaller than that of the He-Ne laser in Fig. 4. The high frequency noise also improves by about two orders of magnitude. The detection limit at $S/N = 3$ is 4 μ g (0.02%) and 1.2 μ g (0.006%) for the use of the He-Ne laser and the semiconductor laser, respectively, for the direct injection operation. The analytical curves are linear up to 3% and increase monotonically up to 10%. Apparent peaks due to the RI change disturb the signal peak in the high concentration region. The μ g-order detectability for the MOR-based detector is comparable to the conventional RI detector.

The gel chromatography for optically transparent samples is an appropriate demonstration of the usefulness of the MOR flow detector. Figure 6 shows a chromatogram of a 20- μ l injection of 1% (w/w) PEG 6000 and 2000 (average molecular weight: 7400–9000 and 1800–2200, respectively) mixture, using the

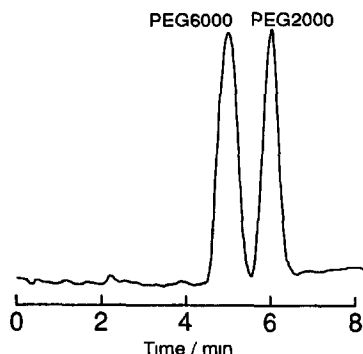


Fig 6 Gel chromatogram of polyethylene glycol (PEG) 6000 and 2000 aqueous solution. Column, Asahipack GS-310M, mobile phase, water, flow-rate, 0.5 ml/min; sample, 1.0% (w/w) each (20- μ l injection)

semiconductor laser. The strength of the magnetic field, the modulation frequency and the time constant of the lock-in amplifier are 200 G, 300 Hz and 3 sec, respectively. The detection limit of PEG 6000 is 8 μg (0.04%) in our chromatography system.

In conclusion, we have demonstrated a HPLC detector with a new principle based on MOR that provides universal response. It will be an alternative to the RI detector. This apparatus is capable of natural optical activity measurement, which is very important in biological studies. In addition, several essential molecules, such as steroids and fatty acids exhibit limited absorptions in the UV and visible spectrum and hence the application of this detector to clinical and environmental research will be useful.

Acknowledgements—The authors thank Dr. Hizkata and T. Sakane of Sharp Corp for supplying the semiconductor laser chips. This work is partially supported by a Grants-in-Aid for Scientific Research (No. 02855180) from the Ministry of Education of Japan.

Following submission of this paper, a report by Xi and Yeung appeared that described the same principle reported here, with differences in instrumentation and performance.¹⁷

REFERENCES

1. E. S. Yeung, in *Analytical Application of Lasers*, E. H. Piepmeier (ed.), Chap 17, p 557. Wiley, New York, 1986.
2. D. O. Hancock and R. E. Synovec *Anal Chem*, 1988, **60**, 1915
3. D. Ishii and T. Takeuchi, *J. Liq. Chromatog*, 1988, **11**, 1865.
4. T. Takeuchi and E. S. Yeung, *J. Chromatog*, 1986, **366**, 145
5. S. R. Erskine and D. R. Bobbitt, *Anal Chem*, 1989, **61**, 910
6. H. Kawazumi, H. Nishimura and T. Ogawa, *Anal Sci*, 1990, **6**, 135
7. E. Hecht, *Optics*, 2nd Ed., p 316, Addison-Wesley, Reading Mass., 1987.
8. E. S. Yeung, L. E. Steenhoek, S. D. Woodruff and J. C. Kuo, *Anal. Chem*, 1980, **52**, 1399
9. V. S. Zapassku, *Opt. Spectrosc. (USSR)*, 1982, **52**, 667
10. D. R. Bobbitt and E. S. Yeung, *Appl. Spectrosc*, 1986, **40**, 407.
11. J. J. Kankare and R. Stephens, *Talanta*, 1986, **33**, 571.
12. D. K. Lloyd, D. M. Goodall and H. Scrivener, *Anal Chem.*, 1989, **61**, 1238.
13. H. Felton, *J. Chromatog. Sci.*, 1969, **7**, 13.
14. E. S. Yeung, *Talanta*, 1985, **32**, 1097.
15. *CRC Handbook of Chemistry and Physics*, 63rd Ed., R. C. Weast (ed.), p E406. CRC Press, Boca Raton, 1982.
16. K. Sauda, T. Imasaka and N. Ishibashi, *Anal Chem*, 1986, **58**, 2649
17. X. Xi and E. S. Yeung, *ibid*, 1991, **63**, 490

SEPARATION OF NIOBIUM AND TANTALUM BY EXTRACTION CHROMATOGRAPHY WITH BIS(2-ETHYLHEXYL)PHOSPHORIC ACID

YI YU VIN and S. M. KHOPKAR*

Department of Chemistry, Indian Institute of Technology, Bombay 400 076, India

(Received 22 January 1990 Revised 24 February 1991. Accepted 5 March 1991)

Summary—A novel method is developed for the reversed-phase extractive chromatographic separation of niobium and tantalum with bis(2-ethylhexyl)phosphoric acid. Niobium is extracted from 1–10*M* hydrochloric acid and can be stripped with 3*M* sulphuric acid containing 2% hydrogen peroxide. Tantalum is extracted from 0.1–2*M* hydrochloric acid and can be stripped with 0.1*M* hydrochloric acid containing 2*M* tartaric acid. It is possible to separate niobium and tantalum, in different ratios, from multicomponent mixtures.

Tributyl phosphate¹⁻⁴ has been used as the stationary phase for the extractive chromatographic separation of niobium and tantalum, with hydrochloric acid and hydrogen peroxide as stripping agents. Aliquat 336^{5,6} and trioctylamine⁷⁻⁹ have also been used to separate niobium and tantalum, with ammonium fluoride and ammonium chloride as stripping agents. Thenoyltrifluoroacetone¹⁰ and methyl isobutyl ketone¹¹ were found not to be effective as extractants for niobium and tantalum.

Bis(2-ethylhexyl)phosphoric acid (HDEHP) gives quantitative extraction of niobium and tantalum from a tartaric/oxalic acid mixture,¹²⁻¹⁶ but this system has not been applied in extraction chromatography.

The present work investigated the extractive chromatographic separation of niobium and tantalum from each other and from other elements. The method was extended to the determination of these metals in real samples.

EXPERIMENTAL

Apparatus

A borosilicate glass chromatography column packed with silica gel was made as described earlier.¹⁷

Reagents

Bis(2-ethylhexyl)phosphoric acid (Schuchardt, Munich) was used without further purification.

The stock solution of niobium was prepared by fusing 100 mg of niobium pentoxide with 5 g of potassium bisulphate in a platinum crucible. The cooled mass was dissolved in 5 ml of 200 mg/ml tartaric acid solution, made up to 100 ml with distilled water and standardized gravimetrically with *N*-benzoyl-*N*-phenylhydroxylamine;¹⁸ it was found to contain 0.68 mg/ml niobium. A solution containing 40 µg/ml niobium was prepared by appropriate dilution.

The stock solution of tantalum was prepared by fusing 100 mg of tantalum pentoxide (Aldrich) with 5 g of potassium pyrosulphate. The cooled melt was dissolved with 2 ml of 50-mg/ml ammonium oxalate solution, diluted to 100 ml with distilled water and standardized gravimetrically with selenious acid;¹⁹ it was found to contain 0.81 mg/ml tantalum. A solution containing 20 µg/ml was prepared by appropriate dilution.

Procedure

Concentrated hydrochloric acid was added to a known volume of solution containing 40 µg of niobium or 20 µg of tantalum. The solution was passed through the column at a flow-rate of 1 ml/min. The extracted niobium or tantalum was stripped with a suitable stripping agent. Twenty 2-ml fractions were collected and analysed spectrophotometrically, for niobium with 4-(2-thiazolylazo)resorcinol²⁰ and tantalum with Brilliant Green.^{21,22}

*Author for correspondence

RESULTS AND DISCUSSION

Extraction conditions

Niobium and tantalum were found to be quantitatively extracted from 1–10 and 0.1–2M hydrochloric acid respectively (Fig. 1).

Stripping agents

None of the mineral acids in any concentration range was effective for stripping niobium and tantalum. However, niobium can be completely stripped with 3–4M sulphuric acid containing 2–3% hydrogen peroxide, and tantalum completely stripped with 0.1M hydrochloric acid containing 1.5–3M tartaric acid, and partially stripped with 3–4M sulphuric acid containing 2–3% hydrogen peroxide.

Separation from binary mixtures

The different conditions required for stripping niobium or tantalum were exploited to devise several separation methods. When niobium was extracted from 2M hydrochloric acid or tantalum was extracted from 0.1M hydrochloric acid in the presence of one of the other ions listed in Table 1, most accompanying ions were not extracted and so passed through the column. When the accompanying ion, *e.g.*, iron, was co-extracted, it was stripped with mineral acid before niobium was stripped with 3M sulphuric acid containing 2% hydrogen peroxide or tantalum with 0.1M hydrochloric acid containing 2M tartaric acid (Table 1).

Separation of niobium from tantalum

As shown in Fig. 1, niobium and tantalum can both be extracted from 1–2M hydrochloric acid

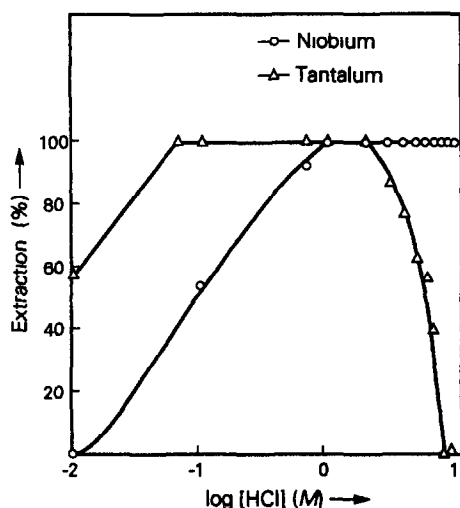


Fig. 1 Effect of hydrochloric acid concentration on extraction of niobium and tantalum

Table 1 Separation of niobium and tantalum from binary mixtures (Nb 40 μ g, stripped with 3M H₂SO₄ + 2% H₂O₂; Ta 20 μ g, stripped with 0.1M HCl + 2M tartaric acid; most other ions pass unextracted through the column)

Foreign ion	Foreign ion amount, mg	Amount found, mg	
		Nb	Ta
Li(I)	5.0	40.1	19.9
Na(I)	4.9	39.8	19.2
K(I)	5.0	41.0	20.1
Rb(I)	5.0	38.5	19.8
Mg(II)	4.8	40.1	19.6
Ca(II)	5.0	40.2	20.2
Sr(II)	5.0	40.4	19.4
Al(II)	5.0	39.6	19.9
Pb(II)	5.4	40.2	19.8
As(V)	5.2	40.1	20.1
Bi(III)	4.5	39.9	19.4
Sb(III)	3.9	38.9	19.3
Se(IV)	4.8	39.9	19.2
Te(IV)	4.6	39.8	20.0
Cr(III)	2.4	41.0	20.1
Mn(II)	5.0	39.9	19.6
Fe(III)*	4.9	39.8	20.0
Co(II)	4.8	38.9	19.8
Ni(II)	4.8	39.9	19.7
Cu(II)	5.2	40.0	19.8
Cd(II)	3.8	39.7	19.9
V(V)	2.4	39.4	19.4

*Co-extracted, stripped with 3M hydrochloric acid before Nb or Ta

acid, but Table 2 shows that they can be separated if the tantalum is stripped first, with 0.1M hydrochloric acid/2M tartaric acid mixture, and then the niobium with 3M sulphuric acid containing 2% hydrogen peroxide (Table 2).

Separation of niobium or tantalum from multi-component mixtures

The optimum conditions for the extraction and stripping of various metals are summarized in Table 3. Gallium, indium, iron, tin, antimony, bismuth, vanadium, titanium, beryllium, molybdenum, tantalum and (partially) niobium are extractable from 0.1M hydrochloric acid, whereas only germanium, thorium and niobium are extracted from 10M hydrochloric acid.

Table 2 Extraction and stripping conditions for niobium and tantalum (Nb 40 μ g; Ta 20 μ g)

Conditions		Nb	Ta
		Extracted, %	
Extraction from	0.1M HCl	54.0	99.6
	1M HCl	99.6	100.2
	2M HCl	99.8	99.9
		Recovery, %	
Stripping with	3M H ₂ SO ₄ + 2% H ₂ O ₂	99.9	40.9
	0.1M HCl + 2M tartaric acid	0	100.4

These differences in behaviour can be exploited for multicomponent analyses, provided proper stripping sequences are used. Table 4 gives some examples.

When a mixture of manganese, iron, thorium, niobium and uranium in 2M hydrochloric acid was passed through the column, all except manganese were extracted. They were then stripped in succession, iron with 3M hydrochloric acid, thorium with 3M phosphoric acid, niobium with 3M sulphuric acid containing 2% hydrogen peroxide and uranium with 6M hydrochloric acid containing 0.1M ascorbic acid.

The separation of a mixture of chromium, iron, tantalum and niobium in 2M hydrochloric acid was similarly achieved; chromium was not extracted, iron was stripped with 3M hydrochloric acid, tantalum with 0.1M hydrochloric acid containing 2M tartaric acid and niobium with 3M sulphuric acid containing 2% hydrogen peroxide.

A five-component mixture (in 0.1M hydrochloric acid) containing nickel, bismuth, antimony, tin and tantalum was separated by passing it through the column. All the components except nickel were extracted. Bismuth was then stripped with 0.5M hydrochloric acid,

antimony with 3M nitric acid, tin with 5M hydrochloric acid and tantalum with 0.1M hydrochloric acid containing 2M tartaric acid.

A mixture of vanadium (or lead or bismuth or chromium), tantalum (or molybdenum) and niobium in 2M hydrochloric acid was separated, only the tantalum, molybdenum and niobium being extracted. Molybdenum was stripped first with 0.1M hydrochloric acid containing 0.2M tartaric acid, or tantalum with 0.1M hydrochloric acid containing 2M tartaric acid, and finally niobium with 3M sulphuric acid containing 2% hydrogen peroxide.

The mixture of copper or bismuth or aluminium with vanadium (or iron), tantalum and titanium was resolved by making it 0.1M in hydrochloric acid before passage through the column. The copper or bismuth or aluminium was not extracted. Vanadium or iron was stripped with 3M hydrochloric acid, tantalum with 0.1M hydrochloric acid containing 2M tartaric acid and finally titanium with 2.5M sulphuric acid containing 3% hydrogen peroxide.

Determination of niobium in stainless steel

About 0.5 g of steel was dissolved in a mixture of hydrochloric and hydrofluoric acids (2:1 v/v).

Table 3 Extraction and stripping conditions for various metals

Element	Extraction from HCl, M	Stripping agents			
		HCl, M	HNO ₃ , M	H ₂ SO ₄ , M	Others
Be(II)	0.01-0.25	1-3	2-3	1-2	—
Ge(IV)	6-10	0.25-3	0.25-3	1-4	0.01M citric acid (pH 3.5) 0.1M oxalic acid (pH 1.0)
Sn(IV)	0.01-0.75	5-7	—	—	—
Sb(III)	0.005-0.5	2-8	1-8	1-8	—
Bi(III)	0.01-0.1	0.5-3	2-3	4-5	—
Pb(II)	0.001-0.05	0.1-4	1-4	—	0.1-4M HClO ₄
Ti(IV)	0.01-4	—	—	2.5 + 3% H ₂ O ₂	—
Th(IV)	1-10	—	—	—	3M H ₃ PO ₄
V(V)	0.1-0.5	2-6	—	—	—
Nb(V)	1-10	—	—	3-5 + 2% H ₂ O ₂	—
Ta(V)	0.05-2	0.1 + 2-3M tartaric acid	—	—	—
Ga(III)	0.01-0.1	0.25	—	—	—
In(III)	0.01-0.1	0.25	—	—	—
Cu(II)	0.01	0.1	—	—	—
Zn(II)	0.01	0.1	—	—	—
Fe(III)	0.01-2	2-6	—	—	—
Co(II)	0.01	0.1	—	—	—
Ni(II)	0.01	0.1	—	—	—
Mn(II)	0.01	0.1	—	—	—
Mo(VI)	0.01-2	0.1 + 0.2M tartaric acid	—	—	—
U(VI)	0.05-2	—	—	—	6M HCl + 0.1M ascorbic acid
Cr(V)	0.01	0.1	—	—	—

Table 4 Separation of niobium and tantalum from multi-component mixtures

No	Mixtures	Amount taken, μg	Recovery, %	Stripping agent	Volume of stripping agent, ml	Determined spectrophotometrically with
1	Mn	100	98.9	Not extracted	16	Formaloxime
	Fe	50	100.4	3M HCl	20	1,10-Phenanthroline
	Th	50	98.8	3M H_3PO_4	20	Arsenazo III
	Nb	40	99.4	3M H_2SO_4 + 2% H_2O_2	20	TAR
	U	25	98.2	6M HCl + 0.1M ascorbic acid	20	Arsenazo III
2	Cr	50	99.8	Not extracted	18	Diphenylcarbazide
	Fe	50	100.6	3M HCl	20	1,10-Phenanthroline
	Ta	20	98.9	0.1M HCl + 2M tartaric acid	20	Brilliant Green
	Nb	40	100	3M H_2SO_4 + 2% H_2O_2	20	TAR
3	Ni	100	99.2	Not extracted	16	PAR
	Bi	100	100.2	0.5M HCl	18	Iodide
	Sb	50	99.0	3M HNO_3	18	Phenylfluorone
	Sn	60	98.3	5M HCl	22	Pyrocatechol Violet
	Ta	20	99.0	0.1M HCl + 2M tartaric acid	20	Brilliant Green
4	V/Pb/Bi/Cr	150	98.5	Not extracted	18	Hydrogen peroxide/dithizone/iodide/diphenylcarbazide
	Ta or Mo	20	99.5	0.1M HCl + 2M tartaric acid	20	Brilliant Green/Tiron
	Nb	40	99.4	3M H_2SO_4 + 2% H_2O_2	20	TAR
5	Cu/Bi/Al	100	99.4	Not extracted	16	Cupral/iodide/Alizarin Red S
	V/Fe	150	100.3	2M HCl	20	Hydrogen peroxide/1,10-phenanthroline
	Ta	20	99.0	0.1M HCl + 2M tartaric acid	20	Brilliant Green
	Ti	150	98.6	2.5M H_2SO_4 + 3% H_2O_2	20	Hydrogen peroxide

The solution was evaporated almost to dryness, the salts were taken up by addition of 2 ml of 200 mg/ml tartaric acid solution and the solution was made up to volume in a 100-ml standard flask with distilled water. An aliquot was made 2M in hydrochloric acid, and passed through the column. Niobium and iron were extracted, and chromium, nickel and manganese passed through the column. The iron was stripped with 3M hydrochloric acid and niobium with 3M sulphuric acid containing 2% hydrogen peroxide. The niobium content was found to be 1.05, 1.03 and 1.04% (certified value 1.02%).

The proposed method is simple, rapid and selective. The separation of niobium and tantalum from each other and from chromium, molybdenum, iron, vanadium and tin is important, as these are associated in various types of steel. The total time required for separation

and determination of niobium and tantalum is 45 min.

REFERENCES

- 1 J. Minczewski and C. Rózycki, *Chem Anal Warsaw*, 1965, **10**, 965
- 2 R. Denig, N. Trautmann and G. Hermann, *J Radioanal Chem*, 1970, **6**, 331
- 3 I. P. Alimarin, I. M. Gibalo and L. A. Lapenko, *Vestn Mosk Univ Khim*, 1972, **13**, 435, *Chem Abstr*, 1973, **78**, 11124e
- 4 R. Caletka and V. Krivan, *Z Anal Chem*, 1985, **321**, 61
- 5 N. R. Das and P. Chattopadhyay, *J. Radioanal Nucl Chem.*, 1987, **109**, 45
- 6 I. Stronski, *Radiochem Radioanal. Lett.*, 1969, **1**, 191.
- 7 I. M. Gibalo and N. A. Mymrik, *Zh Analit Khim.*, 1971, **26**, 918
- 8 T. B. Pierce and W. M. Henry, *J Chromatog*, 1966, **23**, 457.
- 9 I. M. Gibalo and N. A. Mymrik, *Zh Analit Khim*, 1970, **25**, 1744

- 10 R Caletka, *Chem Listy*, 1968, **62**, 669, *Chem Abstr*, 1968, **69**, 40419
- 11 J S Fritz and L H Dahmer, *Anal Chem*, 1968, **40**, 20
- 12 K Kimura, *Bull Chem Soc Japan*, 1960, **33**, 1038
- 13 *Idem, ibid.*, 1961, **34**, 63
- 14 N R Das, B Nandi and S N Bhattacharyya, *Int J Appl Radiat Isot*, 1981, **32**, 205
- 15 S N Bhattacharyya and B N Ganguly, *J Radioanal Nucl Chem*, 1986, **98**, 247
- 16 N R Das, B Nandi and S N Bhattacharyya, *J Radioanal Chem*, 1981, **62**, 53
- 17 Y Y Vin and S. M. Khopkar, *Talanta*, 1989, **36**, 1285
- 18 A K Majumdar and A K. Mukherjee, *Anal. Chim. Acta*, 1958, **19**, 23
- 19 A N Nevzorov, N S. Onoprienko and S. N Mordvinova, *Zavodsk. Lab*, 1970, **36**, 1176; *Anal Abstr.*, 1971, **21**, 1052
- 20 V Patrovský, *Talanta*, 1965, **12**, 971.
- 21 A I Busev, V G Tiptsova and V M. Ivanov, *Analytical Chemistry of Rare Elements*, p. 216 Mir, Moscow, 1981.
- 22 F D Snell, *Photometric and Fluorometric Methods of Analysis*, Parts I and II, Wiley-Interscience, New York, 1978

POLAROGRAPHIC DETERMINATION OF FLUORIDE USING THE ADSORPTION WAVE OF THE Ce(III)-ALIZARIN COMPLEXONE-FLUORIDE COMPLEX

LU GUANGHAN, LI XIAOMING, HE ZHIKE and HU SHUANGLONG

Department of Chemistry, Central China Normal University, Wuhan, 430070, People's Republic of China

(Received 3 January 1991. Revised 3 March 1991. Accepted 13 March 1991)

Summary—A very sensitive electrochemical method for trace measurement of fluoride in water is discussed. The complex of cerium(III) with alizarin complexone (ALC) and fluoride ion is adsorbed at the dropping mercury electrode. In cathodic sweeps, the peak height is directly proportional to the concentration of fluoride over the range 8×10^{-8} – $5 \times 10^{-6}M$ (1.5×10^{-9} – 9.5×10^{-8} g/ml), and the detection limit is $5 \times 10^{-8}M$ (9.5×10^{-10} g/ml). The proposed method was applied to the determination of fluoride in water

Fluorine is a very important element in nature. A large number of methods for the determination of fluoride have been reported, principally colorimetric ones.¹⁻⁷ A fluoride-selective electrode was used for the determination of trace fluoride.^{8,9} However, the sensitivity of these methods is not very high and the range of detection is only about 5×10^{-6} – $2 \times 10^{-5}M$. Recently, a polarographic method for determination of fluoride in the presence of La(III) and alizarin complexone (ALC) has been studied.¹⁰ However, reaction equilibration is required for about 2 hr before the potential scan is carried out. The linear range of the method is 1×10^{-7} – $6 \times 10^{-6}M$. In this report, we have investigated the electrochemical behaviour of the Ce(III)-ALC-F⁻ complex in aqueous solution by single-sweep polarography and cyclic voltammetry. The reaction is equilibrated for about 30 min before the potential scan is carried out. The linear range is 8×10^{-8} – $5 \times 10^{-6}M$ (1.5×10^{-9} – 9.5×10^{-8} g/ml), with a detection limit of $5 \times 10^{-8}M$ (9.5×10^{-10} g/ml).

EXPERIMENTAL

Apparatus

A Model JP-2A oscillopolarograph (Chengdu Instrumental Factory, China) was used. A three-electrode system was used with a dropping mercury working electrode (DME). The reference and counter electrodes were saturated calomel and platinum wire electrodes respectively. A Model 82-1 neopolarograph (Lisui

Electronic Factory, China) was used for cyclic voltammetry, with a three-electrode system consisting of a hanging mercury drop electrode as working electrode, a saturated calomel reference electrode and a platinum counter-electrode. A Model pHs-3 meter (Shanghai, China) was used for pH determinations. The electrolytic cell was a 10-ml beaker

Reagents

All solutions were prepared from analytical-reagent grade chemicals and doubly-distilled water.

Stock solutions of F⁻ were prepared by dissolving sodium fluoride in water. Standard solutions were obtained by diluting the stock solutions with water.

A $5 \times 10^{-4}M$ Ce(III) stock solution was prepared by weighing and dissolving 0.1085 g of cerium nitrate [Ce(NO₃)₃.6H₂O] in 450 ml of water. The pH was adjusted to *ca.* 4.8 with 1M nitric acid and the solution was diluted to 500 ml with water.

A $1 \times 10^{-3}M$ stock solution of alizarin complexone (ALC) was prepared by dissolving 0.0964 g of ALC in 2M sodium hydroxide and neutralizing the solution to a yellow colour with 2M nitric acid,¹¹ and then diluting to 250 ml with water.

A 1M hexamethylene tetramine [(CH₂)₆N₄] solution was prepared by weighing and dissolving 70 g of (CH₂)₆N₄ and 50 g of potassium nitrate in 450 ml of hot water. The pH was adjusted to *ca.* 4.8 with 2M nitric acid.

Procedure

To the standard or sample solution (8×10^{-8} – $5 \times 10^{-6} M$ fluoride), add 1.0 ml of $1 M (CH_2)_6N_4$, 0.1 ml of $1 \times 10^{-3} M$ ALC, 1.0 ml of $5 \times 10^{-4} M$ Ce(III) and 1.0 ml of acetone. Allow to stand for about 30 min and then dilute the solution to 10 ml with water. The derivative single-sweep polarogram is then recorded from $-0.3 V$ to $-0.8 V$ (*vs.* SCE) and the height of the peak measured at $-0.64 V$ (Fig. 1).

RESULTS AND DISCUSSION

Selection of experimental conditions

The effects of pH and the concentrations of Ce(III) and ALC on peak height are shown in Fig. 2. The optimum conditions for the determination are $5 \times 10^{-5} M$ Ce(III) and $1 \times 10^{-5} M$ ALC. The optimum pH is about 4.8. It was also found that acetone can reduce the formation time of the Ce(III)–ALC– F^- complex. The optimum concentration of acetone is 10%.

Effect of standing time

In order to obtain a stable peak height, the solution to be analysed was required to stand for some time; a 30-min period was found to be optimum.

Under the optimum conditions, the relationship between peak height and concentration of F^- was linear from $8 \times 10^{-8} M$ to $5 \times 10^{-6} M$ (correlation coefficient = 0.9976). A detection limit of $5 \times 10^{-8} M$ was obtained (concentration

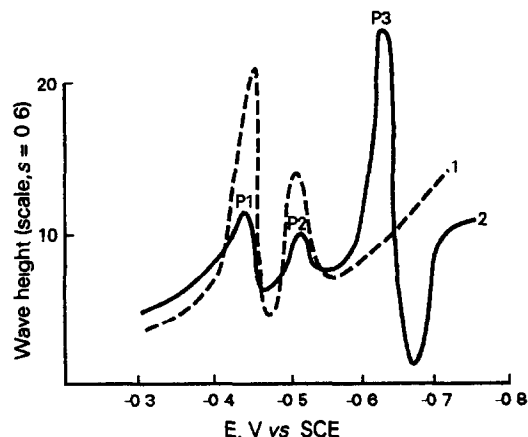


Fig 1 Derivative single sweep polarogram of the Ce(III)–ALC– F^- complex. Curve 1, $0.1 M (CH_2)_6N_4$, 10% acetone, $1 \times 10^{-3} M$ ALC, $5 \times 10^{-5} M$ Ce(III), pH = 4.8. Curve 2, Conditions as for curve 1 plus $3 \times 10^{-6} M F^-$. P₁, ALC; P₂, ALC–Ce(III) complex peak; P₃, Ce(III)–ALC– F^- complex peak.

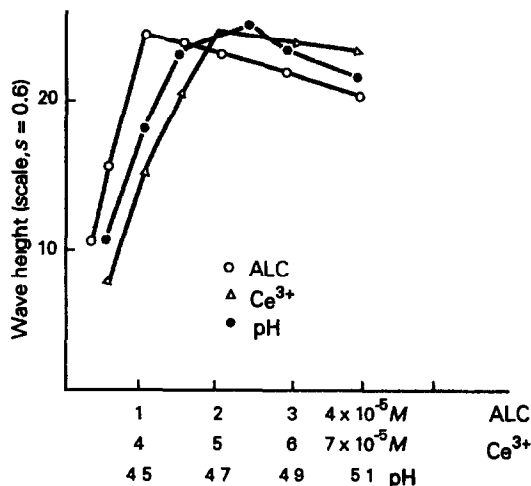


Fig 2 Effect of supporting electrolyte concentration on peak height of Ce(III)–ALC– F^- complex, $F^- = 3 \times 10^{-6} M$

giving a signal equal to three times the standard deviation of the blank).

Effect of foreign ions

The experimental results show that 2000-fold K^+ , Na^+ , Cl^- , NO_3^- and NO_2^- ; 1000-fold Ca(II) and Mg(II); 600-fold Ni(II); 100-fold Pb(II); 70-fold Zn(II), Cu(II) and Co(II); 50-fold Cr(III) and Mo(VI); 40-fold Fe(III) and PO_4^{3-} and 10-fold Cd(II) have no effect on the determination of F^- (0.05 ppm).

Properties of the polarographic wave

Electrocapillary curves. These curves can give some information about the adsorption of a particular species. A solution containing F^- has an electrocapillary curve lower than that of the supporting electrolyte (Fig. 3) because the adsorption of the Ce(III)–ALC– F^- complex on the surface of the DME changes the surface

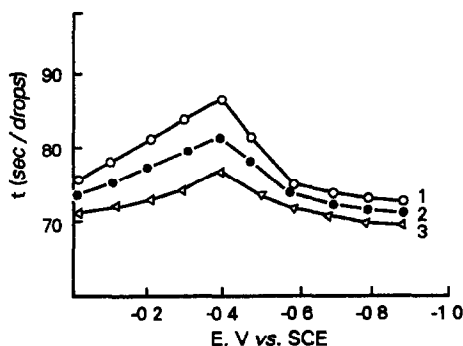


Fig 3 Electrocapillary curves. Curve 1, $0.1 M (CH_2)_6N_4$, 10% acetone, $1 \times 10^{-5} M$ ALC, pH = 4.8. Curve 2, Conditions as for curve 1 plus $5 \times 10^{-5} M$ Ce(III). Curve 3, Conditions as for curve 2 plus $3 \times 10^{-6} M F^-$.

Table 1. Analytical results for fluoride in some natural samples

Sample	n*	Mean value, ppm	sd†, ppm	Recovery of added fluoride, %	Fluoride-selective electrode value, ppm
Tap water	4	0.42	0.03	105	0.43
Lake water	4	0.40	0.05	95	0.41
Well water	4	0.18	0.02	95	0.19

*n = number of determinations.

†sd = standard deviation

tension of the mercury drop. This clearly illustrates the adsorption of Ce(III)-ALC-F^- at the DME.

Effect of accumulation time. The effect of accumulation time at a hanging mercury drop electrode was studied with normal adsorptive voltammetry in $0.1M (\text{CH}_2)_6\text{N}_4-5 \times 10^{-5}M \text{Ce(III)}-1 \times 10^{-5}M \text{ALC}-1 \times 10^{-7}M \text{F}^-$. It was found that the peak height increases with accumulation time and maximum increase occurred with a 2-min accumulation time. If the process is diffusion controlled, with no adsorptive accumulation, the peak height will be independent of the accumulation time before scanning. This proves that the polarographic wave is an adsorption wave.

Effect of starting potential. It was found that the more positive the starting potential, the higher the peak was. The peak height for Ce(III)-ALC-F^- increased with sweeps started from more positive potentials, which allowed more complex to be adsorbed at the electrode. This result shows that the Ce(III)-ALC-F^- complex is negatively charged.

Cyclic voltammetry. The cyclic voltammetry of the system was investigated with a Model 82-1 voltammetric analyser with a hanging mercury drop electrode. The Ce(III)-ALC-F^- complex gives a cathodic peak at about $-0.64 \text{ V (vs. SCE)}$. No peak was observed on the anodic branch, indicating irreversibility of the reduction. The cathodic peak in the first scan with an accumulation time of 1 min was much higher than that in the second scan.

In addition, the polarographic wave shows a decrease in peak height down to zero with addition of surface-active agent, such as tetradecylpyridinium bromide. All these phenomena give evidence of the adsorption character of the wave.

Sample analysis

The procedure for the determination of fluoride in water samples was as follows. Aliquots (0.5 ml) of each water sample were transferred into the 10-ml electrolytic cell. A 1.0-ml portion of $1M (\text{CH}_2)_6\text{N}_4$, 0.1 ml of $1 \times 10^{-3}M \text{ALC}$, 1.0 ml of $5 \times 10^{-4}M \text{Ce(III)}$ and 1.0-ml of acetone were added to each solution in sequence. After shaking and allowing to stand for 30 min, the solutions are diluted to 10 ml with water. The determination is made by the procedure described above. The results obtained are given in Table 1, and are compared with those obtained with a potentiometric fluoride selective method¹² Recovery of spiked fluoride is listed also. The method is sensitive, requiring only 1% of the volume of water sample required for the selective electrode method (50 ml of sample mixed with 20 ml of total ionic strength adjustment buffer solutions and diluted to 100 ml).

REFERENCES

- 1 R Greenhalgh and J P Riley, *Anal Chim Acta*, 1961, **25**, 179
- 2 R Belcher and T S West, *Talanta*, 1961, **8**, 863
- 3 *Idem, ibid*, 1961, **8**, 853
- 4 M A Leonard and T S West, *J Chem Soc*, 1960, 4477
- 5 R Belcher, M A Leonard and T S West, *ibid*, 1959, 3577
- 6 Analytical Methods Committee, *Analyst*, 1971, **96**, 384
- 7 S S Yamamura, M A. Wade and J H Sikes, *Anal Chem.*, 1962, **34**, 1308
- 8 B. L Ingram, *ibid*, 1970, **42**, 1825
- 9 P L Bailey, *Analysis with Ion-selective Electrodes*, 1st Ed, p 95. Heyden, London, 1976
- 10 N Li and X Shang, *Fenxi Shiyanshi*, 1986, **5**, No 8, 12
- 11 W Jin, J Wang, X Zhang and S Wang, *J Electroanal Chem*, 1990, **281**, 221
- 12 Department of Chemistry, Beijing Normal University, Jichuyiqi *Fenxi shiyan*, p 168 Beijing Normal University Press, Beijing, 1984

LABILE SPECIES OF Pb, Zn AND Cd DETERMINED BY ANODIC STRIPPING STAIRCASE VOLTAMMETRY AND THEIR TOXICITY TO *TETRAHYMENA*

JØRGEN LARSEN*

Institute of Cell Biology and Anatomy, The Zoological Institutes, University of Copenhagen,
15 Universitetsparken, DK-2100 Copenhagen Ø, Denmark

BO SVENSMARK

Department of General and Organic Chemistry, The H. C. Ørsted Institute, University of Copenhagen,
Universitetsparken 5, DK-2100 Copenhagen Ø, Denmark

(Received 24 January 1991 Revised 3 March 1991 Accepted 6 March 1991)

Summary—The amounts of free ions and labile complexes of Pb, Zn and Cd have been determined in a complex organic growth medium by use of anodic stripping staircase voltammetry, ASSV. It was possible to determine the labile fractions of metals and to obtain good correlation with data on the toxicity of the metals to *Tetrahymena* when using a specific reduction potential (E_r) for each element, -600 , -800 and -1200 mV vs SCE for Pb, Zn and Cd, respectively. The labile fractions in the organic growth medium were less than 1% for Pb (Pb precipitated), 15% for Zn (as labile complexes) and 30–40% for Cd (as free ions) for total heavy metal concentrations of 0.5 – 2 mM. The toxicity to *Tetrahymena* decreased in the order Cd \gg Zn \gg Pb. The effect of Pb was greater than predicted by ASSV, probably because *Tetrahymena* additionally ingests the lead-containing precipitate and therefore is exposed to concentrations of Pb exceeding those of the soluble species found in the medium. The results stress the importance of using different specific reduction potentials when different elements are compared, instead of one potential common to all elements. The use of a fixed potential may lead to erroneous conclusions regarding the concentrations of labile species in solution.

The speciation of heavy metals in water has been the subject of many studies, as indicated in the review by Florence.¹ Since speciation is known to affect the toxicity to living organisms^{2–5} and to control metal bioavailability, the total metal concentration, as measured by AAS, for example, has little or no meaning for the assessment of toxicity in nature. The free metal ion concentration may be a more useful parameter in determining metal toxicity, although some chelates may be more available and toxic than their corresponding free ions. The complete resolution of all chemical species would be the ideal, but unrealistic goal. The heavy metals of interest in environmental studies are normally present in low concentrations, and since the aquatic environment is complex with unknown constituents, a direct identification of the species is difficult. A more realistic approach is to determine the amounts of metal with the same degree of chemical availability, *i.e.*, complex-bound with similar strength, regardless of the exact nature of the complexes.

In this study anodic stripping staircase voltammetry, ASV,⁶ is the primary method to distinguish labile and bound species of the heavy metals Pb, Zn and Cd. The reduction potential at a mercury electrode is used to differentiate between “free” or “labile” and “bound” forms of the metals. There are several reasons for not using a direct electrochemical method such as cyclic voltammetry. The sensitivity of cyclic voltammetry is too low for many of the measurements, thus the same method could not be used in all cases, making direct comparisons less accurate. Also the organic growth medium may cause deterioration of the electrode surface and affect the cyclic voltammetric response more than the ASSV-response because the oxidation current is significantly lower in cyclic voltammetry. Finally, we are interested in developing a method which can be employed in environmental studies, *i.e.*, at ultra-trace levels of heavy metals.

Another type of fractionation of metals utilizes the particle size distribution of heavy metals in the solution. The particles may be pure metal precipitates, but metals could also be precipitated with particulate matter of the medium.

*Present address Department of Environmental Technology,
Danish Technological Institute, Gregersensvej P O Box
414, DK-2630 Taastrup, Denmark

Such measurements of speciation were performed in an organic growth medium (PP), where the toxic effects on *Tetrahymena* have been studied. *Tetrahymena* is a common freshwater ciliate, often used in assay with heavy metals, see Nilsson for a review.⁷

Zinc has already been investigated in a simple inorganic medium.⁸ It was found that the calculation of speciation may lead to quite erroneous results, even in solution which are much simpler than the natural aquatic environment. Therefore, the present study was undertaken to identify the toxic fractions of heavy metals in an organic growth medium containing a variety of protein fragments, vitamins, salts, *i.e.*, a quite complex medium.

EXPERIMENTAL

Electrochemical measurements

The electrochemical method and the computer controlled instrumentation have been described previously.⁶ Part of the work was done with a new set-up including a Biodata Microline 4000 waveform capture system connected to an Admiral 20286 Personal Computer, using an IEEE 488 interface and ASYST 2.1 software. The new instrumentation was programmed to emulate the old set-up, thus all experiments were performed in exactly the same way. The working electrode was a 3-mm Metrohm 628-10 rotating glassy-carbon electrode rotated at 2000 rpm, the reference electrode was an Ingold mercury sulphate electrode, and a platinum wire served as the counter electrode. The mercury sulphate reference electrode had a potential of +400 mV relative to the SCE electrode and all potentials are given *vs.* SCE. The glassy carbon was covered with a mercury film formed by reduction of 100 ppm Hg^{2+} in 0.2M potassium nitrate at -1100 mV *vs.* SCE for 65 sec.

Samples (10.0 ml of the medium under investigation) were prepared in 0.2M potassium nitrate, the metal ion was added and the pH was readjusted with sodium hydroxide. The oxidation peak current (I_p) was measured after reduction of the metal ions at a plating potential (E_{pl}) for a plating time (p_t) selected according to the actual concentration. Plating times from 0.1 and 10 sec were used in this study.

The plating potential E_p was varied in steps of 100 mV from a value with zero peak current ($I_p = 0$) to a value where the current was independent of potential ($I_p = I_d$). Because of the very low plating time (0.1 sec) in some measure-

ments the reduction current during the stripping scan cannot be neglected. Therefore, plating time was extended such that plating time including scan time was constant at all plating potentials.

The same film was used for measurement both in the medium and in a reference solution of the same metal in 0.2M potassium nitrate in doubly demineralized water deoxygenated with argon. In the proteose peptone (PP) medium very small effects of dissolved oxygen were observed, and as the PP solutions did form a lot of foam when bubbled with argon, the experiments were run in PP saturated with air. In the organic growth medium the electrode deteriorates with time. Therefore, the electrode was only kept in this medium for the minimum time necessary for one measurement.

Size fractionation

The fractionation procedure was initiated by a separation of particulate species by filtration through a 0.45- μm membrane filter. The filtrate was then introduced into an Amicon ultrafiltration system with YM-5 ultrafilters with a cut-off 5000. The ultrafiltration cell and membrane was flushed with doubly distilled water before a sample was introduced and the system pressurized with nitrogen. After filtration the concentration of the three metals was determined by flame atomic-absorption spectrometry on a Perkin-Elmer 2280 instrument.

Toxicity test with Tetrahymena

Tetrahymena pyriformis GL⁹ was grown axenically at 28° in 2% PP enriched with 0.1% yeast extract and inorganic salts.¹⁰ The 100-ml cultures were shaken and aerated and the cells used were in the exponentially multiplying growth phase (about 5×10^4 cells/ml).

Lead, zinc or cadmium was added to the medium in acetate form. Stock solutions used were 100 and 200mM, kept in polyethylene bottles and at least 0.1M in nitric acid. When addition of the metal salts to the medium caused a decrease of pH, sodium hydroxide was used to readjust the pH to 6.8.

The cell density of the cultures was normally determined in triplicate, using an electronic particle counter, Coulter Counter Model ZB, after fixation in a 1:1 (by volume) mixture of 1% glutaraldehyde in an inorganic salt solution.¹¹ Addition of some metals to the medium gave precipitates. In this case the electronic particle counter could not be used directly be-

cause the presence of precipitate resulted in an excess value of the cell density.¹² However, by adding hydrochloric acid to the fixed cell sample the precipitate was dissolved and a homogeneous sample could be obtained for counting. When a high rate of cell mortality was observed the cell density was determined manually in triplicate with a Fuch-Rosenthals cell chamber, because the electronic particle counter could not differentiate between living and dead cells. No difference in the number of cells of untreated control cultures was found with the two methods.

For growth experiments the original 100-ml culture was divided into two portions, the metal was added to one portion, whereas the other served as control. From both cultures cell samples were withdrawn simultaneously for the determination of cell density.

THEORY

On plotting the electrochemical response with the oxidation peak current (I_p) as a function of the reduction potential (E_{pl}), a pseudo-polarogram is obtained.^{13,14} For a free aqua-ion of the investigated metals the curve (Fig. 1, curve a) is an S-shaped wave given by

$$I_p = I_d / \{1 + e[(nF/RT) * (E_{pl} - E_{1/2})]\} \quad (1)$$

The half-wave potential, $E_{1/2}$, is the potential at which the current is one half the limiting current (I_d). $E_{1/2}$ is characteristic of the free metal ions

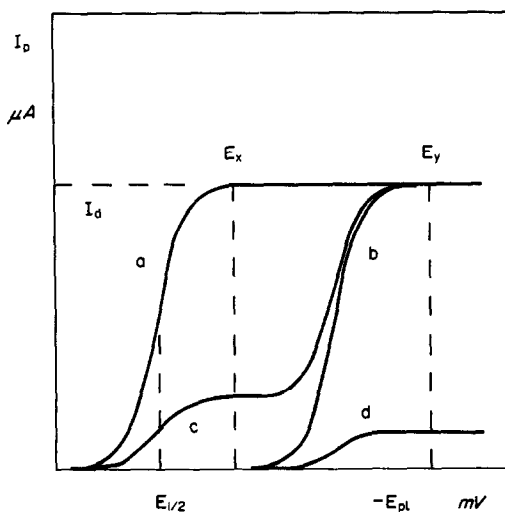


Fig 1 Schematic pseudo-polarograms for (a) free ions, (b) all ions in complex form; (c) both free and complexed ions and (d) medium and very strong complexed ions. $E_{1/2}$: plating potential giving peak currents corresponding to labile forms. E_x : plating potential resulting in peak currents including complex bound ions.

and is close to $E_{M^{2+}/M(Hg)}^0$. In the case of complexation of M^{2+} by ligands L



$$K_f = [ML_m^{2+}] / [M^{2+}][L]^m \quad (2)$$

the curve will be shifted cathodically:

$$\begin{aligned} E_{1/2}(\text{complexed}) - E_{1/2}(\text{free ion}) \\ = -(RT \ln 10/nF) \log(1 + K_f[L]^m) \quad (3) \end{aligned}$$

i.e., the curve is observed at a more negative potential (Fig. 1, curve b).

The term $RT \ln 10/nF$ is equal to $59.16/n$ mV at 25° . For $n = 2$ a shift of 29.6 mV is predicted for each decadic increase in K_f or $[L]^m$, when excess L is present. As an example, for $[L] = 3mM$ and $K_f = 10^{13}M^{-1}$ the shift is 310 mV (Fig. 1, curve b).

When L is deficient, the polarogram consists of two waves, the first for the free ions (height proportional to $[M] - [L]$) and the second for the complexed metal (height proportional to $[L]$), this case is shown in Fig. 1, curve c.

If the reduction potential is shifted beyond the reduction potential of the solvent, the metal complex cannot be determined by ASSV. Figure 1 curve d shows the case of partial reduction at -310 mV relative to $E_{1/2}$ but the main part remaining bound in a strong complex, which cannot be reduced within the available potential range.

Plating at the potential E_x will give a response proportional to the amount of free ion and loose complexes with shifts less than about 60 mV (corresponding to $K_f[L]^m = 100$), whereas the response at E_y will represent both free ions and relatively strong complexes ($K_f[L]^m$ equal to 10^{13}).

It must be stressed that the labile fraction includes the ions, and becomes free when the equilibrium in equation (2) is shifted to the right as a result of the depletion of M^{2+} at the electrode. This amount is limited by the kinetics of the dissociation of the complex, *i.e.*, in general, loose complexes dissociate fast and strong complexes slow, but the mechanism is similar to what might occur when M^{2+} is depleted because of transport through a biological membrane. In this respect, the ASSV-labile fraction is similar to the bioavailable fraction.¹ Thus, at the lowest potential, where I_p is close to I_d , free ions and labile complexes of each element will be reduced. Since this potential depends on the half-wave potential for each element (see Figs. 2 and 3 as an example) we shall denote this potential the specific potential, E_s .

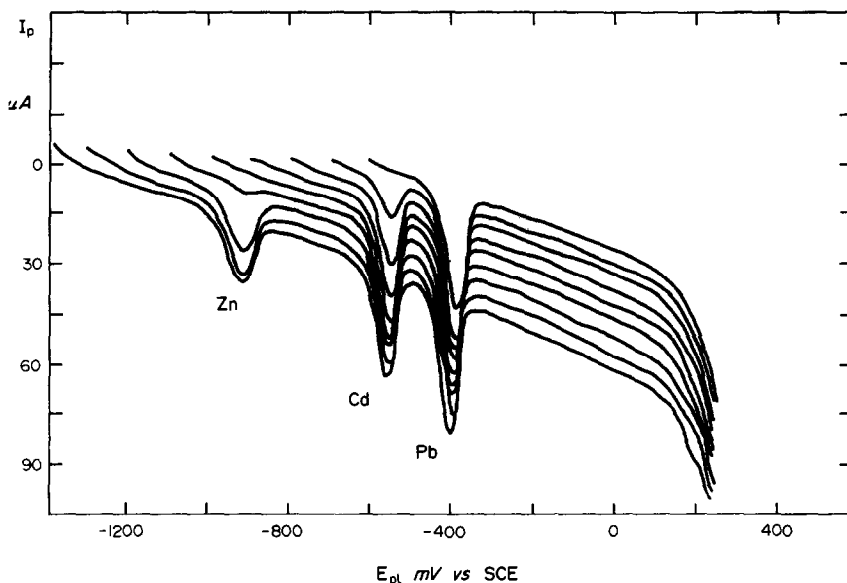


Fig 2 Staircase voltamperograms for $10\mu\text{M}$ Pb, Zn and Cd in 0.2M KNO_3 saturated with air. Plating potentials from -1400 (lefthand, lower curve) to -600 mV vs SCE (righthand upper curve); plating time 1 sec, step-length 10 mV, step-time $256\ \mu\text{sec}$ (i.e., scan-rate 156 mV/sec)

The amount of metal, which can be reduced at a given potential is called ASSV-labile, and the concentration is calculated from the proportion of the response in the medium to the limiting response I_d in water, measured at the same film electrode.

RESULTS

Electrochemical response in 0.2M potassium nitrate

The oxidation current as a function of potential for the free aqua-ions of the three metals in 0.2M potassium nitrate in water is shown in Fig. 2 for plating potentials ranging from -1400 to -600 mV. For each metal a peak is observed at a potential characteristic of the metal. It can be seen that the peak currents depend on the plating potential. The experiments were run in 0.2M potassium nitrate saturated with air. Due to the effect of oxygen the limiting current decreased by 8% for Pb, by 25% for Cd and by 52% for Zn, as compared to deoxygenated solution. A plot of the oxidation peak currents, I_p , as a function of the plating potential, E_{pl} , gives pseudo-polarograms for the three free ions, see Fig. 3. From these pseudo-polarograms the specific potentials for the free ions of Pb, Cd and Zn are taken to be -600 , -800 and -1200 mV vs. SCE respectively.

Electrochemical response in growth medium

In the proteose peptone medium, the electrode response of lead was very low, Table 1. Electrode deterioration resulted in a rapid decrease of the response during repetitive measurements. The addition of lead gave a white precipitate, easily visible at concentrations above 0.5mM lead, and the amount of labile lead increased only slightly from a total concentration of 0.5mM – 2mM . In all cases, the

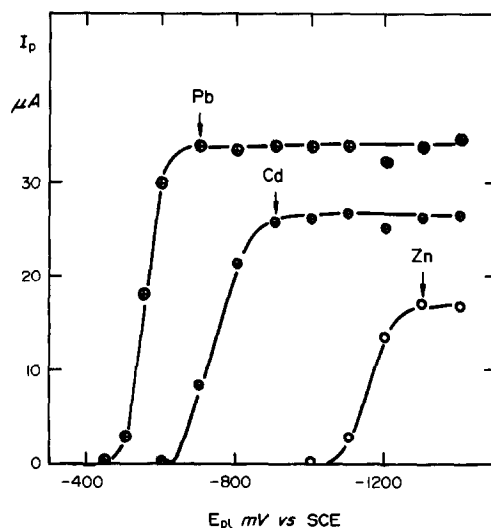


Fig 3 Pseudo-polarograms for $10\mu\text{M}$ Pb, Zn and Cd in 0.2M KNO_3 saturated with air. Plating time 1 sec, step-length 10 mV; step-time $256\ \mu\text{sec}$ (i.e., scan-rate 156 mV/sec)

Table 1 ASSV labile lead in PP-medium

Pb concentration.		500 μM	1000 μM	2000 μM
E^* , <i>mV</i>	E_{pl} , <i>mV vs. SCE</i>	ASSV-labile Pb, μM	ASSV-labile Pb, μM	ASSV-labile Pb, μM
0	-600	0	0	0
-100	-700	0.5	0.4	3
-200	-800	1	2	5
-300	-900	2	2	6
-400	-1000	3	5	7
-500	-1200	3	6	9
-600	-1400	4	7	9

*Potential relative to $E_s(Pb)$

Table 2. ASSV labile zinc in PP-medium

Zn concentration		500 μM	1000 μM	2000 μM
E^* , <i>mV</i>	E_{pl} , <i>mV vs. SCE</i>	ASSV-labile Zn, μM	ASSV-labile Zn, μM	ASSV-labile Zn, μM
+200	-1000	0	0	0
+100	-1100	22	17	83
0	-1200	84	149	220
-100	-1300	396	341	830
-200	-1400	395	805	1220

*Potential relative to $E_s(Zn)$

Table 3 ASSV labile cadmium in PP-medium

Cd concentration		500 μM	1000 μM	2000 μM
E^* , <i>mV</i>	E_{pl} , <i>mV vs. SCE</i>	ASSV-labile Cd, μM	ASSV-labile Cd, μM	ASSV-labile Cd, μM
+200	-600	0	0	0
+100	-700	98	147	552
0	-800	197	307	872
-100	-900	224	371	935
-200	-1000	238	409	920
-300	-1200	251	563	1009
-400	-1400	248	509	975

*Potential relative to $E_s(CD)$

concentration of labile lead is less than $10\mu M$. The potential where I_p reaches a constant value is shifted cathodically about 400mV relative to the potential in 0.2M potassium nitrate indicating that Pb is strongly complex bound.

One wave was also observed for Zn and the amount of labile Zn is given in Table 2. The measurements of Zn were also affected by electrode deactivation in PP. Since the response does not reach a constant value corresponding to I_d it is not possible to assess a single potential shift for Zn. The effect of several overlapping shifted waves with different shifts and heights is seen. Thus, the results indicate the presence of many complexes of varying strengths, but also that a significant part of the Zn is labile in PP.

Cadmium gives a strong and very stable response to PP. The current only decreased slightly because of electrode deterioration, and the levels, Table 3, were quite stable. The potentials do not indicate any shift in the curve

relative to that in water. Thus, in PP nearly half of the Cd is present in a very labile form.

Filtration of growth medium

Atomic-absorption spectrometric determinations, after addition of $24\mu M$ Pb, $76\mu M$ Zn and $44\mu M$ Cd (5 ppm of each of the elements) in samples of PP prior to, and after, filtration through a $0.45\text{-}\mu$ filter and finally after additional ultrafiltration, are given in Table 4. For Pb, 90% was found in the particulate fraction and did not pass the $0.45\text{-}\mu$ filter. Zinc and cadmium did not bind to particles larger

Table 4 AAS of Zn, Cd and Pb in PP-medium*

Treatment	Zn, %	Cd, %	Pb, %
Raw PP	100	100	100
0.45- μ filter	99	100	12
ultrafiltration	82	80	10

*In % of the concentration in raw PP (5 ppm)

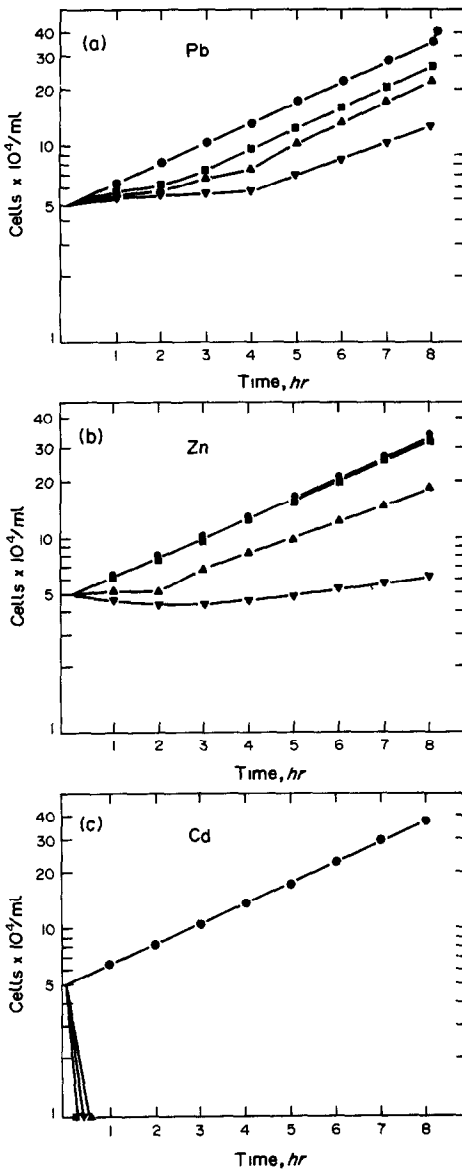


Fig 4 The effect of lead (A), zinc (B) and cadmium (C) on the rate of cell proliferation. Concentrations. 0.5mM (■), 1mM (▲) and 2mM (▼), as compared with the growth rate of untreated cells (●) Mean values of 5 experiments; S D of the mean less than 5%

than $0.45\mu\text{m}$ and only 20% were removed by ultrafiltration.

Toxicity in PP-medium

The effect of different concentrations of Pb, Zn and Cd on the rate of cell proliferation was tested in the PP medium during 24-hr exposures.

Addition of 0.5 and 1mM Pb had no significant effect on cell proliferation which, however, started after a variable lag period, Fig. 4(a). A normal generation time of less than 3 hr was found after 3 and 4 hr exposure to 0.5 and 1mM Pb, respectively. Both cultures reached maxi-

mum cell density (about 1,000,000 cells/ml) after 24 hr, *i.e.*, comparable to control cells. In 2mM Pb, cells exhibit a lag period of about 4 hr, after which the cells start proliferation, but at a decreased rate; the generation time was prolonged by a factor of 1.25 above the control value, and after 24 hr only about 350,000 cells/ml were seen.

Zinc affects cell proliferation in a way comparable to that described for lead with cell proliferation resumed after a variable lag period [Fig. 4(b)]. Addition of 0.5mM Zn had no significant effect on cell proliferation. In the presence of 1mM a lag period of about 2 hr preceded cell proliferation at a decreased rate; the generation time was prolonged by a factor of 1.2 above the rate of control cells but the same final cell density was reached. Although some cells died during the first 3 hr of exposure to 2mM Zn, the survivors were capable of proliferation; the generation time was prolonged by a factor of 3 above the control value during the following 5 hr. A cell density of about 550,000 cells/ml was seen after 24 hr exposure, indicating a further increase in the rate of cell proliferation.

Addition of Cd to cells caused a high rate of cell mortality, thus all cells died within 30, 20 and 15 min exposure to 0.5, 1 and 2mM Cd respectively, see Fig. 4(c).

In vivo observations revealed that *Tetrahymena* ingest the precipitate formed on addition of Pb (in particular) to the organic growth medium. The ingested precipitate was incorporated into food vacuoles and later defecated from the cells as defecation balls. All exposed cells contain small, refractile granules which are not seen in the control cells. Typically, the number of granules increased with time and metal concentrations. In proliferating cells the number of granules reached a stable level, but in the stationary growth phase, where control cells also form the small refractile granules, the metal-treated cells contain an increased number of these granules.

DISCUSSION

When different elements are to be compared it is important to realise that electrochemical stripping methods may lead to erroneous conclusions, when a fixed reduction potential is used for all elements, because the electrochemical labile fractions would be different for different metals. The reduction potential should therefore be selected for each element.

The effect of oxygen on ASSV of Pb, Cd and Zn can be explained in terms of the reduction product, OH^- , which may precipitate $\text{M}(\text{OH})_2$ near the electrode surface. This effect is greater in 0.2M potassium nitrate than in PP, because of the buffer capacity in PP.¹⁵ This effect is most pronounced for Zn, with the most cathodic plating potentials, since the second reduction step of oxygen occurs at -900 mV vs. SCE . The solubility products for the three hydroxides are similar.¹⁶

The concentration of labile Pb species or free Pb^{2+} ions determined in PP is very low: $0\text{--}10 \mu\text{M}$ even after addition of 2mM lead. Precipitation is directly observed, and this explains the low concentrations in labile Pb. The current increases significantly with negative plating potentials indicating that the residual soluble Pb is bound in several complexes.

The observed response for Zn in PP is smaller than in 0.2M potassium nitrate at low potentials, but at more negative potentials the responses increases rapidly. This indicates that Zn is bound in a variety of complexes, of which a substantial part is very labile. At $E_s(\text{Zn})$ we find a current corresponding to a concentration of free ion or very labile complexes of 84, 149 and $220 \mu\text{M}$ at total concentrations of 0.5, 1 and 2mM, respectively. Because of the cathodic shift of the whole response, it is most likely that the current at E_s corresponds to labile complexes rather than to residual free ions. The ASSV-measurements thus indicate that Zn is distributed among several complexes of which about 15% are very labile.

The current for Cd is about half of that in water, and no shift in reduction potential can be seen in the experimental values. This means that half of the Cd is present as free ions or very labile complexes in PP. The remaining part of the Cd must be bound in quite strong complexes.

The filtration experiments followed by determination of total concentrations by AAS support the above findings. Lead is removed to 90% by $0.45 \mu\text{m}$ filtration with no effect of subsequent ultra-filtration. Cadmium stays in solution as does zinc. Thus, the results of filtration support that Pb is active in building aggregates that may precipitate at higher concentrations.

The high tolerance of *Tetrahymena* towards Pb in the organic growth medium is in agreement with the very low ionic concentration of the metal found by ASSV. The protective property of the organic growth medium towards

toxic effects of Pb is also indicated by an increased toxicity of the metal in diluted medium.¹² Although the toxicity of lead is greater than predicted from the ASSV data the growth rate is only slightly affected by 2mM Pb under the present experimental conditions. The discrepancy between the ASSV data and the toxicity could be that *Tetrahymena* ingests the precipitate formed by addition of Pb and therefore becomes exposed to higher amounts of Pb than measured by ASSV. Electron microscopy has revealed that Pb enters *Tetrahymena* through the membrane of digestive vacuoles and through the cell surface;¹⁷ however, in the digestive vacuoles most of the lead-containing precipitate is converted to refractive debris which is defecated.¹² That *Tetrahymena* is able to proliferate in the presence of 2mM lead agrees well with earlier studies in which the cells were maintained under comparable growth conditions.¹² Liu *et al.*,¹⁸ however, found that $48 \mu\text{M}$ Pb was lethal to *Tetrahymena*. The apparent discrepancy between these results and those obtained in the present study may be explained by the use of different organic growth media with different complexing capacity for Pb.

Zinc is an essential metal required in trace amounts by living cells, but toxic in excess amounts. Addition of Zn to the growth medium causes an inhibition of cell proliferation which resembles that described for Pb but the effect is more pronounced. The toxicity of Zn to *Tetrahymena* seems strongly correlated with the amount of organic materials in the medium, a factor which may partly explain some of the disagreement on the concentration of Zn tolerated by this organism.¹⁹⁻²¹ The toxicity of metals may also change with time of exposure as a result of an adaptation. *Tetrahymena* exhibits a certain lag period before cell proliferation takes place in the presence of Pb and Zn. This lag period may be caused by a change in the medium or an adaptation phase during which a metal-regulating system is activated. In *Tetrahymena* this detoxification system may include both a retention of metal within the digestive vacuole and a reduced entry through the plasma membrane. The small refractile granules found in *Tetrahymena* under unfavorable growth conditions have been shown to accumulate Pb, Zn and Cd, when added externally,^{17,19,20} in agreement with their proposed function as ion-regulators.²²⁻²⁴

The toxic effects of Cd, an industrial pollutant, on *Tetrahymena* have been studied extensively.

In the PP medium all cells die within 30 min in 0.5mM Cd which indicates a very high toxicity. About 0.05mM Cd inhibits cell proliferation and produces a high rate of mortality.²⁵⁻²⁷ However, the effect of a given concentration of Cd depends on the initial cell density of the culture.²⁵ Even though most of the cells die in concentrations of about 0.05mM Cd, the surviving cells resume cell proliferation, as if they became adapted.^{25,26,28} A metallothionein-like protein has been found in *Tetrahymena* after exposure to Cd,²⁹⁻³² it may also play an important role in metal detoxification in this organism. The toxicity of Cd seems also to depend on the amount of organic material in the medium; thus, growth is inhibited at 4μM in 0.2% PP,²¹ whereas it is uninhibited at 18μM Cd in 2% PP medium.²⁵ Even though two different strains of *Tetrahymena* was used, the main difference between these studies may well be explained by the different concentrations of organic material. That Cd inhibits cell proliferation in the PP medium at very low concentrations is in agreement with the ASSV data, which indicate that about two-fifths of the added Cd is ASSV-labile.

CONCLUSION

The electrochemical results suggests that Cd is rather (30–40%) free in the organic growth medium, Zn is complexed, but with a substantial amount of quite labile complexes (15%), and Pb are complexed as well as precipitated (less than 1% free). The toxicity of metals towards *Tetrahymena* decreases in the order Cd ≫ Zn > Pb, in agreement with a decreased amount of labile metal. However, the toxicity of Pb is greater than predicted, presumably because the organisms ingest the precipitate formed by addition of lead, and therefore become exposed to a higher concentration of Pb than measured by ASSV.

In conclusion, ASSV can be used to assess the labile fraction of heavy metals by proper selection of specific reduction potentials (E_r) for each element, and good agreement is obtained with the toxicity data. However, an evaluation of the toxicity of heavy metals to aquatic organisms should not be based on the chemical measurements alone, since some complexes may be more toxic than the corresponding free ions. Furthermore, the effect of metals on living organisms are quite complex e.g., different metal ions may show variable toxicity according to different sites of action.

Acknowledgements—Our sincere thanks to Professor Christian Overgaard Nielsen for critical reading of the manuscript. Financial support from the Danish Natural Science Research Council for the electrochemical instrumentation, grant no 511-15013 and 11-7636, is gratefully acknowledged

REFERENCES

1. T. M Florence, *Analyst*, 1986, **111**, 489
2. H. Babich and G Stotzky, *Appl Environ Microbiol.*, 1978, **36**, 906
3. G S Canterford and D R Canterford, *J Mar Biol Assoc, U K*, 1980, **60**, 227.
4. D W Engel and B A Fowler, *Environ. Health Perspect*, 1979, **28**, 81
5. W G Sunda, D W. Engel and R. M. Thuottle, *Environ. Sci. Technol*, 1978, **12**, 409
6. B. Svensmark, *Anal. Chim. Acta*, 1987, **197**, 239
7. J R. Nilsson, *Europ J Protistol*, 1989, **25**, 2.
8. B Svensmark and J Larsen, *Talanta*, 1988, **35**, 953.
9. D L. Nanney and J W McCoy, *Trans Am Microsc Soc.*, 1976, **95**, 664.
10. P Plesner, L Rasmussen and E. Zeuthen, in *Synchrony in Cell Division and Growth*, E Zeuthen (ed.), p. 543. Interscience, New York, 1964
11. K Hamburger and E Zeuthen, *Exp Cell Res.*, 1957, **13**, 443
12. J R. Nilsson, *Protoplasma*, 1978, **95**, 163
13. Š. Komorasky-Lovrić, M. Lovrić and M Branica, *J Electroanal. Chem*, 1986, **214**, 37
14. D L Huizenga and D. R. Kester, *ibid*, 1984, **164**, 229
15. J Larsen, B Svensmark and J R Nilsson, *J. Protozool*, 1988, **35**, 541
16. A. E Martell and R M Smith, *Critical Stability Constants*, Vol 4, Plenum Press, New York, 1976.
17. J. R. Nilsson, *J. Cell Sci.*, 1979, **39**, 383
18. Y -F Liu, R -H Tang, Q -X. Zhang, J -Y. Shi, X -M Li, Z -Q Liu and W. Zhao, *Biol Tr Elem. Res.*, 1986, **9**, 89
19. A R Jones, M. Taylor and K. Simkiss, *Comp Biochem Physiol*, 1984, **78A**, 493
20. S. Dunlop and G Chapman, *Environ Res*, 1981, **24**, 264
21. N. Yamagushi, O Wada, T. Ono, K Yazaki and K Toyokawa, *Ind. Health*, 1973, **11**, 27
22. J R Coleman, J R. Nilsson, R R. Warner and P Batt, *Exp Cell Res*, 1972, **74**, 207.
23. *Idem, ibid*, *Exp Cell Res.*, 1973, **80**, 1.
24. J. R. Nilsson and J. R. Coleman, *J Cell Sci*, 1977, **24**, 311
25. J. Larsen, *Toxicology*, 1989, **58**, 211
26. C K Pyne, F Iftode and J -J Curgy, *Biol. Cell.*, 1983, **48**, 121.
27. C Houba, J Remacle and F De Parmentier, *Europ. J Appl Microbiol Biotechn.*, 1981, **11**, 179
28. F Iftode, J J Curgy, A. Fleury and G Fryd-Versavel, *Acta Protozool.*, 1985, **24**, 273.
29. E Piccinni, P Irato, O Coppellotti and L Gudolin, *J. Cell Sci.*, 1987, **88**, 283.
30. N. Yamaguchi, O. Wada, T. Ono and M. Nagahashi, *Ind Health*, 1978, **16**, 15
31. Y. Nakamura, S. Katayama, Y. Okada, F. Suzuki and Y Nagata, *Agric. Biol Chem*, 1981, **45**, 1167
32. F Suzuki, Y. Nakamura, Y. Kimura, H Muramatsu and Y Nagata, *ibid.*, 1987, **51**, 923

POTASSIUM SODIUM CHLORIDE INTEGRATED MICROCONDUITS IN A POTENTIOMETRIC ANALYTICAL SYSTEM

CUI HONGBO and SUN JUNYAN

Institute of Applied Ecology, Academia Sinica, Shenyang, China

(Received 6 December 1990 Revised 13 February 1991. Accepted 21 March 1991)

Summary—The preparation and application of a K^+ , Na^+ and Cl^- integrated microconduit potentiometric analytical system with tubular ion-selective electrodes (ISEs), microvalve, chemfold, electrostatic and pulse inhibitors is described. Electrochemical characteristics of the tubular ISEs and integrated microconduit FIA-ISEs were studied. The contents of K^+ , Na^+ and Cl^- in soil, water and serum were determined with the device. The analytical results agreed well with those obtained by flame photometric and silver nitrate volumetric methods.

The contents of potassium, sodium and chloride in soil, water and serum are among the determinations which are routinely most often performed in soil chemistry and clinical analytical chemistry. Although flame photometry and silver nitrate volumetry are used as the standard analytical methods for potassium, sodium and chloride, segregated flow and flow-injection analysis-ion selective electrode (FIA-ISE) analytical systems with automatic devices have been used to replace the flame photometer and its fuel gases and gas exhaust, to simplify experimental procedures, to decrease reagent and sample requirements and to increase sampling rate and analytical precision.¹⁻³

We have constructed a new potassium, sodium and chloride integrated microconduit device with micro tubular ISEs, microvalve, coil, chemifold, electrostatic and pulse inhibitors based on Růžička's work.⁴ The size of the device is about one-third smaller than a cigarette pack and about one-third as thick (normally $10 \times 30 \times 50$ mm). In comparison with the Růžička pH integrated microconduits, its specification is as follows:

(1) The device has all solid structure in order to eliminate separation of the adhesive membrane from the perspex piece and solution leakage, at the same time raising the insulating ability of the device and increasing the service life.

(2) The tubular ISEs are well connected to the integrated main piece with a standard channel

to allow replacement of tubular ISEs very simply and to determine more analytes.

The characteristics of the tubular ISEs and the experimental conditions of the integrated microconduit FIA-ISEs were studied. The conditions of K^+ , Na^+ and Cl^- in soil, water and serum samples were determined. The analytical results agreed well with those obtained by flame photometric and silver nitrate volumetric methods.

EXPERIMENTAL

Apparatus

A schematic diagram of the FIA-ISEs manifold used in this study is shown in Figs. 1 and 2. An Orion 901 ionanalyzer connected to a Dahua recorder is used. A Carlo Erba Instrumentazione model 1512 peristaltic pump with Tygon pump tubes was used to propel the carrier and to aspirate the sample solution. The home-made micro-tubular electrodes, microvalve, coil, electrostatic and pulse inhibitors were integrated into the microconduits which allowed the volume between the valve and the electrodes to be reduced to less than $10 \mu\text{l}$ in order to minimize sample dispersion. The connection between the microvalve and the electrode was made with a 0.5-cm long stainless steel tube which was earthed to prevent interference from static electricity created by the pump roller. The connection between the indicator

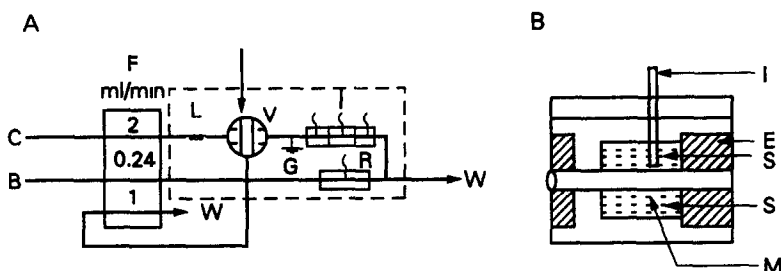


Fig 1(A) Integrated microconduit FIA manifold for potentiometric measurement C, carrier stream, B, solution for the reference electrode, P, pump, V, injection valve, I, indicator electrode, R, reference electrode; L, pulse inhibitor, G, ground, W, waste. (B) Expanded view of tubular flow-through cell I, Ag/AgCl inner reference electrode; M, sensitive membrane; S, internal reference solution, E, epoxy resin

electrode and the reference electrode was made with a micro three-way tube.

Tubular flow-through electrodes

The tubular flow-through potassium, chloride and sodium electrodes were respectively prepared by replacing part of the wall of a small piece of PVC tubing (1.5 cm long, 0.5 mm i.d., 1.5 mm o.d.) with the valinomycin sensing membrane (0.25 mm²), by coating a fine layer of silver chloride onto the inner wall of the silver cylinder (1.0 cm long, 0.5 mm i.d., 0.6 mm o.d.) and by using sensing sodium capillary glass (1.5 cm long, 0.5 mm i.d., 0.7 mm o.d.).⁵⁻⁶ They were placed into the perspex housing respectively as shown in Fig. 1(B). The housings were respectively filled with a suitable inner solution containing the sensing ion and saturated silver chloride into which a Ag/AgCl wire was inserted to serve as the inner reference system. Those pieces of tubing act as potentiometric flow-through detectors with zero dead volume. The dimensions of all the tubular electrodes were 1.5 cm long, 1.0 cm wide and 1.2 cm high.

The prepared tubular electrodes were then integrated into the microconduit with the standard channel (Fig. 2).

Reagents

Doubly distilled water and analytical reagent grade acids and salts were used throughout unless otherwise stated.

The standard solutions and carrier components used for testing the electrode characteristics and calibrating the electrodes prior to K⁺, Na⁺ and Cl⁻ measurements in soil and water are as follows: K⁺: 0.1N hydrochloric acid-triethylamine (1:50) standard solutions, $C_K + = 0.1$ ppm (in carrier). Cl⁻: 0.2M-Cl⁻ standard solutions, $C_{Cl^-} = 10^{-5}M$ (in carrier). Na⁺: 0.25M magnesium acetate-Na⁺ standard solutions, $C_{Na^+} = 10^{-5}M$ (in carrier).

The calibration solutions used for calibrating the electrodes prior to serum K⁺, Na⁺ and Cl⁻ determinations are as follows: (A) 40mM Na⁺-4mM K⁺-136 mM Cl⁻ standard solution. (B) 80mM Na⁺-8mM K⁺-80mM Cl⁻ standard solution.

These solutions are both of pH 7.40 and ionic strength 0.16M.

Sample preparation

Water. K⁺: Pipette 5 ml of water into a 25-ml beaker and add 5 ml of pH 8.5 0.2N HCl-triethanolamine (1:25).

Na⁺: Pipette 5 ml of water into a 25-ml beaker and add 5 ml of 0.4M potassium nitrate.

Cl⁻: Pipette 5 ml of water into a 25-ml beaker and add 5 ml of 0.4M potassium nitrate.

Soil. Weigh 5 g of an air-dried soil sample into a 50-ml flask. Add 25 ml of water and shake for 3 min. Pipette the filtrate and

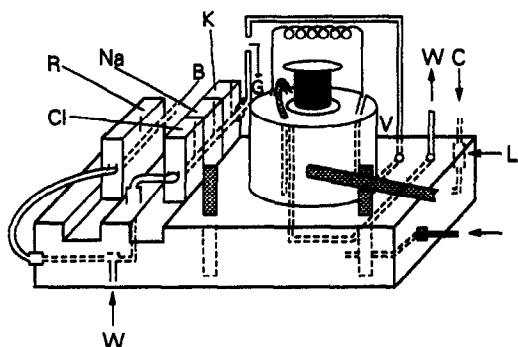


Fig 2. Details of the integrated microconduit shown within the dotted lines in Fig. 1(A).

Table 1 Electrode response characteristics (25°)

Characteristic Type	Condition	Linear range, M	Response time, sec	Repeatability (N = 11), mV	Detection limit, M	Slope, mV/pX	Selectivity coefficient (separate solution method)				
							K ⁺ Na ⁺	K ⁺ Li ⁺	K ⁺ NH ₄ ⁺	K ⁺ Ca ⁺⁺	K ⁺ NH ₄ ⁺
K ⁺	Static	10 ⁻¹ -10 ⁻⁵	10-30	±0.3	10 ⁻⁶	59.1	1.4 × 10 ⁻⁴	2.5 × 10 ⁻⁴	3.4 × 10 ⁻⁵	1.1 × 10 ⁻⁵	3.9 × 10 ⁻³
	Flow	10 ⁻¹ -10 ⁻⁵	5-8	±0.1	2 × 10 ⁻⁶	58.8	1.8 × 10 ⁻⁴	2.4 × 10 ⁻⁴	3.2 × 10 ⁻⁵	2.6 × 10 ⁻⁵	3.5 × 10 ⁻³
Na ⁺	Static	10 ⁻¹ -10 ⁻⁴	10-30	±0.3	2 × 10 ⁻⁶	58.8	10 ³	10 ⁻³			
	Flow	10 ⁻¹ -10 ⁻⁴	5-8	±0.1	5 × 10 ⁻⁶	58.2	10 ³	10 ⁻³			
Cl ⁻	Static	10 ⁻¹ -10 ⁻⁴	10-20	±0.3	5 × 10 ⁻⁵	54.8	4 × 10 ⁻⁴	6 × 10 ⁻³	4 × 10 ⁻³	3 × 10 ⁻³	34
	Flow	10 ⁻¹ -10 ⁻⁴	5-8	±0.1	5 × 10 ⁻⁵	54.2	4 × 10 ⁻⁴	5 × 10 ⁻³	4 × 10 ⁻³	3 × 10 ⁻³	36

prepare the sample as above for the water sample.

Serum. The serum tested originated from the Shenyang hospital and was not diluted.

Electrode characteristics

In order to study the response characteristics of the electrodes in different experimental conditions, a rod electrode and a tubular flow-through electrode in the integrated microconduit with the same sensing membrane were made and tested separately in the static state and in the flow state at 25° (Table 1).

According to the data presented in Table 1, the characteristics for the tubular electrode integrated microconduit under flow conditions had rapid response (5-10 sec), high reproducibility (±0.1 mV) and good stability (overall EMF drift of 0.2 mV/hr over at least 8 hr). This is due to the stable experimental conditions with respect to precise sampling volume, reproducible transport, constant flow and washing in the system.

Flow-injection analysis selectivity coefficient values are slightly different than those obtained in the static state. A plausible explanation is that the contact time between the interference solution and the membrane is much shorter under dynamic conditions than in static measurements. Moreover, the flow of the carrier solution between injections of interference samples provides continuous wash and recondi-

tioning of the membrane. Also, adsorption, desorption and response speed of the sensing membrane may be different. By adjusting experimental conditions, changing carrier components or using FIA treatment on line, the effect of interfering ions on the analytical results may be decreased.

The K⁺, Na⁺ and Cl⁻ flow-through micro-electrode integrated microconduits produce less dispersion, increased sampling rate and analytical precision. Addition of a small amount of the sensing ion to carrier appears to improve the dynamic properties of the electrode, enabling narrower peaks and good linearity to be obtained.

Standard and sample measurement

The integrated microconduit manifold was connected as in Fig. 1. The conditions selected were sampling volume $S_v = 100 \mu\text{l}$, the pumping rate for the indicator electrode $Q = 2.0 \text{ ml/min}$, and for the reference electrode $Q = 0.24 \text{ ml/min}$. The system was calibrated with a series of standard solutions and the samples were analysed. The results summarized in Table 2 show excellent agreement between the integrated microconduit method, flame photometry and silver nitrate volumetry. Typical outputs for calibration series are shown in Figs. 3-5.

For the lower sampling volume with the FIA system, the maximum potentials (peak heights)

Table 2 Comparison of various methods for the determination of K⁺, Na⁺ and Cl⁻

Sample method	Water, mg/l																			
	Soil, mg/100 g				River				Under ground				Well					Serum, mM		
K ⁺	proposed method	54	79	62	71	79	2.03	2.04	1.94	2.23	4.62	5.70	5.42	5.0	4.7	4.2	4.0	4.1	4.9	5.1
	flame photometry	59	77	62	70	76	2.02	2.05	1.98	2.21	4.72	5.87	5.38	4.9	4.6	4.2	4.0	4.0	5.0	4.9
Na ⁺	proposed method	34	39	72	189	123	61.2	50.1	25.8	30.2	49.5	50.7	48.3	134	131	130	129	132	140	139
	flame photometry	38	41	72	182	123	60.9	50.2	25.7	31.8	48.8	52.0	49.2	133	132	132	130	132	138	141
Cl ⁻	proposed method	24	32	54	164	78	26.1	49.3	18.4	14.2	17.8	11.4	16.4	88	100	97	98	104	101	96
	volumetry	21	28	54	161	74	25.9	49.6	17.6	15.0	18.1	12.1	17.1	88	98	98	98	101	99	95

are lower than those obtained by the steady state mode, revealing the influence of the sample dispersion and response time on the readout. The slope of the calibration curve will be the same as that based in steady-state measurements (Fig. 3). The sampling volume S_v required to reach steady state readouts with the integrated microconduit device is only 1/3 of the volume previously required by conventional FIA-ISE methods.

The determination of K^+ , Na^+ and Cl^- in soil, water and serum was carried out separated with the integrated microconduit device shown in Fig. 1. The analytical results agreed well with those obtained by flame photometric and silver nitrate volumetric methods. The following regression equations were obtained for the results.

$$K^+ : C_{FPM} = 0.991 C_{FLA} + 0.129$$

$$Na^+ : C_{FPM} = 0.987 C_{FIA} + 0.118$$

$$Cl^- : C_{VM} = 1.004 C_{FIA} + 0.088$$

where

FPM = flame photometric method

VM = silver nitrate volumetric method

FIA = integrated microconduit FIA-ISE method

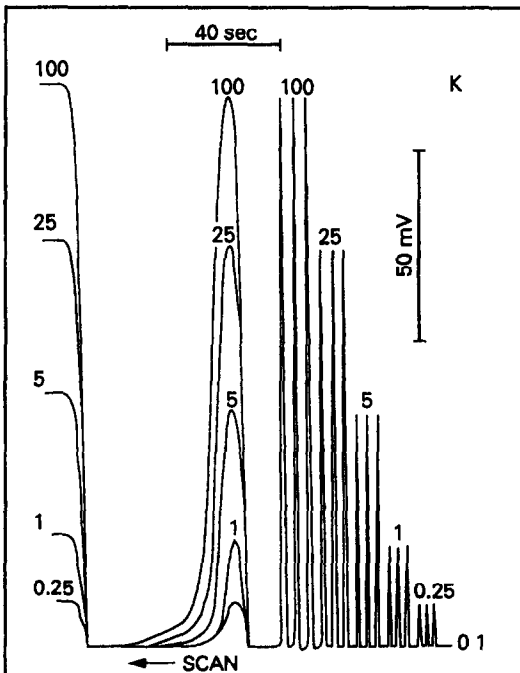


Fig. 3 Response curves obtained by injecting 100 μ l (right, middle) and steady state (left) of standard solutions of different K^+ concentrations into a carrier stream of $C_{K^+} = 0.1$ ppm

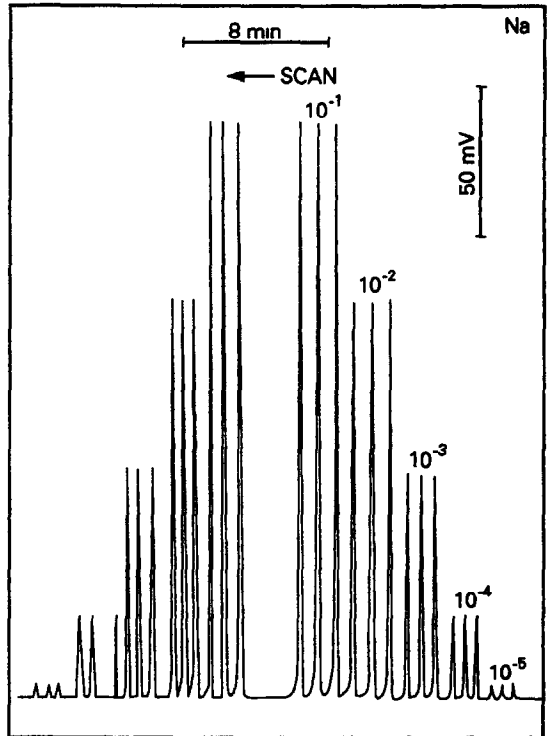


Fig 4 Response curves obtained by injecting 100 μ l standard solutions of different Na^+ concentrations into a carrier stream of $C_{Na^+} = 10^{-6}M$

In general, the detection limit of the integrated microconduit FIA-ISE method appears higher than for the static state method due

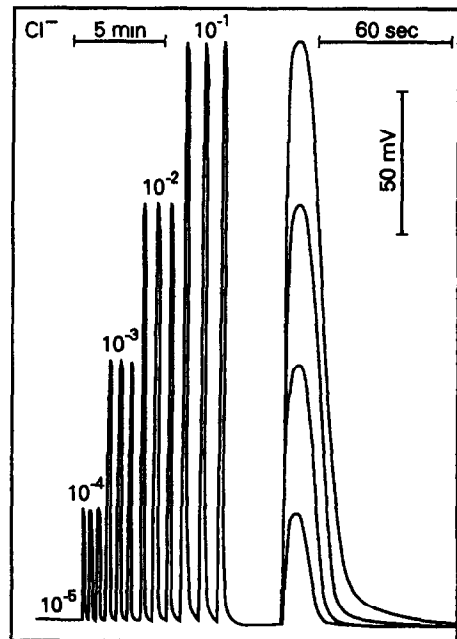


Fig 5 Response curves obtained by 100 μ l standard solutions of different Cl^- concentrations into a carrier stream of $C_{Cl^-} = 10^{-5}M$

to sampling dispersion and slower response of the electrode at very low concentrations. The sampling rate was related to the sample concentration.⁷ The larger the differential value in the concentrations between the carrier and the sample, the more time required to return to the base line. The sampling rate was about 120–200 per hr at almost equilibrium state with carry over of less than 0.7%. The standard deviation over the linear range with tubular electrodes was about 0.1 mV (N = 11).

REFERENCES

- 1 L T Skeggs, *Anal Chem*, 1966, **38**, 31A.
- 2 J Růžicka and E H Hansen, *Anal Chim Acta*, 1975, **78**, 145
- 3 J R Davis, R L Solsky, L Glering and S Malhotra, *Anal. Chem*, 1983, **55**, 202R
- 4 J. Růžicka, *ibid*, 1983 **55**, 1040A
- 5 M. E Meyerhoff and P M Kovach, *J Chem Educ*, 1983, **60**, 76
- 6 J. F Van Staden, *Anal Chim Acta*, 1986, **178**, 407.
- 7 Cui Hongbo and Zhang Sulan, *Anal Chem (Chinese)*, 1985, **4**, 320

THE DETERMINATION OF LEAD IN TOTAL SUSPENDED AIR PARTICULATES BY X-RAY FLUORESCENCE SPECTROSCOPY

THOMAS A. LAFISCA, STUART J. NAGOURNEY and CHARLES PIETARINEN
New Jersey Department of Environmental Protection, 380 Scotch Road, Trenton,
New Jersey 08625, U.S.A

(Received 10 January 1991. Revised 26 March 1991 Accepted 2 April 1991)

Summary—A method has been developed for the measurement of lead in air particulates collected on glass fiber filter paper with wavelength-dispersive x-ray fluorescence spectroscopy (WDXRF). Analyses conducted by both WDXRF and an EPA-approved procedure that employs acid sonication followed by analysis of the extract by atomic-absorption spectroscopy (AAS) shows excellent agreement between the two methods. WDXRF calibration was accomplished with standards prepared from known additions of Pb to unexposed glass fiber filter discs. Method equivalency has also been demonstrated by the analysis of several reference materials and the statistical analysis of quality control data. The WDXRF procedure has also been used to evaluate the distribution of Pb in the particulates across the surface of the filter.

The Clean Air Act of 1970 provided the United States Environmental Protection Agency (EPA) with the authority to establish maximum air concentrations for the most significant pollutants; these are termed National Ambient Air Quality Standards. The pollutants for which standards have been set are particulate matter, carbon monoxide, ozone, nitrogen dioxide, sulfur dioxide and lead. These standards are designed to protect the quality of the environment and provide an adequate margin of safety from adverse impacts on human health.

The New Jersey Air Sampling Network collects samples of either total suspended particulates or only that fraction which is respirable (less than 10 microns in diameter). The total suspended particulate (also known as high volume) filter program collects 24 hour samples of particulates from the air on glass fiber filter paper at least once every six days. There are 28 total suspended particulate samplers in operation at various locations throughout the State. All samples are analyzed for the amount of particulates; selected samples are analyzed for the amounts of benzo-(a)-pyrene, extractable organics, sulfates, nitrates, lead and other metals. Levels of many trace metals are typically in the μm^3 concentration range.

Approved EPA methodology for the analysis of lead on high volume filters involves

sonication of a portion of the filter in dilute *aqua regia*, followed by measurement of Pb in the extract by flame atomic-absorption spectroscopy (AAS). While being sensitive and accurate, the AA method is labour intensive, time consuming and requires the use of large amounts of reagents and glassware. The AA method is also constrained since AA cannot be operated unattended. To overcome these impediments and improve productivity, other methods for the analysis of lead on high volume filters were explored. Analyses of high-volume air filters by wavelength-dispersive x-ray fluorescence (WDXRF) spectroscopy is an attractive alternative, requiring a minimal amount of sample preparation and manpower. There are no reagents or glassware needed and the instrument can be operated unattended to maximize sample throughput.

Application of WDXRF to this media has its own set of analytical problems. This paper describes a procedure for the WDXRF determination of Pb in total particulates collected on glass fiber filters with a direct deposition method for the preparation of calibration standards and the analysis of multiple sections of each sample filter strip. Problems with the application of WDXRF and the remedies that were developed will be presented and comparisons with the EPA-approved sonication-AAS method will be made.

EXPERIMENTAL

Apparatus

Air particulate matter was collected with a General Metal Works Model 2000 high volume sampler. Whatman EPM 2000 glass fiber filter paper (20.24 × 25.40 cm) was used for collection. Filters were weighed with a Torbal Model EA-IAP analytical balance. The acid sonications were made in a L and R Model T28B Sonication bath. AAS analyses were made with a Perkin-Elmer Model 5000 spectrometer equipped with a Model 7500 computer, a Model AS-50 sample changer and a 10.5-cm single-slot burner head for analyses with an air acetylene flame.

WDXRF measurements were made with a Philips Model 1404 wavelength dispersive spectrometer equipped with a Digital Equipment Corporation Model 350 computer and a Herzog Model PW 1500 sample changer. The operating conditions are shown in Table 1.

Reagents

The *aqua regia* for the sonication of the filters was prepared with trace-metal grade nitric and hydrochloric acid (JT Baker Chemical Company). Doubly-demineralized water with a resistivity greater than 18 ohms was used throughout.

A concentration of 10,000 $\mu\text{g/ml}$ lead, obtained from the National Institute for Standards and Technology [Standard Reference Material (SRM) 3128], was used to prepare all calibration standards.

Procedure

Ambient air is drawn into a covered housing and through a glass fiber filter at a flow-rate of (1.13–1.70 m^3/min). Particles within the range of 100–0.1 μm diameter are retained on the filter. An average flow-rate of 1.70 m^3/min for a 24-hr period ensures that a measurable amount of

particulates will be collected. The filters are tared under controlled temperature and humidity before being placed in the field. After exposure, the filter is returned to the laboratory and allowed to stand for 24 hr in the same conditions before being re-weighed and the total mass determined.

Analysis

According to the EPA protocol¹ a 2.54-cm wide by 20.24-cm long strip is cut from each high volume filter with a template and a pizza cutter. The filter strip is folded to fit the inside diameter of a 30-ml glass beaker. Twenty millilitres of dilute *aqua regia* (2.6M nitric acid and 0.9M hydrochloric acid) are added and the beaker is covered with wax paper. The samples are sonicated for 30 min and then filtered through Whatman 41 filter paper into a 100-ml standard flask. Demineralized water is added to cover the filter in the beaker, which is allowed to soak for an additional 30 min before filtration into the standard flask. This soaking procedure is repeated. The flask is brought to volume with demineralized water.

The measurement of Pb in the filter extract by flame atomic-absorption spectroscopy at 217.0 nm has been described elsewhere.²

For our analysis by WDXRF, diameter discs (32 mm) were cut from glass fiber paper with a stainless steel die. The filter discs were placed into aluminum sample cups held in place with a Viton O-ring. A calibration curve was prepared by making known additions of the National Institute for Standards and Technology (NIST) Pb solution at varying concentrations to glass fiber paper discs cut from an unexposed filter. For each filter sample, 5 discs were cut from each filter strip. The concentration of Pb on each filter disc was calculated by comparison of the response to the standard curve. The concentration of Pb on the five discs is summed and a mean calculated. This value is then divided by the area of disc exposed to the x-ray, then multiplied by the area of the original filter and divided by the volume of air sampled to give the concentration of Pb as μm^3 of air sampled. This enables compensation for the inherent inhomogeneous distribution of Pb across the surface of the filter strip.

The calibration curve was generated with spiked filter glass fiber discs prepared by the addition of 50 μl of various concentrations of Pb prepared from serial dilutions of the NIST SRM to blank filter discs. The calibration discs

Table 1 WDXRF instrumental operating conditions

Spectral Line	Pb L-beta
Peak Position	28.235 2-theta, 0.982 nm
Fixed Time Count	50 sec
Tube Target	Cr
Tube Voltage	60 KV
Tube Current	50 MA
Analyzing Crystal	LiF 200
Detector	Scintillation Counter
Collimator	Coarse
Vacuum Path	1 Pascal
Sample Rotation	Yes
Channel Mask	Small

were dried for 10 min at 75° and then measured under the conditions shown in Table 1. A disc without added Pb was included in the calibration curve. The calibration data were fitted with a linear regression algorithm that also corrects for self-absorption and matrix effects.³ The response of the x-ray to lead on glass fiber filters was linear from 0.22 to 22.0 μg of lead per cm^2 .

RESULTS AND DISCUSSION

Calibration standards preparation

The preparation of calibration standards by depositing known amounts of Pb directly onto discs prepared from unexposed glass fiber filter paper was quite successful. Preparation of 6 individual sets of standards by this method showed a mean difference of 3.27% in the response of standards prepared to contain 10 μg of Pb.

The efficacy of this approach to calibration is further demonstrated by the results of the analysis of a filter disc containing 5 μg of Pb, prepared by this direct deposition method from the NIST source, and analyzed with each group of sample filter discs as an unknown. For 12 separate 5 μg additions analyzed over a 6 month period, the mean value of Pb measured is $101.6 \pm 2.8\%$.

Sample homogeneity

Previous analysis of glass fiber filters by the acid sonication/AA procedure have shown that there can be an uneven distribution of material across the entire filter or even within the 2.54-cm wide strip. The AA method extracts and analyzes the entire filter strip. Other XRF applications to the analysis of metals in air particulates collected on filter media involve analysis of various sections of the filter. In all other cases, only a very small fraction of the entire filter is actually subjected to the XRF analysis, taking only one³ or several⁴ filter discs per filter. For our application, analysis of a single filter disc would mean that only 10% of the filter strip would be analyzed.

Table 2. AA/WDXRF comparison

Thrd Quarter 1989		
Sampling Site	No of Samples	Mean \pm SD AA/WDXRF
Newark	16	1.08 \pm 0.10
Newark Boys Club	15	1.01 \pm 0.13
Deepwater	13	1.18 \pm 0.29
New Brunswick	16	1.12 \pm 0.26
Fourth Quarter 1989		
Sampling Site	No of Samples	Mean \pm SD AA/WDXRF
Newark	15	0.94 \pm 0.12
Newark Boys Club	9	0.76 \pm 0.15
Deepwater	7	1.00 \pm 0.18
New Brunswick	21	0.84 \pm 0.14

To compensate for the uneven distribution of Pb across the surface of the filter strip, 5 discs were cut from each filter strip taken from samples which were collected at different locations in New Jersey. The discs from each filter strip were obtained by taking one cut near each end, two between the center and each end and one from the center. Analysis showed significant inhomogeneity in the distribution of Pb; the average deviation of the mean ranged from 1.82 to 16.25%.

Results

Five high volume sampling locations were selected to compare the results of analysis of lead by the standard sonication/AA and WDXRF methods. The sampling locations ranged from urban areas where there are high air particulate concentrations to rural areas where the particulate air concentrations are much lower.

Filter strips from each site from a six month period in 1989 were first analyzed by WDXRF, and then the entire strip analyzed by the sonication/AA method. The values in Table 2 are the mean AA/WDXRF ratios and standard deviations obtained for each sample at each site. The data shows generally good agreement between results generated by the two methods. The lower ambient amounts of Pb collected at the Newark Boys Club and New Brunswick sites may contribute to the lower AA/WDXRF ratios.

Table 3. Analysis of NIST filters

Filter	NIST Value	AAS Value	WDXRF Value	AA/NIST	WDXRF/NIST
1C	7.47	7.22	7.29	0.97	0.97
2C	14.92	16.30	14.27	1.09	0.96
3C	29.81	29.92	24.05	1.00	0.81

All values in μg filter

Table 4 Analysis of polymer film standards

Date of Analysis	Pb Added to Filter μg	Measured Pb, μg
4-10-90	2.00	2.08
5-10-90	2.00	2.00
6-10-90	2.00	2.04
7-10-90	2.00	2.04
4-10-90	10.00	9.45
5-10-90	10.00	9.28
6-10-90	10.00	9.33
7-10-90	10.00	9.13

This quality of the agreement between the results generated by the AA and WDXRF techniques is reinforced by the analyses of filter media containing known amounts by both techniques as discussed below.

Quality assurance

In our WDXRF method of analysis, glass fiber filter discs containing 5 μg of added Pb (prepared as above from the NIST SRM) are analyzed after every 10 measurements. The criteria for data acceptance has been established as $\pm 10\%$ of the added value. Recoveries ranged from 97.8 to 105.0% over the six-month duration of this study.

Several other types of filter media containing known amounts of Pb were analyzed during the course of this study. Samples of cellulose acetate filter paper impregnated with Pb (as well as with known amounts of Cd, Cr and Ni) were analyzed by both the WDXRF and AA/sonication procedures. As shown in Table 3 the data obtained by both methods agreed well with the NIST-certified values for samples 1C and 2C. For sample 3C the solution containing Pb was applied off the center of the disc; the placement of the disc may have resulted in an incomplete exposure to the x-ray beam, accounting for the lower value.

Mylar polyester film impregnated with known amounts of Pb were obtained from Micro Matter Co. Analysis of the materials over a four month period showed good agreement with the known value (not certified), which is another

indicator of the long-term stability of the instrument calibration (Table 4). These results can also be used to decide when re-calibration is necessary.

As mentioned earlier in the paper, samples of glass fiber filters that are impregnated with lead were obtained from EPA's Research and Monitoring Evaluation branch to evaluate the equivalency between the XRF and AA methods of analysis. The filter strips were cut into sections and analyzed by XRF. The total filter strip was then extracted by sonicating in dilute *aqua regia* and analyzed for lead by AA. The results obtained are shown in Table 5, and again indicate the accuracy of both the WDXRF and the sonication/AA methods.

CONCLUSIONS

We have shown that WDXRF is a viable analytical method for the analysis of Pb in air particulates that are collected on glass fiber filter paper with this method for calibration and analysis. Our QA studies suggest that this procedure can be extrapolated to the measurement of Pb on other filter media. We are currently examining the efficacy of this approach to the analysis of other metals on glass fiber and quartz filter media.

REFERENCES

- 1 *Reference Method for the Determination of Pb in Suspended Particulate Matter Collected from Ambient Air*, United States Environmental Protection Agency, United States Federal Register, 1978, 43, 194
- 2 T LaFisca, *Determination of Metals in Suspended Particulate Matter Collected from Ambient Air*, New Jersey Department of Environmental Protection Standard Operating Procedure, DEP-DEQ/AS-031, 1989
- 3 J R. Rhodes, A H. Preadzynski, C. B Hunter, J. S Payne and J L. Lindgren, *Env. Sci. and Tech.*, 1972, 6, 922.
- 4 H. Moore and S Wirtz, *Determination of Pb Concentration in Ambient Particulate Matter by Wavelength-Dispersive X-Ray Fluorescence Spectrometry*, California Department of Health Services, Air and Industrial Hygiene Laboratory, 1980, Report EQL-0581-052

Table 5 Analyses of EPA filters

EPA Value	AA Value	% Difference	WDXRF Value	% Difference
625	607	-2.9	606	-3.0
140	141	0.7	135	-3.6
117	119	2.0	107	-8.2
117	122	4.5	110	-6.0
290	—	—	293	+0.03
780	—	—	792	+1.5

All values in μg filter —Not measured

COMPLEXATION OF Eu AND Tb WITH FULVIC ACIDS AS STUDIED BY TIME-RESOLVED LASER-INDUCED FLUORESCENCE

G. BIDOGLIO, I. GRENTHE*, P. QI†, P. ROBOUCH and N. OMENETTO‡

Commission of the European Communities, Joint Research Centre, Environmental Institute,
21020 Ispra (VA), Italy

(Received 14 February 1990. Revised 24 February 1991 Accepted 26 February 1991)

Summary—Complexation of Eu and Tb with fulvic acids (FA) has been studied by time-resolved laser-induced fluorescence. The lanthanide species are excited by a pulsed Xe/Cl excimer laser and the short-lived luminescence of the fulvic acids is eliminated by time gating. The conditional binding constants (K') and the total metal-binding capacities of the fulvic acids have been determined from the equilibrium titration curves. No significant variations of the $\log K'$ values (about 6) have been found in the pH range investigated (2.7, 5.5, 6.5) at ionic strengths of 0.1 and 1M (NaClO₄). An inverse relationship of K' to total metal concentration is observed. Substitution of Eu for Al has been found to depress the fluorescence signal of the Eu-FA complex. The binding constants of Al³⁺ and Eu³⁺, derived from the competition experiments, are of the same order of magnitude. The effect of competition on metal binding and trace-metal transport is discussed.

The importance of humic/fulvic acids for the transport and bioavailability of trace metals in surface-water systems has been recognized for a long time.^{1,2} Extensive experimental studies have been made on the composition of humic/fulvic acid materials,^{1,3} their acid-base properties,⁴⁻¹³ and their metal-binding characteristics.^{7-9,13-16} Humic/fulvic acids are heterogeneous materials with a large range of molecular weights. It is generally recognized that they are polyelectrolytes containing a set of different functional groups, *cf.* Marinsky and co-workers^{10,11} for a recent literature survey. Their metal and hydrogen-ion binding have been described by means of site-specific binding constants,^{5,12,13} and of a continuous distribution of binding constants.⁷ The stoichiometry of the metal-binding reactions, and their equilibria, are in general described by the equation:



where M denotes a metal ion and HFA the humic/fulvic acid in a state of protonation that is dependent on the pH of the solution. M is in

general not the free metal-ion, Mⁿ⁺, but symbolizes all metal species not bound to the fulvic/humic acid. The equilibrium constant for reaction (1) is thus a *conditional* constant. Some authors have used more elaborate models, involving the stepwise binding of several FA to each metal ion (*e.g.*, Bertha and Choppin⁴ and Torres and Choppin¹⁷), and the formation of ternary complexes such as CuOCuFA (Ephraim and Marinsky¹³).

Traditional solution chemical methods, such as potentiometry (*e.g.*, Buffle *et al.*¹⁴) ion-exchange (*e.g.*, Ephraim *et al.*¹⁸), solvent extraction (*e.g.*, Torres and Choppin¹⁷) and spectrophotometry (*e.g.*, Moulin *et al.*¹⁶) have been used to study the chemical equilibria between humic/fulvic acids and metal ions. The potentiometric studies typically involve direct measurement of the free metal-ion concentration with an ion-selective electrode,¹⁴ rather than an indirect measurement through the hydrogen-ion concentration (*cf.* Ephraim *et al.*,¹¹ Figs. 14-19). The potentiometric methods require a total metal-ion concentration larger than, say, 0.1mM. The ion-exchange and solvent extraction techniques can be used at trace level concentrations, say from 10⁻¹⁰ to 10⁻⁷M. The spectrophotometric method is complicated by the strong light-absorption of the humic/fulvic acids and it seems possible to use light-absorption measurements only for systems

*On leave from the Royal Institute of Technology, Department of Inorganic Chemistry, Stockholm, Sweden.

†On leave from the Institute of Mechanics, Chinese Academy of Sciences, Beijing, People's Republic of China

‡Author to whom all correspondence should be sent

where the metal ion has absorption bands at wavelengths longer than 600 nm, *cf.* Moulin *et al.*¹⁶

Methods based on the quenching of ligand fluorescence were introduced ten years ago¹⁹ and have recently been discussed by Cabaniss and Shuman.²⁰ Laser-induced fluorescence (LIF) is a well established technique that has been extensively used to study metal binding to biomolecules,²¹ as well as for the study of metal binding in humic/fulvic acid systems.²²

During the last two years we have used this method in an exploratory study of metal binding to fulvic acids. We have studied the bonding of europium, terbium and aluminium to a fulvic acid from Bersbo, Sweden. This material has been characterized¹² by Allard and his group. Europium and terbium were chosen because of their fluorescence properties, but also because they are good model ions for trivalent actinides. Humic/fulvic acids are efficient transport vectors for trace metals in ground- and surface-water systems. Information on their role in the transport of actinides is relevant for the understanding of the radioecology of these elements, and also for the possible environmental impact caused, for example, by leakage from nuclear installations of various kinds.

The binding of trace metals, (TM), to the humic/fulvic materials present in ground- and surface-water systems is a competitive process which takes place in the presence of relatively large concentrations of Mg(II), Ca(II), Fe(II,III), Al(III), *etc.*, according to the equilibrium:



The ratio $[(\text{TM})\text{FA}]/[\text{MFA}]$ depends on the equilibrium constant of equation (2) and the ratio $[\text{M}]/[(\text{TM})]$. No experimental measurements of equilibria of type (2) have been published, a fact which makes it difficult to quantify trace-metal binding. We have therefore studied the competition between aluminium and europium in a fulvic acid system. Aluminium is one of the most important humic/fulvic acid binding elements in nature. However, it is difficult to study its binding directly. Such information may be obtained by combining experimental information from the binary Eu-FA and the ternary Al-Eu-FA systems.

We were also interested in developing fluorescence spectroscopy as a diagnostic tool in order to determine whether Eu(III)/Tb(III)

and, hence, trivalent actinides can bind to the organic materials in ground- and surface-water samples. Information of this type is obviously of interest in radioactive-waste management.

The points of main interest in the present study were to use the sensitivity of the LIF method as a tool for

- (i) determining whether Eu(III)/Tb(III) can bind to organic material in its form present in ground-water samples;
- (ii) comparing fluorescence methods with other techniques for the determination of metal-fulvic acid binding constants;
- (iii) exploring the use of competition methods, with Eu/Tb as probes, for the study of metal-fulvic acid interactions.

EXPERIMENTAL

Reagents

Sodium perchlorate, sodium acetate, acetic acid, sodium hydroxide, perchloric acid, and europium and terbium chlorides were all of analytical grade. The stock solutions of the reagents were prepared with doubly distilled water. They were analysed by standard analytical procedures and their concentrations were known with an accuracy better than 0.5%. Solutions used in the measurements were prepared from the stock solutions by use of standard flasks and calibrated Eppendorf pipettes. Their concentrations were calculated from the known volumes and concentrations of the stock solutions used. The fulvic acid was obtained from the University of Linköping, Sweden. Its properties have been described extensively:¹² the material has a titratable acid capacity in water of 4.65 ± 0.15 meq/g and contains several different acid sites (20% with $pK = 1.7$; 25% with $pK = 3.3$; 30% with $pK = 5$; 20% with $pK = 6.5$ and 5% with $pK = 7$). A stock solution of FA was prepared by weighing a suitable amount of the solid fulvic material and dissolving it in distilled water. The solution was analysed by spectrophotometry (extinction coefficient 27 ± 1 $\mu\text{g}^{-1} \cdot \text{cm}^{-1}$, at 250 nm).

Instrumentation

A tunable dye laser pumped by an excimer laser, and the excimer laser alone were used throughout the experiments. The excimer laser (Lambda Physik, Model EMG-102, Göttingen, Germany) was operated with an Xe/Cl mixture, delivering a 20 nsec pulse of about 100 mJ (at 308 nm) at a variable repetition frequency

(1–100 Hz). The rectangular beam, which was conveniently filtered and shaped with a circular aperture (5 mm diameter), was folded by a quartz prism and mildly focused by a spherical quartz lens (25 cm focal length) into the fluorescence cuvette. At the cuvette, the energy of the laser was reduced to 3–5 mJ. When the tunable dye laser (Jobin Yvon, Longjumeau, France) was installed in front of the excimer laser, the latter could be used as a pump laser by diverting part of its output with a beam splitter. The dye laser, consisting of an oscillator section plus an amplifier section, provided the necessary tunability for the various experiments. Its output beam was directed and focused in the same fluorescence cuvette by means of two prisms and a spherical lens, both laser beams (dye and excimer) were used alternatively, according to the experiments to be performed. The fluorescence light, collected at right angles by another lens (15 cm focal length) was dispersed by a grating monochromator and measured with a photomultiplier (Hamamatsu, Model R928S, Hamamatsu Corp., Japan) wired for fast response. Two monochromators were used, having 1.29 m and 10 cm focal lengths, respectively. The former instrument provided good resolution and stray-light rejection, and the latter was used for its simplicity and convenience of operation. Both monochromators were equipped with scanning facilities to obtain a fluorescence spectrum, whenever needed. The photomultiplier signal, after suitable amplification obtained with a preamplifier directly attached to the anode, was sent into one channel of a boxcar integrator (Stanford Research Corp., Model SR250, U.S.A.) and a digital storage oscilloscope (Tektronix, Model 2430, U.S.A.), which was directly interfaced to a computer (Hewlett Packard, Model 9816). The measuring gate of the boxcar could be adjusted to reject completely the fast fluorescence component. However, since the photomultiplier was not operated stroboscopically, the fast fluorescence signal of the fulvic acids was so strong that it caused saturation of the tube and/or preamplifier (with consequent ringing). The gate was then opened after complete recovery of linear operating conditions. This obviously limited the resolution of fast-decay components in the signal and the possibility of deconvolution of multicomponent decay. The energy of both lasers was constantly monitored by a pyroelectric detector positioned near the cuvette: its output was fed into the other channel of the

boxcar integrator and continuously displayed on a strip-chart recorder.

Choice of conditions for fluorescence excitation

We use the fluorescence data for the interpretation of chemical equilibria in metal–fulvic acid systems. The technique used is the same as in other spectrophotometric methods, *cf.* Rossotti and Rossotti.²³ It is of great advantage for the interpretation of such data if the experiment can be done in such a way that only one or a few species will contribute to the measured absorptivity (or fluorescence intensity) of the solution. For precise measurements it is of course also desirable to have a large value of the molar absorptivity (or the corresponding emission coefficient) for the absorbing (emitting) species. Europium is often excited by using a dye laser tuned to 394 nm, which corresponds to a resonant absorption transition in the metal ion. The fluorescence observed corresponds to the $^5D_0 \rightarrow ^7F_2$ “hypersensitive” transition at 616 nm, and the $^5D_0 \rightarrow ^7F_1$ transition at 592 nm. With 394 nm excitation the fluorescence spectrum will contain significant contributions from both free Eu and bound Eu, *cf.* Dobbs *et al.*²² The excitation of the *bound* europium occurs much more efficiently through the excitation of the fulvic acid molecule, followed by an energy transfer to the metal. With such an excitation mechanism, there should be a very strong increase in fluorescence of the bound europium when exciting the ligand at shorter wavelengths, where the molar absorptivity is higher. At the same time the excitation of the free Eu ion should be negligible. This is indeed what happens: a direct excitation at 308 nm with the Xe/Cl excimer laser increases the fluorescence of bound europium (EuFA) and it is only this species which contributes to the measured fluorescence intensity. We have evaluated the decay times of the EuFA complex both with 308 and 394 nm excitation and found them to be the same within experimental error ($\sim 10\%$), indicating a similar excitation mechanism in both cases. The same conclusion seems to hold for the terbium–fulvic acid system, on excitation at 308 and 228 nm. Fulvic acids are known to be sensitizers in photoredox reactions.²⁴ We found no clear evidence of decomposition or redox reactions in the solutions used in our experiments, and both the europium and terbium systems behaved in a similar way. In some cases, however, we observed a transient signal, the fluorescence decreasing noticeably and then stabilizing after

20–30 sec, indicating that some kind of photochemical reaction was occurring. We have no conclusive experimental evidence of such a phenomenon, which certainly deserves a more systematic investigation.

Procedure

Most experiments were titrimetric in nature, two solutions of known composition being mixed in a titration vessel. The two solutions had the same hydrogen-ion concentration, in general obtained by use of an acetate buffer. The hydrogen-ion concentrations of the initial solutions and the solution in the titration vessel were measured by using a combined Ross glass-electrode (Orion, Model 810200, U.S.A.) and a pH-meter (Radiometer, Model PHM84, Denmark). The reference solution of the electrode had the same ionic strength as the test solution (0.1 or 1.0M NaClO₄). The electrode was calibrated in concentration units with an acetate buffer of known [H⁺]. The precision of the pH measurements was better than 0.005, and the accuracy about 0.03. The fluorescence was measured in 1 cm fused-silica cuvettes with 3 ml samples withdrawn from the test solutions. At the lowest metal concentrations (10⁻⁸M or less) we measured the blank correction of pure fulvic acid. The blank correction for free Eu(III) was negligible in the Eu(III)–FA titrations carried out with the excitation set at 308 nm. Sorption on the walls, important at concentrations lower than 10⁻⁷M, was found to be fairly slow (a few hours). The sorbed EuFA could be removed by washing with concentrated mineral acid.

The titrations were in general done at constant metal-ion concentration by mixing a solution S containing 2 × 10⁻⁵ or 2 × 10⁻⁷M M(III), 10mM acetate buffer and sodium perchlorate to give an ionic strength *I*, with a solution T of the same composition as S but containing a known quantity of fulvic acid, usually 50 ppm. The titrations were done at three different hydrogen-ion concentrations, -log[H⁺] = 2.7, 5.5 or 6.5, and two ionic strengths, *I* = [Na⁺] = 0.1 or 1.0M.

A few titrations were done by starting with a solution containing fulvic acid (50 ppm) and no metal, and then increasing the metal-ion concentration by adding a titrant containing only the metal-ion.

The competition experiments had to be done in such a way that the ratio [Al]/[Eu] was larger than 10. In order to avoid too high an Al(III) concentration we had to use

[Eu(III)] = 2 × 10⁻⁷M. The experiments were done as titrations at pH 5.5, at constant Eu(III) concentration, by increasing the fulvic acid concentration. After each addition of FA a 3 ml sample was withdrawn from the test solution and its fluorescence intensity measured. Three successive additions of a concentrated Al(III) solution were made to the solution in the cuvette. After each addition the fluorescence intensity was measured. The additions were so small that the Eu(III) and FA concentrations did not change appreciably (the largest change was 3%). To avoid the formation of a precipitate (detectable through light-scattering) we had to keep [Al(III)] < 2 × 10⁻⁵M.

TREATMENT OF DATA

Binary system: M–FA

It is generally assumed that the reactions with humic/fulvic acids are of the type exemplified by equation (1). As most experimental studies are made with buffers at constant pH, it is practical to write this equation as:



with an equilibrium constant

$$K' = [MFA]/[M][FA] \quad (4)$$

where *K'* is a conditional constant which depends on the pH, the ionic strength and the total concentration of the metal ion. Titrations of M and FA often result in titration curves of the type shown in Fig. 1. In all the figures shown, the intensity of the fluorescence signal (FI) is given in arbitrary units. This curve shape, corresponding to 1:1 stoichiometry, shows that only one species is formed. We prefer to consider the binding in humic/fulvic acids as an ion-exchange process and not a process similar to complex formation with small ligands.

We will use equation (3) as a purely phenomenological description of the equilibrium in metal–fulvic acid systems. The following notations will be used:

μ_{FA}	the maximum fluorescence, in arbitrary units
FI	the fluorescence of the test solution (same units as above)
[M] _t	total metal-ion concentration (<i>M</i>)
[M]	concentration of metal-ion not bound to FA (<i>M</i>)
<i>c</i>	total metal-binding capacity of fulvic acid (mole/g)

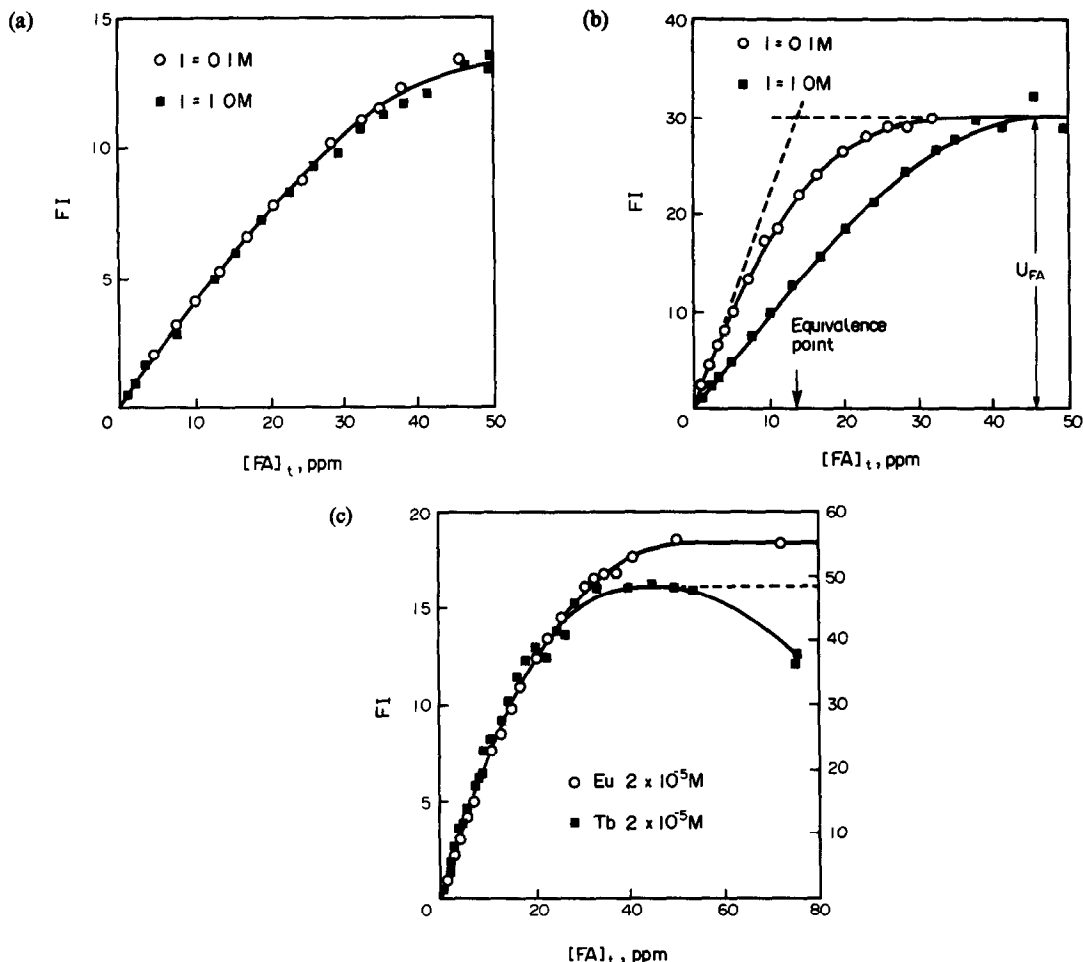


Fig. 1 Equilibrium titration curves of lanthanides with fulvic acids in NaClO_4 solutions at different pH values and ionic strength (I). The fluorescence signal (FI) is given in arbitrary units ($\lambda_{\text{exc}} = 308 \text{ nm}$) (a) $[\text{Eu}]_i = 2 \times 10^{-5} \text{ M}$, pH 2.7, (b) $[\text{Eu}]_i = 2 \times 10^{-5} \text{ M}$, pH 6.5; (c) $I = 0.1 \text{ M}$, pH 5.5.

$[\text{FA}]_t$ total fulvic acid concentration (g/l.)
 $[\text{FA}]$ free fulvic acid concentration (M)
 $[\text{MFA}]$ complex concentration (M).

The following relations can then be written:

$$[\text{MFA}] = [\text{M}]_i \text{FI}/u_{\text{FA}} \quad (5)$$

$$[\text{M}]_i = [\text{M}] + [\text{MFA}] \quad (6)$$

$$c[\text{FA}]_t = [\text{FA}] + [\text{MFA}] \quad (7)$$

By substituting equations (5–7) into (4) we obtain

$$K' = (\text{FI}/u_{\text{FA}})/(1 - \text{FI}/u_{\text{FA}}) \times (c[\text{FA}]_t - [\text{M}]_i \text{FI}/u_{\text{FA}}) \quad (8)$$

Fi and u_{FA} are measured experimentally, and c is measured from the extrapolated equivalence point, as indicated in Fig. 1b. The equilibrium constant K' is then calculated from equation (8). We have in general preferred a curve-fitting method, where a set of curves of FI vs. $[\text{FA}]_t$ is

calculated for given values of the experimental parameters $[\text{M}]_i$, $[\text{FA}]_t$, c , and u_{FA} , with K' as a predictor variable. A set of such curves is shown in Fig. 1b. The results of the experimental studies are shown in Fig. 1 and Table 1 (see later).

Ternary system: competition experiments with Al(III)

Some previous studies of the interaction between aluminium and humic acids were done by using distribution methods such as ion-exchange²⁵ and equilibrium dialysis.²⁶ Laser-induced fluorescence is a convenient non-invasive method to study the competition between Al(III) and Eu(III), i.e., the equilibrium:



The equilibrium constant $K'(\text{Al}/\text{Eu})$ for reaction (9) is also a conditional constant, valid only for the ionic medium and pH investigated.

Table 1 Binding constants and capacities of Eu(III) and Tb(III) for the Bersbo fulvic acid, at various $-\log[H^+]$ values, ionic strengths, I , and total lanthanide concentrations, $[M]$

I	$[M]$	Binding capacity, <i>mmole M(III)/g FA</i>			$\log K'^{\dagger}$		
		2 70*	5 56*	6 51*	2 70*	5 56*	6 51*
0.1 M	Eu, $2 \times 10^{-5} M$	0.60 ± 0.10	0.81 ± 0.08	1.35 ± 0.10	6.20 ± 0.10 (6.20 ± 0.10)	5.95 ± 0.10 (6.3 ± 0.1)	6.00 ± 0.10 (6.5 ± 0.1)
1.0 M	Eu, $2 \times 10^{-5} M$	0.60 ± 0.10	0.91 ± 0.09	0.66 ± 0.06	6.00 ± 0.05 (6.00 ± 0.05)	6.0 ± 0.1 (6.2 ± 0.1)	6.40 ± 0.10 (6.7 ± 0.1)
0.1 M	Eu, $2 \times 10^{-7} M$		0.15 ± 0.09			7.90 ± 0.10 (8.3 ± 0.1)	
0.1 M	Tb, $2 \times 10^{-5} M$		1.04 ± 0.10			5.95 ± 0.10 (6.3 ± 0.1)	

* $-\log[H^+]$

† The values in parentheses are the binding constants corrected for acetate complex formation

However, this is sufficient to obtain information about the relative bonding strengths of Eu(III) and Al(III) to FA, information which is relevant for the transport properties of trace quantities of trivalent lanthanides and actinides in ground- and surface-waters. For the competition experiments, the following additional mass balance and equilibrium conditions have to be considered:

$$[Al]_t = [Al] + [AlFA] \quad (10)$$

$$K'(Al/Eu) = [AlFA][Eu]/[EuFA][Al] \quad (11)$$

It follows that relation (7) must be adapted to give:

$$c[FA]_t = [FA] + [EuFA] + [AlFA] \quad (12)$$

$K'(Al/Eu)$ can be calculated by substituting equations (4)–(6), (10) and (12) in (11); it is then expressed in terms of measurable quantities, as in equation (8). We have calculated theoretical curves for FI *vs.* $[FA]_t$ in given experimental conditions; by comparing the experimental data with such theoretical curves (see Fig. 3, below) we were able to estimate $K'(Al/Eu)$.

RESULTS AND DISCUSSION

Determination of binding constants and binding capacities for Eu(III) and Tb(III) with the Bersbo FA

The binding capacities and binding constants for Eu(III) (and Tb(III)) were determined at different ionic strengths, pH values and total metal-ion concentrations. Some of the experimental results are shown in Fig. 1, and the binding capacities and binding constants are given in Table 1. At high concentrations of fulvic acid, the fluorescence signal of Tb showed a marked decrease in intensity (See Fig. 1c). Since absorption of the fluorescence emission by

the non-complexed FA is stronger at 544 nm (Tb) than at 617 nm (Eu), it is conceivable that an inner-filter effect is responsible for the observed phenomenon.

The experimental conditional equilibrium constants were corrected for acetate complex formation by using the equilibrium constant for the reaction: $Eu^{3+} + Ac^- \rightleftharpoons EuAc^{2+}$, determined in 0.5 M NaClO₄,²⁷ and recalculated to 0.1 and 1.0 M ionic strength by the specific ion interaction theory.²⁸ The following interaction coefficients were used: $\epsilon(Eu^{3+}, ClO_4^-) = 0.49 \pm 0.03$; $\epsilon(Ac^-, Na^+) = 0.08 \pm 0.01$ and $\epsilon(EuAc^{2+}, ClO_4^-) = \epsilon(YHCO_3^{2+}, ClO_4^-) = 0.39 \pm 0.04$. The values corrected in this way are given in Table 1.

In a separate titration we investigated the pH-profile of the fluorescence at $[FA]_t = 50$ ppm and $[Eu]_t = 2 \times 10^{-5} M$. The result is shown in Fig. 2. This curve indicates a pronounced pH-dependence of the fluorescence. However, no further studies have been made in order to

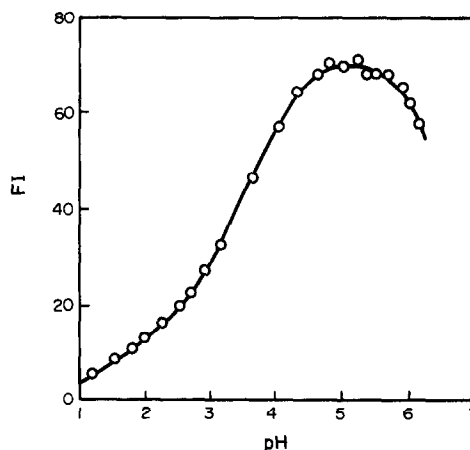


Fig. 2. pH-dependence of the Eu fluorescence signal in a 50 ppm FA solution; $[Eu]_t = 2 \times 10^{-5} M$, $I = 0.1 M$ (NaClO₄); $\lambda_{exc} = 308$ nm

ascribe this effect either to changes in the binding sites of the MFA complex, or to variations in the excited-state number density, caused by collisional quenching.

Competition between Al(III) and Eu(III) for FA

The competition experiments show clearly that the fluorescence intensity of EuFA decreases on addition of Al(III), provided the ratio Al(III)/Eu(III) is larger than 10, *cf.* Fig. 3. This decrease is not due to quenching of the EuFA fluorescence, as the decay-time does not seem to be influenced by the presence of Al(III), but to a chemical competition.

From the experimental data we obtain $\log K'(Al/Eu) = -1.6 \pm 0.2$. It is difficult to obtain a precise value of this exchange constant because of its small value and the experimental difficulties due to the precipitate formation encountered at high $[Al]_t$. By correcting this equilibrium constant for the formation of europium-acetate²⁷ and aluminium-hydroxide²⁹ complexes we obtain $\log K'(Al/Eu)_{corr} = -0.6$, *i.e.*, the binding constants of Al^{3+} and Eu^{3+} are of the same order of magnitude.

Several considerations arising from the matter above are now felt appropriate. First, we consider the technical quality of the binding-constant determinations. A comparison with previously used spectrophotometric methods (*cf.* Moulin *et al.*¹⁶) shows the very obvious advantage that no correction is needed for the light absorption of the ligand, and that the measured fluorescence is dependent only on the concentration of MFA. The change in fluorescence emission throughout the titration is also much larger than the change in light absorption, with a resulting increase in the sensitivity and precision of the fluorescence method. The method is also fast and a complete titration with 15 experimental points takes less than an hour to perform. In our experiments we have used acetate buffers to ensure a good buffer capacity of the chemical system. This is necessary when using low total concentrations of metal ion and ligand. When working at higher total concentrations, it should be quite feasible to use the buffering capacity of the fulvic acid and a much less sophisticated experimental set-up, *e.g.*, a spectrofluorimeter, can then be used. However, a pulsed excitation source and gated detection are necessary to avoid measuring the strong FA fluorescence. The equilibrium constants determined by us are nearly identical with the value for Am(III)-FA obtained by Moulin *et al.*¹⁶

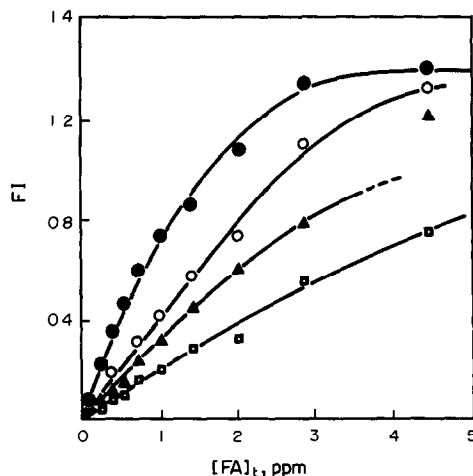


Fig 3. Fluorescence titration curves of $2 \times 10^{-7} M$ Eu in $0.1 M$ $NaClO_4$ at pH 5.5 in the presence of different concentrations of Al: (●) no Al, (○) $3.3 \times 10^{-6} M$; (▲) $10^{-5} M$, (□) $2.3 \times 10^{-5} M$. The solid lines represent the theoretical curves, obtained as described in the text

under similar conditions, with the same FA. Europium, terbium and americium are expected to have similar chemical properties. Many of the other quantitative results also agree well with the known chemical properties of the Bersbo FA. The metal-binding capacity at a given ionic strength increases with pH, in keeping with the presence of functional groups of different acidities. The highest binding capacity, $1.30 \pm 0.10 mM$ Eu/g FA, or 3.90 ± 0.30 meq/g at pH 6.5, is close to the total aqueous titratable exchange capacity, 4.86 ± 0.15 meq/g.

The observation that the binding constant and the binding capacity vary with the total metal concentration, *cf.* Table 1, is also in qualitative agreement with the observations of Ephraim *et al.*¹² The higher the total concentration of metal ion, the greater the number of the protonated functional groups used for metal binding. $[MFA]$ increases more slowly than $[M]_t$, hence the conditional equilibrium constants decrease with increasing $[M]_t$, in agreement with the observations. There is no polyelectrolyte effect at pH 2.7, also in agreement with Ephraim's observations on protonation equilibria.¹² The ionic-strength dependence of the binding constant is small in the pH range investigated, and is largest at pH 6.5, where the degree of dissociation of the ligand is largest.

From the data of Ephraim *et al.*¹² we have estimated that the degree of ionization of the FA at the pH values studied is $\alpha = 0.3, 0.77$ and 0.93 , respectively. However, the binding constants vary fairly little in the same pH range,

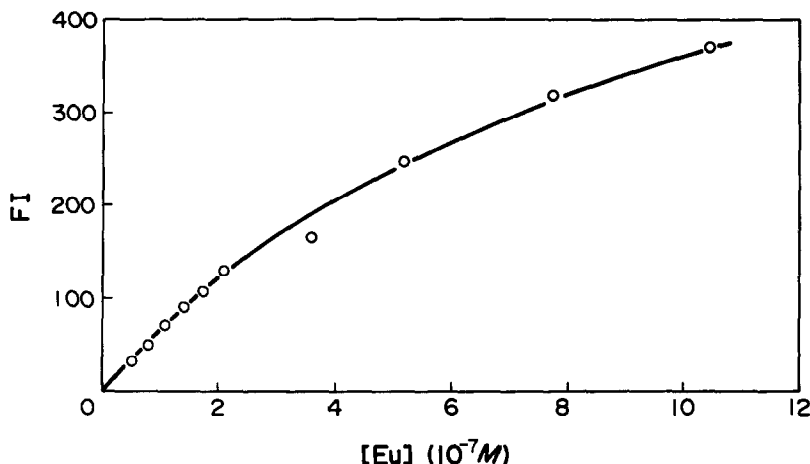


Fig 4 Sensitivity curve of EuFA fluorescence pH = 5.5, $I = 0.1M$ (NaClO_4); 3 ppm FA, $\lambda_{\text{exc}} = 308$ nm; $\lambda_{\text{em}} = 617$ nm

from $\log K' = 6.2 \pm 0.1$ at pH 2.70 to $\log K' = 6.5 \pm 0.1$ at pH 6.51. The magnitude of the binding constants and their pH variation in the range $5.5 < \text{pH} < 6.5$ are in fair agreement with observations on the same system studied by using an ion-exchange method.¹⁸ The pH-dependence of the Eu(III)-FA system seems to be smaller than that observed for humic acid.¹⁷ The observed binding constant for Eu(III)-FA is also in good agreement with the observations of other investigators.^{15,16}

Spectrophotometric data can be used to obtain thermodynamic information and may, in addition, provide information about the chromophore. However, we found no, or only very small, changes in the shape, intensity ratios and peak positions in the emission spectra. This is perhaps not surprising, bearing in mind that the same donor (oxygen) is present in all the different functional groups of the ligand.

It should be pointed out that the shape of the titration curves gives no indication of the stoichiometry of the complex, showing only that the ligand at a given pH contains a given number of sites which can be occupied by the metal ion in an ion-exchange reaction. We do not think it proper to use the concept of step-wise complex formation, as used for example by Choppin *et al.*^{15,17} The polyfunctionality could possibly be studied by the method developed by Fronaeus³⁰ for polyfunctional ion-exchangers.

Identification of lanthanide binding sites in humic/fulvic material (under in situ conditions)

The very high sensitivity of the fluorescence methods made it feasible to study europium

binding to organic material present in ground-water samples. In a preliminary experiment we tested the sensitivity of the europium fluorescence method by using test solutions containing 3 ppm FA, a 10mM acetate buffer of pH 5.5, and I 0.1M. The europium concentration varied from 5×10^{-8} to $10^{-6}M$. The resulting experimental curve is shown in Fig. 4. The deviation from linearity may be due to the fact that, with increasing Eu(III) concentrations, the Eu(III)/FA ratios might shift outside the plateau region, with a consequent decrease of the fluorescence signal.

The presence of lanthanide/actinide-binding organic materials in ground-water systems is easily tested for by adding a few μl of 0.01M EuCl_3 solution to 100 ml of the water sample and recording its emission spectrum immediately. An example of such a test on a ground-water from Gorleben (Germany) is shown in Fig. 5. The source and the characteristics of this water are given in the legend of the figure. The concentrations of metal ions which can compete with Eu(III) for the organic material are very low in this water.

An advantage of the technique is that it provides direct information on the lanthanide/actinide bonding under *in situ* conditions, *i.e.*, in the presence of all competing ions, such as Ca(II), Mg(II), Fe(II,III), Al(III), *etc.* The fluorescence method gives only qualitative information. Quantitative data usually require much more idealized systems such as the chemically separated HA/FA materials used in the present work.

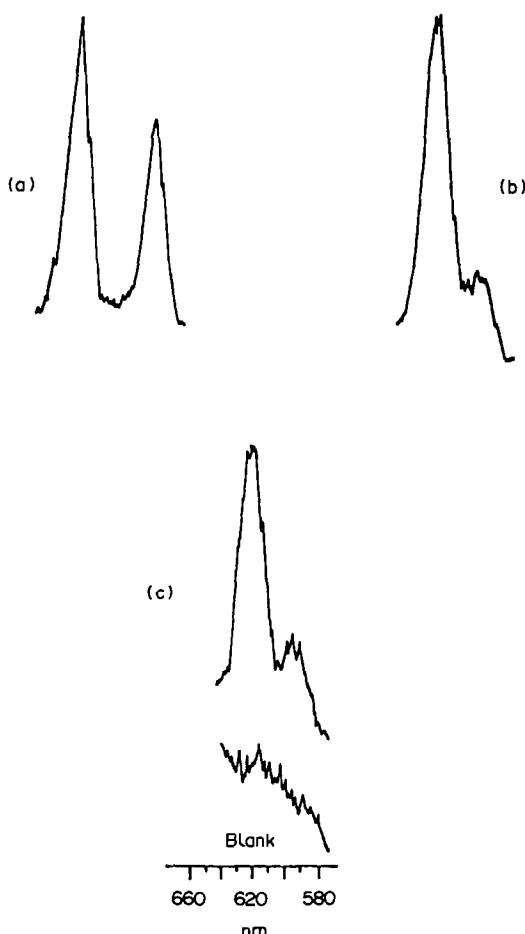


Fig 5 Typical emission spectra of various Eu(III) species (a) Eu free ions in 0.1 M NaClO₄, pH = 5.5, [Eu]_i = 10⁻⁵ M, λ_{exc} = 394 nm, (b) EuFA complex in 0.1 M NaClO₄, pH = 5.5, [Eu]_i = 10⁻⁸ M; [FA]_i = 3 ppm; λ_{exc} = 308 nm, (c) EuFA complex in a Gorleben ground-water (pH = 8, total carbonates 2 × 10⁻³ M), λ_{exc} = 308 nm; [Eu]_i ~ 4 × 10⁻⁸ M. The detection sensitivity has been optimized for each spectrum

Competitive metal binding and its consequences for trace metal transport

It is obvious from equation (9) that the binding of trace metals such as Eu(III) to HA/FA is influenced by the presence of other cations (and competing ligands, such as OH⁻). The *relative load* of cations is important for the transport capacity of the humic/fulvic material. We have made a model of this, using a Gorleben type water with 16 ppm Ca(II) as the main HA/FA-binding metal ion. The conditional binding constants at pH 6.5 are: log *K'*(Eu) = 6.5 and¹⁴ log *K'*(Ca) = 2.4. By using these constants and the total concentrations [Ca]_t = 4 × 10⁻⁴ M (16 ppm), [Eu(III)]_t = 10⁻⁹ M and [FA]_t = 1 and 10 ppm, we have calculated the concentrations of EuFA and CaFA, assum-

ing that the HA/FA has a metal-binding capacity of around 10⁻³ M Eu(III)/g. We find that with 1 ppm HA/FA 64% of the Eu(III) is bonded as EuFA; the corresponding quantity at 10 ppm is 95%. Deep ground-water often contains little organic material (from <0.1 to 1 ppm is not uncommon³¹ and high Ca(II) concentrations (3.5–9 × 10⁻⁴ M in several deep granitic waters in Sweden³¹). Under these conditions Ca(II) may be an efficient competitor for binding the organic material, in comparison with trace metals such as Eu(III) and trivalent actinides, despite the larger binding constants of these trace metals.

The Gorleben water contains approximately 3 ppm of organic materials, but small concentrations of Ca(II). Under these circumstances, Eu(III) is expected to be strongly bonded, as is indeed observed experimentally.

Bivalent metal ions such as Mg(II), Ca(II) and Fe(II) form weaker hydroxide complexes than Eu(III) but also weaker complexes with other ligands (presumably also with FA/HA). At pH 5.35 these bivalent metal ions may not compete with Eu³⁺ aquo ions for FA. The situation may be quite different at pH > 7 where europium hydrolysis is much more pronounced than that of M(II). Qualitative titrations of Eu/Ca at pH 5.5 indeed showed that competition between the two metals for FA was much weaker than that found for the Al/Eu system. In a recent investigation,³² a different behaviour was found for natural organic substances of higher molecular weight (humic acids). This matter therefore seems worth more experimental investigation.

Acid rain changes the trace-metal distribution in the soil layer. One reason for this might be that the *relative* binding constant of Al(III) to HA/FA increases in comparison with the binding constant of less hydrolysed trace metals at lower pH.

Fluorescence decay-time

There is no doubt that investigations such as those discussed in this work would greatly benefit from a simultaneous measurement of the fluorescence decay-time. In fact, it is well known³³ that, in addition to a change in the fluorescence intensity, there is also a drastic change in the fluorescence lifetime as a result of complexation.

In general, the fluorescence lifetime of lanthanide complexes is greater than that of the corresponding aquo-ions. This is due to the very

efficient energy transfer from the aquo-complex through hydrogen bonding to the solvent. In our case, the complexation by the FA system should also result in a fluorescence lifetime different from that of the aquo-ion. At present, however, we cannot claim any conclusive evidence for such an effect, since, as reported earlier, the strong organic fluorescence produces undesirable artifacts in our detection system. Work is now in progress to eliminate this problem.

Acknowledgements—This work was supported by the Joint Research Centre of Ispra and the Swedish Nuclear Fuel and Waste Management Corp. (SKB) We are indebted to Mr Paolo Cavalli for his assistance in the experimental work and to Professors B. Allard and J I Kim for the sample of fulvic acid and the Gorleben ground-water, respectively

REFERENCES

- 1 W Stumm and J J Morgan, *Aquatic Chemistry*, Chaps 6–8, Wiley, New York, 1981
- 2 M. Whitfield and D R Turner, in E A Jenne (ed.), *Chemical Modeling in Aqueous Systems*, p 657 ACS, Washington D C, 1979
- 3 M Schmitzer and S U Khan, *Humic Substances in the Environment*, Dekker, New York, 1972
- 4 M S Shuman, G J Collins, R J Fitzgerald and D L Olson, in *Aquatic and Terrestrial Humic Materials*, R F Christman and E T Gjessing (eds.), p 387 Ann Arbor Sci., Ann Arbor MI, 1983.
- 5 N. Paxéus and M Wedborg, *Anal. Chim Acta*, 1985, **169**, 87
- 6 E M. Perdue, J H Reuter and M Ghosal, *Geochim Cosmochim Acta*, 1980, **44**, 1841
- 7 E M Perdue and C R Lytle, *Environ Sci Technol*, 1983, **17**, 654
- 8 D A. Dzombak, W Fish and F. M M Morel, *ibid*, 1986, **20**, 669
- 9 W Fish, D A Dzombak and F. M. M Morel, *ibid*, 1986, **20**, 676.
- 10 J A Marinsky and J Ephraim, *ibid.*, 1986, **20**, 349
- 11 J Ephraim, S Alegret, A Mathuthu, M Bicking, R L Malcom and J A. Marinsky, *ibid.*, 1986, **20**, 354
- 12 J H Ephraim, H B Boren, C Pettersson, I. Arsenic and B Allard, *ibid*, 1989, **23**, 356
- 13 J Ephraim and J A Marinsky, *ibid.*, 1986, **20**, 367
- 14 J. Buffle, P Deladoey, F L Greter and W Haerdi, *Anal Chim Acta*, 1980, **116**, 255
15. E L Bertha and G R Choppin, *J Inorg. Nucl Chem*, 1978, **40**, 655
- 16 V. Moulin, P Robouch, P Vitorge and B Allard, *Inorg Chim Acta*, 1987, **140**, 303
- 17 R A. Torres and G R Choppin, *Radiochim Acta*, 1984, **35**, 143
- 18 J. H Ephraim, J. A Marinsky and S J Cramer, *Talanta*, 1989, **36**, 437
- 19 R A. Saar and J H Weber, *Anal Chem*, 1980, **52**, 2095
- 20 S E Cabaniss and M S Shuman, *ibid*, 1988, **60**, 2418
- 21 F V Bright, *ibid*, 1988, **60**, 1031
- 22 J C Dobbs, W Susetyo, F E Knight, M A Castles, L A Carreira and L V. Azarraga, *Anal Chem*, 1989, **61**, 483
- 23 F J C Rossotti and H Rossotti, *The Determination of Stability Constants*, McGraw-Hill, New York, 1959
- 24 B C Faust and J Hoigne, *Environ Sci Technol*, 1987, **21**, 957
- 25 D B Pott, J J Alberts and A W Elzerman, *Chem Geol*, 1985, **48**, 293
- 26 C A Backes and E Tipping, *Water Res*, 1987, **21**, 211
- 27 I Grenthe, *Acta Chem Scand.*, 1962, **16**, 1695
- 28 G Biedermann, J Bruno, D Ferni, I Grenthe, F Salvatore and K Spahiu, *Mater Res Soc Symp Proc*, 1982, **11**, 791
- 29 C F Baes, Jr and R. E Mesmer, *The Hydrolysis of Cations*, Wiley, New York, 1976
- 30 S Fronaeus, *Acta Chem Scand.*, 1953, **7**, 469.
- 31 I Puigdomenech and K Nordstrom, *SKB Tech Rep*, 87-15, 1987, *Chem Abstr.*, 1988, **108**, 100732g.
32. G Bidoglio, N Omenetto and P. Robouch, *Radiochim Acta*, 1991, **52/53**, 57
- 33 S P Sinha, (ed.), *Systematics and Properties of the Lanthanides*, pp 451–500 Reidel, Dordrecht, 1983

ELECTROGENERATION OF Hg⁺ IN THE PRESENCE OF TRYPTOPHAN

A. RENUKA* and K. SHAKUNTALA

Department of Physical Chemistry, University of Madras, A. C. College of Technology, Guindy, Madras 600 025, India

(Received 14 November 1989 Revised 7 March 1991 Accepted 19 March 1991)

Summary—In the presence of L-tryptophan, a one-electron oxidation of mercury takes place at the dropping mercury electrode at 0.265 V vs SCE in 0.1M potassium nitrate. The electrogeneration of the monomeric Hg⁺ ion has been established by a.c. polarography, cyclic voltammetry and ultraviolet spectroscopy. A paramagnetic Hg-trp compound has been electrochemically synthesized and characterized.

The first report of the existence of the monomeric mercurous ion, Hg⁺, appeared in 1940.¹ It was based on an electrochemical investigation of the anodic oxidation of the dropping mercury electrode in the presence of cysteine, and stated that at mercury(I) concentrations < 10⁻²⁰M practically all the mercurous ions are present as Hg⁺ and not Hg₂²⁺. Thirty years later, other evidence for the existence of Hg⁺ was obtained by γ -irradiation of solid inorganic compounds doped with mercury(II), or radiolysis and photolysis of solutions of mercury compounds. Symons and co-workers²⁻⁴ detected the Hg⁺ ion in γ -irradiated glasses, samples of cadmium carbonate containing Hg²⁺ impurity, cadmium acetate doped with mercury(II) and in pure mercuric acetate, by the EPR technique. They indicated that Hg⁺ is produced in a covalent environment. Dalal and co-workers^{5,6} showed that Hg⁺ can be substituted for K⁺ and NH₄⁺ in KHSO₄ and NH₄H₂PO₄ respectively. Faraggi and Amozig⁷ characterized the ultraviolet spectrum of Hg⁺, with λ_{max} at 272 nm. They produced Hg⁺ ions by the reaction of hydrogen atoms with Hg²⁺ or Hg₂²⁺. Gupta and Kaur,⁸ who investigated the polarography of *o*-mercaptobenzoic acid, showed that the anodic wave in 60% v/v methanol medium is due to the formation of an Hg⁺ complex, RSHg. In earlier work^{9,10} we obtained polarographic data for a one-electron anodic oxidation of a mercury electrode in presence of L-tryptophan (trp). In this paper, evidence obtained by

cyclic voltammetry, constant-potential macroelectrolysis, and structure analysis of the reaction product is presented.

EXPERIMENTAL

The experimental details for the reagents and d.c. polarography are the same as those reported earlier.⁹ An alternating voltage amplitude of 5 mV and a frequency of 60 Hz were used in the fundamental harmonic a.c. polarography. An alternating voltage amplitude of 10 mV and a frequency of 120 Hz were used in the second harmonic a.c. polarography. A thick-walled blunt capillary having the following characteristics was used as the dropping mercury electrode (DME): drop time, $t = 6.2$ sec in 0.1M potassium nitrate; mercury flow-rate, $m = 1.3$ mg/sec. Cyclic voltamperograms were obtained with a PAR model 173 potentiostat/galvanostat, model 176 current to voltage converter, and model RE008 XY recorder. The hanging mercury drop electrode (HMDE) was fabricated by the procedure of Bellamy.¹¹ Ultraviolet spectra were obtained with a Zeiss spectrophotometer and a Hitachi 320 spectrophotometer with 1-cm fused-silica cells. Infrared spectra were obtained with a Shimadzu IR 408 spectrophotometer with KBr cells in the range 5000–600 cm⁻¹ and polythene cells in the range 600–200 cm⁻¹. A Polytech FIR-30 spectrophotometer was used for FT-FIR measurements. The EPR spectrum of the sample in the powdered form was recorded on an E4 Varian X-band spectrometer. Constant-potential macroelectrolysis was performed

*Author for correspondence. present address, CECRI Unit, CSIR Complex, Taramani, Madras 600113, India

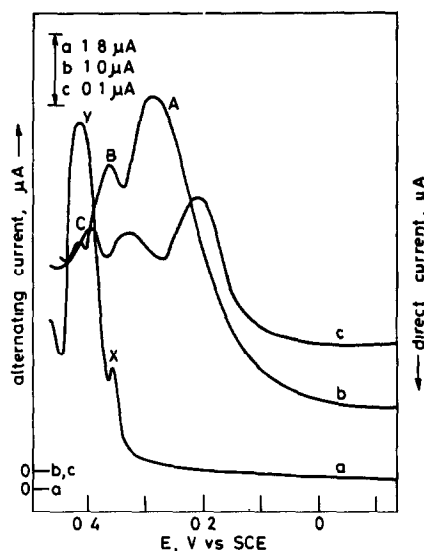


Fig. 1 Fundamental harmonic a.c. (a, b) and second harmonic a.c. (c) polarograms for the anodic dissolution of mercury in the presence of 6mM trp (b, c) and absence of trp (a), in 0.1M KNO₃

with a large mercury pool electrode 10 cm in diameter. The solution was thoroughly de-aerated with purified nitrogen before the electrolysis and purging was continued during the electrolysis. The product was isolated from the electrolyte solution under a nitrogen atmosphere to avoid contact with air. All experiments were performed at $25 \pm 1^\circ$.

RESULTS AND DISCUSSION

Alternating current polarography and cyclic voltammetry

A representative fundamental harmonic a.c. polarogram for the anodic dissolution of mercury in the presence of trp in 0.1M is shown in Fig. 1, curve b. Curve a is the corresponding polarogram of the supporting electrolyte.

The peak current for peak A (I_pA) increases linearly with [trp] in the range 0.1–0.8mM,

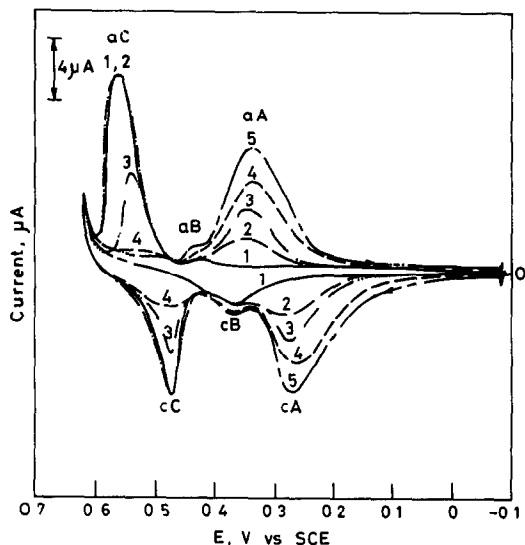


Fig. 2 Cyclic voltamperograms for the anodic dissolution of mercury in the presence of trp in 0.1M KNO₃ at a sweep rate of 50 mV/sec [trp], mM. (1) 0; (2) 2, (3) 4, (4) 8, (5) 20

above which the increase is only slight. The peak potential (E_pA) does not vary with [trp] (Table 1). The peak width at half height is 110 ± 5 mV. The plot of $\log\{(I_p/I)^{1/2} + [(I_p - I)/I]^{1/2}\}$ vs. E is linear, with a slope of 128 mV. The deviation of these values from the theoretical values for a one-electron process (90 mV and 118.2 mV respectively¹²) indicates that peak A corresponds to a quasi-reversible process. It should be mentioned that even slight departures from the theoretical Nernstian conditions will be exhibited as broadening of the a.c. wave.¹³ That the degree of irreversibility is small is shown by the cyclic voltamperogram (Fig. 2) in which $\Delta E_p (= E_{pa} - E_{pc})$ for peak A is 57.5 ± 2.5 mV. E_{pa} is the potential corresponding to the peak labelled aA, and E_{pc} that for peak cA. The second harmonic a.c. polarogram (Fig. 1, curve c) confirms the 1-electron nature of process A, by its possession of two peaks 70 mV apart, and

Table 1. Effect of trp on I_p and E_p of the fundamental harmonic a.c. polarograms for the anodic dissolution of mercury

[trp], mM	I_pA , μA	E_pA , mV	ΔE at $I_pA/2$, mV	Slope*, mV	I_pB , μA	E_pB , V	ΔE at $I_pB/2$, mV	Slope*, mV	I_pC , μA	E_pC , V	ΔE at $I_pC/2$, mV
0.0	—	—	—	—	3.50	0.345	—	—	14.6	0.430	—
0.1	0.10	0.265	—	—	3.50	0.345	—	—	11.4	0.430	—
0.5	0.25	0.265	—	—	2.70	0.350	—	—	9.34	0.435	—
1.0	0.50	0.265	105	—	2.10	0.355	—	—	4.90	0.435	45
2.0	1.02	0.265	105	117	1.80	0.365	80	117	1.80	0.435	45
3.0	1.41	0.265	105	117	1.90	0.365	80	117	1.80	0.435	45
6.0	2.92	0.265	110	128	1.82	0.365	90	120	0.80	0.460	45
8.0	3.64	0.265	110	128	1.95	0.365	80	117	0.50	0.460	45
12.0	4.20	0.265	110	130	1.91	0.365	80	117	0.20	0.465	—
16.0	4.49	0.265	110	130	1.91	0.365	80	117	—	—	—

*Slope of $\log\{(I_p - I)/I\}^{1/2} + (I_p/I)^{1/2}$ vs E_{dc}

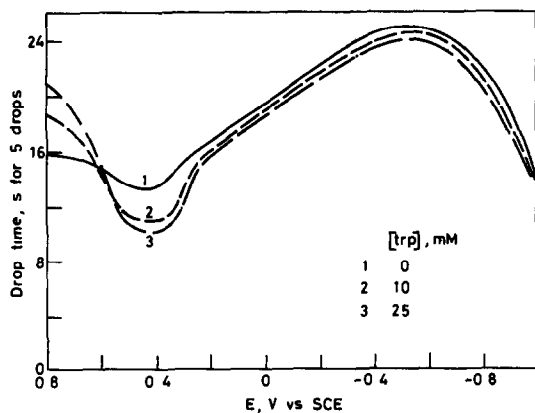


Fig 3 Effect of $[\text{trp}]$ on electrocapillary curves in $0.1M$ KNO_3 .

the minimum in current at E_pA for the fundamental harmonic a.c. polarogram.

E_pB and I_pB do not vary appreciably with $[\text{trp}]$, but I_pB is lower and E_pB more positive than in the absence of trp . Peak C is not seen at high trp concentrations, but begins to appear at about $12mM$ trp and increases in height with decrease of $[\text{trp}]$, together with a shift in its peak potential, E_pC , to less positive values. Thus it is evident that peaks B and C represent only the mercury–nitrate interactions of the supporting electrolyte,^{9,14} which are suppressed in the presence of trp .

The electrocapillary curves (Fig. 3) in the presence of trp show a marked depression in the potential region (0.3–0.5 V) of processes X and Y of the supporting electrolyte. This could result if the Hg – trp product, free trp , or both, get adsorbed on the electrode surface, causing inhibition of the mercury–nitrate interactions.

Constant-potential macroelectrolysis

Constant-potential macroelectrolysis of $0.05mM$ trp in $0.1M$ potassium nitrate was performed sequentially at three potentials:

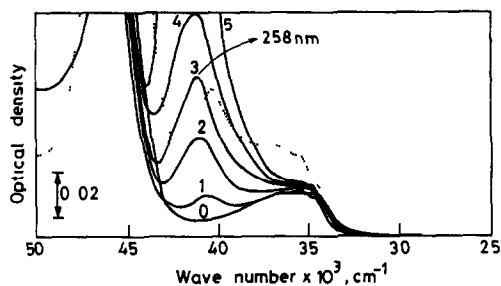


Fig. 4 Difference UV spectra recorded during the macroelectrolysis of $0.05mM$ trp in $0.1M$ KNO_3 at the E_pA potential of 0.265 V. (0) before electrolysis; (1–5) at every 30 min during electrolysis (.. .) is the UV spectrum of the brown solid isolated from macroelectrolysis of trp at E_pA .

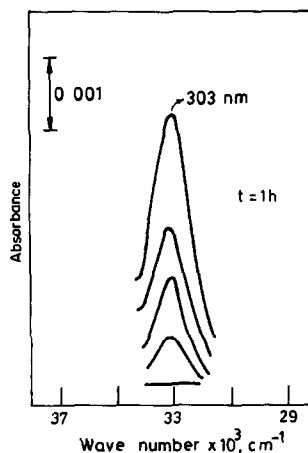


Fig 5 Difference UV spectra recorded during the macroelectrolysis of $0.05mM$ trp in $0.1M$ KNO_3 at the E_pB potential of 0.365 V. 303 nm corresponds to λ_{max} for nitrate.

(a) E_pA , 0.265 V; (b) E_pB , 0.365 V; (c) E_pC , 0.485 V. The ultraviolet spectra of the electrolysed solutions were recorded at regular intervals during the electrolysis.

Macroelectrolysis at 0.265 V. The spectra recorded at 30-min intervals during the macroelectrolysis at 0.265 V are shown in Fig. 4. The indole chromophore of trp exhibits three different λ_{max} values (272 , 279 and 283 nm)¹⁵ and as electrolysis proceeds, the spectrum shifts toward shorter wavelengths. A new peak appears at 258 nm and develops as the electrolysis proceeds. This new peak is attributable to mercury. The ultraviolet absorption spectrum of mercury has been well analysed, and the absorption at 230 – 235 nm is attributed^{16–18} to $\text{Hg}^{2+}/\text{Hg}_2^{2+}$, and that at 272 nm is attributed⁷ to Hg^+ . The λ_{max} value of 258 nm observed in the present study is closer to 272 nm than 235 nm and may be taken as evidence that Hg^+ is formed under the experimental conditions. It should be mentioned here that the value of 272 nm for Hg^+ was for aqueous solutions containing no complexing agent or excess salts.⁷ In the present case, the solution contains $0.1M$ potassium nitrate and trp . This difference in background medium may account for the shift in λ_{max} .

Macroelectrolysis at 0.365 V. The nitrate ion has a characteristic ultraviolet absorption spectrum with a λ_{max} of 302.8 nm.¹⁹ When the difference spectra were recorded with the unelectrolysed solution of $0.05mM$ trp in $0.1M$ potassium nitrate in the sample cell and the corresponding electrolysed solution in the reference cell, the change in the nitrate absorbance at 302.8 nm could be followed (Fig. 5). The difference in recorded absorbance increases as the

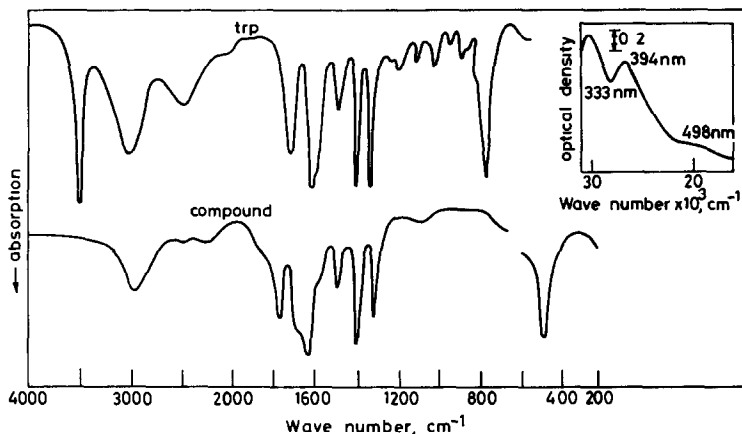


Fig 6 IR spectra of trp and of the brown compound obtained from the macroelectrolysis of trp in 0.1M KNO_3 at 0.265 V. Inset is the visible-region spectrum of the compound in methanol.

electrolysis proceeds, which indicates a decrease in the concentration of nitrate ions. Thus process B is seen to correspond to the mercury–nitrate interactions characteristic of the supporting electrolyte.¹⁴

Macroelectrolysis at 0.485 V. The spectral results obtained were similar to those obtained for the electrolysis at 0.365 V in that the difference absorbance of nitrate increased during the electrolysis. Thus process C is also due to the mercury–nitrate interactions.

Product analysis

A series of constant-potential macroelectrolyses of 0.05mM trp in 0.1M potassium nitrate was conducted in order to collect the product, as follows. The electrolysed solution was removed from the mercury and slowly evaporated to dryness at 60°. The solid left was repeatedly washed with cold doubly-distilled water to remove potassium nitrate and then with hot

doubly-distilled water to remove unreacted trp. The brown solid left behind was dried under reduced pressure. The ultraviolet absorption spectrum of a solution of this compound in methanol is shown by the dotted line in Fig. 4. The spectrum shows shifts in the λ_{max} values for trp and mercury, indicating that the two are bonded to each other. The visible spectrum of the compound in methanol is shown as the inset in Fig. 6. There are two strong absorption peaks at 333 and 394 nm and a weak absorption at 498 nm.

A comparative study of the infrared spectra of the brown compound and trp (Fig. 6) reveals the following features. The characteristic stretching frequency of the NH group of indole at 3500 cm^{-1} is absent in the spectrum of the compound, indicating strong association of the indolyl nitrogen atom with mercury. The NH stretching frequency of the zwitterionic NH_3^+ group shows a minor shift of 30 cm^{-1}

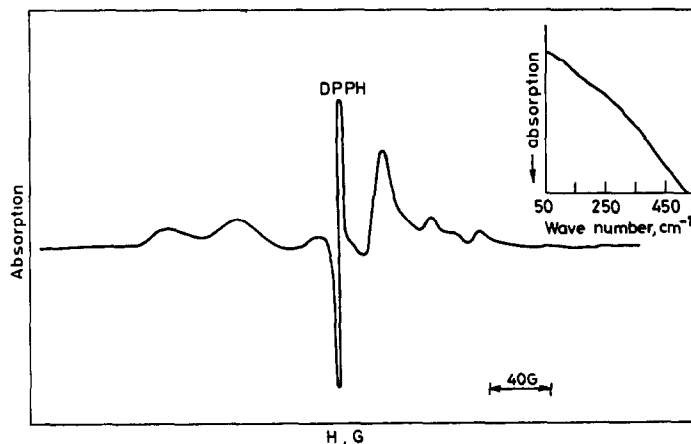
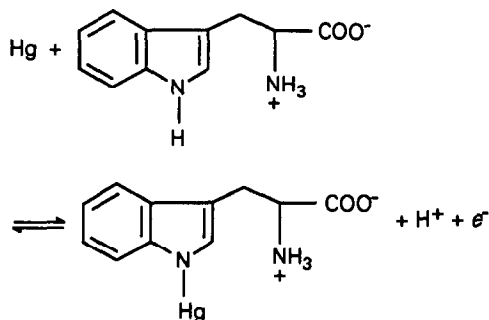


Fig 7 EPR spectrum of compound obtained from the macroelectrolysis of trp in 0.1M KNO_3 at the E_p , A potential of 0.265 V. Inset is the FT-FIR spectrum of the compound. DPPH is diphenylpicrylhydrazyl

from 3010 cm⁻¹ to 2980 cm⁻¹. The stretching frequency of the carboxylic C=O group at 1730 cm⁻¹ is unaffected. The NH in-plane bending vibrations of the -NH₂ or -NH₃⁺ group at 1610 cm⁻¹ are unchanged. Similarly, the carboxylic OH stretching at 1320 cm⁻¹ is also not affected. These observations indicate that the mercury-trp bond is formed at the indolyl nitrogen atom and that other functional groups are not involved in the compound formation. The fingerprint region of trp between 1200 and 600 cm⁻¹ is structureless in the spectrum of the compound. Aromatic compounds in general show a strong absorption at 800 cm⁻¹. CH rocking mode vibration also occurs at 800 cm⁻¹,^{20,21} and trp does show a strong vibration at 800 cm⁻¹ which is absent in the spectrum of the mercury derivative. This observation and the minor shift of the zwitterionic -NH₃⁺ stretching frequency indicate that the binding of mercury at the indolyl nitrogen atom affects the entire molecule. The compound does not show any absorption in the FT-FIR spectrum (Fig. 7, inset).

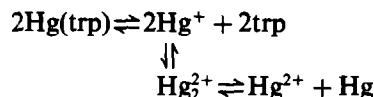
The EPR spectrum of the compound is shown in Fig. 7. This spectrum is similar to that reported by Dalal *et al.*⁶ for the Hg⁺ (6s¹) ion in irradiated mercuric acetate. However, in the present case, the multiplicities of the signals on either side of the reference (DPPH) do not coincide, indicating the anisotropic nature of the mercury-trp compound.

The foregoing spectral data support the following mechanism proposed⁹ for the anodic dissolution of mercury in the presence of trp.



The brown compound was analysed for mercury [determined as mercury(II) thionalide]²² and for nitrogen by the Kjeldahl method,²³ and the N:Hg atomic ratio found was 2.001, in agreement with the formula C₁₁H₁₁N₂O₂Hg. The magnetic moment of the compound was measured by the Gouy method,²⁴ and a freshly prepared sample had a magnetic moment (μ_{eff}) of 1.87 BM.

The brown compound decomposed on standing, expelling fine droplets of mercury with decreased paramagnetism (μ_{eff} of the decomposed sample was 0.32 BM). This shows that Hg⁺ is unstable and dimerizes, followed by disproportionation, according to the following scheme.



CONCLUSION

There has been a remarkable development in the chemistry of unusual oxidation states of mercury, leading to the identification of formal oxidation states of +0.67,^{25,26} and +0.35,²⁷ and the study of the electrochemical oxidation of the complex [Hgcyclam]BF₄ in acetonitrile medium by Deming *et al.*²⁸ provided evidence for the existence of the Hg³⁺ ion. Electrochemical techniques have been extremely useful in the unravelling of unusual oxidation states of mercury. The present work is yet another example, and reports a method of electrochemically preparing a paramagnetic compound of mercury containing the Hg⁺ ion. Further investigation is in progress.

REFERENCES

- 1 I M. Kolthoff and C Barnum, *J Am. Chem Soc*, 1940, **62**, 3061.
- 2 M C R Symons, R. S Eachus and J K Yandell, *J Chem Soc Chem Commun*, 1969, 979
- 3 R. S Eachus and M C R. Symons, *ibid*, 1970, 70.
- 4 *Idem*, *Can. J Chem*, 1971, **49**, 2868
- 5 N S Dalal, J A Hebden and C A McDowell, *J Mag Reson*, 1974, **16**, 289
- 6 N S Dalal, D Nettare and P Grandinetti, *J Am Chem Soc*, 1982, **104**, 2054
- 7 M Faraggi and A Amozig, *Int J Radiat Phys. Chem*, 1972, **4**, 353
- 8 K C Gupta and T Kaur, *J Electrochem Soc*, 1982, **129**, 90
- 9 K Shakuntala, A Renuka and V Nagarajan, *Bull Electrochem*, 1987, **3**, 187.
- 10 K Shakuntala and A Renuka, *Proc Int. Seminar Electroanal Techniques and Instrumentation*, India, November 1987, p. 121
- 11 A J Bellamy, *Anal Chem*, 1980, **52**, 607
- 12 A. M Bond, in A. J Bard (ed), *Modern Polarographic Methods in Analytical Chemistry*, p 302 Dekker, New York, 1980
- 13 *Idem*, *op. cit*, p 305
- 14 A Renuka and K Shakuntala, *Bull Electrochem*, 1990, **6**, 546
- 15 D B Wetlaufer, *Advan Proteom Chem*, 1952, **7**, 319
- 16 W C E Higginson, *J Chem Soc*, 1951, 1438.

17. T. Yamane and N Davidson, *J Am Chem Soc.*, 1960, **82**, 2123.
18. E. Onat, *J Inorg Nucl. Chem* , 1974, **36**, 2029
19. S F Mason, *Quart Rev* , 1961, **15**, 356.
20. J P Greenstein and M Winitz, in *Chemistry of Amino Acids*, Vol 2, Ch 17 Wiley, New York, 1961
21. J. R. Dyer, in *Applications of Absorption Spectroscopy of Organic compounds*, p 31 Prentice-Hall, New Delhi, 1987
22. *Vogel's Text Book of Quantitative Inorganic Analysis*, 4th Ed , p 471. ELBS/Longmans, London
23. J P Greenstein and M. Winitz, *op cit.*, p. 312
24. Gouy, *Compt Rend* , 1889, **109**, 935.
25. G Torsi and G Mamantov, *Inorg Nucl Chem Lett* , 1970, **6**, 843
26. G. Torsi, K W Fung, G. M Begun and G Mamantov, *Inorg Chem.*, 1971, **10**, 2285
27. A. J Schultz, J M Williams, N D. Miro, A G MacDiarmid and A. J Heeger, *ibid* , 1978, **17**, 646.
28. R L. Deming, A L Allred, A. R Dahl, A. L Herlinger and M. O. Kestner, *J Am Chem Soc* , 1976, **98**, 4132

PROTONATION AND SOLVENT EXTRACTION OF *N-p*-TOLYLBENZOHYDROXAMIC ACID IN HYDROCHLORIC ACID MEDIUM

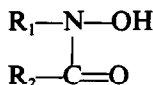
RAMA PANDE and S. G. TANDON

Department of Chemistry, Ravishankar University, Raipur 492010, India

(Received 3 April 1989. Revised 10 January 1991 Accepted 26 March 1991)

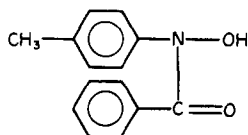
Summary—The protonation of *N-p*-tolylbenzohydroxamic acid (*p*-TBHA) in aqueous hydrochloric acid has been investigated by determination of its distribution between cyclohexane and hydrochloric acid. The pK_a value found was -2.30 ± 0.02 at 30° . The solubility of *p*-TBHA as a function of hydrochloric acid concentration has also been determined. At lower acid concentrations the solubility decreases owing to a salting-out effect, whereas at higher concentrations it increases because of formation of the more hydrophilic protonated species and a salting-in effect. Intramolecular hydrogen-bonding observed in *p*-TBHA provides evidence for protonation of the nitrogen atom.

Substituted hydroxamic acids (HA), of general formula



have been the subject of a large number of physicochemical studies, because of their wide applications in solvent extraction of metals.¹⁻⁵ Nevertheless, it is not clear how distribution of the hydroxamic acids between the organic and aqueous phases is affected by the acidity of the aqueous phase. These reagents might be expected to differ in solubility in different organic solvents, and in their distribution between these solvents and aqueous phases. Another factor that may affect the solubility and distribution ratio, and also the metal-extracting properties of these reagents in acid solutions is the formation of a protonated species ($HA + H^+ \rightleftharpoons H_2^+ A$).

In the present investigation the distribution ratios of *N-p*-tolylbenzohydroxamic acid (*p*-TBHA)



between various organic solvents and aqueous phases were determined, along with the effect of hydrochloric acid concentration on the solubility of *p*-TBHA. The protonation constant was also determined.

EXPERIMENTAL

Absorption spectra were recorded with a Zeiss Specord recording spectrophotometer, and 1-cm path-length matched fused-silica cells. Fixed wavelength measurements were made on an EC model GS 865 spectrophotometer.

Pure *p*-TBHA was prepared by a procedure reported earlier.⁶ The chloroform used was shaken five or six times with equal volumes of water to remove the ethanol (present as preservative) and then distilled. A saturated solution of analytical grade ammonium metavanadate was prepared in distilled water. Analytical grade hydrochloric acid was used to determine the solubilities and distribution ratios, but for the extraction work C.P. grade acid was adequate because any iron(II) present in it did not interfere. Iron(II) is Fe(II). Normally, HCl contains traces of Fe(II) which interfere in the determination of Vanadium V, but in the reverse determination of *p*-TBHA by vanadium V, Fe(II) does not interfere because vanadium V is taken in large excess.

All other organic solvents (BDH, analytical grade) were used without further purification.

Measurement of solubility

Saturated solutions were prepared in different solvents at the desired temperature, and suitable aliquots were used for determining the reagent content.

Table 1 Effect of solvents on the absorption maximum of *p*-TBHA in the ultraviolet

Solvent	λ_{\max} , nm
Water	245–260
Ethanol, 95%	270
Cyclohexane	278
Carbon tetrachloride	279
Chloroform	273
Dioxan	275

Measurement of distribution ratio

A known quantity of *p*-TBHA was dissolved in a known volume (10–25 ml) of organic solvent and shaken vigorously with a known volume (25–100 ml) of water for 30–60 min. The volumes of the two solvents were chosen according to the magnitude of the distribution ratio. The phases were separated by centrifugation and analysed for *p*-TBHA spectrophotometrically with vanadium(V).⁷

For determining the distribution ratio of *p*-TBHA between cyclohexane and hydrochloric acid, a rapid technique was adopted to avoid errors due to acid hydrolysis of the hydroxamic acid. It was observed that with sufficiently vigorous shaking equilibration between the organic and aqueous phases could be achieved within 5 min.

Analysis of the phases

The determination of *p*-TBHA by its absorbance in the ultraviolet gave unsatisfactory results because of the variation of its spectral characteristics with change in the solvent (Table 1) and with the acidity of its aqueous

Table 2. Solubility and distribution ratio of *p*-TBHA in different solvents at 25°

Solvent	Solubility, g/l	<i>D</i>
Water	0.25	—
n-Hexane	1.0	3.85
Cyclohexane	2.4	7.55
Carbon tetrachloride	18.3	62
Methyl isobutyl ketone	87.6	—
Benzene	109	169
Chlorobenzene	116	188
<i>o</i> -Dichlorobenzene	124	184
Ethyl acetate	140	—
Acetone	260	—
Chloroform	375	665

solutions. The *p*-TBHA concentrations were therefore determined spectrophotometrically with vanadium(V)⁷ which gives reproducible and accurate results.

RESULTS AND DISCUSSION

Spectrophotometric study

The ultraviolet spectral characteristics of *p*-TBHA in various organic solvents are presented in Table 1. It is evident that the position of the absorption band shifts according to the solvent used.

In hydrochloric acid media *p*-TBHA hydrolyses into the parent benzoic acid and *N*-*p*-tolylhydroxylamine, the latter being further changed into a variety of complex compounds. Hence the ultraviolet spectrum changes with time and direct spectrophotometry cannot be used to determine the concentration of *p*-TBHA in hydrochloric acid solutions. Figure 1 shows the effect of hydrochloric acid concentration on the ultraviolet spectrum of *p*-TBHA.

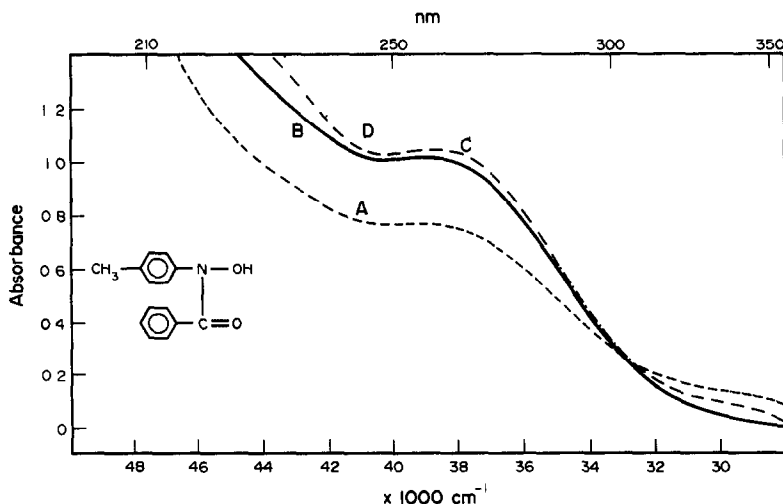
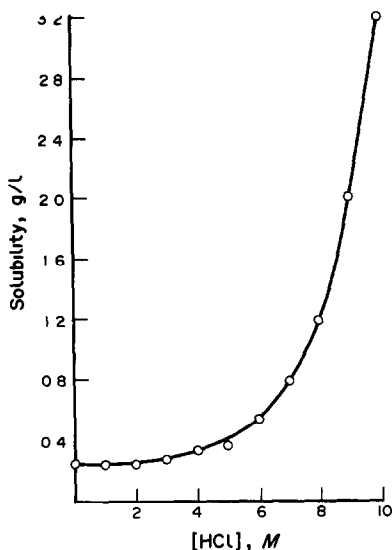


Fig 1 Effect of hydrochloric acid concentration on the ultraviolet spectrum of fresh solutions of *p*-TBHA. [HCl], M: A, 0; B, 0.01; C, 3 and 6; D, 10

Fig. 2 Solubility of *p*-TBHA as a function of [HCl]

Solvent extraction studies

The data presented in Table 2 show that of the solvents tested, chloroform gives the highest solubility of *p*-TBHA and water the lowest. *n*-Hexane and cyclohexane are poor solvents for *p*-TBHA. For purification of the reagent by recrystallization a mixture of benzene and petroleum ether of *n*-hexane has proved very effective.

Solubility and distribution ratio of *p*-TBHA as a function of hydrochloric acid concentration

Figure 2 shows that the solubility of *p*-TBHA increases with increasing hydrochloric acid concentration; this is due to protonation of *p*-TBHA in acidic solutions. The hydrophilic nature of the protonated species is presumably responsible for the enhanced solubility. However, a plot of $\{([HA] + [H_2^+A])/[HA]\} - 1$ vs.

$[H^+]$ is not linear, so protonation alone cannot account for the increased solubility, so other factors such as salting-in may also be involved.

The effect of hydrochloric acid concentration on the distribution into cyclohexane is shown in Table 3. Cyclohexane was chosen for the study because of its favourable physical properties such as adequate difference in density from water, low dielectric constant and vapour pressure, zero dipole moment and very low mutual solubility with water. From Fig. 2 and Table 3 it is inferred that for the system of *p*-TBHA with cyclohexane and hydrochloric acid the solubility and the distribution ratio are constant up to about 2*M* hydrochloric acid concentration and then protonation increases the solubility in aqueous medium and decreases the distribution ratio.

The degree of protonation is only 6.6% in 4*M* hydrochloric acid but 92% in 10*M* hydrochloric acid.

The distribution constant (K_D) for the unprotonated reagent between the aqueous and organic phases is defined by the equation

$$K_D = \frac{[p\text{-TBHA}]_{\text{org}}}{[p\text{-TBHA}]_{\text{aq}}}$$

The distribution between cyclohexane and aqueous hydrochloric acid is affected by the protonation reaction, and the distribution constant (D) is

$$D = \frac{[p\text{-TBHA}]_{\text{org}}}{[p\text{-TBHA}]_{\text{aq}} + [p\text{-TBH}_2^+\text{A}]_{\text{aq}}}$$

The dissociation constant, pK_a , of $p\text{-TBH}_2^+\text{A}$ can be calculated from

$$pK_a = H_0 - \log\left(\frac{K'_D - D}{D}\right)$$

Table 3 Distribution data

[HCl], M	H_0^*	Fraction protonated, %	D	Dh_0	$\log\left(\frac{K'_D - D}{D}\right)$	pK_a
4	-1.40	6.6	7.95	200	-0.8876	-2.29
5	-1.76	13.9	7.00	403	-0.5484	-2.31
6	-2.12	27.1	5.40	712	-0.1785	-2.30
7	-2.50	47.1	3.40	1075	0.2151	-2.29
8	-2.86	67.1	1.96	1420	0.5540	-2.31
9	-3.22	82.4	1.00	1660	0.9020	-2.32
10	-3.59	91.6	0.45	1750	1.2777	-2.31
$K'_D = 8.98$			Average $pK_a = -2.30$			
[HCl], M	0		1	2	3	
D	7.55		9.20	9.20	9.20	
Fraction protonated, %	—		—	1.4	3.1	

*C H Rochester; *Acidity Functions*, pp 39 and 61, Academic Press, New York, 1970

where H_0 is the Hammett acidity function; the data are presented in Table 3. K'_D is the distribution constant of *p*-TBHA between the organic layer and aqueous acid in the acidity region where appreciable protonation is occurring, and is estimated by the relation

$$D = K'_D - \frac{Dh_0}{K_a}$$

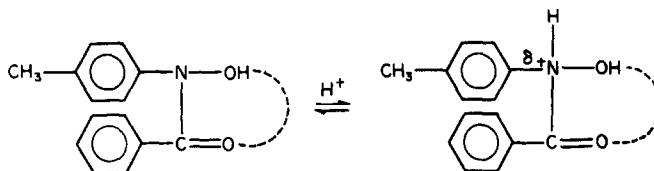
or from the intercept of a plot of D vs. Dh_0 , where $h_0 = 10^{-H_0}$. In the infrared spectra of *p*-TBHA in nujol both $\nu_{\text{O-H}}$ and $\nu_{\text{C=O}}$ appear at lower wavenumbers than expected, namely at 3180 and 3300 cm^{-1} and 1643 and 1623 cm^{-1} , respectively,⁶ and the positions of these bands remain unaffected on dilution. It is thus inferred that there is intramolecular hydrogen bonding in *p*-TBHA, and hence that the nitrogen atom is protonated in acid medium.

determination of the extraction coefficients of its metal chelates.

Acknowledgements—The authors are indebted to UGC, New Delhi for the financial assistance.

REFERENCES

- 1 A. K. Majumdar, *N-Benzoyl-N-phenylhydroxylamine and its Analogues*, Pergamon Press, Oxford, 1972.
- 2 R. Pande and S. G. Tandon, *J. Indian Chem. Soc.*, 1977, **54**, 990.
- 3 F. Vernon and J. H. Khorassani, *Talanta*, 1978, **25**, 410.
- 4 F. Vernon and H. D. Gunawardhana, *Anal. Chim. Acta*, 1978, **98**, 349.
- 5 A. K. De, S. M. Khopkar and R. A. Chalmers, *Solvent Extraction of Metals*, Van Nostrand Reinhold, London, 1970.
- 6 S. G. Tandon and S. C. Bhattacharyya, *J. Chem. Eng. Data*, 1962, **7**, 553.
- 7 R. Pande and S. G. Tandon, *Z. Anal. Chem.*, 1979, **296**, 407.



A knowledge of the protonation constant is of importance to explain the rate data of acid-catalysed hydrolysis of *p*-TBHA and also in

INTERFERENCE IN THE KINETIC DETERMINATION OF ASCORBIC ACID BY SULPHIDE AND SULPHITE

CONSTANTINA N. KONIDARI and MILTIADES I. KARAYANNIS*

Department of Chemistry, University of Ioannina, 451 10 Ioannina, Greece

(Received 12 November 1990 Revised 8 February 1991 Accepted 5 April 1991)

Summary—The reduction of 2,6-dichlorophenolindophenol (DCPI) by sulphides and sulphites has been studied kinetically by the stopped-flow technique. The reaction is first-order with respect to each of the reactants. From the distribution diagrams for the species DH_2^+ , DH and D^- for DCPI and H_2Q , HQ^- and Q^{2-} for sulphides or sulphites, a mechanism is proposed which suggests partial reactions of all possible combinations of the reacting species at any pH. An equation for calculation of the second-order reaction rate constants k at any pH is derived, which gives k as a function of $[\text{H}^+]$, the partial reaction rate constants and the dissociation constants of DCPI and H_2S or H_2SO_3 . Values of the overall reaction rate constants over a wide pH-range have been determined, together with values of k for all possible partial reactions. For particular pH-values the second-order reaction rate constant was determined by four different methods. Mean values of $k = 251 \pm 1$ and $240 \pm 11 \text{ mole}^{-1} \cdot \text{sec}^{-1}$ were obtained for pH 3.15 and 4.17, respectively, for the DCPI- Na_2S reaction and $k = 137 \pm 1$, 127 ± 1 and $136 \pm 11 \text{ mole}^{-1} \cdot \text{sec}^{-1}$ for pH 2.02, 4.25 and 5.10, respectively, for the DCPI- Na_2SO_3 reaction. From the slopes of the linear Arrhenius plots activation energies of 66 ± 0.2 and $40 \pm 0.1 \text{ kcal/mole}$ for the DCPI- Na_2S and DCPI- Na_2SO_3 reactions, respectively were calculated. The effect of ionic strength on the reactions supports the proposed mechanism.

The main chemical method for determination of ascorbic acid in biological samples is the 2,6-dichlorophenolindophenol (DCPI) method.¹ Its simplicity and the relatively close correlation with the results of biological assays have led to its extensive use. Both the equilibrium and reaction-rate procedures are widely employed.² The method works well for colourless fruit juices but has serious drawbacks when other reducing substances such as thiols, hydrogen sulphide, thiosulphates, dithionates, cysteine, homocysteine, reduced glutathione and metal ions in lower oxidation states (*e.g.*, Fe^{2+} , Sn^{2+} , Cu^+) are present.³⁻⁵

Of these interferents, hydrogen sulphide and thiols are of special interest because any dehydroascorbic acid present is measured as ascorbic acid after its reduction by hydrogen sulphide and removal of the excess of reductant. Quinols and thiols may also be formed by hydrogen sulphide reactions with the sample, and interfere with the dye reduction. Thiols reduce DCPI at a rate that depends on pH.⁶

Attempts to suppress the interference by thiols have been made,^{3,5,7} the first by formation of complexes of the interfering substances and

formaldehyde, the second by the use of *p*-chloromercuribenzoic acid, and the third by use of mercuric acetate to precipitate some of the interfering substances, but all are time-consuming and add more steps to the method. Furthermore, complete removal of hydrogen sulphide and/or thiols is not ensured.

Despite the voluminous literature on modifications of the 2,6-dichlorophenolindophenol method to avoid such interferences, many basic questions remain, some of which have already been studied⁸ or are under investigation.⁹

In this paper a kinetic and mechanistic study of the DCPI reduction by hydrogen sulphide and sulphurous acid over a wide pH-range is presented. The results are a good basis for optimization of the reaction pH, and correction of the errors due to these interferences, and the rate constants reported may be useful in other investigations.

EXPERIMENTAL

Reagents

All solutions were prepared in distilled water from analytical-reagent grade reagents without further purification.

Buffer solutions. The buffer solutions used were based on 0.2M potassium chloride and

*Author for correspondence.

hydrochloric acid for pH 1.0–2.2, 0.1M potassium hydrogen phthalate and hydrochloric acid or sodium hydroxide for pH 2.2–6.0, 0.1M potassium dihydrogen phosphate and sodium hydroxide for pH 6.0–8.0 and 0.025M borax and 0.1M hydrochloric acid or sodium hydroxide for pH 8.0–9.5.

Sodium sulphide solution. An approximately 0.05M solution was prepared daily with freshly distilled water, standardized by titration with iodine solution,¹⁰ and diluted further with the appropriate buffer as required.

Sodium sulphite solution. An approximately 0.05M solution was prepared daily with freshly distilled water, standardized by titration with potassium iodate,¹¹ and diluted further with the appropriate buffer as required.

DCPI solution. A stock solution ($\sim 7.5 \times 10^{-4}M$) was prepared in distilled water containing 210 mg/l. sodium bicarbonate, and further diluted with 210 mg/l. sodium bicarbonate solution as required. The stock solution was standardized by titration with freshly prepared ascorbic acid solution, and also spectrophotometrically at 522 nm, the isosbestic point. The molar absorptivity¹² at 522 nm is 8600 l.mole⁻¹.cm⁻¹.

Apparatus

A Durrum Model D-110 stopped-flow spectrophotometer was used; the course of the reaction was displayed on a Textronix 5103N storage oscilloscope and photographed with a Polaroid camera or recorded on a Houston Instrument Omnigraphic 2000 recorder. The path-length of the measuring cell was 2.0 cm. The experimental arrangement is described in detail elsewhere.^{2,13}

A Radiometer pH M 83 Autocal pH-meter was also used.

Procedure

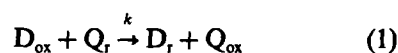
The stopped-flow spectrophotometer was calibrated for 0 and 100% transmittance with the reductant solution in the observation cell. All measurements were made at 522 nm.

The concentrations given in the figures and tables are the initial concentrations in the reacting mixture.

In all experiments the analytical concentration of sulphide or sulphite was held much higher than that of DCPI in order to create pseudo first-order conditions.

Data treatment

For the generalized reaction scheme



absorbance (A) vs time (t) was recorded, with variation of parameters such as pH, reactant concentrations, temperature and ionic strength. D and Q denote DCPI and sulphide or sulphite, respectively, the subscripts ox and r representing the oxidized and reduced forms.

The Guggenheim method¹⁴ was applied to determine the observed reaction rate constants, k_{ob} . Since the reductant concentration (c_q) was always much higher than that of DCPI (c_d), the conditions were pseudo first-order and the k_{ob} was equal to kc_q . The initial slopes R_A were determined graphically from the reaction curves.

From the values of k_{ob} and the initial slopes R_A given by the equation

$$R_A = -(dA/dt)_m = \epsilon b k c_q c_d \quad (2)$$

the second-order reaction rate constants k were calculated by applying four different techniques described in detail elsewhere.⁸ The calculated constants given in the tables are symbolized as k_I , k_{II} , k_{III} and k_{IV} , corresponding to the four evaluation methods I–IV.

RESULTS

Effect of pH

Figure 1 illustrates the dependence of k on pH for the DCPI–Na₂S (a) and DCPI–Na₂SO₃ (b) reactions.

Effect of reactant concentrations

The second-order reaction rate constants at various pH-values and 25° were determined by four evaluation techniques, with one reactant at constant concentration and that of the other varied.

Table 1 gives all the elements for the calculation of the second-order reaction rate constant for the DCPI–sulphite system at pH 3.15 and pH 4.17 by the four different methods mentioned above. Table 2 gives the corresponding information for the DCPI–sulphite system at pH 2.02, 4.25 and 5.10.

The linear dependence of k_{ob} and R_A on the initial concentration of the reductant, when c_d remains constant, suggests first-order kinetics with respect to the reductant. Also, the propor-

DISCUSSION

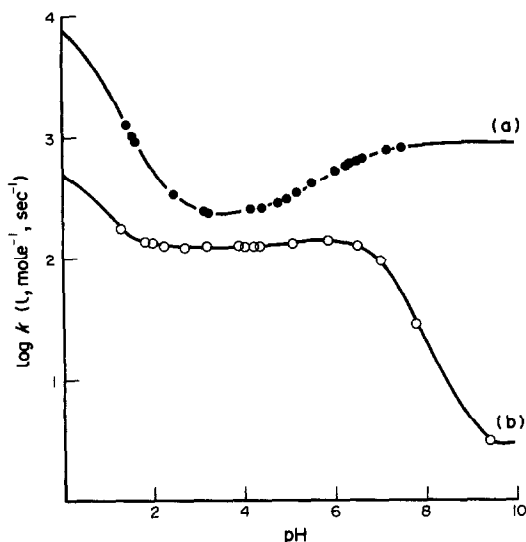


Fig 1 Dependence of the second-order reaction rate constant on pH for the reaction of DCPI with Na_2S (a) and Na_2SO_3 (b) $[\text{DCPI}]_0 = 1.57 \times 10^{-5} M$, $[\text{Na}_2\text{S}]_0 = 6.30 \times 10^{-4} M$, $[\text{Na}_2\text{SO}_3]_0 = 5.00 \times 10^{-4} M$, temperature 25°C

tionality between R_A and the initial concentration of the dye, for constant c_q , and the observed constancy of k_{ob} within experimental error, indicate first-order kinetics with respect to DCPI.

Effect of temperature

Arrhenius plots of $-\log k_{ob}$ vs. $1/T$, and $\log R_A$ vs. $1/T$, where T is the absolute temperature, showed the activation energy to be 6.6 ± 0.2 and 4.0 ± 0.1 kcal/mole for the DCPI- Na_2S and DCPI- Na_2SO_3 reactions, respectively.

The dependence of the reaction rate constant k on pH can be explained, at least qualitatively, by assuming the following mechanism for the reduction of DCPI by Na_2S and Na_2SO_3 . At each pH value the reductant exists as a mixture of three species (H_2Q , HQ^- and Q^{2-}) with stepwise ionization constants $K_{Q1} = 1.07 \times 10^{-7}$ and $K_{Q2} = 1.26 \times 10^{-13}$ for the H_2S and $K_{Q1} = 1.3 \times 10^{-2}$ and $K_{Q2} = 6.17 \times 10^{-8}$ for H_2SO_3 .¹⁶ DCPI also exists in three states. $[\text{DH}_2^+$, DH and $\text{D}^-]$ with stepwise ionization constants $K_{D1} = 0.3$ and $K_{D2} = 2.69 \times 10^{-6}$.¹⁷ Figures 2 and 3 show the distribution diagrams of the H_2S -DCPI and H_2SO_3 -DCPI systems, respectively. From these diagrams it is evident that the overall reaction is a sum of the component reactions between the various species of reductant and DCPI, in all possible combinations whenever they co-exist.

Table 4 shows all possible combinations of the reacting species and the corresponding reaction constants according to the general scheme given in equation (1). The arrows in Figs. 2 and 3 show the different pH ranges and the reaction constants for the component reactions k_i ($i = 1-9$).

Taking these considerations into account, the overall reaction rate constant k can be derived theoretically and expressed as a function of (i) $[\text{H}^+]$, (ii) the ionization constants K_{D1} , K_{D2} , K_{Q1} , K_{Q2} , and (iii) the reaction constants of the component reactions k_i ($i = 1-9$).

For the DCPI- Na_2S reaction the overall reaction rate constant is given by equation (3), and for the DCPI- Na_2SO_3 reaction by equation (4).

$$k = \frac{k_1 \frac{[\text{H}^+]^2}{K_{Q1} K_{D1}} + k_2 \frac{[\text{H}^+]}{K_{Q1}} + k_3 \frac{K_{D2}}{K_{Q1}} + k_5 + k_6 \frac{K_{D2}}{[\text{H}^+]}}{\left[1 + \frac{[\text{H}^+]}{K_{D1}} + \frac{K_{D2}}{[\text{H}^+]}\right] \left[1 + \frac{[\text{H}^+]}{K_{Q1}} + \frac{K_{Q2}}{[\text{H}^+]}\right]} \quad (3)$$

$$k = \frac{k_1 \frac{[\text{H}^+]^2}{K_{Q1} K_{D1}} + k_2 \frac{[\text{H}^+]}{K_{Q1}} + k_4 \frac{[\text{H}^+]}{K_{D1}} + k_5 + k_6 \frac{K_{D2}}{[\text{H}^+]} + k_8 \frac{K_{Q2}}{[\text{H}^+]} + k_9 \frac{K_{Q2} K_{D2}}{[\text{H}^+]^2}}{\left[1 + \frac{[\text{H}^+]}{K_{D1}} + \frac{K_{D2}}{[\text{H}^+]}\right] \left[1 + \frac{[\text{H}^+]}{K_{Q1}} + \frac{K_{Q2}}{[\text{H}^+]}\right]} \quad (4)$$

Effect of ionic strength

The effect¹⁵ of the ionic strength I on k and R_A for the reduction of DCPI by Na_2S and Na_2SO_3 was studied by addition of known amounts of Na_2SO_4 to the reacting mixture. The results are given in Table 3 and show that a change in ionic strength has only a small effect.

Details for the derivation of equations (3) and (4) were given earlier.⁸

To calculate the values of the partial reaction rate constants, shown in Table 5, the overall reaction rate constant was measured in specific pH ranges where only one or two of the reactions take place in parallel.

Table 1 Results for calculated values of k_I , k_{II} , k_{III} and k_{IV} at 25°C for reaction of DCPI with Na₂S

	pH = 3.15				pH = 4.17			
	k_I	k_{II}	k_{III}	k_{IV}	k_I	k_{II}	k_{III}	k_{IV}
Regression equation	$y = -2 \times 10^{-4} + 251x$	—	$y = -1 \times 10^{-4} + 68x$	$y = -1 \times 10^{-4} + 2731x$	$y = 3 \times 10^{-4} + 239x$	—	$y = -2 \times 10^{-4} + 65x$	$y = -1 \times 10^{-5} + 1083x$
r	1.0000	—	0.9999	0.9999	1.0000	—	0.9999	1.0000
k^* , l. mole ⁻¹ . sec ⁻¹	251 ± 0.2	249 ± 1.1	252 ± 1.8	252 ± 1.3	239 ± 0.1	240 ± 0.2	242 ± 0.1	238 ± 0.7
Mean value	$\bar{k} = 251 \pm 11$ mole ⁻¹ . sec ⁻¹							

*Mean \pm standard deviation.

Experimental conditions

pH = 3.15: [DCPI]₀ = $1.57 \times 10^{-5} M$ and [Na₂S]₀ = $(0.63-6.30) \times 10^{-4} M$ [Na₂S]₀ = $6.30 \times 10^{-4} M$ and [DCPI]₀ = $(2.30-23.00) \times 10^{-6} M$ pH = 4.17: [DCPI]₀ = $1.57 \times 10^{-5} M$ and [Na₂S]₀ = $(1.32-5.30) \times 10^{-4} M$ [Na₂S]₀ = $2.65 \times 10^{-4} M$ and [DCPI]₀ = $(2.76-27.64) \times 10^{-6} M$ Table 2 Results for calculated values of k_I , k_{II} , k_{III} and k_{IV} at 25°C for reaction of DCPI with Na₂SO₃

	pH = 2.02				pH = 4.25				pH = 5.10			
	k_I	k_{II}	k_{III}	k_{IV}	k_I	k_{II}	k_{III}	k_{IV}	k_I	k_{II}	k_{III}	k_{IV}
Regression equation	$y = -8 \times 10^{-4} + 138x$	—	$y = -4 \times 10^{-5} + 35x$	$y = 8 \times 10^{-5} + 1106x$	$y = 2 \times 10^{-4} + 127x$	—	$y = -3 \times 10^{-4} + 33x$	$y = 3 \times 10^{-4} + 1006x$	$y = 1 \times 10^{-5} + 137x$	—	$y = 5 \times 10^{-5} + 37x$	$y = 9 \times 10^{-5} + 1180x$
r	0.9999	—	0.9997	0.9998	0.9996	—	0.9991	0.9994	1.0000	—	1.0000	0.9998
k^* , l. mole ⁻¹ . sec ⁻¹	138 ± 0.9	136 ± 0.5	136 ± 2.0	137 ± 2.0	127 ± 2.0	127 ± 2.0	126 ± 0.8	125 ± 2.0	137 ± 0.6	136 ± 0.5	137 ± 0.7	134 ± 1.5
Mean value	$\bar{k} = 137 \pm 11$ mole ⁻¹ . sec ⁻¹											

*Mean \pm standard deviation.

Experimental conditions:

pH = 2.02: [DCPI]₀ = $1.51 \times 10^{-5} M$ and [Na₂SO₃]₀ = $(4.70-11.75) \times 10^{-4} M$ [Na₂SO₃]₀ = $4.70 \times 10^{-4} M$ and [DCPI]₀ = $(7.54-22.62) \times 10^{-6} M$ pH = 4.25: [DCPI]₀ = $1.51 \times 10^{-5} M$ and [Na₂SO₃]₀ = $(4.70-14.10) \times 10^{-4} M$ [Na₂SO₃]₀ = $2.65 \times 10^{-4} M$ and [DCPI]₀ = $(2.76-27.64) \times 10^{-6} M$ pH = 5.10: [DCPI]₀ = $1.57 \times 10^{-5} M$ and [Na₂SO₃]₀ = $(2.56-25.55) \times 10^{-4} M$ [Na₂SO₃]₀ = $5.11 \times 10^{-4} M$ and [DCPI]₀ = $(2.77-36.83) \times 10^{-6} M$

Table 3. Effect of ionic strength on the reaction rate constant k and the initial rate R_A . $[\text{DCPI}]_0 = 1.57 \times 10^{-5} M$, temperature 25°C ; $[\text{Na}_2\text{S}]_0 = 5.50 \times 10^{-4} M$, $\text{pH} = 5.4$; $[\text{Na}_2\text{SO}_3]_0 = 5.11 \times 10^{-4} M$, $\text{pH} = 4.0$

I	Na_2S		Na_2SO_3	
	$k, \text{l. mole}^{-1} \text{sec}^{-1}$	$R_A, A/\text{sec}^*$	$k, \text{l. mole}^{-1} \text{sec}^{-1}$	$R_A, A/\text{sec}^*$
0	393	0.038	127	0.0173
0.24	414	0.040	128	0.0177
0.48	398	0.037	135	0.0187
0.72	440	0.043	139	0.0193
1.20	489	0.047	148	0.0205
1.80	524	0.051	163	0.0223

* A/sec = absorbance change per second.

The theoretical curves for the dependence of the overall reaction rate constant on pH, derived from equation (3) or (4) as appropriate, and the values of k_i , are drawn as solid lines in Fig. 1 for the DCPI- Na_2S (a) and DCPI- Na_2SO_3 (b) reactions, respectively. The experimental values fit the theoretical line satisfactorily.

The type of hydrogen-ion dependence of the DCPI- Na_2S reaction is observed in reacting systems where the following conditions are met: (1) there are more than two species governed by protolytic equilibria, (2) all the species are present in comparable concentrations, (3) all the species are reactive and (4) the middle species is the least reactive.¹⁸ For the oxidation of H_2S with DCPI, all these conditions are satisfied, DH_2^+ , DH and D^- being present in comparable

concentrations and the rate constants ($\text{l. mole}^{-1} \text{sec}^{-1}$) are $k_1 = 9669$, $k_2 = 240$ and $k_3 = 499$. Thus the shape of the curve (a) in Fig. 1 is understandable. The minimum of this curve can be obtained by differentiation of equation (3) with respect to $[\text{H}^+]$. Omitting the term $k_6(K_{\text{D}2}/[\text{H}^+])$ as negligible in this pH range, the first derivative obtained is:

$$\frac{dk}{d[\text{H}^+]} = \frac{k_1}{K_{\text{D}1}} - \frac{1}{[\text{H}^+]^2} (k_3 K_{\text{D}2} + k_5 K_{\text{Q}1}) \quad (5)$$

Because the second derivative

$$\frac{d^2k}{d[\text{H}^+]^2} = 2k_3 \frac{K_{\text{D}2}}{[\text{H}^+]^3} + 2k_5 \frac{K_{\text{Q}1}}{[\text{H}^+]^3} \quad (6)$$

is positive, the dependence of k on pH has a minimum.

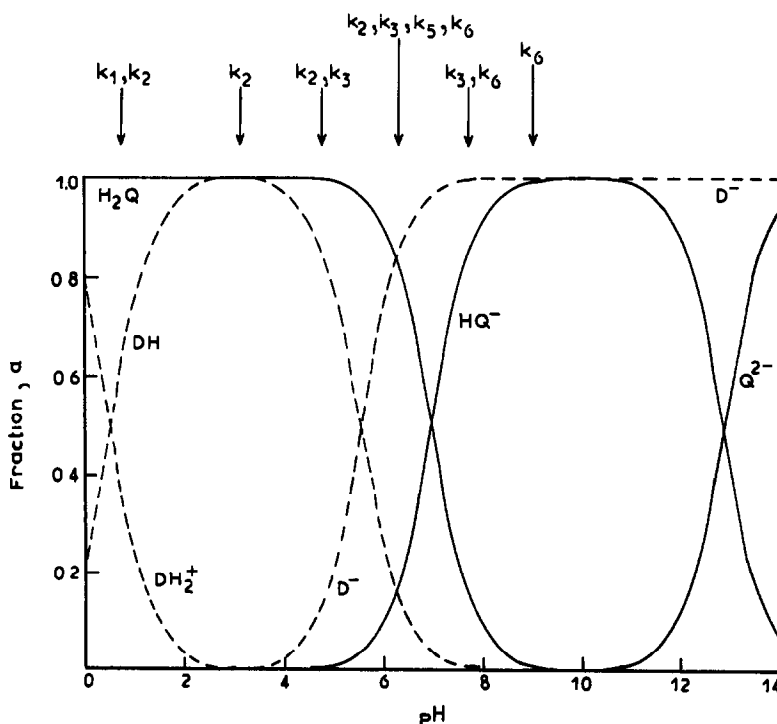


Fig. 2. Distribution diagrams for mixtures of species resulting from DCPI (DH_2^+ , DH , D^-) and sulphide (H_2Q , HQ^- , Q^{2-}), as a function of pH.

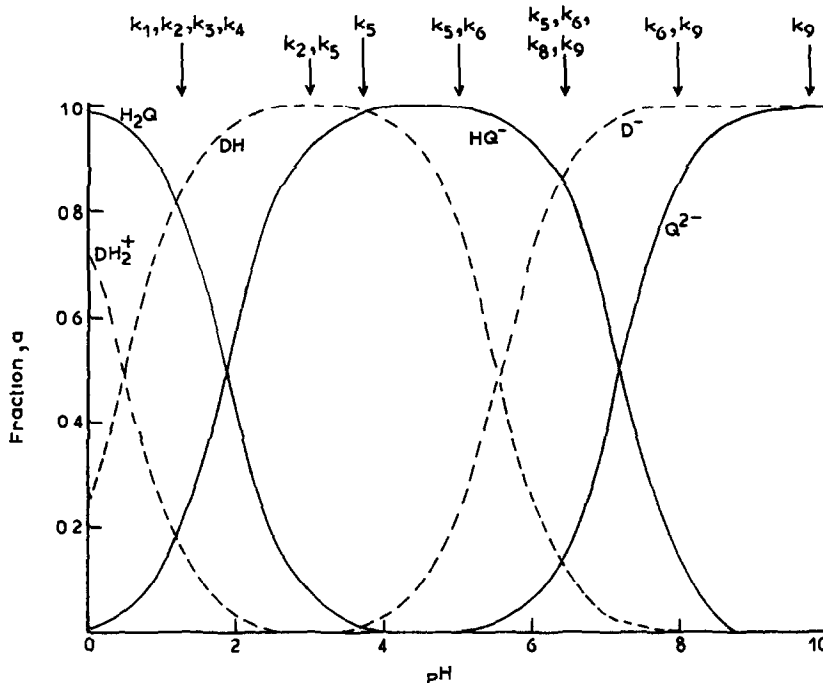


Fig 3 Distribution diagrams for mixtures of species resulting from DCPI (DH_2^+ , DH , D^-) and sulphite (H_2Q , HQ^- , Q^{2-}), as a function of pH

If the first derivative is set equal to zero, the $[\text{H}^+]$ value for the minimum of curve (a) in Fig. 1 is obtained:

$$[\text{H}^+]_{\text{min}} = \sqrt{\frac{K_{\text{D1}}(k_3 K_{\text{D2}} + k_5 K_{\text{Q1}})}{k_1}} = 2.24 \times 10^{-4} \text{M} \quad (7)$$

This value ($\text{pH} = 3.65$) is in good agreement with the experimental value of $\text{pH} = 3.50$. For this $[\text{H}^+]_{\text{min}}$, $k_{\text{min}} = 243 \text{ l. mole}^{-1} \cdot \text{sec}^{-1}$ was calculated by using equation (3).

For the DCPI- Na_2SO_3 reaction the $\log k$ vs. pH curve shows four distinct regions.

(a) pH 0–2.5. Since in this pH-range the species DH_2^+ and DH of DCPI and H_2Q and HQ^- of the reductant predominate, four partial reactions take place, with reaction rate constants k_1 , k_2 , k_4 and k_5 (Table 4). Also, because the relations $1 + [\text{H}^+]/K_{\text{Q1}} \gg K_{\text{Q2}}/[\text{H}^+]$ and $1 +$

$[\text{H}^+]/K_{\text{D1}} \gg K_{\text{D2}}/[\text{H}^+]$ are valid for this pH-range, equation (4) finally gives

$$k = \frac{k_1[\text{H}^+]^2 + (k_2 K_{\text{D1}} + k_4 K_{\text{Q1}})[\text{H}^+] + k_5 K_{\text{D1}} K_{\text{Q1}}}{[\text{H}^+]^2 + (K_{\text{D1}} + K_{\text{Q1}})[\text{H}^+] + K_{\text{D1}} K_{\text{Q1}}} \quad (8)$$

The sigmoid form of curve (b) in Fig. 1 in this pH-range indicates that there are at least two protonated forms of a reactant present and that the fully protonated form is the most reactive. Consequently, the reaction between the species DH_2^+ and H_2Q is much faster ($k_1 = 619 \text{ l. mole}^{-1} \cdot \text{sec}^{-1}$) than that between DH and H_2Q ($k_2 = 57 \text{ l. mole}^{-1} \cdot \text{sec}^{-1}$).

(b) pH 3.5–6.0. In this pH-range the species DH and D^- of DCPI and HQ^- of Na_2SO_3 co-exist. Consequently, k_5 and k_6 are the rate-determining factors. Because of the validity of the relations $1 + K_{\text{D2}}/[\text{H}^+] \gg [\text{H}^+]/K_{\text{D1}}$ and

$$1 \gg \frac{[\text{H}^+]}{K_{\text{Q1}}} + \frac{K_{\text{Q2}}}{[\text{H}^+]}$$

in this pH-range, equation (4) simplifies to

$$k = \frac{k_5[\text{H}^+] + k_6 K_{\text{D2}}}{[\text{H}^+] + K_{\text{D2}}} = k_5 \quad \text{or} \quad k_6 \quad (9)$$

Table 4 Possible combinations of reactions between species of DCPI and Na_2S or Na_2SO_3 , and the corresponding partial reaction rate constants

	Q	H_2S (H_2Q)	HS^- (HQ^-)	H_2SO_3 (H_2Q)	HSO_3^- (HQ^-)	SO_3^{2-} (Q^{2-})
DH_2^+		k_1	—	k_1	k_4	—
DH		k_2	k_5	k_2	k_5	k_8
D^-		k_3	k_6	—	k_6	k_9

Table 5 Second-order reaction rate constants k (at 25°C) for different combinations of reacting species shown in Table 4

Reaction	Partial rate constants, k_i							
	k_1	k_2	k_3	k_4	k_5	k_6	k_8	k_9
DCPI-Na ₂ S	9669	240	499	—	2348	899	—	—
DCPI-Na ₂ SO ₃	619	57	—	1800	128	131	1048	3

Table 6 Interference of sulphide and sulphite in the kinetic determination of ascorbic acid (Asc Ac) $[\text{DCPI}]_0 = 1.09 \times 10^{-5} M$, temperature 25°C

Reaction	pH	$[\text{Q}]_0$, $10^{-4} M$	$[\text{Asc Ac}]_0$, $10^{-4} M$			k_{obs} , sec^{-1}	
			Taken	Found*	Corrected†	Theor.	Exptl
DCPI-Na ₂ S	1.50	5.00	1.25	1.36	1.25	6.968	6.960
	5.70	5.00	1.00	1.41	1.00	0.786	0.783
DCPI-Na ₂ SO ₃	5.60	5.00	1.00	1.12	1.00	0.626	0.626
	5.86	2.51	2.50	2.62	2.51	0.790	0.794

*Without correction for the interference of sulphide or sulphite

†Corrected for the interference of sulphide or sulphites, by using the values of k given in this work

Because k_5 and k_6 have almost the same value (Table 5), the reaction rate constant of the overall reaction reduces to k_5 or k_6 .

(c) pH 6.0–9.5. In view of the partial reactions which take place in this pH-range and the validity of the relations $1 + K_{D2}/[\text{H}^+] \gg [\text{H}^+]/K_{D1}$ and $1 + K_{Q2}/[\text{H}^+] \gg [\text{H}^+]/K_{Q1}$ in this pH-range, equation (4) gives

$$k = \frac{k_5[\text{H}^+]^2 + (k_6K_{D2} + k_8K_{Q2})[\text{H}^+] + k_9K_{D2}K_{Q2}}{[\text{H}^+]^2 + (K_{D2} + K_{Q2})[\text{H}^+] + K_{D2}K_{Q2}} \quad (10)$$

As already explained for the range pH 0–2.5, the most reactive species in this case is DH.

(d) $pH > 9.5$. At pH -values higher than 9.5 only the species D^- and SO_3^{2-} predominate, and owing to the validity of the $K_{Q2}/[\text{H}^+] \gg 1 + [\text{H}^+]/K_{Q1}$ and $K_{D2}/[\text{H}^+] \gg 1 + [\text{H}^+]/K_{D1}$, for this pH , equation (4) gives $k = k_9$.

The simplifications above were applied by taking into account the inequalities $K_{Q1} \gg K_{Q2}$ and $K_{D1} \gg K_{D2}$.

Assay of ascorbic acid in the presence of sulphide

On the basis of the known dependence of the reaction rate constants of the ascorbic acid–DCPI reaction on pH ,^{19,20} and taking into account the results above, a kinetic determination of ascorbic acid (Asc.Ac) in artificial mixtures containing known concentrations of sulphide was undertaken at different pH -values. The theoretically predicted reaction rate constants were calculated and compared with the experimentally determined values for the mixtures. The results are shown in Table 6.

From the rate constant $k_{\text{asc ac}} = 4 \times 10^4$ l.mole⁻¹.sec⁻¹ reported earlier,^{19,20} and $k_{\text{H}_2\text{S}} = 243$ l.mole⁻¹.sec⁻¹ found in this work for $pH_{\text{min}} = 3.50$, it can be estimated that for equimolar concentrations the error due to the hydrogen sulphide interference is less than 0.6%.

Assay of ascorbic acid in the presence of sulphite

At low pH -values (pH 1–2) no interference by sulphites is observed, because the ascorbic acid reacts much faster than sulphite does with the DCPI. At higher pH -values, because the reaction rate constant of sulphite is comparable to that of ascorbic acid, the interference is serious, especially at high concentrations of sulphite and low concentrations of vitamin C. The experimental results are shown in Table 6.

All the results shown in Table 6 reveal that pH -control is very important for minimizing the interfering effect of sulphide or sulphite in the kinetic determination of vitamin C. As can also be seen from Table 6, correction of the observed rate constants for the contribution of the sulphide or sulphite by use of the values of k given in this work, reduced the error in the determination of ascorbic acid at very low levels.

Acknowledgement—The authors gratefully acknowledge partial financial support by the General Secretary of Research and Technology, Greece, Grant No 6254

REFERENCES

1. W. Horowitz (ed.), *Official Methods of Analysis of the Association of Official Analytical Chemists*, 11th Ed., p. 777 A.O.A.C., Washington, D.C., 1970

2. M. I. Karayannis and D. I. Farasoglou, *Analyst*, 1987, **112**, 767
3. J. W. H. Lugg, *Aust. J. Expl. Biol. Med. Sci.*, 1942, **20**, 273
4. R. E. Basford and F. M. Huennekens, *J. Am. Chem. Soc.*, 1955, **77**, 3873.
5. J. A. Owen and B. Iggo, *Biochem J.*, 1956, **62**, 675
6. L. J. Harris and L. W. Mapson, *Brit J Nutr*, 1947, **1**, 7
7. M. van Eekelen and A. Emmerie, *Biochem. J.*, 1936, **30**, 25.
8. C. N. Konidari and M. I. Karayannis, *Anal. Chim. Acta*, 1989, **224**, 199.
9. M. I. Karayannis, S. M. Tzouwara-Karayanni and S. R. Crouch, unpublished results.
10. A. E. Greenberg, J. J. Connors and D. Jenkins (eds), *Standard Methods for the Examination of Water and Wastewater*, 15th Ed., p 448 American Public Health Association, Washington D C., 1981.
11. F. J. Welcher (ed.), *Standard Methods of Chemical Analysis*, 6th Ed., Vol 2B, p 2488. Krieger, New York, 1975.
12. J. McD. Armstrong, *Biochim Biophys. Acta.*, 1964, **86**, 194.
13. M. I. Karayannis, *Anal. Chim. Acta*, 1975, **76**, 121
14. M. G. Fleck, *Chemical Reaction Mechanisms*, p 39. Holt, Rinehart and Winston, New York, 1971
15. A. A. Frost and R. G. Pearson, *Kinetics and Mechanism*, 2nd Ed, p 150. Wiley, New York, 1961.
16. J. A. Dean (ed), *Lange's Handbook of Chemistry*, 12th Ed, 5-15 McGraw-Hill, New York, 1979
17. B. Tonomura, H. Nakatani, M. Ohnishi, J. Yamaguchi-Ito and K. Hiromi, *Anal. Biochem.*, 1978, **84**, 370
18. K. S. Gupta and Y. S. Gupta, *J. Chem. Educ*, 1984, **61**, 972.
19. N. C. Peterson, P. A. Siskos and M. I. Karayannis, *Analyst*, 1987, **112**, 821
20. M. I. Karayannis, *Talanta*, 1976, **23**, 27.

THE RAMESES ALGORITHM FOR MULTIPLE EQUILIBRIA—V. ERROR STATEMENTS

B. W. DARVELL and V. W.-H. LEUNG

Dental Materials Science Unit, University of Hong Kong, Prince Philip Dental Hospital,
34 Hospital Road, Hong Kong

(Received 9 November 1990 Revised 28 January 1991 Accepted 6 February 1991)

Summary—The equations of multiple equilibria systems can be expressed succinctly in matrix algebra terms. This is the basis of the RAMESES algorithm for the solution of those equations. This matrix algebra leads directly to the differential equations for the interdependence of the vector variables of species concentration, component concentration and equilibrium constants, with or without certain constraints. The laws of propagation of errors then give an immediate expression of the covariance matrix for the dependent vector.

In view of the fact that any set of equations representing an equilibrium is a model, and one which is necessarily only as good as its assumptions, the calculation of the errors associated with results is of immediate interest. This is not an easy proposition for anything other than the simplest of systems, due to the non-linearity, non-homogeneity and interdependence of the set of equations which then require elaborate iterative methods of solution to be employed.¹

The RAMESES algorithm¹⁻⁴ arises from a statement of the problem in matrix algebra terms, and it is this expression of the equations that permits direct statements of all relevant errors. The present purpose is to set out the method of the derivation of these error statements, to tabulate a number of results and to give an example. In referring to the original reports, equation numbers will be identified by prefix. *e.g.*, 1.5 refers to equation (5) in Ref. 1.

Errors can arise in source data, predetermined quantities, or in experimental measurements. Whenever speciation is either the focus of a study or crucial to an interpretation, the significance or reliability of the results should be assessed by reference to the errors of the estimates. It is therefore somewhat surprising that, given the large amount of work that has been done on solving the equations of equilibrium, recognition of the value of the calculation of errors has arisen only once.⁵ (It is important to distinguish between errors in the values of variables and those of the solution in the

sense of tolerance. The latter can, in principle, be reduced to near zero, limited only by the precision of the machine/language, by sufficient iterations.) Thus, in addition to those reports previously discussed (with the exception of the two mentioned below),¹⁻⁴ accounts of COMPLEX,⁶ MINEQL,⁷ ITERAT,⁸ COM-PLX,⁹ CHEMEQUIL-2,¹⁰ IONPRODUCT,¹¹ and algorithms from Dudley and Coray¹² and Park,¹³ all failed to consider errors. Similarly, three substantial reviews of such programs¹⁴⁻¹⁶ failed to recognise this omission and made no mention of the effect of any errors or of their calculation.

The question seems first to have been mentioned in the context of the program ES4EC as a practical requirement of such calculations,⁵ and expressions were given for the error (variance) in each solution species concentrations due to errors in both 'analytical' concentrations and formation constants. A later implementation¹⁷ only mentions the derivatives of 'free' (independent species, in our terminology^{1,3}) and analytical concentrations with respect to formation constants and analytical concentrations. These derivatives were expressed in terms of summations of individual derivatives, obtained one by one, and as such they were unable to incorporate the covariance terms of the input error data.⁵ This limitation may be serious, but even so, the notation used does not lend itself to a clear visualization of the underlying algebra. It is the present intention to allow clear and full error statements and to provide the basis for more flexible calculations.

NUMERICAL METHOD

There are just three sources of error to be considered in such systems of equations: (1) most obviously in the values of the logarithmic equilibrium constants themselves, L ; (2) in the ('analytical') component totals, T , whether they are errors of analysis, weighing, or dilution; and (3) in the experimentally determined concentrations of species, X_A , as by a specific ion electrode (pH in particular) or any spectroscopic technique (such as n.m.r.). We may thus enquire about $\partial X/\partial L$, $\partial X/\partial T$, $\partial T/\partial X_A|_L$, $\partial X_B/\partial X_A|_T$ and so on, as well as the log(concentration) equivalents where ∂X is replaced by ∂P in the foregoing. We proceed by first introducing the notation to be used.

The vector partial differentiation operator, ∇ , differentiates one vector, $A(a \times 1)$, with respect to another, $B(b \times 1)$, and is to be understood as implying the following form:

$$\nabla(A, B) = \frac{\partial A}{\partial B} = \begin{bmatrix} \frac{\partial A_1}{\partial B_1} & \dots & \frac{\partial A_1}{\partial B_b} \\ \vdots & \ddots & \vdots \\ \frac{\partial A_a}{\partial B_1} & \dots & \frac{\partial A_a}{\partial B_b} \end{bmatrix} \quad (1)$$

where the resulting partial differential matrix is $(a \times b)$. The generalised inverse or matrix reciprocal operator rec is defined by:^{18,19}

$$\text{rec}(A) = (A^T A)^{-1} A^T \quad (2)$$

where A is $(r \times c)$, $r \geq c$, and superscript T means 'transpose' so that

$$\text{rec}(A)A = I \quad (3)$$

Otherwise, with $A(r \times c)$ but $r \leq c$,

$$\text{rec}(A) = A^T(A \cdot A^T)^{-1} \quad (4)$$

$$A \text{rec}(A) = I \quad (5)$$

The rec operator is convenient because, while $\nabla(A, B)$ may be directly obtainable, $\nabla(B, A)$ may not be. It is to be expected that

$$\nabla(A, B)\nabla(B, A) = \frac{\partial A}{\partial B} \frac{\partial B}{\partial A} = I \quad (6)$$

where $\nabla(B, A)$ is $(b \times a)$. This product is defined when $a \leq b$. If $a = b$

$$\nabla(B, A) = \text{rec}(\nabla(A, B)) = \nabla(A, B)^{-1} \quad (7)$$

For convenience, we define the matrix exponential operator \exp such that for A

and B , both $(a \times b)$, $B = \exp(A)$ is to be read as

$$B_{ij} = \exp(A_{ij}), \quad \text{for all } i, j \quad (8)$$

Thus, the vectors of interest now are related, for concentrations, X , by

$$X = \exp(P) \quad (9)$$

and for equilibrium constants, K , by

$$K = \exp(L) \quad (10)$$

[*c.f.* equations (1.5) and (1.4)]. We also use the 'diagonalised vector' matrix, $A^D(a \times a)$, as before,⁴ where

$$A^D = \text{diag}(A) \quad (11)$$

[see equation (4.3)]. Use is then made of identities of the form

$$\begin{aligned} \partial X_i &= \partial \exp(P_i) \\ &= \exp(P_i) \partial P_i \\ &= X_i \partial P_i \end{aligned}$$

so that we may write

$$\partial X = X^D \partial P \quad (12)$$

where the use of the diag operator preserves the element by element multiplication. Similarly, we obtain

$$\partial P = (X^D)^{-1} \partial X \quad (13)$$

The inverses of equations (12) and (13) are also valid, for example allowing us to write

$$\frac{1}{\partial K} = \frac{1}{\partial L} (K^D)^{-1} \quad (14)$$

We give an example of the method by first noting the basic equations. The fundamental expression of the equilibria and the partition which permits solution¹ is:

$$L = CP \quad (15)$$

$$= C_A P_A + C_B P_B \quad (16)$$

where C is the matrix of coefficients.¹ The component sums, S , are obtained from

$$S = M^T X \quad (17)$$

$$= M_A^T X_A + M_B^T X_B \quad (18)$$

where $S \equiv T$ at the exact solution of the entire system of equations, when the charge error $\Delta = 0$ [equation (2.13)], and where M_A , M_B and M are defined at equations (3.9)–(3.11). [S is now written as a vector, for uniformity of style, see equation (1.12)].

We have immediately from equation (15)

$$\frac{\partial \mathbf{L}}{\partial \mathbf{P}} = \mathbf{C} \frac{\partial \mathbf{P}}{\partial \mathbf{P}} = \mathbf{C} \quad (19)$$

as $\partial \mathbf{P} / \partial \mathbf{P} = \mathbf{I}$ by definition. It then follows by virtue of equation (4) that

$$\frac{\partial \mathbf{P}}{\partial \mathbf{L}} = \text{rec}(\mathbf{C}) \quad (20)$$

This is a result of some interest in that the full effects of errors in all equilibrium constants may be determined directly, and including their interactions, although without regard to maintaining sums. Equally, from equation (17) we have

$$\frac{\partial \mathbf{X}}{\partial \mathbf{S}} = \text{rec}(\mathbf{M}^T) \quad (21)$$

which shows the effect of component concentration changes, albeit without maintaining equilibrium through \mathbf{L} .

The partition of equation (16) yields

$$\frac{\partial \mathbf{L}}{\partial \mathbf{P}_A} = \mathbf{C}_A \frac{\partial \mathbf{P}_A}{\partial \mathbf{P}_A} + \mathbf{C}_B \frac{\partial \mathbf{P}_B}{\partial \mathbf{P}_A} \quad (22)$$

so that fixing \mathbf{P}_B we get

$$\left. \frac{\partial \mathbf{L}}{\partial \mathbf{P}_A} \right|_{\mathbf{P}_B} = \mathbf{C}_A \quad (23)$$

and likewise

$$\left. \frac{\partial \mathbf{P}_A}{\partial \mathbf{L}} \right|_{\mathbf{P}_B} = \text{rec}(\mathbf{C}_A) \quad (24)$$

This approach may be followed for the remaining differentials derived, as appropriate, from either equation (16) or (18). Indeed, it follows that any other partition of equation (15) or (17) may be used as needed; the particular advantage of the generalized inverse is then apparent. However, care must be taken in algebraic manipulation since only one of equations (2) and (4) can be valid if $r \neq c$, and no valid direct inversion of an expression may be possible, hence, another route must be sought.

To take the process a stage further, it must be recognised that there are effectively four vector variables: \mathbf{L} , \mathbf{S} , \mathbf{P}_A , \mathbf{P}_B (or their cognate non-logarithmic equivalents). The purpose now is to construct a set of partial differential equations which take one such vector as being fixed and require information from equations (15) and (17). It may be noted that fixing two such vectors, equivalent to the constraint of charge balance [equation (1.10) or (2.13)],

sets all $\nabla(\mathbf{A}, \mathbf{B})|_{c,d} = 0$, as the system is then fully defined. In a sense, charge balance is the one degree of freedom which is allowed in developing the following results, and this operates in the one unreferenced concentration vector.

Then, equation (18) can be rearranged and expressed as:

$$\exp(\mathbf{P}_A) = \mathbf{S} - \mathbf{M}_B^T \exp(\mathbf{P}_B) \quad (25)$$

dropping $\mathbf{M}_A^T = \mathbf{I}$ [equation (3.11)]. Then

$$\frac{\partial \exp(\mathbf{P}_A)}{\partial \mathbf{L}} = \frac{\partial \mathbf{S}}{\partial \mathbf{L}} - \mathbf{M}_B^T \frac{\partial \exp(\mathbf{P}_B)}{\partial \mathbf{L}} \quad (26)$$

Holding \mathbf{S} constant and expanding [equation (12)]:

$$\mathbf{X}_A^D \left. \frac{\partial \mathbf{P}_A}{\partial \mathbf{L}} \right|_S = -\mathbf{M}_B^T \mathbf{X}_B^D \left. \frac{\partial \mathbf{P}_B}{\partial \mathbf{L}} \right|_S \quad (27)$$

$$\left. \frac{\partial \mathbf{P}_A}{\partial \mathbf{L}} \right|_S = -(\mathbf{X}_A^D)^{-1} \mathbf{M}_B^T \mathbf{X}_B^D \left. \frac{\partial \mathbf{P}_B}{\partial \mathbf{L}} \right|_S \quad (28)$$

From equation (16)

$$\frac{\partial \mathbf{P}_B}{\partial \mathbf{L}} = \mathbf{C}_B^{-1} \left(\frac{\partial \mathbf{L}}{\partial \mathbf{L}} - \mathbf{C}_A \frac{\partial \mathbf{P}_A}{\partial \mathbf{L}} \right) \quad (29)$$

so that substitution from equation (28) gives

$$\left. \frac{\partial \mathbf{P}_B}{\partial \mathbf{L}} \right|_S = \mathbf{C}_B^{-1} \mathbf{I} + \mathbf{C}_B^{-1} \mathbf{C}_A (\mathbf{X}_A^D)^{-1} \mathbf{M}_B^T \mathbf{X}_B^D \left. \frac{\partial \mathbf{P}_B}{\partial \mathbf{L}} \right|_S \quad (30)$$

$$= \mathbf{C}_B^{-1} - \mathbf{M}_B (\mathbf{X}_A^D)^{-1} \mathbf{M}_B^T \mathbf{X}_B^D \left. \frac{\partial \mathbf{P}_B}{\partial \mathbf{L}} \right|_S \quad (31)$$

$$= \mathbf{C}_B^{-1} [\mathbf{I} + \mathbf{M}_B (\mathbf{X}_A^D)^{-1} \mathbf{M}_B^T \mathbf{X}_B^D]^{-1} \quad (32)$$

Then, using the results of identities (12) and (14), the following related result can be written down immediately:

$$\left. \frac{\partial \mathbf{X}_B}{\partial \mathbf{K}} \right|_S = \mathbf{X}_B^D \mathbf{C}_B^{-1} [\mathbf{I} + \mathbf{M}_B (\mathbf{X}_A^D)^{-1} \mathbf{M}_B^T \mathbf{X}_B^D]^{-1} (\mathbf{K}^D)^{-1} \quad (33)$$

In view of the ease of writing down any of the non-logarithmic forms, as exemplified by equation (33), and as the reciprocal differentials are obtained directly by the use of the *rec* operator given at equations (2) and (4), only the basic twelve results of Table 1 need be tabulated for any other result to be readily obtained. Even so, care is required in applying the transformations since the *rec* operator is subject to rules

Table 1. Summary of principal results. Equations (1) and (2) are derived from text equations (15) and (17) respectively, (3)–(5) from text equation (16), (6)–(8) from text equation (18); and (9)–(14) from text equations (16) and (18) combined. For explanation of the notation, see text

$\nabla(\mathbf{P}, \mathbf{L}) = \text{rec}(\mathbf{C})$	(1)
$\nabla(\mathbf{P}, \mathbf{S}) = \text{rec}(\mathbf{M}^T \mathbf{X}^D)$	(2)
$\nabla(\mathbf{P}_A, \mathbf{L}) _{\mathbf{P}_B} = \text{rec}(\mathbf{C}_A)$	(3)
$\nabla(\mathbf{P}_B, \mathbf{L}) _{\mathbf{P}_A} = \mathbf{C}_B^{-1}$	(4)
$\nabla(\mathbf{P}_B, \mathbf{P}_A) _{\mathbf{L}} = \mathbf{M}_B$	(5)
$\nabla(\mathbf{P}_A, \mathbf{S}) _{\mathbf{P}_B} = (\mathbf{X}_A^D)^{-1}$	(6)
$\nabla(\mathbf{P}_B, \mathbf{S}) _{\mathbf{P}_A} = \text{rec}(\mathbf{M}_B^T \mathbf{X}_B^D)$	(7)
$\nabla(\mathbf{P}_A, \mathbf{P}_B) _{\mathbf{S}} = -(\mathbf{X}_A^D)^{-1} \mathbf{M}_B^T \mathbf{X}_B^D$	(8)
$\nabla(\mathbf{P}_A, \mathbf{L}) _{\mathbf{S}} = -(\mathbf{M}^T \mathbf{X}^D \mathbf{M})^{-1} \mathbf{M}_B^T \mathbf{X}_B^D \mathbf{C}_B^{-1}$	(9)
$\nabla(\mathbf{P}_B, \mathbf{L}) _{\mathbf{S}} = [\mathbf{I} + \mathbf{M}_B (\mathbf{X}_A^D)^{-1} \mathbf{M}_B^T \mathbf{X}_B^D]^{-1} \mathbf{C}_B^{-1}$	(10)
$\nabla(\mathbf{S}, \mathbf{L}) _{\mathbf{P}_A} = \mathbf{M}_B^T \mathbf{X}_B^D \mathbf{C}_B^{-1}$	(11)
$\nabla(\mathbf{S}, \mathbf{L}) _{\mathbf{P}_B} = \mathbf{X}_A^D \text{rec}(\mathbf{C}_A)$	(12)
$\nabla(\mathbf{S}, \mathbf{P}_A) _{\mathbf{L}} = \mathbf{M}^T \mathbf{X}^D \mathbf{M}$	(13)
$\nabla(\mathbf{S}, \mathbf{P}_B) _{\mathbf{L}} = -\mathbf{X}_A^D \text{rec}(\mathbf{C}_A) \mathbf{C}_B + \mathbf{M}_B^T \mathbf{X}_B^D$	(14)

of precedence. Thus, for $\mathbf{A}(r \times c)$, $\mathbf{B}(c \times c)$, the following is valid:

$$\text{rec}(\mathbf{AB}) = \mathbf{B}^{-1} \text{rec}(\mathbf{A}), \quad r \geq c \quad (34)$$

and for $\mathbf{A}(r \times c)$, $\mathbf{B}(r \times r)$,

$$\text{rec}(\mathbf{BA}) = \text{rec}(\mathbf{A})\mathbf{B}^{-1}, \quad r \leq c \quad (35)$$

whereas the left hand side of neither equation (34) with $r \leq c$, nor equation (35) with $r \geq c$, has a valid simple equivalent. It is necessary therefore to apply the logarithmic/exponential transformation before the overall inverse is taken.

The results of Table 1 may be converted to the corresponding forms in \mathbf{L}' and \mathbf{C}'_A [equations (3.4)–(3.9)] simply by symbol substitution, noting only that $\mathbf{C}'_B = \mathbf{I}$.

In passing, it may be noted that equation (13) of Table 1, and its non-logarithmic equivalent, are the bases of the Newton–Raphson approaches to the solution of an equilibrium system discussed at equations (4.1) and (4.2).

It only remains to apply the above results to the determination of errors. If we are given the errors in the vector with respect to which the differentiation has been done in the form of the covariance matrix $\sigma^2(\mathbf{B})$, which is $(b \times b)$, the errors in the dependent vector $\sigma^2(\mathbf{A})$, $(a \times a)$, are given directly by the following law of propagation of errors:¹⁹

$$\sigma^2(\mathbf{A}) = \nabla(\mathbf{A}, \mathbf{B})\sigma^2(\mathbf{B})\nabla(\mathbf{A}, \mathbf{B})^T \quad (36)$$

The additivity of variance is also valid for error propagation:

$$\sigma^2(\mathbf{A}) = \sigma^2(\mathbf{B}) + \sigma^2(\mathbf{C}) + \sigma^2(\mathbf{D}) \dots \quad (37)$$

so long as all σ^2 are of the same size and those on the right hand side are mutually independent. We can therefore construct an augmented differential matrix, for example

$$\frac{\partial \mathbf{P}}{\partial (\mathbf{L}|\mathbf{S})} = [\nabla(\mathbf{P}, \mathbf{L})|\nabla(\mathbf{P}, \mathbf{S})] \quad (38)$$

and use this with the augmented error matrix

$$\sigma^2(\mathbf{L}, \mathbf{S}) = \begin{bmatrix} \sigma^2(\mathbf{L}) & \phi \\ \phi & \sigma^2(\mathbf{S}) \end{bmatrix} \quad (39)$$

But combining equations (38) and (39) according to equation (36) is equivalent to writing

$$\sigma^2(\mathbf{P}) = \nabla(\mathbf{P}, \mathbf{L})\sigma^2(\mathbf{L})\nabla(\mathbf{P}, \mathbf{L})^T + \nabla(\mathbf{P}, \mathbf{S})\sigma^2(\mathbf{S})\nabla(\mathbf{P}, \mathbf{S})^T \quad (40)$$

Thus, in computational terms, the augmented matrices at equations (38) and (39) do not actually need to be constructed in computer memory as such so long as the off-diagonal submatrices are null.

EXAMPLE

A simple example will suffice to illustrate the implementation of the above results: phosphoric acid in water. The non-logarithmic equivalent of equation (38) will be solved. The basic data for this system has already been given,³ but we now have to choose to consider a concentration of $10^{-5}M$ $[\text{PO}_4]$ which is almost pH 5. So, given

$$\mathbf{X} = \begin{bmatrix} \text{PO}_4^{3-} \\ \text{H}^+ \\ \text{OH}^- \\ \text{H}_2\text{PO}_4^- \\ \text{HPO}_4^{2-} \\ \text{H}_3\text{PO}_4 \end{bmatrix} = \begin{bmatrix} 2.93\text{E}-15 \\ 1.00\text{E}-5 \\ 1.01\text{E}-9 \\ 9.92\text{E}-6 \\ 6.23\text{E}-8 \\ 1.41\text{E}-8 \end{bmatrix}$$

$$\mathbf{K} = \begin{bmatrix} 4.73\text{E}-13 \\ 6.31\text{E}-8 \\ 1.012\text{E}-14 \\ 7.10\text{E}-3 \end{bmatrix}$$

$$\mathbf{C} = \begin{bmatrix} 1 & 1 & 0 & 0 & -1 & 0 \\ 0 & 1 & 0 & -1 & 1 & 0 \\ 0 & 1 & 1 & 0 & 0 & 0 \\ 0 & 1 & 0 & 1 & 0 & -1 \end{bmatrix}$$

we obtain the following results:

$$\mathbf{V}(\mathbf{X}, \mathbf{K}) = \text{rec}[\mathbf{K}^D \mathbf{C}(\mathbf{X}^D)^{-1}] = \begin{bmatrix} 6.20\text{E}-3 & 4.65\text{E}-8 & -5.82\text{E}-9 & -7.93\text{E}-19 \\ 3.62\text{E}-12 & 6.12\text{E}-3 & 9.97\text{E}+0 & 2.79\text{E}-9 \\ -3.62\text{E}-16 & -6.13\text{E}-7 & 9.95\text{E}+4 & -2.79\text{E}-13 \\ -1.83\text{E}-12 & -6.20\text{E}-3 & 3.68\text{E}-4 & 2.82\text{E}-9 \\ -3.39\text{E}-14 & 9.87\text{E}-1 & -6.18\text{E}-2 & 4.41\text{E}-13 \\ 2.47\text{E}-15 & -2.19\text{E}-7 & 1.40\text{E}-2 & -1.99\text{E}-6 \end{bmatrix}$$

$$\mathbf{V}(\mathbf{X}, \mathbf{S}) = \text{rec}(\mathbf{M}^T) = \begin{bmatrix} 5.71\text{E}-1 & -2.14\text{E}-1 \\ -2.14\text{E}-1 & 1.43\text{E}-1 \\ 2.14\text{E}-1 & -1.43\text{E}-1 \\ 1.43\text{E}-1 & 7.14\text{E}-2 \\ 3.57\text{E}-1 & -7.14\text{E}-2 \\ -7.14\text{E}-2 & 2.14\text{E}-1 \end{bmatrix}$$

Then

$$\mathbf{V}(\mathbf{X}, \mathbf{L} | \mathbf{S}) = [\mathbf{V}(\mathbf{X}, \mathbf{K}) | \mathbf{V}(\mathbf{X}, \mathbf{S})]$$

In the absence of actual data, only guesses can be made at error values. So taking the standard deviations of the values of \mathbf{K} to be ± 1 least significant digit, and arbitrary correlations between them with $r = \pm 0.75$; standard deviations of \mathbf{S} are assumed to be 1% of the total, and the correlations $r = -0.20$. The input covariance matrix is then:

$$\sigma^2(\mathbf{L}, \mathbf{S}) =$$

$$\begin{bmatrix} 1.00\text{E}-30 & -7.50\text{E}-26 & 7.50\text{E}-33 & -7.50\text{E}-21 & 0 & 0 \\ -7.50\text{E}-26 & 1.00\text{E}-20 & -7.50\text{E}-28 & 7.50\text{E}-16 & 0 & 0 \\ 7.50\text{E}-33 & -7.50\text{E}-28 & 1.00\text{E}-34 & -7.5\text{E}-45 & 0 & 0 \\ -7.50\text{E}-21 & -7.50\text{E}-16 & -7.50\text{E}-45 & 1.00\text{E}-10 & 0 & 0 \\ 0 & 0 & 0 & 0 & 1.00\text{E}-14 & -2.00\text{E}-15 \\ 0 & 0 & 0 & 0 & -2.00\text{E}-15 & 1.00\text{E}-14 \end{bmatrix}$$

So that

$$\sigma^2(\mathbf{X}) = \mathbf{V}(\mathbf{X}, \mathbf{L} | \mathbf{S}) \sigma^2(\mathbf{L}, \mathbf{S}) \mathbf{V}(\mathbf{X}, \mathbf{L} | \mathbf{S})^T =$$

$$\begin{bmatrix} 4.21\text{E}-15 & -1.79\text{E}-15 & 1.79\text{E}-15 & 6.43\text{E}-16 & 2.43\text{E}-15 & -1.14\text{E}-15 \\ -1.79\text{E}-15 & 7.86\text{E}-16 & -7.86\text{E}-16 & -2.14\text{E}-16 & -1.10\text{E}-15 & 5.71\text{E}-16 \\ 1.79\text{E}-15 & -7.86\text{E}-16 & 7.86\text{E}-16 & 2.14\text{E}-16 & 1.10\text{E}-15 & -5.71\text{E}-16 \\ 6.43\text{E}-16 & -2.14\text{E}-16 & 2.14\text{E}-16 & 2.14\text{E}-16 & 4.29\text{E}-16 & 8.69\text{E}-24 \\ 2.43\text{E}-15 & -1.10\text{E}-15 & 1.10\text{E}-15 & 4.29\text{E}-16 & 1.43\text{E}-15 & -5.71\text{E}-16 \\ -1.14\text{E}-15 & 5.71\text{E}-16 & -5.71\text{E}-16 & 8.69\text{E}-24 & -5.71\text{E}-16 & 5.71\text{E}-16 \end{bmatrix}$$

DISCUSSION

Although the example given above is artificial, in that the errors in S were deliberately large, it illustrates a point which may, in the absence of such a calculation, pass unnoticed. The calculated standard error of the concentration of the ion PO_4^{3-} is, from the first element of $\sigma^2(\mathbf{X})$, about $6.5\text{E}-8$, rather larger than the calculated concentration itself, the first value of \mathbf{X} . Essentially, the interpretation must be that the sensitivity of the concentration of PO_4^{3-} is so great that nothing can usefully be said about its value in the face of the input uncertainties. The interpretation would perhaps be easier if the calculation were of errors in $\log(\text{concentration})$, when potentially negative concentrations would not be implied, but rather, a large range in the power of ten multiplier. Nevertheless, the danger in basing conclusions on such a calculated concentration is plain: the input data is simply too imprecise.

The relative errors in the means, $\sigma(\mathbf{X}_i)/\mathbf{X}_i$, should therefore be inspected as a matter of course for those species of primary interest in order to determine whether or not confidence can be placed in the results of the speciation calculation. In the reverse sense, such calculations can be used to estimate the precision necessary in analytical concentrations S or in equilibrium constants, \mathbf{K} or \mathbf{L} , to achieve the desired accuracy in a calculated concentration. Indeed, this would enable the feasibility or cost of such knowledge to be calculated. The economic implications of this in areas such as toxicology or pollution control have yet to be considered.

One other point to which attention should be drawn is that even if errors in the input variables are Normally distributed (Gaussian), in general those in the dependent variables will not be. This does not in any way affect the validity of the errors so calculated, but it must be taken as a warning that statistical tests or the calculation of confidence intervals (which rely on the tails of assumed distributions) must be approached with extreme caution. The effects of curvature in the functions being differentiated may be serious if the errors are large but, equally, small errors will tend to approach normality.

The identification of the procedure for the expression of the differential equations of equilibrium systems has made possible more rigorous error statements in respect of any of the quantities of interest. It has not been the pur-

pose here to be exhaustive in the treatment as the number of possibilities is very large indeed and error statements must be tailored to the particular task in hand. For example, second (and higher) differentials, where they exist, can clearly be derived in analogous fashion. It is the particular power of the matrix notation that such statements are possible in succinct and computationally convenient form. They can be used no matter which speciation program was employed.

It can be anticipated that the routine calculation of covariance matrices for calculated values in experimental systems will lead to new insights into the influence of some variables and the avoidance of spurious precision in reported results.

Acknowledgement—We should like to thank Dr W. K. Li of the Department of Statistics, University of Hong Kong for his guidance in our first steps in matrix differentiation.

REFERENCES

- 1 V. W.-H. Leung, B. W. Darvell and A. P.-C. Chan, *Talanta*, 1988, **35**, 713
- 2 B. W. Darvell and V. W.-H. Leung, *ibid*, 1990, **37**, 413
- 3 V. W.-H. Leung and B. W. Darvell, *ibid*, 1990, **37**, 425
- 4 B. W. Darvell and V. W.-H. Leung, *ibid*, in the press
- 5 A. de Robertis, C. de Stefano, S. Sammartano and C. Rigano, *Anal. Chim. Acta*, 1986, **191**, 385.
- 6 G. Ginzburg, *Talanta*, 1976, **23**, 149.
- 7 J. C. Westall, J. L. Zachary and F. M. M. Morel, *MINEQL—A Computer Program for the Calculation of Chemical Equilibrium Composition of Aqueous Systems Technical Note 18*. Department of Civil Engineering, Massachusetts Institute of Technology, Cambridge, MA, 1976
- 8 K. J. Johnson, *Numerical Methods in Chemistry*, p. 219 Dekker, New York, 1980
- 9 *Idem*, *ibid*, p. 226 Dekker, New York, 1980
- 10 V. S. Tripathi, *Talanta*, 1986, **33**, 1015
- 11 R. P. Shellis and G. H. Dibdin, *J. Dent. Res.* 1988, **67**, 438
- 12 L. M. Dudley and C. S. Coray, 1989, *Environ. Sci. Technol.*, **23**, 245.
- 13 D. J. M. Park, *Comput. Chem.*, 1990, **14**, 141
- 14 D. J. Leggett, *Talanta*, 1977, **24**, 535
- 15 D. K. Nordstrom, L. N. Plummer, T. M. L. Wigley, T. J. Wolery, J. W. Ball, E. A. Jenne, R. L. Bassett, D. A. Crerar, T. M. Florence, B. Fritz, M. Hoffman, G. R. Holdren, Jr., G. M. Lafon, S. V. Mattigod, R. E. McDuff, F. Morel, M. M. Reddy, G. Sposito and J. Thraillkill, in *Chemical Modeling in Aqueous Systems*, E. A. Jenne (ed.), p. 857 ACS, Washington DC, 1979
- 16 T. D. Waite, in *Trace Element Speciation Analytical Methods and Problems*, G. E. Batley (ed.), p. 117 CRC, Boca Raton, FL, 1989
- 17 C. de Stefano, P. Princi, C. Rigano and S. Sammartano, *Comput. Chem.*, 1989, **13**, 343
- 18 S. R. Searle, *Matrix Algebra Useful for Statistics*, p. 212 Wiley, New York, 1982
- 19 C. R. Rao and S. K. Mitra, *Generalized Inverse of Matrices and Its Applications*, p. 19 Wiley, New York, 1971.
- 20 S. L. Meyer, *Data Analysis for Scientists and Engineers*, p. 416 Wiley, New York, 1975

SIMULTANEOUS FLOW-INJECTION ANALYSIS OF THREE COMPONENTS WITH ON-LINE DIALYZERS IN SERIES. DETERMINATION OF SODIUM, POTASSIUM AND CHLORIDE IN BLOOD SERUM

JACOBUS F. VAN STADEN

Department of Chemistry, University of Pretoria, Pretoria 0002, South Africa

(Received 15 September 1990 Revised 22 February 1991 Accepted 6 March 1991)

Summary—A fast and reliable fully automated three-component flow-injection procedure for the simultaneous determination of sodium, potassium and chloride in blood serum is described. A single sample injection (100- μ l blood serum) is directed to two different channels by using two dialyzers in series. To avoid interferences and blocking of the fine jet of the atomizer, sodium and potassium are dialyzed by the first dialyzer before measurement by AES with a flame photometer. A second dialyzer in series is used to eliminate interferences and for automated dilution before the dialyzed chloride is measured by UV/VIS spectrophotometry at 485 nm. The results obtained for the sodium, potassium and chloride in blood serum at a sampling rate of 106 samples per hour compared well with data obtained by standard methods.

The large number of electrolyte determinations carried out in the clinical laboratory necessitated an efficient procedure which would reduce the time taken for these determinations. To supply needed data effectively and quickly, it would be an advantage to have a rapid, accurate and reliable method available for the simultaneous determination of sodium, potassium and chloride in blood serum. Conventional automated segmented continuous-flow analysis utilizes sampling rates of up to 60 samples per hour.

The concept of flow-injection analysis (FIA) is now a well defined analytical technique¹⁻⁴ which is suitable to increase the output in some laboratories. Most FIA procedures are however based on the measurement of a single signal of a product formed from a single sample injection which usually involves the determination of a single element or compound carried out on a batch of samples. It is however possible to carry out several measurements from a single sample injection in a FIA system. Simultaneous (or multicomponent) FIA determinations where two or more species are determined in the same sample with a single FIA system, is a relatively unexplored area.² This novel methodology has, however, a great potential in fields such as clinical laboratories where limited numbers of samples are involved.

The concept of mass transfer in on-line analytical dialyzers has been applied in continuous flow systems with suitable membranes for many

years especially in the area of clinical analysis. The use of on-line dialysis in segmented continuous flow systems was probably first described by Skeggs⁵ in his pioneering famous paper in 1957 on automated analysis. Continuous flow dialysis without air segmentation for the determination of glucose was reported in the mid-1960s by Kadish and Hall⁶ and Brown *et al.*⁷ Hansen and Růžička⁸ were the first to exploit this principle in flow-injection analysis in the mid-seventies when applying the technique to the determination of phosphate and chloride in blood serum. The incorporation of flow-through dialyzers as part of the manifold in FIA systems is, however, extremely useful for on-line determination of analytes in biological systems, for example blood serum. van Staden and van Rensburg⁹ studied and compared a number of variables for different semi-permeable dialysis membranes and dialyzers with different dimensions for the determination of inorganic species (Ca^{2+} and Cl^-). A dialyzer as part of the manifold system not only facilitates automated dilution, but the main aim of dialysis so far was to remove interferences like suspended solids, unwanted macromolecules (for example protein) *etc.*, present in the sample channel, by separation from a detector channel where the analyte was detected. To date, dialysis has mainly been used for determination of a single element or compound from a single sample injection. However, it is possible to use dialysis for the simultaneous determination of more than one

component. The main aim is to enable multi-component analysis of a limited amount of blood serum sample with a single sample injection rapidly, accurately and precisely with an on-line dialysis procedure which is also in the working concentration range of all the components involved.

This paper deals with the development of a FIA procedure for the simultaneous determination of sodium, potassium and chloride in blood serum on a single sample injection where two dialyzers were used in series and the dialyzed components were detected with a flame photometer and UV/VIS spectrophotometer.

EXPERIMENTAL

Apparatus

A Carle micro-volume two-position sampling valve with two identical sample loops, each having a volume of 100 μ l, was used with the FIA system together with a Cenco sampler. The valve was operated as follows: samples were aspirated through the valve on a 34-sec cycle. In the first of the two valve positions, the sample was aspirated through loop A to waste, whilst loop B was connected to the carrier stream. On switching to the second position (which was done after 32 sec of the 34-sec cycle) the carrier stream was interrupted and the contents of loop A placed into the carrier stream with loop B now being filled with the next sample from the sample

unit and so on. In this way 100- μ l samples were injected at a rate of one every 34 sec giving an optimum sampling rate of 106 samples per hour. The valve system was synchronized with the operation of the sampler unit, the sampling valve being actuated 32 sec after movement of the sampler probe to the next sample. Carrier, recipient and reagent streams were supplied at constant flow rates with a peristaltic pump operating at 10 rpm. Sodium and potassium were detected with an IL143 flame photometer. Chloride was detected by using UV/VIS spectrophotometric detection with a colour reagent solution, containing mercury(II) thiocyanate and iron(III) nitrate in an aqueous methanolic nitric acid solution, measuring the complex formed at 485 nm. A Bausch and Lomb Spectronic 21 (Rochester, New York) spectrophotometer with a 10-mm Hellma type flow-through cell (volume 80 μ l) was used. The outputs from the different detectors were recorded by a Hitachi Model QPD 53 for sodium, Hitachi Model QPD 54 for potassium and Mettler GA 12 for chloride. Transmission tubing with inner diameters of 0.38 and 0.50 mm (Fig. 1) were used in the flow system. Two slightly modified versions of 12 and 6-inch Technicon AutoAnalyzer II dialyzer units with different dimensions were used. The first dialyzer A consisted of a 160 \times 30 \times 25 module (home-made as a modified version of a 12" Technicon dialyzer) and the second dialyzer B of a 90 \times 30 \times 25 module (home-made as a

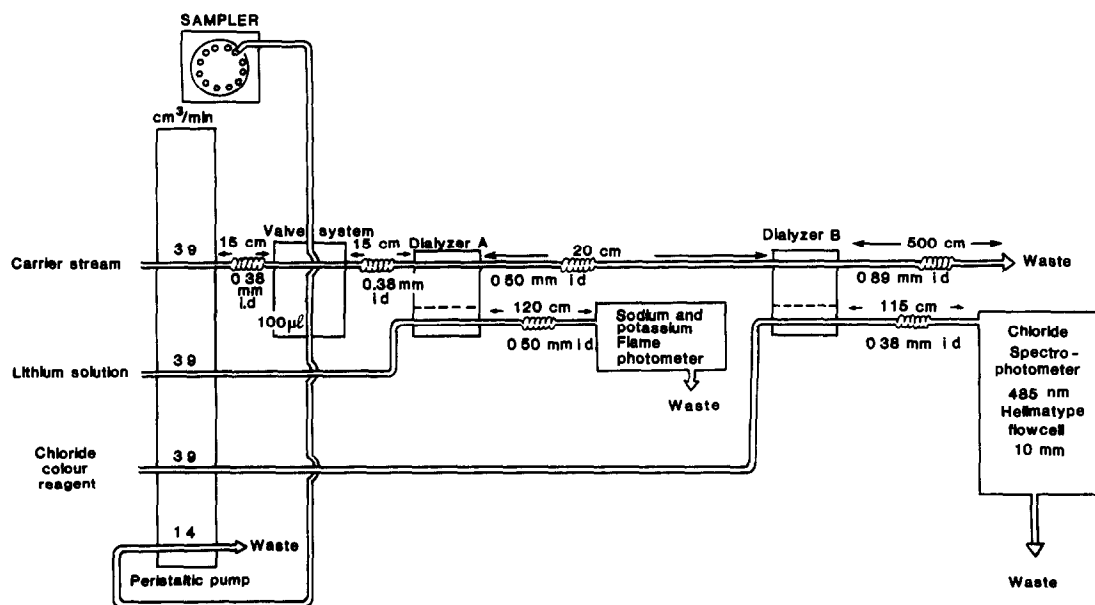


Fig. 1. Flow diagram of the FIA-system for the simultaneous determination of sodium, potassium and chloride. Valve loop size = 100 μ l; sampler = 34 sec; wash = 0 sec; valve actuation at 32 sec; sampling rate = 106 samples per hour. Tube length and i.d. are given in cm and mm respectively

modified version of a 6" Technicon dialyzer). The donor and acceptor channels of both dialyzers consisted of straight semi-tubular grooves with an i.d. of 0.5 mm (*i.e.*, 0.5 mm wide and 0.5 mm deep) and with a distance (width) of 15 mm between the entrance and exit sides of a channel. The path lengths of dialyzer A were 300 mm and of dialyzer B were 150 mm for the donor and acceptor channels of both units respectively. Both dialysis units were equipped with Technicon Pre-mount Dialysis Membranes Type "C".

Reagents

All solutions were prepared from analytical reagent grade chemicals unless otherwise specified. Doubly distilled, demineralized water was used throughout. The water was tested beforehand for traces of chloride. All reagents were degassed before measurement with a vacuum pump.

Carrier stream. Concentrated nitric acid (20 ml, specific gravity = 1.42) (Merck, Darmstadt, Germany) was diluted to 1 litre with water.

Lithium solution. A working solution of 15mM lithium was prepared by dilution of an appropriate aliquot of 1.5M lithium standard stock solution (Instrumentation Laboratory Inc. reagent, Lexington, Massachusetts) with water.

Chloride colour reagent. Mercury(II) thiocyanate (2.4 g) (Merck) was dissolved in 1 litre of distilled water to give a saturated solution which was then filtered. Iron(III) nitrate (7.6 g) (Merck) was dissolved in 5 ml of concentrated nitric acid (Merck, specific gravity = 1.42), 37.5 ml of methanol (Merck) and 0.21–0.22 ml of a solution [containing 68.5 g of mercury(II) nitrate and 10 ml of concentrated nitric acid (specific gravity = 1.42) per litre of water] were added into 250 ml of the saturated filtered mercury(II) thiocyanate solution. This solution should be left overnight to stabilize.

Standard stock solutions

Dried sodium chloride (58.5000 g) (Merck, Darmstadt, Germany) was dissolved in 1 litre of distilled water. Dried potassium chloride (7.4600 g) (Merck, Darmstadt, Germany) was dissolved in 1 litre of distilled water. Anhydrous sodium carbonate (21.2000) (Merck, Darmstadt, Germany) was dissolved in 1 litre of distilled water. Ammonium chloride (53.5000 g) (Merck, Darmstadt, Germany) was dissolved in 1 litre of distilled water.

Standard working solutions

Standard working solutions (each solution containing sodium, potassium and chloride) were prepared by dilution of appropriate aliquots of the standard stock solutions to 100 ml with distilled water to cover the ranges 110–160mM Na⁺, 2–7mM K⁺ and 82–122mM Cl⁻.

RESULTS AND DISCUSSION

A schematic flow diagram of the system used for the simultaneous determination of sodium, potassium and chloride is shown in Fig. 1. As can be seen, the manifold consists of Tygon tubing with tube lengths and inside diameters. The tubing was cut into the required lengths and wound around glass tubes of length 10 cm and width 1 cm. Two on-line dialyzers were incorporated in series into the FIA manifold, separating and channeling the sample plug from a single sample injection via two different channels to the different detectors. The sample plug from the single sample injection was transported to the donor channel of the first dialyzer A where the sodium and potassium were dialyzed to the detector channel for measurement of sodium and potassium by AES with a flame photometer. In this way any interferences as well as blocking of the fine jet of the atomizer were avoided and the sample plug was automatically diluted. The undialyzed plug moved to the second dialyzer B where chloride was dialyzed to eliminate interferences and for automated dilution before detection by UV/VIS spectrophotometry at 485 nm.

With two-cell instruments like the IL143 flame photometer internal standards are often used as a diluting fluid. The diluting fluid contains a suitable metal which is not present in the specimen; lithium is usually chosen. Collected radiation from the flame is directed to photo-sensitive detectors. One detector monitors the sample line (Na or K) and the other the internal Li standard. The photoconductive cells are matched to give proportionally the same change in response to variations in illumination as well as minor variations in gas pressure and spraying. In the proposed flow-injection system the dialysed diluted sample was mixed with standard Li solution from the acceptor stream for Na and K from where it served as an internal standard for the assay of these two species. Univariant optimization indicated that an amount of 15mM lithium at a flow-rate of 3.9 ml/min in the

acceptor stream of dialyzer A was sufficient enough to give a steady photometer output with the required sensitivity for both Na and K in the concentration ranges wanted.

The main aim of this paper was to develop a multicomponent FIA-procedure for the simultaneous determination of sodium, potassium and chloride in blood plasma where a limited amount of sample was available for a single sample injection. To achieve this goal the on-line dialysis FIA-procedure should be applicable in the normal working concentration range of all three species involved to obviate any manual dilution steps. The plasma of normal persons contains about 137–148mM sodium, about 3.9–5.0mM potassium and about 99–108mM chloride. These concentration ranges of sodium, potassium and chloride in blood plasma limited the working range of some of the different operational parameters, such as sample volume, in a multicomponent FIA-serum assay to a certain extent. These factors had to be kept in mind when the actual optimization was performed. Of the various methods of optimization: the univariate, multivariate or simplex optimization, the univariate search (where each variable was optimized, while the others were kept constant) was used because it was more convenient to vary some of the variables in fixed increments. In the proposed multicomponent FIA-procedure it was preferable to distinguish between sample volume optimization and optimization of dialysis efficiency although these two parameters seemed to be mutually interdependent to a certain extent.

The efficiency of on-line continuous dialysis between different dialyzer dimensions and of the different membrane types have been evaluated previously.⁹ van Staden and van Rensburg⁹ studied various factors including flow-injection analysis and continuous flow; the use of concurrent and countercurrent flows between the donor and acceptor streams; concentration of analyte in the donor stream; membrane surface; membrane line-length (dialysis area); membrane porosity; membrane thickness; flow-rate dependence of dialysis (same flow-rates of donor and acceptor streams); flow-rate dependence of dialysis (differences in flow-rates of donor and acceptor streams) and temperature.

The required concentration ranges for sodium, potassium and chloride in the simultaneous determination of all three species placed a restriction in the percentage dialysis necessary for the proposed FIA-system. Keeping this in mind the results obtained in this study revealed that

the Technicon type C membranes were the best suitable for the proposed multicomponent FIA-procedure. Investigation in the present work with the FIA-manifold system shown in Fig. 1, proved that the dialysis efficiency in the present case differed only slightly from the results previously⁹ reported. A percentage dialysis of 2.8% for dialyzer A (membrane pathlength, 300 mm) and 1.4% for dialyzer B (membrane pathlength, 150 mm) were obtained with flow-rates of 3.9 ml/min in the donor and acceptor streams.

A smaller dispersion,⁵ shorter equilibrium time⁹ and higher precision⁹ in a long dialyzer were reported with concurrent flow than with countercurrent flow and as this was confirmed in this study, concurrent flow was preferred in the proposed system.

It was also clear from the results obtained that optimum precise mass transfer of sodium and potassium for the first dialyzer and chloride for the second dialyzer through the semi-permeable Technicon Type C membranes were possible when the same carrier and recipient flow-rates were used in both cases. This ensured that the dialysis process did not alter the geometry of the sample injected, but that the dialysates form identical diluted protein free plugs on the recipient sides of the membranes. Flow-rates of 3.9 ml/min were used for the donor and recipient streams to ensure that an optimum sample

Table 1 Performance of the proposed FIA method for sodium

Sample	Automated standard segmented method, [Na ⁺] in mM	FIA-method, [Na ⁺] in mM	%RSD
Control serum samples			
1	139	141	0.91
2	137	136	0.89
3	143	144	0.80
4	129	133	0.85
5	126	125	0.98
Blood serum			
1	136	136	0.96
2	130	128	0.91
3	145	144	0.81
4	138	137	0.92
5	134	135	0.86
6	142	142	0.82
7	142	141	0.83
8	127	129	0.94
9	147	148	0.79
10	133	133	0.96

%RSD = mean result of 15 tests in each case, with relative standard deviation for the proposed FIA method

Table 2. Performance of the proposed FIA method for potassium

Sample	Automated standard segmented method, [K ⁺] in mM	FIA-method, [K ⁺] in mM	%RSD
Control serum samples			
1	4.2	4.2	0.69
2	3.9	3.9	0.93
3	3.5	3.4	0.92
4	4.6	4.7	0.90
5	2.2	2.3	0.99
Blood serum			
1	4.3	4.3	0.85
2	3.8	3.8	0.97
3	4.0	4.0	0.72
4	5.7	5.7	0.78
5	5.0	4.9	0.69
6	4.1	3.9	0.89
7	3.7	4.0	0.95
8	3.5	3.6	0.82
9	5.1	5.3	0.74
10	4.8	4.7	0.72

%RSD = mean result of 15 tests in each case, with relative standard deviation for the proposed FIA method.

throughput of about 106 samples per hour per determination (that is about 318 measurements for all three components) was still possible and that the correct amounts of sodium, potassium and chloride were dialyzed for determination. The above-mentioned experimental flow-rate conditions used, also tended to equalize diffusion

Table 3. Performance of the proposed FIA method for chloride

Sample	Standard method, [Cl ⁻] in mM	FIA-method, [Cl ⁻] in mM	%RSD
Control serum samples			
1	112	112	0.50
2	100	100	0.61
3	106	106	0.57
4	99	99	0.58
5	84	85	0.70
Blood serum			
1	87	86	0.62
2	97	98	0.66
3	96	94	0.59
4	101	104	0.58
5	105	107	0.61
6	111	109	0.62
7	94	93	0.59
8	107	108	0.56
9	103	103	0.60
10	110	110	0.49

%RSD = mean result of 15 tests in each case, with relative standard deviation for the proposed FIA method

rates between samples and standards. This is all confirmed by the results shown in Tables 1-3.

The chloride colour reagent used in the recipient stream was prepared in nitric acid as part of the reagent because in an univariant search it was found that a concentration of 0.3M nitric acid in the carrier stream gave the best results (accuracy and precision) for chloride.

In the optimization of sample volume with the univariant search method, peak height (as sensitivity measurement) and linearity of all three species (sodium, potassium and chloride) within the normal concentration range in serum were chosen as factors to be maximized. The results revealed that a sample volume of 100 μ l gave optimum performance when both sensitivity and linearity of all three species were considered. After completing the whole optimization procedure, it was clear that the main objectives were achieved and Figs. 2, 3 and 4 show that the proposed FIA-procedure is applicable in the normal working concentration range of all three species involved.

No fouling problems were experienced with any of the dialyses used which is possibly due to the nature of the samples. This was also attributed to the small amount of blood serum samples injected and the procedure of pumping doubly distilled water for about 15 min through both channels of the two membranes during the shutdown period of the FIA system used.

Figures 2, 3 and 4 show representative recorder outputs at an optimum sampling rate of about 106 samples per hour for sodium, potassium and chloride, respectively. Carry-over from one sample to another is less than 1% for every one of the three components measured. Each standard was injected four times followed by single injections of samples and completed by four injections of each standard to control drift. Baseline drift was virtually negligible for sodium, potassium and chloride. The calibration curves (Figs. 2 and 3) for sodium and potassium were linear over the whole working concentration range which indicated that the procedure is also applicable for the determination of concentrations of both species outside the normal concentration range especially in the case of serum sodium values which could fall due to chronic diseases. This is indicated in Fig. 2 by some peaks which lie below the indicated standard sodium value of 120mM. The chloride calibration curve tended to deviate from linearity at the chloride value of 114mM which is the normal case for high chloride concentrations where the

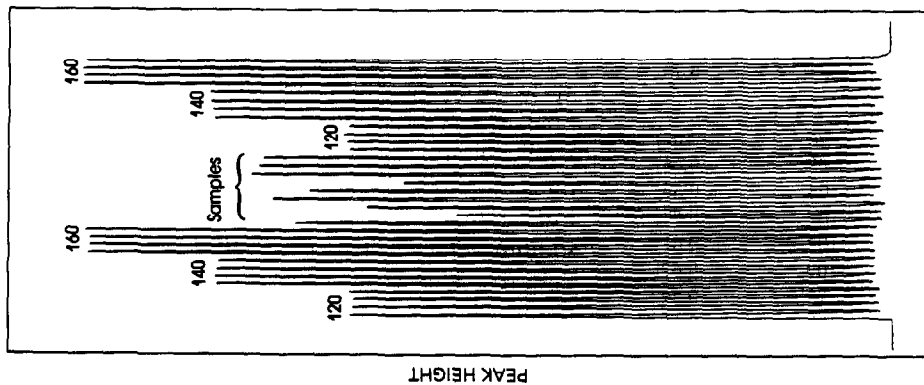


Fig. 2. Typical strip-chart recording for the flow-injection determination of sodium in serum. Recorder paper speed 24 cm/hr. Recorder range 50 mV. From left to right standard sodium solutions, each standard injected four times, followed by single injections of real samples and completed by repetitive standard sodium solutions. Concentrations of standard sodium solutions given as mM above peaks.

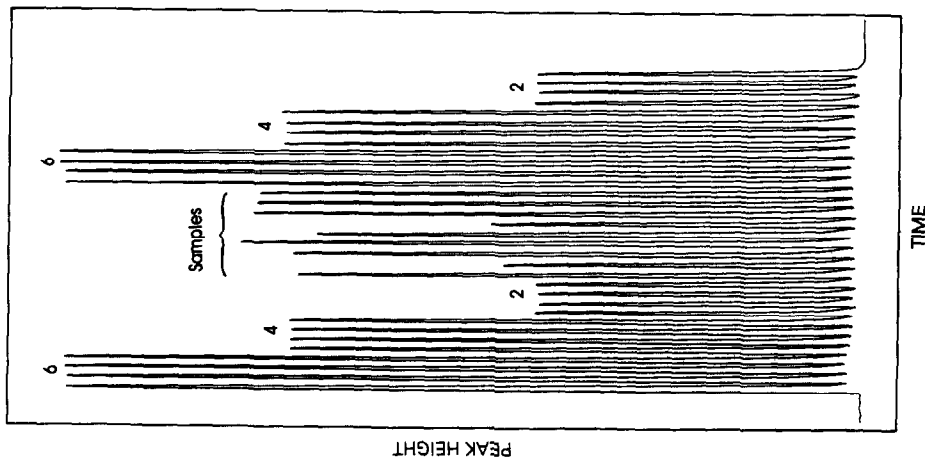


Fig 3 Typical strip-chart recording for the flow-injection determination of potassium in serum. Recorder paper speed 0.5 cm/min. Recorder range 20 mV. From left to right standard potassium solutions, each standard injected four times, followed by single injections of real samples and completed by repetitive potassium standard solutions. Concentrations of standard potassium solutions given as mM on top of peaks

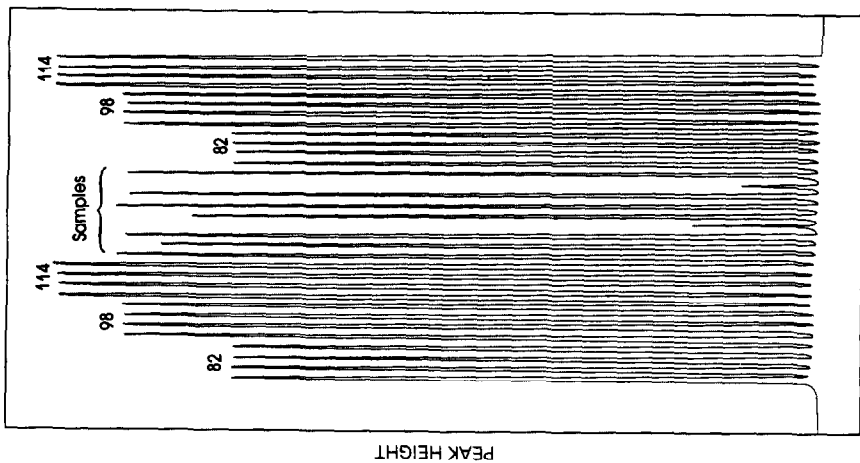


Fig 4 Typical strip-chart recording for the flow-injection determination of chloride in serum. Recorder paper speed 0.4 cm/min Recorder range 1 V. From left to right standard chloride solutions, each standard injected four times, followed by single injections of real samples and completed by repetitive standard chloride solutions. Concentrations of standard chloride solutions given as mM above peaks.

spectrophotometric procedure with mercury(II) thiocyanate and iron(III) nitrate as reagents is used. At lower chloride concentrations, however, the curve becomes more linear and could be used where the chloride concentration range falls below the normal range. This is indicated in Fig. 4 where some peaks lie very well below the indicated chloride value of $82mM$.

The performance of the proposed flow-injection analysis method is shown in Tables 1, 2 and 3 for sodium, potassium and chloride respectively. The values obtained for the three species by the proposed FIA system were also compared with standard methods. The proposed FIA-method compares favourably with a standard automated flame photometric procedure¹⁰ for sodium and potassium and also with a standard chloridometer method¹¹ for chloride as seen from the Tables. Standard control blood serum samples were also used to evaluate the accuracy of the proposed FIA-system. The control samples were interposed at random between the blood serum samples. The results obtained in Tables 1, 2 and 3 for sodium, potassium and chloride compares favourably with the certified values of the control samples. The precision of the proposed method was evaluated by 15 tests on each sample where each sample was analyzed respectively for sodium, potassium and chloride by the proposed FIA-system. With $100\text{-}\mu\text{l}$ samples the relative standard deviation for blood serum samples having different concentrations of sodium ($125\text{--}150mM$), potassium ($2.0\text{--}6.0mM$) and chloride ($80\text{--}110mM$) were better than 1.0% for sodium, 1.0% for potassium and 0.7% for chloride respectively.

CONCLUSION

It seems that the incorporation of flow-through dialyzers as part of the manifold in FIA-systems is extremely useful for on-line simultaneous determination of sodium, potassium and chloride in blood serum. The flow-injection analysis system described here is suitable to carry out simultaneous analysis of sodium, potassium and chloride at a rate of approximately 106 samples per hour. The proposed method should be particularly attractive to small clinical laboratories where a fast and reliable fully automated procedure is needed.

REFERENCES

- 1 J Růžicka and E H Hansen, *Flow Injection Analysis*, 2nd Ed., Wiley, New York, 1988
- 2 M Valcárcel and M. D Luque de Castro, *Flow-injection Analysis Principles and Applications*, Horwood, Chichester, 1987
- 3 J L. Burguera, *Flow-Injection Atomic Spectroscopy*, Dekker, New York, 1989
- 4 B Karlberg and G E Pacey, *Flow-Injection Analysis; A Practical Guide*, Elsevier, Amsterdam, 1989
- 5 L T Skeggs, Jr, *Am J Clin Pathol.*, 1957, **28**, 311
- 6 A H Kadish and D H Hall, *Clin. Chem.*, 1965, **11**, 869
- 7 G M Brown, A Zachwieja and H C Stancer, *Clin Chim Acta*, 1966, **14**, 386
- 8 E H Hansen and J Růžicka, *Anal Chim Acta*, 1976, **87**, 353
- 9 J F van Staden and A van Rensburg, *Analyst*, 1990, **115**, 1049
- 10 G Pennacchia, V G Bethune, M Fleisher and M. K. Schwartz, *Clin Chem.*, 1971, **17**, 339
11. B L Spring, *Am J Med Tech.* 1971, **37**, 361

SPECIFIC SOLID-STATE DETECTION AND SEMIQUANTITATIVE DETERMINATION OF CATECHOL AND *o*-NITROPHENOL AND SOME OF THEIR KINETIC PARAMETERS

K M SHAMSUDDIN and SYED ALI

Department of Applied Chemistry, Aligarh Muslim University, Aligarh 202002, India

PUSHKIN M QURESHI*

Department of Chemistry, P O Box 149, Aligarh Muslim University, Aligarh 202002, India

(Received 4 April 1989 Revised 19 November 1990 Accepted 5 February 1991)

Summary—Catechol and *o*-nitrophenol have been determined successfully in the solid state by means of their solid-state reaction with soda-lime. The glass-wool plug modification has been used with advantage in the determination of *o*-nitrophenol. The reaction mechanism is postulated on the basis of the reflectance electronic spectra. Some solid–solid kinetic parameters have also been studied.

Phenols are important compounds both chemically and biologically, and numerous methods are available for their detection, determination and separation, but few of these are specific for individual members of this class, and none so far has been based on a solid-state reaction.

Qureshi and co-workers¹⁻³ have developed simple solid-state analytical methods on the basis of the work of Voskresenskii⁴ and Rastogi.⁵ Here we report the application of the technique for specific detection of catechol and *o*-nitrophenol.

EXPERIMENTAL

Reagents

o-Nitrophenol and catechol (Sigma) were recrystallized until their melting points were constant and in agreement with reported values. Non-deliquescent soda-lime and sodium chloride (B.D.H.) were used as received.

Procedure

Solid-state detection. *o*-Nitrophenol or catechol (10 mg) was thoroughly ground with 1 g of sodium chloride, and a 200-mg portion of the mixture was similarly mixed thoroughly with 800 mg of sodium chloride. Then 1 mg of this mixture was placed on a spot plate and mixed with a few mg of well powdered soda-lime by

stirring with a glass rod. The colour produced was observed.

Capillary solid-state detection. Well powdered (mesh size 200) test substance and soda-lime were packed in a capillary, one from each end, with two iron rods, with as uniform pressure as possible. The capillary was then heated in an oven at the desired temperature and the colour produced at the junction was noted.

Semiquantitative determination. Fifty mg of a mixture of 8 mg of catechol with 1 g of sodium chloride were tightly packed in a capillary from one end and 500 mg of soda-lime from the other. The capillary was heated for 5 hr in an oven at 80° and the length of the coloured boundary was measured at 1-hr intervals. This procedure was repeated with other mixtures.

For *o*-nitrophenol a glass-wool plug 2 mm in length was placed between the test substance and the reagent and the capillary was heated at $30 \pm 1^\circ$ (*o*-nitrophenol melts at 44°).

Kinetic investigation. Well powdered (mesh size 200) test substance and soda-lime were packed in a capillary as before, and heated at the desired temperature. The length of the coloured boundary was measured as a function of time.

RESULTS

o-Nitrophenol gives a deep red colour with soda-lime and this colour is not given by any other phenol tested. However, since many

*Author for correspondence

phenols give a brown colour, it was thought that they might interfere in detection of low levels of *o*-nitrophenol. However, introduction of a 2-mm long glass-wool plug between the sample and reagent prevents this, as *o*-nitrophenol is the only one of the phenols tested that has a sufficiently high vapour pressure to give a colour reaction at the other side of the glass-wool plug. The limit of detection is 4 μ g, which is comparable to that of solution spot-tests.

Catechol gives a very specific green-blue colour and the limit of detection is 2 μ g.

In the semiquantitative determination catechol gives a length of coloured zone that is linearly related to weight of catechol in the range 0.4–1.2 mg. The slope of the calibration plot increases with the heating time used, but the response is adequate even with heating for 1 hr. An attempt to determine catechol in the presence of phloroglucinol (which does not give any colour with the reagent) was unsuccessful, but it was interesting that when phloroglucinol was present the sharpness and the intensity of the colour given by catechol increased. Hence, either sodium chloride or phloroglucinol can be used as the diluent for the sample, and where conditions permit the latter should be preferred. In either case linear calibration plots are obtained (see Fig. 1).

o-Nitrophenol in the range 0.1–0.5 mg can be determined specifically by the glass-wool plug modification.

Though the sensitivity of determination is not comparable to that of solution methods, it is much higher than that with the capillary method described earlier.^{1,2}

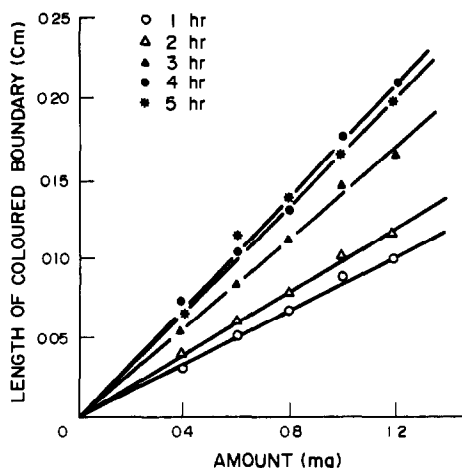


Fig 1 Calibration curves for catechol diluted with phloroglucinol.

Interferences

The following organic compounds do not give any colour with soda-lime.

Amines. Methylamine, dimethylamine, trimethylamine, triethylamine, diethylamine, *o*-, *m*- and *p*-phenylenediamine, α -naphthylamine, β -naphthylamine, diphenylamine, *N*-phenyl-1-naphthylamine, methylaniline, *o*-nitroaniline, *m*-nitroaniline and *p*-nitroaniline.

Ketones. Acetophenone, benzophenone, ethyl methyl ketone, butyrophenone and cyclohexanone.

Aldehydes. Formaldehyde, acetaldehyde, benzaldehyde, *o*-, *m*- and *p*-nitrobenzaldehyde, *p*-chlorobenzaldehyde, *p*-dimethylaminobenzaldehyde, *p*-dimethylaminocinnamaldehyde, salicylaldehyde, paraformaldehyde and paraldehyde.

Ureas. Urea, thiourea, *N*-methylurea, phenylurea, phenylthiourea and allylthiourea.

Carbohydrates. Maltose, glucose, arabinose, rhamnose, sucrose, fructose, lactose, galactose, xylose and starch.

Amino-acids. Adenine, cystine, glycine, β -alanine, sarcosine, glutamine, glutamic acid, L-histidine, L-proline, DL-phenylalanine and L-tryptophan.

Acids. Formic, uric, gallic, malonic, cinnamic, malic, fumaric, phthalic, oxalic, benzoic, barbituric, α -picolinic, *m*- and *p*-nitrobenzoic, nicotinic, monochloroacetic, indolyl-3-acetic, ethylenediaminetetra-acetic and chromotropic (disodium salt).

Amides. Benzamide, salicylamide and acetanilide.

Hydrochlorides. Hydrazine, 2,4-dinitrophenylhydrazine, benzidine and diethylamine hydrochlorides.

Hydrocarbons and their derivatives. Benzene, petroleum ether, nitrobenzene, carbon tetrachloride, chloroform, 2,4-dinitrochlorobenzene, azobenzene and *m*-dinitrobenzene.

Ethers. Diethyl ether and dioxan.

Indoles. Indole and indolyl-3-acetic acid.

Tryptamines. 5-Hydroxytryptamine, 5-methoxytryptamine, 5-benzyloxytryptamine and α -methyltryptamine.

Alkaloids. Brucine, caffeine, quinine and cinchonine.

Miscellaneous. Uracil, 1-nitronaphthalene, urea nitrate, 2,4-dinitrotoluol, dithizone, ammonium purpurate, 1,10-phenanthroline, 4-dimethylaminobenzylidene, rhodanine, diphenylcarbazide, amitrol, ethanoxymercarbide,

saccharin, 8-hydroxyquinoline, galloyanine and safranin.

The reactions of various phenols with anhydrous soda-lime give the following results: phenol (no colour), quinol (light brown), resorcinol (yellow), orcinol (light brown), *o*-methylresorcinol (brown), (+)-catechin (no colour), *m*-nitrophenol (brown), *p*-nitrophenol (yellow), pyrogallol (light brown), phloroglucinol (no colour), α -naphthol (no colour), β -naphthol (no colour), vanillin (no colour) and *o*-vanillin (no colour).

It is therefore apparent that the green-blue colour for catechol and the red colour for *o*-nitrophenol (by the glass-wool modification) are specific for these compounds among those tested, but these colours would be modified by the presence of certain other phenols.

The rate law followed by the reaction of catechol with soda-lime is

$$\xi = kt + c \quad (1)$$

where ξ is the length of the coloured boundary, t is time and k and c are constants. The rate increases with temperature.

A plot of $\log k$ vs. $1/T$ (a standard method for evaluating the activation energy) was linear. The value of E_{act} obtained from it was +8 kcal/mole.

The rate law for the *o*-nitrophenol reaction with soda-lime, with and without a glass-wool plug,

$$\xi = k \log t + c \quad (2)$$

An Arrhenius plot could not be obtained in this case, as *o*-nitrophenol melts at 44°.

DISCUSSION

It is difficult to propose rational mechanisms, owing to the complexity of the systems. However, certain features point to two different mechanisms for *o*-nitrophenol and catechol.

o-Nitrophenol

The reflectance spectrum of *o*-nitrophenol has two maxima, at 300 and 360 nm (Fig. 2). The spectrum of *o*-nitrophenol in the presence of an excess of soda-lime gives a sharp increase in the intensity of both bands and a red shift of the 360-nm band to 430 nm. These electronic spectrum features are consistent with formation of a weak charge-transfer complex. The mechanism probably involves the transformation of

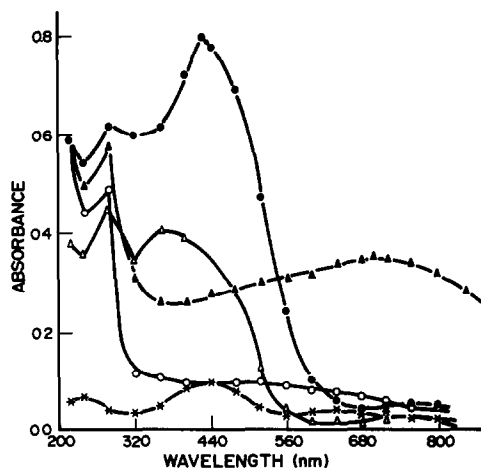


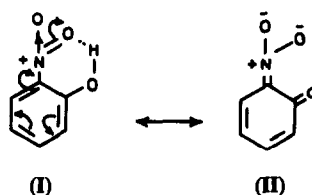
Fig 2 Ultraviolet-visible reflectance spectra of *o*-nitrophenol, catechol and their reaction products with soda-lime: ●, *o*-nitrophenol + soda-lime, *, soda-lime; △, *o*-nitrophenol, ▲, catechol + soda-lime; ○, catechol

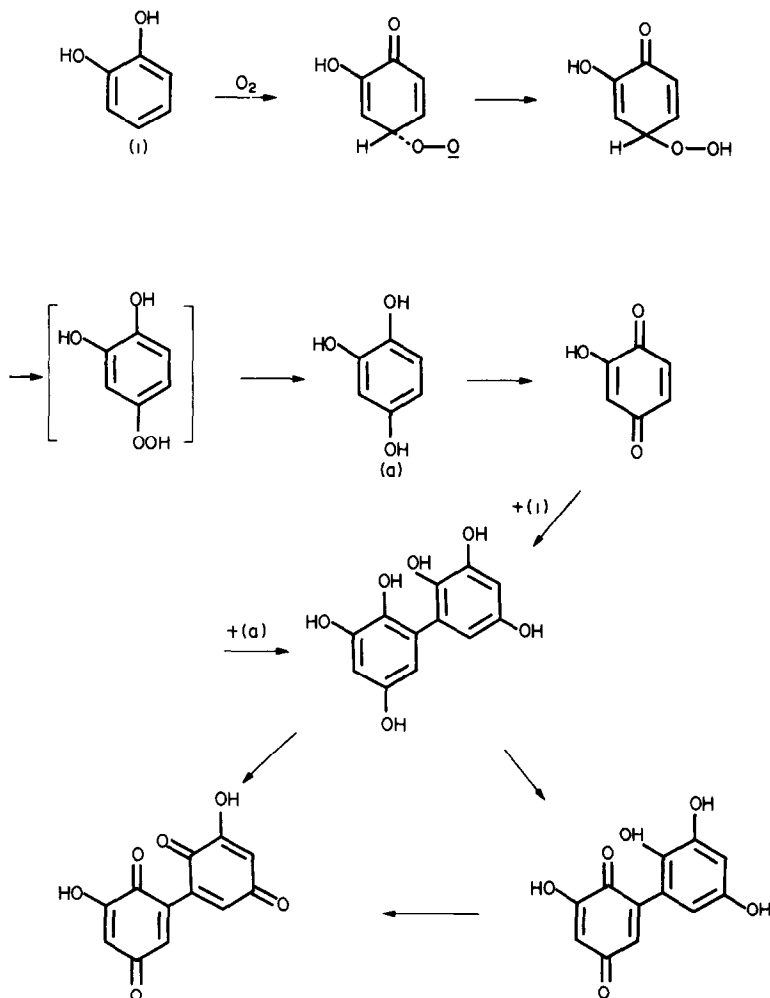
o-nitrophenol (I) into the quinoid structure (II) in the highly basic medium. Form II then complexes with form I to give a charge-transfer complex, probably of 1:1 stoichiometry. The shift of the 360-nm band to 430 nm can be rationalized as follows. According to Mulliken's now widely accepted charge-transfer theory the complex can be described by a wave function as follows:

$$\psi(AD) = a\psi_0(A, D) + b\psi_1(A^-D^+)$$

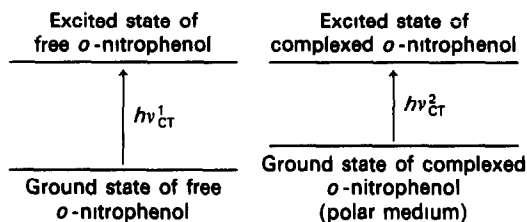
where A is an acceptor and D is a donor, ψ_0 is the non-bonding function, which is mainly due to the dispersion, dipole-dipole, dipole-induced dipole and van der Waals forces, with very little contribution from the dative structure, and ψ_1 is the dative function which signifies transfer of one electron from the donor to the acceptor in such a way that the spin multiplicity is maintained; a and b are constants; A^-D^+ is often called a semipolar double bond.

In the ground state of the complex $a \gg b$, and in the excited state $a \ll b$, and therefore the excited state is usually more ionic than the ground state. Hence, a polar medium will lower (stabilize) the excited state and raise





(destabilize) the ground state, as shown schematically below.



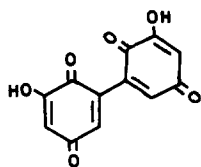
Therefore, $h\nu_{CT}^1 > h\nu_{CT}^2$ and $\lambda_2 > \lambda_1$.

Catechol

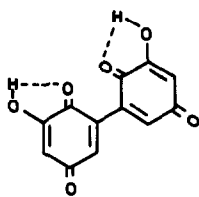
The reflectance spectrum (Fig. 2) of catechol shows a single peak at 300 nm, whereas the spectrum of catechol in the presence of excess of soda-lime has two maxima, one at 300 nm and the other at 700 nm, the intensity of the former being higher than that for catechol alone. The

long-wave band at 700 nm should be due to the result of chemical reaction between catechol and soda lime, and presumably arises from increased conjugation. Formation of such a product is best explained by aerial oxidation of catechol in the presence of base, by a free radical pathway.⁶ To verify this hypothesis, the reaction was performed with rigorous exclusion of air. Both solids were stored under vacuum in a desiccator, with periodic flushing with nitrogen. They were then packed in the capillary in an atmosphere of nitrogen. Under these conditions appearance of the green-blue colour was minimal and even then only on prolonged heating. Reaction scheme 1 can therefore be postulated.

Structure III is a comparatively large conjugated system which seems to be responsible for the green-blue colour. Another fact in support of III is that the increase in intensity of the 300-nm band is much less than that for the



(III)



(IV)

corresponding absorption for *o*-nitrophenol and it may be due to intramolecular hydrogen-bonding within III, as shown in IV.

Acknowledgements—The authors thank Professors K. T. Nasim and S. A. A. Zaidi for facilities

REFERENCES

- 1 M. Qureshi, H. S. Rathore and A. Mohammad, *Talanta*, 1976, **23**, 874
- 2 M. N. Akhtar, H. S. Rathore and M. Qureshi, *ibid.*, 1978, **25**, 235
- 3 M. Qureshi, A. Mohammad and G. G. Raju, *ibid.*, 1981, **28**, 817
- 4 P. I. Voskresenski, *ibid.*, 1965, **12**, 11
- 5 R. P. Rastogi, *J. Sci. Ind. Res. (India)*, 1970, **29**, 177
- 6 H. Musso, *Angew. Chem. Engl. Ed.*, 1963, **2**, 723

SPECTROPHOTOMETRIC DETERMINATION OF PALLADIUM WITH 5,6-DIMETHYL-1,3-INDANEDIONE-2-OXIME

D MALLIKARJUNA RAO, K. HUSSAIN REDDY and D. VENKATA REDDY

Department of Chemistry, Sri Krishnadevaraya University, Anantapur 515003, India

(Received 1 March 1989 Revised 17 January 1990 Accepted 14 March 1991)

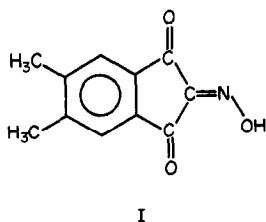
Summary—A rapid, sensitive and selective method has been developed for the determination of palladium with 5,6-dimethyl-1,3-indanedione-2-oxime in acetate buffer (pH 5.5). Beer's law is obeyed over the range 0.15–4.17 $\mu\text{g/ml}$ palladium(II). The molar absorptivity at 370 nm is $2.98 \times 10^4 \text{ l mole}^{-1} \text{ cm}^{-1}$. The method has been applied for the determination of palladium in synthetic mixtures corresponding to Pt–Ir and Oakay alloys. An interesting feature of the system is the abnormal shape of the Job and molar-ratio plots obtained.

Compounds containing a keto group *ortho* to an azomethine nitrogen atom are potential complexing agents. The reactivity of the oxime is dependent, however, on the structural characteristics of the parent aldehyde or ketone.¹ In the work presented here, 5,6-dimethyl-1,3-indanedione-2-oxime was examined as a colorimetric reagent for palladium.

EXPERIMENTAL

Reagents

5,6-Dimethyl-1,3-indanedione-2-oxime (DIDO) was obtained from Beecham Pharmaceuticals Biosciences Research Centre, Epsom, England. Its purity (99%) was checked by elemental and mass spectral analysis. Its infrared spectrum was consistent with the structure I. A 0.005M stock solution was made by dissolving 0.203 g of the reagent in 200 ml of dimethylformamide.



Stock solution of palladium(II). A 0.01M stock solution was prepared by dissolving 177.4 mg of palladium chloride (Johnson Matthey) in a few drops of concentrated hydrochloric acid and diluting to 100 ml. The stock solution was standardized.²

Acetate buffer. Sodium acetate and acetic acid solutions, both 0.2M, were mixed in suitable proportions to give buffers covering the pH-range 3.0–6.5.

All other reagents were of analytical grade and doubly distilled water was used throughout.

Apparatus

Absorption spectra and absorbance measurements were obtained with a Beckman DU-2 spectrophotometer equipped with 1.0-cm fused-silica cells.

Procedure

To a sample solution containing 15–100 μg of Pd(II) add 12 ml of 0.2M acetate buffer (pH 5.5), 2.5 ml of dimethylformamide (DMF) and 1 ml of 0.005M DIDO, in a 25-ml standard flask. Dilute to volume with doubly distilled water and measure the absorbance at 370 nm against a reagent blank in 1.0-cm path-length cells. Prepare a calibration graph similarly.

RESULTS AND DISCUSSION

The reaction is instantaneous and the final product is stable for 12 hr under optimum conditions. The order of addition of the reagents has no effect on the absorbance. In aqueous medium the final complex is precipitated; this is prevented by the presence of at least 10% v/v DMF.

The final complex has two absorption maxima, at 310 and 370 nm (Fig. 1), and latter is used for analytical purposes.

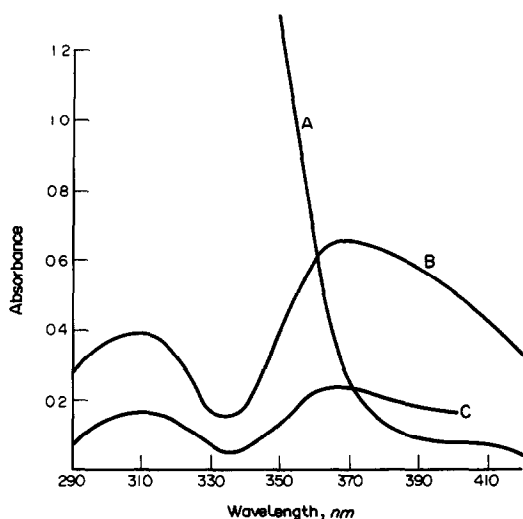


Fig 1 Absorption spectra of (A) reagent solution ($2 \times 10^{-4}M$) vs water blank, (B) Pd-DIDO complex vs DIDO blank, $[DIDO] 2 \times 10^{-4}M$, $[Pd] 2.24 \times 10^{-5}M$, pH 5.5, (C) Pd-DIDO complex vs DIDO blank, $[DIDO] 2 \times 10^{-4}M$, $[Pd] 1 \times 10^{-3}M$, pH 5.5

Maximal and constant absorbance is observed in the pH range 5.0–6.5. Hence the use of a pH-5.5 acetate buffer is recommended. A five-fold molar excess of DIDO is sufficient to develop maximum absorbance of the final complex, so 1.0 ml of 0.005M DIDO is adequate under the recommended conditions.

The absorbance is unaffected by temperature in the range 10–70°, but gradually decreases at temperatures higher than 70°.

Stoichiometry and stability constant of the final complex

The most interesting feature of the system is that the Job plot (Fig. 2) indicates the formation

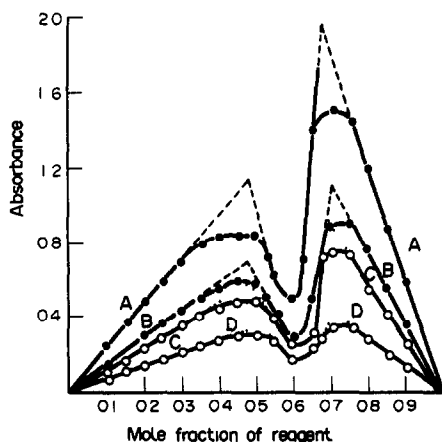


Fig 2 Job plots. A and B, $[Pd] = [DIDO] = 5 \times 10^{-4}M$, C and D, $[Pd] = [DIDO] = 2.5 \times 10^{-4}M$; wavelength = 370 nm (A and C) 310 nm (B and D).

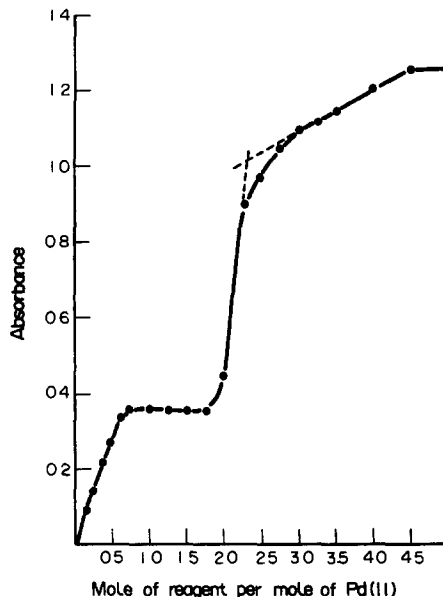


Fig 3 Molar-ratio plot. $[Pd] 4 \times 10^{-5}M$; pH 5.5, $\lambda = 370$ nm

of 1:1 and 1:2 Pd:DIDO complexes, with a marked decrease in absorbance between the two maxima. A similar phenomenon has been reported for the palladium complexes with isonitrosoacetylacetone,³ isonitrosoacetophenone,⁴ isonitrosobenzoylacetone⁵ and *o*-hydroxyacetophenone thiosemicarbazone.⁶ The mole-ratio plot (Fig. 3) is also anomalous, and it may be noted from it that conversion from the 1:1 into the 1:2 complex begins before the 1:1 complex is completely formed. Presumably some sort of rearrangement in the bonding takes place. One possibility is shown in Fig. 4. It is known that $\log k_4$ for formation of $PdCl_4^{2-}$ is only about 2, and from the Job plot it can be estimated that $\log \beta_1$ for the Pd-DIDO system is about 5. As $\log \beta_1$ for the ammine complexes of Pd(II) is 9.6, it seems feasible that an S_N1 reaction (step 1) could be followed by an intramolecular isomerization (step 2) (which could be due to the *trans*-effect or to increased stability caused by charge neutralization, or both), and finally by step 3. The stability constant for the 1:2 complex was estimated as $\log \beta_2 = 9.3$, and pK_a for DIDO was found to be 6.5.

Analytical characteristics

A linear calibration graph for the 1:2 complex was obtained over the concentration range 0.15–3.9 $\mu\text{g/ml}$ palladium, at 370 nm. The molar absorptivity was $2.98 \times 10^4 \text{ l. mole}^{-1} \text{ cm}^{-1}$. Ten replicate analyses of a solution containing 1.50 $\mu\text{g/ml}$ palladium gave a

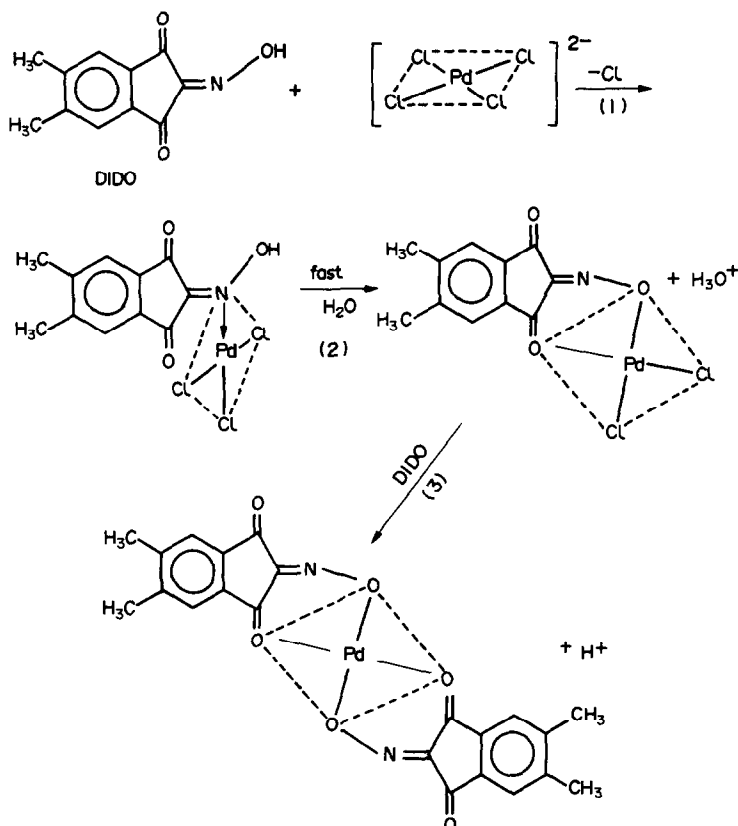


Fig 4 Suggested reaction mechanism

mean absorbance of 0.424 with a standard deviation of 0.005.

Interferences

Various ions were examined for their effect on the determination of 1.5 $\mu\text{g/ml}$ palladium. The tolerance limit was taken as the concentration of foreign ion required to cause $\pm 2\%$ error in the absorbance. The tolerance limit for most of the noble and platinum-group metal ions is fairly high. Larger amounts of platinum(IV) and iron(III) could be masked with oxalate (280 $\mu\text{g/ml}$) and fluoride (1500 $\mu\text{g/ml}$) respectively. The results of the interference and masking studies are summarized in Table 1. EDTA and thiosulphate interfere seriously.

Applications

The method has been applied to the determination of palladium in synthetic mixtures having compositions that correspond to a Pt-Ir alloy and Oakay alloy. Fluoride (1500 $\mu\text{g/ml}$) and oxalate (280 $\mu\text{g/ml}$) were added to mask iron(III) and Pt(IV) respectively. The results are given in Table 2.

Several spectrophotometric methods using oximes have been reported.^{1,7} Most of them

involve an extraction step. The present method is rapid, sensitive and selective and requires no extraction. By comparison with recently

Table 1 Effect of diverse species on the determination of 1.5 ppm palladium

Species*	Tolerance limit, ppm	Species*	Tolerance limit, ppm
Rh(III)	80	Pb(II)	1660
Ir(III)	70	Cd(II)	900
Pt(IV)	18	Hg(II)	4
Pt(IV)†	36	W(VI)	740
Os(VIII)	6	Th(IV)	460
Ru(III)	2	Mo(VI)	380
Au(III)	23	Zr(IV)	360
Ag(I)‡	20	U(VI)	50
Fe(III)§	350	Fluoride	2300
Mn(II)	440	Chloride	350
Al(III)	220	Bromide	30
Cr(III)	28	Iodide	25
Ni(II)	230	Citrate	840
Co(II)	120	Tartrate	1300
Cu(II)	8	Sulphate	760
V(V)	2	Nitrate	600
		Oxalate	350
		Thiourea	2

*Cations added as chloride or sulphate, anions added as sodium or potassium salts, unless otherwise stated.

†In the presence of 280 ppm of oxalate, added as nitrate.

‡Added as nitrate; centrifuged

§In the presence of 1550 ppm fluoride.

Table 2 Determination of palladium in synthetic solutions

Synthetic sample composition, %	Pd, ppm	
	Taken	Found*
55% Pt, 28% Ir,	0.90	0.91
7% Rh, 3.5% Fe,	1.30	1.30
3% Cu, 3.5% Pd	1.80	1.79
	2.70	2.72
	3.90	3.85
60% Ni, 20% Pt	0.90	0.85
9.5% V, 10.5% Pd	1.30	1.31
	1.80	1.82
	2.70	2.71
	3.90	3.87

*Average of five determinations

Table 3. Comparison of some spectrophotometric methods for palladium

Reagent	Molar absorptivity, $l\ mole^{-1}\ cm^{-1}$	Reference
5-Phenylazo-8-aminoquinoline*	7.9×10^4	8
Phenyl α -pyridyl ketoxime*	5.0×10^4	9
9,10-Phenanthroquinone monozime*	2.1×10^4	10
4-(5)-D-Arabinotetrahydroxybutylimidazole-2-thione*	1.99×10^4	11
Thiazole-2-carbaldehyde-2-quinolyldrazone	1.93×10^4	12
2,2'-Bipyridyl 2-pyridylhydrazone*	1.90×10^4	13
3,5-Dichlorosalicylaldehyde-4-phenyl-3-thiosemicarbazone*	1.43×10^4	14
2-(2'-Thiazolylazo)-5-methylanisole	1.13×10^4	15
Thioarbituric acid†	1.00×10^4	16
5,6-Dimethyl-1,3-indanedione-2-oxime	2.98×10^4	Present method

*Methods involving extraction

†Methods involving heating of the reaction mixture

reported spectrophotometric methods for palladium, DIDO is seen to rank among the more sensitive reagents (Table 3). Moreover the colour reaction between palladium(II) and DIDO is fairly selective and free from interferences (Table 1). The colour reaction can be used to provide a rapid, sensitive and specific test for palladium.

Acknowledgements—The authors are thankful to the CSIR, New Delhi, for the award of a Senior Research Fellowship to one of them (DMR), and to Dr P. C. Buxton, Beecham Pharmaceuticals, Great Burgh, for a generous supply of DIDO.

REFERENCES

- R. Singh, B. S. Garg and R. P. Singh, *Talanta*, 1979, **26**, 425
- A. I. Vogel *A Textbook of Quantitative Inorganic Analysis*, 4th Ed., p. 511. Longmans, London 1961
- U. B. Talwar and B. C. Haldar, *Anal. Chem.*, 1966, **38**, 1929
- Idem*, *Anal. Chim. Acta*, 1967, **39**, 264
- D. P. Dave and B. C. Haldar *J. Indian Chem. Soc.*, 1978, **55**, 781.
- G. V. R. Murthy and T. S. Reddy, *Talanta*, in the press.
- Z. Marczenko, *Spectrophotometric Determination of Elements*, p. 437, 1976, Wiley, New York
- M. Blanco and S. Maspoeh, *Mikrochim. Acta*, 1983 **III**, 11
- B. Sen, *Anal. Chem.*, 1959, **31**, 881
- A. Wasey, R. K. Bansal, B. K. Puri and G. Kano, *Mikrochim. Acta*, 1984 **III**, 417
- C. F. Pereira and J. G. Gómez, *ibid*, 1985 **I**, 427
- T. Nakagawa, K. Doi and M. Otomo, *Analyst*, 1985, **110**, 387.
- J. A. Stratus, A. N. Anthemidis and G. S. Vasilikiotis, *ibid*, 1984, **109**, 373
- S. Yamaguchi and K. Uesugi, *ibid*, 1985, **110**, 1241.
- P. Sutthivayakit and A. Ketttrup, *Z. Anal. Chem.*, 1985, **320**, 769.
- B. Morelli, *Analyst*, 1984, **109**, 47.

SIMULTANEOUS SPECTROPHOTOMETRIC DETERMINATION OF THORIUM AND RARE EARTH METALS WITH *m*-CARBOXYCHLOROPHOSPHONAZO (CPAmK) AND CETYLPYRIDINIUM CHLORIDE

CHUNG-GIN HSU,* XI-MAN LIAN and JIAO-MAI PAN

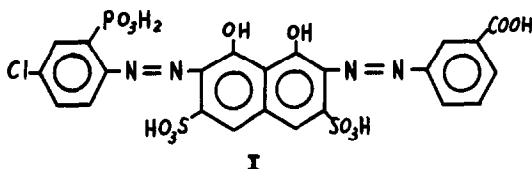
Department of Chemistry, East China Normal University, 3663, Zhong Shan Road (N), Shanghai 200062, People's Republic of China

(Received 12 September 1990 Revised 20 February 1991 Accepted 26 February 1991)

Summary—Th and rare earth elements (REE) react with *m*-carboxychlorophosphonazo (CPAmK) in the absence of cetylpyridinium chloride (CPC) to form colour complexes. The molar absorptivities for Th and Ce are 1.03×10^5 and 1.06×10^5 l. mole⁻¹ cm⁻¹ respectively. In the presence of CPC, REE-complexes are not formed because of micellar masking, while Th gives a more sensitive reaction with CPAmK ($\epsilon = 1.50 \times 10^5$). Most of the foreign ions are tolerated in considerable amounts; 360–1000-fold amounts of rare earths do not interfere with the determination of Th. The optimum conditions of the complex-formation reactions and the compositions of Th–CPAmK complexes are described. A simple method is proposed for simultaneous determination of Th and rare earths without previous separation.

Thorium and rare earths often coexist in their minerals, products and even in waste water. Because of their similar behaviour, determination of thorium and/or rare earths is a problem in analytical chemistry. Although strong claims are made for the specificity and sensitivity of NAA, ICP–AES and ICP–MS, some of the interferences to which these methods are subject are poorly understood and continue to cause problems.¹

Therefore, spectrophotometric methods for thorium and rare earths continue to be of interest.¹ *m*-Carboxychlorophosphonazo (CPAmK, I), an asymmetric derivative of chromotropic acid with one *o*-phosphono-*o*'-hydroxyazo functional group synthesized in this



laboratory has been used for the determination of cerium subgroup rare earths^{2,3} and thorium,⁴ but they interfere with each other when they are present simultaneously.

In this paper, we described the spectrophotometric behaviour of the CPAmK-complexes of

Th and Ce (as well as other rare earths) in the presence and absence of cetylpyridinium chloride (CPC), and a rapid method is proposed for the simultaneous determination of thorium and rare earths without their previous separation.

EXPERIMENTAL

Reagents

All solutions were prepared with distilled, demineralized water.

The standard stock solution of thorium was prepared by dissolving thorium nitrate in a given volume of water, and the solution was standardized by EDTA titration. The working standard solution (10 μ g/ml) was prepared by dilution.

The standard stock solutions of rare earths were prepared by dissolving the oxides of rare earths (Specpure, Johnson Matthey) in hydrochloric acid and the cerium oxide (99.99%, Shanghai Chemicals Factory) in a mixture of sulphuric acid and hydrogen peroxide, evaporating the excess of acid and diluting with hydrochloric acid (1 + 100) to a given volume. The solutions were standardized by EDTA titration with Xylenol Orange as indicator. The working standard solutions were prepared by diluting as required with hydrochloric acid (1 + 100).

*Author for correspondence.

The standard solution of total rare earths (5.0 $\mu\text{g/ml}$) was prepared by mixing the rare earth solutions in the following proportions: $\text{La}_2\text{O}_3:\text{CeO}_2:\text{Nd}_2\text{O}_3:\text{Y}_2\text{O}_3 = 30:40:20:10$.⁵

m-Carboxychlorophosphonazo (CPAmK) solution (0.04%) was prepared by dissolving 0.04 g of CPAmK in 100 ml of water. CPAmK was synthesized as described previously.²

Cetylpyridinium chloride solution (0.2%) was prepared by dissolving 0.2 g of CPC (Fluka) in 100 ml of water.

Apparatus

Absorption spectra and absorbances were recorded and measured with a Beckman DU-7HS spectrophotometer, using 1.0-cm cells.

General procedure

(A). To the mixed solution of Th and Ce (or other REE) in a 25-ml calibrated flask, add 4.0 ml of 2M hydrochloric acid, 2.0 ml of 0.2% CPC and 1.0 ml of 0.04% CPAmK solution successively. Dilute to the mark with water and stand for 20 min. Measure the Th absorbance (A_1) at 685 nm in a 1.0-cm cell against a reagent blank.

(B). To the mixed solution of Th and Ce (or other REE) in a 25-ml calibrated flask, add 2.0 ml of 2M hydrochloric acid, *ca.* 10 ml of water and then 3.0 ml of 0.04% CPAmK solution. Dilute to the mark with water. Measure the absorbance (A_2) for the sum of Th and Ce (or

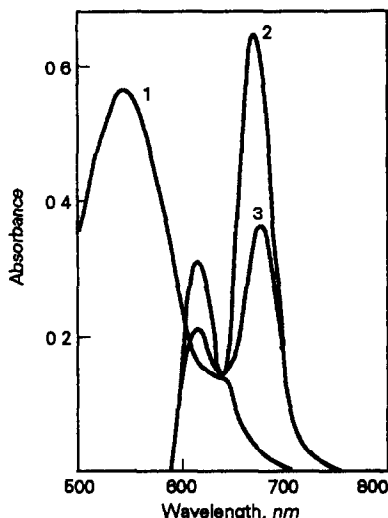


Fig 1 Absorption spectra in the absence of CPC. 1. CPAmK ($1.5 \times 10^{-5}M$); reference, water, 2. Ce-CPAmK, reference, reagent blank, 3 Th-CPAmK; reference, reagent blank; $5.7 \times 10^{-6}M$ Ce, $3.5 \times 10^{-6}M$ Th, $3.8 \times 10^{-5}M$ CPAmK, 0.16M HCl

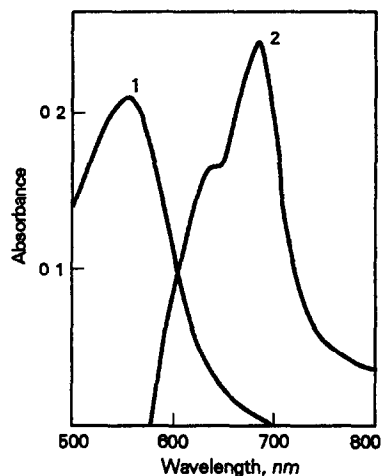


Fig 2 Absorption spectra in the presence of CPC 1 CPAmK ($6.0 \times 10^{-6}M$); reference, water, 2 Th-CPAmK; reference, reagent blank, $1.7 \times 10^{-6}M$ Th, $1.5 \times 10^{-5}M$ CPAmK, 0.32M HCl, $4.5 \times 10^{-4}M$ CPC

other REE), at 669 nm in a 1.0-cm cell against the reagent blank.

RESULTS AND DISCUSSION

Absorption spectra

In the absence of CPC, CPAmK exhibits a maximum absorption at 545 nm (Fig. 1), whereas cerium- and thorium-complexes have maximum absorption peaks at 669 nm and 676 nm, respectively, in hydrochloric acid solution. On addition of CPC, the absorption peak of CPAmK is shifted to 565 nm (Fig. 2); micellar masking⁶ prevents the formation of a Ce-complex, while the thorium complex gives a more sensitive peak at 685 nm.

Optimum conditions for complex formation

In the absence of CPC, 0.04–0.72M hydrochloric acid and $3.0\text{--}7.5 \times 10^{-5}M$ CPAmK gave the highest and most constant absorbance values of cerium- and thorium-complexes. Higher acidity led to the precipitation of CPAmK, and addition of more CPAmK would make the background absorbance too high. Both the complexes of cerium and thorium were formed instantly and their absorbances were stable for at least 24 hr.

In the presence of CPC, the optimum conditions for thorium were 0.28–0.80M hydrochloric acid, $1.13\text{--}3.0 \times 10^{-5}M$ CPAmK and $2.24\text{--}11.2 \times 10^{-4}M$ CPC. Below $2.24 \times 10^{-4}M$ CPC, the solution became turbid, and the absorbance decreased gradually as the concentration of CPC exceeded $11.2 \times 10^{-4}M$. The

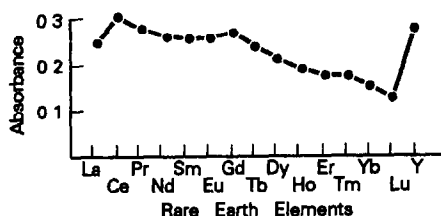


Fig. 3. Absorbances of CPAmK complexes of rare earths at 669 nm 10 μg of rare earth, $3.8 \times 10^{-5}M$ CPAmK, 0.16M HCl

order of addition of CPC (before or after complex formation) did not influence the result. The Th-CPAmK complex formation was completed within 20 min and it remained stable for at least 2 hr. All solutions became turbid after standing for longer periods.

Behaviour of other rare earth elements

The absorbances of the CPAmK complexes of the other rare earths (10 μg each) were also measured at 669 nm against a reagent blank in the absence of CPC. Figure 3 shows that the complexes of cerium sub-group rare earths and yttrium (the major constituents in rare earth mixtures) give higher absorbances. The absorbances from gadolinium to lutetium (the minor constituents) decrease with an increase in atomic number. In the presence of CPC, cerium as well as other rare earths are completely masked. This behaviour enables other rare earths to be determined along with cerium.

Compositions of the complexes

The molar composition of the Th-CPAmK complex formed in the absence of CPC was ascertained by Job's method of continuous variations, slope-ratio and equilibrium shift methods. All three methods indicated that the metal-to-ligand ratio was 1:2. This ratio differs from the value (1:3) found by us in sulphuric acid medium.⁴

In the presence of CPC, the molar composition of the complex was found by the same methods to be 1:5 (Th:CPAmK). It is because

more of the negative-charged CPAmK ions are adsorbed and concentrated on the positive-charged surface of CPC micelle that the formation of a higher order complex is favoured.⁷

The stoichiometry of the Ce-CPAmK complex in the absence of CPC is 1:3, which has been previously estimated.² After addition of CPC, the complex was completely dissociated due to micellar masking.

The characteristics of the complexes mentioned above are listed in Table 1.

Analytical characteristics of the method

Under the conditions employed in procedure (A), cerium as well as other rare earths are completely masked in the presence of CPC, while the absorption of Th-CPAmK is greatly enhanced. Under the conditions for procedure (B), the absorbances of thorium and cerium (as well as other rare earths) are additive. This property can be utilized to create a method for the simultaneous determination of thorium and rare earths. Their amounts were obtained by the following expressions:⁶

$$C_{\text{Th}} = A_1/\epsilon'_{\text{Th}} \quad (1)$$

$$C_{\text{REE}} = (A_2 - A_1\epsilon_{\text{Th}}/\epsilon'_{\text{Th}})/\epsilon_{\text{REE}} \quad (2)$$

Where A_1 and A_2 are the absorbances read [at 685 nm (procedure A) and 669 nm (procedure B) respectively] and ϵ'_{Th} and ϵ_{Th} are the molar absorptivities of thorium found in the presence and absence of CPC. ϵ_{REE} is the molar absorptivity of rare earths found in the absence of CPC.

In the presence of CPC, the calibration graph for thorium was constructed according to procedure (A). Beer's law was obeyed for 0–10 μg of thorium in a 25-ml solution at 685 nm. The apparent molar absorptivity and Sandell sensitivity were found to be 1.50×10^5 l.mole⁻¹.cm⁻¹ and 1.55 ng/cm², respectively. Ten replicate analyses of a test solution containing 10.0 μg of Th gave a coefficient of variation of 1.2%.

Table 1. Characteristics of CPAmK complexes of Th and Ce

Complex	Medium HCl, M	CPC	Composition M CPAmK	λ_{max} , nm	ϵ ($\times 10^{-4}$) l.mole ⁻¹ cm ⁻¹
Th-CPAmK	0.16	Absent	1:2	676	10.3
Th-CPAmK	0.16	Absent	1:2	669*	8.06
Ce-CPAmK	0.16	Absent	1:3	669	10.6
Th-CPAmK	0.32	Present	1:5	685	15.0
Ce-CPAmK	0.32	Present	No complex formed	—	—

*Wavelength of measurement, not maximum absorption

Table 2 Straight-line equations of calibration graphs

Procedure determined	Metal	Straight-line equation†	Correlation coefficient
(A)	Th	A = 0.026C + 0.004	0.9995
(B)	Ce	A = 0.030C + 0.003	0.9999
(B)	REE*	A = 0.029C + 0.006	0.9996
(B)	Th	A = 0.014C + 0.001	0.9997

*Total rare earth elements

†A is absorbance, C is μg in 25-ml solution

In the absence of CPC, calibration graphs of cerium, total rare earths and thorium were constructed according to procedure (B). Beer's law was obeyed for 0–24 μg of cerium, 0–20 μg of total rare earths or 0–28 μg of thorium in 25 ml of solution at 669 nm. The apparent molar absorptivities of cerium and thorium at 669 nm were 1.06×10^5 and 8.06×10^4 $\text{l. mole}^{-1} \cdot \text{cm}^{-1}$, respectively ($\epsilon_{676}^{\text{Th}} = 1.03 \times 10^5$ $\text{l. mole}^{-1} \cdot \text{cm}^{-1}$). The Sandell sensitivities were 1.32 ng/cm^2 and 2.90 ng/cm^2 . The coefficients of variation for the determination of 10.0 μg of cerium or thorium (10 determinations each) were 1.2 and 0.8% respectively. The straight-line equations of the calibration graphs obtained by a least-squares treatment are listed in Table 2.

The difference in absorbance, obtained for equal weights of metals, between the calibration graph for cerium and that for total rare earth

Table 3 Tolerance limits (5% error maximum) for foreign ions in the determination of 5.0 μg of thorium in the presence of CPC

Foreign ion	Tolerance limit μg	Ion/Th w/w
Ca(II), Sr(II), Mg(II), Mn(II)	50000*	10000
Co(II)	25000	5000
Ba(II)	20000*	4000
Al(III)	15000	3000
$\text{NH}_4(\text{I})$, Na(I), K(I)	10000*	2000
Zn(II)	10000	2000
Pb(II), Cr(III)	5000	1000
Yb(III)	5000†	1000
Ni(II)	4000	800
Fe(III)	3500	700
Fe(III)	5000‡	1000
Eu(III)	2200†	440
Ce(III)	1800†	360
Cu(II)	800	160
Ti(IV)	500	100
Ag(I)	100*	20
U(VI)	20	4
Zr(IV)	16	3.2
Ascorbic acid	100000	20000
Nitrate, sulphate, phosphate	10000*	2000
Silicate	7000	1400
Fluoride	500	100

*Not to the maximum amounts

†Add 5.0 ml of 0.2% CPC.

‡Add 100 mg of ascorbic acid.

Table 4. Tolerance limits (5% error maximum) for foreign ions in the determination of 5.0 μg of cerium in the absence of CPC

Foreign ion	Tolerance limit μg	Ion/Ce w/w
Na(I), $\text{NH}_4(\text{I})$, Mg(II)	10000*	2000
Mn(II)	3000	600
Zn(II)	2000*	400
Fe(III)	2000†	400
Cr(III)	1000	200
Zr(IV)	800†	160
Co(II)	700	140
Sr(II), Ni(II), Cu(II)	200	40
U(VI)	120†	24
Ca(II)	100	20
Pb(II)	50	10
Ti(IV)	50†	10
Mo(VI)	40	8
Ag(I), Al(III)	20	4
Nb(V)	10	2
Oxalate	150000	30000
Nitrate, phosphate, fluoride	10000*	2000
Sulphate	8000	1600
Silicate	1500	300

*Not to the maximum amounts.

†Add 3 ml of 5% oxalic acid.

elements is usually not more than 5%, hence the former can be employed for the determination of total rare earths.

Effect of foreign ions

Solutions containing 5.0 μg of thorium or 5.0 μg of cerium, and various amounts of foreign ions were prepared and determined by procedure (A) and procedure (B), respectively. The tolerance limits (5% error maximum) are listed in Tables 3 and 4. As shown in Table 3, 360-fold amounts of cerium, 440-fold amounts of europium and 1000-fold amounts of ytterbium do not interfere with the determination of 5.0 μg of thorium, which is an advantage over the published methods.⁸⁻¹² In the absence of CPC, Table 4 shows that 150 mg of oxalic acid are tolerated, which can be used to mask Fe(III), Zr(IV), U(VI) and Ti(IV), and raise the limits to which they can be tolerated.

Simultaneous determination of thorium and rare earths in waste water

The proposed method was applied to the determination of thorium and rare earths (expressed as cerium) in six industrial waste-water samples taken from chemical works. Place two appropriate aliquots of the sample in 25-ml calibrated flasks, add 6M hydrochloric acid or sodium hydroxide to adjust the solutions to pH ca. 3, then follow the general procedure (A) and

(B)* for the determinations. Thorium values were in the range 0.243–2.21 ppm and cerium values in the range of 0.258–3.92 ppm. The coefficients of variation ranged from 0.6 to 1.8% for thorium and from 0.4 to 2.9% for cerium. The recoveries of thorium and cerium found by standard addition of 2.00 μg of thorium or cerium to each determination averaged 99.4% and 97.3%, respectively, with ranges of 96.0–102% for thorium and 95.0–101.5% for cerium.

REFERENCES

- 1 C J Kantipuly and A D. Westland, *Talanta*, 1988, **35**, 1
- 2 J. M. Pan, L. P. Yang, H. Y. Liu, Y. S. Chen, H. T. Yan, M. L. Wang and F. C. Yu, *Fenxi Huaxue*, 1980, **8**, 298
- 3 J. M. Pan, Y. S. Chen and H. T. Yan, *Chromogenic Reagents and their Applications in Metallurgical Analysis (in Chinese)*, Shanghai Publishing House of Science and Technology, Shanghai, 1981
- 4 J. M. Pan, C. G. Hsu and Y. He, *Microchem. J.*, 1987, **35**, 218
- 5 Q. S. Yang, G. S. Chen, Z. H. Zhang, X. H. Deng and H. X. He, *Fenxi Huaxue*, 1985, **13**, 864.
- 6 J. H. Mendez, B. M. Cordero and J. L. P. Pavon, *Talanta*, 1988, **35**, 293
- 7 H. Kohara, *Bunseki Kagaku*, 1974, **23**, 39.
- 8 S. B. Savvin, *Talanta*, 1961, **8**, 673
- 9 T. Yamamoto, *Anal Chim Acta*, 1973, **63**, 65.
- 10 X. Y. Li, X. M. Yu, Z. H. Chen and Y. E. Zhen, *Huaxue Shiji*, 1981, **4**, 198
- 11 J. M. Pan, W. L. Zhou, H. Zhao and Z. S. Hu, *ibid.*, 1984, **6**, 43.
- 12 J. M. Lin, M. X. Gao and H. C. Liu, *Fenxi Huaxue*, 1984, **12**, 900

*3.0 ml of 5% oxalic acid are added to mask the interfering ions before the addition of CPAmK solution in procedure (B)

SPECTROPHOTOMETRIC DETERMINATION OF NICOUMALONE, ACEBUTOLOL HYDROCHLORIDE AND PROCAINAMIDE HYDROCHLORIDE

C. S. P. SASTRY*, T THIRUPATHI RAO and A SAILAJA

Foods and Drugs Laboratories, School of Chemistry, Andhra University, Visakhapatnam 530 003, India

(Received 5 September 1990 Revised 1 January 1991 Accepted 26 February 1991)

Summary—A sensitive spectrophotometric method is described for the determination of nicoumalone (NIC), acebutolol hydrochloride (ACBH) or procainamide hydrochloride (PAH) either in pure form or in pharmaceutical formulations. The method is based on the oxidative coupling reaction through the involvement of an aromatic primary amino group (released through reduction in NIC or hydrolysis in ACBH or existing free in PAH) in the drug with 3-methyl-2-benzothiazolinone hydrazone hydrochloride (MBTH) in the presence of ferric chloride [Fe(III)]. The resulting chromophores are measured at 620 nm for NIC and ACBH and 580 nm for PAH. The concentration measurements are reproducible within a relative standard deviation of 1%.

Nicoumalone (NIC)^{1,2} is extensively used as an anticoagulant while acebutolol hydrochloride (ACBH) and procainamide hydrochloride (PAH)^{1,2,3} are two widely used anti-arrhythmic agents. They have been officially determined by titrimetry with sodium nitrite (PAH)^{1,2} or ultraviolet spectrophotometry (NIC).^{1,2} Acebutolol hydrochloride is not yet official in any pharmacopoeia. Most of the methods for spectrophotometric determination of NIC,⁴ ACBH⁵⁻⁷ and PAH⁸⁻¹⁰ in the visible region suffer from lack of sensitivity or specificity. After oxidation with Fe(III), MBTH has been used as a chromogenic agent in the estimation of aromatic primary amines.^{11,12} In this paper we report its application to the determination of NIC, ACBH and PAH in bulk samples and pharmaceutical preparations.

EXPERIMENTAL

Apparatus

A Systronics model 106 digital spectrophotometer with 1-cm matched glass cells was used for all the absorbance measurements. An Elico LI-120 digital pH meter was used for pH measurements.

Reagents

Pharmacopoeial grade NIC, ACBH and PAH were obtained as gift samples from Sarabhai

Chemicals, May & Baker (India) Ltd. and Natco-Fine Pharmaceuticals Pvt. Ltd. They were used as working standards without further treatment. All other reagents and solvents were of analytical grade. Commercial dosage forms were purchased from local pharmacies.

MBTH solution (Fluka). Freshly prepared 0.2% solution in distilled water.

Ferric chloride hexahydrate solution (Wilson). Freshly prepared 0.8% solution in 0.01M hydrochloric acid.

Standard solution of nicoumalone (300 µg/ml). An accurately weighed 30 mg sample of NIC was treated with 10 ml of 1M methanolic hydrochloric acid and 0.3 g of zinc dust added in portions. After standing for 45 min at room temperature, the solution was filtered through cotton wool, the residue was washed with 3 × 5-ml portions of methanol (Qualigens, Excellar) and the filtrate was made up to 100 ml with methanol after bringing the pH to 5.5–6.5 with sodium hydroxide.

Standard solution of acebutolol hydrochloride (400 µg/ml). About 40 mg of accurately weighed ACBH in 15 ml of water was treated with 4 ml of concentrated hydrochloric acid and refluxed for 45 min in a waterbath, cooled and the excess of hydrochloric acid removed under vacuum and the remaining mixture diluted to 100 ml with distilled water.

Procainamide hydrochloride solution (500 µg/ml). Prepared by dissolving 50 mg of the drug in 100 ml of distilled water.

*Author for correspondence.

Procedure

Bulk samples. Volumes of the standard solutions of reduced NIC (0.25–2.25 ml, 300 $\mu\text{g/ml}$) or hydrolysed ACBH (0.25–2.0 ml, 400 $\mu\text{g/ml}$) or PAH (0.4–2.8 ml, 500 $\mu\text{g/ml}$) were placed in a series of 25-ml calibrated tubes. Iron(III) chloride (3.0 ml) and MBTH (4.0 ml for NIC, 3.0 ml for ACBH or PAH) were added successively with appropriate time intervals (1 min to ACBH and NIC; 5 min to PAH) to each tube, allowed to stand for 20 min (NIC or PAH) or 25 min (ACBH) and diluted to volume with distilled water. After colour development and final dilution the absorbances were measured at 620 nm (NIC or ACBH) or 580 nm (PAH) against a reagent blank during the stability period (1 min–5 hr for NIC, 1 min–3 hr for ACBH or 1 min–15 hr for PAH). The drug concentration was read from the appropriate calibration graphs prepared under identical conditions

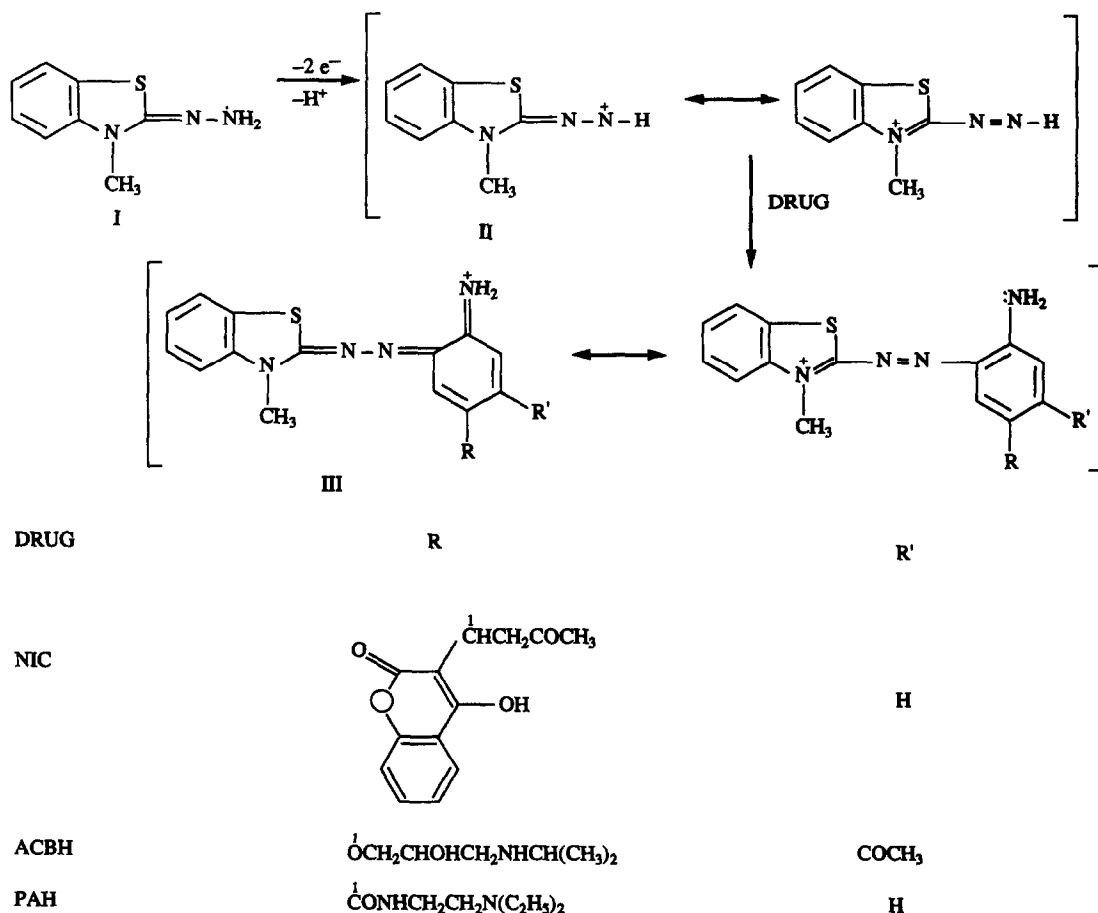
Pharmaceutical preparations. Tablet powder equivalent to 30 mg of NIC was extracted with

3 \times 5-ml portions of acetone, the combined acetone extract was evaporated on a steam bath and the residue was treated as in preparation of the standard drug solution and analysed as in the procedure for bulk samples. For ACBH and PAH, tablet powder equivalent to 40 mg of ACBH or 50 mg of PAH was extracted with 3 \times 5-ml portions of distilled water and filtered. The filtrate was treated as in the preparation of the standard drug solution and analysed as in the procedure for bulk samples.

RESULTS AND DISCUSSION

Nature of the coloured species

The coloured species obtained in this reaction can be considered to be an oxidative coupling product between the drug and MBTH analogous to the products obtained by reaction of MBTH with amines.^{11,12} Under the experimental conditions, MBTH (I) loses two electrons and one proton on oxidation forming the electrophilic



Scheme 1.

Table 1 Optical characteristics and precision

Parameters	NIC	ACBH	PAH
λ_{\max} , nm	620	620	580
Beer's law limits, $\mu\text{g/ml}$	3-27	4-32	8-56
Molar absorptivity, $l.\text{mole}^{-1}\text{cm}^{-1}$	6.38×10^3	4.01×10^3	1.53×10^3
*Regression equation			
Slope (b)	1.91×10^{-2}	1.06×10^{-2}	0.55×10^{-2}
Intercept (a)	1.53×10^{-3}	1.15×10^{-3}	2.53×10^{-3}
Correlation coefficient (r)	0.9999	0.9999	0.9999
Relative standard deviation, †%	0.29	0.37	0.81
Range of Error, †%	± 0.30	± 0.39	± 0.85
(Confidence limits at 0.05 level)			

* $A = a + bC$ where C is the concentration in $\mu\text{g/ml}$

†Six replicate samples

intermediate (II) which has been postulated to be the active coupling species (Scheme 1). The intermediate (II) undergoes electrophilic substitution with amine to form the coloured product (III). Aromatic primary amines react in the *para* position, or the *ortho* position if the *para* position is blocked, to the amino group, which is quite usual in such oxidative coupling reactions. The compounds mentioned above do not possess a free *para* position and so coupling takes place in the less sterically hindered *ortho* position. The variation in λ_{\max} and ϵ_{\max} in the case of oxidative coupling products resulting from NIC, ACBH and PAH appear to be due to the inductive and mesomeric effects of the other substituents (R, R') existing on the aromatic nucleus besides the primary amino group.

Reaction parameters

Since the drugs under investigation have either a free (PAH) or potential (released by reduction of NIC or hydrolytic cleavage of ACBH) aromatic primary amino group, the suitability of MBTH for their estimation was examined. The applicability of MBTH reagent in conjunction with different oxidants [Fe(III) , Ce(IV) , IO_4^- , CAT , $\text{Cr}_2\text{O}_7^{2-}$, $\text{S}_2\text{O}_8^{2-}$, OCl^- or Fe(CN)_6^{3-}] for the determination of each drug was examined, with respect to λ_{\max} and ϵ_{\max} values and stability of the coloured species formed, and the MBTH- Fe(III) combination was preferred for the high sensitivity obtained. Beer's law was found to be valid over the concentration ranges given in Table 1 at appropriate λ_{\max} (Fig. 1). To ascertain the optimum conditions for complete hydrolysis, ACBH was hydrolysed with different concentrations (1-10M) of hydrochloric acid and various time intervals (5-120 min) in a boiling water bath. Concentrations in the range 2.0-3.0M hydrochloric acid and a 45-min hydrolysis time are sufficient to yield maximum absorbance. For the reduction of NIC, use of 0.5-2.0M hydro-

chloric acid and 0.2-1.0 g of zinc dust was found to be optimal. The reduction time was established by increasing it by 5-min intervals. A 45-min period was found to yield maximum absorbance.

For 450 μg of NIC or 600 μg of ACBH or PAH, 3.0 ml (ACBH or PAH) or 4.0 ml (NIC) of 0.2% MBTH solution and 3.0 ml of 0.8% Fe(III) solution were found to be sufficient to give maximum colour intensity. Higher concentrations of reagent and oxidant did not affect the absorption intensity in PAH and NIC, but in the case of ACBH an increase in the volume of both reagent and oxidant decreases the absorbance of the chromophore. Heating the reaction mixture

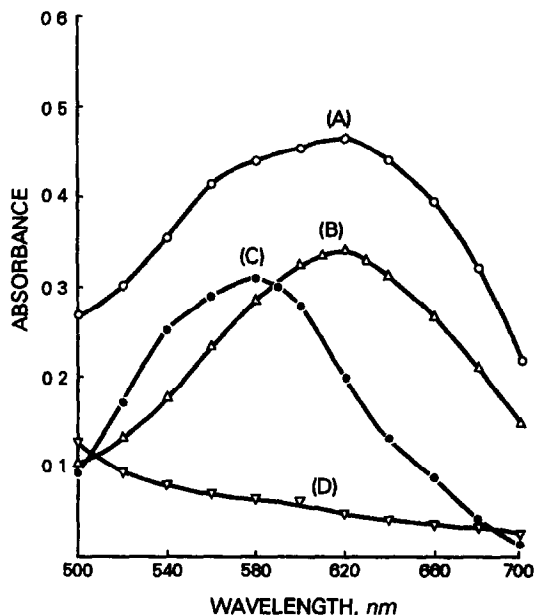


Fig. 1. Absorption spectra of nicoumalone (A), acebutolol hydrochloride (B) and procainamide hydrochloride (C)-MBTH- Fe(III) systems. Concentration of nicoumalone $6.793 \times 10^{-5}M$; acebutolol hydrochloride $8.58 \times 10^{-5}M$, procainamide hydrochloride $2.061 \times 10^{-4}M$; MBTH $1.369 \times 10^{-3}M$ (for NIC), $1.027 \times 10^{-3}M$ (for ACBH and PAH) and ferric chloride $3.552 \times 10^{-3}M$ reagent blank vs distilled water (D)

Table 2 Analysis of dosage forms by proposed and reference methods

Drug	Nominal amount, mg	Proposed method found, %*	Added, mg	Recovery, %*	Reference method† found, %*
NIC-4 mg	4	99.6 ± 0.4 t = 0.477, F = 2.633	5	99.8 ± 0.3	99.2 ± 0.7
NIC-1 mg, SYFCF	1	99.4 ± 0.4 t = 0.407, F = 2.733	5	99.1 ± 0.4	98.8 ± 0.6
ACBH-400 mg	400	100.1 ± 0.6 t = 0.704, F = 1.137	50	99.4 ± 0.7	100.1 ± 0.7
ACBH-200 mg	200	99.6 ± 0.6 t = 0.633, F = 1.976	50	99.5 ± 0.6	99.3 ± 0.4
ACBH-200 mg, HCT-12.5 mg	200	100.2 ± 0.5 t = 0.603, F = 1.202	50	99.3 ± 0.5	100.2 ± 0.5
PAH-250 mg	250	99.6 ± 0.3 t = 0.331, F = 2.464	50	99.8 ± 0.5	99.6 ± 0.2
PAH-250 mg	250	99.7 ± 0.2 t = 0.209, F = 1.472	50	99.6 ± 0.5	99.2 ± 0.2

*Average ± standard deviation of 6 determinations, the *t*- and *F*-values refer to comparison of the proposed method with the reference method. Theoretical values at 95% confidence limit, *t* = 2.57, *F* = 5.05.

†Reported method for ACBH (5), B P method for NIC (2) and PAH (2) HCT = Hydrochlorothiazide, SYFCF = Sunset Yellow FCF

for PAH causes a marked decrease in absorbance. In the case of NIC and ACBH, heating the reaction mixture at 80° for 5–10 min which looks much less critical, gives absorbances that are unstable and less precise. It was observed that when 0.1 and 1.0M hydrochloric acid are added, the absorbance of the solution gradually decreases (due to protonation of the amine group decreasing the oxidative coupling reaction) and hence the addition of hydrochloric acid was discontinued.

The coloured products developed rapidly after addition of the reagents and attained maximum intensity after about 20 min for NIC or PAH and 25 min for ACBH prior to final dilution at room temperature. They were stable for 5 (NIC), 3 (ACBH) or 15 hr (PAH). The solvents studied were water, methanol, ethanol, propan-1-ol, propan-2-ol, acetonitrile, chloroform, butan-1-ol and benzene. Water proved to be the most efficient.

Analytical data. The optical characteristics and figures of merit are given in Table 1. Commercial tablets containing each drug were successfully analysed by the proposed method. The values obtained by the proposed and reference methods for pharmaceutical preparations (Table 2) were compared statistically by the *t*- and *F*-tests and found not to differ significantly. The results of the recovery experiments by the proposed method are also listed in Table 2. Recovery experiments indicated the absence of interference from the commonly encountered pharmaceutical additives and excipients such as lactose, glucose,

starch, gum acacia, magnesium stearate and talc. Hydrochlorothiazide, which is co-formulated with ACBH, also had no effect. The colouring agent Sunset yellow FCF which was added to NIC did not interfere. The proposed method had advantages over other reported methods (including the MBTH-Ce(IV) method⁷ for direct determination of ACBH) in terms of sensitivity and freedom from interferences.

REFERENCES

1. *Pharmacopoeia of India*, pp 334, 413 Ministry of Health and Family Welfare, Government of India, New Delhi, 1985
2. *British Pharmacopoeia*, Vol II, pp. 974, 992 Her Majesty's Stationery Office, London, 1988
3. *United States Pharmacopoeia*, 1985, p. 880. The United States Pharmacopoeial convention, New York, 1985.
4. H. Auterhoff and A. S. Beinroth, *Arch Pharm* 1980, **313**, 807.
5. G. Hakyemez, *Acta Pharm Turc*, 1988, **30**, 153
6. M. A. H. Elsayed, M. Barary, M. A. Salam and S. Mohamed, *Anal Lett*, 1989, **22**, 1665
7. G. Ramana Rao, G. Rajgopalakimi, A. B. Avadhanulu and D. K. Vatsa, *Eastern Pharm*, 1990, **33**, 133
8. C. S. P. Sastry, P. L. Kumari and B. G. Rao, *Chemia Analytyczna*, 1985, **30**, 461
9. A. S. Kvach and V. Ya. Alokサンドロワ, *Khim Farm Zh*, 1987, **21**, 110
10. G. Ramana Rao, A. B. Avadhanulu and Dileep K. Vatsa, *Eastern Pharm*, 1990, **33**, 147
11. E. Sawicki, T. W. Stanley, T. R. Hauser, W. Elbert and J. L. Noe, *Anal Chem*, 1961, **33**, 722
12. M. Pays, R. Bourdon and M. Beljean, *Anal. Chim Acta*, 1969, **47**, 101

NEW REAGENT FOR SPECTROPHOTOMETRIC DETERMINATION OF SALICYLIC ACID

YI-BIN QU

Institute of Precious Metals, China National Nonferrous Metals Industry Corporation, Kunming,
People's Republic of China

(Received 14 August 1990 Revised 15 January 1991. Accepted 6 February 1991)

Summary—In 6M hydrochloric acid solution, salicylic acid reacts with pentachloronitrosyliridate $[\text{Ir}(\text{NO})\text{Cl}_5]^-$ to form a new 1:1 complex giving two absorption maxima at 369 and 446 nm with molar absorptivities both of $1.1 \times 10^4 \text{ l mole}^{-1} \text{ cm}^{-1}$. The reaction is second order with apparent energy, E_a , of 16.8 kJ/mole. At constant temperature, the apparent rate constant k increases to a maximum when the concentration of hydrogen ion is decreased to 4–5M and the concentration of chloride ion is kept at ~6M. The mechanism of the reaction is also discussed. In alkaline solution, the absorption maxima shift to 381 and 506 nm with molar absorptivities of 6.0×10^3 and $2.4 \times 10^4 \text{ l mole}^{-1} \text{ cm}^{-1}$, respectively. Salicylic acid can be determined spectrophotometrically with high sensitivity and precision. Benzoic and boric acids do not interfere.

Salicylic acid is an important antifungal agent and is widely used in pharmaceutical preparations. Although several photometric methods¹⁻⁴ have been developed for its determination, the commonly used method is alkalimetry;⁵ however, this method suffers from interference by benzoic acid. The officially approved photometric method for determination of salicylic acid in pharmaceutical preparation uses ferric nitrate as reagent,⁵ but its application is restricted because of a strict pH value of 2.45 being required for colour development. Recently, a simple spectrophotometric method has been established for the determination of salicylic acid,⁶ but the interference of benzoic acid cannot be eliminated.

Pentachloronitrosyliridate, abbreviated here as PCNI, is a versatile transition metal nitrosyl complex.⁷⁻⁹ We have studied its reaction with diphenylamine¹⁰ and sodium diphenylamine-sulphonate^{11,12} and experimental tests have also indicated that it undergoes a series of reactions with organic and pharmaceutical compounds. Its reaction with salicylic acid is sensitive and selective. Developing a spectrophotometric method for determination of salicylic acid seems to be theoretically and practically promising.

EXPERIMENTAL

Apparatus

A Pye-Unicam PU8800 spectrophotometer with 1-cm cells and a PHS-3 pH meter

equipped with glass-calomel electrodes were used.

Reagents

All chemicals were of analytical-reagent grade.

Standard salicylic acid solution, $1.04 \times 10^{-3}\text{M}$. Prepared by dissolving pure salicylic acid in distilled water, assisted by the addition of a minimum amount of 6M sodium hydroxide.

Standard PCNI solution, $1.0 \times 10^{-3}\text{M}$ in 6M hydrochloric acid. Prepared as described previously¹¹ and kept under dark conditions.

Ascorbic acid solution, 20 mg/ml. Prepared by dissolving colourless ascorbic acid in distilled water and used within 3 days.

Procedures

Procedure 1. To a 10-ml calibrated flask, add 0.2 g of sodium chloride, 0.5 ml of standard or sample solution containing up to 70 μg of salicylic acid, 1.0 ml of $1.0 \times 10^{-3}\text{M}$ PCNI solution and mix thoroughly. Keep in the dark for at least 1 hr. Add 0.2 ml of ascorbic acid and dilute to the mark with 4M hydrochloric acid. Measure the absorbance at 446 nm against a blank prepared under the same conditions.

Procedure 2. Prepare colour development as above. Add 6M sodium hydroxide solution until the colour changes from greenish yellow to red and then add an excess of 0.2 ml. Heat on a water bath for 1.0 min. Immediately cool the flask and its contents to room temperature by

placing in water. Dilute to the mark with water and measure the absorbance at 506 nm against a blank or water.

Kinetic experiments. Use a special glass flask with ground stopper and three side tubes¹³ for mixing solutions. Transfer various amounts of PCNI and salicylic acid solutions respectively into two of the side tubes. Adjust the concentrations of hydrogen ion and chloride ion of the two solutions respectively by adding hydrochloric acid, sodium (or calcium) chloride and water so that their concentrations in the two solutions are identical. Place the glass flask in a thermostat at constant temperature. After 30 min, mix the contents of the flask thoroughly and transfer immediately to a stoppered cell kept at the same temperature. Measure the absorbance at 446 nm against water at regular time intervals.

RESULTS AND DISCUSSION

Absorption spectra

In 6M hydrochloric acid solution, salicylic acid reacted with PCNI forming a colour species exhibiting two absorption maxima at 369 and 446 nm, both with molar absorptivities of 1.1×10^4 l.mole⁻¹ cm⁻¹ as shown in Fig. 1, curve 1.

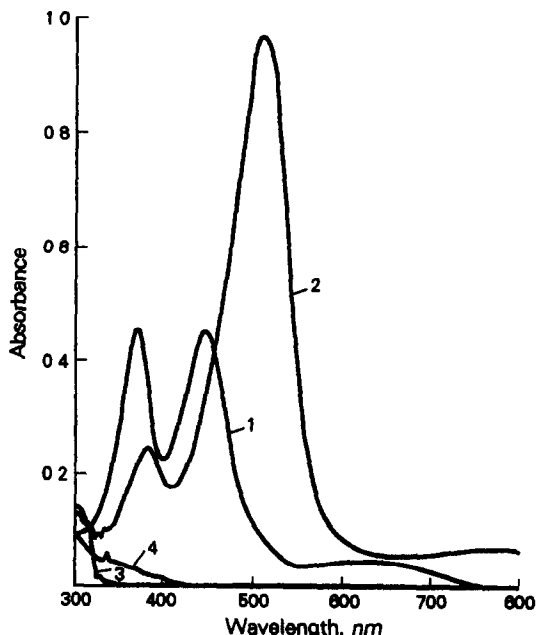


Fig 1 Absorption spectra of 1, salicylic acid-PCNI complex ($4.05 \times 10^{-5}M$) in 6M HCl; 2, salicylic acid-PCNI complex ($4.05 \times 10^{-5}M$) in 0.1M NaOH; 3, salicylic acid ($4.05 \times 10^{-5}M$) in 6M HCl; 4, PCNI ($4.05 \times 10^{-5}M$) and ascorbic acid in excess.

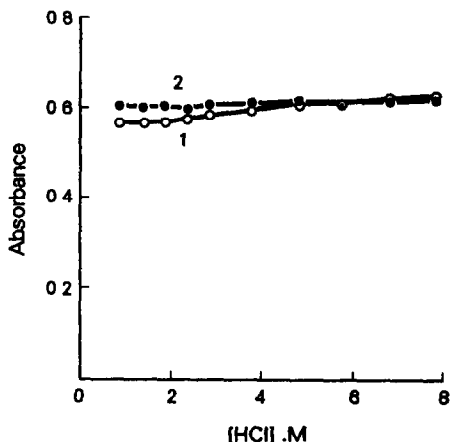


Fig 2. Effect of concentration of HCl on the absorbance of salicylic acid-PCNI complex ($5.2 \times 10^{-5}M$) 1, 446 nm, 2, 369 nm

When the solution was diluted to various concentrations of hydrochloric acid after colour development the absorbance at 446 nm decreased slightly with the decreasing concentration of hydrochloric acid while the absorbance at 369 nm remained nearly constant as shown in Fig. 2. The absorbance at 446 nm varied also with the concentration of sodium chloride and the extent of variation was similar to that with hydrochloric acid.

When the solution was made alkaline after colour development, the colour changed from greenish yellow to red. The absorption spectrum changed gradually over a long time period at room temperature, but quickly became constant on heating. The absorption peak at 446 nm showed an increase and a slight red shift on increasing the solution pH over the range 1-5, and then decreased with a slight hypsochromic shift when the pH of the solution was further increased. This peak disappeared at pH ~ 10 . A new absorption peak occurred at ~ 480 nm when the pH of the solution reached ~ 8 and increased with increasing pH accompanied by a red shift. This peak shifted to 506 nm and its absorptivity reached a constant value when the pH of the solution exceeded 12.7. The absorption peak at 369 nm decreased with increasing pH and shifted to 381 nm when the pH of the solution was greater than ~ 10 . The absorption spectrum in alkaline solution is shown in Fig. 1, curve 2, with molar absorptivities of 0.6×10^4 and 2.4×10^4 l.mole⁻¹ cm⁻¹ at 381 and 506 nm respectively. The effect of pH on the absorbance at 446 and 506 nm is shown in Fig. 3. With a heating time of 1 min, the absorbance at 506 nm remained constant over the pH range 12.7-13.7

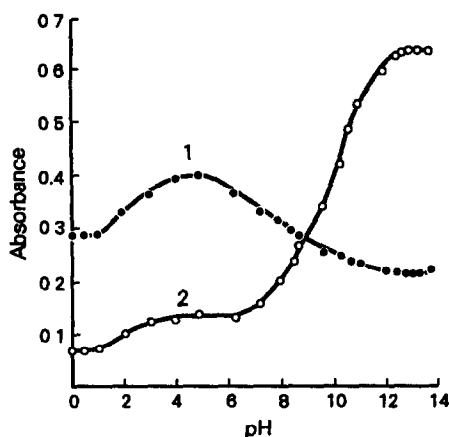


Fig. 3 Effect of pH on the absorbance of salicylic acid-PCNI complex ($2.6 \times 10^{-5}M$, heating, 1 min). 1, 446 nm, 2, 506 nm.

(corresponding to 0.05–0.5M in sodium hydroxide). When the alkalinity of the solution was 0.1M in sodium hydroxide, the optimum heating time was 0.5–2 min as shown in Fig. 4.

Composition and nature of the coloured species

The molar ratio of salicylic acid to PCNI in the coloured species was studied by the continuous variations method and the molar ratio method and found to be 1:1 in each case.

When the solution of the coloured species was passed through ion exchange resins, the greenish yellow species was retained by the anion exchange resin and not by the cation exchange resin, indicating that the species is anionic in nature.

According to Bottomley,^{9,14} a metal nitrosyl complex with $\nu_{NO} \geq 1890 \text{ cm}^{-1}$ may react as an electrophile. The electrophilic substitution reaction products of nitrosyl complexes of ruthenium with phenol and secondary or tertiary

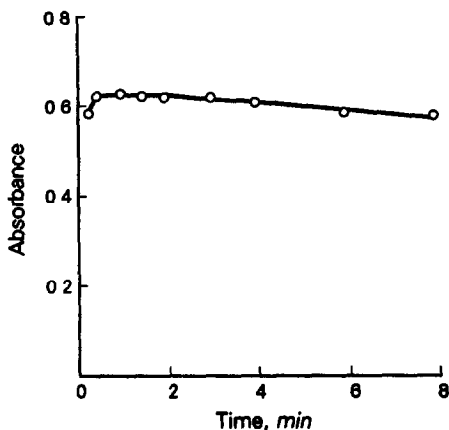
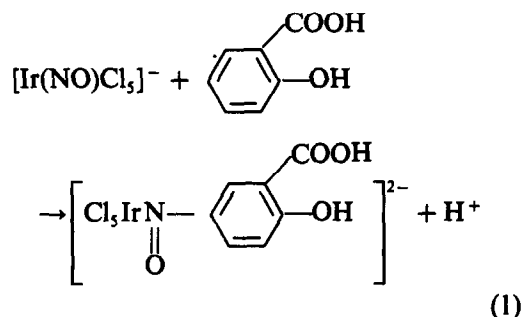


Fig. 4. Effect of heating time on the absorbance of salicylic acid-PCNI complex ($2.6 \times 10^{-5}M$) in 0.1M NaOH. 506 nm.

aromatic amines are nitrosoarene complexes.^{15,16} In our previous work,¹⁰ it was shown that PCNI with a ν_{NO} of 1992 cm^{-1} has electrophilic substitution reactions with diphenylamine and sodium diphenylaminesulphonate and nitrosoarene complexes are also formed. These nitrosoarene complexes are all formed by the electrophilic attack of NO^+ of the nitrosyl complexes on the *para*-position to the amino-group or OH-group of aromatic compounds. It is assumed that the reaction of PCNI with salicylic acid is also an electrophilic substitution reaction which occurs mainly on the *para*-position to the OH-group of salicylic acid. It may be represented by the following equation.



The product formed may also be a nitrosoarene complex.

Origin of the absorption bands in the visible region

Bowden assigned the absorption bands of ruthenium nitrosoarene complexes in the visible region as $d\pi \rightarrow \pi^*$ charge transfer transitions. Because of the similarity between the nitrosoarene complexes of iridium and ruthenium, the absorption band of salicylic acid-PCNI complex at 446 nm may also be a $d\pi \rightarrow \pi^*$ charge transfer transition. When the pH of the solution is changed, the first colour change of the complex over the pH range 1–5 may be due to the dissociation of the carboxyl group and the second colour change over the pH range 8–11 may originate from the loss of hydrogen ion from the hydroxyl group. Both carboxyl group and hydroxyl group are auxochromes.^{17,18} The lone pair of electrons of the hydroxyl group are in conjugation with the π electron system of the aromatic ring. The loss of hydrogen ion from this group will increase its strength of conjugation and lower the energy of the π^* orbital, thus giving a red shift of the $d\pi \rightarrow \pi^*$ band. The carboxyl group operates as an auxochrome through its induction effect and also forms a hydrogen bond with the adjacent hydroxyl

group.¹⁸ The dissociation of this group will affect its inducing strength and the auxochromic ability of the hydroxyl group. The resulting effect of these two factors is reflected in the change of the $d\pi \rightarrow \pi^*$ band.

Kinetics of the reaction

From the preliminary calculation of the kinetic data, the reaction between salicylic acid and PCNI was found to be second order. The absorbance of salicylic acid was zero at 446 nm while that of PCNI was very low but could not be neglected. The precise calculation was carried out as follows.

From the standard equation for a second order reaction,

$$k = \frac{1}{t(a-b)} \ln \frac{b(a-x)}{a(b-x)} \quad (2)$$

let a = initial concentration of salicylic acid and b = initial concentration of PCNI. When $t = 0$, let the absorbance of $a = A_i = 0$ and the absorbance of $b = A_h$. At any intermediate time t , let the total absorbance of the solution = A_d and the absorbance of the product = A_p . When the reaction is completed, let the total absorbance of the solution = A_f and the absorbance of the product = A_m . Then:
When $a > b$,

$$x = b \cdot A_p / A_m. \quad (3)$$

Substitute equation (3) into equation (2):

$$k = \frac{1}{t(a-b)} \ln \frac{a \cdot A_m - b \cdot A_p}{a(A_m - A_p)} \quad (4)$$

where

$$A_m = A_f$$

$$A_p = A_d - A_h(1 - A_p/A_m)$$

$$\approx A_d - A_h(1 - A_d/A_f).$$

Table 1 The apparent rate constant, k , and energy, E_a , of the reaction between salicylic acid and PCNI in 6M HCl

	Temperature, K			Energy, E_a kJ/mole
	303	313	323	
k , $l \text{ mole}^{-1} \text{ sec}^{-1}$	11.8	14.7	17.6	
	11.8	14.7	18.3	
		12.1	14.8	
Mean	11.9	14.7	18.0	16.8

When

$$a < b,$$

$$x = a \cdot A_p / A_m. \quad (5)$$

Substitute equation (5) into equation (2):

$$k = \frac{1}{t(a-b)} \ln \frac{b(A_m - A_p)}{b \cdot A_m - a \cdot A_p} \quad (6)$$

where

$$A_m = A_f - A_h(b - a)/b$$

$$A_p = A_d - A_h[1 - (a \cdot A_p)/(b \cdot A_m)]$$

$$\approx A_d - A_h[1 - (a \cdot A_d)/(b \cdot A_f)].$$

The kinetic experiments were carried out first in 6M hydrochloric acid and the results obtained are summarized in Table 1. The rate of reaction increased slowly with an increase in temperature. The apparent energy was found to be 16.8 kJ/mole.

If the concentration of hydrochloric acid of the solution is decreased, the rate of reaction may be affected in two opposite ways. From equation (1), it is clear that the reaction rate may increase with decreasing concentration of hydrogen ion which is one of the products of the reaction. On the other hand, PCNI is mainly present in $\geq 6M$ hydrochloric acid solution and its concentration decreases rapidly with the

Table 2 Effect of concentration of hydrogen ion and chloride ion on the apparent reaction rate constant, k , at 30°

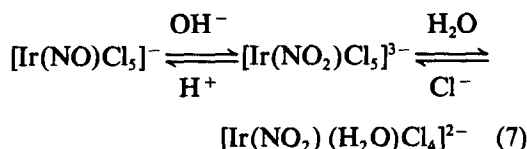
Concentration,* M			Concentration,† M			Concentration,‡ M		
H ⁺	Cl ⁻	k , $l \text{ mole}^{-1} \text{ sec}^{-1}$	H ⁺	Cl ⁻	k , $l \text{ mole}^{-1} \text{ sec}^{-1}$	H ⁺	Cl ⁻	k , $l \text{ mole}^{-1} \text{ sec}^{-1}$
6.0	6.0	11.9						
5.0	5.0	15.3	5.0	6.0	18.4			
4.0	4.0	11.1	4.0	6.0	25.1	4.0	5.0	14.0
3.0	3.0	~5	3.0	6.0	~25	3.0	5.0	~8
2.0	2.0	~1.5	2.0	6.0	irregular results	2.0	5.0	~3

*Maintained with HCl

†Maintained with HCl and CaCl₂

‡Maintained with HCl and NaCl

decreasing concentration of hydrochloric acid according to the following equation,¹⁹



which causes the reaction rate to decrease. The apparent rate constant k will increase or decrease depending on which factor dominates. Thus the data in column 1 of Table 2 can be reasonably explained.

If calcium chloride or sodium chloride is added to the solution to maintain the chloride ion at relatively high levels while the concentration of hydrogen ion is decreased by decreasing the concentration of hydrochloric acid, the concentration of PCNI will be higher than that in solutions of the same acidity without adding salts, and the apparent rate constant, k , will increase. Comparison of the data in columns 2 and 3 of Table 2 with that in column 1 shows that experimental data conform well with theoretical prediction.

Stability of the complex and the optimum conditions for colour development and measurement

It is suitable to develop colour in solutions of 4–5M hydrochloric acid, saturated with sodium chloride. Calcium is not recommended for increasing the reaction rate at lower acidity since it sometimes causes irregular results. The reason is unknown at present.

The complex was stable for at least 72 hr even in 6M hydrochloric acid. Both 369 and 446 nm may be used for measurement, but 446 nm is preferable as there is less interference. Ascorbic acid was added to reduce irregular absorbance caused by a small amount of H_2IrCl_6 in PCNI solution. It also reacted with PCNI and the resulting product gave a small absorbance in

$\geq 4M$ hydrochloric acid solution and larger absorbance in solutions with lower acidity. It is acceptable to adjust the final acidity of the solution to any value between 4 and 6M.

The sensitivity was doubled when measurements were made in alkaline solution with procedure 2. The absorbance at 506 nm was stable for at least 3 hr and the reagent itself gave no absorbance.

Calibration and precision

A calibration graph was constructed by plotting known concentrations of salicylic acid against the corresponding absorbance obtained by using procedure 1 (using longer time for full colour development when the amount of salicylic acid exceeded 70 μg). The resulting graph was linear and passed through the origin. Beer's law was obeyed over the concentration range 0.5–13 $\mu\text{g}/\text{ml}$. To study the precision, a series of determinations was made for 70 μg of salicylic acid and the relative standard deviation was found to be 0.64%.

Interferences

For determination of 69.6 μg of salicylic acid, 500 μg of boric acid, 500 μg of phenacetine, 5000 μg of benzoic acid and 5000 μg of caffeine did not interfere. Wool fat or vaseline was dissolved in ethyl ether and extracted with sodium hydroxide solution. The extract did not interfere with the determination of salicylic acid.

Applications

Results obtained by applying the following procedure to the determination of salicylic acid in synthetic samples of compound benzoic ointment are shown in Table 3.

Dissolve 0.2 g of ointment in 10 ml of diethyl ether. Transfer into a 60-ml separating funnel. Extract the salicylic acid content

Table 3 Determination of salicylic acid in synthetic samples of compound benzoic acid ointment

Content of Sal,* %	Content of other components, %			Sal* found, %	Relative error, %
	Ben†	Wf‡	Vas§		
5.07	12.13	40.4	42.4	5.01	-1.2
7.29	13.41	38.7	40.6	7.12	-2.3
6.10	12.50	39.7	41.7	6.06	-0.7
5.33	11.67	40.5	42.5	5.36	+0.6
6.85	15.45	37.9	39.8	6.81	-0.6
5.48	11.62	40.5	42.4	5.45	-0.5

*Sal = salicylic acid. †Ben = benzoic acid. ‡Wf = wool fat §Vas = vaseline.

with four successive 5-ml portions of 0.5M sodium hydroxide. Wash the extract with 5 ml of petroleum ether (boiling point range 90–120°) and transfer into a 100-ml standard flask. Dilute to the mark with water. Continue the determination according to procedure 1.

REFERENCES

- 1 Uwe Amschler, *Pharm Ztg*, 1980, **125**, 555, *Chem Abstr.*, 1980, **92**, 220749r.
- 2 M E El-Kommos, *Arch Pharm Chemi Sci Ed*, 1982, **10**, 146, *Chem. Abstr.*, 1983, **98**, 95753h
- 3 Y A Beltagy, *Zentralbl Pharm, Pharmakother Laboratoriumsdiagn*, 1977, **116**, 925, *Chem Abstr*, 1978, **88**, 158548m.
- 4 K Velasevic, A Dukanovic, and Z Radovic, *Arh Farm*, 1977, **27**, 163, *Chem Abstr*, 1978, **88**, 158538h
5. *British Pharmacopoeia*, pp 396, 543, 548, 701 HM Stationery Office, London, 1980
6. U Saha and K. Baksı, *Analyst*, 1985, **110**, 739
- 7 K. K. Pandey, *Coordm. Chem. Rev.*, 1983, **51**, 69.
- 8 J. H Swinehart, *ibid.*, 1967, **2**, 385
9. F. Bottomley, S G Clarson and S. B Tong, *J. Chem Soc Dalton*, 1974, 2344
- 10 Y-B Qu, *Journal of Inorganic Chemistry (Chinese)*, 1988, **4**, No 2, 21
- 11 Y-B Qu, J-M Wang and H-Y Chen, *Fenxi Huaxue*, 1985, **13**, 329
12. Y-B Qu and J.-M. Wang, *Analyst*, 1987, **112**, 463
- 13 K B Yatsimirskii, *Kinetic Method of Analysis (in Russian)*, p 47 Goskhimizdat, Moscow, 1963
- 14 F Bottomley, *Acc Chem Res*, 1978, **11**, 158.
- 15 W L Bowden, W F Little and T J. Meyer, *J Am. Chem Soc*, 1974, **96**, 5605.
- 16 *Idem, ibid*, 1976, **98**, 444
- 17 J Griffiths, *Colour and Constitution of Organic Molecules*, p. 82 Academic Press, New York, 1976
18. Ci Yunxiang and Zhou Tianze, *Huaxue Shiji*, 1982, **4**, 33.
- 19 Y-B. Qu and J.-M Wang, *Huaxue Xuebao*, 1986, **44**, 330

BOOK REVIEWS

Continuous-Flow Fast Atom Bombardment Mass Spectrometry: R. M. CAPRIOLI (editor), Wiley, Chichester, 1990 Pages x + 189 £27.50

This book is based on transcripts of papers presented at a workshop on CF-FAB in Annapolis, Maryland in 1989. The papers have been expanded and edited into this small volume detailing recent advances in CF-FAB. It is written very much at a "hands-on" level and provides a valuable reference work for the practical mass spectroscopist.

The first chapter explains the principle of operation and the necessary conditions needed to obtain the best results. The chapters are written by users of different instruments and discuss the practicalities and idiosyncrasies of using CF-FAB with their particular make of instrument. The book covers many uses of the technique, including quantitative and trace analysis, direct monitoring of biological processes, liquid chromatography/mass spectrometry and capillary-zone electrophoresis/mass spectrometry.

This is an excellent book and a new user of CF-FAB, or anyone considering taking it up, will find a wealth of valuable information contained within it. This is definitely a book to be kept handily placed in the laboratory and referred to frequently, not tucked away on a library shelf collecting dust.

M. E. HARRISON

Treatise on Analytical Chemistry, Part 1, Theory and Practice: J. D. WINEFORDER, M. M. BURSEY and I. M. KOLTHOFF (editors), 2nd Ed., Vol. 11, Wiley, New York, 1989 Pages xvii + 311 £59.00

This book is devoted to the practice of analysis by the manipulation of gaseous ions and very properly the most substantial chapter is that devoted to conventional mass spectrometry. Indeed, the mass spectrometer may be considered to be the ideal analytical instrument, providing as it does the molecular weight, atomic constitution and isotopic composition of unknown compounds, the qualitative and quantitative analysis of complex mixtures and structural information on organic molecules, and all this with sample sizes of a few micrograms or less. These aspects of the technique are fully covered in the chapter which examines in detail both instrumental aspects and the interpretation of spectra. Information is also included on the examination of mixtures by tandem and multiple unit spectrometers.

The inclusion of a separate chapter dealing with ion cyclotron resonance and the application of Fourier transform methods in a text devoted to analytical chemistry seems unjustified and the authors have very properly compared it to a stone-age tool. Despite its great potentialities it is of more interest to the physical chemist concerned with the problems of ion dissociation.

If FT-ICR may be considered to be at the very beginning of its development, then Spark Source Mass Spectrometry is at its end. Although the great sensitivity and dynamic range, and its ability to cope with the most refractory materials, are unique, the numbers of analytical problems requiring these abilities are decreasing, and so are the number of operating instruments. The authors describe in detail the theory, construction and operation of spark-source instruments and give an account of their application in geology, forensic studies and environmental science.

The great attractions of Plasma Chromatography are operation at atmospheric pressure and a sensitivity which compares with and sometimes surpasses that of the electron capture detector. The text gives a critical review of the possibilities of the technique and lists its more recent achievements.

The final chapter is concerned with the examination of solid surfaces by the energy analysis of scattered incident noble gas ions. As such the technique competes with Auger spectroscopy and ESCA. It has, however, the additional advantage that both surface layers and interior structure may be examined by the aid of sputtering. The characterization of typical surfaces of conductors, insulators and catalysts is described.

J. R. MAJER

Basic Chemical Thermodynamics: E. B. SMITH, 4th Ed., OUP, Oxford, 1990 Pages xvi + 166 £9.95 (softback), £20.00 (hardback)

Chemical thermodynamics is not the most exciting of subjects for science students, who now, as a group, appear to have even greater difficulty in understanding, and handling, equations. The new edition of this popular book will therefore be greatly welcomed, with its larger format and clearer presentation making it much more pleasant to read. The contents remain essentially as before, with the achieved objective of providing a clear description of the basic concepts of thermodynamics. A discussion of mechanical equilibrium helps the reader to understand the factors involved in chemical equilibrium, and the results are applied to a range of situations. A section is now included on Ellingham diagrams, though this could usefully be expanded to emphasize the industrial relevance of these diagrams.

BOOK REVIEWS

Continuous-Flow Fast Atom Bombardment Mass Spectrometry: R. M. CAPRIOLI (editor), Wiley, Chichester, 1990. Pages x + 189. £27.50

This book is based on transcripts of papers presented at a workshop on CF-FAB in Annapolis, Maryland in 1989. The papers have been expanded and edited into this small volume detailing recent advances in CF-FAB. It is written very much at a "hands-on" level and provides a valuable reference work for the practical mass spectroscopist.

The first chapter explains the principle of operation and the necessary conditions needed to obtain the best results. The chapters are written by users of different instruments and discuss the practicalities and idiosyncrasies of using CF-FAB with their particular make of instrument. The book covers many uses of the technique, including quantitative and trace analysis, direct monitoring of biological processes, liquid chromatography/mass spectrometry and capillary-zone electrophoresis/mass spectrometry.

This is an excellent book and a new user of CF-FAB, or anyone considering taking it up, will find a wealth of valuable information contained within it. This is definitely a book to be kept handily placed in the laboratory and referred to frequently, not tucked away on a library shelf collecting dust.

M. E. HARRISON

Treatise on Analytical Chemistry, Part 1, Theory and Practice: J. D. WINEFORDER, M. M. BURSEY and I. M. KOLTHOFF (editors), 2nd Ed., Vol. 11, Wiley, New York, 1989. Pages xvii + 311. £59.00

This book is devoted to the practice of analysis by the manipulation of gaseous ions and very properly the most substantial chapter is that devoted to conventional mass spectrometry. Indeed, the mass spectrometer may be considered to be the ideal analytical instrument, providing as it does the molecular weight, atomic constitution and isotopic composition of unknown compounds, the qualitative and quantitative analysis of complex mixtures and structural information on organic molecules, and all this with sample sizes of a few micrograms or less. These aspects of the technique are fully covered in the chapter which examines in detail both instrumental aspects and the interpretation of spectra. Information is also included on the examination of mixtures by tandem and multiple unit spectrometers.

The inclusion of a separate chapter dealing with ion cyclotron resonance and the application of Fourier transform methods in a text devoted to analytical chemistry seems unjustified and the authors have very properly compared it to a stone-age tool. Despite its great potentialities it is of more interest to the physical chemist concerned with the problems of ion dissociation.

If FT-ICR may be considered to be at the very beginning of its development, then Spark Source Mass Spectrometry is at its end. Although the great sensitivity and dynamic range, and its ability to cope with the most refractory materials, are unique, the numbers of analytical problems requiring these abilities are decreasing, and so are the number of operating instruments. The authors describe in detail the theory, construction and operation of spark-source instruments and give an account of their application in geology, forensic studies and environmental science.

The great attractions of Plasma Chromatography are operation at atmospheric pressure and a sensitivity which compares with and sometimes surpasses that of the electron capture detector. The text gives a critical review of the possibilities of the technique and lists its more recent achievements.

The final chapter is concerned with the examination of solid surfaces by the energy analysis of scattered incident noble gas ions. As such the technique competes with Auger spectroscopy and ESCA. It has, however, the additional advantage that both surface layers and interior structure may be examined by the aid of sputtering. The characterization of typical surfaces of conductors, insulators and catalysts is described.

J. R. MAJER

Basic Chemical Thermodynamics: E. B. SMITH, 4th Ed., OUP, Oxford, 1990. Pages xvi + 166. £9.95 (softback), £20.00 (hardback)

Chemical thermodynamics is not the most exciting of subjects for science students, who now, as a group, appear to have even greater difficulty in understanding, and handling, equations. The new edition of this popular book will therefore be greatly welcomed, with its larger format and clearer presentation making it much more pleasant to read. The contents remain essentially as before, with the achieved objective of providing a clear description of the basic concepts of thermodynamics. A discussion of mechanical equilibrium helps the reader to understand the factors involved in chemical equilibrium, and the results are applied to a range of situations. A section is now included on Ellingham diagrams, though this could usefully be expanded to emphasize the industrial relevance of these diagrams.

One important point that should be made at an early stage is the necessity to define exactly what change is being considered. The physical states of reactants and products should appear as part of every chemical equation, from the first one onwards, together with a note of the temperature and pressure. It is unfortunate that the recommendations of IUPAC have not been followed, whereby the subscript used to denote a chemical process should be written as a subscript to the Δ symbol and also the standard pressure should be taken as 10^5 N/m². This latter factor could easily have been accommodated in equations by use of a symbol to represent the standard-state pressure.

It is disappointing to find that several errors have crept into this edition, with changes in notation only partly implemented, and references to other sections now incorrect because of alterations that have been made. In addition, there are a number of mistakes in the equations and in the examples given.

Nevertheless, this is still a book to be recommended for the student seeking a sound introduction to the subject.

J. H. DYMOND

Problem Solving with Microbeam Analysis: K. KISS, Elsevier, Amsterdam, 1988. Pages 410. Dfl 255.00

This book attempts to review a whole gamut of analytical techniques, in the fields of optical and laser microscopy and spectroscopy, X-ray spectroscopy, electron diffraction and spectroscopy and heavy-ion probes. It is perhaps inevitable, as the author indicates in the foreword, that the depth to which each technique is covered is not always satisfactory.

Part I of the book is perhaps misleadingly entitled "Theory and Techniques"—the limited coverage of the mathematical background cannot realistically be construed as Theory. For example, I am unconvinced the non-expert reader could understand the principles of electron diffraction from the details given. The Techniques, on the other hand, are comprehensively surveyed, though again a little sketchily. I particularly enjoyed the historical introduction, leading me through the early development of each technique. This theme, repeated in several places, helped place into perspective the logical progression of analytical technique development to its present, profuse nature. The treatment of the techniques, as the author concedes, is reliant on a substantial use of the bibliography for a full appreciation of the details. While accepting the need for conciseness in the context of such a wide-ranging treatment, it is possible to be a touch too concise—some more depth in this section would have been appreciated. I would describe the treatment very much as a practical, non-rigorous guide to the range of analysis techniques available.

In Part II we are treated to a whole series of case studies illustrating the use of the techniques discussed. This again was impressive in its coverage of the range of applications, but as a non-analyst I felt that closer examination of somewhat fewer examples would have benefited the understanding. Apart from a few cases, the presentation was all too brief to give a real flavour of the problem, its solution and importance. This having been said, however, the availability of such a comprehensive case-book is likely to be of use to the practising analyst searching for a clue towards a temporarily intractable problem. Again combination of the sketchy information available in the book with use of the extensive bibliography could well lead, in practice, to a satisfying conclusion and a successful analysis.

In summary, this reviewer was both intimidated and impressed by the range of analysis techniques available and covered in this book. The summaries concluding each section, on the advantages and limitations of each technique, helped clear a path through this veritable forest of alternatives, leading to an awareness of the flexibility available. However, for all but the practising analyst at whom the book is directed, real satisfaction would require a significant amount of further reading.

C. C. WILSON

Gas chromatography—Biochemical, Biomedical and Clinical Applications: R. E. CLEMENT (editor), Wiley Interscience, New York, 1990, Pages x + 393. £70.50

Although it often seems that high-performance liquid chromatography dominates analytical separation methods, over the last 10 years there have been an important series of improvements in the application of gas chromatography (GC) to biomedical and biochemical samples. These developments, primarily in the use of open-tubular columns and coupled mass spectrometric detection, have frequently given gas chromatography a distinct advantage in column efficiency and for qualitative identifications, making it ideal for the examination of complex biological matrices.

These advantages are emphasized in this edited work. The most valuable chapters will be those on the applications of GC. These include GC profiling in biomedical investigations by Rosenfeld, fatty acids and lipids analysis by Muskiet and Van Doormaal, amino-acid separations by MacKenzie and the application of GC-MS to human plasma by Taguchi. More specialized aspects are the role of GC in the identification of micro-organisms by Eiceman, Windig, and Snyder, forensic and clinical toxicology by Beaumier and Leavitt and sport drug testings by Viau. The final chapter covers the analysis of organometallic compounds.

These applications chapters are preceded by a series of introductory chapters on open-tubular columns, modern instrumentation, multidimensional gas chromatography, coupled GC-mass spectrometry, derivatization and methods for qualitative and quantitative analysis. However, these are the weakest part of the book, often being over-simplified, with a number of topics repeated by different contributors. The first chapter in particular contains a number of typographical errors.

R. M. SMITH

One important point that should be made at an early stage is the necessity to define exactly what change is being considered. The physical states of reactants and products should appear as part of every chemical equation, from the first one onwards, together with a note of the temperature and pressure. It is unfortunate that the recommendations of IUPAC have not been followed, whereby the subscript used to denote a chemical process should be written as a subscript to the Δ symbol and also the standard pressure should be taken as 10^5 N/m². This latter factor could easily have been accommodated in equations by use of a symbol to represent the standard-state pressure.

It is disappointing to find that several errors have crept into this edition, with changes in notation only partly implemented, and references to other sections now incorrect because of alterations that have been made. In addition, there are a number of mistakes in the equations and in the examples given.

Nevertheless, this is still a book to be recommended for the student seeking a sound introduction to the subject.

J. H. DYMOND

Problem Solving with Microbeam Analysis: K. KISS, Elsevier, Amsterdam, 1988. Pages 410. Dfl 255.00

This book attempts to review a whole gamut of analytical techniques, in the fields of optical and laser microscopy and spectroscopy, X-ray spectroscopy, electron diffraction and spectroscopy and heavy-ion probes. It is perhaps inevitable, as the author indicates in the foreword, that the depth to which each technique is covered is not always satisfactory.

Part I of the book is perhaps misleadingly entitled "Theory and Techniques"—the limited coverage of the mathematical background cannot realistically be construed as Theory. For example, I am unconvinced the non-expert reader could understand the principles of electron diffraction from the details given. The Techniques, on the other hand, are comprehensively surveyed, though again a little sketchily. I particularly enjoyed the historical introduction, leading me through the early development of each technique. This theme, repeated in several places, helped place into perspective the logical progression of analytical technique development to its present, profuse nature. The treatment of the techniques, as the author concedes, is reliant on a substantial use of the bibliography for a full appreciation of the details. While accepting the need for conciseness in the context of such a wide-ranging treatment, it is possible to be a touch too concise—some more depth in this section would have been appreciated. I would describe the treatment very much as a practical, non-rigorous guide to the range of analysis techniques available.

In Part II we are treated to a whole series of case studies illustrating the use of the techniques discussed. This again was impressive in its coverage of the range of applications, but as a non-analyst I felt that closer examination of somewhat fewer examples would have benefited the understanding. Apart from a few cases, the presentation was all too brief to give a real flavour of the problem, its solution and importance. This having been said, however, the availability of such a comprehensive case-book is likely to be of use to the practising analyst searching for a clue towards a temporarily intractable problem. Again combination of the sketchy information available in the book with use of the extensive bibliography could well lead, in practice, to a satisfying conclusion and a successful analysis.

In summary, this reviewer was both intimidated and impressed by the range of analysis techniques available and covered in this book. The summaries concluding each section, on the advantages and limitations of each technique, helped clear a path through this veritable forest of alternatives, leading to an awareness of the flexibility available. However, for all but the practising analyst at whom the book is directed, real satisfaction would require a significant amount of further reading.

C. C. WILSON

Gas chromatography—Biochemical, Biomedical and Clinical Applications: R. E. CLEMENT (editor), Wiley Interscience, New York, 1990, Pages x + 393. £70.50

Although it often seems that high-performance liquid chromatography dominates analytical separation methods, over the last 10 years there have been an important series of improvements in the application of gas chromatography (GC) to biomedical and biochemical samples. These developments, primarily in the use of open-tubular columns and coupled mass spectrometric detection, have frequently given gas chromatography a distinct advantage in column efficiency and for qualitative identifications, making it ideal for the examination of complex biological matrices.

These advantages are emphasized in this edited work. The most valuable chapters will be those on the applications of GC. These include GC profiling in biomedical investigations by Rosenfeld, fatty acids and lipids analysis by Muskiet and Van Doormaal, amino-acid separations by MacKenzie and the application of GC-MS to human plasma by Taguchi. More specialized aspects are the role of GC in the identification of micro-organisms by Eiceman, Windig, and Snyder, forensic and clinical toxicology by Beaumier and Leavitt and sport drug testings by Viau. The final chapter covers the analysis of organometallic compounds.

These applications chapters are preceded by a series of introductory chapters on open-tubular columns, modern instrumentation, multidimensional gas chromatography, coupled GC-mass spectrometry, derivatization and methods for qualitative and quantitative analysis. However, these are the weakest part of the book, often being over-simplified, with a number of topics repeated by different contributors. The first chapter in particular contains a number of typographical errors.

R. M. SMITH

Principles of Environmental Sampling: L. W. KEITH (editor) ACS, Washington, 1988 Pages xxiv + 458 \$39.95 (softback), \$64.95 (hardback).

Quality Assurance and Quality Control are concepts which have exploded into the day to day affairs of the majority of analysts within the last couple of years, as evidenced by the enormous interest at Euroanalysis 1990 in the QA/QC session. Methodology and laboratory management are being tackled energetically, with good examples to follow and plentiful advice to be had. But what of the most crucial step in any analysis—the sampling?

The ACS Symposium on Environmental Sampling attempted to summarize thinking not only on *how* to sample, but on *what* to consider when planning the sampling. So this book can be divided into those chapters on the philosophy and logic, definitions and interpretation of QA/QC as applied to sampling (perhaps also including the statistics of sampling), on the one hand, and those on the experience of workers who have struggled with the sampling of inhomogeneous “real” situations such as polluted natural waters, soils, sediments, stack gases, biota, sludges and so on. I feel that the first group of chapters could, with skilful editing, and without loss of information, have been condensed considerably, as there is much repetition and generalization which tires the reader and buries the message under a profusion of words. The second group of chapters, in contrast, constitutes fascinating reading from which much benefit can be extracted by the reader, learning from the difficulties encountered, though not always overcome, by many analysts experienced in handling environmental samples. As the good points far outweigh the minor criticisms the book can be strongly recommended for all practising analysts—and the price is very reasonable.

I. L. MARR

Carbon, Nitrogen and Sulphur Pollutants and their Determination in Air and Water: J. GREYSON, Dekker, New York, 1980 Pages xi + 376, \$99.75, (\$119.50 outside North America)

There are several puzzling features of this book. First, the title and contents are totally mismatched, with very few pages devoted to actual determinations, and very many to an attempt to cover all other aspects of chemistry remotely associated with these three elements. Thus over 50 pages take us through the chemistry of these elements, including lengthy yet sketchy accounts of various biochemical pathways, and a further 40 deal with reactions taking place in aqueous and atmospheric environments. Then there are inadequate chapters on various analytical techniques, with brief summaries of applications to environmental samples: 19 pages on theory of titrations and 3 on actual methods, 8 pages on thermodynamics of electrochemical cells and half a page on the silver sulphide electrode, with not a mention of the other kinds of ISEs, and so on.

The second puzzle is simply “who is the book written for?” The author suggests that it is for the engineer or chemist who finds himself having to do some analyses. Such a reader will need real help which he will not find in this book. While the cover note says “this practical reference details procedures available” the contents certainly do not. The book might have been written as a general text for introductory environmental chemistry students, but it repeats too much material which is presented much more clearly in other texts, and the price at \$100 is anyway far beyond the student’s pocket.

The third puzzle is the large number of mistakes: *n*-octane as a GC stationary phase¹, fluorescence emission at shorter wavelengths than the excitation¹, TLC with the spots *descending*¹, $\text{CO}_2 + \text{HCO}_3^- + \text{CO}_3^{2-}$ summing to 120% at pH 8¹, BOD determinations requiring solutions to be *oxygen-saturated*¹, spectrophotometry possible *only between 30% and 60%T* when most modern instruments easily measure 1%T¹, “practically all modern spectrophotometers make use of *photomultipliers*” except all those (very many) which use silicon diodes¹, *p-rosaniline* instead of *pararosaniline* (there is no group to be *para*), and so on.

A puzzling book indeed, but not one that I can recommend, for any class of reader.

I. L. MARR

Chemical Demonstrations—A Sourcebook for Teachers, Volume 1, 2nd Edition: L. R. SUMMERLIN and J. L. EALY JR (editors), ACS, Washington, DC, 1988. Pages xii + 198 \$19.95 (US and Canada), \$23.95 (elsewhere)

Chemical Demonstrations—A Sourcebook for Teachers, Volume 2, 2nd Edition: L. R. SUMMERLIN, C. L. BORGFORD and J. B. EALY (editors), ACS, Washington, DC, 1988. Pages xii + 233 \$19.95 (US and Canada), \$23.95 (elsewhere)

How did *you* become interested in Chemistry? Almost certainly because you had the best kind of teacher—one who aroused your enthusiasm by showing you interesting and exciting chemical changes. Colours! Bright lights! Explosions!!! Remember? The authors of the two volumes of “Chemical Demonstrations” fit nicely into this category themselves. They have chosen over two hundred demonstrations which are designed to be *enjoyed* by students as well as providing subjects for discussion. The experiments cover a wide range of topics—gases, solubility and solution, kinetics and equilibria, oxidation and reduction, colloids, polymers, physical changes, reactions of elements, transition metals and complex ions, and chemical bonding. They range from the very simple proof that air is a substance (Empedocles, 440 BC) to the highly intricate oscillating reactions (which follow chaotic dynamics under certain conditions). For each demonstration the procedure is described in detail, there follows an explanation together with teaching tips and questions. Many perennial favorites, e.g., the starch-iodine clock reaction, are included but for safety reasons the authors have (clearly regretfully) had to exclude several of the more dramatic classical experiments. The few obvious errors intrigue rather than confuse. One ponders over the likelihood of the “light red solution of NH_4^+ (aq)” (Vol. 1, p. 95) and over the electron-deficient

Principles of Environmental Sampling: L. W. KEITH (editor) ACS, Washington, 1988 Pages xxiv + 458 \$39.95 (softback), \$64.95 (hardback).

Quality Assurance and Quality Control are concepts which have exploded into the day to day affairs of the majority of analysts within the last couple of years, as evidenced by the enormous interest at Euroanalysis 1990 in the QA/QC session. Methodology and laboratory management are being tackled energetically, with good examples to follow and plentiful advice to be had. But what of the most crucial step in any analysis—the sampling?

The ACS Symposium on Environmental Sampling attempted to summarize thinking not only on *how* to sample, but on *what* to consider when planning the sampling. So this book can be divided into those chapters on the philosophy and logic, definitions and interpretation of QA/QC as applied to sampling (perhaps also including the statistics of sampling), on the one hand, and those on the experience of workers who have struggled with the sampling of inhomogeneous “real” situations such as polluted natural waters, soils, sediments, stack gases, biota, sludges and so on. I feel that the first group of chapters could, with skilful editing, and without loss of information, have been condensed considerably, as there is much repetition and generalization which tires the reader and buries the message under a profusion of words. The second group of chapters, in contrast, constitutes fascinating reading from which much benefit can be extracted by the reader, learning from the difficulties encountered, though not always overcome, by many analysts experienced in handling environmental samples. As the good points far outweigh the minor criticisms the book can be strongly recommended for all practising analysts—and the price is very reasonable.

I. L. MARR

Carbon, Nitrogen and Sulphur Pollutants and their Determination in Air and Water: J. GREYSON, Dekker, New York, 1980 Pages xi + 376, \$99.75, (\$119.50 outside North America)

There are several puzzling features of this book. First, the title and contents are totally mismatched, with very few pages devoted to actual determinations, and very many to an attempt to cover all other aspects of chemistry remotely associated with these three elements. Thus over 50 pages take us through the chemistry of these elements, including lengthy yet sketchy accounts of various biochemical pathways, and a further 40 deal with reactions taking place in aqueous and atmospheric environments. Then there are inadequate chapters on various analytical techniques, with brief summaries of applications to environmental samples: 19 pages on theory of titrations and 3 on actual methods, 8 pages on thermodynamics of electrochemical cells and half a page on the silver sulphide electrode, with not a mention of the other kinds of ISEs, and so on.

The second puzzle is simply “who is the book written for?” The author suggests that it is for the engineer or chemist who finds himself having to do some analyses. Such a reader will need real help which he will not find in this book. While the cover note says “this practical reference details procedures available” the contents certainly do not. The book might have been written as a general text for introductory environmental chemistry students, but it repeats too much material which is presented much more clearly in other texts, and the price at \$100 is anyway far beyond the student’s pocket.

The third puzzle is the large number of mistakes: *n*-octane as a GC stationary phase¹, fluorescence emission at shorter wavelengths than the excitation¹, TLC with the spots *descending*¹, $\text{CO}_2 + \text{HCO}_3^- + \text{CO}_3^{2-}$ summing to 120% at pH 8¹, BOD determinations requiring solutions to be *oxygen-saturated*¹, spectrophotometry possible *only between 30% and 60%T* when most modern instruments easily measure 1%T¹, “practically all modern spectrophotometers make use of *photomultipliers*” except all those (very many) which use silicon diodes¹, *p-rosaniline* instead of *pararosaniline* (there is no group to be *para*), and so on.

A puzzling book indeed, but not one that I can recommend, for any class of reader.

I. L. MARR

Chemical Demonstrations—A Sourcebook for Teachers, Volume 1, 2nd Edition: L. R. SUMMERLIN and J. L. EALY JR (editors), ACS, Washington, DC, 1988. Pages xii + 198 \$19.95 (US and Canada), \$23.95 (elsewhere)

Chemical Demonstrations—A Sourcebook for Teachers, Volume 2, 2nd Edition: L. R. SUMMERLIN, C. L. BORGFORD and J. B. EALY (editors), ACS, Washington, DC, 1988. Pages xii + 233 \$19.95 (US and Canada), \$23.95 (elsewhere)

How did *you* become interested in Chemistry? Almost certainly because you had the best kind of teacher—one who aroused your enthusiasm by showing you interesting and exciting chemical changes. Colours! Bright lights! Explosions!!! Remember? The authors of the two volumes of “Chemical Demonstrations” fit nicely into this category themselves. They have chosen over two hundred demonstrations which are designed to be *enjoyed* by students as well as providing subjects for discussion. The experiments cover a wide range of topics—gases, solubility and solution, kinetics and equilibria, oxidation and reduction, colloids, polymers, physical changes, reactions of elements, transition metals and complex ions, and chemical bonding. They range from the very simple proof that air is a substance (Empedocles, 440 BC) to the highly intricate oscillating reactions (which follow chaotic dynamics under certain conditions). For each demonstration the procedure is described in detail, there follows an explanation together with teaching tips and questions. Many perennial favorites, e.g., the starch-iodine clock reaction, are included but for safety reasons the authors have (clearly regretfully) had to exclude several of the more dramatic classical experiments. The few obvious errors intrigue rather than confuse. One ponders over the likelihood of the “light red solution of NH_4^+ (aq)” (Vol. 1, p. 95) and over the electron-deficient

nature of a complex containing two *di*-covalent boron atoms (Vol 2, p. 97) Finally, if you are involved in the teaching of chemistry make sure that you have access to both of these books—and *use* them!

O. C. MUSGRAVE

DNA in Forensic Science—Theory, Techniques and Applications: J ROBERTSON, A. M. ROSS and L. M. BURGOYNE (editors), Ellis Horwood, Chichester, 1990 Pages xiii + 197 £39.95

DNA analysis of blood or tissues to identify a donor is of interest to forensic scientists and lawyers. Many, however, may feel that their knowledge of the scientific principles and techniques is inadequate or out of date. If so then this volume should be of considerable help.

The first two chapters describe the nature and occurrence of DNA in tissues and the way information is stored and used in the cell. This section is particularly good at describing the scale of the human genome and putting the various components into context. There are some errors in Table 1.2 in the CU* and AU* amino-acid allocations in the genetic code table and in the descriptions of the different regions of the genes represented in Figs. 1.9 and 1.11.

Having covered the groundwork the next chapters deal more specifically with forensic aspects such as the effects of the environment on, and the means of recovering useful DNA from, various types of forensic sample. The various steps in the DNA analyses are described and the bases of the variations between different individuals are explained. Although the polymerase chain reaction is cited frequently as an important alternative method of analysis and is described in the glossary and in part in various places throughout the book, a more detailed description of the process would be welcome. The application of DNA analysis to paternity testing is considered in a separate chapter.

The final chapter explores the use of this new technology in the courts and some of the legal implications.

The book is clearly written with many illustrations, a glossary, an index and is well supported with references. It should be useful to lawyers and others with an interest in DNA "fingerprinting" as well as to scientists wishing to update their knowledge.

N. D. WATSON

nature of a complex containing two *di*-covalent boron atoms (Vol 2, p. 97) Finally, if you are involved in the teaching of chemistry make sure that you have access to both of these books—and *use* them!

O. C. MUSGRAVE

DNA in Forensic Science—Theory, Techniques and Applications: J ROBERTSON, A. M. ROSS and L. M. BURGOYNE (editors), Ellis Horwood, Chichester, 1990 Pages xiii + 197 £39.95

DNA analysis of blood or tissues to identify a donor is of interest to forensic scientists and lawyers. Many, however, may feel that their knowledge of the scientific principles and techniques is inadequate or out of date. If so then this volume should be of considerable help.

The first two chapters describe the nature and occurrence of DNA in tissues and the way information is stored and used in the cell. This section is particularly good at describing the scale of the human genome and putting the various components into context. There are some errors in Table 1.2 in the CU* and AU* amino-acid allocations in the genetic code table and in the descriptions of the different regions of the genes represented in Figs. 1.9 and 1.11.

Having covered the groundwork the next chapters deal more specifically with forensic aspects such as the effects of the environment on, and the means of recovering useful DNA from, various types of forensic sample. The various steps in the DNA analyses are described and the bases of the variations between different individuals are explained. Although the polymerase chain reaction is cited frequently as an important alternative method of analysis and is described in the glossary and in part in various places throughout the book, a more detailed description of the process would be welcome. The application of DNA analysis to paternity testing is considered in a separate chapter.

The final chapter explores the use of this new technology in the courts and some of the legal implications.

The book is clearly written with many illustrations, a glossary, an index and is well supported with references. It should be useful to lawyers and others with an interest in DNA "fingerprinting" as well as to scientists wishing to update their knowledge.

N. D. WATSON

BROMIDE DETERMINATION AT NANOGRAM LEVELS BY LASER-EXCITED MOLECULAR FLUORESCENCE SPECTROSCOPY IN A GRAPHITE FURNACE*

JAMIL ANWAR,† JESÚS M. ANZANO‡ and JAMES D. WINEFORDNER§

Department of Chemistry, University of Florida, Gainesville, Florida 32611, U.S.A.

(Received 5 March 1991. Accepted 22 April 1991)

Summary—Bromide was determined at nanogram levels by introducing the sample with excess aluminum into a graphite furnace and measuring the laser-excited molecular fluorescence of aluminum bromide. Experimental parameters including excitation and fluorescence wavelengths, thermal conditions and aluminum concentration were optimized. Effects of concomitant ions and of barium hydroxide concentration, as a matrix modifier, have also been checked. The analytical reliability of the described procedure was checked by determining the bromide content in a standard reference material.

Laser-excited fluorescence spectroscopy (LEFS) is one of the most sensitive techniques for ultra-trace element determinations. Detection limits in the femtogram range have been achieved for a number of elements when the technique was employed with high temperature atomizers.¹⁻³ However, LEFS has not been fully exploited for the determination of non-metals mainly because their resonance lines lie in the vacuum UV region and intense laser sources are not yet available in this spectral region. This limitation in the case of non-metals has not only restricted the use of fluorescence methods but has also been considered a serious obstacle in absorption techniques. As an alternative, to achieve good detection limits, research workers developed a number of indirect methods based on molecular emission and absorption of non-metals.⁴

Halogens, an important group of non-metals, have been determined at trace levels by using such molecular emission and absorption methods.^{5,6} Preliminary investigations concerning the quantitative determination of halogens by molecular emission in cool flames were carried out by using copper and indium halide compounds.^{7,8} Later, the use of molecular emission cavity analysis (MECA) improved their detection limits significantly.⁹ Molecular emis-

sion of halogen-containing diatomic molecules in high temperature arcs¹⁰ and microwave-induced plasmas¹¹ were also employed for the determination of halogens. Molecular absorption spectroscopy (MAS) has also been used for the determination of halogens; hence, absorption of halogen-containing diatomic molecules, formed in a graphite furnace, was measured. Different research groups achieved detection limits in the nanogram range for various halogens by MAS.^{12,13}

Molecular emission of halogen-containing molecules¹⁴ in flames and plasmas, and molecular fluorescence of alkaline-earth halides¹⁵ and heavy metal fluorides¹⁶ have been the subject of several physical studies. Recently, fluorescence of such diatomic molecules as indium chloride, magnesium fluoride and aluminum bromide for the analytical determination of halides has been reported.¹⁷ Dittrich and coworkers¹⁸ used a modified graphite furnace for measuring the laser-excited fluorescence of the diatomic molecules of halides with Al, In and Mg.

In the present work, bromide is measured by introducing the sample with an excess of aluminum into a standard graphite furnace tube and measuring the laser-excited non-resonance fluorescence of aluminum bromide. Experimental parameters including excitation and fluorescence wavelengths, thermal conditions and concentration of added aluminum are optimized. The use of barium hydroxide as a matrix modifier and the presence of other concomitant ions have also been evaluated. The analytical usefulness of the described method is evaluated

*This research was supported by NIH-GM 38434-04.

†On leave from University of the Punjab, Lahore, Pakistan.

‡On leave from Department of Analytical Chemistry, University of Zaragoza, Zaragoza, Spain.

§Author for correspondence.

Table 1. Experimental conditions used for measuring the fluorescence of aluminum bromide

Maximum energy obtained from the dye laser after doubling	20 μ J
Dye-laser wavelength used (based on best signal/noise)	278.85 nm
Fluorescence wavelength (at which maximum signal obtained)	284.50 nm
Monochromator slitwidth (based on best signal/noise)	500 μ m (band width = 1 nm)
Photomultiplier tube voltage	-1000 V
Sample drying conditions	150°, 20 sec, Ar flow = 1.5 l./min
Sample ashing conditions	600°, 15 sec, Ar flow = 1.5 l./min
Sample vaporizing conditions	2600°, 2 sec, Ar flow = 0

by determining bromide content in standard samples of wheat flour.

EXPERIMENTAL

Reagents

A $1 \times 10^{-2}M$ solution of Coumarin 540 dye (Exciton Inc. Dayton, 45431) in ethanol was used in the dye laser. Standard solutions of bromide and aluminum were prepared from sodium bromide and aluminum nitrate of 99.99% purity (Aldrich Chemical Co. Wis. 53233) respectively. A $1 \times 10^{-2}M$ solution of barium hydroxide (98+ %, Aldrich Chemical Co.) was used as matrix modifier.

Instrumentation

The dye laser was pumped by a nitrogen laser (7 mJ, 337.13 nm). The laser beam from the dye laser was doubled by a doubling crystal "KDP", passed through the UV filter and then focused into a graphite furnace tube via a pierced mirror.¹⁹ The molecular fluorescence produced after vaporization of the sample in the graphite furnace was collected by the pierced mirror and focused into the entrance slit of the monochromator. The signal from the PMT photomultiplier tube was processed by a boxcar integrator and recorded on a strip chart recorder. A schematic set up of the apparatus used has been described in earlier work.²⁰

Procedure

A 10- μ l aliquot of bromide sample containing bromide and aluminum (in w/w ratio of 2×10^2) was injected into the graphite furnace with a micro syringe. This was followed by the injection of 10 μ l of a $1 \times 10^{-2}M$ solution of barium hydroxide. After introducing the sample and matrix modifier, a controlled heating program of drying, ashing and vaporizing was employed. The experimental conditions used in this work are given in Table 1.

RESULTS AND DISCUSSION

Wavelengths and slitwidth

In previous work,¹⁸ the fluorescence of aluminum bromide was measured at the resonance wavelength *i.e.*, 278.91 nm, but in our system due to severe scattering problems the measurement of resonance fluorescence was not possible; therefore, measurements were made at the non-resonant wavelength. As the literature reveals,²¹ a number of excitation schemes in both the visible and ultra violet regions of the spectrum are possible for measuring the molecular fluorescence of aluminum bromide. The strongest molecular bands representing various transitions of aluminum bromide are closely spaced in the region 279–286 nm.²¹ In the present work, the maximum fluorescence intensity was found by exciting the sample with a laser beam tuned at 278.85 nm (the 0,0 transition) and measuring the fluorescence at 284.5 nm. A number of attempts were made to measure the fluorescence at other possible wavelengths, including 422.5 nm (the 0,0 transition in visible region), after exciting the sample at 278.5 nm, but the fluorescence intensity was far less in all cases than that obtained at 284.5 nm. Hence, all the fluorescence measurements were made at this wavelength.

The effect of spectrometer slitwidth on the signal to noise ratio was evaluated over a range of slitwidths from 100–1000 μ m. The best signal to noise ratio was obtained at 500 μ m slitwidth (=1 nm band width). Greater slitwidths did not improve the signal to noise ratio and so all of the present work was done at a 500- μ m slitwidth.

Thermal conditions

After introducing the sample (10 μ l) and matrix modifier (10 μ l) into the graphite furnace tube, the contents were dried at 150° for 20 sec

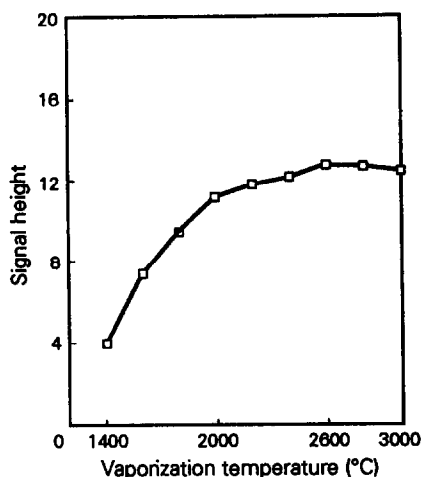


Fig. 1. Effect of vaporization temperature. [10 ng Br/10 μ l; 2 μ g Al; 17 μ g Ba(OH)₂.]

and then ashed at 600° for 15 sec. Drying and ashing time intervals were critical but for the samples larger than 10 μ l an additional 5 sec of drying and ashing at the respective temperatures yielded better results. There was an argon flow of 1.5 l./min during drying and ashing. Higher temperatures and variation in gas flow-rate during drying and ashing did not cause any effect on the signal. Finally, the contents were vaporized at 2600° for 2 sec without any argon flow. The vaporization temperature was optimized by varying it from 1500–3000°. As shown in Fig. 1, the fluorescence intensity increased at about 2000° and reached its maximum at 2600°. A further increase in vaporization temperature did not give any significant increase in the signal. Similarly no noticeable effect resulted by increasing the vaporization time from 2 to 3 sec; rather it increased the noise level after recording the fluorescence signal. After every five sample runs, the graphite furnace was heated to 3000° to eliminate memory effects.

Effects of barium hydroxide

Use of barium hydroxide as a matrix modifier in the determination of bromide by measuring the fluorescence¹⁸ or absorption¹³ of aluminum bromide has already been evaluated by others. It has been suggested¹⁸ that barium ions reduce the loss of bromide as hydrogen bromide during drying and ashing stages and assist the formation of aluminum bromide in the gaseous phase. In our studies a problem arose with the addition of barium hydroxide to a bromide sample which already contained excess aluminum nitrate; precipitation of aluminum hydroxide resulted which not only reduced the

aluminum concentration in the sample but also posed problems in sample injection due to heterogeneity of the solution. To overcome this problem, the barium hydroxide aliquot was directly introduced into the furnace after the sample injection. The influences of the amount of barium hydroxide on the aluminum bromide and in the blank signals are shown in Fig. 2. The best fluorescence sensitivity was achieved by using a bromide to barium hydroxide (w/w) ratio of 1:1700. Further increase in the quantity of barium hydroxide depressed the fluorescence signal significantly probably due to the formation of aluminum hydroxide; therefore, this ratio of bromide to barium hydroxide was used throughout.

Effect of aluminum concentration

The effect of aluminum was studied by adding different quantities of aluminum to a fixed quantity of bromide and barium hydroxide. As can be seen in Fig. 3, the fluorescence intensity of aluminum bromide reached a plateau for the ratio of the amount of aluminum to amount of bromide which exceeded about 200-fold. Aluminum had no appreciable effect on the blank signals.

Effect of concomitant ions

The effect of the number of concomitant ions on the determination of bromide by the described procedure was evaluated. These ions were added in a ten-fold excess of bromide as their sodium salts except iodide and nitrate which were added as their potassium salt. As shown in Table 2 among the halogens, only

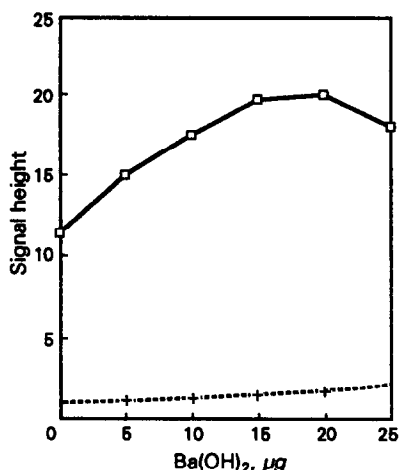


Fig. 2. Effect of Ba(OH)₂ concentration. 10 ng Br/10 μ l; 2 μ g Al. (---- = blank).

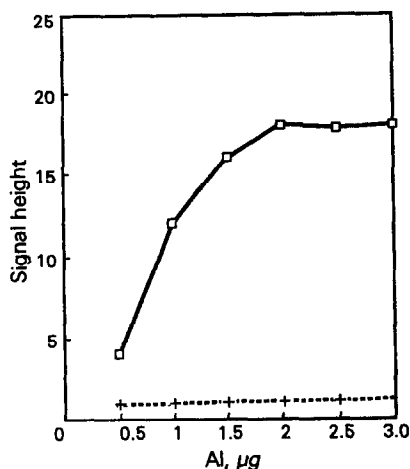


Fig. 3. Effect of Al concentration. 10 ng Br/10 μ l; 17 μ g Ba(OH)₂. (---- = blank).

fluoride increased the fluorescence signal to a considerable extent (10%) which may be due to either bromide contamination in the fluoride salt or more probably to a transition of fluoride in the observation region.²¹ The other ions which depressed the signal of aluminum bromide to a noticeable extent were phosphates and carbonate. This was probably because aluminum and barium also form stable compounds with these ions. An increase in the amount of barium and aluminum ions did not show any significant effect on the interferences due to carbonate and phosphate. Nitrate, acetate, thio-sulfate, sulfite and sulfate did not cause much variation in the fluorescence signal.

Blank signals

Extra large blank signals were seen to appear occasionally. These were mainly due to contamination in reagents, water, glassware and the

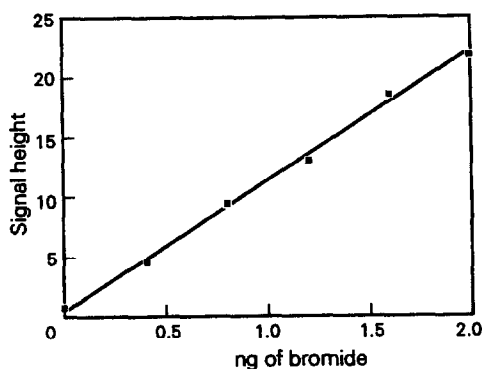


Fig. 4. Calibration curve for bromide. λ_{ex} = 278.5 nm; λ_{fl} = 284.5 nm.

graphite tube. Higher quantities of aluminum and barium hydroxide also contributed blank signals probably due to the formation of stable solid particles in the graphite furnace. However, to minimize the blank signals, doubly-demineralized distilled water and ultra-pure reagents were used. The blank signals were significantly controlled by using adequate quantities of barium and aluminum ions (see Figs. 2 and 3). The graphite tube was replaced after every fifty bromide samples.

Calibration

Under optimum conditions, a linear calibration graph in the range 0.4–2.0 ng of bromide, shown in Fig. 4, with a correlation value of 0.996, was obtained. The relative standard deviation, calculated for nine blank signals, was 5.6%; a detection limit (defined as a signal equal to three times the standard deviation) of 45 pg of bromide was obtained. The calibration graph remained linear up to 100 ng of bromide.

Bromide in standard material

Analytical applicability of the described procedure was evaluated by analyzing the standard sample of wheat flour (from NIST, USA). A known weight of the sample (\approx 200 mg) was decomposed by slow digestion with nitric acid. The desired quantity of aluminum was added and the contents were diluted to a known volume. Aliquots of the sample solution (10 μ l) were injected into the graphite furnace and the fluorescence of aluminum bromide was measured. The bromide content was calculated by comparing the signal with the calibration graph. The average analytical result was in good agreement with the reported value (Br found: 8.85 μ g; reported: 9.00 μ g/g).

Table 2. Effect of concomitant ions on the fluorescence of aluminum bromide

Concomitant ion	Added as	% Recovery
chloride	sodium	102
fluoride	sodium	110
iodide	potassium	101
carbonate	sodium	94
sulphate	sodium	102
phosphate	sodium	92
sulphite	sodium	92
acetate	sodium	98
nitrate	potassium	100
hyd. phosphate	sodium	93
thiosulfate	sodium	97

Signal from 10 ng Br/10 μ g was considered 100%.

Each ion was added in ten fold excess of Br in weight.

CONCLUSION

Bromide at nanogram levels, was determined by using laser-induced molecular fluorescence of aluminum bromide in the graphite furnace. Barium hydroxide was used as a matrix modifier in this work. The parameters, including quantities of aluminum and barium, thermal conditions, excitation and fluorescence wavelengths, and slitwidth, were optimized. A detection limit of 45 pg was obtained under optimum conditions. Among the concomitant ions, only fluoride and phosphate slightly interfered with the determination. The utility of the method was evaluated by determining the bromide content in a standard sample of wheat flour. The analytical results obtained were in good agreement with reported values.

Acknowledgements—Grant from Academy for Education Development (US, AID) to Jamil Anwar is gratefully acknowledged. Jesús M. Anzano thank the Spanish Education & Science Ministry for providing a grant.

REFERENCES

1. H. G. C. Human, N. Omenetto, P. Cavalli and G. Rossi, *Spectrochim. Acta*, 1984, **39B**, 1345.
2. J. P. Dougherty, F. R. Preli, Jr. and R. G. Michel, *J. Anal. At. Spectrom.*, 1987, **2**, 429.
3. M. A. Bolshov, A. V. Zybin and I. I. Smirenkina, *Spectrochim. Acta*, 1981, **36B**, 1143.
4. K. Dittrich, *CRC Critical Rev. Anal. Chem.*, 1986, **16**, 223.
5. K. Fuwa, *4th Int. Conf. Atomic Spectroscopy*, 1973.
6. J. F. Alder, Q. Jin and R. D. Snook, *Anal. Chim. Acta*, 1980, **120**, 147.
7. R. M. Dagnall, K. C. Thompson and T. S. West, *Analyst*, 1969, **94**, 643.
8. G. E. Marsh, *Appl. Spectrosc.*, 1958, **12**, 113.
9. M. Burguera and J. L. Burguera, *Anal. Chim. Acta*, 1983, **153**, 53.
10. I. Schoenfeld, *Appl. Spectrosc.*, 1970, **24**, 359.
11. R. M. Dagnall, T. S. West and P. Whitehead, *Anal. Chem.*, 1972, **44**, 2074.
12. K. Dittrich, B. Vorberg, J. Funk and V. Beyer, *Spectrochim. Acta*, 1984, **39B**, 349.
13. M. G. Gomez, M. A. P. Corvillo and C. C. Rica, *Analyst*, 1988, **113**, 1109.
14. S. J. Davis and S. G. Hatley, *Phys. Rev.*, 1976, **A14**, 1146.
15. J. G. Pruett and R. N. Zare, *J. Chem. Phys.*, 1975, **62**, 2050.
16. R. B. Green, L. Hanko and S. J. Davis, *Chem. Phys. Lett.* 1979, **64**, 461.
17. K. Dittrich, B. Hanisch and H.-J. Stärk, *Acta Phys. Hung.*, 1987, **61**, 79.
18. K. Dittrich and H.-J. Stärk, *Anal. Chim. Acta*, 1987, **200**, 581.
19. M. Leong, J. Vera, B. W. Smith, N. Omenetto and J. D. Winefordner, *Anal. Chem.*, 1988, **60**, 1605.
20. J. Anwar, J. M. Anzano, G. Petrucci and J. D. Winefordner, *Microchem. J.*, in the press.
21. R. W. B. Pearse and A. G. Gaydon, *The Identification of Molecular Spectra*, 3rd Ed., p. 57. Chapman & Hall, London, 1965.

ELECTROCATALYSIS AND AMPEROMETRIC DETECTION OF ORGANIC PEROXIDES AT MODIFIED CARBON-PASTE ELECTRODES

JOSEPH WANG,* LUCIO ANGNES and CHEN LIANG

Department of Chemistry, New Mexico State University, Las Cruces, NM 88003, U.S.A.

OTIS EVANS

Environmental Monitoring Systems, Laboratory, U.S. Environmental Protection Agency, Cincinnati,
OH 45268, U.S.A.

(Received 1 March 1991. Revised 19 April 1991. Accepted 25 April 1991)

Summary—Cobalt-phthalocyanine modified carbon-paste electrodes are shown to catalyze the electro-oxidation of organic peroxides. Cyclic voltammetry offers useful insights into the catalytic behavior. Such behavior is exploited for developing an effective amperometric detection scheme for butanone peroxide, cumene hydroperoxide and tert-butyl hydroperoxide with optimum response at a potential of +0.70 V (*vs.* Ag/AgCl). Highly sensitive and stable flow injection measurements, with detection limits of 2.4–8.3 ng and relative standard deviations of 1.7–1.8% ($n = 30$), are reported. Applicability to measurements in drinking water is illustrated.

The determination of low levels of organic peroxides is of considerable importance due to their widespread use in various industries. In addition, there is growing environmental interest in the identification and quantitation of organic peroxides in drinking water in connection with ozonation disinfection processes.¹ Organic peroxides and hydroperoxides may be formed in water when ozone reacts with natural organic substances and may exhibit adverse health effects. The D.C. polarographic behavior of organic peroxides was explored during the 1960s,^{2,3} and was used to quantitate millimolar concentrations of these compounds. However, methods based on solid electrodes (that are not susceptible to oxygen interferences) may be more desirable for on-line monitoring and other sensing applications. Unfortunately, the anodic oxidation of organic peroxides suffers from high overvoltages.

This paper describes an electrocatalytic chemically modified electrode (CME) system for the voltammetric and amperometric quantitation of organic peroxides. Chemically modified electrodes, containing a surface-bound mediator, can be used to substantially lower the overvoltage for the redox processes of numerous

compounds.^{4,5} In particular, the well-known catalytic activity of metallophthalocyanines has been exploited for facilitating the detection of a wide variety of redox systems.^{6–8} Baldwin and coworkers have incorporated cobalt phthalocyanine (CoPC) into carbon paste electrode (CPEs) for catalyzing the electrooxidation of hydrazines,⁶ keto acids⁷ or sulfhydryl compounds.⁸ Similarly, the faster rates of electron transfer of hydrogen peroxide at CoPC-CMEs,^{9,10} may indicate electrocatalytic activity toward other (organic) compounds containing the peroxide bond. The following sections explore this possibility and its utility for sensitive amperometric detection of organic peroxides.

EXPERIMENTAL

Apparatus

Cyclic voltammetry was performed with a PAR EG&G Model 264A voltammetric analyzer, in conjunction with a Houston Omniscrite X-Y recorder. A Bioanalytical Systems (BAS) Model VC-2 electrochemical cell (10 ml) was employed in these experiments. The working electrode, the reference electrode (Ag/AgCl, Model RE-1, BAS), and the platinum wire auxiliary electrode were inserted into the cell through holes in its Teflon cover.

*Author for correspondence.

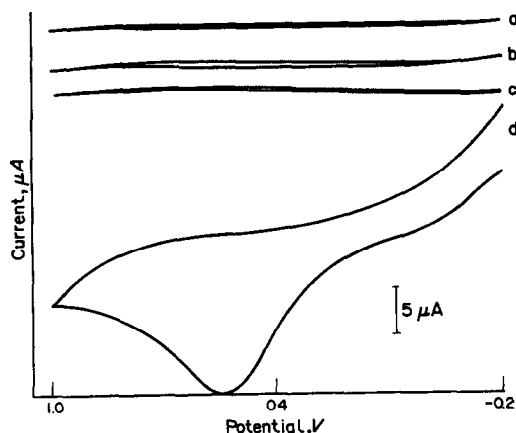


Fig. 1. Cyclic voltamperograms recorded at the ordinary CPE [(a) and (b)] and 1% CoPC-CPE [(c) and (d)], in the absence [(a) and (c)] and presence [(b) and (d)] of 2.8 mM butanone peroxide. Supporting electrolyte, 0.05M potassium nitrate; scan rate, 50 mV/sec.

The flow injection system consisted of the carrier reservoir, a Rainin Model 5041 sample injection valve (20 μ l loop), interconnecting Teflon tubing and a thin-layer amperometric detector (Model TL-4, BAS). A gravity feed of the carrier was used. A PAR EG&G Model 173 Potentiostat/Galvanostat and a Houston Omniscrite chart recorder were used in the flow injection experiments.

Cobalt-phthalocyanine modified carbon paste electrodes were prepared by thoroughly hand mixing CoPC with a slurry of graphite powder (Acheson 38) and mineral oil (Aldrich) (60:40% w/w graphite: oil). Electrodes containing 1 and 10% (w/w) CoPC were used in the batch and flow experiments, respectively. Fresh surfaces were smoothed on a computer card.

Reagents

All solutions were prepared from doubly distilled water. Most of the organic peroxides were purchased from Aldrich, with the exception of tert-butyl peroxyacetate (Atochem, Buffalo). Acetonitrile (LC grade, Aldrich) was used to facilitate the dissolution of some water-insoluble peroxides. All measurements were performed with a 0.05M potassium nitrate (Mallinckrodt) supporting electrolyte. Tap waters were collected in the NMSU laboratory.

RESULTS AND DISCUSSION

Cyclic voltammetry

Figures 1 and 2 show typical cyclic voltamperograms for butanone peroxide and cumene hydroperoxide, respectively, at both plain (b)

and CoPC-containing (d) CPEs. Also shown [curves (a) and (c)] are the corresponding response of the blank (0.05M potassium nitrate) solution. At the conventional CPE, these organic peroxides are not oxidized under the experimental conditions used. The CoPC modifier, in contrast, catalyzes the oxidation of butanone peroxide and cumene hydroperoxide, as is evident from the defined anodic peaks at +0.55 and +0.35 V, respectively. The oxidation process is irreversible. Similar to other CoPC-CMEs,⁶ the background currents are similar to those of the plain surface [(c) vs. (a)], although the Co(II)/Co(III) oxidation process is known to occur around +0.4 V. The catalytic cycle appears to involve a chemical reduction of the cobalt(III) by the peroxides, with subsequent electrochemical oxidation of the cobalt(II) to cobalt(III). In order to obtain and maintain the catalytic current at the level shown in Figs. 1 and 2, the CoPC-CME needed to be exposed to cathodic conditions. A similar requirement was reported for other CoPC-CMEs;^{11,12} it is not clear whether such cathodic activation involves only a change in the oxidation state of the cobalt. (Redox processes of the phthalocyanine ring have also been claimed to affect the catalytic cycle¹¹) The data of Figs. 1 and 2 were thus obtained after holding the electrode at -0.2 V for 30 sec. The use of longer periods (initially) resulted in even larger catalytic currents. Continued cycling of the CoPC-CME in the peroxide solutions resulted in a slow decrease of the peak (down to 60% of its original value over the first eight cycles), followed by a stable response. However, highly stable and large catalytic peaks were obtained for the same peroxides over a

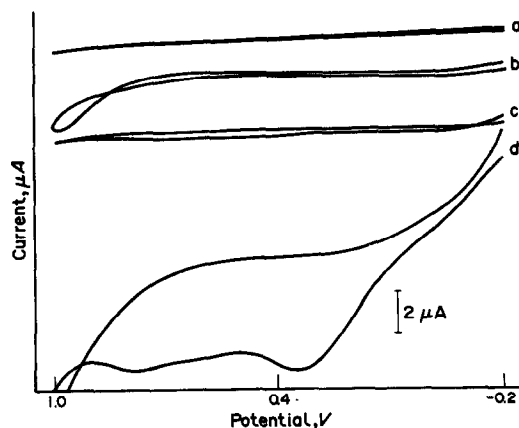


Fig. 2. Cyclic voltamperograms recorded at the ordinary CPE [(a) and (b)] and CoPC-CPE [(c) and (d)] in the absence [(a) and (c)] and presence [(b) and (d)] of 2.7 mM cumene hydroperoxide. Other conditions as in Fig. 1.

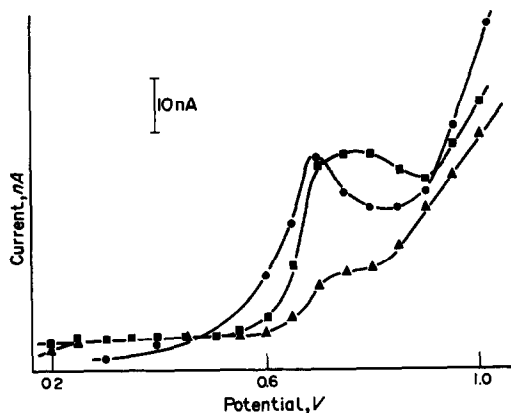


Fig. 3. Hydrodynamic voltammograms for $4 \times 10^{-5} M$ cumene hydroperoxide (\blacktriangle), $2.8 \times 10^{-4} M$ butanone hydroperoxide (\bullet), and $4.5 \times 10^{-4} M$ tert-butyl hydroperoxide (\blacksquare). Flow rate, 1.6 ml/min, electrolyte and carrier, $0.05 M$ KNO_3 .

prolonged period (2 hr) of continued scanning at a slower (10 mV/sec) scan rate and with a more negative (-0.35 V) potential limit (to allow cathodic regeneration of the catalyst). The catalytic activity was also not affected by the solution pH over a wide pH range. Unlike the catalytic detection of other compounds (e.g., 11,12), alkaline media is not required for obtaining the electrocatalytic response. For example, no change in the peak current and potential of cumene hydroperoxide was observed by changing the solution pH between 3.5 and 9. However, the catalytic response disappeared under more acidic conditions.

Similar CV experiments were performed with other organic peroxides. A large catalytic current was observed for the tert-butyl hydroperoxide ($E_p = 0.52$ V), with no response at the plain CPE. Benzoyl peroxide, in contrast, yielded anodic peaks at both CoPC- and plain CPEs, while these electrodes exhibited no response for tertbutyl peroxyacetate (not shown). Apparently, the catalytic activity is not universal toward all compounds containing the peroxide bond. Such differences in the behavior among classes of peroxides can offer improved selectivity.

Flow analysis

The electrocatalytic behavior can be exploited for developing a highly sensitive flow detection scheme for organic peroxides. Such amperometric scheme should benefit the monitoring of chromatographic effluents, the automated flow-injection analysis (FIA) of discrete samples, or on-line assays of environmental matrices.

Anodic detection should be particularly suitable for this task, as it eliminates oxygen interferences and the need for deaeration associated with reductive flow measurements of peroxides.¹¹ Figure 3 shows hydrodynamic voltammograms (HDVs), obtained under flow injection conditions, for the oxidation of butanone peroxide, cumene hydroperoxide and tert-butyl hydroperoxide. For all three compounds, the oxidation starts in the vicinity of $+0.5$ V, with a maximum response around $+0.7$ V. Note also the peak-shaped HDV in the case of butanone peroxide. Such a peak-shaped response was reported previously for CoPC-based flow detectors. Based on the data of Fig. 3, an operating potential of $+0.7$ V was used in all subsequent work. In addition to the operating potential, the amperometric response of the CoPC-detector is influenced by the flow-rate. A gradual (25%) decrease of the FIA response for $2.8 \times 10^{-3} M$ butanone peroxide was observed on increasing the flow-rate from 0.4 to 3.1 ml/min (not shown).

Figure 4 illustrates FIA peaks for increasing (micromolar) levels of different peroxides. The CoP-CPE detector responds very rapidly to

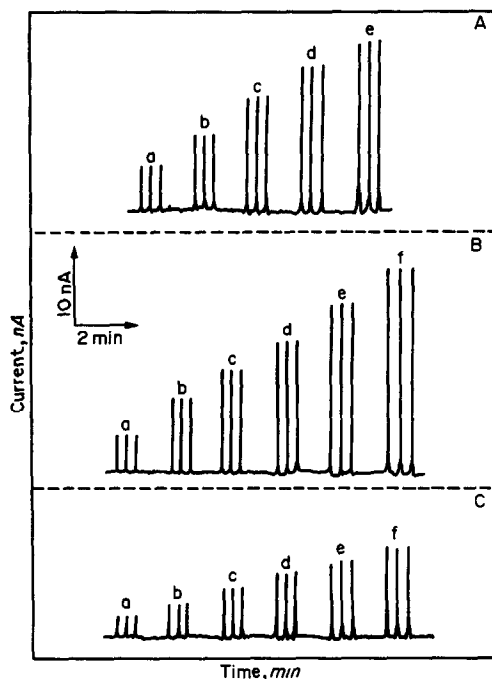


Fig. 4. Detection peaks at 10% CoPC-CPE for successive increments of organic peroxides concentration: [A (a)-(e)] $1.35 \times 10^{-5} M$ steps of cumene hydroperoxide; [B (a)-(f)] $7 \times 10^{-5} M$ steps of butanone peroxide; [C (a)-(f)] $2.25 \times 10^{-5} M$ steps of tert-butyl hydroperoxide. Applied potential, $+0.7$ V; flow rate, 1.2 ml/min. Other conditions are as in Fig. 3.

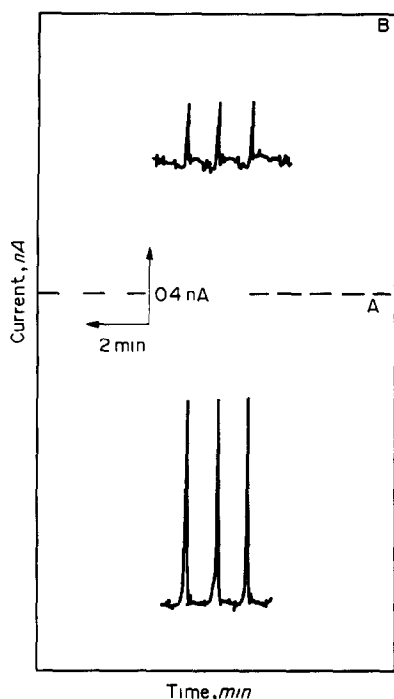


Fig. 5. Detection peaks for $1.3 \times 10^{-5} M$ (A) cumene hydroperoxide and (B) butanone peroxide. Flow rate, 1.4 ml/min. Other conditions are as in Fig. 4.

such dynamic changes in the peroxide concentration. The peak widths are about 5 sec allowing high injection rates (of *ca.* 240 samples/hour). Calibration plots, constructed from these injections, were linear over these entire ranges with slopes of 318, 61.8, 85 nA/mM for cumene hydroperoxide, butanone peroxide and tert-butyl hydroperoxide, respectively (correlation coefficients = 0.996, 0.999 and 0.999).

Amperometric peaks for injections of solutions of $1.3 \times 10^{-5} M$ of cumene hydroperoxide and butanone peroxide were used to estimate the detection limits (Fig. 5). Favorable signal-to-noise (S/N) ratios of 48 and 10 were observed at this level. Based on a S/N of 3, these data correspond to detection limits of $8 \times 10^{-7} M$ (2.4 ng) and $4 \times 10^{-6} M$ (8.3 ng), respectively.

The CoPC-CPE flow detector also offers a high degree of reproducibility. Fig. 6(b) shows 30 repetitive injections (within 10 min) of tert butyl-hydroperoxide (A) and butanone-peroxide (B) solutions. Also shown (for comparison) are analogous measurements at the plain CPE (Fig. 6(a)). The significantly larger FIA response of the CME remained unchanged during this prolonged series (with the last injection producing more than 96–99% of the current exhibited by the first one). The relative standard deviations of these 30 successive runs

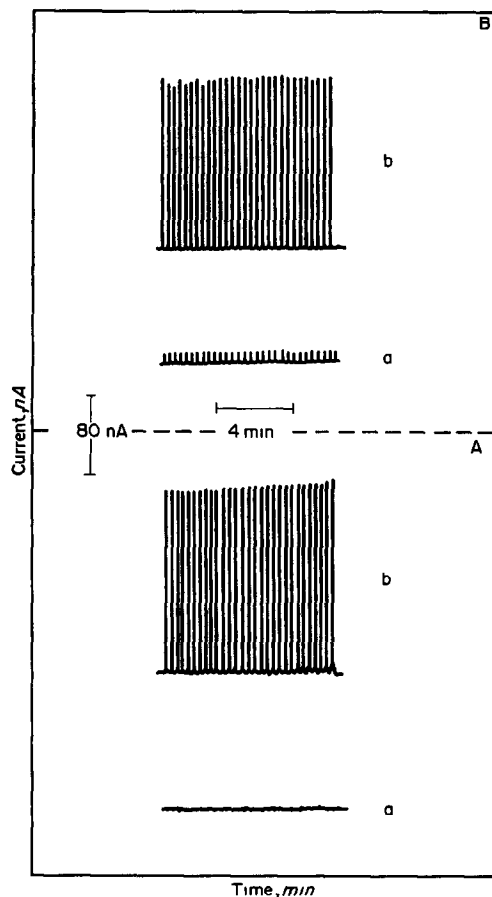


Fig. 6. Detection peaks for repetitive injections of $4.5 \times 10^{-3} M$ tert-butyl hydroperoxide (A) and $2.8 \times 10^{-3} M$ butanone peroxide (B), at ordinary (a) and CoPC (b) CPEs. Conditions, as in Fig. 4.

were 1.7(A) and 1.8 (B)%. As expected for CoPC-CME detectors,⁶⁻⁹ such high reproducibility is obtained only after an initial (3–5 min) exposure of the fresh surface to the flowing solution, during which 10–15 analyte injections are made and a gradual current decrease and stabilization is observed. While no cathodic activation (of the catalyst) was required under the present FIA conditions, operation at higher potentials may lead to passivation of the catalyst.

Reliable measurements of organic peroxides in drinking water supplies are receiving considerable attention in connection with the growing interest in ozonation treatment processes. The suitability of the CoPC-CME for flow measurements of peroxides in drinking water is illustrated in Fig. 7. Only small FIA peaks are observed for the original (unspiked) water (A), indicating a low level of oxidizable constituents. (Since the sample did not undergo ozonation treatment, these peaks are not due to peroxides.)

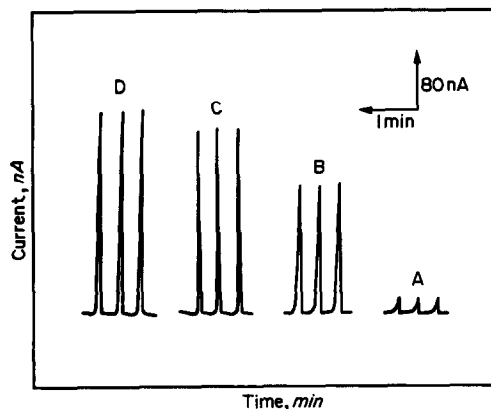


Fig. 7. Measurements of organic peroxides in drinking water: detection peaks for the unspiked sample (A), and upon spiking this sample with 2.7mM butanone peroxide (B), 4.0mM tert-butyl hydroperoxide (C) and 2.6mM cumene hydroperoxide (D). Applied potential: +0.6 V; flow rate: 1.2 ml/min; carrier and sample electrolyte: 0.05M KNO_3 .

In contrast, large and sharp peaks are observed upon spiking this sample with butanone peroxide (B), tert-butyl hydroperoxide (C) and cumene hydroperoxide (D).

In conclusion, the utility of CoPC-modified CPEs for amperometric detection of organic peroxides has been demonstrated. The electrocatalytic surfaces offer marked decreases in overpotentials for the organic-peroxide oxidation. The use of these electrodes in liquid chromatography with electrochemical detection (LCEC) should be attractive for highly selective and sensitive assays of peroxide mixtures. Reverse-phase chromatographic columns have been useful for separating closely-related peroxides.¹³ Such LCEC application should benefit from the recently introduced polymeric CoPC-CMEs,¹⁴ that offer higher stability and compatibility in organic phases (compared to CoPC-CMEs). FIA procedures, in contrast, should be attractive for rapid screening of drinking water. Besides analytical schemes, the diagnostic power of cyclic voltammetry may be useful for gaining insights into ozonation processes leading to the formation of organic peroxides. The nature of these processes and the identity of the resulting peroxides are currently

not clear. The CoPC-containing pastes can be easily adapted to ultramicroelectrode configurations,¹⁵ capable of characterizing and analyzing resistive media such as low-ionic strength drinking water. In addition, the ultrafast scanning capability of such electrodes should be useful for following the fate of peroxide species following ozonation. Cobalt phthalocyanine may mimic the enzymatic activity of horseradish peroxidase, HRP (which is a heme-containing glycoprotein). Work in these laboratories is progressing toward the development of bio-sensing assays for organic peroxides at HRP-based electrodes.

Acknowledgement—The authors acknowledge the financial support of the U.S. Environmental Protection Agency (EPA). L.A. acknowledges a fellowship from Fundação de Amparo à Pesquisa do Estado de São Paulo (FAPESP), Brazil. Mention of trade names or commercial products does not constitute endorsement or recommendation by the U.S. EPA.

REFERENCES

1. W. H. Glaze, *Env. Sci. Technol.*, 1987, **21**, 224.
2. R. H. Johnson and I. W. Siddiqui, *J. Polarogr. Soc.*, 1965, **11**, No. 3, 72.
3. D. Swern and L. S. Silbert, *Anal. Chem.*, 1963, **35**, 880.
4. J. Zak and T. Kuwana, *J. Electroanal. Chem.*, 1983, **150**, 645.
5. S. Dong and Y. Wang, *Electroanalysis*, 1989, **1**, 99.
6. K. M. Korfhage, K. Ravichandran and R. P. Baldwin, *Anal. Chem.*, 1984, **56**, 1514.
7. L. M. Santos and R. P. Baldwin, *ibid.*, 1986, **58**, 848.
8. M. K. Halbert and R. P. Baldwin, *J. Chromatogr.*, 1985, **345**, 43.
9. J. Wang, T. Golden and R. Li, *Anal. Chem.*, 1988, **60**, 1642.
10. G. J. Patriarche, J. M. Kauffman and J. C. Viré in "Redox Chemistry and Interfacial Behavior of Biological Molecules," G. Dryhurst and K. Nike (Eds.), p. 479. Plenum Press, New York, 1988.
11. A. M. Tolbert, R. P. Baldwin and L. M. Santos, *Anal. Lett.*, 1989, **22**, 683.
12. L. M. Santos and R. P. Baldwin, *Anal. Chem.*, 1987, **59**, 1766.
13. M. O. Funk, M. B. Keller and B. Levison, *ibid.*, 1980, **52**, 771.
14. X. H. Qi, R. P. Baldwin, H. W. Li and T. F. Guarr, *Electroanalysis*, 1991, **3**, 119.
15. J. Wang and J. M. Zadeii, *J. Electroanal. Chem.*, 1988, **249**, 339.

DETERMINATION OF BARIUM, STRONTIUM AND NINE MINOR AND TRACE ELEMENTS IN IMPURE BARITE AND STRONTIANITE BY INDUCTIVELY-COUPLED PLASMA ATOMIC-EMISSION SPECTROMETRY AFTER DISSOLUTION IN DISODIUM ETHYLENEDIAMINETETRAACETATE*

J. G. SEN GUPTA

Geological Survey of Canada, Ottawa, Ontario, Canada

(Received 26 December 1990. Revised 18 March 1991. Accepted 29 March 1991)

Summary—A new method has been developed for the determination of barium, strontium, silicon and nine minor and trace elements of barite and strontianite associated with gangue materials. It involves dissolution of the sample by boiling under reflux with a concentrated solution of disodium ethylenediaminetetraacetate (EDTA-2Na) in the presence of ammonium hydroxide. Barite and strontianite dissolve quantitatively under this condition, and any associated silicate and sulphide mineral impurities, remaining insoluble, are filtered off and ignited to constant weight in a platinum crucible. Silica is determined gravimetrically by heating the residue with concentrated sulphuric and hydrofluoric acids, followed by ignition to oxides. The residue is fused with sodium bisulphate and dissolved in dilute sulphuric acid. After suitable dilution of the EDTA-2Na solution, Ba, Sr, Be, Co, Cr, Cu, La, Ni, V, Yb and Zn are determined by inductively-coupled plasma atomic-emission spectrometry (ICP-AES). The bisulphate fusion product is separately analysed by ICP-AES, and the elements found are combined with those obtained from the EDTA-2Na solution. The replicate values of this work compare well with each other and with other values obtained by independent methods.

Recently it has been necessary at the Geological Survey of Canada to analyse a large number of samples of impure barite and strontianite where barium and strontium contents may vary from 0.1 to 40%. Although it is not hard to attack samples containing low amounts of barium or strontium as sulphate by fusion methods,^{1,2} samples containing high barium or strontium as sulphate present difficulties. In these cases, the normal procedure for attack of the sample by fusion with sodium carbonate or lithium metaborate fails because of incomplete decomposition in the case of the former³ and reprecipitation of barium sulphate in solution in the case of the latter.⁴ It was therefore necessary to look for an alternative method for dissolution of these materials.

In previous work,³ an ammoniacal solution of the disodium salt of ethylenediaminetetraacetate has been used for quantitative dissol-

ution of pure barite prior to determination of barium and strontium by flame atomic-absorption and rubidium by graphite-furnace atomic-absorption spectrometry. In the present work, the same procedure with some modification was used for decomposition of impure barite or strontianite, and from the resulting solutions barium, strontium and several minor and trace elements were determined simultaneously by the application of ICP-AES.

EXPERIMENTAL

Apparatus, operating parameters and standards

The instrument used for ICP-AES measurements, and the operating parameters, plasma conditions and the nature of the calibration standards employed are given in Table 1.

Reagents

A.C.S. grade ethylenediaminetetraacetate (disodium salt, dihydrate) was used for sample dissolution, and a blank solution of the reagent was prepared by dissolving 3 g in 25 ml of water.

Freshly prepared ammonia solution was obtained by passing ammonia gas into 500 ml of

*Invited paper presented at 73rd Canadian Chemical Conference and Exhibition, July 15-20, 1990, Halifax, Nova Scotia. Government of Canada copyrights reserved. Geological Survey of Canada Contribution No. 45890.

Table 1. Instrument and operating parameters

<i>Instrument</i> —Jobin-Yvon Model JY 48 equipped with a demountable torch.	
<i>Element and wavelength (nm)</i> —Ba 233.53, Sr 407.77, V 292.40, Cr 267.72, Co 228.62, Ni 231.60, Cu 324.75, Zn 213.86, La 333.75 and Yb 324.94.	
<i>Plasma conditions</i>	
Oscillating frequency, MHz	27
R.f. power, Kw	1.2
Reflected power, W	5
Plasma gas flow-rate, l./min	13
Auxiliary flow-rate, l./min	0.2
Nebulizer flow-rate, l./min	0.7
Sheath gas flow-rate, l./min	0.3
<i>Calibration standards</i>	
Synthetic solutions prepared from high-purity 1000 µg/ml commercial solutions	

water, contained in a 1-litre polyethylene bottle and chilled in ice-cold water, until the volume rose to ~750 ml. The bottle was then tightly closed until used.

Ultrapure water, prepared by reverse osmosis with a Millipore apparatus, was used throughout this work.

Analytical procedure

Accurately weigh 0.1 g of sample into a 150-ml borosilicate beaker, add 60 ml of freshly prepared ammonia solution and 3 g of EDTA-2Na (dihydrate), mix with a glass rod and cover with a watch glass. Place the covered beaker on a hot plate containing an asbestos sheet on its top for even distribution of heat, and boil the solution for 3–4 hr with occasional stirring. Add ammonia solution from time to time to make up losses due to evaporation. Place the covered beaker on a steam bath and allow to stand until the turbidity clears.

Filter through a 5.5-cm Whatman # 40 filter paper and wash with 5% hot ammonia solution.

Table 2. Determination of barium and strontium in impure barite and strontianite samples after dissolution in ethylenediaminetetraacetate (disodium salt) (results in %)

Sample	Ba		Sr	
	This work	Other values	This work	Other values
1	7.0	7.9*	0.059	0.110*
	6.0	7.6	0.044	0.052†
2	2.2, 2.2	4.4*	0.023, 0.021	0.020*
	3.0, 2.5	3.7†	0.023, 0.023	0.026†
3	1.2	2.3†	0.0075	0.011†
	1.7	1.5–2‡	0.0076	0.007‡
4	26.8, 29.4	25.3*	0.8, 0.8	1.12*
	28.5, 27.6		0.7, 0.7	
5	30.5, 29.0	30.1*	0.7, 0.5	0.78*
	31.8, 34.9	25.3†	0.5, 0.5	0.38†
6	15.1	13.5*	0.3	0.4*
	15.0	11.9†	0.3	0.22†
7	1.2, 1.2	1.04*	35.4	33.33*
	1.0, 0.8	0.81†	31.7, 31.5	27.57†
8	0.20	0.04*	0.18	0.55*
	0.16	0.02†	0.18	0.16†
9	0.7, 0.7	0.74*	37.4	41.54*
	0.6, 0.6	0.60†	37.4, 41.1	34.92†
10	4.7	5.2*	0.1	0.16*
	4.8	5.4†	0.1	0.1†
11	42.0	42.5*, 38.5†	0.063	0.15*, 0.11†
	47.0	47.7§	0.067	0.07¶
12	9.9	12.7*	0.062	0.14*
	9.5	11.8†	0.059	0.065†
13	0.072	0.11*	4.9	6.7*
	0.079	0.076†	5.3	4.1†
14	41.0	34.5*, 34.8†	0.18	0.35*, 0.18†
	37.0	40.8 #	0.19	0.11 #

*Commercial laboratory 1 (acid digestion and sodium carbonate fusion, followed by determination of low Ba and Sr by flame AAS and high Ba by gravimetry as barium sulphate).

†GSC-XRF (wavelength dispersive analysis of fused disk^{5,6}).

‡GSC-Flame AAS.

§Commercial laboratory 2—XRF.

¶GSC-ICP.

Commercial laboratory 3—ICP.

Table 3. Determination of SiO₂ in impure barite and strontianite samples after dissolution in disodium ethylenediaminetetraacetate (results in %)

Sample	This work*	Other values†
1	53.7, 53.4	59.7
2	59.1, 59.4, 60.2, 59.7	63.7
3	68.4, 68.5	72.4
4	35.9, 36.0, 35.8, 36.0	—
5	35.5, 34.4, 35.8	36.0
6	24.6, 25.1	26.6
7	8.6, 8.8, 9.0, 9.1	9.7
8	32.7, 32.7	32.3
9	9.7, 9.7, 9.6, 9.1	9.9
10	57.6, 57.7	59.7
11	—‡	8.3
12	64.1, 64.0	70.7
13	68.8, 69.0	69.2
14	20.2, 23.6	25.5

*Determined gravimetrically from the residue after EDTA-2Na dissolution.

†GSC-XRF (wavelength dispersive analysis of fused disk).

‡Not found.

Evaporate the filtrate to ~20 ml and dilute to 25 ml in a standard flask (solution A). Transfer the residue to a 10-ml platinum crucible, ignite the paper at 450° in a muffle furnace, and finally heat at 1000° to constant weight. Determine silica gravimetrically by volatilization with hy-

drofluoric and sulphuric acids on the sand bath, followed by ignition of the residue in a muffle furnace at 1000° to constant weight. Fuse the residue with 1.5 g of sodium bisulphate, cool and dissolve the salts in 10 ml of water (standard flask) adding 1 or 2 drops of 1:1 sulphuric acid, if necessary, to clear the turbidity (solution B).

Determine barium, strontium and other minor and trace elements (Be, Co, Cr, Cu, La, Ni, V, Yb and Zn) from solutions A (after necessary dilution for high Ba and Sr) and B (without dilution) by ICP-AES with suitable standards for calibration and simultaneous measurement of these elements. Wash the nebulizer with plenty of 5% ammonia solution in between aspiration of sample solutions to avoid internal deposition of salts and clogging.

RESULTS AND DISCUSSION

The results for barium and strontium in 14 impure barite and strontianite samples, as obtained by ICP-AES measurements of the EDTA-2Na fraction (solution A) and the bisulphate fusion product (solution B) are combined and the total values for replicate determinations are given in Table 2. Other values on these two elements obtained by independent methods are

Table 4. Determination of beryllium, cobalt and chromium in impure barite and strontianite samples after dissolution in EDTA (disodium salt) and sodium bisulphate fusion of the residue (results in µg/g)

No.	Be			Co			Cr		
	EDTA fraction	Residual fraction	Total	EDTA fraction	Residual fraction	Total	EDTA fraction	Residual fraction	Total
1	0.3	14	14.3	124	472	596	18	107	125
	0.1	14	14.1	130	478	608	18	104	122
2	0.1	1.2	1.3	19	13	32	12	79	91
	<0.1	1.2	1.2	19	12	31	11	81	92
3	<0.1	1.8	1.8	8	13	21	9	98	107
	<0.1	1.8	1.8	10	15	25	10	98	108
4	<0.1	0.9	0.9	100	10	110	14	17	31
	<0.1	0.8	0.8	100	8	108	16	17	33
5	<0.1	1.2	1.2	100	14	114	35	37	72
	<0.1	1.2	1.2	100	7	107	36	33	69
6	0.4	1.6	2.0	55	23	78	9	185	194
	<0.1	1.5	1.5	53	21	74	5	177	182
7	0.3	0.1	0.4	61	31	92	47	43	90
	0.4	0.1	0.5	59	35	94	47	38	85
8	0.2	<0.1	0.2	26	26	52	83	61	144
	0.3	<0.1	0.3	25	27	52	81	64	145
9	0.2	0.1	0.3	51	9	60	24	23	47
	0.1	0.1	0.2	51	8	59	25	20	45
10	0.5	4.0	4.5	38	6	44	81	19	100
	0.5	4.0	4.5	38	5	43	81	22	103
11	<0.1	<0.1	<0.1	165	<1	165	<1	24	24
	<0.1	<0.1	<0.1	190	1	191	<1	21	21
12	<0.1	2.1	2.1	31	3	34	<1	82	82
	<0.1	2.0	2.0	30	2	32	<1	75	75
13	<0.1	<0.1	<0.1	19	22	41	3	32	35
	<0.1	<0.1	<0.1	6	41	47	2	33	35
14	<0.1	0.5	0.5	431	46	477	<1	45	45
	<0.1	0.5	0.5	408	56	464	<1	39	39

Table 5. Determination of copper, lanthanum and nickel in impure barite and strontianite samples after dissolution in EDTA (disodium salt) and sodium bisulphate fusion of the residue (results in $\mu\text{g/g}$)

No.	Cu			La			Ni		
	EDTA fraction	Residual fraction	Total	EDTA fraction	Residual fraction	Total	EDTA fraction	Residual fraction	Total
1	267	643	910	3	8	11	942	133	1075
	200	590	790	2	5	7	960	99	1048
2	22	24	46	4	6	10	437	31	468
	21	25	46	3	5	8	430	31	461
3	15	18	33	1	23	24	210	65	275
	16	111	127	2	21	23	210	167	377
4	110	219	329	2	4	6	3500	41	3541
	98	202	300	4	4	8	3400	14	3414
5	72	49	121	4	<1	4	3600	334	3934
	78	58	136	8	<1	8	3700	13	3713
6	12	12	24	17	13	30	2000	127	2127
	3	12	15	<1	8	8	1900	57	1957
7	12	22	34	19	2	21	270	19	289
	11	6	17	12	2	14	220	19	239
8	12	12	24	16	<1	16	85	24	109
	17	15	32	13	<1	13	74	22	96
9	19	13	32	10	4	14	220	22	242
	9	11	20	9	5	14	190	11	201
10	17	8	25	12	5	17	920	14	934
	16	7	23	9	4	13	920	14	934
11	<1	21	21	<1	<1	<1	6071	12	6083
	<1	23	23	<1	<1	<1	6804	14	6818
12	4	12	16	<1	<1	<1	1412	28	1440
	4	9	13	<1	<1	<1	1360	25	1385
13	<1	<1	<1	<1	<1	<1	25	10	35
	<1	54	54	<1	1	1	12	17	29
14	47	100	147	<1	7	7	5555	30	5585
	29	89	118	<1	1	1	5536	24	5560

Table 6. Determination of vanadium, ytterbium and zinc in impure barite and strontianite samples after dissolution in EDTA (disodium salt) and sodium bisulphate fusion of the residue (results in $\mu\text{g/g}$)

No.	V			Yb			Zn		
	EDTA fraction	Residual fraction	Total	EDTA fraction	Residual fraction	Total	EDTA fraction	Residual fraction	Total
1	12	165	177	0.3	1.3	1.6	400	4727	5127
	12	165	177	0.3	1.3	1.6	412	4593	5005
2	19	181	200	0.4	1.7	2.1	68	462	530
	18	178	196	1.5	1.6	3.1	41	686	727
3	20	235	255	0.1	1.9	2.0	120	1018	1138
	21	234	255	0.3	1.9	2.2	110	1416	1526
4	5	3	8	0.1	0.1	0.2	3300	46680	49980
	5	3	8	0.2	<0.1	0.2	4500	30180	34680
5	16	23	39	0.2	0.1	0.3	72	329	401
	15	26	41	0.2	0.3	0.5	50	157	207
6	3	96	99	<0.1	2.3	2.3	39	479	518
	3	93	96	<0.1	2.2	2.2	25	71	96
7	11	17	28	0.6	0.3	0.9	950	6395	7345
	11	17	28	0.6	0.3	0.9	1000	10520	11520
8	15	17	32	0.4	0.4	0.8	1000	15410	16410
	15	18	33	0.5	0.5	1.0	2000	9510	11510
9	8	8	16	0.4	0.3	0.7	870	5513	6383
	7	8	15	0.4	0.3	0.7	1200	5267	6467
10	26	6	32	0.6	0.2	0.8	330	2251	2581
	25	5	30	0.6	0.2	0.8	430	2263	2693
11	<1	2	2	<0.1	<0.1	<0.1	49	200	249
	<1	3	3	<0.1	<0.1	<0.1	90	69	159
12	21	570	591	<0.1	0.6	0.6	133	400	533
	10	530	540	<0.1	0.4	0.4	98	390	488
13	<1	1	1	<0.1	<0.1	<0.1	5540	24000	29540
	<1	4	4	<0.1	<0.1	<0.1	2460	25000	27460
14	<1	62	62	<0.1	0.7	0.7	131	430	561
	<1	63	63	<0.1	0.1	0.1	165	550	715

also quoted in Table 2 for comparison. For most samples containing low barium and strontium, reasonably good agreement is noted between replicate ICP-AES values of this work and with other values. Greater scatter of values occurs when the concentration of barium or strontium is high. For ICP-AES measurement, this involved up to 100-times dilution of the original solution to be within the scale of calibration standards. This might have caused some dilution errors. There is also significant difference in other values for these samples containing high barium and strontium. However, the average values of this work for high barium and strontium (range ~28–42%) are generally within 2% of the mean values of those obtained by other methods.

Gravimetric values for silica as found in this work are given in Table 3 and are compared with independent X-ray fluorescence values obtained by wavelength dispersive analysis of fused disks. The agreement between replicate values is found to be excellent. Although there is an agreement between gravimetric and X-ray fluorescence values in most cases, the latter values are higher for some samples.

The results for minor and trace elements (Be, Co, Cr, Cu, La, Ni, V, Yb and Zn) in the

EDTA-2Na fraction (solution A) and the residual fraction (solution B) for the same fourteen samples of Tables 2 and 3 are given in Tables 4–6. In the absence of any reference sample of similar nature or trace element data on these samples by other methods, duplicate values of this work are found to compare well with each other in most cases.

Acknowledgements—The author is indebted to I. R. Jonasson for supplying the samples with some previous analytical data, to K. A. Church and R. M. Rousseau for ICP-AES and XRF measurements, respectively, and to D. C. Grégoire and K. N. DeSilva for critical reading of the manuscript.

REFERENCES

1. M. Barbieri, U. Masi and L. Tolomeo, *Chem. Geol.*, 1982, **35**, 351.
2. S. Lange, S. Chaudhuri and N. Clauer, *Econ. Geol.*, 1983, **78**, 1255.
3. J. G. Sen Gupta, *Talanta*, 1987, **34**, 427.
4. J. L. Bouvier, *Private communication*.
5. R. M. Rousseau, *Advances in X-Ray Analysis*, 1989, **32**, 69.
6. *Idem*, in *X-Ray Fluorescence Analysis in the Geological Sciences. Advances in Methodology*, Vol. 7, S. T. Ahmedali (ed.), p. 141. Department of Geological Sciences, McGill University, Montreal, 1989.

APPLICATION OF CHEMICALLY MODIFIED PROBE-ATOMIC ABSORPTION SPECTROMETRY (CMPAAS)—I. DETERMINATION OF Bi IN COPPER ALLOY AND LEAD BY TRIOCTYLPHOSPHINE OXIDE-COATED TUNGSTEN PROBE-AAS

XU BO-XING, SHENG MING-NENG, HUANG CHAO-BIAO* and FANG YU-ZHI
Department of Chemistry, East China Normal University, Shanghai, 200062, China

(Received 4 October 1990. Revised 26 December 1990. Accepted 24 January 1991)

Summary—A trioctylphosphine oxide (TOPO) coated tungsten probe has been prepared and used for the determination of Bi and the $\mu\text{g/g}$ level in copper alloy and lead. Bismuth is preconcentrated on the probe which is placed in a graphite-cup furnace for AA determination of bismuth. The method has good sensitivity and minimises analysis time. Microgram per gram levels of Bi can be determined with good precision and accuracy.

Trioctylphosphine oxide (TOPO) is a typical organic complexant which has been studied intensively as a chemical modification reagent for modified electrodes.¹⁻³ The TOPO-coated electrodes were used widely for determination of electroactive species by electrochemical stripping analysis, because the TOPO film on the surface of the electrode could selectively accumulate different ions, such as Bi(III), Au(III), U(VI), Cr(VI), *etc.*^{2,4-6} In this paper, we attempt to combine the chemical modification technique with AAS to create a new microanalysis technique. We coated TOPO film onto a tungsten wire probe by adsorption, then directly determined the Bi on the probe by GFAAS after preconcentration by soaking the probe in the test solution for a certain period. Since Bi was preconcentrated under optimal conditions, this method can be used for analysis of different samples having complicated matrices. Also, the W wire probe has the behaviour of a L'vov platform in a graphite cup during atomization. For the determination of Bi, the results show that the detection limit (concentration giving an absorbance equal to three times the standard deviation of the background absorbance) is 0.3 ng/ml and the linear range covers 0.5 ng/ml–20 ng/ml. The RSD for 15 determinations of 4 ng/ml Bi is 6.9%.

EXPERIMENTAL

Apparatus

A Hitachi 180-80 Zeeman AAS with programmable heating unit and printer (Hitachi Co., Japan), and an electromagnetic stirrer (Shanghai analytical instrumentation factory) were used.

Chemicals

Hydrochloric acid, TOPO and ethanol were analytical reagent grade and used as received. Demineralized water was used throughout.

Bismuth stock solution. Dissolve pure Bi metal in nitric acid and dilute it with dilute nitric acid solution. A bismuth working solution ($\mu\text{g/ml}$ level) is prepared by diluting the stock solution with 1M hydrochloric acid.

Preparation of TOPO coated tungsten probes

Several researchers reported that preparation of a TOPO modified film was very simple and easy, either by covalent attachment or by adsorption.^{3,5,6} We prepared the modified probe by adsorption. The tungsten probe was made by twisting a W wire of 0.5-mm diameter into a coil (Fig. 1). The W probe was held on the arm of an automatic sampler (Fig. 2) and immersed into 0.1M TOPO-ethanol solution for 5 sec. Then the W probe was raised from the TOPO solution and moved into the graphite cup atomizer by turning the arm towards the cup. The

*Department of Chemistry, ZheJiang Normal University, Jing Hua City, ZheJiang Province, China.



Fig. 1. Tungsten probe. 1. Probe coil. 2. Metallic sleeve.

probe was heated at 120° for 18 sec to evaporate the solvent and make a thin film on the surface of the W probe coil.

Procedure

Add 20 ml of hydrochloric acid acidified test solution to a 50-ml plastic beaker and stir the solution at about 300 rpm. Immerse the TOPO coated probe into the test solution for 1 min to extract trace Bi. Replace the test solution with a 0.1M hydrochloric acid solution containing $20 \mu\text{g/ml Ni}^{2+}$ and allow the probe to soak for 5 sec to wash away the test solution drop which stuck onto the coil during the previous immersion. Turn the arm and move the probe directly into the graphite cup atomizer. Determine the Bi preconcentrated in the TOPO layer under the following conditions:

Dry	120°	20 sec
Ash	600°	25 sec
Atomize	2200°	7 sec (stop gas flow)
Clean	2600°	3 sec
Ar gas flow rate		100 ml/min

RESULTS AND DISCUSSION

Effect of hydrochloric acid concentration

The HCl concentration in the test solution has a significant effect on the preconcentration of Bi, because the interaction of metal ions with TOPO is based on the formation of TOPO

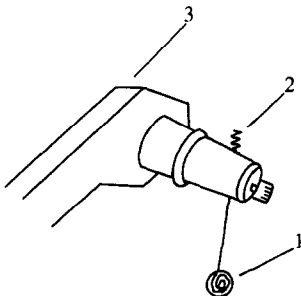


Fig. 2. Schematic diagram of the probe system. 1. W probe. 2. Metallic sleeve. 3. Sampler arm.

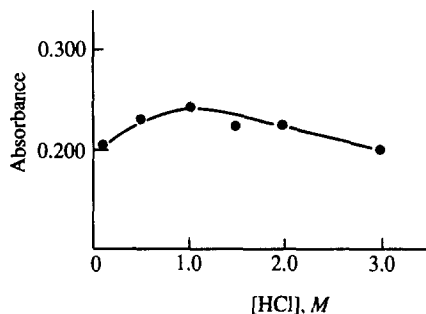


Fig. 3. The effect of HCl concentration on the extraction of Bi.

solvates of salts.² The effect of hydrochloric acid concentration on the extraction of Bi is shown in Fig. 3. We chose 1M hydrochloric acid for an optimal acidity for Bi preconcentration.

Concentration of TOPO-ethanol solution

The thickness of the TOPO film on the probe is a very important parameter during extraction of Bi. However, formation of the TOPO-film on the surface is based on immersing the probe into the TOPO solution followed by other procedures that include evaporation and finally atomization. Therefore, discussion of the thickness of TOPO film is rather complicated. The concentration of the TOPO-ethanol solution is the most important factor. Experimental results indicated (Fig. 4) that the highest Bi extraction efficiency was given when 0.01–0.1M TOPO solution was used. We used 0.1M TOPO solution throughout.

Accumulation time

Lexa and Štulík noted that Bi was accumulated into the TOPO layer very quickly without connection to a potentiostat.⁴ Our experiments show that a period of 60 sec is practical and sufficient for enrichment of Bi at the ng/ml level

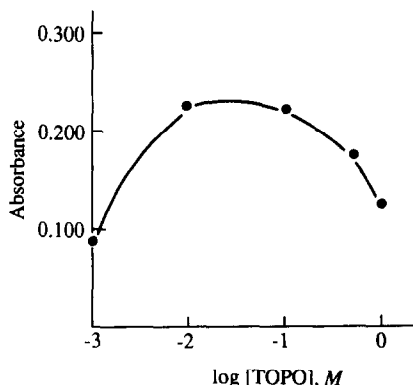


Fig. 4. The effect of TOPO concentration on the extraction of Bi.

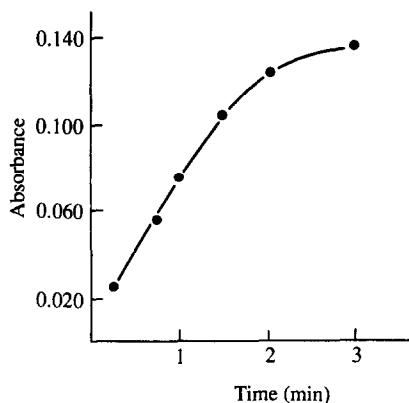


Fig. 5. The effect of preconcentration time on the extraction of Bi. Bi: 4 ng/ml, HCl: 1M, TOPO in ethanol: 0.1M.

(Fig. 5). At more than 3 min, the accumulation rate will be decreased under the experimental conditions.

Charring temperature

To avoid interference of smoke during the AAS measurement of Bi absorbance, the TOPO film on the probe coil must be destroyed by charring and needs to be swept out with Ar flow before atomization. The data show that the optimal charring temperature is 500–600° for 25 sec. Under this charring temperature, the highest absorbance and lowest background were obtained (Fig. 6) and at a temperature over 700°, Bi is seriously lost before atomization. In order to protect Bi from evaporation during the charring step, we used an acidic solution, in which 20 µg/ml Ni²⁺ was contained, as a washing liquid. The probe was soaked in the liquid for 5 sec before the AAS measurement to wash

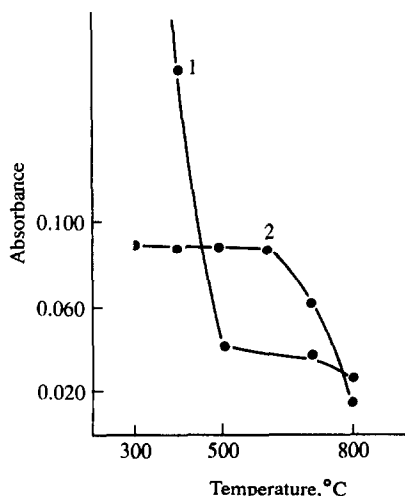


Fig. 6. Effect of temperature. 1. Background signal. 2. Bi absorbance.

Table 1. Effect of foreign ions on determination of 0.125 µg of Bi in 1M HCl solution

Foreign ion	Added, µg	Bi found, µg	Error, %
Pb ²⁺	125.0	0.127	+1.6
Cd ²⁺	28.1	0.128	+2.4
Co ²⁺	67.1	0.123	-1.6
	25.0	0.124	-0.8
Mn ²⁺	50.0	0.116	-7.2
	25.0	0.125	0
	50.0	0.128	+2.4
Fe ²⁺	50.0	0.123	-1.6
Cu ²⁺	31.3	0.117	-6.4
Fe ³⁺	13.0	0.123	-1.6
	62.5	0.114	-8.8
Al ³⁺	25.0	0.118	-5.8
Sn ²⁺	13.0	0.108	-13.6

off the adsorbed test solution drop, at the same time Ni²⁺ is absorbed on the surface of the probe, which allows a higher charring temperature without loss of Bi.

Effect of foreign ions

The effect of several ions on the determination of Bi was examined by the addition method (Table 1). The foreign ions do not affect the signal appreciably at the levels studied, as the errors all seem to be within the precision of the method, with the possible exception of tin and iron(III).

Determination of Bi in samples and their recoveries

To test the accuracy and precision of this method, we analysed two reference standards of copper alloy and a lead sample. The compositions of the two copper references were for BY-1914-2: Cu 57.91%, Bi 0.00290%, Mn 1.41%, Sb 0.0041%, Fe 0.86%, P 0.0093% and Pb 0.079% and for BY-1902-3: Cu 61.34%, Bi 0.0013%, Sb 0.0043%, Fe 0.14%, P 0.0062% and Pb 0.066%. The procedure is as follows: Weigh a certain amount of copper alloy and lead sample. Dissolve the samples with 1:1 nitric acid solution, evaporate to a small volume, transfer to a standard flask and dilute to the mark with water (BY-1914-2: 5.684 mg/ml, BY-1902-3: 5.139 mg/ml, lead sample: 5.430 mg/ml).

In hydrochloric acid solution, Cu²⁺ can be extracted into the TOPO layer and hence interferes with the extraction of Bi. However, the amount of Cu ion extracted and retained in the TOPO layer can be controlled by changing the HCl concentration. In 0.1–0.3M hydrochloric acid, up to 0.3 mg/ml Cu²⁺ did not interfere

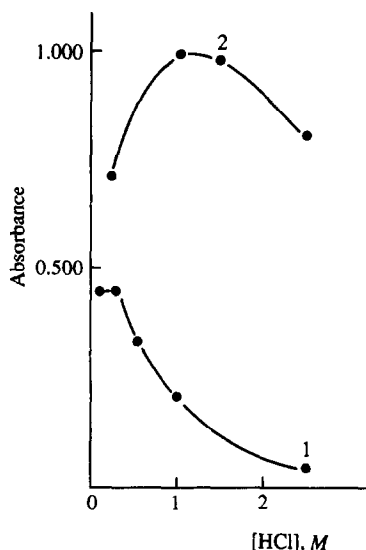


Fig. 7. Effect of HCl concentration on the determination of Bi in copper alloy and lead sample. Curve 1. Copper test solution containing 0.3 mg/ml Cu and 6.0 ng/ml Bi. Curve 2. Lead test solution containing 0.25 mg/ml Pb and 15 ng/ml Bi.

Table 2. Results of determination for Bi in samples

Sample	Bi content by this method, %	Average	RSD	Bi content by ICP, %
BY-1914-2	0.00301	0.00303	6.4	0.00290
	0.00330			
	0.00294			
	0.00285			
BY-1902-3	0.00127	0.00132	9.1	0.00130
	0.00121			
	0.00132			
	0.00149			
Pb sample	0.00708	0.00720	2.4	—
	0.00712			
	0.00740			

Table 3. Addition recoveries

Sample	Volume of sample, ml	Total volume of solution, ml	Added Bi, μg	Found Bi, μg	Average, μg	Recoveries, %
BY-1914-2	1	20.0	0	0.167	0.172	92.5
	1	20.0	0	0.177		
	1	20.0	0.160	0.301		
	1	20.0	0.160	0.339		
BY-1902-3	1	20.0	0	0.077	0.068	87.5
	1	20.0	0	0.059		
	1	20.0	0.160	0.201		
	1	20.0	0.160	0.215		
Pb sample	1	20.0	0	0.378	0.392	100
	1	20.0	0	0.406		
	1	20.0	0.160	0.549		
	1	20.0	0.160	0.555		

with the recovery of 120 ng of Bi (Fig. 7, Curve 1). It seems that, at low hydrochloric acid concentration, the capability of Cu^{2+} to form a solvate with TOPO is lower than that of Bi. For lead, in 1M hydrochloric acid containing 0.25 mg/ml Pb^{2+} , the highest recovery of 300 ng Bi was obtained (Fig. 7, Curve 2). In order to obtain accurate results in the determination of Bi in real samples, we kept the Cu^{2+} and Pb^{2+} concentrations in the sample solution low. A 1-ml volume of the above copper test solution was taken into a 50-ml plastic beaker and diluted with 0.1M hydrochloric acid to 20 ml, and the trace Bi in the solution was determined by using the standard addition method. In the case of the lead sample, 1 ml of the sample solution was diluted by 1M hydrochloric acid and analysed by the same procedure, because

in 1M hydrochloric acid coexisting Pb^{2+} had minimal interference in the determination of Bi.

The results of Bi determinations are shown in Table 2 and are compared with the results from an ICP method. The addition recoveries of Bi in both copper and lead samples are shown in Table 3.

REFERENCES

1. K. Izutsu, T. Nakamura and T. Oku, *Nippon Kagaku Kaishi*, 1980, 1656.
2. K. Izutsu, T. Nakamura, T. Takizawa and H. Hanawa, *Anal. Chim. Acta*, 1983, 149, 147.
3. J. Lexa and K. Štulík, *Talanta*, 1985, 32, 1027.
4. *Idem, ibid.*, 1986, 33, 11.
5. Fang Yu-Zhi, Bai Zhu-Ping and Jin Li-Tong, *Anal. Chem. (Chinese)*, 1989, 4, 307.
6. Fang Yu-Zhi, Wei Ru, He Ping-Gang and Jin Li-Tong, *Anal. Lab. (Chinese)*, 1988, 3, 1.

DETERMINATION OF URANIUM IN TECHNOLOGICAL WATERS BY ION-PAIR LIQUID CHROMATOGRAPHY

IRENA JANČÁŘOVÁ, HANA KŘÍŽOVÁ and VLASTIMIL KUBÁŇ*

Department of Analytical Chemistry, Masaryk University, CS-61137 Brno, Czechoslovakia

(Received 19 November 1990. Revised 11 April 1991. Accepted 16 April 1991)

Summary—U(VI) can be efficiently determined in the range 0.3–10mM after its separation from Th(IV), Zr(IV), Al(III), Fe(III), lanthanides and other ions by ion-pair liquid chromatography on a 3 × 150 mm glass column packed with Separon SGX C18 modified with sorbed ammonium dodecyl sulphate. Traces of uranium can be preconcentrated directly on the analytical column from acidified water solutions and separated from Th, Zr, Al, Fe, lanthanides and other elements, with an enrichment factor of ~100 and recovery of 98 ± 8%, by isocratic or pH or concentration gradient elution with ammonium 2-hydroxy-2-methylpropionate or ammonium citrate solution. Post-column derivatization with 25μM Arsenazo III in 0.1M formate buffer at pH 2.7 is used for detection and quantification.

The need for analytical methods capable of determining uranium at trace and ultratrace levels (from μg to mg per litre) has been steadily growing. Increased awareness of the risks associated with low-level emissions from uranium-handling operations or the storage of spent fuel from nuclear power stations has put increasing demands on uranium determination.

Numerous spectrophotometric and fluorimetric methods based on a wide variety of organic analytical reagents have been developed for the purpose.^{1–6} Only some of these, in particular those using hydroxytriphenylmethane dyes together with cationic surfactants as sensitizing agents,^{2–5} offer the sensitivity needed but their selectivity is usually poor. The low uranium concentrations and large amounts of other dissolved species make existing direct procedures unsuitable for these types of samples.

Better selectivity can be attained by using masking agents or a step such as liquid–liquid extractions^{2,3} or ion-exchange⁷ to separate uranium from interferents and in some cases also to preconcentrate it. However, incomplete separation causes at least a significant impoverishment of the limits of determination and often gives false results.

For these reasons, liquid chromatographic methods^{8–16} have become attractive for the purpose. Metal ions can be separated with either bonded-phase ion-exchangers or dynamically modified reverse-phase (RP) sorbent systems. Among these techniques, ion-pair chromatography with dynamically modified alkylated silica gels has found use for the separation and quantification of a number of metal ions.

U(VI), Th(IV), Zr(IV) and lanthanides can be efficiently separated on C₁₈ alkylated RP silica gel modified by octanesulphonate, pentanesulphonate or butanesulphonate.^{8,9} Slight modification to the standard lanthanides procedure would allow quantification of uranium.^{9–16} Similar systems have also been used for determination of uranium in natural ground waters after its preconcentration on a small (30 mm) C₁₈ RP silica gel enrichment cartridge.¹² The uranium is back-flushed onto an analytical column where it is separated by elution with the ammonium salt of α-hydroxyisobutyric acid (HIBA). Arsenazo III has been used as a sensitive and selective post-column spectrophotometric reagent because the presence of HIBA in the eluent has little effect on the reaction, which can be performed in acidic solution.^{8–16}

During our studies of the ion-pair (IP) HPLC determination of lanthanides, we have found that U, Zr, Th and lanthanides can be efficiently determined in this way after preconcentration on an analytical column, U and Th giving very wide peaks in the region of the peaks for

*Author for correspondence. Present address: c/o Professor P. K. Dasgupta, Department of Chemistry and Biochemistry, Texas Tech University, P.O.B. 4260, Lubbock, Texas, 79409-1061, U.S.A.

Yb–Ho^{15,16} under the same experimental conditions. In the present paper, a modified procedure for preconcentration and direct determination of uranium in technological waters from uranium ore processing is presented.

EXPERIMENTAL

Reagents

A stock solution of uranium (0.1734M) was prepared by dissolving analytical grade $\text{UO}_2(\text{NO}_3)_2 \cdot \text{H}_2\text{O}$ in approximately 0.1M nitric acid. Stock solutions of lanthanides and yttrium ($\sim 0.01M$) in *ca.* 0.1M nitric acid were prepared from the nitrates (La, Ce, Pr, Nd, Tb, Ho), oxides (Sm, Er, Tm, Lu, Y) or carbonates (Eu, Gd, Dy, Yb) of reagent grade purity, supplied by Reakhim, Moscow, (except the Tm and Lu oxides, which were from Fluka). Stock solutions of the other metal ions were prepared by dissolving their analytical grade nitrates in approximately 0.1M nitric acid. The solutions were standardized gravimetrically or by chelometric titration. Working solutions (0.01–1mM) were prepared by diluting the stock solutions with 0.1M nitric acid.

A 1mM Arsenazo III (AA3) solution was prepared by dissolving the chromatographically pure chemical in water. Working solutions of AA3 were obtained by diluting 5 ml of this solution and 20 ml of 1M formate buffer (pH 2.7) to 200 ml.

A 1.0M solution of HIBA was prepared from the reagent grade chemical (m.p. 79.0° Lachema, Brno, Czechoslovakia) and purified by passing it through a 10 × 200 mm column of Dowex 50W × 8 cation-exchanger (50–100 mesh) in the H⁺ form, at a flow-rate of 1 ml/min. A 1M stock solution of reagent grade citric acid was prepared. Working solutions of the ammonium salt of HIBA (0.090 or 0.180M) or citric acid (0.060 or 0.090M) were obtained by neutralization of the stock solutions to the required pH with concentrated ammonia solution, followed by dilution with water.

A 0.1M solution of ammonium dodecyl sulphate (ADS) was obtained by passing an appropriate sodium dodecyl sulphate solution (SDS, from BDH) at 1 ml/min through a 10 × 200 mm column of the Dowex 50W × 8 cation-exchanger in the NH₄⁺ form. The cation-exchanger columns were regenerated by passage of 200 ml of 1M hydrochloric acid (HIBA column) or 2M ammonium nitrate (ADS column) at the same flow-rate.

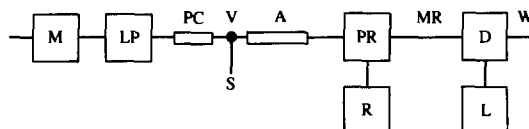


Fig. 1. A block scheme of the chromatographic apparatus. M—mobile phase reservoir, LP—HPLC pump, PC—pre-column, V—injection valve, S—sample, A—analytical column, PR—post-column reactor, R—derivatization reagent reservoir, MR—mixing and reaction coil, D—spectrophotometric detector, L—recorder, W—waste.

Apparatus

The chromatographic apparatus (Fig. 1) consists of a VCM 300 high-pressure chromatographic pump (Development Workshop of Czechoslovak Academy of Sciences, Prague), a 3 × 50 mm glass pre-column packed with Silpearl silica gel sorbent for TLC (Lachema, Brno), a Rheodyne 7125 six-port chromatographic valve (Rheodyne, Cotati, USA) with a 20- μ l sample loop, a 3 × 150 mm glass analytical CGC column, a home-made post-column reactor and a flow-through spectrophotometric detector. A six-way chromatographic switching valve with six inlet ports and a single central outlet port (Mikrotechna, Prague) was placed in front of the VCM 300 pump to create the stepwise concentration or acidity gradients in the low-pressure part of the system.

A CGC glass chromatographic column (3 × 150 mm) packed with Separon SGX C18 RP sorbent (5 μ m particle size, Tessek, Prague) was washed with 10% v/v methanol–water mixture at a flow-rate of 0.01 ml/min for 1 hr and then with 0.005M ADS at a flow-rate of 0.1 ml/min for 2–3 hr. After two weeks of use (or if unused for a period of a week), the column was regenerated by a shortened procedure, the same solutions being passed through it for 30 and 60 min, respectively, especially when the samples had very complex matrices. At the start of each day's work the column was equilibrated with an HIBA solution of appropriate concentration at a flow-rate of 0.4 ml/min for 30–40 min. The precolumn served to trap impurities from the mobile phase before it entered the injection valve and analytical column. The use of this precolumn also prolongs the life-time of the analytical column.

The post-column reactor consisted of a PTFE tee-screen type mixing chamber with a volume of $\sim 0.6 \mu$ l, to which eluate and derivatizing reagent were both fed through Teflon capillaries (0.6 mm i.d.) at a flow-rate of 0.5 ml/min. The homogeneous reaction mixture then flowed

through a reaction coil (0.3×400 mm) to an $18 \mu\text{l}$ flow-cell in the Zeiss Spekol 21 single-beam spectrophotometric detector, connected to a Zeiss K201 recorder. The analytical signal was measured at an absorption maximum of the AA3 chelates with the metal ions of interest, as either peak area or peak height.

RESULTS AND DISCUSSION

Chromatographic separation

The two distinct absorption maxima at 660 and 610 nm attained maximum intensity at pH 2.7 in aqueous mixtures of AAS and U(VI) (each $25 \mu\text{M}$) and their position and amplitude were not affected by the presence of 50mM HIBA or citric acid. The absorption band at $660 \mu\text{m}$ was chosen for the determination because of the higher sensitivity.¹

The quality of the chromatographic separation of uranium(VI) from the other elements depends primarily on the concentration of complexing agent in the mobile phase and on the pH, because of the effect of the latter on the conditional stability constants of the metal chelates formed with the eluting agent in the mobile phase (*cf.* Fig. 2). Under otherwise identical experimental conditions, the retention times increase with increasing acidity of the mobile phase and decreasing concentration of citric acid, over the pH range from 2.4 to 3, and remain constant at higher pH values because of the strong chelates formed with citric acid. The retention times increase with decreasing concentration of HIBA in the mobile phase and reach a minimum at $\sim\text{pH}$ 3.5–3.8. In general, the uranium can be quantitatively separated from other elements under suitable experimental conditions by isocratic elution with either HIBA or citric acid.

Sharper chromatographic peaks, and better and faster separation, were obtained by eluting with 0.090M HIBA at pH 3.5 or with 0.090M citric acid at pH 3.0, than with higher concen-

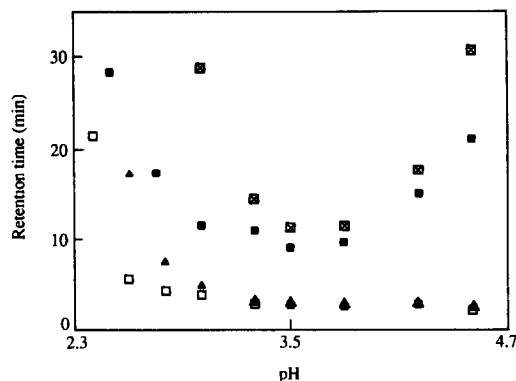


Fig. 2. Dependence of the retention time of U(VI) on the concentration of eluting agent in the mobile phase and the pH of the latter. [U] 0.5mM ; [AA3] $25 \mu\text{M}$. [HIBA]: \square 0.090mM , \blacksquare 0.180mM ; [cit]: \blacktriangle 0.060mM , \square 0.090mM .

trations of these elements (at the same pH). The repeatability of the retention time and peak area (see Table 1 for the statistical parameters)¹⁷ for two different concentrations of U(VI) were satisfactory ($s_r \leq 3\%$). Slightly better repeatability was obtained with HIBA as eluent, than with citric acid. Calibration graphs were linear for 0.3 – 10mM uranium, with detection limits of 0.16 and 0.18mM for elution with HIBA and citric acid respectively (the detection limit being the concentration corresponding to a signal 10 times the noise of the blank signal).

Interferences

Although only Th(IV), Fe(III) and lanthanides [besides U(VI)] gave measurable peaks in the AA3 derivatization reaction,^{1,15,16} possible interference from all elements giving a colour reaction with AA3 was studied. The retention times for uranium and the other elements varied only slightly with changes in the concentration ratios of the individual elements to uranium and with column aging. The separation of U(VI) from the other elements was complete in all cases and no interference was observed over a wide concentration range of the elements (see Table 2).

Table 1. Repeatability¹⁷ of determination of a retention time and a peak area after elution of U(VI) by 0.090M HIBA at pH 3.5 or 0.090M citric acid at pH 3.0: [AA3] = $25 \mu\text{M}$; $n = 10$

HIBA			Citric acid		
[U(VI)], mM	$t_r \pm s(t_r)$, min	$A_p \pm s(A_p)^*$	[U(VI)], mM	$t_r \pm s(t_r)$, min	$A_p \pm s(A_p)^*$
0.3	20.4 ± 0.3	19.2 ± 0.6	0.5	3.9 ± 0.1	15.7 ± 0.5
0.7	12.4 ± 0.2	38.2 ± 0.5	1.0	4.0 ± 0.1	32.3 ± 1.0

* A_p is given in the scale units of the mechanical integrator of the K201 recorder.

Table 2. Chromatographic separation of U(VI) from interfering ions (M) by eluting with 0.090M HIBA or citric acid at pH 3.5 and 2.5, respectively

Ion	[M], mM	t_r (HIBA), min	t_r (cit), min	Ion	[M], mM	t_r (HIBA), min	t_r (CIT), min
U(VI)	0.5	12.4	9.3	Lu(III)	0.3	11.6	—
Th(IV)	0.5	15.8	3.8	Lu(III) ^a	5.0	24.0	15.4
Th(IV)	1.0	16.4	3.6	Yb(III)	0.3	13.8	—
Th(IV)	5.0	25.1 ^b	4.3 ^c	Tm(III)	0.3	19.8	—
Th(IV)	10.0	28.8 ^b	— ^d	Fe(III)	2.0	6.2	4.3
Ba(II)	100	—	29.6	Fe(III)	10.0	8.8	—
U(VI) ^e	0.52	15.1	9.7				
Th(IV) ^e	0.1	—	5.0				
Fe(III) ^f	96	10.8	—				

^a t_r (U) = 15.1 for HIBA at pH 3.3 and 9.4 min for citric acid at pH 2.5, ^b t_r (U) = 15.9 and 16.1 min at pH 3.3, ^c t_r (U) = 9.4 min at pH 2.4, ^dno separation, ^e t_r at pH 3.3 for HIBA and 2.5 for citric acid, for separation of an artificial sample solution [composition (mM): U(VI) 0.52, Th(IV) 0.1, Fe(III) 96, Cu(II) 0.39, Ni(II), 0.49, Cr(III) 0.5, Zr(IV) 0.27, Be(II) 2.8, Mn(II) 0.01, Al(III) 9.3, Ti(IV) 0.52, Cl⁻ 270, NO₃⁻ 31, SO₄²⁻ 3.8].

Al(III) and Cr(III) are eluted at shorter retention times and do not interfere with the elution when present in up to 1000-fold concentration ratio to U(VI). Bivalent species such as Ca(II), Sr(II), Ba(II), Mg(II), also do not interfere at 1000-fold concentration ratio. Pb(II) in equimolar ratio does not interfere, and Cu(II), Ti(IV) and Zr(IV) ions do not interfere when present in up to 2-fold (Cu) or 4-fold (Ti, Zr) concentration ratio.

Th(IV), Lu(III) and Yb(III), which have retention times closest to that for U(VI), are efficiently separated from it when present in 1:1, 20:1 or 10:1 concentration ratio to it, respectively. Other lanthanides do not affect the determination of uranium unless they have a longer retention time than Lu(III), Yb(III) and Tm(III) and are present in >1000-fold ratio to U(VI), because they are eluted after Tm(III) (the retention times increase with decreasing atomic number of the element.^{15,16} If required, the complete group of lanthanides can be efficiently separated from uranium by acidity gradient elution and determination simultaneously.¹⁵

Uranium(VI) can be easily preconcentrated directly on the CGC Separon SGX C18 analytical column from sample solutions at pH 3.5–4.5, with an enrichment factor of up to 100. It is quantitatively sorbed on the analytical column from volumes of 0.1–12.5 ml. The sample solution (at pH 4) is introduced directly into the analytical column by time-controlled pumping (the precolumn and loop injector are not used) via a four-way stopcock. Before and after sorption of the analyte, the column is washed with 10% v/v methanol–water mixture for 10 min to remove the mobile phase and to fill the column with a solvent that does not affect

the sorption or desorption of uranium, and/or to wash out the rest of the sample solution with matrix before the chromatographic separation. The uranium is then eluted and effectively separated from the other elements by isocratic or pH-gradient elution (depending on the matrix composition of the sample and the purpose of the analysis, see above). The repeatability of the method was found to be better than 5%, and the recovery 90–106% for 0.01–0.1mM uranium.

Determination of U(VI) in water samples

Before determination of U(VI) in real samples, the procedure was tested and optimized for an artificial sample containing a selection of elements, at the most probable concentrations (see footnote to Table 2). The best results were obtained by eluting the sample with 0.090M HIBA or citric acid at pH 3.3 and 2.5, respectively. All the peaks appearing in the chromatograms were identified by the standard addition method. Only the lanthanides, Fe(III) and Th(IV) are potential interferents, giving measurable chromatographic peaks under the experimental conditions used, and only their peaks were found when eluting with HIBA or citric acid. None of the above-mentioned elements affects the determination of U(VI) when present at the given concentrations. A U(VI) concentration of 0.53mM (126 mg/l.) with $s_r = 1.9\%$ was found by the standard addition method with linear regression of the function $A_p = f(c)$, for peak area (A_p) vs. U(VI) concentration (c) for successive 1mM additions over the range 1–8mM U(VI), with 5 replicates for each data-point.

Two real samples were analyzed by a similar procedure, and values of 93 and 75 mg/l. with $s_r = 2.2$ and 2.5% were found by the standard addition method. These concentrations agree very well with those obtained by the spectrophotometric method with liquid-liquid extraction,² 99 and 72 mg/l. A very simple in-line preconcentration on the analytical column has to be applied for samples with U(VI) concentrations below the determination limit (35 mg/l.). For 1–20 mg/l. uranium the reproducibility was better than 5% and the results were in good agreement with radiometric analysis (maximum difference 89°).

The proposed method gives precise and correct results. It is relatively fast (around 20 min per analysis) compared to the liquid-liquid extractions,^{2,3,10} ion-exchanger⁷ and other methods. The advantage of the procedure over the extraction-photometric method is its simplicity and the quantitative separation of all interfering elements.

Acknowledgements—The authors wish to thank Dr. M. Radil of the Institute of Nuclear Fuels in Prague-Zbraslav for supplying them with a sample of chromatographically pure Arsenazo III.

REFERENCES

1. S. B. Savvin, *Arsenazo III*, Atomizdat, Moscow, 1966.
2. L. Jančář, B. Slezáčková and L. Sommer, *Talanta*, 1989, **36**, 549.
3. M. Pištělka, B. Stojek and J. Havel, *Collection Czech. Chem. Commun.*, 1984, **49**, 1974.
4. V. Kanický, J. Havel and L. Sommer, *ibid.*, 1980, **45**, 1525.
5. M. Jarosz, *Chem. Anal. (Warsaw)*, 1986, **31**, 553.
6. S. D. Hartenstein, *Anal. Chim. Acta*, 1990, **228**, 279.
7. M. Marhol, *Ion Exchangers in Chemistry and Radiochemistry*, Academia, Prague, 1975.
8. R. M. Cassidy and S. Elchuk, *Anal. Chem.*, 1982, **54**, 1558.
9. C. H. Knight, R. M. Cassidy, B. M. Recoskie and L. W. Green, *ibid.*, 1984, **56**, 474.
10. R. L. Smith and D. J. Pietrzyk, *ibid.*, 1984, **56**, 1572.
11. D. J. Barkley, M. Blanchette, R. M. Cassidy and S. Elchuk, *ibid.*, 1986, **58**, 2222.
12. A. Kerr, W. Kupferschmidt and M. Attas, *ibid.*, 1988, **60**, 2729.
13. K. S. Park, N. B. Kim, Y. S. Kim, K. Y. Lee, H. W. Choi and Y. Y. Yoon, *J. Radioanal. Nucl. Chem.* 1988, **123**, 585.
14. T. Kawamura, *Bunseki Kagaku*, 1988, **37**, 585.
15. V. Kubáň and D. B. Gladilovich, *Collection Czech. Chem. Commun.*, 1988, **53**, 1664.
16. V. Kubáň, L. Sommer and D. B. Gladilovich, *Zh. Analit. Khim.*, 1989, **44**, 292.
17. K. Eckschlager, *Chyby chemických rozborů*, SNTL, Prague, 1971.
18. T. T. Bykhovtsova and I. A. Tserkovnitskaya, *Zh. Analit. Khim.*, 1977, **32**, 745.

INTERACTION OF SERUM ALBUMIN WITH A SULPHONATED AZO DYE IN ACIDIC SOLUTION

MARIA PESAVENTO and ANTONELLA PROFUMO

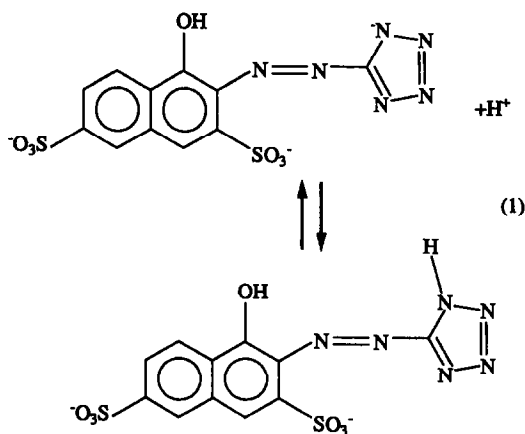
Dipartimento di Chimica Generale, Università di Pavia, Viale Taramelli 12, 27100 Pavia, Italy

(Received 1 October 1990. Revised 14 February 1991. Accepted 25 February 1991)

Summary—The uptake of the sulphonated azo dye [1-(tetrazolylazo)-2-hydroxynaphthalene 3,6-disulphonic acid, or T-azo-R] by bovine serum albumin (BSA) in the pH range 1–4 was investigated by a spectrophotometric method, based on the fact that the absorption spectra of the free and bound dye are different. The effect of increasing concentration of sodium chloride and sodium perchlorate was considered, as well as the influence of the BSA on the protonation equilibria of the dye. The Scatchard model, which has been widely used previously to describe the interaction between small substances and proteins, was not helpful in the treatment of data obtained in the acidity range considered here. Instead a phase distribution model allowed a good quantitative treatment of the experimental findings. The distribution constant of the monoprotonated T-azo-R between aqueous solution and the albumin microphase was found to be $\log K_{d(HL)}/\gamma'_{HL} = 6.3$, while the biprotonated form does not bind to BSA. As a consequence, the protonation constant of T-azo-R is decreased in the presence of BSA, particularly at low salt concentrations in aqueous solution. An equation relating the observed protonation constant to the protonation constant of the dye in solution and to the ionic strength is proposed. It has been found that the effect of salts on the uptake of T-azo-R by BSA can be explained simply by considering the variation of the activity coefficients of the ionic species involved in aqueous solution.

Among the many methods proposed for the quantitative determination of serum albumin, those based on dye binding, and spectrophotometric determination, are commonly used when large numbers of specimens are to be analyzed. The most widely utilized reagents are probably Bromocresol Green (BCG) at pH = 4,¹ or 3.8,² and HABA [2-(4-hydroxyphenylazo) benzoic acid] at pH = 3.2.³ However, no systematic investigation on the interaction between dyes and serum albumin at these acidities has been found in the literature. A study of the albumin-anionic dyes combination at these conditions should be interesting to improve the existing methods or to design new dyes with better performances.

As a first approach, the pH range 1–4 is interesting to investigate, because serum albumin is completely protonated⁴ and is in its expanded conformation.⁵ According to Pinnell and Northam⁶ the best dyes for serum albumin determination are those having protonation constants around the working pH. So the sulphonated azo dye T-azo-R [1-(tetrazolylazo)-2-hydroxynaphthalene-3,6-disulphonic acid]⁷ seemed particularly suitable for this investigation, because its second protonation reaction is as follows:



and its protonation constant is $\log K_a = 2.90$ (in 0.1M sodium perchlorate).

Therefore, this protonation takes place in the acidity range 2–4, which is that investigated in the present study. (In the text ion charges will be omitted for simplicity).

The observations by Pinnell and Northam seem to indicate that the spectrum of the free dye and that of the dye bound to albumin are better differentiated at pH values at which the protonation reaction is at equilibrium. The absorption spectra of T-azo-R bound to BSA at two different pH levels, registered against a solution of T-azo-R at the same conditions, are reported in Fig. 1. It is evident that it is

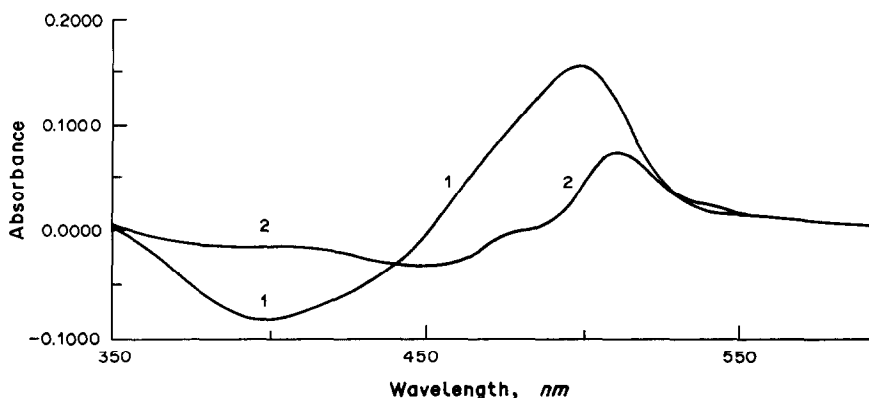


Fig. 1. Absorption spectrum of T-azo-R bound to albumin against free T-azo-R. $c_{\text{T-azo-R}} = 2.16 \times 10^{-5}$ moles/kg; $c_{\text{BSA}} = 1.54 \times 10^{-5}$ moles/kg. Curve 1: 0.0050 moles/kg HCl (pH = 2.30). Curve 2: 0.0050 moles/kg NaCl (pH = 4.10).

much higher at pH = 2.30, when reaction 1 is at equilibrium, than at pH = 4.50 when the deprotonation is complete.

In the present paper it will be shown that this is because the monoprotinated form is bound to albumin much more strongly than the biprotinated one, which shifts the protonation equilibrium (1) to the left in the presence of albumin.

Scatchard *et al.*⁸ treated the reaction of small ions with albumin as a true combination of the ligand with specific sites on the macromolecule. Since then, this model has been widely employed to describe the combination of small ions or molecules with proteins.^{9,10} However, this model doesn't seem appropriate for describing the combination of T-azo-R with BSA in the acidic solutions considered here, because the Scatchard plot $[(n/[L])e^{2.303pZL}]$ vs. n obtained here is completely different from that expected, as will be discussed later on.

Moreover, some previous observations showed that the effects of BSA on the spectrum and protonation constant of T-azo-R were similar to that of cationic surfactant micelles,¹¹ in which evidently specific interaction sites could hardly be detected. Similar behaviour was observed in the case of sulphophthaleinic dyes.¹² Based on this similarity, an attempt was made to interpret the experimental findings with a model based on the assumption that BSA can be considered as a microphase distinct from the aqueous solution in which it is dispersed. Thus, a substance X is distributed between the two phases, according to the equilibrium:



$$K_{d(X)} = \frac{a_{X'}}{a_X} = \frac{n\gamma_{X'}}{[X]\gamma_X} \quad (2)$$

where a_X and γ_X are respectively the activity

(moles/kg) and the activity coefficient of X. Primed symbols refer to species bound to albumin. Concentrations in albumin microphase are in mmoles per mmole of BSA (n).

$K_{d(X)}$ is expected to have a constant value only if the protonation and the conformation of serum albumin are constant, as it is in the pH range 1–4 investigated in the present work. The combination of T-azo-R with albumin was studied by a spectrophotometric method which is more rapid than the usual methods based on dialysis or ultracentrifugation and takes advantage of the fact that the spectra of the free and bound dye are quite different in the acidic solutions considered here, as can be seen from Figs 1 and 2.

EXPERIMENTAL

Reagents

All reagents were of analytical reagent grade. Bovine Serum Albumin (BSA) 98–99%, virtually free from fatty acids (0.005%), was obtained from Sigma Chemical Co. and used without further purification. All calculations reported for BSA are in terms of a molecular weight of 65,000. Concentrations of albumin ranging from 3.0×10^{-7} to 5.0×10^{-5} moles/kg were considered. At higher concentration, a turbidity was formed in the presence of T-azo-R. T-azo-R was synthesized as previously described⁷ and standard solutions were prepared by direct weighing of the solid. In the test solutions its concentration was in the range $1-10 \times 10^{-5}$ moles/kg.

Apparatus

A DMS 100 Varian spectrophotometer with 1-cm quartz cells was used throughout. An Orion 901 potentiometer with a combined Ross

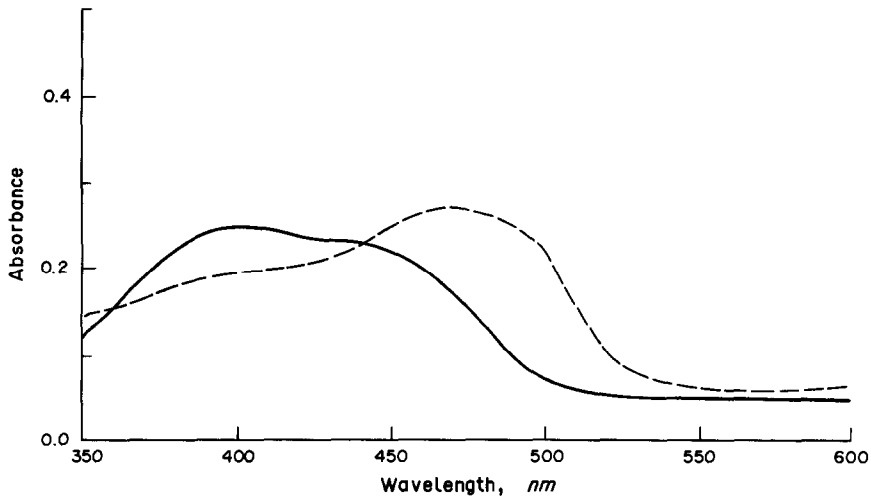


Fig. 2. Absorption spectrum of T-azo-R in HCl 0.0050 moles/kg in the presence of albumin (broken curve: $c_{\text{BSA}} = 1.54 \times 10^{-5}$ moles/kg), and in its absence (continuous line). $c_{\text{T-azo-R}} = 2.16 \times 10^{-5}$ moles/kg.

glass electrode (Orion) was used for pH measurements. The potentiometric cell was standardized by Gran's method, as described previously.¹³ The presence of BSA doesn't change the standard potential or the liquid junction potential of the cell.

Spectrophotometric method

The concentration of the bound and free ligand ($[L']$ and $[L]$ respectively, moles/kg) was calculated on the basis of the following relationships

$$A = \epsilon'_L [L'] + \epsilon_L [L] \quad (3)$$

$$c_L = [L] + [L'] \quad (4)$$

so that

$$[L'] = \frac{A - \epsilon_L c_L}{\epsilon'_L - \epsilon_L} \quad (5)$$

where

$$[L'] = [H_2L'] + [HL']$$

and

$$[L] = [H_2L] + [HL] \quad (6)$$

and A is the absorbance measured at a fixed wavelength ($\lambda = 510$ nm, where T-azo-R combined with albumin absorbs more than the free dye), ϵ'_L is the mean molar absorptivity of the dye bound to albumin ($\text{moles}^{-1} \text{ kg cm}^{-1}$), and ϵ_L is the mean molar absorptivity of the free dye ($\text{moles}^{-1} \text{ kg cm}^{-1}$).

The mean molar absorptivities of the bound and free T-azo-R were determined from the absorbance of solutions containing known amounts of T-azo-R, in the presence of an

excess of BSA, and with no BSA. They can be evaluated from the spectra reported in Fig. 2. In the considered acidity range, T-azo-R can be monoprotonated or diprotonated, depending on the acidity. The two forms absorb differently, so that the mean molar absorptivities also depend on the acidity of the solution. In 0.0050 moles/kg hydrochloric acid, an acidity at which many determinations of the present research were done, the two mean molar absorptivities are respectively $\epsilon'_L = 6.1 \times 10^3$ and $\epsilon_L = 7.5 \times 10^2$ $\text{mole}^{-1} \text{ kg cm}^{-1}$ (standard deviation: 2×10^2 $\text{mole}^{-1} \text{ kg cm}^{-1}$).

RESULTS AND DISCUSSION

Combination of T-azo-R with BSA at constant ionic strength and test of the Scatchard model

A set of experiments was performed, keeping the T-azo-R concentration constant and increasing the BSA concentration. As an example, Fig. 3, reports the absorbance, at 510 nm, of solutions with different concentrations of T-azo-R, with increasing BSA concentration at a pH of 2.5. The absorbance increases linearly with the albumin concentration, according to the Beer-Lambert law, up to $c_{\text{BSA}} < c_{\text{T-azo-R}}/30$. At T-azo-R concentration higher than about 10×10^{-5} moles/kg a turbidity was observed at the considered conditions, so that only lower concentrations can be used for spectrophotometric determinations. As a consequence, the linear range is extended only up to 2.7×10^{-6} moles/kg.

At sufficiently high albumin concentration the absorbance reaches a steady value indicating that the dye is completely bound. ϵ'_L can be

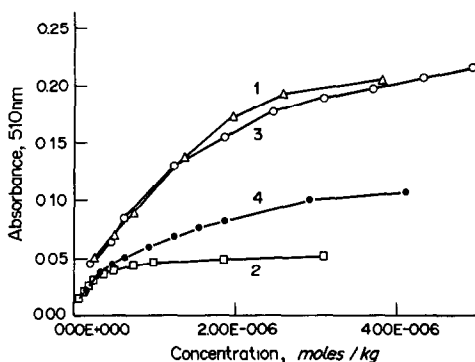


Fig. 3. Absorbance of solutions containing increasing concentration of BSA, $\lambda = 510$ nm. Curve 1: $c_{\text{T-azo-R}} = 3.36 \times 10^{-5}$ moles/kg; 0.0030 moles/kg HCl. Curve 2: $c_{\text{T-azo-R}} = 7.38 \times 10^{-6}$ moles/kg; 0.0030 moles/kg HCl. Curve 3: $c_{\text{T-azo-R}} = 3.36 \times 10^{-5}$ moles/kg; 0.0018 moles/kg H_2SO_4 . Curve 4: $c_{\text{T-azo-R}} = 1.80 \times 10^{-5}$ moles/kg; 0.0018 moles/kg H_2SO_4 .

obtained from this absorbance and ϵ_L from the absorbance at the same wavelength in the absence of BSA. Thus, $[L']$ and $[L]$ are calculated from equations (4) and (5).

At first, an attempt was made to treat these data according to the Scatchard model.⁸ It states that if there were only binding sites of one kind for T-azo-R on serum albumin, with the same intrinsic constant K_L^0 , but electrostatically influenced by other ions already linked to BSA, the observed binding coefficient K_L should not be constant as the combination proceeds, but should depend on the total charge which is actually present on the protein molecule (z_p), according to the relationship.

$$K_L = K_L^0 e^{-2 w z_p z_L} \quad (7)$$

where $z_p = 93 - 3n$, and 93 is the protonation degree of albumin at the considered pH. The term $2 w z_p z_L kT$ is the electrostatic work of

bringing the ion L with charge z_L to the surface of the protein molecule. At the considered acidity, 80% T-azo-R is in the biprotonated form H_2L , which bears a charge of -2 ($z_L = -2$). However, in the presence of albumin the deprotonation is enhanced as will be shown later. In this case, T-azo-R is almost completely deprotonated, so that $z_L = -3$.

According to Scatchard, w in a solution at I ionic strength can be evaluated at 25° according to the relationship

$$w/2.303 = 0.0517 - 0.5085 I^{1/2}/(1 + 10.663 I^{1/2})$$

From equation (7) the following relationship can be derived

$$\frac{n}{[L]} e^{2 w z_p z_L} = K_L \gamma_L N - K_L \gamma_L n \quad (8)$$

where N is the maximum number of interaction sites on serum albumin. Thus by plotting $n e^{2 w z_p z_L}/[L]$ vs. n a straight line with negative slope should be obtained. If more than one kind of interaction site were present on serum albumin, the function should be a curve with negative slope.⁹

As an example, the values obtained for n and $n e^{2 w z_p z_L}/[L]$ in one experiment are reported in Table 1. In contrast to what is expected on the basis of equation (8) when n decreases, $n e^{2 w z_p z_L}/[L]$ decreases too. This could be attributed to an incorrect evaluation of the ionic radius of albumin in the expanded form which prevails in the acidity range considered here. However, even by assuming a radius 20 times higher for albumin, the trend of the curve $n e^{2 w z_p z_L}/[L]$ vs. n is opposite to that expected on the basis of the Scatchard model. For this reason, it is impossible to make use of the Scatchard model in the present case.

Table 1. Effect of increasing concentration of BSA on the absorbance of T-azo-R at 510 nm, in 0.0050 moles/kg hydrochloric acid. T-azo-R: 1.08×10^{-5} moles/kg; $V = 25.0$ cm³. $e = e^{2 w z_p z_L}$; $w = 0.0718$; $z_p = 93 - 3n$; $z_{\text{HL}} = -3$

c_{BSA}	$A(510)$ [L']	n	$n/[L]$	$n e/[L]$
6.16×10^{-8}	0.015	7.88×10^{-7}	12.8	1.28×10^6 7.87×10^{-5}
1.23×10^{-7}	0.021	1.97×10^{-6}	16.0	1.81×10^6 6.98×10^{-3}
1.85×10^{-7}	0.026	2.95×10^{-6}	16.0	2.04×10^6 7.73×10^{-3}
2.46×10^{-7}	0.031	3.94×10^{-6}	16.0	2.33×10^6 8.92×10^{-3}
3.69×10^{-7}	0.037	5.12×10^{-6}	13.9	2.44×10^6 5.92×10^{-4}
4.92×10^{-7}	0.040	5.71×10^{-6}	11.6	2.28×10^6 2.95×10^{-5}
7.38×10^{-7}	0.044	6.49×10^{-6}	8.80	2.04×10^6 7.10×10^{-7}
9.84×10^{-7}	0.046	6.89×10^{-6}	7.00	1.79×10^6 6.07×10^{-8}
1.23×10^{-6}	0.048	7.28×10^{-6}	5.92	1.68×10^6 1.41×10^{-8}
1.85×10^{-6}	0.049	7.48×10^{-6}	4.04	1.22×10^6 9.04×10^{-10}
3.08×10^{-6}	0.052	8.07×10^{-6}	2.62	9.59×10^5 1.13×10^{-10}
6.03×10^{-6}	0.054	8.46×10^{-6}	1.40	6.00×10^5 1.47×10^{-11}

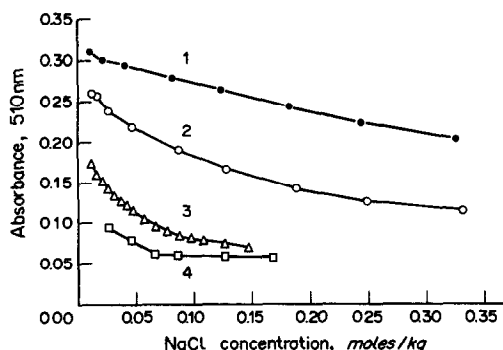


Fig. 4. Effect of increasing concentration of sodium chloride on binding of T-azo-R to BSA in 0.0050 moles/kg HCl. $c_{\text{T-azo-R}} = 5.00 \times 10^{-5}$ moles/kg. Curve 1: $c_{\text{BSA}} = 4.62 \times 10^{-5}$ moles/kg. Curve 2: $c_{\text{BSA}} = 1.54 \times 10^{-5}$ moles/kg. Curve 3: $c_{\text{BSA}} = 1.54 \times 10^{-6}$ moles/kg. Curve 4: $c_{\text{BSA}} = 3.69 \times 10^{-7}$ moles/kg.

However, it can be seen from Table 1 that the ratio $n/[L]$ is practically constant, as predicted by the phase distribution model, according to equation (2) at constant acidity and ionic strength of the solution and if γ_{HL} is constant.

Indeed the following relationships hold:

$$[L] = [\text{H}_2\text{L}] + [\text{HL}] = [\text{HL}] (1 + K_a[\text{H}])$$

$$[L'] = [\text{H}_2\text{L}'] + [\text{HL}'] = [\text{HL}'] (1 + K'_a[\text{H}])$$

$$K_{d(\text{HL})} = \frac{a_{\text{HL}'}}{a_{\text{HL}}} = \frac{n\gamma_{\text{HL}'}}{[L]\gamma_{\text{HL}}} \frac{1 + K_a[\text{H}]}{1 + K'_a[\text{H}]}$$

$$= K_{\text{dc}} \frac{1 + K_a[\text{H}]}{1 + K'_a[\text{H}]} \frac{\gamma_{\text{HL}'}}{\gamma_{\text{HL}}} \quad (9)$$

where $K_{d(\text{HL})}$ is the distribution constant of the dye in the monoprotonated form, and K_{dc} is the global distribution coefficient ($K_{\text{dc}} = n/[L]$). K_a and K'_a are the protonation constants of T-azo-

R in aqueous solution and T-azo-R bound to albumin, respectively, defined as:

$$K_a = \frac{[\text{H}_2\text{L}]}{[\text{HL}][\text{H}]} \quad (9(a))$$

$$K'_a = \frac{[\text{H}_2\text{L}']}{[\text{HL}'][\text{H}]} \quad (9(b))$$

The average value of the distribution coefficient of T-azo-R at the conditions considered here is $\log K_{\text{dc}} = 5.61$.

Influence of the salt composition of the solution

Some experiments were carried out by adding increasing concentrations of sodium chloride to solutions with different BSA and T-azo-R concentrations at constant acidity (5×10^{-3} moles/kg hydrochloric acid, equal to that investigated above).

The absorbance of the solution at $\lambda = 510$ nm was recorded. Some results are reported in Fig. 4. Increasing salt concentration causes a diminution of the absorbance at 510 nm. This is due to a partial release of T-azo-R from BSA, as demonstrated by a few dialysis experiments (Table 2). The concentration of free dye is greatly increased in 0.5 moles/kg sodium chloride.

This effect was also observed in the case of sulphophthaleinic dyes at acidities around neutrality⁹ and was interpreted as competition between anions and dyes for the same binding sites on serum albumin. The ionic strength variations were not taken into account but are, however, important and can justify the observed behaviour according to the phase distribution model.

Table 2. Dialysis of T-azo-R in the presence of BSA at 0.0050 moles/kg HCl and different sodium chloride concentration. HCl and NaCl are at the same concentration inside and outside the bag. $T = 25^\circ$. Dialysis time: 48 hr; bag: SPECTRA/POR molecular membrane; tubing: 18 mm \times 50 ft; Vol: 1.0 cm³; m.w. cut-off: 3500. Concentrations are in moles/kg

Composition of the solution							
inside the bag			outside		[L] (free)	n	log K_{dc}
c_{NaCl}	c_{BSA}	$c_{\text{T-azo-R}}$	$c_{\text{T-azo-R}}$				
0	6.15×10^{-6} (V = 10 cm ³)	5.00×10^{-5}	5.00×10^{-5} (V = 10 cm ³)	1.02×10^{-5}	6.46	6.39	
0	6.15×10^{-6} (V = 10 cm ³)	8.97×10^{-5}	5.00×10^{-5} (V = 10 cm ³)	2.16×10^{-5}	15.72	6.15	
0.50	6.15×10^{-6} (V = 15.2 cm ³)	5.00×10^{-5}	5.00×10^{-5} (V = 42 cm ³)	4.58×10^{-5}	2.60	6.30	
0.50	6.15×10^{-6} (V = 15.2 cm ³)	6.17×10^{-5}	0 (V = 42 cm ³)	1.52×10^{-5}	0.73	6.22	
0.50	6.15×10^{-6} (V = 15.2 cm ³)	1.17×10^{-4}	2.25×10^{-4} (V = 43 cm ³)	1.66×10^{-4}	5.42	6.05	

From equation (9), and by estimating the activity coefficient in the aqueous phase on the basis of the specific interaction theory,¹⁴ the following relationship is obtained

$$\log \frac{n}{[L]} = \log K_d' - \frac{0.51 z_{HL}^2 I^{1/2}}{1 + 1.5 I^{1/2}} + b(L, Na)m_{Na} \quad (10)$$

where z_{HL} is the charge of the dye (-3 in the case of the monoprotonated T-azo-R), and $K_d' = K_{d(HL)}(1 + K_a[H]) / (\gamma_{HL}(1 + K_a[H]))$ includes all the terms of equation (9) which are practically independent of the ionic strength of the aqueous solution. The term $b(L, Na)$ is the coefficient of specific interaction of the monoprotonated dye with sodium which is present at a concentration of m_{Na} (moles/kg).

The parameters of equation (10) can be estimated by a least square procedure. Good values for R^2 were obtained. The interaction coefficient is not significantly different from 0, and a mean $\log K_d'$ value of 6.10 ± 0.17 was obtained, in agreement with the value of $\log K_d' = \log K_{d(HL)} / \gamma_{HL} + \log \gamma_{HL}$ which can be calculated from the experiments reported above where the solution was 5×10^{-3} moles/kg hydrochloric acid so that $\log \gamma_L = -0.29$, and $\log K_d' = 5.90$.

The coefficient of the independent variable $I^{1/2}/(1 + I^{1/2})$ has an average value of $-5.0 (\pm 1.2)$, in fair agreement with -4.5 , corresponding to the charge (-3) of the monoprotonated species HL. It is interesting to notice that the $\log K_d'$ values obtained from the dialysis experiments, shown in Table 2, are in agreement with the values found spectrophotometrically. Thus, the effects of the increasing salt concentration can be well explained on the basis of the phase distribution model, without any

hypothesis on competition of different anions for the same binding sites.

To test the dependance of the conditional distribution constants K_d' on the acidity, an experiment was carried out in more dilute hydrochloric acid 1×10^{-3} moles/kg, by adding increasing concentrations of sodium chloride. The results are reported in Table 3. A higher value of K_d' is obtained, showing that $K_a > K_a'$. An evaluation of $K_{d(HL)} / \gamma_{HL}$ can be made by assuming that $K_d'[H] \ll 1$. A value of 5.7×10^6 is obtained at this acidity, in good agreement with the value in 0.0050 moles/kg hydrochloric acid (6.3×10^6).

According to equation (10), a different anion must have the same effect on T-azo-R binding to BSA. Some results at increasing concentrations of sodium perchlorate are reported in Table 4. The data, treated according to the phase distribution model, gave the same results as in the case of sodium chloride: $\log K_d' = 6.06$, and $0.51z_L^2 = -5.71$ ($R^2 = 0.991$). Perchlorate was chosen to test the effect of an anion having a much higher lipophilic character than chloride, hence supposedly competing with the dye more than chloride for binding to a hydrophobic environment.

Protonation of T-azo-R in presence of BSA

It is well known that macromolecular particles have an influence on the protonation equilibria of indicator dyes.⁶ The same is observed in the BSA/T-azo-R system. This point was investigated here by considering solutions with fixed concentrations of T-azo-R and BSA, at a ligand to albumin molar ratio of 3.25, and by changing the acidity by small additions of concentrated acid or base. The free proton concentration was measured with the glass elec-

Table 3. Effect of increasing concentrations of sodium chloride on binding of T-azo-R to BSA, 0.0010 moles/kg hydrochloric acid. T-azo-R: 5.00×10^{-5} moles/kg; $V = 25.0$ cm³; $c_{BSA} = 1.64 \times 10^{-5}$ moles/kg. $rad I = I^{1/2}/(1 + 1.5 I^{1/2})$

c_{NaCl}	$A(510)$ [L]	n	$rad I$	$\log n[L]$
6.00×10^{-3}	0.316 4.80×10^{-5}	3.12	0.069	6.19
1.10×10^{-2}	0.311 4.69×10^{-5}	3.05	0.091	5.99
1.62×10^{-2}	0.306 4.58×10^{-5}	2.98	0.107	5.85
2.13×10^{-2}	0.304 4.53×10^{-5}	2.95	0.120	5.80
3.14×10^{-2}	0.296 4.35×10^{-5}	2.83	0.140	5.64
4.16×10^{-2}	0.289 4.20×10^{-5}	2.73	0.156	5.53
6.19×10^{-2}	0.274 3.87×10^{-5}	2.52	0.181	5.35
8.20×10^{-2}	0.260 3.56×10^{-5}	2.31	0.200	5.21
1.02×10^{-1}	0.247 3.27×10^{-5}	2.13	0.216	5.09
1.23×10^{-1}	0.236 3.02×10^{-5}	1.96	0.230	4.99
1.63×10^{-1}	0.220 2.67×10^{-5}	1.74	0.251	4.87
3.68×10^{-1}	0.182 1.82×10^{-5}	1.18	0.318	4.57
6.15×10^{-1}	0.170 1.53×10^{-5}	0.99	0.360	4.46

Regression: $\log K_d' = 6.50(0.08)$; $0.51 z_{HL}^2 = -6.15(0.27)$; $R^2, 0.978$.

Table 4. Effect of increasing concentrations of sodium perchlorate on binding of T-azo-R to BSA. Perchloric acid 0.0050 moles/kg. T-azo-R: 5.00×10^{-5} moles/kg; $V = 25.0 \text{ cm}^3$; $c_{\text{BSA}} = 1.54 \times 10^{-6}$ moles/kg. $\text{rad } I = I^{1/2}/(1 + 1.5 I^{1/2})$

c_{NaClO_4}	$A(510)$	$[L^-]$	n	$\text{rad } I$	$\log n/[L]$
5.09×10^{-4}	0.185	2.76×10^{-5}	18.4	2.18×10^{-2}	5.91
1.02×10^{-3}	0.182	2.70×10^{-5}	18.0	3.05×10^{-2}	5.89
2.04×10^{-3}	0.175	2.57×10^{-5}	17.1	4.23×10^{-2}	5.85
4.07×10^{-3}	0.157	2.23×10^{-5}	14.9	5.82×10^{-2}	5.73
1.04×10^{-2}	0.137	1.86×10^{-5}	12.4	8.85×10^{-2}	5.60
1.68×10^{-2}	0.118	1.51×10^{-5}	10.1	1.09×10^{-1}	5.46
2.95×10^{-2}	0.089	9.63×10^{-6}	6.42	1.37×10^{-1}	5.20
8.04×10^{-2}	0.066	5.33×10^{-6}	3.55	1.99×10^{-1}	4.90
1.06×10^{-1}	0.059	4.02×10^{-6}	2.68	2.19×10^{-1}	4.77
1.57×10^{-1}	0.057	3.64×10^{-6}	2.43	2.49×10^{-1}	4.72

Regression: $\log K'_d = 6.06(0.05)$; $0.51 z_1^2 = -5.71(0.19)$; R^2 , 0.991.

trode standardized as described previously.¹³ The pH range 1–4 was studied and absorbances recorded at 510 nm (Fig. 5). Curve 1 corresponds to the deprotonation of T-azo-R in 0.1 moles/kg sodium chloride without albumin. The molar absorptivities of the species H_2L and HL at 510 nm are 4.2×10^2 and 3.9×10^3 moles⁻¹ kg cm⁻¹, respectively. In the presence of BSA and at sodium chloride concentrations lower than 0.05 moles/kg the molar absorptivity of the monoprotonated form is much higher, 7.0×10^3 moles⁻¹ kg cm⁻¹. A large effect of increasing salt

concentration is observed, which agrees with the effect reported above of inorganic salts on dye binding.

The data were treated on the basis of the following relationship:

$$\begin{aligned}
 A &= \epsilon_{\text{H}_2\text{L}'}[\text{H}_2\text{L}'] + \epsilon_{\text{HL}'}[\text{HL}'] \\
 &+ \epsilon_{\text{H}_2\text{L}}[\text{H}_2\text{L}] + \epsilon_{\text{HL}}[\text{HL}] \\
 &= \epsilon_{\text{H}_2\text{L}}([\text{H}_2\text{L}'] + [\text{H}_2\text{L}]) \\
 &+ \epsilon_{\text{HL}}([\text{HL}'] + [\text{HL}]) \quad (11)
 \end{aligned}$$

where $\epsilon_{\text{H}_2\text{L}}$ and ϵ_{HL} are the mean molar absorptivities of the free and bound dye, respectively in the biprotonated and monoprotonated form.

Thus the observed protonation constant of T-azo-R in the presence of albumin is

$$K_{\text{ao}} = \frac{([\text{H}_2\text{L}'] + [\text{H}_2\text{L}])}{([\text{HL}'] + [\text{HL}]) [\text{H}]} = \frac{(c_L \epsilon_{\text{HL}} - A)}{(A - \epsilon_{\text{H}_2\text{L}} c_L) [\text{H}]} \quad (12)$$

K_{ao} , ϵ_{HL} and $\epsilon_{\text{H}_2\text{L}}$ have been determined by a least square procedure and the results are reported in Table 5, for the solution of Fig. 5.

According to the phase distribution model, the following relationship should correlate the protonation constant observed in the presence of albumin K_{ao} with the protonation constant in aqueous solution K_a :

$$K_{\text{ao}} = K_a \frac{1 + K_{\text{d}(\text{H}_2\text{L})} \gamma_{\text{H}_2\text{L}} c_{\text{-BSA}} / \gamma_{\text{H}_2\text{L}'}}{1 + K_{\text{d}(\text{HL})} \gamma_{\text{HL}} c_{\text{BSA}} / \gamma_{\text{HL}'}} \quad (13)$$

The activity coefficients in albumin microphase were assumed to be constant and those in aqueous solution were evaluated by the specific interaction theory.¹⁴ The parameters in equation (13) can be transformed into a linear equation and their best values can be found by a multiple linear regression.

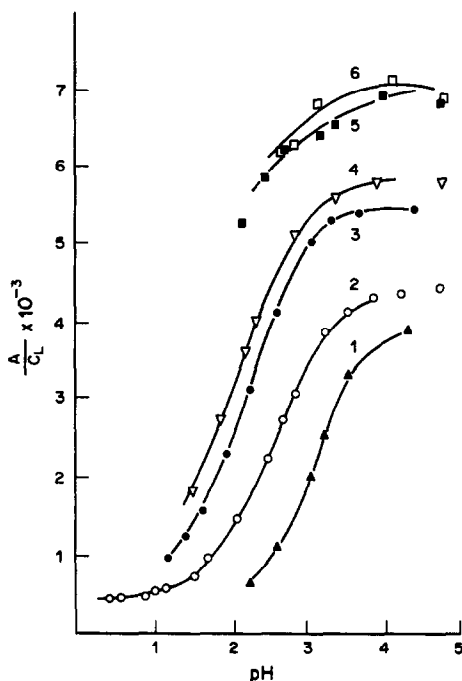


Fig. 5. Protonation of T-azo-R in aqueous solution without BSA (curve 1), and in the presence of BSA. Abscissa: pH; Ordinate: A/c_L ($\lambda = 510 \text{ nm}$). $c_{\text{T-azo-R}} = 5.00 \times 10^{-5}$ moles/kg; $c_{\text{BSA}} = 1.54 \times 10^{-5}$ moles/kg; conc. of HCl initially present. Curve 2: 0.50 moles/kg; Curve 3: 0.10 moles/kg; Curve 4: 0.050 moles/kg; Curve 5: 0.010 moles/kg; Curve 6: 0.0010 moles/kg.

Table 5. Apparent protonation constants of T-azo-R in the presence of BSA at different sodium chloride concentrations. T-azo-R: 5.00×10^{-5} moles/kg, BSA: 1.54×10^{-5} moles/kg. ϵ_{H_2L} : mean molar absorbance of the biprotonated T-azo-R; ϵ_{HL} : mean molar absorbance of the mono-protonated T-azo-R

c_{NaCl}	ϵ_{H_2L}	ϵ_{HL}	K_{a0}	n. obser.	R^2
0.01	410	7138	39	3	
0.05	208	5792	87	7	0.982
0.1	490	5636	146	8	0.999
0.5	327	4219	298	14	0.986

The following results were obtained:

number of observations = 10; $R^2 = 0.878$; $\log K_a = 2.72$; $\log K_{d(HL)}c_{BSA}/\gamma_{HL} = 1.41$, and $\log K_{d(HL)}/\gamma_{HL} = 6.22$. $K_{d(H_2L)}$ is not significantly different from 0. Thus the biprotonated form H_2L does not seem to be significantly distributed in the albumin microphase. K_a is in acceptable agreement with the value found in aqueous solution. Also $\log K_{d(HL)}/\gamma_{HL}$ agrees with the values found in the two completely independent experiments described above.

CONCLUSIONS

The uptake of T-azo-R by BSA in the pH range 1–4 cannot be described with the Scatchard model. Instead it has been demonstrated that a phase distribution model is able to describe the dye/BSA combination under different conditions. This does not require any hypothesis about the nature of the interaction of T-azo-R with albumin (for instance hydrophobic, electrostatic, at a specific site).

The proposed model seems to be useful in practice, because it describes the interaction on the basis of only one parameter, the distribution constant. It allows the prediction of the effects of the ionic strength on the uptake of the ligand by BSA [equation (10)], and the effect of serum albumin on the protonation equilibrium of

the indicator dye under different conditions [equation (13)]. An important point of the phase distribution model is that it is implicitly assumed that the global structure of albumin does not sensibly change when T-azo-R combines. This is supported by the observation that the electrokinetic potentials of albumin and of albumin in the presence of T-azo-R, at a dye to albumin molar ratio equal to 30:1 at pH = 2.3, and in 0.1 moles/kg sodium chloride are $+38(\pm 6)$ mV and $+35(\pm 2)$ mV, respectively (practically identical).

Acknowledgement—This work was financially supported by the National Research Council (CNR) of Italy.

REFERENCES

1. B. T. Doumas, W. A. Watson and H. G. Biggs, *Clin. Chim. Acta*, 1971, **31**, 87.
2. B. E. Northam and G. M. Widdowson, *Assoc. Clin. Biochem., Tech. Bull.*, 1967, No. 11, 1.
3. E. G. Porter and W. J. Waters, *J. Lab. Clin. Med.*, 1966, **67**, 660.
4. C. Tanford, S. A. Swanson and W. S. Shore, *J. Am. Chem. Soc.*, 1955, **77**, 6414.
5. J. F. Foster, in *The Plasma Proteins*, Vol. 1, F. W. Putnam (ed.), p. 194. Academic Press, New York, 1960.
6. A. E. Pinnell and B. E. Northam, *Clin. Chem.*, 1978, **24**, 80.
7. T. F. Soldi, C. B. Riolo, G. Gallotti and M. Pesavento, *Gazz. Chim. It.*, 1877, **107**, 347.
8. G. Scatchard, I. H. Scheinberg and S. H. Armstrong, Jr., *J. Am. Chem. Soc.*, 1950, **72**, 535.
9. U. Kragh-Hansen and J. V. Møller, *Biochim. Biophys. Acta*, 1973, **295**, 438.
10. U. Kragh-Hansen, *Mol. Pharmacol.*, 1988, **34**, 160.
11. M. Pesavento and A. Profumo, *Atti XVI Congresso Nazionale di Chimica, Bologna*, 9–10 October, 1988, p. 51.
12. J. V. Møller and U. Kragh-Hansen, *Biochemistry*, 1975, **14**, 2317.
13. M. Pesavento, C. Riolo, T. Soldi and R. Garzia, *Ann. Chim. (Rome)*, 1982, **72**, 217.
14. G. Biedermann, *Dahlem Workshop on the Nature of Seawater*, p. 339. Dahlem Konferenzen, Berlin, 1975.

MICRO-DETERMINATION OF WARFARIN SODIUM, NICOUMALONE AND ACEBUTOLOL HYDROCHLORIDE IN PHARMACEUTICAL PREPARATIONS

C. S. P. SASTRY,* T. THIRUPATHI RAO, A. SAILAJA and J. VENKATESWARA RAO

Foods and Drugs Laboratories, School of Chemistry, Andhra University, Visakhapatnam 530 003, India

(Received 19 February 1991. Revised 15 April 1991. Accepted 25 April 1991)

Summary—A simple, selective and sensitive spectrophotometric method has been developed for the determination of microgram quantities of warfarin sodium (WS), nicoumalone (NIC) and acebutolol hydrochloride (ACBH), either in pure form or in pharmaceutical preparations. This method is based on the haloform reaction with a known and excess of standard iodine solution under alkaline conditions. The excess of iodine is determined at pH 3.0 with metol—INH. The absorbance of the resulting *p*-*N*-methylbenzoquinonemonoimine—INH charge-transfer complex is measured at 620 nm.

Coumarin derivatives such as warfarin sodium (WS) and nicoumalone (NIC) are extensively used as anticoagulants and the butanamide derivative acebutolol hydrochloride (ACBH) is widely used as an anti-arrhythmic agent. They have been officially determined by U.V. spectrophotometry.^{1,2} Acebutolol hydrochloride is not yet official in any pharmacopoeia. A study of the literature revealed that visible spectrophotometric methods for their determination are scarce. There are none for WS, one for NIC³ and three for ACBH.⁴⁻⁶ Even these methods require some preliminary treatment (reduction or hydrolysis) and are time consuming, tedious and have low sensitive. The methylketone group existing in all three drugs has not been exploited so far. It is well known that methylketones react with iodine under alkaline conditions leading to the formation of iodoform.⁷ Sastry *et al.*^{8,9} suggested a coloured charge-transfer complex (λ_{\max} 620–630 nm) formation at pH 3.0 involving two molecules of *p*-*N*-methylbenzoquinonemonoimine (formed *in situ* from metol and iodine) and one molecule of isonicotinic acid hydrazide (INH). The drug (WS, NIC or ACBH) is treated with standard iodine in excess under alkaline conditions. The consumed iodine corresponding to the drug content in the sample is obtained by estimating the excess of iodine spectrophotometrically at pH 3.0 with metol and INH as the chromogenic agent.

EXPERIMENTAL

Apparatus

A Systronics model 106 digital spectrophotometer with 1-cm matched glass cells was used for absorbance measurements. An Elico model LI-120 digital pH meter was used for pH measurements.

Reagents

All the reagents were of analytical or pharmacopoeial grade and all solutions were freshly prepared in doubly distilled water.

Aqueous solutions of iodine [0.0035*M* I₂ (E. Merck) in 0.05*M* potassium iodide (Loba)], metol (BDH, 0.3%), INH (Wilson, 0.15%), sodium hydroxide (E. Merck, 1*M*), hydrochloric acid (Sarabhai, 1*M*) and potassium hydrogen phthalate—hydrochloric acid buffer (pH 3.0)¹⁰ were prepared.

Standard drug solutions

Standard stock solutions of WS and ACBH were prepared by dissolving 20 mg of drug in 100 ml of distilled water. A stock solution of NIC was prepared by dissolving 20 mg of drug in 30 ml of 0.01*M* sodium hydroxide and diluting to 100 ml with distilled water. The working standard solutions were prepared by suitable dilution of the stock solution with distilled water.

Procedure for bulk samples

Aliquots of standard solution of WS or NIC (0.25–3.0 ml; 100 μ g/ml) or ACBH (0.25–2.0 ml;

*Author for correspondence.

200 $\mu\text{g/ml}$) were transferred into a series of 25-ml graduated test tubes. Then 1.5 ml of iodine and 1 ml of sodium hydroxide were added and the volume was adjusted to 6 ml with distilled water. The mixture was set aside for a designated period at 25–30° (15 min for WS or NIC and 60 min for ACBH) or 45–50° (2 min for WS or NIC and 5 min for ACBH) for completion of reaction. Later 1 ml of hydrochloric acid, 15 ml of pH 3.0 buffer and 2.0 ml of metol solution were added. After 2 min, 1 ml of INH solution was added. The absorbances were measured at 620 nm after 5 min and before 20 min against distilled water. In the same way a corresponding reference solution was prepared simultaneously, containing the sample, but with 1.0 ml of distilled water instead of 1.0 ml of sodium hydroxide solution. The absorbance of the sample solution was subtracted from that of the reference. The difference in absorbance corresponds to the iodine consumed by the drug. The amount of drug present in each pharmaceutical preparation was computed from the corresponding calibration graph or regression equation.

Analysis of pharmaceutical preparations

Tablet powder equivalent to 10 mg of drug was treated with 20 ml of water (ACBH) or 0.01M sodium hydroxide (WS or NIC) and filtered. The filtrate was neutralised with alkali (ACBH) or acid (WS or NIC) and extracted with 3 \times 10-ml portions of chloroform. The combined chloroform layers were extracted with 3 \times 10-ml portions of 0.01M hydrochloric acid (ACBH) or sodium hydroxide (WS or NIC) and diluted to 100 ml with distilled water. These solutions were analysed as described under the procedure for bulk samples.

RESULTS AND DISCUSSION

Since the drugs under investigation have a methyl ketone group, the suitability of the haloform reaction has been examined. In the proposed method, the iodine consumed during the haloform reaction is indirectly determined spectrophotometrically with metol and INH. The experimental conditions have been established through control experiments. The Beer's law limits, molar absorptivity, regression equation, correlation coefficient obtained for each drug by a linear least-squares treatment of the results are given in Table 1. The precision of the method was tested by measuring six replicate samples of the drug within Beer's law limits (2 ml, 100 $\mu\text{g/ml}$ for WS and NIC; 1.5 ml, 200 $\mu\text{g/ml}$ for ACBH). The relative standard deviation and range of error at 95% confidence level are also given in Table 1.

Commercial tablets containing each drug were successfully analysed by the proposed method. The values obtained by the proposed method and reference (WS or NIC)² or reported (ACBH)⁴ method for pharmaceutical preparations are listed in Table 2. In the *t*- and *F* tests, there were no significant differences between the calculated and theoretical values (95% confidence limit) for comparison of the proposed and reference methods, indicating their similar accuracy and precision (Table 2). Recovery experiments indicated the absence of interference from the active ingredient hydrochlorothiazide.

The excipients such as magnesium stearate, talc, gumacacia and sodium phosphate do not interfere. Carbohydrates such as glucose, lactose and starch which are usually present in combination with the drug in pharmaceutical preparations interfere with the determinations of the latter by the proposed procedure. This interference was avoided by extracting the drug

Table 1. Optical characteristics, precision and accuracy

Parameters	WS	NIC	ACBH
Beer's law limits ($\mu\text{g/ml}$)	1–12	1–12	2–16
Molar absorptivity (litre mole ⁻¹ cm ⁻¹)	1.367×10^4	1.70×10^4	1.268×10^4
Sandell's sensitivity ($\mu\text{g/cm}^2/0.001$ absorbance unit)	0.0243	0.0208	0.0294
Regression equation (<i>Y</i>) [*]			
Slope (<i>n</i>)	0.04074	0.04778	0.03383
Intercept (<i>m</i>)	0.003584	0.000992	0.000789
Correlation coefficient (<i>r</i>)	0.9999	0.9999	0.9999
Relative standard deviation† (%)	0.74	0.50	0.33
Range of error† (%; 95% confidence limit)	± 0.80	± 0.53	± 0.36

^{*} $Y = m + nC$ where *C* is the concentration ($\mu\text{g/ml}$).

†Six replicate samples.

Table 2. Determination of tablets by the proposed and official methods

Drug	Nominal content, mg/tablet	Proposed method			Found by Reference† method, %*
		Found, %*	Added, mg/tablet	Recovery, %*	
WS-5 mg, TY	5	99.6 ± 0.54	5	100.3 ± 0.74	99.5 ± 0.33
NIC-1 mg, SYFCF	1	98.3 ± 0.98	5	100.6 ± 0.49	98.8 ± 0.64
NIC-4 mg	4	100.2 ± 0.60	5	99.6 ± 0.53	99.2 ± 0.74
ACBH-200 mg	200	99.4 ± 0.47	50	99.9 ± 0.40	99.3 ± 0.43
ACBH-200 mg; HCT-12.5 mg	200	99.7 ± 0.54	50	99.3 ± 0.65	100.2 ± 0.52
ACBH-400 mg	400	99.6 ± 0.45	50	99.7 ± 0.49	100.1 ± 0.72

*Average ± standard deviation of 6 determinations.

†B.P. method for WS² and NIC², reported method for ACBH.⁴

TY = Tartrazine Yellow; SYFCF: Sunset yellow FCF.

into chloroform from aqueous solution either in slightly acid (WS or NIC) or alkaline (ACBH) conditions. Further, the potential interference of other chloroform soluble reducing compounds, if any, in the determination of the drugs mentioned can be avoided by subtracting the amount of iodine consumed by the drug under neutral or acidic conditions from that consumed under alkaline conditions.

The proposed method is simpler, more accurate and highly sensitive when compared to reported visible spectrophotometric methods for the assay of WS, NIC or ACBH in bulk samples and its dosage forms. It is selective to compounds containing a methyl ketone portion in their molecules.

Acknowledgements—The authors gratefully acknowledge the gift samples from Unichem Laboratories (India), Sarabhai Chemicals and May & Baker (India) Ltd. and also to the authorities of Andhra University for providing research facilities.

REFERENCES

1. *Pharmacopoeia of India*, p. 334. Ministry of Health and Family Welfare, Govt. of India, New Delhi, 1985.
2. *British Pharmacopoeia*, Vol. II, pp. 974, 1017. Her Majesty's Stationary Office, London, 1988.
3. H. Auterhoff and A. S. Beinroth, *Arch. Pharm.*, 1980, **313**, 807; *Chem. Abstr.*, 1981, **94**, 36429b.
4. Gonul Hakyemez, *Acta. Pharm. Turc.*, 1988, **30**, 153; *Chem. Abstr.*, 1989, **110**, 219192n.
5. M. A. H. Elsayed, M. Barary, M. A. Salam and S. Mohamed, *Anal. Lett.*, 1989, **22**, 1665; *Chem. Abstr.*, 1989, **111**, 160396x.
6. G. Ramana Rao, G. Rajagopalakini, A. B. Avadhanulu and D. K. Vatsa, *East. Pharm.*, 1990, **33**, 133; *Chem. Abstr.*, 1990, **113**, 218365w.
7. C. L. Chakrabarti, in *Oxidation in Organic Chemistry*, Trahanovsky, Pt. C., pp. 343–370. Academic Press, New York, 1978.
8. C. S. P. Sastry, B. S. Reddy and B. G. Rao, *Indian J. Pharm. Sci.*, 1981, **43**, 118.
9. *Idem*, *Indian Drugs*, 1984, **21**, 145; *Chem. Abstr.*, 1984, **101**, 43684x.
10. J. Lurie, *Handbook of Analytical Chemistry*, p. 253. Mir, Moscow, 1975.

UPTAKE OF LEAD AND ITS INFLUENCE IN THE ALGA *SELENASTRUM CAPRICORNUTUM* PRINTZ

M. L. S. SIMÕES GONÇALVES and M. F. C. VILHENA

Centro de Química Estrutural, Complexo I, Instituto Superior Técnico, Av. Rovisco Pais,
1096 Lisboa Codex, Portugal

J. M. FERNANDES SOLLIS and J. M. CASTRO ROMERO

Escuela Universitaria Politecnica, Carrera de Serantes Arreiros, 15605 Ferrol, La Coruña, Spain

M. A. SAMPAYO

Instituto Nacional de Investigação das Pescas, Av. Brasília, 1400 Lisboa, Portugal

(Received 26 November 1990. Revised 18 March 1991. Accepted 9 April 1991)

Summary—The influence of nutrient level, hours of light and the flux of air by volume of solution on uptake of lead has been examined from batch growth experiments carried out with the alga *Selenastrum capricornutum* Printz. The organic matter released by the alga has been characterized in terms of absorbance at 285 nm, dissolved organic carbon and maximum intensity of fluorescence at the excitation peak. The lability of lead complexes formed with the alga exudates has been investigated in terms of differential pulse anodic stripping voltammetry (DPASV). It has been noticed that lead inhibits the division of the cells which become bigger in size but with less pigment per cell.

The unicellular green alga *Selenastrum capricornutum* Printz, a chlorophyceas of the order of chlorococcales, has been used because it is a non-mobile, quite resistant species, which allows easy enumeration in the tests. Although the behaviour of the algae in laboratory cultures can be slightly different from that of the natural phytoplankton,¹ cultures normally serve as good models. *Selenastrum capricornutum* has been chosen because it is considered by the U.S. Environmental Agency to be a standard for assaying algae growth potential in natural water samples.

The absorption of heavy metals by unicellular alga is of great importance because they are a primary link in food chains contaminating the organisms that depend directly or indirectly on them, and also are useful in terms of treatment of polluted water.

Following our work about the toxicity of cadmium to the alga *Selenastrum capricornutum* Printz² a study has been undertaken on the influence of nutrients, light and flux of air by volume of solution on the toxicity of lead at different levels. The effect on the growth rate, percentage of pigments and uptake of lead has been analysed.

In order to have a better insight into the type of organics released by the alga at different

experimental conditions, dissolved organic carbon (DOC), absorbance at 285 nm and maximum intensity of fluorescence at the excitation peak (F) have been determined and compared with those obtained in natural freshwaters.^{3,4}

The lability of formation of lead complexes with the exudates in terms of differential pulse anodic stripping voltammetry (DPASV) for different conditions has also been analysed. The results have been interpreted in terms of a possible mechanism to decrease toxicity; this type of mechanism has already been proposed by Williams.⁵

EXPERIMENTAL

Chemicals and solutions

The reagents used were of analytical grade and the content of heavy metals was tested by differential pulse anodic stripping voltammetry (DPASV) and found to be negligible. The standard solution of lead nitrate was prepared from Merck p.a. salt and checked with a standard solution of EDTA.

The distilled and demineralized water used had conductivity values $\leq 0.1 \mu\text{sec}$. In the voltammetric experiments the pH was adjusted with acetate buffer to pH between 4 and 5.

Procedure

The alga *Selenastrum Capricornutum* was isolated from fish ponds at Azambuja, Portugal. The stock monoculture for the experiment is maintained at "Instituto Nacional de Investigação das Pescas". (Fisheries Institute), according to our previous paper.² The average cellular volume was determined by measuring twenty cells from each experiment and considering them to have the form of two cones.

For the biological cultures, flasks of pyrex were used with distilled and demineralized water with concentrations of essential nutrients of 26.5 ppm potassium nitrate (3.67 ppm N) and 2.65 ppm sodium dihydrogen phosphate ($\text{NaH}_2\text{PO}_4 \cdot \text{H}_2\text{O}$) (0.60 ppm P) for the cultures with "more nutrients" and with 5.65 ppm potassium nitrate (0.78 ppm N) and 0.56 ppm $\text{NaH}_2\text{PO}_4 \cdot \text{H}_2\text{O}$ (0.13 ppm P) for those with "less nutrients".

The concentration of iron(III) was always $\sim 10^{-6}M$ and pH ~ 6 . The flasks with the medium were sterilized at 125° for 30 min before inoculation with the alga from a stock culture containing a final value of $\sim 8 \times 10^9$ cells/l. The air bubbled through the flasks was previously passed through activated charcoal. Lead was added two days before inoculation of the algae. Cultures were incubated in a Lab-Line chamber with days and nights simulated. During daytime the temperature was 20° and at night 15° . In the set of experiments with "more light" there were 11 hours of daylight and for those with "less light" the cells were subjected to 8 hours of daylight. The growth curves (number of cells per litre of solution *vs.* time) were determined from counts of cells under the microscope in Burkler Chamber Resistance L/W, Tiefe 0.100 mm, 0.0025/0.04 mm². Aliquots for counting were sampled at intervals of one day until the stationary phase was obtained, generally within 7–8 days.

All the samples of the solution of the growth media were passed through a $0.45\text{-}\mu\text{m}$ filter. For determination of dissolved organic carbon (DOC), absorbance at 285 nm (A_{285}), maximum intensity of fluorescence at maximum excitation of 340 nm (F) (calibrated at 100% for a concentration of 0.2 mg/l. salicylic acid solution according to Buffle and co-workers^{3,4}) and lead concentration without decomposition of the organic matter by DPASV, the samples were kept in the refrigerator at $\sim 4^\circ$ between 1 and 5 days. For the determination of the pigments the pro-

cedure indicated by Simões Gonçalves *et al.*² was followed.

Instruments

The voltammetric experiments were done with a PAR 174 A polarograph under potentiostatic control, with three electrodes: hanging mercury drop electrode, platinum electrode and saturated calomel electrode. A deposition potential of -0.5 V has been used.

The spectrophotometric experiments were done in a Lambda 5 Perkin-Elmer spectrophotometer. The determination of molecular fluorescence was performed with a Perkin-Elmer MPF-3 fluorimeter with a xenon lamp. DOC was determined with a Dohrmann carbon analyser DC-85 A.

The whole procedure was similar to that of our previous work.²

RESULTS AND DISCUSSION

From Fig. 1 it can be seen that the growth curves of the uncontaminated cells are not significantly influenced by the number of hours of exposure to light between 11 and 8 hr (curves B and D).

However, from curves A and C it is apparent that in the presence of a concentration of lead

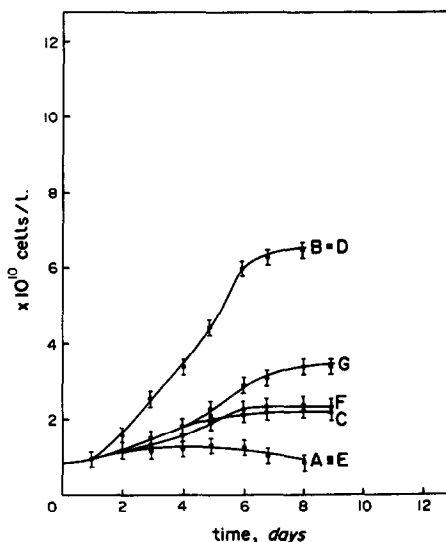


Fig. 1. Growing curves of the alga *Selenastrum capricornutum* with time. Curves B, D without lead with more nutrients and more or less light. Curve G—with lead $3 \times 10^{-8}M$, more light and less nutrients. Curve F— $1 \times 10^{-6}M$ lead, more light and less nutrients. Curve C— $9 \times 10^{-7}M$ lead, more light and more nutrients. Curve A—lead $1 \times 10^{-6}M$, more nutrients, less light. Curve E—lead $2.5 \times 10^{-6}M$, more nutrients, more light. The flux of air by volume of solution was always 1.9×10^{-3} /sec. For more details see Experimental.

of $\sim 10^{-6}M$ the light has influence, the number of cells per litre in the stationary phase being significantly smaller when there is a shorter time of exposure to light. In this situation the increase of lead from 1×10^{-6} to $2.5 \times 10^{-6}M$ in the cultures with 11 hr of exposure to light (by day), causes an effect similar to that which is caused by the decrease of hours of light (by day) from 11 to 8 hr for lead concentrations of $1 \times 10^{-6}M$.

Experiments with 11 hours of light by day and "less nutrients" have also been done and it can be seen from curve G that even with a small concentration of lead ($2.7 \times 10^{-8}M$) the growing curve decreases significantly, which may indicate that for cells not too much affected, or even without lead, the decrease of the concentration of the nutrients from 3.67 ppm N and 0.60 ppm P to 0.78 ppm N and 0.13 ppm P has more influence than the reduction of hours of light (by day) from 11 to 8 hr.

However this effect is not so clear in the presence of $1 \times 10^{-6}M$ lead (curves F and C).

Figure 2 shows the influence of the flux of air (Q) divided by the volume of the culture (V) on the growing curve of the cells. In fact, it can be seen for both cultures, not contaminated (curve A) and contaminated with $\sim 2 \times 10^{-6}M$ (curve B), that after attaining the plateau a new exponential phase can occur after an increase of the ratio Q/V and the response is not instantaneous. As the solution is always saturated with oxygen

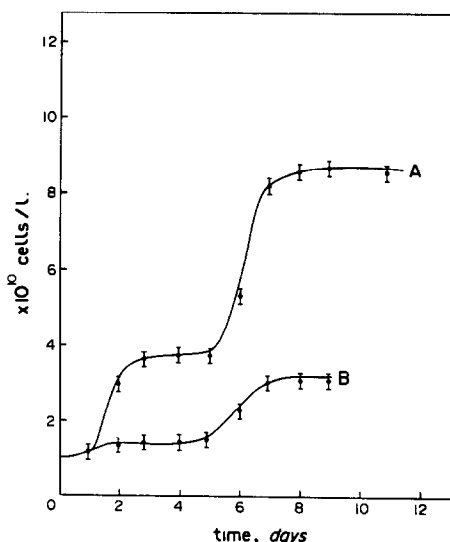


Fig. 2. Influence of the ratio of the flux of air by volume of solution in the growing curve of *Selenastrum capricornutum*. Curve A without lead, "more nutrients" and "more light". Curve B $2 \times 10^{-6}M$ lead, "more nutrients" and "more light". Q/V changed on the 3rd day from $2.5 \times 10^{-3}/\text{sec}$ to $3.5 \times 10^{-3}/\text{sec}$. For more details see Experimental.

Table 1. Influence of nutrients, lead concentration, light and the ratio of flux of the air by the volume Q/V in the growth rate of the alga *Selenastrum capricornutum* ($\ln N_{\text{cel}} = a + \mu t$)

Experimental conditions	C_{Pb}	$\mu \text{ hr}^{-1}$
more nutrients more or less light $Q/V = 1.9 \times 10^{-3}/\text{sec}$	—	$(12 \pm 1) \times 10^{-3}$
more nutrients less light $Q/V = 1.9 \times 10^{-3}/\text{sec}$	1×10^{-6}	$(3.8 \pm 0.5) \times 10^{-3}$
more nutrients more light $Q/V = 1.9 \times 10^{-3}/\text{sec}$	1×10^{-6}	$(8 \pm 1) \times 10^{-3}$
more nutrients more light $Q/V = 3.2 \times 10^{-3}/\text{sec}$	1×10^{-6}	$(14 \pm 1) \times 10^{-3}$

and carbon dioxide from the air, this is probably due to the fact that highly stirred cells are more exposed to light and nutrients. In fact CO_2 is generally not a limiting step in well aerated cultures according to Goldman *et al.*⁶

If we linearize the exponential growth phase in the form $\ln N = a + \mu t$, it can be seen from Table 1 that for the cells contaminated with lead $\sim 1 \times 10^{-6}M$ the ratio Q/V induces a change of the rate constant μ from 8×10^{-3} to $14 \times 10^{-3} \text{ hr}^{-1}$. For the smaller value of Q/V the decrease of hours of light by day from 11 hr to 8 hr leads to a change of μ from $8 \times 10^{-3} \text{ hr}^{-1}$. The increase of Q/V causes a significant increase in μ , even in the presence of lead.

Table 2 summarizes the total values of lead in the alga and in the water together with the labile lead in terms of DPASV, *i.e.*, lead determined directly in samples without the destruction of organic matter (complexes dissociated within a time scale of a few milliseconds⁷). From this table it can be seen that for the experimental conditions of "more nutrients", "more light" and flux of air by volume of solution $Q/V = 3.2 \times 10^{-3} \text{ sec}^{-1}$, the percentage of labile lead is about 70% for the concentration of lead $8 \times 10^{-7}M$ and about 80% for $C_{\text{Pb}} = 2.5 \times 10^{-6}M$ from the beginning until the last day of the experiment (9th day). This means that in the presence of less lead the cation is complexed with the exudates in the form of more inert complexes in terms of DPASV. These species can be physically (due to the size of the molecule) and chemically inert. So in an environment with less lead the alga may have the possibility of releasing organics that can act as a protection.

This has been checked from the results of the last day of the experiment (last column of

Table 2. Influence of the nutrients, light, concentration of lead and the ratio of flux of air by the volume (Q/V) in the uptake of lead by the alga *Selenastrum capricornutum* and lead speciation in the medium

Experimental conditions	3rd day			4th day			7th day			9th day			
	C _{Pb} ^{total}	Pb _{water}	Pb _{lab}	Pb _{alga}	Pb _{water}	Pb _{lab}	Pb _{alga}	Pb _{water}	Pb _{lab}	Pb _{alga}	Pb _{water}	Pb _{lab}	Pb _{alga}
more light more nutrients Q/V = 1.9 × 10 ⁻³ sec ⁻¹	9 × 10 ⁻⁷							1.47 × 10 ⁻⁷	1.40 × 10 ⁻⁷ 95%	7.46 × 10 ⁻⁷ 83%			
less light more nutrients Q/V = 1.9 × 10 ⁻³ sec ⁻¹	1 × 10 ⁻⁶							4.2 × 10 ⁻⁷	4.0 × 10 ⁻⁷ 95%	0.84 × 10 ⁻⁶ 84%			
more light more nutrients Q/V = 3.2 × 10 ⁻³ sec ⁻¹	8 × 10 ⁻⁷				3.7 × 10 ⁻⁷	2.51 × 10 ⁻⁷ 68%		2.34 × 10 ⁻⁷	1.66 × 10 ⁻⁷ 71%	5.59 × 10 ⁻⁷ 70%			
more light more nutrients Q/V = 3.2 × 10 ⁻³ sec ⁻¹	2.5 × 10 ⁻⁶	4.33 × 10 ⁻⁷	3.22 × 10 ⁻⁷ 74%	1.5 × 10 ⁻⁶ 60%	3.16 × 10 ⁻⁷	2.30 × 10 ⁻⁷ 73%		3.63 × 10 ⁻⁷	3.23 × 10 ⁻⁷ 89%	1.93 × 10 ⁻⁶ 77%			
more light less nutrients Q/V = 4.7 × 10 ⁻³ sec ⁻¹	1 × 10 ⁻⁶	2.2 × 10 ⁻⁷	1.6 × 10 ⁻⁷ 73%	0.8 × 10 ⁻⁶ 80%	3.65 × 10 ⁻⁷	2.2 × 10 ⁻⁷ 60%		2.86 × 10 ⁻⁷	1.9 × 10 ⁻⁷ 66%	0.8 × 10 ⁻⁶ 80%			

Table 2) where it can be seen that for the same experimental conditions the percentage of uptake of lead by the cells increases with the level of contamination.

In the experiment with "less nutrients" and higher flux of air by volume $Q/V = 4.7 \text{ sec}^{-1}$ with $C_{Pb} = 10^{-6} M$ the percentage of labile lead between the first and the 9th day is about 70%, which means that the level of nutrients and the charge of Q/V probably compensate each other in terms of a detoxification mechanism, which is checked by the percentage of lead uptake by the alga.

For the concentration of lead $\sim 10^{-6} M$, "more nutrients" and "more or less light" but with a smaller flux of air by volume $Q/V = 1.9 \times 10^{-3} / \text{sec}$ it can be seen that on the last day $\%Pb_{lab} = 95\%$ for both cases. So this probably means that the mechanism of detoxification is less efficient in this case when the value Q/V is smaller. The protection of algae by organics has already been noticed in experiments with the alga *Selenastrum capricornutum* with natural waters contaminated with heavy metals, where it is apparent that the sensitivity of the organism increases with the dilution of the growth medium with distilled water.⁸

We have already noticed in similar experiments with cadmium that the alga *Selenastrum capricornutum* takes more heavy metal and releases a higher percentage of organics forming inert complexes when in more adequate conditions of nutrients, light and temperature.²

In Fig. 3 the evolution of total lead in the culture medium divided by the number of cells *vs.* time is presented for experiments with different concentrations of nutrients, lead and flux of air by volume of solution. From these plots it can be seen that the evolution of the curves is of the same type, the concentration of lead by cell in the medium decreases exponentially with time. It can also be noticed that for the same order of contamination of lead the effect of the decrease of nutrients from 3.67 ppm N and 0.66 ppm P to 0.78 ppm N and 0.13 ppm P is similar to the decrease of Q/V from $4.7 \times 10^{-3} \text{ sec}^{-1}$ to $3.2 \times 10^{-3} \text{ sec}^{-1}$.

The peaks obtained in DPASV generally have potentials that are slightly more negative in the presence of organics than in their absence with a positive shift during the addition of lead. This probably means that the complexes are labile (in terms of formation) within the time scale of the technique.

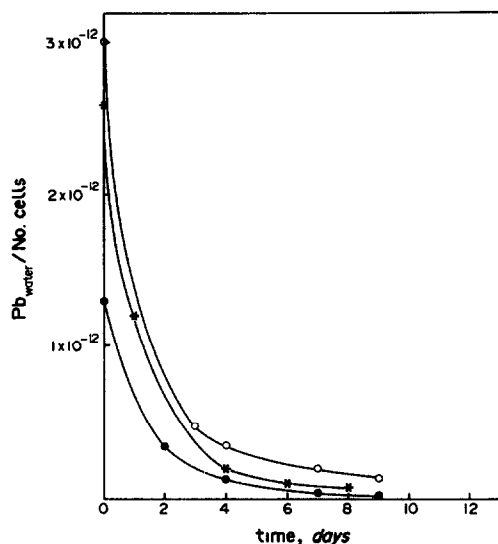


Fig. 3. Plot of the concentration of lead dissolved in the water versus time. ●—experiments with "more nutrients", "more light", $C_{Pb} = 8 \times 10^{-7} M$, $Q/V = 1.9 \times 10^{-3}/sec$. ○—experiments with more nutrients, more light, $C_{Pb} = 2.5 \times 10^{-6} M$, $Q/V = 3.2 \times 10^{-3}/sec$. *—experiments with less nutrients, more light, $C_{Pb} = 1 \times 10^{-6} M$, $Q/V = 4.7 \times 10^{-3}/sec^{-1}$. For more details see Experimental.

It was checked that the peak current (i_p) was proportional to the deposition time between 1 and 15 min, indicating that there was no distortion of the peak due to possible surface effects.⁹

For all experiments it was noticed that both chlorophyll *a* and *b* as well as vegetal carotenoids decrease with the increase in lead concentration on the last day of the experiment (8th–9th day).

On the other hand from Fig. 4 it can be seen that the concentration of pigments divided by the number of cells decreases with the level of lead in the alga, which means that lead accumulated in each cell influences the level of pigments existing in each unit. Once more it can be noticed that the effect of the decrease of nutrients from 3.67 ppm N and 0.60 ppm P to 0.78 ppm N and 0.13 ppm P was compensated by the increase of the value of Q/V from $3.2 \times 10^{-3} sec^{-1}$ to $4.7 \times 10^{-3} sec^{-1}$.

From the results obtained with the experiments with cadmium,² it is also apparent that a decrease of 1/3 of nutrients is roughly compensated (in terms of pigments in the cells) by an increase of 6° of temperature and 4 hr of light.

From the experiments with the highest value of Q/V ($4.7 \times 10^{-3} sec^{-1}$) and in the presence of lead (conc. $\sim 10^{-6}$), it was very clear that the cells, although small in number, had a much higher volume ($V = 31.68 \mu m^3$) than those in

the absence of lead ($V = 19.95 \mu m^3$) (as can be seen in the photograph in Fig. 5). So, in fact, this heavy metal inhibits the division of the cells but increases their size, as already noticed by Christensen *et al.*¹⁰ However, the level of pigments per cell decreases in the presence of lead, which probably means that although bigger, the cells are not so healthy.

In Table 3 the influence of nutrients, light, concentration of lead in the contaminated medium and flux of air by volume of solution has been analysed in terms of DOC, intensity of fluorescence at 400–440 nm at the excitation maximum of 340 nm and intensity of absorbance at 285 nm. This has been done to give a better insight into the organics released by the alga contaminated or not with lead and to compare with the values obtained in natural waters.^{3,4}

From this table it is apparent that the DOC is about ~ 20 mg/l. and the effect of the change of concentration of lead, Q/V , nutrients or number of hours of light is not clear.

The values of A_{285}/DOC and F/DOC are always within 1–2, of the same order as for cadmium,² and as expected, since the concentration of benzenecarboxylic and phenolic compounds for the same DOC is generally smaller

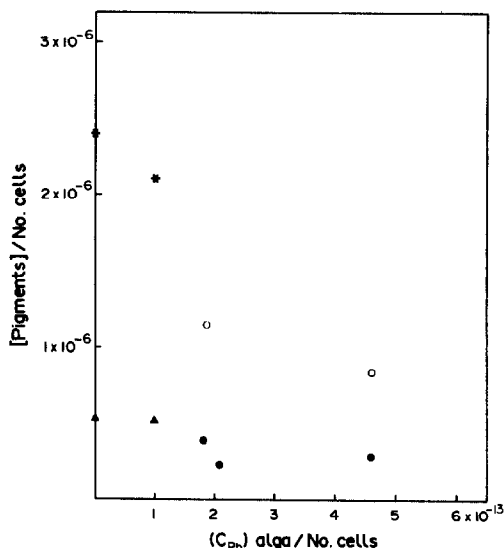


Fig. 4. Plot of chlorophyll *a* and vegetal carotenoids divided by the number of cells vs. the concentration of lead in the alga divided by the number of cells. *—Vegetal carotenoids in experiments with more nutrients, more light and $Q/V = 3.2 \times 10^{-3} s^{-1}$. ○—Vegetal carotenoids in experiments with less nutrients, more light and $Q/V = 4.7 \times 10^{-3} s^{-1}$. ▲—Chlorophyll *a* in experiments with more nutrients, more light and $Q/V = 3.2 \times 10^{-3} s^{-1}$. ●—Chlorophyll *a* in experiments with less nutrients, more light and $Q/V = 4.7 \times 10^{-3} s^{-1}$. For more details see Experimental.

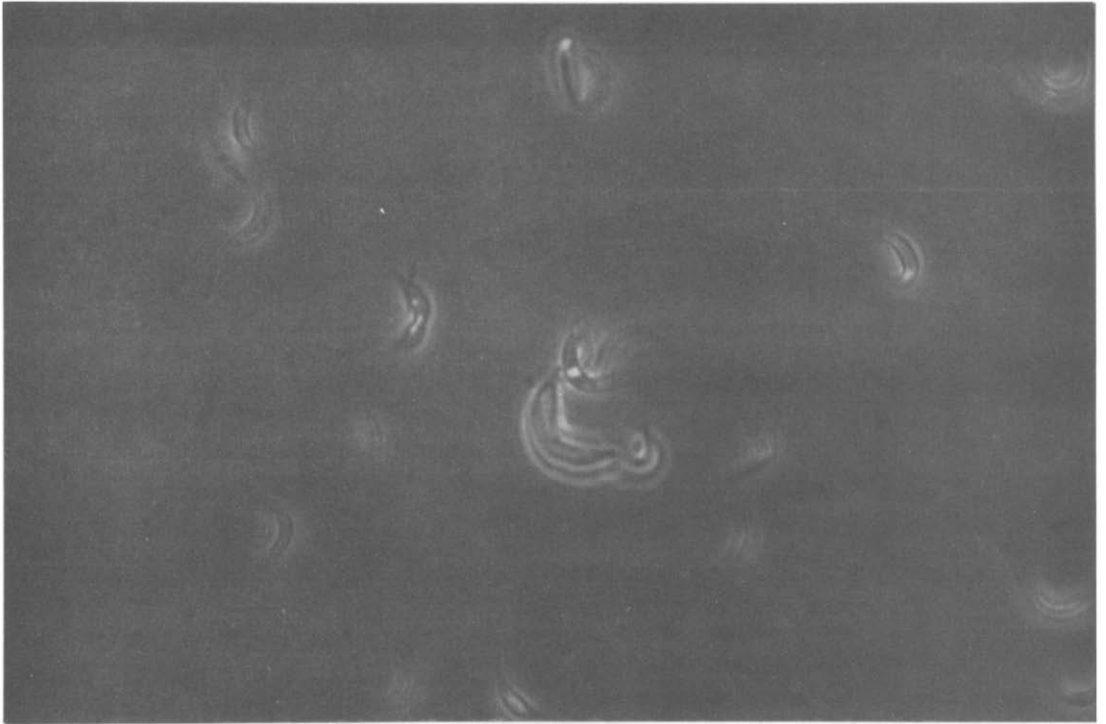


Fig. 5(a)

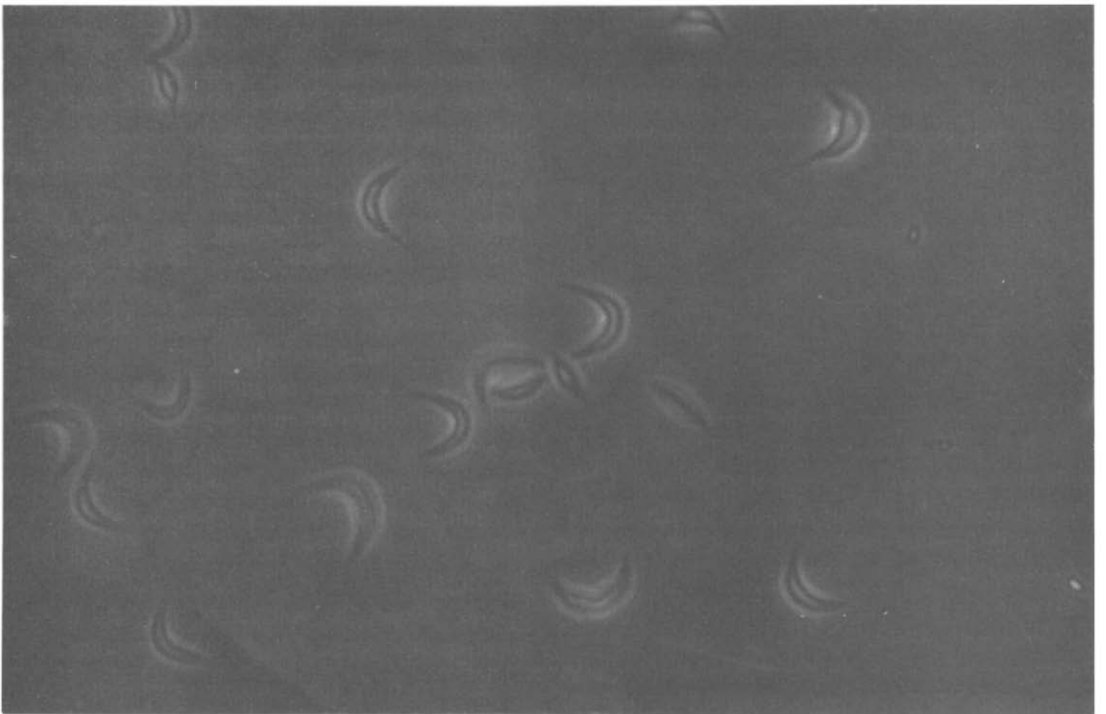


Fig. 5(b)

Fig. 5. Photograph of the alga in the presence and absence of lead. (a) With lead (b) no lead.

in biological models than in natural waters where there are fulvic and humic acids, especially of the pedogenic type. In the alga

culture medium, particularly at the end of the growth phase where higher concentrations of exudates are being produced,^{11,12} the dominant

Table 3. Influence of nutrients, light, concentration of lead and the ratio of the flux of air by the volume of the solution in the type of organics released by the alga *Selenastrum capricornutum*

Experimental conditions	C_{Pb}^{tot}	DOC mg/l.	A_{285}/DOC 1/log	F%	F/DOC 1/log
more nutrients, more light	—	—	—	—	—
1.5 Q/V	—	—	—	—	—
1.5 Q/V	2×10^{-7}	24–36*	~2	32–39	1
1.5 Q/V	8×10^{-7}	17–26	~1	16–22*	1
1.5 Q/V	2.5×10^{-6}	12–17*	~1	16–19*	1
more nutrients, more light	—	8	~3	25	3
Q/V	—	—	—	—	—
Q/V	1×10^{-6}	10	0.5	18	2
more nutrients, less light	—	16.5	~1.5	37.5	2
Q/V	—	—	—	—	—
Q/V	1×10^{-6}	20	0.8	17	1
less nutrients, more light	—	—	—	7–23†	—
3 Q/V	—	—	—	—	—
3 Q/V	1×10^{-6}	—	—	6–10†	—

When not mentioned the values are at the end of the experiment.

*Evolution during the last two days.

†Evolution from the 1st until the 8th day.

organics are low-absorbing aliphatic organic compounds such as carbohydrates, organic acids such as glycollic acid, aminoacids, polypeptides, lipids and organic phosphates.

However, from Fig. 6 it is clear that the fluorescence of the organics released by the non-contaminated cells during the several days is higher than for the alga with lead. Therefore, as noticed with cadmium,² it seems that the organics released by the cells in healthier conditions have a higher fluorescence.

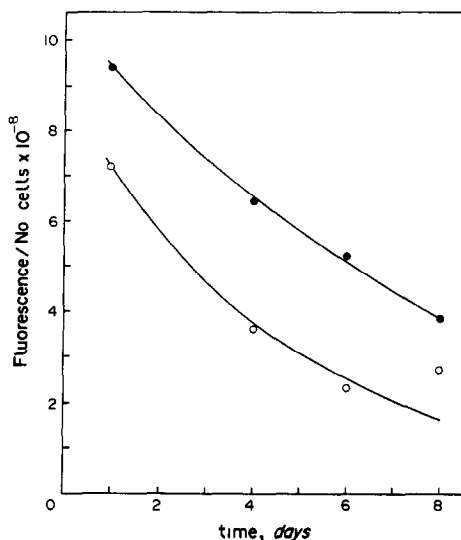


Fig. 6. Plots of the fluorescence intensity of the solution at 400–440 nm (after excitation at 340 nm) divided by the number of cells versus time. ●—experiments with less nutrients, more light, without lead and $Q/V = 4.7 \times 10^{-3} \text{ s}^{-1}$. ○—experiments with less nutrients, more light $1 \times 10^{-6} M$ in lead and $Q/V = 4.7 \times 10^{-3} \text{ s}^{-1}$. For more details see Experimental.

CONCLUSIONS

As a result of the investigations the following conclusions were drawn:

(a) The reduction of the number of hours of light from 11 hr to 8 hr has little influence on the growth curves without lead but clearly affects the cultures with lead.

(b) An increase of the ratio of flux of air by volume of solution (Q/V) at the stationary phase may produce another exponential phase.

(c) The increase of the ratio of Q/V and of nutrients and the decrease of contamination with Pb^{2+} led to a release of exudates by the alga that form more inert complexes in terms of DPASV, with a smaller relative uptake of this heavy metal by the alga.

(d) Although lead inhibits the division of the cells, the average cell volume increases considerably, which is clearer at higher Q/V values. However, the number of pigments by unit decreases in the presence of lead.

The organics released by the alga not contaminated with lead have more fluorescent groups.

Acknowledgement—This work is within the context of research project no. 87/48 MAR of Junta Nacional de Investigação, Científica e Tecnológica.

REFERENCES

1. P. H. Nienhuis, in *Marine Organic Chemistry*, E. K. Duursma and R. Dawson, (eds.), Chap. 3, Elsevier, Amsterdam, 1981.
2. M. L. S. Simões Gonçalves, M. F. C. Vilhena and M. A. Sampayo, *Water Res.*, 1988, **22**, 1429.

3. J. Buffle, P. Deladoey, J. Zumstein and W. Haerdi, *Schweiz Z. Hydrol.*, 1982, **44**, 325.
4. J. Buffle and P. Deladoey, *ibid.*, 1982, **44**, 363.
5. P. J. le B. Williams, in *Chemical Oceanography*, J. P. Riley and G. Skirrow (eds.), 2nd Ed., Vol. 2, Chap. 12, Academic Press, New York, 1975.
6. J. C. Goldman, W. J. Oswald and D. Jenkins, *J. Water Pollut. Control Fed.*, 1974, **46**, 554.
7. W. Davison, *J. Electroanal. Chem.*, 1978, **87**, 395.
8. T. D. Brisbin, *Ph.D. Thesis*, Illinois Institute of Technology, Chicago, 1980; *Chem. Abstr.*, 1981, **94**, 42286u.
9. A. M. A. Mota, J. Buffle, S. P. Kovhaves and M. L. S. Simões Gonçalves, *Anal. Chim. Acta*, 1985, **172**, 13.
10. E. R. Christensen, J. Scherfig and P. S. Dixon, *Water Res.* 1979, **13**, 79.
11. O. Hoyer, B. Lusse and H. Bernhardt, *Z. Wasser Abwasser Forsch.*, 1985, **18**, 76.
12. D. M. McKnight and F. M. M. Morel. *Limnol. Oceanogr.*, 1979, **24**, 823.

FLOW ANALYSIS OF SILICATE ROCKS FOR ZIRCONIUM

R. KURODA, K. OGUMA, K. KITADA and S. KOZUKA

Laboratory for Analytical Chemistry, Faculty of Engineering, University of Chiba, Yayoi-cho,
Chiba 260, Japan

(Received 20 February 1991. Revised 28 March 1991. Accepted 3 April 1991)

Summary—A flow analysis system involving the on-line configuration of an anion-exchange column has been examined to enrich and determine trace concentrations of zirconium of several ppm to hundred ppm levels in silicate rocks and minerals. About 100 mg of sample is decomposed by fusion with a mixture of boric acid and lithium carbonate and taken up with 1M hydrochloric acid to a total of 100 ml. Depending upon the concentration of zirconium, either a 1- or 4-ml aliquot is introduced into an aqueous carrier stream, merged with sulphuric acid and passed through a small volume anion-exchange column. The enriched zirconium is then back eluted with hydrochloric acid, colour-developed with Arsenazo III, and detected spectrophotometrically at 665 nm.

Flow-injection analysis of silicate rocks for major, minor and trace constituents has been reported. For major elements specific spectrophotometric or atomic-absorption spectrometric methods^{1–5} are used for detection. For minor^{6,7} and trace^{8,9} determination, off-line and on-line enrichment techniques have been used. On-line separations are preferable to off-line techniques in view of the obvious advantages of rapidity, reproducibility and elimination of involved manipulation. Continuous on-line precipitation–dissolution techniques coupled with conventional atomic-absorption spectrometric instruments have been developed for preconcentration and determination of trace cobalt⁸ and copper⁹ in silicate rocks. Scant information is available for other trace and minor elements in silicate rocks.

Many spectrophotometric methods for zirconium have been reported in combination with time-consuming ion-exchange chromatographic techniques^{10–17} or with use of masking agents and sample-simulated standard solutions.¹⁸ In this work, a flow analysis method for on-line anion-exchange preconcentration and determination of a few $\mu\text{g/g}$ to hundreds of $\mu\text{g/g}$ quantities of zirconium in silicates has been developed in conjunction with selective spectrophotometry with Arsenazo III. Though the decomposition step is the most labour-intensive and has the lowest throughput, the flow analysis preconcentration/measurement developed in this work for the treated samples takes 17–34 min, depending on the concentration level of zirconium.

EXPERIMENTAL

Reagents

The stock solution of zirconium (1.004 mg Zr per ml of 1M nitric acid) was obtained from Kanto Chemical Co., Tokyo. A working stock solution (100.4 μg Zr per ml of 3M hydrochloric acid) was prepared from this solution. The working standards were made by serial dilution of the working stock solution with 1M hydrochloric acid. Arsenazo III [2,7-bis(2-arsonophenylazo)-1,8-dihydroxynaphthalene-3,6-disulphonic acid] of notified reagent grade (Notification no. 850004) was purchased from Dojindo Laboratories, Kumamoto, Japan) and was used as received. From an Arsenazo III stock solution (0.25% aqueous solution), the working reagent solution was prepared by dilution with 4M hydrochloric acid to yield 0.005% solution. All other chemicals used were of reagent grade.

Apparatus

A schematic of the flow system is shown in Fig. 1. A Shimadzu Model UV-180 double beam spectrophotometer with a 20-mm flow cell (62.8 μl) was used as the detector, the output being fed to a Hitachi Model 561 strip chart recorder.

The ion-exchange column (IC) for on-line use was prepared by packing a strongly basic anion-exchange resin Bio-Rad AG1-X8 (100–200 mesh in the chloride form), into a 9-cm length of 1-mm bore Teflon tube and was plugged with polyester fibre at both ends. The flow channel

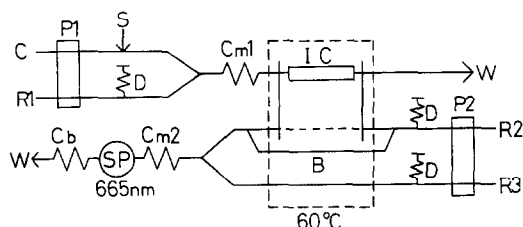


Fig. 1. Block diagram of FIA system. C: carrier (water, 0.2 ml/min); R1: 0.1M sulphuric acid (2.0 ml/min); S: sample (0.945 or 4.13 ml); Cm1 and Cm2: mixing coil (200 cm and 100 cm, respectively); IC: ion-exchange column; W: waste; P1 and P2: double plunger type pump; R2: 4M hydrochloric acid, R3: Arsenazo III solution (see the text for the flow rates of R2 and R3); D: damper coil (1 mm \times 500 cm); B: bypass (0.25 mm \times 100 cm); SP: spectrophotometer; Cb: back pressure coil (200 cm).

was assembled from 0.5-mm bore Teflon tubing and Daiflon connectors except for the ion-exchange column, damper and bypass tubings. Six-way loop injection valves were used for sample injections and switching of the flow path. A reciprocating pump of the double plunger type (Kyowa Seimitsu Model KHU-W-104) (P1) was used for pumping the carrier (C) and 0.1M sulphuric acid solutions (R1). The ion-exchange column eluent (R2) and chromogenic solution (Arsenazo III solution, R3) were propelled by a Sanuki Kogyo Model DM3M-2044 double plunger pump (P2). The ion-exchange column (IC), eluent (R2) and Arsenazo III solution (R3) were heated to 60° in a thermostat to accelerate the elution and indicator reaction.

Procedure

Preparation of sample solution. Place a 100-mg powdered sample in a platinum crucible, add 600 mg of 1:1 lithium carbonate-boric acid mixture and mix. Fuse the mixture for 15 min at 1000°. Dissolve the cooled melt in 1M hydrochloric acid and dilute accurately to 100 ml with the same acid. Subject the solution to FIA measurements within 24 hr.

Flow analysis measurement. Introduce the sample solution into the carrier (C), at point S with the six-way rotary injection valve. Use a sample aliquot of 1 ml (0.945 ml in the valve used) for usual silicate rocks ($> 50 \mu\text{g Zr/g}$) and of 4 ml (4.13 ml in the valve used) for low zirconium minerals. Allow the sample slug to merge with (R1) to form the sulphatocomplex of zirconium. Then, pass through the ion-exchange column (IC), where it is sorbed. By switching the valve at 6 (or 23) min from the start of 1 (or 4) ml sample introduction, place the column

into the eluent flow path (R2) to strip the zirconium in the reverse direction. Merge the stripped zirconium with the chromogenic solution (R3) to develop the colour. Read the absorbance in the flow-through cell at 665 nm. Take measurements three times for each sample. Use the peak height or peak height times band width at the half peak height as a measure of the signal.

RESULTS AND DISCUSSION

In order to separate the zirconium from the complicated matrix in silicate rock and mineral samples, the anion-exchange was carried out in sulphuric acid media because of the high sorption and high selectivity for zirconium of this medium.^{19,20} Major elements in silicate rocks do not exhibit any tendency to sorb on the resin over a wide concentration range of sulphuric acid. The sorbed zirconium can be eluted by 4M hydrochloric acid, which leaves uranium on a conventional anion-exchange resin column as chlorocomplexes.²⁰

Recorded signals for zirconium in the flow system are illustrated in Fig. 2 as a function of sulphuric acid concentration in the on-line anion-exchange column. In these runs the flow-rate of carrier (C) and sulphuric acid (R1) was kept at 0.2 and 2.0 ml/min, respectively, and the concentration of the acid was varied in the range 0.05–0.25M. The sharp peak to the left is a refractive index peak and the subsequent skewed peak is due to the zirconium-Arsenazo III complex. As can be seen, the peak height of the complex increases with decreasing concentration of sulphuric acid, not reaching a plateau under the conditions tested. Owing to a small volume of the ion-exchange column used (0.0707 ml), the retention (elution) volume for the column is low, being calculated to be approximately 9.7 ml for the eluent 0.25M sulphuric acid and 32 ml for 0.1M sulphuric acid by assuming K_D ¹⁹ of 211 (k-prime *ca.* 390) and of 704 (k-prime *ca.* 1309), respectively. (See note for the calculation of elution volume at the end of this section.)

During the 6-min sample loading period, 13 ml of sample/the reagent stream R1 (sulphuric acid solution of varying concentration) is forced to pass through the column. Therefore, the zirconium sorbed at the earlier stage of the sample loading period may be removed from the column partially or to a significant extent, depending on the concentration of sulphuric acid

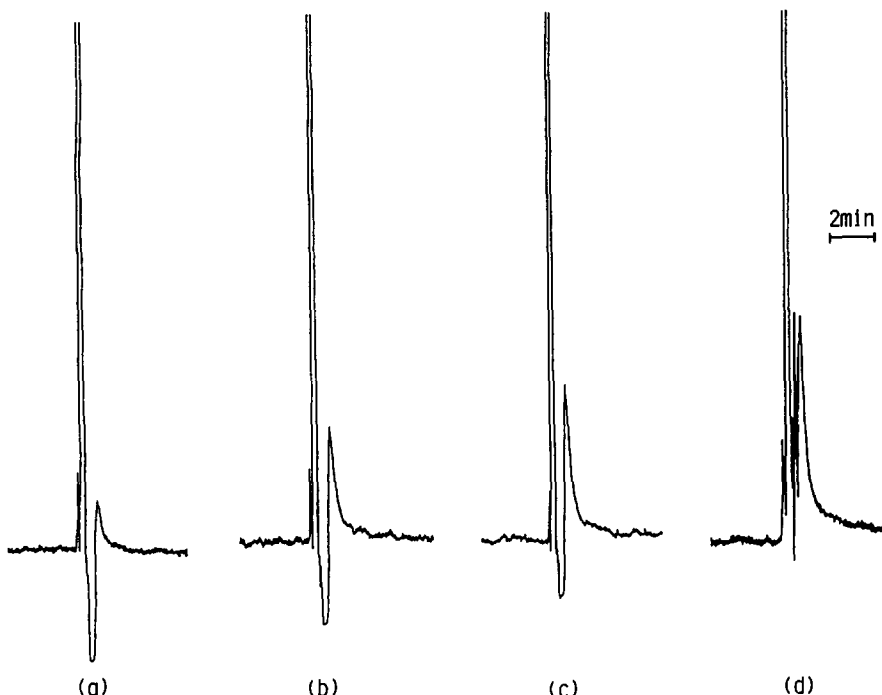


Fig. 2. Signals as a function of concentration of H_2SO_4 (M) in reagent stream R1. Zr concentration: $0.10 \mu\text{g Zr/ml}$. Concentration of H_2SO_4 : (a) $0.25M$, (b) $0.15M$, (c) $0.10M$, (d) $0.05M$. Sample loading: 0.945 ml .

solution (R2), yielding insufficient recoveries, as reflected by the varying peak height (Fig. 2). However, neither homogeneous mixing during chemical reaction nor attainment of chemical equilibrium are essential conditions for flow-injection analysis to be performed successfully. In the present ion-exchange enrichment, the reproducible quantitation of zirconium is possible with production of a coloured complex. We used $0.1M$ sulphuric acid as the reagent stream (R1). Stripping of zirconium is feasible by elution with $4M$ hydrochloric acid (R2) in the opposite direction to reduce band broadening. The temperature of the column, the eluent (R2) and the chromogenic solution (R3) was kept at 60° to avoid the occurrence of ghost peaks and to enhance the sensitivity of detection; in actual fact, heating resulted in a signal with twice the peak area as that obtained at room temperature.

Since the flow-rate of the eluent (R2) affects the detection sensitivity of zirconium with Arsenazo III, we examined the effect of flow-rates of the eluent and chromogenic solution on the peak height, keeping both rates the same, over the range $1.45\text{--}2.50 \text{ ml/min}$ [0.90 to 1.70 ml/min] in the case of 1 ml [4 ml] sample loading. The peak height decreased a little with increasing flow-rate, reaching a constant level at 1.95

ml/min for the 1-ml loading. A similar trend was observed for the 4-ml loading, but the peak height decreased rather rapidly with increasing flow-rate. From the aspect of sensitivity and avoidance of the presence of a neighbouring ghost peak, the flow-rate of 1.70 ml/min and 0.90 ml/min were chosen for 1 and 4 ml sample loadings, respectively.

The effects of other metal ions in the present system is given in Table 1. Actinides and lanthanides are known to interfere seriously with the determination of zirconium with Arsenazo III. However, lanthanides do not sorb on the anion-exchange resin from sulphuric acid media. The distribution coefficients¹⁹ of uranium and thorium on Bio-Rad AG1 at $0.1M$ sulphuric acid are 248 and 21, respectively, but their sorptions are not always quantitative, particularly for thorium during the loading of a large volume of sample + reagent solution (R1) relative to the column volume in the present anion-exchange system. The low sensitivity of Arsenazo III reaction with uranium(VI) also helps to reduce the interference from uranium(VI).

Zirconium becomes hydrolysed at low acid concentrations. The time dependence of stability of the ion-exchangeable zirconium in $1M$ hydrochloric acid of the boric acid-lithium

Table 1. Effect of foreign ions

Ion	Added as	Amount present		Zr amount, $\mu\text{g/ml}$	
		$\mu\text{g/ml}$	Added	Found (peak area)	Found (peak height)
UO_2^{2+}	chloride	0.012	0.120	0.121	0.121
Th(IV)	chloride	0.034	0.120	0.123	0.121
Ti(IV)	sulphate	9.9	0.120	0.122	0.118
Fe(III)	chloride	118	0.120	0.119	0.116
Al(III)	chloride	100	0.120	0.121	0.119
Ca(II)	chloride	80	0.120	0.118	0.120
Mg(II)	chloride	40	0.120	0.121	0.117

Conditions: sample (0.945 ml) and sulphuric acid were passed through the column for 6 min at a flow rate of 2.2 ml/min (see Procedure).

carbonate fusion case was studied. The measurable zirconium decreased relatively rapidly with time (0.5, 2 and 8% decrease after 1, 2 and 8 days respectively), so that the prompt determination of zirconium after the decomposition of sample is of importance. We subjected the sample solution to flow analysis measurements within 24 hr.

The proposed procedure was applied to the analysis of practical silicate samples. The results of two independent determinations for a number of different types of reference rocks and minerals of the Geological Survey of Japan are given in Table 2. As indicated, *ca.* 4–140 ppm of zirconium in these samples can be determined. Comparison with data for the reference samples that have been assigned working values²¹ shows that there is reasonable agreement. At the present time, no recommended values are given to these reference samples, partially because of lack of adequate data for these rocks. Users of

geostandards are solicited to contribute more data, particularly on trace elements.²¹ The reproducibility obtained for the individual sample solutions (RSD, $n = 3$) ranges from 0.27 to 9.6%, averaging at 3.4%.

Note: Calculation of the retention (elution) volume of a column

For any ion-exchanger, k' -prime is defined by the ratio of the amount of material in the exchanger phase to the amount of material in the solution (mobile) phase. The k' -prime value is related to the distribution coefficient K_D by the equation:

$$k' = K_D V_R / V_S \quad (1)$$

where V_R and V_S refer to the volumes of the resin and solution phases in the column. For a column packed with spherical resins, the stationary phase occupies roughly 65% of the column volume, so that the ratio V_R/V_S is about 1.86 (65/35).

$$k' = 1.86 K_D \quad (2)$$

The retention volume V of the sorbed species is related to k' -prime by the equation

$$V = V_S(1 + k') \quad (3)$$

where V_S of the present column is 0.0247 ml. Knowing K_D for a species under the conditions used, we can estimate roughly the retention (elution) volume, where the sorbed species elutes at a maximum concentration.

REFERENCES

1. R. Kuroda, I. Ida and H. Kimura, *Talanta*, 1985, **32**, 353.
2. T. Mochizuki, Y. Toda and R. Kuroda, *ibid.*, 1982, **29**, 659.
3. K. Oguma, Y. Kato and R. Kuroda, *Bunseki Kagaku*, 1985, **34**, T98.

Table 2. Determination of zirconium in rock reference samples

Sample	Found, ppm*	Proposed value, ppm ²¹
JG-2	98, 103	97
JG-1a	115, 127	115
JG-3	143	137
JR-1	98, 99	102
JR-2	87, 90	98.5
JA-1	87, 91	87
JA-2	112, 113	119
JGb-1	27, 28	33
JB-2	46, 45	52
JB-1a	131, 135	144
JB-3	82, 94	99.4
JP-1	5.2, 5.2	6
JF-1	36, 37	41
JF-2	3.7, 3.7	7

*Values obtained by the peak height.

JG-2: Granite; JG-1a, JG-3: Granodiorite; JR-1, JR-2: Rhyolite; JA-1, JA-2, JA-3: Andesite; JGB-1: Gabbro; JV-2, JB-1a, JB-3: Basalt; JP-1: Peridotite, JF-1, JF-2: Feldspar.

4. K. Oguma, T. Nara and R. Kuroda, *ibid.*, 1986, **35**, 690.
5. T. Nara, K. Oguma and R. Kuroda, *ibid.*, 1987, **36**, 851.
6. K. Oguma, K. Nishiyama and R. Kuroda, *Anal. Sci.*, 1987, **3**, 251.
7. R. Kuroda, I. Ida and K. Oguma, *Mikrochim Acta*, 1984 I, 377.
8. R. E. Santelli, M. Gallego and M. Valcárcel, *J. Anal. Atom. Spectrom.*, 1989, **4**, 547.
9. *Idem.*, *Anal. Chem.*, 1989, **61**, 1427.
10. F. W. E. Strelow, C. J. Liebenberg and F. von S. Toerien, *Anal. Chim. Acta*, 1969, **47**, 251.
11. F. W. E. Strelow, in *Ion Exchange and Solvent Extraction*, J. A. Marinsky and Y. Marcus (eds), Vol. 5, p. 121. Dekker, New York, 1973.
12. F. W. E. Strelow, C. J. Liebenberg and A. H. Victor, *Anal. Chem.*, 1974, **46**, 1409.
13. T. Kiriyaama and R. Kuroda, *Anal. Chim. Acta*, 1974, **71**, 375.
14. A. Mazzucotelli, R. Frache, A. Dadone and F. Baffi, *Talanta*, 1977, **24**, 690.
15. R. Frache, A. Mazzucotelli, A. Dadone, F. Baffi and P. Cescon, 1978, *Analisis*, **6**, 294.
16. T. Kiriyaama, *Nippon Kagaku Kaishi*, 1979, 1609.
17. H. Onishi, *Photometric Determination of Traces of Metals*, Part IIB, p. 773. Wiley, New York, 1989.
18. T. Okai, *Bunseki Kagaku*, 1988, **37**, 671.
19. F. W. E. Strelow and C. J. L. Bothma, *Anal. Chem.*, 1967, **39**, 595.
20. H. Hamaguchi, A. Ohuchi, T. Shimizu, N. Onuma and R. Kuroda, *ibid.*, 1964, **36**, 2304.
21. K. Govindaraju, *Geost. Newslet.*, 1989, **13**, Special Issue, (See p. 86).

SUPERCRITICAL FLUID EXTRACTION OF HIGH SULFUR SOILS, WITH USE OF A COPPER SCAVENGER

STEVEN M. PYLE* and MATTHEW M. SETTY

U. S. Environmental Protection Agency, Las Vegas, NV 89119, U.S.A.

(Received 26 October 1990. Revised 28 February 1991. Accepted 5 March 1991)

Summary—Supercritical fluid extraction (SFE) of sulfur-containing soils and sediments was hindered by deposition of elemental sulfur in the restrictor stopping the flow of carbon dioxide. It was found that a copper scavenger column placed after the sample cell removed the elemental sulfur, making SF extraction and quantification possible. Conditions are described for SFE and analysis of two standard reference materials (SRM), with use of a copper scavenger column. Quantification was performed by gas chromatography with mass spectrometric detection and the results were compared with the certified SRM values.

Supercritical fluid extraction (SFE) is a promising method for removing organic chemicals from solid matrices without the use of toxic solvents. Past environmental applications of SFE have used carbon dioxide, which exhibits a viscosity and density intermediate between those of a gas and liquid when at above its critical temperature (31.0°) and pressure (73 atm).¹⁻⁸ Off-line SFE is accomplished by placing a solid matrix (*e.g.*, fly-ash, soil, sludge) in a high-pressure cell and then passing carbon dioxide, pressurized to above its critical point, through the sample with a syringe pump. A post-cell fused-silica restrictor maintains the supercritical pressure within the cell and leads the carbon dioxide containing dissolved organics into an appropriate solvent or cryogenic trap for subsequent analysis by gas chromatography. SFE has been shown to be cheaper and faster than classical methods of extraction (ultrasonication and Soxhlet extraction) for small samples (*ca.* 1 g).

Because the solubility of dissolved materials decreases at lower fluid pressure, the fused-silica restrictor may become plugged with extracted material as the supercritical carbon dioxide is decompressed along the length of the restrictor. Lowering the carbon dioxide pressure reduces the plugging but reduces the extraction rate and the solubility of organics in the supercritical fluid. Heating the restrictor reduces precipitation, thus minimizing obstruction of the restrictor. Unfortunately, neither technique is appropriate when the sample contains appreciable amounts

of elemental sulfur (S_8). Two recent studies^{9,10} have dealt with the presence of elemental sulfur. The more recent⁹ analyzed the cyclohexane-soluble extracts of three sediments and found that 10–20% of the elemental content was sulfur. Restrictor clogging by sulfur is therefore a potential limitation of the use of SFE for environmental applications.

In this note, we describe a technique for using granular copper to remove elemental sulfur from supercritical carbon dioxide extracts of soils. The results of the analysis of a standard reference material (SRM) are compared with the certified value. The use of an SFE scavenger column was developed from a concept by Muragaverl and Vorhees.¹ This paper is intended to inform the scientific community of a potentially useful solution to the problem of extracting samples containing sulfur. It is by no means a complete validation of the technique.

EXPERIMENTAL

Supercritical fluid extraction was performed with a Suprex (Pittsburgh, PA) Model 50 Supercritical Fluid Extractor. SFE-grade carbon dioxide was obtained from Scott Specialty Gases (Plumstead, NY) and passed through a sample cell at 400 atm pressure and 60° for 10 min. The CO₂ flow was estimated to be 3.3 ml/min during extraction, from measurement of the flow of gaseous CO₂ (with a bubble meter) as it left the restrictor at the temperature and pressure of the extraction. This flow-rate was converted into ml/min for liquid CO₂ by dividing it by the

*Author for correspondence.

ratio of the density of liquid CO₂ (0.849 g/ml) to that of gaseous CO₂ (0.00198 g/ml). The sample cell, consisting of an empty 10 cm × 4.6 mm i.d. stainless-steel tube, was made from an HPLC column cartridge (Brownlee, Santa Clara, CA) by removing the inlet frit and column packing. The scavenger column consisted of 2.0 g of granular copper in a 3 cm × 4.6 mm i.d. Brownlee HPLC guard column with the inlet frit removed. The extraction and scavenger cartridge columns were fitted into the Brownlee holders for easy installation and removal. A 0.5 μm by ¼-in. o.d. frit was placed in the inlet of the cell holder to prevent the cell contents from leaving the cell during depressurization. The 50 μm i.d. × 10 cm fused-silica restrictor was connected to the exit of the scavenger column and passed through a Valco Tee into a length of stainless-steel tubing so that the restrictor remained entirely within the oven. As the CO₂ expanded at the end of the restrictor, the Joule-Thompson effect cooled the stainless-steel (SS) tubing and empty 7.4-ml sample vial and cold-trapped the eluted organics. A piece of 0.53 μm i.d. fused-silica tubing carried the spent gaseous carbon dioxide to a molecular sieve/activated charcoal trap, which ensured that no toxic volatiles were released into the laboratory. Figure 1 shows the SFE apparatus.

The sediment used in this work was a commercially available certified standard. SRM 1941 is a marine sediment from the National Institute of Standards and Testing (NIST), Gaithersburg, MD, which contains a high concentration of sulfur and less than 1 μg/g of several polynuclear

aromatics (PNAs). Non-oxidized granular copper was purchased from Mallinckrodt.

A 1-g portion of sediment was placed in the cell and extracted for 10 min. Organic compounds extracted were deposited on the inside of the stainless-steel tubing and the empty 7.4-ml sample vial as the CO₂ was decompressed inside the SS tubing during the extraction. Organics were washed into the sample vial by replacing the plug in the Valco Tee (Valco part # ZT1) with an HPLC injector fitting (Valco screw hub nut; part # ZN1) and injecting 250 μl of hexane through the injector fitting. The vial was removed and capped for subsequent mass spectrometric analysis.

Gas chromatographic/mass spectrometric analysis was performed with an HP 5890 gas chromatograph equipped with an on-column injector and a 30 m × 0.25 μm DB-5 fused silica capillary column (J and W Scientific, Folsom, CA). The initial linear velocity of the helium carrier gas was 45 cm/sec; the linear temperature program started at 60° and ended at 300°, with a total run time of 29 min. A 1 m × 0.53 μm fused-silica retention gap was connected to the head of the analytical column to facilitate injection and to protect the analytical column. The gas chromatograph was connected to a Finnigan Incos 50 mass spectrometer which scanned from *m/z* 64 to 650 in 0.5 sec. Quantification was by the method of external standardization, based on the average response factor for four replicate injections.

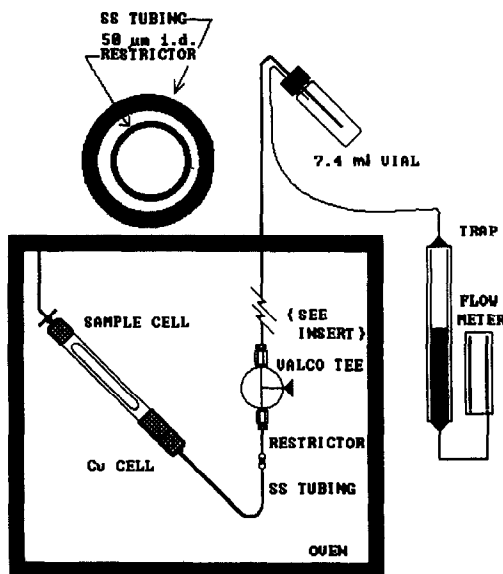


Fig. 1

RESULTS AND DISCUSSION

The SFE system shown in Fig. 1 was designed for speed and ease of use. An initial design, with a 30 cm × 50 μm restrictor, was tested by spiking the empty cell with an appropriate amount of PNA standards and performing the extraction in triplicate under the specified conditions. The resulting SF extracts were compared with PNA standards of equal concentration, and the recoveries calculated. These recoveries were poor (14–65%) for the lighter, more volatile PNAs (naphthalene–fluorene). However, for the remaining PNAs, the recoveries ranged from 68 to 100% with an average recovery of 82.5%. This demonstrated that physical trapping of the less volatile eluting organics was possible with this initial design.

For the SRM 1941 samples, which contain ~25% sulfur, the restrictor was shortened to

Table 1. Results of SF extraction of SRM 1941

Compound	<i>m/z</i>	Found, $\mu\text{g/g}$	Certified value, $\mu\text{g/g}$	Recovery*, %
d8-naphthalene	136	1.2; 1.2	4.0†	30*
d10-acenaphthene	164	2.4; 3.0	4.0†	67
d10-phenanthrene	188	2.8; 3.4	4.0†	78
phenanthrene	178	0.29; 0.32	0.577	52
anthracene	178	0.098; 0.103	0.202	50
fluoranthene	202	0.74; 0.80	1.22	63
pyrene	202	0.72; 0.78	1.08	70
benz(<i>a</i>)anthracene	228	0.28; 0.36	0.55	55
d12-chrysene	240	3.8; 5.0	4.0†	110
benzo(<i>b</i>)fluoranthene	252	0.30; 0.42	0.78	46
benzo(<i>k</i>)fluoranthene	252	0.37; 0.38	0.444	85
benzo(<i>a</i>)pyrene	252	0.23; 0.25	0.67	36
d12-perylene	264	2.7; 5.0	4.0†	96
perylene‡	252	0.08; 0.09	0.422	21
benzo(<i>ghi</i>)perylene	276	0.16; 0.18	0.569	30
indeno(1,2,3- <i>cd</i>)perylene	276	0.18; 0.14	0.516	31

*Recovery = $100 \times \text{mean value/certified value}$.

†Spike value.

‡No standard available; the d12-perylene response factor was used.

4 cm to increase the flow and improve recoveries, since our experience has demonstrated a "matrix effect" when working with soil samples. That is, spiked soil samples show greater recoveries than weathered samples.

The dimensions (length and i.d.) of the restrictor determine the flow of CO_2 and, therefore, the rate of extraction of the organics in the sediment sample. If the restriction is too great (long length and/or narrow i.d.), the extraction recoveries will be low and clogging will tend to occur. However, if the restriction is too little (short length and/or wider i.d.), the pressure may be difficult to maintain and the fast flow of CO_2 , along with aerosol generation, will make trapping of the organics more difficult. Since SRM 1941 did not contain any of the more volatile PNAs, the restrictor length was reduced to 4 cm for faster flow of CO_2 and, therefore, could increase recoveries in the 10 min extraction period.

The certified sediment, SRM 1941, was spiked with five deuterated PNAs (each at $410 \mu\text{g/g}$ level) and duplicate samples were extracted, with use of the copper scavenger column. The recoveries of the PNAs as a fraction of the certified or spike values are provided in Table 1. The recoveries ranged from 21 to 85% for the native PNAs and from 30 to 110% for the deuterated spikes. The recoveries of the heaviest two spikes were quantitative (110 and 96%) compared to those of the other PNAs. This is an indication that the lower PNA recovery was due to the "matrix effect" and not the copper scavenger. No extraction was possible without the copper scavenger column, since the elemental

sulfur deposited during extraction plugged the restrictor and stopped the flow of carbon dioxide. No flow-interruptions were experienced during the two extractions. After the two SF extractions the 2.0 g of copper in the scavenger column had increased in weight by 9 mg and was also totally blackened. The color change and weight gain are consistent with formation of copper sulfide.

Though the recoveries obtained in this study were not quantitative, they were in agreement with the average recoveries reported in a U.S. EPA round robin study of SFE.¹¹

CONCLUSION

The presence of elemental sulfur (S_8) in soil and sediments can degrade the performance of supercritical fluid extraction, by slowing the flow of carbon dioxide or completely plugging the restrictor. A copper scavenger column placed between the extraction column and the restrictor has been shown to effectively remove or reduce sulfur, from the supercritical carbon dioxide, apparently without adversely affecting the recoveries.

Acknowledgement—The authors wish to thank Dr. Mehdi Ashraf-Khorasani of Suprex Corporation and P. Marsden, Chief Methods Branch, EMSL-LV, for their help and suggestions in the course of this work.

Notice—Although the research described in this article has been supported by the United States Environmental Protection Agency, it has not been subjected to Agency review and, therefore, does not necessarily reflect the views of the Agency, and no official endorsement should be inferred. Mention of trade names or commercial products does not constitute endorsement or recommendation for use.

REFERENCES

1. B. Murugaverl and K. J. Voorhees, *Anal. Chem.*, in press.
2. V. Janda, G. Steenbeke and P. Sandra, *J. Chromatog.*, 1989, **479**, 200.
3. S. B. Hawthorne and D. J. Miller, *J. Chromatog. Sci.*, 1989, **27**, 197.
4. B. W. Wright, C. W. Wright, R. W. Gale and R. D. Smith, *Anal. Chem.*, 1987, **59**, 38.
5. M. A. Schneiderman, A. K. Sharma and D. C. Locke, *J. Chromatog. Sci.*, 1988 **26**, 458.
6. H. Engelhardt and A. Gross, *J. High Resolut. Chromatog. Chromatog. Commun.*, 1988, **11**, 726.
7. M. E. P. McNally and J. R. Wheeler, *J. Chromatog.*, 1988, **435**, 63.
8. J. H. Phillips and R. J. Robey, *ibid.*, 1989, **465**, 177.
9. M. Remberger, P.-Å. Hynning and A. H. Neilson, *ibid.*, 1990, **508**, 159.
10. P. D. Clark and K. L. Lesage, *J. Chromatog. Sci.*, 1989, **27**, 259.
11. T. L. Jones, U.S. EPA, *Interlaboratory Evaluation of SFE* (in manuscript).

EXTRACTION OF COPPER(II) WITH THE APCD/DIBK SYSTEM FROM CONCENTRATED HYDROCHLORIC AND NITRIC ACID MEDIA: ESTIMATION OF TRUE LIMIT OF ACIDITY FOR THE EXTRACTION

MASAHIKO MURAKAMI and TAKEO TAKADA

Department of Chemistry, College of Science, Rikkyo (St. Paul's) University, Nishi-Ikebukuro, Toshima-ku, Tokyo 171, Japan

(Received 10 December 1990. Revised 26 February 1991. Accepted 6 March 1991)

Summary—The extraction of copper(II) from strongly acidic solution (0.01–8*M* hydrochloric and 0.01–5*M* nitric acid) with ammonium 1-pyrrolidinecarbodithioate in di-isobutyl ketone has been studied. Compared with the hydrochloric acid system, a considerably larger amount of the reagent is needed for complete extraction of copper chelate from nitric acid solution as the extract is more unstable in the nitric acid system. The decomposition of copper chelates extracted from nitric acid is based on the oxidation of the reagent and the chelate; the spectral change of the extract from nitric acid suggests that the copper(II) chelate is initially oxidized to copper(II) and then decomposes. The upper limit of the acidity of both acids from which the copper chelate can be quantitatively extracted strongly depends on the reagent concentration; the limit with $8 \times 10^{-2}M$ APCD (500-fold reagent: metal molar ratio) was taken as 8 and 4*M* for hydrochloric and nitric acid, respectively.

The extraction of various elements into isobutyl methyl ketone (IBMK) with ammonium 1-pyrrolidinecarbodithioate (APCD) is widely used for increasing the sensitivity of atomic-absorption spectrometry (AAS). Although it is known that APCD is relatively stable in very low pH (< 1) media and has sufficient ability for formation of the chelate with some elements even in such a media, a study of the use of the APCD/IBMK system in strongly acidic media had not been attempted. There are only two reports that suggest the possibility of using this system at very low pH (< 1) or that mention the effect of hydrogen ion concentration on the extraction of various elements,^{1,2} and neither show any positive intention to use this system in such a region.

From a practical point of view, extraction of the metal chelates from such an acidic region has significant advantages. It allows metals to be directly extracted from a sample dissolved in concentrated acid, without pH adjustment, and only requires minimum dilution of the sample solution. Such a direct extraction saves time and is free from contamination by impurities in the buffer. We have investigated the extraction of copper(II) from very acidic solution,^{3–6} based on this concept.

In preceding papers^{4,5} we studied the extraction of copper(II) from 0.01–8*M* hydrochloric acid into IBMK with APCD in order to apply this system to the extraction of some elements from very acidic solution. It was found that IBMK was less suitable for the extraction in strongly acidic media, because a considerable part of the IBMK phase was dissolved into the acidic aqueous phase, and a large amount of free acid contaminated the extract and caused decomposition of the copper chelate. We therefore studied the use of di-isobutyl ketone (DIBK) as an alternative to IBMK and found it to be a more suitable solvent for extraction of the Cu(II)–PCD chelate from strongly acidic media.⁶ In contrast to IBMK, DIBK is virtually insoluble in up to 10*M* hydrochloric acid, and the copper chelate extracted into DIBK exhibits excellent stability. Copper can be quantitatively extracted from up to 8*M* hydrochloric acid with the APCD/DIBK system.

In this paper, to estimate the optimum conditions and true limit of acidity for copper extraction, we have systematically investigated the extraction of copper(II) from 0.01–8*M* hydrochloric acid and 0.01–5*M* nitric acid. From the standpoint of practical analysis, the applicability of this extraction system to nitric acid

media is of interest. Nitric acid is often used for the decomposition of solid samples due to its oxidizing ability. In our earlier work,³ it was suggested that the chelate extracted from nitric acid solution is oxidatively decomposed. Hence, the decomposition behaviour of the copper chelate extracted from nitric acid solution with this system was also studied.

EXPERIMENTAL

Reagents

All chemicals used were of reagent grade. Water was redistilled from an all-glass apparatus. A standard copper stock solution (1000 $\mu\text{g/ml}$) was prepared from 99.99% pure metal. All solvents were used without further purification.

Procedures

Extraction. A 20-ml volume of hydrochloric or nitric acid of desired concentration and 2.5 ml of a 10- $\mu\text{g/ml}$ copper solution were transferred to a 100-ml separating funnel. DIBK (10 ml) and 2.5 ml of APCD solution were added. The mixture was vigorously mechanically shaken.

Washing of the extract. Immediately after the aqueous phase had been withdrawn a 25-ml volume of water was added to the separating funnel and the mixture was mechanically shaken for 180 sec.

Measurements. The absorbance of the DIBK phase was measured at 433.5 nm in a 10-mm silica cell against DIBK as reference. For the kinetic study, the sample was kept in the cell compartment of the spectrophotometer at a constant temperature of 25°. Timing was started when the reagent was added to the mixture.

RESULTS AND DISCUSSION

Extraction of $\text{Cu}(\text{PCD})_2$ in hydrochloric acid media

The effect of hydrochloric acid concentration on the shaking time and the reagent concentration needed for quantitative extraction were studied at 0.01–8M hydrochloric acid. The amount of copper left in the aqueous phase was also checked by using flame atomic-absorption spectrometry to estimate the degree of copper chelate extraction.

Shaking time. In the extraction of copper-PCD chelate from strongly acidic solution, use of a large excess of reagent is recommended

since the kinetic stability of the copper chelate is highly dependent on the concentration of reagent.⁴ Hence, $8 \times 10^{-2}M$ APCD (corresponding to a 500-fold reagent: metal molar ratio in this system; close to the limit of solubility of APCD) was used in this study.

Figure 1 shows that the shaking time needed for completing the extraction depends on the acidity. The minimum shaking time needed for quantitative extraction decreased as the acidity was increased: 120 sec for 0.01M, 90 sec for 1M acid, and 60 sec for 4M and 8M acid. These findings disagree with the generally accepted acidity dependence of the rate of the metal chelate formation and of its extraction; Irving and Williams⁷ reported that the rate at which the metal chelates are formed and extracted decreases as the pH is reduced. However, the same tendency as that observed in this study was also obtained in the copper extraction with the APCD/IBMK system.⁵

It can be considered that this difference in the acidity dependence of the extraction rate between these two systems and others was based on the difference in the methods of adding the reagent. In the general metal chelate extraction system, the reagent is previously dissolved in the organic phase whereas in the APCD/IBMK and APCD/DIBK systems, the reagent is added to the system as an aqueous solution since it is not very soluble in these solvents. The facts suggest that the rate of copper chelate extraction is dependent on the rate of extraction of the reagent into the organic phase. It is expected that the rate of the reagent extraction increases as the acidity is increased since only an acid form of PCD ligand can be extracted and it seems that copper is mainly extracted by the ligand extracted in the organic phase.

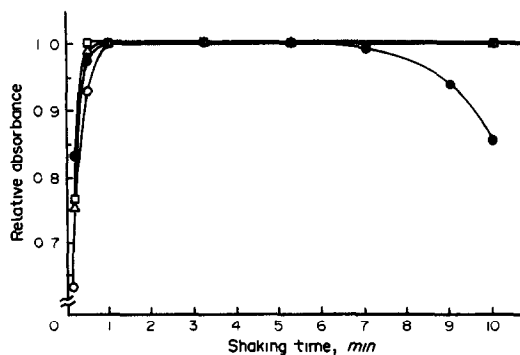


Fig. 1. Effect of shaking time on extraction of $\text{Cu}(\text{PCD})_2$ in DIBK from hydrochloric acid: HCl 0.01M (○), 4M (△), 6M (□), 8M (●); [Cu] $1.6 \times 10^{-5}M$; [APCD] $1.6 \times 10^{-3}M$ (HCl 0.01–6M), $8.0 \times 10^{-3}M$ (HCl 8M).

After extraction the absorbance remained constant, even after a 20-min shaking period, for all concentrations of hydrochloric acid except 8M for which the absorbance gradually decreased above 300 sec of shaking. This indicates that the copper chelate was decomposed by the contact with the acid solution during the period of shaking. Over all the acidities used, the copper chelate could be extracted quantitatively in the range 120–300 sec shaking. Hence, this range was taken as optimum.

APCD concentration. Figure 2 shows the degree of extraction of copper chelate from hydrochloric acid as a function of the reagent concentration. As the acidity is increased the minimum concentration of the reagent needed for complete extraction increases: $4.0 \times 10^{-5}M$ (2.5-fold ratio to copper) for 0.01M, $6.4 \times 10^{-5}M$ (4-fold) for 4M, $2.6 \times 10^{-4}M$ (16-fold) for 6M acid and $2.2 \times 10^{-3}M$ (140-fold) for 8M acid.

For each acidity (except 0.01M), copper chelate was not extracted at all up to a certain concentration of the reagent, and this threshold concentration of the reagent increased as the acidity was increased: $3.2 \times 10^{-5}M$ (2-fold ratio to copper) for 4M, $1.3 \times 10^{-4}M$ (8-fold) for 6M acid, and $1.6 \times 10^{-4}M$ (10-fold) for 8M acid. Both of these findings indicate that there is appreciable decomposition of the chelate during the shaking period, and it becomes more marked as the acidity is increased and the concentration of the reagent is decreased.

Kinetic stability of the extract. The kinetic stability of the chelate extracted from hydrochloric acid into DIBK was studied at various APCD concentrations. As previously reported, the $Cu(PCD)_2$ chelate extracted into IBMK or DIBK from strongly hydrochloric acid media

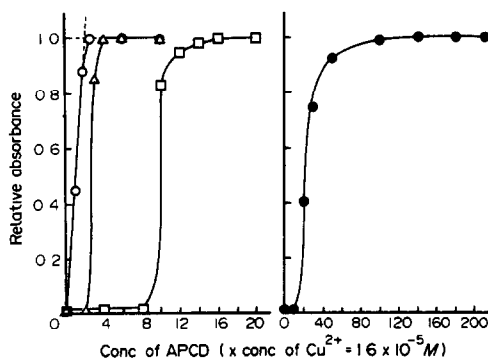


Fig. 2. Effect of APCD concentration on extraction of $Cu(PCD)_2$ in DIBK from hydrochloric acid solution: [HCl] 0.01M (○), 4M (△), 6M (□), 8M (●); [Cu] $1.6 \times 10^{-5}M$; shaking time 300 sec (0.01–6M), 120 sec (8M).

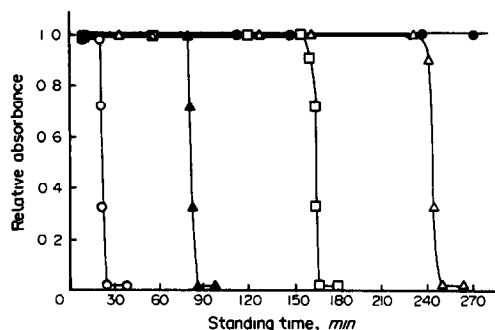


Fig. 3. Kinetic stability of $Cu(PCD)_2$ extracted in DIBK from 4M hydrochloric acid solution: [APCD] $7.0 \times 10^{-5}M$ (○), $1.6 \times 10^{-4}M$ (▲), $2.9 \times 10^{-4}M$ (□), $4.2 \times 10^{-4}M$ (△), $1.6 \times 10^{-3}M$ (●); [Cu] $1.6 \times 10^{-5}M$; shaking time 300 sec.

shows the characteristic behaviour of decomposition.^{5,6} Figure 3 shows the variation in absorbance of copper chelate extracted into DIBK from hydrochloric acid solution with time; the absorbance was constant for a certain time and then suddenly dropped.

Sufficient stability for the determination could be obtained by using a large amount of the reagent. Table 1 gives the time ($t_{1/2}$) needed for the absorbance of the extract to decrease to half its original value. The kinetic stability of copper chelate is strongly dependent on the concentration of the reagent added; the decomposition time ($t_{1/2}$) increases as the concentration of the reagent is increased. It was noted that when $1.6 \times 10^{-3}M$ (100-fold to copper) or more of the reagent was added, the absorbance of the extract remained constant for more than 48 hr.

When the IBMK and DIBK extracts are washed with water or are filtered with dry filter paper, the stability can be considerably increased.^{5,6} In these extraction systems, it was observed that the free hydrochloric acid transferred into the extract by dissolution and by

Table 1. Decomposition time ($t_{1/2}$) of $Cu(II)$ -PCD chelate extracted from 4M HCl

[APCD], M	$t_{1/2}$ min
7.0×10^{-5}	25.0
1.6×10^{-4}	86.0
2.9×10^{-4}	164.5
4.2×10^{-4}	244.7
1.6×10^{-3}	>48 hr
1.6×10^{-2}	>48 hr

With washing or filtration

1.6×10^{-4} >48 hr

[Cu²⁺] $1.6 \times 10^{-5}M$, shaking time 5 min.

very fine droplets of the aqueous phase causes the copper chelate to decompose. The effect of the washing is due to almost complete removal of the free acid contaminated into the extract. In the case of filtration, a large part of the free acid can be removed, and it is considered that the fine droplets of the aqueous hydrochloric acid remaining in the extract can be removed.⁶ Therefore, the free acid is effectively removed by the washing and filtering of the extract. However, in the case of DIBK extraction, the extract exhibited sufficient stability without these treatments, if a large excess of APCD (about 100-fold or more to copper) was added (Table 1).

Acidity range. To estimate the acidity range which can be used for copper extraction, the percentage extraction of copper chelate was studied as a function of concentration of hydrochloric acid, with various concentrations of the reagent. Figure 4 shows the change in the percentage extraction of copper chelate with hydrochloric acid concentration of the aqueous phase, with 1.6×10^{-3} , 3.2×10^{-3} , 8.0×10^{-3} and $8.0 \times 10^{-2}M$ of APCD solution. The acidity range depends on the concentration of the reagent added; for example, although copper chelate can be extracted from $8M$ acid with $8.0 \times 10^{-2}M$ APCD (500-fold ratio of copper), it is not extracted at all above $7M$ acid with $0.0016M$ APCD. The limiting acidities of quantitative extraction of copper chelate were taken as follows: $5M$ with $1.6 \times 10^{-3}M$ APCD (10-fold ratio to copper), $6M$ with $3.2 \times 10^{-3}M$ (20-fold) and $8.0 \times 10^{-3}M$ (50-fold) APCD, $7M$ for $1.6 \times 10^{-2}M$ APCD (100-fold) and $8M$ for $8.0 \times 10^{-2}M$ APCD (500-fold).

These findings suggest that the range of acidity which can be used for the extraction is determined by the concentration of the reagent added; however, this point has been missed in several reports which have commented on these

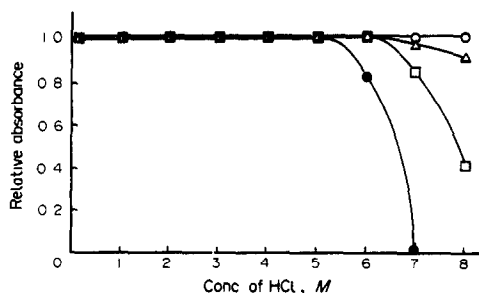


Fig. 4. Extraction range of Cu(II) with APCD/DIBK system in hydrochloric acid media: [APCD] $1.6 \times 10^{-3}M$ (●), $3.2 \times 10^{-3}M$ (□), $8.0 \times 10^{-3}M$ (△), $8.0 \times 10^{-2}M$ (○); [Cu] $1.6 \times 10^{-3}M$; shaking time 300 sec.

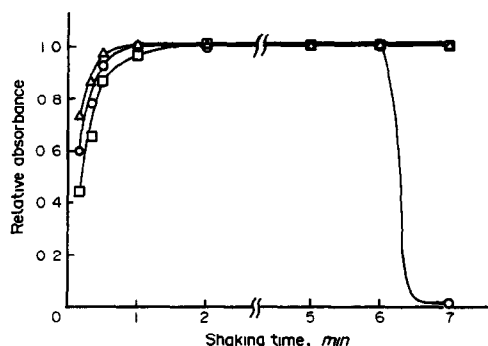


Fig. 5. Effect of shaking time on extraction of $Cu(PCD)_2$ in DIBK from nitric acid: $[HNO_3]$ $0.01M$ (□), $2M$ (○), $4M$ (△); $[Cu]$ $1.6 \times 10^{-3}M$; $[APCD]$ $8.0 \times 10^{-3}M$.

acidity ranges.^{1,2,8,9} Hence, it seems that the range of acidity for the extraction of various metals with APCD must be re-examined.

Extraction of $Cu(PCD)_2$ in nitric acid media

The extraction behaviour and the optimum conditions of copper extraction from 0.01 – $5M$ nitric acid solution were studied.

Shaking time. The shaking time needed for completing the extraction of copper chelate was studied with $8.0 \times 10^{-2}M$ APCD. Figure 5 shows the results in nitric acid media. The minimum shaking time for quantitative extraction decreases as the acidity is increased, similarly to the case in hydrochloric acid media. For 0.01 – $4M$ acid, the minimum shaking time for each acidity was the same as that for hydrochloric acid media: 120 sec for $0.01M$, and 60 sec for 2 and $4M$.

However, in $4M$ acid copper chelate was decomposed and was not extracted when the period of shaking exceeded 420 sec. It was also observed that the decomposition of copper chelate occurred during the shaking period and that the chelate was not extracted for any shaking time at concentrations above $4M$. This suggests that the kinetic stability of copper chelate in nitric acid media is lower than that in hydrochloric acid media, although the formation of the chelate is not dependent on the kind of acid. Hence, the range 120–180 sec was taken as the optimum shaking period.

APCD concentration. The concentration of reagent needed for complete extraction of copper chelate was studied at 2 and $4M$ nitric acid. Figure 6 shows the results with 120 sec of shaking. In nitric acid media, a considerably higher concentration of the reagent was needed for complete extraction compared with that for the same acidity in hydrochloric acid media. To

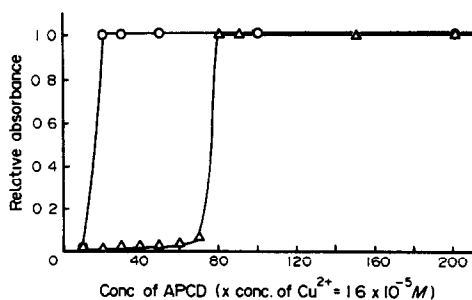


Fig. 6. Effect of APCD concentration on extraction of Cu(PCD)_2 in DIBK from nitric acid solution: $[\text{HNO}_3]$ $2M$ (O), $4M$ (Δ); $[\text{Cu}]$ $1.6 \times 10^{-5}M$; shaking time 120 sec.

complete the extraction, more than $3.2 \times 10^{-4}M$ (20-fold ratio to copper) and $1.3 \times 10^{-3}M$ (80-fold) reagent concentrations were needed for 2 and 4M nitric acid, respectively. In contrast to that of the hydrochloric acid system (Fig. 2), it is noted that copper chelate was not extracted at all with less than these reagent concentrations, suggesting that the decomposition of copper chelate is considerably more rapid when shaken with nitric acid than with hydrochloric acid.

The concentration of the reagent needed for completing the extraction apparently increases with increasing shaking time. When copper chelate was extracted with 300 sec of shaking, $1.6 \times 10^{-2}M$ APCD was needed. On the other hand, copper chelate could be completely extracted with $9.6 \times 10^{-4}M$ APCD, if the shaking period was reduced to 60 sec. These facts suggest that the kinetic stability of copper chelate when shaking with nitric acid solution is not so good as that with hydrochloric acid solution, due to oxidative decomposition of copper chelate and the reagent with nitric acid.

Kinetic stability. The decomposition behaviour and the kinetic stability of the chelate extracted from 2M nitric acid into DIBK were studied. Figure 7 shows the variation in the absorbance of copper chelate extracted into

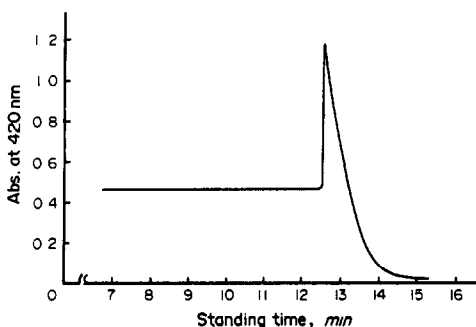


Fig. 7. Kinetic stability of Cu(PCD)_2 extracted in DIBK from 2M nitric acid solution: $[\text{APCD}]$ $1.6 \times 10^{-3}M$; $[\text{Cu}]$ $1.6 \times 10^{-5}M$; shaking time 120 sec.

DIBK from 2M nitric acid solution, with time. The absorbance was constant for a certain time, similarly to the case of hydrochloric acid media; however, beyond this time the absorbance jumped to about twice as much as its original value, and then exponentially decreased with time.

The spectral changes with the decomposition of copper chelate extracted from 2M nitric acid are shown in Fig. 8. The initial absorption spectrum is the same as that of Cu(PCD)_2 chelate extracted from hydrochloric acid media in its shape, wavelength of absorption maximum and molar absorption coefficient. The initial peak at 434 nm [Fig. 8(a)] is enlarged with a shift in the peak wavelength to about 420 nm [Fig. 8(b)], with the isosbestic point at about 460 nm; then the peak gradually disappears without shift in the wavelength [Fig. 8(c)].

Such a spectral change strongly resembles that observed in the spectrophotometric monitoring of the electrochemical oxidation process of some bis-dithiocarbamate Cu(II) complexes $[\text{Cu}(\text{dtc})_2]$. Hendrickson *et al.*¹⁰ reported that $\text{Cu}(\text{dtc})_2$ underwent a single one-electron oxidation step at a platinum electrode: $\text{Cu}(\text{dtc})_2 + e^- \rightarrow [\text{Cu}(\text{dtc})_2]^+$, and the progress of this process was followed by the change in the absorbance spectrum from that of $\text{Cu}(\text{dtc})_2$ to $[\text{Cu}(\text{dtc})_2]^+$ with two isosbestic points at 464 and 328 nm. This report also noted that there

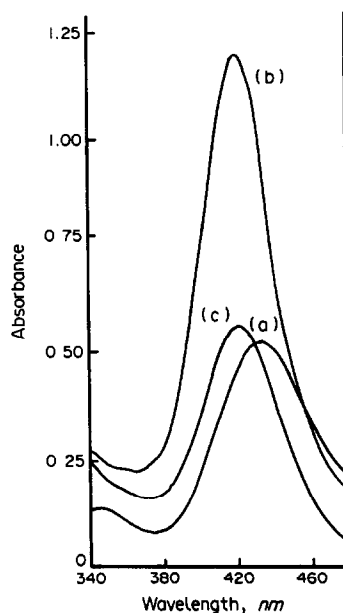


Fig. 8. Change in spectra of Cu(PCD)_2 in DIBK from 2M nitric acid solution: (a) standing time 7 min, (b) 12.5 min, (c) 13.3 min; $[\text{APCD}]$ $1.6 \times 10^{-3}M$; $[\text{Cu}]$ $1.6 \times 10^{-5}M$; shaking time 120 sec.

was an absorption maximum of $[\text{Cu}(\text{dte})_2]^+$ at about 420 nm, and its absorbance was several times larger than that of $\text{Cu}(\text{PCD})_2$. This suggests that $\text{Cu}(\text{PCD})_2$ extracted from nitric acid solution is oxidized, and a trivalent complex, $[\text{Cu}(\text{PCD})_2]^+$, is formed as an intermediate which then decomposes.

Table 2 gives the period of time when the absorbance of the extract remains constant, a so-called "decomposition time", under various conditions. The decomposition time of the chelate increased linearly with increasing concentration of the reagent up to $9.6 \times 10^{-3} M$ (60-fold); however, above this, it did not depend on the reagent concentration. In contrast to the case of the hydrochloric acid system, the kinetic stability of the chelate is not very dependent on the concentration of the reagent added in the relatively higher range of the reagent concentration, such as up to $9.6 \times 10^{-3} M$. It seems that this is due to the oxidative decomposition of copper and the reagent.

Similar to the situation in hydrochloric acid media, the washing of the extract contributed to stabilizing the copper chelate. When it was washed with water, the chelate exhibited sufficient stability for its determination; the absorbance of the extract remained constant for more than 60 min. However, the absorbance of the extract dropped within 15 min when no washing of the extract was done, even though a considerable amount of the reagent (about 500-fold ratio to copper) was added.

When the chelate was extracted from 4M nitric acid, it was observed that the absorbance of the extract increased with time due to scattering of light caused by the suspended particle in the formation of the extract with time, even if the extract had been washed with water. The absorbance of the extract could be returned

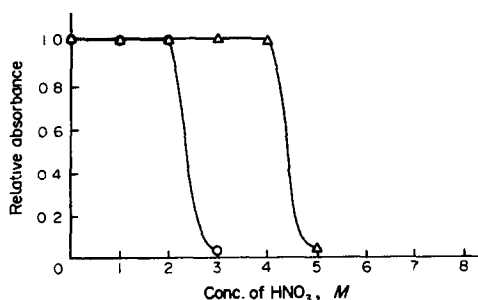


Fig. 9. Extraction range of Cu(II) with APCD/DIBK system in nitric acid media: $[\text{APCD}] 3.2 \times 10^{-3} M$ (O), $1.6 \times 10^{-2} M$ (Δ), $[\text{Cu}] 1.6 \times 10^{-5} M$; shaking time 120 sec.

to its original value by filtering it through a dry filter paper. It was observed also that the formation of suspended particles could be prevented by washing the extract twice, immediately after its extraction. This suspension is perhaps caused by decomposition of free PCD ligand in the extract due to its reaction with the free nitric acid contaminated in the extract. When the chelate was extracted from 4M nitric acid, the absorbance remained constant for over 60 min provided that the extract was washed twice. Hence, the washing of the extract is recommended for the extraction from nitric acid solution.

Acidity range. The range of nitric acid concentration which can be used for copper chelate extraction is shown in Fig. 9. Similar to the hydrochloric acid system, the acidity range depends on the concentration of the reagent, but the extent of this dependence is smaller than that observed in the hydrochloric acid system. The copper chelate could be extracted from 4M nitric acid with $1.6 \times 10^{-2} M$ APCD; however, the acidity range was not extended when the concentration of the reagent was increased to $8.0 \times 10^{-2} M$. Such a saturation of the effect of the reagent concentration on extending the acidity range in nitric acid system can be expected from the kinetic stability of copper chelate in this system.

At concentrations above 4M, it was observed that copper chelate was decomposed during a shaking period of 120 sec, even with $8.0 \times 10^{-2} M$ APCD. If the shaking period is reduced to 60 sec, copper chelate can be quantitatively extracted from up to 5M nitric acid, with $8 \times 10^{-2} M$ APCD; even in this case, provided that the extract was separated from the aqueous phase before the chelate decomposes and was washed twice with water, the absorbance was kept constant for 60 min or more.

Table 2. Decomposition time of Cu(II)-PCD chelate extracted from 2M HNO₃

$[\text{APCD}]$, M	Decomposition time,* min
3.1×10^{-4}	5.8
4.7×10^{-4}	7.4
6.3×10^{-4}	9.2
7.9×10^{-4}	10.5
9.4×10^{-4}	12.0
1.6×10^{-3}	12.8
3.1×10^{-3}	12.2
With washing 1.6×10^{-3}	>1 hr

$[\text{Cu}^{2+}] 1.6 \times 10^{-5} M$, shaking time 2 min.

*Determined by the time at which the absorbance jumps (see Fig.7).

However, such an extraction condition is too critical for practical use, and it was observed that at a concentration greater than 5M, The chelate was decomposed during a shaking period even with any extraction conditions. Hence, about 4M was taken as the practical acidity limit for copper chelate extraction in the nitric acid system.

CONCLUSIONS

With the APCD/DIBK extraction system, copper can be quantitatively extracted from up to 8M hydrochloric and 4M nitric acid. In the nitric acid system, extraction of copper chelate shows "all or nothing" behaviour. Because the decomposition of the chelate when shaken with nitric acid solution is rapid, the chelate is not extracted at all during the shaking period.

On the other hand, when the extract separates from the aqueous phase before the chelate decomposes, the chelate can be completely extracted. The kinetic stability of the chelate in the extract is also not so good as that in the hydrochloric acid system, which is thought to be due to oxidative decomposition of both reagent and copper chelate. However, sufficient kinetic stability can be obtained for its practical use, provided that the extract is washed with water.

It is worth noting that the kinetic stability of Cu(II)-PCD chelates and the acidity range are determined by the amount of the reagent added; hence, the use of a large excess of the reagent is recommended for copper extraction in strongly acidic media. Although several reports have commented on the kinetic stability and the acidity range for their extractions, it seems that they have not accurately estimated them, since they have missed this point. Therefore, in order to estimate the proper acidity range of extraction for these elements, the re-examination of the extraction conditions for each element is required.

REFERENCES

1. I. Dellien and L. Persson, *Talanta*, 1979, **26**, 1101.
2. R. J. Everson and H. E. Parker, *Anal. Chem.*, 1974, **46**, 1966.
3. T. Takada, Y. Okabe and K. Nakano, *Bull. Chem. Soc. Japan.*, 1981, **54**, 3589.
4. T. Takada, *Talanta*, 1982, **29**, 799.
5. M. Murakami and T. Takada, *ibid.*, 1985, **32**, 513.
6. *Idem*, *ibid.*, 1990, **37**, 229.
7. H. Irving and R. J. P. Williams, *J. Chem. Soc.*, 1949, 1841.
8. J. D. Kinrade and J. C. Van Loon, *Anal. Chem.*, 1974, **46**, 1894.
9. R. R. Brooks, M. Hoashi, S. M. Wilson and R. Q. Zhang, *Anal. Chim. Acta*, 1989 **217**, 165.
10. A. R. Hendrickson, R. L. Martin, and N. M. Rohde, *Inorg. Chem.*, 1976, **15**, 2115.

THE EFFECT OF MOLYBDENUM(VI) ON THE PRODUCTION OF ARSINE BY THE TETRAHYDROBORATE(III) REACTION

IAN D. BRINDLE*

Chemistry Department, Brock University, St Catharines, Ontario L2S 3A1, Canada

HENGWU CHEN

Department of Chemistry, Hangzhou University, Hangzhou, Zhejiang, People's Republic of China, 310028

(Received 30 July 1990. Revised 26 March 1991. Accepted 8 April 1991)

Summary—Molybdenum(VI) increases signals in the determination of arsenic after reduction by tetrahydroborate(III). An increase in the signal by up to two-and-a-half fold is observed when arsenic(III) is determined in the presence of sulphuric and hydrochloric acid concentrations of 0.01–0.02M. The enhancement effect disappears at higher acid concentrations and is eliminated by the presence of *L*-cysteine. Signals from other hydride-forming elements (antimony, bismuth and tin) were reduced in the presence of molybdenum(VI). Reduction of interferences in the hydride-forming reaction from nickel and cobalt is observed, so that the range of tolerance of these elements is extended by one and two orders of magnitude, respectively. The interference reducing effect is not as profound as that observed with *L*-cysteine.

A number of papers have been published over recent years which describe interferences in the determination of hydride-forming elements by various ions in solution.^{1–4} Although most papers report that interferences reduce the signal from the hydride-forming element, several describe enhancement of the signal. Thus Kirkbright and Taddia reported that the presence of copper(II) gave rise to enhanced signals from arsenic.² Tin signals have been reportedly increased by the presence of beryllium, thallium and titanium.³ We have reported that peroxodisulphate enhances recovery of germanium.⁴

Enhancement or depression of signals from ions which could be present in solution from the sample or dissolution matrix is an effect which must be taken into account when determining hydride-forming elements. The search for reagents which will eliminate these variations has led to the use of a number of compounds which have some measure of efficacy in reducing interferences. The use of iron(III) as a releasing agent in the determination of selenium by hydride generation has been reported.^{5,6} Brindle *et al.* have reported the use of *L*-cysteine and *L*-cystine to reduce interferences from various metal ions in the determination of arsenic, germanium and tin.^{7–10}

Interference from molybdenum(VI) has been reported to reduce the signal from arsenic in concentrated hydrochloric acid,^{11,12} while other authors have found the effect to be insignificant.¹ In recent investigations into the determination of arsenic, where *L*-cysteine was used to reduce As(V) to As(III)¹³ in dilute acid solution, the presence of Mo(VI) significantly increased the signal from the reduction of As(III) by sodium tetrahydroborate(III) in the absence of *L*-cysteine.

In this paper, we report on our investigations into the effect of molybdenum(VI) and other oxyanions on the enhanced production of arsine by the hydride transfer reaction and on the reduction of interferences in reaction of arsenic with tetrahydroborate(III).

EXPERIMENTAL

Instrumentation

Data were acquired with a Spectraspan V d.c. plasma atomic-emission spectrometer equipped with a Beckman hydride generator modified as described elsewhere.⁹ Signals were recorded on a Fisher Recordall Series 5000 chart recorder. A Brinckman variable volume Macro-Transferpettor was used for all analyte injections with the volume fixed at 5.0 ml.

*Author for correspondence.

The arsenic emission line at 193.7 and 228.8 nm were measured with entrance and exit slit widths of 50 and 100 μm , respectively. The slit heights were matched at 300 μm . Photomultiplier voltage and gain settings were used to provide convenient signals and to minimize noise.

Reagents

Argon of welding grade (Union Carbide, Canada) proved to be sufficiently pure for use without further treatment. All inorganic chemicals were analytical reagent grade or better. *L*-Cysteine was obtained from Sigma (Sigma grade) and BDH. Sodium tetrahydroborate(III) solutions were prepared in 0.2M sodium hydroxide and were filtered before use. Ammonium molybdate $[(\text{NH}_4)_2\text{Mo}_7\text{O}_{24}\cdot 4\text{H}_2\text{O}]$ was obtained from Fisher Scientific, Toronto. Arsenic(V) solutions (1000 $\mu\text{g}/\text{ml}$) and arsenic(III) (1000 $\mu\text{g}/\text{ml}$) solutions were prepared from $\text{Na}_2\text{HAsO}_4\cdot 7\text{H}_2\text{O}$ and As_2O_3 respectively. Since the As(V) solution was prepared from a non-standard reagent, the concentration was verified by comparison with the As(III) solution, prepared from standard arsenic(III) oxide, in the d.c. plasma spectrometer. Solutions for the determinations were subsequently prepared by dilution with the appropriate reagents.

RESULTS AND DISCUSSION

A preliminary survey of oxyanions was carried out to determine which, if any, enhance signals from arsenic(III). Ions were tested in 0.02 and 0.2M hydrochloric acid and the results are shown in Table 1. At the lower acid concentration, molybdenum(VI) at a concentration of 100 $\mu\text{g}/\text{ml}$ gave a two-and-a half fold increase in signal. This enhancement was observed at both

of the arsenic wavelengths. A small (30%) signal enhancement was observed with vanadium(V) in 0.02M hydrochloric acid, while tungsten(VI) had no observable effect on the signal. Of the strongly oxidizing ions, dichromate and peroxodisulphate gave reduced signals while permanganate eliminated the signal completely. At higher acid concentration (0.2M), the enhancement effects disappeared.

Not only acid concentration, but the acid type has a significant effect on the enhancement effect produced by molybdenum. Hydrochloric, nitric, sulphuric and phosphoric acids were investigated over the range of concentrations from 0.01 to 0.2M. Higher concentrations of acids used in the hydride generator produced instability in the plasma and were not investigated. The results of the study are shown in Fig. 1. For all acids, the enhancement effect is most significant at low concentrations and becomes insignificant at a concentration of 0.08M for hydrochloric and nitric acids, and 0.06M for sulphuric acid. The effect was most significant with hydrochloric and sulphuric acids and was somewhat reduced by the nitric acid. Phosphoric acid did not increase the signal from arsenic as much as hydrochloric acid. The most likely reason for this is the formation of the phosphomolybdate complex ion. Evidence for the formation of the ion was the formation of the characteristic blue colour when molybdenum(VI) solution was added to the solution of arsenic(III) in phosphoric acid in the reaction vessel, which retains some reducing capacity even after washing with distilled water. The colour could not be reproduced when sulphuric or hydrochloric acids were used.

Figure 2 illustrates the relationship between peak height and molybdenum(VI) concentration for the generation of arsine from

Table 1. Interference of oxyanions on arsenic(III) signals from tetrahydroborate(III) reduction

Anion	Added as	Concentration, $\mu\text{g}/\text{ml}$	Arsenic* recovery %	
			0.02M HCl	0.2M HCl
MoO_4^{2-}	$(\text{NH}_4)_2\text{Mo}_7\text{O}_{24}\cdot 4\text{H}_2\text{O}$	100	246	101
VO_3^-	NH_4VO_3	50	129	—
		100	143	101
$\text{Cr}_2\text{O}_7^{2-}$	$\text{K}_2\text{Cr}_2\text{O}_7$	100	80	85.3
WO_4^{2-}	Na_2WO_4	100	101	107
		200	98	104
MnO_4^-	KMnO_4	100	n.d.†	—
$\text{S}_2\text{O}_8^{2-}$	$(\text{NH}_4)_2\text{S}_2\text{O}_8$	100	76	—

*A 5 ml aliquot of 200 ng/ml arsenic(III) solution was treated with 1 ml of 1% w/v sodium tetrahydroborate(III) solution.

†n.d. = not detectable.

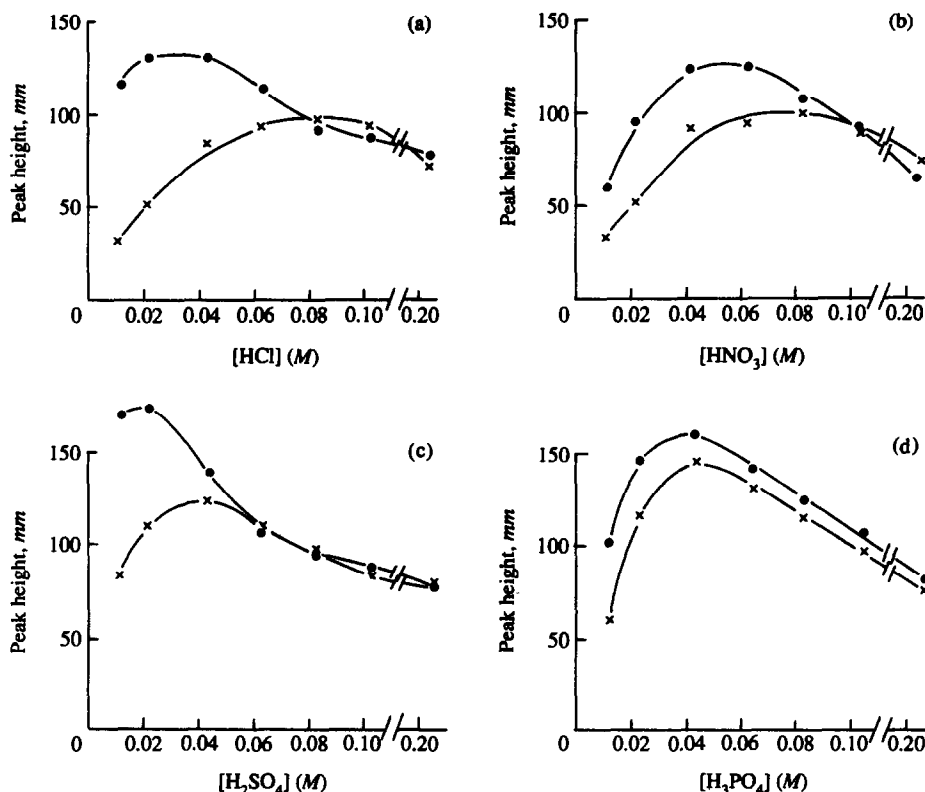


Fig. 1. Molybdenum(VI) interference with arsine generation at different acid concentrations: ●—100 ng/ml As(III) + 50 µg/ml Mo(VI), ×—100 ng/ml As(III) (a) Hydrochloric acid, (b) nitric acid, (c) sulphuric acid and (d) phosphoric acid.

arsenic(III). It is clear from the figure that, in 0.2M hydrochloric acid, molybdenum(VI) has no effect on the peak height over the range of concentrations used. At the lower concentration

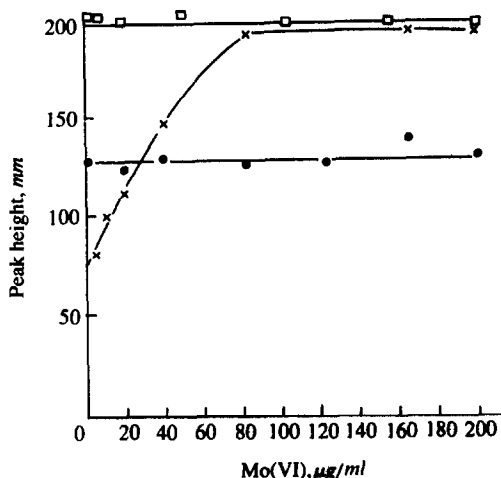


Fig. 2. Influence of molybdenum(VI) on the arsenic signal. ●—5 ml of 200 ng/ml As(III) in 0.2M HCl, ×—5 ml of 200 ng/ml As(III) in 0.02M HCl, □—5 ml of 50 ng/ml As(III) in 0.02M HCl with 0.5% w/v *L*-cysteine (Note: the concentration of arsenic is 1/4 of the concentration compared with the other curves).

of 0.02M hydrochloric acid, the effect is quite striking. Thus the peak height increases almost linearly with molybdenum(VI) concentrations of 0–80 µg/ml, after which the signal remains constant up to a molybdenum(VI) concentration of 200 µg/ml, the limit of these experiments. Although molybdenum(VI) increased the height of the peaks from arsenic, the peak width at half maximum remained the same, suggesting that molybdenum(VI) increases the yield of arsine from the reduction process. The presence of *L*-cysteine in solution, however, served significantly to increase the signal from arsenic(III), while eliminating any effect from the presence of molybdenum(VI). The enhancement of the signal by molybdenum(VI) is only one quarter of that produced by *L*-cysteine.

The relationship between acid concentration, molybdenum(VI) and arsenic(V) is also quite significant. Thus in 0.01M hydrochloric acid, arsenic(V) gives no observable signal whereas in the presence of 20 µg/ml Mo(VI), a substantial peak was obtained. Unfortunately, Mo(VI) does not give similar recoveries for As(V) as it does for As(III). Typically, arsenic(V) gives signals

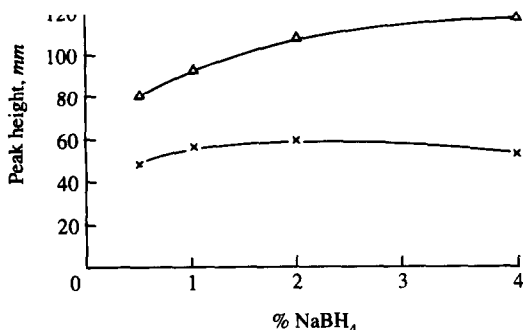


Fig. 3. The effect of tetrahydroborate(III) concentration on the molybdenum(VI) interference. \times —5 ml of 200 ng/ml As(III) in 0.02M HCl, Δ —5 ml of 200 ng/ml As(III) + 20 $\mu\text{g/ml}$ Mo(VI) in 0.02M HCl.

that are only 20–30% of the signals obtained from similar concentrations of arsenic(III).

The effect of tetrahydroborate(III) concentration is also significantly altered by the presence of molybdenum(VI) in the generation of arsine from arsenic(III). From Fig. 3, it is clear that the presence of 20 $\mu\text{g/ml}$ molybdenum(VI) created a different response as the concentration of tetrahydroborate(III) is increased. Thus, in the absence of molybdenum(VI), a relatively constant signal is obtained over the range of concentrations studied. In the presence of 20 $\mu\text{g/ml}$ molybdenum(VI), the signal increases over the same range and starts to level off at a concentration of approximately 4% w/v sodium tetrahydroborate(III).

Welz and Melcher have reported that iron(III) has a releasing effect on nickel(II) in the determination of arsenic and selenium by hydride generation.⁵ Bye has also commented on the same effect in the determination of selenium.⁶ In both cases, the releasing effect was ascribed to the reduction of iron(III) to iron(II),

prior to the reduction of nickel(II) to metallic nickel which, the authors suggest, is the agent responsible for the decomposition of the hydride, before it can be stripped from the solution. The releasing effect of molybdenum(VI) on nickel(II) and cobalt(II) was evaluated, and the results are shown in Fig. 4. It is clear that the presence of 50 $\mu\text{g/ml}$ molybdenum(VI) increased the interference-free level by one to two orders of magnitude.

Evidence for the formation of intermediate oxidation states of molybdenum is supported by the observed colour changes in the reduction reactions. Thus, when tetrahydroborate(III) solution was added to molybdenum(VI) solution in 0.02M hydrochloric acid solution, in the presence or absence of arsenic(III), the colourless solution turned yellow-brown. If the concentration of molybdenum(VI) was greater than 100 $\mu\text{g/ml}$, a small amount of brown precipitate appeared on the frit of the generator. It has been reported that molybdenum(VI) reacts with tetrahydroborate(III) in 0.001M sulphuric acid to form a blue solution of molybdenum(IV).¹⁴ It has also been reported that reduction of the colourless molybdenum(VI) solution by a strong reducing agent in dilute hydrochloric acid turned first blue, then green, and finally brown, due to the formation of molybdenum(III) chloride.¹⁵ Crouthamel and Johnson reported that molybdenum(V) is brown in dilute hydrochloric acid, and that freshly formed molybdenum(V) is unstable.¹⁶ These observations lead us to conclude that the reduction of interferences by molybdenum(VI) is most likely due to the formation of lower oxidation states of molybdenum by the tetrahydroborate(III), and that this reaction competes with

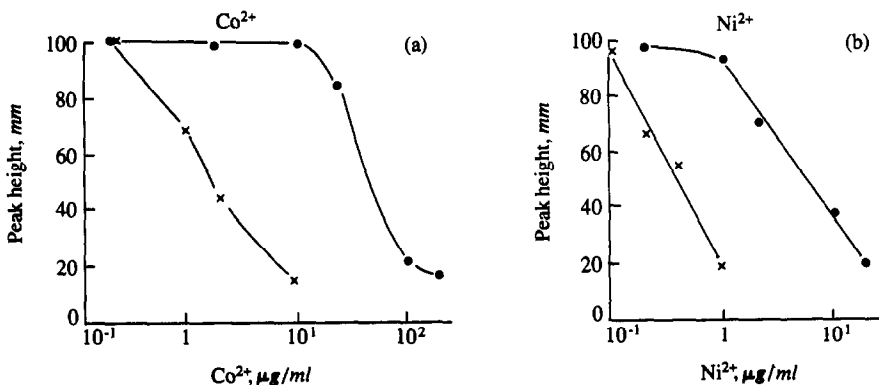


Fig. 4. The releasing effect of molybdenum(VI) on the interference from (a) Co(II) and (b) Ni(II). \times = 5 ml of 200 ng/ml As(III) in 0.04M HCl, \bullet —5 ml of 200 ng/ml As(III) + 50 $\mu\text{g/ml}$ Mo(VI) in 0.04M HCl.

the reduction of Ni(II) and Co(II) to the metals. We have argued elsewhere that intermediate hydrides may be formed that are more efficient hydride transfer reagents than tetrahydroborate(III).¹⁸ Whether this is the case with molybdenum is not clear at this point.

The generality of the method was tested on the hydride-forming elements antimony, bismuth and tin. In all cases, molybdenum(VI) has a depressing effect upon the signals from the hydrides. We have previously reported the depressing effect of molybdenum(VI) on the generation of germane.⁸

It is clear that molybdenum(VI) has an enhancing effect on arsine production at low acid concentrations, and that it reduces interferences from nickel and cobalt. The method is obviously limited in scope for analytical determinations, but may find applications in some limited areas.

Acknowledgements—The authors wish to thank the Ontario Ministry of the Environment for funding this research (Project 434 G). Hangzhou University is thanked for providing a leave of absence for Hengwu Chen.

REFERENCES

1. A. E. Smith, *Analyst*, 1975, **100**, 300.
2. G. F. Kirkbright and M. Taddia, *Anal. Chim. Acta*, 1978, **100**, 145.
3. T. Nakahara, *Applied Spectroscopy*, 1983, **37**, 539.
4. I. D. Brindle and C. M. Ceccarelli Ponzoni, *Analyst*, 1987, **112**, 1547.
5. B. Welz and M. Melcher, *ibid.*, 1984, **109**, 577.
6. R. Bye, *ibid.*, 1986, **111**, 111.
7. C. Boampong, I. D. Brindle, X.-c. Le, L. Pidwerbesky and C. M. Ceccarelli Ponzoni, *Anal. Chem.*, 1988, **60**, 1185.
8. I. D. Brindle and X.-c. Le, *Anal. Chim. Acta*, 1990, **229**, 239.
9. I. D. Brindle, X.-c. Le and X.-f. Li, *J. Anal. Atom. Spectrom.*, 1989, **4**, 227.
10. I. D. Brindle and X.-c. Le, *Analyst*, 1988, **113**, 1377.
11. F. D. Pierce and H. R. Brown, *Anal. Chem.*, 1976, **48**, 693.
12. F. D. Pierce and H. R. Brown, *ibid.*, 1977, **49**, 1417.
13. H. Chen, I. D. Brindle and X.-c. Le, *unpublished results*.
14. M. Dasgupta and M. K. Mahanti, *Transition Met. Chem.*, 1988, **13**, 42.
15. G. Svehla, *Vogel's Qualitative Inorganic Analysis 6th Ed.*, Longmans, Harlow, 1981, p. 250.
16. C. E. Crouthamel and C. E. Johnson, *Anal. Chem.*, 1954, **26**, 1284.

ANALYTICAL APPLICATION OF A NEW THIAZOLYLAZO REAGENT, 2-(2-BENZOTHIAZOLYLAZO)-5- DIMETHYLAMINO-4-TOLYLARSONIC ACID

SPECTROPHOTOMETRIC DETERMINATION OF PALLADIUM

LIU PO and LIU HENGCHUAN

Department of Chemistry, East China Normal University, Shanghai 200062, People's Republic of China

WU CHENG

Shanghai Research Institute for Materials, MMBEI, Shanghai 200433, People's Republic of China

(Received 10 October 1989. Revised 24 February 1991. Accepted 4 March 1991)

Summary—A new thiazolyazo reagent, 2-(2-benzothiazolyazo)-5-dimethylamino-4-tolylarsonic acid, has been synthesized and found to be a good chromogenic reagent for palladium. A 1:1 blue chelate ($\lambda_{\max} = 718$ nm) is formed in a sulphuric or nitric acid medium. The molar absorptivity is 6.65×10^4 l. mole⁻¹. cm⁻¹. Beer's law is obeyed in the range 0–1.6 μ g/ml Pd. Relatively large amounts of co-existing elements, including noble metals, can be tolerated.

The selectivity and stability of the chelates of palladium with many of the thiazolyazo reagents have attracted much attention by analytical chemists. These properties are conferred by the functional group, (—NH₂, —COOH, etc.) *ortho* to the azo group.^{1,2} To improve the selectivity, introduction of an arsonic group *ortho* to the azo group is proposed, and a new compound, 2-(2-benzothiazolyazo)-5-dimethylamino-4-tolylarsonic acid (BTADMTA) has been synthesized and the photometric properties of its chelate with palladium have been studied. A blue 1:1 chelate with palladium can be formed even in strongly acidic medium. The absorption maximum is at 718 nm and the molar absorptivity is 6.65×10^4 l. mole⁻¹. cm⁻¹. Beer's law is obeyed in the concentration range 0–1.6 μ g/ml Pd. Relatively large amounts of vanadium, chromium, manganese, copper, iron, nickel, zinc, molybdenum, silicon, silver, cadmium, and even noble metals such as platinum, gold, ruthenium and iridium can be tolerated. This new reagent is comparable both in sensitivity and selectivity with thiazolyazo compounds reported earlier.³⁻¹³ A simple and rapid spectrophotometric method for determination of palladium is proposed and has been tested in the analysis of industrial samples.

EXPERIMENTAL

Apparatus

Spectra were obtained with a Hitachi Model 557 double-beam dual wavelength spectrophotometer equipped with 1-cm cells. The pH measurements were made with a Model pH-III pH-meter.

Reagents

Pd standard solution A. Pure palladium (99.9% pure, 0.1000 g) was dissolved in *aqua regia*. Sixteen ml of sulphuric acid (1 + 1) were added and the solution was heated till fuming strongly. It was cooled to room temperature, about 30 ml of water were added and the solution was cooled, transferred into a 100-ml standard flask, and diluted to volume with water.

Pd standard solution B. Prepared just before use, by transfer of 1.00 ml of Pd standard solution A into a 100-ml standard flask, addition of 1 ml of sulphuric acid (1 + 1), and dilution to volume with water. One ml of this solution contains 10 μ g of Pd.

BTADMTA solution, 0.1 mg/ml in ethyl alcohol.

Synthesis of BTADMTA

Dissolve 1.5 g (0.01 mole) of 2-aminobenzothiazol in 2 ml of formic acid and 5 ml of

Table 1. Infrared spectrum data for BTADMTA

Group	ν , cm^{-1}
—CH ₃	2930
Ar—H	3030
>C=C<	1600–1400
—N(CH ₃) ₂	2815–2805
—AsO ₃ H ₂	3000–2300

concentrated sulphuric acid and add 8 ml of water. Add a solution of 0.72 g of sodium nitrite in 20 ml of water dropwise to this solution at 0–5°. Dissolve 2.6 g (0.01 mole) of 3-dimethylamino-4-tolylarsonic acid in 25 ml of acetic acid plus 100 ml of methyl alcohol, and cool the solution to 0–5°. Add the diazotized solution dropwise to this solution, with vigorous stirring, and let the mixture stand overnight. Adjust the pH to about 4 to precipitate crude BTADMTA and purify the red product by recrystallization from dimethylformamide (DMF) and water. Its m.p. is 214°, and the yield is about 47%. Its structure has been verified by infrared and NMR spectroscopy. (Tables 1 and 2).

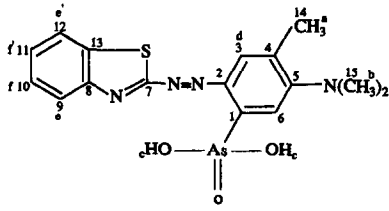
Elemental analysis confirmed its purity (Table 3). The pure product is easily soluble in polar organic solvents, *e.g.*, DMF, dimethylsulphoxide, chloroform, acetone, ethanol and is also soluble in dilute acidic or alkaline solution. It is only slightly soluble in water. It is red in weakly acidic or alkaline solution, and green in strongly acidic solution.

General procedure

In a 25-ml standard flask, place 5 ml of sulphuric acid (1 + 1) and a sample containing not more than 40 μg of Pd, mix well and cool if necessary. Add successively 10 ml of 95%

Table 2. NMR data for BTADMTA

¹ H NMR			¹³ C NMR	
Position	δ , ppm	No. of H atoms	Position	δ , ppm
a	2.30	3	1	179.7
b	2.98	6	2	156.3
c	3.78	2	3	138.4
d	8.10	1	4	124.4
d'	8.12	1	5	123.0
e-f'	7.52–7.58	4	6	137.5
			7	161.5
			8	141.3
			9	130.7
			10	126.0
			11	128.0
			12	131.2
			13	147.5
			14	24.46
			15	46.74

Table 3. Elemental analysis of BTADMTA (C₁₆H₁₇AsN₄O₃S)

	C, %	H, %	N, %
Found	45.8	4.1	13.9
Theory	45.7	4.05	13.3

ethanol and 3 ml of 0.1 mg/ml BTADMTA solution, mix, dilute to the mark with water, mix, and let stand for 10 min. Measure the absorbance at 718 nm, in a 1-cm cell, against water as reference.

RESULTS AND DISCUSSION

Effect of acidity

The colour reaction can be performed in either nitric or sulphuric acid medium. The optimum acid concentrations are 0.1–0.8 and 0.32–3.2M respectively. Perchloric acid medium can also be used but the sensitivity is lower. Since chloride forms a fairly strong complex with palladium, hydrochloric acid medium should not be used. At high nitric acid concentration, *e.g.*, 6M, the sensitivity is even higher than in sulphuric acid medium, but the blue chelate is soon destroyed. A 2M sulphuric acid medium is recommended.

Effect of organic solvents

Addition of appropriate amounts of ethanol, acetone or dimethylformamide increases the solubility of BTADMTA and thus favours the reaction with palladium, and increases the absorbance. Ethanol is the best to use, and the increase in absorbance is constant when more than 8 ml of ethanol is added. Maximum absorbance is attained after 10 min and is stable for at least 24 hr. In the absence of ethanol the reaction system achieves maximum absorbance after 5 min, but the absorbance decreases gradually upon standing. The addition of non-ionic surfactants, *e.g.*, Triton X-100, can also improve the stability but cannot increase the sensitivity (Fig. 1).

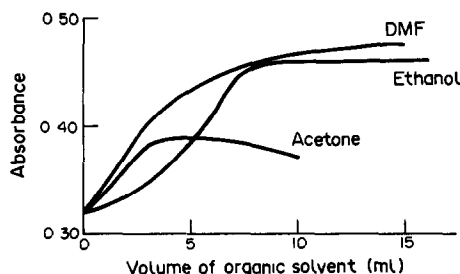


Fig. 1. Effect of organic solvent (20 μg of Pd, 3 ml of 0.1 mg/ml BTADMTA, 2M HNO₃).

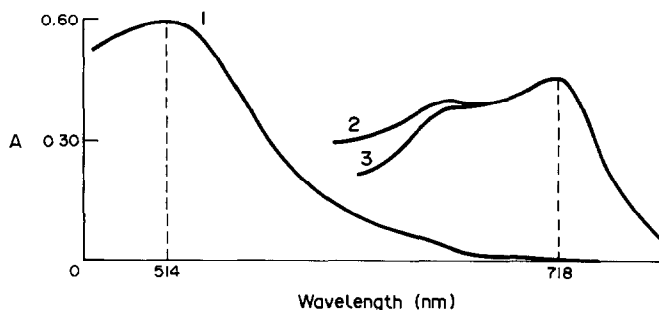


Fig. 2. Absorption spectra (20 μg of Pd, 2M HNO_3 , 10 ml of ethanol, $l = 1$ cm). 1, Reagent vs. H_2O ; 2, Pd-chelate vs. H_2O ; 3, Pd-chelate vs. reagent blank.

Effect of BTADMTA concentration

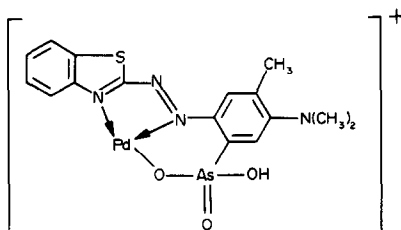
For up to 40 μg of Pd, the addition of more than 0.30 mg of BTADMTA is enough for complete reaction. Hence 3 ml of 0.1-mg/ml reagent solution is specified in the general procedure. Beer's law is obeyed in the concentration range 0–1.6 $\mu\text{g}/\text{ml}$ Pd, and the apparent molar absorptivity is 6.65×10^4 l.mole⁻¹.cm⁻¹. For > 1.6 $\mu\text{g}/\text{ml}$ Pd, addition of a greater amount of BTADMTA will extend the linear range.

Absorption spectra

The absorption spectra of BTADMTA and its Pd-chelate under the optimum conditions are shown in Fig. 2. The absorption maximum of the reagent lies at 514 nm, and the chelate has two maxima, at 660 and 718 nm, the latter being chosen for measurements, as the reagent itself has no absorption.

Composition of the chelate

The mole-ratio and continuous variation methods show that a 1:1 chelate is formed, which may have the structure:



Effect of diverse ions

Under the specified optimum conditions, a 200-fold ratio of Mg(II), Al(III), Cr(III), Mn(II), Co(II), Ni(II), Cu(II), Zn(II), Cd(II), Ag(I), Zr(IV), and Si(IV) to Pd(II) does not

interfere; 100-fold ratio of V(V), Fe(III), Mo(IV), Pt(IV), Au(III), Ru, Ir can be tolerated. Fluoride, borate, citrate and a few drops of 3% hydrogen peroxide solution do not interfere. Chloride forms a stable complex with Pd(II), and ascorbic acid destroys the BTADMTA, thus causing serious interference.

Applications

The proposed method has been applied to the determination of palladium in an Ni–Al catalyst and an active carbon concentrate.

For the Ni–Al catalyst, a 50-mg sample is dissolved in a mixture of nitric acid and hydrochloric acid, 10 ml of concentrated sulphuric acid are added and the mixture is heated until fuming. For complete oxidation of organic matter in the sample, the addition of a few ml of concentrated nitric acid may be necessary during the fuming. The solution is cooled, the salts are taken up in water, and after cooling the solution is transferred to a 50-ml standard flask, and diluted to the mark with water. An appropriate aliquot is analysed as described in the general procedure.

For the active carbon concentrate, a 50-mg sample is ignited in a porcelain crucible in a muffle furnace at 850° until the carbon is completely oxidized. The residue is dissolved in 2 ml of *aqua regia* and the solution is heated to fuming after addition of 2 ml of concentrated sulphuric acid. The solution is cooled, 10 ml of water are added to dissolve the salts, and the solution is diluted to volume in a 50-ml standard flask with water. An appropriate aliquot is then analysed by the general procedure.

The results obtained for some industrial samples are consistent with those obtained by the 1-nitroso-2-naphthol photometric method¹⁴ (Table 4).

Table 4. Results for industrial samples

Sample	Proposed method			1-Nitroso-2-naphthol method	
	Pd, %	\bar{X} , %	Std. devn, %	Pd, %	\bar{X} , %
Ni-Al catalyst	0.185			0.182	
	0.187				
	0.190	0.186	0.004	0.190	0.183
	0.180				
Active carbon concentrate	0.186			0.178	
	0.501			0.510	
	0.497				
	0.503	0.500	0.003	0.498	0.506
	0.498				
	0.502			0.510	

REFERENCES

- G. Zhang and X. Zhang, *Fenxi Shiyanshi*, 1988, 7, No. 8, 35; *Anal. Abstr.*, 1989, 59, 6A5.
- C. Ma and C. Wu, *Lihua Jiannan, Huaxue Fence*, 1988, 24, 311; *Anal. Abstr.*, 1989, 51, 5A4.
- H. Xu and J. Qin, *Fenxi Huaxue*, 1984, 12, 504; *Chem. Abstr.*, 1985, 102, 55248s.
- M. Yu. Yusupov, A. Kh. Alikhodzhaev and D. N. Pachadzhanov, *Zh. Analit. Khim.*, 1985, 40, 844.
- J. Vořtová and L. Sommer, *Collection Czech. Chem. Commun.*, 1976, 41, 1137.
- L. P. Adamovich, A. L. Gershuns, A. A. Oleinik and Nguen Tkhi Zung, *Zh. Analit. Khim.*, 1973, 28, 715.
- P. Sutthivaiyakit and A. Kettrup, *Z. Anal. Chem.*, 1985, 320, 769.
- F. García Montelongo, V. González Díaz and C. R. Tallo González, *Analisis*, 1981, 9, 353.
- G. Zhang, Y. Hu and G. Xu, *Fenxi Huaxue*, 1987, 15, 986; *Chem. Abstr.*, 1988, 108, 231068t.
- F. García Montelongo, V. González Díaz and C. R. Tallo González, *Analyst*, 1979, 104, 1091.
- Y. Li, M. Chen, Y. Liu, X. Shen, J. Xue and C. He, *Fenxi Huaxue*, 1988, 16, 1034; *Chem. Abstr.*, 1989, 111, 32834b.
- F. García Montelongo, V. González Díaz and C. R. Tallo González, *Microchem J.*, 1982, 27, 194.
- T. Katami, T. Hayakawa, M. Furukawa and S. Shibata, *Bunseki Kagaku*, 1984, 33, 676.
- 1984 *Annual Book of ASTM Standards*, Vol. 03.05, pp. 407-408. ASTM, Easton MD.

KINETIC DETERMINATION OF Hg(II) BASED ON ITS ACCELERATING EFFECT ON THE REACTION BETWEEN HEXACYANOFERRATE(II) AND 1,10-PHENANTHROLINE CATALYSED BY MICELLES

DOLORES SICILIA, SOLEDAD RUBIO and DOLORES PEREZ BENDITO

Department of Analytical Chemistry, Faculty of Sciences, University of Córdoba, Córdoba, Spain

(Received 12 September 1990. Revised 14 March 1991. Accepted 25 March 1991)

Summary—A kinetic-photometric method for the determination of Hg(II) over the range 10–80 ng/ml is proposed. It is based on the accelerating effect of this ion on the reaction between hexacyanoferrate(II) and 1,10-phenanthroline which is monitored via the ferriox complex formed. Anionic sodium dodecyl sulphate (SDS) micelles, which catalyse the reaction, allow the ferriox complex to be formed under more acidic conditions. Combination of this pH shift and the development of the reaction in the vicinity of micelles results in improved selectivity in the determination of Hg(II) compared to the reaction occurring in an aqueous medium. Some observations on the effect of SDS on the reaction are reported.

Reactions in micellar media have aroused much attention in the last two decades.^{1–3} Experiments on a variety of systems have shown that remarkable kinetic advantages can be gained upon confining a chemical reaction to a micelle and, more recently, these advantages have begun to be exploited in analytical kinetic methods.^{4–7} Two types of physico-chemical factors are responsible for the efficiency of micellar catalysis on reactions of second and higher orders, namely, the concentration of reactants inside the micellar phase and the change in the reactant reactivities on transfer from water to the micellar phase.

Micellar systems are known⁸ to have a marked effect on the acid–base equilibria of compounds with different ionization states. Changes in the apparent pK_a values can be caused and the direction in which equilibrium will displace depends essentially on electrostatic interactions between one of the species involved and the micelle surface. If both forms of the compound involved in the equilibrium have a charge of the same sign, specific factors such as hydrophobic and micro-solvent interactions and electrostatic forces will determine the displacement direction. As a result the complexes formed between these compounds and metal ions occasionally occur at lower pHs: this phenomenon has been exploited in analytical chemistry to increase the selectivity of metal ion determinations based on complexation reactions with chelometric indicators.⁹

In this work we applied the concept of micelle-induced changes in the pK_a to analytical kinetic methods in order to improve their selectivity. For this purpose, at least one reactant taking part in the reaction must have acid-base properties and one of the forms involved in the equilibrium must concentrate preferentially on the micellar surface. Thus, if a change in the pK_a value is observed and the reaction (complexation, redox or precipitation) is affected by the pH, changes in the pH region where it takes place will be produced. The reaction between hexacyanoferrate(II) and 1,10-phenanthroline, which is accelerated by mercury(II), was selected for this study.¹⁰

EXPERIMENTAL

Apparatus

Kinetic measurements were made on a Perkin–Elmer Lambda 5 spectrophotometer fitted with a Perkin–Elmer C570-0701 digital controller to keep the cell compartment at constant temperature. All measurements were recorded by using slits of 2-nm spectral band-pass. A classical stalagmometer was used for surface tension measurements in order to determine the critical micellar concentrations (cmc) of the surfactants.

Reagents

All reagents used were of analytical grade and utilized as purchased, without further purification.

A stock Hg(II) solution ($4.98 \times 10^{-3} M$) was prepared by dissolving mercury(II) oxide (Merck) in 20 ml of 1:1 hydrochloric acid and making up to one litre with doubly distilled water. Working solutions ($4.98 \times 10^{-6} M$) were prepared daily by appropriate dilution with doubly distilled water. A $5.0 \times 10^{-3} M$ aqueous solution of potassium iron cyanide [$K_4Fe(CN)_6 \cdot 3H_2O$] (Merck) was also prepared daily. A $1.0 \times 10^{-3} M$ aqueous solution of 1,10-phenanthroline was made from 1,10-phenanthroline chloride monohydrate (Merck). A sodium dodecyl sulphate (SDS) solution ($6.94 \times 10^{-2} M$) (Aldrich) was prepared by dissolving the surfactant in doubly distilled water. The other surfactants tested, *viz* sodium dioctylsulphosuccinate (Aerosol OT) (Aldrich), cetyltrimethylammonium bromide (CTAB) (Sigma), dodecyltrimethylammonium bromide (DTAB) (Sigma), cetylpyridinium chloride (CPC) (Serva), Triton X-100 (Serva), Brij-35 (Merck) and N-dodecyl-N,N-dimethylammonium-3 propane-sulphonate (SB-12, sulphobetaine) (Serva) were prepared in a similar way. Less soluble surfactants were dissolved with warming.

Procedure for the kinetic photometric determination of mercury

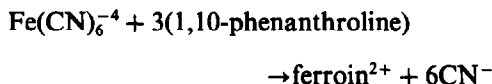
In a 10-ml standard flask were placed, in sequence, 1 ml of $K_4Fe(CN)_6$ ($4.997 \times 10^{-3} M$), 2 ml of 1,10 phenanthroline ($1.0 \times 10^{-3} M$), 0.7 ml of SDS ($6.94 \times 10^{-2} M$), the volume of hydrochloric acid (0.2M) required to obtain a final pH of 2.0 and appropriate volumes of mercury(II) standard solution ($4.98 \times 10^{-6} M$) to give a mercury(II) final concentration between 10 and 80 ng/ml. The stopclock was started immediately after mercury(II) was added and the solution was then diluted to the mark with doubly distilled water. An aliquot of the reaction mixture was transferred to a cell kept at $60 \pm 0.1^\circ$ and the absorbance ($\lambda = 500$ nm) was recorded as a function of time. Measurements were started exactly 3 min after the addition of mercury(II). The reaction rate was calculated by the tangent method from the absorbance-time curves and the rate corresponding to a blank solution, containing no mercury(II), was subtracted.

RESULTS AND DISCUSSION

Selection and influence of the micellar system on the mercury(II)-accelerated reaction between hexacyanoferrate(II) and 1,10-phenanthroline

The ligand-exchange reaction between hexacyanoferrate(II) and 1,10-phenanthroline, which

is accelerated by mercury(II), was used to determine this ion by measuring the rate of formation of ferriin spectrophotometrically¹¹⁻¹² according to the following system:



The 1,10-phenanthroline reagent has acid-base properties, so it yields a typical uniequivalent titration curve on titration with strong acids.¹³ The acid dissociation constant of the phenantrolium ion in aqueous solutions has been measured by several different methods and pK_a values of *ca.* 5 have been reported. Although, the UV spectra obtained from concentrated sulphuric acid solutions reveal the formation of the diprotic species, the pK_a values reported for phen.2H⁺ (about -1.6)¹⁴ indicate that the phen.2H⁺ concentration is negligible at the pH where the above reaction takes place. Therefore, only the phen.H⁺/phen. equilibrium will be considered. This can be displaced to the acid form by anionic micellar systems, which can alter the pH at which the reaction develops.

The effect of surfactants of different nature [anionic (SDS, Aerosol OT), cationic (DTAB, CTAB, CPC), nonionic (Brij 35, Triton X-100) and zwitterionic (SB-12)] on the analytical reaction was tested at three surfactant concentrations, namely, below, close to and above their cmc, and at different pH values. Micellar catalysis was found to occur in the presence of anionic and zwitterionic micelles at pH values where the aqueous reaction hardly developed. The most significant rate increase was due to SDS, which was thus chosen for subsequent experiments. Nonionic micelles had no effect on the reaction rate and the influence of cationic micelles could not be established because a precipitate was formed on addition of the cationic surfactant.

Figure 1 shows the effect of the SDS concentration on the rate of the non-catalysed hexacyanoferrate-1,10-phenanthroline system (curve a) and that catalysed by different mercury(II) concentrations (curves b and c) at pH 2. The rate was scarcely affected by surfactant concentrations below the cmc ($5 \times 10^{-4} M$, calculated under our reaction conditions), but, close to the cmc, the rates started to rise sharply to a maximum value, above which they decreased with increasing SDS concentration, the final rate decrease being the effect of dilution of the reactants over the increasing concentration of micelles in the solution. Sodium dodecyl

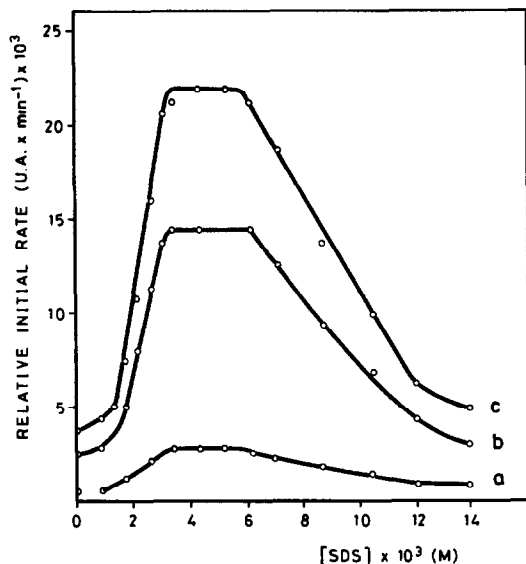


Fig. 1. Influence of the SDS concentration on the rate of the non-catalysed (curve a) and the mercury(II)-catalysed (curve b, c) reaction between hexacyanoferrate(II) and 1,10-phenanthroline. Mercury(II) concentration: (b) 0.05 $\mu\text{g/ml}$; (c) 0.1 $\mu\text{g/ml}$. The concentrations of the other reactants are given under Experimental.

sulphate enhances the accelerating effect of mercury, as can be inferred from Fig. 1 by comparing the reaction rate increments of the different

curves at the SDS concentrations 0 and $4 \times 10^{-3} \text{M}$. Therefore, the kinetic determination of mercury(II) in the presence of this surfactant will be more sensitive at the working pH (pH = 2).

Study of the optimum reaction conditions

The effect of different variables affecting the reaction rate was studied in the presence and absence of SDS in order to compare the behaviour of the reaction in micellar and aqueous media and optimize the conditions for the determination of mercury(II). The optimum conditions chosen were those yielding a minimum relative standard deviation for the initial rate measurement under conditions in which the reaction order was zero, or as close to zero as possible, with respect to the variable concerned.

Figure 2 shows the variation of the initial rate as a function of different variables [temperature (A); pH (B); 1,10-phenanthroline (C) and hexacyanoferrate(II) (D)] for the SDS + Hg-(curve 2) and Hg(II)-accelerated (curve 1) reactions. The initial rates yielded by the blanks [without Hg(II)] were subtracted prior to plotting.

The dependence of the initial rate of the SDS-Hg(II) accelerated reaction [Fig. 2(A),

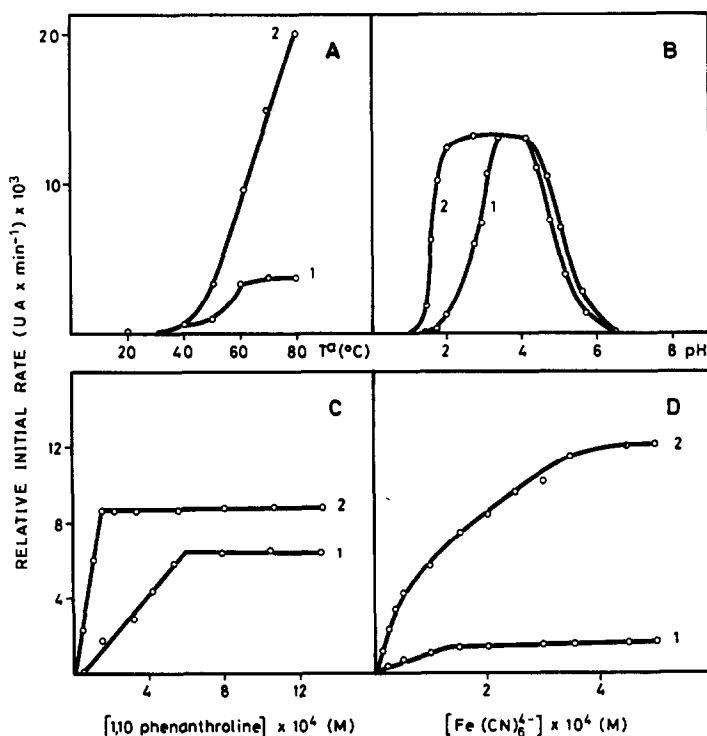


Fig. 2. Influence of (A) temperature, (B) pH, (C) 1,10-phenanthroline concentration and (D) hexacyanoferrate(II) concentration on the rate of the Hg(II)- (curve 1) and Hg(II) + SDS-accelerated (curve 2) reaction between hexacyanoferrate(II) and 1,10-phenanthroline. The concentrations of reactants are given under Experimental.

curve 2] on the temperature was exponential over the range tested (20–80°) and was greater than that corresponding to the Hg(II)-accelerated reaction. Temperatures above 60° were not advisable for the determination of mercury because of the decreased precision of the measurements.

The presence of anionic micelles of SDS allowed ferroin to be formed under more acidic conditions. As can be seen from Fig. 2(B), this complex is optimally formed at pH 2–4 and 3.5–4 in the presence and absence, respectively, of the anionic micellar system. Its analytical advantage lies in the fact that it allows the complex to be formed over a wider pH region, which increases the possibility of choosing a pH allowing the reduction or elimination of interferences. The pH selected for the determination of mercury(II) in the presence of SDS micelles was the minimum value which resulted in the maximum reaction rate in order to improve the selectivity. The optimum pH (2.0) was adjusted with hydrochloric acid; none of the buffers tested (tartrate, glycine and phthalate) was effective at this working pH.

The curves in Fig. 2(C) show the variation of the initial rate of the aqueous (curve 1) and micellar (curve 2) reaction with the phenanthroline concentration. The reaction reaches pseudozero order with respect to this variable at lower phenanthroline concentrations.

The influence of the hexacyanoferrate(II) concentration is illustrated in Fig. 2(D). The curves corresponding to the Hg(II)- and SDS + Hg-accelerated reactions show a first-order dependence on hexacyanoferrate(II) at low concentrations of this ion. As the hexacyanoferrate(II) concentration increases, this dependence tails off to zero for the Hg(II)- and SDS-Hg(II)- accelerated reactions rapidly and gradually, respectively. The concentration of hexacyanoferrate(II) corresponding to a zero-order dependence is a function of both the absolute concentrations of 1,10-phenanthroline and hexacyanoferrate(II) and of the ratio between the two (a hexacyanoferrate(II):1,10-phenanthroline ratio above 2:1 is required).

The reaction rate remained maximal on varying the order of addition of reagents and the ionic strength (adjusted with potassium chloride or potassium nitrate) at least up to $2 \times 10^{-2}M$.

Analytical features

A calibration graph for the determination of Hg(II) in the SDS micellar medium was run

Table 1. Analytical features of the determination of Hg(II) by its accelerating effect on the hexacyanoferrate(II)-1,10-phenanthroline system in the presence and absence of SDS

Parameter	With SDS	Without SDS
Sensitivity, M^{-1}/min	$(32.4 \pm 0.6) \times 10^3$	$(4.3 \pm 0.3) \times 10^3$
*Detection limit, ng/ml	4	23
†RSD, %	4.5	10.8

* 3σ .

† $n = 11$, for 40 ng/ml Hg(II).

under the optimal conditions described earlier. The determination of this ion was feasible over the range 10–80 ng/ml. Analytical features such as sensitivity, detection limit and precision (expressed as relative standard deviation) are summarized in Table 1, which also includes the same analytical features for the determination of Hg(II) in the absence of SDS at pH 2 for contrast. On the basis of these features, the determination of Hg(II) at pH 2 is more favourable in the micellar medium. At pH 3.5, and in the absence of SDS, the sensitivity and detection limit are similar to those obtained at pH 2 in the presence of SDS, as can be seen from Fig. 2(B). Only a net gain in precision in the determination of Hg(II) was observed at any pH values tested when the reaction was developed in the SDS micellar medium.

In order to elucidate whether micellar catalysis resulted in increased selectivity towards the determination of Hg(II), the effect of various ions on the hexacyanoferrate(II)-1,10-phenanthroline system in the presence and absence of SDS was studied at pH 2. The ions tested were those normally found in biological fluids, which are among the matrices most frequently used for the determination of Hg(II). Table 2 summarizes some of the results obtained. The selectivity factor, defined as the ratio between the tolerated concentrations of foreign species in the presence of SDS to that found when the surfactant was absent is also included in this table. The maximum mole ratio of ion to Hg(II) tested was 2000. The selectivity was significantly improved with respect to some cations present in biological fluids. Since the experiment was carried at the same pH values in the presence and absence of SDS, the micelles must be responsible for such an improvement. An identical experiment was done at pH 3.5 and the results obtained for the main interferents are also listed in Table 2. Logically, the selectivity decreased as pH increased for ions such as Cu(II) and Zn(II). Improved selectivity was also obtained at pH

Table 2. Effect of foreign ions on the determination of $5 \times 10^{-7} M$ Hg(II) at two pH values

Ion tested	Tolerated mole ratio of ion to Hg(II)		Selectivity factor (with SDS/without SDS)
	with SDS	without SDS	
		pH = 2	
Cu(II)	10^{-2}	10^{-3}	10
Ca(II)	≥ 2000	50	≥ 40
Fe(III)	10	1	10
Zn(II)	30	1	30
I ⁻	5	5	1
		pH = 3.5	
Cu(II)	10^{-3}	10^{-4}	10
Ca(II)	≥ 2000	50	≥ 40
Fe(III)	10	1	10
Zn(II)	10	1	10

Mg(II), K(I), Cl⁻, F⁻, HCO₃⁻, PO₄³⁻ and SO₄²⁻ ions are tolerated up to a mole ratio of ion to Hg(II) of 2000 in both methods.

3.5 in the SDS micellar medium. Therefore, micelles probably enhance the selectivity of kinetic methods, especially if they permit the reaction to occur at lower pH values than in the aqueous medium. Nevertheless, further studies must be made in this direction to determine the real applicability of micelles in analytical kinetic methods.

Some observations on the action of SDS on the reaction

In order to determine the mechanism via which SDS acts on the hexacyanoferrate(II)-1,10-phenanthroline system we must first consider the net changes that this surfactant induces on the reaction features. The observed alterations were:

- the pH over which the reaction took place [Fig. 2(B)].
- the acceleration of the reaction over a given pH range [Fig. 2(B)].

Since the hexacyanoferrate(II) ion is negatively charged and thus cannot be concentrated on the micellar surface, only 1,10-phenanthroline-micelle and ferroin-micelle interactions were investigated in order to determine the origin of the above changes.

1,10-Phenanthroline-micelle interaction. Only the phen.H⁺/phen. equilibrium was considered because the diprotic species phen.2H⁺ (pK_a about -1.6)¹⁴ was considered to be present at a negligible concentration over the pH range where the reaction took place. The pK_a of the phen.H⁺/phen. equilibrium was found to be different for the SDS micellar (6.0 ± 0.1) and aqueous (5.0 ± 0.1) media when calculated under the same conditions. Therefore, the SDS anionic micelles displace the equilibrium to the acid form and 1,10-phenanthroline becomes a

weaker acid in the micellar medium. This results in phen.H⁺ being preferentially concentrated on the micellar surface and, although hydrophobic interactions could be significant, ionic interactions are definitive.

Ferroin-micelle interaction. Micelles are known to increase the molar absorptivity of complexes, which results in apparently increased reaction rates if reaction development is monitored via the formation or disappearance of the complex. To clarify this point several experiments were done in which the potential sensitization of ferroin by SDS was investigated. The experiments were carried out by mixing Fe(II) ($4.99 \times 10^{-4} M$) with 1,10-phenanthroline ($3 \times 10^{-4} M$) at pH 2. Once the reaction was complete, the absorbance was found to decrease very slightly with time. If SDS was added to this solution 1 hr after the reaction was started, the maximum absorbance was restored, but no net increment in the absorbance was obtained under the reaction conditions. Therefore, no sensitization of ferroin by SDS micelles occurred.

In order to determine the net influence of SDS micelles on the formation of ferroin at different pH values, Fe(II) ($2.0 \times 10^{-5} M$) and 1,10-phenanthroline ($2.6 \times 10^{-4} M$) were mixed in the presence ($4.85 \times 10^{-3} M$) and absence of SDS at 60°, the temperature chosen to monitor the development of the reaction between hexacyanoferrate(II) and 1,10-phenanthroline. Figure 3 shows the maximum absorbance values obtained as a function of pH. It is clearly seen that the ferroin complex begins to be formed at lower pH values in the micellar medium compared to the aqueous medium. Therefore SDS seems to have a concomitant effect on the Fe(II)-1,10 phenanthroline and hexacyanoferrate(II)-1,10-phenanthroline systems.

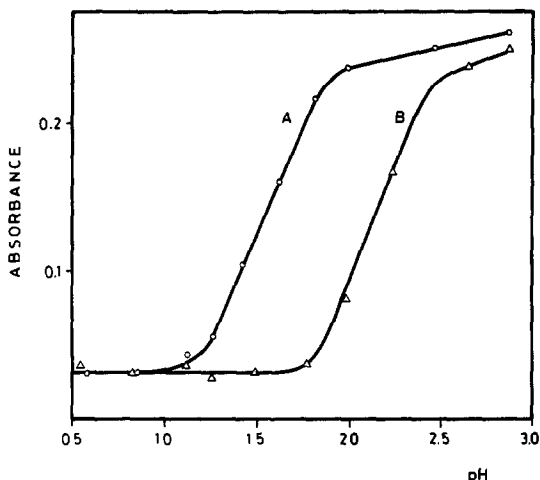


Fig. 3. Influence of the pH on the final absorbance of the Fe(II)-1,10-phenanthroline system in the presence (curve A) and absence (curve B) of SDS.

Since phen.H⁺ is concentrated on the micellar surface, the effective concentration of this reactant will be increased compared to that in the aqueous medium. In addition to an increased rate of ferroin formation this increased effective concentration, may result in an increased overall concentration of the complex formed. Figure 4 shows kinetic curves for the formation of ferroin from Fe(II) and 1,10-phenanthroline at different ligand concentrations. When the ligand concentration in solution was a limiting factor for the total ferroin complex produced [Figs 4(A) and (B)], more complex was produced under the same conditions in the micellar medium. When the ligand concentration was not a limiting factor [Figure 4(C)], differences in the reaction rate of formation of ferroin only were observed in the presence and absence of SDS.

The results obtained in the above experiments allow some considerations to be made on the effect of SDS on the reaction between

hexacyanoferrate(II) and 1,10-phenanthroline. If micellar catalysis occurs when one or more reactants are concentrated on the micellar surface, at least phen.H⁺ is concentrated on SDS micelles. Since ionic interaction is the decisive factor in this association (phen.H⁺ is preferentially concentrated from the phen.H⁺/phen. equilibrium) the ionic group of the phen.H⁺ molecule must be oriented towards the micellar surface. Therefore, for ferroin to be formed, Fe(II) must approach the micellar surface. Because of the negative charge carried by hexacyanoferrate, a direct interaction between this reagent and phen.H⁺ is impossible when the reaction takes place in the micelle. As a result, a reaction intermediate with positive or null charge must be formed from hexacyanoferrate(II) or, as suggested elsewhere¹⁵ the iron-bound cyanide is released under the catalytic action of Hg(II), which forms acid-resistant cyanides, and then the free iron(II) is complexed by 1,10-phenanthroline. This could account for the similar effects of SDS on the Fe(II)-1,10-phenanthroline and hexacyanoferrate(II)-1,10-phenanthroline systems.

From Fig. 3 it is apparent that under the working conditions used the reaction between 1,10-phenanthroline and Fe(II) on the micellar surface involves phen.H⁺ since the reaction takes place at lower pH values compared to in an aqueous medium in spite of the fact that 1,10-phenanthroline is a weaker acid in the presence of SDS micelles ($pK_a = 6$). On the other hand, the reaction in the aqueous medium must involve the basic form phen since the conditional formation constant decreases with pH. Although both reactions, that on the micellar surface and that in aqueous medium, can occur concomitantly in solution the relative significance of one over the other will depend on the concentration ratio of phen.H⁺ to phen.

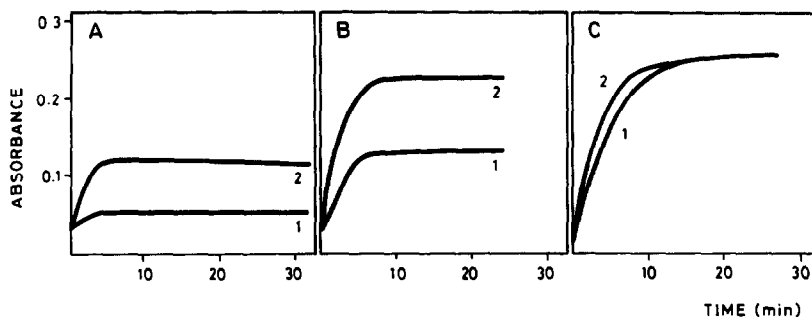


Fig. 4. Influence of the 1,10-phenanthroline concentration on the rate and final absorbance of the Fe(II)-1,10-phenanthroline system at pH 2 in the presence (curve 2) and absence (curve 1) of SDS. [Fe(II)] = $2 \times 10^{-5} M$ pH = 2. Ligand concentration: (A) 4×10^{-5} ; (B) 2×10^{-4} ; (C) $8 \times 10^{-4} M$.

CONCLUSIONS

The features of some analytical kinetic methods can be improved by developing the reactions involved in micellar media. Thus we have shown improved selectivity to be obtained when a reactant has acid-base properties and these are modified appropriately by the presence of surfactants. Further research is required in order to establish the advantages that micellar media can bring to kinetic methods of analysis but, in principle, improved sensitivity, selectivity and/or experimental convenience are to be expected from some reactions.

Acknowledgement—The authors are grateful to the CICYT for financial support (Project No. PB87-0821).

REFERENCES

1. E. H. Cordes, *Reaction Kinetics in Micelles*, Plenum Press, New York, 1973.
2. J. H. Fendler and E. J. Fendler, *Catalysis in Micellar and Macromolecular Systems*, Academic Press, New York, 1975.
3. J. H. Fendler, *Membrane Mimetic Chemistry*, Wiley-Interscience, New York, 1982.
4. E. Athanasiou-Malaki and M. A. Koupparis, *Anal. Chim. Acta*, 1989, **219**, 295.
5. H. A. Archontaki M. A. Koupparis and C. E. Efstathiou, *Analyst*, 1989, **114**, 591.
6. S. Rubio and D. Pérez-Bendito, *Anal. Chim. Acta*, 1989, **224**, 185.
7. M. L. Lunar, S. Rubio and D. Pérez-Bendito, *ibid.*, 1990, **237**, 207.
8. G. S. Hartley, *Trans. Faraday Soc.*, 1934, **30**, 444.
9. W. L. Hinze, in *Solution Chemistry of Surfactants*, K. L. Mittal (ed.), Vol. 1, p. 79. Plenum Press, New York, 1979.
10. T. J. Rohm and W. C. Purdy, *Anal. Chim. Acta*, 1974, **72**, 177.
11. S. Raman, *Indian J. Chem.*, 1975, **13**, 1229.
12. N. D. Lis and N. E. Katz, *Anal. Asoc. Quim. Argentina*, 1981, **69**, No. 1, 1.
13. A. A. Schilt, *Analytical Applications of 1,10-Phenanthroline and Related Compounds*, Pergamon Press, London, 1969.
14. R. H. Linnell and A. Kaczmarczyk, *J. Phys. Chem.*, 1961, **65**, 1196.
15. T. J. Rohm, H. C. Nipper and W. C. Purdy, *Anal. Chem.*, 1972, **44**, 869.

NEW SPECTROPHOTOMETRIC METHODS FOR DETERMINATION OF CAPTOPRIL BULK DRUG AND TABLETS

HASSAN F. ASKAL

University of Assiut, Department of Pharmaceutical Chemistry, Faculty of Pharmacy, Assiut, Egypt

(Received 11 February 1991. Revised 21 April 1991. Accepted 21 May 1991)

Summary—Three simple, rapid and sensitive methods for the assay of captopril which is an effective alternative to digitalis were developed. These methods are based on the oxidation reaction in aqueous solution of captopril with either ferric chloride or iodine. The indirect quantitation of the product was carried out at 523, 351 and 620 nm for ferro-bipyridyl, residual iodine and residual iodine-starch complex, respectively. All variables were studied to optimize the reaction conditions. Regression analysis of Beer's plot showed good correlation in a general concentration range of 0.25–25 µg captopril/ml. No interference was observed from hydrochlorothiazide diuretic which was recently introduced in combination with captopril or other common pharmaceutical adjuvants. The validity of the methods was tested by analysing capoten and capozide tablets. Recoveries were 99.1–102.8%.

Captopril, 1-[(2S)-3-mercapto-2-methylpropionyl]-L-proline, was made generally available for treatment of hypertensive diseases in 1981.¹ It can be used alone or in combination with thiazide diuretics or digoxin²⁻⁵ in patients with moderate heart failure. As several methods have been reported for the quantitative determination of captopril in pure form or in biological fluids, including titrimetry,⁶ amperometry,^{7,8} HPLC,⁹⁻¹⁵ gas-liquid chromatography,¹⁶⁻¹⁹ radioimmunoassay,²⁰⁻²² fluorometry²³⁻²⁵ and colourimetry.²⁶⁻²⁸ Due to the absence of chromophores and/or auxochromes in the captopril molecule, it shows no distinct absorption in the ultraviolet range above 200 nm. Therefore UV spectrophotometry is not the method of choice for the determination of this thiol compound. The reported procedures are sophisticated and time consuming, thus unsuitable for the analysis of a large number of samples.

The development of simple chemical procedures for the determination of captopril in pure and in pharmaceutical dosage forms is therefore necessary.

In the present work, three new, simple, sensitive and rapid spectrophotometric procedures were developed with Fe(III)-bipyridyl and aqueous iodine solution, alone or with starch.

EXPERIMENTAL

Apparatus

The spectrophotometer used was a Uvidex 320 (JASCO, Tokyo, Japan) with two matched 1-cm quartz cells.

Reagents

2,2'-Bipyridyl solution (0.2% w/v) (prolabo Rhone poulenc) in distilled water.

Ferric chloride solution (0.1% w/v in 0.5% hydrochloric acid).

Sodium fluoride solution (1.0% w/v) in distilled water.

Iodine solution ($1.5 \times 10^{-3}M$). Prepared by dissolving 38 mg of resublimed iodine and 80 mg of potassium iodide in 100 ml of distilled water.

Starch solution 0.5% w/v soluble starch in distilled water.

Captopril. Obtained from Squibb-Egypt and hydrochlorothiazide from Kahira Co-Egypt.

Dosage form. Capoten tablets (Squibb-Egypt) containing 25 mg captopril per tablet and capozide tablets (Squibb-Egypt) containing 50 mg captopril and 25 mg hydrochlorothiazide per tablet.

Synthetic mixtures. Captopril combined with common tablet excipients (e.g., starch, glucose, lactose, sucrose, magnesium stearate and acacia) together with hydrochlorothiazide.

Preparation of standards

Dissolve an accurately weighed amount of captopril in water and dilute quantitatively with water to obtain dilutions containing from 2.5 to 250 $\mu\text{g/ml}$.

Preparation of samples

Powdered forms. Accurately weigh *ca.* 10 mg of captopril and dissolve in 50 ml of distilled water. Dilute this solution to contain 200 μg captopril/ml.

Tablets. Weigh and finely powder 20 tablets. Accurately weigh a portion of powder, equivalent to *ca.* 10 mg of captopril, and shake with 15 ml of distilled water for 10 min. Filter the resulting mixture and dilute the filtrate and washings to 50 ml with distilled water to contain 200 μg captopril/ml.

Synthetic mixtures. Accurately weigh a portion of thoroughly mixed components of each ingredient with *ca.* 50 mg of captopril, shake with 15 ml of water for 10 min, and then complete the analysis as described under tablets, "Filter the resulting . . .".

Recovery study

Add an accurately weighed amount of captopril for each preparation in a 50-ml standard flask containing an accurately weighed quantity of mixed contents of powdered tablets. Dissolve the contents of the flask in distilled water and treat as described for tablets.

Procedure A

Pipette 1.0 ml of the standard or pharmaceutical preparations into a 10-ml standard flask and add 1.0 ml of ferric chloride solution. Mix

well and allow to stand for 5 min at $20 \pm 5^\circ$. Add 1.0 ml of sodium fluoride solution, dilute to the mark with distilled water and measure the absorbance at 523 nm against the reagent blank.

Procedure B

(i) Pipette 1.0 ml of the standard or pharmaceutical preparations into a 10-ml standard flask, add 1.0 ml of iodine solution and dilute to the mark with distilled water. Mix well and measure the absorbance at 351 nm against a reagent blank.

(ii) Repeat the same procedure, adding 1.0 ml of starch solution before diluting to the mark with distilled water. Measure the absorbance at 620 nm against the reagent blank.

RESULTS AND DISCUSSION

Of the eight closely related antihypertensive drugs (captopril, enalapril, lisinapril, ramipril, pentopril, qunapril, zofenopril and fentiapril) only captopril possesses a sulfhydryl group.²⁹

Captopril, as a reducing agent, reacts with ferric chloride and the resulting ferrous ion produces an intense colour ($\lambda_{\text{max}} = 523 \text{ nm}$) with 2,2'-bipyridyl (Fig. 1). The resulting colour is due to the formation of the stable complex cation $[\text{Fe}(2,2'\text{-bip})_3]^{2+}$.³⁰

Captopril also reacts with aqueous iodine and the excess iodine could be measured either as its triiodide ($\lambda_{\text{max}} \sim 290, 351 \text{ nm}$) or its starch complex ($\lambda_{\text{max}} = 620 \text{ nm}$) as shown in Fig. 1. The bleaching action of the thiol drug on iodine can be illustrated as follows:

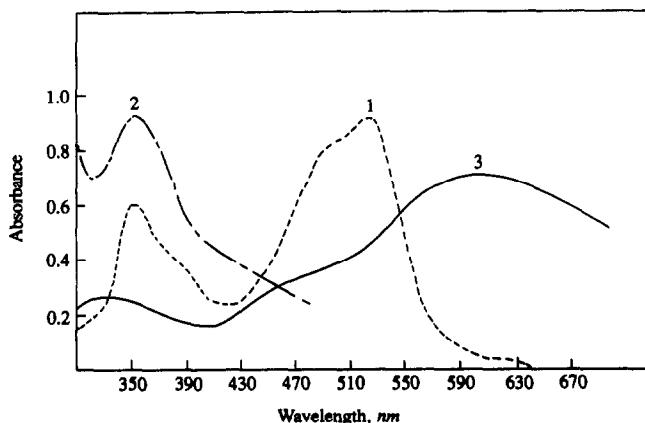


Fig. 1. Absorption spectra of 1-FeIII-bipy, 2-aqueous-iodine and 3-iodine-starch with 20, 5 and 0.5 μg captopril/ml respectively.

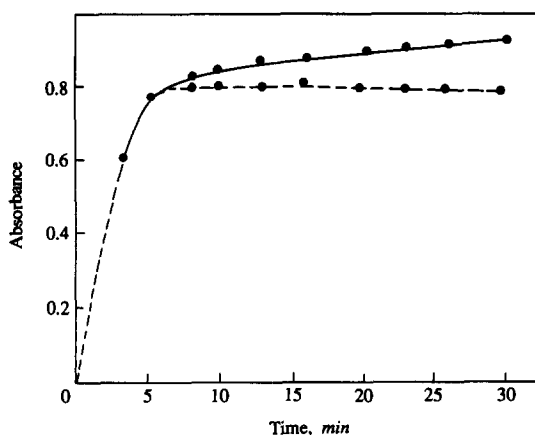


Fig. 2. Effect of time on the colour development at 523 nm with 20 µg captopril/ml (----) with and (—) without sodium fluoride.

Although these very sensitive colour reactions are completely new for captopril, it can be postulated that the oxidation of captopril with either ferric chloride or iodine proceed via the thiol group.³¹

Investigations were carried out to establish the most favourable conditions for the assay procedure. The absorbance readings of the resulting solutions were found to increase with increasing ferric chloride and 2,2'-bipyridyl concentrations up to 1.0 ml of 0.1 and 0.2 g% respectively for procedure A. The use of 1.0 ml of $1.5 \times 10^{-3}M$ iodine solution was considered satisfactory for the proposed concentration levels of captopril in procedure B.

The reaction between the drug and ferric ion goes rapidly at 20–25° within 5 min and then proceeds very slowly; therefore, the use of sodium fluoride is necessary after 5 min for quenching the interaction and obtain stable absorbance readings (Fig. 2). The best diluting solvent among the solvents studied was water (methanol, ethanol and isopropanol).

A linear correlation was found between absorbance and concentration of captopril (Table 1). Regression analysis of Beer's plot gave the following linear regression equations:

$$A_{523} = -0.0331 + 0.0432C$$

$$\Delta A_{351} = -0.0005 + 0.0237C$$

$$\Delta A_{620} = 0.1256 + 0.2365C$$

Table 2. Replicate analysis of captopril standard solutions by different methods

Replicates	Absorbance, nm			
	Fe(III)-bipy 523*	Aqueous iodine 290†	351†	I ₂ -Starch 620‡
1	0.382	0.771	0.513	0.586
2	0.375	0.782	0.496	0.594
3	0.380	0.788	0.515	0.599
4	0.378	0.780	0.517	0.593
5	0.374	0.780	0.515	0.593
Mean	0.378	0.780	0.511	0.593
SD±	0.003	0.006	0.008	0.004
CV%	0.79	0.70	1.57	0.70

*10 µg/ml.

†15 µg/ml.

‡2.5 µg/ml.

These equations can be used to calculate the concentration of an unknown sample. The use of starch makes the iodine method about eleven times more sensitive than that of the triiodide, as seen from its higher molar absorptivities.

To examine the precision of the procedures, replicate determinations were made on the same solution containing the specified amount of captopril stated in Table 2, by different procedures. The percentage coefficients of variation at these concentration levels ranged between 0.7–1.57.

We investigated the influence of frequently encountered excipients and additives on the assay of captopril. No interference was observed from the presence of hydrochlorothiazide, starch, sucrose, glucose, lactose, acacia and magnesium stearate (Table 3). Under the specified reaction conditions, reducing sugars and starch do not interfere, since iodine reacts with reducing sugars only in alkaline medium.

The suggested methods were applied to the quantitative determination of captopril in bulk and in capotin or capozide tablets (Table 4).

Table 1. Comparative statistical evaluation for captopril analysis by the suggested procedures

Method	λ_{max} , nm	ϵ , l. mole. ⁻¹ cm ⁻¹	Linear range, µg/ml	Corr. coeff., r	Intercept,* a	Slope,* b
Fe(III)-bipyridyl	523	8.65×10^3	2–20	0.9990	-0.0331	0.0432
Aqueous iodine	351	5.09×10^3	5–25	0.9991	-0.0005	0.0237
Iodine starch	620	6.31×10^4	0.25–3	0.9994	0.1256	0.2365

*In all cases, n = 5.

Table 3. Determination of captopril in the presence of hydrochlorothiazide (HCTZ) and common excipients by different methods

Ingredients,* mg	Fe(III)-bipy		Aqueous iodine		I ₂ -Starch	
	Found,† mg	% Recovery ± SD	Found,† mg	% Recovery ± SD	Found, † mg	% Recovery ± SD
HCTZ (25)	50.00	100.0 ± 0.40	50.25	100.5 ± 0.76	49.90	99.8 ± 0.66
Starch (50)	49.90	99.8 ± 0.81	49.85	99.7 ± 0.89	50.00	100.0 ± 1.5
Sucrose (50)	50.10	100.2 ± 0.98	50.15	100.3 ± 1.40	49.80	99.6 ± 1.21
Glucose (10)	49.85	99.7 ± 1.02	49.75	99.5 ± 0.84	50.05	100.1 ± 0.96
Lactose (10)	50.00	100.0 ± 0.32	49.90	99.8 ± 0.53	50.05	100.1 ± 1.11
Acacia (10)	49.95	99.9 ± 0.40	50.00	100.0 ± 1.21	49.80	99.6 ± 0.79
MG-stearate (10)	50.50	101.0 ± 1.23	49.70	99.4 ± 1.04	50.00	100.0 ± 0.81
Mean % recov.		100.1		99.9		99.9
Pool SD (±SP)%		0.336		0.269		0.268

*Added in mg per 50 mg of captopril.

†Mean of three determinations.

Table 4. Assay of captopril in local market pharmaceutical formulations

Formulation	Claimed (mg/tab.)	% Found, ± SD*		
		Fe(III)-bipy	Aqueous iodine	I ₂ -starch
Capoten tab.	25	99.1 ± 0.451	100.6 ± 0.605	102.8 ± 0.540
Capozide tab.	50	101.1 ± 0.323	101.7 ± 0.115	100.0 ± 0.100

*Average of 5 determinations.

REFERENCES

1. K. Florey (ed.), *Analytical Profiles of Drug Substances*, Vol. 11, pp. 81-136. Academic Press, New York, 1982.
2. A. D'Angelo, L. Sartori, G. Gambaro, S. Giannini, L. Malvasi, P. Benetollo, T. Lavagnini and G. Grepaldi, *Postgrad. Med. J.* 1986, **62**, Suppl. 1, 69.
3. R. M. Lederle, *J. Cardiovasc. Pharmacol.*, 1985, Suppl. 1, S63.
4. E. Ambrosioni, C. Borghi and F. V. Costa, *Brit. J. Clin. Pharmacol.*, 1987, **23**, Suppl. 1, 43S.
5. The Captopril-Digoxin Multicenter Research Group, *J. Am. Med. Assoc.*, 1989, **259**, 539.
6. M. E. Mohamed, H. Y. Aboul-Enein and E. A. Gad-Kariem, *Anal. Lett.*, 1983, **16**, 45.
7. M. E. Mohamed and H. Y. Aboul-Enein, *ibid.*, 1985, **18**, 2591.
8. K. Nikolic and K. Velasevic, *Pharmazie*, 1989, **44**, 155.
9. B. Jarrott, A. Anderson, R. Hooper and W. J. Louis, *J. Pharm. Sci.*, 1981, **70**, 665.
10. K. Shimada, M. Tanaka, T. Nambara, Y. Imai, K. Abe and T. Yoshinaga, *J. Chromatog.*, 1982, **227**, 445.
11. K. Hayashi, M. Miyamoto and Y. Sekine, *ibid.*, 1985, **338**, 161.
12. V. Cavrini, R. Gatti, A. M. DiPietra and M. A. Raggi, *Chromatographia*, 1987, **23**, 680.
13. C. M. Pereira, Y. K. Tam, R. L. Collins, R. Nakai and P. Ng, *J. Chromatog.*, 1988, **452**, 208.
14. H. Bökens, M. Foullois and R. F. Müller, *Z. Anal. Chem.*, 1988, **330**, 431.
15. P. Colin and E. Scherer, *J. Liq. Chromatog.*, 1989, **12**, 629.
16. A. I. Cohen, R. G. Devlin, E. Ivashkiv, P. T. Funke and T. McCormick, *J. Pharm. Sci.*, 1982, **71**, 1251.
17. O. H. Drummer, B. Jarrott and W. J. Louis, *J. Chromatog.*, 1984, **305**, 83.
18. E. Ivashkiv, B. N. McKinstry and A. I. Cohen, *J. Pharm. Sci.*, 1984, **73**, 1113.
19. T. Ito, Y. Matsuki, H. Kurihara and T. Nambara, *J. Chromatog.*, 1987, **417**, 79.
20. J. Tu, E. Liu and E. L. Nickoloff, *Ther. Drug Monit.*, 1986, **6**, 59.
21. F. M. Duncan, V. I. Martin, B. C. Williams, E. A. S. Al-Dujaili and C. R. W. Edwards, *Clin. Chim. Acta*, 1983, **131**, 295.
22. H. Kinoshita, R. Nakamaru, S. Tanaka, Y. Tohira and M. Sawada, *J. Pharm. Sci.*, 1986, **75**, 711.
23. K. Imai, T. Toyoka and Y. Watanabe, *Anal. Biochem.*, 1983, **128**, 471.
24. E. Ivashkiv, *J. Pharm. Sci.*, 1984, **73**, 1427.
25. V. Cavrini, R. Gatti, P. Roveri and M. R. Cesaroni, *Analyst*, 1988, **113**, 1447.
26. M. E. Mohamed, M. S. Tawakkol and H. Y. Aboul-Enein, *Zentralbl. Pharm., Pharmakother. Laboratoriumsdign*, 1983, **122**, 1163.
27. M. A. Raggi, V. Cavrini, A. M. DiPietra and D. Lacche, *Pharm. Acta Helv.*, 1988, **63**, 19.
28. J. Emmanuel and S. D. Halankar, *Indian Drugs*, 1989, **26**, 319.
29. P. Nuhn, *Die Pharmazie*, 1990, **45**, 457.
30. M. R. F. Ashworth, *The Determination of Sulphur-Containing Groups*, Vol. 2, pp. 22, 62. Academic Press, New York, 1976.
31. S. Patai (ed.), *The Chemistry of the Thiol Group*, Part I, pp. 271-324. Wiley-Interscience, New York, 1974.

SIMULTANEOUS DETERMINATION OF IRON(III) AND VANADIUM(V) BY USE OF A KINETIC-SPECTROPHOTOMETRIC AND RAPID MIXING FLOW SYSTEM

HONG-BIN HE, YUN-XIANG CI,* WEN-BAO CHANG and WEN-LING GONG

Department of Chemistry, Peking University, Beijing 100871, People's Republic of China

(Received 1 March 1991. Revised 8 April 1991. Accepted 17 April 1991)

Summary—The quantitative spectrophotometric determination of V(V) by its catalytic effect on the oxidation of chromotropic acid [the disodium salt of 4,5-dihydroxynaphthalene-2,7-disulphonic acid (CS)] by potassium bromate has been adapted to a flow system employing a rapid sample and reagent introduction manifold, in which valves and carrier streams are omitted without decreasing the precision or increasing the sample consumption relative to flow-injection analysis (FIA). Measurements are made at 420 nm. Coexisting Fe(III) can be determined simultaneously at the same wavelength by its more rapid colour chelate formation with CS. An accurate determination of V(V) and Fe(III) in the mixture was developed with a sample throughput of about 60 hr.

The flow pulsations caused by pumps can have a dramatic effect on signal profiles in flow systems. Therefore, numerous measures have been taken to lessen pulsations and their effects.¹ Stopped-flow methods record the signal after the flow comes to a halt and, as a result, pulsation effects are eliminated. Along with other advantages, such as longer reaction time and high tolerance to background signals, stopped-flow has become an important form of flow-injection analysis (FIA).^{2,3} Removal of the sampling valve and the replacement of the peristaltic pump with a pulsed pump (a home-made syringe-like pump) lead to the formation of a new sample introduction system. According to A. Gomez-Hens and Perez-Bendito, a high flow-rate of reactants through the mixing chamber was very important in the stopped-flow technique.⁴ In our work reported here, we have found that this sample introducer not only retains most of the advantages of the stopped-flow FIA method, but also displays some others, such as simplicity and especially a much wider reaction inspection time, from as little as 0.1 sec to what a conventional stopped-flow FIA can reach. This merit is particularly useful in the measurements of differences in kinetic reactions of some metal ions.

The sodium salt of 4,5-dihydroxynaphthalene-2,7-disulphonic acids (CS) forms a coloured complex with Fe(III) at a much faster

rate than the oxidation of CS by potassium bromate under the catalysis of V(V), using the same wavelength of 420 nm for monitoring. Its reaction with Fe(III) is virtually complete by the time the V(V) catalyzed reaction is initiated. The new sample introducer was adopted in this work because the conventional FIA method cannot mix the sample with reagents within 0.2 sec, which is required to discriminate these two reactions. Satisfactory results have been obtained in the simultaneous determination of Fe(III) by its colour reaction and V(V) by its catalytic effect, using this new sample introducer.

EXPERIMENTAL

Apparatus

The schematic view of the system is shown in Fig. 1 and it consisted of the units described below.

Pump. The pump used was designed and made in our laboratory. Figure 2 shows one of the three lines of the pump. A time of 0.3 sec was needed for filling the chamber C with solution via valve V_2 while V_1 was closed, and 30 μ l of solution was pushed out of the chamber within 0.2 sec via V_1 toward the mixing point while V_2 was closed. The total average flow-rate for all of the three lines was about 11 ml/min. The space from the joint point of the three lines to the farther end of the light path in the flow cell was calculated to be less than 60 μ l,

*Author for correspondence.

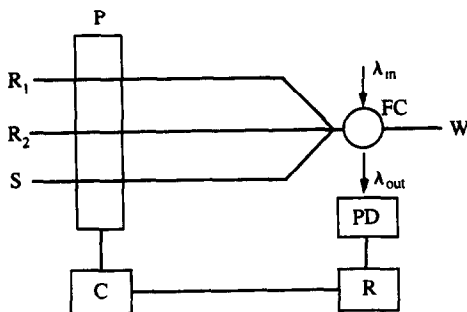


Fig. 1. Schematic diagram of the sample introducer. P: pump; R₁: CS; R₂:KBrO₃; S: sample; λ_{in}, λ_{out}: light; C: controller; FC: flow cell; W: waste; PD: photo detector; R: recorder.

therefore, the solution from every pulsation of the pump (90 μl) could not only fill the flow cell but also wash away the waste in the cell. About 10–15 pulsations were needed to refresh the three lines and the flow cell with new sample solutions. Therefore, total sample consumption was about 0.4 ml, no more than that consumed in a conventional FIA apparatus including loading of the injection valve.

Tubing. Poly(tetrafluoroethylene) (PTFE) tubing (0.5 mm i.d.) was used throughout the experiment. The length from the joint point of the three lines to the beginning of the light path in the flow cell is 35 mm long and 1.0 mm in diameter.

Flow cell. The glass flow cell was made to give a path 1.0 cm long and 2.0 mm in diameter.

Photometric detector. A model 722 Spectrophotometer (No. 3 Analytical Instrument Factory, Shanghai, PR China) was used to measure reaction signals.

Chart recorder. An LKB Bromma 2212 Recorder was used to record signals.

The control diagram of this sample introducer is shown in Fig. 3. This introducer worked under the following procedure: when the push-button PB was first pressed, the pump pushed

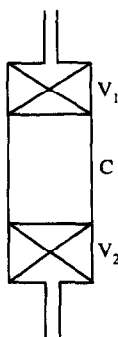


Fig. 2. General diagram of the components of the pump. V₁, V₂: valves; C: chamber.

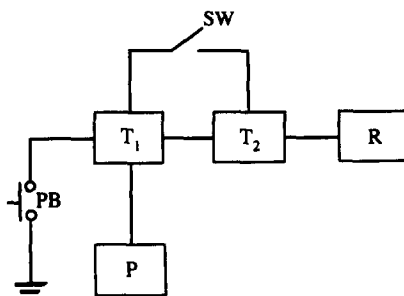


Fig. 3. Control diagram of the sample introducer. PB: push-button; T₁: timer₁; T₂: timer₂; SW: switch; R: recorder.

the solutions in the three channels into the flow cell. After a preset time (usually 5–7 sec for refreshing the three channels and the flow cell), timer T₁ stopped the pump, and timer T₂ started the chart recorder immediately after the last pulsation. After the preset time for T₂ had elapsed, the recorder was stopped so that the end point of the measurement could be examined easily. By closing the switch SW, the pump could be restarted, and the cycle T₁ (pump) → T₂ (recorder) → T₁ (pump) could go on automatically until SW was opened. The experiment for each sample was repeated until peak height repeatability to within 1 mm on the chart recorder was obtained (typically three experiments). Before and after experiments, hydrochloric acid (pH 1.7) was pumped through the three lines for cleaning.

The absorbance spectra were recorded on a Shimadzu UV-300 double/difference/dual-wavelength recording spectrophotometer.

Reagents

The following solutions were prepared: Fe(III) solution (2.25 × 10⁻³ g/ml, pH 1.7); V(V) solution (5.0 × 10⁻⁵ g/ml, pH 1.7); Chromotropic acid (CS) solution (0.5%, pH 1.7) which was kept in a refrigerator; potassium bromate solution (5.0%); hydrochloric acid and sodium hydroxide were used to adjust the pH. A mixed acid (67% HNO₃:70% HClO₄ = 1:1) was used to dissolve the food samples.

All reagents were of reagent grade and solutions were made up with double ion-exchanged water.

Procedure

Two of the three lines were inserted into the solutions of CS and potassium bromate, respectively, and the third into the sample solution. The absorbance at 420 nm was measured within the first 30 sec.

The food samples were prepared by the following procedure: 2.00 g of food sample was treated with 20 ml of mixed acid (67% HCO_3 :70% $\text{HClO}_4 = 1:1$) and was heated on an electric heater until almost dry. This food sample was finally diluted to 25 ml with 0.01M hydrochloric acid. Four measurements were done for each sample.

RESULTS AND DISCUSSION

Spectral characteristics

The absorbance spectra at reaction equilibrium are shown in Fig. 4. Curve (a) shows the absorbance of CS with Fe(III). Experiments showed that CS alone did not present any absorbance in the range 400–750 nm, and the mixture of CS with potassium bromate did not absorb significantly in the first 60 sec. Curve (b) is the spectrum of CS with potassium bromate recorded 20 min after the two reactants were mixed. Curve (c) shows the spectrum of CS, potassium bromate and V(V). The CS/ KBrO_3 /V(V) system has a maximum absorbance at 420 nm. The CS–Fe(III) has a peak absorbance at 740 nm, but it also presents significant absorbance at 420 nm. Considering the simplicity and the reproducibility of the system, 420 nm was selected as the optimal wavelength in the experiment to allow simultaneous measurement of Fe(III) and V(V).

Dynamic characteristics

The dynamic isotherms of the reactions are shown in Fig. 5. Since the mixture of CS and potassium bromate did not present any significant absorbance in the first 60 sec, all the

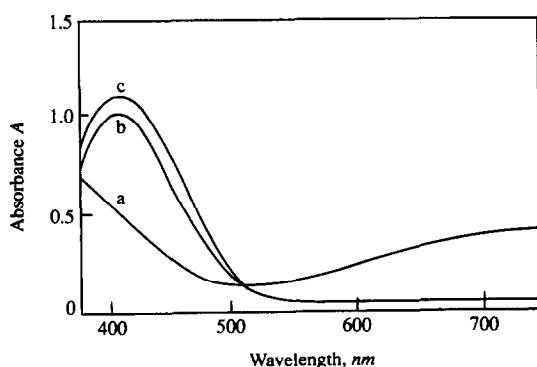


Fig. 4. Spectra for Fe(III) and V(V). (a) CS: 0.5%; Fe(III): 1.0×10^{-4} g/ml; (b) CS: 0.5%; KBrO_3 : 5.0%; (c) CS: 0.5%; KBrO_3 : 5.0%; V(V): 2.0×10^{-8} g/ml. All of the above spectra were recorded against water. Curve (b) was recorded 20 min after the two reactants were mixed.

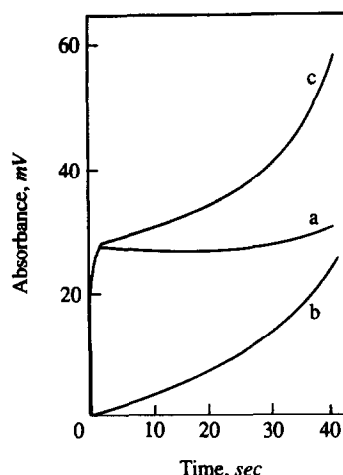


Fig. 5. Plot of absorbance against reaction time. (a) CS: 0.5%; KBrO_3 : 5.0%; Fe(III): 7.4×10^{-6} g/ml; (b) CS: 0.5%; KBrO_3 : 5.0% (20 min after mixing); (c) CS: 0.5%; KBrO_3 : 5.0%; V(V): 2.9×10^{-7} g/ml. All of the curves were recorded against water.

measurements were done against water instead of the CS and potassium bromate solution. Curve (a) shows that the signal from Fe(III) rises steeply in the first second and then remains constant for about 30 sec, followed by another increase. The output from V(V) goes up gradually with reaction time up to 30 sec [curve (b)].

Table 1. Effect of various ions on the determinations of $5.4 \times 10^{-5}M$ (30×10^{-6} g/ml) Fe(III) and $3.3 \times 10^{-6}M$ (1.7×10^{-7} g/ml) V(V)

Ion added*	Tolerance ratio of ion to Fe ^{III} , molar ratio
NH_4^+ , SO_4^{2-} , NO_3^-	500
Mn^{II} , Mg^{II}	150
Br^- , Ca^{II}	50
F^-	20
Zn^{II} , Ni^{II} , Al^{III} , I^-	5
Sn^{IV} , Zr^{IV} , Nb^V , Cr^{III} , PO_4^{3-} , Cu^{II}	3
V^V , Au^{III}	1.5
Fe^{II} , Mo^VI	1
CrO_4^{2-} , CO^{II}	0.5
Sn^{II}	0.01
	Tolerance ratio of ion to V ^V , molar ratio
Ion added*	
NH_4^+ , I^-	10000
PO_4^{3-}	5000
HCO_3^- , Na^+ , F^-	2500
Ac^- , K^+ , Cr^{III} , Nb^V	200
Ni^{II} , Co^{II} , Fe^{II}	
Br^-	100
Al^{III}	50
Cu^{II}	30
Ag^+	20
Fe^{III}	16
Mn^{II}	10

*The stated ratio of these ions caused a relative error of less than 5%.

Table 2. Results of Fe(III) and V(V) Determinations in Food Samples*

Sample	Fe(III)		V(V)	
	Content	Recovery†	Content	Recovery†
Raisin	100 ± 4 ^c	99%	0.77 ± 0.04 ^c	98%
Milk Powder	76 ± 0 ^d	105%	1.15 ± 0.07	102%
Biscuit	98.4 ± 0	103%	0.65 ± 0.02	101%

*Concentrations expressed in mg/kg. †The recovery is for 9 mg/kg of Fe(III) and 0.1 mg/kg of V(V). ‡Standard deviation. §The concentration stated in the label is 90 mg/kg.

Curve (c) suggests that these two isotherms could be added linearly in the first 30 sec. The increase between the initial Fe(III) signal and the next 30 sec is not correlated to the concentration of Fe(III) but correlated to that of V(V). Therefore, the reaction time for vanadium measurement was selected to be 30 sec and used throughout the experiment. The iron(III) was measured from the height of the initial rapid rise portion of the signal (at about 2 sec).

Effects of reaction variables

In order to optimize the system, the effects of pH and concentration of CS and potassium bromate on the absorbance were studied. The optimal pH for both Fe(III) and V(V) was 1.7–2.0. The optimum concentration of CS was 0.3–0.8% for Fe(III) and 0.4–1.0% for V(V). Potassium bromate should be 5.0% for V(V) and can be 0–5.0% for Fe(III). A pH of 1.7, 0.5% CS and 5.0% KBrO₃ were selected for measurements.

Calibration graphs for Fe(III) and V(V)

Under the optimal conditions, a simple spectrophotometric method for the simultaneous determination of Fe(III) and V(V) has been developed. The method was used to determine the Fe(III) and V(V) contents of some foods. Calibration curves were constructed with standard Fe(III) and V(V) solutions. The calibration graph of Fe(III) covers two orders of magnitude, from 1.5×10^{-7} to 1.5×10^{-5} g/ml Fe(III). The correlation coefficient was $r = 0.9974$. The calibration curve of V(V) is linear over the range 3.0×10^{-9} – 7.0×10^{-7} g/ml V(V), with a correlation coefficient of 0.9975. The relative standard deviation obtained for 10 samples of

3.0×10^{-6} g/ml Fe(III) was 0.6% and 2% for 10 samples of 5.7×10^{-9} g/ml V(V).

Interferences

The selectivity was assessed by studying the effect of foreign ions on the kinetic determinations of Fe(III) and V(V). The results are summarized in Table 1.

Table 1 shows that Sn^{II}, Co^{II} and CrO₄²⁻ interfere strongly in the determination of Fe(III). However, these ions do not exceed the tolerance ratio in raisins, milk powder, biscuit and some other food samples. All of the tolerance ratios of foreign ions in the determination of V(V) are over 10. Therefore, this method can be applied to the determination of V(V) in food samples.

Application

Finally, to test the applicability of the method, some food and fruit samples were analyzed with the calibration curves. The results are presented in Table 2. Results of added Fe(III) and V(V) were excellent. The determined iron content of the milk powder agrees well with the labelled content.

Acknowledgements—The authors express thanks to Prof. Gary D. Christian, joint Editor-in chief of *Talanta*, for technical and literal assistance.

REFERENCES

1. H. Wada, Y. Sawa, M. Morimoto, T. Ishizuki and G. Nakagawa, *Anal. Chim. Acta*, 1989, **220**, 293.
2. H. B. Filho, B. F. Reis, E. A. G. Zagatto, *ibid.*, 1978, **97**, 427.
3. N. Hanaoka, R. S. Givens and T. Kuwana, *Anal. Chem.*, 1988, **60**, 219.
4. A. Gomez-Hens and D. Perez-Bendito, *Anal. Chim. Acta*, 1991, **242**, 147.

MALACHITE GREEN AS A REAGENT FOR DETECTION AND SPECTROPHOTOMETRIC DETERMINATION OF CHROMIUM(VI)

RAM PARKASH, REETA BANSAL, AJIT KAUR and S. K. REHANI
Department of Chemistry, Panjab University, Chandigarh-160014, India

(Received 7 March 1991. Accepted 3 April 1991)

Summary—A sensitive and inexpensive method of spectrophotometric determination of chromium(VI), based on the absorbance of its complex with malachite green and acetic acid at pH 2.5 is reported. The complex shows a molar absorptivity of 8×10^4 l. mole⁻¹ cm⁻¹ at 560 nm, using malachite green and acetic acid as reference solution. The effect of time, temperature, pH and reagent concentration is studied and optimum operating conditions are established. Beer's law is applicable in the concentration range 2.0–22.8 µg/ml chromium(VI). The resin beads act as a catalyst and as little as 1.6 µg of chromium(VI) is detected in the resin phase as compared to 4.1 µg in the solution phase. The standard deviation in the determinations is ± 0.40 µg/ml for a 10.35 µg/ml solution.

Feigl and Anger,¹ Sandell,² and Snell and Snell³ reviewed the earlier work on the detection and determination of chromium(VI) as chromate or dichromate ions. Microamounts of chromium(VI) have also been determined spectrophotometrically with varamine blue,⁴ diphenylcarbazine,^{5,6} alizarin,⁷ 3,3'-diaminobenzidine,⁸ pyridine-2,4,6-tricarboxylic acid,⁹ triethylenetetraaminehexaacetic acid,¹⁰ *O*-toluidine,¹¹ α -naphthyl,¹² crystal violet,¹³ cesium iodide¹⁴ and 2-(5-bromo-2-pyridylazo)-5-diethylaminophenol.¹⁵ Indirect determination of chromium(VI) was achieved by using iron(II) and ferrozine.¹⁶ However, most of these methods are either time consuming or less selective than desired and are subject to interference from common ions.

Chromium(VI) is a moderate to severe toxic agent. Determination of its microquantities is of increasing interest to analytical chemists, particularly environmental scientists. We report here a rapid, sensitive and inexpensive method for detection and spectrophotometric determination of micro amounts of chromium(VI) based on its colour reaction with acetic acid and malachite green. The method is not only superior to most of the reported methods in simplicity, rapidity and selectivity but is also suitable for chromium determination in industrial waste water.

EXPERIMENTAL

Reagents

Analytical grade reagents and doubly distilled water were used throughout. Strongly acidic

cation-exchange resin Amberlite IR 120 (standard grade, B.D.H.) was used in the H⁺ form. Potassium dichromate stock solution (10⁻¹M) and acetic acid solution (10% v/v) were prepared by dissolving appropriate amounts of the reagents in demineralized water. Malachite green (0.1%) was prepared by dissolving an appropriate amount of reagent in distilled methanol. Working solutions of potassium dichromate of appropriate dilutions were stored in the dark.

Apparatus

A Hitachi model 330 double-beam recording spectrophotometer with 10-mm cells was used for absorbance measurements.

Detection

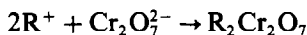
About 5–10 resin beads (H⁺ form) are placed on a white spot-plate and blotted dry with filter paper. One drop of test solution is added, followed by a drop of acetic acid and malachite green. Green colour develops on the bead surface within 10 min if the test solution contains chromium(VI).

Determination

Shake dichromate (20.0–228.4 µg), acetic acid (2.5 ml of 10% solution) and malachite green (1.0 ml 0.1% solution) for about 10 min for complete colour development. Make the volume up to 10 ml with water. Measure the absorbance at 560 nm against a blank solution at room temperature (25–30°).

RESULTS AND DISCUSSION

Malachite green (R^+X^-) and dichromate react without destroying the quinoidal structure of the dye. On the analogy of the reaction between antimony(III) and malachite green,¹⁷ the tentative mechanisms may be written as



Two types of ion-exchange resins, Amberlite IR 120 (H^+ form) and Amberlite IRA 400 (OH^- form) were added in two different microtest tubes containing, the coloured complex formed by the recommended procedure. The positively charged resin beads turn green, indicating that the complex formed is positively charged.

The plot of absorbance of the green complex as a function of wavelengths shows a plateau with a maximum absorbance ($\epsilon = 8 \times 10^4$ l. mole⁻¹ cm⁻¹) at 560 nm. Beer's law is obeyed for solutions containing 2.0–22.8 $\mu\text{g/ml}$ of chromium(VI) under the optimum conditions. The stability of the complex was studied by measuring the absorbance as a function of time. A green colour developed after 10 min, was stable for about 2 hr at room temperature (25–30°) and then started to fade. The absorbance of the solution decreases with the increase in temperature. However, the colour takes more time to develop at lower temperatures.

The effect of acetic acid or malachite green concentration and variation in pH on the absorption of the green complex was examined. It was revealed that 2.5 ml of 10% solution of acetic acid is the most suitable. Absorbance decreases if the volume of acetic acid is increased further. Similarly, 1 ml of 0.1% malachite green solution gives maximum absorbance. Further increase in the amount of malachite green has no effect on the absorbance. The absorbance was maximum and constant at pH 2.5 at 560 nm. On increasing the pH, the absorbance of the green complex decreases.

Chromium(VI) is detected in the presence of large amounts of foreign substances; no interference was given by Cu(II), Mn(II), Co(II), Ni(II), Zn(II), Ca(II), Mg(II), Cr(III), Fe(III), Ce(IV), V(V), chloride, nitrate, sulphate, acetate, phosphate, citrate, permanganate and tartarate in solution phase and in bead test even when present in 100 times excess. The identification limit of chromium(VI) at room temperature (25–30°) is 4.1 μg in solution phase (10 ml) and 1.6 μg in resin phase. Ion-exchange resin beads, thus, serve to concentrate the chromium product and act as detection medium to improve the sensitivity of the test.

The tolerance limits (mg) of the following elements in the determination of chromium(VI) for $\leq 0.80\%$ error are given in parentheses: Ag(I) (84.5), Cu(II) (74.8), Mn(II) (37.7), Co(II) (87.3), Ni(II) (116.0), Zn(II) (59.4), Cd(II) (184.8), Mg(II) (20.5), Ca(II) (98.4), Hg(II) (128.0), Cr(III) (60.0), Fe(III) (32.4), Al(III) (150.0) and Mo(VI) (163.8) in 80 $\mu\text{g}/10$ ml of dichromate solution. The standard deviation (10 replicates) was ± 0.40 $\mu\text{g/ml}$ for a 10.35 $\mu\text{g/ml}$ solution. In the absence of determinate error, the true value fell within 9.40–10.28 μg with a confidence interval of 95%.

This method is highly sensitive, selective, precise, accurate and quick. It offers certain advantages over several other methods. The colour reaction of chromium(VI) with 2-(5-bromo-2-pyridylazo)-5-diethylaminophenol occurs on heating the reactants in a boiling water bath for 45 min,¹⁵ whereas the reaction is complete in ~ 10 min at room temperature in the present case. The procedure suggested by Malik *et al.*¹³ also requires 2 hr for complete colour reaction. In the method of Bet-Pera and Jaselskis,¹⁶ permanganate and Fe(III) interfere. Low results are obtained in the presence of Co(II) and Ni(II) because these ions form ferrozine complexes. There is no such difficulty with the present procedure. Various oxidants such as permanganate, Ce(IV), V(V) and Fe(III) interfere in the

Table 1. Spectrophotometric determination of Cr(VI) in waste water samples

Sample	Cr(VI), (μg)		Mean recovery, %	Relative standard deviation, %	Found by reference procedure, ⁵ mean recovery, %
	Added	Found			
Chromium plating electrolyte	0.0	65.2	—	0.43	—
	20.0	85.6	102	1.85	103
waste water	0.0	64.4	—	0.85	—
	20.0	84.2	99.0	1.65	101

method proposed by Cheng and Goydish,⁸ but these oxidants do not interfere in the present studies.

The present procedure is suitable for detection and determination of Cr(VI) in industrial waste water and chromium plating electrolyte waste water without prior separation. The relative standard deviation calculated from six replicate analyses of the samples, is in the range 0.85–1.65% and 0.43–1.85% respectively. The mean recovery of Cr(VI) is 102% and 99%, respectively (Table 1).

The results obtained by this procedure agree satisfactorily with those obtained by the method reported in the literature.¹⁵

Acknowledgement—One of the authors (Reeta Bansal) is thankful to the U.G.C., New Delhi, India for financial assistance.

REFERENCES

1. F. Feigl and V. Anger, *Spot Tests in Inorganic Analysis*, 6th Ed., p. 188 Elsevier, Amsterdam, 1972.
2. E. B. Sandell, *Colorimetric Determination of Traces of Metals*, 3rd Ed., p. 390. Interscience, New York, 1959.
3. F. D. Snell and C. T. Snell, *Colorimetric Methods of Analysis*, Vol. IIA, p. 212. Van Nostrand, Princetown, 1959.
4. L. Erdey and F. Szabadváry, *Acta Chim. Acad. Sci. Hung.*, 1958, **13**, 335.
5. D. O. Miller and J. H. Yoe, *Clin. Chim. Acta*, 1959, **4**, 378.
6. G. A. Sereda, *Gig. Tr. Prof. Zabol*, 1967, **11**, No. 10, 60.
7. G. C. Bhattacharya, *J. Sci. Ind. Res. (India)*, 1961, **20B**, 351.
8. K. L. Cheng and B. L. Goydish, *Chemist-Analyst*, 1963, **52**, 7.3
9. I. Morimoto, H. Shinoda and Y. Yabashi, *Bunseki Kagaku*, 1964, **13**, 692.
10. F. Bermejo Martinez and A. Longarde Pena, *Acta Cient. Compostelana*, 1971, **8**, 95.
11. I. Florea, *Rev. Roum. Chim.*, 1973, **18**, 1993.
12. S. V. Vartanyan and V.M. Tarayan, *Arm. Khim. Zh.*, 1976, **29**, 303.
13. W. U. Malik, R. Bembi, P. P. Bhargava and R. Singh, *Z. Anal. Chem.*, 1976, **282**, 140.
14. A. B. Blank and L. P. Eksperiandov, *Zh. Anal. Khim.*, 1982, **37**, 940.
15. G.-Z. Fang and C.-Y. Miao, *Analyst*, 1985, **110**, 65.
16. F. Bet-Pera and B. Jaselskis, *ibid.*, 1981, **106**, 1234.
17. R. W. Burke and O. Menis, *Anal. Chem.*, 1966, **36**, 11719.

RAPID SPECTROPHOTOMETRIC DETERMINATION OF TRACE COPPER IMPURITY IN *N,N'*-DI(2-BUTYL)-*p*-PHENYLENEDIAMINE

J. K. GUPTA

Petrochemistry Division, Indian Institute of Petroleum, Dehradun 248005, U.P., India

(Received 18 October 1988. Revised 28 February 1991. Accepted 11 March 1991)

Summary—The trace copper is separated from the matrix by extraction of the latter (an antioxidant of *N*-alkylated *p*-phenylenediamine type) from ammoniacal medium and then determined spectrophotometrically.

For determination of trace copper contamination in organic products, the matrix can be removed by ashing or chemically.^{1,2} The latter is generally preferred, but ashing is particularly appropriate for coloured products. During synthesis of butylated *p*-phenylenediamine in our laboratory, the product was found to be contaminated with copper at ppm level, from the hydrogenation catalyst (copper chromite; CuO 46%, Cr₂O₃ 46%). It was desired to find a rapid process for determining the copper, but the existing non-ashing methods were unsuitable because of the dark colour and alkaline nature of the product. Therefore, an alternative non-ashing method has been developed for the purpose and could be used for determining copper in similar amine-type antioxidants.

EXPERIMENTAL

Reagents

All chemicals used were of analytical reagent grade.

Standard copper solution. Wash pure copper metal with petroleum ether to remove any surface grease and dry it at 100°. Prepare a 1-mg/ml solution by dissolving the metal in concentrated nitric acid, boiling off brown fumes, cooling and diluting accurately to known volume. Prepare a 10-μg/ml solution from this by accurate dilution.

Buffer (pH 10). Dissolve 39 g of ammonium chloride in 100 ml of water plus 100 ml of concentrated ammonia solution.

Sodium diethyldithiocarbamate solution. 0.1 g per 100 ml.

Citric acid solution. 5 g per 100 ml.

Procedure

Weigh accurately about 0.25 g of sample, dissolve it in 15 ml of 4*M* hydrochloric acid and transfer the solution into a 250-ml separatory funnel. Add 10 ml of concentrated ammonia solution, cool the mixture, and shake it vigorously with 25 ml of chloroform for about 1 min. Allow the layers to separate and then discard the chloroform layer. Repeat the extraction, if necessary, with another 25 ml of chloroform for complete removal of the organic compound.

Add 5 ml of citric acid solution, and then 4 drops of Thymol Blue solution as indicator to check that the pH is ~9 (which is indicated by a colour change from yellow to blue). Add 10 ml of buffer solution and 10 ml of the sodium diethyldithiocarbamate solution, mixing after each addition.

Transfer exactly 25 ml of chloroform to the funnel and shake the mixture for 2 min. Allow the layers to separate, transfer part of the chloroform layer into a clean, dry 1-cm path-length cell and measure the absorbance at 440 nm against a reagent blank similarly prepared (by the whole procedure). Read the copper content from a calibration graph covering the range up to 100 μg.

RESULTS AND DISCUSSION

Conventional non-ashing methods could not be used, because dissolving the copper-contaminated product (*N*-alkylated *p*-phenylenediamine) in hydrochloric acid resulted in an aqueous solution of the hydrochloride, from which the protonated organic base was not extractable into an organic solvent.

However, it was realized that alkalizing this solution by addition of ammonia solution would free the organic base and also convert any copper present into its tetraammine complex. Extraction with an organic solvent would remove the organic base and leave the copper in the aqueous phase, where it could be determined by any convenient method, such as the diethyldithiocarbamate method. Citric acid is added to mask any metal ions that might be co-extracted and interfere.

The method is rapid and simple; one determination takes about half an hour. It is reproducible and the results compare favourably with those obtained by an ashing method. Ten repli-

cate analyses of a product sample gave a copper content of 207 $\mu\text{g/g}$, with a standard deviation of 0.6 $\mu\text{g/g}$. The comparison method gave a value of 206 $\mu\text{g/g}$, with a standard deviation of 0.5 $\mu\text{g/g}$.

Acknowledgements—The author thanks Dr K. K. Bhattacharya and Dr. S. Bhattacharjee for helpful discussions during the course of this work. Thanks are also due to Shri R. S. Gaharwar and research colleagues for their co-operation.

REFERENCES

1. O. I. Milner, *Analysis of Petroleum for Trace Elements*, p. 51. Pergamon Press, Oxford, 1963.
2. J. W. McCoy, *The Inorganic Analysis of Petroleum*, p. 11. Chemical Publishing Co., New York, 1962.

PROMOTION OF TIN OXIDE GAS SENSOR BY ALUMINUM DOPING

CHAONAN XU, JUN TAMAKI, NORIO MIURA and NOBORU YAMAZOE

Department of Materials Science and Technology, Graduate School of Engineering Sciences,
Kyushu University 39, Kasuga, Fukuoka 816, Japan

(Received 29 November 1990. Accepted 4 February 1991)

Summary—Effects of Al-doping on tin oxide based elements were investigated in the Al content range 0.001–5.000%. Gas sensitivity to H₂ and *i*-C₄H₁₀ was found to be promoted extensively when 1 or 5% Al was doped, while promotion was modest with doping up to 0.1% Al. Seebeck coefficients indicated that carrier concentration decreased with Al-doping, resulting in an increase in Debye length. At the same time, the crystallite size of tin oxide was found to decrease especially drastically when Al was doped excessively. It was concluded that the increased Debye lengths and decreased crystallite sizes were combined to produce the microstructure responsible for extremely high gas sensitivity of 1 and 5% Al-doped elements.

Gas sensors based on semiconductive oxides, represented by tin oxide, are very important devices for detecting the leakage of inflammable gases. Research on semiconductor gas sensors is being directed more and more towards their use in monitoring lower levels of gaseous components such as odours and harmful gases generated from various origins. To measure such low level components, however, the sensors need to be improved in several respects and gas sensitivity in particular should be promoted. Our recent investigation has revealed that this type of sensor is strongly influenced by the microstructure of sensor elements.^{1,2} The gas sensitivity (*S*) of SnO₂-based elements increases steeply as the grain size (*D*) of SnO₂ decreases down to *ca.* 6 nm. A simple model analysis has shown that such a grain size effect shows up when *D* decreases to be comparable with $2L$, where *L* is the depth of space charge layer. This shows the importance of controlling *D* to a size comparable with or less than $2L$. At the same time, this also suggests that control of *L* instead of *D* would give rise to a similar effect. It is known that *L* of a semiconductor can be controlled by doping impurities inside the lattice.³ In the case of SnO₂, *L* will increase with Al³⁺-doping, while it will decrease with Sb⁵⁺-doping, for example, according to the vacancy control principle. In fact, our preliminary study has confirmed that Al³⁺- or Sb⁵⁺-doping leads to a drastic change in gas sensitivity in accordance with the expectation. These findings have

prompted us to investigate the doping effects in more detail. This paper deals with the effects of Al³⁺-doping on SnO₂-based sensors. First we have examined how the gas sensitivity is modified with varying extents of Al³⁺-doping and then we carried out the measurements of Seebeck coefficients in order to estimate important parameters for understanding the doping effects.

EXPERIMENTAL

Hydrous SnO₂ powder was prepared by neutralizing a cold solution of SnCl₄ with an aqueous ammonia solution, followed by thorough washing with demineralized water, drying at 100° and grinding. It was calcined at a prescribed temperature for 1 hr in air to obtain undoped SnO₂ powder. To dope Al³⁺ into SnO₂ lattice (Al³⁺-SnO₂), an aqueous chloride mixture (SnCl₄ + AlCl₃) was treated with an aqueous ammonia solution. Aluminium content was varied in the range 0.001–5.000% in the atomic composition Al/(Al + Sn). The resulting coprecipitate was washed, dried and calcined at a temperature of 1100°. The mean size of SnO₂ crystallites was evaluated from the width of the X-ray diffraction (XRD) line of the (101) plane, based on Scherrer's equation.

To fabricate porous sensor elements, each powder sample prepared above was mixed with water, and the resulting paste was applied on an alumina tube with Pt wire electrodes and

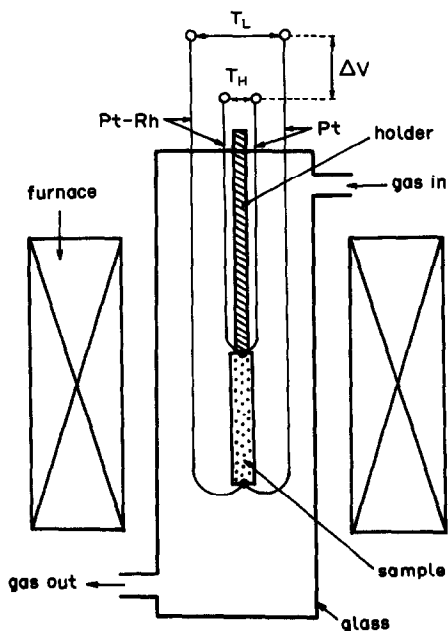


Fig. 1. Apparatus for Seebeck effect measurements. T_H and T_L denote temperatures at the high and low temperature ends of the specimen.

sintered at 700° for 4 hr in air unless otherwise stated. The gas sensing properties of each element were examined in a heated chamber through which air or a sample gas was allowed to flow at a rate of 150 cm³/min. The gas sensitivity was defined as the ratio of electric resistance in air (R_a) to that in the sample gas (R_g).

Measurement of the Seebeck effect was carried out in an apparatus shown in Fig. 1. Each powder sample was pressed into a ribbon-shaped specimen (3 × 15 × 0.3 mm) under a pressure of 1000 kg/cm², and calcined at 800 or 1100°. The two ends of the specimen were fixed onto a quartz rod with silver paste, together with two Pt/Pt-Rh thermocouples as shown in Fig. 1. The assembly was set in a quartz chamber located inside an electric furnace. The temperature difference of the specimen was measured with the two thermocouples, while the difference in electric potential (thermoelectric motive force) was measured between the Pt

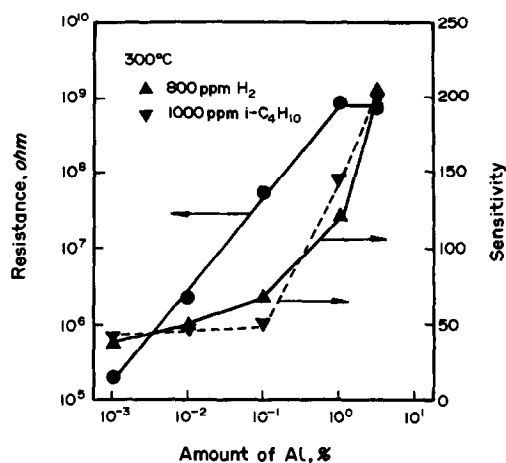


Fig. 2. Electrical resistance and gas sensitivity towards 800 ppm H₂ and 1000 ppm *i*-C₄H₁₀ correlated with the amount of Al doped into SnO₂ elements.

wire electrodes of the thermocouples in a flow of dry air.

RESULTS AND DISCUSSION

Properties of Al-doped sensors

Figure 2 shows the electric resistance (R_a) of the sensor elements at 300° in dry air as a function of Al content. R_a increased with increasing Al content up to 1% Al, above which R_a was saturated. This behaviour suggests that the solubility of Al in SnO₂ is 1% or less under these conditions. On the other hand, gas sensitivity (S) showed quite different dependence on Al content. As also shown in Fig. 2, S to both H₂ (800 ppm) and *i*-C₄H₁₀ (1000 ppm) increased only slightly up to 0.1% Al, and then increased dramatically. These properties of doped elements are summarized in Table 1, together with the data of the undoped one. The gas sensitivity could be promoted greatly when Al was doped by 1 and 5%.

We have reported that for undoped SnO₂ elements the crystallite size of SnO₂ (D) seriously affects the electric resistance and gas sensitivity. The crystallite size data for the present elements are also shown in Table 1. It is seen that D decreases with an increase in Al

Table 1. Properties of the Al-doped SnO₂

Amount of Al	Calcination conditions	Grain size D/nm	$\log R_a/\text{ohm}$ (300°)	Gas sensitivity	
				H ₂	<i>i</i> -C ₄ H ₁₀
0 (undoped)	800C·4 hr	25	5.30	30	41
0.001%	1100C·3 hr	>60	5.63	37	41
0.01%	1100C·3 hr	>60	6.34	50	45
0.1%	1100C·3 hr	60	7.74	69	48
1%	1100C·3 hr	43	8.93	118	145
5%	1100C·3 hr	19	8.84	204	201

content. This suggests that the properties of Al-doped elements are affected not only by the dissolution of Al into the lattice of SnO₂ but also by a change in D . As seen in Table 1, D was as small as 43 and 19 nm at Al contents of 1 and 5%, respectively, even under the severe calcination conditions applied. For those particular samples, the part of Al content in excess of solubility limit seems to have acted as a stabilizer of the ultrafine crystallites of SnO₂.

In order to examine the crystallite size effect in Al-doped elements, the resistance (R_a) and the gas sensitivity (S) to 800 ppm H₂ are shown as a function of D in Fig. 3 together with the data of undoped elements already reported. Only two elements doped with 1 and 5% Al were available for this correlation because the other elements had D values too large to be determined from XRD. The R_a vs. D relation for undoped elements is divided into two regions: R_a decreases steeply with increasing D in the small D region, while R_a increases slightly in the large D region. As has already been pointed out,¹ such D dependency of R_a results from whether D is smaller or larger than twice the depth of space charge layer ($2L$). From the D value bordering the two regions, L is estimated to be *ca.* 3 nm for the undoped SnO₂. For 1 and

5% Al doped elements, on the other hand, R_a was very large (10⁹ ohm) and exhibited no such dependency on D . As shown in Fig. 3(b), the gas sensitivity (S) of undoped elements increases drastically when D decreases down to 6 nm or less. When compared with these elements, the gas sensitivity of Al-doped elements was still very high at D as large as 20 nm or more. These data clearly show that both crystallite size (D) and impurity levels of SnO₂ bulk are important in determining S of Al-doped elements.

Seebeck coefficients

The valence control principle predicts that when trivalent ions (Al³⁺) are partially introduced into the lattice, the carrier concentration (n) of SnO₂ will decrease, leading to an increase in Debye length. In addition to such a change in the electronic structure in the bulk, however, actual Al-doped elements showed a change in the size of SnO₂ crystallites depending on Al content, as just mentioned. Furthermore, one cannot know *a priori* what portion of doped Al ions would in fact have entered the SnO₂ lattice. Under such conditions it seems imperative to separate the electronic structure factor from the microstructure factor for a basic understanding of the effect of Al-doping. For this purpose, we tried for the first time to evaluate the electronic structure of polycrystalline SnO₂ from the measurements of Seebeck effect.

The Seebeck effect is defined as the generation of a thermo-emf (electromotive force) between two points of a semiconductor when a temperature difference is applied between these points.⁴ The Seebeck coefficient (Q) is defined as a temperature derivative of thermoelectric potential (V). Under the condition that both electric field and temperature gradient are uniform between the two points, Q can be obtained as the ratio of emf (ΔV) to the temperature difference (ΔT).

$$Q = \frac{dV}{dT} = \frac{\Delta V}{\Delta T} \quad (1)$$

Thus Q was evaluated by measuring ΔV while applying ΔT between the two ends of the ribbon-like specimen. In all measurements, the lower temperature end was fixed to 300° and ΔT was set to be 10° or less. Prior to each measurement, the specimen was heat-treated at 500° for 30 min in dry air to eliminate possible surface contaminants like water and CO₂, and then kept at the temperature of measurement for 2 hr for stabilization.

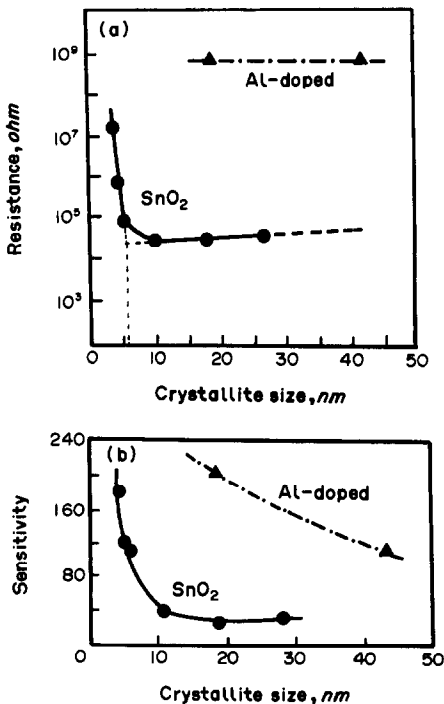


Fig. 3. Influence of crystallite size in Al-doped and undoped elements on (a) electric resistance and (b) gas sensitivity towards 800 ppm H₂.

Table 2. Seebeck coefficients and related characteristics of Al-doped SnO₂

Amount of Al	ΔV , mV	ΔT , °C	Q , $\mu V/K$	n , cm^{-3}	L_D , nm
0 (undoped)	-2.045	10	-205	4×10^{18}	2.8
0.001%	-2.302	9	-256	2×10^{18}	4.0
0.01%	-3.052	9	-339	8×10^{17}	6.4
0.1%	-4.600	8	-575	5×10^{16}	25.0
1%	-6.400	8	-800	(4×10^{15})	(88.5)

The values of ΔV , ΔT and Seebeck coefficient, Q , obtained are listed for each specimen in Table 2. For an n -type semiconductor, Q is known to be negative in sign. All the specimens showed negative coefficients and the absolute values were larger for larger amounts of Al-doping. For 5% Al-doped specimen this measurement was not possible because of too large a noise.

It should be noted that in the above procedure the assumption of a uniform electric field is an important approximation. For a polycrystalline system, this assumption may not always be verified because of the surface barrier. This matter will be discussed later.

Carrier concentration

For an n -type semiconductor of a single carrier system, the carrier concentration (n) is assumed to obey a Boltzmann distribution, $n = N_c \cdot \exp[-(E_C - E_F)/k]$, where E_C and E_F are the electronic potentials at the conduction band edge and Fermi level, respectively, and N_c is the density of states in the conduction band. Then Q can be related with n by the following equation.^{5,6}

$$n = N_c / \exp[-(eQ/kT) - A] \quad (2)$$

Here A is a constant associated with the transport of energy and e is elementary electric charge. For a non-degenerate semiconductor, $A = 2$ and $N_c = 2(2\pi m^* kT/h^2)^{3/2}$, where m^* is the ratio of effective mass to mass of electron and *ca.* 0.2 for SnO₂.^{7,8}

In this way, one can evaluate the concentration of carriers from Q data by using equation (2). Resulting carrier concentrations (n) are shown in Table 2 and Fig. 4. It is seen that n decreases steeply with an increase in doping amount of Al³⁺, from 4×10^{18} (cm⁻³) for undoped SnO₂ to 4×10^{15} (cm⁻³) for 1% Al³⁺ doped sample. The n value of undoped SnO₂ coincides well with that reported for porous SnO₂ thin films which falls in the range of 10^{18} – 10^{19} (cm⁻³) depending on the preparation methods.^{9–11} This seems to verify the

evaluation of n from Seebeck coefficients. The decrease of n with Al-doping is in accordance with the valence control principle. When it is assumed that each Al ion introduced in the lattice of SnO₂ traps a conduction electron, the observed decreases in n suggest that all Al ions enter the SnO₂ lattice up to 0.01% Al-doping, while only small portions of Al ions do so for larger amounts of Al-doping.

Debye length and the depth of space charge layer

When an n -type semiconductor has a carrier concentration of n , the Debye length is given as follows.

$$L_D = (\epsilon kT/e^2 n)^{1/2} \quad (3)$$

Here ϵ is the dielectric constant of the semiconductor and is *ca.* 10^{-10} F/cm for SnO₂.¹² Thus L_D can be directly derived from the data of n , as shown in Table 2 and Fig. 4. An increase in Al content is seen to increase L_D drastically; while L_D was 3 nm for undoped SnO₂, it was 25 nm at 0.1% Al. The L_D value at 1% Al (88 nm) apparently far exceeded one half of the crystallite size (43 nm), but because the various assumptions used for deriving it may not always be justified under such conditions this is not definite. Nevertheless, it can be concluded clearly that L_D is rather close to $1/2 D$ at 0.1%

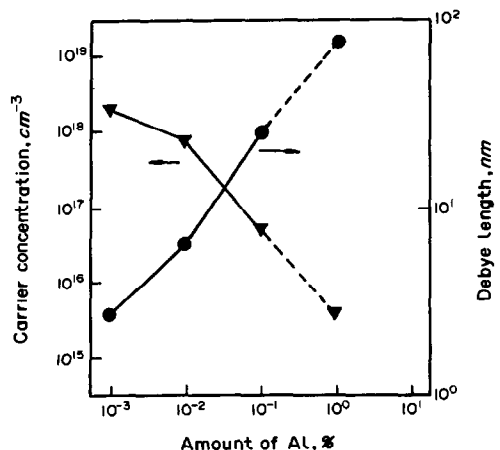


Fig. 4. Influence of Al content on carrier concentration and Debye length of Al-doped SnO₂.

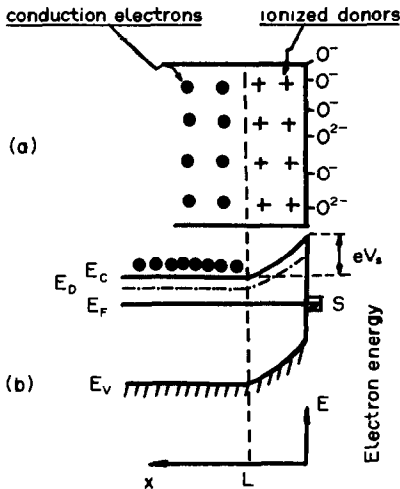


Fig. 5. Idealized model for oxygen adsorption on an *n*-type semiconductor. (a) Charge distribution. (b) Energy band structure.

Al while it is far larger than $1/2 D$ at 1% and 5% Al.

L_D is an important parameter in determining the depth of space charge layer (L) when a semiconductor interacts with a gas. In our case, oxygen would be adsorbed on the surface of SnO_2 crystallites. Figure 5 shows carrier distribution and energy band structure schematically, in the surface region. In the simplest case where all donors are ionized and all conduction electrons in the space charge layer are depleted, to be trapped by surface states (adsorbed oxygen), L is proportional to L_D with a proportionality constant being determined by surface potential (eV_s) and thermal energy as follows.³

$$L = (2eV_s/kT)^{1/2} L_D \quad (4)$$

Thus one needs the surface potential data for estimating L , but unfortunately no reliable data are available for SnO_2 . At 300° , the proportionality constant of equation (4) is close to unity for $eV_s = 0.03$ eV and increases with the square root of increasing eV_s . Considering that the surface potentials are often of the order of 0.1 eV for other oxides,¹³⁻¹⁵ L does not seem to be much different from L_D for SnO_2 . It is noted that for undoped SnO_2 , L_D (3 nm) coincides well with the empirical value of L (3 nm) estimated from Fig. 3(a).

Polycrystalline state of SnO_2

Equation (1), used for the measurements of Seebeck coefficients, assumes the uniformity of both temperature gradient and electric field between the two measuring points. These requirements would be easily satisfied with a

single crystal or a densely sintered specimen but not with a porously sintered specimen, as used in the present study, because of the surface potential. Nevertheless, the measurements were found to bring about rather reasonable values of carrier concentration and Debye length, especially for undoped SnO_2 . This suggests that the specimens, though porous and polycrystalline, have a microstructure which somehow meets the requirements.

According to our previous study with TEM observation and other techniques,¹⁶ the microstructure of SnO_2 -based elements can be pictured as composed of three dimensional arrays of SnO_2 crystallites. Each crystallite is co-ordinated with 4 neighbours, on average, through necks of a diameter of $0.8 D$ (D = crystallite diameter), whereas a far fewer number of grain boundary contacts are also included in the array. For simplicity, such a microstructure can be reduced to a one-dimensional chain as schematically shown in Fig. 6. The connections between neighbouring crystallites are provided almost exclusively by necks and only scarcely by grain boundary contacts. If D is larger than $2L$, the space charge layer forms only in the surface region of each crystallite. The core region, undisturbed by the surface effect, can extend through necks in the chain until it terminates at the grain boundary contacts. When a temperature gradient is applied in the chain direction the resulting electric field inside the core region can be uniform as long as neck contacts are available. In this situation, therefore, the Seebeck effect can be measured without being disturbed by the surface effect if grain boundary contacts are scarce compared with neck contacts. This situation was probably achieved in the present specimens when Al contents were low. For 1 and 5% Al-doped samples which had D smaller than $2L$, however, Seebeck effects could possibly be seriously disturbed by the surface effect.

Implication of Al-doping for gas sensitivity

As mentioned above, the gas sensitivity of SnO_2 -based elements towards H_2 (and $i\text{-C}_4\text{H}_{10}$)

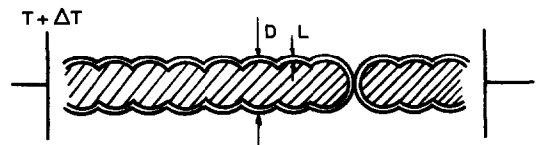


Fig. 6. One dimensional model for interconnection of SnO_2 crystallites in polycrystalline elements.

could be promoted with Al-doping, with best results at Al contents of 1 and 5%. Subsequent analyses revealed that Al-doping had two effects on the elements: the increase of Debye length of SnO₂ as a result of valence control and the stabilization of microcrystalline particles of SnO₂. Both effects are quite favourable from the viewpoint of gas sensitivity, since gas sensitivity has been shown to increase when the crystallite size of SnO₂ is comparable with or smaller than twice the depth of space charge layer.

It is often asserted that gas sensitivity should increase with increasing electric resistance of the element on the grounds that a change in conduction electron concentration would bring about a larger resistance change with increasing resistance. Figure 7 shows the relation between electric resistance (R_a) and gas sensitivity (S) for Al-doped SnO₂ in the present experiments. Although S tends to increase with an increase in R_a , the relation does not seem to be as simple as the above assertion. The increase of S is only gradual in the R_a range below 10⁸ ohm, while it is quite steep above it. This tendency is well coincident with whether $D > 2L$ (gradual increase) or $D < 2L$ (steep increase), in agreement with what was observed for undoped SnO₂. This strongly suggests that the observed increase of S with Al-doping should be understood on the basis of microstructure of the elements rather than R_a .

The present study indicates that the doping of impurities in semiconductive oxides can be an important method for promoting semiconductor gas sensors. As illustrated above, the doping affects not only the electronic structure but also the microstructure of the elements,

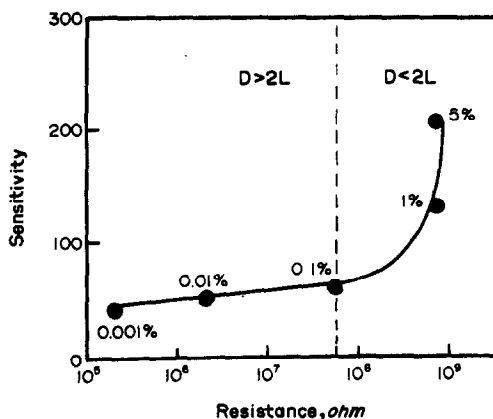


Fig. 7. Relationship between electric resistance in air and gas sensitivity to 800 ppm H₂ at 300° for Al-doped elements. Figures attached indicates Al contents.

both being critically important for gas sensing properties. There are many oxides which exhibit semiconductive properties, but very few of them have actually been used for gas sensors. As the doping method can modify the properties of oxides rather drastically, it is possible that new sensing materials are developed by this method. Although this method has hardly been applied so far, research in this direction is desired for further development of gas sensors.

CONCLUSION

The effects of Al-doping on SnO₂ elements were investigated with respect to gas sensing properties as well as electronic and physical structure of the elements. Gas sensitivity to H₂ and i-C₄H₁₀ is promoted tremendously when Al is doped by 1 and 5% although promotion remains slight up to 0.1% Al. Seebeck effect measurements indicate that Debye length increases with Al-doping, while XRD shows that SnO₂ crystallite size (D) decreases with Al-doping. As a result of these two effects, the relation $D < 2L$ (L = the depth of space charge layer) is achieved when 1% or more Al is doped and this is a reason for the high gas sensitivity of these elements.

REFERENCES

1. C. Xu, J. Tamaki, N. Miura and N. Yamazoe, *J. Electrochem. Soc. Jpn.*, 1990, **58**, in the press.
2. *Idem*, *Chem. Lett.*, 1990, 441.
3. H. K. Henisch, *Semiconductor Contacts*, p. 45. Clarendon Press, Oxford, 1984.
4. See *e.g.*, W. D. Kingery, H. K. Bowen and D. R. Uhlmann, *Introduction to Ceramics*, 2nd Ed., p. 871. Wiley, New York, 1976.
5. I. Bransky and N. M. Tallen in *Physics of Electronic Ceramics*, Part A, L. L. Hench and D. B. Dove (eds.), p. 67. Dekker, New York, 1971.
6. R. N. Blumenthal and M. A. Seitz, in *Electrical Conductivity in Ceramics and Glass*, Part A, N. M. Tallen (ed.), Chap. 4. Dekker, New York, 1974.
7. J. A. Marley and R. C. Dockerty, *Phys. Rev. A*, 1965, **140**, 304.
8. C. G. Fonstad and R. H. Rediker, *J. Appl. Phys.*, 1971, **42**, 2911.
9. H. Ogawa, M. Nishikawa and A. Abe, *ibid.*, 1982, **53**, 4448.
10. S. C. Chang and D. B. Hicks, in *Fundamentals and Application of Chemical Sensors*, D. Schuetzle and R. Hammerle (eds.), p. 58. ACS, Washington DC, 1986.
11. M. Kojima, H. Kato, A. Imai and A. Yoshida, *J. Appl. Phys.*, 1988, **64**, 1902.

12. J. F. McAleer, P. T. Moseley, J. O. W. Norris and D. E. Williams, *J. Chem., Soc. Faraday Trans. I*, 1987, **83**, 1323.
13. D. F. Cox, T. B. Fryberger and S. Semancik, *Phys. Rev. B*, 1988, **38**, 2072.
14. V. E. Henrich, *Rep. Prog. Phys.*, 1985, **48**, 1481.
15. W. Göpel, U. Kirner, H. D. Wiemhöfer and G. Rocker, *Solid State Ion.*, 1988, **28-30**, 1423.
16. C. Xu, J. Tamaki, N. Miura and N. Yamazoe, *J. Mater. Sci.*, to be published.

DETERMINATION OF IRON(II) WITH CHEMICALLY-MODIFIED CARBON-PASTE ELECTRODES

ZHIQIANG GAO

Department of Chemistry and Chemical Engineering, Henan University, Kaifeng, Henan, 475001,
People's Republic of China

PEIBIAO LI* and ZAOFAN ZHAO

Department of Chemistry, Wuhan University, Wuhan, Hubei, 430072, People's Republic of China

(Received 27 June 1990. Revised 24 September 1990. Accepted 3 November 1990)

Summary—The utility of carbon-paste electrodes modified with 2,2'-bipyridyl and Nafion for the differential pulse voltammetric determination of iron(II) in aqueous medium is demonstrated. The method is based on formation of the 2,2'-bipyridyl complex of iron(II) and its accumulation by the Nafion. The differential pulse voltammetric response of the accumulated complex is used as the analytical signal. The response was evaluated with respect to carbon-paste composition, preconcentration time, pH, iron(II) concentration and other variables. A 3-min accumulation period permits measurement of iron(II) down to $10^{-8}M$, and a relative standard deviation of 3.8% for $2 \times 10^{-6}M$ iron(II). Rapid and convenient chemical renewal allows use of a single modified carbon-paste electrode in multiple analytical measurements over several days. The proposed procedure was applied to the determination of iron in certified standard reference materials and trace iron in natural waters.

The application of chemically-modified electrodes (CMEs) in analytical chemistry has attracted considerable attention in recent years. A number of CMEs have proved suitable as sensors in the electrochemical determination of metal ions¹⁻⁵ and organic and bio-organic species.⁶⁻⁸ Various methods have been demonstrated, including complexation,¹ precipitation,² electrostatic preconcentration,⁹ bio-accumulation,³ potentiometry,¹⁰ permselectivity¹¹ and others.¹²⁻¹⁶ Of these, the application that is currently the most widely developed and the closest to practical use in analytical chemistry is probably that involving analyte preconcentration. Concentrating the analyte in the modified film greatly improves the sensitivity and selectivity of voltammetric determination. This approach is analogous in some respects to traditional electrochemical stripping voltammetry in that a preconcentration step is employed to enhance the sensitivity and selectivity, but with the difference that in the CME approach these characteristics are governed by the chemical reactivity of the modifier rather than by the reduction potential of the analyte. As a result, the nature of the analytes that can be accumulated on the CME surface can be rationally

predicted for a given modifier, and electrodes can be designed for particular analytes. As CMEs utilize a chemical step for analyte accumulation, their use can often be more selective than electrochemical stripping voltammetry.

In addition, many methods have been used to immobilize chemically active species on the electrode surface. The carbon-paste electrode appears especially advantageous for modification. CME fabrication with this electrode involves only the addition of a sparingly soluble modifier to an otherwise conventional graphite powder/nujol oil mixture and has several attractive features. Chemically-modified carbon-paste electrodes (CMCPes) are very easy to make, and can readily be prepared with a variety of modifier loading levels. More importantly, fresh modified-electrode surfaces can be generated rapidly and reproducibly. The low background current is another advantage for practical analytical applications.

Various chemically active species (preconcentration reagents) have been introduced into carbon-paste electrodes to produce CMCPes. Baldwin and co-workers have described the use of carbon-paste electrodes modified with dimethylglyoxime and 2,9-dimethyl-1,10-phenanthroline² for the determination of nickel(II) and copper(I), respectively. Gardea-Torresday

*Author for correspondence.

et al. proposed a micro-organism-modified CPE for the bio-accumulation and subsequent voltammetric determination of copper(II).³ Ion-exchangers have also been used to modify CPEs.^{9,17-20} We have employed CPEs modified with chelating resins for the determination of silver(I)²¹ and gold(III).²²

There are several studies on the use of CMEs in the electrochemical determination of iron. Wang and Martinez²³ reported that carbon-paste electrodes modified with montmorillonite clay can be used for the collection of iron(III) from dilute solutions, followed by voltammetric quantification of the surface-bound iron(III) ion. This method suffers from poor sensitivity, however, having a detection limit of only $3.6 \times 10^{-6} M$. Guadalupe and Abruña²⁴ proposed an approach based on the use of functionalized polymer films for determining iron(II) with CMEs. In addition to taking advantage of the favourable aspects of CMEs, this method circumvents the difficulties associated with surface saturation and matrix effects. Modification of platinum electrodes with quaternized poly(4-vinylpyridine) cross-linked with 4,7-diphenyl-1,10-phenanthroline disulphonic acid has recently been reported by Gehron and Brajter-Toth.²⁵ The modified electrodes were applied to the determination of iron(II) in aqueous solution. The ligand-loaded CMEs generally offer low detection limits, but are often difficult to regenerate and suffer from poor reproducibility.

In this paper we describe a new concept for the accumulation/determination approach, based on complexation of the metal ion by a ligand (2,2'-bipyridyl)²⁶ and then accumulation by an ion-exchanger (Nafion) incorporated in the carbon-paste electrode. In the work described below, the CME was easily prepared by simply mixing the required amounts of the two modifiers with a carbon-paste matrix. This allows easy variation of the two modifier contents and regeneration of the modified electrode surface. For a 3-min accumulation period, the detection limit could be extended to $10^{-8} M$ and the relative standard deviation was 3.8%. In addition, rapid chemical renewal of the modified electrode surface was possible and the CME stability was such that the surface retained its performance for several days' use.

EXPERIMENTAL

Reagents

An iron(II) stock solution ($10^{-2} M$) was prepared by dissolving the required amount of

ammonium ferrous sulphate (analytical grade, Shanghai Chemicals Factory) in 0.01M sulphuric acid. Working solutions were prepared by diluting the stock solution with water just before use.

Graphite powder and nujol oil were of reagent grade (Beijing Chemicals Factory). Nafion solution (5%) was obtained from Dupont. 2,2'-Bipyridyl and all other chemicals were of certified analytical grade and used without further purification. Doubly-distilled water from a fused-silica still was used to prepare all solutions. It was unnecessary to remove dissolved oxygen from solutions.

Electrodes

Unmodified carbon paste was made by mixing 1.0 g of graphite powder and 0.60 g of nujol oil in a mortar. Modified carbon paste was prepared similarly, except that the graphite was first mixed with the desired weights of 2,2'-bipyridyl and Nafion solutions. Uniform dispersion of the modifiers was obtained by ultrasonication of a slurry of the graphite/modifier mixture in ethanol for 15–20 min, and evaporation of the alcohol under an infrared lamp. Finally, the carbon paste was packed into one end of a glass tube (4 mm i.d., 6 mm o.d.) and a copper wire (≤ 4 mm diameter) was inserted through the opposite end to establish electrical contact. The carbon paste surface was polished on smooth paper until shiny, and then conditioned by exposure to a Britton–Robinson buffer solution (pH 5.0) containing $5 \times 10^{-5} M$ iron(II) for 60 sec, then to 1.0M potassium thiocyanate for 10 min to remove accumulated iron(II) and finally to pure Britton–Robinson buffer solution (pH 5.0) for 2 min. The conditioning cycle was repeated 3–5 times. The modified electrode could easily be resurfaced by removing some carbon paste extruded by pushing down the copper contact wire, and repolishing.

Apparatus

A PAR 174A polarographic analyser was used for cyclic and differential pulse voltammetric measurements, together with an EG&G PAR Model 0089 X–Y recorder. Unless otherwise indicated, the pulse amplitude in the differential pulse voltammetric experiments was 50 mV and the scan-rate was 10 mV/sec. A three-electrode system consisting of a CMCP working electrode, a platinum wire auxiliary electrode and a saturated calomel reference electrode

(SCE) and a 1.0M potassium chloride salt bridge was used for all voltammetric measurements. All potentials are referred to the SCE. A magnetic stirrer with a 1.5-cm stirrer bar was used in the preconcentration and electrode renewal steps. The electrolytic cell was a 20-ml beaker. All experiments were performed at room temperature (22–25°).

Procedure

A preconcentration/medium-exchange/voltammetric determination/renewal scheme¹ was used in all experiments. The preconcentration was applied to 20 ml of Britton–Robinson buffer solution (pH 5.0) containing the iron(II); the voltammetric scan was performed in iron-free buffer solution (pH 5.0). After each electrochemical determination, the electrode was kept in stirred 0.5–1.0M potassium thiocyanate for several minutes and then thoroughly washed with water and pH 5.0 buffer solution. The cleaned electrode was placed in the preconcentration cell for the next cycle.

RESULTS AND DISCUSSION

Electrochemical behaviour of iron(II) on CMCPEs

CMCPEs intended for use in routine analysis ideally involve a permanently immobilized and stable species. In practice, however, the modifier need only be insoluble enough to ensure that the rate of bleeding into the solution is very low, and slow bleeding can even have a beneficial effect for surface renewal and continuous use. The solubilities²⁶ of 2,2'-bipyridyl and its iron(II) complex are not low enough, however, for a 2,2'-bipyridyl-modified carbon-paste electrode to work well. However, because the iron(II) complex is positively charged, incorporation of a cation-exchanger as an additional modifier will reduce the rate of bleeding to an acceptable level. Nafion polymers are perfluoro-sulphonate cation-exchange polymers with good selectivity for large organic cations,²⁸ Sharp²⁹ has reported that the 2,2'-bipyridyl-iron(II) complex is strongly retained in a Nafion film on a glassy-carbon electrode. The experimental results reported in the present paper are part of an effort to evaluate this type of CMCPE and its applications in analytical chemistry.

Initial experiments showed that carbon-paste electrodes incorporating 2,2'-bipyridyl alone were unstable when immersed in aqueous solution. After a few minutes exposure to water,

the polished electrode surface became noticeably rough and subsequently exhibited little or no complexing capabilities. Furthermore, when the 2,2'-bipyridyl-modified CPE was immersed in a relatively high concentration of iron(II) solution (10^{-3} – $10^{-4}M$), a reddish colour gradually developed, undoubtedly because of loss of the modifier to the aqueous medium. In contrast, the CPE modified with Nafion and 2,2'-bipyridyl was stable and remained chemically active in aqueous medium. Therefore, only this combination of modifiers was used in further experiments.

Figure 1 shows cyclic voltamperograms obtained with the bipyridyl/Nafion modified electrode in pH 5.0 Britton–Robinson buffer in the presence and absence of iron(II). With the buffer solution alone, there is a stable and fairly low residual current over a wide potential scan range (0.3–1.3 V) and no distinct redox waves are observed for either 2,2'-bipyridyl or Nafion. The voltamperogram is not significantly different from one obtained with a plain carbon-paste electrode in the same solution except that the residual current for the CMCPE is 40–50% larger.

In contrast, the cyclic voltamperogram obtained with a CMCPE that had been immersed for 3 min in buffer solution containing $1 \times 10^{-4}M$ iron(II) and then washed with water,

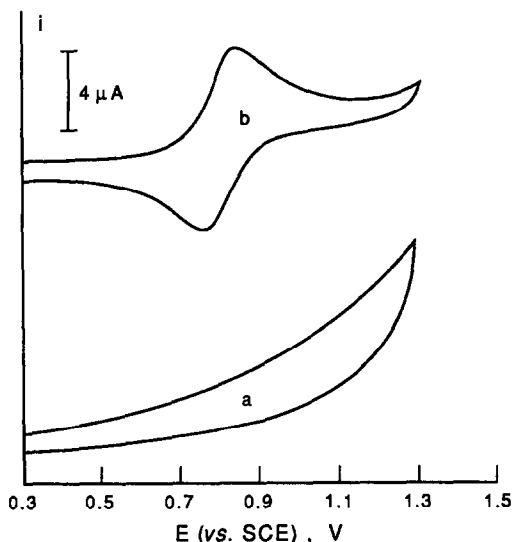


Fig. 1. Cyclic voltammetric response of iron(II) on the modified electrode. (a) Blank Britton–Robinson buffer solution (pH 5), and (b) potential scan following 3-min stirring in $1 \times 10^{-4}M$ iron(II) in Britton–Robinson buffer, rinsing with water and 60-sec electrolysis at 0.3 V (vs. SCE) in pure Britton–Robinson buffer solution. Potential scan rate 100 mV/sec.

before transfer into pure buffer solution in the determination cell, had a pair of well-defined redox waves with $E_m = \frac{1}{2}(E_{pa} + E_{pc})$ of ca. 0.79 V *vs.* SCE. These waves could be obtained not only by exposure of the modified electrode to iron(II) but also for iron(III) in the same buffer solution. However, when the modified electrode was briefly immersed in an iron(II) or an iron(III) solution (each at the same concentration) under the same conditions, then rinsed and placed in the determination cell as before, the voltammetric scan exhibited larger redox waves for iron(II) ($i_{pFe^{2+}}/i_{pFe^{3+}} = 1.5-2.0$), which are more suitable for practical use. The shapes of the cyclic voltamperograms and the peak potentials of the iron(II) and iron(III) redox waves were almost identical. Because the waves occurred in the same potential region as those obtained with a glassy carbon electrode coated with Nafion and 2,2'-bipyridyl-iron(II) complex in weakly acidic solution,²⁹ they were assigned to the oxidation of the surface-accumulated iron(II) complex and reduction of the oxidized form. The cyclic voltamperogram in Fig. 1(b) indicates that there is considerable diffusion of the iron(II) complex within the Nafion matrix ($\Delta E_p = 90-100$ mV). This behaviour is attributable to the mass-transfer and charge-transfer limitations within the Nafion film and at the substrate/film interface.^{30,31} Furthermore, when the CMCPE was immersed in a more concentrated iron(II) solution in the buffer solution or a longer preconcentration time was employed, a red colour appeared on the surface of the modified electrode before the voltammetric scan.

Figure 2 shows differential pulse voltamperograms obtained after immersing the plain CPE (a) and the Nafion-2,2'-bipyridyl modified CPE (b) in a buffered $2 \times 10^{-3} M$ iron(II) solution (pH 5.0) for 3 min, at open circuit, washing, and transferring into pure buffer. The iron(II) uptake from such a dilute solution is clear. The oxidation of the surface-accumulated iron(II)-2,2'-bipyridyl complex yields a well-defined differential-pulse peak current with a peak potential of 0.83 V *vs.* SCE. No such iron(II) peak current was observed with the plain CPE. Furthermore, the differential pulse voltammetric method is more suitable than cyclic voltammetry for practical analysis: the sensitivity is greatly improved, there is better discrimination, and the peak current is easier to measure. Normal linear sweep voltammetry or cyclic voltammetry can also be used, but the detection

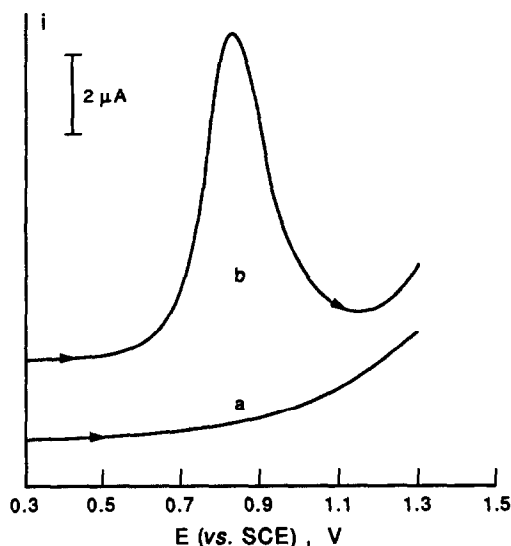


Fig. 2. Differential pulse voltammetric response of iron(II) on different electrodes. (a) Unmodified CPE, (b) Nafion/2,2'-bipyridyl-modified CPE. Preconcentration of $2 \times 10^{-3} M$ iron(II) in Britton-Robinson buffer solution (pH 5.0), other conditions as for Fig. 1(b). Potential scan rate 10 mV/sec, pulse amplitude 50 mV, repetition time 1 sec.

limit is much higher (e.g., $5 \times 10^{-7} M$ for a 3-min accumulation).

These results show that fabrication of a CMCPE by use of 2,2'-bipyridyl and Nafion as modifiers is based on forming and accumulating the iron(II)-2,2'-bipyridyl complex on the CPE surface. The cationic iron(II) complex is then collected by an ion-association complex with the SO_3^- site of the Nafion. The uptake properties of large organic cations such as the iron(II)-2,2'-bipyridyl complex can thus be utilized for a very efficient preconcentration step prior to electrochemical measurement.

Convenient regeneration of an analyte-free surface is particularly attractive for analytical applications of CMEs. Effective renewal combines with reproducible preconcentration and a robust electrode surface to give highly reproducible results. The utility of various cleaning methods for renewal of the modified electrode surface was evaluated. It was found that renewal was easily accomplished by dipping the electrode into 0.5–1.0 M thiocyanate solution for a certain period, usually 5–10 min, depending on the amount of iron(II) accumulated on the surface. A subsequent differential pulse voltammetric scan should show no redox waves; if it does, the renewal step must be repeated. The effective cleaning and reproducible accumulation are illustrated by the precision obtained during a series of eight preconcentration/

determination/renewal cycles with $2 \times 10^{-6} M$ iron(II) during 2 hr of continuous operation. The complete series yielded a mean peak current of $0.75 \mu A$ with a relative standard deviation of 3.8% (conditions as for Fig. 2). These results indicate that the modification method described results in a stable electrode surface with very low leaching of the modifiers into the aqueous medium.

The ability of an individual electrode to perform multiple analytical determinations with highly reproducible results is an important feature of CPEs modified with complexing agents. In the present work, the same electrode could be used for several days, performing 25–35 preconcentration/determination/renewal cycles with no noticeable loss of sensitivity or stability. Different portions of the same modified carbon paste (stored at room temperature) yielded repeatable results over a period of at least 6 months.

The differential pulse voltammetric response of a virgin modified electrode during repetitive accumulation/determination/renewal cycles is shown in Fig. 3. It is obvious that virgin CME surfaces were somewhat less effective for iron(II) accumulation than surfaces that had been previously exposed to iron(II) solutions [Fig. 2(b)]. After several cycles, however, highly

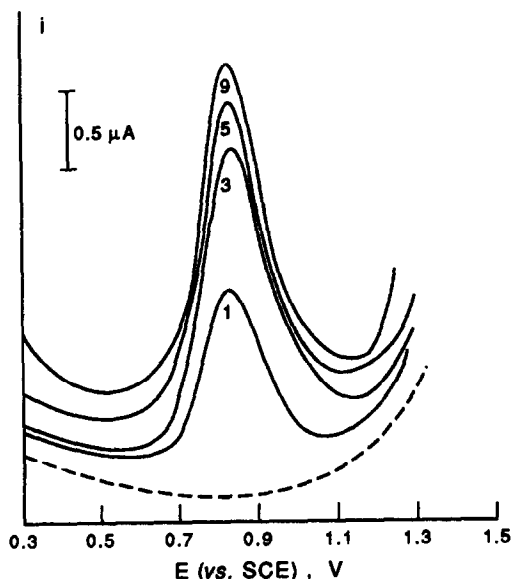


Fig. 3. Differential pulse voltammetric response of virgin CMCPE during repetitive accumulation/determination/renewal cycles. Preconcentration of $5 \times 10^{-6} M$ iron(II) in Britton–Robinson buffer solution, other conditions as for Fig. 2; (1), (3), (5) and (9) are the cycle numbers for the same electrode; dashed trace represents the voltamperogram obtained after renewal procedure.

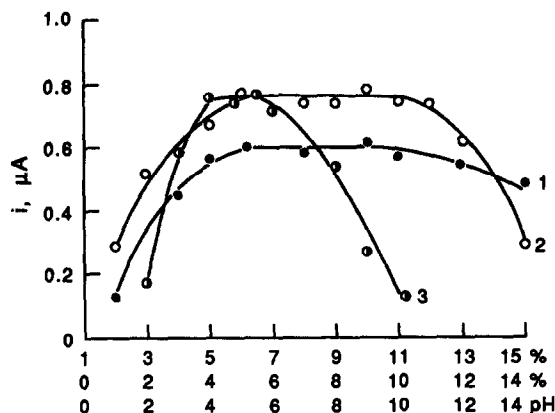


Fig. 4. Effect of CPE composition and pH on differential pulse response for $2 \times 10^{-6} M$ iron(II). (1) Nafion, (2) 2,2'-bipyridyl, (3) pH of preconcentration electrolyte. Other conditions as for Fig. 2.

reproducible responses can be obtained when the preconcentration/determination/renewal cycles are performed under identical conditions. Enhancement of the sensitivity during the initial cycles has been found by other authors in studying other CPEs modified with organic complexing agents.^{1,2,32} The reason for the enhancement might be that the surface chelating groups of the complexing agent, after complexation with the analyte, attain a certain degree of ordering and orientation that facilitates subsequent complexation.¹ As a consequence of this behaviour, to avoid a time-dependent sensitivity in subsequent determinations virgin modified-electrode surfaces require conditioning as described in the experimental section. Similar sequences have been found essential for successful operation of other CPEs modified with complexing agents.^{1,2,32}

Optimum experimental conditions for analysis

The effect of the carbon-paste composition on the differential pulse voltammetric response of the accumulated iron(II) was tested, with the results in Fig. 4. Curve (1) shows the effect of Nafion in carbon paste (containing 13% 2,2'-bipyridyl) on the electrochemical response. The reason for the non-linear relationship is not yet certain, but may either be a greater extent of intercalation at high Nafion loading, or increasing electrode resistance. Other possible reasons are mass-transfer and charge-transfer limitations within the polymer film and at the substrate/film interface.^{30,31} The considerable change in the background current at high Nafion loading made it very difficult to determine traces of iron(II), so carbon paste with

6–10% Nafion was employed in all subsequent experiments.

The effect of 2,2'-bipyridyl in carbon paste loaded with 6% Nafion was also tested. It was found that the largest differential-pulse peak current for iron(II) occurred when the carbon paste contained 5–10% w/w 2,2'-bipyridyl [Fig. 4, curve (2)].

The solution employed in the determination step has a profound effect on the differential-pulse voltammetric response. Various electrolyte and buffer solutions were tested. Britton-Robinson buffer (pH 5.0) proved to be better than the other solutions tested (0.1M KCl, 0.1M CH₃COONa, 0.1M NH₄Cl, 0.1M Na₂CO₃, 0.1M KNO₃, 0.1M HCl, 0.2M KCl-HCl, Na₂B₄O₇-NaOH buffer, CH₃COONa-CH₃COOH buffer, 0.1M NaOH, Na₂HPO₄-KH₂PO₄ buffer, 0.05M Na₂B₄O₇ and 0.1M NaH₂PO₄), yielding the largest and sharpest peak. A 0.2M acetate buffer (pH 5.0–5.8) was also suitable for accumulating iron(II). The effect of the pH of the Britton-Robinson buffer solution on the differential-pulse voltammetric response of iron(II) is shown in Fig. 4, curve (3); the optimum pH range is 4.0–5.6. As with 2,2'-bipyridyl alone, attempting accumulation from a more acidic medium caused a drastic decrease in the peak current. At the same time, the use of a preconcentration medium more alkaline than pH 8 often resulted in premature precipitation of iron(II) hydroxide when relatively high iron(II) concentrations were encountered and the accumulation efficiency decreased

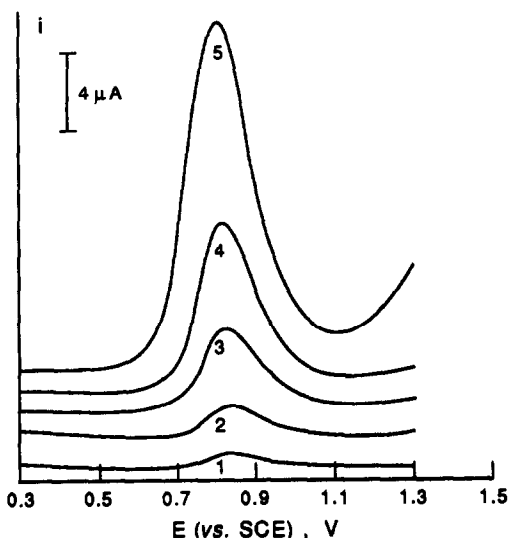


Fig. 5. Dependence of differential pulse voltammetric response of CMCPE on pulse amplitude. (1) 5, (2) 10, (3) 25, (4) 50 and (5) 100 mV. Other conditions as for Fig. 2.

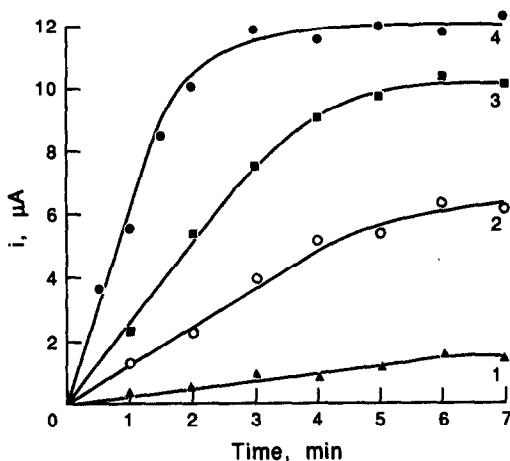


Fig. 6. Dependence of differential pulse voltammetric response of CMCPE on the accumulation time. Iron(II) concentrations: (1) 2×10^{-6} , (2) 1×10^{-5} , (3) 2×10^{-5} and (4) 5×10^{-5} M. Other conditions as for Fig. 2.

drastically. Hydrogen ion is not involved directly in either the complex or the ion-association. However, owing to the basicity of 2,2'-bipyridyl, protons compete with iron(II), reducing the formation of the complex and therefore the differential-pulse response of iron(II). In alkaline solution, because of hydrolysis of the analyte, the preconcentration of iron(II) on the modified electrode surface is also less effective.

The differential-pulse voltammetric waveform offered better response characteristics than did linear-sweep voltammetry and was used in practical measurements (as shown in Fig. 2). The peak current increased quasi-linearly with the pulse amplitude over the range 5–100 mV (Fig. 5). The best signal-to-background current ratio and high sensitivity can be obtained with 50-mV pulse amplitude and this was therefore used in all other measurements.

The dependence of the differential-pulse voltammetric peak current on accumulation time for different iron(II) concentrations is shown in Fig. 6. The rate of iron(II) uptake is dependent on concentration. The peak current increased rapidly at first, then gradually more slowly until a steady-state current was reached. The steady-state currents increased with the concentration of iron(II), but non-linearly. In all cases, the preconcentration process was relatively rapid, more than 80% of the final response being generated within the first few minutes of accumulation. Such profiles were observed at the different concentrations of iron(II) employed and appeared to represent the kinetics of the cation uptake by the ion-ex-

changer. This behaviour of electrodes modified with ion-exchanger is in agreement with common models for the rates of ion accumulation in ion-exchangers.³³

Under the optimum experimental conditions, the differential-pulse voltammetric peak current increased linearly with $[\text{Fe(II)}]$ from 3×10^{-7} to $2 \times 10^{-5} M$ (3-min accumulation period) and the detection limit was $8 \times 10^{-8} M$. Because of trace amounts of iron(II) in the chemicals and water used, lower detection limits could not be reached by using longer accumulation times. The linear response may be extended by the use of shorter accumulation times. At higher concentrations the response started to level off; a possible explanation for this may be saturation of the binding sites of the Nafion film. Another possibility is mass-transfer and charge-transfer limitations in the Nafion.^{30,31}

Interferences

The most significant potential advantage of using CMEs in analytical chemistry is the opportunity that the modifier-analyte interaction affords for greatly improved sensitivity and/or selectivity. If a highly selective modifier is used, the CME should allow interferences from co-existing species possessing electrochemical behaviour similar to that of the analyte to be by-passed in a straightforward fashion. It is precisely this kind of interference that poses a nearly insurmountable problem for conventional voltammetric stripping analysis. Furthermore, because of the high selectivity toward the target analyte, a number of co-existing species have little or no effect on its determination. Co-existing ions can interfere with the determination of iron(II) if they compete for surface binding sites and reaction with the modifier or yield an overlapping response. For the specific case of 2,2'-bipyridyl, Co(II), Cu(I), Cu(II), Ni(II), Ru(III), Ag(I) and Fe(III) are potential interferences. In these studies the response of the CMCPes to $5 \times 10^{-7} M$ iron(II) was investigated as a function of increasing concentrations of these ions. It was found that additions of $5 \times 10^{-6} M$ Co(II), Cu(I), Cu(II), Ni(III), Ru(III) and Ag(I) to the iron(II) solution resulted in 28, 25, 23, 18, 20 and 15% depression of the peak current for iron(II), respectively. Addition of $5 \times 10^{-7} M$ iron(III) results in 60% enhancement of the iron(II) peak current. Anions such as CN^- and SCN^- can form complexes with iron(II) and seriously interfere with the determination. Electroactive but non-

accumulated metal ions do not interfere, because of the use of the medium-exchange procedure. Reductants such as ascorbic acid, hydroxylamine hydrochloride and hydroxylamine sulphate, which may be used to reduce iron(III) in the sample solution to iron(II) for total iron determination, have no effect on the determination of iron(II). However, in practical use, thousandfold excesses of co-existing ions (such as Al^{3+} ions) could be tolerated before the iron(II) quantification began to be affected. In these cases, no new peak currents indicative of complex or co-precipitation formation and carry-over of the interferences were observed, but a gradual suppression of the iron(II) peak became evident. This implies that, in unknown samples, large excesses of such indirectly interacting interferences might produce erroneously low results. In such instances, more accurate determination would probably be achieved by using a standard-addition method instead of a calibration graph, or by use of a prior separation step. Alternatively, selective masking of the most important co-existing ions might also be useful.

Practical applications

The Nafion/2,2'-bipyridyl-modified CPE was applied to the determination of iron in certified standard reference materials and natural waters by a standard-addition method. Aluminium samples (0.1–0.3 g) were dissolved with a mixture of 6M hydrochloric acid and 30% hydrogen peroxide in a beaker; the solutions were carefully heated (under a cover) on a hot-plate until nearly dry, then treated with concentrated hydrochloric acid and evaporated to dryness. The residues were dissolved in 7M hydrochloric acid and the iron was extracted with a benzene/methyl isobutyl ketone mixture as proposed by Jackson and Philips.³⁴

Aqueous samples were acidified with hydrochloric acid and filtered through a fine filter paper.

An aliquot of the test solution was taken and iron(III) was reduced by adding 0.2–0.4 ml of 10 mg/ml hydrochloride hydroxylamine solution; the iron(II) was then determined by the procedure above. The results agreed well with the reference values and the recovery was good enough for practical use, as shown in Table 1.

CONCLUSIONS

Although this study should be considered preliminary, the results demonstrate the feasi-

Table 1. Determination of iron in samples

Sample	Found	Standard value	Addition, $\mu\text{g/ml}$	Found, $\mu\text{g/ml}$	Recovery, %
LF ₃ aluminium alloy	0.49%	0.50%	1.0	0.94	94
ZL ₁₀ aluminium alloy	0.23%	0.23%	1.0	0.98	98
Pure aluminium Al-1	0.23%	0.24%	1.0	0.94	94
Water (reference sample)	0.079 $\mu\text{g/ml}$	0.078 $\mu\text{g/ml}$	0.10	0.103	103
Water I	0.26 $\mu\text{g/ml}$	—	0.10	0.096	96
Water II	0.083 $\mu\text{g/ml}$	—	0.10	0.105	105
Water III	0.14 $\mu\text{g/ml}$	—	0.10	0.097	97

bility of using an ion-exchanger such as Nafion to immobilize a large and fairly soluble organic modifier such as 2,2'-bipyridyl and its complexes for performing trace analysis by preconcentration and determination. Carbon paste is shown to be a suitable matrix for the immobilization of Nafion and 2,2'-bipyridyl in a stable, reproducible and responsive form. This kind of CME is simple and inexpensive to prepare and the modified electrodes can be easily miniaturized by using the method developed by Wang and Brennstainer³⁵ and the manual batch procedure can also be easily automated with a computerized flow system as described by Thomsen *et al.*³⁶ A variety of potential analytical applications for this kind of CME exist, based on a judicious choice of the ion-exchanger and organic complexing reagent and control of the experimental conditions. The present work can thus serve as a basis for further research in this area.

Acknowledgements—This work was supported by the National Natural Science Foundation of China, the aid of which is gratefully acknowledged. We are thankful to Mr Sheng for helpful discussions.

REFERENCES

- R. P. Baldwin, J. K. Christensen and L. Kryger, *Anal. Chem.*, 1988, **58**, 1790.
- S. V. Prabhu, R. P. Baldwin and L. Kryger, *ibid.*, 1987, **59**, 1074.
- J. Gardea-Torresdey, D. Darnall and J. Wang, *ibid.*, 1988, **60**, 72.
- D. M. T. O'Riordan and G. G. Wallace, *ibid.*, 1986, **58**, 128.
- J. Wang and M. Bonakdar, *Talanta*, 1988, **35**, 277.
- G. A. Gerhardt, A. F. Oke, G. Nagy, B. Moghaddam and R. N. Adams, *Brain Res.*, 1983, **290**, 390.
- J. Wang, T. Golden and P. Tuzhi, *Anal. Chem.*, 1987, **59**, 740.
- Y. Ohnuki, H. Matsuda, T. Ohsaka and N. Oyama, *J. Electroanal. Chem.*, 1983, **158**, 55.
- J. Wang, B. Greene and C. Morgan, *Anal. Chim. Acta*, 1984, **158**, 15.
- W. R. Heineman, H. J. Wieck and A. M. Yacynych, *Anal. Chem.*, 1980, **52**, 345.
- J. Wang, P. Tuzhi and T. Golden, *Anal. Chim. Acta*, 1987, **194**, 129.
- J. Ye, R. P. Baldwin and J. W. Schlager, *Electroanalysis*, 1989, **1**, 133.
- K. N. Thomsen and R. P. Baldwin, *Anal. Chem.*, 1989, **61**, 2594.
- J. Wang and M. S. Lin, *ibid.*, 1988, **60**, 1545.
- K. E. Liu and H. D. Abruña, *ibid.*, 1989, **61**, 2599.
- L. A. Coury, E. M. Birch and W. R. Heineman, *ibid.*, 1988, **60**, 553.
- K. Kalcher, *Anal. Chim. Acta*, 1985, **177**, 175.
- Idem*, *Z. Anal. Chem.*, 1985, **321**, 666.
- G. T. Cheek and R. F. Nelson, *Anal. Lett.*, 1978, **11**, 393.
- L. Hernández, J. M. Melguizo, M. H. Blanco and P. Hernández, *Analyst*, 1989, **114**, 397.
- P. Li, Z. Gao, Y. Xu, G. Wang and Z. Zhao, *Anal. Chim. Acta*, 1990, **229**, 213.
- Z. Gao, P. Li, S. Dong and Z. Zhao, *ibid.*, 1990, **232**, 367.
- J. Wang and T. Martinez, *Electroanalysis*, 1989, **1**, 167.
- A. R. Guadalupe and H. D. Abruña, *Anal. Chem.*, 1985, **57**, 142.
- M. J. Gehron and A. Brajter-Toth, *ibid.*, 1986, **58**, 1488.
- K. L. Cheng, K. Ueno and T. Imamura (eds.), *CRC Handbook of Organic Analytical Reagents*, Chapter 4, CRC Press, Boca Raton, 1982.
- T. Kuwana and W. G. French, *Anal. Chem.*, 1964, **36**, 241.
- C. R. Martin and H. Freiser, *ibid.*, 1981, **53**, 902.
- M. Sharp, *J. Electroanal. Chem.*, 1987, **230**, 109.
- I. Rubinstein and A. J. Bard, *J. Am. Chem. Soc.*, 1981, **103**, 5007.
- H. S. White, J. Leddy and A. J. Bard, *J. Am. Chem. Soc.*, 1982, **104**, 4811.
- J. Wang, P. Tuzhi, R. Li and J. Zadeii, *Anal. Lett.*, 1989, **22**, 719.
- T. Qian (ed.), *Application and Technology of Ion-Exchange*, p. 84. Tianjin Keji Press, Tianjin, 1985.
- N. Jackson and D. S. Philips, *Analyst*, 1962, **87**, 718.
- J. Wang and A. Brennstainer, *Anal. Lett.*, 1988, **21**, 1773.
- K. N. Thomsen, L. Kryger and R. P. Baldwin, *Anal. Chem.*, 1988, **60**, 151.

POTENTIOMETRIC DETERMINATION OF TRACE SILVER BASED ON THE USE OF A CARBON PASTE ELECTRODE

JIANHONG PEI, QUAN YIN and JIAYUE ZHONG

Chemistry Department, Wuhan University, Wuhan, People's Republic of China

(Received 12 October 1990. Revised 6 February 1991. Accepted 5 March 1991)

Summary—A carbon paste electrode used as a sensor for silver has been developed and electrode response characteristics have been investigated. The electrode exhibits linear response to the logarithm of the concentration of silver from $5 \times 10^{-7}M$ to $1 \times 10^{-2}M$, with a response slope of 63 ± 2 mV. The detection limit according to IUPAC recommendations is $1 \times 10^{-7}M$. This electrode has been used to determine trace silver in fixing solutions and waste electroplate solutions with good results.

There are many electroactive materials that can be used in Ag^+ -ion selective electrodes, but the selectivity and sensitivity of Ag_2S -based electrodes are by far the best.^{1,2} Recently, many new types of crown ethers have been synthesized and involved in the field of ion selective electrodes (ISE).^{3,4} These substances form polar cavities in which certain ions can be enclosed because of ion-dipole interactions, with the formation of a charged mobile complex which is soluble in organic solvents. This process exhibits a high degree of selectivity. Some crown ethers containing thiol have been used as ion-carriers for silver determination.^{5,6}

The idea of mixing redox couples into carbon paste electrode was introduced by Kuwana and French⁷ in 1964, with subsequent further studies by several groups.^{8,9} Although the complex issue of transport of the electroactive species to the carbon-solvent interface is not satisfactorily explained, the electrode is very useful to analysts for the determination of many trace ions.¹⁰ Considerable attention has been focused on electrochemical determinations using chemically modified carbon paste electrodes, with the pre-concentration agent mixed into a carbon paste matrix in order to react with and bind the target solute.^{11,12} The electrochemical responses are very stable and the electrode can be easily renewed by removing an outer layer of the paste and resmoothing the surface. But so far, the applications of carbon paste electrodes are mainly defined in the field of voltammetric determination and very few have been used in potentiometry. A carbon paste electrode prepared from graphite powder and Aliquat 336, a

liquid quaternary ammonium chloride, was used as a chloride ion-selective electrode.¹³

In this paper, we report a carbon paste electrode prepared from carbon graphite and Nujol oil which is used as a potentiometric Ag^+ -selective electrode. This analyte was chosen because graphite powder has a tendency to absorb silver.¹⁴ The carbon paste electrode is simple to prepare and its surface is easy to renew in a reproducible manner, which makes it very useful as an electrochemical sensor. We have investigated its response to silver and the results show that the carbon paste electrode is very sensitive and selective, using suitable masking procedures, for silver determination. The potential response of the electrode is found to be linear to the logarithm of the concentration of silver from $5 \times 10^{-7}M$ to $1 \times 10^{-2}M$, with a response slope of 63 ± 2 mV per decade concentration and a detection limit of $1 \times 10^{-7}M$. Because of the good conductivity of carbon paste, this type of electrode is a promising new form of ion-electrode, with different modifiers mixed into the matrix. The small resistance and rapid response would be welcomed in clinical analysis.¹⁵

EXPERIMENTAL

Reagents and apparatus

Graphite powder (Hongxin Chemical Reagents Factory, Beijing, China) and Nujol oil (Wuhan Chemical Reagents Factory, China) were used for the preparation of the carbon paste electrode. A 0.100M Ag^+ standard stock solution was prepared by dissolving 1.6987 g of silver nitrate (analytical grade) in a standard

100-ml flask with doubly-distilled water. The solution was placed in the shade and protected against light. The working solutions were prepared daily by suitable dilution of this solution. Sodium nitrate (1M) and sodium fluoride (1M) solutions were prepared and used as supporting electrolyte and masking agent, respectively. All other solutions used in interference studies were prepared from analytical grade salts of nitrate. Doubly distilled water was used throughout.

The electromotive force (EMF) measurements were performed at 23.1° with a PHS-10A Digital Ion-pH Meter (Xiaoshan Scientific Instrumental Factory, China). A PHS-2 pH Meter (Shanghai Analytical Instrumental Factory No. 2, China) was used for pH determination. A 314 S²⁻ ion-selective electrode (Jiangsu Electro-analytical Instrumental Factory, China) was used to determine trace silver, which gave a reference value for the carbon paste electrode.

Cyclic voltamperograms were recorded with a PAR 174A polarographic analyser equipped with a Model 0089 X-Y recorder. The three electrode system was used with a carbon paste electrode, a saturated calomel reference electrode and a platinum auxiliary electrode.

Preparation and renewal of carbon paste electrode

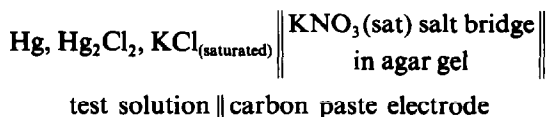
A carbon paste electrode was prepared by mixing 5 g of graphite powder and 3 ml of Nujol oil in a mortar. Electrode bodies were made from disposable 1-ml polyethylene syringes (3 mm i.d.), the tip of which had been cut off with a razor blade. These bodies were filled with approximately 0.3 ml of carbon paste. Smooth surfaces were obtained by applying manual pressure to the piston while holding the electrode surface against a smooth, solid support. The electrode connection to the carbon paste was established via a thin copper wire.

A fresh electrode surface was obtained by dipping the electrode into dilute ammonia solution for one minute and rinsing in water several times to remove the residual ammonium; or squeezing out a small amount of paste, scraping off the excess with a glass rod and polishing the electrode on paper until the surface had a shiny appearance.

Procedure

The carbon paste electrode was used as indicator electrode. The reference electrode was a saturated calomel electrode (SCE) which was connected to the test solution with a salt bridge

of saturated potassium nitrate in agar gel. The measurement cell was as follows:



The carbon paste electrode was immersed in 30 ml of silver test solution containing 0.3M sodium nitrate and 3×10^{-2} M sodium fluoride with stirring, using a magnetic stirrer (100 rpm), for 30 sec. Potentials were measured at rest.

Sample analysis

Transfer two milliliters of photographic fixing solution or waste electroplate solution to a 50-ml beaker containing 1 ml of concentrated nitric acid, 1 ml of concentrated hydrochloric acid and several drops of 1M sulphuric acid. Heat until gas is no longer evolved. Repeat this addition and evaporation, then dissolve the residue in 0.1M nitric acid and adjust the pH value of the solution to about 6. Transfer this solution into a 100-ml standard flask and dilute to volume with water. The concentration of silver was determined by the procedure described above, with a calibration curve.

RESULTS AND DISCUSSION

The compositions of supporting electrolyte solution

Ideal potentiometric measurements, especially in analytical chemistry, require that only the composition of the analyte solution affects the potential of the indicating electrode. This would occur only if the liquid-junction potential could be neglected. Therefore, an indifferent electrolyte of much larger concentration has to be contained in the system. Sodium nitrate (0.3M) was chosen in this system to maintain the ionic strength and minimize the liquid-junction potential. Some multi-valent ions, such as Fe³⁺, Al³⁺ and Cr²⁺, interfered with the determination, and 3×10^{-2} M sodium fluoride was used to eliminate these interferences. Potentiometric measurements also require the potential of the reference electrode to be fixed and, in this system, silver can affect the potential of the SCE. Therefore, the saturated potassium nitrate agar gel salt bridge was used to connect the solution to the reference electrode (SCE).

Effect of pH

The effect of the test solution pH on the electrode response was investigated at

$1 \times 10^{-4}M$ silver solution. The experimental results are shown in Fig. 1. At the pH range of 4.5–7, the potential remains unchanged. At higher pH values, the solution becomes turbid due to silver hydrolysis and the response decreases. At lower pH, the response decreases and dramatically becomes unstable.

The electrode response curves at different pH values are shown in Fig. 2. At a value of about 6, the electrode gives good linearity and low detection limit. The electrode exhibits little or no response to silver at much lower pH. Thus, the data shown in Fig. 2(a) can be used to calculate the selectivity coefficient for the silver ion to the hydrogen ion with the constant interference concentration method.¹⁶ The value calculated, $K^{Ag^+,H^+} = 3.98 \times 10^{-4}$ (at pH = 1.1).

Response characteristics of carbon paste electrode

The response time of the carbon paste electrode is measured in the usual way. It was found that a long response time is required for attaining a constant potential in dilute solution (below $10^{-5}M$) without stirring. In order to decrease response time it is important to stir the sample solution for a period of time prior to measurement. The test solutions are magnetically stirred for 30 sec (100 rpm). It is not recommended to measure the potential while stirring because of potential instability. The response time (to 95% of steady reading) for different concentrations of silver are shown in Table 1 (including a 30 sec stirring time). The carbon paste electrode exhibits a sufficiently stable EMF response for several months and the drift of measurement is

Table 1. The response time of the carbon electrode (95% of steady reading)

C_{Ag^+} , (M)	10^{-6}	10^{-5}	10^{-3}
Response time, (sec)	100	60	40

less than 1 mV over four hours in $10^{-3}M$ silver solution.

The ISE potential depends directly on the test ionic activity. But in analytical practice concentration values are more often required than activity values. In this paper, concentrations are used rather than activities because of the supporting electrolyte ($0.3M$ $NaNO_3$) used to maintain the ionic strength.

Figure 2(b) shows the response curve of the carbon paste electrode at pH 6. The potential of the cell assembly exhibits a linear response to the logarithm of silver concentration from $5 \times 10^{-7}M$ to $1 \times 10^{-2}M$, with a response slope of 63 ± 2 mV per decade of silver concentration. A higher silver solution concentration was not tested. The regression equation is $E(mV) = (546.6 \pm 1.5) + (63 \pm 2) \log C_{Ag^+}$ and the correlation coefficient is 0.996. According to the IUPAC recommendations¹⁷ for ion-selective electrodes, the practical detection limit may be taken as the concentration corresponding to the point of intersection of two extrapolated lines as shown in Fig. 2 and hence the detection limit is $1 \times 10^{-7}M$.

Selectivity and interferences

In $0.3M$ sodium nitrate solution, Fe^{3+} , Cr^{3+} and Al^{3+} severely interfere with the determination of Ag^+ . A concentration of $3 \times 10^{-2}M$ F

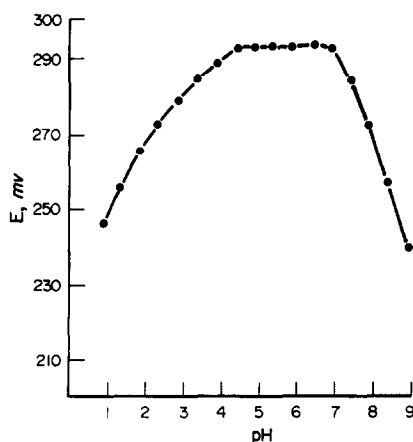


Fig. 1. The effect of pH on the response of the carbon paste electrode; $3 \times 10^{-2}M$ NaF, $0.3M$ $NaNO_3$ and $1 \times 10^{-4}M$ Ag^+ .

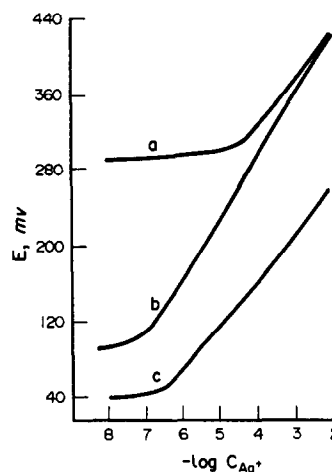


Fig. 2. Carbon paste electrode response curves at different pH values. (a) pH = 1.1, (b) pH = 6, (c) pH = 11.5. $3 \times 10^{-2}M$ NaF, $0.3M$ $NaNO_3$.

Table 2. Selectivity coefficients of the carbon paste electrode

Interference ions K^{As+}, K^{m+}		Interference ions K^{m+}, K^{As+}, K^{m+}	
Na^+	$< 10^{-6}$	Fe^{3+}	4.5×10^{-4}
Li^+	2.3×10^{-4}	K^+	$< 10^{-6}$
Al^{3+}	4.9×10^{-4}	Co^{2+}	6.9×10^{-4}
Fe^{2+}	1.7×10^{-4}	Ca^{2+}	$< 10^{-6}$
Mg^{2+}	10^{-6}	Ni^{2+}	6.9×10^{-4}
Cu^{2+}	7.8×10^{-3}	Sn^{2+}	5.1×10^{-4}
Zn^{2+}	6.9×10^{-4}	Hg^{2+}	0.21
Cr^{3+}	5×10^{-4}	Cd^{2+}	10^{-5}
Pb^{2+}	4.9×10^{-3}		

Table 3. Measurements of $1 \times 10^{-4}M$ silver solution with six different carbon paste electrodes

Electrode	1	2	3	4	5	6	\bar{X}	$X\delta_{n-1}$
Potential value, <i>mV</i>	295	294	294	293	295	294	294	0.75

Table 4. Alternating measurements in $1 \times 10^{-5}M$ and $1 \times 10^{-3}M$ silver solutions

Determination		1	2	3	4	5	6	\bar{X}	$X\delta_{n-1}$
Response value, <i>mV</i>	$1 \times 10^{-5}M$	228	229	230	228	231	228	229	1.25
	$1 \times 10^{-3}M$	256	355	356	356	354	355	355	0.82

is added as a masking agent to eliminate these interferences.

The selectivity coefficients of the carbon paste electrode were evaluated by the constant interference concentration method.^{17,18} The concentrations of the interference ions used were as follows: $0.1M$ Na^+ , K^+ , Ca^{2+} , Mg^{2+} , Zn^{2+} and Cd^{2+} ; $1 \times 10^{-2}M$ Li^+ , Fe^{2+} , Co^{2+} , Ni^{2+} and Sn^{2+} ; $1 \times 10^{-3}M$ Fe^{3+} , Cr^{3+} , Al^{3+} and Pb^{2+} and $1 \times 10^{-4}M$ Hg^{2+} and Cu^{2+} . After each interferent is investigated, the electrode is washed with water thoroughly and carefully dried with a fine filter paper. The experimental results are shown in Table 2.

Electrode renewal and its reproducibility

It is important to renew the electrode surface when the silver solution is changed from high concentration to a dilute solution because residual silver will still be adsorbed on the surface of the carbon paste electrode which will lead to poor reproducibility. The appropriate renewal process is described above. Renewal with ammonia water solution is recommended as the same electrode surface is utilized for a series of consecutive determinations. In this manner, the surface-to-surface variability occurring when the carbon paste is manually refreshed could be avoided and at the same time, an improvement in speed and flexibility of the procedure is achieved.

Six different carbon paste electrodes were used at the same time to determine $1 \times 10^{-4}M$ silver solution in order to test parallel results (Table 3).

To evaluate the reproducibility of emf response of the cell assembly, alternating

measurements were performed in $1 \times 10^{-5}M$ and 1×10^{-3} silver solution (ion background: $0.3M$ sodium nitrate, $3 \times 10^{-2}M$ sodium fluoride). The procedure was repeated six times and the results are shown in Table 4. (The electrode surface is renewed for each high/low concentration measurement cycle).

Practical applications

Trace silver in the fixing solution and waste electroplate solution was determined with this electrode. The treatment of samples was described above. The commercial $314 S^{2-}$ ion-selective electrode was used to give the reference values¹⁸ and the results are given in Table 5.

Possible response mechanism of carbon paste electrode to silver

The carbon paste electrode was immersed in $0.3M$ sodium nitrate and $2 \times 10^{-3}M$ Ag^+ solution, which was stirred with a magnetic stirrer. After 5 min, the electrode was removed from the solution and rinsed thoroughly with water, then dipped in $0.3M$ sodium nitrate solution (oxygen

Table 5. Determination trace silver in fixing solution and waste electroplate solution (all determinations were carried out in triplicate)

	Fixing solution, ppm	Electroplate solution, ppm
Carbon paste electrode, <i>mV</i>	13.2	8.98
Recovery of added Ag^+ , %	97	94
$314 S^{2-}$ ion-selective* electrode, <i>mV</i>	13.4	9.03

*Measured by the method of Zhou *et al.*¹⁸

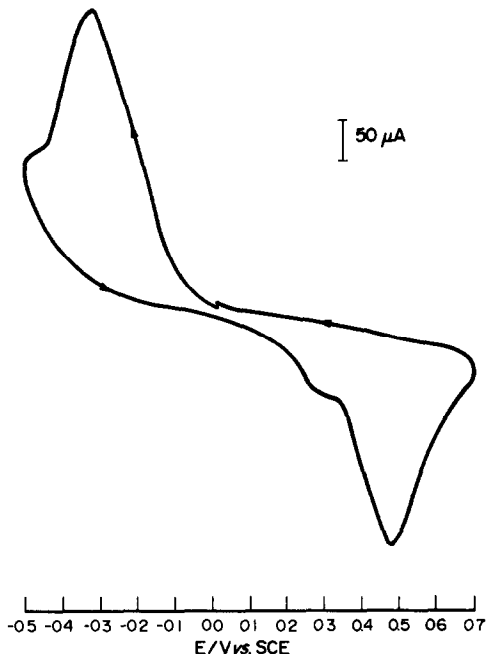


Fig. 3. Cyclic voltamperogram. scan rate: 250 mV/sec.

free) and the cyclic voltamperogram was recorded. Figure 3 indicates that carbon paste has a tendency to adsorb the silver ion. This phenomenon has been noted by Cheek and Nelson.¹⁴ The phase boundary potential may originate from the adsorption of silver at the surface of the carbon paste electrode. Further evidence arises from the fact that dilute ammo-

nia water easily refreshes the electrode surface. At the phase boundary and electrical double layer is formed as a result of the distribution equilibrium of the silver ion.

REFERENCES

1. J. Veselý, O. J. Jensen and B. Nicolaisen, *Anal. Chim. Acta*, 1972, **62**, 1.
2. R. Bock and H. J. Putt, *Z. Anal. Chem.* 1968 **240**, 381.
3. O. Ryba and J. Petránek, *J. Electroanal. Chem.*, 1973, **44**, 425.
4. J. Petránek and O. Ryba, *Anal. Chim. Acta*, 1974, **72**, 375.
5. M. Oue, K. Kimura, K. Akama, M. Tanaka and T. Shono, *Chem. Lett.*, 1988, 409.
6. Z. Xi, J. Li, L. Yu, D. Zhang, J. Yang, S. Luo, B. Wu and L. Cun, *Huaxue Xuebao*, 1986, **44**, 951.
7. T. Kuwana and W.G. French, *Anal. Chem.*, 1964, **36**, 241.
8. M. Lamache and D. Bauer, *J. Electroanal. Chem.*, 1977, **79**, 359.
9. T. Yao and S. Musha, *Anal. Chim. Acta*, 1979, **110**, 203.
10. J. Wang and T. Martinez, *ibid.*, 1988, **207**, 95.
11. P. R. Baldwin, J. K. Christensen and L. Kryger, *Anal. Chem.* 1986, **58**, 1790.
12. K. E. Liu and H. D. Abruña, *ibid.*, 1989, **61**, 2599.
13. J. P. Sapiro, J. F. Colaruotolo and J. M. Bobbitt, *Anal. Chim. Acta*, 1973, **67**, 240.
14. G. T. Cheek and R. F. Nelson, *Anal. Lett.*, 1978, **11**, 393.
15. T. A. Nieman and G. Horvai, *Anal. Chim. Acta*, 1985, **170**, 359.
16. E. Pungor and K. Tóth, *ibid.*, 1969, **47**, 291.
17. *Pure Appl. Chem.*, 1976, **48**, 127.
18. A. Zhou, G. Zhang and H. Wang, *Huaxue Tongbao*, 1976, **5**, 299.

POLY-SALICYLIC ACID MODIFIED GLASSY-CARBON ELECTRODE AND ITS APPLICATION

JINRUI XU and XIURUN ZHUANG

Department of Applied Chemistry, Huaqiao University, Quanzhou, Fujian, 362011,
People's Republic of China

(Received 3 January 1991. Revised 25 March 1991. Accepted 26 March 1991)

Summary—A poly-salicylic acid modified glassy-carbon electrode (PSAMGCE) was prepared by electropolymerisation. The behaviour of copper on this electrode was investigated by anodic stripping voltammetry. The electrode is about 40 times more sensitive than the unmodified glassy-carbon electrode. It was applied to the determination of trace copper(II) in water, and shows a 96–106% recovery and a relative standard deviation of ca. 3%.

The modification of electrode surfaces is currently an active area of research. A variety of methods for preparing modified electrodes have been reported.¹⁻⁸ In recent years electrodes modified by electropolymerisation have become of great interest.⁹⁻¹⁴ In the present work, salicylic acid was electrochemically polymerised on the surface of a glassy-carbon electrode in an aqueous solution containing salicylic acid, formaldehyde and sodium hydroxide. The electrochemical properties of the poly-salicylic acid modified glassy-carbon electrode (PSAMGCE) have been investigated by anodic stripping voltammetry. The modified electrode was applied to the determination of copper(II) in water, and its sensitivity for copper(II) is about 40 times higher than that of the unmodified glassy-carbon electrode.

EXPERIMENTAL

Apparatus

Current-potential curves were obtained by a Model 79-1 voltammetric analyzer (Jinan No. 4 Radio Factory, Shandong, China), and voltamperograms were recorded on an X-Y recorder (Shanghai Dahua Instrument Factory, China). A simple three-electrode electrochemical cell with a saturated calomel electrode (SCE, Model 232, Shanghai Tien Kuang Scientific Instruments Works, China) as reference electrode, a platinum wire as an auxiliary electrode and a PSAMGCE as working electrode were used for all the electrochemical experiments. Infra-red spectra were recorded with a Perkin-Elmer 983 IR Spectrometer (Perkin-Elmer Corp., U.S.A.).

Reagents

All reagents used were of analytical grade. All water used was doubly-distilled water from a quartz apparatus. The standard stock solution of copper(II) was 1 mg/ml and diluted as required. An aqueous solution containing 0.5 g of salicylic acid (Shanghai Wulian Chemical Factory, China), 0.5 g of formaldehyde (Shanghai Solvents Factory, China) and 0.5 g of sodium hydroxide (Beijing Chemical Factory, China) in 50 ml of water was used in the electropolymerisation.

Surface modification

The glassy-carbon disk electrode (Model AD-2, area = 0.1 cm², Jintan Analytical Instrument Factory, China) was first polished to a mirror finish with a paper tissue and then washed with ethanol and doubly-distilled water for 2 min with each, in an ultrasonic bath. The glassy-carbon working electrode was immersed in 50 ml of aqueous solution containing 0.5 g of salicylic acid, 0.5 g of formaldehyde and 0.5 g of sodium hydroxide, with the SCE and Pt wire as reference and auxiliary electrodes respectively. The electropolymerisation on the glassy-carbon electrode was carried out by sweeping the electrode potential between -0.1 and +1.3 V (*vs.* SCE), with a scan-rate of 100 mV/sec and a scan-time of 5 min, while stirring. Finally, the electrode prepared was rinsed thoroughly with doubly-distilled water, and a poly-salicylic acid modified glassy-carbon electrode (PSAMGCE) was made.

Procedure

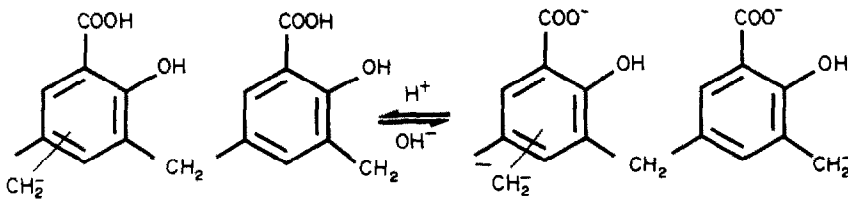
Nitrogen gas was passed through the test solutions containing sodium acetate-acetic acid to remove dissolved oxygen before the measurements, and over the solutions during the measurements. On the PSAMGCE, the pre-electrolysis was conducted at -0.6 V (*vs.* SCE) for 2 min, while stirring. After a rest period of 30 sec, the 2nd order differential anodic stripping voltamperogram was recorded with a scan rate of 100 mV/sec. After each determination, the PSAMGCE potential was shifted at $+0.6$ V (*vs.* SCE) and the electrolysis was done for 5 min with strong stirring. The regenerated PSAMGCE is used in the next determination.

RESULTS AND DISCUSSION

Composition of the modified film

The modified film obtained from electropolymerisation of salicylic acid was insoluble in water, dilute acid and base solutions.

According to DeGeiso *et al.*,¹⁵ salicylic acid could be condensed with formaldehyde, and a poly-salicylic acid could be prepared by refluxing a mixture containing salicylic acid, formaldehyde and oxalic acid. The polymer could then be treated with dilute sodium hydroxide solution and dried. The infrared spectrum of the resulting polymer was about the same as that of the modified film and does not change on heating the polymer under reflux with rapid stirring. This indicates that the treatment with the electrochemical method indeed results in the formation of a salicylic acid-formaldehyde copolymer on the electrode surface which may be represented by the following formula:¹⁵



Voltammetric properties of Cu(II) on PSAMGCE

The voltammetric properties of PSAMGCE were studied by cyclic voltammetry in 0.05M sodium acetate-0.05M acetic acid containing copper(II). Figure 1 shows a cyclic voltamperogram of the redox reaction of copper on the PSAMGCE between -0.5 and $+0.5$ V (*vs.* SCE) at 100 mV/sec. The oxidation and reduction peaks of copper appear at -0.05 and

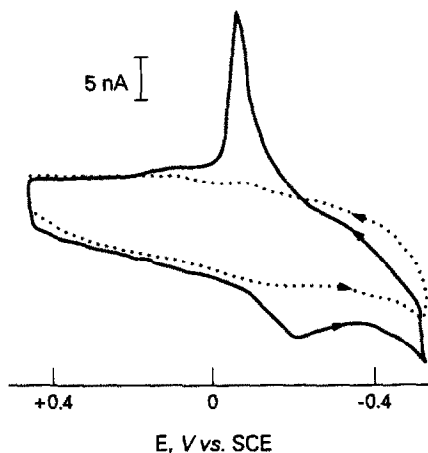


Fig. 1. Cyclic voltamperogram of copper on PSAMGCE (—) and unmodified glassy-carbon electrode (···). $[Cu^{2+}] = 100$ ng/ml, supporting electrolytes 0.05M sodium acetate-0.05M acetic acid, scan-rate 100 mV/sec.

-0.2 V (*vs.* SCE), respectively. The peak separation for the redox reaction of the copper is about 0.15 V. It shows that the redox process of the copper on the PSAMGCE is an irreversible redox reaction. When the PSAMGCE is placed in 0.05M sodium acetate-0.05M acetic acid that does not contain copper(II), no electrochemical peaks occur between -0.5 and $+0.5$ V (*vs.* SCE).

According to the procedure described in the experimental section, a 2nd differential anodic stripping voltamperogram for the solution containing 0.05M sodium acetate-0.05M acetic acid and 5 μ g/ml copper(II) was recorded (Fig. 2). The sensitivity of the PSAMGCE for copper(II) is about 40 times higher than that of the unmodified glassy-carbon electrode. This results from the formation of complexes be-

tween copper(II) and the salicylic acid polymer film which act as a linking agent on the electrode surface. In other words, the modified polymer film results in the transport of more copper(II) ions to the electrode surface during pre-electrolysis.

Electropolymerisation conditions

According to the modified method described in the experimental section, cyclic voltampero-

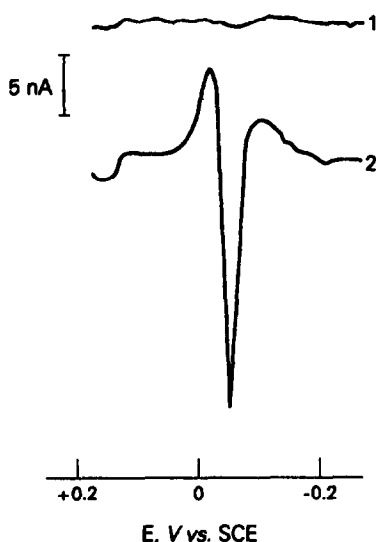


Fig. 2. Second-differential anodic stripping voltamperogram of copper on unmodified glassy-carbon electrode (1) and PSAMGCE (2). $[Cu^{2+}] = 5 \text{ ng/ml}$, supporting electrolytes $0.05M$ sodium acetate- $0.05M$ acetic acid, pre-electrolysis for 2 min at -0.6 V (*vs.* SCE), scan-rate 100 mV/sec .

grams of successive potential sweeps in a solution containing salicylic acid, formaldehyde and sodium hydroxide were recorded (Fig. 3). It shows an oxidation peak at $+0.5 \text{ V}$ (*vs.* SCE)

for the solution containing the salicylic acid, formaldehyde and sodium hydroxide. In this work, a potential sweep between -0.1 and $+1.3 \text{ V}$ (*vs.* SCE) was selected for electropolymerisation of the salicylic acid. Sweeping potentials more positive than $+1.3 \text{ V}$ (*vs.* SCE) will lead to the formation of gas which will interfere with electrode modification.

Figure 3 also indicates that the oxidation peak decreases with scan time. The peak height stabilizes after about 5 min. Therefore an electropolymerisation time of about 5 min was used in the above experiments.

Effect of composition of the solution used for modification

The solution used for modification was composed of salicylic acid, formaldehyde and sodium hydroxide. The amount of salicylic acid was 0.5 g in 50 ml of aqueous solution and the effects of formaldehyde and sodium hydroxide on the peak height for copper(II) are summarized in Table 1. These results indicate that the highest peak was found with 0.5 g of formaldehyde (36%) and 0.5 g of sodium hydroxide.

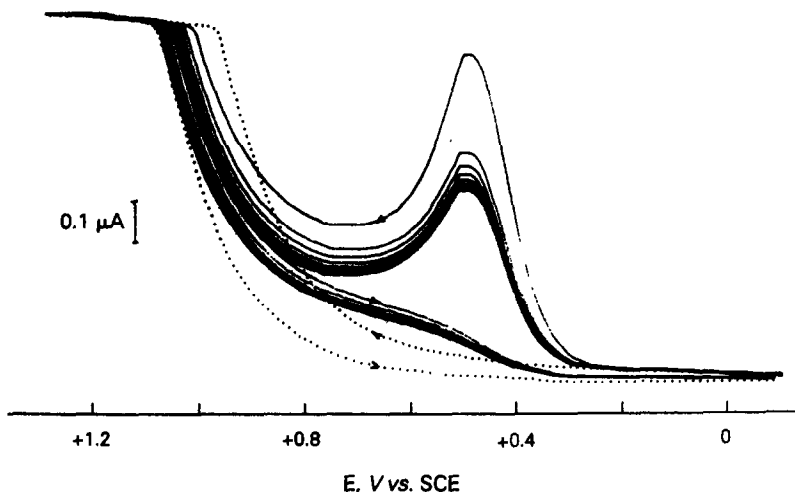


Fig. 3. Cyclic voltamperogram of electrode modification in 50 ml of aqueous solution containing 0.5 g of salicylic acid, 0.5 g of formaldehyde and 0.5 g of sodium hydroxide (—), containing only 0.5 g of formaldehyde and 0.5 g of sodium hydroxide (···), scan-rate 100 mV/sec .

Table 1. Effect of the composition of the modification solution (50 ml) on the anodic stripping peak height of copper. Salicylic acid = 0.5 g

Experimental No.		1	2	3	4	5	6
Composition	Formaldehyde (36%), g	0.5	0.8	0.5	0.8	0.2	0.5
	NaOH, g	0.5	0.5	0.8	0.8	0.5	0.2
Peak current,* nA		51	45	14	12	27	21

* $[Cu^{2+}] = 5 \text{ ng/ml}$, supporting electrolytes $0.05M$ sodium acetate- $0.05M$ acetic acid, pre-electrolysis for 2 min at -0.6 V (*vs.* SCE).

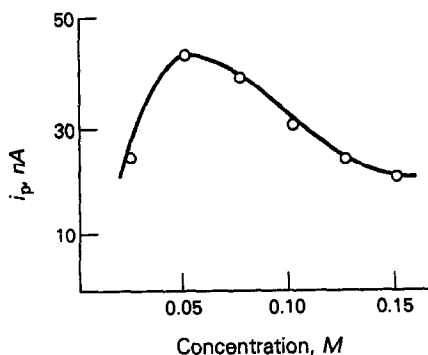


Fig. 4. Effect of the concentration of sodium acetate-acetic acid on stripping peak height of copper. $[Cu^{2+}] = 5 \text{ ng/ml}$, pre-electrolysis for 2 min at -0.6 V (*vs.* SCE), scan-rate 100 mV/sec .

Effect of supporting electrolytes

For comparison, the seven supporting electrolytes chosen were ammonium sulphate, ammonium acetate, sodium acetate, ammonium chloride, sodium acetate-acetic acid, potassium chloride and potassium nitrate. The effect of these supporting electrolytes on the anodic stripping peak height of copper at the modified electrode was examined by the procedure described in the experimental section. The results show that a well-formed peak appears at -0.05 V (*vs.* SCE) and its peak height is highest if sodium acetate-acetic acid is used as supporting electrolyte.

When the sodium acetate-acetic acid ratio is 1:1, the highest peak is obtained with $0.05M$ sodium acetate- $0.05M$ acetic acid as shown in Fig. 4.

Influence of pH, pre-electrolysis potential and pre-electrolysis time

When the pH is varied by addition of hydrochloric acid or sodium hydroxide to the solution

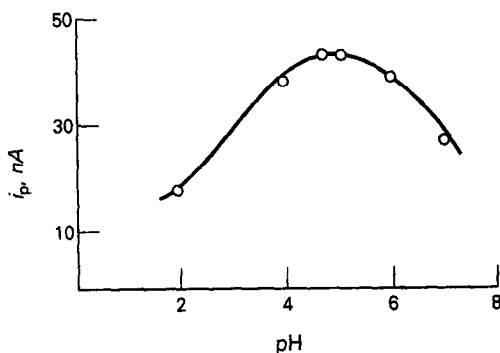


Fig. 5. Effect of pH on stripping peak height of copper. $[Cu^{2+}] = 5 \text{ ng/ml}$, supporting electrolytes $0.05M$ sodium acetate- $0.05M$ acetic acid, pre-electrolysis for 2 min at -0.6 V (*vs.* SCE), scan-rate 100 mV/sec .

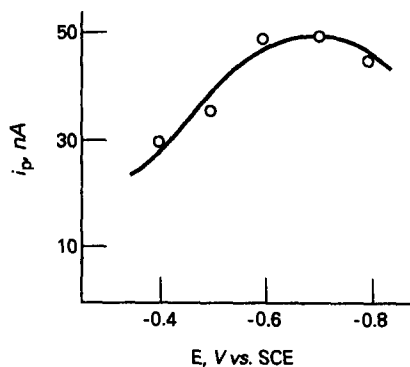


Fig. 6. Effect of pre-electrolysis potential on stripping peak height of copper. $[Cu^{2+}] = 5 \text{ ng/ml}$, supporting electrolytes $0.05M$ sodium acetate- $0.05M$ acetic acid, pre-electrolysis for 2 min, scan-rate 100 mV/sec .

containing 5 ng/ml copper(II) and the $0.05M$ sodium acetate- $0.05M$ acetic acid supporting electrolyte, the higher peak is found near pH 4-6 (Fig. 5). At pH values lower than 4, the height of the peaks decreased very sharply. The explanation is probably that the formation and stability of copper(II)-salicylic acid chelates decreases at low pH. At $\text{pH} > 6$, the peak height also decreased, which is possibly due to hydrolysis of copper(II).

The peak height also depends on the pre-electrolysis potential. Figure 6 shows that the anodic stripping peak height of copper at the PSAMGCE is higher and more stable from -0.6 to -0.7 V (*vs.* SCE).

The peak height is linearly related to the pre-electrolysis time up to 4 min. In the present experiment adequate sensitivity for the determination of trace copper(II) in water can be obtained with a pre-electrolysis time of 2 min. The detection limit is 0.27 ng/ml .

Dependence of peak height on the Cu(II) concentration

The anodic stripping peak height measured by the preceding method was plotted against the copper(II) concentration. It shows that the peak height depends linearly on the copper(II) concentration up to 20 ng/ml . The quantitative detection limit with this electrode was 0.3 ng/ml .

Reproducibility and selectivity of the PSAMGCE for Cu(II)

The PSAMGCE shows excellent reproducibility. The anodic stripping peak height of copper measured with a 2-min pre-electrolysis time at -0.6 V (*vs.* SCE) in a solution containing 5 ng/ml of copper(II), resulted in a relative standard deviation of only 2.7% ($n = 10$).

Table 2. Determination of copper(II) in water samples

Sample	Dam water	Tap water	Lake water	Single distilled water*
Concentration found†, ng/ml	6.28	7.08	4.36	10.22
Concentration added, ng/ml	6.00	2.00	2.00	4.00
Total concentration found, ng/ml	12.40	9.04	6.48	14.08
Recovery, %	102	98.0	106	96.5

*Distilled with distiller No. 34-4 (Shanghai Medical Apparatus and Instruments Factory, China).

†Mean of five replicate measurements.

The stripping peak of copper can tolerate 50-fold amounts of Cd^{2+} , Mn^{2+} and Pb^{2+} ; 35-fold amounts of Ni^{2+} , Zn^{2+} , Co^{2+} and Ag^{+} ; 25-fold amounts of Sn^{2+} , Cr^{3+} and Sb^{3+} ; 10-fold amounts of Fe^{3+} and Hg^{2+} and any amount of Cl^{-} , NO_3^{-} , K^{+} and Na^{+} .

Application of the PSAMGCE

From the experimental results it can be concluded that traces of copper(II) in water samples can be determined at the PSAMGCE. The best experimental conditions are: a water sample containing 0.05M sodium acetate-0.05M acetic acid (pH = 4-6), a pre-electrolysis potential of -0.6 V (vs. SCE) and a pre-electrolysis time of 2 min.

Quantitative data obtained with the previous experimental procedures are presented in Table 2. The PSAMGCE can be used in the determination of trace copper(II) in water with a satisfactory recovery of 96-106%. The relative standard deviation for five parallel determinations of the tap water is lower than 3%.

REFERENCES

1. B. Hoyer, T. M. Florence and G. E. Batley, *Anal. Chem.*, 1987, **59**, 1608.
2. X. R. Zhuang and J. R. Xu, *J. Huaqiao Univ.*, (Nat. Sci.), 1988, **9**, 452.
3. M. Karayama and S. Suzuki, *Nippon Kagaku Kaishi*, 1982, No. 1, 66.
4. L. T. Jin, J. R. Xu and Y. Z. Fang, *Fenxi Huaxue*, 1986, **14**, 513.
5. G. H. Heider, Jr., M. B. Gelbert and A. M. Yacynych, *Anal. Chem.*, 1982, **54**, 322.
6. R. J. Nowak, F. A. Schultz, M. Umaña, R. Lam and R. W. Murray, *ibid.*, 1980, **52**, 315.
7. R. M. Ianniello, T. J. Lindsay and A. M. Yacynych, *Anal. Chim. Acta*, 1982, **141**, 23.
8. J. A. Cox and P. J. Kulesza, *Anal. Chem.*, 1984, **56**, 1021.
9. I. Rubinstein, *ibid.*, 1984, **56**, 1135.
10. P. G. Pickup and R. A. Osteryoung, *J. Am. Chem. Soc.*, 1984, **106**, 2294.
11. X. R. Zhuang and J. R. Xu, *J. Huaqiao Univ. (Nat. Sci.)*, 1989, **10**, 24.
12. B. Zinger, *J. Electroanal. Chem.*, 1988, **244**, 115.
13. M. D. Imisides and G. G. Wallace, *ibid.*, 1988, **246**, 181.
14. G. Zotti, S. Cattarin and N. Comisso, *ibid.*, 1988, **239**, 387.
15. R. C. DeGeiso, L. G. Donaruma and E. A. Tomic, *J. Org. Chem.*, 1962, **27**, 1424.

DETERMINATION OF UREA IN SERUM BY A FIBER-OPTIC FLUORESCENCE BIOSENSOR

XIANGFANG XIE, AHMAD A. SULEIMAN and GEORGE G. GUILBAULT

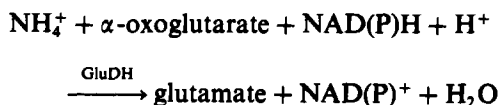
Chemistry Department, University of New Orleans, New Orleans, LA 70148, U.S.A.

(Received 14 August 1990. Revised 12 December 1990. Accepted 10 January 1991)

Summary—A new fiber-optic biosensor for urea has been developed, based on immobilized urease coupled to a fluorescence ammonia sensor. The enzymatically generated ammonia diffuses through the membrane into a solution of the fluorescent pH indicator trisodium 8-hydroxypyrene-1,3,6-trisulfonate. The sensor has been successfully used for the determination of urea in serum samples, with results in good agreement with those reported by a local hospital. The proposed sensor is reversible and selective to urea. The ease of construction of the sensor tip offers the possibility of designing disposable tips for use in clinical applications.

There has been increasing interest in the development of fiber-optic biosensors. Of special importance are applications in clinical analysis (because of the possibility of miniaturizing the sensor), the safety factor (direct electrical connections with the body are not required), and the ability to be used in a remote mode. Different types of fiber-optic biosensors based on fluorescence or absorption measurements have been developed, for O₂, glucose, pH, CO₂ and ammonia.¹

Urea is the chief nitrogenous end-product of protein catabolism in humans and other mammals.² The determination of urea concentration in blood and urine is important in the diagnosis of liver and kidney diseases. There are several indirect methods for urea determination based on the use of urease, which hydrolyzes urea to ammonia and carbon dioxide. These methods differ only in the measurement of the generated ammonia. The oldest method used Nessler's reagent, K₂HgI₄, which gives an orange-red color when it reacts with ammonia in alkaline solution.³ Later the Berthelot reaction, where the ammonium ion reacts with phenol and hypochlorite in alkaline medium to form indophenol, was used.⁴ Absorbance of dissociated indophenol, a blue chromophore, is measured at 630 nm. The third method for the determination of ammonia is based on the following reaction catalyzed by glutamate dehydrogenase (GluDH):^{5,6}



where NAD(P)H and NAD(P)⁺ are the reduced and oxidized forms, respectively, of nicotinamide adenine dinucleotide (phosphate). The decrease in absorbance is monitored at 340 nm in either an end-point or kinetic mode. One direct method used in most clinical laboratories is the diacetyl monoxime method.² In an acidic solution, diacetyl monoxime is converted into diacetyl hydroxylamine which reacts with urea at high temperature to form diazine which absorbs strongly at 520 nm. Thiosemicarbazide and Fe(III) are usually added to the system to enhance and stabilize the color. All of the above-mentioned methods involve the use of unpleasant reagents, high temperature or stabilizers.

Since 1986, several urea fiber-optic sensors based on the use of urease and of different pH-indicator phases to measure ammonia have been reported. The urea sensor developed by Yerian *et al.*^{7,8} was based on commercial non-bleeding acid-base indicator papers situated in a flow stream in an integrated micro-conduit at the tip of a fiber-optic bundle. The urease was adsorbed on the indicator paper and the analyte solution was directly in contact with the pH indicator, hence the sensor suffered from interference by the serum sample. Rhines and Arnold⁹ developed a urea sensor based on the immobilization of urease at the sensing tip of an ammonia gas-sensing fiber-optic chemical sensor. The indicator solution used was a mixture of 2',7'-bis(carboxyethyl)-5(and 6)-carboxyfluorescein and 5(and 6)-carboxyfluorescein, held by a Teflon membrane. Luo and Walt¹⁰ used a new technique called Avidin-Biotin

coupling for the immobilization of both indicator and urease. The indicator was a pH-sensitive fluorescein isothiocyanate isomer. Although the response time was significantly decreased, the sensor was not very sensitive to urea and the immobilization process involved extensive chemical treatments. Therefore, it is very difficult to make replicate sensors.

In this paper, a fluorescence fiber-optic urea sensor based on the use of trisodium 8-hydroxypyrene-1,3,6-trisulfonate (HPTS) as indicator is described. The indicator solution was held at the fiber tip by a membrane permeable to ammonia, which formed the bottom of a Teflon cap. The urease was immobilized on the membrane. HPTS has a pK_a of 7.3 and is highly stable with respect to photodegradation.¹ It was previously used in an ammonia gas-fiber optic sensor.¹¹ Both excitation (470 nm) and emission (518 nm) wavelengths of the basic form of HPTS are in the visible region, facilitating measurement with a glass fiber. One limitation of HPTS is its high sensitivity to ionic strength. However, in the present study, the indicator phase is separated from the analyte solution by the ammonia membrane, which is only gas-permeable, so the ionic strength of the indicator solution will not change significantly when different urea test solutions or serum samples are measured. Several characteristics of this urea sensor have been investigated. The practical application for the determination of urea in human serum has been demonstrated.

EXPERIMENTAL

Apparatus

Fluorescence measurements were made with a Perkin-Elmer model 650-10s fluorescence spectrophotometer modified to accommodate a fiber-optic arrangement. The bifurcated fiber-optic bundle used was an Oriel model 77533. A recorder was used to record the fluorescence intensity, which was converted into an electrical potential by a photomultiplier. A research pH-meter (Radiometer, model PHM 84) was used for all the pH measurements. A Beckman model DB-G grating spectrophotometer was also employed to measure the urea concentration by the diacetyl monoxime method in the comparison study.

Reagents

The indicator, trisodium 8-hydroxypyrene-1,3,6-trisulfonate (HPTS), was purchased from

Molecular Probes (Eugene, OR). Urease (E.C. 3.5.1.5) (Sigma u-2125) containing 7.1×10^4 units/g, urea, glutaraldehyde solution (25%), bovine serum albumin (BSA), diacetyl monoxime and thiosemicarbazide were purchased from Sigma (St Louis, MO). The Orion gas-permeable Teflon ammonia membranes (cat. no. 951204) were obtained from VWR Scientific.

The indicator solution was composed of 0.01M sodium chloride, 0.01M ammonium chloride, and 2.5mM HPTS. The working buffer, either for testing urea solution or serum sample, was 0.1M Tris buffer at pH 7.5.

All other chemicals were of reagent grade and were used without further purification. All solutions were prepared with doubly distilled demineralized water.

Configuration of enzyme cap

A Teflon tube (i.d. 6 mm) with two open ends was used to construct the cap. It was 6 mm in length, with an internal diameter to give a tight fit on the common end of the fibers. The ammonia membrane was mounted on one end of the tube with an O-ring and a Teflon "TEEZE"-strip was used to seal the rest of the membrane around the O-ring. Enzyme solution (15 μ l, containing 64.8 units of urease and 0.45 mg of BSA) and 2.5 μ l of 2.5% glutaraldehyde solution were added on the outside of the ammonia membrane, mixed gently for a few seconds and allowed to dry for 4 hr in air. The membrane was washed by immersing it in 0.1M glycine phosphate buffer solution for 15 min and was stored in 0.1M Tris buffer at 4° overnight.

Configuration of urea sensor

The common end of the fiber bundle was held upward, and the indicator solution (usually 4 μ l) was added onto it. The solution was evenly spread to cover the whole surface of the fiber end, then the fiber was pushed slowly into the cap described above.

Measurement procedure

The excitation wavelength was set at 470 nm and the emission wavelength at 518 nm. Working buffer (900 μ l) was added to the glass reaction cell. The cell compartment was covered and the output, which is proportional to the fluorescence intensity, was monitored until a stable baseline was achieved. Then the compartment was opened, 100 μ l of standard urea solution or serum sample were added and the

cell compartment was covered again. An increase in potential, proportional to the urea concentration, was observed. After the measurement, the sensor tip was immersed in buffer solution, and recovery was usually achieved in 15 min for a steady-state mode and 6–10 min for a kinetic mode.

RESULTS AND DISCUSSION

Concentration of HPTS

A study of the effect of HPTS concentration on sensor response (Fig. 1), showed that the response increased with increasing HPTS concentration up to 3 mM, then decreased drastically at above about 5 mM. Since the basic form of HPTS can be excited at 470 nm and emits fluorescence at 518 nm, the fluorescence intensity is proportional to the concentration of deprotonated HPTS, which is related to the amount of ammonia that diffuses through the membrane. At high HPTS concentration, the decrease in signal is probably due to the self-absorption of the fluorescence by the indicator itself.

Response and recovery times

The response time of the proposed urea sensor depends on the rates of the following steps: (1) the urease enzyme reaction, which is affected by several factors, including urease activity, the ratio of urease, BSA and glutaraldehyde in the immobilized matrix, pH, composition of working buffer, and urea concentration; (2) diffusion rate of ammonia through the membrane, which is controlled by the thickness of the immobilized enzyme layer as well as the inside pressure of the cap (usually the looser the cap, the less the pressure inside it). Because there is a 0.5-mm distance between the fiber end and the membrane, where the indicator solution is held, this inside pressure does not change the volume of

indicator solution, it only affects the diffusion of ammonia. The recovery time depends on the diffusion rate of ammonia outside the cap and the reversibility of HPTS. In our study, we found the following optimum parameters for this urea sensor: about 60 units of urease, 0.45 mg of BSA and 2.5 μ l of 2.5% glutaraldehyde solution as immobilization matrix; 4 μ l of 2.5mM HPTS indicator solution containing 0.01M sodium chloride and 0.01M ammonium chloride; 0.1M Tris buffer, pH 7.5, as working buffer. The higher the urea concentration, the shorter the response time and the longer the recovery time. The average response time for a steady-state mode was about 15 min, with a complete baseline recovery in about 15 min. However, measurement after 6 min was found suitable in the kinetic mode analysis.

Calibration curve

A calibration curve for the urea fiber-optic sensor was constructed by measuring the change of fluorescence intensity 6 min after addition of urea solution to the cell. The calibration curve was sigmoidal and the useful response range for urea was from 1×10^{-4} to 5×10^{-3} M. A calibration curve obtained by the standard-addition method showed the same characteristics, except that the response range was only from 1×10^{-4} to 1×10^{-3} M.

Reproducibility and stability

The reproducibility of this urea sensor has been investigated by making 10 measurements of a 1×10^{-3} M urea solution within one day with the same sensor. The standard deviation was 2.2 mV and the coefficient of variation was 2.9%. The long-term stability of this sensor depends only on the activity of the immobilized urease. No significant activity loss was found after one month, but after two months the activity was 80% of its initial value. Approximately 200 assays were performed with the same sensor during those two months. The whole enzyme cap was stored at 4° when not in use. The reproducibility of different sensors was also studied. A coefficient of variation of 4.2% was obtained when 5 different sensors were used for measurement of a 1×10^{-3} M urea solution. The ease of sensor tip construction and the reproducibility between the different sensor tips suggest the possibility of designing disposable tips for use in clinical application. It is worth mentioning that such disposable tips would probably cost only about \$1.50 each.

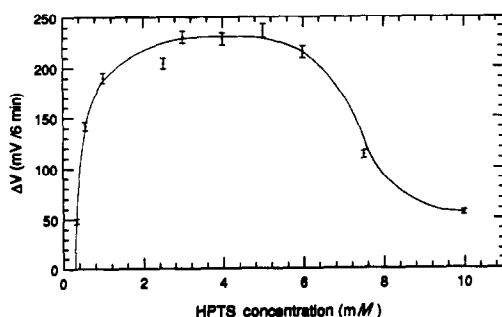


Fig. 1. Effect of HPTS concentration on response. Urea concentration was 2.5mM; 4 μ l of indicator solution containing 0.01M NaCl and 0.01M NH_4Cl .

Interference study

The interference study was performed by testing the response of the sensor to several potential interferents, as reported in the literature.¹² Glucose, uric acid, creatinine, creatine, cholesterol, potassium, sodium and chloride are the major components (besides urea) in blood which may cause interference in blood urea determination. For the selectivity study, 100 μ l of 6.0mM glucose, 0.3mM uric acid, 0.18mM creatinine, 0.5mM creatine, 0.15M sodium chloride and 5.0mM cholesterol were added to 900 μ l of 0.5mM urea solution, separately. None of these gave significant changes from the response for 0.5mM urea, and it was concluded that no interference need be expected in the determination of urea in serum with the proposed sensor.

Comparison study

The urea fiber-optic biosensor was tested for the determination of urea concentration in human serum. The blood samples were obtained from the Chemistry Laboratory of Louisiana Charity Hospital two days after these samples were taken from patients. They were stored in a freezer and centrifuged and only the sera were used for the measurements. Serum samples (100 μ l) were added to 900 μ l of working buffer, except for serum samples with a high urea concentration, where 50- μ l samples were added to 950 μ l of buffer. The calibration curve was constructed by measurement of mixtures of 100 μ l of various standard urea solutions with 900 μ l of working buffer. The change in fluorescence intensity was measured 6 min after addition of the urea solution or serum sample to the cell. The urea concentrations of the samples were obtained from the regression equation of the calibration curve by a series of calculations. The direct diacetyl monoxime method was also applied. Table 1 shows the comparison of the urea-nitrogen concentrations measured with the present urea sensor, the values from a hospital report and the results of the diacetyl monoxime method, for some serum samples. There is good agreement, suggesting that this sensor can be successfully used for urea determination in serum. The performance of this urea sensor is similar to that of the sensor reported by Rhines

Table 1. Comparison study of urea-nitrogen concentration of present urea sensor, hospital values, and diacetyl monoxime method for serum samples

Test No.	Present fiber-optic urea sensor,* mg/100 ml (mM)	Hospital report, mg/100 ml	Diacetyl monoxime†, mg/100 ml
1	13.7 (4.89)	14	12.6
2	28.6 (10.2)	30	26.0
3	4.5 (1.6)	4	3.4
4	8.0 (2.9)	8	7.0
5	36.3 (13.0)	36	35.0
6	18.7 (6.68)	19	18.2
7	23.2 (8.28)	22	23.5
8	25.0 (8.93)	26	24.1
9	48.5 (17.3)	50	45.8
10	10.7 (3.82)	11	10.4
11	31.0 (11.1)	32	30.0
12	14.3 (5.11)	14	13.6

*The standard deviations for the present fiber optic urea sensor ranged from 0.3 to 1.2 mg/100 ml ($n = 3$).

†The standard deviations for the diacetyl monoxime method ranged from 0.4 to 1.5 mg/100 ml ($n = 3$).

and Arnold,⁹ but the dye HPTS (used in the present sensor) is highly stable with respect to photodegradation and the construction of the present sensor tip seems more suitable for designing disposable tips.

Acknowledgements—The financial assistance of the LEQSF (Grant RD-8-17) is gratefully acknowledged. Also we wish to thank Dr W. T. Wu of the Chemistry Laboratory of Louisiana Charity Hospital for providing the serum samples and Dr S. S. Kuan of Food and Drug Administration, New Orleans, for his helpful discussions.

REFERENCES

1. W. R. Seitz, *CRC Crit. Rev. Anal. Chem.*, 1988, **19**, 135.
2. G. Toro and P. Ackermann, *Practical Clinical Chemistry*, Little and Brown, Boston, 1975.
3. F. C. Koch and T. L. McMeekin, *J. Am. Chem. Soc.*, 1924, **46**, 2066.
4. E. D. Noble, *Anal. Chem.*, 1955, **27**, 1413.
5. C. J. Hallett and J. G. H. Cook, *Clin. Chim. Acta*, 1971, **35**, 33.
6. N. W. Tietz, *Fundamentals of Clinical Chemistry*, Saunders, Philadelphia, 1987.
7. T. D. Yerian, G. D. Christian and J. Růžička, *Analyst*, 1986, **111**, 865.
8. *Idem*, *Anal. Chim. Acta*, 1988, **204**, 7.
9. T. Rhines and M. A. Arnold, *ibid.*, 1989, **227**, 387.
10. S. Luo and D. R. Walt, *Anal. Chem.*, 1989, **61**, 1069.
11. O. S. Wolfbeis and H. Posch, *Anal. Chim. Acta*, 1986, **185**, 321.
12. R. M. Schultz, *Chemistry for the Health Sciences*, MacMillan, New York, 1973.

BOOK REVIEWS

The Scientific Examination of Documents: Methods and Techniques: D. ELLEN, Ellis Horwood, Chichester, 1989. Pages 182. £42.95.

Questioned Document Examination is an area of forensic science providing evidence for courts of law on subjects such as handwriting, typewriting and printing. Much of this work depends on "the experience and ability of the analyst". Mr Ellen, with 35 years experience in forensic science and a founder member of the Metropolitan Police Documents Section is perhaps the best qualified to write a book on the subject.

This book is aimed primarily at those who may need to use documentary evidence during the investigation, prosecution or defence of a case. Handwriting is the most difficult area of this work and occupies four chapters. The author is keen to show the reasoning behind handwriting evidence and first describes those features that can be observed in the reader's own writing, such as natural variation and letter structure, before moving on to discuss the scientific principles on which a document examiner bases his or her conclusions.

The typewriting section deals in detail with conventional typewriters but is less informative about more modern methods. Other chapters include simple and easy to follow descriptions of printing processes, photocopying and the use of light to compare inks. In particular the chapter on incidental marks may provide investigators with fresh ideas for solving a problem, and explains the mysterious and much publicised FSDA machine.

The use of frequent headings and a comprehensive index makes this a valuable reference book for the investigator and a useful starting point for would-be document examiners.

S. P. DAY

Handbook of Thin-Layer Chromatography: J. SHERMA and B. FRIED (editors), Dekker, New York, 1991. Pages viii + 1047. \$165.00 (US and Canada), \$198.00 (elsewhere).

Volume 55 in the Chromatography Science Series by Dekker is a large work containing contributions from 43 different authors. It is not a collection of papers from a symposium but purports to be an organized work by recognized, international experts. The co-editor, Professor Sherma, is well known for his biennial reviews of progress in TLC and this practical, comprehensive handbook is to be welcomed.

The book is divided into two parts, with Chapters 1-13 covering the principles and practice of TLC and Chapters 14-31 dealing with some specific applications. There is some inevitable overlap between contributions but the references (totalling over 2700) at the ends of each of each chapter appear to be selective.

Part 1 includes details of the theory, apparatus and techniques used in the different variations of planar chromatography. There are chapters on optimization, sorbents and instrumental methods such as TLC coupled with mass spectrometry. Preparative TLC is covered as well as qualitative and quantitative analysis. Part 1 is of general interest for all those who dabble with TLC, whereas part 2 concentrates on the analysis of specific chemical substances. It is probable that users of the handbook will just select those chapters in part 2 which are of relevance to their own work. Here the compounds covered include amino-acids, antibiotics, carbohydrates, pesticides, steroids, vitamins, toxins and many others. An important chapter on enantiomer separations is included and this is a useful addition, owing to the increased awareness of the importance of enantiomeric purity in pharmaceutical compounds. Throughout part 2 numerous tables are presented that give details of separations performed with various solvent systems, *e.g.*, the chapter on TLC of inorganics and organometallics contains 69 Tables and 217 references. At the end of the book a glossary of terms is provided together with a directory of suppliers and a competent index.

The book is extremely useful for those who wish to discover how a TLC separation has been performed. If you can cope with the weight and price of this work then it is to be recommended to the beginner and the advanced user of TLC.

P. J. Cox

Methods of Biochemical Analysis, Volume 34—Biomedical Applications of Mass Spectrometry: C. H. SUELTER and J. T. WATSON (editors), Wiley Interscience, New York, 1990. Pages xiii + 396. £39.80.

This is the latest book in a series covering techniques of biochemical analysis, and this volume focuses specifically on mass spectrometry. The book is comprised of five chapters each covering different aspects of the application of mass spectrometry in biomedical research.

Chapter 1 gives a comprehensive introduction which would give anyone new to this field a broad knowledge of mass spectrometry. This ranges from the mechanics of the vacuum pumps, through the many techniques available on modern instruments, to the interpretation of the spectra produced.

BOOK REVIEWS

The Scientific Examination of Documents: Methods and Techniques: D. ELLEN, Ellis Horwood, Chichester, 1989. Pages 182. £42.95.

Questioned Document Examination is an area of forensic science providing evidence for courts of law on subjects such as handwriting, typewriting and printing. Much of this work depends on "the experience and ability of the analyst". Mr Ellen, with 35 years experience in forensic science and a founder member of the Metropolitan Police Documents Section is perhaps the best qualified to write a book on the subject.

This book is aimed primarily at those who may need to use documentary evidence during the investigation, prosecution or defence of a case. Handwriting is the most difficult area of this work and occupies four chapters. The author is keen to show the reasoning behind handwriting evidence and first describes those features that can be observed in the reader's own writing, such as natural variation and letter structure, before moving on to discuss the scientific principles on which a document examiner bases his or her conclusions.

The typewriting section deals in detail with conventional typewriters but is less informative about more modern methods. Other chapters include simple and easy to follow descriptions of printing processes, photocopying and the use of light to compare inks. In particular the chapter on incidental marks may provide investigators with fresh ideas for solving a problem, and explains the mysterious and much publicised FSDA machine.

The use of frequent headings and a comprehensive index makes this a valuable reference book for the investigator and a useful starting point for would-be document examiners.

S. P. DAY

Handbook of Thin-Layer Chromatography: J. SHERMA and B. FRIED (editors), Dekker, New York, 1991. Pages viii + 1047. \$165.00 (US and Canada), \$198.00 (elsewhere).

Volume 55 in the Chromatography Science Series by Dekker is a large work containing contributions from 43 different authors. It is not a collection of papers from a symposium but purports to be an organized work by recognized, international experts. The co-editor, Professor Sherma, is well known for his biennial reviews of progress in TLC and this practical, comprehensive handbook is to be welcomed.

The book is divided into two parts, with Chapters 1-13 covering the principles and practice of TLC and Chapters 14-31 dealing with some specific applications. There is some inevitable overlap between contributions but the references (totalling over 2700) at the ends of each of each chapter appear to be selective.

Part 1 includes details of the theory, apparatus and techniques used in the different variations of planar chromatography. There are chapters on optimization, sorbents and instrumental methods such as TLC coupled with mass spectrometry. Preparative TLC is covered as well as qualitative and quantitative analysis. Part 1 is of general interest for all those who dabble with TLC, whereas part 2 concentrates on the analysis of specific chemical substances. It is probable that users of the handbook will just select those chapters in part 2 which are of relevance to their own work. Here the compounds covered include amino-acids, antibiotics, carbohydrates, pesticides, steroids, vitamins, toxins and many others. An important chapter on enantiomer separations is included and this is a useful addition, owing to the increased awareness of the importance of enantiomeric purity in pharmaceutical compounds. Throughout part 2 numerous tables are presented that give details of separations performed with various solvent systems, *e.g.*, the chapter on TLC of inorganics and organometallics contains 69 Tables and 217 references. At the end of the book a glossary of terms is provided together with a directory of suppliers and a competent index.

The book is extremely useful for those who wish to discover how a TLC separation has been performed. If you can cope with the weight and price of this work then it is to be recommended to the beginner and the advanced user of TLC.

P. J. Cox

Methods of Biochemical Analysis, Volume 34—Biomedical Applications of Mass Spectrometry: C. H. SUELTER and J. T. WATSON (editors), Wiley Interscience, New York, 1990. Pages xiii + 396. £39.80.

This is the latest book in a series covering techniques of biochemical analysis, and this volume focuses specifically on mass spectrometry. The book is comprised of five chapters each covering different aspects of the application of mass spectrometry in biomedical research.

Chapter 1 gives a comprehensive introduction which would give anyone new to this field a broad knowledge of mass spectrometry. This ranges from the mechanics of the vacuum pumps, through the many techniques available on modern instruments, to the interpretation of the spectra produced.

The bulk of the book focuses on specific applications: carbohydrates, peptide sequencing, nucleic acids, and the role of mass spectrometry in pharmacology. These four chapters explain in greater detail those particular techniques applicable to each study area. The bulk of these chapters is concerned with the practical details of performing the analysis. Very detailed information is given enabling the reader to repeat the analyses and interpret the results obtained. Each chapter also contains a large number of figures and references to back up the text.

I feel that the book has two faults, the introductory chapter covers too much of the "nut and bolts" of mass spectrometry, and that as each chapter is written by a different author, some details about ionisation techniques are repeated in several chapters.

M. E. HARRISON

Chromatographic Analysis of Alkaloids: M. POPL, J. FAHRICH and V. TATAR, Dekker, New York, 1990. Pages 664. \$150.00 (U.S. and Canada), \$180.00 (elsewhere).

For anyone wishing to enter the field of alkaloid chemistry, reading this book will be a great help. It will give the reader an insight into how alkaloids are grouped (Chapter 1) as well as describing the general properties of these natural products (Chapter 2). This latter section is particularly useful as the data on basicity, solubility, dissociation constants, main chromophoric groupings, and electrochemical properties help one to appreciate the general behaviour of alkaloids. These criteria are necessary for their chromatographic properties to be assessed for selection of the best chromatographic procedure. These procedures are summarized in Chapter 3.

The next three chapters outline the techniques of gas, liquid and thin-layer chromatography, respectively, with well chosen examples explaining each chromatographic method. Derivatization reactions such as acylation, alkylation and silylation, which are required to improve volatility and thermal stability, are well covered in the chapters on gas chromatography and thin-layer chromatography. However, derivatization as a means of allowing the utilization of specific methods of detection, such as fluorescence, is not discussed under liquid chromatography.

In the penultimate chapter—Applications,—is where the "meat" of this book is located. First there are details of simple preparation—for materials from biological, plant and pharmaceutical sources—with tables summarizing preparative procedures. Then follows a sixteen-section tabulation on alkaloidal families in groupings starting with the simple, e.g., phenylethylamines, through to the complex, e.g., *Strychnos*, *Vinca* types. The dominant position of liquid chromatography, particularly reversed-phase HPLC, in the analysis of alkaloids is well exemplified. This list is comprehensive enough to allow the reader to make a rapid assessment in a selected field.

The final chapter (3 pages) is very much a critique of existing methodology with some pointers as to the future, including supercritical fluid chromatography.

The main index is sufficiently detailed to give rapid access to individual alkaloids and to plant genera. I would have liked each chapter to be prefaced by its own index—this would have been particularly helpful in the seventh chapter for locating areas for general perusal.

Although the price is somewhat prohibitive for individual purchase, this book makes a useful contribution to natural product chemistry and is to be recommended as a work of reference on the application of chromatographic techniques.

JOHN R. LEWIS

The Analytical Chemistry of Silicones: A. L. SMITH (editor), Wiley-Interscience, New York, 1991. Pages xxii + 551. £97.35.

This book is a recent addition to the highly successful and authoritative Wiley Chemical Analysis series, updating *Analysis of Silicones* edited by A. L. Smith and published in 1974. Silicones have a wide variety of commercial uses, from adhesives and sealants to textile finishes. Not unexpectedly, all the authors included in this book are affiliated with Dow Corning, and in some ways the book may be seen as a tribute to the impressive, multidisciplinary approach to silicone analysis at the company. Like Gaul, the book is divided into three parts: a very brief introductory chapter by Smith, a series of chapters on problem-solving in silicone analysis, followed by chapters on the basic techniques: physical properties, chemical analysis, microscopy, chromatography spectroscopy (IR, UV-Vis, NMR, MS, atomic) and X-ray methods. Useful tables of physical properties of silicones are provided at the back of the book. While some chapters are illustrated by a disappointingly brief range of applications, others are extremely well-written (especially the chromatography, solution NMR and MS chapters). For the general reader, the microscopy chapter presents a fascinating series of images ranging from contact lenses to finger implant tissue. Essential reading for the specialist and newcomer, of course, but at nearly £100, the non-specialist would be wise to view the book carefully before making a purchase.

J. A. CRAYSTON

Mössbauer Spectroscopy of Frozen Solutions: A. VERTES and D. L. NAGY (editors). Akadémiai Kiadó, Budapest, 1990. Pages 303. £22.50

The book is concerned with the use of Mössbauer spectroscopy to investigate structures and coordination, mainly in solutions but also in glasses. If during rapid freezing of solutions no structural changes occur, then Mössbauer spectroscopy (a solid state technique) can indeed be an excellent probe of solution structures.

The bulk of the book focuses on specific applications: carbohydrates, peptide sequencing, nucleic acids, and the role of mass spectrometry in pharmacology. These four chapters explain in greater detail those particular techniques applicable to each study area. The bulk of these chapters is concerned with the practical details of performing the analysis. Very detailed information is given enabling the reader to repeat the analyses and interpret the results obtained. Each chapter also contains a large number of figures and references to back up the text.

I feel that the book has two faults, the introductory chapter covers too much of the "nut and bolts" of mass spectrometry, and that as each chapter is written by a different author, some details about ionisation techniques are repeated in several chapters.

M. E. HARRISON

Chromatographic Analysis of Alkaloids: M. POPL, J. FAHRICH and V. TATAR, Dekker, New York, 1990. Pages 664. \$150.00 (U.S. and Canada), \$180.00 (elsewhere).

For anyone wishing to enter the field of alkaloid chemistry, reading this book will be a great help. It will give the reader an insight into how alkaloids are grouped (Chapter 1) as well as describing the general properties of these natural products (Chapter 2). This latter section is particularly useful as the data on basicity, solubility, dissociation constants, main chromophoric groupings, and electrochemical properties help one to appreciate the general behaviour of alkaloids. These criteria are necessary for their chromatographic properties to be assessed for selection of the best chromatographic procedure. These procedures are summarized in Chapter 3.

The next three chapters outline the techniques of gas, liquid and thin-layer chromatography, respectively, with well chosen examples explaining each chromatographic method. Derivatization reactions such as acylation, alkylation and silylation, which are required to improve volatility and thermal stability, are well covered in the chapters on gas chromatography and thin-layer chromatography. However, derivatization as a means of allowing the utilization of specific methods of detection, such as fluorescence, is not discussed under liquid chromatography.

In the penultimate chapter—Applications,—is where the "meat" of this book is located. First there are details of simple preparation—for materials from biological, plant and pharmaceutical sources—with tables summarizing preparative procedures. Then follows a sixteen-section tabulation on alkaloidal families in groupings starting with the simple, e.g., phenylethylamines, through to the complex, e.g., *Strychnos*, *Vinca* types. The dominant position of liquid chromatography, particularly reversed-phase HPLC, in the analysis of alkaloids is well exemplified. This list is comprehensive enough to allow the reader to make a rapid assessment in a selected field.

The final chapter (3 pages) is very much a critique of existing methodology with some pointers as to the future, including supercritical fluid chromatography.

The main index is sufficiently detailed to give rapid access to individual alkaloids and to plant genera. I would have liked each chapter to be prefaced by its own index—this would have been particularly helpful in the seventh chapter for locating areas for general perusal.

Although the price is somewhat prohibitive for individual purchase, this book makes a useful contribution to natural product chemistry and is to be recommended as a work of reference on the application of chromatographic techniques.

JOHN R. LEWIS

The Analytical Chemistry of Silicones: A. L. SMITH (editor), Wiley-Interscience, New York, 1991. Pages xxii + 551. £97.35.

This book is a recent addition to the highly successful and authoritative Wiley Chemical Analysis series, updating *Analysis of Silicones* edited by A. L. Smith and published in 1974. Silicones have a wide variety of commercial uses, from adhesives and sealants to textile finishes. Not unexpectedly, all the authors included in this book are affiliated with Dow Corning, and in some ways the book may be seen as a tribute to the impressive, multidisciplinary approach to silicone analysis at the company. Like Gaul, the book is divided into three parts: a very brief introductory chapter by Smith, a series of chapters on problem-solving in silicone analysis, followed by chapters on the basic techniques: physical properties, chemical analysis, microscopy, chromatography spectroscopy (IR, UV-Vis, NMR, MS, atomic) and X-ray methods. Useful tables of physical properties of silicones are provided at the back of the book. While some chapters are illustrated by a disappointingly brief range of applications, others are extremely well-written (especially the chromatography, solution NMR and MS chapters). For the general reader, the microscopy chapter presents a fascinating series of images ranging from contact lenses to finger implant tissue. Essential reading for the specialist and newcomer, of course, but at nearly £100, the non-specialist would be wise to view the book carefully before making a purchase.

J. A. CRAYSTON

Mössbauer Spectroscopy of Frozen Solutions: A. VERTES and D. L. NAGY (editors). Akadémiai Kiadó, Budapest, 1990. Pages 303. £22.50

The book is concerned with the use of Mössbauer spectroscopy to investigate structures and coordination, mainly in solutions but also in glasses. If during rapid freezing of solutions no structural changes occur, then Mössbauer spectroscopy (a solid state technique) can indeed be an excellent probe of solution structures.

The bulk of the book focuses on specific applications: carbohydrates, peptide sequencing, nucleic acids, and the role of mass spectrometry in pharmacology. These four chapters explain in greater detail those particular techniques applicable to each study area. The bulk of these chapters is concerned with the practical details of performing the analysis. Very detailed information is given enabling the reader to repeat the analyses and interpret the results obtained. Each chapter also contains a large number of figures and references to back up the text.

I feel that the book has two faults, the introductory chapter covers too much of the "nut and bolts" of mass spectrometry, and that as each chapter is written by a different author, some details about ionisation techniques are repeated in several chapters.

M. E. HARRISON

Chromatographic Analysis of Alkaloids: M. POPL, J. FAHRICH and V. TATAR, Dekker, New York, 1990. Pages 664. \$150.00 (U.S. and Canada), \$180.00 (elsewhere).

For anyone wishing to enter the field of alkaloid chemistry, reading this book will be a great help. It will give the reader an insight into how alkaloids are grouped (Chapter 1) as well as describing the general properties of these natural products (Chapter 2). This latter section is particularly useful as the data on basicity, solubility, dissociation constants, main chromophoric groupings, and electrochemical properties help one to appreciate the general behaviour of alkaloids. These criteria are necessary for their chromatographic properties to be assessed for selection of the best chromatographic procedure. These procedures are summarized in Chapter 3.

The next three chapters outline the techniques of gas, liquid and thin-layer chromatography, respectively, with well chosen examples explaining each chromatographic method. Derivatization reactions such as acylation, alkylation and silylation, which are required to improve volatility and thermal stability, are well covered in the chapters on gas chromatography and thin-layer chromatography. However, derivatization as a means of allowing the utilization of specific methods of detection, such as fluorescence, is not discussed under liquid chromatography.

In the penultimate chapter—Applications,—is where the "meat" of this book is located. First there are details of simple preparation—for materials from biological, plant and pharmaceutical sources—with tables summarizing preparative procedures. Then follows a sixteen-section tabulation on alkaloidal families in groupings starting with the simple, e.g., phenylethylamines, through to the complex, e.g., *Strychnos*, *Vinca* types. The dominant position of liquid chromatography, particularly reversed-phase HPLC, in the analysis of alkaloids is well exemplified. This list is comprehensive enough to allow the reader to make a rapid assessment in a selected field.

The final chapter (3 pages) is very much a critique of existing methodology with some pointers as to the future, including supercritical fluid chromatography.

The main index is sufficiently detailed to give rapid access to individual alkaloids and to plant genera. I would have liked each chapter to be prefaced by its own index—this would have been particularly helpful in the seventh chapter for locating areas for general perusal.

Although the price is somewhat prohibitive for individual purchase, this book makes a useful contribution to natural product chemistry and is to be recommended as a work of reference on the application of chromatographic techniques.

JOHN R. LEWIS

The Analytical Chemistry of Silicones: A. L. SMITH (editor), Wiley-Interscience, New York, 1991. Pages xxii + 551. £97.35.

This book is a recent addition to the highly successful and authoritative Wiley Chemical Analysis series, updating *Analysis of Silicones* edited by A. L. Smith and published in 1974. Silicones have a wide variety of commercial uses, from adhesives and sealants to textile finishes. Not unexpectedly, all the authors included in this book are affiliated with Dow Corning, and in some ways the book may be seen as a tribute to the impressive, multidisciplinary approach to silicone analysis at the company. Like Gaul, the book is divided into three parts: a very brief introductory chapter by Smith, a series of chapters on problem-solving in silicone analysis, followed by chapters on the basic techniques: physical properties, chemical analysis, microscopy, chromatography spectroscopy (IR, UV-Vis, NMR, MS, atomic) and X-ray methods. Useful tables of physical properties of silicones are provided at the back of the book. While some chapters are illustrated by a disappointingly brief range of applications, others are extremely well-written (especially the chromatography, solution NMR and MS chapters). For the general reader, the microscopy chapter presents a fascinating series of images ranging from contact lenses to finger implant tissue. Essential reading for the specialist and newcomer, of course, but at nearly £100, the non-specialist would be wise to view the book carefully before making a purchase.

J. A. CRAYSTON

Mössbauer Spectroscopy of Frozen Solutions: A. VERTES and D. L. NAGY (editors). Akadémiai Kiadó, Budapest, 1990. Pages 303. £22.50

The book is concerned with the use of Mössbauer spectroscopy to investigate structures and coordination, mainly in solutions but also in glasses. If during rapid freezing of solutions no structural changes occur, then Mössbauer spectroscopy (a solid state technique) can indeed be an excellent probe of solution structures.

The book of ca. 300 pages consists of seven chapters, all written by East European scientists. The English is generally very good, but rather formal in style. Individual chapters are concerned with (i) the physical and technical basis of Mössbauer spectroscopy, (ii) Mössbauer spectra in frozen solutions, (iii) relaxation phenomena in frozen solutions, (iv) short range order in frozen aqueous solutions of Fe(III) salts, (v) chemical structure of liquid solutions, (vi) after-effects of nuclear transformations in frozen solutions and (vii) Mössbauer effects as applied to investigations of glassy material. Adequate references are listed at the end of each chapter and a collected subject index appears at the end of the book. There are numerous figures and tables.

There is a strong mathematical presence in the book; experimental details also are featured. However, the bulk of the book is concerned with experimental results and their interpretation.

The book was published in 1990 and a cursory look through the reference lists reveals a few references dated in the 1980s and even one dated 1988. There are a few references to conference proceedings and lectures in the 1960s and 1970s; presumably such work has never been published in refereed journals.

The price of the book just has to be noted; at £22.50 it makes many books published in western Europe look very expensive.

Overall the book is a useful one, and has suggested several ideas to this reviewer.

J. L. WARDELL

Infrared Spectroscopy of Adsorbed Species on the Surface of Transition Metal Oxides: A. A. DAVYDOV, Wiley, Chichester, 1990. Pages xii + 243. £65.00.

Although a number of texts are currently available on the IR spectroscopy of adsorbed species on the surfaces of transition metals, there is a marked shortage of books discussing the equally important field of adsorption on transition metal *oxide* surfaces. This book, therefore, makes a welcome and long needed contribution in this area. Essentially, the book is a summary of the author's investigations of the surface chemistry of simple and complex oxide catalysts. Throughout, the emphasis is on elucidating the relationships between the structure and function of oxide catalysts.

Chapters 1 and 2 discuss the use of IR spectra of probe molecules such as ammonia, CO and NO to investigate the nature and adsorption properties of surface centres such as hydroxyl groups, electron-donating oxygen ions and electron-acceptor metal cations. Of particular use to a surface IR spectroscopist is the discussion of a scheme for interpretation of the adsorption site occupied, based on the frequency of the CO and NO stretching vibrations.

Chapter 3 progresses to the use of more complex probe molecules, such as alkenes, to demonstrate the role of the surface centre in determining the adsorption characteristics of a system. This is a particularly relevant system of study since many catalytic hydrocarbon conversions occur on oxide surfaces. This chapter is also valuable for its discussion of the problems that confront a researcher when interpreting IR spectra from complex adsorbates. The author has developed a range of strategies to overcome these problems, with notable success achieved by combining IR spectroscopy with thermal desorption and chromatographic analysis of the desorption products.

Finally, Chapter 4 discusses the use of IR spectroscopy in elucidating the mechanisms of heterogeneous catalytic processes on oxide surfaces. In particular, the mechanistic aspects of the CO oxidation reaction, the water-gas shift reaction, the CO + NO reaction, the oxidation reactions of acrolein and methanol and the reactions of alkenes are discussed in detail.

The book was first published in Russian in 1984 and has been widely researched up to that date, totalling some 400 references. This is the English translation, hence the lack of references after 1984. Despite this, the book makes a valuable and timely contribution to the literature in this area and will prove to be an invaluable guide to researchers in this field.

R. RAVAL

Determination of the Precious Metals: Selected Instrumental Methods: J. C. VAN LOON and R. R. BAREFOOT, Wiley, Chichester, 1991. Pages x + 276. £45.00.

The book basically consists of two parts, the first dealing (sometimes too briefly) with the physical and chemical properties of the precious metals, the principles of the instruments used, sampling, sample processing, equipment, safety, reference materials and so on. The second gives detailed procedures for the determination of the precious metals in various types of sample by different instrumental methods, and as it consists mainly of information reprinted from the literature, it will save the practising analyst a great amount of library work. Useful comments are made on the methods selected. Because the nature of the instrumental methods generally makes the oxidation state of the metal of little or no consequence, the discussion of the chemistry of the metals concerned is rather cursory, and it would have been useful to have had more complete information given, especially with regard to the kinetic behaviour of the metal ions, and their hydrolysis and polymerization. However, the information given is doubtless adequate for the purposes for which the book will be used, and it forms a welcome addition to the literature on analysis for the platinum metals and gold.

R. A. CHALMERS

The book of ca. 300 pages consists of seven chapters, all written by East European scientists. The English is generally very good, but rather formal in style. Individual chapters are concerned with (i) the physical and technical basis of Mössbauer spectroscopy, (ii) Mössbauer spectra in frozen solutions, (iii) relaxation phenomena in frozen solutions, (iv) short range order in frozen aqueous solutions of Fe(III) salts, (v) chemical structure of liquid solutions, (vi) after-effects of nuclear transformations in frozen solutions and (vii) Mössbauer effects as applied to investigations of glassy material. Adequate references are listed at the end of each chapter and a collected subject index appears at the end of the book. There are numerous figures and tables.

There is a strong mathematical presence in the book; experimental details also are featured. However, the bulk of the book is concerned with experimental results and their interpretation.

The book was published in 1990 and a cursory look through the reference lists reveals a few references dated in the 1980s and even one dated 1988. There are a few references to conference proceedings and lectures in the 1960s and 1970s; presumably such work has never been published in refereed journals.

The price of the book just has to be noted; at £22.50 it makes many books published in western Europe look very expensive.

Overall the book is a useful one, and has suggested several ideas to this reviewer.

J. L. WARDELL

Infrared Spectroscopy of Adsorbed Species on the Surface of Transition Metal Oxides: A. A. DAVYDOV, Wiley, Chichester, 1990. Pages xii + 243. £65.00.

Although a number of texts are currently available on the IR spectroscopy of adsorbed species on the surfaces of transition metals, there is a marked shortage of books discussing the equally important field of adsorption on transition metal *oxide* surfaces. This book, therefore, makes a welcome and long needed contribution in this area. Essentially, the book is a summary of the author's investigations of the surface chemistry of simple and complex oxide catalysts. Throughout, the emphasis is on elucidating the relationships between the structure and function of oxide catalysts.

Chapters 1 and 2 discuss the use of IR spectra of probe molecules such as ammonia, CO and NO to investigate the nature and adsorption properties of surface centres such as hydroxyl groups, electron-donating oxygen ions and electron-acceptor metal cations. Of particular use to a surface IR spectroscopist is the discussion of a scheme for interpretation of the adsorption site occupied, based on the frequency of the CO and NO stretching vibrations.

Chapter 3 progresses to the use of more complex probe molecules, such as alkenes, to demonstrate the role of the surface centre in determining the adsorption characteristics of a system. This is a particularly relevant system of study since many catalytic hydrocarbon conversions occur on oxide surfaces. This chapter is also valuable for its discussion of the problems that confront a researcher when interpreting IR spectra from complex adsorbates. The author has developed a range of strategies to overcome these problems, with notable success achieved by combining IR spectroscopy with thermal desorption and chromatographic analysis of the desorption products.

Finally, Chapter 4 discusses the use of IR spectroscopy in elucidating the mechanisms of heterogeneous catalytic processes on oxide surfaces. In particular, the mechanistic aspects of the CO oxidation reaction, the water-gas shift reaction, the CO + NO reaction, the oxidation reactions of acrolein and methanol and the reactions of alkenes are discussed in detail.

The book was first published in Russian in 1984 and has been widely researched up to that date, totalling some 400 references. This is the English translation, hence the lack of references after 1984. Despite this, the book makes a valuable and timely contribution to the literature in this area and will prove to be an invaluable guide to researchers in this field.

R. RAVAL

Determination of the Precious Metals: Selected Instrumental Methods: J. C. VAN LOON and R. R. BAREFOOT, Wiley, Chichester, 1991. Pages x + 276. £45.00.

The book basically consists of two parts, the first dealing (sometimes too briefly) with the physical and chemical properties of the precious metals, the principles of the instruments used, sampling, sample processing, equipment, safety, reference materials and so on. The second gives detailed procedures for the determination of the precious metals in various types of sample by different instrumental methods, and as it consists mainly of information reprinted from the literature, it will save the practising analyst a great amount of library work. Useful comments are made on the methods selected. Because the nature of the instrumental methods generally makes the oxidation state of the metal of little or no consequence, the discussion of the chemistry of the metals concerned is rather cursory, and it would have been useful to have had more complete information given, especially with regard to the kinetic behaviour of the metal ions, and their hydrolysis and polymerization. However, the information given is doubtless adequate for the purposes for which the book will be used, and it forms a welcome addition to the literature on analysis for the platinum metals and gold.

R. A. CHALMERS

Detection-Oriented Derivatization Techniques in Liquid Chromatography: H. LINGEMAN and W. J. M. UNDERBERG (editors), Dekker, 1990. Pages xvi + 389. \$99.75 (U.S. and Canada), \$119.50 (elsewhere).

This volume is an excellent addition to the Chromatographic Science Series. It reviews how derivatization can extend high performance liquid chromatography applications and gives general coverage of the various types of analyte derivatization for all major detection techniques.

The text is well organized and arranged, starting with basic ideas and advantages of derivatization followed by a survey of the physical and chemical effects pertinent to the kinetics of derivatization reactions. A chapter is included on sample pretreatment which, although a bit removed from the general content of the volume, provides an excellent overview of the common and not so common techniques used for preparing analytes for injection. There is an interesting chapter on the theory and practical aspects of homogeneous and solid state post-column reactors.

The remainder of the book consists of a series of chapters covering derivatization procedures used to augment various detection methods. Where appropriate, for example in electrochemical detection and in enzyme derivatization, the principles of the detection method are also outlined.

As a result of its very complete coverage of derivatization related topics this will prove a very useful text both for general reading and for use in solving specific chromatographic problems. The balance of principles, practical and examples has been well struck.

R. B. TAYLOR

Analytical Methods in Forensic Chemistry: M. H. Ho, Ellis Horwood, Chichester, 1990. Pages XVII + 440. £56.00.

This book attempts to bring together in its 29 chapters various analytical methods available. In doing so the bias is towards drug analyses at the expense of inorganic techniques. However, this is not altogether a shortcoming since the vast majority of forensic work involves analysis and comparison of drugs and related samples.

Modern instrumental techniques (GC-MS, capillary GC, HPLC, *etc.*) are covered along with some of the more exotic and less well used methods (chiroptical), with quotation of case examples and methodology where necessary. I found the chapters on drug profiling by gas chromatography particularly interesting, as well as the chapter on the use of GCMS in arson analysis.

With the increasing incidence of firearms-related offences in the United Kingdom and world wide terrorism it is perhaps one criticism that the detection of explosives residues and firearms residues is not given more exposure. A chapter on computerization or data handling would also have been useful.

The book has been attractively presented and all the chapters appear clear and concise. I strongly recommend the book to students of forensic science, toxicology, science in general, the legal profession and to the experienced forensic scientist and it should be regarded as good reference material.

R. M. STEWART

Analytical Instrumentation Handbook: G. W. EWING (editor), Dekker, New York, 1990. Pages xi + 1071. \$195.00 (U.S. and Canada). \$234.00 (All other countries).

This book describes the modern instrumentation required for a very wide range of currently used analytical techniques. The readily understandable introductory chapter is on the use of computers in the laboratory. The computing aspect, particularly with regard to the collection and processing of acquired data, is emphasised throughout the book. The book is divided into five sections, *viz.* the measurement of mass, spectrochemical instrumentation, electrochemical instrumentation, chromatographic instrumentation and miscellaneous methods (which include mass spectrometry, thermoanalytical instrumentation, automatic titration and continuous flow analysis). In general, theoretical considerations are minimised but adequately referenced. The text concentrates on the description of the particular instrumental components, and on the description and discussion of the complete instruments, their limitations, and the errors associated with their practical use. The presentation is of high standard throughout, but for content, quality and references the chapters on IR, EPR, NMR, molecular fluorescence and phosphorescence, and continuous flow analysis deserve special mention.

This book represents a valuable reference source which will aid analysts in their selection of the most appropriate instrumentation to solve a particular analytical problem.

R. R. MOODY

Chemometrics: Experimental Design: E. MORGAN, Wiley, Chichester, 1991. Pages xviii + 275. £25.00.

Near the beginning of this book, Ed Morgen writes: "Often we waste time and effort by rushing into experimental work, and, most important, we frequently do not have any idea of the significance of the results we have obtained". So his purpose is to lay a sound foundation of rational experimental design for beginners, and there is no doubt that he succeeds. The book is in the ACOL series (Analytical Chemistry by Open Learning) with all that that implies, but unlike previous volumes it carries an index, although it is only a little over two pages long.

There are a lot of good things here. The writing is clear, with few typographical errors; at the start of the book there is a reading list as well as a brief survey of some suitable statistics computer programs that are currently available. The use of spreadsheets for experimental design is also mentioned. Sometimes the author is inconsistent with significant figures in his worked examples—trailing zeros are often omitted—and this could confuse students who are learning in isolation.

Detection-Oriented Derivatization Techniques in Liquid Chromatography: H. LINGEMAN and W. J. M. UNDERBERG (editors), Dekker, 1990. Pages xvi + 389. \$99.75 (U.S. and Canada), \$119.50 (elsewhere).

This volume is an excellent addition to the Chromatographic Science Series. It reviews how derivatization can extend high performance liquid chromatography applications and gives general coverage of the various types of analyte derivatization for all major detection techniques.

The text is well organized and arranged, starting with basic ideas and advantages of derivatization followed by a survey of the physical and chemical effects pertinent to the kinetics of derivatization reactions. A chapter is included on sample pretreatment which, although a bit removed from the general content of the volume, provides an excellent overview of the common and not so common techniques used for preparing analytes for injection. There is an interesting chapter on the theory and practical aspects of homogeneous and solid state post-column reactors.

The remainder of the book consists of a series of chapters covering derivatization procedures used to augment various detection methods. Where appropriate, for example in electrochemical detection and in enzyme derivatization, the principles of the detection method are also outlined.

As a result of its very complete coverage of derivatization related topics this will prove a very useful text both for general reading and for use in solving specific chromatographic problems. The balance of principles, practical and examples has been well struck.

R. B. TAYLOR

Analytical Methods in Forensic Chemistry: M. H. Ho, Ellis Horwood, Chichester, 1990. Pages XVII + 440. £56.00.

This book attempts to bring together in its 29 chapters various analytical methods available. In doing so the bias is towards drug analyses at the expense of inorganic techniques. However, this is not altogether a shortcoming since the vast majority of forensic work involves analysis and comparison of drugs and related samples.

Modern instrumental techniques (GC-MS, capillary GC, HPLC, *etc.*) are covered along with some of the more exotic and less well used methods (chiroptical), with quotation of case examples and methodology where necessary. I found the chapters on drug profiling by gas chromatography particularly interesting, as well as the chapter on the use of GCMS in arson analysis.

With the increasing incidence of firearms-related offences in the United Kingdom and world wide terrorism it is perhaps one criticism that the detection of explosives residues and firearms residues is not given more exposure. A chapter on computerization or data handling would also have been useful.

The book has been attractively presented and all the chapters appear clear and concise. I strongly recommend the book to students of forensic science, toxicology, science in general, the legal profession and to the experienced forensic scientist and it should be regarded as good reference material.

R. M. STEWART

Analytical Instrumentation Handbook: G. W. EWING (editor), Dekker, New York, 1990. Pages xi + 1071. \$195.00 (U.S. and Canada). \$234.00 (All other countries).

This book describes the modern instrumentation required for a very wide range of currently used analytical techniques. The readily understandable introductory chapter is on the use of computers in the laboratory. The computing aspect, particularly with regard to the collection and processing of acquired data, is emphasised throughout the book. The book is divided into five sections, *viz.* the measurement of mass, spectrochemical instrumentation, electrochemical instrumentation, chromatographic instrumentation and miscellaneous methods (which include mass spectrometry, thermoanalytical instrumentation, automatic titration and continuous flow analysis). In general, theoretical considerations are minimised but adequately referenced. The text concentrates on the description of the particular instrumental components, and on the description and discussion of the complete instruments, their limitations, and the errors associated with their practical use. The presentation is of high standard throughout, but for content, quality and references the chapters on IR, EPR, NMR, molecular fluorescence and phosphorescence, and continuous flow analysis deserve special mention.

This book represents a valuable reference source which will aid analysts in their selection of the most appropriate instrumentation to solve a particular analytical problem.

R. R. MOODY

Chemometrics: Experimental Design: E. MORGAN, Wiley, Chichester, 1991. Pages xviii + 275. £25.00.

Near the beginning of this book, Ed Morgen writes: "Often we waste time and effort by rushing into experimental work, and, most important, we frequently do not have any idea of the significance of the results we have obtained". So his purpose is to lay a sound foundation of rational experimental design for beginners, and there is no doubt that he succeeds. The book is in the ACOL series (Analytical Chemistry by Open Learning) with all that that implies, but unlike previous volumes it carries an index, although it is only a little over two pages long.

There are a lot of good things here. The writing is clear, with few typographical errors; at the start of the book there is a reading list as well as a brief survey of some suitable statistics computer programs that are currently available. The use of spreadsheets for experimental design is also mentioned. Sometimes the author is inconsistent with significant figures in his worked examples—trailing zeros are often omitted—and this could confuse students who are learning in isolation.

There are times also when I would have preferred a more detailed description of the underlying assumptions of a given technique, and more mathematical formulae, but these are relatively small matters.

The book begins with revision of *t*- and *F*-tests, which leads naturally to simple analysis of variance techniques. Experimental design methods are then described for systems of increasing complexity. Factorial design then follows, and then fractional factorial design. The book concludes with a chapter on response surfaces. This is the right subject matter, well handled, and I recommend this book as a good introduction to chemometrics.

C. J. GILMORE

High Performance Liquid Chromatography in Biotechnology: W. S. HANCOCK (editor), Wiley-Interscience, New York, 1990. Pages x + 564, £74.35.

Lavoisier's axiom that only pure substances would yield information of significance is as true today as it was in his day. We now possess the techniques to enable us to isolate well-defined compounds that satisfy the most stringent of purity. There can be no doubt that high performance liquid chromatography has proved to be one of the most important and rapidly advancing of these techniques. Since biotechnology is another branch of science which is making rapid strides and which offers considerable promise for the future, this book, which examines the various applications of HPLC to biotechnology is very timely indeed. It is worth noting that the majority of papers published recently which are concerned with HPLC have concentrated on biological applications.

The book nicely reflects the multifaceted nature of the subject and the important interplay between its analytical and preparative aspects. The range of applications stretches from the nanogram scale, for characterization studies of novel proteins, to the kilogram amounts required for a manufacturing process.

Chapter 1 by the Editor is a useful introduction which provides an overview of the role of HPLC in biotechnology and a guide to subsequent chapters. Chapter 2, which deals with the design and synthesis of silica-based bonded phases for reversed-phase, ion-exchange and hydrophobic interaction chromatography, includes details for the purification of lysozyme, ovalbumin and other proteins.

Chapter 3 deals with nature of the sorption forces and the thermodynamics of protein adsorption. The next chapter addresses the important question of how much denaturation of proteins by organic solvents and consequent loss of biological activity occurs as a result of reversed-phase HPLC (RP-HPLC). The success of the technique depends very much on the particular protein—for example it can be used successfully for the isolation of human insulin without damage to the molecule, whereas with many other proteins reduced bioactivity may occur. This links in with Chapter 8 which deals in some detail with the use of analytical RP-HPLC in biosynthetic insulin production.

Chapter 5 deals with the physical properties and applications of new synthetic hydrophilic vinyl polymer packing materials for industrial separation of biopolymers. Next follows a substantial chapter on the scale-up of protein chromatographic separation, which contains some introductory material on the basic principles of chromatography which would not have been out of place in the introductory chapter. The subject of Chapter 7 is the HPLC of antigenic proteins and vaccines. Chapter 9 deals very specifically with the application of RP-HPLC to the separation of human growth hormone, and a more general review of methods and mechanisms of high performance ion-exchange chromatography of proteins is the subject of the next chapter. In Chapter 11 the complementary nature of ion-exchange HPLC and reversed-phase HPLC for polypeptide purification is pointed out—complementary in the sense that their combined use can provide the optimal separation or purity assessment of a peptide.

Hydrophobic interaction HPLC is the subject of Chapter 12, and Chapter 13 deals with high performance affinity chromatography (HPAC) or high performance liquid affinity chromatography (HPLAC) whichever one prefers to call it.

The next chapter on the purification of synthetic oligonucleotides provides a change from other chapters, which seem to concentrate almost exclusively on peptides and proteins. At first glance, one might consider a single chapter on oligonucleotides to represent an imbalance in the book, but on closer inspection one quickly realizes that it is a very extensive and detailed chapter (100 pages, 248 references). The emphasis of most chapters on the application of HPLC to polypeptide purification reflects the enormous effort which goes into the production of polypeptides which are antigenically or physiologically active. The final chapter deals with the chemical synthesis of peptides and the contribution of mass spectrometry to their analysis.

There is such a bewildering number of terms used in this book that a glossary of terms would not have been out of place and indeed it would have been welcomed. It does not help when alternative names for the same technique (gel filtration and size exclusion chromatography) are used in different chapters—the latter term is much preferred.

All chapters of the book are well-referenced and are illustrated with clear line drawings and photographs. The book is very broad in coverage, both of techniques and applications.

This is not a book for the newcomer to HPLC but I am certain that it will prove to be a valuable source-book to meet the needs of all workers in the field, whether they be analytical chemists, biochemists or chemical engineers.

A. K. DAVIES

Pharmaceutical Chemicals in Perspective: B. G. REUBEN and H. A. WITTCOFF, Wiley, Chichester, 1989. Pages xviii + 518. £59.00.

The aim of this book is to provide an overview of the pharmaceutical industry and its more important products. This is a somewhat ambitious goal to achieve within a mere five hundred pages.

The book is divided into three parts. The first part includes as an introductory chapter a brief review of the chronological introduction of drugs, coupling this to statistical data on changing patterns of mortality. This is followed by a wide-ranging

There are times also when I would have preferred a more detailed description of the underlying assumptions of a given technique, and more mathematical formulae, but these are relatively small matters.

The book begins with revision of *t*- and *F*-tests, which leads naturally to simple analysis of variance techniques. Experimental design methods are then described for systems of increasing complexity. Factorial design then follows, and then fractional factorial design. The book concludes with a chapter on response surfaces. This is the right subject matter, well handled, and I recommend this book as a good introduction to chemometrics.

C. J. GILMORE

High Performance Liquid Chromatography in Biotechnology: W. S. HANCOCK (editor), Wiley-Interscience, New York, 1990. Pages x + 564, £74.35.

Lavoisier's axiom that only pure substances would yield information of significance is as true today as it was in his day. We now possess the techniques to enable us to isolate well-defined compounds that satisfy the most stringent of purity. There can be no doubt that high performance liquid chromatography has proved to be one of the most important and rapidly advancing of these techniques. Since biotechnology is another branch of science which is making rapid strides and which offers considerable promise for the future, this book, which examines the various applications of HPLC to biotechnology is very timely indeed. It is worth noting that the majority of papers published recently which are concerned with HPLC have concentrated on biological applications.

The book nicely reflects the multifaceted nature of the subject and the important interplay between its analytical and preparative aspects. The range of applications stretches from the nanogram scale, for characterization studies of novel proteins, to the kilogram amounts required for a manufacturing process.

Chapter 1 by the Editor is a useful introduction which provides an overview of the role of HPLC in biotechnology and a guide to subsequent chapters. Chapter 2, which deals with the design and synthesis of silica-based bonded phases for reversed-phase, ion-exchange and hydrophobic interaction chromatography, includes details for the purification of lysozyme, ovalbumin and other proteins.

Chapter 3 deals with nature of the sorption forces and the thermodynamics of protein adsorption. The next chapter addresses the important question of how much denaturation of proteins by organic solvents and consequent loss of biological activity occurs as a result of reversed-phase HPLC (RP-HPLC). The success of the technique depends very much on the particular protein—for example it can be used successfully for the isolation of human insulin without damage to the molecule, whereas with many other proteins reduced bioactivity may occur. This links in with Chapter 8 which deals in some detail with the use of analytical RP-HPLC in biosynthetic insulin production.

Chapter 5 deals with the physical properties and applications of new synthetic hydrophilic vinyl polymer packing materials for industrial separation of biopolymers. Next follows a substantial chapter on the scale-up of protein chromatographic separation, which contains some introductory material on the basic principles of chromatography which would not have been out of place in the introductory chapter. The subject of Chapter 7 is the HPLC of antigenic proteins and vaccines. Chapter 9 deals very specifically with the application of RP-HPLC to the separation of human growth hormone, and a more general review of methods and mechanisms of high performance ion-exchange chromatography of proteins is the subject of the next chapter. In Chapter 11 the complementary nature of ion-exchange HPLC and reversed-phase HPLC for polypeptide purification is pointed out—complementary in the sense that their combined use can provide the optimal separation or purity assessment of a peptide.

Hydrophobic interaction HPLC is the subject of Chapter 12, and Chapter 13 deals with high performance affinity chromatography (HPAC) or high performance liquid affinity chromatography (HPLAC) whichever one prefers to call it.

The next chapter on the purification of synthetic oligonucleotides provides a change from other chapters, which seem to concentrate almost exclusively on peptides and proteins. At first glance, one might consider a single chapter on oligonucleotides to represent an imbalance in the book, but on closer inspection one quickly realizes that it is a very extensive and detailed chapter (100 pages, 248 references). The emphasis of most chapters on the application of HPLC to polypeptide purification reflects the enormous effort which goes into the production of polypeptides which are antigenically or physiologically active. The final chapter deals with the chemical synthesis of peptides and the contribution of mass spectrometry to their analysis.

There is such a bewildering number of terms used in this book that a glossary of terms would not have been out of place and indeed it would have been welcomed. It does not help when alternative names for the same technique (gel filtration and size exclusion chromatography) are used in different chapters—the latter term is much preferred.

All chapters of the book are well-referenced and are illustrated with clear line drawings and photographs. The book is very broad in coverage, both of techniques and applications.

This is not a book for the newcomer to HPLC but I am certain that it will prove to be a valuable source-book to meet the needs of all workers in the field, whether they be analytical chemists, biochemists or chemical engineers.

A. K. DAVIES

Pharmaceutical Chemicals in Perspective: B. G. REUBEN and H. A. WITTCOFF, Wiley, Chichester, 1989. Pages xviii + 518. £59.00.

The aim of this book is to provide an overview of the pharmaceutical industry and its more important products. This is a somewhat ambitious goal to achieve within a mere five hundred pages.

The book is divided into three parts. The first part includes as an introductory chapter a brief review of the chronological introduction of drugs, coupling this to statistical data on changing patterns of mortality. This is followed by a wide-ranging

There are times also when I would have preferred a more detailed description of the underlying assumptions of a given technique, and more mathematical formulae, but these are relatively small matters.

The book begins with revision of *t*- and *F*-tests, which leads naturally to simple analysis of variance techniques. Experimental design methods are then described for systems of increasing complexity. Factorial design then follows, and then fractional factorial design. The book concludes with a chapter on response surfaces. This is the right subject matter, well handled, and I recommend this book as a good introduction to chemometrics.

C. J. GILMORE

High Performance Liquid Chromatography in Biotechnology: W. S. HANCOCK (editor), Wiley-Interscience, New York, 1990. Pages x + 564, £74.35.

Lavoisier's axiom that only pure substances would yield information of significance is as true today as it was in his day. We now possess the techniques to enable us to isolate well-defined compounds that satisfy the most stringent of purity. There can be no doubt that high performance liquid chromatography has proved to be one of the most important and rapidly advancing of these techniques. Since biotechnology is another branch of science which is making rapid strides and which offers considerable promise for the future, this book, which examines the various applications of HPLC to biotechnology is very timely indeed. It is worth noting that the majority of papers published recently which are concerned with HPLC have concentrated on biological applications.

The book nicely reflects the multifaceted nature of the subject and the important interplay between its analytical and preparative aspects. The range of applications stretches from the nanogram scale, for characterization studies of novel proteins, to the kilogram amounts required for a manufacturing process.

Chapter 1 by the Editor is a useful introduction which provides an overview of the role of HPLC in biotechnology and a guide to subsequent chapters. Chapter 2, which deals with the design and synthesis of silica-based bonded phases for reversed-phase, ion-exchange and hydrophobic interaction chromatography, includes details for the purification of lysozyme, ovalbumin and other proteins.

Chapter 3 deals with nature of the sorption forces and the thermodynamics of protein adsorption. The next chapter addresses the important question of how much denaturation of proteins by organic solvents and consequent loss of biological activity occurs as a result of reversed-phase HPLC (RP-HPLC). The success of the technique depends very much on the particular protein—for example it can be used successfully for the isolation of human insulin without damage to the molecule, whereas with many other proteins reduced bioactivity may occur. This links in with Chapter 8 which deals in some detail with the use of analytical RP-HPLC in biosynthetic insulin production.

Chapter 5 deals with the physical properties and applications of new synthetic hydrophilic vinyl polymer packing materials for industrial separation of biopolymers. Next follows a substantial chapter on the scale-up of protein chromatographic separation, which contains some introductory material on the basic principles of chromatography which would not have been out of place in the introductory chapter. The subject of Chapter 7 is the HPLC of antigenic proteins and vaccines. Chapter 9 deals very specifically with the application of RP-HPLC to the separation of human growth hormone, and a more general review of methods and mechanisms of high performance ion-exchange chromatography of proteins is the subject of the next chapter. In Chapter 11 the complementary nature of ion-exchange HPLC and reversed-phase HPLC for polypeptide purification is pointed out—complementary in the sense that their combined use can provide the optimal separation or purity assessment of a peptide.

Hydrophobic interaction HPLC is the subject of Chapter 12, and Chapter 13 deals with high performance affinity chromatography (HPAC) or high performance liquid affinity chromatography (HPLAC) whichever one prefers to call it.

The next chapter on the purification of synthetic oligonucleotides provides a change from other chapters, which seem to concentrate almost exclusively on peptides and proteins. At first glance, one might consider a single chapter on oligonucleotides to represent an imbalance in the book, but on closer inspection one quickly realizes that it is a very extensive and detailed chapter (100 pages, 248 references). The emphasis of most chapters on the application of HPLC to polypeptide purification reflects the enormous effort which goes into the production of polypeptides which are antigenically or physiologically active. The final chapter deals with the chemical synthesis of peptides and the contribution of mass spectrometry to their analysis.

There is such a bewildering number of terms used in this book that a glossary of terms would not have been out of place and indeed it would have been welcomed. It does not help when alternative names for the same technique (gel filtration and size exclusion chromatography) are used in different chapters—the latter term is much preferred.

All chapters of the book are well-referenced and are illustrated with clear line drawings and photographs. The book is very broad in coverage, both of techniques and applications.

This is not a book for the newcomer to HPLC but I am certain that it will prove to be a valuable source-book to meet the needs of all workers in the field, whether they be analytical chemists, biochemists or chemical engineers.

A. K. DAVIES

Pharmaceutical Chemicals in Perspective: B. G. REUBEN and H. A. WITTCOFF, Wiley, Chichester, 1989. Pages xviii + 518. £59.00.

The aim of this book is to provide an overview of the pharmaceutical industry and its more important products. This is a somewhat ambitious goal to achieve within a mere five hundred pages.

The book is divided into three parts. The first part includes as an introductory chapter a brief review of the chronological introduction of drugs, coupling this to statistical data on changing patterns of mortality. This is followed by a wide-ranging

outline of the characteristics of the pharmaceutical industry. A third chapter deals with the distribution chain through physician to patient and highlights some emergent trends in drug prescribing. The section concludes with a chapter on pharmacological concepts.

The second part details the top one hundred prescribed drugs in the United States, classifying them into therapeutic categories and discussing aspects of their modes of action and production. The third part deals with other important therapeutic groups of drugs which do not fall under the aegis of Part II. This section is concluded by a chapter on problems that confront the drug industry and likely future developments.

For the serious reader much of the treatment is superficial, with even the limited statistical data overwhelming in the context. The laborious details of drug syntheses would only be appreciated by a chemist with a considerable depth of training in synthetic methodology. It is difficult therefore to adequately identify the audience to whom the book is addressed.

However within these limitations, the book contains a wealth of information, is readable, and amply illustrated with clear diagrams and tables. A minor irritation is the "wrap around" layout presentation of some figures. Particularly useful are the bibliography and notes (Appendix 3) which act as a "launch pad" for more extended study. A useful addition to most library shelves for undergraduate chemists with an interest in the pharmaceutical industry.

D. G. DURHAM

NMR, NQR, EPR, and Mössbauer Spectroscopy in Inorganic Chemistry: R. V. PARISH, Ellis Horwood, Chichester, 1990. Pages 223. £29.95.

Spectroscopy is one of those branches of science that can be made as easy or as difficult as we like. Some extremists look on it as a beautiful intellectual exercise in which quantum mechanics is really put to work, whilst others, equally extreme, regard it as a tool to be used by chemists, whether it is understood or not. Extremists always run into problems of one kind or another, so most chemists tend to find their own optimized spectroscopic level somewhere in between these extreme points of view. It is not true to say that this book belongs to either of the extreme spectroscopy camps, but it certainly lies closer to the latter than to the former.

In his preface the author explains, "... what this book is *not*. It is not a spectroscopic textbook, nor is it written for those with a need for detailed theory. Such books and reviews exist in abundance already. Rather, being written by a simple-minded inorganic chemist, it is intended to give an introduction to the *interpretation* of some of the types of spectra often met with in the inorganic laboratory."

Chapter 1 forms an introduction to features that are common to most of the four branches of spectroscopy with which the book is concerned, and Chapters 2, 3, 4 and 5 are concerned with nuclear magnetic resonance, nuclear quadrupole resonance, Mössbauer spectroscopy and electron paramagnetic resonance spectroscopy, respectively. The introduction, and the treatment of some of the more theoretical aspects of the other chapters, tend to be superficial, sometimes inaccurate, and occasionally quite wrong. The treatment is also somewhat out-dated, but the book does come into its own when the author applies each of the four branches of spectroscopy to inorganic chemistry. The inorganic applications, the bibliographies at the end of each chapter and the problems, with detailed answers, at the end of Chapters 2-5 are well-chosen and are particularly clearly presented.

Most of my inorganic friends are slick high-powered chemists, who are anything but simple-minded and are more than able to keep up with these four parts of spectroscopy. They will all learn quite a lot from this book. Its subject matter is changing fast and I look forward to a second, unblemished, up-dated edition. It cannot be far away.

A. L. PORTE

outline of the characteristics of the pharmaceutical industry. A third chapter deals with the distribution chain through physician to patient and highlights some emergent trends in drug prescribing. The section concludes with a chapter on pharmacological concepts.

The second part details the top one hundred prescribed drugs in the United States, classifying them into therapeutic categories and discussing aspects of their modes of action and production. The third part deals with other important therapeutic groups of drugs which do not fall under the aegis of Part II. This section is concluded by a chapter on problems that confront the drug industry and likely future developments.

For the serious reader much of the treatment is superficial, with even the limited statistical data overwhelming in the context. The laborious details of drug syntheses would only be appreciated by a chemist with a considerable depth of training in synthetic methodology. It is difficult therefore to adequately identify the audience to whom the book is addressed.

However within these limitations, the book contains a wealth of information, is readable, and amply illustrated with clear diagrams and tables. A minor irritation is the "wrap around" layout presentation of some figures. Particularly useful are the bibliography and notes (Appendix 3) which act as a "launch pad" for more extended study. A useful addition to most library shelves for undergraduate chemists with an interest in the pharmaceutical industry.

D. G. DURHAM

NMR, NQR, EPR, and Mössbauer Spectroscopy in Inorganic Chemistry: R. V. PARISH, Ellis Horwood, Chichester, 1990. Pages 223. £29.95.

Spectroscopy is one of those branches of science that can be made as easy or as difficult as we like. Some extremists look on it as a beautiful intellectual exercise in which quantum mechanics is really put to work, whilst others, equally extreme, regard it as a tool to be used by chemists, whether it is understood or not. Extremists always run into problems of one kind or another, so most chemists tend to find their own optimized spectroscopic level somewhere in between these extreme points of view. It is not true to say that this book belongs to either of the extreme spectroscopy camps, but it certainly lies closer to the latter than to the former.

In his preface the author explains, "... what this book is *not*. It is not a spectroscopic textbook, nor is it written for those with a need for detailed theory. Such books and reviews exist in abundance already. Rather, being written by a simple-minded inorganic chemist, it is intended to give an introduction to the *interpretation* of some of the types of spectra often met with in the inorganic laboratory."

Chapter 1 forms an introduction to features that are common to most of the four branches of spectroscopy with which the book is concerned, and Chapters 2, 3, 4 and 5 are concerned with nuclear magnetic resonance, nuclear quadrupole resonance, Mössbauer spectroscopy and electron paramagnetic resonance spectroscopy, respectively. The introduction, and the treatment of some of the more theoretical aspects of the other chapters, tend to be superficial, sometimes inaccurate, and occasionally quite wrong. The treatment is also somewhat out-dated, but the book does come into its own when the author applies each of the four branches of spectroscopy to inorganic chemistry. The inorganic applications, the bibliographies at the end of each chapter and the problems, with detailed answers, at the end of Chapters 2-5 are well-chosen and are particularly clearly presented.

Most of my inorganic friends are slick high-powered chemists, who are anything but simple-minded and are more than able to keep up with these four parts of spectroscopy. They will all learn quite a lot from this book. Its subject matter is changing fast and I look forward to a second, unblemished, up-dated edition. It cannot be far away.

A. L. PORTE

TALANTA MEDAL

PROFESSOR WILHELM SIMON

The Publisher and Editorial Board of *Talanta* take great pleasure in announcing that, with the approval of the Advisory Board, the Thirteenth Award of the Talanta Medal has been made to Professor Wilhelm Simon, of the Department of Chemistry, Eidgenössische Technische Hochschule, Zürich, in recognition of his outstanding contributions in the field of ion-selective electrodes, especially with regard to the use of neutral carriers.

The previous winners of the Talanta Medal are as follows:

1961	F. FEIGL	1974	B. V. L'VOV
1963	G. SCHWARZENBACH	1977	R. BELCHER
1965	I. P. ALIMARIN	1981	J. RŮŽIČKA
1967	E. STAHL	1983	T. FUJINAGA
1969	A. WALSH	1986	E. PUNGOR
1971	R. PŘIBIL	1988	H. A. LAITINEN

THE LOUIS GORDON MEMORIAL AWARD

The Louis Gordon Memorial Award for 1990 (for the paper judged to be the best written of those appearing in *Talanta* during the year) will be made to Mrs. Elsie M. Donaldson, of the Canada Centre for Mineral and Energy Technology, for her paper "Determination of antimony in ores and related materials by continuous hydride-generation atomic-absorption spectrometry after separation by xanthate extraction" (*Talanta*, 1990, 37, 955).

THE PHARMACIA PRIZE

The Pharmacia Prize for the paper published in *Talanta* and judged to be the best contributed from an industrial laboratory has been awarded to Dr. Jun'ichi Toei, of the Tosoh Corporation, Kanagawa, Japan, for his paper "Potential of the flow-gradient function in FIA with a multifunction pump delivery system" (*Talanta*, 1988, 36, 425).

SOLUTION INFRARED SPECTROELECTROCHEMISTRY: A REVIEW

KEVIN ASHLEY

Department of Chemistry, San Jose State University, San Jose, California 95192, U.S.A.

(Received 30 November 1990. Revised 20 February 1991. Accepted 13 March 1991)

Summary—Infrared (IR) spectroelectrochemical techniques have seen extensive use in studies of electrode surface processes. They have also been employed, albeit less frequently, to investigations of redox species dissolved in solution. The application of IR spectroscopy to electrochemical solution processes represents a special challenge, for absorption of IR radiation by the solvent is a significant interference to detection of vibrational modes of dissolved analytes. It is also difficult to maintain potentiostatic control of the system in specially designed thin-layer spectroelectrochemical cells. Solution IR spectroelectrochemical experiments are important for investigations of redox systems in which it is desired to spectroscopically monitor the structures of dissolved products, intermediates and reactants involved in electrode reactions. Such experiments have been conducted on biochemical, inorganic, organic, and other systems. In this paper some examples of applications of IR spectroelectrochemical studies of solution species in the above areas are presented, and experimental aspects are discussed.

In situ spectroscopic techniques for studying electrode processes were first introduced in the 1960's in an effort to provide a better means to elucidate electrode reaction mechanisms and kinetics. These first experiments employed UV-visible spectroscopy coupled with an electrochemical cell,¹ and were used to monitor solution concentrations of redox species dissolved in solution. By using a UV-visible probe, it became possible to follow the time- and potential-dependent spectra of reactants, intermediates, and products of electrode reactions. Species in the diffusion layer could be monitored spectroscopically, and therefore it was possible to elucidate electrode reaction mechanisms and kinetics; investigations of this kind were previously much more difficult without the advantage of an optical probe. A tremendous amount of activity in the area of UV-visible spectroelectrochemistry followed for the next several years,^{2,3} but the experimental emphasis later shifted to phenomena occurring at the electrode surface. Since UV-visible spectroelectrochemical methods are largely insensitive to surface species, other techniques were required for surface studies. This change in emphasis led to the development of surface infrared spectroelectrochemistry, as well as other surface-sensitive methods. Much less emphasis has been placed on infrared studies of solution species, but in the past five years or so a few examples of such investigations have appeared.

The past decade has seen numerous advances in the development of infrared (IR) spectroscopy as applied to electrochemical systems. Much of the progress in this field has been due to the development of the Fourier transform instrument, which was unavailable during the first UV-visible experiments in the mid-1960's. Most of the effort has focused on the characterization of electrode surfaces by IR techniques,^{4,5} since surface phenomena are supremely important in electrochemical systems. These surface infrared studies have the advantage of being conducted *in situ*, and have served to complement other *in situ* surface spectroscopic probes such as surface-enhanced Raman scattering (SERS),⁶ optical second-harmonic generation (SHG),⁷ and x-ray methods.⁸ These *in situ* techniques are seen as having an advantage over *ex situ* methods which require that the spectroscopy be performed in air, gas, or in ultra-high vacuum (*i.e.*, outside the electrochemical cell). The reason for this is that in an *ex situ* experiment the electrode environment might be different from its environment *in situ*. In addition to being an *in situ* technique, IR spectroelectrochemistry also has an advantage over other *in situ* spectroscopic techniques in that experiments can be performed on either smooth or rough electrodes, and a great deal of information concerning identities and orientation of species at electrode surfaces is obtainable. Thus IR spectroscopy, as applied to electrode sur-

faces, has emerged as a very powerful probe of electrochemical surface processes.

Applications of IR spectroscopy to electrochemical processes occurring in solution (*i.e.*, in the diffusion layer near the electrode surface) have been relatively few when compared to surface studies. The principal reason for this is that the strong absorption of IR radiation by the solvent can interfere with the absorption by the dissolved redox species. Studies of solution processes in electrochemical systems are extremely important in such fields as organic, inorganic, and biological chemistry. Other spectroscopic techniques to monitor solution electrochemical processes *in situ* have been limited to methods such as UV-visible spectroelectrochemistry (mentioned above),⁹ electron spin resonance (ESR),¹⁰ and Mossbauer spectroscopy.¹¹ IR spectroscopy offers an advantage over these and other spectroscopic methodologies in that much more detail regarding molecular structure of products, intermediates and reactants of electrode processes is attainable when IR radiation is employed as a spectroscopic probe. While ESR and Mossbauer techniques can give detailed structural information in many cases, it is generally difficult to conduct these types of experiments on electrochemical systems. UV-visible spectroelectrochemical methods are much more straightforward, but other spectroscopies (such as IR) are better suited for providing structural information regarding species involved in electrode-mediated reactions.

In this paper, some examples of applications of IR spectroelectrochemistry to studies of redox species dissolved in solution are presented. Also, considerations on the design of IR spectroelectrochemical cells for solution studies, as well as instrumental considerations, are presented. The systems chosen for discussion represent examples of solution IR spectroelectrochemical investigations in the areas of inorganic, organic and biological chemistry.

CELL DESIGN AND INSTRUMENTATION

Two principle IR spectroelectrochemical cell designs which have been employed for investigation of solution redox species in electrochemical systems are external reflectance and transmission cells. It is also possible to use internal reflectance, but this sampling technique is generally not feasible owing to the low electrical conductivities of available internal reflection elements. A special internal reflection IR spec-

troelectrochemical cell design has been demonstrated to be quite useful for surface studies,¹² but applications of this design to solution studies are not recommended due to the possibility of interference from surface adsorbed species. Prime considerations in the design of a useful cell for solution applications include high electrode conductivity and optimized throughput of the IR radiation through the solution chamber of the electrochemical cell.

External reflection cells

The external reflection IR spectroelectrochemical cell is amenable to investigations of solution redox species. This cell, which was first used about a decade ago,¹³ has seen a number of refinements and improvements.¹⁴⁻¹⁷ Figure 1 shows the design of a reflectance IR spectroelectrochemical cell.¹⁻⁴ An IR transparent window is mounted at one end of the cell; this window may be flat or bevelled (as shown) to minimize reflection losses.¹⁸ The working electrode, which is usually a flat metal disk polished to a mirror finish, is positioned close to the window. For surface IR applications the mirror electrode is pushed up against the window, and a thin solution layer several microns thick is trapped between the electrode surface and the back side of the window. However, for solution applications the electrode is pulled back so that a thicker "thin layer" of electrolyte solution, say 50 microns thick, exists between the metal surface and the IR window. Incident radiation passes through the window and the thin solution layer, strikes the electrode surface and is then reflected back out of the cell to be focussed on a detector. The external reflection geometry serves to minimize absorption of IR radiation

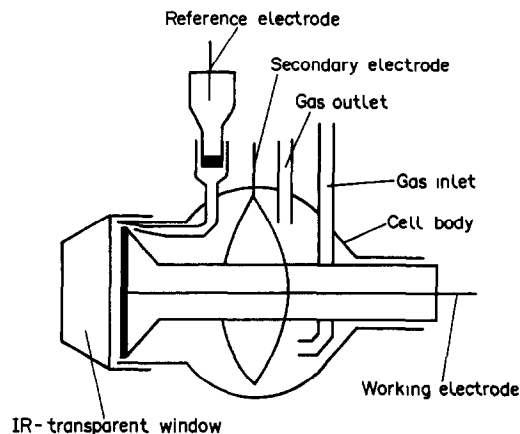


Fig. 1. Configuration of an external reflectance cell for IR spectroelectrochemistry. Reproduced from Ref. 4.

by the solvent, while maximizing the sampling efficiency of absorbing analyte species present within the diffusion layer near the electrode surface.

The IR window material chosen depends on the spectral region of interest and on the solvent. For mid-IR applications calcium fluoride, silicon, or zinc selenide windows are used most often, while polyethylene or Mylar window materials are used in the far-IR region.

The cell housing can be comprised of inert materials such as glass^{2,16,18,19}, Teflon^{17,20}, or Kel-F^{14,21}. It is important that the cell material be inert so that the solution does not become contaminated. The electrode is mounted onto the end of a metal rod which is generally sheathed in glass, Teflon, or Kel-F so that the connecting metal rod is insulated from solution. This rod is then inserted into the cell body so that the polished mirror electrode may be positioned as desired (Fig. 1). A Luggin capillary reference probe or microreference electrode is positioned near the edge ($\sim 1mM$) of the working (mirror) electrode. The secondary (counter) electrode is usually a platinum wire which is placed behind the working electrode in a configuration that minimizes the solution resistance. The geometry of the secondary electrode is circular (see Fig. 1); this gives a symmetric current distribution pattern to the working electrode. Inlets and outlets for de-gassing of the cell must also be provided.

Adaptations to the basic reflectance cell design described above have provided for control of temperature and maintenance of the cell within an evacuated sample chamber.²⁰ Another cell design enables the use of a carbon dioxide laser source.²² Flow cells have also been contrived so that one may control the flow of electrolyte through the thin layer,^{16,17} such cells have applications in both surface and solution studies.

Transmittance cells

Just as in the external reflectance cells described above, the design for a transmittance IR spectroelectrochemical cell is based on the requirement of a thin solution layer. Such cells are known as optically transparent thin-layer electrochemical (OTTLE) cells, and are based on a "sandwich" design in which an optically transparent electrode (OTE) is positioned between two IR-transparent windows.²³ Transmittance cells offer an advantage over external reflection cells in that the cell may be placed directly

within the sample chamber of most conventional IR spectrometers. External reflection cells usually require additional optics that allow for the infrared beam path to be directed onto the face of the working electrode, which is positioned outside the sample chamber or within a specially modified sample chamber. This has three disadvantages. First, throughput is decreased since the IR beam must be reflected off a minimum of at least two additional mirrors, and much light is lost due to reflection losses. Second, alignment of the IR beam is much more difficult if a reflection geometry rather than transmission cell is used. Third, there is added expense since additional optical components must be purchased.

Figures 2 and 3 show two recent designs for thin-layer transmittance cells for use in IR spectroelectrochemistry;^{24,25} these cells are similar in design to the transmittance cells originally used in UV-visible spectroelectrochemistry^{2,3} and in some of the first IR spectroelectrochemistry experiments.²³ Other similar designs for solution IR applications have also been reported²⁶⁻²⁹, some requiring the use of O-rings and spacers to sandwich the cell together. Both designs shown in Figs. 2 and 3 avoid the use of adhesives and O-rings, which can cause cell contamination and/or leakage. Besides these advantages, the cells are reusable and robust, and are relatively inexpensive to fabricate. In all cases it is essential to employ a three-electrode design, since it is crucial that solution resistance

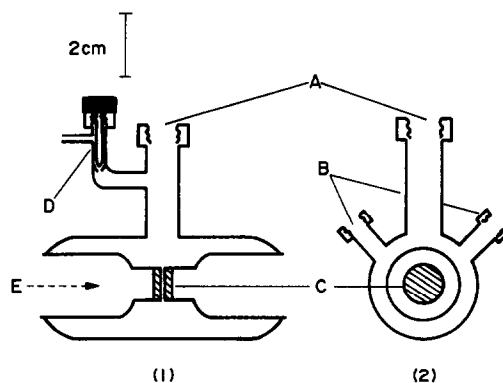


Fig. 2. (1) Side and (2) end views of a glass (Pyrex) thin-layer IR transmittance spectroelectrochemical cell with silicon windows. (A) Port for Pt gauze OTE; (B) ports for reference (saturated calomel) and secondary (Pt foil) electrodes; (C) Si windows; (D) Teflon stopcock assembly; (E) direction of incident light beam. Reference and secondary electrode ports are omitted from the side view, and the Teflon stopcock from the end view, for the sake of clarity. Reproduced with permission from the American Chemical Society from Ref. 24.

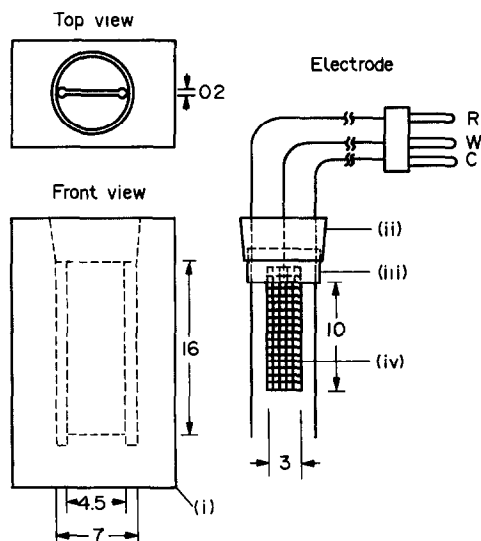


Fig. 3. Schematic illustration of a transmittance IR spectroelectrochemical cell, fabricated from potassium bromide, with a platinum optically transparent electrode. (i) KBr cell body; (ii) Teflon cell cap; (iii) Tefzel insulating film; (iv) Pt gauze working electrode. W: working electrode lead; C: counter electrode; R: Ag wire reference electrode. Reproduced with permission from the American Chemical Society from Ref. 25.

in the thin layer be minimized. The reported percent transmittance attainable with these IR OTTLE cells is as high as 50%,³⁰ representing a very high throughput. The superiority of newer transmission cells partially results from the fact that the measurements were conducted on more favorable systems than those studied early on. For example, organometallic species dissolved in methylene chloride³⁰ are more easily studied by IR than is ninhydrin in water²³ is, especially when an FTIR instrument is made available.

Instrumental considerations

For the most studies Fourier transform instruments are employed for solution IR spectroelectrochemistry owing to the multiplex and throughput advantages of FTIR.³¹ Usually fast scans are required since thin-layer electrochemistry is fraught with inherent instabilities. In many cases electrode reactions within a thin-layer cell can be subject to poisoning by the window material; this is especially a problem with ZnSe, which can foul electrolyte solutions rather quickly. Polarization of the electrode at high applied potentials for long periods can also lead to the formation of undesired impurities and, in some instances, films on the electrode surface. Electrolyte depletion within the thin layer may also be a problem if electrodes are held at high potentials for long periods,^{32,33}

although this is less of a concern in solution applications than in surface studies where the thin layer is much thinner. For these reasons it is desirable to obtain IR spectroelectrochemical spectra as quickly as possible. Signal averaging of numerous scans is virtually always necessary in IR spectroelectrochemical experiments.

Both absolute transmission spectra and difference spectra can be obtained by solution IR spectroelectrochemical techniques. Transmittance spectra may be obtained at desired applied potentials, and difference spectra may be plotted which show the ratio of absolute spectra taken at different potentials. Difference spectra are often used so that spectral interferences from species whose concentrations do not change with potential (e.g., solvent, electrolyte, atmosphere, etc.) are effectively cancelled. It is also possible to obtain time-dependent spectra, conduct spectrocoulometric titrations, and perform other experiments as well. In surface IR applications, usually potential-dependent difference spectra are required, although it is possible to obtain absolute spectra of surface species at a single potential by the technique of polarization modulation.² For solution IR applications no light polarization is required. In surface IR spectroscopy of electrodes¹ [at least for potential-dependent IR spectroscopy (PDIRS)³⁴], the light must be p-polarized. The lack of the necessity for a polarizer is a decided advantage, since polarizers are rather expensive and also serve to attenuate the infrared beam. Solution species can be distinguished from surface species by employing s-polarized radiation.¹⁻⁴ However, since in most cases the signal from surface species is much weaker than that from solution species, polarization of the incident radiation is not typically necessary for solution IR applications. It should also be mentioned that in cases where semiconductor electrodes are employed, the field strengths of p- and s-polarized components near the surface are similar, so there is clearly no benefit in using polarized radiation in this situation to determine between surface and solution species.

APPLICATIONS

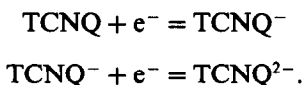
Solution IR spectroelectrochemistry has been used to study electrode reactions involving inorganic, organic, organometallic, and biological systems. Such investigations have also been done in conjunction with surface IR spectroelectrochemistry in efforts to elucidate the identities

of reactants, intermediates, and products of electrode reactions both on the electrode surface and within the diffusion layer. In this section a few examples of studies in which solution IR spectroelectrochemistry has been employed in the above areas are presented, and the utility of the technique is discussed.

Organic systems

The earliest applications of IR spectroelectrochemistry were in studies of the redox behavior of conjugated and aromatic organic molecules^{23,35,36}. Early solution studies employed IR-OTTLE cells,²³ but the electrochemical characteristics of the thin layer cell were poor and spectral quality was substandard due to a number of factors, not the least of which was the unavailability of FTIR instruments. More recent thinlayer cell designs demonstrate much better cell characteristics than were previously attainable. Thin-layer cells were originally subject to severe potential drop problems caused by high solution resistance, but newer thin-layer cells are designed to alleviate effects of solution resistance within the thin layer as much as possible. Furthermore the advent of FTIR instruments enabled spectra to be obtained much faster than was possible with dispersive IR spectrometers.

An OTTLE cell was employed to study the reduction of tetracyanoquinodimethane (TCNQ) to its radical anion and dianion in the aprotic solvent acetonitrile:²⁴



Both electron transfers are nearly reversible, and the radical anion and dianion are stable on the experimental timescale. Figure 4 shows the cyclic voltammetry of this system in the thin-layer transmittance cell illustrated in Fig. 2. The two cathodic waves are well separated and show rather large peak separations compared to the voltammetry that is obtainable in bulk solution³⁷. However, it is important to emphasize that the quality of the voltamperogram is excellent, considering that the thin-layer geometry results in increased solution resistance. The effects of solution resistance in this cell are minimized by careful placement of the working and auxiliary electrodes.

Figure 5 shows potential-difference IR spectra produced by stepping the Pt gauze OTE through the first and second reduction waves.

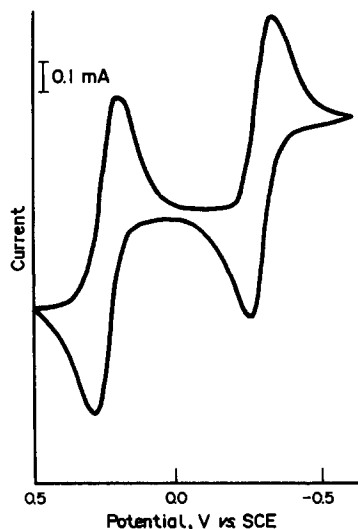


Fig. 4. Thin-layer cyclic voltamperogram of a solution of 5mM TCNQ in acetonitrile (0.1M tetraethylammonium perchlorate supporting electrolyte) obtained in the cell described in Fig. 2. Potentials are vs. SCE, and the sweep rate was 5 mV/sec. Reproduced with permission from the American Chemical Society from Ref. 24.

The upper spectra correspond to the first reduction wave (due to the formation of anion radical from neutral TCNQ), while the lower spectra correspond to the second reduction (dianion formation from the radical anion). Negative bands are due to the disappearance of species present at the base (reference) potential,

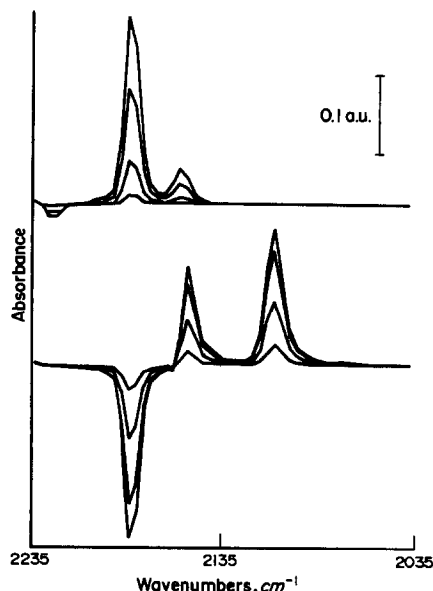


Fig. 5. Potential difference IR spectra obtained during reduction of TCNQ. Upper spectra (referenced to +0.5V): $E = 0.295, 0.255, 0.210,$ and 0.130 V vs. SCE. Lower spectra (referenced to -0.15 V): $E = -0.250, -0.315, -0.350, -0.400, -0.450$ V. Reproduced with permission from the American Chemical Society from Ref. 24.

while positive bands are due to species prevalent at the sample (pulsed) potential. The upper spectrum of Figure 5 shows the disappearance of a weak IR band due to neutral TCNQ, and the appearance of two strong bands due to TCNQ^- ; the spectral features are due to normal $\text{C}\equiv\text{N}$ stretching vibrations. The observation of significantly greater extinction coefficients for radical anions than for neutral reactant species has been made previously for aromatic and/or conjugated organic molecules such as anthracene and tetracyanoethylene (TCNE)^{38,39}. The lower spectra show the appearance of positive bands due to TCNQ^{2-} , concurrent with the disappearance of bands attributed to TCNQ^- . The quality of the different spectra are quite good, and are in agreement with previous studies⁴⁰. This work illustrates the benefits of the thin-layer IR spectroelectrochemical cell design shown in Fig. 2, which has also been employed in solution IR studies of redox reactions in molten salts⁴¹. This cell can therefore be used in severe solution environments. The novel application to molten salt electrochemical measurements is a demonstration of the applicability of solution infrared spectroelectrochemistry to a variety of diverse and previously unforeseen systems. Other applications of these techniques in materials science and engineering may also be forthcoming.

The external reflection technique has been used to study the ion pairing reactions of the dianions of TCNE and TCNQ mentioned above.⁴⁰ A polished mirror electrode was used, and the electrode surface was pulled back from the window to give a thin layer about 50 microns across. PDIRS experiments were then performed by pulsing between potentials at which different species involved in the reduction of TCNE or TCNQ were predominant. Spectra were collected at pulsed and reference potentials, and ratioed as described previously.

The IR bands due to TCNE^{2-} and TCNQ^{2-} ($\text{C}\equiv\text{N}$ stretching modes) were found to be dependent upon the supporting electrolyte. In acetonitrile the $\text{C}\equiv\text{N}$ stretching frequencies of the dianions were observed to shift to higher wavenumbers in the presence of alkali metal salts than in the presence of tetraalkylammonium salts. Figure 6 shows representative IR difference spectra (in the $\text{C}\equiv\text{N}$ stretching region) obtained during the electroreduction of TCNE to TCNE^- at a Pt mirror electrode. While there are differences in reflectance intensities for spectra obtained in lithium perchlorate

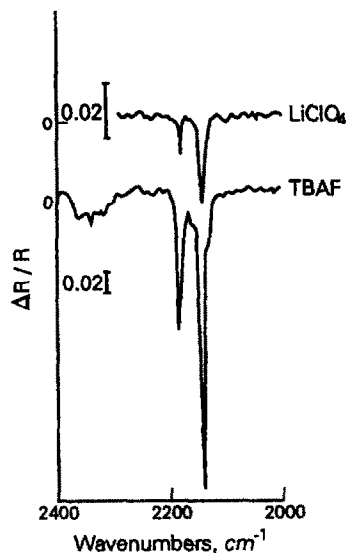


Fig. 6. Potential differential spectra in the C-N stretching region for the reduction of TCNE to TCNE^- at a Pt mirror electrode. Spectra were obtained with an external reflection cell similar to the cell described in Fig. 1. Solutions consisted of 5mM TCNE in CH_3CN with either 0.1M LiClO_4 (top spectrum) or 0.1M TBAF (bottom spectrum) as background electrolyte. The potential was modulated from $+0.5\text{ V}$ to -0.5 V vs. $\text{Ag}/0.01\text{M}$ Ag^+ reference. Reprinted with permission from Elsevier Science Publishers from Ref. 40.

vs. tetrabutylammonium tetrafluoroborate (TBAF) electrolyte, there are no differences in band frequencies for the two bands observed. Figure 7 shows IR difference spectra obtained during the reduction of neutral TCNE to its

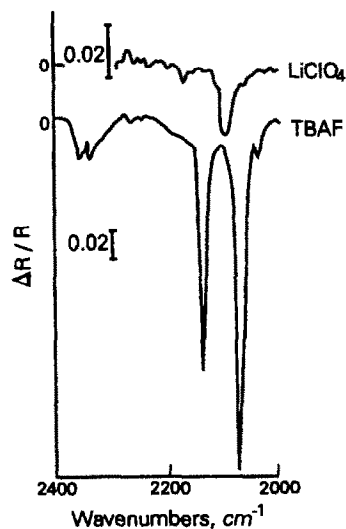


Fig. 7. PDIRS results (obtained in the C-N stretching region) for the reduction of TCNE to TCNE^- at Pt; solution conditions and reference electrode are the same as in Fig. 6. Top spectrum: 0.1M LiClO_4 as supporting electrolyte; potential modulated from $+0.5$ to -1.2 V . Bottom spectrum: 0.1M TBAF as supporting electrolyte; potential modulated from $+0.5$ to -0.2 V . Reproduced with permission from Elsevier Science Publishers from Ref. 40.

dianion. In this case a clear shift in the frequencies of the C≡N stretching modes is observed, suggesting environmental differences in the two electrolytes. Similar effects were seen in PDIRS results for the TCNQ system.

The observed frequency shifts seen during the formation of the TCNE²⁻ species were attributed to ion pairing between the dianion and the alkali metal cation. No shifts of this kind were observed, however, for the radical anion species. The observed frequency shifts (or absence thereof) correlated well with observed voltammetric behaviour, *i.e.*, if ion pairing was observed, the voltammetry indicated shifts in the value of the half-wave potential for the radical anion < = > dianion redox couple. This work was one of the first applications of solution IR spectroelectrochemistry to studies of ion pairing interactions between solute anions and cations dissolved in solution.

Other studies of organic systems have dealt with features from both the solution within the thin layer as well as the electrode surface.^{42,43} Reflectance cells are necessary for such investigations, since surface features can only be elucidated from a bulk electrode surface and not from an OTE. In one study it was possible to use real-time FTIR spectroscopy to monitor the temporal behavior of electrode reactions on a voltammetric timescale.⁴³

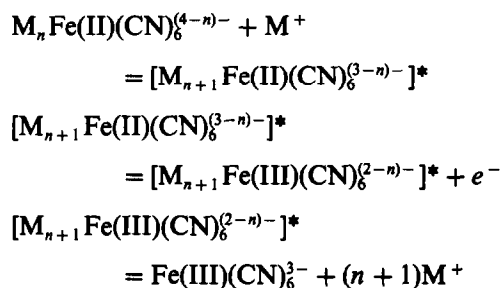
Inorganics and organometallics

A number of solution IR studies have focussed on inorganic and organometallic redox systems. Several investigations have focused on the ferro–ferricyanide redox couple.^{17,44,45} This redox couple is used routinely in electroanalysis as an example of a well-behaved, ‘totally reversible’ couple in most solvent and electrolyte systems. Surface IR spectroelectrochemical studies of this system, however, have shown that adsorbed intermediates exist on the electrode surface, suggesting that the electron transfer reaction is not a simple process involving the formation of an activated transition state complex⁴⁴. These results confirmed radiotracer measurements which indicated the presence of irreversibly adsorbed hexacyanoferrate and cyanide ions at platinum electrode surfaces⁴⁶. Solution IR spectroelectrochemical studies (employing an external reflectance cell) of the ferro/ferricyanide system in aqueous electrolytes showed that the C≡N stretching frequency of the ferrocyanide anion (formed as a result of reduction of the ferricyanide species) was depen-

Table 1. C≡N stretching infrared frequencies for various hexacyanoferrate complexes⁴⁵

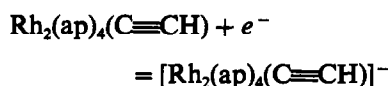
Complex	Wavenumbers, cm ⁻¹
Fe(III)(CN) ₆ ³⁻	2116
K _n Fe(II)(CN) ₆ ⁽⁴⁻ⁿ⁾⁻	2040
K _n HFe(II)(CN) ₆ ⁽³⁻ⁿ⁾⁻	2054
K _n H ₂ Fe(II)(CN) ₆ ⁽²⁻ⁿ⁾⁻	2067
K _n Li _m Fe(II)(CN) ₆ ^{(4-n-m)-}	2040
K _n Mg _m Fe(II)(CN) ₆ ^{(4-n-2m)-}	2038
K _n La _m Fe(II)(CN) ₆ ^{(4-n-3m)-}	2064

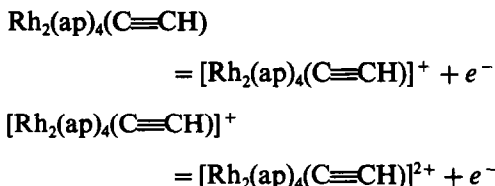
dent on the pH and on the identity of the supporting electrolyte cation. A mechanism was proposed for the overall redox process:



where M⁺ is an electrolyte cation, and the superscript * denotes an activated complex. Table 1 lists the various solution complexes that were detected in the IR spectroelectrochemical study, along with their observed C≡N stretching frequencies. This study shows how solution IR spectroelectrochemistry is useful for detecting dissolved redox species in the diffusion layer which are not otherwise detectable.

Other studies have been concerned with monitoring the redox chemistry of various rhodium organometallic complexes by solution IR spectroscopy.^{25,28} Transmittance spectroelectrochemical cells were used for this work. In one study²⁵ the cell shown in Fig. 3 was employed. The cyclic voltammetry of the ferro–ferricene redox couple was first studied in this cell. At slow sweep rates the peak separation between cathodic and anodic peaks was extremely narrow, indicating a small solution resistance across the thin layer. Subsequently, redox systems of interest were investigated in the cell. A case in particular is that of Rh₂(ap)₄(C≡CH) in CH₂Cl₂ system, where ap = 2-anilinopyridinate. The neutral compound can either be oxidized or reduced reversibly through one-electron transfers, and the product of the first oxidation can in turn be oxidized to a dication:⁴⁷





The cation and anion are stable on the experimental timescale, while the dication is unstable and rapidly forms decomposition products.

PDIRS data were obtained for the first oxidation and reduction waves of the neutral rhodium species in CH_2Cl_2 containing 0.1M tetrabutylammonium perchlorate (TBAP) (Fig. 8). The band at 1954 cm^{-1} is due to the $\text{C}\equiv\text{C}$ stretching mode of the neutral compound, as indicated by the transmission IR spectrum obtained at 0.0V *vs.* Ag/Ag⁺ [Figure 8(a)]. Difference spectra taken during reduction and oxidation [Figures 8(b) and (c), respectively] indicate a $\text{C}\equiv\text{C}$ band shift to 1922 cm^{-1} for the

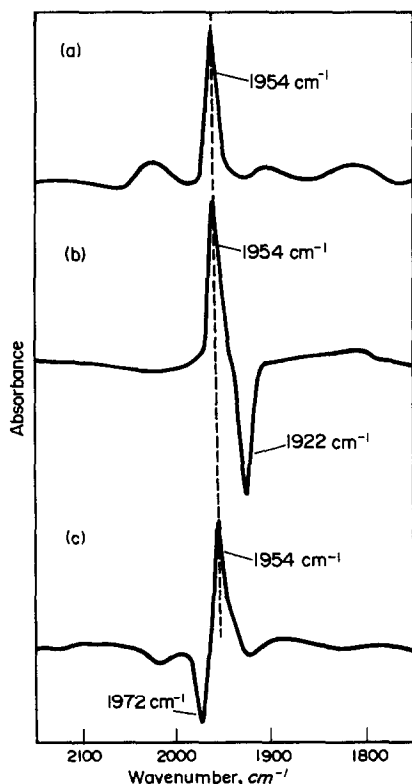


Fig. 8. FTIR spectra of $[\text{Rh}_2(\text{ap})_4(\text{C}\equiv\text{CH})]^x$ (where $x = +1, 0,$ or -1) complexes in 0.1M TBAP/ CH_2Cl_2 . (a) Initial spectrum of the neutral complex; applied potential = 0.0 V *vs.* Ag/Ag⁺. (b) Difference IR spectrum of neutral and singly reduced species; applied (sample) potential = -0.8 V, reference voltage = 0.0 V. (c) Difference IR spectrum of neutral and single oxidized species; applied potential = $+0.7$ V, reference potential = 0.0 V. Reproduced with permission from the American Chemical Society from Ref. 25.

anion and a shift to 1972 cm^{-1} for the cation. While not stated in the original study,²⁵ the shift to lower wavenumber (of the anion) is probably due to higher occupancy of antibonding π^* orbitals of the $\text{C}\equiv\text{C}$ moiety, which causes an overall decrease in bond order and a corresponding decrease in frequency. For the cation, a shift to higher frequency (with respect to neutral species) is attributable to decreased σ -donation to the Rh metal center, which results in an increase in bond order of the $\text{C}\equiv\text{C}$ bond. This work demonstrated the utility of an inexpensive, easily fabricated, and reusable OTTLE cell for solution IR applications. It was determined, however, that use of a thin-layer transmittance cell is not reliable for quantitative purposes in spectral regions where solvent and/or electrolyte absorbance is strong.

Another study concerned the IR spectroelectrochemistry of the Creutz-Taube ion, $[\text{Ru}(\text{NH}_3)_5]_2\text{pyrazine}]^{5+}$, in aqueous solution.⁴⁸ Near- and mid-IR spectroelectrochemical studies of this ion revealed a low frequency electronic transition, which had been postulated previously based on results from other spectroscopic studies. It was shown that each ruthenium center of the Creutz-Taube ion bears a charge of $+2.5$, indicating that on the vibrational timescale the odd electron is fully delocalized between the two metal centers. This work represents the first application of spectroelectrochemical techniques to the study of low energy electronic transitions of mixed-valent compounds.

Several other investigations have been reported^{20,26,27,49} concerning the redox chemistry of organometallic compounds. Other work has focussed on potential-dependent dynamic processes within the thin layer.⁵⁰ It is clear that from the evidence of these few successes, solution IR spectroelectrochemical methods ought to be applicable to studies of many organometallic and inorganic redox systems.

Biological systems and 'model' biosystems

A few IR spectroelectrochemical studies have been concerned with systems of biological interest. In one investigation, an OTTLE cell was used to characterize the electro-oxidation of a series of selected metalloporphyrins.³⁰ Metalloporphyrins form the central redox sites in a number of biomolecules, including heme proteins, chlorophyll, and the cytochromes, to name a few. Analysis of the potential-dependent IR difference spectra of certain metallopor-

phyrins allowed the site of electrooxidation on the metalloporphyrin molecule to be deduced.³⁰ Furthermore, it was possible to determine the oxidation state of the electrogenerated species and the fate of any axially coordinated NO or CO group. Additionally, it was found that other axial ligands oriented *trans* to the electrooxidized metalloporphyrin could be spectrally monitored. Such a degree of spectral characterization had not previously been obtained (for electro-oxidized compounds in solution) prior to the advent of solution IR spectroelectrochemistry.

The redox behavior of (TPP)Co(NO) (where TPP is the dianion of tetraphenylporphyrin) has been studied by a number of electrochemical and spectroscopic techniques, including *in situ* FTIR spectroelectrochemistry in an OTTE cell.⁵⁰ This metalloporphyrin can undergo two one-electron oxidations and three one-electron reductions in CH₂Cl₂ solvent,⁵¹ but the third oxidation is observed only at very high potential scan rates or at low temperature. The voltammetry of the (TPP)Co(NO) system, presented in Fig. 9, clearly shows the first two oxidations and reductions, which are reversible at a microelectrode. IR spectroelectrochemistry was employed to study the first two oxidations of

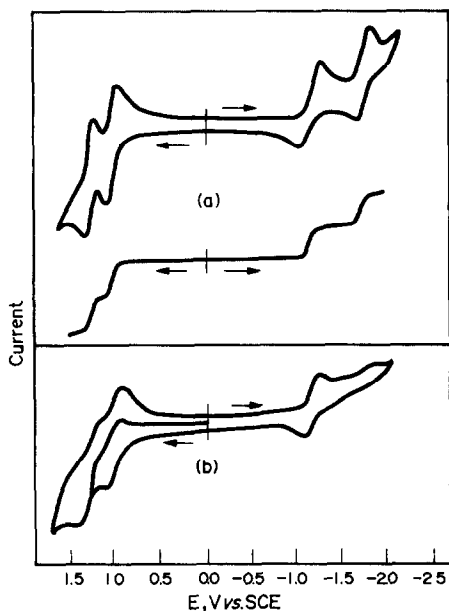


Fig. 9. (a) Top: cyclic voltamperogram (scan rate = 10 V/sec); and bottom: steady-state voltamperogram (scan rate = 50 mV/sec) of (TPP)Co(NO) at a 25-micron diameter Pt microelectrode in 0.1M TBAP/CH₂Cl₂. (b) Conventional cyclic voltamperogram (scan rate = 100 mV/sec) of (TPP)Co(NO) in 0.1M TBAP/CH₂Cl₂. Potentials are vs. the Ag/AgCl reference. Reproduced with permission from the American Chemical Society from Ref. 50.

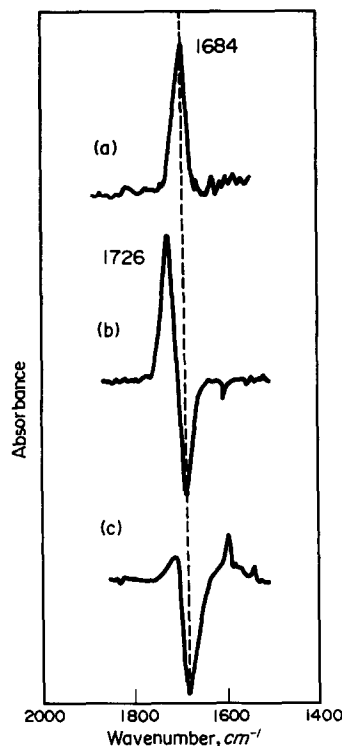


Fig. 10. Solution FTIR difference spectra of (TPP)Co(NO) species. (a) Spectrum of neutral species dissolved in 0.1M TBAP/CH₂Cl₂; reference spectrum is that due to blank electrolyte. (b) Spectrum obtained after controlled potential oxidation at +1.1 V; referenced potential = 0.0 V. (c) Spectrum obtained after controlled potential oxidation at +1.4 V. Reproduced with permission from the American Chemical Society from Ref. 50.

(TPP)Co(NO). Figure 10 shows the *in situ* IR difference spectra taken (in the N-O stretching region) as a result of pulsing to potentials positive enough to effect the first two oxidations. The spectra indicate that the NO moiety remains associated with the singly oxidized species, but dissociates from the dication at a long time scale. Evidence for this dissociation had not been determinable previously.

IR spectroelectrochemical studies of redox biosystems have appeared. A recent study was concerned with the redox chemistry of bacteriochlorophylls and bacteriopheophytins.⁵² IR spectroelectrochemical studies allowed detailed structural analyses of the redox states, and provided for implications concerning the binding of pigments with the reaction centers of photosynthetic bacteria.

CONCLUSION

It is apparent that while surface IR spectroscopy of electrode surfaces is presently a well-developed methodology, solution IR spec-

troelectrochemistry needs expansion. Comparatively few studies have been conducted in which solution IR spectroelectrochemistry was used as a tool. This is rather surprising, considering the wealth of detailed structural, dynamical, and other information that can be gleaned from IR studies of redox species which are dissolved in solution. Numerous advances in this area have been made recently owing to improvements in spectroelectrochemical cell design and instrumental sensitivity. In the next few years it is probable that many redox systems of interest will be investigated with solution IR spectroelectrochemical techniques, and much more elegant experiments than those described in this review are anticipated.

Acknowledgements—This work was supported by the donors of the Petroleum Research Fund (administered by the American Chemical Society) and Research Corporation. The author thanks Dr. Diane Parry for helpful discussions.

REFERENCES

1. T. Kuwana, R. K. Darlington and D. W. Leedy, *Anal. Chem.* 1964, **36**, 2023.
2. W. R. Heineman, F. M. Hawkridge, and H. N. Blount, in *Electroanalytical Chemistry*, Vol. 13; A. J. Bard (ed.), Dekker, New York, 1974, and references therein.
3. T. Kuwana and W. R. Heineman, *Acc. Chem. Res.* 1976, **9**, 241.
4. K. Ashley, *Spectroscopy*, 1990, **5**, No. 1, 22.
5. K. Ashley and B. S. Pons, *Chem. Rev.*, 1988, **88**, 673 and references therein.
6. R. K. Chang and T. E. Furtak (eds.), *Surface Enhanced Raman Scattering*, Plenum Press, New York, 1982.
7. G. L. Richmond, J. M. Robinson, and V. L. Shannon, *Prog. Surf. Sci.*, 1988, **28**, 1.
8. O. R. Melroy, M. G. Samant, G. L. Borges, J. G. Gordon II, L. Blum, J. H. White, M. J. Albarelli, M. McMillan and H. D. Abruna, *Langmuir*, 1988, **4**, 728.
9. K. Ashley and B. S. Pons, *Trends Anal. Chem.*, 1986, **5**, 263.
10. R. G. Compton and A. M. Waller, in *Spectroelectrochemistry*; R. J. Gale (ed.), pp. 349–398. Plenum Press, New York, 1988.
11. D. A. Scherson, in *Spectroelectrochemistry*; R. J. Gale (ed.), pp. 399–446. Plenum Press, New York, 1988.
12. D. B. Parry, J. M. Harris and K. Ashley, *Langmuir*, 1990, **6**, 209.
13. A. Bewick, K. Kunimatsu and B. S. Pons, *Electrochim. Acta*, 1980, **25**, 465.
14. H. Seki, K. Kunimatsu and W. G. Golden, *Appl. Spectrosc.*, 1985, **39**, 437.
15. D. S. Bethune, A. C. Luntz, J. K. Sass and D. K. Roe, *Surf. Sci.*, 1988, **197**, 44.
16. R. J. Nichols and A. Bewick, *Electrochim. Acta*, 1988, **33**, 1691.
17. J. O'M. Bockris and B. Yang, *J. Electroanal. Chem.*, 1988, **252**, 209.
18. J. K. Foley and B. S. Pons, *Anal. Chem.*, 1985, **57**, 945A.
19. K. Ashley, M. G. Samant, H. Seki and M. R. Philpott, *J. Electroanal. Chem.*, 1989, **270**, 349.
20. S. P. Best, R. J. H. Clark, R. C. S. McQueen and R. P. Cooney, *Rev. Sci. Instrum.*, 1987, **58**, 2071.
21. K. Ashley, M. Lazaga, M. G. Samant, H. Seki and M. R. Philpott, *Surf. Sci.*, 1989, **219**, L590.
22. D. K. Roe, J. K. Sass, D. S. Bethune and A. C. Luntz, *J. Electroanal. Chem.*, 1987, **216**, 293.
23. W. R. Heineman, J. N. Burnett and R. W. Murray, *Anal. Chem.*, 1968, **40**, 1974.
24. P. A. Flowers and G. Mamantov, *ibid.*, 1989, **61**, 190.
25. C.-L. Yao, F. J. Capdevielle, K. M. Kadish and J. L. Bear, *ibid.*, 1989, **61**, 2805.
26. D. L. Dubois, *Inorg. Chem.*, 1984 **23**, 2047.
27. W. A. Nevin and A. B. P. Lever, *Anal. Chem.*, 1988, **60**, 727.
28. J. P. Bullock, D. C. Boyd and K. R. Mann, *Inorg. Chem.*, 1987 **26**, 3086.
29. R. S. K. A. Gamage, S. Umapathy and A. J. McQuillan, *J. Electroanal. Chem.*, 1990, **284**, 229.
30. K. M. Kadish, X. H. Mu and X. Q. Lin, *Electroanalysis*, 1989, **1**, 35.
31. S. Pons, *J. Electroanal. Chem.*, 1983, **150**, 495.
32. S. Pons, T. Davidson and A. Bewick, *ibid.*, 1984, **160**, 63.
33. I. Roušar and N. A. Anastasijević, *Electrochim. Acta*, 1988, **33**, 1157.
34. D. S. Corrigan and M. J. Weaver, *J. Phys. Chem.*, 1986, **90**, 5300.
35. B. S. Pons, J. S. Mattson, L. O. Winstrom, and H. B. Mark, Jr., *Anal. Chem.*, 1967, **39**, 685.
36. A. Reed and E. Yeager, *J. Electrochem. Soc.*, 1966, **113**, 1044, (last contribution to discussion).
37. D. L. Jeanmaire and R. P. Van Duyne, *J. Am. Chem. Soc.*, 1976, **98**, 4209.
38. J. J. Hinkel and J. P. Devlin, *J. Chem. Phys.*, 1973, **58**, 4750.
39. B. S. Pons, T. Davidson and A. Bewick, *J. Am. Chem. Soc.*, 1983, **105**, 1802.
40. S. B. Khoo, J. F. Foley, C. Korzeniewski, B. S. Pons and C. Marcott, *J. Electroanal. Chem.*, 1987, **233**, 223.
41. P. A. Flowers and G. Mamantov, *J. Electrochem. Soc.*, 1989, **136**, 2944.
42. C. Korzeniewski and B. S. Pons, *Langmuir*, 1986, **2**, 468.
43. L.-W. H. Leung and M. J. Weaver, *J. Phys. Chem.*, 1988, **92**, 4019.
44. S. Pons, M. Datta, J. F. McAleer, and A. S. Hinman, *J. Electroanal. Chem.*, 1984, **160**, 369.
45. D. J. Blackwood and B. S. Pons, *ibid.*, 1988, **244**, 301.
46. A. Wieckowski and M. Szklarczyk, *ibid.*, 1982, **142**, 157.
47. J. L. Bear, C.-L. Yao, L. M. Liu, F. J. Capdevielle, J. D. Korp, T. A. Albright, S.-K. Kang and K. M. Kadish, *Inorg. Chem.*, 1989, **28**, 1254.
48. S. P. Best, R. J. H. Clark, R. C. S. McQueen and S. Joss, *J. Am. Chem. Soc.*, 1989, **111**, 548.
49. D. L. DuBois and J. A. Turner, *ibid.*, 1982, **104**, 4989.
50. K. M. Kadish, X. H. Mu and X. Q. Lin, *Inorg. Chem.*, 1988, **27**, 1489.
51. S. Kelly, D. Lançon and K. M. Kadish, *ibid.*, 1984, **23**, 1451.
52. W. G. Mäntele, A. M. Wollenweber, E. Nabedryk and J. Breton, *Proc. Nat. Acad. Sci. USA*, 1988, **85**, 8468.

SPECTROPHOTOMETRIC DETERMINATION OF TETRACYCLINE AND OXYTETRACYCLINE IN PHARMACEUTICAL PREPARATIONS

KAMLA M. EMARA, HASSAN F. ASKAL and GAMAL A. SALEH

Department of Pharmaceutical Chemistry, Faculty of Pharmacy, University of Assiut, Assiut, Egypt

(Received 24 October 1990. Revised 12 May 1991. Accepted 27 May 1991)

Summary—A simple, rapid and sensitive spectrophotometric procedure for the assay of tetracycline hydrochloride and oxytetracycline hydrochloride has been developed. 2,2-Diphenyl-1-picrylhydrazyl (DPH), an intensely violet-coloured stable free radical, is changed in colour on reaction with the antibiotics investigated. The decrease in the intensity of the violet colour is used to measure the concentration of the drug. All measurements are made at 520 nm on methanolic solutions of the drug and reagent, buffered at pH 6. Beer's law is obeyed in the concentration ranges 2.5–15 and 2.5–20 $\mu\text{g/ml}$ for tetracycline and oxytetracycline respectively. The proposed method has been successfully applied to analysis of the bulk drugs and their pharmaceutical formulations.

The tetracyclines are broad-spectrum antibiotics that are effective against nearly all gram-positive and gram-negative organisms. However, tetracycline and oxytetracycline are unstable under certain conditions, yielding structurally related decomposition products which have no significant antibacterial activity,¹ and determination of the active drugs in the presence of their decomposition products is therefore of importance.

Various titrimetric,² colorimetric,^{3–10} spectrophotometric,^{11,12} spectrofluorimetric,^{13,14} polarographic,¹⁵ complexometric,^{16,17} voltammetric,¹⁸ radioimmunoassay,¹⁹ TLC²⁰ and HPLC²¹ methods have been reported. The official B.P.,²² and U.S.P.²³ methods are biological assays.

In this work, a simple, rapid and sensitive spectrophotometric method is adopted for the determination of tetracycline and oxytetracycline, in the pure forms and in pharmaceutical preparations, with 2,2-diphenyl-1-picrylhydrazyl (DHP).

EXPERIMENTAL

Reagents

Pharmaceutical grade tetracycline hydrochloride (TC) and oxytetracycline hydrochloride (OTC) (Cid, Cairo, Egypt) were used as working standards.

DPH (Sigma) was used as received. A $1 \times 10^{-3}M$ methanolic solution was used except in the solvent study, where a solution of the

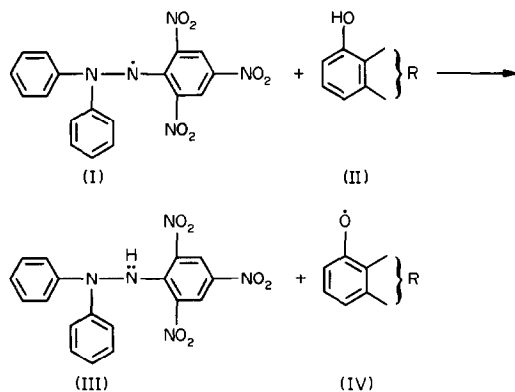
reagent was prepared in the solvent in question. The solution is stable for one week when kept at 4° and protected from sunlight.

A 0.1M acetate buffer was prepared and adjusted to pH 6. A 0.2M calcium chloride solution and a 0.5M 5,5-diethylbarbituric acid solution were prepared, both in distilled water.

All solvents used were of spectroscopic grade (Merck) and analytical grade reagents (or equivalent) were used whenever possible.

Calibration procedure

Weigh 50 mg of TC or OTC into a separating funnel and dissolve the drug in 30 ml of water. Add 2.0 ml of 0.2M calcium chloride and 2.0 ml of 0.5M 5,5-diethylbarbituric acid, and extract the undecomposed drug (as its complex with calcium and the barbituric acid)²⁴ with three 10-ml portions of ethyl acetate. Filter the organic phase through anhydrous sodium sulphate, evaporate the ethyl acetate under reduced pressure, dissolve the residue in methanol and dilute the solution to volume in a 50-ml standard flask. Dilute this solution stepwise with methanol to obtain drug concentrations in the ranges 25–150 $\mu\text{g/ml}$ for tetracycline hydrochloride and 25–200 $\mu\text{g/ml}$ for oxytetracycline hydrochloride. For each solution accurately transfer 1.0 ml into a 10-ml standard flask, add 2 ml of the buffer solution followed by 2 ml of DPH solution, and mix well. Heat the mixture in a water-bath at $60 \pm 5^\circ$ for 12 min. Cool and complete to volume with methanol. Measure the



R = OTC, TC molecule residue

Scheme 1.

absorbance of the test solution and of a reagent blank against methanol at 520 nm. Plot the difference in absorbance (ΔA) against drug concentration to obtain the calibration graph.

Assay of tablets

Weigh and finely powder 20 tablets. Extract an accurately weighed portion of the powder, equivalent to about 50 mg of the drug, with three 10-ml portions of methanol and filter. Transfer the filtrate and washings to a separating funnel and proceed as above, beginning with the addition of 2.0 ml of 0.2M calcium chloride. Use an aliquot containing $\sim 100 \mu\text{g}$ of the drug.

Assay of capsules

Weigh an amount of the mixed contents of 20 capsules that will be equivalent to about 50 mg of the antibiotic drug, extract with two 15-ml portions of methanol, and extract the active drug with calcium *etc.*, as for assay of tablets.

RESULTS AND DISCUSSION

Diphenylpicrylhydrazyl (I) is used for the determination of phenols.²⁵ It is employed here to abstract a hydrogen atom from a phenol group on the tetracycline molecule (II), resulting in the formation of yellow diphenylpicrylhy-

drazine (III) and a phenoxy radical (IV) as shown in Scheme 1.

The decrease in the violet colour of the DPH is proportional to the amount of tetracycline that has reacted.

Optimization of variables

At room temperature, the reaction proceeds very slowly. When mixtures of the drug with DPH and buffer solutions were heated in a water-bath at 60°, the optimum reaction time was found to be 12 min for both tetracycline and oxytetracycline hydrochlorides (Fig. 1). Higher temperatures result in a decrease in ΔA , which may be due to decomposition of DPH and/or the drugs studied.

The most suitable range of pH for the reaction was found to be 5.5–6.5. A 0.1M acetate buffer (pH 6) was used throughout all further experiments. Highly acidic and highly alkaline media led to destruction of the reagent.

Different solvents (methanol, ethanol, 1-butanol, 1-propanol, 2-propanol and mixtures of these with water) were investigated. Methanol was found to be the best solvent and was used for dissolving both the drugs and the reagent.

Interferences. The commonly used tablet excipients, such as starch, talc and magnesium stearate, were found not to interfere with the proposed method.

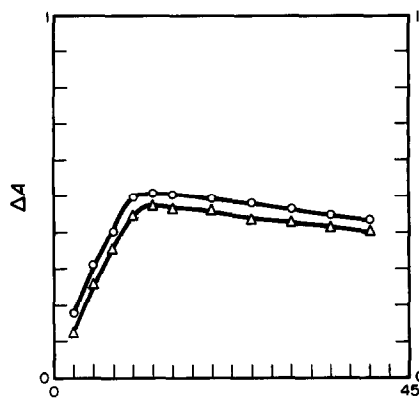


Fig. 1.

Table 1. Spectral characteristics of the products from the reaction between DPH and the drugs studied

Compound	ϵ_{max} , $10^4 \text{ l. mole}^{-1}, \text{ cm}^{-1}$	Linear range, $\mu\text{g/ml}$	Quantitative parameters*		
			Intercept	Slope	Correlation coefficient
Tetracycline hydrochloride	1.92	2.5–15	0.0094	0.0458	0.9993
Oxytetracycline hydrochloride	1.44	2.5–20	0.0233	0.0466	0.9976

*From five determinations.

Table 2. Determination of tetracyclines by DPH and reported methods

Sample	DPH method		Reported method ²⁶		<i>t</i> ‡	<i>F</i> ‡
	Recovery,* %	SD, %	Recovery %	SD, %		
Micycline capsules	98.5	1.3	99.8	1.1	0.72	1.40
Hostacycline tablets	100.3	1.0	99.2	0.9	0.69	1.14
Oxytetracid capsules	99.9	1.6	98.6	1.1	1.55	2.15
Tetracid capsules	100.7	1.3	99.5	1.6	1.53	1.73

*Average of 5 determinations.

†Tabulated *t* for 4 degrees of freedom at *P* 0.05 is 2.776.

‡Tabulated *F* for (4,4) degrees of freedom at *P* 0.05 is 6.39.

Interference by the structurally related decomposition products, as reported, could be eliminated by the use of calcium chloride and 5,5-diethylbarbituric acid, which form a complex with the undecomposed biologically active antibiotics, the complex being extractable with ethyl acetate.²⁴ The decomposition products do not form such complexes.

In examination by thin-layer chromatography, the extracted antibiotics TC or OTC gave single spots corresponding to the undecomposed drugs, whereas several spots were obtained with the original aqueous solutions. These findings are in agreement with those reported by Kohn.²⁴ In addition, the reaction mixture in the proposed analytical method is buffered at pH 6, at which, as reported,¹ there is minimal decomposition of TC and OTC.

Quantification

A linear correlation was found between ΔA at 520 nm and concentration for each drug in the range given in Table 1. The slope of the linear Beer's plots can also be used for calculation of the concentration of the antibiotics.

The precision (coefficient of variation) of ten replicate determinations at the 10- μ g/ml level was 1.9% for tetracycline and 1.5% for oxytetracycline (both as the hydrochlorides).

Application to bulk drugs and dosage form

Table 2 shows the results obtained for determination of the antibiotics in the pure form and in some of their dosage forms by means of the proposed and reported methods. The average recoveries obtained by the proposed method ranged between 98.5 and 100.7% and the relative standard deviations were both 1.3%, indicating good accuracy and precision. In addition, the proposed method, when accompanied by the extraction method, enables the analyst to determine the undecomposed antibiotics in pharmaceutical formulations.

REFERENCES

1. A. Regosz, *Pharmazie*, 1977, **32**, 681.
2. F. Yokoyama and L. G. Chatten, *J. Am. Pharm. Assoc., Sci. Ed.*, 1958, **47**, 548.
3. U. Saha, *J. Assoc. Off. Anal. Chem.*, 1987, **70**, 686.
4. Y. K. Agrawal and D. R. Patel, *Indian J. Pharm. Sci.*, 1986, **48**, 92.
5. M. S. Mahrous and M. M. Abdel-Khalek, *Talanta*, 1984, **31**, 289.
6. M. El-Sadek, M. Ayad and S. Mostaffa, *Anal. Lett.*, 1987, **20**, 1885.
7. M. M. Abdel-Khalek and M. S. Mahrous, *Talanta*, 1983, **30**, 792.
8. T. E. Divakar, M. K. Tummuru and C. S. P. Sastry, *Indian Drugs*, 1984, **22**, 28.
9. D. Veselinovic and M. Jelikic-Stankov, *Pharmazie*, 1987, **42**, 199.
10. M. Ayad, M. El-Sadek and S. Mostaffa, *Anal. Lett.*, 1986, **19**, 2169.
11. A.-A. M. Wahbi, M. H. Barary, H. Mahgoub and M. A.-H. Elsayed, *J. Assoc. Off. Anal. Chem.*, 1985, **68**, 1045.
12. M. A.-H. Elsayed, M. H. Barary and H. Mahgoub, *Anal. Lett.*, 1985, **18**, 1357.
13. J. Winkelman and J. Grossman, *Anal. Chem.*, 1967, **39**, 1007.
14. M. A.-H. Elsayed, M. H. Barary and H. Mahgoub, *Talanta*, 1985, **32**, 1153.
15. S. Sabharwal, K. Kishore and P. N. Moorthy, *J. Pharm. Sci.*, 1988, **77**, 78.
16. S. M. Sultan, I. Z. Alzamil and N. A. Alarfaj, *Talanta*, 1988, **35**, 375.
17. S. S. M. Hassan, M. M. Amer and A. S. Ahmed, *Mikrochim. Acta*, 1984 **III**, 165.
18. Yu. N. Kozlov and J. Koryta, *Anal. Lett.*, 1983, **16**, 255.
19. B. A. Faraj and F. M. Ali, *J. Pharmacol. Exp. Ther.*, 1981, **217**, 10.
20. H. Oka, K. Uno, K. Harada and M. Suzuki, *J. Chromatog.*, 1984, **284**, 227.
21. N. H. Khan, E. Roets, J. Hoogmartens and H. Vanderhaeghe, *ibid.*, 1987, **405**, 229.
22. *British Pharmacopoeia*, Her Majesty's Stationery Office, London, 1989.
23. *United States Pharmacopoeia*, XXIst Revision, *National Formulary*, XVIth Ed., United States Pharmacopoeial Convention, Rockville, 1985.
24. K. W. Kohn, *Anal. Chem.*, 1961, **33**, 862.
25. G. J. Papariello and M. A. M. Janish, *ibid.*, 1966, **38**, 211.
26. H. W. Dibbern, *UV and IR Spectra of Some Important Drugs*, Editio Contor, Aulendorf, 1979.

SUBSTITUTION COMPLEXOMETRIC DETERMINATION OF CADMIUM IN THE PRESENCE OF ZINC IN HOMOGENEOUS WATER-ORGANIC SOLVENT MEDIUM

ASSEN KAROLEV

Institute of Ferrous Metallurgy, Sofia 1870, Bulgaria

(Received 31 July 1989. Revised 16 May 1991. Accepted 29 May 1991)

Summary—A method for substitution complexometric determination of cadmium is based on the decomposition of the Cd-EDTA complex by the combined action of ethylxanthate and zinc. The reaction is performed in a slightly acid homogeneous water-organic solvent medium in which the cadmium ethylxanthate complex is stable and soluble.

In two earlier papers^{1,2} we have described the theoretical basis of some analytical procedures generalized by the equation



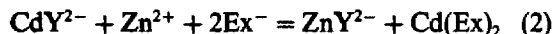
where MY is the complexonate of the metal (M) to be determined, N is the ion used for titrating the complexone (Y) released, and A (or L) is an auxiliary reagent used to form a slightly soluble compound (MA_i) or a soluble complex (ML_i).

The methods are applied in two steps.

1. Determination (direct or by back-titration) of the sum of the elements reacting with the complexone under the given conditions.

2. Selective displacement of the metal to be determined, by formation of a sparingly soluble compound or another complex of M. The Y released is titrated with N. The earliest example of this type of reaction was reported by Pfišil and Veselý.³

In an earlier paper we reported⁴ a complexometric method for determination of cadmium in the presence of zinc, in aqueous solution, by means of the reaction



where CdY²⁻ and ZnY²⁻ are the EDTA complexes of the two metals, Ex⁻ is the ethylxanthate ion and Cd(Ex)₂ is cadmium ethylxanthate.

The sum of cadmium and zinc is first determined by addition of excess of EDTA and back-titration with zinc in acetate-buffered medium at pH 5.1-5.7 with Xylenol Orange as indicator or at pH 5.7-6.2 with Methylthymol

Blue as indicator. Back-titration is preferred to direct titration with Methylthymol Blue as indicator, as the end-point is sharper. Addition of ethylxanthate then produces a precipitate of cadmium ethylxanthate during further titration with zinc. The quantity of zinc required to reach the second end-point is equivalent to the cadmium. By similar procedures Pb, Cu(II), Hg(II) and Bi can be determined.

This cadmium determination is based on the considerable difference between the solubility products of cadmium and zinc ethylxanthates (2.6×10^{-14} and 4.9×10^{-9} respectively⁵).

The equilibrium constant for the reaction in equation (2) is

$$K_{eq} = \frac{[ZnY]}{[CdY][Zn][Ex]^2} \quad (3)$$

Since the activity of a precipitate is conventionally taken as unity, multiplication of equation (3), top and bottom, by [Y][Cd] and substitution of the stability constants for the EDTA complexes and the solubility product of the precipitate will give

$$K_{eq} = \beta_{ZnY} / \beta_{CdY} K_{sp}[Cd(Ex)_2] \quad (4)$$

Because the reaction is done in 0.5M acetate buffer at pH 5, the side-reactions of zinc, cadmium and EDTA must be taken into account, and the conditional concentrations and constants⁶ must be used:

$$K'_{eq} = \beta'_{ZnY} / \beta'_{CdY} K'_{sp}[Cd(Ex)_2] \quad (5)$$

Under the conditions used, the values are $\beta'_{ZnY} = \beta_{ZnY} / \alpha_{Y(H)} \alpha_{Zn(Ac)}$, $\beta'_{CdY} = \beta_{CdY} / \alpha_{Y(H)} \alpha_{Cd(Ac)}$

and $K'_{sp} = K_{sp} \alpha_{Cd(Ac)} \alpha_{Ex(H)}^2$, and substitution into (5) gives

$$K'_{eq} = \beta_{ZnY} / \beta_{CdY} \alpha_{Zn(Ac)} K_{sp} \alpha_{Ex(H)}^2 \quad (6)$$

For 99.9% conversion of CdY into Cd(Ex)₂ and 99.9% conversion of the liberated Y into ZnY, the value of K'_{eq} must be not less than $K'_{99.9}$, given by

$$K'_{99.9} = \frac{[ZnY]}{[CdY][Zn'][Ex']^2} \\ = \frac{[ZnY]}{0.001 C_{Cd} \times 0.001 (C_{Zn} + C_{Cd}) [Ex']^2} \quad (7)$$

where $[Ex'] = (C_{Ex} - 1.998 C_{Cd})$, C_{Zn} , C_{Cd} , and C_{Ex} are the initial concentrations of zinc, cadmium and ethylxanthate respectively. Note that $[ZnY]$ must be the sum of the ZnY formed in the first titration and that formed in the second.

Under the conditions given in the procedure,

$$\alpha_{Zn(Ac)} = 1 + \beta_1 [Ac'] / \alpha_{Ac(H)} \\ + \beta_2 [Ac']^2 / \alpha_{Ac(H)}^2 \\ = 1 + 10^{1.3} \times 0.5 / 1.45 \\ + 10^2 \times 0.25 / 1.45^2 \approx 23$$

$$\alpha_{Ex(H)} = 1 + [H^+] / K_{a(HEX)} \\ = 1 + 10^{-5} / 10^{-3.5} \approx 1$$

Since $K_{sp[Cd(Ex)_2]} = 2.6 \times 10^{-14}$, $K'_{eq} = 1.7 \times 10^{12}$. For $C_{Zn} = C_{Cd} = 0.01M$, and $C_{Ex} = 0.1M$, $K'_{99.9} = 0.02/2 \times 10^{-10} \times 0.08^2 \approx 1.6 \times 10^{10} < K'_{eq}$

It is known that metal xanthate complexes are soluble in certain organic solvents⁷⁻¹¹ and the stability constants of some of them have been determined in aqueous methanol media.¹² It therefore seemed logical to extend the approach indicated by equation (2) by using a medium in which the cadmium ethylxanthate would be soluble.

The experiments showed that cadmium ethylxanthate is readily soluble in ethanol, dioxan, acetone and other organic solvents that are completely miscible with water. At $\leq 10^3M$ cadmium concentration, in the presence of $10^{-2}M$ ethylxanthate, no precipitate is formed in solutions containing not less than 25% v/v ethanol or 20% v/v acetone or dioxan.

EXPERIMENTAL

Apparatus

A Zeiss Specol 10 instrument for photometric titration with 30-ml cells (path-length 20 mm) was used.

Reagents

Analytical grade chemicals were used throughout, and 0.01M disodium EDTA, zinc acetate and cadmium acetate solutions and 10% ammonium acetate solution (adjusted to pH 5.5), were prepared. A 0.02% Xylenol Orange solution (XO) was used as indicator.

Procedure

To a slightly acid solution containing some mg of cadmium and zinc, add 4–5 ml of pH-5.5 ammonium acetate solution and a known and excessive volume of EDTA solution. Add a few drops of XO and back-titrate with zinc solution to a sharp rise in the absorbance measured at 570 nm. This gives the sum of the cadmium and zinc. Then add enough ethanol (or other organic solvent) to keep the cadmium ethylxanthate in solution, followed by ethylxanthate in 10–15-fold ratio to the expected cadmium content, and titrate again with zinc solution to a sharp and stable absorbance change. The zinc required is equivalent to the cadmium content.

RESULTS AND DISCUSSION

Figure 1 shows the back-titration curve and the substitution titration curve obtained with a water-ethanol medium.

The absorbance changes are very sharp at the equivalence points. This permits the very precise determination of the consumption of back-titrant and practically no construction is needed for interpretation of the titration curves (a fact of real importance in routine analysis).

The broken line on the first titration curve marks its shape in the absence of ethylxanthate. Addition of ethylxanthate, however, causes the absorbance to return to nearly its initial value, which is then maintained until just before the equivalence point in the back-titration (in practice, owing to the kinetics of the exchange reaction the absorbance momentarily rises and then falls as each drop of zinc solution is added in this region).

The difference between the titrant consumptions for the second and the first titration, which is equivalent to the cadmium content, is in practice the same whether it is determined by means of the equivalence points E_{eq}^2 and E_{eq}^1 or the end-points E_{ep}^2 and E_{ep}^1 , i.e., by means of $\Delta V = V_2 - V_1 \approx V_4 - V_3$.

The absorbance change in the first titration is smaller than that in the second because at the first titration end-point the indicator colour

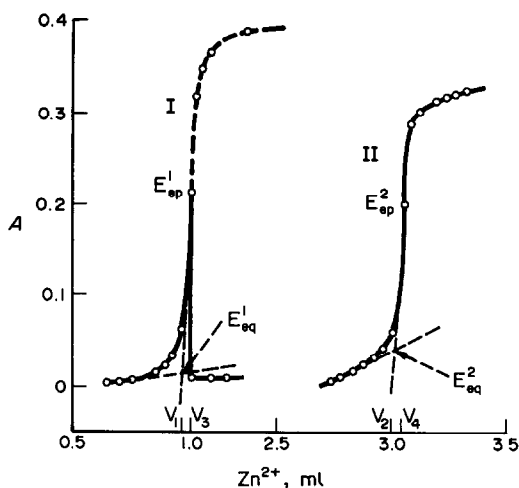


Fig. 1. Photometric titration with $0.01M$ Zn^{2+} ; I, 2.00 ml of $Cd^{2+} + 2.00$ ml of $0.01M$ $Zn^{2+} + 5.00$ ml of $0.01M$ EDTA in the presence of 4.0 ml of 10% ammonium acetate solution and 1.0 ml of 0.02% Xylenol Orange solution; II, the back-titration of the EDTA liberated by addition of 6 ml of ethanol and 1 ml of $0.025M$ potassium ethylxanthate to the titrated solution I.

change will be due to formation of a mixture of the zinc and cadmium XO complexes (owing to the exchange reaction $CdY^{2-} + Zn^{2+} \rightleftharpoons ZnY^{2-} + Cd^{2+}$), and the molar absorptivity of the $Zn-XO$ complex is higher than that of the $Cd-XO$ complex, and only the $Zn-XO$ complex will be formed at the second end-point.

The proposed method can be applied for complexometric titration with photometric end-point detection, especially when a very high zinc concentration is present. The procedure has been used for analysis of "Weltz-oxides". These are intermediate products in zinc production technology, and contain $54-57\%$ Zn, $13-15\%$ Pb, $1.5-3.0\%$ Fe, $0.6-1.0\%$ Cd.

Lead reacts like cadmium and interferes, so should be removed as lead sulphate (a reaction which can be included to allow the complexometric determination of the lead as well). Iron is bound as a very stable EDTA complex, so will not interfere in the determination of cadmium. The Weltz-oxides generally contain $0.1-0.4\%$ copper as impurity. Copper interferes strongly, forming copper ethylxanthate, which has a low solubility even in the mixed solvents. Up to $10-12$ mg/l. concentration, the copper can be

Table 1. Average \pm standard deviation of six determinations of the Cd content (%) in two samples of "Weltz-oxides" ($Cu = 0.36\%$)

Sample	Complexometric method	Polarographic method
1	0.62 ± 0.018	0.61 ± 0.016
2	0.92 ± 0.025	1.05 ± 0.027

reduced to Cu(I) and bound as the thiourea complex, before the first EDTA titration. The thiourea concentration has to be at least $5-6$ g/l. to prevent copper from reacting with both EDTA and ethylxanthate, and the organic solvent concentration has to be increased by about 10% (absolute).

Table 1 gives the results obtained for cadmium in Weltz-oxides by the proposed method and by polarography.

The values obtained by the two methods show that the proposed method has good reproducibility and accuracy.

In conclusion, it has to be stressed that the substitution titration is successful because the stable soluble cadmium ethylxanthate complex is formed whereas the corresponding zinc complex is either not formed in the aqueous organic solution or is less stable than the zinc-Xylenol Orange complex, and hence does not affect correct end-point detection in the back-titration after the substitution reaction.

REFERENCES

1. A. Karolev, *Izvestia po chimia, BAN*, 1987, **20**, 583.
2. *Idem, ibid.*, 1987, **20**, 593.
3. R. Přebil and V. Veselý, *Chem. Listy*, 1953, **47**, 1173.
4. A. Karolev, *Metallurgia*, 1970, **3**, 16.
5. I. A. Kakovskii, *Tsvetnye Metal.*, 1957, **30**, No. 7, 42.
6. A. Ringbom, *Complexation in Analytical Chemistry*, Interscience, New York, 1963.
7. G. H. Morrison and H. Freiser, *Solvent Extraction in Analytical Chemistry*, p. 182. Wiley, New York, 1957.
8. J. Starý, *Extraction*, p. 247, Mir, Moscow, 1966.
9. E. M. Donaldson and E. Mark, *Talanta*, 1982, **29**, 663.
10. N. K. Shakurova, N. A. Ulakhovich and G. K. Budnikov, *Organicheskii reaktivi v analiticheskii khimii: Teoriya deistvia i primenenie v fotometrii*, p. 129. Saratov, 1983.
11. E. A. Mazurenko, *Spravochnik po ekstraksii*, p. 205. Tekhnika, Kiev, 1972.
12. K. Burger, *Organic Reagents in Metal Analysis*, Pergamon Press, Oxford, 1973.

SIMULTANEOUS FLOW-INJECTION DETERMINATION OF CHLORPROMAZINE AND PROMETHAZINE BY PHOTOCHEMICAL REACTION

DANHUA CHEN,* A. RÍOS, M. D. LUQUE DE CASTRO† and M. VALCÁRCEL

Department of Analytical Chemistry, Faculty of Sciences, University of Córdoba, 14004 Córdoba, Spain

(Received 26 November 1990. Revised 1 May 1991. Accepted 15 May 1991)

Summary—Chlorpromazine and promethazine were simultaneously determined by irradiating flow-injection manifolds with ultraviolet light. The simultaneous determination was based on the difference in pH of the media where the photochemical conversion of each phenothiazine into a fluorescent product took place. The choice of the best flow-injection configuration and mathematical treatment for solving the mixtures are discussed. Chlorpromazine and promethazine can be simultaneously determined at the $\mu\text{g/ml}$ level with r.s.d. values between 2 and 4% and sampling frequencies in the range 30–40/hr.

Flow-injection analysis (FIA) has been applied for 16 years in over 2500 pieces of research work. However, little attention has so far been paid to photochemical reactions^{1–4} compared to complex formation, acid-base, redox, ion-pair formation and catalytic reactions. Photochemical reactions have many advantages over other chemical reactions that originate in the great purity, cleanliness, selectivity, availability and affordability of the reagent (UV or visible light).

Phenothiazine compounds are usually employed in medicine as psychotropic drugs in pharmaceutical preparations. Several analytical methods have been developed for their qualitative^{5–7} and quantitative determination.^{8–10} An interesting feature of these compounds is their photochemical instability,^{11,12} which we exploited in previous work for the individual determination of chlorpromazine and promethazine. Both compounds were exposed to UV irradiation and determined at the $\mu\text{g/ml}$ level by two different flow-injection methods. In the present work, chlorpromazine and promethazine were simultaneously determined by using different configurations for implementation of the photochemical reactions involved. The resulting products were sensed fluorimetrically.

EXPERIMENTAL

Reagents

Chlorpromazine and promethazine stock solutions of 1.000 mg/ml each were prepared in distilled water and kept in a refrigerator in the dark. Working solutions were prepared daily by direct dilution with distilled water and also kept in the dark. Both $1 \times 10^{-3}M$ hydrochloric acid and $1 \times 10^{-3}M$ sodium hydroxide were utilized as carriers.

Instruments and apparatus

Fluorescence measurements were made on a Kontron SM25 spectrofluorimeter equipped with a Knauer x-t recorder. UV irradiation on the PTFE reactor was performed by a Uvaton 70 lamp emitting at 50 Hz, 220 V and 254 nm. An external fan was fitted to cool the reactor to room temperature. The analytes were injected by means of a Rheodyne Teflon rotary valve (110- μl loop) and driven through the reactor to the fluorescence flow-cell (1.1 mm path length) by the $1 \times 10^{-3}M$ hydrochloric acid and $1 \times 10^{-3}M$ sodium hydroxide carriers, which were propelled by a Gilson Minipuls-2 peristaltic pump.

RESULTS AND DISCUSSION

Foundation of the simultaneous determination

Chlorpromazine and promethazine undergo photodecomposition to fluorescent products

*Permanent address: Department of Chemistry, Wuhan University, Wuhan, China.

†Author for correspondence.

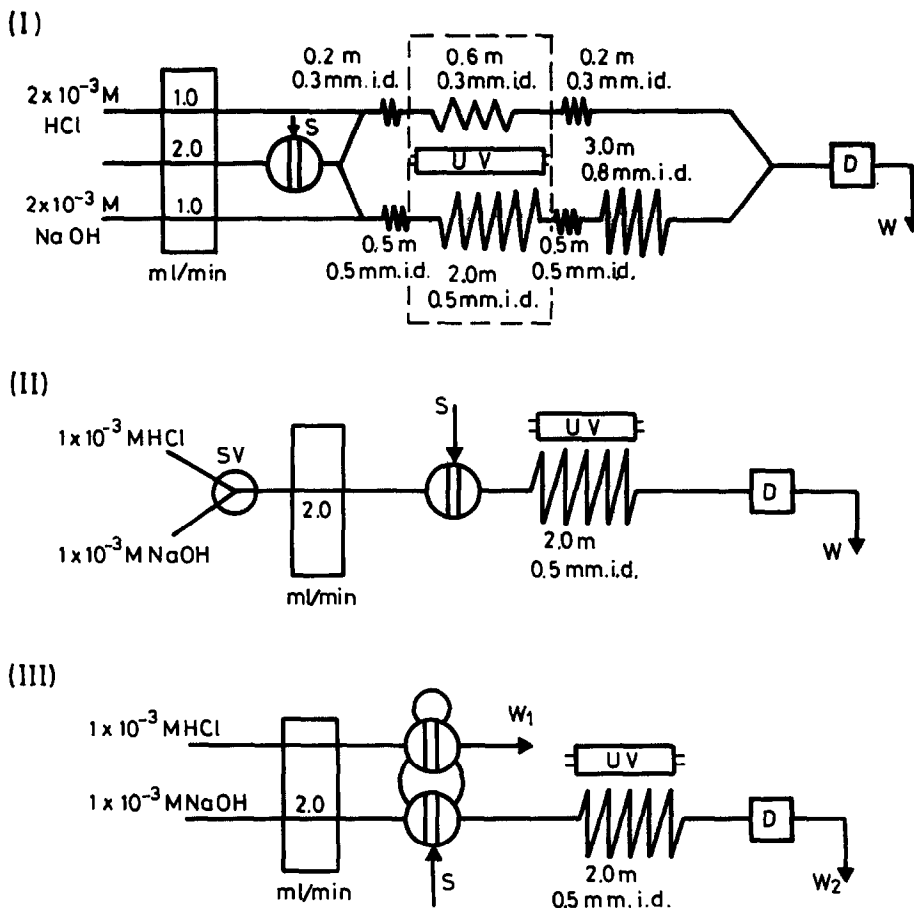


Fig. 1. Configurations for the simultaneous (I and III) and sequential (II) determination of chlorpromazine and promethazine. S denotes sample, SV selecting valve, UV ultraviolet source, D detector and W waste (for details see text).

under different working conditions. Thus, the reaction product of chlorpromazine was highly fluorescent in $1 \times 10^{-3} M$ hydrochloric acid, but scarcely fluorescent in basic medium (sodium hydroxide). On the other hand, promethazine was reactive in both solutions. This distinctive behaviour was the basis for the simultaneous determination of the two phenothiazine compounds.

Configuration designs

The aim of the configuration used for the simultaneous determination was to provide different reaction conditions for the photodecomposition of the two analytes present in the samples. Three configurations were tested for this purpose (Fig. 1).

In configuration I, the sample solution was injected via the valve into a distilled water carrier, then split into two streams, one of which was merged with $2 \times 10^{-3} M$ hydrochloric acid and the other with $2 \times 10^{-3} M$ sodium

hydroxide. Both streams were passed through PTFE reactors under UV irradiation. Arrival of the sub-plug in the sodium hydroxide carrier at the detector was delayed by using a 3-m PTFE tube of 0.8 mm i.d. to achieve complete resolution of the two peaks; *i.e.*, to allow the reaction products in the two reactors to reach the detector sequentially. The different i.d. of the reactors for the two sub-plugs was intended to balance the two channels to a similar pressure and hence to a similar volume. The shorter the reactor used for the acid stream, the smaller the diameter it should have to match its flow resistance to that of the longer reactor (basic stream), of also a larger diameter.

Configuration II included a selection valve for switching between the hydrochloric and sodium hydroxide carrier solutions, hence the sample solution had to be injected twice. Different peaks were obtained on the sample solution in different carriers sequentially passing through

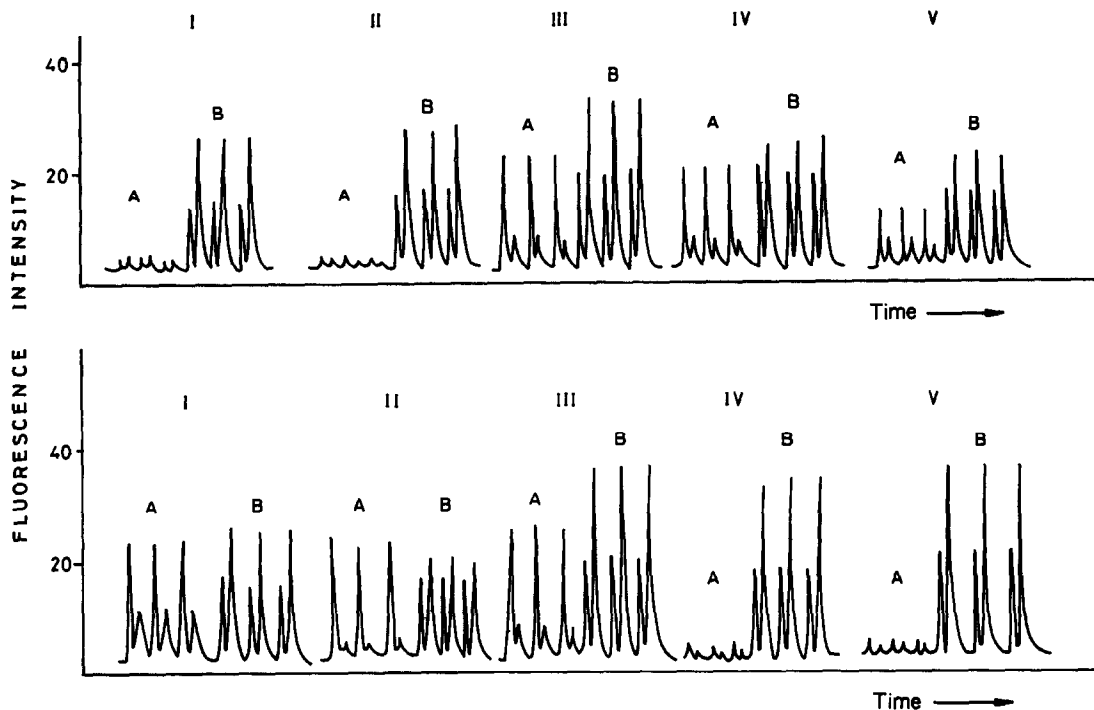


Fig. 2. Influence of the reaction media by using configuration I. (A) 2 $\mu\text{g/ml}$ chlorpromazine, (B) 2 $\mu\text{g/ml}$ promethazine. (a) With $1 \times 10^{-3}M$ NaOH and, (I) $1 \times 10^{-3}M$ HCl, (II) $1 \times 10^{-4}M$ HCl, (III) $1 \times 10^{-3}M$ HCl, (IV) $1 \times 10^{-2}M$ HCl, (V) $0.1M$ HCl. (b) with $1 \times 10^{-3}M$ HCl and, (I) $1 \times 10^{-3}M$ NaOH, (II) $1 \times 10^{-4}M$ NaOH, (III) $1 \times 10^{-3}M$ NaOH, (IV) $1 \times 10^{-2}M$ NaOH, (V) $0.1M$ NaOH.

the reactor under UV irradiation and reaching the detector.

Two injection valves were internally coupled¹³ in configuration III and intended to create two basic medium-sample interfaces (head and tail of the overall injected plug) and two acid medium-sample interfaces in the centre of the injected plug. The sample and hydrochloric acid solutions were injected through the main and secondary valve, respectively, into a sodium hydroxide stream, so the sample volume was divided into two parts by the hydrochloric acid plug. A pH gradient was formed as the plugs passed through the reactor. Instead of the three peaks expected, only two overlapped peaks or a single one were actually obtained even if the injection volumes of the hydrochloric acid and sample solution and the concentrations of the acid and sodium hydroxide were adjusted. This was a result of the maximum concentration of the two gradients (sample and acid medium) lying in different positions and hence of the insufficient fluorescence difference in the middle portion of the plugs.

Configurations I and II were finally chosen for the simultaneous determination as they provided better defined recordings.

Influence of variables

The working irradiation wavelength was 254 nm. The results obtained with light of wavelengths in the range 230–320 nm were similar. Between 320 and 360 nm, the yield of the photochemical reaction clearly decreased. Above 360 nm the reaction does not take place at all. To obtain as high a sensitivity as possible, the reactors were stitched across a frame of steel net which was placed near the UV lamp. A fan was used to remove the heat generated by the light source from the reactor. The optimal reactor lengths (*i.e.*, those resulting in the best peak resolution) are given in Fig. 1. The influence of the hydrochloric acid and sodium hydroxide concentrations were studied from 0.1 to $1 \times 10^{-5}M$, the optimal value being $1 \times 10^{-3}M$ in both cases. The shape and behaviour of the recordings in this study are illustrated in Fig. 2. The energy of the detector was adjusted at 550 V. The photochemical products of both phenothiazines showed maximum emission at 373 nm and four excitation maxima at 253, 273, 295 and 333 nm. The excitation wavelengths at 253 and 333 nm were the most suitable for the formation of the photochemical product of

chlorpromazine, while the amount of product yielded by promethazine increased with an increase in the wavelength. As the signal provided by the product from chlorpromazine was smaller than that of the promethazine product (see Fig. 2) a wavelength of 253 nm was selected for the simultaneous determination; irradiation at 333 nm was applied to samples containing promethazine concentrations much smaller than those of chlorpromazine. The optimal sample volume was 100 μl for both configurations and the flow-rates of the streams were 2.0 ml/min in configuration II, and 2.0 and 1.0 ml/min for the top and bottom channels, respectively, in configuration I. Under the above working conditions, sampling frequencies of 30/hr (60 determinations) for configuration I and 40/hr (40 determinations) for configuration II were achieved.

Features of the simultaneous determination

As the mixture of chlorpromazine and promethazine reacts with a common "reagent" (UV light) to form highly fluorescent products in two different carrier solutions, the total fluorescence can be expressed as:

$$H_j = \sum_{i=1}^2 h_{ij} \quad (j = 1, 2) \quad (1)$$

where i denotes the component and j the carrier solution; h_{ij} stands for the fluorescence contributed by each component, where

$$h_{ij} = a_{ij}C_i + b_{ij} \quad (i = 1, 2 \quad \text{and} \quad j = 1, 2) \quad (2)$$

The values of a_{ij} and b_{ij} were obtained by experiments at known concentration of chlorpromazine and promethazine alone.

(a) *Configuration I.* For chlorpromazine, over the concentration range 0.4–10.0 $\mu\text{g/ml}$, in $10^{-3}M$ hydrochloric acid and $10^{-3}M$ sodium hydroxide,

$$h_{11} = 14.34 C_1 - 5.60 \quad (r^2 = 0.9984)$$

$$h_{12} = 2.61 C_1 - 0.43 \quad (r^2 = 0.9993)$$

For promethazine, over the concentration range of 0.4–10.0 $\mu\text{g/ml}$, in $10^{-3}M$ hydrochloric acid and $10^{-3}M$ sodium hydroxide,

$$h_{21} = 7.63 C_2 + 0.52 \quad (r^2 = 0.9992)$$

$$h_{22} = 14.43 C_2 - 0.16 \quad (r^2 = 0.9979)$$

(b) *Configuration II.* For chlorpromazine, from 0.5 to 4.0 $\mu\text{g/ml}$, in $10^{-3}M$ hydrochloric acid and $10^{-3}M$ sodium hydroxide,

$$h_{11} = 38.03 C_1 + 6.05 \quad (r^2 = 0.9995)$$

$$h_{12} = 2.70 C_1 - 0.60 \quad (r^2 = 0.9998)$$

For promethazine, from 0.5 to 6.0 $\mu\text{g/ml}$, in $10^{-3}M$ hydrochloric acid and $10^{-3}M$ sodium hydroxide.

$$h_{21} = 24.32 C_2 - 7.06 \quad (r^2 = 0.9998)$$

$$h_{22} = 18.40 C_2 + 0.54 \quad (r^2 = 0.9992)$$

Therefore, the concentrations of chlorpromazine (C_1) and promethazine (C_2) in the mixture can be obtained from the total fluorescence in $10^{-3}M$ hydrochloric acid (H_1) and $10^{-3}M$ sodium hydroxide (H_2), by solving equation (1),

$$C_1 = [(H_1 - b_{11} - b_{21}) a_{22} - (H_2 - b_{12} - b_{22}) a_{21}] / (a_{11} a_{22} - a_{12} a_{21}) \quad (3)$$

$$C_2 = [(H_2 - b_{12} - b_{22}) a_{11} - (H_1 - b_{11} - b_{21}) a_{12}] / (a_{11} a_{22} - a_{12} a_{21}) \quad (4)$$

Tables 1 and 2 list the results obtained in the determination of chlorpromazine and promethazine in synthetic samples by using

Table 1. Simultaneous determination of chlorpromazine and promethazine, configuration I (from individual calibration curves)

Added, $\mu\text{g/ml}$		Found, $\mu\text{g/ml}$					
Chlorp.	Promet.	Chlorp.		Promet.			
1.000	1.000	0.763	0.748	0.747	0.715	0.718	0.748
2.000	2.000	1.585	1.608	1.614	1.642	1.667	1.696
4.000	4.000	3.534	3.509	3.469	3.333	3.383	3.465
6.000	6.000	5.595	5.626	5.624	5.360	5.354	5.415
8.000	1.000	7.840	7.917	7.706	0.843	0.858	0.973
8.000	2.000	7.877	7.918	7.964	1.610	1.528	1.549
6.000	4.000	6.002	6.018	5.940	3.419	3.386	3.431
4.000	6.000	3.670	3.695	3.711	5.585	5.536	5.503
2.000	8.000	1.756	1.679	1.677	7.893	7.908	7.983
1.000	8.000	0.907	0.907	0.938	8.058	8.058	8.052

Table 2. Simultaneous determination of chlorpromazine and promethazine, configuration II (from individual calibration curves)

Added, $\mu\text{g/ml}$		Found, $\mu\text{g/ml}$					
Chlorp.	Promet.	Chlorp.		Promet.			
0.500	0.500	0.413	0.506	0.466	0.486	0.484	0.479
1.000	1.000	0.851	0.844	0.960	0.890	0.880	0.885
1.000	2.000	0.695	0.803	0.931	1.815	1.798	1.753
2.000	2.000	1.954	1.887	1.891	1.673	1.667	1.651
0.500	5.000	0.440	0.550	0.525	4.635	4.595	4.611
1.000	5.000	0.852	1.120	0.851	4.465	4.459	4.668
4.000	0.400	4.118	3.699	3.660	0.345	0.417	0.401
4.000	1.000	3.871	3.811	3.799	0.740	0.760	0.740

configurations I and II, respectively, and the above calibration curves. The errors made were generally larger than 10%, as a result of the interaction of the two phenothiazines, which reduced the reaction rate of each other, the effect being more significant on promethazine. Recoveries were usually low; thus, development of the photochemical reaction in isolated standards was more extensive than in the mixtures.

In order to solve the problem caused by the above-mentioned negative synergistic effect, calibration curves were run by using different combinations of known concentrations of the two phenothiazines in mixtures. As C_1 and C_2 were known, H_1 and H_2 were determined; a_{11} , a_{12} , B_1 and B_2 being calculated by multicomponent regression according to the following equations:

$$H_{1k} = a_{11}C_{1k} + a_{21}C_{2k} + B_1 \quad (k = 1, 2, \dots, n) \quad (5)$$

$$H_{2k} = a_{21}C_{1k} + a_{22}C_{2k} + B_2 \quad (k = 1, 2, \dots, n) \quad (6)$$

From the above expressions, the equations for the calibration curves obtained by multicomponent regression from the experimental data were as follows:

(a) Configuration I

For the different combinations of known concentrations of the two phenothiazines in mixtures from 1.0 to 8.0 $\mu\text{g/ml}$ in $10^{-3}M$ hydrochloric acid and $10^{-3}M$ sodium hydroxide for chlorpromazine and promethazine, respectively.

$$H_1 = 14.331C_1 + 7.296C_2 - 6.44 \quad (r = 0.996) \quad (10)$$

$$H_2 = 2.263C_1 + 13.532C_2 - 4.05 \quad (r = 0.996) \quad (11)$$

(b) Configuration II

For the different combinations of known concentrations of the two phenothiazines in

mixtures from 0.5 to 4.0 $\mu\text{g/ml}$ in $10^{-3}M$ hydrochloric acid and $10^{-3}M$ sodium hydroxide for chlorpromazine and promethazine, respectively.

$$H_1 = 39.510C_1 + 22.670C_2 - 5.27 \quad (r = 0.998) \quad (12)$$

$$H_2 = 2.137C_1 + 16.700C_2 - 0.00 \quad (r = 0.999) \quad (13)$$

Hence, the concentration of each component in the mixture (C_1 and C_2) can be obtained from the total fluorescence in $10^{-3}M$ hydrochloric acid (H_1) and $10^{-3}M$ sodium hydroxide (H_2) by solving the corresponding equations.

Tables 3 and 4 list the results obtained in the determination of the analytes in synthetic samples with configurations I and II, calculated from the multicomponent regression equations. The errors made were generally less than 5%; only a few were larger than 10% owing to the large concentration ratio of the two components. However, this was overcome by weighted regression calibration.

The relative standard deviations of configuration I were 3.77% and 2.11 for chlorpromazine and promethazine, respectively (5 $\mu\text{g/ml}$ of each analyte in 11 different samples injected in triplicate), while those of configuration II were 4.23% for chlorpromazine and 3.76% for promethazine (2 $\mu\text{g/ml}$ of each analyte under the same conditions used with configuration I).

The proposed method was also applied to the resolution of mixtures of pharmaceuticals including both phenothiazines. The results obtained (Table 5) are consistent with the certified values.

CONCLUSIONS

Photochemical reactions were used in two flow-injection manifolds to develop a simultaneous determination for two analytes.

Table 3. Simultaneous determination of chlorpromazine and promethazine, configuration I (from multicomponent regression calibration curves)

Added, $\mu\text{g/ml}$		Found, $\mu\text{g/ml}$					
Chlorp.	Promet.	Chlorp.			Promet.		
1.000	1.000	1.062	1.047	1.046	0.934	0.938	0.967
2.000	2.000	1.865	1.887	1.893	1.879	1.905	1.933
4.000	4.000	3.773	3.748	3.707	3.614	3.663	3.743
6.000	6.000	5.788	5.819	5.816	5.686	5.681	5.741
8.000	1.000	8.042	8.117	7.908	1.260	1.277	1.386
		(7.917)	(7.919)	(7.783)	(0.967)	(1.038)	(1.088)
8.000	2.000	8.072	8.113	8.158	2.203	1.943	1.965
6.000	4.000	6.206	6.223	6.149	3.769	3.737	3.771
4.000	6.000	3.888	3.912	3.929	5.856	5.808	5.776
2.000	8.000	1.979	1.903	1.900	8.097	8.109	8.184
1.000	8.000	1.140	1.140	1.171	8.237	8.237	8.232
		(1.090)	(1.090)	(1.122)	(7.966)	(7.966)	(7.965)

Values in parenthesis are from weighted regression calibration curves.

Table 4. Simultaneous determination of chlorpromazine and promethazine, configuration II (from multicomponent regression calibration curves)

Added, $\mu\text{g/ml}$		Found, $\mu\text{g/ml}$					
Chlorp.	Promet.	Chlorp.			Promet.		
0.500	0.500	0.538	0.585	0.593	0.530	0.536	0.523
1.000	1.000	0.984	0.978	1.004	0.988	0.977	0.997
1.000	2.000	0.806	0.841	0.961	2.004	1.998	1.954
2.000	2.000	1.924	2.044	2.135	1.909	1.876	1.894
0.500	5.000	0.493	0.562	0.582	5.109	5.077	5.086
1.000	5.000	0.840	1.091	0.871	4.945	4.949	5.157
4.000	0.400	3.979	3.944	3.904	0.533	0.549	0.530
		(3.983)	(3.949)	(3.911)	(0.423)	(0.429)	(0.385)
4.000	1.000	4.117	4.055	4.042	0.910	0.930	0.908
		(4.103)	(4.043)	(4.031)	(0.999)	(0.997)	(0.961)

Values in parenthesis are from weighted regression calibration curves.

Table 5. Determination of phenothiazines in pharmaceuticals

Sample	Reference value, $\mu\text{g/ml}$		Found, $\mu\text{g/ml}$							
	Chlorpromazine	Promethazine	Chlorpromazine				Promethazine			
Largactil + Fenegan	2.50	5.00	2.46	2.44	2.13	2.34*	5.52	5.36	5.18	5.35*
Largactil + Hemotripsin	2.50	1.20	2.42	2.51	2.25	2.39*	1.52	1.34	1.40	1.42*
Largatrex + Fenegan	2.00	2.50	1.78	1.69	1.96	1.81*	2.82	2.51	2.65	2.66*
Largatrex + Hemotripsin	4.00	1.80	3.88	3.88	3.99	3.92*	2.05	2.16	1.96	2.06*

*Average value.

From our experience,^{1,2,4} light-wavelength is more critical to photochemical reactions than the intensity and irradiation time, just like the features of the reagents are more influential than their concentrations and reactions times. As a rule photochemical reactions do not take place at wavelengths above 360 nm, and start immediately on "addition" of the "reagent" (UV light of a wavelength usually below 320 nm) and stop as this unique reagent is removed. As a result, methods based on this type of reaction (e.g., the proposed method) are quite selective and sensitive.

Acknowledgements—The authors wish to express their gratitude to CICyT for financial support (Grant No. PA86-0146). D.C. is grateful to the Dirección General de

Investigación Científica y Técnica for financing his stay in Spain.

REFERENCES

1. L. E. León, A. Ríos, M. D. Luque de Castro and M. Valcárcel, *Anal. Chim. Acta*, 1990, **234**, 227.
2. Idem, *Lab. Robot. Autom.*, 1989, **1**, 295.
3. J. Růžicka and G. D. Christian, *Analyst*, 1990, **115**, 475.
4. D. Chen, A. Ríos, M. D. Luque de Castro and M. Valcárcel, *ibid.*, in the press.
5. T. J. Mellinger and C. E. Keeler, *Anal. Chem.*, 1963, **35**, 554.
6. J. B. Ragland and V. J. Kiross-Wright, *ibid.*, 1964, **36**, 1357.
7. T. J. Mellinger and C. E. Keeler, *ibid.*, 1964, **36**, 1841.
8. N. E. Larsen, L. B. Hansen and J. Knudson, *J. Chromatog.*, 1985, **42**, 244.
9. M. Jarayama, V. D'Souza, H. S. Yathirajan and M. S. Rangaswamy, *Talanta*, 1986, **33**, 352.

10. M. C. Gutiérrez, A. Gómez-Hens and D. Pérez-Bendito, *Anal. Lett.*, 1987, **20**, 1847.
11. V. R. White, C. S. Frings, J. E. Villafranca and J. M. Fitzgerald, *Anal. Chem.*, 1976, **48**, 1314.
12. A. H. M. T. Scholten, V. A. Brickman and R. W. Frei, *Anal. Chim. Acta*, 1980, **114**, 137.
13. A. Ríos, M. D. Luque de Castro and M. Valcárcel, *Anal. Chem.*, 1986, **58**, 663.

FLOW-INJECTION SUCCESSIVE DETERMINATION OF CYSTEINE AND CYSTINE IN PHARMACEUTICAL PREPARATIONS

TOMÁS PÉREZ-RUIZ, CARMEN MARTÍNEZ-LOZANO, VIRGINIA TOMÁS and GABRIEL LAMBERTOS
Department of Analytical Chemistry, University of Murcia, Murcia, Spain

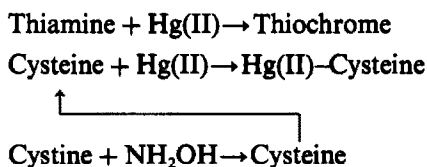
(Received 1 October 1990. Revised 22 March 1991. Accepted 31 March 1991)

Summary—A flow-injection configuration is proposed for the individual determination of cysteine and cystine and for the mixtures of both analytes. The procedure is based on the inhibitory effect of cysteine on the oxidation of thiamine to thiochrome by mercury(II). Linear calibration graphs were obtained between 1.0×10^{-5} and $1.0 \times 10^{-4}M$, with a sampling rate of 22 samples/hr and relative standard deviation of 1.14%. The inclusion of a selecting valve in the configuration, to pump water or hydroxylamine, allows the successive determination of these two analytes. The applicability of the method to the determination of cysteine and cystine in pharmaceutical preparations was demonstrated by investigating the effect of potential interferences and by the analysis of commercial preparations.

The amino acids *L*-cystine and *L*-cysteine are substances of great biological importance. *L*-Cysteine participates in a number of biochemical processes that depend directly on the particular reactivity of thiols. The high nucleophilicity of thiols facilitates the role of cysteine as an active site, covalent catalyst (e.g., in papain¹ and glyceraldehyde-3-phosphate dehydrogenase²) and allows the cysteine residue of glutathione to scavenge and detoxify electrophiles during mercapturic acid biosynthesis^{3,4} and peroxide reduction.⁵ Oxidized derivatives of *L*-cysteine have additional metabolic roles. The disulphide bonds of *L*-cystine residues stabilize the tertiary structure of proteins, for example. As *L*-cystine is hydrolysed to *L*-cysteine in water, and *L*-cysteine is readily oxidized to *L*-cystine in air, they are often presented together (in hair, liver, horn, etc.). Several different methods have been developed for the determination of cysteine and/or cystine.⁶ However, the analysis of cysteine-cystine mixtures has rarely been performed by non-chromatographic techniques. Photometric,^{7,8} electrochemical,⁹ titrimetric,¹⁰ flow-injection¹¹ and catalytic¹² methods have been used with this aim.

Flow-injection analysis offers the chance to determine species in a mixture without prior separation, by several methods based on the different working conditions with the use of a very simple manifold and a flow cell in a single detector.^{13,14} The indicator reaction chosen for

the development of the determination method of cysteine and cystine in mixtures is the oxidation of thiamine to fluorescent thiochrome by mercury(II). Cysteine is an inhibitor of this reaction while cystine requires reduction to cysteine in order to do so. On this basis, a sequential method involving the use of a simple manifold with a diverting valve which provides carriers with water or hydroxylamine for the determination of cysteine or cystine plus cysteine has been applied. Hence, the method will involve the following reactions:



The technique chosen was the reversed FI mode because it enables a higher sensitivity to be reached and wider dynamic concentration range.¹⁴

EXPERIMENTAL

Apparatus

A Gilson Minipuls peristaltic pump was used and the components of the system were linked by polypropylene connectors and 0.5-mm i.d. PTFE tubing. An Omnifit selecting valve was used to select the carrier solution for the simultaneous determination. A Perkin-Elmer 3000

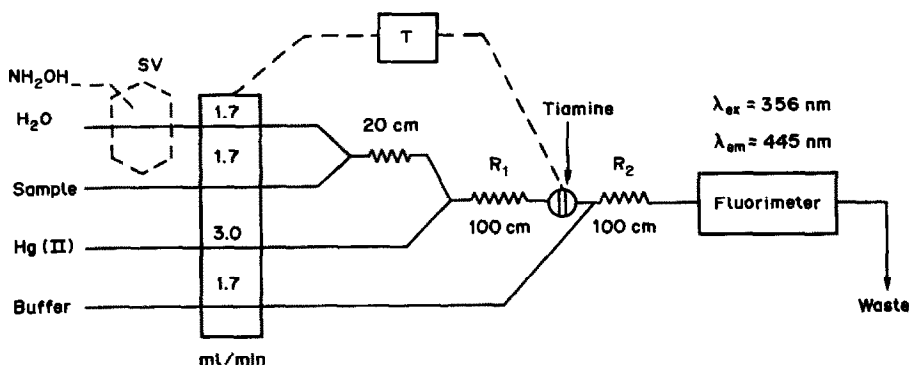


Fig. 1. Reversed FIA mode manifold for the individual determination of cysteine and cystine and for the simultaneous determination of both analytes (inclusion of selecting valve SV).

spectrofluorimeter connected to a Linseis 6512 recorder was used as a detector.

The manifold used is shown in Fig. 1. In the successive determination, valve SV allows switching between the distilled water stream (determination of cysteine) and that of hydroxylamine (joint determination of cysteine and cystine). This selection valve is cancelled for the individual determinations.

Reagents

All reagents were of analytical-reagent grade and solutions were always prepared with doubly-distilled water.

A $10^{-3}M$ stock cysteine solution was prepared daily by dissolving 0.0302 g of *L*-cysteine (Merck) in water and diluting to 250 ml in a calibrated flask. A $10^{-3}M$ stock cystine solution was prepared daily by dissolving 0.0600 g of *L*-cystine (Sigma) in 10 ml of 0.5M sodium hydroxide and diluting with water to 250 ml in a calibrated flask. Working solutions of both analytes were prepared from the stock solutions by appropriate dilution with water.

A $3.5 \times 10^{-3}M$ thiamine solution was prepared by dissolving 0.295 g of thiamine hydrochloride in water, adjusting to pH 4 with hydrochloric acid and diluting to 250 ml in a calibrated flask. This solution was stable for three months if kept refrigerated.

A $10^{-3}M$ mercury(II) solution was prepared from mercuric chloride and adjusted to pH 4 with hydrochloric acid. The working solution, $10^{-5}M$, was prepared daily by appropriate dilution with water.

Phosphate buffers were prepared from 0.2M disodium or dipotassium hydrogen phosphate and sufficient 5M potassium hydroxide to give the desired pH.

RESULTS AND DISCUSSION

Stationary system

Thiamine is oxidized to fluorescent thiochrome (TC) by mercury(II) in basic solutions.^{15,16} The order of addition of the reagents is critical. If the thiamine is mixed with the base first, a low yield of TC is obtained on the addition of Hg(II). The addition of a large excess of Hg(II) to the thiamine solution apparently stabilises the latter by the formation of a complex which can then be oxidised to TC when the base is added. The time taken to reach equilibrium decreases with increasing Hg(II) and HO^- concentrations; optimum values are obtained between pH 11 and 13. The phosphate buffer was selected because it provided a good buffering capacity at this pH range and good precision in the fluorescent measurements.

The formation of a precipitate in a spectrofluorimetric detection is unacceptable because of the lack of reproducibility of the measurements. Therefore, it was necessary to study the solubility of Hg(II) at alkaline pH. It was found that with $1.0 \times 10^{-3}M$ Hg(II) and 0.2M phosphate buffer, precipitation did not occur after 8 min in the pH range 10–13.

When cysteine is present in this system, the formation of TC is decreased because Hg(II) forms a complex with cysteine ($\log \beta = 14.21$),¹⁷ which thus acts as an inhibitor.

Flow system

The inhibitory effect of cysteine on the oxidation of thiamine to TC by Hg(II) was adapted for FIA to achieve a rapid and sensitive method for the determination of this amino acid. Of all the FIA tested, the best results were found with the reversed mode manifold shown in Fig. 1, because it resulted in an increase in sensitivity

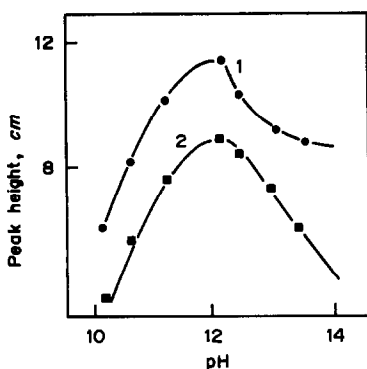


Fig. 2. Influence of pH on the peak height. [Cysteine]: (1) 0; (2) $5 \times 10^{-5} M$.

and a decrease in the number and level of interferences.

Optimization of the chemical variables

To test different pH values, 0.2M phosphate buffers were used, and the optimum pH for measurement was found to be 12.0 (Fig. 2).

The influence of the concentration of thiamine was studied in the range 10^{-4} – $5.0 \times 10^{-3} M$. Maximum signals were obtained with $3.5 \times 10^{-3} M$ thiamine.

The effect of the concentration of Hg(II) is shown in Fig. 3; the optimum concentration of the Hg(II) stream was found to be $10^{-5} M$ because then the highest peaks and the largest concentration range for the determination of cysteine were obtained.

The reaction rate of the oxidation of thiamine by Hg(II) increases with increasing temperature. A temperature of $30 \pm 0.5^\circ$ was found to be suitable to obtain an appropriate peak height.

Optimization of the FIA variables

The reactor R_1 is where the complex formation reaction between Hg(II) and cysteine

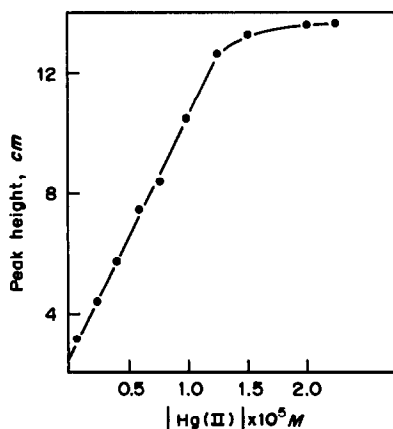


Fig. 3. Influence of Hg(II) concentration on the peak height.

takes place. A length of 100 cm is sufficient for the chemical reaction to reach or come near to completion with a flow-rate between 1.7 and 3 ml/min. Changes in the volume of thiamine injected in the range 90–130 μl yields an almost constant signal, which decreases outside this range; a volume of 100 μl was always used. The peak height increased with increasing residence time because the oxidation of the thiamine to TC by Hg(II) is not fast. The best results were obtained if the pump was stopped when the plug was located in the reaction coil R_2 . After a given period of time the pump was triggered by a timer and the reaction zone was directed towards the detector. A coil length of 100 cm and a timer programmed to stop the flow after 30 sec for 1 min were chosen as a compromise between analytical signal and sampling rate.

Determination of cysteine

A series of standard solutions were pumped in triplicate to test the linearity of the calibration graph. The calibration graph is linear from 1.0×10^{-5} to $1.0 \times 10^{-4} M$ with a correlation coefficient of 0.9997. The sample rate is about 22 samples/hr. The statistical study performed on 11 samples of triplicate pumping of $2.0 \times 10^{-5} M$ concentration yielded a r.s.d. of 1.14%.

Determination of cystine

The determination of cystine involved the previous reduction to cysteine. In the manifold shown in Fig. 1 (with no selecting valve) the cystine stream and hydroxylamine stream merged, after the reduction step, with the mercury(II) solution.

A r.s.d. of 1.23% was obtained when 11 samples of $2.0 \times 10^{-5} M$ cystine were pumped in triplicate.

Interferences

An interference study, aimed at the determination of cysteine in pharmaceutical preparations, was performed. Samples containing a fixed concentration of cysteine ($5.0 \times 10^{-5} M$) and various concentrations of the foreign substance were injected into the FIA system. A substance was considered not to interfere if the variation in the peak height of cysteine was less than 3% in its presence. The results are shown in Table 1.

Table 1. Tolerance of the proposed procedure to other substances*

Substance	Tolerable molar ratio Interferent: cysteine
Leucine, isoleucine, phenylalanine, glycine tryptophan, cystine, serine, alanine	100†
Methionine, valine, tyrosine, threonine, pyridoxine, biotin, calcium pantothenate cyanocobalamin	50
Glutathione, riboflavin	1

* $1.0 \times 10^{-5}M$ cystine added.

†Maximum tested.

Table 2. Analysis of synthetic mixtures of cysteine and cystine

Mixture taken, μM		Found,* μM			
Cysteine	Cystine	Cysteine	Error (%)	Cystine	Error (%)
5.00	—	5.01	+0.2	—	—
5.00	10.00	5.02	+0.5	10.13	+1.3
5.00	15.00	5.03	+0.6	15.16	+1.1
5.00	20.00	5.03	+0.6	20.22	+1.1
5.00	25.00	5.06	+1.2	25.32	+1.3
5.00	30.00	5.05	+1.1	30.48	+1.6
5.00	35.00	5.06	+1.2	35.52	+1.5
5.00	40.00	5.06	+1.2	40.68	+1.7

*Mean of four determinations.

Successive determination of cysteine and cystine

The resolution of the cysteine-cystine mixtures was based on the fact that cystine did not inhibit the oxidation of thiamine by Hg(II). The behaviour of both amino acids with reductants was the basis for their successive determination. The use of a selecting value to pump a distilled water stream or hydroxylamine stream merging with the sample stream in an alternate fashion (Fig. 1) makes possible the determination of the cysteine-cystine mixture to obtain analytical signals due to the contribution of cysteine or both analytes, respectively.

The results for the determination of cysteine and cystine in a series of synthetic mixtures are given in Table 2.

Analysis of pharmaceutical preparations

The method was applied to the determination of cysteine and cystine in pharmaceuticals. Commercially available formulations were analysed and the results obtained are summarized in Table 3. As can be seen for all the formulations the assay results were in good agreement with the declared content.

Table 3. Determination of cysteine and cystine in pharmaceuticals

Sample*	Source	Nominal value, mg		Found,† mg	
		Cysteine	Cystine	Cysteine	Cystine
Pil-Food	Pamies	80	25	79.2	24.6
Tulgrasum	Liade	0.356	—	0.349	—
Cistina	Quim.Med.	—	250	—	249.6
Freamine	Farmiberia	20	—	21.1	—

*Composition of samples—Pil-Food: methionine, 200 mg; cysteine, 80 mg; cystine, 25 mg; millet, 20 mg; calcium pantothenate, 25 mg; riboflavin, 1 mg; pyridoxin, 10 mg; biotin, 0.2 mg; α -tocopherol acetate, 3 mg. Tulgrasum: benzalconium chloride, 0.04 mg; bencil benzoate, 1.58 mg; threonine, 15.8 mg; cysteine, 0.356 mg; glycine, 0.216 mg. Cistina: cystine, 250 mg; excipient, 70 mg. Freamine: isoleucine, 300 mg; leucine, 770 mg; L-lysine acetate, 870 mg; methionine, 450 mg; phenylalanine, 480 mg; threonine, 340 mg; tryptophan, 130 mg; valine, 560 mg; alanine, 600 mg; arginine, 810 mg; histidine, 240 mg; proline, 950 mg; serine, 500 mg; glycine, 1190 mg; cysteine hydrochloride, 20 mg; sodium, 1 meq; acetate, 7.4 meq; phosphate, 2 meq; chloride, 0.2 meq; water and excipient up to 100 ml.

†Average of four determinations.

The accuracy of the proposed method was verified by carrying out recovery studies. When synthetic preparations that reproduced the compositions of the commercial formulations spiked with known amounts of these analytes were analysed, quantitative recoveries, 99.5–100.4% for cysteine and 99.8–100.3% for cystine, were obtained.

Acknowledgements—The authors thank the financial support given by CICYT (Project No. 0053/87).

REFERENCES

1. A. N. Glazer and E. L. Smith, in *The Enzymes*, P. D. Boyer (ed.), 3rd Ed., Vol. 3, p. 502. Academic Press, New York, 1971.
2. J. I. Harris and M. Waters, P. D. Boyer (ed.), 3rd Ed., Vol. 13, p. 1. Academic Press, New York, 1976.
3. S. S. Tate, in *Enzymatic Basis of Detoxification*, W. B. Jakoby (ed.), Vol. 2, p. 95. Academic Press, New York, 1980.
4. W. B. Jakoby, J. L. Stevens, M. W. Duffel and R. A. Weisiger, *Rev. Biochem. Toxicol.*, 1984, **6**, 97.
5. L. Flohé, *Ciba Found Symp.*, 1979, **63**, 95.
6. H. Stern, in *Moderne Methoden der Pflanzenanalyse*, V. Beiss *et al.* (eds.), Springer Verlag, Berlin, 1963.
7. M. H. Malloy, D. K. Rassin and G. E. Gault, *Anal. Biochem.*, 1981, **113**, 407.
8. P. Felker and G. Waines, *Anal. Biochem.*, 1978, **87**, 641.
9. E. G. Sement, M. L. Girard, F. Rousselet and M. Chemla, *Ann. Pharm. Fr.*, 1979, **37**, 509.
10. S. Ikeda and H. Satake, *Anal. Chim. Acta*, 1982, **142**, 289.
11. R. Egli and R. Asper, *ibid.*, 1978, **101**, 253.
12. M. Marquez, M. Silva and D. Pérez-Bendito, *Analyst*, 1988, **113**, 1373.
13. M. Valcárcel and M. D. Luque de Castro, *Flow-Injection Analysis*, Horwood, Chichester, 1987.
14. J. Růžička and E. Hansen, *ibid.*, 2nd Ed., Wiley, New York, 1988.
15. J. Holzbecher and D. E. Ryan, *Anal. Chim. Acta*, 1973, **64**, 333.
16. M. A. Ryan and D. J. Ingle, Jr., *Anal. Chem.* 1980, **52**, 2177.
17. G. R. Lenz and A. E. Martell, *Biochemistry*, 1964, **3**, 745.

DETERMINATION OF BROMAZEPAM BY COUPLING A CONTINUOUS LIQUID-LIQUID EXTRACTOR TO AN ATOMIC-ABSORPTION SPECTROMETER

RICARDO E. SANTELLI,* MERCEDES GALLEGO and MIGUEL VALCARCEL

Department of Analytical Chemistry, Faculty of Sciences, University of Córdoba, Córdoba-14004, Spain

(Received 1 October 1990. Revised 6 May 1991. Accepted 13 May 1991)

Summary—Bromazepam, in the form of the ion-pair (bromazepam)₃Cu(ClO₄)₂, can be extracted into methyl isobutyl ketone, and determined indirectly by atomic-absorption spectrometry with a limit of detection of 0.1 µg/ml bromazepam at the 324.8 nm copper resonance line. The optimum conditions for determining this drug (0.4–4.0 µg/ml) are described. The relative standard deviation achieved is 1.7%. The method is selective and free from the interference of other 1,4-benzodiazepines. It was applied to the determination of bromazepam in pharmaceuticals and was also spiked in plasma samples.

The potential of the 1,4-benzodiazepines as medical drugs was first exploited by Zbinden and Randall in their studies on chlordiazepoxide.¹ Since then, many of these compounds have been synthesised and tested for pharmacological activity. Comprehensive reviews by different authors^{2,3} have compared the pharmacological actions of the therapeutically active members and the methods of analysis of this group. Bromazepam [7-bromo-1,3-dihydro 5-(2-pyridyl)-2H-1,4-benzodiazepin-2-one] is a major sedative-hypnotic drug widely employed in clinical as an anti-anxiety agent. Only the parent compound has been found to occur in blood after therapeutic administration. Both gas and liquid chromatographic methods with electron capture and ultraviolet detection, respectively, have been developed for the determination of bromazepam in plasma with a sensitivity of 5 ng/ml.⁴ Other techniques including spectrophotometry⁵ and voltammetry^{6,7} have been used for its determination.

The occurrence of the α - α' -dipyridyl moiety enables bromazepam to form cationic 3:1 complexes with divalent metal ions such as copper(II), cobalt(II), iron(II), nickel(II) and zinc(II).^{6, 8–10} These complexes have been employed for the indirect determination of bromazepam by spectroscopic techniques such as spectrophotometry and atomic-absorption spectrometry after manual solvent extraction

into methyl isobutyl ketone (MIBK) of the ion-pair formed with perchlorate.

The combination of flow-injection and atomic-absorption spectrometry (FI/AAS) has been shown to be of use in extending the performance of atomic spectrometers, increasing nebulization efficiency and diminishing physical manipulation of the samples by use of continuous separation systems.¹¹ We have conducted research into the use of FI/AAS in conjunction with liquid-liquid extraction for the indirect determination of perchlorate in human urine and serum samples,¹² nitrite and nitrate in meat¹³ and surfactants in waters.^{14,15}

This paper reports a simple and accurate method for the determination of bromazepam in plasma and pharmaceuticals involving the continuous liquid-liquid extraction of the ion-pair formed between the chelate, copper (bromazepam)₃²⁺, and perchlorate (as counter-ion), and the determination of copper in the extract by AAS.

EXPERIMENTAL

Instrumentation

A Perkin-Elmer 380 atomic-absorption spectrometer equipped with a copper hollow-cathode lamp (absorbance measured at 324.8 nm, spectral bandpass 0.7 nm) and an air-acetylene flame was employed with a multi-range Radiometer REC-80 recorder. The flow system comprised two peristaltic pumps (Gilson Minipuls-2), an injection valve (Rheodyne

*Permanent address: Chemistry Institute, University Federal Fluminense, Niterói-24020, Brazil.

5041), an A-10T solvent segmenter and a phase separator furnished with a Fluoropore membrane (1.0- μm pore size, FALP 02500, Millipore) described elsewhere,¹⁴ and displacement bottles for pumping methyl isobutyl ketone (MIBK). Poly(vinyl chloride) pumping tubes and Teflon tubing for the coils were also used.

Reagents

A stock solution of bromazepam (from Sigma) was prepared by dissolving 0.100 g in 100 ml of methanol and was stored at 0–4° in the dark. A 1000-mg/l. copper solution was prepared by dissolving 1.000 g of copper metal in a minimum volume of nitric acid (1 + 1 v/v) and diluting to 1 litre with 1% v/v nitric acid. A 5M perchlorate solution was made from sodium perchlorate.

The carrier solution was prepared by mixing 2.5 ml of 1000 mg/l. copper, 20 ml of 5M sodium perchlorate and 10 ml of 1M acetic acid/1M sodium acetate buffer (pH 4.75) and diluting to 100 ml with distilled water.

Sample preparation

Bromazepam standards with concentrations in the range 0.4–4.0 $\mu\text{g}/\text{ml}$ were made by pipetting appropriate volumes into 50-ml calibrated flasks and diluting to the mark with 1:4 (v/v) methanol–water.

The contents of 2–8 capsules of each Lexatin sample (from Roche, Spain) were placed in a 100-ml vessel, 25 ml of methanol were added, the mixture was shaken electromagnetically for 10 min, filtered, and the residue washed with water. The filtrate was then diluted to volume with water in a 100-ml standard flask. For continuous flow analyses, different aliquots of the sample solution (0.5–2.0 ml) were placed in 50-ml calibrated flasks and diluted to the mark with a 1:4 (v/v) methanol–water mixture.

Bromazepam spiked in plasma (5 ml) was extracted into 20 ml of chloroform, the solvent

was evaporated off at 50° on a water bath, and the residue was diluted to 25-ml with 1:4 (v/v) methanol–water.

Procedure

The manifold used for the extraction is illustrated in Fig. 1. The sample, containing 0.4–4.0 $\mu\text{g}/\text{ml}$ of bromazepam in methanol–water (1:4 v/v) at pH 3.8–9.8, was continuously pumped into the system and mixed with the carrier solution. The ion-pair formed was extracted into MIBK from a displacement bottle. A fraction of the extract, controlled through another displacement bottle, was separated in the membrane phase separator. The determination was effected by injecting 100 μl of the organic extract via injector I into a water stream that was directly aspirated by the nebuliser. The heights of the peaks were proportional to the bromazepam concentration in the sample. No blank extraction was required.

RESULTS AND DISCUSSION

Prior to selecting perchlorate as counter-ion, nitrate, chloride and chlorate were also tested. These anions, however, did not allow the $\text{Cu}(\text{bromazepam})_2^{3+}$ complex to be extracted. MIBK, ethyl acetate and 1,2 dichloroethane were tested as extractants. MIBK was chosen because it yielded a negligible blank absorbance and was neither viscous nor toxic. On the other hand, Fe(II), Zn(II), Co(II), Ni(II) and Cu(II) were also assayed as metal ions forming complexes with bromazepam. The copper ion provided the highest extraction efficiency in terms of sensitivity and reproducibility. Finally, a 1:4 v/v methanol–water medium resulted in a signal 50% greater than that provided by water alone. This was probably the result of the ethanol molecules competing with those of water, thereby hindering the formation of hydrated ions and hence favouring ion-pair formations.

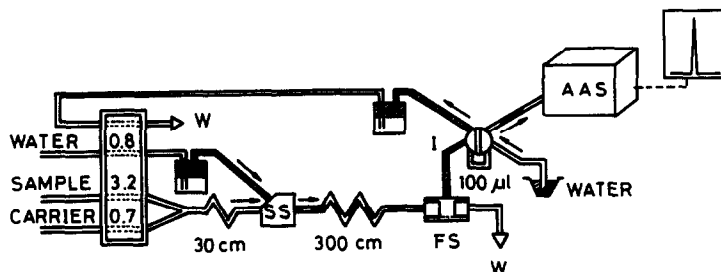


Fig. 1. Manifold for the determination of bromazepam. SS, solvent segmenter; FS, phase separator; I, injector; W, wastes; flow-rates in ml/min.

Influence of chemical variables

This study was performed by introducing a standard solution containing 1 $\mu\text{g/ml}$ of bromazepam into the system. The effect of the carrier and sample pH was studied in the range 1–6 and 3–11, respectively. The pH was found to have no influence on the signals over the ranges 3.5–6.0 and 3.8–9.8 for the carrier and sample, respectively. Above pH 6, the carrier solution (copper) was precipitated. A 1M acetic acid/1M sodium acetate buffer (pH 4.75) was selected to adjust the pH (it was added to the carrier solution). The effect of changing the concentration of the buffer between 0.2–1M was negligible. The concentration of the perchlorate (ion pairing reagent) was varied between 0.1 and 5M in the carrier solution. To study the influence of the concentration of copper on the absorbance, several carrier solutions with concentrations in the range 1–200 $\mu\text{g/ml}$ were investigated. A 10 $\mu\text{g/ml}$ solution of copper was found to be sufficient for maximum response. The absorbance remained constant at higher concentrations (up to 200 $\mu\text{g/ml}$). The ionic strength (adjusted with potassium nitrate or ammonium chloride) had no effect, at least up to 1M.

A carrier solution containing 25 $\mu\text{g/ml}$ Cu^{2+} , 1M in perchlorate and 0.2M buffer was selected for routine analyses.

Influence of flow-injection variables

The flow-rates of the aqueous and organic phases were studied. For this study an extraction coil length of 300 cm (0.7 mm i.d.) and an injected volume of 100 μl were used. The carrier flow-rate was kept at 0.22 times the sample flow-rate in order to avoid excessive dilution of the continuously pumped sample (1.0 $\mu\text{g/ml}$ bromazepam).

First, the sample flow-rate was varied between 1.4 and 3.8 ml/min while keeping that of the organic phase constant at 0.5 ml/min. The absorbance did not increase with increasing sample flow-rate, as one would expect taking into account that it increased the preconcentration ratio. A similar effect was observed by decreasing the organic phase flow-rate (1.0–0.3 ml/min) at a sample flow-rate of 2.5 ml/min. These results were checked by carrying out six experiments at three aqueous/organic phase flow ratios (1, 5 and 10) and two bromazepam concentrations (0.4 and 4.0 $\mu\text{g/ml}$). The blank solutions yielded negligible signals in every

instance and the absorbance of the two samples assayed remained constant at the three flow-ratios used.

The influence of the residence time was also studied by changing the length of the extraction coil in the range 30–500 cm (0.7 mm i.d.) at an aqueous and organic phase flow-rate of 3.9 and 0.8 ml/min, respectively. The absorbance was not affected by extraction coil lengths longer than 200 cm (residence time 10 sec), which ensured the fast extraction of the ion-pair. The tube length between the mixing point for the sample and carrier stream and the segmenter did not affect the signal at values above 30 cm for an inner diameter of 0.7 mm.

The extracted sample volume injected into the water line had a significant effect on the absorbance. The peak height increased with increasing injected sample volume up to 90 μl , above which it remained constant up to 300 μl . The areas of the peaks recorded at a low chart rate increased with increasing injected volume (Fig. 2).

Determination of bromazepam

Under the optimum conditions, a linear calibration graph (absorbance vs. $\mu\text{g/ml}$) for 0.4–4.0 $\mu\text{g/ml}$ bromazepam was obtained. The equation of the graph was:

$$A = 0.004 + 0.052 (\text{bromazepam}) \quad (r = 0.997)$$

where A is the peak height absorbance and the concentration is expressed in $\mu\text{g/ml}$. The detection limit, 0.1 $\mu\text{g/ml}$, was calculated as 3 times the standard deviation of the peak height for 30 injections of the same sample. The precision of the method was checked on 11 samples containing 1.0 $\mu\text{g/ml}$ bromazepam. The relative

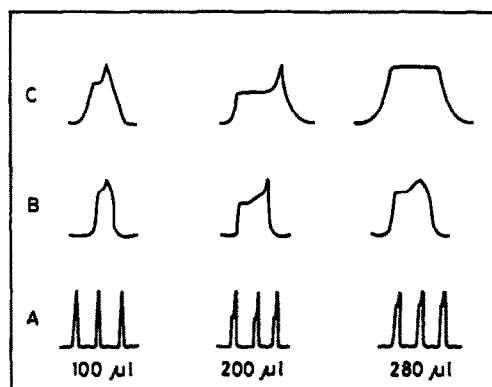


Fig. 2. FIA peaks obtained with different injected volumes at three chart rates. A, B and C: 2 min/cm, 10 sec/cm and 5 sec/cm.

Table 1. Determination of bromazepam in pharmaceutical preparations

Sample	Manufacturer*	Nominal amount	Found	Mean Recovery, † %
Lexatin 1.5	Roche	1.5 mg/capsule	1.51 ± 0.05	100.4
Lexatin 3	Roche	3 mg/capsule	3.03 ± 0.01	98.7
Lexatin 6	Roche	6 mg/capsule	5.8 ± 0.1	101.6

*Spanish; †Mean of 7 determinations.

standard deviation was 1.7% and the sampling frequency was 40/hr.

To test the specificity of the method for bromazepam, other narcotic-analgesics and hypnotic drugs were investigated. The benzodiazepines assayed were chlordiazepoxide (librium), nitrazepam, diazepam, oxazepam, flurazepam, medazepam and lorazepam. Codeine, metamphetamine and pentobarbital were also assayed. Foreign species were added at a maximum level of 1 mg/ml per 1.0 µg/ml of bromazepam. There was no interference from any of the substances studied. (Tolerated ratio 1000:1.)

Applications

The proposed method was applied to the determination of bromazepam in three commercial pharmaceuticals (lexatin) containing 1.5, 3 and 6 mg of bromazepam per capsule. The results found were consistent with the nominal contents, as can be shown in Table 1.

The procedure was also evaluated on the determination of bromazepam spiked in human plasma. A maximum volume of 1 ml of plasma was diluted to 25-ml with methanol-water (1:4 v/v); the recovery was about 99%. Higher volumes of plasma resulted in greater recoveries because of the interfering organic substances present in the fluid, and resulted in incomplete phase separation as a result of the formation of emulsions. Thus, plasma volumes larger than 1 ml must be treated as described in the Experimental section. Blanks of different human plasmas treated like the samples, yielded negligible absorbance values. Different amounts of bromazepam (25, 50 and 100 µg) were added to 5 ml of plasma and subsequently treated as described above. Application of the continuous mode of analysis yielded bromazepam recoveries of about 96% (average of five determinations on the whole amount added).

CONCLUSIONS

The proposed automatic method for the determination of bromazepam allows the direct

assay of formulations. Plasma samples require prior extraction into chloroform for volumes higher than 1 ml (diluted to 25-ml). The procedure yields acceptable results and is subject to no interference from other 1,4-benzodiazepines at concentrations 1000-fold higher than that of bromazepam.

The method compares favourably with its batch counterpart and has several advantages: small sample volume, low reagent consumption, and higher sampling frequency (inherent in the FIA techniques); wide pH range (3.8–9.8 and 4.0–5.4 for the continuous and manual extraction, respectively); higher sensitivity (0.052 and 0.031 ml/µg for the continuous and batch extraction, respectively) and higher precision thanks to the lesser sample manipulation involved.

In this paper it has been demonstrated that liquid-liquid extraction implemented in FIA manifolds is an excellent way for eliminating any influence due to the potential lability of the copper-bromazepam complex formed and the possible negative effects of acetate because of the reproducible and exact timing of this approach.

Acknowledgement—The CICYT (Spain) is acknowledged for financial support (Grant No PA86-0146). R.E.S. is grateful to FAPER J (E-29/170.478/89) and the University of Córdoba for financial support.

REFERENCES

1. G. Zbinden and L. O. Randall, in *Advances in Pharmacology*, S. Garattini and P. A. Shore (eds.), Vol. V, p. 213. Academic Press, New York, 1967.
2. J. M. Clifford and W. F. Smyth, *Analyst*, 1974, **99**, 241.
3. J. Gasparič and J. Zimák, *J. Pharm. Biomed. Anal.*, 1983, **1**, 259.
4. A. C. Moffat, J. V. Jackson, M. S. Mos and B. Widdop (eds.), *Clarke's Isolation and Identification of Drugs*, Pharmaceutical Press, London, 1986.
5. A. Hernández, P. Gutierrez and J. Thomas, *Farmaco, Ed. Prat.*, 1986, **41**, 300.
6. W. F. Smyth, R. Scannell, T. K. Goggin and D. Lucas-Hernández, *Anal. Chim. Acta*, 1982, **141**, 321.
7. L. Hernández, A. Zapardiel, J. A. Pérez López and E. Bermejo, *Talanta*, 1988, **35**, 287.

8. M. Fukumoto, *Chem. Pharm. Bull.*, 1980, **28**, 3678.
9. C. González-Pérez, M. I. González Martín, J. Hernández Méndez and R. Recio Robuster, *Quim. Anal. (Barcelona)*, 1986, **5**, 420.
10. C. González-Pérez, J. Hernández-Méndez and M. I. González-Martín, *Farmaco, Ed. Prat.*, 1983, **38**, 383.
11. J. L. Burguera (ed.), *Flow-Injection Atomic Spectroscopy*, Dekker, New York, 1989.
12. M. Gallego and M. Valcárcel, *Anal. Chim. Acta*, 1985, **169**, 161.
13. M. Silva, M. Gallego and M. Valcárcel, *ibid.*, 1986, **179**, 341.
14. M. Gallego, M. Silva and M. Valcárcel, *Anal. Chem.*, 1986, **58**, 2269.
15. P. Martínez-Jiménez, M. Gallego and M. Valcárcel, *Anal. Chim. Acta*, 1988, **215**, 233.

A FAST METHOD FOR THE DETERMINATION OF LEAD IN PAPRIKA BY ELECTROTHERMAL ATOMIC-ABSORPTION SPECTROMETRY WITH SLURRY SAMPLE INTRODUCTION

MANUEL HERNÁNDEZ CÓRDOBA* and IGNACIO LÓPEZ GARCÍA

Department of Analytical Chemistry, Faculty of Chemistry, University of Murcia, 30071 Murcia, Spain

(Received 15 November 1990. Revised 15 April 1991. Accepted 19 April 1991)

Summary—A rapid procedure for the determination of lead in commercial paprika samples is described. The samples are first calcined at 350°, then suspensions are prepared in water containing 0.1% v/v Triton X-100 and 0.1% w/v ammonium phosphate and injected into the electrothermal atomiser. The use of platform atomisation with a preatomisation cooling step allows for simple calibration with aqueous standards. When using 0.4% suspensions the detection limit is 0.2 µg/g. The results for seven paprika samples agree with those obtained by an alternative method involving calcination and dissolution in acid.

Paprika, the ground dried ripe fruit of *Capsicum annum*, is widely used as a garnish and flavorant in foods. The lead content in paprika is restricted by law to less than 10 µg/g and the products must be periodically analysed to verify this condition. Lead determination in these samples, as well as in other biological materials, involves time-consuming steps and is subject to error due to contamination from reagents and the lengthy processes involved.

On the other hand, the direct analysis of slurries by electrothermal atomisation atomic-absorption spectrometry (ETA-AAS) offers recognized advantages over the conventional methods involving dissolution of the samples, and appears to be a suitable alternative for the rapid determination of a number of elements in a wide range of products, including foods. Thus, this analytical approach has been extensively studied by several researchers to determine lead in a variety of biological materials.¹⁻¹⁰

As far as we know, lead determination in paprika has been carried out with emission spectroscopy,¹¹ voltammetry¹² and ETA-AAS¹³ after a mineralisation and acid digestion step, but no slurry-ETA-AAS procedure has been specifically developed for this purpose. Recently, we were asked for a reliable and fast procedure for the determination of lead in commercial paprika and the slurry-ETA-AAS approach appears to be the most suitable way to

develop such a simple procedure for routine purposes. This paper describes the results of our study and as a consequence, a simple, rapid method for the determination of lead in commercial paprika samples is reported.

EXPERIMENTAL

Apparatus

A Perkin-Elmer Model 1100B atomic-absorption spectrometer with deuterium-arc background correction and an HGA-400 graphite furnace were used. Measurements were performed at the 283.3-nm line of lead with a spectrometer bandpass of 0.7 nm and a hollow-cathode lamp (Perkin-Elmer) operated at 8 mA. Background-corrected absorbance peak areas were measured. Grooved pyrolytically coated graphite tubes were used with pyrolytically coated platforms, unless otherwise stated. The samples were weighed with an analytical balance (Mettler, Model AJ100, precision ± 0.01 mg). Slurries were injected into the graphite furnace with precision micropipettes (Eppendorf).

Reagents

All inorganic chemicals used were of analytical-reagent grade and were used without further purification. Doubly distilled water was used exclusively.

A stock solution of lead (1000 mg/l.) was prepared by dissolving lead nitrate (Fluka Chemie AG, Switzerland) in 1% v/v nitric acid.

*Author for correspondence.

The solution was stored in a polyethylene bottle and working solutions were prepared daily by appropriate dilution.

Triton X-100 (octyl phenoxy polyethoxy-ethanol) and concentrated nitric and sulphuric acids were obtained from Merck (Merck, Germany).

Ammonium dihydrogen phosphate was from Fluka Chemie AG.

Procedure for the determination of lead in paprika with slurries

Weigh 1 g of dried sample (110°) and ash at 350° in a porcelain crucible for 2 hr. Weigh the ash, grind it in an agate ball mill for 10 min and sieve with a 325-mesh sieve. Discard the small fraction containing larger size particles. Take an amount of sieved, ashed sample ranging 10–100 mg and add 25 ml of a solution containing 0.1% Triton X-100 and 0.1% ammonium phosphate. Stir magnetically for a minimum of 10 min. While the suspension is being stirred, take 20- μ l aliquots by means of a micropipette and inject into the furnace. Start the heating programme given in Table 1, where all temperatures quoted are values set on the HGA-400 power supply, and obtain the absorbance peak area values. Prepare a calibration graph up to 2 ng of lead with aqueous lead standard solutions containing 0.1% Triton X-100 and 0.1% ammonium phosphate. If the standard additions procedure is preferred, calibration graphs are easily obtained by adding aliquots of standard lead solution to the slurry.

Determination of lead by dissolution of the samples

For comparative purposes, paprika samples were analysed with the following procedure. The samples were dried, weighed (1 g) and placed in a porcelain crucible. Concentrated sulphuric acid (2.5 ml) was added and the mixture carefully heated to dryness with a sand-bath. The crucibles were then heated in a furnace at 400° for 2 hr. After cooling, 1 ml of concentrated nitric acid was added and the heating steps were repeated. The entire process, addition of nitric acid and heating, was performed three times. Finally, the ashes were dissolved in 1 ml of concentrated nitric acid and small amounts of a solution containing 0.5% ammonium phosphate and 0.5% nitric acid were added to a volume of 50 ml. Aliquots of this solution were taken and analysed for lead by ETA-AAS with the standard additions

Table 1. Recommended furnace programme for the Perkin-Elmer HGA-400; grooved pyrolytic graphite coated tubes with solid pyrolytic graphite L'vov platforms placed inside them; purge gas-argon, the flow- (300 ml/min) stopped during the atomisation step

Stage	Temperature/ $^{\circ}$	Ramp time/sec	Hold time/sec
Dry	120	1	30
Dry	170	1	30
Char	1000	10	20
Cool	200	5	10
Atomise	1900	0	2.5
Clean	2600	1	5

procedure. A reagent blank was performed to correct the results.

RESULTS AND DISCUSSION

There have been several reports of slurry analytical results which depend on particle size. Thus, Fuller *et al.*¹⁴ noted particle size effects for solids with $\geq 25 \mu\text{m}$ diameter and Jackson and co-workers^{15,16} confirmed that successful ETA-AAS determinations required particle size diameters of less than $30 \mu\text{m}$ for slurry preparations of soil. On the other hand, Miller-Ihli⁸ in an elaborate study on slurry sample preparation with ETA-AAS purposes, suggested that very small particle sizes ($< 30 \mu\text{m}$) may not be essential for precise slurry analyses of biological or botanical materials. With this in mind, a number of experiments were performed on two previously analysed commercial paprika samples containing 6.6 and 2.2 $\mu\text{g/g}$ of lead, respectively. The samples were dried and sieved through 200, 100, 50 and 30- μm sieves. The particle size distribution was very similar for the two samples and, as can be seen in Fig. 1, only 2–3% of particles were less than $30 \mu\text{m}$ with the bulk of the particles in the 50–200 μm range. An attempt was made to decrease the particle size by grinding the commercial samples in an agate

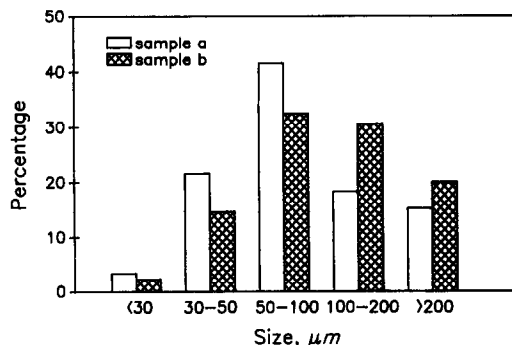


Fig. 1. Particle size distribution for two commercial paprika samples.

ball mill for 15, 30 and 90-min periods. However, because of the physical characteristics of paprika, the particle size distribution was not significantly modified even after 90 min of grinding. Several suspensions were then prepared with the same percentage of the 100–200, 50–100, 30–50 and $<30\ \mu\text{m}$ sieved fractions. Aliquots of $20\ \mu\text{l}$ from these suspensions were injected into the electrothermal atomiser and the signal from lead was obtained in the presence of ammonium phosphate as a chemical modifier with wall atomisation and 1000° and 1900° as charring and atomisation temperatures respectively. The lead signals from the slurries prepared from the 100–200, 50–100 and 30–50 μm fractions were only 1.1, 2.4 and 10.5% of that obtained from the slurry prepared from less than $30\ \mu\text{m}$ fraction, suggesting that in this case a considerable particle size effect occurs. On the other hand, the reproducibility of the signals from the slurries prepared from the coarse fractions was worse than that of the finest (RSD was $\pm 15.6\%$ for the 50–100 fraction and $\pm 5.6\%$ for the less than $30\ \mu\text{m}$ fraction).

These problems appear to be direct consequences of the sampling error which occurs when the aliquots are taken with the micropipette and of an ineffective action of the chemical modifier on the larger particles, leading to premature determinant losses. The latter point was proved when the charring temperature was decreased to 500° and the signal from the slurries prepared from the coarse material (100–200 μm) increased, being 21% of that obtained for the $<30\ \mu\text{m}$ slurries under the same experimental conditions. Furthermore, the separated fractions were mineralised and lead determined as indicated in Experimental, very similar lead contents being obtained in the four fractions. There is no doubt that the determinant is homogeneously distributed throughout the samples and the above quoted problems of low signal and poor reproducibility are exclusively due to an excessive particle size.

Taking into account all the above, the samples were calcined and then ground in an agate ball-mill, as indicated in Experimental, in order to render the particle size diminution possible. Under the recommended conditions, more than 90% of the ground calcined samples was easily sieved through a 325-mesh size. Since the determinant is homogeneously distributed through the sample, the sieved fraction was considered as representative and the small frac-

tion (3–7%) containing larger particles was discarded. The sieved portions were then used for the preparation of the slurries.

When suspensions were prepared from calcined samples, the ashes tended to float on top of the liquid and dispersion was difficult. For this reason, several concentrations of Triton X-100 were tried in order to obtain a stable suspension more rapidly and a 0.1% concentration was found to be the most adequate. Although only partial stabilisation was achieved and the aliquots had to be taken while the suspension was being continuously stirred, it was proved that the presence of the surfactant improved the reproducibility.

In spite of the pre-treatment of the samples at 350° , which allows the decomposition of most of the organic matter, problems from spluttering and high values for the background were encountered. To overcome this, a number of experiments were performed on a 0.2% w/v slurry prepared from a sample containing $6.6\ \mu\text{g/g}$ of lead, using both wall and platform atomisation. The suspension was prepared in the presence of 0.1% w/v ammonium phosphate to avoid premature loss of lead, and a charring step at 1000° with atomisation at 1900° was used. Both maximum power heating and a 1-s ramp for the atomisation step were considered. The best results were found when using platform and maximum power heating. Under these experimental conditions, the background signal was the lowest (0.094 A.s for peak area) with a peak height nearly constant during the development of the signal from lead (0.030 A), which makes the correction by the deuterium device more reliable.

Figure 2 shows char curves for a 0.2% slurry, without addition of a chemical modifier and

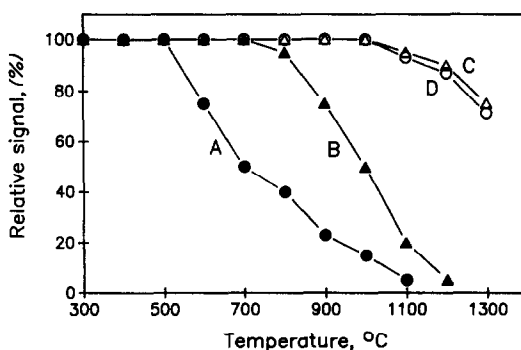


Fig. 2. Effect of the charring temperature on the relative signal for (A) aqueous Pb solution, (B) slurry paprika sample, (C) and (D) as (A) and (B) in the presence of 0.1% w/v ammonium phosphate.

with the addition of 0.1% ammonium phosphate solution. For comparison, curves for aqueous solutions of lead are also included and absorbance peak areas have been normalised, *i.e.*, data on the ordinate are the ratios between the signal obtained when using the charring temperature given in abscissas and the maximum signal obtained. As can be seen, when a 0.2% slurry was used (curve *b*), the charring temperature could be raised to 700° without loss of determinant. It was proved that this matrix auto-stabilising effect depends on the slurry percentage and it is preferable to add 0.1% w/v ammonium phosphate. Under this condition, the maximum char temperatures for slurries and aqueous solutions (curves *d* and *c*) were virtually identical, the charring step could be raised to 1000° and a lower background signal in the atomisation step was obtained.

The atomisation temperature was studied in the range 1400–2300° and the maximum signal for lead was obtained for temperatures ranging between 1800 and 2000°. Only for temperatures higher than 2100° did the signal decrease. This is a similar result to that previously reported by Hoenig and Van Hoeyweghen,⁵ which showed that when using ammonium phosphate as a modifier it was possible to use an atomisation temperature of 2200°. On the other hand, Lynch and Littlejohn⁹ proved that the temperature must not be higher than 1300° for a 4% w/v fish slurry and 1600° for a 4% w/v bovine liver slurry. As indicated by these authors,⁹ the discrepancy may be due to the use of lower slurry concentrations, as is the case reported here.

Because it has been reported that, in some instances, the inclusion of a cooling step before the atomisation stage improves the performance of ETA–AAS procedures, this point was also studied. When this cooling step was included in the programme, the time differentiation between the analyte and background signals increased and the background signal remained very small at the maximum of the analyte, permitting a more reliable background correction by the deuterium device.

Calibration, reproducibility and accuracy

From a practical point of view, it is desirable for calibration to be performed with aqueous standards, avoiding the need for using suspensions from samples of known lead content. Under the above conditions, the background-corrected peak areas obtained from atomisation of aqueous standards and slurries were additive.

Table 2. Slopes of the standard addition graphs with a charring temperature of 1000° and ammonium phosphate as chemical modifier*

Slurry, w/v	Slope, † A · s/ng
0.05	0.1965 ± 0.0008
0.09	0.1970 ± 0.0006
0.16	0.1968 ± 0.0005
0.20	0.1952 ± 0.0010

*Slope for aqueous standard, 0.1960 A · s/ng.

†The slopes were calculated from four-point standard additions. Each addition point was measured three times.

To prove this point, several slurries in the 0.05–0.2% w/v range were prepared from a paprika sample containing $6.6 \pm 0.3 \mu\text{g/g}$ lead and standard addition calibrations graphs were obtained. The results shown in Table 2 demonstrated, as expected, that the slopes of these graphs and the slope from a calibration graph for aqueous standard solutions, obtained under the same experimental conditions, are virtually identical. Therefore, direct calibration against aqueous standards is valid.

A linear relationship between the peak area and the percentage of sample in the slurries in the 0.04–0.4% range was verified for a sample containing $2.2 \pm 0.1 \mu\text{g/g}$ of lead. The background signals were in the 0.04–0.188 A.s range with a peak height nearly constant during the development of the lead signal ranging from 0.006 to 0.039 A. More concentrated suspensions were not studied because the sensitivity is high enough for the routine purposes for which the procedure was designed. Taking into account that the thermal pre-treatment of the sample at 350° involves a weight loss of about 80%, a 0.4% slurry prepared from the calcined sample is equivalent to a 2% slurry from the

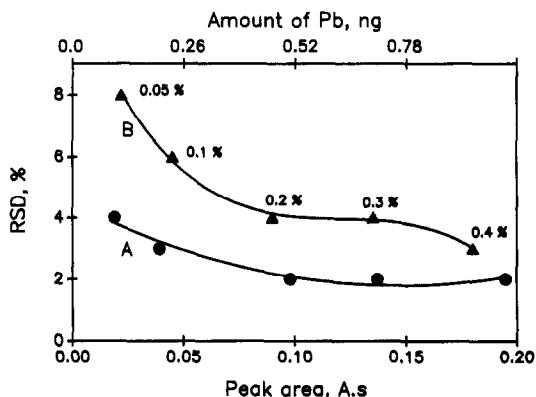


Fig. 3. Reproducibility of the procedure. (A) aqueous Pb solution, (B) paprika slurries. Numbers on the graph indicate the percentage of the slurry.

Table 3. Lead content in paprika samples

Sample	Value (\pm SD) obtained, $\mu\text{g/g}$		
	Proposed method		
	Standard additions	Aqueous calibration	Acid-digestion and ETAAS
1	6.5 \pm 0.2	6.4 \pm 0.2	6.6 \pm 0.3
2	2.3 \pm 0.1	2.4 \pm 0.1	2.2 \pm 0.1
3	7.5 \pm 0.3	7.5 \pm 0.2	7.7 \pm 0.3
4	5.2 \pm 0.2	5.5 \pm 0.2	5.4 \pm 0.3
5	9.6 \pm 0.4	9.5 \pm 0.3	9.7 \pm 0.4
6	3.9 \pm 0.1	3.8 \pm 0.1	4.0 \pm 0.2
7	1.5 \pm 0.1	1.5 \pm 0.1	1.6 \pm 0.2

original vegetal material, which allows a detection limit for lead in paprika of 0.2 $\mu\text{g/g}$, calculated on the basis of 2σ .

Reproducibility was studied with five slurries prepared from the above cited sample covering the 0.05 to 0.4% range. Ten aliquots were taken from each suspension and the signal from lead obtained following the recommended procedure. Figure 3 shows a plot of RSD against the mean value of the peak area. As can be seen in the Figure, the RSD is higher than that obtained for aqueous standards, which are included for comparison, but the reproducibility is adequate for routine purposes.

In order to check the reliability of the method, seven samples of commercial paprika were analysed with the acid dissolution procedure indicated in the Experimental section. Table 3 gives the results obtained for four replicate analyses of each sample. As can be seen from the Table, the results agree with

those obtained by the slurry method reported here, using both direct calibration with aqueous standards and the standard additions procedure.

Acknowledgement—The authors are grateful to the Spanish DGICYT (Project PB87-0053) for financial support.

REFERENCES

1. D. Littlejohn, S. C. Stephen and J. M. Ottaway, *Anal. Proc.*, 1985, **22**, 376.
2. S. C. Stephen, D. Littlejohn and J. M. Ottaway, *Analyst*, 1985, **110**, 1147.
3. F. Fagioli, S. Landi, C. Locatelli and C. Bigli, *At. Spectrosc.*, 1986, **7**, 49.
4. L. Ebdon and A. Lechotycki, *Microchem. J.*, 1986, **34**, 340.
5. M. Hoening and P. Van Hoeyweghen, *Anal. Chem.*, 1986, **58**, 2614.
6. S. C. Stephen, J. M., Ottaway and D. Littlejohn, *Z. Anal. Chem.*, 1987, **328**, 346.
7. N. Carrión, Z. A. de Benzo, B. Moreno, A. Fernández, E. J. Eljuri and D. Flores, *J. Anal. At. Spectrom.*, 1988, **3**, 479.
8. N. J. Miller-Ihli, *ibid.*, 1988, **3**, 73.
9. S. Lynch and D. Littlejohn, *ibid.*, 1989, **4**, 157.
10. U. K. Kunwar, D. Littlejohn and D. J. Halls, *Talanta*, 1990, **37**, 555.
11. J. Borszèki, J. Kepes, L. Koltay and I. Sarudi, *Acta Aliment.*, 1986, **15**, 93.
12. U. Gerhardt and G. Muhr, *Fleischwirtschaft*, 1978, **58**, 857.
13. H. Hecht, *ibid.*, 1978, **58**, 849.
14. C. W. Fuller, R. C. Hutton and B. Preston, *Analyst*, 1981, **106**, 913.
15. K. W. Jackson and A. P. Newman, *ibid.*, 1983, **108**, 261.
16. R. Karwowska and K. W. Jackson, *J. Anal. At. Spectrom.*, 1987, **2**, 125.

POTENTIOMETRIC TITRATION OF PHENOTHIAZINE COMPOUNDS IN CHLOROFORM AND ITS USE IN PHARMACEUTICAL ANALYSIS

S. M. GOLABI* and M. SHOWKATI-SHISHEVAN

Electroanalytical Chemistry Laboratory, Faculty of Chemistry, University of Tabriz, Tabriz, Iran

(Received 23 June 1989. Revised 30 April 1991. Accepted 18 May 1991)

Summary—The potentiometric titration of some phenothiazine drugs in chloroform is described. A standard solution of bromine in chloroform was used as titrant and the end-points were detected with a small platinum indicator electrode, and an Ag/AgCl electrode in 0.01M Et₄NCl in chloroform as reference. A fast redox reaction occurs during the titrations and the phenothiazine ring is oxidized to the phenothiazonium free radical (P⁺). The low dielectric constant of the medium favours the formation of (P⁺Br⁻) ion-pairs or (P⁺Br₃⁻) ion-pairs on further addition of bromine, which has no influence on the position of the first end-point. The method was used for the determination of promethazine, chlorpromazine, trifluoperazine and thioridazine in pharmaceutical preparations after extraction into chloroform. The relative standard deviation for the determination of 5 mg of all these phenothiazines was about 1%.

Numerous electroanalytical methods for the determination of phenothiazines are available in the literature.¹⁻⁹ Potentiometry with ion-selective membrane electrodes has also been reported¹⁰ and is applicable to aqueous buffered solutions, but a specific electrode is needed for each phenothiazine compound.

The official method proposed for the assay of phenothiazines in pharmaceuticals involves their extraction into chloroform and subsequent determination by ultraviolet spectrophotometry.^{11,12} An investigation of the polarographic properties of phenothiazines has shown that they can be anodically oxidized in chloroform medium¹³ and this suggests that they might be determined oxidimetrically in this solvent.

In this work, the potentiometric characteristics of some phenothiazines in chloroform have been studied and the compounds in various pharmaceutical forms were determined by potentiometric titration with bromine.

EXPERIMENTAL

Apparatus

Potentials were measured with a Metrohm recording potentiograph, type E536, equipped with an E578 titration stand. A Metrohm EA201 platinum electrode was used as indicator and the reference electrode was Ag/AgCl in

0.01M tetraethylammonium chloride solution in chloroform.

Reagents

All chemicals were of analytical reagent grade. Chloroform (Merck) was used as solvent without further purification. Stock bromine solution (0.1M) was prepared by dissolving pure bromine in chloroform. Titrant solutions (0.01 or 0.005M) were prepared by dilution just before use. These solutions must be protected from light to avoid the disappearance of bromine. A 0.005M phenothiazine solution in chloroform was prepared from the pure substance (Aldrich). *N*-Substituted phenothiazine solutions were prepared by dissolving an accurately weighed amount of each phenothiazine (as its hydrochloride) in water and then extracting with chloroform. The extracted phase was diluted quantitatively with the same solvent to give a 0.005M solution. The extraction was implemented by the procedure described in the *U.S. Pharmacopeia*,¹¹ except that the ammonia was replaced by 10M sodium hydroxide.¹³ The solutions can be used as standards instead of the phenothiazine solution.

Pharmaceutical preparations were purchased from local sources in various forms (tablet, syrup, injection, drops) and were treated by the dissolution procedures in the *U.S. Pharmacopeia*¹¹ before the phenothiazines were extracted as above.

*Author for correspondence.

Procedure

Standardization of bromine. A 5 or 10 ml portion of standard phenothiazine solution in chloroform (0.005M) was pipetted into the reaction vessel. The bromine titrant (ca. 0.01 or 0.005M) was added at 1 ml/min. The potential ranges from 800 to 1300 mV vs. reference electrode. The variation of electrode potential as a function of the volume of titrant is shown in Fig. 1a and the corresponding differential plot in Fig. 1b.

Potentiometric titration of phenothiazines. The titration is carried out as above with 5 ml of solution obtained from extraction of pharmaceutical samples with chloroform. Quantitative determination of phenothiazine drugs in the extracted phase and therefore in pharmaceutical preparations is achieved in one of the following ways.

(i) Comparison with standard. Another titration is carried out with 5 ml of a standard solution of the *N*-substituted phenothiazine. The quantity of pharmaceutical ingredient is calculated by comparison of the volumes of bromine consumed in the two titrations.

(ii) Standard addition method. Another titration is carried out, with a second 5 ml aliquot of extracted phase and 1 or 2 ml of standard phenothiazine or *N*-substituted phenothiazine solution. The content of phenothiazine is calculated from the ratio of the volumes of bromine consumed in the two titrations, and the amount of standard added.

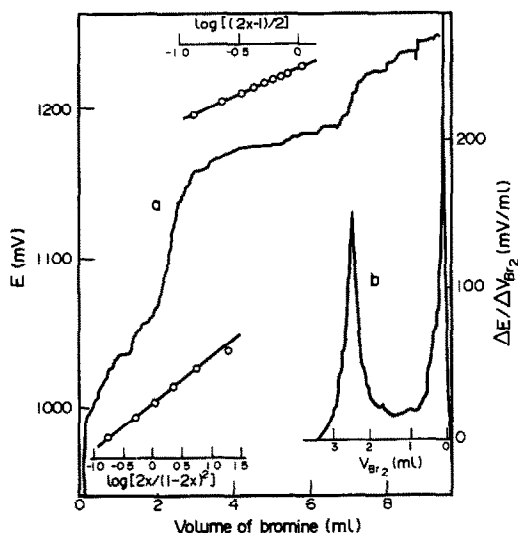


Fig. 1. Titration of 5 ml of 0.005M phenothiazine with 0.005M bromine in chloroform. (a) Plot of E as a function of V_{Br_2} . (b) Plot of $\Delta E/\Delta V_{Br_2}$ as a function of V_{Br_2} .

RESULTS AND DISCUSSION

Reaction stoichiometry

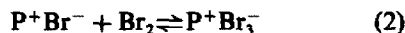
The electron-transfer reaction between phenothiazine (P) and bromine can proceed by the following schemes.

(i) The reaction product is the P^+Br^- ion-pair:



The potentiometric curve for such a reaction is expected to be the first part of curve a in Fig. 1.

(ii) Following the oxidation of phenothiazine to P^+Br^- , the complex $P^+Br_3^-$ is formed:¹⁴



In this case, a second potential jump is expected to appear at $V_2 = 3V_1$ (the second part of curve a in Fig. 1).

In both cases, the low dielectric constant of the solvent ($\epsilon = 6.2$) favours the formation of P^+Br^- and $P^+Br_3^-$ ion-pairs.

In practice, the potentiometric titration of phenothiazine with bromine, curve a in Fig. 1, shows the second end-point expected for formation of $P^+Br_3^-$ following P^+Br^- , when $V_2 = 3V_1$. Alternatively, this can be tested by analysis of the experimental curve. The electrode potentials on the two sides of the equivalence point can be expressed as follows (at 25°).

Before the equivalence point ($P^+Br^- + e \rightleftharpoons P + Br^-$):

$$E = E_1^0 + 0.0591 \log\left(\frac{[P^+Br^-]}{[P][Br^-]}\right) \quad (3)$$

After the equivalence point and assuming the formation of stable $P^+Br_3^-$, ($P^+Br_3^- + 2e \rightleftharpoons P^+Br^- + 2Br^-$):

$$E = E_2^0 + \frac{0.0591}{2} \log \frac{[P^+Br_3^-]}{[P^+Br^-][Br^-]^2} \quad (4)$$

If the $P^+Br_3^-$ ion-pair is not sufficiently stable, the potential after the equivalence point ($x > 0.5$) will be associated with ($Br_2 + 2e \rightleftharpoons 2Br^-$):

$$E = E_3^0 + (0.0591/2) \log\left(\frac{[Br_2]}{[Br^-]^2}\right) \quad (5)$$

For an initial concentration of phenothiazine equal to C_0 , we have the following concentration balance during the titration:

$$xC_0 = C_{Br_2} = \text{bromine added.}$$

$$2xC_0 = C_{P^+Br^-} = \text{ion-pair produced.}$$

$$C_0 - 2xC_0 = C_0(1-2x) = P = \text{concentration of unreacted phenothiazine.}$$

Table 1. Potentiometric determination of phenothiazines in pharmaceutical preparations

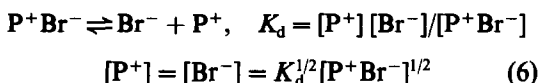
Product*	Nominal content	Found†	
		Potentiometric titration	U.S.P. method
Promethazine syrup	5 mg/5 ml	5.20 mg/5 ml	5.28 mg/5 ml
Promethazine ampoule	50 mg/2 ml	50.6 mg/2 ml	50.5 mg/2 ml
Promethazine tablet	25 mg/tab.	25.2 mg/tab.	25.3 mg/tab.
Chlorpromazine ampoule	50 mg/2 ml	51.4 mg/2 ml	50.8 mg/2 ml
Chlorpromazine drops	1 mg/drop	0.97 mg/drop	0.98 mg/drop
Chlorpromazine tablet	25 mg/tab.	25.8 mg/tab.	25.8 mg/tab.
Trifluoperazine ampoule	1 mg/ml	0.98 mg/ml	1.01 mg/ml
Thioridazine tablet	25 mg/tab.	27.3 mg/tab.	26.1 mg/tab.

*In each case, the active principle is the hydrochloride of the drug.

†All values are the average of 3–5 determinations by the standard addition or reference method.

$x C_0 - C_0/2 = C_0(2x - 1)/2 = P^+Br_3^-$ produced after the equivalence point, or the excess of added bromine, when the $P^+Br_3^-$ is supposed to be nearly dissociated.

The dissociation of P^+Br^- can be considered as follows:



Substituting $[Br^-]$ from equation (6) into equations (3), (4) and (5) and considering the concentration balance, we have:

(i) before the equivalence point ($0.5 > x > 0$):

$$E = A + (0.0591/2)\log[2x/(1 - 2x)^2] \quad (7)$$

with $A = E_1^0 - (0.0591/2)\log K_d C_0$.

(ii) after the equivalence point ($1.5 > x > 0.5$); according to equation (4):

$$E = B + (0.0591/2)\log[(4x - 2)/(3 - 2x)^2] \quad (8)$$

with $B = E_2^0 - (0.0591/2)\log K_d C_0$.

or according to equation (5):

$$E = C + (0.0591/2)\log[(2x - 1)/2] \quad (9)$$

with $C = E_3^0 - (0.0591/2)\log K_d$.

The plots of $\log[2x/(1 - 2x)^2]$ against E for $0.5 > x > 0$ and $\log[(2x - 1)/2]$ against E for $1.5 > x > 0.5$ gave straight lines with slopes of $0.0591/2$ V (see Fig. 1). This agrees with the proposed stoichiometry for the titration reaction and confirms the instability of the $P^+Br_3^-$ ion-pair.

Analysis of pharmaceutical preparations

Several preparations of phenothiazine drugs were analysed by potentiometric titration and

by the U.S.P. spectrophotometric method. The results are given in Table 1. Errors are typically 1–4%, except for thioridazine. Figure 2 illustrates the potentiometric titration curves of chlorpromazine and promethazine in chloroform. The relative standard deviations of five assays of samples containing 5 mg of phenothiazines were about 1%.

CONCLUSIONS

The use of bromine as a convenient titrant in the oxidimetric titration of phenothiazine derivatives in chloroform with potentiometric end-point detection has been demonstrated. The stoichiometry of the titration reaction is the

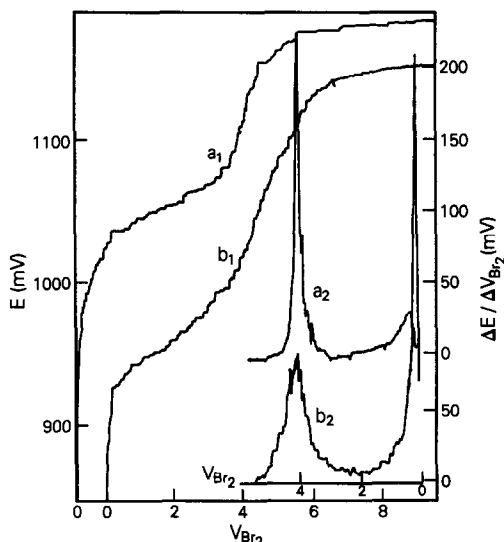


Fig. 2. Potentiometric titration of chlorpromazine (a_1 and a_2) and promethazine (b_1 and b_2) with $0.005M$ bromine in chloroform. The titrands were obtained from pharmaceutical preparations. a_1 and b_1 , E vs. V_{Br_2} ; a_2 and b_2 , $\Delta E/\Delta V_{Br_2}$ vs. V_{Br_2} .

same for all phenothiazines and the reaction product is always a coloured cationic free radical (P^+) which is stabilized by formation of P^+Br^- ion-pairs. The P^+Br^- ion-pairs can be partially transformed into $P^+Br_3^-$ ion-pairs in the presence of excess of bromine. The reaction is adequately rapid and shows a sufficiently large potential jump at the equivalence point to make detection of this easy. However, the use of derivative curves is recommended for precise detection of the end-point at the first equivalence point. The second equivalence point in the derivative method is not quite sharp because the $P^+Br_3^-$ formation reaction is not quantitative and cannot be used for the end-point detection. The method can be used for concentrations as low as 0.2 mg/ml phenothiazine and allows the accurate and precise determination of phenothiazines in pharmaceutical products after extraction into chloroform.

REFERENCES

1. F. H. Merkle and C. A. Discher, *Anal. Chem.*, 1964, **36**, 1639.
2. G. J. Patriarache and J. J. Lingane, *Anal. Chim. Acta*, 1970, **49**, 25.
3. *Idem*, *J. Pharm. Belg.*, 1970, **25**, 57.
4. *Idem*, *Ann. Pharm. Fr.*, 1970, **28**, 511.
5. G. J. Patriarache, *Mikrochim. Acta*, 1970, 950.
6. G. S. Porter, *J. Pharm. Pharmacol.*, 1964, **16**, 24.
7. H. Oelschläger and K. Bunge, *Arch. Pharm. (Weinheim)*, 1974, **307**, 410.
8. M. M. Ellaithy, *Indian J. Pharm. Sci.*, 1980, **2**, 41.
9. F. W. Teare and R. N. Yadav, *Can. J. Pharm. Sci.*, 1978, **13**, 69.
10. V. V. Coşofreţ and R. P. Buck, *Analyst*, 1984, **109**, 1321.
11. *U.S. Pharmacopeia XX*, Mack Co., Easton, Pa., 1980.
12. *British Pharmacopeia*, Vols. I and II, H.M.S.O., London, 1980.
13. S. M. Golabi, M. H. Pournaghi-Azar and M. B. Shabani, *J. Pharm. Belg.*, 1988, **43**, 19.
14. M. Rumeau, in *The Chemistry of Nonaqueous Solvents*, J. J. Lagowski (ed.), Vol. IV, p. 87. Academic Press, New York, 1976.

DETERMINATION OF REDUCED GLUTATHIONE IN HUMAN WHOLE BLOOD BY HIGH-PERFORMANCE LIQUID CHROMATOGRAPHY WITH ELECTROCHEMICAL DETECTION BY A GRAPHITE-EPOXY RESIN ELECTRODE CHEMICALLY MODIFIED WITH COBALT PHTHALOCYANINE

STEPHEN A. WRING and JOHN P. HART*

Science Department, Bristol Polytechnic, Coldharbour Lane, Frenchay, Bristol, BS16 1QY, U.K.

BRIAN J. BIRCH

Unilever Research, Sensors Group, Colworth Laboratory, Colworth House, Sharnbrook, Bedford, MK44 1LQ, U.K.

(Received 12 January 1990. Revised 3 April 1991. Accepted 5 April 1991)

Summary—High-performance liquid chromatography with electrochemical detection by means of a re-polishable graphite-epoxy resin composite electrode, modified with the electrocatalyst cobalt phthalocyanine, has been used for the determination of reduced glutathione (GSH) in 25- μ l samples of whole blood. The mobile phase was 0.05M phosphate buffer (pH 2.3) containing 1 mM EDTA, used in conjunction with a Waters μ Bondapak ODS chromatography column. The use of the electrocatalyst reduced the overpotential for the oxidation of GSH at a carbon electrode by \sim 750 mV, and the applied potential used was +0.5 V vs. Ag/AgCl. The mean recovery of GSH added during the sample pretreatment step was 95%; the assay imprecision was 1-2% for triplicate analyses of the whole blood samples.

Within the human circulation glutathione exists predominantly in the erythrocytes, where it is maintained primarily in the reduced form (GSH, L- γ -glutamyl-L-cysteinylglycine). It is an important factor in conferring protection against toxic effects of reactive oxygen compounds, such as hydrogen peroxide and superoxide, which are produced during normal metabolism and the detoxification of some drugs.¹⁻³

Determination of GSH in whole blood is important since depressed concentrations arising from some types of infection or treatment with oxidant drugs may lead to acute haemolytic anaemias in both neonates and adults.³ These deficiencies may arise from faults in a number of enzyme pathways; the most common involves a deficiency, or reduced activity, of glucose-6-phosphate dehydrogenase (G6PD).^{3,4}

In a previous study we gave some results demonstrating that trace concentrations of GSH in human plasma could be determined

accurately with a graphite-epoxy resin composite electrode modified with the electrocatalyst cobalt phthalocyanine (CoPC),⁵ which reduces the overpotential necessary for the oxidation of GSH at plain graphite electrodes by \sim 750 mV to only +0.45 V vs. SCE.⁶

In the present investigation, we tested this electrode for the determination of GSH in whole blood. In particular, for future clinical use, we required a method that would be applicable to very small volumes of whole blood, taken from neonates without venepuncture.

EXPERIMENTAL

Apparatus

High-performance liquid chromatography with electrochemical detection (HPLC-EC) was performed at room temperature with an LDC Constametric III twin-piston reciprocating pump (flow-rate, 1 ml/min). Samples were injected with a syringe-loading Rheodyne valve (model 7125) fitted with a 10- μ l sample loop, into a Waters μ Bondapak (10 μ m) ODS column (30 cm \times 3.9 mm i.d.). An Uptight guard

*Author for correspondence.

column containing 30–40 μm ODS pellicular packing (kit No. 1602, Upchurch Scientific) was positioned in series before the main column.

For electrochemical detection a three-electrode thin-layer flow-through cell (BAS TL-3) with a 0.05 mm thick gasket was employed; the Ag/AgCl reference electrode was in a separate compartment, and the auxiliary electrode was the stainless-steel outlet tube. The working electrode was incorporated in an acrylic base which fitted the top half of the TL-3 cell. The acrylic base and working electrode were made as described previously.⁶ The electrode surface was washed with a jet of demineralized water and dried with tissue paper at the start of a day's work; it could be used all day without further cleaning. When properly polished and cleaned, individual electrodes could be used for several months.⁶

An EDT LCA15 amperometric detector, in conjunction with a J.J. Instruments PN4 *x/t-y* plotter, was used to record the chromatograms.

Reagents

All chemicals were of analytical-reagent grade and were obtained from BDH unless stated otherwise. The GSH and sulphosalicylic acid (SSA), CoPC, graphite (Ultra "F" grade, UCP-1M) and epoxy resin (CY 1301 GB/HY 1300 GB) were obtained from Sigma, Kodak, Johnson-Matthey, and Ciba-Geigy Plastics, respectively.

The mobile phase used for all studies was 0.05M sodium phosphate buffer (pH 2.3) containing 1 mM Na₂EDTA, filtered through a glass micro-fibre membrane (Whatman GF/F) and deaerated with helium immediately before use.^{6,7} All solutions were prepared with demineralized water obtained from a Millipore Milli-Q system.

Standard solutions of GSH, perchloric acid and SSA were freshly prepared in deaerated mobile phase for each investigation, and protected from light during all studies.

Procedures

Calibration. Calibration graphs were prepared by injecting 10- μl aliquots of standard solutions containing 0.76, 1.52, 3.04, 4.56 and 6.08 $\mu\text{g/ml}$ GSH. Injections of standard GSH solutions and samples were alternated to provide a continual check of electrode response.

Sample collection and analysis. Whole blood samples were collected by finger prick from normal adult males and females. The hands

were thoroughly washed and dried. The index finger was wiped with isopropyl alcohol and allowed to dry, then was pricked with a disposable sterile lancet and a drop of blood was allowed to form; 25 μl of this was drawn into a sterile plastic micropipette and expelled into 2 ml of a 50-mg/ml solution of SSA. This solution was mixed on a vortex mixer and allowed to stand in the dark for 5 min to ensure protein precipitation was complete. It was then centrifuged at ~ 3000 rpm for 10 min. The supernatant was decanted and passed through a 25 mm diameter Metrical filter membrane (5 μm pore size) and an aliquot of the filtrate (10 μl) was loaded onto the HPLC column. Each sample was analysed immediately after pretreatment, to avoid loss of GSH by oxidation during storage.

RESULTS AND DISCUSSION

The optimization of the conditions for the quantification of GSH with the modified electrode has already been reported.⁶ The optimum applied potential was +0.45 V *vs.* Ag/AgCl when the mobile phase was a phosphate buffer at pH 3. However, since the electrocatalytic current was shown to be pH-dependent, and a 1-electron oxidation is involved, an applied potential of +0.5 V is required with the pH 2.3 buffer used in the present investigation.

Comparison of protein precipitating agents

Perchloric acid and SSA have both been used successfully to precipitate proteins and to inhibit oxidation of GSH by endogenous enzymes.^{8,9} However, perchloric acid proved unsuitable in the present method, since it resulted in chromatograms with a large number of anodic peaks at retention times between 2.7 and 4.4 min, followed by a very broad cathodic response lasting for about 4.5 min. In contrast, SSA did not give any interfering peaks, and a 50-mg/ml solution was selected for protein precipitation.

Calibration and recovery

The calibration graphs were linear over the range studied, in agreement with previous investigations;⁶ higher concentrations were not studied, as they were not needed for the proposed application. The limit of detection (3:1 signal to noise ratio) was 450 pg of GSH when a full-scale deflection of 1 nA was used.⁶

To assess the recovery, replicate samples of blood from the same volunteer were subjected to the analytical procedure, and spiked with small volumes of a GSH standard prepared in 50-mg/ml SSA solution. The mean recovery of GSH, calculated from the slope of a recovery graph of amount of GSH added *vs.* GSH recovered, over the range 0.38–3.02 $\mu\text{g/ml}$, was 95%.

Determination of GSH in normal human whole blood

Figure 1 shows chromatograms of (A) normal human blood, and (B) the same blood sample spiked to give a final concentration of 3.4 $\mu\text{g/ml}$ GSH in the SSA solution. The endogenous GSH concentrations were determined in the blood of five normal male and female volunteers (Table 1). The ranges are in agreement with earlier studies on healthy human subjects.^{10,11}

CONCLUSIONS

Other workers have determined GSH in various biological matrices, *e.g.*, animal tissues,^{12,13}

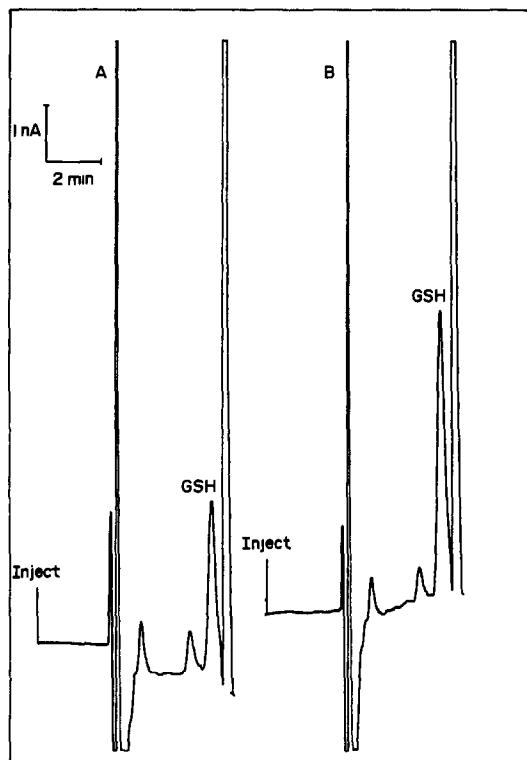


Fig. 1. Chromatograms obtained by HPLC-EC with the CoPC modified carbon-epoxy electrode for (A) a typical normal male human blood sample (GSH in the diluted solution, 2.03 $\mu\text{g/ml}$, equivalent to 0.66 mM in the original sample) and (B) the same blood spiked with GSH to give a final concentration of 3.4 $\mu\text{g/ml}$ in the solution injected onto the column.

Table 1. Replicate whole blood GSH levels determined by HPLC-EC with the modified electrode

Normal male subjects, mM	Normal female subjects, mM
(a) 0.488, 0.455, 0.461	(a) 0.588, 0.606, 0.606
(b) 0.778, 0.791, 0.804	(b) 0.725, 0.698, 0.725
(c) 0.501, 0.501, 0.501	(c) 0.633, 0.646, 0.651
(d) 0.685, 0.692, 0.692	(d) 0.685, 0.685, 0.693
(e) 0.573, 0.567, 0.560	(e) 0.519, 0.527, 0.540

by HPLC-EC with conventional carbon electrodes. In both cases^{12,13} a series dual electrode coulometric cell was used, operated in the screen mode¹⁴ to remove spurious peaks, which probably arise from the oxidation of other naturally occurring species at the high operating potentials necessary for detection of GSH at plain carbon electrodes. Oxidized glutathione (GSSG) was also determined.¹³

Other workers have attempted to improve selectivity by developing methods incorporating pre-column derivatization with electron mediators¹¹ or by including the mediator in carbon paste electrodes.¹⁰ Shimada *et al.*¹¹ studied the use of derivatization reagents containing the ferrocene moiety for pre-column reactions with several biological compounds containing thiol groups. For electrochemical detection these workers still used the coulometric cell, operated in the screen mode, but were able to obtain less complicated chromatograms than those reported later,^{12,13} owing to the lower applied potentials employed. The disadvantage of the procedure was the extra sample pretreatment step, involving incubation of the thiol with the derivatization reagent. Post-column derivatization with *o*-phthalaldehyde has been investigated by Buchberger and Winsauer,¹⁵ who applied the method to liver, eye lens and blood samples; however, no chromatograms or normal values were given for the latter samples.

A similar approach to ours was reported by Halbert and Baldwin¹⁰ who incorporated CoPC into carbon paste electrodes and successfully determined GSH in whole blood. Wang *et al.* have also described a graphite-epoxy resin electrode containing CoPC, which they used for some preliminary studies on standard solutions of hydrazine, cysteine, penicillamine and oxalic acid.¹⁶ We consider our method, using the modified carbon-epoxy resin composite electrode, to provide a significant advantage. The electrode can be used for several hours in a flowing stream without any significant deterioration in the measured current response,⁶ and

only 25 μ l of whole blood is needed for the analysis. The pretreatment with SSA to prevent blood proteins from being loaded into the chromatographic column leads to a significant reduction in extraneous chromatographic peaks and should extend the column's usable life. The simplicity of the procedure permits rapid sample handling, which should minimize losses of GSH prior to analysis.⁷

Acknowledgements—The authors are grateful to the National Advisory Board (NAB) for funding this work. They thank R. Shadwick, M. Norman and colleagues for technical assistance and Mr C. Pallister for his interest. They are also grateful to the staff of the Engineering Department of Bristol Polytechnic for their help in manufacturing the bases for the TL-3 cell.

REFERENCES

1. A. Meister, in *Glutathione—Chemical, Biochemical and Medical Aspects*, Part A, D. Dolphin, R. Poulson and O. Avramovic (eds.), p. 1. Wiley, New York, 1989.
2. *Idem*, *J. Biol. Chem.*, 1988, **263**, 17205.
3. R. Hall and R. G. Malia, *Medical Laboratory Haematology*, p. 294, Butterworths, London, 1986.
4. R. D. Eastman, *Clinical Haematology*, 6th Ed., p. 126, Wright, Bristol, 1984.
5. S. A. Wring, J. P. Hart and B. J. Birch, *Analyst*, 1989, **114**, 1571.
6. *Idem*, *ibid.*, 1989, **114**, 1563.
7. D. Perrett and S. R. Rudge, *J. Pharm. Biomed. Anal.*, 1985, **3**, 3.
8. R. C. Fahley, in *Glutathione—Chemical, Biochemical and Medical Aspects*. Part A, D. Dolphin, R. Poulson and O. Avramovic (eds), p. 303. Wiley, New York, 1989.
9. M. E. Anderson, in *Methods in Enzymology*, Volume 113, A. Meister (ed.), p. 548. Academic Press, London, 1985.
10. M. K. Halbert and R. P. Baldwin, *J. Chromatog.*, 1985, **345**, 43.
11. K. Shimada, T. Oe and T. Nambara, *ibid.*, 1987, **419**, 17.
12. E. Bousquet, N. A. Santagati and T. Lancetta. *J. Pharm. Biomed. Anal.*, 1989, **7**, 643.
13. G. Carro-Ciampi, P. G. Hunt, C. J. Turner and P. G. Wells, *J. Pharm. Meth.*, 1988, **19**, 75.
14. J. P. Hart, *Electroanalysis of Biologically Important Compounds*, p. 35. Horwood, Chichester, 1990.
15. W. Buchberger and K. Winsauer, *Anal. Chim. Acta*, 1987, **196**, 251.
16. J. Wang, T. Golden, K. Varughese and I. El-Rayes, *Anal. Chem.*, 1989, **61**, 508.

DETERMINATION OF SULPHAMETHIZOLE IN THE PRESENCE OF NITROFURANTOINE BY DERIVATIVE SPECTROPHOTOMETRY AND RATIO SPECTRA DERIVATIVE

J. J. BERZAS NEVADO, J. RODRIGUEZ FLORES and M. L. DE LA MORENA PARDO

Department of Analytical Chemistry and Foods Technology, University of Castilla-La Mancha, 13071 Ciudad Real, Spain

(Received 8 March 1991. Revised 23 May 1991. Accepted 27 May 1991)

Summary—Two methods for determining sulphamethizol in the presence of nitrofurantoin in mixtures by first-derivative spectrophotometry and by the first derivative of the ratio spectra are described. The procedures do not require any separation step. In the first method the measurements are obtained in the zero-crossing wavelengths and the calibration graphs were linear up to 32 $\mu\text{g/ml}$ of sulphamethizole at 251 and 278.5 nm. In the second method, the calibration graphs were linear up to 43 $\mu\text{g/ml}$ by measuring at the maximum (263 nm), at the minimum (244 nm) and peak to peak. The methods were applied for determining sulphamethizole in a pharmaceutical product containing nitrofurantoin.

Sulphonamides are widely used in medicine and veterinary practice as antibacterial drugs. Many sulphonamides are now available as pharmaceutical products and numerous methods have been developed for their determination. Different chromatographic techniques have been reported for the analysis of sulphonamide mixtures.¹⁻⁵ Methods for the determination of the total content of sulphonamides have also been reported. These methods involving spectrophotometric techniques based on the Bratton-Marshall procedure⁶ have been studied and have been automated by using an air-segmented continuous flow analyser⁷ and by using flow-injection analysis.⁸ Recently, derivative spectrophotometry has been used for determining the total content of sulphonamides in urine and honey without pretreatment of the samples.⁹

Derivative spectrophotometry can also be used to resolve mixtures with few chromophores without sample pretreatment. This is the case for some pharmaceutical products that contain one sulphonamide mixed with another drug. In this way derivative spectra have been used for resolving the mixture of sulphametoxazole and trimethoprim.¹⁰

Recently, Salinas *et al.*¹¹ developed a new method for resolving mixtures of chromophores with overlapped spectra. This method is based on the use of the first derivative of the ratio of the spectra. The absorption spectrum of the mixture is divided by the absorption spectrum

of a standard solution of one of the chromophores (amplitudes by amplitudes at each wavelength) and the first derivative of the ratio spectrum is obtained. The concentration of the other component is then determined from a calibration graph obtained previously.

In this work, the determination of sulphamethizole (SMT) in the presence of nitrofurantoin (NFT) is proposed by using first-derivative spectra and the first derivative of the ratio spectra for resolving a pharmaceutical product, with good results. The nitrofurantoin is an antibacterial agent that increases the effect of the sulphamethizole.

EXPERIMENTAL

Apparatus

A Beckman Instruments DU-70 spectrophotometer connected to an IBM PS/2 fitted with Beckman Data Leader Software¹² and an Epson FX-850 printer were used for all the measurements and treatment of data.

Solutions

All solvents and reagents were of analytical reagent grade. Sulphamethizole ethanol-water 1:1 solution and nitrofurantoin ethanolic solution were prepared from Sigma products at a concentration of 250 $\mu\text{g/ml}$. Ammonia/ammonium chloride buffer solution (0.5M,

pH = 10) was prepared from analytical reagent grade materials.

Procedures

First derivative spectrophotometry. Samples were prepared in 25-ml calibrated flasks containing up to 32 $\mu\text{g/ml}$ of sulphamethizole (in the presence of nitrofurantoin), 5 ml of buffer solution and were diluted with water and ethanol to the mark (the resulting final solution was 10% ethanol). The absorption spectra of the samples thus prepared were recorded against a reagent blank and stored in the IBM computer. The sulphamethizole content is determined from the first derivative spectrum (obtained with $\Delta\lambda = 6$ nm) by measuring the signal at 251 or 278.5 nm (zero-crossing points for nitrofurantoin) and by using an appropriate calibration graph.

First derivative of the ratio spectra. Samples were prepared and their absorption spectra were recorded and stored in the computer as described above. For determining sulphamethizole, the stored spectra were divided by a standard spectrum of nitrofurantoin of 5.0 $\mu\text{g/ml}$. From the ratio spectra thus obtained, first derivatives were calculated with $\Delta\lambda = 6$ nm. The concentration of sulphamethizole was proportional to the amplitude of the maximum at 263 nm, the minimum at 244 nm and the peak to peak (244–263 nm). The calibration graph can be extended up to 43 $\mu\text{g/ml}$ of sulphamethizole.

RESULTS AND DISCUSSION

Method development

The influence of pH on the absorption spectra of SMT and NFT was studied. The best results for analytical purposes were obtained at pH = 10 (ammonia/ammonium chloride buffer solution) because SMT absorption spectra were stable between pH 7 and 12 and NFT between pH 9 and 12.

The ethanol content slightly affects the absorption spectra of SMT and NFT, and as a result 10% was selected to be optimum. Under these conditions (pH = 10 and ethanol 10%), diluted solutions of SMT and NFT are stable for at least 4 hr.

Derivative spectrophotometry

The zero-order spectra of SMT and NFT in the 200–500 nm wavelength range are shown in Fig. 1. It can be seen that the absorption spectra of nitrofurantoin shows a prominent peak that

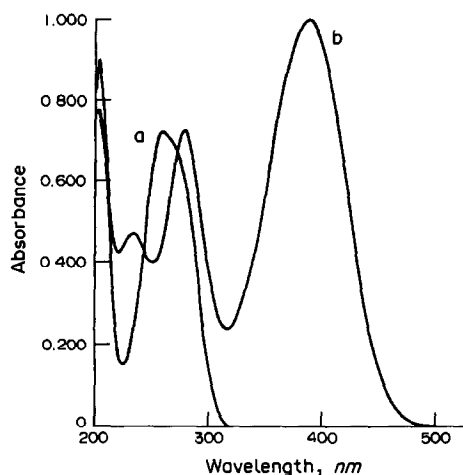


Fig. 1. (a) Absorption spectrum of 10.8 $\mu\text{g/ml}$ SMT, (b) absorption spectrum of 14.3 $\mu\text{g/ml}$ NFT.

can be used for reliable direct absorbance measurements. However, the absorption spectrum of sulphamethizole is completely overlapped with the spectrum of NFT and because of that the determination of SMT in the presence of NFT cannot be used for reliable direct absorbance measurements.

Derivative spectrophotometry can be suitable to obviate this problem. The commonest procedures for the preparation of analytical calibration graphs are "peak to peak" and "base line" measurements (generally called graphical measurements) and "zero-crossing" measurements. In practice, the measurement selected is that which exhibits the best linear response, gives a zero or near zero intercept on the ordinate of the calibration graph, and is less affected by the concentration of any other component. The shape of the first derivative spectra is adequate for determining SMT in the presence of NFT. Figure 2 shows the first derivative absorption spectra of a solution of SMT and other samples with different NFT concentrations.

It can be seen that due to the overlapping spectra of these compounds in a determined region, the zero-crossing method is the most appropriate for resolving mixtures of these compounds and it was used in this work with satisfactory results.

Preliminary experiments showed that the height, h_1 , of the first derivative at 251.0 and 278.5 nm (working zero-crossing wavelength of NFT) was proportional to the SMT concentration. The results obtained for the SMT in the presence of the nitrofurantoin were in accordance with the above calibration graph.

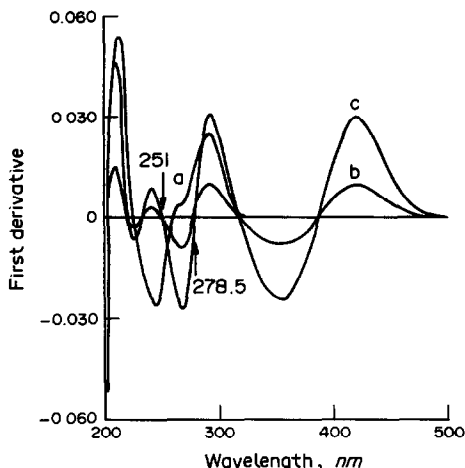


Fig. 2. (a) First derivative spectrum of 10.8 $\mu\text{g/ml}$ SMT, (b) first derivative spectrum of 6.7 $\mu\text{g/ml}$ NFT, (c) first derivative spectrum of 19.0 $\mu\text{g/ml}$ NFT.

Selection of optimal instrumental conditions.

The main instrumental parameters that affect the shape of the derivative spectra are the wavelength scanning speed, the wavelength increment over which the derivative is obtained ($\Delta\lambda$) and smoothing. These parameters need to be optimized to give a well-resolved, large peak *i.e.*, to give good selectivity and larger sensitivity in the determination. Generally, the noise level decreases with an increase in $\Delta\lambda$ thus decreasing the fluctuations in the derivative spectrum. However, if the value of $\Delta\lambda$ is too large, the spectral resolution is very poor.

Therefore, the optimum value of $\Delta\lambda$ should be determined by taking into account the noise level, the resolution of the spectrum and the sample concentration. Some values of $\Delta\lambda$ were tested and 6.0 nm was selected as the optimum in order to give a satisfactory signal to noise ratio. In this way, a smoothing function was not necessary.

Once the experimental conditions were established, the calibration graphs were tested between 2.16 and 32.4 $\mu\text{g/ml}$ SMT concentration at 251.0 and 278.5 nm. Good linearities were observed in both cases.

First derivative of the ratio spectra

When derivative spectrophotometry is used for resolving a mixture of chromophores with overlapped spectra it is often necessary to use zero-crossing, which causes a considerable loss of sensitivity. The name "ratio spectra derivative" permits the use of the wavelengths corresponding to a maximum or minimum and, also, the use of the peak to peak between consecutive maxima and minima.

Figure 3A shows the ratio spectra of different SMT standards (spectra divided by the spectrum of a 5.0 $\mu\text{g/ml}$ NFT solution) in basic medium and in Fig. 3B their first derivatives are calculated. The first derivative amplitudes at a given wavelength are proportional to the SMT concentration. As the noise levels were small a smoothing function was not needed.

The influence of the $\Delta\lambda$ for obtaining the first derivative was tested and $\Delta\lambda$ of 6 nm was considered suitable. The concentration of the NFT solution used as divisor can be modified and different calibration graphs are obtained. A standard spectrum of 5 $\mu\text{g/ml}$ of NFT was considered as suitable.

Calibration graphs were constructed at wavelengths of 263 and 244 nm corresponding to a maximum and minimum, and measuring the

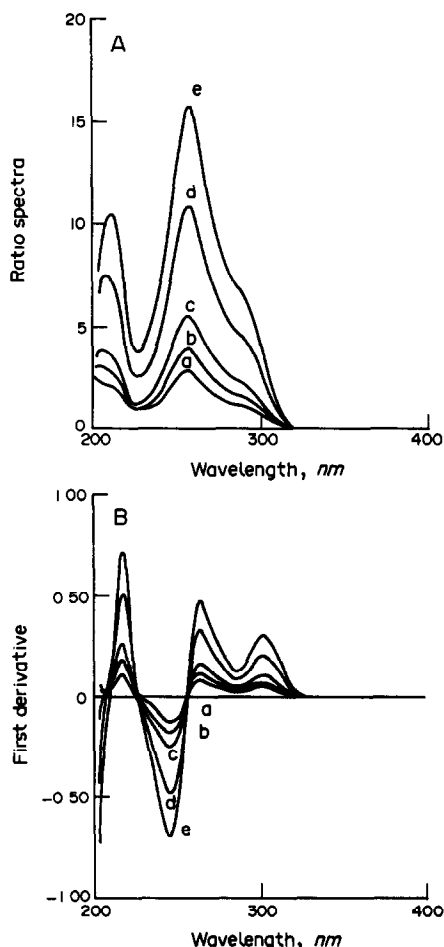


Fig. 3. A. Ratio spectra for different concentrations of SMT when NFT divisor was 5.0 $\mu\text{g/ml}$. (a) 5.4 $\mu\text{g/ml}$, (b) 7.6 $\mu\text{g/ml}$, (c) 10.8 $\mu\text{g/ml}$, (d) 21.6 $\mu\text{g/ml}$, (e) 32.4 $\mu\text{g/ml}$. B. First derivatives for different concentrations of SMT when NFT divisor was 5.0 $\mu\text{g/ml}$. (a) 5.4 $\mu\text{g/ml}$, (b) 7.6 $\mu\text{g/ml}$, (c) 10.8 $\mu\text{g/ml}$, (d) 21.6 $\mu\text{g/ml}$, (e) 32.4 $\mu\text{g/ml}$.

Table 1. Statistical parameters for SMT determination

Equation	Regression coefficient	Detection limit (3σ), $\mu\text{g/ml}$
${}^1D_{251} = 0.0008 + 0.0016C$	0.9991	<0.01
${}^1D_{278.5} = 0.012 + 0.0012C$	0.9988	0.223
${}^1DD_{263} = 0.010 + 0.0142C$	0.9996	0.086
${}^1DD_{244} = 0.012 + 0.0208C$	0.9997	0.059
${}^1DD_{263,244} = 0.023 + 0.0350C$	0.9997	0.035

Table 2. Accuracy of the 20 $\mu\text{g/ml}$ SMT determination

Signal measured	Promedium, $\mu\text{g/ml}$	RSD, %
${}^1D_{251}$	19.6	0.20
${}^1D_{278.5}$	21.2	0.28
${}^1DD_{263}$	20.5	0.10
${}^1DD_{244}$	20.2	0.10
${}^1DD_{263,244}$	20.3	0.05

Table 3. Results obtained for different mixtures by using the proposed methods

Relation NFT/SMT	NFT, $\mu\text{g/ml}$	SMT, $\mu\text{g/ml}$	SMT recovery, %				
			${}^1D_{251}$	${}^1D_{278.5}$	${}^1DD_{244}$	${}^1DD_{263}$	${}^1DD_{244,263}$
5:1	14.29	2.86	79.37	73.43	87.06	107.34	95.10
5:2	14.29	5.72	93.88	94.06	98.42	109.44	102.80
5:3	14.29	8.58	98.72	101.98	102.21	110.49	105.48
5:4	14.29	11.44	95.02	97.90	98.60	103.93	100.69
5:5	14.29	14.29	95.94	98.39	98.88	103.71	100.77

peak to peak between this maximum and minimum. Straight lines were obtained up to 43 $\mu\text{g/ml}$.

Statistical comparative study. Tables 1 and 2 summarize the most characteristic statistical data obtained from the different calibration graphs and from the reproducibility of the reagent-blank and a standard by eight successive scans. In all cases good results were obtained. The best limit quantification was obtained from the first derivative at 251 nm. Nevertheless, in general the methods that used the first derivative of the ratio spectra show a bigger accuracy and comparable limit quantifications.

Applications

The proposed methods were applied for resolving the determination of SMT in the presence of NFT in artificial mixtures. The results corresponding to these determinations are summarized in Table 3. The obtained recoveries were in the range 90–110%. The recoveries by first-derivative spectrophotometry were in the order of 95% except when the ratio of NFT to SMT was 5:2. In this case the recovery was lower. Better results were obtained from the first derivative of the ratio spectra method as can be seen in Table 3. In conclusion, both methods

gave good results for the determination of SMT in the presence of NFT.

The proposed methods were applied to the determination of SMT in the pharmaceutical Micturol from Liade laboratory (Spain) with a content of 50 mg NFT and 100 mg SMT per tablet. The determination of SMT in the pharmaceutical Micturol gave recoveries around at 96%.

REFERENCES

1. M. H. Thomas, R. L. Epstein, R. B. Ashworth and H. Marks, *J. Ass. Off. Anal. Chem.*, 1983, **66**, 884.
2. S. J. Stout, W. A. Steller, A. J. Manuel, M. O. Poeppel and A. R. daCunha, *ibid.*, 1984, **67**, 142.
3. R. M. Simpson, F. B. Suhre and J. W. Schafer, *ibid.*, 1985, **68**, 23.
4. N. Haagsma and C. van de Water, *J. Chromatog.*, 1985, **333**, 256.
5. M. M. L. Aerts, W. M. J. Beekandu and A. Th. Brindkman, *ibid.*, 1988, **435**, 97.
6. A. C. Bratton and E. K. Marshall, *J. Biol. Chem.*, 1939, **128**, 537.
7. A. Bye and A. F. J. Fox, *Clin. Chem.*, 1974, **20**, 288.
8. M. A. Koupparis and P. I. Anagnostopoulou, *Anal. Chim. Acta*, 1988, **204**, 271.
9. F. Salinas, A. Espinosa Mansilla and J. J. Berzas Nevado, *ibid.*, 1988, **233**, 289.
10. P. R. Pal, S. Bhaduri and T. K. Pal, *Indian Drugs*, 1989, **26(7)**, 367.
11. F. Salinas, J. J. Berzas Nevado and A. Espinosa Mansilla, *Talanta*, 1990, **37**, 347.
12. Beckman Instruments, Inc., *Spectroscopy*, 1987, **2**, 16.

CHANGES IN PLASMA CHARACTERISTICS CAUSED BY EASILY IONISABLE ELEMENTS IN HOLLOW CATHODE DISCHARGE EMISSION SPECTROGRAPHY

Zs. SZILVÁSSY-VÁMOS, A. GYÖRFI-BUZÁSI and Zs. PÁSZTOR

Department of Radiochemistry and Physics, University of Veszprém, Veszprém, 158, Hungary

(Received 10 December 1990. Revised 22 April 1991. Accepted 21 May 1991)

Summary—The effect of several concomitant easily ionisable elements (EIE's), Li, Na, K, Rb and Cs on the line intensity of Sr II (first ionised state) and Al I and He I (atomic states) has been studied by atomic emission spectrometry (AES) hollow cathode (HCD) analysis. The spectral line intensities emitted by Sr II, Al I and He I have been measured while varying the volume of the EIE's concentrations, ranging from 0.1 mg ml to 10 mg ml. In the presence of EIE's at higher concentrations than 0.5% a considerable decrease of the line intensities of Sr II at 430.54 nm and 407.71 nm was observed, together with a gradual decrease in the line intensities of both Al I 494.40 nm and 396.15 nm, and He I 412.1 nm. It is demonstrated in the present experiments with a water-cooled HCD source that interference effects caused by EIE's are observed when the ratio of the number of gas atoms (n_g) and atoms with low ionisation energy (n_a)— n_g/n_a —is lower than 10^{12} .

The first publications on emission sources of atomic spectrometry such as various low pressure discharge tubes (*e.g.*, Grimm's lamp) and hollow cathode discharge tubes (HCD) indicated freedom from all sorts of interelement effects.^{1–5}

However, it has been proved in later studies that these spectrochemical emission sources do not offer complete freedom from interelement effects.^{6–7}

The interelement effect may exert its interfering actions in two ways: it may affect the evaporation, *i.e.*, the entrance of the element into the plasma or alternatively it may alter the conditions of excitation prevailing in the plasma.

The sample volatilization of copper-base alloys in hot-type HCD was investigated by Broekaert.⁸ His experiments proved that the sample volatilization is due to thermal evaporation processes and atomic sputtering. It has been pointed out that the volatile elements can only be evaporated quantitatively from a less volatile base when the sample is completely molten and when the cathode temperature is sufficiently high for allowing a quick thermal evaporation of the elements studied.

Broekaert also investigated matrix effects in hot HCD and observed that detection capability decreased in the presence of Mg which, at increasing concentrations, diminished the

number of useful collisions of analyte atoms with argon metastables because it possesses a low ionisation potential and decreases the excitation of the rare earths, except for Sc and Y, which have equal relative atomic masses to Mg and Ar.⁹ Maksimov and co-workers studied the effects of cadmium vapour introduced into the plasma by the HCD excitation processes and he reported that the addition of Cd resulted in increased intensity of some analyte elements.^{10–12} He observed that particular levels of Ca and Na are excited with higher intensity at the optimal Cd concentration of 6%. He assumes that the possible source of the enhancement of the intensity of some Ca and Na lines in the presence of Cd is the resonance transfer of the energy of the metastable levels of Cd atoms and ions.

Analysing biological samples, Caroli and Delle Femine performed a comparative study of matrix effects hollow cathode under conditions and concluded that slight matrix effects can also be observed in HCD, but the HCD emission source is affected by this type of interference to a lesser extent than with graphite furnace AAS and arc-emission spectrography.¹³

Its assay of Al tracers in various organs and brain tissues led to substantially identical considerations, *i.e.*, matrix effects were practically negligible.¹⁴

Typical interelement effects can be found in the excitation of gas mixtures. Thus, the emission

of helium excited in a Geissler-tube is suppressed by introduction of 1% argon, and only the small amount of argon present is excited to emission.¹⁵

The excitation energies of the metastable states of He 1¹S and 2³S are 20.55 and 19.77 eV, respectively. The first ionisation energy of He is 24.77 eV. The metastable state of Ar is 11.83 eV. The presence of Ar in the He discharge, even in an Ar concentration of 1%, quenches the excited and ionised states of He. This can be explained by the collision of Ar atoms with fast electrons, leaving so called slow electrons behind which do not allow high energy He levels to be produced.

All these experiments indicate that some interference effects also occur in the HCD during analyses of multi-component samples, such as the majority of biological and environmental samples, *etc.*

The interference effects can exert positive effects, *e.g.*, the increasing effects of Cd, Zn on line intensity, or negative effects, decreasing line intensities and worsening detection limits.

Similar phenomena can be found in other low pressure discharges such as HCD tubes, that is, elements with higher ionisation potentials are

not excited if the concentration level of EIE's present exceeds a specified value.

In this study, the minimum concentration values of EIE's present causing detectable interferences have been investigated. The effects of EIE's on elementary processes and plasma characteristics of HCD have been studied and changes of spectral line intensities of Sr II, Al I and He I in the presence of EIE's have been interpreted.

EXPERIMENTAL

Instrumentation

The experimental method used has been described by Szilvássy.¹⁶ A brief description is as follows.

The discharge tube applied in our experiments was made of steel. Both the anode and cathode units have double walls and can be cooled by water. The cylindrical cathode cups made of aluminium or spectroscopic grade carbon and having a cylindrical hole can be placed in the cathode unit (Fig. 1).

The secondary discharge is defined as a negative glow light occurring in the hot hollow cathode placed perpendicularly to the main axis

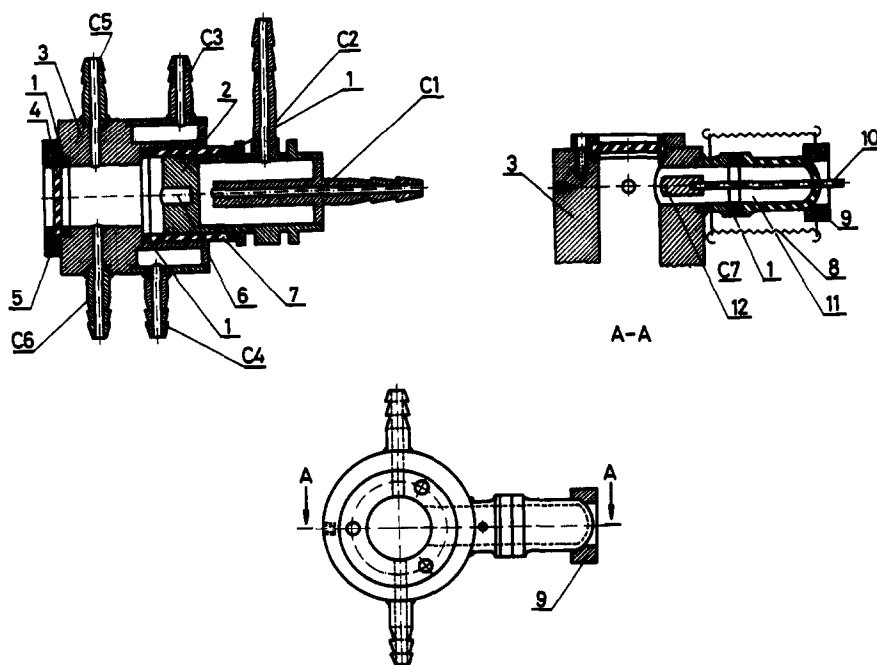


Fig. 1. Cross-section of the improved demountable hollow cathode lamp. Silicon rubber sealing [1], brass cathode block [2], brass anode block [3], quartz window [4], PVC clamping disc [5], cathode hole for negative glow discharge [6], pyrex glass tube [7], steel spring [8], PVC ring clamp [9], tungsten filament [10], auxiliary cathode block [11], carbon cathode cup [12], water cooling system [C, 1-4], gas inlet, outlet [C, 5, 6], connecting branch [C, 7].

of the discharge tube. This cathode consists of a carbon cathode cup on a tungsten wire.

The secondary cathode, which can also contain samples, can be switched on after an appropriate delay, once the main discharge has stabilised. It has been proved in earlier studies that in this case the standard deviation and the detection limits can be decreased.¹⁷

The secondary discharge can function without samples as a source of electrons, ions and metastable state gas atoms. Having no charge, the metastable state gas atoms can reach every part of the discharge tube by diffusion, so they also reach the excitation zone, thus increasing the number of excitation and ionisation processes.

In the present work, the discharge tube shown in Fig. 1 was applied with parameters listed in Table 1.

The discharge tube was mounted on the optical axis of a PGS-2 Zeiss plane-grating spectrograph and connected to a vacuum system, (as described previously)¹⁶ with a dual-rotating-vane pump. A 2 kW D.C. power supply (2000 V, 1 A) was connected to the discharge tube.

Sample preparation

A series of aqueous solutions were prepared containing the analytical element—Sr—at a concentration of 0.1 mg/ml, together with the easily ionisable elements (Li, Na, K, Rb and Cs) in a concentration range of 0.1–10 mg/ml.

A sample volume of 0.1 ml was placed in an aluminium cathode cup. The analytical solutions were dried in a cabinet drier at 40°.

Table 1. Experimental conditions

Excitation: D.C. power supply of 2 kW connected to the modified version of the water-cooled hollow cathode discharge tube
Hollow cathode: material of the cathode cups: at the primary and secondary discharges; aluminium and carbon, respectively
Diameter of cathode holes: 5.5 mm
Depth of the cathode holes: 10 mm
Carrier gas: gas mixture of 75% He and 25% Ne at a pressure of 666 Pa
Discharge current: 500 mA–700 mA
Voltage: 400–500 V
Exposure time: 5 min
Spectrograph: Zeiss/Jena/PGS 2 plane grating
Wavelength scale 1st order 200–780 nm
Dispersion 1st order, 651 lines/mm
Grating: 0.74 nm/mm
Illumination of spectrograph: intermediate focusing
Entrance slit: 0.02 mm
Step filter: 100/50/10% average light transmission
Photographic plate: ORWO WU 3
Developer: KODAK D 19
Developing temperature: 19°
Microdensitometer for spectroscopy: Zeiss G II

Evaluation of spectrograms

“ ℓ ”-Transformation¹⁸ was applied to transform blackening values measured with a Zeiss G-II microphotometer for spectroscopy; “ ℓ ” blackening transformation assigns a quantity to the blackening (s) which remains linearly proportional to the logarithm of intensity (Y), thereby to the logarithm of the concentration also.

The equation of “ ℓ ” transformation is:

$$\ell = s - (k - s)d$$

where: $s = S/\gamma$ (reduced blackening, $\gamma =$ gradation, the slope of the straight portion of the characteristic curve), $k =$ constant of “ ℓ ” transformation (the lowest blackening value on the straight part of the characteristic curve) and $d = s - 1 \text{ g}(10^s - 1)$ (Gaussian subtraction logarithm belonging to s). Therefore, the “ ℓ ” transformation relates only to the underexposed part of the characteristic curve. When $s \geq k$, $s \equiv \ell$, i.e., only in the case of $s < k$ is the transformation necessary.

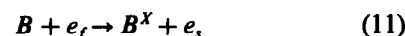
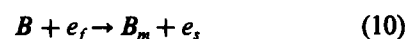
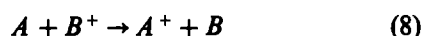
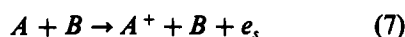
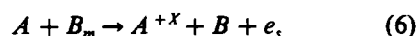
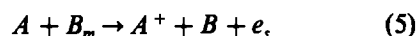
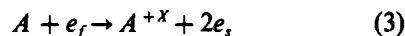
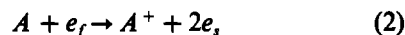
For the determination of relative standard deviations (r.s.d.), 7 parallel measurements were carried out. This value was found to be less than 8%.

RESULTS AND DISCUSSION

Decrease of spectral line intensities

The effects of EIE's were investigated on the spectral line intensities of (i) rare gas atoms having high excitation energies, (ii) Sr⁺ ions having medium excitation energies and (iii) two Al atom lines having low excitation energies.

The excited and ionized states can be formed in the following processes:



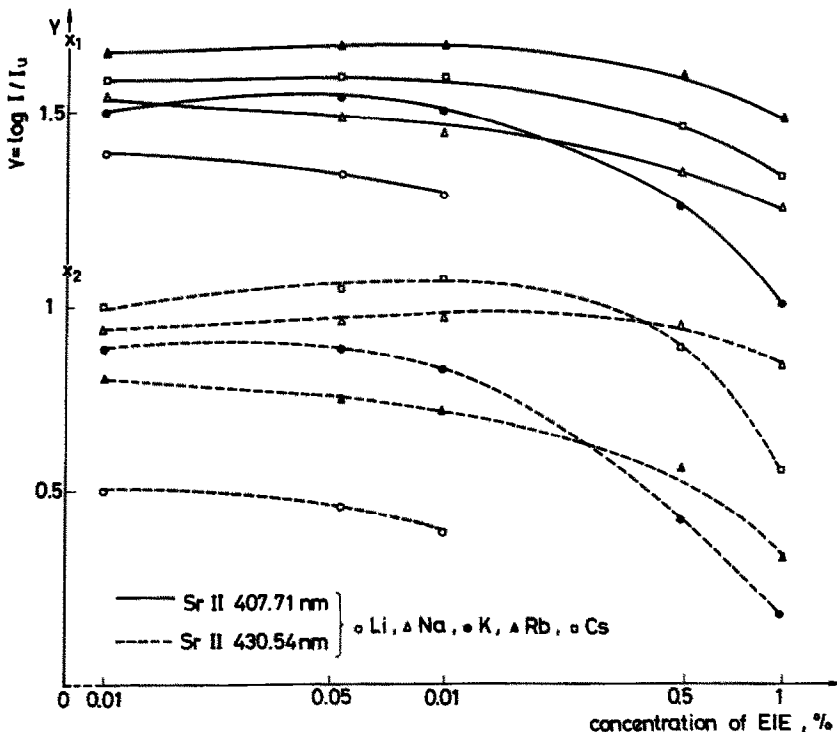
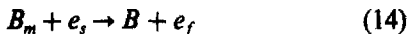
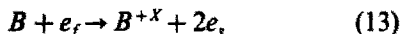


Fig. 2. Background corrected Sr^+ curves as a function of EIE concentration. X_1 and X_2 values on axis Y show Sr^+ Y intensity values without EIE's present; $Y = \log I/I_0$ background corrected relative signal.



Where A is the atom of the sample, A^X is the excited state, A^+ is the ionized state, B is the atom of the rare gas, B_m is the metastable state, e_f is fast electron and e_s is slow electron.

The presence of EIE's in the plasma reduces the number of fast electrons [processes (1)–(9)] and hinders process (10) that is, less metastable rare gas atoms are produced. Process (14) describes a possible form of decay of metastable states of rare gas atoms, which is significant in view of high energy collision processes, because the fast electrons are reproduced in this process.

Decrease of line intensities of He I 412.10 nm (23.97 eV) and He I 447.15 nm (23.73 eV) lines

Figure 2 shows the changes in line intensities of He carrier gases for Li, Na, K, Rb and Cs concentration ranges from 0.01–1%. It can be observed that a decrease in intensity occurs at 0.01% concentration and the intensity of spectral lines further decreases gradually as the EIE's concentration is increased.

Processes (11) and (12) describe the generation of rare gas ions and excited rare gas atoms by collisions. The number of both processes decreases if there are less fast electrons in the discharge zone. Therefore the spectral line intensities of the carrier gas decrease under the effect of EIE's.

The ionization energies of the alkali metals are listed in Table 2.

The effects of EIE's on Sr II 407.71 nm (3.04 eV) and 430.54 nm (5.91 eV) spectral line intensities

For the present investigations two Sr^+ ion lines of the highest intensity were selected from the Sr spectrum. For both spectral lines the decrease of intensity was observed.

The presence of EIE's in the negative glow light results in the decrease of the number of fast electrons participating in processes (1), (2) and (3) thus reducing the number of higher energy

Table 2. First ionisation energies of the alkali metals

Element	Energy, eV
Li	5.390
Na	5.138
K	4.340
Rb	4.176
Cs	3.893

excited atoms and ions, as well as the number of single-step excited ions. [Penning ionisation, Process (3)].

The sum of ionization and excitation energies in the present measurements are higher than 8 eV, the probability of process (3) therefore occurring is less, which causes the intensity of Sr⁺ spectral lines to decrease.

Figure 3 shows the changes of two ion lines of Sr under the effect of EIE's. Detectable decreases in intensity can only be detected when the concentration of EIE's is higher than 0.5%.

Changes in Al I 396.15 nm (3.14 eV) and Al I 394.40 nm (3.14 eV) spectral line intensities due to EIE's

The excitation energy of the above two Al spectral lines is 3.14 eV. The atoms of the cathode cup made of Al are sputtered by the rare gas ions and metastable rare gas atoms into the plasma.

The decrease of Al line intensity in the presence of EIE's—as shown in Fig. 4—can be explained by the lower efficiency of sputtering. The presence of EIE's does not reduce the number of lower energy collisions, the decrease of intensity can be explained by the lower number of sputtered Al atoms.

The decreased sputtering yield indicates that a reduced number of rare gas ions and metastable state atoms with lower energies occur in the plasma due to the EIE's.

The increase of the conductivity does not contradict this phenomenon. Greater numbers of charged particles are present due to the easy ionisation of EIE's, however, the energy distribution of the charged particles changes to the detriment of higher energies.

Changes in current intensity under the effects of Li, Na, K, Rb and Cs

The entrance of EIE's in the plasma is indicated by an increased conductivity, and an increase in current between 10 and 150 mA was noted. Current intensities were measured at constant voltage.

Table 3 contains the changes of the absolute values of current in the presence of Li, Na, K, Rb and Cs at concentrations of 0.01 and 1% for the latter four, and 0.01 and 0.1% for Li. It is well illustrated that the maximum 25% increase of relative current intensity occurs at 1% Cs concentration.

CONCLUSIONS

From the results presented in this paper it is clear that the sputtering, excitation and

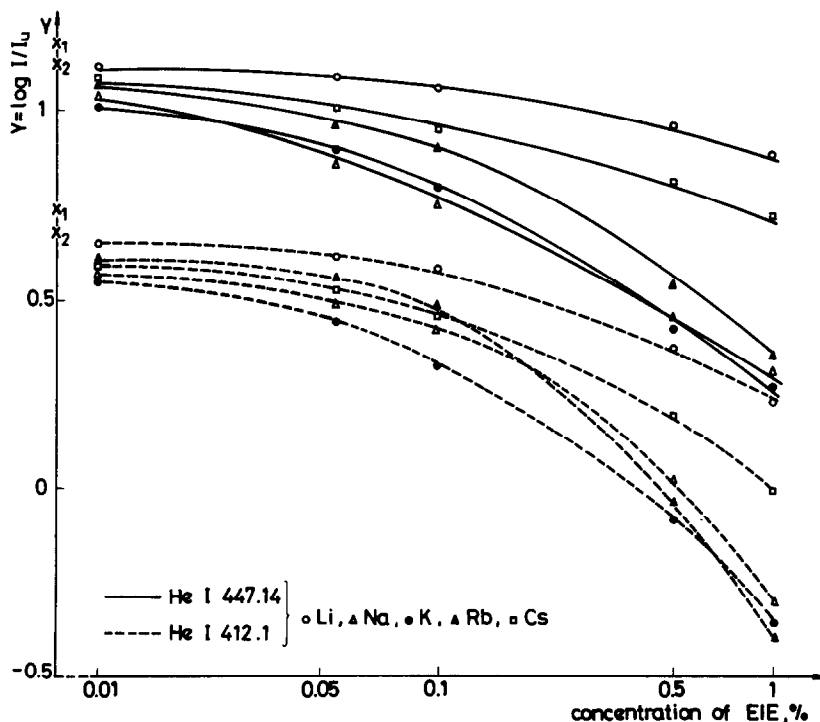


Fig. 3. Background corrected He I curves as a function of EIE concentration. X₁ values on axis Y represent He I Y values obtained using empty Al cathode cup. X₂ values represent He I intensity values in the presence of 0.1% Sr (dried from aqueous solution); Y = log I/I₀ background corrected relative signal.

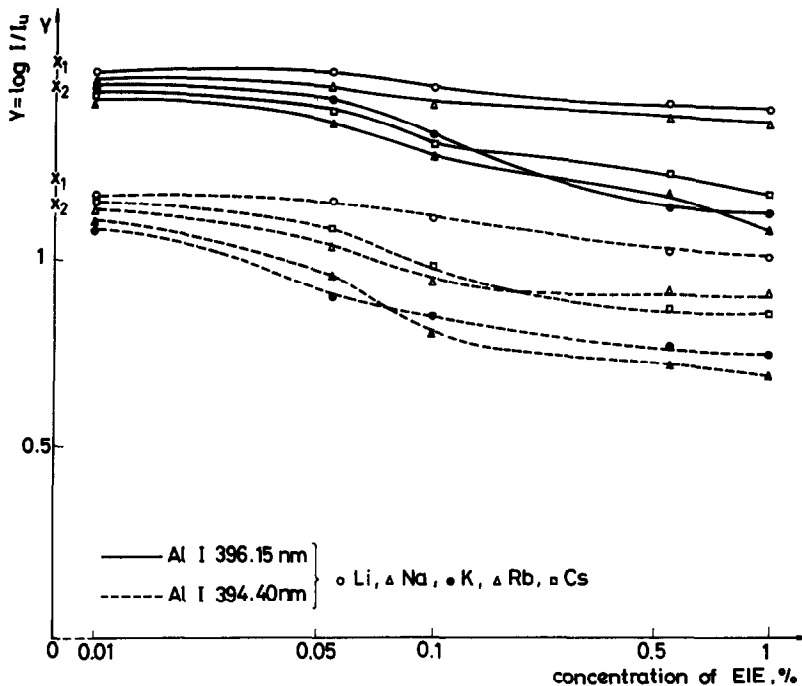


Fig. 4. Background corrected Al I curves as a function of EIE concentration. X_1 values on axis Y represent Y values obtained with empty Al cathode cup. X_2 values represent Al intensities in the presence of 0.1% Sr (dried from aqueous solution); $Y = \log I/I_0$ background corrected relative signal.

ionisation processes in the HCD are not completely free from interelement effects.

The EIE's in the plasma cause ion and electron densities, and electron energies to change, and as a consequence the conditions for the ionization and excitation processes are also changed, a smaller number of metastable state excited gas atoms are produced; all these processes causing changes in the spectrum.

The interelement processes can be detected for Sr, He and Al spectral lines in the presence of concomitant EIE's.

A considerable decrease in Sr^+ ion line intensities measured in the presence of EIE's was observed at concentrations higher than 0.5% for Li, Na, K and over 1% for Rb and Cs.

Table 3. Changes in current intensity under the effect of Li, Na, K, Rb and Cs

	%	i/mA	^{87}Sr (560 mA)	
Li	0.01	570	1.02	
	0.1	580	1.04	
Na	0.01	610	1.09	
	1	630	1.13	
K	0.01	620	1.11	
	1	640	1.14	
Rb	0.01	650	1.16	
	1	670	1.20	
Cs	0.01	680	1.21	
	1	700	1.25	

This phenomenon can be explained by the decreased electron energies and the reduced number of metastable gas atoms. The decrease in the spectral line intensities of He carrier gas clearly indicates a decrease of energy in the plasma. The decrease in spectral line intensities of Al originating from the cathode cup in the presence of EIE's indicate the decrease of the sputtering yield, which may be explained by the decrease in the number and energy of gas ions and metastable gas atoms.

It has been observed that the effect of EIE's is considerable when the ratio between the number of gas atoms (n_g) and the number of atoms with low ionisation energy (n_a) — n_g/n_a — is lower than 10^{12} .

Although a relative standard deviation of less than 5% can generally be achieved with the HCD/AES method, in the present experiments the relative standard deviation obtained from 7 parallel measurements was found to be up to 8% due to the presence of EIE's in the plasma.

REFERENCES

1. H. Schüler, *Z. für Phys.*, 1930, **59**, 149.
2. F. T. Birks, *Spectrochim. Acta*, 1954, **6**, 169.
3. H. J. Eichhoff, *Phys. Chem. Rada*, 1964, **13**, 7.
4. W. Grimm, *Spectrochim. Acta*, 1968, **23B**, 443.

5. G. Milazzo and N. Sporzani, *Appl. Spectrosc.*, 1967, **21**, 172.
6. Zs. Szilvássy-Vámos, *XVI. Ung. Tagung für Spectralanalyse, Balatonszéplak Chem. Sect. II*, 1973, 121.
7. Zs. Szilvássy-Vámos, *XX Coll. Spectr. Inter Prague, Abstracts*, 1977, 513.
8. J. A. C. Broekaert, *Spectrochim. Acta*, 1979, **34B**, 11.
9. *Idem*, *Bull. Soc. Chim. Belg.*, 1976, **85**, 261.
10. D. E. Maksimov and A. N. Rudnevskii, (*USSR*) *Zh. Prikl. Spektrosk.*, 1981, **34**, 406.
11. D. E. Maksimov and A. N. Rudnevskii, *Phys. Chem. (USSR)*, 1981, **256**, 628.
12. A. N. Rudnevskii and P. E. Maksimov, *Zh. Prikl. Spektrosk.*, 1987, **46**, 898.
13. S. Caroli, P. Delle Femine, *Anal. Chim. Acta*, 1982, **15**, 303.
14. S. Caroli and O. Senafonte, *Analyst (London)*, 1983, **108**, 196.
15. T. Török, J. Mika and E. Gegus, *Emission Spectrochemical Analysis Akadémiai Kiadó, Budapest*, 1978, 164.
16. Zs. Szilvássy in *Improved Hollow Cathode Lamps for Atomic Spectroscopy*, S. Caroli (ed.), Chap. 7, pp. 178–203. Ellis Horwood, Chichester, 1985.
17. Zs. Szilvássy-Vámos and A. Buzási, *Mikrochim. Acta*, 1985, **1**, 15.
18. T. Török and K. Zimmer, *Quantitative Evaluation of Spectrograms by Means of "l" Transformation*, Akadémia Kiadó Budapest, 1972.

ENZYMATIC DETERMINATION OF N-METHYLCARBAMATE PESTICIDES AT THE NANOMOLAR LEVEL BY THE STOPPED-FLOW TECHNIQUE

M. C. QUINTERO, M. SILVA and D. PÉREZ-BENDITO

Department of Analytical Chemistry, Faculty of Sciences, University of Córdoba, 14004 Cordoba, Spain

(Received 15 October 1990. Revised 8 April 1991. Accepted 15 April 1991)

Summary—A sensitive and selective kinetic enzymatic method for the determination of N-methylcarbamate pesticides is presented. It is based on their inhibitory effect on electric eel acetylcholinesterase and the use of 5,5'-dithiobis(2-nitrobenzoic) acid (DTNB) as chromogenic reagent for the thiocholine released from the acetylthiocholine iodide substrate. The fast DTNB-thiocholine reaction is monitored photometrically by the stopped-flow technique. Carbaryl, propoxur and carbofuran can be determined at concentrations in the ranges 6.5–120, 2–15 and 0.1–5.0 ng/ml, respectively, by the proposed method. An interference study was also reported.

Pesticides of the carbamate family have become increasingly important in recent years because of their wide ranging biological activity. Among the analytical methods available for their determination, enzymatic methods based on cholinesterase (ChE) inhibition are widely used and can be combined with optical^{1,2} and chromatographic techniques^{3,4} for detection. On the other hand, the inhibitory effect of pesticides (including organophosphorous and chlorinated pesticides) on cholinesterase is known to depend on enzymes sources (human serum, rat liver, electric eel, *etc.*), which also affects the detection limit and sensitivity of determinations. In this context, some attempts have been made^{2,5} at establishing a relationship between the Michaelis-Menten constant (K_m), an index of enzyme-substrate affinity and I_{50} , the inhibitory concentration resulting in 50% inhibition. Kinetic studies of biochemical nature on the inhibition of ChE by carbamate pesticides⁶⁻⁸ or others⁹ have been developed with the aid of stopped-flow instrumentation. However, so far this technique has not been applied to these pesticides for analytical purposes.

This paper reports the use of a single modular stopped-flow system for the kinetic determination of carbaryl, propoxur and carbofuran on the basis of their inhibitory effect on electric eel acetylcholinesterase (AChE), using acetylthiocholine iodide (ATChI) as substrate and 5,5'-dithiobis(2-nitrobenzoic) acid (DTNB) as chromogenic reagent. The use of the above-

mentioned enzyme source, the optimized procedure for the incubation process and the stopped-flow technique to monitor the chromogenic reaction improved already existing methods in terms of sensitivity and selectivity, thereby providing a useful automated means of carrying out analyses for these pesticides.

EXPERIMENTAL

Reagents

All reagents used were analytical-reagent chemicals; solutions were prepared in distilled water and 1,4-dioxane. Carbaryl, propoxur and carbofuran (Chem. Service Inc.) solutions ($6.63 \times 10^{-6} M$) made by dilution of more concentrated stock solutions prepared by dissolving 100.0 mg of the corresponding chemical in 100 ml of 1,4-dioxane, were stored in PTFE bottles in a refrigerator. An acetylthiocholine iodide ($9.4 \times 10^{-3} M$) solution was prepared by dissolving 68 mg of this chemical (Sigma Chemical) in 25 ml of distilled water. A $1 \times 10^{-3} M$ DTNB solution was prepared by dissolving 100 mg in 250 ml of TRIS buffer of pH 7.4. A 0.05M TRIS buffer solution was prepared by dissolving 6.05 g of Tris and 6.64 g of sodium chloride in water and using hydrochloric acid or sodium hydroxide to adjust the pH to 7.4, 8.0 or 9.0 in a final volume of one litre. An electric eel acetylcholinesterase (Sigma Chemical) solution of 4.0 units/ml was prepared from the lyophilized powdered enzyme containing 5% ammonium

sulphate and featuring a protein activity of 200–400 units/mg.

Apparatus

A Perkin–Elmer Lambda 5 spectrophotometer coupled on-line with a stopped-flow module¹⁰ was used. The acquisition and treatment of kinetic data was performed by a Hewlett-Packard 98561AE computer and a 16-bit Hewlett-Packard 98640A analogue-to-digital converter. The software required for application of the kinetic method was written by the authors themselves.

Procedure for kinetic-enzymatic determination of *N*-methyl-carbamate pesticides

Two solutions were prepared and placed in the drive syringes. For solution A, an aliquot of the pesticide solution containing a few nanograms of the compound (32.5–600 ng of carbaryl, 10–75 ng of propoxur and 0.5–25 ng of carbofuran) and 0.5 ml of electric eel acetylcholinesterase solution of 4.0 units/ml were added to a 5-ml standard flask. The mixture was then diluted to the mark with 0.05M TRIS buffer of pH 8.0. This solution was incubated at 37° for 30 min. Solution B was prepared by mixing 0.8 ml of 9.4×10^{-3} M acetylthiocholine iodide solution and 2.5 ml of 10^{-3} M DTNB solution in a 10-ml standard flask and diluting to the mark with 0.05M TRIS buffer of pH 9.0. Equal volumes of both solutions were mixed in the stopped-flow system and the reaction was monitored at 400 nm. The temperature was kept constant at $35 \pm 0.1^\circ$ throughout. The kinetic curve, the initial rate (both in the presence of pesticide and in its absence) and the analyte concentration were automatically acquired by the computer.

RESULTS AND DISCUSSION

Carbamate insecticides, like other pesticides (organochlorine and organophosphorous) are known to inhibit the action of acetylcholinesterase, which acts on the hydrolysis of acetylthiocholine. The inhibitory effect involves the formation of a complex between the enzyme and the pesticide and the subsequent carbamoylation and de-carbamoylation of the enzyme. The overall inhibition process is rather slow and requires several minutes for the incubation step, depending on the specific activity of the inhibitor.

In the proposed method, the amount of the thiocholine released in the hydrolysis reaction of acetylthiocholine, which is a measure of the amount of pesticide-inhibitor present, is monitored photometrically by adding DTNB, which reacts with thiocholine yielding a sulphur derivative of 2-nitrobenzoic acid which is responsible for the colour observed. This compound shows maximum absorption at 400 nm. This reaction is completed in a few seconds, which calls for the use of the stopped-flow technique to make the kinetic measurements. Figure 1 shows the kinetic curves obtained, both for the enzymatic (curve 1) and for the inhibited (curve 2) reaction, which are the basis for the development of this automated kinetic method for *N*-methylcarbamate pesticides.

Three *N*-methylcarbamates, namely carbaryl, propoxur and carbofuran were selected to develop this enzymatic stopped-flow approach by using DTNB as chromogenic reagent. This reagent had previously been used for the kinetic determination of thiofanox with electric eel acetylcholinesterase on a CentrifChem 400 Analyser;¹ however, the sensitivity achieved was lower than that provided by the proposed method.

Influence of variables

The working conditions for application of the method were optimized by using carbaryl only as pesticide-inhibitor to examine the influence of variables on both the incubation and the chromogenic reaction (post-incubation) processes.

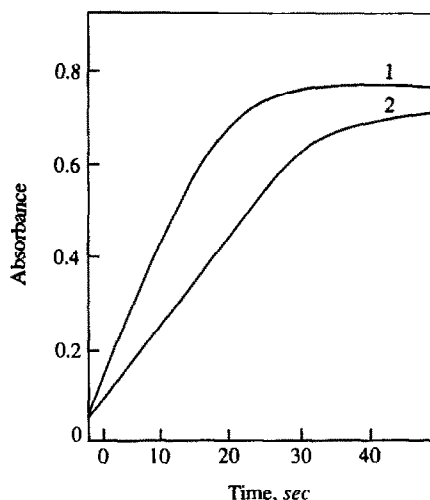


Fig. 1. Inhibitory effect of carbaryl on the enzymatic reaction: (1) enzymatic reaction; (2) reaction inhibited by 120 ng/ml of carbaryl. Reaction conditions as described in Procedure.

The optimal conditions found for carbaryl were applied to propoxur and carbofuran and appropriate corrections were introduced if required.

Incubation process. Variables were optimized so as to obtain the maximum inhibition of the enzymatic activity of the pesticide. The inhibition percentage I (%), the measurement parameter used, is given by:

$$I(\%) = [(V_E - V_I)/V_E] \times 100 \quad (1)$$

where V_E and V_I are the reaction rate in the absence and presence of inhibitor, respectively. There is a linear relationship between I (%) and the concentration of pesticide-inhibitor.

The pH, temperature and incubation time were the factors which most strongly influence the enzyme-pesticide reaction. However, as the pesticide was previously dissolved in an organic solvent (1,4-dioxane), it was necessary to examine the influence of the solvent on the enzyme action in the absence of pesticide. The results of the experiments carried out at 25° and pH 7.4 (with 0.05M TRIS buffer) showed high 1,4-dioxane contents inhibit the action of AChE; the maximum allowed content of this solvent without causing inhibition was 2.8% (14 μ l of 1,4-dioxane per 0.5 ml of electric eel acetylcholinesterase solution of 4.0 unit/ml).

Other variables were also studied at a physiological pH value of 7.4 adjusted with TRIS buffer. By using the procedure described under Experimental, the effect of the temperature on the incubation was examined between 30 and 40° for a constant, arbitrary incubation time of 5 min. The results showed I (%) to increase with the temperature up to about 34°, above which it kept constant up to 37°. At higher temperatures, I (%) decreased owing to the enzyme denaturation [Fig. 2(a)]. An incubation temperature of 37° was thus selected. The effect of the incubation time on I (%) at 37° is shown in Fig. 2(b). An incubation time of 30 min was finally chosen.

In order to check the suitability of the incubation procedure, we studied the stability of the incubated solution under the conditions described above. The inhibition percentage was found not to vary with time, at least up to 2 hours after the incubation step.

Post-incubation step. The working conditions for this step, which involves the fast coloured reaction by mixing the DTNB solution with the incubated solution, was aimed at obtaining the maximum possible rate of the chromogenic reaction. The slope of the initial portion of the

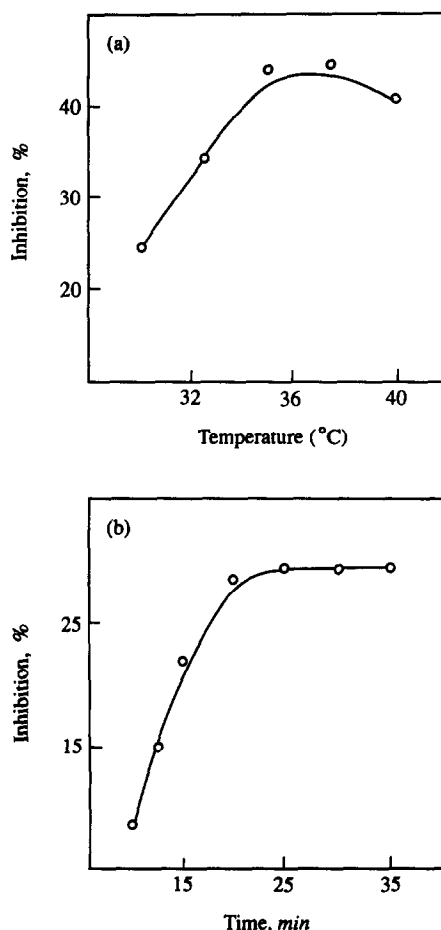


Fig. 2. Effect of (a) temperature and (b) time on the enzyme inhibition by carbaryl in the incubation process (conditions described in Experimental)

absorbance-time curves (initial-rate method) was monitored by the stopped-flow technique and used as a kinetic parameter.

The effect of temperature on the reaction rate was examined between 15 and 45°. The initial rate increased with the temperature up to 35°, above which it remained practically constant but decreased slightly above 40°. A temperature of 35° was chosen as optimal.

The influence of the ATChI substrate concentration was studied over the range 9.43×10^{-5} – $9.43 \times 10^{-4}M$; the reaction rate was found to increase with the ATChI concentration up to $6.5 \times 10^{-4}M$ above which it remained constant [see Fig. 3(a)]. An ATChI concentration of $7.5 \times 10^{-4}M$ (0.8 ml of the $9.4 \times 10^{-3}M$ solution) was selected. From the dependence shown in Fig. 3(a), the Michaelis-Menten constant was found to be $K_m = 2.54 \times 10^{-4}M$.

The effect of the concentration of the chromogenic reagent, DTNB, was studied in the

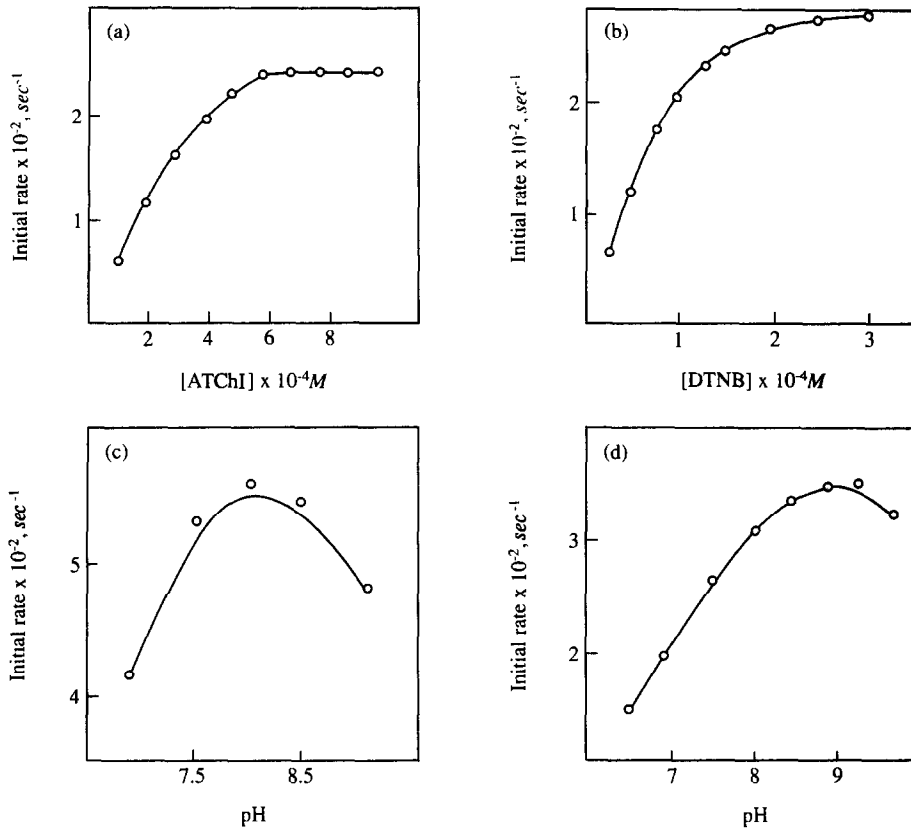


Fig. 3. Effect of (a) ATChI, (b) DTNB concentration, (c) pH of analyte solution and (d) pH of chromogenic reagent solution in the post-incubation step (conditions described in Experimental).

range $0.25\text{--}3.0 \times 10^{-4}M$ [Fig. 3(b)]. A DTNB concentration of $2.5 \times 10^{-4}M$ was selected (2.5 ml of $10^{-3}M$ DTNB solution), corresponding to zero-order zone of the dependence observed.

The study of the effect of pH on the reaction rate was made alternately on the analyte solution (from the incubation process) (solution A) and on the chromogenic reagent solution (solution B) by adjusting the pH between 6.2 and 10.3 with $0.05M$ TRIS buffer in both cases. The influence of the pH of solution A is shown in Fig. 3(c) and a pH of 8.0 was selected as optimum, whereas a pH value of 9.0 was chosen as optimum for solution B according to the results shown in Fig. 3(d). The decreasing of the initial rate at pH higher than 8 is due to hydrolysis of the substrate itself. The optimal concentration of the TRIS buffer was found to be $0.05M$ in both cases.

The influence of the enzyme on the sensitivity of the determination of N-methylcarbamate pesticides (using carbaryl) was studied at three concentrations, 2.4, 4.0 and 5.6 unit/ml under optimal conditions described under Experimental over the linear concentration range of the pesticide. The results obtained are shown in

Fig. 4. Although, with 5.6 unit/ml of the enzyme, the sensitivity was slightly higher, a concentration of 4.0 unit/ml was more than adequate and avoided unnecessary usage of the enzyme.

Analytical features

Under the optimal working conditions, carbaryl, propoxur and carbofuran were determined at the nanomolar level by the proposed

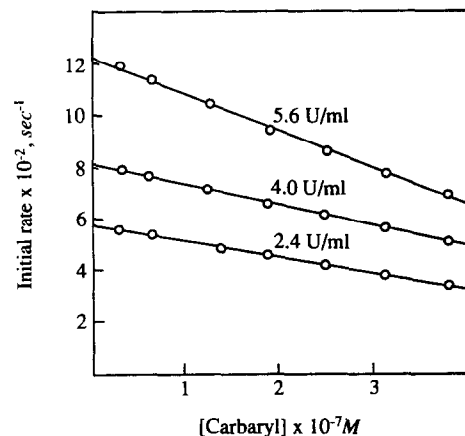


Fig. 4. Calibration graph for carbaryl at various AChE concentrations (conditions described in Experimental).

Table 1. Analytical figures of merit of the determination of N-methylcarbamate pesticides by the proposed kinetic enzymatic stopped-flow method

Feature	Carbaryl	Propoxur	Carbofuran
Dynamic linear range, ng/ml	6-150	2-15	0.1-5.0
Sensitivity, ng/ml	0.398	2.06	13.21
I_{50} , ng/ml	120	40	3.0
Detection limit, ng/ml	4.3	0.8	0.1
Precision (RSD), %	0.61	0.76	0.55

kinetic enzymatic method. The temperature and time used in the incubation of carbaryl also yielded good results for propoxur and carbofuran. Table 1 shows the analytical figures of merit of the determination of these pesticides. The linear range of the calibration graph varied with the pesticide, the concentration quoted being the actual concentration of the analyte in the mixing-observation chamber of the stopped-flow module. The comparative sensitivities, taken as the slope of the respective calibration graphs, and the I_{50} values (the inhibitor concentration for 50% inhibition), varied in the sequence:

Carbofuran > Propoxur > Carbaryl

The detection limit was calculated as the minimum pesticide concentration resulting in a statistically significant I (%) according to the expression:

$$C_{DL} = I_{DL}(\%)/m \quad (2)$$

where $I_{DL}(\%)$ is the minimum value statistically obtained by substituting $V_E - V_I$ in equation (1) by three times the standard deviation (3σ) of the initial rate of the enzyme, V_E , in the absence of pesticide; m is the slope of the calibration graph (analytical sensitivity). The detection limit was experimentally obtained by substituting $I_{DL}(\%)$ in the calibration graph of each pesticide. Taking into account the calculated value of V_E was $9.03 \times 10^{-2} \text{ sec}^{-1}$ and that its $3\sigma = 1.54 \times 10^{-3}$, the minimum detectable value of the inhibition percentage [$I_{DL}(\%)$] found was 1.7%. Substituting this value into equation (2) gave the C_{DL}

Table 2. Selectivity achieved in the kinetic enzymatic stopped-flow determination of 20 ng/ml of carbaryl

Compound assayed	Tolerance ratio
Malathion, methylparathion, aldrin, dieldrin	100†
α -HCH,* lindane, maneb, zineb, ziram	
Fenitrothion	25
Paraoxon, carbofuran, propoxur	< 1

* α -HCH = 1,2,3,4,5,6-hexachlorocyclohexane.

†Maximum ratio tested.

values listed in Table 1. The precision was determined from 11 samples containing 80, 10 and 12 ng/ml of carbaryl, propoxur and carbofuran each, respectively. These results show the method is highly sensitive for the determination of these pesticides, especially carbofuran.

Regarding the selectivity, it is well known that many pesticides, not only those of the carbamate family, inhibit the action of the enzyme ChE,¹¹ the selectivity being strongly dependent on the enzyme source.¹² Thus, it has been claimed² that by using electric eel cholinesterase only chlorinated pesticides inhibit the enzyme activity. However, studies on the influence of organochlorine pesticides on the determination of these N-methylcarbamates pesticides by the proposed method (using electric eel acetylcholinesterase) showed chlorinated pesticides do not interfere at the maximum level tested (see Table 2). This selectivity study also showed the proposed method to be selective against organophosphorous pesticides assayed, except for paraoxon, which interfered at the same concentration level as the pesticide tested.

Taking into account the good selectivity achieved by this method for the determination of these N-methylcarbamate pesticides and their relative reactivity, it is useful for the determination of carbofuran in water samples as well as for the analysis of these pesticides in formulations.

Acknowledgement—The authors gratefully acknowledge financial support from the CICYT (Project No. PB87-0821).

REFERENCES

1. B. H. Chin and N. Spangler, *J. Agric. Food Chem.*, 1980, **28**, 1342.
2. M. H. Sadar, S. S. Kuan and G. G. Guilbault, *Anal. Chem.*, 1970, **42**, 1770.
3. C. E. Mendoza and J. B. Shields, *J. Agric. Food Chem.*, 1973, **21**, 178.
4. M. F. Cranmer and A. Peoples, *Anal. Biochem.*, 1973, **55**, 255.
5. S. U. Bhaskar and N. V. N. Kumar, *J. Assoc. Off. Anal. Chem.*, 1982, **65**, 1297.
6. G. L. Horton, J. R. Lowe and C. N. Lieske, *Anal. Biochem.*, 1977, **78**, 213.
7. L. C. Post, *Biochim. Biophys. Acta*, 1971, **250**, 121.
8. T. Nishioka, K. Kitamura, T. Fujita and M. Nakajima, *Pestic. Biochem. Physiol.*, 1976, **6**, 320.
9. G. J. Hart, *ibid.*, 1974, **4**, 239.
10. A. Loriguillo, M. Silva and D. Pérez-Bendito, *Anal. Chim. Acta*, 1987, **199**, 29.
11. J. R. Corbett, K. Wright and A. C. Baillie, *The Biochemical Mode of Action of Pesticides*, 2nd Ed., Academic Press, London, 1984.
12. R. D. O'Brien, *Biochem. J.*, 1961, **79**, 229.

SEPARATION AND IDENTIFICATION OF VARIOUS VULCANIZATION AGENTS AND ANTIOXIDANTS IN TWO TYPES OF RUBBER BY CHROMATOGRAPHIC AND SPECTROMETRIC METHODS

S. CHAUVEAU and M. HAMON

Laboratoire de Chimie Analytique, Faculté de Pharmacie, 5 rue Jean Baptiste Clément,
92 290 Chatenay Malabry, France

E. LELEU

AKZO Chemicals, BP 217, 60 202 Compiègne Cédex, France

(Received 2 January 1991. Revised 17 April 1991. Accepted 22 April 1991)

Summary—The aim of this study was to separate and identify by chromatographic and spectrometric methods, the various allergenic vulcanization agents and antioxidants used in the manufacture of industrial rubber. Specimens of elastomers were manufactured specially for this study. The specificity of the gas chromatographic method developed allows separation of all the manufacturing additives in the selected rubber types after one injection only, even though they belong to extremely varied chemical categories. The GLC method was coupled with mass spectrometry, which permitted identification of the peaks obtained and the study of the fragmentation of the 4 reference products under various conditions. Separation by TLC was performed in parallel on the same extracts, allowing rapid identification of the products tested for, and showed new spots after vulcanization.

The allergenic potential of rubber items is well known and has been widely investigated in numerous publications. In particular, many cases of reaction to surgical gloves have been reported. It appears, from the literature data, that the allergenic potential of rubber would not be essentially due to the actual polymer, but to secondary constituents, in particular manufacturing agents such as antioxidants and vulcanization accelerators or retardants. The isolated agents have also been tested for potential allergenicity. Such investigations do not however take into account the changes induced by the heat process in vulcanization. Few authors envisaged this issue.^{1,2}

Manufacture of industrial rubber requires an elastomer, sulphur, one or more vulcanization accelerators, an antioxidant and filling material. We have taken an analytical approach to these investigations and carried out a study on specially manufactured experimental specimens containing two accelerators and an antioxidant with each elastomer. Various agents were added to obtain formulations which could be manufactured under normal industrial conditions in the following proportions: elastomer 100, zinc oxide 5, stearic acid 1, carbon black 25, sulfur 2, accelerators 1 + 0.5 and antioxidant 2.

Furthermore, we tested the composition of the mixtures before and after vulcanization, which does not seem to have been done in existing literature. Preparation of the initial mixtures takes place at a temperature of approximately 70°, and the vulcanization process itself around 200°, generally under pressure.

EXPERIMENTAL

Extraction

Extraction was performed on the rubber specimens in a Soxhlet extractor for six hours with a defined amount of acetone at the boiling temperature of the solvent. The samples obtained were stored in a refrigerator after evaporation to dryness in a vacuum, to be recovered extemporaneously with a small amount of acetone for analysis.

Separation

Gas-liquid chromatography. The following operating conditions were used:

Temperature graded from 50 to 230° in levels of 10°/1 min without an initial plateau.

Splitless injector.

Table 1. *R_f* values of the products by TLC with two solvents

Products	Solvent 1	Solvent 2
MBT	0.07	0.25
CBS	0.52	/
DPG	/	0.65
TMTM	0.35	0.88
IPPD	0.31	/
6PPD	0.49	/

Thin-layer chromatography. Two solvents were used:

System 1: Toluene/ethylacetate/ammonia (100/5/1)

System 2: Toluene/acetone/ammonia (45/65/1)

Separation was obtained with the *R_f* values shown in Table 1 for the following products:

solvent 1: CBS, MBT, IPPD, 6PPD, TMTM

solvent 2: DPG, MBT, TMTM.

Operating conditions

Materials. Specimens of elastomers were manufactured specifically for this study. Raw materials were therefore selected with particular regard to their allergenic potential. Two types of elastomers were used: isoprene rubber (IR) and styrene butadiene rubber (SBR).

The following vulcanization accelerators were selected to typify the various chemical categories, since it was observed that the allergic reactions to rubber items are most frequently related to groups of chemicals: cyclohexyl benzothiazyl sulphenamide (CBS), mercaptobenzothiazole (MBT), tetramethyl thiuram monosulphide (TMTM) and diphenylguanidine (DPG).

The two antioxidants used are *para*-phenylene diamine derivatives: *N*-isopropyl *p*-phenylene diamine (IPPD) and *N*-1,3-(dimethyl-butyl) *N'*-phenyl phenylene diamine (DMPPD or 6PPD). The specimens were manufactured with the additives in different formulas. In this way, the role of each of the additives could be derived from the comparison of results observed (Table 2). One half of each sample was vulcanized and the other half left raw to show the effects of vulcanization on the constituents of the mixtures.

Extraction. The method of extraction is derived from the exhaustive study of Vimalasiri

*et al.*³ The duration of the procedure was determined by successive extractions for one hour each and determination by gas chromatography of the amounts present in each extraction.

For a better assessment of possible losses, we also evaluated product degradation resulting from extraction by gas-chromatography in the presence of an internal standard. As a result of the disappearance of CBS, the study of this product was impossible with this extraction method.

Preservation of the obtained organic extracts was evaluated by thin-layer chromatography. In view of the results, it was decided to eliminate the solvent and to store the dried extracts in a refrigerator before analysis. The appearance of additional spots on TLC performed a few hours after storage in the solvent, evidenced degradation of the extracts in the liquid phase.

Separation. The difficulty in isolating each of the additives used and present in the rubber mixtures in one operation arises from their very different polarities.

(i) Gas-liquid chromatography. Separation of the vulcanization agents in rubber extracts was obtained by gas-liquid chromatography coupled with mass spectrometry for identification of the peaks observed. We verified that stearic acid does not interfere with the tested agents. To study the effect of vulcanization, we used chromatographs of raw elastomer extracts previously performed under the same conditions as blanks. Reference mixtures of additives corresponding to the manufactured specimens were also prepared under the same conditions. The addition of measured amounts served to confirm the presence or absence of the test agents. Reproducibility and repeatability of the method were tested before coupling with mass spectrometry.

(ii) Thin-layer chromatography. TLC was performed simultaneously to separate additives in the extracts. Results yielded by each method were found to be complementary. Separation of all test agents required the use of two solvents.

Analysis by mass spectrometry. The reference additives selected for the study were first injected alone under the same conditions as defined for the extracts to obtain reference

Table 2. Formulas of the samples

IR	SBR
IR ₁ = CBS + TMTM	SBR ₁ = MBT + TMTM + 6PPD
IR ₂ = CBS + TMTS + 6PPD	
IR ₃ = CBS + TMTM + IPPD	SBR ₃ = MBT + DPG + 6PPD

chromatograms and groups. The results obtained with a 70 eV electronic impact were for most agents in agreement with those reported by several authors.⁴⁻⁸

However, the mass spectrum of TMTM obtained under these conditions did not give a molecular peak, and therefore identification of the agent in a complex mixture was impossible. Furthermore tests were therefore carried out with a 20-eV impact, at which the molecular peak was obtained.

RESULTS

Thin-layer chromatography

The separation of the products in the extracts were possible, using the two solvents, as shown in Figs. 1 and 2.

Analysis by mass spectrometry of reference samples

The mass spectrum with 70 eV electronic impact and fragmentations of the 5 tested products can be found in the existing literature. To our knowledge, however, no data are available on 6PPD, which was therefore investigated in our study (Fig. 3).

As indicated previously, the conditions selected to obtain the mass spectrum of TMTM did not provide for the molecular peak. Further tests were therefore performed with 20 eV and the molecular peak obtained (Fig. 4). Some of the products were also studied under these

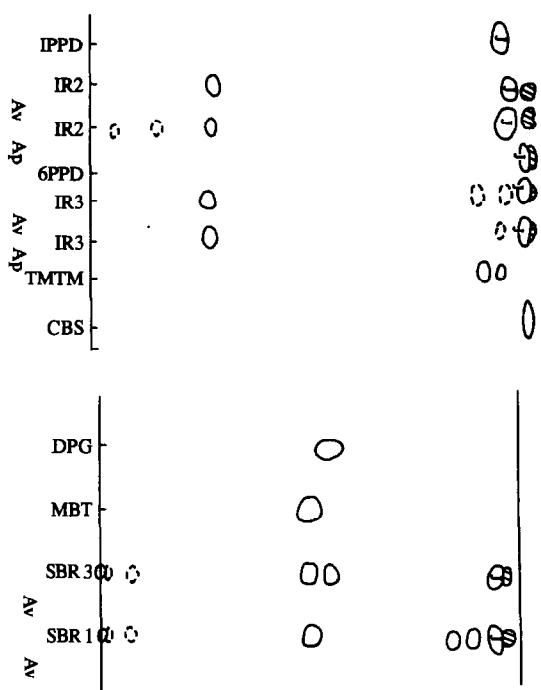


Fig. 2. TLC of the extracts using solvent 2. (⊙) yellow, fluorescent under UV. (⊗) yellow-brown, no fluorescent. (○) fluorescent under UV.

conditions and the new fragmentations give evidence of the preferential terminations; the fragmentation of DPG under 20 eV is given as an example in Fig. 5.

DISCUSSION

The specificity of the chromatographic method used is that it allows separation of all the manufacturing additives in the selected rubber types, although they belong to extremely varied chemical categories and contain inorganic parts which make chromatographic analysis difficult in the polymer compounds. The effects of vulcanization on the extracts could be seen after just one only.

The selected method gives the best extraction of the rubber for our chromatographic conditions while being least drastic in view of the stability of the tested products and of the treatments to which the specimens were submitted prior to analysis. Indeed, acetone reaches boiling point at 66°, a temperature lower than that used to mix the additives into the gum before vulcanization (approximately 70°); besides, exhaustion of the specimens under reflux was found to be the only efficient method of extraction.

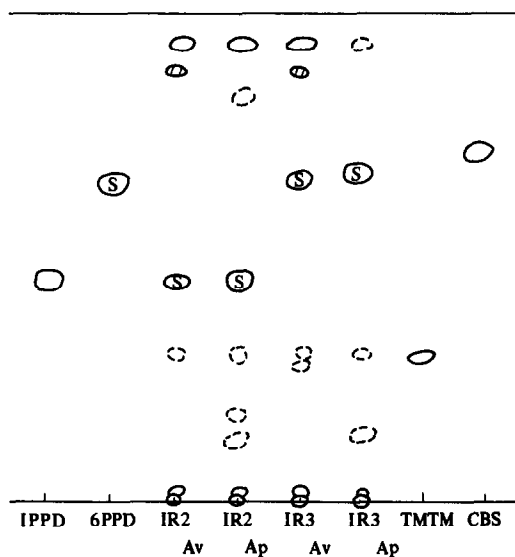


Fig. 1. TLC of the extracts using solvent 1. (⊙) yellow, fluorescent under UV. (⊗) yellow, no fluorescence. (○) fluorescent under UV.

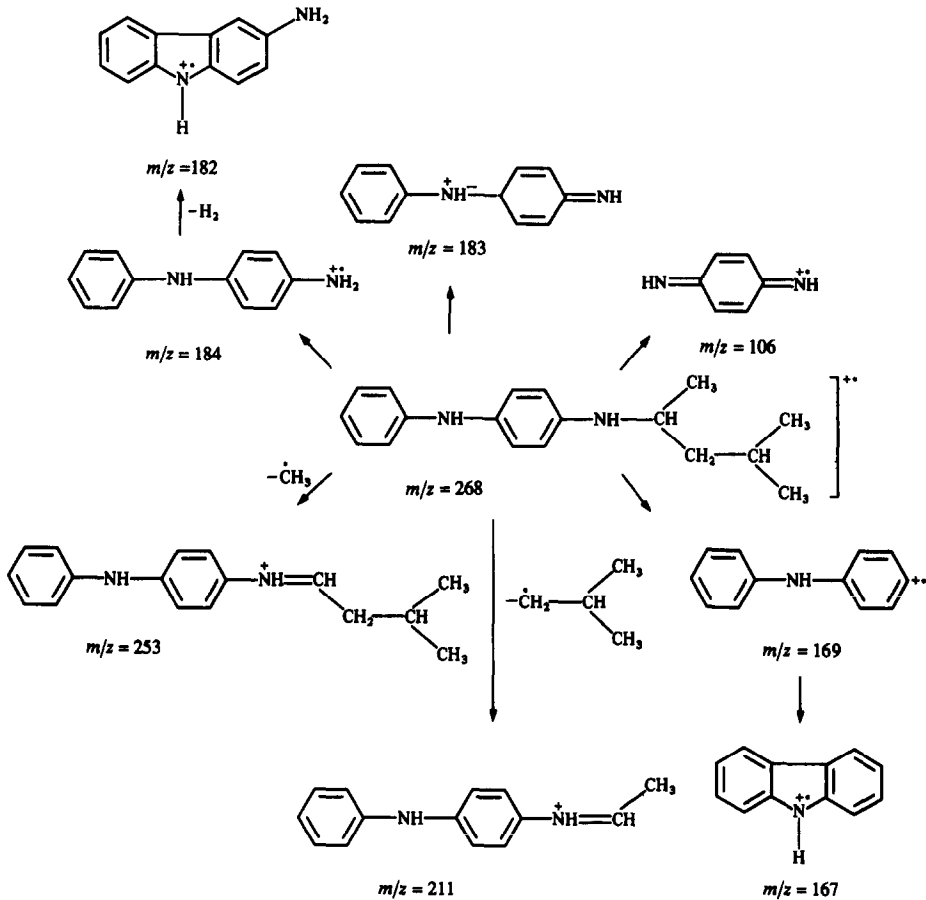


Fig. 3. 6PPD Mass fragmentation.

CBS cannot withstand such temperature conditions and is present in the extracts in a degraded form: degradation may take place during extraction, but it is thought that it occurred previously, since the mixture is prepared under heat.

Our chromatographic study was meant to be exclusively qualitative; the GLC study included

a reproducibility study of the retention time results obtained with the tested products individually and as a mixture. We also tested the peak height relationship in order to detect a possible adsorption of the products on the column or interactions between products, but such phenomena failed to be observed. TMTM, however, shows some particular features with

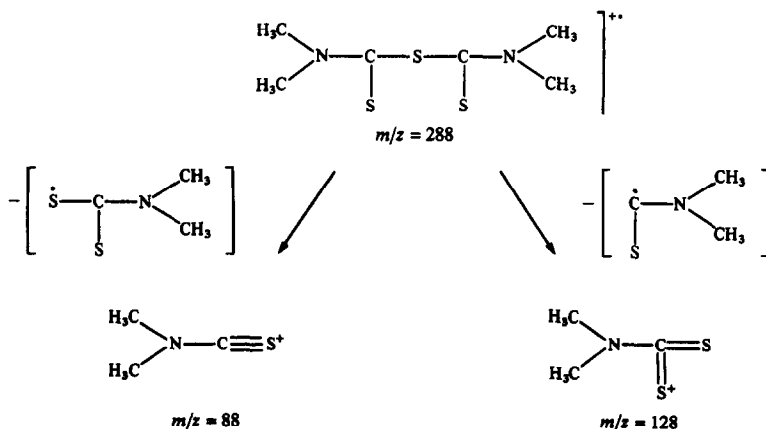


Fig. 4. TMTM Mass fragmentations under 20 eV.

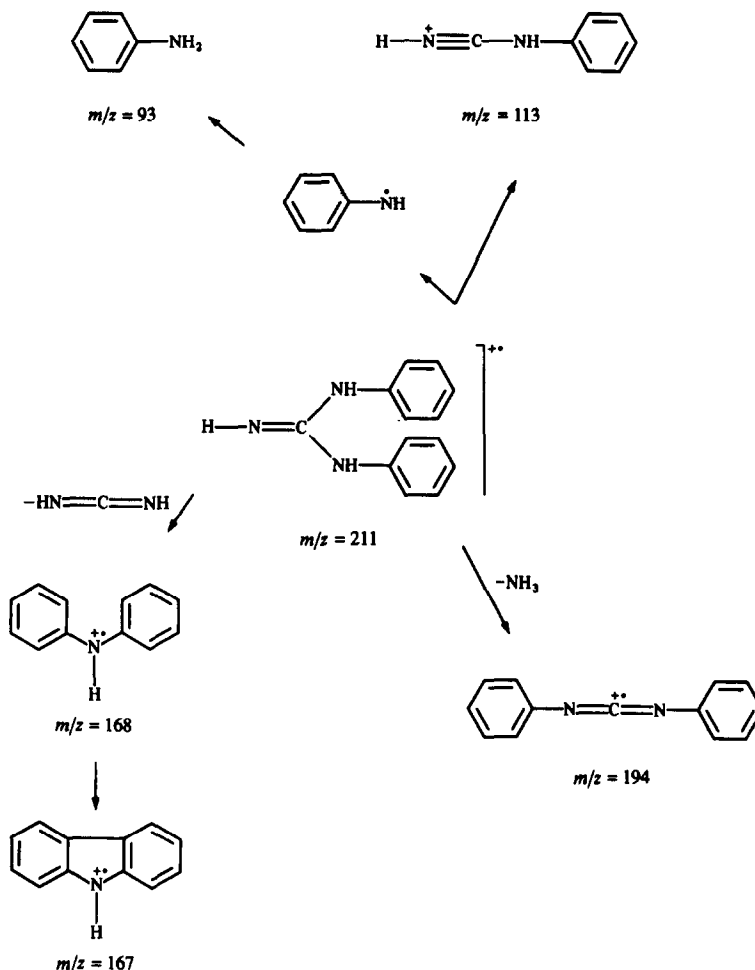


Fig. 5. DPG Mass fragmentations under 20 eV.

chromatography. With TLC, its presence in the extracts before vulcanization is sometimes characterized by several spots, and in GLC by a group of peaks, one of which only has the molecular weight of the initial product as measured by mass spectrometry. The product therefore appears to have undergone partial transformation while being mixed into the rubber in hot air.

Separation by TLC performed in parallel on the same extracts rapidly allowed the products tested to be identified and showed new spots after vulcanisation. The additional advantage of this method is that it allows one to detect, from large deposits, products present in small amounts in the extracts after vulcanization (e.g. MBT).

Mass spectrometry permitted not only to identify the peaks obtained, but also to study the fragmentation of the 4 reference products by applying two different electronic energy levels.

Two examples are shown here of the preferential fragmentations which occur under 20 eV and of the new fragmentations which may occur under 70 eV, an impact too heavy in view of the stability of such fragmentation intermediates.

REFERENCES

1. R. H. Campbell and R. W. Wise, *Rubber Chem. Technol.*, 1964, **37**, 635.
2. S. Fregert, *Acta Derm. Venereol.*, 1969, **49**, 45.
3. P. A. D. T. Vimalasiri, J. K. Haken and R. P. Burford, *J. Chromatog.*, 1984, **300**, 303.
4. G. Salmona, A. Assafa, A. Gayte-Sorbier and C. B. Airaud, *Biomed. Mass Spectrom.*, 1984, **11**, 450.
5. G. Czybulka, H. Dunker, H.-J. Dussel, H. Logeman and D. O. Hummel, *Angew. Makromol. Chem.*, 1981, **100**, 1.
6. D. O. Hummel, G. Czybulka and H.-J. Dussel, *Makromol. Chem. Rapid Commun.*, 1982, **3**, 335.
7. B. J. Millard and A. F. Temple, *Org. Mass Spectrom.*, 1968, **1**, 285.
8. A. S. Hilton and A. G. Alteneau, *Rubber Chem. Technol.*, 1973, **46**, 1035.

FORMATION RATES AND PROTONATION CONSTANTS OF AZO DYES IN A SODIUM DODECYLSULPHATE MICELLAR SOLUTION

J. S. ESTEVE ROMERO, M. C. GARCÍA ALVAREZ-COQUE and G. RAMIS RAMOS*

Departamento de Química Analítica, Facultad de Química, Universitat de Valencia,
46100 Burjassot, Valencia, Spain

(Received 15 October 1990. Revised 15 April 1991. Accepted 18 April 1991)

Summary—The effects of a sodium dodecylsulphate micellar solution on the coupling rates of several diazotized arylamines with *N*-(1-naphthyl)-ethylenediamine and the shifts in the protonation constants of the corresponding azo dyes are quantitatively studied. Aniline, *o*-, *m*- and *p*-aminobenzoic acids, ethyl *p*-aminobenzoate and several sulphadriugs are used, and the relationships among the intensity of the effects and the molecular structure of the diazonium ions and the dyes are discussed. A single simplified procedure for the determination of all the substances at pH = 1.3 ± 0.3, where coupling is quickly completed to directly produce the protonated form of the dyes, is established and applied to the analysis of several pharmaceutical preparations.

Arylamines are frequently determined spectrophotometrically after diazotization and coupling with an adequate substrate such as *N*-(1-naphthyl)-ethylenediamine (NED).¹⁻⁴ The procedures are highly sensitive and widely applicable, but drawbacks are slow reactions, the limited solubility of many analytes or of their corresponding azo dyes, and finally, the necessary pH changes before and after coupling which are needed. Diazonium ions are formed at pH ≈ 1, whereas pH > 4 is necessary for coupling if the diazonium ion lacks a strong activating substituent, and an additional adjustment of pH is usually done to obtain the protonated form of the dye, which has a higher absorptivity and absorbs at longer wavelengths than its basic form.

In a previous paper⁵ we showed that in a sodium dodecylsulphate (SDS) micellar solution the rate of the coupling reactions greatly increases. Also, in this medium, the protonization of the azo dyes is inhibited. Both effects permit the rapid formation of the protonated dyes in an acetate buffer, thus making possible a simplification of the conventional procedures for the determination of arylamines. The possibility of directly analyzing hydrophobic samples, such as vegetable oils, in a microemulsion containing SDS has also been demonstrated.⁶

In this work, the effects of the SDS micellar medium on the coupling rates of several arylamines with NED and the shifts in the protonation constants of the corresponding azo dyes are quantitatively studied. The relationships among the magnitude of the effects and the molecular structure of the diazonium ions and the dyes are discussed, and consequences of analytical interest are drawn.

EXPERIMENTAL

Reagents and apparatus

Analytical-reagent grade aniline, sodium nitrite, sulphamic acid (Probus, Spain), NED dichloride (Scharlau, Spain), *o*- and *m*-aminobenzoic acids (Merck, Germany), SDS, *p*-aminobenzoic acid and ethyl *p*-aminobenzoate (Fluka, Switzerland) were used. Sulphonamides were obtained from several pharmaceutical laboratories. Solutions of the diazotizable substances were prepared in water, as well as in a medium containing 1.25% SDS and 0.15M hydrochloric acid. Distilled demineralized water was used throughout.

A Crison micropH 2001 pH-meter, a Shimadzu UV-240 and a Perkin-Elmer Lambda 9 spectrophotometer were used. All measurements were made at 25°.

Procedures

Acid-base titrations. A mixture of 200 ml of the diazotizable substance solution and 10 ml

*Author for correspondence.

of 1% sodium nitrite was allowed to react for 5 min in a 500-ml standard flask. The nitrite excess was removed by adding 10 ml of 3% sulphamic acid. After 10 min, 200 ml of 0.5M sodium acetate, 10 ml of 0.75% NED, 25 ml of 1.5M sodium hydroxide and water up to the mark were added.

The final 0.5% SDS concentration was above the critical micelle concentration (cmc) which, at low and moderate ionic strengths, is below 0.3%.^{7,8} In addition, it has been shown that, at this SDS concentration, all changes produced by the surfactant on the log *K* values of the azo dyes have been completed.⁹

Titration with 2M hydrochloric acid, in the absence and presence of 0.5% SDS, were done in triplicate with 150-ml aliquots. Simultaneous photometric and potentiometric monitoring was implemented. Protonation constants were evaluated by linear regression with points within the range $\text{pH} = \log K \pm 1$, the ionic strength being 0.3M. Other details have been reported previously.¹⁰

Kinetic studies. The procedure given above was modified as follows: 25-ml standard flasks were used and the volumes were proportionally reduced. After elimination of the nitrite excess, 4 ml of 0.5M sodium acetate, 0–5 ml of concentrated hydrochloric acid, and water were added. The mixture was kept at 25° in a thermostat. Coupling was started by adding 0.5 ml of 0.75% NED and the reaction was spectrophotometrically monitored for at least 20 min.

Analysis of pharmaceutical preparations. Tablets were pulverized and samples of 50–100 mg were taken. Five successive extractions were made by heating, stirring and centrifuging the powder with 5 ml of the 1.25% SDS–0.15M

hydrochloric acid mixture. The same mixture was used to conveniently dilute the extracts. Suspensions were treated similarly with 1 ml of sample. In all cases, a sixth extract was made and treated separately to assure quantitative extraction. Diazotization and coupling was made in 25-ml standard flasks with 10-ml aliquots of the sample, 0.5 ml of 1% sodium nitrate, 0.5 ml of 3% sulphamic acid, 0.5 ml of 0.75% NED, and water up to the mark. The absorbance was measured at 550 nm.

RESULTS AND DISCUSSION

Absorption spectra

The wavelengths and molar absorptivities of the maxima of the dyes, obtained in a hydrochloric acid medium of $\text{pH} = 1$ in the absence and presence of 0.5% SDS, are given in Table 1. Most sulphonamide dyes were not soluble in water but no precipitation was observed in the micellar medium. The micellar medium produces small bathochromic shifts and slightly enhances the sensitivity, indicating that the $\pi \rightarrow \pi^*$ transition must take place in a less polar environment than in water. The dye formed by *o*-aminobenzoic acid shows a significantly smaller sensitivity which decreases in the micellar medium. This particular behaviour can be due to the presence of an intramolecular hydrogen bond.

Protonation constants

The protonation constants of the dyes in water and in a 0.5% SDS micellar medium are also given in Table 1. It has been shown⁹ that in the latter medium, the apparent protonation constants of the dyes correspond to the

Table 1. Absorption maxima and protonation constants of several azo dyes formed with NED in the absence and presence of 0.5% SDS*

Diazotizable substance	$\lambda_{\text{max}}, \text{nm}$		$\epsilon, \text{l. mole}^{-1} \cdot \text{cm}^{-1}$		log <i>K</i>	log K_c^H	log(K_c^{HA}/K_c^H)
	Water	0.5% SDS	Water	0.5% SDS			
Aniline	555	560	38,300 ± 200	44,900 ± 200	3.033 ± 0.015	4.15 ± 0.10	1.1
<i>o</i> -Aminobenzoic acid	546	550	6400 ± 100	4300 ± 100	4.55 ± 0.04	7.45 ± 0.15	2.9
<i>m</i> -Aminobenzoic acid	534	550	35,800 ± 400	42,400 ± 600	2.89 ± 0.08	3.91 ± 0.10	1.0
<i>p</i> -Aminobenzoic acid	538	551	46,800 ± 100	50,200 ± 1900	3.16 ± 0.07	4.47 ± 0.10	1.3
Ethyl <i>p</i> -aminobenzoate	540	556	44,400 ± 1000	49,000 ± 100	3.31 ± 0.15	3.66 ± 0.04	0.35
Sulphanilamide	538	550	50,900 ± 600	47,600 ± 2000	3.16 ± 0.03	3.86 ± 0.06	0.70
Sulphomethoxazole	†	545	†	44,700 ± 100	†	4.18 ± 0.06	—
Sulphadiazine	†	550	†	49,000 ± 100	†	3.77 ± 0.10	—
Sulphametizole	†	555	†	47,900 ± 1100	†	3.64 ± 0.02	—
Sulphathiazole	†	552	†	46,500 ± 500	†	3.81 ± 0.07	—
Sulphadimetoxine	†	545	†	41,100 ± 1000	†	3.97 ± 0.09	—
Sulphametoxypridazine	†	550	†	37,200 ± 2000	†	3.68 ± 0.13	—

*Average of triplicate experiments.

†The dye was not soluble in HCl at $\text{pH} \approx 1$ in the absence of surfactant.

protonation of the dye-surfactant aggregates, $\log K_c^H$, and that:

$$\log(K_c^{HA}/K_c^A) = \log K_c^H - \log K \quad (1)$$

where K is the protonation constant of the dye in the absence of surfactant, and K_c^{HA} and K_c^A are the binding constants of the protonated and unprotonated forms of the dye to the micelles. Equation (1) indicates that the difference between $\log K_c^H$ and $\log K$ is a measure of the selective ability of the surfactant to bind the protonated form of the dye with respect to the unprotonated form. In all instances, the data in Table 1 indicate that the former is more strongly bound than the latter.

This can be explained by assuming that hydrophobic interactions are of the same order of magnitude for both forms of the dye, but binding of the protonated form is strengthened by electrostatic attraction. Consequently, the value of $\log(K_c^{HA}/K_c^A)$ must increase as the basic character of the dye increases. Hydrophobic interactions are probably of similar strength for aniline and the series of aminobenzoic acids and therefore provide a means of checking this. The data in Table 1 show that the values of $\log K$ and $\log(K_c^{HA}/K_c^A)$ follow the same order, which is:

ortho \gg *para*

> non substituted (aniline) > *meta*

In addition, the value of $\log(K_c^{HA}/K_c^A)$ must decrease as the hydrophobicity of the substituents increases, which holds for the series:

aminobenzoic acids

> sulphanilamide > ethyl ester

It can be concluded that, with the exception of the *o*-aminobenzoic acid dye, the shifts in the protonation constants are small, approximately of one pH-unit, increasing with $\log K$ and decreasing as the hydrophobicity of the substituents increases.

Kinetic studies

The coupling reactions were found to be adequately described by the pseudo-first order model:

$$\ln \frac{A_\infty}{A_\infty - A_t} = k't \quad (2)$$

where k' is the rate constant, and A_t and A_∞ are the absorbances at a given time t and at the end of the experiment when a constant

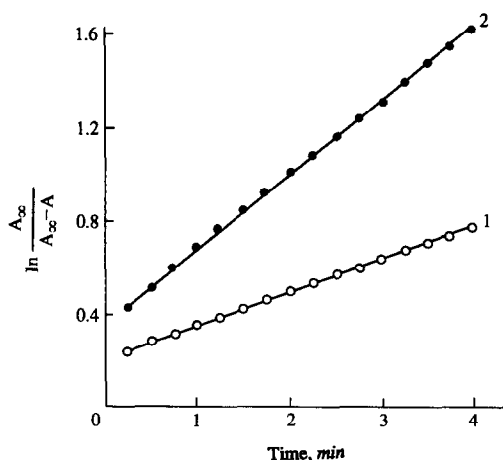


Fig. 1. Plot of equation (2) for coupling of the *p*-aminobenzoic acid dye: (1) in the absence and (2) presence of 0.5% SDS. Hydrochloric acid concentration was 1.92M and 2.16M, respectively.

value has been reached. A plot of equation (2) for *p*-aminobenzoic acid in the absence and presence of 0.5% SDS is shown in Fig. 1.

Some selected values of k' at increasing hydrochloric acid concentrations are given in Table 2. Coupling rates follow the order of the activity of the diazonium ions which is:

sulphadrigs

> aminobenzoic acids > ethyl ester

Diazonium ions are activated by electron withdrawing substituents, such as sulphonic, carboxylate and ester groups, the former having a stronger effect than the others.¹¹ The intensity of the effect of micellar catalysis is also shown in Table 2 and is positive for all dyes with the exception again of the *o*-aminobenzoic acid dye. Micellar catalysis is particularly strong for ethyl *p*-aminobenzoate and *m*-aminobenzoic acid.

Coupling rates slow down when the acid concentration increases due to protonation of NED, which hinders electrophilic substitution. Since NED has two amino groups, the relationship between k' and $[H^+]$ is not simple. As a first approximation, it was assumed that:

$$k' = k/[H^+]^n \quad (3)$$

The values of n , within the hydrochloric acid concentration ranges of Table 2, were higher in the micellar medium than in water. As the hydrochloric acid concentration increased, the values of n decreased, between approximately 4 and 1 in the micellar medium, and 3 and 1 in water. Therefore, when the acid concentration increases, coupling is more rapidly inhibited in

Table 2. Selected values of coupling rate constants (k') in the presence and absence of 0.5% SDS and optimum pH range, to obtain directly the protonated form of the dye by coupling in less than one minute

Diazotizable substance	[HCl], <i>M</i>	Water, $k'_w \times 10^3$, <i>sec</i> ⁻¹	0.5% SDS, $k'_{SDS} \times 10^3$, <i>sec</i> ⁻¹	k'_{SDS}/k'_w	Water pH_{min}	ΔpH^*	0.5% SDS pH_{min}	ΔpH^*
<i>o</i> -Aminobenzoic acid	0.24	0.33	—	—				
	0.96	0.11	0.033	0.3	1-2	†	0-1	≈4
	1.44	0.03	0.020	0.7				
<i>m</i> -Aminobenzoic acid	0.24	4.2	—	—				
	0.96	2.4	20.3	8.5	2-3	†	≈0.5	≈1.5
	1.44	2.6	9.6	3.7				
<i>p</i> -Aminobenzoic acid	0.48	12.9	—	—				
	2.40	1.4	2.6	1.9	0-1	†	≈0	≈2.5
	2.88	—	1.4	—				
Ethyl <i>p</i> -aminobenzoate	0.48	0.014	—	—				
	1.68	0.0025	0.059	24	0-1	†	<0	>2
	2.40	—	0.014	—				
Sulphanilamide	1.44	12.7	14.9	1.2	0-1	≈0.5	0-1	≈1
	2.88	4.8	5.7	1.2				
	2.88	15.2	22.8	1.5	<0	—	≈0	>2
Sulphamethoxazole	2.40	8.7	24.5	2.8	<0	—	≈0	>2
Sulphametizole	2.88	7.2	10.5	1.5				
Sulphathiazole	2.40	6.1	13.6	2.2	<0	—	≈0	>2
	2.88	4.0	10.7	2.7				
	2.88	4.0	10.7	2.7				
Sulphamethoxypyridazine	2.40	7.0	10.5	1.5	<0	—	≈0	>2
	2.88	4.5	14.5	3.2				

* $\Delta pH = pH_{max} - pH_{min}$ (see text).

†An optimum pH range does not exist or it is smaller than 0.5 pH-units.

the micellar medium than in water. However, micellar catalysis was always positive.

Optimum pH range

An optimum pH range for the determination of a diazotizable substance with NED can be deduced as follows. The upper limit can be taken as:

$$pH_{max} = \log K - 2 \quad (4)$$

which corresponds to a 99% protonation of the dye. A practical lower limit, pH_{min} , will be given by the time allowed for coupling to be completed to a satisfactory degree. Values of pH_{min} estimated to reach a 99% degree of coupling in about one min are also given in Table 2. These values were obtained by interpolating or extrapolating the points given in the Table, in some cases with the aid of a few additional measurements of k' .

Table 3. Analysis of pharmaceutical preparations

Compound	Pharmaceutical	Declared	Found*
<i>p</i> -Aminobenzoic acid	Complidermol capsules (Medea)	per capsule: <i>p</i> -aminobenzoic acid, 50 mg; biotin, 150 mcg; vitamin A, 20 000 UI; calcium pantothenate, 25 mg; inositol, 25 mg; vitamin B ₆ , 25 mg; vitamin B ₁₂ , 25 mcg	48.1 ± 0.4
	Ethyl <i>p</i> -aminobenzoate	Cinfaotin drops (Cinfa)	per ml: ethyl <i>p</i> -aminobenzoate, 25 mg; hydrocortisone acetate, 5 mg; neomycin sulphate, 3.5 mg;
Bucometasona tablets (Nezel)		per tablet: ethyl <i>p</i> -aminobenzoate, 20 mg; triamcinolone acetonide, 1 mg; lisozyme chloride, 10 mg; cetyltrimethylammonium bromide, 10 mg, tyrothricin, 10 mg	18.1 ± 0.2
Sulphamethoxazole	Septin Pediatric suspension (Gayoso Wellcome)	per ml: sulphamethoxazole, 40 mg; trimethoprim, 200 mg ethanol, 0.033 ml	41 ± 0.6

*Average from triplicate measurements.

It may be observed that where these criteria are met, an optimum pH range does not exist or is very small in water, but ranges from 1 to 4 pH units in the micellar medium. Furthermore, all the optimum pH ranges overlap between the values $1.0 < \text{pH} < 1.6$, which permits the establishment of a single and simplified procedure for the determination of all the diazotizable substances studied here. Consequently, in the procedure given above, the hydrochloric acid concentration was adjusted to give a final pH of about 1.3 (final hydrochloric acid concentration, $0.06M$), thus avoiding the addition of sodium acetate before coupling and more hydrochloric acid after coupling, as in the conventional procedure.

Analysis of pharmaceutical preparations

Application of the simplified procedure to the analysis of several pharmaceutical preparations led to the results given in Table 3.

CONCLUSION

A simplified procedure which permits the determination of many diazotizable substances in an SDS micellar medium with an optimum pH range of 1.3 ± 0.3 has been developed. The

advantage of micellar catalysis of the coupling reaction particularly concerns analytes giving diazonium ions which lack strong activating substituents rather than sulphadruugs. However, the determination of the latter benefits from the advantage of higher solubility of azo dyes in the micellar medium.

REFERENCES

1. F. J. Bandelin and C. R. Kemp, *Ind. Eng. Chem., Anal. Ed.*, 1946, **18**, 470.
2. M. Montgomery and V. H. Freed, *J. Agric. Food Chem.*, 1959, **7**, 617.
3. J. W. Daniel, *Analyst*, 1961, **86**, 640.
4. G. Norwitz and P. N. Keliher, *Anal. Chem.*, 1981, **53**, 1238.
5. G. Ramis Ramos, J. S. Esteve Romero and M. C. García Alvarez-Coque, *Anal. Chim. Acta*, 1989, **223**, 327.
6. J. S. Esteve Romero, E. F. Simó Alfonso, M. C. García Alvarez-Coque and G. Ramis Ramos, *ibid.*, 1990, **235**, 317.
7. M. J. Rosen, *Surfactants and Interfacial Phenomena*, Wiley, New York, 1978.
8. H. N. Singh and W. L. Hinze, *Analyst*, 1982, **107**, 1073.
9. J. S. Esteve Romero, G. Ramis Ramos and M. C. García Alvarez-Coque, *J. Coll. Interface Sci.*, 1991, **141**, 44.
10. M. C. García, G. Ramis and C. Mongay, *Spectrochim. Acta*, 1982, **38A**, 1005.
11. R. E. Shirmer, *Modern Methods of Pharmaceutical Analysis*, CRC Press, Boca Raton, Florida, 1982.

THE EFFECT OF pH ON A MULTIPROTONATABLE QUINIDINE ION-SELECTIVE ELECTRODE

MA WAN-LI

Research Institute for Material Protection, Wuhan Institute of Technology, Wuhan 430070,
People's Republic of China

(Received 5 February 1991. Revised 11 April 1991. Accepted 17 April 1991)

Summary—The pH effect on the quinidine ion-selective electrode performance and its electroactive material composition were investigated. It was found that variation of the pH in the bulk solution can alter the ion-pair composition in the membrane phase, thus affecting the electrode behaviour. A capacitor model was suggested for the description of the electrode response.

Numerous drugs contain more than one nitrogen atom which can be protonated, e.g., nicotine, quinidine and cinchonine. The pK_{a1} and pK_{a2} values of their relevant protonated acids are different (nicotine $pK_{a1} = 3.15$, $pK_{a2} = 7.87$; quinidine $pK_{a1} = 4.0$, $pK_{a2} = 8.54$; cinchonine $pK_{a1} = 5.85$, $pK_{a2} = 9.92$).¹ Each drug has a pH range in which both its mono- and diprotonated pharmaceutical ions co-exist. The problem that arises here is whether the monoprotonated or the diprotonated ion will show the main response when a corresponding ion-selective electrode is employed. It is well known the more responsive ions are held by the carriers or sites in the ion-pair complex within the membrane; others are interferences. But if the composition of the complex in the electrode membrane varied due to the pH influence of the bulk solution, the electrode behaviour might be affected, Efstathiou *et al.*² reported that the monoprotonated nicotine ion-selective electrode became progressively sensitive to the diprotonated nicotine ions with a decrease in the pH of the sample solution.

The present paper reports a capacitor model built to describe the electrode performance, based on further investigation of the effect of pH on the quinidine electrode performance and on oil/water extraction models of different protonated quinidine ions.

EXPERIMENTAL

Reagents

Demineralized doubly distilled water and A.R. grade chemicals were used throughout unless otherwise stated. Quinidine hydrochlor-

ide was of Chinese Pharmacopoeia quality (>99%).

pH buffers

The method employed for the preparation of pH = 2.2, 2.6, . . . , 7.0 McIlvaine buffers was essentially the same as proposed by Elving *et al.*,³ except that sodium chloride was added instead of potassium chloride to keep the ionic strength constant at 0.1M. The mixture at pH 1.8 was prepared with hydrochloric acid and sodium chloride.

Ion-pair complexes

To investigate the pH effect on the ion-pair composition of the products synthesized in different pH buffers ion-pair complexes, under their corresponding pH conditions, were prepared by continuously adding 0.01M tetraphenylborate (TPB) sodium solution to $1.002 \times 10^{-2}M$ quinidine solution dropwise until no further precipitate appeared when more drops were added. The precipitates were filtered with a sintered glass crucible No. 4 and then washed with distilled water several times. The filtrates were dried at 50° for 10 hr in a vacuum chamber. Each product was carefully weighed. The mole fraction of monoprotonated quinidine-TPB complex (g_1) and the composition ratio of quinidine to TPB [$1:n$, $QH_n^+(TPB)_n^-$] under its corresponding pH condition were calculated.

Extraction

pH effect. The following systems: (1) 2 ml of $2 \times 10^{-4}M$ QH-TPB in chloroform and (2) 10 ml of $1 \times 10^{-5}M$ McIlvaine pH buffered

Table 1. Response slope (S), composition of synthesized ion pair complexes (g_1 , 1:n) and mole fraction of monoprotonated quinidine-TPB complex (h_1) in organic phase under different pH conditions

pH	s ,			
	mv/dec	g_1	1:n	h_1
1.8	29.0	0.003	1:1.997	0.00
2.2	29.0	0.014	1:1.986	0.00
2.6	29.3	0.040	1:1.960	0.01
3.0	30.4	0.100	1:1.960	0.12
3.4	32.1	0.208	1:1.792	0.21
3.8	36.1	0.391	1:1.609	0.39
4.2	42.0	0.612	1:1.388	0.61
4.6	47.8	0.801	1:1.119	0.83
5.0	54.2	0.911	1:1.089	0.92
5.4	56.3	0.962	1:1.028	0.95
5.8	57.6	0.988	1:1.012	0.98
6.2	57.8	0.981	1:1.019	0.98
6.6	58.1	0.990	1:1.010	1.00
7.0	58.0	1.000	1:1.003	1.00

quinidine solution (pH varying from 1.8 to 7.0, in steps of 0.4) were employed to simulate the pH effect on the composition of the electroactive material in the electrode membrane. Originally, only the monoprotonated quinidine-TPB complex was dissolved in chloroform. After mixing with different pH buffered quinidine solutions for thirty minutes, each organic phase was separated and washed with its corresponding pH buffer. The absorbances of 20, 40, 60 and 80- μ l portions of the organic phase, diluted with 2.0 ml of chloroform (giving a concentration series), were determined with a Pye Unicam PU 8800 U/V spectrophotometer at $\lambda_{max} = 334.0$ nm. The slope of absorbance *vs.* carrier concentration was calculated and by dividing this value with the value of the slope obtained when only monoprotonated quinidine-TPB complex existed, the mole fraction of the monoprotonated quinidine-TPB complex (Table 1) under the given pH condition can be calculated (see appendix).

Concentration effect. To study whether the composition of the electroactive material in the electrode membrane remains constant when employed in a given pH series, the influence of concentration on the ion-pair composition was observed in the same simulation system, with the quinidine concentration in pH = 4.2 buffered aqueous phase varying from $1.0 \times 10^{-3}M$ to $1.0 \times 10^{-5}M$ (1×10^{-3} , 5×10^{-4} , 1×10^{-4} , 5×10^{-5} and $1 \times 10^{-5}M$). The mole

fractions of the monoprotonated quinidine-TPB complex in the organic phase under different concentration conditions were determined by the same method. The results are recorded in Table 2.

Electrode system and EMF measurement

Poly(vinylchloride) (PVC) quinidine ion-selective electrodes were prepared by a standard method.⁴ Contained in the membrane were 30% (m/m) PVC and 70% dibutyl-*o*-phthalate (DOP, in which about 5 mM electroactive material was dissolved). The electroactive materials used were either monoprotonated quinidine-TPB complex, diprotonated quinidine-TPB complex or any ratio of their mixtures prepared in the previous step. Cells of the type

Hg; Hg₂Cl₂, KCl(std.)|0.1M KCL|Sample solution

|| membrane || 0.01M KCl, AgCl; Ag

were employed. Potentiometric measurements were performed with an Orion 980 Digital Ion Analyser with the prepared electrode connected with a Model 217 double junction calomel reference electrode (Shanghai, China), with 0.1M potassium chloride in the outer compartment. The pH adjustment was conducted with a Model 231 glass electrode (Shanghai, China). Calibration graphs were obtained for different pH buffered solutions containing quinidine in concentrations ranging from 10^{-2} to $10^{-6}M$.

RESULTS AND DISCUSSION

Effect of pH on electrode performance.

No obvious differences were observed for the electrodes containing the monoprotonated quinidine-TPB complex, diprotonated quinidine-TPB complex or any ratio of their mixtures; only the absolute potential may have a slight variation within 10 mV. The behaviour of quinidine electrodes depends only on the bulk solution conditions. The response slopes obtained in various pH buffered series are summarized in Table 1. Three typical calibration curves for a monoprotonated quinidine-TPB electrode are drawn in Fig. 1. All are linear with regression coefficients higher than 0.996.

Table 2. Influence of quinidine concentration upon ion-pair composition, pH = 4.2

C, M	1.0×10^{-3}	5.0×10^{-4}	1.0×10^{-4}	5.0×10^{-5}	5.0×10^{-5}
h_1	0.62	0.59	0.62	0.60	0.61

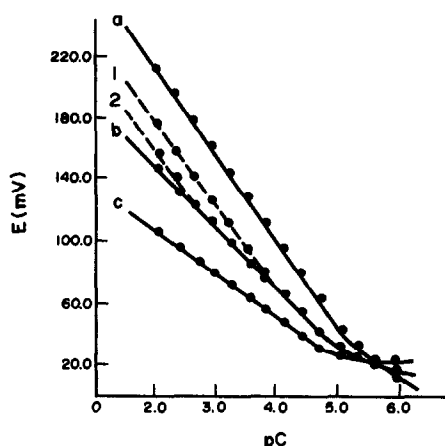


Fig. 1. Calibration curves for a monoprotated quinidine-TPB electrode, (a) pH = 6.6, (b) pH = 4.2, (c) pH = 1.8.

Similar to an ideal univalent ion-selective electrode, the electrode still only responded to monoprotated quinidine ions in approximately neutral solution (pH = 6.6). But with decreasing pH the electrode gradually changed its behaviour to act in a completely different way. Its response slope was no longer a constant value or a step function *vs.* ionic charge (Z) as predicted by the Nernst equation.

$$S = \frac{RT}{F} \ln 10 \frac{1}{Z} \quad (1)$$

but became a continuous function *vs.* pH. It decreased synchronously with decreasing pH, demonstrating a transient process from responding to monoprotated quinidine ions to diprotonated ones. In strongly acidic solution, the electrode responded only to diprotonated quinidine ions (pH \leq 2.2), just like an ideal divalent ion-selective electrode. Also, the apparent charge calculated from the Nernst equation in the transient process was no longer a constant whole number.

When testing a given pH series following a change in pH, the measurements must be performed one or more times until a stable and linear response can be observed. The two dashed curves on Fig. 1 (curves 1 and 2) demonstrate the initial measurement at the 4.2 pH series following the measurement at the 6.6 pH series. The calibration curve gradually approaches linearity, first at the low concentration range and then over the whole range, implying that the electrode itself might have changed; increasing its sensitivity to diprotonated quinidine ions.

The effect of pH on the ion-pair composition of the synthesized products. In the products synthesized under different pH conditions, either the monoprotated quinidine-TPB complex (1:1), diprotonated quinidine-TPB complex (1:2) or their mixture is present. The mole fractions, g , of these two kinds of complexes in a certain product are approximately equal to the distribution fractions, f , of their corresponding quinidine ions under corresponding pH conditions.

$$g_1 = f_1; \quad g_2 = f_2 \quad (2)$$

$$f_1 = \frac{K_{a1}[\text{H}^+]}{[\text{H}^+]^2 + K_{a1}[\text{H}^+] + K_{a1}K_{a2}}; \quad (3)$$

$$f_2 = \frac{[\text{H}^+]^2}{[\text{H}^+]^2 + K_{a1}[\text{H}^+] + K_{a1}K_{a2}}$$

These kinds of ions can react with a given carrier to produce a precipitate, and the corresponding ion-selective electrode can be made with that carrier. So mono- and di-protonated quinidine ion-selective electrodes can be prepared with TPB carrier. Even an electrode which can respond to both mono- and di-protonated quinidine ions can be prepared, by using a mono- and di-protonated quinidine-TPB mixture as the electroactive material.

Existing state of the ion-pair complex in the organic phase

Following the pH variation in the aqueous phase from 7.0 to 1.8, the ion-pair composition in the organic phase varied synchronously. At first, only monoprotated quinidine-TPB complex existed, then the diprotonated quinidine-TPB complex appeared and its proportion increased gradually. Finally, under strong acidic conditions, only the diprotonated quinidine-TPB complex can be observed. Under the same pH conditions, the mole fractions, h , of mono- and di-protonated quinidine-TPB complexes in the organic phase almost equal the distribution fractions of mono- and di-protonated quinidine ions.

$$h_1 = f_1; \quad h_2 = f_2 \quad (4)$$

Three typical spectra are drawn in Fig. 2. The $n - \pi^*$ transition peak diminishes gradually with decreasing aqueous phase pH, directly indicating that the proportion of monoprotated quinidine-TPB complex in the organic phase has comparatively decreased. Since only monoprotated quinidine-TPB complex can generate this peak, an unprotonated nitrogen

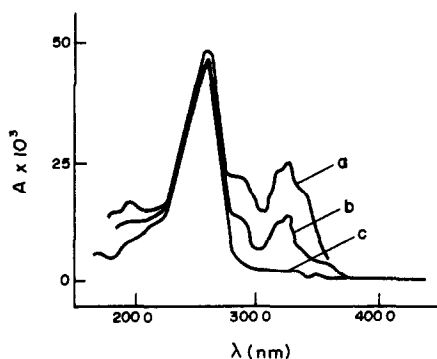


Fig. 2. Three typical spectra. Total concentration of quinidine species = $2.0 \times 10^{-6}M$, (a) pH = 6.6, (b) pH = 4.2, (c) pH = 1.8.

atom on its molecular structure is the source for the $n - \pi^*$ transition.

However, in a series at given pH, the ion-pair composition in the organic phase is essentially constant. The concentration of quinidine in the aqueous phase hardly influences it.

The variation of the ion-pair composition in the organic phase is due to entering ions, and provides information about the states of extracted protonated quinidine ions. The experimental result is that the ratio of mono- and di-protonated quinidine ions "extracted" depend only on the bulk solution conditions. This result requires that the extraction ability of the given electroactive material is strong enough to instantly "extract" either the mono- or the di-protonated quinidine ions reaching the interface and that the extraction process is controlled by the partition diffusion step of protonated quinidine ions from the bulk solution to the interface. This is in agreement with the three-step model proposed by Buck⁵ and Thomas *et al.*⁶ for a single ion system.

Now, it may be concluded that the extraordinary behaviour of the quinidine electrode is due to the variation of the electroactive material composition as a function of the pH. The ions extracted into the electrode membrane depend only on the probability of different protonated quinidine ions reaching the membrane surface or their distributions in the bulk solution, for changes in the mobility of different protonated quinidine ions in the bulk solution phase are negligible due to their large sizes, especially under strong stirring conditions. The roles of mono- and di-protonated quinidine ions as host or guest ions can no longer be identified, since both of them contribute to the membrane potential.

Capacitor model

The electrode membrane separates two aqueous phases. Electroneutrality makes the ions on either side impossible to transfer over completely. But this tendency exists if the electrochemical potentials on the two sides are different. To make the process valid, the existence of electroactive material is crucial. The TPB carriers homogeneously distribute in the electrode membrane, serving as sites to construct a space lattice. The mole fraction of the sites occupied by mono- and di-protonated quinidine ions respectively equals

$$m_1 = \frac{h_1 Z_1}{h_1 Z_1 + h_2 Z_2}; \quad m_2 = \frac{h_2 Z_2}{h_1 Z_1 + h_2 Z_2} \quad (5)$$

The site group held by a certain kind of ion establishes a hopping pathway which only allows this kind of ion to pass. The mono- and di-protonated quinidine hopping pathways distribute on the electrode membrane (surface area, S) respectively at their element areas

$$S_1 = m_1 S; \quad S_2 = m_2 S \quad (6)$$

When the responding ions transport from the bulk solution into the internal reference solution selectively through the corresponding hopping pathways, their counterpart ions with opposite sign (Cl^- , *etc.*) are left in the bulk solution, thus generating a potential difference due to the enrichment of response ions at the internal reference solution side and their counterpart ions at the bulk solution side, much like recharging a parallel-plate capacitor (Fig. 3). When the potential rises to match the original electrochemical potential difference an equilibrium will be established. As a result, on the element capacitors occupied by mono- and di-protonated quinidine the hopping pathway is

$$C_1 = D \frac{S_1}{d}; \quad C_2 = D \frac{S_2}{d} \quad (7)$$

where D and d are the dielectric constant and thickness of the electrode membrane respect-

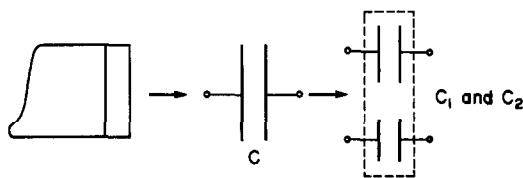


Fig. 3. An electrode membrane treated as two bridging capacitors.

ively, ideal Nernst potentials are generated independently for each element:

$$V_1 = \frac{RT}{Z_1 F} \ln \frac{a_1}{\bar{a}_1}; \quad V_2 = \frac{RT}{Z_2 F} \ln \frac{a_2}{\bar{a}_2} \quad (8)$$

Now the membrane body is separated into two parts, one responding to mono-protonated quinidine ions, the other to di-protonated ones. Actually, the mono- and di-protonated quinidine hopping pathways are alternately and uniformly distributed in the electrode membrane, and so are transported ionic charges. Then for the whole electrode membrane, the apparent potential can be calculated upon the principle of bridging capacitors.

$$CV = C_1 V_1 + C_2 V_2 \quad (9)$$

$$D \frac{S}{d} V = \frac{D}{d} \frac{h_1 Z_1}{h_1 Z_1 + h_2 Z_2} S \frac{RT}{Z_1 F} \ln \frac{a_1}{\bar{a}_1} + \frac{D}{d} \frac{h_2 Z_2}{h_1 Z_1 + h_2 Z_2} S \frac{RT}{Z_2 F} \ln \frac{a_2}{\bar{a}_2} \quad (10)$$

$$V = \frac{RT}{F(h_1 Z_1 + h_2 Z_2)} [(h_1 \ln f_1 + h_2 \ln f_2) - (\ln \bar{a}_1 + \ln \bar{a}_2)] + \frac{h_1 + h_2}{h_1 Z_1 + h_2 Z_2} \frac{RT}{F} \ln a \quad (11)$$

Introducing equation (4), and designating the first term as V_0 since it is constant in a given pH series, then

$$V = V_0 + \frac{RT}{F} \frac{f_1 + f_2}{f_1 Z_1 + f_2 Z_2} \ln a \quad (12)$$

The slope function is

$$s = \frac{\partial V}{\partial (\log a)} = \frac{RT}{F} \ln 10 \frac{f_1 + f_2}{f_1 Z_1 + f_2 Z_2} \quad (13)$$

To define the s -pH function for pH around pK_{a1} , equation (3) is introduced and the term K_{a1} , K_{a2} neglected, yielding

$$s = \frac{RT}{F} \ln 10 \frac{10^{pH - pK_{a1}} + 1}{Z_2 + Z_1 10^{pH - pK_{a1}}} \quad (14)$$

Solving

$$\frac{\partial^2 S}{\partial pH^2} = 0$$

$$pK_{a1} = pH \Big|_{\frac{\partial^2 S}{\partial pH^2} = 0} - \log(Z_2/Z_1) \quad (15)$$

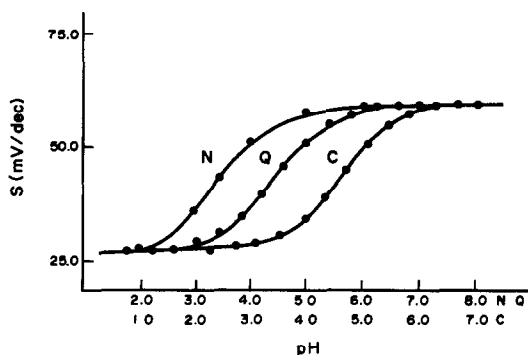


Fig. 4. Comparison of tested and simulated slopes for nicotine (N), quinidine (Q) and cinchonine (C) electrodes.

Model verification

Figure 4 shows experimental and simulated slopes for different electrodes as a function of pH. The dots represent the experimental slope data, and the lines are the computer simulated graphs, using model equation (14). The experimental and simulated data fit quite well (slope data for nicotine and cinchonine were obtained with their corresponding TPB electrodes). McIlvaine pH buffers were not employed for the nicotine electrode due to its lack of selectivity. The pH of a series was controlled by adding 0.01M hydrochloric acid or sodium hydroxide, (pH = 2.0, 3.0, 3.5, 4.0, 5.0, 6.0, 7.0).

The pK_{a1} values obtained from experimental slope data by the numerical differentiation method through equation (15), (Table 3) are close to the literature values.¹ (Note it seems that the pK_{b1} rather than the pK_{a1} value for cinchonine had been mistakenly quoted in the 13th edition of "Lange's Handbook of Chemistry".)

CONCLUSION

Both the mono- and di-protonated quinidine ions can be extracted into the electrode membrane and contribute to the membrane potential. Their individual roles as host or guest ions are impossible to identify, but diprotonated quinidine is dominant in acid solution and the monoprotated form in the mid-pH range. The composition of the electroactive material in

Table 3. Comparison of tested pK_{a1} values with those from Ref. 1

	Nicotine	Quinidine	Cinchonine
Experimental	3.11	4.02	4.10
Literature	3.15	4.0	5.85 (4.04)*

*From 12th edition of "Lange's Handbook of Chemistry".

the electrode membrane is no longer a single kind of ion-pair complex, but a mixture of mono- and di-protonated quinidine-TPB complexes, varying synchronously with the bulk solution conditions. The electrode response is controlled by the partition diffusion process of different protonated quinidine ions from the bulk solution to the membrane surface via a kinetic mechanism. The proposed capacitor model can serve to describe the response.

REFERENCES

1. J. A. Dean, *Lange's Handbook of Chemistry*, 13th ed., McGraw-Hill, 1985.
2. C. E. Efstathiou, E. P. Diammandis and T. P. Hadjiioannou, *Anal. Chim. Acta*, 1981, **127**, 173.
3. P. J. Elving, J. M. Markowitz and I. Rosenthal, *Anal. Chem.*, 1956, **28**, 1179.
4. G. J. Moody, R. B. Oke and J. D. R. Thomas, *Analyst*, 1970, **95**, 910.
5. R. P. Buck, *Crit. Rev. Anal. Chem.*, 1975, **5**, 323.
6. W. Thomas, M. Vladimir, H. Karel and S. Zdenek, *J. Phys. Chem.*, 1989, **93**, 8204.

APPENDIX

Calculation of the Fraction of Monoprotonated quinidine-TPB complex (h_1)

The TPB carriers can be assumed to be held in the organic phase in the simulation system, since both the mono- and di-protonated quinidine complexes are insoluble in water. The mole concentration was defined as T . The mole fraction of total TPB carriers occupied by mono- and di-protonated quinidine ions respectively equals

$$m_1 = \frac{h_1 Z_1}{h_1 Z_1 + h_2 Z_2}; \quad m_2 = \frac{h_2 Z_2}{h_1 Z_1 + h_2 Z_2} \quad (1)$$

The mole concentration of mono- and di-protonated quinidine-TPB complexes can be presented as a function of the TPB carrier concentration

$$t_1 = m_1 T / Z_1; \quad t_2 = m_2 T / Z_2 \quad (2)$$

After 20, 40, 60 and 80- μ l portions of the organic phase were diluted,

$$t'_1 = t_1 \frac{v}{V+v}; \quad t'_2 = t_2 \frac{v}{V+v} \quad (3)$$

($V = 2.0$ ml, the volume of the solvent for dilution, v was the volume of the sample taken from the organic phase.)

Only the mono-protonated quinidine-TPB complex can generate the $n - \pi^*$ transition absorption peak. According to Beer's law, the absorbance under given pH conditions is

$$A = \epsilon b t'_1 \quad (4)$$

$$= \epsilon b m_1 T \frac{v}{V+v} \quad (5)$$

$$= \epsilon b m_1 T' \quad (6)$$

$T' = Tv/(V+v)$ was the TPB concentration after dilution. It depends only on the volume of the sample, and its concentration in the series remains unvaried when the pH in the aqueous phase has varied, so it can serve as a reference to observe the existing state of the protonated quinidine ions associated with the carriers.

The determined slope ratio (r) in the $A - T'$ coordinate system is

$$r = \frac{\epsilon b m_1}{\epsilon b_1} = m_1 \quad (7)$$

or

$$h_1 = \frac{r Z_2}{Z_1 + r(Z_2 - Z_1)} \quad (8)$$

ACID-BASE INDICATORS IN *N,N*-DIMETHYLFORMAMIDE: CHROMATIC PARAMETERS OF TRANSITION RANGES

JOSÉ BARBOSA and CARLES M. BOSCH

Department of Analytical Chemistry, University of Barcelona, 08028 Barcelona, Spain

(Received 30 October 1990. Revised 19 February 1991. Accepted 18 March 1991)

Summary—A series of commercial indicators in *N,N*-dimethylformamide has been established. Their chromaticity coordinates, transition pH ranges, pH of maximum colour change, optimum concentration for titration, quality of colour change and the effect of ionic strength have been determined. A variety of acids and their mixtures have been titrated to test the indicators.

N,N-Dimethylformamide is particularly useful in organic reaction chemistry due to its moderately high dielectric constant, 36.7 at 25^o, and its aprotic nature. It is also useful in electrochemical and coordination chemistry studies. In addition, DMF and to a lesser extent ethylenediamine (EDA) are very popular solvents for the titration of acids and mixtures of acid. The much greater basicity of EDA than DMF is an analytical disadvantage because of the levelling off effect. Also, EDA is toxic and unpleasant in use.

In addition, because of its greater hydrogen bond accepting basicity, with a solvatochromic parameter $\beta = 0.69^2$ the formation of homoconjugation and heteroconjugation complexes occurs to a lesser extent in DMF than in acetonitrile (AN)³ and hence often gives normal shaped titration curves in the buffer region.¹

In DMF indicators have been recommended for acid-base titrations⁴ because visual end-point detection is very precise and accurate for acids. As the neutralization curves for acids can be calculated, if the indicator dissociation constants are known, it is possible to predict which indicators will have a sharp colour change at the end-point.

In connection with our studies of acid-base equilibria and colour change quality of the indicators in several solvents,⁵⁻⁸ a series of commercially available indicators in DMF with pronounced colour change have been studied in this work. The colour changes were characterized by the chromatic parameters in both the CIE and complementary chromaticity systems.⁹⁻¹¹ The optimum concentrations for the

indicators were determined by the Vytras¹² and Kotrly and Vytras¹³ methods. In accordance with CIE recommendations, the CIELAB (L*, a*, b*) and CIELUV (L*, u*, v*) co-ordinates were used to calculate the index of colour change perceptibility. The sensitivity, sharpness of colour change, pH corresponding to maximum colour change, and the transition ranges of each indicator were determined.

In this paper we report the pH value at which an indicator would show a specific colour, at zero ionic strength, taking into account the activity coefficients, as reported earlier.⁶ Finally the behaviour of the indicators was tested by titration of different acids and mixtures of acids.

EXPERIMENTAL

Apparatus

For the determination of chromaticity coordinates a Beckman DU-7 spectrophotometer with cells of 1-cm path length and a Hewlett-Packard 9816 computer were used. For potentiometric titrations, a Crison Digilab 517 pH-meter equipped with a Radiometer G202B glass electrode and a 0.01M AgNO₃(DMF)/Ag reference electrode with 0.1M tetramethylammonium perchlorate in DMF serving as a double salt-bridge similar to that used by Kolthoff *et al.*¹⁶ were used (see Fig. 1). This system of electrodes and salt-bridge (kept at 25^o) gave the best combination of all those tested; stable and reproducible potentials were obtained in 15 min or less. The glass electrode was kept in DMF when not used, as recommended.¹⁶

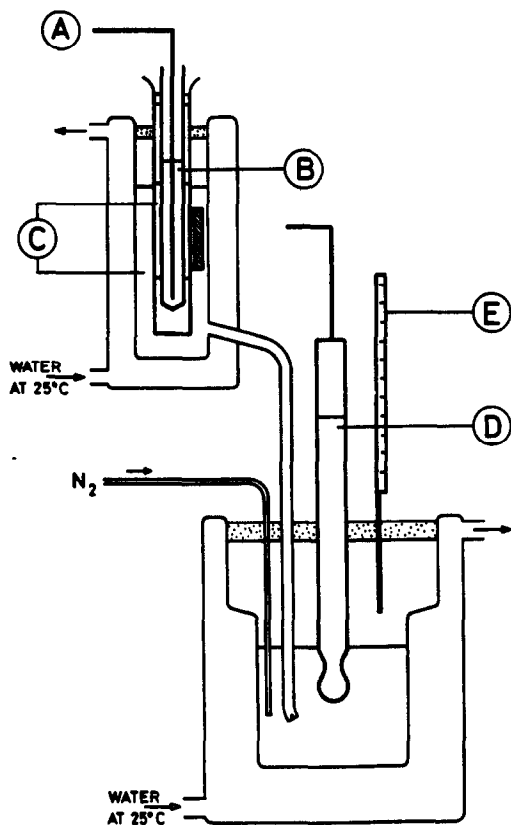


Fig. 1. Potentiometric cell for titrations in DMF with the reference electrode and salt bridge. A, Silver electrode; B, AgNO_3 0.01M in DMF; C, tetramethylammonium perchlorate 0.1M in DMF; D, glass electrode; E, burette with titrant.

The DMF solutions with Ag^+ ions are colourless and clear when prepared, but in about ten days they became crimson and turbid, even though not exposed to light for more than one hour during that period.¹⁷ To minimize possible decomposition of the reference electrode solution, millimolar quantities of perchloric acid were added.¹⁷

Since DMF hydrolyses at a relatively fast rate in the presence of acid or bases, we have been particularly careful to avoid contamination of the solvent by atmospheric moisture. All the experiments have been carried out under a purified nitrogen atmosphere.

Reagents

Tetramethylammonium perchlorate. Carlo Erba, R.S. grade.

Tetrabutylammonium hydroxide (TBAH). A 0.1M solution in propan-2-ol (Carlo Erba, RPE grade).

Benzoic acid. (Carlo Erba, RPE grade).

Acetic acid. (Carlo Erba, RPE grade).

Phenol. (Panreac, AR grade).

Salicylic acid. (Panreac, AR grade)

Malonic acid. (Panreac, AR grade)

Hydrochloric acid gas solution in DMF.

The indicators studied in DMF were: thymol blue (TB), (Scharlau, AR grade); bromocresol green (BCG), (Scharlau, AR grade); bromothymol blue (BTB), (Merck, ACS grade); *m*-Cresol purple (MCP), (Merck, ACS grade); phenol red (PR), (Panreac, AR grade) and azo violet (AV), (Scharlau, AR grade).

Standard potential and DMF autoprotolysis constant

To calibrate the glass electrode in DMF, mixtures of benzoic acid and its tetrabutylammonium salts have been used. The $pK = 12.27$ value of benzoic acids in DMF¹⁶ was taken as a standard reference value.^{16,18-20} The pH values were calculated on the basis of simple dissociation of the acid and complete dissociation of the salts.¹⁶

The glass electrode was calibrated by titration of 0.005M benzoic acid in DMF with 0.1M tetrabutylammonium hydroxide.^{5,6,8} The small quantity of water and alcohols introduced with the titrant have a negligible influence on the chemical potential in DMF.²¹ A computer program, ACETERISO, written in BASIC, was used to calculate the standard potentials in acidic and basic media ($E_a^0 = -51.3$ and $E_b^0 = -1423.6$ mV). From here, the average autoprotolysis constant of the medium was $pK_{ap} = 23.2 \pm 0.3$.

Procedure

Indicator solutions (approximately $10^{-5}M$) were titrated with 0.1M tetrabutylammonium hydroxide solution, in the presence of an appropriate buffer. Hydrochloric and benzoic acid mixture for TB, salicylic acid for BCG, benzoic acid for BTB, a mixture of hydrochloric acid and phenol for MCP, acetic acid for PR and malonic acid for AV were used. Simultaneous potentiometric and spectrophotometric monitoring at 10 nm intervals between 380 and 770 nm was implemented.

The test solution, stirred with a stream of nitrogen, was continuously circulated between the titration vessel and the spectrophotometer cell by means of a peristaltic pump. The temperature was $25 \pm 0.2^\circ$.

Computation method

To calculate the chromaticity parameters, the weighted ordinate method ($\Delta\lambda = 10$ nm), with

the coefficients for the standard illuminant C and "2° standard observer" was used. To compute the optimum concentration of the indicator in the titrations, the chromaticity co-ordinates in a variety of colour spaces,⁶ and the *pK* value of the indicator, the program SUPER-COLOR,²² written in BASIC, was used.

RESULTS AND DISCUSSION

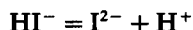
The criteria for selection of the indicators were commercial availability, widespread use, solubility in DMF and sharpness of visual transition. Involved equilibria were:

1. AV1



$$pK = \text{pH} - \log y_{\text{HI}^-} - \log([\text{HI}^-]/[\text{H}_2\text{I}])$$

2. BCG, AV2, BTB, MCP, PR, TB



$$pK = \text{pH} + \log(y_{\text{HI}^-}/y_{\text{I}^{2-}}) - \log([\text{I}^{2-}]/[\text{HI}^-])$$

Table 1 shows the effect of ionic strength (*I*) on activity coefficients in DMF. However, due to the high dielectric constant of DMF (36.7),¹ the activity coefficients have less influence than in other solvents, such as 2-methyl-2-propanol and propan-2-ol and similar influence to that in acetonitrile. Using the pH value at zero ionic strength (*pH*₀) to specify a reference indicator colour⁶ we have:

$$\text{pH}_0 = \text{pH} - \log y_{\text{HI}^-} \quad (1)$$

$$\text{pH}_0 = \text{pH} + \log(y_{\text{HI}^-}/y_{\text{I}^{2-}}) \quad (2)$$

These relationships allow chromaticity parameters to be referred to *pH*₀ values, and colour transitions at different ionic strengths for indicators of various types to be compared. The activity coefficients were calculated by means of the Debye-Hückel equation

$$\log \gamma = -A I^{1/2}/(1 + B a I^{1/2})$$

Table 1. Influence of ionic strength (*I*) on activity coefficients in DMF

<i>I</i>	$\log \gamma_{\text{I}^-}$	$\log(y_{\text{HI}^-}/y_{\text{I}^{2-}})$
10 ⁻⁶		0
10 ⁻⁵	0	0.01
10 ⁻⁴	-0.02	0.05
5 · 10 ⁻³	-0.03	0.10
10 ⁻³	-0.05	0.14
5 · 10 ⁻³	-0.10	0.29
10 ⁻²	-0.13	0.39
10 ⁻¹	-0.29	0.86

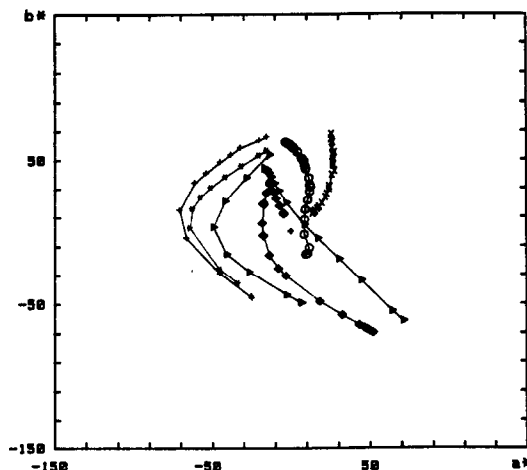


Fig. 2. Chromatic co-ordinates *a'* and *b'* of indicator solutions at optimum concentration. \blacktriangleright TB, \blacktriangleleft PR, \blacksquare MCP, \star BTB + BCG, \times AV1 and \circ AV2. The symbols for AV1 and AV2 correspond to complete transition of the indicator at optimum concentration for equilibria 1 and 2 respectively.

were

$$A = 1.594, B = 0.480 \times 10^8 \text{ and } a = 5 \text{ \AA.}^{23}$$

The pH range of a given colour transition can be calculated from the *pH*₀ range and the ionic strength of the solution.

The CIELAB (see Fig. 2) and CIELUV systems can be used advantageously in calculations of chromaticity.

The complementary chromaticity co-ordinates (*Q*_x, *Q*_y), were used to describe the colour sequence of the indicators, Fig. 3. For all the indicators tested, straight lines denoting mixtures of two pure coloured forms were obtained. The fact that AV gives two linear segments shows the presence of two equilibria,

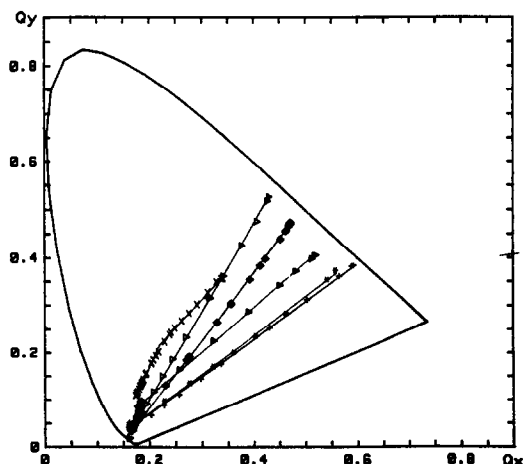


Fig. 3. Colour transitions in the complementary chromaticity diagram. Symbols as in Fig. 2.

Table 2. Colour changes of indicators

Indicator	C_{ref}, M	Optimum concentration M	pK	pK'	Transition pH range	pH_{mcc}	$\Delta pH_{1/2} \text{SCD}$	$pK - pH_{mcc}$
TB	2.0×10^{-5}	8×10^{-5}	15.24 ± 0.17	17.74	13.5–15.9	14.80	1.20	0.44
PR	3.2×10^{-5}	1×10^{-4}	15.37 ± 0.06	17.87	13.5–16.7	14.80	1.60	0.57
MCP	6.9×10^{-5}	1×10^{-4}	15.16 ± 0.15	17.66	14.1–15.8	14.80	0.90	0.36
BTB	7.8×10^{-5}	1×10^{-4}	12.96 ± 0.10	15.46	11.4–13.7	12.40	1.10	0.56
BCG	2.3×10^{-5}	1×10^{-4}	9.06 ± 0.08	11.56	7.2–10.0	8.40	1.40	0.66
AV1	1.4×10^{-5}	4×10^{-4}	9.15 ± 0.05	11.65	8.0–9.1	8.60	0.60	0.55
AV2	1.4×10^{-5}	6×10^{-5}	13.52 ± 0.06	16.02	13.0–13.6	13.50	0.30	0.02

each involving a particular colour change, the first from red to yellow and the second from red to blue.

Thymol blue and *M*-cresol purple show a second colour change at very low pH values, which has no analytical interest. We have, therefore, studied only the transition referring to the colour change from yellow to that of the strongly blue alkaline form.

The indicator dissociation constants were determined from the complementary chromaticity co-ordinates according to Reilley *et al.*²⁴ and by a procedure described by Albert and Serjeant.²⁵ The results of the two methods agree and are shown in Table 2. In the case of TB and MCP, the first protonation equilibria, perceptible as short lines in the complementary chromaticity diagram, Fig. 3, were taken into account in the respective pK computation. The colour point of the pure form HI^- can be found from the intersection of the two linear segments in Fig. 3.²⁶

One of the purposes of studies dealing with the influence of solvents on acid–base equilibria is to obtain a solvent-independent acidity scale. By referring the acid–base character of non-aqueous solvents to the same aqueous standard state, an “absolute” pH scale is obtained, which allows the acidity of aqueous solutions to be compared directly,²⁷

$$pH' = pH_s + p\gamma'_{w \rightarrow s}(H^+)$$

where pH_s is the pH in solvent, s , $p = -\log$ and $\gamma'_{w \rightarrow s}(H^+)$, is the proton transfer activity coefficient, which is closely related to $\Delta G'_{w \rightarrow s}(H^+)$, the standard free energy of transfer of 1 mole of protons from water to the solvent s .

$$\log \gamma'_{w \rightarrow s}(H^+) = [\Delta G'_{w \rightarrow s}(H^+)]/2.303 RT$$

The proton transfer activity coefficient, represents the acid end of the solvent independent pH' scale in each solvent s with ultimate reference to the familiar aqueous pH scale and with physical comparability with the latter. The basic

limit of the pH' scale in any solvent is conventionally defined from its autoprotolysis constant.²⁸

For a solvent s , like DMF, the dissociation constants of a series of indicators in this solvent, pK , were then translated to the absolute scale by the equation:

$$pK' = pK + p\gamma'_{w \rightarrow DMF}(H^+)$$

In recent reviews,²⁹ the various extrathermodynamic assumptions which have been made to find transfer activity coefficients have been discussed. Here, $\log \gamma'_{w \rightarrow DMF}(H^+) = -2.5$, was used, as reported by Kolthoff and Chantooni.³⁰ These data are based on the tetraphenylborate assumption, which with reference to water would appear to yield, γ' values closer to the true values than other assumptions do.²⁹

The pK' values obtained for the indicators studied are shown in Table 2. It must be emphasized that each pK value is valid only for the pH scale relevant to the specific pure solvent considered.²⁸ Values of pK pertaining to different solvents would become physically comparable on an “intersolvental” pH scale with ultimate reference to the familiar pH scale in water³¹ only by being first converted to pK' values.

From Fig. 3, and considering only segments with a similar orientation it can be deduced that the colour change qualities of BCG and BTB are similar. As the orientation of the other segments are different their transitions cannot be compared. Further, complementary data give no information about the ideal concentration for the use of the indicators.

In order to obtain the optimum concentrations of the indicators for the titration arrangement used, the method of Kotrlý and Vytřas¹³ was followed. In this method, the minimum of the plot of $\Delta pH/\Delta E$ (index of colour change perceptibility) *vs.* $\log(c/c_{\text{ref}})$ gives the optimum indicator concentration; c_{ref} is the reference experimental value of the indicator concentration, c is the indicator concentration and ΔE is the

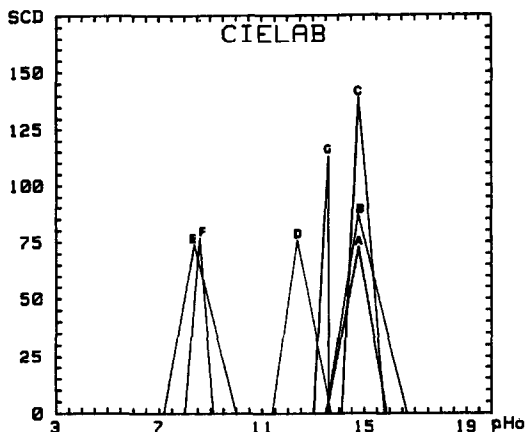


Fig. 4. Changes of SCD values in CIELAB system, with pH at zero ionic strength (pH_0). A-TB, B-PR, C-MCP, D-BTB, E-BCG, F-AV1 and G-AV2.

total difference between two colours, calculated by using the CIELAB and CIELUV systems. The data obtained by the two systems agree and the results (for a 1-cm path-length) are given in Table 2.

To describe the quality of colour change of the indicators objectivity, a modification¹⁵ on the method of Bhuchar and Agrawal¹⁴ based on a plot of $\Delta E/\Delta \text{pH}$ [or the specific colour discrimination (SCD) values] vs. pH (Fig. 4), was used.

In this plot, the band-width, of each peak is the transition pH range, and the pH value at the maximum is the pH for the maximum change of colour (pH_{mcc}). The half band-width ($\Delta \text{pH}_{1/2\text{SCD}}$) is also related to the sharpness of the chromatic transition, and the maximum of each peak (in SCD units) is taken as the sensitivity of the colour change. Table 2 gives the average of the results obtained by the CIELAB and the CIELUV system, except for the SCD values, which are not comparable for different chromatic systems.

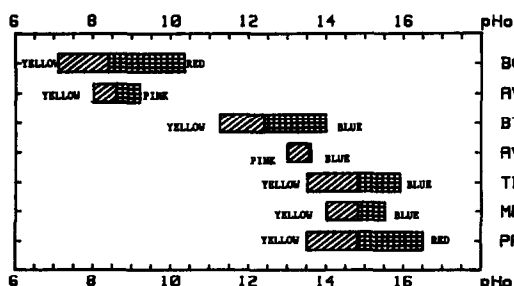


Fig. 5. Indicator transition ranges, at zero ionic strength, for the indicators in DMF. Diagonal hatching, before the pH of maximum colour change; no hatching, after the pH of maximum colour change.

From the SCD values (Fig. 4) it can be deduced that MCP and AV2 show very pronounced colour changes in DMF and the other indicators studied show similar quality of colour changes with adequate sensitivity. These conclusions all agree with visual observations.

Table 2 shows the difference between the $\text{p}K_a$ and pH_{mcc} values that do not agree, as a result of the varying sensitivity of the human eye to different colours. The pH_{mcc} values are displaced, relative to the $\text{p}K$ values, towards pH values at which the concentration of the less intensely coloured form is the higher. Thus the $\text{p}K$ values of all the sulphonephthaleins studied are higher than their pH_{mcc} values, because the blue or violet basic form is more intensely coloured than the yellow acidic form. Values of pH_{mcc} are important because they allow selection of the most suitable indicator for a specific titration.³²

Figure 5 gives the colour-change pH ranges of the indicators studied, the colours before and after the pH of maximum colour change, and the pH_{mcc} value. The series of indicators studied covers the necessary pH range, for acid-base titration of weak acids.

In order to test the proposed indicator scale, suitable amounts of acid were weighed and titrated in DMF with 0.1M tetrabutylammonium solution.

The acids tested were hydrochloric, 2,6-dihydroxybenzoic, salicylic, benzoic and acetic acids with $\text{p}K$ values of 3.2, 3.56, 8.24, 12.27 and 13.5,¹⁶ respectively, and phenol. All tested indicators gave very sharp end-points in titrations of acids with $\text{p}K$ values of about 14 or lower. The titration curve for phenol had no clear inflection at the equivalent point.⁴

Hence, taking into account the $\text{p}K$ values of the indicators, and the quality of the colour change, we suggest the use of MCP, TB and PR for titrations, all of the acids tested, BTB and AV2 for hydrogen chloride, 2,6-dihydroxybenzoic, salicylic and benzoic acids and BCG for strong acids, hydrogen chloride and 2,6-dihydroxybenzoic acid. A binary mixture of 2,6-dihydroxybenzoic and benzoic acids was titrated with AV, with an error smaller than 2%.

REFERENCES

1. I. M. Kolthoff and P. J. Elving, (eds.), *Treatise on Analytical Chemistry*, 2nd Ed., Part 1, Vol. 2, Wiley-Interscience, New York, 1979.
2. M. J. Kamlet, J.-L. M. Abboud, M. H. Abraham and R. W. Taft, *J. Org. Chem.*, 1983, **48**, 2877.

3. I. M. Kolthoff, *Anal. Chem.*, 1974, **46**, 1992.
4. S. S. M. Hassan and M. T. M. Zaki, *Talanta*, 1975, **22**, 843.
5. J. Barbosa, E. Bosch and F. Suárez, *Analyst*, 1985, **110**, 1473.
6. J. Barbosa, E. Bosch and M. Rosés, *ibid.*, 1987, **112**, 179.
7. J. Barbosa, D. Barrón and E. Bosch, *ibid.*, 1987, **112**, 1717.
8. J. Barbosa, M. Rosés and V. Sanz-Nebot, *Talanta*, 1988, **35**, 1013.
9. F. W. Billmeyer, Jr. and M. Saltzman, *Principles of Color Technology*, 2nd Ed., Wiley, New York, 1981.
10. G. J. Chamberlin and D. G. Chamberlin, *Colour: Its Measurements, Computation and Application*, Heyden, London, 1980.
11. C. N. Reilley, H. A. Flaschka, S. Laurent and B. Laurent, *Anal. Chem.*, 1960, **32**, 1218.
12. K. Vytřas, *Chem. Zvesti*, 1974, **28**, 252.
13. S. Kotrlý and K. Vytřas, in *Essays on Analytical Chemistry*, E. Wänninen (ed.), p. 259. Pergamon Press, Oxford, 1977.
14. V. M. Bhuchar and A. K. Agrawal, *Analyst*, 1982, **107**, 1439.
15. J. Barbosa, E. Bosch and R. Carrera, *Talanta*, 1985, **32**, 1077.
16. I. M. Kolthoff, M. K. Chantooni, Jr. and H. Smagowski, *Anal. Chem.*, 1970, **42**, 1622.
17. A. V. Banedetti, C. S. Fugivara, M. Cilense and T. Rabocai, *Anal. Lett.*, 1983, **16A**, 1357.
18. J. Juillard and B. Loubinoux, *C. R. Acad. Sci.*, 1967, **264**, 1680.
19. S. M. Petrov and Yu. I. Umanskii, *Russ. J. Phys. Chem.*, 1967, **41**, 729.
20. B. W. Clare, D. Cook, S. F. Ko, Y. C. Mac and A. J. Parker, *J. Am. Chem. Soc.* 1966, **88**, 1911.
21. A. J. Parker, *Australian J. Chem.*, 1963, **16**, 585.
22. M. Rosés, *Anal. Chim. Acta*, 1988, **204**, 311.
23. J. Juillard, *J. Chim. Phys.*, 1966, **63**, 1190.
24. C. N. Reilley and E. M. Smith, *Anal. Chem.*, 1960, **32**, 1233.
25. A. Albert and E. P. Serjeant, *The Determination of Ionization Constants*, Chapman & Hall, 2nd Ed., London, 1974.
26. J. Barbosa, J. Sánchez and E. Bosch, *Talanta*, 1984, **31**, 279.
27. P. Ugo, S. Daniele, G. A. Mazzochin and G. Bontempelli, *Anal. Chim. Acta*, 1988, **208**, 207.
28. T. Mussini and F. Mazza, *Electrochim. Acta*, 1987, **32**, 855.
29. Y. Marcus, *Pure Appl. Chem.*, 1986, **58**, 1721.
30. I. M. Kolthoff and M. K. Chantooni, Jr., *J. Phys. Chem.*, 1972, **76**, 2024.
31. J. Barbosa, C. M. Bosch and V. Sanz-Nebot, *Mikrochim. Acta*, in press.
32. J. Barbosa, E. Bosch and M. Rosés, *Analisis*, 1990, **18**, 515.

UTILIZATION OF *O*-PHTHALALDEHYDE–SULPHURIC ACID AS A SPRAY REAGENT IN THIN-LAYER CHROMATOGRAPHIC DETECTION OF SOME INDOLEALKYLAMINES AND APPLICATION TO CUTANEOUS SECRETION EXTRACTS OF TOAD SPECIES

CLAUSIUS G. DE LIMA*

Departamento de Química, Universidade de Brasília, Brasília, DF 70910, Brazil

TEREZA C. M. PASTORE

Laboratório de Produtos Florestais, IBAMA, Brasília, DF 70770, Brazil

CARLOS A. SCHWARTZ, JADER S. CRUZ† and ANTONIO SEBEN

Departamento de Ciências Fisiológicas, Universidade de Brasília, Brasília, DF 70910, Brazil

(Received 11 February 1991. Accepted 8 April 1991)

Summary—An expansion of the utilisation of *o*-phthalaldehyde in sulphuric acid medium as spray reagent was carried out when tryptophan and some tryptophan-derived indole alkylamines such as tryptamine, serotonin, bufotenine, dehydrobufotenine and bufotenidine were examined by thin-layer chromatography. *R_f*-values and limits of detection ranging from 20 (serotonin) to 100 (dehydrobufotenine) ng per spot were found. Application of this reagent for the detection of some of these compounds was carried out, using either methanolic extracts or column chromatographic fractions of the skin secretion of the toads *Bufo ictericus* and *Odontophrynus cultripes*.

Paraformaldehyde gas,¹ van Urk's or Ehrlich's reagents (*p*-dimethylaminobenzaldehyde in HCl medium),^{2,3} Prochazka reagent (formaldehyde in HCl: ethanol solution)^{2,3} or *paraformaldehyde* in alkaline medium⁴ are the classical spray reagents for the chromogenic or fluorogenic identification of indolic compounds.

In spite of that, *o*-phthalaldehyde (OPA) has been developed and successfully used for the detection of indole compounds after thin-layer chromatography (TLC),^{5–20} generally in hydrochloric acid conditions. *o*-Phthalaldehyde in hydrochloric acid medium, as proposed by Maickel and Miller,²¹ but modified by the addition of cysteine, was employed by Narasimhachari and Plaut⁵ for the identification of 5-hydroxytryptamine (serotonin), *N*-methylserotonin, 5-hydroxy-*N,N*-dimethyltryptamine (bufotenine) and 5-methoxy-*N,N*-dimethyltryptamine. This technique was later used for the determination of *N*-methyltransferase activity present in human and animal tissues.⁶

5-Hydroxy-3-ylacetic acid was detected under similar conditions after separation by TLC by Korf and Valkenburgh-Sikkema.⁷ Recently, Arqué *et al.*⁸ searched for the optimum hydrochloric acid concentration for the identification and determination of several 5-hydroxy and 5-methoxy indoleamines, including serotonin, employing TLC of the reaction products of these and other compounds with OPA–hydrochloric acid. The limits of detection from the fluorescent intensities of the spots were determined with a chromatograph-spectrofluorometer.⁸ OPA was used in sulphuric acid medium by Szabó and Karacsony¹⁰ for the detection of ergolones and ergolines (indole alkaloids) in TLC conditions. Based on their previous work,²² Pastore and de Lima¹¹ examined the utilization of this spray reagent for the detection of a series of indol-3-ylacids including indol-3-ylacetic acid and 4-(indol-3-yl) butyric acid, both known as phytohormones. OPA has also been proposed as a spray reagent in the determination of tryptophan,^{9,12} histamine,^{9,13,14} histidine^{9,18} and other aminoacids and peptides,^{16–18} hydrazine and substituted hydrazines,¹⁹ amphetamines, mescaline and noradrenaline,²⁰ using TLC, paper chromatography

*Author for correspondence.

†Present address: Departamento de Bioquímica, Universidade Federal de Minas Gerais, Belo Horizonte, MG, Brazil.

or electrophoresis under different reaction conditions. A large number of compounds also react with OPA, depending on the reaction medium, either in chromatographic or solution fluorimetric conditions.⁹

In the present work we examined the possibility of detecting tryptophan and some indolealkylamines such as tryptamine, serotonin, bufotenine, bufotenidine and dehydrobufotenidine with OPA in sulphuric acid and TLC medium. Using OPA-HCl in an investigation with tryptophan or tryptamine, an extremely weak signal was observed.²¹ Similar results were also found by Aures *et al.*¹ after examining OPA as spray reagent in acid (acetic acid in acetone) or basic (potassium hydroxide) conditions. According to our previous work,²² both serotonin and tryptophan react with OPA-sulphuric acid in solution, with a λ_{\max} of emission at 478 and 463 nm, respectively; the latter being shifted to 470 nm after ultraviolet irradiation.

o-Phthalaldehyde, in alkaline medium and in the presence of 2-mercapthoethanol (Roth's reagent),²³ reacted with tryptamine,²⁴ although the reaction was carried out in solution. No reference was found in the literature to the reaction of bufotenidine or dehydrobufotenine with OPA.

Due to the interesting biological behaviour, derived principally from the hallucinogenic action of most of these compounds,²⁵ there is great interest in their detection and determination by TLC. We studied the feasibility of detection of these compounds in 'real' samples and then examined the application of the present method for the detection of some of these compounds, using samples of cutaneous secretion extracts of toad species, either raw or after column and TLC separation.

EXPERIMENTAL

Reagents and apparatus

All reagents used were analytical-grade. Ethanol 99% (Merck S. A., Rio de Janeiro, Brazil) was purified through reflux (12 hr) with Zn-KOH and distillation. Tryptamine (as hydrochloride), tryptophan, serotonin (as hydrochloride) and *o*-phthalaldehyde were purchased from Sigma Chemical Company (St. Louis, MO, USA) and used as received. Bufotenine and dehydrobufotenine were of laboratory origin having been isolated and purified,

using extraction, picrate formation, free base column chromatograph separation and TLC examination of the purity, from different natural sources, such as *Anadenanthera colubrina* (bufotenine), according to Stromberg²⁶ and from a sample (bufotenine) kindly provided by Dr. Nuno A. Pereira (Faculdade de Farmácia, Universidade Federal do Rio de Janeiro, Rio de Janeiro, Brazil), which was isolated from *Piptadenia peregrina* (monopicrate m.p. 176–178; literature 177.5).²⁷ Dehydrobufotenine was isolated from the secretion of a toad (*Bufo ictericus*) according to Slotta and Neisser.²⁸ Bufotenidine was obtained through methylation of bufotenine²⁷ with methyl iodide, in absolute ethanol at a temperature of 60° for 2 hr. Picrates of dehydrobufotenine and bufotenidine were obtained with melting points of 184–186° (literature 186°) and 197–198° (literature 198°),²⁷ respectively. Structural diagrams of bufotenine, dehydrobufotenine and bufotenidine are shown in Fig. 1.

Thin-layer glass plates (50 × 200 mm or 100 × 200 mm) were coated with silica-gel (G, type 60, Merck Darmstadt, FRD). Ascending, one dimension, thin-layer chromatography was carried out at room temperature (*ca.* 25°) in glass tanks, the plates having previously been eluted (washed) with ethyl acetate and air dried. As eluent a solvent mixture (ethyl acetate: propan-2-ol: conc. ammonium hydroxide; concentrations; 45:35:20 v/v) was used, a modification from a known solvent system which uses methyl acetate in place of ethyl acetate, as described by Randerath.²

The indole compound solutions (dissolved in 1 ml of absolute ethanol and diluted to 10 ml with water) were applied to the plates with a 10- μ l Hamilton microsyringe (Hamilton, Reno, NV, USA). For the visual observation of the fluorescent spots, determination of the *R_f*s and estimation of the limits of detection, an ultraviolet viewing box (Ultra Violet Products, San Gabriel, CA, USA) was employed.

Procedure

Classical procedures were used for the preparation of the plates, the chromatographic process and the detection.^{2,3} The volumes of analyte solutions, ranging from 1 to 5 μ l, were applied in the plates at 10 mm from the base. The spots were air dried. The plate was developed (ascending chromatography) 120–140 mm from the starting point with running times of *ca.* 60–80 min.

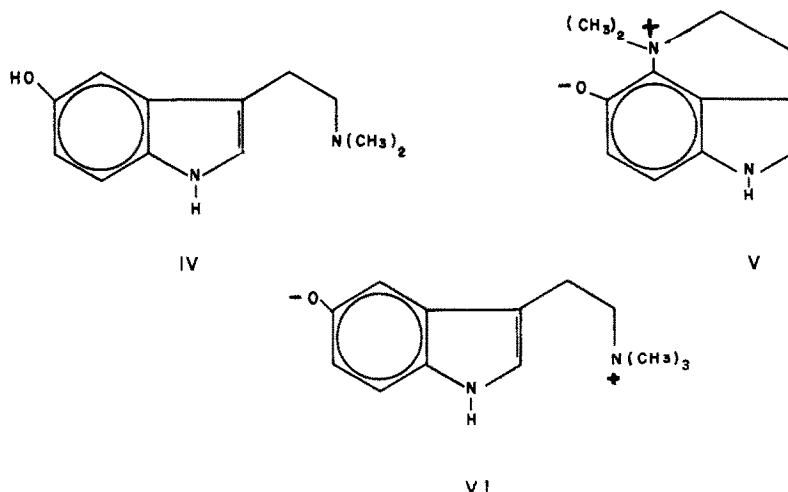


Fig. 1. Structural diagrams of some of the compounds studied: bufotenine (IV), dehydrobufotenine (V) and bufotenidine (VI).

After development, the plates were dried with an air blower. Hot air was avoided. After being dried, the plates were sprayed with an *o*-phthalaldehyde-sulphuric acid solution 0.15% (m/v). The OPA solution was prepared as follows: 0.15 g of OPA was dissolved in 10 ml of absolute ethanol in a standard flask. After dissolution, the volume was made up to the mark with 7.77*M* sulphuric acid, yielding an OPA hydroalcoholic solution of concentration 7*M* sulphuric acid. This solution can be used for 7 days if kept in darkness in a refrigerator.

RESULTS AND DISCUSSION

Solutions of the pure compounds with a known concentration (ranging from 20–350 µg/ml) were spotted on the plates and eluted for the determination of the *R_f*s, limits of detection and colour of the spots. Table 1 shows the results obtained. The *R_f*-values fluctuate as a

function of the distance run. Due to the volatile character of the components of the solvent mixture (principally ammonium hydroxide) a fresh eluent must be used. Otherwise, a much larger spread in the *R_f*-values is found.

Some colour intensities increased with time and ultraviolet exposure (such as the case of tryptophan and 5-OH-tryptamine) and the limits of detection were determined 15–60 min after spraying. The spots were usually stable even after 24 hr, although some bleaching was observed in some cases.

It is interesting to observe that the compounds with the 5-hydroxy substituent or the unprotonated (fenolic) group at the same position showed yellow or yellowish colours. In contrast, compounds in which the 5-hydroxy substituent is absent, such as tryptamine or tryptophan, yields products with blue or bluish colours. In the present case we also observed that when hot air is used in the drying step

Table 1. Analytical characteristics of the compounds studied with OPA-H₂SO₄ spray reagent

Compound	<i>R_f</i> *	Colour	Estimated limit of detection, ng per spot
I Tryptamine	0.68 ± 0.06 (0.77)	Blue	40
II Serotonin (5-Hydroxytryptamine)	0.59 ± 0.05 (0.65)	Whitish-yellow	20
III Thryptophan	0.38 ± 0.01 (0.23)	Bluish-white	50
IV Bufotenine† (5-Hydroxy- <i>N,N</i> -dimethyltryptamine)	0.76 ± 0.04	Yellow	25
V Dehydrobufotenine†	0.36 ± 0.02	Yellow	100
VI Bufotenidine† (5-Hydroxy- <i>N,N,N</i> -trimethyltryptamine)	0.13 ± 0.04	Yellow	50

*In parenthesis are the results described in the literature² with methyl acetate; propan-1-ol: ammonium hydroxide, 25% (45:35:20).

†See Fig. 1.

(after chromatography), the yellow colour may change to blue, possibly due to a thermal reaction. In our previous observation,^{11,22} 5-hydroxyindol-3-ylacetic acid was the sole compound to produce a colour which was different from blue (green) in comparison with some unsubstituted indol-3-ylacids. Even with 5-methoxy-indol-3-ylacetic acid a bluish spot was found. Similar results have also been found by Arqué *et al.*,⁸ when OPA-hydrochloric acid (Maickel and Miller's reagent)²¹ was examined: the 5-hydroxy indoleamines produced orange spots but with 5-methoxyindoleamines blue spots were observed. Using OPA-hydrochloric acid also (but in the presence of cysteine), Narasimhachari and Plaut⁵ found yellow spots with serotonin and bufotenine (which are 5-hydroxy substituted compounds) and blue spots with 5-methoxy-*N,N*-dimethyltryptamine. From these observations we can conclude that different products are obtained and this difference can be useful for the possible characterization of the analyte's chemical structure present in the spot.

The estimated limits of detection were in the range 25–100 ng. The limit of detection of serotonin was equal to that found by Narashimhachari and Plaut (20 ng)⁵ despite being much higher if compared with 0.6 ng, found by Arqué *et al.*⁸ with OPA-hydrochloric acid and a TLC-scanner-spectrofluorometer. The limit of detection found in the present work with tryptophan is higher if compared to the results found by Lindeberg (5–10 ng for each spot),¹⁵ using OPA-2-mercaptoethanol as proposed by Roth.²³ Our result is also higher when compared with 5 ng described by Stahl³ (using formaldehyde) or 1.6 ng found by Toneby⁴ (paraformaldehyde in alkalized ethanol as spray reagent).

With bufotenine a lower result was observed, in comparison with previous work (50 ng).⁵ Cowles *et al.*²⁹ obtained a weak fluorescence signal with bufotenine, using formaldehyde (from paraformaldehyde) as a spray reagent, although with tryptamine, serotonin and tryptophan strong fluorescence signals were present. These authors conclude that an amino terminal group is necessary for reaction completion when formaldehyde is employed.

On the other hand, the reaction with OPA can occur in the presence or absence of such a group. As previously observed by us, OPA either in solution or in thin-layer conditions can react in sulphuric acid medium with compounds

which lack a primary amino group or even with indole compounds without a 5-hydroxy or 5-methoxy substituent. This was demonstrated when indole—substituted at position 3 with an *n*-alkylcarboxylic acid group—reacted with OPA-sulphuric acid.^{11,22} OPA also has the advantage of substituting formaldehyde, a reagent which is suspected of having carcinogenic action.³⁰ Also, it is known that the reaction of formaldehyde with hydrochloric acid in the vapour phase can possibly occur, yielding bis(chloromethyl)ether, a potent carcinogenic compound.³¹

o-Phthalaldehyde in sulphuric acid medium was successfully applied to the detection of serotonin and dehydrobufotenine in fresh cutaneous secretion of the South American toads, *Odontophrynus cultripes* and *Bufo ictericus*,³² by TLC. The results were confirmed with either Ehrlich's reagent or Pauly reagent (sulphanilic acid in the presence of sodium nitrite) after TLC. Some chromatographic fractions of toad extracts—prepared with alumina as the stationary phase and methanol as the eluent followed by TLC separation—were also examined. In such conditions bufotenine and bufotenidine were identified besides serotonin. This spray seems to be extremely useful for the identification of indolealkylamines after chromatography.

REFERENCES

1. D. Aures, R. Fleming and R. Hakanson, *J. Chromatog.*, 1968, **33**, 480.
2. K. Randerath, *Cromatografia de Capa Fina*, Ediciones Urmo, Bilbao, 1974.
3. E. Stahl, *Thin-layer Chromatography*, Academic Press, New York, 1965.
4. M. I. Toneby, *J. Chromatog.*, 1974, **97**, 47.
5. N. Narashimhachari and J. Plaut, *ibid.*, 1971, **57**, 433.
6. N. Narashimhachari, R. L. Lin, J. Plaut and K. Leiner, *ibid.*, 1973, **86**, 123.
7. J. Korf and T. Vankenburgh-Sikkema, *Clin. Chim. Acta*, 1969, **26**, 301.
8. J. M. Arqué, J. Serrano, A. De Leiva and R. Segura, *Anal. Biochem.*, 1988, **174**, 275.
9. T. D. Turner and S. L. Wightman, *J. Chromatog.*, 1968, **32**, 315.
10. A. Szabó and E. M. Karacsony, *ibid.*, 1980, **193**, 500.
11. T. C. M. Pastore and C. G. De Lima, *Analyst*, 1986, **111**, 107.
12. A. R. Patton and E. M. Foreman, *Science*, 1949, **109**, 339.
13. W. B. Shelley and L. Julhin, *J. Chromatog.*, 1966, **22**, 130.
14. R. Hakanson, L. Julhin, C. Owman and B. Sporrang, *J. Histochem. Cytochem.*, 1970, **18**, 93.
15. E. G. G. Lindeberg, *J. Chromatog.*, 1976, **177**, 440.

16. E. Schilts, R. D. Schmackerz and R. W. Gracy, *Anal. Biochem.*, 1977, **79**, 33.
 17. E. Mendez and J. G. Gavilanes, *ibid.*, 1976, **72**, 473.
 18. L. Edvinsson, R. Hakanson, A. L. Rönnerberg and F. Sundler, *J. Chromatog.*, 1972, **67**, 81.
 19. R. W. Weeks Jr., S. K. Yasuda and B. J. Dean, *Anal. Chem.* 1976, **48**, 159.
 20. G. Gübitz, *Chromatographia*, 1979, **12**, 779.
 21. R. P. Maickel and F. P. Miller, *Anal. Chem.*, 1966, **38**, 1967.
 22. T. C. M. Pastore, E. M. De M. Nicola and C. G. De Lima, *Analyst*, 1984, **109**, 243.
 23. M. Roth, *Anal. Chem.*, 1971, **43**, 880.
 24. C. Buteau and C. L. Duitschaever and G. C. Ashton, *J. Chromatog.*, 1984, **284**, 201.
 25. R. E. Schultes and A. Hofmann, *Plant of Gods. Origins of Hallucinogenic Use*. McGraw-Hill, New York, 1979.
 26. V. L. Stromberg, *J. Am. Chem. Soc.*, 1954, **76**, 1707.
 27. V. Deulofeu and E. A. Ruveda, *The Basic Constituents of Toad Venoms in Venomous Animals and their Venoms*, W. Bücherl and E. E. Buckley, (eds.), Vol. II, pp. 475-495. Academic Press, New York, 1971.
 28. C. H. Slotta and C. Neisser, *Mem. Inst. Butantan*, 1937, **11**, 89.
 29. E. J. Cowles, G. M. Christensen and A. C. Hilding, *J. Chromatog.*, 1968, **284**, 201.
 30. B. N. Ames, R. Magaw and L. S. Gold, *Science*, 1987, **236**, 271.
 31. L. Bretherick, (ed.), *Hazards in the Chemical Laboratory*, 3rd Ed., The Royal Society of Chemistry, London, 1981.
 32. A. Sebben, *D.Sc. Thesis*, Instituto de Biociências, Universidade de São Paulo, 1989.
- Note added on proof: Kitzrow *et al.* also examined the reaction of serotonin and bufotenine with OPA in HCl-cysteine medium. W. Kitzrow, L. Franke, R. Uebelhack and K. Seidel, *Acta Biol. Med. Ger.*, 1980, **39**, 489. *Anal. Abstr.*, 1980, **41**, 6D193.

EFFECTS OF SALTS ON THE STABILITY OF THE CATIONIC RADICAL OF PHENOTHIAZINE DERIVATIVES

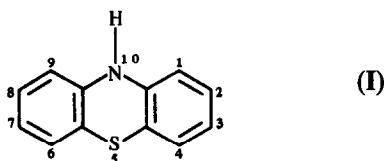
I. JELÍNEK, I. NĚMCOVÁ and P. RYCHLOVSKÝ

Department of Analytical Chemistry, Charles University, Albertov 2030, 128 40 Prague 2, Czechoslovakia

(Received 11 February 1991. Accepted 6 March 1991)

Summary—Effects of cations and anions of various salts on the stability of the diethazine cation radical were studied in various mineral acids. It was found that stability is enhanced in the presence of salts that contain the same anion as that contained in the cation radical salt. Other anions decrease the stability. The influence of salt cations is negligible.

Many derivatives of phenothiazine (I) are used in analytical chemistry, especially those substituted in positions 3 and 7 (dyes of the methylene blue group) as well as those substituted in position 10 alone and positions 2 and 10. The latter substances are also utilized in medicine as antipsychotic pharmaceuticals.



Analytical use of phenothiazine derivatives with substituents in position 10 (A) is usually based on their reversible oxidation to intensely coloured cationic radicals (A^+), which makes it possible to employ them as redox indicators or spectrophotometric reagents.¹ However, this application is complicated by limited stability of these cationic radicals, the rate of their degradation being strongly dependent on the composition of the reaction mixture. The stability of the cationic radical is also considered as an important factor in pharmacological use, as these radicals are often assumed to be the actual pharmacologically active component.

It follows from published studies²⁻⁷ that cationic radicals of most phenothiazine derivatives decompose to yield an approximately equimolar mixture of the original derivative (A) and its sulphoxide (AO), according to the overall equation



However, the decomposition is more complex in some cases and products have not yet been unambiguously identified.

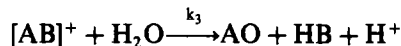
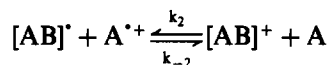
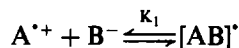
It has been demonstrated that the stability, or the rate of degradation, of cationic radicals strongly depends on the following factors:

(a) type and position of substituents on the phenothiazine skeleton.²⁻⁵

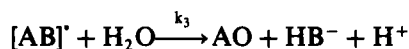
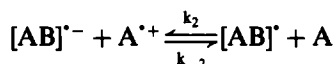
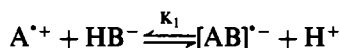
(b) acidity of the reaction medium³—the stability of the cationic radical A^+ increases with increasing acidity, given by the H_3O^+ ion activity rather than its concentration (as correlation with the Hammett acidity function); *i.e.*, the H_3O^+ ion exerts a thermodynamic stabilizing effect rather than a kinetic effect.

(c) in media with low acidities (pH 2–7) the rate of cationic radical decomposition depends on the type and concentration of buffer used.⁵⁻⁷

From the kinetics of decomposition of cationic radicals which are second-order with respect to A^+ , the following reaction mechanisms have been proposed:



(For anions B^- that do not contain acidic hydrogen, *e.g.*, acetate, CH_3COO^-)



(For anions HB^- that contain acidic hydrogen, *e.g.*, dihydrogenphosphate, $H_2PO_4^{2-}$)

Both reactions are specifically base catalysed, *i.e.*, the catalytic effect of a base depends on the chemical structure of the base.

The above kinetic studies employed buffered media (acetate, phosphate, citrate, glycine, *etc.*) and a constant ionic strength obtained with sodium chloride; however, the effect of sodium chloride on the reaction has not been studied. The effect of neutral salts on rate of decomposition of the cationic radical, A^{+} , is also very important from the point of view of practical application (especially in view of the observed specific catalysis of the decomposition) and thus this paper deals with this problem.

Diethazine (10-diethylaminoethylphenothiazine) was selected for the study; this substance is also used in clinical practice as an antiparkinson drug.

EXPERIMENTAL

Chemicals

Diethazine hydrochloride, used for the preparation of the diethazine radical cation, was obtained from Léčivae (Modřany, Czechoslovakia) and its purity was checked by TLC with a methanol-chloroform (1:1) mobile phase.

The diperchlorate salt of the diethazine cationic radical, $DE^{+}ClO_4^{-}HClO_4$ ($M_r = 498.4$), was prepared by oxidation of diethazine hydrochloride with hydrogen peroxide in perchloric acid, according to Levy *et al.*³ A stock solution of $1 \times 10^{-2}M$ $DE^{+}ClO_4^{-}HClO_4$ was prepared by dissolving this substance in concentrated perchloric acid. This solution, stored in the dark, is stable for several weeks.

The dichloride salt of the diethazine cationic radical, $DE^{+}Cl^{-}HCl$ ($M_r = 370.4$), was prepared by electrochemical oxidation of $1 \times 10^{-3}M$ diethazine chloride in concentrated hydrochloric acid. The oxidation was performed coulometrically at a potential of 750 mV *vs.* SCE, the potential was found from an experimental voltammetric curve and the end of the generation was determined from the measured electric charge. Ultra-violet absorption spectra indicated that the oxidation of DE to DE^{+} was quantitative. Bands corresponding to DE hydrochloride and to the higher oxidation state, *i.e.*, the DE sulphoxide, were absent.

Salt solutions were prepared by dissolving these salts, of analytical-grade purity, in distilled water.

Apparatus

Spectrophotometric measurements were performed with a PU 8800 instrument (Pye Unicam, Cambridge, England) in 1.00-cm cuvettes. Solutions were kept at $25 \pm 0.5^{\circ}$.

Procedure

Absorbance was recorded against time at a wavelength of 512 nm corresponding to the absorption maximum of the radical cation, over an interval of 60 min starting from the moment the compounds were mixed. Degradation half-times were found from these curves and these variables were linearized (assuming a second-order reaction, the equation $1/c = k_r t + 1/c_0$ is valid). Values of the rate constant, k_r , were obtained from the slope of a plot of $1/c$ *vs.* t .

The ϵ_{512} value for DE^{+} , which was used to calculate concentration from the measured absorbance, was found from the absorbance of $2 \times 10^{-4}M$ DE^{+} in concentrated (11.0M) perchloric acid where DE^{+} is stable.

RESULTS AND DISCUSSION

Initial time dependent changes of the diethazine cationic radical, DE^{+} were obtained from its UV and visible absorption spectra. It can be seen in Fig. 1 that the absorption maxima of the diethazine cationic radical⁸ ($\lambda = 212, 265$ and 272 nm) decrease with time while maxima of diethazine⁹ ($\lambda = 205, 250$ and 299 nm) and its sulphoxide⁹ ($\lambda = 2332.5, 268$ and 292.5 nm) increase indicating that the latter substances are the final products of DE^{+} , decomposition.

The effect of the non-oxidized diethazine hydrochloride on the rate constant of the DE^{+} decomposition was studied first. As assumed, an addition of diethazine hydrochloride leads to a decrease in the k_r value for decomposition of the diethazine cationic radical (measurements were performed in perchloric acid medium). Dependence of the rate constant on the diethazine hydrochloride concentration is linear. Measurements were performed up to a diethazine hydrochloride concentration of $1 \times 10^{-3}M$; at higher concentrations the solution becomes turbid.

In the study of the influence of ions on the rate of DE^{+} decomposition, phosphoric acid was first selected as the reaction medium, as it is often used in spectrophotometric determinations of metals with phenothiazine derivatives and its effect on the stability of the cationic radicals of phenothiazine derivatives has

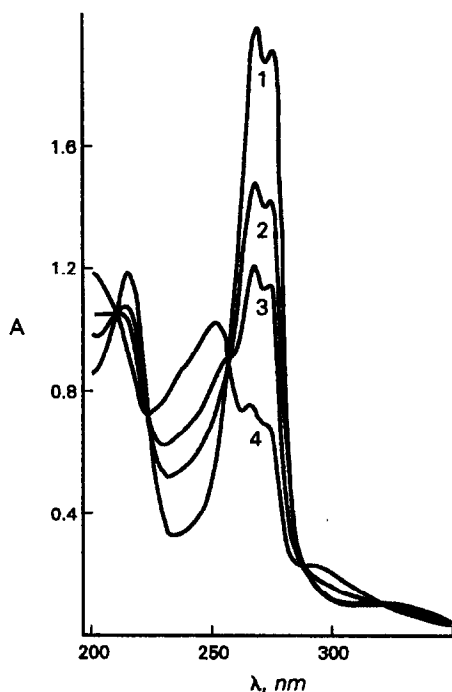


Fig. 1. Time changes in the absorption spectrum of the diethazine radical cation in the UV region. Concentration of $\text{DE}^+ \cdot \text{ClO}_4^- \cdot \text{HClO}_4 = 5 \times 10^{-5} M$. Concentration of $\text{HClO}_4 = 0.23 M$. Curves 1 to 4 were obtained at times of 1, 30, 60 and 180 min, respectively after mixing.

already been studied.¹⁰ In order to interpret the results obtained, the behaviour of DE^+ perchlorate in perchloric acid and DE^+ chloride in hydrochloric acid had to be studied.

Stability of the perchlorate of the diethazine radical cation

Phosphoric acid media. The effect of the concentration of the sodium salts of ClO_4^- , Cl^- , SO_4^{2-} and NO_3^- on the rate constant of DE^+ degradation was studied. The DE^+ species was prepared as the perchlorate salt and dissolved in 3M phosphoric acid. It can be seen from Fig. 2 that the presence of the perchlorate anion increases the DE^+ stability; the rate constant is seen to decrease. On the other hand, Cl^- and SO_4^{2-} decrease the DE^+ stability. The degradation of DE^+ is greatly enhanced in the presence of nitrate; the effect of nitrate is apparently described by a more complex mechanism, as demonstrated by the time dependences of DE^+ degradation that do not correspond to a second-order reaction.

The effect of the salt cations on the resultant k_t value was also studied [LiCl, NaCl, KCl and NH_4Cl , curves 2(a)–(d)]. The cation exerts only a small influence on the resultant rate constant. The ratio increases in the order,

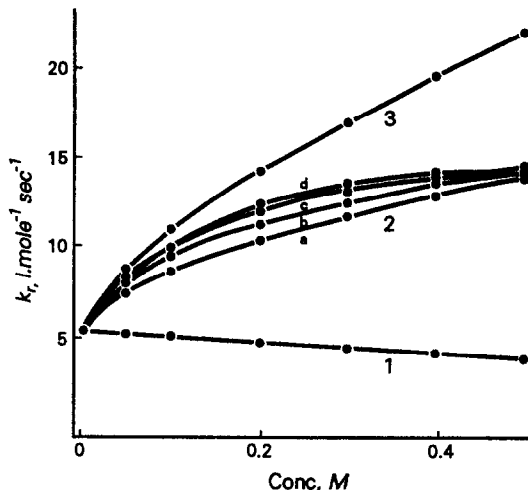


Fig. 2. Dependence on salt concentration of the rate of decay of the perchlorate salt of the diethazine radical cation. Concentration of $\text{DE}^+ \cdot \text{ClO}_4^- \cdot \text{HClO}_4 = 2 \times 10^{-4} M$; medium, 3M H_3PO_4 .

- Curve 1 NaClO_4
 Curve 2(a) LiCl
 (b) NaCl
 (c) KCl
 (d) NH_4Cl
 Curve 3 Na_2SO_4

$\text{Li}^+ < \text{Na}^+ < \text{K}^+ < \text{NH}_4^+$, *i.e.*, with decreasing value of the mean activity coefficient for these salts (γ_{\pm} values for 0.5M solutions of these salts are 0.73, 0.68, 0.65 and 0.62, respectively). Moreover, hydrolysis of ammonium chloride probably also plays a role.

It follows from the above results that only sodium perchlorate, *i.e.*, a salt with the same anion as that of the diethazine cation radical, causes a decrease in the rate of the cation radical degradation. Therefore, a further study of the behaviour of the DE^+ perchlorate was conducted in a medium containing only the ClO_4^- anions.

Perchloric acid media. The effect of perchloric acid concentration, *i.e.*, the influence of H^+ and ClO_4^- ions, on the rate constant of the DE^+ perchlorate decomposition was studied first, from a maximal (11.0M) to a minimal (0.23M) perchloric acid concentration, obtained by dilution of the stock solution.

The dependence of the rate constant on the perchloric acid concentration is given in Fig. 3 (values are averages of five experimental values). It can be seen that the rate constant decreases with increasing perchloric acid concentration. There is a variance on the dependence around 4.0M perchloric acid. The decomposition of the

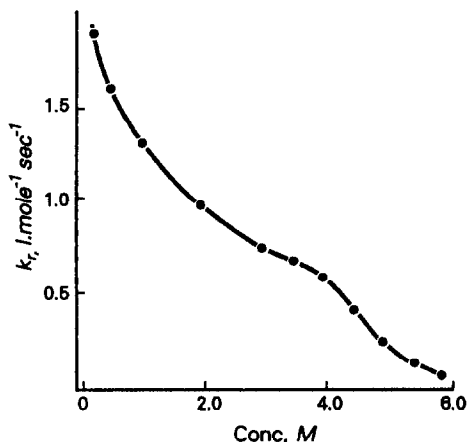


Fig. 3. Dependence of the HClO_4 concentration of the rate of decay of the perchlorate salt of the diethazine radical cation. Concentration of $\text{DE}^{+\cdot}\text{Cl}^- \text{HClO}_4 = 2 \times 10^{-4} M$.

diethazine radical cation probably obeys a more complex mechanism at perchloric acid concentrations higher than $4.0 M$, as the $1/c$ vs. t dependences do not correspond to 2nd order kinetics. The $\text{DE}^{+\cdot}$ perchlorate is stable at a perchloric acid concentration of $6 M$ or higher.

To verify the hypothesis that the perchlorate anion decelerates the decomposition of the perchlorate of the diethazine cationic radical, the effect of sodium perchlorate was studied over the concentration range 0.05 – $1.0 M$. The dependence of the rate constant on the sodium perchlorate concentration is given in Fig. 4, curve 1. The reaction rate is constant up to a

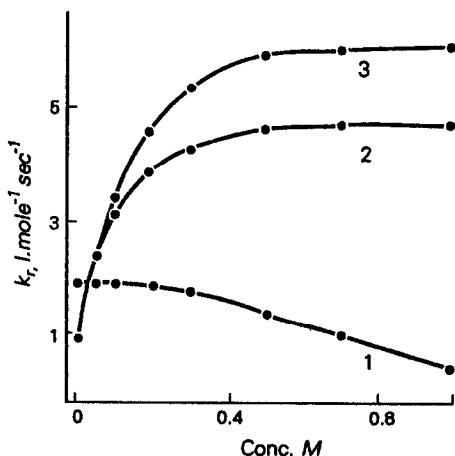


Fig. 4. Dependence on salt concentration of the rate of decay of the perchlorate salt of the diethazine radical cation. Concentration of $\text{DE}^{+\cdot}\text{Cl}^- \text{HClO}_4 = 2 \times 10^{-4} M$; medium, $0.5 M \text{HClO}_4$ for curve 1 and $2.0 M \text{HClO}_4$ for curve 2, 3.

Curve 1 NaClO_4
Curve 2 NaCl
Curve 3 HCl

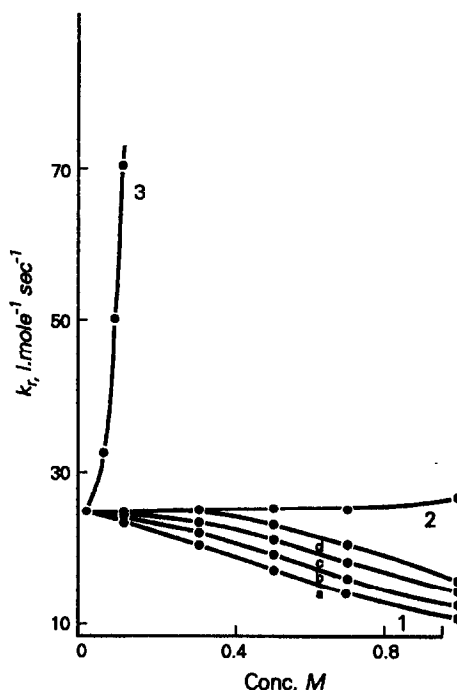


Fig. 5. Dependence on salt concentration of the rate of decay of the hydrochloride salt of the diethazine radical cation. Concentration of $\text{DE}^{+\cdot}\text{Cl}^- \text{HCl} = 2 \times 10^{-4} M$; medium, $2 M \text{HCl}$

Curve 1(a) LiCl
(b) NaCl
(c) KCl
(d) NH_4Cl
Curve 2 Na_2SO_4
Curve 3 NaClO_4

sodium perchlorate concentration of $0.2 M$ and then decreases at higher concentrations.

The effect of chloride anion (sodium chloride) was also followed in a perchlorate medium (curve 2). It can be seen that sodium chloride increases the rate of the $\text{DE}^{+\cdot}$ decomposition, especially at lower concentrations.

To verify this finding, the effect of hydrochloric acid was also studied (curve 3). The decomposition rate increases from 0.01 – $2.0 M$ hydrochloric acid, *i.e.*, the effect of Cl^- predominates over the stabilizing effect of H^+ .

Sodium nitrate affects the $\text{DE}^{+\cdot}$ disproportionation in perchloric acid medium according to a mechanism that is more complex than a 2nd order reaction.

Stability of the chloride of the diethazine radical cation

As above, the effect of selected anions (ClO_4^- , SO_4^{2-} and Cl^-) was studied by following the rate of degradation of the diethazine radical cation

prepared by electrochemical oxidation of the hydrochloride salt. Dependences are given in Fig. 5. It is evident that chloride causes the rate constant for the decomposition of the $DE^{+\cdot}$ radical cation to decrease, *i.e.*, increases the stability of the radical cation. In contrast, sulphate and perchlorate cause an increase in the rate constant; sulphate a slight increase and perchlorate a large one.

The effects of Li^+ , Na^+ , K^+ and NH_4^+ on the resultant rate constant were also followed [curves 1(a)–(d)]. Here, the rate constant of $DE^{+\cdot}$ disproportionation decreases, *i.e.*, the $DE^{+\cdot}$ stability increases as follows: $NH_4^+ < K^+ < Na^+ < Li^+$.

It follows from the above results that the kind of salt present in solution significantly affects the stability of the cationic radicals of phenothiazine derivatives. The stability is strongly enhanced in the presence of salts with the same anion as that contained in the salt of the cation radical, while other salts decrease the stability. This finding can be utilized in analytical deter-

minations based on the formation of coloured cationic radicals of these substances.

Acknowledgement—The authors are grateful to Dr J. Vohlídal for valuable discussions.

REFERENCES

1. I. Němcová, N. Zimová-Šulcová and I. Němec, *Chem. Listy*, 1982, **76**, 142.
2. T. N. Tozer and L. D. Tuck, *J. Pharm. Sci.*, 1965, **54**, 1169.
3. L. Levy, T. N. Tozer, L. D. Tuck and D. B. Loveland, *J. Med. Chem.*, 1972, **15**, 898.
4. A. Ortiz, T. Poyato and J. I. Fernández-Alonso, *J. Pharm. Sci.*, 1983, **72**, 50.
5. P. H. Sackett and R. L. McCreery, *J. Med. Chem.*, 1979, **22**, 1447.
6. H.-Y. Cheng, P. H. Sackett and R. L. McCreery, *J. Am. Chem. Soc.*, 1978, **100**, 962.
7. *Idem*, *J. Med. Chem.*, 1978, **21**, 948.
8. A. Ortiz, H. Pardo and J. I. Fernández-Alonso, *J. Pharm. Sci.*, 1980, **69**, 378.
9. A. De Leenheer, *J. Assoc. Off. Anal. Chem.*, 1973, **56**, 105.
10. I. Němcová, J. Novotný and V. Horská, *Microchem. J.*, 1986, **34**, 180.

CHROMOGENIC BENZO- AND MONOAZA-12-CROWN-4, 13-CROWN-4 AND 14-CROWN-4 LITHIUM-SELECTIVE CROWN ETHERS

K. WILCOX and G. E. PACEY

Department of Chemistry, Miami University, Oxford, Ohio 45056, U.S.A.

(Received 13 February 1990. Revised 19 March 1991. Accepted 29 March 1991)

Summary—Chromogenic benzo-12-crown-4, benzo-13-crown-4 and benzo-14-crown-4 ethers have been compared with monoaza-12-crown-4 and monoaza-13-crown-4 ethers. Of these compounds, monoaza-13-crown-4 exhibited the best analytical characteristics toward the selective determination of lithium. $K_{Li/Na}$ was 525 for the monoaza-crown-4 compound.

The search for a lithium selective ionophore has been continuous over the past two decades. Both open chained¹ and cyclic²⁻¹¹ compounds have been studied. From an analytical viewpoint, the primary difficulty was to develop a colorimetric ionophore that exhibits substantial selectivity for the lithium ion over the sodium ion.

The majority of these investigations have centered around the 12-crown-4 to 14-crown-4 substituted and unsubstituted ether compounds. For example dodecyl-14-crown-4 has exhibited the best selectivity.⁷ However, the addition of a chromogenic tag requires certain structural features which do not exist in some of the alkyl substituted crown ethers. Therefore, the best chromogenic crown ether for lithium has been the chromogenic monoaza-12-crown-4.²

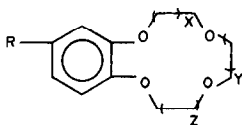
There have been two approaches to color addition in crown ethers. The intermolecular approach uses an azo type dye attached to the crown ether. On complexation, the conformational changes in the crown ring affect the energy levels of the *pi* electron system, usually producing a bathochromic shift. Unfortunately, the majority of the compounds reported exhibit small 5–25 nm shifts upon complexation. The second approach is to synthesize intramolecular ion pair compounds which utilize a functional group that deprotonates upon complexation, to provide the required counter ion. The result is usually an extension of the conjugation of the dye portion of the chromogenic crown ether. This approach is the one used in this study. Some lithium chromogenic crown ethers that have been reported include those such as Misumi "crowned" dinitrophenylazophenols.¹²⁻¹⁵

This paper reports the systematic study of the chromogenic 12-crown-4 through 14-crown-4 unsubstituted and benzo substituted crown ethers versus the monoaza 12 and 13 crown ether substituted compounds (Fig. 1).

EXPERIMENTAL

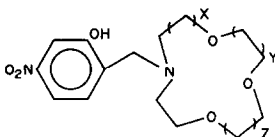
Synthesis

Benzocrown ethers. Chromogenic and nonchromogenic benzo-14-crown-4 compounds have been reported.³ Benzo-12-crown-4 and benzo-13-crown-4 were synthesized by combining the appropriate dichlorodiethyl glycol with catechol in *n*-butanol. Catechol (8.6 g, 0.08 mole), lithium hydroxide (6.6 g, 0.16 mole) and lithium perchlorate (4 g, 0.04 mole) were placed in 500 ml of *n*-butanol and refluxed. The dichloride, 1,2-bis(2-chloroethoxy)ethane for benzo-12-crown-4 or 1,2-bis(2-chloroethoxy)propane for benzo-13-crown-4, (0.08 mole in *n*-butanol), was added dropwise and the reaction was continued for six days. The cooled mixture was rotary evaporated and the residue taken up in 5% potassium hydroxide (250 ml). The aqueous phase was extracted several times with chloroform. The organic layer was combined, washed with water, dried over magnesium sulfate and evaporated. For benzo-12-crown the thick residue was passed through a silica column. The yield was 30% with a melting point of 44–45°. For the benzo-13-crown-4 the residue was distilled under vacuum (95–100°, 0.05 mm Hg). A clear liquid was collected which solidified upon standing. Recrystallization from hexane provided a pure compound in 55% yield.



R	X	Y	Z	Compound
H	O	O	O	Benzo-12-Crown-4
H	O	1	O	Benzo-13-Crown-4
H	1	O	1	Benzo-14-Crown-4
TAG	O	O	O	Chromogenic Benzo-12-Crown-4
TAG	O	1	O	Chromogenic Benzo-13-Crown-4
TAG	1	O	1	Chromogenic Benzo-14-Crown-4

R 2,4-Dinitro-6-Trifluoromethylphenyl



X	Y	Z	Compound
O	1	O	Monoaza-12-Crown-4
1	O	1	Monoaza-13-Crown-4

Fig. 1. Compounds developed and tested in this investigation.

The chromogenic tag was added to both of these compounds by the following procedure. The benzo-12-crown-4 or benzo-13-crown-4 compound (4.5 g or 4.8 respectively, 0.02 mole) was dissolved in 200 ml of chloroform/acetic acid (50:50 v/v). Concentrated nitric acid (20 ml) was dripped into the solution and the reaction mixture was stirred for 24 hr at room temperature. After neutralization with sodium bicarbonate, the separated aqueous layer was extracted with chloroform several times. The combined organic layers were dried over magnesium sulfate, filtered and evaporated to dryness. The pure product crystallized as a yellow solid. The 4'-nitrobenzo-12-crown-4 yield was 60%, mp 134–135°. The 4'-nitrobenzo-13-crown-4 yield was 86% with a mp of 144–145°.

The next step is the conversion of the nitro group to amine. The 4'-nitrobenzo crown ether (0.5 g, 2.0 mmole), 10% palladium on carbon (0.2 g) and freshly distilled ethanol were shaken in a hydrogen atmosphere at 33 psi. After 4 hr the mixture was filtered and the solvent was rotary evaporated. The dark residue was taken up into 40 ml of water and extracted with several portions of chloroform. The combined organic fractions were dried with anhydrous magnesium sulfate, filtered and evaporated to dryness. The product obtained was a dark

brown liquid. Yields were between 80–90%. This compound must be used immediately or kept under a nitrogen atmosphere.

The chromogenic tag was added by placing aminobenzo crown ethers (0.4 g, 1.6 mmole) into 250 ml of methanol and refluxing. Sodium bicarbonate (0.15 g, 1.8 mmole) and 2-chloro-3,5-dinitrobenzene trifluoride (0.48 g, 1.8 mmole) were added together. The stirred mixture was refluxed overnight. The cooled solution was neutralized with 1.0M hydrochloric acid, filtered and extracted with chloroform. The chloroform was dried over magnesium sulfate, filtered and rotary evaporated. The dark oily residue was dissolved in hot isopropanol followed by addition of petroleum ether until a slight cloudiness appeared. The solution was cooled overnight and the pure compound was collected as a darkened crystal. Yields range from 50–70%. Elemental analysis: chromogenic benzo-12-C-4; calc. 48.20% C, 3.81% H, 27.06% O, 8.62% N, 12.05% F; found 48.14% C, 3.14% H, 8.53% N, 11.96% F; chromogenic benzo-13-C-4; calc. 49.28% C, 4.11% H, 26.28% O, 8.62% N, 11.7% F; found 49.19% C, 4.01% H, 8.53% N, 11.43% F.

Monoazacrown ethers. The synthesis of the chromogenic monoazacrown ether has been significantly shortened by eliminating the need for protecting the amine group during the cyclization reaction. The first step is to prepare the two sections—the glycol and the amine—of the cyclic ring. The 1,2-bis(ethoxy)ethanes were synthesized and then tosylated. The tosylation reaction was performed in triethylamine (100 ml). The glycol (16.5 g, 0.1 mole) was cooled with an ice-water bath while *p*-toluenesulfonylchloride (38.4 g, 0.2 mole) was added in small portions. The heterogenous mixture was stirred overnight by an overhead stirrer while warming to room temperature. The resulting white slurry was poured over 100 g of ice, diluted with 75 ml of water and made acidic with dilute hydrochloric acid.

The precipitated ditosylate was filtered off, washed with water and recrystallized from ethanol. The pure product was obtained in 70% yield with a melting point of 89°.

The amines were prepared by using excess 2-aminoethanol (250 ml) with sodium carbonate (15 g, 0.19 mole). The mixture was heated to 150° under a nitrogen atmosphere. Then the appropriate chlorohydroxypropane was added dropwise to the stirred mixture. For monoaza-12-crown-4, 1-chloro-2-hydroxy ethane was

used; for monoaza-13-crown, the 1-chloro-2-hydroxy propane was used. After 30 hr the cooled solution was diluted with methanol (50 ml) and filtered. The precipitate was washed with a minimum amount of methanol and the combined washings and filtrates were concentrated under reduced pressure. The remaining oil was vacuum distilled to remove excess 2-aminoethanol leaving a reddish-gray, taffy-like residue. This was extracted several times with hot tetrahydrofuran. The combined tetrahydrofuran extracts were concentrated under reduced pressure to give a yellow oil which was vacuum distilled. The pure compound was obtained in 80% yields.

The cyclization of the dihydroxamine with the ditosylate was accomplished by dissolving the dihydroxyamine (0.3 mole) into t-butyl alcohol (200 ml) with sodium (0.6 mole). This mixture was heated to 40° under nitrogen pressure. Lithium bromide (0.03 mole) was added to the stirred mixture after the sodium was consumed. The ditosylated glycol (0.03 mole) was dissolved in 50 ml of 1,4-dioxane and dripped into the mixture. After 30 hr, the heterogenous mixture was cooled and filtered. The precipitate was washed with dichloromethane and the combined filtrate and washings were concentrated under reduced pressure. The residue was taken up in 20 ml of water and washed once with hexane and several times with dichloromethane. The combined dichloromethane extracts were concentrated under reduced pressure to give a yellow oil which was vacuum distilled. The final oil product was obtained in a 9% yield.

The chromogenic tag was added by dissolving the monoaza crown ether (0.012 mole) in THF and triethylamine (0.02 mole). This mixture was cooled in an ice water bath before the 2-hydroxy-5-nitrobenzyl bromide (0.012 mole), which was dissolved in THF, was added dropwise to the stirred mixture. The reaction was run under nitrogen at room temperature overnight. The resulting yellow solution was refluxed for 3 hr, cooled and filtered. The precipitate was washed with THF and the combined filtrate and washings concentrated under reduced pressure. The remaining yellow oil was dissolved in 25 ml of water and 2M hydrochloric acid was slowly added until the color turned pale yellow or colorless.

The acidic solution was extracted with chloroform while 2.5M potassium hydroxide was added dropwise until the color remained constant. The aqueous layer was extracted four

times with 30-ml portions of chloroform. All the organic extracts were combined, washed with three 20-ml portions of water, filtered and evaporated to dryness.

The residue was taken into water, filtered and concentrated. This residue was dissolved in chloroform and evaporated to dryness in a vacuum with gentle heating. Yellow crystals were recrystallized in hexane to give final product yields of 80–90% for monoaza-12-crown-4 and 85–87% for monoaza-13-crown-4. Elemental analysis: chromogenic monoaza-12-C-4; calc. 55.21% C, 6.75% H, 29.44% O, 8.59% N; found 55.14% C, 6.70% H, 8.53% N; chromogenic monoaza-13-C-4 calc 56.47% C, 7.06% H, 28.24% O, 8.24% N; found 56.39% C, 7.00% H, 8.13% N.

Extraction procedures for chromogenic benzocrown ethers

Determination of acid dissociation constant. The fact that the acid and base forms of the compound absorb in the ultraviolet and visible regions of the spectrum allows the acid dissociation constant to be determined spectrophotometrically. A weighed quantity of the reagent was dissolved in a 5% acetonitrile/water mixture. A 5-ml aliquot of the standard solution was pipetted into a 50-ml beaker and 2 ml of 1.0M rubidium chloride were added to control the ionic strength. The pH was adjusted with a dilute cesium hydroxide solution. The solution was transferred to a 25-ml standard flask and diluted to volume giving final concentrations of $1.89 \times 10^{-3}M$ crown ether and $8.0 \times 10^{-2}M$ rubidium chloride. The absorbance spectra at several pH values were obtained after which the pH was measured. From the absorbance values at the wavelengths of maximum absorption for the acid and base species the equilibrium concentrations could be calculated by solving simultaneous equations. The pK_a was readily determined from the Henderson-Hasselbach equation.

Determination of extraction constants. Attempts to obtain the extraction constants for the chromogenic reagent followed the experimental methods previously reported.³ Aliquots (4 ml) of the organic phase containing the reagent (6.6×10^{-5} – $2.0 \times 10^{-3}M$) and of the aqueous metal solutions (7.5×10^{-3} – $2.0 \times 10^{-1}M$) were placed in 50-ml flasks. The stoppered flasks were shaken for 15 min at a constant speed. Following phase separation, the absorbance of the organic layer was measured.

Instrumentation. All absorbance spectra were obtained on a Hewlett-Packard 8450A Diode Array spectrophotometer. A Fisher Accumet model 825 mp pH meter with an Orion model 91-05 combination electrode was used to measure the pH. All extractions were performed with a Lab-line multi-wrist shaker model 3587. The titrations of the reagents were done with a Metrohm Dosimet E-535 equipped with the potentiograph E-536.

Extraction procedures for chromogenic monoazacrown ethers

Determination of the acid dissociation constants. An aqueous solution (20–25 ml) containing the monoaza crown being studied ($3.36 \times 10^{-4} M$), hydrochloric acid ($3.6 \times 10^{-3} M$) and cesium chloride (0.1M), was titrated with potassium hydroxide (0.05M below pH 11; 0.9M above pH 11). The titration was stopped every 0.3–0.9 pH unit increase to measure the absorbance of the solution. A 3–4 ml portion was pipetted into a cuvette, and the spectrum recorded. The absorbances were corrected for dilution.

Determination of extraction constants. A 4-ml aliquot of the organic phase under study and a 4-ml aliquot of the aqueous phase containing the monoaza crown, potassium hydroxide, and varying concentration of lithium or sodium were placed in successive 50-ml round bottom flasks. The final concentrations of all species were (4.78–6.36) $10^{-4} M$ crown, 0.1M potassium hydroxide, $0-4.4 \times 10^{-3} M$ lithium, or 0–0.52M sodium. The stoppered flasks were shaken for 15 min at room temperature and left standing. After separation of the two layers, the absorbance of the organic and aqueous phases was recorded.

Interference study. To a series of 50-ml round bottom flasks was added 4 ml of dichloroethane and 4 ml of an aqueous phase containing $6.1 \times 10^{-4} M$ monoaza crown, 0.2M potassium hydroxide, $1.2 \times 10^{-4} M$ lithium bromide and $(0.004-4.0) \times 10^{-2} M$ sodium chloride. The stoppered flasks were shaken for 15 min, the layers were given time to separate and the organic phase absorbance was measured at 400 nm.

RESULTS AND DISCUSSION

Benzocrown ethers. The equations used for these experiments have been reported previously.⁴ Conclusions from the literature²⁻¹¹ would suggest that the best candidates for the

Table 1. Comparison of benzo crown ether ion-pair picrate log extraction constants* (25°)

Reagent/ solvent	Li ⁺	Na ⁺	K ⁺
B12C4/CHCl ₃ †	NE‡	1.10 ± 0.05	2.17 ± 0.05
B12C4/CH ₂ Cl ₂ †	NE	1.92 ± 0.01	2.74 ± 0.01
B13C4/CHCl ₃	1.22 ± 0.02	0.90 ± 0.05	0.87 ± 0.08
B13C4/CH ₂ Cl ₂	0.99 ± 0.03	1.01 ± 0.01	0.67 ± 0.02
B13C4/C ₂ H ₄ Cl ₂	1.46 ± 0.01	1.66 ± 0.01	1.52 ± 0.01
B14C4/CH ₂ Cl ₂	2.77 ± 0.02	2.17 ± 0.04	1.65 ± 0.05

*Triplicate samples †Cotton and Wilkinson¹⁹ ‡NE = No Extraction.

addition of chromophores would be the benzo-12-crown-4, benzo-13-crown-4 and benzo-14-crown-4 ethers. Using these compounds in picrate ion-pairing extraction studies,³ the data in Table 1 were generated. Using the chlorinated solvents, chloroform, methylene chloride and 1,2-dichloroethane as the organic phase, benzo-14-crown-4 exhibited the best selectivity toward the lithium ion. It should be pointed out that in the case of benzo-13-crown, the lithium-to-sodium selectivity was very dependent on the solvent used; chloroform being lithium-selective and methylene chloride and 1,2-dichloroethane sodium selective. This solvent dependence is not unusual.^{1,16} The usual conclusion is that the larger the solvent donor number the lower the formation or stability constant, particularly with the lithium cation because of its high-charge density. That is, the constants are dependent on how effectively the crown ether can desolvate the metal ion. Benzo-12-crown-4 did not extract lithium at all.

A linear response toward lithium was observed in the 3–140 meq/l. range with an equation $y = (5.00 \pm 0.03) \times 10^{-4} X + (7.6 \pm 0.5) \times 10^{-3}$ and a correlation coefficient of 0.999 where y denotes the absorbance and X is the lithium concentration in meq/l. However, as would be expected, sodium interferences began at about 1 meq/l. A linear response for lithium was observed in the 2–100 meq/l. range with an equation $y = (5.69 \pm 0.03) \times 10^{-4} X + (1.23 \pm 0.5) \times 10^{-5}$ and a correlation coefficient of 0.999. In the benzo-14-crown-4 case sodium interference began at 13 meq/l.

It has been shown that the selectivity of the benzocrown ethers is significantly increased by the physical attachment of a chromogenic compound.⁴ Therefore, both the 13- and 14-benzocrown ethers where tagged through an amine attachment to the benzene ring, using 1-chloro-, 4-dinitro-6-trifluoro-methylbenzene.

By tagging the crown ether, an intramolecular ion-pair which is inherently more stable, is formed during the extraction process. In the case of these chromogenic crown ethers, the protonated form exhibits one color while the deprotonated form exhibits another color. For 2'',4''-dinitro-6''-trifluoromethylphenyl-4'-aminobenzo-13-crown-4 the protonated form has a wavelength maximum at 375 nm ($\epsilon = 14,000 \text{ l. mole}^{-1} \cdot \text{cm}^{-1}$) and the deprotonated form has a wavelength maximum at 450 nm ($\epsilon = 18,000 \text{ l. mole}^{-1} \cdot \text{cm}^{-1}$). The 2'',4''-dinitro-6''-trifluoromethylphenyl-4'-aminobenzo-14-crown-4 exhibits a protonated wavelength maximum at 380 nm ($\epsilon = 12,000 \text{ l. mole}^{-1} \cdot \text{cm}^{-1}$) and deprotonated wavelength maximum at 462 nm ($\epsilon = 20,000 \text{ l. mole}^{-1} \cdot \text{cm}^{-1}$). The acid dissociation constants were 10.15 ± 0.02 and 9.99 ± 0.03 .

These acid base properties of both compounds behaved as expected; however, they exhibited very unexpected complexing abilities. The chromogenic benzo-13-crown-4 exhibited no extraction of any alkali metal ions. Single-crystal X-ray studies¹⁷ show that the lithium cation does not fit in the plane of the ring oxygens, but is positioned slightly out of the ring, forming a pyramidal shaped complex. Without the additional coordination from the picrate anion, as in the ion-pair extractions, the cation is exposed to coordination by other species such as water. The same certainly holds true for the rest of the alkali metal ions which are larger. The presence of the water makes the reagent too lipophobic to be extracted back into the organic phase. The fact that the aqueous phase took on the red color of the deprotonated reagent during the extraction process supports this argument.

For chromogenic benzo-14-crown-4, lithium extraction was quite good. The extraction constants for this compound are given in Table 2. A linear calibration curve was obtained for 2–80 meq/l. with a sensitivity of $1.69 \times 10^{-3} \pm 2.2 \times 10^{-5}$. Sodium did not interfere below a concentration of 130 meq/l.

Although this compound is lithium selective, it is not sensitive enough for the intended uses such as test strips and sensors for manic depressives. Previously, a report from this laboratory disclosed that monoaza-12-crown-4 exhibits very good lithium selectivity. It is now clear that the configuration of these monoazacrown ethers is superior to the benzocrown ethers. In other words, the chromogenic benzo-12-crown-4 and

Table 2. Extraction constants for lithium complexing chromogenic and nonchromogenic crown ethers (25°)

Reagent	$-\log K_{ex} \text{Li}$	$-\log K_{ex} \text{Na}$	Selectivity ($K_{ex} \text{Li}/K_{ex} \text{Na}$)
L13C4	NR	NR	2
L14C4	NR	NR	19*
CHRL14C4	11.29	13.66	240†
B13C4	1.22 ± 0.02	0.90 ± 0.05	0.48
CHRB13C4	NE	NE	—
B14C4	2.77 ± 0.02	2.17 ± 0.04	0.25‡
CHRB14C4	11.00	11.43	2.7‡
MA12C4	10.18	12.49	210§
MA13C4	9.98 ± 0.08	12.7 ± 0.02	525
MA15C5	9.15	9.76	4

L = Lipophillic crown ethers.

B = Benzo crown ethers.

CHR = Chromogenic crown ether.

MA = Monoaza crown ethers.

NE = No Extraction.

NR = Not Reported.

*Reference 8.

†Reference 7.

‡Reference 4.

§Reference 2.

||Reference 11.

benzo-13-crown-4 ethers do not compete favorably with the water for the coordination sites of the alkali metal where as the ring nitrogen and phenolic counter ion do compete effectively. Therefore, the chromogenic monoaza-13-crown-4 was investigated.

Nonchromogenic and chromogenic monoaza-crown ethers

Determination of acid dissociation constants.

To determine the K_{a1} and K_{a2} from the experimental data, it is first necessary to define the proton-dissociation process of the system. The equilibria for the chromogenic monoaza crown ethers are summarized in Fig. 2. The HL species can exist in the aqueous phase in two tautomeric forms, *i.e.*, nonionic and zwitterionic forms. Therefore, as reported by Katayama,¹⁸

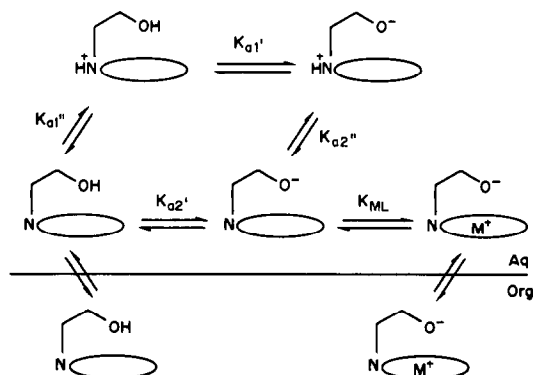


Fig. 2. Schematic representation of the equilibria for the monoazacrown ethers.

coexistence of a small amount of one species or the other cannot be totally excluded, and Ka_1 may be considered as the sum of Ka'_1 and Ka''_1 .

The acidity constants can be described as follows:

$$Ka_1 = \frac{[HL][H^+]}{[HLH^+]} \quad (1)$$

and

$$Ka_2 = \frac{[L^-][H^+]}{[HL]}. \quad (2)$$

Figure 3 shows absorption spectra of the 13-crown-4 reagent in water at various hydrogen ion concentrations. From the spectra it is seen that the reagent exhibits two pH dependent isosbestic points at 343 nm and 402 nm.

Within certain pH regions, $[HL]^- \gg [L^-]$ for Ka_1 and $[HL]^- \gg [HLH^+]$ for Ka_2 , and $[L^-]$ or $[HLH^+]$ can be neglected when compared with $[HL]^-$. In terms of pH, $[HL]^-$ is much greater than $[L^-]$ at pH 6.9, and $[HL]^-$ is much greater than $[HLH^+]$ at pH 9.6.

Working with this knowledge, the acid dissociation constant, Ka_1 was determined by substituting the absorbance data below pH 6.9 in simultaneous equations to obtain the concentrations of, $[HLH^+]$ and $[HL]$. From these equilibrium concentrations and the pH, the first acid dissociation constant could be calculated. In a similar fashion, using the absorbance data above pH 9.6, the second acid dissociation constant was determined. The values obtained for the two chromogenic monoaza crown ethers are reported, along with the literature values of other monoaza crown ethers in Table 3. The values obtained in this study are comparable to the literature values.

Table 3. Acid dissociation constants for chromogenic monoaza crown ethers (25°)

Crown ether	$-\log Ka_1$	$-\log Ka_2$
MA 12-crown-4	5.41	9.80*
MA 13-crown-4	5.65 ± 0.03	10.31 ± 0.2
MA 14-crown-4	5.60 ± 0.7	10.77 ± 0.03
MA 15-crown-5	5.79	9.69†
MA 18-crown-6	5.77	9.59†

*In water (Ref. 2).

†In 10% 1,4-dioxane/water (Ref. 14).

Determination of the extraction constants. The metal extraction processes equilibria can be expressed mathematically as:

$$K_{ex} = \frac{[ML]_0 [H^+]_{aq}}{[HL]_0 [M^+]_{aq}} \quad (3)$$

The analytical concentrations of the reagent and metal ion can be expressed as:

$$[HL]_t = [HL]_{aq} + [HL]_0 + [ML]_{aq} + [ML]_0 + [L^-]_{aq} + [HLH^+]_{aq} \quad (4)$$

$$[M^+]_t = [ML]_{aq} + [ML]_0 + [M^+]_{aq} \quad (5)$$

and molar absorptivity at any wavelength can be expressed by:

$$E = A_0 / ([HL]_0 + [ML]_0) \quad (6)$$

By substituting $A_0 = (\epsilon_{HL}^0 [HL]_0 + \epsilon_{ML}^0 [ML]_0)$ we get

$$E = (\epsilon_{HL}^0 [HL]_0 + \epsilon_{ML}^0 [ML]_0) / ([HL]_0 + [ML]_0) \quad (7)$$

From the experimental conditions at pH 12 it is known that

$$[HL]_t \gg [HLH^+]_{aq} \text{ and } [L^-]_{aq} \gg [HL]_{aq} + [ML]_{aq}.$$

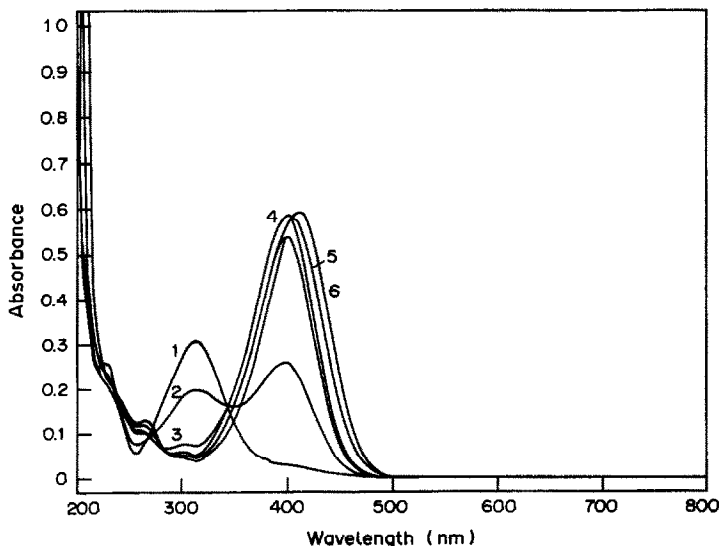


Fig. 3. Absorption spectra for monoaza-13-crown-4 pH = 1 (4.3), 2 (5.2), 3 (6.7), 4 (9.3), 5 (10.8), 6 (1.5).

Therefore, equation (4) simplifies to:

$$[\text{HL}]_t = [\text{HL}]_0 + [\text{ML}]_0 + [\text{L}^-]_{\text{aq}} \quad (8)$$

and the only absorbing species in the aqueous phase is L^- , so that:

$$[\text{L}^-]_{\text{aq}} = A_{\text{aq}}/\epsilon_{\text{L}^-} \quad (9)$$

Equation (7) can be transformed into a linear relationship, as indicated by Sasaki and Pacey,² which allows the extraction constants to be obtained graphically. First subtract the molar absorptivity of the blank, $E^0 = \epsilon_{\text{HL}}^0$, from both sides.

$$E - E^0 = \frac{\epsilon_{\text{ML}}^0 [\text{HL}]_0 + \epsilon_{\text{HL}}^0 [\text{ML}]_0}{[\text{HL}]_0 + [\text{ML}]_0} - \epsilon_{\text{HL}}^0 \quad (10)$$

By taking the reciprocal of both sides and multiplying ϵ_{HL}^0 by $([\text{HL}]_0/[\text{HL}]_0)$ to achieve a common denominator, equation (10) becomes:

$$\frac{1}{E - E^0} = \frac{1}{\left(\frac{\epsilon_{\text{ML}}^0 [\text{HL}]_0 + \epsilon_{\text{HL}}^0 [\text{ML}]_0}{[\text{HL}]_0 + [\text{ML}]_0} \right) - \left(\frac{\epsilon_{\text{HL}}^0 [\text{HL}]_0 + \epsilon_{\text{HL}}^0 [\text{ML}]_0}{[\text{HL}]_0 + [\text{ML}]_0} \right)} \quad (11)$$

If like terms are cancelled and combined over the common denominator, equation (11) becomes:

$$\begin{aligned} \frac{1}{E - E^0} &= \frac{1}{\left(\frac{\epsilon_{\text{ML}}^0 [\text{ML}]_0 - \epsilon_{\text{HL}}^0 [\text{ML}]_0}{[\text{HL}]_0 + [\text{ML}]_0} \right)} \\ &= \frac{[\text{HL}]_0 + [\text{ML}]_0}{\epsilon_{\text{ML}}^0 [\text{ML}]_0 + \epsilon_{\text{HL}}^0 [\text{ML}]_0} \quad (12) \end{aligned}$$

Separating the fraction into individual parts allows:

$$\begin{aligned} \frac{1}{E - E^0} &= \frac{[\text{HL}]_0}{\epsilon_{\text{ML}}^0 [\text{ML}]_0 - \epsilon_{\text{HL}}^0 [\text{ML}]_0} \\ &+ \frac{[\text{ML}]_0}{\epsilon_{\text{ML}}^0 [\text{ML}]_0 - \epsilon_{\text{HL}}^0 [\text{ML}]_0} \quad (13) \end{aligned}$$

By placing like terms outside parentheses we get:

$$\begin{aligned} \frac{1}{E - E^0} &= \frac{[\text{HL}]_0}{(\epsilon_{\text{ML}}^0 - \epsilon_{\text{HL}}^0) [\text{ML}]_0} \\ &+ \frac{[\text{ML}]_0}{(\epsilon_{\text{ML}}^0 - \epsilon_{\text{HL}}^0) [\text{ML}]_0} \quad (14) \end{aligned}$$

Cancelling like terms gives:

$$\frac{1}{E - E^0} = \frac{[\text{HL}]_0}{(\epsilon_{\text{ML}}^0 - \epsilon_{\text{HL}}^0) [\text{ML}]_0} + \frac{1}{(\epsilon_{\text{ML}}^0 - \epsilon_{\text{HL}}^0)} \quad (15)$$

Substituting $[\text{H}^+]_{\text{aq}}/(K_{\text{ex}}[\text{M}^+]_{\text{aq}}) = [\text{HL}]_0/[\text{ML}]_0$ and $\epsilon_{\text{ML}}^0 - \epsilon_{\text{HL}}^0 = \Delta\epsilon$ gives:

$$\frac{1}{E - E^0} = \frac{[\text{H}^+]_{\text{aq}}}{K_{\text{ex}}[\text{M}^+]_{\text{aq}} \Delta\epsilon} + \frac{1}{\Delta\epsilon} \quad (16)$$

For lithium, equation (17) shows that a plot of $1/(E - E^0)$ vs. $1/[\text{M}^+]_{\text{aq}}$ should be linear and K_{ex} can be calculated from the slope, intercept and the pH. By combining equations (6), (8) and (9), the values of E and E^0 (E^0 is determined from the blank absorbance value) can be obtained according to equation (17)

$$\begin{aligned} E &= \frac{A_0}{[\text{HL}]_0 + [\text{ML}]_0} + \frac{A_0}{[\text{HL}]_t - [\text{L}^-]_{\text{aq}}} \\ &= \frac{A_0}{[\text{HL}]_t - (A_{\text{aq}}/\epsilon_{\text{L}^-})_{\text{aq}}} \quad (17) \end{aligned}$$

where A_0 is the absorbance of the organic layer at 400 nm, A_{aq} is the absorbance of the aqueous layer at 412 nm, and ϵ_{L^-} is the molar absorptivity of the aqueous species at 412 nm.

The poor extraction, and the experimental conditions used, allow the assumption $[\text{M}^+]_{\text{aq}} = [\text{M}^+]_t$ for the sodium system, so that:

$$\frac{1}{E - E^0} = \frac{[\text{H}^+]_{\text{aq}}}{K_{\text{ex}}[\text{M}^+]_t \Delta\epsilon} + \frac{1}{\Delta\epsilon} \quad (18)$$

The K_{ex} for sodium can then be determined in a similar fashion by plotting $1/(E - E^0)$ vs. $1/[\text{M}^+]_t$. Typical plots of the data for the respective extraction systems were straight lines as shown in Fig. 4.

Table 2 shows the $-\log K_{\text{ex}}$ values for the monoaza crown ethers together with the $-\log K_{\text{ex}}$ values reported for other ionizable lithium selective reagents.

In comparison to the other reagents, the new reagent exhibits significantly greater selectivity for lithium over sodium. There are several factors which may contribute to this increased selectivity.

A CPK space-filling model shows that the attachment of the chromophore to the nitrogen atom in the ring allows the phenolate anion to

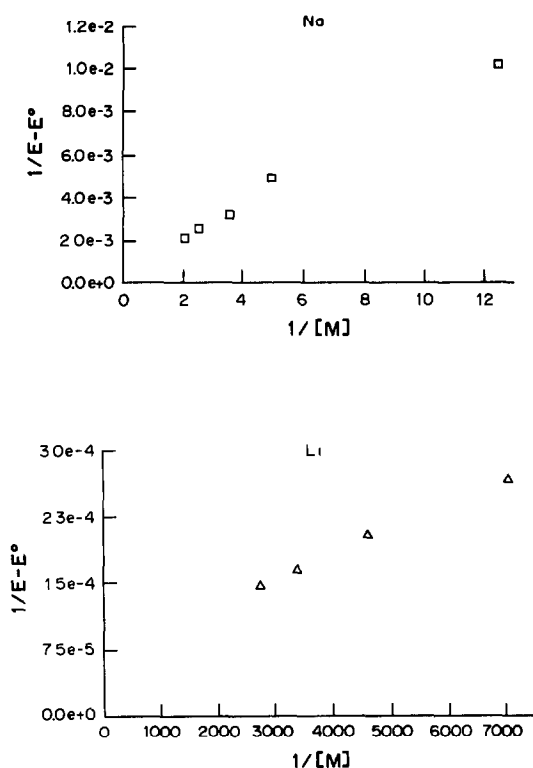


Fig. 4. Typical plots for extraction constant data.

be positioned directly over the cavity of the crown. In such a geometry the interaction of the anion with the metal cation is much greater than the interaction where the chromophore is attached to a carbon atom in the ring. When attached to a carbon atom the chromophore essentially has too short a "tether" to allow the phenolate anion to be positioned above the cavity. Rather, it is off to one side and does not interact as effectively with the cation.

Because of this favourable positioning, the interaction of the phenolate anion and the lithium cation ion should be very strong. In fact, the bond between the two may have considerable covalent character.¹⁹ Katayama¹⁸ has shown that the less basic, more charge-delocalized phenolate anions, such as the 2,4-dinitrophenol used by Kimura,⁷ prefer the extraction of the larger metal ions (lower surface-charge density). In contrast, the more basic, less charge-delocalized phenolate anions prefer the extraction of the use of 4-nitrophenol as the chromophore may enhance the metal:crown complex.

The presence of the nitrogen atom in the crown ether ring may also provide additional stability to the complex. The non-bonding electrons of the nitrogen may be polarized such that

the interaction between the metal ion and the nitrogen may have much covalent character.²⁰ In addition, models show the monoaza crown structure is such that formation of a six-membered chelate ring is possible, comprised of the nitrogen atom, a methylene carbon, two aromatic carbons, the phenolate oxygen, and metal cation, two aromatic carbons, the phenolate oxygen and metal cation within the crown ether cavity. In classical chelating compounds, six-membered rings are usually considered to be ideal in terms of their complex stability.²¹ Such an additional chelate ring should strengthen the initial complexation due to interaction of the metal ion with the ring heteroatoms. Those reagents which have the chromophore attached to a ring carbon cannot form true chelate rings. Thus, the extra stability is not present.

The excellent selectivity exhibited by these monoaza compounds is also illustrated in Fig. 5. This shows the results of competitive extractions performed with a constant lithium ion concentration while increasing the sodium ion concentration.

Analytical characteristics

The reagents were examined in two different solvent systems, chloroform and dichloromethane. Although both systems extracted the lithium cation effectively, the dichloromethane system exhibited better sensitivity as defined by the slope of the sample response curve (Fig. 4). It is interesting to note that Sasaki and Pacey tested several organic solvents and reported that chloroform gave the best results,² while Katayama *et al.* reports using 1,3-dichloroethane in their system.¹⁸

The observed selectivity may be dependent on how the particular organic phase solvates or interacts with the complex. In the monoaza 14-crown-4 the metal ion is probably not fully shielded from the organic phase. This may allow

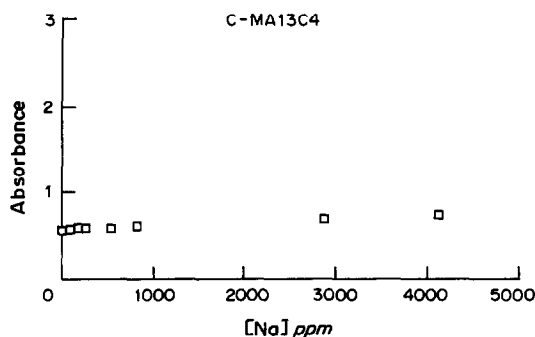


Fig. 5. Selectivity plots for the monoaza crown ether.

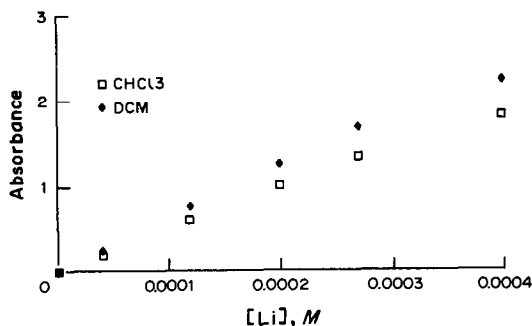


Fig. 6. Sample response curves for monoaza crown ether in the two solvents.

the cation to interact with the solvent significantly, or possibly a water molecule is coordinated to the cation. The larger azacrowns may be more capable of shielding the cation from such interactions and thus the complex prefers different solvents. It is reasonable to assume the more lipophilic complex would extract more easily into the more lipophilic solvent. *i.e.* 1,2-dichloroethane.

The response observed for lithium ion extraction is shown in Figs. 6 and 7. The limited linear range does occur below the physiological concentration of lithium, therefore allowing dilution.

Good precision about triplicate determinations is shown by the error bars. The majority of the error is believed to arise from two areas. First, the method of extraction sometimes leads to incomplete extraction. Second, the absorbance of the organic phase was unstable. Sasaki reported the same difficulty with the absorbance and attempted to correct it but had little success.² No attempt was made, in this study, to eliminate this problem. However, adaptation of this extraction procedure to an automated system such as flow-injection analysis may reduce or remove both sources of error.

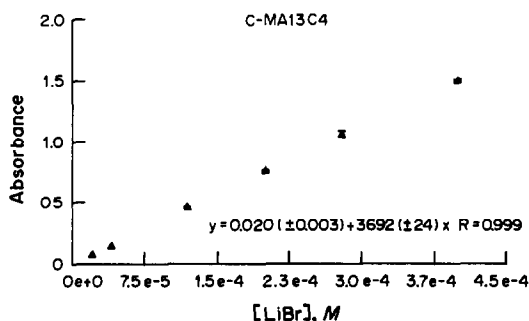


Fig. 7. Optimized sample response curve for monoaza-13-crown-4.

The detection limits for the individual reagents can be theoretically determined from equation (19).²²

$$\text{Detection limit} = KS_{\text{bk}}/M_{\text{rc}} \quad (19)$$

Here K equals some constant, typically 2 or 3, S_{bk} is the standard deviation of the blank and M_{rc} equals the slope of the response curve. The detection limit (K equals 3) calculated for the monoaza 13 was 0.06 ppm.

CONCLUSIONS

It is clear from this work that the chromogenic monoaza crown ethers do possess better selectivity toward lithium ion than the chromogenic benzocrown ethers. This work suggests that further extension of the monoaza-crown system will provide useful information. Compounds such as the isomers of chromogenic monoaza-14-crown-4 may well be even better reagents for the lithium ion.

REFERENCES

1. A. Shanzer, D. Samuel and R. Korenstein, *J. Am. Chem. Soc.*, 1983, **105**, 3815.
2. K. Sasaki and G. E. Pacey, *Anal. Chim. Acta*, 1985, **174**, 141.
3. Y. P. Wu and G. E. Pacey, *ibid.*, 1984, **162**, 285.
4. B. P. Bubnis, J. L. Steger, Y. P. Wu, L. A. Meyers and G. E. Pacey, *ibid.*, 1982, **139**, 307.
5. K. Kimura, M. Tanaka, S. Kitazawa and T. Shono, *Chem. Lett.*, 1985, 1239.
6. H. Nakamura, H. Sakka, M. Takagi and K. Ueno, *ibid.*, 1981, 1305.
7. K. Kimura, M. Tanaka, S. Iketani and T. Shono, *J. Org. Chem.*, 1987, **52**, 836.
8. R. A. Rartsch, B. P. Czech, S. I. Kang, L. E. Stewart, W. Walkowiak, W. A. Charewicz, G. S. Heo and B. Son, *J. Am. Chem. Soc.*, 1985, **107**, 4997.
9. B. Dietrich, J. M. Lehn and J. P. Sauvage, *Tetrahedron Lett.*, 1969, 2885.
10. G. W. Gokel, D. M. Dishong and C. J. Diamond, *J. Chem. Soc. Chem. Commun.*, 1980, 1053.
11. Y. Nakatsuji, R. Wakita, Y. Harada and M. Okahara, *J. Org. Chem.*, 1989, **54**, 2988.
12. K. Nakashima, S. Nakatsuji, S. Akiyama, T. Kaneda and S. Misumi, *Chem. Pharm. Bull.*, 1984, **34**, 168.
13. K. Nakashima, S. Nakatsuji, S. Akiyama, I. Tanigawa, T. Kaneda and S. Misumi, *Talanta*, 1984, **31**, 749.
14. K. Nakashima, N. Michizuki, S. Nakatsuji, S. Akiyama, T. Kaneda and S. Misumi, *Chem. Pharm. Bull.*, 1984, **32**, 2468.
15. K. Nakashima, S. Nakatsuji, S. Akiyama, T. Kaneda and S. Misumi, *Chem. Lett.*, 1982, 1781.
16. B. P. Czech, D. A. Babb, B. Son and R. A. Bartsch, *J. Org. Chem.*, 1984, **49**, 4805.
17. G. Shoham, W. N. Lipscomb and U. Olsher, *J. Am. Chem. Soc.*, 1983, **105**, 1247.
18. Y. Katayama, K. Nita, M. Ueda, H. Nakamura, M. Takagi and K. Ueno, *Anal. Chim. Acta*, 1985, **173**, 193.

19. F. Cotton and G. Wilkinson, *Advanced Inorganic Chemistry*, 4th Ed., pp. 264–268. Wiley, New York, 1980.
20. D. L. Williams, *The Metals of Life*, Camelot Press Ltd., London, 1974.
21. B. E. Douglas, D. H. McDaniel and J. J. Alexander, *Concepts and Models of Inorganic Chemistry*, 2nd Ed., Wiley, New York, 1983.
22. J. Ingle and S. R. Crouch, *Spectrochemical Analysis*, Prentice-Hall, Englewood Cliffs, N.J., 1988.

THERMODYNAMIC STUDY OF SOLVENT EXTRACTION OF 15-CROWN-5- AND 18-CROWN-6-s-BLOCK METAL ION COMPLEXES AND TETRAALKYLAMMONIUM IONS WITH PICRATE ANIONS INTO CHLOROFORM

YASUYUKI TAKEDA,* NOBUYUKI IKEO and NORIKO SAKATA

Department of Chemistry, Faculty of Science, Chiba University, Yayoi-cho, Chiba 260, Japan

(Received 26 November 1990. Revised 22 February 1991. Accepted 26 February 1991)

Summary—Enthalpy and entropy changes for ion-pair extractions of tetraalkylammonium ions (R_4N^+) with picrate anions, overall extractions of s-block metal picrates with 15-crown-5 (15C5) and 18-crown-6 (18C6) and the partition of 15C5 itself were determined between chloroform and water. The distribution behaviour of crown ethers and the extraction process of s-block metal picrates with the crown ethers are discussed in detail on molecular grounds from the thermodynamic point of view. Moreover, enthalpy and entropy changes for ion-pair extractions of 1:1 15C5- and 18C6-s-block metal ion complexes with picrate anions are calculated from these experimental thermodynamic parameters and the literature values for complex-formation reactions of the crown ethers with the s-block metal ions in water. Enthalpy and entropy changes are negative for overall extractions of all the s-block metal picrates with 15C5 and 18C6. The extractions of the metal picrates with 15C5 and 18C6 at 25° are completely enthalpy driven. Plots of thermodynamic parameters for ion-pair extractions of R_4NA vs. the number of carbon atoms of R_4N^+ show a linear relationship. From these experimental data, contributions of a methylene group and an ether oxygen atom to the thermodynamic parameters of the ion-pair extraction of R_4NA and the partition of the crown ethers, respectively, between chloroform and water were obtained. Enthalpy and entropy changes for ion-pair extractions of 15C5- and 18C6-s-block metal picrate complexes were compared with those of R_4NA . A striking difference in the ion-pair extraction process was found between the crown ether complexes and R_4NA .

Since Pedersen conducted extractions of alkali metal picrates with crown ethers for the first time,¹ solvent extraction has been used as one of the least difficult methods for evaluating the complexing abilities of newly synthesized crown compounds with cations.² In general, a crown compound efficiently extracts a cation of suitable size into the cavity of the crown compound. The overall extraction consists of some fundamental processes.³ Thus, in order to elucidate the extraction efficiency and selectivity of a crown compound for a cation, it is necessary to analyse the overall extraction equilibrium in terms of the underlying equilibria; for example, distribution of the free crown compound, complex formation in the aqueous phase and ion-pair extraction of the crown compound complex. The distribution of an uncomplexed crown compound governs the extractability of the crown compound for cations. The stability in water and the ion-pair extractability of the crown compound complex govern both the

extractability and selectivity of the crown compound for cations. In addition, these basic equilibrium constants provide valuable information on solute-solvent interactions of crown compounds and their complexes. For further study of the role of crown compounds in the extraction process and of solvation properties of free crown compounds and their complexes, it is important to obtain thermodynamic parameters for the overall extraction process and the fundamental processes. Some enthalpy and entropy changes of overall extraction processes have been presented, but only a few thermodynamic quantities concerning the basic processes have been reported.⁴⁻⁶

In the present study, enthalpy and entropy changes for ion-pair extractions of tetraalkylammonium ions (R_4N^+) with picrate anions, overall extractions of s-block metal picrates with 15-crown-5 (15C5) and 18-crown-6 (18C6) and the partition of 15C5 itself were determined between chloroform and water. The distribution behaviour of crown ethers and the extraction process of s-block metal picrates with the crown

*Author for correspondence.

ethers are discussed in detail on molecular grounds from the thermodynamic point of view. Moreover, enthalpy and entropy changes for ion-pair extractions of 1:1 15C5- and 18C6-s-block metal ion complexes with picrate anions are calculated from these experimental thermodynamic parameters and the literature values for complex-formation reactions of the crown ethers with the s-block metal ions in water. The thermodynamic quantities for ion-pair extractions of 15C5- and 18C6-s-block metal picrate complexes are compared with those of R_4NA .

EXPERIMENTAL

Materials

Tetramethyl-, tetraethyl-, tetrapropyl-, and tetrabutylammonium hydroxides were purchased from Wako-Pure Chemicals Ltd. and used as received. 15-Crown-5 (Nisso Co., Ltd.) was purified by distillation under vacuum [b.p. 129.0–130.5°, 2.6 mmHg (1 mmHg \approx 133.322 Pa)]. 18-Crown-6 (Nisso Co., Ltd.) was recrystallized from acetonitrile and, prior to use, dried at 80° *in vacuo*. Chloroform, picric acid, lithium hydroxide ($LiOH \cdot H_2O$), sodium hydroxide, potassium hydroxide, strontium hydroxide [$Sr(OH)_2 \cdot 8H_2O$] and barium hydroxide [$Ba(OH)_2 \cdot 8H_2O$] were analytical grade reagents. Rubidium and cesium hydroxides were of reagent grade. Chloroform was purified by distillation and washed three times with distilled water.

Extraction procedure

Ion-pair extraction of tetraalkylammonium picrate. A $CHCl_3$ phase and an aqueous phase of R_4NOH (3.8×10^{-3} – $2.3 \times 10^{-2}M$; lithium hydroxide (0.01M), and picric acid (3.2×10^{-5} – $1.5 \times 10^{-2}M$) in stoppered glass tubes (30 ml) were shaken for 2 hr in a water bath kept at 15, 20, 25, 30 and $35 \pm 0.2^\circ$, and centrifuged. The initial volume of each phase was 10 ml in all cases. Extractions were conducted at pH 11.3–12.1. For the Bu_4NA system, the concentration of the picrate anion in the aqueous phase was determined spectrophotometrically at 356 nm ($\epsilon = 1.45 \times 10^4$ l. mole $^{-1}$. cm $^{-1}$). For Me_4NA , Et_4NA and Pr_4NA systems, an 8-ml portion of the $CHCl_3$ phase was transferred to a beaker and allowed to evaporate over several days. The residue was dissolved in 4 ml of 0.1M aqueous sodium hydroxide and the picrate concentration was determined spectrophotometrically (at 356 nm, $\epsilon = 1.45 \times 10^4$ l. mole $^{-1}$. cm $^{-1}$).

In blank experiments, there was no extraction of picrate anions in the absence of R_4N^+ .

Extraction of metal picrates with 15C5 and 18C6. A $CHCl_3$ phase of crown ether (1.1×10^{-5} – $3.6 \times 10^{-3}M$), and an aqueous phase of metal hydroxide (6.7×10^{-4} – $2.3 \times 10^{-2}M$) and picric acid (2.8×10^{-4} – $1.5 \times 10^{-3}M$) in a stoppered glass tube (30 ml) were agitated in a water bath kept at constant temperature for 2 hr and centrifuged. The initial volume of each phase was 12 ml in all cases. Extractions were performed at 15, 20, 25, 30 and $35 \pm 0.2^\circ$ for 15C5 systems, and at 15, 20, 25, 30 and $32 \pm 0.2^\circ$ for 18C6 systems; carried out at pH 11.2–12.2 for alkali metal ions and at pH 9.1–10.0 for alkaline earth metal ions. The picrate in the $CHCl_3$ phase was back-extracted twice into 0.01M sodium hydroxide aqueous solution, and the picrate concentration was determined by spectrophotometry (at 356 nm, $\epsilon = 1.45 \times 10^4$ l. mole $^{-1}$. cm $^{-1}$). In blank experiments, there was no extraction in the absence of the crown ethers.

Distribution coefficient of 15C5. A 10-ml $CHCl_3$ solution of 15C5 (3.0×10^{-4} – $2.2 \times 10^{-3}M$) and an equal volume of distilled water in a stoppered glass tube (30 ml) were shaken (in a water bath kept at constant temperature) for 2 hr and centrifuged. A 6-ml portion of the aqueous phase and an equal volume of an aqueous solution (pH 10.9–11.8) containing sodium hydroxide ($1.1 \times 10^{-1}M$) and picric acid ($1.0 \times 10^{-1}M$) were placed in a stoppered glass tube and 12 ml of $CHCl_3$ were added. The two phases were agitated for 1 hr at 2–30. After centrifuging, the picrate in the $CHCl_3$ phase was back-extracted into 0.01M sodium hydroxide aqueous solution, and the picrate concentration was determined spectrophotometrically (at 356 nm, $\epsilon = 1.45 \times 10^4$ l. mole $^{-1}$. cm $^{-1}$). Experiments were conducted at 15, 20, 25, 30 and $35 \pm 0.2^\circ$. The distribution coefficient [$K_D(L)$] values of 15C5 are shown in Table 1. Each $K_D(15C5)$ value is the average of about 30 measurements.

Table 1. Summary of $K_D(L)$ values of 15C5 between $CHCl_3$ and water

Temp, °C	$K_D(L)$
15	6.83 \pm 0.02
20	7.42 \pm 0.02
25	8.27 \pm 0.05
30	9.03 \pm 0.08
35	9.86 \pm 0.03

The uncertainties are the standard deviations.

RESULTS

Ion-pair extraction of R_4NA

In an equilibrium between $CHCl_3$ and an aqueous solution of R_4NA , the equilibrium constants are defined as

$$K_A(R_4NA) = [R_4NA]_o/[R_4N^+][A^-], \quad (1)$$

$$K_D(R_4NA) = [R_4NA]_o/[R_4NA], \quad (2)$$

$$K_{ex,ip}(R_4NA) = [R_4NA]_o/[R_4N^+][A^-] \\ = K_A(R_4NA)K_D(R_4NA). \quad (3)$$

The subscript "o" and the absence of a subscript denote the organic and aqueous phases, respectively. The distribution ratio of R_4N^+ is represented by

$$D = [R_4NA]_o/([R_4N^+] + [R_4NA]). \quad (4)$$

Combination of equations (1–4) leads to

$$D^{-1} = K_D(R_4NA)^{-1} \\ + (K_{ex,ip}(R_4NA)[A^-])^{-1}. \quad (5)$$

Plots of D^{-1} vs. $[A^-]^{-1}$ show a linear relationship in every case. Values of $K_{ex,ip}(R_4NA)$ were obtained from the slopes of the straight lines. Since the $K_D(R_4NA)$ value scarcely varied in the range 15–35° in all cases, enthalpy and entropy changes for this process could not be determined.

Plots of $R \ln K_{ex,ip}(R_4NA)$ vs. T^{-1} were found to be linear in every system. The enthalpy change $[\Delta H_{ex,ip}^\circ(R_4NA)]$ and entropy change $[\Delta S_{ex,ip}^\circ(R_4NA)]$ for equation (3) were calculated from these data. The thermodynamic parameters are compiled in Table 2.

Extraction of metal picrates with crown ethers

When an equilibrium occurs between an aqueous phase of a metal ion (M^{m+}) and picrate ion, and a $CHCl_3$ phase of a crown ether (L), the equilibrium constants are defined as

$$K_{ex} = [MLA_m]_o/[M^{m+}][L]_o[A^-]^m, \quad (6)$$

$$K_D(L) = [L]_o/[L], \quad (7)$$

$$K_{ML} = [ML^{m+}]/[M^{m+}][L], \quad (8)$$

$$K_{ex,ip}(MLA_m) = [MLA_m]_o/[ML^{m+}][A^-]^m \quad (9)$$

The overall extraction equilibrium constant, K_{ex} , can be written as

$$K_{ex} = K_{ML} \cdot K_{ex,ip}(MLA_m) \cdot K_D(L)^{-1} \quad (10)$$

The distribution ratio of the metal is represented by

$$D = [MLA_m]_o/([M^{m+}] + [ML^{m+}]) \quad (11)$$

In the case of $[M^{m+}] \gg [ML^{m+}]$, equation (11) is transformed into

$$D = K_{ex}[L]_o[A^-]^m \quad (12)$$

Plots of $\log(D/[A^-]^m)$ vs. $\log[L]_o$ give a straight line with a slope of 1 in every case. This indicates that the crown ether forms a 1:1 complex with the M^{m+} ion.

From the mass balances, $[L]_o$ and $[M^{m+}]$ are given by

$$[L]_o = ([L]_t - [MLA_m]_o)/(\alpha + \beta[M^{m+}]) \quad (13)$$

$$[M^{m+}] = ([M]_t - [MLA_m]_o)/(1 + \beta[L]_o) \quad (14)$$

where the subscript "t" denotes the total concentration, $\alpha = 1 + K_D(L)^{-1}$, and $\beta = K_{ML}K_D(L)^{-1}$. The K_{ex} value was determined by using the $[L]_o$ value of equation (13), the $[M^{m+}]$ value of equation (14), and the $[A^-]$ value of equation (15),

$$[A^-] = [HA]_t - m[MLA_m]_o \quad (15)$$

Equilibrium constants are summarized in Table 3.

$-R \ln K_D(L)$ vs. T^{-1} and $-R \ln K_{ex}$ vs. T^{-1} plots show a linear relationship in every system (Figs. 1, 2 and 3). Enthalpy and entropy change for equations (6) and (7) were calculated from the data in the same manner as that described above. The thermodynamic quantities are listed in Table 4.

Table 2. Thermodynamic quantities for ion-pair extraction of tetraalkylammonium picrates between $CHCl_3$ and water

	$\log [K_{ex,ip}(R_4NA)/M]^*$	$\log [K_A(R_4NA)/M]^*$	$\log K_D(R_4NA)^*$	$\Delta H_{ex,ip}^\circ(R_4NA)$ kJ/mole	$T\Delta S_{ex,ip}^\circ(R_4NA)$ kJ/mole*
Me_4NA	-0.923 ± 0.008	-1.3	0.4 ± 0.1	-19.8	-25.1
Et_4NA	1.294 ± 0.003	-0.75	2.04 ± 0.04	-16.7	-9.3
Pr_4NA	3.677 ± 0.006	1.3	2.4 ± 0.4	-12.7	8.3
Bu_4NA	6.045 ± 0.007	3.3	2.7 ± 0.5	-8.8	25.6

*Temp = 25°. Each $\log K_{ex,ip}(R_4NA)$ and $\log K_D(R_4NA)$ value is the average of 8–12 measurements. The uncertainties are the standard deviations.

Table 3. Equilibrium constants for 15C5 and 18C6 complexes with s-block metal ions at 25°

	$\log K_D(15C5) = 0.91_8^*$		$\log K_D(18C6) = 0.78_6^* \dagger$			
	$\log K_{ex}^*$		$\log K_{ML}^*$		$\log K_{ex,ip}^*$	
	15C5	18C6	15C5†	18C6	15C5	18C6
Na ⁺	4.001 ± 0.005	3.47†	0.70	0.80†	4.22	3.46†
K ⁺	3.523 ± 0.003	6.07†	0.74	2.03†§	3.70	4.83†
Rb ⁺	3.345 ± 0.005	5.65†	0.62	1.56†	3.64	4.88†
Cs ⁺	2.603 ± 0.003	4.62†	0.8	0.99†	2.7	4.42†
Sr ²⁺	4.551 ± 0.003	9.429 ± 0.004	1.95	2.72†	3.52	7.50
Ba ²⁺	5.204 ± 0.004	9.498 ± 0.009	1.71	3.87†	4.41	6.41

*At 25°. †Ref. 5. ‡Ref. 26. §Ref. 27. Each $\log K_{ex}$ value is the average of 6–8 measurements. The uncertainties are the standard deviations.

DISCUSSION

Ion-pair extraction of R_4NA

The $\log K_A(Bu_4NA)$ value at 25° in this study is almost consistent with that (3.1₅) at 25° reported in a previous paper (benzene/water system).⁶ From Table 2, the $\log K_A(R_4NA)$ value sequences are $Me_4N^+ < Et_4N^+ \ll Pr_4N^+ \ll Bu_4N^+$; namely, the $\log K_A(R_4NA)$ value increases with an increase in the R_4N^+ size, which is not compatible with coulombic ionic association theories. In water saturated methylene chloride, however, the order of the $\log K_A(R_4NA)$ value is completely reversed ($Me_4N^+ > Et_4N^+ > Pr_4N^+$).⁷ The trend of the $\log K_A(R_4NA)$ values in water reflects the effect of increasing enforcement of a hydrogen-

bonded structure of water on the R_4N^+ ion ($Me_4N^+ \rightarrow Bu_4N^+$). The $\log K_A(R_4NA)$ value in water is very much smaller than the corresponding $\log K_A(R_4NA)$ value in water saturated methylene chloride [5.021(Me_4NA), 4.276(Et_4NA), 4.117(Pr_4NA)]⁷ ($\epsilon_r = 8.94$ at 25°) which is attributed to water having a very much higher dielectric constant.

The $\log K_D(R_4NA)$ order is $Me_4NA \ll Et_4NA < Pr_4NA < Bu_4NA$ (Table 2); the same tendency is found for benzene⁶ and methylene chloride;⁷ namely, the $\log K_D(R_4NA)$ value increases with an increase in the R_4N^+ size. This is attributable to the effect of increasing enforcement of the hydrogen-bonded structure of water on the R_4NA ($Me_4NA \rightarrow Bu_4NA$). The difference in the $\log K_D(R_4NA)$ values

Table 4. Thermodynamic quantities for extraction of s-block metal picrates with 15C5 and 18C6 between $CHCl_3$ and water

	$\Delta H_D^\circ(L), \text{kJ/mole}$			$T\Delta S_D^\circ(L), \text{kJ/mole}^*$		
	15C5	18C6		15C5	18C6	
		13.7	17.5	19.0	22.0	
	15C5					
	ΔH_{ex}°	$\Delta H_{ML}^\circ \dagger$	$\Delta H_{ex,ip}^\circ$	$T\Delta S_{ex}^\circ^*$	$T\Delta S_{ML}^\circ \dagger \ddagger$	$T\Delta S_{ex,ip}^\circ^*$
	<i>kJ/mole</i>	<i>kJ/mole</i>	<i>kJ/mole</i>	<i>kJ/mole</i>	<i>kJ/mole</i>	<i>kJ/mole</i>
Na ⁺	-58.2	-6.28	-38.2	-35.4	-2.2	-14.2
K ⁺	-30.1	-17	0.6	-10.1	-13.0	21.9
Rb ⁺	-37.6	-7.95	-16.0	-18.6	-4.4	4.8
Cs ⁺	-40.7	-5.4	-21.6	-26.0	-0.6	-6.4
Sr ²⁺	-35.2	-3.8	-17.7	-9.21	7.5	2.2
Ba ²⁺	-61.6	-4.8	-43.1	-31.8	5.0	-17.8
	18C6					
	ΔH_{ex}°	ΔH_{ML}°	$\Delta H_{ex,ip}^\circ$	$T\Delta S_{ex}^\circ^*$	$T\Delta S_{ML}^\circ^*$	$T\Delta S_{ex,ip}^\circ^*$
	<i>kJ/mole</i>	<i>kJ/mole</i>	<i>kJ/mole</i>	<i>kJ/mole</i>	<i>kJ/mole</i>	<i>kJ/mole</i>
Na ⁺	-45.7†	-9.41†	-18.8†	-26.0†	-4.6†	0.6†
K ⁺	-76.4†	-25.01§	-33.9†	-41.8†	-13.33§	-6.6†
Rb ⁺	-79.1†	-16.0†	-45.6†	-46.9†	-7.1†	-17.8†
Cs ⁺	-76.5†	-15.9†	-43.1†	-50.1†	-10†	-18.1†
Sr ²⁺	-92.4	-15.1†	-59.8	-38.7	0.4†	-17.1
Ba ²⁺	-99.8	-31.7†	-50.6	-45.8	-9.9†	-13.9

*Temp = 25°.

†Takeda and Tanaka.⁵

‡Izatt *et al.*²⁶

§Takeda and Arima.²⁷

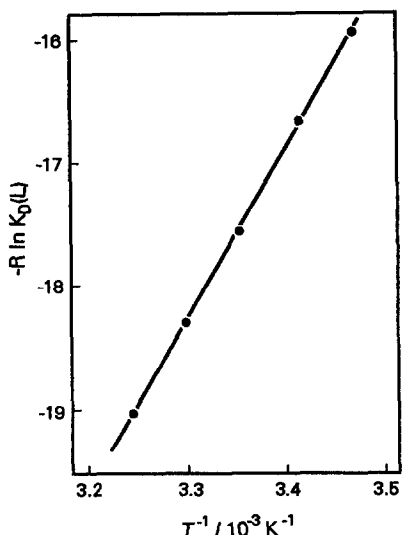


Fig. 1. $-R \ln K_D(L)$ vs. T^{-1} plots for 15C5 between CHCl_3 and H_2O .

$[\Delta \log K_D(\text{R}_4\text{NA})]$ between Pr_4NA and Et_4NA is nearly equal to that between Bu_4NA and Pr_4NA ; but, the $\Delta \log K_D(\text{R}_4\text{NA})$ values are much smaller than the $\Delta \log K_D(\text{R}_4\text{NA})$ value between Et_4NA and Me_4NA . The same trend is also observed for the cases of C_6H_6 and CH_2Cl_2 .⁷ This indicates that the $\log K_D(\text{Me}_4\text{NA})$ value is much lower than that expected based on a contribution to the $\log K_D(\text{R}_4\text{NA})$ value of a methylene group calculated from $\log K_D(\text{R}_4\text{NA})$ values of Et_4NA , Pr_4NA and Bu_4NA . The unexpectedly low $\log K_D(\text{Me}_4\text{NA})$

value is probably due to the fact that the ratio of the number of carbon atoms of R_4N^+ to that of the neighbouring larger R_4N^+ is the smallest for the case of Me_4N^+ and Et_4N^+ (1:2).

It can be seen from the $\log K_{\text{ex,ip}}(\text{R}_4\text{NA})$ values in Table 2 that extractability of the R_4N^+ with a picrate ion into CHCl_3 increases with an increase in the R_4N^+ size. The order of increasing extractability of the R_4N^+ is consistent completely with those of increasing $K_A(\text{R}_4\text{NA})$ and $K_D(\text{R}_4\text{NA})$ values. This is also the case in C_6H_6 and CH_2Cl_2 systems.⁷ It can be concluded from the above discussion that the ion-pair extractability of R_4N^+ with a picrate ion is determined by the strength of enforcement of the hydrogen-bonded structure of water for the R_4N^+ ion. Plots of $\log K_{\text{ex,ip}}(\text{R}_4\text{NA})$ vs. the number of carbon atoms of R_4N^+ give a straight line with a slope of 0.582. This indicates that the contribution of a methylene group to the extraction constant of ion pairs (Π_{CH_2}) at 25° between chloroform and water is 0.582. The Π_{CH_2} value (0.58) determined in this study is consistent with the value of 0.59 reported by Motomizu *et al.*⁸ but is slightly larger than those reported by Modin and Schill⁹ (0.56), Matsunaga and Yotsuyanagi¹⁰ (0.54) and Eksborg and Schill¹¹ (0.52). The difference in $\log K_{\text{ex,ip}}$ values between Me_4N^+ and Et_4N^+ is nearly equal to that between Et_4N^+ and Pr_4N^+ and that between Pr_4N^+ and Bu_4N^+ . This is due to the fact that the unexpectedly large $\log K_A$

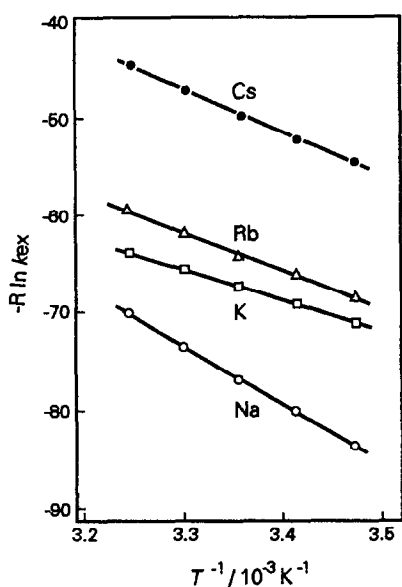


Fig. 2. $-R \ln K_{\text{ex}}$ vs. T^{-1} plots for 15C5-alkali metal picrate complexes between CHCl_3 and H_2O .

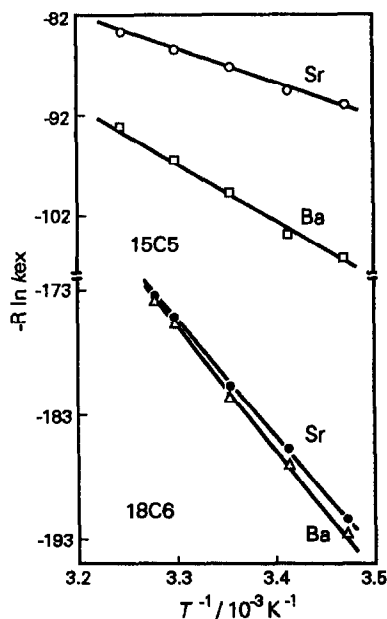


Fig. 3. $-R \ln K_{\text{ex}}$ vs. T^{-1} plots for 15C5- and 18C6-alkaline earth metal picrate complexes between CHCl_3 and H_2O .

and small $\log K_D$ values of Me_4N^+ compensate each other.

Plots of thermodynamic quantities for ion-pair extraction of R_4NA against the number of carbon atoms of R_4N^+ in Fig. 4 show a linear relationship. Contributions of a methylene group to ΔH° and ΔS° of ion-pair extraction [$\Delta H_{\text{ex,ip}}^\circ(\text{CH}_2)$ and $\Delta S_{\text{ex,ip}}^\circ(\text{CH}_2)$] between CHCl_3 and water were obtained from the slopes to be 0.93 kJ/mole and 14 J K^{-1} mole $^{-1}$, respectively. Positive values of $\Delta H_{\text{ex,ip}}^\circ(\text{CH}_2)$ and $\Delta S_{\text{ex,ip}}^\circ(\text{CH}_2)$ indicate that the methylene group undergoes hydrophobic hydration in water. The $T\Delta S_{\text{ex,ip}}^\circ(\text{CH}_2)$ value at 25° is 4.5 times larger than the $\Delta H_{\text{ex,ip}}^\circ(\text{CH}_2)$ value. Thus the larger the size of R_4N^+ , the more entropy- and the less enthalpy-driven the ion-pair extraction process of R_4NA is (Table 2).

Table 2 shows that for Me_2NA , a favourable enthalpy change is completely cancelled by an unfavourable entropy change, resulting in the negative $\log K_{\text{ex,ip}}$ value; for Bu_4NA , favourable enthalpy and more favourable entropy changes lead to the large $\log K_{\text{ex,ip}}$ value. Both $\Delta H_{\text{ex,ip}}^\circ(\text{R}_4\text{NA})$ and $\Delta S_{\text{ex,ip}}^\circ(\text{R}_4\text{NA})$ values increase with an increase in the size of R_4N^+ . This may result from the change from a structure-breaking effect of Me_4N^+ to a structure-making effect of Bu_4N^+ in water.¹²

A linear relationship is found for plots of $\Delta H_{\text{ex,ip}}^\circ$ and $\Delta S_{\text{ex,ip}}^\circ$ of R_4NA *vs.* the reciprocal of the radius of R_4N^+ (correlation coefficient $r = -0.980$ for $\Delta H_{\text{ex,ip}}^\circ$ and -0.986 for $\Delta S_{\text{ex,ip}}^\circ$). Both $\Delta H_{\text{ex,ip}}^\circ$ and $\Delta S_{\text{ex,ip}}^\circ$ of R_4NA are composed mostly of electrostatic interaction.

Distribution of crown ethers

From $\log K_D(\text{L})$ values of 15C5 and 18C6 obtained in our laboratory, the contribution (Π_0) of an ether oxygen atom to $\log K_D(\text{L})$ at 25° between CHCl_3 and water can be calculated by use of the Π_{CH_2} value determined in this study; namely $\Pi_0 = [\log K_D(\text{L}) - \Pi_{\text{CH}_2} \times a]/b$ (a and b denoting the number of methylene groups and ether oxygen atoms, respectively). The Π_0 values from 15C5 and 18C6 are nearly equal, -0.98_0 and -1.03_3 , respectively. The Π_0 value is -1.00 on the average. An ether oxygen atom is hydrophilic, whereas a methylene group is lipophilic. The $\log K_D(\text{L})$ values of 12-crown-4 (12C4), 15C5 and 18C6 can be estimated to be 0.66, 0.82 and 0.98, respectively. They are consistent with the respective experimental $\log K_D(\text{L})$ values [$\log K_D(12\text{C4}) = 0.90(\text{exptl})$]¹³. Contributions of benzo ($\Pi_{\text{C}_6\text{H}_4}$) and methyl

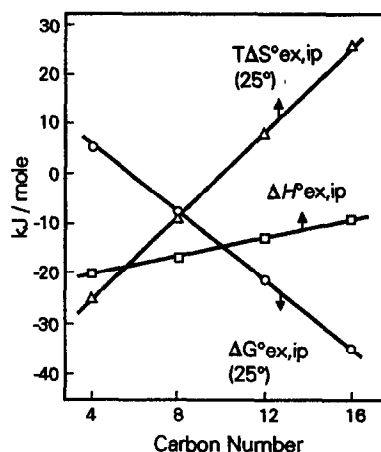


Fig. 4. Plots of thermodynamic quantities for ion-pair extraction of R_4NA *vs.* the number of carbon atoms of R_4N^+ .

(Π_{CH_3}) groups to $\log K_D(\text{L})$ at 25° between CHCl_3 and H_2O can be calculated to be 2.57 and 1.09 from $\log K_D(\text{L})$ values of benzo-18-crown-6 (B18C6) (2.569)¹⁴ and 1,2-bis[2-(2-methoxyethoxy)ethoxy]benzene (AC·B18C6) (3.40),¹⁵ that is, $\Pi_{\text{C}_6\text{H}_4} = 2.569 - 0.582 \times 10 - (-1.00) \times 6$ and $\Pi_{\text{CH}_3} = [3.40 - 0.582 \times 8 - (-1.00) \times 6 - 2.57]/2$. From these empirical parameters, the $\log K_D(\text{L})$ values of benzo-15-crown-5 (B15C5), B18C6, AC·B18C6, and dibenzo-18-crown-6 (DB18C6) can be estimated to be 2.23, 2.39, 3.41 and 3.80, respectively. They are in accord with the respective experimental $\log K_D(\text{L})$ values of B15C5 (2.4),¹⁶ B18C6, AC·B18C6 and DB18C6 (3.9).¹⁷ Using these empirical parameters, $\log K_D(\text{L})$ values of crown ethers at 25° between CHCl_3 and H_2O can be estimated regardless of their shapes.

By using the $\Delta H_{\text{ex,ip}}^\circ(\text{CH}_2)$ and $\Delta S_{\text{ex,ip}}^\circ(\text{CH}_2)$ values determined in this study, contributions of an ether oxygen atom to $\Delta H_D^\circ(\text{L})$ [$\Delta H_D^\circ(\text{o})$] and $\Delta S_D^\circ(\text{L})$ [$\Delta S_D^\circ(\text{o})$] between CHCl_3 and H_2O were calculated from $\Delta H_D^\circ(\text{L})$ and $\Delta S_D^\circ(\text{L})$ of 15C5 and 18C6 (Table 4); namely, $\Delta H_D^\circ(\text{o}) = [\Delta H_D^\circ(\text{L}) - \Delta H_{\text{ex,ip}}^\circ(\text{CH}_2) \times a]/b$ and $\Delta S_D^\circ(\text{o}) = [\Delta S_D^\circ(\text{L}) - \Delta S_{\text{ex,ip}}^\circ(\text{CH}_2) \times a]/b$. $\Delta H_D^\circ(\text{o})$ and $\Delta S_D^\circ(\text{o})$ are 0.8₈ kJ/mole and -15.0_6 J K^{-1} mole $^{-1}$ from 15C5, and 1.5 kJ/mole and -16.0_1 J K^{-1} mole $^{-1}$, respectively, from 18C6. They are almost the same. $\Delta H_D^\circ(\text{o})$ and $\Delta S_D^\circ(\text{o})$ are 0.9₆ kJ/mole and -15.8 J K^{-1} mole $^{-1}$, respectively, on the average. Strong interaction between an ether oxygen atom and water¹⁸ is responsible for the positive $\Delta H_D^\circ(\text{o})$ and negative $\Delta S_D^\circ(\text{o})$ values. The $\Delta H_D^\circ(\text{o})$ and $\Delta S_D^\circ(\text{o})$ values between benzene and water are 2.8 kJ/mole and -13 J K^{-1} mole $^{-1}$, respectively,⁶ and are larger than

those between CHCl_3 and water. This is attributable to the interaction between an ether oxygen atom and CHCl_3 via hydrogen bonding. $\Delta H_D^\circ(\text{L})$ and $\Delta S_D^\circ(\text{L})$ values of 15C5 and 18C6 between CHCl_3 and water can be estimated from these empirical parameters. They are as follows:

	15C5	18C6
$\Delta H_D^\circ(\text{L})/\text{kJ/mole}$	14	17
$\Delta S_D^\circ(\text{L})/\text{J K}^{-1} \text{mole}^{-1}$	61	73

They are consistent with the experimental $\Delta H_D^\circ(\text{L})$ and $\Delta S_D^\circ(\text{L})$ values (Table 4). $\Delta H_D^\circ(\text{L})$ and $\Delta S_D^\circ(\text{L})$ values of a 3m-crown-m ether between CHCl_3 and H_2O can be estimated, regardless of its shape, from the empirical thermodynamic parameters.

Partition of 15C5 and 18C6 from H_2O to CHCl_3 is entropy driven; favourable $T\Delta S_D^\circ(\text{L})$ values at 25° are largely cancelled by unfavourable $\Delta H_D^\circ(\text{L})$ values, resulting in small positive $\log K_D(\text{L})$ values of 15C5 and 18C6. Positive $\Delta H_D^\circ(\text{L})$ values of 15C5 and 18C6 are a result of a sum of the effect of interaction between ether oxygen atoms and water and the effect of hydrophobic hydration of methylene groups in water. The effect of hydrophobic hydration of methylene groups surpasses that of interaction between ether oxygen atoms and water, resulting in positive $\Delta S_D^\circ(\text{L})$ values of 15C5 and 18C6.

Extraction of metal picrates with crown ethers

From Table 3, extraction-selectivity sequences of 15C5 for the alkali metal ions are $\text{Na}^+ > \text{K}^+ > \text{Rb}^+ > \text{Cs}^+$ [ionic radius¹⁹: 1.02 Å (Na^+), 1.38 Å (K^+), 1.49 Å (Rb^+) and 1.70 Å (Cs^+)], indicating that the more closely the metal ion fits into the 15C5 cavity (cavity radius 0.85 Å,²⁰ the more extractable the 15C5-metal ion complex is (size-fit concept). $\log K_{\text{ML}}$ and $\log K_{\text{ex,ip}}$ sequences of 15C5 for the alkali metal ions are $\text{Cs}^+ > \text{K}^+ > \text{Na}^+ > \text{Rb}^+$ and $\text{Na}^+ > \text{K}^+ > \text{Rb}^+ > \text{Cs}^+$, respectively. The $\log K_{\text{ex}}$ sequences of 15C5 are not consistent with the $\log K_{\text{ML}}$ sequences, but are consistent with the $\log K_{\text{ex,ip}}$ sequences. The 15C5- Na^+ and K^+ complexes are more stable than the 15C5- Rb^+ complex in water. This enhances extraction selectivity of 15C5 for Na^+ and K^+ over that for Rb^+ . However, the extraction-selectivity sequences of 15C5 for the alkali metal ions are determined completely by the $\log K_{\text{ex,ip}}$ sequences (equation 10). Whereas extraction-selectivity sequences of 18C6 for the alkali metal ions are governed largely by the $\log K_{\text{ML}}$ sequences. Ion-pair extraction selectivity for

18C6-alkali metal ion complexes partly enhances the extraction selectivity of 18C6 for the alkali metal ions.

The size-fit concept holds for the selectivity of 15C5 and 18C6 (cavity radius 1.38 Å²⁰) for Sr^{2+} and Ba^{2+} (ionic radius¹⁹: 1.13 and 1.36 Å, respectively) in water, but does not hold for the extraction selectivity of 15C5 and 18C6 for Sr^{2+} and Ba^{2+} . The unexpected extraction selectivity is attributed to the higher ion-pair extractability of the 15C5- Ba^{2+} and 18C6- Sr^{2+} complexes compared with the 15C5- Sr^{2+} and 18C6- Ba^{2+} complexes, respectively.

Partition equilibrium between CHCl_3 and H_2O of free 15C5 and 18C6, which are less water-soluble, lowers the extractability for the metal ions of 15C5 and 18C6, respectively. For every crown ether-metal ion system in Table 3, the $\log K_{\text{ex,ip}}$ value is much greater than $\log K_D(\text{L})$ and $\log K_{\text{ML}}$ values. Thus, the magnitude of the $\log K_{\text{ex}}$ value depends largely on that of the $\log K_{\text{ex,ip}}$ value.

All $\Delta H_{\text{ex}}^\circ$ and $\Delta S_{\text{ex}}^\circ$ values in Table 4 are negative. The $T\Delta S_{\text{ex}}^\circ$ value at 25° is much larger than the corresponding $\Delta H_{\text{ex}}^\circ$ value. Thus, all the extractions of the metal picrates with 15C5 and 18C6 are completely enthalpy driven. For 15C5, the difference between $|\Delta H_{\text{ex}}^\circ|$ and $|T\Delta S_{\text{ex}}^\circ|$ is larger for the bivalent metal ion than for the univalent metal ion. The same is true for the case of 18C6. Extraction of the bivalent metal ion is more enthalpy driven than that of the univalent metal ion. For the 15C5- M^+ system, the most favourable $\Delta H_{\text{ex}}^\circ$ of Na^+ is balanced by the most unfavourable $T\Delta S_{\text{ex}}^\circ$, leading to the greatest $\log K_{\text{ex}}$ value.

Ion-pair extraction of crown ether-metal ion complexes with picrate anions.

The $\log K_{\text{ex,ip}}$ value of 15C5 varies with a cation of the same charge except for the cases of K^+ and Rb^+ ; those of the 15C5- K^+ and Rb^+ complexes are nearly equal (Table 3). The same tendency is found for 18C6. For alkali metal ions, the $\log K_{\text{ex,ip}}$ value of 15C5 decreases in the order, $\text{Na}^+ > \text{K}^+ \geq \text{Rb}^+ > \text{Cs}^+$; that is, the 15C5- M^+ complex, where the metal ion has a suitable size for the cavity, is more extractable as an ion pair with a picrate ion. However, this is not true for each case of 15C5- and 18C6-alkaline earth metal ion complex systems; the crown ether complex with a less size-fitting metal ion is more extractable. The higher ion-pair extractability of the less size-fitting alkaline earth metal ion is ascribed entirely to the more

favourable $\Delta H_{\text{ex,ip}}^\circ$ value. For 15C5, the most favourable $\Delta H_{\text{ex,ip}}^\circ$ value of Na^+ among the alkali metal ions is cancelled by the most unfavourable $T\Delta S_{\text{ex,ip}}^\circ$ value, resulting in the greatest $\log K_{\text{ex,ip}}$ value. Ion-pair extraction of $\text{K}(15\text{C5})\text{A}$ is completely entropy driven, whereas ion-pair extractions of $\text{M}(15\text{C5})\text{A}_m$ ($\text{M} = \text{Rb}, \text{Cs}, \text{Sr}, \text{Ba}$) and $\text{M}(18\text{C6})\text{A}_2$ ($\text{M} = \text{Sr}, \text{Ba}$) are enthalpy controlled.

From the structure of the 15C5 complex with the alkali metal ion held in the cavity, anion- and solvent-contact are possible in respective directions perpendicular to the plane of the 15C5 ring. Gibbs free energies of hydration ($\Delta G_{\text{h}}^\circ/\text{kJ/mole}$) of Na^+ , K^+ , Rb^+ and Cs^+ are -411.3 , -338 , -320 and -297 , respectively.²¹ The interaction of the alkali metal ion with water increases in the order, $\text{Cs}^+ < \text{Rb}^+ < \text{K}^+ \ll \text{Na}^+$. The order of the interaction with water of the alkali metal ion trapped in the 15C5 cavity is expected to be $\text{Cs}^+ < \text{Rb}^+ < \text{K}^+ < \text{Na}^+$. The association constant of the alkali metal ion with a picrate ion in water decreases in the order, $\text{Cs}^+ > \text{Rb}^+ > \text{K}^+ > \text{Na}^+$.²² The order of the association constant with a picrate ion of the alkali metal ion held in the 15C5 cavity is expected to be $\text{Cs}^+ > \text{Rb}^+ > \text{K}^+ > \text{Na}^+$. From the above discussion, the $\log K_{\text{ex,ip}}$ -value sequence of the 15C5 complex is expected to be $\text{Cs}^+ > \text{Rb}^+ > \text{K}^+ > \text{Na}^+$. But, the sequence of the experimental $\log K_{\text{ex,ip}}$ value of the 15C5 complex in Table 3 is the reverse. This unexpected result is attributed to a negligible effect of water on association of the alkali metal ion in the 15C5 complex with a picrate ion and/or weak interaction with water of the alkali metal ion in the 15C5 complex. Table 4 shows that, in the cases of the 15C5-alkali metal ion complexes, both $\Delta H_{\text{ex,ip}}^\circ$ and $\Delta S_{\text{ex,ip}}^\circ$ values vary considerably with the cation. This is probably attributed to large differences in interactions of the 15C5 complexes directly with picrate anions in an aqueous phase rather than those with water molecules. It has been reported that, when 15C5 extracts an alkali metal ion into nitrobenzene, the more closely the alkali metal ion fits into the 15C5 cavity, the more water molecules attached to the alkali metal ion are released; and that the number of water molecules coextracted with the uncomplexed alkali metal ion varies appreciably from Na^+ to Cs^+ but those coextracted with the 15C5 complex vary little with the alkali metal ion.²³ This strongly supports the above discussion.

The $\log K_{\text{ex,ip}}$ value of Na^+ is greater for 15C5 than for 18C6, but the reverse holds for the cases of the other metal ions (Table 3); a more favourable $\Delta H_{\text{ex,ip}}^\circ$ value is responsible for the higher ion-pair extractability of the M^{m+} complex with one crown ether compared with the corresponding M^{m+} complex with the other crown ether (Table 4). $K_{\text{ex,ip}}$ consists of two underlying equilibria, $K_{\text{ex,ip}} = K_{\text{MLA}_m} \cdot K_{\text{D}}(\text{MLA}_m)$, where $K_{\text{MLA}_m} = [\text{MLA}_m]/[\text{ML}^{m+}][\text{A}^-]^m$ and $K_{\text{D}}(\text{MLA}_m) = [\text{MLA}_m]_o/[\text{MLA}_m]$. Since $K_{\text{D}}(\text{MLA}_m)$ is a distribution constant of a neutral complex MLA_m between CHCl_3 and H_2O and hydrogen bonding to the ether oxygen atoms when the crown ethers are complexed is greatly decreased as a result of ionic M^{m+} -O bonding,²⁴ the effect of interaction of the MLA_m with water on the partition of the MLA_m is negligible as is stated above. Thus, the $K_{\text{D}}[\text{M}(18\text{C6})\text{A}_m]$ value is expected to be higher than the corresponding $K_{\text{D}}[\text{M}(15\text{C5})\text{A}_m]$ value because of the larger size of 18C6 than that of 15C5. This is one of the dominant factors in determining the larger $\log K_{\text{ex,ip}}$ value of the 15C6- M^{m+} complex compared with the corresponding 15C5- M^{m+} complex except for the case of $\text{M}^{m+} = \text{Na}^+$. It follows from this that the higher $K_{\text{ex,ip}}$ value of the 15C5- Na^+ complex compared with that for the 18C6- Na^+ complex is caused entirely by the larger K_{MLA} value of the 15C5- Na^+ complex. The number of water molecules attached to the 15C5- Na^+ complex (0.9) in nitrobenzene is smaller than that to the 18C6- Na^+ complex (1.2).²³ This supports the above discussion.

Both $\Delta H_{\text{ex,ip}}^\circ$ and $T\Delta S_{\text{ex,ip}}^\circ$ values of 15C5 vary with the cation more than do those of 18C6. This indicates that 15C5 less effectively shields the cation in the cavity from the access of picrate ions and solvents than does 18C6.

Sizes of 15C5- Na^+ and 18C6- K^+ complexes are nearly equal to those of Pr_4N^+ and Bu_4N^+ ions, respectively.²⁵ Since 15C5 and 18C6 have the most suitable cavity sizes for Na^+ and K^+ , respectively, among alkali metal ions, the cation held in the cavity is most effectively shielded by the crown ether. Four alkyl groups of a tetra-alkylammonium ion screen the central nitrogen atom well. The 15C5- Na^+ and 18C6- K^+ complexes are regarded as disks, whereas Pr_4N^+ and Bu_4N^+ are regarded as spheres. Therefore, it is interesting to compare the ion-pair extraction process of $\text{Na}(15\text{C5})\text{A}$ and $\text{K}(18\text{C6})\text{A}$ with that of Pr_4NA and Bu_4NA , respectively. From the standpoint of thermodynamics, a striking

difference in the ion-pair extraction process is observed between the crown ether complexes and the tetraalkylammonium picrates. $\Delta S_{\text{ex,ip}}^{\circ}$ values of Na(15C5)A and K(18C6)A complexes are negative; but, those of Pr₄NA and Bu₄NA are positive. $\Delta H_{\text{ex,ip}}^{\circ}$ and $T\Delta S_{\text{ex,ip}}^{\circ}$ values of Na(15C5)A and K(18C6)A complexes are much smaller than those of Pr₄NA and Bu₄NA, respectively. Ion-pair extraction of the crown ether complexes is completely enthalpy driven, whereas, that of Pr₄NA and Bu₄NA is both enthalpy and entropy driven; in particular, ion-pair extraction of Bu₄NA is dependent largely on the entropy contribution. The log $K_{\text{ex,ip}}$ value of Na(15C5)A is larger than that of Pr₄NA, and the reverse is true for the cases of K(18C6)A and Bu₄NA. This reflects the difference in the solute-solvent and solute-picrate anion interaction caused by the difference in the shape between the crown ether complex and the corresponding R₄N⁺ though they are nearly equal in size.

REFERENCES

1. C. J. Pedersen, *Fed. Proc. Fed. Am. Soc. Exp. Biol.*, 1968, **27**, 1305.
2. Y. Takeda, *The Solvent Extraction of Metal Ions by Crown Compounds, Host Guest Complex Chemistry III, Topics in Current Chemistry*, F. Voegtle and E. Weber (eds.), Vol. 121, pp. 1-38. Springer-Verlag, Berlin, 1984.
3. H. K. Frensdorff, *J. Am. Chem. Soc.*, 1971, **93**, 4684.
4. Y. Takeda, T. Namisaki and S. Fujiwara, *Bull. Chem. Soc. Jpn.*, 1984, **57**, 1055.
5. Y. Takeda and A. Tanaka, *ibid.*, 1986, **59**, 733.
6. Y. Takeda and Y. Matsumoto, *ibid.*, 1987, **60**, 2313.
7. P. Beronius and A. Brändström, *Acta Chem. Scand.*, 1976, **A30**, 687.
8. S. Motomizu, S. Hamada and K. Toei, *Bunseki Kagaku*, 1983, **32**, 648.
9. R. Modin and G. Schill, *Talanta*, 1975, **22**, 1017.
10. H. Matsunaga and T. Yotsuyanagi, *Nippon Kagaku Kaishi*, 1982, 785.
11. S. Eksborg and G. Schill, *Anal. Chem.*, 1973, **45**, 2092.
12. C. V. Krishnan and H. L. Friedman, *J. Phys. Chem.*, 1970, **74**, 2356.
13. Y. Hasegawa, H. Tanabe and S. Yoshida, *Bull. Chem. Soc. Jpn.*, 1985, **58**, 3649.
14. Y. Takeda and M. Nishida, *ibid.*, 1989, **62**, 1468.
15. Y. Takeda, W. Ohson and N. Fukada, *J. Incl. Phenom.*, 1990, **9**, 301.
16. Y. Hasegawa, T. Nakano, Y. Odori and Y. Ishikawa, *Bull. Chem. Soc. Jpn.*, 1984, **57**, 8.
17. Y. Hasegawa, H. Wakabayashi, M. Sakuma and T. Sekine, *ibid.*, 1981, **54**, 2427.
18. Y. Takeda, R. Kohno, Y. Kudo and N. Fukada, *ibid.*, 1989, **62**, 999.
19. R. D. Shannon and C. T. Prewitt, *Acta Crystallogr., Sect. B*, 1969, **25**, 925.
20. J. D. Lamb, R. M. Izatt and J. J. Christensen, *Progress in Macrocyclic Chemistry*, R. M. Izatt and J. J. Christensen (eds), Vol. 2, Chap. 2, p. 54. John Wiley and Sons, New York, 1981.
21. H. L. Friedman and C. V. Krishnan, *Water*, F. Franks (ed.), Vol. 3, Chapter 1, p. 55. Plenum, New York, 1973.
22. M. Yamane, T. Iwachido and K. Toei, *Bull. Chem. Soc. Jpn.*, 1971, **44**, 745.
23. T. Iwachido, M. Minami, M. Kimura, A. Sadakane, M. Kawasaki and K. Toei, *ibid.*, 1980, **53**, 703.
24. M. K. Chantooni, Jr. and I. M. Kolthoff, *Proc. Natl. Acad. Sci. USA*, 1981, **78**, 7245.
25. Y. Takeda, H. Yano, M. Ishibashi and H. Isozumi, *Bull. Chem. Soc. Jpn.*, 1980, **53**, 72.
26. R. M. Izatt, R. E. Terry, B. L. Haymore, L. D. Hansen, N. K. Dalley, A. G. Avondet and J. J. Christensen, *J. Am. Chem. Soc.*, 1976, **98**, 7620.
27. Y. Takeda and O. Arima, *Bull. Chem. Soc. Jpn.*, 1985, **58**, 3403.

SPECTROPHOTOMETRIC DETERMINATION OF THE OXYGEN TO URANIUM RATIO IN URANIUM OXIDES BASED ON DISSOLUTION IN SULPHURIC ACID

B. NARASIMHA MURTY, R. B. YADAV, C. K. RAMAMURTHY and S. SYAMSUNDAR
Control Laboratory, Nuclear Fuel Complex, Hyderabad, India

(Received 8 March 1991. Revised 15 April 1991. Accepted 30 April 1991)

Summary—The oxygen to uranium ratio in uranium oxides such as U_3O_8 , UO_{2+x} powders and UO_2 fuel pellets has been determined by a new spectrophotometric method. The method can be used for determination of O/U ratio in UO_2 pellets and powders on a routine basis. In the described method, uranium oxides in the powder form are dissolved in 2M sulphuric acid containing a few drops of HF. The concentrations of U(IV) and U(VI) are directly determined by means of the absorbances of these species at different wavelengths. For determination of the O/U ratio in U_3O_8 powder samples, 630 and 310 nm are the wavelengths chosen for U(IV) and U(VI), respectively. For UO_{2+x} powder, where the O/U ratio lies between 2.04 to 2.15, U(IV) and U(VI) are determined at 630 and 300 nm respectively, whereas for UO_2 fuel pellets, where the O/U ratio is less than 2.01, 535 and 285 nm are used. The molar absorptivity of U(IV) at 630 and 535 nm is 21.4 and 6.8 l.mole⁻¹.cm⁻¹ and that of U(VI) at 310, 300 and 285 nm is 178.1, 278.6 and 585 l.mole⁻¹.cm⁻¹, respectively. Standard deviations of ± 0.002 O/U ratio units for pellets and ± 0.004 O/U ratio units for powders have been achieved.

The uranium–oxygen system is one of the most complex systems known because of the multiplicity of stable oxidation states of uranium. Because of this, the exact stoichiometry of uranium dioxide is seldom attained, as it usually exists as a hyperstoichiometric oxide which includes excess oxygen in its cubic lattice. One of the most important parameters of nuclear grade uranium dioxide pellets is the O/U ratio, as it is important in the characterization of the sinterability of the powder and its performance as a fuel under reactor conditions. An oxygen-to-uranium ratio closely approaching 2.000 is a frequent requirement for nuclear fuel, so, as a quality control measure, it is essential to know the O/U ratio of the UO_2 powder.

There are many instrumental and chemical methods available for the determination of the O/U ratio. Both destructive and non-destructive methods have been reviewed by Florence.¹ Some of the instrumental methods are X-ray diffraction analysis,² electromotive force measurement of a Ni, NiO electrolyte– UO_{2+x} cell^{3–6} and X-ray photoemission spectrometry.^{7,8} A major disadvantage of these methods, is that they need reference materials having identical composition with that of the sample in order to calibrate the methods. Chemical methods include gravimetry,^{3,9} coulometry,^{10,11} titrimetry^{3,12} and polarography.^{13–15}

All the wet chemical methods for the determination of the O/U ratio are based on the determination of either U(IV) and/or U(VI), since the degree of hyperstoichiometry can be directly related to the concentration of U(VI).¹⁶ Thus, the estimation of U(VI) serves as a measure of the excess oxygen and, coupled with total uranium determination, enables one to determine the exact composition of the oxide. For near stoichiometric UO_2 pellets, where a minute quantity of U(VI) has to be determined in the presence of a large excess of U(IV), polarographic, coulometric and biamperometric methods are preferred.¹⁷ However, for UO_{2+x} powders, where U(VI) is also present in relatively higher concentration, titrimetric procedures^{1,18,19} using potentiometric and/or visual indicator techniques²⁰ are more convenient. However, these methods require that the sample is weighed accurately and dissolved completely.

Spectrophotometric methods for the determination of the O/U ratio do not require weighing and complete dissolution of the sample because both U(VI) and U(IV) are determined in the same aliquot. Our experiments demonstrate that uranium dissolves at the same rate in both oxidation states as evidenced by the same O/U ratio obtained irrespective of whether the sample is partially or completely dissolved. However, spectrophotometric methods which

use phosphoric acid²¹⁻²⁴ reported so far for the determination of O/U ratios of UO_2 pellets are not convenient on a routine basis because they suffer from many disadvantages such as high viscosity, long dissolution time, poor sensitivity and elaborate treatment procedures.²⁵ The present method is based on the dissolution of the sample in 2M sulphuric acid in the presence of a very small quantity of HF, followed by measurement of absorbances at specific wavelengths for U(IV) and U(VI).

Earlier, Takeuchi *et al.*²⁶ have reported the dissolution of uranium oxide in 1M sulphuric acid containing a few drops of HF and subsequent determination of the U(VI) coulometrically by titrating with electrogenerated Ti(III). Stronhill¹⁹ determined uranium(IV) titrimetrically with Fe^{2+} or Ti^{3+} based on sulphuric acid dissolution.

EXPERIMENTAL

Reagents

Uranium dioxide pellets, UO_2 powders and U_3O_8 powders produced at the Nuclear Fuel Complex, Hyderabad, India were used as samples. All dissolution reagents were prepared with reagent grade materials and distilled water.

Instrumentation

Absorbance measurements were carried out on a Shimadzu Model UV-240, Graphicord UV-visible Recording Spectrophotometer. Matched quartz cells of 1-cm path length were used. The base line and digital absorbance readings were adjusted to 0.000 for a reagent blank (2M sulphuric acid) before each set of measurements.

Procedure

In order to obtain a reliable value of the O/U ratio in UO_{2+x} , it is essential that the oxidation states of uranium in the solid be kept unchanged throughout procedures such as the grinding of the UO_{2+x} pellet and the dissolution of the powder obtained. Keeping this in view, the following strategy was adopted for grinding the pellets and dissolution of the powder.

UO_2 pellets. The UO_{2+x} pellet was placed in a cylindrical container and the air was displaced with a jet of argon. After sufficient flushing the lid was tightened, and the sample was ground for about 10–15 sec in a Spex Mixer Mill to provide a mesh size no smaller than 150. If the particles are very fine some oxidation may

occur. Nearly 10–15 g of the ground powder was then dissolved under argon atmosphere in 100–110 ml of 2M sulphuric acid containing 1–2 drops of HF, on a water bath. The dissolution was carried out for about one and half hours. The absorbances for U(IV) and U(VI) were measured at 535 and 285 nm, respectively.

UO_2/U_3O_8 powders. About 80–100 mg of powder was dissolved in 40–50 ml of 2M sulphuric acid containing one drop of HF. Dissolution was carried out on a water bath in ambient air for about half an hour. For UO_2 powders, the absorbances of U(IV) and U(VI) were measured at 630 and 310 nm, respectively, while for U_3O_8 powders they were measured at 630 and 300 nm.

Determination of molar absorptivity of U(IV) at 630 and 535 nm. Nuclear grade uranium metal turnings were degreased with carbon tetrachloride, pickled with 1:1 nitric acid, washed with 1:3 hydrochloric acid followed by distilled water and finally acetone.

A weighed quantity (300–350 mg) of the cleaned and dried uranium metal turnings was dissolved under argon atmosphere in 2M sulphuric acid containing a few drops of HF on a water bath. After complete dissolution of the turnings, the solution was cooled to room temperature under inert atmosphere and transferred to a 100-ml standard flask and diluted to volume with 2M sulphuric acid. The absorbances were recorded immediately.

Determination of molar absorptivity of U(VI) at 310, 300 and 285 nm. An accurately weighed amount of cleaned uranium metal turnings was dissolved in concentrated nitric acid and evaporated to dryness. A few milliliters of concentrated sulphuric acid were added and the solution was heated to dense white fumes. This residue was then dissolved in 2M sulphuric acid and diluted to 100 ml. This solution was used as a stock solution and absorbances were recorded after appropriate dilution of this solution.

RESULTS AND DISCUSSION

From the absorption spectra of U(IV) and U(VI) in 2M sulphuric acid medium (Fig. 1), it is seen that U(IV) has maxima at 535 and 630 nm with no absorption by U(VI) at these wavelengths. U(IV) does not absorb at all in the wavelength region 280–380 nm. Below 275 nm, however, there is a continuous absorption by U(IV) as well as U(VI). U(VI) absorbs in the wavelength region 360–480 nm. Below 340 nm,

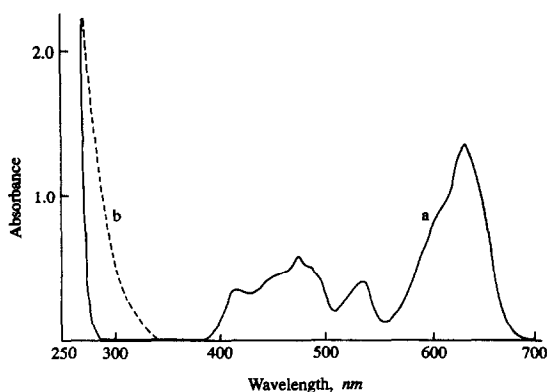


Fig. 1. Absorption spectra of U(IV) and U(VI) in 2M sulphuric acid medium. (a) U(IV), 14.6 mg/ml (b) U(VI) 0.32 mg/ml.

there is no wavelength of maximum absorption for U(VI), but rather is a continuous absorption. However, the Beer-Lambert law is obeyed for solutions of U(VI) at 310, 300 and 285 nm from 0.06–1.2 absorbance units. The molar absorptivities of U(VI) at 310, 300 and 285 nm are 178.1, 278.6 and 585 l.mole⁻¹.cm⁻¹, respectively, whereas the molar absorptivities of U(IV) at 630 and 535 nm are 21.4 and 6.8 l.mole⁻¹.cm⁻¹, respectively. The higher molar absorptivity value of U(VI) at 285 nm and lower molar absorptivity value of U(IV) at 535 nm enables one to determine the O/U ratio in UO₂ pellets close to 2.001, a measurement which is difficult in phosphoric acid medium.

The extent of oxidation of U(IV) in 2M sulphuric acid by air at ~100° within half an hour is 0.1–0.2%, an amount which contributes to a positive bias of 0.001–0.002 O/U ratio units (well within the required precision). Secondly, since stringent O/U specifications are not required in the case of powder samples, purging of

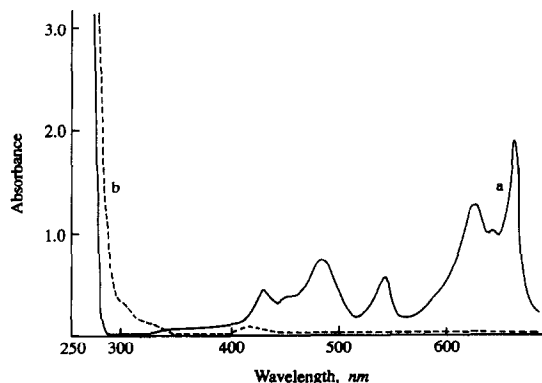


Fig. 2. Absorption spectra of U(IV) and U(VI) in 13M phosphoric acid medium. (a) U(IV), 9.53 mg/ml (b) U(VI), 1.53 mg/ml.

inert gas during dissolution of uranium oxide powders is not necessary. However, in the case of uranium dioxide pellets, the O/U ratio is an important parameter and a precise O/U ratio determination is required. (The O/U ratio specification for powders is normally in the range 2.05–2.15 compared with 2.000–2.015 for pellets. The powder ratio is important for characterizing sinterability of the pellets.) The rate of dissolution in the case of pellet powders is slow compared to uranium oxide powders and therefore a dissolution period of about 1.5 hours is required to dissolve sufficient U(VI). During such extended dissolution periods, oxidation of U(IV) by air becomes significant (1–1.5%) and would result in an increase in the O/U ratio of 0.015 O/U ratio units. Hence, an inert atmosphere is essential during dissolution of the pellet samples. The volume of 2M sulphuric acid to be used for the dissolution purpose should be 100–110 ml with 0.3–0.5% (v/v) HF so that precipitation of uranium(IV) sulphate does not take place, even after slight evaporation during dissolution. This precipitation would cause a higher O/U ratio because of the preferential precipitation of the uranium(IV) sulphate by virtue of its limited solubility in sulphuric acid.

At room temperature, oxidation of U(IV) by air in 2M sulphuric acid medium is not significant within 5–6 hr. However, this rate of oxidation of U(IV) at elevated temperatures (~100°) decreases with an increase in sulphuric acid concentration because of the increased stability of U(IV) in a higher concentration of sulphuric acid. The effect of air oxidation in various concentrations of sulphuric acid at ~100° are shown in Fig. 3. At a sulphuric acid concentration greater than 5M, the oxidation may not be significant and at this acidity an inert atmosphere may not be needed during dissolution of pellet powders also, thus making the procedure still convenient. The drawback of dissolving the uranium dioxide powders in such high concentrated sulphuric acid is the limited solubility of uranium(IV) sulphate. Hence, 2M sulphuric acid is taken as the medium of dissolution, using inert gas purging during dissolution.

It is observed that gadolinium in 2M sulphuric acid medium does not have significant absorbance in the wavelength range 700–250 nm. Hence, the present method is well suited even for determining the O/U ratio of uranium dioxide pellets containing gadolinium as a burnable poison.

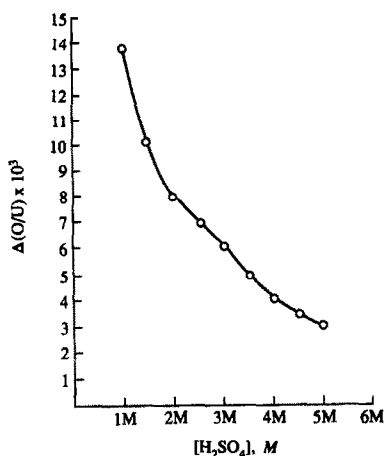


Fig. 3. Effect of concentration of sulphuric acid on air oxidation of U(IV). $\Delta(O/U)$ indicates the difference of O/U ratio values with and without inert atmosphere during dissolution.

Absorption spectra in 2M sulphuric acid. The absorption spectra of U(IV) and U(VI) in 2M sulphuric acid and strong (13M) phosphoric acid (SPA) are shown in Fig. 1 and Fig. 2, respectively. It is clear from the spectra of U(IV) and U(VI) in 2M sulphuric acid and SPA for expected concentrations of U(IV) and U(VI), that the spectral pattern in both media is essentially similar, indicating the similarity between the molecular structure of U(IV) and U(VI) and the nature of transitions involved²⁴ in these two media. In both cases there is a shift towards lower wavelengths and significant difference in

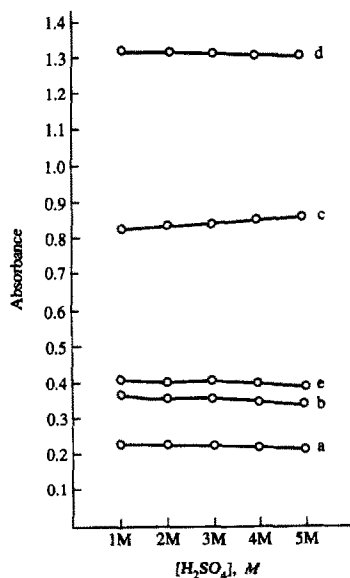


Fig. 4. Absorbances of a mixture of 14.6 mg/ml U(IV) and 0.32 mg/ml U(VI) at varying concentrations of sulphuric acid. U(VI) at (a) 310 nm, (b) 300 nm, (c) 285 nm. U(IV) at (d) 630 nm, (e) 535 nm.

the molar absorptivity, causing better sensitivity in sulphuric acid medium when compared to phosphoric acid medium. The absorbances of U(IV) and U(VI) at the wavelengths considered are independent of the concentration of sulphuric acid between 1 and 5M, which is clear from Fig. 4.

The reported molar absorptivity of U(IV) at 544 nm is 11.66 l.mole⁻¹.cm⁻¹ and that of U(VI) at 290 nm is 215.9 l.mole⁻¹.cm⁻¹ in SPA.²³ Whereas in the present 2M sulphuric acid medium, the molar absorptivity of U(IV) at 535 nm is 6.8 l.mole⁻¹.cm⁻¹ and that of U(VI) at 285 nm is 585 l.mole⁻¹.cm⁻¹. Hence, in the present medium there is an almost five-fold increase in sensitivity with respect to O/U ratio units. This has enabled the work to be extended to the determination of O/U ratio in UO₂ pellets closer to 2.001 O/U units with good accuracy.

The rate of dissolution of UO_{2+x} is greater in 2M sulphuric acid containing a few drops of HF compared to SPA, which makes the present method of analysis more rapid. HF seems to act as a catalyst in the dissolution, as is the case with PuO₂ and ThO₂ dissolution in HNO₃-HF mixture²⁷ where the nature of the intermediate complex is assumed to be MF₂⁺. Most of the HF vaporizes out of solution with the argon stream by the end of the dissolution period. Therefore, the concentration of the residual HF, if any, is too low to attack quartz cells at room temperature during the absorbance measurements. It has been observed that a small quantity of free HF in 2M sulphuric acid does not alter the absorbance values of U(IV) and U(VI) at their respective wavelengths.

The data tabulated in Table 1 shows the precision of the method for UO₂ fuel pellets and UO_{2+x} powders. It is clear from Table 2 that the O/U ratios obtained by the spectrophotometric method are in close agreement with those

Table 1. Data justifying the precision of the method

	Pellets	Powders
	2.005	2.069
	2.005	2.068
	2.004	2.069
	2.004	2.067
	2.005	2.070
	2.008	2.077
	2.007	2.072
	2.007	2.070
	2.006	2.076
	2.005	2.070
Mean	2.006	2.071
Precision ± 0.002		± 0.004

Table 2. O/U ratios in UO_2 and U_3O_8 powders

S. No.	Sample Code No.	O/U ratio value	
		spectrophotometry	volumetry
1	M 370	2.077	2.078
2	M 365	2.058	2.056
3	M 30	2.120	2.118
4	M 31	2.085	2.086
5	M 32	2.148	2.149
6	M 39	2.103	2.101
7	M 36	2.093	2.095
8	M 38	2.078	2.076
9*	M 33	2.683	2.682
10*	M 29	2.677	2.679

* U_3O_8 powder samples

obtained by the volumetric method. This indicates the stability of tetravalent uranium in 2M sulphuric acid medium. The O/U ratios calculated with possible combinations of wavelengths for U(IV) and U(VI) give the same value of O/U ratio for a given sample (Table 3). It is concluded that the combination 535 and 285 nm for U(IV) and U(VI), respectively, is well suited to the determination of the O/U ratio in UO_2 pellets where the O/U ratio lies between 2.001 and 2.010 units.

Comparison of O/U ratios of uranium dioxide pellets obtained by the spectrophotometric method based on dissolution in SPA and 2M sulphuric acid are shown in Table 4. The fair agreement between these results emphasize that the stability of U(IV) towards oxidation in both media is of the same order. The values of O/U

Table 5. Comparison of O/U ratios in uranium dioxide fuel pellets by spectrophotometric and polarographic methods

S. No.	Code No.	Oxygen to uranium ratio	
		Spectrophotometry	Polarography
1	CFFP 21	2.002	2.002
2	CFFP 47	2.003	2.002
3	CFFP 30	2.002	2.002
4	CFFP 26	2.004	2.002
5	CFFP 51	2.004	2.003
6	CFFP 49	2.003	2.003
7	CFFP 44	2.002	2.001
8	CFFP 45	2.000	2.002
9	2604	2.001	2.001
10	2586	2.001	2.001

ratios of UO_2 pellets obtained by polarography and the present spectrophotometric method have been compared and the results are shown in Table 5. This table shows the good agreement between the two methods. The fact that the O/U ratio values obtained by the two independent methods are in good agreement confirms the non-oxidising nature of the present medium, *i.e.*, 2M sulphuric acid, and also the accuracy of the present spectrophotometric method.

CALCULATIONS

Let the absorbances of U(IV) at λ_1 nm be a units and that of U(VI) at λ_2 nm be b units and the corresponding molar absorptivities be ϵ_1 and ϵ_2 respectively. Then, the O/U ratio of the

Table 3. O/U ratio values of UO_2 pellets calculated with various combinations of wavelength

S. No.	1	2	3	4	5	6
Wavelength combination for U(IV), U(VI), (nm)	BR202	M418	BR248III	BR238I	BR252	MB160
630, 310	2.004	2.006	2.003	2.004	2.010	2.007
630, 300	2.005	2.006	2.003	2.004	2.010	2.007
630, 285	2.004	2.005	2.003	2.005	2.009	2.007
535, 310	2.004	2.006	2.004	2.004	2.010	2.007
535, 300	2.004	2.006	2.003	2.004	2.010	2.007
535, 285	2.005	2.005	2.003	2.004	2.009	2.007

Table 4. O/U ratios in UO_2 pellets

S. No.	Oxygen to Uranium ratio	
	13M phosphoric acid medium [544 nm and 290 nm are used for U(IV) and U(VI)]	2M sulphuric acid medium [535 nm and 285 nm are used for U(IV) and U(VI)]
1	2.010	2.009
2	2.007	2.008
3	2.006	2.005
4	2.008	2.006
5	2.008	2.007

various kinds of uranium oxides can be calculated as follows:

$$\begin{aligned} \text{OU} &= 2 + \frac{C_{\text{u(VI)}}}{C_{\text{u(VI)}} + C_{\text{u(IV)}}} \\ &= 2 + \frac{1}{1 + \frac{(\epsilon_2)(a)}{(\epsilon_1)(b)}} \end{aligned}$$

However, in the case of pellets where $C_{\text{u(VI)}} \ll C_{\text{u(IV)}}$, the above expression reduces to

$$\text{O/U} = 2 + \frac{(\epsilon_1)(b)}{(\epsilon_2)(a)}$$

If the observed absorbance for U(IV) at 535 nm is a units and that of U(VI) at 285 nm is b units, then the O/U ratio is given by $\text{O/U} = 2 + 0.0116 b/a$.

Acknowledgements—The authors wish to express their deep gratitude to Dr. T. S. Krishnan, Deputy Chief Executive (Q.A.) for his keen interest and encouragement in the present work. The authors also acknowledge Shri H. R. Ravindra for useful discussions during the course of the present investigation.

REFERENCES

1. T. M. Florence, *IAEA Symp. Anal. Meth. in the Nucl. Fuel Cycle*, Vienna, 1972.
2. R. Conti, *Euratom Rep.*, EUR 4518f, 1970.
3. Hellmann K. W. U., Erlangen, W. Germany, 1982, *Private communications*.
4. K. Kiukkola and C. Wagner, *J. Electrochem. Soc.*, 1957, **104**, 379.
5. S. Aronson and J. Bell, *J. Chem. Phys.*, 1958, **29**, 151.
6. T. M. Florence, *Analytical Methods in the Nuclear Fuel Cycle*, IAEASM—149/64, IAEA: Vienna, 1972, p. 145.
7. B. M. Veal and D. Lam, *J. Phys. Lett. A*, 1974, **49**, 466.
8. G. C. Allen, J. A. Crofts, M. T. Curtis, P. M. Tucker, D. Chadwick and P. J. Hampson, *J. Chem. Soc. Dalton Trans.*, 1974, 1296.
9. E. A. Shaefer and J. O. Hibbits, *Anal. Chem.*, 1969, **41**, 254.
10. R. W. Stromatt and R. E. Connally, *ibid.*, 1961, **33**, 345.
11. S. Kihara, Z. Yoshida, H. Mutto, H. Aoyagi, Y. Baba and H. Hashitani, *ibid.*, 1980, **52**, 1601.
12. J. J. Engelsman, J. Knaape and J. Visser, *Talanta*, 1968, **15**, 171.
13. R. M. Burd and G. M. Goward, USAEC Rep. WAPD-205, 1959.
14. H. Kubota, *Anal. Chem.*, 1960, **32**, 610.
15. K. Matojima and A. Hoshino, *J. At. Energy Soc. Jpn.*, 1960, **2**, 1.
16. P. L. Buldini, D. Ferri, E. Paluzzi and M. Zambianchi, *Analyst*, 1984, **109**, 225.
17. V. Kuvik, J. Kritl and A. Moravec, *Radiochem. Radioanal. Lett.*, 1982, **54**, 209.
18. S. R. Dharwadkar and Chandrasekharaigh, *Anal. Chim. Acta*, 45, **545**, 1969.
19. L. G. Stronhill, *Can. J. Chem.*, 1959, **37**, 454.
20. R. B. Yadav, B. Narasimha Murty and S. Syamsundar, *National Workshop on Testing and Characterisation of Materials TACOM-90*, Bombay, March 15–16, 1990.
21. E. Kuhn, G. Baumgartel and H. Schmieder, *Z. Anal. Chem.*, 1973, **264**, 103.
22. S. Kihara, T. Adachi and H. Hashitani, *ibid.*, 1980, **303**, 28.
23. H. Takeishi, H. Muto, H. Aoyagi, T. Adachi, K. Izawa, Z. Yoshida, H. Kawamura and S. Kihara, *Anal. Chem.*, 1986, **58**, 458.
24. M. K. Ahmed and N. L. Sreenivasan, *ibid.*, 1986, **58**, 2479.
25. A. Tolk and W. A. Lingerak, *Proceedings of a panel on Analytical Chemistry of Nuclear Fuel*; IAEA: Vienna, 1972; STI/PUB/337, pp. 51–58.
26. T. Takeuchi and T. Yoshimori, *Banseki Kagaku* 1963, **12**, 840.
27. O. K. Tallent and J. C. Mailen, *Nuclear Technology*, 1977, **32**, 167.

MULTICOMPONENT ANALYSIS OF CHLOROPHENOLS BY DIODE ARRAY DERIVATIVE SPECTROPHOTOMETRY

F. NAVARRO-VILLOSLADA, L. V. PÉREZ-ARRIBAS, M. E. LEÓN-GONZÁLEZ,
M. J. SANTOS-DELGADO and L. M. POLO-DÍEZ*

Departamento Química Analítica, Facultad de Ciencias Químicas, Universidad Complutense de Madrid,
E-28040 Madrid, Spain

(Received 15 December 1990. Revised 18 April 1991. Accepted 25 April 1991)

Summary—A multicomponent analysis method is proposed for the determination of chlorophenols by diode array derivative spectrophotometry. The method is based on formation of ion-pairs with tetrabutylammonium as counterion and extraction in chloroform at pH 9.1. Quantitative determinations (within the 2–20 mg/l. concentration range) of two-, three- and four-component mixtures were possible, using the first derivative spectra and a least-squares computer programme.

Chlorophenols are widely used in pesticide production. The presence of chlorophenols in water, soil, food and animal foodstuffs presents a potential hazard due to their high toxicity. Spectrophotometric determination of these phenols is of limited use because their absorption bands overlap.¹ The need for reliable determination of these chemicals has led to the development of many analytical methods,^{2–7} mainly using chromatographic techniques (HPLC and GC).

A review of papers published on the spectrophotometric analysis of multicomponent mixtures shows that the quantification of compounds continues to be a difficult problem when there is high spectral overlapping and components have unequal concentration, but also shows that the application of derivative spectroscopy offers a powerful approach to the problem of resolution of mixtures.^{7,8} O'Haver and Green⁹ have evaluated the utility of the derivative spectrometry in multicomponent analysis in reducing band-overlap error of the type often encountered in quantitative spectrometry. This method is useful for reduction of band-overlap errors if the systematic error caused by the overlap is large compared to the random error and the interfering band is either known and constant or is broader than the analyte band. In general, the derivative technique reduces the total error by a factor of at least 3, and usually by much more.

This paper describes the development of a method for the multicomponent determination of chlorophenols by diode array derivative spectrophotometry. The method is based on ion-pair formation with tetrabutylammonium as counterion and extraction in chloroform at pH 9.1. Quantitative determination of two-, three- and four-component mixtures were possible, using the first derivative spectra and a least-squares computer programme.

THEORY

The background and theory of multicomponent analysis have been discussed before.¹⁰ Therefore, only key equations are presented here.

The Beer's Law model can be generalized for multicomponent systems and expressed in matrix notation as:

$$A = C\epsilon \quad (1)$$

where ϵ is the matrix of linear response constants whose elements represent the sensitivity of each wavelength to each analyte. To find a solution for the system expressed in equation (1), the number of wavelengths must be at least equal to the number of analytes. Once the ϵ matrix is calculated, its inverse can be used to determine the concentrations of unknowns from measured absorbances as:

$$C = A\epsilon^{-1} \quad (2)$$

If the number of wavelengths is greater than the number of analytes, ϵ is not a square matrix. C

*Author for correspondence.

is solved by using the generalised inverse of ϵ where according to:

$$C = A\epsilon^T(\epsilon\epsilon^T)^{-1} \quad (3)$$

where

$A = m \times n$ matrix of calibration spectra
 $C = m \times 1$ matrix of component concentrations
 $\epsilon = 1 \times n$ matrix of absorptivity-path length products

The utility of a spectrophotometric method for multicomponent analysis is determined by its selectivity and by all errors inherent in the calibration and prediction procedure. Several statistics may be used to describe the accuracy and precision of a multiple linear least squares regression.

In our research, the spectra of synthetic mixtures of known composition were compared with absorbances calculated from the spectra of the individual components and the composition of the solution to establish the additivity of the absorbances of the pure components. This comparison was made at 2 nm intervals in several wavelength ranges and a standard deviation,¹¹ S.D., was calculated for each synthetic mixture at different wavelength ranges, based on the following relationship:

$$\text{S.D.} = \left[\sum_{h=1}^k (Ah - \hat{A}h)^2/k \right]^{1/2} \quad (4)$$

We used this S.D. to verify the additivity of absorbances of components in a mixture within the limits of experimental error. A more complete statistic also used¹² to quantify the analytical precision in each mixture is the prediction error:

Prediction error (%)

$$= 100 \left[\sum_{i=1}^N (ci - \hat{c}i)^2 / \sum_{i=1}^N Ci^2 \right]^{1/2} \quad (5)$$

S.D. and prediction error can be expressed¹³ for all mixtures and components as follows:

$$\text{S.D.} = \left[\frac{\sum_{i=1}^N \sum_{j=1}^M (cij - \hat{c}ij)^2}{N(M-1)} \right]^{1/2} \quad (6)$$

Prediction error (%)

$$= 100 \left[\frac{\sum_{i=1}^N \sum_{j=1}^M (cij - \hat{c}ij)^2}{\sum \sum c^2ij} \right]^{1/2} \quad (7)$$

Ah = the mixture absorbance at each wavelength

$\hat{A}h$ = the calculated absorbance

k = the number of wavelengths

N = the number of components

M = the number of mixtures

c = the "true" concentration

\hat{c} = the estimated concentration

S.D. and prediction error for one component can be calculated from equations (6) and (7) making $N = 1$.

EXPERIMENTAL

Equipment

A detection system consisting of a diode array HP 8452A spectrophotometer equipped with a 1-cm path length silica cell was used. The spectrophotometer was interfaced to an HP Vectra AT computer and an HP Think Jet printer.

Reagents

All chemicals were of analytical reagent grade and purified water was obtained with a Milli-Q apparatus.

Pentachlorophenol (99% pure, Carlo Erba), 2-chlorophenol (99% pure, Carlo Erba), 2,4-dichlorophenol (99% pure, Aldrich Chemie) and 4-chloro-3-methylphenol (99% pure, Aldrich Chemie) were used for preparing 150.0 and 50.0 mg/l. stock solutions in $10^{-3}M$ sodium hydroxide. Standard working solutions of the chlorophenols were prepared by suitable dilution of the stock solutions with water. A 5000 mg/l. stock solution of tetrabutylammonium nitrate (98% pure, Fluka Chemie AG) was also used. The pH was adjusted with a 0.1M borate buffer (pH 9.1).

Spectrophotometric grade chloroform (Carlo Erba) was used in extraction.

Procedure

To a 100-ml extraction funnel add, in the following order, 3.0 ml of 0.1M $\text{Na}_2\text{B}_4\text{O}_7 \cdot 10\text{H}_2\text{O}$ buffer (pH 9.1), 1.0 ml of 5000 mg/l. tetrabutylammonium nitrate solution, chlorophenol stock solution within the 2–20 mg/l. range in the final volume and the purified water necessary for a 10-ml final volume. Equilibrate with three 3.0-ml portions of chloroform, shaking for 1 min each time. The total organic extract is transferred into a 10-ml standard flask and made up to volume with chloroform. In order to obtain a standard spectrum of pure

components, 40 replicate solutions were prepared for each component. The absorbance spectra of chlorophenols and/or chlorophenol ion-pairs were obtained and normalized to 1.0 mg/l. The Q Dixon or t Student tests were used to exclude the spectra which are outside the 95% confidence interval around the mean. Several mixtures with different ratios of two, three and four components with 5 replicates per composition were prepared from the stock solutions. A home-made multicomponent programme allows the determination of different chlorophenol mixtures with the first derivative normalized standard spectra in the 250–380 nm wavelength range. This programme fits a combination of standard spectra to the spectrum of the mixture by means of the least-squares method.

RESULTS AND DISCUSSION

Optimization of working conditions

The effects of varying chemical conditions in the chlorophenol determination were examined

Variable	Range studied	Value selected
pH	2–10	9.1
Counterion	CTAB Hyamine 3500 TBA TPA TMA	TBA
TBA, mg/l.	0–1500	500
Organic solvent	1,2-Dichloroethane Chloroform Carbon tetrachloride	Chloroform

and the parameter values selected for use are listed in Table 1.

The effect of pH within the range 2–10 and the nature of the counterion was investigated. Several 1500-mg/l. quaternary ammonium salts solutions were studied, *viz.* cetyltrimethylammonium bromide (CTAB), benzyldiisobutylphenoxyethoxydimethylammonium bromide (Hyamine 3500), tetrabutylammonium nitrate (TBA), tetrapropylammonium bromide (TPA) and tetramethylammonium nitrate (TMA).

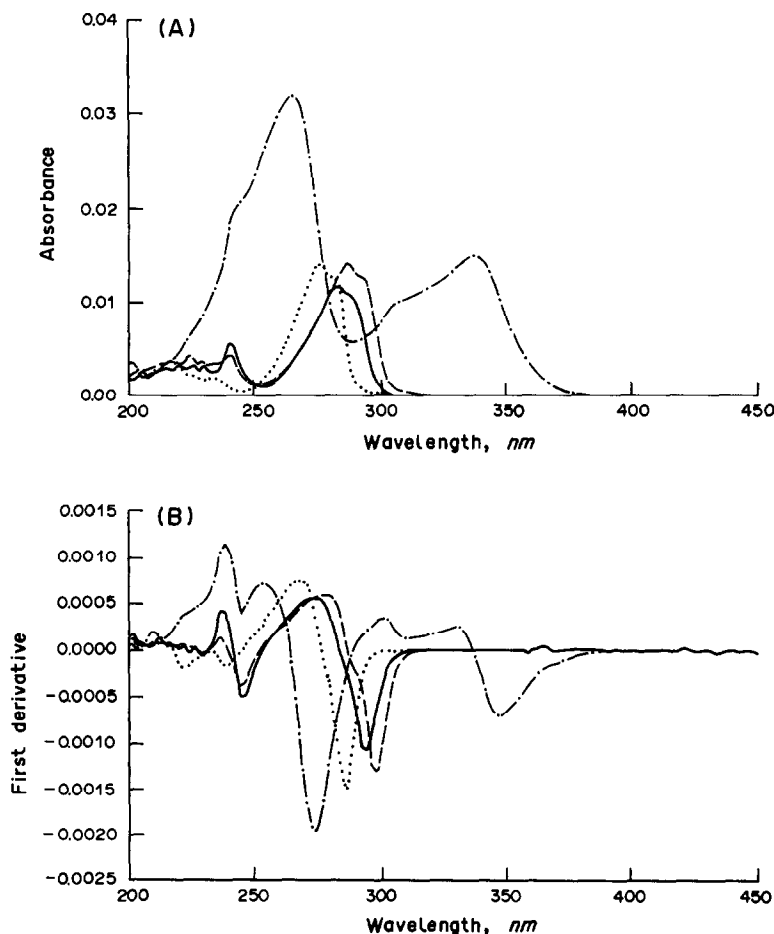


Fig. 1. Normalized absorbance (A) and derivative spectra (B) of: ——— pentachlorophenol. ---- 2-chlorophenol. - - - - 2,4-dichlorophenol. ——— 4-chloro-3-methylphenol.

Table 2. Composition of mixtures

Mixture	Concentration, mg/l.			
	2-chloroph.	4-Cl-3-methylph.	2,4-dichloroph.	pentachlorph.
1	15.0	11.0	7.0	3.0
2	15.0	7.0	3.0	7.0
3	11.0	13.0	15.0	13.0
4	7.0	5.0	3.0	5.0
5	3.0	11.0	13.0	5.0
6	11.0	5.0	5.0	11.0
7	15.0	15.0	9.0	7.0
8	5.0	3.0	13.0	15.0
9	15.0	7.0	7.0	15.0
10	11.0	5.0	11.0	13.0
11	7.0	5.0	15.0	15.0
12	5.0	11.0	3.0	9.0
13	5.0	5.0	9.0	7.0
14	7.0	7.0	9.0	9.0
15	15.0	7.0	9.0	9.0
16	9.0	11.0	9.0	5.0
17	9.0	11.0	13.0	7.0
18	11.0	3.0	3.0	5.0
19	13.0	9.0	9.0	5.0
20	15.0	9.0	3.0	3.0

The effect of counterions on formation and/or extraction of ion-pairs was studied keeping the chlorophenol concentration constant. It was found that the presence of quaternary ammonium salts is necessary to extract chlorophenols at pH values above their respective pK_a values. In the absence of these ammonium salts, the extraction does not take place. The ion-pair formation is more effective in the presence of the bigger counterions and at high pH, but CTAB and Hyamine 3500 produce strong emulsions and hence irreproducible results. Thus, tetrabutylammonium (TBA) was selected for further studies.

The effect of pH on the formation of ion-pairs and on the extraction of chlorophenols and/or chlorophenol ion-pairs was examined with the following buffers in the 2–10 pH range: hydrochloric acid, sodium acetate/acetic acid, Na_2HPO_4/NaH_2PO_4 , borax and sodium hydrox-

ide. It was observed that only pentachlorophenol forms ion-pairs with all counterions studied at pH values higher than 4.7. On the other hand, a small amount of 2,4-dichlorophenol forms ion-pairs only at pH 10, while monochlorophenols do not form ion-pairs at any pH. Figure 1 shows the pentachlorophenol ion-pairs and chlorophenol absorbances, and first derivative spectra at pH 9.1 with TBA as counterion.

The effect of different TBA concentrations on chlorophenol extraction was investigated within

Table 4. Prediction error and standard deviation for each component in quaternary mixtures* at 250–380 nm

Component	S.D., mg/l.	Prediction error, %
2-Chlorophenol	1.82	16.24
4-Chloro-3-methylphenol	0.36	4.05
2,4-Dichlorophenol	0.81	6.42
Pentachlorophenol	1.42	14.96

*Composition shows in Table 2.

Table 3. Prediction error and standard deviation for each wavelength range for the 20 quaternary mixtures in Table 2

Wavelength range, nm	S.D., mg/l.	Prediction error, %
200–450	2.05	20.86
200–380	2.05	20.86
200–400	2.05	20.86
210–380	2.07	21.06
220–380	2.16	21.89
230–380	2.11	21.50
230–400	2.11	21.50
240–380	2.11	21.43
240–400	2.11	21.43
250–380	1.21	12.31
250–500	1.21	12.31
270–400	1.27	12.98
270–380	1.27	12.98

Table 5. Analytical characteristics

Chlorophenol	Beer's Law, mg/l.	Detection limit, mg/l.
2-Chlorophenol	2–20	1.23
4-Chloromethylphenol	2–20	1.30
2,4-Dichlorophenol	2–20	0.98
Pentachlorophenol	2–20	0.23

*Calculated as:

$$c_{1,N} = zs(c_N \rightarrow 0)$$

where: $c_{1,N}$ detection limit of the N component index, z takes the value 3 in UV-vis spectrophotometry for a 99.00% confidence level.¹⁴ $s(c_N \rightarrow 0)$ = standard deviation of the concentration determined for the component blank ($n = 10$), n = number of determinations.

Table 6. Determination of chlorophenols in binary mixtures

Mixture	Added, mg/l.	Found, mg/l.	Error, %
2-Chlorophenol	7.0	6.7	4.3
4-Chloro-3-methylphenol	5.0	4.9	2.0
2,4-Dichlorophenol	7.0	6.8	2.9
Pentachlorophenol	5.0	5.2	4.0
4-Chloro-3-methylphenol	7.0	6.7	4.3
Pentachlorophenol	5.0	5.0	—
4-Chloro-3-methylphenol	5.0	5.2	4.0
2,4-Dichlorophenol	7.0	7.1	1.4
2-Chlorophenol	9.0	8.6	4.4
Pentachlorophenol	5.0	4.9	2.0
2-Chlorophenol	5.0	4.8	4.0
2,4-Dichlorophenol	3.0	3.0	—
2-Chlorophenol	5.0	4.9	2.0
4-Chloro-3-methylphenol	3.0	2.9	3.3
4-Chloro-3-methylphenol	3.0	2.9	3.3
Pentachlorophenol	7.0	6.8	2.9

the 0–1500 mg/l. range. It was found that chlorophenols and/or chlorophenol ion-pair extraction was not significantly increased by using TBA concentrations higher than 500 mg/l.

The effect of organic solvents on the extraction of chlorophenols and/or chlorophenol ion-pairs was examined. Several organic solvents, *viz.* 1,2-dichloroethane, chloroform and carbon tetrachloride, were tested. The pentachlorophenol ion-pair was not extracted with carbon tetrachloride. In 1,2-dichloroethane, an absorption band was observed between 226–230 nm; this band is not characteristic of chlorophenols and is not reproducible. Thus, chloroform was selected for further studies.

Determination of chlorophenols in binary, ternary and quaternary mixtures

The accuracy of results obtained in the multicomponent analysis of overlapping spectra depends on the wavelength range. Several wavelength ranges were studied and the optimum conditions were selected based on standard deviation and prediction error. The study was made on 20 quaternary mixtures (Table 2) containing different concentrations within the 3–15 mg/l. concentration range and the results

Table 7. Determination of chlorophenols in ternary mixtures

	Added, mg/l.	Found, mg/l.	Error, %
2-Chlorophenol	5.0	5.0	—
4-Chloro-3-methylphenol	7.0	7.2	2.8
2,4-Dichlorophenol	5.0	5.1	2.0
2-Chlorophenol	7.0	7.0	—
4-Chloro-3-methylphenol	5.0	5.0	—
Pentachlorophenol	3.0	2.9	3.3
4-Chloro-3-methylphenol	7.0	6.8	2.9
2,4-Dichlorophenol	5.0	5.0	—
Pentachlorophenol	5.0	4.9	2.0
2-Chlorophenol	9.0	8.6	4.4
2,4-Dichlorophenol	7.0	6.9	1.4
Pentachlorophenol	5.0	5.0	—
2-Chlorophenol	5.0	5.0	—
4-Chloro-3-methylphenol	3.0	3.1	3.3
Pentachlorophenol	7.0	7.1	1.4
4-Chloro-3-methylphenol	5.0	5.0	—
2,4-Dichlorophenol	3.0	3.1	3.3
Pentachlorophenol	7.0	7.1	1.4
2-Chlorophenol	5.0	4.8	4.0
2,4-Dichlorophenol	9.0	9.0	—
Pentachlorophenol	7.0	7.2	2.8
2-Chlorophenol	5.0	5.0	—
4-Chloro-3-methylphenol	9.0	9.0	—
2,4-Dichlorophenol	7.0	7.1	1.4

are shown on Table 3. The optimum wavelength range (250–380 nm) is that which provides minimum standard deviation [equation (6)] and minimum prediction error [equation (7)]. Table 4 shows standard deviation and prediction error for each component in quaternary mixtures at 250–380 nm wavelength range.

Table 5 sets out the analytical characteristics for each chlorophenol studied in all mixtures. Detection limit was calculated taking into account the standard deviation of the blank.

Multicomponent determinations of two-, three- and four-component mixtures over the 250–380 nm wavelength range were carried out. Tables 6, 7 and 8 include the results obtained from first derivative spectra and relative errors in the determination of chlorophenols in spiked water.

The multicomponent computer programme allows the determination of each chlorophenol

Table 8. Determination of chlorophenols in quaternary mixtures

2-Chloroph.			4-Chloro-3-methylph.			2,4-Dichloroph.			Pentachloroph.		
A	F	E	A	F	E	A	F	E	A	F	E
15.0	13.8	8.0	7.0	6.6	5.6	3.0	3.0	—	7.0	6.7	4.3
7.0	6.5	7.1	5.0	4.7	6.0	3.0	3.3	10.0	5.0	4.6	8.0
15.0	13.8	8.0	15.0	15.2	1.3	9.0	9.5	5.5	7.0	7.2	2.8
15.0	13.5	9.9	7.0	7.1	1.4	9.0	8.9	1.1	9.0	8.7	3.3
13.0	11.9	8.5	9.0	9.2	2.2	9.0	9.5	5.5	5.0	5.1	2.0

A = added (mg/l.).

F = found (mg/l.).

E = error (%).

in the spiked water in the 250–380 nm wavelength range with relative errors below 4.4% for binary and ternary mixtures and in the 1–10% range for quaternary ones.

When matrix effects are encountered, the prediction error reaches values higher than 50%. The method can be applied to the determination of chlorophenols in the absence of nitrophenols because when the presence of nitrophenols is suspected in the same sample, the calibration method described above is not suitable. We are using the generalized standard addition method, or GSAM, to prevent this problem, but this will be described in a future paper.

CONCLUSIONS

It can be concluded that a photodiode array multi-wavelength detector, together with multi-component analysis, is a very efficient tool for the analysis of multicomponent samples. The overlapping of spectra in the simultaneous determination of a substance can be overcome.

The accuracy of the results depends on the wavelength ranges used.

Acknowledgement—We acknowledge the financial support given by the CAICYT (Project 86/0371).

REFERENCES

1. G. Norwitz, N. Nataro and P. N. Keliher, *Anal. Chem.*, 1986, **58**, 639.
2. T. R. Edgerton, R. F. Moseman, E. M. Lores and L. H. Wright, *ibid.*, 1980, **52**, 1774.
3. D. A. Baldwin and J. K. Debowski, *Chromatographia*, 1988, **26**, 186.
4. C. D. Chriswell, R. C. Chang and J. S. Fritz, *Anal. Chem.*, 1975, **47**, 1325.
5. J. Gawdzik, B. Gawdzik and U. Czerwinska-Bil, *Chromatographia*, 1988, **25**, 504.
6. P. Alarcon, A. Bustos, B. Cañas, M. D. Andrés and L. M. Polo, *ibid.*, 1987, **24**, 613.
7. A. G. Davidson and H. Elsheikh, *Analyst*, 1982, **107**, 879.
8. D. T. Rossi and H. L. Pardue, *Anal. Chim. Acta*, 1985, **175**, 153.
9. T. C. O'Haver and G. L. Green, *Anal. Chem.*, 1976, **48**, 312.
10. M. A. Sharaf, D. L. Illman and B. R. Kowalski, *Chemometrics*, Wiley, New York, 1986.
11. J. C. Sternberg, H. S. Stillo and R. H. Schwendeman, *Anal. Chem.*, 1960, **32**, 84.
12. M. Otto and W. Wegscheider, *ibid.*, 1985, **57**, 63.
13. M. A. Maris, C. W. Brown and D. S. Lavery, *ibid.*, 1983, **55**, 1694.
14. H. Freiser and G. H. Nancollas, *Compendium of Analytical Nomenclature*. Pergamon Press, Oxford, 1978.

STATISTICAL OPTIMISATION APPLIED TO THE SPECTROPHOTOMETRIC STUDY OF THE TOLMETIN-Fe(III) COMPLEX

S. AGATONVIĆ-KUŠTRIN, LJ. ŽIVANOVIĆ, D. RADULOVIĆ and M. VASILJEVIĆ

Institute of Pharmaceutical Chemistry, Faculty of Pharmacy, Dr. Subotica 8,
11000 Belgrade, Yugoslavia

Summary—Tolmetin sodium has been examined and determined from dosage forms as its Fe(III) complex and the method has been optimized by statistical optimization.

Tolmetin [(1-methyl-5-*p*-toluoylpyrrol-2-yl)-acetic acid] is a non-steroidal anti-inflammatory agent with analgesic and antipyretic activities. As the sodium salt dihydrate it is formulated in tablet and capsule forms, both of which are used for the treatment of rheumatoid arthritis and osteoarthritis.

Tolmetin has been determined by a variety of analytical techniques, the most common ones being colorimetry,¹ UV spectrophotometry² and gas and liquid chromatography.³⁻⁷ Other methods include thin-layer chromatography,⁸⁻⁹ fluorimetry¹⁰ and polarography.¹¹ The compendial assay for tablets and capsules entailed lengthy spectrophotometric procedures.¹² Because spectrophotometric techniques offer significant economic advantages over gas and liquid chromatography, the aim of the present work was to establish a new, highly sensitive spectrophotometric method for the determination of tolmetin sodium in bulk drug form and in tablets.

Colorogenic reaction with iron(III) chloride in the presence of ammonium thiocyanate was used to modify the spectrum of tolmetin and enable its detection in the visible spectral region. The method involves the formation of a tolmetin-iron(III) complex which is soluble in chloroform and is stable, but does not absorb in the visible region. The complex can be converted to a red coloured ion-pair, by the addition of ammonium thiocyanate. The ion-pair is extractable with chloroform and can be detected colorimetrically.

The assay was developed with two mathematical statistical models: factorial design and response surface mapping.¹³ The decision to apply experimental design techniques to the development of the method was made after a

series of screening experiments revealed that the complex formation and extraction are maximized as a function of supporting electrolyte concentration, concentration of colour reagents and pH of reaction mixture. One set of two-level four variable factorial experiments were carried out in order to evaluate the main effect, as well as the interaction among factors. The final step was to optimize the values of four variables with response surface design. The best set of conditions was selected for further investigation.

EXPERIMENTAL

Reagents

Tolmetin sodium bulk drug and Tolectin® tablets (200 mg) were obtained by courtesy of McNail Inc. (New York, USA). Iron(III) chloride, potassium chloride, acetic acid and sodium hydroxide were obtained from Merck A. G. (Darmstadt, FRG). Doubly-distilled water was used throughout.

Solutions

For analytical purposes a freshly prepared (1.6 mg/ml; $5.07 \times 10^{-3} M$) aqueous solution of tolmetin sodium bulk drug was used as the standard solution. The calibration curve was prepared with ten standard solutions having concentration in the range 0.2–2.0 mg/ml (6.34×10^{-4} – $6.34 \times 10^{-3} M$). A sample solution containing 1.0 mg/ml ($3.17 \times 10^{-3} M$) tolmetin sodium was prepared by extracting tolmetin sodium from tablets.

Iron(III) chloride solution (27.03 mg/ml; $1 \times 10^{-1} M$) was prepared by dissolving 1.3515 g of iron(III) chloride in 40 ml of water, adding 1 ml of 1M hydrochloric acid and diluting the solution to 50 ml with water.

Ammonium thiocyanate solution (76.12 mg/ml; 1M) was prepared by dissolving 3.806 g of ammonium thiocyanate in 50 ml of water.

The ionic strength of the final solution was kept constant at 0.2M by addition of 2M potassium chloride. Acetate buffer solutions covering the pH range 4.0–6.5 were made by mixing appropriate volumes of 1M sodium hydroxide and 1M acetic acid.

Apparatus

A Specord M 40 Carl Zeiss Jena spectrophotometer, provided with matched 10-mm quartz cells and a Radiometer 22 pH-meter calibrated with appropriate standard buffer solutions were used.

Procedure

To 2 ml of tolmetin sodium solution placed in an Erlenmeyer flask fitted with a ground glass stopper, 2 ml of iron(III) chloride, 2 ml of ammonium thiocyanate, 1 ml of 2M potassium chloride and 3 ml of acetate buffer were added, followed by 5 ml of chloroform. The Erlenmeyer is stoppered and after shaking the reaction mixture for 10 min the red-coloured chloroformic layer is separated with a separating funnel and the absorbance measured at 486 nm, against a reagent blank. This procedure was employed for measuring the absorption spectrum and for determination of tolmetin sodium from bulk drug and tablets.

RESULTS AND DISCUSSION

Absorption spectrum of the tolmetin–iron(III) complex

Tolmetin sodium reacts with iron(III) chloride in the presence of ammonium thiocyanate at pH 4.6–6.8 to form a red, chloroform extractable complex. The absorption spectrum of the extracted complex was measured in the spectrum region from 400–600 nm. The complex shows maximum absorbance at 486 nm (Fig. 1), which can therefore be used as the wavelength for the determinations. Under the same conditions, the chloroformic extract of iron(III) chloride, ammonium thiocyanate, potassium chloride and acetate buffer solution does not absorb in this spectral region. The maximal production and extraction of the complex was reached after 5 min and the colour was stable for 24 hr.

Iron(III) chloride and ammonium thiocyanate were added in excess. Investigation

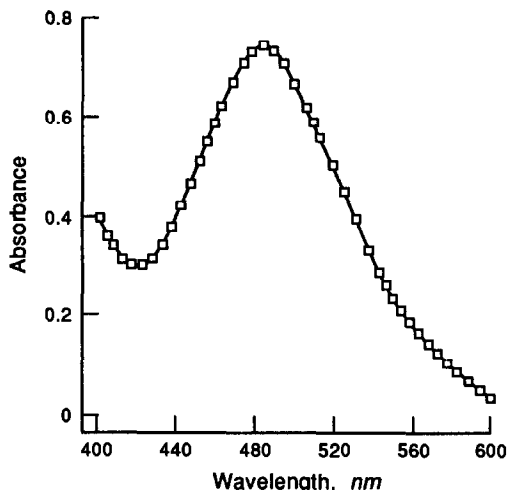


Fig. 1. Absorption spectra of the tolmetin–Fe(III) complex in chloroform. [Tolmetin] = $5.07 \times 10^{-3}M$; [Fe(III)] = $10^{-1}M$; $[NH_4SCN] = 1M$; pH 5.8; $\mu = 0.2M$.

showed that the absorbance increases up to a molar ratio of 20:1 for iron(III)–tolmetin and 9:1 for ammonium thiocyanate–iron(III) chloride.

Effect of pH and ionic strength on complex formation

The complex is only produced at pH values above 4.6. The general trend observed was a gradual increase in absorbance to pH 5.6, followed by a steady decrease in absorbance after pH 5.8 (Fig. 2); therefore, the optimum conditions for complex formation were found to be in the pH range 5.6–5.8.

As the shape of the absorption curves and positions of the absorption maximum do not vary with pH, we assumed that in this pH range only one type of complex is formed (Fig. 3).

The ionic strength also plays a significant role by its influence on the shape and intensity of the

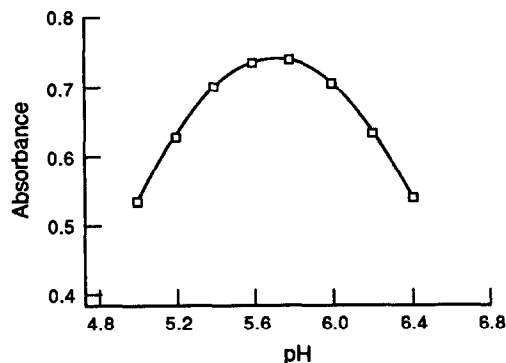


Fig. 2. The effect of pH on complex absorption at 486 nm. [Tolmetin] = $5.07 \times 10^{-3}M$; [Fe(III)] = $10^{-1}M$; $[NH_4SCN] = 1M$; $\mu = 0.2M$.

recorded peaks. The effect of ionic strength and complex formation was followed in the range 0.1–0.4M. At an ionic strength of 0.2M, spectra with optimum shape were recorded.

Optimum conditions for complex formation

Optimization of this spectrophotometric procedure was especially difficult because the absorbance and reproducibility response depend on several variables that interact with each other. In order to investigate the effect of each factor and their interaction, a four variable, two level factorial design was chosen. The variables were: ionic strength (*A*), pH (*B*), iron(III) chloride concentration (*C*) and concentration of ammonium thiocyanate (*D*) in the reaction mixture. Different levels of these variables were selected in order to maximize the information that could be extracted from experimental data. The design matrix (Table 1) shows the 16 treatment combinations of low (–) and high (+) level factors.

From the estimate of factors effect (Table 2) it can be seen that the pH of reaction mixture is the most significant effect. The interaction of the concentration of iron(III) chloride and concentration of ammonium thiocyanate was greater than the other combined effects which indicates that the amount of the formed complex influenced by the concentration of iron(III) chloride is dependent on the concentration of ammonium thiocyanate.

In order to increase the sensitivity of the method response, a surface diagram was chosen to identify the optimum experimental conditions. Response surface can simultaneously

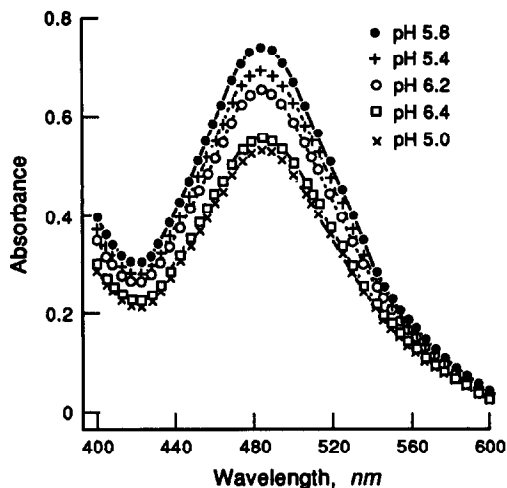


Fig. 3. The effect of pH on complex formation and extraction. [Tolmetin] = $5.07 \times 10^{-3}M$; [Fe(III)] = $10^{-1}M$; $[NH_4SCN] = 1M$; $\mu = 0.2M$.

Table 1. 2^4 factorial design

Trial	Factor level*				Absorbance
	A	B	C	D	
1	–	–	–	–	0.2368
2	+	–	–	–	0.2704
3	–	+	–	–	0.4065
4	+	+	–	–	0.3987
5	–	–	+	–	0.4857
6	+	–	+	–	0.5163
7	–	+	+	–	0.7208
8	+	+	+	–	0.3706
9	–	–	–	+	0.5092
10	+	–	–	+	0.5629
11	–	+	–	+	0.7141
12	+	+	–	+	0.3901
13	–	–	+	+	0.5390
14	+	–	+	+	0.5325
15	–	+	+	+	0.7389
16	+	+	+	+	0.4022

*Low (–) and high (+) levels of the following factors:

Factor	Value	
	Low(–)	High(+)
A (ionic strength)	0.1M	0.2M
B (pH of reaction mixture)	5.0	5.8
C [Fe(III) chloride conc.]	0.01M	0.02M
D (ammonium thiocyanate conc.)	0.10M	0.20M

represent two independent and one dependent variable when a mathematical relationship between variables is known or can be assumed. Ten experimental data were fitted to a polynomial mathematical model so that variables were adjusted until calculated values were in close agreement with the experimental values.¹⁴ The relationship between iron(III) chloride concentration (x_1), ammonium thiocyanate concentration (x_2) and absorbance of chloroform extract (*A*), while holding pH and ionic strength of the reaction mixture constant (pH 5.7 and $\mu = 0.2M$) is shown by model fitting methods which give the equation:

$$A = -1.686 + 77.143x_1 + 17.276x_2 - 764x_1^2 - 32.078x_2^2 - 231.969x_1x_2$$

Table 2.

Estimates of factor effects	
aver	= 0.48374
A	= 0.13116
B	= 0.16736
AB	= 0.02914
C	= 0.13051
AC	= 0.01804
BC	= 0.02389
ABC	= 0.00211
D	= 0.13934
AD	= 0.01761
BD	= 0.03501
ABD	= -0.02411
CD	= -0.10209
ACD	= -0.01416
BCD	= -0.02011
ABCD	= -0.00339

Maximum absorbance of the extracted complex can be obtained with $2 \times 10^{-2} M$ iron(III) chloride and $2 \times 10^{-1} M$ ammonium thiocyanate in the reaction mixture as can be seen from the assumed response surface and contours of constant response for the response surface given in Fig. 4.

For the relationship between pH, ionic strength and absorbance, while holding the concentration of colour reagents constant at optimal concentrations, ten solutions were examined (pH 5.2, 5.8, 6.4 and $\mu = 0.1, 0.2, 0.3 M$, with a replicate at the mid-point pH 5.8, $\mu = 0.2 M$) and model fitting methods give the equation:

$$A = -13.971 + 5.1904\mu + 4.9756 \text{ pH} \\ - 14.0995 \mu^2 - 0.4379 \text{ pH}^2 \\ + 0.1043 \rho \text{ pH}$$

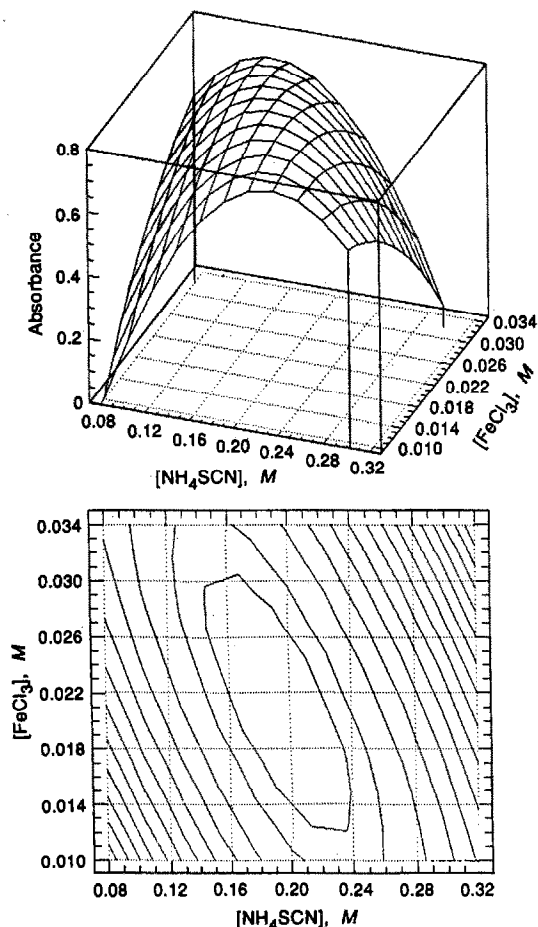


Fig. 4. The absorption response of the tolmetin-Fe(III) complex in chloroform and contours of constant response for the response surface as a function of the concentration of colour reagents. [Tolmetin] = $5.07 \times 10^{-3} M$; pH 5.7; $\mu = 0.2 M$.

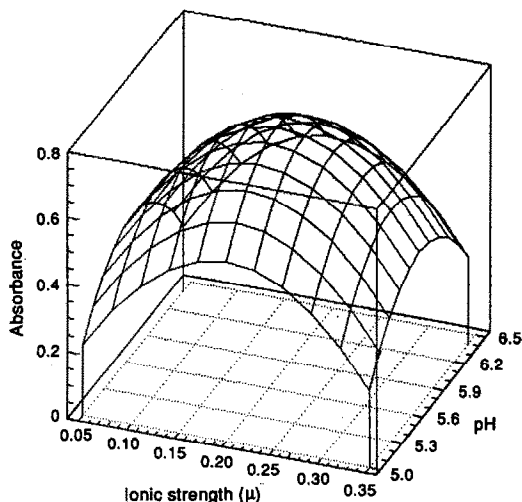


Fig. 5. The absorption response of the tolmetin-Fe(III) complex in chloroform with respect to the pH and ionic strength. [Tolmetin] = $5.07 \times 10^{-3} M$; [Fe(III)] = $10^{-1} M$; $[\text{NH}_4\text{SCN}] = 1 M$.

The equation maximum is obtained with pH 5.7 and $\mu = 0.2 M$. The assumed response surface is shown in Fig. 5. All further measurements were carried out at pH 5.7, ionic strength 0.2 M and a ten-fold excess of ammonium thiocyanate concentration to iron(III) chloride concentration.

Stoichiometry of the complex

The composition of the tolmetin-iron(III) complex was determined by applying Job's method of continuous variation. The concentration of aqueous tolmetin sodium and iron(III) chloride solutions was $5 \times 10^{-3} M$. Nine solutions were prepared containing tolmetin sodium and ferric chloride in various molar ratios so that their volume always amounted to 5 ml with addition of 2 ml of

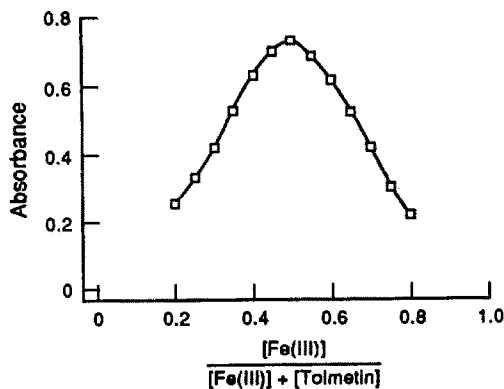


Fig. 6. Job's curve of equimolar solutions for the tolmetin-Fe(III) complex in chloroform. [Tolmetin] = [Fe(III)] = $5 \times 10^{-3} M$; pH = 5.7; $\mu = 0.2 M$.

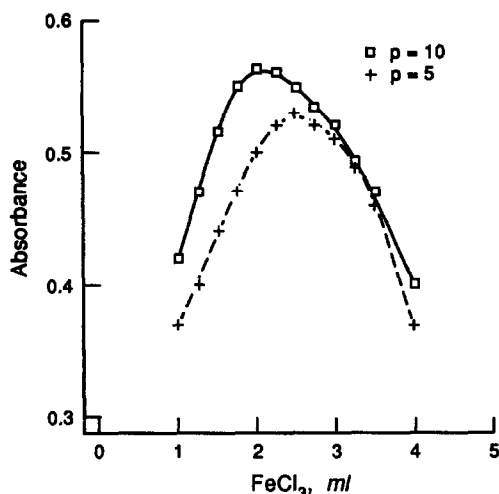


Fig. 7. Job's curve of non-equimolar solution at 486 nm. [Tolmetin] = $2.5 \times 10^{-3} M$; pH 5.7; $\mu = 0.2 M$.

ammonium thiocyanate solution, 1 ml of potassium chloride and 2 ml of acetate buffer solution. The extraction was performed with 5 ml of chloroform and the absorbance measured at 486 nm. The plot reaches maximum value at a mole fraction $X_{\max} = 0.5$ (Fig. 6), which indicates the formation of a 1:1 complex. The composition of the complex was confirmed by the molar ratio method. The curve obtained shows a break point at the iron(III)-tolmetin molar ratio of 1:1.

Relative stability of the complex

The relative stability constant of the complex has been determined by applying the method of Sommer *et al.*¹⁶ on the basis of results obtained by Job's method for the composition of the complex and also by the application of Job's method of non-equimolar solutions¹⁵ (Table 3). By Job's method of non-equimolar solutions the curves for a five- and ten-fold excess of reagent were obtained (Fig. 7).

The conditional stability constant was then calculated in the following way:

$$K' = \frac{(p-1)(1-2X_{\max})}{(C_{\text{tolmetin}})[(1+p)X_{\max}-1]^2}$$

Table 3. Conditional stability constant of the tolmetin-Fe(III) complex*

Job's method of non-equimolar solutions*			
[Fe(III)]	p	X_{\max}	$\log K'$
1.25×10^{-2}	5	0.208	4.18
2.50×10^{-2}	10	0.166	3.78
Mean: 3.98			
Sommer's method*			
$\log K'$	$\log K'_{\min}$	$\log K'_{\max}$	SD RSD, %
3.84	3.71	4.01	0.11 2.37

*Conditions: pH 5.7; $\mu = 0.2$; Temperature = $25 \pm 0.5^\circ$

where $p = 5$ or 10, X_{\max} is projection of the peak maximum divided by the total volume of chloroform used for extraction in each case (12 ml). The values obtained by the two different methods are in good agreement.

Validation

The method was tested for linearity, precision and reproducibility. The Beer-Lambert law was obeyed over the tolmetin sodium concentration range 0.04–0.04 mg/ml; $A_{486} = a + bC$, where C is the concentration of tolmetin sodium in mg/ml (calculated in the final solution for extraction), $a = -0.0172$ and $b = 2.326$; the regression coefficient being $R = 0.999$ ($n = 10$) indicates excellent linearity.

The precision of the method was checked at three different concentrations. The relative standard deviation varied from 1.31–2.33% for concentration of tolmetin sodium from 0.4–1.6 mg/ml.

The applicability of the method for the assay of simple dosage forms was examined by analysing Tolectine[®] tablets. The recovery was 98.6% ($n = 10$) relative to the labelled strength of those preparations and relative standard deviation of 1.62%.

The statistical analysis of the results obtained in the determination of tolmetin as a pure compound and from dosage forms is shown in Table 4.

The colorimetric procedure, based on selective reaction of tolmetin sodium with iron(III) chloride in the presence of ammonium thiocyanate and extraction of the formed complex is

Table 4. Statistical analysis of results in the determination of tolmetin

Sample ($n = 10$)	Concentration	Found	SD,	RSD,	S_x	Recovery,
	solutions					
Tolmetin Sodium bulk drug	0.4	0.40	0.093	2.33	0.003	97–103
	1.0	1.00	0.013	1.31	0.027	98–101
	1.6	1.60	0.021	1.31	0.008	98–102
Tolectine [®] tbl. (200 mg)	1.0	0.986	0.016	1.62	0.005	98.6

suitable for rapid and sensitive analysis of tolmetin sodium in commercial formulations. The lower limit of sensitivity of the method was found to be 11.6 $\mu\text{g/ml}$.

REFERENCES

1. T. Guneri and L. Kirilmaz, *Acta Pharm. Turc.*, 1988, **30**, 149.
2. C. Janicki and K. F. Daly, *J. Pharm. Sci.*, 1980, **69**, 147.
3. M. L. Selley, J. Thomas and E. J. Triggs, *J. Chromatog.*, 1974, **94**, 143.
4. K.-T. Ng, *ibid.*, 1978, **166**, 527.
5. R. Stromberg, *ibid.*, 1988, **448**, 1.
6. R. K. Gilpin and C. A. Janicki, *ibid.*, 1978, **147**, 501.
7. M. L. Hyneck, P. C. Smith, E. Unsel and L. Z. Benet, *ibid.*, 1987, **420**, 349.
8. R. A. Egli, H. Müller and S. Tanner, *Z. Anal. Chem.*, 1981, **305**, 267.
9. C. Sarbu, *J. Chromatog.*, 1986, **367**, 286.
10. J. N. Miller, D. L. Phillips, D. T. Burns and J. W. Bridges, *Talanta*, 1978, **25**, 46.
11. M. Počtová and B. Kakác, *Cesk. Farm.*, 1982, **31**, 116.
12. *United States Pharmacopeia*, XXI Revision, pp. 1070–1071. U.S. Pharmacopeial Convention, Rockville, MD, 1985.
13. S. N. Deming and S. L. Morgan, *Experimental Design: A Chemometric Approach*, Elsevier, Amsterdam, 1987.
14. Statistical Graphics System Statgraphics 3.0, by Statistical Graphics Corporation.
15. W. C. Vosburgh and G. R. Cooper, *J. Am. Chem. Soc.*, 1941, **63**, 437.
16. L. Sommer, V. Kubáň and J. Havel, *Spectrophotometric Studies of Complexation in Solution*, *Folia Fac. Sci Nat., Univ. Purkynianae Brunensis, Chemia* 7, Brno, 1970.

A POTENTIOMETRIC TECHNIQUE FOR KINETIC DETERMINATION OF CITRATE, BASED ON INHIBITION OF CRYSTALLINE GROWTH OF LEAD CARBONATE SEED CRYSTALS

F. GRASES and C. GENESTAR

Department of Chemistry, University of Balearic Islands, 07071 Palma de Mallorca, Spain

(Received 22 April 1991. Revised 6 June 1991. Accepted 25 June 1991)

Summary—The growth of lead carbonate seed crystals is strongly inhibited by the presence of citric acid. The kinetics of crystal growth were followed potentiometrically with a lead ion-selective electrode. The study of different variables on such a process was carried out with the aim of developing kinetic procedures to determine citrate (0.5–2.0 $\mu\text{g/ml}$). The selectivity and sensitivity of these processes allow the application of his crystallization reaction to direct determination of citrate in drinks and in a pharmaceutical product.

Citric acid has aroused notable interest as an additive in food, mainly as an acidifying agent in drinks. Citrate is also widely used in pharmaceutical preparations. It is biologically involved in the well-known Krebs cycle of glucid metabolism¹ and plays an important role in preventing calcium oxalate urolithiasis due to its effective inhibitory effects.²

Determination of citric acid can be accomplished through gravimetric and volumetric methods,³ photometric procedures,⁴ enzymatic analyses⁵ and chromatographic determinations, mainly HPLC.⁶ Recently, an indirect potentiometric method was also presented.⁷ In this paper we propose a kinetic potentiometric technique for kinetic determination of citrate based on its inhibitory effects on the growth of lead carbonate seed crystals. The determination was applied to the direct determination of citrate in drinks. We have demonstrated previously the usefulness of inhibitory processes of crystalline growth with analytical purposes, due to the sensibility and selectivity of such processes. Thus, procedures for phytic acid determination with seed crystals of calcium oxalate monohydrate⁸ and determination of phosphate with calcite (calcium carbonate) seed crystals⁹ were developed.

EXPERIMENTAL

Reagents and apparatus

Solutions of sodium bicarbonate, sodium citrate (both from Panreac) and sodium per-

chlorate (Carlo Erba) were prepared with analytical-reagent grade chemicals. A standard solution of 0.1M lead perchlorate (Orion) was used. Lead carbonate seed crystals of analytical reagent grade (Panreac) were characterized by termogravimetry (with a Perkin-Elmer TGS 2 Electromicroanalytical balance) and scanning electron microscopy (with a Hitachi S-530 SEM). Potentiometric measurements were taken by means of a Crison pH/mV-meter digit 501 with a lead electrode (Orion Model 94-82) coupled with a silver/silver chloride electrode, separated from the cell solution by an intermediate junction containing potassium chloride. The temperature was controlled by a sensor immersed in the working solution.

Procedure

In a 250-ml beaker were placed 2 ml of 5M sodium perchlorate, 0.4 ml of 0.1M lead perchlorate, the volume of citrate solution necessary for a final concentration between 0.5 and 2 ppm of citrate, and water to a final volume of 200 ml (initial pH = 5.8). The solution was immersed in a constant-temperature waterbath and was always magnetically stirred. After the temperature of the working solution was stabilized ($25.0 \pm 0.2^\circ$), 1 ml of a perfectly homogeneous suspension, obtained by mixing 5 g of lead carbonate seed crystals and 20 g of water, was added. Finally, when the potentiometer gave a constant reading (± 0.5 mV), 1 ml of 0.2M sodium bicarbonate solution was added.

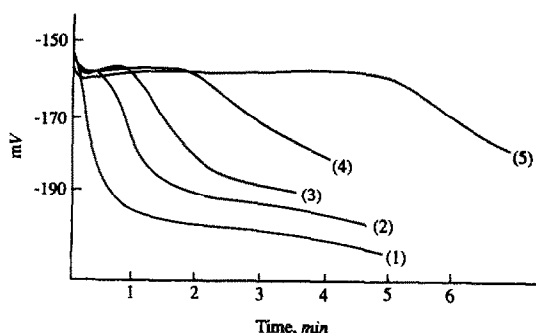


Fig. 1. Lead crystallization runs in the absence and presence of citrate. $[Pb^{2+}]_0 = 2 \times 10^{-4}M$, $[HCO_3^-]_0 = 1 \times 10^{-3}M$, $[NaClO_4] = 0.05M$, initial pH = 5.8; 0.25 g of lead carbonate seed crystals, temperature = 25°. (1) without citrate; (2) [citrate] = $2.5 \times 10^{-6}M$; (3) [citrate] = $3.4 \times 10^{-6}M$; (4) [citrate] = $5.0 \times 10^{-6}M$; (5) [citrate] = $6.8 \times 10^{-6}M$.

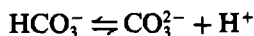
Potential-time curves were obtained whether the induction period method or the fixed-time method of rate measurement was applied (Fig. 1). The duration of each measurement was *ca.* 10 min.

RESULTS AND DISCUSSION

Study of crystalline growth of lead carbonate seed crystals

The crystalline growth of lead carbonate seed crystals was potentiometrically studied with a lead ion-selective electrode in order to obtain optimum conditions to observe inhibitory processes of crystal growth. Thus, the influence of pH, supersaturation, ionic strength, temperature and seed morphology on the reaction rate were studied.

Figure 2 shows the influence of initial pH on the reaction rate. As can be seen the rate of lead carbonate crystal growth increases when initial pH increases. This is directly related to the displacement of the following equilibrium.



giving a higher initial free carbonate concentration at higher pH values and consequently increasing the initial crystallization rate of the lead carbonate. Considering the pH range of the optimum response for the lead ion-selective electrode, a pH of *ca.* 5.8 was chosen as optimum. When the lead carbonate crystallization process took place with working solutions containing lead, hydrogen carbonate and carbonate (without pH buffer), using the above conditions, a continuous increase in the pH of the solution was observed (one unit of pH, approx.) and this

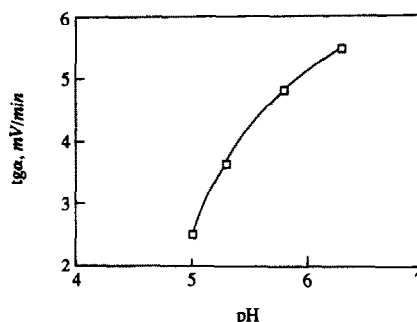


Fig. 2. Influence of the initial pH on the initial rate ($tg \alpha$) of lead carbonate crystallization. $[Pb^{2+}]_0 = 2 \times 10^{-4}M$, $[HCO_3^-]_0 = 5 \times 10^{-4}M$, $[NaClO_4] = 0.05M$; 0.25 g of lead carbonate seed crystals, temperature = 25°.

is explained by considering the existence of basic lead forms at 5.8 initial pH value.

Figure 3 shows the rate of crystallization corresponding to different selected supersaturation values. As can be appreciated for a total initial lead concentration of $2 \times 10^{-4}M$ and bicarbonate concentration of $1 \times 10^{-3}M$, the electrode potential remained constant before seed addition, and after bicarbonate addition the rate of crystalline growth provoked a rapid decrease in the potential with time. These are two essential conditions for exploiting this methodology for analytical purposes. For those reasons the above-mentioned lead and bicarbonate concentrations were chosen as optimum. As can be seen in Fig. 3, it can be assumed that no nucleation processes took place and consequently only crystalline growth on seed crystals was produced.

The study of the ionic strength influence demonstrated that in the studied interval

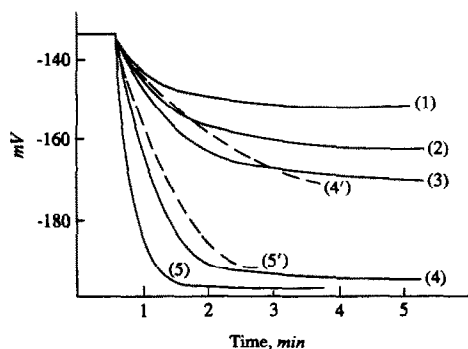


Fig. 3. Lead carbonate crystallization runs at different supersaturation. $[Pb^{2+}]_0 = 2 \times 10^{-4}M$, $[NaClO_4] = 0.05M$, initial pH = 5.8; 0.25 g of lead carbonate seed crystals, temperature = 25°. (1) $[HCO_3^-]_0 = 3 \times 10^{-4}M$; (2) $[HCO_3^-]_0 = 4 \times 10^{-4}M$; (3) $[HCO_3^-]_0 = 5 \times 10^{-4}M$; (4) $[HCO_3^-]_0 = 1 \times 10^{-3}M$; (5) $[HCO_3^-]_0 = 2 \times 10^{-3}M$; (4') and (5') experiments without seed.

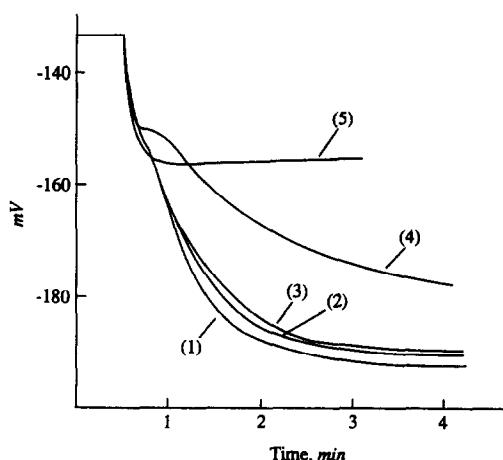


Fig. 4. Effects of several substances in lead carbonate crystal growth. $[Pb^{2+}]_0 = 2 \times 10^{-4}M$, $[HCO_3^-]_0 = 1 \times 10^{-3}M$, $[NaClO_4] = 0.05M$, initial pH = 5.8; 0.25 g of lead carbonate seed crystals, temperature = 25°. (1) Reference, thiamine ($5 \times 10^{-6}M$), threonine ($1.7 \times 10^{-6}M$), sulphate ($2 \times 10^{-5}M$), phosphate ($2 \times 10^{-5}M$), EDTA ($1 \times 10^{-5}M$), fumaric acid ($1.7 \times 10^{-5}M$); (2) ascorbic acid ($1.1 \times 10^{-5}M$); (3) oxalate ($2.3 \times 10^{-5}M$); (4) pyrophosphate ($1.4 \times 10^{-5}M$); (5) citrate ($6.8 \times 10^{-6}M$).

(0.025–0.15M sodium perchlorate) the crystalline growth is only slightly affected. An ionic strength of 0.05M sodium perchlorate was chosen as optimum after consideration of the most appropriate electrode response. Studies of the temperature influence on lead carbonate crystal growth demonstrated that between 25 and 30°, the crystallization runs were practically unmodified.

The size and morphology of seed crystals can in some cases affect the rates of crystal growth.¹⁰ Thus to evaluate the influence of size and morphology of the lead carbonate seed on crystallization runs, experiments were made with seeds of two different surface characteristics (aged and non-aged seed crystals). No significant

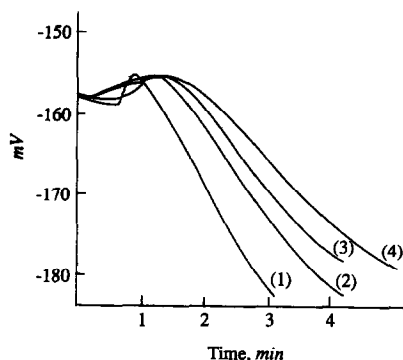


Fig. 5. Influence of the initial pH on the inhibition of citrate in the crystalline growth of lead carbonate. $[Pb^{2+}]_0 = 2 \times 10^{-4}M$, $[HCO_3^-]_0 = 1 \times 10^{-3}M$, $[NaClO_4] = 0.05M$, $[citrate] = 3.4 \times 10^{-6}M$; 0.25 g of lead carbonate seed crystals, temperature = 25°. (1) pH = 6.3; (2) pH = 5.8; (3) pH = 5.3; (4) pH = 5.0.

variations were observed when using the two distinct seeds, in spite of their different morphology, demonstrating that in this case the type of seed used had little influence on the process. The quantity of seed crystals used in each experience was also studied and it was found that 0.25 g of lead carbonate seed crystals caused a rapid and easily measurable decrease in the potential with time.

Finally, the crystalline growth of lead carbonate seed crystals was studied in the presence of several additives. As is shown in Fig. 4, the growth of lead carbonate crystals was notably delayed by the presence of citrate and pyrophosphate, in such a manner that the citrate exhibited the highest effect and ascorbic and oxalic acids the lowest one, whereas, fumaric acid, thiamine, threonine, sulphate, phosphate and EDTA manifested no significant effects in the experimental conditions used. These results demonstrate that the structure of the citric acid

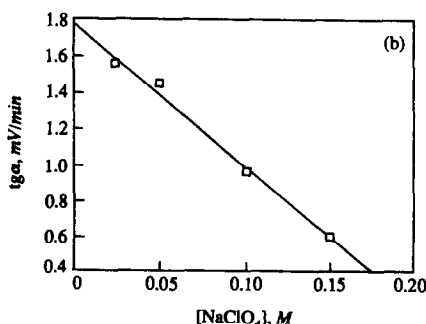
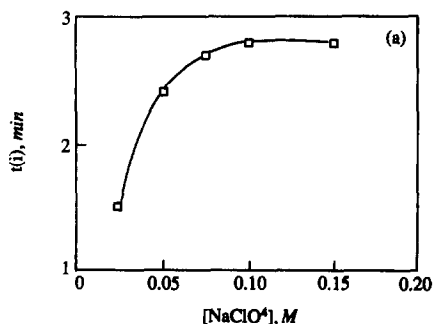


Fig. 6. Influence of the ionic strength on the inhibition of citrate in the crystalline growth of lead carbonate. $[Pb^{2+}]_0 = 2 \times 10^{-4}M$, $[HCO_3^-]_0 = 1 \times 10^{-3}M$, $[citrate] = 3.4 \times 10^{-6}M$, initial pH = 5.8; 0.25 g of lead carbonate seed crystals, temperature = 25°. (a) influence of the ionic strength on the induction period; (b) influence of the ionic strength on the initial rate (mV/min).

Table 1. Characteristics of the analytical methods

	Linear range of logarithmic plots, ppm	RSD, %†
Fixed-time method*	0.5–2	3.9
Induction period method	0.5–2	2.8

*5 min.

† $n = 11$.

permits a very effective adaptation of the substance on the crystal surface. The adsorption of the polyhydroxycarboxylic acid to the active growth sites would be responsible for the reduction in the crystalline growth rates.

Effects of citrate on lead carbonate crystallization

Study of experimental conditions. For the purpose of finding the optimum conditions to develop a kinetic procedure for the determination of citric acid based on its inhibition on lead carbonate crystal growth, the influence of pH and ionic strength on the reaction rate was investigated. Figure 5 shows the study of the pH influence. As can be appreciated when pH increased the citrate inhibitory capacity did not increase. This indicates that deprotonation of the citrate molecule does not affect its inhibitory capacity. On the other hand, when considering the influence of the ionic strength (Fig. 6), the citrate inhibition increases when ionic strength also increases. These findings seem to indicate that the citrate-lead carbonate interaction is not a simple electrostatic interaction. Thus, an initial pH value of 5.8 and an ionic strength of 0.05M were chosen to prepare the calibration graph.

Characteristics of the analytical methods. The fixed-time (5 min) and the induction period methods were applied to the potential (mV)–time curves, recorded in the presence of different amounts of citrate under selected conditions in order to obtain the calibration graph. The

Table 2. Tolerance levels (ppm) for several species in the determination of citrate (1 ppm)

Species	Amount tolerated, ppm
Sulphate, phosphate, EDTA	>2
Fumaric acid	>5
Malic, ascorbic and oxalic acids*	2
Thiamine, threonine	>10
Calcium, sodium, potassium and ammonium ions	>20
Pyrophosphate*	0.5

*Higher concentrations increased the induction period.

Table 3. Determination of citrate in drinks and pharmaceutical products

Sample	Proposed method,* g/l.	Photometric method,* g/l.
Pharmaceutical product	256 ± 3.40	234 ± 2.68
Fruit juice	3.45 ± 0.04	3.13 ± 0.05
Wine	2.80 ± 0.06	2.24 ± 0.04

*Average of 5 determinations.

results obtained are shown in Table 1. As can be seen the induction period method exhibited the best analytical characteristics. The selectivity was tested by obtaining the rate curves in the presence of several species that could potentially act as inhibitors of lead carbonate crystal growth. The results in Table 2 show few interferences, thus only pyrophosphate caused some important disturbance at concentrations similar to that of citrate. The proposed method exhibited a good calcium tolerance, even though this species forms precipitates with carbonate. It is evident that large amounts of species that could precipitate with lead ions must be avoided.

Applications

The proposed method was applied to citrate determination in drinks and in a pharmaceutical product. It was noteworthy that no matrix effects were observed when analysing such real samples. This permitted the methods to be applied without any previous treatment of the samples (except appropriate dilutions). Nevertheless, with the aim of confirming the reliability of the procedure, the standard addition method was applied and the results (Table 3) were compared with those obtained by a spectrophotometric procedure based on the formation of an Fe(III) yellow complex.⁴ As can be seen, there was fair agreement between the present and Fe(III) procedures, confirming the applicability of the method.

Acknowledgement—Financial support by the Dirección General de Investigación Científica y Técnica (Grant PB 89-0423) is gratefully acknowledged.

REFERENCES

1. S. J. Pilkis, R. M. El-Magharabi and T. H. Clause, *Ann. Rev. Biochem.*, 1988, **57**, 755.
2. F. Grases, A. Millán and A. Garcia-Raso, *J. Crystal Growth*, 1988, **89**, 496.
3. S. N. Bhosale and S. M. Khopkar, *Talanta*, 1985, **32**, 15.
4. A. Millan, A. Conte, A. Garcia-Raso and F. Grases, *Clin. Chem.*, 1987, **33**, 1259.

5. H. V. Bergmeyer (ed.), *Methods of Enzymatic Analysis*, Vol. 3, pp. 1563, 1568. Academic Press, London, 1974.
6. S. H. Ashoor and M. J. Knox, *J. Chromatog.*, 1984, **299**, 288.
7. J. G. Pentari, C. E. Efstathion and T. P. Hadjiioannou, *Talanta*, 1991, **38**, 295.
8. F. Grases and P. March, *Anal. Chim. Acta*, 1989, **219**, 89.
9. F. Grases and J. G. March, *ibid.*, 1990, **229**, 249.
10. R. P. Singh, S. S. Gaur, D. J. White and G. H. Nancollas, *J. Colloid Interface Sci.*, 1987, **118**, 379.

EXPLOITING THE HYDRODYNAMIC ASPECTS OF CONTINUOUS-FLOW SYSTEMS

ANGEL RÍOS and MIGUEL VALCÁRCCEL

Department of Analytical Chemistry, Faculty of Sciences, University of Córdoba, Córdoba, Spain

(Received 20 April 1991. Revised 27 June 1991. Accepted 28 June 1991)

Summary—An overview of the analytical potential of the hydrodynamic aspects of unsegmented flow systems is presented. Different approaches involving flow manipulation are described: stopped-flow methodologies, intermittent pumping, selecting-diverting carrier (reagent) streams, open-closed flow systems, flow reversal and flow gradient.

The flow-rate (q) is one of the major variables in flow manifolds. Every method developed is optimized for a characteristic flow rate, which is kept constant throughout analyses through the different available propulsion elements (usually peristaltic pumps). Few methods use variable flow-rates; the best known are probably those based on stopping a pump of the system. The stopped-flow and intermittent pumping techniques are the most representative in this respect.^{1,2} However, other methods based on manipulation of the flow-rate during the analysis step also offer major analytical possibilities as shown below.

The manipulation of hydrodynamic aspects in flow systems allows interesting analytical applications to be developed and a high degree of automation to be accomplished. Several of such applications were recently reported and could strongly influence the future of unsegmented flow analysers. This paper offers a systematic overview of the different modes involving manipulation of hydrodynamic features of flow systems, their applications and analytical potential.

The flow is usually manipulated in its pattern, direction or intensity; thus, pumps and valves are the two key devices allowing the hydrodynamic conditions of flow systems to be suited to one's requirements. Methodologies developed in this way involve stopping the flow, altering the flow pattern without changing the flow-rate, reversing the flow direction or establishing flow rate-gradients (Fig. 1).

Thus, to date, constant flow-rates have dominated the applications of continuous flow systems [Fig. 1(a)]:

$$q_{t_0}^n = \text{constant}$$

where t_0 is the time in which the analysis starts and t_n is the time in which the analysis finishes. Time stopped-flow modes have been used, alternating go/stop steps [Fig. 1(b)]:

$$q_{t_0}^1, q_{t_2}^2, \dots, q_{t_i}^i = q = \text{constant}$$

but

$$q_{t_1}^1, q_{t_3}^3, \dots, q_{t_{i-1}}^{i-1} = 0$$

Flow reversal methodology are based on an analogue flow pattern, but in this case [Fig. 1(c)]:

$$q_{t_0}^1, q_{t_2}^2, \dots, q_{t_i}^i = q$$

and

$$q_{t_1}^1, q_{t_3}^3, \dots, q_{t_{i-1}}^{i-1} = -q$$

Flow rate-gradients [Fig. 1(d)] are characterized by the continuous change of the flow-rate according to a linear function:

$$q = a*t + b \quad (t = \text{time}; a = \text{slope}; b = \text{intercept})$$

or a non-linear function:

$$q = F(t) \quad (\text{polynomic, exponential, etc.})$$

This variability is associated with constant flow gradients for the linear functions:

Flow-gradient = $Q = dq/dt = a = \text{constant}$ and non-constant flow-gradients for the other function, in general:

$$Q = d[F(t)]/dt$$

It is also possible to combine two or more of these methodologies by using different mathematical functions [Fig. 1(e)]. All these alternatives are discussed below.

Stopped-flow modes

The flow can be stopped either in the entire system or only in part of it. These two possibilities are related to stopped-flow methods and intermittent pumping, respectively.

Stopped-flow methods¹ involve an abrupt change in the flow-rate (q) from a $q \neq 0$ to zero. During the period over which $q \neq 0$ the sample plug is mixed with the reagent and transported to the detector [Fig. 2(a)]. When the flow is stopped, the chemical reaction on which the determination is based develops and the detector continuously monitors the signal-time curve. The slopes of the curves obtained are proportional to the analyte concentration. Experimentally, stopped-flow methods can be implemented by synchronizing injection with the pump operation, or by using a three-way valve between the injection unit and the detector. In both cases a timer or microcomputer is used to control and synchronize the operation of the valves and the pump. One of the most outstanding practical advantages of stopped-flow methods is the elimination of background signals from the blank or matrix as they are based on measurements of the signal change during the stop period. In this way, Růžicka and Hansen have developed interesting applications for the determination of sulphur dioxide in wine,³ alcohol in blood or serum without sample pretreatment,⁴ and glucose in serum.⁵ The reduction in the number and level of interfering species is another asset of the stopped-flow methods,⁶ as shown by Lázaro *et al.* with their catalytic-fluorimetric determination of trace copper.⁷

An alternative conception of the stopped-flow technique involves stopping the flow not as the sample reaches the detector, but in the tubing zone (reactor) [Fig. 2(b)], in order to increase the residence time and avoid the dispersion of the injected plug. A significant increase in sensitivity is obtained as a result of the longer reaction time without the dilution of the plug that would ensue with ordinary FIA systems. Several methods have been developed by using this methodology.⁸⁻¹⁰ The term "parallel analysis" used by Růžicka and Hansen¹ also allows the reaction time to be increased by using two or more reaction coils in parallel, but decreasing the dispersion of the sample; the sample is sequentially stored in parallel coils before reaching the detector. The same authors explained a parallel FIA analyser with eight 80- μ l storage

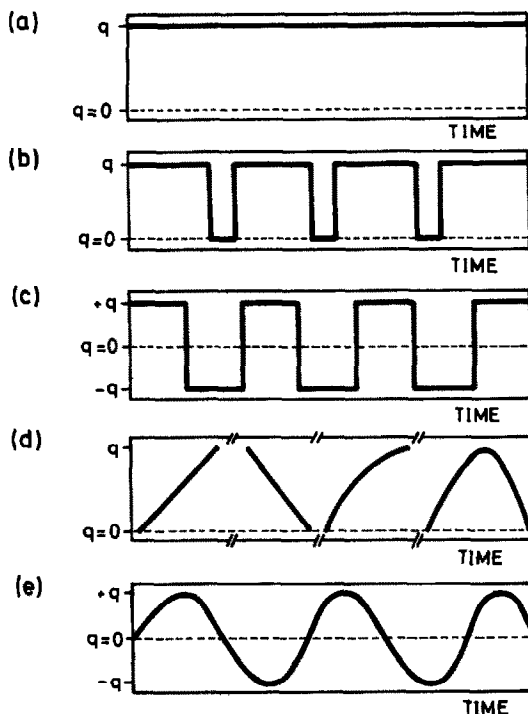


Fig. 1. Characteristic flow rate-time profiles for different methodologies: (a) constant flow-rate modes; (b) stopped-flow; (c) flow reversal; (d) flow-gradient and (e) flow-gradient/flow reversal coupling.

tubes in which several sample zones are stored in parallel (in a rotating drum) for a desired period of time.

An interesting assembly for simultaneous multideterminations by the stopped-flow technique was recently applied to the determination of free and bound sulphur dioxide in wines.¹¹ It uses a doubly stopped-flow manifold and can be considered to be a combination of the two above approaches [Fig. 2(c)]. Free sulphur dioxide directly reacts with formaldehyde and *para*-rosaniline to form a coloured compound which is monitored photometrically, whereas bound sulphur dioxide requires a prior hydrolytic release. Two sample plugs are injected simultaneously. Plug-1 merges with the *para*-rosaniline/formaldehyde mixture. The resulting merging stream is stopped when it reaches the detector, where the indicator reaction is monitored (determination of free sulphur dioxide). Simultaneously, plug-2 is stopped in a previous reactor coil, where its alkaline hydrolysis takes place. Then, on starting the pump, plug-1 is flushed out of the system and plug-2 is driven to the detector after merging with the reacting mixture. The second halting is effected as plug-2 reaches the detector and is followed by the

monitoring of the signal change with time, which is now made up of the contribution of free and bound sulphur dioxide. On starting the pump again, plug-2 is driven to waste.

Intermittent pumping involves stopping and starting one or several pumps from injection and the consequent temporary halting of one or several streams in the course of a determination. According to Růžička and Hansen,¹² two pumps can be incorporated into a manifold in a variety of combinations, especially if one considers different timings of their stop-go intervals, but, to date, little work has been done in this respect. The simplest application of a two-pump FIA system is to increase the sampling frequency by increasing the washout speed from the coils and from the flow-cell. Thus, the Brazilian FIA group, using commutation units, developed an improved procedure for the determination of nitrite in waters,¹³ and the turbidimetric determination of sulphate in natural waters and plant digests.¹⁴

Constant flow rate methodologies

FIA modes involving a constant flow-rate allow one to manipulate hydrodynamic aspects through selecting/diverting valves. These valves are of great interest to unsegmented flow methods.¹⁵

The six-way rotary valves usually employed in injection systems, converted to selecting-diverting valves by an alternative connection of different channels, probably represent the most useful alternative in this context. Olsen *et al.*¹⁶ employed a flow system incorporating three of these valves to preconcentrate heavy metals in a Chelex-100 minicolumn in a first step, followed by an elution step (in a reverse direction) to bring the eluted metal to a flame atomic-absorption detector. These readapted valves can also be used to co-ordinate two FIA subsystems by selecting the stream coming from one of them from a location prior to the detector¹⁷ [Fig. 3(a)]. In other applications, they perform selecting-diverting operations on flow streams.

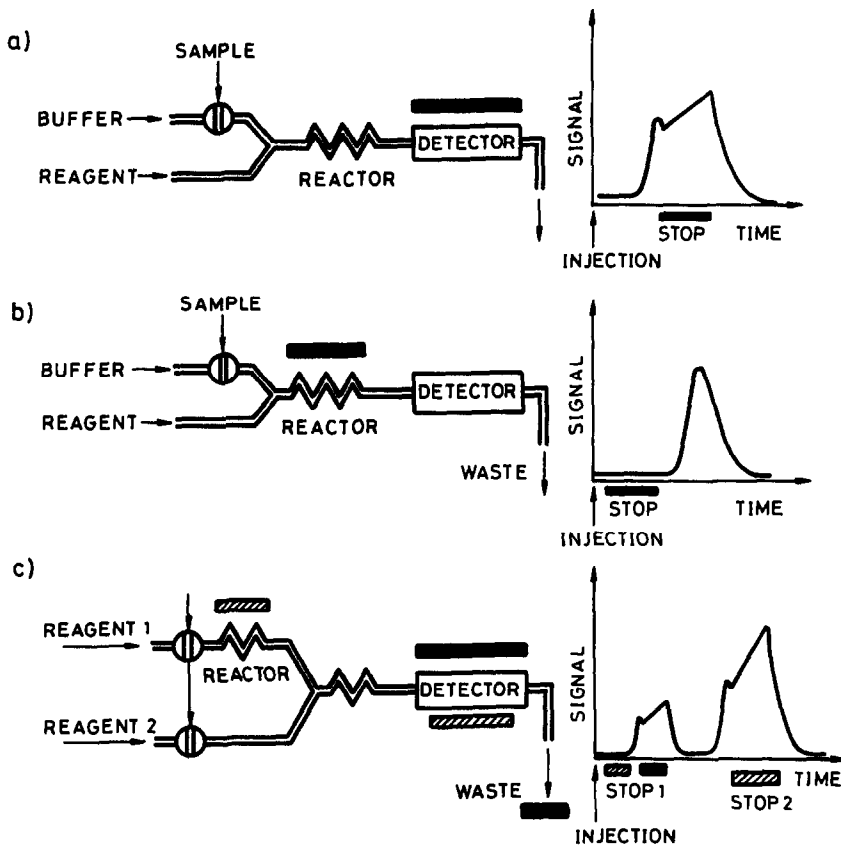


Fig. 2. Different approaches to the implementation of the stopped-flow technique: (a) Stopping the flow as the reacting plug reaches the detector. (b) Stopping the flow while the reacting plug is in the tubing zone (reactor). (c) Doubly stopped flow: first stop when plug-1 (■) reaches the detector and plug-2 (▨) is stopped in the reactor; second stop when plug-2 reaches the detector. [■ and ▨ indicate the position of the plug at the stop times].

One of the streams reaching the valve is selected at its exit; the other is driven to waste or allowed to reach a given point in the FIA configuration [Fig. 3(b)]. One such assembly was employed in speciation studies of chromium.¹⁸ The main channel, which contains sulphuric acid as carrier and into which the sample is injected, is merged with channel C from the selecting-diverting valve. The valve allows the selected stream [1,5-diphenylcarbazide (DPC) or oxidant] to reach the merging point. Initially, the oxidant stream (2) is fed to waste by the valve, whilst DPC (1) flows through channel C, so that the indicator reaction [DPC selectively reacts with Cr(VI)] can take place in the subsequent reactors. When valve selects the oxidant stream, DPC is driven to the second reactor. Thus, Cr(III) is oxidized to Cr(VI) in the first reactor, the indicator reaction takes place in the last reactor and total chromium is determined as a result.

Figure 3(c) shows an alternative possibility recently proposed for simultaneous kinetic determinations.¹⁹ Fe(III) and Co(II) form colourless

complexes with EGTA [reagent 1 in Figure 3(c)], which react at a different rate with PAR (reagent 2) in ligand-displacement reactions, to yield coloured complexes that are monitored photometrically at the same wavelength. In one position, the valve [Figure 3(c)], selects the sample-EGTA mixture and leads the PAR stream to point B (in this case the reaction only occurs along the last reactor). In the other position, the valve selects the PAR stream and leads the sample-EGTA mixture to point A. The reaction occurs now along the two reactors before detection. The two continuous signals obtained correspond to different reaction times and allow one to determine the Fe(III) and Co(II) present in the sample.

Six-way rotary valves adapted as selecting-diverting valves are a key to designing open-closed systems,²⁰ in which multidetection is carried out by repeatedly passing the reacting plug through a single detector. In this case, one of the streams reaching the valve is the carrier solution and the other is that coming from the detector (Fig. 4). In the open position [Fig. 4(a)],

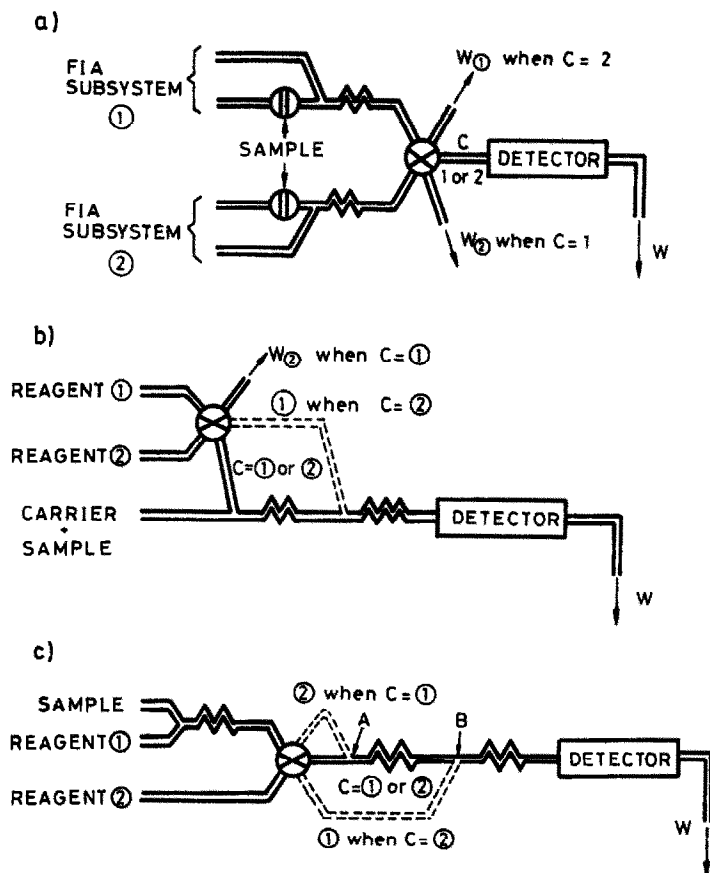


Fig. 3. Different uses of selecting-diverting valves to control the direction of one or two flow streams (see text). C = selected stream; W = waste. ⊗ selecting-diverting valve. ⊕ injection valve.

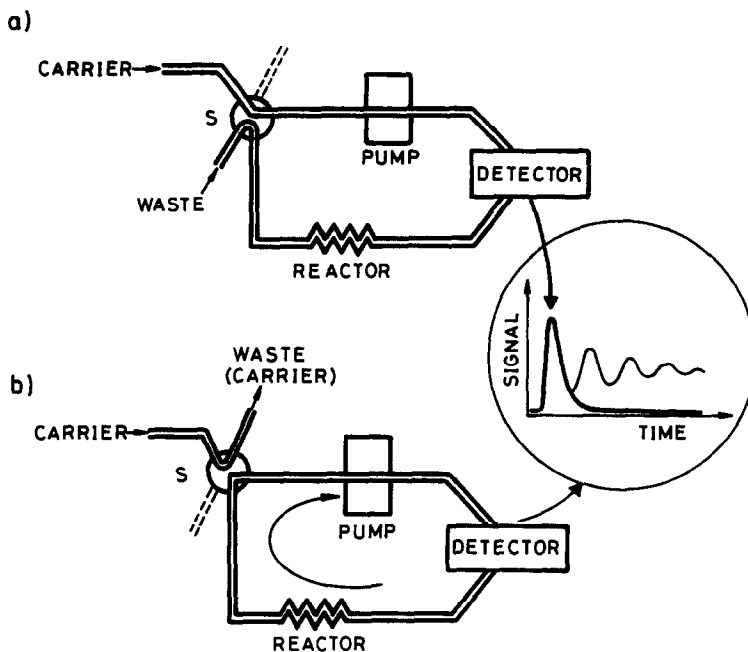


Fig. 4. Role of the selecting-diverting valve (S) in establishing open-closed flow systems. (a) Open-system position; (b) Closed-system position. The signal-time graph shows the response obtained by the detector in the open position configuration (■) (single FIA peak) and in the closed-system configuration (—) (multipeak recording), assuming no chemical reaction takes place (injection of a dye).

the valve selects the carrier solution and drives it to the detector, after which it goes to waste. In the closed-system position [Fig. 4(b)], a closed circuit is established as a result of the selecting-diverting valve selecting the channel coming from the detector. In this latter position the physical and chemical evolution of a sample injected into the flow can be monitored.

The analytical potential of open-closed flow systems has been clearly shown in the last few years. Their most remarkable applications are amplification methods,^{20,21} kinetic^{20,22} and speciation²³ studies, determination of reaction stoichiometries²⁴ and viscosity,²⁵ simultaneous kinetic determinations,²⁶ and determinations of enzymatic activities.^{27,28}

Flow reversal methodology

This methodology is based on the change of flow direction from $+q$ to $-q$, which establishes constant or non-constant time cycles. As pointed out by Betteridge *et al.*,²⁹ flow reversals can be implemented in three different ways (Fig. 5). One involves using two pumps [Fig. 5(a), pump A propels the carrier stream, pump B is unused. Then, the sample is injected and allowed to travel downstream into the reaction coil for a set time. Pump A is then stopped and pump B is started at the same

flow-rate to pull the sample plug back and through the detector and a second coil, and then out to waste. Therefore, this procedure requires two pumps.

The second procedure [Fig. 5(b)] uses a single pump and two valves, one for injecting the sample and the other as a selecting-diverting valve, which is the key to this procedure. First, the sample is injected into a carrier stream flowing at $+q$. After the entire plug has passed through the detector, the flow is reversed (at flow-rate $-q$) by switching the selecting-diverting valve. The peak is passed back through the detector, thereby establishing a cycle reversal.

The simplest procedure to perform flow reversal FIA involves using a single pump and changing the direction of the drum rotation [Fig. 5(c)]. This requires electronic³⁰ or computer³¹ control.

The reversal of the flow direction in continuous automatic analysers was first achieved by the air-segmented mode proposed by Technicon. In the last few years this approach has been used in unsegmented continuous flow analysis (*e.g.*, to control the dispersion and automatic variation of reaction coil length).²⁹ The reaction coil length plays a major role in determining the characteristics of any FIA system and significantly interacts with other factors. Other FIA variables (flow-rate, inner tubing diameter, *etc.*)

play their part in determining the amount of dispersion that a sample plug undergoes as it traverses a flow-injection manifold. Flow reversal may be used in conjunction with choice of flow-rate and sample size to determine the amount of dispersion that a sample undergoes. The flow can be reversed not only by allowing the entire plug to pass through the detector but also by "sampling" a preset zone of the plug, so that the reversal cycles all take place within one FIA peak.³⁰ In a way, this mode can be considered a peculiar variant of the sampling zone mode proposed by Krug *et al.*,³² but intended to obtain a multiplex recording that defines kinetic profiles (Fig. 6) that one can readily manipulate through the flow-rate, sample zone and cycle time.

Toei used flow reversal FIA for the determination of glucose in clinical samples with a

single-³³ and double-pump system.³⁴ The specific enzymatic reaction of glucose oxidase with β -D-glucose was exploited, but straight calibration graphs could not be obtained when the reaction time was short or when using a stopped-flow FIA procedure. A long period (5 min) was needed for the reaction with end-point rate assay. However, in a conventional single-line manifold with sufficiently long tubing to obtain the required delay, the peak analysis time was rather long because of the large dispersion of the samples in the long reaction tubing. The kinetic FIA procedure in which two peaks are obtained by flow reversal offers better results, probably as a consequence of more efficient mixing that in turn results in a higher reaction rate. Moreover, by measuring the difference between the two peaks for a sample, the blank signal of the samples can also be eliminated. Recently, Wang

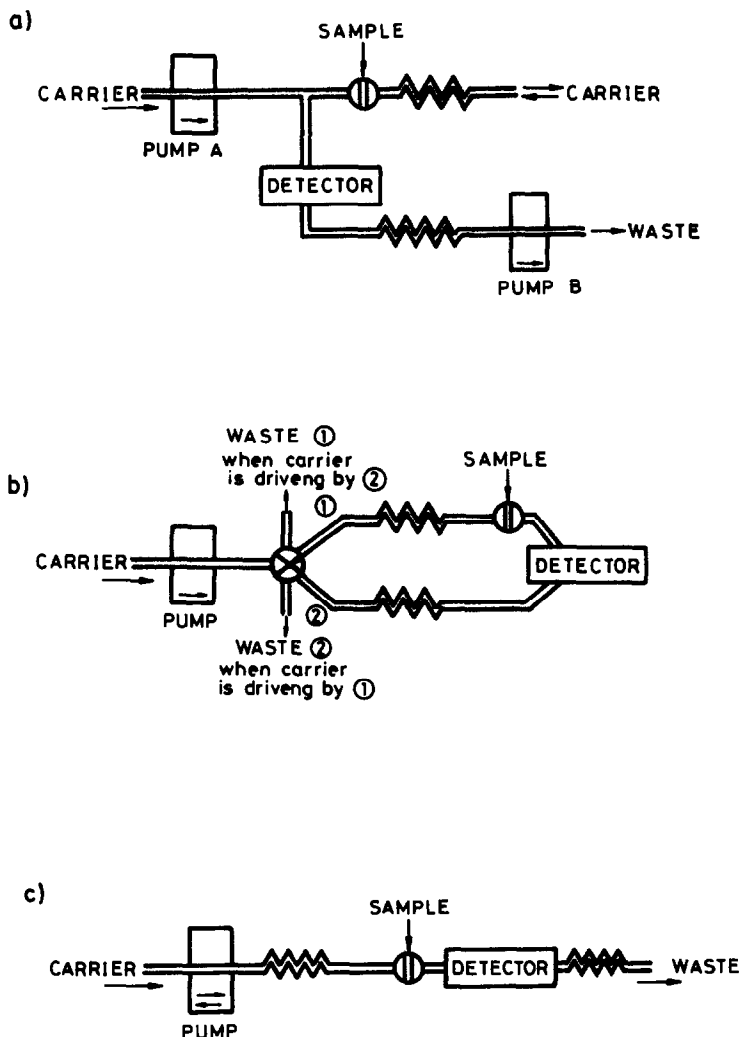


Fig. 5. Different procedures for applying the flow-reversal methodology: (a) by means of two pumps, (b) a selecting-diverting valve or (c) a single pump reversing the direction of the drum.

et al. also showed the use of repeated reversals of the flow direction to significantly improve the sensitivity of flow-injection stripping voltammetric measurements.³⁵ The plating efficiency and the resulting stripping peak currents were greatly enhanced thanks to the repeated passage of the same sample plug over the working electrode, which addressed the time restriction of conventional flow-injection stripping measurements.

The direct analysis of gas samples by flow injection is another interesting approach afforded by flow reversal methods implemented without a debubbler.³⁶ The sample is injected into a liquid carrier-reagent stream and the repeated passage of the liquid zone close to the gas-liquid interface nearest to the detector is monitored to obtain a signal-time multipeak recording. The method lends itself readily to automation and speeds up the analytical process as no prior collection in an absorbent solution or on a filter is required.

Flow reversal is also the foundation of a new methodology for performing liquid-liquid extraction processes in automatic unsegmented flow systems based on simplified configurations with no segmenter or separation units.³⁷ The key to this methodology is the placement of the detector in the loop of an injection valve, which is filled with the organic phase, whereas the aqueous phase containing the analyte makes the carrier. The process (reversal cycles as the two liquid-liquid interfaces are created by switching

the injection valve) is repeated as many times as required to achieve a suitable solute transfer between the two liquid-liquid interfaces; and is favoured by the formation of a thin layer of organic phase on the Teflon coil. The phases are never segmented or separated, and the organic phase plug is continuously monitored. Therefore, the solute transfer between the two phases, and the dispersion of the solute into the organic phase, can be continuously monitored. Some kinetic aspects of extraction in continuous flow systems and the behaviour of different ion pairs have been studied.³⁸ Simultaneous kinetic determinations by flow reversal/liquid-liquid extraction have also been reported.^{31,38}

Clark *et al.* have recently used flow-reversal flow-injection analysis for FIA titrations.³⁹ They employed a single-line manifold for the titration of strong acids (HCl, H₂SO₄ and H₃PO₄). The main advantages were the flexibility in operation and the increase in sensitivity.

Recently, Růžička and Marshall used the movement of the piston of a syringe-type pump coupled with an eight-port valve to generate flow reversal steps and allowing sequential injections in the flow system.⁴⁰ The synchronization between the movement of the piston and the valve allowed sample zone injection, reagent addition, mixing, measurement, and ejection of the reacted mixture took place by a combination of forward and reversed flow steps. The concept of sequential injection analysis, based on the mixing of the sample with a reagent in order to

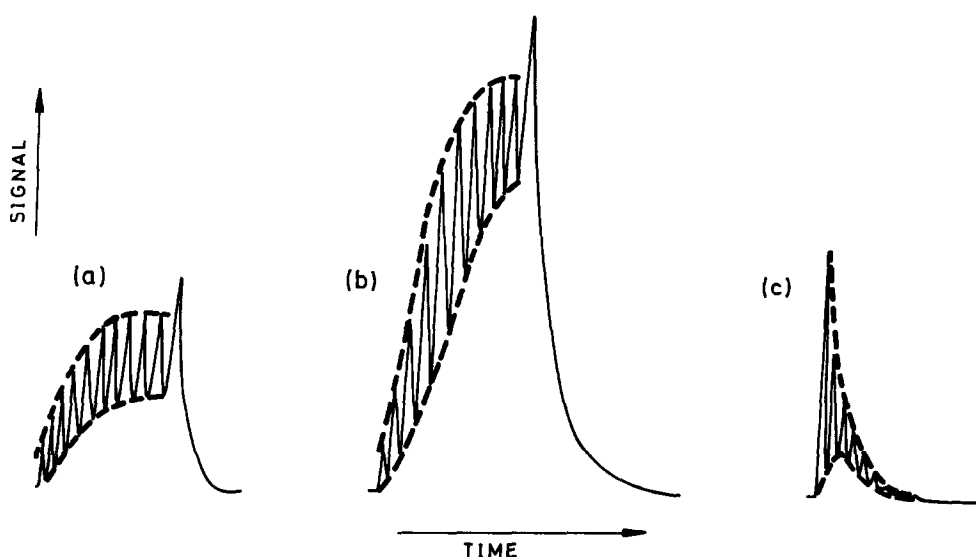


Fig. 6. Multipeak recordings obtained by the flow reversal methodology showing the kinetic profiles defined by their maxima and minima: (a) without chemical reaction; (b) with chemical reaction, by monitoring the formation of a product, or (c) the disappearance of a reactant.

produce a measurable response, was explained through the random walk model, being defined as a new concept for chemical sensors, process analysis and laboratory assays by the authors.

Flow-gradient technique

A flow rate-gradient (flow-gradient) can be defined as the variation of the flow-rate over a given period of time. It has been scantily used in FIA,^{41,42} but is well-known and widely employed in HPLC to increase resolution. Two FIA references describe the effect of flow-gradients on the more characteristic FIA parameters. In one, the flow-gradient was created by means of a hydrostatic head in a single channel.⁴¹ The flow-rate range obtained was limited to 0.7–2.4 ml/min. In later work, a multifunction pump delivery system was used to establish several flow patterns.⁴² The effects of these flow patterns on systems with and without chemical reaction were evaluated. One of the most important applications in this context is the washout effect (Fig. 7), whereby a higher sampling frequency is obtained. Thus, if a positive linear flow-gradient is established as the sample is injected, the peak-width can be dramatically decreased, the baseline restoration time shortened, the time lapse between consecutive injections minimized and the peak-height increased. Agudo *et al.* recently obtained similar results by using some non-constant flow rate-gradients.⁴³ Similar results can be obtained by operating with intermittent pumping, as was reported by Růžička and Hansen¹² and then reviewed by Krug *et al.*,⁴⁴ but in this mode it is necessary to use

two peristaltic pumps (one to propel the reagent stream and another to flush the system with the wash solution).

Different types of gradients were obtained by using a microcomputer which controlled (through an interface) the motion of the peristaltic pump drum.⁴⁵ These flow-gradients can be used to establish concentration-gradients in an easy, fast and accurate way (*e.g.*, to create pH-gradients allowing the photometric determination of acidity constants of compounds active in the UV-visible spectral region with no pH measurements,⁴⁵ and carry out acid–base titrations⁴⁶). Other linear concentration gradients can be created in flow systems for several analytical purposes. The stoichiometries of coloured complexes can be determined and complexometric titrations carried out by establishing ligand concentration gradients.⁴³

An interesting flow pattern combining variable flow-rates and flow reversal modes has been proposed by Růžička *et al.*⁴⁷ establishing sinusoidal flow functions by a cam-driven computer-controlled piston pump. This system controls two syringes (one for the sample and the other for the reagent) and an eight-port valve, generating alternate load and measurement cycles. The authors give an important number of advantages of the sinusoidal flow pump, its main disadvantages are low sampling frequency and the device being less flexible than a peristaltic pump. The establishment of this and other similar flow patterns through a conventional peristaltic pump controlled by a computer may provide higher flexibility, avoiding the refilling reservoir requirements.

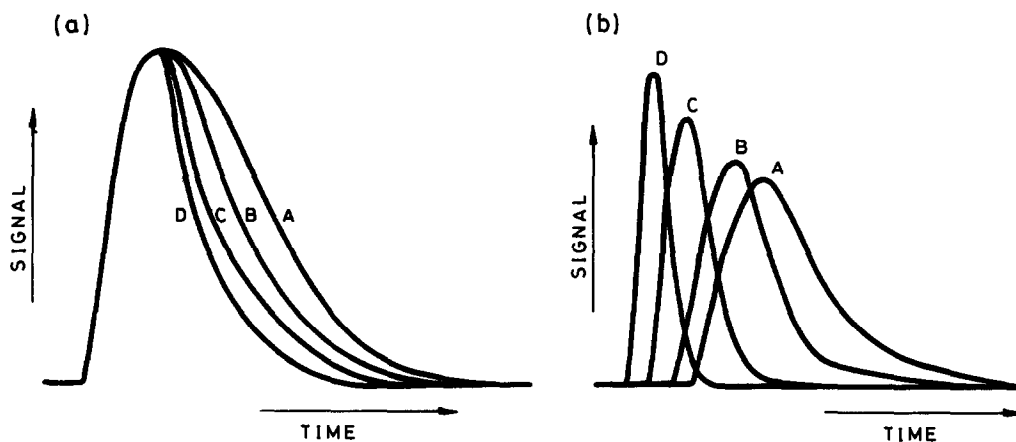


Fig. 7. Washing effect obtained by using positive linear flow-gradients applied at the residence time of FIA peak (a), and starting simultaneously with the injection of the sample (b). The flow-gradient increases from A to D in both cases.

Table 1. Analytical applications of methodologies based on hydrodynamic aspects of unsegmented flow systems

Methodology	Key element to perform the methodology	Analytical applications
Stopped-flow	Peristaltic pump (valves)	Kinetic studies Blank correction Reduction of interferences Increase of sensitivity Simultaneous determinations
Intermittent pumping	Peristaltic pump	Increase of sample frequency
Open-closed flow systems	Selecting-diverting valve	Improvement of sensitivity Kinetic studies Determination of viscosity Determination of stoichiometries Simultaneous determinations Speciation studies Enzymatic activities
Flow reversal	Peristaltic pump Selecting-diverting valve	Dispersion manipulation Improvement of sensitivity Kinetic studies Simultaneous determinations Direct gaseous sample analysis Liquid-liquid extraction
Flow-gradients	Peristaltic pump	Increase of sample frequency Establishment of concentration-gradients Determination of acidity constants Determination of stoichiometries

Another interesting and useful application of non-constant flow patterns was proposed by Růžička and Flossdorf by using variable forward flow with immobilized enzymes.⁴⁸ They employed designs with stopped flow, flow reversals and variable flow for the spectrophotometric determination of glucose with glucose oxidase and peroxidase immobilized on controlled-pore glass in the same reactor. The variable flow pattern was fast/slow/fast cycles to increase both the contact time and contact volume between the sample zone and the immobilized enzymes without increasing the zone dispersion or flow resistance.

CONCLUSIONS

The analytical potential of methodologies based on hydrodynamic features of flow systems offers interesting possibilities briefly discussed in this paper and summarized in Table 1. Pumps and valves are the key elements to these methodologies; they can be controlled by electronic timers or microcomputers (through active interfaces) in order to accomplish the maximum possible degree of automation. In addition to the dynamic foundation of these methodologies, most of them involve kinetic aspects that can be exploited for analytical purposes. Other interesting possibilities are the manipulation of dis-

persion (flow reversal) and sampling frequency (intermittent pumping and flow-gradient techniques). The flow reversal mode has introduced a new conception in flow manipulation with major repercussions on the automation of analytical processes. Thus, direct gas sample analyses and liquid-liquid extraction with no segmenter or separation units are two recent examples in this context. The flow-reversal/flow-gradient coupling is another potentially interesting approach that will offer important applications.

REFERENCES

1. J. Růžička and E. H. Hansen, *Flow Injection Analysis*, 2nd Ed., Wiley, New York, 1988.
2. M. Valcárcel and M. D. Luque de Castro, *Flow Injection Analysis. Principles and Applications*, Ellis Horwood, Chichester, 1987.
3. J. Růžička and E. H. Hansen, *Anal. Chim. Acta*, 1980, **114**, 19.
4. P. J. Worsfold, J. Růžička and E. H. Hansen, *Analyst*, 1981, **106**, 1309.
5. *Idem*, *Anal. Chim. Acta*, 1979, **106**, 207.
6. M. Valcárcel, *Analyst*, 1987, **112**, 729.
7. F. Lázaro, M. D. Luque de Castro and M. Valcárcel, *Anal. Chim. Acta*, 1984, **165**, 177.
8. T. Yamane, *Anal. Chim. Acta*, 1980, **130**, 65.
9. C. S. Lim, J. N. Miller and J. W. Bridges, *ibid.*, 1980, **114**, 183.
10. P. Linares, M. D. Luque de Castro and M. Valcárcel, *ibid.*, 1984, **161**, 257.

11. F. Lázaro, M. D. Luque de Castro and M. Valcárcel, *Anal. Chem.*, 1987, **59**, 950.
12. J. Růžicka and E. H. Hansen, *Flow Injection Analysis*, 2nd Ed., p. 172. Wiley, New York, 1988.
13. E. A. G. Zagatto, A. O. Jacintho, J. Mortatti and H. Bergamin F^o, *Anal. Chim. Acta*, 1980, **120**, 399.
14. F. J. Krug, E. A. G. Zagatto, B. F. Reis, O. Bahia, A. O. Jacintho and S. S. Jorgensen, *ibid.*, 1983, **145**, 179.
15. A. Ríos, M. D. Luque de Castro and M. Valcárcel, *J. Automatic Chem.*, 1987, **9**, 30.
16. S. Olsen, L. C. R. Pessenda, J. Růžicka and E. H. Hansen, *Analyst*, 1983, **108**, 905.
17. A. Ríos, M. D. Luque de Castro and M. Valcárcel, *ibid.*, 1985, **110**, 277.
18. J. Ruz, A. Ríos, M. D. Luque de Castro and M. Valcárcel, *Anal. Chim. Acta*, 1986, **186**, 139.
19. M. Romero-Saldaña, A. Ríos, M. D. Luque de Castro and M. Valcárcel, *Talanta*, 1991, **38**, 291.
20. A. Ríos, M. D. Luque de Castro and M. Valcárcel, *Anal. Chem.*, 1985, **57**, 1803.
21. A. Ríos, F. Lázaro, M. D. Luque de Castro and M. Valcárcel, *Anal. Chim. Acta*, 1987, **199**, 15.
22. S. D. Kolev, A. Ríos, M. D. Luque de Castro and M. Valcárcel, *Talanta*, 1991, **38**, 125.
23. J. Ruz, A. Ríos, M. D. Luque de Castro and M. Valcárcel, *ibid.*, 1986, **33**, 199.
24. A. Ríos, M. D. Luque de Castro and M. Valcárcel, *J. Chem. Education*, 1986, **63**, 552.
25. *Idem*, *Talanta*, 1987, **34**, 915.
26. *Idem*, *Anal. Chim. Acta*, 1986, **179**, 463.
27. J. M. Fernández-Romero, M. D. Luque de Castro and M. Valcárcel, *ibid.*, 1989, **219**, 191.
28. *Idem*, *J. Biotechnology*, 1990, **14**, 43.
29. D. Betteridge, P. B. Oates and A. P. Wade, *Anal. Chem.*, 1987, **59**, 1236.
30. A. Ríos, M. D. Luque de Castro and M. Valcárcel, *ibid.*, 1988, **60**, 1540.
31. L. E. León, A. Ríos, M. D. Luque de Castro and M. Valcárcel, *J. Laboratory and Robotics*, 1989, **1**, 295.
32. A. O. Jacintho, E. A. G. Zagatto, B. F. Reis, L. C. R. Pessenda and F. J. Krug, *Anal. Chim. Acta*, 1981, **130**, 361.
33. J. Toei, *Analyst*, 1988, **113**, 475.
34. *Idem*, *Talanta*, 1989, **36**, 1233.
35. J. Wang, H. Huiliang and W. Kubiak, *Electroanalysis*, 1990, **2**, 127.
36. F. Cañete, A. Ríos, M. D. Luque de Castro and M. Valcárcel, *Anal. Chim. Acta*, 1989, **224**, 127.
37. *Idem*, *Anal. Chem.*, 1988, **60**, 2354.
38. *Idem*, *Anal. Chim. Acta*, 1989, **224**, 169.
39. G. D. Clark, J. Zable, J. Růžicka and G. D. Christian, *Talanta*, 1991, **38**, 119.
40. J. Růžicka and G. D. Marshall, *Anal. Chim. Acta*, 1990, **237**, 329.
41. A. Ríos, M. D. Luque de Castro and M. Valcárcel, *Talanta*, 1985, **32**, 845.
42. J. Toei, *ibid.*, 1988, **35**, 425.
43. M. Agudo, J. Marcos, A. Ríos and M. Valcárcel, *Anal. Chim. Acta*, 1990, **239**, 211.
44. F. J. Krug, H. Bergamin F^o and A. E. G. Zagatto, *ibid.*, 1983, **179**, 103.
45. J. Marcos, A. Ríos and M. Valcárcel, *Anal. Chem.*, 1990, **62**, 2237.
46. J. Marcos, *Private communication*.
47. J. Růžicka, G. D. Marshall and G. D. Christian, *Anal. Chem.*, 1990, **62**, 1861.
48. J. Růžicka and J. Flossdorf, *Anal. Chim. Acta*, 1989, **218**, 291.

A PRACTICAL APPROACH TO HIGH PERFORMANCE CAPILLARY ELECTROPHORESIS WITH BIOSYNTHETIC HUMAN GROWTH HORMONE AS A MODEL PROTEIN

ANDERS VINThER* and HENRIK SØEBERG

The Technical University of Denmark, Department of Chemical Engineering, Building 229,
DK-2800 Lyngby, Denmark

HANS HOLMEGAARD SØRENSEN and ANNE MUNK JESPERSEN

Novo Nordisk A/S, Analytical Development, Lagergårdsvej 2, DL-2820 Gentofte, Denmark

(Received 16 May 1991. Revised 26 June 1991. Accepted 26 June 1991)

Summary—Biosynthetic human Growth Hormone (B-hGH) is a protein comprising 191 amino acids. The molecular weight is 22,125 and the isoelectric point is close to pH 5. Due to the ready availability of closely related analogues B-hGH was used as a model protein thus allowing for the demonstration and evaluation of the high resolution capability of high performance capillary electrophoresis (HPCE). The same apparatus was used throughout the experiments and an optimum signal-to-noise ratio was found at 200 nm. Linearity was observed between peak area, retention time and the hGH concentration or sample introduction time. Baseline separation of hGH, desamido hGH and didesamido hGH was obtained. Examples showing analysis with 1 million theoretical plates per meter, high speed separation, simultaneous analysis of multiple samples, sample stacking, hGH tryptic digest, and hGH lysate are reported. The use of electrophoretic velocities instead of apparent velocities for peak identification is illustrated.

High performance capillary electrophoresis (HPCE) is an analytical technique which permits rapid and efficient charge and/or size based separations of various substances in an automated format. HPCE descends from various electrophoretic and chromatographic techniques, but in its present form it is most often dated back to the 1981–1983 papers by Jorgenson and coworkers.^{1–3}

Since then there has been a growing interest in the technique as judged from the exponentially increasing number of annual publications. At present more than 1000 papers have been published, and the third international meeting on HPCE was held in February 1991 with great success. Reviews of the technique have been presented by Karger *et al.*,⁴ Wallingford and Ewing⁵ and Kuhr,⁶ among others.

Analysis of biomolecules is among the most promising application areas^{7–17} of HPCE (*e.g.*, purity control and identification of byproducts) as high efficiency separations of proteins, peptides, nucleic acid fragments and poly-

saccharides may be obtained. Hence, in the years to come, HPCE is expected to become a major supplement to already existing analytical methods in the biotechnological industries.

Biosynthetic human Growth Hormone (B-hGH) comprises 191 amino acids (Fig. 1), the molecular weight is 22,125 and the isoelectric point is close to pH 5. The hGH is concerned with somatic growth and is produced in the anterior pituitary by the eosinophil or α -cells.¹⁸ As a pharmaceutical, hGH has so far been used primarily in the treatment of retarded growth and dwarfism caused by underproduction of hGH in the growth period.

In this paper B-hGH will be used as a model protein in order to illustrate some of the characteristics of HPCE. By choosing hGH as the model protein the ready availability of closely related analogues allows for the demonstration and evaluation of the high resolution capability of HPCE.

EXPERIMENTAL

Reagents

Biosynthetic human Growth Hormone (B-hGH) was from Novo Nordisk A/S

*Author for correspondence.

(Gentofte, Denmark). The B-hGH samples contained various preservatives. Tricine (N-[Tris-(hydroxymethyl)methyl]glycine) and sodium chloride were purchased from Fluka Chemie AG (Buchs, Switzerland). Citrate and CAPS [3-(Cyclohexylamino)-1-propanesulphonic acid] buffers were from Applied Biosystems (Foster City, CA, USA). Fused-silica capillaries were obtained from Polymicro Technologies (Phoenix, AZ, USA). Peak areas were integrated on a Shimadzu C-R5A integrator (Kyoto, Japan).

Procedures

All the experiments were performed on an Applied Biosystems (ABI) Model 270A CE instrument (Foster City, CA, USA). The fused-silica capillaries had an internal diameter of 50 μm and an outer diameter of 192 μm . Most of the capillary from the introduction end to the detector (termed the effective capillary length) was surrounded by an airbath kept at a constant temperature. Samples were introduced by means of a 4.95-in Hg (16.8 kPa) vacuum. The x-axis values of each electropherogram are

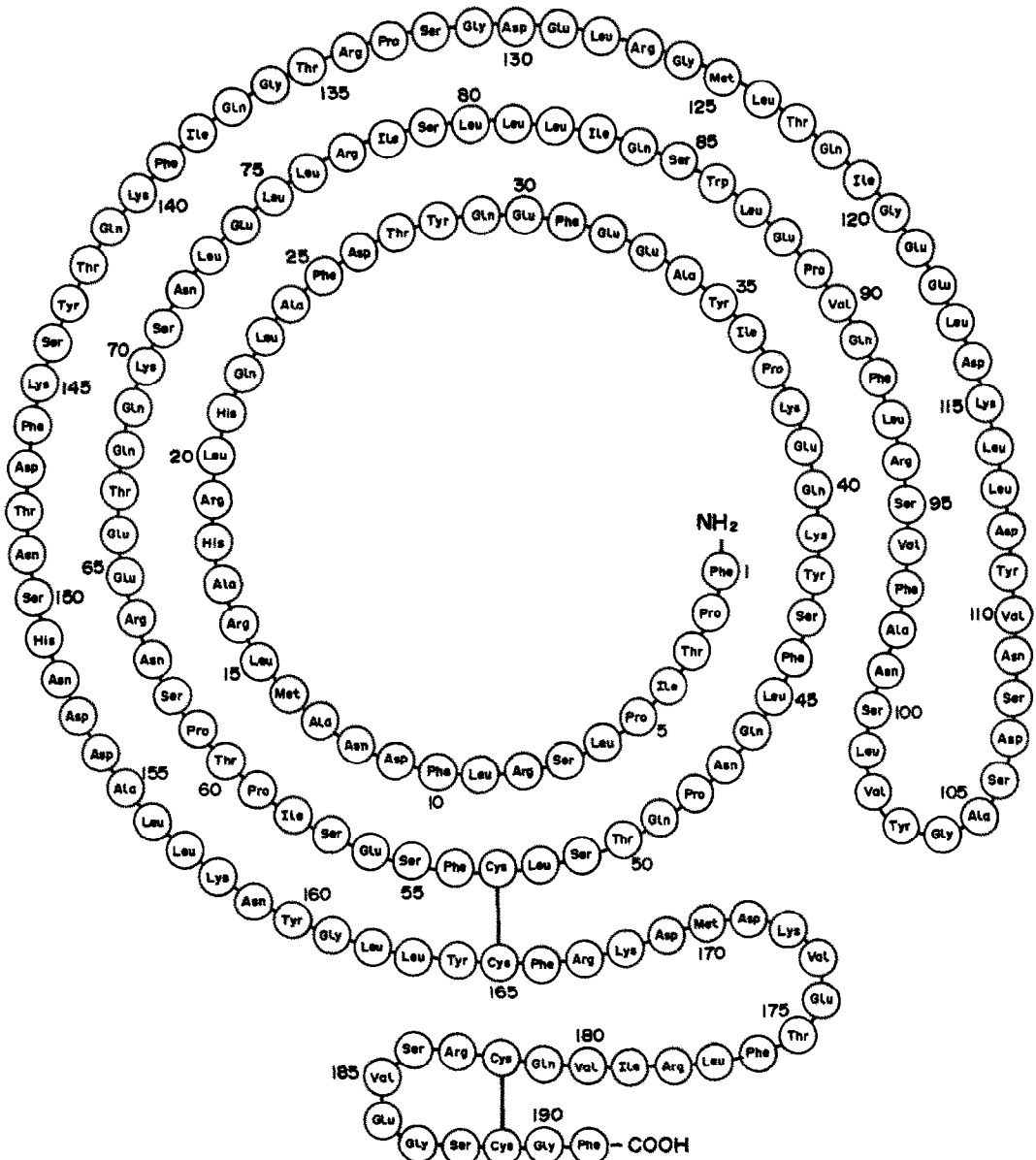


Fig. 1. Primary sequence of human Growth Hormone (hGH). The protein comprises 191 amino acids, the molecular weight is 22,125 and the isoelectric point is close to pH 5.

in minutes. Other experimental conditions are given in the figure legends.

RESULTS AND DISCUSSION

Basically, carrying out HPCE analysis is very simple. A typical sequence comprises four cycles:

- (1) The capillary is flushed with *e.g.*, 0.1M sodium hydroxide, thus ionizing the silanol groups of the fused-silica capillary inner surface.
- (2) The capillary is filled with running buffer.
- (3) Sample is introduced by siphoning or by applying a pressure or voltage gradient between the two capillary ends.
- (4) HPCE analysis/electrophoretic separation of the analytes is initiated by applying a voltage (typically 50–500 V/cm) between the two capillary ends, which are immersed in vials containing the running buffer.

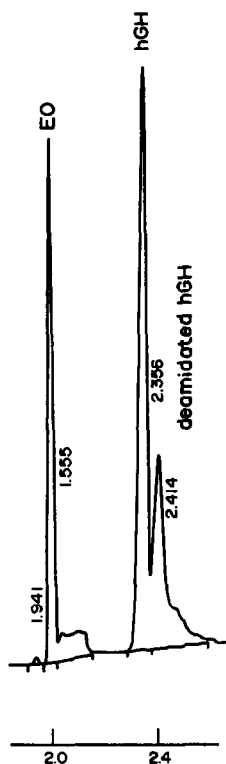


Fig. 2. High speed separation of hGH and deamidated hGH. The total analysis time is less than 3 min. Peak EO marks the electroosmotic flow (flow of neutrals). The x-axis scale is in minutes, while the y-axis scale is in arbitrary absorbance units. Experimental conditions: Buffer; pH 8.0, 10mM tricine, 20mM NaCl. Sample; 0.2 mg/ml B-hGH in distilled water and allowed to degrade several weeks at ambient temperature, introduced for 0.5 sec by 16.8 kPa vacuum. Detection at 200 nm, 0.5 sec risetime. Capillary length 55 cm (total), 30 cm (effective). 20 kV applied. Temperature; 30°.

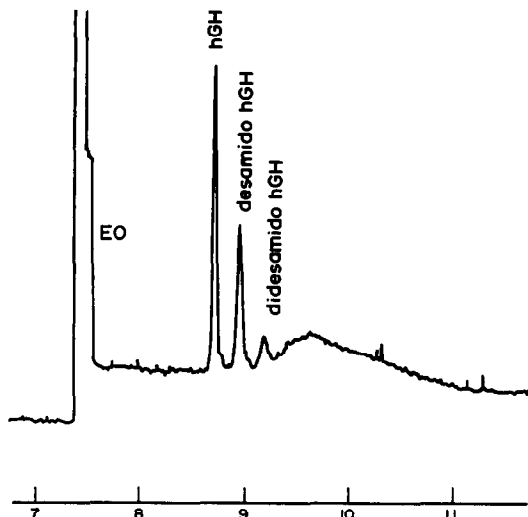


Fig. 3. Baseline separation of hGH, desamido and didesamido hGH. Peak EO marks the neutrals (electroosmotic flow). The x-axis scale is in minutes, while the y-axis scale is in arbitrary absorbance units. Experimental conditions: Buffer; pH 8.0, 10mM tricine. Sample; 0.1 mg/ml B-hGH in distilled water and allowed to degrade several weeks at ambient temperature, introduced for 1.0 sec by 16.8 kPa vacuum. Detection at 200 nm, 0.5 sec risetime. Capillary length 100 cm (total), 75 cm (effective). 20 kV applied. Temperature; 27°.

Detection is most often accomplished on-line by means of UV light,^{19–22} though other detection means have been applied (*e.g.*, fluorescence,^{23–29} mass spectrometry,^{30–36} amperometry,³⁷ conductivity).^{20, 38–39} The detector signal *vs.* analysis time takes the form of an electropherogram. Figure 2 shows the separation of hGH and desamido hGH in pH 8.0 tricine buffer. During deamidation hGH acquires an additional negative charge. This makes separation of hGH and its deamidated form very suitable for capillary electrophoresis. The figure illustrates that high speed separations can be performed in HPCE. However, while total analysis time is less than 3 min, the resolution of hGH and desamido hGH is poor. If more time is allowed for the two peaks to separate, baseline resolution is obtained. This is shown in Fig. 3 for another partly degraded hGH sample. Didesamido hGH elutes shortly after and is baseline resolved from the desamido hGH peak. With a typical analysis time of 5–15 min HPCE can be used on-line to monitor reactions with time constants in the minutes to hours range.

In the free solution capillary electrophoresis (FSCE) mode,⁷ analytes migrate by the combined action of electrophoresis and electroosmosis. Electroosmosis is usually explained

by the Gouy–Chapman–Stern model.⁴⁰ At pH values above *ca.* 2 the silanol groups of the fused-silica capillary inner surface are partly ionized when in contact with the buffer solution. Electroneutrality is attained by hydronium cations in the bulk solution. This results in a bulk flow towards the cathode when voltage is applied. The electroosmotic flow increases with increasing pH and decreasing buffer ionic strength.⁴⁰ At neutral pH values the electroosmotic flow is much stronger than most peptide/protein electrophoretic velocities. Hence, positively as well as negatively charged peptides/proteins can be analysed in the same run as they are both swept towards the detector end (cathodic end) of the capillary. Peak EO in Figs. 2–3 marks the electroosmotic flow. The numerical v_{EO}/v_{EP} ratio (v_{EO} = electroosmotic velocity, v_{EP} = electrophoretic velocity) was *ca.* 5. In Fig. 2 the electroosmotic flow was *ca.* 15 cm/min or *ca.* 0.3 μ l/min, which equals 155 ml/year!

Mostly due to viscosity changes,^{41,42} the electroosmotic velocity increases by 2–3% per °C. The electrophoretic velocity also increases at increasing temperatures. A linear v_{EO} -T and v_{EP} -T relationship was found in the range 25–55°.

When a new running buffer is introduced, an “equilibrium” between the new buffer and the capillary surface must be established. During the equilibrium period (which can last for minutes, hours or even days) the buffer affects

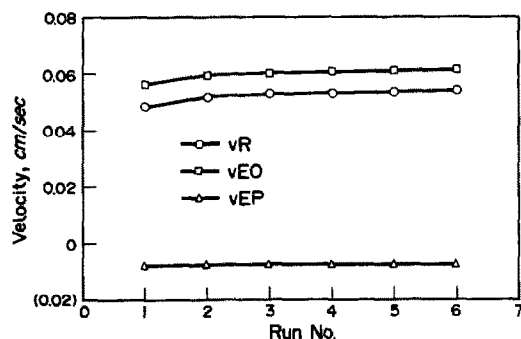


Fig. 4. Electroosmotic (v_{EO} , cm/sec), electrophoretic (v_{EP} , cm/sec), and apparent ($v_R = v_{EO} + v_{EP}$, cm/sec) velocity *vs.* the run number after the capillary had been thoroughly flushed with 0.1M NaOH. The velocity is given relative to the anode. As the negatively charged hGH molecules migrate towards the anode (opposite the electroosmotic flow), negative velocity values are obtained. Experimental conditions: Buffer; pH 8.0, 50mM tricine. Sample; 0.5 mg/ml B-hGH in distilled water, introduced for 0.5 sec by 16.8 kPa vacuum. Detection at 200 nm. Capillary length 50 cm (total), 25 cm (effective). 5 kV applied. Temperature; 30°.

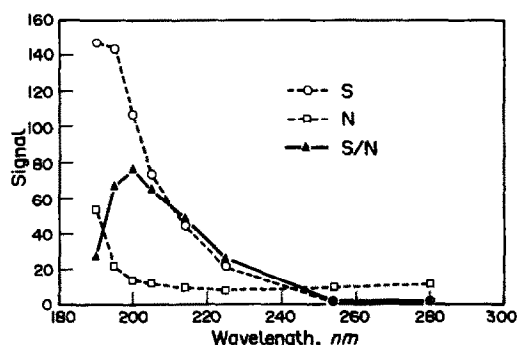


Fig. 5. Signal (S, Peak area/ t_R , arbitrary units), noise level (N, arbitrary units) and S/N ratio on the ABI Model 270A detector *vs.* wavelength. An optimum hGH signal-to-noise (S/N) ratio was obtained at 200 nm. Experimental conditions: Buffer; pH 8.0, 10mM tricine. Sample; 0.1 mg/ml B-hGH in distilled water, introduced for 1.0 sec by 16.8 kPa vacuum. Variable wavelength 190–280 nm, 0.2 sec risetime. Capillary length 70 cm (total), 50 cm (effective). 20 kV applied. Temperature; 30°.

the charge density of the capillary wall and thereby the electroosmotic flow. An example of this is shown in Fig. 4. A 50- μ m inner diameter capillary was rinsed thoroughly with 0.1M sodium hydroxide. First manually by means of a syringe, followed by a 20.35-in Hg (68.9 kPa) vacuum for *ca.* 30 min after the capillary had been aligned in the CE instrument. Immediately following this rinsing procedure 6 identical runs were carried out in a pH 8.0 tricine buffer. Prior to each run the capillary was flushed with 0.1M sodium hydroxide for 2 min by the 20.35-in Hg vacuum. (This results in *ca.* 3 μ l of the sodium hydroxide solution being sucked through the capillary. The internal volume of the capillary was *ca.* 1 μ l). Figure 4 depicts the measured v_{EP} , v_{EO} and v_R ($v_R = v_{EO} + v_{EP}$, the apparent velocity) values. The negatively charged hGH molecules migrate towards the anode while the electroosmotic flow is towards the cathode. As the velocity is written relative to the anode the hGH v_{EP} values are negative. While the v_{EO} value is not constant in the initial runs, v_{EP} is almost constant already from the first or second run. Hence, if absolute v_{EP} values are used instead of the v_R values, velocity based peak identification can be performed already from the first runs. As the residuals are not randomly distributed around the mean v_R value there is no point in comparing v_{EP} and v_R relative standard deviations (RSDs) of the six runs.

The ratio of hGH to total hGH and desamido hGH peak area per retention time was, however, randomly distributed around the mean with a RSD equal to 0.6% for the six runs.

The peptide bond shows a maximum absorbance at 193 nm. However, if the detector wavelength is set below 200 nm the noise level increases dramatically with an optimum signal-to-noise (S/N) level being governed by the quality of the UV absorbance detector. A series of experiments was performed on the ABI Model 270A CE instrument at 190, 195, 200, 205, 214, 225, 254 and 280 nm. The hGH concentration was 0.1 mg/ml. An optimum S/N ratio of 76 was obtained at 200 nm (Fig. 5). Changing the wavelength from 214 nm to 200 nm improved the S/N ratio by more than 50% with this specific detector.

In order to examine whether peak area per retention time (t_R) or peak height should be used for quantitative HPCE analysis two sets of experiments were performed. (Peak area is inversely proportional to the velocity of the analyte zone when it passes the detector. Division of peak area by the analyte zone retention time accounts for this difference.)

In the first set of experiments, sample was introduced for 5 sec (~ 12 nl) while the hGH concentration was varied in the range 7.8–1000 $\mu\text{g/ml}$. Peak area/ t_R and peak height were plotted *vs.* hGH concentration (Fig. 6). Linearity between hGH concentration and peak area/ t_R was observed in the range 16–1000 $\mu\text{g/ml}$. At the lowest hGH concentration, 7.8 $\mu\text{g/ml}$, there was a positive deviation from linearity, which may be ascribed to the integration of hGH and monodesamido hGH as one peak. When plotting peak height *vs.* hGH concentration linearity was only observed in the

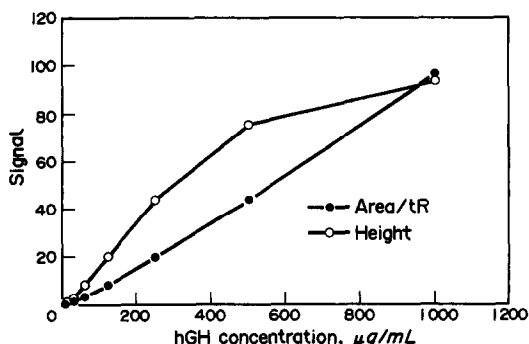


Fig. 6. Peak area/ t_R (arbitrary units) and peak height (arbitrary units) *vs.* the hGH concentration. Linear regression of the area/ t_R points in the range 16–1000 $\mu\text{g/ml}$ gave a correlation coefficient equal to $r = 0.998$. Experimental conditions: Buffer; pH 8.0, 10mM tricine, 20mM NaCl. Sample; 7.8–1000 $\mu\text{g/ml}$ B-hGH in distilled water, introduced for 5.0 sec by 16.8 kPa vacuum. Wavelength; 200 nm, 1.0 sec risetime. Capillary length 109 cm (total), 90 cm (effective). 30 kV applied. Temperature; 30°.

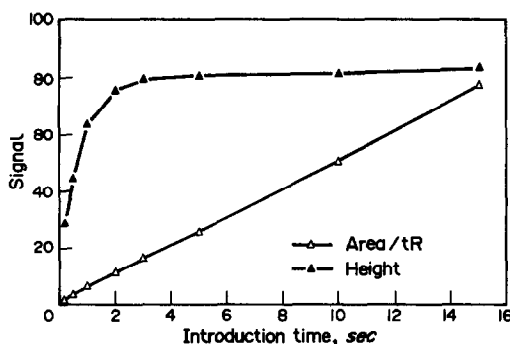


Fig. 7. Peak area/ t_R (arbitrary units) and peak height (arbitrary units) *vs.* sample introduction time (sec.). Linear regression on all peak area/ t_R data points gave a correlation coefficients equal to $r = 1.000$. Experimental conditions: Buffer; pH 8.0, 10mM tricine. Sample; 0.1 mg/ml B-hGH in distilled water, introduced for 0.2–15.0 sec by 16.8 kPa vacuum. Wavelength; 200 nm, 1.0 sec risetime. Capillary length 100 cm (total), 75 cm (effective). 15 kV applied. Temperature; 30°.

range 16–250 $\mu\text{g/ml}$. The reason for the negative deviation from linearity above 250 $\mu\text{g/ml}$ hGH is interpreted to be an effect of sample overload, which causes increased dispersion. Sample overload, which is explained by the use of the Kohlrausch regulation function,^{43,44} occurs when the analyte ion (hGH) concentration cannot be neglected relative to the background electrolyte concentration. Increasing the hGH concentration decreased the number of theoretical plates (the theoretical plate number was higher by a factor of *ca.* 7 at 7.8 $\mu\text{g/ml}$ compared to 1000 $\mu\text{g/ml}$ hGH).

In the second set of experiments the hGH concentration was kept constant at 0.1 mg/ml while the introduction time, t_{inj} , varied in the range 0.2–15.0 sec (~ 0.5 –35.6 ml). Linearity was observed between peak area/ t_R and t_{inj} in the entire t_{inj} range (Fig. 7). When peak height was plotted *vs.* t_{inj} , linearity was only observed in the range 0.2–1.0 sec (Fig. 7). In this set of runs the deviation from linearity is caused by the sample plug originally introduced being a major contributor to the total analyte zone peak width.⁴⁵ Hence, at long introduction times the analyte peak changes appearance from gaussian towards plug shape. The analyte zone length can be compressed by the use of stacking conditions. This is exemplified in a subsequent paragraph.

Based on the analysis of a 0.02 mg/ml hGH sample solution and a detector risetime of 1.0 sec the detection limit was calculated to be 19 pg of hGH (~ 850 attomole). While the mass sensitivity of UV detection in general is higher in HPCE than HPLC, the concentration

sensitivity is poorer as the analyte in HPCE is detected in a very small sample volume (typically 1–10 nl).

One of the attractive features of HPCE is the possibility of obtaining high efficiencies with theoretical plate numbers in the order of 10^5 – 10^7 per meter,¹ *e.g.*, for proteins and peptides. In Fig. 8 one million theoretical plates per meter was obtained for the hGH peak. Sample was introduced for 0.2 sec thus introducing a volume of *ca.* 0.5 nl. One of the reasons for the high number of theoretical plates is that the electroosmotic bulk flow profile is much closer to plug flow than to laminar flow.^{45–47}

The dispersive factors in HPCE can be grouped into six additive variance terms,⁴⁵ axial and radial diffusion, sample zone length, detector size, chromatographic effects and sample overload. All six terms are effected by temperature changes.

Dispersion due to chromatographic effects is caused by electrostatic attractions between the analyte molecule and the negatively charged fused-silica capillary surface. In general proteins and peptides have a strong tendency for adsorption to the capillary wall, thus resulting in severe peak tailing or even total adsorption. The protein-capillary wall coulombic inter-

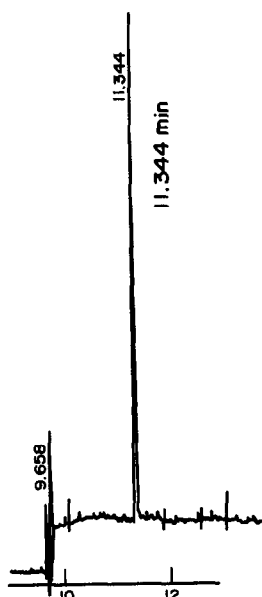


Fig. 8. 1,000,000 theoretical plates (N) per meter was obtained for hGH at 0.2 sec introduction. *Ca.* 0.5 nl was introduced. N was calculated as $5.54 \cdot (t_R/\omega_{1/2})^2$, where t_R is the hGH retention time, while $\omega_{1/2}$ is the peak width at half hGH peak height. The x-axis scale is in minutes and the y-axis scale is in arbitrary absorbance units. Experimental conditions are as for Fig. 7 except that sample was introduced for 0.2 sec.

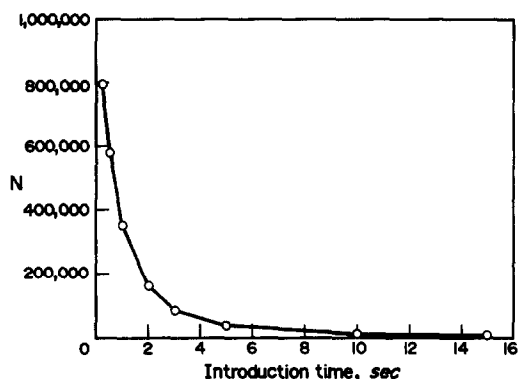


Fig. 9. The number of theoretical plates (N) decreases exponentially with increasing sample introduction time (t_{inj} , sec). Experimental conditions are given in Fig. 7.

actions can be minimized in several ways. If analysis is performed at a pH value above the isoelectric point of the protein, it is negatively charged thus being repelled from the capillary wall. That approach has been used in most of the experiments reported here as the hGH isoelectric point is *ca.* pH 5, while analysis was performed at pH 8.0. Lowering the pH of the running buffer to a value where most of the negative charges are titrated off the capillary wall eliminates most of the electrostatic interactions even though the protein is positively charged.^{9,10} Another approach is to coat the capillary surface either through covalent bonding of chemical agents to the capillary wall^{9,48} or dynamically.^{12,49–52} Dynamic coating of the capillary is performed by the addition of ionic species to the buffer solution. This results in a competition between the cationic ions and the analyte molecules for the adsorption sites on the capillary surface.

Huang *et al.*⁵³ discussed that the introduction term of the total variance could only be neglected at very small sample plug lengths. This is demonstrated in Fig. 9. The introduction time of a 0.1 mg/ml hGH sample was varied in the range 0.2–15.0 sec (\sim 0.5–35.6 nl). The number of theoretical plates decreases exponentially as a function of increasing introduction time. At a 0.2-sec introduction time the introduction term was calculated to contribute *ca.* 7% of the total variance, while at a 15.0-sec introduction time the contribution was *ca.* 99%.⁴⁵

One way of improving the number of theoretical plates is to stack the originally introduced sample zone. Sample stacking (concentration of the analyte zone) is the process occurring when voltage is applied along the capillary tube containing a sample plug with a lower specific

conductivity than the surrounding running buffer. As the electric field strength is inversely proportional to the specific conductivity of the liquid, the field strength is higher along the sample plug than to the running buffer. In this way the electrophoretic velocity, which is proportional to the field strength, increases and the ionic analyte zone is narrowed. This "reversed dispersion" is termed stacking.⁴⁵ An example of stacking is shown in Fig. 10. A hGH sample was either diluted in distilled water (stacking conditions) or in the running buffer (non-stacking conditions) to a concentration of 0.1 mg/ml. At stacking conditions the ratio of the specific conductivity of the running buffer to that of the sample zone was *ca.* 16. Inherently, at non-stacking conditions the corresponding ratio was 1. Identical runs were carried out only differing by the two samples. Figures 10(a) and (b) show part of the two electropherograms with identical co-ordinate scalings. Turning from non-stacking to stacking conditions the number of theoretical plates was improved from 113,000 to 345,000 per meter.

Due to the low dispersion during HPCE analysis the voltage can be shut off for short periods of time with no significant loss of peak efficiency. In Fig. 11(a) the sample was introduced and normal HPCE analysis was carried out with a retention time of *ca.* 8.8 min. In Fig. 11(b) the applied voltage was shut off every 5 min and a new sample introduced. This means that there were always several hGH sample zones in the capillary. No significant peak broadening caused by the power shut-off period was observed. Hence, multiple samples can be run simultaneously in the capillary (provided the sample components elute closely) thus reducing the average analysis time.

At Novo Nordisk A/S recombinant hGH is produced intracellularly by *E. coli* cells. During the fermentation period the microorganisms produce hGH extended with 4 amino acids (4aa-hGH). During down-stream processing the 4 amino acids are removed thus yielding a molecule having an amino acid sequence, which is identical to that produced in humans. Figure 12 is an electropherogram showing baseline resolution of B-hGH and 4aa-hGH. Furthermore, monodeamidated forms of hGH and 4aa-hGH are also seen in the electropherograms.

During the down-stream processing after the hGH fermentation period the cells are lysed and

filtrated. Figure 13 shows an electropherogram of a fermentation broth sample after 4aa-hGH had been "extracted" with acetic acid and filtrated. 4aa-hGH was spiked to the sample. The running buffer was a pH-11.0 CAPS solution. The retention time of the 4aa-hGH peak was *ca.* 14 min but no baseline separation of 4aa-hGH and the other sample components was obtained. In order to use this method for reliable quantitative calculations further improvements in resolution should be made. The figure illustrates that HPCE can be used (on-line) to monitor, *e.g.*, products and metabolites

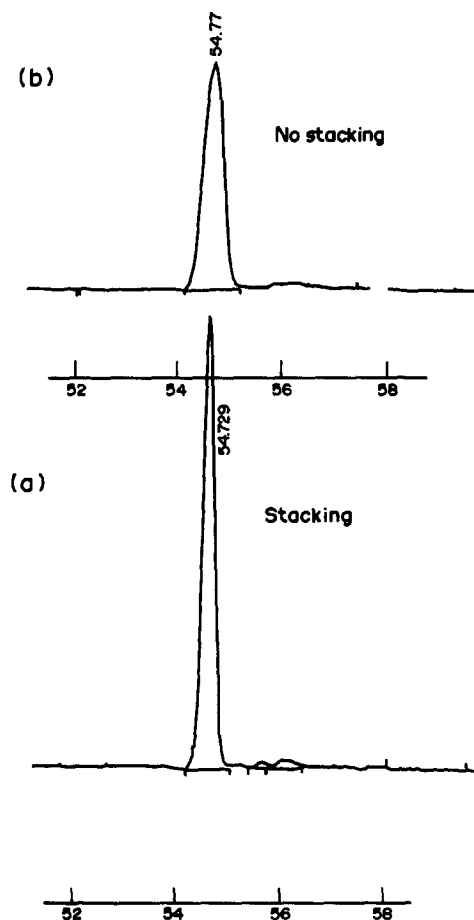
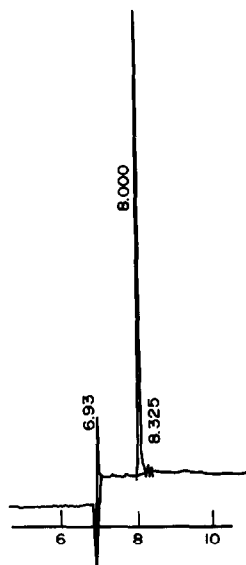


Fig. 10. A lower specific conductivity of the sample solution relative to the running buffer results in sample stacking when voltage is applied. The analyte zone is reduced in length and a higher number of theoretical plates is obtainable. (a) Stacking and (b) non-stacking conditions. The x-axis scale is in minutes, while the y-axis scale is in arbitrary absorbance units. Experimental conditions: Buffer; pH 8.0, 10mM tricine, 25mM NaCl. Sample; 0.1 mg/ml B-hGH in (a) distilled water (stacking) or (b) running buffer (no stacking), introduced for 3.0 sec by 16.8 kPa vacuum. Detection at 200 nm, 1.0 sec risetime. Capillary length 100 cm (total), 75 cm (effective). 5 kV applied. Temperature; 27°.

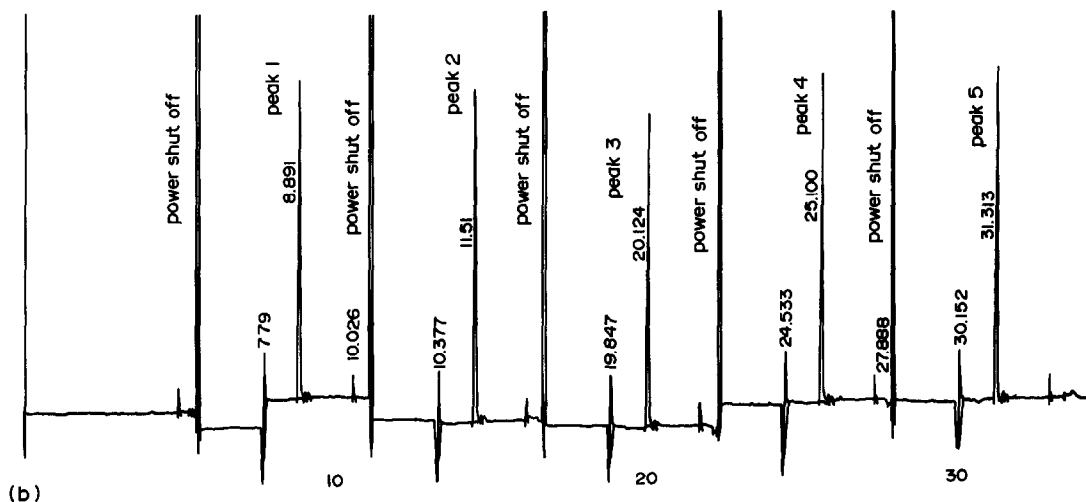
in fermentation broths. In general, only filtration or centrifugation is required as sample pretreatment.

Trypsin splits peptide bonds on the carboxyl side of lysine and arginine residues.⁵⁴ Trypsin digested hGH contains 21 fragments, two of which are crosslinked by disulphide bridges.⁵⁵ The fragments range in size from 147 to 3763D. Reversed phase HPLC (RP-HPLC) is often used to make a chromatographic fingerprint of

the tryptic digest peptide mixture thus yielding, *e.g.*, purity information on the hGH molecule. Fingerprints can also be obtained by FSCE. As analytes are separated according to fundamentally different principles in RP-HPLC and FSCE the two methods are orthogonal,^{14,15} and analytes which are not separated by RP-HPLC might be separated by FSCE and vice versa. If no differences are found it increases the confidence level of the first result. If differences



(d)



(b)

Fig. 11. Multiple sample analysis. Due to low dispersion in FSCE the voltage can be shut off for short periods of time with no significant loss of peak efficiency. The x-axis scale is in minutes, while the y-axis scale is in arbitrary absorbance units. In (a) the sample was introduced and analysis was carried out with a retention time of *ca.* 8.8 min. In (b) the applied potential was shut off every 5 min and a new sample introduced. Hence, multiple samples were run simultaneously in the capillary. Experimental conditions: Buffer; pH 8.0, 10mM tricine. Sample; 0.1 mg/ml B-hGH in distilled water, introduced for 1.0 sec by 16.8 kPa vacuum. Detection at 200 nm, 0.5 sec risetime. Capillary length 100 cm (total), 75 cm (effective). 20 kV applied. Temperature; 27°.

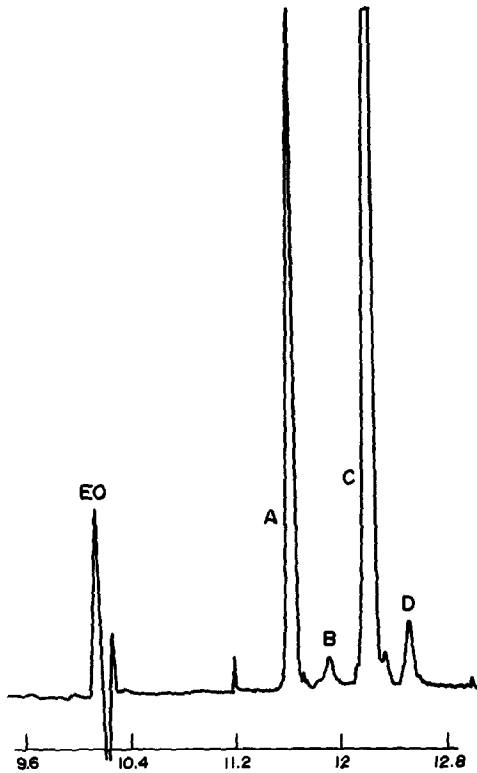


Fig. 12. Separation of hGH (peak A), desamido hGH (peak B), hGH extended with 4 amino acids (4aa-hGH, peak C) and desamido 4aa-hGH (peak D). Peak EO marks the neutrals. The x-axis scale is in minutes, while the y-axis scale is in arbitrary absorbance units. Experimental conditions: Buffer; pH 8.0, 10mM tricine, 20mM NaCl. Sample; 0.1 mg/ml B-hGH and 0.2 mg/ml 4aa-hGH in distilled water, introduced for 1.0 sec by 16.8 kPa vacuum. Detection at 200 nm, 1.0 sec risetime. Capillary length 105 cm (total), 80 cm (effective). 20 kV applied. Temperature; 27°.

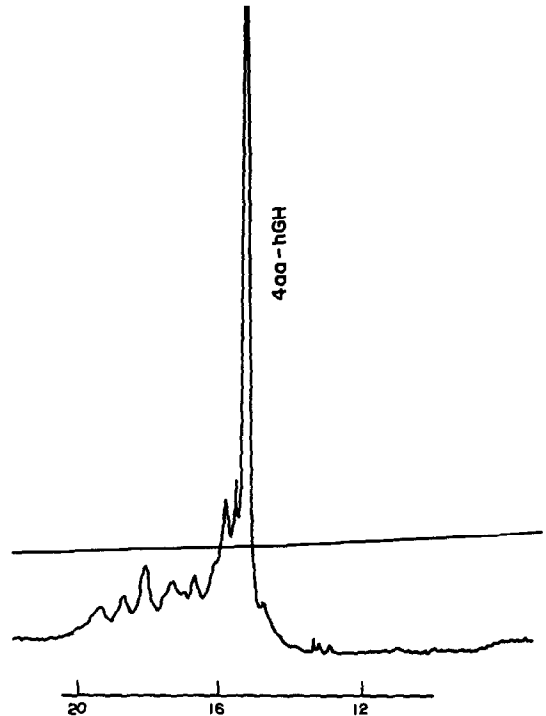


Fig. 13. 4aa-hGH fermentation broth. 4aa-hGH was "extracted" by the addition of acetic acid and filtrated before being subjected to HPCE analysis. The x-axis scale is in minutes, while the y-axis scale is in arbitrary absorbance units. Experimental conditions: Buffer; pH 11.0, 10mM CAPS. Sample; 4aa-hGH lysate after filtration. 4aa-hGH was spiked to the sample, introduced for 1.0 sec by 16.8 kPa vacuum. Detection at 200 nm, 1.0 sec risetime. Capillary length 109 cm (total), 90 cm (effective). 30 kV applied. Temperature; 27°.

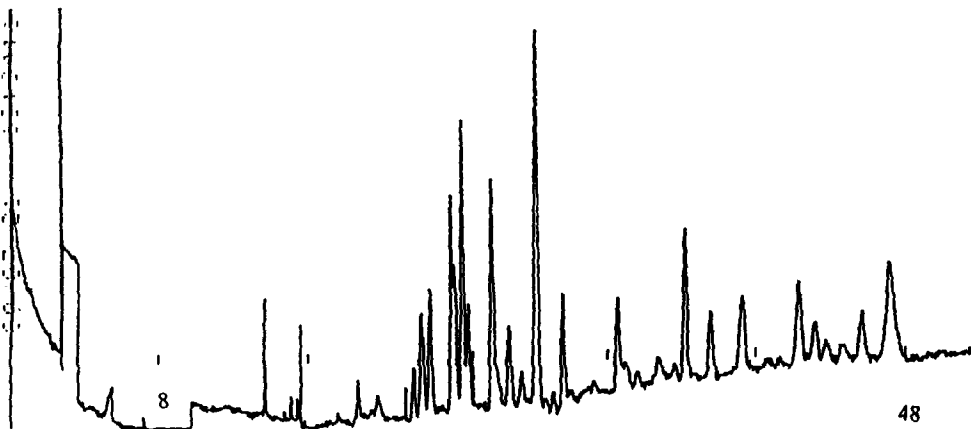


Fig. 14. Tryptic digest of hGH. Nothing was done in order to identify the individual peaks in the electropherogram. The x-axis scale is in minutes, while the y-axis scale is in arbitrary absorbance units. Experimental conditions: Buffer; pH 2.5, 20mM citrate. Sample; tryptic digest of B-hGH in pH 7.8 50mM tris, 2mM CaCl₂, introduced for 1.0 sec by 16.8 kPa vacuum. Detection at 200 nm, 1.0 sec risetime. Capillary length 109 cm (total), 90 cm (effective). 25 kV applied. Temperature; 30°.

are discovered it suggests further action maybe needed subject to the circumstance.

A 1-ml volume of 1 mg/ml hGH sample was digested with 10 μ l of 1 mg/ml trypsin for 6 hr at 37° and subjected to FSCE analysis. Figure 14 is an electropherogram of the trypsin digested hGH sample obtained in a pH 2.5 buffer. Nothing was done to identify the individual peaks of the electropherograms (*e.g.*, by spiking analysis) or to improve separations.

CONCLUSIONS

We have looked at some of the characteristics of HPCE by illustrative example electropherograms of "pure" as well as fermentation broth samples. The characteristics include:

(i) Low sample and reagent consumption. Typically: 1–10 nl sample for introduction; 50–150 ml reagent per year.

(ii) High speed separations. Typically: 1–15 min analysis time.

(iii) High separation efficiencies. Typically: 10^4 – 10^6 theoretical plates per meter.

(iv) High mass (but poor concentration) sensitivity. hGH: 20 pg (1 fmole).

(v) Non-toxic chemicals are usually employed.

(vi) Experimental conditions are changed by changing the running buffer rather than changing the column.

(vii) The presence of a strong electroosmotic flow towards the cathode in untreated fused silica capillaries.

Furthermore the following parameters were examined:

(i) Linearity between hGH concentration/introduction time and the peak area per retention time/peak height.

(ii) Absorbance at various wavelengths.

(iii) Stacking as a means to increase the number of theoretical plates.

(iv) Equilibrium period when introducing a new buffer.

We found that one of the major advantages of HPCE is the possibility of obtaining high efficiency separations (of *e.g.*, large molecules, fermentation broth) at high speed, which makes it an obvious on-line analytical technique.

REFERENCES

- J. W. Jorgenson and K. D. Lukacs, *Anal. Chem.*, 1981, **53**, 1298.
- Idem*, *J. Chromatog.*, 1981, **218**, 209.
- Idem*, *Science*, 1983, **222**, 266.
- B. L. Karger, A. S. Cohen and A. Guttman, *J. Chromatog.*, 1989, **492**, 585.
- R. A. Wallingford and A. G. Ewing, *Adv. Chromatog.*, 1989, **29**, 1.
- W. G. Kuhr, *Anal. Chem.*, 1990, **62**, 403R.
- P. D. Grossman, J. C. Colburn, H. H. Lauer, R. G. Nielsen, R. M. Riggin, G. S. Sittampalam and E. C. Rickard, *ibid.*, 1989, **61**, 1186.
- H. H. Lauer and D. McManigill, *ibid.*, 1986, **58**, 166.
- R. M. McCormick, *ibid.*, 1988, **60**, 2322.
- A. Vinther, S. E. Bjørn, H. H. Sørensen and H. Sæberg, *J. Chromatog.*, 1990, **516**, 175.
- M. V. Novotny, K. A. Cobb and J. Liu, *Electrophoresis*, 1990, **11**, 735.
- M. M. Bushey and J. W. Jorgenson, *J. Chromatog.*, 1989, **480**, 301.
- H. Lüdi, E. Gassmann, H. Grossenbacher and W. Märki, *Anal. Chim. Acta*, 1988, **213**, 215.
- J. Frenz, S.-L. Wu and W. S. Hancock, *J. Chromatog.*, 1989, **480**, 379.
- R. G. Nielsen, R. M. Riggin and E. C. Rickard, *ibid.*, 1989, **480**, 393.
- P. D. Grossman, J. C. Colburn and H. H. Lauer, *Anal. Biochem.*, 1989, **179**, 28.
- N. Banke and K. Hansen, Submitted to *J. Chromatog.*
- J. H. Green, *An Introduction to Human Physiology*, 4th Ed., p. 161. Oxford University Press, Oxford, 1985.
- Y. Walbroehl and J. W. Jorgenson, *J. Chromatog.*, 1984, **315**, 135.
- F. Foret, M. Deml, V. Kahle and P. Bocek, *Electrophoresis*, 1986, **7**, 430.
- A. E. Bruno, E. Gassmann, N. Periclé and K. Anton, *Anal. Chem.*, 1989, **61**, 876.
- S. R. Weinberger, Poster TP-120, *1st International Symposium on High Performance Capillary Electrophoresis*, HPCE'89, Boston, 1989, April 10–12.
- J. S. Green and J. W. Jorgenson, *J. Chromatog.*, 1986, **352**, 337.
- B. Nickerson and J. W. Jorgenson, *ibid.*, 1989, **480**, 157.
- S. Wu and N. J. Dovichi, *ibid.*, 1989, **480**, 141.
- A. S. Cohen, D. R. Najarian and B. L. Karger, *ibid.*, 1990, **516**, 49.
- D. J. Rose and J. W. Jorgenson, *ibid.*, 1988, **447**, 117.
- W. G. Kuhr and E. S. Yeung, *Anal. Chem.*, 1988, **60**, 1832.
- L. Gross and E. S. Yeung, *J. Chromatog.*, 1989, **480**, 169.
- R. D. Smith and H. R. Udseth, *Nature*, 1988, **331**, 639.
- R. D. Smith and C. J. Barinaga and H. R. Udseth, *Anal. Chem.*, 1988, **60**, 1948.
- R. D. Smith, J. A. Loo, C. J. Barinaga, C. G. Edmonds and H. R. Udseth, *J. Chromatog.*, 1989, **480**, 211.
- E. D. Lee, W. Mück, J. D. Henion and T. R. Covey, *ibid.*, 1988, **458**, 313.
- M. A. Moseley, L. J. Deterding, K. B. Tomer and J. W. Jorgenson, *Rapid Commun. Mass Spectrom.*, 1989, **3**, 87.
- R. M. Caprioli, W. T. Moore, M. Moore, B. B. DaGue, K. Wilson and S. Moring, *J. Chromatog.*, 1989, **480**, 247.
- R. W. Hallen, C. B. Shumate, W. F. Siems, T. Tsuda and H. H. Hill Jr, *ibid.*, 1989, **480**, 233.
- R. A. Wallingford and A. G. Ewing, *Anal. Chem.*, 1987, **59**, 1762.

38. F. E. P. Mikkers, F. M. Everaerts and Th. P. E. M. Verheggen, *J. Chromatog.*, 1979, **169**, 11.
39. X. Huang, T. K. J. Pang, M. J. Gordon and R. N. Zare, *Anal. Chem.* 1987, **59**, 2747.
40. A. W. Adamson, *Physical Chemistry of Surfaces*, Chapter 5, John Wiley & Sons, 1982.
41. A. Vinther and H. Sørenberg, *J. Chromatog.*, 1991, **559**, 27.
42. E. Grushka, R. M. McCormick and J. J. Kirkland, *Anal. Chem.*, 1989, **61**, 241.
43. F. Kohlrausch, *Ann. Phys. Chem.*, 1897, **62**, 209.
44. F. M. Everaerts, J. L. Beckers and Th. P. E. M. Verheggen, *Isotachopheresis, Theory, Instrumentation and Applications*, Elsevier, Amsterdam, 1976.
45. A. Vinther and H. Sørenberg, *J. Chromatog.*, 1991, **559**, 3.
46. C. L. Rice and R. Whitehead, *J. Phys. Chem.*, 1965, **69**, 4017.
47. M. Martin, G. Guiochon, Y. Walbroehl and J. W. Jorgenson, *Anal. Chem.*, 1985, **57**, 559.
48. S. Hjertén, *J. Chromatog.*, 1985, **347**, 191.
49. J. S. Green and J. W. Jorgenson, *ibid.*, 1989, **478**, 63.
50. K. D. Altria and C. F. Simpson, *Chromatographia*, 1987, **24**, 527.
51. T. Tsuda, *J. High Res. Chromatog. & Chromatog. Commun.* 1987, **10**, 622.
52. K. D. Altria and C. F. Simpson, *Anal. Proc.*, 1988, **25**, 85.
53. X. Huang, W. F. Coleman and R. N. Zare, *J. Chromatog.*, 1989, **480**, 95.
54. L. Stryer, *Biochemistry*, 2nd Ed., W. H. Freeman and Company, San Francisco, 1981.
55. T. Christensen, J. J. Hansen, H. H. Sørensen and J. Thomsen, *High Performance Liquid Chromatography in Biotechnology*, Chapter 9, John Wiley & Sons, Inc., W. S. Hancock (ed.), 1990.

PERMEATION-SOLID ADSORBENT SAMPLING AND GC ANALYSIS OF FORMALDEHYDE

CHANSA MUNTUTA-KINYANTA and JAMES K. HARDY*

Department of Chemistry, The University of Akron, Akron, Ohio 44325-3601, U.S.A.

(Received 9 April 1991. Revised 25 June 1991. Accepted 26 June 1991)

Summary—A passive method with membrane permeation sampling for the determination of time-weighted-average (TWA) concentration of formaldehyde in air is described. The sampling device was constructed by affixing an unbacked dimethyl silicone membrane to the base of a glass tube and by sealing the top with a rubber stopper. Formaldehyde permeates the membrane and reacts with 2-(hydroxymethyl)piperidine (2-HMP) coated on the surface of XAD-2. Sampling times from 15 min to 8 hr have been used. The formaldehyde-oxazolidine produced is thermally desorbed and determined by a packed column gas chromatograph equipped with a flame ionization detector (FID). The response of the monitor is directly proportional to the external concentration of formaldehyde over the concentration range 0.050–100 ppm. The permeation constant (the slope of the permeation curve) of the membrane is $0.333 \mu\text{g ppm}^{-1} \cdot \text{hr}$, and the detection limit of the method is 0.03 ppm for an 8-hr sampling period. Relative humidity (RH) (35–94%), temperature (0–82°) and storage period (0–25 days) do not affect the permeation process for sample collection. Moreover, potential chemical interferences, 10 ppm acetone or acrolein, respectively, have no detectable effect on the process. The method gives TWA concentration directly from the measurements, and the equipment is economical and convenient for personal or multi-location sample collections.

Exposure to formaldehyde in air results from a number of commercial and non-commercial users.¹⁻⁸ Due to the toxic, carcinogenic and mutagenic effects of formaldehyde,^{2-4, 6-9} the Occupational Safety and Health Administration (OSHA) has established new limits: (a) an 8-hr time-weighted-average (TWA) action level of 0.5 ppm; (b) a permissible exposure limit (PEL) of 1 ppm and (c) a 2 ppm 15-min short term exposure limit (STEL).¹⁰ These changes have led to increased interest in determining formaldehyde.

One particular difficulty is the sampling method. Although methods using real-time area monitors, impingers, and active adsorbents are currently used for the collection of formaldehyde, they are not convenient for personal monitoring.¹¹⁻¹³ The major drawbacks of the recommended active sampling method¹⁰ are the use of a toxic solvent desorption, CS₂ in benzene,¹⁴ and the lack of the sensitivity needed for the determination of nanogram levels of formaldehyde.^{12,15-18}

Permeation sampling has been used for sampling vinyl chloride,¹⁹ hydrogen sulfide,²⁰ and ethylene oxide in air,²¹ as well as phenols²²

and six volatile priority pollutants from aqueous solutions.²³ The technique relies on the selective permeability of materials through a polymeric membrane, where the rate of permeation is directly proportional to the external concentration of the permeating gas, or:

$$M_t = KC_{\text{ef}}t \quad (1)$$

where M_t is the mass of formaldehyde (μg) collected at any time; C_{ef} is the external concentration of formaldehyde in ppm; t is sampling time in hr and K is the permeation constant which is characteristic of the membrane. Moreover, the magnitude of the response (M_t) depends on interferences, the reactivity of the analyte with the reagent used, the stability and the detectability of the product as well. By exposing calibrated samplers for known sampling periods, it is possible to determine the TWA of formaldehyde, or:

$$C_{\text{TWA}} = M_t/Kt \quad (2)$$

The conversion of carbonyl compounds to oxazolidines^{24,25} with 2-HMP has been used for quantification of acrolein²⁶ and acetaldehyde;²⁷ the gas chromatographic determination detected no evidence of formaldehyde interferences.^{26,27} Other conversion reagents suffer

*Author for correspondence.

interferences and/or the instability of the products.²⁹⁻³¹ This paper reports a (2-HMP)-coated solid sorbent/permeation sampling method followed by gas chromatography determination of formaldehyde in air. The effects of relative humidity, temperature, storage period and interferences on the sampling technique are also reported. The method is simple, sensitive, efficient and allows a TWA level to be directly obtained from the measurements of formaldehyde. The sampling device, which responds within 3 min, is economical, lightweight and lends itself to repeated uses for personal or area monitoring.

EXPERIMENTAL

Apparatus

The investigation used a previously described^{21,22} sampling chamber and sampling device. The membrane affixed to the sampling device (Fig. 1) was a 0.025-mm thick unbacked polymeric dimethylsilicone membrane (General Electric Company, Schenectady, New York). The sorbent throughout the study was Amberlite XAD-2, a nonionic polymeric porous resin, 80/100 mesh size (Supelco, Inc., Supelco Park, Bellefonte, PA, U.S.A.), coated with 2-(hydroxymethyl)piperidine (2-HMP) (Aldrich Chemical Company, Inc., Milwaukee, Wisconsin USA). A Supelco thermal desorption unit, thermal tube desorber (TTD) Model 850, and desorption sample tubes (DST), 6 mm o.d. \times 4 mm

i.d. \times 11.50 cm, were used for the introduction of samples into the GC. A Hewlett-Packard gas chromatograph Model 5890A equipped with a flame ionization detector (FID) and a Supelco stainless steel packed column, 10% UCON 50-HB-5100/2% KOH on 80/100 chromosorb W-AW, 15 m \times 2 mm i.d., were used for the determination of formaldehyde in the collected sample. A water bath, a 300-ml round-bottomed flask with three \$24/40 ground glass joints, a 20-cm glass tube, and gas dispersion tubes were used to produce formaldehyde from paraformaldehyde. An Airguide Instrument Company humidity indicator Model 605 was required for monitoring the humidity of the system. A 4 cm \times 30 cm glass tube, a rotary evaporator and a Thermolyne Sybron Corporation furnace, TEMCOMETER Model CP-12915, were necessary for drying the adsorbent.

Reagents

Adsorbent preparation. Dry acetone (100 ppm) and dry acrolein (100 ppm) lecture size cylinders were purchased from the Akron Gas Specialities, in Akron, Ohio. All other chemicals were American Chemical Society (ACS) certified to be more than 95% pure, and used without purification. Paraformaldehyde was purchased from the Aldrich Chemical Company. About 250 g of XAD-2 were placed in a 300-ml round-bottomed evaporating flask to which 25% (w/w) of 2-HMP and 200 ml of methanol were added. The solution was vigorously shaken for several minutes to mix well and let sit for 8 hr at ambient temperature. A rotary evaporator was used to remove the solvent. The adsorbent was then transferred to a 30-cm glass tube and was continuously purged with a 20 ml/min helium flow at 80°, to remove residual formaldehyde and impurities. The sorbent was routinely analyzed for the detection of residual formaldehyde and/or contaminants, which were not specifically identified, from the chemical treatment of the adsorbent.

Procedure

Standard formaldehyde atmosphere. A temperature controlled depolymerization of paraformaldehyde was used to produce standards of formaldehyde. The components of the apparatus were: (1) a standard 300-ml round-bottomed flask with three \$24/40 ground glass joints as the mixing chamber; (2) a glass tube containing paraformaldehyde, 20 cm long, fitted to the middle joint of the flask as the diffusion

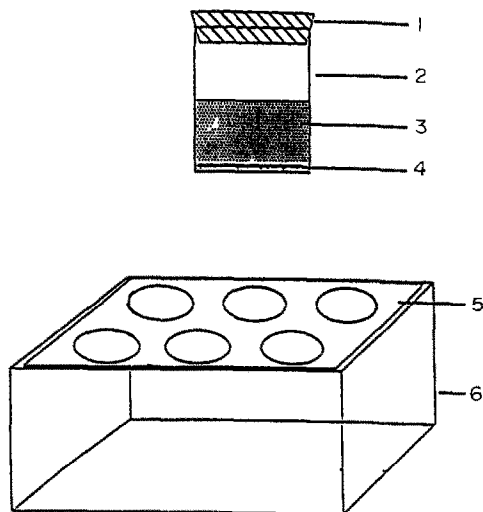


Fig. 1. Apparatus for sampling. Top, sampling device: (1) rubber stopper (2) glass tubing (3) adsorbent, (4) single backed dimethylsilicone membrane. Bottom, exposure chamber: (5) holes to support sampling devices (6) aluminum box.

tube; (3) two Fisher scientific dispersion tubes, extra course frit, 12 mm × 22 mm frit × 8 mm o.d., were used as the inlet and outlet, respectively, and prevented the carrier gas from disturbing the paraformaldehyde in the diffusion tube. A range of concentrations of formaldehyde up to several ppm was produced by immersing the diffusion tube in a water bath at a known temperature (30–60°). By passing a metered flow of dry air over the diffusion tube, 20–500 ml/min, a series of formaldehyde standards was produced. The flow rate of the dilution air was calibrated with both a flow sensor of the gas chromatograph and a bubbler flowmeter, and was routinely sampled with a syringe for the determination of the produced formaldehyde.

Sampling and analysis. The calibration of sampling devices was conducted at 22° and 27% RH. Two hundred milligrams of the treated Amberlite XAD-2 were transferred to a sampling device and exposed to a standard of formaldehyde in the sampling chamber for a sampling period ranging from 0.25–8 hr. Formaldehyde was trapped on the XAD-2 via a reaction between 2-HMP and formaldehyde forming a stable, slightly volatile product, which was readily detected by an FID. After sampling, the sample was spiked with formamide as an internal standard, transferred to a thermal desorption tube and analyzed for formaldehyde. The parameters of the instrument were as follows: sample desorption set at 300° for 2 min; the gas chromatograph initial temperature was 140° for 2 min, which was then increased to 200° at 16°/min. The flow-rate of the helium carrier gas was 20 ml/min. Figure 2 shows a typical chromatogram resulting from the above settings.

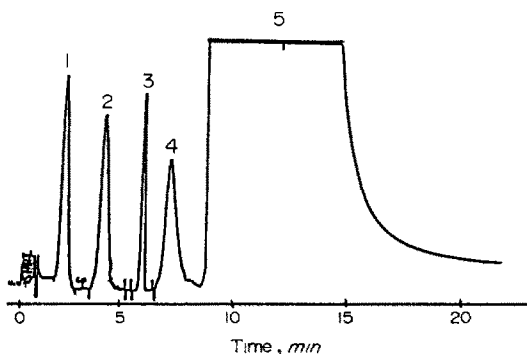


Fig. 2. A representative chromatogram: the parameters of the instrument are described in the text. The peaks are the oxazolidines of: (1) formaldehyde (2) acrolein (3) acetone and (4) formamide; and (5) 2-(hydroxymethyl)piperidine.

Table 1. Membranes investigated; the concentration of formaldehyde was 10 ppm, temperature 21° and RH = 35%

Membrane	Relative response (%) at steady state*	Response time, min
Unbacked dimethylsilicone	100	2.67
Single backed dimethylsilicone	87	33
Silicone Polycarbonate	65	57
Polyethylene	53	64
Polyvinylfluoride	9	83
Mylar	ND	$t > 120$
Teddlar	ND	$t > 120$
Polystyrene	ND	$t > 120$
Polyethylene terephthylate	ND	$t > 120$

*The highest response made was 100%.

ND = not detected.

t = time

RESULTS AND DISCUSSION

Permeation through membrane.

Initial permeation evaluation involved membrane screening and the calibration of sampling devices. A constant flow of formaldehyde was produced by a thermal decomposition of paraformaldehyde. By using a flow-through permeation cell,^{22,23} it was possible to determine the steady state permeation time. Results of membrane screening (Table 1) and the study of the breakthrough time (Fig. 3) indicate that the unbacked dimethylsilicone membrane has high formaldehyde permeability, with the lag time equal to 2.67 ± 0.08 min. The rapid transport is attributed to the flexibility of the silicon-oxygen-silicon chain and the absence of crystallinity in this membrane material.³²⁻³⁴ Additional advantages of the membrane are high thermal stability, high separation factors for many gases, inertness, the lack of pin holes and hydrophobicity.³²

Figure 4 shows a representative calibration plot of the sampling devices for the methods, which covers the concentration range from 0.050–100 ppm, for sampling periods over

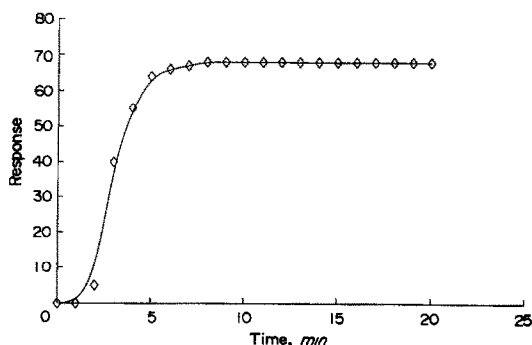


Fig. 3. Breakthrough time.

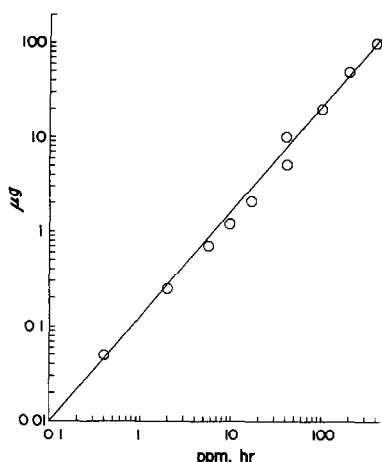


Fig. 4. The detection or calibration curve.

0.25–8 hr. The result indicates that the rate of permeation of formaldehyde through the unbacked dimethylsilicone membrane is directly proportional to the external concentration of the toxin and sampling time. The calibration constant for the method, K , determined as the slope of the calibration curve, has been calculated to be $0.333 \mu\text{g ppm}^{-1} \cdot \text{hr}$, with the correlation coefficient being 0.99998. Representative results for TWA and K values are shown in Table 2.

Factors affecting sampling. Figure 5 is a representative result of environmental including stability studies, which indicated there were no detectable losses or response variations for the factors and the ranges covered. Temperature and RH variations, the presence of other chemi-

Table 2. TWA concentration and permeation constant values

Time, hr*	Sampling device	K , $\text{ng ppm}^{-1} \cdot \text{hr} \dagger$	TWA, $\text{ppm} \dagger$
1	1	336.70	1.165
	2	330.30	1.037
	3	335.50	1.149
	4	332.60	1.017
	5	328.89	1.015
	average	332.80 ± 3.82	1.077 ± 0.085
	K (the slope)	333.33	
2	1		1.096
	2		1.012
	3		1.109
	4		1.024
	5		1.009
	average		1.05 ± 0.056
8	1		1.253
	2		1.114
	3		1.099
	4		1.047
	5		1.004
	average		1.103 ± 0.108

*Concentration = 1.0 ppm.

†At 95% confidence limit.

cals in air, and the storage period can be expected to alter device performance. To determine the effects of temperature, the mixing and sampling chambers were placed in a temperature controlled bath, and the exposure study was performed with a 1.89-ppm standard for 4 hr over the range 0–82°. The analysis was conducted as stated above. The result showed no detectable variations for the temperature range covered.

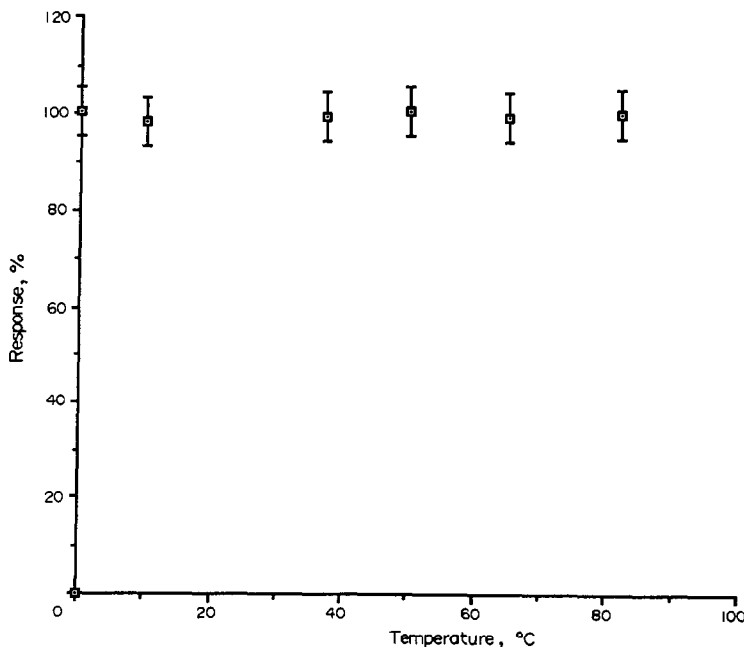


Fig. 5. A typical result of environmental factors and stability studies.

Studying the influence of RH, from 30–95%, on the permeation of formaldehyde involved adding moisture to the above dry standard of formaldehyde, and sampling for 4 hr. The relative humidity of the system was continuously monitored with the humidity indicator placed at the outlet of the sampling chamber. The determination was conducted as measured earlier, after 30 min of equilibration. Again, no change in the relative humidity was observed (Fig. 5).

Any chemical capable of reacting with formaldehyde and/or 2-HMP, thereby depleting the derivatizing reagent or degrading the membrane, is a possible interference. Similarly, any compound having the same retention time as formaldehyde and giving a detector response is a potential analytical interference. Analytical interference can usually be overcome by adjusting the gas chromatographic parameters to resolve component peaks. As acetone and acrolein contain a functional group (carbonyl) present in formaldehyde, sampling devices were exposed to a flow containing 20 ppm formaldehyde and up to 10 ppm acetone or acrolein, respectively. After 30 min of equilibration, sample collection and determination were performed as described above. Spiked samples showed a recovery above 99%, indicating there were no detectable losses of formaldehyde due to interferences (Fig. 5), which supports other researchers' findings.^{26,27}

To examine sample stability, samples were collected with the above standard and sampling period, and stored at ambient temperature in sealed thermal desorption sample tubes for a period of 0–25 days. At daily intervals, the determination was performed on a sample set (3 samples) as described above. The results showed samples can be stored up to 25 days without any deterioration (Fig. 5).

CONCLUSION

A permeation sampler for formaldehyde with Amberlite XAD-2 coated with 2-HMP has been found to be an effective sampling device. The calculated permeation constant (the slope) for a prototype monitor was $0.333 \mu\text{g ppm}^{-1}\text{hr}$, within the concentration range 0.050 ppm–100 ppm. The detection limit for an 8-hr sampling period was determined to be $0.039 \mu\text{g}$. Storage time and environmental variables have no detectable effects on the sampling rate or on the collected sample, *i.e.*, recovery was better than 99% at the 95% confidence limit. The lag

time of the sampling device and the minimum sampling time tested are about 3 and 15 min, respectively, which indicate the rapid response of the sampler. TWA concentration can be obtained directly from the calibration curve. The sampling method and the monitor can be an alternative technique for the determination of exposure to organic vapors in air.

REFERENCES

1. M. S. Reisch, *C & E News*, April 9, p. 11, 1990.
2. Omori, *Chemistry*, 1977, **32**, 184.
3. R. W. Hart, A. Terturro and L. Neimeth, Eds. *Environ. Health Perspect.*, 1984, **58**, 334.
4. *Idem, ibid.*, 1984, **58**, 325.
5. T. H. Stock and S. R. Mendez, *Am. Ind. Hyg. Assoc. J.*, 1985, **46**, 313.
6. NIOSH, *Current Intelligence Bulletin No. 34*, Cincinnati, 1981.
7. R. J. Fielder, *Toxicity Review 2, Formaldehyde*, HMSO 1981.
8. *The Assessment of Data on the Effects of Formaldehyde on Humans*, European Chemical Industries Ecology and Toxicology Centre, Brussels, 1982.
9. *Threshold Limit Values for Chemical Substances and Physical Agents in the Workroom Environment*, American Conference of Government Industrial Hygienists, Cincinnati, 1983.
10. *Code of Federal Regulations*, 29 CFR, 1988, 1901, 1048.
11. Walter S. Kim, Charles L. Geraci, Jr. and Richard E. Kupel, *Am. Ind. Hyg. Assoc. J.*, 1980, **41**, 334.
12. J. O. Levin, R. Lindhal and K. Andersson, *Environ. Sci. Technol.*, 1986, **20**, 1273.
13. B. Coyne, R. E. Cook, J. R. Mann, S. Bouyoucos, O. McDonald and E. L. Baldwin, *Am. Ind. Hyg. Assoc. J.*, 1985, **46**, 609.
14. *NIOSH Pocket Guide to Chemical Hazards, DHEW (NIOSH) No. 78-210*, 1985.
15. J. N. Driscoll, *US Patent No. 4, 801*, 841, January 31, 1989.
16. J. O. Levin, R. Lindhal, K. Andersson and C. A. Nilsson, *Anal. Chem.*, 1985, **57**, 1032.
17. P. Bisgaard, L. Molhave, B. Rietz and P. Wilhardt, *Am. Ind. Hyg. Assoc. J.*, 1984, **45**, 425.
18. I. Ahonen, E. Priha and M.-L. Aijala, *Chemosphere*, 1984, **13**, 521.
19. P. W. West and K. D. Reiszener, *Environ. Sci. Technol.*, 1973, **7**, 526.
20. J. K. Hardy, D. T. Strecker, C. P. Savariar and P. W. West, *Am. Ind. Hyg. Assoc. J.*, 1981, **42**, 283.
21. J. K. Hardy and Chansa Muntuta-Kinyanta, *ibid.*, in the press.
22. J. K. Hardy and Guo-Zheng Zhang, *J. Environ. Sci. Health*, 1989, **A24**, 279.
23. R. D. Blanchard and J. K. Hardy, *Anal. Chem.*, 1985, **57**, 2349.
24. E. D. Bergmann, *Chem. Rev.*, 1953, **53**, 309.
25. G. Hilgetag and A. Martini, *Preparative Organic Chemistry*, pp. 412–413, 504–527. John Wiley and Sons, 1972.
26. Eugen R. Kennedy, Ph.D. and Paula Fey O'Connor, *Acrolein: NIOSH Manual of Analytical Methods: NIOSH/DPSE, No. 2501*, 1984.

27. Karen J. Williams, *Acetaldehyde: NIOSH Manual of Analytical Methods: NIOSH/DPSE No. 2539*, 1989.
28. *NIOSH Manual of Analytical Methods*, 2nd Ed., Vol. 4, p. 327. U.S. Department of Health and Welfare (NIOSH), 78-175, 1978.
29. *Idem.*, 2nd ed., Vol. 1, P & CAM, p. 125. U.S. Department of Health and Welfare (NIOSH), 77-157A, 1977.
30. *Idem.*, 2nd ed., Vol. 4, P & CAM, p. 354. U.S. Department of Health and Welfare (NIOSH), 82-100, 1982.
31. S. F. Sleva, *Determination of Formaldehyde: Chromotropic Acid Method*, PHS Publication 999-AP-11, H-1, 1965.
32. *Manual: General Electric Permselective Membranes*, General Electric Co., Membrane Products Operation, Schnectady, New York, USA.
33. Mears Patric, *Membrane Separation Processes*, p. 307. Elsevier Scientific Publishing Company, 1976.
34. S. A. Michaels and H. J. Bixler, *Progress in Separation and Purification*, E. S. Perry (ed.), Vol. 1, pp. 143-186. Interscience, New York, 1968.

ON-LINE ALUMINIUM PRECONCENTRATION ON CHELATING RESIN AND ITS FIA-SPECTROFLUORIMETRIC DETERMINATION IN FOODS AND DIALYSIS CONCENTRATES

P. FERNÁNDEZ, C. PÉREZ CONDE, A. GUTIÉRREZ and C. CÁMARA*

Departamento de Química Analítica, Facultad de Ciencias Químicas de la Universidad Complutense,
28040 Madrid, Spain

(Received 19 March 1991. Revised 31 May 1991. Accepted 17 June 1991)

Summary—A new, sensitive and rapid spectrofluorimetric flow-injection method, is presented for the determination of trace levels of aluminium based on the formation of a fluorescent complex between aluminium and 5,7-dibromo-8-quinolinol (DBQ) and its extraction into diethylether ($\lambda_{exc} = 400$ nm, $\lambda_{em} = 525$ nm). Experimental conditions such as pH, reagent concentration, flow-rates, sample volume, extraction coil length, *etc.*, have been optimized for on-line and batch procedures. The detection limits are 1 ppb and 0.3 ppb for batch and on-line systems respectively. The coefficient of variation is 3.0% at the 4 ppb level for the FIA system. To remove interferences and to preconcentrate aluminium, a chelating resin microcolumn which was able to selectively complex Al(III) and was obtained by immobilizing Chromotrope 2B on AG1-X8 ion-exchange resin, was incorporated into the FIA system. The proposed method was successfully applied to determine aluminium in tap water, food samples and dialysis solutions.

Aluminium has been proven to be toxic to certain "at-risk humans",¹ including patients with chronic renal failure. The main sources of aluminium for the human organism are foods and drinking water as well as dialysis fluids for people undergoing renal treatment; therefore, monitoring of this element in such materials is necessary. Since aluminium is toxic at very low concentrations for the above-mentioned group of humans, the availability of sensitive analytical methods for this element is essential.

Several methods are available to determine aluminium in biological materials and dialysis fluids; none being fully satisfactory. In particular, atomic-absorption spectrometry with electrothermal atomization (ETAAS) is widely used²⁻⁴ for sample solutions with concentrations below 30 ppb. However, large discrepancies still exist in the results obtained² most probably due to contamination problems. Furthermore, the high salt content in dialysis concentrates interferes with the determination of Al by this technique.⁵ Other alternatives are the ICP-AES and FAAS techniques, which are less sensitive and need a preconcentration of the analyte.^{5,6}

Fluorimetric methods are very sensitive and require readily available instrumentation. Particularly sensitive are those based on the complexation with Morin⁷ and with 8-hydroxyquinoline-5-sulphonic acid (HQS) in the presence of surfactants,⁸ although both lack adequate selectivity. In the Morin method better selectivity is achieved by using a previous extraction with isobutyl methyl ketone. However, the reaction between Morin and aluminium is slow and does not allow the automatization of the process.

The method based on complexing with HQS in micellar medium does not require extraction which is an important advantage, but to overcome selectivity problems, the use of a complex high pressure liquid chromatography system is needed.⁹

As already mentioned, both selectivity and sensitivity problems need to be considered to satisfactorily determine aluminium in the required biological samples and dialysis concentrates. We thought that passing the sample through a chelating resin that could selectively retain the aluminium could simultaneously solve the two mentioned problems and therefore allow the analysis of the samples under study. It has been reported that aluminium is in fact strongly complexed by sulphonated azo dyes

*Author for correspondence.

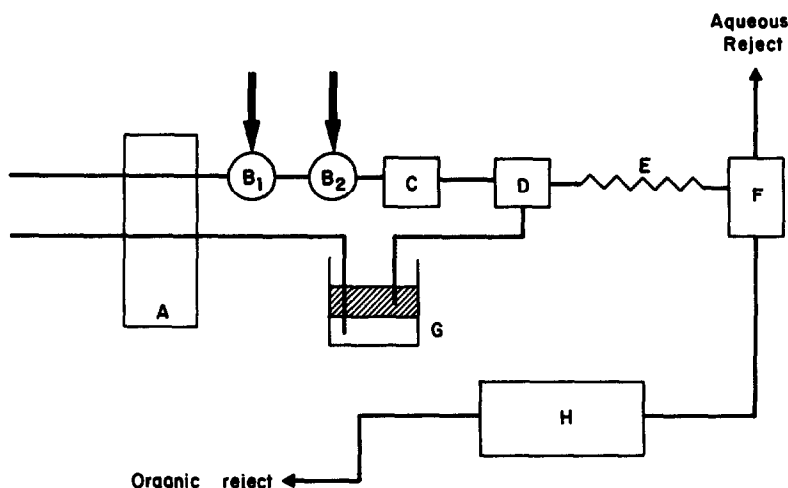


Fig. 1. Scheme of the FIA system for removing interferences with a chelating microcolumn

Fig. 1. Scheme of the FIA system for removing interferences with a chelating microcolumn

possessing dihydroxylic groups.¹⁰ In particular, 1,8-dihydroxy-2-(*p*-nitro-phenylazo)-naphthalene-3,6-disulphonic acid (Chromotrope 2B) forms an extremely strong complex with Al(III) allowing its separation from the rest of the matrix¹¹ and simultaneously preconcentrating it.

If a microcolumn of chelating resin were prepared, it could be inserted in a flow-injection system with the known advantages of increased speed of analysis and decreased risk of sample contamination thus improving reproducibility of the results.

This paper describes a new, rapid, selective and sensitive method that allows the determination of aluminium in biological samples and dialysis concentrates. The method is based on the separation of the element in a chelating microcolumn followed by a spectrofluorimetric determination of the complex Al(III)-5,7-dibromo-8-quinolinol extracted into diethylether. In addition the conditions for automatization of the process by FIA have been established and samples of food, drinking water and dialysis concentrates analysed.

EXPERIMENTAL

Apparatus

A Perkin-Elmer Model MPF-44A Spectrofluorimeter equipped with a Hellma flow-cell (optical path 1 cm; inner volume 18 μ l) was used connected to a Perkin-Elmer 56 recorder.

Two Omnifit injection valves (six-way) were employed. Teflon tubes (i.d. 0.5 mm) and connectors were employed to build the reaction coils and transmission lines. A displacement flask (Omnifit), a laboratory-made phase separator and a teflon column of 35-mm length and 5-mm i.d. were also used.

Reagents

Aluminium standard solution (1000 μ g/ml). Prepared by dissolving aluminium metal (Merck) in 2% hydrochloric acid.

5,7-Dibromo-8-quinolinol (DBQ) (Flucka) solution, 0.05% (w/v) in diethylether (Carlo Erba).

2-Methyl-8-quinolinol (Scharlau) solution, 0.05% (w/v) in diethylether (Carlo Erba).

5-Sulphonic-8-quinolinol acid (Merck) solution, 0.05% (w/v) in demineralized water.

AG1-X8 anion-exchange resin, 100-200 Mesh (Bio-Rad).

Chromotrope 2B (Aldrich).

Acetate buffer carrier solution 0.05M (pH = 3.5-5.5).

Buffer 0.5M hexamethylenetetramine (HMTA) (Merck). Acidified with perchloric or hydrochloric acid (Merck) to pH = 5.5-7.5. All chemicals were of analytical reagent grade and demineralized water (Milli-Q) was used throughout.

Procedures

Batch method. A volume of solution containing up to 100 ng of aluminium was placed in a polypropylene test tube. DBQ solution (0.5 ml

of 0.5% (w/v) DBQ in acetone) and 1 ml of $\text{H}_2\text{MTA}^+/\text{HMTA}$ buffer (pH = 6.0) were added, and the final volume of the aqueous phase was made up to 2.5 ml with water. After adding 2.5 ml of diethylether, the mixture was shaken for 2 min and the fluorescence intensity of the organic extract was measured ($\lambda_{\text{exc}} = 400$ nm, $\lambda_{\text{em}} = 525$ nm) against a blank prepared in parallel.

Flow-injection method. The system for on-line preconcentration with a microcolumn is shown in Fig. 1.

The procedure is as follows: A 185- μl volume of the sample solution containing less than 100 ng/ml was injected from the first injection valve (B_1) into the acetate buffer carrier solution, pH = 5.5, at 0.6 ml/min.

This solution passed through a microcolumn (C) filled with immobilized Chromotrope 2B, in which the aluminium was retained. To remove the immobilized aluminium, 100 μl of 0.1M hydrochloric acid was injected from the second injection valve (B_2). The carrier solution was mixed with the organic phase [0.05% DBQ in diethylether from the displacement flask (G)] in segmenter (D), whose flow-rate was 0.36 ml/min. The alternative aqueous and organic phase segments were separated in the membrane separator (F) after passing through the reaction coil (E). The organic phase passed through the flow-cell (H) and the fluorescence peaks were recorded.

Full-column preparation. Chromotrope 2B was immobilized on the anionic AG1-X8 resin by soaking 1 g of wet resin in 25 ml of a solution containing about 6.6×10^{-3} millimoles of Chromotrope 2B. The suspension was shaken until the aqueous phase became colourless (30 min).

The chelating resin was placed in a microcolumn made of a teflon tube 35 mm long and 5 mm i.d. The column end-caps were teflon screws; a fibre glass membrane of 3- μm pore size to prevent loss of resin particles was used.

RESULTS AND DISCUSSION

Batch method

The properties to complex Al shown by three different derivatives of 8-hydroxyquinoline (5,7-dibromo, 2-methyl and 5-sulphonic acid) were studied in order to select the one showing the best analytical characteristics. Different organic media (n-butanol, chloroform and diethylether) were tested for extraction of the complex. The last, in spite of its notoriously inconvenient

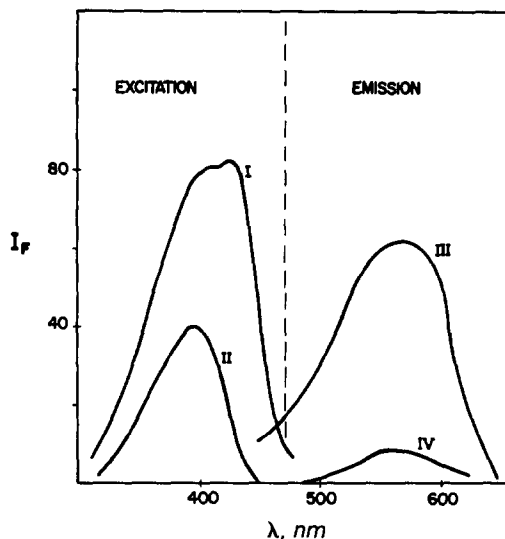


Fig. 2. Uncorrected excitation and emission spectra of Al(III)-DBQ complex (I, III) and DBQ blank (II, IV). Conditions: [Al(III)] = 0.1 ppm; [DBQ] = 0.5% (w/v) in acetone; $\text{H}_2\text{MTA}^+/\text{HMTA}$ (pH = 6.0) medium.

handling, was chosen because it appreciably increased fluorescence intensity. The complex showing the best sensitivity was Al(III)-5,7-dibromo-8-quinolinol (DBQ) extracted into diethylether.

The Al(III)-5,7-dibromo-8-quinolinol complex in diethyl ether showed maximum fluorescence intensity at 525 nm when excited at 400 nm. Uncorrected excitation and emission spectra are given in Fig. 2.

To determine the optimum extraction pH, several regulatory media were tested: HCl (pH = 1), HAc/Ac⁻ (pH = 3.5-5.5), $\text{H}_2\text{MTA}^+/\text{HMTA}$ (pH = 5.5-7.5), $\text{NH}_4\text{Cl}/\text{NH}_3$ (pH = 8.0-9.0) and NaOH (pH > 10). The results given in Fig. 3 show that the optimum pH range is 5.5-7.5. It was noted that the presence of HMTA significantly increased the sensitivity compared to that obtained with HAc/Ac⁻ and therefore $\text{H}_2\text{MTA}^+/\text{HMTA}$ was chosen as optimum medium.

The effect of ionic strength was studied by adding increasing amounts of ammonium nitrate and sodium chloride as strong electrolytes to a solution containing 0.02 ppm aluminium. It was found that up to an ionic strength of 0.25M, the fluorescence intensity of the complex remained constant, and that above this value it decreased.

Changes in temperature over the range 0-25° had no effect on the fluorescence complex.

The analytical characteristics are as follows. The calibration graph is linear from 1 to 75 ppb.

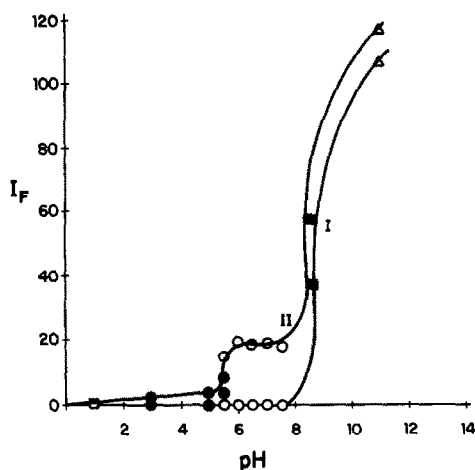


Fig. 3. Effect of pH on fluorescence intensity for: (I) DBQ blank and (II) Al(III)-DBQ complex. pH was adjusted with (□) HCl, (●) HAc/Ac⁻, (○) H₂MTA⁺/HMTA, (■) NH₄⁺/NH₃ and (△) NaOH. Conditions: [Al(III)] = 50 ppb; [DBQ] = 0.05% (w/v) in diethylether.

The coefficient of variation, evaluated from ten independent determinations, was 6% at the 30 ppb level. The limit of detection was 1 ppb. A study of several potential interfering species showed that elements usually present at relatively high concentrations, such as Zn, Ca, Mg and Fe, seriously interfere. Thus, in spite of the fact that the proposed (batch) method is very sensitive, its selectivity is very low.

Flow-injection method

Both chemical and physical experimental conditions, affecting Al-DBQ formation and extraction into the FIA system were optimized.

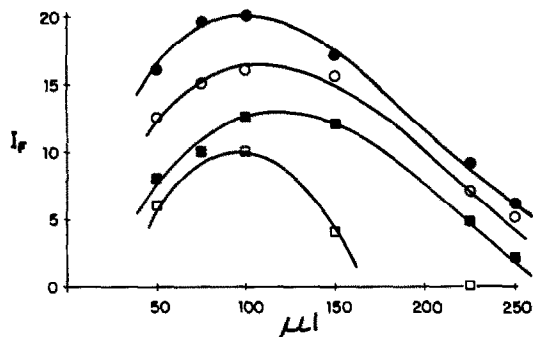


Fig. 4. Fluorescence emission of Al(III)-DBQ complex with different volumes and concentrations of HCl eluant (■) 0.01M, (○) 0.05M, (●) 0.1M, (□) 0.5M. Conditions: [Al(III)] = 50 ppb; [DBQ] = 0.05% (w/v) in diethylether; HAc/Ac⁻ 5.10⁻³M (pH = 5.9) medium.

Table 1. Optimum values of FIA system physical and chemical variables. Liquid-liquid extraction followed by fluorimetric determination of Al(III) with DBQ

Variable	Optimum value
pH	6.5*
Regulating medium	0.5M H ₂ MTA ⁺ /HMTA*
DBQ concentration in diethylether	0.05% (w/v)
Aqueous flow-rate	0.62 ml/min
Organic flow-rate	0.36 ml/min
Injection volume	185 μl
Reactor length	300 cm
Coil shape	82 knots
Reactor inner diameter	0.5 mm
Segmenter angle	45°
Phase separator	Membrane

*Acetate buffer 0.05M pH = 5.5 was used when a chelating microcolumn was inserted into the FIA systems.

The optimum medium was, as in the batch method, HMTA buffer solution at pH 5.5–7.5. The optimum DBQ concentration in diethylether was 0.05%.

To choose the optimum organic and aqueous flow-rates, the range 0.3–2.1 ml/min was tested and 0.62 ml/min and 0.36 ml/min were chosen for aqueous and organic flow-rates respectively, using 185 μl as optimum sample injection volume. The effect of different lengths of extraction coil, inner diameter and shape were also tested, the optimum extraction coil having a 300-cm length, 0.5-mm inner diameter and 82 knots. It was found that knots in the extraction coil increased the yield of extraction by 300%. Optimum values for physical and chemical variables are summarized in Table 1.

The selectivity of the FIA method is substantially higher than that batch method, but not so high that it can be applied to determine Al(III) in complicated matrices such as food and dialysis fluids.

To increase the selectivity of the method, a chelating resin microcolumn was inserted in the FIA system (Fig. 1). Chromotrope 2B immobilized on the AG1-X8 anion exchange resin was used. This reagent is able to retain the aluminium present in the sample as a chelate. Previous studies¹¹ showed that this chelating resin completely separates aluminium from lead, nickel, cadmium, calcium and magnesium, although copper and iron were in part retained on the resin.

This microcolumn makes it necessary to use HAc/Ac⁻ carrier because the H₂MTA⁺/HMTA carrier acidified with both, perchloric acid or hydrochloric acid significantly increased blank fluorescence emission intensity due to its reaction with eluated Chromotrope 2B. The lower

Table 2. Determination of Al(III) content of several samples by FIA-spectrofluorimetric method (FIA-SFM) and electrothermal atomic-absorption spectrometry (ETAAS)

Sample	FIA-SFM,		ETAAS,		Addition,† ppb	Recovery,† %
	µg/g*	CV	µg/g*	CV		
Water	149	3	142	7	10	95.5
					20	100
					30	105
Fresh tomato	7.57	5	7.70	7	10	110
					20	99.3
					30	97.7
Dialysis fluid 920	1.75	9	—	—	10	111
					20	99.3
					30	102

*Average of six determinations.

†For FIA-SFM only.

fluorescence intensity with a HAc/Ac⁻ carrier was compensated by the aluminium preconcentration obtained with the chelating micro-column.

Optimum Al(III) retention in the micro-column and Al-DBQ fluorescence development were obtained at pH 5.5 with $5 \times 10^{-2} M$ HAc/Ac⁻.

Varying concentrations and volumes of hydrochloric acid eluant were studied. The results (Fig. 4) show that maximum fluorescence intensity is reached between 75 and 100 µl of $10^{-1} M$ hydrochloric acid. A volume of 100 µl was selected as optimum for further experiments.

The effect of varying the amount of Chromotrope 2B immobilized in the column from 1.3×10^{-4} to 1.6 mmoles was studied. For amounts higher than 6.6×10^{-3} mmoles, the retained aluminium could not be completely removed. For complete removal, it was necessary to raise the hydrochloric acid concentration above 0.5M which made it more difficult to reach the optimum pH for Al-DBQ complex formation. As a compromise, 6.6×10^{-3} mmoles of Chromotrope 2B per gram of AG1-X8 dry resin was used. The results of the preconcentration study showed that the fluorescence intensity of the signal increased proportionally with increasing volume of injected sample up to the maximum volume assayed of 1000 µl. Thus, using the optimum eluant volume of 100 µl it was possible to achieve a 10-fold sample preconcentration.

The calibration graph was linear from 1 to 50 ng/ml aluminium. The limit of detection for the sample solution is 0.3 ppb aluminium and the coefficient of variation at the 4 ppb level is about 3%.

Sample analysis

Various dialysis fluids, foods and tap water were analysed. Tap water was analysed without any sample pretreatment and dialysis fluid with a 1:25 sample:water dilution. Freeze dried fresh tomato was mineralized by the following dry ashing procedure: About 0.25 g of sample was placed in a porcelain crucible and held at 500° for 2 hr. The residue was dissolved in 0.5 ml of 65% (w/v) nitric acid and the final volume was made up to 25 ml.¹²

In all cases, the slope of the standard additions line was parallel to the slope obtained from the Al(III) standard solutions. It was concluded that the analysed samples did not show matrix effects.

The results obtained for tap water and fresh tomato with the proposed method agreed with those obtained by the ETAAS method; the differences were not significant at the 5% level. For dialysis fluids the mean value of recovery, obtained by adding different known amounts of aluminium to the samples, was 104%. The results obtained for six replicate determinations are summarized in Table 2.

CONCLUSIONS

The new spectrofluorimetric FIA method proposed for the determination of aluminium is very sensitive and selective, because interfering ions are removed by passage through a chelating resin microcolumn incorporated into the FIA system. Furthermore, samples can be preconcentrated at least 10-fold by retaining the Al(III) contained in 1000 µl of sample solution and eluting it with 100 µl of 0.1M hydrochloric acid. It is therefore a

valid alternative method to determine traces of aluminium in biological materials. It has been successfully applied to determine aluminium in tap water, food samples and dialysis fluids.

Acknowledgements—The authors wish to thank CICYT for their financial support under contract No. PB 88/0094 and Max Gorman for the revision of this manuscript.

REFERENCES

1. J. Savory, R. L. Bertholf and M. R. Wills, *Clinics Endocrinol. Metabolism*, 1985, **14**, 681.
2. A. Cedergren and W. Frech, *Pure Appl. Chem.*, 1987, **59**, 221.
3. M. Bettinelli, U. Baroni, F. Fontana and P. Poisetti, *Analyst*, 1985, **110**, 19.
4. A. D. Woolfson and G. M. Gracey, *ibid.*, 1987, **112**, 1387.
5. M. R. Pereiro, A. López, M. E. Diaz and A. Sanz Medel, *J. Anal. At. Spectrom.*, 1990, **5**, 15.
6. S. Hirata, K. Honda and T. Kumamaru, *Anal. Chim. Acta*, 1989, **221**, 65.
7. F. Hernández Hernández and J. Medina Escriche, *Analyst*, 1984, **109**, 1585.
8. A. Sanz-Medel, M. R. Fernández de la Campa and J. I. Garcia Alonso, *ibid.*, 1987, **112**, 493.
9. J. I. Garcia Alonso, A. López Garcia, A. Sanz Medel, E. Blanco González, L. Ebdon and P. Jones, *Anal. Chim. Acta*, 1989, **225**, 339.
10. M. Pesavento, C. Riolo, T. Soldi and R. Garcia, *Ann. Chim. (Rome)*, 1982, **72**, 217.
11. M. Pesavento, A. Profumo, C. Riolo and T. Soldi, *Analyst*, 1989, **114**, 623.
12. P. Fernández, C. Pérez Conde, A. Gutiérrez and C. Cámara, *Talanta*, 1989, **36**, 960.

UNSEGMENTED FLOW ANALYSIS WITH ION-SELECTIVE ELECTRODES BY USE OF A LARGE-VOLUME WALL-JET CELL

CONTINUOUS ELECTRODE REACTIVATION IN THE DETERMINATION OF FLUORIDE AND CHLORIDE

Jiří LEXA

Chemical Laboratories, Central Research Institute, Škoda Works, 316 00 Pilsen, Czechoslovakia

KAREL ŠTULÍK

Department of Analytical Chemistry, Charles University, Albertov 2030, 128 40 Prague 2, Czechoslovakia

(Received 30 July 1990. Revised 3 June 1991. Accepted 11 June 1991)

Summary—A simple, large-volume wall-jet cell was designed for unsegmented flow analysis. The working electrode is immersed in a solution that reactivates the electrode surface. During the sample measurement, the working electrode is screened from the reactivation solution by the streaming sample solution; between the individual samples, air is pumped through the jet and agitates the reactivating solution at the electrode surface. The properties of the cell were investigated with the fluoride and chloride ion-selective electrodes and the method was applied to determination of fluoride and chloride in steel corrosion products and in a reference sample of the fly dust from electric-arc furnaces. The method permits about 90 measurements per hour, the results are reproducible and the limits of determination (6.3×10^{-8} and $2.3 \times 10^{-7} M$ for fluoride and chloride, respectively) are substantially lower than the values commonly obtained in batch experiments. At least 150 measurements can be carried out without significant changes in the reliability of determination and the reactivation solution can then be replaced.

Various techniques of flow analysis have rapidly gained importance, as they exhibit many advantages that are thoroughly discussed in the literature.^{1,2} In addition to the most common spectrophotometric detection, some electrochemical methods are being progressively used more (primarily potentiometry, amperometry and coulometry), in view of their high sensitivity and selectivity that can, to a certain extent, be varied by judicious control of the experimental conditions.³ Potentiometry with ion-selective electrodes (ISE's) is very popular because it is highly selective and simple. However, problems may arise in flow detection due to rather sluggish response of many ISE's which, to make it worse, is dependent on the analyte activity (the response time generally increases with decreasing activity).³⁻⁵ Another difficulty, common to all the electrochemical methods except for high-frequency impedance measurements, stems from the interactions between the electrode surface and the test solution and leads to electrode passivation, memory effects and enhanced noise.^{3,6}

On the other hand, an advantage of flow measurements with ISE's lies in the fact that the measuring sensitivity is often somewhat higher than in batch experiments⁶ and that many operations required for the sample pretreatment and electrode reactivation are easy to carry out.

The cells for flow potentiometry are mostly low-volume thin-layer, wall-jet and tubular cells or open wall-jet systems with the working electrode placed above a solution containing a reference electrode.³ All these cells often suffer from noise and random interruptions to the electric circuit, due to air bubbles trapped in small cells or breakage of the thin film of liquid connecting the working electrode with the solution containing the reference electrode in the open systems. Moreover, if the working electrode is to be reactivated, it must either be taken out of the cell, or a different solution must be pumped through the cell, which is awkward and time consuming.

A large-volume wall-jet cell, in which the test solution is fed from a jet onto the working electrode surface and the whole system is placed

in a large vessel containing a suitable solution, was first described by Horvai *et al.*⁷ and later studied in detail by Gunasingham *et al.*⁸⁻¹⁰ The detector has primarily been used for amperometric detection in HPLC⁸⁻¹¹ and recently also for flow-injection potentiometric stripping analysis,¹² flow-injection potentiometry¹³⁻¹⁵ and potentiometric detection in ion chromatography.^{16,17}

It has been shown⁸⁻¹¹ that the liquid beam coming from the jet remains intact even at 10-mm distances of the jet orifice to the electrode surface, that the effective working volume of the cell is small (less than the volume of the hydrodynamic boundary layer at the electrode surface) and that the impinging test solution shields the electrode from the effects of the liquid in the cell, so that it is, *e.g.*, possible to perform amperometric reductive measurements without removal of oxygen from the solution in the cell.

The present paper describes a large-volume wall-jet cell of a very simple design and its application to unsegmented flow ISE potentiometry. The favourable properties of the cell are utilized for continuous reactivation of the working electrode surface and the method is applied to determination of fluoride and chloride in the products of steel corrosion and in a reference sample of fly dust from electric-arc furnaces.

EXPERIMENTAL

Apparatus

The potentiometric measurements were performed with an ION-85 instrument and a REC-80 chart recorder with a REA-120 module (all from Radiometer, Copenhagen, Denmark). The fluoride and Chloride ISE's and the saturated silver/silver chloride reference electrode were Crytur types 09-27, 17-27 and RAE-112, respectively, obtained from Monokrystaly, Turnov, Czechoslovakia. In order to suppress the noise caused by the high impedance of the chloride ISE, an impedance convertor based on a WSH-220 operational amplifier (Tesla, Lanškroun, Czechoslovakia) was placed inside the electrode body.¹⁸

The test solutions were propelled by a Type 315 peristaltic pump (Zalimp, Warsaw, Poland). In the measurement of the detector time constant dependence on the solution flow-rate, an ABU-80 autoburette (Radiometer, Copenhagen, Denmark) was used for pumping.

The sample solutions were aspirated from polypropylene beakers and the sample size was controlled by controlling the aspiration time. The solutions were aspirated through a PTFE tubing (1 mm in internal diameter) and led to the detection cell by silicone rubber tubing (40 cm long and 2 mm in internal diameter). Unless stated otherwise, the flow-rate was 3 ml/min.

The detection cell is schematically depicted in Fig. 1. The cell consists of a cylindrical glass vessel (1) with an opening for the working electrode (2) and reference (3) electrode and for the jet (4) which are fixed in place by polyethylene O-rings. The horizontal position of the ISE and the jet prevents gas bubbles from adhering to the ISE surface. The polyethylene jet is 0.3 mm in internal diameter and its distance from the ISE can be varied. The vessel is provided with a solution outlet stop-cock (5) and is placed in the neck of a waste bottle (7). Tube (6) maintains a constant solution level (a solution volume of 50 ml).

Reagents

Analytical-grade chemicals were employed as received from Lachema, Brno, Czechoslovakia.

Stock solutions of the analytes, 0.1M, were prepared by dissolving solid sodium fluoride and sodium chloride in water, and used as primary standards.

Buffer solution A [0.5M in sodium nitrate, acetic acid and sodium acetate and 0.1M in diaminocyclohexanetetraacetic acid (DCTA)], pH 4.3, was prepared as follows. A 36-g amount of DCTA was dissolved in *ca.* 500 ml of an aqueous solution of 15 g of sodium hydroxide,

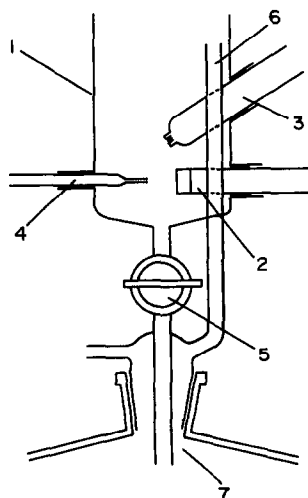


Fig. 1. The large-volume wall-jet cell (for description see text).

then 43 g of sodium nitrate and 30 ml of acetic acid ($\rho = 1.060$) were added and the mixture was made up with water to 1000 ml.

Buffer solution B (pH 4.3) was 0.5M in sodium nitrate, acetic acid and sodium acetate, and was prepared by dissolving 6.0 g of sodium hydroxide in water, adding 30 ml of acetic acid ($\rho = 1.060$) and 43 g of sodium nitrate, and diluting with water to 1000 ml. Solutions A and B were filtered before use. Buffer solutions A and B were mixed with the sample solutions at a volume ratio of 1:5.

A reactivation solution, 0.1M in Al^{3+} and nitric acid, was prepared by dissolving 3.3 g of $\text{Al}_2(\text{SO}_4)_3 \cdot 18\text{H}_2\text{O}$ in 100 ml of 0.1M nitric acid.

General measuring procedure

The detection cell is prepared for measurement by directing the jet to the centre of the working electrode and adjusting its distance from the electrode. The jet is placed excentrically in a plastic stopper, so that its proper position is attained by turning the stopper, while pumping water onto the electrode surface through the jet in the empty vessel. The vessel is then filled with 50 ml of an appropriate reactivation solution and the ISE potential is allowed to stabilize.

The test solution is pumped for 5–10 sec, thus obtaining sample solution volumes from 0.25 to 0.5 ml at a flow-rate of 3 ml/min. When a sample is not aspirated, air is pumped through the jet and the reactivation solution is thus stirred at the electrode, hastening the reactivation process.

Procedure for determination of fluoride and chloride in the steel corrosion products and in the fly dust from electric-arc furnaces

A sample of 10–25 mg is fused in a platinum crucible with 0.5 g of sodium carbonate; 20 mg of silica may be added to assist the sample decomposition. The melt is extracted with 5 ml of cold water in an ultrasonic bath, the extract acidified with 2 ml of 5M nitric acid, degassed in an ultrasonic bath and diluted with water to 10 ml. A part of this solution is measured in a polyethylene beaker and diluted with water to 20 ml. A volume of 5 ml of buffer A (determination of fluoride) or buffer B (determination of chloride) is added to the beaker, the mixture is stirred and the determination is carried out according to the above measuring procedure. The vessel contains the appropriate

reactivation solution, *i.e.*, 0.1M Al^{3+} + 0.1M HNO_3 (fluoride) or 0.1M NaNO_3 + 0.1M CH_3COOH + 0.1M CH_3COONa + 0.02M DCTA, pH 4.3 (chloride). The samples are pumped for 10 sec at a flow-rate of 3 ml/min; the reactivation interval is 30 sec.

RESULTS AND DISCUSSION

So far, when the activity of a measuring ISE in a flow cell changed, the electrode was either removed from the cell and reactivated by a suitable mechanical or chemical procedure, or a chemical reactivation was carried out directly in the cell, by passage of a reactivating solution. In both cases, the sequence of analytical measurements had to be interrupted. However, the favourable properties of the large-volume wall-jet cell, primarily the fact that the solution impinging on the electrode efficiently separates the electrode surface from the bulk solution in the cell, make it possible to continuously reactivate the electrode by placing the reactivating solution in the cell. During passage of a sample solution, the reactivating solution has no access to the electrode surface; between samples, air is pumped through the jet and stirs the reactivating solution at the electrode.

The most efficient way of reactivating solid-membrane ISE's is removal of a very thin layer of the electrode surface, either by mechanical polishing or chemical etching. In this work, complexation reactions are used for the purpose—an acidic solution of aluminium ions for the fluoride ISE and a weakly acidic solution of DCTA for the chloride ISE. The action of these solutions is efficient but gentle and no mechanical damage is done to the electrode surface.

Basic properties of the cell

The results are in agreement with those published earlier.⁸⁻¹¹ The optimal distance of the jet orifice from the electrode surfaces lies within an interval of 2–12 mm. The higher the flow-rate, the greater is the optimal distance. At distances shorter than 2 mm, the noise sharply increases; at distances longer than *ca.* 12 mm, the beam of the liquid coming from the jet ceases to be intact. For the flow-rate used in further experiments, 3 ml/min, a distance of 3–6 mm was found optimal and was maintained within this interval throughout. At this or greater distance, there was also no danger of air bubbles being trapped between the jet and the electrode.

Table 1. Dependence of the time constant, T_k , of the detector with the chloride ISE on the flow-rate of the test solution

Flow rate, ml/min	T_k , sec
1	4.60
2	1.93
3	1.14
4	0.73
6	0.55
8	0.40

The T_k value is the time required for the signal to increase to 63.2% of the maximum value on a step change in the chloride concentration; the test solution, $0.1M HNO_3 + 2.5 \times 10^{-5}$ or $2.5 \times 10^{-4}M Cl^-$; the cell solution, $0.1M HNO_3$.

As can be expected, the response time decreases with increasing flow-rate (for the dependence with the chloride ISE see Table 1). From the points of view of electrode response and sample consumption, a flow-rate of 3 ml/min is a useful compromise.

Determination of fluoride and chloride

Whereas the response rate of the chloride ISE is independent of the solution pH from 1.1 to 4.6 and of the chloride concentration within the range of 2.5×10^{-4} – $2.5 \times 10^{-5}M Cl^-$, the response rate of the fluoride ISE increases with increasing concentration of fluoride and decreasing pH (see Table 2). Moreover, the linear dynamic range increases with decreasing pH (see Fig. 2). However, measurement in strongly acidic solutions is inconvenient because the potential stabilization is slow and the selectivity of measurement is poorer. Therefore, it is better to work at a pH between 4 and 5 (we further used

Table 2. Dependence of the time constant, T_k , of the detector with the fluoride ISE on the fluoride concentration and the solution pH

pH	c_{F^-} , $\mu g/25 ml$	T_k , sec
6.7	1.9	4.8
6.7	19	1.5
4.6	1.9	2.7
4.6	19	0.6
1.1	1.9	1.3
1.1	19	0.6

For the definition of T_k see Table 1; the test and the cell solutions were identical, either $0.1M HCl$ (pH 1.1), or $0.1M NaCl + 0.08M CH_3COOH$ with the pH adjusted between 4.6 and 6.7 by additions of NaOH.

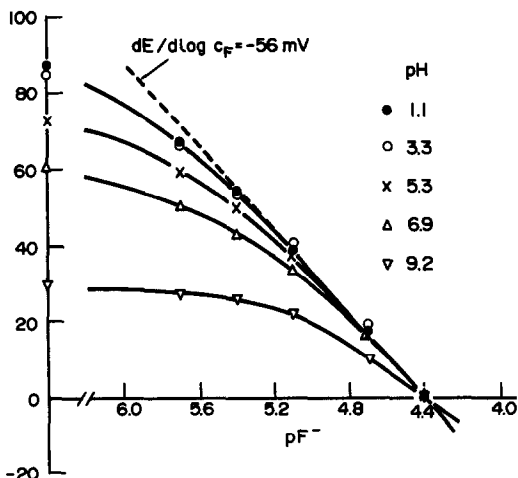


Fig. 2. The effect of the test solution pH on the fluoride calibration plot. The test and the cell solution were identical: $0.1M$ sulphosalicylic acid + $0.02M$ EDTA with the pH adjusted with an NaOH solution, or a $0.1M HCl$ (pH 1.1).

a pH of 4.3), and add aluminium(III) ions to the cell solution to enhance the electrode reactivation ($0.1M HNO_3 + 0.1M Al^{3+}$). We further added DCTA to the sample solution, to improve the measuring selectivity.⁶

The calibration dependences obtained under these conditions are given in Fig. 3. It can be seen that the slope of the dependence is higher for the flow measurement (68 mV per concentration decade) than for the batch measurements under identical conditions (60 mV per concentration decade). The reason for this phenomenon is not only a somewhat higher sensitivity of measurement attained under flow conditions, but also the fact that a nonsteady-

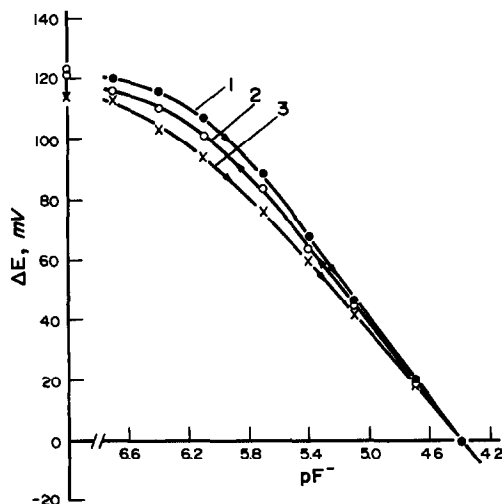


Fig. 3. The calibration plots for fluoride obtained in flow (1, 2) and batch (3) experiments. Buffer solution A; reactivation solution of $0.1M Al^{3+}$ and HNO_3 .

state signal is measured in the flow system and that the electrode response is slower at low analyte concentrations. Therefore, the values obtained at low fluoride concentrations are further removed from the respective steady-state values than those obtained at higher analyte concentrations. The hysteresis region in the flow measurements is wider at low analyte concentrations (*ca.* 6 mV) and it only occurs in the presence of DCTA (this confirms the earlier observations that DCTA makes the response of the fluoride ISE slower⁶).

Typical recordings of repeated flow determinations of fluoride are given in Fig. 4. It can be seen that the baseline is usually subject to a drift and thus it is more convenient to measure the difference between the peaks corresponding to the highest and the actual analyte concentration. Hence the signal for the highest analyte concentration defines the working baseline, which is stable for several hours.

The limit of determination was determined as follows: A regression straight line was constructed for a narrow range of the lowest concentrations ($0-4 \times 10^{-7}$ and $0-4 \times 10^{-6}$ for fluoride and chloride, respectively), and the value was found on this line that corresponded to triple the standard deviation of the intercept divided by the straight line slope. The limit of determination for fluoride under the above flow conditions is $1.2 \mu\text{g/l.}$ ($6.3 \times 10^{-8} M$), which is a value about 30 times lower than that obtained in common batch measurements.¹⁹ An

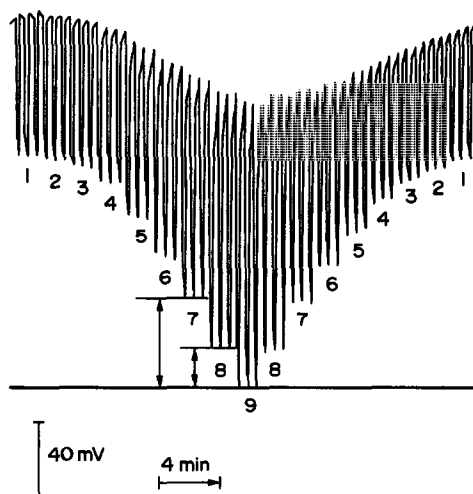


Fig. 4. A recording of a series of flow determinations of fluoride. Measurements were always made in triplicate (for conditions see Fig. 3 and text). c_F ($\mu\text{g}/25 \text{ ml}$): 0 (1), 0.095 (2), 0.19 (3), 0.38 (4), 0.95 (5), 1.9 (6), 3.8 (7), 9.5 (8) and 19 (9).

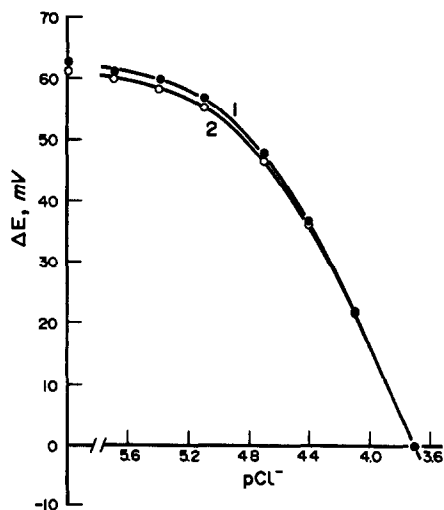


Fig. 5. The calibration plots for chloride. Flow measurement with (1) and without (2) DCTA (for conditions see text).

analogous situation is with the determination of chloride, where the limit of determination equals $8 \mu\text{g/l.}$ (2.3×10^{-7}), about 14 times lower than in common batch measurements.¹⁹

In measurements with the chloride ISE, the optimal pH range lies between 2.5 and 4.5, as expected and thus a solution of buffer B was selected for the measurement. The electrode can be reactivated in the blank sample solution, but somewhat better results are obtained when this solution is made $0.02 M$ in DCTA. The slope of the calibration plot (Fig. 5) then slightly increases (from 61.4 mV per concentration decade in the absence of DCTA to 62.7 mV in its presence) and the linear correlation coefficient is somewhat improved (from 0.9996 to 0.9999). The cleaning effect of DCTA probably depends on the complexation reaction with the Ag^+ ions on the surface of the membrane. Moreover, DCTA improves the selectivity of determination, similar to the determination of fluoride.

Rather high concentrations of the reactivation solutions were used to prevent rapid loss of their function on dilution with the samples. Under the given experimental conditions, at least 150 measurements could be carried out without significant deterioration in the measuring reliability. The reactivation solution was then replaced.

The results of the application of the flow-through method to determination of fluoride and chloride in steel corrosion products and in a reference sample of an electric-arc furnace fly

Table 3. Determination of fluoride and chloride in the steel corrosion products and in a reference sample of the electric-arc furnace fly dust (for procedures see Experimental)

Sample	Decomposition procedure	Fluoride content	n	Chloride content	n	Turbidimetry
		(%) Confidence interval		(%) Confidence interval		
Corrosion products I	without SiO ₂	0.017 ± 0.003	3	0.21 ± 0.04	3	0.28 ± 0.05
Corrosion products II	without SiO ₂	0.053 ± 0.005	3	1.29 ± 0.04	4	1.3 ± 0.03
Fly dust	without SiO ₂	0.26 ± 0.04	4	1.35 ± 0.17	3	1.5 ± 0.08
	with SiO ₂	0.24 ± 0.04	4	1.39 ± 0.17	3	0.43 ± 0.10

dust are given in Table 3 (for the procedures see Experimental). The determination of chloride was compared with the results obtained by a turbidimetric method²⁰ employing a surfactant for stabilization of the turbidity and the agreement was satisfactory (see Table 3), except for the procedure in which SiO₂ was added to the fusion mixture. The turbidimetric determination is, of course, much more sensitive to colouration of the test solution and to cloudiness, which is caused in this case by a high content of hydrated silicon dioxide. The results indicate that the method yields good results and permits about 90 individual measurements per hour. There was no suitable reference method available for the determination of fluoride.

REFERENCES

1. J. Růžička and E. H. Hansen, *Flow Injection Analysis*, 2nd Ed., Wiley, New York, 1988.
2. M. Valcárcel and M. D. Luque de Castro, *Flow Injection Analysis. Principles and Applications*, Horwood, Chichester, 1987.
3. K. Štulík and V. Pacáková, *Electroanalytical Measurements in Flowing Liquids*, Horwood, Chichester 1987.
4. J. Koryta and K. Štulík, *Ion Selective Electrodes*, 2nd Ed., Cambridge University Press, 1983.
5. P. Peták and K. Štulík, *Anal. Chim. Acta*, 1986, **185**, 171.
6. J. Veselý, D. Weiss and K. Štulík, *Analysis with Ion-Selective Electrodes*, Horwood, Chichester, 1978.
7. G. Horvai, K. Tóth, J. Fekete and E. Pungor, *Euro-analysis IV*, Helsinki, 1981.
8. H. Gunasingham and B. Fleet, *Anal. Chem.*, 1983, **55**, 1409.
9. H. Gunasingham, B. T. Tay, K. P. Ang and L. L. Koh, *J. Chromatog.*, 1984, **285**, 103.
10. H. Gunasingham, *Anal. Chim. Acta*, 1984, **159**, 139.
11. Z. Niegreis, L. Szűcs, J. Fekete, G. Horvai, K. Tóth and E. Pungor, *J. Chromatog.*, 1984, **316**, 451.
12. W. Matuszewski, M. Trojanowicz and W. Frenzel, *Z. Anal. Chem.*, 1988, **332**, 148.
13. L. Ilcheva, M. Trojanowicz and T. Krawczynski vel Krawczyk, *ibid.*, 1987, **328**, 27.
14. M. Trojanowicz and W. Frenzel, *ibid.*, 1987, **328**, 653.
15. W. Frenzel, *Analyst*, 1988, **113**, 1039.
16. M. Trojanowicz and M. E. Mayerhoff, *Anal. Chem.*, 1989, **61**, 787.
17. *Idem*, *Anal. Chim. Acta*, 1989, **222**, 95.
18. J. Langmaier, K. Štulík and R. Kalvoda, *ibid.*, 1983, **148**, 19.
19. J. Lexa and K. Štulík, *Chem. Listy*, 1988, **82**, 1287.
20. J. Lexa and J. Liška, *Czech Pat. Appl. PV 4021-88*, 1988: AO 270 057.

CHLOROQUINE POLYMERIC MEMBRANE ELECTRODES: DEVELOPMENT AND APPLICATIONS

BAHRUDDIN SAAD,* KANAGI KANAPATHY and MOHD NOOR AHMAD

School of Chemical Sciences, Universiti Sains Malaysia, 11800 Penang, Malaysia

ABAS HAJI HUSSIN and ZHARI ISMAIL

School of Pharmaceutical Sciences, Universiti Sains Malaysia, 11800 Penang, Malaysia

(Received 30 December 1990. Revised 13 May 1991. Accepted 18 June 1991)

Summary—Three main types of PVC solvent polymeric membrane ion-selective electrodes for chloroquine are described. They are based on three ion-pairing agents namely dipicrylamine (DPA), tetraphenylborate (TPB) or tetrakis(4-chlorophenyl)borate (TCPB) with either dioctylphenyl phosphonate (DOPP) or trioctyl phosphate (TOP) solvent mediator. All electrodes exhibit Nernstian responses, fast dynamic response times and a wide useful pH range. The best all-round electrode is based on TPB and TOP plasticizing solvent mediators with a limit of detection of $7.1 \times 10^{-6}M$ and was utilized for the assay of chloroquine in tablets. Direct potentiometric determinations with either the analyte addition method or the normal calibration method gave results comparable to the official method.

Malaria is a mosquito-borne disease and one of the major killers of the world, currently causing an estimated one million deaths annually.¹ In 1983, a report estimated the number of new malaria infections annually throughout the world was 210–230 million,² most of these (85%) being malignant malaria caused by the most dangerous of all the malaria parasites, *Plasmodium falciparum*.

Anti-malaria drugs are usually classified in terms of the action against the different stages of the life-cycle of the parasite. Chloroquine [7-chloro-4-(4-diethylamine-1-methylbutylamino)-quinoline] the most widely used anti-malarial drug is an example of a schizonticidal agent which is effective against the erythrocytic forms of the plasmodial organism and is used to cure the clinical attack of malaria.³ Chloroquine is effective against the erythrocytic forms of all types of malaria parasites with the exception of resistant strains of *Plasmodium falciparum* in South America and South-East Asia. With the exception of this resistant strain, they completely cure falciparum malaria.

Chloroquine in pharmaceutical preparations may be determined by two rather laborious methods: the U.S. Pharmacopoeia⁴ which involves extraction with chloroform followed by spectrophotometry at 343 nm; or the British

Pharmacopoeia⁵ which involves extraction of the chloroquine in sodium hydroxide with ether and back titration of excess base with hydrochloric acid, using bromocresol green as indicator.

Ion-selective electrodes have been advocated as simple, fast responding and sensitive devices for the monitoring of various biochemical and pharmaceutical species.^{6–8} In this context, a PVC membrane chloroquine selective electrode containing chloroquine–dinonylnaphthalene sulphonate (DNNS) as the electroactive material and 2-nitrophenyl octyl ether (NPOE) solvent mediator has been proposed.⁹ Here we report the development of chloroquine solvent polymeric membrane electrodes based on three other ion-pairing agents namely DPA, TCPB and TPB.

EXPERIMENTAL

Reagents

Sodium tetraphenylborate, potassium tetrakis(4-chlorophenyl)borate and high molecular mass poly(vinyl chloride) were obtained from Aldrich. The other reagents were obtained from the following sources: dioctylphenyl phosphonate (Lanchester Synthesis); chloroquine diphosphate, glucose, starch (Sigma); hydrochlorides of berberine and cinchonine, dipicrylamine (Tokyo Kogyo Kasei); trioctyl phosphate (Pfaltz and Bauer). Chloroquine tablets were

*Author for correspondence.

purchased from a local drug store. AnalaR-grade chlorides of calcium, magnesium, sodium, potassium and copper(II) were used.

Electrode preparation and use

Chloroquine-TPB ion-pair was formed by precipitation of an aqueous solution of sodium tetraphenylborate (0.1M) and chloroquine diphosphate (0.1M). The white precipitate was isolated by filtration, thoroughly washed with demineralized water and dried overnight at 30°. The dried salt (40 mg) was added to PVC (170 mg) and plasticizing solvent mediator (360 mg) dissolved in tetrahydrofuran (6.0 cm³). The homogeneous cocktail was next cast with a glass plate and glass ring (30 mm i.d.) as described elsewhere.¹⁰

For potassium tetrakis(4-chlorophenyl)borate and dipicrylamine which are both insoluble in water, it was necessary to prepare their master membranes by entrapping the ion-pairing agent without chloroquine (30 mg) plus plasticizing solvent in PVC, in an equal amount as for the TPB membrane. The TCPB- and DPA-chloroquine ion-pair was generated *in situ* by conditioning the assembled electrode¹⁰ in 10⁻²M chloroquine diphosphate (pH 4.70, ionic strength 0.03M) overnight. Similar chloroquine diphosphate concentration was used as the internal filling solution for all the electrodes. After overnight storage, the DPA-based membrane turned from orange to dark brown, indicating the formation of a DPA-chloroquine ion-pair.

Electrochemical measurements were made with an Orion digital ionanalyser (Model 701A). A double junction reference electrode (Orion model 90-02) was used. Electrode calibrations were effected by spiking with successive aliquots of a known concentration of sample into doubly demineralized water (20 cm³). All samples were prepared in doubly demineralized water. The chloroquine standard solution was prepared fresh and protected from light by wrapping the standard flasks with aluminium foil.

Selectivity coefficients, $k_{i,j}^{\text{pot}}$ were measured with the separate solution method at a cation concentration of 10⁻²M, unless otherwise stated, using the equation;

$$\log k_{i,j}^{\text{pot}} = (E_2 - E_1)/S$$

where E_1 and E_2 are the measurements on separate solutions of the primary ion (i) and interferent ion (j), respectively, at the same

concentration, and S is the slope of the chloroquine calibration curve.

Tablet analysis

All analysis was done in 0.10M acetate buffer; pH adjusted to 5 with sodium hydroxide. Ten chloroquine tablets were finely ground and thoroughly mixed. A mean mass of each tablet of 0.4131 g was dissolved in acetate buffer in a standard flask (100 cm³) up to the mark. The analyte addition method was based on:

$$C_o = C_s [10^{\Delta E/S} (1 + V_s/V_o) - V_s/V_o]$$

where ΔE is the emf difference after spiking the tablet solution of volume V_o (150 μ l) of unknown concentration C_o into a chloroquine solution in buffer of volume V_s (15 cm³) and concentration C_s (10⁻⁴M).

RESULTS AND DISCUSSION

All electrodes prepared with TPB, TCPB and DPA as ion-pairing agents in a plasticized PVC liquid membrane gave functional chloroquine electrodes with almost Nernstian responses (Table 1) and a long linear range. Even though these electrodes possessed slightly inferior detection limits as compared to the reported chloroquine electrode based on dinonylnaphthalene sulphonate, this is sufficiently low for many analytical applications. These electrodes exhibit fast dynamic response times (= 10 sec), although at lower concentrations (< 10⁻⁶M), the response time is expectedly sluggish (30–60 sec). The electrode responses were found to be pH-independent in the pH range of about 3.5–8.0 (Fig. 1). This was studied by varying the pH of 10⁻³M chloroquine by addition of minute amounts of concentrated hydrochloric acid and/or sodium hydroxide. At higher pH values, the potential decreased due to the gradual increase in the concentration of unprotonated chloroquine resulting in the precipitation of chloroquine base, while at low pH, a triprotonated chloroquine species [ChlH_3^{3+}] is probably formed. The chloroquine base and the triprotonated chloroquine are presumably not detected by the electrode. Such pH-mV profiles are also observed for electrodes based on other ion-pairing agents.¹¹

When tested for possible interferents that might be present in pharmaceutical preparations, the electrodes were essentially interferent-free from the alkali and alkaline earth metal ions tested (Table 2). The electrode

Table 1. Comparison of electrochemical characteristics of chloroquine membrane electrodes

Electrode no. (ion-pairing agent)	Solvent mediator	Slope*, <i>mV/decade</i>	Detection limit*, <i>M</i>	Useful pH range
1 (TPB)	DOPP	32.0	4.3×10^{-6}	
2 (TPB)	TOP	33.0	7.1×10^{-6}	3.5–8.0
3 (TCPB)	DOPP	31.2	3.5×10^{-5}	
4 (TCPB)	TOP	32.6	8.6×10^{-5}	4.0–8.0
5 (DPA)	DOPP	31.3	7.0×10^{-6}	
6 (DPA)	TOP	33.0	2.8×10^{-5}	3.5–8.0
7† (DNNS)	NPOE	28.6	2.0×10^{-7}	2.0–8.0

*Mean of three determinations.

†From Reference 9. Key to abbreviations: TPB = Sodium tetraphenylborate. DOPP = Dioctyl phenylphosphonate. TOP = Trioctyl phosphate. TCPB = Potassium tetrakis(4-chlorophenyl)borate. DPA = Dipicrylamine. DNNS = Dinonyl naphthalenesulphonic acid.

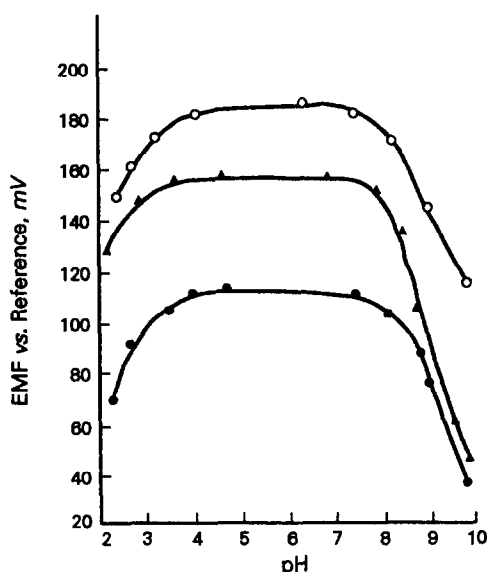


Fig. 1. pH-emf profiles of chloroquine electrodes (all at $10^{-3}M$ chloroquine) based on TPB (○), TCPB (●) and DPA (▲); all plasticized with trioctyl phosphate.

responses were also not affected by glucose or binders such as starch. Indeed, the electrode response was unaffected even up to 500 ppm starch. However, alkaloids such as cinchonine and berberine cause serious interferences. This

is expected of electrodes based on ion-pairing agents where larger lipophilic species will also be efficiently extracted into the membranes,¹² hence the interference phenomena. Interference from lipophilic amines were also observed for the DNNS-based chloroquine electrode.⁹ However, this is of no deterrent to the use of these electrodes in the analysis of pharmaceutical preparations as these alkaloids are not present together with chloroquine.

The use of trioctyl phosphate plasticizing solvent also yields a good quality electrode (Table 1) with Nernstian response and fast response times. The use of TOP yields electrodes of slightly improved selectivity characteristics, especially for the TPB-based membrane (Table 2). Hence this electrode (electrode 2) was studied further.

Potentiometric determination of standard chloroquine solutions utilizing this electrode yields an average recovery of 103.0 and 100.9% with the normal calibration and the analyte addition methods, respectively (Table 3). When used for the analysis of chloroquine in tablets, the potentiometric normal calibration and analyte addition methods yield 252.0 and 250.0 mg per tablet of the base, respectively, as

Table 2. Selectivity coefficients* k_{ij}^{Pot} of chloroquine membrane electrodes

Electrode No.	Ca ²⁺	Mg ²⁺	Na ⁺	K ⁺	Cu ²⁺	Glucose	Cinchonine	Berberine
1	5.43×10^{-3}	1.83×10^{-3}	2.28×10^{-3}	1.28×10^{-3}	9.02×10^{-2}	6.12×10^{-4}	47.2	38.0
2	5.37×10^{-3}	1.99×10^{-3}	7.88×10^{-4}	5.67×10^{-4}	1.63×10^{-3}	3.56×10^{-4}	69.0	14.1
3	4.29×10^{-2}	7.94×10^{-3}	2.06×10^{-3}	2.72×10^{-4}	1.39×10^{-2}	8.84×10^{-5}	0.26	29.2
4	5.78×10^{-2}	7.81×10^{-3}	1.85×10^{-2}	9.82×10^{-3}	4.78×10^{-2}	1.49×10^{-2}	2.79	65.34
5	2.94×10^{-2}	7.18×10^{-3}	1.97×10^{-3}	8.16×10^{-4}	1.54×10^{-2}	1.12×10^{-4}	3.05	22.53
6	2.02×10^{-2}	7.37×10^{-3}	3.25×10^{-3}	1.05×10^{-3}	1.22×10^{-3}	2.89×10^{-4}	8.50	87.29
7†	$<10^{-4}$	$<10^{-4}$	$<10^{-4}$	$<10^{-4}$	—	—	—	—

*Separate solution method, evaluated at $10^{-2}M$ except for cinchonine and berberine, ($10^{-3}M$).

†Fixed interferent method ($10^{-2}M$), from Ref. 9.

Table 3. Potentiometric determination of chloroquine using the tetraphenylborate (TPB) chloroquine electrode*

Chloroquine spiked, ppm	Normal calibration, ppm	Analyte addition, ppm
3.2	3.4 (106.0%)†	—
16.0	16.9 (105.0%)	—
32.0	33.2 (103.4%)	—
160.0	163.1 (101.9%)	—
319.9	323.1 (101.0%)	323.1 (101.0%)
1599.5	1609.0 (100.5%)	1612.2 (100.8%)

*Mean of triplicate determinations.

†All data in brackets denote per cent recovery.

compared to the British pharmacopoeia method of 246.0 mg.

CONCLUSIONS

The electrodes developed showed good prospects for the analysis of chloroquine in pharmaceutical preparations. Although the detection limit ($7.1 \times 10^{-6}M$) is slightly inferior as compared to the DNNS-based electrode ($2 \times 10^{-7}M$), good agreement was found between both the calibration and analyte

addition potentiometric methods and the official method, using the proposed electrode. The proposed electrode method has the advantage of being much simpler than the official method.

Acknowledgements—The authors would like to express their gratitude to the Universiti Sains Malaysia for a short-term grant and the Federal Government of Malaysia for funding this work.

REFERENCES

1. D. J. Wyler, *N. Eng. J. Med.*, 1983, **308**, 875.
2. *Idem, ibid.*, 1983, **308**, 934.
3. World Health Organization Technical Report, 1984, Series 711.
4. United States Pharmacopoeia, XX Rev., U.S. Pharmacopoeial Convention, Rockville, MD, 1980.
5. British Pharmacopoeia 1980, Vol. 1, p. 103. HMSO, London, 1980.
6. V. V. Cosofret, *Ion-Selective Electrode Rev.*, 1980, **2**, 159.
7. V. V. Cosofret and R. P. Buck, *ibid.*, 1984, **6**, 59.
8. L. Campanella and M. Tomassetti, *Selective Electrode Rev.* 1989, **11**, 69.
9. V. V. Cosofret and R. P. Buck, *Anal. Chim. Acta*, 1985, **174**, 299.
10. A. Craggs, G. J. Moody and J. D. R. Thomas, *J. Chem. Educ.*, 1974, **51**, 541.
11. S. S. M. Hassan and E. M. Elnemma, *Analyst*, 1989, **114**, 1033.
12. W. E. Morf, *The Principles of Ion-Selective Electrodes and of Membrane Transport*, p. 11. Elsevier, Amsterdam, 1981.

EXTRACTION AND COMPLEX FORMATION OF NIOBIUM(V) WITH 3-HYDROXY-2-METHYL-1-(4-TOLYL)-4-PYRIDONE

A. GOJMERAC IVŠIĆ and B. TAMHINA

Laboratory of Analytical Chemistry, Faculty of Science, University of Zagreb, Strossmayerov trg 14,
41000 Zagreb, Yugoslavia

(Received 1 October 1990. Revised 4 June 1991. Accepted 4 June 1991)

Summary—The extraction of niobium(V) from aqueous hydrochloric and sulphuric acid solutions with 3-hydroxy-2-methyl-1-(4-tolyl)-4-pyridone (HY) dissolved in chloroform is described. Niobium(V) can be quantitatively extracted with HY in the form of two different complexes depending on the chloride ion concentration in the aqueous phase. At a low chloride concentration or without chloride in the aqueous phase niobium(V) is extracted with HY in the form of $\text{Nb}(\text{OH})_3\text{Y}_2$ and at a high chloride concentration as a mixed $\text{Nb}(\text{OH})_3\text{ClY}$ complex. Niobium extraction with HY enables the separation of niobium(V) from zirconium(IV) and hafnium(IV). The formation of a mixed chloro-4-pyridone complex is also applicable for the spectrophotometric determination of niobium in the organic phase at the maximum absorption at 350 nm.

In continuation of our investigations of metal extraction with 4-pyridone derivatives: 3-hydroxy-2-methyl-1-phenyl-4-pyridone (HX) and 3-hydroxy-2-methyl-1-(4-tolyl)-4-pyridone (HY)¹⁻⁵ the present experiments were undertaken to study the extraction of niobium(V) with HY from different aqueous solutions. The results described here show that the extraction of niobium(V) with HY is preferable to that with HX¹ because it is feasible from solutions without the presence of large amounts of chloride or thiocyanate ions. Niobium(V) can be quantitatively extracted with HX only in the presence of an excess of chloride or thiocyanate ions in the form of a mixed $\text{Nb}(\text{OH})_3\text{ClX}$ [$\text{Nb}(\text{OH})_3\text{NCSX}$] complex.¹ However, niobium(V) can be quantitatively extracted with HY in the form of two different complexes depending on the chloride ion concentration in the aqueous phase. At a low chloride concentration or without chloride in the aqueous phase niobium is extracted with HY in the form of $\text{Nb}(\text{OH})_3\text{Y}_2$ and at a high chloride concentration as a mixed $\text{Nb}(\text{OH})_3\text{ClY}$ complex. For some other metal ions, as for niobium(V), HY is a more effective extractant than HX.²⁻⁵ With some metal ions the tolyl analogue (HY) reacts at higher acid concentration than the phenyl analogue (HX), quantitatively extracted with less excess of extractant, and sometimes causes a change in the composition of extracted complexes.

Based on conditions of niobium(V) extraction with HY described here and those of zirconium(IV) and hafnium(IV) extraction with HY dealt with earlier,⁵ a simple and fast separation of niobium(V) from zirconium(IV) and hafnium(IV) is feasible by extraction with HY from 1M hydrochloric acid.

EXPERIMENTAL

Reagents and radioactive tracer

A standard solution of niobium(V) (about $2 \times 10^{-2}M$) was prepared in hydrochloric and sulphuric acid solutions as described earlier.¹ The ⁹⁵Nb isotope supplied from the Radiochemical Centre, Amersham, England, in the form of an oxalato complex in a 0.5% solution of oxalic acid was used as tracer. ⁹⁵Nb in the form of chloride and sulphate was prepared as described earlier.¹ HY was synthesized as described previously⁶ and used in a chloroform solution. All other chemicals used were of analytical reagent grade.

Apparatus and procedures

Radioactivity measurements were performed with a well-type gamma scintillation counter (NaI/Tl) from Ecko Electronic. Gamma-ray spectrophotometry was carried out with a computerized multichannel analyzer, Model 8100, Canberra. For extraction, a Griffin flask shaker with a time switch was used. Absorption spectra

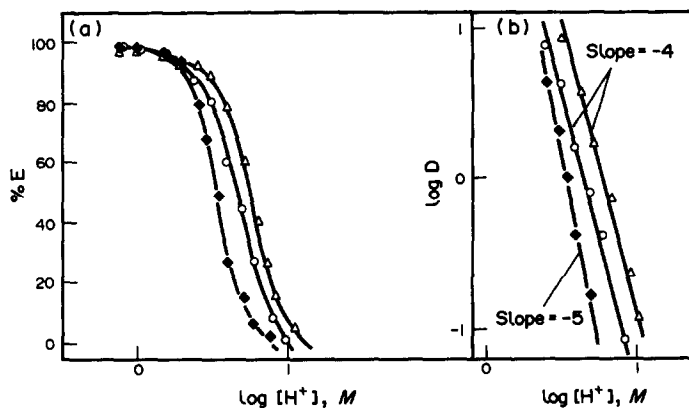


Fig. 1. The dependence of the percentage of extraction (a) and the distribution ratio (b) of niobium on initial hydrogen ion concentration. Concentration: $6 \times 10^{-5} M$ Nb(V); \blacklozenge , sulphuric acid solution, without addition of Cl^- ; \circ , \triangle , hydrochloric acid solution, $(\text{H}, \text{Li})\text{Cl} = 10M$; \circ , $1.5 \times 10^{-3} M$ HY; \triangle , $3 \times 10^{-3} M$ HY.

and absorbance measurements of solutions were made with a Perkin-Elmer Hitachi-200 spectrophotometer.

Determination of the distribution ratio and spectrophotometric determination of niobium in the organic phase were performed by the same procedure as used for the HX method.¹

The testing of the separation of niobium(V) from zirconium(IV) and hafnium(IV) has been described earlier.⁵

RESULTS AND DISCUSSION

Optimum conditions for extraction

The extraction of niobium(V) from aqueous hydrochloric and sulphuric acid with HY dissolved in chloroform was examined at different acidities and ionic strengths. Niobium(V) can be quantitatively extracted with HY from aqueous

hydrochloric or sulphuric acid solution in the range 0.8–1.2M hydrogen ion concentration [Fig. 1(a)] if chloride concentration is less than 3M (Table 1). With an increase in chloride ion concentration in the range 3–6M the percentage of extracted niobium gradually decreases, but with an increase in chloride concentration above 6M it increases again and at a chloride ion concentration higher than 8M, niobium(V) is quantitatively extracted from hydrochloric acid solutions. From sulphuric acid solution and at a chloride ion concentration above 8M, the maximum niobium concentration is about 83%. The optimal hydrochloric acid concentration for quantitative extraction of niobium(V) at a chloride concentration higher than 8M is also 0.8–1.2M, and is the same for extraction of niobium(V) at a low chloride concentration or without chloride in the aqueous phase

Table 1. The dependence of niobium extraction on chloride ion concentration in the aqueous phase

Conc. LiCl, M	Hydrochloric acid solution		Sulphuric acid solution
	E, %	A_{350}	E, %
—	99.6		99.5
0.5	99.7		99.7
1.0	99.6		99.5
1.5	99.6		99.6
2.0	99.7		99.6
2.5	99.7		99.7
3.0	99.2		99.4
4.0	98.0		95.3
5.0	95.2		89.0
6.0	92.8	0.390	73.2
7.0	95.3	0.455	78.3
8.0	99.2	0.515	79.5
9.0	99.6	0.516	82.3
10.0	99.7	0.515	83.2

Organic phase: $3 \times 10^{-3} M$ HY.

Aqueous phase: $6 \times 10^{-5} M$ Nb(V), 1.0M H^+ .

Table 2. The dependence of niobium extraction on HY concentration in the organic phase

Conc. HY, <i>M</i>	HY:Nb (molar ratio)	Chloride conc.,		<i>A</i> ₃₅₀
		2 <i>M</i>	10 <i>M</i>	
2×10^{-5}	0.34	1.1	25.0	
5×10^{-5}	0.83	1.6	49.0	
1×10^{-4}	1.67	11.1	69.2	0.112
3×10^{-4}	5.00	39.9	90.7	0.213
5×10^{-4}	8.34	66.6	93.7	0.250
8×10^{-4}	13.34	82.3	96.7	0.358
1×10^{-3}	16.67	87.1	98.3	0.458
2×10^{-3}	33.34	99.1	99.8	0.498
3×10^{-3}	50.00	99.8	99.7	0.512
6×10^{-3}	100.00	99.7	99.8	0.516
1×10^{-2}	166.67	99.7	99.7	0.515

Aqueous phase: $6 \times 10^{-5}M$ Nb(V), $1M$ H⁺.

[Fig. 1(a)]. These results suggest that niobium(V) can be extracted with HY in the form of two different complexes depending on the chloride ion concentration in the aqueous phase and also suggest that hydrochloric acid solutions are more suitable for extraction of niobium than sulphuric acid solutions. In order to extract niobium(V) quantitatively from an optimal hydrochloric acid concentration the HY concentration must be at least 17 times higher than that of niobium if extraction takes place from solution at a chloride concentration higher than $8M$ and 40 times higher if extraction is from solution without chloride or at a chloride concentration less than $3M$ (Table 2).

The niobium(V) extracted in the presence of an excess of chloride or at low chloride concentration, or without the presence of chloride can be quantitatively stripped with $10M$ hydrochloric or sulphuric acid. At optimum extracting conditions only citrate, tartrate, fluoride and oxalate minimize niobium extraction. These anions mask niobium(V) but do not interfere if present in moderate quantities. Citrate and tartrate may not exceed a 100-fold amount and fluoride and oxalate a 10-fold amount with respect to niobium(V).

Absorption spectra of the extracted complexes

The absorption maximum of the extracted complexes depends on chloride concentration and lies between 310 and 350 nm (Fig. 2). With an increase in chloride concentration it is shifted towards higher wavelengths. With chloride concentrations less than $3M$ the absorption maximum of the extracted complex is in the range 310–320 nm. With a chloride concentration between 3 and $5M$ the absorbance at

310–320 nm gradually decreases and, simultaneously, another absorption maximum appears at 350 nm. At a chloride concentration higher than $6M$ the absorption maximum of the organic phase is at 350 nm. At this wavelength there is no shift of either the absorption maximum or the absorbance values with an increase in chloride concentration. The absorbance of the organic phase obtained with an excess of chloride in the aqueous phase is stable for about 30 min. With prolonged standing the absorption maximum appears at 310–320 nm and the absorbance values at 310–320 nm increase with time. After 120 min, the maximum at 350 nm is still visible and after one day, the spectrum shows a maximum at 320 nm only (Fig. 3).

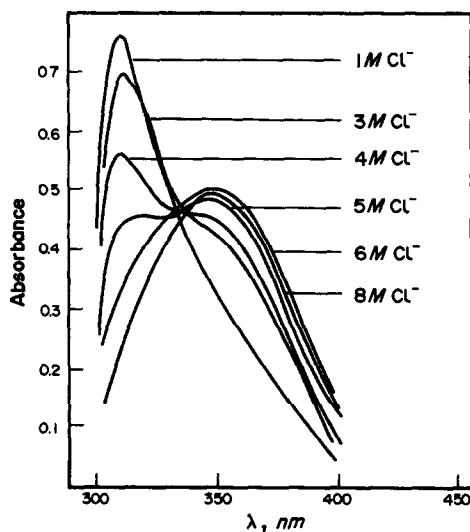


Fig. 2. The dependence of the absorption spectra of the organic phase on chloride ion concentration. $6 \times 10^{-5}M$ Nb(V); $1M$ H⁺; $3 \times 10^{-3}M$ HY.

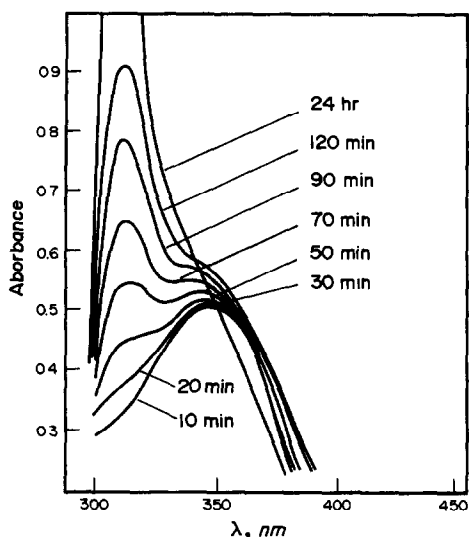
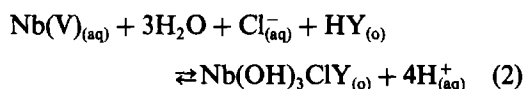
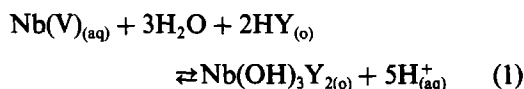


Fig. 3. The dependence of the absorption spectrum of the organic phase on standing time. $6 \times 10^{-5} M$ Nb(V); $1 M$ H^+ ; $10 M$ Cl^- ; $3 \times 10^{-3} M$ HY.

Identification of extractable niobium(V) complexes

The compositions of the extracted niobium(V) complexes have been studied by radiometric and spectrophotometric methods. Distribution studies (Fig. 4) show that at a low chloride concentration or without the presence of chloride in the aqueous phase niobium(V) can be extracted as a complex with two HY molecules bonded to a single niobium atom and at a high chloride concentration as a mixed chloro-HY complex with one HY molecule bonded to a single niobium atom. The ratio of niobium to HY was also determined on the basis of the dependence of niobium extraction on its initial concentration in the aqueous phase and spectrophotometrically by Job's method.

The results also indicate that niobium can be extracted as a complex with two HY molecules bonded to a single niobium atom or as a mixed chloro complex with one HY molecule bonded to a single niobium atom. Distribution studies also show that four protons are released in the formation of the mixed Nb-Cl-HY complex and five protons in the formation of the Nb-HY complex [Fig. 1(b)]. It was not possible to determine the ratio of niobium to chloride in the mixed chloro-HY complex, but the ratio was determined at extraction of niobium with HX as a mixed chloro-HX complex.¹ Comparison of those results and the results described here shows the compositions of the mixed Nb-Cl-HX and Nb-Cl-HY complexes to be identical. On the basis of all the results obtained and the fact that niobium(V) in an acidic solution can exist in the form of various hydroxo and oxo ions whose composition depends on the acidity as well as on the kind and concentration of anion present⁷⁻⁹ we suggest that complexes having the stoichiometries $Nb(OH)_3Y_2$ and $Nb(OH)_3ClY$ can be quantitatively extracted. The formation of these complexes may be shown as:



The formation of the complex at low chloride concentration or without chloride in the aqueous phase shown in equation (1) is fundamentally different from the extraction of niobium with HX. With HX, niobium is

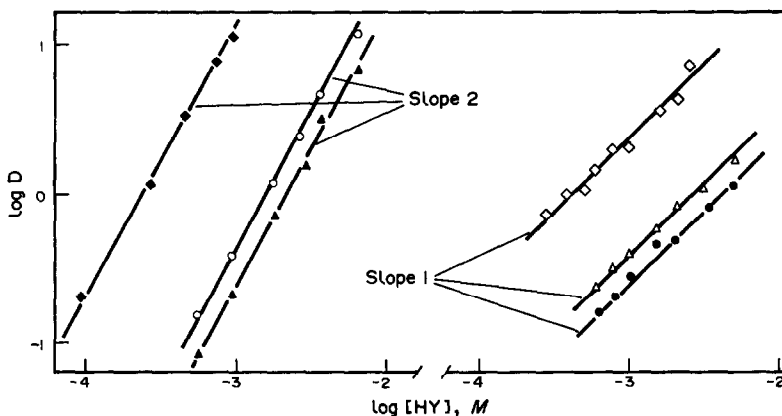
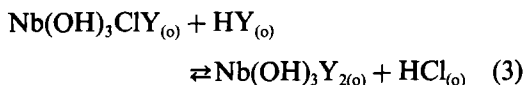


Fig. 4. The dependence of the distribution ratio of niobium(V) on initial HY concentration; \blacklozenge , \circ , \blacktriangle , without addition of Cl^- ; \diamond , \triangle , \bullet , $10 M$ Cl^- ; \blacklozenge , $1 M$ H^+ ; \circ , $3.2 M$ H^+ ; \blacktriangle , $3.5 M$ H^+ ; \diamond , $4.5 M$ H^+ ; \triangle , $6 M$ H^+ ; \bullet , $6.5 M$ H^+ .

quantitatively extracted only as a mixed ligand complex.¹ Based on the absorption spectra of the extracted complexes (Figs. 2 and 3) it is also suggested that the mixed ligand complex produced from a high chloride concentration in the aqueous phase shown in equation (2) with maximum absorption at 350 nm by prolonged standing reacts with the excess of undissociated HY molecules in the organic phase giving $\text{Nb}(\text{OH})_3\text{Y}_2$ with maximum absorption at 310–320 nm as shown in equation (3):



Spectrophotometric determination of niobium in the organic phase

The formation of a mixed ligand Nb–Cl–HY complex is applicable to the spectrophotometric determination of niobium in the organic phase at the maximum absorption of 350 nm. Optimum conditions for extraction and spectrophotometric determination are: 0.8–1.2M hydrogen ion concentration and 10M chloride concentration ($\text{HCl} + \text{LiCl} = 10M$) in the aqueous phase and $3 \times 10^{-3}M$ HY in the organic phase. The optimum concentration range for niobium is 1–20 $\mu\text{g}/\text{ml}$. Beer's law is obeyed over this range. The effective molar absorptivity is $8.7 \times 10^3 \text{ l. mole}^{-1} \cdot \text{cm}^{-1}$. The absorbance of the organic phase is stable for 30 min (Fig. 3). The reproducibility of the method, expressed as a relative standard deviation, is 1–5% depending on niobium concentration. The influence of foreign ions on the absorbance at 350 nm was studied. A large concentration of ions can be present in the aqueous solution of niobium. Acetate, bromide, sulphate, nitrate, perchlorate, ammonium, sodium, potassium, magnesium, cadmium, manganese(II), nickel, barium, strontium, chromium(III), lead and zinc ions do not interfere in amounts exceeding 1000-fold those of niobium. Thorium, uranyl, tin(II), europium, mercury(II), copper, citrate and tartrate are tolerated in 100-fold and molybdenum(VI), titanium, fluoride and oxalate in a 10-fold molar ratio to niobium. Uranyl, zirconium, thorium, copper and molybdenum can be found in large amounts if a higher HY concentration is present in the organic phase, because these metals con-

sume HY for their own extraction and decrease the extraction of niobium.

Separation of niobium(V) from zirconium(IV) and hafnium(IV)

The varying behaviours of niobium(V), zirconium(IV) and hafnium(IV), in extraction with HY can be utilized for their separation. From 1M hydrochloric acid, niobium is quantitatively extracted (Fig. 1) while zirconium and hafnium remain in the aqueous phase.⁵ The separation of zirconium and niobium is of large practical importance because of the radiochemical equilibrium $^{95}\text{Zr}/^{95}\text{Nb}$. The separation of zirconium and niobium was tested with $^{95}\text{Zr}/^{95}\text{Nb}$ and that of hafnium and niobium with a mixture of ^{181}Hf and ^{95}Nb . A 0.1-ml volume of $^{95}\text{Zr}/^{95}\text{Nb}$ in 5M hydrochloric acid or 0.1 ml of a mixture of ^{95}Nb and ^{181}Hf in 5M hydrochloric acid, 0.9 ml of 5M hydrochloric acid and 4 ml of water were shaken mechanically for 20 min with 5 ml of $5 \times 10^{-3}M$ HY in chloroform. For quantitative separation the HY concentration in the organic phase must be at least 40 times higher than that of niobium (Table 2). After centrifugation the phases were separated. The results show that the radiochemical purity of niobium in the organic phase was 98% and in the aqueous phase 98% for zirconium and hafnium. The radiochemical purity of the separated ^{95}Zr and ^{181}Hf in the aqueous phase and of ^{95}Nb in the organic phase was verified by a gamma counting system consisting of a 40-cm³ Ge(Li) semiconductor crystal attached to a multichannel (4096) analyser (Canberra). The precision of this measurement was $\pm 2\%$.

REFERENCES

1. B. Tamhina and A. Gojmerac Ivšić, *Solvent Extr. Ion Exch.*, 1987, **5**, 909.
2. B. Tamhina and V. Vojković, *Mikrochim. Acta*, 1986, 135.
3. V. Vojković and B. Tamhina, *Solvent Extr. Ion Exch.*, 1986, **4**, 27.
4. *Idem, ibid.*, 1987, **5**, 245.
5. B. Tamhina and V. Vojković, *Analisis*, 1988, **16**, Suppl. 9–10, 151.
6. K. Jakopčić, B. Tamhina, F. Zorko and M. J. Herak, *J. Inorg. Nucl. Chem.*, 1977, **39**, 1201.
7. C. J. Hardy and D. Scargill, *ibid.*, 1960, **13**, 174.
8. T. Omori and N. Suzuki, *Bull. Chem. Soc. Japan*, 1962, **35**, 1633.
9. B. I. Nabivanec, *Zh. Neorg. Khim.*, 1964, **9**, 1079.

JESS, A JOINT EXPERT SPECIATION SYSTEM—I. RAISON D'ÊTRE

PETER M. MAY

School of Mathematical and Physical Sciences, Murdoch University, Murdoch, Western Australia 6150

KEVIN MURRAY

Division of Water Technology, CSIR, P.O. Box 395, Pretoria, South Africa 0001

(Received 19 March 1991. Revised 10 June 1991. Accepted 14 June 1991)

Summary—JESS is a new computer package for modelling chemical systems in solution and performing numerical analyses on associated experimental data. It was developed to solve problems requiring specialist knowledge of chemical speciation. It currently comprises over 150 programs, 1200 subroutines and 120,000 lines of Fortran code. The main reasons for the development of JESS, and the principles which underpin it, are described. Subsequent papers detail the major facilities which JESS now provides.

This paper introduces a large computer package, written in Fortran 77, called JESS (for "Joint Expert Speciation System"). The package has been designed to minimize the expertise needed to carry out various calculations concerned with chemical species in solution. In particular, the aims have been to make JESS as "user-friendly" as possible and to embody in it a more comprehensive knowledge of solution chemistry than has hitherto characterized speciation computer programs. Whilst one purpose of this is to help inexperienced users, it is also intended for accomplished researchers who wish to perform their calculations more easily and/or with fewer errors. Such assistance can be of benefit to many scientists.¹

The specific reasons why speciation calculations can cause difficulties, even for those with a good basic training in chemistry, are numerous and inter-dependent. In essence, however, most of them boil down to a single problem: to use existing computer programs successfully requires considerable judgement guided by experience.² Reaching the overall goal may be simple enough in principle but, in practice, it always entails many sub-tasks, each of which demands some detailed knowledge. Often the information to be supplied to the program is peripheral to the chemical issue but, nevertheless, it is used to make decisions that can substantially influence the program's chemical predictions. Attempts to perform speciation calculations without sufficient expertise may accordingly yield deceptive or overtly incorrect results. All too frequently these are accepted at face value because it is

virtually impossible to identify and check all the assumptions upon which the calculations depend.

It is worth listing briefly the main difficulties that are encountered. First, there are significant technical obstacles in preparing input data. All existing programs have an implicit way of formulating the description of chemical systems which is computationally convenient but far from what might be termed "a natural chemical approach". Rarely are the program's requirements well documented and particular idiosyncrasies abound to trap the unwary or the uninitiated. Secondly, many applications of speciation modelling inherently require sophisticated chemical expertise. This includes the need to know about definition of components, methods of expressing equilibria, effects of background electrolytes, choice of standard state, changes of temperature and pressure, *etc.* Whilst each of these specific issues may be well enough understood individually, dealing with all of them simultaneously in complicated systems is not so easy.³ There are also subtle conceptual questions like how best to handle metastable chemical systems or the redox potential of solutions.¹ Thirdly, obtaining reliable thermodynamic data from the literature can be a formidable undertaking; considerable insight is required to discriminate properly between the large number of inconsistent equilibrium constants that have been published. All too often there is a paucity of critically-evaluated data for a particular system of interest.

Worrying evidence of the consequences of the above difficulties is provided by the recent CHEMVAL/MIRAGE report on the verification of speciation models used to describe the chemistry of radionuclides in the geosphere.⁴ CHEMVAL is an international project concerned with predictive simulations of radioactive waste disposal; it involves fourteen organizations from the European Community, Finland, Sweden and Switzerland. The verification exercise was "essentially a test that the mathematical models accurately perform the calculations for which they were written" (Reference 4, p. 11); in this comparison between organizations, no experimental measurements were performed, just simulations. Despite this, and despite the fact that the participants were all very well-experienced practitioners in the area of research, striking discrepancies in results were often obtained. For example, consider the data for species of Fe(II) and Fe(III) in the "straight-forward" case of a groundwater assuming no equilibration with solid phases, as shown in Fig. 1. Differences in database compilations, followed by individual decisions about data input, were found by the authors of the report to be the most frequent source of variation in the modelling results. There are also grounds for thinking some blame rests with dependence on computational procedures that demand too much from users: an intimate control over the calculations combined with the need for a good

grasp of all the relevant chemistry is a recipe for making mistakes.

In the area of solution chemistry, few computer programs to date can justifiably be called "user-friendly". This is illustrated in the complexities of program input requirements documented in Reference 5. Neither has a single standard program or approach emerged. This is surprising because computational methods have been utilized for equilibrium calculations and the determination of equilibrium constants since their introduction by Sillén and co-workers in the early 1960's.⁶⁻⁹ However, the codes and techniques in standard use today offer little improvement over the originals. Although new programs are regularly reported in the literature, the majority of these can, at best, be considered refinements.¹ Apart from a few notable exceptions,^{2,10-12} applications of novel numerical methods and/or artificial intelligence are conspicuous by their absence. Moreover, scant advantage has been taken of the modern, interactive computing environments which have become available over the last decade.

This is in stark contrast to other areas of chemistry where it has been evident for a long while that computer technology is making an impact in many ways other than by just performing traditional calculations more rapidly.^{13,14} For example, the emergence of "chemometrics" as a major activity in contemporary analytical research^{15,16} is based on the

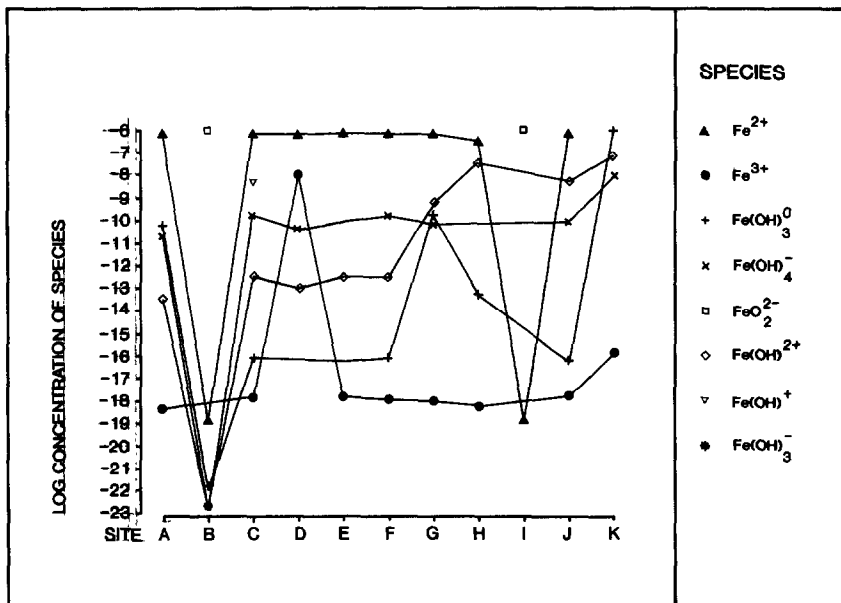


Fig. 1. Example of result from CHEMVAL/MIRAGE verification exercises for groundwater speciation. Test case B. 1.—concentration of iron species—redrawn from Ref. 4.

additional information which can be obtained from experimental data with modern numerical techniques. So-called "expert systems"^{17,18} provide another example where chemistry has been expanded by new computing methods: these are decision-making computer programs which can assist the inexperienced in areas requiring specialist knowledge. Expert systems such as SYNCHEM¹⁹ and DENDRAL²⁰ have demonstrated unequivocally that, in certain limited contexts, computers can interpret chemical phenomena as well as, and often even better than, a competent person. It seems clear that, as performance-to-cost ratios continue to improve, so will the scope and effectiveness of this kind of computer application.

When work on JESS commenced in 1985, we decided to tackle the above difficulties with speciation calculations by exploiting developments in computing that, at that time, had either just occurred or could be foreseen. The newly-available computing power permitted an entirely novel approach. We wanted to generalize the way the calculations were performed, permitting the widest possible variety of simulations and avoiding dependence on particular numerical methods. As already mentioned, we sought to integrate chemical knowledge more intimately into the calculations. We also made a commitment to pay more attention than was conventional in scientific programming to the methodology of computer science.

CHEMICAL OBJECTIVES

This section outlines how our broad general vision translates into a variety of specific chemical goals.

A unified thermodynamic data depository

To perform speciation simulations successfully, inexperienced users must obviously have a source of equilibrium constants that is reliable, comprehensive and can be accessed automatically *i.e.*, without direct user-intervention.

A number of thermodynamic solution-chemistry databases in machine-readable form already exist. To our knowledge, all of these are associated with particular speciation programs, examples being GEOCHEM,^{21,22} MINEQL,²³ PHREEQE,²⁴ EQ3/6,³ SOLMINEQ.88²⁵ and ECCLES.²⁶ Unfortunately, these databases all exhibit serious weaknesses, as will be discussed in Part II of this series. Hence, a supremely important objective of JESS is to develop a large

on-line database of thermodynamic parameters which, by design, will evolve progressively to satisfy the majority of users regarding the data it ought to contain.

The accumulation over an extended period of time of critically-selected data into a unified primary source for speciation calculations is, unquestionably, an ambitious goal but, in our opinion, it is nevertheless feasible. Part II describes in detail how it has been tackled in the development of the JESS Thermodynamic Database. It is sufficient here to say that, clearly, success will depend on the extent to which the new database:

- (i) proves convenient to use;
- (ii) respects conflicts in expert opinion;
- (iii) encourages informed feedback.

Estimating unmeasured equilibrium constants

Large numbers of chemical reactions remain without measured equilibrium constants. At the same time there are a variety of methods which make it possible to estimate values for a significant proportion of these reactions. For example, "mixed-ligand" or "ternary" metal-ion complexes are formed in such plentiful combinations that to investigate them all would be a Herculean labour; however, it is often possible to calculate their formation constants quite precisely from a knowledge of the reactions forming their "binary" parent species.^{27,28} Estimating equilibrium constants from certain established chemical trends is another common way to obtain values when they have not yet been experimentally determined.²⁹

It is pertinent to note that if such estimates are to be used satisfactorily in speciation calculations, the method by which they are obtained must be visible, well-defined and reproducible. However, these ideals have seldom, if ever, been achieved. The large volume of the information that has to be recorded has been one pitfall and the temptation to resort to subjective judgments has been another.

Accordingly, the automation of procedures for estimating equilibrium constants that are not available in the thermodynamic database is another high priority of JESS. In some instances, this should be accomplished fairly readily. The calculation of formation constants for mixed-ligand complexes following the approach adopted for the model of low-molecular-weight equilibria in blood plasma²⁶ is the obvious example. It will not be as easy in other

cases. Our intention, therefore, is to introduce these facilities as soon as possible, just as long as there is some sound chemical basis for making the predictions.

Automatic generation of speciation models

Setting up the input for a speciation calculation has been identified in the introduction as being a major obstacle for the inexperienced and a significant cause of errors, even for more knowledgeable users. Thus, for the goals of JESS to be accomplished, automating these procedures is essential.

One difficulty here is to span the varying requirements users have, depending on their level of expertise.³⁰ Simplicity is the key to helping some users whereas speed and convenience are more important to others. Beginners should be able to specify a chemical system in very general terms, just by naming the substances present in the solution of interest. However, once they have the knowledge to do so, users must be able to exert a greater degree of control over the calculation. This goes beyond simply determining the model's parameters. Recasting the entire simulation to address various "what if" questions is a routine requirement. Resolving this conflict between the needs of novices and of experts has been a dominant theme of JESS development.

A second difficulty in setting up speciation calculations is associated with the choice of component set and the formulation of reaction equilibria. Although widely regarded as straightforward once understood, these tasks involve manipulations which are generally tedious and prone to careless mistakes. A good illustration of this is the interconversion of reactions and equilibrium constants made necessary by different assignments for the "number of dissociable protons" on ligands such as citric acid. Similar interconversions are also required when reactions reported in the literature are not expressed in the way demanded by the speciation computer program, *e.g.*, most programs only accept formation reactions, with a single species on the right-hand side of the chemical equation. As described in subsequent parts of this series, in JESS there are no program restrictions placed on the form which reactions can take or on which species can be regarded as components when data are entered into the database. Procedures have been developed to carry out all interconversions of reactions and equilibrium constants as required.

It is therefore possible to store all experimental data in the exact representation of its measurement but, nevertheless, to perform speciation calculations for any mathematically-feasible formulation of the reactions.

Correcting for changes in ionic strength and temperature

How to deal with changes in ionic strength and temperature is, in principle, well understood. Nevertheless these corrections cause profound difficulties in practice. First of all, there are well-known deficiencies in the theoretical expressions describing how the equilibrium constants change. Functions for ionic strength, especially, are rarely valid over an extended range. Resulting errors can be significant because many existing databases use "infinite dilution" as their reference ionic strength and no single alternative having presented itself as a better standard condition. Secondly, there isn't any uniformity regarding the best type of Debye-Hückel function to use. The Davies equation is widely employed despite almost universal reservations.³¹ This is because the theoretically superior Pitzer equations³²⁻³⁴ and other specific ion interaction models³⁵⁻³⁸ are frequently impractical due to a lack of data. Thus, an inadequate theoretical base is worsened by a widespread inconsistency of approach. Thirdly, the exact ionic strength of the solution only becomes known when the speciation has been calculated; this therefore requires an iterative approach which, in turn, implies slowness. Fourthly, in those computer programs which attempt such corrections simultaneously, *e.g.*, ESTA,³⁹ the chosen correction functions have to be imbedded very deeply into the equation-solving code. Modifying the functions, even in minor ways, can consequently be a big undertaking which tends not to get done, regardless of any deficiencies that might emerge. A new approach towards these problems has been developed and is now fully incorporated into JESS. Details will be given in Part III.

Improving model verification

In an effort to address some of the problems mentioned in the introduction concerning verification of results, special output should be produced automatically at each major stage of the modelling procedure to summarize the important assumptions made and, where any options are available, the particular methods used. The combined output from each stage would thus

provide a full description of all the relevant information, from start to finish, that may have affected the predictions of the model. It is envisaged that such information would be published routinely along with the results of the model, making detailed inter-model comparisons feasible. An important characteristic of expert systems is that they should be able to show how they arrived at their results.⁴⁰

Comprehensive modelling capability

The industrial, physiological or environmental applications for which many speciation calculations are performed cannot be adequately addressed by simulations limited to simple equilibria. Whilst it has been possible to include a broad variety of physico-chemical phenomena such as adsorption, transport and diffusion with equilibrium calculations for some time,^{41,42} models of such processes are still relatively imperfect and uncommon. Moreover, other much-needed capabilities are not yet available. The coupling of general speciation models with a variety of kinetic calculations and the ability to deal generally with metal ion binding by macromolecules fall into this category. Ways must still be found to link the different parts of such computations together intimately and efficiently. An inability to evaluate rigorously the sensitivity of speciation models to errors is another serious current weakness.¹

Although it is too soon to know how all these necessary features will eventually be provided, a large effort has been made to ensure that JESS is highly amenable to change and to extension. This should enable it to evolve into a comprehensive modelling package for simulating all kinds of systems in a far less restricted manner than is possible with the older program codes.

COMPUTATIONAL DESIGN

In any substantial software project, there are always a number of design decisions which have to be made at an early stage. Such decisions cannot later be reversed because this would generally mean rewriting too large an amount of code. This section describes the basis for the main computational design decisions on which JESS was based.

Modular program units

Since our main objectives could obviously only be accomplished by a large and complex

computer system, one of our first decisions was to implement JESS as a collection of many computer programs rather than as a single one. Certain benefits of tackling the project piecemeal are obvious: problems can be digested in whatever order and at whatever rate are most convenient; it is not necessary for the whole system to be operational before parts of it can be useful; solutions to intricate questions can be developed gradually. Moreover, even with the virtual memory capabilities of some modern computer operating systems, huge multi-purpose programs are still far from being a practical proposition. Inordinately long "link" times during the development cycle are a particular problem.

On the other hand, segmentation of the system into many units implies that all but the most simple of tasks need to be accomplished by sequential execution of programs. This has to be co-ordinated at a higher level, by involving the computer operating system. It also requires that knowledge of both the chemical and the computational goals be encoded and subsequently applied by some kind of artificial intelligence. For this reason, amongst others, we concluded that an expert-system capability was essential. To distinguish it from the user-interface provided by individual programs, we call the level controlling program execution and intended to supply expert-system guidance, the command interface.

Segmentation of the system into many programs also raises the need for effective inter-program communication. Substantial quantities of data must be transferred, as must information used to control, assist and check on progress towards current goals and subgoals. Putting all this into a conventional sequential formatted computer file would be highly inappropriate. Accordingly, a special mechanism has had to be developed which allows various data types (integers, reals, arrays, strings, files and so on) to be stored as nodes in a hierarchical tree structure. We have called this assembly of information "Resident Data".

User interface

The need to be helpful implies at least three things: the system must be consistent, it has to be tolerant of but not permissive towards errors and, where necessary, it should suggest how to proceed. We decided this could only be effectively achieved if it were tackled differently at command and program levels.

For various reasons including user-simplicity and system-portability (as discussed below), the command interface needs to be as basic as possible. Little more than a facility to select and execute sequences of programs is necessary; all the sophisticated capabilities of the system can then be embodied in specialized programs which are summoned up at the appropriate time. From the user's viewpoint however, the system at this level should appear to be driven by a small set of commands. These permit the user to exercise overall control but, at the same time, novices need only be aware of a few of the broader choices available. A comprehensive "help facility" ought to be apparent at this level. Likewise, expert system guidance regarding what goals can be reached and how best to reach them must be provided here. In reality, however, all these functions can be achieved by executing appropriate independent programs.

At program level, much more detailed interaction with users is required. In particular, this is where the convenience of the system is either accomplished or it is not. Consistency of messages/prompts issued, of input expected, of consequent program behaviour and of output displayed is one of the most important keys to helping new users. Thorough checking of user responses, as immediately as possible, is another. Using menus to indicate options available and supplying sensible defaults on prompts, are further aids that should be routinely implemented.

The conflicting priorities of experts and novices mentioned earlier is another of the challenges at design stage. Experts want speed and convenience; knowing where to go and what to do are not their main concern. Novices want help and do not mind if this means proceeding more slowly. In principle, we believe the solution to this lies in developing a "black box" system, but one which is sufficiently modular to permit intervention at appropriate stages by more knowledgeable users. Initially, such a system can produce results with a minimum of user involvement. Then, if and when the need to modify calculations or to change assumptions becomes apparent, the beginner is motivated to learn more about driving the system. This is made easier because the focus of attention falls on an individual aspect of the calculation—thus making it unnecessary to master the whole system in advance.

Computer portability

It is difficult to overstate our concern to ensure that JESS software is independent of the computers on which it will operate. The reasons are twofold:

- (i) with such a long term endeavour, it seems imperative to produce code that will work far into the future, well after the hardware on which it was developed has become obsolete;
- (ii) to succeed, JESS must become widely available.

The latter goal will not be achieved if JESS only runs under one or two computer operating systems. In our experience, most individuals interested in speciation calculations are as yet unable to acquire computers specifically for this purpose, even though this will probably change in time as microcomputers grow powerful enough to support larger software packages.

Writing portable software is difficult, much more difficult than is commonly supposed. Moreover, in the present context, the problem is intensified because the catholic requirements of JESS make it far more demanding than simple number-crunching programs.

Fortran 77 is the only scientific computer language which offers any realistic prospect of achieving the degree of hardware independence that we desire. It is fundamentally more efficient than the large majority of more recent computer languages, in particular Pascal. As well as being superior for numerical processing, it is far more portable than C. Fortran 77 therefore represents the language of choice for our purpose. However, it nonetheless suffers from a number of serious disadvantages. Perhaps the worst of these is that it is inherently very poorly structured, so that without great care, large amounts of code may easily become unmanageable. In particular, if programming gets too complicated, errors are impossible to eradicate and the system is impractical to maintain (*i.e.*, to modify and/or extend). Furthermore, compared with some languages that are now available, standard Fortran is technically deficient in many areas. For instance, there is no indexed file capability—something which is essential for our database applications. Limitations with the way Fortran handles character string manipulations is another profound weakness. Much of the early construction of JESS consequently had to be devoted to producing code which rectifies

these deficiencies in a rigorously portable manner. We had, for example, at the very earliest stage to define our own JESS collating sequence as a subset of printable ASCII and EBCDIC characters, to guarantee the compatibility of ordered data at all JESS sites.

IMPLEMENTATION

Although it may still be many years before the ambitions of JESS are all addressed, let alone fully realized, development has now reached the stage where the package can be used effectively for its essential purposes. To be specific, it is now possible to perform speciation calculations from a primary database of over 12,000 reactions in aqueous solution. There are no program-imposed constraints regarding the kinds of equations to be solved, the presence of other phases, the form in which reactions are represented, the choice of electrolyte medium or changes to ionic strength and temperature. Limits to the number of chemical species and number of reactions do exist but are probably in excess of 100,000. The entire procedure is automated so that it can be carried out with a minimum of user intervention; at the same time, each stage can be isolated and its input modified if greater control or flexibility is desired.

The JESS package presently comprises over 150 programs, most of these being interactive. Only relatively few are actually used for speciation modelling. Some exist specifically for thermodynamic database management. Yet others provide a range of facilities to help with everyday tasks. These include a portable general-purpose editor, a spelling-checker and a suite of programs to manage large numbers of literature references. The remainder are for general JESS development purposes.

This gamut of programs is made possible by extensive sharing of lower-level code. In total there are now over 1200 subroutines and 120,000 lines of Fortran code. The present computer storage requirement is generally about 25MB. The thermodynamic data, other data, Fortran code, object libraries and executable images each need about 5MB. It should be noted, however, that some computer systems require considerably more than this.

So far, the amount of experience we have had with JESS is necessarily patchy. Most of the common subroutines, and certain facilities like the JESS Literature databases, have been operational for several years but we have only

recently completed the software for equilibrium modelling. The thermodynamic database programs fall between these two extremes, having been initiated about 18 months ago but exercised intensively since then. The system seems to be evolving as planned, although at present it remains difficult to judge whether or not it will prove as helpful to inexperienced users as we hope. This is because the development of the final tiers of the system, especially at the command level, has only just commenced.

At program level, the user interface is well advanced. A substantial degree of consistency has been achieved. For example, simple commands like "View", "Insert", "Modify" and "Delete" operate in the same way everywhere, regardless of the program or the kind of database. The use of menus to present other choices is ubiquitous. Control is always implemented in a hierarchical way so that, for instance, entering "Back" generally causes the previous prompt to be re-issued. Likewise, entering "Quit" terminates the current context whatever it may be, first returning the program to its highest level of command and then exiting the program. Identical methods of editing data operate universally throughout the system. Similar methods of abbreviation are also widely implemented, although we have found it desirable to permit a few context-dependent differences. Low-level error detection (*e.g.*, if entered data are of the wrong type or happen to be outside present limits) is diagnosed and handled in the same way by all programs. The input stream can be redirected to accept data from a named sequential file at all interactive prompts. Database house-keeping mechanisms are completely independent of the kind of database. None of these features depend on the capabilities of the computer operating system external to the JESS programs themselves.

We have attempted to display sensible default responses on prompts for input wherever possible; however, this is not a trivial matter and it is already clear that improvements will have to be made as experience dictates. We are also conscious that until the command level is fully developed, users will need a knowledge of their computer operating system and an understanding of the relationships between JESS programs beyond our stated objectives.

From a computational viewpoint, the JESS code now available is highly structured. A hierarchy of interfaces has been constructed which deals with the various levels of processing in a

Table 1. Basic JESS interfaces

Name	Purpose
CHR	universal collating sequence
FIL	file manipulation
GEQ	general equation solving
JAR	storage and retrieval of large arrays of numbers
JED	editing
JIF	storage and retrieval of strings by key
JLR	storage and retrieval of literature references
JPF	general text formatting
LST	manipulating of character string lists
NOD	tree-structure storage
NUM	character-to-number interconversions
OPD	numerical optimization
PLT	graphical facilities
PLY	polynomial storage and manipulation
PWD	authorization facilities
RAN	random number generators
RSD	inter-program data storage
SRT	sorting facilities
STR	character string operators
TYM	time and date facilities
VDU	interaction with visual display units

strictly modular way. The common routines, providing standard facilities such as checking user responses, sorting data, list processing, generating random numbers have already been briefly described.⁴³ Table 1 shows how the system is subdivided and gives the purposes of the different sections of code. Two of the more notable features in this respect are:

- (i) the JIF (JESS Indexed File) subsystem, on which depends all database activity;
- (ii) the RSD (Resident Data) mechanism by which information is generally transferred between sequentially-executed programs.

The effort that has been put into producing portable Fortran has enabled us to implement

*Interested readers can obtain details of how to acquire the latest version of JESS (currently V3.0) by writing to either of the authors. Email inquiries can be sent to "may@murdoch.edu.au".

JESS on a wide variety of computer systems. These are listed in Table 2 to indicate the kind of facility required to support JESS. We have established that there are no compatibility problems associated with character sets (particularly control characters) when JESS data are transferred between different types of machine, or when interactive JESS programs are operated across computer networks.

Documentation is fairly extensive (>500 pages) and comes in two main parts. The User's manual describes how to operate the system and gives a certain amount of background chemical theory. The developer's manual contains specific information about the Fortran code and the algorithms applied therein. The developer's manual also contains a detailed statement of the Fortran coding conventions we have adopted and a specification of the minimum computer facilities required to implement JESS. Both manuals are extensively indexed and cross-referenced.*

CONCLUSIONS

For the future, completion of the command level interface is our highest priority, but this should become operational shortly. Work will also soon commence on the programs for automatic estimation of equilibrium constants and checking of the thermodynamic database for internal consistency. We have already written a prototype code for modelling systems in which compartmentalization and/or reaction kinetics are involved⁴⁴ and this is now ready to be integrated with the equilibrium modelling programs. Methods of dealing properly with macromolecular interactions are presently under investigation and will also be incorporated into JESS in due course.

Table 2. Computer systems running JESS

System	Compiler	Operating System	JESS Version
Commodore Amiga 2000	Absoft Inc.	Amiga-CLI	2
Cyber 860	ftn	NOS/VE 1.4.2	2
Data General	f77	AOS/VS	1
Honeywell	Fortran	CP6	2†
Honeywell	Fortran	Multics	1
ICL 2980	ICL Fortran 77 Plus	VME	1
MicroVAXII	MicroVAX Fortran	MicroVMS (V.4)	3
MicroVAXIII	f77	Unix Berkley (V4.3) Tahoe	3
Prime	Salford Univ.	Primos	1†
Sun IPC SPARCstation	Sun FORTRAN 1.3	SunOS 4.1.1	3
Total Peripherals 80386/7	Lahey	MS-DOS/OS386	3
VAX-11	VAX Fortran	VAX-VMS (v.3)	1

†Compiled but not fully tested.

Thus far we have given little attention to the benefits which can be derived from the application of JESS to the analysis of experimental data, especially from potentiometric titrations. We have previously noted that an entirely new approach to the computation of solution equilibria is needed to extract the maximum information available from such data.¹² JESS has been designed as a foundation for this. Given other demands, however, there seems a while to go before we can embark in earnest on such an undertaking. In the meantime, we are distributing ESTA as part of the JESS package even though it does not conform to the JESS program specifications (many of which were formulated directly as a result of problems we experienced with ESTA portability).

Acknowledgements—We are grateful for the many suggestions regarding JESS development that have been made by colleagues in discussions over the past five years. Thanks go especially to Ria Jooste, Ruth May, Julius Pretorius, Marita Roos, Grahame Strong and Peter Verhoeven for their particular contributions to the overall project. The advice of Dr Sid Wright (Murdoch University) on computational matters is appreciated.

REFERENCES

- R. L. Bassett and D. C. Melchior, in *Am. Chem. Soc. Symp. Ser. 416*, D. C. Melchior and R. L. Bassett (eds.), pp. 1–14. ACS, Washington, 1990.
- F. J. Pearson, Jr., B. S. Jensen and A. Haug, *ibid.*, D. C. Melchior and R. L. Bassett (eds.) pp. 330–338. ACS, Washington, 1990.
- T. J. Wolery, K. J. Jackson, W. L. Bourcier, C. J. Briton, B. E. Viani, K. G. Krauss and J. M. Delany, *ibid.*, D. C. Melchior and R. L. Bassett (eds.), pp. 104–116. ACS, Washington, 1990.
- D. Read and T. W. Broyd, *Report on Stage 1 of Project CHEMVAL/MIRAGE, Verification of Speciation Models*, WS Atkins Eng. Services under CEC contract FI.IW0077. UK(H), Epsom, UK, 1988.
- D. J. Leggett (ed.), *Computational Methods for the Determination of Formation Constants*, Plenum, New York, 1985.
- L. G. Sillén, *Acta Chem. Scand.*, 1962, **16**, 159.
- N. Ingri and L. G. Sillén, *ibid.*, 1962, **16**, 173.
- N. Ingri and L. G. Sillén, *Arkiv Kemi*, 1964, **23**, 97.
- L. G. Sillén, *Acta Chem. Scand.*, 1964, **18**, 1085.
- A. Avdeef and D. L. Kearney, *J. Am. Chem. Soc.*, 1982, **104**, 7212.
- H. Gamp, M. Maeder, C. J. Meyer and A. D. Zuberhuhler, *Talanta*, 1986, **33**, 943.
- P. M. May and K. Murray, *ibid.*, 1988, **35**, 933.
- J. G. Liscouski, *Computers in the Laboratory, Current Practice and Future Trends*, ACS Symp. Ser. 265, Am. Chem. Soc., Washington, 1984.
- P. C. Jurs, *Science*, 1986, **232**, 1219.
- L. S. Ramos, K. R. Beebe, W. P. Carey, E. Sanchez, B. C. Erickson, B. E. Wilson, L. E. Wangen and B. R. Kowalski, *Anal. Chem.*, 1986, **58**, 294R.
- G. Kateman, *Analyst* 1990, **115**, 487.
- T. P. Bridge, M. H. Williams and A. F. Fell, *Chem. Br.*, 1987, **23**, 1085.
- K. Parsaye and M. Chignell, *Expert Systems for Experts*, John Wiley, New York, 1988.
- H. L. Gelernter, A. F. Sanders and D. L. Larsen, *Science*, 1977, **197**, 1041.
- B. G. Buchanan, D. H. Smith, W. C. White, R. J. Gritter, E. A. Feigenbaum, J. Lederberg and C. Djerassi, *J. Am. Chem. Soc.*, 1976, **98**, 6168.
- S. V. Mattigod and G. Sposito, in *Am. Chem. Soc. Symp. Ser. 93*, E. A. Jenne (ed.), pp. 837–856. ACS, Washington, 1979.
- G. Sposito and S. V. Mattigod, *Univ. California, Dept. Soil Environ. Report*, 1980, 1.
- J. C. Westall, J. L. Zachary and F. M. M. Morel, *Users Manual: MINEQL, A Computer Program for the Calculation of Chemical Composition of Aqueous Systems. Tech. Note 18, Dept. Civil Eng., M.I.T.*, Cambridge, MA, 1976.
- D. L. Parkhurst, D. C. Thorstenson and L. N. Plummer, *Users Manual: PHREEQE, NTIS Tech. Rep., PB81-167801*, 1980. Revised 1985.
- E. H. Perkins, Y. K. Kharaka, W. D. Gunter and J. D. DeBraul, in *Am. Chem. Soc. Symp. Ser. 416*, D. C. Melchior and R. L. Bassett (eds.), pp. 117–127. ACS, Washington, 1990.
- P. M. May, P. W. Linder and D. R. Williams, *J. Chem. Soc. Dalton Trans.*, 1977, 588.
- S. H. Laurie and C. James, *Inorg. Chim. Acta*, 1983, **78**, 225.
- S. H. Laurie, *ibid.*, 1983, **80**, L27.
- R. D. Hancock, *Acc. Chem. Res.*, 1990, **23**, 253.
- M. Visvalingam, *Univ. Comput.*, 1988, **10**, 80.
- B. W. Darvell and V. W.-H. Leung, *Chem. Br.*, 1991, **27**, 29.
- K. S. Pitzer, *J. Phys. Chem.*, 1973, **77**, 268.
- F. J. Millero, *Marine Chem.*, 1990, **30**, 205.
- L. N. Plummer and D. L. Parkhurst, in *Am. Chem. Soc. Symp. Ser. 416*, D. C. Melchior and R. L. Bassett (eds.), pp. 128–137. ACS Washington, 1990.
- J. N. Bronsted, *J. Am. Chem. Soc.*, 1922, **44**, 877.
- G. Scatchard, *Chem. Rev.*, 1933, **13**, 7.
- Idem, ibid.*, 1936, **19**, 309.
- G. Biedermann, in *The Nature of Seawater*, E. D. Goldberg (ed.), pp. 339–362. 1975.
- P. M. May, K. Murray and D. R. Williams, *Talanta*, 1988, **35**, 825.
- D. M. Cleal and N. O. Heaton, *Knowledge-Based Systems: Implications for Human-Computer Interfaces*, p. 132. Ellis Horwood, Chichester, 1988.
- C. W. Miller, in *Mat. Res. Soc. Symp. Proc.*, Vol. 15, pp. 481–488, 1983.
- D. S. Brown and J. D. Allison, Report EPA/600/3-87/012, MINTEQA1, *An Equilibrium Metal Speciation Model: Users Manual*, U.S. Environmental Protection Agency, Athens, Georgia 30613, 1987.
- P. M. May and K. Murray, *Talanta*, 1987, **34**, 821.
- P. Verhoeven, P. M. May and K. Murray, *unpublished work*.

JESS, A JOINT EXPERT SPECIATION SYSTEM—II. THE THERMODYNAMIC DATABASE

PETER M. MAY

School of Mathematical and Physical Sciences, Murdoch University, Murdoch, Western Australia 6150

KEVIN MURRAY

Division of Water Technology, CSIR, P.O. Box 395, Pretoria, South Africa 0001

(Received 19 March 1991. Revised 10 June 1991. Accepted 14 June 1991)

Summary—The thermodynamic database of the JESS (Joint Expert Speciation System) software package is described. It overcomes many existing problems associated with solution-chemistry databases. The system is fully interactive. Reactions can be expressed in any form. Any number of equilibrium constants, enthalpy, entropy and Gibbs-free energy values can be associated with a reaction. Supplementary data such as background electrolyte, temperature, ionic strength, method of determination and original literature reference are also stored. Data can be readily transferred between databases. Currently, the thermodynamic database that is being distributed with JESS contains over 12,000 reactions and over 20,000 equilibrium constants. These data span interactions in aqueous solution of some 100 metal ions with more than 650 ligands.

As is well recognized, one of the most serious weaknesses with equilibrium calculations is the reliability of thermodynamic data.^{1,2} The preparation and handling of such data are major contributors to this unreliability. The process tends to be time-consuming and prone to human error. Accordingly, one of the most important objectives of JESS is to produce programs that will facilitate the development of a large, on-line database of reliable thermodynamic parameters.³

Many existing equilibrium calculation programs⁴⁻⁹ do supply some sort of thermodynamic data set. However, these systems were mostly written many years ago, when there was much less computer power than is now available. As a result, they suffer from a variety of limitations which tend to contribute to the problem of unreliable data rather than help to alleviate it. Common weaknesses include a lack of versatility in the calculations they can perform (increasing the need for manual intervention), technical difficulties with preparing their input, poor or non-existent error detection and an inherent tendency to divergence of their data sets across various sites running the same program. The last of these is especially troublesome and difficult to correct. Differing priorities and opinions make it inevitable that modifications to databases will vary from one location to another. Since none of the existing computer

systems offers a mechanism to resolve such differences, it has become prohibitively time-consuming to re-establish any kind of uniformity, and therefore authority, using currently-available speciation software.

Moreover, the data associated with these programs are themselves inherently limited. The sets are all relatively small, none possessing more than a few thousand reactions. Nearly always, only a single equilibrium constant can be stored for each reaction, *i.e.*, the value applies to a particular temperature and ionic strength (usually 25° and zero, respectively). Reactions are invariably expressed in a fixed form. The “components” or basis species are pre-defined and all “complexes” must be expressed in terms of these components. Changing the component set is tedious, necessarily requiring constants to be re-evaluated manually.

Some programs⁹ supply enthalpy data and others⁷ permit the storage of functions describing how enthalpy changes with temperature. However, these functions usually have to be determined prior to their insertion in the database. If new primary data become available the appropriate function needs to be re-determined manually and re-entered. A better approach is to preprocess the data, replacing the equilibrium constants with equivalent interpolating polynomials,¹⁰ but this is not yet widely done.

Another common limitation is the lack of information on what methods and/or publications were used to obtain a constant. This makes it difficult, and sometimes impossible, to assess the correctness of a value. Given the many problems that can be encountered in critically assessing the literature, or estimating constants for conditions under which no measurements are available, omission of such information does little to enhance confidence in the database and hence in the results of any calculations based on it. Inconsistencies between various results reported in the literature are a largely unsolved problem for those currently building thermodynamic databases.¹⁰

Finally, there are at present no convenient mechanisms by which data in solution-chemistry computer systems can readily be transferred from one database to another. This has led to a divergence of equilibrium constant values (and hence of results of equilibrium calculations) that has surely damaged the credibility in general of speciation modelling.³ There has also been much wasteful duplication of effort since the same primary data are often entered in more than one location. As a corollary, the databases tend to remain restricted in size, with only a small fraction of all the equilibrium constants that could usefully be included. An important reason for these problems is that the identity of every chemical entity is not unambiguously established within the database itself. In other words, the abbreviated symbols used to represent chemical species are not definitive. Consequently, it is impossible to automate the transfer process securely.

This paper describes how these various issues have been addressed in the development of the JESS thermodynamic database.

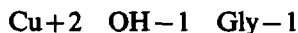
USER INTERFACE

Data definition

Every attempt has been made to ensure the interface of the database with the user is as clear as possible. One of the main ways this has been done is by using symbols directly recognizable in terms of the chemistry they represent. To achieve this, we have classified the data into four fundamental types.

The first is the unique symbol used to represent a chemical species in any input or output, referred to hereafter as an I/O symbol. Two types of I/O symbol exist, primitive and composite. The latter are comprised of two or more

primitive symbols in any order separated by underscore characters. Typical primitive symbols might be as follows:



The following are some examples of composite symbols:



These combinations of symbols permit a large number of chemical species to be represented, using relatively few primitives. However, users entering new data always have the choice. Any species, even complexes, can be represented by a single primitive symbol if this is deemed appropriate. For example, the above composite species could equally well be expressed as the following primitives:

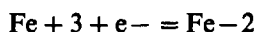
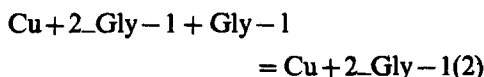
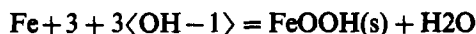


This is particularly useful when a composite symbol would contain so many primitives that it might not clearly convey the identity of the species. In some cases a primitive symbol may be the only option because the species cannot be written in terms of any combination of existing primitives.

The second data type is "species". This term is used to describe both the I/O symbol (primitive or composite) and various data characteristics of the associated chemical entity. The molecular formula and the charge of each species are always determined for this purpose (although they only need to be entered specifically for primitive species). The CAS registry number and any number of names (common, IUPAC, Chemical Abstracts, *etc.*) can also be associated with species, as can certain other species-specific data, *e.g.*, regarding ionic strength corrections.

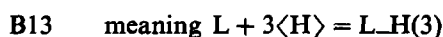
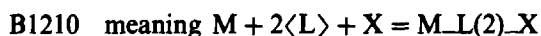
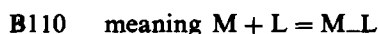
Since I/O symbols can be readily modified to suit any individual need, they cannot be used as unique identifiers, *e.g.*, when data are being transferred from one database to another. To overcome this problem, the CAS registry number serves as the primary means of unambiguous identification. Indeed, we carefully maintain the distinction between I/O symbols and species to emphasize that species are the real chemical entities whereas I/O symbols are just arbitrarily-formulated tokens.

The third data type is the reaction. This is expressed in terms of interacting species. The species are delimited within a reaction by plus or minus signs (surrounded by blanks) with reactants and products being separated by an equals sign. Species preceded by a stoichiometric coefficient are enclosed in angle brackets. The following are some examples:

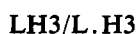


Reactions may be entered with any number of reactants and products. Stoichiometric coefficients may be integers or real numbers. These conventions permit the insertion of all reactions in the exact form in which they are published, irrespective of what might be required for subsequent equilibrium calculations. A check is made to ensure that each reaction is balanced with respect to charge and mass when it is being inserted.

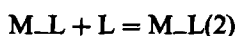
Two other, abbreviated, methods for expressing reactions are available which greatly simplify the specification of certain reactions and speed up their insertion. First, the conventional "beta formulation" is permitted, *i.e.*, overall formation reactions of simple binary and ternary complexes can be expressed as follows:



where the identity of M, L and X is given only once, prior to specifying the reaction or, more usually, sequences of related reactions. The second option permits specification of diverse reactions with the letters M, L, X, H and the pair OH. Thus, having once established the identity of each letter, the three reactions above could also be entered as follows:



The advantage of this second abbreviated method is that it also encompasses many step-wise reactions, for example:



ML2X/ML2.X meaning



LH3/LH2.H meaning



It is worth noting how easily ternary complexes (MLX, ML2X, *etc.*) are handled since these are somewhat inconvenient to classify in printed compilations of formation constants.

The fourth and final data type is the thermodynamic data itself. Such data may include equilibrium constants, standard enthalpy, entropy and Gibbs free energy values.

Any number of constants can be associated with a reaction although to help establish internal consistency only one value may exist for a given combination of medium, temperature and ionic strength. For the same reason, a constant is considered to exist if it can be determined from other existing data, using the following thermodynamic relationships:

$$\Delta G = -RT \ln K = \Delta H - T\Delta S$$

Each thermodynamic constant is characterized by certain supplementary data.

- (i) Each is associated with a medium (background electrolyte), a temperature and an ionic strength. The temperature and the ionic strength can both be represented as ranges if necessary. In addition to conventional mediums, *e.g.*, NaCl or KNO₃, we also often use this item to indicate particular groupings of equilibrium constants. For instance, all the values estimated for the simulation of metal-ligand equilibria in human blood plasma⁸ have been inserted in the database under the medium "Blood Plasma". The procedures for automatic extraction of the data, to be described in a subsequent paper, select constants according to an order of priority which is assigned to the various mediums as appropriate for each application. This mechanism also permits different sets of equilibrium constants to be held simultaneously in the database where there are irreconcilable differences in expert opinion regarding which ought to be used, *e.g.*, one might establish two mediums, NaCl (Toulouse) and NaCl (Cardiff), so that by specifying different medium-priority orders each centre could preferentially determine the data to be selected for their

simulations, *even though both centres were using the same database.*

- (ii) A three-character code is also associated with each constant indicating the method by which it was obtained. This distinguishes between experimentally measured, estimated and critically assessed (*e.g.*, averaged) constants. It also indicates the actual experimental technique used; for example, two such codes are MGL "Measured, Glass Electrode" and MSP "Measured, Spectrophotometry".
- (iii) An error is associated with each constant. It can be expressed as a standard deviation, maximum error or in terms of the number of significant figures. A three-character code can also be associated with the error describing how it was obtained.
- (iv) The literature publications from which the data are obtained are entered into a corresponding literature reference database (with cross-references between publications, if required). The unique number of the publication in this database is then stored in the thermodynamic database alongside each of its corresponding thermodynamic constants. In this way, the publications on which every constant in the database depends can always be ascertained.

Data display and modification

Data can be displayed on the VDU with a program that opens the database for read-only access. No modification of data is then possible; this serves as a useful protection mechanism (allowing for write-access to be restricted to certain users and minimizing the occasions when the database is open to corruption). Species (with any associated data) and reactions (with their thermodynamic data) can be displayed. Various facilities are available which permit rapid searching of the database. For example, all reactions containing specified species (or combinations thereof) can be displayed; species with a given name, CAS registry number or molecular formula can be located and so on.

Updating is done by a separate program which permits new species, reactions or data to be inserted, as well as allowing existing data to be modified or deleted.

Various miscellaneous facilities like producing lists of reactions whose data have been modified since a specified date and obtaining printed lists of specific species and reactions with their data are also provided by individual programs.

Database housekeeping

Physically, the database consists of eight JIFs (JESS Indexed Files [Part I]³). Each JIF contains a particular data type and/or certain links between the data items. Some of these links, called inverted lists, make it possible to provide those capabilities requiring rapid searching of the database.

Unfortunately, links such as these inherently make the database open to corruption. For example, if the computer's power supply happens to be interrupted while internal links are being updated, the database may be left in a badly-defined state. Although all programs operating on the database have built-in mechanisms that aim to minimize the chance of such corruption, a special set of programs has been developed to provide a convenient means of keeping backups of the database, from which it may be restored if necessary.

Such backups consist of all the data written out sequentially, with individual items existing more-or-less independently of other items, yet from which the whole original database can be reconstructed automatically. Indeed, regular reconstruction in this way is recommended as part of the routine housekeeping required to maintain a high level of efficiency in accessing databases that are frequently modified. Another advantage of this backup system is that the storage required to make a direct sequential copy of all the information is always considerably less than to make a copy of the database JIFs themselves.

Data transfer between databases

Although the process of inserting data from original publications into a JESS thermodynamic database is made as easy as possible, it nonetheless remains a time-consuming business. For this reason, at least, it is highly desirable that entry of data into local databases is not duplicated at different sites. One way to minimize this is to transfer data directly from one JESS database to another, making use of an intermediate set of sequential files. A set of programs exists to facilitate this.

The program that produces the set of “transfer files” processes *all* reactions and their data in the source database. The reactions, thermodynamic data, species, species data, literature references, *etc.*, are handled *en bloc*. If only a subset of the reactions in a database needs to be transferred, another program is available by which a sub-database, containing only the required reactions, can first be produced.

Usually, the owner of the “target database” checks the incoming data before they are inserted. In particular, synchronization may be necessary to ensure that the same data item is not being referred to by two different names or descriptions in the two databases. This also permits the deletion of any reactions or data that ought not to be transferred into the target database. The program which loads transferred data into the target database checks for such errors but overall control resides with the database owner.

Database management and responsibility

Within JESS, a thermodynamic database represents the starting point in the automation of equilibrium calculations leading to the final display of results. From this perspective, both the entry of data and the management of the database are different from subsequent steps in that there is no need for any involvement by completely inexperienced users. It nevertheless remains important that the knowledge required to perform these tasks should relate mainly to chemical rather than computational issues. Sooner or later many users will want either to insert new data or to modify copies of the database distributed with JESS. In practice we have found that chemical expertise is mostly required to define and enter new primitive species; entering composite species and reactions is relatively straightforward because the program can deduce most of its essential requirements. Regarding the input of primitive species, the user must at least be able to determine both the molecular formula and the appropriate charge. This is simple enough if the source publication is well-written but, unfortunately, all too frequently the details supplied are not as clear as they could be.

It is important to realize that control over the contents of a database cannot therefore be divorced from the possibility of introducing errors, no matter how expert the user. Accordingly, we envisage that wherever there are multiple users of a single JESS system, a variety of databases may be established. This will provide the flexibility required to deal with applications that are inevitably more diverse than can be accommodated by a single database. On the other hand, convenient exchanges between databases can and should be made whenever there are data which can usefully be shared.

The proliferation of JESS databases, locally and globally, makes it essential that the responsibility for each is clearly demarcated to the person mainly making changes to it. It also seems likely that, at each location there ought to be a single person in charge of the database distributed with JESS. In itself this will require little expertise, for housekeeping is only necessary if a database is extended or modified. However, where different research projects generate many individual databases, some co-ordination may become desirable to maintain local coherence.

IMPLEMENTATION

Although we expect many users to build JESS thermodynamic databases for their own specific needs, we have ourselves constructed a master set, pertaining to aqueous solutions, which we intend to distribute widely as part of the JESS package. This has two purposes:

- (i) to serve as a source of thermodynamic parameters for those who do not have the time or expertise to provide their own; and
- (ii) to provide a substantial amount of common data as a nucleus for those who wish to contribute their data and opinions to a unified primary source for speciation models.³

At the time of writing (Feb. 1991), the master database* contains over 12,000 reactions and over 20,000 equilibrium constants. Table 1 lists the metal ions for which more than 10 reactions exist. More than 25 inorganic ligands and over 600 organic ligands are involved. Data for about 250 solid species have so far also been included.

In an effort to achieve a practical database, best suited to the needs of speciation modelling, we have decided not to be overly restrictive concerning the reactions and constants which

*Interested readers can obtain details of how to acquire copies of this database by writing to either of the authors. Email inquiries can be sent to “may@murdoch.edu.au”.

Table 1. Number of reactions for various metal ions in the JESS master database

Ag ⁺ 209	Fe ³⁺ 299	Pu ⁴⁺ 124
Al ³⁺ 265	Ga ³⁺ 49	Rh ³⁺ 29
Au ⁺ 10	Gd ³⁺ 24	Ru ²⁺ 21
Au ³⁺ 29	Hf ⁴⁺ 14	Ru ⁴⁺ 19
Ba ²⁺ 23	Hg ²⁺ 111	Sc ³⁺ 27
Be ²⁺ 52	Ho ³⁺ 23	Sm ³⁺ 27
Bi ³⁺ 19	In ³⁺ 59	Sn ²⁺ 28
Ca ²⁺ 316	Ir ⁴⁺ 12	Sr ²⁺ 58
Cd ²⁺ 411	K ⁺ 47	Th ⁴⁺ 93
Ce ³⁺ 31	La ³⁺ 83	Ti ³⁺ 11
Co ²⁺ 308	Li ⁺ 23	Tl ⁺ 14
Co ³⁺ 20	Mg ²⁺ 283	Tl ³⁺ 16
Cr ²⁺ 38	Mn ²⁺ 268	U ⁴⁺ 18
Cr ³⁺ 65	Mn ³⁺ 24	UO ₂ ²⁺ 39
CrO ₄ ²⁻ 20	Na ⁺ 54	VO ₂ ⁺ 30
Cu ⁺ 51	Ni ²⁺ 645	VO ₂ ²⁺ 101
Cu ²⁺ 1565	Np ⁴⁺ 15	Y ³⁺ 57
Dy ³⁺ 25	Pb ²⁺ 321	Zn ²⁺ 719
Eu ³⁺ 29	Pd ²⁺ 40	Zr ⁴⁺ 15
Fe ²⁺ 227	Pt ²⁺ 23	

we include. Our aim is to construct the best possible representation of reactions occurring in solution, regardless of experimental or other practical constraints. There are three aspects to this:

(a) *Methods of determining constants.* A constant may be inserted into the database if: (i) it has been experimentally measured; (ii) it is an average of values determined experimentally by more than one worker; or (iii) it has been estimated empirically, based on "expert" knowledge in this field (*e.g.*, using graphical methods, linear free energy relationships, Irving-Williams series, *etc.*). The use of method codes (*vide supra*) ensures that the distinction between measured and estimated values is always apparent. Of course, critical assessments which cast sufficient doubt on published values to justify them being excluded, override all of these selection criteria. Moreover, as mentioned above, only one constant is permitted under a single set of conditions (medium, ionic strength and temperature). Constants are not inserted into the database if they can be calculated automatically from data already existing in the database with a simple mathematical formula (like the van't Hoff equation).

(b) *Dealing with inadequacies of data in the literature.* Given the seriousness of the errors which pervade the formation-constant literature,¹¹ it is obviously important to establish a strategy for dealing with discrepancies in published values. The two most commonly-used sources of thermodynamic constants adopt different approaches, neither of them ideal. On

the one hand, the Chemical Society and certain IUPAC compilations¹²⁻¹⁵ strive to be comprehensive, leaving all assessment to the user. This makes things very difficult for everyone but the highly-specialized expert. On the other hand, the critical volumes of Smith and Martell¹⁶ are selective—they average values and omit outliers, for example. The problem with this is that the data available in the literature are often insufficient to make definitive judgements. One of the most common difficulties is to reconcile different sets of species reported by various investigators. Sometimes it is reasonable to pick the results of the work appearing to be of the highest standard but, all too frequently, objective criteria for judging this are inadequate. Another difficulty lies in distinguishing between the effects of electrolyte medium and differences due solely to the investigators' experimental errors. Consequently, the Smith and Martell tabulations largely disregard the effects of an electrolyte medium.

We are attempting to find a compromise between these two approaches, in which much of the evident experimental noise is filtered out but without arbitrarily selecting between sets of constants or neglecting the systematic effects of electrolyte mediums. We thus hope to compile an unbiased collection of constants, accurate and practical enough for automatic utilization by non-experts yet comprehensive enough to satisfy the needs of the more specialized researcher.

The principal means whereby we deal with unresolvable differences in the literature is to categorize each species in the database with respect to its likelihood of existence. Users can later select which reactions are extracted automatically from the database in a way similar to that for handling constants from different research groups, using the medium classification [see User Interface section 1(i)]. In this instance, we employ terms like "assured" (meaning found by every investigation of good standing), "probable" (found by most), "controversial" (no clear-cut agreement) and "improbable" (found by a minority, often only one investigation, but with otherwise insufficient reason for exclusion). In addition, where significant grounds exist regarding poor analytical techniques or in adequate computational methods, anomalous species can simply be omitted. However, when there is doubt, we prefer to include species in the database (as "improbable") rather than omit them. This is because (i) omission is tantamount

to an estimate for the formation constant of zero—it is generally possible to be more accurate than that; and (ii) omission is likely to mean a possible species is subsequently overlooked—it is better instead to exclude uncertain species later, during the equilibrium modelling process.

At present it is not feasible to employ the error estimates associated with each thermodynamic constant for automatic assessment and selection purposes. Errors are sometimes not reported and, even when they are, they tend neither to be reliable nor comparable from one system to another. For example, so-called “internal standard deviations” of formation constants (as computed by least squares programs) are invariably underestimates since they take no account of systematic errors in the titration parameters.¹⁷ This is not to say that the error estimate data are without value: they have been included in the database because (i) realistic values are occasionally available, *e.g.*, from various IUPAC critical reviews,^{18–23} (ii) reported errors may be indicative of the relative internal consistency of constants determined by a single investigator, and (iii) large estimated errors can be used to flag constants which can only be very roughly estimated.

(c) *Correcting errors introduced during the compilation of data.* Given that a reliable thermodynamic database is the cornerstone of all JESS procedures to help inexperienced users, a strategy for detecting and eliminating errors is essential. Many programmed checks are carried out when the data are being entered, particularly with the aim of preventing duplication of a species. However, these checks clearly cannot entirely prevent the entry of mistaken information or careless errors. We intend to pursue this problem in two ways, over and above being as systematic and as careful as we can be.

The first of these ways is to develop programs that predict equilibrium constants automatically; these will be used to search for internal inconsistencies, as foreshadowed in Part I of this series.³ Intra-reaction checking would confirm that the data for a particular reaction obey various established relationships, such as govern the effect of electrolyte mediums and changes in ionic strength or temperature. Inter-reaction checking would involve two approaches:

- (i) different linear combinations of reactions giving a particular reaction of interest, should give rise to constants in agreement with those of that reaction; and

- (ii) a given series of reactions, *e.g.*, with a common ligand or metal ion, can be expected to show characterizable trends in their equilibrium constants.

Of course, none of these approaches can be perfect; their usefulness will very much depend on quantifying the tolerance within which differences between observed and calculated values are considered acceptable. However, it seems likely that any gross discrepancies introduced by errors made whilst the data are being compiled or entered will thus be detectable.

Our second way of dealing with such errors in the master database is to invite input and feedback from all users of it. One of the great advantages of a computerized source of data compared with a printed compilation, is that it readily affords modification. Our hope is that users will see the benefits not only of sending us new data but also of notifying us of errors. Convenient mechanisms for transferring data make this feasible. There is also a strong incentive for anyone receiving regular updates of the system: they can avoid repeatedly having to modify each new copy of the enlarged database by having their improvements made centrally just once. Of course, all such suggestions will be assessed by us to preserve the integrity of the data distributed with JESS but this scheme should considerably reduce the workload involved in keeping the JESS master database up-to-date, comprehensive and as error-free as possible.

CONCLUSIONS

The various classifications and cross-linking of data in a JESS thermodynamic database make it potentially far more useful than either a printed compilation or a computerized list of equilibrium constants. The main purpose for which the system has been designed is to facilitate the automatic extraction of data for equilibrium speciation calculations following pre-determined selection criteria. This is essential for JESS to meet its primary objectives.³ However, it is clear, even as the system is currently developing, that the thermodynamic database will also serve in other ways. In a stand-alone capacity, it can provide solution-chemistry researchers with the means of accessing the formation-constant literature in a convenient and powerful manner. The whole master database can now readily be installed on certain commonly-available workstations (*e.g.*,

on a 386 desktop microcomputer). This only requires about 10 MB of hard disk, including space for the appropriate programs. At the same time, at the other end of the spectrum of potential applications, it is now possible to search through a large and growing body of integrated thermodynamic data, using special-purpose computer programs. Interesting new chemical relationships might well be revealed as such programs systematically quantify the collective properties of metals and ligands interacting in solution.

REFERENCES

1. D. K. Nordstrom, L. N. Plummer, T. M. L. Wigley, T. J. Wolery, J. W. Ball, E. A. Jenne, R. L. Bassett, D. A. Crerar, T. M. Florence, B. Fritz, M. Hoffman, G. R. Holdren Jr., G. M. Lafon S. V. Mattigod, G. C. Smith, F. Morel, M. M. Reddy, G. Sposito and J. Thraillkill, *Am. Chem. Soc. Symp. Ser.*, 1979, **93**, 857.
2. D. K. Nordstrom and J. W. Ball, In *Complexation of Trace Metals in Natural Waters*, pp. 194–164. 1984.
3. P. M. May and K. Murray, Part I, *Talanta*, 1991, **38**, 1409.
4. S. V. Mattigod and G. Sposito, in *Am. Chem. Soc. Symp. Ser. 93*, E. A. Jenne (ed.), pp. 837–856. ACS, Washington, 1979.
5. G. Sposito and S. V. Mattigod, *Univ. California, Dept. Soil Environ. Report*, 1980, 1.
6. J. C. Westall, J. L. Zachary and F. M. M. Morel, *Users Manual: MINEQL, A Computer Program for the Calculation of Chemical Composition of Aqueous Systems. Tech. Note 18, Dept. Civil Eng., M.I.T., Cambridge, Massachusetts*, 1976.
7. D. L. Parkhurst, D. C. Thorstenson and L. N. Plummer, *Users Manual: PHREEQE, NTIS Tech. PB81-167801, 1980*. Revised 1985.
8. P. M. May, P. W. Linder and D. R. Williams, *J. Chem. Soc. Dalton Trans.*, 1977, 588.
9. D. S. Brown and J. D. Allison, *MINTEQA1, An Equilibrium Metal Speciation Model: Users Manual. US Environ. Protection Agency Report EPA/600/3-87/012*, 1987.
10. T. J. Wolery, K. J. Jackson, W. L. Boucier, C. J. Britton, B. E. Viani, K. G. Krauss and J. M. Delany, in *Am. Chem. Soc. Symp. Ser. 416*, D. C. Melchior and R. L. Bassett (eds.), pp. 104–116. ACS, Washington, 1990.
11. P. M. May, K. Murray and D. R. Williams, *Talanta*, 1988, **35**, 825.
12. J. Bjerrum, G. Schwartzbach and L. G. Sillén, *Stability Constants of Metal Ion Complexes*, Special Publications Nos. 6 and 7, Chem. Soc., London 1957, 1958.
13. L. G. Sillén and A. E. Martell, *Stability Constants of Metal Ion Complexes*, Special Publications Nos. 17 and 25, Chem. Soc., London 1964, 1971.
14. E. Högfeldt, *Stability Constants of Metal Ion Complexes, Part A: Inorganic Ligands, IUPAC, Chem. Data Ser. No. 21*, Pergamon Press, Oxford, 1982.
15. D. D. Perrin, *Stability Constants of Metal Ion Complexes, Part B: Organic Ligands, IUPAC, Chem. Data Ser. No. 22*, Pergamon Press, Oxford, 1979.
16. R. M. Smith and A. E. Martell, *Critical Stability Constants*, Vol. 1–6, Plenum Press, New York, 1974, 1975, 1976, 1977, 1982, 1989.
17. P. M. May and K. Murray, *Talanta*, 1988, **35**, 933.
18. W. A. E. McBryde, *A Critical Review of Equilibrium Data for Proton- and Metal Complexes of 1,10-Phenanthroline, 2,2' Bipyridyl and Relation Compounds, IUPAC Chem. Data Ser. No. 17*, Pergamon Press, Oxford, 1975.
19. G. Anderegg, *Critical Survey of Stability Constants of EDTA Complexes, IUPAC Chem. Data. Ser. No. 14*, Pergamon Press, Oxford, 1977.
20. A. M. Bond and G. T. Hefter, *Critical Survey of Stability Constants and Related Thermodynamic Data of Fluoride Complexes in Aqueous Solution, IUPAC, Chem. Data. Ser. No. 27*, Pergamon Press, Oxford, 1980.
21. G. Anderegg, *Pure Appl. Chem.*, 1982, **54**, 2693.
22. L. D. Pettit, *ibid.*, 1984, **56**, 247.
23. M. T. Beck, *ibid.*, 1987, **59**, 1703.

ASSAY OF SULPHUR COMPOUNDS WITH 1-CHLOROBENZOTRIAZOLE

C. CHANNE GOWDA and S. M. MAYANNA*

Department of Chemistry, Central College, Bangalore University, Bangalore-560 001, India

(Received 20 March 1991. Revised 29 May 1991. Accepted 13 June 1991)

Summary—A simple but accurate potentiometric method for the estimation of certain sulphur containing organic compounds has been developed, based on their oxidation with 1-chlorobenzotriazole. A back-titration procedure can also be used. The nature of oxidation in different media is discussed and the oxidation products have been identified.

Thioureas find extensive application in rubber vulcanization, electrodeposition and corrosion inhibition of metals, photography, polymers, textiles and agriculture. Dithiocarbamates and thioamides are well known analytical reagents. Methionine is one of the essential amino acids present in a large number of biological systems. A review of the literature reveals the use of a few procedures for the assay of thioureas,¹ dithiocarbamates,² thioamides³ and methionine.⁴ However, these methods have limitations due to time consumption, narrow range of developed experimental conditions and in some cases over oxidation of reductants.

Recently, 1-chlorobenzotriazole (1-CBT), an *N*-halogeno compound, has attracted the attention of organic chemists as a novel organic reagent in organic synthesis because of its reactivity towards a number of functional groups.⁵ However, its analytical application is scarce. As part of our investigations of potential oxidative reagents, we have studied its utility as an analytical reagent for the assay of a few industrially important organic compounds.^{6,7} In this communication we report titrimetric procedures for the assay of thiourea (TU), allylthiourea (ATU), phenylthiourea (PTU), tolythiourea (TTU), thioacetamide (TA), thiobenzamide (TB), diethyldithiocarbamate (DDC), ethylphenyldithiocarbamate (EPDC), diisopropylthiocarbamate (DIDC) and methionine (Met) with CBT.

EXPERIMENTAL

CBT was prepared by the method of Johnson *et al.*⁸ and recrystallized (m.p. 105.0–106.0 ±

0.1°) from dichloromethane. Its purity was checked (>99%) by the iodometric method. The sulphur compounds (Sigma or Aldrich, U.S.A.) were used after purification with suitable solvents. Comparative assay of these compounds showed acceptable purity (>99%). Solutions were prepared from analytical reagent grade chemicals and distilled water. The experiments were repeated to check reproducibility. The detailed procedures for preliminary studies, back titration and potentiometric titration are similar to those described earlier.⁶

The rate of oxidation at different temperatures and pH values prior to back titration are depicted in Fig. 1. Oxidation reactions are reproducible in 0.1M sodium hydroxide with stoichiometries of 1:4 for thioureas and thioamides, and 1:6 and 1:8 for methionine and dithiocarbamates, respectively (Table 1). Hence, 0.1M sodium hydroxide is used for the analysis.

Back-titration. Prepare accurately a solution containing about 1 mg/ml of the sulphur compound. Add an aliquot of this solution to 50.00 ml of $2 \times 10^{-3}M$ CBT solution in an iodine flask. Add enough sodium hydroxide to obtain the required concentration (0.1M). Set the reaction mixture aside at 30° for 15–20 min (40 min for PTU) and shake at intervals. Add 25.0 ml of 1.0M sulphuric acid and 5.00 ml of 2% (w/v) KI solution and titrate with standard thiosulphate solution ($1 \times 10^{-3}M$) to a starch end-point. Run a blank under the same conditions. The amount of sulphur compound in the solution (% mg) is given by the equation,

$$x = \frac{MY(V_2 - V_1)}{E}$$

*Author for correspondence.

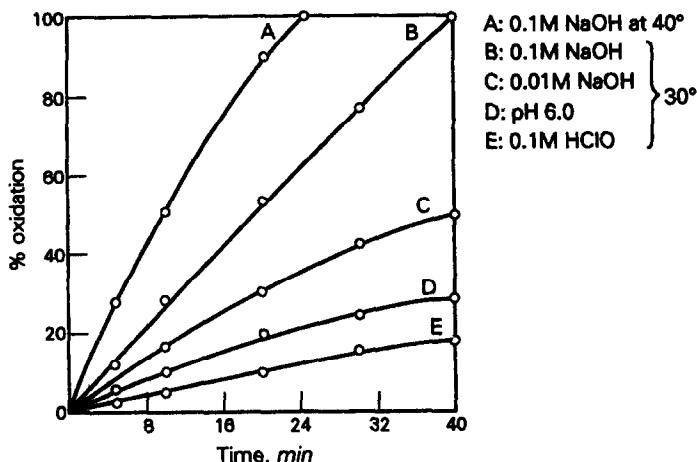


Fig. 1. Rate of oxidation of phenylthiourea under different conditions. $[CBT] = 2 \times 10^{-3}M$, $[PTU] = 1 \times 10^{-4}M$.

where M is the molecular weight of the sulphur compound, Y the molarity of the sodium thio-sulphate solution, E is the number of electrons per mole of sulphur compound, V_2 ml is the blank titre and V_1 ml is the sample titre, respectively.

Potentiometric titration

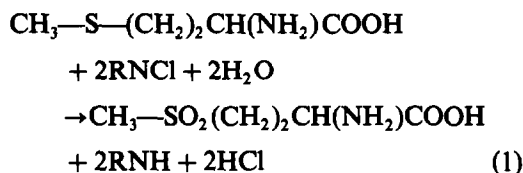
During potentiometric titration the change in potential at the end-point on addition of 0.1 ml of $2.0 \times 10^{-3}M$ CBT was appreciable (50–120 mV) and reproducible in the pH range 1–5 (Fig. 2). The number of electrons involved in the stoichiometric reactions depends on the nature of the reductant and the medium (Table 2). In buffer solution of pH 5.0, it is 6 for TU and ATU, 4 for PTU and TTU, 5 for TA and TB, and 2 for Met.

RESULTS AND DISCUSSION

Some of the results obtained during back-titration and potentiometric titration are given

in Table 3. The present method (especially the potentiometric method) seems to be superior to the back-titration method.

The four-electron stoichiometry obtained for oxidation of Met in 0.1M perchloric acid can be represented by equation 1.



The respective 1:1, 1:2, 1:3, 2:5 stoichiometries for the oxidation of Met, arylthioureas, alkylthioureas and thioamides with CBT in pH 5 buffer can be represented by equations (2) to (5).

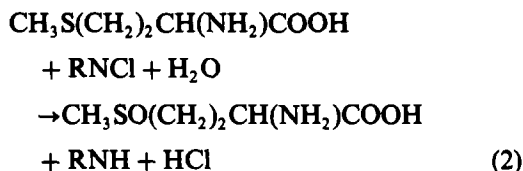


Table 1. Extent of oxidation of thioureas, thioamides, dithiocarbamates and methionine ($1 \times 10^{-4}M$) in different media (buffers, acid and base) with excess of 1-chlorobenzotriazole ($2 \times 10^{-3}M$) (back-titration)

Medium	mmols CBT/mmoles reductant									
	TU	ATU	PTU	TTU	TA	TB	Met	DDC	EPDC	DIDC
0.1M HClO ₄	1.10	1.52	1.55	1.68	1.70	1.72	2.05			
0.01M HClO ₄	1.15	1.60	1.85	1.70	2.00	2.02	2.00			
pH 3	1.20	1.73	2.20	2.25	2.30	2.15	2.66			
pH 4	2.30	2.55	2.31	2.35	2.50	2.43	2.75			
pH 5	2.65	2.96	2.50	2.56	2.50	2.50	3.10			
pH 6	2.70	3.05	2.55	2.58	2.87	2.80	3.15			
pH 7	3.72	3.80	3.50	3.55	3.40	3.31	3.30			
pH 8	3.90	3.85	3.60	3.72	3.50	3.40	3.86	6.05	5.90	6.11
pH 9	3.92	3.90	3.65	3.75	3.51	3.42	4.80	6.21	6.00	6.35
pH 10	3.94	3.91	3.70	3.80	3.90	3.78	4.85	7.30	7.10	7.50
0.01M NaOH	3.95	3.99	3.80	3.89	3.98	3.88	6.01	7.80	7.50	7.90
0.1M NaOH	4.00	4.05	3.98	3.99	4.00	4.01	6.00	8.00	8.01	7.99

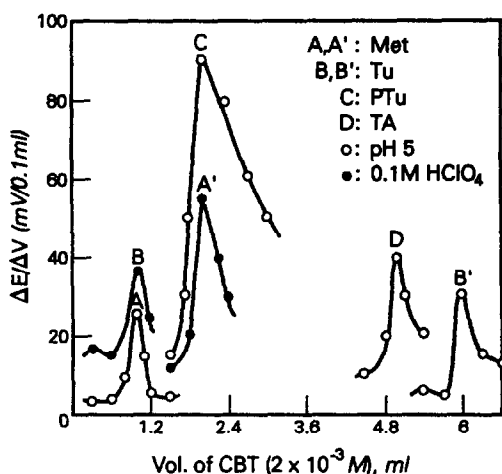
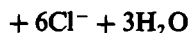
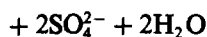
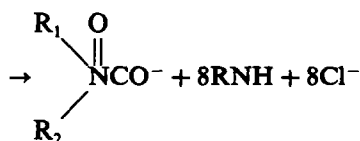
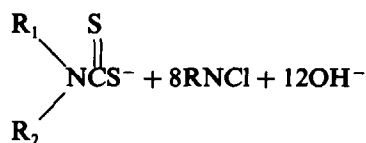


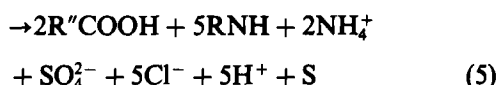
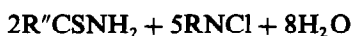
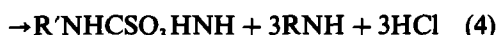
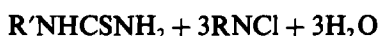
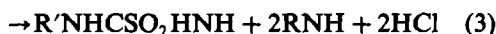
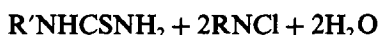
Fig. 2. Variation of $\Delta E/\Delta V$ vs volume of CBT under different conditions. [Reductant] = 1 mg/10 ml. Temperature = 30°.



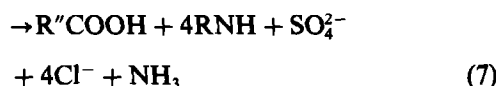
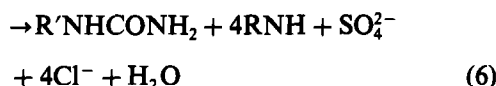
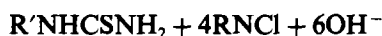
(8)



(9)



The 1:4 (thioureas and thioamides), 1:6 (Met) and 1:8 (dithiocarbamates) stoichiometry in 0.1M sodium hydroxide can be represented by equations (6) to (9).



where; $\text{R}=\text{C}_6\text{H}_4\text{N}_2$ for CBT and 1H-benzotriazole (BTA); $\text{R}'=\text{H}$ for TU, $\text{CH}_2\text{CH}=\text{CH}_2$ for ATU, C_6H_5 for PTU, $\text{CH}_3\text{C}_6\text{H}_5$ for TTU; $\text{R}''=\text{CH}_3$ for TA, C_6H_5 for TB; $\text{R}_1=\text{R}_2=\text{C}_2\text{H}_5$ for DDC, CH_3CHCH_3 for DIDC and $\text{R}_1=\text{C}_6\text{H}_5$ for EPDC.

The reaction products such as $\text{CH}_3\text{SO}(\text{CH}_2)_2\text{CH}(\text{NH}_2)\text{COOH}^{13}$ [equation (2)], $\text{CH}_3\text{SO}_2(\text{CH}_2)_2\text{CH}(\text{NH}_2)\text{COOH}^{14}$ [equation (1)], $\text{R}'\text{NHSO}_2\text{CHNH}^{15}$ [equation (3)] $\text{R}'\text{NHSO}_3\text{CHNH}^{15}$ [equation (4)], HCHO^{15} [equation (8)], $\text{R}'\text{NHCONH}_2$ [equation (6)], $\text{R}_1\text{R}_2\text{NCOO}^{-15}$ [equation (9)] and $^-\text{O}_3\text{S}(\text{CH}_2)_2\text{CN}^{16}$ [equation (8)] have been identified with standard procedures. The carboxylic acids [equations (5) and (7)] have been identified by TLC (R_f 0.68) with toluene/dichloromethane/methanol (25:10:1) as solvent, SO_4^{2-} in the form of barium sulphate and NH_3 with Nessler's reagent. The UV spectrum of one of the products (RNH) in methanol showed bands at 275, 258 and 253 nm similar to those for 1H-benzotriazole.

Table 2. Extent of oxidation of thioureas, thioamides and methionine ($1 \times 10^{-4}\text{M}$) in different media (buffers, acid and base) at 30° with 1-CBT ($2 \times 10^{-3}\text{M}$) (Potentiometric titration)

Medium	mmoles CBT/mmoles reductant						
	TU	ATU	PTU	TTU	TA	TB	Met
0.1M HClO ₄	1.00	1.06	1.55	1.52	1.95	1.76	2.00
0.01M HClO ₄	1.06	1.21	1.51	1.50	2.00	1.98	1.80
pH 3	2.48	2.50	1.46	1.43	2.26	2.30	1.36
pH 4	2.90	2.73	1.49	1.45	2.40	2.33	1.20
pH 5	3.00	3.01	2.00	2.00	2.50	2.50	1.00
pH 6	3.06	3.11	2.00	2.06	2.87	2.58	1.01
pH 7	3.46	3.66	2.50	2.65	3.48	3.35	1.11

Table 3. Estimation of thioureas, thioamides, dithiocarbamates and methionine with 1-CBT at 30°

Compound (0.5–10 mg)	Recovery, %		Comparison method	Reagent for comparison method
	Back titration	Potentiometric		
TU	99.6 ± 0.1	99.8 ± 0.1	99.7 ± 0.2	NaOI ¹⁰
ATU	99.5 ± 0.2	99.7 ± 0.1	98.8 ± 0.1	NaOI ¹⁰
PTU	98.4 ± 0.3	98.6 ± 0.2	98.2 ± 0.3	Iodine ¹⁰
TTU	98.6 ± 0.2	98.8 ± 0.2	98.5 ± 0.2	Iodine ¹⁰
TA	99.3 ± 0.1	99.6 ± 0.2	99.2 ± 0.3	Chloramine-T ³
TB	98.9 ± 0.2	99.2 ± 0.2	98.6 ± 0.3	Chloramine-T ³
Met	99.7 ± 0.1	99.9 ± 0.1	99.6 ± 0.1	Acetous perchloric acid ¹¹
DDC	98.4 ± 0.3		97.6 ± 0.3	Iodine ¹²
EPDC	98.8 ± 0.2		98.2 ± 0.2	Hg(II) ¹²
DIDC	99.3 ± 0.2		98.8 ± 0.2	Hg(II) ¹²

*Mean ± standard deviation of 10 determinations.

From the detailed investigations of the above compounds, it was found that Mg^{2+} , Ba^{2+} , Zn^{2+} , Cu^{2+} , K^+ , Na^+ , PO_4^{3-} , ClO_4^- and SO_4^{2-} had no effect on the rate of oxidation. [Chloride (>0.35 mg/ml) particularly in appreciably acidic media interferes in the estimation.] In the case of the back-titration procedure, the stoichiometry was unaffected by the reversal of the order of addition of CBT and reductant. 1-CBT showed stoichiometric reactivity towards the reductants and also in many occasions behaved as a powerful oxidizing agent when compared to other similar *N*-halogeno compounds like chloramine-T and chloramine-B.

REFERENCES

1. K. V. Uma and S. M. Mayanna, *J. Indian Chem. Soc.*, 1980, **58**, 655.
2. A. Stevenson, *J. Sci. Food Agr.*, 1964, **15**, 505.
3. T. P. Hadjiioannou and E. A. Piperaki, *Anal. Chim. Acta*, 1977, **190**, 329.
4. K. K. Tiwari and R. M. Verma, *Talanta*, 1983, **30**, 440.
5. R. C. Hiremath, S. M. Mayanna and N. Venkatasubramanian, *J. Sci. Ind. Res.*, 1990, **49**, 122.
6. C. Channegowda and S. M. Mayanna, *Mikrochim. Acta*, 1990 **III**, 271.
7. R. C. Hiremath, *Ph.D. Thesis*, 1988, Bangalore University, India.
8. C. R. Johnson, C. C. Bacon and W. D. Kingsbury, *Tetrahedron Lett.*, 1972, **6**, 501.
9. A. Findlay, *Practical Physical Chemistry*, p. 268. Longmans, London, 1954.
10. P. C. Gupta, *Z. Anal. Chem.*, 1963, **196**, 412.
11. A. I. Vogel, *Quantitative Organic Analysis*, Part III, p. 698. Longmans, 1958.
12. F. P. Przybylowicz and L. B. Rogers, *Anal. Chim. Acta*, 1958, **18**, 596.
13. K. B. Goswami, G. Chandra and S. N. Srivastava, *J. Indian Chem. Soc.*, 1981, **58**, 252.
14. N. M. M. Gowda and D. S. Mahadevappa, *Talanta*, 1977, **24**, 470.
15. F. Feigl, *Spot Test in Organic Analysis*, Elsevier, London, 1966.
16. S. Soloway and A. Lipschitz, *Anal. Chem.*, 1952, **24**, 898.

ADSORBING COLLOID FLOTATION SEPARATION AND POLAROGRAPHIC DETERMINATION OF Mo(VI) IN WATER

BHARATHIBAI J. BASU, D. K. PADMA* and S. R. RAJAGOPALAN†

Materials Science Division, National Aeronautical Laboratory, Bangalore-560017, India

(Received 1 February 1991. Revised 19 June 1991. Accepted 19 June 1991)

Summary—A method is described for the flotation and determination of Mo(VI) in water at ng/ml levels. Mo(VI) is preconcentrated and separated by adsorbing colloid flotation employing aluminium(III) hydroxide as collector and sodium lauryl sulphate as surfactant at pH 5.3 ± 0.1 . The molybdenum content in the froth is estimated by using the catalytic wave of Mo(VI) in the presence of nitrate by charging current compensated d.c. polarography (CCDCP) or differential pulse polarography (DPP). The effect of variables such as pH, ionic strength, concentration of collector and surfactant, time of stirring and gas flow-rate on the recovery of Mo by flotation is reported. The effects of various cations and anions on the flotation and determination of Mo are studied. This method is employed for the determination of molybdenum in natural fresh water samples.

Adsorbing colloid flotation (ACF) has been applied to the separation and preconcentration of trace elements in many aqueous systems during the past two decades.¹⁻¹³ Analytical applications of flotation have been reviewed recently.¹⁴ Adsorbing colloid flotation has some advantages over ion flotation (IF) such as (i) surfactant needed in ACF is smaller compared to the stoichiometric or greater amount required in IF and (ii) the flotation is achieved in a few seconds in ACF whereas gas has to be bubbled for a longer duration in IF.

Kim and Zeitlin¹ have separated Mo by ACF with ferric hydroxide as collector and sodium lauryl sulphate (SLS) as surfactant and estimated Mo by spectrophotometry. Recently Hidalgo *et al.*² have preconcentrated Mo in sea water by flotation with iron(III) hydroxide and hexadecyl trimethyl ammonium bromide. They estimated Mo in the floated layer (after removing iron by ion exchange) by differential pulse polarography employing the catalytic wave in nitrate medium. In all the ACF separations of Mo reported so far, iron(III) hydroxide has been used as the collector.^{1,2} Iron interferes with the polarographic estimation of Mo when the Fe:Mo ratio is greater than 100. Hence iron has to be separated by ion-exchange or any other suitable method. This additional separation step

can be avoided if iron(III) hydroxide is replaced by aluminium(III) hydroxide. But previous efforts to use aluminium(III) hydroxide as collector were not successful.² The present study is aimed at finding out a method of preconcentrating Mo by ACF with aluminium(III) hydroxide as collector.

EXPERIMENTAL

Apparatus

Polarographic measurements were made with a model CL-90 Pulse Polarograph of Elico (P) Ltd., Hyderabad. A Metrohm polarographic cell with mercury pool as counter electrode and SCE as reference electrode was used with a Sargeant capillary having a 3-sec natural droptime as DME. The rate of flow of mercury was found to be 2.30 mg/sec. For DPP measurements, the pulse duration was 0.04 sec and the pulse amplitude was 50 mV. The droptime was mechanically controlled.

The flotation apparatus was similar to that described by Nakashima.⁶ The flotation cell was a tall glass cylinder with a 500-ml capacity fitted with a G-4 porosity sintered glass disc to generate small gas bubbles. A side arm was provided near the bottom of the cell to drain the mother liquor rapidly after flotation.

Purified nitrogen (free from oxygen) was used for deaeration of the solution prior to polarographic measurements as well as for bubbling through the flotation cell.

*Department of Inorganic and Physical Chemistry, Indian Institute of Science, Bangalore-560003, India.

†Author for correspondence.

Hitachi UV-Visible spectrophotometer (model 139) was used for spectrophotometric determination of some of the added ions present in the froth.

Reagents

All reagents used were of analytical grade. A Mo(VI) (1 mg Mo/ml) stock solution was prepared from ammonium molybdate, Al(III) (10 mg Al/ml) solution from aluminium nitrate and Fe(III) (2 mg Fe/ml) solution by dissolving pure iron powder in diluted hydrochloric acid. Standard solutions of other metals were prepared either by dissolving the pure metal in nitric acid or by dissolving the nitrate salt in water. Eighty per cent (v/v) ethanolic solutions of sodium lauryl sulphate (SLS) (1 mg/ml), sodium oleate (SO) (4 mg/ml) and cetyl trimethyl ammonium bromide (CTAB) (1 mg/ml) were employed. Sodium chloride, sodium nitrate and sodium sulphate were used to study the effect of ionic strength. For the study of anionic interferences, standard solutions of Na_2CO_3 , sodium carbonate, sodium hydrogen carbonate and sodium phosphate were used. A standard silicate solution is prepared by dissolving pure silica in sodium hydroxide solution and diluting to volume.

Procedures

Flotation step. Place 400 ml of water containing trace amounts of Mo(VI) in a beaker and add 2 ml of Al(III) solution. Adjust the pH to 5.3 ± 0.1 with aqueous ammonia solution while stirring with a magnetic stirrer. Continue stirring for 10 min. Add 2 ml of SLS solution to the beaker and then transfer the contents to the flotation cell, quantitatively. Pass nitrogen at a moderate rate for 1 min. Allow the froth to settle for 2 min. Drain most of the mother liquor through the side arm. The remaining mother liquor is sucked off through the sintered disc. Dissolve the froth in the cell with 10 ml of 2M nitric acid and collect it quantitatively in a beaker. Heat this solution to boiling and simmer until the volume is reduced to 1 ml. Make up to 10 ml with water. For the separation of Mo from natural water samples, the above procedure is modified by increasing the solution volume to 1000 ml and Al^{3+} and SLS concentrations to 100 mg and 5 mg respectively.

Polarographic measurement. Transfer a suitable aliquot of the preconcentrated Mo(VI)

solution to a polarographic cell. Add 10 ml of a solution containing 2M sodium nitrate and 0.5M sulphuric acid and dilute to 20 ml so that the solution is 1M in sodium nitrate and 0.25M in sulphuric acid. After deaeration, record the polarogram from 0.0 to -0.40 V vs. SCE at 25° . Determine the concentration of Mo(VI) by making standard additions of comparable amounts of Mo(VI).

RESULTS AND DISCUSSION

Effect of pH on the flotation behaviour of collectors with surfactants

The flotation behaviour of iron(III) hydroxide and aluminium(III) hydroxide with SLS, SO and CTAB was studied. This was done by adjusting the pH of solutions containing Al(III) and Fe(III) by means of dilute ammonia and nitric acid and floating with an ethanolic solution of surfactant. After flotation, a visual evaluation of the completeness of flotation was made by observing the residual solution and the froth. A clear residual solution, which is free from the collector as shown by quantitative testing, and a stable froth indicate complete flotation. If the flotation is incomplete, the precipitate remains dispersed in the solution. It was found that SLS was able to float ferric hydroxide completely in the pH range 4.5–8.0. Aluminium(III) hydroxide was completely floated in the pH range 5.0–7.5. The flotation was incomplete above pH 7.5 for aluminium(III) hydroxide and above pH 8.0 for iron(III) hydroxide. This was expected, because the isoelectric points (IEP) of the hydroxides of Al(III) and Fe(III) are 7.5 and 8.0, respectively.¹⁵ Flotation of these colloids with other surfactants like SO and CTAB was also dependent on pH. SO floats both aluminium(III) and iron(III) hydroxides completely above pH 7. CTAB floats iron(III) hydroxide partially at low pH values and completely at pH 9–10. With aluminium(III) hydroxide and CTAB, no flotation occurs in the pH range 4–10 and the precipitate remains dispersed in solution.

The results obtained for ferric hydroxide are in agreement with the results of Grieves and Bhattacharya.¹⁶ Matsuzaki and Zeitlin⁹ had studied the effect of pH on the ability of various surfactants to float the collectors from artificial sea water. Their results showed that ferric hydroxide could easily be floated with a number of surfactants while the flotation efficiency was

poor for aluminium hydroxide. The negative results for aluminium hydroxide were probably due to the effect of high ionic strength as found in sea water. No work has been reported on the flotation behaviour of collectors with surfactants from fresh water or water with low ionic strength. We have found that aluminium(III) hydroxide can be completely floated from fresh water samples by SLS in the pH range of 5–7.5 and by SO in the pH range 7–10. When the ionic strength is increased, complete flotation can be achieved by increasing the amount of surfactant to some extent. Above a particular limit, flotation remains incomplete. Further experiments on the flotation of Mo(VI) with aluminium(III) and iron(III) hydroxides were carried out with SLS as surfactant.

Effect of pH on the recovery of Mo(VI) by ACF

Figure 1 shows the effect of pH on the recovery of Mo(VI) using aluminium and ferric hydroxides as collectors and SLS as surfactant. A 100% recovery of Mo(VI) is achieved with aluminium(III) hydroxide in the pH range 5.2–5.5. As the pH is increased, the recovery of Mo(VI) decreases even though the flotation is complete. At higher pH values, the colloid becomes negatively charged and the recovery of molybdate decreases to zero. With iron(III) hydroxide as collector, 100% recovery is obtained in the pH range 4.5–6.0.

In ACF, the mechanism of collection of the analyte on the colloidal precipitate is either adsorption or coprecipitation. In the case of Mo(VI), the pH range for maximum recovery is quite narrow and in this pH range, the colloidal precipitate has a charge opposite to that of the analyte. Hence, it appears that the mechanism governing the separation of Mo(VI) from solution is adsorption. Since Mo(VI) is present as an anion at $\text{pH} > 1.0$, adsorption of this species can be expected to occur at a positively charged colloid. Fe(III) hydroxide and Al(III) hydroxide have positive charges at pH values lower than their IEP's. Above the IEP, there is no electrostatic attraction as both molybdate and the colloidal precipitates are negatively charged. Therefore the adsorption of Mo(VI) decreases almost to zero as the pH is increased to a value above the IEP of the colloidal precipitates (Fig. 1).

Kim and Zeitlin¹⁷ found that Mo(VI) could be completely coprecipitated with colloidal ferric and thorium hydroxides but the recovery of

Mo(VI) by coprecipitation on aluminium(III) hydroxide was very poor. They attributed this to the relatively higher solubility of aluminium molybdate compared to ferric and thorium molybdates. The Paneth–Fajans–Hahn rule for the coprecipitation mechanism requires that the collector must contain an ion which forms a compound of low solubility with the counter ion adsorbed. In the light of the above discussion, it may be concluded that the nearly complete recovery of molybdate on aluminium(III) hydroxide by flotation at pH 5.2–5.5 should be due to adsorption.

Effect of ionic strength

The effect of nitrate, chloride and sulphate ions on the recovery of Mo(VI) by ACF with aluminium(III) hydroxide as collector was investigated. The concentrations used for this study were 0.1 ppm Mo(VI), 50 ppm aluminium(III) and 5 ppm SLS. The inert ion concentrations were varied from 0.01 to 0.20M. The pH was adjusted to 5.3 ± 0.1 in all these experiments (Fig. 2). It was found that the doubly charged sulphate ions decreased the percentage recovery of Mo(VI) to a greater extent than singly charged nitrate or chloride ions. When the ionic strength was increased, the recovery of Mo(VI) decreased and the flotation was incomplete at concentrations higher than 0.1M for chloride and nitrate and 0.03M for sulphate. The flotation efficiency was very poor above 0.06M sulphate and 0.2M nitrate or chloride. In the presence of 0.1M chloride or nitrate, 64% of molybdate was recovered by flotation as seen from Fig. 2. The precipitate

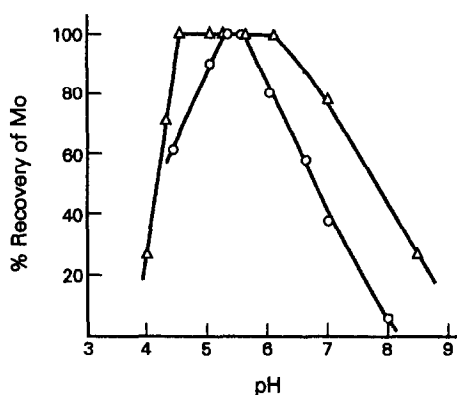


Fig. 1. Effect of pH on the recovery of Mo(IV) with SLS as surfactant and aluminium(III) hydroxide (○) and iron(III) hydroxide (△) as collectors. [Mo(IV)] = 0.20 ppm; [Al(III)] = 50 ppm; [Fe(III)] = 50 ppm; [SLS] = 5 ppm; solution volume = 200 ml.

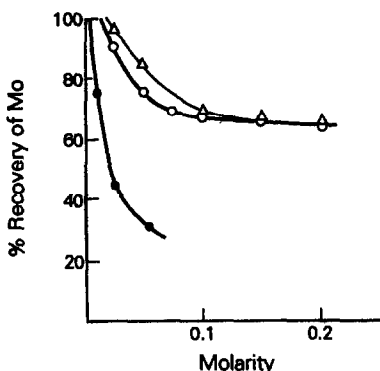


Fig. 2. Effect of ionic strength on the recovery of Mo(VI) with SLS as surfactant and aluminium(III) hydroxide as collector; (Δ) NaNO_3 , (\circ) NaCl and (\bullet) Na_2SO_4 . $[\text{Mo(VI)}] = 0.20$ ppm; $[\text{Al(III)}] = 50$ ppm; $[\text{SLS}] = 5$ ppm; $\text{pH} = 5.3 \pm 0.1$.

of aluminium(III) hydroxide remaining in the residual solution after flotation was separated by filtration and Mo(VI) in this residue was estimated. It was found that about 30% molybdate could be recovered from this precipitate showing that Mo(VI) is adsorbed by aluminium(III) hydroxide in the presence of 0.1M chloride or nitrate but the flotation of the collector by the surfactant is affected. The presence of sulphate seriously affected both the adsorption of Mo(VI) and the flotation of aluminium(III) hydroxide.

Effect of the concentrations of surfactant and collector

The effect of SLS on the ACF of Mo(VI) with Al(III) and Fe(III) hydroxides was studied by varying the SLS concentration from 0.2–10 mg. Concentrations of 0.1 ppm Mo(VI) and 50 ppm Al(III) or Fe(III) were used. The pH was maintained at 5.3 ± 0.1 . It was found that 1 mg of SLS was sufficient to float precipitates containing up to 40 mg of Fe(III) or Al(III) in a solution volume of 400 ml (when the ionic strength was less than 0.02M). Recovery of Mo(VI) was maximum when the SLS concentration was in the range 1–4 mg. Higher amounts of surfactant result in the formation of an excess of foam which is not beneficial. If the surfactant concentration exceeds the critical micelle concentration (cmc), the flotation tends to become incomplete. At very low concentrations of surfactant, the foam layer was thin and unstable and could not support the precipitate. Hence a surfactant concentration of 2 mg for a solution volume of 400 ml was used in this work.

The concentrations of Al(III) and Fe(III) were varied from 2–100 mg in a solution volume of 400 ml. SLS concentration was 5 ppm and the pH was adjusted to 5.3 ± 0.1 . When the Mo(VI) concentration was 1–40 μg , an optimum concentration of 10–20 mg Al(III) or Fe(III) was enough to bring about complete recovery of Mo(VI).

Effect of stirring time

The relation between stirring time and recovery of Mo(VI) was investigated. The concentrations of Mo(VI), Al(III) and SLS used were 0.2, 50 and 5 ppm, respectively. The pH was maintained at 5.3 ± 0.1 . It was found that at very low concentrations of colligend (less than 50 μg of Mo), the adsorption of Mo(VI) on the colloidal precipitate was rapid whereas at higher concentrations of Mo(VI), stirring time had an effect on the recovery of Mo(VI). The results obtained are shown in Fig. 3. It is seen that a stirring time of 15 min was needed to get 100% recovery for floating 500 μg of Mo(VI) with 10 mg of aluminium(III) hydroxide. Mo(VI) concentrations of 4, 10 and 40 μg could be collected almost instantaneously. This can be readily explained in terms of the adsorption since it is well known that the rate of adsorption increases when the ratio of adsorbent to adsorbate is large.

The other parameters like gas flow-rate, duration of gas flow and volume of solution had little effect on the recovery of Mo(VI). Gas was bubbled at a moderate rate for 1 min. The solution volume was changed from 100 to 1000 ml. A quantitative recovery of Mo(VI) was obtained.

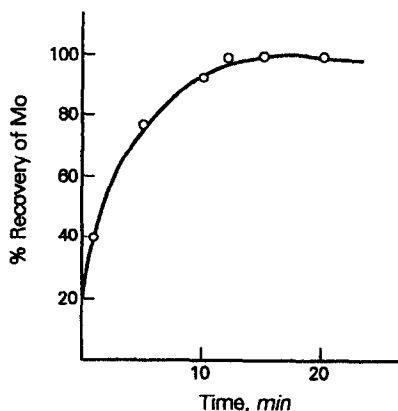


Fig. 3. Effect of stirring time on the recovery of Mo(VI) with SLS as surfactant and aluminium(III) hydroxide as collector; $[\text{Mo(VI)}] = 500$ μg ; $[\text{Al(III)}] = 10$ mg; $[\text{SLS}] = 1$ mg; solution volume = 200 ml.

Catalytic wave of Mo(VI) in the presence of surfactants

Following Kannan and Rajagopalan,¹⁸ a supporting electrolyte of 1M sodium nitrate and 0.25M sulphuric acid was chosen for the catalytic wave polarographic determination of Mo(VI). The catalytic current is sensitive to temperature and hence all the polarograms were recorded at 25°. Hidalgo *et al.*² studied the effect of various surfactants on the catalytic wave of Mo(VI) and found that many of them suppress the peak current. Their report did not include the effect of SLS. In this work, the effect of 5–50 ppm surfactant on the catalytic current (both dc and DPP) of 1 ppm Mo(VI) was investigated (Fig. 4). It was found that in the presence of 30 ppm SLS, the catalytic current of Mo(VI) was suppressed to about half its original value. But at SLS concentrations less than 10 ppm, the reduction of catalytic current was <20%. However, it was noticed that the catalytic current was virtually unaffected after treatment of the froth with nitric acid. This might be due to the oxidative degradation of SLS into products that are not surface active. The catalytic current of Mo(VI) is affected to a lesser extent by the addition of SO and CTAB as seen from Fig. 4.

Comparison of DPP and CCCDCP for the determination of Mo(VI)

In order to arrive at the best technique from the point of view of improved sensitivity for the estimation of Mo(VI) by the catalytic wave, CCCDCP and DPP were compared both experimentally and theoretically. Typical polarograms (both CCCDCP and DPP) are shown in Fig. 5. Our experiments show that the dc catalytic current is 2.75 times more sensitive than the DPP catalytic current for a droptime of 0.5 sec. When the droptime is increased to 2.0 sec, the ratio of $i(\text{CCCDCP})$ to $i(\text{DPP})$ is increased to 3.4. The pulse duration was 0.04 sec in all the experiments. The ratio of dc catalytic current to DPP catalytic current was calculated with the expression derived by Rodriguez-Monge *et al.*¹⁹ for EC processes and the values were 2.77 and 3.76 for droptimes of 0.5 and 2.0 sec respectively. Thus it can be seen that the experimental values are in good agreement with the theoretical values. Therefore it may be concluded that the catalytic reduction of Mo(VI) by nitrate is more sensitive by CCCDCP than by DPP. This conclusion contradicts that stated

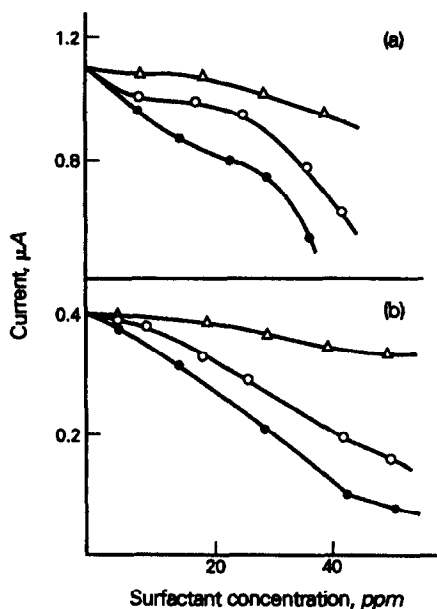


Fig. 4. Effect of variation of surfactant concentration on the catalytic current of Mo(VI); [Mo] = 1 ppm, time = 0.5 sec (a) dc catalytic current (b) DPP catalytic current; (Δ) SO, (\circ) CTAB and (\bullet) SLS.

by Lanza *et al.*²⁰ They found DPP to be 4.7 times more sensitive than DCP. This result is difficult to understand since it is contrary to theoretical expectations.

Effects of diverse cations and anions on the flotation and determination of Mo(VI)

The flotation of Mo(VI) was carried out in the presence of various cations and anions. This was done by adding known amounts of these ions to a synthetic solution before flotation.

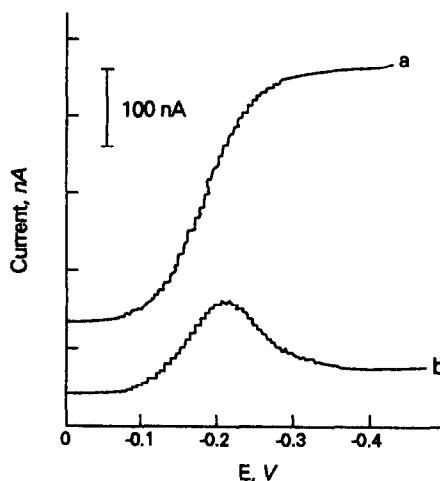


Fig. 5. Typical polarograms of Mo(VI) in a supporting electrolyte of 1M NaNO₃ and 0.25M H₂SO₄. [Mo] = 0.1 ppm; $m = 2.30$ mg/sec; time = 2 sec (a) CCCDCP and (b) DPP, $\Delta E = 50$ mV.

The results are summarized in Tables 1 and 2. The amounts of added ions in the froth after flotation at $\text{pH } 5.3 \pm 0.1$ were determined either by polarography or by spectrophotometry. Cu(II), Pb(II), Ni(II), Co(II), Bi(III), Sb(III), Zn(II) and Cd(II) in the froth were estimated by polarography. Fe(III), Ti(IV), Zr(IV) and Cr(III) in the froth after flotation were determined by conventional spectrophotometric methods. Fe(III), Bi(III), Ti(IV), Cr(III) and Zr(IV) were floated completely along with Mo(VI). These elements with the exception of Fe(III) do not interfere with the polarographic determination of Mo. The recoveries of Cu(II) and Pb(II) were 75–80%. Co(II), Ni(II), Zn(II), Cd(II) and Sb(II) were partially floated.

Table 2 gives the results obtained on studying the effect of anions on the flotation of Mo. The flotation efficiency of Mo was affected by the presence of phosphate and silicate. Thus the recovery of Mo is reduced to 56 and 61% by 50 ppm levels of silicate and phosphate respectively. The interference was found to be negligible at or below 5 ppm silicate and phosphate. At higher concentrations, these multivalent anions compete with molybdate in the process of adsorption on the collector and thus cause a lower recovery for Mo(VI). Anions like carbonate and bicarbonate could be tolerated to a level of 1000 ppm in the solution.

The effect of various cations and anions on the catalytic wave of Mo(VI) was investigated.

Table 1. Effect of the addition of other metallic ions on the flotation of Mo with Al(OH)_3 as collector and SLS as surfactant. $[\text{Mo(VI)}] = 40 \mu\text{g}$; $[\text{Al(III)}] = 20 \text{mg}$; $[\text{SLS}] = 1 \text{mg}$; $\text{pH} = 5.3 \pm 0.1$; solution volume = 200 ml

Ion	Ratio of Mo(VI) to the added ion	% Recovery	
		Mo(VI)	Added ion
Pb(II)	1:1	100	80
	1:10	>95	75
	1:25	>95	75
Cu(II)	1:1	100	75
	1:10	>95	75
	1:25	>95	75
Fe(III)	1:1	100	100
	1:100	95	>95
Bi(III)	1:1	100	>95
	1:25	96	>95
Ti(IV)	1:10	100	100
	1:100	>95	>95
Zr(IV)	1:100	>95	>95
Cr(III)	1:1	100	>95
	1:10	>95	>95
Cr(IV)	1:1	>95	—
Co(II)	1:1	>95	7
Ni(II)	1:1	>95	12
Cd(II)	1:10	>95	5
Zn(II)	1:10	>95	50

Table 2. Effect of the presence of anions on the flotation of Mo. $[\text{Mo(VI)}] = 40 \mu\text{g}$; $[\text{Al(III)}] = 20 \text{mg}$; $[\text{SLS}] = 1 \text{mg}$; $\text{pH} = 5.3 \pm 0.1$; solution volume = 200 ml

Ion	Amount of ion added, mg	Mo recovery, μg	Recovery, %
SiO_3^{2-}	1.0	38.0	95.0
	2.0	35.0	87.5
	4.0	32.8	82.0
	10.0	22.4	56.0
PO_4^{3-}	1.0	38.4	96.0
	2.0	36.0	90.0
	4.0	35.0	87.5
	10.0	24.4	61.0
CO_3^{2-}	10.0	39.2	98.0
	50.0	39.1	97.8
	100.0	38.0	95.0
	200.0	38.4	96.0
HCO_3^-	100.0	39.0	97.5
	200.0	38.0	95.0

The concentration of Mo(VI) in the supporting electrolyte was 0.2 ppm. The results are given in Table 3. The catalytic current of Mo(VI) is not affected by the presence of a 100-fold excess of silicate and phosphate. A 100-fold excess of metallic ions such as Pb(II), Cd(II), Zn(II), Ni(II) and Co(II) do not interfere as their reduction potentials are more negative than that of Mo(VI). A 1000-fold excess of Al(III) and 100-fold excess of Ti(IV) and Zr(IV) also do not interfere. Cu(II) and Bi(III) peaks occur at a more positive potential than that of Mo(VI). But since the peaks are separated by more than 150 mV and the sensitivities of copper and bismuth are much less than that of Mo(VI)

Table 3. Interferences due to foreign species in the polarographic determination of Mo. $[\text{Mo(VI)}] = 0.2 \text{ppm}$; time = 0.5 sec; $\Delta E = 50 \text{mV}$

Ion	Concentration ratio,	
	ion: Mo(VI)	Error %
Pb(II), Cd(II), Zn(II), Co(II), Ni(II), Cr(III), Ti(IV), Zr(IV)	100:1	nil
	1000:1	nil
	25:1	nil
	10:1	nil
Fe(III)	50:1	-13
	40:1	nil
	100:1	-10
Cr(VI)	200:1	-25
	400:1	-55
	10:1	-6
	10:1	-6
Sb(III)	1:1	+13
	2:1	+25
Sb(V)	10:1	nil
SiO_3^{2-}	100:1	nil
PO_4^{3-}	100:1	nil

in nitrate medium, it is possible to determine Mo(VI) in the presence of a 25-fold excess of Cu(II) and Bi(III). In such cases, DPP offers better resolution than CCCDCP. Hence in the presence of an excess of Cu(II) and Bi(III), it is preferable to use DPP for the determination of Mo. A 10-fold excess of Cr(III), Cr(VI), Tl(I) and Sn(IV) does not interfere. Fe(III) does not interfere if present in small amounts but a 100-fold excess of Fe(III) causes a decrease in the Mo catalytic current by 10%. When the Fe:Mo ratio is 400, there is a significant reduction in the catalytic current of Mo(VI) as seen from Table 3. Sb(III) interferes as its reduction peak coincides with that of Mo(VI). It is seen that Sb(III) gets partially floated with Mo(VI). The interference was overcome by oxidizing Sb(III) to the electroinactive Sb(V) by adding a few drops of potassium permanganate solution to the solution of froth.

Recovery of Mo(VI) from synthetic solutions

Initial experiments were carried out with 1 ppm Mo(VI), 10 mg Al(III) and 1 mg SLS in a solution volume of 400 ml to standardize the experimental conditions. Then under the standardized conditions, the flotation was done at lower Mo(VI) concentrations and the results are given in Table 4. Thus it was seen that 1 μg of Mo in 400 ml of water could be preconcentrated by this method.

The detection limit (at a signal-to-noise ratio of 3) is 5.0 $\mu\text{g/l}$. for CCCDCP and DPP at a droptime of 2 sec. When the initial volume of water for flotation was increased to 1000 ml, the concentration factor was 50. Thus it was possible to achieve a detection limit of 0.1 $\mu\text{g/l}$. for Mo(VI) in water by this flotation-polarographic method. This value is comparable to the detection limit obtained by adsorption voltammetry.²¹ The relative standard deviation for 8 replicate analyses of a solution containing 2 $\mu\text{g/l}$. Mo was found to be 3.0%.

Recovery of Mo from natural fresh water samples

It was noticed that the recovery of Mo from natural fresh water by ACF under the experimental conditions standardized for synthetic solutions [50 ppm Al(III), 5 ppm SLS and pH 5.3 ± 0.1] was about 50%. Fresh water samples often contain anions like carbonate, bicarbonate, chloride, silicate and phosphate in addition to some metal ions. The approximate ranges and typical values for some metals and ligands in fresh waters have been reported elsewhere.²²

Table 4. Results for the analysis of synthetic water samples*

No.	Mo(IV) added, μg	Mo(IV) found, μg	Recovery %
1	1.0	1.0	100
2	1.6	1.56	97.5
3	8.0	7.84	98.0
4	40.0	39.0	97.5
5	500.0	495.0	99.0

*Solution volume = 400 ml.

The results of the study of anionic interference on the flotation of Mo(VI) are already given in Table 2. The concentrations of Mo(VI), Al(III) and SLS used for this study were 0.2 ppm, 100 ppm and 5 ppm. It can be seen from Table 2 that up to 1000 ppm of carbonate and bicarbonate do not interfere with the flotation of Mo whereas the recovery of Mo is affected by silicate and phosphate at concentrations higher than 10 ppm. But the typical concentrations of phosphate and silicate in fresh water are of the order of 1 and 5 ppm respectively. We found that the recovery of Mo from natural water samples could be improved by increasing the collector concentration to 100 ppm. The alternative method is to repeat the flotation until all the Mo was recovered. The recovery of Mo was about 90% in a single flotation by employing 100 ppm Al(III). Two consecutive flotations with 50 ppm Al(III) also enabled us to recover 90% Mo but a single flotation with increased amount of collector and surfactant was less time consuming than double flotations.

Iron and copper present in natural water were also floated along with molybdenum. Copper does not interfere in the determination of Mo. The iron to molybdenum ratio was often higher than 100 in the froth and this decreased the sensitivity of molybdenum determination by catalytic wave polarography. By examining water samples from different sources like wells, lakes and borewells, we found that the Fe(III) to Mo(VI) ratio in the froth often exceeded 500. This suppresses the polarographic signal considerably and results in lower values for Mo. Hence it is essential to remove iron which is done by incorporating an additional flotation step prior to the flotation for the preconcentration of Mo.

Since the recovery of Mo(VI) falls to zero at pH values above 8.0, it is possible to separate Fe(III) from Mo(VI) by employing a flotation step. Therefore, for the determination of Mo in natural water samples containing considerable amounts of Fe(III), the procedure is modified

Table 5. Results for the determination of Mo(VI) in fresh water samples

No.	Sample*	Mo(VI) found† ($\mu\text{g/l}$)
1	A	0.42 ± 0.04
2	B	0.50 ± 0.04
3	C	0.64 ± 0.05
4	D	0.31 ± 0.03

*A = laboratory tap water; B = well water;

C = bore-well water; D = lake water.

†Mean \pm standard deviation ($n = 4$).

as follows: add 20 mg of Al(III) to 1000 ml of the sample solution, adjust the pH to 8.5 with dilute ammonia, add an ethanolic solution containing 5 mg of sodium oleate and float by bubbling nitrogen through the solution for 2 min. Fe(III) and other cations like Cu(II) and Pb(II) if present are separated in the froth. To the residual solution, add 100 mg of Al(III), adjust the pH to 5.3 ± 0.1 , add 5 mg of SLS and continue as described earlier in the experimental section. Mo(VI) in four natural water samples from different sources was estimated with this procedure and the results obtained are shown in Table 5. The reproducibility was good. Thus the method is found to have great potential in determining nanogram levels of Mo(VI) in natural fresh water samples.

REFERENCES

1. Y. S. Kim and H. Zeitlin, *Sep. Sci.*, 1971, **6**, 505.
2. J. L. Hidalgo, M. A. Gomez, M. Caballero, R. Cela and J. A. Perez-Bustamante, *Talanta*, 1988, **35**, 301.
3. Y. S. Kim and H. Zeitlin, *Sep. Sci.*, 1972, **7**, 861.
4. G. Leung, Y. S. Kim and H. Zeitlin, *Anal. Chim. Acta*, 1972, **60**, 229.
5. M. Hiraide, Y. Yoshida and A. Mizuike, *ibid.*, 1976, **81**, 185.
6. S. Nakashima, *Anal. Chem.*, 1979, **51**, 654.
7. M. Hiraide, T. Ito, M. Baba, H. Kawaguchi and A. Mizuike, *ibid.*, 1980, **52**, 804.
8. E. H. DeCarlo and H. Zeitlin, *ibid.*, 1981, **53**, 1104.
9. C. Matsuzaki and H. Zeitlin, *Sep. Sci.*, 1973, **8**, 185.
10. R. Lemlich, *Adsorptive Bubble Separation Techniques*, p. 1-331. Academic Press, New York, 1972.
11. A. N. Clarke and D. J. Wilson, *Sepr. Purif. Methods*, 1978, **7**, 55.
12. M. Hiraide and A. Mizuike, *Rev. Anal. Chem.*, 1982, **6**, 151.
13. A. Mizuike and M. Hiraide, *Pure. Appl. Chem.*, 1982, **54**, 1956.
14. M. Caballero, R. Cela and J. A. Perez-Bustamante, *Talanta*, 1990, **37**, 275.
15. G. A. Parks, *Chem. Rev.*, 1965, **65**, 177.
16. R. B. Grieves and D. Bhattacharya, *J. Appl. Chem.*, 1968, **18**, 149.
17. Y. S. Kim and H. Zeitlin, *Anal. Chim. Acta*, 1970, **51**, 516.
18. R. Kannan and S. R. Rajagopalan, *Proceedings of the Second International Symposium on Industrial and Oriented Basic Electrochemistry at IIT*, p. 471. Madras, December 1980.
19. L. M. Rodriguez-Monge, E. Munoz, J. L. Avila and L. Camacho, *Anal. Chem.*, 1988, **60**, 2269.
20. P. Lanza, D. Ferri and P. L. Buldini, *Analyst*, 1980, **105**, 379.
21. C. M. G. van den Berg, *Anal. Chem.*, 1985, **57**, 1532.
22. P. C. Singer, *Trace Metals and Metal—Organic Interactions in Natural Waters*; p. 165. Ann Arbor Science Publishers, 1973.

ANALYTICAL DATA

MICROSCOPIC ACID–BASE EQUILIBRIA OF ARGININE

BÉLA NOSZÁL and RÓZSA KASSAI-TÁNCZOS

Department of Inorganic and Analytical Chemistry, L. Eötvös University, H-1518 Budapest 112, Pf. 32,
 Hungary

(Received 25 April 1991. Accepted 30 May 1991)

Summary—Three and two protonation macroconstants as well as twelve and four microconstants have been determined for arginine and citrulline, respectively. These data include microscopic basicity values of the arginine guanidino group, for which no reliable constants have been reported earlier. The determinations were carried out by a combination of potentiometric and deductive methods. The guanidino basicity proved to be extremely high, and can be characterized by microconstants between 14.7 and 15.0 log k units. The interactivity parameters could also be determined from the microscopic protonation constants. These values for the guanidino–amino and the guanidino–carboxylate interactions are 0.2 and 0.1 log k units, respectively. The pH-dependent distribution of all eight arginine microspecies is made visual by a microspeciation diagram. The microspeciation diagram is the most useful tool to predict bidentate binding isomerism in metal complex formation and site-specific bioligand–bioligand associations.

Arginine is a semi-essential amino acid, which plays an important role as a binding moiety in proteins¹ and also as a metal–complexing agent.²

Of the twenty “classical” amino acids, however, arginine is the only one for which no microscopic protonation constants (microconstants) have been published.³ Microconstants are submolecular thermodynamic parameters, quantitating the proton-binding capability of basic groups, when the protonation states of all other basic sites are definite in the molecule. Thus, microconstants are the proper terms for the thorough and exact characterization of the basicity of multidentate (bio)ligands^{4–6} and also the tools for the analytical determination of all protonation forms in the solution (microspeciation).^{7,8}

Concerning proton-binding sites, arginine is a tridentate ligand, which contains guanidino (G), amino (A) and carboxylate (C) groups. The protonation scheme can be seen in Fig. 1. The relationships between the arginine macro- and microconstants are as follows:

$$K_1 = k^G + k^A + k^C \quad (1)$$

$$\begin{aligned} K_1 K_2 &= k^G k_G^A + k^G k_G^C + k^A k_A^C \\ &= k^A k_A^G + k^C k_C^G + k^C k_C^A \end{aligned} \quad (2)$$

$$\begin{aligned} K_1 K_2 K_3 &= k^G k_G^A k_{GA}^C = k^G k_G^C k_{GC}^A \\ &= k^A k_A^G k_{GA}^C = \dots \end{aligned} \quad (3)$$

where K_1 , K_2 and K_3 are the stepwise macroconstants, k^G , k^A , k^C , k_G^A , k_{GA}^C , etc., are the microconstants. Superscripts of microconstants indicate the group protonating in the given microequilibrium protonation process, whereas subscript(s) (if any) stand for the group(s) already attached to the proton. Arg[−], HArg, H₂Arg⁺ and H₃Arg²⁺ are macrospecies, of which HArg and H₂Arg⁺ are composites of three protonation isomers each:

$$[\text{HArg}] = [\text{HArg}_G] + [\text{HArg}_A] + [\text{HArg}_C] \quad (4)$$

$$\begin{aligned} [\text{H}_2\text{Arg}^+] &= [\text{H}_2\text{Arg}_{G,A}^+] + [\text{H}_2\text{Arg}_{G,C}^+] \\ &\quad + [\text{H}_2\text{Arg}_{A,C}^+] \end{aligned} \quad (5)$$

where entries on the right-hand sides are protonation isomer microspecies. The subscripts G, A and C indicate the site(s) of protonation.

The protonation at one basic site modifies the basicity of the other site. The measure of this basicity-modifying (mostly decreasing) effect can be quantitated in terms of interactivity parameters. For example, the interactivity parameter for the guanidino and amino groups can be written as:

$$\Delta \log k_{G-A} = \log k^G - \log k_A^G = \log k^A - \log k_G^A \quad (6)$$

For arginine, it has long been recognized that the group-basicity gradually and significantly

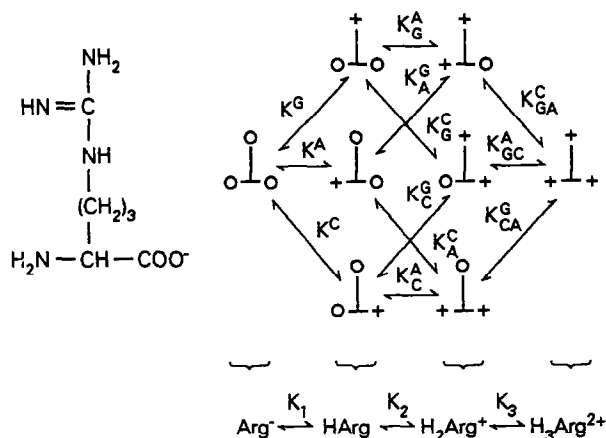


Fig. 1. Microscopic protonation scheme of arginine.

decreases in the order guanidino, amino, carboxylate. Accordingly, the predominating protonations proceed along the k^G , k_G^A and k_{GA}^C microconstants. Nevertheless, it is important to determine all the microconstants and the microspecies concentrations, because the predominant species are not necessarily the reactive ones.⁹

Due to its biological significance, the acid-base properties of arginine have been studied in several cases.¹⁰⁻³¹ In the vast majority of papers, however, two stepwise macroconstants have been determined only, which essentially refer to the amino and carboxylate protonations (see Table 1). All three stepwise equilibria

(including the one for the guanidino group) have been studied only rarely.^{10,11,16,27,29-31} Unfortunately, the critical survey of equilibrium constants³² has accepted none of these data and the recent values also contain several controversies.²⁹⁻³¹ Owing to lack of basicity data and interactivity parameters for the guanidino group, the arginine microequilibria could not previously be characterized.

We therefore aimed at determining all the macro- and microconstants of arginine. The two major difficulties of the determinations were (i) the extremely high guanidino basicity and (ii) the concomitant need for a model compound which mimics those minor protonation isomers

Table 1. Literature protonation macroconstants of arginine

Reference	Temperature, °C	Ionic strength, <i>M</i>	log K_1	log K_2	log K_3
10.	25	0	12.48	9.04	2.02
11.	23	0	13.2	9.09	2.18
12.	25	0.1		9.04	2.17
13.	25	0.1		9.01	1.807
14.	25	0.1		9.04	
15.	25	0.1		9.07	2.10
16.	20	0.1	12.48	9.08	2.17
17.	19	0.01		9.11	
18.	25.15	0.015		9.11	
19.	20	1.0		9.21	2.19
20.	20	0.01		9.13	
21.				9.05	1.98
22.*	25			9.05	1.97
23.*	25			8.994	1.822
24.	25	0.1		9.03	
25.	25	0.1	11.5	9.36	
26.	25	0.15		8.92	2.02
27.	25	1.0	12.28	9.27	2.21
28.	25	0.2		8.99	1.82
29.	37	0.15	11.43	8.79	2.08
30.	35	0.1	12.00	9.00	2.00
31.	25	0.1	11.58	8.98	2.22

*Data at several temperatures are reported, from which we took the 25° values.

of arginine where the guanidino group is not protonated.

The extremely high basicity of the guanidino group allows only partial deprotonation even at the upper limit of the pH-scale. To provide sufficiently high hydroxide ion concentration, we performed potentiometric titrations at several ionic strengths, including 5.0 and 2.0*M*. The hydroxide ion concentrations were calculated from acid-base titration data rather than from emf values. The latter always bear a considerable alkali and matrix error at high pH. The degree of guanidinium deprotonation was also calculated as Δ ml volume difference of titrant added to solutions with and without arginine. The emf values were only used to identify the corresponding potential values in the blank and the arginine-containing acid-base titrations.

Due to the very high guanidino basicity, the concentration of those microspecies is very low where the guanidino group bears no positive charge. Consequently, the combination of pH-metry and NMR or UV spectrometry (the most widely used methods for the determination of microconstants) can not be applied here. The only available means is a deductive method which needs a model compound of the minor protonation isomer. Our model compound was citrulline, a very close analogue of arginine. The carbamoyl locus of citrulline is isoelectronic and isosteric with the guanidyl group of arginine. The rest of the molecules are the same. An important difference between the carbamoyl and guanidyl moieties is that the carbamoyl group remains unprotonated throughout the entire pH-range. It has recently been shown that the isoelectronic, isosteric $-\text{COOH}$ and $-\text{CONH}_2$ residues⁶ have the same effect on the NMR parameters, rotamer populations and the basicity. In general, such analogous moieties in the same state of protonation influence equally the rest of the molecule. We applied the above principle to the guanidyl and carbamoyl groups and treated the citrulline protonation constants as constants for the corresponding minor microspecies of arginine.

In this paper we report the 3 and 2 macroscopic as well as the 12 and 4 microscopic protonation constants for arginine and citrulline, respectively, determined by potentiometry and using the principles described above. From microconstants of the same group the guanidino-amino and the guanidino-carboxylate interactivity parameters could be calculated. A microspeciation diagram is also presented here.

EXPERIMENTAL

Arginine and citrulline were products of Reanal and used as received. All chemicals were of analytical reagent grade. A microtitration technique was developed for the determination of equilibrium constants,³² with a combined microelectrode suitable in an initial volume of 0.6–1.0 ml. Potentiometric titrations were carried out with an ABU 12 Radiometer automatic buret, Ingold combined microelectrode and a Radiometer pHM 64 pH-mV meter. Arginine and citrulline were dissolved in 0.8 ml of hydrochloric acid, and potassium hydroxide solution was used as titrant. Both the initial and the titrant potassium hydroxide solutions contained potassium chloride as auxiliary electrolyte to provide constant ionic strength. All measurements were made at $25.0 \pm 0.1^\circ$. A n-pentane layer separated the solutions from the atmospheric carbon dioxide. The potentiometric measurements were made under various conditions, varying the arginine concentration at constant ionic strength and varying the ionic strength at constant arginine concentration (Table 2). The wide variety of ionic strengths and arginine concentrations were used to make sure that no significant intermolecular association occurs and also to provide sufficiently high OH^- concentration for the guanidinium group deprotonation. Prior to the pH-metric measurements the emf cells were calibrated by the following standard solutions: 0.01*M* HCl, 0.09*M* KCl (declared pH at $25^\circ = 2.075$); 0.05*M* KHphtalate ($\text{pH}_{25^\circ} = 4.008$); 0.01*M*

Table 2. Stepwise protonation macroconstants and circumstances of determination. Data are valid in H_2O at 25.0°

Ionic strength	Concentration of titrant		Arginine	Citrulline
	<i>M</i>	<i>M</i>		
			Macroconstants	
0.3	0.3		$\log K_2 = 9.28$	$\log K_1 = 9.48$
			$\log K_3 = 2.20$	$\log K_2 = 2.30$
0.5	0.3		$\log K_2 = 9.25$	$\log K_1 = 9.49$
			$\log K_3 = 2.23$	$\log K_2 = 2.33$
1.0	0.3		$\log K_2 = 9.30$	$\log K_1 = 9.50$
			$\log K_3 = 2.18$	$\log K_2 = 2.30$
1.5	0.3		$\log K_2 = 9.36$	$\log K_1 = 9.55$
			$\log K_3 = 2.20$	$\log K_2 = 2.31$
1.0	0.1		$\log K_2 = 9.35$	$\log K_1 = 9.52$
			$\log K_3 = 2.17$	$\log K_2 = 2.33$
1.0	0.6		$\log K_2 = 9.32$	$\log K_1 = 9.56$
			$\log K_3 = 2.20$	$\log K_2 = 2.32$
1.0	1.0		$\log K_2 = 9.31$	$\log K_1 = 9.53$
			$\log K_3 = 2.15$	$\log K_2 = 2.32$
2.0	2.0		$\log K_1 = 15$	$\log K_1 = 9.51$
			$\log K_2 = 9.30$	$\log K_2 = 2.30$
			$\log K_2 = 2.17$	

$\text{Na}_2\text{B}_4\text{O}_7 \cdot 10\text{H}_2\text{O}$ ($\text{pH}_{25^\circ} = 9.180$); $0.025M$ NaHCO_3 , $0.025M$ Na_2CO_3 ($\text{pH}_{25^\circ} = 10.012$). The pH-meter readings were used in the 1.0–12.0 pH range. Above pH 12 the hydroxide and hydrogen ion concentrations were calculated from acid–base titration data.

RESULTS AND DISCUSSION

The protonation macroconstants of arginine and citrulline as well as the conditions of determination are reported in Table 2. The estimated ambiguity of the data is 0.02–0.06 log K units (based upon standard deviations) except for the log K_1 value of arginine which equals 15 at $I = 2.0M$, where the ambiguity is 0.1–0.2 log K units. The same value was obtained at $5.0M$ (potassium chloride) ionic strength. The log K_1 values of arginine at 2.0 and $5.0M$ ionic strengths are concentration constants. All others are activity constants, based upon pH calibration by standard buffer solutions. The arginine total concentration was always approximately one third of the titrant potassium hydroxide concentration. Data in Table 2 show no differences in the function of ionic strength or potassium hydroxide concentrations, thus no intermolecular associations had to be hypothesized.

Table 3 contains the microconstants of arginine and citrulline. From the view-point of protonation, citrulline is a bifunctional ligand (containing amino and carboxylate groups), since the carbamoyl moiety does not associate with protons. The microscopic protonation scheme of citrulline is essentially the same as the bottom-left cyclic section of Fig. 1, which involves four microspecies and the k^A , k^C , k^A_C and k^C_A microconstants. In this thermodynamic sys-

tem the following relationships are valid between the macro- and microconstants:

$$K_1 = k^A + k^C \quad (7)$$

$$K_1 K_2 = k^A k^C_A = k^C k^A_C \quad (8)$$

To calculate all four microconstants, one more independent item of information in addition to the values of the two macroconstants is required. The most appropriate additional information is the interactivity parameter for the amino and carboxylate groups, which was basically determined for glycine,³³ but it proved to be valid for other amino acids as well.^{3,8} Introducing this $\Delta \log k_{A-C} = 2.18$ value into equations (7) and (8), all citrulline microconstants could be calculated.

All arginine microconstants could be calculated once the citrulline microconstants, the amino–carboxylate interactivity parameter and the relationships between the macro- and microconstants [equations (1)–(3)], were known.

Owing to the significantly different inherent basicities of the arginine guanidino, amino and carboxylate protonation sites, the k^G , k^A_G and k^C_{GA} microconstants indicate the major protonation pathway and are essentially equal to the K_1 , K_2 and K_3 macroconstants, respectively. For the k^A , k^C_A , k^C and k^A_C values, the corresponding citrulline constants were taken as described above. The k^G_{AC} microconstant then could be calculated as $k^G_{AC} = K_1 K_2 K_3 (k^A k^C_A)^{-1} = K_1 K_2 K_3 (k^C k^A_C)^{-1}$. The k^G_A value was obtained from the cyclic system as $k^G_A = k^G k^A_G (k^A)^{-1}$. A comparison of k^G_A and k^G_{AC} as well as k^C_A and k^C_{GA} values yielded the guanidino–carboxylate interactivity parameter ($\Delta \log k_{G-C} = \log k^G_A - \log k^G_{AC} = \log k^C_A - \log k^C_{GA}$) which could then be used to calculate k^C_G and k^G_C from k^C and k^G , respectively. Finally, k^A_{GC} was obtained as $k^A_{GC} = K_1 K_2 K_3 (k^G k^C_G)^{-1} = K_1 K_2 K_3 (k^C k^G_C)^{-1}$. Due to the inevitable proliferation of the errors, the estimated ambiguity of the microconstants varies between 0.04 and 0.3 log k units. The greatest ambiguities obviously belong to microconstants of the guanidino group. The amino–guanidino interactivity parameter can be calculated as 0.21 log k units, thus the more realistic rounded value is 0.2. The analogous guanidino–carboxylate value is equal to 0.1 ~ 0.13 log k units.

Data in Table 3 show that the guanidino microconstants (including the smallest k^G_{AC}) are extremely large values. This is in full agreement with the qualitative observation that even in

Table 3. Microscopic protonation constants of arginine and citrulline

Arginine	Citrulline
Microconstants	
log $k^G = 15.0$	log $k^A = 9.51$
log $k^A = 9.51$	log $k^C = 4.48$
log $k^C = 4.48$	log $k^A_C = 7.33$
log $k^A_G = 14.8$	log $k^C_A = 2.30$
log $k^G_{AC} = 14.9$	
log $k^G_A = 9.30$	
log $k^A_C = 7.33$	
log $k^C_G = 4.35$	
log $k^C_A = 2.30$	
log $k^G_{AC} = 14.7$	
log $k^A_{GC} = 7.12$	
log $k^C_{GA} = 2.17$	

1.0M strong base solutions no more than 10% guanidinium deprotonation can be reached.

The apparent reason why the guanidino basicity was underestimated in earlier works is methodical. On one hand, there are no standard buffer solutions to provide reliable calibration pH values at the upper extreme of the pH scale. Consequently, concentration constants are adequate to quantitate basicity here. On the other hand, the previous values were measured by glass electrode pH-metry, which produces distorted pH-meter readings at high concentration, high ionic strength alkali solutions, due to alkali, matrix and diffusion potential errors.

The occurrence probability (p) of arginine microspecies can be expressed by means of microspecies concentrations or by micro- and macroconstants and hydrogen ion concentrations. For example, the occurrence probability (relative concentration) for the non-protonated (Arg^-) and one of the three diprotonated ($\text{H}_2\text{Arg}_{\text{G,C}}^+$) microspecies can be expressed as follows in equations (9) and (10), respectively:

$$p_{\text{Arg}^-} = \frac{[\text{Arg}^-]}{([\text{Arg}^-] + [\text{HArg}] + [\text{H}_2\text{Arg}^+] + [\text{H}_3\text{Arg}^{2+}])^{-1}} \quad (9)$$

$$p_{\text{H}_2\text{Arg}_{\text{G,C}}^+} = \frac{[\text{H}_2\text{Arg}_{\text{G,C}}^+]}{([\text{Arg}^-] + [\text{HArg}] + [\text{H}_2\text{Arg}^+] + [\text{H}_3\text{Arg}^{2+}])^{-1}} \quad (10)$$

All macro- and microspecies can be expressed in terms of macro- and microconstants, Arg^- and H^+ concentrations. After reduction by $[\text{Arg}^-]$, (9) and (10) take the following forms:

$$p_{\text{Arg}^-} = (1 + K_1[\text{H}^+] + K_1K_2[\text{H}^+]^2 + K_1K_2K_3[\text{H}^+]^3)^{-1} \quad (11)$$

$$p_{\text{H}_2\text{Arg}_{\text{G,C}}^+} = k^{\text{G}} k_{\text{G}}^{\text{C}} [\text{H}^+]^2 (1 + K_1[\text{H}^+] + K_1K_2[\text{H}^+]^2 + K_1K_2K_3[\text{H}^+]^3)^{-1} \quad (12)$$

Relative concentrations for any other microspecies can be expressed in an analogous way. The relative concentrations can be converted into real solution concentrations if we multiply them by the total (analytical concentration of arginine).

A more visual representation of the microspecies distribution can be seen in Fig. 2, where the parallel running curves stand for the protonation isomers. This microspeciation diagram is a useful tool to predict binding isomerism in

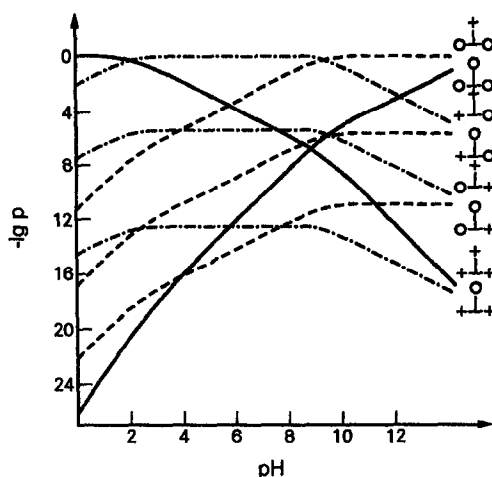


Fig. 2. The pH-dependent distribution of the 8 arginine microspecies.

metal complex formation, where arginine can act as a mono-, bi- or tridentate Lewis-acid and in site-specific interactions with other biomolecules, where arginine can take part as mono-, di- or trivalent proton-donor or acceptor.

REFERENCES

1. J. D. Bell, J. C. C. Brown, G. Kubal and P. J. Sadler, *FEBS Letters*, 1988, **235**, 81.
2. R. B. Martin, *Complexes of α -Amino Acids with Chelatable Side Chain Donor Atoms*, in *Metal Ions in Biological Systems*. H. Sigel (ed.), Vol. 9, p. 6. Marcel Dekker Inc., New York, Basel, 1979.
3. B. Noszál, *Acid-Base Properties of Bioligands*, in *Biocoordination Chemistry: Coordination Equilibria in Biologically Active Systems*. K. Burger (ed.), pp. 49–51. Ellis Horwood, Chichester, 1990.
4. R. B. Martin, *J. Phys. Chem.*, 1971, **75**, 2657.
5. D. L. Rabenstein and T. L. Sayer, *Anal. Chem.*, 1976, **48**, 1141.
6. B. Noszál and P. Sándor, *ibid.*, 1989, **61**, 2631.
7. B. Noszál, *J. Phys. Chem.*, 1986, **90**, 6345.
8. B. Noszál and D. L. Rabenstein, *J. Phys. Chem.*, 1991, **95**, 4761.
9. B. Noszál, V. Scheller-Krattiger and R. B. Martin, *J. Am. Chem. Soc.*, 1982, **104**, 1078.
10. C. L. A. Schmidt, W. K. Appelmann and P. L. Kirk, *J. Biol. Chem.*, 1930, **88**, 285.
11. T. W. Birch and L. J. Harris, *Biochem. J.*, 1930, **24**, 564.
12. E. J. Cohn, *Ergebn. d. Physiol.*, 1933, **33**, 781.
13. A. C. Batchelder and D. L. A. Schmidt, *J. Phys. Chem.*, 1940, **44**, 893.
14. N. C. Li and E. Doody, *J. Am. Chem. Soc.*, 1952, **74**, 4184.
15. E. Ellenbogen, *ibid.*, 1952, **74**, 5198.
16. A. Albert, *Biochem. J.*, 1952, **55**, 690.
17. D. J. Perkins, *ibid.*, 1953, **55**, 649.
18. C. Tanford and W. S. Shore, *J. Am. Chem. Soc.*, 1953, **75**, 816.
19. D. D. Perrin, *J. Chem. Soc.*, 1958, 3125.
20. S. P. Datta and A. K. Grzybowski, *ibid.*, 1959, 1091.

21. S. Pelletier, *Ph.D. Thesis*, University of Paris, 1960.
22. *Idem*, *J. Chim. Phys.*, 1960, **57**, 318.
23. S. P. Datta and A. K. Grzybowski, *Biochem. J.*, 1961, **78**, 289.
24. J. Israeli and M. Cecchetti, *Canad. J. Chem.*, 1968, **46**, 3821.
25. E. R. Clarke and A. E. Martell, *J. Inorg. Nucl. Chem.*, 1970, **32**, 911.
26. C. V. Phan, L. Tosi and A. Garnier, *ibid.*, 1975, **37**, 2385.
27. L. B. Pfeudt and D. Spasojevic, *Glas. Hem. Drus. Beograd*, 1976, **41(9-10)**, 391.
28. C. M. Metzler, A. Cahill and D. E. Metzler, *J. Am. Chem. Soc.*, 1980, **102**, 6075.
29. M. S. Nair and M. Santappa, *Indian J. Chem. Soc. Sect. A*, 1982, **21A(1)**, 58.
30. A. K. Bajpai and H. Yadava, *Afinidad*, 1988, **45(414)**, 149.
31. A. Albourine, M. Petit-Ramel, G. Thomas-David and J. J. Vallon, *Can. J. Chem.*, 1989, **67**, 959.
32. B. Noszál and M. Juhász, *Talanta*, 1987, **34**, 397.
33. E. J. Cohn and J. T. Edsall, *Proteins, Amino Acids and Peptides*, p. 99. Reinhold Publishing Corp., New York, 1943.

AN ION-EXCHANGE SEPARATION OF Cu^{2+} , Cd^{2+} , Pb^{2+} AND Tl^{+} ON SILICA GEL WITH POLAROGRAPHIC DETECTION

PAVEL JANOŠ

The Research Institute of Inorganic Chemistry, 400 60 Ústí nad Labem, Czechoslovakia

KAREL ŠTULFÍK and VĚRA PACÁKOVÁ

Department of Analytical Chemistry, Charles University, Albertov 2030, 128 40 Prague 2, Czechoslovakia

(Received 1 December 1990. Revised 24 May 1991. Accepted 27 May 1991)

Summary—The HPLC separation of heavy metal cations was studied with a column packed with Separon SGX silica gel. The retention of the cations is controlled by an ion-exchange mechanism. The ion-exchange capacity is primarily dependent on the mobile phase pH. The analyte retention is further affected by the type and concentration of the complexing agent present and of the counterion. The effect of acetate, tartrate and α -hydroxyisobutyrate as complexing agents and that of methanol as the organic modifier were studied in detail and the results were compared with the theoretical model of ion-exchange separation. Simple mixtures of metals can be rapidly separated on a short column (30×3.3 mm i.d.), e.g., with a mobile phase containing $10^{-2}M$ tartrate at pH 6.0. The metals separated can be detected by dc amperometry at a hanging mercury drop electrode. The limits of detection at an electrode potential of -0.95 V (Ag/AgCl) are in the units-tens of ng range with $20\text{-}\mu\text{l}$ samples with satisfactory precision (RSD values of 2-6%). The main advantages of the method are rapidly and simplicity because derivatization of the analytes is not required.

Silica gel is one of the oldest and most common chromatographic sorbents.¹ It has been extensively used for separations of substances of medium polarity in normal-phase chromatography and even more so as an ion exchanger²⁻⁵ in gravity-feed separations of inorganic cations.⁶⁻¹² The ion-exchange properties of silica gel are rather rarely utilized in HPLC, because of the complicated behaviour of silica gel and gaps in the theoretical model.

Iwachido and co-workers^{13,14} used a silica gel column for separation of the alkali and alkaline earth metal cations and determination of Na^+ , K^+ , NH_4^+ , Ca^{2+} and Mg^{2+} ions in river and rain waters with a mobile phase containing lithium acetate or oxalate. Smith and Pietrzyk¹⁵ studied the separation of the alkali metals, the alkaline earths and the rare earth metals. A mixed column containing silica gel as cation exchanger and alumina as the anion exchanger was used¹⁶ for separation of monovalent cations and anions with a lithium acetate mobile phase of pH 6.65. Conductometric detection was employed in all these cases.

In addition to almost universal conductometric detection, potentiometry with a copper elec-

trode¹⁷ and measurement of fluorescence¹⁸ have been employed in HPLC of metal cations. The transition and heavy metal cations have most often been detected photometrically, after post-column derivatization (e.g., with PAR¹⁹⁻²¹).

In view of the favourable polarographic characteristics,²² Cu^{2+} , Cd^{2+} , Pb^{2+} and Tl^{+} can be detected by amperometry at mercury electrodes. There is the problem of interference by oxygen dissolved in the mobile phase and/or the sample injected.²³ Many procedures and devices have been proposed for removal of dissolved oxygen, but they complicate the chromatographic procedure. Therefore, reversed-pulse voltammetry²³⁻²⁵ is preferable, as it discriminates between the reversible reduction of the test metals and the irreversible reduction of oxygen. However, with a suitable arrangement of the polarographic detector it is also possible to attain a sufficient low limit of detection in d.c. amperometric measurements.²⁶

The present paper studies HPLC separation of heavy metals on silica gel. On the basis of previous works,⁶⁻¹² possible main components of the mobile phases were selected, i.e., acetic acid which has also been successfully applied to

TLC separation of metal ions on silica gel,²⁷ tartrate that has been used in ion chromatography^{28,29} and micelle exclusion chromatography³⁰ and α -hydroxyisobutyric acid (HIB) that is often employed in HPLC of the rare earth metals.³⁰⁻³³ The effects on analyte retention of the mobile phase ionic strength, the pH, the type of counterion and the organic modifier were studied and the results compared with theoretical assumptions. The measurements were carried out on a short column (30×3.3 mm i.d.) which permits rapid analysis and a low pressure drop, thus improving the baseline stability and suppressing peak broadening of strongly retained analytes. The metal cations were detected amperometrically at a hanging mercury drop electrode.

EXPERIMENTAL

Apparatus

The liquid chromatograph consisted of a HPP 5001 high-pressure pump, an LCI 30-sample injection valve with $20\text{-}\mu\text{l}$ loop, an EDLC electrochemical detector and a TZ 4261 chart recorder (all from Laboratorní Přístroje, Prague, Czechoslovakia). The detection cell with a hanging mercury drop working electrode, a saturated silver/silver chloride reference electrode and a platinum counter electrode is described in detail elsewhere.³⁴ The glass analytical column, 30×3.3 mm i.d., was packed with silica gel Separon SGX ($5\ \mu\text{m}$) and placed between the pump and the sample injection valve to presaturate the mobile phase with dissolved silica. The columns were products of Tessek, Prague.

Reagents

Stock solutions ($0.1M$) of sodium acetate (NaAc), sodium tartrate (Na_2Tart) and sodium α -hydroxyisobutyrate (NaHIB) were prepared by neutralization of the acids with sodium hydroxide to a pH of 7.0. The mobile phases were obtained by diluting these stock solutions, mixing them with $0.1M$ stock solutions of sodium perchlorate and cerous nitrate, and with methanol and then adjusting the pH by addition of dilute perchloric acid.

Stock solutions of the test metal cations, $0.1M$, were prepared from the appropriate chlorides, nitrates or sulphates and were diluted to a concentration of $10^{-4}M$ unless stated otherwise.

All the chemicals were analytical grade (Lachema, Brno, Czechoslovakia): α -hydroxy-

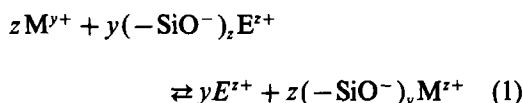
isobutyric acid, *puriss.*, was obtained from Fluka, Switzerland.

The mobile phases were degassed in an ultrasonic bath. The flow-rate was $0.3\ \text{ml/min}$. All the electrode potentials refer to the saturated aqueous Ag/AgCl electrode. The measurements were performed at laboratory temperature ($20 \pm 2^\circ$).

RESULTS AND DISCUSSION

Separation

In the separation of the metal cations, silica gel acts as a weak cation exchanger whose properties depend on the degree of dissociation of the exchange sites (the silanol groups $-\text{SiOH}$). These groups make the silica gel surface acidic, with a $\text{p}K_a$ value³⁵ of 7.1. Therefore, dissociation of protons from the silanol groups occurs above a pH of *ca.* 4 and silica gel is then able to bind cations.³⁶ The corresponding ion-exchange equilibrium is described by



where M^{y+} is the cation to be separated and E^{z+} is the cation of the eluting agent. Analogous to the equation derived by Haddad and Foley,³⁷ equation (1) yields a relationship for the capacity factor in the form,

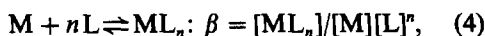
$$\log k = \frac{y}{z} \log(\text{cap}/z) + \frac{1}{z} \log K_M^E + \log(w/V_m) - \frac{y}{z} \log[\text{E}^{z+}] \quad (2)$$

where cap is the exchange capacity, K_M^E is the selectivity coefficient and w/V_m is the ratio of the stationary phase weight, w , to the mobile phase volume, V_m .

If cation M^{y+} participates in a complexation equilibrium, equation (2) assumes the form,³⁷

$$\log k = \log \alpha_M + \frac{y}{z} \log(\text{cap}/z) + \frac{1}{z} \log K_m^E + \log(w/V_m) - \frac{y}{z} \log[\text{E}^{z+}] \quad (3)$$

where α_M is the ratio of the concentration of the free cation and the overall cation concentration in the solution. Therefore, for the complexation equilibrium,



the α_M value is given by

$$\alpha_M = 1/(1 + \beta[L]^n), \quad (5)$$

provided that the $[L]$ value is sufficiently large, so that the concentrations of the lower complexes, ML , $\text{ML}_2, \dots, \text{ML}_{n-1}$, are negligible.

The exchange capacity of silica gel depends primarily on the pH.¹⁵ If the capacity is assumed to be constant at a given pH, then combination of equations (3) and (5) yields

$$\log k = \text{constant}$$

$$-\frac{y}{z} \log \{[E^{z+}] \cdot (1 + \beta[L]^n)^{z/y}\} \quad (6)$$

where all the constants are summarized in a single term.

It should be pointed out that the above relationships assume a negligible concentration of the positively charged (cationic) complexes.³⁷ This assumption should be satisfied in the Na_2Tart medium, but not necessarily in NaAc and NaHIB .

When the pH is not constant, then the variations in the dissociation of the $-\text{SiOH}$ groups must be considered; the relationship for the capacity factor has been derived for univalent cations by Smith and Pietrzyk.¹⁵

$$1/k = \frac{1}{qK_0} \left\{ \frac{[\text{H}^+](1 + K_{\text{app}})}{K\text{H}^M} + [\text{M}^+] + \frac{[\text{E}^+]}{K\text{E}^M} \right\} \quad (7)$$

where q is the ratio of the volumes of the stationary and mobile phases, K_0 is the exchange

capacity available, K_{app} is the apparent ionization constant of the $-\text{SiOH}$ group and K_{H^M} and K_{E^M} are the selectivity coefficients for exchange of the analyte with proton and the eluent cation, respectively.

It clearly follows from this simple theoretical model that the retention of metal cations on silica gel is primarily influenced by the type and concentration of the eluent cation (counterion), the type and concentration of the complexing agent and the mobile phase pH. Equation (7) also predicts a dependence of the capacity factor on the analyte concentration; however, the dependence is insignificant at analyte concentrations common in HPLC, as confirmed experimentally,¹⁵ and thus we did not study it here.

If the mobile phase contains a complexing agent, then the analyte retention depends on the two effects: The eluent cation (counterion) competes for the exchange sites with the analyte cation (the pushing effect of the E^{z+} ion). The ligand anion enhances the analyte affinity to the mobile phase (the pulling effect of ligand L^-). Both the two effects cause a decrease in the analyte retention. It follows from equation (6) that, at a constant ligand concentration and a constant pH, there is a linear relationship between the logarithm of the analyte capacity factor and the eluent cation concentration.

This experimental dependence is shown in Fig. 1. The concentration of the counterion (Na^+) was varied by adding sodium perchlorate

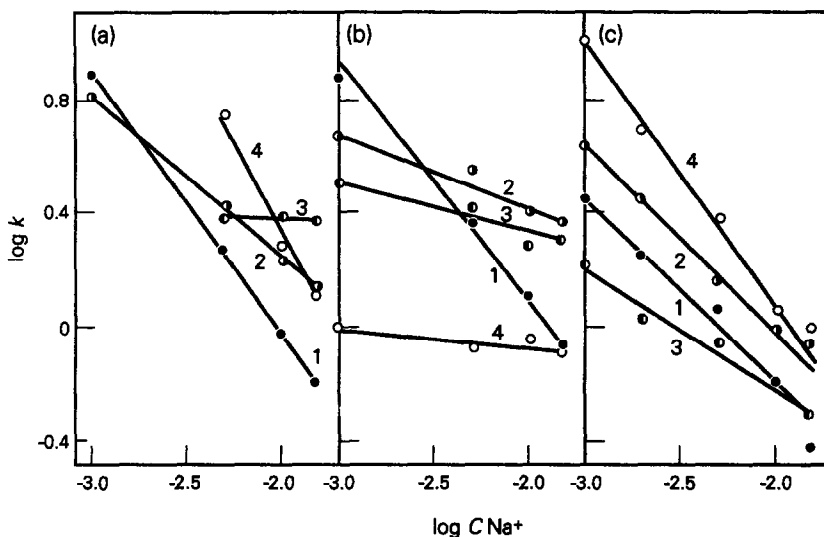


Fig. 1. Log-log dependence of the capacity factors on the Na^+ concentration in the mobile phase. (a) $5 \times 10^{-4} \text{M}$ NaAc , pH 5.0; (b) $2.5 \times 10^{-4} \text{M}$ Na_2Tart , pH 5.0; (c) $5 \times 10^{-4} \text{M}$ NaHIB , pH 6.0, -0.95V (Ag/AgCl), flow-rate, 0.3 ml/min. 1— Cd^{2+} ; 2— Tl^+ ; 3— Pb^{2+} ; 4— Cu^{2+} .

Table 1. Slopes of the experimental $\log k$ vs. $\log c_{\text{Na}^+}$ dependences

Cation	Slope		
	NaAc [Fig. 1(a)]	Na ₂ Tart [Fig. 1(b)]	NaHIB [Fig. 1(c)]
Cu ²⁺	-1.11	-0.06	-0.92
Cd ²⁺	-0.92	-0.80	-0.62
Pb ²⁺	-0.05	-0.16	-0.42
Tl ⁺	-0.59	-0.26	-0.63

to the mobile phases of a constant pH, containing constant concentrations of NaAc [Fig. 1(a)], Na₂Tart [Fig. 1(b)] or NaHIB [Fig. 1(c)], assuming that the complexation ability of perchlorate is negligible. It can be seen that the dependences are linear, but the experimental slopes are substantially smaller than the predicted value of -2.0 for divalent analyte cations and a monovalent eluent cation or -1.0 for monovalent analyte cations (see Table 1). The most probable reasons for this deviation are a substantial decrease in the effective charge on the analyte cation in real systems due to non-negligible content of lower complexes, *e.g.*, $M(\text{Ac})^+$, and the effect of the ionic strength, a contribution from interactions other than ion exchange, *e.g.*, non-specific interactions with the siloxane groups, molecular adsorption and hydrogen bonding and variations in the silica gel ion-exchange capacity with changing experimental conditions.

In some cases (Pb²⁺ with the NaAc mobile phase or Cu²⁺ with the Na₂Tart mobile phase),

the slope of the $\log k$ vs. $\log c_{\text{Na}^+}$ plot approaches zero: apparently, ion exchange does not control the retention in these systems and the cations are retained in the form of neutral or negatively charged complexes through a combination of various interactions.

It can be seen from Fig. 2 that the sodium perchlorate concentration affects not only the analyte retention time but also the peak shape. With low perchlorate concentrations the retention times are large and the peaks exhibit strong tailing. According to Giddings,³⁸ peak tailing most often stems from the presence of active sites of several different types on the surface of the stationary phase. This really is the case with silica gel;¹ the increase in the ionic strength with increasing concentration of perchlorate suppresses dissociation of minority exchange sites and enhances the complex formation in the mobile phase, thus suppressing the tailing and decreasing the retention time.

As can be expected, the replacement of the univalent counterion by a cation of a higher valence leads to a pronounced decrease in the retention (see Table 2), as the affinity toward an ion exchanger increases with increasing charge of the ion.

The capacity factor dependence on the concentration of the complexing agent also follows from equation (6): if the pH is maintained constant and the complexing agent is a salt of a weak acid, E_xL_x , where E is the counterion

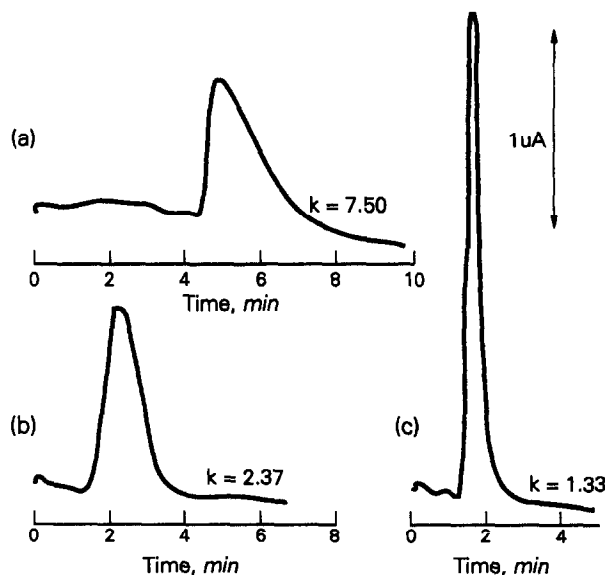


Fig. 2. The effect of the NaClO_4 concentration in the mobile phase on the shape of the Cd^{2+} peak. Mobile phase: $2.5 \times 10^{-4} \text{M}$ Na₂Tart + $x \text{M}$ NaClO₄. (a) $x = 10^{-3}$; (b) 5×10^{-3} ; (c) 10^{-2} . Other conditions as for Fig. 1.

Table 2. The effect of NaClO_4 and $\text{Ce}(\text{NO}_3)_3$ on the test cation retention

Cation	k	
	$2.5 \times 10^{-4}M \text{ Na}_2\text{Tart}$, $\text{pH } 5.0 + 10^{-3}M \text{ NaClO}_4$	$2.5 \times 10^{-4}M \text{ Na}_2\text{Tart}$, $\text{pH } 5.0 + 10^{-3}M \text{ Ce}(\text{NO}_3)_3$
Cd^{2+}	7.50	1.00
Cu^{2+}	1.00	1.00
Pb^{2+}	3.15	1.50
Tl^+	4.69	1.25

and L is the ligand in equation (4), then equation (6) can be rewritten as

$$\log k = \text{constant}$$

$$-\frac{y}{z} \log \left\{ \frac{z}{x} [L] \cdot (1 + \beta [L]^n)^{z/y} \right\} \quad (8)$$

where the charge of the ligand is omitted for simplicity. Equation (8) is simplified when the numeral 1 in the term $(1 + \beta [L]^n)$ can be neglected with respect to the product $\beta [L]^n$, i.e., when the ligand concentration is sufficiently high and/or the β value is large, obtaining

$$\log k = \text{constant} - \frac{y}{z} \left(n \frac{z}{y} + 1 \right) \log [L] \quad (9)$$

Hence there should be a linear relationship between the logarithm of the capacity factor and the ligand concentration. The stability constants for the complexes studied (except for those of thallium) are typically³¹⁻⁴¹ in the range of 10^2 – 10^3 and thus the above simplified equation should be valid for ligand concentrations greater than *ca.* $10^{-3}M$.

The experimental dependences are given in Fig. 3. It can be seen that the condition of linearity is satisfied, while the experimental slopes (Table 3) are again much smaller than expected: the probable reasons are the same as with the $\log k$ vs. $\log c_E$ plots.

The dependence of capacity ratio on the buffer concentration is most pronounced in the Na_2Tart medium. The slopes of the $\log k$ vs. $\log c_L$ dependences are greater in this system than those of the $\log k$ vs. $\log c_{\text{Na}^+}$ plots (Table 1), which is in agreement with equation (9). Hence the retention of the test cations is most effectively controlled by varying the tartrate concentration in the mobile phase. Equation (9) suggests that the retention of monovalent cations is more strongly affected by the presence of a ligand than that of divalent cations (relative increase in the slope is greater), as demonstrated by the $\log k$ vs. $\log c_L$ plot for Tl^+ in Fig. 3(b). It can also be seen from this figure that a change in the buffer concentration may also lead to changes in the eluting order. The slopes of the $\log k$ vs. $\log c_L$ dependences

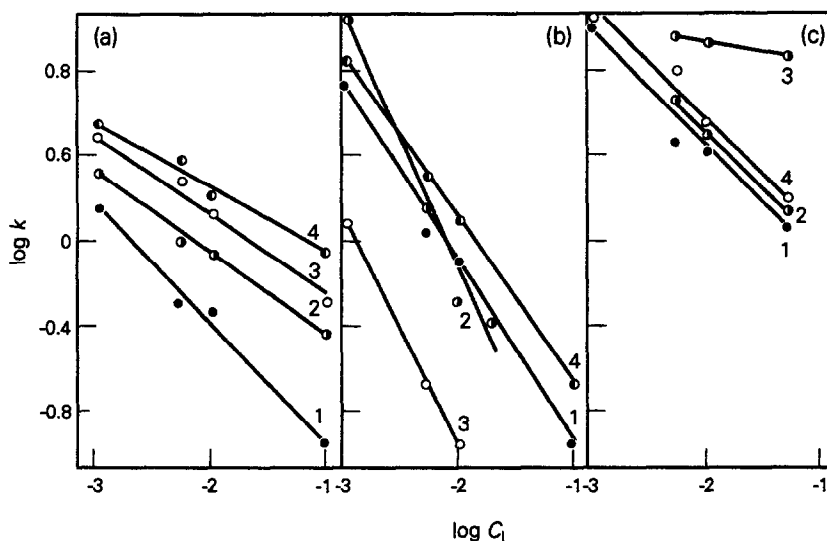


Fig. 3. Log-log dependence of the capacity factors on the ligand concentration in the mobile phase. (a) NaAc , $\text{pH } 5.0$; (b) Na_2Tart , $\text{pH } 5.0$; (c) NaHIB , $\text{pH } 6.0$. 1— Cd^{2+} ; 2— Tl^+ ; 3— Cu^{2+} ; 4— Pb^{2+} . Other conditions as for Fig. 1.

Table 3. The slopes of the experimental $\log k$ vs. $\log c_L$ dependences

Cation	Slope		
	NaAc [Fig. 3(a)]	Na ₂ Tart [Fig. 3(b)]	NaHIB [Fig. 3(c)]
Cu ²⁺	-0.38	-1.04	-0.09
Cd ²⁺	-0.55	-0.84	-0.54
Pb ²⁺	-0.30	-0.77	-0.54
Tl ⁺	-0.37	-1.18	-0.54

Table 4. Dependence of the capacity factors on the presence of methanol in the mobile phase

Cation	k	
	$5 \times 10^{-4}M$ NaAc (pH 5.0)	$5 \times 10^{-4}M$ NaAc (pH 5.0) + 5% (v/v) methanol
Cd ²⁺	1.44	0.75
Cu ²⁺	3.11	1.15
Pb ²⁺	3.61	1.00
Tl ⁺	2.04	1.00

cannot be calculated rigorously, in view of the above simplifications and the lack of data on the composition and stability of the complexes involved in real systems. Deviations from the theory are greater in the NaAc and NaHIB media, mainly because of the presence of lower cationic complexes; other possible factors are discussed with the $\log k$ vs. $\log c_E$ dependence.

The theory predicts a strong dependence of the capacity factors on the mobile phase pH, through the effects of the pH on the dissociation of the mobile phase components and of the silanol groups. Equation (7) predicts an exponential relationship between the capacity factor and the hydrogen ion concentration. Figure 4 demonstrates that the experimental dependences correspond to equation (7) with NaAc [Fig. 4(a)] and Na₂Tart [Fig. 4(b)]. The dependences with NaHIB [Fig. 4(c)] are more complicated, indicating that the separation mechanism is more complex. (Similar plots were obtained in separations of the rare earths on silica gel.¹⁵)

It is clear from Fig. 4 that analyte retention becomes negligible under a pH of *ca.* 4. At pH values greater than *ca.* 7, the retention rapidly

increases and the peaks exhibit tailing, due to dissociation of minority exchange sites (see above). Above a pH of *ca.* 7.5, the silica gel matrix is damaged and the column efficiency decreases.

Addition of methanol to the mobile phase causes a decrease in the column efficiency²⁸ and enhanced complexation in the mobile phase, resulting in a shortening of the retention times, peak broadening and a poorer resolution, even with low methanol contents (5% vol.). Older magnetochemical measurements³ also demonstrate suppression of ion exchange on silica gel when the relative permittivity of the solvent decreases. The capacity factors in the presence and absence of methanol are compared in Table 4.

The dependences indicate that separation of metal cations on silica gel is affected by many factors and thus optimization of the separation conditions is difficult. Moreover, separations of complex mixtures are complicated by the fact that the elution curves exhibit tailing, especially with strongly retained components.

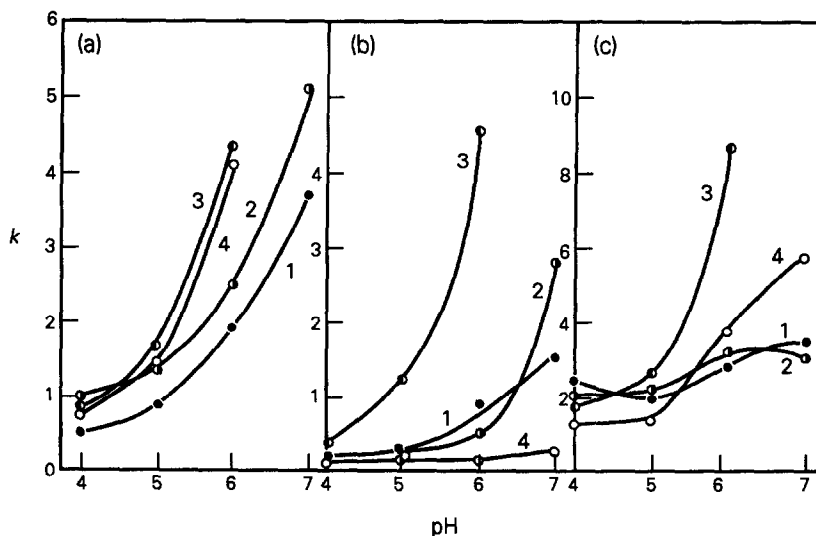


Fig. 4. Capacity factor dependence on the mobile phase pH. (a) $10^{-2}M$ NaAc; (b) $10^{-2}M$ Na₂Tart; (c) $10^{-2}M$ NaHIB. 1—Cd²⁺; 2—Tl⁺; 3—Pb²⁺; 4—Cu²⁺. Other conditions as for Fig. 1.

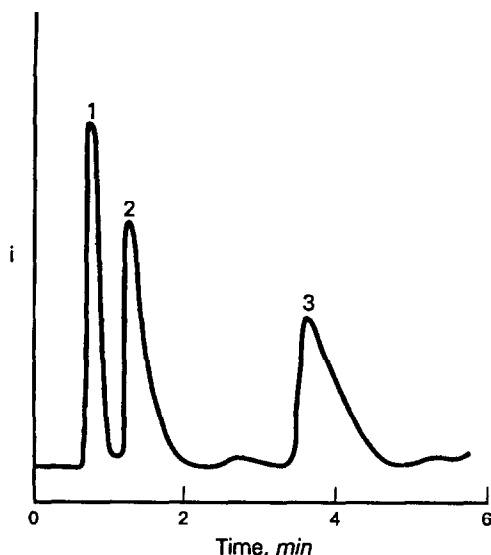


Fig. 5. Separation of Cu^{2+} (1), Cd^{2+} (2) and Pb^{2+} (3). Mobile phase: $10^{-2}M$ Na_2Tart , pH 6.0. Flow-rate, 0.3 ml/min; -0.95 V (Ag/AgCl).

For example, divalent cations, Cu^{2+} , Cd^{2+} and Pb^{2+} , can be successfully separated with a mobile phase of $10^{-2}M$ Na_2Tart , pH 6 (Fig. 5). However, Tl^{+} is co-eluted with Cd^{2+} under these conditions.

Detection

The dc hydrodynamic polarograms of Cd^{2+} , Cu^{2+} , Pb^{2+} and Tl^{+} are given in Fig. 6 for the three mobile phases used. In these experiments the analytical column was replaced by a capillary 50 cm long and 0.2 mm in internal diameter. The limits of detection were determined at a potential of -0.95 V and are summarized in Table 5. These values are comparable with the results obtained by using reversed-pulse polarography.²⁵

In real chromatographic systems, the limits of detection are somewhat higher, owing to poorer baseline stability and peak broadening, e.g., 5.4, 8.8, 53.1 and 36.6 ng for Cd^{2+} , Cu^{2+} , Pb^{2+} and Tl^{+} , respectively, in a mobile phase of $10^{-2}M$

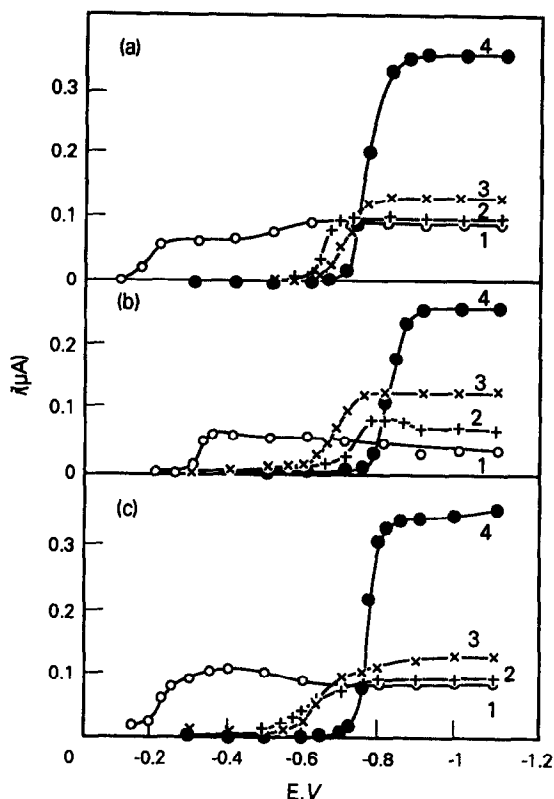


Fig. 6. Hydrodynamic polarograms of Cu^{2+} (1), Pb^{2+} (2), Tl^{+} (3) and Cd^{2+} (4). Mobile phase: (a) $10^{-2}M$ NaAc , pH 5.0; (b) $10^{-2}M$ Na_2Tart , pH 5.0; (c) $10^{-2}M$ NaHIB , pH 5.0. Sample concentration, $1.5 \times 10^{-4}M$; injected amounts, $20 \mu\text{l}$; flow rate, 0.3 ml/min.

Na_2Tart , pH 6.0 and with $20\text{-}\mu\text{l}$ samples. The reproducibility of measurement is satisfactory: at concentrations equal to about 10 times the limit of detection, the relative standard deviations are 2.2, 3.1, 6.4 and 2.9% for $\text{Cu}(\text{II})$, $\text{Tl}(\text{I})$, $\text{Pb}(\text{II})$ and $\text{Cd}(\text{II})$, respectively, for six parallel measurements. Typical calibration plot parameters are given in Table 6.

CONCLUSION

Heavy metal cations are retained on silica gel by a mechanism in which ion exchange

Table 5. Polarographic limits of detection for some cations

Cation	Limit of detection, ng		
	$10^{-2}M$ NaAc (pH 5.0)	$10^{-2}M$ Na_2Tart (pH 5.0)	$10^{-2}M$ NaHIB (pH 5.0)
Cd^{2+}	3.2	2.8	4.5
Cu^{2+}	3.3	4.3	2.9
Pb^{2+}	2.5	16.5	31.1
Tl^{+}	3.8	9.5	17.2

Flow-rate, 0.3 ml/min; $20\text{-}\mu\text{l}$ samples; -0.95 V (Ag/AgCl); without analytical column. The limit of detection is the absolute amount of the analyte that produces a signal equal to three times the baseline noise.

Table 6. Calibration plot parameters for determination of Cd²⁺, Cu²⁺, Pb²⁺ and Tl⁺

Cation	Slope, nA/ng	Intercept, nA	Coefficient of correlation
Cd ²⁺	0.950	0.234	0.9996
Cu ²⁺	0.220	0.116	0.9987
Pb ²⁺	0.121	-0.008	0.9990
Tl ⁺	0.212	0.096	0.9895

Mobile phase: 10⁻²M Na₂Tart, pH 5.0; 0.3 ml/min; -0.95 V (Ag/AgCl)

predominates, although other interactions, *e.g.*, molecular adsorption,⁶⁻¹² may also play a role. The retention can be described by relationships that are analogous to those derived for classical ion exchangers.^{28,37} The heterogeneity of the silica gel surface and the presence of several types of ion-exchange site cause peak tailing which can be suppressed by increasing the mobile phase ionic strength and decreasing its pH, which also leads to reduced retention times. Methanol substantially decreases the efficiency of separation and the resolution and thus purely aqueous mobile phases are preferable. The separation is improved by complexing agents: tartrate seems to be most suitable.

The main advantages of the method, using polarographic detection that is sufficiently sensitive, are the rapidity and simplicity of determination, as very short columns can be used and there is no need for derivatization. Another advantage is the very small amount of sample required for analysis, compared with polarographic and stripping voltammetric methods of analysis.

REFERENCES

1. K. K. Unger, *Porous Silica, J. Chromatog. Lib.*, Vol. 16, Elsevier, Amsterdam, 1979.
2. F. Vydra and V. Marková, *J. Inorg. Nucl. Chem.*, 1964, **26**, 1319.
3. C. M. French and J. P. Howard, *Trans. Faraday Soc.*, 1956, **52**, 712.
4. R. W. Dalton, J. L. McClanahan and R. W. Maatman, *J. Colloid. Sci.*, 1962, **17**, 207.
5. L. H. Allen and E. Matijevic, *J. Colloid. Interface Sci.*, 1970, **33**, 420.
6. Z. Šulcek, J. Doležal and J. Michal, *Coll. Czech. Chem. Commun.*, 1961, **26**, 246.
7. Z. Šulcek, J. Doležal, J. Michal and V. Sychra, *Talanta*, 1963, **10**, 3.
8. Z. Šulcek, J. Kremer and J. Doležal, *Coll. Czech. Chem. Commun.*, 1969, **34**, 1720.
9. Z. Šulcek, M. Vašák and J. Doležal, *Microchem. J.*, 1971, **16**, 210.
10. F. Vydra and J. Galba, *Coll. Czech. Chem. Commun.*, 1967, **32**, 3530.
11. *Idem*, *ibid.*, 1968, **34**, 3471.
12. *Idem*, *Z. Anal. Chem.*, 1968, **235**, 166.
13. T. Iwachido, K. Ishimaru and S. Motomizu, *Anal. Sci.*, 1988, **4**, 81.
14. T. Iwachido, T. Ikeda and M. Zenki, *ibid.*, 1990, **6**, 593.
15. R. L. Smith and D. J. Pietrzyk, *Anal. Chem.*, 1984, **56**, 610.
16. D. M. Brown and D. J. Pietrzyk, *J. Chromatog.*, 1989, **466**, 291.
17. P. R. Haddad, P. W. Alexander and M. Trojanowicz, *ibid.*, 1985, **324**, 319.
18. B. D. Karcher and I. S. Krull, *J. Chromatog. Sci.*, 1987, **25**, 472.
19. J. R. Jezorek and H. Freiser, *Anal. Chem.*, 1979, **51**, 373.
20. R. M. Cassidy, S. Elchuk and P. K. Dasgupta, *ibid.*, 1987, **59**, 85.
21. D. Yan and G. Schwedt, *Z. Anal. Chem.*, 1987, **327**, 503.
22. A. A. Vlček, *Chem. Listy*, 1956, **50**, 400.
23. P. Jandik, P. R. Haddad and P. E. Sturrock, *CRC Crit. Rev. Anal. Chem.*, 1988, **20**, 1.
24. F. A. Schultz and D. E. Mathis, *Anal. Chem.*, 1974, **46**, 2253.
25. T. Hsi and D. C. Johnson, *Anal. Chim. Acta*, 1985, **175**, 23.
26. K. Štulík and V. Pacáková, *Electroanalytical Measurements in Flowing Liquids*, Horwood, Chichester, 1987.
27. L. F. Druding, *Anal. Chem.*, 1963, **35**, 1582.
28. G. J. Sewenich and J. S. Fritz, *ibid.*, 1983, **55**, 12.
29. D. T. Gjerde, *J. Chromatog.*, 1988, **439**, 49.
30. T. Okada, *Anal. Chem.*, 1988, **60**, 2116.
31. K. Robards, S. Clarke and E. Patsalides, *Analyst*, 1988, **113**, 1757.
32. V. Kubáň and D. B. Gládilovich, *Coll. Czech. Chem. Commun.*, 1988, **53**, 1664.
33. R. M. Cassidy, *Chem. Geol.*, 1988, **67**, 185.
34. K. Štulík, V. Pacáková and M. Podolák, *J. Chromatog.*, 1983, **262**, 85.
35. M. L. Hair and W. Hertt, *J. Phys. Chem.*, 1970, **74**, 91.
36. L. G. Daignault, D. C. Jackman and P. D. Rillema, *J. Chromatog.*, 1989, **462**, 71.
37. P. R. Haddad and R. C. Foley, *ibid.*, 1990, **500**, 301.
38. J. C. Giddings, *Dynamics of Chromatography, Part I, Principles and Theory*, pp. 75-79. Dekker, New York, 1965.
39. L. G. Sillén and A. E. Martell, *Stability Constants of Metal-Ion Complexes*, 2nd Ed., The Chemical Society, London, 1964.
40. S. Kotrlý and L. Šucha, *Handbook of Chemical Equilibria in Analytical Chemistry*, Horwood, Chichester, 1985.
41. T. Hirokawa, T. Matsuki, H. Takemi and Y. Kiso, *J. Chromatog.*, 1983, **280**, 233.

EFFECT OF STRUCTURAL VARIATION WITHIN SYM-(R)DIBENZO-16-CROWN-5-OXYACETIC ACID RESINS UPON THE SELECTIVITY AND EFFICIENCY OF ALKALI-METAL CATION SORPTION

TAKASHI HAYASHITA, MI-JA GOO, JONG SEUNG KIM and RICHARD A. BARTSCH*

Department of Chemistry and Biochemistry, Texas Tech University, Lubbock, Texas 79409-1061, U.S.A.

(Received 31 May 1991. Accepted 17 June 1991)

Summary—Five new crown ether carboxylic acid resins have been prepared by condensation polymerization of *sym*-(R)dibenzo-16-crown-5-oxyacetic acids with formaldehyde. Competitive alkali-metal cation sorption by these novel resins, which contain both ion-exchange and crown ether binding sites for metal ions, has been investigated. As the R-group was varied (methyl, ethyl, propyl, butyl, hexyl and decyl) both the alkali-metal cation sorption selectivity and efficiency were affected. The highest efficiency (loading) and Na⁺ sorption selectivity were obtained when R = methyl, ethyl and propyl. The longer alkyl groups were found to be detrimental to both sorption efficiency and selectivity.

The development of chelating resins for separation of selected metal cations from aqueous solutions has received considerable attention. In general, these resins are prepared by immobilization of a chelating reagent which has an affinity for the desired metal ion into a polymeric matrix.¹ In the design of such resins, several factors must be taken into account. Interactions of the metal cation with the resin matrix as well as the chelating reagent may affect sorption behavior. The geometry and microenvironments of chelating resins are important factors for metal separation processes.²

In a recent study, we synthesized carboxylic acid resins **1**, **2** and **5** (Scheme 1) which contain integral acyclic or cyclic polyether units and evaluated their alkali-metal cation sorption behavior.³ These novel resins possess both ion-exchange and polyether binding sites for metal ions. It was found that the sorption selectivity for the cyclic polyether (crown ether) carboxylic acid resins was controlled by the relationship between the crown ether cavity and metal ion diameters. Thus the Li⁺ sorption selectivity observed for the acyclic polyether carboxylic acid resin **1** changed to Na⁺ selectivity for the *sym*-dibenzo-16-crown-5-oxyacetic acid resins **2** and **5**. The Na⁺ selectivity for resin **5** in which there is a propyl group attached to the same crown ether ring carbon as the side arm was much higher than that of resin **2**. It was postu-

lated that in resin **5** the lipophilic propyl group is directed away from the polar polyether ring.³ This orients the side arm over the crown ether cavity and enhances selectivity by pre-organization of the binding site.⁴ In an analytical application, crown ether carboxylic acid resin **5** has been utilized for the column concentration of alkali metal-cations from dilute aqueous solutions.^{3,5}

Since the introduction of an alkyl group into crown ether carboxylic acid resin **2** could affect not only the positioning of the carboxylic acid group but also the microenvironment of the resin, a study of the influence of alkyl group variation was undertaken. A series of *sym*-(R)dibenzo-16-crown-5-oxyacetic acid resins **3**, **4** and **6-8** in which the alkyl group is systematically varied (methyl, ethyl, butyl, hexyl, decyl, respectively) has been prepared and their alkali-metal cation sorption behavior evaluated and compared with that reported for resins **1**, **2** and **5**.

EXPERIMENTAL

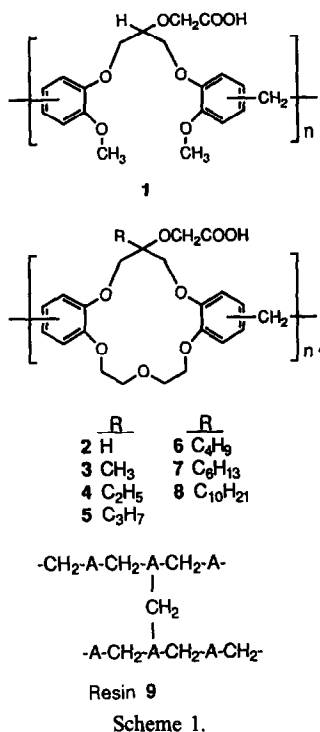
Apparatus

The apparatus was the same as that in the previous study.³

Reagents

Unless specified otherwise, reagent grade reactants and solvents were obtained from chemical suppliers and used as received. Aqueous

*Author for correspondence.



stock solutions of 0.50M alkali-metal chlorides (NaCl, KCl, RbCl and CsCl, 0.50M in each), 0.50M LiCl and 0.50M LiOH were stored in polyethylene bottles. Sample solutions were prepared by mixing and diluting these stock solutions. Purified water for sample solutions was prepared by passing distilled water through three Barnsted D8922 combination cartridges in series. *sym*-Ketodibenzo-16-crown-5, *sym*-(butyl)dibenzo-16-crown-5-oxyacetic acid, and *sym*-(decyl)-dibenzo-16-crown-5-oxyacetic acid were prepared by the reported methods.^{6,7}

Preparation of *sym*-(hydroxy)(methyl)dibenzo-16-crown-5

To 0.84 g (34.5 mmoles) of magnesium turnings in 150 ml of anhydrous Et₂O under nitrogen was added dropwise 4.90 g (34.5 mmoles) of methyl iodide. The reaction mixture was refluxed until the magnesium disappeared. A solution of *sym*-ketodibenzo-16-crown-5 (4.00 g, 11.6 mmoles) in 300 ml of THF was added dropwise and refluxing was continued for 24 hr. The reaction mixture was cooled in an ice-bath, 90 ml of 5% aqueous ammonium chloride solution was added, and the mixture was stirred for 2 hr. The solvent was evaporated in vacuo and extracted with CH₂Cl₂ (2 × 100 ml). The CH₂Cl₂ solution was dried over magnesium sulfate and evaporated *in vacuo*. The crude product was recrystallized from pentane and

then subjected to column chromatography on silica gel with CH₂Cl₂ as eluent to give 1.73 g (41%) of the title compound as a white solid with mp. 110–111°, lit. mp. 109–110°.⁸

Preparation of *sym*-(hydroxy)(ethyl)- and *sym*-(hydroxy)(hexyl)-dibenzo-16-crown-5

By the procedure reported for the preparation of *sym*-(hydroxy)(propyl)-dibenzo-16-crown-5³ but replacing 1-bromopropane with 1-bromoethane and 1-bromohexane, the title compounds were prepared.

sym-(Hydroxy)(ethyl)dibenzo-16-crown-5, mp. 101–102°, 91% yield. IR (deposit) 3461 (OH), 1257, 1122 (CO) cm⁻¹. ¹H NMR (CDCl₃) δ 1.05 (t, 3), 1.90 (q, 2), 3.11 (s, 1), 3.89–4.27 (m, 12), 6.83–7.26 (m, 8). Analysis calculated for C₂₁H₂₆O₆: C 67.36; H, 7.00. Found: C, 67.55; H, 7.01.

sym-(Hydroxy)(hexyl)dibenzo-16-crown-5, mp. 126–127°, 85% yield. IR (deposit) 3395 (OH), 1122, 1039 (CO) cm⁻¹. ¹H NMR (CDCl₃) δ 0.88 (t, 3), 1.15–1.55 (m, 8), 1.80–1.92 (m, 2); 3.45 (br s, 1), 3.90–4.30 (m, 12), 6.84–7.02 (m, 8). Analysis calculated for C₂₅H₃₄O₆: C, 69.74; H, 7.96. Found: C, 69.63; H, 7.61.

Preparation of *sym*-(methyl)-, *sym*-(ethyl)-, and *sym*-(hexyl)-dibenzo-16-crown-5-oxyacetic acids

By the procedure reported for the preparation of *sym*-(propyl)dibenzo-16-crown-5-oxyacetic acid from *sym*-(hydroxyl)(propyl)dibenzo-16-crown-5,³ the appropriate crown ether alcohols were converted into the title compounds.

sym-(Methyl)dibenzo-16-crown-5-oxyacetic acid, mp. 100–102°, 80% yield. IR (deposit) 3400–3000 (COOH), 1766, 1736 (C=O), 1122, 1053 (CO) cm⁻¹. ¹H NMR (CDCl₃) δ 1.50 (s, 3), 3.80–4.15 (m, 10), 4.60 (d, 2), 4.85 (s, 2), 6.84–7.02 (m, 8), 8.88 (br s, 1). Analysis calculated for C₂₂H₂₆O₈: C, 63.15; H, 6.26. Found: C, 62.81; H, 6.34.

sym-(Ethyl)dibenzo-16-crown-5-oxyacetic acid, mp. 112–113°, 69% yield. IR (deposit) 3363 (COOH), 1738 (C=O), 1255, 1128 (CO) cm⁻¹. ¹H NMR (CDCl₃) δ 1.09 (t, 3), 2.00 (q, 2), 3.79–4.22 (m, 10), 4.57 (d, 2), 4.85 (s, 2), 6.70–7.01 (m, 8). Analysis calculated for C₂₃H₂₈O₈: C 63.88; H, 6.53. Found: C, 64.28; H, 6.62.

sym-(Hexyl)dibenzo-16-crown-5-oxyacetic acid, mp 139–141°, 85% yield. IR (deposit) 3400–3000 (COOH), 1735, 1699 (C=O), 1122, 1053 (CO) cm⁻¹. ¹H NMR (CDCl₃) δ 0.93 (t, 3), 1.25–1.50 (m, 8), 1.93–1.97 (m, 2), 3.80–4.15 (m,

10), 4.60 (d, 2), 4.85 (s, 2), 6.84–7.02 (m, 8), 9.90 (br s, 1). Analysis calculated for $C_{27}H_{36}O_8$: C, 66.38; H, 7.43. Found: C, 66.46; H, 7.87.

Preparation of crown ether carboxylic acid resins 3, 4 and 6–8

The crown ether carboxylic acid resins were synthesized by condensation polymerization of the *sym*-(R)dibenzo-16-crown-5-oxyacetic acid monomers with formaldehyde in formic acid as described in detail previously.^{3,9} The resins were ground and used in powder form (finer than 100 mesh).

Resin 3, 65% yield. IR (KBr) 3448 (COOH), 1719 (C=O), 1282, 1105 (CO) cm^{-1} . Analysis calculated for 9–1.5 H_2O : C, 63.68; H, 6.11. Found: C, 63.44; H, 5.80.

Resin 4, 65% yield. IR (KBr) 3448 (COOH), 1735 (C=O), 1282, 1102 (CO) cm^{-1} . Analysis calculated for 9–0.5 H_2O : C, 64.83; H, 6.29. Found: C, 64.57; H, 5.85.

Resin 6, 67% yield. IR (KBr) 3442 (COOH), 1720 (C=O), 1278, 1108 (CO) cm^{-1} . Analysis calculated for 9–3 H_2O : C, 64.80; H, 6.89. Found: C, 64.72; H, 6.64.

Resin 7, 65% yield. IR (KBr) 3448 (COOH), 1735 (C=O), 1274, 1132 (CO) cm^{-1} . Analysis calculated for 9: C, 67.31; H, 7.22. Found: C, 67.21; H, 7.02.

Resin 8, 83% yield. IR (KBr) 3448 (COOH), 1735 (C=O), 1277, 1120 (CO) cm^{-1} . Analysis calculated for 9: C, 69.15; H, 7.94. Found: C, 69.69; H, 7.84.

Procedure

The procedure was the same as that utilized in the earlier study.³ A resin (0.050 g) and 5.0 ml of an aqueous solution containing the alkali-metal chlorides with hydroxides for pH adjustment (0.10M in each) were shaken for 3 hr in a 30-ml separating funnel at room temperature (23–24°) with a Burrell wrist-action shaker. The aqueous phase was filtered with a sintered glass filter funnel (15 ml, medium porosity) and the equilibrium pH of the aqueous phase was measured. The resin was washed with 100 ml of distilled, demineralized water and dried. Of the dried resin, a 0.020-g sample was shaken with 5.0 ml of a 0.10M hydrochloric acid solution to strip the alkali-metal cations from the resin into an aqueous solution for analysis by ion chromatography.

RESULTS AND DISCUSSION

Preparation of crown ether carboxylic acid resins

Crown ether carboxylic acid resins 3, 4 and 6–8 were prepared by condensation of the appropriate *sym*-(R)dibenzo-16-crown-5-oxyacetic acid monomer with formaldehyde in formic acid. Previously it was shown for the synthesis of resin 5 by this method that the IR spectra of the crown ether carboxylic acid monomer and resin were nearly the same.³ Also it was demonstrated that the alkali-metal cation sorption behavior of two different independent preparations of resin 5 was very similar. As expected, the IR spectra for resins 3, 4 and 6–8 (see Experimental) showed very little change from those of the crown ether carboxylic acid monomers.

The structural representations for crown ether carboxylic acid resins 3, 4 and 6–8 imply polymers with no cross-linking. This is most certainly an oversimplification since some level of cross-linking is anticipated.¹⁰ A possible structure for the partially cross-linked resins is given by 9 in which A is the polyether carboxylic acid unit in the resin. Elemental analysis results for resins 7 and 8 agree with the formulation. For resins 3, 4 and 6, the elemental analysis results are consistent with that of 9 as 1.5, 0.5 and 3.0 hydrates, respectively. [Resin 5 which was prepared in the previous study analyzed as a dihydrate.³]

Alkali metal cation sorption by crown ether carboxylic acids

To provide more relevance to actual metal separation systems, competitive, rather than single species, alkali-metal cation sorption behavior of crown ether carboxylic acid resins 3, 4 and 6–8 was investigated.

An aqueous solution of the five alkali-metal cations (0.10M in each) as the chlorides and hydroxides was shaken with the crown ether carboxylic acid resin for 3 hr [even though sorption may be complete in a matter of minutes³]. The resin was filtered, washed with water, and dried. Of the dried resin a weighed portion was shaken with 0.10M hydrochloric acid to strip the alkali-metal cations from the resin into aqueous solution for analysis by ion chromatography. For a resin, sorption of a given alkali-metal cation at a given pH was found to be reproducible within 5 percent of the stated value.

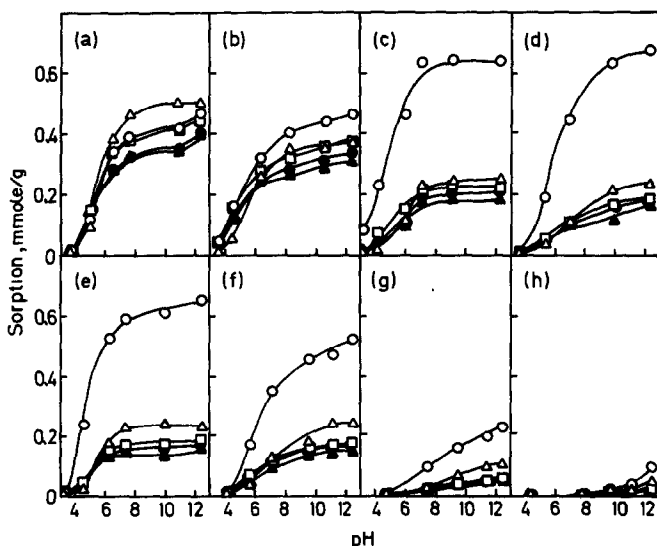


Fig. 1. Sorption of alkali-metal cations by the polyether carboxylic acid *vs.* the equilibrium pH of the aqueous phase for (a) 1, (b) 2, (c) 3, (d) 4, (e) 5, (f) 6, (g) 7, (h) 8: (Δ) Li⁺, (○) Na⁺, (□) K⁺, (▲) Rb⁺, (●) Cs⁺.

The influence of the equilibrium pH of the aqueous phase upon the competitive sorption of alkali-metal cations for crown ether carboxylic acid resins 3, 4 and 6–8 is shown in Figs. 1(c), (d), (f)–(h), respectively. For comparison, data reported³ for acyclic polyether carboxylic acid resin 1 and crown ether carboxylic acid resins 2 and 5 are included as Figs. 1(a), (b), (e), respectively. The curve shapes for alkali-metal cation sorption by the resins *vs.* the equilibrium pH are typical for metal sorption by a weak acid resin.¹¹ Thus the negligible alkali-metal cation sorption observed when the aqueous solution is quite acidic (pH ≤ 3) increases markedly as the pH is enhanced.

As noted earlier,³ the Li⁺ sorption selectivity exhibited by acyclic polyether carboxylic acid resin 1 changes to modest Na⁺ selectivity for the *sym*-dibenzo-16-crown-5-oxyacetic acid resin 2.

Complexation selectivity for Na⁺ is anticipated for the dibenzo-16-crown-5 ring system.¹² Attachment of a methyl group to the crown ether ring carbon which bears the side arm causes a marked change in Na⁺ selectivity for resin 3 [Fig. 1(c)] compared with resin 2 [Fig. 1(b)]. Thus the introduction of the smallest alkyl group is sufficient to produce a major change in sorption selectivity. This enhanced Na⁺ selectivity remains virtually unchanged as the alkyl group is varied from methyl to ethyl [Fig. 1(d)] to propyl [Fig. 1(e)]. Further elongation of the alkyl group to butyl [Fig. 1(f)] produces a noticeable decrease in Na⁺ sorption selectivity. When the alkyl group is changed to hexyl a further decrease in selectivity is noted [Fig. 1(g)]

Table 1. Alkali-metal cation sorption efficiency of polyether carboxylic acid resins 1–8.

Resin	Alkyl chain	Ion-exchange capacity,* mmole/g	Sorption, mmole/g	Percent loading, %
1	none†	2.66	2.22	83
2	none	2.39	1.85	77
3	methyl	2.31	1.49	65
4	ethyl	2.23	1.43	64
5	propyl	2.17	1.40	65
6	butyl	2.11	1.27	60
7	hexyl	1.93	0.49	25
8	decyl	1.79	0.21	12

*Calculated from elemental analysis data.

†Acyclic polyether carboxylic acid resin.

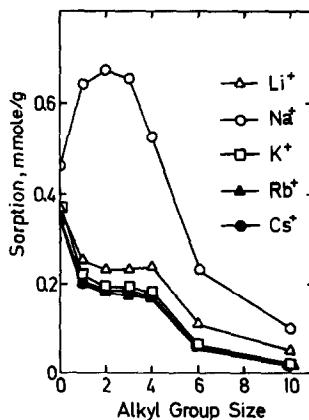


Fig. 2. Effect of alkyl group chain length upon alkali-metal cation sorption by *sym*-(R)dibenzo-16-crown-5-oxyacetic acid resins at equilibrium pH = 12.5.

and for a decyl group only slight Na^+ selectivity is observed [Fig. 1(h)].

The total alkali-metal cation sorptions and loadings for polyether resins 1–8 at equilibrium $\text{pH} = 12.5$ are presented in Table 1. The loading is defined as the total alkali-metal cation sorption by the resin divided by the ion-exchange capacity calculated from the elemental analysis data. The loading decreases from 77% for crown ether carboxylic acid resin 2 to 65% when a methyl group is attached to the crown ether ring which bears the side arm. The efficiency then remains constant as the alkyl group is varied from methyl to ethyl to propyl. The loading shows a slight decrease for the butyl group then plummets to 25% for the hexyl group and only 12% for the decyl group.

The low alkali-metal cation loadings observed for resins 7 and 8 may be attributed to enhanced hydrophobicity which hinders penetration of the aqueous solution into the resin and diminishes effective interactions between the metal cations and the ion exchange sites. In agreement, when the solvent for the alkali-metal cations was changed from water to methanol-water (4:1), the percent loading for resin 8 changed from 12 to 44% with no variation in the sorption selectivity.¹³ This enhanced loading is consistent with better penetration of the alkali-metal cation solution into the resin with the mixed aqueous-organic solvent.

Figure 2 compares the influence of alkyl group variation upon the sorption of each alkali-metal cation by resins 2–8 at equilibrium $\text{pH} = 12.5$. The curve for Na^+ sorption is markedly different than those for sorptions for the other alkali-metal cations. Thus the sorption of Li^+ , K^+ , Rb^+ and Cs^+ shows a sharp decrease when the methyl group is introduced into the crown ether carboxylic acid unit and then remains nearly constant as the alkyl group is varied from methyl to ethyl to propyl to butyl. Elongation of the alkyl group from butyl to hexyl causes an abrupt diminution of sorption with a further decrease when the alkyl group is changed to decyl. In contrast, the Na^+ sorption is strongly enhanced when the methyl group is introduced. The Na^+ sorption then remains virtually the same as the alkyl group is varied from methyl to ethyl to propyl. However the change to a butyl group produces a substantial

decrease in Na^+ sorption and the decline continues for the hexyl and decyl groups. It should be noted that even though the sorption efficiency for crown ether carboxylic acid resin 8 which has a decyl alkyl group is very low its Na^+ selectivity is higher than that of resin 2 which has no alkyl group. Thus the predominant influence of the longer alkyl groups is to decrease sorption efficiency by making the resins more hydrophobic.

CONCLUSIONS

This study of structural variation within *sym*-(R)dibenzo-16-crown-5-oxyacetic acid resins reveals that the highest alkali-metal cation sorption efficiency and Na^+ selectivity is obtained when the alkyl group is methyl, ethyl or propyl. The incorporation of longer alkyl groups diminishes sorption efficiency by increasing the hydrophobicity of the resins.

Acknowledgement—This research was supported by the Division of Chemical Sciences of the Office of Basic Energy Sciences of the U.S. Department of Energy (Grant DE-FG05-88ER13832) and the Advanced Technology Program of the State of Texas.

REFERENCES

1. F. Helfferich, *Ion Exchange*, pp. 43–47. McGraw-Hill, New York, 1962.
2. P. H. Gramain in P. A. Williams and M. J. Hudson, *Developments in Ion Exchange*, pp. 300–314. Elsevier Applied Science, New York, 1987.
3. T. Hayashita, M.-J. Goo, J. C. Lee, J. S. Kim and R. A. Bartsch, *Anal. Chem.*, 1990, **62**, 2283.
4. D. J. Cram, *Angew. Chem., Int. Ed. Engl.*, 1986, **25**, 1039.
5. T. Hayashita, J. H. Lee, S. Chen and R. A. Bartsch, *Anal. Chem.*, 1991, **63**, 1844.
6. R. A. Bartsch, Y. Liu, S. I. Kang, B. Son, G. S. Heo, P. G. Hipes and L. J. Bills, *J. Org. Chem.*, 1983, **48**, 4864.
7. P. R. Brown, J. L. Hallman, L. W. Whaley, D. H. Desai, M. J. Pugia and R. A. Bartsch, *J. Membrane Sci.*, 1991, **56**, 195.
8. M. J. Pugia, B. E. Knudsen, C. V. Cason and R. A. Bartsch, *J. Org. Chem.*, 1987, **52**, 541.
9. T. Hayashita, H. Noguchi, M. Igawa and M. Takagi, *J. Appl. Polym. Sci.*, 1990, **39**, 561.
10. E. Blasius, W. Adrian, K.-P. Janzen and G. J. Kalutke, *J. Chromatogr.*, 1974, **96**, 89.
11. Reference 1, p. 86.
12. J. Strzelbicki and R. A. Bartsch, *Anal. Chem.*, 1981, **53**, 1894.
13. T. Hayashita, J. H. Lee, J. C. Lee, J. Krzykawski and R. A. Bartsch, *Talanta*, in press.

INFRARED EMISSION SPECTROSCOPY OF LIQUID SAMPLES WITH MULTIVARIATE CALIBRATION AS A MODEL FOR PROCESS ANALYTICAL APPLICATIONS

BRICE C. ERICKSON*, RANDY J. PELL† and BRUCE R. KOWALSKI‡

Department of Chemistry, University of Washington, Laboratory for Chemometrics, Seattle, Wa. 98195

(Received 9 November 1990. Revised 17 May 1991. Accepted 21 May 1991)

Summary—Infrared emission spectroscopy and multivariate calibration are used to provide a method for the quantitative analysis of liquid samples. Differing forms of the data including second derivative and interferogram representation are used for prediction of sample composition, thickness and temperature. Comparisons are made with transmission measurements of the same samples. In some situations emission measurements may be the preferred method of analysis.

Many products made by the chemical industry are above ambient temperatures at some or all points in the manufacturing process. Some of these products are considerably higher in temperature as they are produced, *e.g.*, glass, metal, synthetic fibers, polymers and coatings. A non-invasive, remote method of monitoring the composition or quality of the product would be desirable,¹ but conditions and hazards in the plant environment may make spectroscopic absorption or reflectance measurements difficult to obtain. Any sample which absorbs IR radiation emits at the same wavelengths when heated, implying that the information in an absorption or transmission spectrum used for chemical analysis should also be present in the emission spectrum. Infrared emission spectroscopy (IES), therefore, may have several advantages over transmission spectroscopy in some situations, especially where remote monitoring is desirable such as process analysis applications.¹ However, its use has been limited due to lack of suitable instrumentation of the required sensitivity and ruggedness, and the difficulty in interpreting the complex spectra obtained. Emission spectra are much more complex than transmission spectra since they are affected not only by sample composition, but by several other effects as well such as background blackbody radiation, in-

ternal reflection and self-reabsorption, refractive index, sample thickness and geometry, and most importantly temperature and temperature gradients.² The recent innovations in process qualified Fourier transform infrared spectrophotometers have provided great progress on the limitations of instrumentation, but spectral interpretation—especially for quantitation—has remained a problem. Griffiths³ and Hirschfeld⁴ have both pointed out that IES could be a powerful quantitative tool if a general method or algorithm could be developed to aid in data interpretation.

Some potential advantages of IES over the more traditional spectroscopies include the fact that there is no need to use an external source of radiation since the hot sample acts as its own source; requirements for optical alignment are minimized; there is less sensitivity to effects such as reflections or diffractions which may occur at the surface of the sample; measurement can be made remotely, measurement is non-invasive and non-destructive; and information about sample temperature is contained in the spectrum.

Limitations of IES include the lower radiation levels available for detection, especially at shorter wavelengths, resulting in the need for cooled detectors; the requirement that the sample must be at a temperature different than the detector and its surroundings; and a decrease in spectral information as the sample becomes more opaque.

Infrared emission spectroscopy has been used in a number of different applications in the past. Most of these applications relate to temperature

*Present address: 3M Chemolite Center, P.O. Box 33131, Saint Paul, Minnesota 55133-3131.

†Present address: Analytical Sciences Laboratory, The Dow Chemical Company, 1897 Building, Midland, MI 48667.

‡Author for correspondence.

measurements by optical pyrometry, or to qualitative analysis of optically thin samples, although there have been attempts to use IES quantitatively. Quantitative applications of IES in the chemistry literature generally involve optically thin samples under carefully controlled laboratory conditions, usually with known temperature. Some examples of samples types on which IES has been used are thin films of oils⁵ and lubricants,⁶ molten salts^{7,8} and oxide coatings on metals.^{9,10} A number of reviews or general papers are available of applications of IES in the chemistry literature.^{11,12}

Multivariate calibration methods, and specifically the Partial Least Squares (PLS) method, have been found useful for quantitative analysis in a number of spectroscopic techniques.¹³ For example, these methods have been applied to absorption or reflectance spectroscopy in the mid- and near-IR regions.^{14,15} In an earlier paper,¹⁶ the applicability of multivariate calibration methods, specifically partial least squares (PLS) calibration, was demonstrated for quantitation from infrared emission spectra of polymer film samples in spite of these non-linearities. The results of that work demonstrate the ability of multivariate calibration to extract not only information concerning the composition of the sample, but thickness and temperature as well, from emission data. This work is a further study on use of PLS for the analysis of IES data from liquid samples. The study was conducted to better understand the limitation for determining thickness, temperature and composition since these parameters can be better controlled with liquid samples.

EXPERIMENTAL

A Perkin-Elmer model 1720 FTIR spectrometer was modified to allow use of the instrument for either emission or transmission studies. For emission studies, the focal plane of the optical system is changed from the normal instrument source to an external sample mount by changing one reflector. With the instrument source turned off, the sample then becomes the source of radiation which eventually reaches the detector. No sample is placed in the normal sample compartment. A medium band MCT (Hg-Cd-Te) detector was used to provide the required sensitivity.

A model system was desired for IES studies which would allow more precise control of the parameters of sample composition, thickness

and temperature to further evaluate the effectiveness of the method. The samples studied are binary mixtures squalene and di(2-ethylhexyl)sebacate. These compounds were chosen for their low vapor pressures and thermal stability over a wide range of temperatures. Since they are complex organic molecules, they have a large number of strongly absorbing bands in the infrared. They may also serve as a model of organic systems that might be encountered in process situations.

For emission studies, mixtures containing 60, 70, 80 and 90% squalene were prepared by weight. Samples were placed in a variable pathlength liquid cell. Cell windows were potassium bromide, and no reflecting backplate was used. The cell pathlength was adjustable from 50 micrometers to 5 mm, and pathlengths of 0.1, 0.2, 0.4, 0.6, 1, 3 and 5 mm were used. The circumference of the cell was wrapped with a heating tape with temperature controlled by a variable voltage power supply. Sample temperature was accurately measured by an RTD temperature sensor placed against the back window of the cell. For longer pathlength samples, a thermocouple was also placed inside the cell to verify the measurements, and temperatures were in agreement within 1°. The single beam infrared emission spectrum, second derivative of the single beam emission spectrum and raw interferogram from the instrument were recorded for each concentration and thickness at 4 random temperatures in the range 45–80°. A 500-point spectrum was used for the PLS analysis from 3000–500 cm⁻¹ at 5 cm⁻¹ intervals for emission and derivative spectra; the 200 point interferogram was used for interferogram predictions.

For transmission and absorption spectra, squalene/di(2-ethylhexyl) sebacate mixture samples were prepared as above with concentrations of 60, 65, 70, 75, 80, 85 and 90% squalene; the three additional concentrations were added to assure a sufficiently large calibration data set. Temperature was not varied or predicted for transmission or absorption spectra, since it has minimal effect on the spectra obtained. Transmission spectra were obtained for the samples in the variable pathlength cell for the thicknesses used earlier from 0.1 to 5.0 mm on the same instrument, using the instrument source and the DTGS detector with the sample placed in the usual sample compartment. Spectra were saved in both transmission and absorbance units. The Perkin-Elmer data system does not record absorbance values

greater than 5 so these data points were given the value 5. The PLS method was applied for data analysis, using 500-point spectra from 3000–500 cm^{-1} at 5 cm^{-1} intervals.

The intention of this work was to investigate the use of multivariate calibration for quantitation using infrared emission data. Although the application of certain *a priori* information in the form of wavelength selection/deletion may have helped to optimize the data analysis, this approach was not taken. Minimal preprocessing of the data was performed to provide an approach that could easily be automated with little expert interaction. This approach provides a worst case scenario and any intelligent application of wavelength selection may only serve to further refine the method and improve the results.

RESULTS AND DISCUSSION

The PLS regression method and algorithm are described in the literature.¹³ A calibration set is used to develop the multivariate model, which can then be used to predict properties such as concentration for similar samples not included in the calibration. A method must be chosen to determine the number of latent variables or factors to be retained for the model. Since our main concern was the ability of the model to predict unknown samples, predictive ability was determined with a cross-validation procedure.¹⁷

In order to evaluate the effectiveness of the model in predicting the unknown, the SEP (standard error prediction, or average prediction error) is calculated to give a meaningful expression of how well the method is able to predict relative to the true values.

$$\text{SEP} = \left(\sum_{i=1}^N (y_i - \hat{y}_i)^2 / N \right)^{1/2}$$

where y_i 's are the reference values obtained by an independent method of analysis and the \hat{y}_i 's are the values predicted by PLS. The number of factors retained is the lowest number of factors with a SEP within the uncertainties of the lowest SEP obtained, that is, the lowest number of factors with a prediction which is not significantly worse than the best SEP obtained. The SEP then gives an indication of how well the model will predict a sample not contained in the calibration set. A number of diagnostics were used with the algorithm to detect samples which are outliers relative to the calibration (not to be discussed here).

Figure 1 shows typical spectra obtained on our instrument. The low intensities above 2000 cm^{-1} are due to the relatively low temperature of the samples related to Planck's equation. The sharp drop in intensity from 550 to 450 cm^{-1} and some of the additional apparent "structure" in the spectrum are actually due to variable instrument responses over the wavelength range. Some of the observable fine structure, especially between 1350 and 1800 and between 2300 and 2400 cm^{-1} , is due to absorption by atmosphere H_2O and CO_2 in the radiation path between the sample and instrument. No attempt is made to correct for these various response factors; they are assumed to be constant so that they will not affect the calibration from PLS. Figures 1(a), (b) and (c) show typical spectral changes due to changing sample composition, temperature and thickness respectively. Of the three sample properties studied, temperature has the greatest effect on the intensities in the spectra.

Table 1 summarizes the predictive ability of the method for certain subsets of the data, along with the number of latent variables (factors) found to be significant in the calibration. When samples with thicknesses in the 0.6–5 mm range are used, the SEP for concentration predictions is 3.4% absolute over the 60–90% range. Prediction of the thickness of these samples gives a SEP of 0.43 mm over the 0.6–5 mm range. Temperature in this case is predicted quite well, with a SEP of 0.7° over the 45–80° range. This verifies that temperature prediction is possible from emission spectra, using PLS, when temperature values are known to sufficient precision in the calibration set; this point was unclear in the earlier study.¹⁶

For thinner samples in the 0.1–0.6 mm range, of the 64 possible spectra (4 concentrations at 4 thicknesses and 4 temperatures), 3 were removed due to known experimental problems. An additional 3 were found statistically to be spectral outliers. These six samples were removed from the calibration set. Concentration predictions showed a SEP of 1.6% absolute over the 60–90% range. Sample thickness had a SEP of 0.03 over the 0.1–0.6 mm range. Temperature was predicted with a SEP of 0.9°. While a large number of factors were used for this prediction, it should be noted that a single factor predicted temperature with a SEP of 1.6, so it appears that the main temperature effect is easily modeled while additional factors make slight corrections for the non-linearities.

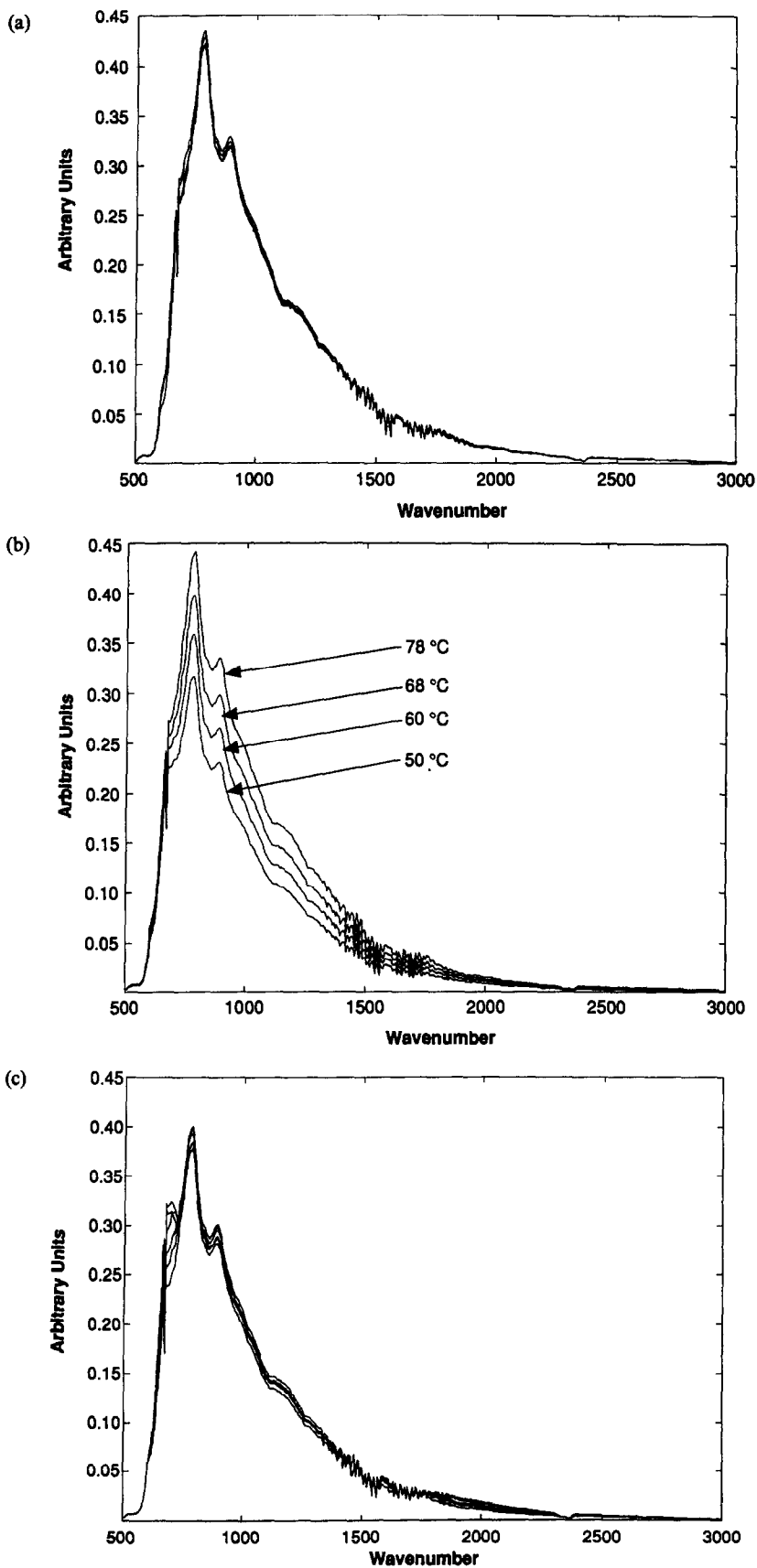


Fig. 1. Emission spectra. (a) Concentration variation: samples 0.4 mm thick at about 77° with concentrations of 60%, 70%, 80% and 90% squalene. (b) Temperature variation: samples 80% squalene and 0.2 mm thick at 50, 60, 68 and 78°. (c) Thickness variation: samples 80% squalene at about 67° and 0.1, 0.2, 0.4, 0.6, 1.0, 3.0 and 5.0 mm thickness.

Table 1. Summary of prediction results for emission spectra of liquids

Data type	Standard error of prediction					
	Conc., (%)	Factors	Thickness, mm	Factors	Temp., °C	Factors
Thick (0.6–5 mm) samples emission spectra	3.4	10	0.43	11	0.7	14
Thin (0.1–0.6 mm) samples emission spectra	1.6	16	0.03	15	0.9	13
Thin (0.1–0.6 mm) samples 2nd deriv. spectra	3.0	11	0.05	10	1.0	9
Thin (0.1–0.6 mm) samples interferograms	2.8	10	0.05	14	0.7	12

Table 1 also shows that the use of second derivative spectra for the prediction resulted in roughly the same prediction results for thickness and temperature but somewhat poorer results for composition, although 4 or 5 fewer latent variables were used for optimal prediction. It is interesting to note that the prediction can also be made directly from the interferogram,

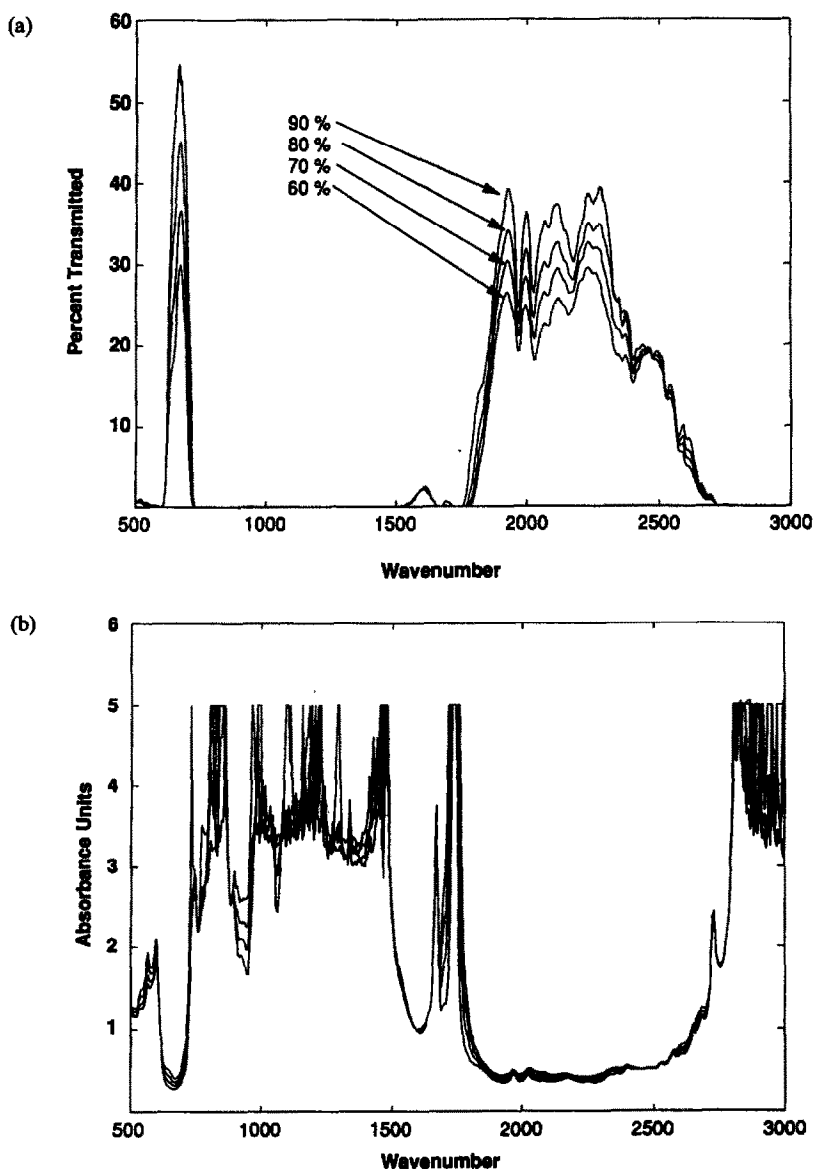


Fig. 2. Concentration variations. Transmission (a) and absorbance (b) spectra of 0.4-mm samples containing 60%, 70%, 80% and 90% squalene.

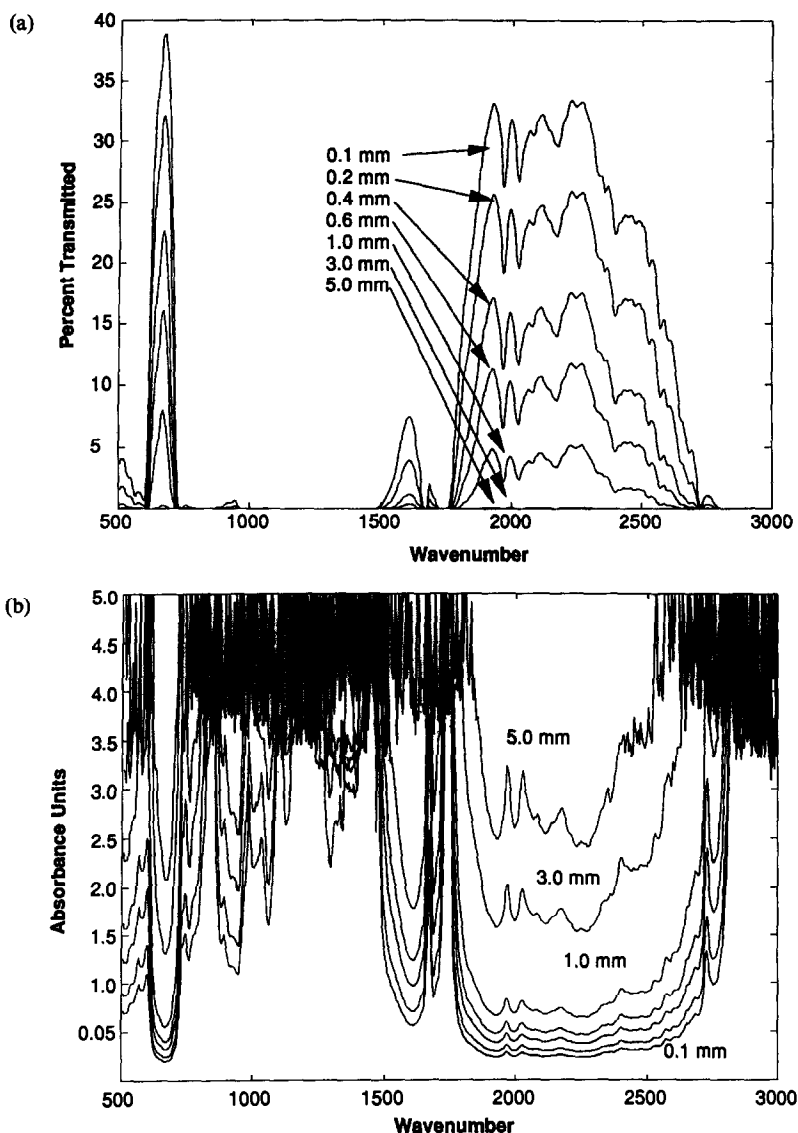


Fig. 3. Thickness variations. Transmission (a) and absorbance (b) spectra of 80% squalene sample with thicknesses of 0.1, 0.2, 0.4, 0.6, 1.0, 3.0 and 5.0 mm.

without transforming to the spectral domain. The concentration and thickness predictions are slightly worse than the prediction from the emission spectra, but still as good or better than the second derivative prediction.

The success of the PLS method in predicting composition, sample thickness and sample temperature with these liquid samples verifies the validity of the results of the earlier polymer studies that IR emission shows great promise as an analytical tool for certain process situation.

In the more typical transmission experiments, response is linearized for concentration and thickness effects by converting data to absorbance units. Spectra of the liquid samples were taken in the transmission mode and a

comparison is made in the number of factors retained and predictive ability for transmission, absorption and emission spectra of these samples.

Typical transmission and absorption spectra of samples with changing concentration are shown in Figs. 2(a) and (b). Figures 3(a) and (b) show spectra with changing thickness at constant composition. Results from the PLS analysis are summarized in Table 2, along with the earlier results from the emission experiments. For samples in the 0.6–5 mm thickness range, the emission spectra showed the best prediction of sample concentration with a SEP of 3.4 *vs.* 6.6 for absorption and 4.0 for transmission. Thickness, however, was predicted

Table 2. Summary of prediction results for emission, transmission and absorbance spectra of liquid samples

Data type	Standard error of prediction			
	Conc., %	Factors	Thickness mm	Factors
Thick (0.6–5 mm) samples emission spectra	3.4	10	0.43	11
Thick (0.6–5 mm) samples transmission spectra	4.0	10	0.1	11
Thick (0.6–5 mm) samples absorbance spectra	6.6	3	0.21	2
Thin (0.1–0.6 mm) samples emission spectra	1.6	16	0.03	15
Thin (0.1–0.6 mm) samples transmission spectra	0.1	13	0.002	12
Thin (0.1–0.6 mm) samples absorbance spectra	2.5	5	0.02	4
Thin (0.1–0.6 mm) samples absorbance trunc. at 3	0.77	9	0.003	11
Thin (0.1–0.6 mm) samples absorbance trunc. at 2	0.51	10	0.002	13

better by absorption (SEP of 0.21) than emission (SEP of 0.43), and better yet by transmission (SEP of 0.1). The absorption spectra, which are expected to be more linear with respect to concentration and thickness, require fewer latent variables to make the predictions, requiring only 3 for concentration and 2 for thickness. Emission and transmission both require 10 for concentration and 11 for thickness for their optimal predictions. This implies that the number of factors retained for prediction for emission spectra are reasonable, using about the same number as the less complex transmission spectra.

Figure 4(a) shows the SEP *vs.* number of factors used in prediction for the three types of spectra. The optimal prediction is reached quickly by absorbance calibration, and predictive ability is not significantly improved as additional factors are added. Emission and transmission predictions continue to improve until they reach their optimal predictions between 10 and 15 factors. A similar trend is seen in Fig. 4(b) for thickness predictions.

For the thinner set of samples in the 0.1–0.6 mm range, the emission spectra (SEP = 1.6) still have an advantage over absorption spectra (SEP = 2.5) in predicting concentration, but surprisingly the transmission calibration (SEP = 0.1) is an order of magnitude better than both. For thickness prediction, absorption (SEP = 0.02) is slightly better than emission (SEP = 0.03), but again transmission (SEP = 0.002) is an order of magnitude better than both. Again, absorption calibrations use far fewer factors for prediction.

Apparently the transformation of the data from transmittance to absorbance values expands the noise in the high absorption regions, due to the logarithmic relationship. To check this assumption, values in the absorption data set were truncated at 3 absorbance units; that is, all values greater than 3 were reassigned the value 3. The prediction for concentration was improved from a SEP of 2.5 to about 0.8, and thickness from 0.02 to 0.003. Thus removing those values suspected of being in a “noisy” portion of the spectrum greatly improves the predictive ability of the calibration. Truncating the data at 2 absorbance units results in slightly better prediction. In addition, over 98% of the spectral variance is now explained by the model for data with absorbances truncated at 3, and over 99% for data truncated at 2. Figure 4(c) shows the trends in the SEP for emission, transmission, absorption and truncated (at 3) absorption data over number of factors retained in the model for thin samples.

This result is significant for multivariate calibration in that it implies great care must be taken in preprocessing of data to be sure that the transformation used does not scale the noise level of the data up to intolerable levels.

While transmission and absorption spectra do predict better than emission for thin samples, this does not imply that emission will not be useful. The reasons cited earlier for using IES methods in process situations have more to do with other considerations which make emission methods more attractive than transmission methods. As long as predictive ability is sufficient for the application, IES should remain

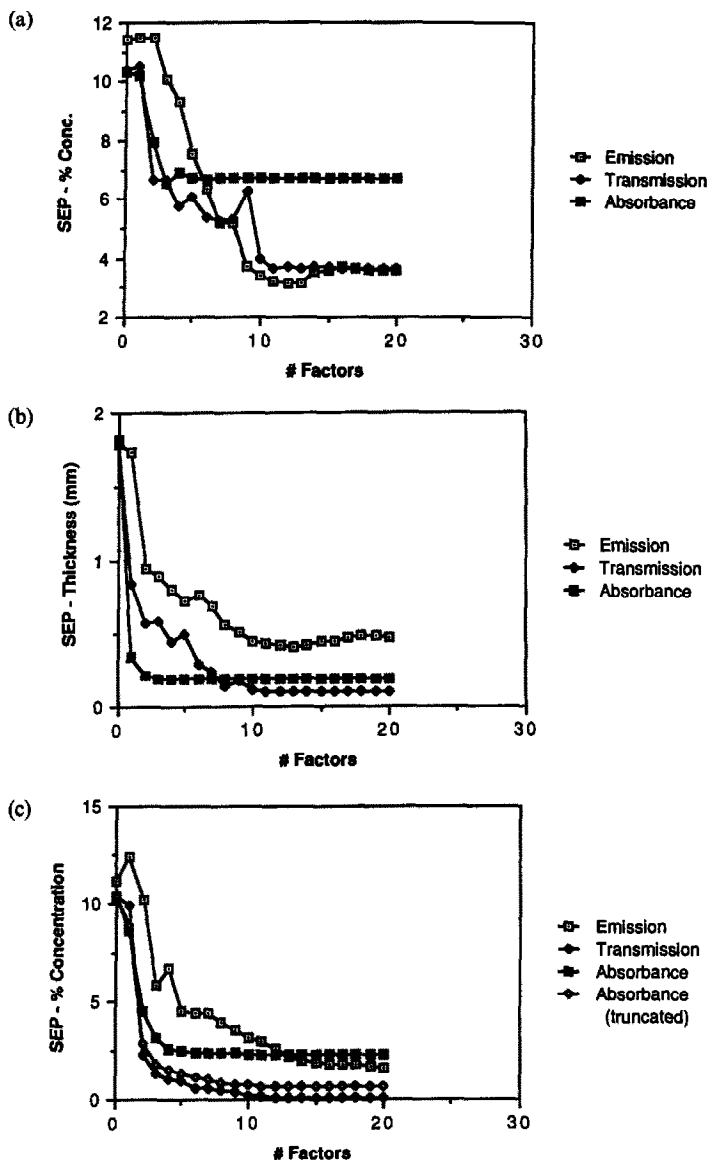


Fig. 4. Standard error of prediction (SEP) vs. number of factors retained in the model used for prediction. (a) Prediction of squalene concentration (%) in samples 0.6–5 mm thick for absorbance, transmission and emission spectra. (b) Prediction of thickness of samples 0.6–5 mm thick for absorbance, transmission and emission spectra. (c) Prediction of squalene concentration (%) in samples 0.1–0.6 mm thick for emission, transmission, and absorbance spectra, including absorbance spectra truncated at 3.

a viable tool. And the better prediction observed for emission spectra on the thicker samples indicates that it may in fact be the best method for prediction in some applications.

Acknowledgements—This work was supported by the Center for Process Analytical Chemistry (CPAC), a National Science Foundation Industry/University Cooperative Research Center at the University of Washington.

REFERENCES

1. J. B. Callis, D. L. Illman and B. R. Kowalski, *Anal. Chem.*, 1987, **59**, 624R.
2. J. Hvistendahl, E. Rytter and H. A. Oye, *Appl. Spectrosc.*, 1983, **37**, 182.
3. P. R. Griffiths, *ibid.*, 1972, **26**, 73.
4. T. Hirschfeld, *Appl. Opt.*, 1978, **17**, 1400.
5. S. F. Kapff, *J. Chem Phys.*, 1948, **16**, 446.
6. J. L. Lauer and V. W. King, *Infrared Physics*, 1979, **19**, 395.
7. T. R. Kozlowski, *Appl. Opt.*, 1968, **7**, 795.
8. J. B. Bates and G. E. Boyd, *Appl. Spectrosc.*, 1973, **27**, 204.
9. G. E. Guazzoni, *ibid.*, 1972, **26**, 60.
10. D. Kember and N. Sheppard, *ibid.*, 1975, **29**, 496.
11. N. Sheppard, in *Analytical Applications of FT-IR to Molecular and Biological Systems: Proceedings of the NATO Advanced Study Institute held at Florence, Italy*,

- August 31 to September 12, 1979*, J. R. Durig (ed.), p. 125. D. Reidel Pub. Co., Hingham, Massachusetts, 1980.
12. P. R. Griffiths and J. A. deHaseth, *Fourier Transform Infrared Spectrometry*, p. 202–208. John Wiley & Sons, New York, 1986.
 13. D. M. Haaland and E. V. Thomas, *Anal. Chem.*, 1988, **60**, 1193.
 14. B. R. Buchanan and D. E. Honigs, *Spectrosc.*, 1986, **1**, 40.
 15. D. M. Haaland, *Anal. Chem.*, 1988, **60**, 1208.
 16. R. J. Pell, B. C. Erickson, R. W. Hannah, J. B. Callis and B. R. Kowalski, *ibid.*, 1988, **60**, 2824.
 17. S. Wold, *Technometrics*, 1978, **20**, 397.

POLAROGRAPHIC BEHAVIOUR OF URANIUM β -DIKETONATES IN CHLOROFORM

APPLICATION OF AC POLAROGRAPHY TO THE ANALYSIS OF URANIUM MINERALS

M. H. POURNAGHI-AZAR* and J. ORDOUKHANIAN

Electroanalytical Chemistry Laboratory, Faculty of Chemistry, University of Tabriz, Tabriz, Iran

(Received 15 December 1990. Revised 23 April 1991. Accepted 14 May 1991)

Summary—The polarographic behaviour of U(VI) β -diketonates has been studied in chloroform. The conditions for reversible electrochemical reduction of U(VI) acetylacetonate and benzoylacetonate at a dropping mercury electrode was optimized by using a suitable ratio of piperidinium perchlorate and piperidine mixture as supporting electrolyte in chloroform. The one-electron nature of the reduction wave of U(VI) complexes was confirmed by controlled potential coulometry. The ac method preceded by a solvent extraction of U(VI) benzoylacetonate in chloroform was used for the determination of uranium. The calibration curve was linear over the range 0.5–20 $\mu\text{g/ml}$. The correlation coefficient was 0.9998 and the detection limit was about 0.2 $\mu\text{g/ml}$. The interference of some concomitant ions were examined and EDTA was used as an effective masking agent to separate uranium from other metals. The proposed method has been applied to the determination of uranium in uranium minerals.

In general a preliminary separation by solvent extraction provides good selectivity for instrumental methods of analysis that tend to be subject to matrix effects or interferences from concomitant elements. Analytical determination of metal ions following solvent extraction based on electrochemical methods, involving either direct measurement of the amount of the analyte in the organic phase diluted with a convenable supporting electrolyte solution,^{1–5} back-extraction into aqueous phase,⁶ or evaporation of the extracted phase and redissolution of the residue in some other polar solvent.

Such methods are however time-consuming and it is often very difficult to destroy the chelating agents. In addition, the large number of steps involved in the analytical process and the dilution of the extracted phase affect the precision and sensitivity of analytical methods.

Direct application of electroanalytical methods to the determination of analytes in pure extracts seem to be simple and sensitive.^{7–11} To carry out this, it is necessary to provide conditions for the electrochemical studies in extracting solvents with a low dielectric constant.

The study of electrochemical behaviour of organic and inorganic compounds in non-aqueous media was limited to solvents with high

dielectric constant; solvents with low dielectric constant which are used in liquid–liquid extraction (e.g., chloroform, dichloromethane, benzene etc.) have been rarely used.

Application of common methods such as cyclic voltammetry, polarography and controlled potential coulometry for the study of electrochemical behaviour of some organic compounds with several supporting electrolytes at the bright platinum and dropping mercury electrodes in chloroform have been reported recently.^{11–14}

In this paper we describe the study of polarographic behaviour of metal ion complexes such as uranium β -diketonates in chloroform. The alternating current (ac) polarography was applied as a convenable technique for the determination of uranium in mineral ores at the ppm level after optimization of polarographic conditions.

EXPERIMENTAL

Chemicals and reagents

Chloroform, piperidine, perchloric acid, acetylacetone, benzoylacetonate and thenoyltrifluoroacetone were Merck p.a grade. The supporting electrolyte, piperidinium perchlorate, was prepared by gradual neutralization of a given volume of piperidine with the required amount of

*Author for correspondence.

perchloric acid while cooling the solution in iced water. The neutral solution obtained was crystallized by successive concentration on the water bath and cooling at room temperature. The white crystals formed were dried at 50°.

Standard uranium solution. A $10^{-2}M$ aqueous solution of uranyl nitrate, $UO_2(NO_3)_2 \cdot 6H_2O$, from BDH was prepared as a stock solution. The standard solutions were prepared by successive dilutions of this stock solution.

Extraction solution. A 50% solution of acetylacetone, 1M benzoylacetone and 0.15M thenoyltrifluoroacetone solutions in chloroform were used.

Apparatus

A polarograph E 506 was used with an E 505 mercury dropping-electrode (METROHM) to plot the polarograms in connection with a V.A scanner E 612 and an X-Y recorder to record the cyclic voltamperograms. An E 524 coulostat connected to an E 478 recorder was used for coulometry at controlled potential.

Procedure

Transfer 10 ml of aqueous standard or uranium sample solution into a 100-ml separating funnel. Adjust the pH of aqueous solution with 0.01N sodium hydroxide or ammonia and 0.01N nitric acid to a pH at which the extraction of complexes are complete (optimum pH for quantitative extraction of acetylacetonate, benzoylacetone and thenoyltrifluoroacetone of uranium(VI) are 3, 4 and 7 respectively¹⁵). Shake with an equal volume of chloroformic solution of β -diketone for 10 min on a shaker. Separate the chloroform extract and transfer it into a polarographic cell, add 1.40 g of piperidinium perchlorate and 0.25 ml of piperidine (0.75M PP + 0.25M P) as supporting electrolyte. Bubble nitrogen through the solution for 20 min, record the ac polarogram by sweeping the potential from 0 to -500 mV vs. Ag/AgI reference electrode at 2 mV/sec. When other metals were also present, 1 ml of 0.05M EDTA was added before the chloroformic solution of β -diketone.

RESULTS AND DISCUSSION

In chloroform in the presence of extracting agents and with 0.5M TBAP as supporting electrolyte, the uranium(VI) β -diketonates were not reducible at the dropping mercury electrode, but with piperidinium perchlorate (0.75M) and piperidine (0.25M) merged as supporting elec-

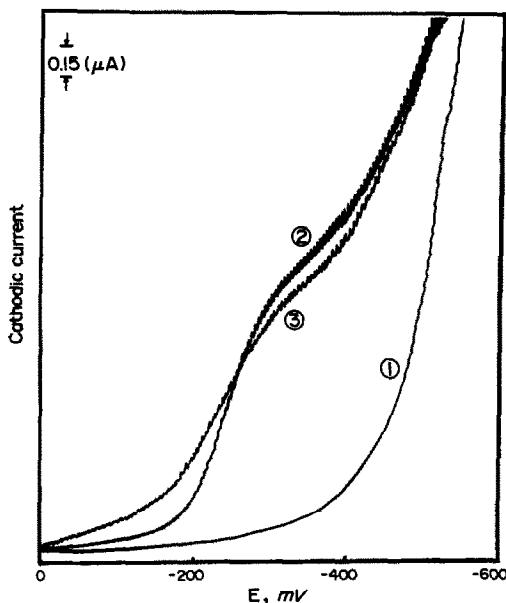


Fig. 1. Direct current (dc) polarograms of (1) 0.75M PP/0.25M P + 50% Acetylacetone, (2) (1) + 1mM U(VI) acetylacetonate, (3) (1) + 1mM U(VI) benzoylacetone.

trolyte, the reduction of acetylacetonate and benzoylacetone of U(VI) gives each one reduction wave with a half-wave potential of -0.240, -0.200 V, respectively (Fig. 1). The reduction wave of thenoyltrifluoroacetone was not a well-defined one. Controlled potential coulometry shows that the single cathodic wave of U(VI) β -diketonates corresponds to a one electron reduction process. A plot of $\log [(i_d - i)/i]$ vs. E gives a straight line with a slope of about 64 mV. Cyclic voltamperograms of U(VI) β -diketonates are shown in Fig. 2. For all scan-rates between 0 and -0.5 V one cathodic peak and one anodic peak are observed. Peak heights, as expected, increased with increasing scan-rate. The current function ($i_{pc}/V^{1/2}$) remains constant. The peak separation $E_{pa} - E_{pc}$ for scan-rates less than 20 mV/sec are 75 and 73 mV for U(VI) acetylacetonate and benzoylacetone respectively. The ratio of anodic to cathodic peak currents as a function of voltage scan-rate is unity and remains constant. These confirm that there is no kinetic complication for the reduction of U(VI) β -diketonates under optimized polarographic conditions.

Alternating current (ac) polarography presents well-defined peaks with E_p equal to $E_{1/2}$ of dc waves. The half-width of peaks are 90 mV. The calibration graphs were linear over the range 10^{-5} - $2 \times 10^{-4}M$ for acetylacetonate and 4×10^{-6} - $2 \times 10^{-4}M$ for benzoylacetone (Fig. 3). Correlation coefficient is 0.9998 and

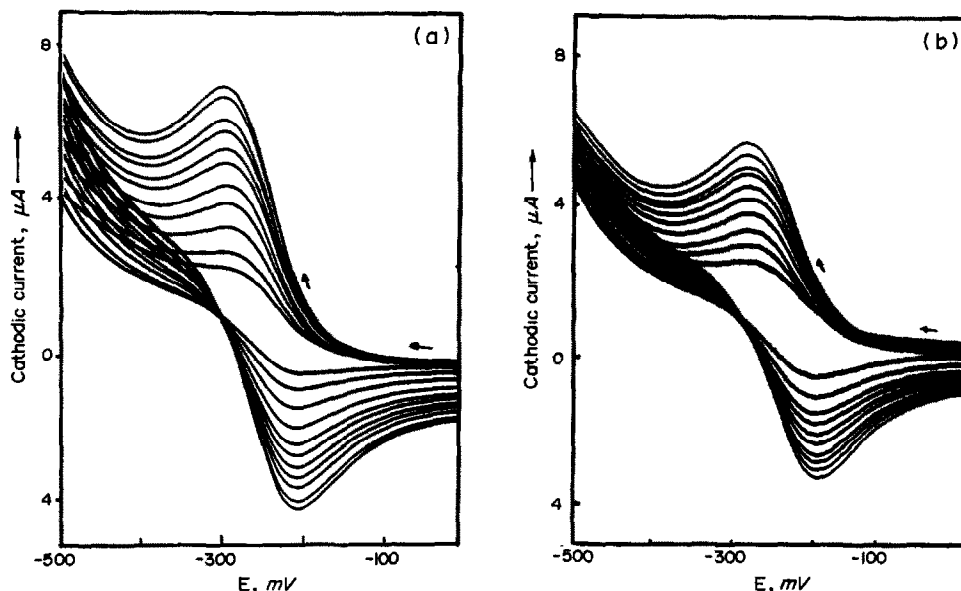


Fig. 2. Cyclic voltamperograms of (a) 1mM U(VI) acetylacetonate (b) 1mM U(VI) benzoylacetonate in the presence of 0.75M PP/0.25M P as supporting electrolyte, scan-rate 5–100 mV/sec.

the detection limit for U(VI) benzoylacetonate is 10^{-6} or 0.2 $\mu\text{g/ml}$ of uranium in the original aqueous solution. The relative standard deviation for five replicate determinations of 1 $\mu\text{g/ml}$ uranium was 2.5%.

With the 0.75M PP/0.25M P as supporting electrolyte the differential pulse polarogram of U(VI) β -diketonates coalesce with the reduction wall of the solvent and therefore an accurate and quantitative measurement of these peaks cannot be made.

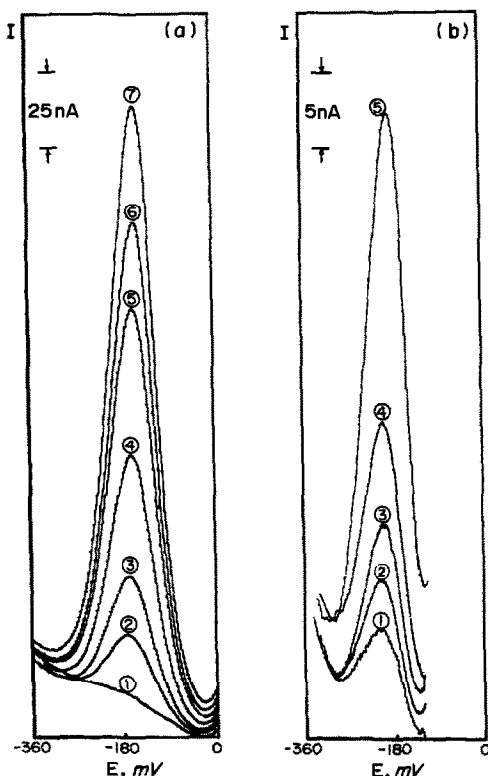


Fig. 3. Alternating current (ac) polarograms of (a) U(VI) acetylacetonate 1.5×10^{-3} – $1.5 \times 10^{-6}M$ (b) U(VI) benzoylacetonate (2×10^{-6} – $10^{-5}M$) in the presence of 0.75M PP/0.25M P $V = 10 \text{ mV}$ $t = 1 \text{ sec}$, $f = 75 \text{ Hz}$.

Interferences

The interferences from some concomitant elements such as V(V), Pd(II), Mo(VI), Cu(II), Fe(III), etc., have been examined. The experimental results show that among the concomitant elements extractable with β -diketonates in chloroform, only Fe(III) and Cu(II) are electroactive under the polarographic conditions of uranium. The potential of the copper(II) reduction peak is sufficiently positive in comparison with uranium and hence does not cause any severe interference. However, the presence of iron(III) is undesirable (Fig. 4). In this event, extraction at pH 7 with 1M benzoylacetonate solution in the presence of 0.05M EDTA masks Fe(III) and prevents the interference of 1000-fold molar excesses of this ion. Thus the extraction of uranium(VI) remains totally unaffected. The presence of F^- ion in aqueous solution prevents the extraction of U(VI), therefore decomposition of uranium minerals in the presence of hydrofluoric acid is undesirable (Fig. 5).

Application to the analysis of uranium minerals

Several sensitive electrochemical methods have been developed for the determination of U(VI), including polarography preceded by

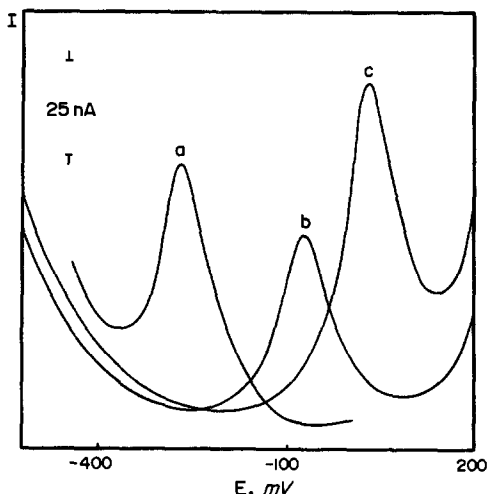


Fig. 4. Alternating current (ac) polarograms of metal benzoylacetonate (a), U(VI), (b), Fe(III), (c), Cu(II) in the presence of 0.75M PP/0.25M P as supporting electrolyte $t = 1$ sec, $f = 75$ Hz, $V = 10$ mV.

liquid-liquid extraction,^{7,10,16} voltammetry after preconcentration on the surface of solid electrodes^{17,18} and cathodic stripping voltammetry preceded by adsorptive collection of surface active metal complexes on the hanging mercury drop electrode.¹⁹⁻²² But this method may not be suited to the determination of uranium in mineral ores.



Fig. 5. Polarograms of uranium mineral extracts, in chloroform in the presence of 0.75M PP/0.25M P as supporting electrolyte (1) decomposed with HNO₃, (2) decomposed with HNO₃ + HF $V = 10$ mV $f = 75$ Hz $t = 1$ sec.

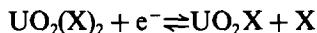
The proposed ac polarographic method in this work was checked by analysing the uranium sample (from Ssagand-Iran), containing a certified amount of uranium. The samples were decomposed by the following procedure.

Transfer a powdered sample into a 100-ml beaker, add about 15 ml of 12N hydrochloric acid and boil on a hot plate, then add 5 ml of 16N nitric acid, boil the solution almost to dryness. Take the residue with a solution (1.1) of nitric acid and boil for 15 min. Filter and wash with a 5% hot solution of nitric acid. Transfer the filtrate into a 100-ml standard flask and dilute to volume. Subject an aliquot of the sample solution (10 ml) to the polarographic determination of uranium as described above.

The results of replicate determinations (3890 ± 25.5 ppm) confirm that the uranium content of such samples is consistent. The proposed extraction polarographic method is applicable to the rapid determination of uranium in rocks, minerals and uranium concentrates with sufficient accuracy and precision.

CONCLUSION

On the basis of results obtained from dc and ac polarography and controlled potential coulometry, the reduction of acetylacetonate and benzoylacetonate of uranium(VI) in the presence of 0.75M PP/0.25M P can be shown to be:



where X is the β -diketonate ion.

The plot of $\log[(i_d - i)/i]$ vs. E for the dc polarograms, the half-peak width in the ac polarograms and ΔE_p values in cyclic voltammetry are three criteria which indicate that the reduction of uranium β -diketonate is a one-electron reversible process. The reversible reduction of U(VI) in chloroform, the linear relationship between i_p and the concentration of uranium in the original aqueous phase, provide the possibility of determination of uranium by extraction polarography of its β -diketonates in chloroform at the μg level. The proposed method for U(VI) determination is highly selective, without any interference from concomitant elements.

REFERENCES

1. B. K. Afghan and R. M. Dagnall, *Talanta*, 1966, 13, 1097.
2. *Idem, ibid.*, 1967, 14, 239.
3. B. K. Afghan, R. M. Dagnall and K. C. Thompson, *ibid.*, 1967, 14, 715.

4. R. M. Dagnall and S. K. Hasanuddin, *ibid.*, 1968, **15**, 1025.
5. P. Bosserman, D. T. Sawyer and A. L. Page, *Anal. Chem.*, 1978, **50**, 1300.
6. R. Pffibil, Jr. and J. Adam, *Talanta*, 1973, **20**, 1338.
7. T. Fujinaga and H. L. Lee, *ibid.*, 1977, **24**, 395.
8. S. M. Golabi and M. H. Pournaghi-Azar, *Proc. 6th Intern. Conf. Non-aqueous Solutions*, Canada, 1978, p. 97.
9. J. D. Wilson, R. K. Webster, G. W. C. Milner, G. A. Barnett and A. A. Smales, *Anal. Chim. Acta*, 1960, **23**, 505.
10. Y. Nagaosa and K. Kobayashi, *Talanta*, 1984, **31**, 593.
11. S. M. Golabi and M. H. Pournaghi-Azar, *Electrochim. Acta*, 1987, **32**, 425.
12. M. H. Pournaghi-Azar and S. M. Golabi, *J. Pharm. Belg.*, 1987, **42**, 315.
13. S. M. Golabi, M. H. Pournaghi and M. B. Shabani, *ibid.*, 1988, **43**, 19.
14. M. H. Pournaghi-Azar and S. M. Golabi, *Talanta*, 1988, **35**, 959.
15. A. K. De, S. M. Khopkar and R. A. Chalmers, *Solvent Extraction of Metals*, Van Nostrand, London, 1970.
16. G. W. C. Milner, J. D. Wilson, G. A. Barnett and A. A. Smales, *J. Electroanal. Chem.*, 1967, **2**, 25.
17. K.-H. Lubert, M. Schnurrbusch and A. Thomas, *Anal. Chim. Acta*, 1982, **144**, 123.
18. K. Izutsu, T. Nakamura and T. Ando, *ibid.*, 1983, **152**, 285.
19. N. K. Lam, R. Kalvoda and M. Kopanica, *ibid.*, 1983, **154**, 79.
20. C. M. G. van den Berg and Z. Q. Huang, *ibid.*, 1984, **164**, 209.
21. *Idem*, *Anal. Chem.*, 1984, **56**, 2383.
22. C. M. G. van den Berg and M. Nimmo, *ibid.*, 1987, **59**, 924.

AUTOMATIC KINETIC DETERMINATION OF Hg(II) BY ANODIC STRIPPING POTENTIOMETRY WITH CONSTANT CURRENT OXIDATION

A. CLADERA, J. M. ESTELA and V. CERDÁ

Department of Chemistry, Faculty of Sciences, University of the Balearic Islands,
E-07071 Palma de Mallorca, Spain

(Received 15 November 1990. Revised 12 April 1991. Accepted 13 May 1991)

Summary—A new kinetic method for the determination of Hg(II) is proposed. It is based on the kinetic evolution of the anodic stripping potentiometric curves yielded by a gold electrode previously coated with mercury upon passage of constant electrical currents. The method features a linear determination range between 40 and 800 ppb of Hg(II) and a relative standard deviation of 5% ($n = 9$) for a mercury concentration of 200 ppb. The experiments were conducted on a customized automatic set-up, and instrumentation, data acquisition and processing were all governed by means of a QBASIC program (PSAKINEL) written by the authors.

Anodic stripping potentiometry (ASP) was originally developed by Jagner,¹⁻³ who proposed its use for the determination of heavy metals such as Cd, Pb, Bi, Cu, Tl and Zn. This technique relies on recording anodic stripping potentiometric curves generated upon the deposition of metals on mercury-coated graphite electrodes caused by the presence of oxidants such as Hg(II) and oxygen¹⁻⁷ or the passage of a constant electric current.⁸⁻¹¹ Jagner¹² addressed the determination of mercury by using a variation of the original technique involving the deposition of the metal in the presence of copper and the joint stripping of the two metals with an oxidant such as potassium permanganate or dichromate. In both variants, the analytical signal typically obtained is a potentiometric $E-t$ curve where the potential changes rapidly in the absence of an oxidation process and remains constant and parallel to the time axis in its presence. The length of the plateau is proportional to the analyte concentration and is also related to the pre-electrolysis potential and time, the concentration and nature of the oxidant, the stirring rate, pH and background of the working electrode.

Anodic stripping potentiometry equals its voltammetric counterpart in sensitivity and even surpasses it in instrumental simplicity and scope as it can be applied to multideterminations. However, its low reproducibility and the time-consuming operations involved in its appli-

cation are two major weaknesses. The sluggishness of ASP determinations has so far been overcome by automating the process involved¹³ or by using powerful collection systems allowing data to be acquired at rates as high as 30 kHz,^{8-11,14} which in turn allow the analytical and blank signals to be discerned by using short pre-electrolysis times.

With the aim of improving the reproducibility of this technique—particularly in the automatic determination of several samples—without resorting to the electrode repolishing and regeneration we studied the optimal acidity, nature and concentration of various oxidants and types of electrodes. In the course of the study we found that the potentiometric oxidation curves yielded upon oxidation of mercury with the periodate/iodide system at a gold electrode deviated from the typical behaviour of ASP curves and resemble those normally obtained with kinetic methods (spectrophotometric, fluorimetric and thermometric). As we found no literature reference accounting for this phenomenon, we tackled its study in order to interpret this anomalous behaviour and develop a kinetic method for the determination of mercury by ASP.^{15,16} Since preliminary experiments showed that the use of chemical oxidants complicated the application of the method, we assayed the kinetic determination by ASP with an electric current for oxidation. The instrumentation required for this purpose and the results thus obtained are discussed below.

EXPERIMENTAL

Apparatus

All experiments were carried out on a fully automatic set-up designed and constructed by the authors. It consisted of the following elements: a PC-compatible system, a Metrabyte DASH-8 A/D converter board, a custom-made optocoupling system for triggering relays, a CRISON autoburette furnished with an RS-232C interface, a CRISON autosampler also furnished with an RS-232C interface, two custom-made potentiostats/galvanostats, and an electrode system composed of gold (working, $S = 0.2 \text{ cm}^2$), calomel (reference) and platinum wire (counter-electrode). The complete assembly is depicted in Fig. 1.

The instrumentation was governed by a computer system which controlled the operation of the automatic burette and the sampler via their respective RS-232C interfaces by using the manufacturer's communication protocol. The pre-electrolysis and electric oxidation steps were carried out by using a potentiostat and a galvanostat, respectively, which were switched via two relays actuated by the computer through the digital outlets of the DASH-8 board and the optocoupling system. Finally, experimental data were acquired through one of the analogical lines of the DASH-8 board (sampling rate = 10/sec) connected to the working and reference electrodes via an RC filter ($R = 500 \text{ kohm}$, $C = 1 \mu\text{F}$).

Reagents

The reagents used, all of which were pro-analysis grade, included a standard 1000 ppm Hg(II) solution prepared from $\text{Hg}(\text{NO}_3)_2$, H_2O and 4M and 2.5M sodium chloride and hydrochloric acids respectively.

Procedure

In a 50-ml standard flask were placed 5 ml of 4M sodium chloride and 2 ml of 2.5M hydrochloric acid; the solution was made to the mark with distilled water. The solution was then transferred to the autosampler and a blank signal was obtained by using a pre-electrolysis potential of -0.5 V and an oxidation current of $15 \mu\text{A}$. The Hg(II) was added and the pre-electrolysis repeated to obtain the analytical signal. The whole process was performed automatically via an automatic burette for adding the sample.

Software

The instrumentation, data acquisition and processing were controlled by means of a QBASIC program written specifically for this purpose by the authors; the original BASIC code was compiled and linked to the subroutines for handling of the DASH-8 board supplied by the manufacturer.

The program performed two distinct functions, namely:

Experimental control. The software allows a specific procedure to be applied to the same

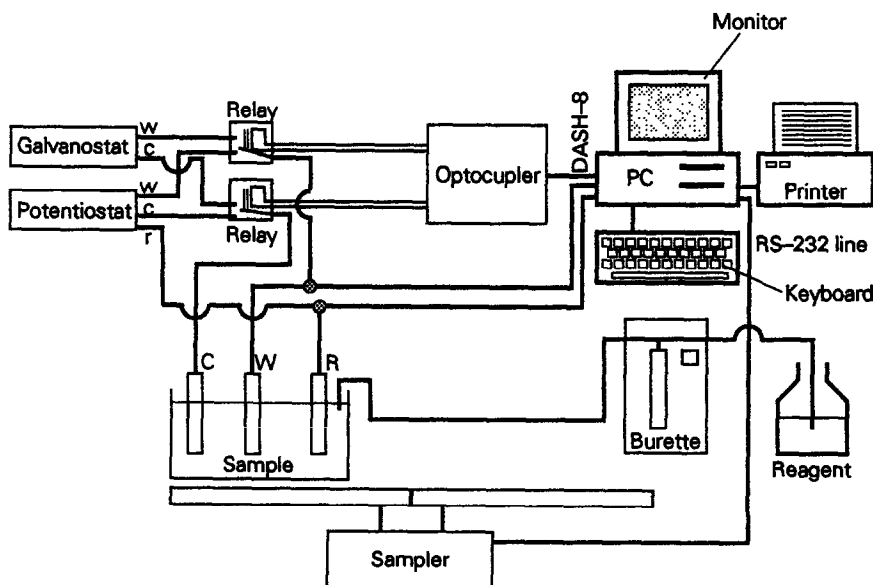


Fig. 1. Block diagram of the automatic set-up.

sample by having the automatic burette add preset volumes between measurements. The acquisition of experimental data is started by setting the autosampler to the required position and—if required—adding some reagent from the burette and switching the potentiostat on for a preset time (pre-electrolysis step). Next, the computer switches the potentiostat off and the galvanostat on and starts experimental data acquisition (potential of the working electrode as a function of time).

Additions from the autoburette can be effected from an external reservoir or even from one of the autosampler cups. In the latter case, the sample is aspirated and discarded through the same burette channel, the loop volume of which is somewhat larger than the injected volume. The aspirated sample volume is always slightly larger than that to be added to include a few milliliters for flushing to avoid sample carry-over.

Thus, by loading one half of the sampler with blanks and the other with samples, up to six samples can be analyzed completely automatically by using their respective blanks. Each experiment involves applying the above-described procedure to the blank, which is subsequently added to the sample to be assayed. The difference between the sample and blank response yields the analytical measurement sought. The acquired data can be processed at once or stored on disk for later treatment.

Data processing. The PSAKINEL program allows experimental data to be processed by the three typical procedures for kinetic data, namely the initial-rate (slope of the $E-t$ curve), fixed-time (potential reached at a prefixed time) and fixed-potential (time passed between the start of the stripping and a prefixed potential is reached).

Prior to the treatment proper, the experimental curves can be smoothed by the Sawitzki-Golay method,¹⁷ and their first and second derivative readily obtained.

The treatment can be effected manually or fully automatically. The manual processing option is included on the corresponding menu in order to establish the most suitable criteria for obtaining results or as an alternative to the automatic procedure when this yields spurious results for some reason.

Trials on the different treatments possible revealed that the fixed-potential option yielded the most satisfactory results as the initial-rate method involved the difficulty arising from the

drawing of the tangent to the $E-t$ curve at the most appropriate point, and the fixed-time method required finding a time suitable for quite a wide concentration range.

RESULTS

The influence of the different experimental variables on the system was investigated.

pH. Figure 2 shows the time results obtained at a fixed-potential by changing the hydrochloric acid concentration in the blank and a sample containing 800 ppb Hg(II). As can be seen, the H^+ hardly influences the signal over the pH range tested. We thus chose 0.1M hydrochloric acid for subsequent experiments.

Oxidation current. Figure 3 shows the variation of the signal with the oxidation current. As expected, the sensitivity decreased with increasing current. However, small currents resulted in the ill-defined, difficult-to-process curves shown in Fig. 4, which displays the potentiograms obtained at different oxidation currents for a sample containing 800 ppb Hg(II). A current of 15 μA was chosen for subsequent experiments.

Pre-electrolysis time. Figure 5 reflects the variation of the blank signal and that provided by a sample containing 800 ppb Hg(II) with the pre-electrolysis time. As can be seen, the sensitivity increased with the pre-electrolysis time up to 5 min, where the $E-t$ curve became a plateau and the blank and sample signals ran virtually parallel. Thus, we chose a pre-electrolysis time of 5 min as optimum to ensure maximum sensitivity while avoiding reaching the aforesaid plateau.

Effect of foreign ions. The effect of various ions on the shape of the kinetic curves was studied. When the Cu^{2+} ion is present in the sample, the kinetic effects disappear and potentiometric curves with two typical plateaus were

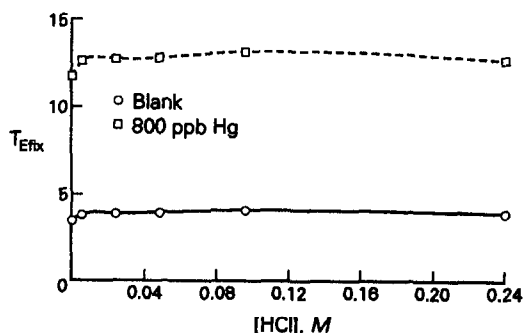


Fig. 2. Influence of HCl concentration on the signal (T_{Efx}). $[NaCl] = 0.4M$; $I = 15 \mu A$; 1 min pre-electrolysis at $-0.5 V$.

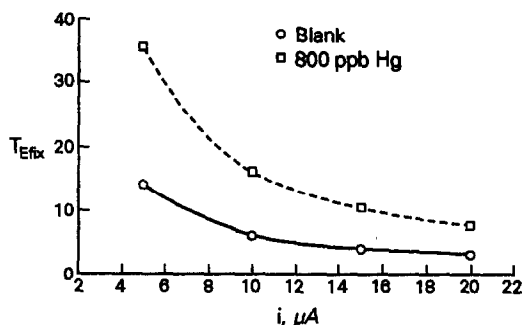


Fig. 3. Influence of the oxidation current on the signal (T_{Efix}). $[\text{HCl}] = 0.1\text{M}$; $[\text{NaCl}] = 0.4\text{M}$; $I = 15 \mu\text{A}$; 30 sec pre-electrolysis at -0.5V .

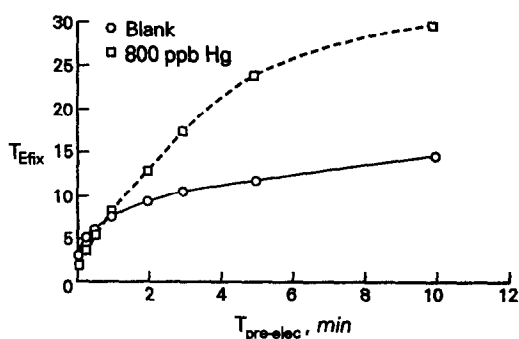


Fig. 5. Influence of the pre-electrolysis time on the signal (T_{Efix}). $[\text{HCl}] = 0.1\text{M}$; $[\text{NaCl}] = 0.4\text{M}$; $I = 15 \mu\text{A}$; pre-electrolysis voltage, -0.5V .

obtained. This effect can be avoided by performing the pre-electrolysis step at a greater potential where the Cu^{2+} is not reduced. This solution, however, causes an important diminution in the sensibility of the kinetic method. Another interfering ion is the As^{3+} which causes an important diminution in the slope of the kinetic curves. Other ions like the Sn^{2+} don't affect the kinetic curves obtained.

Analytical parameters. We studied the linearity and applicability range of the proposed method. For a given, fixed potential, the time and the slope of the linear portion of the potentiometric curve were found to vary linearly with the concentration and its logarithm, respectively. In the fixed-potential method, the measurement potential is chosen from the linear range of the kinetics curves of all of the standards (see Fig. 6) which is 300–400 mV. A potential of 400 mV was chosen. The most representative parameters of the curves obtained are summarized in Table 1.

The reproducibility of the method was checked on 9 individual samples containing 200 ppb by applying the above-described procedure. The relative standard deviation thus obtained

was 4.9 and 4.2% for the fixed-time and slope methods, respectively.

DISCUSSION

A careful study of the working conditions and influence of the different variables affecting the experimental system allowed us to interpret the overall process involved in the ASP of mercury as follows: in the electrolysis step, mercury is reduced on the gold surface, with which it amalgamates according to



Once the amount of deposited mercury is large enough, we may assume the formation of an additional layer of unamalgamated mercury.

When the amount of mercury present is quite large, the metal cannot fully penetrate the electrode surface, so, in the first few moments, the situation is equivalent to working with a pure mercury electrode which gives rise to the typical plateau of ASP curves during the stripping. Once the entire mercury surface has been depleted or if the deposited amount is small enough to penetrate the gold electrode, the redox process may be limited by the kinetics of

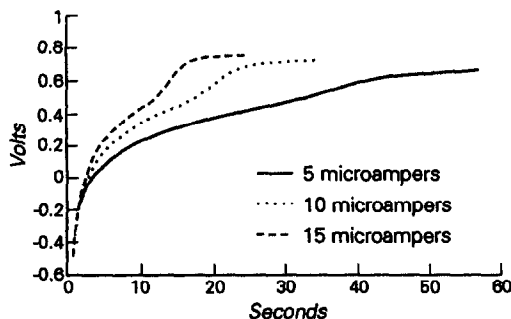


Fig. 4. Potentiograms obtained at different oxidation currents. $[\text{Hg}(\text{II})] = 800\text{ppb}$; $[\text{HCl}] = 0.1\text{M}$; $[\text{NaCl}] = 0.4\text{M}$; 30 sec pre-electrolysis at -0.5V .

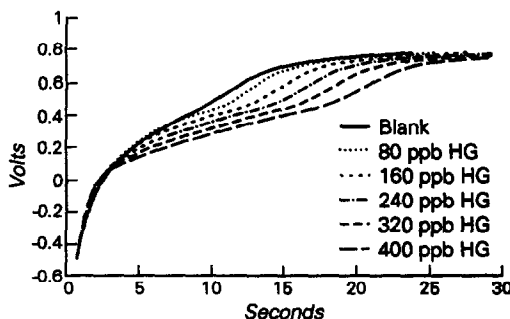


Fig. 6. Potentiograms obtained at different $\text{Hg}(\text{II})$ concentrations. $[\text{HCl}] = 0.1\text{M}$; $[\text{NaCl}] = 0.4\text{M}$; $I = 15 \mu\text{A}$; 5 min pre-electrolysis at -0.5V .

Table 1. Parameters of interest of the potentiometric curves

Method	Equation	<i>r</i>	Linear range, ppb
Slope	$T_{g\infty} = -0.0156 + 6.98 \times 10^3 \ln(\text{conc})$	0.993	80-400
Fixed-potential	$T_{\text{Eax}} = 0.116 + 0.0196 \text{ conc}$	0.998	80-400

transfer from the bulk of the electrode to the interface. This phenomenon, together with slower transfer kinetics than that of the chemical oxidation reaction, accounts for the attainment of kinetic curves after the typical plateau or even from the beginning of the stripping if the amount of deposited mercury is rather small. This interpretation is supported by the fact that the copperized graphite electrode only gives rise to the expected plateau, *i.e.*, that of copper, followed by that of mercury.¹⁶ As the copper has already been stripped before the mercury, the latter does not have to diffuse throughout the electrode and is only reoxidized in a step controlled by the chemical process and oxidant diffusion. On the other hand, experiments carried out with a gold thin film electrode¹⁶ gives curves with a smaller kinetic effect than that obtained with the gold electrode.

The shape of the kinetic curves, which show two distinct slopes, can be interpreted by first assuming the electrode potential to be determined by the Hg concentration at the electrode surface, which in turn depends on its rate of diffusion through the gold. Once all the mercury has been oxidized, the slope changes again and becomes steeper as it reaches the plateau yielded by the blank.

The kinetic curves obtained with the gold electrode disappear when important quantities of Cu²⁺ are present in the sample. This means that the deposition of Cu on the electrode surface reduces the diffusion of the Hg into the Au bulk.

From the results given it must, however, be concluded that the kinetic approach does not give very satisfactory results from an analytical point of view as compared to other stripping techniques.

Acknowledgements—The authors wish to express their gratitude to the DGIcyT (Spanish Council for Research in Science and Technology) for financial support granted through Project PA 86-0033.

REFERENCES

1. D. Jagner and A. Granéli, *Anal. Chim. Acta*, 1976, **83**, 19.
2. D. Jagner, *Anal. Chem.*, 1978, **50**, 1924.
3. *Idem*, *Analyst*, 1982, **107**, 539.
4. D. Jagner and K. Årén, *Anal. Chim. Acta*, 1979, **107**, 29.
5. D. Jagner, *Anal. Chem.*, 1979, **51**, 342.
6. D. Jagner and S. Westerlund, *Anal. Chim. Acta*, 1980, **117**, 159.
7. D. Jagner and K. Årén, *ibid.*, 1978, **100**, 375.
8. L. Renman, D. Jagner and R. Berglund, *ibid.*, 1986, **188**, 137.
9. H. Huang, D. Jagner and L. Renman, *ibid.*, 1988, **207**, 17.
10. *Idem*, *ibid.*, 1988, **207**, 37.
11. *Idem*, *ibid.*, 1988, **207**, 27.
12. D. Jagner, *ibid.*, 1979, **105**, 33.
13. T. Anfält and M. Strandberg, *ibid.*, 1978, **103**, 379.
14. A. Granéli, D. Jagner and M. Josefson, *Anal. Chem.*, 1980, **52**, 2220.
15. A. Cladera, J. M. Estela and V. Cerdá, *3rd Inter. Symp. Kin. Anal. Chem., Cavtat (Yugoslavia)*, September 1989.
16. A. Cladera, J. M. Estela and V. Cerdá, *J. Electroanal. Chem.*, 1990, **288**, 99.
17. A. Savitzky and M. J. E. Golay, *Anal. Chem.*, 1964, **36**, 1627.

ADSORPTIVE VOLTAMMETRIC DETERMINATION OF COPPER WITH A BENZOIN OXIME GRAPHITE PASTE ELECTRODE

GUORONG ZHANG and CHONGGANG FU

Department of Chemistry, Liaocheng Teachers' College, Shandong, People's Republic of China

(Received 2 January 1991. Revised 12 April 1991. Accepted 23 April 1991)

Summary—A method for the determination of trace amounts of copper with a chemically modified carbon press-formed electrode is described. Copper could be accumulated at the electrode by complexing with benzoïn oxime in ammonia buffer, then reduced at a constant potential of -0.4 V (*vs.* SCE) in nitric acid solution. Finally, a well-defined stripping peak could be obtained by scanning the potential in a positive direction. The response depends on the concentration of copper and accumulation time. For an accumulation time of 5 min the detection limit is about 1 ng/ml and the linear range is from 2 ng/ml to 4000 ng/ml, with a relative standard deviation of 5%. Many common metal ions have little or no effect on the determination of copper. The recommended procedure was applied to the determination of trace amounts of copper in natural water, and the results are in agreement with those of atomic-absorption spectrometry.

In electroanalysis the most sensitive and commonly used approach for trace metal analysis is undoubtedly stripping voltammetry. However, because of problems ranging from inordinately negative reduction potentials and slow electron transfer kinetics to the formation of intermetallic compounds upon electrodeposition, widespread utilization of this approach for practical solution analysis problems has been limited. Recently, a number of investigators have described a new variation of this approach in which analyte preconcentration is carried out at chemically modified electrodes (CMEs) possessing surfaces specifically designed for the ability to react with and bind the target solute.¹⁻¹² In this approach, the CMEs preconcentrate via a non-electrochemical mechanism and overcome disadvantages arising from electrochemical preconcentration. Further, preconcentration can be extended to analytes that cannot be reductively deposited directly or that require excessively negative deposition potentials. Also, the selectivity of the chemical step involved in the preconcentration can be used to increase overall selectivity of the analysis.

In our work, we describe the construction and behaviour of a chemically modified carbon press-formed electrode (CMCPFE) system appropriate for the chemical preconcentration and voltammetric quantitation of copper. Here, the electrode was prepared by pressing a mixture of benzoïn oxime (BO), graphite powder

and liquid paraffin into a glass tube (4 mm i.d.). Such CMCPFEs are simple to prepare and permit convenient variation of the modifier surface coverage, and they have small resistance and long lifetime. Also, a fresh modifier surface can be easily regenerated in a rapid and reproducible fashion. The principal characteristic required for the success of the modification approach is that the solubility of the modifier must be sufficiently slight in the solvents employed so that it remains stably incorporated in the carbon paste mixture. The reason for choosing BO as a modifier was because BO and its complexes all possess very limited solubility in the aqueous solvents commonly used in connection with carbon paste electrodes.^{13,14}

EXPERIMENTAL

Apparatus

An MP-1 stripping analyzer was used for voltammetric measurements (Shandong Electronic 7th Factory, Jining). A magnetic stirrer (Taixian Electronic Factory) was used in the accumulation step. The three-electrode system used was a CMCPFE working electrode, a platinum wire auxiliary electrode and a SCE (with a 0.1M nitric acid bridge). All potentials were referred to the SCE. A model PHS-3c pH meter (Shanghai Second Analyzer Factory) was used for measurement of pH. A Hitachi model 180-80 polarized Zeeman atomic-absorption

spectrometer equipped with pyrolytically coated graphite tubes was used for atomic absorption measurements.

Reagents and chemicals

A copper stock solution (1 g/l.) was prepared by dissolving pure copper (99.999%, Germany) in nitric acid, and working solutions were prepared by diluting the stock solution. Graphite powder (Shanghai Graphite Factory) was spectroscopic grade. Benzoin oxime (Beijing Chemical Reagent Institute) and all other reagents were analytical-reagent grade. Triply distilled water was used in all experiments.

Preparation of the CMCPFE

Take 0.8 g of pure graphite powder and 0.2 g of BO in a mortar with a pestle, grind and mix well, add 0.16 ml of liquid paraffin and mix well again. The mixture is filled into the end of a glass tube (50 mm length, 6 mm o.d., 4 mm i.d.) and pressed with a steel bar (4 mm o.d.) under a pressure of 6.2 Mpa. Make the electrical connection with a nickel-chromium wire which is passed through a rubber plug. The electrode surface (0.13 cm²) was polished on transparent paper until the surface had a shiny appearance. The renewal of the electrode surface was achieved by pushing the rubber plug 0.5–1.0 mm, scraping off the mixture with a blade and then polishing the surface of the electrode.

Procedure

Chemical accumulation. The electrode was immersed in 20 ml of copper sample solution containing 0.16M ammonium chloride and 0.02M ammonia which was stirred with a magnetic stirrer (500 rpm) for a fixed period of time.

Electrochemical reduction. After accumulation, the electrode was removed from the solution and rinsed thoroughly with water, then dipped into 0.015M nitric acid and electrolysed at -0.4 V for a fixed time without stirring.

Anodic stripping. The electrode was scanned anodically from -0.4 to $+0.5$ V and the wave height was measured at about $+0.2$ V.

Following measurements, the electrode was cleaned at $+0.5$ V for 20 sec.

RESULTS AND DISCUSSION

Composition of the electrode

The effect of the amount of BO on accumulations of copper was investigated by altering the weight ratio of BO to graphite powder. The

height of the peak increased with increasing amounts of BO up to 15% and then remained constant. The resistance of the electrode increased when the amount of BO was increased. A ratio of BO to graphite powder of 1:4 was used for most of this work. The resistance of the electrode is in the range 2–10 ohms.

Behaviour of the CMCPFE

Figure 1 shows the cyclic voltamperograms in 0.015M nitric acid, showing stable and relatively low residual current over a wide potential range recorded at the CMCPFE. The anodic wave at about $+0.2$ V is the oxidation current of copper electrochemically reduced at the CMCPFE, following the chemical accumulation. The cyclic voltamperograms had no obvious cathodic wave, showing that the oxidation of copper is irreversible and means that the electrochemically deposition rate is much less than the stripping rate. The first scan (designated as 1) exhibits a large anodic peak, due to the oxidation of the

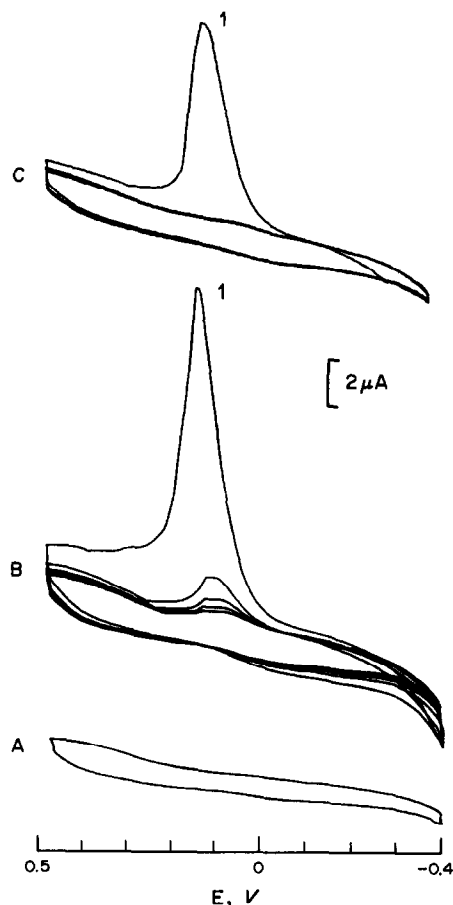


Fig. 1. Cyclic voltamperograms in 0.015M nitric acid: A—blank; B—500 ng/ml copper, T_a —120 sec, T_r —80 sec, without stirring; C—500 ng/ml copper, T_a —60 sec, T_r —80 sec, under stirring; scan rate -100 mv/sec.

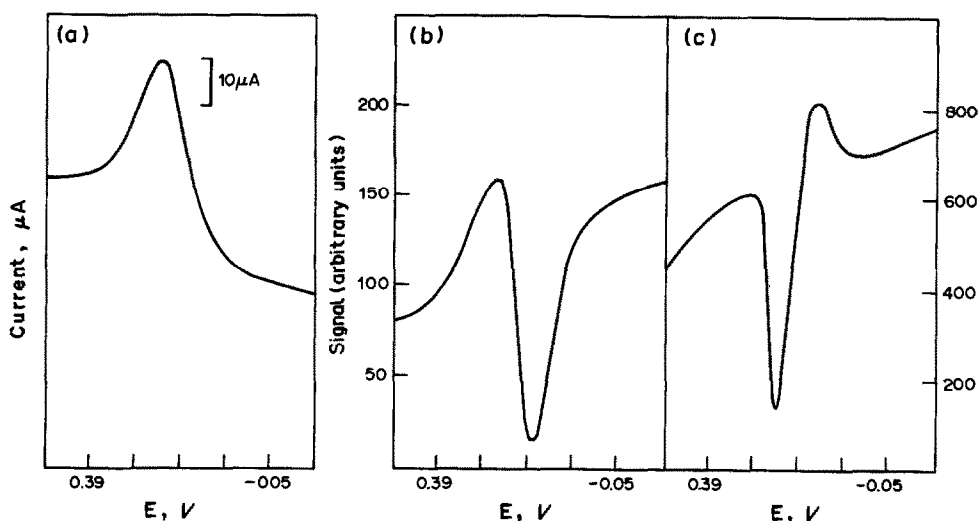


Fig. 2. Various linear sweep voltamperograms for ASV of copper. (a) Normal linear sweep voltamperogram; (b) First-order derivative voltamperogram; (c) Second-order derivative voltamperogram. Other conditions as in Fig. 1.

accumulated copper. The anodic peak decreases gradually on continued scanning without stirring, reflecting the gradual diffusion of the product from the surface of the CMCPFE (Fig. 1, B). If the scan is carried out with stirring, the anodic peak disappears on continued scanning (Fig. 1, C).

Various voltammetric measurements methods for the ASV of copper are illustrated in Fig. 2. The sensitivity is greatly improved by using second-order derivative voltammetry; a better discrimination against background is obtained and the sharper anodic stripping peak is easier to measure, so the sensitivity for the determination of copper was greatly increased. Hence, it is more suitable for practical analysis. Figure

3 gives the second-order derivative voltamperograms of 4–8 ng/ml copper.

Reduction time

The effect of the reduction time, T_r , on the peak height is illustrated in Fig. 4. It confirmed that the reduction of copper was easily accomplished, so that when the concentration of copper is less than 100 ng/ml, the T_r chosen is 30 sec; for 100–500 ng/ml it is 50 sec; 500–1000 ng/ml, 80 sec, 1000–4000 ng/ml, 100 sec.

Effect of pH

The effect of the pH on the peak height is illustrated in Fig. 5. The optimum pH range

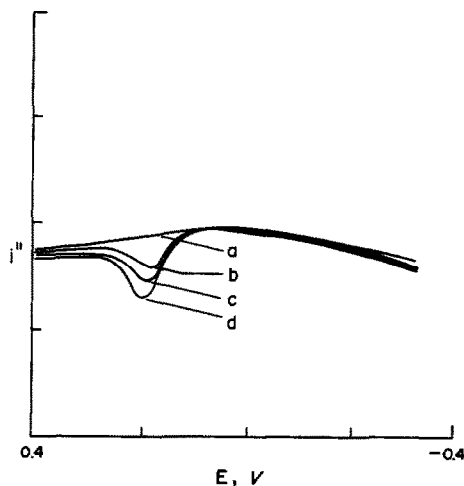


Fig. 3. The second-order derivative voltamperograms of copper in 0.015M nitric acid: (a) 0; (b) 4; (c) 6; (d) 8 ng/ml copper. T_a —5 min, T_r —30 sec, scan rate -332 mv/sec.

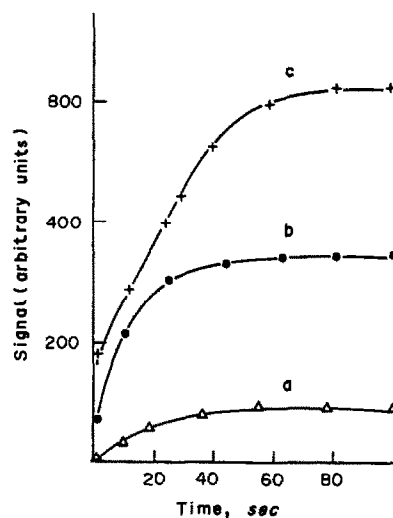


Fig. 4. The effect of T_r on the peak height. (a) 100; (b) 500 and (c) 1000 ng/ml copper. T_a —2 min, T_r —100 sec, other conditions as in Fig. 1.

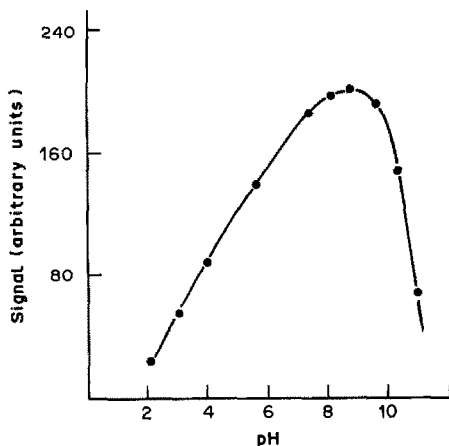


Fig. 5. The effect of pH on the peak height. 250 ng/ml copper T_a —4 min., other conditions as in Fig. 1.

is 7.0–10.0, so that 0.16M ammonium chloride–0.02M ammonia medium (pH 8.5) was selected for chemical accumulation.¹⁵

Working range

Under the selected conditions, the linear range of peak height *vs.* copper concentration is from 2 ng/ml to 4000 ng/ml for an accumulation time of 5 min, and the detection limit is 1 ng/ml with a relative standard deviation of 5% ($n = 10$). For a 10-min accumulation time, the detection limit can be lowered to 0.5 ng/ml.

Interference effects

Many common cations and anions were examined as possible interferents in the determination of 50 ng/ml copper by second-order derivative voltammetry. The results showed that 500-fold Al^{3+} , Fe^{3+} , Fe^{2+} , Pb^{2+} , Cd^{2+} , Zn^{2+} , Cr^{3+} , Sn^{2+} , In^{3+} , Ti^{4+} , Tl^+ , V^{5+} , 400-fold Co^{2+} , Ni^{2+} , Hg^{2+} , Bi^{3+} , Ag^+ , 100-fold Mn^{2+} , Mo(VI) , W(VI) , 40-fold Sb(III) , Se(IV) , and 500-fold PO_4^{3-} , SO_4^{2-} , NO_3^- , ClO_4^- , Ac^- , F^- , Br^- , Cl^- , 80-fold S^{2-} , I^- , CNS^- , do not interfere under the experimental conditions (less than 10% different). In the determination of copper by conventional ASV with an unmodified CPE, Bi(III) , Ag^+ and Sb(III) interfere seriously, because their ASV peaks overlap with that of copper. However, with the CMCPFE, Bi(III) , Ag^+ and Sb(III) show no interference.

Reproducibility

The analytical responses obtained after 30 sec chemical accumulation from 50 ng/ml copper in ammonia buffer were measured and compared for a series of different CMCPFE surfaces. Fresh electrode surfaces were generated simply by scraping off the old surface and polishing the newly exposed layer in the same manner as above. The reproducibility measured in this manner as the relative standard deviation of the peak height was typically in the 10% range (for 10 measurements). Alternatively, the same-initially conditioned-electrode surface, subjected after each preconcentration/reduction/oxidation to the cleaning procedure, was used for a series of consecutive determinations of copper employing the same deposition conditions. In this manner, the surface-to-surface variability occurring when the electrode surface was manually refreshed could be avoided, the resulting reproducibility, again computed as the relative standard deviation, of 10 consecutive measurements, was only 5%.

Life-time

The CMCPFE must be kept from sunlight when not in use. The first CMCPFE prepared has not exhibited significant changes in performance over half a year.

Practical application

The proposed method has been used for the determination of trace amounts of copper in natural waters. Any sample treatment is not necessary. The results agreed well with those obtained by atomic-absorption spectrometry, as shown in Table 1.

REFERENCES

1. R. W. Murray, A. G. Ewing and R. A. Durst, *Anal. Chem.*, 1987, **59**, 379A.
2. R. W. Murray, in A. J. Bard (ed.), *Electroanal. Chem.*, Vol. 13, pp. 191–368. Dekker New York, 1984.
3. S. Tanaka and H. Yoshida, *Talanta*, 1989, **36**, 1044.
4. S. Dong, *Fenxi Huaxue*, 1988, **16**, 951.
5. M. Trojanowicz and W. Matuszewski, *Talanta*, 1989, **36**, 680.

Table 1. Determination of copper in sample ($n = 5$)

Sample	Proposed method		Graphite furnace AAS	
	Mean, ng/ml	RSD, %	Mean, ng/ml	RSD, %
Lake water	12.8	3.9	13.5	5.2
River water	15.5	3.2	15.9	5.0
Tap water	9.7	4.1	11.3	7.1

6. O. Chastel, J. M., Kauffmann and G. J. Patriarcho, *ibid.*, 1990, **37**, 213.
7. P. Li, Z. Gao, Y. Xu, G. Wang and Z. Zhao, *Anal. Chim. Acta*, 1990, **229**, 213.
8. R. P. Baldwin, J. K. Christensen and L. Kryger, *Anal. Chem.*, 1986, **58**, 1790.
9. A. R. Guadalupe and H. D. Abruna, *ibid.*, 1985, **57**, 142.
10. S. V. Prabhu, R. P. Baldwin and L. Kryger, *ibid.*, 1987, **59**, 1074.
11. J. Wang, B. Greene and C. Morgan, *Anal. Chim. Acta.*, 1984, **158**, 15.
12. L. Hernandez, P. Hernandez, M. H. Blanco and M. Sanchez, *Analyst*, 1988, **113**, 41.
13. Z. L. Li and X. F. Huang, *Hunan Science and Technology Publishing House*, Changsha, 1986.
14. Z. Holzbecher, L. Divis, L. Sucha and F. Vlacil, *Handbook of Organic Reagents in Inorganic Analysis*, Ellis Horwood, 1976.
15. Hangzhou University, *Handbook of Analytical Chemistry* (No. 2), Beijing 1982, 24.

5-[(*p*-METHYL-PHENYL)AZO]-8-AMINOQUINOLINE AS A NEW REAGENT FOR TRACE DETERMINATION OF NICKEL BY ADSORPTIVE CATHODIC STRIPPING VOLTAMMETRY

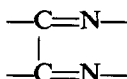
ZHENG-QI ZHANG, ZHAO-PENG CHENG, SHENG-ZONG CHENG and GUI-FA YANG

Department of Chemistry and Chemical Engineering, Hunan University,
Changsha, People's Republic of China

(Received 15 January 1991. Revised 11 March 1991. Accepted 29 March 1991)

Summary—The synthesis of *p*-MPAQ and the electroanalytical chemical properties of the nickel(II)-*p*-MPAQ complex are reported in this paper. A sensitive adsorptive cathodic stripping procedure for trace nickel determination was developed. For a 3-min preconcentration time the detection limit is $3.0 \times 10^{-11}M$.

Adsorptive stripping voltammetry is widely recognised as one of the most sensitive methods in electroanalytical chemistry.¹⁻⁷ It has been shown that adsorption of metal chelates can be used as a preconcentration step to improve the detection limit of the electroanalytical determination. The surface concentration of a metal complex at a mercury electrode is related to the structure of the ligand. The synthesis of new organic chelating agents is one of the available approaches for increasing the sensitivity of adsorptive stripping voltammetry.⁸ Dimethylglyoxime (DMG) has been used as a complexing agent for the voltammetric determination of cobalt and nickel with a detection limit of $5.0 \times 10^{-11}M$.^{2,9,10} Dimethylglyoxime has the functional group



The ligands suitable for adsorptive stripping voltammetry are characterized by the presence of aromatic rings.¹ 8-Aminoquinoline and its derivatives possess not only the above-mentioned functional group but aromatic rings as well. Recently we have synthesized a series of azo compounds derived from 8-aminoquinoline, including 5-[(*p*-methylphenyl)azo]-8-aminoquinoline (*p*-MPAQ), 5-[(*p*-acetylphenyl)azo]-8-aminoquinoline (*p*-APAQ), 5-[(*p*-nitrophenyl)azo]-8-aminoquinoline (*p*-NPAQ), 5-[(*m*-nitrophenyl)azo]-8-aminoquinoline (*m*-NPAQ) and 5-[(*o*-nitrophenyl)azo]-8-aminoquinoline (*o*-NPAQ). The reagent *p*-MPAQ has been used as

a spectrophotometric reagent for palladium and a fluorogenic reagent for iron.¹¹ It also possesses excellent electroanalytical characteristics. The adsorptivity of *p*-MPAQ is stronger than that of DMG because its π -orbital interaction is greater than DMG's. The experimental results show that the reduction potential of *p*-MPAQ (−0.55 V under optimum conditions) is more positive than that of the Ni(II)-*p*-MPAQ complex (−0.95 V) but the reduction potential of DMG (−1.63 V) is more negative than that of Ni(DMG)₂. Therefore, at the adsorption potential the excessive *p*-MPAQ doesn't compete with the Ni-*p*-MPAQ complex for the adsorption site on the electrode surface, but DMG does. Our previous works show that the greater the ratio of the coverage of the complex to the ligand, the lower the detection limit of the adsorptive-complex wave.¹² Obviously, using *p*-MPAQ as a ligand is advantageous as it lowers the detection limit of nickel. The present paper describes a very sensitive cathodic stripping procedure for the determination of nickel by adsorptive accumulation and reduction of its *p*-MPAQ complex at the hanging mercury drop electrode, the detection limit being 3.0×10^{-11} for an adsorption time of 3.0 min.

EXPERIMENTAL

Apparatus

The single-sweep polarograms were recorded on a JP-1A polarograph. The polarographic cell has the three electrode system: a dropping

mercury electrode (DME), a working electrode, a silver/silver chloride (saturated potassium chloride) reference electrode and a platinum wire auxiliary electrode. An XJP-821 neopolarograph in connection with an LZ3-100 X-Y recorder and a JM-01 (manual micrometric screw delivery) hanging mercury drop electrode (HMDE) were used for linear scan voltammetry and cyclic voltammetry measurements. The solution was stirred with a Model GSP-84-01 stirrer.

Reagents

Standard nickel solution. A stock solution of nickel (II) was prepared by dissolving 0.291 g of nickel nitrate $\text{Ni}(\text{NO}_3)_2 \cdot 6\text{H}_2\text{O}$ in 50 ml of 0.1M hydrochloric acid and diluting to 1 litre. The solution was standardized volumetrically with EDTA. Prepare solutions of lower concentration by serial dilution.

***p*-MPAQ ethanolic solution, 10^{-3}M .** Dissolve 0.262 g of *p*-MPAQ in 1 litre of absolute ethanol.

Synthesis of *p*-MPAQ. Dissolve 1.2 g of *p*-methyl-aniline (0.01 mole) in 20 ml of 5M hydrochloric acid solution and cool to below 5°C in ice. While stirring, add dropwise 20 ml of ice-cold water containing 4.0 g of sodium nitrite. The mixture is stirred for a further 30 min and the diazonium salt is poured in a thin stream, with constant stirring, into 10 ml of cold *N,N*-dimethylformamide containing 1.4 g of 8-aminoquinoline. After standing aside for 1 hr the resulting mixture is neutralized by adding dilute alkaline solution and allowing to stand for 24 hr. The separated crystals are recrystallized from 1:1 ethanol solution and dried at room temperature under vacuum. The product is a red solid yield of about 70%. The purity of the product was examined by thin-layer chromatography with ethanol-benzene (1:3). It was considered pure if the chromatogram showed only a yellow spot at $R_f = 0.74$. Analysis: $\text{C}_{16}\text{H}_{14}\text{N}_4$ requires 73.26% C, 5.38% H, 21.36% N; found, 72.93% C, 5.58% H, 20.73% N. The principal infrared bands were at 3420, 3302, 3030, 1332, 1280, 1430 and 1385 cm^{-1} .

Other reagents were of suprapure or analytical-reagent grade. Water, redistilled in a fused-silica apparatus, was used throughout.

Procedure

Adsorptive cathodic stripping voltammetry of pure nickel solution. Mix 0.10 ml of $1.0 \times 10^{-3}\text{M}$

p-MPAQ solution, 2.0 ml of buffer solution (pH 6.8) and a varied amount of nickel standard solution. Dilute to 10 ml with redistilled water. After standing for 15 min for complete complex formation the solution was transferred to the voltammetric cell, and purged with oxygen-free nitrogen for 10 min. A flow of nitrogen was maintained over the cell throughout the analysis to prevent interference from oxygen. The adsorption potential (usually -0.70 V) was applied to a fresh mercury drop while the solution was stirred. Following the adsorption step, the stirring was stopped, and after 30 sec the voltamperogram was recorded by applying a linear scan terminating at -1.2 V . The stripping voltammetric peak of the complex of nickel with *p*-MPAQ appears at about $-0.95\text{ V vs. Ag-AgCl-KCl(satd)}$.

Analysis of samples. Blood serum was prepared by centrifuging blood samples three times followed by digestion in perchloric acid at 200° with a digester until the sample was colourless. Market milk was digested with $\text{HNO}_3\text{-HClO}_4\text{-H}_2\text{SO}_4$. Transfer a moderate amount of natural water, the digested blood serum or the treated milk sample into a 10-ml standard flask, and continue as above.

Recovery experiment. Add the amounts of nickel shown in Table 1 into a 50-ml beaker containing the samples and treat as described above.

RESULTS AND DISCUSSION

Adsorptive stripping voltammetry

The five synthesized azo compounds all give one or two polarographic reduction waves, the peak potentials shifting to negative direction with increasing pH value of test solution. In a neutral or weakly basic solution these reagents form with nickel(II) purple-red complexes which give a new polarographic reduction wave. Among them, the $\text{Ni(II)-}p\text{-MPAQ}$ complex [$\text{Ni}(p\text{-MPAQ})_2$] from continuous variation and molar ratio measurements, shows higher sensitivity. Figure 1 shows linear scan voltamperograms for $1.0 \times 10^{-8}\text{M}$ nickel(II), in the presence of $5.0 \times 10^{-6}\text{M}$ *p*-MPAQ after different preconcentration periods. The $\text{Ni(II)-}p\text{-MPAQ}$ complex yields a well-defined cathodic stripping peak at -0.95 V . Its peak height increases rapidly with increasing preconcentration time. A concentration of $3.0 \times 10^{-11}\text{M}$ can be detected if a preconcentration time of 180 sec is used; the detection

Table 1. Determination of nickel in some samples

Samples	Ni added, ng/ml	Ni found, ng/ml	Recovery,* %	Ni content,† ng/ml
Xiang River water	0	5.40		5.63
	5.00	10.1	94	
	1.00	6.50	110	
	0.80	6.10	88	
Blood serum	0	21.3		—
	20.0	41.0	99	
	15.0	36.8	103	
	5.00	25.8	90	
	0	11.7		11.0
Market milk	0	11.7		
	10.0	21.4	93	
	5.00	16.6	98	

*Mean of three parallel determinations.

†Determined by ICP-AES.

limit was taken as the concentration that gave a signal equal to three times the standard deviation of the blank signal, calculated from the calibration slopes. The reproducibility was evaluated by ten repetitive experiments on a $1.0 \times 10^{-8} M$ nickel(II) solution with a preconcentration time of 120 sec. The relative standard deviation was 2.3%.

Effect of pH and buffer concentration. The buffer concentration and pH are the important factors influencing the peak height and the stability of the complex. The pH doesn't affect the peak potential of the Ni(II)-*p*-MPAQ complex, but strongly affects its peak current. If the pH is less than 3, no wave appears. If the pH is 5.5–8.0, the peak current is the largest; after that, the wave height decreases gradually with an increase in pH and finally disappears. In our experiments pH is kept at 6.8, using ammonium acetate as buffer. The peak current increases

linearly with increasing buffer concentration from 0.01 to 0.05 *M* and decreases slightly when the buffer concentration exceeds 0.10 *M*. In this paper the ammonium acetate concentration is 0.08 *M*.

Effect of *p*-MPAQ concentration. The concentration of *p*-MPAQ affects both peak height and linear range. The peak currents increase rapidly with *p*-MPAQ concentration and maximum values are attained from 3.0×10^{-6} to $1.0 \times 10^{-5} M$ *p*-MPAQ. As *p*-MPAQ concentration is larger than $1.0 \times 10^{-5} M$, the peak currents decrease and the linear range becomes narrower. A $5.0 \times 10^{-6} M$ *p*-MPAQ concentration is suitable for the experiment.

Effect of the preconcentration potential. The dependence of the stripping peak current on the preconcentration potential was examined over the range from -0.1 to -0.8 V (Fig. 2, curve A). Potentials ranging from -0.1 to -0.6 V yielded similar peak heights. At potentials more negative than -0.6 V the peak height increased rapidly. The maximum peak current was

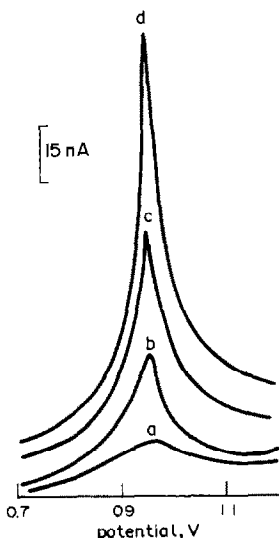


Fig. 1

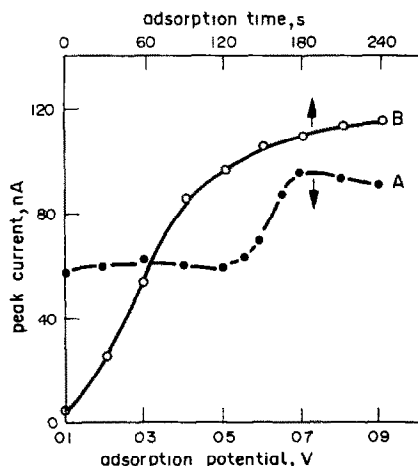


Fig. 2

obtained at -0.7 V, which was used in all subsequent work.

Effect of the preconcentration time. The accumulated amount on the surface depends on the length of time over which the adsorption is allowed to proceed. Figure 2 curve B shows the dependence of the adsorptive stripping peak current on the adsorption time for nickel present at the 0.60 ng/ml level. The peak current increases non-linearly with preconcentration time and then remains constant after 4 min. Obviously, a compromise between increase in sensitivity and speed is required in selecting the optimum preconcentration time. The preconcentration time was chosen to be 180 sec in all subsequent work.

Interferences

Interference by diverse ions was investigated by adding appropriate amounts of various ion solutions to 10 ml of solution containing 5.0 ng of nickel. Interference was taken as causing an error in excess of 10%. The amounts of some foreign ions which did not interfere are as follows: 4.0 mg of K^+ and Na^+ ; 10 μ g of Al^{3+} ; 5 μ g each of Ca^{2+} , Ba^{2+} and Mg^{2+} ; 0.5 μ g each of Be^{2+} , Mn^{2+} , Pb^{2+} and Bi^{3+} ; 0.3 μ g of Cr^{3+} and Fe^{3+} ; 0.1 μ g of Pd^{2+} ; 0.08 μ g each of Cd^{2+} , Cu^{2+} and Zn^{2+} ; 0.05 μ g of Co^{2+} ; 8.0×10^{-5} mmol of tartrate and citrate; 2.0×10^{-5} mmol of PO_4^{3-} , $C_2O_4^{2-}$ and EDTA. The reduction potential of the $Co(II)$ - p -MPAQ complex is -1.34 V, well removed from the nickel peak. But the cobalt competes with the nickel for the ligand, causing a negative interference above 0.05 μ g: -14 – 45% and -73% at 0.10, 0.50 and 5.0 μ g $Co(II)$, respectively.

Adsorptive characters of $Ni(II)$ - p -MPAQ complex

The adsorption of the complex of nickel(II) with p -MPAQ at the mercury drop electrode was demonstrated by constructing electrocapillary curves and by carrying out medium-exchange experiments.

The electrocapillary curve of a buffer solution containing p -MPAQ is lower than that of the pure buffer, and the electrocapillary curve of the solution containing the $Ni(II)$ - p -MPAQ complex was lower still than the p -MPAQ solution, indicating that p -MPAQ and its nickel(II) complex are both adsorbed at the mercury drop electrode.

For medium-exchange studies, the static mercury drop electrode (SMDE) used as a

working electrode, was kept in contact with a solution containing the $Ni(II)$ - p -MPAQ complex for 240 sec with stirring. Following this, the electrode was cleaned carefully and transferred into another cell containing the background solution only. The reduction process shown in the voltamperogram obtained in the new cell closely resembled those in the original cell.

Cyclic voltammetry

The redox and interfacial behaviour of chelate of nickel(III) with p -MPAQ can be evaluated by using cyclic voltammetry. Figure 3 shows cyclic voltamperograms for 1.0×10^{-8} nickel(II) in 5.0×10^{-6} M p -MPAQ solution in 0.08 M ammonium acetate (pH 6.8). Stirring the solution for 3 min at -0.35 V before starting the first scan (Fig. 3 curve 1), resulted in two distinct cathodic peaks due to the reduction of the adsorbed dye (at -0.55 V) and of the adsorbed chelate (at -0.95 V). The oxidation peak of the chelate was observed in the anodic branch. Subsequent repetitive scans yielded significantly smaller (but stable) cathodic peaks corresponding to the reduction of dissolved species. This behaviour indicates that the adsorption of dye and chelate at the mercury electrode is reactant adsorption.¹³ The difference in peak potentials between E_{p_2} and $E_{p_2'}$ is 30 mV, which shows that the number reacted electrons of the complex equals two.

Application

The proposed method has been applied to the determination of nickel in natural water, human blood and milk samples.

Calibration graphs. Treat the standard nickel(II) solutions used for preparation of the

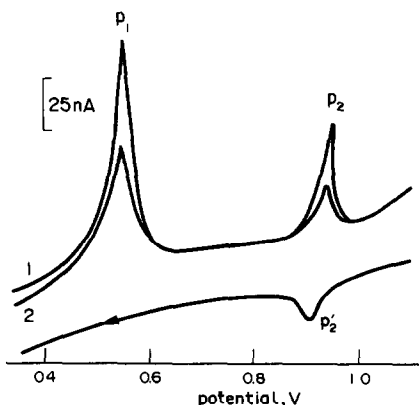


Fig. 3

calibration line in the procedure as described in the section of analysis of samples. The regression equation of the calibration line has the form:

$$Y = 5.13X - 0.008 \quad (1)$$

where Y is the stripping peak current in nA and X is the concentration of nickel(II) in ng ml. The correlation coefficient was 0.996. The results of the determination of nickel and recovery of added nickel by using the recommended method are summarized in Table 1.

REFERENCES

1. J. Arcos, J.-C. Viré, A. El Jammal, G. J. Patriarche and G. D. Christian, *Talanta*, 1990, **37**, 661.
2. C. M. G. van den Berg, *Analyst*, 1989, **114**, 1527.
3. H. Zhang, R. Wollast, J.-C. Viré and G. J. Patriarche, *Analyst*, 1989, **114**, 1597.
4. J. Wang, P. A. M. Farias and J. S. Mahmoud, *Anal. Chim. Acta*, 1985, **171**, 215.
5. H. Xu, Z. Zhang and Z. Liu, *Fenxi Huaxue*, 1989, **17**, 257.
6. J. Wang and J. M. Zadeii, *Talanta*, 1986, **33**, 321.
7. *Idem, ibid.*, 1987, **34**, 247.
8. Z.-Q. Zhang, *Mikrochim. Acta*, 1991, **I**, 89.
9. H. Zhang, J.-C. Viré, G. J. Patriarche and R. Wollast, *Anal. Lett.*, 1988, **21**, 1409.
10. B. Pihlar, P. Valenta and H. W. Nürnberg, *Z. Anal. Chem.*, 1981, **307**, 337.
11. G. Shi, *Application of the Azocompounds Derived from 8-Aminoquinoline in Analytical Chemistry*, Thesis, Hunan University, 1989.
12. Z.-Q. Zhang and R.-Q. Yu, *Science in China*, 1989, **32**, 278.
13. S. Dong, *Fenxi Yiqi*, 1984, No. 1, 1.

DETERMINATION OF GERMANIUM BY POTENTIOMETRIC STRIPPING ANALYSIS AND ADSORPTION POTENTIOMETRIC STRIPPING ANALYSIS

FENG DEXIONG, YANG PEIHUI and YANG ZHAOLIANG

Department of Chemistry, Jinan University, Guangzhou, People's Republic of China

(Received 24 July 1990. Revised 27 November 1990. Accepted 14 December 1990)

Summary—Potentiometric stripping analysis was applied to determination of germanium(IV) in 0.2M $\text{NH}_3\text{-NH}_4\text{Cl}$ (pH 8.4) buffer solution at -1.8 V (vs. Ag/AgCl), with dissolved oxygen or Hg(II) as oxidant. The sensitivity was 8.5×10^{-9} M in the presence of 2.0×10^{-5} M Hg(II) with plating for 15 min after deaeration for 20 min. Cyclic voltammetry revealed that Ge(IV) \rightarrow Ge at the surface of the mercury-film electrode in a one-step irreversible reduction reaction, and the Ge at the electrode was oxidized by dissolved oxygen in the solution. The presence of complexing agents such as Alizarin Red (ARS), which forms a Ge(IV) complex adsorbed at the electrode, improved the sensitivity by one order of magnitude. The presence of adsorption was revealed by the temperature coefficient, the electrocapillary curve and cyclic voltammetry. Ge-containing samples were analysed by the proposed methods and agreement with the results obtained by other methods was excellent.

In the last decade potentiometric stripping analysis (PSA)^{1,2} has become of increasing interest because of certain advantages it possesses (e.g., no interference by oxygen, less susceptibility to adsorption phenomena, and cheapness and simplicity of instrumentation).³ It has been recognized as an electroanalytical technique for the determination of trace amounts of heavy metals such as Cu, Pb, Zn, Cd, Bi, Tl, Ga and Hg. The high sensitivity and specificity and the possibility of simultaneous determinations inherent in stripping analysis are distinctive features that make it attractive in environmental, clinical, industrial and other fields of analytical chemistry. However, potentiometric stripping analysis of germanium has not yet been reported.

In an early study of the polarographic behaviour of germanium,⁴ it was observed that germanium(IV) could be reduced to elemental germanium in two steps in 6M hydrochloric acid. Sauvenier and Duyckaerts⁵ and Dhar⁶ found that germanium(IV) could be reduced to elemental germanium at the dropping mercury electrode in ammonia or boric acid buffer solution with a half-wave potential of -1.5 V. Recently, several electroanalytical techniques have been applied to the determination of germanium. Kalvoda⁷ observed that adsorptive accumulation of the germanium–Pyrocatechol

complex on a hanging mercury drop electrode produced increased sensitivity in differential pulse polarography. An analogous procedure using the germanium complex with pyrogallol has been described.⁸ Li *et al.*^{9,10} studied the polarographic adsorptive complex wave of the germanium–Alizarin Red (ARS) and germanium–Alizarin systems, which were applied to the determination of germanium(IV) down to 0.1 mg/l. Deng *et al.*¹¹ used a gold-film electrode for an anodic stripping voltammetric study of the reduction of Ge(IV). Two stripping peaks were reported, the first corresponding to the oxidation of Ge to Ge(II) and the second to the oxidation of Ge(II) to Ge(IV), detection limits of 5 $\mu\text{g/l}$. being observed when the first peak was used for quantification. No report of potentiometric stripping analysis for Ge(IV) at a mercury-film electrode has been found.

The aims of the present work are to offer another simple and sensitive method of analysis for germanium and to extend the application of potentiometric stripping analysis. The paper deals with the study of the potentiometric stripping behaviour of germanium and adsorption potentiometric stripping analysis (APSA) for germanium, in which an ARS complex is formed and adsorbed at the electrode to increase the sensitivity. Some generally applicable conditions for this method are discussed. The

Table 1. τ values in different media

Medium	τ , sec
0.2M Na ₂ CO ₃	N.S.
0.4M Na ₂ CO ₃ + 0.01M EDTA	N.S.
0.2M KH ₂ PO ₄ + Na ₂ HPO ₄ (pH 8)	N.S.
0.2M Citric acid + Na ₂ HPO ₄ (pH 8)	24.0
0.2M Borax + NaOH (pH 8)	12.5
0.2M NH ₃ + NH ₄ Cl (pH 8)	31.0
0.1M KCl	N.S.

N.S. = no signal.

method is applied to the analysis of samples from plants and mineral water.

EXPERIMENTAL

Apparatus

A Metrohm E-524 potentiostat was used for constant-potential electrolysis. The potentiometric stripping curve was recorded with an LZ 3-04 $x-y$ recorder (Shanghai), which was connected to a meter with high input-impedance (pH s-3, Shanghai). A model FA-1 cyclic voltammetry instrument (Changchun) was used. A rotating glassy-carbon disc electrode (ATA-1A, Jiangsu) with a mercury film was used as the working electrode (diameter 4 mm). A spiral Ag/AgCl electrode was used as the reference electrode, with a saturated potassium nitrate agar salt bridge. A platinum wire was used as the counter-electrode.

Reagents

All reagents were of general or analytical reagent grade and were prepared with doubly distilled water. A stock standard solution of $1.0 \times 10^{-2} M$ germanium(IV) was prepared by dissolving 0.0726 g of Ge powder (99.999% pure) in a beaker containing 1 g of sodium hydroxide and 10 ml of 30% hydrogen peroxide solution, then adding 15 ml of 1:1 v/v sulphuric acid to the beaker, heating gently to expel excess of hydrogen peroxide, cooling, and diluting accurately to 100 ml. Ammonia buffers of different pH were prepared from mixtures of 0.2M ammonia and 0.2M ammonium chloride.

Preparation of the working electrode

The working electrode must be coated with mercury before the start of the analysis. This was achieved by keeping the working electrode

rotating for 4 min at $-0.90 V$ vs. Ag/AgCl in 50 ml of 0.1M hydrochloric acid containing 25 mg/l. mercury(II). The rotation was stopped and at the same time the working and reference electrodes were connected to a recorder. A stripping curve was registered and a steady baseline established. After that, the working electrode was washed immediately with distilled water and stored in distilled water for later use.

Procedure

Measure 50 ml of germanium solution in 0.2M ammonia buffer (pH 8.4) into an electrolysis cell. In routine analysis, dissolved oxygen is preferred as the oxidant in order to save time. If it is necessary to enhance the sensitivity, add Hg(II) as oxidant to the solution and deaerate with purified nitrogen for 20 min. After that, let the stream of nitrogen pass over the surface of the solution to prevent oxygen from redissolving in the solution. Immerse a glassy-carbon electrode coated with a mercury film in the solution and connect the cell to an Ag/AgCl reference electrode. Electrolyse at $-1.8 V$ with the electrode rotating at 2000 rpm, then stop the rotation and at the same time connect the electrodes to a recorder to trace the potential-time curve.

RESULTS AND DISCUSSION

PSA for germanium(IV)

Selection of supporting electrolyte. Values for the stripping time, τ , in different media are shown in Table 1 and indicate that ammonia buffer is the optimum supporting electrolyte.

Effect of pH. The sample pH was adjusted to the optimum value (8.4), which gives the maximum signal, as shown in Fig. 1.

Plating potential E_p . Table 2 demonstrates that there was no signal at potentials more positive than $-1.55 V$, because Ge(IV) cannot then be reduced to Ge. The signal increased with more cathodic potentials in the range from -1.55 to $-1.80 V$ and stayed constant for $E_p < -1.80 V$. Therefore E_p was chosen to be $-1.80 V$.

Dependence of τ on concentration. The stripping signals increased linearly with the concentration of Ge(IV). Figure 2 illustrates the effect

Table 2. Dependence of τ on E_p for $2.0 \times 10^{-5} M$ Ge(IV), t_p 4 min, pH 8.4

$-E_p, V$	1.50	1.55	1.60	1.65	1.70	1.75	1.80	1.85	1.90	1.95
τ, sec	N.S.	8.2	24.0	35.0	63.8	82.0	105.0	101.0	104.0	100.0

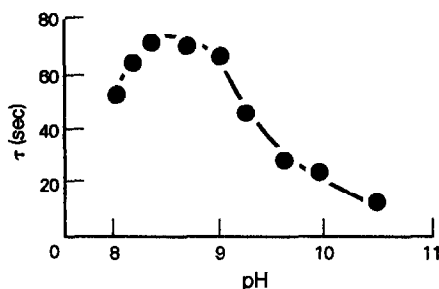


Fig. 1. Dependence of τ on pH: $10^{-4}M$ Ge(IV); $0.2M$ NH_3-NH_4Cl ; E_p -1.6 V; pre-electrolysis time 2 min; dissolved oxygen as oxidant.

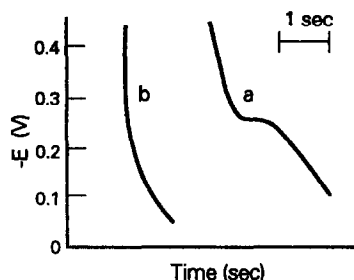


Fig. 3. Typical stripping curve for (a) $8.5 \times 10^{-9}M$ Ge(IV) and (b) the corresponding blank: t_p 15 min, $2 \times 10^{-5}M$ Hg(II), deaeration for 20 min.

of standard additions to a $1.0 \times 10^{-8}M$ Ge(IV) solution in $0.2M$ NH_3-NH_4Cl (pH 8.4).

The detection limit in PSA depends on the plating time, the oxidant concentration and, to some extent, the recording speed. Figure 3 gives a typical set of stripping curves for $8.5 \times 10^{-9}M$ Ge(IV) and $2.0 \times 10^{-5}M$ Hg(II), with plating for 15 min after deaeration with purified nitrogen for 20 min.

Interferences. The interfering action of 10-fold or 100-fold excesses of co-existing ions on the determination of $1.0 \times 10^{-6}M$ Ge(IV) was investigated. Decreases in the Ge(IV) signal were caused by Sn(IV), Fe(III) and Mn(II) and increases by Co(II) and Cu(II) when these ions were present in 10-fold molar ratio to Ge(IV). No interference was observed from Tl(III), Bi(III), Zn(II), Pb(II), Cd(II), Se(IV), even in 100-fold molar ratio to Ge(IV).

The interferences may be classified into three categories.

(i) An increase in the analytical signal is caused by overlapping of the stripping signals owing to similarity of the stripping potentials of the interferent ion and Ge(IV). An example is

the interference by copper, which can be eliminated by employing plating potentials of -0.90 and -1.80 V and obtaining the difference in stripping time ($\Delta\tau$).

(ii) A decrease in the analytical signal is caused by simultaneous oxidation of the deposited Ge(Hg) by the interferent ion, e.g., by Sn(IV) and Fe(III).

(iii) An increase or decrease in the analytical signal may be caused by formation of an intermetallic compound or by chemical interaction between the interferent and germanium. Co(II) and Mn(II) do not fit into class (i) or (ii) and are probably to be included in this class.

Studies on the electrode processes

Cyclic voltamperograms of the supporting electrolyte and the Ge(IV)-containing solution at the mercury-film electrode are shown in Fig. 4. There is a cathodic peak at -1.45 V during the negative potential scan and no peak during the positive scan. The cathodic peak height decreases with continued scanning. If the circuit is broken and the electrode allowed to rotate for a few seconds, and the circuit is then

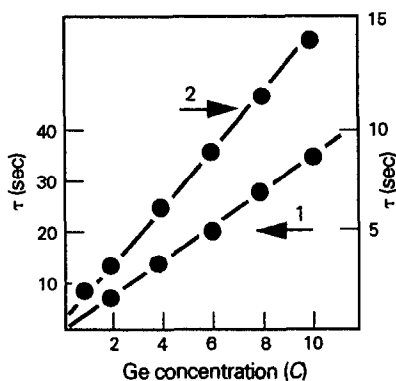


Fig. 2. The relationship between τ and concentration (C): 1, $C = (2-10) \times 10^{-7}M$, t_p 4 min; 2, $C = (1-10) \times 10^{-8}M$, t_p 8 min; $2 \times 10^{-5}M$ Hg(II), deaeration for 20 min.

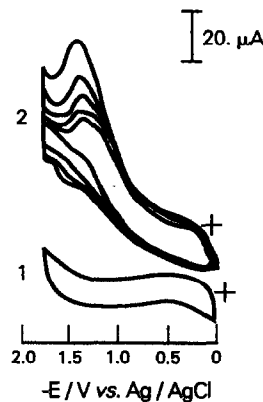


Fig. 4. Cyclic voltamperograms: (1) without and (2) with $10^{-4}M$ Ge(IV) in $0.2M$ NH_3-NH_4Cl buffer at pH 8.4; sweep rate 200 mV/sec.

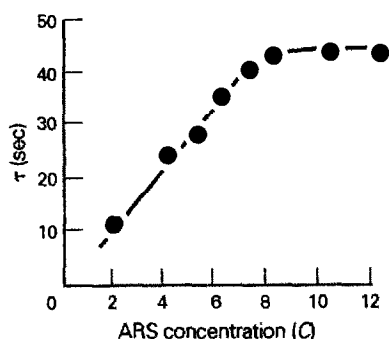


Fig. 5. The effect of ARS concentration (C) on τ : $C = (2-12) \times 10^{-5}M$; $2 \times 10^{-6}M$ Ge(IV); $0.2M$ NH_3-NH_4Cl (pH 8.8); $E_p = -1.6$ V; $t_p = 2$ min; $3 \times 10^{-5}M$ Hg(II).

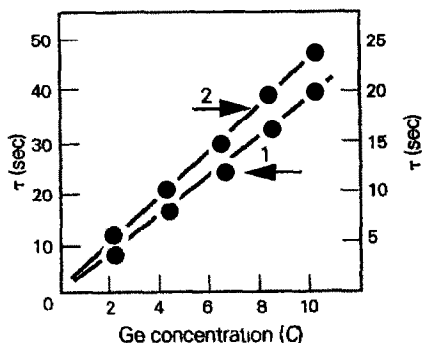


Fig. 7. Relationship between τ and concentration (C): (1) $C = (2-10) \times 10^{-7}M$, $t_p = 3$ min; (2) $C = (2-10) \times 10^{-9}M$, $t_p = 8$ min; $3 \times 10^{-5}M$ Hg(II); deaeration for 20 min.

closed and the scan repeated, the peak height increases to its previous value. The same phenomenon occurs after deaeration of the solution, but finally the peak disappears. It can be deduced that $Ge(IV) \rightarrow Ge$ is an irreversible one-step reaction and dissolved oxygen in the solution can oxidize Ge at the surface of the electrode. This is why oxygen dissolved in the solution can be used as the oxidant in PSA for Ge(IV).

APSA for germanium(IV)

A complex may be formed and adsorbed at the electrode when the germanium solution contains a complexing agent such as ARS. The stripping signal increases significantly and the sensitivity for Ge(IV) can be enhanced. Optimization of the experimental conditions and the characteristics of the adsorption are discussed below.

pH and concentration of ARS. The stripping time in ammonia buffer media of different pH was measured and was shown to be constant in

the pH range 8.4–9.1. Therefore the pH value was chosen to be 8.8.

Figure 5 gives the dependence of τ on the concentration of ARS; τ reaches a constant value when $C_{ARS} > 8.0 \times 10^{-5}M$, which is, therefore, the concentration of ARS necessary to saturate the electrode surface.

Effect of plating potential. The $\tau-E_p$ curve takes on a peak shape in the potential range from -1.35 to -1.60 V. As shown in Fig. 6, τ is maximal when E_p is -1.5 V under the experimental conditions and this indicates an adsorption effect which will be verified later. From comparison of Fig. 6 with Table 2, we can see that the Ge-ARS complex adsorbed at the electrode is reduced at a more positive potential (-1.5 V) than germanium itself (-1.8 V). It is probable that ARS adsorbed at the electrode catalyses the reduction of germanium.

Effect of electrode speed. Rotation at 570 rpm during pre-concentration and stripping gives a satisfactory signal without sacrifice of sensitivity.

Relationship between τ and concentration. A linear relationship between τ and concentration, C , was obtained (Fig. 7) and extended down to $10^{-9}M$. A typical stripping curve for $8.0 \times 10^{-10}M$ Ge(IV) is shown in Fig. 8.

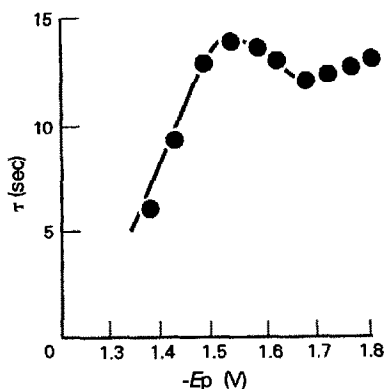


Fig. 6. The effect of plating potential on τ : $5 \times 10^{-7}M$ Ge(IV); $10^{-4}M$ ARS; $3 \times 10^{-5}M$ Hg(II); $t_p = 3$ min.

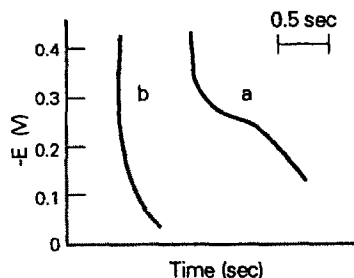


Fig. 8. Stripping curves for (a) $8 \times 10^{-10}M$ Ge(IV) and (b) blank; $t_p = 12$ min; $3 \times 10^{-5}M$ Hg(II); deaeration for 20 min.

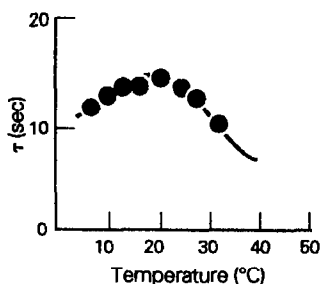


Fig. 9. Effect of temperature on stripping time: $2 \times 10^{-6}M$ Ge(IV); $0.2M$ NH_3-NH_4Cl (pH 8.8), $3 \times 10^{-5}M$ Hg(II); t_p 1 min.

Verification of adsorption characteristics

Effect of temperature. The τ -temperature curve (Fig. 9) is characteristic of a general adsorption wave. At temperatures $<18^\circ$ the adsorptive capacity is controlled by adsorption kinetics. The adsorption rate increases with temperature and the temperature coefficient is positive. At $18-25^\circ$ the adsorptive capacity is controlled by the equilibrium between adsorption and desorption. At temperatures $>25^\circ$, the equilibrium shifts toward desorption and the adsorptive capacity decreases. The temperature coefficient then becomes negative.

Electrocapillary curves. The change in the electrocapillary curves (Fig. 10) shows that ARS and the Ge-ARS complex are adsorbed in the potential range from -0.2 to -1.5 V.

Cyclic voltammetry. Cyclic voltamperograms of ARS, Ge(IV) and ARS + Ge(IV) at a mercury-film electrode are shown in Fig. 11. Figure 11(a) shows a pair of redox peaks, in which the potential is -0.62 V for the reduction

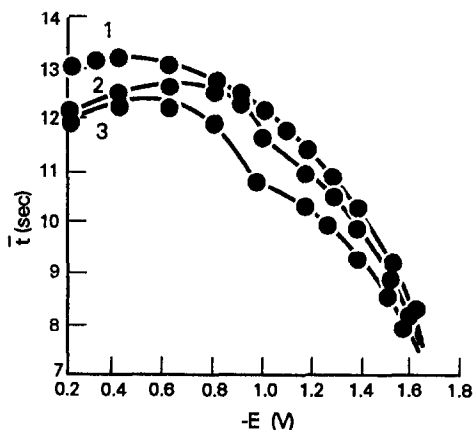


Fig. 10. Electrocapillary curves in $0.2M$ NH_3-NH_4Cl (pH 8.8); (1) blank; (2) with $3 \times 10^{-4}M$ ARS; (3) with $10^{-4}M$ Ge(IV) and $3 \times 10^{-4}M$ ARS; \bar{t} mean time for 20 drops of mercury.

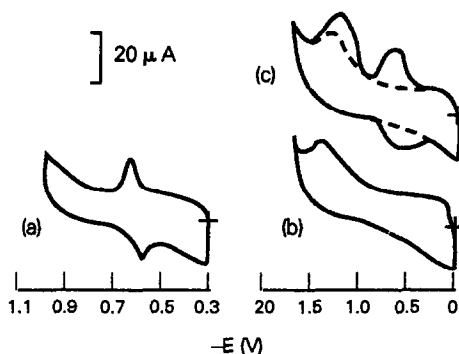


Fig. 11. Cyclic voltamperograms in $0.2M$ NH_3-NH_4Cl (pH 8.8) at 100 mV/sec: (a) $10^{-4}M$ ARS, (b) $5 \times 10^{-5}M$ Ge(IV), and (c) — $5 \times 10^{-5}M$ Ge(IV) + $2 \times 10^{-4}M$ ARS; --- $5 \times 10^{-5}M$ Ge(IV).

peak and -0.56 V for oxidation. The plot of the peak height, h , vs. the square root of scan rate, \sqrt{v} , as in Fig. 12, shows some deviation from the linear relationship predicted by the Randles-Ševčík equation. This behaviour is characteristic of adsorption at the electrode, the product being adsorbed more weakly than the reactant. An irreversible reduction peak for Ge(IV) appears at -1.43 V [Fig. 11(b)], which is shifted to -1.18 V in the presence of ARS (Fig. 11(c)), with an increase in reduction current. This is consistent with the discussion of the dependence of τ on E_p shown in Fig. 6. It is deduced that a Ge-ARS complex is formed and adsorbed at the mercury-film electrode. Figure 11(c) presents a pair of redox peaks with similar peak potentials to those in Fig. 11(a), but with broader shapes. This is probably caused by overlap with the adsorption wave of the complex. Furthermore, the deviation from linearity of the $h-\sqrt{v}$ curve is more serious for the Ge-ARS complex (Fig. 13) than for ARS itself (Fig. 12), indicating that the complex is more strongly adsorbed than ARS. These results agree with those for the electrocapillarity.

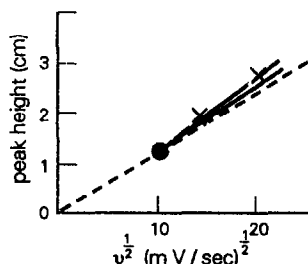


Fig. 12. Effect of scan rate on peak height for $10^{-4}M$ ARS: (●) reduction peak, (×) oxidation peak.

Table 3. Determination of germanium in samples

Sample	Germanium content*, $\mu\text{g/g}$ or $\mu\text{g/l.}\dagger$			
	PSA	APSA	FIPSA	ASV
Garlic	2.17 ± 0.02	1.98 ± 0.03	2.13 ± 0.04	2.00 ± 0.02
<i>Lycium chinense</i>	0.11 ± 0.02	0.19 ± 0.02	0.10 ± 0.02	0.14 ± 0.02
Mineral water 1	4.64 ± 0.03	4.57 ± 0.02	4.80 ± 0.05	4.77 ± 0.03
Mineral water 2	1.14 ± 0.01	1.18 ± 0.01	1.09 ± 0.02	1.01 ± 0.02

*Mean \pm mean deviation of three measurements.

$\dagger\mu\text{g/g}$ for garlic and *lycium chinense* and $\mu\text{g/l.}$ for mineral waters.

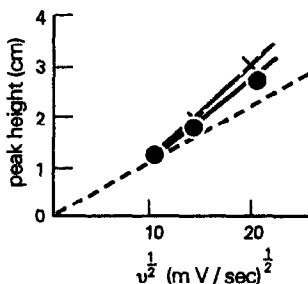


Fig. 13. Effect of scan rate on peak height for $10^{-4}M$ ARS + $5 \times 10^{-5}M$ Ge(IV): (●) reduction peak, (×) oxidation peak.

Analysis of samples

Samples of garlic and *lycium chinense* were digested in a minimum volume of a 3:1 v/v mixture of concentrated nitric and perchloric acids until the first appearance of perchloric acid fumes, after which the samples were cooled and diluted accurately to 100 ml. The final H^+ concentration of the sample solutions was approximately $0.7M$. The samples of mineral water were concentrated prior to analysis.

The samples were analysed by the proposed methods, and by anodic-stripping voltammetry (ASV)¹¹ and flow-injection potentiometric stripping analysis (FIPSA).¹² The results are compared in Table 3.

CONCLUSIONS

In a Ge(IV) solution containing ARS, both ARS and its Ge-complex are adsorbed at the mercury-film electrode, enhancing the sensitivity of determining Ge by PSA. The enhancement has two main causes: (a) in the deposition step adsorption raises the preconcentration efficiency and (b) in the stripping step the metallic Ge in the mercury film is oxidized with more difficulty than expected (shown by the more positive stripping potential in the cyclic voltammetry, which means that adsorption persists during stripping).

REFERENCES

1. D. Jagner, *Analyst*, 1982, **107**, 593.
2. S. Jaya and T. P. Rao, *Rev. Anal. Chem.*, 1982, **6**, 343.
3. T. M. Florence, *J. Electroanal. Chem.*, 1984, **168**, 207.
4. T. Österud and M. Prytz, *Arch. Math. Naturvidensk.*, 1943, **47**, 73.
5. Gh. Sauvenier and G. Duyckaerts, *Anal. Chim. Acta*, 1955, **13**, 396.
6. S. K. Dhar, *ibid.*, 1956, **15**, 91.
7. R. Kalvoda, *ibid.*, 1982, **138**, 11.
8. X. Wang and X. Du, *Proc. Electroanal. Chem. Symp. (China)*, 1981, 334.
9. N. Li and Y. Cui, *Acta Chim. Sinica*, 1985, **43**, 1155; *Chem. Abstr.*, 1986, **104**, 141353v.
10. N. Li and X. Shang, *Kexue Tongbao*, 1986, **9**, 667; *Chem. Abstr.*, 1987, **107**, 69851y.
11. J. Deng, Q. Zhang and Z. Wang, *Acta Chim. Sinica*, 1982, **40**, 151; *Chem. Abstr.*, 1982, **97**, 65582p.
12. D. Feng, P. Yang and Z. Yang, *J. Jinan Univ.*, 1990, **11**, 41.

BOOK REVIEWS

SolvEq: FOSTER ROEGIERS, BIOSOFT, Cambridge, 1990. £149, US\$299.

SolvEq is described as "a general purpose equation solver and numerical modelling tool for science and technology". It runs on IBM PC and compatible computers with 640K of memory and DOS 3.1 or later. A math coprocessor is used if present. Output can be to an IBM, Epson or HP Laserjet printer, or to an HPGL plotter. The program runs best from hard disc, but can also be used on a double floppy system provided that at least one drive has a capacity of 720K or more.

I found the manual excellent. It offers an extended tutorial section, followed by a reference section covering all the possible options and variations. I therefore found it quick and easy to learn to use SolvEq.

The program operates from submenus that drop down from the main menu bar. The equations to be solved are first of all entered in the EDIT screen. Later, they can be reLOAded from files that have previously been SAVEed. Equations are entered in algebraic form just as they would be written down on paper. A single equation can be entered, or several equations can be solved simultaneously. The equations may involve real, vector, and/or complex numbers; they may include integrals, summations, differentials; and many algebraic, trigonometric, hyperbolic and exponential functions. Arrays of variables are possible, but matrix operations are not supported.

In the VALUES screen, variables are designated as known or unknown, and values are assigned to those that are known. A known variable can be made to take a whole series of values (a "parametric study"); and an unknown variable can be designated as an optimization variable, which the program can either maximize or minimize.

I tested solvEq by using it to solve many of the equations for acid-base equilibria commonly found in analytical text-books. The usual book approach is to give the exact equation, then show how it can be simplified to allow solution. For every case I tried, SolvEq was able easily to solve the exact equation; solutions could be found in just a few seconds for entire titration curves. It was also easily possible to calculate values of Ringbom alpha-coefficients and conditional stability constants.

When solutions had been obtained for a series of values of a variable (a "parametric study"), the output could be presented as a graph, and the axes could be transformed if desired into log-lin, lin-log or log-log form.

The following equations for the titration of a dibasic acid were solved in about thirty seconds for 65 values of Vb, and a graph of the titration curve was obtained by plotting pH against Vb.

$$H^4 + (Cb \cdot Vb \div V_{tot} + K_1) \cdot H^3 + K_1 \cdot \left(-K_w \div K_1 + \frac{Cb \cdot Vb - Ca \cdot Va}{V_{tot}} \right) \cdot H^2 + \dots$$

$$K_1 \cdot K_2 \cdot \left(-K_w \div K_2 + \frac{Cb \cdot Vb - 2 \cdot Ca \cdot Va}{V_{tot}} \right) \cdot H - K_1 \cdot K_2 \cdot K_w = 0$$

$$H = 10^{-pH}$$

$$V_{tot} = Va + Vb$$

I very much enjoyed using SolvEq, and I feel that I can still discover many more applications for it in analytical chemistry, particularly for optimization. I think, too, that SolvEq could find a useful place in the teaching of analytical chemistry.

MARY MASSON

P. FIT: FIG.P Software Corporation, BIOSOFT, Cambridge, 1990. £125, US\$199.

P. Fit is a non-linear curve-fitting program for IBM PC and compatible computers with at least 512K of RAM, DOS 2.0 or later, and a hard disk. The program is controlled from a main menu screen which gives the various options in the order in which they should be performed. Data are entered in a spreadsheet-type format, and can be saved before further processing. Data can instead be imported from ASCII files produced by other applications.

A varied selection of possible equations for curve-fitting is built into the program, and others can easily be added, either temporarily or permanently.

I tested a range of types of data—linear, curved, and sigmoid—and was always satisfied with the fit obtained. I was pleased with the statistical reports produced by P. Fit, particularly with the plots of residuals, but also with the confidence limits, goodness-of-fit index, correlation, chi-squared, sign-test and run-test. The print-out I obtained from a laser printer was of excellent quality, though the range of styles was limited.

The only thing that worries me about P. Fit is the manual, in that it assumes that the reader already has a good knowledge of statistics. My feeling is that an easy-to-use program like P. Fit is likely to attract many users with virtually no statistical knowledge, and I think that the manual should have catered for such users by providing more basic background information. I hope that the publishers will give some thought to improving the manual, perhaps initially by adding references to suitable statistical text-books, but later by providing a much more extensive guide to the practice of curve-fitting.

MARY MASSON

Electrochemistry, Past and Present: J. T. STOCK and M. V. ORNA (editors), ACS, Washington, DC, 1989. Pages ix + 606. \$89.95 (US and Canada), \$107.95 (elsewhere).

This book consists of 38 chapters "developed" from a symposium held in 1988 and unequally spread between *Foundations of Electrochemistry*, *Organic and Biochemical Electrochemistry* (the smallest and weakest section), *Electroanalytical Chemistry* and *Industrial Electrochemistry*. With such an arrangement and so many authors, variability of material and writing must be expected. The most obviously historical pieces, centred on chemists from Faraday to Heyrovský, are good and also reveal curiosities such as Wilmore's role in the hydrogen electrode debate. I commend Leddy's piece on industrial electrochemistry, as it is very instructive and does not depend on the cachet of Great Names. The chapters on analytical instrumentation were generally interesting, but some of those on recent developments were curiously flat and inhibited, amounting to no more than sketchy literature reviews, as if the authors were not really interested in this type of writing. I counted 13 very good chapters, 12 that were worthwhile, 5 that were rather poor and 8 that were either suspiciously idiosyncratic or a courtesy to the author rather than the reader. That is not a bad score and the book as a whole meets the editors' claim to "educate and engage" the reader. For camera-ready copy, the book is not cheap and I wish it had been published in paperback (with some chapters omitted) to widen the readership, for this is as near a bedside book as the chemist is likely to get. Recommended.

D. MIDGLEY

Spectroscopic and Structural Studies of Biomaterials—I Proteins: J. TWARDOWSKI (editor). Sigma Press, Wilmslow, Cheshire, 1988. Pages viii + 289.

This book contains a collection of lectures and selected communications presented at the Third International Scientific School, entitled "Spectroscopic and structural studies of materials and systems of fundamental importance to biology and medicine" in Ustron, Poland, 1987. The authors' original manuscripts are reproduced for this book, which gives a mixture of print types, sizes and quality. The book also suffers from numerous spelling and linguistic mistakes which have not been corrected.

It has a very heterogenous content and covers a wide range of topics and research fields. Some papers describe new work carried out by the authors but many are review articles within a particular field. The topics include sections on methodology, medical aspects, hemeproteins, membrane proteins and protein complexes. As such, it is considered by the reviewer to be a book for the library, where it will be of interest to and can be read by multi-discipline users, rather than a book for individuals.

M. L. DUFFIELD

Talanta

The International Journal of Pure and Applied Analytical Chemistry

Editors-in-Chief

PROFESSOR G.D.CHRISTIAN,
Department of Chemistry, BG-10,
University of Washington,
Seattle, WA 98195, U.S.A.

PROFESSOR E.H.HANSEN,
Chemistry Department A, Building 207,
Technical University of Denmark,
DK-2800 Lyngby, Denmark

Consultant Editor

DR. R.A.CHALMERS, Department of Chemistry, University of Aberdeen, Old Aberdeen, Scotland, U.K.

Assistant Editors

DR. W.A.J.BRYCE, University of Aberdeen, Scotland, U.K.

DR. D.MIDGLEY, National Power, Leatherhead, U.K.

DR. P.J.COX, Robert Gordon's Institute of Technology, Aberdeen, Scotland, U.K.

Computing Editor

DR. MARY R.MASSON, University of Aberdeen, Scotland, U.K.

Book Review Editor

DR. P.J.COX, Robert Gordon's Institute of Technology, Aberdeen, Scotland, U.K.

Technical Editor

MISS C.R.HIGGINSON, B.Sc.

U.S. Review Editor

PROFESSOR LINDA MCGOWN, Duke University, N.C., U.S.A.

Editorial Board

Chairman: PROFESSOR J.D.WINEFORDNER

DR. R.A.CHALMERS

PROFESSOR G.D.CHRISTIAN

PROFESSOR E.H.HANSEN

DR. M.R.MASSON

DR. D.MIDGLEY

PROFESSOR R.SEITZ

Advisory Board

Chairman: PROFESSOR J.D.WINEFORDNER, Gainesville,
Florida, U.S.A.

Talanta

PROFESSOR A.G.ASUERO, Seville, Spain

PROFESSOR P.R.BONTCHEV, Sofia, Bulgaria

PROFESSOR DR. P.W.J.M.BOUMANS, Eindhoven,

The Netherlands (Liaison member for *Spectrochimica Acta B*)

PROFESSOR D.T.BURNS, Belfast, N. Ireland, U.K.

PROFESSOR R.G.COOKS, West Lafayette, Indiana, U.S.A.

PROFESSOR A.CORSINI, Ontario, Canada

PROFESSOR S.R.CROUCH, East Lansing, Michigan, U.S.A.

DR. P.DASGUPTA, Texas, U.S.A.

PROFESSOR H.FALK, Kleve, F.R.G.

PROFESSOR J.F.FRITZ, Iowa, U.S.A.

PROFESSOR R.GJBELS, Wilrijk, Belgium

PROFESSOR M.GROSS, Strassbourg, France

PROFESSOR T.HORI, Kyoto, Japan

PROFESSOR A.HULANICKI, Warsaw, Poland

PROFESSOR J.INCZÉDY, Veszprém, Hungary

PROFESSOR J.D.INGLE, Corvallis, Oregon, U.S.A.

PROFESSOR A.IVASKA, Åbo, Finland

DR. K.IZUTSU, Matsumoto, Japan

PROFESSOR D.JAGNER, Gothenburg, Sweden

DR. H.KRAGTEN, Amsterdam, The Netherlands

DR. L.J.KRICKA, Philadelphia, Pennsylvania, U.S.A.

DR. L.KRYGER, Aarhus, Denmark

PROFESSOR D.MALJKOVIĆ, Zagreb, Yugoslavia

DR. J.MATOUSEK, Kensington, Australia

DR. T.NIEMCZYK, Albuquerque, New Mexico, U.S.A.

PROFESSOR M.NOVTNY, Bloomington, Indiana, U.S.A.

DR. N.OMENETTO, Ispra, Italy

DR. S.PERONE, San Jose, California, U.S.A.

PROFESSOR E.PUNGOR, Budapest, Hungary

PROFESSOR I.ROELANDTS, Liège, Belgium

PROFESSOR M.SMYTH, Dublin, Ireland

PROFESSOR L.SOMMER, Brno, Czechoslovakia

DR. B.YA.SPIVAKOV, Moscow, U.S.S.R.

PROFESSOR K.ŠTULÍK, Prague, Czechoslovakia

DR. J.D.R.THOMAS, Cardiff, Wales, U.K.

(Liaison member for *Selective Electrode Reviews*)

PROFESSOR G.TÖLG, Dortmund, F.R.G.

PROFESSOR M.VALCARCEL, Córdoba, Spain

DR. T.VODINH, Oak Ridge, Tennessee, U.S.A.

DR. J.WANG, Las Cruces, New Mexico, U.S.A.

DR. I.WARNER, Atlanta, Georgia, U.S.A.

PROFESSOR E.L.WEHRY, JR., Knoxville, Tennessee, U.S.A.

DR. B.WELZ, Uberlingen, F.R.G.

Talanta: Chemical Sensors

DR. A.FOGG, Fukuoka, Japan

PROFESSOR J.JANATA, Salt Lake City, Utah, U.S.A.

DR. S.MARTIN, Albuquerque, New Mexico, U.S.A.

PROFESSOR M.MASCINI, Florence, Italy

DR. T.SHONO, Osaka, Japan

PROFESSOR M.THOMPSON, Toronto, Canada

PROFESSOR N.YAMAZOE, Fukuoka, Japan

ERRATA

In the article entitled "Kinetic determination of EDTA and citrate by the displacement of fluoride from $Al^{3+}-F^-$ complexes and use of a fluoride ion-selective electrode" by Pentari *et al.* (*Talanta*, 1991, 38, 295) equation (12) should have been

$$[F^-] \left(1 + \frac{[H^+]}{K_{HF}} \right) + \frac{\sum_{i=1}^4 \left(i [F^-]^i \prod_{j=1}^i K_j \right)}{1 + K_h/[H^+] + \sum_{i=1}^4 \left([F^-]^i \prod_{j=1}^i K_j \right)} C_{Al} = C_F$$

and in the article entitled "Analytical applications of 1,10-anthraquinones: A review" by Diaz (*Talanta*, 1991, 38, 571) "1,10-anthraquinones" should have been "9,10-anthraquinones".

NOTICES

European Analytical Column 14 (Sept. 1990)

Letter of Information of the Working Party on Analytical Chemistry of the Federation of European Chemical Societies (WPAC/FECS)

Chairman: L. NIINISTÖ, Helsinki

Secretary: R. KELLNER, Vienna

WPAC held its 21st meeting on 26 August 1990 in connection with Euroanalysis VII in Vienna. The attendance was 38 delegates from chemical societies in 24 countries, the highest number so far and an almost complete representation. FECS and WPAC cover practically the whole of Europe, as the Romanian Society of Analytical Chemistry joined FECS as a full member this year.

The major event of WPAC this year was Euroanalysis VII, held at the University of Technology, Vienna (26–31 August 1990). A very high attendance of 1100 active participants was recorded for this latest event of the triennial series of European conferences of Analytical Chemistry.

The conference was organized on behalf of the WPAC by the Austrian Society for Analytical Chemistry with Prof. J. F. K. Huber as chairman and Prof. M. Grasserbauer as secretary general. The opening session was held in the beautiful golden hall of the Vienna Musikverein with a programme consisting of short addresses by Prof. Huber, Dr. Fritsche, Chairman of FECS, and Prof. Niinistö and much Viennese music. The traditional historic lecture was given by Prof. H. Malissa. Numerous awards and prizes were also given at this occasion including the H. E. Merck Prize for Analytical Chemistry to Dr. B. A. Bidlingmeyer and Prof. R. Nießner and the Robert Boyle Gold Medal to Prof. H. Malissa.

Euroanalysis conferences are broad-scope Analytical Chemistry meetings and consequently the Vienna meeting covered all main fields in Analytical Chemistry, with 95 invited lecturers and 618 contributed papers in oral and poster sessions. For compiling the programme, the "convener-system" was used and this and the high number of invited lectures were the key features which guaranteed an interesting high-level programme.

Euroanalysis VII was not only characterized by a record attendance right up to the closing session, but by the active participation of numerous delegates in the "Special Sessions" (Quality Assurance, Education, Computer Based Analytical Chemistry and Sampling) that are among the key areas in the field today. Special reports about these fields will follow.

Besides the discussion of regular technical questions (a detailed report will appear in TRAC, Analytical Chemistry and most other Analytical Chemistry journals, proceedings will appear in Mikrochimica Acta, contributed papers in Fresenius Journal of Analytical Chemistry) Euroanalysis VII was a forum for 2 important resolutions:

1. Recommendations for the future in Education in Analytical Chemistry
2. Declarations of Vienna by the members of WPAC

Both resolutions were unanimously supported by WPAC at its meeting on 26 August 1990 (38 participants) and accepted by Euroanalysis VII.

Further—facing the fact that Analytical Chemistry has developed worldwide into "a key for a safer future for mankind" by controlling technological progress, food and the environment—closer formal contacts were established between WPAC and the Analytical Divisions of IUPAC, ACS, the Japanese Chemical Society and the Chinese Academy of Sciences.

NOTICES

THE RONALD BELCHER MEMORIAL AWARD FOR 1992

Applications are invited for the Ronald Belcher memorial Award, in commemoration of the late Professor Belcher's outstanding contributions to analytical chemistry, international relations and understanding, his interest in student welfare, and continued association with *Talanta* from his conception of the journal in 1957 right up to his death. The award takes the form of a travel grant of US\$1000 to enable a young analytical scientist to undertake travel abroad and is made in even-numbered years. Candidates may be of either sex and any nationality, but must be under 30 years of age at the time of application, and not have had more than one year of post-doctoral experience. Applications may be sent by the candidates themselves, or on their behalf by a responsible senior (*e.g.*, Head of Department, research supervisor), and must be submitted by the end of the year preceding the award. They must include a brief curriculum vitae, a short statement of the purpose of travel and the places to be visited, a testimonial of ability, and a recommendation from a senior research worker.

Applications for the 1992 award should be sent to

Professor J. D. Winefordner
Department of Chemistry
University of Florida
Gainesville, Florida 32611, U.S.A.

to arrive before 31 December 1991.

4th INTERNATIONAL SYMPOSIUM ON DRUG ANALYSIS

5-8 May 1992
Palais des Congrès
LIEGE, BELGIUM
FIRST CIRCULAR

Scope

The purpose of DRUG ANALYSIS '92 is to bring together people from Industry, Universities, Control Laboratories and Hospitals to discuss the current status of analytical techniques including instrumental applications and theoretical developments.

Topics

1. Fundamental Aspects of Drug Analysis.
2. Quality Control of Natural and Synthetic Raw Materials.
3. Analysis of Pharmaceutical Preparations.
4. Determination of Drugs in Biological Media.
5. Automation in Drug Analysis.

Programme

Plenary and keynote lectures will be given by invited speakers. A limited number of contributed papers will be presented as oral communications. The preference will be given to poster presentations. Discussion sessions will also be organized.

Language

The official language of the Symposium is English. No simultaneous translation will be provided.

CORRIGENDUM

In the announcement of the Ronald Belcher Memorial Award winners (*Talanta*, 1990, 37, No. 11, V) there was an error in the name of one of them, "Dr. R. Kobinski" should have been "Dr. R. Łobiński", and we apologise to him for the error.

NOTICES

THE RONALD BELCHER MEMORIAL AWARD FOR 1992

Applications are invited for the Ronald Belcher memorial Award, in commemoration of the late Professor Belcher's outstanding contributions to analytical chemistry, international relations and understanding, his interest in student welfare, and continued association with *Talanta* from his conception of the journal in 1957 right up to his death. The award takes the form of a travel grant of US\$1000 to enable a young analytical scientist to undertake travel abroad and is made in even-numbered years. Candidates may be of either sex and any nationality, but must be under 30 years of age at the time of application, and not have had more than one year of post-doctoral experience. Applications may be sent by the candidates themselves, or on their behalf by a responsible senior (*e.g.*, Head of Department, research supervisor), and must be submitted by the end of the year preceding the award. They must include a brief curriculum vitae, a short statement of the purpose of travel and the places to be visited, a testimonial of ability, and a recommendation from a senior research worker.

Applications for the 1992 award should be sent to

Professor J. D. Winefordner
Department of Chemistry
University of Florida
Gainesville, Florida 32611, U.S.A.

to arrive before 31 December 1991.

4th INTERNATIONAL SYMPOSIUM ON DRUG ANALYSIS

5-8 May 1992
Palais des Congrès
LIEGE, BELGIUM
FIRST CIRCULAR

Scope

The purpose of DRUG ANALYSIS '92 is to bring together people from Industry, Universities, Control Laboratories and Hospitals to discuss the current status of analytical techniques including instrumental applications and theoretical developments.

Topics

1. Fundamental Aspects of Drug Analysis.
2. Quality Control of Natural and Synthetic Raw Materials.
3. Analysis of Pharmaceutical Preparations.
4. Determination of Drugs in Biological Media.
5. Automation in Drug Analysis.

Programme

Plenary and keynote lectures will be given by invited speakers. A limited number of contributed papers will be presented as oral communications. The preference will be given to poster presentations. Discussion sessions will also be organized.

Language

The official language of the Symposium is English. No simultaneous translation will be provided.

Publications

All registered participants will receive a copy of the book of abstracts. All invited and submitted papers will be considered for publication in a 1992 special Symposium issue of the *Journal of Pharmaceutical and Biomedical Analysis*.

An exhibition of scientific equipment books and periodicals will be held during the congress.

The deadline for receipt of abstracts is 15 November 1991.

For further information, please contact:

Dr. J. CROMMEN
DRUG ANALYSIS '92—LIEGE
University of Liège
Institute of Pharmacy
rue Fusch 5
B-4000 LIEGE
BELGIUM

Phone: +32-41-23 70 02

Fax: +32-41-22 18 55

1992 WINTER CONFERENCE ON FLOW INJECTION ANALYSIS

12–15 January 1992
Scottsdale, Arizona

WCFA 92 will be held in Scottsdale, Arizona, 12–15 January, 1992. It will focus on how industrial FIA techniques have helped solve real world problems. New hardware and software-driven applications will be presented. The following areas will be highlighted: process chemistry, biotechnology, instrument design, new methods, atomic spectroscopy, electrochemistry. There will be a vendor exhibition. Deadline for abstracts for presentation (20 min.) and posters, and for preregistration, is 3 December, 1991.

For information, write to:

WCFA 92
Gary D. Christian
University of Washington, BG-10
Seattle, WA 98195
TEL: 206-543-1635
FAX: 206-685-3478

Publications

All registered participants will receive a copy of the book of abstracts. All invited and submitted papers will be considered for publication in a 1992 special Symposium issue of the *Journal of Pharmaceutical and Biomedical Analysis*.

An exhibition of scientific equipment books and periodicals will be held during the congress.

The deadline for receipt of abstracts is 15 November 1991.

For further information, please contact:

Dr. J. CROMMEN
DRUG ANALYSIS '92—LIEGE
University of Liège
Institute of Pharmacy
rue Fusch 5
B-4000 LIEGE
BELGIUM

Phone: +32-41-23 70 02

Fax: +32-41-22 18 55

1992 WINTER CONFERENCE ON FLOW INJECTION ANALYSIS

12–15 January 1992

Scottsdale, Arizona

WCFA 92 will be held in Scottsdale, Arizona, 12–15 January, 1992. It will focus on how industrial FIA techniques have helped solve real world problems. New hardware and software-driven applications will be presented. The following areas will be highlighted: process chemistry, biotechnology, instrument design, new methods, atomic spectroscopy, electrochemistry. There will be a vendor exhibition. Deadline for abstracts for presentation (20 min.) and posters, and for preregistration, is 3 December, 1991.

For information, write to:

WCFA 92
Gary D. Christian
University of Washington, BG-10
Seattle, WA 98195
TEL: 206-543-1635
FAX: 206-685-3478

Euroanalysis VII was a further landmark in the development of this conference series. After Euroanalysis I in Heidelberg (1972) where WPAC was founded (spiritus rector: Dr. W. Fritsche, GDCh, Frankfurt) this triennial event has taken place in Budapest (1975), Dublin (1978), Helsinki (1981), Cracow (1984) and Paris (1987). WPAC is most grateful to the Austrian Society for Analytical Chemistry (ASAC) for having hosted this most successful Viennese Congress of Analytical Chemistry, which was also a social event to be remembered.

The next Euroanalysis will take place in Edinburgh, 5–11 September 1993 (Chairman: Prof. D. T. Burns). Details about Euroanalysis and other WPAC activities (e.g., in Quality Assurance and Education) are available from the WPAC secretariat upon request:

Prof. R. Kellner
Institute for Analytical Chemistry
Technical University Vienna
Getreidemarkt 9
A-1060 Vienna
Fax. +43-1-567813

The following motions have been proposed by the members of the Working Party on Analytical Chemistry of the Federation of European Chemical Societies (WPAC/FECS) and approved in the closing session of Euroanalysis VII on Friday, August 31, 1990.

“Declarations of Vienna”

Motion 1

The delegates of Euroanalysis VII strongly affirm that only a good and sound *education in Analytical Chemistry* gives proper provision for adequate progress in science and research, and for control of production, consumable goods and the environment.

Motion 2

With respect to progress in the political and economic integration of Europe, Euroanalysis VII recommends that the WPAC takes the necessary steps towards advancing harmonization of analytical chemistry curricula according to the recommendations of the WPAC based on the survey of 1989/90 as reported to Euroanalysis VII in session C4 on Tuesday, 28 August 1990.

Motion 3

Since high standards of analytical quality in any one European country directly concern and benefit every other country, Euroanalysis VII strongly recommends that in order to ensure and enhance the quality of analysis the WPAC aims to encourage that consistent rules and commitments for analytical quality assurance are valid throughout Europe by the harmonization of existing and new “accreditation systems” within Europe.

Vienna, August 31, 1990

Prof. Dr. L. Niinistö
(Chairman WPAC/FECS)

European Analytical Column 15 (Jan. 1991)

Letter of information of the Working Party on Analytical Chemistry of the Federation of European Chemical Societies (WPAC/FECS).

Chairman: L. Niinistö, Helsinki

Secretary: R. Kellner, Vienna

Education in Analytical Chemistry—New Developments

In addition to the publication of the “WPAC-Recommendations for the Future in Education in Analytical Chemistry” (see European Analytical Column 14) we are happy to inform you about

very positive comments about this major WPAC activity from outside Europe (see editorial by G. Morrison, *Analytical Chemistry*, 1 Nov. 1990) and about further actions:

- The complete Special Session on Education will be documented in a convener-edited part of the proceedings of EUROANALYSIS VII (to appear in *Mikrochimica Acta*, 1991).
- The WPAC-secretariat will stimulate activities in the field of new textbooks of Analytical Chemistry.
- A high-level postgraduate training system in Europe was proposed under the name "WPAC-Euro-Courses". Final statutes are under discussion.
- Further aspects of education in Analytical Chemistry at university level will be discussed at depth at the "2nd FEICHEM Conference on Education in Analytical Chemistry" to be held in Prague, at the famous Charles University in the beginning of September 1992. Professor Štulík has already obtained support from the Czechoslovak Chemical Society which will organize the conference in connection with the 16th International Competition in Analytical Chemistry (ICAC 16).
- We would like to thank Professor Krofta and his colleagues from the ICAC for their personal efforts to make the 15th ICAC 1990 a success, and we finish the column with their report.

Report of the 15th International Competition in Analytical Chemistry

From 3rd to 7th September 1990 the Department of Analytical Chemistry of the Prague Institute of Chemical Technology again organized the 15th ICAC—International Competition in Analytical Chemistry.

The Competition was held under the sponsorship of the Rector of the Prague Institute of Chemical Technology, the Ministry of Education, Youth and Sports of the Czech Republic, and the Czechoslovak Chemical Society. The Competition is one of the events supported by the Working Party on Analytical Chemistry (WPAC) of the Federation of European Chemical Societies (FECS).

The official opening of the Competition, which took place in the Schooling Club, was attended by the chairman of the Working Party on Analytical Chemistry of FECS, Professor L. Niinistö, and its secretary, Professor R. Kellner, the Rector of the Prague Institute of Chemical Technology Professor Cerny, and a representative of the Czechoslovak Chemical Society, Professor Horak.

The Competition was attended by students from 24 universities and technical universities, guided by their teachers, from 9 European countries: Poland (1), USSR (4), GDR (5), Hungary (5), Romania (1), Yugoslavia (1), Italy (1), Holland (1), and Czechoslovakia (5).

The Competition involved a theoretical part and a practical one. In the theoretical part the students were solving 25 tasks and problems covering the most widely used analytical methods. In the practical part they were determining the contents of copper and nickel in a mixture, by titration with EDTA. The time limit for solving the set tasks in both parts of the Competition was 150 minutes. The official language of the Competition was English.

The results of the respective parts of the Competition were evaluated by an International Jury formed by the university teachers who guided the individual teams. The chairman of the Jury was Associate-Professor Popl from the Prague Institute of Chemical Technology, the vice-chairman was Dr. F. Gerhartl (Arrhem, Holland). Intermediate results, after being evaluated by the International Jury, were always made public on notice boards.

In the individuals competition Mr. A. Kotschy won 1st place, Mr. Hantosi Zolt the 2nd (both are from Lorand Eötvös University in Budapest) and Mr. A. Granovski from the Moscow State University won 3rd place.

In the team competition the placement was as follows: 1. Lorand Eötvös University, Budapest; 2. Lajos Kossuth University, Debrecen; 3. Moscow State University.

Besides the Competition, the organizers provided for the participants a social programme including a sightseeing tour of Prague, attendance at a performance of *Laterna Magica*, a social evening and a closing festive dinner following by music and dancing.

The participants highly appreciated the organization and the professional programme as well as the Competition itself.

Organization Committee of the 15th ICAC

NOTICES

THIRD INTERNATIONAL SYMPOSIUM ON PHARMACEUTICAL AND BIOMEDICAL ANALYSIS

28 April-1 May 1991

Boston, Mass., U.S.A.

The Third International Symposium on Pharmaceutical and Biomedical Analysis will be held in the Boston Park Plaza Hotel, Boston, U.S.A. from Sunday 28 April to Wednesday 1 May 1991. This Symposium continues the series of successful meetings held in Barcelona, Spain (1987) and York, U.K. (1990). All those involved in the analysis of drugs, related materials and endogenous compounds, in any area of the pharmaceutical and biomedical sciences, are invited to participate. The principal scientific themes include:

- Analytical aspects of biotechnology
- Current analytical issues in TDM and sports medicine
- Novel methods for ADME studies
- Novel chromatographic methods for the analysis of enantiomeric drugs
- Advances in drug analysis by high-resolution NMR and MS
- Advances in detector technology, including UV, FL, EC and MS
- New approaches to sample handling and sample pre-treatment
- Novel analytical techniques and applications for QC, QA, drug formulations, assay validation, stability testing, bioanalysis, pharmacokinetics, biopharmaceutics, clinical chemistry, toxicology, drug metabolism and environmental control

The meeting will consist of opening and closing Plenary Lectures and 14 invited Keynote Lectures given by internationally renowned scientists in their respective fields. There will be a limited number of Oral Presentations available. Preference will be given to Poster Presentations, as the central feature of the Symposium. A unique feature will be the Poster Discussion Sessions, based on short presentations by each author, and structured around topical themes. A series of Workshops will also be presented on Chiral Separations; Capillary Electrophoresis; Sample Preparation; Detector Technology; and Microdialysis.

All papers presented will be published, after refereeing, in a special issue of the *Journal of Pharmaceutical and Biomedical Analysis*. Registered participants will receive a complimentary copy of the Proceedings, the Book of Abstracts, and entry to the Exhibition.

For further information contact:

Shirley Schlessinger, PBA'91
Suite 1015, 400 East Randolph Street
Chicago, IL 60661, U.S.A.
Tel.: (312) 527-2011
Fax: (312) 527-3437

LIST OF CONTENTS

JANUARY

SENSOR ELECTRODES

Editorial	V
Lars Kryger	VII Foreword
Richard P. Baldwin and Karsten N. Thomsen	1 Chemically modified electrodes in liquid chromatography detection: a review
Derek H. Craston, Christopher P. Jones, David E. Williams and Nabil El Murr	17 Microband electrodes fabricated by screen printing processes: applications in electroanalysis
Debra R. Rolison, Robert J. Nowak, Timothy A. Welsh and Catherine G. Murray	27 Analytical implications of zeolites in overlayers at electrodes
Kiamars Hajizadeh, H. Brian Halsall and William R. Heineman	37 Immobilization of lactate oxidase in a poly(vinyl alcohol) matrix on platinized graphite electrodes by chemical cross-linking with isocyanate
Rhodora L. Villarta, David D. Cunningham and George G. Gullbault	49 Amperometric enzyme electrodes for the determination of L-glutamate
P. N. Bartlett, V. Q. Bradford and R. G. Whitaker	57 Enzyme electrode studies of glucose oxidase modified with a redox mediator
Darryl L. Luscombe and Alan M. Bond	65 Determination of tocopherols by reverse-phase liquid chromatography and electrochemical detection at a surface-oxide modified platinum micro- electrode, without added electrolyte
Huamin Ji and Erkang Wang	73 Amperometric detection at a carbon-fibre array ring/glassy-carbon disk electrode in a wall-jet cell
Joseph Wang, Ziad Taha and Najih Naser	81 Electroanalysis at modified carbon-paste electrodes containing natural ionic polysaccharides
Seong K. Cha, Kasem K. Kasem and Héctor D. Abruña	89 Effects of competitive binding on the amperometric determination of copper with electrodes modified with Chromotrope 2B
M. Freund, L. Bodalbhai and A. Brajter-Toth	95 Anion-excluding polypyrrole films
Kong Ling Dong, Lars Kryger, Joan K. Christensen and Karsten N. Thomsen	101 Preconcentration and determination of bismuth(III) at a chemically modified electrode containing 1-(2-pyridylazo)-2-naphthol
A. Amine, J.-M. Kauffmann and G. J. Patriarche	107 Amperometric biosensors for glucose based on carbon paste modified electrodes
Shaojun Dong and Guangli Che	111 An electrochemical microsensor for chloride
Boy Hoyer	115 Calibration of solid-state copper ion-selective electrode in cupric ion buffers containing chloride
<i>Questionnaire: Software Survey Section</i>	i

FEBRUARY

Louis Gordon Memorial Award	V
Gregory D. Clark, John Zable, Jaromír Růžička and Gary D. Christian	119 Flow-reversal flow-injection analysis. Enhancement of flow-injection titrations
S. D. Kolev, A. Ríos, M. D. Luque de Castro and M. Valcárcel	125 Determination of rate constants and reaction orders with an open-closed flow-injection configuration

Shen Dong and Purnendu K. Dasgupta	133	Automated determination of total phosphorus in aqueous samples
Takeshi Yamane and Eiichi Goto	139	Simultaneous determination of calcium and magnesium by using a flow-injection system with simultaneous injection of two sample plugs and a masking agent plug
G. Gordon, D. L. Sweetin, K. Smith and G. E. Pacey	145	Improvements in the <i>N,N</i> -diethyl- <i>p</i> -phenylenediamine method for the determination of free and combined residual chlorine through the use of FIA
M. J. Hemmings and E. A. Jones	151	The speciation of arsenic(V) and arsenic(III), by ion-exclusion chromatography, in solutions containing iron and sulphuric acid
C. L. Chakrabarti and S. J. Cathum	157	Arrhenius plots for activation energy of atomization in graphite-furnace atomic-absorption spectrometry
Raja H. Atallah and David A. Kalman	167	On-line photo-oxidation for the determination of organoarsenic compounds by atomic-absorption spectrometry with continuous arsine generation
D. Ramesh Babu and P. R. Naidu	175	A solvent extraction-atomic absorption technique for the simultaneous determination of low concentrations of iron, nickel, chromium and manganese in drinking water
Ki-Min Bark and R. Ken Forcé	181	Analysis of polynuclear aromatic hydrocarbon mixtures in various environments by time-resolved fluorescence spectroscopy
Xiang Yuan and Ray von Wandruszka	189	Precapacitive processes in single potential-step chronoamperometry
Tapio Kotiaho, Anita K. Lister, Mark J. Hayward and R. Graham Cooks	195	On-line monitoring of chloramine reactions by membrane introduction mass spectrometry
Alan R. Katritzky, G. Paul Savage and Maria Pilarska	201	The response of some organic microsensor coatings to a variety of vapors
Robert D. Braun	205	Solubility of iron(II) carbonate at temperatures between 30 and 80°
O. E. S. Godinho, J. J. R. Rohwedder, M. N. Eberlin, L. M. Aleixo and G. de Oliveira Neto	213	Determination of lead(II) by argentimetry
B. C. Verma, S. B. Kalia, V. S. Jamwal, Sudhir Kumar, D. K. Sharma and Anila Sud	217	Redox reactions in non-aqueous media: determination of organic isothiocyanates alone, in formulations and in important mixtures
N. M. Sundaramurthi and V. M. Shinde	223	Extraction and separation of uranium and lead with liquid anion-exchangers
A. Safavi, A. A. Ensafi and A. Massoumi	229	Spectrophotometric determination of nickel in vegetable oil with ammonium 2-amino-1-cyclohexene-1-dithiocarboate
<i>Analytical Data</i>		
J. E. Kountourellis, C. K. Markopoulou, F. A. Underwood and B. Chapman	233	X-Ray powder diffraction data for nine analgesics
<i>Corrigendum</i>	i	
<i>Notices</i>	iii	
<i>Questionnaire: Software Survey Section</i>	v	
MARCH		
<i>Talanta Advisory Board</i>	V	
Peter T. Ying and John G. Dorsey	237	Characterization of retentivity of reversed phase liquid chromatography columns
Dean A. Martens and William T. Frankenberger, Jr.	245	Determination of aminosaccharides by high-performance anion-exchange chromatography with pulsed amperometric detection

Mark V. Main and James S. Fritz	253	Determination of metal ions by liquid chromatographic separation of their 2-acetylpyridine-4-ethyl-3-thiosemicarbazone chelates
J. W. Morgan, D. W. Golightly and A. F. Dorrzapf, Jr.	259	Methods for the separation of rhenium, osmium and molybdenum applicable to isotope geochemistry
T. I. Tikhomirova, V. I. Fadeeva, G. V. Kudryavtsev, P. N. Nesterenko, V. M. Ivanov, A. T. Savitchev and N. S. Smirnova	267	Sorption of noble-metal ions on silica with chemically bonded nitrogen-containing ligands
Elo H. Hansen, Lars Nørgaard and Mikael Pedersen	275	Optimization of flow-injection systems for determination of substrates by means of enzyme amplification reactions and chemiluminescence detection
Krishna K. Verma, Kent K. Stewart, Archana Jain, Dayashanker Gupta and Sunil K. Sanghi	283	Manual and flow-injection spectrophotometric assay of thiols, based on their <i>S</i> -nitrosation
M. Romero-Saldaña, A. Ríos, M. D. Luque de Castro and M. Valcárcel	291	Simple unsegmented flow configurations for simultaneous kinetic determinations
J. G. Pentari, C. E. Efstathiou and T. P. Hadjiioannou	295	Kinetic determination of EDTA and citrate by the displacement of fluoride from Al^{3+} - F^{-} complexes and use of a fluoride ion-selective electrode
A. Velasco, M. Silva and M. Valcárcel	303	Kinetic spectrophotometric determination of nanogram amounts of cyanide
F. Reber Brown, Quintus Fernando and Tetsuya Ogura	309	Kinetics of the dissolution of copper metal in aqueous solutions containing unsaturated organic ligands and copper(II)
L. García Rodenas and S. J. Liberman	313	Hydrolysis of gadolinium(III) in light and heavy water
He Xing-Cun	319	Ion flotation of rhodium(III) and palladium(II) with anionic surfactants
Kiyohisa Ohta, Syn-ichi Itoh and Takayuki Mizuno	325	Electrothermal atomic-emission spectrometric determination of lithium with a metal-tube atomizer and a matrix modifier
M. S. Rathi, P. P. Khanna and Pulok Kumar Mukherjee	329	Determination of ten rare-earth elements and yttrium in silicate rocks by ICP-AES without separation and preconcentration
Randjel P. Mihajlović, Vilim V. Vajgand and Ljiljana N. Jakšić	333	Coulometric generation of H^{+} and D^{+} ions in aqueous media by anodic oxidation of hydrogen and deuterium dissolved in palladium
J. B. Puschett, B. S. Rao, B. M. Karandikar and K. Matyjaszewski	335	Indicator characteristics of Bromothymol Blue derivatives
Liliana Fernández and Roberto Olsina	339	Synthesis and characterization of 2-(3,5-dichloro-2-pyridylazo)-5-dimethylaminophenol as a reagent for determination of lanthanum
Itsuo Mori, Yoshikazu Fujita, Minako Toyoda, Keiji Kato, Kazumi Fujita and Yuji Okazaki	343	Spectrophotometric determination of antimony with vanillylfluorone in the presence of poly(vinyl alcohol)
C. Mohana Das	347	Determination of some sulphur compounds with <i>N</i> -bromoimides
<i>Book Reviews</i>	351	
<i>Questionnaire: Software Survey Section</i>	i	

APRIL

H. K. Chung and J. D. Ingle, Jr.	355	Kinetic fluorometric FIA determination of total ascorbic acid, based on use of two serial injection valves
M. C. Quintero, M. Silva and D. Pérez-Bendito	359	Kinetic determination of zineb in agricultural samples by continuous addition of reagent
Russell L. Dills, Stuart D. Kent, Harvey Checkoway and David A. Kalman	365	Quantification of volatile solvents in blood by static headspace analysis

Juwadee Shiowatana and Jaroslav P. Matousek	375	Electrodeposition on pyrolytic graphite platforms for electrothermal atomic-absorption spectroscopic determination of labile lead in saline water
Marit Andersson and Åke Olin	385	Determination of lead in household refuse fly-ash by X-ray fluorescence spectrometry and a modified standard-addition technique
José M. Fernández Alvarez, Malcolm R. Smyth and Richard O'Kennedy	391	Adsorptive voltammetric behaviour of immunoglobulin M
Akiharu Hioki, Masaaki Kubota and Akira Kawase	397	Accuracy in the precise coulometric titration of ammonia and ammonium ion with electrogenerated hypobromite
A. Lapolla, C. Gerhardinger, G. Crepaldi, D. Fedele, M. Palumbo, D. Dalzoppo, C. J. Porter, E. Ghezzi, R. Seraglia and P. Traldi	405	Mass spectrometric approaches in structural identification of the reaction products arising from the interaction between glucose and lysine
Jean Pettersson and Åke Olin	413	The rate of reduction of selenium(VI) to selenium(IV) in hydrochloric acid
Stephen N. Brune and Donald R. Bobbitt	419	Effect of pH on the reaction of tris(2,2'-bipyridyl)ruthenium(III) with amino-acids: implications for their detection
José Barbosa, Victoria Sanz-Nebot and Elena Torrero	425	Equilibrium constants and assay of bases in acetonitrile
G. Bidoglio, P. Cavalli, I. Grenthe, N. Omenetto, Pan Qi and G. Tanet	433	Studies on metal carbonate equilibria—Part 21. Study of the U(VI)-H ₂ O-CO ₂ (g) system by thermal lensing spectrophotometry
Alessandro De Robertis and Concetta De Stefano	439	Studies of polyfunctional <i>O</i> -ligands: formation and stability of Mg ²⁺ and Ca ²⁺ complexes of 1,2,4,5-benzenetetracarboxylic acid in aqueous solution at 25°
E. Cristofol, F. Sanchez Rojas and J. M. Cano-Pavón	445	Evaluation of various <i>N</i> -phenylthiosemicarbazones as chromogenic reagents in spectrophotometric analysis
<i>Analytical Data</i> Lorenzo Abate, Riccardo Maggiore, Carmelo Rigano and Concetta De Stefano	449	Protonation and complex formation constants of 3-amino-1,2,4-triazole in NaCl and CaCl ₂ media at different temperatures and ionic strengths
Predrag Djurdjević, Dusan Radanović, Milica Cvijović and Dragan Veselinović	455	Potentiometric determination of the protonation constants of 1,3-propanediamine- <i>N,N'</i> -diacetate- <i>N,N'</i> -di-3-proprionate
<i>Book Reviews</i>	461	
<i>Software Survey Section</i>	465	
<i>Questionnaire: Software Survey Section</i>	i	

MAY

<i>Editorial</i>	V	
<i>Talanta: Chemical Sensors Advisory Board</i>	VII	
A. R. Timerbaev, O. M. Petrakhin, I. P. Alimarin* and T. A. Bol'shova	467	High-performance liquid chromatography of metal chelates: Environmental and industrial trace metal control
Koichi Yamamoto and Shoji Motomizu	477	Liquid-liquid distribution of ion-associates of acidic dyes with quaternary ammonium counter-ions
M. Hidalgo, A. Masana, V. Salvadó, M. Muñoz and M. Vallente	483	Extraction of palladium with tri-isobutylphosphine sulphide (Cyanex 471) in toluene from chloride solutions containing thiocyanate
Joseph Wang and Ziad Taha	487	Trace measurements of rhodium by adsorptive stripping voltammetry

Agnes Yoo and Carl E. Moore	493	The synthesis of some lipophilic tetra-arylborates for use in membrane electrode preparation
Christopher P. Loran and Ray Von Wandruszka	497	Nucleation in premicellar aggregation
Mo Shengjun and James A. Holcombe	503	Preconcentration of nickel and cobalt on algae and determination by slurry graphite-furnace atomic-absorption spectrometry
Hajime Ishii and Katsunori Kohata	511	Indirect spectrophotometric determination of trace cyanide with cationic porphyrins
Nobutaka Yoshikuni	515	Rapid dissolution of chromite with sulphuric acid-lithium sulphate mixture containing ceric sulphate, manganese dioxide or periodate, and spectrophotometric determination of chromium
Reiko Fujita	521	The influence of hydrogen peroxide and pH on the Mohr titration
R. Raghavan and Subhir Raha	525	A rapid turbidimetric method for the determination of total sulphur in zinc concentrate
<i>Chemical Sensors Section</i>		
J. P. Alarie and T. Vo-Dinh	529	A fiber-optic cyclodextrin-based sensor
Alan R. Katritzky, Jamshed N. Lam and Hassan M. Faid-Allah	535	Synthesis of new microsensor coatings, and their response to test vapors
Orlando Fatibello-Filho, Ahmad A. Suleiman and George G. Guilbault	541	Piezoelectric crystal sensor for the determination of formaldehyde in air
Jianxun Zhou and Erkang Wang	547	Liquid chromatography amperometric detection of carboxylic acids and phenolic acids with a copper-based chemically-modified electrode
Weiyang Hou and Erkang Wang	557	A glassy-carbon electrode modified by dispersed α -alumina as an enhanced electrochemical detector in liquid chromatography for cysteine and glutathione
Saad S. M. Hassan, Eman M. Elnemma and Marawan A. Hamada	561	Nitron tetrachloroaurate(III) electrodes with poly(vinyl chloride) and liquid membranes for the selective determination of gold
<i>Book Reviews</i>	567	

JUNE

Aurora Navas Diaz	571	Analytical applications of 1,10-anthraquinones: A review
S. Wayne Kubala, David C. Tilotta, Marianna A. Busch and Kenneth W. Busch	589	Design and performance of a direct-reading, multichannel spectrometer for the determination of chlorinated purgeable organic compounds by flame infrared-emission spectrometry
Mohammad S. Iqbal, Farooq Rashid and Naimat A. Javed	603	An electrolytic device for preparation of hydrogen and oxygen from water for isotopic analysis
Les Ebdon, Steve J. Hill and Philip Jones	607	HPLC coupled with in-line photolysis, hydride generation and flame atomic-absorption spectrometry for the speciation of tin in natural waters
Zhaolun Fang, Tiezheng Guo and Bernhard Welz	613	Determination of cadmium, lead and copper in water samples by flame atomic-absorption spectrometry with preconcentration by flow-injection on-line sorbent extraction
Jiang Zhi-Liang	621	Catalytic determination of ultratrace amounts of ruthenium with oscillopolarographic detection
Surendra Prasad and Prem C. Nigam	627	Catalytic kinetic determination of ultratrace amounts of ruthenium(III), based on the oxidation of benzylamine by alkaline hexacyanoferrate(III)
James W. Dunning, Jr. and James T. Stewart	631	Some new acridinium trifluoromethanesulfonates as spectrophotometric derivatization reagents for aromatic and aliphatic primary amines

Saidul Zafar Qureshi, Ahsan Saeed, Seema Hague and Mubeen Ahmad Khan	637	Extraction spectrophotometric method for the determination of ascorbic acid in pharmaceutical preparations, urine and fruit juices with potassium iodate
B. Chiswell and K. R. O'Halloran	641	Comparison of three colorimetric methods for the determination of manganese in freshwaters
Neesha Shah, M. N. Desai, S. K. Menon and Y. K. Agrawal	649	Ion-exchange separation and spectrophotometric determination of vanadium in environmental samples
Shigeo Umetani, Naoki Shigemura, Sorin Kihara and Masakazu Matsui	653	Precipitation and extraction of some bivalent metal ions with bis(di-phenylphosphinyl)methane and perchlorate
Walter Lengauer	659	On the application of the Dumas technique for the determination of nitrogen in refractory nitrides
D. K. Sharma and R. D. Sharma	665	Non-aqueous cerimetric determination of dithiocarbamates and its application to the determination of amines
Liu Qiping, Zhang Huashan and Cheng Jieke	669	Reversed-phase HPLC determination of some noble metals as their thiazolylazoresorcinol chelates
R. P. Mihajlović, V. J. Vajgand and R. M. Džudović	672	The application of deuterium-palladium electrodes in the coulometric-potentiometric determination of bases in ketone media
C. Sánchez-Pedreño, M. I. Albero, M. S. García and A. Saez	677	Kinetic determination of selenium, based on inhibition of the Pd(II)-catalysed reaction between Pyronine G and hypophosphite
Itsuo Mori, Yoshikazu Fujita, Minako Toyoda, Keiji Kato, Naomi Yoshida and Masao Akagi	683	Fluorimetric determination of hydrogen peroxide by use of the fluorescence reaction between <i>N</i> -(4'-hydroxyphenyl)- <i>N</i> -(4-methylquinolinyl)-amine and cobalt(II) in the presence of trimethylstearylammmonium chloride
<i>Book Reviews</i>	687	
<i>Questionnaire: Software Survey Section</i>	i	

JULY

Constantinos A. Georgiou, Michael A. Koupparis and Themistocles P. Hadjiioannou	689	Flow-injection stopped-flow kinetic spectrophotometric determination of drugs, based on micellar-catalysed reaction with 1-fluoro-2,4-dinitrobenzene
Paolo Uguagliati and Luciano Canovese	697	Macroscopic and microscopic acid dissociation constants of diprotic acids—a potentiometric and spectrophotometric study
S. Koch and G. Ackermann	705	Spectrophotometric examination of redox equilibria by use of logarithmic transformations
Nai-Xing Wang	711	Direct spectrophotometric determination of Nd in mixed rare earths with Semi-Xylenol Orange and cetylpyridinium chloride
David K. Gosser Jr. and Feng Zhang	715	A PC-based general program for the simulation and analysis of cyclic voltammetric experiments
Marcin Palys, Tomas Korba, Martinus Bos and Willem E. van der Linden	723	The separation of overlapping peaks in cyclic voltammetry by means of semi-differential transformation
Aldalea Lopes Brandes Marques and Gilberto Orivaldo Chierice	735	Elimination of the copper-zinc interference in anodic stripping voltammetry by addition of a complexing agent
Peng Tuzhi, Yang Zhongping and Lu Rongshan	741	Voltammetric measurement of haloperidol following adsorptive accumulation at glassy-carbon electrodes
Mercedes Sánchez, Domingo Gázquez and Paloma García	747	Determination of molybdenum by atomic-absorption spectrometry after separation by 5,5'-methylenedisalicylohydroxamic acid extraction and further reaction with thiocyanate and tin(II)
Rajesh Purohit and Surekha Devi	753	Determination of copper at ng levels by in-line preconcentration and flow-injection analysis coupled with flame atomic-absorption spectrometry
Anatoly B. Volynsky, Eveline M. Sedykh and Lidilya N. Bannykh	761	Ascorbic acid as a matrix modifier for determination of tin in concentrated boric acid solutions by electrothermal atomic-absorption spectrometry

J. C. Coria-García and T. M. Niemezyk	767	Determination of nitric acid concentration by using europium ion fluorescence
Lawrence C. Thomas and Rashid Al Othman	773	Comparisons of integration <i>vs.</i> rate measurements for oxidase enzymatic analyses
Masaki Mifune, Junichi Odo, Akimasa Iwado, Yutaka Saito, Noriko Motohashi, Masahiko Chikuma and Hisashi Tanaka	779	Uricase-like catalytic activity of ion-exchange resins modified with metalloporphyrins
K. Brodersen, U. Werner, Y. A. Gawargious and S. Huang	785	Indirect determination of traces of thiosulphate by differential-pulse polarography
S. K. Sahoo	789	Extractive-chromatographic separation of bismuth with Aliquat 336S from citrate solutions
K. M. M. Krishna Prasad and S. Raheem	793	Specification of colour changes of metallochromic indicators in the titration of bismuth with EDTA
Liu Shaopu and Wang Fuchang	801	A highly sensitive colour reaction for chromium(VI) with the iodide-basic xanthene dye-PVA system
<i>Annotation</i>		
Madeleine Štulíková	805	Is nitrate really an inert electrolyte? A brief review
<i>Book Reviews</i>	809	
Questionnaire: Software Survey Section	i	

AUGUST

V Obituary

Akheel A. Syed and Maravattickal K. Dinesan	815	Review: Polyaniline—A novel polymeric material
Mollie L. E. TeVrucht and Peter R. Griffiths	839	Quantitative investigation of matrices for diffuse reflectance infrared Fourier transform spectrometry
Thomas Gübell, Jaromír Růžička and Gary D. Christian	851	Determination of trace amounts of a proteolytic enzyme by FIA with a stopped-flow and an on-line preconcentration technique
Oroncio Jiménez de Blas, José Luis Pereda de Paz and Jesús Hernández Méndez	857	Indirect determination of the pesticide dimethoxydithiophosphate in an FIA-AAS system with liquid-liquid back-extraction
U. Richts, J. A. C. Broekaert, P. Tschöpel and G. Tölg	863	Comparative study of a Beenakker cavity and a surfatron in combination with electrothermal evaporation from a tungsten coil for microwave plasma optical emission spectrometry (MIP-AES)
Kiyohisa Ohta, Syn-Ichi Itoh and Takayuki Mizuno	871	Electrothermal atomization atomic absorption spectrometry of cadmium with a platinum tube atomizer
B. W. Darvell and V. W.-H. Leung	875	The RAMESES algorithm for multiple equilibria—IV. Strategies for improvement (RAMESES III)
W. D. Scott, T. J. Wrigley and K. M. Webb	889	A computer model of struvite solution chemistry
Sajid Husain, M. Kifayatullah and R. Nageswara Rao	897	Computer-assisted ¹³ C NMR spectroscopic identification and determination of chlorohydrins in reaction mixtures formed during the manufacture of glycerol
P. A. Snyder and E. Voigtman	903	Functional group effects in laser-excited multi-photon photoionization of organics in liquid solutions
Zhao Jianwei and Xu Qibeng	909	Colour reaction of platinum(II) with 5-(4-nitrophenylazo)-8-(<i>p</i> -toluenesulphonamido)quinoline and its analytical applications
Bhagwandas M. Patel, H. Anson Moyo and Robert Weinberger	913	Postcolumn formation of fluorophores from nitrogenous pesticides by UV photolysis
F. W. E. Strelow	923	Separation of traces and larger amounts of bismuth from gram amounts of thallium, mercury, gold and platinum by cation-exchange chromatography on a macroporous resin

A. El-Jammal, A. A. Bouklouze, G. J. Patriarche and G. D. Christian	929	Use of ethylene-vinyl-acetate as a new membrane matrix for calcium ion-selective electrode preparation
M. S. Prasada Rao, A. Rama Mohan Rao, Karri V. Ramana and S. R. Sagi	937	Thallimetric oxidations—VI. Titrimetric and spectrophotometric methods for the determination of phosphite and analysis of binary mixtures of phosphite and oxalate
Ashok Kumar Malik and A. L. J. Rao	941	Spectrophotometric determination of ziram, ferbam and zineb with diphenylcarbazone
K. Krishnan Namboothiri, N. Balasubramanian and T. V. Ramakrishna	945	Spectrophotometric determination of thallium after its extraction as an ion-pair of the chloro-complex and pyronine G
<i>Notices</i>	i	
<i>Software Survey Section</i>	iii	
<i>Questionnaire: Software Survey Section</i>	v	

SEPTEMBER

D. S. Forsyth and C. Cl��roux	951	Determination of butyltin, methyltin and tetraalkyltin in marine food products with gas chromatography-atomic absorption spectrometry
J. V. Gimeno Adelantado, V. Peris Mart��nez, A. Pastor Garcia and F. Bosch Reig	959	Atomic-absorption spectrometric determination of calcium, magnesium and potassium in leaf samples after decomposition with molten sodium hydroxide
Hirofumi Kawazumi, Hideki Nishimura, Yukiaki Otsubo and Teichiro Ogawa	965	Universal on-line detector for high-performance liquid chromatography via magneto-optical rotation
Yi Yu Vin and S. M. Khopkar	971	Separation of niobium and tantalum by extraction chromatography with bis(2-ethylhexyl)phosphoric acid
Lu Guanghan, Li Xiaoming, He Zhilke and Hu Shuanglong	977	Polarographic determination of fluoride using the adsorption wave of the Ce(III)-alizarin complexone-fluoride complex
J��rgen Larsen and Bo Svensmark	981	Labile species of Pb, Zn and Cd determined by anodic stripping staircase voltammetry and their toxicity to <i>Tetrahymena</i>
Cui Hongbo and Sun Junyan	989	Potassium sodium chloride integrated microconduits in a potentiometric analytical system
Thomas A. LaFisca, Stuart J. Nagourney and Charles Pietarinen	995	The determination of lead in total suspended air particulates by x-ray fluorescence spectroscopy
G. Bidoglio, I. Grenthe, P. Qi, P. Robouch and N. Omenetto	999	Complexation of Eu and Tb with fulvic acids as studied by time-resolved laser-induced fluorescence
A. Renuka and K. Shakuntala	1009	Electrogeneration of Hg ⁺ in the presence of tryptophan
Rama Pande and S. G. Tandon	1015	Protonation and solvent extraction of <i>N-p</i> -tolylbenzohydroxamic acid in hydrochloric acid medium
Constantina N. Konidari and Miltiades I. Karayannis	1019	Interference in the kinetic determination of ascorbic acid by sulphide and sulphite
B. W. Darvell and V. W.-H. Leung	1027	The RAMESES algorithm for multiple equilibria—V. Error statements
Jacobus F. van Staden	1033	Simultaneous flow-injection analysis of three components with on-line dialyzers in series. Determination of sodium, potassium and chloride in blood serum
K. M. Shamsuddin, Syed Ali and Pushkin M. Qureshi	1041	Specific solid-state detection and semiquantitative determination of catechol and <i>o</i> -nitrophenol and some of their kinetic parameters
D. Mallikarjuna Rao, K. Hussain Reddy and D. Venkata Reddy	1047	Spectrophotometric determination of palladium with 5,6-dimethyl-1,3-indanedione-2-oxime
Chung-Gin Hsu, Xi-Man Lian and Jiao-Mai Pan	1051	Simultaneous spectrophotometric determination of thorium and rare earths with <i>m</i> -carboxychlorophosphonazo (CPAmK) and cetylpyridinium chloride (CPC)

C. S. P. Sastry, T. Thirupathi Rao and A. Sallaja	1057	Spectrophotometric determination of nicoumalone, acebutolol hydrochloride and procainamide hydrochloride
Yi-Bin Qu	1061	New reagent for spectrophotometric determination of salicylic acid
<i>Book Reviews</i>	1065	
<i>Notices</i>	i	
<i>Questionnaire: Software Survey Section</i>	ix	

OCTOBER

V Obituary

Jamil Anwar, Jesús M. Anzano and James D. Winefordner	1071	Bromide determination at nanogram levels by laser-excited molecular fluorescence spectroscopy in a graphite furnace
Joseph Wang, Lucio Angnes and Chen Liang	1077	Electrocatalysis and amperometric detection of organic peroxides at modified carbon-paste electrodes
J. G. Sen Gupta	1083	Determination of barium, strontium and nine minor and trace elements in impure barite and strontianite by inductively-coupled plasma atomic-emission spectrometry after dissolution in disodium ethylenediaminetetraacetate
Xu Bo-Xing, Sheng Ming-Neng, Huang Chao-Biao and Fang Yu-Zhi	1089	Application of chemically modified probe-atomic absorption spectrometry (CMPAAS)—I. Determination of Bi in copper alloy and lead by trioctylphosphine oxide-coated tungsten probe-AAS
Irena Jančářová, Hana Křížová and Vlastimil Kubáň	1093	Determination of uranium in technological waters by ion-pair liquid chromatography
Maria Pesavento and Antonella Profumo	1099	Interaction of serum albumin with a sulphonated azo dye in acidic solution
C. S. P. Sastry, T. Thirupathi Rao, A. Sallaja and J. Venkateswara Rao	1107	Micro-determination of warfarin sodium, nicoumalone and acebutolol hydrochloride in pharmaceutical preparations
M. L. S. Simões Gonçalves, M. F. C. Vilhena, J. M. Fernandes Sollis, J. M. Castro Romero and M. A. Sampayo	1111	Uptake of lead and its influence in the alga <i>Selenastrum capricornutum</i> Printz
R. Kuroda, K. Oguma, K. Kitada and S. Kozuka	1119	Flow analysis of silicate rocks for zirconium
Steven M. Pyle and Matthew M. Setty	1125	Supercritical fluid extraction of high sulfur soils, with use of a copper scavenger
Masahiko Murakami and Takeo Takada	1129	Extraction of copper(II) with the APCD/DIBK system from concentrated hydrochloric and nitric acid media: estimation of true limit of acidity for the extraction
Ian D. Brindle and Hengwu Chen	1137	The effect of molybdenum(VI) on the production of arsine by the tetrahydroborate(III) reaction
Liu Po, Liu Hengchuan and Wu Cheng	1143	Analytical application of a new thiazolylazo reagent, 2-(2-benzothiazolylazo)-5-dimethylamino-4-tolylarsonic acid
Dolores Sicilia, Soledad Rubio and Dolores Perez Bendito	1147	Kinetic determination of Hg(II) based on its accelerating effect on the reaction between hexacyanoferrate(II) and 1,10-phenanthroline catalysed by micelles
Hassan F. Askal	1155	New spectrophotometric methods for determination of captopril bulk drug and tablets
Hong-Bin He, Yun-Xiang Ci, Wen-Bao Chang and Wen-Ling Gong	1159	Simultaneous determination of iron(III) and vanadium(V) by use of a kinetic-spectrophotometric and rapid mixing flow system

Ram Parkash, Reeta Bansal, Ajit Kaur and S. K. Rehani	1163	Malachite green as a reagent for detection and spectrophotometric determination of chromium(VI)
J. K. Gupta	1167	Rapid spectrophotometric determination of trace copper impurity in <i>N,N'</i> -di(2-butyl)- <i>p</i> -phenylenediamine
<i>Chemical Sensors Section</i> Chaonan Xu, Jun Tamaki, Norio Miura and Noboru Yamazoe	1169	Promotion of tin oxide gas sensor by aluminum doping
Zhiqiang Gao, Peibiao Li and Zaofan Zhao	1177	Determination of iron(II) with chemically-modified carbon-paste electrodes
Jianhong Pei, Quan Yin and Jiayue Zhong	1185	Potentiometric determination of trace silver based on the use of a carbon paste electrode
Jinrui Xu and Xiurun Zhuang	1191	Poly-salicylic acid modified glassy-carbon electrode and its application
Xiangfang Xie, Ahmad A. Saleiman and George G. Guilbault	1197	Determination of urea in serum by a fiber-optic fluorescence biosensor
<i>Book Reviews</i>	1201	
<i>Errata</i>	i	
<i>Questionnaire: Software Survey Section</i>	iii	

NOVEMBER

<i>Talanta Medal</i>	1207	
Kevin Ashley	1209	Solution infrared spectroelectrochemistry: A review
Kamla M. Emara, Hassan F. Askal and Gamal A. Saleh	1219	Spectrophotometric determination of tetracycline and oxytetracycline in pharmaceutical preparations
Assen Karolev	1223	Substitution complexometric determination of cadmium in the presence of zinc in homogeneous water-organic solvent medium
Danhua Chen, A. Ríos, M. D. Luque de Castro and M. Valcárcel	1227	Simultaneous flow-injection determination of chlorpromazine and promethazine by photochemical reaction
Tomás Pérez-Ruiz, Carmen Martínez-Lozano, Virginia Tomás and Gabriel Lambertos	1235	Flow-injection successive determination of cysteine and cystine in pharmaceutical preparations
Ricardo E. Santelli, Mercedes Gallego and Miguel Valcárcel	1241	Determination of bromazepam by coupling a continuous liquid-liquid extractor to an atomic-absorption spectrometer
Manuel Hernández Córdoba and Ignacio López García	1247	A fast method for the determination of lead in paprika by electrothermal atomic-absorption spectrometry with slurry sample introduction
S. M. Golabi and M. Showkati-Shishevan	1253	Potentiometric titration of phenothiazine compounds in chloroform and its use in pharmaceutical analysis
Stephen A. Wring, John P. Hart and Brian J. Birch	1257	Determination of reduced glutathione in human whole blood by high-performance liquid chromatography with electrochemical detection by a graphite-epoxy resin electrode chemically modified with cobalt phthalocyanine
J. J. Berzas Nevado, J. Rodríguez Flores and M. L. de la Morena Pardo	1261	Determination of sulphamethizole in the presence of nitrofurantoin by derivative spectrophotometry and ratio spectra derivative
Zs. Szilvássy-Vámos, A. Györfi-Buzási and Zs. Pásztor	1265	Changes in plasma characteristics caused by easily ionisable elements in hollow cathode discharge emission spectrography
M. C. Quintero, M. Silva and D. Pérez-Bendito	1273	Enzymatic determination of <i>N</i> -methylcarbamate pesticides at the nanomolar level by the stopped-flow technique

- S. Chauveau, M. Hamon and E. Lelou 1279 Separation and identification of various vulcanization agents and anti-oxidants in two types of rubber by chromatographic and spectrometric methods
- J. S. Esteve Romero, M. C. García Álvarez-Coque and G. Ramis Ramos 1285 Formation rates and protonation constants of azo dyes in a sodium dodecylsulphate micellar solution
- Ma Wan-Li 1291 The effect of pH on a multiprotonatable quinidine ion-selective electrode
- José Barbosa and Carles M. Bosch 1297 Acid-base indicators in *N,N*-dimethylformamide: chromatic parameters of transition ranges
- Clausius G. De Lima, Tereza C. M. Pastore, Carlos A. Schwartz, Jader S. Cruz and Antonio Sebben 1303 Utilization of *o*-phthalaldehyde-sulphuric acid as a spray reagent in thin-layer chromatographic detection of some indolealkylamines and application to cutaneous secretion extracts of toad species
- I. Jelinek, I. Němcová and P. Rychlovský 1309 Effect of salts on the stability of the cationic radical of phenothiazine derivatives
- K. Wilcox and G. E. Pacey 1315 Chromogenic benzo- and monoaza-12-crown-4, 13-crown-4 and 14-crown-4 lithium selective crown ethers
- Yasuyuki Takeda, Nobuyuki Ikeo and Noriko Sakata 1325 Thermodynamic study of solvent extraction of 15-crown-5- and 18-crown-6-*s*-block metal ion complexes and tetraalkylammonium ions with picrate anions into chloroform
- B. Narasimha Murty, R. B. Yadav, C. K. Ramamurthy and S. Syamsundar 1335 Spectrophotometric determination of the oxygen to uranium ratio in uranium oxides based on dissolution in sulphuric acid
- F. Navarro-Villoslada, L. V. Pérez-Arribas, M. E. León-González, M. J. Santos-Delgado and L. M. Polo-Díez 1341 Multicomponent analysis of chlorophenols by diode array derivative spectrophotometry
- S. Agatonović-Kuštrin, Lj. Živanović D. Radulović and M. Vasiljević 1347 Statistical optimisation applied to the spectrophotometric study of the tolmetin-Fe(III) complex

Questionnaire: Software Survey Section i

DECEMBER

- F. Grases and C. Genestar 1353 A potentiometric technique for kinetic determination of citrate, based on inhibition of crystalline growth of lead carbonate seed crystals
- Angel Ríos and Miguel Valcárcel 1359 Exploiting the hydrodynamic aspects of continuous-flow systems
- Anders Vinther, Henrik Sæberg, Hans Holmegaard Sørensen and Anne Munk Jespersen 1369 A practical approach to high performance capillary electrophoresis with biosynthetic human growth hormone as a model protein
- Chansa Muntuta-Kinyanta and James K. Hardy 1381 Permeation-solid adsorbent sampling and GC analysis of formaldehyde
- P. Fernández, C. Pérez Conde, A. Gutiérrez and C. Cámara 1387 On-line aluminium preconcentration on chelating resin and its FIA-spectrofluorimetric determination in foods and dialysis concentrates
- Jiří Lexa and Karel Štulík 1393 Unsegmented flow analysis with ion-selective electrodes by use of a large-volume wall-jet cell
- Bahrudin Saad, Kanagi Kanapathy and Mohd Noor Ahmad 1399 Chloroquine polymeric membrane electrodes: development and applications
- A. Gojmerac Ivšić and B. Tambina 1403 Extraction and complex formation of niobium(V) with 3-hydroxy-2-methyl-1-(4-tolyl)-4-pyridone
- Peter M. May and Kevin Murray 1409 JESS, a joint expert speciation system—I. Raison d'être
- Peter M. May and Kevin Murray 1419 JESS, a joint expert speciation system—II. The thermodynamic database
- C. Channe Gowda and S. M. Mayanna 1427 Assay of sulphur compounds with 1-chlorobenzotriazole

Bharathibai J. Basu, D. K. Padma and S. R. Rajagopalan	1431	Adsorbing colloid flotation separation and polarographic determination of Mo(VI) in water
<i>Analytical Data</i>		
Béla Noszál and Rózsa Kassai-Tánczos	1439	Microscopic acid–base equilibria of arginine
Pavel Janoš, Karel Štullk and Věra Pacáková	1445	An ion-exchange separation of Cu ²⁺ , Cd ²⁺ , Pb ²⁺ and Tl ⁺ on silica gel with polarographic detection
Takashi Hayashita, Mi-Ja Goo, Jong Seung Kim and Richard A. Bartsch	1453	Effect of structural variation within <i>sym</i> -(R)dibenzo-16-crown-5-oxyacetic acid resins upon the selectivity and efficiency of alkali-metal cation sorption
Brice C. Erickson, Randy J. Pell and Bruce R. Kowalski	1459	Infrared emission spectroscopy of liquid samples with multivariate calibration as a model for process analytical applications
M. H. Pournaghi-Azar and J. Ordoukhanian	1469	Polarographic behaviour of uranium β -diketonates in chloroform
A. Cladera, J. M. Estela and V. Cerdá	1475	Automatic kinetic determination of Hg(II) by anodic stripping potentiometry with constant current oxidation
Guorong Zhang and Chonggang Fu	1481	Adsorptive voltammetric determination of copper with a benzoin oxime graphite paste electrode
Zheng-Qi Zhang, Zhao-Peng Cheng, Sheng-Zong Cheng and Gui-Fa Yang	1487	5-[(<i>p</i> -methyl-phenyl)azo]-8-aminoquinoline as a new reagent for trace determination of nickel by adsorptive cathodic stripping voltammetry
Feng Dexiong, Yang Peihui and Yang Zhaoliang	1493	Determination of germanium by potentiometric stripping analysis and adsorption potentiometric stripping analysis
<i>Book Reviews</i>	1499	
<i>Questionnaire: Software Survey Section</i>	i	

THIRD INTERNATIONAL SYMPOSIUM

Under the aegis of IUPAC

Analytical chemistry in the exploration, mining, and processing of materials

2-7 August 1992, Sandton Sun Hotel, Sandton, South Africa

The organizers cordially invite you to attend this, the third symposium in the series, which will be held at the Sandton Sun Hotel, Sandton, from Sunday 2 to Friday 7 August 1992. The occasion will once again provide an opportunity for analytical scientists and their counterparts in the mining and metallurgical fields worldwide to exchange experiences.

The technical programme will consist of plenary lectures, parallel sessions of oral presentations and poster presentations. Detailed information and instructions to participants and to those presenting papers will be given in the Second Circular.

Those interested in presenting papers and/or posters are invited to submit preliminary abstracts. The general theme will be

The role of contemporary chemical analysis in mining and industrial technology.

The following topics will be covered:

- (1) Geochemical exploration
- (2) Extraction and beneficiation of materials
- (3) Value-added products
- (4) Environmental aspects
- (5) Coal
- (6) Metals and alloys
- (7) Rare earths
- (8) Noble and base metals
- (9) Analytical assurance and laboratory management
- (10) Automation and process control
- (11) High-technology materials.

Innovation in analytical techniques will be particularly welcome.

For further information please contact:

The Symposium Secretariat
Mintek
Private Bag X3015
RANDBURG
2125 South Africa.
Telephone: (27) (11) 793-3511
Mrs. Pam Baartman
Miss Yvonne Arnold
Facsimile: (27) (11) 793-2413
Telex: 424867 SA.

COMPANA '92

5th Conference
Computer Application in Analytical Chemistry
24-27 August 1992
Jena/Thuringia

The 5th Conference Computer Applications in Analytical Chemistry—COMPANA '92 continues the conferences organized in 1977 in Leipzig, 1980 in Dresden, 1985 and 1988 in Jena.

**THE 3rd INTENSIVE COURSE ON PRINCIPLES & APPLICATIONS
OF CHEMICAL SENSORS**

11–14 June 1991

Wildbad Kreuth, Bavaria, Germany

Lecturers for this course will include:

S. Brukenstein, E. Hall, J. Janata, M. Josowicz, H. D. Liess, D. Lubbers, H. L. Schmidt and E. Obermeier.

For further information contact:

Dr. Mira Josowicz
Inst. für Physik
Universität der Bundeswehr München
D-8014 Neubiberg
Germany
Tel.: 089 6004 3793
Fax: 089 6004 3560
E-Mail: K1401AC%DMOLRZ01,BITNET

THIRD INTERNATIONAL SYMPOSIUM

Under the aegis of IUPAC

Analytical chemistry in the exploration, mining, and processing of materials

2-7 August 1992, Sandton Sun Hotel, Sandton, South Africa

The organizers cordially invite you to attend this, the third symposium in the series, which will be held at the Sandton Sun Hotel, Sandton, from Sunday 2 to Friday 7 August 1992. The occasion will once again provide an opportunity for analytical scientists and their counterparts in the mining and metallurgical fields worldwide to exchange experiences.

The technical programme will consist of plenary lectures, parallel sessions of oral presentations and poster presentations. Detailed information and instructions to participants and to those presenting papers will be given in the Second Circular.

Those interested in presenting papers and/or posters are invited to submit preliminary abstracts. The general theme will be

The role of contemporary chemical analysis in mining and industrial technology.

The following topics will be covered:

- (1) Geochemical exploration
- (2) Extraction and beneficiation of materials
- (3) Value-added products
- (4) Environmental aspects
- (5) Coal
- (6) Metals and alloys
- (7) Rare earths
- (8) Noble and base metals
- (9) Analytical assurance and laboratory management
- (10) Automation and process control
- (11) High-technology materials.

Innovation in analytical techniques will be particularly welcome.

For further information please contact:

The Symposium Secretariat
Mintek
Private Bag X3015
RANDBURG
2125 South Africa.
Telephone: (27) (11) 793-3511
Mrs. Pam Baartman
Miss Yvonne Arnold
Facsimile: (27) (11) 793-2413
Telex: 424867 SA.

COMPANA '92

5th Conference
Computer Application in Analytical Chemistry
24-27 August 1992
Jena/Thuringia

The 5th Conference Computer Applications in Analytical Chemistry—COMPANA '92 continues the conferences organized in 1977 in Leipzig, 1980 in Dresden, 1985 and 1988 in Jena.

The Conference is organized by the Institute of Inorganic and Analytical Chemistry of the Friedrich Schiller University in collaboration with the Chemical Society of GDR, particularly the group of Analytical Chemistry and the group of Chemometrics and takes place in the main building of the Friedrich Schiller University, Goetheallee 1.

Language: The Conference languages will be German and English.

No simultaneous translation or interpretation will be provided.

Topics

- Chemometrics for environmental analysis and monitoring. Quality control/assurance of the environment
- Expert systems, principles of artificial intelligence in analytical chemistry
- Explorative and statistical data analysis, interactive scientific processing
- Multivariate experimental design and optimization
- Structure-activity and composition-quality relations
- Simulation and modelling of processes
- Complex application of chemometric procedures
- Evaluation of spectroscopic and chromatographic data
- Computer-coupled tandem methods in analytical chemistry
- Laboratory automation and information management
- Principles of image analysis in analytical chemistry
- Schooling and further training in the field of computer chemistry and chemometrics.

Key dates:

Return of preliminary application	to JUNE 1991
Distribution of 2nd Circular	SEPTEMBER 1991
Submission of contributions	NOVEMBER 1991
Deadline for submission of abstracts	FEBRUARY 1992
Notification of acceptance	APRIL 1992
Distribution of final programme	JUNE 1992

Address: COMPANA '92
 Friedrich Schiller University Jena
 Institute of Inorganic and Analytical Chemistry
 Steiger 3, Haus 3, Jena, Germany 6900
 Prof. Dr. K. Danzer (Scientific Committee) Tel.: 82-25467
 Dr. W. Ludwig (Organizing Committee) Tel.: 82-25029

SAC 92

An International Conference on Analytical Chemistry

20–26 SEPTEMBER 1992

UNIVERSITY OF READING

Organized by the Analytical Division of The Royal Society of Chemistry
 and the

Laboratory of the Government Chemist in its 150th year

An International Conference on Analytical Chemistry (SAC 92) organised jointly by the Analytical Division of The Royal Society of Chemistry and the Laboratory of the Government Chemist will be held in the Palmer building at the University of Reading. This is the tenth in the series of triennial Conferences originally started by the Society for Analytical Chemistry (hence SAC) and on this occasion also celebrates the 150th anniversary of the founding of the Laboratory of the Government Chemist (LGC). The conference will be held from Sunday 20 to Saturday 26 September 1992.

OBITUARY

PROFESSOR HERBERT A. LAITINEN

Professor Herbert A. Laitinen, one of the world's premier analytical chemists, died at his home in Gainesville, Florida, on 22 March 1991 at the age of 76. He was born on a farm in Ottertail County, Minnesota, of second-generation Finnish parents from whom he learned to speak Finnish before English. He attended the University of Minnesota, receiving the Ph.D. degree in 1940, having studied with Professor I. M. Kolthoff.

Dr Laitinen joined the chemistry faculty of the University of Illinois in 1940, becoming Head of Division of Analytical Chemistry in 1953. During World War II, he was a group leader in synthetic rubber research. An outstanding educator, he trained many of the analytical chemists presently influential in industry and academia. He lectured widely in Europe, Japan, China, and was a visiting professor at UCLA, Birmingham (England), Nanking, Seoul, and Munich, as well as an exchange visitor to Yugoslavia. A considerable number of scientists from abroad were attracted to Urbana for advanced study under his direction. His advanced text *Chemical Analysis* (second edition co-authored with W. E. Harris) is well known to two generations of chemists. In 1974, Dr Laitinen accepted an appointment as Graduate Research Professor at the University of Florida, a position he occupied at the time of his death. From 1966 to 1979, he served as editor of *Analytical Chemistry*.

Dr Laitinen's interests covered a wide spectrum of analytical chemistry. His major research interests were in electroanalytical chemistry, and in the early years he addressed problems in potentiometry and voltammetry. Later he emphasized the properties of molten salts, surface phenomena and catalysis. He had much to do with the revitalization of electroanalytical chemistry in the 1970s-1980s.

His career brought him numerous awards and honorary appointments. These include the American Chemistry Society's Award in Analytical Chemistry, the SOCMA Gold Medal in Environmental Chemistry, the Pittsburgh Society for Analytical Chemistry Award, the Kuebler Award of Alpha Chi Sigma, the Gadolin Medal Award of the Finnish Chemical Society, the ACS Analytical Chemistry Division Award for excellence in Teaching, The Talanta Medal in 1989, and the outstanding Alumni Achievement Award of the University of Minnesota. He was an honorary member of the Finnish Academy of Sciences, The Japan Society for Analytical Chemistry, and the Royal Society of Chemistry (London). He was a fellow of the AAAS and a member of the Electrochemical Society and the ACS, having been chairman of the latter's Division of Analytical Chemistry. He had also served as Secretary of the Commission on Electrochemical Data of the International Union of Pure and Applied Chemistry.

Although his personal research accomplishments were immeasurable and ground-breaking in many cases, I feel Herb Laitinen's major contributions to science were in the areas of teaching and analytical chemistry as a discipline. As an undergraduate and graduate student at the University of Illinois, I remember well the elegance, rigor, enthusiasm, and interest shown by Herb in his undergraduate and graduate classes at the U of I. I still have my notes from his courses, even though I discarded long ago the notes from most other courses. His books have greatly affected the teaching of analytical chemistry and his *History of Analytical Chemistry* with Galen Ewing as co-editor was a labor of love and a major accomplishment. Herb received in 1986 the American Chemical Society Analytical Division Award for Excellence in Teaching. Herb's contribution to analytical chemistry as a discipline is perhaps even more significant. As the Editor of the journal *Analytical Chemistry*, he brought new respect to the journal and to the discipline.

Herb Laitinen was always all business. He imparted his own enthusiasm, interest, and excitement to his students, even those who initially had little interest in the subject. At the University of Illinois

and the University of Florida Herb's wide-ranging scientific curiosity was always apparent in the stimulating and significant questions asked by him at seminars. Finally, within the last several months of his life, Herb had gone back into the laboratory to do his own research. I'll remember Herb Laitinen not only as a great scientist, scholar, and teacher but also as a friend, who gave me and many others excellent advice and support.

JIM WINEFORDNER

EDITORIAL

SENSORS PROVIDE IMMEDIATE ANALYTICAL RESULTS ON A CONTINUOUS OR REPETITIVE BASIS

Starting with this issue, Talanta will publish papers dealing with chemical sensors in a separate section. I will be serving as the first editor of this section, assisted by a distinguished board of sensor scientists who are introduced in this issue.

To decide what manuscripts will be appropriate for the new section, it is necessary to develop a working definition of a "chemical sensor". The "traditional" types of chemical sensors include electrodes and acoustic devices. More recently fiber optic devices have been widely accepted as chemical sensors. These devices share two common features; they are relatively low in cost, and they involve insertion of a device into the sample. However, there are many differences among "traditional" sensors. Some respond continuously. Others can be used for multiple single measurements with a "recharging" step in between. Still others can only be used for a single measurement. A few devices can be inserted directly into a sample. Many others require the addition of reagents to modify the sample, such as buffers to adjust pH and salt solutions to control ionic strength.

Rigor can be introduced into the definition of a chemical sensor by restricting the term to devices that have a specific set of properties. For example, an "ideal" sensor may be described as a device which is low in cost, responds continuously, does not perturb the sample and does not require the addition of reagents to the sample. However, many devices that are widely considered to be sensors do not satisfy this definition.

I prefer to define sensors, not in terms of device properties, but rather in terms of the kinds of problems that they solve. These problems have two elements. One is the need for multiple measurement. This can be met by continuous measurement or repetitive single measurements. The crucial parameter is the response time, either the intrinsic response time of a continuous sensor or the time between multiple single measurements. Low cost, frequently considered to be a property of a chemical sensor, is implicit in this aspect of single measurement devices since it is rarely practical to make multiple measurements by techniques having a high cost per measurement.

The second element of sensing is that analytical results are required immediately, *i.e.*, there is not a significant time interval between taking the sample and making the measurement. Making the measurement directly on the sample is the most effective way of accomplishing this. However, on site measurements, *e.g.*, field measurements of pollutants or home measurements of blood glucose, also involve a minimal interval between taking the sample and making the measurement.

I look forward to seeing how this guideline works out in practice. I invite you, my colleagues, to share with me your thoughts about chemical sensing. I also invite you to contribute manuscripts to Talanta: Chemical Sensors. I hope that together we will define and advance "chemical sensors" as a subdiscipline within analytical chemistry.

W. RUDOLF SEITZ

LOUIS GORDON MEMORIAL AWARD

Their Louis Gordon Memorial Awards were presented to Professor Yu. A. Zolotov (Kurnakov Institute of General and Inorganic Chemistry, U.S.S.R. Academy of Sciences, Moscow) and Dr. J. Šrámková and Dr. S. Kotrlý (University of Chemical Technology, Pardubice, Czechoslovakia) by Dr. R. A. Chalmers.



EDITORIAL

The Publisher and Editorial Board of *Talanta* regret to announce that owing to pressure of work Professor David Littlejohn has felt obliged to resign as joint Editor-in-Chief, and they take this opportunity to thank him on behalf of contributors and readers for the valuable work done by him for the journal during his all too brief tenure of the position, and for his enthusiasm in making innovations in it. From 1 January 1991 he will be replaced as joint Editor-in-Chief by Professor Elo H. Hansen, of the Technical University of Denmark, whose name will be well known to all in connection with flow-injection analysis. Papers that would previously have been sent to Professor Littlejohn should now be sent to:

Professor E. H. Hansen
Chemistry Department A
Building 207
Technical University of Denmark
DK-2800 Lyngby
Denmark

This issue is the first in the year that will see the introduction of a new feature in the journal, the Chemical Sensors Section, which will be edited by Professor Rudolf Seitz, of the University of New Hampshire, with the assistance of a separate Advisory Board, so it is particularly fitting that it should be a Special Issue on Sensor Electrodes, organized by Professor Lars Kryger, of Aarhus University, Denmark, who is warmly thanked for his work in compiling it. This special issue may be regarded as the forerunner of the new Chemical Sensors Section, giving a taste of things to come. The aims and scope of the new section appear elsewhere in this issue. Papers intended as contributions to this section should be sent to:

Professor W. Rudolf Seitz
Department of Chemistry
University of New Hampshire
Durham, NH 03824
U.S.A.

The Conference is organized by the Institute of Inorganic and Analytical Chemistry of the Friedrich Schiller University in collaboration with the Chemical Society of GDR, particularly the group of Analytical Chemistry and the group of Chemometrics and takes place in the main building of the Friedrich Schiller University, Goetheallee 1.

Language: The Conference languages will be German and English.

No simultaneous translation or interpretation will be provided.

Topics

- Chemometrics for environmental analysis and monitoring. Quality control/assurance of the environment
- Expert systems, principles of artificial intelligence in analytical chemistry
- Explorative and statistical data analysis, interactive scientific processing
- Multivariate experimental design and optimization
- Structure-activity and composition-quality relations
- Simulation and modelling of processes
- Complex application of chemometric procedures
- Evaluation of spectroscopic and chromatographic data
- Computer-coupled tandem methods in analytical chemistry
- Laboratory automation and information management
- Principles of image analysis in analytical chemistry
- Schooling and further training in the field of computer chemistry and chemometrics.

Key dates:

Return of preliminary application	to JUNE 1991
Distribution of 2nd Circular	SEPTEMBER 1991
Submission of contributions	NOVEMBER 1991
Deadline for submission of abstracts	FEBRUARY 1992
Notification of acceptance	APRIL 1992
Distribution of final programme	JUNE 1992

Address: COMPANA '92
 Friedrich Schiller University Jena
 Institute of Inorganic and Analytical Chemistry
 Steiger 3, Haus 3, Jena, Germany 6900
 Prof. Dr. K. Danzer (Scientific Committee) Tel.: 82-25467
 Dr. W. Ludwig (Organizing Committee) Tel.: 82-25029

SAC 92

An International Conference on Analytical Chemistry

20–26 SEPTEMBER 1992

UNIVERSITY OF READING

Organized by the Analytical Division of The Royal Society of Chemistry
 and the

Laboratory of the Government Chemist in its 150th year

An International Conference on Analytical Chemistry (SAC 92) organised jointly by the Analytical Division of The Royal Society of Chemistry and the Laboratory of the Government Chemist will be held in the Palmer building at the University of Reading. This is the tenth in the series of triennial Conferences originally started by the Society for Analytical Chemistry (hence SAC) and on this occasion also celebrates the 150th anniversary of the founding of the Laboratory of the Government Chemist (LGC). The conference will be held from Sunday 20 to Saturday 26 September 1992.

The scientific programme will be organized around plenary, invited and contributed papers and posters covering the whole field of analytical chemistry. The language will be English and the programme will include workshops where research workers can demonstrate new apparatus and techniques. An opportunity will be made for all participants to visit The Laboratory of the Government Chemist and other scientific establishments.

As for previous SAC Conferences a special issue of *The Analyst* will be published, and intending authors who would like their papers to be published therein are invited to include novel or relevant review material to satisfy the normal criteria for *The Analyst*. Papers may also be offered for publication in *The Journal of Analytical Atomic Spectrometry* and *Analytical Proceedings*.

All aspects of analytical science can be included in SAC 92, some suggested areas are:

Accreditation	Enzyme techniques	Preconcentration and separation
Agricultural	Flow injection methods	Probe methods
Atomic spectrometries	Food and drink	Process analysis
Atmospheric	Forensic	Professional and technical aspects of 1992
Automation and robotics	Genetic fingerprinting	Quality assurance
Bioanalytical techniques	Geological	Radiochemistry
Biochemical methods	Immunoassay	Reference materials
Biological and microbiological	Industrial	Remote sensing
Biotechnology	Instrumentation	Sample preparation
Catalytic and kinetic methods	Ion exchange	Sampling
Chemicals and petrochemicals	Laboratory design	Sensors
Chemometrics	Laboratory information	Standards
Chromatography	Management systems	Statistics in analysis
Clinical	Mass spectrometry	Surfaces
Collaborative analytical studies	Metallurgical	The integrated laboratory
Consumer protection	Methods of validation	Thermal methods
Data processing	Microanalysis	Toxicology
Drugs in sport	Molecular recognition	Water and effluents
Education	Molecular spectrometries	X-Ray methods
Electroanalytical methods	Nuclear magnetic resonance	
Electrophoresis	Pharmaceutical	
Environmental	Plastics, rubbers and textiles	

For further information please contact:

The Secretary
Analytical Division
Royal Society of Chemistry
Burlington House
Piccadilly
London W1V 0BN, U.K.

EUROANALYSIS VIII

5-11 September 1993
Edinburgh, U.K.

The Working Party on Analytical Chemistry of the Federation of European Chemical Societies and the Analytical Division of the Royal Society of Chemistry cordially invite your participation in the eighth triennial European Conference on Analytical Chemistry to be held at the University of Edinburgh from 5 to 11 September 1993.

Euroanalysis VIII will emphasise the role of analytical chemistry as a tool for problem solving in major areas of science as well as methodological developments. The programme will be designed to appeal both to practising analytical chemists in industry and to those in academia who are teaching and undertaking research.

OBITUARY



On March 11, 1991, Professor Gaston Jules Patriarche, internationally known in the field of electroanalytical and pharmaceutical chemistry, passed away.

G. J. Patriarche was born in Obaix-Buzet, near Brussels, on March 10, 1930. He studied at the Free University of Brussels (ULB) to become a pharmacist in 1956. Remaining faithful to his "Alma Mater", all his academic career has been devoted to ULB. Starting this career in 1957 as an assistant to Professor Louis Maricq in the analytical chemistry department of the Pharmaceutical Institute, he became immediately interested in electrochemical techniques which were being developed in the department. Encouraged by Professor James Lingane, visiting professor at the Faculty of Sciences, he was among the first European scientists to conduct coulometric measurements. Investigating the electrogeneration of bromine and iodine, he was able to determine about twenty different metal ions, directly or after complexation with 8-hydroxyquinoline, as well as numerous pharmaceutically interesting organic compounds. These studies allowed him to acquire

his Ph.D. in Pharmaceutical Sciences in 1963 with a thesis entitled "Contribution to coulometric analysis. Application to pharmaceutical sciences". Three subsidiary works were presented at the same time, devoted to polarimetry of antimony, polarographic separation of cobalt and nickel and thin layer chromatographic separation of As, Sb and Sn. He completed his education in Saclay, France where he acquired a radioelements manipulator degree.

Becoming a Main Assistant at ULB in 1964, he developed polarographic techniques and created a research unit in electrochemistry in the analytical department. He was a Research Associate in Chemistry at Harvard University in the laboratory of Professor J. Lingane in 1966 and 1969 and Visiting Professor in 1976. Promoted to Associate Professor in 1969 and Full Professor in 1977 at the Pharmaceutical Institute of ULB, he divided his time between teaching general chemistry, analytical chemistry and electrochemistry, and the development of his research laboratory. While modern polarographic techniques and voltammetry as solid electrodes remained the basis for his activities, he rapidly understood and developed considerable interest in modified electrodes and enzyme electrodes in pharmaceutical research. He was particularly fond of developing new biosensors and their application to pharmaceutical and biomedical analysis. He also contributed to the development of spectrophotometric and chromatographic techniques. Undefatigable in his approach to research, his whole life can be characterized by a need for knowledge

Professor Patriarche is author or co-author, with Ph.D. students and colleagues, of more than 250 scientific papers, including book chapters. All his publications as well as the hundreds of lectures given around the world were characterized by the will to demonstrate that electrochemical techniques are well adapted to pharmaceutical analysis. It was in this way that he directed the research work of his students in which he was always attentive and ready to assist.

The important role played by Professor Patriarche in scientific research is reflected by the positions he has occupied. He was the youngest member of the Belgian Royal Academy of Medicine, past-president of the Belgian Society of Pharmaceutical Sciences and the Analytical Section of the Belgian Royal Chemical Society. Among others, he was a member of the American Chemical Society since 1966, the Electrochemical Society, the International Society for Electrochemistry, the Society for Electroanalytical Chemistry and the Analytical Division of the International Union of Pure and Applied Chemistry. He was also a member of the Commission of the Belgian Pharmacopoeia and of the Scientific Council of the Belgian Department of Drug Control.

He was an active member of scientific committees of numerous international congresses devoted to electrochemistry or to pharmaceutical sciences, and he was the organizer of several.

His outstanding activity in the analytical, electroanalytical and pharmaceutical field was also reflected by his membership on the editorial boards of *Electroanalytical Abstracts*, *Clinical Letters*, *Analytical Letters*, *Journal of Pharmaceutical and Biomedical Analysis*, *Trends in Analytical Chemistry* and *Journal de Pharmacie de Belgique*. He was also Regional Editor for Europe of *Electroanalysis* at the time of his death.

He was awarded the Quinquennial Prize of the Belgian Royal Academy of Medicine and Doctor Honoris Causa of the Complutena University of Madrid.

The fruitful life of this outstanding electroanalytical pharmacist has been interrupted too early. However, he will remain in the memory of everybody who knew him.

Jean-Claude Viré
Institut de Pharmacie
Université Libre de Bruxelles

Editor's Note: Professor Patriarche was a close personal friend and colleague, and was a frequent referee for *Talanta* as well as contributor. Those who knew him will remember his jovial nature and his devotion to his family as well as to his teaching and science.

G.D.C.

The scientific programme will be organized around plenary, invited and contributed papers and posters covering the whole field of analytical chemistry. The language will be English and the programme will include workshops where research workers can demonstrate new apparatus and techniques. An opportunity will be made for all participants to visit The Laboratory of the Government Chemist and other scientific establishments.

As for previous SAC Conferences a special issue of *The Analyst* will be published, and intending authors who would like their papers to be published therein are invited to include novel or relevant review material to satisfy the normal criteria for *The Analyst*. Papers may also be offered for publication in *The Journal of Analytical Atomic Spectrometry* and *Analytical Proceedings*.

All aspects of analytical science can be included in SAC 92, some suggested areas are:

Accreditation	Enzyme techniques	Preconcentration and separation
Agricultural	Flow injection methods	Probe methods
Atomic spectrometries	Food and drink	Process analysis
Atmospheric	Forensic	Professional and technical aspects of 1992
Automation and robotics	Genetic fingerprinting	Quality assurance
Bioanalytical techniques	Geological	Radiochemistry
Biochemical methods	Immunoassay	Reference materials
Biological and microbiological	Industrial	Remote sensing
Biotechnology	Instrumentation	Sample preparation
Catalytic and kinetic methods	Ion exchange	Sampling
Chemicals and petrochemicals	Laboratory design	Sensors
Chemometrics	Laboratory information	Standards
Chromatography	Management systems	Statistics in analysis
Clinical	Mass spectrometry	Surfaces
Collaborative analytical studies	Metallurgical	The integrated laboratory
Consumer protection	Methods of validation	Thermal methods
Data processing	Microanalysis	Toxicology
Drugs in sport	Molecular recognition	Water and effluents
Education	Molecular spectrometries	X-Ray methods
Electroanalytical methods	Nuclear magnetic resonance	
Electrophoresis	Pharmaceutical	
Environmental	Plastics, rubbers and textiles	

For further information please contact:

The Secretary
Analytical Division
Royal Society of Chemistry
Burlington House
Piccadilly
London W1V 0BN, U.K.

EUROANALYSIS VIII

5-11 September 1993
Edinburgh, U.K.

The Working Party on Analytical Chemistry of the Federation of European Chemical Societies and the Analytical Division of the Royal Society of Chemistry cordially invite your participation in the eighth triennial European Conference on Analytical Chemistry to be held at the University of Edinburgh from 5 to 11 September 1993.

Euroanalysis VIII will emphasise the role of analytical chemistry as a tool for problem solving in major areas of science as well as methodological developments. The programme will be designed to appeal both to practising analytical chemists in industry and to those in academia who are teaching and undertaking research.

The programme will consist of invited plenary and keynote lectures, contributed papers, and posters and workshops. In order to ensure the high quality of the programme all contributed papers will be refereed by an international panel.

The conference organizer to whom all correspondence should be addressed is:

Miss P. E. Hutchinson
Analytical Division
The Royal Society of Chemistry
Burlington House
Piccadilly
London W1V 0BN, U.K.

XXI. European Congress on Molecular Spectroscopy

EUCMOS XXI

23–28 August 1992

Technical University Vienna, Physics Department, Vienna, Austria

This 21st event in the well established series of EUCMOS-conferences will be organized by the Working Group Molecular Spectroscopy of the Austrian Society for Analytical Chemistry (ASAC) in the GÖCh, in the historic mid-European city of Vienna on behalf of the International Committee of EUCMOS. EUCMOS XXI is supported by the Working Party on Analytical Chemistry of the Federation of European Chemical Societies (WPAC/FECS) and will highlight modern trends and recent developments in the rapidly expanding field of molecular spectroscopy. Methods and applications will be treated in 9 sessions including plenary, keynote and contributed oral and poster presentations.

Main Topics:

- 1 Molecular Structure and Interactions
- 2 Surface Analysis—Methods and Applications
- 3 Hyphenated Techniques (Chromatography–Spectroscopy)
- 4 Optical Sensors
- 5 Computer Aided Molecular Spectroscopy
- 6 Theoretical Aspects
- 7 Biological Pathways
- 8 Phase Transition and Order Phenomena
- 9 General

Conveners:

- (A. J. Barnes)
(M. Grasserbauer)
(J. F. K. Huber)
(R. Kellner)
(W. Wegscheider)
(A. Karpfen)
(A. Müller)
(H. Ratajczak)

International Committee:

- President: W. J. Orville-Thomas (GB)
President Elect: A. J. Barnes (GB)
Vice Presidents: A. Müller (D), H. Ratajczak (P)

Organizing Committee:

- R. Kellner (Chairman) (A)
A. J. Barnes (GB)
J. Bellanato (E)
J. G. Grasselli (USA)
J. A. Lercher (A)
J. van der Maas (NL)
H. H. Mantsch (CDN)
Z. Meic (YU)
J. Mink (H)
A. Neckel (A)
B. Schrader (D)
K. Taga (Secretary) (A)

Programme Committee:

- W. Landvoigt (Chairman) (A)
A. Benninghoven (D)
M. Grasserbauer (A)
E. H. Korte (D)
J. Lascombe (F)
H. Malissa (A)
E. Pretsch (CH)
C. N. R. Rao (IND)
M. Tasumi (J)
L. A. Gribov (USSR)
W. Wegscheider (A)
G. Zerbi (I)

FOREWORD

This special issue of *Talanta* is devoted to sensor electrodes for amperometric, potentiometric, and voltammetric analysis.

Over the past few years electrochemical probes have received a significant share of the attention which is currently focused on the construction of chemical sensors. Several types of ultramicro-electrodes, for instance, have been developed, and many have proved useful in the analysis of solutions with low electrolyte content, as low capacitance voltammetric sensors, and as sensors in the electroanalysis of microvolumes of solutions. A large variety of chemically modified electrodes, with functional groups incorporated on their surfaces, have been constructed for non-electrolytic preconcentration of trace analytes and for utilization of catalytic electrode processes. Also new potentiometric electrodes and calibration procedures have been introduced. As a result of these activities, electroanalytical approaches have progressively become more selective and sensitive, and the class of species which can be accessed by means of electroanalysis has been steadily expanding. The fifteen research papers and reviews in this issue are all written by authors who have contributed significantly in the area of sensor electrode research. It is my hope that the publication of their results and points of view will actuate further research and intensify the flow of knowledge between research and routine analytical laboratories.

I take this opportunity to thank the research groups who have contributed to this issue. Also, I wish to thank the Consultant Editor of *Talanta*, Dr. R. A. Chalmers, for his helpful suggestions, and Mrs. Anne-Lise Mikkelsen for her friendly and patient help with correspondence and coordination.

LARS KRYGER

The programme will consist of invited plenary and keynote lectures, contributed papers, and posters and workshops. In order to ensure the high quality of the programme all contributed papers will be refereed by an international panel.

The conference organizer to whom all correspondence should be addressed is:

Miss P. E. Hutchinson
Analytical Division
The Royal Society of Chemistry
Burlington House
Piccadilly
London W1V 0BN, U.K.

XXI. European Congress on Molecular Spectroscopy

EUCMOS XXI

23–28 August 1992

Technical University Vienna, Physics Department, Vienna, Austria

This 21st event in the well established series of EUCMOS-conferences will be organized by the Working Group Molecular Spectroscopy of the Austrian Society for Analytical Chemistry (ASAC) in the GÖCh, in the historic mid-European city of Vienna on behalf of the International Committee of EUCMOS. EUCMOS XXI is supported by the Working Party on Analytical Chemistry of the Federation of European Chemical Societies (WPAC/FECS) and will highlight modern trends and recent developments in the rapidly expanding field of molecular spectroscopy. Methods and applications will be treated in 9 sessions including plenary, keynote and contributed oral and poster presentations.

Main Topics:

- 1 Molecular Structure and Interactions
- 2 Surface Analysis—Methods and Applications
- 3 Hyphenated Techniques (Chromatography–Spectroscopy)
- 4 Optical Sensors
- 5 Computer Aided Molecular Spectroscopy
- 6 Theoretical Aspects
- 7 Biological Pathways
- 8 Phase Transition and Order Phenomena
- 9 General

Conveners:

- (A. J. Barnes)
(M. Grasserbauer)
(J. F. K. Huber)
(R. Kellner)
(W. Wegscheider)
(A. Karpfen)
(A. Müller)
(H. Ratajczak)

International Committee:

- President: W. J. Orville-Thomas (GB)
President Elect: A. J. Barnes (GB)
Vice Presidents: A. Müller (D), H. Ratajczak (P)

Organizing Committee:

- R. Kellner (Chairman) (A)
A. J. Barnes (GB)
J. Bellanato (E)
J. G. Grasselli (USA)
J. A. Lercher (A)
J. van der Maas (NL)
H. H. Mantsch (CDN)
Z. Meic (YU)
J. Mink (H)
A. Neckel (A)
B. Schrader (D)
K. Taga (Secretary) (A)

Programme Committee:

- W. Landvoigt (Chairman) (A)
A. Benninghoven (D)
M. Grasserbauer (A)
E. H. Korte (D)
J. Lascombe (F)
H. Malissa (A)
E. Pretsch (CH)
C. N. R. Rao (IND)
M. Tasumi (J)
L. A. Gribov (USSR)
W. Wegscheider (A)
G. Zerbi (I)

For further information please contact:

Mrs. E. M. Schaup
c/o Interconvention
Austria Center Vienna
A-1450 Vienna
Austria
Tel: +43-222-2369-2647
Fax: +43-222-2369-648
Telex: 11 18 03 icos a

Copenhagen Opt(r)ode Workshop: Opt(r)odes for charged species

4 November 1991

Risø and Radiometer A/S, Denmark.

For further information contact:

Dr. B. Skytte Jensen
MODECS, Risø National Laboratory
P.O. Box 49
DK-4000 Roskilde
Denmark

Sixth Biennial National Atomic Spectroscopy Symposium

will be held at

Polytechnic South West, Plymouth, UK

22–24 July 1992

The symposium will provide a forum where interesting and useful applications of atomic spectroscopy can be reported and discussed. In addition to plenary, invited and submitted lectures, a particular feature of the meeting will be the presentation of posters. There will also be an exhibition and a social programme for delegates and their guests.

Scientific programme will include:

Plenary Lecturers—

M. W. Blades (Vancouver, BC, Canada)
B. V. L'vov (Leningrad, USSR)
J. W. McLaren (Ottawa, Ontario, Canada)

K. Niemax (Dortmund, Germany)
B. L. Sharp (Loughborough, UK)

Invited Lecturers—

J. S. Crighton (Sunbury-on-Thames, UK)
H. Falk (Kleve, Germany)
S. J. Hill (Plymouth, UK)
D. Littlejohn (Glasgow, UK)
C. McLeod (Sheffield, UK)

G. Schlemmer (Überlingen, Germany)
P. Stockwell (Sevenoaks, UK)
J. F. Tyson (Amherst, MA, USA)
A. M. Ure (Glasgow, UK)
J. G. Williams (Egham, UK)

This meeting is organized by the Atomic Spectroscopy Group, Analytical Division of The Royal Society of Chemistry.

Further information can be obtained from the Chairman of the organizing committee:

Dr S. J. Hill, Department of Environmental Sciences, Polytechnic South West, Drake Circus, Plymouth, Devon PL4 8AA, UK.

TALANTA: CHEMICAL SENSORS ADVISORY BOARD

The Publisher and Editorial Board of *Talanta* welcome the following as members of the Advisory Board of *Talanta*: Chemical Sensors, a new feature that is inaugurated in this issue of the journal.

A. G. FOGG M. MASCINI
J. JANATA T. SHONO
S. J. MARTIN M. THOMPSON
 N. YAMAZOE

After working for ICI (Dyestuffs Division) in Manchester on pharmaceutical analysis, in the days before ICI had a pharmaceuticals division, Arnold Fogg obtained an external degree from the University of London, partly by part-time study. He then studied under Bob Chalmers and Wolf Moser at the University of Aberdeen and obtained a Ph.D. degree in 1961. From Aberdeen he came to the institution which is now Loughborough University of Technology, where he has been Reader in Analytical Chemistry since 1981. He has published 180 papers from his research. He obtained a D.Sc. degree from the University of London in 1986 and was awarded the Royal Society of Chemistry (RSC) Electroanalytical Chemistry Award in 1989. In 1988-90 he was a Vice-President of the Analytical Division of the RSC. In various roles in the RSC Electroanalytical Group, including that of Chairman, he has helped organize numerous international conferences, including the series of Anglo-Czech Electroanalytical meetings. He is a member of the Portuguese Electrochemical Society. His main interests are in electroanalytical chemistry, UV/visible spectrophotometric methods, automatic methods, and analytical solution chemistry. Current research interests are in the development of amperometric and spectrophotometric flow-injection monitors and disposable sensor devices, and the chemistries related to these. Complementary studies are of the direct adsorptive stripping voltammetry of pharmaceuticals and other large and small molecules of biological significance, and of their labelled compounds and metal complexes.

Jiri Janata received his Ph.D. in analytical chemistry from Charles University, Prague, in 1965. After postdoctoral studies at the University of Michigan he spent six years in the Corporate Laboratory of ICI in England, and in 1976 joined the faculty of the University of Utah. In 1986/85 he was on sabbatical leave at UKAEA Harwell in England, and at the Universität der Bundeswehr Munich, Germany, where he holds a Visiting Professorship in the Department of Physics. He is Professor of Materials Science and Engineering and Director of the HEDCO Microengineering Facility at the University of Utah. In 1987 he received the Senior Scientist Alexander von Humboldt Prize. His research interests include chemical sensors and electrochemistry. In this area he has published over 100 research papers, 16 chapters in co-authored books and one textbook: *Principles of Chemical Sensors*. He is inventor or co-inventor of 15 patented devices.

Stephen J. Martin received his B.S. degree in electrical engineering from Rensselaer Polytechnic Institute, Troy, New York, in 1978. He received his M.S. and Ph.D. degrees in electrical engineering from Purdue University, West Lafayette, Indiana, graduating in 1983. Since then he has been a member of Sandia National Laboratories' Microsensor Research Division in Albuquerque, NM. His current research focuses on the use of acoustic wave devices for physical and chemical sensing and for thin-film materials characterization. These sensors include surface acoustic wave (SAW) devices, acoustic plate mode (APM) devices and quartz crystal microbalances (QCMs). His sensor research has been directed towards characterization and development of novel gas and liquid phase microsensors for species detection, viscosity sensing, and corrosion monitoring. Material characterization studies have included the investigation of polymer viscoelastic properties, cross-linking reactions, as well as determination of surface area and pore size distributions in porous films. He is particularly interested in interaction mechanisms between acoustic devices and the environment.

Marco Mascini is now full Professor of Analytical Chemistry at the University of Florence. From 1963 till 1986 he was Associate Professor at the University La Sapienza and at the University Tor Vergata in Rome. In Florence he is also the co-ordinator of Ph.D. courses in Analytical Chemistry. He was among the early researchers on ion-selective electrodes, being engaged on their preparation, characterization and analytical applications. He then directed his research interests to the development of electrochemical biosensors by coupling immobilized enzymes, bacteria and whole tissues with ion-selective electrodes and amperometric probes, to obtain new devices for clinical applications, especially in the field of continuous monitoring by developing probes and procedures for *ex vivo* and *in vivo* biosensors. He is also concerned in applying biosensors for the analysis of food and drugs and developing optical biosensors. He has published over 100 papers in these areas. He was the organizer of several international meetings on Chemical Sensors and Biosensors in Italy.

Toshiyuki Shono graduated on 1954 and received his Ph.D. (Dr. of Engineering) in 1960 from the Department of Applied Chemistry, Faculty of Engineering, Osaka University. He remained at Osaka University as an Associate Professor and became Professor for Analytical Chemistry in 1974 and moved to the Osaka Institute of Technology in 1990. He was recipient of the 1984 award presented by the Japan Society for Analytical Chemistry for his contribution to the host-guest chemistry of synthetic ionophores. His current research interests lie in analytical reagents, that is, development and synthesis of ionophores, application of ion-selective membrane electrodes and derivatization in chromatography. He has co-authored more than 250 articles on these topics.

Michael Thompson was born in Rotherham, U.K., in 1942. He received the B.Sc. degree in chemistry from the University College of Swansea, U.K. in 1966, and the Ph.D. degree in analytical chemistry from McMaster University, Canada in 1970. After a period as Science Research Council Post-Doctoral Fellow at the University College of Swansea, working on vacuum ultraviolet photoelectron spectroscopy, he became a Lecturer in Instrumental Analysis at Loughborough University of Technology, U.K. In 1976 he moved to the University of Toronto where he is now Professor of Analytical Chemistry. Currently, he also holds the position of Staff Research Scientist at Toronto General Hospital. Over recent years his research interests have been in photoelectron and Auger electron spectroscopy, lipid bilayer and Langmuir-Blodgett monolayer chemistry, and chemical and biosensor technology in general. Dr. Thompson is a fellow of the Royal Society of Chemistry and the Chemical Institute of Canada. In 1982 he was presented with the Ontario Confederation of University Faculty Associations Teaching Award for his efforts in education in analytical chemistry. The D.Sc. degree was awarded by the University of Wales in 1986. Dr. Thompson received the 1989 Fisher Scientific Lecture Award of the Canadian Society for Chemistry for his research in analytical chemistry. He serves on the Editorial Boards of several international journals.

Noboru Yamazoe, born in 1940, obtained his Dr. Eng. degree from Kyushu University in 1968 after majoring in applied chemistry. He became a Research Associate in 1968, an Associate Professor in 1969, and a full Professor in 1981 at Kyushu University. He has been interested in materials science and application of functional inorganic materials such as oxide semiconductors, solid electrolytes, and oxide catalysts, and is deeply concerned with chemical sensors. His laboratory has housed the office of the Japan Association of Chemical Sensors since the foundation of the Association. He has received awards from the Electrochemical Society of Japan (1988) and the Chemical Society of Japan (1990).

For further information please contact:

Mrs. E. M. Schaup
c/o Interconvention
Austria Center Vienna
A-1450 Vienna
Austria
Tel: +43-222-2369-2647
Fax: +43-222-2369-648
Telex: 11 18 03 icos a

Copenhagen Opt(r)ode Workshop: Opt(r)odes for charged species

4 November 1991

Risø and Radiometer A/S, Denmark.

For further information contact:

Dr. B. Skytte Jensen
MODECS, Risø National Laboratory
P.O. Box 49
DK-4000 Roskilde
Denmark

Sixth Biennial National Atomic Spectroscopy Symposium

will be held at

Polytechnic South West, Plymouth, UK

22–24 July 1992

The symposium will provide a forum where interesting and useful applications of atomic spectroscopy can be reported and discussed. In addition to plenary, invited and submitted lectures, a particular feature of the meeting will be the presentation of posters. There will also be an exhibition and a social programme for delegates and their guests.

Scientific programme will include:

Plenary Lecturers—

M. W. Blades (Vancouver, BC, Canada)
B. V. L'vov (Leningrad, USSR)
J. W. McLaren (Ottawa, Ontario, Canada)

K. Niemax (Dortmund, Germany)
B. L. Sharp (Loughborough, UK)

Invited Lecturers—

J. S. Crighton (Sunbury-on-Thames, UK)
H. Falk (Kleve, Germany)
S. J. Hill (Plymouth, UK)
D. Littlejohn (Glasgow, UK)
C. McLeod (Sheffield, UK)

G. Schlemmer (Überlingen, Germany)
P. Stockwell (Sevenoaks, UK)
J. F. Tyson (Amherst, MA, USA)
A. M. Ure (Glasgow, UK)
J. G. Williams (Egham, UK)

This meeting is organized by the Atomic Spectroscopy Group, Analytical Division of The Royal Society of Chemistry.

Further information can be obtained from the Chairman of the organizing committee:

Dr S. J. Hill, Department of Environmental Sciences, Polytechnic South West, Drake Circus, Plymouth, Devon PL4 8AA, UK.

AUTHOR INDEX

- Abate L., 449
 Abruña H. D., 89
 Ackermann G., 705
 Adelantado J. V. G., 959
 Agatonović-Kuštrin S., 1347
 Agrawal Y. K., 649
 Ahmad M. N., 1399
 Akagi M., 683
 Alarie J. P., 529
 Albero M. I., 677
 Aleixo L. M., 213
 Ali S., 1041
 Alimarin I. P., 467
 Alvarez J. M. F., 391
 Alvarez-Coque M. C. G., 1285
 Amine A., 107
 Andersson M., 385
 Angnes L., 1077
 Anwar J., 1071
 Anzano J. M., 1071
 Ashley K., 1209
 Askal H. F., 1155, 1219
 Atallah R. H., 167
- Babu D. R., 175
 Balasubramanian N., 945
 Baldwin R. P., 1
 Bannykh L. N., 761
 Bansal R., 1163
 Barbosa J., 425, 1297
 Bark K.-M., 181
 Bartlett P. N., 57
 Bartsch R. A., 1453
 Basu B. J., 1431
 Bendito D. P., 1147
 Bidoglio G., 433, 999
 Birch B. J., 1257
 de Blas O. J., 857
 Bo-Xing X., 1089
 Bobbitt D. R., 419
 Bodalbhai L., 95
 Bol'shova T. A., 467
 Bond A. M., 65
 Bos M., 723
 Bosch C. M., 1297
 Bouklouze A. A., 929
 Bradford V. Q., 57
 Brajter-Toth A., 95
 Braun R. D., 205
 Brindle I. D., 1137
 Brodersen K., 785
 Broekaert J. A. C., 863
 Brown F. R., 309
 Brune S. N., 419
 Busch K. W., 589
 Busch M. A., 589
- Cámara C., 1387
 Cano-Pavón J. M., 445
 Canovese L., 697
 de Castro M. D. L., 125, 291, 1227
 Cathum S. J., 157
 Cavalli P., 433
 Cerdá V., 1475
 Cha S. K., 89
 Chakrabarti C. L., 157
 Chang W.-B., 1159
 Chao-Biao H., 1089
 Chapman B., 233
 Chauveau S., 1279
 Che G., 111
- Checkoway H., 365
 Chen D., 1227
 Chen H., 1137
 Cheng S.-Z., 1487
 Cheng W., 1143
 Cheng Z.-P., 1487
 Chierice G. O., 735
 Chikuma M., 779
 Chiswell B., 641
 Christensen J. K., 101
 Christian G. D., 119, 851, 929
 Chung H. K., 355
 Ci Y.-X., 1159
 Cladera A., 1475
 Clark G. D., 119
 Cléroux C., 951
 Conde C. P., 1387
 Cooks R. G., 195
 Córdoba M. H., 1247
 Coria-García J. C., 767
 Craston D. H., 17
 Crepaldi G., 405
 Cristofol E., 445
 Cruz J. S., 1303
 Cunningham D. D., 49
 Cvijović M., 455
- Dalzoppo D., 405
 Darvell B. W., 875, 1027
 Das C. M., 347
 Dasgupta P. K., 133
 De Lima C. G., 1303
 Desai M. N., 649
 Devi S., 753
 Dexiong F., 1493
 Diaz A. N., 571
 Dills R. L., 365
 Dinesan M. K., 815
 Djurdjević P., 455
 Dong K. L., 101
 Dong S., 111, 133
 Dorrzapf Jr. A. F., 259
 Dorsey J. G., 237
 Dunning Jr. J. W., 631
 Džudović R. M., 672
- Ebdon L., 607
 Eberlin M. N., 213
 Efstathiou C. E., 295
 El-Jammal A., 929
 Elnemma E. M., 561
 Emara K. M., 1219
 Ensafi A. A., 229
 Erickson B. C., 1459
 Estela J. M., 1475
- Fadeeva V. I., 267
 Faid-Allah H. M., 535
 Fang Z., 613
 Fatibello-Filho O., 541
 Fedele D., 405
 Fernández L., 339
 Fernández P., 1387
 Fernando Q., 309
 Flores J. R., 1261
 Forcé R. K., 181
 Forsyth D. S., 951
 Frankenberger Jr. W. T., 245
 Freund M., 95
 Fritz J. S., 253
 Fu C., 1481
- Fuchang W., 801
 Fujita K., 343
 Fujita R., 521
 Fujita Y., 343, 683
- Gallego M., 1241
 Gao Z., 1177
 García A. P., 959
 García P., 747
 García I. L., 1247
 García M. S., 677
 Gawargious Y. A., 785
 Gázquez D., 747
 Genestar C., 1353
 Georgiou C. A., 689
 Gerhardinger C., 405
 Ghezze E., 405
 Godinho O. E. S., 213
 Golabi S. M., 1253
 Golightly D. W., 259
 Gonçalves M. L. S. S., 1111
 Gong W.-L., 1159
 Goo M.-J., 1453
 Gordon G., 145
 Gosser Jr. D. K., 715
 Goto E., 139
 Gowda C. C., 1427
 Grases F., 1353
 Grenthe I., 433, 999
 Griffiths P. R., 839
 Guanghan L., 977
 Gübeli T., 851
 Guilbault G. G., 49, 541, 1197
 Guo T., 613
 Gupta D., 283
 Gupta J. G. S., 1083
 Gupta J. K., 1167
 Gutiérrez A., 1387
 Györfi-Buzási A., 1265
- Hadjiioannou T. P., 295, 689
 Hague S., 637
 Hajizadeh K., 37
 Halsall H. B., 37
 Hamada M. A., 561
 Hamon M., 1279
 Hansen E. H., 275
 Hardy J. K., 1381
 Hart J. P., 1257
 Hassan S. S. M., 561
 Hayashita T., 1453
 Hayward M. J., 195
 He H.-B., 1159
 Heineman W. R., 37
 Hemmings M. J., 151
 Hengchuan L., 1143
 Hidalgo M., 483
 Hill S. J., 607
 Hioki A., 397
 Holcombe J. A., 503
 Hongbo C., 989
 Hou W., 557
 Hoyer B., 115
 Hsu C.-G., 1051
 Huang S., 785
 Huashan Z., 669
 Husain S., 897
- Ikeo N., 1325
 Ingle Jr. J. D., 355
 Iqbal M. S., 603

- Ishii H., 511
 Itoh S.-I., 325, 871
 Ivanov V. M., 267
 Ivšić A. G., 1403
 Iwado A., 779
- Jain A., 283
 Jakšić L. N., 333
 Jamwal V. S., 217
 Jančářová I., 1093
 Janoš P., 1445
 Javed N. A., 603
 Jelinek I., 1309
 Jespersen A. M., 1369
 Ji H., 73
 Jianwei Z., 909
 Jieke C., 669
 Jones C. P., 17
 Jones E. A., 151
 Jones P., 607
 Junyan S., 989
- Kalia S. B., 217
 Kalman D. A., 167, 365
 Kanapathy K., 1399
 Karandikar B. M., 335
 Karayannis M. I., 1019
 Karolev A., 1223
 Kasem K. K., 89
 Kassai-Tánczos R., 1439
 Kato K., 343, 683
 Katritzky A. R., 201, 535
 Kauffmann J.-M., 107
 Kaur A., 1163
 Kawase A., 397
 Kawazumi H., 965
 Kent S. D., 365
 Khan M. A., 637
 Khanna P. P., 329
 Khopkar S. M., 971
 Kifayatullah M., 897
 Kihara S., 653
 Kim J. S., 1453
 Kitada K., 1119
 Koch S., 705
 Kohata K., 511
 Kolev S. D., 125
 Konidari C. N., 1019
 Korba T., 723
 Kotiaho T., 195
 Kountourellis J. E., 233
 Koupparis M. A., 689
 Kowalski B. R., 1459
 Kozuka S., 1119
 Křížová H., 1093
 Kryger L., VII, 101
 Kubala S. W., 589
 Kubáň V., 1093
 Kubota M., 397
 Kudryavtsev G. V., 267
 Kumar S., 217
 Kuroda R., 1119
- Lafisca T. A., 995
 Laitinen P. H. A., v
 Lam J. N., 535
 Lambertos G., 1235
 Lapolla A., 405
 Larsen J., 981
 Leleu E., 1279
 Lengauer W., 659
 León-González M. E., 1341
 Leung V. W.-H., 875, 1027
- Lexa J., 1393
 Li P., 1177
 Lian X.-M., 1051
 Liang C., 1077
 Liberman S. J., 313
 van der Linden W. E., 723
 Lister A. K., 195
 Lorán C. P., 497
 Luscombe D. L., 65
- Maggiore R., 449
 Main M. V., 253
 Malik A. K., 941
 Markopoulou C. K., 233
 Marques A. L. B., 735
 Martens D. A., 245
 Martínez V. P., 959
 Martínez-Lozano C., 1235
 Masana A., 483
 Massoumi A., 229
 Matousek J. P., 375
 Matsui M., 653
 Matyjaszewski K., 335
 May P. M., 1409, 1419
 Mayanna S. M., 1427
 Méndez J. H., 857
 Menon S. K., 649
 Mifune M., 779
 Mihajlović R. P., 333, 672
 Mikael P., 275
 Ming-Neng S., 1089
 Miura N., 1169
 Mizuno T., 325, 871
 Moore C. E., 493
 de la Morena Pardo M. L., 1261
 Morgan J. W., 259
 Mori I., 343, 683
 Motohashi N., 779
 Motomizu S., 477
 Moye H. A., 913
 Mukherjee P. K., 329
 Muñoz M., 483
 Muntuta-Kinyanta C., 1381
 Murakami M., 1129
 Murr N. E., 17
 Murray C. G., 27
 Murray K., 1409, 1419
 Murty B. N., 1335
- Nagourney S. J., 995
 Naidu P. R., 175
 Namboothiri K. K., 945
 Naser N., 81
 Navarro-Villoslada F., 1341
 Němcová I., 1309
 Nesterenko P. N., 267
 Neto G. de O., 213
 Nevado J. J. B., 1261
 Niemczyk T. M., 767
 Nigam P. C., 627
 Nishimura H., 965
 Nørgaard L., 275
 Noszál B., 1439
 Nowak R. J., 27
- O'Halloran K. R., 641
 O'Kennedy R., 391
 Odo J., 779
 Ogawa T., 965
 Oguma K., 1119
 Ogura T., 309
 Ohta K., 325, 871
 Okazaki Y., 343
- Olin A., 385, 413
 Olsina R., 339
 Omenetto N., 433, 999
 Ordoukhanian J., 1469
 Othman R. A., 773
 Otsubo Y., 965
- Pacáková V., 1445
 Pacey G. E., 145, 1315
 Padma D. K., 1431
 Palumbo M., 405
 Palys M., 723
 Pan J.-M., 1051
 Pande R., 1015
 Parkash R., 1163
 Pastore T. C. M., 1303
 Pásztor Zs., 1265
 Patel B. M., 913
 Patriarche G. J., 107, 929
 de Paz J. L. P., 857
 Pei J., 1185
 Peihui Y., 1493
 Pell R. J., 1459
 Pentari J. G., 295
 Pérez-Arribas L. V., 1341
 Pérez-Bendito D., 359, 1273
 Pérez-Ruiz T., 1235
 Pesavento M., 1099
 Petrukhin O. M., 467
 Pettersson J., 413
 Pietarinen C., 995
 Pilarska M., 201
 Po L., 1143
 Polo-Díez L. M., 1341
 Porter C. J., 405
 Pournaghi-Azar M. H., 1469
 Prasad K. M. M. K., 793
 Prasad S., 627
 Profumo A., 1099
 Purohit R., 753
 Puschett J. B., 335
 Pyle S. M., 1125
- Qi P., 433, 999
 Qiheng X., 909
 Qiping L., 669
 Qu Y.-B., 1061
 Quintero M. C., 359, 1273
 Qureshi P. M., 1041
 Qureshi S. Z., 637
- Radanović D., 455
 Radulović Lj. Z. D., 1347
 Raghavan R., 525
 Raha S., 525
 Raheem S., 793
 Rajagopalan S. R., 1431
 Ramakrishna T. V., 945
 Ramamurthy C. K., 1335
 Ramana K. V., 937
 Ramos G. R., 1285
 Rao A. L. J., 941
 Rao A. R. M., 937
 Rao B. S., 335
 Rao D. M., 1047
 Rao J. V., 1107
 Rao M. S. P., 937
 Rao R. N., 897
 Rao T. T., 1057, 1107
 Rashid F., 603
 Rathi M. S., 329
 Reddy D. V., 1047
 Reddy K. H., 1047

- Rehani S. K., 1163
 Reig F. B., 959
 Renuka A., 1009
 Richts U., 863
 Rigano C., 449
 Ríos A., 125, 291, 1227, 1359
 de Robertis A., 439
 Robouch P., 999
 Rodenas L. G., 313
 Rohwedder J. J. R., 213
 Rojas F. S., 445
 Rolison D. R., 27
 Romero J. M. C., 1111
 Romero J. S. E., 1285
 Romero-Saldaña M., 291
 Rongshan L., 741
 Rubio S., 1147
 Růžička J., 119, 851
 Rychlovský P., 1309
- Saad B., 1399
 Saeed A., 637
 Saez A., 677
 Safavi A., 229
 Sagi S. R., 937
 Sahoo S. K., 789
 Sailaja A., 1057, 1107
 Saito Y., 779
 Sakata N., 1325
 Saleh G. A., 1219
 Salvadó V., 483
 Sampayo M. A., 1111
 Sánchez M., 747
 Sánchez-Pedreño C., 677
 Sanghi S. K., 283
 Santelli R. E., 1241
 Santos-Delgado M. J., 1341
 Sanz-Nebot V., 425
 Sastry C. S. P., 1057, 1107
 Savage G. P., 201
 Savitchev A. T., 267
 Schwartz C. A., 1303
 Scott W. D., 889
 Sebben A., 1303
 Sedykh E. M., 761
 Seraglia R., 405
 Setty M. M., 1125
 Shah N., 649
 Shakuntala K., 1009
 Shamsuddin K. M., 1041
 Shaopu L., 801
 Sharma D. K., 217, 665
 Sharma R. D., 665
 Shengjun M., 503
 Shigemura N., 653
 Shinde V. M., 223
 Shiowatana J., 375
 Showkati-Shishevan M., 1253
 Shuanglong H., 977
- Sicilia D., 1147
 Silva M., 303, 359, 1273
 Smirnova N. S., 267
 Smith K., 145
 Smyth M. R., 391
 Snyder P. A., 903
 Sørenberg H., 1369
 Sollis J. M. F., 1111
 Sørensen H. H., 1369
 van Staden J. F., 1033
 de Stefano C., 439, 449
 Stewart J. T., 631
 Stewart K. K., 283
 Strelow F. W. E., 923
 Štulík K., 1393, 1445
 Štulíková M., 805
 Sud A., 217
 Suleiman A. A., 541, 1197
 Sundaramurthi N. M., 223
 Svensmark B., 981
 Sweetin D. L., 145
 Syamsundar S., 1335
 Syed A. A., 815
 Szilvássy-Vámos Zs., 1265
- Taha Z., 81, 487
 Takada T., 1129
 Takeda Y., 1325
 Tamaki J., 1169
 Tamhina B., 1403
 Tanaka H., 779
 Tandon S. G., 1015
 Tanet G., 433
 TeVrucht M. L. E., 839
 Thomas L. C., 773
 Thomsen K. N., 1, 101
 Tikhomirova T. I., 267
 Tilotta D. C., 589
 Timerbaev A. R., 467
 Tölg G., 863
 Tomás V., 1235
 Torrero E., 425
 Toyoda M., 343, 683
 Traldi P., 405
 Tschöpel P., 863
 Tuzhi P., 741
- Uguagliati P., 697
 Umetani S., 653
 Underwood F. A., 233
- Vajgand V. J., 672
 Vajgand V. V., 333
 Valcárcel M., 125, 291, 303, 1227, 1241, 1359
 Valiente M., 483
 Vasiljević M., 1347
 Velasco A., 303
 Verma B. C., 217
- Verma K. K., 283
 Veselinović D., 455
 Vilhena M. F. C., 1111
 Villarta R. L., 49
 Vin Y. Y., 971
 Vinther A., 1369
 Vo-Dinh T., 529
 Voigtman E., 903
 Volynsky A. B., 761
- Wan-Li M., 1291
 von Wandruszka R., 189, 497
 Wang E., 73, 547, 557
 Wang J., 81, 487, 1077
 Wang N.-X., 711
 Webb K. M., 889
 Weinberger R., 913
 Welsh T. A., 27
 Weiz B., 613
 Werner U., 785
 Whitaker R. G., 57
 Wilcox K., 1315
 Williams D. E., 17
 Winefordner J. D., 1071
 Wrigley T. J., 889
 Wring S. A., 1257
- Xiaoming L., 977
 Xie X., 1197
 Xing-Cun H., 319
 Xu C., 1169
 Xu J., 1191
- Yadav R. B., 1335
 Yamamoto K., 477
 Yamane T., 139
 Yamazoe N., 1169
 Yang G.-F., 1487
 Yin Q., 1185
 Ying P. T., 237
 Yoo A., 493
 Yoshida N., 683
 Yoshikuni N., 515
 Yu-Zhi F., 1089
 Yuan X., 189
- Zable J., 119
 Zhang F., 715
 Zhang G., 1481
 Zhang Z.-Q., 1487
 Zhao Z., 1177
 Zhaoliang Y., 1493
 Zhi-Liang J., 621
 Zhike H., 977
 Zhong J., 1185
 Zhongping Y., 741
 Zhou J., 547
 Zhuang X., 1191